Sun. May 26, 2019

[E] Poster | P (Space and Planetary Sciences)：P-PS Planetary Sciences

3:30 PM - 5:00 PM JST | 6:30 AM - 8:00 AM UTC | Poster Hall International Exhibition Hall8, Makuhari Messe_3

[P-PS04] Mars and Mars system: results from a broad spectrum of Mars studies and aspects for future missions

convener:Hideaki Miyamoto(University of Tokyo), Tomohiro Usui(Earth-Life Science Institute, Tokyo Institute of Technology), Ayako Matsuoka(Research Division for Space Plasma, Institute of Space and Astronautical Science, Japan Aerospace Exploration Agency), Sushil K Atreya(University of Michigan Ann Arbor)

[PPS04-P01] Observation of the O_2^+ first negative band (1,0) emissions in the Mars ionosphere with a visible spectrograph on Haleakala T60

*Toshihisa Suzuki[1], Masato Kagitani[1], Takeshi Sakanoi[1] (1.PPARC, Graduate School of Science, Tohoku University)

[PPS04-P02] Search of shallow subsurface reflectors around RSLs in Martian Chryse and Acidalia planitiae by the MRO/SHARAD public data

*Aina Oura[1], Yasumasa Kasaba[1], Atsushi Kumamoto[1], Rina Noguchi[2], Tomohiro Usui[2], Ken Ishiyama[2], Chihiro Uemura[3] (1.Tohoku University, 2.Institute of Space and Astronautical Science, 3.SOKENDAI)

[PPS04-P03] Detecting surface changes on Mars using principle component analysis of repeat imagery

*Reid Parsons[1], Hideaki Miyamoto[1] (1.University of Tokyo)

[PPS04-P04] Evaluation of the detectability of hydrated salts on recurring slope lineae on Mars.

*Shoko Imamura[1,2], Yasuhito Sekine[2], Hiroyuki Kurokawa[2] (1.University of Tokyo, 2.Earth-Life Science Institute, Tokyo Institute of Technology)

[PPS04-P05] Frequency of ice sheet growth recorded on Mons Pavonis, Mars

*Tomohiro Kanzaki[1], Reid Parsons[1,2], Ryodo Hemmi[1], Hideaki Miyamoto[1] (1.University of Tokyo, 2.Fitchburg State University)

[PPS04-P06] Development of Life Detection Microscope (LDM) for *in situ* imaging of living cells on Mars surface

*Yoshitaka Yoshimura[1], Akihiko Yamagishi[2], Takehiko Satoh[3], Atsuo Miyakawa[2], Eiichi Imai[4], Satoshi Sasaki[5], Kensei Kobayashi[6], Yoko Kebukawa[6], Tomoka Okada[6], Keigo Enya[3], Hikaru Yabuta[7], Takeshi Naganuma[7], Hajime Mita[8], Kazuhisa Fujita[3], Tomohiro Usui[3] (1.College of Agriculture, Tamagawa University, 2.Tokyo University of Pharmacy and Life Science, 3.Japan Aerospace Exploration Agency, 4.Nagaoka University of Technology, 5.Tokyo University of Technology, 6.Yokohama National University, 7.Hiroshima University, 8.Fukuoka Institute of Technology)

[PPS04-P07] Development of a Mars Web-GIS for viewing multiple kinds of spectral data from orbiters

*Yuya Matsubara[1], Hironori Fukuchi[1], Yoshiko Ogawa[1], Yohei Hayashi[2] (1.The University of Aizu, 2.National Astronomical Observatory of Japan)

[PPS04-P08] **Visualization and Analysis of the Surface of Mars with NASA's Mars Trek Portal**

*Brian Hamilton Day[1], Emily Law[2] (1.NASA Solar System Exploration Research Virtual Institute, NASA Ames Research Center, 2.NASA Jet Propulsion Laboratory, California Institute of Technology)

[PPS04-P09] Increase in Dissolved Iron Concentration from Fayalite by UltravioletA・C Irradiation

*Nobuo Komori[1] (1.The United Graduate School of Education Tokyo Gakugei University)

[PPS04-P10] Small-scale ridges newly identified on the equatorial region of the Phobos nearside

*Ryodo Hemmi[1], Hiroshi Kikuchi[1], Hideaki Miyamoto[1] (1.The University of Tokyo)

[PPS04-P11] Development of a compact Muography instrument for future Mars exploration missions

*Hiroaki Kamiyoshihara[1], Tetsuro Ninomiya[1], Yuri Yoshihara[1], Kenji Shimazoe[1], Hiroyuki Takahashi[1], Hiroyuki Tanaka[1], Hideaki Miyamoto[1] (1.University of Tokyo)

[E] Poster | P (Space and Planetary Sciences)：P-PS Planetary Sciences

5:15 PM - 6:30 PM JST | 8:15 AM - 9:30 AM UTC | Poster Hall International Exhibition Hall8, Makuhari Messe_4

[P-PS04] Mars and Mars system: results from a broad spectrum of Mars studies and aspects for future missions

convener:Hideaki Miyamoto(University of Tokyo), Tomohiro Usui(Earth-Life Science Institute, Tokyo Institute of Technology), Ayako Matsuoka(Research Division for Space Plasma, Institute of Space and Astronautical Science, Japan Aerospace Exploration Agency), Sushil K Atreya(University of Michigan Ann Arbor)

[PPS04-P01] Observation of the O_2^+ first negative band (1,0) emissions in the Mars ionosphere with a visible spectrograph on Haleakala T60

*Toshihisa Suzuki[1], Masato Kagitani[1], Takeshi Sakanoi[1] (1.PPARC, Graduate School of Science, Tohoku University)

[PPS04-P02] Search of shallow subsurface reflectors around RSLs in Martian Chryse and Acidalia planitiae by the MRO/SHARAD public data

*Aina Oura[1], Yasumasa Kasaba[1], Atsushi Kumamoto[1], Rina Noguchi[2], Tomohiro Usui[2], Ken Ishiyama[2], Chihiro Uemura[3] (1.Tohoku University, 2.Institute of Space and Astronautical Science, 3.SOKENDAI)

[PPS04-P03] Detecting surface changes on Mars using principle component analysis of repeat imagery

*Reid Parsons[1], Hideaki Miyamoto[1] (1.University of Tokyo)

[PPS04-P04] Evaluation of the detectability of hydrated salts on recurring slope lineae on Mars.

*Shoko Imamura[1,2], Yasuhito Sekine[2], Hiroyuki Kurokawa[2] (1.University of Tokyo, 2.Earth-Life Science Institute, Tokyo Institute of Technology)

[PPS04-P05] Frequency of ice sheet growth recorded on Mons Pavonis, Mars

*Tomohiro Kanzaki[1], Reid Parsons[1,2], Ryodo Hemmi[1], Hideaki Miyamoto[1] (1.University of Tokyo, 2.Fitchburg State University)

[PPS04-P06] Development of Life Detection Microscope (LDM) for *in situ* imaging of living cells on Mars surface

*Yoshitaka Yoshimura[1], Akihiko Yamagishi[2], Takehiko Satoh[3], Atsuo Miyakawa[2], Eiichi Imai[4], Satoshi Sasaki[5], Kensei Kobayashi[6], Yoko Kebukawa[6], Tomoka Okada[6], Keigo Enya[3], Hikaru Yabuta[7], Takeshi Naganuma[7], Hajime Mita[8], Kazuhisa Fujita[3], Tomohiro Usui[3] (1.College of Agriculture, Tamagawa University, 2.Tokyo University of Pharmacy and Life Science, 3.Japan Aerospace Exploration Agency, 4.Nagaoka University of Technology, 5.Tokyo University of Technology, 6.Yokohama National University, 7.Hiroshima University, 8.Fukuoka Institute of Technology)

[PPS04-P07] Development of a Mars Web-GIS for viewing multiple kinds of spectral data from orbiters

*Yuya Matsubara[1], Hironori Fukuchi[1], Yoshiko Ogawa[1], Yohei Hayashi[2] (1.The University of Aizu, 2.National Astronomical Observatory of Japan)

[PPS04-P08] Visualization and Analysis of the Surface of Mars with NASA's Mars Trek Portal

*Brian Hamilton Day[1], Emily Law[2] (1.NASA Solar System Exploration Research Virtual Institute, NASA Ames Research Center, 2.NASA Jet Propulsion Laboratory, California Institute of Technology)

[PPS04-P09] Increase in Dissolved Iron Concentration from Fayalite by UltravioletA・C Irradiation

*Nobuo Komori[1] (1.The United Graduate School of Education Tokyo Gakugei University)

[PPS04-P10] Small-scale ridges newly identified on the equatorial region of the Phobos nearside

*Ryodo Hemmi[1], Hiroshi Kikuchi[1], Hideaki Miyamoto[1] (1.The University of Tokyo)

[PPS04-P11] Development of a compact Muography instrument for future Mars exploration missions

*Hiroaki Kamiyoshihara[1], Tetsuro Ninomiya[1], Yuri Yoshihara[1], Kenji Shimazoe[1], Hiroyuki Takahashi[1], Hiroyuki Tanaka[1], Hideaki Miyamoto[1] (1.University of Tokyo)

[E] Poster | P (Space and Planetary Sciences)：P-EM Solar-Terrestrial Sciences, Space Electromagnetism & Space Environment

10:45 AM - 12:15 PM JST | 1:45 AM - 3:15 AM UTC | Poster Hall International Exhibition Hall8, Makuhari Messe_2

[P-EM14] Recent Advances in Ionosphere Observation and Modeling for Monitoring and Forecast

convener:Yang-Yi Sun(China University of Geosciences), CHIYEN LIN(Center for Astronautical Physics and Engineering, National Central University, TAIWAN), MINYANG CHOU(National Cheng Kung University)

[PEM14-P01] **The Daytime and Nighttime Mapped Whistler Plasmapause Observed by DEMETER**

*ChaoYen Chen[1,2], Tiger J. Y. Liu[1,2,3] (1.Institute of Space Science, National Central University, Taiwan, 2.Center for Astronautical Physics and Engineering, National Central University, Taiwan , 3.Center for Space and Remote Sensing Research, National Central University, Taiwan)

[PEM14-P02] Global Plasma Density Irregularity Distributions Observed by Advanced Ionospheric Probe Onboard FORMOSAT-5 Satellite

*Chi-Kuang Chao[1], Yi-Wun Chen[1] (1.Graduate Institute of Space Science, National Central University)

[PEM14-P03] The First Result on Ionospheric Space Weather of FORMOSAT-5/AIP Ion Density

*FU-YUAN CHANG[1], JANN-YENQ Liu[1], Chi-Kuang Chao[1] (1.National Central University)

[PEM14-P04] **The global total electron content reconstruction in the local time frame**

*Tsung-Che Tsai[1,2], Hau-Kun Jhuang[3], Lou-Chuang Lee[3,4,5], Yi-Ying Ho[4] (1.National Center for High-Performance Computing, National Applied Research Laboratories, Hsinchu, Taiwan, 2.Department of Civil Engineering, National Chiao Tung University, Hsinchu, Taiwan., 3.Department of Geoscience, National Taiwan University, Taipei, Taiwan., 4.Institute of Earth Science, Academia Sinica, Nankang, Taipei, Taiwan., 5.Institute of Space Science, National Central University, Jhongli, Taiwan.)

[PEM14-P05] Research on impacts of power line harmonic radiation on ionospheric parameters

*Qiang Guo[1], Jing Wu[1], Ling Yang[1] (1.Beihang University)

[PEM14-P06] **Analysis of cosmic rays dynamics and ionospheric parameters during increased solar activity and magnetic storms**

*Oksana Mandrikova[1], Yurii Polozov[1], Bogdana Mandrikova[1,2] (1.Institute of Cosmophysical Research and Radio Wave Propagation, Far Eastern Branch of the Russian Academy of Sciences, 2.Saint Petersburg Electrotechnical University "LETI")

[PEM14-P07] King Tidal Effects on the ionosphere during the period of 2000 to 2017

*TsungYu Wu[1], JANN-YENQ Liu[1] (1.Institute of Space Science, NCU, Taiwan)

[PEM14-P08] SuperDARN near range echoes and higher resolution measurement - recent improvement and future

*Akira Sessai Yukimatu[1,2] (1.National Institute of Polar Research, 2.SOKENDAI)

[PEM14-P09] **The ionospheric wave peak structures in the low latitude region and their seasonal, and solar activity dependence based on Global Ionosphere Maps**

*Hau-Kun Jhuang[1], Tsung-Che Tsai[2,3], Lou-Chuang Lee[1,4,5], Yi-Ying Ho[4] (1.Department of Geosciences, National Taiwan University, Taipei, Taiwan, 2.National Center for High-performance Computing, National Applied Research Laboratories, Hsinchu, Taiwan, 3.Department of Civil Engineering, National Chiao Tung University, Hsinchu, Taiwan, 4.Institute of Earth Science, Academia Sinica, Nankang, Taipei, Taiwan, 5.Institute of Space Science, National Central University, Jhongli, Taiwan)

[E] Poster | P (Space and Planetary Sciences)：P-EM Solar-Terrestrial Sciences, Space Electromagnetism & Space Environment

5:15 PM - 6:30 PM JST | 8:15 AM - 9:30 AM UTC | Poster Hall International Exhibition Hall8, Makuhari Messe_5

[P-EM14] Recent Advances in Ionosphere Observation and Modeling for Monitoring and Forecast

convener:Yang-Yi Sun(China University of Geosciences), CHIYEN LIN(Center for Astronautical Physics and Engineering, National Central University, TAIWAN), MINYANG CHOU(National Cheng Kung University)

[PEM14-P01] **The Daytime and Nighttime Mapped Whistler Plasmapause Observed by DEMETER**

*ChaoYen Chen[1,2], Tiger J. Y. Liu[1,2,3] (1.Institute of Space Science, National Central University, Taiwan, 2.Center for Astronautical Physics and Engineering, National Central University, Taiwan , 3.Center for Space and Remote Sensing Research, National Central University, Taiwan)

[PEM14-P02] Global Plasma Density Irregularity Distributions Observed by Advanced Ionospheric Probe Onboard FORMOSAT-5 Satellite

*Chi-Kuang Chao[1], Yi-Wun Chen[1] (1.Graduate Institute of Space Science, National Central University)

[PEM14-P03] The First Result on Ionospheric Space Weather of FORMOSAT-5/AIP Ion Density

*FU-YUAN CHANG[1], JANN-YENQ Liu[1], Chi-Kuang Chao[1] (1.National Central University)

[PEM14-P04] **The global total electron content reconstruction in the local time frame**

*Tsung-Che Tsai[1,2], Hau-Kun Jhuang[3], Lou-Chuang Lee[3,4,5], Yi-Ying Ho[4] (1.National Center for High-Performance Computing, National Applied Research Laboratories, Hsinchu, Taiwan, 2.Department of Civil Engineering, National Chiao Tung University, Hsinchu, Taiwan., 3.Department of Geoscience, National Taiwan University, Taipei, Taiwan., 4.Institute of Earth Science, Academia Sinica, Nankang, Taipei, Taiwan., 5.Institute of Space Science, National Central University, Jhongli, Taiwan.)

[PEM14-P05] Research on impacts of power line harmonic radiation on ionospheric parameters

*Qiang Guo[1], Jing Wu[1], Ling Yang[1] (1.Beihang University)

[PEM14-P06] **Analysis of cosmic rays dynamics and ionospheric parameters during increased solar activity and magnetic storms**

*Oksana Mandrikova[1], Yurii Polozov[1], Bogdana Mandrikova[1,2] (1.Institute of Cosmophysical Research and Radio Wave Propagation, Far Eastern Branch of the Russian Academy of Sciences, 2.Saint Petersburg Electrotechnical University "LETI")

[PEM14-P07] King Tidal Effects on the ionosphere during the period of 2000 to 2017

*TsungYu Wu[1], JANN-YENQ Liu[1] (1.Institute of Space Science, NCU, Taiwan)

[PEM14-P08] SuperDARN near range echoes and higher resolution measurement - recent improvement and future

*Akira Sessai Yukimatu[1,2] (1.National Institute of Polar Research, 2.SOKENDAI)

[PEM14-P09] **The ionospheric wave peak structures in the low latitude region and their seasonal, and solar activity dependence based on Global Ionosphere Maps**

*Hau-Kun Jhuang[1], Tsung-Che Tsai[2,3], Lou-Chuang Lee[1,4,5], Yi-Ying Ho[4] (1.Department of Geosciences, National Taiwan University, Taipei, Taiwan, 2.National Center for High-performance Computing, National Applied Research Laboratories, Hsinchu, Taiwan, 3.Department of Civil Engineering, National Chiao Tung University, Hsinchu, Taiwan, 4.Institute of Earth Science, Academia Sinica, Nankang, Taipei, Taiwan, 5.Institute of Space Science, National Central University, Jhongli, Taiwan)

[E] Poster | P (Space and Planetary Sciences)：P-CG Complex & General

3:30 PM - 5:00 PM JST | 6:30 AM - 8:00 AM UTC | Poster Hall International Exhibition Hall8, Makuhari Messe_5

[P-CG21] Future Missions and instrumentation for space and planetary science

convener:Mitsunori Ozaki(Faculty of Electrical and Computer Engineering, Institute of Science and Engineering, Kanazawa University), Satoshi Kasahara(The university of Tokyo), Shingo Kameda(School of Science, Rikkyo University), Kazuo Yoshioka(Graduate School of frontier Science, The University of Tokyo)

[PCG21-P01] Visible and ultraviolet imagers for auroral and airglow observations by FACTORS - a future satellite mission for understanding the coupling and transportation processes in the upper atmosphere

*Takeshi Sakanoi[1], Masafumi Hirahara[2], Takuo T. Tsuda[3], Kazushi Asamura[4], Yoshizumi Miyoshi[2], Tomo-Hiko Watanabe[5], Takanori Nishiyama[6], Shin-ichiro Oyama[2,7], Yoshifumi Saito[4], Keisuke Hosokawa[3], Hirotsugu Kojima[8], Naritoshi Kitamura[9], Yasunobu Ogawa[5], Masatoshi Yamauchi[10], Ayako Matsuoka[4], Naoshi Yagi[1], Fukizawa Fukizawa[1], Genki Ishizawa[11] (1.Planetary Plasma and Atmospheric Research Center, Graduate School of Science, Tohoku University, 2.ISEE, Nagoya University, 3.Graduate School of Informatics and Engineering, School of Informatics and Engineering, The University of Electro-Communications, 4.ISAS/JAXA, 5.Graduate School of Science, Nagoya University, 6.National Institute for Polar Research, 7.University of Oulu, Finland, 8.RISH, Kyoto University, 9.Graduate School of Science, the University of Tokyo, Tokyo, 10.IRF Kiruna, Sweden, 11.Graduate School of Science, Tohoku University)

[PCG21-P02] Spatio-temporal analysis of flash aurora using Convolutional Neural Network

*Toki Genda[1], Takumi Inoue[1], Mitsunori Ozaki[1], Satoshi Yagitani[1], Imamura Kousuke[1], Kazuo Shiokawa[2], Yoshizumi Miyoshi[2], Shin-ichiro Oyama[2], Ryuho Kataoka[3], Yusuke Ebihara[4], Keisuke Hosokawa[5] (1.Kanazawa Univ., 2.Nagoya Univ., 3.NIPR, 4.Kyoto Univ., 5.UEC)

[PCG21-P03] Study on the pulse noise removal technique for Pc1 geomagnetic pulsations on the ground by signal processing

*Fumiya Komase[1], Tomohiro Inoue[1], Mitsunori Ozaki[1], Satoshi Yagitani[1], Kazuo Shiokawa[2], Masahito Nose[2], Tsutomu Nagatsuma[3] (1.Kanazawa Univ., 2.Nagoya Univ., 3.NICT)

[PCG21-P04] Application of magneto-impedance sensor to geomagnetic field measurements

*Masahito Nose[1], Reiko Nomura[2], Kazushi Asamura[3], Hitoshi Aoyama[4], Takeshi Kawano[4], Ayako Matsuoka[3], Kentarou Kitamura[5], Yukinobu Koyama[6], Haruhisa Matsumoto[7], Masafumi Hirahara[1] (1.Institute for Space-Earth Environmental Research, Nagoya University, 2.National Astronomical Observatory of Japan, 3.Institute of Space and Astronautical Science, Japan Aerospace Exploration Agency, 4.Aichi Steel Corporation, 5.National Institute of Technology, Tokuyama College, 6.National Institute of Technology, Oita College, 7.Research and Development Directorate, Japan Aerospace Exploration Agency)

[PCG21-P05] Observation of the Ionospheric Currents by the CubeSat at the Low and Middle Latitude

*Kentarou Kitamura[1], Kazumasa Imai[2], Taku Takada[2], Manabu Shinohara[3], Makoto Wakabayashi[4], KOSEN Space Collaboration Group (1.National Institute of Technology, Tokuyama Collge, 2.National Institute of Technology, Kochi Collge, 3.National Institute of Technology, Kagoshima Collge, 4.National Institute of Technology, Niihama Collge)

[PCG21-P06] Basic study on miniaturization of electric field instrument for plasma wave observations by ASIC technology

*Yuya Tokunaga[1], Mitsunori Ozaki[1], Keigo Ishisaka[2], Hirotsugu Kojima[3], Satoshi Yagitani[1], Takahiro Zushi[3] (1.Kanazawa University, 2.Toyama Prefectural University, 3.Kyoto University)

[PCG21-P07] Evaluation of radiation tolerance of electronics parts used for the ultra-small mission

*Riku Katsuse[1], Kazuo Yoshioka[1], Masaki Kuwabara[2], Reina Hikida[1], Shogo Arao[1], Ichiro Yoshikawa[1] (1.The university of Tokyo , 2.Institute of Space and Astronautical Science)

[PCG21-P08] A method to quantitatively evaluate Non-evaporable-getter pump for use in space science mission

*Seiya Nishimura[1], Ichiro Yoshikawa[1], Kazuo Yoshioka[1], Shogo Arao[1], Zhang Tianxu[1] (1.The university of tokyo)

[PCG21-P09] Interpretation on slight asymmetry of analyzer characteristics of MIA onboard the Mio by means of a model calculation of 3-D potential distribution

*Wataru Miyake[1], Yoshifumi Saito[2], Shoichiro Yokota[3] (1.Tokai University, 2.ISAS, 3.Osaka University)

[PCG21-P10] Construction of impact testing machine for small satellites and evaluation of mechanical resistance of MCPs by the impact test

*Junya Fukuba[1] (1.Graduate school of Tokyo)

[PCG21-P11] Innovative design of double-shell type energy analyzer for simultaneous electron and ion measurements in space

*Tomomi Takei[1], Masafumi Hirahara[1] (1.Institute for space-earth environmental research, Nagoya university)

[PCG21-P12] Microsatellite Development and Education of Space Science and Technology at Kanazawa University

*Tomohiko Imachi[1], Satoshi Yagitani[1], Daisuke Yonetoku[1], Yoshiya Kasahara[1], Tatsuya Sawano[1], Makoto Arimoto[1], Yoshitaka Goto[1], Mitsunori Ozaki[1], Ryuichi Fujimoto[1] (1.Kanazawa University)

[PCG21-P13] Attitude Control System for Kanazawa-SAT3 Microsatellite

Takuya Nakajima[1], Yuuki Yasuda[1], Hirofumi Segawa[1], *Tomohiko Imachi[1], Satoshi Yagitani[1], Yoshiya Kasahara[1], Daisuke Yonetoku[1], Tatsuya Sawano[1], Makoto rimoto[1] (1.Kanazawa University)

[PCG21-P14] Communications System and Antennas for Kanazawa-SAT3 Microsatellite

Teruya Minamoto[1], Koyo Ina[1], Kohei Kawagoshi[1], *Tomohiko Imachi[1], Satoshi Yagitani[1], Yoshitaka Goto[1], Daisuke Yonetoku[1], Yoshiya Kasahara[1], Tatsuya Sawano[1], Makoto Arimoto[1] (1.Kanazawa University)

[PCG21-P15] Development of micrometeoroid impact sensor within a multi-layered insulation (CLOTH) onboard 6U deep-space explorer EQUULEUS

*Takayuki Hirai[1], Hajime Yano[2], Ritsuko Jitsukawa[3], Eigo Ishioka[3], Haruki Nakano[3], Kazuyoshi Arai[3], Sunao Hasegawa[2] (1.Planetary Exploration Research Center, Chiba Institute of Technology, 2.Institute of Space and Astronautical Science, Japan Aerospace Exploration Agency, 3.Faculty of Science and Engineering, Hosei University)

[PCG21-P16] Breadboard model of asteroid tracking system for DESTINY$^+$ mission

*Peng Hong[1], Ko Ishibashi[1], Shunsuke Sato[2], Kazutoshi Takemura[3], Kotaro Fujiwara[4], Kanako Machii[5], Hiroyuki Toyota[2], Kazutaka Nishiyama[2], Masatsugu Otsuki[2], Osamu Okudaira[1], Takeshi Takashima[2] (1.Planetary Exploration Research Center, Chiba Institute of Technology, 2.Institute of Space and Astronautical Science, Japan Aerospace Exploration Agency, 3.Department of Applied Mechanics, Graduate School of Fundamental Science and Engineering, Waseda University, 4.Division of Mechanical and Space Engineering, Graduate School of Engineering, Hokkaido University, 5.Department of Mechanical Engineering and Intelligent Systems, Faculty of Informatics and Engineering, The University of Electro-Communications)

[PCG21-P17] Development of telescopic camera (TENGOO) performance evaluation device in MMX

*Hiroki Kato[1], Shingo Kameda[1], Keigo Enya[2], Osada Naoya[1] (1.Rikkyo University, 2.Japan Aerospace Exploration Agency)

[PCG21-P18] Observation Plans in the Cruising-Phase of the Solar Power Sail: OKEANOS

*Takahiro Iwata[1], Shuji Matsuura[2], KOHJI TSUMURA[3], Hajime Yano[1], Takayuki Hirai[4], Ayako Matsuoka[1], Daisuke Yonetoku[5], Tatehiro Mihara[6], Tatsuaki Okada[1], Osamu Mori[1], Toshihiro Chujo[1] (1.Institute of Space and Astronautical Science, Japan Aerospace Exploration Agency, 2.Kwansei Gakuin University, 3.Tohoku University, 4.Chiba Institute of Technology, 5.Kanazawa University, 6.RIKEN)

[E] Poster | P (Space and Planetary Sciences)：P-CG Complex & General

5:15 PM - 6:30 PM JST | 8:15 AM - 9:30 AM UTC | Poster Hall International Exhibition Hall8, Makuhari Messe_8

[P-CG21] Future Missions and instrumentation for space and planetary science

convener:Mitsunori Ozaki(Faculty of Electrical and Computer Engineering, Institute of Science and Engineering, Kanazawa University), Satoshi Kasahara(The university of Tokyo), Shingo Kameda(School of Science, Rikkyo University), Kazuo Yoshioka(Graduate School of frontier Science, The University of Tokyo)

[PCG21-P01] Visible and ultraviolet imagers for auroral and airglow observations by FACTORS - a future satellite mission for understanding the coupling and transportation processes in the upper atmosphere

*Takeshi Sakanoi[1], Masafumi Hirahara[2], Takuo T. Tsuda[3], Kazushi Asamura[4], Yoshizumi Miyoshi[2], Tomo-Hiko Watanabe[5], Takanori Nishiyama[6], Shin-ichiro Oyama[2,7], Yoshifumi Saito[4], Keisuke Hosokawa[3], Hirotsugu Kojima[8], Naritoshi Kitamura[9], Yasunobu Ogawa[5], Masatoshi Yamauchi[10], Ayako Matsuoka[4], Naoshi Yagi[1], Fukizawa Fukizawa[1], Genki Ishizawa[11] (1.Planetary Plasma and Atmospheric Research Center, Graduate School of Science, Tohoku University, 2.ISEE, Nagoya University, 3.Graduate School of Informatics and Engineering, School of Informatics and Engineering, The University of Electro-Communications, 4.ISAS/JAXA, 5.Graduate School of Science, Nagoya University, 6.National Institute for Polar Research, 7.University of Oulu, Finland, 8.RISH, Kyoto University, 9.Graduate School of Science, the University of Tokyo, Tokyo, 10.IRF Kiruna, Sweden, 11.Graduate School of Science, Tohoku University)

[PCG21-P02] Spatio-temporal analysis of flash aurora using Convolutional Neural Network

*Toki Genda[1], Takumi Inoue[1], Mitsunori Ozaki[1], Satoshi Yagitani[1], Imamura Kousuke[1], Kazuo Shiokawa[2], Yoshizumi Miyoshi[2], Shin-ichiro Oyama[2], Ryuho Kataoka[3], Yusuke Ebihara[4], Keisuke Hosokawa[5] (1.Kanazawa Univ., 2.Nagoya Univ., 3.NIPR, 4.Kyoto Univ., 5.UEC)

[PCG21-P03] Study on the pulse noise removal technique for Pc1 geomagnetic pulsations on the ground by signal processing

*Fumiya Komase[1], Tomohiro Inoue[1], Mitsunori Ozaki[1], Satoshi Yagitani[1], Kazuo Shiokawa[2], Masahito Nose[2], Tsutomu Nagatsuma[3] (1.Kanazawa Univ., 2.Nagoya Univ., 3.NICT)

[PCG21-P04] Application of magneto-impedance sensor to geomagnetic field measurements

*Masahito Nose[1], Reiko Nomura[2], Kazushi Asamura[3], Hitoshi Aoyama[4], Takeshi Kawano[4], Ayako Matsuoka[3], Kentarou Kitamura[5], Yukinobu Koyama[6], Haruhisa Matsumoto[7], Masafumi Hirahara[1] (1.Institute for Space-Earth Environmental Research, Nagoya University, 2.National Astronomical Observatory of Japan, 3.Institute of Space and Astronautical Science, Japan Aerospace Exploration Agency, 4.Aichi Steel Corporation, 5.National Institute of Technology, Tokuyama College, 6.National Institute of Technology, Oita College, 7.Research and Development Directorate, Japan Aerospace Exploration Agency)

[PCG21-P05] Observation of the Ionospheric Currents by the CubeSat at the Low and Middle Latitude

*Kentarou Kitamura[1], Kazumasa Imai[2], Taku Takada[2], Manabu Shinohara[3], Makoto Wakabayashi[4], KOSEN Space Collaboration Group (1.National Institute of Technology, Tokuyama Collge, 2.National Institute of Technology, Kochi Collge, 3.National Institute of Technology, Kagoshima Collge, 4.National Institute of Technology, Niihama Collge)

[PCG21-P06] Basic study on miniaturization of electric field instrument for plasma wave observations by ASIC technology

*Yuya Tokunaga[1], Mitsunori Ozaki[1], Keigo Ishisaka[2], Hirotsugu Kojima[3], Satoshi Yagitani[1], Takahiro Zushi[3] (1.Kanazawa University, 2.Toyama Prefectural University, 3.Kyoto University)

[PCG21-P07] Evaluation of radiation tolerance of electronics parts used for the ultra-small mission

*Riku Katsuse[1], Kazuo Yoshioka[1], Masaki Kuwabara[2], Reina Hikida[1], Shogo Arao[1], Ichiro Yoshikawa[1] (1.The university of Tokyo , 2.Institute of Space and Astronautical Science)

[PCG21-P08] A method to quantitatively evaluate Non-evaporable-getter pump for use in space science mission

*Seiya Nishimura[1], Ichiro Yoshikawa[1], Kazuo Yoshioka[1], Shogo Arao[1], Zhang Tianxu[1] (1.The university of tokyo)

[PCG21-P09] Interpretation on slight asymmetry of analyzer characteristics of MIA onboard the Mio by means of a model calculation of 3-D potential distribution

*Wataru Miyake[1], Yoshifumi Saito[2], Shoichiro Yokota[3] (1.Tokai University, 2.ISAS, 3.Osaka University)

[PCG21-P10] Construction of impact testing machine for small satellites and evaluation of mechanical resistance of MCPs by the impact test

*Junya Fukuba[1] (1.Graduate school of Tokyo)

[PCG21-P11] Innovative design of double-shell type energy analyzer for simultaneous electron and ion measurements in space

*Tomomi Takei[1], Masafumi Hirahara[1] (1.Institute for space-earth environmental research, Nagoya university)

[PCG21-P12] Microsatellite Development and Education of Space Science and Technology at Kanazawa University

*Tomohiko Imachi[1], Satoshi Yagitani[1], Daisuke Yonetoku[1], Yoshiya Kasahara[1], Tatsuya Sawano[1], Makoto Arimoto[1], Yoshitaka Goto[1], Mitsunori Ozaki[1], Ryuichi Fujimoto[1] (1.Kanazawa University)

[PCG21-P13] Attitude Control System for Kanazawa-SAT3 Microsatellite

Takuya Nakajima[1], Yuuki Yasuda[1], Hirofumi Segawa[1], *Tomohiko Imachi[1], Satoshi Yagitani[1], Yoshiya Kasahara[1], Daisuke Yonetoku[1], Tatsuya Sawano[1], Makoto rimoto[1] (1.Kanazawa University)

[PCG21-P14] Communications System and Antennas for Kanazawa-SAT3 Microsatellite

Teruya Minamoto[1], Koyo Ina[1], Kohei Kawagoshi[1], *Tomohiko Imachi[1], Satoshi Yagitani[1], Yoshitaka Goto[1], Daisuke Yonetoku[1], Yoshiya Kasahara[1], Tatsuya Sawano[1], Makoto Arimoto[1] (1.Kanazawa University)

[PCG21-P15] Development of micrometeoroid impact sensor within a multi-layered insulation (CLOTH) onboard 6U deep-space explorer EQUULEUS

*Takayuki Hirai[1], Hajime Yano[2], Ritsuko Jitsukawa[3], Eigo Ishioka[3], Haruki Nakano[3], Kazuyoshi Arai[3], Sunao Hasegawa[2] (1.Planetary Exploration Research Center, Chiba Institute of Technology, 2.Institute of Space and Astronautical Science, Japan Aerospace Exploration Agency, 3.Faculty of Science and Engineering, Hosei University)

[PCG21-P16] Breadboard model of asteroid tracking system for DESTINY$^+$ mission

*Peng Hong[1], Ko Ishibashi[1], Shunsuke Sato[2], Kazutoshi Takemura[3], Kotaro Fujiwara[4], Kanako Machii[5], Hiroyuki Toyota[2], Kazutaka Nishiyama[2], Masatsugu Otsuki[2], Osamu Okudaira[1], Takeshi Takashima[2] (1.Planetary Exploration Research Center, Chiba Institute of Technology, 2.Institute of Space and Astronautical Science, Japan Aerospace Exploration Agency, 3.Department of Applied Mechanics, Graduate School of Fundamental Science and Engineering, Waseda University, 4.Division of Mechanical and Space Engineering, Graduate School of Engineering, Hokkaido University, 5.Department of Mechanical Engineering and Intelligent Systems, Faculty of Informatics and Engineering, The University of Electro-Communications)

[PCG21-P17] Development of telescopic camera (TENGOO) performance evaluation device in MMX

*Hiroki Kato[1], Shingo Kameda[1], Keigo Enya[2], Osada Naoya[1] (1.Rikkyo University, 2.Japan Aerospace Exploration Agency)

[PCG21-P18] Observation Plans in the Cruising-Phase of the Solar Power Sail: OKEANOS

*Takahiro Iwata[1], Shuji Matsuura[2], KOHJI TSUMURA[3], Hajime Yano[1], Takayuki Hirai[4], Ayako Matsuoka[1], Daisuke Yonetoku[5], Tatehiro Mihara[6], Tatsuaki Okada[1], Osamu Mori[1], Toshihiro Chujo[1] (1.Institute of Space and Astronautical Science, Japan Aerospace Exploration Agency, 2.Kwansei Gakuin University, 3.Tohoku University, 4.Chiba Institute of Technology, 5.Kanazawa University, 6.RIKEN)

[E] Poster | A (Atmospheric and Hydrospheric Sciences)：A-OS Ocean Sciences & Ocean Environment

3:30 PM - 5:00 PM JST | 6:30 AM - 8:00 AM UTC | Poster Hall International Exhibition Hall8, Makuhari Messe_7

[A-OS09] Ocean Mixing Processes: Impact on Biogeochemistry, Climate and Ecosystem

convener:Ichiro Yasuda(Atmosphere and Ocean Research Institute, The University of Tokyo), Toshiyuki Hibiya(Department of Earth and Planetary Science, Graduate School of Science, University of Tokyo), Jun Nishioka(Hokkaido University, Institute of low temperature sciences), Shin-ichi Ito(Atmosphere and Ocean Research Institute, The University of Tokyo)

[AOS09-P01] Correction method of fast-response thermistors data to estimate turbulence intensity

*kimura shino[1], Yasutaka Goto[2], Koenjong Lee[1], Ichiro Yasuda[1] (1.The Univercity of Tokyo, 2.Meteorological Agency)

[AOS09-P02] Observation of turbulent mixing using a deep float with microstructure sensors

*Shuo Zhai[1], Ichiro Yasuda[1], Masaaki Kikuchi[1], Yasutaka Goto[1], Koenjong Lee[1], Takahiro Tanaka[2], Ken Yamaki[3], Yutaka Imamura[4] (1.Atmosphere and Ocean Research Institute, The University of Tokyo, 2.Japan Fisheries Research Agency, 3.TSK Tsurumi-Seiki Co., Ltd., 4.Aomori Prefectural Industrial Thechnology Research Center, Fisheries Research Insititute)

[AOS09-P03] Evaluation of the underwater glider flight model using the electromagnetic current sensor

*Takahiro Tanaka[1], Daisuke Hasegawa[1], Takeshi Okunishi[1], Ichiro Yasuda[2] (1.Tohoku National Fisheries Research Institute, Japan Fisheries Research and Education Agency, 2.Atmosphere and Ocean Research Institute, University of Tokyo)

[AOS09-P04] Mixing processes observed by a slocum glider at the Oyashio-TWC front

*Daisuke Hasegawa[1], Takahiro Tanaka[1], Takeshi Okunishi[1], Ichiro Yasuda[2] (1.Tohoku National Fisheries Research Institute, Japan Fisheries Research and Education Agency, 2.Atmosphere and Ocean Research Institute, The University of Tokyo)

[AOS09-P05] Impact of the astronomical lunar 18.6-yr tidal cycle on El-Niño and Southern Oscillation

*Ichiro Yasuda[1] (1.Atmosphere and Ocean Research Institute, The University of Tokyo)

[AOS09-P06] The effect of 18.6-year period lunar nodal cycle on Pacific Decadal Oscillation (PDO)

*Masaki Hamamoto[1], Ichiro Yasuda[1] (1.Atmosphere and Ocean Research Institute, The University of Tokyo)

[AOS09-P07] A comparison of ocean deoxygenation between CMIP5 models and an observational dataset

*Yumi Abe[1], Shoshiro Minobe[1,5], Takamitsu Ito[2], Curtis Deutsch[3], Matthew C. Long[4] (1.Department of Natural History Sciences, Graduate School of Science,Hokkaido University, Sapporo, Japan, 2.School of Earth and Atmospheric Sciences, Georgia Institute of Technology, Atlanta, Georgia, USA, 3.School of Oceanography, University of Washington, Seattle, Washington, USA, 4.Climate and Global Dynamics Laboratory, National Center for Atmospheric Research, Boulder, Colorado, USA, 5.Department of Earth and Planetary Sciences, Faculty of Science, Hokkaido University, Sapporo, Japan)

[AOS09-P08] Pacific Ocean State Estimation and Clarification of Mechanism of Ocean Circulation by Data Synthesis of Global Observations

*Shuhei Masuda[1] (1.Japan Agency for Marine-Earth Science and Technology)

[AOS09-P09] Impact of Tidal Vertical Mixing to Barotropic Water Exchange between the Sea of Okhotsk and Pacific through Diffusive Adjustment with Turbulent Closure Scheme

*Hung Wei Chou[1], Humio Mitsudera[1], Hatsumi Nishikawa[1], Kaihe Yamazaki[2] (1.Hokkaido University, Institute of Low Temperature Science, 2.Hokkaido University, Graduate School of Environmental Science)

[AOS09-P10] Distributions of organic Fe-binding ligands in the eastern and western subarctic North Pacific

*Yoshiko Kondo[1,2], Yudai Sunahara[2], Jun Nishioka[3], Hajime Obata[4], Shigenobu Takeda[1,2] (1.Graduate School of Fisheries and Environmental Sciences, Nagasaki University, 2.Faculty of Fisheries, Nagasaki University, 3.Institute of Low Temperature Science, Hokkaido University, 4.Atmosphere and Ocean Research Institute, The University of Tokyo)

[AOS09-P11] Chemical and physical speciation of copper in the subarctic North Pacific

*Kuo Hong Wong[1], Hajime Obata[1], Taejin Kim[2], Yoshiko Kondo[3], Jun Nishioka[4] (1.Atmosphere and Ocean Research Institute, The University of Tokyo, 2.Seoul National University, Korea, 3.Nagasaki University, 4.Institute of Low

Temperature Science, Hokkaido University)

[AOS09-P12] Latitudinal and temporal variations in phytoplankton size structure within mesoscale eddies from space

*Hisatomo Waga[1], Toru Hirawake[1], Ueno Hiromichi[1] (1.Hokkaido University)

[AOS09-P13] Structure and impact of the Kuroshio nutrient stream

*Kosei Komatsu[1,2], Yutaka Hiroe[3] (1.Graduate School of Frontier Sciences, The University of Tokyo, 2.Atmosphere and Ocean Research Institute, The University of Tokyo, Kashiwa, Japan, 3.Seikai National Fisheries Research Institute, Japan Fisheries Research and Education Agency, Nagasaki, Japan)

[AOS09-P14] Enhanced nutrient supply and biogeochemical impacts induced by internal waves in the oligotrophic northern South China Sea

*Chin-chang Hung[1], Dewang Li[2], Wen-Chen Chou[3], Yung-Yen Shih[1,4], Guan-Yu Chen[1] (1.Department of Oceanography, National Sun Yat Sen University, Kaohsiung, Taiwan, 2.Second Institute of Oceanography, State Oceanic Administration, Hangzhou, PRC, 3.Institute of Marine Environmental Chemistry and Ecology, National Taiwan Ocean University, Taiwan, 4.Department of Applied Science, R.O.C Naval Academy, Kaohsiung, Taiwan)

[AOS09-P15] Mixing over the eastern ridge in the Luzon Strait caused by high-mode internal waves

*Akie Sakai[1], Tomoharu Senjyu[2], Eisuke Tsutsumi[2], Takeshi Matsuno[2], Takahiro Endo[2], Ichiro Yasuda[3], Daigo Yanagimoto[3] (1.Department of Earth System Science and Technology, Interdisciplinary Graduate School of Engineering Sciences, Kyushu University, 2.Research Institute for Applied Mechanics , 3.Atmosphere and Ocean Reserch Institute The University of Tokyo)

[AOS09-P16] **From the Luzon Strait to the Tsushima Strait: Water masses and nutrient transports approached using ^{137}Cs**

*Siteng Zhu[1], JING ZHANG[1], Shota Kambayashi[2], Takeshi Matsuno[3], Eisuke Tsutsumi[3], Shigenobu Takeda[4], Seiya Nagao[5], Hiroshi Inoue[5], Hiroshi Ogawa[6], Ichiro Yasuda[6] (1.University of Toyama, 2.Fukushima university, 3.Kyushu university, 4.Nagasaki university, 5.Kanazawa university, 6.The University of Tokyo)

[AOS09-P17] Impact of cyclonic eddies and typhoons on biogeochemistry in the oligotrophic ocean based on time-series observation at the western Pacific subtropical station KEO

*Makio Honda[1], Yoshikazu Sasai[1], Eko Siswanto[1], Akira Kuwano-Yoshida[2], Hidenori AIKI[3], Meghan Cronin[4] (1.Japan Agency for Marine-Earth Science and Technology, 2.Disaster Prevention Laboratory, Kyoto University, 3.Nagoya University, 4.NOAA Pacific Marine Environmental Laboratory)

[AOS09-P18] Island-mass effect on the phytoplankton and zooplankton community in south of Japan

*Kiyotaka Hidaka[1], Kazuaki Tadokoro[1], Hiroomi Miyamoto[1], Tadafumi Ichikawa[1] (1.Japan Fisheries Research and Education Agency)

[AOS09-P19] Influence of enhanced deep circulation due to geothermal heat on biogeochemical cycle in the Pacific Ocean

*Shogo Urakawa[1], Hideyuki Nakano[1], Hiroyuki Tsujino[1], Kei Sakamoto[1], Takahiro Toyoda[1], Goro Yamanaka[1] (1.Meteorological Research Institute, Japan Meteorological Agency)

[AOS09-P20] The Parameterization of the Pressure-Strain Correlations in the Stably or Unstably Stratified Ocean Surface Layer.

*Yusuke Ushijima[1], Yutaka Yoshikawa[1] (1.Graduate School of Science, Kyoto University)

[AOS09-P21] Numerical studies on asymmetric responses of the upper ocean to tropical cyclone

*Daiki Okura[1], Yutaka Yoshikawa[1] (1.Graduate School of Science, Kyoto University)

[AOS09-P22] Influence of the distortion of the internal wave field on estimates of turbulent mixing using fine-scale parameterizations

*Anne Takahashi[1], Toshiyuki Hibiya[1], Alberto C. Naveira Garabato[2] (1.Department of Earth and Planetary Science, Graduate School of Science, University of Tokyo, 2.National Oceanography Centre, University of Southampton)

[E] Poster | A (Atmospheric and Hydrospheric Sciences)：A-OS Ocean Sciences & Ocean Environment

5:15 PM - 6:30 PM JST | 8:15 AM - 9:30 AM UTC | Poster Hall International Exhibition Hall8, Makuhari Messe_11

[A-OS09] Ocean Mixing Processes: Impact on Biogeochemistry, Climate and Ecosystem

convener:Ichiro Yasuda(Atmosphere and Ocean Research Institute, The University of Tokyo), Toshiyuki Hibiya(Department of Earth and Planetary Science, Graduate School of Science, University of Tokyo), Jun Nishioka(Hokkaido University, Institute of low temperature sciences), Shin-ichi Ito(Atmosphere and Ocean Research Institute, The University of Tokyo)

[AOS09-P01] Correction method of fast-response thermistors data to estimate turbulence intensity

*kimura shino[1], Yasutaka Goto[2], Koenjong Lee[1], Ichiro Yasuda[1] (1.The Univercity of Tokyo, 2.Meteorological Agency)

[AOS09-P02] Observation of turbulent mixing using a deep float with microstructure sensors

*Shuo Zhai[1], Ichiro Yasuda[1], Masaaki Kikuchi[1], Yasutaka Goto[1], Koenjong Lee[1], Takahiro Tanaka[2], Ken Yamaki[3], Yutaka Imamura[4] (1.Atmosphere and Ocean Research Institute, The University of Tokyo, 2.Japan Fisheries Research Agency, 3.TSK Tsurumi-Seiki Co., Ltd., 4.Aomori Prefectural Industrial Thechnology Research Center, Fisheries Research Insititute)

[AOS09-P03] Evaluation of the underwater glider flight model using the electromagnetic current sensor

*Takahiro Tanaka[1], Daisuke Hasegawa[1], Takeshi Okunishi[1], Ichiro Yasuda[2] (1.Tohoku National Fisheries Research Institute, Japan Fisheries Research and Education Agency, 2.Atmosphere and Ocean Research Institute, University of Tokyo)

[AOS09-P04] Mixing processes observed by a slocum glider at the Oyashio-TWC front

*Daisuke Hasegawa[1], Takahiro Tanaka[1], Takeshi Okunishi[1], Ichiro Yasuda[2] (1.Tohoku National Fisheries Research Institute, Japan Fisheries Research and Education Agency, 2.Atmosphere and Ocean Research Institute, The University of Tokyo)

[AOS09-P05] Impact of the astronomical lunar 18.6-yr tidal cycle on El-Niño and Southern Oscillation

*Ichiro Yasuda[1] (1.Atmosphere and Ocean Research Institute, The University of Tokyo)

[AOS09-P06] The effect of 18.6-year period lunar nodal cycle on Pacific Decadal Oscillation (PDO)

*Masaki Hamamoto[1], Ichiro Yasuda[1] (1.Atmosphere and Ocean Research Institute, The University of Tokyo)

[AOS09-P07] A comparison of ocean deoxygenation between CMIP5 models and an observational dataset

*Yumi Abe[1], Shoshiro Minobe[1,5], Takamitsu Ito[2], Curtis Deutsch[3], Matthew C. Long[4] (1.Department of Natural History Sciences, Graduate School of Science,Hokkaido University, Sapporo, Japan, 2.School of Earth and Atmospheric Sciences, Georgia Institute of Technology, Atlanta, Georgia, USA, 3.School of Oceanography, University of Washington, Seattle, Washington, USA, 4.Climate and Global Dynamics Laboratory, National Center for Atmospheric Research, Boulder, Colorado, USA, 5.Department of Earth and Planetary Sciences, Faculty of Science, Hokkaido University, Sapporo, Japan)

[AOS09-P08] Pacific Ocean State Estimation and Clarification of Mechanism of Ocean Circulation by Data Synthesis of Global Observations

*Shuhei Masuda[1] (1.Japan Agency for Marine-Earth Science and Technology)

[AOS09-P09] Impact of Tidal Vertical Mixing to Barotropic Water Exchange between the Sea of Okhotsk and Pacific through Diffusive Adjustment with Turbulent Closure Scheme

*Hung Wei Chou[1], Humio Mitsudera[1], Hatsumi Nishikawa[1], Kaihe Yamazaki[2] (1.Hokkaido University, Institute of Low Temperature Science, 2.Hokkaido University, Graduate School of Environmental Science)

[AOS09-P10] Distributions of organic Fe-binding ligands in the eastern and western subarctic North Pacific

*Yoshiko Kondo[1,2], Yudai Sunahara[2], Jun Nishioka[3], Hajime Obata[4], Shigenobu Takeda[1,2] (1.Graduate School of Fisheries and Environmental Sciences, Nagasaki University, 2.Faculty of Fisheries, Nagasaki University, 3.Institute of Low Temperature Science, Hokkaido University, 4.Atmosphere and Ocean Research Institute, The University of Tokyo)

[AOS09-P11] Chemical and physical speciation of copper in the subarctic North Pacific

*Kuo Hong Wong[1], Hajime Obata[1], Taejin Kim[2], Yoshiko Kondo[3], Jun Nishioka[4] (1.Atmosphere and Ocean Research Institute, The University of Tokyo, 2.Seoul National University, Korea, 3.Nagasaki University, 4.Institute of Low

Temperature Science, Hokkaido University)

[AOS09-P12] Latitudinal and temporal variations in phytoplankton size structure within mesoscale eddies from space

*Hisatomo Waga[1], Toru Hirawake[1], Ueno Hiromichi[1] (1.Hokkaido University)

[AOS09-P13] Structure and impact of the Kuroshio nutrient stream

*Kosei Komatsu[1,2], Yutaka Hiroe[3] (1.Graduate School of Frontier Sciences, The University of Tokyo, 2.Atmosphere and Ocean Research Institute, The University of Tokyo, Kashiwa, Japan, 3.Seikai National Fisheries Research Institute, Japan Fisheries Research and Education Agency, Nagasaki, Japan)

[AOS09-P14] Enhanced nutrient supply and biogeochemical impacts induced by internal waves in the oligotrophic northern South China Sea

*Chin-chang Hung[1], Dewang Li[2], Wen-Chen Chou[3], Yung-Yen Shih[1,4], Guan-Yu Chen[1] (1.Department of Oceanography, National Sun Yat Sen University, Kaohsiung, Taiwan, 2.Second Institute of Oceanography, State Oceanic Administration, Hangzhou, PRC, 3.Institute of Marine Environmental Chemistry and Ecology, National Taiwan Ocean University, Taiwan, 4.Department of Applied Science, R.O.C Naval Academy, Kaohsiung, Taiwan)

[AOS09-P15] Mixing over the eastern ridge in the Luzon Strait caused by high-mode internal waves

*Akie Sakai[1], Tomoharu Senjyu[2], Eisuke Tsutsumi[2], Takeshi Matsuno[2], Takahiro Endo[2], Ichiro Yasuda[3], Daigo Yanagimoto[3] (1.Department of Earth System Science and Technology, Interdisciplinary Graduate School of Engineering Sciences, Kyushu University, 2.Research Institute for Applied Mechanics , 3.Atmosphere and Ocean Reserch Institute The University of Tokyo)

[AOS09-P16] **From the Luzon Strait to the Tsushima Strait: Water masses and nutrient transports approached using ^{137}Cs**

*Siteng Zhu[1], JING ZHANG[1], Shota Kambayashi[2], Takeshi Matsuno[3], Eisuke Tsutsumi[3], Shigenobu Takeda[4], Seiya Nagao[5], Hiroshi Inoue[5], Hiroshi Ogawa[6], Ichiro Yasuda[6] (1.University of Toyama, 2.Fukushima university, 3.Kyushu university, 4.Nagasaki university, 5.Kanazawa university, 6.The University of Tokyo)

[AOS09-P17] Impact of cyclonic eddies and typhoons on biogeochemistry in the oligotrophic ocean based on time-series observation at the western Pacific subtropical station KEO

*Makio Honda[1], Yoshikazu Sasai[1], Eko Siswanto[1], Akira Kuwano-Yoshida[2], Hidenori AIKI[3], Meghan Cronin[4] (1.Japan Agency for Marine-Earth Science and Technology, 2.Disaster Prevention Laboratory, Kyoto University, 3.Nagoya University, 4.NOAA Pacific Marine Environmental Laboratory)

[AOS09-P18] Island-mass effect on the phytoplankton and zooplankton community in south of Japan

*Kiyotaka Hidaka[1], Kazuaki Tadokoro[1], Hiroomi Miyamoto[1], Tadafumi Ichikawa[1] (1.Japan Fisheries Research and Education Agency)

[AOS09-P19] Influence of enhanced deep circulation due to geothermal heat on biogeochemical cycle in the Pacific Ocean

*Shogo Urakawa[1], Hideyuki Nakano[1], Hiroyuki Tsujino[1], Kei Sakamoto[1], Takahiro Toyoda[1], Goro Yamanaka[1] (1.Meteorological Research Institute, Japan Meteorological Agency)

[AOS09-P20] The Parameterization of the Pressure-Strain Correlations in the Stably or Unstably Stratified Ocean Surface Layer.

*Yusuke Ushijima[1], Yutaka Yoshikawa[1] (1.Graduate School of Science, Kyoto University)

[AOS09-P21] Numerical studies on asymmetric responses of the upper ocean to tropical cyclone

*Daiki Okura[1], Yutaka Yoshikawa[1] (1.Graduate School of Science, Kyoto University)

[AOS09-P22] Influence of the distortion of the internal wave field on estimates of turbulent mixing using fine-scale parameterizations

*Anne Takahashi[1], Toshiyuki Hibiya[1], Alberto C. Naveira Garabato[2] (1.Department of Earth and Planetary Science, Graduate School of Science, University of Tokyo, 2.National Oceanography Centre, University of Southampton)

[E] Poster | H (Human Geosciences)：H-GG Geography

3:30 PM - 5:00 PM JST | 6:30 AM - 8:00 AM UTC | Poster Hall International Exhibition Hall8, Makuhari Messe_8

[H-GG01] Human-Natural system interactions and solutions for environmental management

convener:Yuei-An Liou(National Central University)

[HGG01-P01] **Feasibility assessment of constructing high-resolution 3D panoramic images using the VLP-16 LiDAR Puck**

*Yan-Jyun Lin[1], Shen Yu Hsiao[1], REN-JHIH YANG[1], Zhen-Yu Wu[1] (1.National Chung Hsing University)

[HGG01-P02] **The environmental impact of mountaineering in the Mt. Manaslu region**

*Hijiri SHIMOJIMA[1] (1.Tokyo University of Agriculture)

[HGG01-P03] Understanding human system vulnerability to typhoon for Improved Adaptive Capacity

*Kim-Anh Nguyen[1], Yuei-An Liou[1] (1.Center for Space and Remote Sensing Research, National Central University)

[HGG01-P04] Environmental Impact Evaluation of Solar Park Project in Western Desert, Minia, Egypt.

*Ramadan Gamal Abdelrehim[1], Josaphat Tetuko Sri Sumantyo[1] (1.Center for Environmental Remote Sensing, Chiba University)

[HGG01-P05] Peatland Assessment Based on DInSAR approach by using ALOS-2 PALSAR-2 Data in Kalimantan, Indonesia

*Joko Widodo[1], Josaphat Tetuko Sri Sumantyo[1], Daniele Perissin[2], Katsunoshin Nishi[1], Pakhrur Rozi[1] (1.JMRSL - Josaphat Microwave Remote Sensing Laboratory Center for Environmental Remote Sensing Graduate School of Advanced Integration Science Chiba University, 2.Sarproz, Razer Limited, Hongkong)

[HGG01-P06] Development of Nanosatellite for Ionospheric Measurement for Earthquake Prediction

*Peberlin Parulian Sitompul[1], Josaphat Tetuko Sri Sumantyo[2] (1.Chiba University, and Indonesia National Institute of Aeronautic and Space, 2.Center for Environmental Remote Sensing, Chiba University)

[E] Poster | H (Human Geosciences)：H-GG Geography

5:15 PM - 6:30 PM JST | 8:15 AM - 9:30 AM UTC | Poster Hall International Exhibition Hall8, Makuhari Messe_14

[H-GG01] Human-Natural system interactions and solutions for environmental management

convener:Yuei-An Liou(National Central University)

[HGG01-P01] **Feasibility assessment of constructing high-resolution 3D panoramic images using the VLP-16 LiDAR Puck**

*Yan-Jyun Lin[1], Shen Yu Hsiao[1], REN-JHIH YANG[1], Zhen-Yu Wu[1] (1.National Chung Hsing University)

[HGG01-P02] **The environmental impact of mountaineering in the Mt. Manaslu region**

*Hijiri SHIMOJIMA[1] (1.Tokyo University of Agriculture)

[HGG01-P03] Understanding human system vulnerability to typhoon for Improved Adaptive Capacity

*Kim-Anh Nguyen[1], Yuei-An Liou[1] (1.Center for Space and Remote Sensing Research, National Central University)

[HGG01-P04] Environmental Impact Evaluation of Solar Park Project in Western Desert, Minia, Egypt.

*Ramadan Gamal Abdelrehim[1], Josaphat Tetuko Sri Sumantyo[1] (1.Center for Environmental Remote Sensing, Chiba University)

[HGG01-P05] Peatland Assessment Based on DInSAR approach by using ALOS-2 PALSAR-2 Data in Kalimantan, Indonesia

*Joko Widodo[1], Josaphat Tetuko Sri Sumantyo[1], Daniele Perissin[2], Katsunoshin Nishi[1], Pakhrur Rozi[1] (1.JMRSL - Josaphat Microwave Remote Sensing Laboratory Center for Environmental Remote Sensing Graduate School of Advanced Integration Science Chiba University, 2.Sarproz, Razer Limited, Hongkong)

[HGG01-P06] Development of Nanosatellite for Ionospheric Measurement for Earthquake Prediction

*Peberlin Parulian Sitompul[1], Josaphat Tetuko Sri Sumantyo[2] (1.Chiba University, and Indonesia National Institute of Aeronautic and Space, 2.Center for Environmental Remote Sensing, Chiba University)

[E] Poster | H (Human Geosciences)：H-SC Social Earth Sciences & Civil/Urban System Sciences

3:30 PM - 5:00 PM JST | 6:30 AM - 8:00 AM UTC | Poster Hall International Exhibition Hall8, Makuhari Messe_10

[H-SC06] Role of Geosciences for sustainable use of marine and coastal ecosystems in urbanized world.

convener:Kalpana Chaudhari(Institute For Sustainable Development and Research)

[HSC06-P01] Research on Diffusion Method of Factor in Urban Land Classification

★Invited Papers

*Jun Zhou[1] (1.Tianjin Normal University)

[HSC06-P02] Assessment of facilities for green tourism in Japan: Fifty-six indices in eight regions using online data

*Hanqiu Zhang[1], Qiongying Xiang[1], Jiaying Shi[1], Junchi Zhang[1], Yingming Mao[1], Kyung-hun Min[1], Ge Chen, Tokiya Oka[1], Zijiao Xie[1], Minami Kashima[1], I Made Pradnyan Dana Natawiguna, Katsunori Furuya[1] (1.Graduate School of Horticulture, Chiba University)

[HSC06-P03] Study on Green Tourism Experience —— Cases of Popular Strawberry Farms in Chiba Prefecture

*Yilin Wu[1], Mengying Gao[1], Kazuhei Sato[1], Tingyu Lu[1], Fumeng Zhang[1], Siqi Xing[1], Karolina Brandt[1], Mai Uemura, Katsunori Furuya[1] (1.Graduate School of Horticulture, Chiba University)

[HSC06-P04] **Ritual plant utilization in landscapes planning. Case study: Riverside in Denpasar City.**

*I Made Pradnyan Natawiguna[1], Katsunori Furuya[1] (1.Graduate School of Horticulture, Chiba University)

[E] Poster | H (Human Geosciences)：H-SC Social Earth Sciences & Civil/Urban System Sciences

5:15 PM - 6:30 PM JST | 8:15 AM - 9:30 AM UTC | Poster Hall International Exhibition Hall8, Makuhari Messe_17

[H-SC06] Role of Geosciences for sustainable use of marine and coastal ecosystems in urbanized world.

convener:Kalpana Chaudhari(Institute For Sustainable Development and Research)

[HSC06-P01] Research on Diffusion Method of Factor in Urban Land Classification

★Invited Papers

*Jun Zhou[1] (1.Tianjin Normal University)

[HSC06-P02] Assessment of facilities for green tourism in Japan: Fifty-six indices in eight regions using online data

*Hanqiu Zhang[1], Qiongying Xiang[1], Jiaying Shi[1], Junchi Zhang[1], Yingming Mao[1], Kyung-hun Min[1], Ge Chen, Tokiya Oka[1], Zijiao Xie[1], Minami Kashima[1], I Made Pradnyan Dana Natawiguna, Katsunori Furuya[1] (1.Graduate School of Horticulture, Chiba University)

[HSC06-P03] Study on Green Tourism Experience —— Cases of Popular Strawberry Farms in Chiba Prefecture

*Yilin Wu[1], Mengying Gao[1], Kazuhei Sato[1], Tingyu Lu[1], Fumeng Zhang[1], Siqi Xing[1], Karolina Brandt[1], Mai Uemura, Katsunori Furuya[1] (1.Graduate School of Horticulture, Chiba University)

[HSC06-P04] **Ritual plant utilization in landscapes planning. Case study: Riverside in Denpasar City.**

*I Made Pradnyan Natawiguna[1], Katsunori Furuya[1] (1.Graduate School of Horticulture, Chiba University)

[E] Poster | H (Human Geosciences)：H-TT Technology & Techniques

3:30 PM - 5:00 PM JST | 6:30 AM - 8:00 AM UTC | Poster Hall International Exhibition Hall8, Makuhari Messe_11

[H-TT20] Environmental Remote Sensing

convener:Wei Yang(Chiba University), Akihiko Kondoh(Center for Environmental Remote Sensing, Chiba University)

[HTT20-P01] **Classification of Winter Wheat using high spatial resolution data in North China Plain**

*Chunyang Wang[1,2], Wei Yang[2], Xifang Wu[3], Zhichao Chen[1], Junjun Lu[1], Zongze Zhao[1], Hebing Zhang[1] (1.School of Surveying and Land Information Engineering, Henan Polytechnic University, 2.Center for Environmental Remote Sensing, Chiba University, 3.Graduate School of Science and Engineering, Chiba University)

[HTT20-P02] Normalized Difference Greenness Index (NDGI): A new vegetation index for improved estimation of vegetation phenology

*Wei Yang[1], Hideki Kobayashi[2], Akihiko Kondoh[1] (1.Chiba University, 2.JAMSTEC)

[HTT20-P03] ***Characteristics of manual and automatically tree species classification in mixed forest (Yamagata University Research Forest)***

*Sarah Kentsch[1,2], Larry Maximo Lopez Caceres[1], Yago Diez[1], Motohisa Fukuda[1] (1.Yamagata University, 2.United Graduate School of Agricultural Sciences)

[HTT20-P04] Land subsidence detection by SBAS-InSAR technology and its factor analysis in the inland area of Chiba Prefecture

*HALIPU AYIHUMAIER[1], Richa Bhattarai[1], Wen - LIU[1], Akihiko - Kondoh[1,2] (1.Graduate School of Science and Engineering, 2.Center for Environmental Remote Sensing, Chiba University)

[HTT20-P05] Development of a novel data fusion model to generate high spatiotemporal resolution NDVI time series

*Wei Yang[1], Jin Chen[2] (1.Chiba University, 2.Beijing Normal University)

[E] Poster | H (Human Geosciences)：H-TT Technology & Techniques

5:15 PM - 6:30 PM JST | 8:15 AM - 9:30 AM UTC | Poster Hall International Exhibition Hall8, Makuhari Messe_18

[H-TT20] Environmental Remote Sensing

convener:Wei Yang(Chiba University), Akihiko Kondoh(Center for Environmental Remote Sensing, Chiba University)

[HTT20-P01] **Classification of Winter Wheat using high spatial resolution data in North China Plain**

*Chunyang Wang[1,2], Wei Yang[2], Xifang Wu[3], Zhichao Chen[1], Junjun Lu[1], Zongze Zhao[1], Hebing Zhang[1] (1.School of Surveying and Land Information Engineering, Henan Polytechnic University, 2.Center for Environmental Remote Sensing, Chiba University, 3.Graduate School of Science and Engineering, Chiba University)

[HTT20-P02] Normalized Difference Greenness Index (NDGI): A new vegetation index for improved estimation of vegetation phenology

*Wei Yang[1], Hideki Kobayashi[2], Akihiko Kondoh[1] (1.Chiba University, 2.JAMSTEC)

[HTT20-P03] ***Characteristics of manual and automatically tree species classification in mixed forest (Yamagata University Research Forest)***

*Sarah Kentsch[1,2], Larry Maximo Lopez Caceres[1], Yago Diez[1], Motohisa Fukuda[1] (1.Yamagata University, 2.United Graduate School of Agricultural Sciences)

[HTT20-P04] Land subsidence detection by SBAS-InSAR technology and its factor analysis in the inland area of Chiba Prefecture

*HALIPU AYIHUMAIER[1], Richa Bhattarai[1], Wen - LIU[1], Akihiko - Kondoh[1,2] (1.Graduate School of Science and Engineering, 2.Center for Environmental Remote Sensing, Chiba University)

[HTT20-P05] Development of a novel data fusion model to generate high spatiotemporal resolution NDVI time series

*Wei Yang[1], Jin Chen[2] (1.Chiba University, 2.Beijing Normal University)

[E] Poster | S (Solid Earth Sciences)：S-SS Seismology

3:30 PM - 5:00 PM JST | 6:30 AM - 8:00 AM UTC | Poster Hall International Exhibition Hall8, Makuhari Messe_13

[S-SS04] New methods for seismicity characterization

convener:Francesco Grigoli(ETH-Zurich, Swiss Seismological Service), Aitaro Kato(Earthquake Research Institute, the University of Tokyo), Yosuke Aoki(Earthquake Research Institute, University of Tokyo), Claudio Satriano(Institut de Physique du Globe de Paris)

[SSS04-P01] **Constraint of focal mechanisms of induced seismicity by using misfit angles based on known *in-situ* stress**

*Yusuke Mukuhira[1], Makoto Naoi[2], Michael C Fehler[3], Hirokazu Moriya[5], Takatoshi Ito[1], Hiroshi Asanuma[4], Markus O Häring[6] (1.Institute of Fluid Science, Tohoku University, 2.Disaster Prevention Research Institute, Kyoto University, 3.Earth Resources Laboratory, MIT, 4.FREA, AIST, 5.School of Engineering, Tohoku University, 6.Häring GeoProject)

[SSS04-P02] Kinematic slip imaging of the Mw 3.3 earthquake in the St. Gallen 2013 geothermal reservoir, Switzerland, using an isochrone back projection approach

*Claudio Satriano[1], Eszter Király-Proag[2], Pascal Bernard[1], Stefan Wiemer[2] (1.Institut de Physique du Globe de Paris, France, 2.ETH Swiss Federal Institute of Technology Zurich, Switzerland)

[SSS04-P03] **Monitoring induced seismicity with a single seismic station by combining coda wave interferometry with distance geometry solvers**

*Francesco Grigoli[1], Simone Cesca[2], Alessandro Vuan[3], Filippo Broggini[1], John Clinton[1], Stefan Wiemer[1] (1.ETH-Zurich, Switzerland, 2.GFZ-Potsdam, Germany, 3.OGS-Trieste, Italy)

[SSS04-P04] Automatic Earthquake Locating by Stacking Characteristic Functions in a Source Scanning Method

★Invited Papers

*Hilary Chang[1], Alison Malcolm[1], Frédérick Massin[2], Francesco Grigoli[2] (1.Memorial University of Newfoundland, Earth Sciences, Canada, 2. ETH Zurich, Department of Earth Sciences, Zürich, Switzerland)

[SSS04-P05] Earthquake nowcasting: further development and application to Japan

*Kazuyoshi Nanjo[1], John B. Rundle[2], Tetsuo Sakurada[3] (1.University of Shizuoka, 2.University of California at Davis, 3.SAKURADA&Company)

[E] Poster | S (Solid Earth Sciences)：S-SS Seismology

5:15 PM - 6:30 PM JST | 8:15 AM - 9:30 AM UTC | Poster Hall International Exhibition Hall8, Makuhari Messe_24

[S-SS04] New methods for seismicity characterization

convener:Francesco Grigoli(ETH-Zurich, Swiss Seismological Service), Aitaro Kato(Earthquake Research Institute, the University of Tokyo), Yosuke Aoki(Earthquake Research Institute, University of Tokyo), Claudio Satriano(Institut de Physique du Globe de Paris)

[SSS04-P01] **Constraint of focal mechanisms of induced seismicity by using misfit angles based on known *in-situ* stress**

*Yusuke Mukuhira[1], Makoto Naoi[2], Michael C Fehler[3], Hirokazu Moriya[5], Takatoshi Ito[1], Hiroshi Asanuma[4], Markus O Häring[6] (1.Institute of Fluid Science, Tohoku University, 2.Disaster Prevention Research Institute, Kyoto University, 3.Earth Resources Laboratory, MIT, 4.FREA, AIST, 5.School of Engineering, Tohoku University, 6.Häring GeoProject)

[SSS04-P02] Kinematic slip imaging of the Mw 3.3 earthquake in the St. Gallen 2013 geothermal reservoir, Switzerland, using an isochrone back projection approach

*Claudio Satriano[1], Eszter Király-Proag[2], Pascal Bernard[1], Stefan Wiemer[2] (1.Institut de Physique du Globe de Paris, France, 2.ETH Swiss Federal Institute of Technology Zurich, Switzerland)

[SSS04-P03] **Monitoring induced seismicity with a single seismic station by combining coda wave interferometry with distance geometry solvers**

*Francesco Grigoli[1], Simone Cesca[2], Alessandro Vuan[3], Filippo Broggini[1], John Clinton[1], Stefan Wiemer[1] (1.ETH-Zurich, Switzerland, 2.GFZ-Potsdam, Germany, 3.OGS-Trieste, Italy)

[SSS04-P04] Automatic Earthquake Locating by Stacking Characteristic Functions in a Source Scanning Method

★Invited Papers

*Hilary Chang[1], Alison Malcolm[1], Frédérick Massin[2], Francesco Grigoli[2] (1.Memorial University of Newfoundland, Earth Sciences, Canada, 2. ETH Zurich, Department of Earth Sciences, Zürich, Switzerland)

[SSS04-P05] Earthquake nowcasting: further development and application to Japan

*Kazuyoshi Nanjo[1], John B. Rundle[2], Tetsuo Sakurada[3] (1.University of Shizuoka, 2.University of California at Davis, 3.SAKURADA&Company)

[E] Poster | S (Solid Earth Sciences)：S-SS Seismology

10:45 AM - 12:15 PM JST | 1:45 AM - 3:15 AM UTC | Poster Hall International Exhibition Hall8, Makuhari Messe_6

[S-SS05] Induced and triggered seismicity: case-studies, monitoring and modeling techniques

convener:Luca Urpi(Swiss Seismological Service - ETH Zurich), Bogdan Enescu(Department of Geophysics, Kyoto University), Yosuke Aoki(Earthquake Research Institute, University of Tokyo), Francesco Grigoli(ETH-Zurich, Swiss Seismological Service)

[SSS05-P01] Harmonic seismic waves excited by far-field earthquakes

*Osamu Murakami[1] (1.Tono Rearch Institute of Earthquake Science, Association for the Development of Earthquake Prediction)

[SSS05-P02] **Dynamic triggering of microseismicity around Yunnan following the 2004 Sumatra and 2012 Indian Ocean Earthquakes**

*Lu Li[1], Baoshan Wang[1,4], Zhigang Peng[2], Danning Li[3] (1.Institute of Geophysics, CEA, 2.Georgia Tech, 3.Yunnan Earthquake Agency, 4.USTC)

[SSS05-P03] Megathrust-inducing azimuthal seismic anisotropy in local and regional crusts

*Tae-Kyung Hong[1], Junhyung Lee[1], Ilgoo Kim[1], Seongjun Park[1] (1.Department of Earth System Sciences, Yonsei University)

[SSS05-P04] **A Novel Method to Estimate Fracture Permeability: Combining microseismic observational data and reservoir engineering model**

*Meihua Yang[1,2], Yusuke Mukuhira[2], Takatoshi Ito[2] (1.State Key Laboratory of Oil and Gas Geology and Exploitation, Chendu University of Technology (China) , 2.Institute of Fluid Science, Tohoku University (Japan))

[SSS05-P05] Doublet Earthquake Triggering for the April 2014 Events in the Solomon Islands

*Calvin Luiramo Qwana[1], Masatoshi Miyazawa[2], James Mori[2] (1.Graduate School of Science, Kyoto University, 2.DPRI, Kyoto Univ.)

[SSS05-P06] Thermal pressurization in a deep geological repository as a possible mechanism for fault reactivation

*Luca Urpi[1], Antonio Pio Rinaldi[1], Jonny Rutqvist[2], Stefan Wiemer[1] (1.Swiss Seismological Service, ETH Zurich, Switzerland, 2.Energy Geosceinces Division, LBNL, USA)

[E] Poster | S (Solid Earth Sciences)：S-SS Seismology

5:15 PM - 6:30 PM JST | 8:15 AM - 9:30 AM UTC | Poster Hall International Exhibition Hall8, Makuhari Messe_25

[S-SS05] Induced and triggered seismicity: case-studies, monitoring and modeling techniques

convener:Luca Urpi(Swiss Seismological Service - ETH Zurich), Bogdan Enescu(Department of Geophysics, Kyoto University), Yosuke Aoki(Earthquake Research Institute, University of Tokyo), Francesco Grigoli(ETH-Zurich, Swiss Seismological Service)

[SSS05-P01] Harmonic seismic waves excited by far-field earthquakes

*Osamu Murakami[1] (1.Tono Rearch Institute of Earthquake Science, Association for the Development of Earthquake Prediction)

[SSS05-P02] **Dynamic triggering of microseismicity around Yunnan following the 2004 Sumatra and 2012 Indian Ocean Earthquakes**

*Lu Li[1], Baoshan Wang[1,4], Zhigang Peng[2], Danning Li[3] (1.Institute of Geophysics, CEA, 2.Georgia Tech, 3.Yunnan Earthquake Agency, 4.USTC)

[SSS05-P03] Megathrust-inducing azimuthal seismic anisotropy in local and regional crusts

*Tae-Kyung Hong[1], Junhyung Lee[1], Ilgoo Kim[1], Seongjun Park[1] (1.Department of Earth System Sciences, Yonsei University)

[SSS05-P04] **A Novel Method to Estimate Fracture Permeability: Combining microseismic observational data and reservoir engineering model**

*Meihua Yang[1,2], Yusuke Mukuhira[2], Takatoshi Ito[2] (1.State Key Laboratory of Oil and Gas Geology and Exploitation, Chendu University of Technology (China) , 2.Institute of Fluid Science, Tohoku University (Japan))

[SSS05-P05] Doublet Earthquake Triggering for the April 2014 Events in the Solomon Islands

*Calvin Luiramo Qwana[1], Masatoshi Miyazawa[2], James Mori[2] (1.Graduate School of Science, Kyoto University, 2.DPRI, Kyoto Univ.)

[SSS05-P06] Thermal pressurization in a deep geological repository as a possible mechanism for fault reactivation

*Luca Urpi[1], Antonio Pio Rinaldi[1], Jonny Rutqvist[2], Stefan Wiemer[1] (1.Swiss Seismological Service, ETH Zurich, Switzerland, 2.Energy Geosceinces Division, LBNL, USA)

[E] Poster | S (Solid Earth Sciences)：S-IT Science of the Earth's Interior & Techtonophysics

3:30 PM - 5:00 PM JST | 6:30 AM - 8:00 AM UTC | Poster Hall International Exhibition Hall8, Makuhari Messe_16

[S-IT20] Property and role of liquids inside terrestrial planets

convener:Tatsuya Sakamaki(Department of Earth Science, Tohoku University), Yoichi Nakajima(Kumamoto University, Priority Organization for Innovation and Excellence)

[SIT20-P01] Melting relations in the Fe-P system at high pressures

*Yoichi Nakajima[1,2], Haruki Obata[2], Daisuke Kinoshita[2], Shigehiko Tateno[3], Kei Hirose[3,4], Naohisa Hirao[5], Saori I. Kawaguchi[5], Yasuo Ohishi[5] (1.Priority Organization for Innovation and Excellence, Kumamoto University, 2.Department of Phsyics, Kumamoto University,, 3.Earth-Life Science Institue, Tokyo Institute of Technology, 4.Department of Earth and Planertary Science, The University of Tokyo, 5.JASRI)

[SIT20-P02] Elastic property and structure of pyrope glass at high pressure

*Naoki Hisano[1], Tatsuya Sakamaki[1], Tomonori Ohashi[1], Ken-ichi Funakoshi[2], Yuji Higo[3], Yuki Shibazaki[4], Akio Suzuki[1] (1.Department of Earth Science, Graduate School of Science, Tohoku University, 2.Neutron Science & Technology Center, Comprehensive Research Organization for Science and Society (CROSS), 3.Japan Synchrotron Radiation Research Institute, 4.International Center for Young Scientists, National Institute for Materials Science)

[SIT20-P03] The effect of water and redox state on melting at the top of the lower mantle

*Ayano Nakajima[1], Tatsuya Sakamaki[1], Akio Suzuki[1] (1.Tohoku University)

[SIT20-P04] Sound velocity measurements on liquid Fe-P alloy up to 80 GPa

*Daisuke Kinoshita[1], Yoichi Nakajima[1,2], Yasuhiro Kuwayama[2,3], Kei Hirose[3], Daisuke Ishikawa[2,4], Baron Q.R. Alfred[2] (1.Kumamoto University, 2.RIKEN MDL, 3.Tokyo University, 4.JASRI)

[SIT20-P05] High-pressure structural investigations for hydrous sodium silicate melts

*Tomonori Ohashi[1], Tatsuya Sakamaki[1], Ken-ichi Funakoshi[2], Miki Muranushi[1], Chikara Shito[1], Yuki Shibazaki[3], Akio Suzuki[1] (1.Department of Earth Science, Tohoku University, 2.Neutron Science and Technology Center, Comprehensive Research Organization for Science and Society (CROSS), 3.National Institute for Materials Science (NIMS))

[SIT20-P06] Inelastic X-ray scattering measurements of liquid Fe-N alloy under high pressure

*Asaki Iwamoto[1], Yoichi Nakajima[1,2], Daisuke Kinoshita[1], Yasuhiro Kuwayama[2,3], Kei Hirose[3], Daisuke Ishikawa[2,4], Alfred Q.R. Baron[2] (1.Kumamoto University, 2.RIKEN MDL, 3.The University of Tokyo, 4.JASRI)

[SIT20-P07] Formation of highly pure anorthite crust on the low-volatile astral bodies by low-viscous magma ocean

*Tatsuya Sakamaki[1], Yoshio Kono[2] (1.Graduate School of Science, Tohoku University, 2.Geodynamics Research Center, Ehime University)

[E] Poster | S (Solid Earth Sciences)：S-IT Science of the Earth's Interior & Techtonophysics

5:15 PM - 6:30 PM JST | 8:15 AM - 9:30 AM UTC | Poster Hall International Exhibition Hall8, Makuhari Messe_28

[S-IT20] Property and role of liquids inside terrestrial planets

convener:Tatsuya Sakamaki(Department of Earth Science, Tohoku University), Yoichi Nakajima(Kumamoto University, Priority Organization for Innovation and Excellence)

[SIT20-P01] Melting relations in the Fe-P system at high pressures

*Yoichi Nakajima[1,2], Haruki Obata[2], Daisuke Kinoshita[2], Shigehiko Tateno[3], Kei Hirose[3,4], Naohisa Hirao[5], Saori I. Kawaguchi[5], Yasuo Ohishi[5] (1.Priority Organization for Innovation and Excellence, Kumamoto University, 2.Department of Phsyics, Kumamoto University,, 3.Earth-Life Science Institue, Tokyo Institute of Technology, 4.Department of Earth and Planertary Science, The University of Tokyo, 5.JASRI)

[SIT20-P02] Elastic property and structure of pyrope glass at high pressure

*Naoki Hisano[1], Tatsuya Sakamaki[1], Tomonori Ohashi[1], Ken-ichi Funakoshi[2], Yuji Higo[3], Yuki Shibazaki[4], Akio Suzuki[1] (1.Department of Earth Science, Graduate School of Science, Tohoku University, 2.Neutron Science & Technology Center, Comprehensive Research Organization for Science and Society (CROSS), 3.Japan Synchrotron Radiation Research Institute, 4.International Center for Young Scientists, National Institute for Materials Science)

[SIT20-P03] The effect of water and redox state on melting at the top of the lower mantle

*Ayano Nakajima[1], Tatsuya Sakamaki[1], Akio Suzuki[1] (1.Tohoku University)

[SIT20-P04] Sound velocity measurements on liquid Fe-P alloy up to 80 GPa

*Daisuke Kinoshita[1], Yoichi Nakajima[1,2], Yasuhiro Kuwayama[2,3], Kei Hirose[3], Daisuke Ishikawa[2,4], Baron Q.R. Alfred[2] (1.Kumamoto University, 2.RIKEN MDL, 3.Tokyo University, 4.JASRI)

[SIT20-P05] High-pressure structural investigations for hydrous sodium silicate melts

*Tomonori Ohashi[1], Tatsuya Sakamaki[1], Ken-ichi Funakoshi[2], Miki Muranushi[1], Chikara Shito[1], Yuki Shibazaki[3], Akio Suzuki[1] (1.Department of Earth Science, Tohoku University, 2.Neutron Science and Technology Center, Comprehensive Research Organization for Science and Society (CROSS), 3.National Institute for Materials Science (NIMS))

[SIT20-P06] Inelastic X-ray scattering measurements of liquid Fe-N alloy under high pressure

*Asaki Iwamoto[1], Yoichi Nakajima[1,2], Daisuke Kinoshita[1], Yasuhiro Kuwayama[2,3], Kei Hirose[3], Daisuke Ishikawa[2,4], Alfred Q.R. Baron[2] (1.Kumamoto University, 2.RIKEN MDL, 3.The University of Tokyo, 4.JASRI)

[SIT20-P07] Formation of highly pure anorthite crust on the low-volatile astral bodies by low-viscous magma ocean

*Tatsuya Sakamaki[1], Yoshio Kono[2] (1.Graduate School of Science, Tohoku University, 2.Geodynamics Research Center, Ehime University)

[E] Poster | S (Solid Earth Sciences)：S-IT Science of the Earth's Interior & Techtonophysics

10:45 AM - 12:15 PM JST | 1:45 AM - 3:15 AM UTC | Poster Hall International Exhibition Hall8, Makuhari Messe_7

[S-IT23] Structure and Dynamics of Earth and Planetary Mantles

convener:Takashi Nakagawa(Department of Earth Sciences, The University of Hong Kong), Takashi Yoshino(Institute for Planetary Materials, Okayama University), Dapeng Zhao(Department of Geophysics, Tohoku University)

[SIT23-P01] Interaction between volcanisms inland and the spreading center: example of Galápagos archipelago

*Walid Ben Mansour[1], Guust Nolet[2], Mario Ruiz[3], Juan Carlos Afonso[1] (1.Department of Earth and Planetary Sciences, Macquarie University, Sydney (Australia), 2.Geoazur, Université Cote d'Azur, Sophia Antipolis (France), 3.Instituto Geofisco, Escuela Politecnica Nacional, Quito (Ecuador))

[SIT23-P02] **Effect of iron content on thermal conductivity of olivine with implications for cooling history of rocky planets**

*Youyue Zhang[1], Takashi Yoshino[1], Akira Yoneda[1], Masahiro Osako[2] (1.Institute for Planetary Materials, Okayama University, 2.Division of Physical Sciences, National Museum of Nature and Science)

[SIT23-P03] **The distribution of Cenozoic conglomerates and its sedimentological constraint on the uplift of the South Tianshan, NW China**

*SUN HAITAO[1] (1.China University of Petroluem-Beijing)

[SIT23-P04] **Electrical conductivity of diaspore, δ-AlOOH and ε-FeOOH**

*Ran Wang[1] (1.Institute for Planetary Materials, Okayama University)

[SIT23-P05] Multi-mode surface wave tomography for azimuthal anisotropy in the Australasian upper mantle

*Yuka Nishimura[1], Kazunori Yoshizawa[2] (1. Graduate School of Science, Hokkaido University, 2.Faculty of Science, Hokkaido University)

[SIT23-P06] Mapping multi-mode surface wave phase speeds in North America using mode-branch waveforms decomposed by linear Radon transform

*Hitoshi Matsuzawa[1], Kazunori Yoshizawa[2] (1.Graduate School of Science, Hokkaido University, 2.Faculty of Science, Hokkaido University)

[SIT23-P07] Radial anisotropy in the upper mantle using multi-mode surface waves incorporating the η_K parameter: Application to the Pacific and Australian regions

Shuya Okuyama[1], *Kazunori Yoshizawa[1,2], Hitoshi Kawakatsu[3], Takehi Isse[3] (1.Graduate School of Science, Hokkaido University, 2.Faculty of Science, Hokkaido University, 3.Earthquake Research Institute, University of Tokyo)

[SIT23-P08] Pure to impure and dry to wet olivine rheology based on high temperature dependency of diffusion creep

*Kosuke Yabe[1], Takehiko Hiraga[1] (1.School of Science, The University of Tokyo)

[SIT23-P09] Finite frequency S wave tomography model beneath the Ontong Java Plateau using data recorded by broadband ocean bottom seismographs

*Misaki Horiuchi[3], Hiroko Sugioka[3], Masayuki Obayashi[1], Daisuke Suetsugu[1], Hajime Shiobara[2], Aki Ito[1], Yasushi Ishihara[1], Satoru Tanaka[1], Takehi Isse[2], Takashi Tonegawa[1], Junko Yoshimitsu[1], Takumi Kobayashi[3] (1.Japan Agency for Marine-Earth Science and Technology, Yokosuka, Japan, 2.Earthquake Research Institute, The University of Tokyo, Tokyo, Japan, 3.The University of Kobe, Hyogo, Japan)

[SIT23-P10] Shear wave structure of the upper mantle beneath the Ontong Java Plateau

*Takehi Isse[1], Daisuke Suetsugu[2], Hajime Shiobara[1], Hiroko Sugioka[3], Aki Ito[2], Yasushi Ishihara[2], Satoru Tanaka[2], Masayuki Obayashi[2], Takashi Tonegawa[2], Junko Yoshimitsu[2], Takumi Kobayashi[3], Kazunori Yoshizawa[4] (1.Earthquake Research Institute University of Tokyo, 2.Japan Agency for Marine-Earth Science and Technology, 3.Kobe University, 4.Faculty of Science, Hokkaido University)

[SIT23-P11] Effect of impurity on post-post-perovskite transition of $MgSiO_3$ by first principles

*Koichiro Umemoto[1] (1.Earth-Life Science Institute, Tokyo Institute of Technology)

[SIT23-P12] Unsusual high-Ti corundum recovered from the Horoman peridotites, Hokkaido, Japan

*oosawa takumi[1], Shinji Yamamoto[1] (1.yokohama national university)

[SIT23-P13] Deformation experiments on akimotoite

*Longli Guan[1], Daisuke Yamazaki[1], Noriyoshi Tsujino[1] (1.Institute for Planetary Materials, Okayama University, Misasa, Japan)

[SIT23-P14] Fate of water in subducted hydrous sediments deduced from stability fields of FeOOH and AlOOH up to 20 GPa

*Takashi Yoshino[1], Edward Baker[2], Kyle Duffey[3] (1.Institute for Planetary Materials, Okayama University, 2.Department of Earth Sciences, University of Oxford, 3.Department of Geosciences, Princeton University)

[E] Poster | S (Solid Earth Sciences)：S-IT Science of the Earth's Interior & Techtonophysics

5:15 PM - 6:30 PM JST | 8:15 AM - 9:30 AM UTC | Poster Hall International Exhibition Hall8, Makuhari Messe_29

[S-IT23] Structure and Dynamics of Earth and Planetary Mantles

convener:Takashi Nakagawa(Department of Earth Sciences, The University of Hong Kong), Takashi Yoshino(Institute for Planetary Materials, Okayama University), Dapeng Zhao(Department of Geophysics, Tohoku University)

[SIT23-P01] Interaction between volcanisms inland and the spreading center: example of Galápagos archipelago

*Walid Ben Mansour[1], Guust Nolet[2], Mario Ruiz[3], Juan Carlos Afonso[1] (1.Department of Earth and Planetary Sciences, Macquarie University, Sydney (Australia), 2.Geoazur, Université Cote d'Azur, Sophia Antipolis (France), 3.Instituto Geofisco, Escuela Politecnica Nacional, Quito (Ecuador))

[SIT23-P02] **Effect of iron content on thermal conductivity of olivine with implications for cooling history of rocky planets**

*Youyue Zhang[1], Takashi Yoshino[1], Akira Yoneda[1], Masahiro Osako[2] (1.Institute for Planetary Materials, Okayama University, 2.Division of Physical Sciences, National Museum of Nature and Science)

[SIT23-P03] **The distribution of Cenozoic conglomerates and its sedimentological constraint on the uplift of the South Tianshan, NW China**

*SUN HAITAO[1] (1.China University of Petroluem-Beijing)

[SIT23-P04] **Electrical conductivity of diaspore, δ-AlOOH and ε-FeOOH**

*Ran Wang[1] (1.Institute for Planetary Materials, Okayama University)

[SIT23-P05] Multi-mode surface wave tomography for azimuthal anisotropy in the Australasian upper mantle

*Yuka Nishimura[1], Kazunori Yoshizawa[2] (1. Graduate School of Science, Hokkaido University, 2.Faculty of Science, Hokkaido University)

[SIT23-P06] Mapping multi-mode surface wave phase speeds in North America using mode-branch waveforms decomposed by linear Radon transform

*Hitoshi Matsuzawa[1], Kazunori Yoshizawa[2] (1.Graduate School of Science, Hokkaido University, 2.Faculty of Science, Hokkaido University)

[SIT23-P07] Radial anisotropy in the upper mantle using multi-mode surface waves incorporating the η_K parameter: Application to the Pacific and Australian regions

Shuya Okuyama[1], *Kazunori Yoshizawa[1,2], Hitoshi Kawakatsu[3], Takehi Isse[3] (1.Graduate School of Science, Hokkaido University, 2.Faculty of Science, Hokkaido University, 3.Earthquake Research Institute, University of Tokyo)

[SIT23-P08] Pure to impure and dry to wet olivine rheology based on high temperature dependency of diffusion creep

*Kosuke Yabe[1], Takehiko Hiraga[1] (1.School of Science, The University of Tokyo)

[SIT23-P09] Finite frequency S wave tomography model beneath the Ontong Java Plateau using data recorded by broadband ocean bottom seismographs

*Misaki Horiuchi[3], Hiroko Sugioka[3], Masayuki Obayashi[1], Daisuke Suetsugu[1], Hajime Shiobara[2], Aki Ito[1], Yasushi Ishihara[1], Satoru Tanaka[1], Takehi Isse[2], Takashi Tonegawa[1], Junko Yoshimitsu[1], Takumi Kobayashi[3] (1.Japan Agency for Marine-Earth Science and Technology, Yokosuka, Japan, 2.Earthquake Research Institute, The University of Tokyo, Tokyo, Japan, 3.The University of Kobe, Hyogo, Japan)

[SIT23-P10] Shear wave structure of the upper mantle beneath the Ontong Java Plateau

*Takehi Isse[1], Daisuke Suetsugu[2], Hajime Shiobara[1], Hiroko Sugioka[3], Aki Ito[2], Yasushi Ishihara[2], Satoru Tanaka[2], Masayuki Obayashi[2], Takashi Tonegawa[2], Junko Yoshimitsu[2], Takumi Kobayashi[3], Kazunori Yoshizawa[4] (1.Earthquake Research Institute University of Tokyo, 2.Japan Agency for Marine-Earth Science and Technology, 3.Kobe University, 4.Faculty of Science, Hokkaido University)

[SIT23-P11] Effect of impurity on post-post-perovskite transition of $MgSiO_3$ by first principles

*Koichiro Umemoto[1] (1.Earth-Life Science Institute, Tokyo Institute of Technology)

[SIT23-P12] Unsusual high-Ti corundum recovered from the Horoman peridotites, Hokkaido, Japan

*oosawa takumi[1], Shinji Yamamoto[1] (1.yokohama national university)

[SIT23-P13] Deformation experiments on akimotoite

*Longli Guan[1], Daisuke Yamazaki[1], Noriyoshi Tsujino[1] (1.Institute for Planetary Materials, Okayama University, Misasa, Japan)

[SIT23-P14] Fate of water in subducted hydrous sediments deduced from stability fields of FeOOH and AlOOH up to 20 GPa

*Takashi Yoshino[1], Edward Baker[2], Kyle Duffey[3] (1.Institute for Planetary Materials, Okayama University, 2.Department of Earth Sciences, University of Oxford, 3.Department of Geosciences, Princeton University)

[E] Poster | S (Solid Earth Sciences)：S-IT Science of the Earth's Interior & Techtonophysics

3:30 PM - 5:00 PM JST | 6:30 AM - 8:00 AM UTC | Poster Hall International Exhibition Hall8, Makuhari Messe_17

[S-IT24] Attenuation from crust to core: in situ experiments, observaions and implications

convener:Konishi Kensuke(Institute of Earth Sciences, Academia Sinica), Ikuo Katayama(Department of Earth and Planetary Systems Science, Hiroshima University), Takashi Yoshino(Institute for Planetary Materials, Okayama University), Alexandre Schubnel(CNRS)

[SIT24-P01] **Attenuation of seismic wave in water-saturated granite during triaxial deformation**

*Ikuo Katayama[1], Keiya Yamada[1], Kanta Zaima[1] (1.Department of Earth and Planetary Systems Science, Hiroshima University)

[SIT24-P02] Waveform inversion for the radial elastic and anelastic structure of the lowermost mantle beneath Central America and the Caribbean

*Anselme F. E. Borgeaud[1,2], Frederic Deschamps[1], Kensuke Konishi[1], Kenji Kawai[2], Robert J. Geller[2] (1.Institute of Earth Sciences, Academia Sinica, 2.Department of Earth and Planetary Science, Graduate School of Science, University of Tokyo)

[SIT24-P03] 3-D elastic and anelastic structure of the lowermost mantle beneath the western Pacific from finite-frequency tomography

*Konishi Kensuke[1], Nobuaki Fuji[2], Frederic Deschamps[1] (1.Institute of Earth Sciences, Academia Sinica, 2.Institut de Physique du Globe de Paris)

[SIT24-P04] **Inferring the lowermost mantle thermo-chemical structure beneath the Western Pacific with seismic attenuation and shear-wave speed anomalies**

*Frederic Deschamps[1], Kensuke Konishi[1], Nobuaki Fuji[2], Laura J Cobden[3] (1.Academia Sinica, 2.Institut de Physique du Globe de Paris, 3.Utrecht University)

[SIT24-P05] Intrinsic attenuation factor Q of partially molten Fe–S–O system

*Chao Liu[1], Takashi Yoshino[1] (1.Institute for Planetary Materials, Okayama University)

[SIT24-P06] Effect of pore pressure on attenuation of seismic waves in thermally cracked granite

*Keiya Yamada[1], Kazuki Sawayama[2], Ikuo Katayama[1] (1.Hiroshima University, 2.Kyushu University)

[E] Poster | S (Solid Earth Sciences)：S-IT Science of the Earth's Interior & Techtonophysics

5:15 PM - 6:30 PM JST | 8:15 AM - 9:30 AM UTC | Poster Hall International Exhibition Hall8, Makuhari Messe_30

[S-IT24] Attenuation from crust to core: in situ experiments, observaions and implications

convener:Konishi Kensuke(Institute of Earth Sciences, Academia Sinica), Ikuo Katayama(Department of Earth and Planetary Systems Science, Hiroshima University), Takashi Yoshino(Institute for Planetary Materials, Okayama University), Alexandre Schubnel(CNRS)

[SIT24-P01] **Attenuation of seismic wave in water-saturated granite during triaxial deformation**

*Ikuo Katayama[1], Keiya Yamada[1], Kanta Zaima[1] (1.Department of Earth and Planetary Systems Science, Hiroshima University)

[SIT24-P02] Waveform inversion for the radial elastic and anelastic structure of the lowermost mantle beneath Central America and the Caribbean

*Anselme F. E. Borgeaud[1,2], Frederic Deschamps[1], Kensuke Konishi[1], Kenji Kawai[2], Robert J. Geller[2] (1.Institute of Earth Sciences, Academia Sinica, 2.Department of Earth and Planetary Science, Graduate School of Science, University of Tokyo)

[SIT24-P03] 3-D elastic and anelastic structure of the lowermost mantle beneath the western Pacific from finite-frequency tomography

*Konishi Kensuke[1], Nobuaki Fuji[2], Frederic Deschamps[1] (1.Institute of Earth Sciences, Academia Sinica, 2.Institut de Physique du Globe de Paris)

[SIT24-P04] **Inferring the lowermost mantle thermo-chemical structure beneath the Western Pacific with seismic attenuation and shear-wave speed anomalies**

*Frederic Deschamps[1], Kensuke Konishi[1], Nobuaki Fuji[2], Laura J Cobden[3] (1.Academia Sinica, 2.Institut de Physique du Globe de Paris, 3.Utrecht University)

[SIT24-P05] Intrinsic attenuation factor Q of partially molten Fe–S–O system

*Chao Liu[1], Takashi Yoshino[1] (1.Institute for Planetary Materials, Okayama University)

[SIT24-P06] Effect of pore pressure on attenuation of seismic waves in thermally cracked granite

*Keiya Yamada[1], Kazuki Sawayama[2], Ikuo Katayama[1] (1.Hiroshima University, 2.Kyushu University)

[E] Poster | S (Solid Earth Sciences)：S-TT Technology & Techniques

3:30 PM - 5:00 PM JST | 6:30 AM - 8:00 AM UTC | Poster Hall International Exhibition Hall8, Makuhari Messe_19

[S-TT42] Recent Advances in Exploration Geophysics 2019

convener:Hitoshi Mikada(Kyoto University), Yoshihisa Iio(Disater Prevention Research Institute, Kyoto University), Nobukazu Seama(Department of Planetology, Graduate School of Science, Kobe University), Junichi Takekawa(Graduate School of Science, Kyoto University)

[STT42-P01] DISCRIMINATION OF HYDRATE BEARING MARINE SEDIMENTS BY USING FREQUENCY BASED ATTENUATION

*Nisar Ahmed[1], Mubasher Ahmad[1], Perveiz Khalid[1] (1.Institute of Geology, University of the Punjab, Lahore 54590, Pakistan)

[STT42-P02] Evaluation of methane hydrate based on attenuation parameter in seismic exploration

*Mizuki Kawabe[1], Hitoshi Mikada[1], Junichi Takekawa[1] (1.Kyoto Unibercity)

[STT42-P03] Estimating the earthquake source mechanism using full waveform inversion

*Jang Iktae[1], Hitoshi Mikada[1], Junichi Takekawa[1] (1.Kyoto University)

[STT42-P04] A quantitative analysis of the passive seismic emission tomography using the lattice Boltzmann method

*Sakemi Yuichi[1], Hitoshi Mikada[1], Junichi Takekawa[1] (1.Kyoto University)

[STT42-P05] A feasibility study for supercritical geothermal energy in enhanced geothermal system

*Tatsuki Ueda[1], Hitoshi Mikada[1], Junichi Takekawa[1] (1.Kyoto University)

[E] Poster | S (Solid Earth Sciences)：S-TT Technology & Techniques

5:15 PM - 6:30 PM JST | 8:15 AM - 9:30 AM UTC | Poster Hall International Exhibition Hall8, Makuhari Messe_32

[S-TT42] Recent Advances in Exploration Geophysics 2019

convener:Hitoshi Mikada(Kyoto University), Yoshihisa Iio(Disater Prevention Research Institute, Kyoto University), Nobukazu Seama(Department of Planetology, Graduate School of Science, Kobe University), Junichi Takekawa(Graduate School of Science, Kyoto University)

[STT42-P01] DISCRIMINATION OF HYDRATE BEARING MARINE SEDIMENTS BY USING FREQUENCY BASED ATTENUATION

*Nisar Ahmed[1], Mubasher Ahmad[1], Perveiz Khalid[1] (1.Institute of Geology, University of the Punjab, Lahore 54590, Pakistan)

[STT42-P02] Evaluation of methane hydrate based on attenuation parameter in seismic exploration

*Mizuki Kawabe[1], Hitoshi Mikada[1], Junichi Takekawa[1] (1.Kyoto Unibercity)

[STT42-P03] Estimating the earthquake source mechanism using full waveform inversion

*Jang Iktae[1], Hitoshi Mikada[1], Junichi Takekawa[1] (1.Kyoto University)

[STT42-P04] A quantitative analysis of the passive seismic emission tomography using the lattice Boltzmann method

*Sakemi Yuichi[1], Hitoshi Mikada[1], Junichi Takekawa[1] (1.Kyoto University)

[STT42-P05] A feasibility study for supercritical geothermal energy in enhanced geothermal system

*Tatsuki Ueda[1], Hitoshi Mikada[1], Junichi Takekawa[1] (1.Kyoto University)

[E] Poster | B (Biogeosciences)：B-PT Paleontology

3:30 PM - 5:00 PM JST | 6:30 AM - 8:00 AM UTC | Poster Hall International Exhibition Hall8, Makuhari Messe_22

[B-PT04] Biomineralization and the Geochemistry of Proxies

convener:Takashi Toyofuku(Japan Agency for Marine-Earth Science and Technology (JAMSTEC)), Hiroshi Kitazato(Tokyo University of Marine Science and Technology (TUMSAT)), Jelle Bijma(Alfred-Wegener-Institut Helmholtz-Zentrum f?r Polar- und Meeresforschung), Kotaro Hirose(Faculty of Science & Engineering, Waseda University)

[BPT04-P01] Living (stained) benthic foraminifera in the West-Gironde mud patch (Bay of Biscay, France): An ongoing survey for the European Community.

*Christophe Fontanier[1,2], Bruno Deflandre[1], Sylvain Rigaud[3], Sabine Schmidt[1], Bastien Lamarque[1], Pascal Lebleu[1], Dominique Poirier[1], Antoine Grémare[1] (1. Bordeaux University, EPOC Laboratory, UMR CNRS 5805 OASU, F-33615 Pessac, FRANCE, 2.FORAM Research Group, F-49140 Villevêque, FRANCE, 3.Nîmes University, GIS Laboratory, EA 7352 CHROME, F-30035 Nïmes, FRANCE)

[BPT04-P02] Biomonitoring in the Cassidaigne Canyon (NW Mediterranean): the resilience and recovery of deep-sea benthic foraminifera at a bauxite industrial waste site

*Pauline Duros[1], Christophe Fontanier[1,2,3], Briony Mamo[4,5], Deborah Mille[6], Olivier Herlory[6] (1.FORAM Research Group, F-49140 Villevêque, FRANCE, 2.Bordeaux University, EPOC Laboratory, UMR CNRS 5805 OASU, F-33615 Pessac, FRANCE, 3.Angers University, 4 boulevard Lavoisier, F-49000 Angers, FRANCE., 4.School of Biological Sciences, University of Hong Kong, Pokfulam Road Sai Wan, Hong Kong SAR, CHINA. , 5.Department of Biology, Macquarie University, North Ryde, NSW, 2109, AUSTRALIA., 6.CREOCEAN, Agence PACA Corse, 230 Avenue de Rome, Valparc-Bât B, F-83500 La Seyne sur Mer, FRANCE.)

[BPT04-P03] Comparison between assemblages of diatom fossil and biomarkers in surface sediments from Seto Inland Sea

*Kotaro Hirose[1], Hideto Nakamura[2], Takuto Ando[4], Satoshi Asaoka[3], Ken Sawada[5] (1.Faculty of Science & Engineering, Waseda University, 2.Faculty of Science, Osaka City University, 3.Research Center for Inland Seas & Department of Planetology, Kobe University, 4.Arctic Research Center, Hokkaido University, 5.Department of Earth & Planetary Science, Faculty of Science, Hokkaido University)

[BPT04-P04] Combined impacts of ocean acidification and desalination: culture experiments on the coastal species *Ammonia* sp. and *Elphidium crispum*

*Laurie Marie Charrieau[1], Helena L. Filipsson[2], Yukiko Nagai[1], Sachiko Kawada[1], Karl Ljung[2], Emma Kritzberg[3], Takashi Toyofuku[1,4] (1.Japan Agency for Marine-Earth Science and Technology, 2.Department of Geology, Lund University, Sweden, 3.Department of Biology, Lund University, Sweden, 4.Tokyo University of Marine Science and Technology (TUMSAT), Japan)

[BPT04-P05] Effects on larger benthic foraminiferal shell density under global warming

★Invited Papers

*Shunichi Kinoshita[1], Azumi Kuroyanagi[2], Hiroshi Nishi[2], Osamu Sasaki[2], Kazuhiko Fujita[3], Atsushi Suzuki[4], Hodaka Kawahata[5] (1.Graduate School of Science, Tohoku University, 2.The Tohoku University Museum, The Center for Academic Resources and Archives, Tohoku Univerity, 3.Department of Physics and Earth Sciences, Faculty of Science and Tropical Biosphere Research Center, University of the Ryukyus, 4.Geological Survey of Japan National Institute of Advanced Industrial Science and Technology, 5.Atmosphere and Ocean Research Institute, the University of Tokyo)

[BPT04-P06] Estimation of the calcification rate of foraminifera -exceptionally fast extending of the shell-

*Yukiko Nagai[1,2], Katsuyuki Uematsu[3], Takashi Toyofuku[2,4] (1.National Museum of Nature and Science of Tokyo, 2.Japan Agency for Marine-Earth Science and Technology, 3.Marine Works Japan Enterprise, 4.Tokyo university of Marine Science and Technology)

[BPT04-P07] Estimation of foraminiferal calcification process from live imaging and FIB-SEM approach

*Takashi Toyofuku[1,2], Yukiko Nagai[1,3] (1.Japan Agency for Marine-Earth Science and Technology (JAMSTEC), 2.Tokyo University of Marine Science and Technology, 3.National Museum of Nature and Science,Tokyo)

[BPT04-P08] Toward a better understanding of planktic foraminiferal proxies: Are they photosymbiotic or not?

*Haruka TAKAGI[1], Katsunori KIMOTO[2], Tetsuichi FUJIKI[2], Kazuyoshi MORIYA[3], Hiroaki SAITO[1] (1.Atmosphere and Ocean Research Institute, The University of Tokyo, 2.Japan Agency for Marine-Earth Science and Technology,

3.School of Education, Waseda University)

[BPT04-P09] Evaluation of geochemistry in hypercalcified demosponges as a paleoceanographic proxy

*Ryuji Asami[1], Tohru Naruse[2], Masaru Mizuyama[3], Ryu Uemura[3], Ryuichi Shinjo[3], Yuji Ise[4], Yoshihisa Fujita[5], Takashi Sakamaki[6] (1.Graduate School of Science, Tohoku University, 2.Tropical Biosphere Research Center, University of the Ryukyus, 3.Faculty of Science, University of the Ryukyus, 4.Centre for Marine and Coastal Studies, Universiti Sains Malaysis, 5.Okinawa Prefectural University of Arts, 6.Graduate School of Engineering, Tohoku University)

[E] Poster | B (Biogeosciences)：B-PT Paleontology

5:15 PM - 6:30 PM JST | 8:15 AM - 9:30 AM UTC | Poster Hall International Exhibition Hall8, Makuhari Messe_36

[B-PT04] Biomineralization and the Geochemistry of Proxies

convener:Takashi Toyofuku(Japan Agency for Marine-Earth Science and Technology (JAMSTEC)), Hiroshi Kitazato(Tokyo University of Marine Science and Technology (TUMSAT)), Jelle Bijma(Alfred-Wegener-Institut Helmholtz-Zentrum f?r Polar- und Meeresforschung), Kotaro Hirose(Faculty of Science & Engineering, Waseda University)

[BPT04-P01] Living (stained) benthic foraminifera in the West-Gironde mud patch (Bay of Biscay, France): An ongoing survey for the European Community.

*Christophe Fontanier[1,2], Bruno Deflandre[1], Sylvain Rigaud[3], Sabine Schmidt[1], Bastien Lamarque[1], Pascal Lebleu[1], Dominique Poirier[1], Antoine Grémare[1] (1. Bordeaux University, EPOC Laboratory, UMR CNRS 5805 OASU, F-33615 Pessac, FRANCE, 2.FORAM Research Group, F-49140 Villevêque, FRANCE, 3.Nîmes University, GIS Laboratory, EA 7352 CHROME, F-30035 Nïmes, FRANCE)

[BPT04-P02] Biomonitoring in the Cassidaigne Canyon (NW Mediterranean): the resilience and recovery of deep-sea benthic foraminifera at a bauxite industrial waste site

*Pauline Duros[1], Christophe Fontanier[1,2,3], Briony Mamo[4,5], Deborah Mille[6], Olivier Herlory[6] (1.FORAM Research Group, F-49140 Villevêque, FRANCE, 2.Bordeaux University, EPOC Laboratory, UMR CNRS 5805 OASU, F-33615 Pessac, FRANCE, 3.Angers University, 4 boulevard Lavoisier, F-49000 Angers, FRANCE., 4.School of Biological Sciences, University of Hong Kong, Pokfulam Road Sai Wan, Hong Kong SAR, CHINA. , 5.Department of Biology, Macquarie University, North Ryde, NSW, 2109, AUSTRALIA., 6.CREOCEAN, Agence PACA Corse, 230 Avenue de Rome, Valparc-Bât B, F-83500 La Seyne sur Mer, FRANCE.)

[BPT04-P03] Comparison between assemblages of diatom fossil and biomarkers in surface sediments from Seto Inland Sea

*Kotaro Hirose[1], Hideto Nakamura[2], Takuto Ando[4], Satoshi Asaoka[3], Ken Sawada[5] (1.Faculty of Science & Engineering, Waseda University, 2.Faculty of Science, Osaka City University, 3.Research Center for Inland Seas & Department of Planetology, Kobe University, 4.Arctic Research Center, Hokkaido University, 5.Department of Earth & Planetary Science, Faculty of Science, Hokkaido University)

[BPT04-P04] Combined impacts of ocean acidification and desalination: culture experiments on the coastal species *Ammonia* sp. and *Elphidium crispum*

*Laurie Marie Charrieau[1], Helena L. Filipsson[2], Yukiko Nagai[1], Sachiko Kawada[1], Karl Ljung[2], Emma Kritzberg[3], Takashi Toyofuku[1,4] (1.Japan Agency for Marine-Earth Science and Technology, 2.Department of Geology, Lund University, Sweden, 3.Department of Biology, Lund University, Sweden, 4.Tokyo University of Marine Science and Technology (TUMSAT), Japan)

[BPT04-P05] Effects on larger benthic foraminiferal shell density under global warming

★Invited Papers

*Shunichi Kinoshita[1], Azumi Kuroyanagi[2], Hiroshi Nishi[2], Osamu Sasaki[2], Kazuhiko Fujita[3], Atsushi Suzuki[4], Hodaka Kawahata[5] (1.Graduate School of Science, Tohoku University, 2.The Tohoku University Museum, The Center for Academic Resources and Archives, Tohoku Univerity, 3.Department of Physics and Earth Sciences, Faculty of Science and Tropical Biosphere Research Center, University of the Ryukyus, 4.Geological Survey of Japan National Institute of Advanced Industrial Science and Technology, 5.Atmosphere and Ocean Research Institute, the University of Tokyo)

[BPT04-P06] Estimation of the calcification rate of foraminifera -exceptionally fast extending of the shell-

*Yukiko Nagai[1,2], Katsuyuki Uematsu[3], Takashi Toyofuku[2,4] (1.National Museum of Nature and Science of Tokyo, 2.Japan Agency for Marine-Earth Science and Technology, 3.Marine Works Japan Enterprise, 4.Tokyo university of Marine Science and Technology)

[BPT04-P07] Estimation of foraminiferal calcification process from live imaging and FIB-SEM approach

*Takashi Toyofuku[1,2], Yukiko Nagai[1,3] (1.Japan Agency for Marine-Earth Science and Technology (JAMSTEC), 2.Tokyo University of Marine Science and Technology, 3.National Museum of Nature and Science,Tokyo)

[BPT04-P08] Toward a better understanding of planktic foraminiferal proxies: Are they photosymbiotic or not?

*Haruka TAKAGI[1], Katsunori KIMOTO[2], Tetsuichi FUJIKI[2], Kazuyoshi MORIYA[3], Hiroaki SAITO[1] (1.Atmosphere and Ocean Research Institute, The University of Tokyo, 2.Japan Agency for Marine-Earth Science and Technology,

3.School of Education, Waseda University)

[BPT04-P09] Evaluation of geochemistry in hypercalcified demosponges as a paleoceanographic proxy

*Ryuji Asami[1], Tohru Naruse[2], Masaru Mizuyama[3], Ryu Uemura[3], Ryuichi Shinjo[3], Yuji Ise[4], Yoshihisa Fujita[5], Takashi Sakamaki[6] (1.Graduate School of Science, Tohoku University, 2.Tropical Biosphere Research Center, University of the Ryukyus, 3.Faculty of Science, University of the Ryukyus, 4.Centre for Marine and Coastal Studies, Universiti Sains Malaysis, 5.Okinawa Prefectural University of Arts, 6.Graduate School of Engineering, Tohoku University)

[E] Poster | M (Multidisciplinary and Interdisciplinary)：M-IS Intersection

10:45 AM - 12:15 PM JST | 1:45 AM - 3:15 AM UTC | Poster Hall International Exhibition Hall8, Makuhari Messe_9

[M-IS01] Environmental, socio-economic and climatic changes in Northern Eurasia

convener:Pavel Groisman(NC State University Research Scholar at NOAA National Centers for Environmental Information, Asheville, North Carolina, USA), Shamil Maksyutov(National Institute for Environmental Studies), Evgeny P Gordov(Institute of Monitoring of Climatic and Ecological Systems SB RAS), Dmitry A Streletskiy(George Washington University)

[MIS01-P01] Effects of clear-cutting on carbon dioxide fluxes in a boreal forest ecosystem - results of numerical experiments with a three-dimensional turbulent exchange model

Yulia Mukhartova[3], Maria Dyachenko[3], Polina Mangura[3], Alexander Krupenko[3], *Alexander Olchev[1,2] (1.Faculty of Geography, Lomonosov Moscow State University, 2.A.N. Severtsov Institute of Ecology and Evolution, Russian Academy of Sciences, 3.Faculty of Physics, Lomonosov Moscow State University)

[MIS01-P02] Retrieving the forest species composition from remote sensing data using a three-dimensional radiative transfer model

*Alexander Olchev[1,2], Natalia Levashova[3], Dmitry Lukyanenko[3] (1.Faculty of Geography, Lomonosov Moscow State University , 2.Severtsov Institute of Ecology and Evolution, Russian Academy of Science, 3.Faculty of Physics, Lomonosov Moscow State University)

[MIS01-P03] Satellite-derived Burned Area for Siberia (1979 – 2000)

*Amber Jeanine Soja[1], Brian J. Stocks[2], Stefano Potter[3], Brendan Rogers[3], Donald R. Cahoon[4], Natasha Jurko[5], Susan G. Conard[6], William 'Bill' deGroot[5], Nadezhda Tchebakova[7] (1.National Iinstitute of Aerospace / NASA Langley Research Center, 2.B.J. Stocks Wildfire Investigations Ltd., 3.Woods Hole Research Center , 4.Terra Systems Research, 5.Canadian Forest Service/Service canadien des forêts, 6.George Mason University,Fairfax, VA, 7.Sukachev Institute of Forestry, Siberian Branch of the Russian Academy of Sciences)

[MIS01-P04] Analysis and prediction of hazardous hydrometeorological phenomena in the coastal areas of the Arctic

*Irina Repina[1,2] (1.A.M.Obukhov Institute of Atmospheric Physics RAS, 2.Lomonosov Moscow State University)

[MIS01-P05] Recent baric and climatic conditions over East Europe with a focus on Belarus

*Irina Danilovich[1], Vladimir Loginov[1], Pavel Groisman[2] (1. Institute for Nature Management National Academy of Science, Minsk, Belarus, 2. NC State University at NOAA National Centers for Environmental Information, Asheville, USA)

[MIS01-P06] Assessment of climatic and environmental conditions along the track of projected Kyzyl-Kuragino railway line (the Western Sayan Mountains)

★Invited Papers

*Aleksandra Alekseevna Mikheeva[1], Margarita Syromyatina[1], Yurii Kurochkin[1] (1.Institute of Earth Sciences, Saint Petersburg State University, Russia)

[MIS01-P07] Assessment of interlinkages among industrialization, climate change, and forest fire activity: Thematic study of the Republic of Sakha (Yakutia), Russia

*Kiunnei Kirillina[1], Wanglin Yan[1] (1.Graduate School of Media and Governance, Keio University SFC)

[MIS01-P08] Quantitative Evaluation of Winter Daily Precipitation over Northern Japan

*Minami Masuda[1], Akiyo Yatagai[1], Toshiyuki Nakaegawa[2], Kenji Kamiguchi[3] (1.Graduate School of Science and Technology, Hirosaki University, 2.Meteorological Research Institute/Japan Meteorological Agency, 3.Japan Meteorological Agency)

[MIS01-P09] Seasonal variation of wetland carbon dioxide and methane fluxes measured by automatic chambers at the Bakchar bog, West Siberia

*Shamil Maksyutov[1], Alexandre Fofonov[2], Denis Davydov[2], Oleg Krasnov[2], Tadanobu Nakayama[1], Mikhail Glagolev[3] (1.National Institute for Environmental Studies, 2.V.E. Zuev Institute of Atmospheric Optics, 3.M.V. Lomonosov Moscow State University)

[MIS01-P10] Climatic distances between origin and labor locations for migrants in a changing climate in Siberia by the end of the 21st century

*Elena I. Parfenova[1], Nadezhda M. Tchebakova[1] (1.V.N.Sukachev Institute of Forest SB RAS, FRC SB RAS)

[E] Poster | M (Multidisciplinary and Interdisciplinary)：M-IS Intersection

5:15 PM - 6:30 PM JST | 8:15 AM - 9:30 AM UTC | Poster Hall International Exhibition Hall8, Makuhari Messe_40

[M-IS01] Environmental, socio-economic and climatic changes in Northern Eurasia

convener:Pavel Groisman(NC State University Research Scholar at NOAA National Centers for Environmental Information, Asheville, North Carolina, USA), Shamil Maksyutov(National Institute for Environmental Studies), Evgeny P Gordov(Institute of Monitoring of Climatic and Ecological Systems SB RAS), Dmitry A Streletskiy(George Washington University)

[MIS01-P01] Effects of clear-cutting on carbon dioxide fluxes in a boreal forest ecosystem - results of numerical experiments with a three-dimensional turbulent exchange model

Yulia Mukhartova[3], Maria Dyachenko[3], Polina Mangura[3], Alexander Krupenko[3], *Alexander Olchev[1,2] (1.Faculty of Geography, Lomonosov Moscow State University, 2.A.N. Severtsov Institute of Ecology and Evolution, Russian Academy of Sciences, 3.Faculty of Physics, Lomonosov Moscow State University)

[MIS01-P02] Retrieving the forest species composition from remote sensing data using a three-dimensional radiative transfer model

*Alexander Olchev[1,2], Natalia Levashova[3], Dmitry Lukyanenko[3] (1.Faculty of Geography, Lomonosov Moscow State University , 2.Severtsov Institute of Ecology and Evolution, Russian Academy of Science, 3.Faculty of Physics, Lomonosov Moscow State University)

[MIS01-P03] Satellite-derived Burned Area for Siberia (1979 – 2000)

*Amber Jeanine Soja[1], Brian J. Stocks[2], Stefano Potter[3], Brendan Rogers[3], Donald R. Cahoon[4], Natasha Jurko[5], Susan G. Conard[6], William 'Bill' deGroot[5], Nadezhda Tchebakova[7] (1.National Iinstitute of Aerospace / NASA Langley Research Center, 2.B.J. Stocks Wildfire Investigations Ltd., 3.Woods Hole Research Center , 4.Terra Systems Research, 5.Canadian Forest Service/Service canadien des forêts, 6.George Mason University,Fairfax, VA, 7.Sukachev Institute of Forestry, Siberian Branch of the Russian Academy of Sciences)

[MIS01-P04] Analysis and prediction of hazardous hydrometeorological phenomena in the coastal areas of the Arctic

*Irina Repina[1,2] (1.A.M.Obukhov Institute of Atmospheric Physics RAS, 2.Lomonosov Moscow State University)

[MIS01-P05] Recent baric and climatic conditions over East Europe with a focus on Belarus

*Irina Danilovich[1], Vladimir Loginov[1], Pavel Groisman[2] (1. Institute for Nature Management National Academy of Science, Minsk, Belarus, 2. NC State University at NOAA National Centers for Environmental Information, Asheville, USA)

[MIS01-P06] Assessment of climatic and environmental conditions along the track of projected Kyzyl-Kuragino railway line (the Western Sayan Mountains)

★Invited Papers

*Aleksandra Alekseevna Mikheeva[1], Margarita Syromyatina[1], Yurii Kurochkin[1] (1.Institute of Earth Sciences, Saint Petersburg State University, Russia)

[MIS01-P07] Assessment of interlinkages among industrialization, climate change, and forest fire activity: Thematic study of the Republic of Sakha (Yakutia), Russia

*Kiunnei Kirillina[1], Wanglin Yan[1] (1.Graduate School of Media and Governance, Keio University SFC)

[MIS01-P08] Quantitative Evaluation of Winter Daily Precipitation over Northern Japan

*Minami Masuda[1], Akiyo Yatagai[1], Toshiyuki Nakaegawa[2], Kenji Kamiguchi[3] (1.Graduate School of Science and Technology, Hirosaki University, 2.Meteorological Research Institute/Japan Meteorological Agency, 3.Japan Meteorological Agency)

[MIS01-P09] Seasonal variation of wetland carbon dioxide and methane fluxes measured by automatic chambers at the Bakchar bog, West Siberia

*Shamil Maksyutov[1], Alexandre Fofonov[2], Denis Davydov[2], Oleg Krasnov[2], Tadanobu Nakayama[1], Mikhail Glagolev[3] (1.National Institute for Environmental Studies, 2.V.E. Zuev Institute of Atmospheric Optics, 3.M.V. Lomonosov Moscow State University)

[MIS01-P10] Climatic distances between origin and labor locations for migrants in a changing climate in Siberia by the end of the 21st century

*Elena I. Parfenova[1], Nadezhda M. Tchebakova[1] (1.V.N.Sukachev Institute of Forest SB RAS, FRC SB RAS)

[E] Poster | M (Multidisciplinary and Interdisciplinary)：M-GI General Geosciences, Information Geosciences & Simulations

1:45 PM - 3:15 PM JST | 4:45 AM - 6:15 AM UTC | Poster Hall International Exhibition Hall8, Makuhari Messe_7

[M-GI31] Open Science in Action: Research Data Sharing, Infrastructure, Transparency, and International Cooperation

convener:Yasuhiro Murayama(Strategic Program Produce Office, National Institute of Information and Communications Technology), Yasuhisa Kondo(Research Institute for Humanity and Nature), Shelley Stall(American Geophysical Union), Baptiste Cecconi(LESIA, Observatoire de Paris, CNRS, PSL Research University)

[MGI31-P01] Open Science, Community Science, and AGU's Thriving Earth Exchange.

*Shelley Stall[1], Raj Pandya[1] (1.American Geophysical Union)

[MGI31-P02] RDUF (Research Data Utilization Forum): an arena for community discussion of international and regional research data sharing and management

Hideaki Takeda[2], *Yasuhiro Murayama[1], RDUF secretary office[3] (1.Strategic Program Produce Office, National Institute of Information and Communications Technology, 2.National Institute of Informatics, 3.Japan Science and Technology Agency)

[MGI31-P03] Query string-controlled web service for sharable and reproducible data visualization of earth, planetary and space sciences

*Koji Imai[1], Yasuhiro Murayama[1] (1.National Institute of Information and Communications Technology)

[MGI31-P04] Development of ground pipeline system for high-level scientific data products of the Hisaki satellite mission and its application to planetary space weather

*Tomoki Kimura[1], Atsushi Yamazaki[2], Kazuo Yoshioka[3], Go Murakami[2], Fuminori Tsuchiya[4], Hajime Kita[2], Chihiro Tao[5], Ichiro Yoshikawa[3], Atsushi Kumamoto[6], Yamauchi Chisato[7] (1.Frontier Research Institute for Interdisciplinary Sciences, Tohoku University, 2.Institute of Space and Astronautical Science, Japan Aerospace Exploration Agency, 3.Department of Complexity Science and Engineering, University of Tokyo, 4.Planetary Plasma and Atmospheric Research Center, Tohoku University, 5.National Institute of Information and Communications Technology, 6.Space and Terrestrial Plasma Physics Laboratory, Tohoku University, 7.Misato Observatory)

[MGI31-P05] Recent activities of the IUGONET for accelerating the integrated solar terrestrial science

*Shuji Abe[1], Yoshimasa Tanaka[2], Norio Umemura[3], Atsuki Shinbori[3], Satoru UeNo[4], Masahito Nose[3] (1.International Center for Space Weather Science and Education, Japan, 2.National Institute of Polar Research, 3.Institute for Space-Earth Environmental Research, Nagoya University, 4.Kwasan & Hida Observatories, School of Science, Kyoto University)

[MGI31-P06] Attempt for Research Data Sharing and Citation in context of Open Science - Sharing Atmospheric MF Radar Observation Database as a Case Study

*Isoda Fusako[1], Yasuhiro Murayama[1], Koji Imai[1] (1.National Institute of Information and Communications Technology)

[MGI31-P07] A case example of sharing meteor radio observational data by small laboratory

*Yukinobu Koyama[1], Yusuke Miyanari[1] (1.National Institute of Technology, Oita College)

[MGI31-P08] Promotion of an Open-Science Activity of the Earth Science - Coordinated Observations and Data Analyses of meteor-associated Low-Frequency Radio Emission and Anomalous Hearing

*Takashi Watanabe[1] (1.ISC World Data System International Programme Office)

[MGI31-P09] Current status of minting DOIs for research data in JAMSTEC

*Kazuyo Fukuda[1], Hajime Kawakami[1], Tomoki Sasaki[1], Hiroki Horikawa[1], Hideaki Saito[1], Chizuru Saito[1], Sonoda Akira[1] (1.Japan Agency for Marine-Earth Science and Technology)

[MGI31-P10] Application of Web and GIS Technology to Develop Military's Differential Action Information Platform

*Chien Hao Chang[1], Ch Yu Liu[1], Chun Ta Wei[1] (1.Department of Computer Science and Information Engineering,CCIT)

[E] Poster | M (Multidisciplinary and Interdisciplinary)：M-GI General Geosciences, Information Geosciences & Simulations

5:15 PM - 6:30 PM JST | 8:15 AM - 9:30 AM UTC | Poster Hall International Exhibition Hall8, Makuhari Messe_43

[M-GI31] Open Science in Action: Research Data Sharing, Infrastructure, Transparency, and International Cooperation

convener:Yasuhiro Murayama(Strategic Program Produce Office, National Institute of Information and Communications Technology), Yasuhisa Kondo(Research Institute for Humanity and Nature), Shelley Stall(American Geophysical Union), Baptiste Cecconi(LESIA, Observatoire de Paris, CNRS, PSL Research University)

[MGI31-P01] Open Science, Community Science, and AGU's Thriving Earth Exchange.

*Shelley Stall[1], Raj Pandya[1] (1.American Geophysical Union)

[MGI31-P02] RDUF (Research Data Utilization Forum): an arena for community discussion of international and regional research data sharing and management

Hideaki Takeda[2], *Yasuhiro Murayama[1], RDUF secretary office[3] (1.Strategic Program Produce Office, National Institute of Information and Communications Technology, 2.National Institute of Informatics, 3.Japan Science and Technology Agency)

[MGI31-P03] Query string-controlled web service for sharable and reproducible data visualization of earth, planetary and space sciences

*Koji Imai[1], Yasuhiro Murayama[1] (1.National Institute of Information and Communications Technology)

[MGI31-P04] Development of ground pipeline system for high-level scientific data products of the Hisaki satellite mission and its application to planetary space weather

*Tomoki Kimura[1], Atsushi Yamazaki[2], Kazuo Yoshioka[3], Go Murakami[2], Fuminori Tsuchiya[4], Hajime Kita[2], Chihiro Tao[5], Ichiro Yoshikawa[3], Atsushi Kumamoto[6], Yamauchi Chisato[7] (1.Frontier Research Institute for Interdisciplinary Sciences, Tohoku University, 2.Institute of Space and Astronautical Science, Japan Aerospace Exploration Agency, 3.Department of Complexity Science and Engineering, University of Tokyo, 4.Planetary Plasma and Atmospheric Research Center, Tohoku University, 5.National Institute of Information and Communications Technology, 6.Space and Terrestrial Plasma Physics Laboratory, Tohoku University, 7.Misato Observatory)

[MGI31-P05] Recent activities of the IUGONET for accelerating the integrated solar terrestrial science

*Shuji Abe[1], Yoshimasa Tanaka[2], Norio Umemura[3], Atsuki Shinbori[3], Satoru UeNo[4], Masahito Nose[3] (1.International Center for Space Weather Science and Education, Japan, 2.National Institute of Polar Research, 3.Institute for Space-Earth Environmental Research, Nagoya University, 4.Kwasan & Hida Observatories, School of Science, Kyoto University)

[MGI31-P06] Attempt for Research Data Sharing and Citation in context of Open Science - Sharing Atmospheric MF Radar Observation Database as a Case Study

*Isoda Fusako[1], Yasuhiro Murayama[1], Koji Imai[1] (1.National Institute of Information and Communications Technology)

[MGI31-P07] A case example of sharing meteor radio observational data by small laboratory

*Yukinobu Koyama[1], Yusuke Miyanari[1] (1.National Institute of Technology, Oita College)

[MGI31-P08] Promotion of an Open-Science Activity of the Earth Science - Coordinated Observations and Data Analyses of meteor-associated Low-Frequency Radio Emission and Anomalous Hearing

*Takashi Watanabe[1] (1.ISC World Data System International Programme Office)

[MGI31-P09] Current status of minting DOIs for research data in JAMSTEC

*Kazuyo Fukuda[1], Hajime Kawakami[1], Tomoki Sasaki[1], Hiroki Horikawa[1], Hideaki Saito[1], Chizuru Saito[1], Sonoda Akira[1] (1.Japan Agency for Marine-Earth Science and Technology)

[MGI31-P10] Application of Web and GIS Technology to Develop Military's Differential Action Information Platform

*Chien Hao Chang[1], Ch Yu Liu[1], Chun Ta Wei[1] (1.Department of Computer Science and Information Engineering,CCIT)

[E] Poster | M (Multidisciplinary and Interdisciplinary)：M-SD Space Development & Earth Observation from Space

1:45 PM - 3:15 PM JST | 4:45 AM - 6:15 AM UTC | Poster Hall International Exhibition Hall8, Makuhari Messe_8

[M-SD42] A new era of international space collaboration using microsatellites

convener:Junichi Kurihara(Graduate School of Science, Hokkaido University), Joel Joseph Jr Marciano(Advanced Science and Technology Institute, Department of Science and Technology, Philippines), Huy Xuan Le(Vietnam National Space Center)

[MSD42-P01] A high spatial resolution multispectral remote sensing by the RISESAT microsatellite

*Junichi Kurihara[1], Toshinori Kuwahara[2], Shinya Fujita[2], Yuji Sakamoto[2], Yukihiro Takahashi[1] (1.Graduate School of Science, Hokkaido University, 2.Graduate School of Engineering)

[MSD42-P02] Initial check out and experiment plan of Very Small Optical Transmitter (VSOTA) on board a micro satellite RISESAT for Space-Ground Optical Communication

*Hiroo Kunimori[1], Hideki Takenaka[1], Toshinori Kuwahara[2], Yuji Sakamoto[2], Shinya Fujita[2], Hannah Tomio[2], MOROKOT SAKAL[2], Junichi Kurihara[3] (1.National Institute of Information and Communications Technology, 2.Tohoku Univ., 3.Hokkaido Univ.)

[MSD42-P03] Ten years history of Tohoku University ground station and operation system for micro and nano satellites

*Yuji Sakamoto[1], Toshinori Kuwahara[1], Shinya Fujita[1] (1.Tohoku University)

[MSD42-P04] Development of Thermal Infrared Sensor Camera on board LAPAN-A4 for Thunderstorm Cloud Observation

*Purwadi Purwadi[1,2], Yukihiro Takahashi[1], Junichi Kurihara[1], M. Arif Saifudin[3] (1.Department of Cosmosciences, Hokkaido University, Sapporo 0600810, Japan, 2.Agency for Assessment and Application of Technology (BPPT), Jakarta 10340, Indonesia, 3.Indonesian National Institute of Aeronautics and Space (LAPAN), Jawa Barat, 16310, Indonesia)

[E] Poster | M (Multidisciplinary and Interdisciplinary)：M-SD Space Development & Earth Observation from Space

5:15 PM - 6:30 PM JST | 8:15 AM - 9:30 AM UTC | Poster Hall International Exhibition Hall8, Makuhari Messe_47

[M-SD42] A new era of international space collaboration using microsatellites

convener:Junichi Kurihara(Graduate School of Science, Hokkaido University), Joel Joseph Jr Marciano(Advanced Science and Technology Institute, Department of Science and Technology, Philippines), Huy Xuan Le(Vietnam National Space Center)

[MSD42-P01] A high spatial resolution multispectral remote sensing by the RISESAT microsatellite

*Junichi Kurihara[1], Toshinori Kuwahara[2], Shinya Fujita[2], Yuji Sakamoto[2], Yukihiro Takahashi[1] (1.Graduate School of Science, Hokkaido University, 2.Graduate School of Engineering)

[MSD42-P02] Initial check out and experiment plan of Very Small Optical Transmitter (VSOTA) on board a micro satellite RISESAT for Space-Ground Optical Communication

*Hiroo Kunimori[1], Hideki Takenaka[1], Toshinori Kuwahara[2], Yuji Sakamoto[2], Shinya Fujita[2], Hannah Tomio[2], MOROKOT SAKAL[2], Junichi Kurihara[3] (1.National Institute of Information and Communications Technology, 2.Tohoku Univ., 3.Hokkaido Univ.)

[MSD42-P03] Ten years history of Tohoku University ground station and operation system for micro and nano satellites

*Yuji Sakamoto[1], Toshinori Kuwahara[1], Shinya Fujita[1] (1.Tohoku University)

[MSD42-P04] Development of Thermal Infrared Sensor Camera on board LAPAN-A4 for Thunderstorm Cloud Observation

*Purwadi Purwadi[1,2], Yukihiro Takahashi[1], Junichi Kurihara[1], M. Arif Saifudin[3] (1.Department of Cosmosciences, Hokkaido University, Sapporo 0600810, Japan, 2.Agency for Assessment and Application of Technology (BPPT), Jakarta 10340, Indonesia, 3.Indonesian National Institute of Aeronautics and Space (LAPAN), Jawa Barat, 16310, Indonesia)

Mon. May 27, 2019

[E] Poster | P (Space and Planetary Sciences)：P-PS Planetary Sciences

3:30 PM - 5:00 PM JST | 6:30 AM - 8:00 AM UTC | Poster Hall International Exhibition Hall8, Makuhari Messe_1

[P-PS05] Recent advances of Venus science

convener:Takehiko Satoh(Institute of Space and Astronautical Science, Japan Aerospace Exploration Agency), Takeshi Horinouchi(Faculty of Environmental Earth Science, Hokkaido University), Masaru Yamamoto(Research Institute for Applied Mechanics, Kyushu University), Kevin McGouldrick(University of Colorado Boulder)

[PPS05-P01] New thermal infrared camera for fine horizontal brightness temperature structures at the cloud-top level of Venus

*Tetsuya Fukuhara[1], Makoto Taguchi[1], Takeshi Imamura[2], Sanjay S Limaye[3] (1.Rikkyo University, 2.The University of Tokyo, 3.University of Wisconsin)

[PPS05-P02] Temperature and wind variations in Venusian mesosphere and lower thermosphere by mid-infrared heterodyne spectrometer in 2018

*Kosuke Takami[1], Hiromu Nakagawa[1], Hideo Sagawa[2], Isao Murata[1], Yasumasa Kasaba[1] (1.Graduate School of Science, Tohoku University, 2.Division of Science, Kyoto Sangyo University)

[PPS05-P03] Local time dependence of limb darkening seen in the thermal infrared Venus disk

*Masahiro Akiba[1] (1.Rikkyo University)

[PPS05-P04] Stationary wavy features and Banded structures at Venusian cloud top extracted by averaging multiple LIR images

*Kiichi Fukuya[1], Takeshi Imamura[1], Makoto Taguchi[2], Tetsuya Fukuhara[2], Toru Kouyama[3] (1.Univ. of Tokyo, 2.Rikkyo Univ., 3.AIST)

[PPS05-P05] Akatsuki's IR2 Nightside Photometry Restoration by Deconvolution

*Choon Wei Vun[1], Takehiko Satoh[2,1], Kevin McGouldrick[3], Takeshi Horinouchi[4], Takao M. Sato[5] (1.SOKENDAI, 2.ISAS/JAXA, 3.University of Colorado Boulder, 4.Hokkaido University, 5.Hokkaido Information University)

[PPS05-P06] Enormous cloud cover as seen by Akatsuki/IR2 on the night-side disk of Venus

*Takehiko Satoh[1,2], Choon Wei Vun[2], Takao M. Sato[3], Takeshi Horinouchi[4], George HASHIMOTO[5], Kevin McGouldrick[6] (1.Institute of Space and Astronautical Science, Japan Aerospace Exploration Agency, 2.Department of Space Science, SOKENDAI, 3.Department of Business and Information Systems, Hokkaido Information University, 4.Faculty of Environmental Earth Science, Hokkaido University, 5.Department of Earth Science, Okayama University, 6.LASP, University of Colorado Boulder)

[PPS05-P07] The global variation of Venus cloud obtained from IR1 camera onboard AKATSUKI

*Seiko Takagi[1], Naomoto Iwagami, Yukihiro Takahashi[1], Mitsuteru Sato[1] (1.Hokkaido University, Graduate School of Science)

[PPS05-P08] Development of a Venus' cloud formation scheme for a convection resolving model

*Ko-ichiro SUGIYAMA[1], Nozomu Fukuhara[1], Masatsugu Odaka[2], Kensuke Nakajima[3], Masaki Ishiwatari[2], Takeshi Imamura[4], Yoshi-Yuki Hayashi[5] (1.National Institute of Technology, Matsue College, 2.Department of Cosmoscience, Graduate School of Science, Hokkaido University, 3.Department of Earth and Planetary Sciences,Flculty of Sciences,Kyushu University, 4.Graduate School of Frontier Sciences, The University of Tokyo, 5.Department of Planetology, Graduate School of Science, Kobe University / Center for Planetary Science (CPS))

[PPS05-P09] Zonal mean structure of Venus atmosphere observed in a Venus general circulation model with explicit radiative transfer

★Invited Papers

*Yoshi-Yuki Hayashi[1], Chisato Shiojiri[1], Hiroki Kashimura[1], Yoshiyuki O. Takahashi[1] (1.Department of Planetology/CPS, Graduate School of Science, Kobe University)

[PPS05-P10] Gravity wave packets detected in radio occultation temperature profiles of the Venus atmosphere

*Ryota Mori[1], Takeshi Imamura[1], Javier Peralta[2] (1.The University of Tokyo, 2.Japan Aerospace Exploration Agency)

[PPS05-P11] **Status of lightning hunt in Venus with Akatsuki/LAC and Pirka telescope**

*Yukihiro Takahashi[1,2], Mitsuteru Sato[1,2], Masataka Imai[3], Ralph Lorenz[4], Seiko Takagi[1,2], Ono Tatsuharu[1] (1.Graduate School of Science, Hokkaido University, 2.Faculty of Science, Hokkaido University, 3.National Institute of Advanced Industrial Science and Technology,, 4.Applied Physics Laboratory, Johns Hopkins University)

[PPS05-P12] **Possibility of electric discharge in the Venusian atmosphere due to the super-rotation of clouds**

*Adhithiyan Neduncheran[1], Ugur Guven[1,2], Ananyo Bhattacharya[3] (1.University of Petroleum and Energy Studies, India, 2.United Nations Centre for Space Science and Technology Education in Asia and the Pacific, 3.Sardar Vallabhbhai National Institute of Technology,India)

[E] Poster | P (Space and Planetary Sciences)：P-PS Planetary Sciences

5:15 PM - 6:30 PM JST | 8:15 AM - 9:30 AM UTC | Poster Hall International Exhibition Hall8, Makuhari Messe_2

[P-PS05] Recent advances of Venus science

convener:Takehiko Satoh(Institute of Space and Astronautical Science, Japan Aerospace Exploration Agency), Takeshi Horinouchi(Faculty of Environmental Earth Science, Hokkaido University), Masaru Yamamoto(Research Institute for Applied Mechanics, Kyushu University), Kevin McGouldrick(University of Colorado Boulder)

[PPS05-P01] New thermal infrared camera for fine horizontal brightness temperature structures at the cloud-top level of Venus

*Tetsuya Fukuhara[1], Makoto Taguchi[1], Takeshi Imamura[2], Sanjay S Limaye[3] (1.Rikkyo University, 2.The University of Tokyo, 3.University of Wisconsin)

[PPS05-P02] Temperature and wind variations in Venusian mesosphere and lower thermosphere by mid-infrared heterodyne spectrometer in 2018

*Kosuke Takami[1], Hiromu Nakagawa[1], Hideo Sagawa[2], Isao Murata[1], Yasumasa Kasaba[1] (1.Graduate School of Science, Tohoku University, 2.Division of Science, Kyoto Sangyo University)

[PPS05-P03] Local time dependence of limb darkening seen in the thermal infrared Venus disk

*Masahiro Akiba[1] (1.Rikkyo University)

[PPS05-P04] Stationary wavy features and Banded structures at Venusian cloud top extracted by averaging multiple LIR images

*Kiichi Fukuya[1], Takeshi Imamura[1], Makoto Taguchi[2], Tetsuya Fukuhara[2], Toru Kouyama[3] (1.Univ. of Tokyo, 2.Rikkyo Univ., 3.AIST)

[PPS05-P05] Akatsuki's IR2 Nightside Photometry Restoration by Deconvolution

*Choon Wei Vun[1], Takehiko Satoh[2,1], Kevin McGouldrick[3], Takeshi Horinouchi[4], Takao M. Sato[5] (1.SOKENDAI, 2.ISAS/JAXA, 3.University of Colorado Boulder, 4.Hokkaido University, 5.Hokkaido Information University)

[PPS05-P06] Enormous cloud cover as seen by Akatsuki/IR2 on the night-side disk of Venus

*Takehiko Satoh[1,2], Choon Wei Vun[2], Takao M. Sato[3], Takeshi Horinouchi[4], George HASHIMOTO[5], Kevin McGouldrick[6] (1.Institute of Space and Astronautical Science, Japan Aerospace Exploration Agency, 2.Department of Space Science, SOKENDAI, 3.Department of Business and Information Systems, Hokkaido Information University, 4.Faculty of Environmental Earth Science, Hokkaido University, 5.Department of Earth Science, Okayama University, 6.LASP, University of Colorado Boulder)

[PPS05-P07] The global variation of Venus cloud obtained from IR1 camera onboard AKATSUKI

*Seiko Takagi[1], Naomoto Iwagami, Yukihiro Takahashi[1], Mitsuteru Sato[1] (1.Hokkaido University, Graduate School of Science)

[PPS05-P08] Development of a Venus' cloud formation scheme for a convection resolving model

*Ko-ichiro SUGIYAMA[1], Nozomu Fukuhara[1], Masatsugu Odaka[2], Kensuke Nakajima[3], Masaki Ishiwatari[2], Takeshi Imamura[4], Yoshi-Yuki Hayashi[5] (1.National Institute of Technology, Matsue College, 2.Department of Cosmoscience, Graduate School of Science, Hokkaido University, 3.Department of Earth and Planetary Sciences,Flculty of Sciences,Kyushu University, 4.Graduate School of Frontier Sciences, The University of Tokyo, 5.Department of Planetology, Graduate School of Science, Kobe University / Center for Planetary Science (CPS))

[PPS05-P09] Zonal mean structure of Venus atmosphere observed in a Venus general circulation model with explicit radiative transfer

★Invited Papers

*Yoshi-Yuki Hayashi[1], Chisato Shiojiri[1], Hiroki Kashimura[1], Yoshiyuki O. Takahashi[1] (1.Department of Planetology/CPS, Graduate School of Science, Kobe University)

[PPS05-P10] Gravity wave packets detected in radio occultation temperature profiles of the Venus atmosphere

*Ryota Mori[1], Takeshi Imamura[1], Javier Peralta[2] (1.The University of Tokyo, 2.Japan Aerospace Exploration Agency)

[PPS05-P11] Status of lightning hunt in Venus with Akatsuki/LAC and Pirka telescope

*Yukihiro Takahashi[1,2], Mitsuteru Sato[1,2], Masataka Imai[3], Ralph Lorenz[4], Seiko Takagi[1,2], Ono Tatsuharu[1] (1.Graduate School of Science, Hokkaido University, 2.Faculty of Science, Hokkaido University, 3.National Institute of

Advanced Industrial Science and Technology,, 4.Applied Physics Laboratory, Johns Hopkins University)

[PPS05-P12] Possibility of electric discharge in the Venusian atmosphere due to the super-rotation of clouds

*Adhithiyan Neduncheran[1], Ugur Guven[1,2], Ananyo Bhattacharya[3] (1.University of Petroleum and Energy Studies, India, 2.United Nations Centre for Space Science and Technology Education in Asia and the Pacific, 3.Sardar Vallabhbhai National Institute of Technology,India)

[E] Poster | P (Space and Planetary Sciences)：P-EM Solar-Terrestrial Sciences, Space Electromagnetism & Space Environment

1:45 PM - 3:15 PM JST | 4:45 AM - 6:15 AM UTC | Poster Hall International Exhibition Hall8, Makuhari Messe_1

[P-EM10] Multi-scale Coupling in the Magnetosphere-Ionosphere-Thermosphere System

convener:Yue Deng(University of Texas at Arlington), Toshi Nishimura(Boston University), Huixin Liu(Earth and Planetary Science Division, Kyushu University SERC, Kyushu University), Yanshi Huang(Harbin Institute of Technology, Shenzhen)

[PEM10-P01] Atmospheric responses in both hemispheres to relativistic electron precipitation

*Yoshimasa Tanaka[1,13,14], Takanori Nishiyama[1,14], Akira Kadokura[1,13,14], Mitsunori Ozaki[2], Yoshizumi Miyoshi[3], Shin-ichiro Oyama[3,15], Ryuho Kataoka[1,14], Masaki Tsutsumi[1,14], Koji Nishimura[1,13,14], Kaoru Sato[4], Yoshiya Kasahara[2], Atsushi Kumamoto[5], Fuminori Tsuchiya[5], Mizuki Fukizawa[5], Mitsuru Hikishima[6], Shoya Matsuda[6], Ayako Matsuoka[6], Iku Shinohara[6], Masahito Nose[3], Tsutomu Nagatsuma[7], Manabu Shinohara[8], Akiko Fujimoto[9], Mariko Teramoto[3], Reiko Nomura[10], Akira Sessai Yukimatu[1,14], Keisuke Hosokawa[11], Masafumi Shoji[3], Ralph Latteck[12] (1.National Institute of Polar Research, 2.Institute of Science and Engineering, Kanazawa University, 3.Institute for Space-Earth Environmental Research, Nagoya University, 4.Graduate School of Science, The University of Tokyo, 5.Graduate School of Science, Tohoku University, 6.Japan aerospace exploration agency, Institute of space and astronautical science, 7.National Institute of Information and Communications Technology, 8.Kagoshima National College of Technology, 9.Kyushu Institute of Technology, 10.National Observatory of Japan, 11.Department of Communication Engineering and Informatics, University of Electro-Communications, 12.Leibniz-Institute of Atmospheric Physics e.V. at the University Rostock, Germany, 13.Polar Environment Data Science Center, Joint-Support Center for Data Science Research, Research Organization of Information and Systems, 14.The Graduate University for Advanced Studies (SOKENDAI), 15.University of Oulu, Finland)

[PEM10-P02] Comparison of precipitating particle energy of proton aurora at geomagnetic conjugate points

*Makoto Taguchi[1], Tatsuki Nishijima[1], Akira Kadokura[2] (1.Rikkyo University, 2.Research Organization of Information and Systems)

[PEM10-P03] A regularized deep convolutional general adversarial network (R-DCGAN) for total electron content map completion

*Mingwu Jin[1], Zhou Chen[2,3], Yue Deng[1], Yang Pan[1], Jin-Song Wang[2] (1.University of Texas at Arlington, 2.Institute of Space Science and Technology, Nanchang University, Nanchang, China, 3.Key Laboratory of Space Weather, National Center for Space Weather, China Meteorological Administration, Beijing, China)

[PEM10-P04] A long-lasting auroral bright spot around magnetic north pole: Is it the evidence of stable magnetic reconnection?

*Qing-He Zhang[1], Guo-Cheng Shen[1], Yong-Liang Zhang[2], Kjellmar Oksavik[3], Michael Lockwood[4], Zan-Yang Xing[1], Yu-Zhang Ma[1] (1.Institute of Space Sciences, Shandong University, Weihai, China, 2.The Johns Hopkins University Applied Physics Laboratory, Laurel, Maryland, USA, 3.Birkeland Centre for Space Science, University of Bergen, Bergen, Norway, 4.Department of Meteorology, University of Reading, Earley Gate, Post Office Box 243, RG6 6BB, UK.)

[PEM10-P05] Statistical study of the relationship between ion upflow and field-aligned current in the topside ionosphere for both hemispheres during disturbed and quiet times

Shan-Yu Zhou[1], *Qing-He Zhang[1], P. T. Jayachandran[2], Kjellmar Oksavik[3], Larry Lyons[4], Zan-Yang Xing[1], Yu-Zhang Ma[1], Marc Hairston[5], Yong Wang[1] (1.Institute of Space Sciences, Shandong University, Weihai, China, 2.Physics Department, University of New Brunswick, Fredericton, New Brunswick, Canada, 3.Birkeland Centre for Space Science, University of Bergen, Bergen, Norway, 4.Department of Atmospheric and Oceanic Sciences, University of California, Los Angeles, California, USA, 5.William B. Hanson Center for Space Sciences, University of Texas at Dallas, Richardson, Texas, USA)

[PEM10-P06] SAPS in the 2013 March 17 Storm Event: Initial Results from the Coupled Magnetosphere-Ionosphere-Thermosphere Model

*Dong Lin[1,2], Wenbin Wang[2], Wayne Scales[1], Kevin Pham[2], Jing Liu[2], Binzheng Zhang[2], Viacheslav Merkin[3], Xueling Shi[1] (1.Virginia Tech, 2.High Altitude Observatory, NCAR, 3.APL, John Hopkins Univ.)

[PEM10-P07] Westward turning motions of nighttime medium-scale traveling ionospheric disturbances (MSTIDs) at the equatorward side of the dusk side auroral oval associated with auroral brightening

*Sneha Yadav[1,2], Kazuo Shiokawa[1], Shin-ichiro Oyama[1,3,4], Yuichi Otsuka[1] (1.ISEE, Nagoya University, Nagoya, Japan, 2.SPL, VSSC, India, 3.Ionosphere Research Unit, University of Oulu, Oulu, Finland, 4.NIPR, Tachikawa, Japan)

[E] Poster | P (Space and Planetary Sciences)：P-EM Solar-Terrestrial Sciences, Space Electromagnetism & Space Environment

5:15 PM - 6:30 PM JST | 8:15 AM - 9:30 AM UTC | Poster Hall International Exhibition Hall8, Makuhari Messe_4

[P-EM10] Multi-scale Coupling in the Magnetosphere-Ionosphere-Thermosphere System

convener:Yue Deng(University of Texas at Arlington), Toshi Nishimura(Boston University), Huixin Liu(Earth and Planetary Science Division, Kyushu University SERC, Kyushu University), Yanshi Huang(Harbin Institute of Technology, Shenzhen)

[PEM10-P01] Atmospheric responses in both hemispheres to relativistic electron precipitation

*Yoshimasa Tanaka[1,13,14], Takanori Nishiyama[1,14], Akira Kadokura[1,13,14], Mitsunori Ozaki[2], Yoshizumi Miyoshi[3], Shin-ichiro Oyama[3,15], Ryuho Kataoka[1,14], Masaki Tsutsumi[1,14], Koji Nishimura[1,13,14], Kaoru Sato[4], Yoshiya Kasahara[2], Atsushi Kumamoto[5], Fuminori Tsuchiya[5], Mizuki Fukizawa[5], Mitsuru Hikishima[6], Shoya Matsuda[6], Ayako Matsuoka[6], Iku Shinohara[6], Masahito Nose[3], Tsutomu Nagatsuma[7], Manabu Shinohara[8], Akiko Fujimoto[9], Mariko Teramoto[3], Reiko Nomura[10], Akira Sessai Yukimatu[1,14], Keisuke Hosokawa[11], Masafumi Shoji[3], Ralph Latteck[12] (1.National Institute of Polar Research, 2.Institute of Science and Engineering, Kanazawa University, 3.Institute for Space-Earth Environmental Research, Nagoya University, 4.Graduate School of Science, The University of Tokyo, 5.Graduate School of Science, Tohoku University, 6.Japan aerospace exploration agency, Institute of space and astronautical science, 7.National Institute of Information and Communications Technology, 8.Kagoshima National College of Technology, 9.Kyushu Institute of Technology, 10.National Observatory of Japan, 11.Department of Communication Engineering and Informatics, University of Electro-Communications, 12.Leibniz-Institute of Atmospheric Physics e.V. at the University Rostock, Germany, 13.Polar Environment Data Science Center, Joint-Support Center for Data Science Research, Research Organization of Information and Systems, 14.The Graduate University for Advanced Studies (SOKENDAI), 15.University of Oulu, Finland)

[PEM10-P02] Comparison of precipitating particle energy of proton aurora at geomagnetic conjugate points

*Makoto Taguchi[1], Tatsuki Nishijima[1], Akira Kadokura[2] (1.Rikkyo University, 2.Research Organization of Information and Systems)

[PEM10-P03] A regularized deep convolutional general adversarial network (R-DCGAN) for total electron content map completion

*Mingwu Jin[1], Zhou Chen[2,3], Yue Deng[1], Yang Pan[1], Jin-Song Wang[2] (1.University of Texas at Arlington, 2.Institute of Space Science and Technology, Nanchang University, Nanchang, China, 3.Key Laboratory of Space Weather, National Center for Space Weather, China Meteorological Administration, Beijing, China)

[PEM10-P04] A long-lasting auroral bright spot around magnetic north pole: Is it the evidence of stable magnetic reconnection?

*Qing-He Zhang[1], Guo-Cheng Shen[1], Yong-Liang Zhang[2], Kjellmar Oksavik[3], Michael Lockwood[4], Zan-Yang Xing[1], Yu-Zhang Ma[1] (1.Institute of Space Sciences, Shandong University, Weihai, China, 2.The Johns Hopkins University Applied Physics Laboratory, Laurel, Maryland, USA, 3.Birkeland Centre for Space Science, University of Bergen, Bergen, Norway, 4.Department of Meteorology, University of Reading, Earley Gate, Post Office Box 243, RG6 6BB, UK.)

[PEM10-P05] Statistical study of the relationship between ion upflow and field-aligned current in the topside ionosphere for both hemispheres during disturbed and quiet times

Shan-Yu Zhou[1], *Qing-He Zhang[1], P. T. Jayachandran[2], Kjellmar Oksavik[3], Larry Lyons[4], Zan-Yang Xing[1], Yu-Zhang Ma[1], Marc Hairston[5], Yong Wang[1] (1.Institute of Space Sciences, Shandong University, Weihai, China, 2.Physics Department, University of New Brunswick, Fredericton, New Brunswick, Canada, 3.Birkeland Centre for Space Science, University of Bergen, Bergen, Norway, 4.Department of Atmospheric and Oceanic Sciences, University of California, Los Angeles, California, USA, 5.William B. Hanson Center for Space Sciences, University of Texas at Dallas, Richardson, Texas, USA)

[PEM10-P06] SAPS in the 2013 March 17 Storm Event: Initial Results from the Coupled Magnetosphere-Ionosphere-Thermosphere Model

*Dong Lin[1,2], Wenbin Wang[2], Wayne Scales[1], Kevin Pham[2], Jing Liu[2], Binzheng Zhang[2], Viacheslav Merkin[3], Xueling Shi[1] (1.Virginia Tech, 2.High Altitude Observatory, NCAR, 3.APL, John Hopkins Univ.)

[PEM10-P07] Westward turning motions of nighttime medium-scale traveling ionospheric disturbances (MSTIDs) at the equatorward side of the dusk side auroral oval associated with auroral brightening

*Sneha Yadav[1,2], Kazuo Shiokawa[1], Shin-ichiro Oyama[1,3,4], Yuichi Otsuka[1] (1.ISEE, Nagoya University, Nagoya, Japan, 2.SPL, VSSC, India, 3.Ionosphere Research Unit, University of Oulu, Oulu, Finland, 4.NIPR, Tachikawa, Japan)

[E] Poster | A (Atmospheric and Hydrospheric Sciences)：A-OS Ocean Sciences & Ocean Environment

3:30 PM - 5:00 PM JST | 6:30 AM - 8:00 AM UTC | Poster Hall International Exhibition Hall8, Makuhari Messe_3

[A-OS12] Marine ecosystems and biogeochemical cycles: theory, observation and modeling

convener:Shin-ichi Ito(Atmosphere and Ocean Research Institute, The University of Tokyo), Takafumi Hirata(Faculty of Environmental Earth Science, Hokkaido University), Enrique N Curchitser(Rutgers University New Brunswick), Eileen E Hofmann(Old Dominion University)

[AOS12-P01] Impact of the nutrient transport through the Tsushima Strait on the ecosystem in the Japan Sea

*Ryota Shibano[1], Akihiko Morimoto[1], Katsumi Takayama[2], Tetsutaro Takikawa[3], Masashi Ito[4] (1.Center for Marine Environmental Studies, Ehime University, 2.Research Institute for Applied Mechanics, Kyushu University, 3.Graduate School of Fisheries and Environmental Sciences, Nagasaki University, 4.Fisheries Oceanography Department, Japan Sea National Fisheries Research Institute)

[AOS12-P02] Revisiting vertical variations in stoichiometry during oceanic organic matter decomposition

*Masahito Shigemitsu[1], Michio Aoyama[1], Toshimasa Doi[1], Taichi Yokokawa[1], Akihiko Murata[1] (1.Japan Agency for Marine-Earth Science and Technology)

[AOS12-P03] Reproduction of iron-rich intermediate water in the Sea of Okhotsk by high resolution biogeochemical model.

*Hatsumi Nishikawa[1], Humio Mitsudera[1], Hiroshi Yoshinari[2], Takuya Nakanowatari[3], Tomohiro Nakamura[1], Keisuke Uchimoto[4], Hiroyasu Hasumi[5] (1.Institute of Low Temperature Science, Hokkaido University, 2.National Institute for Environmental Studies, 3.Tohoku National Fisheries Research Institute, Japan Fisheries Research and Education Agency, 4.Research Institute of Innovative Technology for the Earth, 5.Atmosphere and Ocean Research Institute, University of Tokyo)

[AOS12-P04] The global oceanic iron distribution estimated by data assimilation approach

*Doi Toshimasa[1], Satoshi Osafune[1], Shuhei Masuda[1], Hajime Obata[2], Kazuhiro Misumi[3], Jun Nishioka[4] (1.Japan Agency for Marine-Earth Science and Technology, 2.The University of Tokyo, 3.Central Research Institute of Electric Power Industry, 4.Hokkaido University)

[AOS12-P05] A high-resolution multi-purpose particle tracking framework for coastal areas near Japan

*Yoshimasa Matsumura[1], Shota Katsura[1], Masao Kurogi[2], Hideyuki Nakano[3], Takateru Yamagishi[4] (1.Atmosphere and Ocean Research Institute, University of Tokyo, 2.Japan Agency for Marine-Earth Science and Technology, 3.Meteorological Research Institute, Japan Meteorological Agency , 4.Research organization for Information Science and Technology)

[AOS12-P06] Numerical study on seasonality of ocean litters collected at the Dongsha Island in the northern South China Sea

*Yi-Chia Hsin[1], Chia-Ying Ko[2], Ming-Shiou Jeng[3] (1.Research Center for Environmental Changes, Academia Sinica, 2.Institute of Fisheries Science, National Taiwan University, 3.Biodiversity Research Center, Academia Sinica)

[AOS12-P07] A key spot and timing to monitor chlorophyll-a in the Kuroshio western boundary current

*Takafumi Hirata[1] (1.Faculty of Environmental Earth Science, Hokkaido University)

[AOS12-P08] **Impacts of cyclonic eddies on phytoplankton biomass and phenology in the Kuroshio Extension region**

*Eko Siswanto[1], Yoshikazu Sasai[1] (1.Japan Agency for Marine-Earth Science and Technology)

[AOS12-P09] Diagnostic estimation and uncertainties of nutrient limitation of phytoplankton growth in Michaelis-Menten functional form

*Taketo Hashioka[1], Maki Noguchi Aita[1] (1.Japan Agency for Marine-Science and Technology)

[AOS12-P10] Modeling productivity in lower trophic levels in Otsuchi Bay, northeast of Japan, using a nested OGCM with a biogeochemical component

*Takashi T Sakamoto[1], L. Shogo Urakawa[2], Sachihiko Itoh[1], Hiroyasu Hasumi[1], Kiyoshi Tanaka[1] (1.Atmosphere and Ocean Research Institute, the University of Tokyo, 2.Meteorological Research Institute, Japan Meteorologica Agancy)

[AOS12-P11] Change in lower trophic level ecosystems to decadal scale variation of climate system in the North Pacific Ocean

*Maki Noguchi Aita[1], Kazuaki Tadokoro[2], Yoshiki Komuro[3], Taketo Hashioka[1], Naomi Harada[1] (1.Research and Development Center for Global Change, Japan Agency for Marine-Earth Science and Technology, 2.Tohoku National Fisheries Research Institute, Japan Fisheries Research and Education Agency, 3.Institute of Arctic Climate and Environment Research, Japan Agency for Marine-Earth Science and Technology)

[AOS12-P12] Estimation of experienced environment of jack mackerel in the East China Sea

*Tomihiko Higuchi[1], Motomitsu Takahashi[2], Kotaro Shirai[1], Shin-ichi Ito[1] (1.Atmosphere and Ocean Research Institute, The University of Tokyo, 2.Seikai National Fisheries Research Institute,FRA)

[E] Poster | A (Atmospheric and Hydrospheric Sciences)：A-OS Ocean Sciences & Ocean Environment

5:15 PM - 6:30 PM JST | 8:15 AM - 9:30 AM UTC | Poster Hall International Exhibition Hall8, Makuhari Messe_5

[A-OS12] Marine ecosystems and biogeochemical cycles: theory, observation and modeling

convener:Shin-ichi Ito(Atmosphere and Ocean Research Institute, The University of Tokyo), Takafumi Hirata(Faculty of Environmental Earth Science, Hokkaido University), Enrique N Curchitser(Rutgers University New Brunswick), Eileen E Hofmann(Old Dominion University)

[AOS12-P01] Impact of the nutrient transport through the Tsushima Strait on the ecosystem in the Japan Sea

*Ryota Shibano[1], Akihiko Morimoto[1], Katsumi Takayama[2], Tetsutaro Takikawa[3], Masashi Ito[4] (1.Center for Marine Environmental Studies, Ehime University, 2.Research Institute for Applied Mechanics, Kyushu University, 3.Graduate School of Fisheries and Environmental Sciences, Nagasaki University, 4.Fisheries Oceanography Department, Japan Sea National Fisheries Research Institute)

[AOS12-P02] Revisiting vertical variations in stoichiometry during oceanic organic matter decomposition

*Masahito Shigemitsu[1], Michio Aoyama[1], Toshimasa Doi[1], Taichi Yokokawa[1], Akihiko Murata[1] (1.Japan Agency for Marine-Earth Science and Technology)

[AOS12-P03] Reproduction of iron-rich intermediate water in the Sea of Okhotsk by high resolution biogeochemical model.

*Hatsumi Nishikawa[1], Humio Mitsudera[1], Hiroshi Yoshinari[2], Takuya Nakanowatari[3], Tomohiro Nakamura[1], Keisuke Uchimoto[4], Hiroyasu Hasumi[5] (1.Institute of Low Temperature Science, Hokkaido University, 2.National Institute for Environmental Studies, 3.Tohoku National Fisheries Research Institute, Japan Fisheries Research and Education Agency, 4.Research Institute of Innovative Technology for the Earth, 5.Atmosphere and Ocean Research Institute, University of Tokyo)

[AOS12-P04] The global oceanic iron distribution estimated by data assimilation approach

*Doi Toshimasa[1], Satoshi Osafune[1], Shuhei Masuda[1], Hajime Obata[2], Kazuhiro Misumi[3], Jun Nishioka[4] (1.Japan Agency for Marine-Earth Science and Technology, 2.The University of Tokyo, 3.Central Research Institute of Electric Power Industry, 4.Hokkaido University)

[AOS12-P05] A high-resolution multi-purpose particle tracking framework for coastal areas near Japan

*Yoshimasa Matsumura[1], Shota Katsura[1], Masao Kurogi[2], Hideyuki Nakano[3], Takateru Yamagishi[4] (1.Atmosphere and Ocean Research Institute, University of Tokyo, 2.Japan Agency for Marine-Earth Science and Technology, 3.Meteorological Research Institute, Japan Meteorological Agency , 4.Research organization for Information Science and Technology)

[AOS12-P06] Numerical study on seasonality of ocean litters collected at the Dongsha Island in the northern South China Sea

*Yi-Chia Hsin[1], Chia-Ying Ko[2], Ming-Shiou Jeng[3] (1.Research Center for Environmental Changes, Academia Sinica, 2.Institute of Fisheries Science, National Taiwan University, 3.Biodiversity Research Center, Academia Sinica)

[AOS12-P07] A key spot and timing to monitor chlorophyll-a in the Kuroshio western boundary current

*Takafumi Hirata[1] (1.Faculty of Environmental Earth Science, Hokkaido University)

[AOS12-P08] **Impacts of cyclonic eddies on phytoplankton biomass and phenology in the Kuroshio Extension region**

*Eko Siswanto[1], Yoshikazu Sasai[1] (1.Japan Agency for Marine-Earth Science and Technology)

[AOS12-P09] Diagnostic estimation and uncertainties of nutrient limitation of phytoplankton growth in Michaelis-Menten functional form

*Taketo Hashioka[1], Maki Noguchi Aita[1] (1.Japan Agency for Marine-Science and Technology)

[AOS12-P10] Modeling productivity in lower trophic levels in Otsuchi Bay, northeast of Japan, using a nested OGCM with a biogeochemical component

*Takashi T Sakamoto[1], L. Shogo Urakawa[2], Sachihiko Itoh[1], Hiroyasu Hasumi[1], Kiyoshi Tanaka[1] (1.Atmosphere and Ocean Research Institute, the University of Tokyo, 2.Meteorological Research Institute, Japan Meteorologica Agancy)

[AOS12-P11] Change in lower trophic level ecosystems to decadal scale variation of climate system in the North Pacific Ocean

*Maki Noguchi Aita[1], Kazuaki Tadokoro[2], Yoshiki Komuro[3], Taketo Hashioka[1], Naomi Harada[1] (1.Research and Development Center for Global Change, Japan Agency for Marine-Earth Science and Technology, 2.Tohoku National Fisheries Research Institute, Japan Fisheries Research and Education Agency, 3.Institute of Arctic Climate and Environment Research, Japan Agency for Marine-Earth Science and Technology)

[AOS12-P12] Estimation of experienced environment of jack mackerel in the East China Sea

*Tomihiko Higuchi[1], Motomitsu Takahashi[2], Kotaro Shirai[1], Shin-ichi Ito[1] (1.Atmosphere and Ocean Research Institute, The University of Tokyo, 2.Seikai National Fisheries Research Institute,FRA)

[E] Poster | H (Human Geosciences)：H-DS Disaster geosciences

1:45 PM - 3:15 PM JST | 4:45 AM - 6:15 AM UTC | Poster Hall International Exhibition Hall8, Makuhari Messe_3

[H-DS11] Subaqueous Landslides and Their Anthropogenic Impact for Coastal Regions

convener:Yujin Kitamura(Department of Earth and Environmental Sciences, Graduate School of Science and Engineering, Kagoshima University), Yasuhiro Yamada(Japan Agency for Marine-Earth Science and Technology (JAMSTEC), R&D Center for Ocean Drilling Science (ODS))

[HDS11-P01] Deformed sediment gravity flow deposits associated with bypassing slides:an example from the Miocene Ushikiri Formation, Southwest Japan

*Miki Kobayashi[1], Tetsuya Sakai[2] (1.Nippon Koei, 2.Shimane University)

[HDS11-P02] Submarine Landslide and Resulting Tsunami on the Continental Shelf Slope off Shikoku

*Youdai Gon[1], Toshitaka Baba[1], Tetsuo Matsuno, Mitsuru Hayashi, Hiroshi Ichihara (1.Tokushima University graduate school)

[HDS11-P03] Sedimentary environment estimated from physical properties of sediment core collected during the cruise of Hakuho-maru KH-18-3 in the South Yatsushiro sea, western Kyushu.

*Koki Hori[1], Yujin Kitamura[2], Hakuho-maru KH-18-3 Scientists (1.Department of Earth and Planetary Sciences, Graduate School of Science, Kyushu University , 2.Department of Earth and Environmental Sciences, Graduate School of Science and Engineering , Kagoshima University)

[HDS11-P04] Variation in vane shear strength and magnetic susceptibility in the cores recovered by Hakuho-maru KH-18-3 cruise in Yatsushiro sea

*Yujin Kitamura[1], Haruka Kageyama[2], Kaede Yamasaki[2], Ryoya Goto[2], Koki Hori[2], Yuta Ikebata[2], Kuniyo Kawabata[1], Daiki Oyama[2], Hakuho-maru KH-18-3 Scientists (1.Department of Earth and Environmental Sciences, Graduate School of Science and Engineering, Kagoshima University, 2.Department of Earth and Environmental Sciences, Faculty of Science, Kagoshima University)

[HDS11-P05] Identification of turbidites in the Yatsushiro Sea surface sediment core samples from non-destructive measurements: Hakuho-maru KH-18-3 Cruise, Yatsushiro Sea, Western Kyushu, Japan

*Ryoya Goto[1], Yujin Kitamura[2], Hakuho-maru KH-18-3 Cruise Scientist (1.Atmosphere and Ocean Research Institute, The University of Tokyo, 2.Department of Earth and Environmental Sciences, Graduate School of Science, Kagoshima University)

[HDS11-P06] Revised columnar section based on grain size distribution analysis of samples from Hakuho-maru KH-18-3 in Yatsushiro sea

*Yuta Ikebata[1], Yujin Kitamura[2], Hakuho-maru KH-18-3 Scientists Family (1.Kyusyu University Graduate School Of Science Earth and Planetary Science, 2.Graduate school of science, Kagoshima University)

[E] Poster | H (Human Geosciences)：H-DS Disaster geosciences

5:15 PM - 6:30 PM JST | 8:15 AM - 9:30 AM UTC | Poster Hall International Exhibition Hall8, Makuhari Messe_13

[H-DS11] Subaqueous Landslides and Their Anthropogenic Impact for Coastal Regions

convener:Yujin Kitamura(Department of Earth and Environmental Sciences, Graduate School of Science and Engineering, Kagoshima University), Yasuhiro Yamada(Japan Agency for Marine-Earth Science and Technology (JAMSTEC), R&D Center for Ocean Drilling Science (ODS))

[HDS11-P01] Deformed sediment gravity flow deposits associated with bypassing slides:an example from the Miocene Ushikiri Formation, Southwest Japan

*Miki Kobayashi[1], Tetsuya Sakai[2] (1.Nippon Koei, 2.Shimane University)

[HDS11-P02] Submarine Landslide and Resulting Tsunami on the Continental Shelf Slope off Shikoku

*Youdai Gon[1], Toshitaka Baba[1], Tetsuo Matsuno, Mitsuru Hayashi, Hiroshi Ichihara (1.Tokushima University graduate school)

[HDS11-P03] Sedimentary environment estimated from physical properties of sediment core collected during the cruise of Hakuho-maru KH-18-3 in the South Yatsushiro sea, western Kyushu.

*Koki Hori[1], Yujin Kitamura[2], Hakuho-maru KH-18-3 Scientists (1.Department of Earth and Planetary Sciences, Graduate School of Science, Kyushu University , 2.Department of Earth and Environmental Sciences, Graduate School of Science and Engineering , Kagoshima University)

[HDS11-P04] Variation in vane shear strength and magnetic susceptibility in the cores recovered by Hakuho-maru KH-18-3 cruise in Yatsushiro sea

*Yujin Kitamura[1], Haruka Kageyama[2], Kaede Yamasaki[2], Ryoya Goto[2], Koki Hori[2], Yuta Ikebata[2], Kuniyo Kawabata[1], Daiki Oyama[2], Hakuho-maru KH-18-3 Scientists (1.Department of Earth and Environmental Sciences, Graduate School of Science and Engineering, Kagoshima University, 2.Department of Earth and Environmental Sciences, Faculty of Science, Kagoshima University)

[HDS11-P05] Identification of turbidites in the Yatsushiro Sea surface sediment core samples from non-destructive measurements: Hakuho-maru KH-18-3 Cruise, Yatsushiro Sea, Western Kyushu, Japan

*Ryoya Goto[1], Yujin Kitamura[2], Hakuho-maru KH-18-3 Cruise Scientist (1.Atmosphere and Ocean Research Institute, The University of Tokyo, 2.Department of Earth and Environmental Sciences, Graduate School of Science, Kagoshima University)

[HDS11-P06] Revised columnar section based on grain size distribution analysis of samples from Hakuho-maru KH-18-3 in Yatsushiro sea

*Yuta Ikebata[1], Yujin Kitamura[2], Hakuho-maru KH-18-3 Scientists Family (1.Kyusyu University Graduate School Of Science Earth and Planetary Science, 2.Graduate school of science, Kagoshima University)

[E] Poster | H (Human Geosciences)：H-DS Disaster geosciences

1:45 PM - 3:15 PM JST | 4:45 AM - 6:15 AM UTC | Poster Hall International Exhibition Hall8, Makuhari Messe_4

[H-DS12] Advanced Remote Sensing toward Mega-Disaster Response

convener:Young-Joo Kwak(ICHARM-UNESCO: International Centre for Water Hazard And Risk Management), Wataru Takeuchi(Institute of Industrial Science, The University of Tokyo)

[HDS12-P01] Satellite-based assessment of electricity restoration efforts in Puerto Rico after Hurricane Maria

*Miguel O Roman[1], Eleanor Stokes[2,3], Zhuosen Wang[2,3], Virginia Kalb[3], Ranjay Shrestha[4,3] (1.Earth from Space Institute, Universities Space Research Association, 2.Earth System Science Interdisciplinary Center, University of Maryland, 3.NASA Goddard Space Flight Center, 4.Science Systems and Applications, Inc)

[HDS12-P02] **Flood inundation forecasting coupled with in-situ water level and satellite data**

*Young-Joo Kwak[1], Jonggeol Park[2], Wataru Takeuchi[3] (1.ICHARM-UNESCO: International Centre for Water Hazard And Risk Management, 2.Tokyo University of Information and Sciences, 3.University of Tokyo)

[HDS12-P03] Long term monitoring of flood damage in the coastal area of Bangladesh

★Invited Papers

*Park Jonggeol[1], Young-Joo Kwak[2] (1.Tokyo University of Information Sciences, 2.ICHARM-UNESCO)

[HDS12-P04] Automatic shoreline detection and coastal change detection using multiple satellite data in Bangladesh

*Young-Joo Kwak[1] (1.ICHARM-UNESCO: International Centre for Water Hazard And Risk Management)

[E] Poster | H (Human Geosciences)：H-DS Disaster geosciences

5:15 PM - 6:30 PM JST | 8:15 AM - 9:30 AM UTC | Poster Hall International Exhibition Hall8, Makuhari Messe_14

[H-DS12] Advanced Remote Sensing toward Mega-Disaster Response

convener:Young-Joo Kwak(ICHARM-UNESCO: International Centre for Water Hazard And Risk Management), Wataru Takeuchi(Institute of Industrial Science, The University of Tokyo)

[HDS12-P01] Satellite-based assessment of electricity restoration efforts in Puerto Rico after Hurricane Maria

*Miguel O Roman[1], Eleanor Stokes[2,3], Zhuosen Wang[2,3], Virginia Kalb[3], Ranjay Shrestha[4,3] (1.Earth from Space Institute, Universities Space Research Association, 2.Earth System Science Interdisciplinary Center, University of Maryland, 3.NASA Goddard Space Flight Center, 4.Science Systems and Applications, Inc)

[HDS12-P02] **Flood inundation forecasting coupled with in-situ water level and satellite data**

*Young-Joo Kwak[1], Jonggeol Park[2], Wataru Takeuchi[3] (1.ICHARM-UNESCO: International Centre for Water Hazard And Risk Management, 2.Tokyo University of Information and Sciences, 3.University of Tokyo)

[HDS12-P03] Long term monitoring of flood damage in the coastal area of Bangladesh

★Invited Papers

*Park Jonggeol[1], Young-Joo Kwak[2] (1.Tokyo University of Information Sciences, 2.ICHARM-UNESCO)

[HDS12-P04] Automatic shoreline detection and coastal change detection using multiple satellite data in Bangladesh

*Young-Joo Kwak[1] (1.ICHARM-UNESCO: International Centre for Water Hazard And Risk Management)

[E] Poster | H (Human Geosciences)：H-CG Complex & General

3:30 PM - 5:00 PM JST | 6:30 AM - 8:00 AM UTC | Poster Hall International Exhibition Hall8, Makuhari Messe_9

[H-CG26] Deltas and estuaries: multidisciplinary analyses of complex river-mouth systems

convener:Yoshiki Saito(Estuary Research Center, Shimane University), Guan-Hong Lee(Inha University), David L Dettman(University of Arizona), Kazuaki Hori(Department of Geography, Graduate School of Environmental Studies, Nagoya University)

[HCG26-P01] Deltafront Clinoform of Abandoned Yellow River Delta in Jiangsu Province, China

*LIANGYONG ZHOU[1] (1.Qingdao Institute of Marine Geology China Geological Survey)

[HCG26-P02] Holocene evolution and Anthropocene destruction of the Krishna delta, east coast of India: delta lobe shifts, human impact, and sea-level history

Kakani Nageswara Rao[2], *Yoshiki Saito[1], K.Ch.V. Nagakumar[4], Sumiko Kubo[3], Shilpa Pandey[5], Zhen Li[6], G. Demudu[2], A.S. Rajawat[7] (1.Estuary Research Center, Shimane University, 2.Andhra University, 3.Waseda University, 4.Centre for Water Resources and Management, 5.Birbal Sahni Institute of Palaeosciences, 6.University of Victoria, 7.Space Applications Centre)

[HCG26-P03] Offset in radiocarbon ages between marine bioclast and terrestrial plant pairs in the Holocene sediments around Japan

*Nakanishi Toshimichi[1,2], Futoshi Nanayama[3,4], Atsushi Urabe[5], Kazuaki Hori[6], Wan Hong[7] (1.Kyoto Univ., 2.JAEA, 3.AIST, 4.Kumamoto Univ., 5.Niigata Univ., 6.Nagoya Univ., 7.KIGAM)

[HCG26-P04] Assessment of MEIS for Marine Spatial Planning in the Nakdong River Estuary, Busan Metropolitan City, South Korea

*Jun-Ho Lee[1], Han Jun Woo[1], Hoi-Soo Jung[1], Chan Mi Park[1] (1.Korea Institute of Ocean Science and Technology)

[HCG26-P05] Tidal changes at Asian deltas in response to future sea-level rise

*Katsuto Uehara[1] (1.Kyushu University)

[HCG26-P06] **A governing equation of non-deltaic transgressive profile: 2D numerical simulation and flume experiments**

*Junhui Wang[1,2,3], Tetsuji Muto[3] (1.China University of Petroleum (Beijing), 2.State Key Laboratory of Petroleum Resources and Prospecting, China, 3.Nagasaki University)

[E] Poster | H (Human Geosciences)：H-CG Complex & General

5:15 PM - 6:30 PM JST | 8:15 AM - 9:30 AM UTC | Poster Hall International Exhibition Hall8, Makuhari Messe_16

[H-CG26] Deltas and estuaries: multidisciplinary analyses of complex river-mouth systems

convener:Yoshiki Saito(Estuary Research Center, Shimane University), Guan-Hong Lee(Inha University), David L Dettman(University of Arizona), Kazuaki Hori(Department of Geography, Graduate School of Environmental Studies, Nagoya University)

[HCG26-P01] Deltafront Clinoform of Abandoned Yellow River Delta in Jiangsu Province, China

*LIANGYONG ZHOU[1] (1.Qingdao Institute of Marine Geology China Geological Survey)

[HCG26-P02] Holocene evolution and Anthropocene destruction of the Krishna delta, east coast of India: delta lobe shifts, human impact, and sea-level history

Kakani Nageswara Rao[2], *Yoshiki Saito[1], K.Ch.V. Nagakumar[4], Sumiko Kubo[3], Shilpa Pandey[5], Zhen Li[6], G. Demudu[2], A.S. Rajawat[7] (1.Estuary Research Center, Shimane University, 2.Andhra University, 3.Waseda University, 4.Centre for Water Resources and Management, 5.Birbal Sahni Institute of Palaeosciences, 6.University of Victoria, 7.Space Applications Centre)

[HCG26-P03] Offset in radiocarbon ages between marine bioclast and terrestrial plant pairs in the Holocene sediments around Japan

*Nakanishi Toshimichi[1,2], Futoshi Nanayama[3,4], Atsushi Urabe[5], Kazuaki Hori[6], Wan Hong[7] (1.Kyoto Univ., 2.JAEA, 3.AIST, 4.Kumamoto Univ., 5.Niigata Univ., 6.Nagoya Univ., 7.KIGAM)

[HCG26-P04] Assessment of MEIS for Marine Spatial Planning in the Nakdong River Estuary, Busan Metropolitan City, South Korea

*Jun-Ho Lee[1], Han Jun Woo[1], Hoi-Soo Jung[1], Chan Mi Park[1] (1.Korea Institute of Ocean Science and Technology)

[HCG26-P05] Tidal changes at Asian deltas in response to future sea-level rise

*Katsuto Uehara[1] (1.Kyushu University)

[HCG26-P06] **A governing equation of non-deltaic transgressive profile: 2D numerical simulation and flume experiments**

*Junhui Wang[1,2,3], Tetsuji Muto[3] (1.China University of Petroleum (Beijing), 2.State Key Laboratory of Petroleum Resources and Prospecting, China, 3.Nagasaki University)

[E] Poster | S (Solid Earth Sciences)：S-SS Seismology

1:45 PM - 3:15 PM JST | 4:45 AM - 6:15 AM UTC | Poster Hall International Exhibition Hall8, Makuhari Messe_5

[S-SS07] Rigorous Seismicity Modelling and Hypothesis Testing

convener:Jiancang Zhuang(Institute of Statistical Mathematics), Danijel Schorlemmer(GFZ German Research Centre for Geosciences), Matt Gerstenberger(GNS Science), Hiroshi Tsuruoka(Earthquake Research Institute, Tokyo Univ.)

[SSS07-P01] Development of Physics-based Ground Motion Simulation in A Hybrid Approach and Applications to Seismic Hazard Assessment in Taiwan

*Ming-Che Hsieh[1], Yin-Tung Yen[1], Kuo-Fong Ma[2,3] (1.Disaster Prevention Technology Research Center, Sinotech Engineering Consultants (Inc.), Taiwan, 2.Department of Earth Sciences, National Central University, Taiwan, 3.Earthquake-Disaster & Risk Evaluation and Management Center, National Central University, Taiwan)

[SSS07-P02] Increasing Earthquake Forecast Testability - CSEP Future Developments

*Danijel Schorlemmer[1], Naoshi Hirata[2], Fabrice Cotton[1], Matt Gerstenberger[3], Thomas Jordan[7], Warner Marzocchi[4], William Savran[7], Maximilian Werner[5], Stefan Wiemer[6], Thomas Beutin[1], David D Jackson[8], Philip Maechling[7], Sum Mak[1], Kazuyoshi Nanjo[9], Yosihiko Ogata[10], David Rhoades[3], Hiroshi Tsuruoka[2], Graeme Weatherill[1], Jiancang Zhuang[10] (1.GFZ German Research Centre for Geosciences, 2.Earthquake Research Institute, University of Tokyo, Japan, 3.GNS Science, Lower Hutt, New Zealand, 4.University of Naples, Naples, Italy, 5.University of Bristol, Bristol, United Kingdom, 6.ETH Zurich, Zurich, Switzerland, 7.University of Southern California, Los Angeles, USA, 8.University of California Los Angeles, Los Angeles, USA, 9.University of Shizuoka, Shizuoka, Japan, 10.Institute of Statistical Mathematics, Tachikawa, Japan)

[SSS07-P03] Precision versus uncertainty in regional seismic hazard mapping

*Matt Gerstenberger[1], Danijel Schorlemmer[2] (1.GNS Science, 2.GFZ-Potsdam)

[SSS07-P04] An extreme value analysis of seismograms designed for early forecast of aftershocks

*Kaoru Sawazaki[1] (1.National Research Institute for Earth Science and Disaster Resilience)

[SSS07-P05] Spatio-temporal clustering of successive earthquakes: data analyses of global data.

*THYSTERE MATONDO BANTIDI[1], Takeshi Nishimura[1] (1.Tohoku University)

[SSS07-P06] Kanto 3 month testing class results of CSEP Japan

*Hiroshi Tsuruoka[1], Naoshi Hirata[1] (1.Earthquake Research Institute, Tokyo Univ.)

[SSS07-P07] Long-term earthquake risk in North China estimated from a modern catalogue

Ziyao Xiong[2], *Jiancang Zhuang[1], Shiyong Zhou[2] (1.Institute of Statistical Mathematics, 2.Peking University)

[SSS07-P08] Distributions of focal mechanisms in background seismicity and earthquake clusters in Japan

*Jiancang Zhuang[1,2], Eri Maita[2] (1.Institute of Statistical Mathematics, 2.Graduate University for Advanced Studies)

[SSS07-P09] New Ground Motion Prediction Equations for Western Saudi Arabia

*Ryota Kiuchi[1,2], Walter Mooney[1], Hani Zahran[3] (1.U.S. Geological Survey, 2.Disaster Prevenetion Research Institute, Kyoto University, 3.Saudi Geological Survey)

[SSS07-P10] Study on the spatial and temporal change of velocity structure before and after 2003 Chengkung earthquake, Taiwan

*TING YA LIANG[1], Wen-Yen Chang[1,2,3], Strong Wen[4] (1.National DONG HWA University, 2.Eastern Taiwan Earthquake Research Center, 3.National Center for Research on Earthquake Engineering, 4.National Chung Cheng University)

[E] Poster | S (Solid Earth Sciences)：S-SS Seismology

5:15 PM - 6:30 PM JST | 8:15 AM - 9:30 AM UTC | Poster Hall International Exhibition Hall8, Makuhari Messe_19

[S-SS07] Rigorous Seismicity Modelling and Hypothesis Testing

convener:Jiancang Zhuang(Institute of Statistical Mathematics), Danijel Schorlemmer(GFZ German Research Centre for Geosciences), Matt Gerstenberger(GNS Science), Hiroshi Tsuruoka(Earthquake Research Institute, Tokyo Univ.)

[SSS07-P01] Development of Physics-based Ground Motion Simulation in A Hybrid Approach and Applications to Seismic Hazard Assessment in Taiwan

*Ming-Che Hsieh[1], Yin-Tung Yen[1], Kuo-Fong Ma[2,3] (1.Disaster Prevention Technology Research Center, Sinotech Engineering Consultants (Inc.), Taiwan, 2.Department of Earth Sciences, National Central University, Taiwan, 3.Earthquake-Disaster & Risk Evaluation and Management Center, National Central University, Taiwan)

[SSS07-P02] Increasing Earthquake Forecast Testability - CSEP Future Developments

*Danijel Schorlemmer[1], Naoshi Hirata[2], Fabrice Cotton[1], Matt Gerstenberger[3], Thomas Jordan[7], Warner Marzocchi[4], William Savran[7], Maximilian Werner[5], Stefan Wiemer[6], Thomas Beutin[1], David D Jackson[8], Philip Maechling[7], Sum Mak[1], Kazuyoshi Nanjo[9], Yosihiko Ogata[10], David Rhoades[3], Hiroshi Tsuruoka[2], Graeme Weatherill[1], Jiancang Zhuang[10] (1.GFZ German Research Centre for Geosciences, 2.Earthquake Research Institute, University of Tokyo, Japan, 3.GNS Science, Lower Hutt, New Zealand, 4.University of Naples, Naples, Italy, 5.University of Bristol, Bristol, United Kingdom, 6.ETH Zurich, Zurich, Switzerland, 7.University of Southern California, Los Angeles, USA, 8.University of California Los Angeles, Los Angeles, USA, 9.University of Shizuoka, Shizuoka, Japan, 10.Institute of Statistical Mathematics, Tachikawa, Japan)

[SSS07-P03] Precision versus uncertainty in regional seismic hazard mapping

*Matt Gerstenberger[1], Danijel Schorlemmer[2] (1.GNS Science, 2.GFZ-Potsdam)

[SSS07-P04] An extreme value analysis of seismograms designed for early forecast of aftershocks

*Kaoru Sawazaki[1] (1.National Research Institute for Earth Science and Disaster Resilience)

[SSS07-P05] Spatio-temporal clustering of successive earthquakes: data analyses of global data.

*THYSTERE MATONDO BANTIDI[1], Takeshi Nishimura[1] (1.Tohoku University)

[SSS07-P06] Kanto 3 month testing class results of CSEP Japan

*Hiroshi Tsuruoka[1], Naoshi Hirata[1] (1.Earthquake Research Institute, Tokyo Univ.)

[SSS07-P07] Long-term earthquake risk in North China estimated from a modern catalogue

Ziyao Xiong[2], *Jiancang Zhuang[1], Shiyong Zhou[2] (1.Institute of Statistical Mathematics, 2.Peking University)

[SSS07-P08] Distributions of focal mechanisms in background seismicity and earthquake clusters in Japan

*Jiancang Zhuang[1,2], Eri Maita[2] (1.Institute of Statistical Mathematics, 2.Graduate University for Advanced Studies)

[SSS07-P09] New Ground Motion Prediction Equations for Western Saudi Arabia

*Ryota Kiuchi[1,2], Walter Mooney[1], Hani Zahran[3] (1.U.S. Geological Survey, 2.Disaster Prevenetion Research Institute, Kyoto University, 3.Saudi Geological Survey)

[SSS07-P10] Study on the spatial and temporal change of velocity structure before and after 2003 Chengkung earthquake, Taiwan

*TING YA LIANG[1], Wen-Yen Chang[1,2,3], Strong Wen[4] (1.National DONG HWA University, 2.Eastern Taiwan Earthquake Research Center, 3.National Center for Research on Earthquake Engineering, 4.National Chung Cheng University)

[E] Poster | S (Solid Earth Sciences)：S-IT Science of the Earth's Interior & Techtonophysics

3:30 PM - 5:00 PM JST | 6:30 AM - 8:00 AM UTC | Poster Hall International Exhibition Hall8, Makuhari Messe_12

[S-IT21] Interaction and Coevolution of the Core and Mantle in the Earth and Planets

convener:Kenji Kawai(Department of Earth and Planetary Science, School of Science, University of Tokyo), Tsuyoshi Iizuka(University of Tokyo), Kenji Ohta(Department of Earth and Planetary Sciences, Tokyo Institute of Technology), Taku Tsuchiya(Geodynamics Research Center, Ehime University)

[SIT21-P01] Sample-scale compositional variation of the Inada granite, Ibaraki, Japan -toward the reduction of geoneutrino flux estimation errors from the Japanese crust-

★Invited Papers

*Kenta Ueki[1], Minami Kazuki[2], Tsuyoshi Iizuka[3], Sanshiro Enomoto[4], Hiroyuki Tanaka[2] (1.Japan Agency for Marine-Earth Science and Technology, 2.Earthquake Research Institute, University of Tokyo, 3.Department of Earth and Planetary Science, University of Tokyo, 4.Center for Experimental Nuclear Physics and Astrophysics, University of Washington)

[SIT21-P02] Towards a better estimation of the temperature distribution beneath the Japanese Islands

*Akiko Tanaka[1], Makoto Yamano[2], Hideki Hamamoto[3], Shusaku Goto[4], Takumi Matsumoto[5] (1.Geological Survey of Japan, National Institute of Advanced Industrial Science and Technology, 2.Earthquake Research Institute, The University of Tokyo, 3.Center for Environmental Science in Saitama, 4.Institute for Geo-Resources and Environment National Institute of Advanced Industrial Science and Technology, 5.National Research Institute for Earth Science and Disaster Resilience)

[SIT21-P03] The estimation of the neutrino flux from the crust of the Japanese islands using the geochemical database

*Satoru Haraguchi[1], Kenta Ueki[1], Hikaru Iwamori[1,2,3] (1.Japan Agency for Marine-Earth Science and Technology, 2.Earthquake Research Institute, the University of Tokyo, 3.Tokyo Institute of Technology)

[SIT21-P04] **Viscosity of potassium titanosilicate melt at high pressure**

*Akio Suzuki[1] (1.Department of Earth Science, Graduate School of Science, Tohoku University)

[SIT21-P05] **Lattice thermal conductivity of wadsleyite and ringwoodite at the mantle transition zone pressures**

*seiji kimura[1], Kenji Ohta[6], Takaaki Kawazoe[2], Kei Hirose[3], Hiroyuki Kagi[4], Takashi Yagi[5] (1.Department of Earth and Planetary Sciences Tokyo Institute of Technology, 2.Department of Earth and Planetary Systems Science, Hiroshima University, 3.Earth-Life Science Institute, Tokyo Institute of Technology, 4.Geochemical Research Center, Graduate School of Science, University of Tokyo, 5.National Institute of Advanced Industrial Science and Technology, 6.Department of Earth and Planetary Sciences, Tokyo Institute of Technology)

[SIT21-P06] In-situ X-ray observations of the olivine-spinel transformation under shear deformation: preliminary results on the reaction-induced weakening

*Tomoaki Kubo[1], Moriyama Kazuya[1], Yuichiro Mori[1], Masahiro Imamura[1], Sanae Koizumi[2], Yu Nishihara[3], Akio Suzuki[4], Yuji Higo[5] (1.Kyushu Univ., 2.ERI, 3.GRC Ehime Univ., 4.Tohoku Univ., 5.JASRI)

[SIT21-P07] Internally resistive heated diamond anvil cell experiments with metal encapsulated minerals

*YAMAMOTO TOMONARI[1], Kenji Ohta[1], Sho Suehiro[1], Hayato Inoue[1] (1.Tokyo Institute of Technology)

[SIT21-P08] Shear deformation on post-spinel

*Daisuke Yamazaki[1], Noriyoshi Tsujino[1], Yu Nishihara[2] (1.Institute for Planetary Materials, Okayama University, 2.GRC, Ehime University)

[SIT21-P09] **Lattice thermal conductivity of $CaSiO_3$ perovskite at high pressures and high temperatures**

*Kotaro Onga[1], Kenji Ohta[1], Akira Hasegawa[1,2], Takashi Yagi[2], Kei Hirose[3,4], Yasuo Ohishi[5] (1.Department of Earth and Planetary Sciences, Tokyo Institute of Technology, 2.National Institute of Advanced Industrial Science and Technology, 3.Earth-Life Science Institute, Tokyo Institute of Technology, 4.Department of Earth and Planetary Science, The University of Tokyo, 5.Japan Synchrotron Radiation Research Institute)

[SIT21-P10] **Polycrystalline diamond sintered from ultradispersed nanodiamonds**

*Masayuki Nishi[1,2], Koichiro Yamamoto[1], Youmo Zhou[1], Tetsuo Irifune[2,1] (1.Geodynamics Research Center, Ehime University, 2.Earth-Life Science Institute, Tokyo Institute of Technology)

[SIT21-P11] Thermal conductivity measurements on iron and MgO periclase at high pressure and high temperature similar to the Earth's mid-lower mantle conditions

*Akira Hasegawa[1,2], Kenji Ohta[2], Takashi Yagi[1], Kei Hirose[3,4] (1.National Institute of Advanced Industrial Science and Technology, 2.Tokyo Institude of Technology, 3.Earth-Life Science Institute, Tokyo Institude of Technology, 4.The University of Tokyo)

[SIT21-P12] Azimuthal anisotropy in the lowermost mantle beneath Philippine from ScS-S times

*Satoru Tanaka[1] (1.Department of Deep Earth Structure and Dynamics Research Japan Agency for Marine-Earth Science and Technology)

[SIT21-P13] Detailed 3-D S-velocity structure within D" at the western Pacific LLSVP margin: smaller scale plumes and paleoslabs

*Yuki Suzuki[1], Kenji Kawai[1], Robert J. Geller[1], Satoru Tanaka[2], Weerachai Siripuvaraporn[3], Songkhun Boonchaisuku[3], Noisagool Sutthipong[3], Yasushi Ishihara[2], Taweoon Kim, Koji MIYAKAWA[4], Nozomu Takeuchi[4] (1.The University of Tokyo, 2.Japan Agency for Marine-Earth Science and Technology, 3.Mahidol University, 4.Earthquake Research Institute, The University of Tokyo)

[SIT21-P14] Possible interaction between the core and mantle inferred from a core surface flow model

*Masaki Matsushima[1] (1.Department of Earth and Planetary Sciences, School of Science, Tokyo Institute of Technology)

[SIT21-P15] Determination of the noble gas partition coefficients between metal-silicate melts under high-pressure and high-temperature conditions

*Tomotaka Tanaka[1], Hideharu Kuwahara[2], Satoshi Kishi[1], Ryuichi Nomura[3], Kenji Mibe[5], Hiroyuki Kagi[4], Shigehiko Tateno[6], Hirochika Sumino[1] (1.Department of Basic Science, Graduate School of Arts and Sciences, The University of Tokyo , 2.Geodynamics Research Center, Ehime University, 3.Kyoto University, 4.Geochemical Research Center, Graduate School of Science, University of Tokyo, 5.Earthquake Research Institute, University of Tokyo, 6.Earth-Life Science Institute, Tokyo Institute of Technology)

[SIT21-P16] **Measurement of T-dependent electrical resistivity of solid and liquid Fe and Pt at fixed P**

*Innocent Ezenwa[1], Takashi Yoshino[1] (1.Institute for Planetary Materials, Okayama University)

[SIT21-P17] Ancient, highly depleted mantle constrained by Re-Os isotope and highly-siderophile element compositions of French Polynesian xenoliths

*Norikatsu Akizawa[1], Akira Ishikawa[2], Katsuhiko Suzuki[3], Tetsu Kogiso[4] (1.Atmosphere and Ocean Research Institute, The University of Tokyo, 2.Department of Earth and Planetary Sciences, Tokyo Institute of Technology, 3.Research and Development Center for Submarine Resources, Japan Agency for Marine-Earth Science and Technology (JAMSTEC), 4.Graduate School of Human and Environmental Studies, Kyoto University)

[SIT21-P18] First-principles prediction of hydrogen partitioning between the core and mantle

*Atsuroh Ohba[1], Taku Tsuchiya[1] (1.Ehime University Geodynamics Research Center)

[SIT21-P19] Microvolume stable isotope measuremetns and its applicaiton for high-pressure high-temperature experimental run products

*Madhusoodhan Satish-Kumar[1], Shinnosuke Aoyama[1] (1.Department of Geology, Faculty of Science, Niigata University)

[SIT21-P20] Electrical resistivity of hcp Fe-Si alloys at high pressure and temperature

*Hayato Inoue[1], Sho Suehiro[1], Kenji Ohta[1], Kei Hirose[2,3], Yasuo Ohishi[4] (1.Department of Earth and Planetary Sciences, Tokyo Institute of Technology, 2.Earth-Life Science Institute, Tokyo Institute of Technology, 3.Department of Earth and Planetary Science, The University of Tokyo, 4.Japan Synchrotron Radiation Research Institute)

[SIT21-P21] Electrical resistivity and thermal conductivity of fcc Fe: Implications for the Mercury's core

★Invited Papers

*Hitoshi Gomi[1], Takashi Yoshino[1] (1.Okayama University)

[SIT21-P22] Lateral heterogeneity in the lowermost outer core (F layer) of the Earth revealed by seismic analyses

*Toshiki Ohtaki[1], Satoshi Kaneshima[2], Taku Tsuchiya[3] (1.Geological Survey of Japan, National Institute of Advanced Industrial Science and Technology (AIST), 2.Department of Earth and Planetary Sciences, Kyushu University,

3.Geodynamics Research Center, Ehime University)

[SIT21-P23] Flows and light element distribution in the outer core associated with heterogeneous growth of the inner core of the Earth

*Shin-ichi Takehiro[1], Youhei SASAKI[2] (1.Research Institute for Mathematical Sciences, Kyoto University, 2.Department of Mathematics, Kyoto University)

[SIT21-P24] Sharpness of the hemispherical boundary in the inner core beneath the northern Pacific

*Ryohei Iritani[1], Hitoshi Kawakatsu[1], Nozomu Takeuchi[1] (1.Earthquake Research Institute, Univ. of Tokyo)

[SIT21-P25] Stable carbon isotope fractionation in Fe-C system from first principles

*Haruhiko Dekura[1], Taku Tsuchiya[1] (1.Geodynamics Research Center, Ehime University)

[E] Poster | S (Solid Earth Sciences)：S-IT Science of the Earth's Interior & Techtonophysics

5:15 PM - 6:30 PM JST | 8:15 AM - 9:30 AM UTC | Poster Hall International Exhibition Hall8, Makuhari Messe_22

[S-IT21] Interaction and Coevolution of the Core and Mantle in the Earth and Planets

convener:Kenji Kawai(Department of Earth and Planetary Science, School of Science, University of Tokyo), Tsuyoshi Iizuka(University of Tokyo), Kenji Ohta(Department of Earth and Planetary Sciences, Tokyo Institute of Technology), Taku Tsuchiya(Geodynamics Research Center, Ehime University)

[SIT21-P01] Sample-scale compositional variation of the Inada granite, Ibaraki, Japan -toward the reduction of geoneutrino flux estimation errors from the Japanese crust-

★Invited Papers

*Kenta Ueki[1], Minami Kazuki[2], Tsuyoshi Iizuka[3], Sanshiro Enomoto[4], Hiroyuki Tanaka[2] (1.Japan Agency for Marine-Earth Science and Technology, 2.Earthquake Research Institute, University of Tokyo, 3.Department of Earth and Planetary Science, University of Tokyo, 4.Center for Experimental Nuclear Physics and Astrophysics, University of Washington)

[SIT21-P02] Towards a better estimation of the temperature distribution beneath the Japanese Islands

*Akiko Tanaka[1], Makoto Yamano[2], Hideki Hamamoto[3], Shusaku Goto[4], Takumi Matsumoto[5] (1.Geological Survey of Japan, National Institute of Advanced Industrial Science and Technology, 2.Earthquake Research Institute, The University of Tokyo, 3.Center for Environmental Science in Saitama, 4.Institute for Geo-Resources and Environment National Institute of Advanced Industrial Science and Technology, 5.National Research Institute for Earth Science and Disaster Resilience)

[SIT21-P03] The estimation of the neutrino flux from the crust of the Japanese islands using the geochemical database

*Satoru Haraguchi[1], Kenta Ueki[1], Hikaru Iwamori[1,2,3] (1.Japan Agency for Marine-Earth Science and Technology, 2.Earthquake Research Institute, the University of Tokyo, 3.Tokyo Institute of Technology)

[SIT21-P04] **Viscosity of potassium titanosilicate melt at high pressure**

*Akio Suzuki[1] (1.Department of Earth Science, Graduate School of Science, Tohoku University)

[SIT21-P05] **Lattice thermal conductivity of wadsleyite and ringwoodite at the mantle transition zone pressures**

*seiji kimura[1], Kenji Ohta[6], Takaaki Kawazoe[2], Kei Hirose[3], Hiroyuki Kagi[4], Takashi Yagi[5] (1.Department of Earth and Planetary Sciences Tokyo Institute of Technology, 2.Department of Earth and Planetary Systems Science, Hiroshima University, 3.Earth-Life Science Institute, Tokyo Institute of Technology, 4.Geochemical Research Center, Graduate School of Science, University of Tokyo, 5.National Institute of Advanced Industrial Science and Technology, 6.Department of Earth and Planetary Sciences, Tokyo Institute of Technology)

[SIT21-P06] In-situ X-ray observations of the olivine-spinel transformation under shear deformation: preliminary results on the reaction-induced weakening

*Tomoaki Kubo[1], Moriyama Kazuya[1], Yuichiro Mori[1], Masahiro Imamura[1], Sanae Koizumi[2], Yu Nishihara[3], Akio Suzuki[4], Yuji Higo[5] (1.Kyushu Univ., 2.ERI, 3.GRC Ehime Univ., 4.Tohoku Univ., 5.JASRI)

[SIT21-P07] Internally resistive heated diamond anvil cell experiments with metal encapsulated minerals

*YAMAMOTO TOMONARI[1], Kenji Ohta[1], Sho Suehiro[1], Hayato Inoue[1] (1.Tokyo Institute of Technology)

[SIT21-P08] Shear deformation on post-spinel

*Daisuke Yamazaki[1], Noriyoshi Tsujino[1], Yu Nishihara[2] (1.Institute for Planetary Materials, Okayama University, 2.GRC, Ehime University)

[SIT21-P09] **Lattice thermal conductivity of $CaSiO_3$ perovskite at high pressures and high temperatures**

*Kotaro Onga[1], Kenji Ohta[1], Akira Hasegawa[1,2], Takashi Yagi[2], Kei Hirose[3,4], Yasuo Ohishi[5] (1.Department of Earth and Planetary Sciences, Tokyo Institute of Technology, 2.National Institute of Advanced Industrial Science and Technology, 3.Earth-Life Science Institute, Tokyo Institute of Technology, 4.Department of Earth and Planetary Science, The University of Tokyo, 5.Japan Synchrotron Radiation Research Institute)

[SIT21-P10] **Polycrystalline diamond sintered from ultradispersed nanodiamonds**

*Masayuki Nishi[1,2], Koichiro Yamamoto[1], Youmo Zhou[1], Tetsuo Irifune[2,1] (1.Geodynamics Research Center, Ehime University, 2.Earth-Life Science Institute, Tokyo Institute of Technology)

[SIT21-P11] Thermal conductivity measurements on iron and MgO periclase at high pressure and high temperature similar to the Earth's mid-lower mantle conditions

*Akira Hasegawa[1,2], Kenji Ohta[2], Takashi Yagi[1], Kei Hirose[3,4] (1.National Institute of Advanced Industrial Science and Technology, 2.Tokyo Institude of Technology, 3.Earth-Life Science Institute, Tokyo Institude of Technology, 4.The University of Tokyo)

[SIT21-P12] Azimuthal anisotropy in the lowermost mantle beneath Philippine from ScS-S times

*Satoru Tanaka[1] (1.Department of Deep Earth Structure and Dynamics Research Japan Agency for Marine-Earth Science and Technology)

[SIT21-P13] Detailed 3-D S-velocity structure within D" at the western Pacific LLSVP margin: smaller scale plumes and paleoslabs

*Yuki Suzuki[1], Kenji Kawai[1], Robert J. Geller[1], Satoru Tanaka[2], Weerachai Siripuvaraporn[3], Songkhun Boonchaisuku[3], Noisagool Sutthipong[3], Yasushi Ishihara[2], Taweoon Kim, Koji MIYAKAWA[4], Nozomu Takeuchi[4] (1.The University of Tokyo, 2.Japan Agency for Marine-Earth Science and Technology, 3.Mahidol University, 4.Earthquake Research Institute, The University of Tokyo)

[SIT21-P14] Possible interaction between the core and mantle inferred from a core surface flow model

*Masaki Matsushima[1] (1.Department of Earth and Planetary Sciences, School of Science, Tokyo Institute of Technology)

[SIT21-P15] Determination of the noble gas partition coefficients between metal-silicate melts under high-pressure and high-temperature conditions

*Tomotaka Tanaka[1], Hideharu Kuwahara[2], Satoshi Kishi[1], Ryuichi Nomura[3], Kenji Mibe[5], Hiroyuki Kagi[4], Shigehiko Tateno[6], Hirochika Sumino[1] (1.Department of Basic Science, Graduate School of Arts and Sciences, The University of Tokyo , 2.Geodynamics Research Center, Ehime University, 3.Kyoto University, 4.Geochemical Research Center, Graduate School of Science, University of Tokyo, 5.Earthquake Research Institute, University of Tokyo, 6.Earth-Life Science Institute, Tokyo Institute of Technology)

[SIT21-P16] **Measurement of T-dependent electrical resistivity of solid and liquid Fe and Pt at fixed P**

*Innocent Ezenwa[1], Takashi Yoshino[1] (1.Institute for Planetary Materials, Okayama University)

[SIT21-P17] Ancient, highly depleted mantle constrained by Re-Os isotope and highly-siderophile element compositions of French Polynesian xenoliths

*Norikatsu Akizawa[1], Akira Ishikawa[2], Katsuhiko Suzuki[3], Tetsu Kogiso[4] (1.Atmosphere and Ocean Research Institute, The University of Tokyo, 2.Department of Earth and Planetary Sciences, Tokyo Institute of Technology, 3.Research and Development Center for Submarine Resources, Japan Agency for Marine-Earth Science and Technology (JAMSTEC), 4.Graduate School of Human and Environmental Studies, Kyoto University)

[SIT21-P18] First-principles prediction of hydrogen partitioning between the core and mantle

*Atsuroh Ohba[1], Taku Tsuchiya[1] (1.Ehime University Geodynamics Research Center)

[SIT21-P19] Microvolume stable isotope measuremetns and its applicaiton for high-pressure high-temperature experimental run products

*Madhusoodhan Satish-Kumar[1], Shinnosuke Aoyama[1] (1.Department of Geology, Faculty of Science, Niigata University)

[SIT21-P20] Electrical resistivity of hcp Fe-Si alloys at high pressure and temperature

*Hayato Inoue[1], Sho Suehiro[1], Kenji Ohta[1], Kei Hirose[2,3], Yasuo Ohishi[4] (1.Department of Earth and Planetary Sciences, Tokyo Institute of Technology, 2.Earth-Life Science Institute, Tokyo Institute of Technology, 3.Department of Earth and Planetary Science, The University of Tokyo, 4.Japan Synchrotron Radiation Research Institute)

[SIT21-P21] Electrical resistivity and thermal conductivity of fcc Fe: Implications for the Mercury's core

★Invited Papers

*Hitoshi Gomi[1], Takashi Yoshino[1] (1.Okayama University)

[SIT21-P22] Lateral heterogeneity in the lowermost outer core (F layer) of the Earth revealed by seismic analyses

*Toshiki Ohtaki[1], Satoshi Kaneshima[2], Taku Tsuchiya[3] (1.Geological Survey of Japan, National Institute of Advanced Industrial Science and Technology (AIST), 2.Department of Earth and Planetary Sciences, Kyushu University,

3.Geodynamics Research Center, Ehime University)

[SIT21-P23] Flows and light element distribution in the outer core associated with heterogeneous growth of the inner core of the Earth

*Shin-ichi Takehiro[1], Youhei SASAKI[2] (1.Research Institute for Mathematical Sciences, Kyoto University, 2.Department of Mathematics, Kyoto University)

[SIT21-P24] Sharpness of the hemispherical boundary in the inner core beneath the northern Pacific

*Ryohei Iritani[1], Hitoshi Kawakatsu[1], Nozomu Takeuchi[1] (1.Earthquake Research Institute, Univ. of Tokyo)

[SIT21-P25] Stable carbon isotope fractionation in Fe-C system from first principles

*Haruhiko Dekura[1], Taku Tsuchiya[1] (1.Geodynamics Research Center, Ehime University)

[E] Poster | B (Biogeosciences)：B-BG Biogeosciences & Geosphere-Biosphere Interactions

1:45 PM - 3:15 PM JST | 4:45 AM - 6:15 AM UTC | Poster Hall International Exhibition Hall8, Makuhari Messe_6

[B-BG01] Elemental cycling in terrestrial and coastal ecosystems- Carbon and Nitrogen perspectives

convener:Punyasloke Bhadury(Indian Institute of Science Education and Research Kolkata)

[BBG01-P01] Forest-CEW: A Forest Ecosystems Model for Carbon-Energy-Water Processes.

*Zhenghong Tan[1] (1.Hainan University China)

[BBG01-P02] **Interdependent Dynamics of LAI-ET across Roofing Landscapes: the Mongolian and Tibetan Plateaus**

*Li Tian[1] (1.Institute of Geographic Sciences and Natural Resources Research, Chinese Academy of Sciences)

[BBG01-P03] **Particle Phase Organic compounds (PAHs and VOCs) at Two Big Cities (Dhaka and Rajshahi) in Bangladesh**

*Islam Nazrul nazrulislam6727@gmail.com[1], Tanzina Tul Karim[1], Rasheda Nahida[1], Nusrat Mousume[1], Farha Jeba[1], Abdus Salam[1] (1.Department of Chemistry, University of Dhaka, Dhaka-1000, Bangladesh)

[BBG01-P04] **Diversity and activity of diazotrophs in the coastal waters of Southeastern Arabian Sea (SEAS)**

*JABIR THAJUDEEN[1], Mohamed Hatha Abdullah (1.Cochin University of Science and Technology India)

[BBG01-P05] **Bloom of *Palmerina hardmaniana*, a marine centric planktonic diatom in a coastal mangrove ecosystem- implication for coastal carbon cycling**

*Punyasloke Bhadury[1] (1.Centre for Climate and Environmental Studies and Department of Biological Sciences, Indian Institute of Science Education and Research Kolkata)

[BBG01-P06] Dynamics of Carbon and Nitrogen influx in large river system: Isotopic study from river Ganga, India

*Anurag Kumar[1], Prasanta Sanyal[1,2], Punyasloke Bhadury[3,2] (1.Department of Earth Sciences, Indian Institute of Science Education and Research Kolkata, Mohanpur 741246, India, 2.Centre for Climate and Environmental studies, Indian Institute of Science Education and Research Kolkata, Mohanpur 741246, India, 3.Department of Biological Sciences, Indian Institute of Science Education and Research Kolkata, Mohanpur 741246, India)

[E] Poster | B (Biogeosciences)：B-BG Biogeosciences & Geosphere-Biosphere Interactions

5:15 PM - 6:30 PM JST | 8:15 AM - 9:30 AM UTC | Poster Hall International Exhibition Hall8, Makuhari Messe_31

[B-BG01] Elemental cycling in terrestrial and coastal ecosystems- Carbon and Nitrogen perspectives

convener:Punyasloke Bhadury(Indian Institute of Science Education and Research Kolkata)

[BBG01-P01] Forest-CEW: A Forest Ecosystems Model for Carbon-Energy-Water Processes.

*Zhenghong Tan[1] (1.Hainan University China)

[BBG01-P02] **Interdependent Dynamics of LAI-ET across Roofing Landscapes: the Mongolian and Tibetan Plateaus**

*Li Tian[1] (1.Institute of Geographic Sciences and Natural Resources Research, Chinese Academy of Sciences)

[BBG01-P03] **Particle Phase Organic compounds (PAHs and VOCs) at Two Big Cities (Dhaka and Rajshahi) in Bangladesh**

*Islam Nazrul nazrulislam6727@gmail.com[1], Tanzina Tul Karim[1], Rasheda Nahida[1], Nusrat Mousume[1], Farha Jeba[1], Abdus Salam[1] (1.Department of Chemistry, University of Dhaka, Dhaka-1000, Bangladesh)

[BBG01-P04] **Diversity and activity of diazotrophs in the coastal waters of Southeastern Arabian Sea (SEAS)**

*JABIR THAJUDEEN[1], Mohamed Hatha Abdullah (1.Cochin University of Science and Technology India)

[BBG01-P05] **Bloom of *Palmerina hardmaniana*, a marine centric planktonic diatom in a coastal mangrove ecosystem- implication for coastal carbon cycling**

*Punyasloke Bhadury[1] (1.Centre for Climate and Environmental Studies and Department of Biological Sciences, Indian Institute of Science Education and Research Kolkata)

[BBG01-P06] Dynamics of Carbon and Nitrogen influx in large river system: Isotopic study from river Ganga, India

*Anurag Kumar[1], Prasanta Sanyal[1,2], Punyasloke Bhadury[3,2] (1.Department of Earth Sciences, Indian Institute of Science Education and Research Kolkata, Mohanpur 741246, India, 2.Centre for Climate and Environmental studies, Indian Institute of Science Education and Research Kolkata, Mohanpur 741246, India, 3.Department of Biological Sciences, Indian Institute of Science Education and Research Kolkata, Mohanpur 741246, India)

[E] Poster | M (Multidisciplinary and Interdisciplinary)：M-IS Intersection

3:30 PM - 5:00 PM JST | 6:30 AM - 8:00 AM UTC | Poster Hall International Exhibition Hall8, Makuhari Messe_19

[M-IS02] Drilling Earth Science

convener:Yasuhiro Yamada(Japan Agency for Marine-Earth Science and Technology (JAMSTEC), R&D Center for Ocean Drilling Science (ODS)), Yumiko Harigane(Geological Survey of Japan, National Institute of Advanced Industrial Science and Technology (AIST)), Azumi Kuroyanagi(Tohoku University Museum, The Center for Academic Resources and Archives, Tohoku University), Kosei E. Yamaguchi(Toho University and NASA Astrobiology Institute)

[MIS02-P01] Utilization and curation of frozen core samples in IODP and implementation of the Nagoya Protocol in ocean drilling science

*Nan XIAO[1] (1.Japan Agency for Marine Earthe Science and Technology)

[MIS02-P02] In-situ rock strength calculated from drilling parameters. Comparison of results from various sites.

*Adam Wspanialy[1], Yasuhiro Yamada[1], Saneatsu Saito[1], KYAW MOE[1] (1.Japan Agency for Marine-Earth Science and Technology)

[MIS02-P03] Interaction between submarine landslides and subseafloor sedimentary microbiome: Chikyu SCORE Expedition 910 off Cape Erimo

*Tatsuhiko Hoshino[1], Go-Ichiro Uramoto[2], Satoshi Tonai[2], Yuki Morono[1], Akira Ijiri[1], Shino Suzuki[1], Yusuke Kubo[1], Fumio Inagaki[1], Chikyu SCORE Exp. 910 Scientists . (1.Japan Agency for Marine-Earth Science and Technology, 2.Kochi University)

[MIS02-P04] High-resolution continuous records of the chemical composition of the marine sediment off Cape Erimo, Hokkaido, Japan

*Masafumi MURAYAMA[1], Shinsuke Yagyu[3], Satoshi Tonai[2], Go-Ichiro Uramoto[3], Yasuhiro Yamada[4], Fumio Inagaki[4], Yusuke Kubo[5] (1.Faculty of Agriculture and Marine Science, Kochi University, 2.Faculty of Science and Technology, Kochi University, 3.Center for Advanced Marine Core Research, Kochi University, 4.Research and Development Center for Ocean Drilling Science, JAMSTEC, 5.Center for Deep Earth Exploration, JAMSTEC)

[MIS02-P05] Thermal property measurements of core samples retrieved from Futagawa fault drilling

*Terasu Sano[1], Weiren Lin[1], Susumu Shibutani[1,2], Nana Kamiya[1], Tatsuhiro Sugimoto[1], Kazuya Ishitsuka[1], Aiming Lin[3] (1.Graduate School of Engineering, Kyoto University, 2.Chi-ken Sogo Consultants Co., Ltd.,, 3.Graduate School of Science, Kyoto University)

[MIS02-P06] Results of geotechnical tests on shallow sediment cores recovered from Lord Howe Rise, off eastern Australia: Implications for future Lord Howe Rise riser drilling

*Takamitsu Sugihara[1], Kan Aoike[1], Saneatsu Saito[2], Tatsuya Murayama[1], Kentaro Takeda[1], Takuya Onodera[3], Ayumi Sumikawa[3], Yukari Kido[1], Yoshinori Sanada[1] (1.Center for deep earth exploration, Japan Agency for Marine-Science and Technology, 2.Research and development center for ocean drilling science, Japan Agency for Marine-Science and Technology, 3.Nippon Marine Enterprises, Ltd.)

[MIS02-P07] ICDP DSeis 4: Drilling, core logging, and in-hole geophysical logging of ICDP DSeis drilling into the M5.5 aftershock zones in a South African gold mines.

*Shunsuke YOSHIDA[1], Tadokoro Ryogo[1], Kosuke Sugimura[1], Kanematsu Makoto[1], Mitsuya Higashi[1], Benni Liebenberg[2], Esterhuizen van Heerden[2], Stephen Tau[3], Siyanda Mngadi[3], Ray Durrheim[3], Martin Ziegler[4], Yusuke Mukuhira[5], Ronald Conze[6], Yasuo Yabe[7], Shunya Kaneki[8], Yuki Yokoyama[9], Nomqhele Nkosi[10], Dave Roberts[10], Sifiso Buccio[11], Hiroshi Ogasawara[1] (1.Graduate school of science and engineering, Ritsumeikan , 2.Moab Khotsong mine, Vijoenskroon, 3.Univ. Witwatersrand, School of Geoscience, 4.ETH, Zurich Dep. Earth Sciences, 5.Inst. Fluid Science, Tohoku Univ., 6.GFZ, Potzdam, 7.Graduate School of Science, Tohoku Univ., 8.Disaster Prevention Research Inst., Kyoto Univ., 9.Graduate School of Science,Osaka Univ., 10.Mandela Mining Precinct, CSIR, 11.Council for Geoscience)

[MIS02-P08] ICDP DSeis 5: Diametrical Core Deformation Analysis of the M5.5 aftershock zone core - stress concentration at reflective intrusives and transition in stress regimes.

*Kosuke Sugimura[1], Shunsuke YOSHIDA[1], Ryogo Tadokoro[1], Hiroshi Ogasawara[2], Akimasa Ishida, Yasuo Yabe[3], Takatoshi Ito[4], Akio Funato[5], Siyanda Mngadi[6], Ray Durrheim[6] (1.Graduate school of science and engineering, Ritsumeikan, 2.College of Science and Engineering, Ritsumeikan Univ., 3.Graduate School of Science, Tohoku Univ., 4.Inst. Fluid Science, Tohoku Univ., 5.Fukada Geological Institute, 6.Univ. Witwatersrand, School of Geoscience)

[MIS02-P09] ICDP DSeis 6: Deformation Rate Analysis of the M5.5 aftershock zone core - stress concentration at reflective intrusives

*Kanematsu Makoto[1], Mitsuya Higashi[1], Yasuo Yabe[2], Shuhei Abe[2], Bryan Watson[3], Ray Durrheim[3], Hiroshi Ogasawara[1] (1.Ritsumeikan Univ., 2.Tohoku Univ., 3.Univ. Witwatersrand)

[MIS02-P10] ICDP DSeis 7: compilation of stress information and comparison with calculated stresses in the M5.5 aftershock zones

*Mitsuya Higashi[1], Yasuo Yabe[2], Kosuke Sugimura[1], Akimasa Ishida, Makoto Kanematsu[1], Shunsuke YOSHIDA[1], Ryogo Tadokoro[1], Takatoshi Ito[4], Akio Funato[5], Hiroshi Ogasawara[3] (1.Graduate School of Science and Engineering, Ritsumeikan Univ., 2.Research Center for Prediction of Earthquakes and Volcanic Eruptions, Graduate School of Science, Tohoku University, 3.College of Science and Engineering, Ritsumeikan Univ., 4.Inst. Fluid Science, Tohoku Univ., 5.Fukada Geological Institute)

[MIS02-P11] ICDP DSeis 8: the M5.5 fault structure and reflective intrusives in legacy 3D seismic reflection data

*Noda Taku[1], Musa Manzi[2], Hiroyuki Ogasawara[1], Lindsay Linzer[2], Stephanie Enslin[2], Ray Durrheim[2], Hiroshi Ogasawara[1] (1.Ritsumeikan Univ., 2.Univ. Witwatersrand)

[MIS02-P12] ICDP DSeis 9: are streaks in the M5.5 aftershocks potentially located on highly stressed intrusive?

*Ryogo Tadokoro[1], Katsuya Ishibashi[2], Horiuchi Shigeki[3], Hiroshi Ogasawara[4] (1.Graduate School of Science and Engineering, Ritsumeikan Univ., 2.School of Science and Engineering, Ritsumeikan Univ., 3.Homeseismo ltd., 4.College of Science and Engineering, Ritsumeikan Univ.)

[E] Poster | M (Multidisciplinary and Interdisciplinary)：M-IS Intersection

5:15 PM - 6:30 PM JST | 8:15 AM - 9:30 AM UTC | Poster Hall International Exhibition Hall8, Makuhari Messe_32

[M-IS02] Drilling Earth Science

convener:Yasuhiro Yamada(Japan Agency for Marine-Earth Science and Technology (JAMSTEC), R&D Center for Ocean Drilling Science (ODS)), Yumiko Harigane(Geological Survey of Japan, National Institute of Advanced Industrial Science and Technology (AIST)), Azumi Kuroyanagi(Tohoku University Museum, The Center for Academic Resources and Archives, Tohoku University), Kosei E. Yamaguchi(Toho University and NASA Astrobiology Institute)

[MIS02-P01] Utilization and curation of frozen core samples in IODP and implementation of the Nagoya Protocol in ocean drilling science

*Nan XIAO[1] (1.Japan Agency for Marine Earthe Science and Technology)

[MIS02-P02] In-situ rock strength calculated from drilling parameters. Comparison of results from various sites.

*Adam Wspanialy[1], Yasuhiro Yamada[1], Saneatsu Saito[1], KYAW MOE[1] (1.Japan Agency for Marine-Earth Science and Technology)

[MIS02-P03] Interaction between submarine landslides and subseafloor sedimentary microbiome: Chikyu SCORE Expedition 910 off Cape Erimo

*Tatsuhiko Hoshino[1], Go-Ichiro Uramoto[2], Satoshi Tonai[2], Yuki Morono[1], Akira Ijiri[1], Shino Suzuki[1], Yusuke Kubo[1], Fumio Inagaki[1], Chikyu SCORE Exp. 910 Scientists . (1.Japan Agency for Marine-Earth Science and Technology, 2.Kochi University)

[MIS02-P04] High-resolution continuous records of the chemical composition of the marine sediment off Cape Erimo, Hokkaido, Japan

*Masafumi MURAYAMA[1], Shinsuke Yagyu[3], Satoshi Tonai[2], Go-Ichiro Uramoto[3], Yasuhiro Yamada[4], Fumio Inagaki[4], Yusuke Kubo[5] (1.Faculty of Agriculture and Marine Science, Kochi University, 2.Faculty of Science and Technology, Kochi University, 3.Center for Advanced Marine Core Research, Kochi University, 4.Research and Development Center for Ocean Drilling Science, JAMSTEC, 5.Center for Deep Earth Exploration, JAMSTEC)

[MIS02-P05] Thermal property measurements of core samples retrieved from Futagawa fault drilling

*Terasu Sano[1], Weiren Lin[1], Susumu Shibutani[1,2], Nana Kamiya[1], Tatsuhiro Sugimoto[1], Kazuya Ishitsuka[1], Aiming Lin[3] (1.Graduate School of Engineering, Kyoto University, 2.Chi-ken Sogo Consultants Co., Ltd.,, 3.Graduate School of Science, Kyoto University)

[MIS02-P06] Results of geotechnical tests on shallow sediment cores recovered from Lord Howe Rise, off eastern Australia: Implications for future Lord Howe Rise riser drilling

*Takamitsu Sugihara[1], Kan Aoike[1], Saneatsu Saito[2], Tatsuya Murayama[1], Kentaro Takeda[1], Takuya Onodera[3], Ayumi Sumikawa[3], Yukari Kido[1], Yoshinori Sanada[1] (1.Center for deep earth exploration, Japan Agency for Marine-Science and Technology, 2.Research and development center for ocean drilling science, Japan Agency for Marine-Science and Technology, 3.Nippon Marine Enterprises, Ltd.)

[MIS02-P07] ICDP DSeis 4: Drilling, core logging, and in-hole geophysical logging of ICDP DSeis drilling into the M5.5 aftershock zones in a South African gold mines.

*Shunsuke YOSHIDA[1], Tadokoro Ryogo[1], Kosuke Sugimura[1], Kanematsu Makoto[1], Mitsuya Higashi[1], Benni Liebenberg[2], Esterhuizen van Heerden[2], Stephen Tau[3], Siyanda Mngadi[3], Ray Durrheim[3], Martin Ziegler[4], Yusuke Mukuhira[5], Ronald Conze[6], Yasuo Yabe[7], Shunya Kaneki[8], Yuki Yokoyama[9], Nomqhele Nkosi[10], Dave Roberts[10], Sifiso Buccio[11], Hiroshi Ogasawara[1] (1.Graduate school of science and engineering, Ritsumeikan , 2.Moab Khotsong mine, Vijoenskroon, 3.Univ. Witwatersrand, School of Geoscience, 4.ETH, Zurich Dep. Earth Sciences, 5.Inst. Fluid Science, Tohoku Univ., 6.GFZ, Potzdam, 7.Graduate School of Science, Tohoku Univ., 8.Disaster Prevention Research Inst., Kyoto Univ., 9.Graduate School of Science,Osaka Univ., 10.Mandela Mining Precinct, CSIR, 11.Council for Geoscience)

[MIS02-P08] ICDP DSeis 5: Diametrical Core Deformation Analysis of the M5.5 aftershock zone core - stress concentration at reflective intrusives and transition in stress regimes.

*Kosuke Sugimura[1], Shunsuke YOSHIDA[1], Ryogo Tadokoro[1], Hiroshi Ogasawara[2], Akimasa Ishida, Yasuo Yabe[3], Takatoshi Ito[4], Akio Funato[5], Siyanda Mngadi[6], Ray Durrheim[6] (1.Graduate school of science and engineering, Ritsumeikan, 2.College of Science and Engineering, Ritsumeikan Univ., 3.Graduate School of Science, Tohoku Univ., 4.Inst. Fluid Science, Tohoku Univ., 5.Fukada Geological Institute, 6.Univ. Witwatersrand, School of Geoscience)

[MIS02-P09] ICDP DSeis 6: Deformation Rate Analysis of the M5.5 aftershock zone core - stress concentration at reflective intrusives

*Kanematsu Makoto[1], Mitsuya Higashi[1], Yasuo Yabe[2], Shuhei Abe[2], Bryan Watson[3], Ray Durrheim[3], Hiroshi Ogasawara[1] (1.Ritsumeikan Univ., 2.Tohoku Univ., 3.Univ. Witwatersrand)

[MIS02-P10] ICDP DSeis 7: compilation of stress information and comparison with calculated stresses in the M5.5 aftershock zones

*Mitsuya Higashi[1], Yasuo Yabe[2], Kosuke Sugimura[1], Akimasa Ishida, Makoto Kanematsu[1], Shunsuke YOSHIDA[1], Ryogo Tadokoro[1], Takatoshi Ito[4], Akio Funato[5], Hiroshi Ogasawara[3] (1.Graduate School of Science and Engineering, Ritsumeikan Univ., 2.Research Center for Prediction of Earthquakes and Volcanic Eruptions, Graduate School of Science, Tohoku University, 3.College of Science and Engineering, Ritsumeikan Univ., 4.Inst. Fluid Science, Tohoku Univ., 5.Fukada Geological Institute)

[MIS02-P11] ICDP DSeis 8: the M5.5 fault structure and reflective intrusives in legacy 3D seismic reflection data

*Noda Taku[1], Musa Manzi[2], Hiroyuki Ogasawara[1], Lindsay Linzer[2], Stephanie Enslin[2], Ray Durrheim[2], Hiroshi Ogasawara[1] (1.Ritsumeikan Univ., 2.Univ. Witwatersrand)

[MIS02-P12] ICDP DSeis 9: are streaks in the M5.5 aftershocks potentially located on highly stressed intrusive?

*Ryogo Tadokoro[1], Katsuya Ishibashi[2], Horiuchi Shigeki[3], Hiroshi Ogasawara[4] (1.Graduate School of Science and Engineering, Ritsumeikan Univ., 2.School of Science and Engineering, Ritsumeikan Univ., 3.Homeseismo ltd., 4.College of Science and Engineering, Ritsumeikan Univ.)

[E] Poster | M (Multidisciplinary and Interdisciplinary)：M-TT Technology & Techniques

1:45 PM - 3:15 PM JST | 4:45 AM - 6:15 AM UTC | Poster Hall International Exhibition Hall8, Makuhari Messe_10

[M-TT46] New phase of GPS/GNSS application as an integrated earth observation system

convener:Yoshinori Shoji(The Second Laboratory of Meteorological Satellite and Observation System Research Department, Meteorological Research Institute), Kaoru Ichikawa(Research Institute for Applied Mechanics, Kyushu University), Yusaku Ohta(Research Center for Prediction of Earthquakes and Volcanic Eruptions, Graduate School of Science, Tohoku University), Takuya Tsugawa(National Institute of Information and Communications Technology)

[MTT46-P01] Continuous acoustic ranging from a GNSS buoy for the new method of seafloor crustal deformation measurements

*Keiichi Tadokoro[1], Natsuki Kinugasa[1], Teruyuki Kato[2], Yukihiro Terada[3], Akira Futamura[4], Kenjiro Matsuhiro[1] (1.Research Center for Seismology, Volcanology and Earthquake and Volcano Research Center, Nagoya University, 2.Hot Springs Research Institute of Kanagawa Prefecture, 3.Kochi National College of Technology, 4.National Institute of Technology, Yuge College)

[MTT46-P02] Accuracy and precision assessment of the real-time kinematic GNSS time series for moored buoy using three-axis programable moving table

*Yusaku Ohta[1], Misae Imano[1], Motoyuki Kido[2] (1.Research Center for Prediction of Earthquakes and Volcanic Eruptions, Graduate School of Science, Tohoku University, 2.IRIDeS, Tohoku University)

[MTT46-P03] GNSS-R altimetry using a Geostationary Satellite

*Kaoru Ichikawa[1], Tatsuki Okumura[2], Masanori Konda[3], Yasuyuki Baba[4] (1.Res. Inst. Appl. Mech., Kyushu Univ., 2.Dept. ESST, Interdicipl. Grad. School Eng. Sc., Kyushu Univ., 3.Graduate School of Science, Kyoto Univ., 4.Disaster Prevention Res. Inst., Kyoto Univ.)

[MTT46-P04] Estimation of typhoon wind speed using CYGNSS observations: A case study of Typhoon Lan in 2017

*Kako Shinichiro[1], Hiroyuki Tomita[2], Kaoru Ichikawa[3] (1.Graduate School of Science and Engineering, Kagoshima University, 2.Institute for Space-Earth Environment, Nagoya University, 3.Research institute for Applied Mechanics, Kyushu University)

[MTT46-P05] Ionospheric and seismic effects caused by the North Korea nuclear tests realized on 2006-2017

Nataliia Perevalova[2], *Nikolai Shestakov[1], Anna Dobrynina[3,4], Dmitry Kostylev[7], Meng Guojie[5], Wei-Wei Wu[5,6] (1.Institute for Applied Mathematics FEB RAS, Vladivostok, Russia; Far Eastern Federal University, Vladivostok, Russia, 2.Institute of Solar-Terrestrial Physics SB RAS, Irkutsk, Russia, 3.Institute of the Earth's Crust SB RAS, Irkutsk, Russia , 4.Geological institute SB RAS, Ulan-Ude, Russia , 5.Institute of Earthquake Forecasting, China Earthquake Administration, Beijing, China, 6.College of Surveying and Geo-informatics, Tongji University, Shanghai, China, 7.Sakhalin Branch of Federal Research Center Geophysical Survey RAS, Yuzhno_Sakhalinsk, Russia)

[MTT46-P06] Relationships between Water Vapor Concentration Index derived from GNSS and Surface Wind Convergence during Localized Heavy Rainfall in Tokyo in Summer

*Yoshihito Seto[1], Yoshinori Shoji[2], Nobumitsu Tsunematsu[3], Hideo Takahashi[1] (1.Department of Geography, Graduate School of Urban Environmental Sciences, Tokyo Metropolitan University, 2.Meteorological Research Institute, 3.Tokyo Metropolitan Research Institute for Environmental Protection)

[MTT46-P07] Development of novel ground-based microwave radiometer for earth science -preliminary report-

*Ryuichi Ichikawa[1], Hideki Ujihara[1], Shinsuke Satoh[1], Jun Amagai[1], Yusaku Ohta[2], Basara Miyahara[3], Hiroshi Munekane[3], Taketo Nagasaki[4], Osamu Tajima[5], Kentaro Araki[6], Takuya Tajiri[6], Hiroshi Takiguchi[7], Takeshi Matsushima[8], Nobuo Matsushima[9], Tatsuya Momotani[10], Kenji Utsunomiya[10] (1.National Institute of Information and Communications Technology, 2.Tohoku University, 3.Geospatial Information Authority of Japan, 4.High Energy Accelerator Research Organization, 5.Kyoto University, 6.Meteorological Research Institute, JMA, 7.Japan Aerospace eXploration Agency, 8.Kyushu University, 9.National Institute of Advanced Industrial Science and Technology, 10.Japan Weather Association)

[MTT46-P08] Refractivity Distributions over the Kanto Plain Obtained by Dual-polarization Radar

*Hiromu Seko[1], Eiichi Sato[1], Hiroshi Yamauchi[2] (1.Meteorological Research Institute, 2.Japan Meteorological Agency)

[MTT46-P09] Spatial and temporal distribution of tropospheric water vapor observed by a Raman lidar and a GNSS receiver network over Shigaraki, Japan

*Masanori Yabuki[1], Toshitaka Tsuda[1], Yuya Kawano[2], Yusaku Tottori[2], Makoto Tsukamoto[2], Eiji Takeuchi[2] (1.Research Institute for Sustainable Humanosphere, Kyoto University, 2.EKO Instruments Co., Ltd.)

[MTT46-P10] **Study of the Mechanisms of Severe Thunderstorm in Tokyo Metropolitan Area using High Frequent Assimilation of GNSS and Other Ground-based Observations**

*Yoshinori Shoji[1], Tetsu Sakai[2], Ahoro Adachi[1], Satoru Yoshida[2], Tomohiro Nagai[2] (1.The Second Laboratory of Meteorological Satellite and Observation System Research Department, Meteorological Research Institute, 2.The Third Laboratory of Meteorological Satellite and Observation System Research Department, Meteorological Research Institute)

[E] Poster | M (Multidisciplinary and Interdisciplinary)：M-TT Technology & Techniques

5:15 PM - 6:30 PM JST | 8:15 AM - 9:30 AM UTC | Poster Hall International Exhibition Hall8, Makuhari Messe_43

[M-TT46] New phase of GPS/GNSS application as an integrated earth observation system

convener:Yoshinori Shoji(The Second Laboratory of Meteorological Satellite and Observation System Research Department, Meteorological Research Institute), Kaoru Ichikawa(Research Institute for Applied Mechanics, Kyushu University), Yusaku Ohta(Research Center for Prediction of Earthquakes and Volcanic Eruptions, Graduate School of Science, Tohoku University), Takuya Tsugawa(National Institute of Information and Communications Technology)

[MTT46-P01] Continuous acoustic ranging from a GNSS buoy for the new method of seafloor crustal deformation measurements

*Keiichi Tadokoro[1], Natsuki Kinugasa[1], Teruyuki Kato[2], Yukihiro Terada[3], Akira Futamura[4], Kenjiro Matsuhiro[1] (1.Research Center for Seismology, Volcanology and Earthquake and Volcano Research Center, Nagoya University, 2.Hot Springs Research Institute of Kanagawa Prefecture, 3.Kochi National College of Technology, 4.National Institute of Technology, Yuge College)

[MTT46-P02] Accuracy and precision assessment of the real-time kinematic GNSS time series for moored buoy using three-axis programable moving table

*Yusaku Ohta[1], Misae Imano[1], Motoyuki Kido[2] (1.Research Center for Prediction of Earthquakes and Volcanic Eruptions, Graduate School of Science, Tohoku University, 2.IRIDeS, Tohoku University)

[MTT46-P03] GNSS-R altimetry using a Geostationary Satellite

*Kaoru Ichikawa[1], Tatsuki Okumura[2], Masanori Konda[3], Yasuyuki Baba[4] (1.Res. Inst. Appl. Mech., Kyushu Univ., 2.Dept. ESST, Interdicipl. Grad. School Eng. Sc., Kyushu Univ., 3.Graduate School of Science, Kyoto Univ., 4.Disaster Prevention Res. Inst., Kyoto Univ.)

[MTT46-P04] Estimation of typhoon wind speed using CYGNSS observations: A case study of Typhoon Lan in 2017

*Kako Shinichiro[1], Hiroyuki Tomita[2], Kaoru Ichikawa[3] (1.Graduate School of Science and Engineering, Kagoshima University, 2.Institute for Space-Earth Environment, Nagoya University, 3.Research institute for Applied Mechanics, Kyushu University)

[MTT46-P05] Ionospheric and seismic effects caused by the North Korea nuclear tests realized on 2006-2017

Nataliia Perevalova[2], *Nikolai Shestakov[1], Anna Dobrynina[3,4], Dmitry Kostylev[7], Meng Guojie[5], Wei-Wei Wu[5,6] (1.Institute for Applied Mathematics FEB RAS, Vladivostok, Russia; Far Eastern Federal University, Vladivostok, Russia, 2.Institute of Solar-Terrestrial Physics SB RAS, Irkutsk, Russia, 3.Institute of the Earth's Crust SB RAS, Irkutsk, Russia , 4.Geological institute SB RAS, Ulan-Ude, Russia , 5.Institute of Earthquake Forecasting, China Earthquake Administration, Beijing, China, 6.College of Surveying and Geo-informatics, Tongji University, Shanghai, China, 7.Sakhalin Branch of Federal Research Center Geophysical Survey RAS, Yuzhno_Sakhalinsk, Russia)

[MTT46-P06] Relationships between Water Vapor Concentration Index derived from GNSS and Surface Wind Convergence during Localized Heavy Rainfall in Tokyo in Summer

*Yoshihito Seto[1], Yoshinori Shoji[2], Nobumitsu Tsunematsu[3], Hideo Takahashi[1] (1.Department of Geography, Graduate School of Urban Environmental Sciences, Tokyo Metropolitan University, 2.Meteorological Research Institute, 3.Tokyo Metropolitan Research Institute for Environmental Protection)

[MTT46-P07] Development of novel ground-based microwave radiometer for earth science -preliminary report-

*Ryuichi Ichikawa[1], Hideki Ujihara[1], Shinsuke Satoh[1], Jun Amagai[1], Yusaku Ohta[2], Basara Miyahara[3], Hiroshi Munekane[3], Taketo Nagasaki[4], Osamu Tajima[5], Kentaro Araki[6], Takuya Tajiri[6], Hiroshi Takiguchi[7], Takeshi Matsushima[8], Nobuo Matsushima[9], Tatsuya Momotani[10], Kenji Utsunomiya[10] (1.National Institute of Information and Communications Technology, 2.Tohoku University, 3.Geospatial Information Authority of Japan, 4.High Energy Accelerator Research Organization, 5.Kyoto University, 6.Meteorological Research Institute, JMA, 7.Japan Aerospace eXploration Agency, 8.Kyushu University, 9.National Institute of Advanced Industrial Science and Technology, 10.Japan Weather Association)

[MTT46-P08] Refractivity Distributions over the Kanto Plain Obtained by Dual-polarization Radar

*Hiromu Seko[1], Eiichi Sato[1], Hiroshi Yamauchi[2] (1.Meteorological Research Institute, 2.Japan Meteorological Agency)

[MTT46-P09] Spatial and temporal distribution of tropospheric water vapor observed by a Raman lidar and a GNSS receiver network over Shigaraki, Japan

*Masanori Yabuki[1], Toshitaka Tsuda[1], Yuya Kawano[2], Yusaku Tottori[2], Makoto Tsukamoto[2], Eiji Takeuchi[2] (1.Research Institute for Sustainable Humanosphere, Kyoto University, 2.EKO Instruments Co., Ltd.)

[MTT46-P10] **Study of the Mechanisms of Severe Thunderstorm in Tokyo Metropolitan Area using High Frequent Assimilation of GNSS and Other Ground-based Observations**

*Yoshinori Shoji[1], Tetsu Sakai[2], Ahoro Adachi[1], Satoru Yoshida[2], Tomohiro Nagai[2] (1.The Second Laboratory of Meteorological Satellite and Observation System Research Department, Meteorological Research Institute, 2.The Third Laboratory of Meteorological Satellite and Observation System Research Department, Meteorological Research Institute)

[E] Poster | M (Multidisciplinary and Interdisciplinary) : M-TT Technology & Techniques

1:45 PM - 3:15 PM JST | 4:45 AM - 6:15 AM UTC | Poster Hall International Exhibition Hall8, Makuhari Messe_11

[M-TT47] GEOSCIENTIFIC APPLICATIONS OF HIGH-DEFINITION TOPOGRAPHY AND GEOPHYSICAL DATA IN THE ANTHROPOCENE

convener:Yuichi S. Hayakawa(Faculty of Environmental Earth Science, Hokkaido University), Shigekazu Kusumoto(Graduate School of Science and Engineering for Research, University of Toyama), Christopher A Gomez(Kobe University Faculty of Maritime Sciences Volcanic Risk at Sea Research Group)

[MTT47-P01] High-definition topography monitoring after riverbed cultivation in the Echi River, central Japan

*Takuro Ogura[1,2], Satoshi Asano[3], Toshiaki Mizuno[3], Yoshihiro Azuma[3], Takeshi Kitai[4], Yuichi S Hayakawa[5,6], Kotaro Iizuka[6] (1.Graduate School of Frontier Sciences, The University of Tokyo, 2.Graduate School of Environmental Science, Hokkaido University, 3.Lake Biwa Environmental Research Institute , 4.Lake Biwa Museum, 5.Faculty of Environmental Earth Science, Hokkaido University, 6.Center for Spatial information Science, The University of Tokyo)

[MTT47-P02] **Spatial distribution of land surface displacements in the crater of Tateyama Midagahara Volcano using high-definition topographic data**

*Yuichi S. Hayakawa[1], Shigekazu Kusumoto[2], Takuro Ogura[3,4] (1.Faculty of Environmental Earth Science, Hokkaido University, 2.Graduate School of Science and Engineering for Research, University of Toyama, 3.Graduate School of Frontier Science, The University of Tokyo, 4.Graduate School of Environmental Science, Hokkaido University)

[MTT47-P03] Study on a simplified measurement of water depth and reconstruction of the riverbed form by using SfM and MVS.

*OSAWA KOTA[1], Tadafumi Niizato [2], Katsuaki Mitachi[3], Makoto Kawamura[1], Masahiro Ohkawa[1] (1.Mitsubishi Materials Techno corporation , 2.Japan Atomic Energy Agency, 3.ATOM TRANSPORT SERVICE CO., LTD)

[MTT47-P04] Ground Penetrating Radar Imaging of Moisture and Water movement in volcanic soil

*Christopher A Gomez[1] (1.Kobe University Faculty of Maritime Sciences Volcanic Risk at Sea Research Group)

[MTT47-P05] **Estimating Eruptive Volumes of Mud Volcano Southwestern Taiwan by Using UAV and SfM-MVS Photogrammetry**

*CHIA-YING LIU[1], Ray Y Chuang[1], Horng-Yue Chen[2] (1.Department of Geography, National Taiwan University, 2.Academia Sinica, Institute of Earth Sciences)

[MTT47-P06] Increasing temporal depth of urban Land-Use Regression Models by wind-data driven dynamic buffer generation

*Tilman Leo Hohenberger[1], King Wai Leung[1] (1.Division of Environment and Sustainability, Hong Kong University of Science and Technology)

[E] Poster | M (Multidisciplinary and Interdisciplinary)：M-TT Technology & Techniques

5:15 PM - 6:30 PM JST | 8:15 AM - 9:30 AM UTC | Poster Hall International Exhibition Hall8, Makuhari Messe_44

[M-TT47] GEOSCIENTIFIC APPLICATIONS OF HIGH-DEFINITION TOPOGRAPHY AND GEOPHYSICAL DATA IN THE ANTHROPOCENE

convener:Yuichi S. Hayakawa(Faculty of Environmental Earth Science, Hokkaido University), Shigekazu Kusumoto(Graduate School of Science and Engineering for Research, University of Toyama), Christopher A Gomez(Kobe University Faculty of Maritime Sciences Volcanic Risk at Sea Research Group)

[MTT47-P01] High-definition topography monitoring after riverbed cultivation in the Echi River, central Japan

*Takuro Ogura[1,2], Satoshi Asano[3], Toshiaki Mizuno[3], Yoshihiro Azuma[3], Takeshi Kitai[4], Yuichi S Hayakawa[5,6], Kotaro Iizuka[6] (1.Graduate School of Frontier Sciences, The University of Tokyo, 2.Graduate School of Environmental Science, Hokkaido University, 3.Lake Biwa Environmental Research Institute , 4.Lake Biwa Museum, 5.Faculty of Environmental Earth Science, Hokkaido University, 6.Center for Spatial information Science, The University of Tokyo)

[MTT47-P02] **Spatial distribution of land surface displacements in the crater of Tateyama Midagahara Volcano using high-definition topographic data**

*Yuichi S. Hayakawa[1], Shigekazu Kusumoto[2], Takuro Ogura[3,4] (1.Faculty of Environmental Earth Science, Hokkaido University, 2.Graduate School of Science and Engineering for Research, University of Toyama, 3.Graduate School of Frontier Science, The University of Tokyo, 4.Graduate School of Environmental Science, Hokkaido University)

[MTT47-P03] Study on a simplified measurement of water depth and reconstruction of the riverbed form by using SfM and MVS.

*OSAWA KOTA[1], Tadafumi Niizato [2], Katsuaki Mitachi[3], Makoto Kawamura[1], Masahiro Ohkawa[1] (1.Mitsubishi Materials Techno corporation , 2.Japan Atomic Energy Agency, 3.ATOM TRANSPORT SERVICE CO., LTD)

[MTT47-P04] Ground Penetrating Radar Imaging of Moisture and Water movement in volcanic soil

*Christopher A Gomez[1] (1.Kobe University Faculty of Maritime Sciences Volcanic Risk at Sea Research Group)

[MTT47-P05] **Estimating Eruptive Volumes of Mud Volcano Southwestern Taiwan by Using UAV and SfM-MVS Photogrammetry**

*CHIA-YING LIU[1], Ray Y Chuang[1], Horng-Yue Chen[2] (1.Department of Geography, National Taiwan University, 2.Academia Sinica, Institute of Earth Sciences)

[MTT47-P06] Increasing temporal depth of urban Land-Use Regression Models by wind-data driven dynamic buffer generation

*Tilman Leo Hohenberger[1], King Wai Leung[1] (1.Division of Environment and Sustainability, Hong Kong University of Science and Technology)

Tue. May 28, 2019

[E] Poster | P (Space and Planetary Sciences)：P-PS Planetary Sciences

3:30 PM - 5:00 PM JST | 6:30 AM - 8:00 AM UTC | Poster Hall International Exhibition Hall8, Makuhari Messe_1

[P-PS01] Outer Solar System Exploration Today, and Tomorrow

convener:Jun Kimura(Osaka University), Yasumasa Kasaba(Planetary Plasma and Atmospheric Research Center, Tohoku University), Kunio M. Sayanagi(Hampton University)

[PPS01-P01] Critical Role of Entry Probes in Giant Planet Exploration

*Sushil K Atreya[1], Olivier Mousis[2] (1.University of Michigan Ann Arbor, 2.Laboratoire d'Astrophysique de Marseille)

[PPS01-P02] OKEANOS – Jupiter Trojan Asteroid Rendezvous and Landing Experiments Using a Solar Power Sail

*Tatsuaki Okada[1,2], Takahiro Iwata[1], Yoko Kebukawa[3], Motoo Ito[4], Jun Aoki[5], Yosuke Kawai[5], Shoichiro Yokota[5], Yoshifumi Saito[1], Kentaro Terada[5], Michisato Toyoda[5], Hikaru Yabuta[6], Hisayoshi Yurimoto[1,7], Shuji Matsuura[8], Kohji Tsumura[9], Daisuke Yonetoku[10], Tatehiro Mihara[11], Ayako Matsuoka[1], Reiko Nomura[12], Hajime Yano[1], Takayuki Hirai[13], Atsushi Kumamoto[9], Ryosuke Nakamura[14], Stephan Ulamec[15], Ralf Jaumann[15], Jean-Pierre Bibring[16], Noel Grand[17], Cyril Szopa[18], Ernesto Palomba[19], Jorn Helbert[15], Alain Herique[20], Matthias Grott[15], Hans-Ulrich Auster[21], Goester Klingelhoefer[22], Fumi Yoshida[13], Makoto Yoshikawa[1], Jun Matsumoto[1], Toshihiro Chujo[1], Masanori Matsushita[1], Takanao Saiki[1], Hideki Kato[1], Osamu Mori[1], Junichiro Kawaguchi[1] (1.Japan Aerospace Exploration Agency, 2.University of Tokyo, 3.Yokohama National University, 4.Japan Agency for Marine-Earth Science and Technology, 5.Osaka University, 6.Hiroshima University, 7.Hokkaido University, 8.Kwansei Gakuin University, 9.Tohoku University, 10.Kanazawa University, 11.RIKEN, 12.National Astronomical Observatory of Japan, 13.Chiba Institute of Technology, 14.National Institute of Advanced Industrial Science and Technology, 15.German Aerospace Center, 16.Institut d'Astrophysique Spatiale, 17.LISA, 18.LATMOS, 19.INAF-IAPS, 20.IPAG, 21.TU Braunschweig, 22.Leibniz Universität Hannover)

[PPS01-P03] Magnetic field model of Jovian magnetosphere

*Naoya Momoki[1], Hiroaki TOH[1] (1.Division of Earth and Planetary Sciences, Graduate School of Science, Kyoto University)

[PPS01-P04] Enhancement of the Jovian thermospheric temperature above the Great Red Spot based on the infrared spectroscopic data obtained with IRTF/iSHELL

*Ayumu Kambara[1], Hajime Kita[2], Takeshi Sakanoi[1], Yasumasa Kasaba[1], Masato Kagitani[1], Haruna Watanabe[1] (1.Planetary Plasma and Atmospheric Research Center, Graduate School of Science, Tohoku University, 2.Institute of Space and Astronautical Science, Japan Aerospace Exploration Agency)

[PPS01-P05] Pulsation-like variation of Jovian infrared polar emission observed by Subaru 8-m: H3+ and methane emissions

*Yasumasa Kasaba[1], Haruna Watanabe[1], Hajime Kita[2], Chihiro Tao[3], Takeshi Sakanoi[1], Masato Kagitani[1], Orton Glenn[1,4], James Sinclair[4] (1.Planetary Plasma and Atmospheric Research Center, 2.ISAS/JAXA, 3.NICT, 4.NASA/JPL)

[PPS01-P06] Structure of Io plasma torus observed with the Tohoku 60-cm telescope

*Masato Kagitani[1], Fuminori Tsuchiya[1], Kazuo Yoshioka[2], Go Murakami[3], Tomoki Kimura[1], Ryoichi Koga[1], Reina Hikida[4], Takeshi Sakanoi[1] (1.Graduate School of Science, Tohoku University, 2.Graduate School of frontier Science, The University of Tokyo, 3.Institute of Space and Astronautical Science, Japan Aerospace Exploration Agency, 4.Department of Earth and Planetary Science, Graduate School of Science, Tokyo University)

[PPS01-P07] Ion Scale Height Variability in Hisaki Io Torus Observations

*Nicholas McCord Schneider[1], Carl Schmidt[2], Masato Kagitani[3], Yasumasa Kasaba[3], Tomoki Kimura[3], Go Murakami[4], Fuminori Tsuchiya[3], Hajime Kita[3], Reina Hikida[5], Ichiro Yoshikawa[5], Kazuo Yoshioka[5] (1.LASP, University of Colorado Boulder, 2.Boston University, 3.Tohoku University, 4.ISAS/JAXA, 5.University of Tokyo)

[PPS01-P08] Size of the Smallest Particles in Saturn's Rings

*Keiji Ohtsuki[1], Hiroshi Kawamura[1], Naoyuki Hirata[1], Hiroshi Daisaka[2], Hiroshi Kimura[3] (1.Graduate School of Science, Kobe University, 2.Graduate School of Commerce and Management, Hitotsubashi University, 3.Planetary Exploration Research Center, Chiba Institute of Technology)

[PPS01-P09] The Radio & Plasma Wave Investigation (RPWI) for JUICE for the investigation of Jupiter and Icy Moons System: Contributions from Japan

*Yasumasa Kasaba[1], Hiroaki Misawa[1], Fuminori Tsuchiya[1], Atsushi Kumamoto[2], Yuto Katoh[2], Tomoki Kimura[2], Hajime Kita[3], J.-E. Wahlund[4] (1.Planetary Plasma and Atmospheric Research Center, Tohoku University, 2.Department of Geophysics, Tohoku University, 3.ISAS/JAXA, 4.IRF Uppsala, Sweden)

[PPS01-P10] Magnetic field experiment at Jupiter icy moons (JUICE J-MAG) and in-flight alignment calibration

*Ayako Matsuoka[1], Michele Karen Dougherty[2], Patrick Brown[2], Futoshi Takahashi[3], Hisayoshi Shimizu[4], Masaki Matsushima[5] (1.Research Division for Space Plasma, Institute of Space and Astronautical Science, Japan Aerospace Exploration Agency, 2.Imperial College London, 3.Kyushu University, 4.University of Tokyo, 5.Tokyo Institute of Technology)

[PPS01-P11] Science targets of the GAnymede Laser Altimeter (GALA) for the JUICE mission

*Jun Kimura[1], Shunichi Kamata[2], Koji Matsumoto[3], Noriyuki Namiki[3], Keigo Enya[4], Masanori Kobayashi[5], Hiroshi Araki[3], Hirotomo Noda[3], Ko Ishibashi[5], Hauke Hussmann[6], Kay Lingenauber[6] (1.Osaka University, 2.Hokkaido University, 3.National Astronomical Observatory Japan, 4.ISAS/JAXA, 5.Chiba Institute of Technology, 6.German Aerospace Center (DLR), Berlin)

[PPS01-P12] Current status of the antenna developments, the data processing, scientific target for JUICE/SWI JAPAN.

*YASUKO KASAI[1], JUICE SWI Japanese Team (1.National Institute of Information and Communications Technology (NICT))

[E] Poster | P (Space and Planetary Sciences)：P-PS Planetary Sciences

5:15 PM - 6:30 PM JST | 8:15 AM - 9:30 AM UTC | Poster Hall International Exhibition Hall8, Makuhari Messe_1

[P-PS01] Outer Solar System Exploration Today, and Tomorrow

convener:Jun Kimura(Osaka University), Yasumasa Kasaba(Planetary Plasma and Atmospheric Research Center, Tohoku University), Kunio M. Sayanagi(Hampton University)

[PPS01-P01] Critical Role of Entry Probes in Giant Planet Exploration

*Sushil K Atreya[1], Olivier Mousis[2] (1.University of Michigan Ann Arbor, 2.Laboratoire d'Astrophysique de Marseille)

[PPS01-P02] OKEANOS – Jupiter Trojan Asteroid Rendezvous and Landing Experiments Using a Solar Power Sail

*Tatsuaki Okada[1,2], Takahiro Iwata[1], Yoko Kebukawa[3], Motoo Ito[4], Jun Aoki[5], Yosuke Kawai[5], Shoichiro Yokota[5], Yoshifumi Saito[1], Kentaro Terada[5], Michisato Toyoda[5], Hikaru Yabuta[6], Hisayoshi Yurimoto[1,7], Shuji Matsuura[8], Kohji Tsumura[9], Daisuke Yonetoku[10], Tatehiro Mihara[11], Ayako Matsuoka[1], Reiko Nomura[12], Hajime Yano[1], Takayuki Hirai[13], Atsushi Kumamoto[9], Ryosuke Nakamura[14], Stephan Ulamec[15], Ralf Jaumann[15], Jean-Pierre Bibring[16], Noel Grand[17], Cyril Szopa[18], Ernesto Palomba[19], Jorn Helbert[15], Alain Herique[20], Matthias Grott[15], Hans-Ulrich Auster[21], Goester Klingelhoefer[22], Fumi Yoshida[13], Makoto Yoshikawa[1], Jun Matsumoto[1], Toshihiro Chujo[1], Masanori Matsushita[1], Takanao Saiki[1], Hideki Kato[1], Osamu Mori[1], Junichiro Kawaguchi[1] (1.Japan Aerospace Exploration Agency, 2.University of Tokyo, 3.Yokohama National University, 4.Japan Agency for Marine-Earth Science and Technology, 5.Osaka University, 6.Hiroshima University, 7.Hokkaido University, 8.Kwansei Gakuin University, 9.Tohoku University, 10.Kanazawa University, 11.RIKEN, 12.National Astronomical Observatory of Japan, 13.Chiba Institute of Technology, 14.National Institute of Advanced Industrial Science and Technology, 15.German Aerospace Center, 16.Institut d'Astrophysique Spatiale, 17.LISA, 18.LATMOS, 19.INAF-IAPS, 20.IPAG, 21.TU Braunschweig, 22.Leibniz Universität Hannover)

[PPS01-P03] Magnetic field model of Jovian magnetosphere

*Naoya Momoki[1], Hiroaki TOH[1] (1.Division of Earth and Planetary Sciences, Graduate School of Science, Kyoto University)

[PPS01-P04] Enhancement of the Jovian thermospheric temperature above the Great Red Spot based on the infrared spectroscopic data obtained with IRTF/iSHELL

*Ayumu Kambara[1], Hajime Kita[2], Takeshi Sakanoi[1], Yasumasa Kasaba[1], Masato Kagitani[1], Haruna Watanabe[1] (1.Planetary Plasma and Atmospheric Research Center, Graduate School of Science, Tohoku University, 2.Institute of Space and Astronautical Science, Japan Aerospace Exploration Agency)

[PPS01-P05] Pulsation-like variation of Jovian infrared polar emission observed by Subaru 8-m: H3+ and methane emissions

*Yasumasa Kasaba[1], Haruna Watanabe[1], Hajime Kita[2], Chihiro Tao[3], Takeshi Sakanoi[1], Masato Kagitani[1], Orton Glenn[1,4], James Sinclair[4] (1.Planetary Plasma and Atmospheric Research Center, 2.ISAS/JAXA, 3.NICT, 4.NASA/JPL)

[PPS01-P06] Structure of Io plasma torus observed with the Tohoku 60-cm telescope

*Masato Kagitani[1], Fuminori Tsuchiya[1], Kazuo Yoshioka[2], Go Murakami[3], Tomoki Kimura[1], Ryoichi Koga[1], Reina Hikida[4], Takeshi Sakanoi[1] (1.Graduate School of Science, Tohoku University, 2.Graduate School of frontier Science, The University of Tokyo, 3.Institute of Space and Astronautical Science, Japan Aerospace Exploration Agency, 4.Department of Earth and Planetary Science, Graduate School of Science, Tokyo University)

[PPS01-P07] Ion Scale Height Variability in Hisaki Io Torus Observations

*Nicholas McCord Schneider[1], Carl Schmidt[2], Masato Kagitani[3], Yasumasa Kasaba[3], Tomoki Kimura[3], Go Murakami[4], Fuminori Tsuchiya[3], Hajime Kita[3], Reina Hikida[5], Ichiro Yoshikawa[5], Kazuo Yoshioka[5] (1.LASP, University of Colorado Boulder, 2.Boston University, 3.Tohoku University, 4.ISAS/JAXA, 5.University of Tokyo)

[PPS01-P08] Size of the Smallest Particles in Saturn's Rings

*Keiji Ohtsuki[1], Hiroshi Kawamura[1], Naoyuki Hirata[1], Hiroshi Daisaka[2], Hiroshi Kimura[3] (1.Graduate School of Science, Kobe University, 2.Graduate School of Commerce and Management, Hitotsubashi University, 3.Planetary Exploration Research Center, Chiba Institute of Technology)

[PPS01-P09] The Radio & Plasma Wave Investigation (RPWI) for JUICE for the investigation of Jupiter and Icy Moons System: Contributions from Japan

*Yasumasa Kasaba[1], Hiroaki Misawa[1], Fuminori Tsuchiya[1], Atsushi Kumamoto[2], Yuto Katoh[2], Tomoki Kimura[2], Hajime Kita[3], J.-E. Wahlund[4] (1.Planetary Plasma and Atmospheric Research Center, Tohoku University, 2.Department of Geophysics, Tohoku University, 3.ISAS/JAXA, 4.IRF Uppsala, Sweden)

[PPS01-P10] Magnetic field experiment at Jupiter icy moons (JUICE J-MAG) and in-flight alignment calibration

*Ayako Matsuoka[1], Michele Karen Dougherty[2], Patrick Brown[2], Futoshi Takahashi[3], Hisayoshi Shimizu[4], Masaki Matsushima[5] (1.Research Division for Space Plasma, Institute of Space and Astronautical Science, Japan Aerospace Exploration Agency, 2.Imperial College London, 3.Kyushu University, 4.University of Tokyo, 5.Tokyo Institute of Technology)

[PPS01-P11] Science targets of the GAnymede Laser Altimeter (GALA) for the JUICE mission

*Jun Kimura[1], Shunichi Kamata[2], Koji Matsumoto[3], Noriyuki Namiki[3], Keigo Enya[4], Masanori Kobayashi[5], Hiroshi Araki[3], Hirotomo Noda[3], Ko Ishibashi[5], Hauke Hussmann[6], Kay Lingenauber[6] (1.Osaka University, 2.Hokkaido University, 3.National Astronomical Observatory Japan, 4.ISAS/JAXA, 5.Chiba Institute of Technology, 6.German Aerospace Center (DLR), Berlin)

[PPS01-P12] Current status of the antenna developments, the data processing, scientific target for JUICE/SWI JAPAN.

*YASUKO KASAI[1], JUICE SWI Japanese Team (1.National Institute of Information and Communications Technology (NICT))

[E] Poster | P (Space and Planetary Sciences)：P-EM Solar-Terrestrial Sciences, Space Electromagnetism & Space Environment

3:30 PM - 5:00 PM JST | 6:30 AM - 8:00 AM UTC | Poster Hall International Exhibition Hall8, Makuhari Messe_3

[P-EM12] Space Weather and Space Climate

convener:Ryuho Kataoka(National Institute of Polar Research), Antti A Pulkkinen(NASA Goddard Space Flight Center), Kanya Kusano(Institute for Space-Earth Environmental Research, Nagoya University), Kaori Sakaguchi(National Institute of Information and Communications Technology)

[PEM12-P01] Reconnection signatures in solar magnetograms during the solar storms of 4-10 September 2017

*Robert Dean Loper[1,2] (1.Air Force Institute of Technology, Department of Engineering Physics, 2.National Center for Atmospheric Research, High Altitude Observatory)

[PEM12-P02] Statistical Relation between Solar Flares and Coronal Mass Ejections with Respect to Sigmoidal Structures in Active Regions

*Yusuke Kawabata[1,2], Yusuke Iida[3], Takafumi Doi, Sachiko Akiyama[4], Seiji Yashiro[4], Toshifumi Shimizu[2] (1.Earth and Planetary Science, The University of Tokyo, 2.Institute of Space and Astronautical Science, JAXA, 3.Kwansei Gakuin University, 4.The Catholic University of America)

[PEM12-P03] Multi-wavelength Observations of Pre-flare Quasi-periodic Pulsation in the C2.2 Flare on 2012 October 15

*Yung-Chi Yang[1], Ya-Hui Yang[1], Baolin Tan[2], Chengming Tan[2], Y.H. Yan[2] (1.Graduate Institute of Space Science National Central University, 2.Key Laboratory of Solar Activities, National Astronomical Observatories)

[PEM12-P04] Investigation of pre-flare type III solar radio bursts and their potential solar origins

*Shao-Fu Hsieh[1], Ya-Hui Yang[1], Baolin Tan[2], Chengming Tan[2], Y.H. Yan[2] (1.Graduate Institute of Space Science National Central University, 2.Key Laboratory of Solar Activities, National Astronomical Observatories, Chinese Academy of Sciences)

[PEM12-P05] Statistical and observational research of solar flare for constructing total emission spectra prediction model

*Shohei Nishimoto[1], kyoko Watanabe[1], Shinsuke Imada[2], Tomoko Kawate[3], Kyoung-Sun Lee[4] (1.National Defense Academy, 2.Institute for Space-Earth Environmental Research, Nagoya University, 3.Institute Of Space And Astronautical Science, Japan Aerospace Exploration Agency, 4.National Astronomical Observatory of Japan)

[PEM12-P06] Modeling of solar active regions using local linear force-free fields to estimate magnetic twist

*Kento Nakatani[1], Kanya Kusano[1], Sung-Hong Park[1], Leka KD[2] (1.Institute for space-Earth Environmental Research, Nagoya University, 2.North West Reserch Associates)

[PEM12-P07] **Magnetohydrodynamic Simulation of an Erupting Magnetic Flux Rope on February 13 2009: Journey to Coronal Mass Ejection**

*Satoshi Inoue[1], Antonia Savcheva[2] (1.Institute for Space-Earth Environmental Research, Nagoya University, 2.Harvard-Smithsonian Center for Astrophysics)

[PEM12-P08] Investigation of flow structures in the solar interior through the surface magnetic elements' tracking

*Yusuke Iida[1] (1.Kwansei Gakuin University)

[PEM12-P09] High-precision measurement of carbon-14 in tree rings around the onset of the Maunder Minimum

*Hiroko Miyahara[1], Fuyuki Tokanai[2], Toru Moriya[2], Hideyuki Hotta[3] (1.Musashino Art University, 2.Yamagata University, 3.Chiba University)

[PEM12-P10] Examination of ^{10}Be in travertine sediment as a possible tool to reconstruct past solar activity

*Hongyang Xu[1,2], Hiroko Miyahara[2], Kazuho Horiuchi[3], Hiroyuki Matsuzaki[4], Hailong Sun[5], Weijun Luo[5], Xiangmin Zheng[1], Yusuke Suganuma[6,7], Shijie Wang[5], Limin Zhou[1] (1.East China Normal University, 2.Musashino Art University,

3.Hirosaki University, 4.University of Tokyo, 5.Chinese Academy of Sciences, 6.National Institute of Polar Research, 7.The Graduate University for Advanced Studies (SOKENDAI))

[PEM12-P11] Examination of ^{10}Be in travertine sediment as a possible tool to reconstruct past solar activity II

*Hongyang Xu[1,2], Hiroko Miyahara[2], Kazuho Horiuchi[3], Hiroyuki Matsuzaki[4], Hailong Sun[5], Weijun Luo[5], Xiangmin Zheng[1], Yusuke Suganuma[6,7], Shijie Wang[5], Limin Zhou[1] (1.East China Normal University, 2.Musashino Art University, 3.Hirosaki University, 4.University of Tokyo, 5.Chinese Academy of Sciences, 6.National Institute of Polar Research, 7.The Graduate University for Advanced Studies (SOKENDAI))

[PEM12-P12] 1 year of CR observation at Syowa Station in the Antarctic.

*Chihiro Kato[1], Kazuoki Munakata[1], Akira Kadokura[2], Ryuho Kataoka[2], Paul Evenson[3] (1.Shinshu University, 2.National Institute of Polar Research, 3.University of Delaware)

[PEM12-P13] Space weather forecast archives at NICT: handwritten solar activity charts

*Kaori Sakaguchi[1], Daikou Shiota[1], Kaori Fukunaga[1], Katsuhide Marubashi[1], Hiromitsu Ishibashi[1], Yuki Kubo[1], Mamoru Ishii[1] (1.National Institute of Information and Communications Technology)

[PEM12-P14] IMF dependence on solar wind parameters

*Tohru Araki, Yuki Harada[1] (1.Kyoto University)

[PEM12-P15] **Dipole Tilt Effect of Geomagnetic Activity from Low- to High-latitudes**

*Nowada Motoharu[1] (1.Shandong University at Weihai)

[PEM12-P16] A New Prediction Model for Solar Wind-Triggered Magnetospheric Disturbances Based on Potential Learning (Neural Network)

*Ryozo Kitajima[1], Motoharu Nowada[2], Ryotaro Kamimura[3] (1.Seikei University, 2.Shandong University at Weihai, 3.Tokai University)

[PEM12-P17] Real-time magnetosphere simulator for space weather using REProduce Plasma Universe code

*Yasubumi Kubota[1], Aoi Nakamizo[1], Kaori Sakaguchi[1], Mitsue Den[1], Yuki Kubo[1], Tsutomu Nagatsuma[1], Takashi Tanaka[1,2] (1.National Institute of Information and Communications Technology, 2.Kyushu University)

[PEM12-P18] **Simulation of GIC flowing through the power transmission network (187 kV-500 kV) in Japan**

*Nishida Yuichiro[1,6], Yusuke Ebihara[1], Satoko Nakamura[1], Shinichi Watari[2], Kumiko Hashimoto[3], Kentaro Kitamura[4], Takashi Kikuchi[5] (1.Kyoto University Reserch Institute for Sustainable Humanosphere, 2.National Institute of Information and Communications Technology, 3.Kibi International University, 4.National Insutitute of Technology, Tokuyama College, 5.Nagoya University, 6.Kyoto University Department of Electrical Engineering)

[PEM12-P19] Climatological features of the upper atmosphere reproduced by a revised version of a whole atmosphere-ionosphere coupled model GAIA

*Hidekatsu Jin[1], Yasunobu Miyoshi[2], Chihiro Tao[1], Hiroyuki Shinagawa[1], Hitoshi Fujiwara[3] (1.National Institude of Information and Communications Technology, 2.Kyushu University, 3.Seikei University)

[PEM12-P20] Investigation of the thermospheric mass density variations below 200 km

*Hitoshi Fujiwara[1], Yasunobu Miyoshi[2], Masayoshi Utashima[1], Huixin Liu[2] (1.Faculty of Science and Technology, Seikei University, 2.Department of Earth and Planetary Sciences, Faculty of Sciences, Kyushu University)

[PEM12-P21] Low-latitude HF Doppler observations of magnetospheric electric fields during space weather disturbances

*Kumiko K. Hashimoto[1], Takashi Kikuchi[2], Ichiro Tomizawa[3], Keisuke Hosokawa[3], Jaroslav Chum[4] (1.Kibi International University, 2.Nagoya University, 3.University of Electro-Commnunications, 4.Institute of Atmospheric Physics, Prague)

[PEM12-P22] Stratospheric ionization during magnetic storms

*Ryuho Kataoka[1] (1.National Institute of Polar Research)

[PEM12-P23] Calculating propagation time of HF radio wave using ray-tracing method and simple comparison with the observation.

*Ryo Nakao[1], Hiroyuki Nakata[1], Hiroyo Ohya[1], Toshiaki Takano[1], Kornyanat Hozumi[2], Takuya Tsugawa[2], Susumu Saito[3], Mamoru Ishii[2] (1.Graduate School of Engineering, Chiba University, 2.National Institute of imformation and Communications Technology, 3.Electronic Navigation Research Institute)

[PEM12-P24] Why do some probabilistic forecasts lack reliability?

*Yuki Kubo[1] (1.National Institute of Information and Communications Technology)

[PEM12-P25] An estimation method of GEO spacecraft surface charging for a real-time spacecraft risk assessment

*Masao Nakamura[1], Ryota Kawachi[1], Go Takahashi[1], Tsutomu Nagatsuma[2], Mamoru Ishii[2] (1.Osaka Prefecture University, 2.NICT)

[PEM12-P26] A network of HF Doppler sounding systems in Japan

*Keisuke Hosokawa[1], Hiroyuki Nakata[2], Kumiko K. Hashimoto[3], Ichiro Tomizawa[1], Jun Sakai[1], Takashi Kikuchi[4] (1.University of Electro-Communications, 2.Chiba University, 3.Kibi International University, 4.ISEE, Nagoya University)

[E] Poster | P (Space and Planetary Sciences)：P-EM Solar-Terrestrial Sciences, Space Electromagnetism & Space Environment

5:15 PM - 6:30 PM JST | 8:15 AM - 9:30 AM UTC | Poster Hall International Exhibition Hall8, Makuhari Messe_3

[P-EM12] Space Weather and Space Climate

convener:Ryuho Kataoka(National Institute of Polar Research), Antti A Pulkkinen(NASA Goddard Space Flight Center), Kanya Kusano(Institute for Space-Earth Environmental Research, Nagoya University), Kaori Sakaguchi(National Institute of Information and Communications Technology)

[PEM12-P01] Reconnection signatures in solar magnetograms during the solar storms of 4-10 September 2017

*Robert Dean Loper[1,2] (1.Air Force Institute of Technology, Department of Engineering Physics, 2.National Center for Atmospheric Research, High Altitude Observatory)

[PEM12-P02] Statistical Relation between Solar Flares and Coronal Mass Ejections with Respect to Sigmoidal Structures in Active Regions

*Yusuke Kawabata[1,2], Yusuke Iida[3], Takafumi Doi, Sachiko Akiyama[4], Seiji Yashiro[4], Toshifumi Shimizu[2] (1.Earth and Planetary Science, The University of Tokyo, 2.Institute of Space and Astronautical Science, JAXA, 3.Kwansei Gakuin University, 4.The Catholic University of America)

[PEM12-P03] Multi-wavelength Observations of Pre-flare Quasi-periodic Pulsation in the C2.2 Flare on 2012 October 15

*Yung-Chi Yang[1], Ya-Hui Yang[1], Baolin Tan[2], Chengming Tan[2], Y.H. Yan[2] (1.Graduate Institute of Space Science National Central University, 2.Key Laboratory of Solar Activities, National Astronomical Observatories)

[PEM12-P04] Investigation of pre-flare type III solar radio bursts and their potential solar origins

*Shao-Fu Hsieh[1], Ya-Hui Yang[1], Baolin Tan[2], Chengming Tan[2], Y.H. Yan[2] (1.Graduate Institute of Space Science National Central University, 2.Key Laboratory of Solar Activities, National Astronomical Observatories, Chinese Academy of Sciences)

[PEM12-P05] Statistical and observational research of solar flare for constructing total emission spectra prediction model

*Shohei Nishimoto[1], kyoko Watanabe[1], Shinsuke Imada[2], Tomoko Kawate[3], Kyoung-Sun Lee[4] (1.National Defense Academy, 2.Institute for Space-Earth Environmental Research, Nagoya University, 3.Institute Of Space And Astronautical Science, Japan Aerospace Exploration Agency, 4.National Astronomical Observatory of Japan)

[PEM12-P06] Modeling of solar active regions using local linear force-free fields to estimate magnetic twist

*Kento Nakatani[1], Kanya Kusano[1], Sung-Hong Park[1], Leka KD[2] (1.Institute for space-Earth Environmental Research, Nagoya University, 2.North West Reserch Associates)

[PEM12-P07] **Magnetohydrodynamic Simulation of an Erupting Magnetic Flux Rope on February 13 2009: Journey to Coronal Mass Ejection**

*Satoshi Inoue[1], Antonia Savcheva[2] (1.Institute for Space-Earth Environmental Research, Nagoya University, 2.Harvard-Smithsonian Center for Astrophysics)

[PEM12-P08] Investigation of flow structures in the solar interior through the surface magnetic elements' tracking

*Yusuke Iida[1] (1.Kwansei Gakuin University)

[PEM12-P09] High-precision measurement of carbon-14 in tree rings around the onset of the Maunder Minimum

*Hiroko Miyahara[1], Fuyuki Tokanai[2], Toru Moriya[2], Hideyuki Hotta[3] (1.Musashino Art University, 2.Yamagata University, 3.Chiba University)

[PEM12-P10] Examination of ^{10}Be in travertine sediment as a possible tool to reconstruct past solar activity

*Hongyang Xu[1,2], Hiroko Miyahara[2], Kazuho Horiuchi[3], Hiroyuki Matsuzaki[4], Hailong Sun[5], Weijun Luo[5], Xiangmin Zheng[1], Yusuke Suganuma[6,7], Shijie Wang[5], Limin Zhou[1] (1.East China Normal University, 2.Musashino Art University,

3.Hirosaki University, 4.University of Tokyo, 5.Chinese Academy of Sciences, 6.National Institute of Polar Research, 7.The Graduate University for Advanced Studies (SOKENDAI))

[PEM12-P11] Examination of ^{10}Be in travertine sediment as a possible tool to reconstruct past solar activity II

*Hongyang Xu[1,2], Hiroko Miyahara[2], Kazuho Horiuchi[3], Hiroyuki Matsuzaki[4], Hailong Sun[5], Weijun Luo[5], Xiangmin Zheng[1], Yusuke Suganuma[6,7], Shijie Wang[5], Limin Zhou[1] (1.East China Normal University, 2.Musashino Art University, 3.Hirosaki University, 4.University of Tokyo, 5.Chinese Academy of Sciences, 6.National Institute of Polar Research, 7.The Graduate University for Advanced Studies (SOKENDAI))

[PEM12-P12] 1 year of CR observation at Syowa Station in the Antarctic.

*Chihiro Kato[1], Kazuoki Munakata[1], Akira Kadokura[2], Ryuho Kataoka[2], Paul Evenson[3] (1.Shinshu University, 2.National Institute of Polar Research, 3.University of Delaware)

[PEM12-P13] Space weather forecast archives at NICT: handwritten solar activity charts

*Kaori Sakaguchi[1], Daikou Shiota[1], Kaori Fukunaga[1], Katsuhide Marubashi[1], Hiromitsu Ishibashi[1], Yuki Kubo[1], Mamoru Ishii[1] (1.National Institute of Information and Communications Technology)

[PEM12-P14] IMF dependence on solar wind parameters

*Tohru Araki, Yuki Harada[1] (1.Kyoto University)

[PEM12-P15] **Dipole Tilt Effect of Geomagnetic Activity from Low- to High-latitudes**

*Nowada Motoharu[1] (1.Shandong University at Weihai)

[PEM12-P16] A New Prediction Model for Solar Wind-Triggered Magnetospheric Disturbances Based on Potential Learning (Neural Network)

*Ryozo Kitajima[1], Motoharu Nowada[2], Ryotaro Kamimura[3] (1.Seikei University, 2.Shandong University at Weihai, 3.Tokai University)

[PEM12-P17] Real-time magnetosphere simulator for space weather using REProduce Plasma Universe code

*Yasubumi Kubota[1], Aoi Nakamizo[1], Kaori Sakaguchi[1], Mitsue Den[1], Yuki Kubo[1], Tsutomu Nagatsuma[1], Takashi Tanaka[1,2] (1.National Institute of Information and Communications Technology, 2.Kyushu University)

[PEM12-P18] **Simulation of GIC flowing through the power transmission network (187 kV-500 kV) in Japan**

*Nishida Yuichiro[1,6], Yusuke Ebihara[1], Satoko Nakamura[1], Shinichi Watari[2], Kumiko Hashimoto[3], Kentaro Kitamura[4], Takashi Kikuchi[5] (1.Kyoto University Reserch Institute for Sustainable Humanosphere, 2.National Institute of Information and Communications Technology, 3.Kibi International University, 4.National Insutitute of Technology, Tokuyama College, 5.Nagoya University, 6.Kyoto University Department of Electrical Engineering)

[PEM12-P19] Climatological features of the upper atmosphere reproduced by a revised version of a whole atmosphere-ionosphere coupled model GAIA

*Hidekatsu Jin[1], Yasunobu Miyoshi[2], Chihiro Tao[1], Hiroyuki Shinagawa[1], Hitoshi Fujiwara[3] (1.National Institude of Information and Communications Technology, 2.Kyushu University, 3.Seikei University)

[PEM12-P20] Investigation of the thermospheric mass density variations below 200 km

*Hitoshi Fujiwara[1], Yasunobu Miyoshi[2], Masayoshi Utashima[1], Huixin Liu[2] (1.Faculty of Science and Technology, Seikei University, 2.Department of Earth and Planetary Sciences, Faculty of Sciences, Kyushu University)

[PEM12-P21] Low-latitude HF Doppler observations of magnetospheric electric fields during space weather disturbances

*Kumiko K. Hashimoto[1], Takashi Kikuchi[2], Ichiro Tomizawa[3], Keisuke Hosokawa[3], Jaroslav Chum[4] (1.Kibi International University, 2.Nagoya University, 3.University of Electro-Commnunications, 4.Institute of Atmospheric Physics, Prague)

[PEM12-P22] Stratospheric ionization during magnetic storms

*Ryuho Kataoka[1] (1.National Institute of Polar Research)

[PEM12-P23] Calculating propagation time of HF radio wave using ray-tracing method and simple comparison with the observation.

*Ryo Nakao[1], Hiroyuki Nakata[1], Hiroyo Ohya[1], Toshiaki Takano[1], Kornyanat Hozumi[2], Takuya Tsugawa[2], Susumu Saito[3], Mamoru Ishii[2] (1.Graduate School of Engineering, Chiba University, 2.National Institute of imformation and Communications Technology, 3.Electronic Navigation Research Institute)

[PEM12-P24] Why do some probabilistic forecasts lack reliability?

*Yuki Kubo[1] (1.National Institute of Information and Communications Technology)

[PEM12-P25] An estimation method of GEO spacecraft surface charging for a real-time spacecraft risk assessment

*Masao Nakamura[1], Ryota Kawachi[1], Go Takahashi[1], Tsutomu Nagatsuma[2], Mamoru Ishii[2] (1.Osaka Prefecture University, 2.NICT)

[PEM12-P26] A network of HF Doppler sounding systems in Japan

*Keisuke Hosokawa[1], Hiroyuki Nakata[2], Kumiko K. Hashimoto[3], Ichiro Tomizawa[1], Jun Sakai[1], Takashi Kikuchi[4] (1.University of Electro-Communications, 2.Chiba University, 3.Kibi International University, 4.ISEE, Nagoya University)

[E] Poster | P (Space and Planetary Sciences)：P-CG Complex & General

10:45 AM - 12:15 PM JST | 1:45 AM - 3:15 AM UTC | Poster Hall International Exhibition Hall8, Makuhari Messe_1

[P-CG22] Shock responses of planetary materials elucidated from meteorites and dynamic compression experiments

convener:Toshimori Sekine(Center for High Pressure Science and Technology Advanced Research), Takuo Okuchi(Institute for Planetary Materials, Okayama University)

[PCG22-P01] discussion

*Takuo Okuchi[1], Toshimori Sekine[2] (1.Institute for Planetary Materials, Okayama University, 2.Center for High Pressure Science and Technology Advanced Research)

[PCG22-P02] Shock-compressed behavior of quartz by XFEL

*Tomoko Sato[1], Yoshinori Tange[2], Yusuke Seto[3], Toshimori Sekine[4,5], Norimasa Ozaki[4], Toyohito Nishikawa[4], Kohei Miyanishi[4], Kensuke Matsuoka[4], Ryosuke Kodama[4], Tadashi Togashi[2], Yuichi Inubushi[2], Toshinori Yabuuchi[6], Makina Yabashi[6] (1.Hiroshima University, 2.Japan Synchrotron Radiation Research Institute, 3.Kobe University, 4.Osaka University, 5.Center for High Pressure Science &Technology Advanced Research, 6.RIKEN)

[PCG22-P04] **Laser-shock experiments of dense polymorphs of Mg_2SiO_4: technical developments using synthetic single crystals**

*Narangoo Purevjav[1], Takuo Okuchi[1], Norimasa Ozaki[2], Takayoshi Sano[3], Yuhei Umeda[2], Shintaro Morioka[2], Nobuki Kamimura[2] (1.Institute for Planetary Materials, Okayama University, 2.Graduate School of Engineering, Osaka University, 3.Institute of Laser Engineering, Osaka University)

[PCG22-P05] Richtmyer-Meshkov instability in inhomogeneous density materials and its application to planetary science

*Takayoshi Sano[1] (1.Institute of Laser Engineering, Osaka University)

[PCG22-P06] Impact-induced dehydration reactions of Fe- and Al-hydrates as potential storage, carrier and source of water

*Tsubasa Tobase[1], Toshimori Sekine[1], Ginga Kitahara[2], Makoto Tokuda[2], Akira Yoshiasa[2], Makoto Takafuji[2], Tsutomu Mashimo[2], Nobuaki Kawai[2] (1.HPSTAR, 2.Graduate School of Science and Technology, Kumamoto University)

[PCG22-P07] Crystallization of amorphous $MgSiO_3$ by shock compression

*Akane Arasuna[1], Masayuki Okuno[1], Nobuaki Kawai[2] (1.Kanazawa University, 2.Kumamoto University)

[PCG22-P08] First-principle study of the structural and electronic properties of N-doped $MgAl_2O_4$ spinel

*Chi Pui Tang[1], Pak Kin Leong[1], Toshimori Sekine[2,3] (1.State Key Laboratory of Lunar and Planetary Sciences, Macau University of Science and Technology, 2.Center for High Pressure Science and Technology Advanced Research (HPSTAR) Shanghai Laboratory of HPSTAR, Shanghai, P.R. China, 3.Graduate School of Engineering, Osaka University)

[PCG22-P09] Transparency of shock-compressed single crystal diamond

*Kento Katagiri[1], Norimasa Ozaki[1,2], Kohei Miyanishi[2], Yuhei Umeda[1], Shintaro Morioka[1], Takayoshi Sano[2], Ryosuke Kodama[1,2] (1.Osaka University, 2.Institute of Laser Engineering, Osaka Unversity)

[PCG22-P10] Pb-Pb dating of the NWA 7203 angrite and relationship to its shock metamorphism

*Hideyuki Hayashi[1], Takashi Mikouchi[1], Yuji Sano[1], Martin Bizzarro[2] (1.The university of Tokyo, 2.University of Copenhagen)

[PCG22-P11] Shock recovery of high-pressure phase of SiO_2 using high-power laser

*Tadashi Kondo[1], Hiromoto Kengo[1], Tatsuhiro Sakaiya[1], Hidenori Terasaki[1], Keisuke Shigemori[2], Youichiro Hironaka[2] (1.Department of Earth and Space Science, Graduate School of Science Osaka University, 2.Institute of Laser Engineering, Osaka University)

[PCG22-P12] Hugoniot measurement of calcite under meteorite collision condition

*Fukui Keiya[1], Norimasa Ozaki[1,2], Yuhei Umeda[1], Kohei Miyanishi[3], Kento Katagiri[1], Shintaro Morioka[1], Takayoshi Sano[3], Ryosuke Kodama[1,2,3] (1.Graduate School of Engineering,Osaka univ., 2.PPC, Osaka Univ., 3.ILE, Osaka Univ.)

[PCG22-P13] Direct observation of the transformation toughening of tetragonal stabilized zirconia under shock deformation condition by ns time-resolved XRD.

*Sota Takagi[1,2], Kouhei Ichiyanagi[2,3], Nobuaki Kawai[4], Ryo Fukaya[2], Shunsuke Nozawa[2], Atsushi Kyono[1], Nobumasa Funamori[2], Shin-ichi Adachi[2] (1.University of Tsukuba, 2.KEK PF, 3.Jichi Medical University, 4.Kumamoto University)

[E] Poster | P (Space and Planetary Sciences)：P-CG Complex & General

5:15 PM - 6:30 PM JST | 8:15 AM - 9:30 AM UTC | Poster Hall International Exhibition Hall8, Makuhari Messe_4

[P-CG22] Shock responses of planetary materials elucidated from meteorites and dynamic compression experiments

convener:Toshimori Sekine(Center for High Pressure Science and Technology Advanced Research), Takuo Okuchi(Institute for Planetary Materials, Okayama University)

[PCG22-P01] discussion

*Takuo Okuchi[1], Toshimori Sekine[2] (1.Institute for Planetary Materials, Okayama University, 2.Center for High Pressure Science and Technology Advanced Research)

[PCG22-P02] Shock-compressed behavior of quartz by XFEL

*Tomoko Sato[1], Yoshinori Tange[2], Yusuke Seto[3], Toshimori Sekine[4,5], Norimasa Ozaki[4], Toyohito Nishikawa[4], Kohei Miyanishi[4], Kensuke Matsuoka[4], Ryosuke Kodama[4], Tadashi Togashi[2], Yuichi Inubushi[2], Toshinori Yabuuchi[6], Makina Yabashi[6] (1.Hiroshima University, 2.Japan Synchrotron Radiation Research Institute, 3.Kobe University, 4.Osaka University, 5.Center for High Pressure Science &Technology Advanced Research, 6.RIKEN)

[PCG22-P04] **Laser-shock experiments of dense polymorphs of Mg_2SiO_4: technical developments using synthetic single crystals**

*Narangoo Purevjav[1], Takuo Okuchi[1], Norimasa Ozaki[2], Takayoshi Sano[3], Yuhei Umeda[2], Shintaro Morioka[2], Nobuki Kamimura[2] (1.Institute for Planetary Materials, Okayama University, 2.Graduate School of Engineering, Osaka University, 3.Institute of Laser Engineering, Osaka University)

[PCG22-P05] Richtmyer-Meshkov instability in inhomogeneous density materials and its application to planetary science

*Takayoshi Sano[1] (1.Institute of Laser Engineering, Osaka University)

[PCG22-P06] Impact-induced dehydration reactions of Fe- and Al-hydrates as potential storage, carrier and source of water

*Tsubasa Tobase[1], Toshimori Sekine[1], Ginga Kitahara[2], Makoto Tokuda[2], Akira Yoshiasa[2], Makoto Takafuji[2], Tsutomu Mashimo[2], Nobuaki Kawai[2] (1.HPSTAR, 2.Graduate School of Science and Technology, Kumamoto University)

[PCG22-P07] Crystallization of amorphous $MgSiO_3$ by shock compression

*Akane Arasuna[1], Masayuki Okuno[1], Nobuaki Kawai[2] (1.Kanazawa University, 2.Kumamoto University)

[PCG22-P08] First-principle study of the structural and electronic properties of N-doped $MgAl_2O_4$ spinel

*Chi Pui Tang[1], Pak Kin Leong[1], Toshimori Sekine[2,3] (1.State Key Laboratory of Lunar and Planetary Sciences, Macau University of Science and Technology, 2.Center for High Pressure Science and Technology Advanced Research (HPSTAR) Shanghai Laboratory of HPSTAR, Shanghai, P.R. China, 3.Graduate School of Engineering, Osaka University)

[PCG22-P09] Transparency of shock-compressed single crystal diamond

*Kento Katagiri[1], Norimasa Ozaki[1,2], Kohei Miyanishi[2], Yuhei Umeda[1], Shintaro Morioka[1], Takayoshi Sano[2], Ryosuke Kodama[1,2] (1.Osaka University, 2.Institute of Laser Engineering, Osaka Unversity)

[PCG22-P10] Pb-Pb dating of the NWA 7203 angrite and relationship to its shock metamorphism

*Hideyuki Hayashi[1], Takashi Mikouchi[1], Yuji Sano[1], Martin Bizzarro[2] (1.The university of Tokyo, 2.University of Copenhagen)

[PCG22-P11] Shock recovery of high-pressure phase of SiO_2 using high-power laser

*Tadashi Kondo[1], Hiromoto Kengo[1], Tatsuhiro Sakaiya[1], Hidenori Terasaki[1], Keisuke Shigemori[2], Youichiro Hironaka[2] (1.Department of Earth and Space Science, Graduate School of Science Osaka University, 2.Institute of Laser Engineering, Osaka University)

[PCG22-P12] Hugoniot measurement of calcite under meteorite collision condition

*Fukui Keiya[1], Norimasa Ozaki[1,2], Yuhei Umeda[1], Kohei Miyanishi[3], Kento Katagiri[1], Shintaro Morioka[1], Takayoshi Sano[3], Ryosuke Kodama[1,2,3] (1.Graduate School of Engineering,Osaka univ., 2.PPC, Osaka Univ., 3.ILE, Osaka Univ.)

[PCG22-P13] Direct observation of the transformation toughening of tetragonal stabilized zirconia under shock deformation condition by ns time-resolved XRD.

*Sota Takagi[1,2], Kouhei Ichiyanagi[2,3], Nobuaki Kawai[4], Ryo Fukaya[2], Shunsuke Nozawa[2], Atsushi Kyono[1], Nobumasa Funamori[2], Shin-ichi Adachi[2] (1.University of Tsukuba, 2.KEK PF, 3.Jichi Medical University, 4.Kumamoto University)

[E] Poster | A (Atmospheric and Hydrospheric Sciences)：A-AS Atmospheric Sciences, Meteorology & Atmospheric Environment

10:45 AM - 12:15 PM JST | 1:45 AM - 3:15 AM UTC | Poster Hall International Exhibition Hall8, Makuhari Messe_2

[A-AS03] Large-scale moisture and organized cloud systems

convener:Hiroaki Miura(The University of Tokyo), Atsushi Hamada(University of Toyama), Satoru Yokoi(Japan Agency for Marine-Earth Science and Technology), Masaki Satoh(Atmosphere and Ocean Research Institute, The University of Tokyo)

[AAS03-P01] Numerical investigation on the shape, terminal velocity, and drag coefficient of a small raindrop by the improved immersed boundary method

*Ong Chia Rui[1], Hiroaki Miura[1] (1.The University of Tokyo)

[AAS03-P02] **A diagnostic study of water vapor during an extreme precipitation event in Yili river valleyA diagnostic study of water vapor during an extreme precipitation event in Yili river valley**

*Jing LiU[1], Yushu Zhou[2], Lianmei Yang[1] (1.Institute of Desert Meteorology,CMA, 2.Institute of Atmospheric Physics,CAS)

[AAS03-P03] **The Study on the Characteristics of Weather and Cloud Types in the Summer and Winter Seasons of the South China Sea**

*Jou Ping Hou[1], Bo-Shiou Wei[1], Li-Zhen Su[1] (1.Chung Cheng Institute of Technology)

[AAS03-P04] **Linkages between the South and East Asian Monsoon water vapor transport during boreal summer**

*Yong Liu[1] (1.Institute of Atmospheric Physics, Beijing , China)

[AAS03-P05] Interannual Modulation of the Local Hadley Circulation on Clouds, Radiation and Diagnostic Fields over the Western North Pacific

*Xinyue Wang[1], Hironobu Iwabuchi[1] (1.Tohoku Univ.)

[AAS03-P06] Seasonal and Regional Variation of Diurnal Cycle of Rainfall over Java Island and the Surrounding Area

*Madam Taqiyya Maulana[1], Takeshi Yamazaki[1] (1.Tohoku University)

[AAS03-P07] **Study on atmospheric circulation characteristics of precipitation anomalies in arid region of Central Asia**

*Lianmei Yang[1], Xuefeng Guan[1] (1.Institute of Desert Meteorology, China Meteorological Administration,)

[AAS03-P08] Mechanisms for northward propagation of boreal summer intraseasonal oscillation

*Kanta Nakae[1], Masaki Satoh[1], Daisuke Takasuka[1] (1.Atmosphere and Ocean Research Institute, The University of Tokyo)

[AAS03-P09] Fractality in the perimeter of tropical clouds observed by Himawari-8 or simulated by a high-resolution model

*Takuya Jinno[1] (1.Graduate School of Science, The University of Tokyo)

[AAS03-P10] **Large-scale deformation of tropical cloud band in the ITCZ detected in NICAM simulations**

*Noriyuki Nishi[1], Atsushi Hamada[4], Yohei Yamada[2], Tomoe Nasuno[2], Reona Satoh[5], Masaki Satoh[3] (1.Faculty of Science, Fukuoka Universtiy, 2.JAMSTEC, 3.AORI, University of Tokyo, 4.Graduate School of Science and Engineering for Education, University of Toyama, 5.Graduate School of Science, Fukuoka University)

[AAS03-P11] **Improvement of single-moment bulk microphysics for super-cooled water clouds over the Southern Ocean in NICAM using Joint simulator and double-moment microphysics**

*Woosub Roh[1], Tatsuya Seiki[2], Masaki Satoh[1], Tempei Hashino[3] (1.AORI, the university of Tokyo, 2.JAMSTEC, 3.Kochi university of technology)

[AAS03-P12] High-cloud property responses to SST change: sensitivity study using a global nonhydrostatic model

*Tomoki Ohno[1], Masaki Satoh[2] (1.Japan Agency for Marine-Earth Science and Technology, 2.Atmosphere and Ocean Research Institute, The University of Tokyo)

[AAS03-P13] Effects of different cloud overlapping parameters on simulated total cloud fraction over the globe and East Asian region

*bo hai Wang[1], hua Zhang[2] (1.Institute of Atmospheric Physics, Chinese Academy of Sciences, 2.State Key Laboratory of Severe Weather, Chinese Academy of Meteorological Sciences)

[E] Poster | A (Atmospheric and Hydrospheric Sciences)：A-AS Atmospheric Sciences, Meteorology & Atmospheric Environment

5:15 PM - 6:30 PM JST | 8:15 AM - 9:30 AM UTC | Poster Hall International Exhibition Hall8, Makuhari Messe_6

[A-AS03] Large-scale moisture and organized cloud systems

convener:Hiroaki Miura(The University of Tokyo), Atsushi Hamada(University of Toyama), Satoru Yokoi(Japan Agency for Marine-Earth Science and Technology), Masaki Satoh(Atmosphere and Ocean Research Institute, The University of Tokyo)

[AAS03-P01] Numerical investigation on the shape, terminal velocity, and drag coefficient of a small raindrop by the improved immersed boundary method

*Ong Chia Rui[1], Hiroaki Miura[1] (1.The University of Tokyo)

[AAS03-P02] **A diagnostic study of water vapor during an extreme precipitation event in Yili river valleyA diagnostic study of water vapor during an extreme precipitation event in Yili river valley**

*Jing LiU[1], Yushu Zhou[2], Lianmei Yang[1] (1.Institute of Desert Meteorology,CMA, 2.Institute of Atmospheric Physics,CAS)

[AAS03-P03] **The Study on the Characteristics of Weather and Cloud Types in the Summer and Winter Seasons of the South China Sea**

*Jou Ping Hou[1], Bo-Shiou Wei[1], Li-Zhen Su[1] (1.Chung Cheng Institute of Technology)

[AAS03-P04] **Linkages between the South and East Asian Monsoon water vapor transport during boreal summer**

*Yong Liu[1] (1.Institute of Atmospheric Physics, Beijing , China)

[AAS03-P05] Interannual Modulation of the Local Hadley Circulation on Clouds, Radiation and Diagnostic Fields over the Western North Pacific

*Xinyue Wang[1], Hironobu Iwabuchi[1] (1.Tohoku Univ.)

[AAS03-P06] Seasonal and Regional Variation of Diurnal Cycle of Rainfall over Java Island and the Surrounding Area

*Madam Taqiyya Maulana[1], Takeshi Yamazaki[1] (1.Tohoku University)

[AAS03-P07] **Study on atmospheric circulation characteristics of precipitation anomalies in arid region of Central Asia**

*Lianmei Yang[1], Xuefeng Guan[1] (1.Institute of Desert Meteorology, China Meteorological Administration,)

[AAS03-P08] Mechanisms for northward propagation of boreal summer intraseasonal oscillation

*Kanta Nakae[1], Masaki Satoh[1], Daisuke Takasuka[1] (1.Atmosphere and Ocean Research Institute, The University of Tokyo)

[AAS03-P09] Fractality in the perimeter of tropical clouds observed by Himawari-8 or simulated by a high-resolution model

*Takuya Jinno[1] (1.Graduate School of Science, The University of Tokyo)

[AAS03-P10] **Large-scale deformation of tropical cloud band in the ITCZ detected in NICAM simulations**

*Noriyuki Nishi[1], Atsushi Hamada[4], Yohei Yamada[2], Tomoe Nasuno[2], Reona Satoh[5], Masaki Satoh[3] (1.Faculty of Science, Fukuoka Universtiy, 2.JAMSTEC, 3.AORI, University of Tokyo, 4.Graduate School of Science and Engineering for Education, University of Toyama, 5.Graduate School of Science, Fukuoka University)

[AAS03-P11] **Improvement of single-moment bulk microphysics for super-cooled water clouds over the Southern Ocean in NICAM using Joint simulator and double-moment microphysics**

*Woosub Roh[1], Tatsuya Seiki[2], Masaki Satoh[1], Tempei Hashino[3] (1.AORI, the university of Tokyo, 2.JAMSTEC, 3.Kochi university of technology)

[AAS03-P12] High-cloud property responses to SST change: sensitivity study using a global nonhydrostatic model

*Tomoki Ohno[1], Masaki Satoh[2] (1.Japan Agency for Marine-Earth Science and Technology, 2.Atmosphere and Ocean Research Institute, The University of Tokyo)

[AAS03-P13] Effects of different cloud overlapping parameters on simulated total cloud fraction over the globe and East Asian region

*bo hai Wang[1], hua Zhang[2] (1.Institute of Atmospheric Physics, Chinese Academy of Sciences, 2.State Key Laboratory of Severe Weather, Chinese Academy of Meteorological Sciences)

[E] Poster | A (Atmospheric and Hydrospheric Sciences)：A-CG Complex & General

10:45 AM - 12:15 PM JST | 1:45 AM - 3:15 AM UTC | Poster Hall International Exhibition Hall8, Makuhari Messe_3

[A-CG32] Global Carbon Cycle Observation and Analysis

convener:Kazuhito Ichii(Chiba University), Prabir Patra(Research Institute for Global Change, JAMSTEC), Forrest M. Hoffman(Oak Ridge National Laboratory), Makoto Saito(National Institute of Environmental Studies)

[ACG32-P01] Regional budgets of 3 major greenhouse gases using inverse modelling of atmospheric data

*Prabir Patra[1], Naveen Chandra[1], Jagat Bisht[1] (1.Japan Agency for Marine-Earth Science and Technology (JAMSTEC))

[ACG32-P02] Analysis of hot summer in 2018

*Kazutaka Murakami[1], Kazuhito Ichii[1,2], Yukio Yoshida[1], Haruki Oshio[1], Makoto Saito[1] (1.National Institute for Environmental Studies, 2.Chiba University)

[ACG32-P03] Updated Data-Driven GPP and NEE Estimation Using Machine Learning Algorithms with Remote Sensing and Flux Data

*Zhiyan Liu[1], Kazuhito Ichii[1], Yusuke Hayasi[1], Riku Kawase[1], Masahito Ueyama[2], Yuji Kominami[3] (1.Chiba University, 2.Osaka Prefecture University, 3.Forest Research and Management Organization)

[ACG32-P04] **Response of a Bornean Rainforest to the Climatic Changes imposed by ENSO during 2009-2016**

*Julie Karine Michelon[1], Tomo'omi Kumagai[2,3], Tetsuya Hiyama[3], Hatsuki Fujinami[3], Kazuho Matsumoto[4], Tomonori Kume[5], Takami Saito[6] (1.Graduate School of Environmental Studies, Nagoya University, 2.Graduate School of Agricultural and Life Sciences, The University of Tokyo, 3.Institute for Space-Earth Environmental Research, Nagoya University, 4.Faculty of Agriculture, University of the Ryukyus, 5.Faculty of Agriculture, Kyushu University, 6.Forest Research and Management Organization)

[ACG32-P05] **Monitoring and Evaluating CO2 Flux in the Grassland Areas of Mongolia**

*Qinxue Wang[1], Tomohiro Okadera[1], Deni Eer[1], Masataka Watanabe[2], Tomohiro Shishime[2], Akihiro Oba[2], Ochirbat Batkhishig[3] (1.National Institute for Environmental Studies, 2.Research and Development Initiative, Chuo University, 3.Institute of Geography and Geoecology, Mongolian Academy of Sciences)

[ACG32-P06] Data-driven monitoring of terrestrial carbon cycle in Mongolia

*ZAYA MART[1], Zhiyan Liu[1], Riku Kawase[1], Kazuhito Ichii[1] (1.Chiba University)

[E] Poster | A (Atmospheric and Hydrospheric Sciences)：A-CG Complex & General

5:15 PM - 6:30 PM JST | 8:15 AM - 9:30 AM UTC | Poster Hall International Exhibition Hall8, Makuhari Messe_13

[A-CG32] Global Carbon Cycle Observation and Analysis

convener:Kazuhito Ichii(Chiba University), Prabir Patra(Research Institute for Global Change, JAMSTEC), Forrest M. Hoffman(Oak Ridge National Laboratory), Makoto Saito(National Institute of Environmental Studies)

[ACG32-P01] Regional budgets of 3 major greenhouse gases using inverse modelling of atmospheric data

*Prabir Patra[1], Naveen Chandra[1], Jagat Bisht[1] (1.Japan Agency for Marine-Earth Science and Technology (JAMSTEC))

[ACG32-P02] Analysis of hot summer in 2018

*Kazutaka Murakami[1], Kazuhito Ichii[1,2], Yukio Yoshida[1], Haruki Oshio[1], Makoto Saito[1] (1.National Institute for Environmental Studies, 2.Chiba University)

[ACG32-P03] Updated Data-Driven GPP and NEE Estimation Using Machine Learning Algorithms with Remote Sensing and Flux Data

*Zhiyan Liu[1], Kazuhito Ichii[1], Yusuke Hayasi[1], Riku Kawase[1], Masahito Ueyama[2], Yuji Kominami[3] (1.Chiba University, 2.Osaka Prefecture University, 3.Forest Research and Management Organization)

[ACG32-P04] **Response of a Bornean Rainforest to the Climatic Changes imposed by ENSO during 2009-2016**

*Julie Karine Michelon[1], Tomo'omi Kumagai[2,3], Tetsuya Hiyama[3], Hatsuki Fujinami[3], Kazuho Matsumoto[4], Tomonori Kume[5], Takami Saito[6] (1.Graduate School of Environmental Studies, Nagoya University, 2.Graduate School of Agricultural and Life Sciences, The University of Tokyo, 3.Institute for Space-Earth Environmental Research, Nagoya University, 4.Faculty of Agriculture, University of the Ryukyus, 5.Faculty of Agriculture, Kyushu University, 6.Forest Research and Management Organization)

[ACG32-P05] **Monitoring and Evaluating CO2 Flux in the Grassland Areas of Mongolia**

*Qinxue Wang[1], Tomohiro Okadera[1], Deni Eer[1], Masataka Watanabe[2], Tomohiro Shishime[2], Akihiro Oba[2], Ochirbat Batkhishig[3] (1.National Institute for Environmental Studies, 2.Research and Development Initiative, Chuo University, 3.Institute of Geography and Geoecology, Mongolian Academy of Sciences)

[ACG32-P06] Data-driven monitoring of terrestrial carbon cycle in Mongolia

*ZAYA MART[1], Zhiyan Liu[1], Riku Kawase[1], Kazuhito Ichii[1] (1.Chiba University)

[E] Poster | H (Human Geosciences)：H-DS Disaster geosciences

3:30 PM - 5:00 PM JST | 6:30 AM - 8:00 AM UTC | Poster Hall International Exhibition Hall8, Makuhari Messe_12

[H-DS09] Landslides and related phenomena

convener:Masahiro Chigira(Disaster Prevention Research Institute, Kyoto University), Gonghui Wang(Disaster Prevention Research Institute, Kyoto University), Fumitoshi Imaizumi(Faculty of Agriculture, Shizuoka University)

[HDS09-P01] **Fluidized landslides triggered by the liquefaction of subsurface volcanic deposits during the 2018 Iburi–Tobu earthquake, Hokkaido**

*Jun Kameda[1], Hiro Kamiya[2], Hirokazu Masumoto[1], Tomonori Morisaki[1], Toru Hiratsuka[2], Chisaki Inaoi (1.Department of Natural History Sciences, Graduate School of Science, Hokkaido University, 2.Department of Earth and Planetary Sciences, School of Science, Hokkaido University)

[HDS09-P02] A comparison between the acoustic signals and seismic signals generated during a dam-break test

★Invited Papers

*Zheng-yi Feng[1], Hao-yang Huang[1], Chia-Ming Chuang[1] (1.Department of Soil and Water Conservation, National Chung Hsing University, Taichung, Taiwan)

[HDS09-P03] Evaluation of factors of safety and landslide risk for a watershed by Scoops3D

*Zheng-yi Feng[1], Chia-Ming Chuang[1], Hao-yang Huang[1] (1.Department of Soil and Water Conservation, National Chung Hsing University, Taichung, Taiwan)

[HDS09-P04] **Fuzzy Clustering Algorithms for Establishing Landslide Susceptibility Map**

*Pei-hsun Tsai[1], Syuan-yi Wang[1], Jie-shin Cheng[1] (1.Chaoyang University of Technology)

[HDS09-P05] **A Study on Landslides and Debris Flows Susceptibility Mapping Using Unmanned Aerial Vehicles**

*Sheng-Jia Liu[1] (1.qwepoi13@gmail.com)

[HDS09-P06] Largescale landslide induced by AD1586 Tensho-Earthquake in Gifu Prefecture, central Japan

*Takahiro Kurimoto[1], Yoshihiko Kariya[2], Kuniyasu Mokudai[3], Ryuji Yamada[4], Takashi Kimura[4] (1.Undergraduate Senshu University, 2.Department of Geography, Senshu University, 3.Japan Geoservice Incorporated, 4.National Research Institute for Earth Science and Disaster Resilience)

[HDS09-P07] Failure Probability of Lushan Landslide, Taiwan

*Wei-Ting Lin[1], Kuang-Tsung Chang[1] (1.National Chung Hsing University)

[HDS09-P08] Interpretation of landslide surface deformation in Kali Gandaki River watershed, Nepal using ALOS-2/PALSAR-2 InSAR image

*Hiroshi, P. Sato[1] (1.College of Humanities and Sciences, Nihon University)

[HDS09-P09] A depth-integrated model for granular flows on the transition of different bed conditions

*Ling-Yi Hsu[1], Chi-Yao Hung[1] (1.National Chung Hsing University)

[HDS09-P10] A viscous granular flow experiment with new refractive index matching material

*Tsai-Jung Lin[1], Chi-Yao Hung[1] (1.National Chung Hsing University)

[HDS09-P11] Sandbox experiments of submarine landslide caused by water film in low permeability layer

*Shogo Kawakita[1], Daisuke Asahina[2], Keiji Kitajima[3], Mitsukazu Nakanishi[3] (1.Graduate School of Science & Technology, Nihon Univ., 2.National Institute of Advanced Industrial Science and Technology, 3.College of Science & Technology, Nihon Univ.)

[HDS09-P12] **Study on Creep Properties of Sand and Cemented Sand**

*JIN-YI YU[1], KUANG-TSUNG CHANG[1] (1.National Chung Hsing University)

[HDS09-P13] The effects of seepage force and the Poisson’s ratio on slope stability

*Hirokazu Fukui[1], Tomomi Terajima[2] (1.Graduate school of Science, Kyoto University, 2.Disaster Prevention Research Institute, Kyoto University)

[HDS09-P14] Study on the factors of seepage erosion

*Szu-Wei Fu[1], Kuang-Tsung Chang[1] (1.National Chung Hsing University)

[HDS09-P15] Deformation of slope models with different orientations of weak planes

*taeyuan tseng[1], Kuang-Tsung Chang[1] (1.National Chung Hsing University)

[E] Poster | H (Human Geosciences)：H-DS Disaster geosciences

5:15 PM - 6:30 PM JST | 8:15 AM - 9:30 AM UTC | Poster Hall International Exhibition Hall8, Makuhari Messe_20

[H-DS09] Landslides and related phenomena

convener:Masahiro Chigira(Disaster Prevention Research Institute, Kyoto University), Gonghui Wang(Disaster Prevention Research Institute, Kyoto University), Fumitoshi Imaizumi(Faculty of Agriculture, Shizuoka University)

[HDS09-P01] **Fluidized landslides triggered by the liquefaction of subsurface volcanic deposits during the 2018 Iburi–Tobu earthquake, Hokkaido**

*Jun Kameda[1], Hiro Kamiya[2], Hirokazu Masumoto[1], Tomonori Morisaki[1], Toru Hiratsuka[2], Chisaki Inaoi (1.Department of Natural History Sciences, Graduate School of Science, Hokkaido University, 2.Department of Earth and Planetary Sciences, School of Science, Hokkaido University)

[HDS09-P02] A comparison between the acoustic signals and seismic signals generated during a dam-break test

★Invited Papers

*Zheng-yi Feng[1], Hao-yang Huang[1], Chia-Ming Chuang[1] (1.Department of Soil and Water Conservation, National Chung Hsing University, Taichung, Taiwan)

[HDS09-P03] Evaluation of factors of safety and landslide risk for a watershed by Scoops3D

*Zheng-yi Feng[1], Chia-Ming Chuang[1], Hao-yang Huang[1] (1.Department of Soil and Water Conservation, National Chung Hsing University, Taichung, Taiwan)

[HDS09-P04] **Fuzzy Clustering Algorithms for Establishing Landslide Susceptibility Map**

*Pei-hsun Tsai[1], Syuan-yi Wang[1], Jie-shin Cheng[1] (1.Chaoyang University of Technology)

[HDS09-P05] **A Study on Landslides and Debris Flows Susceptibility Mapping Using Unmanned Aerial Vehicles**

*Sheng-Jia Liu[1] (1.qwepoi13@gmail.com)

[HDS09-P06] Largescale landslide induced by AD1586 Tensho-Earthquake in Gifu Prefecture, central Japan

*Takahiro Kurimoto[1], Yoshihiko Kariya[2], Kuniyasu Mokudai[3], Ryuji Yamada[4], Takashi Kimura[4] (1.Undergraduate Senshu University, 2.Department of Geography, Senshu University, 3.Japan Geoservice Incorporated, 4.National Research Institute for Earth Science and Disaster Resilience)

[HDS09-P07] Failure Probability of Lushan Landslide, Taiwan

*Wei-Ting Lin[1], Kuang-Tsung Chang[1] (1.National Chung Hsing University)

[HDS09-P08] Interpretation of landslide surface deformation in Kali Gandaki River watershed, Nepal using ALOS-2/PALSAR-2 InSAR image

*Hiroshi, P. Sato[1] (1.College of Humanities and Sciences, Nihon University)

[HDS09-P09] A depth-integrated model for granular flows on the transition of different bed conditions

*Ling-Yi Hsu[1], Chi-Yao Hung[1] (1.National Chung Hsing University)

[HDS09-P10] A viscous granular flow experiment with new refractive index matching material

*Tsai-Jung Lin[1], Chi-Yao Hung[1] (1.National Chung Hsing University)

[HDS09-P11] Sandbox experiments of submarine landslide caused by water film in low permeability layer

*Shogo Kawakita[1], Daisuke Asahina[2], Keiji Kitajima[3], Mitsukazu Nakanishi[3] (1.Graduate School of Science & Technology, Nihon Univ., 2.National Institute of Advanced Industrial Science and Technology, 3.College of Science & Technology, Nihon Univ.)

[HDS09-P12] **Study on Creep Properties of Sand and Cemented Sand**

*JIN-YI YU[1], KUANG-TSUNG CHANG[1] (1.National Chung Hsing University)

[HDS09-P13] The effects of seepage force and the Poisson’s ratio on slope stability

*Hirokazu Fukui[1], Tomomi Terajima[2] (1.Graduate school of Science, Kyoto University, 2.Disaster Prevention Research Institute, Kyoto University)

[HDS09-P14] Study on the factors of seepage erosion

*Szu-Wei Fu[1], Kuang-Tsung Chang[1] (1.National Chung Hsing University)

[HDS09-P15] Deformation of slope models with different orientations of weak planes

*taeyuan tseng[1], Kuang-Tsung Chang[1] (1.National Chung Hsing University)

[E] Poster | H (Human Geosciences)：H-TT Technology & Techniques

3:30 PM - 5:00 PM JST | 6:30 AM - 8:00 AM UTC | Poster Hall International Exhibition Hall8, Makuhari Messe_13

[H-TT18] Development and application of environmental traceability methods

convener:Ichiro Tayasu(Research Institute for Humanity and Nature), Nobuhito Ohte(Department of Social Informatics, Graduate School of Informatics, Kyoto University), Gabriel J Bowen(University of Utah)

[HTT18-P01] Isotopic study on seasonal nitrogen dynamics at Lake Biwa

*Takaaki Ishibashi[1], Ken'ichi Osaka[1], Keisuke Koba[2], Takashi Nakamura[3], Kei Nishida[3] (1.Department of ecosystem study, University of Shiga Prefecture, 2.Center for Ecological Research, Kyoto University, 3.International Research Center for River Basin Environment, University of YAMANASHI)

[HTT18-P02] Relationship between residence time, water quality, and stable isotopes of spring water and groundwater in coastal area of Fukushima prefecture

*Shiho Yabusaki[1], Kazuyoshi Asai[2] (1. Research Institute for Humanity and Nature・Faculty of Symbiotic Systems Science, Fukushima University, 2.Geo Science Laboratory)

[HTT18-P03] Applicability evaluation of CIA due to river and lake

*yusuke hataya[1], SEIKI KAWAGOE[1], Shiho Yabusaki[2], KEN Suzuki[1] (1.fukushima university, 2.Research Institute for Humanity and Nature)

[HTT18-P04] Chemical property analysis of short time scale to determine snowfall source

*Suzuki hiromichi[1], SEIKI KAWAGOE[1], SHO ADACHI[1], Shiho Yabusaki[2] (1.Fukushima University, 2.Research Institute for Humanity and Nature)

[HTT18-P05] Analyzing the origin of surface water in the Saijo Plain, Japan, based on the antimony concentration in the water

*Minoru TOKUMASU[1,2], Ki-Cheol SHIN[3], Yoshihiro YAMADA[4] (1.The United Graduate School of Agricultural Sciences, Ehime University, 2.Saijo City, 3.The Research Institute for Humanity and Nature (RIHN) , 4.Kagawa University, Faculty of Agriculture)

[HTT18-P06] Basic kinetic study on stable isotope ratios of nitrogen compounds: a case study for groundwater in the Kathmandu Valley, Nepal

*Ken Yokozawa[1,2], Kei Nishida[1,3], Takashi Nakamura[1,3], Ken'ichi Osaka[4] (1.University of Yamanashi, 2.Special Graduate Program on River Basin Environmental Science,, 3.ICRE, 4.Department of ecosystem study Univercity of Shiga prefecture)

[HTT18-P07] Usefulness of strontium isotope composition for determining the geographical origin of wasabi and potato

*Takafumi Kamitani[1], Ki-Cheol Shin[2], Sachiko Nakamura[1], Rika Koda[1], Tomoya Oka[1], Noriaki Fushimi[1], Yasuhide Muranaka[1] (1.Shizuoka Institute of Environment and Hygiene, 2.Research Institute for Humanity and Nature)

[HTT18-P08] Reconstruction of sea surface temperature and salinity for the Medieval Climatic Anomaly using a long-lived fossil coral collected at Ishigaki Island, southwestern Japan

*Osamu Abe[1], Maki Morimoto[2], Ryuji Asami[3], Takeshi Nakatsuka[1,4] (1.Graduate School of Environmental Studies, Nagoya University, 2.School of Education, Gifu University, 3.Graduate School of Science, Tohoku University, 4.Research Institute for Humanity and Nature)

[HTT18-P09] Development of the analytical method for sulfur isotope in SO_2 gas

*Masaaki Takahashi[1], Hiroyuki Sase[1], Tsuyoshi Ohizumi[1] (1.Asia Center for Air Pollution Research)

[HTT18-P10] Zinc isotope analysis on human tooth enamel samples to reconstruct diet of the Jomon period.

*Soichiro Kusaka[1], Ki-Cheol Shin[2] (1.Tokai Univ., 2.Research Institute for Humanity and Nature)

[HTT18-P11] Zinc stable isotope analysis of environmental reference materials

*Ki-Cheol Shin[1] (1.Research Institute for Humanity and Nature)

[E] Poster | H (Human Geosciences)：H-TT Technology & Techniques

5:15 PM - 6:30 PM JST | 8:15 AM - 9:30 AM UTC | Poster Hall International Exhibition Hall8, Makuhari Messe_23

[H-TT18] Development and application of environmental traceability methods

convener:Ichiro Tayasu(Research Institute for Humanity and Nature), Nobuhito Ohte(Department of Social Informatics, Graduate School of Informatics, Kyoto University), Gabriel J Bowen(University of Utah)

[HTT18-P01] **Isotopic study on seasonal nitrogen dynamics at Lake Biwa**

*Takaaki Ishibashi[1], Ken'ichi Osaka[1], Keisuke Koba[2], Takashi Nakamura[3], Kei Nishida[3] (1.Department of ecosystem study, University of Shiga Prefecture, 2.Center for Ecological Research, Kyoto University, 3.International Research Center for River Basin Environment, University of YAMANASHI)

[HTT18-P02] Relationship between residence time, water quality, and stable isotopes of spring water and groundwater in coastal area of Fukushima prefecture

*Shiho Yabusaki[1], Kazuyoshi Asai[2] (1. Research Institute for Humanity and Nature・Faculty of Symbiotic Systems Science, Fukushima University, 2.Geo Science Laboratory)

[HTT18-P03] Applicability evaluation of CIA due to river and lake

*yusuke hataya[1], SEIKI KAWAGOE[1], Shiho Yabusaki[2], KEN Suzuki[1] (1.fukushima university, 2.Research Institute for Humanity and Nature)

[HTT18-P04] Chemical property analysis of short time scale to determine snowfall source

*Suzuki hiromichi[1], SEIKI KAWAGOE[1], SHO ADACHI[1], Shiho Yabusaki[2] (1.Fukushima University, 2.Research Institute for Humanity and Nature)

[HTT18-P05] Analyzing the origin of surface water in the Saijo Plain, Japan, based on the antimony concentration in the water

*Minoru TOKUMASU[1,2], Ki-Cheol SHIN[3], Yoshihiro YAMADA[4] (1.The United Graduate School of Agricultural Sciences, Ehime University, 2.Saijo City, 3.The Research Institute for Humanity and Nature (RIHN) , 4.Kagawa University, Faculty of Agriculture)

[HTT18-P06] Basic kinetic study on stable isotope ratios of nitrogen compounds: a case study for groundwater in the Kathmandu Valley, Nepal

*Ken Yokozawa[1,2], Kei Nishida[1,3], Takashi Nakamura[1,3], Ken'ichi Osaka[4] (1.University of Yamanashi, 2.Special Graduate Program on River Basin Environmental Science,, 3.ICRE, 4.Department of ecosystem study Univercity of Shiga prefecture)

[HTT18-P07] Usefulness of strontium isotope composition for determining the geographical origin of wasabi and potato

*Takafumi Kamitani[1], Ki-Cheol Shin[2], Sachiko Nakamura[1], Rika Koda[1], Tomoya Oka[1], Noriaki Fushimi[1], Yasuhide Muranaka[1] (1.Shizuoka Institute of Environment and Hygiene, 2.Research Institute for Humanity and Nature)

[HTT18-P08] Reconstruction of sea surface temperature and salinity for the Medieval Climatic Anomaly using a long-lived fossil coral collected at Ishigaki Island, southwestern Japan

*Osamu Abe[1], Maki Morimoto[2], Ryuji Asami[3], Takeshi Nakatsuka[1,4] (1.Graduate School of Environmental Studies, Nagoya University, 2.School of Education, Gifu University, 3.Graduate School of Science, Tohoku University, 4.Research Institute for Humanity and Nature)

[HTT18-P09] Development of the analytical method for sulfur isotope in SO_2 gas

*Masaaki Takahashi[1], Hiroyuki Sase[1], Tsuyoshi Ohizumi[1] (1.Asia Center for Air Pollution Research)

[HTT18-P10] Zinc isotope analysis on human tooth enamel samples to reconstruct diet of the Jomon period.

*Soichiro Kusaka[1], Ki-Cheol Shin[2] (1.Tokai Univ., 2.Research Institute for Humanity and Nature)

[HTT18-P11] Zinc stable isotope analysis of environmental reference materials

*Ki-Cheol Shin[1] (1.Research Institute for Humanity and Nature)

[E] Poster | H (Human Geosciences)：H-CG Complex & General

1:45 PM - 3:15 PM JST | 4:45 AM - 6:15 AM UTC | Poster Hall International Exhibition Hall8, Makuhari Messe_6

[H-CG28] Implementing Integrated Research for Sustainable Future

convener:Yukio Himiyama(Emeritus Professor, Hokkaido University of Education), Akihiko Kondoh(Center for Environmental Remote Sensing, Chiba University), Takeshi Sakurai(Graduate School of Agricultural and Life Sciences, The University of Tokyo), Kenichi Abe(Research Institute for Humanity and Nature)

[HCG28-P01] **Ground Motion Instrumentation Network and Earthquake Early Warning System for Uttarakhand**

*Pankaj Kumar[1,2], Ashok - Kumar[1,2], Ajay - Gairola[1,2] (1.Indian Institute of Technology Roorkee, India, 2.Earthquake Early Warning Laboratory, Centre of Excellence in Disaster Mitigation & Management, IIT Roorkee)

[HCG28-P02] Linking Socioeconomic and Geographical Model to Analyze Land Use Changes in the Jakarta - Bandung Mega Urban Regions

*Didit Okta Pribadi[1,2] (1.Center for Regional Systems Analysis, Planning and Development (CrestPent) - IPB University, 2.Research Center for Plant Conservation and Botanic Gardens - Indonesian Institute of Sciences)

[HCG28-P03] **Development of an Integrated Model for Evaluation of Pasture Carrying Capacity and its Vulnerability based on Water Resources in Arid and Semi-arid Regions- - - - -A Case Study in Mongolia**

★Invited Papers

*Qinxue Wang[1], Tomohiro Okadera[1], Tadanobu Nakayama[1], Deni Eer[1], Ochirbat Batkhishig[2], Dorjgotov Battogtokh[2], Uudus Bayasaikhan[3] (1.National Institute for Environmental Studies, 2.Institute of Geography and Geoecology, Mongolian Academy of Sciences, 3.School of Arts and Sciences, National University of Mongolia)

[HCG28-P04] Influence of land use histories on vegetation and ecosystem services of restored wetlands in Tumen River basin, China

*CAO GUANGLAN[1], Kazuaki Tsuchiya[1], Weihong Zhu[2], OKURO TOSHIYA[1] (1.The University of Tokyo, 2.Yanbian University)

[HCG28-P05] The spatial flow of freshwater ecosystem services: A case study of Tumen River watershed

*JIAN ZHANG[1], Shizuka hashimoto[1], Kazuaki Tsuchiya[1], Weihong Zhu[2], OKURO TOSHIYA[1] (1.The University of Tokyo, 2.Yanbian University)

[E] Poster | H (Human Geosciences)：H-CG Complex & General

5:15 PM - 6:30 PM JST | 8:15 AM - 9:30 AM UTC | Poster Hall International Exhibition Hall8, Makuhari Messe_25

[H-CG28] Implementing Integrated Research for Sustainable Future

convener:Yukio Himiyama(Emeritus Professor, Hokkaido University of Education), Akihiko Kondoh(Center for Environmental Remote Sensing, Chiba University), Takeshi Sakurai(Graduate School of Agricultural and Life Sciences, The University of Tokyo), Kenichi Abe(Research Institute for Humanity and Nature)

[HCG28-P01] **Ground Motion Instrumentation Network and Earthquake Early Warning System for Uttarakhand**

*Pankaj Kumar[1,2], Ashok - Kumar[1,2], Ajay - Gairola[1,2] (1.Indian Institute of Technology Roorkee, India, 2.Earthquake Early Warning Laboratory, Centre of Excellence in Disaster Mitigation & Management, IIT Roorkee)

[HCG28-P02] Linking Socioeconomic and Geographical Model to Analyze Land Use Changes in the Jakarta - Bandung Mega Urban Regions

*Didit Okta Pribadi[1,2] (1.Center for Regional Systems Analysis, Planning and Development (CrestPent) - IPB University, 2.Research Center for Plant Conservation and Botanic Gardens - Indonesian Institute of Sciences)

[HCG28-P03] **Development of an Integrated Model for Evaluation of Pasture Carrying Capacity and its Vulnerability based on Water Resources in Arid and Semi-arid Regions- - - - -A Case Study in Mongolia**

★Invited Papers

*Qinxue Wang[1], Tomohiro Okadera[1], Tadanobu Nakayama[1], Deni Eer[1], Ochirbat Batkhishig[2], Dorjgotov Battogtokh[2], Uudus Bayasaikhan[3] (1.National Institute for Environmental Studies, 2.Institute of Geography and Geoecology, Mongolian Academy of Sciences, 3.School of Arts and Sciences, National University of Mongolia)

[HCG28-P04] Influence of land use histories on vegetation and ecosystem services of restored wetlands in Tumen River basin, China

*CAO GUANGLAN[1], Kazuaki Tsuchiya[1], Weihong Zhu[2], OKURO TOSHIYA[1] (1.The University of Tokyo, 2.Yanbian University)

[HCG28-P05] The spatial flow of freshwater ecosystem services: A case study of Tumen River watershed

*JIAN ZHANG[1], Shizuka hashimoto[1], Kazuaki Tsuchiya[1], Weihong Zhu[2], OKURO TOSHIYA[1] (1.The University of Tokyo, 2.Yanbian University)

[E] Poster | S (Solid Earth Sciences)：S-SS Seismology

3:30 PM - 5:00 PM JST | 6:30 AM - 8:00 AM UTC | Poster Hall International Exhibition Hall8, Makuhari Messe_16

[S-SS06] Nankai Trough Seismogenic Zone Experiment: Logging and sampling the seismogenic megathrust

convener:Kyuichi Kanagawa(Graduate School of Science, Chiba University), Demian M Saffer(Pennsylvania State University), Masataka Kinoshita(Earthquake Research Institute, University of Tokyo)

[SSS06-P01] Crustal structure in the Nankai Trough seismogenic zone based on renewed depth images and seismic attribute analysis

*Kazuya Shiraishi[1], Yasuhiro Yamada[1], Masataka Kinoshita[2], Gaku Kimura[3] (1.Japan Agency for Marine-Earth Science and Technology, 2.Earthquake Research Institute, The University of Tokyo, 3.Tokyo University of Marine Science and Technology)

[SSS06-P02] Along-strike variations in protothrust zone characteristics at the Nankai Trough subduction margin

*Hannah Tilley[1], Gregory F Moore[1], Mikiya Yamashita[2], Shuichi Kodaira[2] (1.University of Hawaii at Manoa, 2.JAMSTEC)

[SSS06-P03] Temporal change in seismic velocity in the Nankai subduction zone from cross-correlation analysis of ambient noise

*Tatsunori Ikeda[1], Takeshi Tsuji[1] (1.Kyushu University)

[SSS06-P04] Strength profile of the Nankai accretionary prism evaluated from drilling parameters

★Invited Papers

*Yohei Hamada[1], Manami Kitamura[2], Takehiro Hirose[1], Yasuhiro Yamada[1], Yoshinori Sanada[1], Takamitsu Sugihara[1], Saneatsu Saito[1], KYAW MOE[1] (1.Japan Agency for Marine-Earth Science and Technology, 2.National Institute of Advanced Industrial Science andTechnology)

[SSS06-P05] Paleotemperature anomalies deduced from thermal-maturity parameters within the décollement, off Cape of Muroto, Japan

*Nana Kamiya[1,2], Takehiro Hirose[2], Yuzuru Yamamoto[2], Yohei Hamada[2], Stephen A Bowden[3], Man-Yin Tsang[4], Kiho Yang[5], Satoshi Tonai[6], Weiren Lin[1,2] (1.Graduate School of Engineering, Kyoto University, 2.JAMSTEC, 3.University of Aberdeen, 4.University of Toronto, 5.Yonsei University, 6.Kochi University)

[SSS06-P06] Modelling thermal maturity of an accretionary wedge

Utsav Mannu[2], *Masataka Kinoshita[1], Taras Gerya[3] (1.Earthquake Research Institute, University of Tokyo, 2.Department of Earth and Climate Science, IISER Pune, 3.Institute of Geophysics, ETH Zürich)

[E] Poster | S (Solid Earth Sciences)：S-SS Seismology

5:15 PM - 6:30 PM JST | 8:15 AM - 9:30 AM UTC | Poster Hall International Exhibition Hall8, Makuhari Messe_28

[S-SS06] Nankai Trough Seismogenic Zone Experiment: Logging and sampling the seismogenic megathrust

convener:Kyuichi Kanagawa(Graduate School of Science, Chiba University), Demian M Saffer(Pennsylvania State University), Masataka Kinoshita(Earthquake Research Institute, University of Tokyo)

[SSS06-P01] Crustal structure in the Nankai Trough seismogenic zone based on renewed depth images and seismic attribute analysis

*Kazuya Shiraishi[1], Yasuhiro Yamada[1], Masataka Kinoshita[2], Gaku Kimura[3] (1.Japan Agency for Marine-Earth Science and Technology, 2.Earthquake Research Institute, The University of Tokyo, 3.Tokyo University of Marine Science and Technology)

[SSS06-P02] Along-strike variations in protothrust zone characteristics at the Nankai Trough subduction margin

*Hannah Tilley[1], Gregory F Moore[1], Mikiya Yamashita[2], Shuichi Kodaira[2] (1.University of Hawaii at Manoa, 2.JAMSTEC)

[SSS06-P03] Temporal change in seismic velocity in the Nankai subduction zone from cross-correlation analysis of ambient noise

*Tatsunori Ikeda[1], Takeshi Tsuji[1] (1.Kyushu University)

[SSS06-P04] Strength profile of the Nankai accretionary prism evaluated from drilling parameters

★Invited Papers

*Yohei Hamada[1], Manami Kitamura[2], Takehiro Hirose[1], Yasuhiro Yamada[1], Yoshinori Sanada[1], Takamitsu Sugihara[1], Saneatsu Saito[1], KYAW MOE[1] (1.Japan Agency for Marine-Earth Science and Technology, 2.National Institute of Advanced Industrial Science andTechnology)

[SSS06-P05] Paleotemperature anomalies deduced from thermal-maturity parameters within the décollement, off Cape of Muroto, Japan

*Nana Kamiya[1,2], Takehiro Hirose[2], Yuzuru Yamamoto[2], Yohei Hamada[2], Stephen A Bowden[3], Man-Yin Tsang[4], Kiho Yang[5], Satoshi Tonai[6], Weiren Lin[1,2] (1.Graduate School of Engineering, Kyoto University, 2.JAMSTEC, 3.University of Aberdeen, 4.University of Toronto, 5.Yonsei University, 6.Kochi University)

[SSS06-P06] Modelling thermal maturity of an accretionary wedge

Utsav Mannu[2], *Masataka Kinoshita[1], Taras Gerya[3] (1.Earthquake Research Institute, University of Tokyo, 2.Department of Earth and Climate Science, IISER Pune, 3.Institute of Geophysics, ETH Zürich)

[E] Poster | S (Solid Earth Sciences)：S-MP Mineralogy & Petrology

10:45 AM - 12:15 PM JST | 1:45 AM - 3:15 AM UTC | Poster Hall International Exhibition Hall8, Makuhari Messe_7

[S-MP29] Oceanic and Continental Subduction Processes

convener:REHMAN Ur Hafiz(Department of Earth and Environmental Sciences, Graduate School of Science and Engineering, Kagoshima University), Tatsuki Tsujimori(Tohoku University), Chin-Ho Tsai(Department of Natural Resources and Environmental Studies, National Dong Hwa University), Kazuaki Okamoto(Faculty of Education, Saitama University)

[SMP29-P01] Zircon U-Pb ages of metasedimentary rocks in the Hakogase (Hida Marginal) area, Fukui Prefecture.

*Atsushi MIYASHITA[1], Tatsuki Tsujimori[2], Daniel Pastor-Galán[3], Yi Keewook[4] (1.Seikei University, 2.Tohoku University, 3.Salamanca University, 4.Korea Basic Science Institue)

[SMP29-P02] Late Permian to Early Triassic back-arc type volcanism in the southern Mongolia volcano-plutonic belt of the Central Asian Orogenic Belt: Implication for timing of the final closure of the Palaeo-Asian Ocean

*Takeshi Imayama[1], Yoichiro Koh[2], Kazumasa Aoki[3], Mototaka Saneyoshi[4], Koshi Yagi[5], Shogo Aoki[4], Yoshihiro Sawada[6], Chiaki Ikawa[5], Tomoya Terada[4], Shinobu Ishigaki[4], Shin Toyoda[3], Khishigjav Tsogtbaatar[7], Buuvei Mainbayar[7] (1.Research Institute of Natural Sciences, Okayama University of Science, 2.Graduate School of Environmental Science, Hokkaido University, 3.Faculty of Science, Okayama University of Science, 4.Faculty of Biosphere - Geosphere Science, Okayama University of Science, 5.Hiruzen Institute for Geology and Chronology, 6.Emeritus Professor of Shimane University, 7.Institute of Paleontology and Geology, Mongolian Academy of Sciences)

[SMP29-P03] Mantle dynamics of slab breakoff constrained from the temporal change of the melting depth estimated from the Cumulate Member of the Ordovician Hayachine-Miyamori Ophiolite

*Takafumi Kimura[1], Kazuhito Ozawa[1] (1.Department of Earth and Planetary Science, The University of Tokyo)

[SMP29-P04] **Evidence of HIMU seamount on the Farallon Plate: Application of *in-situ* Sr-Pb isotope analysis to Franciscan lawsonite-bearing metagreywacke**

*Tomomi Hara[1], Tatsuki Tsujimori[1], Jun-Ichi Kimura[2] (1.Tohoku University, 2.Japan Agency for Marine-Earth Science and Technology)

[SMP29-P05] Boron isotope variations of antigorite serpentinites associated with high-pressure metamorphic rocks: A case study in the Itoigawa–Omi area of the Hida-Gaien Belt, Japan

*Chinatsu Yamada[1], Tatsuki Tsujimori[1], King Chang[2], Jun-Ichi Kimura[2] (1.Tohoku University, 2.Japan Aegency for Marine-Earth Science and Technology)

[SMP29-P06] **Study of zircons structures from the Miocene Shibi-san Granodiorite, Kagoshima Prefecture, Japan**

*Nakabayashi Marimo[1], REHMAN Ur Hafiz[1] (1.Kagoshima University)

[SMP29-P07] **Experimental modeling of eclogite and C-O-H fluid interaction in the subduction zones**

*Nadezda Chertkova[1], Shigeru Yamashita[2], Hiroaki Ohfuji[1], Tetsuo Irifune[1], Hirokazu Kadobayashi[1], Yoshitaka Yamamoto[3] (1.Ehime University, Geodynamics Research Center, 2.Okayama University, Institute for Planetary Materials, 3.National Institute of Advanced Industrial Science and Technology)

[SMP29-P08] Microfabrics of omphacite and garnet in eclogite from the Lanterman Range, northern Victoria Land, Antarctica

*Daeyeong Kim[1], Taehwan Kim[2], Jungmin Kim[3] (1.Division of Polar-Earth Sciences, Korea Polar Research Institute, 2.School of Earth and Environmental Sciences, Seoul National University, 3.Earth and Environmental Sciences, Korea University)

[SMP29-P09] Primordial Apatite from Ophiolite in Taiwan

*Nobuaki Niitsuma[1], Reishi Takashima[2], Yuan Hsi Lee[3] (1.Institute of Geosciences,Shizuoka University, 2.Tohoku University Museum, 3.National Chung-Cheng University, Taiwan)

[SMP29-P10] The evolution of the Cretaceous Jinan Basin in South Korea and the age and tectonic setting for the volcanic rocks in it

*Seung Hwan LEE[1], Chang Whan Oh[1] (1.Department of earth and environmental sciences Chonbuk national university)

[SMP29-P11] GEOCHORONOLOGY AND PETROCHEMISTREY OF LATE PALEOZOIC MAGMATIC ROCKS OF THE MANDAKH AREA, SOUTHEAST MONGOLIA

*Undarmaa Batsaikhan[1], Noriyoshi Tsuchiya[1], Masaoki Uno[1], Yukio Isozaki[2], Uyanga Bold[2], Hikaru Sawada[2] (1.Graduate School of Environmental Studies, Tohoku University, 2.Graduate School of Arts and Sciences The University of Tokyo)

[SMP29-P12] Feedbacks Offshore the Cascadia Margin

*Joan S Gomberg[1] (1.USGS Earthquake Science Center)

[E] Poster | S (Solid Earth Sciences)：S-MP Mineralogy & Petrology

5:15 PM - 6:30 PM JST | 8:15 AM - 9:30 AM UTC | Poster Hall International Exhibition Hall8, Makuhari Messe_32

[S-MP29] Oceanic and Continental Subduction Processes

convener:REHMAN Ur Hafiz(Department of Earth and Environmental Sciences, Graduate School of Science and Engineering, Kagoshima University), Tatsuki Tsujimori(Tohoku University), Chin-Ho Tsai(Department of Natural Resources and Environmental Studies, National Dong Hwa University), Kazuaki Okamoto(Faculty of Education, Saitama University)

[SMP29-P01] Zircon U-Pb ages of metasedimentary rocks in the Hakogase (Hida Marginal) area, Fukui Prefecture.

*Atsushi MIYASHITA[1], Tatsuki Tsujimori[2], Daniel Pastor-Galán[3], Yi Keewook[4] (1.Seikei University, 2.Tohoku University, 3.Salamanca University, 4.Korea Basic Science Institue)

[SMP29-P02] Late Permian to Early Triassic back-arc type volcanism in the southern Mongolia volcano-plutonic belt of the Central Asian Orogenic Belt: Implication for timing of the final closure of the Palaeo-Asian Ocean

*Takeshi Imayama[1], Yoichiro Koh[2], Kazumasa Aoki[3], Mototaka Saneyoshi[4], Koshi Yagi[5], Shogo Aoki[4], Yoshihiro Sawada[6], Chiaki Ikawa[5], Tomoya Terada[4], Shinobu Ishigaki[4], Shin Toyoda[3], Khishigjav Tsogtbaatar[7], Buuvei Mainbayar[7] (1.Research Institute of Natural Sciences, Okayama University of Science, 2.Graduate School of Environmental Science, Hokkaido University, 3.Faculty of Science, Okayama University of Science, 4.Faculty of Biosphere - Geosphere Science, Okayama University of Science, 5.Hiruzen Institute for Geology and Chronology, 6.Emeritus Professor of Shimane University, 7.Institute of Paleontology and Geology, Mongolian Academy of Sciences)

[SMP29-P03] Mantle dynamics of slab breakoff constrained from the temporal change of the melting depth estimated from the Cumulate Member of the Ordovician Hayachine-Miyamori Ophiolite

*Takafumi Kimura[1], Kazuhito Ozawa[1] (1.Department of Earth and Planetary Science, The University of Tokyo)

[SMP29-P04] **Evidence of HIMU seamount on the Farallon Plate: Application of *in-situ* Sr-Pb isotope analysis to Franciscan lawsonite-bearing metagreywacke**

*Tomomi Hara[1], Tatsuki Tsujimori[1], Jun-Ichi Kimura[2] (1.Tohoku University, 2.Japan Agency for Marine-Earth Science and Technology)

[SMP29-P05] Boron isotope variations of antigorite serpentinites associated with high-pressure metamorphic rocks: A case study in the Itoigawa–Omi area of the Hida-Gaien Belt, Japan

*Chinatsu Yamada[1], Tatsuki Tsujimori[1], King Chang[2], Jun-Ichi Kimura[2] (1.Tohoku University, 2.Japan Aegency for Marine-Earth Science and Technology)

[SMP29-P06] **Study of zircons structures from the Miocene Shibi-san Granodiorite, Kagoshima Prefecture, Japan**

*Nakabayashi Marimo[1], REHMAN Ur Hafiz[1] (1.Kagoshima University)

[SMP29-P07] **Experimental modeling of eclogite and C-O-H fluid interaction in the subduction zones**

*Nadezda Chertkova[1], Shigeru Yamashita[2], Hiroaki Ohfuji[1], Tetsuo Irifune[1], Hirokazu Kadobayashi[1], Yoshitaka Yamamoto[3] (1.Ehime University, Geodynamics Research Center, 2.Okayama University, Institute for Planetary Materials, 3.National Institute of Advanced Industrial Science and Technology)

[SMP29-P08] Microfabrics of omphacite and garnet in eclogite from the Lanterman Range, northern Victoria Land, Antarctica

*Daeyeong Kim[1], Taehwan Kim[2], Jungmin Kim[3] (1.Division of Polar-Earth Sciences, Korea Polar Research Institute, 2.School of Earth and Environmental Sciences, Seoul National University, 3.Earth and Environmental Sciences, Korea University)

[SMP29-P09] Primordial Apatite from Ophiolite in Taiwan

*Nobuaki Niitsuma[1], Reishi Takashima[2], Yuan Hsi Lee[3] (1.Institute of Geosciences,Shizuoka University, 2.Tohoku University Museum, 3.National Chung-Cheng University, Taiwan)

[SMP29-P10] The evolution of the Cretaceous Jinan Basin in South Korea and the age and tectonic setting for the volcanic rocks in it

*Seung Hwan LEE[1], Chang Whan Oh[1] (1.Department of earth and environmental sciences Chonbuk national university)

[SMP29-P11] GEOCHORONOLOGY AND PETROCHEMISTREY OF LATE PALEOZOIC MAGMATIC ROCKS OF THE MANDAKH AREA, SOUTHEAST MONGOLIA

*Undarmaa Batsaikhan[1], Noriyoshi Tsuchiya[1], Masaoki Uno[1], Yukio Isozaki[2], Uyanga Bold[2], Hikaru Sawada[2] (1.Graduate School of Environmental Studies, Tohoku University, 2.Graduate School of Arts and Sciences The University of Tokyo)

[SMP29-P12] Feedbacks Offshore the Cascadia Margin

*Joan S Gomberg[1] (1.USGS Earthquake Science Center)

[E] Poster | S (Solid Earth Sciences)：S-MP Mineralogy & Petrology

10:45 AM - 12:15 PM JST | 1:45 AM - 3:15 AM UTC | Poster Hall International Exhibition Hall8, Makuhari Messe_8

[S-MP30] Crust-Mantle Connections

convener:Yoshihiko Tamura(Research Institute for Marine Geodynamics, Japan Agency for Maine-Earth Science and Technology), Osamu Ishizuka(Geological Survey of Japan, AIST), Chris Conway(Geological Survey of Japan)

[SMP30-P01] Secular evolution of proto-Izu-Bonin-Mariana arc volcanism: Constraints from statistical analysis of melt inclusion compositions

*Morihisa Hamada[1], Hikaru Iwamori[1,2], Philipp A. Brandl[3], Takayuki Ushikubo[4], Kenji Shimizu[4], Motoo Ito[4], He Li[5], Ivan P. Savov[6] (1.Department of Solid Earth Geochemistry, Japan Agency for Marine-Earth Science and Technology, 2.Earthquake Research Institute, University of Tokyo, 3.GEOMAR Helmholtz Centre for Ocean Research Kiel, 4.Kochi Institute for Core Sample Research, Japan Agency for Marine-Earth Science and Technology, 5.Institute of Oceanology, Chinese Academy of Sciences, 6.School of Earth and Environment, University of Leeds)

[SMP30-P02] The Jurassic magmatism of protoliths of Mikabu greenstones in SW Japan: zircon U-Pb dating and trace element analysis

*Hikaru Sawada[1], Yukio Isozaki[1], Shogo Aoki[3], Shuhei Sakata[2], Ryo Hasegawa[1], Yasuo Nakamura[1] (1.Department of General Systems Studies, the University of Tokyo, 2.Department of Chemistry, Gakushuin Universtiy, 3.Department of Applied Science, Okayama University of Science)

[SMP30-P03] **Origin of variable CaO/Al_2O_3 in olivine-hosted melt inclusions from Kibblewhite Volcano, Kermadec Arc**

*Yasuhiro Hirai[1], Yoshihiko Tamura[2], Kaj Hoernle[3], Christian Timm[4], Folkmar Hauff[3], Reinhard Werner[3], Takeshi Hanyu[2], Bogdan Vaglarov[2], Qing Chang[2], Takashi Miyazaki[2], Jun-Ichi Kimura[2] (1.Graduate School of Natural Science and Technology, Kanazawa University, Japan, 2.Japan Agency for Marine-Earth Science and Technology (JAMSTEC), Yokosuka, Kanagawa, Japan, 3.GEOMAR Helmholtz Centre for Ocean Research, Kiel, Germany, 4.GNS Science, Lower Hutt, New Zealand)

[SMP30-P04] Ankaramite from Doyo seamount in the Izu-Ogasawara arc: A precursor of continents?

*Yoshihiko Tamura[1], Tomoki Sato[1], Osamu Ishizuka[1,2], Takashi Miyazaki[1], Yasuhiro Hirai[1,3], Mami Takehara[4], Eri Sakamoto[5] (1.JAMSTEC, 2.AIST, 3.Kanazawa Univ., 4.NIPR, 5.NME)

[SMP30-P05] Different Moho reflections adjacent to Minami-Tori Shima and their petrologic origins

*Yoshihiko Tamura[1], Kentaro Kaneda[2], Gou Fujie[1], Akane Ohira[1], Eiichi TAKAZAWA[3], Georges Ceuleneer[4], Katsuyoshi Michibayashi[5], Tomoki Sato[1], Shuichi Kodaira[1], Seiichi Miura[1] (1.Japan Agency for Maine-Earth Science and Technology, 2.Japan Coast Guard, 3.Niigata University, 4.Universite de Toulouse, 5.Nagoya University)

[SMP30-P06] **Melt-rock interaction in plagioclase peridotites from the southern Palawan Ophiolite, Philippines**

*FLORENCE ANNETTE CRUSPERO LABIS[1], BETCHAIDA D PAYOT[1], GABRIEL THEOPHILUS V VALERA[1], JULIUS A PASCO[1], JESLEY MEI A DYCOCO[1] (1.UNIVERSITY OF THE PHILIPPINES)

[SMP30-P07] Intra-oceanic arc magma genesis: a case study from Havre volcano, Kermadec arc

*Chris Conway[1], Kenichiro Tani[2] (1.Geological Survey of Japan, 2.National Museum of Nature and Science)

[E] Poster | S (Solid Earth Sciences)：S-MP Mineralogy & Petrology

5:15 PM - 6:30 PM JST | 8:15 AM - 9:30 AM UTC | Poster Hall International Exhibition Hall8, Makuhari Messe_33

[S-MP30] Crust-Mantle Connections

convener:Yoshihiko Tamura(Research Institute for Marine Geodynamics, Japan Agency for Maine-Earth Science and Technology), Osamu Ishizuka(Geological Survey of Japan, AIST), Chris Conway(Geological Survey of Japan)

[SMP30-P01] Secular evolution of proto-Izu-Bonin-Mariana arc volcanism: Constraints from statistical analysis of melt inclusion compositions

*Morihisa Hamada[1], Hikaru Iwamori[1,2], Philipp A. Brandl[3], Takayuki Ushikubo[4], Kenji Shimizu[4], Motoo Ito[4], He Li[5], Ivan P. Savov[6] (1.Department of Solid Earth Geochemistry, Japan Agency for Marine-Earth Science and Technology, 2.Earthquake Research Institute, University of Tokyo, 3.GEOMAR Helmholtz Centre for Ocean Research Kiel, 4.Kochi Institute for Core Sample Research, Japan Agency for Marine-Earth Science and Technology, 5.Institute of Oceanology, Chinese Academy of Sciences, 6.School of Earth and Environment, University of Leeds)

[SMP30-P02] The Jurassic magmatism of protoliths of Mikabu greenstones in SW Japan: zircon U-Pb dating and trace element analysis

*Hikaru Sawada[1], Yukio Isozaki[1], Shogo Aoki[3], Shuhei Sakata[2], Ryo Hasegawa[1], Yasuo Nakamura[1] (1.Department of General Systems Studies, the University of Tokyo, 2.Department of Chemistry, Gakushuin Universtiy, 3.Department of Applied Science, Okayama University of Science)

[SMP30-P03] Origin of variable CaO/Al_2O_3 in olivine-hosted melt inclusions from Kibblewhite Volcano, Kermadec Arc

*Yasuhiro Hirai[1], Yoshihiko Tamura[2], Kaj Hoernle[3], Christian Timm[4], Folkmar Hauff[3], Reinhard Werner[3], Takeshi Hanyu[2], Bogdan Vaglarov[2], Qing Chang[2], Takashi Miyazaki[2], Jun-Ichi Kimura[2] (1.Graduate School of Natural Science and Technology, Kanazawa University, Japan, 2.Japan Agency for Marine-Earth Science and Technology (JAMSTEC), Yokosuka, Kanagawa, Japan, 3.GEOMAR Helmholtz Centre for Ocean Research, Kiel, Germany, 4.GNS Science, Lower Hutt, New Zealand)

[SMP30-P04] Ankaramite from Doyo seamount in the Izu-Ogasawara arc: A precursor of continents?

*Yoshihiko Tamura[1], Tomoki Sato[1], Osamu Ishizuka[1,2], Takashi Miyazaki[1], Yasuhiro Hirai[1,3], Mami Takehara[4], Eri Sakamoto[5] (1.JAMSTEC, 2.AIST, 3.Kanazawa Univ., 4.NIPR, 5.NME)

[SMP30-P05] Different Moho reflections adjacent to Minami-Tori Shima and their petrologic origins

*Yoshihiko Tamura[1], Kentaro Kaneda[2], Gou Fujie[1], Akane Ohira[1], Eiichi TAKAZAWA[3], Georges Ceuleneer[4], Katsuyoshi Michibayashi[5], Tomoki Sato[1], Shuichi Kodaira[1], Seiichi Miura[1] (1.Japan Agency for Maine-Earth Science and Technology, 2.Japan Coast Guard, 3.Niigata University, 4.Universite de Toulouse, 5.Nagoya University)

[SMP30-P06] Melt-rock interaction in plagioclase peridotites from the southern Palawan Ophiolite, Philippines

*FLORENCE ANNETTE CRUSPERO LABIS[1], BETCHAIDA D PAYOT[1], GABRIEL THEOPHILUS V VALERA[1], JULIUS A PASCO[1], JESLEY MEI A DYCOCO[1] (1.UNIVERSITY OF THE PHILIPPINES)

[SMP30-P07] Intra-oceanic arc magma genesis: a case study from Havre volcano, Kermadec arc

*Chris Conway[1], Kenichiro Tani[2] (1.Geological Survey of Japan, 2.National Museum of Nature and Science)

[E] Poster | S (Solid Earth Sciences)：S-MP Mineralogy & Petrology

3:30 PM - 5:00 PM JST | 6:30 AM - 8:00 AM UTC | Poster Hall International Exhibition Hall8, Makuhari Messe_18

[S-MP31] Supercontinents and Crustal Evolution

convener:Madhusoodhan Satish-Kumar(Department of Geology, Faculty of Science, Niigata University), Tomokazu Hokada(National Institute of Polar Research), Krishnan Sajeev(Centre for Earth Sciences, Indian Institute of Science), Yasuhito Osanai(Division of Evolution of Earth Environments, Faculty of Social and Cultural Studies, Kyushu University)

[SMP31-P01] Re-examination of metamorphic and geochronologic events in Rayner Complex and Western Rayner Complex in Antarctica

*Tomokazu Hokada[1,2], Sotaro Baba[3], Atsushi Kamei[4], Ippei Kitano[5], Kenji Horie[1,2], Yoshikuni Hiroi[1,6], Yoichi Motoyoshi[1,2], Mami Takehara[1], Kazuyuki Shiraishi[1] (1.National Institute of Polar Research, 2.The Graduate University for Advanced Studies (SOKENDAI), 3.University of the Ryukyus, 4.Shimane University, 5.Kyushu University, 6.Chiba University)

[SMP31-P02] Composition of constituent minerals in corona-bearing and -free mafic gneisses from the Lützow-Holm Complex at Skallen, East Antarctica

*Yuki Mori[1], Takeshi Ikeda[2] (1.Department of Earth and Planetary Sciences, Graduate School of Sciences, Kyushu University, 2.Department of Earth and Planetary Sciences, Faculty of Sciences, Kyushu University)

[SMP31-P03] “Pseudo-concordance” of U-Pb system in zircon at Harvey Nunatak, Napier Complex, East Antarctica

*Mami Takehara[1] (1.National Institute of Polar Research)

[SMP31-P04] Rapid UHT metamorphism and exhumation of the Lützow-Holm Complex in Antarctica

*Yoshikuni Hiroi[1], Tomokazu Hokada[2], Tatsuro Adachi[3], Yasuhito Osanai[3], Yoichi Motoyoshi[2], Kazuyuki Shiraishi[2] (1.Chiba Univ, 2.National Institute of Polar Research, 3.Kyushu University)

[SMP31-P05] Tectonic History of Hiroo Complex and its implication inpaleo-Kuril Arc evolution

*Sreehari Lakshmanan[1], Tsuyoshi Toyoshima[2], Futoshi Nanayama[3] (1.Graduate School of Science and Technology, Niigata University, Niigata, Japan, 2.Department of Geology, Faculty of Science, Niigata Univ. , 3.Geological Survey of Japan, AIST)

[SMP31-P06] **Behaviour of C, O, Sr, Nd and Pb isotopes in high-grade metacarbonate rocks**

*Madhusoodhan Satish-Kumar[1], Akari Imura[1], Momoko Shirakawa[2], Gen Shimoda[3], Kosuke T. Goto[3], M A Sanjeewa P K Malaviarachchi[4] (1.Department of Geology, Faculty of Science, Niigata University, 2.Graduate School of Science and Technology, Niigata University, 3.Geological Survey of Japan, 4.University of Peradeniya, Sri Lanka)

[E] Poster | S (Solid Earth Sciences)：S-MP Mineralogy & Petrology

5:15 PM - 6:30 PM JST | 8:15 AM - 9:30 AM UTC | Poster Hall International Exhibition Hall8, Makuhari Messe_34

[S-MP31] Supercontinents and Crustal Evolution

convener:Madhusoodhan Satish-Kumar(Department of Geology, Faculty of Science, Niigata University), Tomokazu Hokada(National Institute of Polar Research), Krishnan Sajeev(Centre for Earth Sciences, Indian Institute of Science), Yasuhito Osanai(Division of Evolution of Earth Environments, Faculty of Social and Cultural Studies, Kyushu University)

[SMP31-P01] Re-examination of metamorphic and geochronologic events in Rayner Complex and Western Rayner Complex in Antarctica

*Tomokazu Hokada[1,2], Sotaro Baba[3], Atsushi Kamei[4], Ippei Kitano[5], Kenji Horie[1,2], Yoshikuni Hiroi[1,6], Yoichi Motoyoshi[1,2], Mami Takehara[1], Kazuyuki Shiraishi[1] (1.National Institute of Polar Research, 2.The Graduate University for Advanced Studies (SOKENDAI), 3.University of the Ryukyus, 4.Shimane University, 5.Kyushu University, 6.Chiba University)

[SMP31-P02] Composition of constituent minerals in corona-bearing and -free mafic gneisses from the Lützow-Holm Complex at Skallen, East Antarctica

*Yuki Mori[1], Takeshi Ikeda[2] (1.Department of Earth and Planetary Sciences, Graduate School of Sciences, Kyushu University, 2.Department of Earth and Planetary Sciences, Faculty of Sciences, Kyushu University)

[SMP31-P03] “Pseudo-concordance” of U-Pb system in zircon at Harvey Nunatak, Napier Complex, East Antarctica

*Mami Takehara[1] (1.National Institute of Polar Research)

[SMP31-P04] Rapid UHT metamorphism and exhumation of the Lützow-Holm Complex in Antarctica

*Yoshikuni Hiroi[1], Tomokazu Hokada[2], Tatsuro Adachi[3], Yasuhito Osanai[3], Yoichi Motoyoshi[2], Kazuyuki Shiraishi[2] (1.Chiba Univ, 2.National Institute of Polar Research, 3.Kyushu University)

[SMP31-P05] Tectonic History of Hiroo Complex and its implication inpaleo-Kuril Arc evolution

*Sreehari Lakshmanan[1], Tsuyoshi Toyoshima[2], Futoshi Nanayama[3] (1.Graduate School of Science and Technology, Niigata University, Niigata, Japan, 2.Department of Geology, Faculty of Science, Niigata Univ. , 3.Geological Survey of Japan, AIST)

[SMP31-P06] **Behaviour of C, O, Sr, Nd and Pb isotopes in high-grade metacarbonate rocks**

*Madhusoodhan Satish-Kumar[1], Akari Imura[1], Momoko Shirakawa[2], Gen Shimoda[3], Kosuke T. Goto[3], M A Sanjeewa P K Malaviarachchi[4] (1.Department of Geology, Faculty of Science, Niigata University, 2.Graduate School of Science and Technology, Niigata University, 3.Geological Survey of Japan, 4.University of Peradeniya, Sri Lanka)

[E] Poster | S (Solid Earth Sciences)：S-CG Complex & General

3:30 PM - 5:00 PM JST | 6:30 AM - 8:00 AM UTC | Poster Hall International Exhibition Hall8, Makuhari Messe_19

[S-CG49] Hard-Rock Drilling Science: From Continental to Deep Sea Drilling, and Oman Project

convener:Katsuyoshi Michibayashi(Department of Earth and Planetary Sciences, Nagoya University), Eiichi TAKAZAWA(Department of Geology, Faculty of Science, Niigata University), Norikatsu Akizawa(Department of Ocean Floor Geoscience, Atmosphere and Ocean Research Institute, The University of Tokyo)

[SCG49-P01] **Permeability profile in the Oman Drilling Project inferred from resistivity measurements**

*Ikuo Katayama[1], Keishi Okazaki[2], Natsue Abe[2], Ole Ivar Ulven[3], Gilbert Hong[4], Wenlu Zhu[5], Benoit Cordonnier[3], Kohei Hatakeyama[1], Yuya Akamatsu[1], Katsuyoshi Michibayashi[6], Marguerite Godard[7], Peter Kelemen[8], Science Party The Oman Drilling Project Phase 2 (1.Hiroshima University, 2.JAMSTEC, 3.University of Oslo, 4.Seoul National University, 5.University of Maryland, 6.Nagoya University, 7.Universitè Montpellier, 8.Columbia University)

[SCG49-P02] Relationship between alteration intensity and elastic wave velocity of gabbroic rocks from ICDP Hole CM1A, Oman Drilling Project Phase II

*Kosuke Kimura[1], Ikuo Katayama[1], Kohei Hatakeyama[1], Yuya Akamatsu[1], Natsue Abe[2], Keishi Okazaki[2], The Oman Drilling Project Phase II Science Party (1.Hiroshima University, 2.JAMSTEC)

[SCG49-P03] Physical property of the fossilized crust-mantle transition zone from ICDP Oman Drilling Project Hole CM1A and CM2B measured onboard D/V Chikyu

*Keishi Okazaki[1], Natsue Abe[1], Kohei Hatakeyama[2], Yuya Akamatsu[2], Ikuo Katayama[2], Eiichi TAKAZAWA[3], Damon A H Teagle[4], Peter B Kelemen[5], Jude Coggon[4], The Oman Drilling Project Phase 2 Science Party (1.Japan Agency for Marine-Earth Science and Technology, 2.Hiroshima University, 3.Niigata University, 4.University of Southampton, 5.Columbia University)

[SCG49-P04] Microstructures of lower crust gabbros from the Oman Ophiolite: Analyses of the drilled cores of the Oman Drilling Project

*Koki Iida[1], Takahiro Fudai[1], Susumu Umino[1], Yuki Kusano[2] (1.Kanazawa University, 2.Geological Survey of Japan)

[SCG49-P05] Olivine fabric and mineral compositions in the Maqsad area of the Samail massif, the southern Oman ophiolite

*Kaho Takahashi[1], Eiichi TAKAZAWA[2,3], Katsuyoshi Michibayashi[4], Kakihata Yuki[4], Ryoko Senda[5] (1.Graduate School of Science and Technology, Niigata University, 2.Department of Geology, Faculty of Science, Niigata University, 3.JAMSTEC, 4.Nagoya University, 5.Kyushu University)

[SCG49-P06] The evolution of melt inclusions in podiform chromitite in Oman

*Yuan YAO[1], Eiichi TAKAZAWA[2,3], Oman Drilling Project Phase 2 Science Party (1.Graduate School of Sciences& Technology, Niigata University, Japan, 2.Department of Geology, Faculty of Science, Niigata University, Japan, 3.Research and Development Center for Ocean Drilling Science, JAMSTEC, Japan)

[SCG49-P07] Melt/fluid - rock reaction inferred from the Wadi Tayin mantle section in the southern Oman ophiolite

*Keisuke ISHII[1], Eiichi TAKAZAWA[2], Akihiro kuriyama[2], Kyouka Someya[2], Yoshihiko Tamura[3] (1.Graduate School of Science and Technology, Niigata University, 2.Department of Geology, Faculty of Science, Niigata University , 3.R&D Center for Ocean Drilling Science, Japan Agency for Marine-Earth Science and Technology)

[SCG49-P08] Numerical simulations for reaction-induced fracture formation of layered gabbro during hydration process

*Kazuki Yoshida[1], Hiroyuki Shimizu[2], Noriyoshi Tsuchiya[1], Atsushi Okamoto[1], Phase 2 Science Party Oman Drilling Project[3] (1.Tohoku university, 2.Geotechnical Analysis Group, Advanced Analysis Department, Civil Engineering Design Division, Kajima Corporation, 3.Oman Drilling Project Phase 2 Science Party)

[SCG49-P09] X-ray CT images of oceanic lithologies obtained on Oman Drilling Project drillcores during ChikyuOman 2017 and 2018

*Katsuyoshi Michibayashi[1], Peter B Kelemen[2], Margurette Godard[3], Eiichi TAKAZAWA[4], Damon A H Teagle[5], The Oman Drilling Project Science Party[6] (1.Department of Earth and Planetary Sciences, Nagoya University, 2.Columbia University, 3.Université Montpellier, 4.Niigata University, 5.Southampton University, 6.ICDP)

[SCG49-P10] Re-examination of the crystallization process of clinopyroxene oikocrysts in layered gabbros at Hess Deep Rift, EPR

*Akane Yasui[1], Takashi Hoshide[1] (1.Graduate School of International Resource Sciences, Akita University)

[SCG49-P11] Structural petrology of peridotites from the Kalaymyo ophiolite

*Kouhei Asano[1,2], Katsuyoshi Michibayashi[1], Jung-Woo Park[3] (1.Graduate School of Environmental Studies, Nagoya University, 2.Shizuoka University, 3.Seoul National University)

[SCG49-P12] Reevaluation of the origin of mafic layers in the Upper Zone of the Horoman Peridotite

*Yumeto KOGURE[1], Eiichi TAKAZAWA[1] (1.Department of Geology, Faculty of Science, Niigata University)

[SCG49-P13] A structural and petrological study of "Shibukawa ultramafic body" in the Sanbagawa belt, western Shizuoka, Japan

*Hikaru Shioya[1,2], Katsuyoshi Michibayashi[1], Ken-ichi Hirauchi[2] (1.Graduate School of Environmental Studies, Nagoya University, 2.Institute of Geosciences, Shizuoka University)

[E] Poster | S (Solid Earth Sciences)：S-CG Complex & General

5:15 PM - 6:30 PM JST | 8:15 AM - 9:30 AM UTC | Poster Hall International Exhibition Hall8, Makuhari Messe_35

[S-CG49] Hard-Rock Drilling Science: From Continental to Deep Sea Drilling, and Oman Project

convener:Katsuyoshi Michibayashi(Department of Earth and Planetary Sciences, Nagoya University), Eiichi TAKAZAWA(Department of Geology, Faculty of Science, Niigata University), Norikatsu Akizawa(Department of Ocean Floor Geoscience, Atmosphere and Ocean Research Institute, The University of Tokyo)

[SCG49-P01] **Permeability profile in the Oman Drilling Project inferred from resistivity measurements**

*Ikuo Katayama[1], Keishi Okazaki[2], Natsue Abe[2], Ole Ivar Ulven[3], Gilbert Hong[4], Wenlu Zhu[5], Benoit Cordonnier[3], Kohei Hatakeyama[1], Yuya Akamatsu[1], Katsuyoshi Michibayashi[6], Marguerite Godard[7], Peter Kelemen[8], Science Party The Oman Drilling Project Phase 2 (1.Hiroshima University, 2.JAMSTEC, 3.University of Oslo, 4.Seoul National University, 5.University of Maryland, 6.Nagoya University, 7.Universitè Montpellier, 8.Columbia University)

[SCG49-P02] Relationship between alteration intensity and elastic wave velocity of gabbroic rocks from ICDP Hole CM1A, Oman Drilling Project Phase II

*Kosuke Kimura[1], Ikuo Katayama[1], Kohei Hatakeyama[1], Yuya Akamatsu[1], Natsue Abe[2], Keishi Okazaki[2], The Oman Drilling Project Phase II Science Party (1.Hiroshima University, 2.JAMSTEC)

[SCG49-P03] Physical property of the fossilized crust-mantle transition zone from ICDP Oman Drilling Project Hole CM1A and CM2B measured onboard D/V Chikyu

*Keishi Okazaki[1], Natsue Abe[1], Kohei Hatakeyama[2], Yuya Akamatsu[2], Ikuo Katayama[2], Eiichi TAKAZAWA[3], Damon A H Teagle[4], Peter B Kelemen[5], Jude Coggon[4], The Oman Drilling Project Phase 2 Science Party (1.Japan Agency for Marine-Earth Science and Technology, 2.Hiroshima University, 3.Niigata University, 4.University of Southampton, 5.Columbia University)

[SCG49-P04] Microstructures of lower crust gabbros from the Oman Ophiolite: Analyses of the drilled cores of the Oman Drilling Project

*Koki Iida[1], Takahiro Fudai[1], Susumu Umino[1], Yuki Kusano[2] (1.Kanazawa University, 2.Geological Survey of Japan)

[SCG49-P05] Olivine fabric and mineral compositions in the Maqsad area of the Samail massif, the southern Oman ophiolite

*Kaho Takahashi[1], Eiichi TAKAZAWA[2,3], Katsuyoshi Michibayashi[4], Kakihata Yuki[4], Ryoko Senda[5] (1.Graduate School of Science and Technology, Niigata University, 2.Department of Geology, Faculty of Science, Niigata University, 3.JAMSTEC, 4.Nagoya University, 5.Kyushu University)

[SCG49-P06] The evolution of melt inclusions in podiform chromitite in Oman

*Yuan YAO[1], Eiichi TAKAZAWA[2,3], Oman Drilling Project Phase 2 Science Party (1.Graduate School of Sciences& Technology, Niigata University, Japan, 2.Department of Geology, Faculty of Science, Niigata University, Japan, 3.Research and Development Center for Ocean Drilling Science, JAMSTEC, Japan)

[SCG49-P07] Melt/fluid - rock reaction inferred from the Wadi Tayin mantle section in the southern Oman ophiolite

*Keisuke ISHII[1], Eiichi TAKAZAWA[2], Akihiro kuriyama[2], Kyouka Someya[2], Yoshihiko Tamura[3] (1.Graduate School of Science and Technology, Niigata University, 2.Department of Geology, Faculty of Science, Niigata University , 3.R&D Center for Ocean Drilling Science, Japan Agency for Marine-Earth Science and Technology)

[SCG49-P08] Numerical simulations for reaction-induced fracture formation of layered gabbro during hydration process

*Kazuki Yoshida[1], Hiroyuki Shimizu[2], Noriyoshi Tsuchiya[1], Atsushi Okamoto[1], Phase 2 Science Party Oman Drilling Project[3] (1.Tohoku university, 2.Geotechnical Analysis Group, Advanced Analysis Department, Civil Engineering Design Division, Kajima Corporation, 3.Oman Drilling Project Phase 2 Science Party)

[SCG49-P09] X-ray CT images of oceanic lithologies obtained on Oman Drilling Project drillcores during ChikyuOman 2017 and 2018

*Katsuyoshi Michibayashi[1], Peter B Kelemen[2], Margurette Godard[3], Eiichi TAKAZAWA[4], Damon A H Teagle[5], The Oman Drilling Project Science Party[6] (1.Department of Earth and Planetary Sciences, Nagoya University, 2.Columbia University, 3.Université Montpellier, 4.Niigata University, 5.Southampton University, 6.ICDP)

[SCG49-P10] Re-examination of the crystallization process of clinopyroxene oikocrysts in layered gabbros at Hess Deep Rift, EPR

*Akane Yasui[1], Takashi Hoshide[1] (1.Graduate School of International Resource Sciences, Akita University)

[SCG49-P11] Structural petrology of peridotites from the Kalaymyo ophiolite

*Kouhei Asano[1,2], Katsuyoshi Michibayashi[1], Jung-Woo Park[3] (1.Graduate School of Environmental Studies, Nagoya University, 2.Shizuoka University, 3.Seoul National University)

[SCG49-P12] Reevaluation of the origin of mafic layers in the Upper Zone of the Horoman Peridotite

*Yumeto KOGURE[1], Eiichi TAKAZAWA[1] (1.Department of Geology, Faculty of Science, Niigata University)

[SCG49-P13] A structural and petrological study of "Shibukawa ultramafic body" in the Sanbagawa belt, western Shizuoka, Japan

*Hikaru Shioya[1,2], Katsuyoshi Michibayashi[1], Ken-ichi Hirauchi[2] (1.Graduate School of Environmental Studies, Nagoya University, 2.Institute of Geosciences, Shizuoka University)

[E] Poster | B (Biogeosciences)：B-CG Complex & General

3:30 PM - 5:00 PM JST | 6:30 AM - 8:00 AM UTC | Poster Hall International Exhibition Hall8, Makuhari Messe_22

[B-CG06] Earth and Planetary Science Frontiers for Life and Global Environment

convener:Yoshinori Takano(Japan Agency for Marine-Earth Science and Technology (JAMSTEC)), Yohey Suzuki(Graduate School of Science, The University of Tokyo), Shingo Kato(RIKEN), Keisuke Fukushi(Institute of Nature & Environmental Technology, Kanazawa University)

[BCG06-P01] Dynamisms and characteristics of dissolved organic matter (DOM) in deep aquifer: A scope for deep biosphere

*Atsushi Urai[1,2], Yoshinori Takano[2], Naohiko Ohkouchi[2] (1.Department of Science and Technology, Graduate School of Medicine, Science and Technology, Shinshu University, 2.Department of Biogeochemistry, Japan Agency for Marine-Earth Science and Technology)

[BCG06-P02] Correlations of magnetosome-related genes in Nitrospirae genomes to magnetosome geometry and redox stratification in deep-sea environments

*Shinsaku Nakano[1], Shingo Kato[2], Mariko Kouduka[1], Toshitsugu Yamazaki[3], Yohey Suzuki[1] (1.Graduate School of Science, The University of Tokyo, 2.RIKEN, 3.Atmosphere and Ocean Research Institute, The University of Tokyo)

[BCG06-P03] Reconstruction of key ecological responses leading to the most recent dead zone formations in Japan Sea through ancient DNA metabarcodring

*Mariko Kouduka[1], Yohey Suzuki[1] (1.Department of Earth and Planetary Science, The University of Tokyo, 7-3-1 Hongo, Bunkyo-ku, Tokyo, Japan.)

[BCG06-P04] Search for microbial CH_4 production processes in lake sediments and surface water associated with cyanobacterial bloom

*Makoto Matsushita[1], Yoshinori Takano[1], Hiroyuki Imachi[1], Atsushi Urai[2], Ho-Dong Park[3], Hiroki Iwata[3], Naohiko Ohkouchi[1] (1.Japan Agency for Marine-Earth Science and Technology, 2.Department of Science and Technology, Graduate School of Medicine, Science and Technology, Shinshu University, 3.Department of Environmental Sciences, Faculty of Science, Shinshu University)

[BCG06-P05] Did life emerge in a deep-sea metal sulfide chimney? New insights from an archaeal genome and a nanoscale microbe-silicate assemblage

*Hinako Takamiya[1], Hiroki Mukai[2], Mariko Kouduka[1], Shingo Kato[4], Motoo Ito[3], Yohey Suzuki[1] (1.Earth and Planetary Science Graduate School of Science, The University of Tokyo , 2.National Institute of Advanced Industrial Science and Technology, 3.Kochi Institute for Core Sample Research JAMSTEC, 4.RIKEN)

[BCG06-P06] X-ray computed nano-tomography for visualizing microbial cells and their surrounding environments

*Yuki Morono[1], Go-Ichiro Uramoto[2,1], Kentaro Uesugi[3], Nobuhisa Takeuchi[3], Masayuki Uesugi[3], Kengo Kubota[4], Tatsuhiko Hoshino[1], Fumio Inagaki[1] (1.Japan Agency for Marine-Earth Science and Technology, 2.Kochi University, 3.Japan Synchrotron Radiation Research Institute, 4.Tohoku University)

[BCG06-P07] Carbon signatures in amino acids during deep-sea anoxic methanotrophy

*Yoshinori Takano[1] (1.Japan Agency for Marine-Earth Science and Technology (JAMSTEC))

[E] Poster | B (Biogeosciences)：B-CG Complex & General

5:15 PM - 6:30 PM JST | 8:15 AM - 9:30 AM UTC | Poster Hall International Exhibition Hall8, Makuhari Messe_40

[B-CG06] Earth and Planetary Science Frontiers for Life and Global Environment

convener:Yoshinori Takano(Japan Agency for Marine-Earth Science and Technology (JAMSTEC)), Yohey Suzuki(Graduate School of Science, The University of Tokyo), Shingo Kato(RIKEN), Keisuke Fukushi(Institute of Nature & Environmental Technology, Kanazawa University)

[BCG06-P01] Dynamisms and characteristics of dissolved organic matter (DOM) in deep aquifer: A scope for deep biosphere

*Atsushi Urai[1,2], Yoshinori Takano[2], Naohiko Ohkouchi[2] (1.Department of Science and Technology, Graduate School of Medicine, Science and Technology, Shinshu University, 2.Department of Biogeochemistry, Japan Agency for Marine-Earth Science and Technology)

[BCG06-P02] Correlations of magnetosome-related genes in Nitrospirae genomes to magnetosome geometry and redox stratification in deep-sea environments

*Shinsaku Nakano[1], Shingo Kato[2], Mariko Kouduka[1], Toshitsugu Yamazaki[3], Yohey Suzuki[1] (1.Graduate School of Science, The University of Tokyo, 2.RIKEN, 3.Atmosphere and Ocean Research Institute, The University of Tokyo)

[BCG06-P03] Reconstruction of key ecological responses leading to the most recent dead zone formations in Japan Sea through ancient DNA metabarcodring

*Mariko Kouduka[1], Yohey Suzuki[1] (1.Department of Earth and Planetary Science, The University of Tokyo, 7-3-1 Hongo, Bunkyo-ku, Tokyo, Japan.)

[BCG06-P04] Search for microbial CH_4 production processes in lake sediments and surface water associated with cyanobacterial bloom

*Makoto Matsushita[1], Yoshinori Takano[1], Hiroyuki Imachi[1], Atsushi Urai[2], Ho-Dong Park[3], Hiroki Iwata[3], Naohiko Ohkouchi[1] (1.Japan Agency for Marine-Earth Science and Technology, 2.Department of Science and Technology, Graduate School of Medicine, Science and Technology, Shinshu University, 3.Department of Environmental Sciences, Faculty of Science, Shinshu University)

[BCG06-P05] Did life emerge in a deep-sea metal sulfide chimney? New insights from an archaeal genome and a nanoscale microbe-silicate assemblage

*Hinako Takamiya[1], Hiroki Mukai[2], Mariko Kouduka[1], Shingo Kato[4], Motoo Ito[3], Yohey Suzuki[1] (1.Earth and Planetary Science Graduate School of Science, The University of Tokyo , 2.National Institute of Advanced Industrial Science and Technology, 3.Kochi Institute for Core Sample Research JAMSTEC, 4.RIKEN)

[BCG06-P06] X-ray computed nano-tomography for visualizing microbial cells and their surrounding environments

*Yuki Morono[1], Go-Ichiro Uramoto[2,1], Kentaro Uesugi[3], Nobuhisa Takeuchi[3], Masayuki Uesugi[3], Kengo Kubota[4], Tatsuhiko Hoshino[1], Fumio Inagaki[1] (1.Japan Agency for Marine-Earth Science and Technology, 2.Kochi University, 3.Japan Synchrotron Radiation Research Institute, 4.Tohoku University)

[BCG06-P07] Carbon signatures in amino acids during deep-sea anoxic methanotrophy

*Yoshinori Takano[1] (1.Japan Agency for Marine-Earth Science and Technology (JAMSTEC))

[E] Poster | M (Multidisciplinary and Interdisciplinary)：M-IS Intersection

10:45 AM - 12:15 PM JST | 1:45 AM - 3:15 AM UTC | Poster Hall International Exhibition Hall8, Makuhari Messe_10

[M-IS05] New technologies to monitor thunderstorm and severe weather activities

convener:Mitsuteru Sato(Department of Cosmoscience, Hokkaido University), Yukihiro Takahashi(Department of Cosmosciences, Graduate School of Science, Hokkaido University), Hisayuki Kubota(Hokkaido University), Kozo Yamashita(Ashikaga University, Department of Engineering.)

[MIS05-P01] Study on monitoring of thunderstorm activity based on multiple electrostatic measurement

*Kozo Yamashita[1], Kakeru Kanno[1], Mitsuteru Sato[2], Yukihiro Takahashi[2] (1.Ashikaga Univ., 2.Hokkaido Univ.)

[MIS05-P02] **Contribution of Rainfall and Lightning Activities to the Fair Weather Electric Field Evaluated by 3D GEC Model**

*Kittanapat Bandholnopparat[1], Mitsuteru Sato[2], Yukihiro Takahashi[2], Toru Adachi[3], Masashi Kamogawa[5], Yasuhiro Minamoto[5], Akira Kadokura[6], Tomoo Ushio[4] (1.Department of Cosmosciences, Hokkaido University, Sapporo, Japan, 2.Faculty of Science, Hokkaido University, Sapporo, Japan, 3.Meteorological Research Institute, Tsukuba, Japan, 4.Department of Aerospace Engineering, Tokyo Metropolitan University, Hino, Japan, 5.Tokyo Gakugei University, Tokyo, Japan, 6.National Institute of Polar Research, Tokyo, Japan)

[MIS05-P03] A method for locating lightning discharges using tweek atmospherics

*Masafumi Kanno[1], Hiroyo Ohya[2], Kazuo Shiokawa[3], Hiroyuki Nakata[2], Toshiaki Takano[2] (1.Graduate School of Science and Engineering, Chiba University, 2.Graduate School of Engineering, Chiba University, 3.Institute for Space-Earth Environmental Research, Nagoya University)

[MIS05-P04] Monitoring for lightning activities and thunder cloud development over the Tokyo metropolitan area during the 2018 summer

*Jun-Ichi Hamada[1], Jun Matsumoto[1], Kozo Yamashita[2], Masashi Kamogawa[3], Yukihiro Takahashi[4] (1.Faculty of Urban Environmental Sciences, Tokyo Metropolitan University, 2.Department of Engineering, Ashikaga University, 3.Department of Physics, Tokyo Gakugei University, 4.Department of Cosmosciences, Graduate School of Science, Hokkaido University)

[E] Poster | M (Multidisciplinary and Interdisciplinary)：M-IS Intersection

5:15 PM - 6:30 PM JST | 8:15 AM - 9:30 AM UTC | Poster Hall International Exhibition Hall8, Makuhari Messe_42

[M-IS05] New technologies to monitor thunderstorm and severe weather activities

convener:Mitsuteru Sato(Department of Cosmoscience, Hokkaido University), Yukihiro Takahashi(Department of Cosmosciences, Graduate School of Science, Hokkaido University), Hisayuki Kubota(Hokkaido University), Kozo Yamashita(Ashikaga University, Department of Engineering.)

[MIS05-P01] Study on monitoring of thunderstorm activity based on multiple electrostatic measurement

*Kozo Yamashita[1], Kakeru Kanno[1], Mitsuteru Sato[2], Yukihiro Takahashi[2] (1.Ashikaga Univ., 2.Hokkaido Univ.)

[MIS05-P02] **Contribution of Rainfall and Lightning Activities to the Fair Weather Electric Field Evaluated by 3D GEC Model**

*Kittanapat Bandholnopparat[1], Mitsuteru Sato[2], Yukihiro Takahashi[2], Toru Adachi[3], Masashi Kamogawa[5], Yasuhiro Minamoto[5], Akira Kadokura[6], Tomoo Ushio[4] (1.Department of Cosmosciences, Hokkaido University, Sapporo, Japan, 2.Faculty of Science, Hokkaido University, Sapporo, Japan, 3.Meteorological Research Institute, Tsukuba, Japan, 4.Department of Aerospace Engineering, Tokyo Metropolitan University, Hino, Japan, 5.Tokyo Gakugei University, Tokyo, Japan, 6.National Institute of Polar Research, Tokyo, Japan)

[MIS05-P03] A method for locating lightning discharges using tweek atmospherics

*Masafumi Kanno[1], Hiroyo Ohya[2], Kazuo Shiokawa[3], Hiroyuki Nakata[2], Toshiaki Takano[2] (1.Graduate School of Science and Engineering, Chiba University, 2.Graduate School of Engineering, Chiba University, 3.Institute for Space-Earth Environmental Research, Nagoya University)

[MIS05-P04] Monitoring for lightning activities and thunder cloud development over the Tokyo metropolitan area during the 2018 summer

*Jun-Ichi Hamada[1], Jun Matsumoto[1], Kozo Yamashita[2], Masashi Kamogawa[3], Yukihiro Takahashi[4] (1.Faculty of Urban Environmental Sciences, Tokyo Metropolitan University, 2.Department of Engineering, Ashikaga University, 3.Department of Physics, Tokyo Gakugei University, 4.Department of Cosmosciences, Graduate School of Science, Hokkaido University)

[E] Poster | M (Multidisciplinary and Interdisciplinary)：M-GI General Geosciences, Information Geosciences & Simulations

3:30 PM - 5:00 PM JST | 6:30 AM - 8:00 AM UTC | Poster Hall International Exhibition Hall8, Makuhari Messe_28

[M-GI29] Near Surface Investigation and Modeling for Groundwater Resources Assessment and Conservation

convener:Jui-Pin Tsai(National Cheng Kung University, Taiwan), Hwa-Lung Yu(National Taiwan University), Ching-Chung Cheng(National Chiao Tung University Taiwan), Jing-Sen Cai(China University of Geosciences)

[MGI29-P01] Modelling of self-potential signals associated with groundwater flows

*ayaka ishikawa[1], Katsumi Hattori[1] (1.chiba university)

[MGI29-P02] Estimating the Hydraulic Conductivity and Heat Capacity of the Aquifer between the River and Well Site Using Joint Inversion Approach

*Jui-Pin Tsai[1], Chin-Tsai Hsiao[4], Liang-Cheng Chang[2], You-Cheng Chen[2], Chun-Hung Chen[3], Yun-Ta Cheng[3], Jen-Hung Yu[3] (1.National Cheng Kung University, Taiwan , 2.National Chiao Tung University, Taiwan , 3.Water Resources Planning Institute, Water Resources Agency, Taiwan, 4.Department of Information Management, Chung Chou University of Science and Technology)

[MGI29-P03] Evaluation on Soil Permeability Using Electrical Resistant Tomography

*CHIHPING KUO[1], BONIAN SHEN[1], CHIHWEI HUANG[1], YUCHIAO LEE[1], SHENXIANG HUANG[1], YENLIN CHEN[1] (1.Department and Institute of Civil Engineering and Environmental Informatics, Minghsin University of Science and Technology)

[MGI29-P04] The Potential Study of Open Loop System Geothermal Heat Pump in Gifu City, Japan

*Randa Permanda[1], Tomoyuki Ohtani[2] (1.Department of Civil and Environmental Engineering, Gifu University, 2.Department of Civil Engineering, Gifu University)

[MGI29-P05] Application of TL-CHERT Smart Characterization Method to Investigate a Groundwater Contaminated Site

*Tzu-Pin Wang[1,2,5], Yao-Tsung Chen[3], Tien-Hsing Tung[3], Chih-Hung Cheng[2], Jie Wang[4] (1.NCU TW, 2.Geophysical Technology and Engineering Co.,Ltd. R.O.C, 3.Apollo Technology Co.,Ltd. R.O.C., 4.Department of Civil Engineering, Chien Hsin University of Science and Technology, Taoyuan City, Taiwan, 5.Disaster Reduction Research Center, Chien Hsin University of Science and Technology, Taoyuan City, Taiwan)

[MGI29-P06] Data Assimilation in Hydraulic Conductivity Identification using Bayesian Statistical Method

*Shih-Yang Cheng[1], Kuo-Chin Hsu[1] (1.National Cheng Kung Univ.)

[MGI29-P07] Groundwater recharge estimation by using empirical orthogonal function method

Hua-Ting Zeng [1], *Hwa-Lung Yu[1] (1. National Taiwan University)

[MGI29-P08] The Application of Drought Early Warning Index for Regional Hydrological Circumstance Analysis

*Chih Chao Ho[1], Ta Wei Chen[2] (1.Construction and Disaster Prevention Research Center, Feng Chia Univ., 2.Taiwan Hsin-Chu Irrigation Association)

[E] Poster | M (Multidisciplinary and Interdisciplinary)：M-GI General Geosciences, Information Geosciences & Simulations

5:15 PM - 6:30 PM JST | 8:15 AM - 9:30 AM UTC | Poster Hall International Exhibition Hall8, Makuhari Messe_47

[M-GI29] Near Surface Investigation and Modeling for Groundwater Resources Assessment and Conservation

convener:Jui-Pin Tsai(National Cheng Kung University, Taiwan), Hwa-Lung Yu(National Taiwan University), Ching-Chung Cheng(National Chiao Tung University Taiwan), Jing-Sen Cai(China University of Geosciences)

[MGI29-P01] Modelling of self-potential signals associated with groundwater flows

*ayaka ishikawa[1], Katsumi Hattori[1] (1.chiba university)

[MGI29-P02] Estimating the Hydraulic Conductivity and Heat Capacity of the Aquifer between the River and Well Site Using Joint Inversion Approach

*Jui-Pin Tsai[1], Chin-Tsai Hsiao[4], Liang-Cheng Chang[2], You-Cheng Chen[2], Chun-Hung Chen[3], Yun-Ta Cheng[3], Jen-Hung Yu[3] (1.National Cheng Kung University, Taiwan , 2.National Chiao Tung University, Taiwan , 3.Water Resources Planning Institute, Water Resources Agency, Taiwan, 4.Department of Information Management, Chung Chou University of Science and Technology)

[MGI29-P03] Evaluation on Soil Permeability Using Electrical Resistant Tomography

*CHIHPING KUO[1], BONIAN SHEN[1], CHIHWEI HUANG[1], YUCHIAO LEE[1], SHENXIANG HUANG[1], YENLIN CHEN[1] (1.Department and Institute of Civil Engineering and Environmental Informatics, Minghsin University of Science and Technology)

[MGI29-P04] The Potential Study of Open Loop System Geothermal Heat Pump in Gifu City, Japan

*Randa Permanda[1], Tomoyuki Ohtani[2] (1.Department of Civil and Environmental Engineering, Gifu University, 2.Department of Civil Engineering, Gifu University)

[MGI29-P05] Application of TL-CHERT Smart Characterization Method to Investigate a Groundwater Contaminated Site

*Tzu-Pin Wang[1,2,5], Yao-Tsung Chen[3], Tien-Hsing Tung[3], Chih-Hung Cheng[2], Jie Wang[4] (1.NCU TW, 2.Geophysical Technology and Engineering Co.,Ltd. R.O.C, 3.Apollo Technology Co.,Ltd. R.O.C., 4.Department of Civil Engineering, Chien Hsin University of Science and Technology, Taoyuan City, Taiwan, 5.Disaster Reduction Research Center, Chien Hsin University of Science and Technology, Taoyuan City, Taiwan)

[MGI29-P06] Data Assimilation in Hydraulic Conductivity Identification using Bayesian Statistical Method

*Shih-Yang Cheng[1], Kuo-Chin Hsu[1] (1.National Cheng Kung Univ.)

[MGI29-P07] Groundwater recharge estimation by using empirical orthogonal function method

Hua-Ting Zeng [1], *Hwa-Lung Yu[1] (1. National Taiwan University)

[MGI29-P08] The Application of Drought Early Warning Index for Regional Hydrological Circumstance Analysis

*Chih Chao Ho[1], Ta Wei Chen[2] (1.Construction and Disaster Prevention Research Center, Feng Chia Univ., 2.Taiwan Hsin-Chu Irrigation Association)

[E] Poster | M (Multidisciplinary and Interdisciplinary)：M-ZZ Others

1:45 PM - 3:15 PM JST | 4:45 AM - 6:15 AM UTC | Poster Hall International Exhibition Hall8, Makuhari Messe_10

[M-ZZ50] Governance for Trans-boundary Volcanic Disaster

convener:Mayumi Sakamoto(Graduate School of Disaster Resilience and Governance, University of Hyogo), Haruhisa Nakamichi(Sakurajima Volcano Research Center, Disaster Prevention Research Institute, Kyoto University), MASARU ARAKIDA(Asian Disaster Reduction Center)

[MZZ50-P01] Governance for Trans-boundary Volcanic Disaster -a case of 2010 Eyjafjallajökull Eruption-

*Mayumi Sakamoto[1] (1.Graduate School of Disaster Resilience and Governance, University of Hyogo)

[MZZ50-P02] Regional Cooperation against Cross-border Disasters

*MASARU ARAKIDA[1] (1.Asian Disaster Reduction Center)

[MZZ50-P03] Issues of Japan's volcanic disaster prevention system as viewed from overseas alert systems

*Erika Ishimizu[1], Mayumi Sakamoto[1] (1.Graduate School of Disaster Resilience and Governance University of Hyogo)

[E] Poster | M (Multidisciplinary and Interdisciplinary)：M-ZZ Others

5:15 PM - 6:30 PM JST | 8:15 AM - 9:30 AM UTC | Poster Hall International Exhibition Hall8, Makuhari Messe_50

[M-ZZ50] Governance for Trans-boundary Volcanic Disaster

convener:Mayumi Sakamoto(Graduate School of Disaster Resilience and Governance, University of Hyogo), Haruhisa Nakamichi(Sakurajima Volcano Research Center, Disaster Prevention Research Institute, Kyoto University), MASARU ARAKIDA(Asian Disaster Reduction Center)

[MZZ50-P01] Governance for Trans-boundary Volcanic Disaster -a case of 2010 Eyjafjallajökull Eruption-

*Mayumi Sakamoto[1] (1.Graduate School of Disaster Resilience and Governance, University of Hyogo)

[MZZ50-P02] Regional Cooperation against Cross-border Disasters

*MASARU ARAKIDA[1] (1.Asian Disaster Reduction Center)

[MZZ50-P03] Issues of Japan's volcanic disaster prevention system as viewed from overseas alert systems

*Erika Ishimizu[1], Mayumi Sakamoto[1] (1.Graduate School of Disaster Resilience and Governance University of Hyogo)

Wed. May 29, 2019

[E] Poster | P (Space and Planetary Sciences)：P-PS Planetary Sciences

10:45 AM - 12:15 PM JST | 1:45 AM - 3:15 AM UTC | Poster Hall International Exhibition Hall8, Makuhari Messe_2

[P-PS02] Regolith Science

convener:Koji Wada(Planetary Exploration Research Center, Chiba Institute of Technology), Akiko Nakamura(Graduate School of Science, Kobe University), Patrick Michel(Observatoire De La Cote D'Azur), Kevin John Walsh(Southwest Research Institute Boulder)

[PPS02-P01] Abrasion experiments of mineral and meteorite grains: Dependence of particle size and vibration rate on abrasion rate and its application to Itokawa and lunar regolith particles.

*Hirotaka Yamaguchi[1], Akira Tsuchiyama[1], Akiko Nakamura[2] (1.National University Corporation, Kyoto University, 2.National University Corporation,Kobe University)

[PPS02-P02] Measurements of adhesive force of meteorite powders using centrifugal method

*Yuuya Nagaashi[1], Akiko Nakamura[1] (1.Kobe University)

[PPS02-P03] Laboratory impact penetration experiments conducted at simulated reduced gravity

*Akiko Nakamura[1], Kana Morizono[2], Yuuya Nagaashi[1] (1.Graduate School of Science, Kobe University, 2.Faculty of Science, Kobe University)

[PPS02-P04] MARAUDERS: Using instrumented nano-impactors to probe the icy properties of Lunar permanently shadowed regions

*Ronald Ballouz[1], Sarah T Crites[2], Naoya Ozaki[2], Shun Arahata[3], Nicola Baresi[2], Ralf Bolden, Onur Celik[4,2], Yu Himeno[3], Lucie Riu[2], Kevin J Walsh[5] (1.Lunar and Planetary Lab, University of Arizona, Tucson, AZ, USA, 2.Institute of Space and Astronautical Science, Sagamihara, Japan, 3.University of Tokyo, Tokyo, Japan, 4.Sokendai Graduate University, Japan, 5.Southwest Research Institute, Boulder, CO, USA)

[PPS02-P05] Surface size-frequency distribution of accumulating boulders using discrete element simulations of spherical particles in 3D

*Hiroshi Kikuchi[1], Hideaki Miyamoto[1] (1.The University of Tokyo)

[PPS02-P06] Experimental Study to Determine the Best Compression Ratio of High-Resolution Images of Small Bodies for the Martian Moons eXploration (MMX) Mission

*Yuta Shimizu[1], Hiroaki Kamiyoshihara[1], Takafumi Niihara[1], Hideaki Miyamoto[1] (1.University of Tokyo)

[E] Poster | P (Space and Planetary Sciences)：P-PS Planetary Sciences

5:15 PM - 6:30 PM JST | 8:15 AM - 9:30 AM UTC | Poster Hall International Exhibition Hall8, Makuhari Messe_2

[P-PS02] Regolith Science

convener:Koji Wada(Planetary Exploration Research Center, Chiba Institute of Technology), Akiko Nakamura(Graduate School of Science, Kobe University), Patrick Michel(Observatoire De La Cote D'Azur), Kevin John Walsh(Southwest Research Institute Boulder)

[PPS02-P01] Abrasion experiments of mineral and meteorite grains: Dependence of particle size and vibration rate on abrasion rate and its application to Itokawa and lunar regolith particles.

*Hirotaka Yamaguchi[1], Akira Tsuchiyama[1], Akiko Nakamura[2] (1.National University Corporation, Kyoto University, 2.National University Corporation,Kobe University)

[PPS02-P02] Measurements of adhesive force of meteorite powders using centrifugal method

*Yuuya Nagaashi[1], Akiko Nakamura[1] (1.Kobe University)

[PPS02-P03] Laboratory impact penetration experiments conducted at simulated reduced gravity

*Akiko Nakamura[1], Kana Morizono[2], Yuuya Nagaashi[1] (1.Graduate School of Science, Kobe University, 2.Faculty of Science, Kobe University)

[PPS02-P04] MARAUDERS: Using instrumented nano-impactors to probe the icy properties of Lunar permanently shadowed regions

*Ronald Ballouz[1], Sarah T Crites[2], Naoya Ozaki[2], Shun Arahata[3], Nicola Baresi[2], Ralf Bolden, Onur Celik[4,2], Yu Himeno[3], Lucie Riu[2], Kevin J Walsh[5] (1.Lunar and Planetary Lab, University of Arizona, Tucson, AZ, USA, 2.Institute of Space and Astronautical Science, Sagamihara, Japan, 3.University of Tokyo, Tokyo, Japan, 4.Sokendai Graduate University, Japan, 5.Southwest Research Institute, Boulder, CO, USA)

[PPS02-P05] Surface size-frequency distribution of accumulating boulders using discrete element simulations of spherical particles in 3D

*Hiroshi Kikuchi[1], Hideaki Miyamoto[1] (1.The University of Tokyo)

[PPS02-P06] Experimental Study to Determine the Best Compression Ratio of High-Resolution Images of Small Bodies for the Martian Moons eXploration (MMX) Mission

*Yuta Shimizu[1], Hiroaki Kamiyoshihara[1], Takafumi Niihara[1], Hideaki Miyamoto[1] (1.University of Tokyo)

[E] Poster | P (Space and Planetary Sciences)：P-PS Planetary Sciences

3:30 PM - 5:00 PM JST | 6:30 AM - 8:00 AM UTC | Poster Hall International Exhibition Hall8, Makuhari Messe_1

[P-PS03] Solar System Small Bodies: A New Frontier Arising Hayabusa 2, OSIRIS-REx and Other Projects

convener:Masateru Ishiguro(Department of Physics and Astronomy, Seoul National University), Taishi Nakamoto(Tokyo Institute of Technology), Masanao Abe(Institute of Space and Astronautical Science, Japan Aerospace Exploration Agency), Olivier S Barnouin(Johns Hopkins University Applied Physics Laboratory)

[PPS03-P01] Impact experiments on low strength coarse-grained regolith simulating surface materials on asteroid Ryugu

*Yuya Yamamoto[1], Masahiko Arakawa[1], Minami Yasui[1], Sunao Hasegawa[2], Ryo Sugimura[1] (1.Graduate School of Science, Kobe University, 2.ISAS, JAXA)

[PPS03-P02] Reflectance estimation of asteroid Ryugu using MASCOT

*Marika Ishida[1], Koto Amano[1], Keiichi Moroi[1], ERI TATSUMI[2], Tra-Mi Ho[10], Shingo Kameda[1], Seiji Sugita[2], Rie Honda[3], Tomokatsu Morota[4], yokota yasuhiro[5], Toru Kouyama[6], Hidehiko Suzuki[7], Manabu Yamada[8], Naoya Sakatani[5], Chikatoshi Honda[9], Masahiko Hayakawa[5], Kazuo Yoshioka[2], Moe Matsuoka[5], Yuichiro Cho[2], Hirotaka Sawada[5] (1.Rikkyo Univ., 2.Univ. of Tokyo, 3.Kochi Univ., 4.Nagoya Univ., 5.JAXA/ISAS, 6.AIST, 7.Meiji Univ., 8.Chiba Inst. Tech, 9.Univ. of Aizu, 10.DLR)

[PPS03-P03] Flyby observation of Asteroid (3200) Phaethon by DESTINY$^+$ onboard cameras

*Ko Ishibashi[1], Shingo Kameda[2], Masato Kagitani[3], Peng Hong[1], Manabu Yamada[1], Osamu Okudaira[1], Tomoko Arai[1], Fumi Yoshida[1], Shunsuke Sato[4], Takahiro Ishimaru[4], Takaya Okamoto[4], Takahiro Iwata[4], Tatsuaki Okada[4], Takeshi Takashima[4] (1.Chiba Institute of Technology, 2.Rikkyo University, 3.Tohoku Universtiy, 4.Japan Aerospace Exploration Agency)

[PPS03-P04] Polarimetric Study of Asteroids in Comet-Like Orbits (ACOs)

*Jooyeon Geem[1], Masateru Ishiguro[1], Yoonsoo P. Bach[1], Daisuke Kuroda[2], Hiroyuki Naito[3], Hidekazu Hanayama[4], yoonyoung kim[10], Yuna G. Kwon[1], Sunho Jin[1], Tomohiko Sekiguchi[5], Ryo Okazaki[5], Jeremie J. Vaubaillon[6], Masataka Imai[7], Tatsuharu Oono[8], Yuki Futamuts[8], Seiko Takagi[8], Mitsuteru Sato[8], Kiyoshi Kuramoto[8], Makoto Watanabe[9] (1.Astronomy program, Dept of Physics and Astronomy, Seoul National University, 2.Okayama Observatory, Kyoto University, 3.Nayoro Observatory, 4.Ishigakijima Astronomical Observatory, National Astronomical Observatory of Japan, 5.Hokkaido University of Education, 6.Observatoire de Paris, I.M.C.C.E., 7.National Institute of Advanced Industrial Science and Technology, 8.Department of Cosmosciences, Graduate School of Science, Hokkaido University, 9.Department of Applied Physics, Okayama University of Science, 10.Max Planck Institute for Solar System Research)

[PPS03-P05] Dynamical lifetime of the Oort Cloud new comets under planetary perturbation

*Ito Takashi[1], Arika Higuchi[1] (1.National Astronomical Observatory of Japan)

[PPS03-P06] Thermal Infrared Imaging of C-type Asteroid 162173 Ryugu with Porous Surfaces

*Tatsuaki Okada[1,2], Tetsuya Fukuhara[3], Satoshi Tanaka[1], Makoto Taguchi[3], Takehiko Arai[4], Naoya Sakatani[1], Yuri Shimaki[1], Hiroki Senshu[5], Yoshiko Ogawa[6], Hirohide Demura[6], Kentaro Suko[6], Kohei Kitazato[6], Toru Kouyama[7], Tomohiko Sekiguchi[8], Jun Takita[9], Sunao Hasegawa[1], Tsuneo Matsunaga[10], Takehiko Wada[1], Takeshi Imamura[2], Jorn Helbert[11], Thomas G. Mueller[12], Axel Hagermann[13], Jens Biele[11], Matthias Grott[11], Maximiliam Hamm[11], Marco Delbo[14], Yukio Yamamoto[1], Naru Hirata[6], Naoyuki Hirata[15], Fuyuto Terui[1], Takanao Saiki[1], Satoru Nakazawa[1], Makoto Yoshikawa[1], Sei-ichiro WATANABE[1,16], Yuichi Tuda[1] (1.Institute of Space and Astronautical Science, Japan Aerospace Exploration Agency, 2.University of Tokyo, 3.Rikkyo University, 4.Ashikaga University, 5.Chiba Institute of Technology, 6.University of Aizu, 7.National Institute of Advanced Industrial Science and Technology, 8.Hokkaido University of Education, 9.Hokkaido Kitami-Hokuto High School, 10.National Institute for Environmental Studies, 11.German Aerospace Center, 12.Max-Planck Institute for Extraterrestrial Physics, 13.University of Stirling, 14.Observatoire de la Côte d'Azur, 15.Kobe University, 16.Nagoya University)

[PPS03-P07] Data Release of Asteroid 162173 Ryugu by Observation of Thermal Infrared Imager onboard Hayabusa2

*Takehiko Arai[1], Hirohide Demura[2], Toru Kouyama[7], Naoya Sakatani[3], Kentaro Suko[2], Yuri Shimaki[3], Hiroki Senshu[5], Tomohiko Sekiguchi[6], Yoshiko Ogawa[2], Sunao Hasegawa[3], Takehiko Wada[3], Takeshi Imamura[10], Tsuneo Matsunaga[9], Jun Takita[8], Kohei Kitazato[2], Makoto Taguchi[4], Tetsuya Fukuhara[4], Satoshi Tanaka[3], Tatsuaki Okada[3] (1.Ashikaga University, 2.The University of Aizu, 3.Japan Aerospace Exploration Agency (JAXA), 4.Rikkyo University,

5.Chiba Institute of Technology, 6.Hokkaido University of Education, 7.National Institute of Advanced Industrial Science and Technology (AIST), 8.Hokkaido Kitami Hokuto High School, 9.National Institute for Environmental Studies (NIES), 10.The University of Tokyo)

[PPS03-P08] Multi-mission capability of HARMONICS

*Shintaro Tsunoda[1], Hirohide Demura[1], Naru Hirata[1] (1.The University of Aizu)

[PPS03-P09] New interface of verification for calibration and conversion in HEAT : Hayabusa2 Exploration Assistant for TIR

*Tatsuro Kobayashi[1], Kentaro Suko[1], Hirohide Demura[1], Yoshiko Ogawa[1], Takehiko Arai[2], Naoya Sakatani[3], Tatsuaki Okada[3], Satoshi Tanaka[3], Tetsuya Fukuhara[4] (1.The University of Aizu, 2.Ashikaga University, 3.Institute of Space and Astronautical Science, Japan Aerospace Exploration Agency, 4.Rikkyo University)

[PPS03-P10] **Dust particle evolution of a near-Earth object 252P/LINEAR from near-infrared polarimetric observations in 2016**

*Yuna G Kwon[1], Masateru Ishiguro[1], Jungmi Kwon[2], Daisuke Kuroda[3], Myungshin Im[1], Changsu Choi[1], Motohide Tamura[4], Takahiro Nagayama[5], Nobuyuki Kawai[6], Jun-ichi Watanabe[7] (1.Seoul National Univ., 2.ISAS/Japan Aerospace Exploration Agency, 3.Okayama Astrophysical Observatory, 4.The Univ. of Tokyo, 5.Kagoshima Univ., 6.Tokyo Institute of Technology, 7.National Astronomical Observatory of Japan)

[PPS03-P11] **Performance Evaluation of TRIPOL on the 61-cm Telescope at Seoul National University for Polarimetric Observations of Solar System Small Bodies**

*Sunho Jin[1], Masateru Ishiguro[1], Yuna G Kwon[1], Jooyeon Geem[1], Yoonsoo P. Bach[1], Jinguk Seo[1], Hiroshi Sasago[2], Shuji Sato[3] (1.Seoul National University, 2.Sasago Co.,Ltd, 3.Nagoya University)

[PPS03-P12] Smart Interface of HEAT: Hayabusa2 Exploration Assistant for TIR

*Kentaro Suko[1], Tatsuro Kobayashi[1], Hirohide Demura[1], Takehiko Arai[2], Naoya Sakatani[3], Tatsuaki Okada[3], Satoshi Tanaka[3], Tetsuya Fukuhara[4] (1.The University of Aizu, 2.Ashikaga University, 3.Institute of Space and Astronautical Science, Japan Aerospace Exploration Agency, 4.Rikkyo University)

[PPS03-P13] Experimental Study on Collision Crater Formed on Bulge Geography

*Yusaku Yokota[1], Yuya Yamamoto[2], Minami Yasui[2], Masahiko Arakawa[2] (1.Faculty of Science, Kobe University, 2.Graduate School of Science, Kobe University)

[PPS03-P14] Initial analysis plan of soluble organic compounds for the Hayabusa2 sample from asteroid Ryugu

*Hiroshi Naraoka[1], Yoshinori Takano[2], Jason P. Dworkin[3], SOM Analysis Team (1.Department of Earth and Planetary Sciences, Research Center for Planetary Trace Organic Compounds, Kyushu University, 2.Japan Agency for Marine-Earth Science and Technology, 3.Astrochemistry Laboratory NASA Goddard Space Flight Center, Greenbelt, MD 20771 USA)

[PPS03-P15] Radar and optical simultaneous observations of faint meteors with MU radar and Tomo-e Gozen

*Ryou Ohsawa[1], Akira Hirota[2], Shinsuke Abe[2], Daniel Kastinen[3], Kero Johan[3], yasunori Fujiwara[4], Takuji Nakamura[5], Shigeyuki Sako[1], Yuto Kojima[1], Jun-ichi Watanabe[6] (1.Institute of Astronomy, Graduate School of Science, The University of Tokyo, 2.Department of Aerospace Engineering, College of Science & Technology, Nihon University, 3.Swedish Institute of Space Physics, 4.SOKENDAI (The Graduate University for Advanced Studies), 5.National Institute of Polar Research, 6.National Astronomical Observatory of Japan)

[PPS03-P16] Global distribution and spectral characteristics of bright spots on asteroid Ryugu

*Masanori Suemitsu[1], Tomokatsu Morota[1], Rie Honda[2], Singo Kameda[15], Eri Tatsumi[3], Manabu Yamada[4], Naoya Sakatani[5], Toru Kouyama[6], Yokota Yasuhiro[7], Yuichiro Cho[8], Hidehiko Suzuki[9], Masahiko Hayakawa[10], Moe Matsuoka[10], Chikatoshi Honda[11], Tatsuhiro Michikami[12], Kazuo Yoshioka[13], Kazunori Ogawa[14], Hirotaka Sawada[5], Seiji Sugita[3] (1.Graduate School of Environmental Studies, Nagoya University, 2.Department of Science and Technology, System of Natural Science, Kochi Unicversity, 3.Graduate School of Earth and Planetary Science, Tokyo Unicversity, 4.Planetary Exploration Reserch Center, Chiba Institute of Technology, 5.Institute of Space and Astoronautical Science, Japan Aerospace Exploration Agency, 6.National Institute of Advanced Industrial Science and Technology, 7.Kochi University, 8.Department of Earth and Planetary Science, Tokyo University, 9.Depertment of physics, Meiji University , 10.Department of Solar System Science, Institute of Space and Astoronautical Science, Japan Aerospace Exploration Agency, 11.Aizu University, 12.Faculty of Engineering, Kindai University, 13.Graduate School of frontier Science, Tokyo University, 14.Kobe University, 15.Rikkyo University)

[PPS03-P17] Polarimetry of (155140) 2005 UD: the Dynamical Association with (3200) Phaethon

*Masateru Ishiguro[1], Jooyeon Geem[1], Hiroyuki Naito[2], Yoonsoo P. Bach[1], Daisuke Kuroda[3], Tatsuharu Ono[4], Seiko Takagi[4], Mitsuteru Sato[4], Kiyoshi Kuramoto[4], Tomohiko Sekiguchi[5], Masataka Imai[6], Makoto Watanabe[7], Katsuhito Ohtsuka[8], Sunao Hasegawa[9], Takashi Ito[10], Fumi Yoshida[11], Tomoko Arai[11] (1.Department of Physics and Astronomy, Seoul National University, 2.Nayoro Observatory, 3.Okayama Observatory, Kyoto University, 4.Department of Cosmosciences, Graduate School of Science, Hokkaido University, 5.Hokkaido University of Education, 6.National Institute of Advanced Industrial Science and Technology, 7.Department of Applied Physics, Okayama University of Science, 8.Tokyo Meteor Network, 9.Japan Aerospace Exploration Agency, 10.National Astronomical Observatory of Japan, 11.Planetary Exploration Research Center, Chiba Institute of Technology)

[PPS03-P18] **Follow-up observations for AKARI/IRC near-infrared asteroid spectroscopic survey (AcuA-spec)**

*Sunao Hasegawa[1], Daisuke KURODA[2], Kenshi YANAGISAWA[3], Fumihiko Usui[4] (1.Japan Aerospace Exploration Agency, 2.Kyoto University, 3.National Astronomical Observatory of Japan, 4.Kobe University)

[PPS03-P19] Amino acids on witness coupons collected from the ISAS/JAXA curation facility for the assessment and quality control of the Hayabusa2 sampling procedure

*Haruna Sugahara[1,2], Yoshinori Takano[1], Yuzuru Karouji[3], Kazuya Kumagai[4], Toru Yada[3], Naohiko Ohkouchi[1], Masanao Abe[3], Hayabusa2 project team (1.Japan Agency for Marine-Earth Science and Technology (JAMSTEC), 2. Institut de Chimie de Nice, Universite Cote dAzur, 3.Japan Aerospace Exploration Agency (JAXA), 4.Marine Works Japan Ltd.)

[PPS03-P20] Hayabusa2 orbit determination using c5++ software

*Keiko Yamamoto[1], Toshimichi Otsubo[2], Koji Matsumoto[1], Hirotomo Noda[1], Noriyuki Namiki[1], Hiroki Senshu[3], Takahide Mizuno[4], Naoko Ogawa[4], Go Ono[4], Yuya Mimasu[4], Kent Yoshikawa[4], Tadateru Takahashi[4], Yuto Takei[4], Atsushi Fujii[4], Fuyuto Terui[4], Takanao Saiki[4], Satoru Nakazawa[4], Makoto Yoshikawa[4], Yuichi Tsuda[4] (1.National Astronomical Observatory of Japan, 2.Hitotsubashi University, 3.Chiba Institute of Technology, 4.Japan Aerospace Exploration Agency)

[PPS03-P21] **Landing Site Selection for Hayabusa2: Scientific Evaluation of the Candidate Sites on Asteroid (162173) Ryugu**

*Hikaru Yabuta[1], Sei-ichiro WATANABE[2], Tomoki Nakamura[3], Naru Hirata[4], Seiji Sugita[5], Tatsuaki Okada[6], Kohei Kitazato[4], Yoshiaki Ishihara[7], Tomokatsu Morota[2], Naoya Sakatani[6], Koji Matsumoto[8], Koji Wada[9], Shogo Tachibana[5], Mutsumi Komatsu[10], ERI TATSUMI[5], Moe Matsuoka[6], Chikatoshi Honda[4], Takahiro Hiroi[11], Hiroki Senshu[9], Rie Honda[12], Yasuhiro Yokota[6], Rina Noguchi[6], Yuri Shimaki[6], Deborah Lorin Domingue[13], Lucille Le Corre[13], Antonella Barucci[14], Ernest Palomba[15], Shota Kikuchi[6], Akira Miura[6], Tomohiro Yamaguchi[6], Yukio Yamamoto[6], Takanao Saiki[6], Satoshi Tanaka[6], Makoto Yoshikawa[6], Yuichi Tsuda[6] (1.Hiroshima University, Department of Earth and Planetary Systems Science, 2.Nagoya University, 3.Tohoku University, 4.University of Aizu, 5.The University of Tokyo, 6.ISAS/JAXA, 7.NIES, 8.NAOJ, 9.Chiba Institute of Technology, Planetary Exploration Research Center (PERC), 10.Sokendai, 11.Brown University, 12.Kochi University, 13.Planetary Science Institute, USA, 14.Observatoire Paris-Site de Meudon, LESIA, France, 15.INAF-IAPS, Italy.)

[PPS03-P22] Visible Photometric, Spectroscopic and Polarimetric observations of an inactive comet, P/2016 BA14 with the 1.6m Pirka Telescope

*Ryo Yamagata[1], Tomohiko Sekiguchi[1], Ryo Okazaki[1], Kazuya Doi[1], Daisuke Kuroda[2], Masateru Ishiguro[3], Hiroyuki Naito[4] (1.Hokkaido University of Education, 2.Kyoto University, 3.Seoul National University, 4.Nayoro Observatory)

[PPS03-P23] **Polycyclic aromatic hydrocarbons and aliphatic hydrocarbons in Jbilet Winselwan carbonaceous chondrite : Attempt to evaluate the thermal metamorphism degree on the parent body**

Hiroki Kato[1], *Hikaru Yabuta[1] (1.Hiroshima University, Department of Earth and Planetary Systems Science)

[PPS03-P24] Disk-Resolved Photometry Analysis of the Asteroid Ryugu Images Obtained by Hayabusa2 Visible Camera ONC

*yokota yasuhiro[1,2], Rie Honda[1], ERI TATSUMI[3], Deborah Domingue[4], Stefanus E. Schroeder[5], Moe Matsuoka[2], Seiji Sugita[3], Tomokatsu Morota[6], Shingo Kameda[7], Toru Kouyama[8], Hidehiko Suzuki[9], Manabu Yamada[10], Naoya Sakatani[2], Chikatoshi Honda[11], Masahiko Hayakawa[2], Kazuo Yoshioka[3], Yuichiro Cho[3], Hirotaka Sawada[2] (1.Kochi University, 2.ISAS/JAXA, 3.Univ. of Tokyo, 4.Planetary Science Institute, 5.DLR, 6.Nagoya Univ., 7.Rikkyo Univ., 8.AIST, 9.Meiji Univ., 10.Chiba Institute od Technology, 11.Aizu Univ.)

[E] Poster | P (Space and Planetary Sciences)：P-PS Planetary Sciences

5:15 PM - 6:30 PM JST | 8:15 AM - 9:30 AM UTC | Poster Hall International Exhibition Hall8, Makuhari Messe_3

[P-PS03] Solar System Small Bodies: A New Frontier Arising Hayabusa 2, OSIRIS-REx and Other Projects

convener:Masateru Ishiguro(Department of Physics and Astronomy, Seoul National University), Taishi Nakamoto(Tokyo Institute of Technology), Masanao Abe(Institute of Space and Astronautical Science, Japan Aerospace Exploration Agency), Olivier S Barnouin(Johns Hopkins University Applied Physics Laboratory)

[PPS03-P01] Impact experiments on low strength coarse-grained regolith simulating surface materials on asteroid Ryugu

*Yuya Yamamoto[1], Masahiko Arakawa[1], Minami Yasui[1], Sunao Hasegawa[2], Ryo Sugimura[1] (1.Graduate School of Science, Kobe University, 2.ISAS, JAXA)

[PPS03-P02] Reflectance estimation of asteroid Ryugu using MASCOT

*Marika Ishida[1], Koto Amano[1], Keiichi Moroi[1], ERI TATSUMI[2], Tra-Mi Ho[10], Shingo Kameda[1], Seiji Sugita[2], Rie Honda[3], Tomokatsu Morota[4], yokota yasuhiro[5], Toru Kouyama[6], Hidehiko Suzuki[7], Manabu Yamada[8], Naoya Sakatani[5], Chikatoshi Honda[9], Masahiko Hayakawa[5], Kazuo Yoshioka[2], Moe Matsuoka[5], Yuichiro Cho[2], Hirotaka Sawada[5] (1.Rikkyo Univ., 2.Univ. of Tokyo, 3.Kochi Univ., 4.Nagoya Univ., 5.JAXA/ISAS, 6.AIST, 7.Meiji Univ., 8.Chiba Inst. Tech, 9.Univ. of Aizu, 10.DLR)

[PPS03-P03] Flyby observation of Asteroid (3200) Phaethon by DESTINY$^+$ onboard cameras

*Ko Ishibashi[1], Shingo Kameda[2], Masato Kagitani[3], Peng Hong[1], Manabu Yamada[1], Osamu Okudaira[1], Tomoko Arai[1], Fumi Yoshida[1], Shunsuke Sato[4], Takahiro Ishimaru[4], Takaya Okamoto[4], Takahiro Iwata[4], Tatsuaki Okada[4], Takeshi Takashima[4] (1.Chiba Institute of Technology, 2.Rikkyo University, 3.Tohoku Universtiy, 4.Japan Aerospace Exploration Agency)

[PPS03-P04] Polarimetric Study of Asteroids in Comet-Like Orbits (ACOs)

*Jooyeon Geem[1], Masateru Ishiguro[1], Yoonsoo P. Bach[1], Daisuke Kuroda[2], Hiroyuki Naito[3], Hidekazu Hanayama[4], yoonyoung kim[10], Yuna G. Kwon[1], Sunho Jin[1], Tomohiko Sekiguchi[5], Ryo Okazaki[5], Jeremie J. Vaubaillon[6], Masataka Imai[7], Tatsuharu Oono[8], Yuki Futamuts[8], Seiko Takagi[8], Mitsuteru Sato[8], Kiyoshi Kuramoto[8], Makoto Watanabe[9] (1.Astronomy program, Dept of Physics and Astronomy, Seoul National University, 2.Okayama Observatory, Kyoto University, 3.Nayoro Observatory, 4.Ishigakijima Astronomical Observatory, National Astronomical Observatory of Japan, 5.Hokkaido University of Education, 6.Observatoire de Paris, I.M.C.C.E., 7.National Institute of Advanced Industrial Science and Technology, 8.Department of Cosmosciences, Graduate School of Science, Hokkaido University, 9.Department of Applied Physics, Okayama University of Science, 10.Max Planck Institute for Solar System Research)

[PPS03-P05] Dynamical lifetime of the Oort Cloud new comets under planetary perturbation

*Ito Takashi[1], Arika Higuchi[1] (1.National Astronomical Observatory of Japan)

[PPS03-P06] Thermal Infrared Imaging of C-type Asteroid 162173 Ryugu with Porous Surfaces

*Tatsuaki Okada[1,2], Tetsuya Fukuhara[3], Satoshi Tanaka[1], Makoto Taguchi[3], Takehiko Arai[4], Naoya Sakatani[1], Yuri Shimaki[1], Hiroki Senshu[5], Yoshiko Ogawa[6], Hirohide Demura[6], Kentaro Suko[6], Kohei Kitazato[6], Toru Kouyama[7], Tomohiko Sekiguchi[8], Jun Takita[9], Sunao Hasegawa[1], Tsuneo Matsunaga[10], Takehiko Wada[1], Takeshi Imamura[2], Jorn Helbert[11], Thomas G. Mueller[12], Axel Hagermann[13], Jens Biele[11], Matthias Grott[11], Maximiliam Hamm[11], Marco Delbo[14], Yukio Yamamoto[1], Naru Hirata[6], Naoyuki Hirata[15], Fuyuto Terui[1], Takanao Saiki[1], Satoru Nakazawa[1], Makoto Yoshikawa[1], Sei-ichiro WATANABE[1,16], Yuichi Tuda[1] (1.Institute of Space and Astronautical Science, Japan Aerospace Exploration Agency, 2.University of Tokyo, 3.Rikkyo University, 4.Ashikaga University, 5.Chiba Institute of Technology, 6.University of Aizu, 7.National Institute of Advanced Industrial Science and Technology, 8.Hokkaido University of Education, 9.Hokkaido Kitami-Hokuto High School, 10.National Institute for Environmental Studies, 11.German Aerospace Center, 12.Max-Planck Institute for Extraterrestrial Physics, 13.University of Stirling, 14.Observatoire de la Côte d'Azur, 15.Kobe University, 16.Nagoya University)

[PPS03-P07] Data Release of Asteroid 162173 Ryugu by Observation of Thermal Infrared Imager onboard Hayabusa2

*Takehiko Arai[1], Hirohide Demura[2], Toru Kouyama[7], Naoya Sakatani[3], Kentaro Suko[2], Yuri Shimaki[3], Hiroki Senshu[5], Tomohiko Sekiguchi[6], Yoshiko Ogawa[2], Sunao Hasegawa[3], Takehiko Wada[3], Takeshi Imamura[10], Tsuneo Matsunaga[9], Jun Takita[8], Kohei Kitazato[2], Makoto Taguchi[4], Tetsuya Fukuhara[4], Satoshi Tanaka[3], Tatsuaki Okada[3] (1.Ashikaga University, 2.The University of Aizu, 3.Japan Aerospace Exploration Agency (JAXA), 4.Rikkyo University,

5.Chiba Institute of Technology, 6.Hokkaido University of Education, 7.National Institute of Advanced Industrial Science and Technology (AIST), 8.Hokkaido Kitami Hokuto High School, 9.National Institute for Environmental Studies (NIES), 10.The University of Tokyo)

[PPS03-P08] Multi-mission capability of HARMONICS

*Shintaro Tsunoda[1], Hirohide Demura[1], Naru Hirata[1] (1.The University of Aizu)

[PPS03-P09] New interface of verification for calibration and conversion in HEAT : Hayabusa2 Exploration Assistant for TIR

*Tatsuro Kobayashi[1], Kentaro Suko[1], Hirohide Demura[1], Yoshiko Ogawa[1], Takehiko Arai[2], Naoya Sakatani[3], Tatsuaki Okada[3], Satoshi Tanaka[3], Tetsuya Fukuhara[4] (1.The University of Aizu, 2.Ashikaga University, 3.Institute of Space and Astronautical Science, Japan Aerospace Exploration Agency, 4.Rikkyo University)

[PPS03-P10] **Dust particle evolution of a near-Earth object 252P/LINEAR from near-infrared polarimetric observations in 2016**

*Yuna G Kwon[1], Masateru Ishiguro[1], Jungmi Kwon[2], Daisuke Kuroda[3], Myungshin Im[1], Changsu Choi[1], Motohide Tamura[4], Takahiro Nagayama[5], Nobuyuki Kawai[6], Jun-ichi Watanabe[7] (1.Seoul National Univ., 2.ISAS/Japan Aerospace Exploration Agency, 3.Okayama Astrophysical Observatory, 4.The Univ. of Tokyo, 5.Kagoshima Univ., 6.Tokyo Institute of Technology, 7.National Astronomical Observatory of Japan)

[PPS03-P11] **Performance Evaluation of TRIPOL on the 61-cm Telescope at Seoul National University for Polarimetric Observations of Solar System Small Bodies**

*Sunho Jin[1], Masateru Ishiguro[1], Yuna G Kwon[1], Jooyeon Geem[1], Yoonsoo P. Bach[1], Jinguk Seo[1], Hiroshi Sasago[2], Shuji Sato[3] (1.Seoul National University, 2.Sasago Co.,Ltd, 3.Nagoya University)

[PPS03-P12] Smart Interface of HEAT: Hayabusa2 Exploration Assistant for TIR

*Kentaro Suko[1], Tatsuro Kobayashi[1], Hirohide Demura[1], Takehiko Arai[2], Naoya Sakatani[3], Tatsuaki Okada[3], Satoshi Tanaka[3], Tetsuya Fukuhara[4] (1.The University of Aizu, 2.Ashikaga University, 3.Institute of Space and Astronautical Science, Japan Aerospace Exploration Agency, 4.Rikkyo University)

[PPS03-P13] Experimental Study on Collision Crater Formed on Bulge Geography

*Yusaku Yokota[1], Yuya Yamamoto[2], Minami Yasui[2], Masahiko Arakawa[2] (1.Faculty of Science, Kobe University, 2.Graduate School of Science, Kobe University)

[PPS03-P14] Initial analysis plan of soluble organic compounds for the Hayabusa2 sample from asteroid Ryugu

*Hiroshi Naraoka[1], Yoshinori Takano[2], Jason P. Dworkin[3], SOM Analysis Team (1.Department of Earth and Planetary Sciences, Research Center for Planetary Trace Organic Compounds, Kyushu University, 2.Japan Agency for Marine-Earth Science and Technology, 3.Astrochemistry Laboratory NASA Goddard Space Flight Center, Greenbelt, MD 20771 USA)

[PPS03-P15] Radar and optical simultaneous observations of faint meteors with MU radar and Tomo-e Gozen

*Ryou Ohsawa[1], Akira Hirota[2], Shinsuke Abe[2], Daniel Kastinen[3], Kero Johan[3], yasunori Fujiwara[4], Takuji Nakamura[5], Shigeyuki Sako[1], Yuto Kojima[1], Jun-ichi Watanabe[6] (1.Institute of Astronomy, Graduate School of Science, The University of Tokyo, 2.Department of Aerospace Engineering, College of Science & Technology, Nihon University, 3.Swedish Institute of Space Physics, 4.SOKENDAI (The Graduate University for Advanced Studies), 5.National Institute of Polar Research, 6.National Astronomical Observatory of Japan)

[PPS03-P16] Global distribution and spectral characteristics of bright spots on asteroid Ryugu

*Masanori Suemitsu[1], Tomokatsu Morota[1], Rie Honda[2], Singo Kameda[15], Eri Tatsumi[3], Manabu Yamada[4], Naoya Sakatani[5], Toru Kouyama[6], Yokota Yasuhiro[7], Yuichiro Cho[8], Hidehiko Suzuki[9], Masahiko Hayakawa[10], Moe Matsuoka[10], Chikatoshi Honda[11], Tatsuhiro Michikami[12], Kazuo Yoshioka[13], Kazunori Ogawa[14], Hirotaka Sawada[5], Seiji Sugita[3] (1.Graduate School of Environmental Studies, Nagoya University, 2.Department of Science and Technology, System of Natural Science, Kochi Unicversity, 3.Graduate School of Earth and Planetary Science, Tokyo Unicversity, 4.Planetary Exploration Reserch Center, Chiba Institute of Technology, 5.Institute of Space and Astoronautical Science, Japan Aerospace Exploration Agency, 6.National Institute of Advanced Industrial Science and Technology, 7.Kochi University, 8.Department of Earth and Planetary Science, Tokyo University, 9.Depertment of physics, Meiji University , 10.Department of Solar System Science, Institute of Space and Astoronautical Science, Japan Aerospace Exploration Agency, 11.Aizu University, 12.Faculty of Engineering, Kindai University, 13.Graduate School of frontier Science, Tokyo University, 14.Kobe University, 15.Rikkyo University)

[PPS03-P17] Polarimetry of (155140) 2005 UD: the Dynamical Association with (3200) Phaethon

*Masateru Ishiguro[1], Jooyeon Geem[1], Hiroyuki Naito[2], Yoonsoo P. Bach[1], Daisuke Kuroda[3], Tatsuharu Ono[4], Seiko Takagi[4], Mitsuteru Sato[4], Kiyoshi Kuramoto[4], Tomohiko Sekiguchi[5], Masataka Imai[6], Makoto Watanabe[7], Katsuhito Ohtsuka[8], Sunao Hasegawa[9], Takashi Ito[10], Fumi Yoshida[11], Tomoko Arai[11] (1.Department of Physics and Astronomy, Seoul National University, 2.Nayoro Observatory, 3.Okayama Observatory, Kyoto University, 4.Department of Cosmosciences, Graduate School of Science, Hokkaido University, 5.Hokkaido University of Education, 6.National Institute of Advanced Industrial Science and Technology, 7.Department of Applied Physics, Okayama University of Science, 8.Tokyo Meteor Network, 9.Japan Aerospace Exploration Agency, 10.National Astronomical Observatory of Japan, 11.Planetary Exploration Research Center, Chiba Institute of Technology)

[PPS03-P18] **Follow-up observations for AKARI/IRC near-infrared asteroid spectroscopic survey (AcuA-spec)**

*Sunao Hasegawa[1], Daisuke KURODA[2], Kenshi YANAGISAWA[3], Fumihiko Usui[4] (1.Japan Aerospace Exploration Agency, 2.Kyoto University, 3.National Astronomical Observatory of Japan, 4.Kobe University)

[PPS03-P19] Amino acids on witness coupons collected from the ISAS/JAXA curation facility for the assessment and quality control of the Hayabusa2 sampling procedure

*Haruna Sugahara[1,2], Yoshinori Takano[1], Yuzuru Karouji[3], Kazuya Kumagai[4], Toru Yada[3], Naohiko Ohkouchi[1], Masanao Abe[3], Hayabusa2 project team (1.Japan Agency for Marine-Earth Science and Technology (JAMSTEC), 2. Institut de Chimie de Nice, Universite Cote dAzur, 3.Japan Aerospace Exploration Agency (JAXA), 4.Marine Works Japan Ltd.)

[PPS03-P20] Hayabusa2 orbit determination using c5++ software

*Keiko Yamamoto[1], Toshimichi Otsubo[2], Koji Matsumoto[1], Hirotomo Noda[1], Noriyuki Namiki[1], Hiroki Senshu[3], Takahide Mizuno[4], Naoko Ogawa[4], Go Ono[4], Yuya Mimasu[4], Kent Yoshikawa[4], Tadateru Takahashi[4], Yuto Takei[4], Atsushi Fujii[4], Fuyuto Terui[4], Takanao Saiki[4], Satoru Nakazawa[4], Makoto Yoshikawa[4], Yuichi Tsuda[4] (1.National Astronomical Observatory of Japan, 2.Hitotsubashi University, 3.Chiba Institute of Technology, 4.Japan Aerospace Exploration Agency)

[PPS03-P21] **Landing Site Selection for Hayabusa2: Scientific Evaluation of the Candidate Sites on Asteroid (162173) Ryugu**

*Hikaru Yabuta[1], Sei-ichiro WATANABE[2], Tomoki Nakamura[3], Naru Hirata[4], Seiji Sugita[5], Tatsuaki Okada[6], Kohei Kitazato[4], Yoshiaki Ishihara[7], Tomokatsu Morota[2], Naoya Sakatani[6], Koji Matsumoto[8], Koji Wada[9], Shogo Tachibana[5], Mutsumi Komatsu[10], ERI TATSUMI[5], Moe Matsuoka[6], Chikatoshi Honda[4], Takahiro Hiroi[11], Hiroki Senshu[9], Rie Honda[12], Yasuhiro Yokota[6], Rina Noguchi[6], Yuri Shimaki[6], Deborah Lorin Domingue[13], Lucille Le Corre[13], Antonella Barucci[14], Ernest Palomba[15], Shota Kikuchi[6], Akira Miura[6], Tomohiro Yamaguchi[6], Yukio Yamamoto[6], Takanao Saiki[6], Satoshi Tanaka[6], Makoto Yoshikawa[6], Yuichi Tsuda[6] (1.Hiroshima University, Department of Earth and Planetary Systems Science, 2.Nagoya University, 3.Tohoku University, 4.University of Aizu, 5.The University of Tokyo, 6.ISAS/JAXA, 7.NIES, 8.NAOJ, 9.Chiba Institute of Technology, Planetary Exploration Research Center (PERC), 10.Sokendai, 11.Brown University, 12.Kochi University, 13.Planetary Science Institute, USA, 14.Observatoire Paris-Site de Meudon, LESIA, France, 15.INAF-IAPS, Italy.)

[PPS03-P22] Visible Photometric, Spectroscopic and Polarimetric observations of an inactive comet, P/2016 BA14 with the 1.6m Pirka Telescope

*Ryo Yamagata[1], Tomohiko Sekiguchi[1], Ryo Okazaki[1], Kazuya Doi[1], Daisuke Kuroda[2], Masateru Ishiguro[3], Hiroyuki Naito[4] (1.Hokkaido University of Education, 2.Kyoto University, 3.Seoul National University, 4.Nayoro Observatory)

[PPS03-P23] **Polycyclic aromatic hydrocarbons and aliphatic hydrocarbons in Jbilet Winselwan carbonaceous chondrite : Attempt to evaluate the thermal metamorphism degree on the parent body**

Hiroki Kato[1], *Hikaru Yabuta[1] (1.Hiroshima University, Department of Earth and Planetary Systems Science)

[PPS03-P24] Disk-Resolved Photometry Analysis of the Asteroid Ryugu Images Obtained by Hayabusa2 Visible Camera ONC

*yokota yasuhiro[1,2], Rie Honda[1], ERI TATSUMI[3], Deborah Domingue[4], Stefanus E. Schroeder[5], Moe Matsuoka[2], Seiji Sugita[3], Tomokatsu Morota[6], Shingo Kameda[7], Toru Kouyama[8], Hidehiko Suzuki[9], Manabu Yamada[10], Naoya Sakatani[2], Chikatoshi Honda[11], Masahiko Hayakawa[2], Kazuo Yoshioka[3], Yuichiro Cho[3], Hirotaka Sawada[2] (1.Kochi University, 2.ISAS/JAXA, 3.Univ. of Tokyo, 4.Planetary Science Institute, 5.DLR, 6.Nagoya Univ., 7.Rikkyo Univ., 8.AIST, 9.Meiji Univ., 10.Chiba Institute od Technology, 11.Aizu Univ.)

[E] Poster | P (Space and Planetary Sciences)：P-EM Solar-Terrestrial Sciences, Space Electromagnetism & Space Environment

10:45 AM - 12:15 PM JST | 1:45 AM - 3:15 AM UTC | Poster Hall International Exhibition Hall8, Makuhari Messe_3

[P-EM09] Vertical coupling in the atmosphere and Ionosphere

convener:Huixin Liu(Earth and Planetary Science Division, Kyushu University SERC, Kyushu University), Loren Chang(Institute of Space Science, National Central University), Yuichi Otsuka(Institute for Space-Earth Environmental Research, Nagoya University)

[PEM09-P01] **Local-time Variabilities of SABER CO_2 in the Mesosphere and Lower Thermosphere Region**

*Cornelius Csar Jude Salinas[1], Loren Chang[1], Danie Liang[2], Jia Yue[3], Liying Qian[4], Quan Gan[5], James Russel III[3], Martin G Mlynczak[6] (1.Institute of Space Science, National Central University, 2.Institute of Earth Science, Academia Sinica, 3.Department of Atmospheric Sciences, Hampton University, 4.High Altitude Observatory, National Center for Atmospheric Research, 5.Department of Physics and Astronomy, Clemson University, 6.NASA Langley Research Center)

[PEM09-P02] Enhanced dynamo electric field as a possible cause of ionosphere disturbance before Large Earthquake

*Koichiro Oyama[1,2,3] (1.Institute of Plasma and Space Sciences,National Cheng Kung Univ., Taiwan, 2.International Ceneter for Space Weather Sudy and Education, Kyushu Univ.,, 3.CoLtd. Asia Space Environment Research Consortium, Japan)

[PEM09-P03] Morphology of E1 and E2 Kelvin waves from ECMWF reanalysis

*Chen-Jeih Pan[1], Wei-Sheng Chen[1], Uma Das[2] (1.Institute of Space Science, National Central University, 2.Department of Physics, Indian Institute of Information Technology, Kalyani, India)

[PEM09-P04] Impact of strong ENSO on TEC activity disturbed by ultra-fast Kelvin waves

*Wei-Sheng Chen[1], C.J. Pan[1], Uma Das[2], Chian-Chiau Lin[3] (1.Institute of Space Science, National Central University, Taiwan, 2.Department of Physics, Indian Institute of Information Technology, Kalyani, India, 3.Environmental Research and Information Center, Chang Jung Christian University, Taiwan)

[PEM09-P05] **Observation and simulation of propagation of coseismic infrasound to the ionosphere**

*Jaroslav Chum[1] (1.Institute of Atmospheric Physics of the Czech Academy of Sciences)

[PEM09-P06] Solar wind influence on tropical cyclones mediated by atmospheric gravity waves

*Paul Prikryl[1,2], Iurii Cherniak[3], Irina Zakharenkova[4,5], James M. Weygand[6], Bharat S. R. Kunduri[7] (1.Physics Department, University of New Brunswick, Fredericton, NB, Canada, 2.Geomagnetic Laboratory, Natural Resources Canada, Ottawa, ON, Canada, 3.COSMIC Program Office, University Corporation for Atmospheric Research, Boulder, CO, USA, 4.West Department of IZMIRAN, Kaliningrad, Russia, 5.University of Warmia and Mazury in Olsztyn, Poland, 6.Earth Planetary and Space Sciences, University of California, Los Angeles, CA, USA, 7.Bradley Dept. of Electrical and Computer Engineering, Virginia Tech, Blacksburg, VA, USA)

[PEM09-P07] VIPIR ionospheric observations in Japan

*Takuya Tsugawa[1], Hideo Maeno[1], Michi Nishioka[1], Takumi Kondo[1], Mamoru Ishii[1] (1.National Institute of Information and Communications Technology)

[PEM09-P08] Simulation Results and Performance Analysis of Phase Velocity Spectral Analysis Software (M-Transform) for Airglow Imaging Data

*Septi Perwitasari[1], Takuji Nakamura[2], Masaru Kogure[2], Yoshihiro Tomikawa[2], Mitsumu K. Ejiri[2] (1.LAPAN, 2.NIPR)

[PEM09-P09] Comparisons of Co-incident Ionospheric Plasma Observations Between FORMOSAT-5/AIP and Millstone Hill Incoherent Scatter Radar

*Yi-Wun Chen[1], Chi-Kuang Chao[1] (1.Graduate Institute of Space Science, National Central University, Taiwan)

[PEM09-P10] Sub-ionospheric effects of volcano eruptions using VLF/LF standard radio waves

*Kei Maruyama[1], Hiroyo Ohya[1], Fuminori Tsuchiya[2], Kenro Nozaki[5], Kozo Yamashita[3], Yukihiro Takahashi[4], Hiroyuki Nakata[1], Toshiaki Takano[1] (1.Chiba University, 2.Tohoku University, 3.Ashikaga University, 4.Hokkaido University, 5.National Institute of Information and Communications Technology)

[PEM09-P11] Observations of ionospheric and mesospheric wave structures by a low-cost airglow imaging system

*Keisuke Hosokawa[1], Nanami Kusuyama[1], Yuta Hozumi[1], Kohei Takami[1], Susumu Saito[2], Yasunobu Ogawa[3], Mamoru Ishii[4], Yuichi Otsuka[5], Takuya Tsugawa[4] (1.University of Electro-Communications, 2.ENRI, 3.NIPR, 4.NICT, 5.ISEE, Nagoya University)

[PEM09-P12] Analysis of characteristics of ionospheric parameters, Sq index and neutral winds over Taiwan

*Yu-Jung Chuo[1] (1.Department of Information Technology, Ling Tung University)

[PEM09-P13] Statistical study on daytime Es observed by ground-ionosonde and RO-COSMIC in magnetic Equator region in 2010

*Zheng Wang [1,2], Huixin Liu[1] (1.Department of Earth and Planetary Sciences, School of Science, Kyushu University, Japan. , 2.National Space Science Center, Chinese Academy of Sciences, China.)

[PEM09-P14] The statistical study of the growth rates of Medium-Scale Traveling Ionospheric Disturbances observed with GPS-TEC

*Takafumi Ikeda[1], Akinori Saito[1], Takuya Tsugawa[2], Hiroyuki Shinagawa[2] (1.Department of Geophysics, Graduate School of Science, Kyoto University, 2.National Institutes of Information and Communications Technology)

[PEM09-P15] Comparison of Gravity Wave Activity in the Mesosphere Observed by OH Airglow Imagers and MF Radars over the Antarctic (Syowa & Davis).

*Masaru Kogure[1], Takuji Nakamura[1,2], Yoshihiro Tomikawa[1,2], Mitsumu K. Ejiri[1,2], Takanori Nishiyama[2,1], Masaki Tsutsumi[1,2], Michael J. Taylor[3], Yucheng Zhao[3], P.-Dominique Pautet[3], Damian Murphy[4] (1.National Institute of Polar Research, 2.Department of Polar Science, Sokendai, 3.Physics Department, Utah State University, 4.Australian Antarctic Division)

[E] Poster | P (Space and Planetary Sciences)：P-EM Solar-Terrestrial Sciences, Space Electromagnetism & Space Environment

5:15 PM - 6:30 PM JST | 8:15 AM - 9:30 AM UTC | Poster Hall International Exhibition Hall8, Makuhari Messe_4

[P-EM09] Vertical coupling in the atmosphere and Ionosphere

convener:Huixin Liu(Earth and Planetary Science Division, Kyushu University SERC, Kyushu University), Loren Chang(Institute of Space Science, National Central University), Yuichi Otsuka(Institute for Space-Earth Environmental Research, Nagoya University)

[PEM09-P01] Local-time Variabilities of SABER CO_2 in the Mesosphere and Lower Thermosphere Region

*Cornelius Csar Jude Salinas[1], Loren Chang[1], Danie Liang[2], Jia Yue[3], Liying Qian[4], Quan Gan[5], James Russel III[3], Martin G Mlynczak[6] (1.Institute of Space Science, National Central University, 2.Institute of Earth Science, Academia Sinica, 3.Department of Atmospheric Sciences, Hampton University, 4.High Altitude Observatory, National Center for Atmospheric Research, 5.Department of Physics and Astronomy, Clemson University, 6.NASA Langley Research Center)

[PEM09-P02] Enhanced dynamo electric field as a possible cause of ionosphere disturbance before Large Earthquake

*Koichiro Oyama[1,2,3] (1.Institute of Plasma and Space Sciences,National Cheng Kung Univ., Taiwan, 2.International Ceneter for Space Weather Sudy and Education, Kyushu Univ.,, 3.CoLtd. Asia Space Environment Research Consortium, Japan)

[PEM09-P03] Morphology of E1 and E2 Kelvin waves from ECMWF reanalysis

*Chen-Jeih Pan[1], Wei-Sheng Chen[1], Uma Das[2] (1.Institute of Space Science, National Central University, 2.Department of Physics, Indian Institute of Information Technology, Kalyani, India)

[PEM09-P04] Impact of strong ENSO on TEC activity disturbed by ultra-fast Kelvin waves

*Wei-Sheng Chen[1], C.J. Pan[1], Uma Das[2], Chian-Chiau Lin[3] (1.Institute of Space Science, National Central University, Taiwan, 2.Department of Physics, Indian Institute of Information Technology, Kalyani, India, 3.Environmental Research and Information Center, Chang Jung Christian University, Taiwan)

[PEM09-P05] Observation and simulation of propagation of coseismic infrasound to the ionosphere

*Jaroslav Chum[1] (1.Institute of Atmospheric Physics of the Czech Academy of Sciences)

[PEM09-P06] Solar wind influence on tropical cyclones mediated by atmospheric gravity waves

*Paul Prikryl[1,2], Iurii Cherniak[3], Irina Zakharenkova[4,5], James M. Weygand[6], Bharat S. R. Kunduri[7] (1.Physics Department, University of New Brunswick, Fredericton, NB, Canada, 2.Geomagnetic Laboratory, Natural Resources Canada, Ottawa, ON, Canada, 3.COSMIC Program Office, University Corporation for Atmospheric Research, Boulder, CO, USA, 4.West Department of IZMIRAN, Kaliningrad, Russia, 5.University of Warmia and Mazury in Olsztyn, Poland, 6.Earth Planetary and Space Sciences, University of California, Los Angeles, CA, USA, 7.Bradley Dept. of Electrical and Computer Engineering, Virginia Tech, Blacksburg, VA, USA)

[PEM09-P07] VIPIR ionospheric observations in Japan

*Takuya Tsugawa[1], Hideo Maeno[1], Michi Nishioka[1], Takumi Kondo[1], Mamoru Ishii[1] (1.National Institute of Information and Communications Technology)

[PEM09-P08] Simulation Results and Performance Analysis of Phase Velocity Spectral Analysis Software (M-Transform) for Airglow Imaging Data

*Septi Perwitasari[1], Takuji Nakamura[2], Masaru Kogure[2], Yoshihiro Tomikawa[2], Mitsumu K. Ejiri[2] (1.LAPAN, 2.NIPR)

[PEM09-P09] Comparisons of Co-incident Ionospheric Plasma Observations Between FORMOSAT-5/AIP and Millstone Hill Incoherent Scatter Radar

*Yi-Wun Chen[1], Chi-Kuang Chao[1] (1.Graduate Institute of Space Science, National Central University, Taiwan)

[PEM09-P10] Sub-ionospheric effects of volcano eruptions using VLF/LF standard radio waves

*Kei Maruyama[1], Hiroyo Ohya[1], Fuminori Tsuchiya[2], Kenro Nozaki[5], Kozo Yamashita[3], Yukihiro Takahashi[4], Hiroyuki Nakata[1], Toshiaki Takano[1] (1.Chiba University, 2.Tohoku University, 3.Ashikaga University, 4.Hokkaido University, 5.National Institute of Information and Communications Technology)

[PEM09-P11] Observations of ionospheric and mesospheric wave structures by a low-cost airglow imaging system

*Keisuke Hosokawa[1], Nanami Kusuyama[1], Yuta Hozumi[1], Kohei Takami[1], Susumu Saito[2], Yasunobu Ogawa[3], Mamoru Ishii[4], Yuichi Otsuka[5], Takuya Tsugawa[4] (1.University of Electro-Communications, 2.ENRI, 3.NIPR, 4.NICT, 5.ISEE, Nagoya University)

[PEM09-P12] Analysis of characteristics of ionospheric parameters, Sq index and neutral winds over Taiwan

*Yu-Jung Chuo[1] (1.Department of Information Technology, Ling Tung University)

[PEM09-P13] Statistical study on daytime Es observed by ground-ionosonde and RO-COSMIC in magnetic Equator region in 2010

*Zheng Wang [1,2], Huixin Liu[1] (1.Department of Earth and Planetary Sciences, School of Science, Kyushu University, Japan. , 2.National Space Science Center, Chinese Academy of Sciences, China.)

[PEM09-P14] The statistical study of the growth rates of Medium-Scale Traveling Ionospheric Disturbances observed with GPS-TEC

*Takafumi Ikeda[1], Akinori Saito[1], Takuya Tsugawa[2], Hiroyuki Shinagawa[2] (1.Department of Geophysics, Graduate School of Science, Kyoto University, 2.National Institutes of Information and Communications Technology)

[PEM09-P15] Comparison of Gravity Wave Activity in the Mesosphere Observed by OH Airglow Imagers and MF Radars over the Antarctic (Syowa & Davis).

*Masaru Kogure[1], Takuji Nakamura[1,2], Yoshihiro Tomikawa[1,2], Mitsumu K. Ejiri[1,2], Takanori Nishiyama[2,1], Masaki Tsutsumi[1,2], Michael J. Taylor[3], Yucheng Zhao[3], P.-Dominique Pautet[3], Damian Murphy[4] (1.National Institute of Polar Research, 2.Department of Polar Science, Sokendai, 3.Physics Department, Utah State University, 4.Australian Antarctic Division)

[E] Poster | P (Space and Planetary Sciences)：P-EM Solar-Terrestrial Sciences, Space Electromagnetism & Space Environment

1:45 PM - 3:15 PM JST | 4:45 AM - 6:15 AM UTC | Poster Hall International Exhibition Hall8, Makuhari Messe_1

[P-EM11] Dynamics of Magnetosphere and Ionosphere

convener:Aoi Nakamizo(Applied Electromagnetic Research Institute, National Institute of Information and Communications Technology), Mitsunori Ozaki(Faculty of Electrical and Computer Engineering, Institute of Science and Engineering, Kanazawa University), Akiko Fujimoto(Kyushu Institute of Technology), Tomoaki Hori(Institute for Space-Earth Environmental Research, Nagoya University)

[PEM11-P01] Effects of Inclination/Rotation of Earth's Magnetic Axis on Magnetosphere Simulated by Global MHD Model

*Aoi Nakamizo[1] (1.Applied Electromagnetic Research Institute, National Institute of Information and Communications Technology)

[PEM11-P02] Asymmetric deformation of the magnetosphere under low-density solar wind

*Masaki N Nishino[1,2], Yoshifumi Saito[2], Kazuo Shiokawa[1], Masaki Fujimoto[2] (1.Institute for Space-Earth Environmental Research, Nagoya University, 2.JAXA/ISAS)

[PEM11-P03] New perspectives on coupling processes in solar-terrestrial system obtained by comprehensive data analysis

*Yoshimasa Tanaka[1], Norio Umemura[2], Shuji Abe[3], Satoru UeNo[4], Masahito Nose[2], Yumi Nakagawa[5] (1.National Institute of Polar Research, 2.Institute for Space-Earth Environmental Research, Nagoya University, 3.International Center for Space Weather Science and Education, 4.Kwasan & Hida Observatories, School of Science, Kyoto University, 5.Ibaraki University)

[PEM11-P04] The interaction between the magnetosphere-ionosphere compound system and the magnetic field topology

*Shigeru Fujita[1], Takashi Tanaka[2], Masakazu Watanabe[2] (1.Meteorological College, Japan Meteorological Agency/ Nationa Institute of Polar Research, 2.Kyushu University)

[PEM11-P05] Effects of the dipole tilt and the interplanetary magnetic field Bx component on the dawn-dusk and interhemispheric asymmetries of the interchange convection cycle

*Masakazu Watanabe[1,2], Takashi Tanaka[2], Shigeru Fujita[3,4] (1.Graduate School of Science, Kyushu University, 2.International Center for Space Weather Science and Education, Kyushu University, 3.Meteorological College, 4.National Institute of Polar Research)

[PEM11-P06] Transient polar ionospheric convection response to negative dynamic pressure pulse

*Jianjun Liu[1] (1.Polar Research Institute of China)

[PEM11-P07] An active ionosphere: a new perspective of field line dipolarization

*Osuke Saka[1] (1.Office Geophysik)

[PEM11-P08] Toward the automatic identification of FLR signals in the SuperDARN data by using the gradient method

*Hideaki Kawano[1,2], Akira Sessai Yukimatu[3,4], Nozomu Nishitani[5], Yoshimasa Tanaka[3,4], Satoko Saita[6], Tomoaki Hori[5] (1.Dept. Earth Planet. Sci., Kyushu Univ., 2.ICSWSE, Kyushu University, 3.National Institute of Polar Research, 4.SOKENDAI, 5.ISEE, Nagoya University, 6.Kitakyushu College)

[PEM11-P09] A statistical study of Pi2 pulsations observed in the upper ionosphere using Swarm magnetic field data

*Park Jaehee[1], Khan-Hyuk Kim[1], Junga Hwang[2] (1.School of Space Research, Kyung Hee University, Gyeonggi, South Korea, 2.Korea Astronomy and Space Science Institute, Daejeon,South Korea)

[PEM11-P10] Study on the global distribution characteristics of Pc 1-2 geomagnetic pulsation with the 10Hz data of the MAGDAS system

*Taisei Kabasawa[1], Akimasa Yoshikawa[1], Teiji Uozumi[1], Akiko Fujimoto[1], Shuji Abe[1] (1.Kyushu University)

[PEM11-P11] In-situ Observations of Reconnection Separatrix Regions in the near-Earth Magnetotail

*Mizuho Araki[1], Masahiro Hoshino[1], Kunihiro Keika[1], Yoshifumi Saito[2] (1.Graduate School of Science, The University of Tokyo, 2.Institude of Space and Astronautical Science)

[PEM11-P12] Flow speed dependence of ion temperature, electron temperature, and their ratio in the near-Earth magnetotail reconnection region

*Kaori Watanabe[1], Masahiro Hoshino[1], Kunihiro Keika[1], Yoshifumi Saito[2], Naritoshi Kitamura[1] (1.Univ. of Tokyo, 2.ISAS/JAXA)

[PEM11-P13] **Examining Minimum Cyclotron Resonant Electron Energy of EMIC Waves with MMS**

*Si Liu[1] (1.Changsha University of Science and Technology)

[PEM11-P14] Small scale whistler mode waves near the magnetic field intensity minimum in the magnetosheath

*Naritoshi Kitamura[1], Takanobu Amano[1], Yoshiharu Omura[2], Satoko Nakamura[2], Chika Umegaki[1], Scott A Boardsen[3,4], Narges Ahmadi[5], Robert E Ergun[5], Olivier Le Contel[6], Per-Arne Lindqvist[7], Yoshifumi Saito[8], Shoichiro Yokota[9], Daniel J Gershman[3], Barbara L Giles[3], Thomas E Moore[3], William R Paterson[3], Craig J Pollock[10], Christopher T Russell[11], Robert J Strangeway[11], James L Burch[12] (1.Department of Earth and Planetary Science, Graduate School of Science, The University of Tokyo, 2.Research Institute for Sustainable Humanosphere, Kyoto University, 3.NASA Goddard Space Flight Center, 4.University of Maryland, 5.Laboratory for Atmospheric and Space Physics, University of Colorado, 6.Laboratoire de Physique des Plasmas, UMR7648 CNRS/Ecole Polytechnique/UPMC/Université Paris-Sud/Observatoire de Paris, 7.Royal Institute of Technology, 8.Institute of Space and Astronautical Science, Japan Aerospace Exploration Agency, 9.Department of Earth and Space Science, Graduate School of Science, Osaka University, 10.Denali Scientific, 11.Institute of Geophysics and Planetary Physics, University of California, Los Angeles, 12.Southwest Research Institute)

[PEM11-P15] Spatial characteristics of the internal modulation of pulsating aurora: multi-point high-speed optical observations in Scandinavia

*Yuki Kawamura[1], Keisuke Hosokawa[1], Shin-ichiro Oyama[2,3], Yoshizumi Miyoshi[2], Yasunobu Ogawa[3], Satoshi Kurita[2], Satoshi Ebukuro[1], Ryoichi Fujii[4] (1.Department of Communication Engineering and Informatics, University of Electro-Communications, 2.Institute for Space-Earth Environmental Research, Nagoya University, 3.National Institute of Polar Research, 4.Research Organization of Information and Systems)

[PEM11-P16] **Large-scale characteristics of pulsating aurora periodicities:multi-point high-speed optical observations in Scandinavia**

*Satoshi Ebukuro[1], Keisuke Hosokawa[1], Shin-ichiro Oyama[2,3,5], Yoshizumi Miyoshi[2], Yasunobu Ogawa[3], Satoshi Kurita[2], Yuki Kawamura[1], Ryoichi Fujii[4] (1.Department of Communication Engineering and Informatics, University of Electro-Communications, 2.Institute for Space-Earth Environmental Research, Nagoya University, 3.National Institute of Polar Research, 4.Research Organization of Information and Systems, 5.University of Oulu)

[PEM11-P17] Variations of cosmic noise absorption (CNA) by energetic electron precipitation (EEP) and changes of the auroral morphology

*Miyamoto Taishiro[1], Shin-ichiro Oyama[1,4,5], Yasunobu Ogawa[2], Keisuke Hosokawa[3], Satoshi Kurita[1], Yoshizumi Miyoshi[1], Ryuho Kataoka[2], Hiroshi Miyaoka[2], Tero Raita[4] (1. Institute for Space-Earth Environmental Research,Nagoya University, 2.National Institute of Polar Research, 3.Department of Communication Engineering and Informatics, University of Electro-Communications, 4.Sodankylä Geophysical Observatory, University of Oulu, 5.Ionosphere Research Unit, University of Oulu)

[PEM11-P18] Spatiotemporal characteristics on the source region of flash aurora using ray tracing analysis

*Tomohiro Inoue[1], Mitsunori Ozaki[1], Yoshitaka Goto[1], Satoshi Yagitani[1], Yoshiya Kasahara[1], Kazuo Shiokawa[2], Yoshizumi Miyoshi[2], Ryuho Kataoka[3], Yusuke Ebihara[4] (1.Kanazawa University , 2.Nagoya University, 3.National Institute of Polar Research, 4.Kyoto University)

[PEM11-P19] Molecular ion supply mechanisms from the low-altitude ionosphere to magnetosphere observed by EISCAT and Arase(ERG)

*Masayoshi Takada[1], Kanako Seki[1], Yasunobu Ogawa[2], Kunihiro Keika[3], Satoshi Kasahara[4], Shoichiro Yokota[5], Tomoaki Hori[7], Kazushi Asamura[6], Yoshizumi Miyoshi[7] (1.Graduate School of Science, Tokyo University, 2.National Institute of Polar Research, 3.Department of Earth and Planetary Science, Graduate School of Science, Tokyo University, 4.The University of Tokyo, 5.Graduate School of Science, Osaka University, 6.Institute of Space and Astronautical Science, Japan Aerospace Exploration Agency, 7.Institute for Space-Earth Environmental Research, Nagoya University)

[PEM11-P20] Optical and radar observation of the dynamic auroral forms

*Yunosuke Nagafusa[1], Tima Sergienko[2], Satoshi Taguchi[1], Urban Braendstroem[2], Masatoshi Yamauchi[2] (1.Graduate School of Science, Kyoto University, 2.Swedish Institute of Space Physics, Kiruna)

[PEM11-P21] Observations of MF/HF auroral radio emissions at three ground-based stations

*Yuka Sato[1], Atsushi Kumamoto[2], Yuto Katoh[2], Akira Kadokura[3,4], Yasunobu Ogawa[3,4], Atsuki Shinbori[5] (1.Nippon Institute of Technology (NIT), 2.Graduate School of Science, Tohoku University, 3.National Institute of Polar Research (NIPR), 4.The Graduate University for Advanced Studies, 5.Institute for Space-Earth Environmental Research (ISEE), Nagoya University)

[PEM11-P22] **Ionospheric F-region Drift Measurements Derived from DPS-4D at Zhongshan Station, Antarctic**

*Xiangcai Chen[1] (1.Polar Research Institute of China)

[PEM11-P23] PARM-HEP Observation of Precipitating High Energy Electrons over Pulsating Aurora

*Taku Namekawa[1], Takefumi Mitani[2], Kazushi Asamura[2], Yoshifumi Saito[2] (1.Department of Earth and Planetary Science, Graduate school of Science, The University of Tokyo, 2.Institute of Space and Astronautical Science, Japan Aerospace Exploration Agency)

[PEM11-P24] Development of the medium-energy electron detector with hemispherical field-of-view and the flight test in the PARM (Pulsating AuRora and Microburst) mission

*Shin Sugo[1], Oya Kawashima[1], Kazushi Asamura[2], Reiko Nomura[3], Yasunobu Ogawa[4], Keisuke Hosokawa[5], Yoshizumi Miyoshi[6], Takefumi Mitani[2], Taku Namekawa[1,2], Takeshi Sakanoi[7], Mizuki Fukizawa[7], Naoshi Yagi[7], Satoshi Kasahara[1] (1.The University of Tokyo, 2.Institute of Space and Astronautical Science, Japan Aerospace Exploration Agency, 3.National Astronomical Observatory of Japan, 4.National Institute of Polar Research, 5.The University of Electro-Communications, 6.Institute for Space-Earth Environmental Research, Nagoya University, 7.Tohoku University)

[PEM11-P25] Auroral substorm onset in satellite-based global images and ground-based all-sky images

*Akimasa Ieda[1], Kirsti Kauristie[2], Yukitoshi Nishimura[3], Yukinaga Miyashita[4], Harald U Frey[5], Liisa Juusola[2], Daniel Whiter[6], Masahito Nose[7], Matthew O Fillingim[5], Farideh Honary[8], Neil C Rogers[8], Yoshizumi Miyoshi[1], Shinobu Machida[1] (1.Institute for Space-Earth Environmental Research, Nagoya University, 2.Finnish Meteorological Institute, 3.Boston university, 4.Korea Astronomy and Space Science Institute, 5.University of California Berkeley, 6.University of Southampton, 7.Graduate School of Science, Kyoto University, 8.Lancaster University)

[PEM11-P26] Automatic Classification of Auroral images using optical flow feature

*Naoto Kashiwagi[1], Akiko Fujimoto[1], Terumasa Tokunaga[1], Yoshizumi Miyoshi[2], Yasunobu Ogawa[3], Keisuke Hosokawa[4] (1.Kyushu Institute of Technology, 2.Nagoya University, 3.National Institute of Polar Research, 4.The University of Electro-Communications)

[PEM11-P27] Fine-scale visualization of aurora in a wide area using color digital camera images from the International Space Station

*Sota Nanjo[1], Yuta Hozumi[1], Keisuke Hosokawa[1] (1.The University of Electro-Communications)

[PEM11-P28] Geospace Imaging via the soft X-ray imager: GEO-X mission

*Yoshizumi Miyoshi[1], Yuichiro Ezoe[2], Satoshi Kasahara[3], Yosuke Matsumoto[4], Kumi Ishikawa[5], Ryuho Kataoka[6], Hiroki Ito[1], Daiki Ishi[2], Masaki Numazawa[2], Atsushi Yamazaki[5], Hiroshi Hasegawa[5], Masaki Fujimoto[5], Kazuhisa Mitsuda[5] (1.Institute for Space-Earth Environmental Research, Nagoya University, 2.Tokyo Metropolitan University, 3.University of Tokyo, 4.Chiba University, 5.ISAS/JAXA, 6.NIPR)

[E] Poster | P (Space and Planetary Sciences)：P-EM Solar-Terrestrial Sciences, Space Electromagnetism & Space Environment

5:15 PM - 6:30 PM JST | 8:15 AM - 9:30 AM UTC | Poster Hall International Exhibition Hall8, Makuhari Messe_5

[P-EM11] Dynamics of Magnetosphere and Ionosphere

convener:Aoi Nakamizo(Applied Electromagnetic Research Institute, National Institute of Information and Communications Technology), Mitsunori Ozaki(Faculty of Electrical and Computer Engineering, Institute of Science and Engineering, Kanazawa University), Akiko Fujimoto(Kyushu Institute of Technology), Tomoaki Hori(Institute for Space-Earth Environmental Research, Nagoya University)

[PEM11-P01] Effects of Inclination/Rotation of Earth's Magnetic Axis on Magnetosphere Simulated by Global MHD Model

*Aoi Nakamizo[1] (1.Applied Electromagnetic Research Institute, National Institute of Information and Communications Technology)

[PEM11-P02] Asymmetric deformation of the magnetosphere under low-density solar wind

*Masaki N Nishino[1,2], Yoshifumi Saito[2], Kazuo Shiokawa[1], Masaki Fujimoto[2] (1.Institute for Space-Earth Environmental Research, Nagoya University, 2.JAXA/ISAS)

[PEM11-P03] New perspectives on coupling processes in solar-terrestrial system obtained by comprehensive data analysis

*Yoshimasa Tanaka[1], Norio Umemura[2], Shuji Abe[3], Satoru UeNo[4], Masahito Nose[2], Yumi Nakagawa[5] (1.National Institute of Polar Research, 2.Institute for Space-Earth Environmental Research, Nagoya University, 3.International Center for Space Weather Science and Education, 4.Kwasan & Hida Observatories, School of Science, Kyoto University, 5.Ibaraki University)

[PEM11-P04] The interaction between the magnetosphere-ionosphere compound system and the magnetic field topology

*Shigeru Fujita[1], Takashi Tanaka[2], Masakazu Watanabe[2] (1.Meteorological College, Japan Meteorological Agency/ Nationa Institute of Polar Research, 2.Kyushu University)

[PEM11-P05] Effects of the dipole tilt and the interplanetary magnetic field Bx component on the dawn-dusk and interhemispheric asymmetries of the interchange convection cycle

*Masakazu Watanabe[1,2], Takashi Tanaka[2], Shigeru Fujita[3,4] (1.Graduate School of Science, Kyushu University, 2.International Center for Space Weather Science and Education, Kyushu University, 3.Meteorological College, 4.National Institute of Polar Research)

[PEM11-P06] Transient polar ionospheric convection response to negative dynamic pressure pulse

*Jianjun Liu[1] (1.Polar Research Institute of China)

[PEM11-P07] An active ionosphere: a new perspective of field line dipolarization

*Osuke Saka[1] (1.Office Geophysik)

[PEM11-P08] Toward the automatic identification of FLR signals in the SuperDARN data by using the gradient method

*Hideaki Kawano[1,2], Akira Sessai Yukimatu[3,4], Nozomu Nishitani[5], Yoshimasa Tanaka[3,4], Satoko Saita[6], Tomoaki Hori[5] (1.Dept. Earth Planet. Sci., Kyushu Univ., 2.ICSWSE, Kyushu University, 3.National Institute of Polar Research, 4.SOKENDAI, 5.ISEE, Nagoya University, 6.Kitakyushu College)

[PEM11-P09] A statistical study of Pi2 pulsations observed in the upper ionosphere using Swarm magnetic field data

*Park Jaehee[1], Khan-Hyuk Kim[1], Junga Hwang[2] (1.School of Space Research, Kyung Hee University, Gyeonggi, South Korea, 2.Korea Astronomy and Space Science Institute, Daejeon,South Korea)

[PEM11-P10] Study on the global distribution characteristics of Pc 1-2 geomagnetic pulsation with the 10Hz data of the MAGDAS system

*Taisei Kabasawa[1], Akimasa Yoshikawa[1], Teiji Uozumi[1], Akiko Fujimoto[1], Shuji Abe[1] (1.Kyushu University)

[PEM11-P11] In-situ Observations of Reconnection Separatrix Regions in the near-Earth Magnetotail

*Mizuho Araki[1], Masahiro Hoshino[1], Kunihiro Keika[1], Yoshifumi Saito[2] (1.Graduate School of Science, The University of Tokyo, 2.Institude of Space and Astronautical Science)

[PEM11-P12] Flow speed dependence of ion temperature, electron temperature, and their ratio in the near-Earth magnetotail reconnection region

*Kaori Watanabe[1], Masahiro Hoshino[1], Kunihiro Keika[1], Yoshifumi Saito[2], Naritoshi Kitamura[1] (1.Univ. of Tokyo, 2.ISAS/JAXA)

[PEM11-P13] **Examining Minimum Cyclotron Resonant Electron Energy of EMIC Waves with MMS**

*Si Liu[1] (1.Changsha University of Science and Technology)

[PEM11-P14] Small scale whistler mode waves near the magnetic field intensity minimum in the magnetosheath

*Naritoshi Kitamura[1], Takanobu Amano[1], Yoshiharu Omura[2], Satoko Nakamura[2], Chika Umegaki[1], Scott A Boardsen[3,4], Narges Ahmadi[5], Robert E Ergun[5], Olivier Le Contel[6], Per-Arne Lindqvist[7], Yoshifumi Saito[8], Shoichiro Yokota[9], Daniel J Gershman[3], Barbara L Giles[3], Thomas E Moore[3], William R Paterson[3], Craig J Pollock[10], Christopher T Russell[11], Robert J Strangeway[11], James L Burch[12] (1.Department of Earth and Planetary Science, Graduate School of Science, The University of Tokyo, 2.Research Institute for Sustainable Humanosphere, Kyoto University, 3.NASA Goddard Space Flight Center, 4.University of Maryland, 5.Laboratory for Atmospheric and Space Physics, University of Colorado, 6.Laboratoire de Physique des Plasmas, UMR7648 CNRS/Ecole Polytechnique/UPMC/Université Paris-Sud/Observatoire de Paris, 7.Royal Institute of Technology, 8.Institute of Space and Astronautical Science, Japan Aerospace Exploration Agency, 9.Department of Earth and Space Science, Graduate School of Science, Osaka University, 10.Denali Scientific, 11.Institute of Geophysics and Planetary Physics, University of California, Los Angeles, 12.Southwest Research Institute)

[PEM11-P15] Spatial characteristics of the internal modulation of pulsating aurora: multi-point high-speed optical observations in Scandinavia

*Yuki Kawamura[1], Keisuke Hosokawa[1], Shin-ichiro Oyama[2,3], Yoshizumi Miyoshi[2], Yasunobu Ogawa[3], Satoshi Kurita[2], Satoshi Ebukuro[1], Ryoichi Fujii[4] (1.Department of Communication Engineering and Informatics, University of Electro-Communications, 2.Institute for Space-Earth Environmental Research, Nagoya University, 3.National Institute of Polar Research, 4.Research Organization of Information and Systems)

[PEM11-P16] **Large-scale characteristics of pulsating aurora periodicities:multi-point high-speed optical observations in Scandinavia**

*Satoshi Ebukuro[1], Keisuke Hosokawa[1], Shin-ichiro Oyama[2,3,5], Yoshizumi Miyoshi[2], Yasunobu Ogawa[3], Satoshi Kurita[2], Yuki Kawamura[1], Ryoichi Fujii[4] (1.Department of Communication Engineering and Informatics, University of Electro-Communications, 2.Institute for Space-Earth Environmental Research, Nagoya University, 3.National Institute of Polar Research, 4.Research Organization of Information and Systems, 5.University of Oulu)

[PEM11-P17] Variations of cosmic noise absorption (CNA) by energetic electron precipitation (EEP) and changes of the auroral morphology

*Miyamoto Taishiro[1], Shin-ichiro Oyama[1,4,5], Yasunobu Ogawa[2], Keisuke Hosokawa[3], Satoshi Kurita[1], Yoshizumi Miyoshi[1], Ryuho Kataoka[2], Hiroshi Miyaoka[2], Tero Raita[4] (1. Institute for Space-Earth Environmental Research,Nagoya University, 2.National Institute of Polar Research, 3.Department of Communication Engineering and Informatics, University of Electro-Communications, 4.Sodankylä Geophysical Observatory, University of Oulu, 5.Ionosphere Research Unit, University of Oulu)

[PEM11-P18] Spatiotemporal characteristics on the source region of flash aurora using ray tracing analysis

*Tomohiro Inoue[1], Mitsunori Ozaki[1], Yoshitaka Goto[1], Satoshi Yagitani[1], Yoshiya Kasahara[1], Kazuo Shiokawa[2], Yoshizumi Miyoshi[2], Ryuho Kataoka[3], Yusuke Ebihara[4] (1.Kanazawa University , 2.Nagoya University, 3.National Institute of Polar Research, 4.Kyoto University)

[PEM11-P19] Molecular ion supply mechanisms from the low-altitude ionosphere to magnetosphere observed by EISCAT and Arase(ERG)

*Masayoshi Takada[1], Kanako Seki[1], Yasunobu Ogawa[2], Kunihiro Keika[3], Satoshi Kasahara[4], Shoichiro Yokota[5], Tomoaki Hori[7], Kazushi Asamura[6], Yoshizumi Miyoshi[7] (1.Graduate School of Science, Tokyo University, 2.National Institute of Polar Research, 3.Department of Earth and Planetary Science, Graduate School of Science, Tokyo University, 4.The University of Tokyo, 5.Graduate School of Science, Osaka University, 6.Institute of Space and Astronautical Science, Japan Aerospace Exploration Agency, 7.Institute for Space-Earth Environmental Research, Nagoya University)

[PEM11-P20] Optical and radar observation of the dynamic auroral forms

*Yunosuke Nagafusa[1], Tima Sergienko[2], Satoshi Taguchi[1], Urban Braendstroem[2], Masatoshi Yamauchi[2] (1.Graduate School of Science, Kyoto University, 2.Swedish Institute of Space Physics, Kiruna)

[PEM11-P21] Observations of MF/HF auroral radio emissions at three ground-based stations

*Yuka Sato[1], Atsushi Kumamoto[2], Yuto Katoh[2], Akira Kadokura[3,4], Yasunobu Ogawa[3,4], Atsuki Shinbori[5] (1.Nippon Institute of Technology (NIT), 2.Graduate School of Science, Tohoku University, 3.National Institute of Polar Research (NIPR), 4.The Graduate University for Advanced Studies, 5.Institute for Space-Earth Environmental Research (ISEE), Nagoya University)

[PEM11-P22] **Ionospheric F-region Drift Measurements Derived from DPS-4D at Zhongshan Station, Antarctic**

*Xiangcai Chen[1] (1.Polar Research Institute of China)

[PEM11-P23] PARM-HEP Observation of Precipitating High Energy Electrons over Pulsating Aurora

*Taku Namekawa[1], Takefumi Mitani[2], Kazushi Asamura[2], Yoshifumi Saito[2] (1.Department of Earth and Planetary Science, Graduate school of Science, The University of Tokyo, 2.Institute of Space and Astronautical Science, Japan Aerospace Exploration Agency)

[PEM11-P24] Development of the medium-energy electron detector with hemispherical field-of-view and the flight test in the PARM (Pulsating AuRora and Microburst) mission

*Shin Sugo[1], Oya Kawashima[1], Kazushi Asamura[2], Reiko Nomura[3], Yasunobu Ogawa[4], Keisuke Hosokawa[5], Yoshizumi Miyoshi[6], Takefumi Mitani[2], Taku Namekawa[1,2], Takeshi Sakanoi[7], Mizuki Fukizawa[7], Naoshi Yagi[7], Satoshi Kasahara[1] (1.The University of Tokyo, 2.Institute of Space and Astronautical Science, Japan Aerospace Exploration Agency, 3.National Astronomical Observatory of Japan, 4.National Institute of Polar Research, 5.The University of Electro-Communications, 6.Institute for Space-Earth Environmental Research, Nagoya University, 7.Tohoku University)

[PEM11-P25] Auroral substorm onset in satellite-based global images and ground-based all-sky images

*Akimasa Ieda[1], Kirsti Kauristie[2], Yukitoshi Nishimura[3], Yukinaga Miyashita[4], Harald U Frey[5], Liisa Juusola[2], Daniel Whiter[6], Masahito Nose[7], Matthew O Fillingim[5], Farideh Honary[8], Neil C Rogers[8], Yoshizumi Miyoshi[1], Shinobu Machida[1] (1.Institute for Space-Earth Environmental Research, Nagoya University, 2.Finnish Meteorological Institute, 3.Boston university, 4.Korea Astronomy and Space Science Institute, 5.University of California Berkeley, 6.University of Southampton, 7.Graduate School of Science, Kyoto University, 8.Lancaster University)

[PEM11-P26] Automatic Classification of Auroral images using optical flow feature

*Naoto Kashiwagi[1], Akiko Fujimoto[1], Terumasa Tokunaga[1], Yoshizumi Miyoshi[2], Yasunobu Ogawa[3], Keisuke Hosokawa[4] (1.Kyushu Institute of Technology, 2.Nagoya University, 3.National Institute of Polar Research, 4.The University of Electro-Communications)

[PEM11-P27] Fine-scale visualization of aurora in a wide area using color digital camera images from the International Space Station

*Sota Nanjo[1], Yuta Hozumi[1], Keisuke Hosokawa[1] (1.The University of Electro-Communications)

[PEM11-P28] Geospace Imaging via the soft X-ray imager: GEO-X mission

*Yoshizumi Miyoshi[1], Yuichiro Ezoe[2], Satoshi Kasahara[3], Yosuke Matsumoto[4], Kumi Ishikawa[5], Ryuho Kataoka[6], Hiroki Ito[1], Daiki Ishi[2], Masaki Numazawa[2], Atsushi Yamazaki[5], Hiroshi Hasegawa[5], Masaki Fujimoto[5], Kazuhisa Mitsuda[5] (1.Institute for Space-Earth Environmental Research, Nagoya University, 2.Tokyo Metropolitan University, 3.University of Tokyo, 4.Chiba University, 5.ISAS/JAXA, 6.NIPR)

[E] Poster | P (Space and Planetary Sciences)：P-EM Solar-Terrestrial Sciences, Space Electromagnetism & Space Environment

3:30 PM - 5:00 PM JST | 6:30 AM - 8:00 AM UTC | Poster Hall International Exhibition Hall8, Makuhari Messe_2

[P-EM13] Inner magnetosphere: Recent understanding and new insights

convener:Yusuke Ebihara(Research Institute for Sustainable Humanosphere, Kyoto University), Danny Summers(Memorial University of Newfoundland), Yoshizumi Miyoshi(Institute for Space-Earth Environmental Research, Nagoya University), Shinji Saito(Graduate School of Science, Nagoya University)

[PEM13-P01] Evaluation of wave normal and Poynting vector analyses for whistler mode waves observed by the waveform capture (WFC) on board the Arase

*Yoshiya Kasahara[1], Satoshi Ikarashi[1], Hiroyuki Nishizawa[1], Shoya Matsuda[2], Fuminori Tsuchiya[3], Atsushi Kumamoto[3], Yasumasa Kasaba[3], Mitsunori Ozaki[1], Ayako Matsuoka[2] (1.Kanazawa University, 2.ISAS/JAXA, 3.Tohoku University)

[PEM13-P02] Calibration of electric fields dedicated to the measurement of the S-WPIA of the Arase Satellite

*Miki Jumpei[1], Hirotsugu Kojima[2], Yuto Katoh[3], Shoya Matsuda[4], Yoshiya Kasahara[5], Mitsuru Hikishima[4], Satoshi Kurita[6], Masahiro Kitahara[3], Satoshi Kasahara[7], Yoshizumi Miyoshi[6], Atsushi Kumamoto[3], Ayako Matsuoka[4], Shoichiro Yokota[8], Tomoaki Hori[6], Kunihiro Keika[7] (1.Space Radio Engineering Laboratory, Division of Electrical Engineering, Kyoto University Graduated School, 2.Research Institute for Sustainable Humanosphere, Kyoto University, 3.Graduate School of Science and Faculty of Science, Tohoku University, 4.Institute of Space and Astronautical Science, JAXA, 5.Information Media Center, Kanazawa University, 6.Institute for Space-Earth Environmental Research, Nagoya University, 7.School of Science, The University of Tokyo, 8.School of Science, Osaka University)

[PEM13-P03] Enhancement of whistler-mode chorus in association with Pc 4-5 ULF waves and related variation of high energy electrons

*Atsuhiro Ono[1], Yuto Katoh[1], Atsushi Kumamoto[1], Fuminori Tsuchiya[1], Mariko Teramoto[2], Yoshiya Kasahara[3], Shoya Matsuda[4], Ayako Matsuoka[4], Takefumi Mitani[4], Tomoaki Hori[2], Satoshi Kasahara[5], Shoichiro Yokota[6], Kunihiro Keika[5], Yoshizumi Miyoshi[2], Iku Shinohara[4] (1.Tohoku University, 2.Nagoya University, 3.Kanazawa University, 4.ISAS/JAXA, 5.The University of Tokyo, 6.Osaka University)

[PEM13-P04] Sudden enhancements of electron cyclotron harmonic waves observed by the Arase satellite

*Shinjo Airi[1], Hirotsugu Kojima[1], Yoshiya Kasahara[2], Yoichi Kazama[3], Hideyuki Usui[4], Yoshizumi Miyoshi[5], Yasumasa Kasaba[6], Shoya Matsuda[7], Tomoaki Hori[5], S. -Y. Wang[8], Sunny W.Y. Tam[9], Atsushi Kumamoto[10], Ayako Matsuoka[11] (1.Research institute for sustainable humanosphere, Kyoto University, 2.Information Media Center, Kanazawa University, 3.ASIAA, 4.Graduate school of system informatics Kobe University, 5.Institute for Space-Earth Environmental Research, Nagoya University, 6.Planetary Plasma and Atmospheric Research Center, Tohoku University, 7.Institute of Space and Astronautical Science/Japan Aerospace Exploration Agency, 8.ASIAA, Taiwan, 9.ISAPS, NCKU, Taiwan, 10.Department of Geophysics, Graduate School of Science, Tohoku University, 11.Research Division for Space Plasma, Institute of Space and Astronautical Science, Japan Aerospace Exploration Agency)

[PEM13-P05] Correlation between pulsating aurora and electrostatic electron cyclotron harmonic waves obtained from coordinated Arase and ground data

*Mizuki Fukizawa[1], Takeshi Sakanoi[1], Yoshizumi Miyoshi[2], Keisuke Hosokawa[3], Yoichi Kazama[4], Yoshiya Kasahara[5], Shoya Matsuda[6], Ayako Matsuoka[7], Wang Shiang-Yu[4], Sunny Wing-Yee Tam[8], Ryuho Kataoka[9] (1.Planetary Plasma and Atmospheric Research Center, Graduate School of Science, Tohoku University, 2.Institute for Space-Earth Environmental Research, Nagoya University, 3.Department of Communication Engineering and Informatics, University of Electro-Communications, 4.Academia Sinica Institute of Astronomy and Astrophysics, 5.Information Media Center, Kanazawa University, 6.Institute of Space and Astronautical Science/Japan Aerospace Exploration Agency, 7.Research Division for Space Plasma, Institute of Space and Astronautical Science, Japan Aerospace Exploration Agency, 8.Institute of Space and Plasma Sciences, College of Sciences, National Cheng Kung University , 9.National Institute of Polar Research)

[PEM13-P06] Automatic determination of Upper Hybrid Resonance Frequencies by Convolutional Neural Network.

*Shoya Matsuda[1], Tatsuhito Hasegawa[2], Atsushi Kumamoto[3], Fuminori Tsuchiya[3], Yoshiya Kasahara[4], Yoshizumi Miyoshi[5], Yasumasa Kasaba[3], Ayako Matsuoka[1] (1.Institute of Space and Astronautical Science/Japan Aerospace Exploration Agency, 2.University of Fukui, 3.Tohoku University, 4.Kanazawa University, 5.ISEE, Nagoya University)

[PEM13-P07] Amplitude dependence of whistler wave motion on electron scattering process

*Yoshiki Ito[1], Yoshizumi Miyoshi[1], Shinji Saito[1] (1.Nagoya University, ISEE)

[PEM13-P08] Two-dimensional simulation of whistler mode wave packets interacting with energetic electrons

*Takeshi Nogi[1], Yoshiharu Omura[1] (1.Reserch Institute for Sustainable Humanosphere, Kyoto University)

[PEM13-P09] Relativistic electron acceleration by whistler-mode chorus waves in 1D, 2D, and 3D magnetic field models.

*Keita Takahashi[1], Yoshiharu Omura[1], Yikai HSIEH[1], Danny Summers[2] (1.Research Institute for Sustainable Humanosphere, Kyoto University , 2.Department of Mathematics and Statistics, Memorial University of Newfoundland)

[PEM13-P10] Study of global spatio-temporal development of magnetospheric ELF/VLF waves for the 26-30 March 2017 storm based on ground and satellite observations and the RAM simulations

*Yuhei Takeshita[1], Kazuo Shiokawa[1], Yoshizumi Miyoshi[1], Mitsunori Ozaki[2], Yoshiya Kasahara[2], Martine Connors[3], Jyrki Manninen[4], Craig Kletzing[5], Vania Jordanova[6] (1.Nagoya University, Institute for Space-Earth Environmental Resarch, 2.Kanazawa University, 3.Athabasca University, 4.Sodankylä Geophysical Observatory, 5.The University of Iowa, 6.Los Alamos National Laboratory)

[PEM13-P11] Flux decrease of outer radiation belt electrons associated with solar wind pressure pulse: A Code coupling simulation of GEMSIS-RB and GEMSIS-GM

*Ito Hiroki[1], Yoshizumi Miyoshi[1], Shinji Saito[2], Yosuke Matsumoto[3], Takanobu Amano[4] (1.Institute for Space-Earth Environmental Research, Nagoya University, 2. Graduate School of Science, Nagoya University, 3. Graduate School of Science, Chiba University, 4.Department of Earth and Planetary Science, University of Tokyo)

[PEM13-P12] Non-diffusive response of outer belt electrons on interplanetary shock

Takuma Toishi[1], *Yusuke Ebihara[1], Takashi Tanaka[2] (1.Research Institute for Sustainable Humanosphere, Kyoto University, 2.Kyushu University)

[PEM13-P13] PARM: Initial result of the auroral camera on the G-CHASER (RockSat-XN) rocket and status of the development of auroral cameras for the LAMP rocket experiment

*Naoshi Yagi[1], Takeshi Sakanoi[1], Fukizawa Mizuki[1], Kazushi Asamura[2], Yoshizumi Miyoshi[3], Keisuke Hosokawa[4], Genki Ishizawa[5] (1.Planetary Plasma and Atmospheric Research Center, Graduate School of Science, Tohoku University, 2.Institute of Space and Astronautical Science, Japan Aerospace Exploration Agency, 3.Institute for Space-Earth Environmental Research, Nagoya University, 4.Department of Communication Engineering and Informatics, University of Electro-Communications, 5.Space & terrestrial plasma pyhsics)

[PEM13-P14] First simultaneous observation of a SAR arc at subauroral latitudes using a ground all-sky camera and the Arase satellite in the inner magnetosphere

*Yudai Inaba[1], Kazuo Shiokawa[1], Shin-ichiro Oyama[1,8,9], Yuichi Otsuka[1], Atsuki Shinbori[1], Yoichi Kazama[2], Shiang-Yu Wang[2], Sunny W. Y. Tam[2], Shoichiro Yokota[3], Satoshi Kasahara[4], Kunihiro Keika[4], Tomoaki Hori[1], Ayako Matsuoka[5], Yoshiya Kasahara[6], Atsushi Kumamoto[7], Yasumasa Kasaba[7], Yoshizumi Miyoshi[1], Iku Shinohara[5], Arto Oksanen[10] (1.Institute for Space-Earth Environmental Research, 2.Academia Sinica, 3.Osaka Univ, 4.Tokyo Univ, 5.JAXA, 6.Kanazawa University, 7.Tohoku University, 8.University of Oulu, Finland, 9.National Institute of Polar Research, 10.Jyväskylän Sirius ry, Finland)

[PEM13-P15] Pi2 pulsations observed by the Arase satellite inside and outside the plasmapause

*Mariko Teramoto[1], Ayako Matsuoka[2], Reiko Nomura[5], Yoshiya Kasahara[3], Yasumasa Kasaba[4], Atsushi Kumamoto[4], Fuminori Tsuchiya[4], Shoya Matsuda[2], Masahito Nose[1], Masafumi Shoji[1], Yasunori Tsugawa[1], Shun Imajo[1], Yoshizumi Miyoshi[1], Iku Shinohara[2] (1.Institute for Space-Earth Environmental Research Nagoya University, 2.Institute of Space and Astronautical Science, Japan Aerospace eXploration Agency, 3.Kanazawa University, 4.Tohoku University, 5.National Astronomical Observatory of Japan)

[PEM13-P16] An extreme erosion of the plasmasphere during the 7–10 September 2017 storm

*Yuki Obana[1], Naomi Maruyama[2,3], Atsuki Shinbori[4], Kumiko K. Hashimoto[5], Mariangel Fedrizzi[2,3], Masahito Nose[4], Yuichi Otsuka[4], Nozomu Nishitani[4], Tomoaki Hori[4], Atsushi Kumamoto[6], Fuminori Tsuchiya[6], Shoya Matsuda[7], Ayako Matsuoka[7], Yoshiya Kasahara[8], Akimasa Yoshikawa[9], Yoshizumi Miyoshi[4], Iku Shinohara[7] (1.Osaka Electro-Communication University, 2.University of Colorado Boulder, 3.NOAA Space Weather Prediction Center, 4.Nagoya

University, 5.Kibi International University, 6.Tohoku University, 7.Japan Aerospace Exploration Agency, 8.Kanazawa University, 9.Kyushu University)

[PEM13-P17] Relative contribution of ULF and chorus waves to the radiation belt variation: Comparison between multi-point observations and BATSRUS + CRCM simulation

*Naoko Takahashi[1], Kanako Seki[1], Mei-Ching Fok[2], Yihua Zheng[2], Yoshizumi Miyoshi[3], David Hartley[4], Ayako Matsuoka[5], Yoshiya Kasahara[6], Yasumasa Kasaba[7], Nana Higashio[8] (1.Graduate School of Science, University of Tokyo, 2.NASA Goddard Space Flight Center, 3.Institute for Space-Earth Environmental Research, Nagoya University, 4.Department of Physics and Astronomy, University of Iowa, 5.Institute of Space and Astronautical Science, Japan Aerospace Exploration Agency, 6.Information Media Center, Kanazawa University, 7.Planetary Plasma and Atmospheric Research Center, Tohoku University, 8.Japan Aerospace Exploration Agency)

[PEM13-P18] Modulation of the D-region ionosphere by Pc5 waves observed by VLF/LF standard radio waves

*Miyashita Takuya[1], Hiroyo Ohya[1], Fuminori Tsuchiya[2], Hiroyuki Nakata[1], Toshiaki Takano[1], Kazuo Shiokawa[3], Yoshizumi Miyoshi[3] (1.Chiba University, 2.Tohoku University, 3.Nagoya University)

[PEM13-P19] Oxygen-proton differences in ion energies dominating plasma pressure: Dependence on storm phases and solar wind drivers

*Kunihiro Keika[1], Satoshi Kasahara[1], Shoichiro Yokota[2], Masahiro Hoshino[1], Kanako Seki[1], Masahito Nose[3], Yoshizumi Miyoshi[3], Iku Shinohara[4] (1.Graduate School of Science, The University of Tokyo , 2.Graduate School of Science, Osaka University, 3.Institute for Space-Earth Environmental Research, Nagoya University, 4.Institute of Space and Astronautical Science, Japan Aerospace Exploration Agency)

[PEM13-P20] Mass dependence of penetration depth of multi-energy ions in the inner magnetosphere during magnetic storms: Arase observations

*Ryosuke Fujii[1], Yoshizumi Miyoshi[1], Masafumi Shoji[1], Kazushi Asamura[2], Lynn Kistler[1,8], Vania Jordanova[9], Tomoaki Hori[1], Satoshi Kurita[1], Mariko Teramoto[1], Yasunori Tsugawa[1], Yoshiya Kasahara[3], Yasumasa Kasaba[4], Atsushi Kumamoto[5], Fuminori Tsuchiya[4], Shoichiro Yokota[6], Kunihiro Keika[7], Ayako Matsuoka[2], Iku Shinohara[2] (1.Institute for Space-Earth Environmental Research, Nagoya University, 2.Institute of Space and Astronautical Science, Japan Aerospace Exploration Agency, 3.Information Media Center, Kanazawa University, 4.Planetary Plasma and Atmospheric Research Center, Tohoku University, 5.Department of Geophysics, Graduate School of Science, Tohoku University, 6.Graduate School of Science, Osaka University, 7.Department of Earth and Planetary Science, Graduate School of Science, The University of Tokyo, 8.University of New Hampshire, 9.Los Alamos National Laboratory)

[PEM13-P21] Relativistic Acceleration of Energetic Protons by Electromagnetic Ion Cyclotron Waves in the Jovian Magnetosphere

*Tomohiro Sekine[1], Yoshiharu Omura[1], Danny Summers[2], Yikai HSIEH[1], Satoko Nakamura[1] (1.Reserach Institute for Sustainable Humanosphere, Kyoto University, 2.Memorial University of Newfoundland)

[PEM13-P22] Statistical study of IPDP type EMIC wave-related electron precipitation at subauroral latitude

*Asuka Hirai[1], Fuminori Tsuchiya[1], Takahiro Obara[1], Yasumasa Kasaba[1], Yuto Katoh[2], Hiroaki Misawa[1], Kazuo Shiokawa[3], Yoshizumi Miyoshi[3], Satoshi Kurita[3], Martin G Connors[4] (1.Planetary Plasma and Atmospheric Research Center, Graduate School of Science, Tohoku Univ. , 2.Department of Geophysics, Graduate School of Science, Tohoku University, 3.Institute for Space-Earth Environmental Research, Nagoya University, 4.Athabasca University)

[PEM13-P23] Meridional distributions of proton plasma and pressure-driven currents in the nightside inner magnetosphere: Arase observations

*Shun Imajo[1], Masahito Nose[1], Satoshi Kasahara[2], Shoichiro Yokota[3], Ayako Matsuoka[4], Kunihiro Keika[2], Tomoaki Hori[1], Mariko Teramoto[1], Kazuhiro Yamamoto[5], Oimatsu Satoshi[5], Reiko Nomura[6], Akiko Fujimoto[7], Iku Shinohara[4], Yoshizumi Miyoshi[1] (1.Institute for Space-Earth Environmental Research, Nagoya University, 2.Graduate School of Science, The University of Tokyo, 3.Graduate School of Science, Osaka University, 4.Institute of Space and Astronautical Science, Japan Aerospace Exploration Agency, 5.Graduate School of Science, Kyoto University, 6.National Astronomical Observatory of Japan, 7.Kyushu Institute of Technology)

[PEM13-P24] Space Weather Effects on Energetic Proton Flux Response in South Atlantic Anomaly

*Kirolosse Mina GIRGIS[1,2], Tohru Hada[1], Shuichi Matsukiyo[1] (1.Earth System Science and Technology (ESST) Department, Interdisciplinary Graduate School of Engineering Sciences (IGSES), Kyushu University, Japan, 2.Aerospace Engineering Department, Faculty of Engineering, Cairo University, Egypt)

[PEM13-P25] Solar-cycle variations of >30 keV electron flux enhancements under the inner radiation belt

*ALLA SUVOROVA[1] (1.National Central University)

[PEM13-P26] Energy spectra variations of high energy electrons in the inner magnetosphere observed by HEP/XEP on ARASE and SEDA-e on HIMAWARI

*Takeshi Takashima[1], Takefumi Mitani[1], Nana Higashio[2], Tsutomu Nagatsuma[3] (1. ISAS/JAXA, 2.Research and Development Directorate/JAXA, 3.NiCT)

[PEM13-P27] Inter-channel calibration of the high-energy electron experiments (HEP) instrument onboard the Arase satellite

*Tomoaki Hori[1], Takefumi Mitani[2], Takeshi Takashima[2], Park Inchun[1], Satoshi Kurita[1], Mariko Teramoto[1], Nana Higashio[3], Satoshi Kasahara[4], Shoichiro Yokota[5], Yoshizumi Miyoshi[1], Iku Shinohara[2] (1.Institute for Space-Earth Environmental Research, Nagoya University, 2.Japan Aerospace Exploration Agency, Institute of Space and Astronautical Science, 3.Japan Aerospace Exploration Agency, 4.Graduate School of Science, The University of Tokyo, 5.Graduate School of Science, Osaka University)

[PEM13-P28] Particle simulation for calibrating the HEP data onboard the ARASE satellite

*PARK INCHUN[1], Yoshizumi Miyoshi[1], Takefumi Mitani[2], Tomoaki Hori[1], Satoshi Kurita[1], Mariko Teramoto[1], Takeshi Takashima[2], Nana Higashio[3], Iku Shinohara[2] (1.Nagoya University Institute for Space-Earth Environmental Research, 2.Japan Aerospace Exploration Agency Institute of Space and Astronautical Science , 3.Japan Aerospace Exploration Agency)

[PEM13-P29] Geant4 model calculation and energetic particle observation with HEP/Arase in the inner radiation belt

*Honoka Toda[1], Wataru Miyake[1], Takefumi Mitani[3], Takeshi Takashima[3], Yoshizumi Miyoshi[2], PARK INCHUN[2], Tomoaki Hori[2] (1.Tokai University, 2.ISEE/Nagoya University, 3.ISAS/JAXA)

[PEM13-P30] Validation of High-energy electron detector simulator for the HEP instruments onboard Arase

*Takefumi Mitani[1], PARK INCHUN[2], Tomoaki Hori[2], Taku Namekawa[1,3], Kazushi Asamura[1], Takeshi Takashima[1], Satoshi Kasahara[3], Satoshi Kurita[2], Mariko Teramoto[2], Nana Higashio[1], Yoshizumi Miyoshi[2], Iku Shinohara[1] (1.Japan Aerospace Exploration Agency, Institute of Space and Astronautical Science, 2.Institute for Space-Earth Environmental Research, Nagoya Univ., 3.The university of Tokyo)

[E] Poster | P (Space and Planetary Sciences)：P-EM Solar-Terrestrial Sciences, Space Electromagnetism & Space Environment

5:15 PM - 6:30 PM JST | 8:15 AM - 9:30 AM UTC | Poster Hall International Exhibition Hall8, Makuhari Messe_6

[P-EM13] Inner magnetosphere: Recent understanding and new insights

convener:Yusuke Ebihara(Research Institute for Sustainable Humanosphere, Kyoto University), Danny Summers(Memorial University of Newfoundland), Yoshizumi Miyoshi(Institute for Space-Earth Environmental Research, Nagoya University), Shinji Saito(Graduate School of Science, Nagoya University)

[PEM13-P01] Evaluation of wave normal and Poynting vector analyses for whistler mode waves observed by the waveform capture (WFC) on board the Arase

*Yoshiya Kasahara[1], Satoshi Ikarashi[1], Hiroyuki Nishizawa[1], Shoya Matsuda[2], Fuminori Tsuchiya[3], Atsushi Kumamoto[3], Yasumasa Kasaba[3], Mitsunori Ozaki[1], Ayako Matsuoka[2] (1.Kanazawa University, 2.ISAS/JAXA, 3.Tohoku University)

[PEM13-P02] Calibration of electric fields dedicated to the measurement of the S-WPIA of the Arase Satellite

*Miki Jumpei[1], Hirotsugu Kojima[2], Yuto Katoh[3], Shoya Matsuda[4], Yoshiya Kasahara[5], Mitsuru Hikishima[4], Satoshi Kurita[6], Masahiro Kitahara[3], Satoshi Kasahara[7], Yoshizumi Miyoshi[6], Atsushi Kumamoto[3], Ayako Matsuoka[4], Shoichiro Yokota[8], Tomoaki Hori[6], Kunihiro Keika[7] (1.Space Radio Engineering Laboratory, Division of Electrical Engineering, Kyoto University Graduated School, 2.Research Institute for Sustainable Humanosphere, Kyoto University, 3.Graduate School of Science and Faculty of Science, Tohoku University, 4.Institute of Space and Astronautical Science, JAXA, 5.Information Media Center, Kanazawa University, 6.Institute for Space-Earth Environmental Research, Nagoya University, 7.School of Science, The University of Tokyo, 8.School of Science, Osaka University)

[PEM13-P03] Enhancement of whistler-mode chorus in association with Pc 4-5 ULF waves and related variation of high energy electrons

*Atsuhiro Ono[1], Yuto Katoh[1], Atsushi Kumamoto[1], Fuminori Tsuchiya[1], Mariko Teramoto[2], Yoshiya Kasahara[3], Shoya Matsuda[4], Ayako Matsuoka[4], Takefumi Mitani[4], Tomoaki Hori[2], Satoshi Kasahara[5], Shoichiro Yokota[6], Kunihiro Keika[5], Yoshizumi Miyoshi[2], Iku Shinohara[4] (1.Tohoku University, 2.Nagoya University, 3.Kanazawa University, 4.ISAS/JAXA, 5.The University of Tokyo, 6.Osaka University)

[PEM13-P04] Sudden enhancements of electron cyclotron harmonic waves observed by the Arase satellite

*Shinjo Airi[1], Hirotsugu Kojima[1], Yoshiya Kasahara[2], Yoichi Kazama[3], Hideyuki Usui[4], Yoshizumi Miyoshi[5], Yasumasa Kasaba[6], Shoya Matsuda[7], Tomoaki Hori[5], S. -Y. Wang[8], Sunny W.Y. Tam[9], Atsushi Kumamoto[10], Ayako Matsuoka[11] (1.Research institute for sustainable humanosphere, Kyoto University, 2.Information Media Center, Kanazawa University, 3.ASIAA, 4.Graduate school of system informatics Kobe University, 5.Institute for Space-Earth Environmental Research, Nagoya University, 6.Planetary Plasma and Atmospheric Research Center, Tohoku University, 7.Institute of Space and Astronautical Science/Japan Aerospace Exploration Agency, 8.ASIAA, Taiwan, 9.ISAPS, NCKU, Taiwan, 10.Department of Geophysics, Graduate School of Science, Tohoku University, 11.Research Division for Space Plasma, Institute of Space and Astronautical Science, Japan Aerospace Exploration Agency)

[PEM13-P05] Correlation between pulsating aurora and electrostatic electron cyclotron harmonic waves obtained from coordinated Arase and ground data

*Mizuki Fukizawa[1], Takeshi Sakanoi[1], Yoshizumi Miyoshi[2], Keisuke Hosokawa[3], Yoichi Kazama[4], Yoshiya Kasahara[5], Shoya Matsuda[6], Ayako Matsuoka[7], Wang Shiang-Yu[4], Sunny Wing-Yee Tam[8], Ryuho Kataoka[9] (1.Planetary Plasma and Atmospheric Research Center, Graduate School of Science, Tohoku University, 2.Institute for Space-Earth Environmental Research, Nagoya University, 3.Department of Communication Engineering and Informatics, University of Electro-Communications, 4.Academia Sinica Institute of Astronomy and Astrophysics, 5.Information Media Center, Kanazawa University, 6.Institute of Space and Astronautical Science/Japan Aerospace Exploration Agency, 7.Research Division for Space Plasma, Institute of Space and Astronautical Science, Japan Aerospace Exploration Agency, 8.Institute of Space and Plasma Sciences, College of Sciences, National Cheng Kung University , 9.National Institute of Polar Research)

[PEM13-P06] Automatic determination of Upper Hybrid Resonance Frequencies by Convolutional Neural Network.

*Shoya Matsuda[1], Tatsuhito Hasegawa[2], Atsushi Kumamoto[3], Fuminori Tsuchiya[3], Yoshiya Kasahara[4], Yoshizumi Miyoshi[5], Yasumasa Kasaba[3], Ayako Matsuoka[1] (1.Institute of Space and Astronautical Science/Japan Aerospace Exploration Agency, 2.University of Fukui, 3.Tohoku University, 4.Kanazawa University, 5.ISEE, Nagoya University)

[PEM13-P07] Amplitude dependence of whistler wave motion on electron scattering process

*Yoshiki Ito[1], Yoshizumi Miyoshi[1], Shinji Saito[1] (1.Nagoya University, ISEE)

[PEM13-P08] Two-dimensional simulation of whistler mode wave packets interacting with energetic electrons

*Takeshi Nogi[1], Yoshiharu Omura[1] (1.Reserch Institute for Sustainable Humanosphere, Kyoto University)

[PEM13-P09] Relativistic electron acceleration by whistler-mode chorus waves in 1D, 2D, and 3D magnetic field models.

*Keita Takahashi[1], Yoshiharu Omura[1], Yikai HSIEH[1], Danny Summers[2] (1.Research Institute for Sustainable Humanosphere, Kyoto University , 2.Department of Mathematics and Statistics, Memorial University of Newfoundland)

[PEM13-P10] Study of global spatio-temporal development of magnetospheric ELF/VLF waves for the 26-30 March 2017 storm based on ground and satellite observations and the RAM simulations

*Yuhei Takeshita[1], Kazuo Shiokawa[1], Yoshizumi Miyoshi[1], Mitsunori Ozaki[2], Yoshiya Kasahara[2], Martine Connors[3], Jyrki Manninen[4], Craig Kletzing[5], Vania Jordanova[6] (1.Nagoya University, Institute for Space-Earth Environmental Resarch, 2.Kanazawa University, 3.Athabasca University, 4.Sodankylä Geophysical Observatory, 5.The University of Iowa, 6.Los Alamos National Laboratory)

[PEM13-P11] Flux decrease of outer radiation belt electrons associated with solar wind pressure pulse: A Code coupling simulation of GEMSIS-RB and GEMSIS-GM

*Ito Hiroki[1], Yoshizumi Miyoshi[1], Shinji Saito[2], Yosuke Matsumoto[3], Takanobu Amano[4] (1.Institute for Space-Earth Environmental Research, Nagoya University, 2. Graduate School of Science, Nagoya University, 3. Graduate School of Science, Chiba University, 4.Department of Earth and Planetary Science, University of Tokyo)

[PEM13-P12] Non-diffusive response of outer belt electrons on interplanetary shock

Takuma Toishi[1], *Yusuke Ebihara[1], Takashi Tanaka[2] (1.Research Institute for Sustainable Humanosphere, Kyoto University, 2.Kyushu University)

[PEM13-P13] PARM: Initial result of the auroral camera on the G-CHASER (RockSat-XN) rocket and status of the development of auroral cameras for the LAMP rocket experiment

*Naoshi Yagi[1], Takeshi Sakanoi[1], Fukizawa Mizuki[1], Kazushi Asamura[2], Yoshizumi Miyoshi[3], Keisuke Hosokawa[4], Genki Ishizawa[5] (1.Planetary Plasma and Atmospheric Research Center, Graduate School of Science, Tohoku University, 2.Institute of Space and Astronautical Science, Japan Aerospace Exploration Agency, 3.Institute for Space-Earth Environmental Research, Nagoya University, 4.Department of Communication Engineering and Informatics, University of Electro-Communications, 5.Space & terrestrial plasma pyhsics)

[PEM13-P14] First simultaneous observation of a SAR arc at subauroral latitudes using a ground all-sky camera and the Arase satellite in the inner magnetosphere

*Yudai Inaba[1], Kazuo Shiokawa[1], Shin-ichiro Oyama[1,8,9], Yuichi Otsuka[1], Atsuki Shinbori[1], Yoichi Kazama[2], Shiang-Yu Wang[2], Sunny W. Y. Tam[2], Shoichiro Yokota[3], Satoshi Kasahara[4], Kunihiro Keika[4], Tomoaki Hori[1], Ayako Matsuoka[5], Yoshiya Kasahara[6], Atsushi Kumamoto[7], Yasumasa Kasaba[7], Yoshizumi Miyoshi[1], Iku Shinohara[5], Arto Oksanen[10] (1.Institute for Space-Earth Environmental Research, 2.Academia Sinica, 3.Osaka Univ, 4.Tokyo Univ, 5.JAXA, 6.Kanazawa University, 7.Tohoku University, 8.University of Oulu, Finland, 9.National Institute of Polar Research, 10.Jyväskylän Sirius ry, Finland)

[PEM13-P15] Pi2 pulsations observed by the Arase satellite inside and outside the plasmapause

*Mariko Teramoto[1], Ayako Matsuoka[2], Reiko Nomura[5], Yoshiya Kasahara[3], Yasumasa Kasaba[4], Atsushi Kumamoto[4], Fuminori Tsuchiya[4], Shoya Matsuda[2], Masahito Nose[1], Masafumi Shoji[1], Yasunori Tsugawa[1], Shun Imajo[1], Yoshizumi Miyoshi[1], Iku Shinohara[2] (1.Institute for Space-Earth Environmental Research Nagoya University, 2.Institute of Space and Astronautical Science, Japan Aerospace eXploration Agency, 3.Kanazawa University, 4.Tohoku University, 5.National Astronomical Observatory of Japan)

[PEM13-P16] An extreme erosion of the plasmasphere during the 7–10 September 2017 storm

*Yuki Obana[1], Naomi Maruyama[2,3], Atsuki Shinbori[4], Kumiko K. Hashimoto[5], Mariangel Fedrizzi[2,3], Masahito Nose[4], Yuichi Otsuka[4], Nozomu Nishitani[4], Tomoaki Hori[4], Atsushi Kumamoto[6], Fuminori Tsuchiya[6], Shoya Matsuda[7], Ayako Matsuoka[7], Yoshiya Kasahara[8], Akimasa Yoshikawa[9], Yoshizumi Miyoshi[4], Iku Shinohara[7] (1.Osaka Electro-Communication University, 2.University of Colorado Boulder, 3.NOAA Space Weather Prediction Center, 4.Nagoya

University, 5.Kibi International University, 6.Tohoku University, 7.Japan Aerospace Exploration Agency, 8.Kanazawa University, 9.Kyushu University)

[PEM13-P17] Relative contribution of ULF and chorus waves to the radiation belt variation: Comparison between multi-point observations and BATSRUS + CRCM simulation

*Naoko Takahashi[1], Kanako Seki[1], Mei-Ching Fok[2], Yihua Zheng[2], Yoshizumi Miyoshi[3], David Hartley[4], Ayako Matsuoka[5], Yoshiya Kasahara[6], Yasumasa Kasaba[7], Nana Higashio[8] (1.Graduate School of Science, University of Tokyo, 2.NASA Goddard Space Flight Center, 3.Institute for Space-Earth Environmental Research, Nagoya University, 4.Department of Physics and Astronomy, University of Iowa, 5.Institute of Space and Astronautical Science, Japan Aerospace Exploration Agency, 6.Information Media Center, Kanazawa University, 7.Planetary Plasma and Atmospheric Research Center, Tohoku University, 8.Japan Aerospace Exploration Agency)

[PEM13-P18] Modulation of the D-region ionosphere by Pc5 waves observed by VLF/LF standard radio waves

*Miyashita Takuya[1], Hiroyo Ohya[1], Fuminori Tsuchiya[2], Hiroyuki Nakata[1], Toshiaki Takano[1], Kazuo Shiokawa[3], Yoshizumi Miyoshi[3] (1.Chiba University, 2.Tohoku University, 3.Nagoya University)

[PEM13-P19] Oxygen-proton differences in ion energies dominating plasma pressure: Dependence on storm phases and solar wind drivers

*Kunihiro Keika[1], Satoshi Kasahara[1], Shoichiro Yokota[2], Masahiro Hoshino[1], Kanako Seki[1], Masahito Nose[3], Yoshizumi Miyoshi[3], Iku Shinohara[4] (1.Graduate School of Science, The University of Tokyo , 2.Graduate School of Science, Osaka University, 3.Institute for Space-Earth Environmental Research, Nagoya University, 4.Institute of Space and Astronautical Science, Japan Aerospace Exploration Agency)

[PEM13-P20] Mass dependence of penetration depth of multi-energy ions in the inner magnetosphere during magnetic storms: Arase observations

*Ryosuke Fujii[1], Yoshizumi Miyoshi[1], Masafumi Shoji[1], Kazushi Asamura[2], Lynn Kistler[1,8], Vania Jordanova[9], Tomoaki Hori[1], Satoshi Kurita[1], Mariko Teramoto[1], Yasunori Tsugawa[1], Yoshiya Kasahara[3], Yasumasa Kasaba[4], Atsushi Kumamoto[5], Fuminori Tsuchiya[4], Shoichiro Yokota[6], Kunihiro Keika[7], Ayako Matsuoka[2], Iku Shinohara[2] (1.Institute for Space-Earth Environmental Research, Nagoya University, 2.Institute of Space and Astronautical Science, Japan Aerospace Exploration Agency, 3.Information Media Center, Kanazawa University, 4.Planetary Plasma and Atmospheric Research Center, Tohoku University, 5.Department of Geophysics, Graduate School of Science, Tohoku University, 6.Graduate School of Science, Osaka University, 7.Department of Earth and Planetary Science, Graduate School of Science, The University of Tokyo, 8.University of New Hampshire, 9.Los Alamos National Laboratory)

[PEM13-P21] Relativistic Acceleration of Energetic Protons by Electromagnetic Ion Cyclotron Waves in the Jovian Magnetosphere

*Tomohiro Sekine[1], Yoshiharu Omura[1], Danny Summers[2], Yikai HSIEH[1], Satoko Nakamura[1] (1.Reserach Institute for Sustainable Humanosphere, Kyoto University, 2.Memorial University of Newfoundland)

[PEM13-P22] Statistical study of IPDP type EMIC wave-related electron precipitation at subauroral latitude

*Asuka Hirai[1], Fuminori Tsuchiya[1], Takahiro Obara[1], Yasumasa Kasaba[1], Yuto Katoh[2], Hiroaki Misawa[1], Kazuo Shiokawa[3], Yoshizumi Miyoshi[3], Satoshi Kurita[3], Martin G Connors[4] (1.Planetary Plasma and Atmospheric Research Center, Graduate School of Science, Tohoku Univ. , 2.Department of Geophysics, Graduate School of Science, Tohoku University, 3.Institute for Space-Earth Environmental Research, Nagoya University, 4.Athabasca University)

[PEM13-P23] Meridional distributions of proton plasma and pressure-driven currents in the nightside inner magnetosphere: Arase observations

*Shun Imajo[1], Masahito Nose[1], Satoshi Kasahara[2], Shoichiro Yokota[3], Ayako Matsuoka[4], Kunihiro Keika[2], Tomoaki Hori[1], Mariko Teramoto[1], Kazuhiro Yamamoto[5], Oimatsu Satoshi[5], Reiko Nomura[6], Akiko Fujimoto[7], Iku Shinohara[4], Yoshizumi Miyoshi[1] (1.Institute for Space-Earth Environmental Research, Nagoya University, 2.Graduate School of Science, The University of Tokyo, 3.Graduate School of Science, Osaka University, 4.Institute of Space and Astronautical Science, Japan Aerospace Exploration Agency, 5.Graduate School of Science, Kyoto University, 6.National Astronomical Observatory of Japan, 7.Kyushu Institute of Technology)

[PEM13-P24] Space Weather Effects on Energetic Proton Flux Response in South Atlantic Anomaly

*Kirolosse Mina GIRGIS[1,2], Tohru Hada[1], Shuichi Matsukiyo[1] (1.Earth System Science and Technology (ESST) Department, Interdisciplinary Graduate School of Engineering Sciences (IGSES), Kyushu University, Japan, 2.Aerospace Engineering Department, Faculty of Engineering, Cairo University, Egypt)

[PEM13-P25] Solar-cycle variations of >30 keV electron flux enhancements under the inner radiation belt

*ALLA SUVOROVA[1] (1.National Central University)

[PEM13-P26] Energy spectra variations of high energy electrons in the inner magnetosphere observed by HEP/XEP on ARASE and SEDA-e on HIMAWARI

*Takeshi Takashima[1], Takefumi Mitani[1], Nana Higashio[2], Tsutomu Nagatsuma[3] (1. ISAS/JAXA, 2.Research and Development Directorate/JAXA, 3.NiCT)

[PEM13-P27] Inter-channel calibration of the high-energy electron experiments (HEP) instrument onboard the Arase satellite

*Tomoaki Hori[1], Takefumi Mitani[2], Takeshi Takashima[2], Park Inchun[1], Satoshi Kurita[1], Mariko Teramoto[1], Nana Higashio[3], Satoshi Kasahara[4], Shoichiro Yokota[5], Yoshizumi Miyoshi[1], Iku Shinohara[2] (1.Institute for Space-Earth Environmental Research, Nagoya University, 2.Japan Aerospace Exploration Agency, Institute of Space and Astronautical Science, 3.Japan Aerospace Exploration Agency, 4.Graduate School of Science, The University of Tokyo, 5.Graduate School of Science, Osaka University)

[PEM13-P28] Particle simulation for calibrating the HEP data onboard the ARASE satellite

*PARK INCHUN[1], Yoshizumi Miyoshi[1], Takefumi Mitani[2], Tomoaki Hori[1], Satoshi Kurita[1], Mariko Teramoto[1], Takeshi Takashima[2], Nana Higashio[3], Iku Shinohara[2] (1.Nagoya University Institute for Space-Earth Environmental Research, 2.Japan Aerospace Exploration Agency Institute of Space and Astronautical Science , 3.Japan Aerospace Exploration Agency)

[PEM13-P29] Geant4 model calculation and energetic particle observation with HEP/Arase in the inner radiation belt

*Honoka Toda[1], Wataru Miyake[1], Takefumi Mitani[3], Takeshi Takashima[3], Yoshizumi Miyoshi[2], PARK INCHUN[2], Tomoaki Hori[2] (1.Tokai University, 2.ISEE/Nagoya University, 3.ISAS/JAXA)

[PEM13-P30] Validation of High-energy electron detector simulator for the HEP instruments onboard Arase

*Takefumi Mitani[1], PARK INCHUN[2], Tomoaki Hori[2], Taku Namekawa[1,3], Kazushi Asamura[1], Takeshi Takashima[1], Satoshi Kasahara[3], Satoshi Kurita[2], Mariko Teramoto[2], Nana Higashio[1], Yoshizumi Miyoshi[2], Iku Shinohara[1] (1.Japan Aerospace Exploration Agency, Institute of Space and Astronautical Science, 2.Institute for Space-Earth Environmental Research, Nagoya Univ., 3.The university of Tokyo)

[E] Poster | A (Atmospheric and Hydrospheric Sciences)：A-AS Atmospheric Sciences, Meteorology & Atmospheric Environment

3:30 PM - 5:00 PM JST | 6:30 AM - 8:00 AM UTC | Poster Hall International Exhibition Hall8, Makuhari Messe_5

[A-AS01] High performance computing for next generation weather, climate, and environmental sc iences

convener:Hiromu Seko(Meteorological Research Institute), Takemasa Miyoshi(RIKEN), Chihiro Kodama(Japan Agency for Marine-Earth Science and Technology), Masayuki Takigawa(Japan Agency for Marine-Earth Science and Technology)

[AAS01-P01] **Categorized correction forecast for accumulative precipitation of heavy rainfall processes based on optimal probability (OPPF) in medium-extended-range forecast time**

*Ruoyun Niu[1] (1.National Meteorological Center)

[AAS01-P02] **Characteristics of temporal and spatial distribution of regional rainstorm processes to the east of 95°E in China during 1981-2015**

*Ruoyun Niu[1], Couhua Liu[1] (1.National Meteorological Center)

[AAS01-P03] Near-real-time SCALE-LETKF forecasts of the record breaking rainfall in Japan in July 2018

*Takumi Honda[1], Guo-Yuan Lien[2,1], Takemasa Miyoshi[1] (1.RIKEN Center for Computational Science, 2.Central Weather Bureau)

[AAS01-P04] An objective Frontal Analysis Techniques and Application in Model Verification

*couhua liu[1] (1.National Meteorology Centre of China Meteorological Administration)

[AAS01-P05] Assimilating every 30-second phased array weather radar data in a torrential rainfall event on July 6, 2018 around Kobe city

*Yasumitsu Maejima[1], Shigenori Otsuka[1], Takemasa Miyoshi[1,2] (1.RIKEN Center for Computational Science, 2.University of Maryland, College Park)

[AAS01-P06] The impact of range sidelobes from phased array weather radar observations to short-range convective forecasts

*James David Taylor[1], Guo-Yuan Lien[1], Shinsuke Satoh[2], Takemasa Miyoshi[1] (1.RIKEN Research center for computational science, 2.NICT National Institute of Information and Communications Technology)

[AAS01-P07] Development of Hydro-debris 2D model for larger area

*Yosuke Alexandre Yamashiki[1], Tsutao OIZUMI[2], Bruno Ribeiro[1], Ryusuke Kuroki[1] (1.Earth & Planetary Water Resources Assessment Laboratory Graduate School of Advanced Integrated Studies in Human Survivability Kyoto University, 2.Japan Association of Marine-Earth Science and Tecnology)

[AAS01-P08] **Research on the application of an improved terrain-following vertical coordinates on GRAPES model**

*chao li[1] (1.NWPC.CMA)

[AAS01-P09] Development of a parallel spherical harmonic transform library: design and performance

*Fuyuki SAITO[1] (1.Japan Agency for Marine-Earth Science and Technology)

[AAS01-P10] Global data assimilation of multi-species satellite measurements for atmospheric chemistry analysis

*Takashi Sekiya[1], Kazuyuki Miyazaki[2,1], Koji Ogochi[1], Kengo Sudo[3,1], Masayuki Takigawa[1] (1.Japan Agency for Marine-Earth Science and Technology, 2.Jet Propulsion Laboratory/California Institute for Technology, 3.Graduate School of Environmental Studies, Nagoya University)

[AAS01-P11] The sensitivity to WRF shortwave radiation parameterizations in prediction of global horizontal irradiance for investigating interactions of atmosphere with croplands

*Ankur Srivastava[1], Sarita Kumari[1], Rajkumar Dhakar[2] (1.Indian Institute of Technology Delhi, 2.Indian Agriculture Research Institute)

[AAS01-P12] The development of an atmospheric aerosol/chemistry–climate model, BCC_AGCM_CUACE2.0, and simulated effective radiative forcing of nitrate aerosols

*QI AN[1,2,4], Hua Zhang[2], Zhili Wang[2], Yi Liu[1,4], Bing Xie[3], Qianxia Liu[3], Zaizhi Wang[3], Sunling Gong[2] (1.LAGEO, IAP, CAS, 2.LaSW, CAMS, 3.NCC,CMA, 4.UCAS)

[AAS01-P13] **Impacts of different types and intensities of El Niño events on winter aerosols over China**

*Xiaochao Yu[1,2], Zhili Wang[2,1], Hua Zhang[2], Shuyun Zhao[3] (1.Collaborative Innovation Center on Forecast and Evaluation of Meteorological Disasters, Nanjing University of Information Science and Technology, Nanjing, 210044, China, 2.State Key Laboratory of Severe Weather and Key Laboratory of Atmospheric Chemistry of CMA, Chinese Academy of Meteorological Sciences, Beijing, 100081, China., 3.National Climate Center, China Meteorological Administration, Beijing, 100081, China)

[AAS01-P14] High Cloud Annual Variation and Its Responses to Global Warming in the NICAM AMIP Experiment

*Ying-Wen Chen[1], Masaki Satoh[1,2], Chihiro Kodama[2], Akira Noda[2], Yohei Yamada[2] (1.Atmospheric and Ocean Research Institute, The University of Tokyo , 2.Japan Agency for Marine-Earth Science and Technology)

[AAS01-P15] Improvements in Simulating the Relationship between ENSO and East Asian Summer Rainfall in the CMIP5 Models

*Yuanhai FU[1], Riyu Lu[1] (1.IAP, CAS)

[E] Poster | A (Atmospheric and Hydrospheric Sciences)：A-AS Atmospheric Sciences, Meteorology & Atmospheric Environment

5:15 PM - 6:30 PM JST | 8:15 AM - 9:30 AM UTC | Poster Hall International Exhibition Hall8, Makuhari Messe_9

[A-AS01] High performance computing for next generation weather, climate, and environmental sc iences

convener:Hiromu Seko(Meteorological Research Institute), Takemasa Miyoshi(RIKEN), Chihiro Kodama(Japan Agency for Marine-Earth Science and Technology), Masayuki Takigawa(Japan Agency for Marine-Earth Science and Technology)

[AAS01-P01] **Categorized correction forecast for accumulative precipitation of heavy rainfall processes based on optimal probability (OPPF) in medium-extended-range forecast time**

*Ruoyun Niu[1] (1.National Meteorological Center)

[AAS01-P02] **Characteristics of temporal and spatial distribution of regional rainstorm processes to the east of 95°E in China during 1981-2015**

*Ruoyun Niu[1], Couhua Liu[1] (1.National Meteorological Center)

[AAS01-P03] Near-real-time SCALE-LETKF forecasts of the record breaking rainfall in Japan in July 2018

*Takumi Honda[1], Guo-Yuan Lien[2,1], Takemasa Miyoshi[1] (1.RIKEN Center for Computational Science, 2.Central Weather Bureau)

[AAS01-P04] An objective Frontal Analysis Techniques and Application in Model Verification

*couhua liu[1] (1.National Meteorology Centre of China Meteorological Administration)

[AAS01-P05] Assimilating every 30-second phased array weather radar data in a torrential rainfall event on July 6, 2018 around Kobe city

*Yasumitsu Maejima[1], Shigenori Otsuka[1], Takemasa Miyoshi[1,2] (1.RIKEN Center for Computational Science, 2.University of Maryland, College Park)

[AAS01-P06] The impact of range sidelobes from phased array weather radar observations to short-range convective forecasts

*James David Taylor[1], Guo-Yuan Lien[1], Shinsuke Satoh[2], Takemasa Miyoshi[1] (1.RIKEN Research center for computational science, 2.NICT National Institute of Information and Communications Technology)

[AAS01-P07] Development of Hydro-debris 2D model for larger area

*Yosuke Alexandre Yamashiki[1], Tsutao OIZUMI[2], Bruno Ribeiro[1], Ryusuke Kuroki[1] (1.Earth & Planetary Water Resources Assessment Laboratory Graduate School of Advanced Integrated Studies in Human Survivability Kyoto University, 2.Japan Association of Marine-Earth Science and Tecnology)

[AAS01-P08] **Research on the application of an improved terrain-following vertical coordinates on GRAPES model**

*chao li[1] (1.NWPC.CMA)

[AAS01-P09] Development of a parallel spherical harmonic transform library: design and performance

*Fuyuki SAITO[1] (1.Japan Agency for Marine-Earth Science and Technology)

[AAS01-P10] Global data assimilation of multi-species satellite measurements for atmospheric chemistry analysis

*Takashi Sekiya[1], Kazuyuki Miyazaki[2,1], Koji Ogochi[1], Kengo Sudo[3,1], Masayuki Takigawa[1] (1.Japan Agency for Marine-Earth Science and Technology, 2.Jet Propulsion Laboratory/California Institute for Technology, 3.Graduate School of Environmental Studies, Nagoya University)

[AAS01-P11] The sensitivity to WRF shortwave radiation parameterizations in prediction of global horizontal irradiance for investigating interactions of atmosphere with croplands

*Ankur Srivastava[1], Sarita Kumari[1], Rajkumar Dhakar[2] (1.Indian Institute of Technology Delhi, 2.Indian Agriculture Research Institute)

[AAS01-P12] The development of an atmospheric aerosol/chemistry–climate model, BCC_AGCM_CUACE2.0, and simulated effective radiative forcing of nitrate aerosols

*QI AN[1,2,4], Hua Zhang[2], Zhili Wang[2], Yi Liu[1,4], Bing Xie[3], Qianxia Liu[3], Zaizhi Wang[3], Sunling Gong[2] (1.LAGEO, IAP, CAS, 2.LaSW, CAMS, 3.NCC,CMA, 4.UCAS)

[AAS01-P13] **Impacts of different types and intensities of El Niño events on winter aerosols over China**

*Xiaochao Yu[1,2], Zhili Wang[2,1], Hua Zhang[2], Shuyun Zhao[3] (1.Collaborative Innovation Center on Forecast and Evaluation of Meteorological Disasters, Nanjing University of Information Science and Technology, Nanjing, 210044, China, 2.State Key Laboratory of Severe Weather and Key Laboratory of Atmospheric Chemistry of CMA, Chinese Academy of Meteorological Sciences, Beijing, 100081, China., 3.National Climate Center, China Meteorological Administration, Beijing, 100081, China)

[AAS01-P14] High Cloud Annual Variation and Its Responses to Global Warming in the NICAM AMIP Experiment

*Ying-Wen Chen[1], Masaki Satoh[1,2], Chihiro Kodama[2], Akira Noda[2], Yohei Yamada[2] (1.Atmospheric and Ocean Research Institute, The University of Tokyo , 2.Japan Agency for Marine-Earth Science and Technology)

[AAS01-P15] Improvements in Simulating the Relationship between ENSO and East Asian Summer Rainfall in the CMIP5 Models

*Yuanhai FU[1], Riyu Lu[1] (1.IAP, CAS)

[E] Poster | A (Atmospheric and Hydrospheric Sciences)：A-OS Ocean Sciences & Ocean Environment

10:45 AM - 12:15 PM JST | 1:45 AM - 3:15 AM UTC | Poster Hall International Exhibition Hall8, Makuhari Messe_4

[A-OS08] ECS-Kuroshio and Ryukyu Current System -Observation, modeling and theory-

convener:Hirohiko Nakamura(Kagoshima University, Faculy of Fisheries), Xiao-Hua Zhu(Second Institute of Oceanography)

[AOS08-P01] **Impact of the mesosacle eddies on the western boundary current over the entire western North Pacific**

*Kako Shinichiro[1], Hirohiko Nakamura[2] (1.Graduate School of Science and Engineering, Kagoshima University, 2.Faculty of Fisheries, Kagoshima University)

[AOS08-P02] Glider observations of interleaving layers in the Kuroshio

*Sen Jan[1], Shih-Hong Wang[1], Kai-Chieh Yang[1], Yiing Jang Yang[1], Ming-Huei Chang[1] (1.Institute of Oceanography, National Taiwan Univ.)

[AOS08-P03] Bottom Pressure in the East China Sea -Observation and modeling

*Hua Zheng[1], Xiao-Hua Zhu[1], Hirohiko Nakamura[2], Jae-Hun Park[3], Chanhyung Jeon[4], Ruixiang Zhao[1], Ayako Nishina[2], Chuanzheng Zhang[1], Hanna Na[5], Ze-Nan Zhu[1], Hong Sik Min[6] (1.Second Institute of Oceanography, Ministry of Natural Resources, China, 2.Faculty of Fisheries, Kagoshima University, Kagoshima, Japan, 3.Department of Ocean Sciences, Inha University, Incheon, South Kore, 4.Department of Marine Science and Biological Engineering, Inha University, Incheon, Korea, 5.School of Earth and Environmental Sciences, Seoul National University, Seoul, Korea, 6.Ocean Circulation and Climate Research Center, Korea Institute of Ocean Science and Technology, Busan, Korea)

[AOS08-P04] A numerical study on the dynamics of seasonal velocity variation in the East China Sea

*ZHENLONG ZHANG[1], Nakamura Hirohiko[1], Xiao-Hua Zhu[2] (1.Kagoshima University, 2.Ministry of Natural Resources, CHINA.)

[AOS08-P05] Temporal and spatial velocity variations over the Kuroshio Extension, Kuroshio and Ryukyu Current System in 1982-2014

*YUXIANG QIAO[1], Hirohiko Nakamura[2], AYAKO NISHINA[2] (1.Kagoshima University, Graduate School of Fisheries, 2.Kagoshima University, Faculty of Fishries)

[AOS08-P06] Characteristics of water in the southern Okinawa Trough.

*Ayako Nishina[1], Hirohiko Nakamura[1], Jae-Hun Park[2], Xiao-Hua Zhu[3], Hong Sik Min[4], Hanna Na[5] (1.Kagoshima University, 2.Inha University, 3.Second Institute of Oceanography, 4.Korea Institute of Ocean Science and Technology, 5.Seoul National University)

[E] Poster | A (Atmospheric and Hydrospheric Sciences)：A-OS Ocean Sciences & Ocean Environment

5:15 PM - 6:30 PM JST | 8:15 AM - 9:30 AM UTC | Poster Hall International Exhibition Hall8, Makuhari Messe_11

[A-OS08] ECS-Kuroshio and Ryukyu Current System -Observation, modeling and theory-

convener:Hirohiko Nakamura(Kagoshima University, Faculy of Fisheries), Xiao-Hua Zhu(Second Institute of Oceanography)

[AOS08-P01] Impact of the mesosacle eddies on the western boundary current over the entire western North Pacific

*Kako Shinichiro[1], Hirohiko Nakamura[2] (1.Graduate School of Science and Engineering, Kagoshima University, 2.Faculty of Fisheries, Kagoshima University)

[AOS08-P02] Glider observations of interleaving layers in the Kuroshio

*Sen Jan[1], Shih-Hong Wang[1], Kai-Chieh Yang[1], Yiing Jang Yang[1], Ming-Huei Chang[1] (1.Institute of Oceanography, National Taiwan Univ.)

[AOS08-P03] Bottom Pressure in the East China Sea -Observation and modeling

*Hua Zheng[1], Xiao-Hua Zhu[1], Hirohiko Nakamura[2], Jae-Hun Park[3], Chanhyung Jeon[4], Ruixiang Zhao[1], Ayako Nishina[2], Chuanzheng Zhang[1], Hanna Na[5], Ze-Nan Zhu[1], Hong Sik Min[6] (1.Second Institute of Oceanography, Ministry of Natural Resources, China, 2.Faculty of Fisheries, Kagoshima University, Kagoshima, Japan, 3.Department of Ocean Sciences, Inha University, Incheon, South Kore, 4.Department of Marine Science and Biological Engineering, Inha University, Incheon, Korea, 5.School of Earth and Environmental Sciences, Seoul National University, Seoul, Korea, 6.Ocean Circulation and Climate Research Center, Korea Institute of Ocean Science and Technology, Busan, Korea)

[AOS08-P04] A numerical study on the dynamics of seasonal velocity variation in the East China Sea

*ZHENLONG ZHANG[1], Nakamura Hirohiko[1], Xiao-Hua Zhu[2] (1.Kagoshima University, 2.Ministry of Natural Resources, CHINA.)

[AOS08-P05] Temporal and spatial velocity variations over the Kuroshio Extension, Kuroshio and Ryukyu Current System in 1982-2014

*YUXIANG QIAO[1], Hirohiko Nakamura[2], AYAKO NISHINA[2] (1.Kagoshima University, Graduate School of Fisheries, 2.Kagoshima University, Faculty of Fishries)

[AOS08-P06] Characteristics of water in the southern Okinawa Trough.

*Ayako Nishina[1], Hirohiko Nakamura[1], Jae-Hun Park[2], Xiao-Hua Zhu[3], Hong Sik Min[4], Hanna Na[5] (1.Kagoshima University, 2.Inha University, 3.Second Institute of Oceanography, 4.Korea Institute of Ocean Science and Technology, 5.Seoul National University)

[E] Poster | A (Atmospheric and Hydrospheric Sciences)：A-OS Ocean Sciences & Ocean Environment

3:30 PM - 5:00 PM JST | 6:30 AM - 8:00 AM UTC | Poster Hall International Exhibition Hall8, Makuhari Messe_7

[A-OS11] Continental-Oceanic Mutual Interaction: Planetary scale Material Circulation

convener:Yosuke Alexandre Yamashiki(Earth & Planetary Water Resources Assessment Laboratory Graduate School of Advanced Integrated Studies in Human Survivability Kyoto University), Yukio Masumoto(Graduate School of Science, The University of Tokyo), Swadhin Behera(Climate Variation Predictability and Applicability Research Group, Application Laboratory, JAMSTEC, 3173-25 Showa-machi, Yokohama 236-0001), Takanori Sasaki(Department of Astronomy, Kyoto University)

[AOS11-P01] Remote Sensing of Chlorophyll-a and Submerged Aquatic Vegetation for a Freshwater Lake in Japan

*Shweta Yadav[1], Yamashiki Yosuke[1], Junichi Susaki[1], Kanako Ishikawa[2] (1.Kyoto University, 2.Lake Biwa Environmental Research Institute)

[AOS11-P02] Hydrological and Debris-flow simulation of Martian Surface in Hesperian & early Amazonian epoch

*Hiroaki Sato[2], Yosuke Alexandre Yamashiki[1], Ryusuke Kuroki[1], Hideaki Miyamoto[3], Ryodo Hemmi[3] (1.Earth & Planetary Water Resources Assessment Laboratory Graduate School of Advanced Integrated Studies in Human Survivability Kyoto University, 2.Faculty of Engineering, Kyoto University, 3.Graduate School of Engineering, The University of Tokyo)

[AOS11-P03] Global Lakes & reservoirs Repository and their application for terrestrial surface environment

*Yosuke Alexandre Yamashiki[1], Ryusuke Kuroki[1], Botong Gao[1], Hina Bando[2], Fuka Takagi[3], Shweta Yadav[4] (1.Earth & Planetary Water Resources Assessment Laboratory Graduate School of Advanced Integrated Studies in Human Survivability Kyoto University, 2.Faculty of Science, Kyoto University, 3.Faculty of Agriculture, Kyoto University, 4.Educational Unit for Studies on Connectivity of Hills, Humans and Ocean, Kyoto University)

[AOS11-P04] Numerical simulation of Tidal Heating using SPH and its application to inner sea formation

*keiya murashima[1], Yosuke Alexandre Yamashiki[1], Natsuki Hosono[2] (1.Kyoto University, 2.Japan Agency for Marine-Earth Science and Technology)

[E] Poster | A (Atmospheric and Hydrospheric Sciences)：A-OS Ocean Sciences & Ocean Environment

5:15 PM - 6:30 PM JST | 8:15 AM - 9:30 AM UTC | Poster Hall International Exhibition Hall8, Makuhari Messe_12

[A-OS11] Continental-Oceanic Mutual Interaction: Planetary scale Material Circulation

convener:Yosuke Alexandre Yamashiki(Earth & Planetary Water Resources Assessment Laboratory Graduate School of Advanced Integrated Studies in Human Survivability Kyoto University), Yukio Masumoto(Graduate School of Science, The University of Tokyo), Swadhin Behera(Climate Variation Predictability and Applicability Research Group, Application Laboratory, JAMSTEC, 3173-25 Showa-machi, Yokohama 236-0001), Takanori Sasaki(Department of Astronomy, Kyoto University)

[AOS11-P01] Remote Sensing of Chlorophyll-a and Submerged Aquatic Vegetation for a Freshwater Lake in Japan

*Shweta Yadav[1], Yamashiki Yosuke[1], Junichi Susaki[1], Kanako Ishikawa[2] (1.Kyoto University, 2.Lake Biwa Environmental Research Institute)

[AOS11-P02] Hydrological and Debris-flow simulation of Martian Surface in Hesperian & early Amazonian epoch

*Hiroaki Sato[2], Yosuke Alexandre Yamashiki[1], Ryusuke Kuroki[1], Hideaki Miyamoto[3], Ryodo Hemmi[3] (1.Earth & Planetary Water Resources Assessment Laboratory Graduate School of Advanced Integrated Studies in Human Survivability Kyoto University, 2.Faculty of Engineering, Kyoto University, 3.Graduate School of Engineering, The University of Tokyo)

[AOS11-P03] Global Lakes & reservoirs Repository and their application for terrestrial surface environment

*Yosuke Alexandre Yamashiki[1], Ryusuke Kuroki[1], Botong Gao[1], Hina Bando[2], Fuka Takagi[3], Shweta Yadav[4] (1.Earth & Planetary Water Resources Assessment Laboratory Graduate School of Advanced Integrated Studies in Human Survivability Kyoto University, 2.Faculty of Science, Kyoto University, 3.Faculty of Agriculture, Kyoto University, 4.Educational Unit for Studies on Connectivity of Hills, Humans and Ocean, Kyoto University)

[AOS11-P04] Numerical simulation of Tidal Heating using SPH and its application to inner sea formation

*keiya murashima[1], Yosuke Alexandre Yamashiki[1], Natsuki Hosono[2] (1.Kyoto University, 2.Japan Agency for Marine-Earth Science and Technology)

[E] Poster | A (Atmospheric and Hydrospheric Sciences)：A-HW Hydrology & Water Environment

3:30 PM - 5:00 PM JST | 6:30 AM - 8:00 AM UTC | Poster Hall International Exhibition Hall8, Makuhari Messe_8

[A-HW23] Hydrology & Water Environment

convener:Isao Machida(Geological Survey of Japan), Dai Yamazaki(Institute of Industrial Sciences, The University of Tokyo), Takeshi Hayashi(Faculty of Education and Human Studies, Akita University), Keisuke Fukushi(Institute of Nature & Environmental Technology, Kanazawa University)

[AHW23-P01] **A multiobjective risk management model for real-time reservoir flood control operation**

*Juan Chen[1,2], Ping-An Zhong[2], XinYu Wan[2], Yu Zhang[2] (1.College of Earth Sciences and Engineering, Hohai University, 2.College of Hydrology and Water Resources, Hohai University)

[AHW23-P02] **Assessment of the Flow Regime of Roanoke River due to Climatic and Anthropogenic Activities**

*Rahul Kumar Singh[1], Dr. Manoj Kumar Jain[1] (1.Indian Institute of Technology, Roorkee, India)

[AHW23-P03] Predictive Analysis of Climate, Water, Health and the Environment Nexus

*Abhishek [1], Deepika [2] (1.Technical University Dresden, GERMANY, 2.BPS Government Medical College for Women, Sonepat, INDIA)

[AHW23-P05] Severe droughts provide huge fuel for widespread wildfires in California in USA

*Linghua Qiu[1], Ji Chen[1], Haiyun Shi[2], Liqun Sun[3], Jun Niu[4] (1.the University of Hong Kong, 2.Southern University of Science and Technology, 3.Shenzhen Institutes of Advanced Technology, Chinese Academy of Sciences, 4.China Agricultural University)

[AHW23-P06] A comprehensive evaluation of MODIS-based water use efficiency with global eddy covariance flux data and a process model

*Shanshan YANG[1,2], Jiahua ZHANG[1], Sha ZHANG[1,2], Jingwen WANG[1,2], Yun BAI[1,2], Fengmei YAO[2], Huadong GUO[1] (1.Institute of Remote Sensing and Digital Earth, Chinese Academy of Sciences, 2.University of Chinese Academy of Sciences, Beijing, China)

[AHW23-P07] Impact of variability and anisotropy in the correlation decay distance for precipitation spatial interpolation in China

*yingxian zhang[1] (1.National Climate Center, China Meteorological Administration)

[AHW23-P08] New Record-Breaking Frequency of Annual Maximum Daily Precipitation of 58 stations in the whole Japan, an increasing of extreme values.

*Chhay Ngorn SEANG[1], Tomohito YAMADA[1] (1.Hokkaido University)

[AHW23-P09] Quantifying stemflow to better express its ecohydrological significance

*Shin'ichi Iida[1], Darryl E. Carlye-Moses[2], Sonja Germer[3], Pilar Llorens[4], Beate Michalzik[5], Kazuki Nanko[1], Alexander Tischer[5], Delphis F. Levia[6] (1.Department of Disaster Prevention, Meteorology and Hydrology, Forestry and Forest Products Research Institute, 2.Department of Geography and Environmental Studies, Thompson Rivers University, Kamloops, British Columbia, Canada, 3.Department of Bioengineering, Leibniz Institute for Agricultural Engineering and Bioeconomy, Potsdam, Germany, 4.Institute of Environmental Assessment and Water Research (IDAEA-CSIC), Barcelona, Spain, 5.Soil Science, Institute of Geography, Friedrich Schiller University Jena, Jena, Germany, 6.Department of Geography and Department of Plant and Soil Sciences, University of Delaware, Newark, DE, USA)

[AHW23-P10] **Hydraulic analysis of overland flow caused by temporally varying rainfall**

*PING-CHENG HSIEH[1], Ming-Chang Wu[1] (1.National Chung Hsing University)

[AHW23-P11] A comparative Study on Water Environment of Isolated Islands - Focusing on Islands in Nagasaki Prefecture - (3)

*Go Yamaki[1], Koji Kodera[2], Kazuki Asami[1], Yoshihiro IGARI[1], Masaki Horiuchi[1] (1.Grad. Student, Hosei Univ., 2.Dep. of Geography, Hosei Univ.)

[AHW23-P12] **Water environment around Kusatsu-Shirane volcano and consideration of the effect of eruption in January 2018**

*Igari Yoshihiro[1], Koji Kodera[2], Kazuki Asami[1] (1.Grad.Student,Hosei Univ., 2.Dep.of Geography Hosei Univ.)

[AHW23-P13] Re-consideration of discharge rate of spring water in Lake Ezu, Kumamoto

*Kimpei Ichiyanagi[1], Kiyoshi Ide[1], Jun Shimada[1], Tsutomu Ichikawa[2] (1.Kumamoto University, 2.Tokai University)

[AHW23-P14] **Evaluating the efficacy of hydrologically and hydrodynamically driven methods of e-flow assessment for Upper Godavari River Basin, India**

*GAURAV KALIDAS PAKHALE[1], Jyoti Punjahari Nale[2], Ashvin Kumar Gosain[3], Rakesh Khosa[3] (1.PhD Research Scholar, Civil Engineering Department, Indian Institute of Technology, Delhi, 2.Project Advisor, IEWP, GIZ India, New Delhi, India, 3.Professor, Civil Engineering Department, Indian Institute of Technology, Delhi)

[AHW23-P15] Presence of pharmaceutical compounds in freshwater lakes and their impact on phytoplankton

*Nandakumar Kanavillil[1], Cassandra Fligg[1], Sreekumari Kurissery[1] (1.Lakehead University, Canada)

[AHW23-P16] **Novel approximate solutions for solute transport due to injections: considering the scale-dependent dispersion and non-integer flow dimension**

*Ye-Chen Lin[1], Hund-Der Yeh[1] (1.National Chiao Tung Univ.)

[AHW23-P17] Experimemtal study on the residual saturation of Porous Media using Pore Doublets Micromodel

*Chun-Wei Peng[1] (1.Taiwan National Chiao Tung University)

[AHW23-P18] Assessment of Synergy between Biomedical Waste and Shallow Groundwater Pollution

*Deepika [1], Abhishek [2] (1.BPS Government Medical College for Women, Sonepat, INDIA, 2.Technical University Dresden, GERMANY)

[AHW23-P19] Erosion and transport processes of earth surface materials in a reservoir-catchment system inferred from atmospheric radionuclides ^{7}Be and ^{210}Pb

*Mikiya Tsuruoka[1], Shinya Ochiai[2], Atsushi Matsuki[2], Seiya Nagao[2] (1.Graduate School of Natural Science and Technology, Kanazawa University, 2.Institute of Nature and Environmental Technology, Kanazawa University)

[AHW23-P20] Fluctuation of groundwater level in a sloping unconfined aquifer due to time varying recharge

*Ming-Chang Wu[1], Ping-Cheng Hsieh[1] (1.National Chung Hsing University)

[AHW23-P21] **Effect of cutoff wall on recharge water storage volume**

*Pei-hsun Tsai[1], Jung-hsing Tai[1] (1.Chaoyang University of Technology)

[AHW23-P22] **Studying Operation Parameters on Flat-Plate Membrane Bioreactor for Sewage Treatment**

*Jen Hung Chiu[1], Wen Chin Chen[1] (1.Studying Operation Parameters on Flat-Plate Membrane Bioreactor for Sewage Treatment)

[AHW23-P23] **Mine-water quality at a tertiary coalfield in India: Characterisation and treatment using novel polyvinyl alcohol (PVA) gel bioreactor**

*Aparna Dutta[1], Sudipta Sarkar[1] (1.Indian Institute of Technology Roorkee)

[E] Poster | A (Atmospheric and Hydrospheric Sciences)：A-HW Hydrology & Water Environment

5:15 PM - 6:30 PM JST | 8:15 AM - 9:30 AM UTC | Poster Hall International Exhibition Hall8, Makuhari Messe_14

[A-HW23] Hydrology & Water Environment

convener:Isao Machida(Geological Survey of Japan), Dai Yamazaki(Institute of Industrial Sciences, The University of Tokyo), Takeshi Hayashi(Faculty of Education and Human Studies, Akita University), Keisuke Fukushi(Institute of Nature & Environmental Technology, Kanazawa University)

[AHW23-P01] **A multiobjective risk management model for real-time reservoir flood control operation**

*Juan Chen[1,2], Ping-An Zhong[2], XinYu Wan[2], Yu Zhang[2] (1.College of Earth Sciences and Engineering, Hohai University, 2.College of Hydrology and Water Resources, Hohai University)

[AHW23-P02] **Assessment of the Flow Regime of Roanoke River due to Climatic and Anthropogenic Activities**

*Rahul Kumar Singh[1], Dr. Manoj Kumar Jain[1] (1.Indian Institute of Technology, Roorkee, India)

[AHW23-P03] Predictive Analysis of Climate, Water, Health and the Environment Nexus

*Abhishek [1], Deepika [2] (1.Technical University Dresden, GERMANY, 2.BPS Government Medical College for Women, Sonepat, INDIA)

[AHW23-P05] Severe droughts provide huge fuel for widespread wildfires in California in USA

*Linghua Qiu[1], Ji Chen[1], Haiyun Shi[2], Liqun Sun[3], Jun Niu[4] (1.the University of Hong Kong, 2.Southern University of Science and Technology, 3.Shenzhen Institutes of Advanced Technology, Chinese Academy of Sciences, 4.China Agricultural University)

[AHW23-P06] A comprehensive evaluation of MODIS-based water use efficiency with global eddy covariance flux data and a process model

*Shanshan YANG[1,2], Jiahua ZHANG[1], Sha ZHANG[1,2], Jingwen WANG[1,2], Yun BAI[1,2], Fengmei YAO[2], Huadong GUO[1] (1.Institute of Remote Sensing and Digital Earth, Chinese Academy of Sciences, 2.University of Chinese Academy of Sciences, Beijing, China)

[AHW23-P07] Impact of variability and anisotropy in the correlation decay distance for precipitation spatial interpolation in China

*yingxian zhang[1] (1.National Climate Center, China Meteorological Administration)

[AHW23-P08] New Record-Breaking Frequency of Annual Maximum Daily Precipitation of 58 stations in the whole Japan, an increasing of extreme values.

*Chhay Ngorn SEANG[1], Tomohito YAMADA[1] (1.Hokkaido University)

[AHW23-P09] Quantifying stemflow to better express its ecohydrological significance

*Shin'ichi Iida[1], Darryl E. Carlye-Moses[2], Sonja Germer[3], Pilar Llorens[4], Beate Michalzik[5], Kazuki Nanko[1], Alexander Tischer[5], Delphis F. Levia[6] (1.Department of Disaster Prevention, Meteorology and Hydrology, Forestry and Forest Products Research Institute, 2.Department of Geography and Environmental Studies, Thompson Rivers University, Kamloops, British Columbia, Canada, 3.Department of Bioengineering, Leibniz Institute for Agricultural Engineering and Bioeconomy, Potsdam, Germany, 4.Institute of Environmental Assessment and Water Research (IDAEA-CSIC), Barcelona, Spain, 5.Soil Science, Institute of Geography, Friedrich Schiller University Jena, Jena, Germany, 6.Department of Geography and Department of Plant and Soil Sciences, University of Delaware, Newark, DE, USA)

[AHW23-P10] **Hydraulic analysis of overland flow caused by temporally varying rainfall**

*PING-CHENG HSIEH[1], Ming-Chang Wu[1] (1.National Chung Hsing University)

[AHW23-P11] A comparative Study on Water Environment of Isolated Islands - Focusing on Islands in Nagasaki Prefecture - (3)

*Go Yamaki[1], Koji Kodera[2], Kazuki Asami[1], Yoshihiro IGARI[1], Masaki Horiuchi[1] (1.Grad. Student, Hosei Univ., 2.Dep. of Geography, Hosei Univ.)

[AHW23-P12] **Water environment around Kusatsu-Shirane volcano and consideration of the effect of eruption in January 2018**

*Igari Yoshihiro[1], Koji Kodera[2], Kazuki Asami[1] (1.Grad.Student,Hosei Univ., 2.Dep.of Geography Hosei Univ.)

[AHW23-P13] Re-consideration of discharge rate of spring water in Lake Ezu, Kumamoto

*Kimpei Ichiyanagi[1], Kiyoshi Ide[1], Jun Shimada[1], Tsutomu Ichikawa[2] (1.Kumamoto University, 2.Tokai University)

[AHW23-P14] **Evaluating the efficacy of hydrologically and hydrodynamically driven methods of e-flow assessment for Upper Godavari River Basin, India**

*GAURAV KALIDAS PAKHALE[1], Jyoti Punjahari Nale[2], Ashvin Kumar Gosain[3], Rakesh Khosa[3] (1.PhD Research Scholar, Civil Engineering Department, Indian Institute of Technology, Delhi, 2.Project Advisor, IEWP, GIZ India, New Delhi, India, 3.Professor, Civil Engineering Department, Indian Institute of Technology, Delhi)

[AHW23-P15] Presence of pharmaceutical compounds in freshwater lakes and their impact on phytoplankton

*Nandakumar Kanavillil[1], Cassandra Fligg[1], Sreekumari Kurissery[1] (1.Lakehead University, Canada)

[AHW23-P16] **Novel approximate solutions for solute transport due to injections: considering the scale-dependent dispersion and non-integer flow dimension**

*Ye-Chen Lin[1], Hund-Der Yeh[1] (1.National Chiao Tung Univ.)

[AHW23-P17] Experimemtal study on the residual saturation of Porous Media using Pore Doublets Micromodel

*Chun-Wei Peng[1] (1.Taiwan National Chiao Tung University)

[AHW23-P18] Assessment of Synergy between Biomedical Waste and Shallow Groundwater Pollution

*Deepika [1], Abhishek [2] (1.BPS Government Medical College for Women, Sonepat, INDIA, 2.Technical University Dresden, GERMANY)

[AHW23-P19] Erosion and transport processes of earth surface materials in a reservoir-catchment system inferred from atmospheric radionuclides ^{7}Be and ^{210}Pb

*Mikiya Tsuruoka[1], Shinya Ochiai[2], Atsushi Matsuki[2], Seiya Nagao[2] (1.Graduate School of Natural Science and Technology, Kanazawa University, 2.Institute of Nature and Environmental Technology, Kanazawa University)

[AHW23-P20] Fluctuation of groundwater level in a sloping unconfined aquifer due to time varying recharge

*Ming-Chang Wu[1], Ping-Cheng Hsieh[1] (1.National Chung Hsing University)

[AHW23-P21] **Effect of cutoff wall on recharge water storage volume**

*Pei-hsun Tsai[1], Jung-hsing Tai[1] (1.Chaoyang University of Technology)

[AHW23-P22] **Studying Operation Parameters on Flat-Plate Membrane Bioreactor for Sewage Treatment**

*Jen Hung Chiu[1], Wen Chin Chen[1] (1.Studying Operation Parameters on Flat-Plate Membrane Bioreactor for Sewage Treatment)

[AHW23-P23] **Mine-water quality at a tertiary coalfield in India: Characterisation and treatment using novel polyvinyl alcohol (PVA) gel bioreactor**

*Aparna Dutta[1], Sudipta Sarkar[1] (1.Indian Institute of Technology Roorkee)

[E] Poster | A (Atmospheric and Hydrospheric Sciences)：A-CG Complex & General

10:45 AM - 12:15 PM JST | 1:45 AM - 3:15 AM UTC | Poster Hall International Exhibition Hall8, Makuhari Messe_6

[A-CG35] Projection and detection of global environmental change

convener:Michio Kawamiya(Japan Agency for Marine-Earth Science and Technology), Hiroaki Tatebe(Japan Agency for Marine-Earth Science and Technology), Kaoru Tachiiri(Japan Agency for Marine-Earth Science and Technology)

[ACG35-P01] **World Regionalization of Climate Change (1961–2010)**

*Shao Sun[1,2], Peijun Shi[2,3,4], Daoyi Gong[2], Tao Zhou[2] (1.National Climate Center, China Meteorological Administration, Beijing 100081, China, 2.State Key Laboratory of Earth Surface Processes and Resource Ecology, Beijing Normal University, Beijing 100875, China, 3.Key Laboratory of Environmental Change and Natural Disaster of Ministry of Education, Beijing Normal University, Beijing 100875, China, 4.Academy of Disaster Reduction and Emergency Management, Ministry of Civil Affairs & Ministry of Education, Beijing 100875, China)

[ACG35-P02] Quantifying and identifying future climate signal, noise, and internal variability at finer temporal scales

*Jongho Kim[1], Manh Van Doi[1] (1.University of Ulsan)

[ACG35-P03] Basic evaluation of MIROC6 and current status of CMIP6 experiments

*Hiroaki Tatebe[1] (1.Japan Agency for Marine-Earth Science and Technology)

[ACG35-P04] **Synchronized increase of extreme cold and warm events in China during the recent global warming slowdown**

*Xiubao Sun[1,3], Chunzai Wang[1], Guoyu Ren[2,3], Panfeng Zhang[2] (1.State Key Laboratory of Tropical Oceanography (LTO), South China Sea Institute of Oceanology(SCSIO), Chinese Academy of Sciences (CAS), 2.Department of Atmospheric Science, School of Environmental Studies, China University of Geosciences (CUG), 3.Laboratory for Climate Studies, National Climate Center (NCC), China Meteorological Administration (CMA))

[ACG35-P05] Quantification of thermodynamical and dynamical contributions to the anthropogenic influences on tropical cyclone rainfall extremes

*Cheng-Ta Chen[1], Shih-How Lo[1], Chung-Chieh Wang[1], Kazuhisa Tsuboki[2] (1.Department of Earth Sciences, National Taiwan Normal University, 2.Hydrospheric-Atmospheric Research Center, Nagoya University)

[ACG35-P06] **Temporal Evolution of the Long-Term Distributional Biases of Climate Models as a Parameter for the Regional Evaluation of the Simulation of Climate Change**

*Martin Gomez-Garcia[1], Akiko Matsumura[1], Shiro Hishinuma[1], Daikichi Ogawada[1] (1.Nippon Koei Co. Ltd., Reasearch and Development Center)

[ACG35-P07] A global simulation of bioenergy crop yield

*Zhipin Ai[1], Naota Hanasaki[1] (1.National Institute for Environmental Studies)

[ACG35-P08] Integrated Research Program for Advancing Climate Models - Theme B: national research program in Japan on earth system modeling

*Michio Kawamiya[1], Tomohiro Hajima[1], Kaoru Tachiiri[1], Jun'ichi Tsutsui[2], Tokuta Yokohata[3], Takashi Arakawa[4], Takahiro Inoue[4] (1.Japan Agency for Marine-Earth Science and Technology, 2.Central Research Institute of Electric Power Industry, 3.National Institute for Environmental Studies, 4.Research Organization for Information Science and Technology)

[ACG35-P09] Towards probabilistic climate projections based on the CMIP6 multi-model ensemble

*Junichi Tsutsui[1] (1.Central Research Institute of Electric Power Industry)

[ACG35-P10] Effect on the earth system of realizing 1.5 degree climate target by overshooting after reaching 2 degree level

*Kaoru Tachiiri[1], Herran Diego Silva[2], Xuanming Su[1], Michio Kawamiya[1] (1.Japan Agency for Marine-Earth Science and Technology, 2.Institute for Global Environmental Strategies)

[ACG35-P11] **Historical regional and sectoral contributions to climate change**

*Xuanming Su[1], Kaoru Tachiiri[1], Katsumasa TANAKA[2], Michio Watanabe[1] (1.Japan Agency for Marine-Earth Science and Technology, 2.National Institute for Environmental Studies)

[ACG35-P12] **Future projection of global climate, water, food, bio-energy, and land investigated with MIROC-INTEG: a global bio-geophysical land surface model with human components**

*Tokuta Yokohata[1], Yusuke Satoh[1], Tsuguki Kinoshita[2], Gen Sakurai[3], Yadu Pokhrel[4], Akihiko Ito[1], Etsushi Kato[5], Masashi Okada[1], Naota Hanasaki[1], Tomoko Nitta[6], Seita Emori[1] (1.National Institute for Environmental Studies, 2.Ibaraki University, 3.National Agriculture and Food Research Organization, 4.Michigan State University, 5.The Institute of Applied Energy, 6.University of Tokyo)

[ACG35-P13] **Downscaling a global agricultural land use model to country level for national SSP analysis**

*Wenchao Wu[1], Tomoko Hasegawa[1], Kiyoshi Takahashi[1], Shinichiro Fujimori[2] (1.National Institute for Environmental Studies, 2.Kyoto Univ.)

[ACG35-P14] Extreme Events and Emergent Trends in Marine Ecosystem Stressors under a historical/RCP8.5 Climate Change Pathway

*Keith Bradley Rodgers[1,2], Sarah Schlunegger[3], Richard Slater[3], Burke Hales[4], Axel Timmermann[1,2] (1.IBS Center for Climate Physics, Busan, South Korea, 2.Pusan National University, Busan, South Korea, 3.AOS Program, Princeton University, Princeton NJ, USA, 4.College of Ocean and Atmospheric Sciences, Oregon State Universitym, Corvallis, OR, USA)

[E] Poster | A (Atmospheric and Hydrospheric Sciences)：A-CG Complex & General

5:15 PM - 6:30 PM JST | 8:15 AM - 9:30 AM UTC | Poster Hall International Exhibition Hall8, Makuhari Messe_16

[A-CG35] Projection and detection of global environmental change

convener:Michio Kawamiya(Japan Agency for Marine-Earth Science and Technology), Hiroaki Tatebe(Japan Agency for Marine-Earth Science and Technology), Kaoru Tachiiri(Japan Agency for Marine-Earth Science and Technology)

[ACG35-P01] **World Regionalization of Climate Change (1961–2010)**

*Shao Sun[1,2], Peijun Shi[2,3,4], Daoyi Gong[2], Tao Zhou[2] (1.National Climate Center, China Meteorological Administration, Beijing 100081, China, 2.State Key Laboratory of Earth Surface Processes and Resource Ecology, Beijing Normal University, Beijing 100875, China, 3.Key Laboratory of Environmental Change and Natural Disaster of Ministry of Education, Beijing Normal University, Beijing 100875, China, 4.Academy of Disaster Reduction and Emergency Management, Ministry of Civil Affairs & Ministry of Education, Beijing 100875, China)

[ACG35-P02] Quantifying and identifying future climate signal, noise, and internal variability at finer temporal scales

*Jongho Kim[1], Manh Van Doi[1] (1.University of Ulsan)

[ACG35-P03] Basic evaluation of MIROC6 and current status of CMIP6 experiments

*Hiroaki Tatebe[1] (1.Japan Agency for Marine-Earth Science and Technology)

[ACG35-P04] **Synchronized increase of extreme cold and warm events in China during the recent global warming slowdown**

*Xiubao Sun[1,3], Chunzai Wang[1], Guoyu Ren[2,3], Panfeng Zhang[2] (1.State Key Laboratory of Tropical Oceanography (LTO), South China Sea Institute of Oceanology(SCSIO), Chinese Academy of Sciences (CAS), 2.Department of Atmospheric Science, School of Environmental Studies, China University of Geosciences (CUG), 3.Laboratory for Climate Studies, National Climate Center (NCC), China Meteorological Administration (CMA))

[ACG35-P05] Quantification of thermodynamical and dynamical contributions to the anthropogenic influences on tropical cyclone rainfall extremes

*Cheng-Ta Chen[1], Shih-How Lo[1], Chung-Chieh Wang[1], Kazuhisa Tsuboki[2] (1.Department of Earth Sciences, National Taiwan Normal University, 2.Hydrospheric-Atmospheric Research Center, Nagoya University)

[ACG35-P06] **Temporal Evolution of the Long-Term Distributional Biases of Climate Models as a Parameter for the Regional Evaluation of the Simulation of Climate Change**

*Martin Gomez-Garcia[1], Akiko Matsumura[1], Shiro Hishinuma[1], Daikichi Ogawada[1] (1.Nippon Koei Co. Ltd., Reasearch and Development Center)

[ACG35-P07] A global simulation of bioenergy crop yield

*Zhipin Ai[1], Naota Hanasaki[1] (1.National Institute for Environmental Studies)

[ACG35-P08] Integrated Research Program for Advancing Climate Models - Theme B: national research program in Japan on earth system modeling

*Michio Kawamiya[1], Tomohiro Hajima[1], Kaoru Tachiiri[1], Jun'ichi Tsutsui[2], Tokuta Yokohata[3], Takashi Arakawa[4], Takahiro Inoue[4] (1.Japan Agency for Marine-Earth Science and Technology, 2.Central Research Institute of Electric Power Industry, 3.National Institute for Environmental Studies, 4.Research Organization for Information Science and Technology)

[ACG35-P09] Towards probabilistic climate projections based on the CMIP6 multi-model ensemble

*Junichi Tsutsui[1] (1.Central Research Institute of Electric Power Industry)

[ACG35-P10] Effect on the earth system of realizing 1.5 degree climate target by overshooting after reaching 2 degree level

*Kaoru Tachiiri[1], Herran Diego Silva[2], Xuanming Su[1], Michio Kawamiya[1] (1.Japan Agency for Marine-Earth Science and Technology, 2.Institute for Global Environmental Strategies)

[ACG35-P11] **Historical regional and sectoral contributions to climate change**

*Xuanming Su[1], Kaoru Tachiiri[1], Katsumasa TANAKA[2], Michio Watanabe[1] (1.Japan Agency for Marine-Earth Science and Technology, 2.National Institute for Environmental Studies)

[ACG35-P12] **Future projection of global climate, water, food, bio-energy, and land investigated with MIROC-INTEG: a global bio-geophysical land surface model with human components**

*Tokuta Yokohata[1], Yusuke Satoh[1], Tsuguki Kinoshita[2], Gen Sakurai[3], Yadu Pokhrel[4], Akihiko Ito[1], Etsushi Kato[5], Masashi Okada[1], Naota Hanasaki[1], Tomoko Nitta[6], Seita Emori[1] (1.National Institute for Environmental Studies, 2.Ibaraki University, 3.National Agriculture and Food Research Organization, 4.Michigan State University, 5.The Institute of Applied Energy, 6.University of Tokyo)

[ACG35-P13] **Downscaling a global agricultural land use model to country level for national SSP analysis**

*Wenchao Wu[1], Tomoko Hasegawa[1], Kiyoshi Takahashi[1], Shinichiro Fujimori[2] (1.National Institute for Environmental Studies, 2.Kyoto Univ.)

[ACG35-P14] Extreme Events and Emergent Trends in Marine Ecosystem Stressors under a historical/RCP8.5 Climate Change Pathway

*Keith Bradley Rodgers[1,2], Sarah Schlunegger[3], Richard Slater[3], Burke Hales[4], Axel Timmermann[1,2] (1.IBS Center for Climate Physics, Busan, South Korea, 2.Pusan National University, Busan, South Korea, 3.AOS Program, Princeton University, Princeton NJ, USA, 4.College of Ocean and Atmospheric Sciences, Oregon State Universitym, Corvallis, OR, USA)

[E] Poster | H (Human Geosciences)：H-GM Geomorphology

3:30 PM - 5:00 PM JST | 6:30 AM - 8:00 AM UTC | Poster Hall International Exhibition Hall8, Makuhari Messe_11

[H-GM03] Geomorphology

convener:Tsuyoshi Hattanji(Faculty of Life and Environmental Sciences, University of Tsukuba), Masayuki Seto(Fukushima Future Center for Regional Revitalization, Fukushima University)

[HGM03-P01] Honeycomb Weathering (Tafoni) of Sandstone and Environmental Factors in Yonaguni Island, Okinawa Prefecture, Japan

*Takayuki Ogata[1] (1.Disaster Prevention Research Center for Island Regions, University of the Ryukyus)

[HGM03-P02] Colluvial deposits in first-order streams and channel head migration by shallow landslides: Case study in granitic basins, Asaminami, Hiroshima, Japan

*Tsuyoshi Hattanji[1], Ryuya Kodama[2], Takahisa Furuichi[3], Shoji Doshida[4], Yasushi Tanaka[5] (1.Faculty of Life and Environmental Sciences, University of Tsukuba, 2.former College of Geoscience, University of Tsukuba, 3.Hokkaido University, 4.National Research Institute of Fire and Disaster, 5.Komazawa University)

[HGM03-P03] Rock restrictions on topographical features of rivers: model experiment

*Yuta Takase[1], Noritaka Endo[1] (1.Kanazawa University)

[HGM03-P04] Stream power incision model and the stage of topographic equilibrium, using physical experiments

*Imamura Akihiro[1], Noritaka Endo[1] (1.Kanazawa University)

[HGM03-P05] Downstream variation in gravel size of the Tenjin River system

*Kazuaki Hori[1], Kazuya Yonehara[1] (1.Department of Geography, Graduate School of Environmental Studies, Nagoya University)

[HGM03-P06] Talus slope development in the time of deglaciation: a case study of the Rev Valley, SW Spitsbergen

*Krzysztof Senderak[1], Marta Kondracka[1], Bogdan Gądek[1] (1.Faculty of Earth Sciences, University of Silesia)

[HGM03-P07] **Distribution of Large Benthic Foraminifers in one of Majuro's Conservation Areas – Drenmeo Island**

*Benedict Yamamura[1], Kazuhiko Fujita[2], Melba White[3], Kyotak Ishiguro[3], Hironobu Kan[1] (1.Kyushu University, Integrated Sciences for Global Society - Research Center for Coastal Seafloor , 2.Department of Physics and Earth Sciences, University of the Ryukyus, 3.Marshall Islands Marine Resources Authority)

[HGM03-P08] Luminescence chronology of fluvial and marine records from subsurface sediment cores: An insight into the geomorphic evolution of Kaveri delta, India

*kartika goswami[1], Anbarasu Kumaresan[2], Sivakumar Krishnan[2], Senthil K. Sadasivam[2], Manoj Kumar Jaiswal[1] (1.Department of Earth Sciences, Indian Institute of Science Education and Reserach Kolkata, 2.National College Tiruchirappalli, India)

[E] Poster | H (Human Geosciences)：H-GM Geomorphology

5:15 PM - 6:30 PM JST | 8:15 AM - 9:30 AM UTC | Poster Hall International Exhibition Hall8, Makuhari Messe_18

[H-GM03] Geomorphology

convener:Tsuyoshi Hattanji(Faculty of Life and Environmental Sciences, University of Tsukuba), Masayuki Seto(Fukushima Future Center for Regional Revitalization, Fukushima University)

[HGM03-P01] Honeycomb Weathering (Tafoni) of Sandstone and Environmental Factors in Yonaguni Island, Okinawa Prefecture, Japan

*Takayuki Ogata[1] (1.Disaster Prevention Research Center for Island Regions, University of the Ryukyus)

[HGM03-P02] Colluvial deposits in first-order streams and channel head migration by shallow landslides: Case study in granitic basins, Asaminami, Hiroshima, Japan

*Tsuyoshi Hattanji[1], Ryuya Kodama[2], Takahisa Furuichi[3], Shoji Doshida[4], Yasushi Tanaka[5] (1.Faculty of Life and Environmental Sciences, University of Tsukuba, 2.former College of Geoscience, University of Tsukuba, 3.Hokkaido University, 4.National Research Institute of Fire and Disaster, 5.Komazawa University)

[HGM03-P03] Rock restrictions on topographical features of rivers: model experiment

*Yuta Takase[1], Noritaka Endo[1] (1.Kanazawa University)

[HGM03-P04] Stream power incision model and the stage of topographic equilibrium, using physical experiments

*Imamura Akihiro[1], Noritaka Endo[1] (1.Kanazawa University)

[HGM03-P05] Downstream variation in gravel size of the Tenjin River system

*Kazuaki Hori[1], Kazuya Yonehara[1] (1.Department of Geography, Graduate School of Environmental Studies, Nagoya University)

[HGM03-P06] Talus slope development in the time of deglaciation: a case study of the Rev Valley, SW Spitsbergen

*Krzysztof Senderak[1], Marta Kondracka[1], Bogdan Gądek[1] (1.Faculty of Earth Sciences, University of Silesia)

[HGM03-P07] **Distribution of Large Benthic Foraminifers in one of Majuro's Conservation Areas – Drenmeo Island**

*Benedict Yamamura[1], Kazuhiko Fujita[2], Melba White[3], Kyotak Ishiguro[3], Hironobu Kan[1] (1.Kyushu University, Integrated Sciences for Global Society - Research Center for Coastal Seafloor , 2.Department of Physics and Earth Sciences, University of the Ryukyus, 3.Marshall Islands Marine Resources Authority)

[HGM03-P08] Luminescence chronology of fluvial and marine records from subsurface sediment cores: An insight into the geomorphic evolution of Kaveri delta, India

*kartika goswami[1], Anbarasu Kumaresan[2], Sivakumar Krishnan[2], Senthil K. Sadasivam[2], Manoj Kumar Jaiswal[1] (1.Department of Earth Sciences, Indian Institute of Science Education and Reserach Kolkata, 2.National College Tiruchirappalli, India)

[E] Poster | H (Human Geosciences)：H-DS Disaster geosciences

10:45 AM - 12:15 PM JST | 1:45 AM - 3:15 AM UTC | Poster Hall International Exhibition Hall8, Makuhari Messe_7

[H-DS10] Natural hazards impacts on human society, economics and technological systems

convener:ELENA PETROVA(Lomonosov Moscow State University, Faculty of Geography), Hajime Matsushima(Research Faculty of Agriculture, Hokkaido University)

[HDS10-P01] **The 2018 Activity of Kamchatka Volcanoes and Danger to Aviation**

*Olga Girina[1], Dmitry Melnikov[1], Alexander Manevich[1], Anton Nuzhdaev[1], Elena Petrova[2] (1.Institute of Volcanology and Seismology, Far East Division, Russian Academy of Sciences, 2.M.V. Lomonosov Moscow State University)

[HDS10-P02] Planning Methodology on the Effective Use of Green Infrastructure for Disaster Risk Reduction

★Invited Papers

*Keita Aragane[1], Satoshi Funakubo[1] (1.National Institute for Land Infrastructure Management)

[HDS10-P03] EMERGENCY CALL PATTERN IN PETROZAVODSK

*Boris Zalmanovich Belashev[1], Natalia Vladimirovna Krutskikh[1], Anna Aleksandrovna Gerasimova[1] (1.Karelian research center of Russian academy of science)

[HDS10-P04] IDENTIFYING “REGIMES” IN THE TIME SEQUENCES OF PROCESSES

*Boris Zalmanovich Belashev[1] (1.Karelian research center of Russian academy of science)

[HDS10-P05] **Investigation of status and demand on public service of earthquake disaster mitigation in China**

*Lina Dong[1], Weiping Lian[1], Weitao Chen[1] (1.Development Research Center, China Earthquake Administration)

[HDS10-P06] Analysis of Eco-DRR and Ecological Services using InVEST at the Disaster Areas of Kumamoto Earthquake

*Minghui Tang[1], Naoko Fujita[1] (1.Kyushu University)

[HDS10-P07] Transformation as praxis: Exploring socially just and transdisciplinary pathways to sustainability in marginal environments (TAPESTRY)

*Nobuhito Ohte[1], Lyla Mehta[2], Synne Movik[3], Devanathan Parthasarathy[4] (1.Department of Social Informatics, Graduate School of Informatics, Kyoto University, 2.Institute of Development Studies at the University of Sussex, 3.Department of Urban and Regional Planning, Norwegian University of Life Sciences, 4.Department of Humanities and Social Sciences, Indian Institute of Technology)

[HDS10-P08] Study for the Establishment of the Design for Disaster prevention through the survey of Recognition of tsunami disaster prevention from the viewpoint of green infrastructure in the coastal area of Kyushu-Pacific region.

*Shanshan Xu[1], Naoko Fujita[1], Minghui Tang[1] (1.Kyushu University)

[HDS10-P09] Design for Green Infrastructure: Analysis of Landscape change in the Kumamoto earthquake area

★Invited Papers

*Naoko Fujita[1] (1.Kyushu University)

[E] Poster | H (Human Geosciences)：H-DS Disaster geosciences

5:15 PM - 6:30 PM JST | 8:15 AM - 9:30 AM UTC | Poster Hall International Exhibition Hall8, Makuhari Messe_21

[H-DS10] Natural hazards impacts on human society, economics and technological systems

convener:ELENA PETROVA(Lomonosov Moscow State University, Faculty of Geography), Hajime Matsushima(Research Faculty of Agriculture, Hokkaido University)

[HDS10-P01] **The 2018 Activity of Kamchatka Volcanoes and Danger to Aviation**

*Olga Girina[1], Dmitry Melnikov[1], Alexander Manevich[1], Anton Nuzhdaev[1], Elena Petrova[2] (1.Institute of Volcanology and Seismology, Far East Division, Russian Academy of Sciences, 2.M.V. Lomonosov Moscow State University)

[HDS10-P02] Planning Methodology on the Effective Use of Green Infrastructure for Disaster Risk Reduction

★Invited Papers

*Keita Aragane[1], Satoshi Funakubo[1] (1.National Institute for Land Infrastructure Management)

[HDS10-P03] EMERGENCY CALL PATTERN IN PETROZAVODSK

*Boris Zalmanovich Belashev[1], Natalia Vladimirovna Krutskikh[1], Anna Aleksandrovna Gerasimova[1] (1.Karelian research center of Russian academy of science)

[HDS10-P04] IDENTIFYING “REGIMES” IN THE TIME SEQUENCES OF PROCESSES

*Boris Zalmanovich Belashev[1] (1.Karelian research center of Russian academy of science)

[HDS10-P05] **Investigation of status and demand on public service of earthquake disaster mitigation in China**

*Lina Dong[1], Weiping Lian[1], Weitao Chen[1] (1.Development Research Center, China Earthquake Administration)

[HDS10-P06] Analysis of Eco-DRR and Ecological Services using InVEST at the Disaster Areas of Kumamoto Earthquake

*Minghui Tang[1], Naoko Fujita[1] (1.Kyushu University)

[HDS10-P07] Transformation as praxis: Exploring socially just and transdisciplinary pathways to sustainability in marginal environments (TAPESTRY)

*Nobuhito Ohte[1], Lyla Mehta[2], Synne Movik[3], Devanathan Parthasarathy[4] (1.Department of Social Informatics, Graduate School of Informatics, Kyoto University, 2.Institute of Development Studies at the University of Sussex, 3.Department of Urban and Regional Planning, Norwegian University of Life Sciences, 4.Department of Humanities and Social Sciences, Indian Institute of Technology)

[HDS10-P08] Study for the Establishment of the Design for Disaster prevention through the survey of Recognition of tsunami disaster prevention from the viewpoint of green infrastructure in the coastal area of Kyushu-Pacific region.

*Shanshan Xu[1], Naoko Fujita[1], Minghui Tang[1] (1.Kyushu University)

[HDS10-P09] Design for Green Infrastructure: Analysis of Landscape change in the Kumamoto earthquake area

★Invited Papers

*Naoko Fujita[1] (1.Kyushu University)

[E] Poster | H (Human Geosciences)：H-TT Technology & Techniques

1:45 PM - 3:15 PM JST | 4:45 AM - 6:15 AM UTC | Poster Hall International Exhibition Hall8, Makuhari Messe_2

[H-TT21] Non-destructive techniques applied to stone cultural heritage

convener:Chiaki T. Oguchi(Institute for Environmental Science and Technology, Graduate School of Science and Engineering, Saitama University), Celine Elise Thomachot-Schneider(Groupe d'etude des environnements naturels, anthropiques et archeologiques - Universite de Reims-Champagne-Ardenne (France)), Wonsuh Song(Waseda University), Miguel Gomez-Heras(Universidad Autonoma de Madrid)

[HTT21-P01] **Comparison and Analysis of GNSS-RTK Combined with 3D LiDAR Technology on Monument Maintenance Project**

*Lih-Shinn Hwang[1], Chien-Hua Chiu[1], Chien-Wen Wang[1], Hsiao-Hung Chen[1] (1.National Defense Univ.)

[HTT21-P02] Non-destructive field measurement for investigation of deteriorated parts of an artificial cave

Kaisei Sakane[1], *Chiaki T. Oguchi[1], Yasuhiko TAMURA[2] (1.Institute for Environmental Science and Technology, Graduate School of Science and Engineering, Saitama University, 2.The Exective Committee for the Preservation of Taya Cavern)

[HTT21-P03] Ultra-portable thermal cameras for moisture detection

*Miguel Gomez-Heras[1], Laura Lopez-Gonzalez[2], Maria Teresa Gil-Muñoz[3] (1.Universidad Autonoma de Madrid, 2.Artfabrik, 3.Universidad Complutense de Madrid)

[HTT21-P04] A laboratory experiment on stone decay by combination of salt and ice crystallization

*Masato Sato[1], Tsuyoshi Hattanji[2] (1.Graduate School of Life and environmental Sciences, 2.Faculty of Life and EnvironmentalSciences, University of Tsukuba)

[HTT21-P05] Study of the micro-climatic monitoring on the Saint-Remi Basilica (Rheims, France)

*Emilie Huby[1], Celine Elise Thomachot-Schneider[1], Patricia Vazquez[1], Gilles Fronteau[1] (1.Universite de Reims-Champagne-Ardenne)

[E] Poster | H (Human Geosciences)：H-TT Technology & Techniques

5:15 PM - 6:30 PM JST | 8:15 AM - 9:30 AM UTC | Poster Hall International Exhibition Hall8, Makuhari Messe_23

[H-TT21] Non-destructive techniques applied to stone cultural heritage

convener:Chiaki T. Oguchi(Institute for Environmental Science and Technology, Graduate School of Science and Engineering, Saitama University), Celine Elise Thomachot-Schneider(Groupe d'etude des environnements naturels, anthropiques et archeologiques - Universite de Reims-Champagne-Ardenne (France)), Wonsuh Song(Waseda University), Miguel Gomez-Heras(Universidad Autonoma de Madrid)

[HTT21-P01] **Comparison and Analysis of GNSS-RTK Combined with 3D LiDAR Technology on Monument Maintenance Project**

*Lih-Shinn Hwang[1], Chien-Hua Chiu[1], Chien-Wen Wang[1], Hsiao-Hung Chen[1] (1.National Defense Univ.)

[HTT21-P02] Non-destructive field measurement for investigation of deteriorated parts of an artificial cave

Kaisei Sakane[1], *Chiaki T. Oguchi[1], Yasuhiko TAMURA[2] (1.Institute for Environmental Science and Technology, Graduate School of Science and Engineering, Saitama University, 2.The Exective Committee for the Preservation of Taya Cavern)

[HTT21-P03] Ultra-portable thermal cameras for moisture detection

*Miguel Gomez-Heras[1], Laura Lopez-Gonzalez[2], Maria Teresa Gil-Muñoz[3] (1.Universidad Autonoma de Madrid, 2.Artfabrik, 3.Universidad Complutense de Madrid)

[HTT21-P04] A laboratory experiment on stone decay by combination of salt and ice crystallization

*Masato Sato[1], Tsuyoshi Hattanji[2] (1.Graduate School of Life and environmental Sciences, 2.Faculty of Life and EnvironmentalSciences, University of Tsukuba)

[HTT21-P05] Study of the micro-climatic monitoring on the Saint-Remi Basilica (Rheims, France)

*Emilie Huby[1], Celine Elise Thomachot-Schneider[1], Patricia Vazquez[1], Gilles Fronteau[1] (1.Universite de Reims-Champagne-Ardenne)

[E] Poster | H (Human Geosciences)：H-CG Complex & General

3:30 PM - 5:00 PM JST | 6:30 AM - 8:00 AM UTC | Poster Hall International Exhibition Hall8, Makuhari Messe_15

[H-CG25] International Comparison of Landscape Appreciation

convener:Anastasia Petrova(Institute of Oriental Studies of the Russian Academy of Sciences), yoji aoki(Open University of Japan)

[HCG25-P01] **The Globally Important Agricultural Heritage of Aso from the perspective of landscape and its supporting systems**

*REIKO MACHIDA[1] (1.TOKYO UNIVERSITY OF AGRICULTURE)

[HCG25-P02] **Hazardous natural phenomena and weather conditions appreciation in Russian landscape painting**

*ELENA PETROVA[1] (1.Lomonosov Moscow State University, Faculty of Geography)

[HCG25-P03] Trends of evaluation items to landscape appreciation until 2017 in the English journals

*yoji aoki[1], keisuke mukagai[2], Anastasia Petrova[3] (1.Open University of Japan, 2.Nagano University, 3.Institute of Oriental Studies, Russian Academy of Sciences)

[E] Poster | H (Human Geosciences)：H-CG Complex & General

5:15 PM - 6:30 PM JST | 8:15 AM - 9:30 AM UTC | Poster Hall International Exhibition Hall8, Makuhari Messe_24

[H-CG25] International Comparison of Landscape Appreciation

convener:Anastasia Petrova(Institute of Oriental Studies of the Russian Academy of Sciences), yoji aoki(Open University of Japan)

[HCG25-P01] **The Globally Important Agricultural Heritage of Aso from the perspective of landscape and its supporting systems**

*REIKO MACHIDA[1] (1.TOKYO UNIVERSITY OF AGRICULTURE)

[HCG25-P02] **Hazardous natural phenomena and weather conditions appreciation in Russian landscape painting**

*ELENA PETROVA[1] (1.Lomonosov Moscow State University, Faculty of Geography)

[HCG25-P03] Trends of evaluation items to landscape appreciation until 2017 in the English journals

*yoji aoki[1], keisuke mukagai[2], Anastasia Petrova[3] (1.Open University of Japan, 2.Nagano University, 3.Institute of Oriental Studies, Russian Academy of Sciences)

[E] Poster | S (Solid Earth Sciences)：S-IT Science of the Earth's Interior & Techtonophysics

10:45 AM - 12:15 PM JST | 1:45 AM - 3:15 AM UTC | Poster Hall International Exhibition Hall8, Makuhari Messe_8

[S-IT26] New perspectives on the geodynamics of East Asia

convener:Timothy B Byrne(University of Connecticut), Asuka Yamaguchi(Atomosphere and Ocean Research Institute, The University of Tokyo), Jonny Wu(University of Houston), Kyoko Okino(Atmosphere and Ocean Research Institute, The University of Tokyo)

[SIT26-P01] Geochemical characteristics of effusive rocks (greenstones) in the Hidaka Belt, Hokkaido, Japan

*Toru Yamasaki[1], Futoshi Nanayama[1] (1.Geol. Survey of Japan (AIST))

[SIT26-P02] Large gas reservoir in continental back-arc basin, revealed by automatic seismic velocity analysis in the Okinawa Trough

*Kota Mukumoto[1], Takeshi Tsuji[1], Andri Hendriyana[1] (1.Kyushu University)

[SIT26-P03] Characterize coseismic deformation of Mw 7.5 Palu earthquake in a triple junction in Sulawesi, Indonesia

*MIN-CHIEN TSAI[1], Ying-Hui Yang[2], Chun-Ying Chiu[3], Jyr-Ching Hu[3] (1.Seismological center, Central Weather Bureau, Taipei, Taiwan, R.O.C., 2.School of Civil Engineering and Architecture, Southwest Petroleum University, Chengdu, China, 3.Department of Geosciences, National Taiwan University, Taipei, Taiwan, R.O.C.)

[E] Poster | S (Solid Earth Sciences)：S-IT Science of the Earth's Interior & Techtonophysics

5:15 PM - 6:30 PM JST | 8:15 AM - 9:30 AM UTC | Poster Hall International Exhibition Hall8, Makuhari Messe_28

[S-IT26] New perspectives on the geodynamics of East Asia

convener:Timothy B Byrne(University of Connecticut), Asuka Yamaguchi(Atomosphere and Ocean Research Institute, The University of Tokyo), Jonny Wu(University of Houston), Kyoko Okino(Atmosphere and Ocean Research Institute, The University of Tokyo)

[SIT26-P01] Geochemical characteristics of effusive rocks (greenstones) in the Hidaka Belt, Hokkaido, Japan

*Toru Yamasaki[1], Futoshi Nanayama[1] (1.Geol. Survey of Japan (AIST))

[SIT26-P02] Large gas reservoir in continental back-arc basin, revealed by automatic seismic velocity analysis in the Okinawa Trough

*Kota Mukumoto[1], Takeshi Tsuji[1], Andri Hendriyana[1] (1.Kyushu University)

[SIT26-P03] Characterize coseismic deformation of Mw 7.5 Palu earthquake in a triple junction in Sulawesi, Indonesia

*MIN-CHIEN TSAI[1], Ying-Hui Yang[2], Chun-Ying Chiu[3], Jyr-Ching Hu[3] (1.Seismological center, Central Weather Bureau, Taipei, Taiwan, R.O.C., 2.School of Civil Engineering and Architecture, Southwest Petroleum University, Chengdu, China, 3.Department of Geosciences, National Taiwan University, Taipei, Taiwan, R.O.C.)

[E] Poster | S (Solid Earth Sciences)：S-GC Geochemistry

10:45 AM - 12:15 PM JST | 1:45 AM - 3:15 AM UTC | Poster Hall International Exhibition Hall8, Makuhari Messe_9

[S-GC40] Volatile Cycles in the Deep Earth - from Subduction Zone to Hot Spot

convener:Hirochika Sumino(Department of Basic Science, Graduate School of Arts and Sciences, The University of Tokyo), Takeshi Hanyu(Japan Agency for Marine-Earth Science and Technology, Department of Solid Earth Geochemistry), Yuji Sano(Division of Ocean and Earth Systems, Atmosphere and Ocean Research Institute, University of Tokyo), Gray E Bebout(Lehigh University)

[SGC40-P01] Continental growth models demystified

*Jun Korenaga[1] (1.Department of Geology and Geophysics, Yale University)

[SGC40-P02] Mass-independent sulfur isotope signature from the 2.7 Ga Belingwe komatiite: Recycling of crustal material in Archean

*Yusuke Kubota[1], Yuichiro Ueno[1,2,3], Kenji Shimizu[3], Fumihiro Matsuura[2], Akira Ishikawa[1,3] (1.Department of Earth and Planetary Sciences, Tokyo Institute of Technology, 2.Earth-Life Science Institute, Tokyo Institute of Technology, 3.Japan Agency for Marine-Earth Science and Technology (JAMSTEC))

[SGC40-P03] Determination of halogens in some standard materials using the neutron irradiation noble gas mass spectrometric technique

*Hirochika Sumino[1], Masahiro Kobayashi[2], Takehiko Saito[3], Keisuke Nagao[3] (1.Department of Basic Science, Graduate School of Arts and Sciences, The University of Tokyo, 2.Tokyo Metropolitan Industrial Technology Research Institute, 3.Geochemical Research Center, Graduate School of Science, University of Tokyo)

[SGC40-P04] FTIR spectroscopy and noble gas mass spectrometry for a single olivine grain

*Sota Niki[1], Hirochika Sumino[2], Masahiro Kobayashi[3], Hiroyuki Kagi[1], Takafumi Hirata[1], Chris J. Ballentine[4] (1.Geochemical Research Center, Grad. School of Science, Univ. of Tokyo, 2.Dept. of Basic Science, Grad. School of Arts and Sciences, Univ. of Tokyo, 3.Tokyo Metropolitan Industrial Technology Research Institute, 4.Dept. of Earth Sciences, Univ. of Oxford)

[SGC40-P05] New halogen incorporation mechanism in serpentine group minerals: Crystal chemical consideration

*Masami Kanzaki[1] (1.Institute for Planetary Matereials, Okayama University)

[SGC40-P06] Mineralogical and geochemical characteristics of cuttings from Taketomi hot spring

*Noriyuki Shingaki[1], Tomohiro Toki[1], Syogo Oshima[2], Masaaki chinen[3], Arito Sakaguchi[4], Naoto Takahata[5], Yuji Sano[5], Shirai Kotaro[5], Kentaro Tanaka[5] (1.University of the Ryukyus , 2.West Japan Engineering Consultants, Inc., 3.MicroRange, 4.Faculty of Science, Yamaguchi University, 5.Atmosphere and Ocean Research Institute, The University of Tokyo)

[SGC40-P07] Variation of helium isotope compositions at Lake Mashu

*Takanori Kagoshima[1], Yuji Sano[1], Atsushi Tanaka[2] (1.Atmosphere and Ocean Research Institute, University of Tokyo, 2.National Institute for Environmental Studies)

[SGC40-P08] Helium isotopes in Tachibana Bay and Shimabara Bay, Nagasaki

*Ma. Teresa Escobar[1], Yama Tomonaga[2], Hajime Obata[1], Shigenobu Takeda[3], Naoto Takahata[1], Yuji Sano[1] (1.Atmosphere and Ocean Research Institute, University of Tokyo, Kashiwanoha, Kashiwa, Chiba, Japan, 2.Eawag,, Swiss Federal Institute of Aquatic Science and Technology, Department of Water Resources and Drinking Water, Überlandstrasse 133 CH-8600 ,Dübendorf, Switzerland, 3.Graduate School of Fisheries and Environmental Sciences, Nagasaki University, Nagasaki, Japan)

[E] Poster | S (Solid Earth Sciences)：S-GC Geochemistry

5:15 PM - 6:30 PM JST | 8:15 AM - 9:30 AM UTC | Poster Hall International Exhibition Hall8, Makuhari Messe_31

[S-GC40] Volatile Cycles in the Deep Earth - from Subduction Zone to Hot Spot

convener:Hirochika Sumino(Department of Basic Science, Graduate School of Arts and Sciences, The University of Tokyo), Takeshi Hanyu(Japan Agency for Marine-Earth Science and Technology, Department of Solid Earth Geochemistry), Yuji Sano(Division of Ocean and Earth Systems, Atmosphere and Ocean Research Institute, University of Tokyo), Gray E Bebout(Lehigh University)

[SGC40-P01] Continental growth models demystified

*Jun Korenaga[1] (1.Department of Geology and Geophysics, Yale University)

[SGC40-P02] Mass-independent sulfur isotope signature from the 2.7 Ga Belingwe komatiite: Recycling of crustal material in Archean

*Yusuke Kubota[1], Yuichiro Ueno[1,2,3], Kenji Shimizu[3], Fumihiro Matsuura[2], Akira Ishikawa[1,3] (1.Department of Earth and Planetary Sciences, Tokyo Institute of Technology, 2.Earth-Life Science Institute, Tokyo Institute of Technology, 3.Japan Agency for Marine-Earth Science and Technology (JAMSTEC))

[SGC40-P03] Determination of halogens in some standard materials using the neutron irradiation noble gas mass spectrometric technique

*Hirochika Sumino[1], Masahiro Kobayashi[2], Takehiko Saito[3], Keisuke Nagao[3] (1.Department of Basic Science, Graduate School of Arts and Sciences, The University of Tokyo, 2.Tokyo Metropolitan Industrial Technology Research Institute, 3.Geochemical Research Center, Graduate School of Science, University of Tokyo)

[SGC40-P04] FTIR spectroscopy and noble gas mass spectrometry for a single olivine grain

*Sota Niki[1], Hirochika Sumino[2], Masahiro Kobayashi[3], Hiroyuki Kagi[1], Takafumi Hirata[1], Chris J. Ballentine[4] (1.Geochemical Research Center, Grad. School of Science, Univ. of Tokyo, 2.Dept. of Basic Science, Grad. School of Arts and Sciences, Univ. of Tokyo, 3.Tokyo Metropolitan Industrial Technology Research Institute, 4.Dept. of Earth Sciences, Univ. of Oxford)

[SGC40-P05] New halogen incorporation mechanism in serpentine group minerals: Crystal chemical consideration

*Masami Kanzaki[1] (1.Institute for Planetary Matereials, Okayama University)

[SGC40-P06] Mineralogical and geochemical characteristics of cuttings from Taketomi hot spring

*Noriyuki Shingaki[1], Tomohiro Toki[1], Syogo Oshima[2], Masaaki chinen[3], Arito Sakaguchi[4], Naoto Takahata[5], Yuji Sano[5], Shirai Kotaro[5], Kentaro Tanaka[5] (1.University of the Ryukyus , 2.West Japan Engineering Consultants, Inc., 3.MicroRange, 4.Faculty of Science, Yamaguchi University, 5.Atmosphere and Ocean Research Institute, The University of Tokyo)

[SGC40-P07] Variation of helium isotope compositions at Lake Mashu

*Takanori Kagoshima[1], Yuji Sano[1], Atsushi Tanaka[2] (1.Atmosphere and Ocean Research Institute, University of Tokyo, 2.National Institute for Environmental Studies)

[SGC40-P08] Helium isotopes in Tachibana Bay and Shimabara Bay, Nagasaki

*Ma. Teresa Escobar[1], Yama Tomonaga[2], Hajime Obata[1], Shigenobu Takeda[3], Naoto Takahata[1], Yuji Sano[1] (1.Atmosphere and Ocean Research Institute, University of Tokyo, Kashiwanoha, Kashiwa, Chiba, Japan, 2.Eawag,, Swiss Federal Institute of Aquatic Science and Technology, Department of Water Resources and Drinking Water, Überlandstrasse 133 CH-8600 ,Dübendorf, Switzerland, 3.Graduate School of Fisheries and Environmental Sciences, Nagasaki University, Nagasaki, Japan)

[E] Poster | S (Solid Earth Sciences)：S-CG Complex & General

10:45 AM - 12:15 PM JST | 1:45 AM - 3:15 AM UTC | Poster Hall International Exhibition Hall8, Makuhari Messe_10

[S-CG48] Science of slow earthquakes: Toward unified understandings of whole earthquake process

convener:Satoshi Ide(Department of Earth an Planetary Science, University of Tokyo), Hitoshi Hirose(Research Center for Urban Safety and Security, Kobe University), Kohtaro Ujiie(Graduate School of Life and Environmental Sciences, University of Tsukuba), Takahiro Hatano(Earthquake Research Institute, University of Tokyo)

[SCG48-P01] Off the Kii Peninsula Shallow Low Frequency Earthquake in 2004 revealed by Ocean Bottom Seismometer

*Koji Tamaribuchi[1], Akio Kobayashi[1], Takahito Nishimiya[1], Satoshi Annoura[2] (1.Meteorological Research Institute, 2.Japan Meteorological Agency)

[SCG48-P02] The development of pressure vessel on gouges for rock deformation at seismic rates under water-saturated conditions

*Wei-Ting Lin[1], Li-Wei Kuo[1], Wen-Jie Wu[1], Jia-Jyun Dong[1], Yi-Hung Huang[2] (1.National Central University, 2.MATSUKI HYDRAULIC INDUSTRIAL CO. LTD)

[SCG48-P03] Spatial variations of shallow very low-frequency earthquake activity along the Nankai Trough based on CMT inversion using the 3D heterogeneous model

*Shunsuke Takemura[1], Takanori Matsuzawa[1], Akemi Noda[1], Takashi Tonegawa[2], Youichi Asano[1], Takeshi Kimura[1], Katsuhiko Shiomi[1] (1.National Research Institute for Earth Science and Disaster Resilience, 2.Japan Agency for Marine-Earth Science and Technology)

[SCG48-P04] Evaluation of Magnitude and Characteristics of Seismicity of Low Frequency Earthquakes in Parkfield

*Miki Aso[1,3], Naofumi Aso[2], Satoshi Ide[1] (1.Department of Earth and Planetary Science, The University of Tokyo, 2.Tokyo Institute of Technology, School of Science, 3.OYO RMS Corporation)

[SCG48-P05] Tectonic tremor catalog in the Tohoku-Hokkaido-Oki region using S-net

*Satoshi Ide[1], Tomoaki Nishikawa[2], Takanori Matsuzawa[3], Kazuaki Ohta[2], Naoki Uchida[4], Takuya NISHIMURA[2] (1.Department of Earth an Planetary Science, University of Tokyo, 2.Disaster Prevention Research Institute, Kyoto University, 3.National Research Institute for Earth Science and Disaster Resilience, 4.Graduate School of Science and International Research Institute of Disaster Science, Tohoku University)

[SCG48-P06] Spontaneous Slow Slip and Runaway Slip in Laboratory

*Miki Takahashi[1] (1.Institute of Earthquake and Volcano Geology, Geological Survey of Japan, AIST)

[SCG48-P07] Hydration and amorphization of quartz rocks during high-velocity frictional sliding: An examination of fault gouge from friction experiments of synthetic quartz

*Yuko Onoe[1], Hirotaka Iida[2], Akito Tsutsumi[1], Aki Takigawa[1] (1.Graduate School of Science, Kyoto University, 2.Geothermal Engineering Co., Ltd.)

[SCG48-P08] Constraining S Wave Velocity of the Source Region of Shallow Very Low-Frequency Earthquakes

*Takeshi Akuhara[1], Takashi Tonegawa[2] (1.Earthquake Research Institute, The University of Tokyo, 2.Research and Development center for Earthquake and Tsunami, Japan Agency for Marine-Earth Science and Technology)

[SCG48-P09] Quantitative relationship between aseismic slip propagation speed and frictional properties

*Keisuke Ariyoshi[1], Jean-Paul Ampuero[2,3], Roland Burgmann[4], Toru Matsuzawa[5], Akira Hasegawa[5], Ryota Hino[5], Takane Hori[1] (1.Japan Agency for Marine-Earth Science and Technology, 2.Université Côte d'Azur, 3.California Institute of Technology, 4.University of California, Berkeley, 5.Graduate School of Science, Tohoku University)

[SCG48-P10] Comprehensive detection of very low frequency earthquakes off the Pacific coasts of Hokkaido and Tohoku, northeastern Japan

*Satoru Baba[1], Akiko Takeo[1], Kazushige Obara[1], Takanori Matsuzawa[2], Takuto Maeda[3] (1.Earthquake Research Institute, University of Tokyo, 2.National Research Institute for Earth Science and Disaster Resilience, 3.Graduate School of Science and Technology, Hirosaki University)

[SCG48-P11] **Spatio-temporal evolution of long- and short-term slow slip events in the Tokai region, central Japan estimated from a very dense GNSS network, during 1997-2017**

*Hiromu Sakaue[1], Takuya NISHIMURA[2], Jun'ichi Fukuda[3], Teruyuki Kato[4] (1.Graduate School of Science, Kyoto University, 2.Disaster Prevention Research Institute Kyoto University, 3.Earthquake Research Institute,The University of Tokyo, 4.Hot Springs Research Institute of Kanagawa Prefecture)

[SCG48-P12] Broadband excitation of acoustic emission in granular stick-slip : experiments and spectral analyses

*Hidekazu Fukumizu[1], Ikuro Sumita[2] (1.Earth and Environmental Science Course, Division of Natural System, Graduate school of Natural Science and Technology, Kanazawa University, 2.School of Geosciences and Civil Engineering, Kanazawa University)

[SCG48-P13] Episodic tremor and slip silently invades strongly locked megathrust in the Nankai Trough

*Masayuki Kano[1], Aitaro Kato[2], Kazushige Obara[2] (1.Graduate school of science, Tohoku University, 2.Earthquake Research Institute, The University of Tokyo)

[SCG48-P14] Spatial distribution of the electrical resistivity beneath western part of Shikoku Island where long-term SSE events have repeatedly occurred

*Makoto Uyeshima[1], Maki Hata[1], Hiroshi Ichihara[2], Ryokei Yoshimura[3], Koki Aizawa[4] (1.Earthquake Research Institute, The University of Tokyo, 2.Graduate School of Environmental Studies, Nagoya University, 3.Disaster Prevention Research Institute, Kyoto University, 4.Institute of Seismology and Volcanology, Faculty of Sciences, Kyushu University)

[SCG48-P15] Variations of scaling relationships for shallow tremor observed along the Nankai trough

*Masaru Nakano[1], Suguru Yabe[1] (1.Japan Agency for Marine-Earth Science and Technology)

[SCG48-P16] Low-frequency earthquakes triggered by teleseismic surface waves by Ryukyu subduction zone.

Ayumi Kinjo[1], *Mamoru Nakamura[1] (1.Faculty of Science, University of the Ryukyus)

[SCG48-P17] Detection of small surface displacement accompanying deep low-frequency tremor in Shikoku region, southwest Japan

*Yutaro Okada[1], Takao Tabei[2] (1.Faculty of Science, Kochi University, 2.Faculty of Science and Technology, Kochi University)

[SCG48-P18] Long-term temporal change in crustal resistivity beneath western Shikoku

*Futoshi Yamashita[1], Yoshimori Honkura[1] (1.National Research Institute for Earth Science and Disaster Resilience)

[SCG48-P19] Slow decay of postseismic deformation compared with aftershocks following the 2011 Tohoku-oki Earthquake

*Yuta Mitsui[1], Shunsuke Morikami[2] (1.Department of Geosciences, Shizuoka University, 2.Formerly at Graduate School of Science and Technology, Shizuoka University)

[SCG48-P20] Serpentinite dehydration in subduction shear zones formed at source depths of slow earthquakes

*Yasushi Mori[1], Miki Shigeno[1], Kohtaro Ujiie[2], Kazuya Noro[2], Tadao Nishiyama[3] (1.Kitakyushu Museum of Natural History and Human History, 2.University of Tsukuba, 3.Kumamoto University)

[SCG48-P21] Earthquake swarms following very low-frequency earthquakes in the central Ryukyu Trench

*Mamoru Nakamura[1] (1.Faculty of Science, University of the Ryukyus)

[SCG48-P22] Seismic imaging in the central Nankai trough, off Shionomisaki to Kii channel

*Yasuyuki Nakamura[1], Shuichi Kodaira[1], Tetsuo No[1], Yuka Kaiho[1], Gou Fujie[1], Seiichi Miura[1], Kazuya Shiraishi[1] (1.Japan Agency for Marine Earth Science and Technology)

[SCG48-P23] Attempt to Detect Intra-plate SSEs Based on F3 Solution of GEONET

*Yusaku Tanaka[1] (1.Earthquake Research Institute)

[SCG48-P24] A new hydrothermal, low to high speed rotary-shearing apparatus: Reproduction of slow/megathrust earthquakes in laboratory

*Takehiro Hirose[1], Wataru Tanikawa[1], Yohei Hamada[1], Keishi Okazaki[1] (1.Kochi Institute for Core Sample Research, Japan Agency for Marine-Earth Science and Technology)

[SCG48-P25] Very low-frequency earthquakes in western Shikoku remotely triggered by the 2016 Mw5.9 off-Kii Peninsula earthquake

*Masatoshi Miyazawa[1] (1.Disaster Prevention Research Institute, Kyoto University)

[SCG48-P26] **Underground structure around source region of slow earthquakes in western Shikoku obtained by receiver function analysis**

Akira Hikita[1], Aitaro Kato[1], *Kazushige Obara[1], Akiko Takeo[1], Takeshi Akuhara[1] (1.Earthquake Research Institute, The University of Tokyo)

[SCG48-P27] Hypocenter determination of deep low frequency tremors beneath the Kii Peninsula by backprojection of seismic array data

*Kodai Sagae[1], Hisashi Nakahara[1], Takeshi Nishimura[1], Kazutoshi Imanishi[2] (1.Graduate School of Science,Tohoku University, 2.National Institute of Advanced Industrial Science and Technology (AIST))

[SCG48-P28] Triggered tremors and stress perturbations due to surface waves

*Ryohei Ikeda[1], Naoki Suda[1] (1.Hiroshima University)

[SCG48-P29] Numerical modeling of long- and shallow slow slip events including shallow region in Hyuganada and western Nankai, Japan

*Takanori Matsuzawa[1], Bunichiro Shibazaki[2] (1.National Research Institute for Earth Science and Disaster Resilience, 2.Building Research Institute)

[SCG48-P30] Further evidence for the influence of a subducting-ridge on the spatial strain accumulation and release pattern in the shallow eastern Nankai Trough, based on VLFE distribution

*Akiko Toh[1], Chen Wan-Jou [2], Doug Dreger[3], Wu-Cheng Chi[2], Satoshi Ide[1] (1.University of Tokyo, 2.Institute of Earth Sciences, Academia Sinica, 3.UC Berkeley)

[SCG48-P31] Evidence for semi-brittle flow in mantle-wedge serpentinites under high pore fluid pressure and their implications for deep low frequency earthquakes

Kengo Kataoka[1], Yurina Nagata[1], *Ken-ichi Hirauchi[1], Ryosuke Oyanagi[2], Atsushi Okamoto[3], Katsuyoshi Michibayashi[4] (1.Department of Geosciences, Faculty of Science, Shizuoka University, 2.Japan Agency for Marine-Earth Science and Technology, 3.Graduate School of Environmental studies, Tohoku University, 4.Department of Earth and Planetary Sciences, Nagoya University)

[SCG48-P32] Spatial distribution of slow slip events off the Boso peninsula from 1996 to 2018 under sparsity constraints

*Ryoko Nakata[1], Hideitsu Hino[2], Tatsu Kuwatani[3,4], Takahiro Akiyama[5], Shoichi Yoshioka[6], Masato Okada[7], Takane Hori[1] (1.Japan Agency for Marine-Earth Science and Technology, 2.The Institute of Statistical Mathematics, 3.Department of Solid Earth Geochemistry, Japan Agency for Marine-Earth Science and Technology, 4.PRESTO, Japan Science and Technology Agency, 5.Graduate School of Science, Kobe University, 6.Research Center for Urban Safety and Security, Kobe University, 7.Graduate School of Frontier Sciences, The University of Tokyo)

[SCG48-P33] Marine electromagnetic observations around a slow earthquake region in the western Nankai trough

*Hiroshi Ichihara[1], Tada-nori Goto[2], Tetsuo Matsuno[3], Noriko Tada[4], Shinya Sato[2] (1.Earthquake and Volcano Research Center, Nagoya University, 2.Graduate School of Engineering, Kyoto University, 3.Ocean Bottom Exploration Center, Kobe University, 4.JAMSTEC)

[SCG48-P34] Dynamics of precipitating injection fronts inside of structured medium

*Yutaka Sumino[1], Shunsuke Tanaka[1], Miyuki Kunihiro[1] (1.Tokyo University of Science)

[SCG48-P35] Permeability changes of simulated low permeable fault rocks induced by intermediate velocity friction test

*Wataru Tanikawa[1] (1.Japan Agency for Marine-Earth Science and Technology, Kochi Instutute for Core Sample Research)

[SCG48-P36] Modified relation between the coupling and tremor rates around the Shikoku region

*Tadafumi Ochi[1] (1.Institute of Earthquake and Volcano Geology, Geological Survey of Japan, The National Institute of Advanced Industrial Science and Technology)

[SCG48-P37] Spatiotemporal distribution of regular and very low-frequency earthquakes in the northern part of the Ryukyu subduction zone

*Youichi Asano[1], Kazuhiko Goto[2], Hiroshi Yakiwara[3], Shuichiro Hirano[3] (1.National Research Institute for Earth Science and Disaster Resilience, 2.Association for the development of earthquake prediction, 3.Nansei-toko Observatory for Earthquakes and Volcanoes, Kagoshima University)

[SCG48-P38] Possible tectonic tremor activities near the VLFE epicenters in the Sanriku-Oki region in 2011

*Hidenobu Takahashi[1], Ryota Hino[1], Yusaku Ohta[1], Naoki Uchida[1], Syuichi Suzuki[1], Masanao Shinohara[2], Takanori Matsuzawa[3] (1.Graduate school of Science Tohoku University , 2.Earthquake Research Institute, University of Tokyo, 3.National Research Institute for Earth Science and Disaster Resilience)

[SCG48-P39] Heterogeneous structure around a region of slow earthquake activity off Ibaraki prefecture along the Japan Trench

*Kimihiro Mochizuki[1], Tomoaki Yamada[1], Masanao Shinohara[1], Ryota Hino[2], Ryosuke Azuma[2], Yoshihiro Ito[3], Yoshio Murai[4], Kenji Uehira[5], Toshinori Sato[6] (1.ERI, Univ. of Tokyo, 2.Graduate School of Science, Tohoku Univ., 3.DPRI, Kyoto Univ., 4.Faculty of Science, Hokkaido Univ., 5.NIED, 6.Graduate School of Science, Chiba Univ.)

[SCG48-P40] Shallow low-frequency tremor triggered by nearby moderate earthquakes off Sanriku

*Sachiko Tanaka[1], Takanori Matsuzawa[1], Youichi Asano[1] (1.National Research Institute for Earth Science and Disaster Resilience)

[SCG48-P41] Slow slip events in the Bungo Channel over 15 years as inferred from GNSS data (1996-2011)

Takatoshi Yokoi[1], *SHINICHI MIYAZAKI[1], Hiromu Sakaue[1], Jun'ichi Fukuda[2] (1.Graduate School of Science, Kyoto University, 2.Earthquake Research Institute, The University of Tokyo)

[SCG48-P42] Investigations of sensor orientation and a possibility of detecting crustal deformation based on accelerometer records of S-net

*Ryota Takagi[1], Naoki Uchida[1], Takashi NAKAYAMA[1], Ryosuke Azuma[1], Akira Ishigami[1], Tomomi Okada[1], Yusaku Ohta[1], Ryota Hino[1] (1.Research Center for Prediction of Earthquakes and Volcanic Eruptions, Graduate School of Science, Tohoku University)

[SCG48-P43] Spatiotemporal variation of released seismic energy from shallow low-frequency tremor in Hyuga-nada, revealed by ocean bottom seismological observation

*Yusuke Yamashita[1], Saki Watanabe[2], Tomoaki Yamada[3], Masanao Shinohara[3], Takeshi Matsushima[2] (1.Disaster Prevention Research Institute, Kyoto University, 2.Institute of Seismology and Volcanology, Kyushu University, 3.Earthquake Research Institute, The University of Tokyo)

[SCG48-P44] Unified description of fast and slow earthquakes using velocity strengthening patches

*So Ozawa[1], Takahiro Hatano[1] (1.Earthquake Research Institute, the University of Tokyo)

[SCG48-P45] The b-value of the earthquake swarm activities accompanied by the Boso slow slip events

*Yuki Noda[1], Hitoshi Hirose[2,1] (1.Department of Planetology, Faculty of Science, Kobe University , 2.Research Center for Urban Safety and Security, Kobe University)

[SCG48-P46] **Three-dimensional thermal modeling associated with subduction of the Philippine Sea plate at the Ryukyu Trench, and its relation to the occurrence of interplate seismic events**

*Nobuaki Suenaga[1], Shoichi Yoshioka[2,1], Yinfeng Ji[3] (1.Graduate School of Science, Kobe University, Japan, 2.Research Center for Urban Safety and Security, Kobe University, Japan, 3.Chinese Academy of Science, Beijin, China)

[E] Poster | S (Solid Earth Sciences)：S-CG Complex & General

5:15 PM - 6:30 PM JST | 8:15 AM - 9:30 AM UTC | Poster Hall International Exhibition Hall8, Makuhari Messe_33

[S-CG48] Science of slow earthquakes: Toward unified understandings of whole earthquake process

convener:Satoshi Ide(Department of Earth an Planetary Science, University of Tokyo), Hitoshi Hirose(Research Center for Urban Safety and Security, Kobe University), Kohtaro Ujiie(Graduate School of Life and Environmental Sciences, University of Tsukuba), Takahiro Hatano(Earthquake Research Institute, University of Tokyo)

[SCG48-P01] Off the Kii Peninsula Shallow Low Frequency Earthquake in 2004 revealed by Ocean Bottom Seismometer

*Koji Tamaribuchi[1], Akio Kobayashi[1], Takahito Nishimiya[1], Satoshi Annoura[2] (1.Meteorological Research Institute, 2.Japan Meteorological Agency)

[SCG48-P02] The development of pressure vessel on gouges for rock deformation at seismic rates under water-saturated conditions

*Wei-Ting Lin[1], Li-Wei Kuo[1], Wen-Jie Wu[1], Jia-Jyun Dong[1], Yi-Hung Huang[2] (1.National Central University, 2.MATSUKI HYDRAULIC INDUSTRIAL CO. LTD)

[SCG48-P03] Spatial variations of shallow very low-frequency earthquake activity along the Nankai Trough based on CMT inversion using the 3D heterogeneous model

*Shunsuke Takemura[1], Takanori Matsuzawa[1], Akemi Noda[1], Takashi Tonegawa[2], Youichi Asano[1], Takeshi Kimura[1], Katsuhiko Shiomi[1] (1.National Research Institute for Earth Science and Disaster Resilience, 2.Japan Agency for Marine-Earth Science and Technology)

[SCG48-P04] Evaluation of Magnitude and Characteristics of Seismicity of Low Frequency Earthquakes in Parkfield

*Miki Aso[1,3], Naofumi Aso[2], Satoshi Ide[1] (1.Department of Earth and Planetary Science, The University of Tokyo, 2.Tokyo Institute of Technology, School of Science, 3.OYO RMS Corporation)

[SCG48-P05] Tectonic tremor catalog in the Tohoku-Hokkaido-Oki region using S-net

*Satoshi Ide[1], Tomoaki Nishikawa[2], Takanori Matsuzawa[3], Kazuaki Ohta[2], Naoki Uchida[4], Takuya NISHIMURA[2] (1.Department of Earth an Planetary Science, University of Tokyo, 2.Disaster Prevention Research Institute, Kyoto University, 3.National Research Institute for Earth Science and Disaster Resilience, 4.Graduate School of Science and International Research Institute of Disaster Science, Tohoku University)

[SCG48-P06] **Spontaneous Slow Slip and Runaway Slip in Laboratory**

*Miki Takahashi[1] (1.Institute of Earthquake and Volcano Geology, Geological Survey of Japan, AIST)

[SCG48-P07] Hydration and amorphization of quartz rocks during high-velocity frictional sliding: An examination of fault gouge from friction experiments of synthetic quartz

*Yuko Onoe[1], Hirotaka Iida[2], Akito Tsutsumi[1], Aki Takigawa[1] (1.Graduate School of Science, Kyoto University, 2.Geothermal Engineering Co., Ltd.)

[SCG48-P08] Constraining S Wave Velocity of the Source Region of Shallow Very Low-Frequency Earthquakes

*Takeshi Akuhara[1], Takashi Tonegawa[2] (1.Earthquake Research Institute, The University of Tokyo, 2.Research and Development center for Earthquake and Tsunami, Japan Agency for Marine-Earth Science and Technology)

[SCG48-P09] **Quantitative relationship between aseismic slip propagation speed and frictional properties**

*Keisuke Ariyoshi[1], Jean-Paul Ampuero[2,3], Roland Burgmann[4], Toru Matsuzawa[5], Akira Hasegawa[5], Ryota Hino[5], Takane Hori[1] (1.Japan Agency for Marine-Earth Science and Technology, 2.Université Côte d'Azur, 3.California Institute of Technology, 4.University of California, Berkeley, 5.Graduate School of Science, Tohoku University)

[SCG48-P10] Comprehensive detection of very low frequency earthquakes off the Pacific coasts of Hokkaido and Tohoku, northeastern Japan

*Satoru Baba[1], Akiko Takeo[1], Kazushige Obara[1], Takanori Matsuzawa[2], Takuto Maeda[3] (1.Earthquake Research Institute, University of Tokyo, 2.National Research Institute for Earth Science and Disaster Resilience, 3.Graduate School of Science and Technology, Hirosaki University)

[SCG48-P11] **Spatio-temporal evolution of long- and short-term slow slip events in the Tokai region, central Japan estimated from a very dense GNSS network, during 1997-2017**

*Hiromu Sakaue[1], Takuya NISHIMURA[2], Jun'ichi Fukuda[3], Teruyuki Kato[4] (1.Graduate School of Science, Kyoto University, 2.Disaster Prevention Research Institute Kyoto University, 3.Earthquake Research Institute,The University of Tokyo, 4.Hot Springs Research Institute of Kanagawa Prefecture)

[SCG48-P12] Broadband excitation of acoustic emission in granular stick-slip : experiments and spectral analyses

*Hidekazu Fukumizu[1], Ikuro Sumita[2] (1.Earth and Environmental Science Course, Division of Natural System, Graduate school of Natural Science and Technology, Kanazawa University, 2.School of Geosciences and Civil Engineering, Kanazawa University)

[SCG48-P13] Episodic tremor and slip silently invades strongly locked megathrust in the Nankai Trough

*Masayuki Kano[1], Aitaro Kato[2], Kazushige Obara[2] (1.Graduate school of science, Tohoku University, 2.Earthquake Research Institute, The University of Tokyo)

[SCG48-P14] Spatial distribution of the electrical resistivity beneath western part of Shikoku Island where long-term SSE events have repeatedly occurred

*Makoto Uyeshima[1], Maki Hata[1], Hiroshi Ichihara[2], Ryokei Yoshimura[3], Koki Aizawa[4] (1.Earthquake Research Institute, The University of Tokyo, 2.Graduate School of Environmental Studies, Nagoya University, 3.Disaster Prevention Research Institute, Kyoto University, 4.Institute of Seismology and Volcanology, Faculty of Sciences, Kyushu University)

[SCG48-P15] Variations of scaling relationships for shallow tremor observed along the Nankai trough

*Masaru Nakano[1], Suguru Yabe[1] (1.Japan Agency for Marine-Earth Science and Technology)

[SCG48-P16] Low-frequency earthquakes triggered by teleseismic surface waves by Ryukyu subduction zone.

Ayumi Kinjo[1], *Mamoru Nakamura[1] (1.Faculty of Science, University of the Ryukyus)

[SCG48-P17] Detection of small surface displacement accompanying deep low-frequency tremor in Shikoku region, southwest Japan

*Yutaro Okada[1], Takao Tabei[2] (1.Faculty of Science, Kochi University, 2.Faculty of Science and Technology, Kochi University)

[SCG48-P18] Long-term temporal change in crustal resistivity beneath western Shikoku

*Futoshi Yamashita[1], Yoshimori Honkura[1] (1.National Research Institute for Earth Science and Disaster Resilience)

[SCG48-P19] Slow decay of postseismic deformation compared with aftershocks following the 2011 Tohoku-oki Earthquake

*Yuta Mitsui[1], Shunsuke Morikami[2] (1.Department of Geosciences, Shizuoka University, 2.Formerly at Graduate School of Science and Technology, Shizuoka University)

[SCG48-P20] Serpentinite dehydration in subduction shear zones formed at source depths of slow earthquakes

*Yasushi Mori[1], Miki Shigeno[1], Kohtaro Ujiie[2], Kazuya Noro[2], Tadao Nishiyama[3] (1.Kitakyushu Museum of Natural History and Human History, 2.University of Tsukuba, 3.Kumamoto University)

[SCG48-P21] Earthquake swarms following very low-frequency earthquakes in the central Ryukyu Trench

*Mamoru Nakamura[1] (1.Faculty of Science, University of the Ryukyus)

[SCG48-P22] Seismic imaging in the central Nankai trough, off Shionomisaki to Kii channel

*Yasuyuki Nakamura[1], Shuichi Kodaira[1], Tetsuo No[1], Yuka Kaiho[1], Gou Fujie[1], Seiichi Miura[1], Kazuya Shiraishi[1] (1.Japan Agency for Marine Earth Science and Technology)

[SCG48-P23] Attempt to Detect Intra-plate SSEs Based on F3 Solution of GEONET

*Yusaku Tanaka[1] (1.Earthquake Research Institute)

[SCG48-P24] A new hydrothermal, low to high speed rotary-shearing apparatus: Reproduction of slow/megathrust earthquakes in laboratory

*Takehiro Hirose[1], Wataru Tanikawa[1], Yohei Hamada[1], Keishi Okazaki[1] (1.Kochi Institute for Core Sample Research, Japan Agency for Marine-Earth Science and Technology)

[SCG48-P25] Very low-frequency earthquakes in western Shikoku remotely triggered by the 2016 Mw5.9 off-Kii Peninsula earthquake

*Masatoshi Miyazawa[1] (1.Disaster Prevention Research Institute, Kyoto University)

[SCG48-P26] **Underground structure around source region of slow earthquakes in western Shikoku obtained by receiver function analysis**

Akira Hikita[1], Aitaro Kato[1], *Kazushige Obara[1], Akiko Takeo[1], Takeshi Akuhara[1] (1.Earthquake Research Institute, The University of Tokyo)

[SCG48-P27] Hypocenter determination of deep low frequency tremors beneath the Kii Peninsula by backprojection of seismic array data

*Kodai Sagae[1], Hisashi Nakahara[1], Takeshi Nishimura[1], Kazutoshi Imanishi[2] (1.Graduate School of Science,Tohoku University, 2.National Institute of Advanced Industrial Science and Technology (AIST))

[SCG48-P28] Triggered tremors and stress perturbations due to surface waves

*Ryohei Ikeda[1], Naoki Suda[1] (1.Hiroshima University)

[SCG48-P29] Numerical modeling of long- and shallow slow slip events including shallow region in Hyuganada and western Nankai, Japan

*Takanori Matsuzawa[1], Bunichiro Shibazaki[2] (1.National Research Institute for Earth Science and Disaster Resilience, 2.Building Research Institute)

[SCG48-P30] Further evidence for the influence of a subducting-ridge on the spatial strain accumulation and release pattern in the shallow eastern Nankai Trough, based on VLFE distribution

*Akiko Toh[1], Chen Wan-Jou [2], Doug Dreger[3], Wu-Cheng Chi[2], Satoshi Ide[1] (1.University of Tokyo, 2.Institute of Earth Sciences, Academia Sinica, 3.UC Berkeley)

[SCG48-P31] Evidence for semi-brittle flow in mantle-wedge serpentinites under high pore fluid pressure and their implications for deep low frequency earthquakes

Kengo Kataoka[1], Yurina Nagata[1], *Ken-ichi Hirauchi[1], Ryosuke Oyanagi[2], Atsushi Okamoto[3], Katsuyoshi Michibayashi[4] (1.Department of Geosciences, Faculty of Science, Shizuoka University, 2.Japan Agency for Marine-Earth Science and Technology, 3.Graduate School of Environmental studies, Tohoku University, 4.Department of Earth and Planetary Sciences, Nagoya University)

[SCG48-P32] Spatial distribution of slow slip events off the Boso peninsula from 1996 to 2018 under sparsity constraints

*Ryoko Nakata[1], Hideitsu Hino[2], Tatsu Kuwatani[3,4], Takahiro Akiyama[5], Shoichi Yoshioka[6], Masato Okada[7], Takane Hori[1] (1.Japan Agency for Marine-Earth Science and Technology, 2.The Institute of Statistical Mathematics, 3.Department of Solid Earth Geochemistry, Japan Agency for Marine-Earth Science and Technology, 4.PRESTO, Japan Science and Technology Agency, 5.Graduate School of Science, Kobe University, 6.Research Center for Urban Safety and Security, Kobe University, 7.Graduate School of Frontier Sciences, The University of Tokyo)

[SCG48-P33] Marine electromagnetic observations around a slow earthquake region in the western Nankai trough

*Hiroshi Ichihara[1], Tada-nori Goto[2], Tetsuo Matsuno[3], Noriko Tada[4], Shinya Sato[2] (1.Earthquake and Volcano Research Center, Nagoya University, 2.Graduate School of Engineering, Kyoto University, 3.Ocean Bottom Exploration Center, Kobe University, 4.JAMSTEC)

[SCG48-P34] Dynamics of precipitating injection fronts inside of structured medium

*Yutaka Sumino[1], Shunsuke Tanaka[1], Miyuki Kunihiro[1] (1.Tokyo University of Science)

[SCG48-P35] Permeability changes of simulated low permeable fault rocks induced by intermediate velocity friction test

*Wataru Tanikawa[1] (1.Japan Agency for Marine-Earth Science and Technology, Kochi Instutute for Core Sample Research)

[SCG48-P36] Modified relation between the coupling and tremor rates around the Shikoku region

*Tadafumi Ochi[1] (1.Institute of Earthquake and Volcano Geology, Geological Survey of Japan, The National Institute of Advanced Industrial Science and Technology)

[SCG48-P37] Spatiotemporal distribution of regular and very low-frequency earthquakes in the northern part of the Ryukyu subduction zone

*Youichi Asano[1], Kazuhiko Goto[2], Hiroshi Yakiwara[3], Shuichiro Hirano[3] (1.National Research Institute for Earth Science and Disaster Resilience, 2.Association for the development of earthquake prediction, 3.Nansei-toko Observatory for Earthquakes and Volcanoes, Kagoshima University)

[SCG48-P38] Possible tectonic tremor activities near the VLFE epicenters in the Sanriku-Oki region in 2011

*Hidenobu Takahashi[1], Ryota Hino[1], Yusaku Ohta[1], Naoki Uchida[1], Syuichi Suzuki[1], Masanao Shinohara[2], Takanori Matsuzawa[3] (1.Graduate school of Science Tohoku University , 2.Earthquake Research Institute, University of Tokyo, 3.National Research Institute for Earth Science and Disaster Resilience)

[SCG48-P39] Heterogeneous structure around a region of slow earthquake activity off Ibaraki prefecture along the Japan Trench

*Kimihiro Mochizuki[1], Tomoaki Yamada[1], Masanao Shinohara[1], Ryota Hino[2], Ryosuke Azuma[2], Yoshihiro Ito[3], Yoshio Murai[4], Kenji Uehira[5], Toshinori Sato[6] (1.ERI, Univ. of Tokyo, 2.Graduate School of Science, Tohoku Univ., 3.DPRI, Kyoto Univ., 4.Faculty of Science, Hokkaido Univ., 5.NIED, 6.Graduate School of Science, Chiba Univ.)

[SCG48-P40] Shallow low-frequency tremor triggered by nearby moderate earthquakes off Sanriku

*Sachiko Tanaka[1], Takanori Matsuzawa[1], Youichi Asano[1] (1.National Research Institute for Earth Science and Disaster Resilience)

[SCG48-P41] Slow slip events in the Bungo Channel over 15 years as inferred from GNSS data (1996-2011)

Takatoshi Yokoi[1], *SHINICHI MIYAZAKI[1], Hiromu Sakaue[1], Jun'ichi Fukuda[2] (1.Graduate School of Science, Kyoto University, 2.Earthquake Research Institute, The University of Tokyo)

[SCG48-P42] Investigations of sensor orientation and a possibility of detecting crustal deformation based on accelerometer records of S-net

*Ryota Takagi[1], Naoki Uchida[1], Takashi NAKAYAMA[1], Ryosuke Azuma[1], Akira Ishigami[1], Tomomi Okada[1], Yusaku Ohta[1], Ryota Hino[1] (1.Research Center for Prediction of Earthquakes and Volcanic Eruptions, Graduate School of Science, Tohoku University)

[SCG48-P43] Spatiotemporal variation of released seismic energy from shallow low-frequency tremor in Hyuga-nada, revealed by ocean bottom seismological observation

*Yusuke Yamashita[1], Saki Watanabe[2], Tomoaki Yamada[3], Masanao Shinohara[3], Takeshi Matsushima[2] (1.Disaster Prevention Research Institute, Kyoto University, 2.Institute of Seismology and Volcanology, Kyushu University, 3.Earthquake Research Institute, The University of Tokyo)

[SCG48-P44] Unified description of fast and slow earthquakes using velocity strengthening patches

*So Ozawa[1], Takahiro Hatano[1] (1.Earthquake Research Institute, the University of Tokyo)

[SCG48-P45] The b-value of the earthquake swarm activities accompanied by the Boso slow slip events

*Yuki Noda[1], Hitoshi Hirose[2,1] (1.Department of Planetology, Faculty of Science, Kobe University , 2.Research Center for Urban Safety and Security, Kobe University)

[SCG48-P46] **Three-dimensional thermal modeling associated with subduction of the Philippine Sea plate at the Ryukyu Trench, and its relation to the occurrence of interplate seismic events**

*Nobuaki Suenaga[1], Shoichi Yoshioka[2,1], Yinfeng Ji[3] (1.Graduate School of Science, Kobe University, Japan, 2.Research Center for Urban Safety and Security, Kobe University, Japan, 3.Chinese Academy of Science, Beijin, China)

[E] Poster | M (Multidisciplinary and Interdisciplinary)：M-GI General Geosciences, Information Geosciences & Simulations

10:45 AM - 12:15 PM JST | 1:45 AM - 3:15 AM UTC | Poster Hall International Exhibition Hall8, Makuhari Messe_11

[M-GI30] Data assimilation: A fundamental approach in geosciences

convener:Shin ya Nakano(The Institute of Statistical Mathematics), Yosuke Fujii(Meteorological Research Institute, Japan Meteorological Agency), SHINICHI MIYAZAKI(Graduate School of Science, Kyoto University), Takemasa Miyoshi(RIKEN)

[MGI30-P01] Superposition of atmospheric states using information redundancy for Numerical Weather Prediction

*Toshiyuki Ishibashi[1] (1.Meteorological Research Institute/Japan Meteorological Agency)

[MGI30-P02] **Numerical Weather Prediction Experiments using a Coupled Atmosphere-Ocean Data Assimilation System in JMA/MRI** (3)

*Toshiyuki Ishibashi[1], Takeshi Iriguchi[1], Yosuke Fujii[1], Tamaki Yasuda[1], Yuhei Takaya[1], Naoki Saito[1], Toshikazu Onogi[1] (1.Meteorological Research Institute/Japan Meteorological Agency)

[MGI30-P03] **Accurate estimation of posterior error covariance in a 4D-Var inverse analysis**

*Yosuke Niwa[1,2], Yosuke Fujii[2,3] (1.National Institute for Environmental Studies, 2.Meteorological Research Institute, Japan Meteorological Agency, 3.The Institute of Statistical Mathematics)

[MGI30-P04] Assimilation CO_2 concentration data in the Kanto region using AIST-MM model and for the estimation of CO_2 emissions

*Yutaka Arai[1], Ryoichi Imasu[1], Hiroaki Kondo[2], Yosuke Niwa[3] (1.Atmosphere and Ocean Research Institute, The University of Tokyo, 2.National Institute of Advanced Industrial Science and Technology, 3.National Institute for Environmental Studies, Independent Administrative Institutions)

[MGI30-P05] **Application of data assimilation method on parameter estimation of flow and nutrient behavior in watershed model**

*Yosuke Horie[1] (1.Nippon Koei Co., Ltd.)

[MGI30-P06] Bayesian inference of grain growth prediction via multi-phase-field models

*Shin-ichi Ito[1], Hiromichi Nagao[1], Takashi Kurokawa[1], Tadashi Kasuya[1], Junya Inoue[1] (1.The University of Tokyo)

[MGI30-P07] GNSS data assimilation for the Bungo channel Long-term SSEs using Ensemble Kalman Filter (EnKF)

*Megumi Fujita[1], Takuya NISHIMURA[2], Kazuro Hirahara[3], SHINICHI MIYAZAKI[1] (1.Graduate School of Science , Kyoto University, 2.Disaster Prevention Research Institute, Kyoto University, 3.Institute of Education, Research and Regional Cooperation for crisis Management Shikoku, Kagawa University)

[MGI30-P08] A data assimilation library with Python for parallel computing

*Shin ya Nakano[1], Yuya Ariyoshi[2], Tomoyuki Higuchi[1] (1.The Institute of Statistical Mathematics, 2.Faculty of Engineering, Nippon Bunri University)

[E] Poster | M (Multidisciplinary and Interdisciplinary)：M-GI General Geosciences, Information Geosciences & Simulations

5:15 PM - 6:30 PM JST | 8:15 AM - 9:30 AM UTC | Poster Hall International Exhibition Hall8, Makuhari Messe_37

[M-GI30] Data assimilation: A fundamental approach in geosciences

convener:Shin ya Nakano(The Institute of Statistical Mathematics), Yosuke Fujii(Meteorological Research Institute, Japan Meteorological Agency), SHINICHI MIYAZAKI(Graduate School of Science, Kyoto University), Takemasa Miyoshi(RIKEN)

[MGI30-P01] Superposition of atmospheric states using information redundancy for Numerical Weather Prediction

*Toshiyuki Ishibashi[1] (1.Meteorological Research Institute/Japan Meteorological Agency)

[MGI30-P02] **Numerical Weather Prediction Experiments using a Coupled Atmosphere-Ocean Data Assimilation System in JMA/MRI** (3)

*Toshiyuki Ishibashi[1], Takeshi Iriguchi[1], Yosuke Fujii[1], Tamaki Yasuda[1], Yuhei Takaya[1], Naoki Saito[1], Toshikazu Onogi[1] (1.Meteorological Research Institute/Japan Meteorological Agency)

[MGI30-P03] **Accurate estimation of posterior error covariance in a 4D-Var inverse analysis**

*Yosuke Niwa[1,2], Yosuke Fujii[2,3] (1.National Institute for Environmental Studies, 2.Meteorological Research Institute, Japan Meteorological Agency, 3.The Institute of Statistical Mathematics)

[MGI30-P04] Assimilation CO_2 concentration data in the Kanto region using AIST-MM model and for the estimation of CO_2 emissions

*Yutaka Arai[1], Ryoichi Imasu[1], Hiroaki Kondo[2], Yosuke Niwa[3] (1.Atmosphere and Ocean Research Institute, The University of Tokyo, 2.National Institute of Advanced Industrial Science and Technology, 3.National Institute for Environmental Studies, Independent Administrative Institutions)

[MGI30-P05] **Application of data assimilation method on parameter estimation of flow and nutrient behavior in watershed model**

*Yosuke Horie[1] (1.Nippon Koei Co., Ltd.)

[MGI30-P06] Bayesian inference of grain growth prediction via multi-phase-field models

*Shin-ichi Ito[1], Hiromichi Nagao[1], Takashi Kurokawa[1], Tadashi Kasuya[1], Junya Inoue[1] (1.The University of Tokyo)

[MGI30-P07] GNSS data assimilation for the Bungo channel Long-term SSEs using Ensemble Kalman Filter (EnKF)

*Megumi Fujita[1], Takuya NISHIMURA[2], Kazuro Hirahara[3], SHINICHI MIYAZAKI[1] (1.Graduate School of Science , Kyoto University, 2.Disaster Prevention Research Institute, Kyoto University, 3.Institute of Education, Research and Regional Cooperation for crisis Management Shikoku, Kagawa University)

[MGI30-P08] A data assimilation library with Python for parallel computing

*Shin ya Nakano[1], Yuya Ariyoshi[2], Tomoyuki Higuchi[1] (1.The Institute of Statistical Mathematics, 2.Faculty of Engineering, Nippon Bunri University)

[E] Poster | M (Multidisciplinary and Interdisciplinary)：M-TT Technology & Techniques

1:45 PM - 3:15 PM JST | 4:45 AM - 6:15 AM UTC | Poster Hall International Exhibition Hall8, Makuhari Messe_6

[M-TT45] Cryoseismology - a new proxy for detecting surface environmental variations of the Earth -

convener:Genti Toyokuni(Research Center for Prediction of Earthquakes and Volcanic Eruptions, Graduate School of Science, Tohoku University), Masaki Kanao(National Institute of Polar Research), Seiji Tsuboi(JAMSTEC, Center for Earth Information Science and Technology)

[MTT45-P01] Application of neural network and theoretical seismograms as training data to locate ice quakes

*Seiji Tsuboi[1], DAISUKE SUGIYAMA[1] (1.JAMSTEC, Center for Earth Information Science and Technology)

[MTT45-P02] **P-wave tomography beneath Greenland**

*Takaya Matsuno[1], Genti Toyokuni[1], Dapeng Zhao[1] (1.Research Center for Prediction of Earthquakes and Volcanic Eruptions, Graduate School of Science, Tohoku University)

[MTT45-P03] **Seismic observations in Greenland by a joint USA and Japanese GLISN team (2011–2018)**

*Genti Toyokuni[1], Masaki Kanao[2], Seiji Tsuboi[3], Yoko Tono[4] (1.RCPEVE, Tohoku Univ., 2.NIPR, 3.JAMSTEC, 4.ERI, Univ. Tokyo)

[E] Poster | M (Multidisciplinary and Interdisciplinary)：M-TT Technology & Techniques

5:15 PM - 6:30 PM JST | 8:15 AM - 9:30 AM UTC | Poster Hall International Exhibition Hall8, Makuhari Messe_40

[M-TT45] Cryoseismology - a new proxy for detecting surface environmental variations of the Earth -

convener:Genti Toyokuni(Research Center for Prediction of Earthquakes and Volcanic Eruptions, Graduate School of Science, Tohoku University), Masaki Kanao(National Institute of Polar Research), Seiji Tsuboi(JAMSTEC, Center for Earth Information Science and Technology)

[MTT45-P01] Application of neural network and theoretical seismograms as training data to locate ice quakes

*Seiji Tsuboi[1], DAISUKE SUGIYAMA[1] (1.JAMSTEC, Center for Earth Information Science and Technology)

[MTT45-P02] **P-wave tomography beneath Greenland**

*Takaya Matsuno[1], Genti Toyokuni[1], Dapeng Zhao[1] (1.Research Center for Prediction of Earthquakes and Volcanic Eruptions, Graduate School of Science, Tohoku University)

[MTT45-P03] **Seismic observations in Greenland by a joint USA and Japanese GLISN team (2011–2018)**

*Genti Toyokuni[1], Masaki Kanao[2], Seiji Tsuboi[3], Yoko Tono[4] (1.RCPEVE, Tohoku Univ., 2.NIPR, 3.JAMSTEC, 4.ERI, Univ. Tokyo)

Thu. May 30, 2019

[E] Poster | P (Space and Planetary Sciences)：P-EM Solar-Terrestrial Sciences, Space Electromagnetism & Space Environment

3:30 PM - 5:00 PM JST | 6:30 AM - 8:00 AM UTC | Poster Hall International Exhibition Hall8, Makuhari Messe_2

[P-EM15] Study of coupling processes in solar-terrestrial system

convener:Mamoru Yamamoto(Research Institute for Sustainable Humanosphere, Kyoto University), Yasunobu Ogawa(National Institute of Polar Research), Satonori Nozawa(Institute for Space-Earth Environment Research), Akimasa Yoshikawa(Department of Earth and Planetary Sciences, Kyushu University)

[PEM15-P01] Study on adaptive clutter rejection system using external receiving antennas for the MU radar

*Hiroyuki Hashiguchi[1], Issei Terada[1], Mamoru Yamamoto[1] (1.Research Institute for Sustainable Humanosphere, Kyoto University)

[PEM15-P02] Detached cusp aurora for southward IMF

*Kohei Takasu[1], Satoshi Taguchi[1], Keisuke Hosokawa[2] (1.Department of Geophysics, Graduate School of Science, Kyoto University, 2.Department of Communication Engineering and Informatics, University of Electro-Communications)

[PEM15-P03] Motion of the inverted-V structure during an isolated substorm

*Morio Tanaka[1], Satoshi Taguchi[1], Kohei Takasu[1], Tomokazu Oigawa[1], Keisuke Hosokawa[2] (1.Department of Geophysics, Graduate school of science, Kyoto University, 2.Department of Communication Engineering and Informatics, University of Electro-Communications)

[PEM15-P04] Observation and modeling of Na layer response to energetic particle precipitation

*Takuo T. Tsuda[1], Kyogo Takizawa[1], Ryo Tozu[1], Takuya Kawahara[2], Yoshimasa Tanaka[3], Mitsumu K. Ejiri[3], Takanori Nishiyama[3], Takuji Nakamura[3] (1.The University of Electro-Communications, 2.Shinshu University, 3.National Institute of Polar Research)

[PEM15-P05] Lidar data analysis of the sodium atoms in the thermosphere observed at Tromsoe, Norway

*Takuya Kawahara[1], Satonori Nozawa[2], Norihito Saito[3], Takuo T. Tsuda[4], Toru Takahashi[5], Testuya Kawabata[2], Miki Nishimura[1], Yoshitaka Kobayashi[1] (1.Faculty of Engineering, Shinshu University, 2.ISEE, Nagoya University, 3.RIKEN, Center for Advanced Photonics, 4.The University of Electro-Communications, 5.National Institute of Polar Research)

[PEM15-P06] Spatial-temporal distribution of anomalous enhancement of ambipolar diffusion coefficient observed by meteor radars installed in the polar region

*Toru Takahashi[1], Masaki Tsutsumi[1,2], Yasunobu Ogawa[1,2,3], Satonori Nozawa[3], Chris Hall[4], Hiroshi Miyaoka[1,2] (1.National Institute of Polar Research, 2.SOKENDAI, 3.Institute for Space-Earth Environmental Research, 4.TGO, The Arctic University of Norway)

[PEM15-P07] Progress of ICSWSE and MAGDAS project in recent years

*Shuji Abe[1], Akimasa Yoshikawa[2,1], Teiji Uozumi[1], Akiko Fujimoto[3] (1.International Center for Space Weather Science and Education, Japan, 2.Department of Earth and Planetary Sciences, Kyushu University, 3.Kyushu Institute of Technology)

[PEM15-P08] Status of GNU Radio Beacon Receiver 2 (GRBR2) development

*Mamoru Yamamoto[1], Mayumi Matsunaga[2], Roland Tsunoda[3] (1.Research Institute for Sustainable Humanosphere, Kyoto University, 2.Tokyo University of Technology, 3.SRI International)

[PEM15-P09] Statistical comparison between plasma bubble day-to-day variability and neutral atmosphere by using GPS scintillation and GAIA model

*Mamoru Yamamoto[1], Keigo Kono[1] (1.Research Institute for Sustainable Humanosphere, Kyoto University)

[PEM15-P10] Redevelopment of the MU radar transceiver-module control system

*Mamoru Yamamoto[1], Koki Kurokawa[1], Hiroyuki Hashiguchi[1] (1.Research Institute for Sustainable Humanosphere, Kyoto University)

[E] Poster | P (Space and Planetary Sciences)：P-EM Solar-Terrestrial Sciences, Space Electromagnetism & Space Environment

5:15 PM - 6:30 PM JST | 8:15 AM - 9:30 AM UTC | Poster Hall International Exhibition Hall8, Makuhari Messe_2

[P-EM15] Study of coupling processes in solar-terrestrial system

convener:Mamoru Yamamoto(Research Institute for Sustainable Humanosphere, Kyoto University), Yasunobu Ogawa(National Institute of Polar Research), Satonori Nozawa(Institute for Space-Earth Environment Research), Akimasa Yoshikawa(Department of Earth and Planetary Sciences, Kyushu University)

[PEM15-P01] Study on adaptive clutter rejection system using external receiving antennas for the MU radar

*Hiroyuki Hashiguchi[1], Issei Terada[1], Mamoru Yamamoto[1] (1.Research Institute for Sustainable Humanosphere, Kyoto University)

[PEM15-P02] Detached cusp aurora for southward IMF

*Kohei Takasu[1], Satoshi Taguchi[1], Keisuke Hosokawa[2] (1.Department of Geophysics, Graduate School of Science, Kyoto University, 2.Department of Communication Engineering and Informatics, University of Electro-Communications)

[PEM15-P03] Motion of the inverted-V structure during an isolated substorm

*Morio Tanaka[1], Satoshi Taguchi[1], Kohei Takasu[1], Tomokazu Oigawa[1], Keisuke Hosokawa[2] (1.Department of Geophysics, Graduate school of science, Kyoto University, 2.Department of Communication Engineering and Informatics, University of Electro-Communications)

[PEM15-P04] Observation and modeling of Na layer response to energetic particle precipitation

*Takuo T. Tsuda[1], Kyogo Takizawa[1], Ryo Tozu[1], Takuya Kawahara[2], Yoshimasa Tanaka[3], Mitsumu K. Ejiri[3], Takanori Nishiyama[3], Takuji Nakamura[3] (1.The University of Electro-Communications, 2.Shinshu University, 3.National Institute of Polar Research)

[PEM15-P05] Lidar data analysis of the sodium atoms in the thermosphere observed at Tromsoe, Norway

*Takuya Kawahara[1], Satonori Nozawa[2], Norihito Saito[3], Takuo T. Tsuda[4], Toru Takahashi[5], Testuya Kawabata[2], Miki Nishimura[1], Yoshitaka Kobayashi[1] (1.Faculty of Engineering, Shinshu University, 2.ISEE, Nagoya University, 3.RIKEN, Center for Advanced Photonics, 4.The University of Electro-Communications, 5.National Institute of Polar Research)

[PEM15-P06] Spatial-temporal distribution of anomalous enhancement of ambipolar diffusion coefficient observed by meteor radars installed in the polar region

*Toru Takahashi[1], Masaki Tsutsumi[1,2], Yasunobu Ogawa[1,2,3], Satonori Nozawa[3], Chris Hall[4], Hiroshi Miyaoka[1,2] (1.National Institute of Polar Research, 2.SOKENDAI, 3.Institute for Space-Earth Environmental Research, 4.TGO, The Arctic University of Norway)

[PEM15-P07] Progress of ICSWSE and MAGDAS project in recent years

*Shuji Abe[1], Akimasa Yoshikawa[2,1], Teiji Uozumi[1], Akiko Fujimoto[3] (1.International Center for Space Weather Science and Education, Japan, 2.Department of Earth and Planetary Sciences, Kyushu University, 3.Kyushu Institute of Technology)

[PEM15-P08] Status of GNU Radio Beacon Receiver 2 (GRBR2) development

*Mamoru Yamamoto[1], Mayumi Matsunaga[2], Roland Tsunoda[3] (1.Research Institute for Sustainable Humanosphere, Kyoto University, 2.Tokyo University of Technology, 3.SRI International)

[PEM15-P09] Statistical comparison between plasma bubble day-to-day variability and neutral atmosphere by using GPS scintillation and GAIA model

*Mamoru Yamamoto[1], Keigo Kono[1] (1.Research Institute for Sustainable Humanosphere, Kyoto University)

[PEM15-P10] Redevelopment of the MU radar transceiver-module control system

*Mamoru Yamamoto[1], Koki Kurokawa[1], Hiroyuki Hashiguchi[1] (1.Research Institute for Sustainable Humanosphere, Kyoto University)

[E] Poster | A (Atmospheric and Hydrospheric Sciences)：A-AS Atmospheric Sciences, Meteorology & Atmospheric Environment

1:45 PM - 3:15 PM JST | 4:45 AM - 6:15 AM UTC | Poster Hall International Exhibition Hall8, Makuhari Messe_1

[A-AS02] Advances in Tropical Cyclone Research: Past, Present, and Future

convener:Sachie Kanada(Nagoya University), Akiyoshi Wada(Department of Typhoon and Severe Weather Research, Meteorological Research Institute), Kosuke Ito(University of the Ryukyus), Yoshiaki Miyamoto(Faculty of Environment and Information Studies, Keio University)

[AAS02-P01] Numerical study on lightning frequency in a tropical cyclone

*Yousuke Sato[1,3], Yoshiaki Miyamoto[2,3], Tomita Hirofumi[3] (1.Department of Applied Energy, Nagoya University, 2.Faculty of Environment and Information Studies, Keio University, 3.RIKEN Center for Computational Science)

[AAS02-P02] **Sensitivity of Numerical Simulation of Typhoon Nepartak (2016) to Cloud Condensation Nuclei Concentration**

*Yu-De Wu[1], Jian-Liang Wang[1] (1.Dept. of Environmental Informational and Engineering, Chung Cheng Institute of Technology, National Defense University, Taiwan)

[AAS02-P03] Moisture Budget Analysis for Hurricane Precipitation on Texas

*Satoshi Iizuka[1], Naoki Sakai[1] (1.National Research Institute for Earth Science and Disaster Resilience)

[AAS02-P04] Remote response of a developing tropical cyclone over the western North Pacific to large-scale vapor transport from the Kuroshio in boreal fall

*Keita Fujiwara[1], Ryuichi Kawamura[2], Tetsuya Kawano[2] (1.Graduate School of Science, Kyushu University, 2.Faculty of Science, Kyushu University)

[AAS02-P05] Asymmetrically Intensifying Processes of a Category 4 Super Typhoon Lan (2017) during High Vertical Wind Shear

*Sachie Kanada[1], Akiyoshi Wada[2], Kazuhisa Tsuboki[1] (1.Nagoya University, 2.Meteorological Research Institute)

[AAS02-P06] Roles of preexisting oceanic condition and ocean coupling processes in the intensity prediction during the mature phase of Typhoon Trami (2018)

*Akiyoshi Wada[1] (1.Typhoon Research Department Meteorological Research Institute)

[AAS02-P07] Development and assessment of the probabilistic storm surge forecast system in Taiwan: Case Study of Typhoon Maria in 2018

*Chun-Wei Lin[1], Tso-Ren Wu[1], Yu-Lin Tsai[1], Shu-Chun Chuang[1], Chi-Hao Chu[2], Chuen-Teyr Terng[2] (1.Graduate Institute of Hydrological and Oceanic Sciences, National Central University, Chungli, Taiwan, 2.Marine Meteorology Center, Central Weather Bureau, Taipei, Taiwan)

[AAS02-P08] Basic Data Construction for a Typhoon Disaster Prevention Model : Analysis and Changes by El Nino and La Nina year

*HANA NA[1], Woo-Sik Jung[1] (1.Department of Atmospheric Environment Information Engineering, Atmospheric Environment Information Research Center, Inje University, Gimhae 50834, Korea)

[AAS02-P09] Basic Data Construction for a Typhoon Disaster Prevention Model : Analysis According to the Typhoon Path Type

*HANA NA[1], Woo-Sik JUNG[1] (1.Department of Atmospheric Environment Information Engineering, Atmospheric Environment Information Research Center, Inje University, Gimhae 50834, Korea)

[AAS02-P10] Basic Data Construction for a Typhoon Disaster Prevention Model : Monthly Characteristics of Typhoon Rusa, Maemi, Kompasu, and Bolaven

*HANA NA[1], Woo-Sik Jung[1] (1.Department of Atmospheric Environment Information Engineering, Atmospheric Environment Information Research Center, Inje University, Gimhae 50834, Korea)

[AAS02-P11] The mechanism of typhoon generated in the earth that rotates in the space where the solar wind blows

*Shinji Karasawa[1] (1.Miyagi National College of Technology Professor emeritus)

[E] Poster | A (Atmospheric and Hydrospheric Sciences)：A-AS Atmospheric Sciences, Meteorology & Atmospheric Environment

5:15 PM - 6:30 PM JST | 8:15 AM - 9:30 AM UTC | Poster Hall International Exhibition Hall8, Makuhari Messe_5

[A-AS02] Advances in Tropical Cyclone Research: Past, Present, and Future

convener:Sachie Kanada(Nagoya University), Akiyoshi Wada(Department of Typhoon and Severe Weather Research, Meteorological Research Institute), Kosuke Ito(University of the Ryukyus), Yoshiaki Miyamoto(Faculty of Environment and Information Studies, Keio University)

[AAS02-P01] Numerical study on lightning frequency in a tropical cyclone

*Yousuke Sato[1,3], Yoshiaki Miyamoto[2,3], Tomita Hirofumi[3] (1.Department of Applied Energy, Nagoya University, 2.Faculty of Environment and Information Studies, Keio University, 3.RIKEN Center for Computational Science)

[AAS02-P02] **Sensitivity of Numerical Simulation of Typhoon Nepartak (2016) to Cloud Condensation Nuclei Concentration**

*Yu-De Wu[1], Jian-Liang Wang[1] (1.Dept. of Environmental Informational and Engineering, Chung Cheng Institute of Technology, National Defense University, Taiwan)

[AAS02-P03] Moisture Budget Analysis for Hurricane Precipitation on Texas

*Satoshi Iizuka[1], Naoki Sakai[1] (1.National Research Institute for Earth Science and Disaster Resilience)

[AAS02-P04] Remote response of a developing tropical cyclone over the western North Pacific to large-scale vapor transport from the Kuroshio in boreal fall

*Keita Fujiwara[1], Ryuichi Kawamura[2], Tetsuya Kawano[2] (1.Graduate School of Science, Kyushu University, 2.Faculty of Science, Kyushu University)

[AAS02-P05] Asymmetrically Intensifying Processes of a Category 4 Super Typhoon Lan (2017) during High Vertical Wind Shear

*Sachie Kanada[1], Akiyoshi Wada[2], Kazuhisa Tsuboki[1] (1.Nagoya University, 2.Meteorological Research Institute)

[AAS02-P06] Roles of preexisting oceanic condition and ocean coupling processes in the intensity prediction during the mature phase of Typhoon Trami (2018)

*Akiyoshi Wada[1] (1.Typhoon Research Department Meteorological Research Institute)

[AAS02-P07] Development and assessment of the probabilistic storm surge forecast system in Taiwan: Case Study of Typhoon Maria in 2018

*Chun-Wei Lin[1], Tso-Ren Wu[1], Yu-Lin Tsai[1], Shu-Chun Chuang[1], Chi-Hao Chu[2], Chuen-Teyr Terng[2] (1.Graduate Institute of Hydrological and Oceanic Sciences, National Central University, Chungli, Taiwan, 2.Marine Meteorology Center, Central Weather Bureau, Taipei, Taiwan)

[AAS02-P08] Basic Data Construction for a Typhoon Disaster Prevention Model : Analysis and Changes by El Nino and La Nina year

*HANA NA[1], Woo-Sik Jung[1] (1.Department of Atmospheric Environment Information Engineering, Atmospheric Environment Information Research Center, Inje University, Gimhae 50834, Korea)

[AAS02-P09] Basic Data Construction for a Typhoon Disaster Prevention Model : Analysis According to the Typhoon Path Type

*HANA NA[1], Woo-Sik JUNG[1] (1.Department of Atmospheric Environment Information Engineering, Atmospheric Environment Information Research Center, Inje University, Gimhae 50834, Korea)

[AAS02-P10] Basic Data Construction for a Typhoon Disaster Prevention Model : Monthly Characteristics of Typhoon Rusa, Maemi, Kompasu, and Bolaven

*HANA NA[1], Woo-Sik Jung[1] (1.Department of Atmospheric Environment Information Engineering, Atmospheric Environment Information Research Center, Inje University, Gimhae 50834, Korea)

[AAS02-P11] The mechanism of typhoon generated in the earth that rotates in the space where the solar wind blows

*Shinji Karasawa[1] (1.Miyagi National College of Technology Professor emeritus)

[E] Poster | A (Atmospheric and Hydrospheric Sciences)：A-OS Ocean Sciences & Ocean Environment

10:45 AM - 12:15 PM JST | 1:45 AM - 3:15 AM UTC | Poster Hall International Exhibition Hall8, Makuhari Messe_2

[A-OS07] Climate variability and predictability on subseasonal to decadal timescales

convener:Takashi Mochizuki(Japan Agency for Marine-Earth Science and Technology), V Ramaswamy(NOAA GFDL), Doug Smith(Met Office), Yushi Morioka(Japan Agency for Marine-Earth Science and Technology)

[AOS07-P01] Changes in North American and European Heatwave Characteristics

*Szandra A. Peter[1], Ben Kirtman[1] (1.Rosenstiel School of Marine and Atmospheric Science)

[AOS07-P02] **The effects of the "New Climate" Warming on Western Mediterranean: Situation of the Recent Extreme Events**

*Mohammed-Said KARROUK[1] (1.Hassan II University of Casablanca)

[AOS07-P03] **Month-to-month Difference of the Western Pacific Subtropical High Simulated by CMIP5 Models**

*Xiao Dong[1], Renping Lin[1] (1.Institute of Atmospheric Physics)

[AOS07-P04] Potential regulation on the climatic effect of Tibetan Plateau heating by tropical air–sea coupling

*Ziqian Wang[1], Anmin Duan[2], Song Yang[1] (1.School of Atmospheric Sciences, Sun Yat-sen University, 2.Institute of Atmospheric Physics, Chinese Academy of Sciences)

[AOS07-P05] Intraseasonal variation of the South Asian high and its role in connecting the Indian and East Asian summer monsoons

*Wei Wei[1] (1.Sun Yat-sen University)

[AOS07-P06] Mean Surface Air Temperatures in Japan - Regional Classification and Interranual Variability

*Pascal Oettli[1], Masami Nonaka[1], Swadhin Behera[1] (1.Japan Agency for Marine-Earth Science and Technology)

[AOS07-P07] Inter-Annual Variability of the Indonesian Rainfall and Air-Sea Interaction over the Indian-Pacific Ocean Associated with Regime Shift

*Murni Ngestu Nurutami[1], Tadahiro Hayasaka[1] (1.Center for Atmospheric and Oceanic Studies, Graduate School of Science, Tohoku University)

[AOS07-P08] Exploring synoptic-scale drivers of interannual rainfall variability over Africa

*Piotr Wolski[1], Chris Jack[1], Waarith Abrahams[1], Stefaan Conradie[1] (1.University of Cape Town)

[AOS07-P09] **Effect of El Niño on the response ratio of Hadley circulation to different SST meridional structures**

*Juan Feng[1] (1.Beijing Normal University)

[AOS07-P10] **Novel data-driven approach for ENSO prediction**

*Dmitri Kondrashov[1], Evgeniy Loskutov[2], Andrei Gavrilov[2], Dmitry Mukhin[2], Alexander Feigin[2] (1.University of California, Los Angeles, United States, 2.Institute of Applied Physics of the Russian Academy of Sciences, Nizhny Novgorod, Russian Federation)

[AOS07-P11] Experimental seasonal climate prediction using CFES: Comparison with the SINTEX-F systems

*Nobumasa Komori[1], Bunmei Taguchi[2], Akira Kuwano-Yoshida[3,1], Takeshi Doi[1], Masami Nonaka[1] (1.Japan Agency for Marine-Earth Science and Technology, 2.Research Center for Advanced Science and Technology, The University of Tokyo, 3.Disaster Prevention Research Institute, Kyoto University)

[AOS07-P12] Exploring the SST error growth during ENSO developing phase by using BCC_CSM1.1(m)

*Ben Tian[1], Hongli Ren[1] (1.National Climate Center, China Meteorological Administration)

[AOS07-P13] Role of sea-ice initialization in climate predictability over the Weddell Sea

*Yushi Morioka[1], Takeshi Doi[1], Doroteaciro Iovino[2], Simona Masina[2], Swadhin Behera[1] (1.Japan Agency for Marine-Earth Science and Technology (JAMSTEC), 2.Centro Euro-Mediterraneo sui Cambiamenti Climatici (CMCC))

[AOS07-P14] Observed and hindcasted subdecadal variability of the tropical Pacific climate

*Takashi Mochizuki[1], Masahiro Watanabe[2] (1.Japan Agency for Marine-Earth Science and Technology, 2.Atmosphere-Ocean Research Institute, The University of Tokyo)

[E] Poster | A (Atmospheric and Hydrospheric Sciences)：A-OS Ocean Sciences & Ocean Environment

5:15 PM - 6:30 PM JST | 8:15 AM - 9:30 AM UTC | Poster Hall International Exhibition Hall8, Makuhari Messe_7

[A-OS07] Climate variability and predictability on subseasonal to decadal timescales

convener:Takashi Mochizuki(Japan Agency for Marine-Earth Science and Technology), V Ramaswamy(NOAA GFDL), Doug Smith(Met Office), Yushi Morioka(Japan Agency for Marine-Earth Science and Technology)

[AOS07-P01] Changes in North American and European Heatwave Characteristics

*Szandra A. Peter[1], Ben Kirtman[1] (1.Rosenstiel School of Marine and Atmospheric Science)

[AOS07-P02] **The effects of the "New Climate" Warming on Western Mediterranean: Situation of the Recent Extreme Events**

*Mohammed-Said KARROUK[1] (1.Hassan II University of Casablanca)

[AOS07-P03] **Month-to-month Difference of the Western Pacific Subtropical High Simulated by CMIP5 Models**

*Xiao Dong[1], Renping Lin[1] (1.Institute of Atmospheric Physics)

[AOS07-P04] Potential regulation on the climatic effect of Tibetan Plateau heating by tropical air–sea coupling

*Ziqian Wang[1], Anmin Duan[2], Song Yang[1] (1.School of Atmospheric Sciences, Sun Yat-sen University, 2.Institute of Atmospheric Physics, Chinese Academy of Sciences)

[AOS07-P05] Intraseasonal variation of the South Asian high and its role in connecting the Indian and East Asian summer monsoons

*Wei Wei[1] (1.Sun Yat-sen University)

[AOS07-P06] Mean Surface Air Temperatures in Japan - Regional Classification and Interranual Variability

*Pascal Oettli[1], Masami Nonaka[1], Swadhin Behera[1] (1.Japan Agency for Marine-Earth Science and Technology)

[AOS07-P07] Inter-Annual Variability of the Indonesian Rainfall and Air-Sea Interaction over the Indian-Pacific Ocean Associated with Regime Shift

*Murni Ngestu Nurutami[1], Tadahiro Hayasaka[1] (1.Center for Atmospheric and Oceanic Studies, Graduate School of Science, Tohoku University)

[AOS07-P08] Exploring synoptic-scale drivers of interannual rainfall variability over Africa

*Piotr Wolski[1], Chris Jack[1], Waarith Abrahams[1], Stefaan Conradie[1] (1.University of Cape Town)

[AOS07-P09] **Effect of El Niño on the response ratio of Hadley circulation to different SST meridional structures**

*Juan Feng[1] (1.Beijing Normal University)

[AOS07-P10] **Novel data-driven approach for ENSO prediction**

*Dmitri Kondrashov[1], Evgeniy Loskutov[2], Andrei Gavrilov[2], Dmitry Mukhin[2], Alexander Feigin[2] (1.University of California, Los Angeles, United States, 2.Institute of Applied Physics of the Russian Academy of Sciences, Nizhny Novgorod, Russian Federation)

[AOS07-P11] Experimental seasonal climate prediction using CFES: Comparison with the SINTEX-F systems

*Nobumasa Komori[1], Bunmei Taguchi[2], Akira Kuwano-Yoshida[3,1], Takeshi Doi[1], Masami Nonaka[1] (1.Japan Agency for Marine-Earth Science and Technology, 2.Research Center for Advanced Science and Technology, The University of Tokyo, 3.Disaster Prevention Research Institute, Kyoto University)

[AOS07-P12] Exploring the SST error growth during ENSO developing phase by using BCC_CSM1.1(m)

*Ben Tian[1], Hongli Ren[1] (1.National Climate Center, China Meteorological Administration)

[AOS07-P13] Role of sea-ice initialization in climate predictability over the Weddell Sea

*Yushi Morioka[1], Takeshi Doi[1], Doroteaciro Iovino[2], Simona Masina[2], Swadhin Behera[1] (1.Japan Agency for Marine-Earth Science and Technology (JAMSTEC), 2.Centro Euro-Mediterraneo sui Cambiamenti Climatici (CMCC))

[AOS07-P14] Observed and hindcasted subdecadal variability of the tropical Pacific climate

*Takashi Mochizuki[1], Masahiro Watanabe[2] (1.Japan Agency for Marine-Earth Science and Technology, 2.Atmosphere-Ocean Research Institute, The University of Tokyo)

[E] Poster | A (Atmospheric and Hydrospheric Sciences)：A-OS Ocean Sciences & Ocean Environment

3:30 PM - 5:00 PM JST | 6:30 AM - 8:00 AM UTC | Poster Hall International Exhibition Hall8, Makuhari Messe_4

[A-OS10] Atlantic climate variability, and its global impacts and predictability

convener:Ingo Richter(JAMSTEC Japan Agency for Marine-Earth Science and Technology), Hiroki Tokinaga(Research Institute for Applied Mechanics, Kyushu University), Noel S Keenlyside(Geophysical Institute Bergen), Carlos R Mechoso(University of California Los Angeles)

[AOS10-P01] The strengthening of Amazonian precipitation during the wet season driven by tropical sea surface temperature forcing

*Xinyue Wang[1], Xichen Li[1], Jiang Zhu[1], Clemente A S Tanajura[2] (1.Institute of Atmospheric Physics, Chinese Academy of Sciences, 2.Institute of Physics, Federal University of Bahia, Salvador, Brazil)

[AOS10-P02] **Linear inverse modeling of the tropical Atlantic**

*Ingo Richter[1], Ping Chang[2] (1.JAMSTEC Japan Agency for Marine-Earth Science and Technology, 2.Texas A&M University)

[AOS10-P03] Relationships Among Inter-model Spread and Biases in Tropical Atlantic Sea Surface Temperatures

Elsa - Mohino Harris[1], *Belen Rodriguez-Fonseca[1,2], Teresa - Losada[1], Irene - Polo[1], Roberto - Mechoso[3] (1.Department of Physics of the Earth and Astrophysics, Universidad Complutense de Madrid, 28040, Madrid, Spain. , 2.Institute of Geosciences IGEO,UCM-CSIC, 28040, Madrid, Spain., 3.Department of Atmospheric and Oceanic Sciences, UCLA, Los Angeles, USA)

[AOS10-P04] **Revisiting the CMIP5 Thermocline in the Equatorial Pacific and Atlantic Oceans**

Antonio - Castaño[1,2], Elsa - Mohino[1], *Belen Rodriguez-Fonseca[1,2], Teresa - Losada[1] (1.Department of Physics of the Earth and Astrophysics, Universidad Complutense de Madrid, 28040, Madrid, Spain., 2.Institute of Geosciences, IGEO, UCM-CSIC 28040, Madrid, Spain.)

[AOS10-P05] Lagged Effects of North Atlantic SST Anomalies on Weather in Remote Areas

*Natalia Gnatiuk[1], Timo Vihma[2], Leonid Bobylev[1] (1.Nansen International Environmental and Remote Sensing Centre, 2.Finnish Meteorological Institute)

[AOS10-P06] **SST anomalies in the northern tropical Atlantic as a negative feedback to ENSO development**

*Ingo Richter[1], Hiroki Tokinaga[2], Yu Kosaka[3], Takeshi Doi[1] (1.JAMSTEC Japan Agency for Marine-Earth Science and Technology, 2.Kyoto University, 3.University of Tokyo)

[E] Poster | A (Atmospheric and Hydrospheric Sciences)：A-OS Ocean Sciences & Ocean Environment

5:15 PM - 6:30 PM JST | 8:15 AM - 9:30 AM UTC | Poster Hall International Exhibition Hall8, Makuhari Messe_8

[A-OS10] Atlantic climate variability, and its global impacts and predictability

convener:Ingo Richter(JAMSTEC Japan Agency for Marine-Earth Science and Technology), Hiroki Tokinaga(Research Institute for Applied Mechanics, Kyushu University), Noel S Keenlyside(Geophysical Institute Bergen), Carlos R Mechoso(University of California Los Angeles)

[AOS10-P01] The strengthening of Amazonian precipitation during the wet season driven by tropical sea surface temperature forcing

*Xinyue Wang[1], Xichen Li[1], Jiang Zhu[1], Clemente A S Tanajura[2] (1.Institute of Atmospheric Physics, Chinese Academy of Sciences, 2.Institute of Physics, Federal University of Bahia, Salvador, Brazil)

[AOS10-P02] **Linear inverse modeling of the tropical Atlantic**

*Ingo Richter[1], Ping Chang[2] (1.JAMSTEC Japan Agency for Marine-Earth Science and Technology, 2.Texas A&M University)

[AOS10-P03] Relationships Among Inter-model Spread and Biases in Tropical Atlantic Sea Surface Temperatures

Elsa - Mohino Harris[1], *Belen Rodriguez-Fonseca[1,2], Teresa - Losada[1], Irene - Polo[1], Roberto - Mechoso[3] (1.Department of Physics of the Earth and Astrophysics, Universidad Complutense de Madrid, 28040, Madrid, Spain. , 2.Institute of Geosciences IGEO,UCM-CSIC, 28040, Madrid, Spain., 3.Department of Atmospheric and Oceanic Sciences, UCLA, Los Angeles, USA)

[AOS10-P04] **Revisiting the CMIP5 Thermocline in the Equatorial Pacific and Atlantic Oceans**

Antonio - Castaño[1,2], Elsa - Mohino[1], *Belen Rodriguez-Fonseca[1,2], Teresa - Losada[1] (1.Department of Physics of the Earth and Astrophysics, Universidad Complutense de Madrid, 28040, Madrid, Spain., 2.Institute of Geosciences, IGEO, UCM-CSIC 28040, Madrid, Spain.)

[AOS10-P05] Lagged Effects of North Atlantic SST Anomalies on Weather in Remote Areas

*Natalia Gnatiuk[1], Timo Vihma[2], Leonid Bobylev[1] (1.Nansen International Environmental and Remote Sensing Centre, 2.Finnish Meteorological Institute)

[AOS10-P06] **SST anomalies in the northern tropical Atlantic as a negative feedback to ENSO development**

*Ingo Richter[1], Hiroki Tokinaga[2], Yu Kosaka[3], Takeshi Doi[1] (1.JAMSTEC Japan Agency for Marine-Earth Science and Technology, 2.Kyoto University, 3.University of Tokyo)

[E] Poster | A (Atmospheric and Hydrospheric Sciences)：A-HW Hydrology & Water Environment

3:30 PM - 5:00 PM JST | 6:30 AM - 8:00 AM UTC | Poster Hall International Exhibition Hall8, Makuhari Messe_5

[A-HW22] Materials transport and nutrient cycles in watersheds; from headwaters to coastal seas

convener:Masahiro Kobayashi(Forestry and Forest Products Research Institute), Seiko Yoshikawa(Institute for Agro-environmental Sciences, National Agriculture and Food Research Organization), Jun Yasumoto(University of the Ryukyus, Faculty of Agriculuture), Adina Paytan(University of California Santa Cruz)

[AHW22-P01] Phosphate Enrichment Hampers Development of Juvenile Acropora digitifera Coral by Inhibiting Skeleton Formation

Mariko Iijima[1], *Yasumoto Ko[1], Jun Yasumoto[2], Mina Hirose[3], Mitsuru Jimbo[1], Shugo Watabe[1] (1.Kitasato University School of Marine Biosciences, 2.Faculty of Agriculture, University of the Ryukyus, 3.Tropical Technology Plus)

[AHW22-P02] Modeling chlorophyll-a concentration using remote sensing in shallow water systems: Comparison of sensors

*Assefa M Melesse[1], Tara Blakey[1], Mohammad Haji Gholizadeh[1], Mohd Manzar Abbas[1] (1.Florida International University)

[AHW22-P03] Dynamics in groundwater flow system with seasonal water table variation in a coastal and island

*Yusuke Tomozawa[1], Shin-ichi Onodera[1], Mitsuyo Saito[2] (1.Graduate School of Integrated Arts and Sciences Hiroshima University, 2.Graduate School of Environmental and Life Science, Okayama University)

[AHW22-P04] **The Tracing of Groundwater Contamination Sources in Indonesian Coastal Alluvial Groundwater using $\delta^{34}S$ and $\delta^{15}N$ Isotopes**

*Anna Fadliah Rusydi[1,4], Mitsuyo Saito[2], Seiichiro Ioka[3], Shin-ichi Onodera[1] (1.Graduate School of Integrated Arts and Sciences, Hiroshima University, Japan, 2.Graduate School of Environmental and Life Sciences, Okayama University, Japan, 3.Research Institute for Sustainable Energy, Hirosaki University, Japan, 4.Research Center for Geotechnology, Indonesian Institute of Sciences, Indonesia)

[AHW22-P05] Spatio-temporal dynamics of orthophosphate with implications for limitation of phytoplankton growth in north basin of Lake Biwa, Japan

*Xin Liu[1], Rong Yi[1], Masahiro Maruo[1], Syuhei Ban[1] (1.The University of Shiga Prefecture)

[AHW22-P06] Microbial phase analysis in aquifer of Ryukyu Limestone Zone using next generation sequencer

*Umi Murao[1], Jun Yasumoto[1], Yasumoto Ko[3], Mina Hirose[2], Nanami Mizusawa[3], Ryo Iguchi[4], Bam H.N. Razafindrabe[5], Syugo Watabe[3] (1.University of the Ryukyus, Faculty of Agriculuture Department of Regional Agricultural Engineering, 2.Tropical Tecnology Plus, 3.Kitasato University School of Marine Biosciences, 4.National Institute of Advanced Industrial Science and Technology, 5.University of the Ryukyus, Faculty of Agriculuture Department of Subtropical Agro-Environmental Sciences)

[AHW22-P07] Evaluation for temporal variation in groundwater inflow to the lagoons connected to Lake Biwa by radon (^{222}Rn) tracer analysis

*Mitsuyo Saito[1], Shin-ichi Onodera[2], Yusuke Tomozawa[2], Kunyang Wang[2], Syuhei Ban[3], Noboru Okuda[4] (1.Graduate School of Environmental and Life Science, Okayama University, 2.Graduate School of Integrated Arts and Sciences, Hiroshima University, 3.School of Environmental Sciences, The University of Shiga Prefecture, 4.Research Institute for Humanity and Nature)

[AHW22-P08] Br/Cl ratio characteristics of groundwater in coastal areas in Indonesia

*Seiichiro Ioka[1], Shin-ichi Onodera[2], Mitsuyo Saito[3], Anna Fadliah Rusydi[2,4] (1.Institute of Regional Innovation, Hirosaki University, Japan, 2.Graduate School of Integrated Arts and Sciences, Hiroshima University, Japan, 3.Graduate School of Environmental and Life Sciences, Okayama University, Japan, 4.Research Center for Geotechnology, Indonesian Institute of Sciences, Indonesia)

[AHW22-P09] Estimation of groundwater recharge and phosphorus transport under different precipitation conditions in a suburban catchment, using SWAT model

*Kunyang Wang[1,2], Shin-ichi Onodera[1], Mitsuyo Saito[3], Noboru Okuda[4], Takuya Okubo[5] (1.Graduate School of Integrated Arts and Science, Hiroshima University, 2.Capital Normal University, 3.Okayama University, 4.Research

Institute for Humanity and Nature, 5.University of the Shiga Prefecture)

[AHW22-P10] Losses of phosphorus with soil erosion and nitrate with groundwater recharge in an agricultural catchment, subtropical small island

*Shin-ichi Onodera[1], Mitsuyo Saito[2], Yang Cao[1], Anna Fadliah Rusydi[1], Hide Omae[3], Yoshiko Iizumi[4], Yusuke Tomozawa[1] (1.Graduate School of Integrated and Arts Sciences, Hiroshima University, 2.Graduate School of Environmental and Life Science, Okayama University, 3.JIRCAS TARF, 4.JIRCAS HQ)

[AHW22-P11] Phosphate solubilizing bacteria as an indicator of sediment phosphorus in freshwater lakes

*Sreekumari Kurissery[1], Katelynn Crawford[1], Nandakumar Kanavillil[1] (1.Lakehead University, Canada)

[AHW22-P12] A Study on the dynamics of various phosphate forms in soil and groundwater in Ryukyu limestone regions

*Masashi Nozaki[1], Jun Yasumoto[2], Yasumoto Ko[3], Hirose Mina[4], Iijima Mariko[3], Ryuichi Shinjo[5], Bam H.N. Razafindrabe[6] (1.University of The Ryukyus, Graduate School of Agriculture,, 2.University of the Ryukyus, Faculty of Agriculture, Department of Regional Agricultural Engineering, 3.Kitasato University School of Marine Biosciences, 4.Tropical Technology Plus, 5.Department of Physics and Earth Sciences, University of the Ryukyus, 6.University of the Ryukyus, Faculty of Agriculture, Department of Subtropical Agro-Environmental Sciences)

[AHW22-P13] Impacts of highly concentrated turbid water on the groundwater in the Tedori River alluvial fan, Japan

*Yoichi Fujihara[1], Shunsuke Chono[1], Keiji Takase[1], Eiji Ichion[1] (1.Department of Environmental Science, Ishikawa Prefectural University)

[AHW22-P14] Altitude effect of water stable isotopic ratio of ravine water and its contribution to groundwater in alluvial plains - Comparison in east and west side catchments of Lake Biwa –

*Yusuke Tomozawa[1], Kunyang Wang[1], Mitsuyo Saito[2], Syuhei Ban[3], Noboru Okuda[4], Shin-ichi Onodera[1] (1.Graduate School of Integrated Arts and Sciences Hiroshima University, 2.Graduate School of Environmental and Life Science, Okayama University, 3.School of Environmental Science, The University of Shiga Prefecture, 4.Research Institute for Humanity and Nature)

[AHW22-P15] Calculation of TN and TP concentration coefficients of river water for each land use by a simple watershed model.

*Seiko Yoshikawa[1], Donglai Ma[1,4], Tadamasa Saito[1,5], Kenji Matsumori[2], Yuko Itoh[3], Masahiro Kobayashi[3] (1.Institute for Agro-environmental Sciences, National Agriculture and Food Research Organization, 2.Western Region Agricultural Research Center, National Agriculture and Food Research Organization, 3.Forestry and Forest Products Research Institute, 4.Graduate school,Tsukuba University, 5.Faculty of Agriculture, Ibaraki University)

[AHW22-P16] **Possibility of nutrients transportation from littoral slope for enhancement of phytoplankton growth in north basin of Lake Biwa**

*Syuhei Ban[1], Rong YI[1], Xin Liu[1], Masahiro Maruo[1], Miki Sudo[1], Naoshige Goto[1], Jun Murase[2] (1.The University of Shiga Prefecture, 2.Nagoya University)

[AHW22-P17] SWAT model analysis for confirming the effects of crop growth on the suspended sediment concentration from a settling basin catchment on Ishigaki island

*Yang Cao[1], Shin-ichi Onodera[1], Mitsuyo Saito[2], Hide Omae[3], Yoshiko Iizumi[3] (1.Graduate School of Integrate Arts and Sciences, Hiroshima University, 2.Graduate School of Environmental and life Science, Okayama University, 3.Tropical Agriculture Research Front (TARF), Japan International Research Center for Agricultural Sciences (JIRCAS))

[AHW22-P18] Estimating the runoff of water, sediment, and nutrient using SWAT model in Kikuchi-river watershed, Kumamoto, and the influence of the forest

*Soichiro Fujii[1], Masahiko Kanamori[1], Yuko Nagano[1], Maki Kinoshita[2], Yuta Shimizu[3], Shin-ichi Onodera[4] (1.Japan Forest Technology Association, 2.PASCO Corporation, 3.Western Region Agricultural Research Center, National Agriculture and Food Research Organization, 4.Graduate School of Integrated and Arts Sciences, Hiroshima University)

[AHW22-P19] Atmospheric depositions on forest ecosystems in areas along the Sea of Japan

*Yuko Itoh[1], Keiji Takase[2], Yoichi Fujihara[2], Toru Okamoto[1] (1.Forestry and Forest Products Research Institute, Japan, 2.Ishikawa Prefectural University)

[AHW22-P20] Continuous and simultaneous flux measurement of N_2O and CO_2 from agricultural soil using a portable multi-turn time-of-flight mass spectrometer

*Noriko Nakayama[1], Yusuke Iwai[1], Yo Toma[2], Hiroshi Furutani[1], Ryusuke Hatano[3], Michisato Toyoda[1] (1.Osaka University, 2.Ehime University, 3.Hokkaido University)

[AHW22-P21] Effects of introduction of cyclic irrigation system on mass balances of SS and T-P in Lake Inbanuma, Chiba, Japan

*Tomijiro Kubota[1] (1.National Agriculture and Food Research Organization, Institute for Rural Engineering)

[E] Poster | A (Atmospheric and Hydrospheric Sciences)：A-HW Hydrology & Water Environment

5:15 PM - 6:30 PM JST | 8:15 AM - 9:30 AM UTC | Poster Hall International Exhibition Hall8, Makuhari Messe_9

[A-HW22] Materials transport and nutrient cycles in watersheds; from headwaters to coastal seas

convener:Masahiro Kobayashi(Forestry and Forest Products Research Institute), Seiko Yoshikawa(Institute for Agro-environmental Sciences, National Agriculture and Food Research Organization), Jun Yasumoto(University of the Ryukyus, Faculty of Agriculuture), Adina Paytan(University of California Santa Cruz)

[AHW22-P01] Phosphate Enrichment Hampers Development of Juvenile Acropora digitifera Coral by Inhibiting Skeleton Formation

Mariko Iijima[1], *Yasumoto Ko[1], Jun Yasumoto[2], Mina Hirose[3], Mitsuru Jimbo[1], Shugo Watabe[1] (1.Kitasato University School of Marine Biosciences, 2.Faculty of Agriculture, University of the Ryukyus, 3.Tropical Technology Plus)

[AHW22-P02] Modeling chlorophyll-a concentration using remote sensing in shallow water systems: Comparison of sensors

*Assefa M Melesse[1], Tara Blakey[1], Mohammad Haji Gholizadeh[1], Mohd Manzar Abbas[1] (1.Florida International University)

[AHW22-P03] Dynamics in groundwater flow system with seasonal water table variation in a coastal and island

*Yusuke Tomozawa[1], Shin-ichi Onodera[1], Mitsuyo Saito[2] (1.Graduate School of Integrated Arts and Sciences Hiroshima University, 2.Graduate School of Environmental and Life Science, Okayama University)

[AHW22-P04] **The Tracing of Groundwater Contamination Sources in Indonesian Coastal Alluvial Groundwater using $\delta^{34}S$ and $\delta^{15}N$ Isotopes**

*Anna Fadliah Rusydi[1,4], Mitsuyo Saito[2], Seiichiro Ioka[3], Shin-ichi Onodera[1] (1.Graduate School of Integrated Arts and Sciences, Hiroshima University, Japan, 2.Graduate School of Environmental and Life Sciences, Okayama University, Japan, 3.Research Institute for Sustainable Energy, Hirosaki University, Japan, 4.Research Center for Geotechnology, Indonesian Institute of Sciences, Indonesia)

[AHW22-P05] Spatio-temporal dynamics of orthophosphate with implications for limitation of phytoplankton growth in north basin of Lake Biwa, Japan

*Xin Liu[1], Rong Yi[1], Masahiro Maruo[1], Syuhei Ban[1] (1.The University of Shiga Prefecture)

[AHW22-P06] Microbial phase analysis in aquifer of Ryukyu Limestone Zone using next generation sequencer

*Umi Murao[1], Jun Yasumoto[1], Yasumoto Ko[3], Mina Hirose[2], Nanami Mizusawa[3], Ryo Iguchi[4], Bam H.N. Razafindrabe[5], Syugo Watabe[3] (1.University of the Ryukyus, Faculty of Agriculuture Department of Regional Agricultural Engineering, 2.Tropical Tecnology Plus, 3.Kitasato University School of Marine Biosciences, 4.National Institute of Advanced Industrial Science and Technology, 5.University of the Ryukyus, Faculty of Agriculuture Department of Subtropical Agro-Environmental Sciences)

[AHW22-P07] Evaluation for temporal variation in groundwater inflow to the lagoons connected to Lake Biwa by radon (^{222}Rn) tracer analysis

*Mitsuyo Saito[1], Shin-ichi Onodera[2], Yusuke Tomozawa[2], Kunyang Wang[2], Syuhei Ban[3], Noboru Okuda[4] (1.Graduate School of Environmental and Life Science, Okayama University, 2.Graduate School of Integrated Arts and Sciences, Hiroshima University, 3.School of Environmental Sciences, The University of Shiga Prefecture, 4.Research Institute for Humanity and Nature)

[AHW22-P08] Br/Cl ratio characteristics of groundwater in coastal areas in Indonesia

*Seiichiro Ioka[1], Shin-ichi Onodera[2], Mitsuyo Saito[3], Anna Fadliah Rusydi[2,4] (1.Institute of Regional Innovation, Hirosaki University, Japan, 2.Graduate School of Integrated Arts and Sciences, Hiroshima University, Japan, 3.Graduate School of Environmental and Life Sciences, Okayama University, Japan, 4.Research Center for Geotechnology, Indonesian Institute of Sciences, Indonesia)

[AHW22-P09] Estimation of groundwater recharge and phosphorus transport under different precipitation conditions in a suburban catchment, using SWAT model

*Kunyang Wang[1,2], Shin-ichi Onodera[1], Mitsuyo Saito[3], Noboru Okuda[4], Takuya Okubo[5] (1.Graduate School of Integrated Arts and Science, Hiroshima University, 2.Capital Normal University, 3.Okayama University, 4.Research

Institute for Humanity and Nature, 5.University of the Shiga Prefecture)

[AHW22-P10] Losses of phosphorus with soil erosion and nitrate with groundwater recharge in an agricultural catchment, subtropical small island

*Shin-ichi Onodera[1], Mitsuyo Saito[2], Yang Cao[1], Anna Fadliah Rusydi[1], Hide Omae[3], Yoshiko Iizumi[4], Yusuke Tomozawa[1] (1.Graduate School of Integrated and Arts Sciences, Hiroshima University, 2.Graduate School of Environmental and Life Science, Okayama University, 3.JIRCAS TARF, 4.JIRCAS HQ)

[AHW22-P11] Phosphate solubilizing bacteria as an indicator of sediment phosphorus in freshwater lakes

*Sreekumari Kurissery[1], Katelynn Crawford[1], Nandakumar Kanavillil[1] (1.Lakehead University, Canada)

[AHW22-P12] A Study on the dynamics of various phosphate forms in soil and groundwater in Ryukyu limestone regions

*Masashi Nozaki[1], Jun Yasumoto[2], Yasumoto Ko[3], Hirose Mina[4], Iijima Mariko[3], Ryuichi Shinjo[5], Bam H.N. Razafindrabe[6] (1.University of The Ryukyus, Graduate School of Agriculture,, 2.University of the Ryukyus, Faculty of Agriculture, Department of Regional Agricultural Engineering, 3.Kitasato University School of Marine Biosciences, 4.Tropical Technology Plus, 5.Department of Physics and Earth Sciences, University of the Ryukyus, 6.University of the Ryukyus, Faculty of Agriculture, Department of Subtropical Agro-Environmental Sciences)

[AHW22-P13] Impacts of highly concentrated turbid water on the groundwater in the Tedori River alluvial fan, Japan

*Yoichi Fujihara[1], Shunsuke Chono[1], Keiji Takase[1], Eiji Ichion[1] (1.Department of Environmental Science, Ishikawa Prefectural University)

[AHW22-P14] Altitude effect of water stable isotopic ratio of ravine water and its contribution to groundwater in alluvial plains - Comparison in east and west side catchments of Lake Biwa –

*Yusuke Tomozawa[1], Kunyang Wang[1], Mitsuyo Saito[2], Syuhei Ban[3], Noboru Okuda[4], Shin-ichi Onodera[1] (1.Graduate School of Integrated Arts and Sciences Hiroshima University, 2.Graduate School of Environmental and Life Science, Okayama University, 3.School of Environmental Science, The University of Shiga Prefecture, 4.Research Institute for Humanity and Nature)

[AHW22-P15] Calculation of TN and TP concentration coefficients of river water for each land use by a simple watershed model.

*Seiko Yoshikawa[1], Donglai Ma[1,4], Tadamasa Saito[1,5], Kenji Matsumori[2], Yuko Itoh[3], Masahiro Kobayashi[3] (1.Institute for Agro-environmental Sciences, National Agriculture and Food Research Organization, 2.Western Region Agricultural Research Center, National Agriculture and Food Research Organization, 3.Forestry and Forest Products Research Institute, 4.Graduate school,Tsukuba University, 5.Faculty of Agriculture, Ibaraki University)

[AHW22-P16] **Possibility of nutrients transportation from littoral slope for enhancement of phytoplankton growth in north basin of Lake Biwa**

*Syuhei Ban[1], Rong YI[1], Xin Liu[1], Masahiro Maruo[1], Miki Sudo[1], Naoshige Goto[1], Jun Murase[2] (1.The University of Shiga Prefecture, 2.Nagoya University)

[AHW22-P17] SWAT model analysis for confirming the effects of crop growth on the suspended sediment concentration from a settling basin catchment on Ishigaki island

*Yang Cao[1], Shin-ichi Onodera[1], Mitsuyo Saito[2], Hide Omae[3], Yoshiko Iizumi[3] (1.Graduate School of Integrate Arts and Sciences, Hiroshima University, 2.Graduate School of Environmental and life Science, Okayama University, 3.Tropical Agriculture Research Front (TARF), Japan International Research Center for Agricultural Sciences (JIRCAS))

[AHW22-P18] Estimating the runoff of water, sediment, and nutrient using SWAT model in Kikuchi-river watershed, Kumamoto, and the influence of the forest

*Soichiro Fujii[1], Masahiko Kanamori[1], Yuko Nagano[1], Maki Kinoshita[2], Yuta Shimizu[3], Shin-ichi Onodera[4] (1.Japan Forest Technology Association, 2.PASCO Corporation, 3.Western Region Agricultural Research Center, National Agriculture and Food Research Organization, 4.Graduate School of Integrated and Arts Sciences, Hiroshima University)

[AHW22-P19] Atmospheric depositions on forest ecosystems in areas along the Sea of Japan

*Yuko Itoh[1], Keiji Takase[2], Yoichi Fujihara[2], Toru Okamoto[1] (1.Forestry and Forest Products Research Institute, Japan, 2.Ishikawa Prefectural University)

[AHW22-P20] Continuous and simultaneous flux measurement of N_2O and CO_2 from agricultural soil using a portable multi-turn time-of-flight mass spectrometer

*Noriko Nakayama[1], Yusuke Iwai[1], Yo Toma[2], Hiroshi Furutani[1], Ryusuke Hatano[3], Michisato Toyoda[1] (1.Osaka University, 2.Ehime University, 3.Hokkaido University)

[AHW22-P21] Effects of introduction of cyclic irrigation system on mass balances of SS and T-P in Lake Inbanuma, Chiba, Japan

*Tomijiro Kubota[1] (1.National Agriculture and Food Research Organization, Institute for Rural Engineering)

[E] Poster | A (Atmospheric and Hydrospheric Sciences)：A-CG Complex & General

1:45 PM - 3:15 PM JST | 4:45 AM - 6:15 AM UTC | Poster Hall International Exhibition Hall8, Makuhari Messe_3

[A-CG34] Satellite Earth Environment Observation

convener:Riko Oki(Japan Aerospace Exploration Agency), Yoshiaki HONDA(Center for Environmental Remote Sensing, Chiba University), Yukari Takayabu(Atmosphere and Ocean Research Institute, the University of Tokyo), Tsuneo Matsunaga(Center for Global Environmental Research and Satellite Observation Center, National Institute for Environmental Studies)

[ACG34-P01] **Impact of usage of multiple-satellite sensors on accuracy of daily-mean sea surface wind data**

*Ayumi Koizumi[1], Masahisa Kubota[2], Kunio Kutsuwada[3], Hiroyuki Tomita[4], Tsutomu Hihara[5] (1.Tokai University, 2.Tokai University, Institute of Ocean Research and Development, 3.School of Marine Science and Technology, Tokai University, 4.Institute for Space-Earth Environmental, Nagoya University, 5.Japan Agency for Marine-Erth Science and Technology)

[ACG34-P02] Temperature and Size Variability of Warm Pools in the Global Oceans

*ChunYi Lin[1] (1.National Museum of Marine Science & Technology)

[ACG34-P03] Sea surface temperature from SGLI aboard the GCOM-C satellite of JAXA

*Yukio Kurihara[1], Kazunori Ogata[2], Hiroshi Murakami[2], Misako Kachi[2] (1.Tripli-I Co., Ltd., 2.JAXA EORC)

[ACG34-P04] Concept of small satellite UV/visible imaging spectrometer optimized for tropospheric NO_2 measurements in air quality monitoring

*Tamaki Fujinawa[1,5], Katsuyuki Noguchi[2], Akihiko Kuze[3], Andreas Richter[4], John P. Burrows[4], Andreas C. Meier[4], Tomohiro Sato[1], Takeshi Kuroda[1], Naohiro Yoshida[5], YASUKO KASAI[1,5] (1.National Institute of Information and Communications Technology, 2.Nara Women's University, 3.Japan Aerospace Exploration Agency, 4.University of Bremen, 5.Tokyo Institute of Technology)

[ACG34-P05] EarthCARE L2 algorithms for cloud and precipitation

*Kaori Sato[1], Hajime Okamoto[1], Hiroshi Ishimoto[2] (1.Research Institute for Applied Mechanics, Kyushu University, 2.Meteorological Research Institute)

[ACG34-P06] Analysis of the Surface Echo Characteristics Derived from GPM/DPR Wide Swath Observation Experiment

*Kosuke Yamamoto[1], Kinji Furukawa[1], Nobuhiro Takahashi[2], Takuji Kubota[1] (1.Japan Aerospace Exploration Agency, 2.Nagoya University)

[ACG34-P07] The Recent Results from the Global Precipitation Measurement (GPM) mission in Japan

*Riko Oki[1], Takuji Kubota[1], Kinji Furukawa[1], Yuki Kaneko[1], Moeka Yamaji[1], Kosuke Yamamoto[1], Toshio Iguchi[2], Yukari Takayabu[3] (1.Japan Aerospace Exploration Agency, 2.NICT, 3.the University of Tokyo)

[ACG34-P08] **Verification of Global Satellite Mapping of precipitation (GSMaP) for providing its error information**

*Moeka Yamaji[1], Takuji Kubota[1] (1.Earth Observation Research Center, Japan Aerospace Exploration Agency)

[ACG34-P09] Detection of the mixed phase top using the measured dual-frequency ratio of reflectivity with GPM/DPR

*Yuki Kaneko[1], Toshio Iguchi[2] (1.Japan Aerospace Exploration Agency, 2.National Institute of Information and Communications Technology)

[ACG34-P10] **Comparison between high frequency satellite rainfall estimation and APHRODITE-2 ground rain gauge observation**

*Hitoshi Hirose[1], Koichi Toyoshima[1], Atsushi Higuchi[1], Akiyo Yatagai[2], Natsuko Yasutomi[3] (1.Center for Environmental Remote Sensing, Chiba University, 2.Hirosaki University, 3.Disaster Prevention Research Institute, Kyoto University)

[ACG34-P11] Development of the high resolution GSMaP by the Himawari-8

*Tomoaki Mega[1], Tomoo Ushio[1] (1.Tokyo Metropolitan University)

[ACG34-P12] Preliminary results of on-orbit estimation for polarization sensitivity of GCOM-C/SGLI

*Risa Miyazaki[1], Hiroshi Murakami[1], Masahiro Hori[1] (1.Japan Aerospace Exploration Agency)

[ACG34-P13] Analysis of SGLI validation datas based on the effects of the growth and ground types for the AGB development

*Ryota Ishibashi[1], Koji KAJIWARA[1], Yoshiaki HONDA[1] (1.Center for environmental remote sensing, Chiba University)

[ACG34-P14] Remote sensing of aerosol optical properties and water-leaving radiance based on the optimal estimation approach

*Chong Shi[1], Teruyuki Nakajima[1], Makiko Hashimoto[1], Hideaki Takenaka[1] (1.Japan Aerospace Exploration Agency)

[ACG34-P15] Aerosol retrieval and PM2.5 from space using GOSAT/TANSO-CAI

*Makiko Hashimoto[1], Hideaki Takenaka[1], Teruyuki Nakajima[1], Akiko Higurashi[2] (1.Japan Aerospace Explortion Agency, 2.NIES)

[ACG34-P16] **Establishing a high resolution road fugitive dust emission inventory in Kaifeng City, China**

*Yiming Xu[1], Shili Liu[1], Xinyue Cao[1], Xianbao Shen[1], Zhiliang Yao[1] (1.Department of Environmental Science and Engineering, Beijing Technology and Business University)

[ACG34-P17] A Relationship between Diurnal Change Patterns of Land Surface Temperature and Spatial Configuration of the Osaka Metropolitan Area Captured by Himawari-8

*Yuhei Yamamoto[1], Hirohiko Ishikawa[1] (1.Disaster Prevention Research Institute, Kyoto University)

[E] Poster | A (Atmospheric and Hydrospheric Sciences)：A-CG Complex & General

5:15 PM - 6:30 PM JST | 8:15 AM - 9:30 AM UTC | Poster Hall International Exhibition Hall8, Makuhari Messe_12

[A-CG34] Satellite Earth Environment Observation

convener:Riko Oki(Japan Aerospace Exploration Agency), Yoshiaki HONDA(Center for Environmental Remote Sensing, Chiba University), Yukari Takayabu(Atmosphere and Ocean Research Institute, the University of Tokyo), Tsuneo Matsunaga(Center for Global Environmental Research and Satellite Observation Center, National Institute for Environmental Studies)

[ACG34-P01] **Impact of usage of multiple-satellite sensors on accuracy of daily-mean sea surface wind data**

*Ayumi Koizumi[1], Masahisa Kubota[2], Kunio Kutsuwada[3], Hiroyuki Tomita[4], Tsutomu Hihara[5] (1.Tokai University, 2.Tokai University, Institute of Ocean Research and Development, 3.School of Marine Science and Technology, Tokai University, 4.Institute for Space-Earth Environmental, Nagoya University, 5.Japan Agency for Marine-Erth Science and Technology)

[ACG34-P02] Temperature and Size Variability of Warm Pools in the Global Oceans

*ChunYi Lin[1] (1.National Museum of Marine Science & Technology)

[ACG34-P03] Sea surface temperature from SGLI aboard the GCOM-C satellite of JAXA

*Yukio Kurihara[1], Kazunori Ogata[2], Hiroshi Murakami[2], Misako Kachi[2] (1.Tripli-I Co., Ltd., 2.JAXA EORC)

[ACG34-P04] Concept of small satellite UV/visible imaging spectrometer optimized for tropospheric NO_2 measurements in air quality monitoring

*Tamaki Fujinawa[1,5], Katsuyuki Noguchi[2], Akihiko Kuze[3], Andreas Richter[4], John P. Burrows[4], Andreas C. Meier[4], Tomohiro Sato[1], Takeshi Kuroda[1], Naohiro Yoshida[5], YASUKO KASAI[1,5] (1.National Institute of Information and Communications Technology, 2.Nara Women's University, 3.Japan Aerospace Exploration Agency, 4.University of Bremen, 5.Tokyo Institute of Technology)

[ACG34-P05] EarthCARE L2 algorithms for cloud and precipitation

*Kaori Sato[1], Hajime Okamoto[1], Hiroshi Ishimoto[2] (1.Research Institute for Applied Mechanics, Kyushu University, 2.Meteorological Research Institute)

[ACG34-P06] Analysis of the Surface Echo Characteristics Derived from GPM/DPR Wide Swath Observation Experiment

*Kosuke Yamamoto[1], Kinji Furukawa[1], Nobuhiro Takahashi[2], Takuji Kubota[1] (1.Japan Aerospace Exploration Agency, 2.Nagoya University)

[ACG34-P07] The Recent Results from the Global Precipitation Measurement (GPM) mission in Japan

*Riko Oki[1], Takuji Kubota[1], Kinji Furukawa[1], Yuki Kaneko[1], Moeka Yamaji[1], Kosuke Yamamoto[1], Toshio Iguchi[2], Yukari Takayabu[3] (1.Japan Aerospace Exploration Agency, 2.NICT, 3.the University of Tokyo)

[ACG34-P08] **Verification of Global Satellite Mapping of precipitation (GSMaP) for providing its error information**

*Moeka Yamaji[1], Takuji Kubota[1] (1.Earth Observation Research Center, Japan Aerospace Exploration Agency)

[ACG34-P09] Detection of the mixed phase top using the measured dual-frequency ratio of reflectivity with GPM/DPR

*Yuki Kaneko[1], Toshio Iguchi[2] (1.Japan Aerospace Exploration Agency, 2.National Institute of Information and Communications Technology)

[ACG34-P10] **Comparison between high frequency satellite rainfall estimation and APHRODITE-2 ground rain gauge observation**

*Hitoshi Hirose[1], Koichi Toyoshima[1], Atsushi Higuchi[1], Akiyo Yatagai[2], Natsuko Yasutomi[3] (1.Center for Environmental Remote Sensing, Chiba University, 2.Hirosaki University, 3.Disaster Prevention Research Institute, Kyoto University)

[ACG34-P11] Development of the high resolution GSMaP by the Himawari-8

*Tomoaki Mega[1], Tomoo Ushio[1] (1.Tokyo Metropolitan University)

[ACG34-P12] Preliminary results of on-orbit estimation for polarization sensitivity of GCOM-C/SGLI

*Risa Miyazaki[1], Hiroshi Murakami[1], Masahiro Hori[1] (1.Japan Aerospace Exploration Agency)

[ACG34-P13] Analysis of SGLI validation datas based on the effects of the growth and ground types for the AGB development

*Ryota Ishibashi[1], Koji KAJIWARA[1], Yoshiaki HONDA[1] (1.Center for environmental remote sensing, Chiba University)

[ACG34-P14] Remote sensing of aerosol optical properties and water-leaving radiance based on the optimal estimation approach

*Chong Shi[1], Teruyuki Nakajima[1], Makiko Hashimoto[1], Hideaki Takenaka[1] (1.Japan Aerospace Exploration Agency)

[ACG34-P15] Aerosol retrieval and PM2.5 from space using GOSAT/TANSO-CAI

*Makiko Hashimoto[1], Hideaki Takenaka[1], Teruyuki Nakajima[1], Akiko Higurashi[2] (1.Japan Aerospace Explortion Agency, 2.NIES)

[ACG34-P16] **Establishing a high resolution road fugitive dust emission inventory in Kaifeng City, China**

*Yiming Xu[1], Shili Liu[1], Xinyue Cao[1], Xianbao Shen[1], Zhiliang Yao[1] (1.Department of Environmental Science and Engineering, Beijing Technology and Business University)

[ACG34-P17] A Relationship between Diurnal Change Patterns of Land Surface Temperature and Spatial Configuration of the Osaka Metropolitan Area Captured by Himawari-8

*Yuhei Yamamoto[1], Hirohiko Ishikawa[1] (1.Disaster Prevention Research Institute, Kyoto University)

[E] Poster | H (Human Geosciences)：H-TT Technology & Techniques

10:45 AM - 12:15 PM JST | 1:45 AM - 3:15 AM UTC | Poster Hall International Exhibition Hall8, Makuhari Messe_3

[H-TT19] Geographic Information Systems and Cartography

convener:Takashi Oguchi(Center for Spatial Information Science, The University of Tokyo), Yuji Murayama(Graduate School of Life and Environmental Sciences), Yoshiki Wakabayashi(Graduate School of Urban Environmental Sciences, Tokyo Metropolitan University)

[HTT19-P01] **Monitoring and Simulating Land Use/Cover Changes and its Impact on Land Surface Temperature in Sapporo City, Japan**

*RUCI WANG[1], YUJI MURAYAMA[1] (1.University of Tsukuba)

[HTT19-P02] **Spatiotemporal Variations of Land Cover/Use and Sustainable Urban Heat Island (UHI) Mitigation Strategies: A Case Study of Chinese Bay Megacities**

★Invited Papers

*Fei LIU[1], Yuji MURAYAMA[1] (1. University of Tsukuba)

[HTT19-P03] A LST Study of the Seoul Metropolitan City, South Korea, Based on Landsat Data (1996 – 2017)

*Prabath Priyankara[1,3], Manjula Ranagalage[1,4], DMSLB Dissanayake[1,4], Takehiro Morimoto[1,2], Yuji Murayama[1,2] (1.Graduate School of Life and Environmental Sciences, University of Tsukuba, Japan, 2.Faculty of Life and Environmental Sciences, University of Tsukuba, Japan, 3.Faculty of Agriculture, University of Ruhuna, Sri Lanka, 4.Faculty of Social Sciences and Humanities, Rajarata University of Sri Lanka, Sri Lanka)

[HTT19-P04] Improvement of GIS exercise classes using the GIS open educational resources based on questionnaire surveys

★Invited Papers

*Hiroyuki Yamauchi[1], Takashi Oguchi[1], Yuichi S. Hayakawa[2,1], Kotaro Iizuka[1] (1.Center for Spatial Information Science, The University of Tokyo, 2.Environmental Geography, Faculty of Environmental Earth Science, Hokkaido University)

[HTT19-P05] **The Development of COP for Tzu Chi Disaster Prevention System by Using QGIS-Taking 2018 Hualien Earthquake as an Example**

*kuan-wen tseng[1], Ming-Ta Tsai[1], Yun-Ching Wang[1], Ming-Chih Wang[1], Chien-Hsien Liu[1] (1.03-3809093)

[HTT19-P06] Comparative study on shape and distribution of landslides caused by the 2012 Northern Kyushu heavy rainfall and the 2016 Kumamoto earthquake in the Aso region, Kumamoto, Japan

*Yasutaka Haneda[1], Takashi Oguchi[2], Kotaro Iizuka[2], Hitoshi SAITO[3,2], Yuichi S. Hayakawa[4,2], Shoichiro Uchiyama[5] (1.Graduate School of Frontier Science, The University of Tokyo, 2.Center for Spatial Information Science, The University of Tokyo, 3.College of Economics, Kanto Gakuin University, 4.Faculty of Environmental Earth Science, Hokkaido University, 5.National Research Institute for Earth Science and Disaster Resilience)

[HTT19-P07] Using GIS and remote sensing to assess relationships between landslides and land cover changes in the Sanbagawa and Mikabu Belts, Shikoku, Japan

*Roxanne Lai[1], Takashi Oguchi[1] (1.University of Tokyo)

[HTT19-P08] **Analysis of Morphometric Parameters for Mountains Ranges and Landslides due to the July 2018 Heavy Rain in Western Japan Using GIS Data**

*Toshikazu Fukuba[1], Takashi Oguchi[2] (1.Department of Earth and Planetary Environmental Science, The University of Tokyo, 2.Center for Spatial Information Science, The University of Tokyo)

[HTT19-P09] Analyzing short-term topographic change in coastal sand dunes using UAS-SfM photogrammetry: A case study in Northern Kujukuri, Japan

*Seulgi Lee[1], Yasutaka Nakata[2], Kotaro Iizuka[3], Takashi Oguchi[3] (1.Graduate School of Frontier Sciences, The University of Tokyo, 2.Forest Research Department, Forestry Research Institute, Hokkaido Research Organization, 3.Center for Spatial Information Science, The University of Tokyo)

[HTT19-P10] **Responses of suspended sediment yield to precipitation, topography and dam control in the Yellow River Basin, China**

*Ruiqi Zhang[1], Takashi Oguchi[2] (1. Department of Natural Environmental Studies, Graduate School of Frontier Sciences, The University of Tokyo, 2.Center for Spatial Information Science, The University of Tokyo)

[E] Poster | H (Human Geosciences)：H-TT Technology & Techniques

5:15 PM - 6:30 PM JST | 8:15 AM - 9:30 AM UTC | Poster Hall International Exhibition Hall8, Makuhari Messe_16

[H-TT19] Geographic Information Systems and Cartography

convener:Takashi Oguchi(Center for Spatial Information Science, The University of Tokyo), Yuji Murayama(Graduate School of Life and Environmental Sciences), Yoshiki Wakabayashi(Graduate School of Urban Environmental Sciences, Tokyo Metropolitan University)

[HTT19-P01] **Monitoring and Simulating Land Use/Cover Changes and its Impact on Land Surface Temperature in Sapporo City, Japan**

*RUCI WANG[1], YUJI MURAYAMA[1] (1.University of Tsukuba)

[HTT19-P02] **Spatiotemporal Variations of Land Cover/Use and Sustainable Urban Heat Island (UHI) Mitigation Strategies: A Case Study of Chinese Bay Megacities**

★Invited Papers

*Fei LIU[1], Yuji MURAYAMA[1] (1. University of Tsukuba)

[HTT19-P03] A LST Study of the Seoul Metropolitan City, South Korea, Based on Landsat Data (1996 – 2017)

*Prabath Priyankara[1,3], Manjula Ranagalage[1,4], DMSLB Dissanayake[1,4], Takehiro Morimoto[1,2], Yuji Murayama[1,2] (1.Graduate School of Life and Environmental Sciences, University of Tsukuba, Japan, 2.Faculty of Life and Environmental Sciences, University of Tsukuba, Japan, 3.Faculty of Agriculture, University of Ruhuna, Sri Lanka, 4.Faculty of Social Sciences and Humanities, Rajarata University of Sri Lanka, Sri Lanka)

[HTT19-P04] Improvement of GIS exercise classes using the GIS open educational resources based on questionnaire surveys

★Invited Papers

*Hiroyuki Yamauchi[1], Takashi Oguchi[1], Yuichi S. Hayakawa[2,1], Kotaro Iizuka[1] (1.Center for Spatial Information Science, The University of Tokyo, 2.Environmental Geography, Faculty of Environmental Earth Science, Hokkaido University)

[HTT19-P05] **The Development of COP for Tzu Chi Disaster Prevention System by Using QGIS-Taking 2018 Hualien Earthquake as an Example**

*kuan-wen tseng[1], Ming-Ta Tsai[1], Yun-Ching Wang[1], Ming-Chih Wang[1], Chien-Hsien Liu[1] (1.03-3809093)

[HTT19-P06] Comparative study on shape and distribution of landslides caused by the 2012 Northern Kyushu heavy rainfall and the 2016 Kumamoto earthquake in the Aso region, Kumamoto, Japan

*Yasutaka Haneda[1], Takashi Oguchi[2], Kotaro Iizuka[2], Hitoshi SAITO[3,2], Yuichi S. Hayakawa[4,2], Shoichiro Uchiyama[5] (1.Graduate School of Frontier Science, The University of Tokyo, 2.Center for Spatial Information Science, The University of Tokyo, 3.College of Economics, Kanto Gakuin University, 4.Faculty of Environmental Earth Science, Hokkaido University, 5.National Research Institute for Earth Science and Disaster Resilience)

[HTT19-P07] Using GIS and remote sensing to assess relationships between landslides and land cover changes in the Sanbagawa and Mikabu Belts, Shikoku, Japan

*Roxanne Lai[1], Takashi Oguchi[1] (1.University of Tokyo)

[HTT19-P08] **Analysis of Morphometric Parameters for Mountains Ranges and Landslides due to the July 2018 Heavy Rain in Western Japan Using GIS Data**

*Toshikazu Fukuba[1], Takashi Oguchi[2] (1.Department of Earth and Planetary Environmental Science, The University of Tokyo, 2.Center for Spatial Information Science, The University of Tokyo)

[HTT19-P09] Analyzing short-term topographic change in coastal sand dunes using UAS-SfM photogrammetry: A case study in Northern Kujukuri, Japan

*Seulgi Lee[1], Yasutaka Nakata[2], Kotaro Iizuka[3], Takashi Oguchi[3] (1.Graduate School of Frontier Sciences, The University of Tokyo, 2.Forest Research Department, Forestry Research Institute, Hokkaido Research Organization, 3.Center for Spatial Information Science, The University of Tokyo)

[HTT19-P10] **Responses of suspended sediment yield to precipitation, topography and dam control in the Yellow River Basin, China**

*Ruiqi Zhang[1], Takashi Oguchi[2] (1. Department of Natural Environmental Studies, Graduate School of Frontier Sciences, The University of Tokyo, 2.Center for Spatial Information Science, The University of Tokyo)

[E] Poster | S (Solid Earth Sciences)：S-IT Science of the Earth's Interior & Techtonophysics

3:30 PM - 5:00 PM JST | 6:30 AM - 8:00 AM UTC | Poster Hall International Exhibition Hall8, Makuhari Messe_10

[S-IT25] Planetary cores: Structure, formation, and evolution

convener:Hidenori Terasaki(Graduate School of Science, Osaka University), Eiji Ohtani(Department of Earth and Planetary Materials Science, Graduate School of Science, Tohoku University), William F McDonough(University of Maryland College Park), George Helffrich(Earth-Life Science Institute, Tokyo Institute of Technology)

[SIT25-P01] Stratification of the Earth's core by SiO_2 crystallisation

*George Helffrich[1], Satoshi Kaneshima[2], Kei Hirose[1,3] (1.Earth-Life Science Institute, Tokyo Institute of Technology, 2.Earth and Planetary Sciences, Kyushu University, 3.Earth and Planetary Sciences Department, University of Tokyo)

[SIT25-P02] Relation between sound velocity and density for liquid iron alloys under Earth's core pressures by laser-shock compression

*Tatsuhiro Sakaiya[1], Tadashi Kondo[1], Hidenori Terasaki[1], Keisuke Shigemori[2], Yoichiro Hironaka[2] (1.Graduate School of Science, Osaka University, 2.Institute of Laser Engineering, Osaka University)

[SIT25-P03] Geochemical estimates of Earth's core heat content at the end of accretion

*Vincent Clesi[1], Renaud Deguen[1] (1.Laboratoire de Geologie de Lyon - Terre, Planètes, Environnement, Université Claude Bernard Lyon 1, CNRS, ENS-Lyon, 69622 Villeurbanne, France.)

[SIT25-P04] The effect of temperature on density of solid metals

*Asaka Kamiya[1], Hidenori Terasaki[1], Tadashi Kondo[1] (1.Osaka University)

[SIT25-P05] Phase relations in the Fe-Ni-Si system at high pressures and high temperatures

*Daijo Ikuta[1], Eiji Ohtani[1], Saori Kawaguchi[2], Naohisa Hirao[2], Yasuo Ohishi[2] (1.Department of Earth Science, Tohoku University, 2.JASRI)

[E] Poster | S (Solid Earth Sciences)：S-IT Science of the Earth's Interior & Techtonophysics

5:15 PM - 6:30 PM JST | 8:15 AM - 9:30 AM UTC | Poster Hall International Exhibition Hall8, Makuhari Messe_21

[S-IT25] Planetary cores: Structure, formation, and evolution

convener:Hidenori Terasaki(Graduate School of Science, Osaka University), Eiji Ohtani(Department of Earth and Planetary Materials Science, Graduate School of Science, Tohoku University), William F McDonough(University of Maryland College Park), George Helffrich(Earth-Life Science Institute, Tokyo Institute of Technology)

[SIT25-P01] Stratification of the Earth's core by SiO_2 crystallisation

*George Helffrich[1], Satoshi Kaneshima[2], Kei Hirose[1,3] (1.Earth-Life Science Institute, Tokyo Institute of Technology, 2.Earth and Planetary Sciences, Kyushu University, 3.Earth and Planetary Sciences Department, University of Tokyo)

[SIT25-P02] Relation between sound velocity and density for liquid iron alloys under Earth's core pressures by laser-shock compression

*Tatsuhiro Sakaiya[1], Tadashi Kondo[1], Hidenori Terasaki[1], Keisuke Shigemori[2], Yoichiro Hironaka[2] (1.Graduate School of Science, Osaka University, 2.Institute of Laser Engineering, Osaka University)

[SIT25-P03] Geochemical estimates of Earth's core heat content at the end of accretion

*Vincent Clesi[1], Renaud Deguen[1] (1.Laboratoire de Geologie de Lyon - Terre, Planètes, Environnement, Université Claude Bernard Lyon 1, CNRS, ENS-Lyon, 69622 Villeurbanne, France.)

[SIT25-P04] The effect of temperature on density of solid metals

*Asaka Kamiya[1], Hidenori Terasaki[1], Tadashi Kondo[1] (1.Osaka University)

[SIT25-P05] Phase relations in the Fe-Ni-Si system at high pressures and high temperatures

*Daijo Ikuta[1], Eiji Ohtani[1], Saori Kawaguchi[2], Naohisa Hirao[2], Yasuo Ohishi[2] (1.Department of Earth Science, Tohoku University, 2.JASRI)

[E] Poster | S (Solid Earth Sciences)：S-VC Volcanology

3:30 PM - 5:00 PM JST | 6:30 AM - 8:00 AM UTC | Poster Hall International Exhibition Hall8, Makuhari Messe_12

[S-VC34] Connecting magma dynamics in vent-conduit system with surface expression of volcanic eruption

convener:Takahiro Miwa(National research institute for earth science and disaster prevention), Nobuo Geshi(Geological Survey of Japan, The National Institute of Advanced Industrial Science and Technology)

[SVC34-P01] A new formulation of viscosity-included bubble nucleation rate in ascending magmas and re-estimation of bubble number density (2)

*Mizuki Nishiwaki[1], Atsushi Toramaru[2] (1.Department of Earth and Planetary Sciences, Graduate School of Sciences, Kyushu University, 2.Department of Earth and Planetary Sciences, Faculty of Sciences, Kyushu University)

[SVC34-P02] Kinetic delay of crystal growth controls plagioclase-basaltic melt apparent disequilibrium

*Ryoya Oida[1], Hidemi Ishibashi[1], ATSUSHI YASUDA[2], Natsumi Hokanishi[2] (1.Faculty of Science, Shizuoka University, 2.Earthquake Research Institute, University of Tokyo)

[SVC34-P03] **Eruptive trends and dynamics of remote volcanoes detected form space-based thermal data and SO_2 emissions: a comparative analysis of Stromboli, Batu Tara and Tinakula volcanoes**

*Corrado CIGOLINI[1], Marco Laiolo[1], Francesco Massimetti[1,2], Maurizio Ripepe[2], Diego Coppola[1] (1.Department of Earth Sciences, University of Torino, Italy, 2.Department of Earth Sciences, University of Firenze, Italy)

[SVC34-P04] The source depth of Strombolian explosions: a multiparametric approach and comparison

*Jacopo Taddeucci[1], Miguel Angel Alatorre-Ibarguengoitia[2], Valeria Cigala[3], Elisabetta Del Bello[1], Damien Gaudin[4], Ulrich Kueppers[4], Tullio Ricci[1], Valentino Salvatore[5], Piergiorgio Scarlato[1] (1.Istituto Nazionale di Geofisica e Vulcanologia, Rome, Italy, 2.Centro de Investigación en Gestión de Riesgo y Cambio Climático, Universidad de Ciencias y Artes de Chiapas, Tuxtla Gutiérrez, Mexico, 3.Department of Geosciences, Università degli Studi di Padova, Padua, Italy, 4.Department of Earth and Environmental Sciences. Ludwig-Maximilians-Universität (LMU). Munich, Germany, 5.Dipartimento di Scienze della Terra, Sapienza Università di Roma, Rome, Italy)

[SVC34-P05] Magmatic aggregate of basaltic ash particles

*Takahiro Miwa[1], Nobuo Geshi[2] (1.National research institute for earth science and disaster prevention, 2.National Institute of Advanced Industrial Science and Technology)

[SVC34-P06] Melt inclusion study on the eruption process of Izu-Omuroyama monogenetic volcano, Japan

Risako Hatada[1], *Hidemi Ishibashi[1], Yusuke Suzuki[2], ATSUSHI YASUDA[3], Natsumi Hokanishi[3] (1.Faculty of Science, Shizuoka University, 2.Izu Peninsula Geopark, 3.Earthquake Research Institute, University of Tokyo)

[SVC34-P07] Time-series variation in the textures of ejecta of the An'ei eruption, Izu-Oshima

*Yuya Ikenaga[1], Fukashi Maeno[1], ATSUSHI YASUDA[1] (1.Earthquake Research Institute, The University of Tokyo)

[SVC34-P08] The textural analysis of pumice from the Plinian eruption of Taupo volcano: implications for tube pumice

*Masatoshi Ohashi[1], Mie Ichihara[2], Fukashi Maeno[2], Ben Kennedy[3], Darren Gravley[3] (1.Department of Earth and Planetary Science, Graduate School of Science, The University of Tokyo, 2.Earthquake Research Institute, The University of Tokyo, 3.Department of Geological Sciences, The University of Canterbury)

[E] Poster | S (Solid Earth Sciences)：S-VC Volcanology

5:15 PM - 6:30 PM JST | 8:15 AM - 9:30 AM UTC | Poster Hall International Exhibition Hall8, Makuhari Messe_23

[S-VC34] Connecting magma dynamics in vent-conduit system with surface expression of volcanic eruption

convener:Takahiro Miwa(National research institute for earth science and disaster prevention), Nobuo Geshi(Geological Survey of Japan, The National Institute of Advanced Industrial Science and Technology)

[SVC34-P01] A new formulation of viscosity-included bubble nucleation rate in ascending magmas and re-estimation of bubble number density (2)

*Mizuki Nishiwaki[1], Atsushi Toramaru[2] (1.Department of Earth and Planetary Sciences, Graduate School of Sciences, Kyushu University, 2.Department of Earth and Planetary Sciences, Faculty of Sciences, Kyushu University)

[SVC34-P02] Kinetic delay of crystal growth controls plagioclase-basaltic melt apparent disequilibrium

*Ryoya Oida[1], Hidemi Ishibashi[1], ATSUSHI YASUDA[2], Natsumi Hokanishi[2] (1.Faculty of Science, Shizuoka University, 2.Earthquake Research Institute, University of Tokyo)

[SVC34-P03] **Eruptive trends and dynamics of remote volcanoes detected form space-based thermal data and SO_2 emissions: a comparative analysis of Stromboli, Batu Tara and Tinakula volcanoes**

*Corrado CIGOLINI[1], Marco Laiolo[1], Francesco Massimetti[1,2], Maurizio Ripepe[2], Diego Coppola[1] (1.Department of Earth Sciences, University of Torino, Italy, 2.Department of Earth Sciences, University of Firenze, Italy)

[SVC34-P04] The source depth of Strombolian explosions: a multiparametric approach and comparison

*Jacopo Taddeucci[1], Miguel Angel Alatorre-Ibarguengoitia[2], Valeria Cigala[3], Elisabetta Del Bello[1], Damien Gaudin[4], Ulrich Kueppers[4], Tullio Ricci[1], Valentino Salvatore[5], Piergiorgio Scarlato[1] (1.Istituto Nazionale di Geofisica e Vulcanologia, Rome, Italy, 2.Centro de Investigación en Gestión de Riesgo y Cambio Climático, Universidad de Ciencias y Artes de Chiapas, Tuxtla Gutiérrez, Mexico, 3.Department of Geosciences, Università degli Studi di Padova, Padua, Italy, 4.Department of Earth and Environmental Sciences. Ludwig-Maximilians-Universität (LMU). Munich, Germany, 5.Dipartimento di Scienze della Terra, Sapienza Università di Roma, Rome, Italy)

[SVC34-P05] Magmatic aggregate of basaltic ash particles

*Takahiro Miwa[1], Nobuo Geshi[2] (1.National research institute for earth science and disaster prevention, 2.National Institute of Advanced Industrial Science and Technology)

[SVC34-P06] Melt inclusion study on the eruption process of Izu-Omuroyama monogenetic volcano, Japan

Risako Hatada[1], *Hidemi Ishibashi[1], Yusuke Suzuki[2], ATSUSHI YASUDA[3], Natsumi Hokanishi[3] (1.Faculty of Science, Shizuoka University, 2.Izu Peninsula Geopark, 3.Earthquake Research Institute, University of Tokyo)

[SVC34-P07] Time-series variation in the textures of ejecta of the An'ei eruption, Izu-Oshima

*Yuya Ikenaga[1], Fukashi Maeno[1], ATSUSHI YASUDA[1] (1.Earthquake Research Institute, The University of Tokyo)

[SVC34-P08] The textural analysis of pumice from the Plinian eruption of Taupo volcano: implications for tube pumice

*Masatoshi Ohashi[1], Mie Ichihara[2], Fukashi Maeno[2], Ben Kennedy[3], Darren Gravley[3] (1.Department of Earth and Planetary Science, Graduate School of Science, The University of Tokyo, 2.Earthquake Research Institute, The University of Tokyo, 3.Department of Geological Sciences, The University of Canterbury)

[E] Poster | S (Solid Earth Sciences)：S-CG Complex & General

3:30 PM - 5:00 PM JST | 6:30 AM - 8:00 AM UTC | Poster Hall International Exhibition Hall8, Makuhari Messe_14

[S-CG50] Intraslab and intraplate earthquakes

convener:Saeko Kita(International Institute of Seismology and Earthquake Engineering, BRI), Tomohiro Ohuchi(Geodynamics Research Center, Ehime University), Marcel Thielmann(Bavarian Geoinstitute, University of Bayreuth), Ryo Okuwaki(Research Institute of Earthquake and Volcano Geology, Geological Survey of Japan, National Institute of Advanced Industrial Science and Technology)

[SCG50-P01] Changes in seismicity rate, stress orientations, and b-values before and after ETS events in the Philippine sea plate under Kii Peninsula

*Saeko Kita[1], Heidi Houston[2], Sachiko Tanaka[3], Youichi Asano[3], Takuo Shibutani[4], Naoki Suda[5] (1.Building Research Institute, 2.USC, 3.NIED, 4.DPRI, Kyoto University, 5.Hiroshima University)

[SCG50-P02] **Inhomogeneous conduit across slab controlled by intraslab stress heterogeneity in the Nankai subduction zone**

*Makoto Otsubo[1], Ayumu Miyakawa[2], Ikuo Katayama[3], Keishi Okazaki[4] (1.Geological Survey of Japan, Research Institute of Earthquake and Volcano Geology, 2.Geological Survey of Japan, Research Institute of Geology and Geoinformation, 3.Hiroshima University, 4.JAMSTEC)

[SCG50-P03] New insights into the mechanism of deep-focus earthquakes

*Ayako Tsuchiyama[1], Junichi Nakajima[1] (1.Tokyo Institute of Technology)

[SCG50-P04] Faulting in deforming harzburgite under wet conditions

*Tomohiro Ohuchi[1], Xinglin Lei[2], Yuji Higo[3], Yoshinori Tange[3], Takeshi Sakai[1] (1.Geodynamics Research Center, Ehime University, 2.National Institute of Advanced Industrial Science and Technology, 3.Japan Synchrotron Radiation Research Institute)

[SCG50-P05] Semi-brittle behavior of olivine single crystals under the conditions of Earth's mantle transition zone

Yoshihisa Naruse[1], *Tomohiro Ohuchi[1] (1.Geodynamics Research Center, Ehime University)

[SCG50-P06] High-pressure deformation experiments on peridotite gouges under hydrothermal conditions, using a deformation-DIA apparatus

*Maki Semba[1], Ken-ichi Hirauchi[1], Tomohiro Ohuchi[2], Katsuyoshi Michibayashi[3] (1.Department of Geosciences, Faculty of Science, Shizuoka University, 2.Geodynamics Research Center, Ehime University, 3.Department of Earth and Planetary Sciences, Nagoya university)

[SCG50-P07] Stable fault slip in antigorite-olivine aggregates at high pressures

Mai Ikehara[1], *Tomoaki Kubo[1], Takuya Iwasato[2], Yuji Higo[3], Masahiro Imamura[1], Yoshinori Tange[3] (1.Kyushu University, 2.Shin-Nippon Nondestructive Inspection Co., Ltd., 3.JASRI)

[SCG50-P08] Rheology and frictional instability of lawsonite in high pressure deformation experiments

*Rei Shiraishi[1], Jun Muto[1], Akihiro Tsunoda[2], Sando Sawa[1], Akio Suzuki[1] (1.Department of Earth Science, Graduate School of Science, Tohoku University, 2.Earthquake Research Institute, University of Tokyo)

[SCG50-P09] Grain Size Dependency of Olivine-Spinel Phase Transformational Mechanism Responsible for Deep-focus Earthquakes

*Sando Sawa[1], Jun Muto[1], Nobuyoshi Miyajima[2], Hiroyuki Nagahama[1] (1.Department of Earth Science, Tohoku University, 2.Bayerisches Geoinstitut, University of Bayreuth)

[SCG50-P10] **Seismicity and mineral destabilizations in the subducting mantle up to 6 GPa, 200 km depth**

*Thomas P. Ferrand[1] (1.Earthquake Research Institute)

[SCG50-P11] Receiver function imaging of subducting Pacific plate and mantle wedge under Japanese islands using denser network of stations

*HyeJeong Kim[1], Hitoshi Kawakatsu[1], Takeshi Akuhara[1], Masanao Shinohara[1] (1.Earthquake Research Institute, The University of Tokyo)

[SCG50-P12] Strong S-wave attenuation in the mantle wedge beneath the NE Japan and interpretations of high-frequency wave propagation path of intraslab earthquakes

*Takahiro Shiina[1,2], Kei Katsumata[2], Kiyoshi Yomogida[3], Aitaro Kato[1] (1.Earthquake Research Institute, The University of Tokyo, 2.Institute of Seismology and Volcanology, Graduate School of Science, Hokkaido University, 3.Graduate School of Science, Hokkaido University)

[E] Poster | S (Solid Earth Sciences)：S-CG Complex & General

5:15 PM - 6:30 PM JST | 8:15 AM - 9:30 AM UTC | Poster Hall International Exhibition Hall8, Makuhari Messe_26

[S-CG50] Intraslab and intraplate earthquakes

convener:Saeko Kita(International Institute of Seismology and Earthquake Engineering, BRI), Tomohiro Ohuchi(Geodynamics Research Center, Ehime University), Marcel Thielmann(Bavarian Geoinstitute, University of Bayreuth), Ryo Okuwaki(Research Institute of Earthquake and Volcano Geology, Geological Survey of Japan, National Institute of Advanced Industrial Science and Technology)

[SCG50-P01] Changes in seismicity rate, stress orientations, and b-values before and after ETS events in the Philippine sea plate under Kii Peninsula

*Saeko Kita[1], Heidi Houston[2], Sachiko Tanaka[3], Youichi Asano[3], Takuo Shibutani[4], Naoki Suda[5] (1.Building Research Institute, 2.USC, 3.NIED, 4.DPRI, Kyoto University, 5.Hiroshima University)

[SCG50-P02] **Inhomogeneous conduit across slab controlled by intraslab stress heterogeneity in the Nankai subduction zone**

*Makoto Otsubo[1], Ayumu Miyakawa[2], Ikuo Katayama[3], Keishi Okazaki[4] (1.Geological Survey of Japan, Research Institute of Earthquake and Volcano Geology, 2.Geological Survey of Japan, Research Institute of Geology and Geoinformation, 3.Hiroshima University, 4.JAMSTEC)

[SCG50-P03] New insights into the mechanism of deep-focus earthquakes

*Ayako Tsuchiyama[1], Junichi Nakajima[1] (1.Tokyo Institute of Technology)

[SCG50-P04] Faulting in deforming harzburgite under wet conditions

*Tomohiro Ohuchi[1], Xinglin Lei[2], Yuji Higo[3], Yoshinori Tange[3], Takeshi Sakai[1] (1.Geodynamics Research Center, Ehime University, 2.National Institute of Advanced Industrial Science and Technology, 3.Japan Synchrotron Radiation Research Institute)

[SCG50-P05] Semi-brittle behavior of olivine single crystals under the conditions of Earth's mantle transition zone

Yoshihisa Naruse[1], *Tomohiro Ohuchi[1] (1.Geodynamics Research Center, Ehime University)

[SCG50-P06] High-pressure deformation experiments on peridotite gouges under hydrothermal conditions, using a deformation-DIA apparatus

*Maki Semba[1], Ken-ichi Hirauchi[1], Tomohiro Ohuchi[2], Katsuyoshi Michibayashi[3] (1.Department of Geosciences, Faculty of Science, Shizuoka University, 2.Geodynamics Research Center, Ehime University, 3.Department of Earth and Planetary Sciences, Nagoya university)

[SCG50-P07] Stable fault slip in antigorite-olivine aggregates at high pressures

Mai Ikehara[1], *Tomoaki Kubo[1], Takuya Iwasato[2], Yuji Higo[3], Masahiro Imamura[1], Yoshinori Tange[3] (1.Kyushu University, 2.Shin-Nippon Nondestructive Inspection Co., Ltd., 3.JASRI)

[SCG50-P08] Rheology and frictional instability of lawsonite in high pressure deformation experiments

*Rei Shiraishi[1], Jun Muto[1], Akihiro Tsunoda[2], Sando Sawa[1], Akio Suzuki[1] (1.Department of Earth Science, Graduate School of Science, Tohoku University, 2.Earthquake Research Institute, University of Tokyo)

[SCG50-P09] Grain Size Dependency of Olivine-Spinel Phase Transformational Mechanism Responsible for Deep-focus Earthquakes

*Sando Sawa[1], Jun Muto[1], Nobuyoshi Miyajima[2], Hiroyuki Nagahama[1] (1.Department of Earth Science, Tohoku University, 2.Bayerisches Geoinstitut, University of Bayreuth)

[SCG50-P10] **Seismicity and mineral destabilizations in the subducting mantle up to 6 GPa, 200 km depth**

*Thomas P. Ferrand[1] (1.Earthquake Research Institute)

[SCG50-P11] Receiver function imaging of subducting Pacific plate and mantle wedge under Japanese islands using denser network of stations

*HyeJeong Kim[1], Hitoshi Kawakatsu[1], Takeshi Akuhara[1], Masanao Shinohara[1] (1.Earthquake Research Institute, The University of Tokyo)

[SCG50-P12] Strong S-wave attenuation in the mantle wedge beneath the NE Japan and interpretations of high-frequency wave propagation path of intraslab earthquakes

*Takahiro Shiina[1,2], Kei Katsumata[2], Kiyoshi Yomogida[3], Aitaro Kato[1] (1.Earthquake Research Institute, The University of Tokyo, 2.Institute of Seismology and Volcanology, Graduate School of Science, Hokkaido University, 3.Graduate School of Science, Hokkaido University)

[E] Poster | S (Solid Earth Sciences)：S-CG Complex & General

10:45 AM - 12:15 PM JST | 1:45 AM - 3:15 AM UTC | Poster Hall International Exhibition Hall8, Makuhari Messe_6

[S-CG51] Role of volatiles on Earth and planetary dynamics

convener:Takayuki Ishii(Bavarian Research Institute, University of Bayreuth), Eiji Ohtani(Department of Earth and Planetary Materials Science, Graduate School of Science, Tohoku University), Michihiko Nakamura(Division of Earth and Planetary Materials Science, Department of Earth Science, Graduate School of Science, Tohoku University), Bjorn Mysen(Geophysical Laboratory, Carnegie Inst. Washington)

[SCG51-P01] Permeability prediction of porous media with the finite difference Stokes solver LaMEM

*Philipp Eichheimer[1], Wakana Fujita[2], Marcel Thielmann[1], Anton Popov[3], Gregor Golabek[1], Boris Kaus[3], Maximilian Kottwitz[3] (1.Bayerisches Geoinstitut, University of Bayreuth, 2.Department of Earth Science, Tohoku University, Sendai, 3.Institute of Geosciences, Johannes Gutenberg University Mainz)

[SCG51-P02] Grain growth-induced fluid localization and permeability reduction

*Wakana Fujita[1], Michihiko Nakamura[1], Kentaro Uesugi[2] (1.Graduate School of Science, Tohoku University, 2.JASRI/SPring-8)

[SCG51-P03] Pargasite stability in the upper mantle at H_2O-undersaturated conditions

*Marija Putak Juricek[1], Hans Keppler[1] (1.BGI)

[SCG51-P04] **Constraining the water content at the top of the mantle transition zone with the elasticity of wadsleyite and olivine**

*Zhongqing Wu[1] (1.University of Science and Technology of China)

[SCG51-P05] ***Single crystal elasticity of Fe-bearing phase E by Brillouin spectroscopy***

*Niccolo Satta[1], Hauke Marquardt [2], Alexander Kurnosov[1], Tiziana Boffa Ballaran [1], Johannes Buchen[3], Catherine McCammon[1], Takaaki Kawazoe[4] (1.Bayerisches Geoinstitut, University of Bayreuth, 95440 Bayreuth, Germany, 2.Department of Earth Sciences, University of Oxford, South Parks Road, Oxford, UK., 3.Seismological Laboratory, California Institute of Technology, Pasadena, CA 91125, USA., 4.Department of Earth and Planetary Systems Science, Hiroshima University, Hiroshima 739-8526, Japan.)

[SCG51-P06] Discovery of two hexagonal phases in (Fe,Al)OOH under the P-T conditions of the deep lower mantle

*Lu Liu[1,2], Li Zhang[1], Hongsheng Yuan[1] (1.Center for High Pressure Science and Technology Advanced Research, 2.University of Science and Technology of China)

[SCG51-P07] **Effect of grid resolution on tectonic regimes in global-scale convection models**

*Enrico Marzotto[1], Marcel Thielmann[1], Gregor Golabek[1] (1.Bayerisches Geoinstitut)

[SCG51-P08] A 3-D crust and uppermost mantle electrical conductivity model of subduction zone beneath NE Japan

*Masahiro Ichiki[1,2], Toshiki Kaida[1], Yasuo Ogawa[3] (1.Graduate School of Science, Tohoku University, 2.International Research Institute of Disaster Science, 3.School of Science, Tokyo Institute of Technology)

[SCG51-P09] *The conditions of sublithospheric diamond formation constrained from ferric iron-rich exsolution from ferropericlase inclusions.*

*Caterina Melai[1], Daniel Frost[1], Tiziana Boffa Ballaran[1], Catherine McCammon[1] (1.Bayerisches Geoinstitute)

[SCG51-P10] **Probing the variation of the oxygen fugacity in diamond anvil cells using the Fe-Ir alloy as redox sensor**

*Serena Dominijanni[1], Catherine McCammon[1], Leonid Dubrovinsky[1], Dan Frost[1], Nobuyoshi Miyajima[1] (1.Bayerisches Geoinstitut)

[SCG51-P11] Goethite behavior at Earth's lower mantle conditions

*Egor Gennadievich Koemets[1], Maxim Bykov[1], George Aprilis[2], Timofey Fedotenko[2], Stella Chariton[1], Saiana Khandarkhaeva[1], Iuliia Koemets[1], Marcel Thielmann[1], Natalia Dubrovinsaia[2], Leonid Dubrovinsky[1] (1.BGI (Bayerisches Geoinstitut), Universität Bayreuth, Germany, 2.Material Physics and Technology at Extreme Conditions, Laboratory of Crystallography, Universität Bayreuth, Germany)

[SCG51-P12] The oxygen content of sulphides in the mantle and a geothermometer for diamond formation

*Sumith Abeykoon[1], Dan Frost[1], Vera Laurenz[1] (1.Bayerisches Geoinstitut, University of Bayreuth)

[E] Poster | S (Solid Earth Sciences)：S-CG Complex & General

5:15 PM - 6:30 PM JST | 8:15 AM - 9:30 AM UTC | Poster Hall International Exhibition Hall8, Makuhari Messe_27

[S-CG51] Role of volatiles on Earth and planetary dynamics

convener:Takayuki Ishii(Bavarian Research Institute, University of Bayreuth), Eiji Ohtani(Department of Earth and Planetary Materials Science, Graduate School of Science, Tohoku University), Michihiko Nakamura(Division of Earth and Planetary Materials Science, Department of Earth Science, Graduate School of Science, Tohoku University), Bjorn Mysen(Geophysical Laboratory, Carnegie Inst. Washington)

[SCG51-P01] Permeability prediction of porous media with the finite difference Stokes solver LaMEM

*Philipp Eichheimer[1], Wakana Fujita[2], Marcel Thielmann[1], Anton Popov[3], Gregor Golabek[1], Boris Kaus[3], Maximilian Kottwitz[3] (1.Bayerisches Geoinstitut, University of Bayreuth, 2.Department of Earth Science, Tohoku University, Sendai, 3.Institute of Geosciences, Johannes Gutenberg University Mainz)

[SCG51-P02] Grain growth-induced fluid localization and permeability reduction

*Wakana Fujita[1], Michihiko Nakamura[1], Kentaro Uesugi[2] (1.Graduate School of Science, Tohoku University, 2.JASRI/SPring-8)

[SCG51-P03] Pargasite stability in the upper mantle at H_2O-undersaturated conditions

*Marija Putak Juricek[1], Hans Keppler[1] (1.BGI)

[SCG51-P04] **Constraining the water content at the top of the mantle transition zone with the elasticity of wadsleyite and olivine**

*Zhongqing Wu[1] (1.University of Science and Technology of China)

[SCG51-P05] ***Single crystal elasticity of Fe-bearing phase E by Brillouin spectroscopy***

*Niccolo Satta[1], Hauke Marquardt [2], Alexander Kurnosov[1], Tiziana Boffa Ballaran [1], Johannes Buchen[3], Catherine McCammon[1], Takaaki Kawazoe[4] (1.Bayerisches Geoinstitut, University of Bayreuth, 95440 Bayreuth, Germany, 2.Department of Earth Sciences, University of Oxford, South Parks Road, Oxford, UK., 3.Seismological Laboratory, California Institute of Technology, Pasadena, CA 91125, USA., 4.Department of Earth and Planetary Systems Science, Hiroshima University, Hiroshima 739-8526, Japan.)

[SCG51-P06] Discovery of two hexagonal phases in (Fe,Al)OOH under the P-T conditions of the deep lower mantle

*Lu Liu[1,2], Li Zhang[1], Hongsheng Yuan[1] (1.Center for High Pressure Science and Technology Advanced Research, 2.University of Science and Technology of China)

[SCG51-P07] **Effect of grid resolution on tectonic regimes in global-scale convection models**

*Enrico Marzotto[1], Marcel Thielmann[1], Gregor Golabek[1] (1.Bayerisches Geoinstitut)

[SCG51-P08] A 3-D crust and uppermost mantle electrical conductivity model of subduction zone beneath NE Japan

*Masahiro Ichiki[1,2], Toshiki Kaida[1], Yasuo Ogawa[3] (1.Graduate School of Science, Tohoku University, 2.International Research Institute of Disaster Science, 3.School of Science, Tokyo Institute of Technology)

[SCG51-P09] *The conditions of sublithospheric diamond formation constrained from ferric iron-rich exsolution from ferropericlase inclusions.*

*Caterina Melai[1], Daniel Frost[1], Tiziana Boffa Ballaran[1], Catherine McCammon[1] (1.Bayerisches Geoinstitute)

[SCG51-P10] **Probing the variation of the oxygen fugacity in diamond anvil cells using the Fe-Ir alloy as redox sensor**

*Serena Dominijanni[1], Catherine McCammon[1], Leonid Dubrovinsky[1], Dan Frost[1], Nobuyoshi Miyajima[1] (1.Bayerisches Geoinstitut)

[SCG51-P11] Goethite behavior at Earth's lower mantle conditions

*Egor Gennadievich Koemets[1], Maxim Bykov[1], George Aprilis[2], Timofey Fedotenko[2], Stella Chariton[1], Saiana Khandarkhaeva[1], Iuliia Koemets[1], Marcel Thielmann[1], Natalia Dubrovinsaia[2], Leonid Dubrovinsky[1] (1.BGI (Bayerisches Geoinstitut), Universität Bayreuth, Germany, 2.Material Physics and Technology at Extreme Conditions, Laboratory of Crystallography, Universität Bayreuth, Germany)

[SCG51-P12] The oxygen content of sulphides in the mantle and a geothermometer for diamond formation

*Sumith Abeykoon[1], Dan Frost[1], Vera Laurenz[1] (1.Bayerisches Geoinstitut, University of Bayreuth)

[E] Poster | M (Multidisciplinary and Interdisciplinary)：M-IS Intersection

10:45 AM - 12:15 PM JST | 1:45 AM - 3:15 AM UTC | Poster Hall International Exhibition Hall8, Makuhari Messe_9

[M-IS03] Evolution and variability of the Asian monsoon in Cenozoic global climate changes

convener:Masanobu Yamamoto(Faculty of Environmental Earth Science, Hokkaido University), Ryuji Tada(Department of Earth and Planetary Science, Graduate School of Science, The Univeristy of Tokyo)

[MIS03-P01] Asian dust source variability since 10 Ma based on grain size specific mineral composition at IODP Site U1425 in the Japan Sea

*Mui Fa Alison Lee[1], Tomohisa Irino[1] (1.Faculty of Environmental Earth Science, Hokkaido University)

[MIS03-P02] Sources and formation environment of biomass burning products in Pliocene and Pleistocene marine sediments in the Japan Sea

*Song Lu[1], Youhei Yamashita[2], Tomohisa Irino[2] (1.Graduate School of Environmental Science, Hokkaido University , 2.Faculty of Environmental Earth Science, Hokkaido University)

[MIS03-P03] Variation of mineral dust flux in peat at a high moor on the Mt. Daisetsu during Holocene

*Tomohisa Irino[1], Keisuke Hirai[1], Osamu Seki[1], James Hooper[2], Samuel Marx[2] (1.Hokkaido University, 2.University of Wollongong)

[MIS03-P04] Variations in sea surface environments recorded by algal biomarkers in the Japan Sea off the western coast of Hokkaido (IODP Site U1422) over the last 250 ka

*Asako Suzuki[1], Ken Sawada[2], Satoshi Furota[3], Yaeko Igarashi[4], Tomohisa Irino[5] (1.Graduate School of Science, Hokkaido University, 2.Department of Earth and Planetary Sciences, Faculty of Science, Hokkaido University, 3.Japan Agency for Marine-Earth Science and Technology, 4.Institute for Paleoenvironment of Northern Regions, 5.Faculty of Environmental Earth Science, Hokkaido University)

[MIS03-P05] **Decadal oscillation in hydrogen stable isotope ratio of long chain fatty acids in Lake Suigetsu sediment core**

*Masaya Inagaki[1], Masanobu Yamamoto[1,2], Takeshi Nakagawa[3] (1.Graduate School of Environmental Science, Hokkaido University, 2.Faculty of Environmental Earth Science, Hokkaido University, 3.Research Center for Palaeoclimatology, Ritsumeikan University)

[MIS03-P06] **Amplitude modulation of sea surface temperature variability in the Bay of Bengal by 400-kyr eccentricity cycle**

*Masanobu Yamamoto[1], Yuko Tsuchiya[1], Steven Clemens[2] (1.Faculty of Environmental Earth Science, Hokkaido University, 2.Department of Earth, Planetary and Environmental Sciences, Brown University)

[E] Poster | M (Multidisciplinary and Interdisciplinary)：M-IS Intersection

5:15 PM - 6:30 PM JST | 8:15 AM - 9:30 AM UTC | Poster Hall International Exhibition Hall8, Makuhari Messe_34

[M-IS03] Evolution and variability of the Asian monsoon in Cenozoic global climate changes

convener:Masanobu Yamamoto(Faculty of Environmental Earth Science, Hokkaido University), Ryuji Tada(Department of Earth and Planetary Science, Graduate School of Science, The Univeristy of Tokyo)

[MIS03-P01] Asian dust source variability since 10 Ma based on grain size specific mineral composition at IODP Site U1425 in the Japan Sea

*Mui Fa Alison Lee[1], Tomohisa Irino[1] (1.Faculty of Environmental Earth Science, Hokkaido University)

[MIS03-P02] Sources and formation environment of biomass burning products in Pliocene and Pleistocene marine sediments in the Japan Sea

*Song Lu[1], Youhei Yamashita[2], Tomohisa Irino[2] (1.Graduate School of Environmental Science, Hokkaido University , 2.Faculty of Environmental Earth Science, Hokkaido University)

[MIS03-P03] Variation of mineral dust flux in peat at a high moor on the Mt. Daisetsu during Holocene

*Tomohisa Irino[1], Keisuke Hirai[1], Osamu Seki[1], James Hooper[2], Samuel Marx[2] (1.Hokkaido University, 2.University of Wollongong)

[MIS03-P04] Variations in sea surface environments recorded by algal biomarkers in the Japan Sea off the western coast of Hokkaido (IODP Site U1422) over the last 250 ka

*Asako Suzuki[1], Ken Sawada[2], Satoshi Furota[3], Yaeko Igarashi[4], Tomohisa Irino[5] (1.Graduate School of Science, Hokkaido University, 2.Department of Earth and Planetary Sciences, Faculty of Science, Hokkaido University, 3.Japan Agency for Marine-Earth Science and Technology, 4.Institute for Paleoenvironment of Northern Regions, 5.Faculty of Environmental Earth Science, Hokkaido University)

[MIS03-P05] **Decadal oscillation in hydrogen stable isotope ratio of long chain fatty acids in Lake Suigetsu sediment core**

*Masaya Inagaki[1], Masanobu Yamamoto[1,2], Takeshi Nakagawa[3] (1.Graduate School of Environmental Science, Hokkaido University, 2.Faculty of Environmental Earth Science, Hokkaido University, 3.Research Center for Palaeoclimatology, Ritsumeikan University)

[MIS03-P06] **Amplitude modulation of sea surface temperature variability in the Bay of Bengal by 400-kyr eccentricity cycle**

*Masanobu Yamamoto[1], Yuko Tsuchiya[1], Steven Clemens[2] (1.Faculty of Environmental Earth Science, Hokkaido University, 2.Department of Earth, Planetary and Environmental Sciences, Brown University)

[E] Poster | M (Multidisciplinary and Interdisciplinary)：M-IS Intersection

10:45 AM - 12:15 PM JST | 1:45 AM - 3:15 AM UTC | Poster Hall International Exhibition Hall8, Makuhari Messe_10

[M-IS04] Interdisciplinary studies on pre-earthquake processes

convener:Katsumi Hattori(Department of Earth Sciences, Graduate School of Science, Chiba University), JANN-YENQ Liu(Institute of Space Science, National Central University, Taiwan), Dimitar Ouzounov(Center of Excellence in Earth Systems Modeling & Observations (CEESMO) , Schmid College of Science & Technology Chapman University, Orange, California, USA), Qinghua Huang(Peking University)

[MIS04-P01] Statistical analysis and Evaluation of ULF seismo-magnetic phenomena at Kakioka, Japan, during 1983-2017

*Kei Takahashi[1], Katsumi Hattori[2], Peng Han[3] (1.Faculty of Science, Chiba University, 2.Graduate School of Science, Chiba University, 3.Southern University of Science and Technology, China)

[MIS04-P02] Pre-seismic anomalies on Earth's magnetic field and ionosphere electron density using Swarm data

*Amune Yamazaki[1], Katsumi Hattori[1], Rui Song[1] (1.Chiba University)

[MIS04-P03] Measurement of radon density in the atmosphere at Okayama, Kochi, Choshi and Kiyosumi, II

*Tohru Okabayashi[1], Kiyotaka Ninagawa[2], Isao Yamamoto[3], Katsumi Hattori[4], Chie Yoshino[4], Haruna Kojima[4], Nobuhiro Maeda (1.Department of Merical Risk and Crisis Management, Faculty of Risk and Crisis Management, Chiba Institute of Science, 2.Faculty of Science, Okayama University of Science, 3.Falcuty of Engineering, Okayama University of Science, 4.Graduate school of Science, Chiba University)

[MIS04-P04] Possible anomalous changes in solar quiet-daily geomagnetic variation *Sq* related to the 2011 off the Pacific coast of Tohoku earthquake (Mw 9.0)

*Xiaocan Liu[1], Katsumi Hattori[2,3], Peng Han[4], Huaran Chen[1] (1.Institute of geophysics China Earthquake Administrition, 2.Graduate School of Science, Chiba University, Chiba, Japan, 3. Center for Environmental Remote Sensing, Chiba University, Chiba, Japan, 4.Department of Earth and Space Sciences, Southern University of Science and Technology, ShenZhen, China)

[MIS04-P05] Co-seismic geomagnetic fluctuations and atmospheric disturbances during the 2018 M6.2 Hualien Earthquake

*Chun-Rong Chen[1], JANN-YENQ Liu[1] (1.Graduate Institute of Space Science, National Central University)

[MIS04-P06] Multi-sensor monitoring network for earthquake precursor study near subduction zone at Boso, Japan

*Katsumi Hattori[1], Chie Yoshino[1], WEIYUN XIE[2], Sanaka Saito[2], Haruna Kojima[2], Rui Song[2], Peng Han[3], Toru Mogi[4], Tada-nori Goto[5], Ichi Takumi[6], Hiroshi Yasukawa[7], Motoaki Mouri[8], Jun Izutsu[9], Tadashi Takano[10], Chihiro Yamanaka[11], Masashi Kamogawa[12], Yoshiaki Ando[13], JANN-YENQ Liu[14], Dimitar Ouzounov[15], Valery Tramutoli[16] (1.Department of Earth Sciences, Graduate School of Science, Chiba University, 2.Graduate School of Science and Engineering, Chiba University, 3.Southern University of Science and Technology, China, 4.Hokkaido University, 5.Kyoto University, 6.Nagoya Institute of Technology, 7.Aichi Prefectural University, 8.Aichi University, 9.Chubu University, 10.Nihon University, 11.Osaka University, 12.Tokyo Gakugei University, 13.The University of Electro-Communications, 14.National Central University, Taiwan, 15.Chapman University, US, 16.University of Basilicagta, Italy)

[MIS04-P07] Transient Effects in Atmosphere and Ionosphere Associated with 2018 Mw 7.5 Sulawesi Indonesia Earthquake and Triggered Tsunami and Volcano Activities

★Invited Papers

*Dimitar Ouzounov[1], Sergey Pulinets[2], Dmitry Davidenko[2], Alexander Rozhnoi[3], Maria Solovieva[3], Tiger Liu[4] (1.Center of Excellence in Earth Systems Modeling & Observations (CEESMO) , Schmid College of Science & Technology Chapman University, Orange, California, USA, 2.Space Research Institute, RAS, Moscow, Russia, 3.The Schmidt Institute of Physics of the Earth, RAS, Moscow, Russia, 4.Center for Astronautical Physics and Engineering, National Central University, Taoyuan City, Taiwan)

[MIS04-P08] Seismicity change and b value variation prior to the Wenchuan earthquake (*Ms 8.0*)

*Peng Han[1], Rui Wang[1], Ying Chang[1], Miao Miao[1], Haixia Shi[2], Lingyuan Meng[2], Xuemei Zhang[2], Weiyun Xie[3], Katsumi Hattori[3] (1.Southern University of Science and Technology, Shenzhen, China, 2.China Earthquake Networks

Center, Beijing 100045, China, 3.Chiba University, Chiba, Japan)

[E] Poster | M (Multidisciplinary and Interdisciplinary)：M-IS Intersection

5:15 PM - 6:30 PM JST | 8:15 AM - 9:30 AM UTC | Poster Hall International Exhibition Hall8, Makuhari Messe_35

[M-IS04] Interdisciplinary studies on pre-earthquake processes

convener:Katsumi Hattori(Department of Earth Sciences, Graduate School of Science, Chiba University), JANN-YENQ Liu(Institute of Space Science, National Central University, Taiwan), Dimitar Ouzounov(Center of Excellence in Earth Systems Modeling & Observations (CEESMO) , Schmid College of Science & Technology Chapman University, Orange, California, USA), Qinghua Huang(Peking University)

[MIS04-P01] Statistical analysis and Evaluation of ULF seismo-magnetic phenomena at Kakioka, Japan, during 1983-2017

*Kei Takahashi[1], Katsumi Hattori[2], Peng Han[3] (1.Faculty of Science, Chiba University, 2.Graduate School of Science, Chiba University, 3.Southern University of Science and Technology, China)

[MIS04-P02] Pre-seismic anomalies on Earth's magnetic field and ionosphere electron density using Swarm data

*Amune Yamazaki[1], Katsumi Hattori[1], Rui Song[1] (1.Chiba University)

[MIS04-P03] Measurement of radon density in the atmosphere at Okayama, Kochi, Choshi and Kiyosumi, II

*Tohru Okabayashi[1], Kiyotaka Ninagawa[2], Isao Yamamoto[3], Katsumi Hattori[4], Chie Yoshino[4], Haruna Kojima[4], Nobuhiro Maeda (1.Department of Merical Risk and Crisis Management, Faculty of Risk and Crisis Management, Chiba Institute of Science, 2.Faculty of Science, Okayama University of Science, 3.Falcuty of Engineering, Okayama University of Science, 4.Graduate school of Science, Chiba University)

[MIS04-P04] Possible anomalous changes in solar quiet-daily geomagnetic variation *Sq* related to the 2011 off the Pacific coast of Tohoku earthquake (Mw 9.0)

*Xiaocan Liu[1], Katsumi Hattori[2,3], Peng Han[4], Huaran Chen[1] (1.Institute of geophysics China Earthquake Administrition, 2.Graduate School of Science, Chiba University, Chiba, Japan, 3. Center for Environmental Remote Sensing, Chiba University, Chiba, Japan, 4.Department of Earth and Space Sciences, Southern University of Science and Technology, ShenZhen, China)

[MIS04-P05] Co-seismic geomagnetic fluctuations and atmospheric disturbances during the 2018 M6.2 Hualien Earthquake

*Chun-Rong Chen[1], JANN-YENQ Liu[1] (1.Graduate Institute of Space Science, National Central University)

[MIS04-P06] Multi-sensor monitoring network for earthquake precursor study near subduction zone at Boso, Japan

*Katsumi Hattori[1], Chie Yoshino[1], WEIYUN XIE[2], Sanaka Saito[2], Haruna Kojima[2], Rui Song[2], Peng Han[3], Toru Mogi[4], Tada-nori Goto[5], Ichi Takumi[6], Hiroshi Yasukawa[7], Motoaki Mouri[8], Jun Izutsu[9], Tadashi Takano[10], Chihiro Yamanaka[11], Masashi Kamogawa[12], Yoshiaki Ando[13], JANN-YENQ Liu[14], Dimitar Ouzounov[15], Valery Tramutoli[16] (1.Department of Earth Sciences, Graduate School of Science, Chiba University, 2.Graduate School of Science and Engineering, Chiba University, 3.Southern University of Science and Technology, China, 4.Hokkaido University, 5.Kyoto University, 6.Nagoya Institute of Technology, 7.Aichi Prefectural University, 8.Aichi University, 9.Chubu University, 10.Nihon University, 11.Osaka University, 12.Tokyo Gakugei University, 13.The University of Electro-Communications, 14.National Central University, Taiwan, 15.Chapman University, US, 16.University of Basilicagta, Italy)

[MIS04-P07] Transient Effects in Atmosphere and Ionosphere Associated with 2018 Mw 7.5 Sulawesi Indonesia Earthquake and Triggered Tsunami and Volcano Activities

★Invited Papers

*Dimitar Ouzounov[1], Sergey Pulinets[2], Dmitry Davidenko[2], Alexander Rozhnoi[3], Maria Solovieva[3], Tiger Liu[4] (1.Center of Excellence in Earth Systems Modeling & Observations (CEESMO) , Schmid College of Science & Technology Chapman University, Orange, California, USA, 2.Space Research Institute, RAS, Moscow, Russia, 3.The Schmidt Institute of Physics of the Earth, RAS, Moscow, Russia, 4.Center for Astronautical Physics and Engineering, National Central University, Taoyuan City, Taiwan)

[MIS04-P08] Seismicity change and b value variation prior to the Wenchuan earthquake (*Ms 8.0*)

*Peng Han[1], Rui Wang[1], Ying Chang[1], Miao Miao[1], Haixia Shi[2], Lingyuan Meng[2], Xuemei Zhang[2], Weiyun Xie[3], Katsumi Hattori[3] (1.Southern University of Science and Technology, Shenzhen, China, 2.China Earthquake Networks Center, Beijing 100045, China, 3.Chiba University, Chiba, Japan)

[E] Poster | M (Multidisciplinary and Interdisciplinary)：M-IS Intersection

3:30 PM - 5:00 PM JST | 6:30 AM - 8:00 AM UTC | Poster Hall International Exhibition Hall8, Makuhari Messe_19

[M-IS06] Conservation of geoparks, natural geosites and cultural heritage: weathering process and damage assessment

convener:Chiaki T. Oguchi(Institute for Environmental Science and Technology, Graduate School of Science and Engineering, Saitama University), Tetsuya Waragai(Graduate School of Science and Engineering, Nihon University), Kuniyasu Mokudai(Tohoku Gakuin University), Magdalini Theodoridou(School of Engineering, Cardiff University)

[MIS06-P01] The artistic qualities of religion reliefs in Taya-cave.Japan

*OGATA KEISUKE[1] (1.TSURUMI UNIVERSITY)

[MIS06-P02] Effect of stress concentration on the Weathering Mechanism of Sandstone Pillars of Angkor Wat, Cambodia by means of numerical simulation

*Takato Takemura[1], Tetsuya Waragai[2] (1.Nihon Univ., 2.Nihon University)

[MIS06-P03] Meaning to preserve evidence of large scale landslide

*Kuniyasu Mokudai[1], Hidekazu Sato[2] (1.Japan Geoservice Incorporated, 2.Mt. Kurikoma Area Geopark)

[E] Poster | M (Multidisciplinary and Interdisciplinary)：M-IS Intersection

5:15 PM - 6:30 PM JST | 8:15 AM - 9:30 AM UTC | Poster Hall International Exhibition Hall8, Makuhari Messe_36

[M-IS06] Conservation of geoparks, natural geosites and cultural heritage: weathering process and damage assessment

convener:Chiaki T. Oguchi(Institute for Environmental Science and Technology, Graduate School of Science and Engineering, Saitama University), Tetsuya Waragai(Graduate School of Science and Engineering, Nihon University), Kuniyasu Mokudai(Tohoku Gakuin University), Magdalini Theodoridou(School of Engineering, Cardiff University)

[MIS06-P01] The artistic qualities of religion reliefs in Taya-cave.Japan

*OGATA KEISUKE[1] (1.TSURUMI UNIVERSITY)

[MIS06-P02] Effect of stress concentration on the Weathering Mechanism of Sandstone Pillars of Angkor Wat, Cambodia by means of numerical simulation

*Takato Takemura[1], Tetsuya Waragai[2] (1.Nihon Univ., 2.Nihon University)

[MIS06-P03] Meaning to preserve evidence of large scale landslide

*Kuniyasu Mokudai[1], Hidekazu Sato[2] (1.Japan Geoservice Incorporated, 2.Mt. Kurikoma Area Geopark)

[E] Poster | M (Multidisciplinary and Interdisciplinary)：M-IS Intersection

3:30 PM - 5:00 PM JST | 6:30 AM - 8:00 AM UTC | Poster Hall International Exhibition Hall8, Makuhari Messe_20

[M-IS07] Astrobiology

convener:Hikaru Yabuta(Hiroshima University, Department of Earth and Planetary Systems Science), Seiji Sugita(Department of Earth and Planetary Science, Graduate School of Science Sciece, The University of Tokyo), Misato Fukagawa(National Astronomical Observatory of Japan), Fujishima Kosuke(Tokyo Institute of Technology, Earth-Life Science Institute)

[MIS07-P01] Exoplanets Revealed by High-Precision Infrared Doppler Technique Using IRD: Large Exploration for Planets around Cool M-type Stars Begins

*Masayuki Kuzuhara[1,3], Bunei Sato[4], Motohide Tamura[2,1,3], Takayuki Kotani[1,3,5], Nagayoshi Ohashi[3,6], Masashi Omiya[1,3], Teruyuki Hirano[4], Hiroki Harakawa[6,3,1], Wako Aoki[3,5], Norio Narita[2,1], Yasunori Hori[1,3], Akitoshi Ueda[3,5], Akihiko Fukui[2], Hiroyuki Tako Ishikawa[5,3], Ishizuka Masato[2], Takashi Kurokawa[1,7], Nobuhiko Kusakabe[1,3], Tomoyuki Kudo[6,3,1], Eiichiro Kokubo[3], Mihoko Konishi[1,3], Tadashi Nakajima[1,3,5], Jun Nishikawa[3,5,1], Masahiro Ogihara[3], Takuma Serizawa[7] (1.Astrobiology Center of NINS, 2.The University of Tokyo, Graduate School of Science, 3.National Astronomical Observatory of Japan, 4.Tokyo Institute of Technology, 5.SOKENDAI, 6.Subaru Telescope, 7.Tokyo University of Agriculture and Technology)

[MIS07-P02] Discrimination of organic compounds and mineral particles by fluorescent microscopy for the detection of Martian life.

*Tomoka Okada[1], Yoshitaka Yoshimura[2], Atsuo Miyakawa[3], Yuka Murano[3], Shin-ichi Yokobori[3], Akihiko Yamagishi[3], Kensei Kobayashi[1], Yoko Kebukawa[1] (1.YOKOHAMA National university, 2.Tamagawa University, 3.Tokyo University of Pharmacy and Life Sciences)

[MIS07-P03] Morphological and spectroscopic characteristics of organic matter in Banded Iron Formation, Barberton Greenstone Belt, South Africa

*Hiroki Amemiya[1], Ryo Nakajima[1], Yoko Ohtomo[1], Tsubasa Otake[1], Tsutomu Sato[1] (1.Division of sustainable Resources Engineering, Faculty of Engineering, Hokkaido University)

[MIS07-P04] Understanding peptide sequence selectivity on iron sulfide (FeS) nanoparticle surfaces

*Fujishima Kosuke[1], Norio Kitadai[1], Kenji Kasama[1] (1.Earth-Life Science Institute, Tokyo Institute of Technology)

[MIS07-P05] A process model of L-homochiral peptides formation initiated with L-alanine

*Toratane Munegumi[1], Taisuke Yamaga[1] (1.Department of Science Education, Naruto University of Education)

[MIS07-P06] Possible Formation of Amino Acids and Carboxylic Acids in Slightly-Reducing Primitive Earth Atmospheres

*Miei Kinoshita[1], Shintaro Ikeda[1], Kimitaka Kawamura[2], Bhagawati Kunwar[2], Hitoshi Fukuda[3], Yoshiyuki Oguri[3], Hiromi Shibata[4], Junichi Takahashi[1], Vladimir Airapetian[5], Yoko Kebukawa[1], Kensei Kobayashi[1] (1.Yokohama National University, 2.Chubu University, 3.Tokyo Institute of Technology, 4.Osaka University, 5.NASA Goddard SFC)

[MIS07-P07] Application of Machine learning and software development for initial analysis in the TANPOPO mission

*Kyoko Okudaira[1], Yuto Toda[1], Takashi Sonoke[1], Yuichi Yaguchi[1], Masashi Yoshida[1], Junya Imani[2], Satoshi Sasaki[3], Hajime Yano[4], Hirohide Demura[1], Makoto Tabata[5], Akihiko Yamagishi[6] (1.The University of Aizu, 2.YUKI Precision, 3.Tokyo University of Technology, 4.JAXA, 5.Chiba University, 6.Tokyo University of Pharmacy and Life Science)

[MIS07-P08] Structure analysis of the hyper velocity impact tracks of the particles captured by silica aerogel on the International Space Station

*Mizuho Nishi[1], Akira Tsuchiyama[1], Hajime Yano[2], Hikaru Yabuta[3], Kyoko Okudaira[4], Junya Matsuno[1], Masayuki Uesugi[5], Uesugi Kentaro[5], Nakano Tukasa[6], Takaaki Noguchi[7], MITA Hajime[8], Akihiko Yamagishi[9] (1.Kyoto University, 2.Institute of Space and Astronautical Science, Japan Aerospace Exploration Agency, 3.Hiroshima University, 4.The University of Aizu, 5.JASRI/SPring-8, 6.National Institute of Advanced Industrial Science and Technology, 7.Kyusyu University, 8.Fukuoka Institute of Technology, 9.Tokyo University of Pharmacy and Life Science)

[MIS07-P09] High-Angular-Resolution Observations of Protoplanetary Disks

*Misato Fukagawa[1] (1.National Astronomical Observatory of Japan)

[MIS07-P10] Characterization of high molecular weight amino acid precursors formed in interstellar ice analog

*Soushi Kuramoto[1], Tomohito Sato[1], Hitoshi Fukuda[2], Yoshiyuki Oguri[2], Kotaro Kondo[2], Hiromi Shibata[3], Yoko Kebukawa[1], Kensei Kobayashi[1], Satoshi Yoshida[4] (1.Yokohama National University, 2.Tokyo Institute of Technology, 3.University of Osaka, 4.National Institutes for Quantum Radiological Science and Technology)

[MIS07-P11] Theoretical elucidation of prebiotic formation processes into nucleobases

*Yu Komatsu[1,2], Taiki Suzuki[1,2] (1.Astrobiology Center, 2.National Astronomical Observatory of Japan)

[MIS07-P12] Formation Process of A Glycine's Precursor Candidate, CH3NH2

*Taiki Suzuki[1,2], Liton Majumdar[3], Masatoshi Ohishi[2] (1.National Institutes of Natural Sciences Astrobiology Center, 2.National Astronomical Observatory of Japan, 3.NASA Jet Propulsion Laboratory (JPL))

[MIS07-P13] Numerical study on the stellar atmosphere & wind of Cool Stars

*Takahito Sakaue[1], Kazunari Shibata[1] (1.Kyoto University)

[MIS07-P14] Design of space exposure experiments of organic matter in Tanpopo 2

*Takuya Yokoo[1], tomohito sato[1], Itsuki Sakon[2], Kazumichi Nakagawa[3], Hajime Yano[4], Miki Nakayama[5], Hajime Mita[5], Yoko Kebukawa[1], Kensei Kobayashi[1] (1.Yokohama National University, 2.University of Tokyo, 3.Kobe University, 4.JAXA, 5.Fukuoka Institute of Technology)

[E] Poster | M (Multidisciplinary and Interdisciplinary)：M-IS Intersection

5:15 PM - 6:30 PM JST | 8:15 AM - 9:30 AM UTC | Poster Hall International Exhibition Hall8, Makuhari Messe_37

[M-IS07] Astrobiology

convener:Hikaru Yabuta(Hiroshima University, Department of Earth and Planetary Systems Science), Seiji Sugita(Department of Earth and Planetary Science, Graduate School of Science Sciece, The University of Tokyo), Misato Fukagawa(National Astronomical Observatory of Japan), Fujishima Kosuke(Tokyo Institute of Technology, Earth-Life Science Institute)

[MIS07-P01] Exoplanets Revealed by High-Precision Infrared Doppler Technique Using IRD: Large Exploration for Planets around Cool M-type Stars Begins

*Masayuki Kuzuhara[1,3], Bunei Sato[4], Motohide Tamura[2,1,3], Takayuki Kotani[1,3,5], Nagayoshi Ohashi[3,6], Masashi Omiya[1,3], Teruyuki Hirano[4], Hiroki Harakawa[6,3,1], Wako Aoki[3,5], Norio Narita[2,1], Yasunori Hori[1,3], Akitoshi Ueda[3,5], Akihiko Fukui[2], Hiroyuki Tako Ishikawa[5,3], Ishizuka Masato[2], Takashi Kurokawa[1,7], Nobuhiko Kusakabe[1,3], Tomoyuki Kudo[6,3,1], Eiichiro Kokubo[3], Mihoko Konishi[1,3], Tadashi Nakajima[1,3,5], Jun Nishikawa[3,5,1], Masahiro Ogihara[3], Takuma Serizawa[7] (1.Astrobiology Center of NINS, 2.The University of Tokyo, Graduate School of Science, 3.National Astronomical Observatory of Japan, 4.Tokyo Institute of Technology, 5.SOKENDAI, 6.Subaru Telescope, 7.Tokyo University of Agriculture and Technology)

[MIS07-P02] Discrimination of organic compounds and mineral particles by fluorescent microscopy for the detection of Martian life.

*Tomoka Okada[1], Yoshitaka Yoshimura[2], Atsuo Miyakawa[3], Yuka Murano[3], Shin-ichi Yokobori[3], Akihiko Yamagishi[3], Kensei Kobayashi[1], Yoko Kebukawa[1] (1.YOKOHAMA National university, 2.Tamagawa University, 3.Tokyo University of Pharmacy and Life Sciences)

[MIS07-P03] Morphological and spectroscopic characteristics of organic matter in Banded Iron Formation, Barberton Greenstone Belt, South Africa

*Hiroki Amemiya[1], Ryo Nakajima[1], Yoko Ohtomo[1], Tsubasa Otake[1], Tsutomu Sato[1] (1.Division of sustainable Resources Engineering, Faculty of Engineering, Hokkaido University)

[MIS07-P04] Understanding peptide sequence selectivity on iron sulfide (FeS) nanoparticle surfaces

*Fujishima Kosuke[1], Norio Kitadai[1], Kenji Kasama[1] (1.Earth-Life Science Institute, Tokyo Institute of Technology)

[MIS07-P05] A process model of L-homochiral peptides formation initiated with L-alanine

*Toratane Munegumi[1], Taisuke Yamaga[1] (1.Department of Science Education, Naruto University of Education)

[MIS07-P06] Possible Formation of Amino Acids and Carboxylic Acids in Slightly-Reducing Primitive Earth Atmospheres

*Miei Kinoshita[1], Shintaro Ikeda[1], Kimitaka Kawamura[2], Bhagawati Kunwar[2], Hitoshi Fukuda[3], Yoshiyuki Oguri[3], Hiromi Shibata[4], Junichi Takahashi[1], Vladimir Airapetian[5], Yoko Kebukawa[1], Kensei Kobayashi[1] (1.Yokohama National University, 2.Chubu University, 3.Tokyo Institute of Technology, 4.Osaka University, 5.NASA Goddard SFC)

[MIS07-P07] Application of Machine learning and software development for initial analysis in the TANPOPO mission

*Kyoko Okudaira[1], Yuto Toda[1], Takashi Sonoke[1], Yuichi Yaguchi[1], Masashi Yoshida[1], Junya Imani[2], Satoshi Sasaki[3], Hajime Yano[4], Hirohide Demura[1], Makoto Tabata[5], Akihiko Yamagishi[6] (1.The University of Aizu, 2.YUKI Precision, 3.Tokyo University of Technology, 4.JAXA, 5.Chiba University, 6.Tokyo University of Pharmacy and Life Science)

[MIS07-P08] Structure analysis of the hyper velocity impact tracks of the particles captured by silica aerogel on the International Space Station

*Mizuho Nishi[1], Akira Tsuchiyama[1], Hajime Yano[2], Hikaru Yabuta[3], Kyoko Okudaira[4], Junya Matsuno[1], Masayuki Uesugi[5], Uesugi Kentaro[5], Nakano Tukasa[6], Takaaki Noguchi[7], MITA Hajime[8], Akihiko Yamagishi[9] (1.Kyoto University, 2.Institute of Space and Astronautical Science, Japan Aerospace Exploration Agency, 3.Hiroshima University, 4.The University of Aizu, 5.JASRI/SPring-8, 6.National Institute of Advanced Industrial Science and Technology, 7.Kyusyu University, 8.Fukuoka Institute of Technology, 9.Tokyo University of Pharmacy and Life Science)

[MIS07-P09] High-Angular-Resolution Observations of Protoplanetary Disks

*Misato Fukagawa[1] (1.National Astronomical Observatory of Japan)

[MIS07-P10] Characterization of high molecular weight amino acid precursors formed in interstellar ice analog

*Soushi Kuramoto[1], Tomohito Sato[1], Hitoshi Fukuda[2], Yoshiyuki Oguri[2], Kotaro Kondo[2], Hiromi Shibata[3], Yoko Kebukawa[1], Kensei Kobayashi[1], Satoshi Yoshida[4] (1.Yokohama National University, 2.Tokyo Institute of Technology, 3.University of Osaka, 4.National Institutes for Quantum Radiological Science and Technology)

[MIS07-P11] Theoretical elucidation of prebiotic formation processes into nucleobases

*Yu Komatsu[1,2], Taiki Suzuki[1,2] (1.Astrobiology Center, 2.National Astronomical Observatory of Japan)

[MIS07-P12] Formation Process of A Glycine's Precursor Candidate, CH3NH2

*Taiki Suzuki[1,2], Liton Majumdar[3], Masatoshi Ohishi[2] (1.National Institutes of Natural Sciences Astrobiology Center, 2.National Astronomical Observatory of Japan, 3.NASA Jet Propulsion Laboratory (JPL))

[MIS07-P13] Numerical study on the stellar atmosphere & wind of Cool Stars

*Takahito Sakaue[1], Kazunari Shibata[1] (1.Kyoto University)

[MIS07-P14] Design of space exposure experiments of organic matter in Tanpopo 2

*Takuya Yokoo[1], tomohito sato[1], Itsuki Sakon[2], Kazumichi Nakagawa[3], Hajime Yano[4], Miki Nakayama[5], Hajime Mita[5], Yoko Kebukawa[1], Kensei Kobayashi[1] (1.Yokohama National University, 2.University of Tokyo, 3.Kobe University, 4.JAXA, 5.Fukuoka Institute of Technology)

[E] Poster | M (Multidisciplinary and Interdisciplinary)：M-AG Applied Geosciences

10:45 AM - 12:15 PM JST | 1:45 AM - 3:15 AM UTC | Poster Hall International Exhibition Hall8, Makuhari Messe_11

[M-AG38] Satellite Land Physical Processes Monitoring at Medium/High/Very High Resolution

convener:Jean-Claude Roger(University of Maryland College Park), Shinichi Sobue(Japan Aerospace Exploration Agency), Eric Vermote(NASA Goddard Space Flight Center)

[MAG38-P01] Improving the AVHRR LTDR BRDF correction

*Jose Luis Villaescusa[1,2], Belen Franch[1,2], Jean-Claude Roger[1,2], Eric Vermote[2] (1.University of Maryland College Park, 2.NASA Goddard Space Flight Center)

[MAG38-P02] Winter wheat yield model based on remote sensing data

*Belen Franch[1,2], Eric Vermote[2,1], Sergii Skakun[1,2], Jean-Claude Roger[1,2], Inbal Becker-Reshef[1], Chris Justice[1] (1.Department of Geographical Sciences, University of Maryland, 2.NASA Goddard Space Flight Center)

[MAG38-P03] Agricultural monitoring from Optical and SAR data

*Andrés Eduardo Santamaría-Artigas[1,2], Sergii Skakun[1,2], Belen Franch[1,2], Jean-Claude Roger[1,2], Eric Vermote[2] (1.University of Maryland College Park, 2.NASA Goddard Space Flight Center)

[MAG38-P04] **Eco-hydrological modeling using field-based and Earth Observations to assess water use efficiency and support agricultural water resources management**

pierre Guillevic[2,1], *Jean-Claude Roger[1,2] (1.University of Maryland, College Park, USA, 2.NASA Goddard Space flight Center, Greenbelt, USA)

[MAG38-P05] Detecting and quantifying forest dynamics using SAR time-series data in Indonesia

*Pedro Rodriguez-Veiga[1,2,3], Narumasa Tsutsumida[3] (1.Centre for Landscape and Climate Research, University of Leicester, Leicester, UK, 2.NERC National Centre for Earth Observation (NCEO), Leicester, UK, 3.Graduate School of Global Environmental Studies, Kyoto University, Japan)

[E] Poster | M (Multidisciplinary and Interdisciplinary)：M-AG Applied Geosciences

5:15 PM - 6:30 PM JST | 8:15 AM - 9:30 AM UTC | Poster Hall International Exhibition Hall8, Makuhari Messe_43

[M-AG38] Satellite Land Physical Processes Monitoring at Medium/High/Very High Resolution

convener:Jean-Claude Roger(University of Maryland College Park), Shinichi Sobue(Japan Aerospace Exploration Agency), Eric Vermote(NASA Goddard Space Flight Center)

[MAG38-P01] Improving the AVHRR LTDR BRDF correction

*Jose Luis Villaescusa[1,2], Belen Franch[1,2], Jean-Claude Roger[1,2], Eric Vermote[2] (1.University of Maryland College Park, 2.NASA Goddard Space Flight Center)

[MAG38-P02] Winter wheat yield model based on remote sensing data

*Belen Franch[1,2], Eric Vermote[2,1], Sergii Skakun[1,2], Jean-Claude Roger[1,2], Inbal Becker-Reshef[1], Chris Justice[1] (1.Department of Geographical Sciences, University of Maryland, 2.NASA Goddard Space Flight Center)

[MAG38-P03] Agricultural monitoring from Optical and SAR data

*Andrés Eduardo Santamaría-Artigas[1,2], Sergii Skakun[1,2], Belen Franch[1,2], Jean-Claude Roger[1,2], Eric Vermote[2] (1.University of Maryland College Park, 2.NASA Goddard Space Flight Center)

[MAG38-P04] **Eco-hydrological modeling using field-based and Earth Observations to assess water use efficiency and support agricultural water resources management**

pierre Guillevic[2,1], *Jean-Claude Roger[1,2] (1.University of Maryland, College Park, USA, 2.NASA Goddard Space flight Center, Greenbelt, USA)

[MAG38-P05] Detecting and quantifying forest dynamics using SAR time-series data in Indonesia

*Pedro Rodriguez-Veiga[1,2,3], Narumasa Tsutsumida[3] (1.Centre for Landscape and Climate Research, University of Leicester, Leicester, UK, 2.NERC National Centre for Earth Observation (NCEO), Leicester, UK, 3.Graduate School of Global Environmental Studies, Kyoto University, Japan)

[E] Poster | M (Multidisciplinary and Interdisciplinary)：M-AG Applied Geosciences

3:30 PM - 5:00 PM JST | 6:30 AM - 8:00 AM UTC | Poster Hall International Exhibition Hall8, Makuhari Messe_25

[M-AG40] CTBT IMS Technologies for Detecting Nuclear Explosion and Their Applications to Earth Science

convener:Nurcan Meral Ozel(Comprehensive Nuclear-Test-Ban Treaty Organization), Hiroyuki Matsumoto(Japan Agency for Marine-Earth Science and Technology), Yosuke Naoi(Japan Atomic Energy Agency)

[MAG40-P01] Overview of the Japanese National Data Centre-1 (NDC-1)

*RYOHEI EMURA[1], Takayuki Otsu[1], Toyomi Sakamoto[1], Soshi Iwata[1], Takanari Fujii[1], Mami Nogami[1], Makiko Iwakuni[1], Masashi Motohashi[1] (1.Japan Weather Association)

[MAG40-P02] Challenging to utilize the infrasound technologies for civil and science application

*Masashi Motohashi[1], Nobuo Arai[2], Takayuki Otsu[1], Mami Nogami[1], Makiko Iwakuni[1], Ryohei Emura[1] (1.Japan Weather Association, 2.Disaster Mitigation Research Center, Nagoya Unicersity)

[MAG40-P03] CTBT IMS hydroacoustic signal detections from the Ioto volcanic island in the northwest Pacific Ocean

*Hiroyuki Matsumoto[1,2], Mario Zampolli[1], Georgios Haralabus[1], Jerry Stanley[1], James Mattila[1], Nurcan Meral Ozel[1] (1.Comprehensive Nuclear-Test-Ban Treaty Organization (CTBTO), 2.Japan Agency for Marine-Earth Science and Technology (JAMSTEC))

[MAG40-P04] Installation of a floating hydrophone system within the SOFAR channel

*Hiroko Sugioka[1], Masayuki Obayashi[2] (1.Kobe University, 2.JAMSTEC)

[MAG40-P05] Fin whale signals observed at S-net seismic stations

*Takeshi Nakamura[1], Ryoichi Iwase[2] (1.National Research Institute for Earth Science and Disaster Resilience, 2.Japan Agency for Marine-Earth Science and Technology)

[MAG40-P06] Implementation of integrated observation from seafloor through atmosphere – past, current, and future plans

*Keisuke Ariyoshi[1], Akira Nagano[1], Hiroyuki Matsumoto[1], Nurcan Meral Ozel[2] (1.Japan Agency for Marine-Earth Science and Technology, 2.Comprehensive Nuclear-Test-Ban Treaty Organization)

[E] Poster | M (Multidisciplinary and Interdisciplinary)：M-AG Applied Geosciences

5:15 PM - 6:30 PM JST | 8:15 AM - 9:30 AM UTC | Poster Hall International Exhibition Hall8, Makuhari Messe_45

[M-AG40] CTBT IMS Technologies for Detecting Nuclear Explosion and Their Applications to Earth Science

convener:Nurcan Meral Ozel(Comprehensive Nuclear-Test-Ban Treaty Organization), Hiroyuki Matsumoto(Japan Agency for Marine-Earth Science and Technology), Yosuke Naoi(Japan Atomic Energy Agency)

[MAG40-P01] Overview of the Japanese National Data Centre-1 (NDC-1)

*RYOHEI EMURA[1], Takayuki Otsu[1], Toyomi Sakamoto[1], Soshi Iwata[1], Takanari Fujii[1], Mami Nogami[1], Makiko Iwakuni[1], Masashi Motohashi[1] (1.Japan Weather Association)

[MAG40-P02] Challenging to utilize the infrasound technologies for civil and science application

*Masashi Motohashi[1], Nobuo Arai[2], Takayuki Otsu[1], Mami Nogami[1], Makiko Iwakuni[1], Ryohei Emura[1] (1.Japan Weather Association, 2.Disaster Mitigation Research Center, Nagoya Unicersity)

[MAG40-P03] CTBT IMS hydroacoustic signal detections from the Ioto volcanic island in the northwest Pacific Ocean

*Hiroyuki Matsumoto[1,2], Mario Zampolli[1], Georgios Haralabus[1], Jerry Stanley[1], James Mattila[1], Nurcan Meral Ozel[1] (1.Comprehensive Nuclear-Test-Ban Treaty Organization (CTBTO), 2.Japan Agency for Marine-Earth Science and Technology (JAMSTEC))

[MAG40-P04] Installation of a floating hydrophone system within the SOFAR channel

*Hiroko Sugioka[1], Masayuki Obayashi[2] (1.Kobe University, 2.JAMSTEC)

[MAG40-P05] Fin whale signals observed at S-net seismic stations

*Takeshi Nakamura[1], Ryoichi Iwase[2] (1.National Research Institute for Earth Science and Disaster Resilience, 2.Japan Agency for Marine-Earth Science and Technology)

[MAG40-P06] Implementation of integrated observation from seafloor through atmosphere – past, current, and future plans

*Keisuke Ariyoshi[1], Akira Nagano[1], Hiroyuki Matsumoto[1], Nurcan Meral Ozel[2] (1.Japan Agency for Marine-Earth Science and Technology, 2.Comprehensive Nuclear-Test-Ban Treaty Organization)

[E] Poster | P (Space and Planetary Sciences)：P-PS Planetary Sciences

Sun. May 26, 2019 3:30 PM - 5:00 PM JST | Sun. May 26, 2019 6:30 AM - 8:00 AM UTC | Poster Hall International Exhibition Hall8, Makuhari Messe_3

[P-PS04] Mars and Mars system: results from a broad spectrum of Mars studies and aspects for future missions

convener:Hideaki Miyamoto(University of Tokyo), Tomohiro Usui(Earth-Life Science Institute, Tokyo Institute of Technology), Ayako Matsuoka(Research Division for Space Plasma, Institute of Space and Astronautical Science, Japan Aerospace Exploration Agency), Sushil K Atreya(University of Michigan Ann Arbor)

In view of unprecedented advances in our understanding of Mars, primarily due to new and ongoing observations of the planet with a number of spacecraft missions of the US, Europe and Asia, we propose a session on Mars. Mars is an object of intense scrutiny. Currently, eight spacecraft are operating at Mars, with six in orbit (Odyssey, MRO, MAVEN, Mars Express, Mangalyaan and TGO) and two on the surface (MSL-Curiosity and MER-Opportunity), the largest number ever at any given time. In addition, InSight is on track to land on Mars in November 2018, and several spacecraft are in various stages of implementation with launches scheduled for 2020 (Mars 2020, ExoMars 2020, Emirates Mars Mission Hope, Chinese Mars Mission and the Japanese Mars Terahertz Microsatellite), 2022 (ISRO's Mangalyaan 2), and 2024 (JAXA's MMX mission to explore Phobos, Deimos, and Mars). All this is a clear demonstration of public's strong fascination with and commitment to Mars exploration and the resulting scientific bonanza. Synergistic investigations with ongoing and already completed missions along with modeling studies and earth-based observations are gradually revealing the nature of Earth's most closely resembling planet that took on a different evolutionary track than our home planet. Morphology and variable phenomena seen on the surface (RSLs, e.g.) and in the atmosphere (methane) indicate that Mars is possibly currently active. Available data are providing a better understanding of Mars' present geologic and atmospheric state, climate evolution, and habitability. Thus, the scope of this session will be the recent results from a broad spectrum of Mars studies encompassing the interior, surface, atmosphere, plasma environment, and the Mars system including its two satellites. Abstracts on modelling, instrumentation and future mission plans are also encouraged.

[PPS04-P01] Observation of the O_2^+ first negative band (1,0) emissions in the Mars ionosphere with a visible spectrograph on Haleakala T60

*Toshihisa Suzuki[1], Masato Kagitani[1], Takeshi Sakanoi[1] (1.PPARC, Graduate School of Science, Tohoku University)

[PPS04-P02] Search of shallow subsurface reflectors around RSLs in Martian Chryse and Acidalia planitiae by the MRO/SHARAD public data

*Aina Oura[1], Yasumasa Kasaba[1], Atsushi Kumamoto[1], Rina Noguchi[2], Tomohiro Usui[2], Ken Ishiyama[2], Chihiro Uemura[3] (1.Tohoku University, 2.Institute of Space and Astronautical Science, 3.SOKENDAI)

[PPS04-P03] Detecting surface changes on Mars using principle component analysis of repeat imagery

*Reid Parsons[1], Hideaki Miyamoto[1] (1.University of Tokyo)

[PPS04-P04] Evaluation of the detectability of hydrated salts on recurring slope lineae on Mars.

*Shoko Imamura[1,2], Yasuhito Sekine[2], Hiroyuki Kurokawa[2] (1.University of Tokyo, 2.Earth-Life Science Institute, Tokyo Institute of Technology)

[PPS04-P05] Frequency of ice sheet growth recorded on Mons Pavonis, Mars

*Tomohiro Kanzaki[1], Reid Parsons[1,2], Ryodo Hemmi[1], Hideaki Miyamoto[1] (1.University of Tokyo, 2.Fitchburg State University)

[PPS04-P06] Development of Life Detection Microscope (LDM) for *in situ* imaging of living cells on Mars surface

*Yoshitaka Yoshimura[1], Akihiko Yamagishi[2], Takehiko Satoh[3], Atsuo Miyakawa[2], Eiichi Imai[4], Satoshi Sasaki[5], Kensei Kobayashi[6], Yoko Kebukawa[6], Tomoka Okada[6], Keigo Enya[3], Hikaru Yabuta[7], Takeshi Naganuma[7], Hajime Mita[8], Kazuhisa Fujita[3], Tomohiro Usui[3] (1.College of Agriculture, Tamagawa University, 2.Tokyo University of Pharmacy and Life Science, 3.Japan Aerospace Exploration Agency, 4.Nagaoka University of Technology, 5.Tokyo University of Technology, 6.Yokohama National University, 7.Hiroshima University, 8.Fukuoka Institute of Technology)

[PPS04-P07] Development of a Mars Web-GIS for viewing multiple kinds of spectral data from orbiters

*Yuya Matsubara[1], Hironori Fukuchi[1], Yoshiko Ogawa[1], Yohei Hayashi[2] (1.The University of Aizu, 2.National Astronomical Observatory of Japan)

[PPS04-P08] **Visualization and Analysis of the Surface of Mars with NASA's Mars Trek Portal**

*Brian Hamilton Day[1], Emily Law[2] (1.NASA Solar System Exploration Research Virtual Institute, NASA Ames Research Center, 2.NASA Jet Propulsion Laboratory, California Institute of Technology)

[PPS04-P09] Increase in Dissolved Iron Concentration from Fayalite by UltravioletA・C Irradiation

*Nobuo Komori[1] (1.The United Graduate School of Education Tokyo Gakugei University)

[PPS04-P10] Small-scale ridges newly identified on the equatorial region of the Phobos nearside

*Ryodo Hemmi[1], Hiroshi Kikuchi[1], Hideaki Miyamoto[1] (1.The University of Tokyo)

[PPS04-P11] Development of a compact Muography instrument for future Mars exploration missions

*Hiroaki Kamiyoshihara[1], Tetsuro Ninomiya[1], Yuri Yoshihara[1], Kenji Shimazoe[1], Hiroyuki Takahashi[1], Hiroyuki Tanaka[1], Hideaki Miyamoto[1] (1.University of Tokyo)

Observation of the O_2^+ first negative band (1,0) emissions in the Mars ionosphere with a visible spectrograph on Haleakala T60

*Toshihisa Suzuki[1], Masato Kagitani[1], Takeshi Sakanoi[1]

1. PPARC, Graduate School of Science, Tohoku University

We carried out ground-based telescope observations of Martian ionospheric O_2^+ emission to obtain global distribution of Martian O_2^+ ionosphere and its variation for understanding Martian atmospheric escape process. After verifying the analysis method, the result suggests that the O_2^+ first negative bands (1NG) (1, 0) emissions are successfully detected, and calculated O_2^+ emission intensity and column density.
Mars has tenuous atmosphere compared with the Earth. One possible model for Martian tenuous atmosphere is caused by atmospheric escape to space for a long time. In addition, present Mars has only weak crustal magnetic fields for limited area, and therefore, it is likely that solar wind strongly affects Martian atmosphere escape. In recent years, ion composition and densities in the Martian ionosphere are revealed by Mars probes (e.g. Mars Express, MAVEN). In the Martian ionosphere, main ion is O_2^+ [M. Benna et al., 2015]. Moreover O_2^+ recombines with an electron, and as a result of a neutral molecule dissociation, neutral atomic oxygens are generated. Since the neutral atomic oxygen energy is higher than escape velocity of Mars, it can be escaped from Martian gravity. This process is important in Martian atmosphere escape. However, it is difficult to detect atomic oxygen by Mars probe in-situ observation, and escape quantity is indirectly estimated by plasma temperature and density from in-situ observations. On the other hand, remote-sensing of Martian ionosphere is useful to obtain global distribution and its time and spatial variations. It is essential to combine in-situ plasma data with global remote sensing for understanding Martian atmospheric escape, such as solar wind impact and/or crustal magnetic field effect on the escape process.
We carried out Martian ionosphere O_2^+ emission observation using Tohoku University T60 telescope (located at the summit of Mt. Haleakala in Maui) with Vispec (Visual imager and Spectrograph with Coronagraphy) from September 10 to 19, 2018. This is the first attempt to detect Martian O_2^+ emission with a ground-based telescope. We focused O_2^+ 1NG (1, 0) bands emission with a peak wavelength of about 561 nm. Visible Echelle spectrograph Vispec (wavelength resolution was 10,000) covered wavelength range from 550 nm to 570 nm. Vispec slit (width 2” ×length 90”) was located near Martian dayside limb parallel to the Martian rotation axis, and exposure time of one frame was 2 minutes. Total exposure time in observation period was 450 minutes. To refer sunlight spectrum reflecting by Martian surface, we acquired spectrum of disk center by Martian surface. First analysis process (subtraction dark, revision by flat-field, wavelength and space) was conducted on each frame, and each frame was added to gain S/N. Finally, sunlight spectrum was subtracted using disk center to obtain O_2^+ 1NG (1, 0) bands emission spectrum. Next, we compared observed O_2^+ spectrum with O_2^+ 1NG (1, 0) model spectrum given by Henriksen and Veseth [1987]. Focusing on only short period wavelength variations, we performed high-pass filter analysis on the both of observed and model spectrum. After that, we calculated the correlation coefficient between observed spectrum and model spectrum, and found that the coefficient maximum is 0.40 with no wavelength lag between two spectra. Data points, i.e., wavelength range, using correlation coefficient analysis were selected so that model O_2^+ emission is relatively intense and the contamination of solar fraunhofer absorption line is negligible. We estimated O_2^+ 1NG (1, 0) emission intensity with a least-square method to be 691 +/- 171 $\times 10^3$ Rayleighs, and the column density to be 4.4 +/- 1.1 $\times 10^{13}$ /cm^2. The estimated column density was greater than that of simulation. In this presentation, we compare O_2^+ emission observation spectrum with model spectrum, and give the estimation of O_2^+ emission intensity and column density in detail. We also give discussion about the

©2019. Japan Geoscience Union. All Right Reserved.

results.

Keywords: Mars, ionosphere, ground-based telescope

©2019. Japan Geoscience Union. All Right Reserved.

Search of shallow subsurface reflectors around RSLs in Martian Chryse and Acidalia planitiae by the MRO/SHARAD public data

*Aina Oura[1], Yasumasa Kasaba[1], Atsushi Kumamoto[1], Rina Noguchi[2], Tomohiro Usui[2], Ken Ishiyama[2], Chihiro Uemura[3]

1. Tohoku University, 2. Institute of Space and Astronautical Science, 3. SOKENDAI

One of recent discoveries on Mars is the recurring slope lineae (RSL), which are certain features on the surface invoking current icy processes. RSLs are distributed on Mars and these narrow features incrementally lengthen down steep slopes, fade in colder seasons, and recur annually. Candidate and confirmed RSL sites are distributed in four regions, (1) southern mid-latitudes (SML), (2) Valles Marineris (VM), (3) equatorial highlands, and (4) northern Chryse Planitia and southwestern Acidalia Planitia (CAP). The RSLs in (2) VM and (4) CAP are more densely located than other two areas.
This study tries to identify the subsurface structures of the northern mid-latitude RSL in (4) Chryse and Acidalia Planitiae by the public data of Mars shallow radar sounder (SHARAD) onboad the Mars Reconnaissance Orbiter opened on the PDS Geosciences Node. That is because CAP RSLs are densely distributed compared to other regions. CAP RSLs are found on the steep slopes of craters. Their source zones are at or below the elevation of the surrounding plains. We used the Java Mission-planning and Analysis for Remote Sensing (JMARS, https://jmars.asu.edu/) in order to investigate the geological information of the RSL sites and the MRO locations at the SHARAD observed data. We then picked up the location correspond to the RSL sites and generated radargrams from SHARAD data. The observation frequency of SHARAD is 15-25 MHz with the bandwidth of 10 MHz, and the subsurface close to the surface can potentially be resolved with the depth resolution of 15 m in vacuum. Using MOLA data, we generated the virtual radargrams with the surface clutter emulated by the Kirchhoff approximation. Then, we compared both observed radargrams with emulated ones to identify whether there are subsurface reflectors or not.
We surveyed about 12 orbits close to the confirmed RSLs. We could find the hypothetical detection of the subsurface reflector in ‘orbit.00688101’ (Jan 14 2008, N10.0-44.7˚, E313.6-318.3˚) and ‘orbit.00673602’ (Jan 03 2008, N10.1-44.7˚, E312.7-317.4˚). In this abstract, we concentrated the characteristics of the former candidate. In this sample, the closest RSL located at N34.1˚, E317.0˚ and nadir line from the orbit was 13.8 km. Another RSL close to this orbit located N34.8˚, E318.6˚ and nadir line from the orbit was 85.2 km. Apparent elevation of closest RSL was about -3,763 ±10 m. The deepest elevation of the crater was about -4,744 ±10 m and the highest elevation of it was about -3,640 ±10 m. The radargram of this orbit showed that the elevation of surface echo was in the range from -3720 to -3780 m and that of subsurface echo ranged from -3750 to -3800 m. This means that the closest RSL height was almost the same as the depth of subsurface reflector. The subsurface echo located 25 m below the surface, and it had a little bit weak echo strength compared to surface one. If this subsurface echo shows the underground reflection, the subsurface layer will be 180 km wide along the orbit. Although this depth is marginal for the depth resolution of SHARAD, we could not identify such an echo in the emulated radargram.
In the presentation, we will summarize the results of this region including other orbits.

Keywords: Mars, RSL, SHARAD

©2019. Japan Geoscience Union. All Right Reserved.

Detecting surface changes on Mars using principle component analysis of repeat imagery

*Reid Parsons[1], Hideaki Miyamoto[1]

1. University of Tokyo

Change detection is an analytical tool of Remote Sensing in which repeat observations of a particular location can be overlain, subtracted, or ratioed to detect differences between images. High-resolution, repeat imagery on Mars has led to several discoveries of ongoing geologic processes operating at the sub-kilometer scale such as recurring slope lineae (RSL) [1-3], new, small impacts [4], aeolian dune migration [5], sublimation of polar ice [6], and gully formation [7]. Generally, the detection of these changes is done manually by overlaying, and “flipping” between the two images. As planetary remote sensing data sets continue to grow, so does the need for a more efficient means of change detection.

Principle component analysis (PCA) offers an advantageous means for detecting change because it considers the values of all pixels in all the repeat images to extract the most statistically significant variations. These variations are then isolated from one another as a hierarchical set of “principle components” of the image dataset. The user can quickly identify patterns or features of interest which are present in one or more of these components. To illustrate this method, nine HiRISE images [8] collected from Palikir crater on Mars between November 2007 and June 2011 documenting RSL formation will be used.

PCA changes the values of the pixels in each image by plotting the pixel data on a set of axes which capture the maximum variance in the dataset. In our example image set, each pixel in the image stack can be treated as a 9-dimensional vector since there is a value for that pixel in each of the nine images. However, each pixel can be plotted on a new set of axes that capture the most important, or PCs of the image stack.

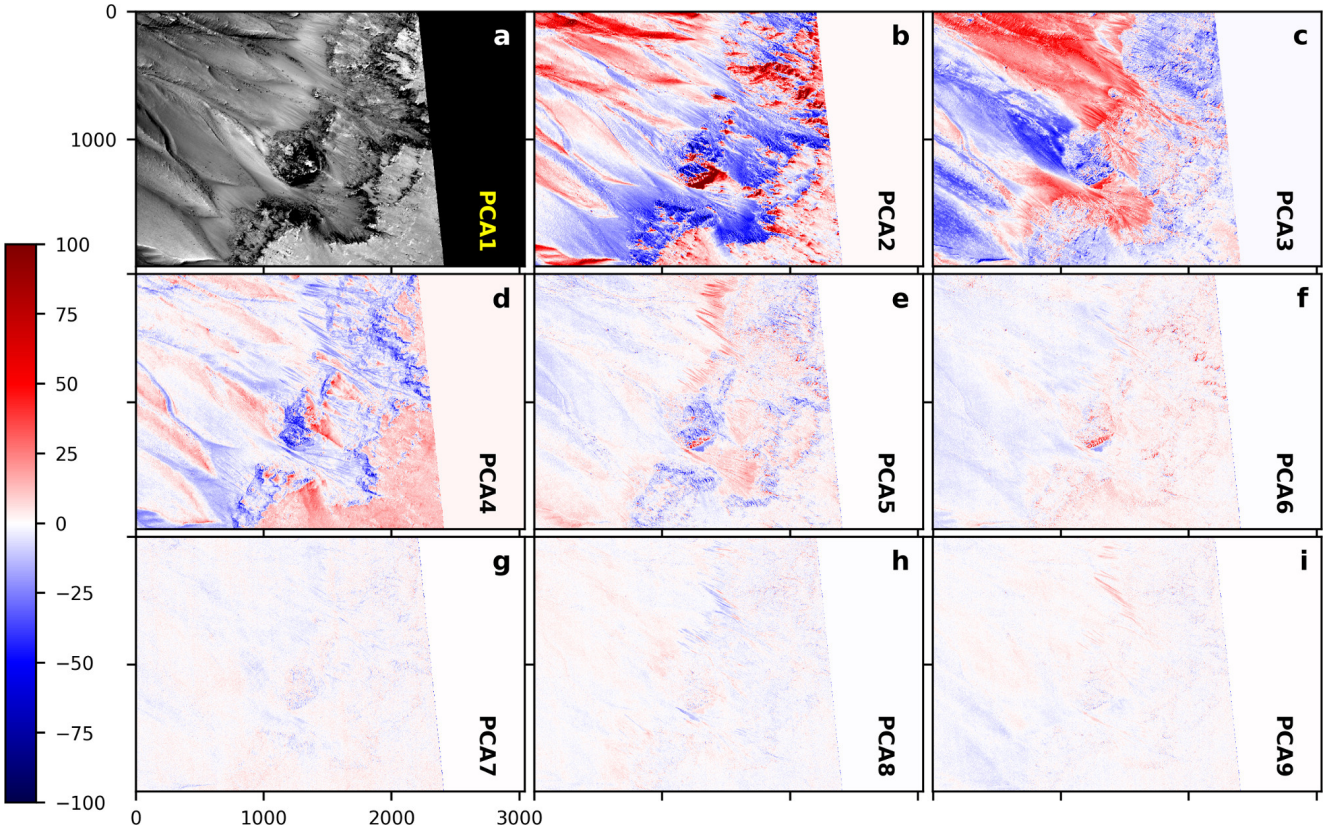
The figure shows the result of the PC transform (performed using ENVI® software) on the stacked time-series. Because most of the variation in the images is captured in the first PC (PCA1), it uses a grayscale color bar spanning 0-255 pixel values. Generally, variations covering a large spatial extent or variations causing a big shift in pixel values will be captured in the lower PCA components. Higher components, on the other hand, will depict smaller amplitude variations occurring in fewer images (or over smaller spatial extents). Thus, components 2 and 3 (panels b and c, respectively) are dominated by variations caused by differences in lighting (sun direction and elevation angle) and possibly dust or frost deposition/erosion. RSL features are identifiable in PCA4 (panel d) as elongated blue “fingers” and become more dominant and appear red in PCA5 (panel e). Subsequent components capture smaller variations caused either by changes in lighting, RSL shape (in PCA 8 and 9), or camera noise.

After identifying the PCs which contain the feature of interest, the feature can be traced back to the original images via an inverting from PC coordinates to image coordinates. Although this step is not completely reliable, it is successful in determining which images contain the most prominent RSL. Eventual combination of this method with machine-learning algorithms may permit a more automated means of detecting interesting surface changes on Mars and other planetary bodies. Note this work was previously published in [9].

©2019. Japan Geoscience Union. All Right Reserved.

References:
[1] McEwen A. S., et al. (2011) Science 333 740–743
[2] Sullivan R., et al. (2001) JGR 106 23607–23633
[3] Ojha L., et al. (2014) Icarus 231 365 –376
[4] Daubar I., et al. (2013) Icarus 225 506 –516
[5] Bourke M., et al. (2008) Geomorph. 94 247–255
[6] Thomas P., et al. (2005) Icarus 174 535 –559
[7] Diniega S., et al. (2009) AGU Fall Meeting Abstracts
[8] HiRISE Operations Center Gullies in palikir crater
https://www.uahirise.org/dtm/dtm.php?ID=PSP_005943_1380 accessed: 2017-07-03
[9] Parsons, R.A. & Miyamoto, H. (2018) J. of Physics: Conf. Series 1036 (012004).

Keywords: Mars, Change, Detection



©2019. Japan Geoscience Union. All Right Reserved.

Evaluation of the detectability of hydrated salts on recurring slope lineae on Mars.

*Shoko Imamura[1,2], Yasuhito Sekine[2], Hiroyuki Kurokawa[2]

1. University of Tokyo, 2. Earth-Life Science Institute, Tokyo Institute of Technology

On present-day Mars, pure liquid water is thermodynamically unstable; whereas, high-salinity brine can exist on the surface, at least temporally, due to freezing point depression [1]. Deliquescence and melting of subsurface ice are proposed as being the major processes of formation of liquid brine on Mars [2, 3]. Although liquid brine is suggested to form upon Mars' daily and seasonal changes [2, 3], generation of brine flow has not been confirmed on current Mars. Our previous study suggests that cycles of formation and evaporation of liquid brine can generate characteristic morphological features of downward-elongated flows on steep slopes [4]. This happens because precipitated salts within soil dramatically decrease the porosity and permeability, leading generation of surface flows [4]. Our study also suggests that precipitation of salts reaches up to ~30% in volume within the soil, implying that any detection of such salt may be evidence for the occurrence of brine flow on current Mars [4]. Proposed morphological features formed by current brine activity include recurring slope lineae (RSL) [5, 6]. Although hydrated salts are suggested to exist on RSL at a few locations [6], identification of salt compositions is still challenging. Additionally, there are no reports on detection of hydrated salts at most of the RSL sites across Mars.

In the present study, we investigate the conditions of identification of hydrated salt compositions on RSL using Compact Reconnaissance Imaging Spectrometer for Mars (CRISM) onboarded on Mars Reconnaissance Orbiter (MRO). We calculate synthesized spectra of mixtures of basaltic soil and various hydrated salts (such as $MgCl_2 \cdot 2H_2O$) with the different mixing ratios using a linear combination method and an addition of random noise with a Gaussian distribution. We evaluate the threshold mixing ratios of salt for the identification of the salt compositions based on the analyses of the synthesized spectra. Our results show that if the mixing ratio of hydrated salt exceeds 20% in volume, O-H bands attributed from hydrated salts can be detected with CRISM. We discuss the observational conditions, such as the observational altitude from the surface, for the identification of salt compositions on RSL in future missions.

[1] McEwen et al. (2011) Science, 333, 740. [2] Martin-Torres et al. (2015) Nature Geoscience 8, 357. [3] Chevrier & Rivera-Valentin (2012) Geophysical Research Letters, 39, 21. [4] Imamura et al. (2018) Planetary People, 27, 163. [5] Hecht et al. (2009) Science, 325, 5936. [6] Ojha et al., (2015) 8, 829.

Keywords: Mars, CRISM, salt

©2019. Japan Geoscience Union. All Right Reserved.

Frequency of ice sheet growth recorded on Mons Pavonis, Mars

*Tomohiro Kanzaki[1], Reid Parsons[1,2], Ryodo Hemmi[1], Hideaki Miyamoto[1]

1. University of Tokyo, 2. Fitchburg State University

On present-day Mars, large scale ice bodies are only found at each pole. However, in mid latitudinal areas, LDA (lobate debris apron), LVF (lineated valley fill), CCF (concentric crater fill) are reported and interpreted to have a glacial origin (Levy et al., 2014). Also, inequatorial areas, fan-shaped deposits at northwestern rim of three shield volcanos in Tharsis region though to have a glacial origin (e.g. Fastook et al., 2008).
Fan-shaped deposits sit beside three Tharsis montes and have characteristic geomorphologies extending for roughly 100-500 km from the foot of mountain, typically consisting of three facies: Smooth facies at the top, Knobby facies at the middle, and Ridged facies at the rim. Smooth facies are smooth-surfaced mounds which superpose on other facies, Knobby facies are collective hillocks a few hundred meters in radius, and Ridged facies are linear ridges (moraine-like features) parallel to the rim of the fan. At Arsia (Kadish et al., 2014) and Pavonis (Shean et al., 2005) Mons, ridged facies are especialy well-developed - containing tens to few hundreds of ridges interpreted to be moraines that indicates the varying extent of a former ice sheet. Such geomorphologies potentially record the advance and retreat of ice sheet for tens of kilometers during the Amazonian adjacent to Arsia and Pavonis Mons.
The association of these geomorphologic features to glacial processes is supported by global climate simulations of Mars during high-obliquity (Forget, 2006). The obliquity of the rotation axis of Mars is considered not stable as on the Earth, reaching 45˚ in the past 20 Myrs (Laskar et al., 2004). Such high obliquity can cause sublimation of the polar cap, enhancing the water vapor content in the atmosphere compared to present-day Mars. By diffusion and condensation model, Mellon & Jakosky (1995) found that in the surface environment of present-day Martian obliquity (25.2˚) water ice is stable only at 40˚ latitude or higher, however, when obliquity gets higher than 32.3˚, with enough amount of atmospheric water vapor, water ice becomes stable globally. This result suggests Martian surface environment has experienced such climate condition that water ice condenses and deposits in mid and low latitudinal areas. Therefore, the existence of Martian “ice age” during Amazonian high-obliquity periods is being proposed (Head et al., 2003).
If ice sheet growth and disappearance on the flanks of Tharsis Montes are an indication of the climate change caused by orbital parameters, each of moraine-like features should correspond to a paleoclimate cycle. However, fluctuation of its spacing, scale and correlation to orbital parameter have not yet been discussed. Hence, as basic study to associate distribution of moraine-like features to extent of the ice sheet, we made DEM data from CTX imagery at the rim of fan-shaped deposits at the foot of Mons Pavonis, and using the DEM data, we measured spacing and cross-sectional area of each moraine, and conducted frequency analysis on the cross section of DEM data.
As a result, spacing of moraine-like feature appeared to fluctuate from few hundred meters to 4.5 km, showing drastic change of the density. Also, cross sectional area of moraine-like feature fluctuates up to 1.4×10^4 m^2. These fluctuations potentially record the change of frequency of events that caused accumulation and ablation of ice sheet or change of velocity of ice sheet flow. In Tharsis region, these two periodic events are assumed to affect ice sheet: global climate change caused by orbital parameter, and local volcanic activity. To prove the spacing and moraine-size are driven by global climate forcings, there should be similarities between the ridges found at Pavonis, Arsia, and a correlation to orbital parameters. Therefore, frequency analysis of cross- sectional view of the terrain is being conducted. The result will be shown in the presentation.

©2019. Japan Geoscience Union. All Right Reserved.

Keywords: Mars, Martian climate, Tharsis region, Milankovich cycle

©2019. Japan Geoscience Union. All Right Reserved.

Development of Life Detection Microscope (LDM) for *in situ* imaging of living cells on Mars surface

*Yoshitaka Yoshimura[1], Akihiko Yamagishi[2], Takehiko Satoh[3], Atsuo Miyakawa[2], Eiichi Imai[4], Satoshi Sasaki[5], Kensei Kobayashi[6], Yoko Kebukawa[6], Tomoka Okada[6], Keigo Enya[3], Hikaru Yabuta[7], Takeshi Naganuma[7], Hajime Mita[8], Kazuhisa Fujita[3], Tomohiro Usui[3]

1. College of Agriculture, Tamagawa University, 2. Tokyo University of Pharmacy and Life Science, 3. Japan Aerospace Exploration Agency, 4. Nagaoka University of Technology, 5. Tokyo University of Technology, 6. Yokohama National University, 7. Hiroshima University, 8. Fukuoka Institute of Technology

Past trial of direct detection of life on Mars by 1970's Viking mission ended up with a negative conclusion [1]. Whereas, numbers of new finding provided by Mars exploration missions in the last decade indicate that there are good reasons to perform another life detection program. The sensitivity of the gas chromatograph mass spectrometer onboard the Viking mission was not very high, and was not able to detect the microbes 10^6 cells in 1 gram clay [2,3]. Resent observations on Mars have found the evidences of past water activities. MSL Curiosity has found the temporal increase of methane concentration in Martian atmosphere [4]. The presence of reduced sulfur compound such as pyrite in Martian soil was also detected by MSL [5]. Methane and reduced sulfur compound can be the energy source to support the growth of chemoautotrophic microbes [6]. Possible presence of liquid water at Recurring Slope Lineae has been supported by the detection of hydrated salts [7]. The presence of organic compounds of Martian origin has been reported [8]. These evidences tend to support the possible presence of living microbes near the surface of Mars.

Physical and chemical limits for terrestrial life have been major foci in astrobiology [9], and are summarized in ref. [6]. Combining the environmental factors, anywhere in the Martian environment where we can find the three components, water molecules, reducing compounds and oxidative compounds could be an environment where life can be sustained for long periods of time, if other factors such as temperature, pressure, UV and other radiations permit [6]. Among these factors, most of the factors including ionic radiation, can be endured by terrestrial extremophiles. Only UV can kill the most UV-resistant microbes within minutes. However, UV can be shielded by a few centimeters soil layer. These evaluations lead to the conclusion that the Martian soil under a few cm can be the place to support the growth of microbes, if the water activity is higher than 0.6.

For exploring extant life on Mars, we have proposed to search cells from a depth of about 5 - 10 cm below the surface by the Life Detection Microscope (LDM) [6, 10]. LDM has the potential to detect single cells in the resolution of 1 micrometer and could detect less than 10^4 cells in 1 gram clay, which is much higher sensitivity than the instrument onboard Viking. We have developed the solution and combination of fluorescence pigments to detect organic compounds, and to differentiate organic compounds surrounded by membrane, which we think to be the most fundamental features that a cell should possess to constitute life. Our investigation goals are the followings. 1) Identify cell-like structure in which organic compounds are enveloped by membrane, which may represent Martian life. 2) Search for any type of organic compounds in Mars surface samples. The compounds include cells, other biological materials, and abiotic polycyclic aromatic hydrocarbon (PAH). 3) High-resolution characterization of regolith and dust particles. The current status of development of LDM will be presented.

©2019. Japan Geoscience Union. All Right Reserved.

References

[1] Margulis, L. et al. *J. Mol. Evol.* 14, 223-232 (1979)

[2] Glavin, et al, *Earth Planet. Sci. Let.*, 185, 1-5 (2001)

[3] Navarro-González, et al., *Proc. Natl. Acad. Sci. USA*. 103 (2006)

[4] Webster, C. R., et al., *Science*, 360 (2018).

[5] Ming, D., et al., *Science*, 343 (2014)

[6] Yamagishi, A. et al. *Biol. Sci. Space*, 24 (2010)

[7] Ojha, L. et al. *Nature Geosci.*, 8 (2015)

[8] Freissient, C. et al. *J. Geophys. Res. Planets* (2015)

[9] Marion, G.M. et al. *Astrobiol*. 3 (2003)

[10] Yamagishi, A., et al., *Trans. JSASS, Aerospace Tech. Japan*, 16 (2018)

Keywords: fluorescent microscope, extraterrestrial life

©2019. Japan Geoscience Union. All Right Reserved.

Development of a Mars Web-GIS for viewing multiple kinds of spectral data from orbiters

*Yuya Matsubara[1], Hironori Fukuchi[1], Yoshiko Ogawa[1], Yohei Hayashi[2]

1. The University of Aizu, 2. National Astronomical Observatory of Japan

The VIS-NIR reflectance spectra observed during latest Mars orbiter missions are of high quality and cover the whole globe. Such data sets are very informative for understanding the materials and their distribution on the surface. Each mineral has unique absorption bands in the spectra. We can identify which minerals are present by comparing the absorption bands of the observed spectra with the known absorption bands in the spectra measured in laboratories. In the case of Mars, we can estimate the type and distribution of hydrous minerals which leads to important clues to understand the water environment.

However, the VIS-NIR spectral data observed on Mars are not well utilized among the community. There are huge volume of accumulated data due to an increasing number of missions and various kinds of instruments with higher accuracy. It is not easy to process huge data and understand the relevance of them visually and intuitively.

We develop a new Mars web-GIS application, "Red Ace", to view and download the Mars observation data, especially the VIS-NIR spectra (image cube data format), easily and intuitively. The Red Ace handles multiple kinds of observation data: the Compact Reconnaissance Imaging Spectrometers for Mars (CRISM) data, the Thermal Emission Imaging System (THEMIS) data and DEM (Digital Elevation Model) data at the same time. Additionally, we use the DEM data from the Mars Orbiter Laser Altimeter (MOLA) to display 3D map of Mars with the Red Ace.

The Red Ace is developed based on CesiumJS that is an open source JavaScript library for 2D/3D maps. The user can choose the dimension of the map. In the Red Ace, the spectral observation points are displayed on the surface image layers. When the user clicks any point on the footprint of the layer, the color of the selected footprint changes and the thumbnail image appears. When the user selects any pixel on the thumbnail image, the Red Ace provides reflectance spectral data and ancillary data as graphs and tables. In response to user operation, multiple kinds of spectral data are displayed on the same window. The Red Ace also provides band- ratio images of THEMIS. The user can download band-ratio images, spectral data and ancillary data as files of PNG, CSV, JSON, XLSX and PVL formats. The user can move the windows displaying thumbnail image and graph freely. In addition, the Red Ace provides the function to control the Mars base map changing the exaggeration of height of the Mars globe. The user can change the order of layers and transparency of layers arbitrarily. The user can also jump to the region of interest directly by setting the coordinates and the zoom level. The user can handle these functions smoothly.

In the case of THEMIS, published data from the mission data archive are not reflectance data but radiance data. Therefore, the Red Ace derives reflectance data from radiance data and ancillary data, in order to compare them with CRISM spectra observed in the same spot.
In this study, considering the portability and extension of the application, the Docker was used for the development environment. Docker is an open source software platform that allow the user to develop applications quickly using containers. JSON format is adopted for data handling to make it easier to add new observation data from new observation equipments in the future. In the JSON format, it is unnecessary to associate item order and item meaning. Hence, it has high reusability and freedom. In the

©2019. Japan Geoscience Union. All Right Reserved.

Red Ace, by standardizing the structure of JSON format data in advance, it is possible to store and handle diverse data by using the same data structure.

Keywords: Mars, Spectral data, Web-GIS

©2019. Japan Geoscience Union. All Right Reserved.

Visualization and Analysis of the Surface of Mars with NASA's Mars Trek Portal

*Brian Hamilton Day[1], Emily Law[2]

1. NASA Solar System Exploration Research Virtual Institute, NASA Ames Research Center, 2. NASA Jet Propulsion Laboratory, California Institute of Technology

Originally released in June, 2015 as a public outreach tool, Mars Trek is currently being enhanced to support site selection and analysis for upcoming human and robotic missions to Mars. Many new data products are being added, with emphasis on providing detailed information for proposed exploration zones. Data products can be loaded and even combined from many different instruments aboard many different Mars-orbiting spacecraft including Viking, Mars Global Surveyor, Mars Odyssey, Mars Reconnaissance Orbiter, and Mars Express. Users can download data products from Mars Trek and access metadata for each product. Web services and APIs allow other clients to access data from Mars Trek's servers. A standardized interface across the Trek portals provides for advanced 3D visualization and navigation. Standard keyboard gaming controls allow the user to maneuver a first-person visualization of "flying" across the surface of the Mars. User-specified bounding boxes can be used to generate STL and/or OBJ files to create physical models of surface features with 3D printers. A new VR capability allows users to generate their own virtual reality flyovers for any user-defined paths along the Mars' surface.

Mars Trek's power as a tool for education and outreach is exemplified by its being designated as key supporting infrastructure for NASA Science Mission Directorate's STEM Activation Initiative, and its serving of data to a growing community of digital planetariums.

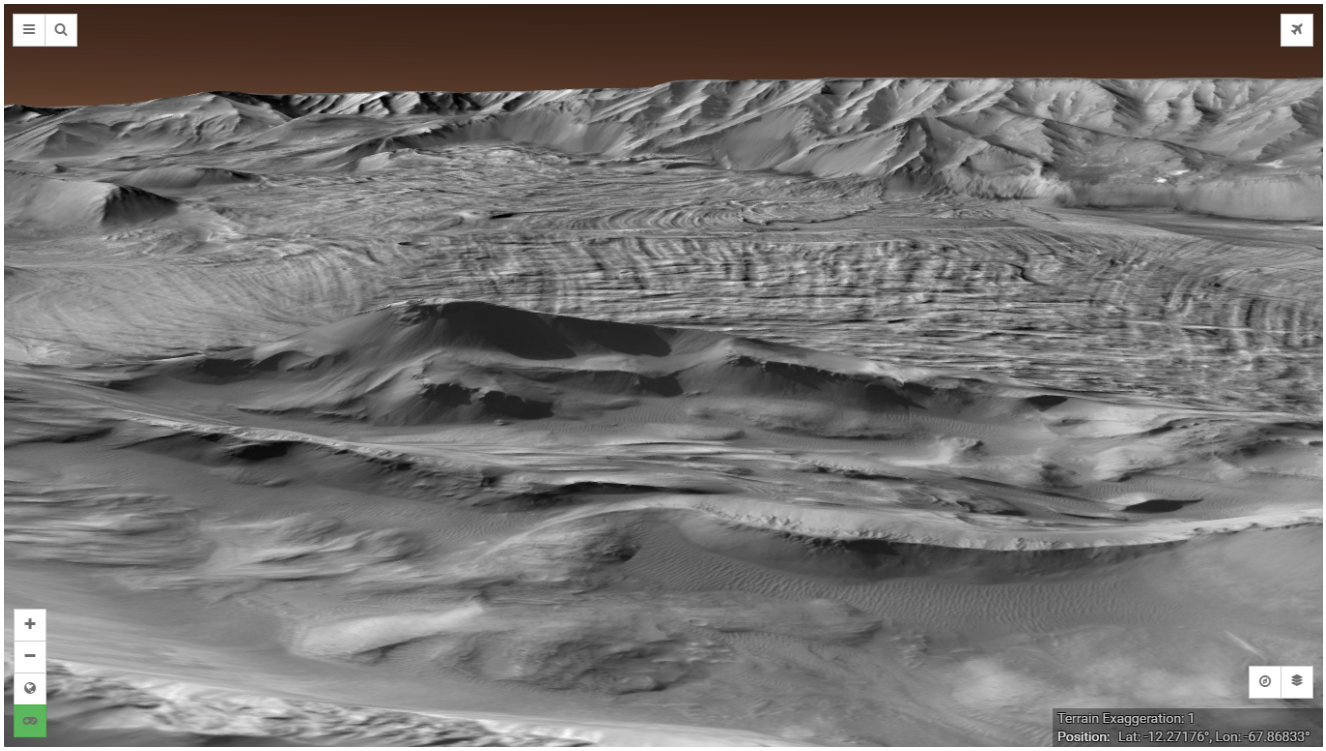
As private industry and space agencies of a growing number of nations plan new missions to Mars, detailed maps and models of Mars' surface and climate will be essential for mission planning. Mars Trek's generalized suite of tools are being designed to meet the needs of this new generation of missions. The portal will also provide an outstanding means of dissemination of data from these missions. Layering and blending many different data products and putting individual products in the context of many others will facilitate mining of information going far beyond what individual products can provide separately. In addition to mission planning and planetary science, Mars Trek will continue supporting the essential task of engaging the public in this great adventure. Mars Trek is developed at NASA's Jet Propulsion Laboratory (JPL) and managed as a project of NASA's Solar System Exploration Research Virtual Institute (SSERVI) at NASA Ames Research Center.

At the request of the Planetary Science Division of NASA's Science Mission Directorate, we are extending the technologies of our existing Trek platforms to create a new portal for Mars' largest moon, Phobos. In this effort, we are working with the International Phobos/Deimos Landing Site Working Group and with JAXA, with JAXA's MMX mission as a primary driver.
Mars Trek is one of the portals in the NASA Solar System Treks Project (SSTP), available at https://trek.nasa.gov. NASA's Solar System Trek online portals provide web-based suites of interactive data visualization and analysis tools to enable mission planners, planetary scientists, students, and the general public to access mapped data products from past and current missions for a growing number of planetary bodies including the Moon, Mars, Vesta, etc. These portals are being used for site selection and analysis by NASA and a number of its international partners, supporting upcoming missions. In addition to demonstrating the capabilities of Mars Trek in this presentation and providing a preview of Phobos Trek,

©2019. Japan Geoscience Union. All Right Reserved.

we will solicit input from the community for ideas for future enhancements to the portals.

Keywords: Mars



©2019. Japan Geoscience Union. All Right Reserved.

Increase in Dissolved Iron Concentration from Fayalite by UltravioletA・C Irradiation

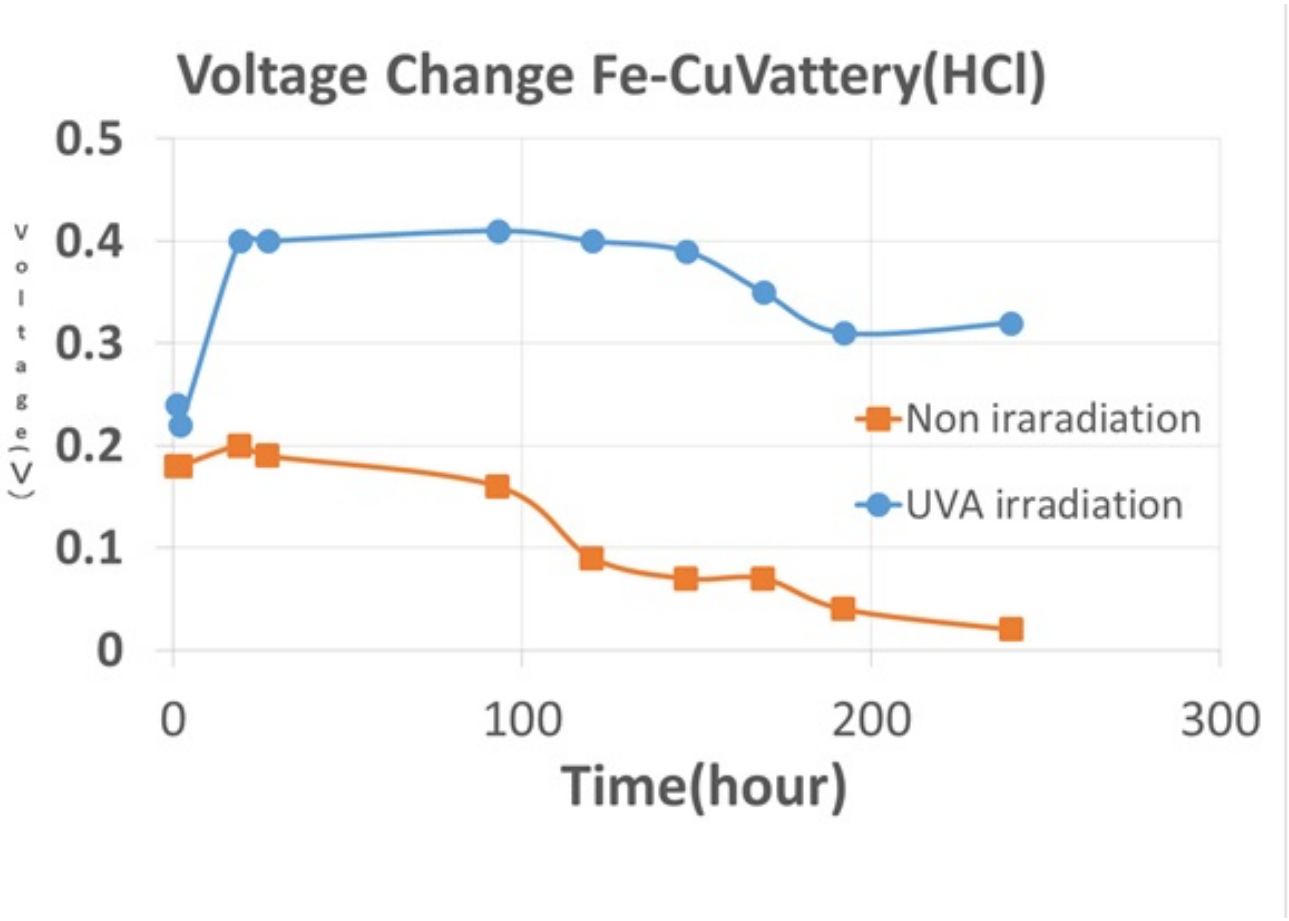
*Nobuo Komori[1]

1. The United Graduate School of Education Tokyo Gakugei University

To investigate the mystery of “Why the Mars' surface with poor oxgen has so much iron oxide" I have led student experiments at junior high schools. I will show my recent experiments and their results.
A.S.Yen (1999) showed that reactive oxygen species can also be formed on mineral grains under Martian conditions by irradiating ultraviolet C to quartz samples. Furthermore he irradiated ultraviolet C to thin iron films in the air and showed that exposure to ultraviolet radiation increases the rate of oxide formation. My experiments was irradiating ultraviolet A and C to fayalites and iron in acid water. This results indicated the possibility that iron oxides might be formed because of ultraviolet rays other than the cause of reactive oxygen species in the past.
Experiment no.1:
I had students irradiate ultraviolet rays A and C to Fayalite in hydrochloric acid.I had students irradiate ultraviolet rays A and C to Fayalite in hydrochloric acid. In this experiment, I used Fayalite from Kawamata-machi, Fukushima.
Fayalite, which is about 1g and not formatted was put in the test tube in the test tube filled with hydrochloric acid pH2.After the experiment, I had students check the concentration of iron ions in the water solution by using a digital pack test. This experiment with ultraviolet rays A was carried out 7 times and the experiment with ulttaviolet rays was carried out 3times.According to the results of the experiment with ultraviolet rays A, the quantity of iron elution increased more in the case of ultraviolet rays irradiating 6 times out of 7 than with the result of no irradiation.The results of the experiment with ultraviolet rays C were idential (3 times out of 3). The peak of wavelength ultraviolet rays A is generated by black lite is 365 nm. The peak of wavelength ultraviolet rays C is generated by germicidal lamp is 245 nm.
Experiments no.2:
I had the students irradiate ultraviolet rays A to a battery that has the iron cathode copper anode in hydrochloric acid. The Students then measured the occured voltage of the battery. I compared the voltage between ultla violet rays irradiation and non irradiation.The irradiated battery’s voltage stayed over 0.2V and the voltage did not decrease after 150hours.Another non-irradiated battery’s voltage decreased lower little by little and the voltage was close to 0V after 150 hours.This experiment was carried out 4times. In all cases the voltage of the battery that was irradiated by ultraviolet rays was higher than the non-irradiated battery.
It seems that electrons dissociate from iron atoms by ultlaviolet energy and form iron ions.
Consideration
From my experiments results, I would infer that ultraviolet rays advance the dissolution of iron ion from fayalite and iron. I think ultraviolet rays are one of the causes of iron oxide and hidroxide existing on Mars’ surface besides reactive oxygen species.It seems that there was water on Mars’ surface. There was a possibility that advancing of iron dissolution from rocks on Mars by ultraviolet rays irradiation.

Keywords: ultraviolet rays, fayalite , hydrochloric acid, iron, elution increase

©2019. Japan Geoscience Union. All Right Reserved.



©2019. Japan Geoscience Union. All Right Reserved.

Small-scale ridges newly identified on the equatorial region of the Phobos nearside

*Ryodo Hemmi[1], Hiroshi Kikuchi[1], Hideaki Miyamoto[1]

1. The University of Tokyo

Although the craters and grooves on Phobos are indicative of widespread and abundant surface modification during Phobos' geologic history [Basilevsky et al., 2014], little definitive evidence exists for geologically recent regolith migration other than down-slope mass-wasting [Shi et al., 2016]. Here we report newly found small-scale sinuous ridges identified in Mars Reconnaissance Orbiter's High Resolution Imaging Science Experiment (HiRISE [McEwen et al., 2007]) images of the nearside of Phobos. These ridges are spatially focused within the equatorial region (-5° to 20° N). Some of them superpose on craters and grooves, which is consistent with a geologically recent activity. They are ~200 m to ~1 km in length, several 10's m in width, and most of them are roughly parallel to each other and are generally oriented in NE-SW direction. To extract detailed topographic profiles, we constructed a high-resolution (~5-6 m/pixel; almost same as the original image) digital elevation model (DEM) by using shape-from-shading [Alexandrov and Beyer, 2018] in the selected regions of a HiRISE image and a stereo-derived HiRISE DEM (20 m/pixel) [Hemmi and Miyamoto, 2019]. Our preliminary analysis shows these ridges are less than several meters high. Their morphology and topography are unlikely to be formed by impact cratering, extensional stress fields, or mass wasting processes. In this presentation, we provide initial results of geological mapping of the small-scale ridges and discuss their possible origins.

References

Alexandrov, O., and R. A. Beyer (2018), Multiview Shape-From-Shading for Planetary Images, *Earth and Space Science*, 5(10).

Basilevsky, A. T., C. A. Lorenz, T. V. Shingareva, J. W. Head, K. R. Ramsley, and A. E. Zubarev (2014), The surface geology and geomorphology of Phobos, *Planetary and Space Science*, 102, 95-118.

Hemmi, R., and H. Miyamoto (2019), HiRISE digital elevation model of Phobos: Implications for morphological analysis of grooves, *Proceedings of the 50th Lunar and Planetary Science Conference*, Abstract No. 1759.

McEwen, A. S., et al. (2007), Mars Reconnaissance Orbiter's High Resolution Imaging Science Experiment (HiRISE), Journal of Geophysical Research: Planets, 112(E5), E05S02.

Shi, X., J. Oberst, and K. Willner (2016), Mass wasting on Phobos triggered by an evolving tidal environment, *Geophysical Research Letters*, 43(24), 12,371-312,379.

Keywords: Phobos, HiRISE, Digital Elevation Model

©2019. Japan Geoscience Union. All Right Reserved.

Development of a compact Muography instrument for future Mars exploration missions

*Hiroaki Kamiyoshihara[1], Tetsuro Ninomiya[1], Yuri Yoshihara[1], Kenji Shimazoe[1], Hiroyuki Takahashi[1], Hiroyuki Tanaka[1], Hideaki Miyamoto[1]

1. University of Tokyo

Muography is a technique that uses cosmic ray muons for visualizing the interior of large-scale structures in much the same way as standard X-ray radiography is used to image the interior of smaller objects. Muography has been successfully applied to explore the internal structure of geological targets on earth. Because exploring the inner structure of the shallow subsurface of celestial bodies is important to understand their origin and evolution, we are planning to operate muography instrument in the extraterrestrial environment, especially on the surface of Mars. Applying muography to planetary explorations has some advantages over conventional internal exploration methods: (1) it is able to observe the absolute linear density of objects; (2) the passive nature of the measurements provides low power consumption; (3) the instrument size is arbitral [1]. However, in order to mount muography instrument on a spacecraft, it is essential to downsize the instrument and investigate the radiation environment on the surface of the celestial body. In this study, we designed and developed a compact muography instrument based on the knowledge of compact gamma ray detectors for nuclear medicine imaging. At the same time, we theoretically estimated the muon production on Mars and evaluated the validity of using muography instrument on Mars.

The detection device of developing muography instrument consists of 64-channel silicon photomultipliers (SiPM), plastic scintillators, dynamic Time-Over-Threshold (dTOT) boards [2], data-acquisition (DAQ) board, and high-voltage power supply units. Incident muons react with the scintillator to emit weak light, and the light is amplified by SiPM attached to the both ends of the scintillator and read out with dTOT boards. The depth of interaction (DOI) in the scintillator is analyzed by measuring the pulse-height ratio of dual-sided readout. The size of the detector is 26.2 mm×26.2 mm×31.4 mm.

We first evaluated DOI resolution of this detector using a point beta-decay source of ^{90}Sr. The result indicates that the DOI resolution (FWHM) is 7.2 mm for the emitted beta rays with a spread of 2.2 mm. Then, we performed a Geant4 [3] simulation to examine the muon angular distribution that would be detected on the ground by this instrument. The result suggests that the structure of the detector makes the observation bias (Fig. 1). There are two solutions that can be considered to solve this problem: (1) developing one more detector and analyzing the coincident signals from dual-sided readout; (2) improving DOI resolution by performing accurate calibration.

We also performed a theoretical estimation to evaluate the muon production on Mars. Although the chemical composition and the density of Martian atmosphere are different from Earth's, the known muon flux in the upper earth atmosphere can be used for estimating the muon rates on Mars [4]. The result shows that the horizontal muon flux is greater than that on Earth (Fig. 2), which means that muography is more suitable for exploration of geological targets on Mars than on Earth.

In this presentation, we report the development status of the detection device and the concrete result of numerical calculation of radiation environment on Mars.

©2019. Japan Geoscience Union. All Right Reserved.

References
[1] Kedar et al., Muon radiography for exploration of Mars geology, Geosci 2, 2013. p.157-164.
[2] Shimazoe et al., Dynamic time over threshold method, IEEE trans. nucl. sci 59, no. 6, 2012. p.3213-3217.
[3] Agostinelli et al., Nuclear Instruments and Methods in Physics Research, A 506, 2003. p.250-303.
[4] Berringer et al., Cosmic Rays At Earth, Elsevier, ISBN 0-444-50710-8, 2001.

Keywords: Muography, Muon, Internal exploration, Mars exploration

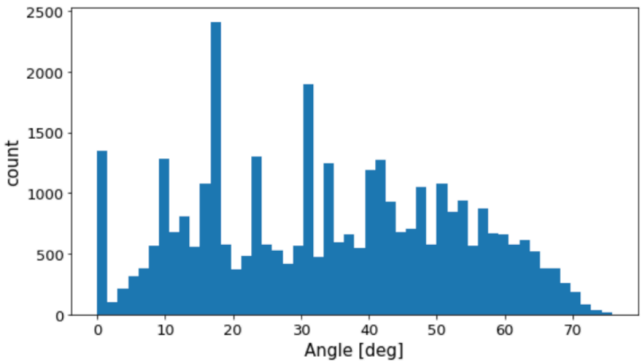


Fig. 1 The simulation result of muon zenith angular distribution that would be detected by developing instrument. The structure of detector makes the observation bias at 0°, 17° and 31°.

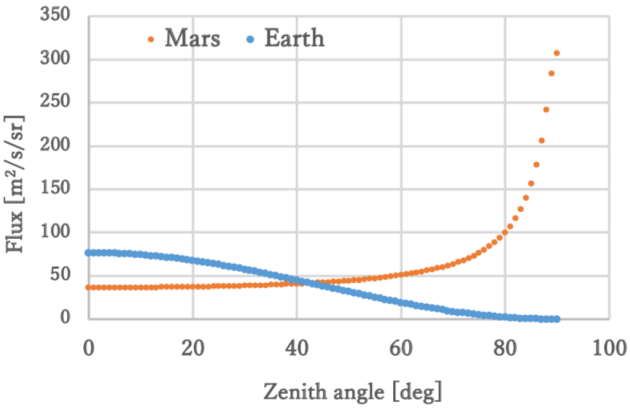


Fig. 2 Zenith angle dependence of muon flux on Mars and Earth. Horizontal muon flux on Mars is greater than that on Earth.

©2019. Japan Geoscience Union. All Right Reserved.

[E] Poster | P (Space and Planetary Sciences)：P-PS Planetary Sciences

Sun. May 26, 2019 5:15 PM - 6:30 PM JST | Sun. May 26, 2019 8:15 AM - 9:30 AM UTC | Poster Hall International Exhibition Hall8, Makuhari Messe_4

[P-PS04] Mars and Mars system: results from a broad spectrum of Mars studies and aspects for future missions

convener:Hideaki Miyamoto(University of Tokyo), Tomohiro Usui(Earth-Life Science Institute, Tokyo Institute of Technology), Ayako Matsuoka(Research Division for Space Plasma, Institute of Space and Astronautical Science, Japan Aerospace Exploration Agency), Sushil K Atreya(University of Michigan Ann Arbor)

In view of unprecedented advances in our understanding of Mars, primarily due to new and ongoing observations of the planet with a number of spacecraft missions of the US, Europe and Asia, we propose a session on Mars. Mars is an object of intense scrutiny. Currently, eight spacecraft are operating at Mars, with six in orbit (Odyssey, MRO, MAVEN, Mars Express, Mangalyaan and TGO) and two on the surface (MSL-Curiosity and MER-Opportunity), the largest number ever at any given time. In addition, InSight is on track to land on Mars in November 2018, and several spacecraft are in various stages of implementation with launches scheduled for 2020 (Mars 2020, ExoMars 2020, Emirates Mars Mission Hope, Chinese Mars Mission and the Japanese Mars Terahertz Microsatellite), 2022 (ISRO's Mangalyaan 2), and 2024 (JAXA's MMX mission to explore Phobos, Deimos, and Mars). All this is a clear demonstration of public's strong fascination with and commitment to Mars exploration and the resulting scientific bonanza. Synergistic investigations with ongoing and already completed missions along with modeling studies and earth-based observations are gradually revealing the nature of Earth's most closely resembling planet that took on a different evolutionary track than our home planet. Morphology and variable phenomena seen on the surface (RSLs, e.g.) and in the atmosphere (methane) indicate that Mars is possibly currently active. Available data are providing a better understanding of Mars' present geologic and atmospheric state, climate evolution, and habitability. Thus, the scope of this session will be the recent results from a broad spectrum of Mars studies encompassing the interior, surface, atmosphere, plasma environment, and the Mars system including its two satellites. Abstracts on modelling, instrumentation and future mission plans are also encouraged.

[PPS04-P01] Observation of the O_2^+ first negative band (1,0) emissions in the Mars ionosphere with a visible spectrograph on Haleakala T60

*Toshihisa Suzuki[1], Masato Kagitani[1], Takeshi Sakanoi[1] (1.PPARC, Graduate School of Science, Tohoku University)

[PPS04-P02] Search of shallow subsurface reflectors around RSLs in Martian Chryse and Acidalia planitiae by the MRO/SHARAD public data

*Aina Oura[1], Yasumasa Kasaba[1], Atsushi Kumamoto[1], Rina Noguchi[2], Tomohiro Usui[2], Ken Ishiyama[2], Chihiro Uemura[3] (1.Tohoku University, 2.Institute of Space and Astronautical Science, 3.SOKENDAI)

[PPS04-P03] Detecting surface changes on Mars using principle component analysis of repeat imagery

*Reid Parsons[1], Hideaki Miyamoto[1] (1.University of Tokyo)

[PPS04-P04] Evaluation of the detectability of hydrated salts on recurring slope lineae on Mars.

*Shoko Imamura[1,2], Yasuhito Sekine[2], Hiroyuki Kurokawa[2] (1.University of Tokyo, 2.Earth-Life Science Institute, Tokyo Institute of Technology)

[PPS04-P05] Frequency of ice sheet growth recorded on Mons Pavonis, Mars

*Tomohiro Kanzaki[1], Reid Parsons[1,2], Ryodo Hemmi[1], Hideaki Miyamoto[1] (1.University of Tokyo, 2.Fitchburg State University)

[PPS04-P06] Development of Life Detection Microscope (LDM) for *in situ* imaging of living cells on Mars surface

*Yoshitaka Yoshimura[1], Akihiko Yamagishi[2], Takehiko Satoh[3], Atsuo Miyakawa[2], Eiichi Imai[4], Satoshi Sasaki[5], Kensei Kobayashi[6], Yoko Kebukawa[6], Tomoka Okada[6], Keigo Enya[3], Hikaru Yabuta[7], Takeshi Naganuma[7], Hajime Mita[8], Kazuhisa Fujita[3], Tomohiro Usui[3] (1.College of Agriculture, Tamagawa University, 2.Tokyo University of Pharmacy and Life Science, 3.Japan Aerospace Exploration Agency, 4.Nagaoka University of Technology, 5.Tokyo University of Technology, 6.Yokohama National University, 7.Hiroshima University, 8.Fukuoka Institute of Technology)

[PPS04-P07] Development of a Mars Web-GIS for viewing multiple kinds of spectral data from orbiters

*Yuya Matsubara[1], Hironori Fukuchi[1], Yoshiko Ogawa[1], Yohei Hayashi[2] (1.The University of Aizu, 2.National Astronomical Observatory of Japan)

[PPS04-P08] **Visualization and Analysis of the Surface of Mars with NASA's Mars Trek Portal**

*Brian Hamilton Day[1], Emily Law[2] (1.NASA Solar System Exploration Research Virtual Institute, NASA Ames Research Center, 2.NASA Jet Propulsion Laboratory, California Institute of Technology)

[PPS04-P09] Increase in Dissolved Iron Concentration from Fayalite by UltravioletA・C Irradiation

*Nobuo Komori[1] (1.The United Graduate School of Education Tokyo Gakugei University)

[PPS04-P10] Small-scale ridges newly identified on the equatorial region of the Phobos nearside

*Ryodo Hemmi[1], Hiroshi Kikuchi[1], Hideaki Miyamoto[1] (1.The University of Tokyo)

[PPS04-P11] Development of a compact Muography instrument for future Mars exploration missions

*Hiroaki Kamiyoshihara[1], Tetsuro Ninomiya[1], Yuri Yoshihara[1], Kenji Shimazoe[1], Hiroyuki Takahashi[1], Hiroyuki Tanaka[1], Hideaki Miyamoto[1] (1.University of Tokyo)

Observation of the O_2^+ first negative band (1,0) emissions in the Mars ionosphere with a visible spectrograph on Haleakala T60

*Toshihisa Suzuki[1], Masato Kagitani[1], Takeshi Sakanoi[1]

1. PPARC, Graduate School of Science, Tohoku University

We carried out ground-based telescope observations of Martian ionospheric O_2^+ emission to obtain global distribution of Martian O_2^+ ionosphere and its variation for understanding Martian atmospheric escape process. After verifying the analysis method, the result suggests that the O_2^+ first negative bands (1NG) (1, 0) emissions are successfully detected, and calculated O_2^+ emission intensity and column density.
Mars has tenuous atmosphere compared with the Earth. One possible model for Martian tenuous atmosphere is caused by atmospheric escape to space for a long time. In addition, present Mars has only weak crustal magnetic fields for limited area, and therefore, it is likely that solar wind strongly affects Martian atmosphere escape. In recent years, ion composition and densities in the Martian ionosphere are revealed by Mars probes (e.g. Mars Express, MAVEN). In the Martian ionosphere, main ion is O_2^+ [M. Benna et al., 2015]. Moreover O_2^+ recombines with an electron, and as a result of a neutral molecule dissociation, neutral atomic oxygens are generated. Since the neutral atomic oxygen energy is higher than escape velocity of Mars, it can be escaped from Martian gravity. This process is important in Martian atmosphere escape. However, it is difficult to detect atomic oxygen by Mars probe in-situ observation, and escape quantity is indirectly estimated by plasma temperature and density from in-situ observations. On the other hand, remote-sensing of Martian ionosphere is useful to obtain global distribution and its time and spatial variations. It is essential to combine in-situ plasma data with global remote sensing for understanding Martian atmospheric escape, such as solar wind impact and/or crustal magnetic field effect on the escape process.
We carried out Martian ionosphere O_2^+ emission observation using Tohoku University T60 telescope (located at the summit of Mt. Haleakala in Maui) with Vispec (Visual imager and Spectrograph with Coronagraphy) from September 10 to 19, 2018. This is the first attempt to detect Martian O_2^+ emission with a ground-based telescope. We focused O_2^+ 1NG (1, 0) bands emission with a peak wavelength of about 561 nm. Visible Echelle spectrograph Vispec (wavelength resolution was 10,000) covered wavelength range from 550 nm to 570 nm. Vispec slit (width 2” ×length 90”) was located near Martian dayside limb parallel to the Martian rotation axis, and exposure time of one frame was 2 minutes. Total exposure time in observation period was 450 minutes. To refer sunlight spectrum reflecting by Martian surface, we acquired spectrum of disk center by Martian surface. First analysis process (subtraction dark, revision by flat-field, wavelength and space) was conducted on each frame, and each frame was added to gain S/N. Finally, sunlight spectrum was subtracted using disk center to obtain O_2^+ 1NG (1, 0) bands emission spectrum. Next, we compared observed O_2^+ spectrum with O_2^+ 1NG (1, 0) model spectrum given by Henriksen and Veseth [1987]. Focusing on only short period wavelength variations, we performed high-pass filter analysis on the both of observed and model spectrum. After that, we calculated the correlation coefficient between observed spectrum and model spectrum, and found that the coefficient maximum is 0.40 with no wavelength lag between two spectra. Data points, i.e., wavelength range, using correlation coefficient analysis were selected so that model O_2^+ emission is relatively intense and the contamination of solar fraunhofer absorption line is negligible. We estimated O_2^+ 1NG (1, 0) emission intensity with a least-square method to be 691 +/- 171 $\times 10^3$ Rayleighs, and the column density to be 4.4 +/- 1.1 $\times 10^{13}$ /cm^2. The estimated column density was greater than that of simulation. In this presentation, we compare O_2^+ emission observation spectrum with model spectrum, and give the estimation of O_2^+ emission intensity and column density in detail. We also give discussion about the

©2019. Japan Geoscience Union. All Right Reserved.

results.

Keywords: Mars, ionosphere, ground-based telescope

©2019. Japan Geoscience Union. All Right Reserved.

Search of shallow subsurface reflectors around RSLs in Martian Chryse and Acidalia planitiae by the MRO/SHARAD public data

*Aina Oura[1], Yasumasa Kasaba[1], Atsushi Kumamoto[1], Rina Noguchi[2], Tomohiro Usui[2], Ken Ishiyama[2], Chihiro Uemura[3]

1. Tohoku University, 2. Institute of Space and Astronautical Science, 3. SOKENDAI

One of recent discoveries on Mars is the recurring slope lineae (RSL), which are certain features on the surface invoking current icy processes. RSLs are distributed on Mars and these narrow features incrementally lengthen down steep slopes, fade in colder seasons, and recur annually. Candidate and confirmed RSL sites are distributed in four regions, (1) southern mid-latitudes (SML), (2) Valles Marineris (VM), (3) equatorial highlands, and (4) northern Chryse Planitia and southwestern Acidalia Planitia (CAP). The RSLs in (2) VM and (4) CAP are more densely located than other two areas.
This study tries to identify the subsurface structures of the northern mid-latitude RSL in (4) Chryse and Acidalia Planitiae by the public data of Mars shallow radar sounder (SHARAD) onboad the Mars Reconnaissance Orbiter opened on the PDS Geosciences Node. That is because CAP RSLs are densely distributed compared to other regions. CAP RSLs are found on the steep slopes of craters. Their source zones are at or below the elevation of the surrounding plains. We used the Java Mission-planning and Analysis for Remote Sensing (JMARS, https://jmars.asu.edu/) in order to investigate the geological information of the RSL sites and the MRO locations at the SHARAD observed data. We then picked up the location correspond to the RSL sites and generated radargrams from SHARAD data. The observation frequency of SHARAD is 15-25 MHz with the bandwidth of 10 MHz, and the subsurface close to the surface can potentially be resolved with the depth resolution of 15 m in vacuum. Using MOLA data, we generated the virtual radargrams with the surface clutter emulated by the Kirchhoff approximation. Then, we compared both observed radargrams with emulated ones to identify whether there are subsurface reflectors or not.
We surveyed about 12 orbits close to the confirmed RSLs. We could find the hypothetical detection of the subsurface reflector in ‘orbit.00688101’ (Jan 14 2008, N10.0-44.7˚, E313.6-318.3˚) and ‘orbit.00673602’ (Jan 03 2008, N10.1-44.7˚, E312.7-317.4˚). In this abstract, we concentrated the characteristics of the former candidate. In this sample, the closest RSL located at N34.1˚, E317.0˚ and nadir line from the orbit was 13.8 km. Another RSL close to this orbit located N34.8˚, E318.6˚ and nadir line from the orbit was 85.2 km. Apparent elevation of closest RSL was about -3,763 ±10 m. The deepest elevation of the crater was about -4,744 ±10 m and the highest elevation of it was about -3,640 ±10 m. The radargram of this orbit showed that the elevation of surface echo was in the range from -3720 to -3780 m and that of subsurface echo ranged from -3750 to -3800 m. This means that the closest RSL height was almost the same as the depth of subsurface reflector. The subsurface echo located 25 m below the surface, and it had a little bit weak echo strength compared to surface one. If this subsurface echo shows the underground reflection, the subsurface layer will be 180 km wide along the orbit. Although this depth is marginal for the depth resolution of SHARAD, we could not identify such an echo in the emulated radargram.
In the presentation, we will summarize the results of this region including other orbits.

Keywords: Mars, RSL, SHARAD

©2019. Japan Geoscience Union. All Right Reserved.

Detecting surface changes on Mars using principle component analysis of repeat imagery

*Reid Parsons[1], Hideaki Miyamoto[1]

1. University of Tokyo

Change detection is an analytical tool of Remote Sensing in which repeat observations of a particular location can be overlain, subtracted, or ratioed to detect differences between images. High-resolution, repeat imagery on Mars has led to several discoveries of ongoing geologic processes operating at the sub-kilometer scale such as recurring slope lineae (RSL) [1-3], new, small impacts [4], aeolian dune migration [5], sublimation of polar ice [6], and gully formation [7]. Generally, the detection of these changes is done manually by overlaying, and “flipping” between the two images. As planetary remote sensing data sets continue to grow, so does the need for a more efficient means of change detection.

Principle component analysis (PCA) offers an advantageous means for detecting change because it considers the values of all pixels in all the repeat images to extract the most statistically significant variations. These variations are then isolated from one another as a hierarchical set of “principle components” of the image dataset. The user can quickly identify patterns or features of interest which are present in one or more of these components. To illustrate this method, nine HiRISE images [8] collected from Palikir crater on Mars between November 2007 and June 2011 documenting RSL formation will be used.

PCA changes the values of the pixels in each image by plotting the pixel data on a set of axes which capture the maximum variance in the dataset. In our example image set, each pixel in the image stack can be treated as a 9-dimensional vector since there is a value for that pixel in each of the nine images. However, each pixel can be plotted on a new set of axes that capture the most important, or PCs of the image stack.

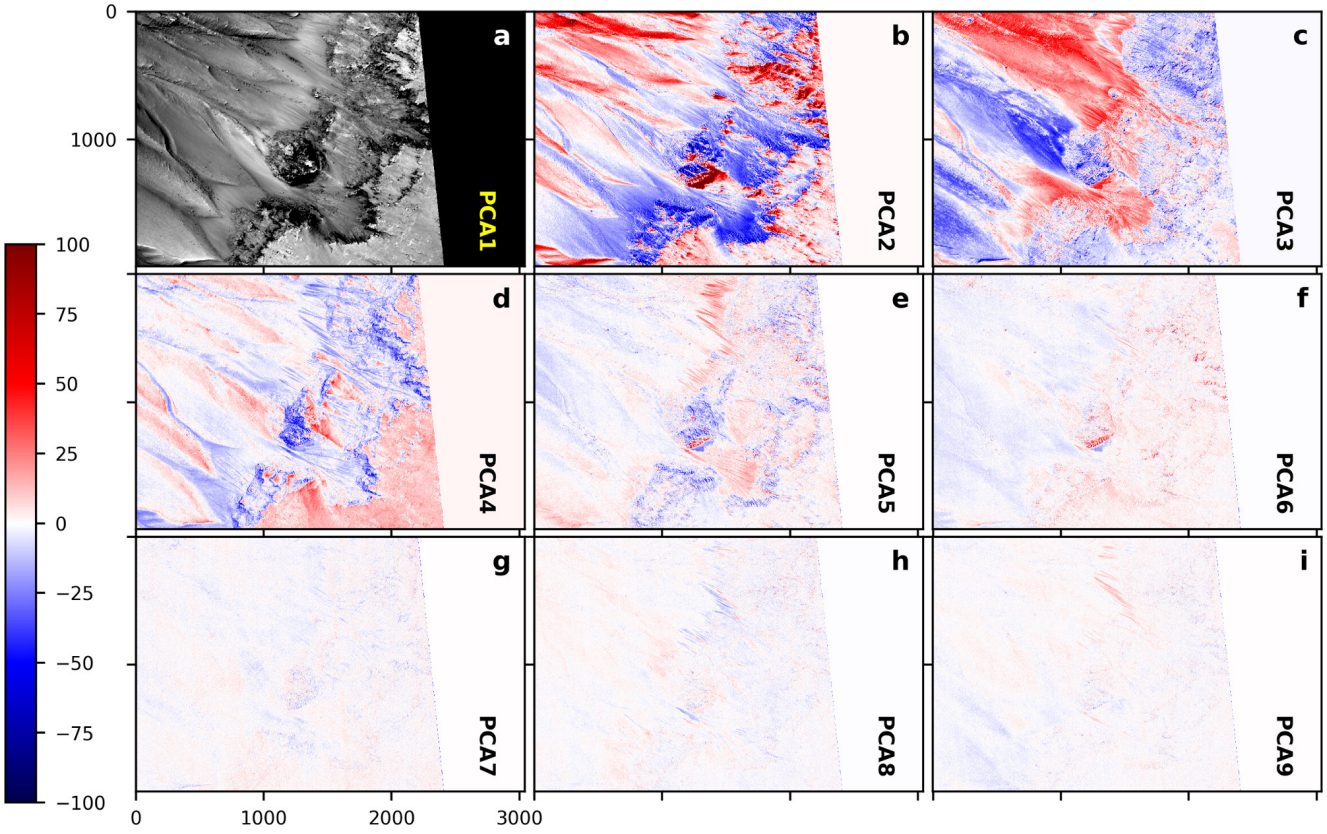
The figure shows the result of the PC transform (performed using ENVI® software) on the stacked time-series. Because most of the variation in the images is captured in the first PC (PCA1), it uses a grayscale color bar spanning 0-255 pixel values. Generally, variations covering a large spatial extent or variations causing a big shift in pixel values will be captured in the lower PCA components. Higher components, on the other hand, will depict smaller amplitude variations occurring in fewer images (or over smaller spatial extents). Thus, components 2 and 3 (panels b and c, respectively) are dominated by variations caused by differences in lighting (sun direction and elevation angle) and possibly dust or frost deposition/erosion. RSL features are identifiable in PCA4 (panel d) as elongated blue “fingers” and become more dominant and appear red in PCA5 (panel e). Subsequent components capture smaller variations caused either by changes in lighting, RSL shape (in PCA 8 and 9), or camera noise.

After identifying the PCs which contain the feature of interest, the feature can be traced back to the original images via an inverting from PC coordinates to image coordinates. Although this step is not completely reliable, it is successful in determining which images contain the most prominent RSL. Eventual combination of this method with machine-learning algorithms may permit a more automated means of detecting interesting surface changes on Mars and other planetary bodies. Note this work was previously published in [9].

©2019. Japan Geoscience Union. All Right Reserved.

References:
[1] McEwen A. S., et al. (2011) Science 333 740–743
[2] Sullivan R., et al. (2001) JGR 106 23607–23633
[3] Ojha L., et al. (2014) Icarus 231 365 –376
[4] Daubar I., et al. (2013) Icarus 225 506 –516
[5] Bourke M., et al. (2008) Geomorph. 94 247–255
[6] Thomas P., et al. (2005) Icarus 174 535 –559
[7] Diniega S., et al. (2009) AGU Fall Meeting Abstracts
[8] HiRISE Operations Center Gullies in palikir crater
https://www.uahirise.org/dtm/dtm.php?ID=PSP_005943_1380 accessed: 2017-07-03
[9] Parsons, R.A. & Miyamoto, H. (2018) J. of Physics: Conf. Series 1036 (012004).

Keywords: Mars, Change, Detection



©2019. Japan Geoscience Union. All Right Reserved.

Evaluation of the detectability of hydrated salts on recurring slope lineae on Mars.

*Shoko Imamura[1,2], Yasuhito Sekine[2], Hiroyuki Kurokawa[2]

1. University of Tokyo, 2. Earth-Life Science Institute, Tokyo Institute of Technology

On present-day Mars, pure liquid water is thermodynamically unstable; whereas, high-salinity brine can exist on the surface, at least temporally, due to freezing point depression [1]. Deliquescence and melting of subsurface ice are proposed as being the major processes of formation of liquid brine on Mars [2, 3]. Although liquid brine is suggested to form upon Mars' daily and seasonal changes [2, 3], generation of brine flow has not been confirmed on current Mars. Our previous study suggests that cycles of formation and evaporation of liquid brine can generate characteristic morphological features of downward-elongated flows on steep slopes [4]. This happens because precipitated salts within soil dramatically decrease the porosity and permeability, leading generation of surface flows [4]. Our study also suggests that precipitation of salts reaches up to ~30% in volume within the soil, implying that any detection of such salt may be evidence for the occurrence of brine flow on current Mars [4]. Proposed morphological features formed by current brine activity include recurring slope lineae (RSL) [5, 6]. Although hydrated salts are suggested to exist on RSL at a few locations [6], identification of salt compositions is still challenging. Additionally, there are no reports on detection of hydrated salts at most of the RSL sites across Mars.

In the present study, we investigate the conditions of identification of hydrated salt compositions on RSL using Compact Reconnaissance Imaging Spectrometer for Mars (CRISM) onboarded on Mars Reconnaissance Orbiter (MRO). We calculate synthesized spectra of mixtures of basaltic soil and various hydrated salts (such as $MgCl_2 \cdot 2H_2O$) with the different mixing ratios using a linear combination method and an addition of random noise with a Gaussian distribution. We evaluate the threshold mixing ratios of salt for the identification of the salt compositions based on the analyses of the synthesized spectra. Our results show that if the mixing ratio of hydrated salt exceeds 20% in volume, O-H bands attributed from hydrated salts can be detected with CRISM. We discuss the observational conditions, such as the observational altitude from the surface, for the identification of salt compositions on RSL in future missions.

[1] McEwen et al. (2011) Science, 333, 740. [2] Martin-Torres et al. (2015) Nature Geoscience 8, 357. [3] Chevrier & Rivera-Valentin (2012) Geophysical Research Letters, 39, 21. [4] Imamura et al. (2018) Planetary People, 27, 163. [5] Hecht et al. (2009) Science, 325, 5936. [6] Ojha et al., (2015) 8, 829.

Keywords: Mars, CRISM, salt

©2019. Japan Geoscience Union. All Right Reserved.

Frequency of ice sheet growth recorded on Mons Pavonis, Mars

*Tomohiro Kanzaki[1], Reid Parsons[1,2], Ryodo Hemmi[1], Hideaki Miyamoto[1]

1. University of Tokyo, 2. Fitchburg State University

On present-day Mars, large scale ice bodies are only found at each pole. However, in mid latitudinal areas, LDA (lobate debris apron), LVF (lineated valley fill), CCF (concentric crater fill) are reported and interpreted to have a glacial origin (Levy et al., 2014). Also, inequatorial areas, fan-shaped deposits at northwestern rim of three shield volcanos in Tharsis region though to have a glacial origin (e.g. Fastook et al., 2008).
Fan-shaped deposits sit beside three Tharsis montes and have characteristic geomorphologies extending for roughly 100-500 km from the foot of mountain, typically consisting of three facies: Smooth facies at the top, Knobby facies at the middle, and Ridged facies at the rim. Smooth facies are smooth-surfaced mounds which superpose on other facies, Knobby facies are collective hillocks a few hundred meters in radius, and Ridged facies are linear ridges (moraine-like features) parallel to the rim of the fan. At Arsia (Kadish et al., 2014) and Pavonis (Shean et al., 2005) Mons, ridged facies are especialy well-developed - containing tens to few hundreds of ridges interpreted to be moraines that indicates the varying extent of a former ice sheet. Such geomorphologies potentially record the advance and retreat of ice sheet for tens of kilometers during the Amazonian adjacent to Arsia and Pavonis Mons.
The association of these geomorphologic features to glacial processes is supported by global climate simulations of Mars during high-obliquity (Forget, 2006). The obliquity of the rotation axis of Mars is considered not stable as on the Earth, reaching 45˚ in the past 20 Myrs (Laskar et al., 2004). Such high obliquity can cause sublimation of the polar cap, enhancing the water vapor content in the atmosphere compared to present-day Mars. By diffusion and condensation model, Mellon & Jakosky (1995) found that in the surface environment of present-day Martian obliquity (25.2˚) water ice is stable only at 40˚ latitude or higher, however, when obliquity gets higher than 32.3˚, with enough amount of atmospheric water vapor, water ice becomes stable globally. This result suggests Martian surface environment has experienced such climate condition that water ice condenses and deposits in mid and low latitudinal areas. Therefore, the existence of Martian “ice age” during Amazonian high-obliquity periods is being proposed (Head et al., 2003).
If ice sheet growth and disappearance on the flanks of Tharsis Montes are an indication of the climate change caused by orbital parameters, each of moraine-like features should correspond to a paleoclimate cycle. However, fluctuation of its spacing, scale and correlation to orbital parameter have not yet been discussed. Hence, as basic study to associate distribution of moraine-like features to extent of the ice sheet, we made DEM data from CTX imagery at the rim of fan-shaped deposits at the foot of Mons Pavonis, and using the DEM data, we measured spacing and cross-sectional area of each moraine, and conducted frequency analysis on the cross section of DEM data.
As a result, spacing of moraine-like feature appeared to fluctuate from few hundred meters to 4.5 km, showing drastic change of the density. Also, cross sectional area of moraine-like feature fluctuates up to 1.4×10^4 m^2. These fluctuations potentially record the change of frequency of events that caused accumulation and ablation of ice sheet or change of velocity of ice sheet flow. In Tharsis region, these two periodic events are assumed to affect ice sheet: global climate change caused by orbital parameter, and local volcanic activity. To prove the spacing and moraine-size are driven by global climate forcings, there should be similarities between the ridges found at Pavonis, Arsia, and a correlation to orbital parameters. Therefore, frequency analysis of cross- sectional view of the terrain is being conducted. The result will be shown in the presentation.

©2019. Japan Geoscience Union. All Right Reserved.

Keywords: Mars, Martian climate, Tharsis region, Milankovich cycle

©2019. Japan Geoscience Union. All Right Reserved.

Development of Life Detection Microscope (LDM) for *in situ* imaging of living cells on Mars surface

*Yoshitaka Yoshimura[1], Akihiko Yamagishi[2], Takehiko Satoh[3], Atsuo Miyakawa[2], Eiichi Imai[4], Satoshi Sasaki[5], Kensei Kobayashi[6], Yoko Kebukawa[6], Tomoka Okada[6], Keigo Enya[3], Hikaru Yabuta[7], Takeshi Naganuma[7], Hajime Mita[8], Kazuhisa Fujita[3], Tomohiro Usui[3]

1. College of Agriculture, Tamagawa University, 2. Tokyo University of Pharmacy and Life Science, 3. Japan Aerospace Exploration Agency, 4. Nagaoka University of Technology, 5. Tokyo University of Technology, 6. Yokohama National University, 7. Hiroshima University, 8. Fukuoka Institute of Technology

Past trial of direct detection of life on Mars by 1970's Viking mission ended up with a negative conclusion [1]. Whereas, numbers of new finding provided by Mars exploration missions in the last decade indicate that there are good reasons to perform another life detection program. The sensitivity of the gas chromatograph mass spectrometer onboard the Viking mission was not very high, and was not able to detect the microbes 10^6 cells in 1 gram clay [2,3]. Resent observations on Mars have found the evidences of past water activities. MSL Curiosity has found the temporal increase of methane concentration in Martian atmosphere [4]. The presence of reduced sulfur compound such as pyrite in Martian soil was also detected by MSL [5]. Methane and reduced sulfur compound can be the energy source to support the growth of chemoautotrophic microbes [6]. Possible presence of liquid water at Recurring Slope Lineae has been supported by the detection of hydrated salts [7]. The presence of organic compounds of Martian origin has been reported [8]. These evidences tend to support the possible presence of living microbes near the surface of Mars.

Physical and chemical limits for terrestrial life have been major foci in astrobiology [9], and are summarized in ref. [6]. Combining the environmental factors, anywhere in the Martian environment where we can find the three components, water molecules, reducing compounds and oxidative compounds could be an environment where life can be sustained for long periods of time, if other factors such as temperature, pressure, UV and other radiations permit [6]. Among these factors, most of the factors including ionic radiation, can be endured by terrestrial extremophiles. Only UV can kill the most UV-resistant microbes within minutes. However, UV can be shielded by a few centimeters soil layer. These evaluations lead to the conclusion that the Martian soil under a few cm can be the place to support the growth of microbes, if the water activity is higher than 0.6.

For exploring extant life on Mars, we have proposed to search cells from a depth of about 5 - 10 cm below the surface by the Life Detection Microscope (LDM) [6, 10]. LDM has the potential to detect single cells in the resolution of 1 micrometer and could detect less than 10^4 cells in 1 gram clay, which is much higher sensitivity than the instrument onboard Viking. We have developed the solution and combination of fluorescence pigments to detect organic compounds, and to differentiate organic compounds surrounded by membrane, which we think to be the most fundamental features that a cell should possess to constitute life. Our investigation goals are the followings. 1) Identify cell-like structure in which organic compounds are enveloped by membrane, which may represent Martian life. 2) Search for any type of organic compounds in Mars surface samples. The compounds include cells, other biological materials, and abiotic polycyclic aromatic hydrocarbon (PAH). 3) High-resolution characterization of regolith and dust particles. The current status of development of LDM will be presented.

©2019. Japan Geoscience Union. All Right Reserved.

References

[1] Margulis, L. et al. *J. Mol. Evol.* 14, 223-232 (1979)

[2] Glavin, et al, *Earth Planet. Sci. Let.*, 185, 1-5 (2001)

[3] Navarro-González, et al., *Proc. Natl. Acad. Sci. USA*. 103 (2006)

[4] Webster, C. R., et al., *Science*, 360 (2018).

[5] Ming, D., et al., *Science*, 343 (2014)

[6] Yamagishi, A. et al. *Biol. Sci. Space*, 24 (2010)

[7] Ojha, L. et al. *Nature Geosci.*, 8 (2015)

[8] Freissient, C. et al. *J. Geophys. Res. Planets* (2015)

[9] Marion, G.M. et al. *Astrobiol*. 3 (2003)

[10] Yamagishi, A., et al., *Trans. JSASS, Aerospace Tech. Japan*, 16 (2018)

Keywords: fluorescent microscope, extraterrestrial life

©2019. Japan Geoscience Union. All Right Reserved.

Development of a Mars Web-GIS for viewing multiple kinds of spectral data from orbiters

*Yuya Matsubara[1], Hironori Fukuchi[1], Yoshiko Ogawa[1], Yohei Hayashi[2]

1. The University of Aizu, 2. National Astronomical Observatory of Japan

The VIS-NIR reflectance spectra observed during latest Mars orbiter missions are of high quality and cover the whole globe. Such data sets are very informative for understanding the materials and their distribution on the surface. Each mineral has unique absorption bands in the spectra. We can identify which minerals are present by comparing the absorption bands of the observed spectra with the known absorption bands in the spectra measured in laboratories. In the case of Mars, we can estimate the type and distribution of hydrous minerals which leads to important clues to understand the water environment.

However, the VIS-NIR spectral data observed on Mars are not well utilized among the community. There are huge volume of accumulated data due to an increasing number of missions and various kinds of instruments with higher accuracy. It is not easy to process huge data and understand the relevance of them visually and intuitively.

We develop a new Mars web-GIS application, "Red Ace", to view and download the Mars observation data, especially the VIS-NIR spectra (image cube data format), easily and intuitively. The Red Ace handles multiple kinds of observation data: the Compact Reconnaissance Imaging Spectrometers for Mars (CRISM) data, the Thermal Emission Imaging System (THEMIS) data and DEM (Digital Elevation Model) data at the same time. Additionally, we use the DEM data from the Mars Orbiter Laser Altimeter (MOLA) to display 3D map of Mars with the Red Ace.

The Red Ace is developed based on CesiumJS that is an open source JavaScript library for 2D/3D maps. The user can choose the dimension of the map. In the Red Ace, the spectral observation points are displayed on the surface image layers. When the user clicks any point on the footprint of the layer, the color of the selected footprint changes and the thumbnail image appears. When the user selects any pixel on the thumbnail image, the Red Ace provides reflectance spectral data and ancillary data as graphs and tables. In response to user operation, multiple kinds of spectral data are displayed on the same window. The Red Ace also provides band- ratio images of THEMIS. The user can download band-ratio images, spectral data and ancillary data as files of PNG, CSV, JSON, XLSX and PVL formats. The user can move the windows displaying thumbnail image and graph freely. In addition, the Red Ace provides the function to control the Mars base map changing the exaggeration of height of the Mars globe. The user can change the order of layers and transparency of layers arbitrarily. The user can also jump to the region of interest directly by setting the coordinates and the zoom level. The user can handle these functions smoothly.

In the case of THEMIS, published data from the mission data archive are not reflectance data but radiance data. Therefore, the Red Ace derives reflectance data from radiance data and ancillary data, in order to compare them with CRISM spectra observed in the same spot.
In this study, considering the portability and extension of the application, the Docker was used for the development environment. Docker is an open source software platform that allow the user to develop applications quickly using containers. JSON format is adopted for data handling to make it easier to add new observation data from new observation equipments in the future. In the JSON format, it is unnecessary to associate item order and item meaning. Hence, it has high reusability and freedom. In the

©2019. Japan Geoscience Union. All Right Reserved.

Red Ace, by standardizing the structure of JSON format data in advance, it is possible to store and handle diverse data by using the same data structure.

Keywords: Mars, Spectral data, Web-GIS

©2019. Japan Geoscience Union. All Right Reserved.

Visualization and Analysis of the Surface of Mars with NASA's Mars Trek Portal

*Brian Hamilton Day[1], Emily Law[2]

1. NASA Solar System Exploration Research Virtual Institute, NASA Ames Research Center, 2. NASA Jet Propulsion Laboratory, California Institute of Technology

Originally released in June, 2015 as a public outreach tool, Mars Trek is currently being enhanced to support site selection and analysis for upcoming human and robotic missions to Mars. Many new data products are being added, with emphasis on providing detailed information for proposed exploration zones. Data products can be loaded and even combined from many different instruments aboard many different Mars-orbiting spacecraft including Viking, Mars Global Surveyor, Mars Odyssey, Mars Reconnaissance Orbiter, and Mars Express. Users can download data products from Mars Trek and access metadata for each product. Web services and APIs allow other clients to access data from Mars Trek's servers. A standardized interface across the Trek portals provides for advanced 3D visualization and navigation. Standard keyboard gaming controls allow the user to maneuver a first-person visualization of "flying" across the surface of the Mars. User-specified bounding boxes can be used to generate STL and/or OBJ files to create physical models of surface features with 3D printers. A new VR capability allows users to generate their own virtual reality flyovers for any user-defined paths along the Mars' surface.

Mars Trek's power as a tool for education and outreach is exemplified by its being designated as key supporting infrastructure for NASA Science Mission Directorate's STEM Activation Initiative, and its serving of data to a growing community of digital planetariums.

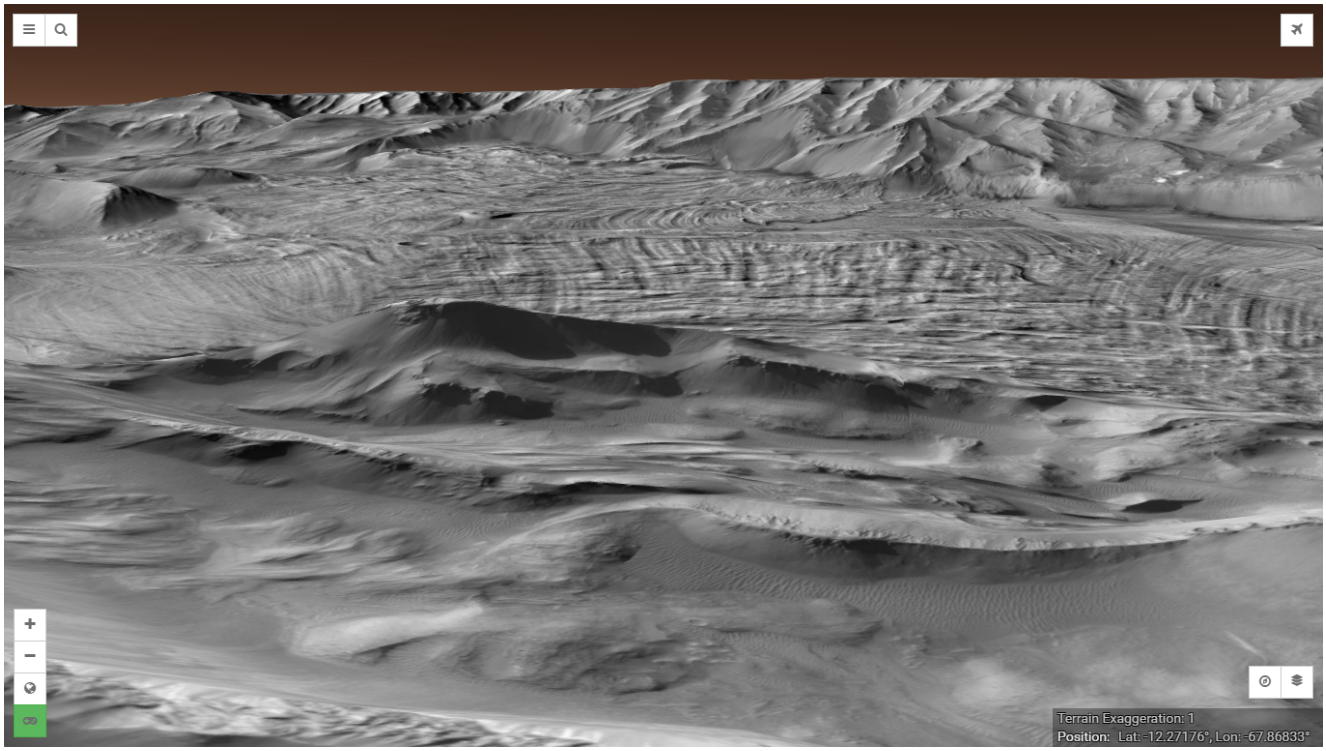
As private industry and space agencies of a growing number of nations plan new missions to Mars, detailed maps and models of Mars' surface and climate will be essential for mission planning. Mars Trek's generalized suite of tools are being designed to meet the needs of this new generation of missions. The portal will also provide an outstanding means of dissemination of data from these missions. Layering and blending many different data products and putting individual products in the context of many others will facilitate mining of information going far beyond what individual products can provide separately. In addition to mission planning and planetary science, Mars Trek will continue supporting the essential task of engaging the public in this great adventure. Mars Trek is developed at NASA's Jet Propulsion Laboratory (JPL) and managed as a project of NASA's Solar System Exploration Research Virtual Institute (SSERVI) at NASA Ames Research Center.

At the request of the Planetary Science Division of NASA's Science Mission Directorate, we are extending the technologies of our existing Trek platforms to create a new portal for Mars' largest moon, Phobos. In this effort, we are working with the International Phobos/Deimos Landing Site Working Group and with JAXA, with JAXA's MMX mission as a primary driver.
Mars Trek is one of the portals in the NASA Solar System Treks Project (SSTP), available at https://trek.nasa.gov. NASA's Solar System Trek online portals provide web-based suites of interactive data visualization and analysis tools to enable mission planners, planetary scientists, students, and the general public to access mapped data products from past and current missions for a growing number of planetary bodies including the Moon, Mars, Vesta, etc. These portals are being used for site selection and analysis by NASA and a number of its international partners, supporting upcoming missions. In addition to demonstrating the capabilities of Mars Trek in this presentation and providing a preview of Phobos Trek,

©2019. Japan Geoscience Union. All Right Reserved.

we will solicit input from the community for ideas for future enhancements to the portals.

Keywords: Mars



©2019. Japan Geoscience Union. All Right Reserved.

Increase in Dissolved Iron Concentration from Fayalite by UltravioletA・C Irradiation

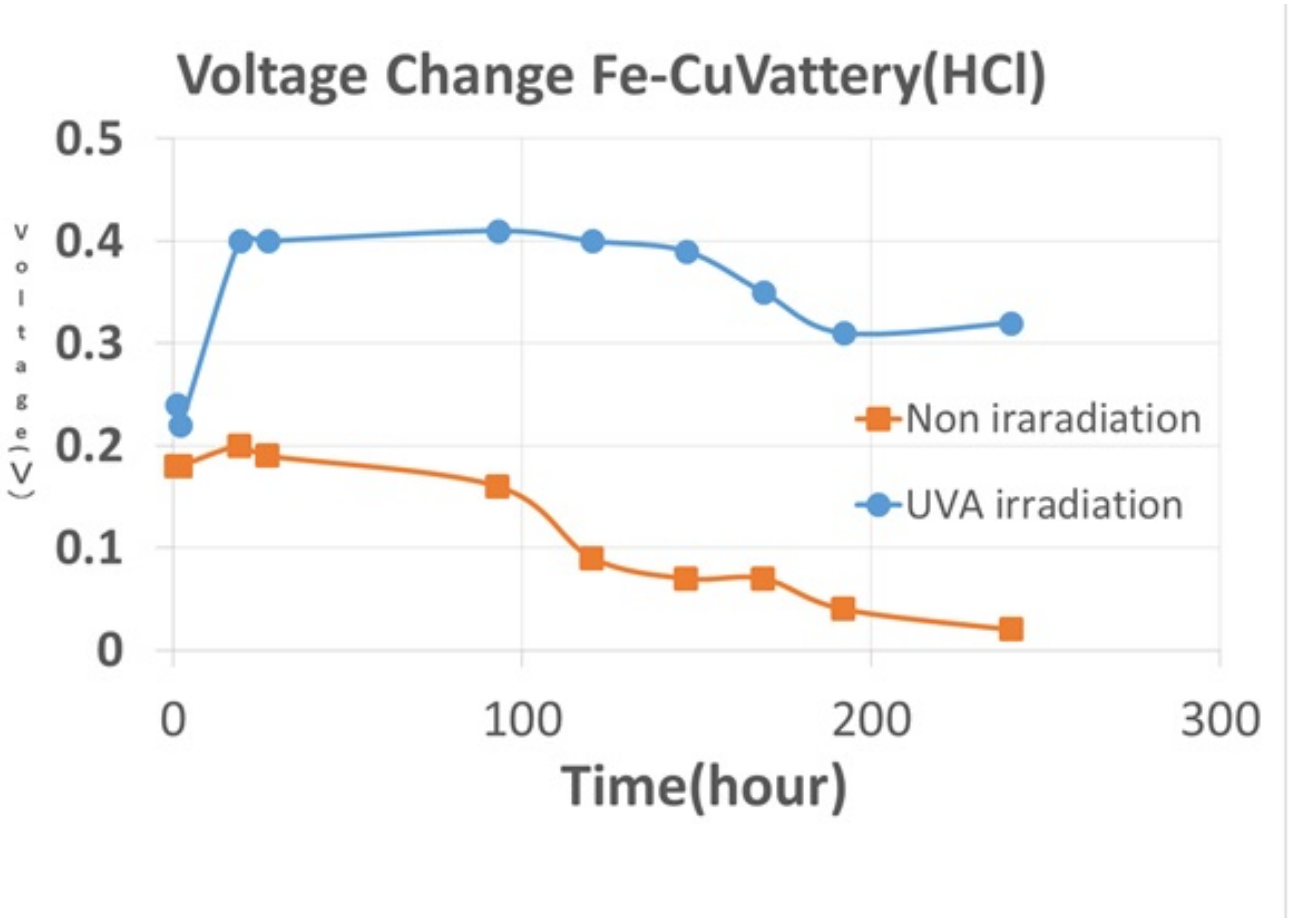
*Nobuo Komori[1]

1. The United Graduate School of Education Tokyo Gakugei University

To investigate the mystery of “Why the Mars' surface with poor oxgen has so much iron oxide" I have led student experiments at junior high schools. I will show my recent experiments and their results.
A.S.Yen (1999) showed that reactive oxygen species can also be formed on mineral grains under Martian conditions by irradiating ultraviolet C to quartz samples. Furthermore he irradiated ultraviolet C to thin iron films in the air and showed that exposure to ultraviolet radiation increases the rate of oxide formation. My experiments was irradiating ultraviolet A and C to fayalites and iron in acid water. This results indicated the possibility that iron oxides might be formed because of ultraviolet rays other than the cause of reactive oxygen species in the past.
Experiment no.1:
I had students irradiate ultraviolet rays A and C to Fayalite in hydrochloric acid.I had students irradiate ultraviolet rays A and C to Fayalite in hydrochloric acid. In this experiment, I used Fayalite from Kawamata-machi, Fukushima.
Fayalite, which is about 1g and not formatted was put in the test tube in the test tube filled with hydrochloric acid pH2.After the experiment, I had students check the concentration of iron ions in the water solution by using a digital pack test. This experiment with ultraviolet rays A was carried out 7 times and the experiment with ulttaviolet rays was carried out 3times.According to the results of the experiment with ultraviolet rays A, the quantity of iron elution increased more in the case of ultraviolet rays irradiating 6 times out of 7 than with the result of no irradiation.The results of the experiment with ultraviolet rays C were idential (3 times out of 3). The peak of wavelength ultraviolet rays A is generated by black lite is 365 nm. The peak of wavelength ultraviolet rays C is generated by germicidal lamp is 245 nm.
Experiments no.2:
I had the students irradiate ultraviolet rays A to a battery that has the iron cathode copper anode in hydrochloric acid. The Students then measured the occured voltage of the battery. I compared the voltage between ultla violet rays irradiation and non irradiation.The irradiated battery’s voltage stayed over 0.2V and the voltage did not decrease after 150hours.Another non-irradiated battery’s voltage decreased lower little by little and the voltage was close to 0V after 150 hours.This experiment was carried out 4times. In all cases the voltage of the battery that was irradiated by ultraviolet rays was higher than the non-irradiated battery.
It seems that electrons dissociate from iron atoms by ultlaviolet energy and form iron ions.
Consideration
From my experiments results, I would infer that ultraviolet rays advance the dissolution of iron ion from fayalite and iron. I think ultraviolet rays are one of the causes of iron oxide and hidroxide existing on Mars’ surface besides reactive oxygen species.It seems that there was water on Mars’ surface. There was a possibility that advancing of iron dissolution from rocks on Mars by ultraviolet rays irradiation.

Keywords: ultraviolet rays, fayalite , hydrochloric acid, iron, elution increase

©2019. Japan Geoscience Union. All Right Reserved.



©2019. Japan Geoscience Union. All Right Reserved.

Small-scale ridges newly identified on the equatorial region of the Phobos nearside

*Ryodo Hemmi[1], Hiroshi Kikuchi[1], Hideaki Miyamoto[1]

1. The University of Tokyo

Although the craters and grooves on Phobos are indicative of widespread and abundant surface modification during Phobos' geologic history [Basilevsky et al., 2014], little definitive evidence exists for geologically recent regolith migration other than down-slope mass-wasting [Shi et al., 2016]. Here we report newly found small-scale sinuous ridges identified in Mars Reconnaissance Orbiter's High Resolution Imaging Science Experiment (HiRISE [McEwen et al., 2007]) images of the nearside of Phobos. These ridges are spatially focused within the equatorial region (-5° to 20° N). Some of them superpose on craters and grooves, which is consistent with a geologically recent activity. They are ~200 m to ~1 km in length, several 10's m in width, and most of them are roughly parallel to each other and are generally oriented in NE-SW direction. To extract detailed topographic profiles, we constructed a high-resolution (~5-6 m/pixel; almost same as the original image) digital elevation model (DEM) by using shape-from-shading [Alexandrov and Beyer, 2018] in the selected regions of a HiRISE image and a stereo-derived HiRISE DEM (20 m/pixel) [Hemmi and Miyamoto, 2019]. Our preliminary analysis shows these ridges are less than several meters high. Their morphology and topography are unlikely to be formed by impact cratering, extensional stress fields, or mass wasting processes. In this presentation, we provide initial results of geological mapping of the small-scale ridges and discuss their possible origins.

References

Alexandrov, O., and R. A. Beyer (2018), Multiview Shape-From-Shading for Planetary Images, *Earth and Space Science*, 5(10).

Basilevsky, A. T., C. A. Lorenz, T. V. Shingareva, J. W. Head, K. R. Ramsley, and A. E. Zubarev (2014), The surface geology and geomorphology of Phobos, *Planetary and Space Science*, 102, 95-118.

Hemmi, R., and H. Miyamoto (2019), HiRISE digital elevation model of Phobos: Implications for morphological analysis of grooves, *Proceedings of the 50th Lunar and Planetary Science Conference*, Abstract No. 1759.

McEwen, A. S., et al. (2007), Mars Reconnaissance Orbiter's High Resolution Imaging Science Experiment (HiRISE), Journal of Geophysical Research: Planets, 112(E5), E05S02.

Shi, X., J. Oberst, and K. Willner (2016), Mass wasting on Phobos triggered by an evolving tidal environment, *Geophysical Research Letters*, 43(24), 12,371-312,379.

Keywords: Phobos, HiRISE, Digital Elevation Model

©2019. Japan Geoscience Union. All Right Reserved.

Development of a compact Muography instrument for future Mars exploration missions

*Hiroaki Kamiyoshihara[1], Tetsuro Ninomiya[1], Yuri Yoshihara[1], Kenji Shimazoe[1], Hiroyuki Takahashi[1], Hiroyuki Tanaka[1], Hideaki Miyamoto[1]

1. University of Tokyo

Muography is a technique that uses cosmic ray muons for visualizing the interior of large-scale structures in much the same way as standard X-ray radiography is used to image the interior of smaller objects. Muography has been successfully applied to explore the internal structure of geological targets on earth. Because exploring the inner structure of the shallow subsurface of celestial bodies is important to understand their origin and evolution, we are planning to operate muography instrument in the extraterrestrial environment, especially on the surface of Mars. Applying muography to planetary explorations has some advantages over conventional internal exploration methods: (1) it is able to observe the absolute linear density of objects; (2) the passive nature of the measurements provides low power consumption; (3) the instrument size is arbitral [1]. However, in order to mount muography instrument on a spacecraft, it is essential to downsize the instrument and investigate the radiation environment on the surface of the celestial body. In this study, we designed and developed a compact muography instrument based on the knowledge of compact gamma ray detectors for nuclear medicine imaging. At the same time, we theoretically estimated the muon production on Mars and evaluated the validity of using muography instrument on Mars.

The detection device of developing muography instrument consists of 64-channel silicon photomultipliers (SiPM), plastic scintillators, dynamic Time-Over-Threshold (dTOT) boards [2], data-acquisition (DAQ) board, and high-voltage power supply units. Incident muons react with the scintillator to emit weak light, and the light is amplified by SiPM attached to the both ends of the scintillator and read out with dTOT boards. The depth of interaction (DOI) in the scintillator is analyzed by measuring the pulse-height ratio of dual-sided readout. The size of the detector is 26.2 mm×26.2 mm×31.4 mm.

We first evaluated DOI resolution of this detector using a point beta-decay source of ^{90}Sr. The result indicates that the DOI resolution (FWHM) is 7.2 mm for the emitted beta rays with a spread of 2.2 mm. Then, we performed a Geant4 [3] simulation to examine the muon angular distribution that would be detected on the ground by this instrument. The result suggests that the structure of the detector makes the observation bias (Fig. 1). There are two solutions that can be considered to solve this problem: (1) developing one more detector and analyzing the coincident signals from dual-sided readout; (2) improving DOI resolution by performing accurate calibration.

We also performed a theoretical estimation to evaluate the muon production on Mars. Although the chemical composition and the density of Martian atmosphere are different from Earth's, the known muon flux in the upper earth atmosphere can be used for estimating the muon rates on Mars [4]. The result shows that the horizontal muon flux is greater than that on Earth (Fig. 2), which means that muography is more suitable for exploration of geological targets on Mars than on Earth.

In this presentation, we report the development status of the detection device and the concrete result of numerical calculation of radiation environment on Mars.

©2019. Japan Geoscience Union. All Right Reserved.

References
[1] Kedar et al., Muon radiography for exploration of Mars geology, Geosci 2, 2013. p.157-164.
[2] Shimazoe et al., Dynamic time over threshold method, IEEE trans. nucl. sci 59, no. 6, 2012. p.3213-3217.
[3] Agostinelli et al., Nuclear Instruments and Methods in Physics Research, A 506, 2003. p.250-303.
[4] Berringer et al., Cosmic Rays At Earth, Elsevier, ISBN 0-444-50710-8, 2001.

Keywords: Muography, Muon, Internal exploration, Mars exploration

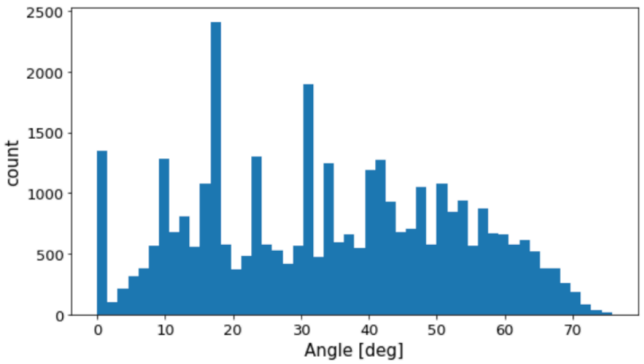


Fig. 1 The simulation result of muon zenith angular distribution that would be detected by developing instrument. The structure of detector makes the observation bias at 0°, 17° and 31°.

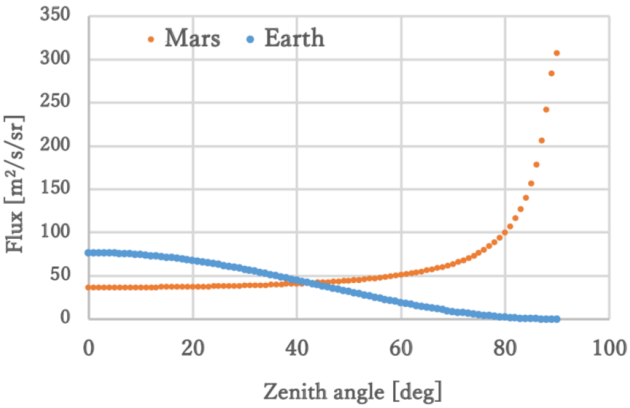


Fig. 2 Zenith angle dependence of muon flux on Mars and Earth. Horizontal muon flux on Mars is greater than that on Earth.

©2019. Japan Geoscience Union. All Right Reserved.

[E] Poster | P (Space and Planetary Sciences)：P-EM Solar-Terrestrial Sciences, Space Electromagnetism & Space Environment

Sun. May 26, 2019 10:45 AM - 12:15 PM JST | Sun. May 26, 2019 1:45 AM - 3:15 AM UTC | Poster Hall International Exhibition Hall8, Makuhari Messe_2

[P-EM14] Recent Advances in Ionosphere Observation and Modeling for Monitoring and Forecast

convener:Yang-Yi Sun(China University of Geosciences), CHIYEN LIN(Center for Astronautical Physics and Engineering, National Central University, TAIWAN), MINYANG CHOU(National Cheng Kung University)

Over the past few decades, rapid developments in space technology have advanced the research of ionospheric space weather by increasing a great number of ground- and space-based observations. In the ground segment, the dense ground-based GNSS networks, radars, and airglow instruments have greatly extended the observational coverages. In the space segment, the extraordinary satellite missions with payloads onboard the satellites providing radio occultation soundings of vertical electron density structure and in-situ observations of airglow, temperature, neutral winds, and electron density contribute to the understanding of middle and upper atmospheric dynamics. With the large amount and diversity of datasets, theoretical and empirical models can be validated and implemented for inclusion of new thermosphere and ionosphere phenomena. Furthermore, remarkable breakthrough of data assimilation techniques advances the ionosphere monitoring and forecast. The recent innovations in observations and models reinterpret the studies of ionospheric space weather. The purpose of this session is to solicit studies providing observations, theoretical and empirical modeling and data assimilation on the multiple scales of ionospheric phenomena, from global morphology to small-scale irregularities and traveling ionospheric disturbances. Studies on magnetically quiescent and disturbed conditions will be both addressed.

[PEM14-P01] The Daytime and Nighttime Mapped Whistler Plasmapause Observed by DEMETER

*ChaoYen Chen[1,2], Tiger J. Y. Liu[1,2,3] (1.Institute of Space Science, National Central University, Taiwan, 2.Center for Astronautical Physics and Engineering, National Central University, Taiwan , 3.Center for Space and Remote Sensing Research, National Central University, Taiwan)

[PEM14-P02] Global Plasma Density Irregularity Distributions Observed by Advanced Ionospheric Probe Onboard FORMOSAT-5 Satellite

*Chi-Kuang Chao[1], Yi-Wun Chen[1] (1.Graduate Institute of Space Science, National Central University)

[PEM14-P03] The First Result on Ionospheric Space Weather of FORMOSAT-5/AIP Ion Density

*FU-YUAN CHANG[1], JANN-YENQ Liu[1], Chi-Kuang Chao[1] (1.National Central University)

[PEM14-P04] The global total electron content reconstruction in the local time frame

*Tsung-Che Tsai[1,2], Hau-Kun Jhuang[3], Lou-Chuang Lee[3,4,5], Yi-Ying Ho[4] (1.National Center for High-Performance Computing, National Applied Research Laboratories, Hsinchu, Taiwan, 2.Department of Civil Engineering, National Chiao Tung University, Hsinchu, Taiwan., 3.Department of Geoscience, National Taiwan University, Taipei, Taiwan., 4.Institute of Earth Science, Academia Sinica, Nankang, Taipei, Taiwan., 5.Institute of Space Science, National Central University, Jhongli, Taiwan.)

[PEM14-P05] Research on impacts of power line harmonic radiation on ionospheric parameters

*Qiang Guo[1], Jing Wu[1], Ling Yang[1] (1.Beihang University)

[PEM14-P06] Analysis of cosmic rays dynamics and ionospheric parameters during increased solar activity and magnetic storms

*Oksana Mandrikova[1], Yurii Polozov[1], Bogdana Mandrikova[1,2] (1.Institute of Cosmophysical Research and Radio Wave Propagation, Far Eastern Branch of the Russian Academy of Sciences, 2.Saint Petersburg

Electrotechnical University "LETI")

[PEM14-P07] King Tidal Effects on the ionosphere during the period of 2000 to 2017

*TsungYu Wu[1], JANN-YENQ Liu[1] (1.Institute of Space Science, NCU, Taiwan)

[PEM14-P08] SuperDARN near range echoes and higher resolution measurement - recent improvement and future

*Akira Sessai Yukimatu[1,2] (1.National Institute of Polar Research, 2.SOKENDAI)

[PEM14-P09] **The ionospheric wave peak structures in the low latitude region and their seasonal, and solar activity dependence based on Global Ionosphere Maps**

*Hau-Kun Jhuang[1], Tsung-Che Tsai[2,3], Lou-Chuang Lee[1,4,5], Yi-Ying Ho[4] (1.Department of Geosciences, National Taiwan University, Taipei, Taiwan, 2.National Center for High-performance Computing, National Applied Research Laboratories, Hsinchu, Taiwan, 3.Department of Civil Engineering, National Chiao Tung University, Hsinchu, Taiwan, 4.Institute of Earth Science, Academia Sinica, Nankang, Taipei, Taiwan, 5.Institute of Space Science, National Central University, Jhongli, Taiwan)

The Daytime and Nighttime Mapped Whistler Plasmapause Observed by DEMETER

*ChaoYen Chen[1,2], Tiger J. Y. Liu[1,2,3]

1. Institute of Space Science, National Central University, Taiwan, 2. Center for Astronautical Physics and Engineering, National Central University, Taiwan , 3. Center for Space and Remote Sensing Research, National Central University, Taiwan

This paper investigates the plasmapause positions in the ionosphere by measurement of the whistler count probed by DEMETER (Detection of Electro-Magnetic Emissions Transmitted from Earthquake Regions) satellite in the daytime at 1030 LT (local time) and the nighttime at 2230 LT during 2005-2010. The whistler finds the plasmapause position which can be clearly allocated in both daytime and nighttime. We examine the nighttime/daytime plasmapause in various longitudes, solar activities, seasons, and geomagnetic actives. Results show that the daytime plasmapause appears in the equatorward side of the nighttime one. Both the daytime and nighttime plasmapause are sensitive to solar activity, which move equatorward form the low to high solar activity in the study period. The seasonal variation of the plasmapause are rather random and insignificant. During magnetic disturbed condition, the plasmapause tend to move equatorward.

Keywords: Plasmapause position, Whistler, DEMETER satellite

©2019. Japan Geoscience Union. All Right Reserved.

Global Plasma Density Irregularity Distributions Observed by Advanced Ionospheric Probe Onboard FORMOSAT-5 Satellite

*Chi-Kuang Chao[1], Yi-Wun Chen[1]

1. Graduate Institute of Space Science, National Central University

A FORMOSAT-5 satellite has been launched on25 August 2017 CST into a 98.28° inclination sun-synchronous circular orbit at 720 km altitude along the 1030/2230 local time sectors. The orbital coverage provides a great opportunity to survey terrestrial ionosphere from equatorial to polar region every two days. Advanced Ionospheric Probe (AIP) is a piggyback science payload developed by National Central University for the FORMOSAT-5 satellite to measure ionospheric plasma concentrations, velocities, and temperatures. It is also capable of measuring ionospheric plasma density irregularities at a sample rate up to 8,192 Hz over a wide range of spatial scales. In this presentation/poster, distributions and structures of pre-midnight low-latitude ionospheric plasma density irregularities will be shown from AIP science data collected since winter 2017. Especially, seasonal variations of the distributions will be compared with ROCSAT-1/Ionospheric Plasma and Electrodynamics Instrument dataset (1999-2004) to understand their trends. Meanwhile, high resolution data measured at a BURST rate (8,192 Hz) in some longitudinal sectors with high plasma density irregularity occurrence rates will also be investigated by spectral analysis to understand their characteristics.

Keywords: AIP, FORMOSAT-5, Irregularities

©2019. Japan Geoscience Union. All Right Reserved.

The First Result on Ionospheric Space Weather of FORMOSAT-5/AIP Ion Density

*FU-YUAN CHANG[1], JANN-YENQ Liu[1], Chi-Kuang Chao[1]

1. National Central University

The science payload of Advantage Ionosphere Probe (AIP) onboard FORMOSAT-5 (F5) launched on 24 August 2017 has being operated in a Sun synchronous orbit at 720km altitude with an inclination angle of 98.28 degrees and the revisit period every 2-day. The global distribution of F5/AIP ion density (Ni) in nighttime of 2200LT during November 2017-October 2018 is examined and reported. F5/AIP ion densities show that equatorial plasma depletions frequently appear over South America, Africa, and Asia sectors; four-peaked EIA (non-migrating tide) structures prominently occur in September-March; and plasma depletion bays (PDBs) at low-latitudes in April-August. It is found that prominent locations of the plasma depletions slightly differ from those of equatorial irregularities, while non-migrating tide and PDBs result from different physical mechanisms.

Keywords: topside ionosphere, equatorial plasma depletion bay, plasma drift

©2019. Japan Geoscience Union. All Right Reserved.

The global total electron content reconstruction in the local time frame

*Tsung-Che Tsai[1,2], Hau-Kun Jhuang[3], Lou-Chuang Lee[3,4,5], Yi-Ying Ho[4]

1. National Center for High-Performance Computing, National Applied Research Laboratories, Hsinchu, Taiwan, 2. Department of Civil Engineering, National Chiao Tung University, Hsinchu, Taiwan., 3. Department of Geoscience, National Taiwan University, Taipei, Taiwan., 4. Institute of Earth Science, Academia Sinica, Nankang, Taipei, Taiwan., 5. Institute of Space Science, National Central University, Jhongli, Taiwan.

The total electron content (TEC) data from Global Ionosphere Maps provide a global TEC map in the region between latitude 87.5˚S to 87.5˚N, and longitude 180˚W to 180˚E. The TEC data in geographic coordinates are first transformed into geomagnetic coordinates through Altitude-Adjusted Corrected Geomagnetic Model (AACGM). We then use 2-dimensional (longitude, 180˚W~180˚E and time, 10 days) Fourier transform (FT) of TEC variations along different geomagnetic latitude to obtain all wave modes for the period from November 18, to October 15, 2014. By the summation of all non-migrating tides, migrating tides, and zonal mean, the TEC global map in the local time frame is reconstructed. Again, the AACGM is applied to transform from geomagnetic coordinates back to geographic coordinates. The local time evolution in geographic coordinates of TEC is then produced. The features of TEC peaks in the local time frame are presented.

Keywords: geomagnetic coordinates, Global Ionospheric Maps, Fourier transform, Ionospheric tides

©2019. Japan Geoscience Union. All Right Reserved.

Research on impacts of power line harmonic radiation on ionospheric parameters

*Qiang Guo[1], Jing Wu[1], Ling Yang[1]

1. Beihang University

Introduction: Power line harmonic radiation (PLHR) refers to a kind of electromagnetic wave phenomena at harmonic frequencies of 50 or 60 Hz, which are the working frequencies of terrestrial power systems. Since the 1970s, PLHR events have been detected with several magnetically conjugate pairs of receivers and different satellites [1, 2, 3]. With the increase of global power consumption, PLHR has become more serious. Already, many scientific satellites have observed such anthropogenic electromagnetic waves in the ionosphere, and some possible typical impacts of those waves on the ionosphere have been reported [4]. However, reaching a final conclusion as to the impacts has been proven to be a difficult task. To further understand PLHR and its impacts, we utilize the data of three scientific payloads of DEMETER satellite collected with the Langmuir probe (ISL), thermal plasma analyzer (IAP), and energetic particle detector (IDP) to study the variation of ionospheric parameters due to the occurrence of PLHR.

Analytical Methods: DEMETER is a French seismo-electromagnetic microsatellite that was in operation from June 29, 2004 to December 9, 2010. The ISL onboard measured the electron density (N_e), electron temperature (T_e), and ion density (N_i). The IAP measured the density of H^+ (N_{H+}), He^+ (N_{He+}), O^+ (N_{O+}), and ion temperature (T_i). The IDP measured the electron fluxes in the range from 70 keV to 2.5 MeV. The variations of ionospheric parameters are affected by many factors, including latitude, longitude, altitude, daytime or nighttime, season, and solar activity. To minimize these impacts, we proposed an approach that compares the data from the PLHR-orbit and quiet-period orbit ($AE \leqq 50$ nT, AE is an index to evaluate the level of geomagnetic activity).

Among the 133 PLHR events detected by Wu et al. [5] when DEMETER flew over China, one quiet-period orbit, covering most of China's latitudes, was found for each year (2004-2010) according to AE index. In each PLHR-orbit, three-segment dataset were obtained: 30s before, at, and 30s after the occurrence region of PLHR event. By subtracting data of quiet-period orbit with corresponding latitudes from each-segment data of PLHR-orbit, we statistically analyzed the variation trend of ionospheric parameter in each PLHR-orbit due to PLHR.

Results & Discussion: With ISL and IAP data, it was found that both N_e and T_e were at a low level, N_{H+} was at a high level, and N_{O+} was at a low level when PLHR occurred. These results were generally helpful for understanding the formation behaviors of PLHR and were consistent with the theoretical results. From the analysis of IDP data, obvious variations of pitch angles before and after PLHR were occasionally observed to occur, and the variation did not exceed 10°. Its corresponding equatorial pitch-angle may not have fallen into a loss-cone, so the variation tendency of the electron flux did not have a definite connection with the pitch angle. The statistical results indicate that when PLHR occurs, the electron flux in the high-band (>1 MeV) tends to decrease and the decremental magnitude is very large, while the electron flux in the middle-band tends to increase and the incremental magnitude is relatively large.

Reference: [1] R. A. Helliwell, et al. (1975) *J. Geophys. Res-Space Phys.*, 80, 4249-4258. [2] J. P. Matthews, et al. (1981) *Planet. Space Sci.*, 29, 97-106. [3] M. Parrot, et al. (2014) *J. Geophys. Res-Space Phys.*, 119, 5744-5754. [4] M. Parrot, et al. (1996) *Surv. Geophys.*, 17, 67-100. [5] J. Wu, et al. (2017) *J. Geophys.*

©2019. Japan Geoscience Union. All Right Reserved.

Res-Space Phys., 122, 3448-3458.

Keywords: power line harmonic radiation, ionospheric parameters, DEMETER

©2019. Japan Geoscience Union. All Right Reserved.

Analysis of cosmic rays dynamics and ionospheric parameters during increased solar activity and magnetic storms

*Oksana Mandrikova[1], Yurii Polozov[1], Bogdana Mandrikova[1,2]

1. Institute of Cosmophysical Research and Radio Wave Propagation, Far Eastern Branch of the Russian Academy of Sciences, 2. Saint Petersburg Electrotechnical University "LETI"

Based on the ground station data, the paper makes complex analysis of cosmic ray dynamics and of ionospheric parameters during strong and moderate magnetic storms in 2015-2018. During the investigation, new methods of modeling and data analysis were applied. A neural network model for neutron monitor data classification was presented. This model makes it possible to evaluate galactic cosmic ray flux state and to detect periods of sporadic effect occurrences in automatic mode. By the use of this model, sporadic effects preceding and accompanying strong and moderate magnetic storms were detected. The model showed its efficiency when applied for data on-line analysis and for detection of sporadic effects including those of small amplitude. Ionospheric data were analyzed on the bases of multi-component modeling method and ionospheric parameter analysis [1, 2]. It allowed us to detect ionospheric disturbances of different intensity and to estimate their characteristics. The results of the work confirmed the possibility of ionospheric electron concentration increase effect preceding magnetic storm commencements [3]. Comparison with cosmic ray data showed the correlation of the effects in the ionospehre with anomalous changes in cosmic ray dynamics that was first mentioned in the paper [3].

1. Mandrikova O.V., Fetisova N.V., Polozov Y.A., Solovev I.S., Kupriyanov M.S. Method for modeling of the components of ionospheric parameter time variations and detection of anomalies in the ionosphere coupling of the high and mid latitude ionosphere and its relation to geospace dynamics // Earth, Planets and Space. 2015. Vol. 67. No 1. pp. 131-146. DOI: 10.1186/s40623-015-0301-4
2. O. Mandrikova, Yu. Polozov, V. Geppener Method of ionospheric data analysis based on a combination of wavelet transform and neural networks // «Procedia Engineering», Elsevier, Amsterdam, Netherlands, V.201, Pp. 756–766, DOI. https://doi.org/10.1016/j.proeng.2017.09.622.
3. Mandrikova O., Polozov Yu., Fetisova N., Zalyaev T. Analysis of the dynamics of ionospheric parameters during periods of increased solar activity and magnetic storms // Journal of Atmospheric and Solar-Terrestrial Physics. –2018. –Vol. 181. –Pp. 116-126. Doi: https://doi.org/10.1016/j.jastp.2018.10.019.

Keywords: cosmic rays, ionospheric parameters, data analysis

©2019. Japan Geoscience Union. All Right Reserved.

King Tidal Effects on the ionosphere during the period of 2000 to 2017

*TsungYu Wu[1], JANN-YENQ Liu[1]

1. Institute of Space Science, NCU, Taiwan

This study examines the spring tide signature of the 14.7-day period in concurrent/co-located measurements of the ionosphere total electron content (TEC) and sea level in an 18-year period of 2000-2017. A discrete Fourier transform is applied to find amplitude and phase of the spring tide in the TEC and sea level. Results show that the spring tide amplitude in the sea level is clear and steady, while that in the ionospheric TEC is rather fluctuated and proportional to the ambient TEC value. The relative amplitude of TEC in the 18-year is a function of the solar local time and become prominent in the daytime of 08:00-19:00. and however that in the nighttime 00:00-06:00 LT becomes prominent in 2002, 2005, 2009, and 2015, when the perihelion and perigee simultaneously occur. On the other hand, the phase of the spring tide signature in the sea level and TEC yield a 3-year period, which is close to the time interval of the above prominent spring tide signature in the nighttime. More detailed discussions and results will be presented.

©2019. Japan Geoscience Union. All Right Reserved.

SuperDARN near range echoes and higher resolution measurement - recent improvement and future

*Akira Sessai Yukimatu[1,2]

1. National Institute of Polar Research, 2. SOKENDAI

SuperDARN (Super Dual Auroral Radar Network) is an international high-frequency radar network originally intended to cover a wide range of polar ionosphere in both hemispheres by its fields-of-view and to monitor global ionospheric plasma convection in high temporal resolution of about 1-2 minitues in quasi real time mainly for space weather research. It can observe not only basic and important ionospheric plasma Doppler velocity and electric field, a variety of geomagnetic waves, ionospheric disturbances and irregularities, but also properties of neutral atmosphere, e.g., traveling ionospheric disturbances (TIDs), mesoepheric echoes like PMSEs and neutral wind around mesopause region. As it is originally designed to measure global large-scale ionospheric plasma parameters, the spatial resolution has been rather coarse, and it was originally difficult to obtain height information of echoes, high temporal resolution less than 1 second, and high spatial resolution of less than 15km in radial direction. Echo height information is very important especially to distinguish those among D, E and F regions as the properties of plasma among them are considerably different and also to obtain precise altitude of meteor echoes around mesopause due to existence of thin layers of neutral wind shear. Recent development in calibrating radar interferometry in SuperDARN community is an important step to improve much the reliability of height information especially in near range echoes and also of region identification for further echoes as well. Combining raw I/Q time series analysis method (Yukimatu and Tsutsumi, GRL, 2002) to be applied to extract underdense meteor echoes precisely, frequency domain interferometry (FDI) and/or over-sampling technique (Tsutsumi et al., 2009) with the appropriate interferometer calibration will improve the reliability and height resolution of the neutral wind measurement possibly leading to global neutral wind observing network around mesopause region with SuperDARN which will contribute to many studies on mesosphere-lower-thermosphere (MLT) or mesoephere-thermosphere-ionosphere (MTI) region dynamics and vertical coupling between ionosphere and neutral upper atmosphere. Another issue possibly critical for some specific studies, e.g., on short period electro-magnetic waves is possibility to achieve higher temporal resolution within a second as well as higher spatial resolution in range direction. (Higher spatial resolution in azimuth direction has been already tried and achieved by some radars using general imaging or spatial domain interferometry (SDI) technique.) There have been some trial against these possibilities with some success depending on the cases of the applied phenomena and the conditions of echoes, but have still been thought to be difficult to be overcome. This presentation will describe the evolution of SuperDARN near range echo measurement after last JpGU meeting, and will also discuss about the reliability of high temporal resolution measurement and the possible method to obtain reliable high temporal resolution data to extend the ability of SuperDARN.

Keywords: SuperDARN, near range echoes, electromagnetic waves, high temporal resolution

©2019. Japan Geoscience Union. All Right Reserved.

The ionospheric wave peak structures in the low latitude region and their seasonal, and solar activity dependence based on Global Ionosphere Maps

*Hau-Kun Jhuang[1], Tsung-Che Tsai[2,3], Lou-Chuang Lee[1,4,5], Yi-Ying Ho[4]

1. Department of Geosciences, National Taiwan University, Taipei, Taiwan, 2. National Center for High-performance Computing, National Applied Research Laboratories, Hsinchu, Taiwan, 3. Department of Civil Engineering, National Chiao Tung University, Hsinchu, Taiwan, 4. Institute of Earth Science, Academia Sinica, Nankang, Taipei, Taiwan, 5. Institute of Space Science, National Central University, Jhongli, Taiwan

The total electron content (TEC) data from Global Ionosphere Maps (GIM) are used to obtain the wave modes in both UT (universal time) and LT (local time) frames through the Fourier transform. The summation of contributing wave modes at a given local time provides the longitudinal variation of the wave peak structure. The phases of wave modes lead to a constructive or destructive interference of contributing wave modes, which gives different wave peak structure at different local time. The dependence of the wave peak structures on latitudinal, seasonal, and solar activity is studied.

Keywords: Global Ionosphere Maps, Ionospheric tides, Atmosphere Ionosphere coupling

©2019. Japan Geoscience Union. All Right Reserved.

[E] Poster | P (Space and Planetary Sciences)：P-EM Solar-Terrestrial Sciences, Space Electromagnetism & Space Environment

Sun. May 26, 2019 5:15 PM - 6:30 PM JST | Sun. May 26, 2019 8:15 AM - 9:30 AM UTC | Poster Hall International Exhibition Hall8, Makuhari Messe_5

[P-EM14] Recent Advances in Ionosphere Observation and Modeling for Monitoring and Forecast

convener:Yang-Yi Sun(China University of Geosciences), CHIYEN LIN(Center for Astronautical Physics and Engineering, National Central University, TAIWAN), MINYANG CHOU(National Cheng Kung University)

Over the past few decades, rapid developments in space technology have advanced the research of ionospheric space weather by increasing a great number of ground- and space-based observations. In the ground segment, the dense ground-based GNSS networks, radars, and airglow instruments have greatly extended the observational coverages. In the space segment, the extraordinary satellite missions with payloads onboard the satellites providing radio occultation soundings of vertical electron density structure and in-situ observations of airglow, temperature, neutral winds, and electron density contribute to the understanding of middle and upper atmospheric dynamics. With the large amount and diversity of datasets, theoretical and empirical models can be validated and implemented for inclusion of new thermosphere and ionosphere phenomena. Furthermore, remarkable breakthrough of data assimilation techniques advances the ionosphere monitoring and forecast. The recent innovations in observations and models reinterpret the studies of ionospheric space weather. The purpose of this session is to solicit studies providing observations, theoretical and empirical modeling and data assimilation on the multiple scales of ionospheric phenomena, from global morphology to small-scale irregularities and traveling ionospheric disturbances. Studies on magnetically quiescent and disturbed conditions will be both addressed.

[PEM14-P01] The Daytime and Nighttime Mapped Whistler Plasmapause Observed by DEMETER

*ChaoYen Chen[1,2], Tiger J. Y. Liu[1,2,3] (1.Institute of Space Science, National Central University, Taiwan, 2.Center for Astronautical Physics and Engineering, National Central University, Taiwan , 3.Center for Space and Remote Sensing Research, National Central University, Taiwan)

[PEM14-P02] Global Plasma Density Irregularity Distributions Observed by Advanced Ionospheric Probe Onboard FORMOSAT-5 Satellite

*Chi-Kuang Chao[1], Yi-Wun Chen[1] (1.Graduate Institute of Space Science, National Central University)

[PEM14-P03] The First Result on Ionospheric Space Weather of FORMOSAT-5/AIP Ion Density

*FU-YUAN CHANG[1], JANN-YENQ Liu[1], Chi-Kuang Chao[1] (1.National Central University)

[PEM14-P04] The global total electron content reconstruction in the local time frame

*Tsung-Che Tsai[1,2], Hau-Kun Jhuang[3], Lou-Chuang Lee[3,4,5], Yi-Ying Ho[4] (1.National Center for High-Performance Computing, National Applied Research Laboratories, Hsinchu, Taiwan, 2.Department of Civil Engineering, National Chiao Tung University, Hsinchu, Taiwan., 3.Department of Geoscience, National Taiwan University, Taipei, Taiwan., 4.Institute of Earth Science, Academia Sinica, Nankang, Taipei, Taiwan., 5.Institute of Space Science, National Central University, Jhongli, Taiwan.)

[PEM14-P05] Research on impacts of power line harmonic radiation on ionospheric parameters

*Qiang Guo[1], Jing Wu[1], Ling Yang[1] (1.Beihang University)

[PEM14-P06] Analysis of cosmic rays dynamics and ionospheric parameters during increased solar activity and magnetic storms

*Oksana Mandrikova[1], Yurii Polozov[1], Bogdana Mandrikova[1,2] (1.Institute of Cosmophysical Research and Radio Wave Propagation, Far Eastern Branch of the Russian Academy of Sciences, 2.Saint Petersburg

Electrotechnical University "LETI")

[PEM14-P07] King Tidal Effects on the ionosphere during the period of 2000 to 2017

*TsungYu Wu[1], JANN-YENQ Liu[1] (1.Institute of Space Science, NCU, Taiwan)

[PEM14-P08] SuperDARN near range echoes and higher resolution measurement - recent improvement and future

*Akira Sessai Yukimatu[1,2] (1.National Institute of Polar Research, 2.SOKENDAI)

[PEM14-P09] **The ionospheric wave peak structures in the low latitude region and their seasonal, and solar activity dependence based on Global Ionosphere Maps**

*Hau-Kun Jhuang[1], Tsung-Che Tsai[2,3], Lou-Chuang Lee[1,4,5], Yi-Ying Ho[4] (1.Department of Geosciences, National Taiwan University, Taipei, Taiwan, 2.National Center for High-performance Computing, National Applied Research Laboratories, Hsinchu, Taiwan, 3.Department of Civil Engineering, National Chiao Tung University, Hsinchu, Taiwan, 4.Institute of Earth Science, Academia Sinica, Nankang, Taipei, Taiwan, 5.Institute of Space Science, National Central University, Jhongli, Taiwan)

The Daytime and Nighttime Mapped Whistler Plasmapause Observed by DEMETER

*ChaoYen Chen[1,2], Tiger J. Y. Liu[1,2,3]

1. Institute of Space Science, National Central University, Taiwan, 2. Center for Astronautical Physics and Engineering, National Central University, Taiwan , 3. Center for Space and Remote Sensing Research, National Central University, Taiwan

This paper investigates the plasmapause positions in the ionosphere by measurement of the whistler count probed by DEMETER (Detection of Electro-Magnetic Emissions Transmitted from Earthquake Regions) satellite in the daytime at 1030 LT (local time) and the nighttime at 2230 LT during 2005-2010. The whistler finds the plasmapause position which can be clearly allocated in both daytime and nighttime. We examine the nighttime/daytime plasmapause in various longitudes, solar activities, seasons, and geomagnetic actives. Results show that the daytime plasmapause appears in the equatorward side of the nighttime one. Both the daytime and nighttime plasmapause are sensitive to solar activity, which move equatorward form the low to high solar activity in the study period. The seasonal variation of the plasmapause are rather random and insignificant. During magnetic disturbed condition, the plasmapause tend to move equatorward.

Keywords: Plasmapause position, Whistler, DEMETER satellite

©2019. Japan Geoscience Union. All Right Reserved.

Global Plasma Density Irregularity Distributions Observed by Advanced Ionospheric Probe Onboard FORMOSAT-5 Satellite

*Chi-Kuang Chao[1], Yi-Wun Chen[1]

1. Graduate Institute of Space Science, National Central University

A FORMOSAT-5 satellite has been launched on25 August 2017 CST into a 98.28° inclination sun-synchronous circular orbit at 720 km altitude along the 1030/2230 local time sectors. The orbital coverage provides a great opportunity to survey terrestrial ionosphere from equatorial to polar region every two days. Advanced Ionospheric Probe (AIP) is a piggyback science payload developed by National Central University for the FORMOSAT-5 satellite to measure ionospheric plasma concentrations, velocities, and temperatures. It is also capable of measuring ionospheric plasma density irregularities at a sample rate up to 8,192 Hz over a wide range of spatial scales. In this presentation/poster, distributions and structures of pre-midnight low-latitude ionospheric plasma density irregularities will be shown from AIP science data collected since winter 2017. Especially, seasonal variations of the distributions will be compared with ROCSAT-1/Ionospheric Plasma and Electrodynamics Instrument dataset (1999-2004) to understand their trends. Meanwhile, high resolution data measured at a BURST rate (8,192 Hz) in some longitudinal sectors with high plasma density irregularity occurrence rates will also be investigated by spectral analysis to understand their characteristics.

Keywords: AIP, FORMOSAT-5, Irregularities

©2019. Japan Geoscience Union. All Right Reserved.

The First Result on Ionospheric Space Weather of FORMOSAT-5/AIP Ion Density

*FU-YUAN CHANG[1], JANN-YENQ Liu[1], Chi-Kuang Chao[1]

1. National Central University

The science payload of Advantage Ionosphere Probe (AIP) onboard FORMOSAT-5 (F5) launched on 24 August 2017 has being operated in a Sun synchronous orbit at 720km altitude with an inclination angle of 98.28 degrees and the revisit period every 2-day. The global distribution of F5/AIP ion density (Ni) in nighttime of 2200LT during November 2017-October 2018 is examined and reported. F5/AIP ion densities show that equatorial plasma depletions frequently appear over South America, Africa, and Asia sectors; four-peaked EIA (non-migrating tide) structures prominently occur in September-March; and plasma depletion bays (PDBs) at low-latitudes in April-August. It is found that prominent locations of the plasma depletions slightly differ from those of equatorial irregularities, while non-migrating tide and PDBs result from different physical mechanisms.

Keywords: topside ionosphere, equatorial plasma depletion bay, plasma drift

©2019. Japan Geoscience Union. All Right Reserved.

The global total electron content reconstruction in the local time frame

*Tsung-Che Tsai[1,2], Hau-Kun Jhuang[3], Lou-Chuang Lee[3,4,5], Yi-Ying Ho[4]

1. National Center for High-Performance Computing, National Applied Research Laboratories, Hsinchu, Taiwan, 2. Department of Civil Engineering, National Chiao Tung University, Hsinchu, Taiwan., 3. Department of Geoscience, National Taiwan University, Taipei, Taiwan., 4. Institute of Earth Science, Academia Sinica, Nankang, Taipei, Taiwan., 5. Institute of Space Science, National Central University, Jhongli, Taiwan.

The total electron content (TEC) data from Global Ionosphere Maps provide a global TEC map in the region between latitude 87.5˚S to 87.5˚N, and longitude 180˚W to 180˚E. The TEC data in geographic coordinates are first transformed into geomagnetic coordinates through Altitude-Adjusted Corrected Geomagnetic Model (AACGM). We then use 2-dimensional (longitude, 180˚W~180˚E and time, 10 days) Fourier transform (FT) of TEC variations along different geomagnetic latitude to obtain all wave modes for the period from November 18, to October 15, 2014. By the summation of all non-migrating tides, migrating tides, and zonal mean, the TEC global map in the local time frame is reconstructed. Again, the AACGM is applied to transform from geomagnetic coordinates back to geographic coordinates. The local time evolution in geographic coordinates of TEC is then produced. The features of TEC peaks in the local time frame are presented.

Keywords: geomagnetic coordinates, Global Ionospheric Maps, Fourier transform, Ionospheric tides

©2019. Japan Geoscience Union. All Right Reserved.

Research on impacts of power line harmonic radiation on ionospheric parameters

*Qiang Guo[1], Jing Wu[1], Ling Yang[1]

1. Beihang University

Introduction: Power line harmonic radiation (PLHR) refers to a kind of electromagnetic wave phenomena at harmonic frequencies of 50 or 60 Hz, which are the working frequencies of terrestrial power systems. Since the 1970s, PLHR events have been detected with several magnetically conjugate pairs of receivers and different satellites [1, 2, 3]. With the increase of global power consumption, PLHR has become more serious. Already, many scientific satellites have observed such anthropogenic electromagnetic waves in the ionosphere, and some possible typical impacts of those waves on the ionosphere have been reported [4]. However, reaching a final conclusion as to the impacts has been proven to be a difficult task. To further understand PLHR and its impacts, we utilize the data of three scientific payloads of DEMETER satellite collected with the Langmuir probe (ISL), thermal plasma analyzer (IAP), and energetic particle detector (IDP) to study the variation of ionospheric parameters due to the occurrence of PLHR.

Analytical Methods: DEMETER is a French seismo-electromagnetic microsatellite that was in operation from June 29, 2004 to December 9, 2010. The ISL onboard measured the electron density (N_e), electron temperature (T_e), and ion density (N_i). The IAP measured the density of H^+ (N_{H+}), He^+ (N_{He+}), O^+ (N_{O+}), and ion temperature (T_i). The IDP measured the electron fluxes in the range from 70 keV to 2.5 MeV. The variations of ionospheric parameters are affected by many factors, including latitude, longitude, altitude, daytime or nighttime, season, and solar activity. To minimize these impacts, we proposed an approach that compares the data from the PLHR-orbit and quiet-period orbit ($AE \leqq 50$ nT, AE is an index to evaluate the level of geomagnetic activity).

Among the 133 PLHR events detected by Wu et al. [5] when DEMETER flew over China, one quiet-period orbit, covering most of China's latitudes, was found for each year (2004-2010) according to AE index. In each PLHR-orbit, three-segment dataset were obtained: 30s before, at, and 30s after the occurrence region of PLHR event. By subtracting data of quiet-period orbit with corresponding latitudes from each-segment data of PLHR-orbit, we statistically analyzed the variation trend of ionospheric parameter in each PLHR-orbit due to PLHR.

Results & Discussion: With ISL and IAP data, it was found that both N_e and T_e were at a low level, N_{H+} was at a high level, and N_{O+} was at a low level when PLHR occurred. These results were generally helpful for understanding the formation behaviors of PLHR and were consistent with the theoretical results. From the analysis of IDP data, obvious variations of pitch angles before and after PLHR were occasionally observed to occur, and the variation did not exceed 10°. Its corresponding equatorial pitch-angle may not have fallen into a loss-cone, so the variation tendency of the electron flux did not have a definite connection with the pitch angle. The statistical results indicate that when PLHR occurs, the electron flux in the high-band (>1 MeV) tends to decrease and the decremental magnitude is very large, while the electron flux in the middle-band tends to increase and the incremental magnitude is relatively large.

Reference: [1] R. A. Helliwell, et al. (1975) *J. Geophys. Res-Space Phys.*, 80, 4249-4258. [2] J. P. Matthews, et al. (1981) *Planet. Space Sci.*, 29, 97-106. [3] M. Parrot, et al. (2014) *J. Geophys. Res-Space Phys.*, 119, 5744-5754. [4] M. Parrot, et al. (1996) *Surv. Geophys.*, 17, 67-100. [5] J. Wu, et al. (2017) *J. Geophys.*

©2019. Japan Geoscience Union. All Right Reserved.

Res-Space Phys., 122, 3448-3458.

Keywords: power line harmonic radiation, ionospheric parameters, DEMETER

©2019. Japan Geoscience Union. All Right Reserved.

Analysis of cosmic rays dynamics and ionospheric parameters during increased solar activity and magnetic storms

*Oksana Mandrikova[1], Yurii Polozov[1], Bogdana Mandrikova[1,2]

1. Institute of Cosmophysical Research and Radio Wave Propagation, Far Eastern Branch of the Russian Academy of Sciences, 2. Saint Petersburg Electrotechnical University "LETI"

Based on the ground station data, the paper makes complex analysis of cosmic ray dynamics and of ionospheric parameters during strong and moderate magnetic storms in 2015-2018. During the investigation, new methods of modeling and data analysis were applied. A neural network model for neutron monitor data classification was presented. This model makes it possible to evaluate galactic cosmic ray flux state and to detect periods of sporadic effect occurrences in automatic mode. By the use of this model, sporadic effects preceding and accompanying strong and moderate magnetic storms were detected. The model showed its efficiency when applied for data on-line analysis and for detection of sporadic effects including those of small amplitude. Ionospheric data were analyzed on the bases of multi-component modeling method and ionospheric parameter analysis [1, 2]. It allowed us to detect ionospheric disturbances of different intensity and to estimate their characteristics. The results of the work confirmed the possibility of ionospheric electron concentration increase effect preceding magnetic storm commencements [3]. Comparison with cosmic ray data showed the correlation of the effects in the ionospehre with anomalous changes in cosmic ray dynamics that was first mentioned in the paper [3].

1. Mandrikova O.V., Fetisova N.V., Polozov Y.A., Solovev I.S., Kupriyanov M.S. Method for modeling of the components of ionospheric parameter time variations and detection of anomalies in the ionosphere coupling of the high and mid latitude ionosphere and its relation to geospace dynamics // Earth, Planets and Space. 2015. Vol. 67. No 1. pp. 131-146. DOI: 10.1186/s40623-015-0301-4
2. O. Mandrikova, Yu. Polozov, V. Geppener Method of ionospheric data analysis based on a combination of wavelet transform and neural networks // «Procedia Engineering», Elsevier, Amsterdam, Netherlands, V.201, Pp. 756–766, DOI. https://doi.org/10.1016/j.proeng.2017.09.622.
3. Mandrikova O., Polozov Yu., Fetisova N., Zalyaev T. Analysis of the dynamics of ionospheric parameters during periods of increased solar activity and magnetic storms // Journal of Atmospheric and Solar-Terrestrial Physics. –2018. –Vol. 181. –Pp. 116-126. Doi: https://doi.org/10.1016/j.jastp.2018.10.019.

Keywords: cosmic rays, ionospheric parameters, data analysis

©2019. Japan Geoscience Union. All Right Reserved.

King Tidal Effects on the ionosphere during the period of 2000 to 2017

*TsungYu Wu[1], JANN-YENQ Liu[1]

1. Institute of Space Science, NCU, Taiwan

This study examines the spring tide signature of the 14.7-day period in concurrent/co-located measurements of the ionosphere total electron content (TEC) and sea level in an 18-year period of 2000-2017. A discrete Fourier transform is applied to find amplitude and phase of the spring tide in the TEC and sea level. Results show that the spring tide amplitude in the sea level is clear and steady, while that in the ionospheric TEC is rather fluctuated and proportional to the ambient TEC value. The relative amplitude of TEC in the 18-year is a function of the solar local time and become prominent in the daytime of 08:00-19:00. and however that in the nighttime 00:00-06:00 LT becomes prominent in 2002, 2005, 2009, and 2015, when the perihelion and perigee simultaneously occur. On the other hand, the phase of the spring tide signature in the sea level and TEC yield a 3-year period, which is close to the time interval of the above prominent spring tide signature in the nighttime. More detailed discussions and results will be presented.

©2019. Japan Geoscience Union. All Right Reserved.

SuperDARN near range echoes and higher resolution measurement - recent improvement and future

*Akira Sessai Yukimatu[1,2]

1. National Institute of Polar Research, 2. SOKENDAI

SuperDARN (Super Dual Auroral Radar Network) is an international high-frequency radar network originally intended to cover a wide range of polar ionosphere in both hemispheres by its fields-of-view and to monitor global ionospheric plasma convection in high temporal resolution of about 1-2 minitues in quasi real time mainly for space weather research. It can observe not only basic and important ionospheric plasma Doppler velocity and electric field, a variety of geomagnetic waves, ionospheric disturbances and irregularities, but also properties of neutral atmosphere, e.g., traveling ionospheric disturbances (TIDs), mesoepheric echoes like PMSEs and neutral wind around mesopause region. As it is originally designed to measure global large-scale ionospheric plasma parameters, the spatial resolution has been rather coarse, and it was originally difficult to obtain height information of echoes, high temporal resolution less than 1 second, and high spatial resolution of less than 15km in radial direction. Echo height information is very important especially to distinguish those among D, E and F regions as the properties of plasma among them are considerably different and also to obtain precise altitude of meteor echoes around mesopause due to existence of thin layers of neutral wind shear. Recent development in calibrating radar interferometry in SuperDARN community is an important step to improve much the reliability of height information especially in near range echoes and also of region identification for further echoes as well. Combining raw I/Q time series analysis method (Yukimatu and Tsutsumi, GRL, 2002) to be applied to extract underdense meteor echoes precisely, frequency domain interferometry (FDI) and/or over-sampling technique (Tsutsumi et al., 2009) with the appropriate interferometer calibration will improve the reliability and height resolution of the neutral wind measurement possibly leading to global neutral wind observing network around mesopause region with SuperDARN which will contribute to many studies on mesosphere-lower-thermosphere (MLT) or mesoephere-thermosphere-ionosphere (MTI) region dynamics and vertical coupling between ionosphere and neutral upper atmosphere. Another issue possibly critical for some specific studies, e.g., on short period electro-magnetic waves is possibility to achieve higher temporal resolution within a second as well as higher spatial resolution in range direction. (Higher spatial resolution in azimuth direction has been already tried and achieved by some radars using general imaging or spatial domain interferometry (SDI) technique.) There have been some trial against these possibilities with some success depending on the cases of the applied phenomena and the conditions of echoes, but have still been thought to be difficult to be overcome. This presentation will describe the evolution of SuperDARN near range echo measurement after last JpGU meeting, and will also discuss about the reliability of high temporal resolution measurement and the possible method to obtain reliable high temporal resolution data to extend the ability of SuperDARN.

Keywords: SuperDARN, near range echoes, electromagnetic waves, high temporal resolution

©2019. Japan Geoscience Union. All Right Reserved.

The ionospheric wave peak structures in the low latitude region and their seasonal, and solar activity dependence based on Global Ionosphere Maps

*Hau-Kun Jhuang[1], Tsung-Che Tsai[2,3], Lou-Chuang Lee[1,4,5], Yi-Ying Ho[4]

1. Department of Geosciences, National Taiwan University, Taipei, Taiwan, 2. National Center for High-performance Computing, National Applied Research Laboratories, Hsinchu, Taiwan, 3. Department of Civil Engineering, National Chiao Tung University, Hsinchu, Taiwan, 4. Institute of Earth Science, Academia Sinica, Nankang, Taipei, Taiwan, 5. Institute of Space Science, National Central University, Jhongli, Taiwan

The total electron content (TEC) data from Global Ionosphere Maps (GIM) are used to obtain the wave modes in both UT (universal time) and LT (local time) frames through the Fourier transform. The summation of contributing wave modes at a given local time provides the longitudinal variation of the wave peak structure. The phases of wave modes lead to a constructive or destructive interference of contributing wave modes, which gives different wave peak structure at different local time. The dependence of the wave peak structures on latitudinal, seasonal, and solar activity is studied.

Keywords: Global Ionosphere Maps, Ionospheric tides, Atmosphere Ionosphere coupling

©2019. Japan Geoscience Union. All Right Reserved.

[E] Poster | P (Space and Planetary Sciences)：P-CG Complex & General

Sun. May 26, 2019 3:30 PM - 5:00 PM JST | Sun. May 26, 2019 6:30 AM - 8:00 AM UTC | Poster Hall International Exhibition Hall8, Makuhari Messe_5

[P-CG21] Future Missions and instrumentation for space and planetary science

convener:Mitsunori Ozaki(Faculty of Electrical and Computer Engineering, Institute of Science and Engineering, Kanazawa University), Satoshi Kasahara(The university of Tokyo), Shingo Kameda(School of Science, Rikkyo University), Kazuo Yoshioka(Graduate School of frontier Science, The University of Tokyo)

Not only national space agencies but some universities and even companies in the world are now leading a number of space science and exploration missions and also energetically initiating new research activities for satellite and rocket developments and international collaborations in these days because the Earth observations from the space and the space explorations could be achieved much easier than a few decades ago. The deployment to the space, which itself is not purely a scientific purpose but one of methods for better sciences, is vigorously motivating the technical innovation and the educational development. For successful space missions, it is also crucial to research and develop aim-oriented on-board instruments, and the fundamental research and development of observational instrumentation with future perspectives could totally lead space missions in some case. Detailed investigation and evaluation on various on-board instruments are needed during their proposals, selections, and fabrications in order to promote the missions, and inevitably we have to make multi-sided arrangements and evolution at every process and aspect of any type of space missions, independently of their mission sizes. In this session, we focus on these comprehensive research activities in the space and astronomical missions, including the mission integrations and the individual instrumental developments, and we also call many presentations showing the uniqueness and renovation regarding the mission strategy and methodology, and the status and latest results in the related state-of-the-art researches and developments, which would provide all of researchers and developers with invaluable opportunities for active discussion, information sharing, and collaboration toward the realization of more missions for more fruitful space sciences and explorations in nearer future.

[PCG21-P01] Visible and ultraviolet imagers for auroral and airglow observations by FACTORS - a future satellite mission for understanding the coupling and transportation processes in the upper atmosphere

*Takeshi Sakanoi[1], Masafumi Hirahara[2], Takuo T. Tsuda[3], Kazushi Asamura[4], Yoshizumi Miyoshi[2], Tomo-Hiko Watanabe[5], Takanori Nishiyama[6], Shin-ichiro Oyama[2,7], Yoshifumi Saito[4], Keisuke Hosokawa[3], Hirotsugu Kojima[8], Naritoshi Kitamura[9], Yasunobu Ogawa[5], Masatoshi Yamauchi[10], Ayako Matsuoka[4], Naoshi Yagi[1], Fukizawa Fukizawa[1], Genki Ishizawa[11] (1.Planetary Plasma and Atmospheric Research Center, Graduate School of Science, Tohoku University, 2.ISEE, Nagoya University, 3.Graduate School of Informatics and Engineering, School of Informatics and Engineering, The University of Electro-Communications, 4.ISAS/JAXA, 5.Graduate School of Science, Nagoya University, 6.National Institute for Polar Research, 7.University of Oulu, Finland, 8.RISH, Kyoto University, 9.Graduate School of Science, the University of Tokyo, Tokyo, 10.IRF Kiruna, Sweden, 11.Graduate School of Science, Tohoku University)

[PCG21-P02] Spatio-temporal analysis of flash aurora using Convolutional Neural Network

*Toki Genda[1], Takumi Inoue[1], Mitsunori Ozaki[1], Satoshi Yagitani[1], Imamura Kousuke[1], Kazuo Shiokawa[2], Yoshizumi Miyoshi[2], Shin-ichiro Oyama[2], Ryuho Kataoka[3], Yusuke Ebihara[4], Keisuke Hosokawa[5] (1.Kanazawa Univ., 2.Nagoya Univ., 3.NIPR, 4.Kyoto Univ., 5.UEC)

[PCG21-P03] Study on the pulse noise removal technique for Pc1 geomagnetic pulsations on the ground by signal processing

*Fumiya Komase[1], Tomohiro Inoue[1], Mitsunori Ozaki[1], Satoshi Yagitani[1], Kazuo Shiokawa[2], Masahito Nose[2], Tsutomu Nagatsuma[3] (1.Kanazawa Univ., 2.Nagoya Univ., 3.NICT)

[PCG21-P04] Application of magneto-impedance sensor to geomagnetic field measurements

*Masahito Nose[1], Reiko Nomura[2], Kazushi Asamura[3], Hitoshi Aoyama[4], Takeshi Kawano[4], Ayako Matsuoka[3], Kentarou Kitamura[5], Yukinobu Koyama[6], Haruhisa Matsumoto[7], Masafumi Hirahara[1] (1.Institute for Space-Earth Environmental Research, Nagoya University, 2.National Astronomical Observatory of Japan, 3.Institute of Space and Astronautical Science, Japan Aerospace Exploration Agency, 4.Aichi Steel Corporation, 5.National Institute of Technology, Tokuyama College, 6.National Institute of Technology, Oita College, 7.Research and Development Directorate, Japan Aerospace Exploration Agency)

[PCG21-P05] Observation of the Ionospheric Currents by the CubeSat at the Low and Middle Latitude

*Kentarou Kitamura[1], Kazumasa Imai[2], Taku Takada[2], Manabu Shinohara[3], Makoto Wakabayashi[4], KOSEN Space Collaboration Group (1.National Institute of Technology, Tokuyama Collge, 2.National Institute of Technology, Kochi Collge, 3.National Institute of Technology, Kagoshima Collge, 4.National Institute of Technology, Niihama Collge)

[PCG21-P06] Basic study on miniaturization of electric field instrument for plasma wave observations by ASIC technology

*Yuya Tokunaga[1], Mitsunori Ozaki[1], Keigo Ishisaka[2], Hirotsugu Kojima[3], Satoshi Yagitani[1], Takahiro Zushi[3] (1.Kanazawa University, 2.Toyama Prefectural University, 3.Kyoto University)

[PCG21-P07] Evaluation of radiation tolerance of electronics parts used for the ultra-small mission

*Riku Katsuse[1], Kazuo Yoshioka[1], Masaki Kuwabara[2], Reina Hikida[1], Shogo Arao[1], Ichiro Yoshikawa[1] (1.The university of Tokyo , 2.Institute of Space and Astronautical Science)

[PCG21-P08] A method to quantitatively evaluate Non-evaporable-getter pump for use in space science mission

*Seiya Nishimura[1], Ichiro Yoshikawa[1], Kazuo Yoshioka[1], Shogo Arao[1], Zhang Tianxu[1] (1.The university of tokyo)

[PCG21-P09] Interpretation on slight asymmetry of analyzer characteristics of MIA onboard the Mio by means of a model calculation of 3-D potential distribution

*Wataru Miyake[1], Yoshifumi Saito[2], Shoichiro Yokota[3] (1.Tokai University, 2.ISAS, 3.Osaka University)

[PCG21-P10] Construction of impact testing machine for small satellites and evaluation of mechanical resistance of MCPs by the impact test

*Junya Fukuba[1] (1.Graduate school of Tokyo)

[PCG21-P11] Innovative design of double-shell type energy analyzer for simultaneous electron and ion measurements in space

*Tomomi Takei[1], Masafumi Hirahara[1] (1.Institute for space-earth environmental research, Nagoya university)

[PCG21-P12] Microsatellite Development and Education of Space Science and Technology at Kanazawa University

*Tomohiko Imachi[1], Satoshi Yagitani[1], Daisuke Yonetoku[1], Yoshiya Kasahara[1], Tatsuya Sawano[1], Makoto Arimoto[1], Yoshitaka Goto[1], Mitsunori Ozaki[1], Ryuichi Fujimoto[1] (1.Kanazawa University)

[PCG21-P13] Attitude Control System for Kanazawa-SAT3 Microsatellite

Takuya Nakajima[1], Yuuki Yasuda[1], Hirofumi Segawa[1], *Tomohiko Imachi[1], Satoshi Yagitani[1], Yoshiya Kasahara[1], Daisuke Yonetoku[1], Tatsuya Sawano[1], Makoto rimoto[1] (1.Kanazawa University)

[PCG21-P14] Communications System and Antennas for Kanazawa-SAT3 Microsatellite

Teruya Minamoto[1], Koyo Ina[1], Kohei Kawagoshi[1], *Tomohiko Imachi[1], Satoshi Yagitani[1], Yoshitaka Goto[1], Daisuke Yonetoku[1], Yoshiya Kasahara[1], Tatsuya Sawano[1], Makoto Arimoto[1] (1.Kanazawa University)

[PCG21-P15] Development of micrometeoroid impact sensor within a multi-layered insulation (CLOTH) onboard 6U deep-space explorer EQUULEUS

*Takayuki Hirai[1], Hajime Yano[2], Ritsuko Jitsukawa[3], Eigo Ishioka[3], Haruki Nakano[3], Kazuyoshi Arai[3], Sunao Hasegawa[2] (1.Planetary Exploration Research Center, Chiba Institute of Technology, 2.Institute of Space and Astronautical Science, Japan Aerospace Exploration Agency, 3.Faculty of Science and Engineering, Hosei University)

[PCG21-P16] Breadboard model of asteroid tracking system for DESTINY$^+$ mission

*Peng Hong[1], Ko Ishibashi[1], Shunsuke Sato[2], Kazutoshi Takemura[3], Kotaro Fujiwara[4], Kanako Machii[5], Hiroyuki Toyota[2], Kazutaka Nishiyama[2], Masatsugu Otsuki[2], Osamu Okudaira[1], Takeshi Takashima[2] (1.Planetary Exploration Research Center, Chiba Institute of Technology, 2.Institute of Space and Astronautical Science, Japan Aerospace Exploration Agency, 3.Department of Applied Mechanics, Graduate School of Fundamental Science and Engineering, Waseda University, 4.Division of Mechanical and Space Engineering, Graduate School of Engineering, Hokkaido University, 5.Department of Mechanical Engineering and Intelligent Systems, Faculty of Informatics and Engineering, The University of Electro-Communications)

[PCG21-P17] Development of telescopic camera (TENGOO) performance evaluation device in MMX

*Hiroki Kato[1], Shingo Kameda[1], Keigo Enya[2], Osada Naoya[1] (1.Rikkyo University, 2.Japan Aerospace Exploration Agency)

[PCG21-P18] Observation Plans in the Cruising-Phase of the Solar Power Sail: OKEANOS

*Takahiro Iwata[1], Shuji Matsuura[2], KOHJI TSUMURA[3], Hajime Yano[1], Takayuki Hirai[4], Ayako Matsuoka[1], Daisuke Yonetoku[5], Tatehiro Mihara[6], Tatsuaki Okada[1], Osamu Mori[1], Toshihiro Chujo[1] (1.Institute of Space and Astronautical Science, Japan Aerospace Exploration Agency, 2.Kwansei Gakuin University, 3.Tohoku University, 4.Chiba Institute of Technology, 5.Kanazawa University, 6.RIKEN)

Visible and ultraviolet imagers for auroral and airglow observations by FACTORS - a future satellite mission for understanding the coupling and transportation processes in the upper atmosphere

*Takeshi Sakanoi[1], Masafumi Hirahara[2], Takuo T. Tsuda[3], Kazushi Asamura[4], Yoshizumi Miyoshi[2], Tomo-Hiko Watanabe[5], Takanori Nishiyama[6], Shin-ichiro Oyama[2,7], Yoshifumi Saito[4], Keisuke Hosokawa[3], Hirotsugu Kojima[8], Naritoshi Kitamura[9], Yasunobu Ogawa[5], Masatoshi Yamauchi[10], Ayako Matsuoka[4], Naoshi Yagi[1], Fukizawa Fukizawa[1], Genki Ishizawa[11]

1. Planetary Plasma and Atmospheric Research Center, Graduate School of Science, Tohoku University, 2. ISEE, Nagoya University, 3. Graduate School of Informatics and Engineering, School of Informatics and Engineering, The University of Electro-Communications, 4. ISAS/JAXA, 5. Graduate School of Science, Nagoya University, 6. National Institute for Polar Research, 7. University of Oulu, Finland, 8. RISH, Kyoto University, 9. Graduate School of Science, the University of Tokyo, Tokyo, 10. IRF Kiruna, Sweden, 11. Graduate School of Science, Tohoku University

We report science subject, design, development plan and identification of issues to be solved on the visible and ultraviolet imagers for a future satellite mission called FACTORS that aims to understand the coupling processes in the terrestrial magnetosphere/ionosphere/thermosphere and the acceleration and transportation of the space plasma and neutral atmospheric particles. FACTORS stands for Frontiers of Formation, Acceleration, Coupling, and Transport Mechanisms Observed by Outer Space Research System that is proposed as a multi-satellite formation flight mission. This will be a community exploration mission in Japanese apace research after the success of the ERG mission. The working group was approved by ISAS, JAXA this year, and we have started the discussion on detailed science targets, instrumental design, feasibility and so on. We mainly concern on visible and ultraviolet remote imaging of aurora and airglow for this mission. A visible imager (VISAI) on FACTORS will measure small-scale auroral structures at a wavelength of auroral prompt emission line, such as N2 1st PG, with high-time (~0.1s) and high-spatial (~1km) resolutions using a science CMOS or EMCCD. The FOV of 8 x 8 deg covers an area of 400 x 400 km viewed from 3000 km altitude. The high-spatial and high-time resolution imaging data is essential to understand small-scale variations of Alfven aurora, pulsating aurora, etc. Combined with particle and electric/magnetic field data by FACTORS, we will reveal the time and spatial variations of acceleration/scattering process in the complicated magnetosphere-ionosphere coupling system. A far-ultraviolet imager (FUVI) adopts a wide (~40 x 40 deg.) FOV objective mirror system which covers ~2500 x 2500 km area viewed from 3000 km altitude. We plan to adopt a filter wheal in FUV imager to change the wavelength between O 135.6 nm and the N2 LBH band at 140-160 nm. Wide-field multi-wavelength FUV images enable us to examine large-scale auroral dynamics like westward-travelling surge during substorm, omega-bands, and provide us to understand the global thermospheric activity from O/N2 airglow ratio. This year we plan to carry out specific studies for CMOS/EMCCD detectors suited for this mission, and perform radiation tests of detectors.
Related to the future FACTORS mission, we are now carrying out the developments of aural cameras for two sounding rocket projects, G-CHASER (Rocksat-XN) and LAMP. The G-CHASER (Rocksat-XN) rocket was successfully launched from Andøya, Norway on January 13, 2019. We installed an auroral camera (AIC) on this rocket to measure N2 1st PG emission with wide-angle FOV lens(96x75 deg), RG-665 filter, and CCD (WAT-910HX). In addition, we are developing two CMOS cameras AIC2 on the LAMP rocket that is scheduled to be launched at Poker Flat Research Range in winter of 2019. AIC2 will be installed on a despun platform to derotate rocket spin. One CMOS camera AIC2-S1 measures N2 1st PG emission with a narrow FOV lens (F-number=0.95, f=17mm, FOV=27x27deg.), and another CMOS camera AIC-S2

©2019. Japan Geoscience Union. All Right Reserved.

measures OI 844.6nm emission with a wide-angle lens (F-number=1.6, f=3.5mm, FOV=120x120deg.). Both cameras adopt the ZWO ASI 180 MM CMOS detector. AIC2-S1 will take fine structure of PsA in the region more than 100 x 100 km area around the magnetic footprint with a few kilo-meter resolution, while AIC2-S2 will obtain an altitude distribution of pulsating aurora in the F-region as well as distribution of PsA in wide-range. The precise imaging and altitude distribution of PsA are obtained with AIC2 at two wavelengths with 10Hz sampling. The imaging data combined with precipitating electron data in the wide energy range enable us to investigate the relativistic electron precipitation called microbursts that is probably caused by chorus waves in the magnetosphere.

Keywords: magnetosphere, aurora, imager, ultra violet, visible, ionosphere

©2019. Japan Geoscience Union. All Right Reserved.

Spatio-temporal analysis of flash aurora using Convolutional Neural Network

*Toki Genda[1], Takumi Inoue[1], Mitsunori Ozaki[1], Satoshi Yagitani[1], Imamura Kousuke[1], Kazuo Shiokawa[2], Yoshizumi Miyoshi[2], Shin-ichiro Oyama[2], Ryuho Kataoka[3], Yusuke Ebihara[4], Keisuke Hosokawa[5]

1. Kanazawa Univ., 2. Nagoya Univ., 3. NIPR, 4. Kyoto Univ., 5. UEC

High energy electrons in the magnetosphere travel along geomagnetic field lines and precipitate into the Earth's atmosphere, then auroras are shown on the ground. We can investigate indirectly the behavior of precipitating electrons in the magnetosphere by deducing auroras on the ground. We focus on flash auroras, which illuminate suddenly at less than 1 s. It is difficult to detect a lot of flash aurora events by visually looking because the duration of flash aurora is very short. In this study, we developed an automatic detection of flash auroral position using Convolutional Neural Network (CNN) and performed statistical analysis of the spatio-temporal variations of flash aurora taken by an EMCCD camera (100 Hz sampling, 256 * 256 pixels) at Gakona (Alaska).

The learning data was obtained by dividing the keogram images (2400 * 720 pixels, 1-minute period) along the north-south direction of all-sky EMCCD data into square blocks (30 * 30 pixels, 750-ms period), then the learning data was visually classified to four classes. Four classes are, "pulsating aurora", "flash aurora", "noise", and "no aurora or noise". We classified the test data using the CNN, its accuracy was 91.2%.

The flash aurora data (about 100 events) are collected by CNN and we extracted flash auroral region using Otsu's method, which is a basic method of contour extraction. We performed statistical analysis about luminous duration, luminous point, spatial size, and spatial extent of flash aurora. The averaged luminescence duration was 0.21±0.08 seconds, and did not depend on magnetic longitudes and latitudes in the field-of-view of camera. We confirmed that most events (about 70%) expand earthward with an average spatial extent of 0.027 Re. We think that the earthward extension can be caused by wave propagation effects of whistler mode waves and the nonuniformity of spatial distribution of loss cones in the magnetosphere.
In this presentation, we will report on our automatic detection method and statistical results of spatio-temporal analysis of flash aurora in detail.

Keywords: Convolutional Neural Network, pulsating aurora, flash aurora

©2019. Japan Geoscience Union. All Right Reserved.

Study on the pulse noise removal technique for Pc1 geomagnetic pulsations on the ground by signal processing

*Fumiya Komase[1], Tomohiro Inoue[1], Mitsunori Ozaki[1], Satoshi Yagitani[1], Kazuo Shiokawa[2], Masahito Nose[2], Tsutomu Nagatsuma[3]

1. Kanazawa Univ., 2. Nagoya Univ., 3. NICT

An electromagnetic ion cyclotron (EMIC) wave, which is a type of plasma waves generated in the magnetosphere, propagates along the geomagnetic field line and we can observe it as the fluctuation in the geomagnetic field on the ground called Pc1 geomagnetic pulsation (0.2 to 5 Hz). We observe Pc1 pulsations at Kapuskasing (Canada). The ground observation is carried out using an induction magnetometer, and the Pc1 pulsations are observed with a high sensitivity and a high time resolution (64 Hz). However, when the observation instrument vibrates due to a strong wind, pulse noise is included in the observed waveforms.
We have been studying an extracting method of Pc1 pulsation by removing the pulse noise included in observed waveform using signal processing technique. Pulse noise shows in a wider frequency range (0.1 to 10 Hz) than the frequency range of Pc1 pulsation and its duration is shorter than the duration of Pc1 pulsation. Pulse noise removal consists of detecting the pulse noise candidate, classifying the pulse noise candidates into pulse noises and others by Neural Network (NN), and interpolating the waveform at the pulse noise domain. In the first step, we set an amplitude threshold for the differential waveform to detect pulse noise candidates. In the second step, as learning data for classification, we use waveform applied a High Pass Filter (HPF) to emphasize pulse noises. In the third step, we use an average energy around the pulse noise in the interpolation. We use random phase, observation phase including the pulse noises, and estimated phase by nonlinear least squares method. For each phase, we evaluated the SNR before and after the pulse noise removal. As a result, the SNR improved with 22dB using the estimated phase, but it requires a huge calculation time.
In this presentation, we will report on the pulse noise removal of Pc1 pulsation using signal processing technique in detail. Conventionally it was necessary to examine and construct the observation environment which suppresses the vibration of the observation equipment as much as possible, we think that our signal processing will be useful for reducing the ground observation costs and a more detailed analysis of Pc1 pulsation.

Keywords: Pc1 geomagnetic pulsation, Noise removal, Signal processing

©2019. Japan Geoscience Union. All Right Reserved.

Application of magneto-impedance sensor to geomagnetic field measurements

*Masahito Nose[1], Reiko Nomura[2], Kazushi Asamura[3], Hitoshi Aoyama[4], Takeshi Kawano[4], Ayako Matsuoka[3], Kentarou Kitamura[5], Yukinobu Koyama[6], Haruhisa Matsumoto[7], Masafumi Hirahara[1]

1. Institute for Space-Earth Environmental Research, Nagoya University, 2. National Astronomical Observatory of Japan, 3. Institute of Space and Astronautical Science, Japan Aerospace Exploration Agency, 4. Aichi Steel Corporation, 5. National Institute of Technology, Tokuyama College, 6. National Institute of Technology, Oita College, 7. Research and Development Directorate, Japan Aerospace Exploration Agency

Magneto-impedance (MI) effect was discovered about 25 years ago and a micro-size magnetic sensor that utilizes this effect becomes commercially available. We made some modifications to the commercially available MI sensors as they can cover the range of the geomagnetic field. For the period of March 30 to April 27, 2018, we conducted experimental observations of geomagnetic field variations with the MI sensors at Mineyama observation site, which is located about 100 km north-west of Kyoto. Data obtained with the MI sensors were compared with those from the fluxgate magnetometer that has been working at the site. Results showed that the MI sensor recorded geomagnetic variations with amplitudes of ~1 nT that were also detected with the fluxgate magnetometer. This suggests that MI sensors are useful for researches in geomagnetism or space physics, although they are much less expensive than fluxgate magnetometers.

We consider developing two different kinds of systems to measure the geomagnetic field using the MI sensor: a system for ground-based observation and a system for a sounding rocket. In presentation, we will display observation data from the MI sensors and the fluxgate magnetometers at Mineyama and other observatories. Future plans of the system onboard sounding rocket will be also presented and discussed.

©2019. Japan Geoscience Union. All Right Reserved.

Observation of the Ionospheric Currents by the CubeSat at the Low and Middle Latitude

*Kentarou Kitamura[1], Kazumasa Imai[2], Taku Takada[2], Manabu Shinohara[3], Makoto Wakabayashi[4], KOSEN Space Collaboration Group

1. National Institute of Technology, Tokuyama Collge, 2. National Institute of Technology, Kochi Collge, 3. National Institute of Technology, Kagoshima Collge, 4. National Institute of Technology, Niihama Collge

The ionospheric currents flowing in the dayside ionosphere have been considered as a significant subsequence of Mesosphere-Ionosphere-Magnetosphere coupling. These currents were well detected in the Solar quiet conditions and named Sq currents. In particular, it is well known that the flow pattern of Sq currents shows the north-south hemispheric asymmetry due to the different ionospheric conductivities in the winter and summer hemispheres. This indicates that the asymmetry of the potential must be kept by the energy balance between each hemisphere through the field line.
An InterHemispheric Field Aligned Current (IHFAC) was theoretically predicted by Maeda [1974] and Fukushima [1979, 1991] to interpret the north-south asymmetry in the potential pattern. Several ground magnetic observations and satellite observations suggested an existence of the IHFAC in the noon sector and both the morning and evening terminators. However, the detailed morphology of the IHFAC have not been well understood yet, despite that the direct detection of the IHFAC at Low Earth Orbit (LEO) was reported in the observation by several satellites.
In order to investigate the Sq current system including the IHFAC, the in-situ observation by a CubeSat (2U size satellite emitted from ISS) is proposed in collaboration with 10 national colleges which belong to National Institute of Technology (KOSEN). The fluxgate magnetometer is onboard the CubeSat to observe small perturbations of the magnetic field. After the ejection from the ISS, the CubeSat will gradually glide down to the upper atmosphere due to the strong atmospheric drag and finally burn up in it. The duration of possible observation is estimated for more than 50 days.
The CubeSat can be characterized by the short duration of development (less than 3 years) and low cost (less than 100,000USD). We are considering an actual utilization of this extremely low-cost CubeSat to more realistic science mission. This concept enables us to conduct the multi-satellite in-situ observation in fairly low budget compared to conventional satellite missions.

Keywords: Ionospheric Current, Interhemispheric Field Aligned Current, CubeSat

©2019. Japan Geoscience Union. All Right Reserved.

Basic study on miniaturization of electric field instrument for plasma wave observations by ASIC technology

*Yuya Tokunaga[1], Mitsunori Ozaki[1], Keigo Ishisaka[2], Hirotsugu Kojima[3], Satoshi Yagitani[1], Takahiro Zushi[3]

1. Kanazawa University, 2. Toyama Prefectural University, 3. Kyoto University

We have been measuring electric fields of the plasma waves (a few Hz to several hundred Hz) to understand the magnetospheric dynamics. The spatial resolutions of electric field measurements are not enough because we cannot launch a lot of satellites due to the large size and mass of satellites. Demands of micro satellites like a 1U (10 cubic centimeters) cube satellites are increasing. We need to miniaturize measurement instruments for probing the plasma waves.

This study deals with an electric field instrument in plasma wave observations. We use the electric field instrument for capturing the electric fields detected by wire probe antennas. In this study, the purpose is to miniaturize the electric field instrument with a high radiation tolerance (300 krad) using Application Specific Integrated Circuit (ASIC) technology.

We designed a based amplifier for a new electric field instrument. In the new based amplifier, the equivalent input noise is 50 nV/sqrt(Hz) at 1 kHz, which is 3.9 dB-larger than that of conventional based amplifier (OP-41). The noise performance of new based amplifier is acceptable for capturing the plasma waves. To confirm the radiation tolerance of new based amplifier, we did the radiation tests up to 300 krad using the gamma ray. From the radiation test results, the gain was no change before and after the radiation tests. The output noise was degraded with 5.05 dB at 100 Hz by total ionizing dose effects. However, the based amplifier was not breakdown by the gamma ray. The electric field instrument consisted of new based amplifier could operate with a high radiation tolerance.

We conducted the transient analysis for the new electric field instrument by a circuit simulator (Tanner EDA). In the simulation, rectangular waves of 1 Vpp with 10 Hz input to the new electric field instrument via a sheath impedance (10 MOhms and 100 pF). From the simulation results, the output waveforms of new electric field instrument showed similar output waveforms in comparison with the conventional electric field instrument. The power consumption of new electric field instrument can decrease with approximately 67% than that of the conventional electric field instrument. From the simulation results, we confirmed the basic operations as the electric field instrument for detecting the plasma waves. In the future work, we will need to improve the temperature operating range because the new electric field instrument cannot operate at minus 60 Celsius degrees from the temperature simulation results.

In this presentation, we will present the basic study on electric field instrument for plasma wave observation by ASIC technology in detail.

Keywords: ASIC, Electric field instrument, Plasma wave observation

©2019. Japan Geoscience Union. All Right Reserved.

Evaluation of radiation tolerance of electronics parts used for the ultra-small mission

*Riku Katsuse[1], Kazuo Yoshioka[1], Masaki Kuwabara[2], Reina Hikida[1], Shogo Arao[1], Ichiro Yoshikawa[1]

1. The university of Tokyo , 2. Institute of Space and Astronautical Science

In the space environment, spacecraft is exposed to radiation and degrades the data. For example, the increase of dark current, and change in current consumption.

Recently, the university-made ultra-small spacecraft mission become popular. The mission in this class can reduce the cost and time by using commercial products. However, these commercial products are thought to have no radiation tolerance. Then, it is necessary to be tested with the radiation total dose which is calculated using the Monte Carlo simulation.

We are developing the extreme ultraviolet imager PHOENIX onboard the ultra-small satellite EQUULEUS which will be launched in 2020. Helium ions in the Earth’ s plasmasphere emit extreme ultraviolet light (wavelength of 30.4 nm) through the solar resonance scattering. PHOENIX observes them from the moon (Earth-Moon L2 point).

The radiation tolerance has been evaluated with a gamma irradiation facility with cesium 137. In this presentation, we show the gain characteristics and change of electric noise with respect to radiation of semiconductor elements used in PHOENIX instrument.

©2019. Japan Geoscience Union. All Right Reserved.

A method to quantitatively evaluate Non-evaporable-getter pump for use in space science mission

*Seiya Nishimura[1], Ichiro Yoshikawa[1], Kazuo Yoshioka[1], Shogo Arao[1], Zhang Tianxu[1]

1. The university of tokyo

Observation instruments are known to deteriorate under atmospheric condition. Deterioration are mainly caused by reaction with water vapor and oxygen. To prevent this, observation instruments must be maintained under vacuum. The problem is that the conventional vacuum pump are too heavy to carry to the launching site. The need of continuous power supply makes the transport more difficult. Also the vacuum pump must be removed before the launch. These problems are not only making it difficult to maintain observation instruments under vacuum but also causing extra costs. Non-evaporable-getter (NEG) pumps are able to solve these problems. NEG pumps are light weight, compact, oil free, vibration free, and able to operate without energy supply after activation. Considering the utilization of NEG pump for space science missions, we need to quantitatively evaluate the NEG pump to optimize its size, shape, material, and mounting position for each mission. In this study, a method to measure pumping speed of NEG pump for carbon monoxide (as substitute to water vapor and oxygen) was established by using the orifice method. By using this method, it will be able to develop a NEG pump which best applies the case for each mission.

Keywords: Non-evaporable-getter pump, vacuum pump

©2019. Japan Geoscience Union. All Right Reserved.

Interpretation on slight asymmetry of analyzer characteristics of MIA onboard the Mio by means of a model calculation of 3-D potential distribution

*Wataru Miyake[1], Yoshifumi Saito[2], Shoichiro Yokota[3]

1. Tokai University, 2. ISAS, 3. Osaka University

MIA (Mercury Ion Analyzer) on board Mio employs a top-hat electrostatic analyzer, which has axisymmetric toroidal electrodes and is designed to have no dependence in its characteristics on azimuthal direction of incident ions. However, our ground calibration experiments have revealed that it has a slight dependence. We have tried to explain the dependence by means of three dimensional model calculations. We assumes that all parts of electrode are manufactured precisely. Our results shows that a slight relative rotation (or tilt) of electrodes can lead to a slight dependence on incident azimuthal direction similar to that obtained from the ground experiments.

Keywords: Mio, tophat electrostatic analyzer , MIA

©2019. Japan Geoscience Union. All Right Reserved.

Construction of impact testing machine for small satellites and evaluation of mechanical resistance of MCPs by the impact test

*Junya Fukuba[1]

1. Graduate school of Tokyo

Small satellites have been developed in recent years. Environmental tests at the development stage play an important role in improving reliability of small satellites. These include a vibration test, an impact test, and a thermal vacuum test. Especially, the impact test is one of the most difficult tests and a reliable method has not yet been established. Against such a background, we constructed an impact testing machine for small satellites. Required performance of the impact testing machine is a controllability and a reproducibility. The controllability means the performance of applying a targeted impact level accurately. This is important to avoid applying excessive impacts on a test target. The reproducibility means the performance of applying same impact level repeatedly and this is also important because if it is possible to apply an unintended impact under the same condition, it degrades the test accuracy. Our impact testing machine is designed to be able to easily adjust the impact level and have high reproducibility. Furthermore, we tested for mechanical resistance of the MCP (micro-channel plate) which is used for optical observation instruments. In this test, we used an impact level assuming the EQUULEUS mission which will be launched by NASA’ s rocket in 2020. In my presentation, I will introduce the details of our impact testing machine and the impact test results of MCP.

Keywords: impact test

©2019. Japan Geoscience Union. All Right Reserved.

Innovative design of double-shell type energy analyzer for simultaneous electron and ion measurements in space

*Tomomi Takei[1], Masafumi Hirahara[1]

1. Institute for space-earth environmental research, Nagoya university

It is well known that the terrestrial and planetary magnetospheres and the interplanetary space are filled with charged particles such as electrons and ions, which are so-called the space plasma, and in-situ observations of the space plasmas have been conducted by using satellites carrying particle instruments, such as the top-hat type electrostatic energy analyzer. Essentially, obtaining three-dimensional velocity distributions of the space plasmas or energy-pitch angle distributions help us understand the dynamics of the space plasmas. Because the top-hat type analyzer is cylindrically symmetric and has a 2π-radian planar field of view, it can independently measure the wide angular and energy distributions of incident particles. Also, three-dimensional velocity or energy-pitch angle distributions can be obtained by utilizing the satellite spin motion.
The top-hat type electrostatic energy analyzers can measure the ions when a negative potential is applied to the inner electrode and the electrons by a positive potential with the outer electrode grounded. Therefore, in the prevailing design of the top-hat type analyzer, the sensor heads separate for the ion and electron observations, respectively. Because of the recent miniaturization of the satellites, the weight and space of the instruments mounted on the small and micro satellites are getting severely restricted. However, if two sensors for electron and ion observations are combined into one sensor head, it is possible to save both weight and space on the small and micro satellites. Therefore, we have been developing double-shell type energy analyzer which can simultaneously measure the ions and the electrons with one sensor head.
We designed the shapes of the collimator and the double-layered dome-shaped electrodes so that the electrons and the ions with appropriate energies pass through the inner gap and the outer gap by applying a negative potential to the central electrode with the inner and outer electrodes grounded, respectively. We made the numerical simulations using SIMION which is a charged particle simulator program and investigated the performance and characteristics as the electrostatic analyzer. Consequently, we confirmed that the electrons and the ions can be analyzed with one sensor head by only applying negative high voltage to the electrodes. So far, we consider the detection unit using Time-Of-Flight velocity spectrometer for the discrimination of the ion species as the part where the ions are detected, and an assembly of micro channel plates is expected for the electron detection. The design of TOF-type mass analysis unit as ion mass analysis unit is one of subjects for future work.

©2019. Japan Geoscience Union. All Right Reserved.

Microsatellite Development and Education of Space Science and Technology at Kanazawa University

*Tomohiko Imachi[1], Satoshi Yagitani[1], Daisuke Yonetoku[1], Yoshiya Kasahara[1], Tatsuya Sawano[1], Makoto Arimoto[1], Yoshitaka Goto[1], Mitsunori Ozaki[1], Ryuichi Fujimoto[1]

1. Kanazawa University

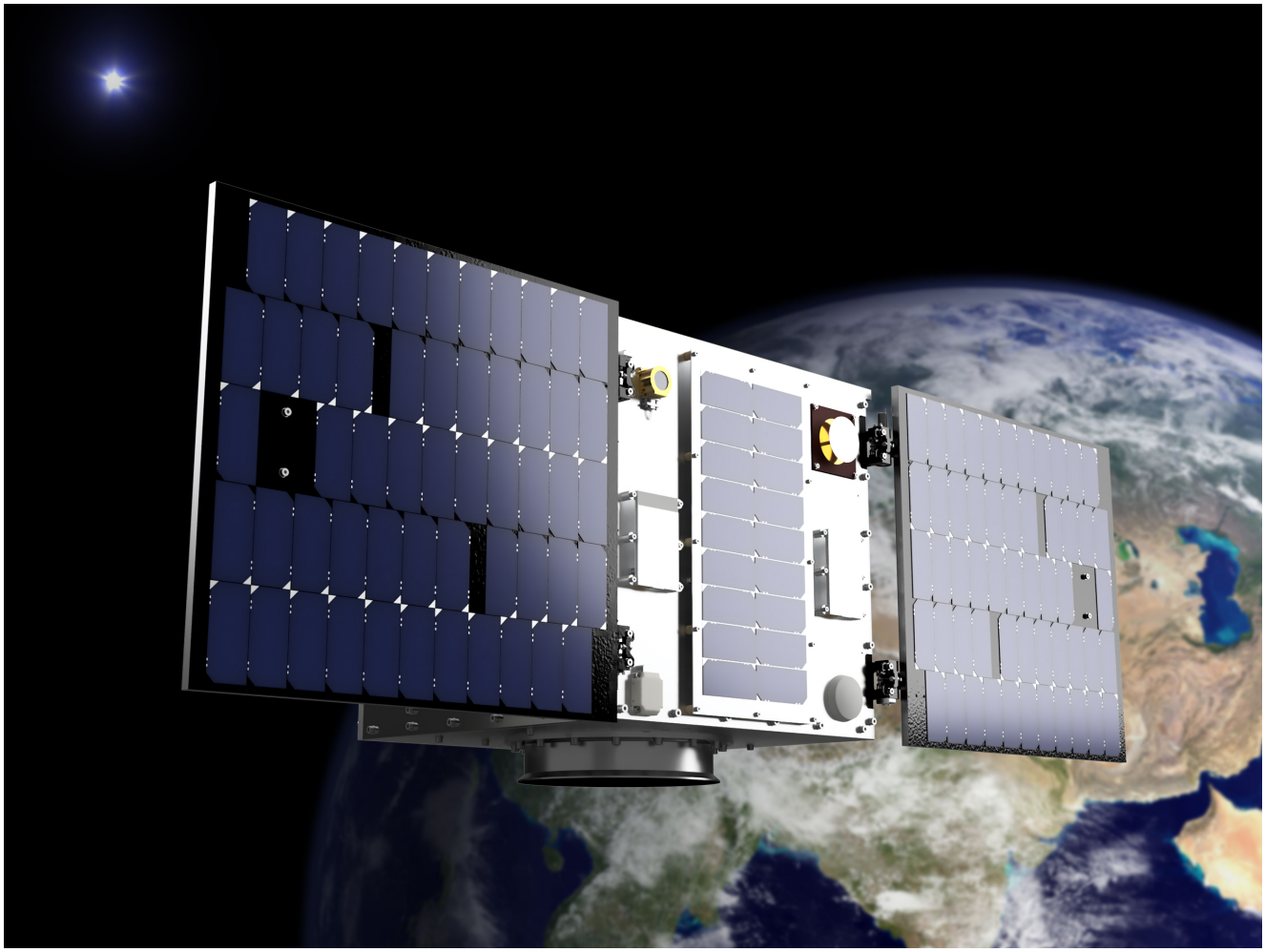
At Kanazawa University, researchers from engineering and science are cooperating to promote the "Kanazawa University Satellite Project (Kanazawa-SAT3: Study and Training in Space Science and Technology for Kanazawa Cube-Satellites)". In this project, a microsatellite is being developed by staff and students of Kanazawa University. It is a scientific satellite which will contribute to the elucidation of the mechanism of gravitational wave generation by identifying the source of gravitational wave by detecting the arrival direction of gamma rays and X rays radiated at the same time when a gravitational waves are generated by collision of astronomical objects The satellite will be inserted into a solar synchronous orbit at about 660 km altitude. It is a microsatellite with a total weight of 50 kg or less, and its size is cubic with a side of 50 cm, and it is designed to be a piggyback on an HII-A rocket.

Also related to this project, a space science and engineering course has been newly established in the Graduate School of Natural Sciences in April 2018. This course is based on the 'satellite development by students', and students are actually involved in the design, fabrication, ground tests, and operation of scientific satellites, aiming to train personnel who are familiar with space science and space engineering, with satellite-development skills.

Ground tests with the thermal and structural model of Kanazawa-SAT3 have been completed , and the unit tests for almost all components are being conducted. Currently, we are completing the design of the flight model. In the presentation, we will report the details of Kanazawa-SAT3 and its development status.

Keywords: Microsatellite, Gravitational wave, Kanazawa SAT3

©2019. Japan Geoscience Union. All Right Reserved.



©2019. Japan Geoscience Union. All Right Reserved.

Attitude Control System for Kanazawa-SAT3 Microsatellite

Takuya Nakajima[1], Yuuki Yasuda[1], Hirofumi Segawa[1], *Tomohiko Imachi[1], Satoshi Yagitani[1], Yoshiya Kasahara[1], Daisuke Yonetoku[1], Tatsuya Sawano[1], Makoto rimoto[1]

1. Kanazawa University

Kanazawa University has been developing a microsatellite. This satellite is equipped with a device to observe celestial bodies emitting gravitational waves with X rays, and aims to elucidate the mechanism of black hole formation by estimating the time of arrival and direction of arrival of gravitational waves.
In this research, the attitude control system is being developed using GAS (Geomagnetic Aspect Sensor) and MTQ (Magnetic Torque). We have constructed the environment for the unit test of RW (Reaction Wheel) also used for attitude control of the satellite.

MTQ is a device that controls the attitude of the satellite by generating a magnetic torque against the geomagnetic field by applying a voltage (an electric current) to a magnetic coil. GAS is a device for detecting the direction of the geomagnetic vector. OBC (On Board Computer) which controls all devices mounted on the satellite receives the geomagnetic field data detected by GAS, and transmits commands to control MTQ. GAS and MTQ cannot be connected to OBC directly, because OBC has just a digital interface, but the output of GAS and the input to MTQ are analog voltages. Therefore, we have developed a control device for on-board equipment using a microcontroller. For the GAS, the voltages are A/D-converted by the microcontroller and transmitted to the OBC. For the MTQ, OBC transmits control commands to the microcontroller, which generates a PWM (Pulse Width Modulation) signal according to the received command that determines the effective voltage to be given to the MTQ. For the system development and operation tests, a PC is used instead of OBC and we carried out experiments of control equipment. For the GAS, we have confirmed the linearity between the analog magnetic field and the corresponding digital values transmitted to the PC. For the MTQ, we have confirmed that the voltage to be given to MTQ were precisely controlled by the duty ratio of the PWM signal output from the microcontroller.

RW is a device to generate a control torque around the rotation axis by accelerating a rotor by a motor and is controlled by transmitting a command from the OBC via an RS-422 serial communication line. The unit test has been carried out by using a PC as a substitute of OBC, but the cable had a influence on the rotation operation of RW. Therefore, we have constructed a system for wirelessly connecting the RW with the PC via a wireless RS-422 communication. Specifically, commands from the PC are wirelessly transmitted to an Arduino microprocessor by a low-power radio module XBee, and the RW is controlled via an RS-422 transceiver. With this system, we demonstrated the basic functions for command and data between the PC and the Arduino via the wireless RS-422 transceiver.

We plan to construct a system that applies appropriate PWM signals to MTQ according to the value detected by GAS. We will also evaluate RW performance by the unit test using the wireless RS-422 communication system.

Keywords: Microsatellite, ACS, Kanazawa SAT3

©2019. Japan Geoscience Union. All Right Reserved.

Communications System and Antennas for Kanazawa-SAT3 Microsatellite

Teruya Minamoto[1], Koyo Ina[1], Kohei Kawagoshi[1], *Tomohiko Imachi[1], Satoshi Yagitani[1], Yoshitaka Goto[1], Daisuke Yonetoku[1], Yoshiya Kasahara[1], Tatsuya Sawano[1], Makoto Arimoto[1]

1. Kanazawa University

Kanazawa University is developing the first Kanazawa University's microsatellite, named as Kanazawa-SAT3. Kanazawa-SAT3 is planned to be launched within FY2019, and its observation mission is to identify the source of gravitational waves by detecting the occurrence time and arrival direction of the X-rays and gamma rays observed simultaneously with gravity waves from distant astronomical objects.

In this research, we are developing a communications system for Kanazwa-SAT3. Kanazawa-SAT3 has three different communication systems using S band, UHF band and Iridium, and the link design of each of them has generally been completed. We summarize each communication system in detail as the following.

The S-band communication system, will use 2-GHz frequency band. Kanazawa-SAT3 is equipped with two types of antennas: S-band patch antennas and S-beacon antennas. S-band system is a main communication system between the satellite and a ground station, and plays a role of high speed data communication and beacon transmission. On the satellite side, two S-band patch antennas designed for both transmission and reception are mounted on the front and rear panels of the satellite. Two S-beacon antennas for transmission are also mounted on the front and rear panels of the satellite. On the ground side, we will send and receive by the signals using a 2.4-m parabolic dish installed at Kanazawa University.

The UHF communication system will use 400-MHz frequency bands. This system transmits commands from the ground to the satellite and telemetry information from the satellite to the ground. On the satellite side, four inverted-F type antennas we developed are mounted (two for receiving and two for transmitting) on the front and rear panels of the satellite. On the ground side, we will send and receive data by using a Yagi antenna with 14 crossed elements installed at Kanazawa University. We have also constructed an automatic satellite tracking system using the Yagi antenna.

A communication system using the Iridium satellite network uses a frequency band around 1.6 GHz. In this system, communications are performed via Iridium satellite, so that the communication can be established even when our ground station is not visible from the satellite. The data is exchanged between the satellite and the ground by using e-mail. This system can transmit and receive data in almost real time so emergency command and data transmission will be available. On the satellite side, two antennas for both transmission and reception are mounted on the front and rear panels of the satellite. A system has been constructed that exchanges data between a laptop computer simulating an onboard computer (OBC) mounted on a satellite and an iridium satellite.

From now on, for the communication systems using the S band and the UHF band, it is necessary to develop the communication software. For In addition, we need to improve the automatic satellite tracking system of Kanazawa-SAT3. For the communication system using Iridium satellite, it is necessary to implement a system on the OBC and conduct a communication experiment.

©2019. Japan Geoscience Union. All Right Reserved.

Keywords: Microsatellite, Communications System, Kanazawa SAT3

©2019. Japan Geoscience Union. All Right Reserved.

Development of micrometeoroid impact sensor within a multi-layered insulation (CLOTH) onboard 6U deep-space explorer EQUULEUS

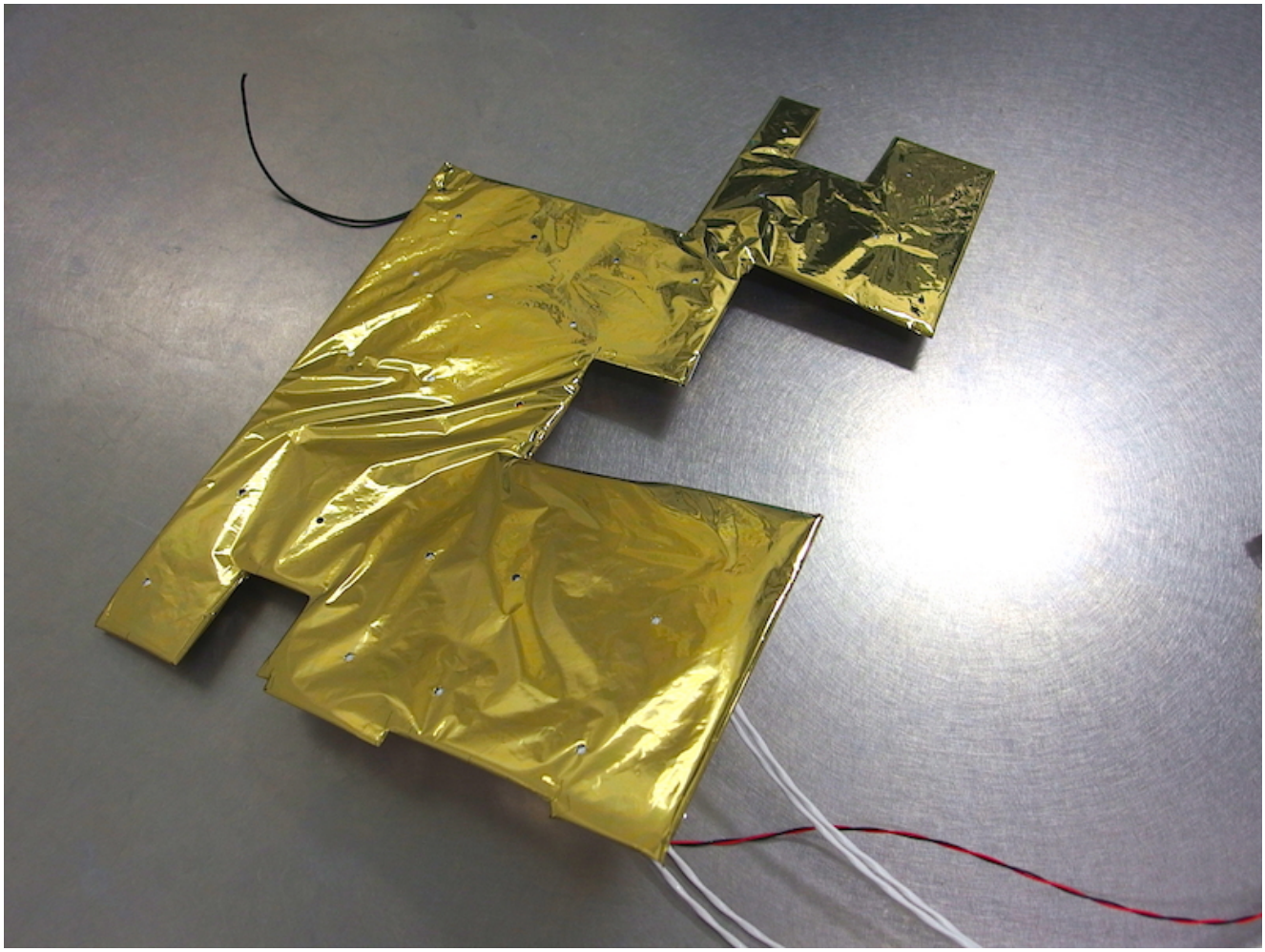
*Takayuki Hirai[1], Hajime Yano[2], Ritsuko Jitsukawa[3], Eigo Ishioka[3], Haruki Nakano[3], Kazuyoshi Arai[3], Sunao Hasegawa[2]

1. Planetary Exploration Research Center, Chiba Institute of Technology, 2. Institute of Space and Astronautical Science, Japan Aerospace Exploration Agency, 3. Faculty of Science and Engineering, Hosei University

In recent years, the use of CubeSat for deep-space exploration is remarkably expanding. Equilibrium Lunar-Earth point 6U Spacecraft (EQUULEUS) project led by the University of Tokyo and JAXA is one of 13 sub payloads which will be launched by the NASA’ s new rocket, Space Launch System (SLS) in 2019 or later. In addition to the engineering mission of orbital maneuvering, EQUULEUS will perform 3 scientific missions consisted of geo-corona, lunar impact flash, and micrometeoroid observations on the way to the Earth-Lunar libration point 2. Our Cis-Lunar Object detector within THermal Insulation (CLOTH) is a piezoelectric film sensor integrated with the EQUULEUS’ s multi-layer insulation (MLI). CLOTH can detect micrometeoroid which impacts and penetrates the outermost layer of EQUULEUS's MLI. The space flight demonstration of CLOTH will expand the possibility of deep-space exploration by CubeSat. In this presentation, we introduce the concept of CLOTH, i.e. micrometeoroid detector integrated with a spacecraft bus component, and the detection performance estimated by hypervelocity microparticle impact test on the ground.

Keywords: Piezoelectric film, PVDF, Thermal insulation, CubeSat, Micrometeoroid, Hypervelocity impact

©2019. Japan Geoscience Union. All Right Reserved.



©2019. Japan Geoscience Union. All Right Reserved.

Breadboard model of asteroid tracking system for DESTINY^{+} mission

*Peng Hong[1], Ko Ishibashi[1], Shunsuke Sato[2], Kazutoshi Takemura[3], Kotaro Fujiwara[4], Kanako Machii[5], Hiroyuki Toyota[2], Kazutaka Nishiyama[2], Masatsugu Otsuki[2], Osamu Okudaira[1], Takeshi Takashima[2]

1. Planetary Exploration Research Center, Chiba Institute of Technology, 2. Institute of Space and Astronautical Science, Japan Aerospace Exploration Agency, 3. Department of Applied Mechanics, Graduate School of Fundamental Science and Engineering, Waseda University, 4. Division of Mechanical and Space Engineering, Graduate School of Engineering, Hokkaido University, 5. Department of Mechanical Engineering and Intelligent Systems, Faculty of Informatics and Engineering, The University of Electro-Communications

DESTINY^{+} (Demonstration and Experiment of Space Technology for Interplanetary voYage, Phaethon fLyby and dUst Science) is a mission proposed for JAXA/ISAS Epsilon class small program, currently in the pre-project phase (Phase-A) with a launch targeted for 2023. The mission plans to conduct high-resolution imaging during close flyby of asteroid (3200) Phaethon, which is considered as a parent body of Geminid meteor shower. Two cameras are planned to be onboard DESTINY^{+}, the Telescopic Camera for Phaethon (TCAP) and the Multiband Camera for Phaethon (MCAP). While MCAP is designed for low spatial resolution imaging, TCAP is planned to perform high-resolution imaging, especially from ~40 seconds before to ~9 seconds after the closest approach with an imaging rate of more than 1 frame per second and the surface of Phaethon will be imaged with a spatial resolution up to 3.5 m/px at closest approach. Both cameras will be mounted and installed on the wall of spacecraft bus, thus orientations of the cameras are mainly controlled by the attitude of spacecraft. However, since the relative flyby speed and closest distance to Phaethon are expected to be 30 to 40 km/s and about 500 km, it is significantly difficult to track the asteroid only by the rotation of the spacecraft itself. Therefore, an asteroid tracking system is required for TCAP to obtain unblurred high-resolution images. The tracking system is also required to operate autonomously during the high-speed flyby. We have conducted conceptual studies of the tracking mirror as well as control algorithms to properly navigate the mirror based on feedforward or feedback loop. To realize the designed concept, we have developed a simple breadboard model focusing on the rotating mechanism which is the most important part of tracking mirror. The breadboard model consists of a rotating mirror, a 2-phase stepping motor and its driver, a motor reducer, and a FPGA board to control the driver. Required performances for the breadboard model of tracking system are (1) the rotating mirror should be able to orient a desired direction with an enough accuracy, (2) the mirror should be able to rotate smoothly with an enough accuracy during the exposure of TCAP. We will report the current development status of breadboard model of asteroid tracking system for TCAP and show its initial results of the performance test.

Keywords: DESTINY+, camera, flyby, tracking system

©2019. Japan Geoscience Union. All Right Reserved.

Development of telescopic camera (TENGOO) performance evaluation device in MMX

*Hiroki Kato[1], Shingo Kameda[1], Keigo Enya[2], Osada Naoya[1]

1. Rikkyo University, 2. Japan Aerospace Exploration Agency

Mars has two satellites, Phobos and Deimos, and there are currently two hypotheses for the origin of these satellites. The first of these hypotheses is that the moons are captured primitive asteroids, and the second is that they formed because of a giant impact event on Mars. The Japan Aerospace Exploration Agency (JAXA) is planning the Martian Moon eXploration (MMX) mission, which is a sample-return mission for Phobos, to determine which hypothesis is correct and reveal the origin of these two satellites.

The TElescopic Nadir imager for GeOmOrphology (TENGOO), which will be installed in MMX, has the purpose of measuring the geographical features of Phobos to locate a suitable landing site less influenced by space weathering. The design of TENGOO was optimized for achieving this goal. In the optical design, the instantaneous Field of View (iFoV) is 5.8 μrad/pix and the Modulation Transfer Function (MTF) is 0.3 at the Nyquist frequency.The design performance of the manufactured TENGOO needs to be confirmed. We evaluate the performance of TENGOO by measuring the Point Spread Function (PSF). Therefore, a low divergence collimated light is needed for a ground experiment to obtain the PSF with sufficient accuracy. We succeeded at making a collimated light source with divergence less than 11.6 μrad.

The Full Width of Half Maximum (FWHM) of PSF obtained with this collimated light is approximately 2x2 pixels in TENGOO. Therefore, the sampling interval becomes wider than FWHM of PSF, and the error of PSF estimation due to Gaussian fitting increases. To solve this problem, we measured the Line Spread Function (LSF) with diagonal lines and complemented the measuring points by obtaining multiple PSFs.

Keywords: Mars, MMX, camera

©2019. Japan Geoscience Union. All Right Reserved.

Observation Plans in the Cruising-Phase of the Solar Power Sail: OKEANOS

*Takahiro Iwata[1], Shuji Matsuura[2], KOHJI TSUMURA[3], Hajime Yano[1], Takayuki Hirai[4], Ayako Matsuoka[1], Daisuke Yonetoku[5], Tatehiro Mihara[6], Tatsuaki Okada[1], Osamu Mori[1], Toshihiro Chujo[1]

1. Institute of Space and Astronautical Science, Japan Aerospace Exploration Agency, 2. Kwansei Gakuin University, 3. Tohoku University, 4. Chiba Institute of Technology, 5. Kanazawa University, 6. RIKEN

The solar power sail mission: OKEANOS (Oversize Kite-craft for Exploration and AstroNautics in the Outer Solar system) is a Japanese candidate deep-space probe that will be powered by hybrid propulsion of solar photon acceleration and ion engines. The main scientific objectives are studies of Trojan asteroids in the Jovian L4 or L5 regions. The long distance and period from the launch to the swing-by at Jupiter will give us a good opportunity to explore the solar system between the Earth and the Jupiter to elucidate the solar system disc structure. We define the cruising-phase sciences of the OKEANOS mission as the scientific theme that will be explored or observed from the launch to the swing-by at Jupiter. Candidates of instruments for the cruising phase are: the EXo-Zodiacal Infrared Telescope (EXZIT), the Arrayed Large-area Dust detectors in INterplanetary space (ALADDIN)-2, the MaGnetic Field experiment (MGF), and the GAmma-ray burst Polarimeter (GAP)-2. In this paper, we report scientific purpose and observation plans of them.

Zodiacal light observed at visible and near-infrared wavelengths is thought to be sunlight scattered by interplanetary dust. The two-dimensional distribution of zodiacal light reflects the three-dimensional structure of interplanetary dust. However, it is still controversial that how the ratio of asteroid-origin to comet-origin changes by the heliocentric distance. Therefore, the comparison of the radial distribution of zodiacal light and the in-situ dust observation will help clarify the distribution and components of solid particles in our solar system. These results are expected to provide precise distribution of the interplanetary dust in our solar-system discs.
The temperature of the solar wind, which depends on the heliocentric distance, has been observed to be greater than that predicted by the adiabatic model. Therefore, the existence of heating processes, such as plasma turbulence or magnetic reconnection, could be predicted. The observation of the magnetic field by the devices separated in the scale of the membrane of the Solar Power Sail provides the resolution of the plasma turbulence on the electron scale. Thus, the intermittent observation of the magnetic field between the Earth and Jupiter would determine the heating mechanism of the solar wind. The synergy of the magnetic field and dust observation may show the interaction between interplanetary dust and solar wind. By analyzing the environments on the dust surface, the chemical evolutions of molecules caused by solar wind and cosmic radiation can be investigated. We are investigating the possibilities to detect gamma-rays and particles from the solar-system shocks.

Keywords: OKEANOS, zodiacal light, dust, plasma, gamma-ray

©2019. Japan Geoscience Union. All Right Reserved.

[E] Poster | P (Space and Planetary Sciences)：P-CG Complex & General

Sun. May 26, 2019 5:15 PM - 6:30 PM JST | Sun. May 26, 2019 8:15 AM - 9:30 AM UTC | Poster Hall International Exhibition Hall8, Makuhari Messe_8

[P-CG21] Future Missions and instrumentation for space and planetary science

convener:Mitsunori Ozaki(Faculty of Electrical and Computer Engineering, Institute of Science and Engineering, Kanazawa University), Satoshi Kasahara(The university of Tokyo), Shingo Kameda(School of Science, Rikkyo University), Kazuo Yoshioka(Graduate School of frontier Science, The University of Tokyo)

Not only national space agencies but some universities and even companies in the world are now leading a number of space science and exploration missions and also energetically initiating new research activities for satellite and rocket developments and international collaborations in these days because the Earth observations from the space and the space explorations could be achieved much easier than a few decades ago. The deployment to the space, which itself is not purely a scientific purpose but one of methods for better sciences, is vigorously motivating the technical innovation and the educational development. For successful space missions, it is also crucial to research and develop aim-oriented on-board instruments, and the fundamental research and development of observational instrumentation with future perspectives could totally lead space missions in some case. Detailed investigation and evaluation on various on-board instruments are needed during their proposals, selections, and fabrications in order to promote the missions, and inevitably we have to make multi-sided arrangements and evolution at every process and aspect of any type of space missions, independently of their mission sizes. In this session, we focus on these comprehensive research activities in the space and astronomical missions, including the mission integrations and the individual instrumental developments, and we also call many presentations showing the uniqueness and renovation regarding the mission strategy and methodology, and the status and latest results in the related state-of-the-art researches and developments, which would provide all of researchers and developers with invaluable opportunities for active discussion, information sharing, and collaboration toward the realization of more missions for more fruitful space sciences and explorations in nearer future.

[PCG21-P01] Visible and ultraviolet imagers for auroral and airglow observations by FACTORS - a future satellite mission for understanding the coupling and transportation processes in the upper atmosphere

*Takeshi Sakanoi[1], Masafumi Hirahara[2], Takuo T. Tsuda[3], Kazushi Asamura[4], Yoshizumi Miyoshi[2], Tomo-Hiko Watanabe[5], Takanori Nishiyama[6], Shin-ichiro Oyama[2,7], Yoshifumi Saito[4], Keisuke Hosokawa[3], Hirotsugu Kojima[8], Naritoshi Kitamura[9], Yasunobu Ogawa[5], Masatoshi Yamauchi[10], Ayako Matsuoka[4], Naoshi Yagi[1], Fukizawa Fukizawa[1], Genki Ishizawa[11] (1.Planetary Plasma and Atmospheric Research Center, Graduate School of Science, Tohoku University, 2.ISEE, Nagoya University, 3.Graduate School of Informatics and Engineering, School of Informatics and Engineering, The University of Electro-Communications, 4.ISAS/JAXA, 5.Graduate School of Science, Nagoya University, 6.National Institute for Polar Research, 7.University of Oulu, Finland, 8.RISH, Kyoto University, 9.Graduate School of Science, the University of Tokyo, Tokyo, 10.IRF Kiruna, Sweden, 11.Graduate School of Science, Tohoku University)

[PCG21-P02] Spatio-temporal analysis of flash aurora using Convolutional Neural Network

*Toki Genda[1], Takumi Inoue[1], Mitsunori Ozaki[1], Satoshi Yagitani[1], Imamura Kousuke[1], Kazuo Shiokawa[2], Yoshizumi Miyoshi[2], Shin-ichiro Oyama[2], Ryuho Kataoka[3], Yusuke Ebihara[4], Keisuke Hosokawa[5] (1.Kanazawa Univ., 2.Nagoya Univ., 3.NIPR, 4.Kyoto Univ., 5.UEC)

[PCG21-P03] Study on the pulse noise removal technique for Pc1 geomagnetic pulsations on the ground by signal processing

*Fumiya Komase[1], Tomohiro Inoue[1], Mitsunori Ozaki[1], Satoshi Yagitani[1], Kazuo Shiokawa[2], Masahito Nose[2], Tsutomu Nagatsuma[3] (1.Kanazawa Univ., 2.Nagoya Univ., 3.NICT)

[PCG21-P04] Application of magneto-impedance sensor to geomagnetic field measurements

*Masahito Nose[1], Reiko Nomura[2], Kazushi Asamura[3], Hitoshi Aoyama[4], Takeshi Kawano[4], Ayako Matsuoka[3], Kentarou Kitamura[5], Yukinobu Koyama[6], Haruhisa Matsumoto[7], Masafumi Hirahara[1] (1.Institute for Space-Earth Environmental Research, Nagoya University, 2.National Astronomical Observatory of Japan, 3.Institute of Space and Astronautical Science, Japan Aerospace Exploration Agency, 4.Aichi Steel Corporation, 5.National Institute of Technology, Tokuyama College, 6.National Institute of Technology, Oita College, 7.Research and Development Directorate, Japan Aerospace Exploration Agency)

[PCG21-P05] Observation of the Ionospheric Currents by the CubeSat at the Low and Middle Latitude

*Kentarou Kitamura[1], Kazumasa Imai[2], Taku Takada[2], Manabu Shinohara[3], Makoto Wakabayashi[4], KOSEN Space Collaboration Group (1.National Institute of Technology, Tokuyama Collge, 2.National Institute of Technology, Kochi Collge, 3.National Institute of Technology, Kagoshima Collge, 4.National Institute of Technology, Niihama Collge)

[PCG21-P06] Basic study on miniaturization of electric field instrument for plasma wave observations by ASIC technology

*Yuya Tokunaga[1], Mitsunori Ozaki[1], Keigo Ishisaka[2], Hirotsugu Kojima[3], Satoshi Yagitani[1], Takahiro Zushi[3] (1.Kanazawa University, 2.Toyama Prefectural University, 3.Kyoto University)

[PCG21-P07] Evaluation of radiation tolerance of electronics parts used for the ultra-small mission

*Riku Katsuse[1], Kazuo Yoshioka[1], Masaki Kuwabara[2], Reina Hikida[1], Shogo Arao[1], Ichiro Yoshikawa[1] (1.The university of Tokyo , 2.Institute of Space and Astronautical Science)

[PCG21-P08] A method to quantitatively evaluate Non-evaporable-getter pump for use in space science mission

*Seiya Nishimura[1], Ichiro Yoshikawa[1], Kazuo Yoshioka[1], Shogo Arao[1], Zhang Tianxu[1] (1.The university of tokyo)

[PCG21-P09] Interpretation on slight asymmetry of analyzer characteristics of MIA onboard the Mio by means of a model calculation of 3-D potential distribution

*Wataru Miyake[1], Yoshifumi Saito[2], Shoichiro Yokota[3] (1.Tokai University, 2.ISAS, 3.Osaka University)

[PCG21-P10] Construction of impact testing machine for small satellites and evaluation of mechanical resistance of MCPs by the impact test

*Junya Fukuba[1] (1.Graduate school of Tokyo)

[PCG21-P11] Innovative design of double-shell type energy analyzer for simultaneous electron and ion measurements in space

*Tomomi Takei[1], Masafumi Hirahara[1] (1.Institute for space-earth environmental research, Nagoya university)

[PCG21-P12] Microsatellite Development and Education of Space Science and Technology at Kanazawa University

*Tomohiko Imachi[1], Satoshi Yagitani[1], Daisuke Yonetoku[1], Yoshiya Kasahara[1], Tatsuya Sawano[1], Makoto Arimoto[1], Yoshitaka Goto[1], Mitsunori Ozaki[1], Ryuichi Fujimoto[1] (1.Kanazawa University)

[PCG21-P13] Attitude Control System for Kanazawa-SAT3 Microsatellite

Takuya Nakajima[1], Yuuki Yasuda[1], Hirofumi Segawa[1], *Tomohiko Imachi[1], Satoshi Yagitani[1], Yoshiya Kasahara[1], Daisuke Yonetoku[1], Tatsuya Sawano[1], Makoto rimoto[1] (1.Kanazawa University)

[PCG21-P14] Communications System and Antennas for Kanazawa-SAT3 Microsatellite

Teruya Minamoto[1], Koyo Ina[1], Kohei Kawagoshi[1], *Tomohiko Imachi[1], Satoshi Yagitani[1], Yoshitaka Goto[1], Daisuke Yonetoku[1], Yoshiya Kasahara[1], Tatsuya Sawano[1], Makoto Arimoto[1] (1.Kanazawa University)

[PCG21-P15] Development of micrometeoroid impact sensor within a multi-layered insulation (CLOTH) onboard 6U deep-space explorer EQUULEUS

*Takayuki Hirai[1], Hajime Yano[2], Ritsuko Jitsukawa[3], Eigo Ishioka[3], Haruki Nakano[3], Kazuyoshi Arai[3], Sunao Hasegawa[2] (1.Planetary Exploration Research Center, Chiba Institute of Technology, 2.Institute of Space and Astronautical Science, Japan Aerospace Exploration Agency, 3.Faculty of Science and Engineering, Hosei University)

[PCG21-P16] Breadboard model of asteroid tracking system for DESTINY$^+$ mission

*Peng Hong[1], Ko Ishibashi[1], Shunsuke Sato[2], Kazutoshi Takemura[3], Kotaro Fujiwara[4], Kanako Machii[5], Hiroyuki Toyota[2], Kazutaka Nishiyama[2], Masatsugu Otsuki[2], Osamu Okudaira[1], Takeshi Takashima[2] (1.Planetary Exploration Research Center, Chiba Institute of Technology, 2.Institute of Space and Astronautical Science, Japan Aerospace Exploration Agency, 3.Department of Applied Mechanics, Graduate School of Fundamental Science and Engineering, Waseda University, 4.Division of Mechanical and Space Engineering, Graduate School of Engineering, Hokkaido University, 5.Department of Mechanical Engineering and Intelligent Systems, Faculty of Informatics and Engineering, The University of Electro-Communications)

[PCG21-P17] Development of telescopic camera (TENGOO) performance evaluation device in MMX

*Hiroki Kato[1], Shingo Kameda[1], Keigo Enya[2], Osada Naoya[1] (1.Rikkyo University, 2.Japan Aerospace Exploration Agency)

[PCG21-P18] Observation Plans in the Cruising-Phase of the Solar Power Sail: OKEANOS

*Takahiro Iwata[1], Shuji Matsuura[2], KOHJI TSUMURA[3], Hajime Yano[1], Takayuki Hirai[4], Ayako Matsuoka[1], Daisuke Yonetoku[5], Tatehiro Mihara[6], Tatsuaki Okada[1], Osamu Mori[1], Toshihiro Chujo[1] (1.Institute of Space and Astronautical Science, Japan Aerospace Exploration Agency, 2.Kwansei Gakuin University, 3.Tohoku University, 4.Chiba Institute of Technology, 5.Kanazawa University, 6.RIKEN)

Visible and ultraviolet imagers for auroral and airglow observations by FACTORS - a future satellite mission for understanding the coupling and transportation processes in the upper atmosphere

*Takeshi Sakanoi[1], Masafumi Hirahara[2], Takuo T. Tsuda[3], Kazushi Asamura[4], Yoshizumi Miyoshi[2], Tomo-Hiko Watanabe[5], Takanori Nishiyama[6], Shin-ichiro Oyama[2,7], Yoshifumi Saito[4], Keisuke Hosokawa[3], Hirotsugu Kojima[8], Naritoshi Kitamura[9], Yasunobu Ogawa[5], Masatoshi Yamauchi[10], Ayako Matsuoka[4], Naoshi Yagi[1], Fukizawa Fukizawa[1], Genki Ishizawa[11]

1. Planetary Plasma and Atmospheric Research Center, Graduate School of Science, Tohoku University, 2. ISEE, Nagoya University, 3. Graduate School of Informatics and Engineering, School of Informatics and Engineering, The University of Electro-Communications, 4. ISAS/JAXA, 5. Graduate School of Science, Nagoya University, 6. National Institute for Polar Research, 7. University of Oulu, Finland, 8. RISH, Kyoto University, 9. Graduate School of Science, the University of Tokyo, Tokyo, 10. IRF Kiruna, Sweden, 11. Graduate School of Science, Tohoku University

We report science subject, design, development plan and identification of issues to be solved on the visible and ultraviolet imagers for a future satellite mission called FACTORS that aims to understand the coupling processes in the terrestrial magnetosphere/ionosphere/thermosphere and the acceleration and transportation of the space plasma and neutral atmospheric particles. FACTORS stands for Frontiers of Formation, Acceleration, Coupling, and Transport Mechanisms Observed by Outer Space Research System that is proposed as a multi-satellite formation flight mission. This will be a community exploration mission in Japanese apace research after the success of the ERG mission. The working group was approved by ISAS, JAXA this year, and we have started the discussion on detailed science targets, instrumental design, feasibility and so on. We mainly concern on visible and ultraviolet remote imaging of aurora and airglow for this mission. A visible imager (VISAI) on FACTORS will measure small-scale auroral structures at a wavelength of auroral prompt emission line, such as N2 1st PG, with high-time (~0.1s) and high-spatial (~1km) resolutions using a science CMOS or EMCCD. The FOV of 8 x 8 deg covers an area of 400 x 400 km viewed from 3000 km altitude. The high-spatial and high-time resolution imaging data is essential to understand small-scale variations of Alfven aurora, pulsating aurora, etc. Combined with particle and electric/magnetic field data by FACTORS, we will reveal the time and spatial variations of acceleration/scattering process in the complicated magnetosphere-ionosphere coupling system. A far-ultraviolet imager (FUVI) adopts a wide (~40 x 40 deg.) FOV objective mirror system which covers ~2500 x 2500 km area viewed from 3000 km altitude. We plan to adopt a filter wheal in FUV imager to change the wavelength between O 135.6 nm and the N2 LBH band at 140-160 nm. Wide-field multi-wavelength FUV images enable us to examine large-scale auroral dynamics like westward-travelling surge during substorm, omega-bands, and provide us to understand the global thermospheric activity from O/N2 airglow ratio. This year we plan to carry out specific studies for CMOS/EMCCD detectors suited for this mission, and perform radiation tests of detectors.
Related to the future FACTORS mission, we are now carrying out the developments of aural cameras for two sounding rocket projects, G-CHASER (Rocksat-XN) and LAMP. The G-CHASER (Rocksat-XN) rocket was successfully launched from Andøya, Norway on January 13, 2019. We installed an auroral camera (AIC) on this rocket to measure N2 1st PG emission with wide-angle FOV lens(96x75 deg), RG-665 filter, and CCD (WAT-910HX). In addition, we are developing two CMOS cameras AIC2 on the LAMP rocket that is scheduled to be launched at Poker Flat Research Range in winter of 2019. AIC2 will be installed on a despun platform to derotate rocket spin. One CMOS camera AIC2-S1 measures N2 1st PG emission with a narrow FOV lens (F-number=0.95, f=17mm, FOV=27x27deg.), and another CMOS camera AIC-S2

©2019. Japan Geoscience Union. All Right Reserved.

measures OI 844.6nm emission with a wide-angle lens (F-number=1.6, f=3.5mm, FOV=120x120deg.). Both cameras adopt the ZWO ASI 180 MM CMOS detector. AIC2-S1 will take fine structure of PsA in the region more than 100 x 100 km area around the magnetic footprint with a few kilo-meter resolution, while AIC2-S2 will obtain an altitude distribution of pulsating aurora in the F-region as well as distribution of PsA in wide-range. The precise imaging and altitude distribution of PsA are obtained with AIC2 at two wavelengths with 10Hz sampling. The imaging data combined with precipitating electron data in the wide energy range enable us to investigate the relativistic electron precipitation called microbursts that is probably caused by chorus waves in the magnetosphere.

Keywords: magnetosphere, aurora, imager, ultra violet, visible, ionosphere

©2019. Japan Geoscience Union. All Right Reserved.

Spatio-temporal analysis of flash aurora using Convolutional Neural Network

*Toki Genda[1], Takumi Inoue[1], Mitsunori Ozaki[1], Satoshi Yagitani[1], Imamura Kousuke[1], Kazuo Shiokawa[2], Yoshizumi Miyoshi[2], Shin-ichiro Oyama[2], Ryuho Kataoka[3], Yusuke Ebihara[4], Keisuke Hosokawa[5]

1. Kanazawa Univ., 2. Nagoya Univ., 3. NIPR, 4. Kyoto Univ., 5. UEC

High energy electrons in the magnetosphere travel along geomagnetic field lines and precipitate into the Earth's atmosphere, then auroras are shown on the ground. We can investigate indirectly the behavior of precipitating electrons in the magnetosphere by deducing auroras on the ground. We focus on flash auroras, which illuminate suddenly at less than 1 s. It is difficult to detect a lot of flash aurora events by visually looking because the duration of flash aurora is very short. In this study, we developed an automatic detection of flash auroral position using Convolutional Neural Network (CNN) and performed statistical analysis of the spatio-temporal variations of flash aurora taken by an EMCCD camera (100 Hz sampling, 256 * 256 pixels) at Gakona (Alaska).

The learning data was obtained by dividing the keogram images (2400 * 720 pixels, 1-minute period) along the north-south direction of all-sky EMCCD data into square blocks (30 * 30 pixels, 750-ms period), then the learning data was visually classified to four classes. Four classes are, "pulsating aurora", "flash aurora", "noise", and "no aurora or noise". We classified the test data using the CNN, its accuracy was 91.2%.

The flash aurora data (about 100 events) are collected by CNN and we extracted flash auroral region using Otsu's method, which is a basic method of contour extraction. We performed statistical analysis about luminous duration, luminous point, spatial size, and spatial extent of flash aurora. The averaged luminescence duration was 0.21±0.08 seconds, and did not depend on magnetic longitudes and latitudes in the field-of-view of camera. We confirmed that most events (about 70%) expand earthward with an average spatial extent of 0.027 Re. We think that the earthward extension can be caused by wave propagation effects of whistler mode waves and the nonuniformity of spatial distribution of loss cones in the magnetosphere.
In this presentation, we will report on our automatic detection method and statistical results of spatio-temporal analysis of flash aurora in detail.

Keywords: Convolutional Neural Network, pulsating aurora, flash aurora

©2019. Japan Geoscience Union. All Right Reserved.

Study on the pulse noise removal technique for Pc1 geomagnetic pulsations on the ground by signal processing

*Fumiya Komase[1], Tomohiro Inoue[1], Mitsunori Ozaki[1], Satoshi Yagitani[1], Kazuo Shiokawa[2], Masahito Nose[2], Tsutomu Nagatsuma[3]

1. Kanazawa Univ., 2. Nagoya Univ., 3. NICT

An electromagnetic ion cyclotron (EMIC) wave, which is a type of plasma waves generated in the magnetosphere, propagates along the geomagnetic field line and we can observe it as the fluctuation in the geomagnetic field on the ground called Pc1 geomagnetic pulsation (0.2 to 5 Hz). We observe Pc1 pulsations at Kapuskasing (Canada). The ground observation is carried out using an induction magnetometer, and the Pc1 pulsations are observed with a high sensitivity and a high time resolution (64 Hz). However, when the observation instrument vibrates due to a strong wind, pulse noise is included in the observed waveforms.
We have been studying an extracting method of Pc1 pulsation by removing the pulse noise included in observed waveform using signal processing technique. Pulse noise shows in a wider frequency range (0.1 to 10 Hz) than the frequency range of Pc1 pulsation and its duration is shorter than the duration of Pc1 pulsation. Pulse noise removal consists of detecting the pulse noise candidate, classifying the pulse noise candidates into pulse noises and others by Neural Network (NN), and interpolating the waveform at the pulse noise domain. In the first step, we set an amplitude threshold for the differential waveform to detect pulse noise candidates. In the second step, as learning data for classification, we use waveform applied a High Pass Filter (HPF) to emphasize pulse noises. In the third step, we use an average energy around the pulse noise in the interpolation. We use random phase, observation phase including the pulse noises, and estimated phase by nonlinear least squares method. For each phase, we evaluated the SNR before and after the pulse noise removal. As a result, the SNR improved with 22dB using the estimated phase, but it requires a huge calculation time.
In this presentation, we will report on the pulse noise removal of Pc1 pulsation using signal processing technique in detail. Conventionally it was necessary to examine and construct the observation environment which suppresses the vibration of the observation equipment as much as possible, we think that our signal processing will be useful for reducing the ground observation costs and a more detailed analysis of Pc1 pulsation.

Keywords: Pc1 geomagnetic pulsation, Noise removal, Signal processing

©2019. Japan Geoscience Union. All Right Reserved.

Application of magneto-impedance sensor to geomagnetic field measurements

*Masahito Nose[1], Reiko Nomura[2], Kazushi Asamura[3], Hitoshi Aoyama[4], Takeshi Kawano[4], Ayako Matsuoka[3], Kentarou Kitamura[5], Yukinobu Koyama[6], Haruhisa Matsumoto[7], Masafumi Hirahara[1]

1. Institute for Space-Earth Environmental Research, Nagoya University, 2. National Astronomical Observatory of Japan, 3. Institute of Space and Astronautical Science, Japan Aerospace Exploration Agency, 4. Aichi Steel Corporation, 5. National Institute of Technology, Tokuyama College, 6. National Institute of Technology, Oita College, 7. Research and Development Directorate, Japan Aerospace Exploration Agency

Magneto-impedance (MI) effect was discovered about 25 years ago and a micro-size magnetic sensor that utilizes this effect becomes commercially available. We made some modifications to the commercially available MI sensors as they can cover the range of the geomagnetic field. For the period of March 30 to April 27, 2018, we conducted experimental observations of geomagnetic field variations with the MI sensors at Mineyama observation site, which is located about 100 km north-west of Kyoto. Data obtained with the MI sensors were compared with those from the fluxgate magnetometer that has been working at the site. Results showed that the MI sensor recorded geomagnetic variations with amplitudes of ~1 nT that were also detected with the fluxgate magnetometer. This suggests that MI sensors are useful for researches in geomagnetism or space physics, although they are much less expensive than fluxgate magnetometers.

We consider developing two different kinds of systems to measure the geomagnetic field using the MI sensor: a system for ground-based observation and a system for a sounding rocket. In presentation, we will display observation data from the MI sensors and the fluxgate magnetometers at Mineyama and other observatories. Future plans of the system onboard sounding rocket will be also presented and discussed.

©2019. Japan Geoscience Union. All Right Reserved.

Observation of the Ionospheric Currents by the CubeSat at the Low and Middle Latitude

*Kentarou Kitamura[1], Kazumasa Imai[2], Taku Takada[2], Manabu Shinohara[3], Makoto Wakabayashi[4], KOSEN Space Collaboration Group

1. National Institute of Technology, Tokuyama Collge, 2. National Institute of Technology, Kochi Collge, 3. National Institute of Technology, Kagoshima Collge, 4. National Institute of Technology, Niihama Collge

The ionospheric currents flowing in the dayside ionosphere have been considered as a significant subsequence of Mesosphere-Ionosphere-Magnetosphere coupling. These currents were well detected in the Solar quiet conditions and named Sq currents. In particular, it is well known that the flow pattern of Sq currents shows the north-south hemispheric asymmetry due to the different ionospheric conductivities in the winter and summer hemispheres. This indicates that the asymmetry of the potential must be kept by the energy balance between each hemisphere through the field line.
An InterHemispheric Field Aligned Current (IHFAC) was theoretically predicted by Maeda [1974] and Fukushima [1979, 1991] to interpret the north-south asymmetry in the potential pattern. Several ground magnetic observations and satellite observations suggested an existence of the IHFAC in the noon sector and both the morning and evening terminators. However, the detailed morphology of the IHFAC have not been well understood yet, despite that the direct detection of the IHFAC at Low Earth Orbit (LEO) was reported in the observation by several satellites.
In order to investigate the Sq current system including the IHFAC, the in-situ observation by a CubeSat (2U size satellite emitted from ISS) is proposed in collaboration with 10 national colleges which belong to National Institute of Technology (KOSEN). The fluxgate magnetometer is onboard the CubeSat to observe small perturbations of the magnetic field. After the ejection from the ISS, the CubeSat will gradually glide down to the upper atmosphere due to the strong atmospheric drag and finally burn up in it. The duration of possible observation is estimated for more than 50 days.
The CubeSat can be characterized by the short duration of development (less than 3 years) and low cost (less than 100,000USD). We are considering an actual utilization of this extremely low-cost CubeSat to more realistic science mission. This concept enables us to conduct the multi-satellite in-situ observation in fairly low budget compared to conventional satellite missions.

Keywords: Ionospheric Current, Interhemispheric Field Aligned Current, CubeSat

©2019. Japan Geoscience Union. All Right Reserved.

Basic study on miniaturization of electric field instrument for plasma wave observations by ASIC technology

*Yuya Tokunaga[1], Mitsunori Ozaki[1], Keigo Ishisaka[2], Hirotsugu Kojima[3], Satoshi Yagitani[1], Takahiro Zushi[3]

1. Kanazawa University, 2. Toyama Prefectural University, 3. Kyoto University

We have been measuring electric fields of the plasma waves (a few Hz to several hundred Hz) to understand the magnetospheric dynamics. The spatial resolutions of electric field measurements are not enough because we cannot launch a lot of satellites due to the large size and mass of satellites. Demands of micro satellites like a 1U (10 cubic centimeters) cube satellites are increasing. We need to miniaturize measurement instruments for probing the plasma waves.

This study deals with an electric field instrument in plasma wave observations. We use the electric field instrument for capturing the electric fields detected by wire probe antennas. In this study, the purpose is to miniaturize the electric field instrument with a high radiation tolerance (300 krad) using Application Specific Integrated Circuit (ASIC) technology.

We designed a based amplifier for a new electric field instrument. In the new based amplifier, the equivalent input noise is 50 nV/sqrt(Hz) at 1 kHz, which is 3.9 dB-larger than that of conventional based amplifier (OP-41). The noise performance of new based amplifier is acceptable for capturing the plasma waves. To confirm the radiation tolerance of new based amplifier, we did the radiation tests up to 300 krad using the gamma ray. From the radiation test results, the gain was no change before and after the radiation tests. The output noise was degraded with 5.05 dB at 100 Hz by total ionizing dose effects. However, the based amplifier was not breakdown by the gamma ray. The electric field instrument consisted of new based amplifier could operate with a high radiation tolerance.

We conducted the transient analysis for the new electric field instrument by a circuit simulator (Tanner EDA). In the simulation, rectangular waves of 1 Vpp with 10 Hz input to the new electric field instrument via a sheath impedance (10 MOhms and 100 pF). From the simulation results, the output waveforms of new electric field instrument showed similar output waveforms in comparison with the conventional electric field instrument. The power consumption of new electric field instrument can decrease with approximately 67% than that of the conventional electric field instrument. From the simulation results, we confirmed the basic operations as the electric field instrument for detecting the plasma waves. In the future work, we will need to improve the temperature operating range because the new electric field instrument cannot operate at minus 60 Celsius degrees from the temperature simulation results.

In this presentation, we will present the basic study on electric field instrument for plasma wave observation by ASIC technology in detail.

Keywords: ASIC, Electric field instrument, Plasma wave observation

©2019. Japan Geoscience Union. All Right Reserved.

Evaluation of radiation tolerance of electronics parts used for the ultra-small mission

*Riku Katsuse[1], Kazuo Yoshioka[1], Masaki Kuwabara[2], Reina Hikida[1], Shogo Arao[1], Ichiro Yoshikawa[1]

1. The university of Tokyo , 2. Institute of Space and Astronautical Science

In the space environment, spacecraft is exposed to radiation and degrades the data. For example, the increase of dark current, and change in current consumption.

Recently, the university-made ultra-small spacecraft mission become popular. The mission in this class can reduce the cost and time by using commercial products. However, these commercial products are thought to have no radiation tolerance. Then, it is necessary to be tested with the radiation total dose which is calculated using the Monte Carlo simulation.

We are developing the extreme ultraviolet imager PHOENIX onboard the ultra-small satellite EQUULEUS which will be launched in 2020. Helium ions in the Earth’ s plasmasphere emit extreme ultraviolet light (wavelength of 30.4 nm) through the solar resonance scattering. PHOENIX observes them from the moon (Earth-Moon L2 point).

The radiation tolerance has been evaluated with a gamma irradiation facility with cesium 137. In this presentation, we show the gain characteristics and change of electric noise with respect to radiation of semiconductor elements used in PHOENIX instrument.

©2019. Japan Geoscience Union. All Right Reserved.

A method to quantitatively evaluate Non-evaporable-getter pump for use in space science mission

*Seiya Nishimura[1], Ichiro Yoshikawa[1], Kazuo Yoshioka[1], Shogo Arao[1], Zhang Tianxu[1]

1. The university of tokyo

Observation instruments are known to deteriorate under atmospheric condition. Deterioration are mainly caused by reaction with water vapor and oxygen. To prevent this, observation instruments must be maintained under vacuum. The problem is that the conventional vacuum pump are too heavy to carry to the launching site. The need of continuous power supply makes the transport more difficult. Also the vacuum pump must be removed before the launch. These problems are not only making it difficult to maintain observation instruments under vacuum but also causing extra costs. Non-evaporable-getter (NEG) pumps are able to solve these problems. NEG pumps are light weight, compact, oil free, vibration free, and able to operate without energy supply after activation. Considering the utilization of NEG pump for space science missions, we need to quantitatively evaluate the NEG pump to optimize its size, shape, material, and mounting position for each mission. In this study, a method to measure pumping speed of NEG pump for carbon monoxide (as substitute to water vapor and oxygen) was established by using the orifice method. By using this method, it will be able to develop a NEG pump which best applies the case for each mission.

Keywords: Non-evaporable-getter pump, vacuum pump

©2019. Japan Geoscience Union. All Right Reserved.

Interpretation on slight asymmetry of analyzer characteristics of MIA onboard the Mio by means of a model calculation of 3-D potential distribution

*Wataru Miyake[1], Yoshifumi Saito[2], Shoichiro Yokota[3]

1. Tokai University, 2. ISAS, 3. Osaka University

MIA (Mercury Ion Analyzer) on board Mio employs a top-hat electrostatic analyzer, which has axisymmetric toroidal electrodes and is designed to have no dependence in its characteristics on azimuthal direction of incident ions. However, our ground calibration experiments have revealed that it has a slight dependence. We have tried to explain the dependence by means of three dimensional model calculations. We assumes that all parts of electrode are manufactured precisely. Our results shows that a slight relative rotation (or tilt) of electrodes can lead to a slight dependence on incident azimuthal direction similar to that obtained from the ground experiments.

Keywords: Mio, tophat electrostatic analyzer , MIA

©2019. Japan Geoscience Union. All Right Reserved.

Construction of impact testing machine for small satellites and evaluation of mechanical resistance of MCPs by the impact test

*Junya Fukuba[1]

1. Graduate school of Tokyo

Small satellites have been developed in recent years. Environmental tests at the development stage play an important role in improving reliability of small satellites. These include a vibration test, an impact test, and a thermal vacuum test. Especially, the impact test is one of the most difficult tests and a reliable method has not yet been established. Against such a background, we constructed an impact testing machine for small satellites. Required performance of the impact testing machine is a controllability and a reproducibility. The controllability means the performance of applying a targeted impact level accurately. This is important to avoid applying excessive impacts on a test target. The reproducibility means the performance of applying same impact level repeatedly and this is also important because if it is possible to apply an unintended impact under the same condition, it degrades the test accuracy. Our impact testing machine is designed to be able to easily adjust the impact level and have high reproducibility. Furthermore, we tested for mechanical resistance of the MCP (micro-channel plate) which is used for optical observation instruments. In this test, we used an impact level assuming the EQUULEUS mission which will be launched by NASA’ s rocket in 2020. In my presentation, I will introduce the details of our impact testing machine and the impact test results of MCP.

Keywords: impact test

©2019. Japan Geoscience Union. All Right Reserved.

Innovative design of double-shell type energy analyzer for simultaneous electron and ion measurements in space

*Tomomi Takei[1], Masafumi Hirahara[1]

1. Institute for space-earth environmental research, Nagoya university

It is well known that the terrestrial and planetary magnetospheres and the interplanetary space are filled with charged particles such as electrons and ions, which are so-called the space plasma, and in-situ observations of the space plasmas have been conducted by using satellites carrying particle instruments, such as the top-hat type electrostatic energy analyzer. Essentially, obtaining three-dimensional velocity distributions of the space plasmas or energy-pitch angle distributions help us understand the dynamics of the space plasmas. Because the top-hat type analyzer is cylindrically symmetric and has a 2π-radian planar field of view, it can independently measure the wide angular and energy distributions of incident particles. Also, three-dimensional velocity or energy-pitch angle distributions can be obtained by utilizing the satellite spin motion.
The top-hat type electrostatic energy analyzers can measure the ions when a negative potential is applied to the inner electrode and the electrons by a positive potential with the outer electrode grounded. Therefore, in the prevailing design of the top-hat type analyzer, the sensor heads separate for the ion and electron observations, respectively. Because of the recent miniaturization of the satellites, the weight and space of the instruments mounted on the small and micro satellites are getting severely restricted. However, if two sensors for electron and ion observations are combined into one sensor head, it is possible to save both weight and space on the small and micro satellites. Therefore, we have been developing double-shell type energy analyzer which can simultaneously measure the ions and the electrons with one sensor head.
We designed the shapes of the collimator and the double-layered dome-shaped electrodes so that the electrons and the ions with appropriate energies pass through the inner gap and the outer gap by applying a negative potential to the central electrode with the inner and outer electrodes grounded, respectively. We made the numerical simulations using SIMION which is a charged particle simulator program and investigated the performance and characteristics as the electrostatic analyzer. Consequently, we confirmed that the electrons and the ions can be analyzed with one sensor head by only applying negative high voltage to the electrodes. So far, we consider the detection unit using Time-Of-Flight velocity spectrometer for the discrimination of the ion species as the part where the ions are detected, and an assembly of micro channel plates is expected for the electron detection. The design of TOF-type mass analysis unit as ion mass analysis unit is one of subjects for future work.

©2019. Japan Geoscience Union. All Right Reserved.

Microsatellite Development and Education of Space Science and Technology at Kanazawa University

*Tomohiko Imachi[1], Satoshi Yagitani[1], Daisuke Yonetoku[1], Yoshiya Kasahara[1], Tatsuya Sawano[1], Makoto Arimoto[1], Yoshitaka Goto[1], Mitsunori Ozaki[1], Ryuichi Fujimoto[1]

1. Kanazawa University

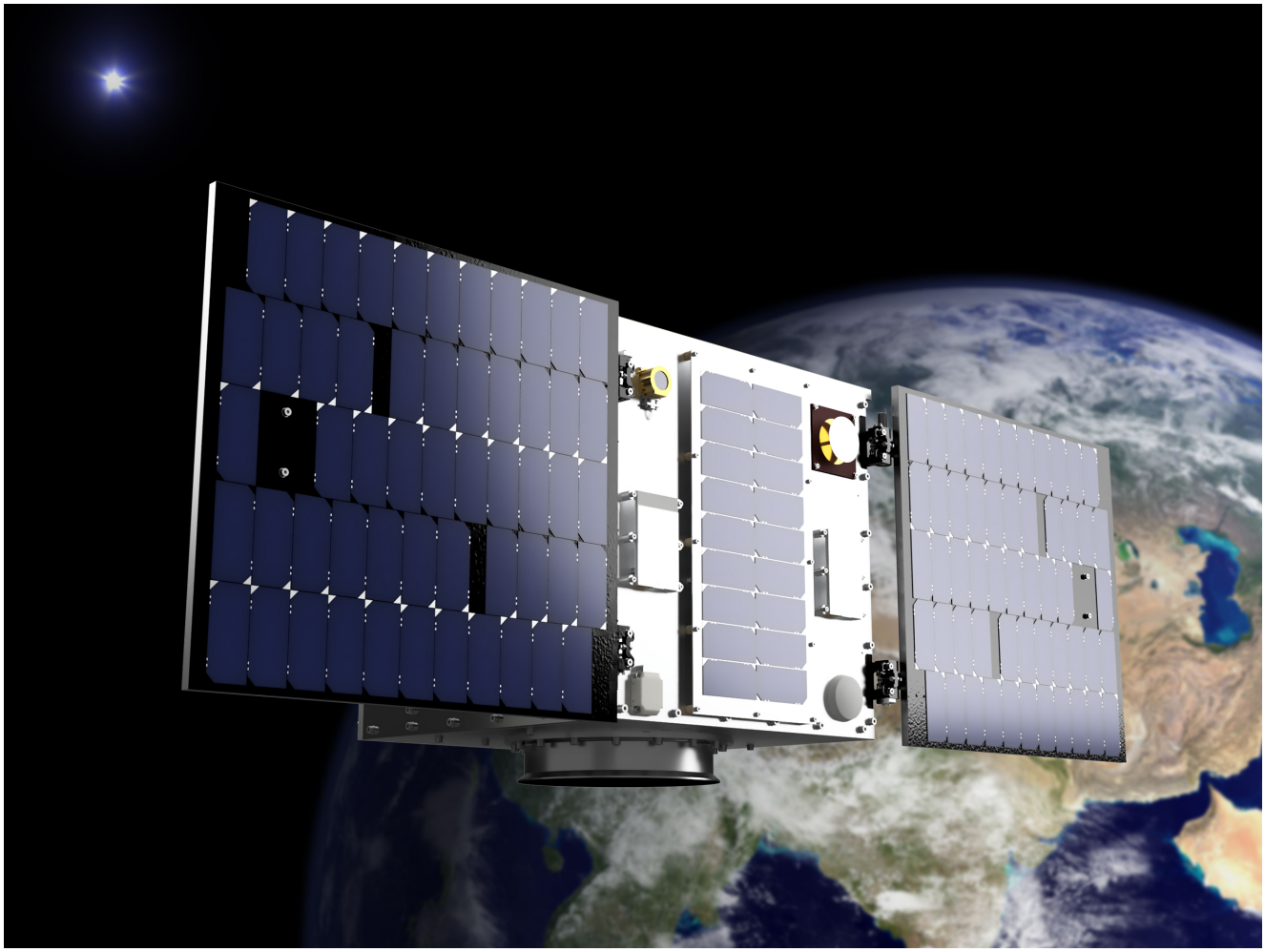
At Kanazawa University, researchers from engineering and science are cooperating to promote the "Kanazawa University Satellite Project (Kanazawa-SAT3: Study and Training in Space Science and Technology for Kanazawa Cube-Satellites)". In this project, a microsatellite is being developed by staff and students of Kanazawa University. It is a scientific satellite which will contribute to the elucidation of the mechanism of gravitational wave generation by identifying the source of gravitational wave by detecting the arrival direction of gamma rays and X rays radiated at the same time when a gravitational waves are generated by collision of astronomical objects The satellite will be inserted into a solar synchronous orbit at about 660 km altitude. It is a microsatellite with a total weight of 50 kg or less, and its size is cubic with a side of 50 cm, and it is designed to be a piggyback on an HII-A rocket.

Also related to this project, a space science and engineering course has been newly established in the Graduate School of Natural Sciences in April 2018. This course is based on the 'satellite development by students', and students are actually involved in the design, fabrication, ground tests, and operation of scientific satellites, aiming to train personnel who are familiar with space science and space engineering, with satellite-development skills.

Ground tests with the thermal and structural model of Kanazawa-SAT3 have been completed , and the unit tests for almost all components are being conducted. Currently, we are completing the design of the flight model. In the presentation, we will report the details of Kanazawa-SAT3 and its development status.

Keywords: Microsatellite, Gravitational wave, Kanazawa SAT3

©2019. Japan Geoscience Union. All Right Reserved.



©2019. Japan Geoscience Union. All Right Reserved.

Attitude Control System for Kanazawa-SAT3 Microsatellite

Takuya Nakajima[1], Yuuki Yasuda[1], Hirofumi Segawa[1], *Tomohiko Imachi[1], Satoshi Yagitani[1], Yoshiya Kasahara[1], Daisuke Yonetoku[1], Tatsuya Sawano[1], Makoto rimoto[1]

1. Kanazawa University

Kanazawa University has been developing a microsatellite. This satellite is equipped with a device to observe celestial bodies emitting gravitational waves with X rays, and aims to elucidate the mechanism of black hole formation by estimating the time of arrival and direction of arrival of gravitational waves.
In this research, the attitude control system is being developed using GAS (Geomagnetic Aspect Sensor) and MTQ (Magnetic Torque). We have constructed the environment for the unit test of RW (Reaction Wheel) also used for attitude control of the satellite.

MTQ is a device that controls the attitude of the satellite by generating a magnetic torque against the geomagnetic field by applying a voltage (an electric current) to a magnetic coil. GAS is a device for detecting the direction of the geomagnetic vector. OBC (On Board Computer) which controls all devices mounted on the satellite receives the geomagnetic field data detected by GAS, and transmits commands to control MTQ. GAS and MTQ cannot be connected to OBC directly, because OBC has just a digital interface, but the output of GAS and the input to MTQ are analog voltages. Therefore, we have developed a control device for on-board equipment using a microcontroller. For the GAS, the voltages are A/D-converted by the microcontroller and transmitted to the OBC. For the MTQ, OBC transmits control commands to the microcontroller, which generates a PWM (Pulse Width Modulation) signal according to the received command that determines the effective voltage to be given to the MTQ. For the system development and operation tests, a PC is used instead of OBC and we carried out experiments of control equipment. For the GAS, we have confirmed the linearity between the analog magnetic field and the corresponding digital values transmitted to the PC. For the MTQ, we have confirmed that the voltage to be given to MTQ were precisely controlled by the duty ratio of the PWM signal output from the microcontroller.

RW is a device to generate a control torque around the rotation axis by accelerating a rotor by a motor and is controlled by transmitting a command from the OBC via an RS-422 serial communication line. The unit test has been carried out by using a PC as a substitute of OBC, but the cable had a influence on the rotation operation of RW. Therefore, we have constructed a system for wirelessly connecting the RW with the PC via a wireless RS-422 communication. Specifically, commands from the PC are wirelessly transmitted to an Arduino microprocessor by a low-power radio module XBee, and the RW is controlled via an RS-422 transceiver. With this system, we demonstrated the basic functions for command and data between the PC and the Arduino via the wireless RS-422 transceiver.

We plan to construct a system that applies appropriate PWM signals to MTQ according to the value detected by GAS. We will also evaluate RW performance by the unit test using the wireless RS-422 communication system.

Keywords: Microsatellite, ACS, Kanazawa SAT3

©2019. Japan Geoscience Union. All Right Reserved.

Communications System and Antennas for Kanazawa-SAT3 Microsatellite

Teruya Minamoto[1], Koyo Ina[1], Kohei Kawagoshi[1], *Tomohiko Imachi[1], Satoshi Yagitani[1], Yoshitaka Goto[1], Daisuke Yonetoku[1], Yoshiya Kasahara[1], Tatsuya Sawano[1], Makoto Arimoto[1]

1. Kanazawa University

Kanazawa University is developing the first Kanazawa University's microsatellite, named as Kanazawa-SAT3. Kanazawa-SAT3 is planned to be launched within FY2019, and its observation mission is to identify the source of gravitational waves by detecting the occurrence time and arrival direction of the X-rays and gamma rays observed simultaneously with gravity waves from distant astronomical objects.

In this research, we are developing a communications system for Kanazwa-SAT3. Kanazawa-SAT3 has three different communication systems using S band, UHF band and Iridium, and the link design of each of them has generally been completed. We summarize each communication system in detail as the following.

The S-band communication system, will use 2-GHz frequency band. Kanazawa-SAT3 is equipped with two types of antennas: S-band patch antennas and S-beacon antennas. S-band system is a main communication system between the satellite and a ground station, and plays a role of high speed data communication and beacon transmission. On the satellite side, two S-band patch antennas designed for both transmission and reception are mounted on the front and rear panels of the satellite. Two S-beacon antennas for transmission are also mounted on the front and rear panels of the satellite. On the ground side, we will send and receive by the signals using a 2.4-m parabolic dish installed at Kanazawa University.

The UHF communication system will use 400-MHz frequency bands. This system transmits commands from the ground to the satellite and telemetry information from the satellite to the ground. On the satellite side, four inverted-F type antennas we developed are mounted (two for receiving and two for transmitting) on the front and rear panels of the satellite. On the ground side, we will send and receive data by using a Yagi antenna with 14 crossed elements installed at Kanazawa University. We have also constructed an automatic satellite tracking system using the Yagi antenna.

A communication system using the Iridium satellite network uses a frequency band around 1.6 GHz. In this system, communications are performed via Iridium satellite, so that the communication can be established even when our ground station is not visible from the satellite. The data is exchanged between the satellite and the ground by using e-mail. This system can transmit and receive data in almost real time so emergency command and data transmission will be available. On the satellite side, two antennas for both transmission and reception are mounted on the front and rear panels of the satellite. A system has been constructed that exchanges data between a laptop computer simulating an onboard computer (OBC) mounted on a satellite and an iridium satellite.

From now on, for the communication systems using the S band and the UHF band, it is necessary to develop the communication software. For In addition, we need to improve the automatic satellite tracking system of Kanazawa-SAT3. For the communication system using Iridium satellite, it is necessary to implement a system on the OBC and conduct a communication experiment.

©2019. Japan Geoscience Union. All Right Reserved.

Keywords: Microsatellite, Communications System, Kanazawa SAT3

©2019. Japan Geoscience Union. All Right Reserved.

Development of micrometeoroid impact sensor within a multi-layered insulation (CLOTH) onboard 6U deep-space explorer EQUULEUS

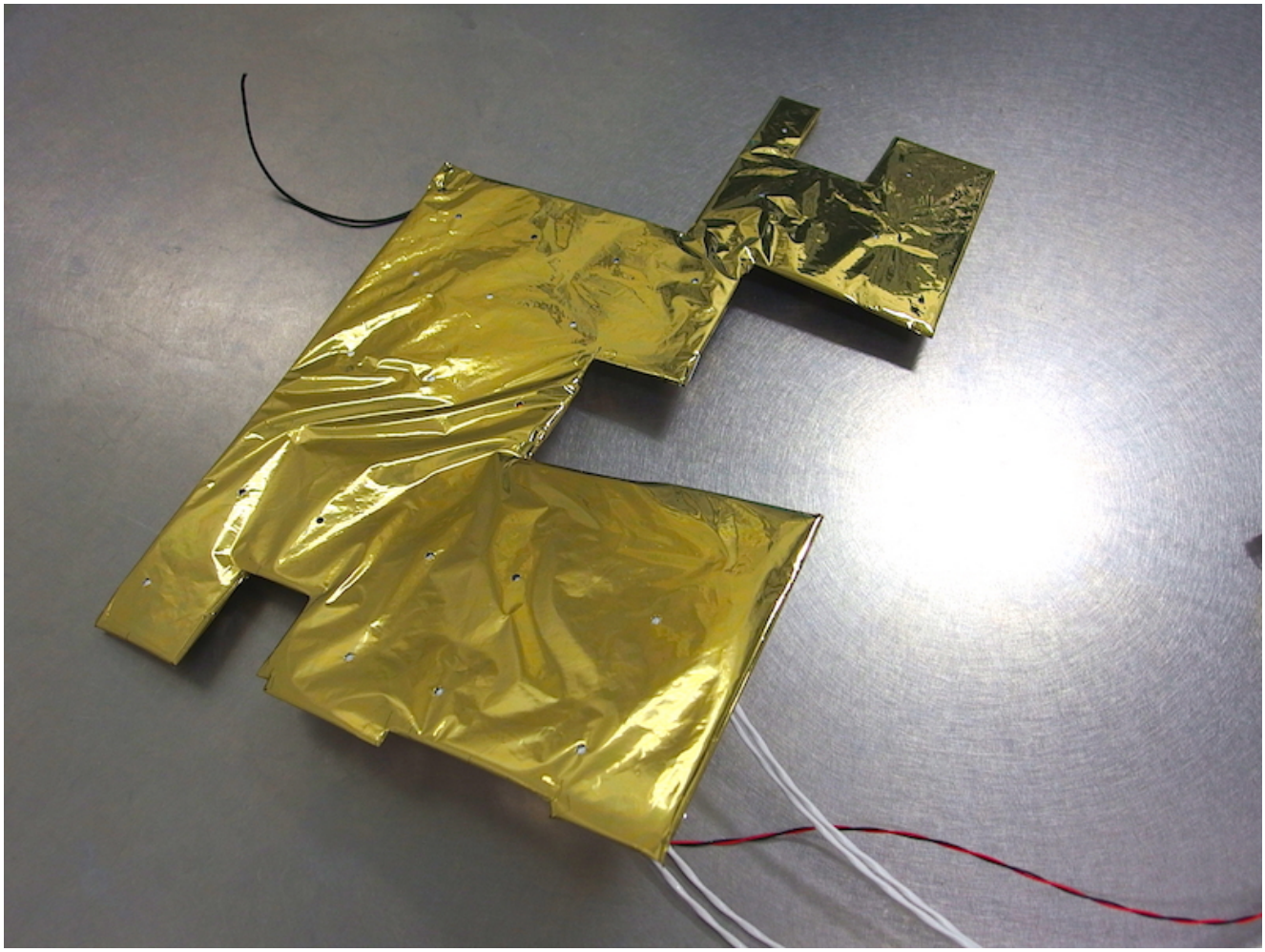
*Takayuki Hirai[1], Hajime Yano[2], Ritsuko Jitsukawa[3], Eigo Ishioka[3], Haruki Nakano[3], Kazuyoshi Arai[3], Sunao Hasegawa[2]

1. Planetary Exploration Research Center, Chiba Institute of Technology, 2. Institute of Space and Astronautical Science, Japan Aerospace Exploration Agency, 3. Faculty of Science and Engineering, Hosei University

In recent years, the use of CubeSat for deep-space exploration is remarkably expanding. Equilibrium Lunar-Earth point 6U Spacecraft (EQUULEUS) project led by the University of Tokyo and JAXA is one of 13 sub payloads which will be launched by the NASA’ s new rocket, Space Launch System (SLS) in 2019 or later. In addition to the engineering mission of orbital maneuvering, EQUULEUS will perform 3 scientific missions consisted of geo-corona, lunar impact flash, and micrometeoroid observations on the way to the Earth-Lunar libration point 2. Our Cis-Lunar Object detector within THermal Insulation (CLOTH) is a piezoelectric film sensor integrated with the EQUULEUS’ s multi-layer insulation (MLI). CLOTH can detect micrometeoroid which impacts and penetrates the outermost layer of EQUULEUS's MLI. The space flight demonstration of CLOTH will expand the possibility of deep-space exploration by CubeSat. In this presentation, we introduce the concept of CLOTH, i.e. micrometeoroid detector integrated with a spacecraft bus component, and the detection performance estimated by hypervelocity microparticle impact test on the ground.

Keywords: Piezoelectric film, PVDF, Thermal insulation, CubeSat, Micrometeoroid, Hypervelocity impact

©2019. Japan Geoscience Union. All Right Reserved.



©2019. Japan Geoscience Union. All Right Reserved.

Breadboard model of asteroid tracking system for DESTINY^{+} mission

*Peng Hong[1], Ko Ishibashi[1], Shunsuke Sato[2], Kazutoshi Takemura[3], Kotaro Fujiwara[4], Kanako Machii[5], Hiroyuki Toyota[2], Kazutaka Nishiyama[2], Masatsugu Otsuki[2], Osamu Okudaira[1], Takeshi Takashima[2]

1. Planetary Exploration Research Center, Chiba Institute of Technology, 2. Institute of Space and Astronautical Science, Japan Aerospace Exploration Agency, 3. Department of Applied Mechanics, Graduate School of Fundamental Science and Engineering, Waseda University, 4. Division of Mechanical and Space Engineering, Graduate School of Engineering, Hokkaido University, 5. Department of Mechanical Engineering and Intelligent Systems, Faculty of Informatics and Engineering, The University of Electro-Communications

DESTINY^{+} (Demonstration and Experiment of Space Technology for Interplanetary voYage, Phaethon fLyby and dUst Science) is a mission proposed for JAXA/ISAS Epsilon class small program, currently in the pre-project phase (Phase-A) with a launch targeted for 2023. The mission plans to conduct high-resolution imaging during close flyby of asteroid (3200) Phaethon, which is considered as a parent body of Geminid meteor shower. Two cameras are planned to be onboard DESTINY^{+}, the Telescopic Camera for Phaethon (TCAP) and the Multiband Camera for Phaethon (MCAP). While MCAP is designed for low spatial resolution imaging, TCAP is planned to perform high-resolution imaging, especially from ~40 seconds before to ~9 seconds after the closest approach with an imaging rate of more than 1 frame per second and the surface of Phaethon will be imaged with a spatial resolution up to 3.5 m/px at closest approach. Both cameras will be mounted and installed on the wall of spacecraft bus, thus orientations of the cameras are mainly controlled by the attitude of spacecraft. However, since the relative flyby speed and closest distance to Phaethon are expected to be 30 to 40 km/s and about 500 km, it is significantly difficult to track the asteroid only by the rotation of the spacecraft itself. Therefore, an asteroid tracking system is required for TCAP to obtain unblurred high-resolution images. The tracking system is also required to operate autonomously during the high-speed flyby. We have conducted conceptual studies of the tracking mirror as well as control algorithms to properly navigate the mirror based on feedforward or feedback loop. To realize the designed concept, we have developed a simple breadboard model focusing on the rotating mechanism which is the most important part of tracking mirror. The breadboard model consists of a rotating mirror, a 2-phase stepping motor and its driver, a motor reducer, and a FPGA board to control the driver. Required performances for the breadboard model of tracking system are (1) the rotating mirror should be able to orient a desired direction with an enough accuracy, (2) the mirror should be able to rotate smoothly with an enough accuracy during the exposure of TCAP. We will report the current development status of breadboard model of asteroid tracking system for TCAP and show its initial results of the performance test.

Keywords: DESTINY+, camera, flyby, tracking system

©2019. Japan Geoscience Union. All Right Reserved.

Development of telescopic camera (TENGOO) performance evaluation device in MMX

*Hiroki Kato[1], Shingo Kameda[1], Keigo Enya[2], Osada Naoya[1]

1. Rikkyo University, 2. Japan Aerospace Exploration Agency

Mars has two satellites, Phobos and Deimos, and there are currently two hypotheses for the origin of these satellites. The first of these hypotheses is that the moons are captured primitive asteroids, and the second is that they formed because of a giant impact event on Mars. The Japan Aerospace Exploration Agency (JAXA) is planning the Martian Moon eXploration (MMX) mission, which is a sample-return mission for Phobos, to determine which hypothesis is correct and reveal the origin of these two satellites.

The TElescopic Nadir imager for GeOmOrphology (TENGOO), which will be installed in MMX, has the purpose of measuring the geographical features of Phobos to locate a suitable landing site less influenced by space weathering. The design of TENGOO was optimized for achieving this goal. In the optical design, the instantaneous Field of View (iFoV) is 5.8 μrad/pix and the Modulation Transfer Function (MTF) is 0.3 at the Nyquist frequency.The design performance of the manufactured TENGOO needs to be confirmed. We evaluate the performance of TENGOO by measuring the Point Spread Function (PSF). Therefore, a low divergence collimated light is needed for a ground experiment to obtain the PSF with sufficient accuracy. We succeeded at making a collimated light source with divergence less than 11.6 μrad.

The Full Width of Half Maximum (FWHM) of PSF obtained with this collimated light is approximately 2x2 pixels in TENGOO. Therefore, the sampling interval becomes wider than FWHM of PSF, and the error of PSF estimation due to Gaussian fitting increases. To solve this problem, we measured the Line Spread Function (LSF) with diagonal lines and complemented the measuring points by obtaining multiple PSFs.

Keywords: Mars, MMX, camera

©2019. Japan Geoscience Union. All Right Reserved.

Observation Plans in the Cruising-Phase of the Solar Power Sail: OKEANOS

*Takahiro Iwata[1], Shuji Matsuura[2], KOHJI TSUMURA[3], Hajime Yano[1], Takayuki Hirai[4], Ayako Matsuoka[1], Daisuke Yonetoku[5], Tatehiro Mihara[6], Tatsuaki Okada[1], Osamu Mori[1], Toshihiro Chujo[1]

1. Institute of Space and Astronautical Science, Japan Aerospace Exploration Agency, 2. Kwansei Gakuin University, 3. Tohoku University, 4. Chiba Institute of Technology, 5. Kanazawa University, 6. RIKEN

The solar power sail mission: OKEANOS (Oversize Kite-craft for Exploration and AstroNautics in the Outer Solar system) is a Japanese candidate deep-space probe that will be powered by hybrid propulsion of solar photon acceleration and ion engines. The main scientific objectives are studies of Trojan asteroids in the Jovian L4 or L5 regions. The long distance and period from the launch to the swing-by at Jupiter will give us a good opportunity to explore the solar system between the Earth and the Jupiter to elucidate the solar system disc structure. We define the cruising-phase sciences of the OKEANOS mission as the scientific theme that will be explored or observed from the launch to the swing-by at Jupiter. Candidates of instruments for the cruising phase are: the EXo-Zodiacal Infrared Telescope (EXZIT), the Arrayed Large-area Dust detectors in INterplanetary space (ALADDIN)-2, the MaGnetic Field experiment (MGF), and the GAmma-ray burst Polarimeter (GAP)-2. In this paper, we report scientific purpose and observation plans of them.

Zodiacal light observed at visible and near-infrared wavelengths is thought to be sunlight scattered by interplanetary dust. The two-dimensional distribution of zodiacal light reflects the three-dimensional structure of interplanetary dust. However, it is still controversial that how the ratio of asteroid-origin to comet-origin changes by the heliocentric distance. Therefore, the comparison of the radial distribution of zodiacal light and the in-situ dust observation will help clarify the distribution and components of solid particles in our solar system. These results are expected to provide precise distribution of the interplanetary dust in our solar-system discs.
The temperature of the solar wind, which depends on the heliocentric distance, has been observed to be greater than that predicted by the adiabatic model. Therefore, the existence of heating processes, such as plasma turbulence or magnetic reconnection, could be predicted. The observation of the magnetic field by the devices separated in the scale of the membrane of the Solar Power Sail provides the resolution of the plasma turbulence on the electron scale. Thus, the intermittent observation of the magnetic field between the Earth and Jupiter would determine the heating mechanism of the solar wind. The synergy of the magnetic field and dust observation may show the interaction between interplanetary dust and solar wind. By analyzing the environments on the dust surface, the chemical evolutions of molecules caused by solar wind and cosmic radiation can be investigated. We are investigating the possibilities to detect gamma-rays and particles from the solar-system shocks.

Keywords: OKEANOS, zodiacal light, dust, plasma, gamma-ray

©2019. Japan Geoscience Union. All Right Reserved.

[E] Poster | A (Atmospheric and Hydrospheric Sciences)：A-OS Ocean Sciences & Ocean Environment

Sun. May 26, 2019 3:30 PM - 5:00 PM JST | Sun. May 26, 2019 6:30 AM - 8:00 AM UTC | Poster Hall International Exhibition Hall8, Makuhari Messe_7

[A-OS09] Ocean Mixing Processes: Impact on Biogeochemistry, Climate and Ecosystem

convener:Ichiro Yasuda(Atmosphere and Ocean Research Institute, The University of Tokyo), Toshiyuki Hibiya(Department of Earth and Planetary Science, Graduate School of Science, University of Tokyo), Jun Nishioka(Hokkaido University, Institute of low temperature sciences), Shin-ichi Ito(Atmosphere and Ocean Research Institute, The University of Tokyo)

The interdisciplinary study on ocean diapycnal mixing and its impacts (Ocean Mixing Processes: Impact on Biogeochemistry, Climate and Ecosystem (OMIX) 2015-2020) is opening the integrated sciences from physical, chemical, biological oceanography to climate and fisheries sciences. In this section, results during the four years of OMIX projects and other related presentations are all welcome to be summarized and to facilitate plans of next projects.

[AOS09-P01] Correction method of fast-response thermistors data to estimate turbulence intensity

*kimura shino[1], Yasutaka Goto[2], Koenjong Lee[1], Ichiro Yasuda[1] (1.The Univercity of Tokyo, 2.Meteorological Agency)

[AOS09-P02] Observation of turbulent mixing using a deep float with microstructure sensors

*Shuo Zhai[1], Ichiro Yasuda[1], Masaaki Kikuchi[1], Yasutaka Goto[1], Koenjong Lee[1], Takahiro Tanaka[2], Ken Yamaki[3], Yutaka Imamura[4] (1.Atmosphere and Ocean Research Institute, The University of Tokyo, 2.Japan Fisheries Research Agency, 3.TSK Tsurumi-Seiki Co., Ltd., 4.Aomori Prefectural Industrial Thechnology Research Center, Fisheries Research Insititute)

[AOS09-P03] Evaluation of the underwater glider flight model using the electromagnetic current sensor

*Takahiro Tanaka[1], Daisuke Hasegawa[1], Takeshi Okunishi[1], Ichiro Yasuda[2] (1.Tohoku National Fisheries Research Institute, Japan Fisheries Research and Education Agency, 2.Atmosphere and Ocean Research Institute, University of Tokyo)

[AOS09-P04] Mixing processes observed by a slocum glider at the Oyashio-TWC front

*Daisuke Hasegawa[1], Takahiro Tanaka[1], Takeshi Okunishi[1], Ichiro Yasuda[2] (1.Tohoku National Fisheries Research Institute, Japan Fisheries Research and Education Agency, 2.Atmosphere and Ocean Research Institute, The University of Tokyo)

[AOS09-P05] Impact of the astronomical lunar 18.6-yr tidal cycle on El-Niño and Southern Oscillation

*Ichiro Yasuda[1] (1.Atmosphere and Ocean Research Institute, The University of Tokyo)

[AOS09-P06] The effect of 18.6-year period lunar nodal cycle on Pacific Decadal Oscillation (PDO)

*Masaki Hamamoto[1], Ichiro Yasuda[1] (1.Atmosphere and Ocean Research Institute, The University of Tokyo)

[AOS09-P07] A comparison of ocean deoxygenation between CMIP5 models and an observational dataset

*Yumi Abe[1], Shoshiro Minobe[1,5], Takamitsu Ito[2], Curtis Deutsch[3], Matthew C. Long[4] (1.Department of Natural History Sciences, Graduate School of Science,Hokkaido University, Sapporo, Japan, 2.School of Earth and Atmospheric Sciences, Georgia Institute of Technology, Atlanta, Georgia, USA, 3.School of Oceanography, University of Washington, Seattle, Washington, USA, 4.Climate and Global Dynamics

Laboratory, National Center for Atmospheric Research, Boulder, Colorado, USA, 5.Department of Earth and Planetary Sciences, Faculty of Science, Hokkaido University, Sapporo, Japan)

[AOS09-P08] Pacific Ocean State Estimation and Clarification of Mechanism of Ocean Circulation by Data Synthesis of Global Observations

*Shuhei Masuda[1] (1.Japan Agency for Marine-Earth Science and Technology)

[AOS09-P09] Impact of Tidal Vertical Mixing to Barotropic Water Exchange between the Sea of Okhotsk and Pacific through Diffusive Adjustment with Turbulent Closure Scheme

*Hung Wei Chou[1], Humio Mitsudera[1], Hatsumi Nishikawa[1], Kaihe Yamazaki[2] (1.Hokkaido University, Institute of Low Temperature Science, 2.Hokkaido University, Graduate School of Environmental Science)

[AOS09-P10] Distributions of organic Fe-binding ligands in the eastern and western subarctic North Pacific

*Yoshiko Kondo[1,2], Yudai Sunahara[2], Jun Nishioka[3], Hajime Obata[4], Shigenobu Takeda[1,2] (1.Graduate School of Fisheries and Environmental Sciences, Nagasaki University, 2.Faculty of Fisheries, Nagasaki University, 3.Institute of Low Temperature Science, Hokkaido University, 4.Atmosphere and Ocean Research Institute, The University of Tokyo)

[AOS09-P11] Chemical and physical speciation of copper in the subarctic North Pacific

*Kuo Hong Wong[1], Hajime Obata[1], Taejin Kim[2], Yoshiko Kondo[3], Jun Nishioka[4] (1.Atmosphere and Ocean Research Institute, The University of Tokyo, 2.Seoul National University, Korea, 3.Nagasaki University, 4.Institute of Low Temperature Science, Hokkaido University)

[AOS09-P12] Latitudinal and temporal variations in phytoplankton size structure within mesoscale eddies from space

*Hisatomo Waga[1], Toru Hirawake[1], Ueno Hiromichi[1] (1.Hokkaido University)

[AOS09-P13] Structure and impact of the Kuroshio nutrient stream

*Kosei Komatsu[1,2], Yutaka Hiroe[3] (1.Graduate School of Frontier Sciences, The University of Tokyo, 2.Atmosphere and Ocean Research Institute, The University of Tokyo, Kashiwa, Japan, 3.Seikai National Fisheries Research Institute, Japan Fisheries Research and Education Agency, Nagasaki, Japan)

[AOS09-P14] Enhanced nutrient supply and biogeochemical impacts induced by internal waves in the oligotrophic northern South China Sea

*Chin-chang Hung[1], Dewang Li[2], Wen-Chen Chou[3], Yung-Yen Shih[1,4], Guan-Yu Chen[1] (1.Department of Oceanography, National Sun Yat Sen University, Kaohsiung, Taiwan, 2.Second Institute of Oceanography, State Oceanic Administration, Hangzhou, PRC, 3.Institute of Marine Environmental Chemistry and Ecology, National Taiwan Ocean University, Taiwan, 4.Department of Applied Science, R.O.C Naval Academy, Kaohsiung, Taiwan)

[AOS09-P15] Mixing over the eastern ridge in the Luzon Strait caused by high-mode internal waves

*Akie Sakai[1], Tomoharu Senjyu[2], Eisuke Tsutsumi[2], Takeshi Matsuno[2], Takahiro Endo[2], Ichiro Yasuda[3], Daigo Yanagimoto[3] (1.Department of Earth System Science and Technology, Interdisciplinary Graduate School of Engineering Sciences, Kyushu University, 2.Research Institute for Applied Mechanics , 3.Atmosphere and Ocean Reserch Institute The University of Tokyo)

[AOS09-P16] **From the Luzon Strait to the Tsushima Strait: Water masses and nutrient transports approached using ^{137}Cs**

*Siteng Zhu[1], JING ZHANG[1], Shota Kambayashi[2], Takeshi Matsuno[3], Eisuke Tsutsumi[3], Shigenobu Takeda[4], Seiya Nagao[5], Hiroshi Inoue[5], Hiroshi Ogawa[6], Ichiro Yasuda[6] (1.University of Toyama,

2.Fukushima university, 3.Kyushu university, 4.Nagasaki university, 5.Kanazawa university, 6.The University of Tokyo)

[AOS09-P17] Impact of cyclonic eddies and typhoons on biogeochemistry in the oligotrophic ocean based on time-series observation at the western Pacific subtropical station KEO

*Makio Honda[1], Yoshikazu Sasai[1], Eko Siswanto[1], Akira Kuwano-Yoshida[2], Hidenori AIKI[3], Meghan Cronin[4] (1.Japan Agency for Marine-Earth Science and Technology, 2.Disaster Prevention Laboratory, Kyoto University, 3.Nagoya University, 4.NOAA Pacific Marine Environmental Laboratory)

[AOS09-P18] Island-mass effect on the phytoplankton and zooplankton community in south of Japan

*Kiyotaka Hidaka[1], Kazuaki Tadokoro[1], Hiroomi Miyamoto[1], Tadafumi Ichikawa[1] (1.Japan Fisheries Research and Education Agency)

[AOS09-P19] Influence of enhanced deep circulation due to geothermal heat on biogeochemical cycle in the Pacific Ocean

*Shogo Urakawa[1], Hideyuki Nakano[1], Hiroyuki Tsujino[1], Kei Sakamoto[1], Takahiro Toyoda[1], Goro Yamanaka[1] (1.Meteorological Research Institute, Japan Meteorological Agency)

[AOS09-P20] The Parameterization of the Pressure-Strain Correlations in the Stably or Unstably Stratified Ocean Surface Layer.

*Yusuke Ushijima[1], Yutaka Yoshikawa[1] (1.Graduate School of Science, Kyoto University)

[AOS09-P21] Numerical studies on asymmetric responses of the upper ocean to tropical cyclone

*Daiki Okura[1], Yutaka Yoshikawa[1] (1.Graduate School of Science, Kyoto University)

[AOS09-P22] Influence of the distortion of the internal wave field on estimates of turbulent mixing using fine-scale parameterizations

*Anne Takahashi[1], Toshiyuki Hibiya[1], Alberto C. Naveira Garabato[2] (1.Department of Earth and Planetary Science, Graduate School of Science, University of Tokyo, 2.National Oceanography Centre, University of Southampton)

Correction method of fast-response thermistors data to estimate turbulence intensity

*kimura shino[1], Yasutaka Goto[2], Koenjong Lee[1], Ichiro Yasuda[1]

1. The Univercity of Tokyo, 2. Meteorological Agency

Fast-response thermistors (FP07) can be used to estimate turbulent energy dissipation rate ε and temperature dissipation rate χ. However, correction is necessary because the insufficient response of FP07 causes underestimate for relatively strong turbulence and individual FP07 sensors have different response. In this study, using simultaneously observed shear probe and FP07 data from a free fall microstructure profiler descending at the speed of 0.6-0.7 m/s, ε_T from various FP07 are compered with ε_S from shear probe to estimate how much correction is necessary for FP07 data. For 3 (7) msec time constant of FP07 for double-pole (single-pole) correction, ε_T is consistent with ε_S within a factor of 3 in the range of ε_S =10^-10 ~10^-7 W/kg. In the presentation we also discuss the impact of correction on χ and the validity of ε_T under double diffusion.

Keywords: vertical mixing, turbulence

©2019. Japan Geoscience Union. All Right Reserved.

Observation of turbulent mixing using a deep float with microstructure sensors

*Shuo Zhai[1], Ichiro Yasuda[1], Masaaki Kikuchi[1], Yasutaka Goto[1], Koenjong Lee[1], Takahiro Tanaka[2], Ken Yamaki[3], Yutaka Imamura[4]

1. Atmosphere and Ocean Research Institute, The University of Tokyo, 2. Japan Fisheries Research Agency, 3. TSK Tsurumi-Seiki Co., Ltd., 4. Aomori Prefectural Industrial Thechnology Research Center, Fisheries Research Insititute

Automated microstructure obsevation method using a deep float (DeepNINJA) with velocity shear probe and fast-response thermistor is being elaborated. From the field test observation in August 2016, availability of shear probe data was tested by comparing turbulent dissipation rates from thermistor. Shear probe data were found to be worse by vibration from motor operartions at buoyancy adjustment and by noise at slow ascending speed of the float. Vertical profiles of turbulent energy dissipation rate could be obtained with the hybrid use of shear probe and thermistor data by correcting time-constant of the termistor with reliable shear probe data and filling gaps of unavailable shear probe data. Data will be reported for the deep float which was deployed on December 12, 2018, in the western slope of Japan Trench off Aomori. The float is observing 0 - 4000 m turbulence profile every 10 days and will be recovered in April R/V Shinsei-maru cruise.

Keywords: vertical mixing , deep float, energy dissipation rate

©2019. Japan Geoscience Union. All Right Reserved.

Evaluation of the underwater glider flight model using the electromagnetic current sensor

*Takahiro Tanaka[1], Daisuke Hasegawa[1], Takeshi Okunishi[1], Ichiro Yasuda[2]

1. Tohoku National Fisheries Research Institute, Japan Fisheries Research and Education Agency, 2. Atmosphere and Ocean Research Institute, University of Tokyo

Turbulence measurement by underwater gliders has become more common in recent years. For the accurate estimation of energy dissipation rates, the accurate measurement of the fall rate and gliding path angle is necessary. The gliding path angle should take the angle of attack (AOA) into account, which is the difference between the gliding path angle and the pitch angle. AOA calculation has been done by using the so-called flight model assuming dynamical force balance in the quasi-steady state. Due to the difficulty in measuring AOA directly, the validity of AOA derived from the flight model and the flight model itself has not been adequately evaluated so far. In this study, we put the electromagnetic current sensor (EM sensor) on the turbulence package to obtain AOA directly and to compare the AOA from EM sensor with that from the flight model. Using the dataset obtained by a Slocum glider in Jul. - Aug. 2017, we found that AOA from the EM sensor during descent and ascent has a mean (standard deviation) of 0.7 (1.2) deg. and -0.7 (1.1) deg., respectively, while AOA from the flight model is 4.9 (0.4) deg. and -4.5 (0.5) deg., respectively. In order to know what cause this difference, we discuss the validity of parameters given in the flight model. It is suggested that a drag coefficient due to parasite drag given in the flight model may be somewhat larger than that calculated using the EM sensor.

Keywords: underwater glider, flight model, electromagnetic current sensor, angle of attack

©2019. Japan Geoscience Union. All Right Reserved.

Mixing processes observed by a slocum glider at the Oyashio-TWC front

*Daisuke Hasegawa[1], Takahiro Tanaka[1], Takeshi Okunishi[1], Ichiro Yasuda[2]

1. Tohoku National Fisheries Research Institute, Japan Fisheries Research and Education Agency, 2. Atmosphere and Ocean Research Institute, The University of Tokyo

In order to grasp the detailed mixing processes along the frontal region between the Oyashio and the Tsugaru Warm Current (TWC), we conducted a zigzag survey crossing the front several times from the merging region of the two current systems to the down stream by an underwater glider (Slocum G2 Glider) equipped with a turbulence sensor, from July 24thto August 29thin 2017. The observed frontal structure indicated the subduction and the intrusion processes of the cold and fresh Oyashio water under the warm and salty TWC water, along layer between 26.5 to 26.8 sigma-theta, which resulted the favorable conditions to the salt finger convection at the upper interface along the 26.5 sigma-theta, and the diffusive convection at the lower interface along the 26.8 sigma-theta where the fresh and cold Oyashio water lying above the warm and salty water. The strong turbulence intensity is observed around the intruded layer, and the mean temperature and the salinity in the layer became warmer and saltier with the increase of the distance from the front, which suggested the time evolution of the vertical mixing driven by double diffusive convections between the three different water masses. Though the strongest turbulence intensity was observed around the frontal region, which may suggest the importance of the cabbeling effect as the additional source of the turbulent mixing.

Keywords: double diffusion, mixing, cabbeling

©2019. Japan Geoscience Union. All Right Reserved.

Impact of the astronomical lunar 18.6-yr tidal cycle on El-Niño and Southern Oscillation

*Ichiro Yasuda[1]

1. Atmosphere and Ocean Research Institute, The University of Tokyo

Even though El-Niño and Southern Oscillation (ENSO) has a tremendous impact on global climate and society, its long-term forecast remains difficult. In this study, we discovered a statistically significant relationship between ENSO timing and the 18.6-year period lunar tidal cycle in the mature-phase (December –February) ENSO time-series during 1867–2015 and extending back to 1706 with proxy data. It was found that El-Niño tended to occur in the 1st, 10th, and 13th years after the maximum diurnal tide in the 18.6-yr cycle, and La-Niña tended to occur in the 3rd, 12th, and 16th years. These tendencies were also confirmed by corresponding sea-surface temperature (SST) and sea-level pressure (SLP) distributions; particularly Pacific SST and SLP spatial patterns in the third La-Niña and the tenth El-Niño year well resemble those of Pacific Decadal Oscillation (PDO). These findings contribute to understanding and forecasting long-term ENSO variability.

Keywords: El-Niño and Southern Oscillation, air-sea interaction, tide, mixing, climate

©2019. Japan Geoscience Union. All Right Reserved.

The effect of 18.6-year period lunar nodal cycle on Pacific Decadal Oscillation (PDO)

*Masaki Hamamoto[1], Ichiro Yasuda[1]

1. Atmosphere and Ocean Research Institute, The University of Tokyo

Pacific Decadal Oscillation (PDO) is the most dominant decadal-inter-decadal ocean-climate variability over the North Pacific; however, the periodicity and cause have not been fully understood. Previous studies suggested that 18.6-year period lunar tidal cycle ($T_{18.6}$) regulate bi-decadal PDO variability through changes in the strength of diapycnal mixing of ocean around the Kuril Islands to result in ocean variability, together with air-sea interactions in the mid-latitude North Pacific and/or equatorial Pacific. In the present study, 297yr-long reconstructed PDO timeseries was re-examined, and 27.9yr (3/2 times 18.6-yr, henceforth, $T_{27.9}$) period variability was significantly detected, and the zero-crossing from minus to plus was found to occur simultaneously with $T_{18.6}$ variability in the interval of 55.4 years (3 times $T_{18.6}$). In the PDO spectrum, a broad multi-decadal 50-80-yr peak (corresponding to 3-5 times $T_{18.6}$, henceforth T_M) was also detected with the zero-crossing synchronized with $T_{18.6}$; this is the extension of previous studies during 1900-2000 back to 1700s on the synchronous changes of bi-decadal and penta-decadal variabilities. These $T_{18.6}$, $T_{27.9}$ and T_M explain 71% of the 10-year low-passed PDO variability. These imply that the 27.9-yr and the multi-decadal variabilities could be related to $T_{18.6}$ tide-induced variability, and may be excited by $T_{18.6}$ tidal forcing, considering that external periodic forcing for delayed oscillator models could excite 3 times period of the external forcing and some non-linear processes may make the half-period variability.

Keywords: 18.6-year period lunar nodal cycle, Pacific Decadal Oscillation

©2019. Japan Geoscience Union. All Right Reserved.

A comparison of ocean deoxygenation between CMIP5 models and an observational dataset

*Yumi Abe[1], Shoshiro Minobe[1,5], Takamitsu Ito[2], Curtis Deutsch[3], Matthew C. Long[4]

1. Department of Natural History Sciences, Graduate School of Science,Hokkaido University, Sapporo, Japan, 2. School of Earth and Atmospheric Sciences, Georgia Institute of Technology, Atlanta, Georgia, USA, 3. School of Oceanography, University of Washington, Seattle, Washington, USA, 4. Climate and Global Dynamics Laboratory, National Center for Atmospheric Research, Boulder, Colorado, USA, 5. Department of Earth and Planetary Sciences, Faculty of Science, Hokkaido University, Sapporo, Japan

Recent studies revealed that the ocean deoxygenation has been accelerating since the 1980s over the global oceans (Schmidtko et al. 2017; Ito et al. 2017), and the observed trend in the last half-century appears to be much larger than the model simulations conducted for CMIP5 (Bopp et al. 2013). This discrepancy is an important issue of the ocean deoxygenation researches as highlighted by a review paper published in the last year (Oschlies et al. 2018).

In order to understand better the relations of oxygen variations between CMIP5 models and observations, we compare oxygen concentration simulated by CMIP5 models and gridded oxygen anomaly dataset used by Ito et al. (2017). For the global oceans, the observed oxygen reduction rate for the historical experiment period appears to be within uncertainty of the models, though this result can be sensitive to the choice of the analysis period associated with the rapid recent oxygen reduction. We also closely examined the two basins that are relatively well sampled, i.e., the North Pacific and the North Atlantic. It is found that the observed North Pacific oxygen reduction is much stronger than the simulated ones, but such a strong reduction of observed oxygen does not occur in the North Atlantic. These results suggest that there are substantial spatio-temporal variations of oxygen concentration on decadal timescales and their mechanism in each basin should be explored in future studies.

Keywords: North Pacific, North Atlantic

©2019. Japan Geoscience Union. All Right Reserved.

Pacific Ocean State Estimation and Clarification of Mechanism of Ocean Circulation by Data Synthesis of Global Observations

*Shuhei Masuda[1]

1. Japan Agency for Marine-Earth Science and Technology

Our aim is to synthesize pre-existing ocean data with newly-acquired turbulence data using state-of-art assimilation technique. Available observations of turbulence strength in the ocean, will be “blended” with pre-existing ocean data applying dynamically self-consistent state estimation approach with 4D-VAR adjoint system. We propose some new techniques and schemes to assimilate turbulence data, which tends to include unique features. The obtained state estimation will provide improved description of ocean circulation, its heat and salt transports, and oceanic ecosystem at lower trophic level.

Keywords: OMIX, ocean , mixing , data assimilation

©2019. Japan Geoscience Union. All Right Reserved.

Impact of Tidal Vertical Mixing to Barotropic Water Exchange between the Sea of Okhotsk and Pacific through Diffusive Adjustment with Turbulent Closure Scheme

*Hung Wei Chou[1], Humio Mitsudera[1], Hatsumi Nishikawa[1], Kaihe Yamazaki[2]

1. Hokkaido University, Institute of Low Temperature Science, 2. Hokkaido University, Graduate School of Environmental Science

The pattern of exchange flow between the Sea of Okhotsk and Pacific is a system composed by an Okhotsk-ward inflow through Kruzenshtern strait in north and a Pacific-ward outflow through Bussol strait in south. One of major theories for explaining the dynamic of water exchange through Kuril Island Chain is the turbulence induced by tidal vertical mixing. Turbulence is an important physical process in geostrophic boundary layer, and because of the complexity of topographic in Kuril island chain, the breaking of internal tides in island coast area leads to increase the thickness of surface mixing layer and causes tilting of isopycnal layer in vicinity. The tilting of isopycnal layer around islands forms a clockwise flow along the shore by geostrophic adjustment. However, above process is majorly broclinicly, and how can it impact to barotropic component is still unknown.

By setting the tidal force as a controlled variable, results from realistic OGCM model COCO show only the case with tidal forcing can consistent with the exchange flow pattern as historical observation (Fig.1). Besides, the vertical diffusivity values also show the magnitude difference in summer time, which the flow in north strait in non-tidal case is opposite to tidal one (Fig.2). Therefore, we designed four experiments for understanding the impact of tidal diffusive adjustment in summer: 1. install vertical diffusivity value generated by tidal case into non-tidal run; 2. install vertical diffusivity value generated by non-tidal case into tidal run; 3. set the vertical diffusivity value as zero in tidal case and 4. in non-tidal case as well. Further, for preventing the underestimates the depth of the mixing layer in Mellor-Yamada turbulence closure scheme, two more experiments with the larger vertical diffusivity mask are applied in both tidal and non-tidal case. After calculating the fraction of baroclinic and barotropic components in either north strait or southern strait, results show the vertical mixing dose influence the strength of volume transported but not the direction as original tidal and non-tidal case shows. Hence, for further understanding the impact of vertical diffusivity, we start a tidal forcing run with non-tidal initial conditions to detect the relationship between the flow direction and magnitiude of vertical diffusivity values by time developing. But the baroclinic result implies that the vertical mixing might not be the main reason to control the flow direction (Fig.3).

This study also implies the tidal impacts in OGCM is not only the vertical mixing, but other geostrophic fluid dynamics might occur, especially the interaction of topography with tidal waves. Therefore, for reproducing the real ocean phenomena, movement of tidal waves should be considered.

Keywords: OGCM, tidal mixing , Okhotsk, cross-basin exchange system

©2019. Japan Geoscience Union. All Right Reserved.

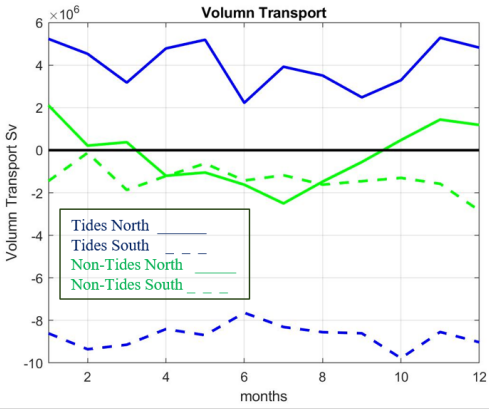


Fig.1: volume transportation in tidal and non-tidal run.
Positive value is Okhotsk-ward and negative value is Pacific-ward flow.

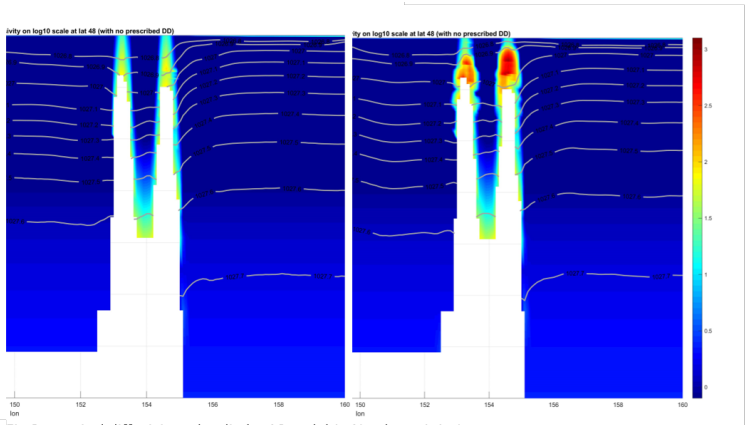


Fig.2: vertical diffusivity value (in log10 scale) in North strait in June, left one is non-tidal run and right is tidal run.

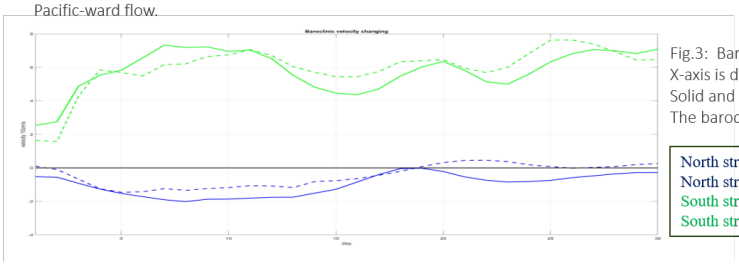


Fig.3: Baroclinic components in the tidal run with non-tidal initial condition.
X-axis is day and y-axis is velocity. Blue line is north strait and green line is south strait.
Solid and dot line are upper and lower isopycal layer, respectively.
The baroclinic velocity is stable after a week running.

©2019. Japan Geoscience Union. All Right Reserved.

Distributions of organic Fe-binding ligands in the eastern and western subarctic North Pacific

*Yoshiko Kondo[1,2], Yudai Sunahara[2], Jun Nishioka[3], Hajime Obata[4], Shigenobu Takeda[1,2]

1. Graduate School of Fisheries and Environmental Sciences, Nagasaki University, 2. Faculty of Fisheries, Nagasaki University, 3. Institute of Low Temperature Science, Hokkaido University, 4. Atmosphere and Ocean Research Institute, The University of Tokyo

Iron (Fe) is well known as a key parameter for primary productivity in the ocean. To understand the distributions and biogeochemical cycle of Fe in the ocean, we need to investigate the sources and sinks of Fe. A recent study has demonstrated a concentration gradient of dissolved Fe in the North Pacific Intermediate Water (NPIW) between western and eastern areas (Nishioka and Obata, 2017), suggesting that Fe-rich intermediate water was transported laterally across the western subarctic gyre. Moreover, it has been demonstrated that most dissolved Fe in seawater is complexed with natural organic ligands. Since bioavailability of Fe in seawater depends on its species, the chemical speciation of Fe is needed to evaluate the nutrient status for phytoplankton. However, the distribution of natural organic ligands has not been revealed yet in the subarctic North Pacific. In this study, vertical distributions of organic Fe-binding ligands were investigated in the eastern and western subarctic North Pacific to clarify its impact on Fe cycle. Seawater samples were obtained through the whole water column during GEOTRACES-Japan cruise KH-17-03 using trace metal clean technique to avoid metal contaminations. Filtered seawater samples (<0.2 μm) for organic Fe-binding ligands analysis were collected in acid-washed bottles inside a laminar-flow clean booth, then they were stored at -20°C until just before analysis. The organic Fe-binding ligands' concentration and their conditional stability constants were determined by competitive ligand equilibration-adsorptive cathodic stripping voltammetry (CLE-ACSV) method using salicylaldoxime (Abualhaija and van den Berg, 2014). The concentration and conditional stability constants of organic ligands ranged from 0.7 nM to 5.9 nM and from $10^{10.1}$ M^{-1} to $10^{12.3}$ M^{-1}, respectively. The concentrations of organic ligands exceeded those of dissolved Fe concentration more than 1 nM in all samples except for the surface (10-m) at the Oyashio-Kuroshio transition zone station; consequently >99% of dissolved Fe was estimated to be complexed with these natural organic ligands. At the western station, high concentrations of organic ligands were observed in the intermediate layers (400 –600 m), which hydrographic data (27.2 σ_θ –27.3 σ_θ) were corresponding to the lower NPIW (Yasuda et al., 2004), suggesting that organic Fe-binding ligands might be transported within the lower NPIW.

Keywords: iron, organic ligand, subarctic North Pacific, GEOTRACES

©2019. Japan Geoscience Union. All Right Reserved.

Chemical and physical speciation of copper in the subarctic North Pacific

*Kuo Hong Wong[1], Hajime Obata[1], Taejin Kim[2], Yoshiko Kondo[3], Jun Nishioka[4]

1. Atmosphere and Ocean Research Institute, The University of Tokyo, 2. Seoul National University, Korea, 3. Nagasaki University, 4. Institute of Low Temperature Science, Hokkaido University

Organic complexation of Cu in seawater plays a major role in controlling the toxicity and bioavailability of Cu for marine microorganism. In this study, we determined the concentrations of Cu and its organic ligands in the soluble and dissolved phases in the subarctic North Pacific. Samples were taken from three stations in the subarctic NorthPacific, CL-2 (western), CL-5 (central) and CL-16 (eastern), during summer 2017.

Concentrations of total dissolved and soluble Cu ranged from 1.28 nM –4.82 nM, and 0.47 nM –2.75 nM, respectively, in the subarctic North Pacific. At both CL-2 and CL-16, soluble Cu accounted for 30% - 100% of total dissolved Cu. The proportion of the soluble Cu fraction was low in surface waters, increased a maximum in the intermediate waters, and decreased slightly in deep waters. Two classes of organic ligands were detected in the surface and intermediate waters of CL-5 and CL-16, and in the intermediate waters of CL-2. In all other depths, only one class of ligand was detected. Concentrations of the stronger ligand (L_1) and weaker ligand (L_2) ranged from 1.02 nM –2.95 nM, and 0.77 nM –8.78 nM, respectively. The distributions of L_1 followed closely that of total dissolved Cu in the surface waters, and no clear trend was observed in the intermediate waters. At CL-2, L_1 mainly existed in the soluble phase, whereas for CL-16, soluble L_1 accounted for 50% - 100% of total dissolved L_1. Concentrations of L_2 were relatively constant throughout the water column but elevated concentrations were detected in the surface waters of CL-5 and in the surface and intermediate waters of CL-16. On the other hand, there were a slight depletion of L_2 in the intermediate waters of CL-2.

Keywords: copper, organic ligands, subarctic North Pacific

©2019. Japan Geoscience Union. All Right Reserved.

Latitudinal and temporal variations in phytoplankton size structure within mesoscale eddies from space

*Hisatomo Waga[1], Toru Hirawake[1], Ueno Hiromichi[1]

1. Hokkaido University

Phytoplankton plays a critical role in a number of key ocean processes. One of the most important functions of phytoplankton is to determine the energy transfer efficiency in marine ecosystems. Although the energy flow from the base of the food web to higher trophic levels depends on both the biomass and size structure of phytoplankton community, phytoplankton size structure is particularly important because energy flow in marine pelagic food webs is largely based on size specific predator-prey relationships. Therefore, spatiotemporal dynamics in size structure of phytoplankton community can trigger changes in the ecosystem’ s functioning through trophic cascade effects in the trophic chain. With the development of remote sensing techniques, mesoscale eddies, nearly ubiquitous features of the World Ocean, has been recognizing as important feature for the distribution of phytoplankton not only the direct transport of phytoplankton and eddy trapping, but also the vertical flux of nutrients. Recent studies have examined regional variations in the influence of mesoscale eddies on phytoplankton community. Namely, phytoplankton production is enhanced in cyclonic eddies (CEs) than that of anticyclonic eddies (ACEs) because of upwelling inside the eddy; this view, on the other hand, does not hold for a substantial portion of eddies within oceanic subtropical gyres, the largest ecosystems in the ocean. However, previous efforts have focused mainly on variations in chl*a*, whereas quite a few studies have worked on that in the size structure of phytoplankton community because remote estimations of phytoplankton size structure are newly established techniques during the last decade. Here we improved a chl*a* size distribution (CSD) model which estimates the synoptic size structure of phytoplankton community, to assess the impact of mesoscale eddies on spatiotemporal variations in phytoplankton size structure. Original CSD model was based on the spectral features of the phytoplankton absorption coefficient ($a_{ph}(\lambda)$), which estimation accuracy becomes poor in areas of the low productivity, such as subtropical gyres. To avoid this, we used not only $a_{ph}(\lambda)$ but also chl*a* to improve estimation accuracy of the CSD model. The resulting estimation error of the improved CSD model was the median absolute percent difference of 26.0% between the measured and satellite-matched values, and global distribution of the phytoplankton size structure was reliable even in subtropical gyres. The phytoplankton size structure showed a clear latitudinal variation: larger and smaller assemblages in temperate (>30˚S and >30˚N) and low latitudes (30˚S–30˚N) latitudes, respectively. When comparing the phytoplankton size structure within ACEs and CEs, a larger phytoplankton size structure was found in ACEs especially in low latitudes. This result was consistent with a previous report that ACEs are more productive than CEs in subtropical gyres because of winter mixing. In addition, we found increasing trends ($p < 0.05$) in differences between the phytoplankton size structure within ACEs and CEs in low latitudes for the years 2003–2014, suggesting a growing importance of ACEs for phytoplankton and in turn marine ecosystem. Consequently, this study demonstrates significant advantages of satellite remote sensing for biogeochemical and ecological studies.

Keywords: Satellite, Mesoscale eddy, Phytoplankton

©2019. Japan Geoscience Union. All Right Reserved.

Structure and impact of the Kuroshio nutrient stream

*Kosei Komatsu[1,2], Yutaka Hiroe[3]

1. Graduate School of Frontier Sciences, The University of Tokyo, 2. Atmosphere and Ocean Research Institute, The University of Tokyo, Kashiwa, Japan, 3. Seikai National Fisheries Research Institute, Japan Fisheries Research and Education Agency, Nagasaki, Japan

Recently the Kuroshio has drawn attention as an important supply route of nutrients in the western North Pacific. However, it is unknown whether nutrient concentrations are enhanced along the jet on isopycnal surfaces, as is the case for the “nutrient stream” along the Gulf Stream. We aim to ascertain the structure of nutrient concentration enhancement along the Kuroshio jet and to estimate the impact of nutrient transport downstream to the Kuroshio-Oyashio interfrontal zone (KOIZ), which is a highly productive region and a major global fishing ground. Recent multiple- transects and retrospective analyses of historic hydrographic data have revealed that the along-jet maximum nitrate concentration appears only in spring on the isopycnal surface $25<\sigma_\theta<26$ in the downstream region of the Kuroshio. The Kuroshio nutrient stream contributes significantly to productivity in the euphotic layer along its downstream trajectory, in conjunction with enhanced vertical turbulence. Analysis of the budget of epipycnal nitrate transport across transects that enclosed the KOIZ suggests that the Kuroshio nutrient stream has a non-negligible potential to significantly impact high productivity in the KOIZ.

Keywords: Kuroshio nutrient stream, Kuroshio-Oyashio interfrontal zone, epipycnal transport

©2019. Japan Geoscience Union. All Right Reserved.

Enhanced nutrient supply and biogeochemical impacts induced by internal waves in the oligotrophic northern South China Sea

*Chin-chang Hung[1], Dewang Li[2], Wen-Chen Chou[3], Yung-Yen Shih[1,4], Guan-Yu Chen[1]

1. Department of Oceanography, National Sun Yat Sen University, Kaohsiung, Taiwan, 2. Second Institute of Oceanography, State Oceanic Administration, Hangzhou, PRC, 3. Institute of Marine Environmental Chemistry and Ecology, National Taiwan Ocean University, Taiwan, 4. Department of Applied Science, R.O.C Naval Academy, Kaohsiung, Taiwan

To understand nutrient supply and the biogeochemical response induced by internal waves in the deep basin of the northern South China Sea (NSCS), nitrate, chlorophyll *a* (Chl *a*), particulate organic carbon (POC) fluxes were measured during the passage of large internal waves using drifting sediment traps attached with hydrographic sensors. Results revealed large variations in temperature, nitrate and chlorophyll *a* (Chl *a*) concentrations during and after internal waves, suggesting that cold nutrient-replete waters may be brought to the euphotic zone in the dissipation zone during and after the passage of internal wave packets, resulted in phytoplankton flourished in oligotrophic water. The result reveals that ocean mixing triggered by internal waves in warm water of the NSCS may be important for phytoplankton species composition. Most importantly, POC fluxes (110.9±10.7 mg C m^{-2} d^{-1}) were significantly enhanced after internal waves compared to non-internal wave area (32.6–73.0 mg C m^{-2} d^{-1}) in the NSCS. Such elevated POC fluxes may be induced by downward flourished biogenic particles, particle aggregation or converged particles from mixed layer triggered by internal waves.

Keywords: internal waves, ocean mixing, South China Sea, nutrient dynamics

©2019. Japan Geoscience Union. All Right Reserved.

Mixing over the eastern ridge in the Luzon Strait caused by high-mode internal waves

*Akie Sakai[1], Tomoharu Senjyu[2], Eisuke Tsutsumi[2], Takeshi Matsuno[2], Takahiro Endo[2], Ichiro Yasuda[3], Daigo Yanagimoto[3]

1. Department of Earth System Science and Technology, Interdisciplinary Graduate School of Engineering Sciences, Kyushu University, 2. Research Institute for Applied Mechanics , 3. Atmosphere and Ocean Reserch Institute The University of Tokyo

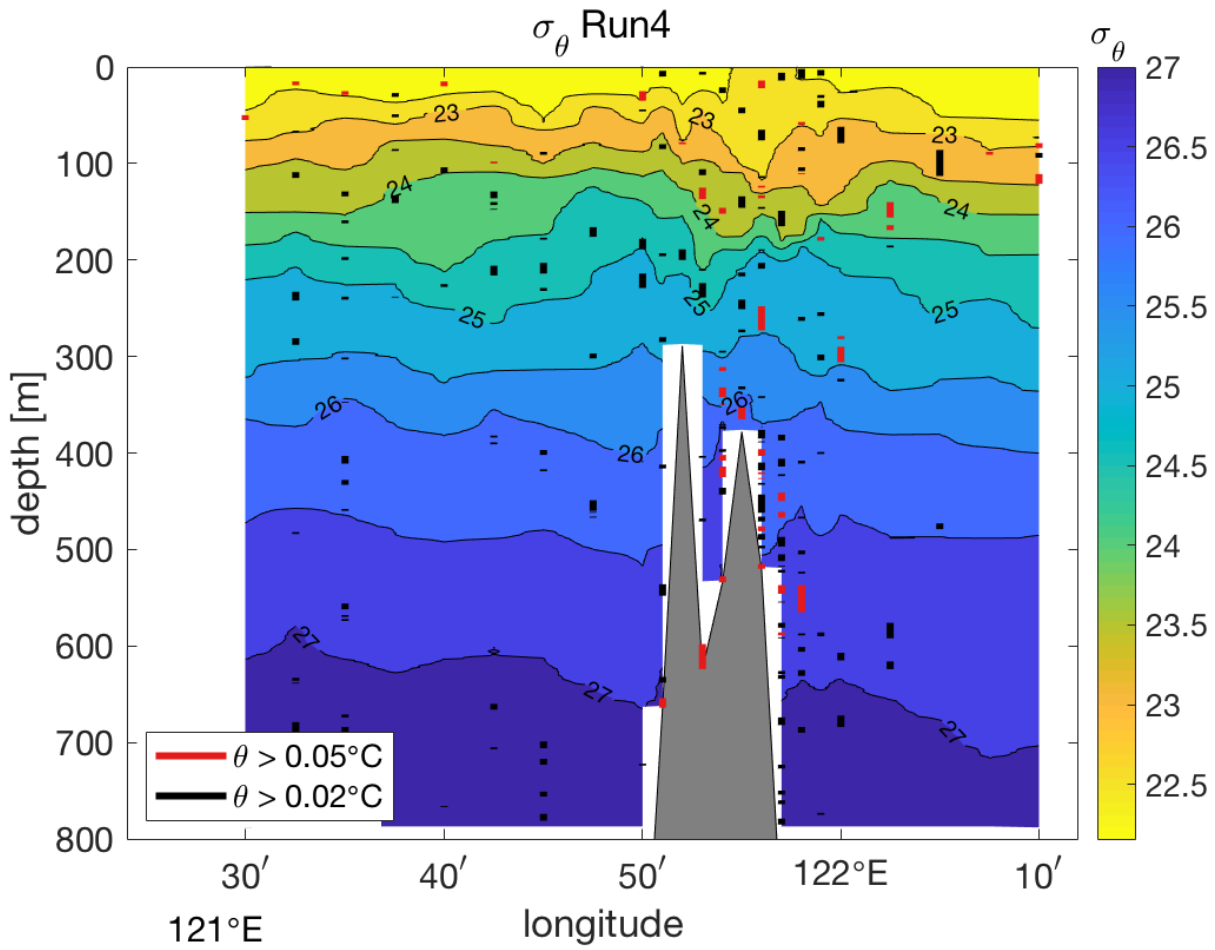
The Luzon Strait has two parallel ridges running from north to south, which is known to create large amplitude internal tides. To investigate the mixing processes accompanied by the internal tides, we carried out repeated observations with XBT, XCTD, CTD, and ADCP in the cruise of R/V Hakuho-maru KH-17-5, Leg-2, in November 2017 as part of the OMIX project. We obtained 6 cross sections around the eastern ridge between 121° 30’ E and 122° 10’ E along the line of 21° N.

The cross sections showed wavy structures of isopycnals over the ridge, with 4-7 km of horizontal scale and about 50 m of vertical scale. Velocity distributions by the shipboard ADCP showed strong vertical shear over the ridge, suggesting high-mode internal waves. Froude number of the high-mode internal waves exceeds unity around two summits of the ridge during the periods of strong tidal flow. This suggests that the high-mode internal waves stay over the ridge.

Many temperature inversions, especially large inversions ($\theta > 0.05$ °C) were formed near the ridge (figure). Therefore, energy dissipation rate and vertical diffusivity assuming the model of Osborn (1980) were estimated by calculating Thorpe scale from the temperature profiles. Relatively large energy dissipation rate and vertical diffusivity were distributed over the ridge from surface to the bottom, as well as unstable regions of $Ri < 0.25$. These results reflect strong mixing over the ridge due to the high-mode internal waves.

Keywords: internal waves, Luzon Strait

©2019. Japan Geoscience Union. All Right Reserved.



©2019. Japan Geoscience Union. All Right Reserved.

From the Luzon Strait to the Tsushima Strait: Water masses and nutrient transports approached using ^{137}Cs

*Siteng Zhu[1], JING ZHANG[1], Shota Kambayashi[2], Takeshi Matsuno[3], Eisuke Tsutsumi[3], Shigenobu Takeda[4], Seiya Nagao[5], Hiroshi Inoue[5], Hiroshi Ogawa[6], Ichiro Yasuda[6]

1. University of Toyama, 2. Fukushima university, 3. Kyushu university, 4. Nagasaki university, 5. Kanazawa university, 6. The University of Tokyo

More than 95% of the water flowing into the Sea of Japan comes from the Tsushima Strait, and 80% of it is Kuroshio Intimidate Water (KIW), which is rich in nutrients compared with Kuroshio surface Water and Kuroshio Tropical Water. However, there is a lack of direct evidence based on surveys or measurement data. ^{137}Cs in the subtropical mode water (STMW) that originated in the Fukushima Dai-ichi Nuclear Power Plant (FNPP1) accident is an excellent tracer which can be transported from the Kuroshio upstream to the Sea of Japan crossing the shelf edge of the East China Sea (ECS) via the KIW. It is also useful for research on the transport of nutrients from the KIW.

Data and water samples were collected during the Hakuho-Maru KH-17-5 Cruise and the Nagasaki-Maru 464 Cruise in November and July 2017, respectively. Data from the KH-17-5 Cruise was used for the study of the area around the Luzon Strait and those of the Nagasaki-maru 464 Cruise was used for the study of area around the outer shelf region of the East China Sea and the Tsushima Strait. The ^{137}Cs active concentration was analyzed by γ-Ray spectrometry after preconcentration. The turbulence intensity was measured using TurboMAP and VMP2000.

The maximum ^{137}Cs concentration shows the existence of the subtropical mode water (STMW) in the Luzon Strait, the ECS and the Tsushima Strait, respectively, at the similar density (25.2-25.7 kg/m^3), temperature (15-17℃) and salinity (34.60-34.75). Although their depth changes from 400 m in the Luzon Strait to 150 m at the shelf edge of the ECS and 100m in the East Channel of the Tsushima Strait, they can all be identified as the KIW because of the similar density. It is noteworthy that around Luzon Strait, the distribution of ^{137}Cs is influenced by strong vertical mixing. The percentage of nutrients transported to the Sea of Japan by KIW is estimated and this is meaningful to the ecosystem of the Sea of Japan.

Keywords: 137Cs, subtropical mode water, water masses, KIW, nutrients

©2019. Japan Geoscience Union. All Right Reserved.

Impact of cyclonic eddies and typhoons on biogeochemistry in the oligotrophic ocean based on time-series observation at the western Pacific subtropical station KEO

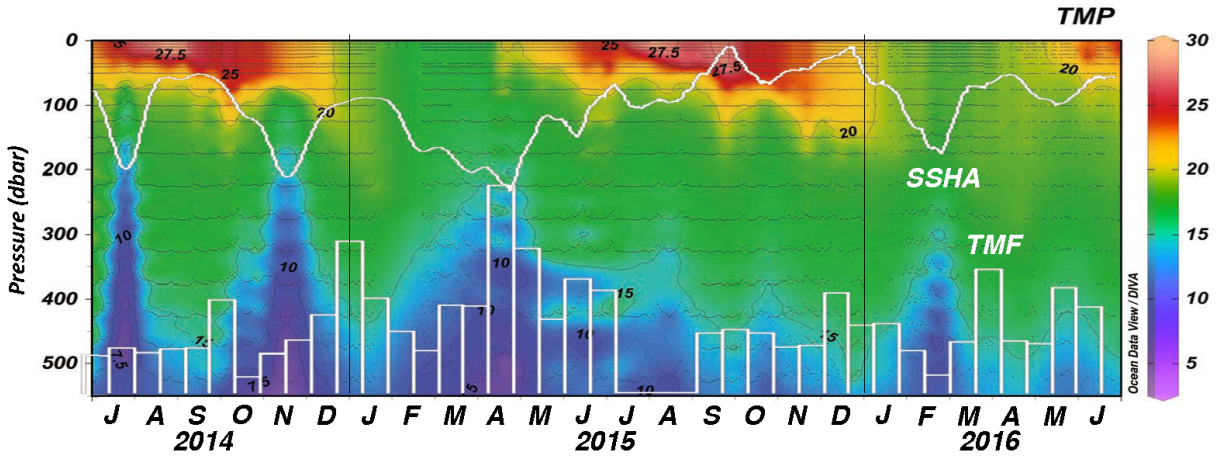
*Makio Honda[1], Yoshikazu Sasai[1], Eko Siswanto[1], Akira Kuwano-Yoshida[2], Hidenori AIKI[3], Meghan Cronin[4]

1. Japan Agency for Marine-Earth Science and Technology, 2. Disaster Prevention Laboratory, Kyoto University, 3. Nagoya University, 4. NOAA Pacific Marine Environmental Laboratory

In 2014, a sediment trap mooring experiment started adjacent to station Kuroshio Extension Observatory (KEO)' s National Ocean and Atmosphere Administration (NOAA) surface mooring. Two-years long sediment trap data show that biogenic material fluxes at ~ 5000 m increased between late winter (March) and late spring (June). Based on sea surface temperature and upper ocean water temperature profiles, from the NOAA surface buoy, and satellite-based surface chlorophyll-a , this increase was likely due to an increase of ocean productivity in early spring (March) that was supported by nutrients supplied by winter mixing. On the other hand, biogenic material fluxes also increased in October 2014, and between late December 2014 and January 2015 when concentrations of nutrients near the surface typically are low. Sea surface height anomalies and vertical profiles of water temperature in the upper 500 m showed cyclonic eddies passing station KEO and causing upwelling of middle-layer water in late July–early August 2014 and November 2014. It appears that these events supplied nutrients to the upper layer, which then caused ocean productivity in the subsurface layer to temporally increase, resulting in increased deep biogenic material fluxes in autumn and winter. This interpretation of the data is consistent with a simple 3D physical-biological model simulation that shows meso-scale cyclonic eddies can supply nutrient to support new production at KEO. During the 2-year-long sediment trap deployments, several typhoons also passed near station KEO and near-inertial internal waves were observed near the nitracline depth after the typhoons passed. Although turbulent mixing caused by near-inertial internal wave could have possibly supplied nutrient to upper oligotrophic euphotic layer, numerical simulations of the turbulent nutrient supply indicate that enhanced turbulent diffusion across the nutrient concentration gradient did not supply enough nitrate to support the increase in biogenic material flux in autumn.

Keywords: KEO, Oligotrophic, Sediment trap, Cyclonic eddy, Nutrient, Typhoon

©2019. Japan Geoscience Union. All Right Reserved.



©2019. Japan Geoscience Union. All Right Reserved.

Island-mass effect on the phytoplankton and zooplankton community in south of Japan

*Kiyotaka Hidaka[1], Kazuaki Tadokoro[1], Hiroomi Miyamoto[1], Tadafumi Ichikawa[1]

1. Japan Fisheries Research and Education Agency

The Izu Ridge brings high plankton production via its island-mass effect, which brings up subsurface nutrients to surface layer. Previous reports on island-mass effect around the ridge have been based on observation in the summer-early autumn and reports in spring, when many small pelagic fish species spawn, are scarce. As the Kuroshio flow through the ridge, island-mass effect on zooplankton, which takes more time to glow than phytoplankton, should be appear in eastern (downstream) area. Thus wider area around the ridge should be examined for the effect on zooplankton. In the present study, we examined island-mass effect of the Izu-Ridge on phytoplankton and zooplankton, based on satellite data and zooplankton data in the broad area south of the Honshu.
The Sea surface chlorophyll concentration (SSChl, MODIS-Aqua) in the area bounded by 135.5-142.0 E and 30.0-37.0 N was examined for the grids with depths of > 500 m. Zooplankton samples were collected by vertical tow (0-150 m) of the NORPAC net with 0.335 mm mesh in the area south of Honshu in February to March of 1963-2017. Samples were fixed in 5% formalin-sea water and copepod biomass was estimated in the laboratory by Bench-top Video Plankton Recorder. The relationships between plankton biomass and distance to the Honshu coast and to the Izu Ridge were examined.
The SSChl declined as distance to the Honshu coast increased. But high SSChl was observed in several areas 150-250 km away to the coast. These areas were mainly located around the Izu Ridge, 32-33.5N, and interpreted as caused by island-mass effect when the Kuroshio flowed in offshore path. The copepod biomass was high around the Honshu coast (<50 km). Stations with high copepod biomass were observed in the 100-200 km north-east (downstream) of the Izu Ridge, but they were located near the Honshu, around the Boso peninsula. Island-mass effect of the Izu-ridge on zooplankton biomass thus cannot be distinguished from the coastal effect and the effect should be examined by rate process (spawning rate and/or growth rate) in species level.

Keywords: zooplankton, island-mass effect

©2019. Japan Geoscience Union. All Right Reserved.

Influence of enhanced deep circulation due to geothermal heat on biogeochemical cycle in the Pacific Ocean

*Shogo Urakawa[1], Hideyuki Nakano[1], Hiroyuki Tsujino[1], Kei Sakamoto[1], Takahiro Toyoda[1], Goro Yamanaka[1]

1. Meteorological Research Institute, Japan Meteorological Agency

There exists heat conduction from the oceanic lithosphere to the abyssal ocean. Its heat flux amounts to about 0.1 W m^{-2} in the global average. It is much smaller than the heat exchange between the atmosphere and ocean in the order of 10 W m^{-2}. However, it is known that this geothermal heat significantly enhances the deep circulation especially in the Pacific Ocean. For example, Adcroft et al. (2001) conduct numerical experiments with/without geothermal heating using an ocean general circulation model and report that constant heat flux at the sea bottom by 0.05 W m^{-2} results in enhancement of the Pacific meridional overturning circulation (PMOC) by 25 %. Other studies also report that the geothermal heat significantly enhances the oceanic deep circulation (e.g., Emile-Geay and Madec, 2009; Urakawa and Hasumi, 2009; Downes et al., 2016). The importance of the geothermal heat seems to be robust from the viewpoint of ocean dynamics but it has not been investigated to what extent the geothermal heat influences the biogeochemical cycle of the ocean. Here, we conduct two numerical experiments with/without the geothermal heat using an ocean general circulation model developed for the CMIP6 and investigate the effect of the geothermal heat on the biogeochemical tracer fields.
The geothermal heating enhances PMOC at 30º S by 17 % in this model, which leads to stronger ventilation in the North Pacific Ocean. This stronger ventilation results in increase of delta ^{14}C by more than 10 per mille, which means younger water masses, at the bottom of the North Pacific. The stronger PMOC also results in higher dissolved oxygen in the abyss especially in the eastern tropical Pacific. The geothermal heat leads to dissolved oxygen increase by more than 10 micro mol L^{-1} there, which corresponds to 10–70 % of hypoxic water in the control experiment without geothermal heating. This oxygenation near the sea bottom affects the oxygen-deficient water in the surface of the eastern tropical Pacific. Its thickness becomes thinner by around 100 m. The geothermal heat also plays an important role in the biogeochemical cycle in the Pacific Ocean.

©2019. Japan Geoscience Union. All Right Reserved.

The Parameterization of the Pressure-Strain Correlations in the Stably or Unstably Stratified Ocean Surface Layer.

*Yusuke Ushijima[1], Yutaka Yoshikawa[1]

1. Graduate School of Science, Kyoto University

Turbulence in the ocean surface layer mixes momentum, heat, and nutrient vertically. It is therefore important for air-sea interaction, phytoplankton blooming, and other oceanic processes (e.g., Roxy et al. 2013; Obata et al. 1996). However, large-scale models such as ocean general circulation models cannot explicitly resolve small-scale turbulence because of their coarse resolution. For this reason, the vertical mixing should be parameterized using the turbulent closure scheme that successfully parameterizes the turbulent mixing. Recently, attention is paid to pressure-strain correlations, which redistribute stress due to fluctuating pressure, in the parameterization scheme used for engineering purposes (Jakilic and Hanjalic 2013). In the present study, therefore, the validity of the pressure-strain correlation parameterization used in the ocean (or atmosphere) (Rotta 1951, Gibson and Launder 1978, Gertski et al. 1992) was examined. To this end, we performed Large-eddy simulations of ocean surface boundary layer to simulate pressure-strain correlations and compared it with parameterized correlations. Here, we focused on the effects of stratification on the correlations, because the stratification is an essential factor in the ocean and atmospheric boundary layers but previous schemes did not include the stratification effects sufficiently. Results show that the parameterizations of the pressure-strain correlations had systematic errors depending on the stability (or stratification). It was also found that the error can be reduced by introducing new parameters related to the stability into the scheme.

Keywords: Parameterization of Pressure-Strain Correlations, Turbulent Closure Model, Turbulence in the Ocean Surface Layer

©2019. Japan Geoscience Union. All Right Reserved.

Numerical studies on asymmetric responses of the upper ocean to tropical cyclone

*Daiki Okura[1], Yutaka Yoshikawa[1]

1. Graduate School of Science, Kyoto University

Tropical cyclones (TCs) decrease sea surface temperature (SST), and the decreased SST weakens TC intensity. This SST decrease is asymmetric with respect to the TC track, known as “rightward bias”. Preceding numerical studies suggested that this asymmetry may influence on the course of the TC. The interaction between TC and the upper ocean is one of key ingredients for precisely predicting TC's development, and the upper ocean response to TC should also be clarified.
The SST decrease during TC passage is mainly caused by two processes; vertical turbulent mixing and advection (Ekman suction). The rightward bias is associated with the mixing which is more intense on the right side of the TC track due to resonant inertial currents with winds. Magnitude and distribution of SST decrease induced by the mixing should vary with parameters characterizing TC; transition speed U_T, radius of maximum wind R_{max}, the friction velocity U_*, and the Coriolis coefficient f. However, detailed physical processes of the mixing and its dependence on these parameters have not been well quantified, because of lack of in-situ data and complicated processes involved in the mixing.

The present study focuses on the vertical turbulent mixing effects on asymmetric SST response. To this aim, vertically one-dimensional model was used in which the vertical turbulent mixing was parameterized with the Nakanishi-Niino-Mellor-Yamada scheme modified by Kitamura (2010). We considered TC-like wind stress of magnitude U_*^2 at radius R_{max} from the TC center moving with transition speed U_T and investigated the mixing on both sides of TC track at distance *r*. Experiments with several friction velocities U_*, maximum wind radii R_{max}, transition speeds U_T and distances *r* were performed. No surface heat flux was considered for simplicity.
The results showed that the rightward bias of the SST response depended on these parameters. The location of the largest SST decrease moved away from the axis as U_T increased, but it depended less on U_*. The SST decreased more with larger U_* and smaller U_T. These results can be explained by energy flux at the surface. In our model configuration, the energy flux depends on two non-dimensional parameters, U_T/fR_{max} and U_*/U_T, and the energy flux had maximum and turbulent kinetic energy penetrated deeper at larger U_*/U_T and at U_T/fR_{max}~1, suggesting the resonance between wind and the inertial current. The SST decrease corresponded with the energy flux, but it depended largely on U_*/U_T, implying importance of wind forcing duration.
Thus, the asymmetric SST response due to the vertical turbulent mixing can be characterized with U_T/fR_{max} and U_*/U_T. Additional advection effects on the SST response will be discussed at the conference using three-dimensional simulation in which the advection as well as the mixing are fully included.

Keywords: Tropical cyclone, Vertical turbulent mixing, Ekman suction, Rightward bias

©2019. Japan Geoscience Union. All Right Reserved.

Influence of the distortion of the internal wave field on estimates of turbulent mixing using fine-scale parameterizations

*Anne Takahashi[1], Toshiyuki Hibiya[1], Alberto C. Naveira Garabato[2]

1. Department of Earth and Planetary Science, Graduate School of Science, University of Tokyo, 2. National Oceanography Centre, University of Southampton

Although the Southern Ocean is one of the turbulent mixing hotspots, we have not yet clarified quantitatively the turbulent mixing processes in this region, where the Antarctic Circumpolar Current (ACC) coexists with near-inertial internal waves generated by wind forcing and internal lee waves radiated by the impingement of eddy flows on topography.

Fine-scale parameterizations, based on the theory of energy cascade from internal waves to turbulence, are most widely used to estimate the turbulent dissipation rate, ε. It has been reported, however, that these fine-scale parameterizations tend to overestimate ε in the ACC (Waterman et al. 2014). Although Takahashi and Hibiya (2019) have suggested that "the distorted fine-scale shear and strain spectra" caused by the existence of eddies trapping near-inertial waves or upward-propagating internal lee waves might be responsible for the overestimates, the problem remains unresolved.

In this study, we use "eikonal" simulations (Henyey et al. 1986), which trace the propagation, refraction and breaking of test waves within a background internal wave field, to assess the evolution of the energy cascade in vertical wavenumber space. Our objective is to examine how the distortion of the vertical wavenumber spectrum affects the performance of fine-scale parameterizations.

In our simulations, in contrast to high vertical wavenumber test waves that are efficiently Doppler-shifted to their breaking limit, low vertical wavenumber test waves are not subject to dissipation processes. In the existing fine-scale parameterizations, however, the energy flux to dissipation scale is estimated using the integrated vertical wavenumber spectral values. This means that, if the range of this integration includes a spectral bump at the low-wavenumber end of the spectrum, the estimated energy flux and hence the resulting ε might be overestimated by these fine-scale parameterizations.

From the simulation results, it is confirmed that fine-scale parameterizations significantly overestimate ε in spectra with a low-wavenumber bump, in particular as the internal wave energy level becomes large and the shear/strain ratio becomes small. These results are supported by the microstructure and fine-structure dataset from the SOFine experiment carried out in the Kerguelen Plateau.

Keywords: Turbulent Mixing, Fine-scale parameterizations, Antarctic Circumpolar Current region

©2019. Japan Geoscience Union. All Right Reserved.

[E] Poster | A (Atmospheric and Hydrospheric Sciences)：A-OS Ocean Sciences & Ocean Environment

Sun. May 26, 2019 5:15 PM - 6:30 PM JST | Sun. May 26, 2019 8:15 AM - 9:30 AM UTC | Poster Hall International Exhibition Hall8, Makuhari Messe_11

[A-OS09] Ocean Mixing Processes: Impact on Biogeochemistry, Climate and Ecosystem

convener:Ichiro Yasuda(Atmosphere and Ocean Research Institute, The University of Tokyo), Toshiyuki Hibiya(Department of Earth and Planetary Science, Graduate School of Science, University of Tokyo), Jun Nishioka(Hokkaido University, Institute of low temperature sciences), Shin-ichi Ito(Atmosphere and Ocean Research Institute, The University of Tokyo)

The interdisciplinary study on ocean diapycnal mixing and its impacts (Ocean Mixing Processes: Impact on Biogeochemistry, Climate and Ecosystem (OMIX) 2015-2020) is opening the integrated sciences from physical, chemical, biological oceanography to climate and fisheries sciences. In this section, results during the four years of OMIX projects and other related presentations are all welcome to be summarized and to facilitate plans of next projects.

[AOS09-P01] Correction method of fast-response thermistors data to estimate turbulence intensity

*kimura shino[1], Yasutaka Goto[2], Koenjong Lee[1], Ichiro Yasuda[1] (1.The Univercity of Tokyo, 2.Meteorological Agency)

[AOS09-P02] Observation of turbulent mixing using a deep float with microstructure sensors

*Shuo Zhai[1], Ichiro Yasuda[1], Masaaki Kikuchi[1], Yasutaka Goto[1], Koenjong Lee[1], Takahiro Tanaka[2], Ken Yamaki[3], Yutaka Imamura[4] (1.Atmosphere and Ocean Research Institute, The University of Tokyo, 2.Japan Fisheries Research Agency, 3.TSK Tsurumi-Seiki Co., Ltd., 4.Aomori Prefectural Industrial Thechnology Research Center, Fisheries Research Insititute)

[AOS09-P03] Evaluation of the underwater glider flight model using the electromagnetic current sensor

*Takahiro Tanaka[1], Daisuke Hasegawa[1], Takeshi Okunishi[1], Ichiro Yasuda[2] (1.Tohoku National Fisheries Research Institute, Japan Fisheries Research and Education Agency, 2.Atmosphere and Ocean Research Institute, University of Tokyo)

[AOS09-P04] Mixing processes observed by a slocum glider at the Oyashio-TWC front

*Daisuke Hasegawa[1], Takahiro Tanaka[1], Takeshi Okunishi[1], Ichiro Yasuda[2] (1.Tohoku National Fisheries Research Institute, Japan Fisheries Research and Education Agency, 2.Atmosphere and Ocean Research Institute, The University of Tokyo)

[AOS09-P05] Impact of the astronomical lunar 18.6-yr tidal cycle on El-Niño and Southern Oscillation

*Ichiro Yasuda[1] (1.Atmosphere and Ocean Research Institute, The University of Tokyo)

[AOS09-P06] The effect of 18.6-year period lunar nodal cycle on Pacific Decadal Oscillation (PDO)

*Masaki Hamamoto[1], Ichiro Yasuda[1] (1.Atmosphere and Ocean Research Institute, The University of Tokyo)

[AOS09-P07] A comparison of ocean deoxygenation between CMIP5 models and an observational dataset

*Yumi Abe[1], Shoshiro Minobe[1,5], Takamitsu Ito[2], Curtis Deutsch[3], Matthew C. Long[4] (1.Department of Natural History Sciences, Graduate School of Science,Hokkaido University, Sapporo, Japan, 2.School of Earth and Atmospheric Sciences, Georgia Institute of Technology, Atlanta, Georgia, USA, 3.School of Oceanography, University of Washington, Seattle, Washington, USA, 4.Climate and Global Dynamics

Laboratory, National Center for Atmospheric Research, Boulder, Colorado, USA, 5.Department of Earth and Planetary Sciences, Faculty of Science, Hokkaido University, Sapporo, Japan)

[AOS09-P08] Pacific Ocean State Estimation and Clarification of Mechanism of Ocean Circulation by Data Synthesis of Global Observations

*Shuhei Masuda[1] (1.Japan Agency for Marine-Earth Science and Technology)

[AOS09-P09] Impact of Tidal Vertical Mixing to Barotropic Water Exchange between the Sea of Okhotsk and Pacific through Diffusive Adjustment with Turbulent Closure Scheme

*Hung Wei Chou[1], Humio Mitsudera[1], Hatsumi Nishikawa[1], Kaihe Yamazaki[2] (1.Hokkaido University, Institute of Low Temperature Science, 2.Hokkaido University, Graduate School of Environmental Science)

[AOS09-P10] Distributions of organic Fe-binding ligands in the eastern and western subarctic North Pacific

*Yoshiko Kondo[1,2], Yudai Sunahara[2], Jun Nishioka[3], Hajime Obata[4], Shigenobu Takeda[1,2] (1.Graduate School of Fisheries and Environmental Sciences, Nagasaki University, 2.Faculty of Fisheries, Nagasaki University, 3.Institute of Low Temperature Science, Hokkaido University, 4.Atmosphere and Ocean Research Institute, The University of Tokyo)

[AOS09-P11] Chemical and physical speciation of copper in the subarctic North Pacific

*Kuo Hong Wong[1], Hajime Obata[1], Taejin Kim[2], Yoshiko Kondo[3], Jun Nishioka[4] (1.Atmosphere and Ocean Research Institute, The University of Tokyo, 2.Seoul National University, Korea, 3.Nagasaki University, 4.Institute of Low Temperature Science, Hokkaido University)

[AOS09-P12] Latitudinal and temporal variations in phytoplankton size structure within mesoscale eddies from space

*Hisatomo Waga[1], Toru Hirawake[1], Ueno Hiromichi[1] (1.Hokkaido University)

[AOS09-P13] Structure and impact of the Kuroshio nutrient stream

*Kosei Komatsu[1,2], Yutaka Hiroe[3] (1.Graduate School of Frontier Sciences, The University of Tokyo, 2.Atmosphere and Ocean Research Institute, The University of Tokyo, Kashiwa, Japan, 3.Seikai National Fisheries Research Institute, Japan Fisheries Research and Education Agency, Nagasaki, Japan)

[AOS09-P14] Enhanced nutrient supply and biogeochemical impacts induced by internal waves in the oligotrophic northern South China Sea

*Chin-chang Hung[1], Dewang Li[2], Wen-Chen Chou[3], Yung-Yen Shih[1,4], Guan-Yu Chen[1] (1.Department of Oceanography, National Sun Yat Sen University, Kaohsiung, Taiwan, 2.Second Institute of Oceanography, State Oceanic Administration, Hangzhou, PRC, 3.Institute of Marine Environmental Chemistry and Ecology, National Taiwan Ocean University, Taiwan, 4.Department of Applied Science, R.O.C Naval Academy, Kaohsiung, Taiwan)

[AOS09-P15] Mixing over the eastern ridge in the Luzon Strait caused by high-mode internal waves

*Akie Sakai[1], Tomoharu Senjyu[2], Eisuke Tsutsumi[2], Takeshi Matsuno[2], Takahiro Endo[2], Ichiro Yasuda[3], Daigo Yanagimoto[3] (1.Department of Earth System Science and Technology, Interdisciplinary Graduate School of Engineering Sciences, Kyushu University, 2.Research Institute for Applied Mechanics , 3.Atmosphere and Ocean Reserch Institute The University of Tokyo)

[AOS09-P16] **From the Luzon Strait to the Tsushima Strait: Water masses and nutrient transports approached using ^{137}Cs**

*Siteng Zhu[1], JING ZHANG[1], Shota Kambayashi[2], Takeshi Matsuno[3], Eisuke Tsutsumi[3], Shigenobu Takeda[4], Seiya Nagao[5], Hiroshi Inoue[5], Hiroshi Ogawa[6], Ichiro Yasuda[6] (1.University of Toyama,

2.Fukushima university, 3.Kyushu university, 4.Nagasaki university, 5.Kanazawa university, 6.The University of Tokyo)

[AOS09-P17] Impact of cyclonic eddies and typhoons on biogeochemistry in the oligotrophic ocean based on time-series observation at the western Pacific subtropical station KEO

*Makio Honda[1], Yoshikazu Sasai[1], Eko Siswanto[1], Akira Kuwano-Yoshida[2], Hidenori AIKI[3], Meghan Cronin[4] (1.Japan Agency for Marine-Earth Science and Technology, 2.Disaster Prevention Laboratory, Kyoto University, 3.Nagoya University, 4.NOAA Pacific Marine Environmental Laboratory)

[AOS09-P18] Island-mass effect on the phytoplankton and zooplankton community in south of Japan

*Kiyotaka Hidaka[1], Kazuaki Tadokoro[1], Hiroomi Miyamoto[1], Tadafumi Ichikawa[1] (1.Japan Fisheries Research and Education Agency)

[AOS09-P19] Influence of enhanced deep circulation due to geothermal heat on biogeochemical cycle in the Pacific Ocean

*Shogo Urakawa[1], Hideyuki Nakano[1], Hiroyuki Tsujino[1], Kei Sakamoto[1], Takahiro Toyoda[1], Goro Yamanaka[1] (1.Meteorological Research Institute, Japan Meteorological Agency)

[AOS09-P20] The Parameterization of the Pressure-Strain Correlations in the Stably or Unstably Stratified Ocean Surface Layer.

*Yusuke Ushijima[1], Yutaka Yoshikawa[1] (1.Graduate School of Science, Kyoto University)

[AOS09-P21] Numerical studies on asymmetric responses of the upper ocean to tropical cyclone

*Daiki Okura[1], Yutaka Yoshikawa[1] (1.Graduate School of Science, Kyoto University)

[AOS09-P22] Influence of the distortion of the internal wave field on estimates of turbulent mixing using fine-scale parameterizations

*Anne Takahashi[1], Toshiyuki Hibiya[1], Alberto C. Naveira Garabato[2] (1.Department of Earth and Planetary Science, Graduate School of Science, University of Tokyo, 2.National Oceanography Centre, University of Southampton)

Correction method of fast-response thermistors data to estimate turbulence intensity

*kimura shino[1], Yasutaka Goto[2], Koenjong Lee[1], Ichiro Yasuda[1]

1. The Univercity of Tokyo, 2. Meteorological Agency

Fast-response thermistors (FP07) can be used to estimate turbulent energy dissipation rate ε and temperature dissipation rate χ. However, correction is necessary because the insufficient response of FP07 causes underestimate for relatively strong turbulence and individual FP07 sensors have different response. In this study, using simultaneously observed shear probe and FP07 data from a free fall microstructure profiler descending at the speed of 0.6-0.7 m/s, ε_T from various FP07 are compered with ε_S from shear probe to estimate how much correction is necessary for FP07 data. For 3 (7) msec time constant of FP07 for double-pole (single-pole) correction, ε_T is consistent with ε_S within a factor of 3 in the range of ε_S =10^-10 ~10^-7 W/kg. In the presentation we also discuss the impact of correction on χ and the validity of ε_T under double diffusion.

Keywords: vertical mixing, turbulence

©2019. Japan Geoscience Union. All Right Reserved.

Observation of turbulent mixing using a deep float with microstructure sensors

*Shuo Zhai[1], Ichiro Yasuda[1], Masaaki Kikuchi[1], Yasutaka Goto[1], Koenjong Lee[1], Takahiro Tanaka[2], Ken Yamaki[3], Yutaka Imamura[4]

1. Atmosphere and Ocean Research Institute, The University of Tokyo, 2. Japan Fisheries Research Agency, 3. TSK Tsurumi-Seiki Co., Ltd., 4. Aomori Prefectural Industrial Thechnology Research Center, Fisheries Research Insititute

Automated microstructure obsevation method using a deep float (DeepNINJA) with velocity shear probe and fast-response thermistor is being elaborated. From the field test observation in August 2016, availability of shear probe data was tested by comparing turbulent dissipation rates from thermistor. Shear probe data were found to be worse by vibration from motor operartions at buoyancy adjustment and by noise at slow ascending speed of the float. Vertical profiles of turbulent energy dissipation rate could be obtained with the hybrid use of shear probe and thermistor data by correcting time-constant of the termistor with reliable shear probe data and filling gaps of unavailable shear probe data. Data will be reported for the deep float which was deployed on December 12, 2018, in the western slope of Japan Trench off Aomori. The float is observing 0 - 4000 m turbulence profile every 10 days and will be recovered in April R/V Shinsei-maru cruise.

Keywords: vertical mixing , deep float, energy dissipation rate

©2019. Japan Geoscience Union. All Right Reserved.

Evaluation of the underwater glider flight model using the electromagnetic current sensor

*Takahiro Tanaka[1], Daisuke Hasegawa[1], Takeshi Okunishi[1], Ichiro Yasuda[2]

1. Tohoku National Fisheries Research Institute, Japan Fisheries Research and Education Agency, 2. Atmosphere and Ocean Research Institute, University of Tokyo

Turbulence measurement by underwater gliders has become more common in recent years. For the accurate estimation of energy dissipation rates, the accurate measurement of the fall rate and gliding path angle is necessary. The gliding path angle should take the angle of attack (AOA) into account, which is the difference between the gliding path angle and the pitch angle. AOA calculation has been done by using the so-called flight model assuming dynamical force balance in the quasi-steady state. Due to the difficulty in measuring AOA directly, the validity of AOA derived from the flight model and the flight model itself has not been adequately evaluated so far. In this study, we put the electromagnetic current sensor (EM sensor) on the turbulence package to obtain AOA directly and to compare the AOA from EM sensor with that from the flight model. Using the dataset obtained by a Slocum glider in Jul. - Aug. 2017, we found that AOA from the EM sensor during descent and ascent has a mean (standard deviation) of 0.7 (1.2) deg. and -0.7 (1.1) deg., respectively, while AOA from the flight model is 4.9 (0.4) deg. and -4.5 (0.5) deg., respectively. In order to know what cause this difference, we discuss the validity of parameters given in the flight model. It is suggested that a drag coefficient due to parasite drag given in the flight model may be somewhat larger than that calculated using the EM sensor.

Keywords: underwater glider, flight model, electromagnetic current sensor, angle of attack

©2019. Japan Geoscience Union. All Right Reserved.

Mixing processes observed by a slocum glider at the Oyashio-TWC front

*Daisuke Hasegawa[1], Takahiro Tanaka[1], Takeshi Okunishi[1], Ichiro Yasuda[2]

1. Tohoku National Fisheries Research Institute, Japan Fisheries Research and Education Agency, 2. Atmosphere and Ocean Research Institute, The University of Tokyo

In order to grasp the detailed mixing processes along the frontal region between the Oyashio and the Tsugaru Warm Current (TWC), we conducted a zigzag survey crossing the front several times from the merging region of the two current systems to the down stream by an underwater glider (Slocum G2 Glider) equipped with a turbulence sensor, from July 24thto August 29thin 2017. The observed frontal structure indicated the subduction and the intrusion processes of the cold and fresh Oyashio water under the warm and salty TWC water, along layer between 26.5 to 26.8 sigma-theta, which resulted the favorable conditions to the salt finger convection at the upper interface along the 26.5 sigma-theta, and the diffusive convection at the lower interface along the 26.8 sigma-theta where the fresh and cold Oyashio water lying above the warm and salty water. The strong turbulence intensity is observed around the intruded layer, and the mean temperature and the salinity in the layer became warmer and saltier with the increase of the distance from the front, which suggested the time evolution of the vertical mixing driven by double diffusive convections between the three different water masses. Though the strongest turbulence intensity was observed around the frontal region, which may suggest the importance of the cabbeling effect as the additional source of the turbulent mixing.

Keywords: double diffusion, mixing, cabbeling

©2019. Japan Geoscience Union. All Right Reserved.

Impact of the astronomical lunar 18.6-yr tidal cycle on El-Niño and Southern Oscillation

*Ichiro Yasuda[1]

1. Atmosphere and Ocean Research Institute, The University of Tokyo

Even though El-Niño and Southern Oscillation (ENSO) has a tremendous impact on global climate and society, its long-term forecast remains difficult. In this study, we discovered a statistically significant relationship between ENSO timing and the 18.6-year period lunar tidal cycle in the mature-phase (December –February) ENSO time-series during 1867–2015 and extending back to 1706 with proxy data. It was found that El-Niño tended to occur in the 1st, 10th, and 13th years after the maximum diurnal tide in the 18.6-yr cycle, and La-Niña tended to occur in the 3rd, 12th, and 16th years. These tendencies were also confirmed by corresponding sea-surface temperature (SST) and sea-level pressure (SLP) distributions; particularly Pacific SST and SLP spatial patterns in the third La-Niña and the tenth El-Niño year well resemble those of Pacific Decadal Oscillation (PDO). These findings contribute to understanding and forecasting long-term ENSO variability.

Keywords: El-Niño and Southern Oscillation, air-sea interaction, tide, mixing, climate

©2019. Japan Geoscience Union. All Right Reserved.

The effect of 18.6-year period lunar nodal cycle on Pacific Decadal Oscillation (PDO)

*Masaki Hamamoto[1], Ichiro Yasuda[1]

1. Atmosphere and Ocean Research Institute, The University of Tokyo

Pacific Decadal Oscillation (PDO) is the most dominant decadal-inter-decadal ocean-climate variability over the North Pacific; however, the periodicity and cause have not been fully understood. Previous studies suggested that 18.6-year period lunar tidal cycle ($T_{18.6}$) regulate bi-decadal PDO variability through changes in the strength of diapycnal mixing of ocean around the Kuril Islands to result in ocean variability, together with air-sea interactions in the mid-latitude North Pacific and/or equatorial Pacific. In the present study, 297yr-long reconstructed PDO timeseries was re-examined, and 27.9yr (3/2 times 18.6-yr, henceforth, $T_{27.9}$) period variability was significantly detected, and the zero-crossing from minus to plus was found to occur simultaneously with $T_{18.6}$ variability in the interval of 55.4 years (3 times $T_{18.6}$). In the PDO spectrum, a broad multi-decadal 50-80-yr peak (corresponding to 3-5 times $T_{18.6}$, henceforth T_M) was also detected with the zero-crossing synchronized with $T_{18.6}$; this is the extension of previous studies during 1900-2000 back to 1700s on the synchronous changes of bi-decadal and penta-decadal variabilities. These $T_{18.6}$, $T_{27.9}$ and T_M explain 71% of the 10-year low-passed PDO variability. These imply that the 27.9-yr and the multi-decadal variabilities could be related to $T_{18.6}$ tide-induced variability, and may be excited by $T_{18.6}$ tidal forcing, considering that external periodic forcing for delayed oscillator models could excite 3 times period of the external forcing and some non-linear processes may make the half-period variability.

Keywords: 18.6-year period lunar nodal cycle, Pacific Decadal Oscillation

©2019. Japan Geoscience Union. All Right Reserved.

A comparison of ocean deoxygenation between CMIP5 models and an observational dataset

*Yumi Abe[1], Shoshiro Minobe[1,5], Takamitsu Ito[2], Curtis Deutsch[3], Matthew C. Long[4]

1. Department of Natural History Sciences, Graduate School of Science,Hokkaido University, Sapporo, Japan, 2. School of Earth and Atmospheric Sciences, Georgia Institute of Technology, Atlanta, Georgia, USA, 3. School of Oceanography, University of Washington, Seattle, Washington, USA, 4. Climate and Global Dynamics Laboratory, National Center for Atmospheric Research, Boulder, Colorado, USA, 5. Department of Earth and Planetary Sciences, Faculty of Science, Hokkaido University, Sapporo, Japan

Recent studies revealed that the ocean deoxygenation has been accelerating since the 1980s over the global oceans (Schmidtko et al. 2017; Ito et al. 2017), and the observed trend in the last half-century appears to be much larger than the model simulations conducted for CMIP5 (Bopp et al. 2013). This discrepancy is an important issue of the ocean deoxygenation researches as highlighted by a review paper published in the last year (Oschlies et al. 2018).

In order to understand better the relations of oxygen variations between CMIP5 models and observations, we compare oxygen concentration simulated by CMIP5 models and gridded oxygen anomaly dataset used by Ito et al. (2017). For the global oceans, the observed oxygen reduction rate for the historical experiment period appears to be within uncertainty of the models, though this result can be sensitive to the choice of the analysis period associated with the rapid recent oxygen reduction. We also closely examined the two basins that are relatively well sampled, i.e., the North Pacific and the North Atlantic. It is found that the observed North Pacific oxygen reduction is much stronger than the simulated ones, but such a strong reduction of observed oxygen does not occur in the North Atlantic. These results suggest that there are substantial spatio-temporal variations of oxygen concentration on decadal timescales and their mechanism in each basin should be explored in future studies.

Keywords: North Pacific, North Atlantic

©2019. Japan Geoscience Union. All Right Reserved.

Pacific Ocean State Estimation and Clarification of Mechanism of Ocean Circulation by Data Synthesis of Global Observations

*Shuhei Masuda[1]

1. Japan Agency for Marine-Earth Science and Technology

Our aim is to synthesize pre-existing ocean data with newly-acquired turbulence data using state-of-art assimilation technique. Available observations of turbulence strength in the ocean, will be “blended” with pre-existing ocean data applying dynamically self-consistent state estimation approach with 4D-VAR adjoint system. We propose some new techniques and schemes to assimilate turbulence data, which tends to include unique features. The obtained state estimation will provide improved description of ocean circulation, its heat and salt transports, and oceanic ecosystem at lower trophic level.

Keywords: OMIX, ocean , mixing , data assimilation

©2019. Japan Geoscience Union. All Right Reserved.

Impact of Tidal Vertical Mixing to Barotropic Water Exchange between the Sea of Okhotsk and Pacific through Diffusive Adjustment with Turbulent Closure Scheme

*Hung Wei Chou[1], Humio Mitsudera[1], Hatsumi Nishikawa[1], Kaihe Yamazaki[2]

1. Hokkaido University, Institute of Low Temperature Science, 2. Hokkaido University, Graduate School of Environmental Science

The pattern of exchange flow between the Sea of Okhotsk and Pacific is a system composed by an Okhotsk-ward inflow through Kruzenshtern strait in north and a Pacific-ward outflow through Bussol strait in south. One of major theories for explaining the dynamic of water exchange through Kuril Island Chain is the turbulence induced by tidal vertical mixing. Turbulence is an important physical process in geostrophic boundary layer, and because of the complexity of topographic in Kuril island chain, the breaking of internal tides in island coast area leads to increase the thickness of surface mixing layer and causes tilting of isopycnal layer in vicinity. The tilting of isopycnal layer around islands forms a clockwise flow along the shore by geostrophic adjustment. However, above process is majorly broclinicly, and how can it impact to barotropic component is still unknown.

By setting the tidal force as a controlled variable, results from realistic OGCM model COCO show only the case with tidal forcing can consistent with the exchange flow pattern as historical observation (Fig.1). Besides, the vertical diffusivity values also show the magnitude difference in summer time, which the flow in north strait in non-tidal case is opposite to tidal one (Fig.2). Therefore, we designed four experiments for understanding the impact of tidal diffusive adjustment in summer: 1. install vertical diffusivity value generated by tidal case into non-tidal run; 2. install vertical diffusivity value generated by non-tidal case into tidal run; 3. set the vertical diffusivity value as zero in tidal case and 4. in non-tidal case as well. Further, for preventing the underestimates the depth of the mixing layer in Mellor-Yamada turbulence closure scheme, two more experiments with the larger vertical diffusivity mask are applied in both tidal and non-tidal case. After calculating the fraction of baroclinic and barotropic components in either north strait or southern strait, results show the vertical mixing dose influence the strength of volume transported but not the direction as original tidal and non-tidal case shows. Hence, for further understanding the impact of vertical diffusivity, we start a tidal forcing run with non-tidal initial conditions to detect the relationship between the flow direction and magnitiude of vertical diffusivity values by time developing. But the baroclinic result implies that the vertical mixing might not be the main reason to control the flow direction (Fig.3).

This study also implies the tidal impacts in OGCM is not only the vertical mixing, but other geostrophic fluid dynamics might occur, especially the interaction of topography with tidal waves. Therefore, for reproducing the real ocean phenomena, movement of tidal waves should be considered.

Keywords: OGCM, tidal mixing , Okhotsk, cross-basin exchange system

©2019. Japan Geoscience Union. All Right Reserved.

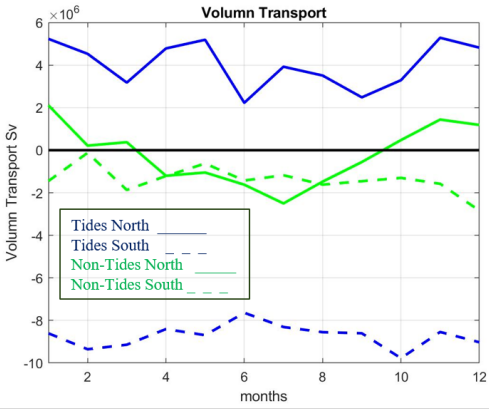


Fig.1: volume transportation in tidal and non-tidal run.
Positive value is Okhotsk-ward and negative value is Pacific-ward flow.

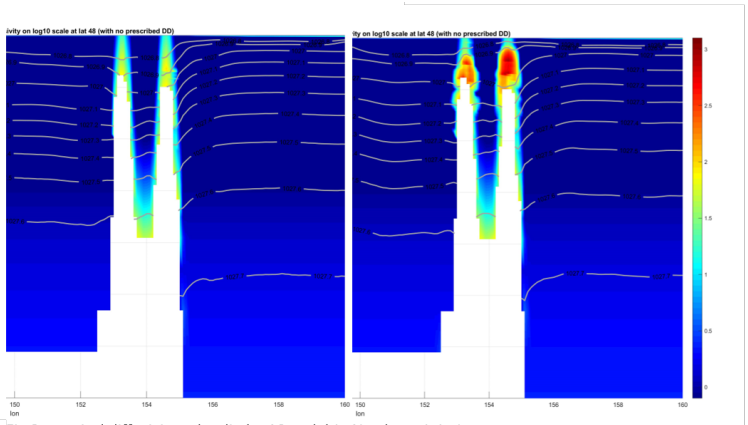


Fig.2: vertical diffusivity value (in log10 scale) in North strait in June, left one is non-tidal run and right is tidal run.

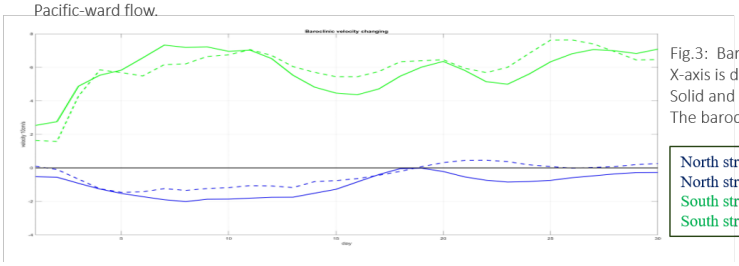


Fig.3: Baroclinic components in the tidal run with non-tidal initial condition.
X-axis is day and y-axis is velocity. Blue line is north strait and green line is south strait.
Solid and dot line are upper and lower isopycal layer, respectively.
The baroclinic velocity is stable after a week running.

©2019. Japan Geoscience Union. All Right Reserved.

Distributions of organic Fe-binding ligands in the eastern and western subarctic North Pacific

*Yoshiko Kondo[1,2], Yudai Sunahara[2], Jun Nishioka[3], Hajime Obata[4], Shigenobu Takeda[1,2]

1. Graduate School of Fisheries and Environmental Sciences, Nagasaki University, 2. Faculty of Fisheries, Nagasaki University, 3. Institute of Low Temperature Science, Hokkaido University, 4. Atmosphere and Ocean Research Institute, The University of Tokyo

Iron (Fe) is well known as a key parameter for primary productivity in the ocean. To understand the distributions and biogeochemical cycle of Fe in the ocean, we need to investigate the sources and sinks of Fe. A recent study has demonstrated a concentration gradient of dissolved Fe in the North Pacific Intermediate Water (NPIW) between western and eastern areas (Nishioka and Obata, 2017), suggesting that Fe-rich intermediate water was transported laterally across the western subarctic gyre. Moreover, it has been demonstrated that most dissolved Fe in seawater is complexed with natural organic ligands. Since bioavailability of Fe in seawater depends on its species, the chemical speciation of Fe is needed to evaluate the nutrient status for phytoplankton. However, the distribution of natural organic ligands has not been revealed yet in the subarctic North Pacific. In this study, vertical distributions of organic Fe-binding ligands were investigated in the eastern and western subarctic North Pacific to clarify its impact on Fe cycle. Seawater samples were obtained through the whole water column during GEOTRACES-Japan cruise KH-17-03 using trace metal clean technique to avoid metal contaminations. Filtered seawater samples (<0.2 μm) for organic Fe-binding ligands analysis were collected in acid-washed bottles inside a laminar-flow clean booth, then they were stored at -20°C until just before analysis. The organic Fe-binding ligands' concentration and their conditional stability constants were determined by competitive ligand equilibration-adsorptive cathodic stripping voltammetry (CLE-ACSV) method using salicylaldoxime (Abualhaija and van den Berg, 2014). The concentration and conditional stability constants of organic ligands ranged from 0.7 nM to 5.9 nM and from $10^{10.1}$ M^{-1} to $10^{12.3}$ M^{-1}, respectively. The concentrations of organic ligands exceeded those of dissolved Fe concentration more than 1 nM in all samples except for the surface (10-m) at the Oyashio-Kuroshio transition zone station; consequently >99% of dissolved Fe was estimated to be complexed with these natural organic ligands. At the western station, high concentrations of organic ligands were observed in the intermediate layers (400 –600 m), which hydrographic data (27.2 σ_θ –27.3 σ_θ) were corresponding to the lower NPIW (Yasuda et al., 2004), suggesting that organic Fe-binding ligands might be transported within the lower NPIW.

Keywords: iron, organic ligand, subarctic North Pacific, GEOTRACES

©2019. Japan Geoscience Union. All Right Reserved.

Chemical and physical speciation of copper in the subarctic North Pacific

*Kuo Hong Wong[1], Hajime Obata[1], Taejin Kim[2], Yoshiko Kondo[3], Jun Nishioka[4]

1. Atmosphere and Ocean Research Institute, The University of Tokyo, 2. Seoul National University, Korea, 3. Nagasaki University, 4. Institute of Low Temperature Science, Hokkaido University

Organic complexation of Cu in seawater plays a major role in controlling the toxicity and bioavailability of Cu for marine microorganism. In this study, we determined the concentrations of Cu and its organic ligands in the soluble and dissolved phases in the subarctic North Pacific. Samples were taken from three stations in the subarctic NorthPacific, CL-2 (western), CL-5 (central) and CL-16 (eastern), during summer 2017.

Concentrations of total dissolved and soluble Cu ranged from 1.28 nM –4.82 nM, and 0.47 nM –2.75 nM, respectively, in the subarctic North Pacific. At both CL-2 and CL-16, soluble Cu accounted for 30% - 100% of total dissolved Cu. The proportion of the soluble Cu fraction was low in surface waters, increased a maximum in the intermediate waters, and decreased slightly in deep waters. Two classes of organic ligands were detected in the surface and intermediate waters of CL-5 and CL-16, and in the intermediate waters of CL-2. In all other depths, only one class of ligand was detected. Concentrations of the stronger ligand (L_1) and weaker ligand (L_2) ranged from 1.02 nM –2.95 nM, and 0.77 nM –8.78 nM, respectively. The distributions of L_1 followed closely that of total dissolved Cu in the surface waters, and no clear trend was observed in the intermediate waters. At CL-2, L_1 mainly existed in the soluble phase, whereas for CL-16, soluble L_1 accounted for 50% - 100% of total dissolved L_1. Concentrations of L_2 were relatively constant throughout the water column but elevated concentrations were detected in the surface waters of CL-5 and in the surface and intermediate waters of CL-16. On the other hand, there were a slight depletion of L_2 in the intermediate waters of CL-2.

Keywords: copper, organic ligands, subarctic North Pacific

©2019. Japan Geoscience Union. All Right Reserved.

Latitudinal and temporal variations in phytoplankton size structure within mesoscale eddies from space

*Hisatomo Waga[1], Toru Hirawake[1], Ueno Hiromichi[1]

1. Hokkaido University

Phytoplankton plays a critical role in a number of key ocean processes. One of the most important functions of phytoplankton is to determine the energy transfer efficiency in marine ecosystems. Although the energy flow from the base of the food web to higher trophic levels depends on both the biomass and size structure of phytoplankton community, phytoplankton size structure is particularly important because energy flow in marine pelagic food webs is largely based on size specific predator-prey relationships. Therefore, spatiotemporal dynamics in size structure of phytoplankton community can trigger changes in the ecosystem’ s functioning through trophic cascade effects in the trophic chain. With the development of remote sensing techniques, mesoscale eddies, nearly ubiquitous features of the World Ocean, has been recognizing as important feature for the distribution of phytoplankton not only the direct transport of phytoplankton and eddy trapping, but also the vertical flux of nutrients. Recent studies have examined regional variations in the influence of mesoscale eddies on phytoplankton community. Namely, phytoplankton production is enhanced in cyclonic eddies (CEs) than that of anticyclonic eddies (ACEs) because of upwelling inside the eddy; this view, on the other hand, does not hold for a substantial portion of eddies within oceanic subtropical gyres, the largest ecosystems in the ocean. However, previous efforts have focused mainly on variations in chl*a*, whereas quite a few studies have worked on that in the size structure of phytoplankton community because remote estimations of phytoplankton size structure are newly established techniques during the last decade. Here we improved a chl*a* size distribution (CSD) model which estimates the synoptic size structure of phytoplankton community, to assess the impact of mesoscale eddies on spatiotemporal variations in phytoplankton size structure. Original CSD model was based on the spectral features of the phytoplankton absorption coefficient ($a_{ph}(\lambda)$), which estimation accuracy becomes poor in areas of the low productivity, such as subtropical gyres. To avoid this, we used not only $a_{ph}(\lambda)$ but also chl*a* to improve estimation accuracy of the CSD model. The resulting estimation error of the improved CSD model was the median absolute percent difference of 26.0% between the measured and satellite-matched values, and global distribution of the phytoplankton size structure was reliable even in subtropical gyres. The phytoplankton size structure showed a clear latitudinal variation: larger and smaller assemblages in temperate (>30˚S and >30˚N) and low latitudes (30˚S–30˚N) latitudes, respectively. When comparing the phytoplankton size structure within ACEs and CEs, a larger phytoplankton size structure was found in ACEs especially in low latitudes. This result was consistent with a previous report that ACEs are more productive than CEs in subtropical gyres because of winter mixing. In addition, we found increasing trends ($p < 0.05$) in differences between the phytoplankton size structure within ACEs and CEs in low latitudes for the years 2003–2014, suggesting a growing importance of ACEs for phytoplankton and in turn marine ecosystem. Consequently, this study demonstrates significant advantages of satellite remote sensing for biogeochemical and ecological studies.

Keywords: Satellite, Mesoscale eddy, Phytoplankton

©2019. Japan Geoscience Union. All Right Reserved.

Structure and impact of the Kuroshio nutrient stream

*Kosei Komatsu[1,2], Yutaka Hiroe[3]

1. Graduate School of Frontier Sciences, The University of Tokyo, 2. Atmosphere and Ocean Research Institute, The University of Tokyo, Kashiwa, Japan, 3. Seikai National Fisheries Research Institute, Japan Fisheries Research and Education Agency, Nagasaki, Japan

Recently the Kuroshio has drawn attention as an important supply route of nutrients in the western North Pacific. However, it is unknown whether nutrient concentrations are enhanced along the jet on isopycnal surfaces, as is the case for the “nutrient stream” along the Gulf Stream. We aim to ascertain the structure of nutrient concentration enhancement along the Kuroshio jet and to estimate the impact of nutrient transport downstream to the Kuroshio-Oyashio interfrontal zone (KOIZ), which is a highly productive region and a major global fishing ground. Recent multiple- transects and retrospective analyses of historic hydrographic data have revealed that the along-jet maximum nitrate concentration appears only in spring on the isopycnal surface $25<\sigma_\theta<26$ in the downstream region of the Kuroshio. The Kuroshio nutrient stream contributes significantly to productivity in the euphotic layer along its downstream trajectory, in conjunction with enhanced vertical turbulence. Analysis of the budget of epipycnal nitrate transport across transects that enclosed the KOIZ suggests that the Kuroshio nutrient stream has a non-negligible potential to significantly impact high productivity in the KOIZ.

Keywords: Kuroshio nutrient stream, Kuroshio-Oyashio interfrontal zone, epipycnal transport

©2019. Japan Geoscience Union. All Right Reserved.

Enhanced nutrient supply and biogeochemical impacts induced by internal waves in the oligotrophic northern South China Sea

*Chin-chang Hung[1], Dewang Li[2], Wen-Chen Chou[3], Yung-Yen Shih[1,4], Guan-Yu Chen[1]

1. Department of Oceanography, National Sun Yat Sen University, Kaohsiung, Taiwan, 2. Second Institute of Oceanography, State Oceanic Administration, Hangzhou, PRC, 3. Institute of Marine Environmental Chemistry and Ecology, National Taiwan Ocean University, Taiwan, 4. Department of Applied Science, R.O.C Naval Academy, Kaohsiung, Taiwan

To understand nutrient supply and the biogeochemical response induced by internal waves in the deep basin of the northern South China Sea (NSCS), nitrate, chlorophyll *a* (Chl *a*), particulate organic carbon (POC) fluxes were measured during the passage of large internal waves using drifting sediment traps attached with hydrographic sensors. Results revealed large variations in temperature, nitrate and chlorophyll *a* (Chl *a*) concentrations during and after internal waves, suggesting that cold nutrient-replete waters may be brought to the euphotic zone in the dissipation zone during and after the passage of internal wave packets, resulted in phytoplankton flourished in oligotrophic water. The result reveals that ocean mixing triggered by internal waves in warm water of the NSCS may be important for phytoplankton species composition. Most importantly, POC fluxes (110.9±10.7 mg C m^{-2} d^{-1}) were significantly enhanced after internal waves compared to non-internal wave area (32.6–73.0 mg C m^{-2} d^{-1}) in the NSCS. Such elevated POC fluxes may be induced by downward flourished biogenic particles, particle aggregation or converged particles from mixed layer triggered by internal waves.

Keywords: internal waves, ocean mixing, South China Sea, nutrient dynamics

©2019. Japan Geoscience Union. All Right Reserved.

Mixing over the eastern ridge in the Luzon Strait caused by high-mode internal waves

*Akie Sakai[1], Tomoharu Senjyu[2], Eisuke Tsutsumi[2], Takeshi Matsuno[2], Takahiro Endo[2], Ichiro Yasuda[3], Daigo Yanagimoto[3]

1. Department of Earth System Science and Technology, Interdisciplinary Graduate School of Engineering Sciences, Kyushu University, 2. Research Institute for Applied Mechanics , 3. Atmosphere and Ocean Reserch Institute The University of Tokyo

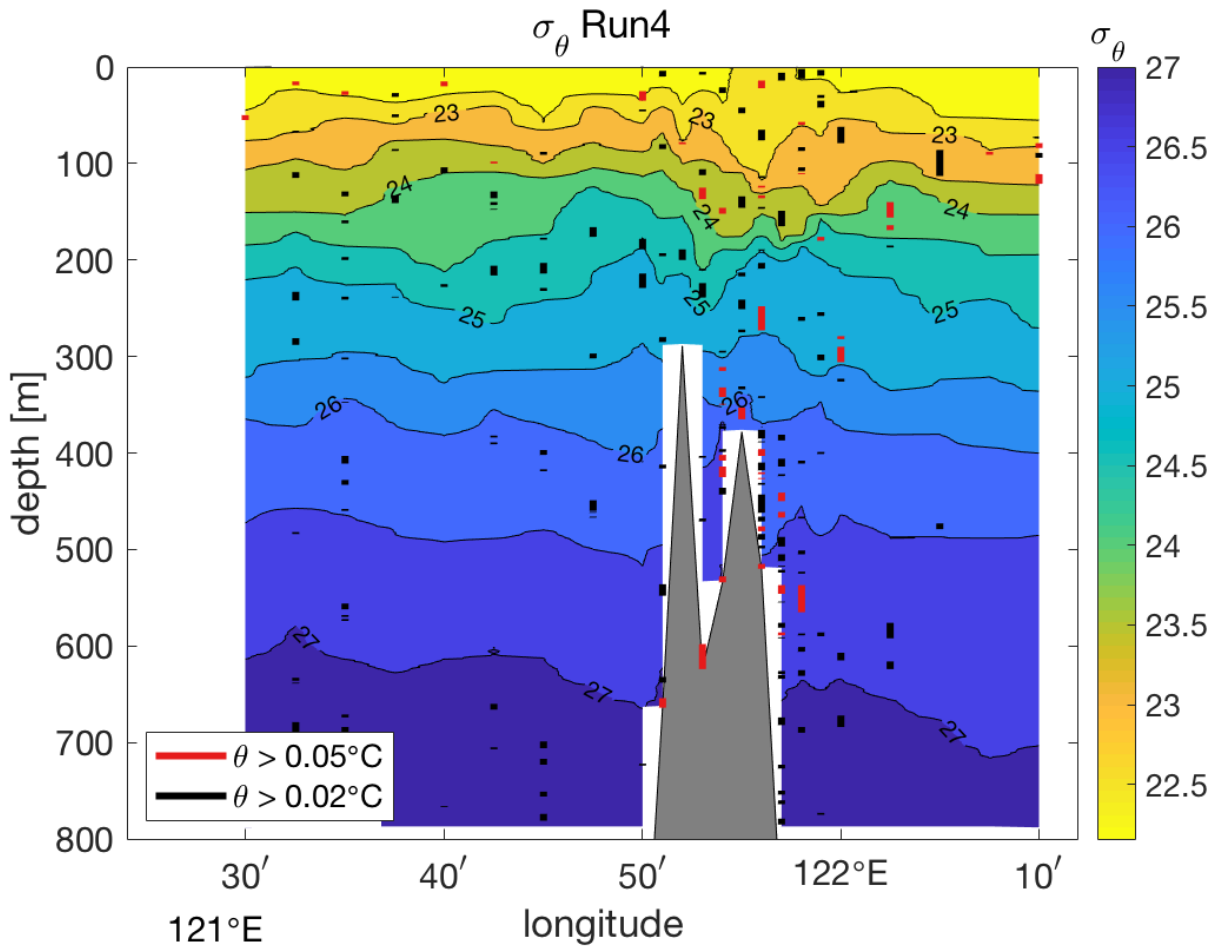
The Luzon Strait has two parallel ridges running from north to south, which is known to create large amplitude internal tides. To investigate the mixing processes accompanied by the internal tides, we carried out repeated observations with XBT, XCTD, CTD, and ADCP in the cruise of R/V Hakuho-maru KH-17-5, Leg-2, in November 2017 as part of the OMIX project. We obtained 6 cross sections around the eastern ridge between 121° 30’ E and 122° 10’ E along the line of 21° N.

The cross sections showed wavy structures of isopycnals over the ridge, with 4-7 km of horizontal scale and about 50 m of vertical scale. Velocity distributions by the shipboard ADCP showed strong vertical shear over the ridge, suggesting high-mode internal waves. Froude number of the high-mode internal waves exceeds unity around two summits of the ridge during the periods of strong tidal flow. This suggests that the high-mode internal waves stay over the ridge.

Many temperature inversions, especially large inversions ($\theta > 0.05$ °C) were formed near the ridge (figure). Therefore, energy dissipation rate and vertical diffusivity assuming the model of Osborn (1980) were estimated by calculating Thorpe scale from the temperature profiles. Relatively large energy dissipation rate and vertical diffusivity were distributed over the ridge from surface to the bottom, as well as unstable regions of $Ri < 0.25$. These results reflect strong mixing over the ridge due to the high-mode internal waves.

Keywords: internal waves, Luzon Strait

©2019. Japan Geoscience Union. All Right Reserved.



©2019. Japan Geoscience Union. All Right Reserved.

From the Luzon Strait to the Tsushima Strait: Water masses and nutrient transports approached using ^{137}Cs

*Siteng Zhu[1], JING ZHANG[1], Shota Kambayashi[2], Takeshi Matsuno[3], Eisuke Tsutsumi[3], Shigenobu Takeda[4], Seiya Nagao[5], Hiroshi Inoue[5], Hiroshi Ogawa[6], Ichiro Yasuda[6]

1. University of Toyama, 2. Fukushima university, 3. Kyushu university, 4. Nagasaki university, 5. Kanazawa university, 6. The University of Tokyo

More than 95% of the water flowing into the Sea of Japan comes from the Tsushima Strait, and 80% of it is Kuroshio Intimidate Water (KIW), which is rich in nutrients compared with Kuroshio surface Water and Kuroshio Tropical Water. However, there is a lack of direct evidence based on surveys or measurement data. ^{137}Cs in the subtropical mode water (STMW) that originated in the Fukushima Dai-ichi Nuclear Power Plant (FNPP1) accident is an excellent tracer which can be transported from the Kuroshio upstream to the Sea of Japan crossing the shelf edge of the East China Sea (ECS) via the KIW. It is also useful for research on the transport of nutrients from the KIW.

Data and water samples were collected during the Hakuho-Maru KH-17-5 Cruise and the Nagasaki-Maru 464 Cruise in November and July 2017, respectively. Data from the KH-17-5 Cruise was used for the study of the area around the Luzon Strait and those of the Nagasaki-maru 464 Cruise was used for the study of area around the outer shelf region of the East China Sea and the Tsushima Strait. The ^{137}Cs active concentration was analyzed by γ-Ray spectrometry after preconcentration. The turbulence intensity was measured using TurboMAP and VMP2000.

The maximum ^{137}Cs concentration shows the existence of the subtropical mode water (STMW) in the Luzon Strait, the ECS and the Tsushima Strait, respectively, at the similar density (25.2-25.7 kg/m^3), temperature (15-17℃) and salinity (34.60-34.75). Although their depth changes from 400 m in the Luzon Strait to 150 m at the shelf edge of the ECS and 100m in the East Channel of the Tsushima Strait, they can all be identified as the KIW because of the similar density. It is noteworthy that around Luzon Strait, the distribution of ^{137}Cs is influenced by strong vertical mixing. The percentage of nutrients transported to the Sea of Japan by KIW is estimated and this is meaningful to the ecosystem of the Sea of Japan.

Keywords: 137Cs, subtropical mode water, water masses, KIW, nutrients

©2019. Japan Geoscience Union. All Right Reserved.

Impact of cyclonic eddies and typhoons on biogeochemistry in the oligotrophic ocean based on time-series observation at the western Pacific subtropical station KEO

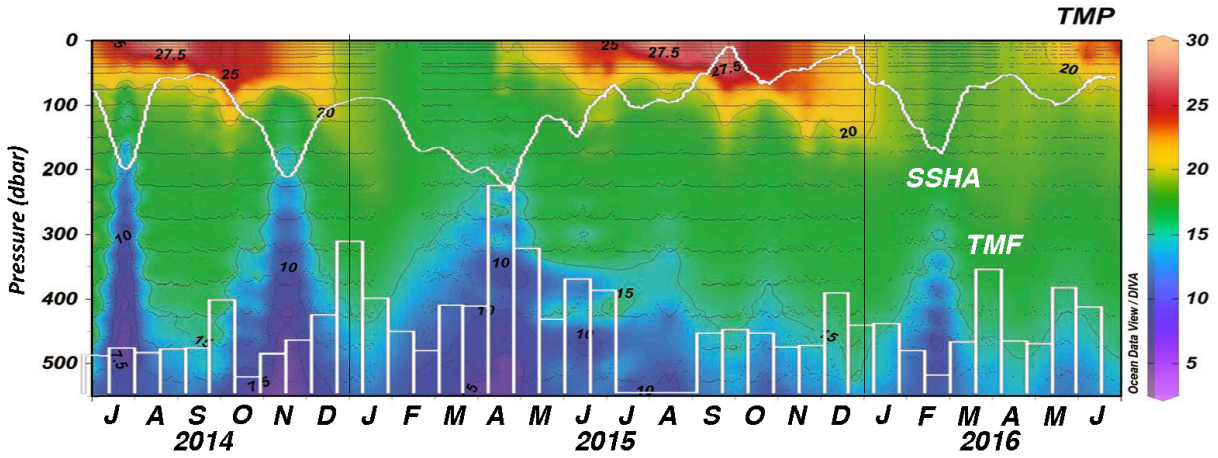
*Makio Honda[1], Yoshikazu Sasai[1], Eko Siswanto[1], Akira Kuwano-Yoshida[2], Hidenori AIKI[3], Meghan Cronin[4]

1. Japan Agency for Marine-Earth Science and Technology, 2. Disaster Prevention Laboratory, Kyoto University, 3. Nagoya University, 4. NOAA Pacific Marine Environmental Laboratory

In 2014, a sediment trap mooring experiment started adjacent to station Kuroshio Extension Observatory (KEO)' s National Ocean and Atmosphere Administration (NOAA) surface mooring. Two-years long sediment trap data show that biogenic material fluxes at ~ 5000 m increased between late winter (March) and late spring (June). Based on sea surface temperature and upper ocean water temperature profiles, from the NOAA surface buoy, and satellite-based surface chlorophyll-a , this increase was likely due to an increase of ocean productivity in early spring (March) that was supported by nutrients supplied by winter mixing. On the other hand, biogenic material fluxes also increased in October 2014, and between late December 2014 and January 2015 when concentrations of nutrients near the surface typically are low. Sea surface height anomalies and vertical profiles of water temperature in the upper 500 m showed cyclonic eddies passing station KEO and causing upwelling of middle-layer water in late July–early August 2014 and November 2014. It appears that these events supplied nutrients to the upper layer, which then caused ocean productivity in the subsurface layer to temporally increase, resulting in increased deep biogenic material fluxes in autumn and winter. This interpretation of the data is consistent with a simple 3D physical-biological model simulation that shows meso-scale cyclonic eddies can supply nutrient to support new production at KEO. During the 2-year-long sediment trap deployments, several typhoons also passed near station KEO and near-inertial internal waves were observed near the nitracline depth after the typhoons passed. Although turbulent mixing caused by near-inertial internal wave could have possibly supplied nutrient to upper oligotrophic euphotic layer, numerical simulations of the turbulent nutrient supply indicate that enhanced turbulent diffusion across the nutrient concentration gradient did not supply enough nitrate to support the increase in biogenic material flux in autumn.

Keywords: KEO, Oligotrophic, Sediment trap, Cyclonic eddy, Nutrient, Typhoon

©2019. Japan Geoscience Union. All Right Reserved.



©2019. Japan Geoscience Union. All Right Reserved.

Island-mass effect on the phytoplankton and zooplankton community in south of Japan

*Kiyotaka Hidaka[1], Kazuaki Tadokoro[1], Hiroomi Miyamoto[1], Tadafumi Ichikawa[1]

1. Japan Fisheries Research and Education Agency

The Izu Ridge brings high plankton production via its island-mass effect, which brings up subsurface nutrients to surface layer. Previous reports on island-mass effect around the ridge have been based on observation in the summer-early autumn and reports in spring, when many small pelagic fish species spawn, are scarce. As the Kuroshio flow through the ridge, island-mass effect on zooplankton, which takes more time to glow than phytoplankton, should be appear in eastern (downstream) area. Thus wider area around the ridge should be examined for the effect on zooplankton. In the present study, we examined island-mass effect of the Izu-Ridge on phytoplankton and zooplankton, based on satellite data and zooplankton data in the broad area south of the Honshu.
The Sea surface chlorophyll concentration (SSChl, MODIS-Aqua) in the area bounded by 135.5-142.0 E and 30.0-37.0 N was examined for the grids with depths of > 500 m. Zooplankton samples were collected by vertical tow (0-150 m) of the NORPAC net with 0.335 mm mesh in the area south of Honshu in February to March of 1963-2017. Samples were fixed in 5% formalin-sea water and copepod biomass was estimated in the laboratory by Bench-top Video Plankton Recorder. The relationships between plankton biomass and distance to the Honshu coast and to the Izu Ridge were examined.
The SSChl declined as distance to the Honshu coast increased. But high SSChl was observed in several areas 150-250 km away to the coast. These areas were mainly located around the Izu Ridge, 32-33.5N, and interpreted as caused by island-mass effect when the Kuroshio flowed in offshore path. The copepod biomass was high around the Honshu coast (<50 km). Stations with high copepod biomass were observed in the 100-200 km north-east (downstream) of the Izu Ridge, but they were located near the Honshu, around the Boso peninsula. Island-mass effect of the Izu-ridge on zooplankton biomass thus cannot be distinguished from the coastal effect and the effect should be examined by rate process (spawning rate and/or growth rate) in species level.

Keywords: zooplankton, island-mass effect

©2019. Japan Geoscience Union. All Right Reserved.

Influence of enhanced deep circulation due to geothermal heat on biogeochemical cycle in the Pacific Ocean

*Shogo Urakawa[1], Hideyuki Nakano[1], Hiroyuki Tsujino[1], Kei Sakamoto[1], Takahiro Toyoda[1], Goro Yamanaka[1]

1. Meteorological Research Institute, Japan Meteorological Agency

There exists heat conduction from the oceanic lithosphere to the abyssal ocean. Its heat flux amounts to about 0.1 W m^{-2} in the global average. It is much smaller than the heat exchange between the atmosphere and ocean in the order of 10 W m^{-2}. However, it is known that this geothermal heat significantly enhances the deep circulation especially in the Pacific Ocean. For example, Adcroft et al. (2001) conduct numerical experiments with/without geothermal heating using an ocean general circulation model and report that constant heat flux at the sea bottom by 0.05 W m^{-2} results in enhancement of the Pacific meridional overturning circulation (PMOC) by 25 %. Other studies also report that the geothermal heat significantly enhances the oceanic deep circulation (e.g., Emile-Geay and Madec, 2009; Urakawa and Hasumi, 2009; Downes et al., 2016). The importance of the geothermal heat seems to be robust from the viewpoint of ocean dynamics but it has not been investigated to what extent the geothermal heat influences the biogeochemical cycle of the ocean. Here, we conduct two numerical experiments with/without the geothermal heat using an ocean general circulation model developed for the CMIP6 and investigate the effect of the geothermal heat on the biogeochemical tracer fields.
The geothermal heating enhances PMOC at 30º S by 17 % in this model, which leads to stronger ventilation in the North Pacific Ocean. This stronger ventilation results in increase of delta ^{14}C by more than 10 per mille, which means younger water masses, at the bottom of the North Pacific. The stronger PMOC also results in higher dissolved oxygen in the abyss especially in the eastern tropical Pacific. The geothermal heat leads to dissolved oxygen increase by more than 10 micro mol L^{-1} there, which corresponds to 10–70 % of hypoxic water in the control experiment without geothermal heating. This oxygenation near the sea bottom affects the oxygen-deficient water in the surface of the eastern tropical Pacific. Its thickness becomes thinner by around 100 m. The geothermal heat also plays an important role in the biogeochemical cycle in the Pacific Ocean.

©2019. Japan Geoscience Union. All Right Reserved.

The Parameterization of the Pressure-Strain Correlations in the Stably or Unstably Stratified Ocean Surface Layer.

*Yusuke Ushijima[1], Yutaka Yoshikawa[1]

1. Graduate School of Science, Kyoto University

Turbulence in the ocean surface layer mixes momentum, heat, and nutrient vertically. It is therefore important for air-sea interaction, phytoplankton blooming, and other oceanic processes (e.g., Roxy et al. 2013; Obata et al. 1996). However, large-scale models such as ocean general circulation models cannot explicitly resolve small-scale turbulence because of their coarse resolution. For this reason, the vertical mixing should be parameterized using the turbulent closure scheme that successfully parameterizes the turbulent mixing. Recently, attention is paid to pressure-strain correlations, which redistribute stress due to fluctuating pressure, in the parameterization scheme used for engineering purposes (Jakilic and Hanjalic 2013). In the present study, therefore, the validity of the pressure-strain correlation parameterization used in the ocean (or atmosphere) (Rotta 1951, Gibson and Launder 1978, Gertski et al. 1992) was examined. To this end, we performed Large-eddy simulations of ocean surface boundary layer to simulate pressure-strain correlations and compared it with parameterized correlations. Here, we focused on the effects of stratification on the correlations, because the stratification is an essential factor in the ocean and atmospheric boundary layers but previous schemes did not include the stratification effects sufficiently. Results show that the parameterizations of the pressure-strain correlations had systematic errors depending on the stability (or stratification). It was also found that the error can be reduced by introducing new parameters related to the stability into the scheme.

Keywords: Parameterization of Pressure-Strain Correlations, Turbulent Closure Model, Turbulence in the Ocean Surface Layer

©2019. Japan Geoscience Union. All Right Reserved.

Numerical studies on asymmetric responses of the upper ocean to tropical cyclone

*Daiki Okura[1], Yutaka Yoshikawa[1]

1. Graduate School of Science, Kyoto University

Tropical cyclones (TCs) decrease sea surface temperature (SST), and the decreased SST weakens TC intensity. This SST decrease is asymmetric with respect to the TC track, known as “rightward bias”. Preceding numerical studies suggested that this asymmetry may influence on the course of the TC. The interaction between TC and the upper ocean is one of key ingredients for precisely predicting TC's development, and the upper ocean response to TC should also be clarified.
The SST decrease during TC passage is mainly caused by two processes; vertical turbulent mixing and advection (Ekman suction). The rightward bias is associated with the mixing which is more intense on the right side of the TC track due to resonant inertial currents with winds. Magnitude and distribution of SST decrease induced by the mixing should vary with parameters characterizing TC; transition speed U_T, radius of maximum wind R_{max}, the friction velocity U_*, and the Coriolis coefficient f. However, detailed physical processes of the mixing and its dependence on these parameters have not been well quantified, because of lack of in-situ data and complicated processes involved in the mixing.

The present study focuses on the vertical turbulent mixing effects on asymmetric SST response. To this aim, vertically one-dimensional model was used in which the vertical turbulent mixing was parameterized with the Nakanishi-Niino-Mellor-Yamada scheme modified by Kitamura (2010). We considered TC-like wind stress of magnitude U_*^2 at radius R_{max} from the TC center moving with transition speed U_T and investigated the mixing on both sides of TC track at distance *r*. Experiments with several friction velocities U_*, maximum wind radii R_{max}, transition speeds U_T and distances *r* were performed. No surface heat flux was considered for simplicity.
The results showed that the rightward bias of the SST response depended on these parameters. The location of the largest SST decrease moved away from the axis as U_T increased, but it depended less on U_*. The SST decreased more with larger U_* and smaller U_T. These results can be explained by energy flux at the surface. In our model configuration, the energy flux depends on two non-dimensional parameters, U_T/fR_{max} and U_*/U_T, and the energy flux had maximum and turbulent kinetic energy penetrated deeper at larger U_*/U_T and at U_T/fR_{max}~1, suggesting the resonance between wind and the inertial current. The SST decrease corresponded with the energy flux, but it depended largely on U_*/U_T, implying importance of wind forcing duration.
Thus, the asymmetric SST response due to the vertical turbulent mixing can be characterized with U_T/fR_{max} and U_*/U_T. Additional advection effects on the SST response will be discussed at the conference using three-dimensional simulation in which the advection as well as the mixing are fully included.

Keywords: Tropical cyclone, Vertical turbulent mixing, Ekman suction, Rightward bias

©2019. Japan Geoscience Union. All Right Reserved.

Influence of the distortion of the internal wave field on estimates of turbulent mixing using fine-scale parameterizations

*Anne Takahashi[1], Toshiyuki Hibiya[1], Alberto C. Naveira Garabato[2]

1. Department of Earth and Planetary Science, Graduate School of Science, University of Tokyo, 2. National Oceanography Centre, University of Southampton

Although the Southern Ocean is one of the turbulent mixing hotspots, we have not yet clarified quantitatively the turbulent mixing processes in this region, where the Antarctic Circumpolar Current (ACC) coexists with near-inertial internal waves generated by wind forcing and internal lee waves radiated by the impingement of eddy flows on topography.

Fine-scale parameterizations, based on the theory of energy cascade from internal waves to turbulence, are most widely used to estimate the turbulent dissipation rate, ε. It has been reported, however, that these fine-scale parameterizations tend to overestimate ε in the ACC (Waterman et al. 2014). Although Takahashi and Hibiya (2019) have suggested that "the distorted fine-scale shear and strain spectra" caused by the existence of eddies trapping near-inertial waves or upward-propagating internal lee waves might be responsible for the overestimates, the problem remains unresolved.

In this study, we use "eikonal" simulations (Henyey et al. 1986), which trace the propagation, refraction and breaking of test waves within a background internal wave field, to assess the evolution of the energy cascade in vertical wavenumber space. Our objective is to examine how the distortion of the vertical wavenumber spectrum affects the performance of fine-scale parameterizations.

In our simulations, in contrast to high vertical wavenumber test waves that are efficiently Doppler-shifted to their breaking limit, low vertical wavenumber test waves are not subject to dissipation processes. In the existing fine-scale parameterizations, however, the energy flux to dissipation scale is estimated using the integrated vertical wavenumber spectral values. This means that, if the range of this integration includes a spectral bump at the low-wavenumber end of the spectrum, the estimated energy flux and hence the resulting ε might be overestimated by these fine-scale parameterizations.

From the simulation results, it is confirmed that fine-scale parameterizations significantly overestimate ε in spectra with a low-wavenumber bump, in particular as the internal wave energy level becomes large and the shear/strain ratio becomes small. These results are supported by the microstructure and fine-structure dataset from the SOFine experiment carried out in the Kerguelen Plateau.

Keywords: Turbulent Mixing, Fine-scale parameterizations, Antarctic Circumpolar Current region

©2019. Japan Geoscience Union. All Right Reserved.

[E] Poster | H (Human Geosciences)：H-GG Geography

Sun. May 26, 2019 3:30 PM - 5:00 PM JST | Sun. May 26, 2019 6:30 AM - 8:00 AM UTC | Poster Hall International Exhibition Hall8, Makuhari Messe_8

[H-GG01] Human-Natural system interactions and solutions for environmental management

convener:Yuei-An Liou(National Central University)

Natural system, environmental quality, and anthropogenic processes interact with each other closely. Environmental changes and their causes increase the needs to address the consequences taking place in the structural and functional ecosystems. Much progress of anthropogenic activities has been made and significantly improves social economics. However, human system has been altering and raising burden on the natural system by alerting land use and land cover, bringing up water, soil and air pollution, changing regional and global climate, and increasing frequency of natural disasters, e.g., floods, landslides. Planners are increasingly pressured by the challenges in balance between demands and development, while lessening the detrimental impact of social processes on environment. Remote sensing and GIS have been proven with their advantages in providing data and tools to model and visualize spatiotemporally environmental changes and influential factors so that practical policy for environmental protection and management can be proposed.
This session seeks for papers on advancements in the development of techniques and models with remote sensing and GIS to contribute environmental applications, to exhibit and visualize influences of human activities on environmental changes, and to improve understanding of the relationship between anthropogenic activities and natural system and climate patterns. Solutions for environmental management in short- and long-term visions are very welcome.

[HGG01-P01] Feasibility assessment of constructing high-resolution 3D panoramic images using the VLP-16 LiDAR Puck

*Yan-Jyun Lin[1], Shen Yu Hsiao[1], REN-JHIH YANG[1], Zhen-Yu Wu[1] (1.National Chung Hsing University)

[HGG01-P02] The environmental impact of mountaineering in the Mt. Manaslu region

*Hijiri SHIMOJIMA[1] (1.Tokyo University of Agriculture)

[HGG01-P03] Understanding human system vulnerability to typhoon for Improved Adaptive Capacity

*Kim-Anh Nguyen[1], Yuei-An Liou[1] (1.Center for Space and Remote Sensing Research, National Central University)

[HGG01-P04] Environmental Impact Evaluation of Solar Park Project in Western Desert, Minia, Egypt.

*Ramadan Gamal Abdelrehim[1], Josaphat Tetuko Sri Sumantyo[1] (1.Center for Environmental Remote Sensing, Chiba University)

[HGG01-P05] Peatland Assessment Based on DInSAR approach by using ALOS-2 PALSAR-2 Data in Kalimantan, Indonesia

*Joko Widodo[1], Josaphat Tetuko Sri Sumantyo[1], Daniele Perissin[2], Katsunoshin Nishi[1], Pakhrur Rozi[1] (1.JMRSL - Josaphat Microwave Remote Sensing Laboratory Center for Environmental Remote Sensing Graduate School of Advanced Integration Science Chiba University, 2.Sarproz, Razer Limited, Hongkong)

[HGG01-P06] Development of Nanosatellite for Ionospheric Measurement for Earthquake Prediction

*Peberlin Parulian Sitompul[1], Josaphat Tetuko Sri Sumantyo[2] (1.Chiba University, and Indonesia National Institute of Aeronautic and Space, 2.Center for Environmental Remote Sensing, Chiba University)

Feasibility assessment of constructing high-resolution 3D panoramic images using the VLP-16 LiDAR Puck

*Yan-Jyun Lin[1], Shen Yu Hsiao[1], REN-JHIH YANG[1], Zhen-Yu Wu[1]

1. National Chung Hsing University

We use the low-cost LiDAR sensor “the VLP-16 LiDAR Puck” to capture the surrounding scene for building high-resolution 360° panoramic images. The VLP-16 LiDAR Puck is mounted on a portable automatic lifting platform(see the attached figure) to increase spatial resolution while doing the experiments. The study locations include buildings, landslide areas, and soil&water conservation structures. The results from the VLP-16 LiDAR Puck will be well compared with those from the high-cost LiDAR sensors “the Trimble TX8” and ”The RIEGL VZ-1000”. The comparisons between three LiDAR sensors include their spatial resolution, accuracy, practicality, convenience, and cost–performance ratio. Overall, the purpose of this research is to analyze the feasibility of constructing high-resolution 3D panoramic images with the VLP-16 LiDAR Puck for applications of soil&water conservation. We also hope this new technique of remote sensing can contribute to environmental monitoring and anthropogenic activities.

Keywords: the VLP-16 LiDAR Puck, 3D panoramic images, remote sensing

©2019. Japan Geoscience Union. All Right Reserved.



©2019. Japan Geoscience Union. All Right Reserved.

The environmental impact of mountaineering in the Mt. Manaslu region

*Hijiri SHIMOJIMA[1]

1. Tokyo University of Agriculture

Manaslu is one of the 8,000-meter peaks ranking as the 8th highest peak in the world, located 130 km northwest of Kathmandu, the capital of Nepal. Since Manaslu's normal route (general climbing route) is relatively less difficult, the number of Manaslu's climbers have increased rapidly over the last 10 years. Sixty years have passed since Manaslu was first conquered by a Japanese expedition. The popularity of its scaling and the rapidly growing tourism in the Nepal Himalayas after 1970 are noticeably affecting natural, social, and cultural environments in the area. This in turn, is creating serious environmental issues at the Manaslu Base Camp (4,800 m above mean sea level), the entry point for climbing Mt. Manaslu.
In this research, we aim to develop a system that can combine high resolution imagery and Digital Surface Model (DSM) in the base camp and simple monitoring into one method in order to estimate the environmental burden associated with the climbing activities in the Manaslu Base Camp. We performed aerial photography of the base camp using Unmanned Aerial Vehicle (UAV) and created DSM from Structure from Motion (SfM) of the obtained images. At the same time, positioning data of the feature was acquired through a Differential Global Positioning System (DGPS) survey, and a 3D topographic map was created.
The geographical area covered in this study is the Manaslu Base Camp in the Manaslu Conservation Area’ s, Gorkha District which is located in Northwest Nepal. In order to elucidate the actual usage of the Manaslu Base Camp, a field survey was carried out in August, 2016 at and around the Manaslu Base Camp using UAV. We conducted the following investigations at the Manaslu Base Camp: survey of the Base Camp, questionnaires to all the mountaineering parties at the Base Camp. We monitored the actual usage of the Manaslu Base Camp in order to clarify the number of tents and their locations by photointerpretation using high resolution satellite images. In the survey of the Base Camp using UAV, we acquired a high resolution image using Phantom 4 of DJI. Using the obtained high resolution image, 3D terrain data and an ortho mosaic image was generated from the SfM, and a map of the Manaslu base camp was created. In the DGPS base camp survey, we recorded location information of features such as tents, toilets and routes in the Manaslu base camp.
A topographical survey of the Base Camp was conducted to pinpoint the location of each tent and to grasp the topographical features of the area. We were probably the first in the world to create a topographical map of the Manaslu Base Camp that shows detailed positioning of the campsite. There were 32 kitchen tents, 58 toilet tents, 42 altars (places to pray for safe climbs) in the post-monsoon season. The resolution of the obtained high-resolution image was 0.009 m.
Inquiries were made to every party staying at the Manaslu Base Camp in 2016 August. The questionnaires enquired about the following information: Number of members in each party; number of belongings brought in and out; number of donkeys used to carry equipment; and environmental considerations taken by each party.
A few of the findings of this study in August 2016 at and around the Manaslu Base Camp are as follows. (1) A topographical map of Base Camp was prepared pinpointing the location of each and every tent of the area. We are the first in the world to prepare such topographical map of the Manaslu Base Camp using UAV. (2) The results of the questionnaires show that during the pre-monsoon period in 2016 an astounding 46 tons of goods were brought into the Base Camp. Furthermore, over 780 donkeys were used for transportation. (3) Water quality research was also conducted at water collection points of the

©2019. Japan Geoscience Union. All Right Reserved.

Base Camp. The water was found to be badly contaminated because of the urine and excrement of donkeys that were found scattered over the Base Camp.

Keywords: Himalaya, GIS, UAV

©2019. Japan Geoscience Union. All Right Reserved.

Understanding human system vulnerability to typhoon for Improved Adaptive Capacity

*Kim-Anh Nguyen[1], Yuei-An Liou[1]

1. Center for Space and Remote Sensing Research, National Central University

Typhoon is one of the most natural disastrous phenomena that have devastating impacts on human system around the world. In the context of climate change, Asian countries particularly in tropical climate zone with high humidity and unevenly-distributed abundant precipitation tend to have frequent occurrence of typhoons and flooding. Here, we present a conceptual framework that incorporates 21 indicators across three dimensions, including vulnerability, exposure/sensitivity, and adaptive capacity to classify vulnerability and adaptive capacity (VAC) using geospatial techniques at regional scales over Vietnam. Results indicate that large spatial differences in VAC are obtained and identify top-priority regions that need enhanced adaptation to typhoons. The Southern Coastal area, South East and Red River Delta exhibit high and very high vulnerability because their physical features tend to be affected by the intensity of typhoons that frequently cross these parts. The lower Mekong Delta and Northern Coastal areas are vulnerable to typhoon-driven flood threats and, in particular, compounded by sea-level rise. Findings of this study are useful in making efficient policy decisions to minimize vulnerability to typhoons in Vietnam. In addition, the framework can be potentially applied to the other regions.

Keywords: human system vulnerability, Typhoon, Adaptive capacity, Geospatial techniques

©2019. Japan Geoscience Union. All Right Reserved.

Environmental Impact Evaluation of Solar Park Project in Western Desert, Minia, Egypt.

*Ramadan Gamal Abdelrehim[1], Josaphat Tetuko Sri Sumantyo[1]

1. Center for Environmental Remote Sensing, Chiba University

More than 95% of the Egyptian lands are desert, Groundwater in this arid desert area is considered as a very valuable and unique source of water for agricultural and manufacturing development projects; therefore environmental impact evaluation of these projects is very important step to protect groundwater from pollution. Three geophysical techniques used for groundwater exploration and upper geological layers evaluation, these techniques are, Vertical electrical sounding, two dimension electrical imaging, and Time Domain electromagnetic techniques. And depending on this study we described the hydro-geological settings of the area, detect the best locations for drilling groundwater wells, safe environmental injection points, and finally safe environmental landfill.

Keywords: Geophysics, Groundwater, Environmental evaluation, Arid Desert lands

©2019. Japan Geoscience Union. All Right Reserved.

Peatland Assessment Based on DInSAR approach by using ALOS-2 PALSAR-2 Data in Kalimantan, Indonesia

*Joko Widodo[1], Josaphat Tetuko Sri Sumantyo[1], Daniele Perissin[2], Katsunoshin Nishi[1], Pakhrur Rozi[1]

1. JMRSL - Josaphat Microwave Remote Sensing Laboratory Center for Environmental Remote Sensing Graduate School of Advanced Integration Science Chiba University, 2. Sarproz, Razer Limited, Hongkong

Indonesia has the lagerst tropical peatland ecosystem in the world around 22 million hectares separate in Sumatera Island, Kalimantan Island, and Papua island. Peatlands can be a source of food, clean water, and provide other benefits for the surrounding community. Peatland is also useful for preventing drought, flooding and mixing salt water for irrigation in agricultural areas. Peatlands are important for biodiversity because they are home to rare species. Peatlands play an important role in climate change mitigation and adaptation. Since subsidence is important phenomenon in peatland, DInSAR provide ability and effective aproach to detect subsidence in peatland area. Subsidence phenomenon in peatland related with groundwater table, carbon emision, and others. In this research, DInSAR is very effective as a basis for an approach to conducting peatland assessment in Kalimantan.

Keywords: DInSAR, Peatland, Assessment, ALOS 2 PALSAR 2

©2019. Japan Geoscience Union. All Right Reserved.

Development of Nanosatellite for Ionospheric Measurement for Earthquake Prediction

*Peberlin Parulian Sitompul[1], Josaphat Tetuko Sri Sumantyo[2]

1. Chiba University, and Indonesia National Institute of Aeronautic and Space, 2. Center for Environmental Remote Sensing, Chiba University

Indonesia is located at equatorial region and also has long coastline that often suffer the earthquakes. In some cases, ionospheric activity level increases just before to an earthquake event and shows a different behaviour 5–10 days before the event, when the seismic event has a magnitude greater than 4–4.5 degrees. The nanosatellite development is very important to get more ionospheric data and reletively cheaper than bigger satellite.

Keywords: Nanosatellite, Circular polarization, Earthquake prediction, Ionosphere

©2019. Japan Geoscience Union. All Right Reserved.

[E] Poster | H (Human Geosciences)：H-GG Geography

Sun. May 26, 2019 5:15 PM - 6:30 PM JST | Sun. May 26, 2019 8:15 AM - 9:30 AM UTC | Poster Hall International Exhibition Hall8, Makuhari Messe_14

[H-GG01] Human-Natural system interactions and solutions for environmental management

convener:Yuei-An Liou(National Central University)

Natural system, environmental quality, and anthropogenic processes interact with each other closely. Environmental changes and their causes increase the needs to address the consequences taking place in the structural and functional ecosystems. Much progress of anthropogenic activities has been made and significantly improves social economics. However, human system has been altering and raising burden on the natural system by alerting land use and land cover, bringing up water, soil and air pollution, changing regional and global climate, and increasing frequency of natural disasters, e.g., floods, landslides. Planners are increasingly pressured by the challenges in balance between demands and development, while lessening the detrimental impact of social processes on environment. Remote sensing and GIS have been proven with their advantages in providing data and tools to model and visualize spatiotemporally environmental changes and influential factors so that practical policy for environmental protection and management can be proposed.
This session seeks for papers on advancements in the development of techniques and models with remote sensing and GIS to contribute environmental applications, to exhibit and visualize influences of human activities on environmental changes, and to improve understanding of the relationship between anthropogenic activities and natural system and climate patterns. Solutions for environmental management in short- and long-term visions are very welcome.

[HGG01-P01] Feasibility assessment of constructing high-resolution 3D panoramic images using the VLP-16 LiDAR Puck

*Yan-Jyun Lin[1], Shen Yu Hsiao[1], REN-JHIH YANG[1], Zhen-Yu Wu[1] (1.National Chung Hsing University)

[HGG01-P02] The environmental impact of mountaineering in the Mt. Manaslu region

*Hijiri SHIMOJIMA[1] (1.Tokyo University of Agriculture)

[HGG01-P03] Understanding human system vulnerability to typhoon for Improved Adaptive Capacity

*Kim-Anh Nguyen[1], Yuei-An Liou[1] (1.Center for Space and Remote Sensing Research, National Central University)

[HGG01-P04] Environmental Impact Evaluation of Solar Park Project in Western Desert, Minia, Egypt.

*Ramadan Gamal Abdelrehim[1], Josaphat Tetuko Sri Sumantyo[1] (1.Center for Environmental Remote Sensing, Chiba University)

[HGG01-P05] Peatland Assessment Based on DInSAR approach by using ALOS-2 PALSAR-2 Data in Kalimantan, Indonesia

*Joko Widodo[1], Josaphat Tetuko Sri Sumantyo[1], Daniele Perissin[2], Katsunoshin Nishi[1], Pakhrur Rozi[1] (1.JMRSL - Josaphat Microwave Remote Sensing Laboratory Center for Environmental Remote Sensing Graduate School of Advanced Integration Science Chiba University, 2.Sarproz, Razer Limited, Hongkong)

[HGG01-P06] Development of Nanosatellite for Ionospheric Measurement for Earthquake Prediction

*Peberlin Parulian Sitompul[1], Josaphat Tetuko Sri Sumantyo[2] (1.Chiba University, and Indonesia National Institute of Aeronautic and Space, 2.Center for Environmental Remote Sensing, Chiba University)

Feasibility assessment of constructing high-resolution 3D panoramic images using the VLP-16 LiDAR Puck

*Yan-Jyun Lin[1], Shen Yu Hsiao[1], REN-JHIH YANG[1], Zhen-Yu Wu[1]

1. National Chung Hsing University

We use the low-cost LiDAR sensor “the VLP-16 LiDAR Puck” to capture the surrounding scene for building high-resolution 360° panoramic images. The VLP-16 LiDAR Puck is mounted on a portable automatic lifting platform(see the attached figure) to increase spatial resolution while doing the experiments. The study locations include buildings, landslide areas, and soil&water conservation structures. The results from the VLP-16 LiDAR Puck will be well compared with those from the high-cost LiDAR sensors “the Trimble TX8” and ”The RIEGL VZ-1000”. The comparisons between three LiDAR sensors include their spatial resolution, accuracy, practicality, convenience, and cost–performance ratio. Overall, the purpose of this research is to analyze the feasibility of constructing high-resolution 3D panoramic images with the VLP-16 LiDAR Puck for applications of soil&water conservation. We also hope this new technique of remote sensing can contribute to environmental monitoring and anthropogenic activities.

Keywords: the VLP-16 LiDAR Puck, 3D panoramic images, remote sensing

©2019. Japan Geoscience Union. All Right Reserved.



©2019. Japan Geoscience Union. All Right Reserved.

The environmental impact of mountaineering in the Mt. Manaslu region

*Hijiri SHIMOJIMA[1]

1. Tokyo University of Agriculture

Manaslu is one of the 8,000-meter peaks ranking as the 8th highest peak in the world, located 130 km northwest of Kathmandu, the capital of Nepal. Since Manaslu's normal route (general climbing route) is relatively less difficult, the number of Manaslu's climbers have increased rapidly over the last 10 years. Sixty years have passed since Manaslu was first conquered by a Japanese expedition. The popularity of its scaling and the rapidly growing tourism in the Nepal Himalayas after 1970 are noticeably affecting natural, social, and cultural environments in the area. This in turn, is creating serious environmental issues at the Manaslu Base Camp (4,800 m above mean sea level), the entry point for climbing Mt. Manaslu.
In this research, we aim to develop a system that can combine high resolution imagery and Digital Surface Model (DSM) in the base camp and simple monitoring into one method in order to estimate the environmental burden associated with the climbing activities in the Manaslu Base Camp. We performed aerial photography of the base camp using Unmanned Aerial Vehicle (UAV) and created DSM from Structure from Motion (SfM) of the obtained images. At the same time, positioning data of the feature was acquired through a Differential Global Positioning System (DGPS) survey, and a 3D topographic map was created.
The geographical area covered in this study is the Manaslu Base Camp in the Manaslu Conservation Area’ s, Gorkha District which is located in Northwest Nepal. In order to elucidate the actual usage of the Manaslu Base Camp, a field survey was carried out in August, 2016 at and around the Manaslu Base Camp using UAV. We conducted the following investigations at the Manaslu Base Camp: survey of the Base Camp, questionnaires to all the mountaineering parties at the Base Camp. We monitored the actual usage of the Manaslu Base Camp in order to clarify the number of tents and their locations by photointerpretation using high resolution satellite images. In the survey of the Base Camp using UAV, we acquired a high resolution image using Phantom 4 of DJI. Using the obtained high resolution image, 3D terrain data and an ortho mosaic image was generated from the SfM, and a map of the Manaslu base camp was created. In the DGPS base camp survey, we recorded location information of features such as tents, toilets and routes in the Manaslu base camp.
A topographical survey of the Base Camp was conducted to pinpoint the location of each tent and to grasp the topographical features of the area. We were probably the first in the world to create a topographical map of the Manaslu Base Camp that shows detailed positioning of the campsite. There were 32 kitchen tents, 58 toilet tents, 42 altars (places to pray for safe climbs) in the post-monsoon season. The resolution of the obtained high-resolution image was 0.009 m.
Inquiries were made to every party staying at the Manaslu Base Camp in 2016 August. The questionnaires enquired about the following information: Number of members in each party; number of belongings brought in and out; number of donkeys used to carry equipment; and environmental considerations taken by each party.
A few of the findings of this study in August 2016 at and around the Manaslu Base Camp are as follows. (1) A topographical map of Base Camp was prepared pinpointing the location of each and every tent of the area. We are the first in the world to prepare such topographical map of the Manaslu Base Camp using UAV. (2) The results of the questionnaires show that during the pre-monsoon period in 2016 an astounding 46 tons of goods were brought into the Base Camp. Furthermore, over 780 donkeys were used for transportation. (3) Water quality research was also conducted at water collection points of the

©2019. Japan Geoscience Union. All Right Reserved.

Base Camp. The water was found to be badly contaminated because of the urine and excrement of donkeys that were found scattered over the Base Camp.

Keywords: Himalaya, GIS, UAV

©2019. Japan Geoscience Union. All Right Reserved.

Understanding human system vulnerability to typhoon for Improved Adaptive Capacity

*Kim-Anh Nguyen[1], Yuei-An Liou[1]

1. Center for Space and Remote Sensing Research, National Central University

Typhoon is one of the most natural disastrous phenomena that have devastating impacts on human system around the world. In the context of climate change, Asian countries particularly in tropical climate zone with high humidity and unevenly-distributed abundant precipitation tend to have frequent occurrence of typhoons and flooding. Here, we present a conceptual framework that incorporates 21 indicators across three dimensions, including vulnerability, exposure/sensitivity, and adaptive capacity to classify vulnerability and adaptive capacity (VAC) using geospatial techniques at regional scales over Vietnam. Results indicate that large spatial differences in VAC are obtained and identify top-priority regions that need enhanced adaptation to typhoons. The Southern Coastal area, South East and Red River Delta exhibit high and very high vulnerability because their physical features tend to be affected by the intensity of typhoons that frequently cross these parts. The lower Mekong Delta and Northern Coastal areas are vulnerable to typhoon-driven flood threats and, in particular, compounded by sea-level rise. Findings of this study are useful in making efficient policy decisions to minimize vulnerability to typhoons in Vietnam. In addition, the framework can be potentially applied to the other regions.

Keywords: human system vulnerability, Typhoon, Adaptive capacity, Geospatial techniques

©2019. Japan Geoscience Union. All Right Reserved.

Environmental Impact Evaluation of Solar Park Project in Western Desert, Minia, Egypt.

*Ramadan Gamal Abdelrehim[1], Josaphat Tetuko Sri Sumantyo[1]

1. Center for Environmental Remote Sensing, Chiba University

More than 95% of the Egyptian lands are desert, Groundwater in this arid desert area is considered as a very valuable and unique source of water for agricultural and manufacturing development projects; therefore environmental impact evaluation of these projects is very important step to protect groundwater from pollution. Three geophysical techniques used for groundwater exploration and upper geological layers evaluation, these techniques are, Vertical electrical sounding, two dimension electrical imaging, and Time Domain electromagnetic techniques. And depending on this study we described the hydro-geological settings of the area, detect the best locations for drilling groundwater wells, safe environmental injection points, and finally safe environmental landfill.

Keywords: Geophysics, Groundwater, Environmental evaluation, Arid Desert lands

©2019. Japan Geoscience Union. All Right Reserved.

Peatland Assessment Based on DInSAR approach by using ALOS-2 PALSAR-2 Data in Kalimantan, Indonesia

*Joko Widodo[1], Josaphat Tetuko Sri Sumantyo[1], Daniele Perissin[2], Katsunoshin Nishi[1], Pakhrur Rozi[1]

1. JMRSL - Josaphat Microwave Remote Sensing Laboratory Center for Environmental Remote Sensing Graduate School of Advanced Integration Science Chiba University, 2. Sarproz, Razer Limited, Hongkong

Indonesia has the lagerst tropical peatland ecosystem in the world around 22 million hectares separate in Sumatera Island, Kalimantan Island, and Papua island. Peatlands can be a source of food, clean water, and provide other benefits for the surrounding community. Peatland is also useful for preventing drought, flooding and mixing salt water for irrigation in agricultural areas. Peatlands are important for biodiversity because they are home to rare species. Peatlands play an important role in climate change mitigation and adaptation. Since subsidence is important phenomenon in peatland, DInSAR provide ability and effective aproach to detect subsidence in peatland area. Subsidence phenomenon in peatland related with groundwater table, carbon emision, and others. In this research, DInSAR is very effective as a basis for an approach to conducting peatland assessment in Kalimantan.

Keywords: DInSAR, Peatland, Assessment, ALOS 2 PALSAR 2

©2019. Japan Geoscience Union. All Right Reserved.

Development of Nanosatellite for Ionospheric Measurement for Earthquake Prediction

*Peberlin Parulian Sitompul[1], Josaphat Tetuko Sri Sumantyo[2]

1. Chiba University, and Indonesia National Institute of Aeronautic and Space, 2. Center for Environmental Remote Sensing, Chiba University

Indonesia is located at equatorial region and also has long coastline that often suffer the earthquakes. In some cases, ionospheric activity level increases just before to an earthquake event and shows a different behaviour 5–10 days before the event, when the seismic event has a magnitude greater than 4–4.5 degrees. The nanosatellite development is very important to get more ionospheric data and reletively cheaper than bigger satellite.

Keywords: Nanosatellite, Circular polarization, Earthquake prediction, Ionosphere

©2019. Japan Geoscience Union. All Right Reserved.

[E] Poster | H (Human Geosciences)：H-SC Social Earth Sciences & Civil/Urban System Sciences

Sun. May 26, 2019 3:30 PM - 5:00 PM JST | Sun. May 26, 2019 6:30 AM - 8:00 AM UTC | Poster Hall International Exhibition Hall8, Makuhari Messe_10

[H-SC06] Role of Geosciences for sustainable use of marine and coastal ecosystems in urbanized world.

convener:Kalpana Chaudhari(Institute For Sustainable Development and Research)

As per the United Nations estimates, the world population reached 7.3 billion as of mid-2015, implying that world has added approximately one billion people in the span of the last 12 years. The total population on earth is predicted to increase by more than one billion people within the next 15 years, reaching 8.5 billion in 2030, and to increase further to 9.7 billion in 2050 and 11.2 billion by 2100. Urban planning and management plays an important role in achieving the social sustainability through geosciences, environmental sustainability for urban transformation. Over the next generation of greatest increase in population, in production and in poverty will occur in cities in Asia and Africa. Due to this rapid urbanization and industrialization, the problems of urban organizational management, which often linked with geosciences and other socio-political aspects include, management of different urban planning and management, disaster management and resources mobilization, coastal zone management etc. for sustainable urban development will need better understanding of geosciences and linked with societal issues .Therefore it would be necessary to study the urban policies for sustainable development in Developed countries in Europe, Asia-Pacific and its impacts on the public life and also on the social-economic development of the urban region through systematic study of geosciences. This joint session will open up the opportunity for the researchers, scientists and students from AGU, EGU and AOGS to present their research/case studies on this topic and to network for future joint research programs. The joint session focuses on policy formulation for resources planning, coastal risk and vulnerability, social-ecological vulnerability and disaster resilience in coastal communities, Human Pressures on Coastal Environments, land water-seawater interactions for sustaining urban development in Asia-Pacific, Europe, South America and Africa region.

[HSC06-P01] Research on Diffusion Method of Factor in Urban Land Classification

★Invited Papers

*Jun Zhou[1] (1.Tianjin Normal University)

[HSC06-P02] Assessment of facilities for green tourism in Japan: Fifty-six indices in eight regions using online data

*Hanqiu Zhang[1], Qiongying Xiang[1], Jiaying Shi[1], Junchi Zhang[1], Yingming Mao[1], Kyung-hun Min[1], Ge Chen, Tokiya Oka[1], Zijiao Xie[1], Minami Kashima[1], I Made Pradnyan Dana Natawiguna, Katsunori Furuya[1] (1.Graduate School of Horticulture, Chiba University)

[HSC06-P03] Study on Green Tourism Experience —— Cases of Popular Strawberry Farms in Chiba Prefecture

*Yilin Wu[1], Mengying Gao[1], Kazuhei Sato[1], Tingyu Lu[1], Fumeng Zhang[1], Siqi Xing[1], Karolina Brandt[1], Mai Uemura, Katsunori Furuya[1] (1.Graduate School of Horticulture, Chiba University)

[HSC06-P04] **Ritual plant utilization in landscapes planning. Case study: Riverside in Denpasar City.**

*I Made Pradnyan Natawiguna[1], Katsunori Furuya[1] (1.Graduate School of Horticulture, Chiba University)

Research on Diffusion Method of Factor in Urban Land Classification

*Jun Zhou[1]

1. Tianjin Normal University

In urban classification, it is rather difficult and complex to calculate the classification factor diffusion. The purpose of this paper is resolve calculation efficiency in more barriers and more pass points condition. Topological processing of obstacle and evaluation extent to generate more evaluation zonings, use Dijkstra algorithm to calculate the shortest distance between any two pass points in advance. The method successfully resolve the spatial operation as distance operation, can effectively resolve calculation efficiency. A case study in Jilin province in 2016 show that the technical roadmap is feasible, and the results are reasonable

Keywords: evaluation zoning, urban land classification, obstacle, diffusion, shortest path

©2019. Japan Geoscience Union. All Right Reserved.

Assessment of facilities for green tourism in Japan: Fifty-six indices in eight regions using online data

*Hanqiu Zhang[1], Qiongying Xiang[1], Jiaying Shi[1], Junchi Zhang[1], Yingming Mao[1], Kyung-hun Min[1], Ge Chen, Tokiya Oka[1], Zijiao Xie[1], Minami Kashima[1], I Made Pradnyan Dana Natawiguna, Katsunori Furuya[1]

1. Graduate School of Horticulture, Chiba University

Background and Objectives

Green tourism is a dynamic and growing global trend. Cities are seeking ways to development by building tourism based on sustainable, environmentally friendly, and responsible activities. City planners are increasingly aware of the great possibilities of the relationship between tourism and cities' natural environments. This study's goal was to develop an objective assessment of green tourism regarding non-human conditions. A scientific evaluation might reveal the specific tourist attractions or places that receive the most tourist attention in Japan.

Methods

The Green Destinations Standard (available on the Green Destinations website) was modified for the purposed assessment. After studying and modifying the standard of green tourism, two types of variables were chosen for the analysis: dichotomous variables (indicators) and continuous variables. The indicators were nature conservation, facilities, popular seasons, management, and resources. The continuous variables were access (types of transportation), capacity/volume (numbers of tourists), and average cost (JPY). We found eight cases of green tourism in eight different regions of Japan and coded their data into the variables for the analysis. Ultimately, 56 indices were created.

The data were analyzed using reliability analysis, binary variables, and descriptive statistics in JASP software. The reliability analysis determined the reliability of the data, and the binary variables assessed the data regarding non-human conditions. The descriptive statistics were used to assess green tourism in the different regions of Japan regarding non-human conditions.

Results

The reliability analytical results were not satisfactory, and the reason might be that the alpha reliability test was not appropriate for binary data. The binary variable and descriptive analyses were performed to assess the data.

©2019. Japan Geoscience Union. All Right Reserved.

First, it seemed that nature conservation was a necessary condition for green tourism because the mean of this variable was 0.88. The data indicated that green tourism in Japan was mainly about the development of nature, and protecting cultural heritage was a less frequent response. Second, most of the areas had perfect and diverse methods of transit, including bicycles, cable cars, boats, walkways, and tourist buses. Although Japan has many mountains and seas, there were just a few cable cars and boats. The tourist attractions were easily reached by walking to them. We concluded that, when Japan developed green tourism, it first considered people's needs and convenience. In addition, most areas were government-managed, although a large proportion was privately administered. Last, the mean amount of tourism for the winter season was low (0.71), which was the lowest mean among the seasons. Apparently, although there are holidays in the winter, green tourist attractions open during the winter is less attractive. (**Table 1.** Descriptive statistics)

Conclusion

In sum, the scores were summarized by region. The highest score computed by the binary variable method was in the Chuba region, and the lowest score was in the Shikoku region. The Kansai cultural center and the Kanto economic center were not major areas of green tourism. If we have an opportunity to conduct in-depth research to explore this phenomenon, our findings might benefit the development of green tourism in Japan. (**Figure 1**. Total scores by region)

Keywords: Green tourism, assessment, binary variable, Japan

Table 1. Descriptive statistics

Descriptive Statistics														
	Nature Protection	Bicycle	Pedestrain	Cable car/ Rope way(Mountain)	Tourism bus/ Train	Water transport	Spring	Summer	Autumn	Winter	Official	Private	Natural	Cultural (Heritage)
Valid	56	56	56	56	56	56	55	56	56	56	56	56	56	56
Missing	0	0	0	0	0	0	1	0	0	0	0	0	0	0
Mean	0.8750	0.5179	0.9643	0.1607	0.6071	0.3750	0.9091	0.9286	0.8929	0.7143	0.8750	0.5536	0.9286	0.6786
Std. Deviation	0.3337	0.5042	0.1873	0.3706	0.4928	0.4885	0.2901	0.2599	0.3121	0.4558	0.3337	0.5016	0.2599	0.4713

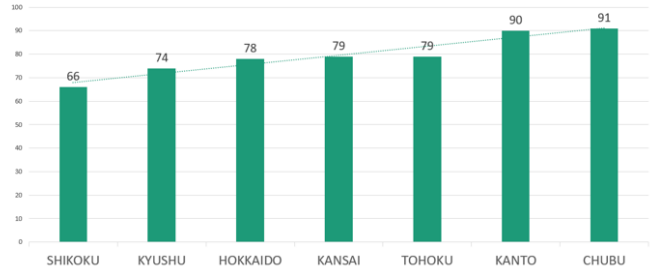


Figure 1. Total scores by region.(The full score is 112 points.)

©2019. Japan Geoscience Union. All Right Reserved.

Study on Green Tourism Experience ——Cases of Popular Strawberry Farms in Chiba Prefecture

*Yilin Wu[1], Mengying Gao[1], Kazuhei Sato[1], Tingyu Lu[1], Fumeng Zhang[1], Siqi Xing[1], Karolina Brandt[1], Mai Uemura, Katsunori Furuya[1]

1. Graduate School of Horticulture, Chiba University

Background and Objectives

The notion of ‘green tourism’, in which people are encouraged to pursue rural leisure activities in a manner that will benefit the countryside, rather than harm, is gaining popularity. (A. Jones, 1987)

Due to today’s enormous social pressure, many people need proximity to nature in order to get recreation in their leisure time. To promote green tourism in cooperation and participation, MAFF (Ministry of Agriculture, Forestry and Fisheries, Japan) arranges green tourism experiences into five categories; farmer restaurants (to taste), local products shops (to buy), farmhouses (to stay), experience of agriculture, forestry and fisheries (to enjoy) and citizen farms (to make). (MAFF HP,2018)

Chiba prefecture is having an advantage in the location as it adjoins to Tokyo metropolitan area, this means that agriculture, fishery experiences and other wide ranges of green-blue tourism activities that can be done on a one-day-trip from the big city. Therefore, it is convenient for urban residents, travelers and visitors to interact and communicate with local farmers and valuable knowledge and experience can easily be exchanged.

Method

The research was conducted in two stages; by collecting literature information and by analysis. Chiba-ken has been chosen as the study area because of the rich nature and beautiful seascape from three sides surrounded. We chose strawberry farms for research because in recent years strawberry picking has received more and more attention and formed a new trend.

Results and Considerations

According to statistics, it is concluded that the largest agricultural experience project in Chiba prefecture is the strawberry picking (Table). The area with the largest distribution of strawberry farms is Kimitsu area, and especially Kimitsu city (Fig.1). Through the study, we found the main reasons for the prosperity of strawberry picking agriculture in this specific area. First, Kimitsu city as a historic strawberry production area has superior geographical conditions. It is possible for the visitors to do the sightseeing in a one-day-trip as the ride is about one hour from Tokyo or Kanagawa when using the Tokyo Bay Aquarain/Tsuchiyama Auto Roadway (Fig.2). Another crucial reason is the strong support from the agricultural office on the improvement of cultivation technology and management improvement of producers. Producers in Kimitsu city are working diligently and making efforts by participating in a

©2019. Japan Geoscience Union. All Right Reserved.

workshop held by ‘JA Kimito Strawberry Committee’.

As a kind of agricultural management, sightseeing farms are often used as a sideline by farmers. Therefore, facilities and services are often inadequate from a tourism perspective. Sightseeing agriculture in Kimitsu city has benefited from the direct sales system of strawberries, and it can be said to be a model in sightseeing agriculture. For the consideration of development within tourism agriculture, more regional characteristics should be combined, and more emphasis should be placed on promoting regional advantages.

Keywords: green tourism, agriculture, tourism agriculture, MAFF

Table over the quantity of experiences in Chiba Prefecture

Activities	Strawberry	Sweet Potato	Bamboo Shoot	Rice	Blueberry
Amount	60	32	27	24	22
Activities	Peanut	Pear	Livestock	Flower Picked	Cauliflower
Amount	20	20	18	16	14
Activities	Corn	Potato	Grapes	Soybeans	Chestnut
Amount	13	13	12	12	12
Activities	Char-grilled	Fishery	Nature	Dairy Farm	Aquatic Food
Amount	11	11	10	9	9
Activities	Orange	Wild Vegetable	Broad Bean	Beach Comb	Shiitake
Amount	9	8	6	6	5
Activities	Loquat	Tomato	Persimmon	Fig	Apple
Amount	5	4	4	4	3
Activities	Taro	Kiwi Fruit	Melon	Carrot	Radish
Amount	3	3	3	3	2
Activities	Broccoli	Onion			
Amount	2	2			

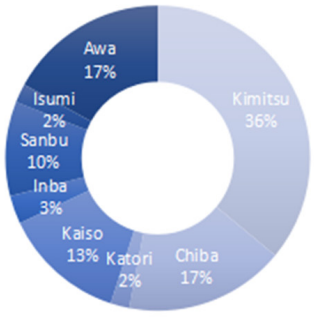


Fig.1 The distribution of strawberry fields



Fig.2 The location of Kimitsu City

©2019. Japan Geoscience Union. All Right Reserved.

Ritual plant utilization in landscapes planning. Case study: Riverside in Denpasar City.

*I Made Pradnyan Natawiguna[1], Katsunori Furuya[1]

1. Graduate School of Horticulture, Chiba University

Background and Purpose of the research

Balinese people used various types of plants for offering ceremonies. This ceremonial activity is based on the beliefs of the Balinese Hindu community, namely the philosophy of *Tri Hita Karana* which upholds the harmonization of the three good relations of fellow human beings, environment, and God. The role of plants is very vital because each ceremony, the community uses plant parts from roots, stems, leaves, flowers, and fruit. The plants used for offering ceremony means are known as ritual plants. The role of the Balinese community in maintaining plant diversity can be seen from the variety of types of ritual facilities. This study will reveal the diversity of plant species used in ceremonial facilities such as *Canang Sari*, *Kwangen*, *Segehan*, *Daksina*, *Pejati*, *Peras*, *Ajuman*, *Sesayut*, and *Penjor*. The existence of ancient ritual plants is effortless to find in the natural environment of Bali. However, the rapid development of tourism led to the conversion of land from agriculture into a built-in space, enabling the loss of the diversity of ritual plant species. Changes in the components of ritual means can occur due to the loss of ritual diversity. Educating the community regarding the importance of the existence of ritual plants is essential to maintain and preserve ritual plants so that in the future Balinese people, especially those living in urban areas, can re-coexist with ritual plants. This study aims to identify plants found in ritual ceremonies, analyzing plant species potentially used in landscape design, and arranging the landscape plan of the riverside in Denpasar by utilizing selected plant species.

Method

Literary studies were carried out to identify the types of plants contained in each ceremonial facility. Descriptive and quantitative analysis of plant species was carried out to determine the value of these plants both functionally and aesthetically. In preparing a landscape plan, a case study was carried out at the border of the *Tukad Mati* River in Denpasar City. The research steps taken are inventory, analysis, synthesis, and planning.

Results

The results of this study revealed that there were 16 plant species in *Canang Sari*, 13 plant species in *Kwangen*, 18 plant species in *Segehan*, 30 plant species in *Daksina*, 43 plant species in *Pejati*, 15 plant species in *Peras*, 23 plant species in *Ajuman*, 21 species plants in *Sesayut*, and 16 plant species at *Penjor* . Several species such as coconut, areca nut, betel and banana are used in 9 types of ritual facilities. Potential plants in landscape design number 25 species, 9 of which fulfill conservation functions, ten species accomplish aesthetic services, and six species perform architectural roles. The green governance plan in the case study carried out at the border of the Tukad Mati River in addition to maintaining existing plants also utilizes potential ritual plant species. The concept of a green governance plan refers to the function of protecting riverside areas, recreational purposes, and public education functions related to the existence of ritual plants.

Conclusion

©2019. Japan Geoscience Union. All Right Reserved.

The diversity of plants has been identified from 9 types of ceremonial facilities of the Balinese Hindu community. *Pejati* ceremony facilities have the highest plant diversity is 43 species of plants and the Kwangen ceremony facilities have the lowest diversity of plants, namely 13 plant species. 25 plant species have the potential to be used as landscape plants. This plant is recommended for riverside landscape planning in Denpasar city. The concept of green governance refers to the function of protecting river areas, recreational functions, and public education functions.

Keywords: ritual plants, plants diversity, bali, landscape plants, green space, riverbank

©2019. Japan Geoscience Union. All Right Reserved.

[E] Poster | H (Human Geosciences)：H-SC Social Earth Sciences & Civil/Urban System Sciences

Sun. May 26, 2019 5:15 PM - 6:30 PM JST | Sun. May 26, 2019 8:15 AM - 9:30 AM UTC | Poster Hall International Exhibition Hall8, Makuhari Messe_17

[H-SC06] Role of Geosciences for sustainable use of marine and coastal ecosystems in urbanized world.

convener:Kalpana Chaudhari(Institute For Sustainable Development and Research)

As per the United Nations estimates, the world population reached 7.3 billion as of mid-2015, implying that world has added approximately one billion people in the span of the last 12 years. The total population on earth is predicted to increase by more than one billion people within the next 15 years, reaching 8.5 billion in 2030, and to increase further to 9.7 billion in 2050 and 11.2 billion by 2100. Urban planning and management plays an important role in achieving the social sustainability through geosciences, environmental sustainability for urban transformation. Over the next generation of greatest increase in population, in production and in poverty will occur in cities in Asia and Africa. Due to this rapid urbanization and industrialization, the problems of urban organizational management, which often linked with geosciences and other socio-political aspects include, management of different urban planning and management, disaster management and resources mobilization, coastal zone management etc. for sustainable urban development will need better understanding of geosciences and linked with societal issues .Therefore it would be necessary to study the urban policies for sustainable development in Developed countries in Europe, Asia-Pacific and its impacts on the public life and also on the social-economic development of the urban region through systematic study of geosciences. This joint session will open up the opportunity for the researchers, scientists and students from AGU, EGU and AOGS to present their research/case studies on this topic and to network for future joint research programs. The joint session focuses on policy formulation for resources planning, coastal risk and vulnerability, social-ecological vulnerability and disaster resilience in coastal communities, Human Pressures on Coastal Environments, land water-seawater interactions for sustaining urban development in Asia-Pacific, Europe, South America and Africa region.

[HSC06-P01] Research on Diffusion Method of Factor in Urban Land Classification

★Invited Papers

*Jun Zhou[1] (1.Tianjin Normal University)

[HSC06-P02] Assessment of facilities for green tourism in Japan: Fifty-six indices in eight regions using online data

*Hanqiu Zhang[1], Qiongying Xiang[1], Jiaying Shi[1], Junchi Zhang[1], Yingming Mao[1], Kyung-hun Min[1], Ge Chen, Tokiya Oka[1], Zijiao Xie[1], Minami Kashima[1], I Made Pradnyan Dana Natawiguna, Katsunori Furuya[1] (1.Graduate School of Horticulture, Chiba University)

[HSC06-P03] Study on Green Tourism Experience —— Cases of Popular Strawberry Farms in Chiba Prefecture

*Yilin Wu[1], Mengying Gao[1], Kazuhei Sato[1], Tingyu Lu[1], Fumeng Zhang[1], Siqi Xing[1], Karolina Brandt[1], Mai Uemura, Katsunori Furuya[1] (1.Graduate School of Horticulture, Chiba University)

[HSC06-P04] **Ritual plant utilization in landscapes planning. Case study: Riverside in Denpasar City.**

*I Made Pradnyan Natawiguna[1], Katsunori Furuya[1] (1.Graduate School of Horticulture, Chiba University)

Research on Diffusion Method of Factor in Urban Land Classification

*Jun Zhou[1]

1. Tianjin Normal University

In urban classification, it is rather difficult and complex to calculate the classification factor diffusion. The purpose of this paper is resolve calculation efficiency in more barriers and more pass points condition. Topological processing of obstacle and evaluation extent to generate more evaluation zonings, use Dijkstra algorithm to calculate the shortest distance between any two pass points in advance. The method successfully resolve the spatial operation as distance operation, can effectively resolve calculation efficiency. A case study in Jilin province in 2016 show that the technical roadmap is feasible, and the results are reasonable

Keywords: evaluation zoning, urban land classification, obstacle, diffusion, shortest path

©2019. Japan Geoscience Union. All Right Reserved.

Assessment of facilities for green tourism in Japan: Fifty-six indices in eight regions using online data

*Hanqiu Zhang[1], Qiongying Xiang[1], Jiaying Shi[1], Junchi Zhang[1], Yingming Mao[1], Kyung-hun Min[1], Ge Chen, Tokiya Oka[1], Zijiao Xie[1], Minami Kashima[1], I Made Pradnyan Dana Natawiguna, Katsunori Furuya[1]

1. Graduate School of Horticulture, Chiba University

Background and Objectives

Green tourism is a dynamic and growing global trend. Cities are seeking ways to development by building tourism based on sustainable, environmentally friendly, and responsible activities. City planners are increasingly aware of the great possibilities of the relationship between tourism and cities' natural environments. This study's goal was to develop an objective assessment of green tourism regarding non-human conditions. A scientific evaluation might reveal the specific tourist attractions or places that receive the most tourist attention in Japan.

Methods

The Green Destinations Standard (available on the Green Destinations website) was modified for the purposed assessment. After studying and modifying the standard of green tourism, two types of variables were chosen for the analysis: dichotomous variables (indicators) and continuous variables. The indicators were nature conservation, facilities, popular seasons, management, and resources. The continuous variables were access (types of transportation), capacity/volume (numbers of tourists), and average cost (JPY). We found eight cases of green tourism in eight different regions of Japan and coded their data into the variables for the analysis. Ultimately, 56 indices were created.

The data were analyzed using reliability analysis, binary variables, and descriptive statistics in JASP software. The reliability analysis determined the reliability of the data, and the binary variables assessed the data regarding non-human conditions. The descriptive statistics were used to assess green tourism in the different regions of Japan regarding non-human conditions.

Results

The reliability analytical results were not satisfactory, and the reason might be that the alpha reliability test was not appropriate for binary data. The binary variable and descriptive analyses were performed to assess the data.

©2019. Japan Geoscience Union. All Right Reserved.

First, it seemed that nature conservation was a necessary condition for green tourism because the mean of this variable was 0.88. The data indicated that green tourism in Japan was mainly about the development of nature, and protecting cultural heritage was a less frequent response. Second, most of the areas had perfect and diverse methods of transit, including bicycles, cable cars, boats, walkways, and tourist buses. Although Japan has many mountains and seas, there were just a few cable cars and boats. The tourist attractions were easily reached by walking to them. We concluded that, when Japan developed green tourism, it first considered people's needs and convenience. In addition, most areas were government-managed, although a large proportion was privately administered. Last, the mean amount of tourism for the winter season was low (0.71), which was the lowest mean among the seasons. Apparently, although there are holidays in the winter, green tourist attractions open during the winter is less attractive. (**Table 1.** Descriptive statistics)

Conclusion

In sum, the scores were summarized by region. The highest score computed by the binary variable method was in the Chuba region, and the lowest score was in the Shikoku region. The Kansai cultural center and the Kanto economic center were not major areas of green tourism. If we have an opportunity to conduct in-depth research to explore this phenomenon, our findings might benefit the development of green tourism in Japan. (**Figure 1**. Total scores by region)

Keywords: Green tourism, assessment, binary variable, Japan

Table 1. Descriptive statistics

Descriptive Statistics														
	Nature Protection	Bicycle	Pedestrain	Cable car/ Rope way(Mountain)	Tourism bus/ Train	Water transport	Spring	Summer	Autumn	Winter	Official	Private	Natural	Cultural (Heritage)
Valid	56	56	56	56	56	56	55	56	56	56	56	56	56	56
Missing	0	0	0	0	0	0	1	0	0	0	0	0	0	0
Mean	0.8750	0.5179	0.9643	0.1607	0.6071	0.3750	0.9091	0.9286	0.8929	0.7143	0.8750	0.5536	0.9286	0.6786
Std. Deviation	0.3337	0.5042	0.1873	0.3706	0.4928	0.4885	0.2901	0.2599	0.3121	0.4558	0.3337	0.5016	0.2599	0.4713

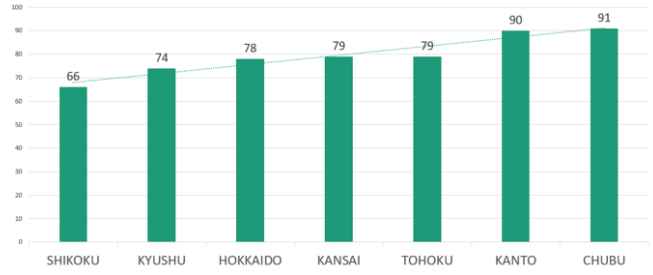


Figure 1. Total scores by region.(The full score is 112 points.)

©2019. Japan Geoscience Union. All Right Reserved.

Study on Green Tourism Experience ——Cases of Popular Strawberry Farms in Chiba Prefecture

*Yilin Wu[1], Mengying Gao[1], Kazuhei Sato[1], Tingyu Lu[1], Fumeng Zhang[1], Siqi Xing[1], Karolina Brandt[1], Mai Uemura, Katsunori Furuya[1]

1. Graduate School of Horticulture, Chiba University

Background and Objectives

The notion of ‘green tourism’, in which people are encouraged to pursue rural leisure activities in a manner that will benefit the countryside, rather than harm, is gaining popularity. (A. Jones, 1987)

Due to today’s enormous social pressure, many people need proximity to nature in order to get recreation in their leisure time. To promote green tourism in cooperation and participation, MAFF (Ministry of Agriculture, Forestry and Fisheries, Japan) arranges green tourism experiences into five categories; farmer restaurants (to taste), local products shops (to buy), farmhouses (to stay), experience of agriculture, forestry and fisheries (to enjoy) and citizen farms (to make). (MAFF HP,2018)

Chiba prefecture is having an advantage in the location as it adjoins to Tokyo metropolitan area, this means that agriculture, fishery experiences and other wide ranges of green-blue tourism activities that can be done on a one-day-trip from the big city. Therefore, it is convenient for urban residents, travelers and visitors to interact and communicate with local farmers and valuable knowledge and experience can easily be exchanged.

Method

The research was conducted in two stages; by collecting literature information and by analysis. Chiba-ken has been chosen as the study area because of the rich nature and beautiful seascape from three sides surrounded. We chose strawberry farms for research because in recent years strawberry picking has received more and more attention and formed a new trend.

Results and Considerations

According to statistics, it is concluded that the largest agricultural experience project in Chiba prefecture is the strawberry picking (Table). The area with the largest distribution of strawberry farms is Kimitsu area, and especially Kimitsu city (Fig.1). Through the study, we found the main reasons for the prosperity of strawberry picking agriculture in this specific area. First, Kimitsu city as a historic strawberry production area has superior geographical conditions. It is possible for the visitors to do the sightseeing in a one-day-trip as the ride is about one hour from Tokyo or Kanagawa when using the Tokyo Bay Aquarain/Tsuchiyama Auto Roadway (Fig.2). Another crucial reason is the strong support from the agricultural office on the improvement of cultivation technology and management improvement of producers. Producers in Kimitsu city are working diligently and making efforts by participating in a

©2019. Japan Geoscience Union. All Right Reserved.

workshop held by ‘JA Kimito Strawberry Committee’.

As a kind of agricultural management, sightseeing farms are often used as a sideline by farmers. Therefore, facilities and services are often inadequate from a tourism perspective. Sightseeing agriculture in Kimitsu city has benefited from the direct sales system of strawberries, and it can be said to be a model in sightseeing agriculture. For the consideration of development within tourism agriculture, more regional characteristics should be combined, and more emphasis should be placed on promoting regional advantages.

Keywords: green tourism, agriculture, tourism agriculture, MAFF

Table over the quantity of experiences in Chiba Prefecture

Activities	Strawberry	Sweet Potato	Bamboo Shoot	Rice	Blueberry
Amount	60	32	27	24	22
Activities	Peanut	Pear	Livestock	Flower Picked	Cauliflower
Amount	20	20	18	16	14
Activities	Corn	Potato	Grapes	Soybeans	Chestnut
Amount	13	13	12	12	12
Activities	Char-grilled	Fishery	Nature	Dairy Farm	Aquatic Food
Amount	11	11	10	9	9
Activities	Orange	Wild Vegetable	Broad Bean	Beach Comb	Shiitake
Amount	9	8	6	6	5
Activities	Loquat	Tomato	Persimmon	Fig	Apple
Amount	5	4	4	4	3
Activities	Taro	Kiwi Fruit	Melon	Carrot	Radish
Amount	3	3	3	3	2
Activities	Broccoli	Onion			
Amount	2	2			

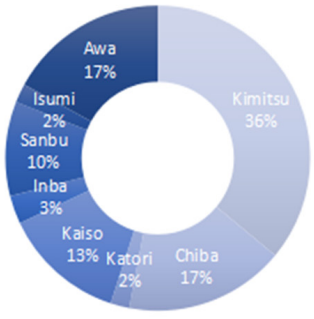


Fig.1 The distribution of strawberry fields



Fig.2 The location of Kimitsu City

©2019. Japan Geoscience Union. All Right Reserved.

Ritual plant utilization in landscapes planning. Case study: Riverside in Denpasar City.

*I Made Pradnyan Natawiguna[1], Katsunori Furuya[1]

1. Graduate School of Horticulture, Chiba University

Background and Purpose of the research

Balinese people used various types of plants for offering ceremonies. This ceremonial activity is based on the beliefs of the Balinese Hindu community, namely the philosophy of *Tri Hita Karana* which upholds the harmonization of the three good relations of fellow human beings, environment, and God. The role of plants is very vital because each ceremony, the community uses plant parts from roots, stems, leaves, flowers, and fruit. The plants used for offering ceremony means are known as ritual plants. The role of the Balinese community in maintaining plant diversity can be seen from the variety of types of ritual facilities. This study will reveal the diversity of plant species used in ceremonial facilities such as *Canang Sari*, *Kwangen*, *Segehan*, *Daksina*, *Pejati*, *Peras*, *Ajuman*, *Sesayut*, and *Penjor*. The existence of ancient ritual plants is effortless to find in the natural environment of Bali. However, the rapid development of tourism led to the conversion of land from agriculture into a built-in space, enabling the loss of the diversity of ritual plant species. Changes in the components of ritual means can occur due to the loss of ritual diversity. Educating the community regarding the importance of the existence of ritual plants is essential to maintain and preserve ritual plants so that in the future Balinese people, especially those living in urban areas, can re-coexist with ritual plants. This study aims to identify plants found in ritual ceremonies, analyzing plant species potentially used in landscape design, and arranging the landscape plan of the riverside in Denpasar by utilizing selected plant species.

Method

Literary studies were carried out to identify the types of plants contained in each ceremonial facility. Descriptive and quantitative analysis of plant species was carried out to determine the value of these plants both functionally and aesthetically. In preparing a landscape plan, a case study was carried out at the border of the *Tukad Mati* River in Denpasar City. The research steps taken are inventory, analysis, synthesis, and planning.

Results

The results of this study revealed that there were 16 plant species in *Canang Sari*, 13 plant species in *Kwangen*, 18 plant species in *Segehan*, 30 plant species in *Daksina*, 43 plant species in *Pejati*, 15 plant species in *Peras*, 23 plant species in *Ajuman*, 21 species plants in *Sesayut*, and 16 plant species at *Penjor* . Several species such as coconut, areca nut, betel and banana are used in 9 types of ritual facilities. Potential plants in landscape design number 25 species, 9 of which fulfill conservation functions, ten species accomplish aesthetic services, and six species perform architectural roles. The green governance plan in the case study carried out at the border of the Tukad Mati River in addition to maintaining existing plants also utilizes potential ritual plant species. The concept of a green governance plan refers to the function of protecting riverside areas, recreational purposes, and public education functions related to the existence of ritual plants.

Conclusion

©2019. Japan Geoscience Union. All Right Reserved.

The diversity of plants has been identified from 9 types of ceremonial facilities of the Balinese Hindu community. *Pejati* ceremony facilities have the highest plant diversity is 43 species of plants and the Kwangen ceremony facilities have the lowest diversity of plants, namely 13 plant species. 25 plant species have the potential to be used as landscape plants. This plant is recommended for riverside landscape planning in Denpasar city. The concept of green governance refers to the function of protecting river areas, recreational functions, and public education functions.

Keywords: ritual plants, plants diversity, bali, landscape plants, green space, riverbank

©2019. Japan Geoscience Union. All Right Reserved.

[E] Poster | H (Human Geosciences)：H-TT Technology & Techniques

Sun. May 26, 2019 3:30 PM - 5:00 PM JST | Sun. May 26, 2019 6:30 AM - 8:00 AM UTC | Poster Hall International Exhibition Hall8, Makuhari Messe_11

[H-TT20] Environmental Remote Sensing

convener:Wei Yang(Chiba University), Akihiko Kondoh(Center for Environmental Remote Sensing, Chiba University)

Our human beings are encountering various environmental issues on the Earth, and it is urgent to find out the solutions. Remote sensing is currently the only feasible means to observe the Earth environment at regional/continental /global scales over long periods, and consequently detects the environmental changes occurred all over the world. This session invites presentations on theory, science, technology, and applications of remote sensing to study the Earth environment from regional to global scales. Both oral and poster presentations are sincerely welcome.

[HTT20-P01] Classification of Winter Wheat using high spatial resolution data in North China Plain

*Chunyang Wang[1,2], Wei Yang[2], Xifang Wu[3], Zhichao Chen[1], Junjun Lu[1], Zongze Zhao[1], Hebing Zhang[1] (1.School of Surveying and Land Information Engineering, Henan Polytechnic University, 2.Center for Environmental Remote Sensing, Chiba University, 3.Graduate School of Science and Engineering, Chiba University)

[HTT20-P02] Normalized Difference Greenness Index (NDGI): A new vegetation index for improved estimation of vegetation phenology

*Wei Yang[1], Hideki Kobayashi[2], Akihiko Kondoh[1] (1.Chiba University, 2.JAMSTEC)

[HTT20-P03] *Characteristics of manual and automatically tree species classification in mixed forest (Yamagata University Research Forest)*

*Sarah Kentsch[1,2], Larry Maximo Lopez Caceres[1], Yago Diez[1], Motohisa Fukuda[1] (1.Yamagata University, 2.United Graduate School of Agricultural Sciences)

[HTT20-P04] Land subsidence detection by SBAS-InSAR technology and its factor analysis in the inland area of Chiba Prefecture

*HALIPU AYIHUMAIER[1], Richa Bhattarai[1], Wen - LIU[1], Akihiko - Kondoh[1,2] (1.Graduate School of Science and Engineering, 2.Center for Environmental Remote Sensing, Chiba University)

[HTT20-P05] Development of a novel data fusion model to generate high spatiotemporal resolution NDVI time series

*Wei Yang[1], Jin Chen[2] (1.Chiba University, 2.Beijing Normal University)

Classification of Winter Wheat using high spatial resolution data in North China Plain

*Chunyang Wang[1,2], Wei Yang[2], Xifang Wu[3], Zhichao Chen[1], Junjun Lu[1], Zongze Zhao[1], Hebing Zhang[1]

1. School of Surveying and Land Information Engineering, Henan Polytechnic University, 2. Center for Environmental Remote Sensing, Chiba University, 3. Graduate School of Science and Engineering, Chiba University

Winter Wheat in North China Plain (NCP) is one of the key food sources for securing food safety of China. Mapping the spatial distributions of winter wheat plays crucial roles in monitoring of planting areas and estimation of winter wheat production, which is usually carried out through classification of satellite images. The traditional classification methods are mainly based on data collection, download storage, and local analysis. However, these approaches are not capable of dealing with the quick mapping of massive satellite data including high spatial-temporal resolutions over large-scale areas. To overcome this challenge, this study developed a processing chain for mapping winter wheat of NCP at 10 m resolution using Sentinel-2-based NDVI time series on the google earth engine (GEE) platform, a cloud computing platform for Earth science data and analysis. First, the influence of phenology between the north and the south of the NCP on classification is eliminated by using the locally selected training data sets. Second, the data contaminated by clouds were all removed. Third, the training sample sets are constructed, and the typical features are searched. Last, two machine learning algorithms were applied to yield the classification result map, that is, Random Forest (RF) method and Regression Trees (CART) method. Validation results showed that the final maps and classification accuracy of RF method was better than SVM and CART method, with total accuracy of 81%. Moreover, this study also demonstrated that the GEE platform can yield dramatically higher efficiency than conventional classification methods by reducing downloading time and local storage capacity. Consequently, we recommend that the GEE cloud computing platform is a more suitable research tool for large-scale geospatial analysis and application.

Keywords: Google earth engine, Cloud computing, Big data, Classification, Sentinel-2, Winter wheat

©2019. Japan Geoscience Union. All Right Reserved.

Normalized Difference Greenness Index (NDGI): A new vegetation index for improved estimation of vegetation phenology

*Wei Yang[1], Hideki Kobayashi[2], Akihiko Kondoh[1]

1. Chiba University, 2. JAMSTEC

Satellite monitoring of vegetation phenology is crucial to understanding the biological impacts of climate change. Nevertheless, satellite-based phenology estimation can be biased by effects of snow using conventional vegetation indices (VIs), such as the normalized difference vegetation index (NDVI). To eliminate effects of snow, snow-free VIs that take advantage of the shortwave infrared (SWIR) band have been proposed (i.e., phenology index [PI] and normalized difference phenology index [NDPI]). However, PI cannot properly capture the presence of sparse vegetation, and NDPI does not account for the influence of dry vegetation. Here, we propose a novel snow-free VI, designated the normalized difference greenness index (NDGI), using reflectance of green, red, and near-infrared (NIR) bands. NDGI is a semi-analytical index deduced based on the linear spectral mixture model and the spectral characteristics of vegetation, snow, soil, and dry grass. Its performance for estimating the start of growing season (SOS) and end of growing season (EOS) was evaluated using simulation datasets, time-lapse camera data of tundra sites, and flux tower gross primary production (GPP) data of grassland sites. Simulation results demonstrated that NDGI can exclude the influence of snow on SOS and EOS estimations. In the camera sites, NDGI markedly outperformed NDVI, PI, and NDPI for SOS estimation with RMSE=6.46 days and Bias=-1.32 days (vs. RMSE range 12.39–14.8 days and Bias>3.5 days for the other VIs), and for EOS estimation with RMSE=8.33 days and Bias=0.11 days (vs. RMSE range 8.00–26.74 days and Bias>2.67 days for the other VIs). In the GPP sites, NDGI also outperformed the other VIs for SOS estimation with RMSE=10.32 days and Bias=-4.91 days (vs. RMSE range 12.9–24.74 days and Bias>6.13 days for the other VIs). Although its performance was lower for monitoring EOS than SOS in GPP sites, it still outperformed the other VIs in EOS estimation. These results indicate the potential of NDGI for operational monitoring of plant phenology in the tundra and grassland ecosystems based on satellite observations.

Keywords: plant phenology, remote sensing, snow, MODIS

©2019. Japan Geoscience Union. All Right Reserved.

Characteristics of manual and automatically tree species classification in mixed forest (Yamagata University Research Forest)

*Sarah Kentsch[1,2], Larry Maximo Lopez Caceres[1], Yago Diez[1], Motohisa Fukuda[1]

1. Yamagata University, 2. United Graduate School of Agricultural Sciences

A low degree of knowledge combined with a complex structure of mixed forests is the reason why researchers still investigate in mixed forest research for getting a deeper understanding. Especially mixed forests in Japan are influenced by the characteristically relief and the climate conditions. There is a high demand on accurate information about tree species of mixed forests. This high demand requires accurate investigation possibilities included by an easier access to the needed information' s (Fritz, 2013). Methods to get accurate information on a large scale with easy access to the desired information are needed. Previous studies show the applicability of drones for forest applications (Torresan et. al, 2016). Images taken with a drone offer new methods to get information of forests like distribution, health condition or automatically classifications of tree species. For example, Onishi & Ise (2018) reached accuracies of up to 90 %. But these studies also illustrated that there are limitations and gaps in knowledge for the applicability of using UAV. Especially, a lot of those high accuracies were reached in forest plantations. There is a need of more detailed information about how to get more accurate information in real forests by using drones (Michez et al., 2016).

The Yamagata Research Forest offers the opportunity to study mixed forests with different conditions in different parts of the forest for doing automatically classifications of tree species. Till now two study sites were defined and image were taken with a camera detecting the visual spectrum of the light. Also, images were taken during different seasons (summer and autumn). After taking the images they needed to be processed. A first step is to generate orthomosaics by merging the images using Photoscan from Agisoft. As a result, DEMs, orthomosaics and 3D models were generated and can be further analyzed. In the next step the segmentation and classification of tree species should be done in an object-based way using feature information of the trees. After processing the images, it should be possible to create a model for deep machine learning which will be able to do the classification on its own.

During the last year the first image taking took place in different seasons in the Yamagata University Research Forest. Also, the image processing with Photoscan was finished. The first images were analyzed manually to check how it is possible to separate tree species automatically. To find out what are the important factors for doing automatically classification is the actual research status. Further, the presentation handles the comparison of manually and automatically ways for doing separations in this research. The results will be first approaches to do automatically classification/separations of tree species.

Literature:

Fritz, A.; Kattenborn, T.; Koch, B., 2013: UAV-based photogrammetric point clouds –tree stem mapping in open stands in comparison to terrestrial laser scanner point clouds; International Archives of the Photogrammetry, Remote Sensing and Spatial Information Sciences, Volume XL-1/W2.

Michez, Adrien et. al, 2016: Classification of riparian forest species and health condition using multi-temporal and hyperspatial imagery from unmanned aerial system; Environ Monit Assess (2016) 188:

©2019. Japan Geoscience Union. All Right Reserved.

146; DOI 10.1007/s10661-015-4996-2; Springer International Publishing Switzerland 2016.

Onishi, Masanori and Ise, Takeshi, 2018: Automatic classification of trees using a UAV onboard camera and deep learning, https://arxiv.org/abs/1804.10390.

Torresan, C. et. al, 2016: Forestry applications of UAVs in Europe: A review, International journal of remote sensing, https://doi.org/10.1080/01431161.2016.1252477

Keywords: tree species classification, UAV, Yamagata Research Forest, Image processing, Photoscan

©2019. Japan Geoscience Union. All Right Reserved.

Land subsidence detection by SBAS-InSAR technology and its factor analysis in the inland area of Chiba Prefecture

*AYIHUMAIER HALIPU[1], Richa Bhattarai[1], Wen - LIU[1], Akihiko - Kondoh[1,2]

1. Graduate School of Science and Engineering, 2. Center for Environmental Remote Sensing, Chiba University

Land subsidence seriously influences the safety of our property. There have been many studies on the deformation of the ground surface due to the groundwater or natural gas extraction. Recently, a large amount of land subsidence had occurred in the Quaternary upland areas in the inland areas of Chiba Prefecture, Japan. There is less evidence of big wells of groundwater or natural gas, and the mechanism of subsidence is not yet clear. So far, SBAS-InSAR (Small Baseline Subset algorithm -Interferometric Synthetic Aperture Radar) technology had been used in the investigation process to clarify the phenomenon of land subsidence in some inland areas of Chiba Prefecture. The ALOS-PALSAR and ALOS-2 PALSAR-2 data for 2006-2010 and 2014-2018 were collected, respectively. The maps of the land subsidence phenomena in Yachimata-Tomisato area are created, and the maps reveal the spatial and temporal distribution of upland area land subsidence. The extent of the subsidence zone are almost consistent with the land survey results. Next step is to reveal the mechanism of land subsidence. At the JpGU2019, we will make a discussion on the possibility of decline of fluid pressure in deep layer.

Keywords: SBAS-InSAR technology, Land subsidence, Chiba Prefecture

©2019. Japan Geoscience Union. All Right Reserved.

Development of a novel data fusion model to generate high spatiotemporal resolution NDVI time series

*Wei Yang[1], Jin Chen[2]

1. Chiba University, 2. Beijing Normal University

Normalized Difference Vegetation Index (NDVI) is one of the most commonly used vegetation indices for monitoring ecosystem dynamics and modeling biosphere processes. However, global NDVI products are usually provided with relatively coarse spatial resolutions that lack important spatial details. Producing NDVI time-series data with high spatiotemporal resolution is indispensable for monitoring land surfaces and ecosystem changes, especially in spatiotemporally heterogeneous areas. We therefore proposed an Improved Flexible Spatiotemporal DAta Fusion (IFSDAF) method to fill this need. In accord with the distinctive characteristics of NDVIs with large data variance and high spatial autocorrelation compared with raw reflectance bands, the IFSDAF method first produces a time-dependent increment with linear unmixing and a space-dependent increment via thin plate spline interpolation. It then makes a final prediction by optimal integration of these two increments with the constrained least squares method. Moreover, the IFSDAF was developed with the capacity to use all available finer-scaled images, including those partly contaminated by clouds. NDVI images with coarse spatial resolution (MODIS) and fine spatial resolution (Landsat and Sentinel) in areas with great spatial heterogeneity and significant land cover changes were used to test the performance of the IFSDAF method. The root mean square error and relative root mean square error of predicted relative to observed results were 0.0884 and 22.12%, respectively, in 3 heterogeneous areas, and 0.0546 and 25.77%, respectively, in areas of land-cover change. These promising results demonstrated the strength and robustness of the IFSDAF method in providing reliable NDVI datasets with high spatial and temporal resolution to support research on land surface processes. The efficiency of the proposed IFSDAF method can be greatly improved by using only the space-dependent increment. This simplification will make IFSDAF a feasible method for monitoring global vegetation.

Keywords: Spatiotemporal data fusion, High spatial and temporal resolution, Weighted integration

©2019. Japan Geoscience Union. All Right Reserved.

[E] Poster | H (Human Geosciences)：H-TT Technology & Techniques

Sun. May 26, 2019 5:15 PM - 6:30 PM JST | Sun. May 26, 2019 8:15 AM - 9:30 AM UTC | Poster Hall International Exhibition Hall8, Makuhari Messe_18

[H-TT20] Environmental Remote Sensing

convener:Wei Yang(Chiba University), Akihiko Kondoh(Center for Environmental Remote Sensing, Chiba University)

Our human beings are encountering various environmental issues on the Earth, and it is urgent to find out the solutions. Remote sensing is currently the only feasible means to observe the Earth environment at regional/continental /global scales over long periods, and consequently detects the environmental changes occurred all over the world. This session invites presentations on theory, science, technology, and applications of remote sensing to study the Earth environment from regional to global scales. Both oral and poster presentations are sincerely welcome.

[HTT20-P01] Classification of Winter Wheat using high spatial resolution data in North China Plain

*Chunyang Wang[1,2], Wei Yang[2], Xifang Wu[3], Zhichao Chen[1], Junjun Lu[1], Zongze Zhao[1], Hebing Zhang[1] (1.School of Surveying and Land Information Engineering, Henan Polytechnic University, 2.Center for Environmental Remote Sensing, Chiba University, 3.Graduate School of Science and Engineering, Chiba University)

[HTT20-P02] Normalized Difference Greenness Index (NDGI): A new vegetation index for improved estimation of vegetation phenology

*Wei Yang[1], Hideki Kobayashi[2], Akihiko Kondoh[1] (1.Chiba University, 2.JAMSTEC)

[HTT20-P03] *Characteristics of manual and automatically tree species classification in mixed forest (Yamagata University Research Forest)*

*Sarah Kentsch[1,2], Larry Maximo Lopez Caceres[1], Yago Diez[1], Motohisa Fukuda[1] (1.Yamagata University, 2.United Graduate School of Agricultural Sciences)

[HTT20-P04] Land subsidence detection by SBAS-InSAR technology and its factor analysis in the inland area of Chiba Prefecture

*HALIPU AYIHUMAIER[1], Richa Bhattarai[1], Wen - LIU[1], Akihiko - Kondoh[1,2] (1.Graduate School of Science and Engineering, 2.Center for Environmental Remote Sensing, Chiba University)

[HTT20-P05] Development of a novel data fusion model to generate high spatiotemporal resolution NDVI time series

*Wei Yang[1], Jin Chen[2] (1.Chiba University, 2.Beijing Normal University)

Classification of Winter Wheat using high spatial resolution data in North China Plain

*Chunyang Wang[1,2], Wei Yang[2], Xifang Wu[3], Zhichao Chen[1], Junjun Lu[1], Zongze Zhao[1], Hebing Zhang[1]

1. School of Surveying and Land Information Engineering, Henan Polytechnic University, 2. Center for Environmental Remote Sensing, Chiba University, 3. Graduate School of Science and Engineering, Chiba University

Winter Wheat in North China Plain (NCP) is one of the key food sources for securing food safety of China. Mapping the spatial distributions of winter wheat plays crucial roles in monitoring of planting areas and estimation of winter wheat production, which is usually carried out through classification of satellite images. The traditional classification methods are mainly based on data collection, download storage, and local analysis. However, these approaches are not capable of dealing with the quick mapping of massive satellite data including high spatial-temporal resolutions over large-scale areas. To overcome this challenge, this study developed a processing chain for mapping winter wheat of NCP at 10 m resolution using Sentinel-2-based NDVI time series on the google earth engine (GEE) platform, a cloud computing platform for Earth science data and analysis. First, the influence of phenology between the north and the south of the NCP on classification is eliminated by using the locally selected training data sets. Second, the data contaminated by clouds were all removed. Third, the training sample sets are constructed, and the typical features are searched. Last, two machine learning algorithms were applied to yield the classification result map, that is, Random Forest (RF) method and Regression Trees (CART) method. Validation results showed that the final maps and classification accuracy of RF method was better than SVM and CART method, with total accuracy of 81%. Moreover, this study also demonstrated that the GEE platform can yield dramatically higher efficiency than conventional classification methods by reducing downloading time and local storage capacity. Consequently, we recommend that the GEE cloud computing platform is a more suitable research tool for large-scale geospatial analysis and application.

Keywords: Google earth engine, Cloud computing, Big data, Classification, Sentinel-2, Winter wheat

©2019. Japan Geoscience Union. All Right Reserved.

Normalized Difference Greenness Index (NDGI): A new vegetation index for improved estimation of vegetation phenology

*Wei Yang[1], Hideki Kobayashi[2], Akihiko Kondoh[1]

1. Chiba University, 2. JAMSTEC

Satellite monitoring of vegetation phenology is crucial to understanding the biological impacts of climate change. Nevertheless, satellite-based phenology estimation can be biased by effects of snow using conventional vegetation indices (VIs), such as the normalized difference vegetation index (NDVI). To eliminate effects of snow, snow-free VIs that take advantage of the shortwave infrared (SWIR) band have been proposed (i.e., phenology index [PI] and normalized difference phenology index [NDPI]). However, PI cannot properly capture the presence of sparse vegetation, and NDPI does not account for the influence of dry vegetation. Here, we propose a novel snow-free VI, designated the normalized difference greenness index (NDGI), using reflectance of green, red, and near-infrared (NIR) bands. NDGI is a semi-analytical index deduced based on the linear spectral mixture model and the spectral characteristics of vegetation, snow, soil, and dry grass. Its performance for estimating the start of growing season (SOS) and end of growing season (EOS) was evaluated using simulation datasets, time-lapse camera data of tundra sites, and flux tower gross primary production (GPP) data of grassland sites. Simulation results demonstrated that NDGI can exclude the influence of snow on SOS and EOS estimations. In the camera sites, NDGI markedly outperformed NDVI, PI, and NDPI for SOS estimation with RMSE=6.46 days and Bias=-1.32 days (vs. RMSE range 12.39–14.8 days and Bias>3.5 days for the other VIs), and for EOS estimation with RMSE=8.33 days and Bias=0.11 days (vs. RMSE range 8.00–26.74 days and Bias>2.67 days for the other VIs). In the GPP sites, NDGI also outperformed the other VIs for SOS estimation with RMSE=10.32 days and Bias=-4.91 days (vs. RMSE range 12.9–24.74 days and Bias>6.13 days for the other VIs). Although its performance was lower for monitoring EOS than SOS in GPP sites, it still outperformed the other VIs in EOS estimation. These results indicate the potential of NDGI for operational monitoring of plant phenology in the tundra and grassland ecosystems based on satellite observations.

Keywords: plant phenology, remote sensing, snow, MODIS

©2019. Japan Geoscience Union. All Right Reserved.

Characteristics of manual and automatically tree species classification in mixed forest (Yamagata University Research Forest)

*Sarah Kentsch[1,2], Larry Maximo Lopez Caceres[1], Yago Diez[1], Motohisa Fukuda[1]

1. Yamagata University, 2. United Graduate School of Agricultural Sciences

A low degree of knowledge combined with a complex structure of mixed forests is the reason why researchers still investigate in mixed forest research for getting a deeper understanding. Especially mixed forests in Japan are influenced by the characteristically relief and the climate conditions. There is a high demand on accurate information about tree species of mixed forests. This high demand requires accurate investigation possibilities included by an easier access to the needed information' s (Fritz, 2013). Methods to get accurate information on a large scale with easy access to the desired information are needed. Previous studies show the applicability of drones for forest applications (Torresan et. al, 2016). Images taken with a drone offer new methods to get information of forests like distribution, health condition or automatically classifications of tree species. For example, Onishi & Ise (2018) reached accuracies of up to 90 %. But these studies also illustrated that there are limitations and gaps in knowledge for the applicability of using UAV. Especially, a lot of those high accuracies were reached in forest plantations. There is a need of more detailed information about how to get more accurate information in real forests by using drones (Michez et al., 2016).

The Yamagata Research Forest offers the opportunity to study mixed forests with different conditions in different parts of the forest for doing automatically classifications of tree species. Till now two study sites were defined and image were taken with a camera detecting the visual spectrum of the light. Also, images were taken during different seasons (summer and autumn). After taking the images they needed to be processed. A first step is to generate orthomosaics by merging the images using Photoscan from Agisoft. As a result, DEMs, orthomosaics and 3D models were generated and can be further analyzed. In the next step the segmentation and classification of tree species should be done in an object-based way using feature information of the trees. After processing the images, it should be possible to create a model for deep machine learning which will be able to do the classification on its own.

During the last year the first image taking took place in different seasons in the Yamagata University Research Forest. Also, the image processing with Photoscan was finished. The first images were analyzed manually to check how it is possible to separate tree species automatically. To find out what are the important factors for doing automatically classification is the actual research status. Further, the presentation handles the comparison of manually and automatically ways for doing separations in this research. The results will be first approaches to do automatically classification/separations of tree species.

Literature:

Fritz, A.; Kattenborn, T.; Koch, B., 2013: UAV-based photogrammetric point clouds –tree stem mapping in open stands in comparison to terrestrial laser scanner point clouds; International Archives of the Photogrammetry, Remote Sensing and Spatial Information Sciences, Volume XL-1/W2.

Michez, Adrien et. al, 2016: Classification of riparian forest species and health condition using multi-temporal and hyperspatial imagery from unmanned aerial system; Environ Monit Assess (2016) 188:

©2019. Japan Geoscience Union. All Right Reserved.

146; DOI 10.1007/s10661-015-4996-2; Springer International Publishing Switzerland 2016.

Onishi, Masanori and Ise, Takeshi, 2018: Automatic classification of trees using a UAV onboard camera and deep learning, https://arxiv.org/abs/1804.10390.

Torresan, C. et. al, 2016: Forestry applications of UAVs in Europe: A review, International journal of remote sensing, https://doi.org/10.1080/01431161.2016.1252477

Keywords: tree species classification, UAV, Yamagata Research Forest, Image processing, Photoscan

©2019. Japan Geoscience Union. All Right Reserved.

Land subsidence detection by SBAS-InSAR technology and its factor analysis in the inland area of Chiba Prefecture

*AYIHUMAIER HALIPU[1], Richa Bhattarai[1], Wen - LIU[1], Akihiko - Kondoh[1,2]

1. Graduate School of Science and Engineering, 2. Center for Environmental Remote Sensing, Chiba University

Land subsidence seriously influences the safety of our property. There have been many studies on the deformation of the ground surface due to the groundwater or natural gas extraction. Recently, a large amount of land subsidence had occurred in the Quaternary upland areas in the inland areas of Chiba Prefecture, Japan. There is less evidence of big wells of groundwater or natural gas, and the mechanism of subsidence is not yet clear. So far, SBAS-InSAR (Small Baseline Subset algorithm -Interferometric Synthetic Aperture Radar) technology had been used in the investigation process to clarify the phenomenon of land subsidence in some inland areas of Chiba Prefecture. The ALOS-PALSAR and ALOS-2 PALSAR-2 data for 2006-2010 and 2014-2018 were collected, respectively. The maps of the land subsidence phenomena in Yachimata-Tomisato area are created, and the maps reveal the spatial and temporal distribution of upland area land subsidence. The extent of the subsidence zone are almost consistent with the land survey results. Next step is to reveal the mechanism of land subsidence. At the JpGU2019, we will make a discussion on the possibility of decline of fluid pressure in deep layer.

Keywords: SBAS-InSAR technology, Land subsidence, Chiba Prefecture

©2019. Japan Geoscience Union. All Right Reserved.

Development of a novel data fusion model to generate high spatiotemporal resolution NDVI time series

*Wei Yang[1], Jin Chen[2]

1. Chiba University, 2. Beijing Normal University

Normalized Difference Vegetation Index (NDVI) is one of the most commonly used vegetation indices for monitoring ecosystem dynamics and modeling biosphere processes. However, global NDVI products are usually provided with relatively coarse spatial resolutions that lack important spatial details. Producing NDVI time-series data with high spatiotemporal resolution is indispensable for monitoring land surfaces and ecosystem changes, especially in spatiotemporally heterogeneous areas. We therefore proposed an Improved Flexible Spatiotemporal DAta Fusion (IFSDAF) method to fill this need. In accord with the distinctive characteristics of NDVIs with large data variance and high spatial autocorrelation compared with raw reflectance bands, the IFSDAF method first produces a time-dependent increment with linear unmixing and a space-dependent increment via thin plate spline interpolation. It then makes a final prediction by optimal integration of these two increments with the constrained least squares method. Moreover, the IFSDAF was developed with the capacity to use all available finer-scaled images, including those partly contaminated by clouds. NDVI images with coarse spatial resolution (MODIS) and fine spatial resolution (Landsat and Sentinel) in areas with great spatial heterogeneity and significant land cover changes were used to test the performance of the IFSDAF method. The root mean square error and relative root mean square error of predicted relative to observed results were 0.0884 and 22.12%, respectively, in 3 heterogeneous areas, and 0.0546 and 25.77%, respectively, in areas of land-cover change. These promising results demonstrated the strength and robustness of the IFSDAF method in providing reliable NDVI datasets with high spatial and temporal resolution to support research on land surface processes. The efficiency of the proposed IFSDAF method can be greatly improved by using only the space-dependent increment. This simplification will make IFSDAF a feasible method for monitoring global vegetation.

Keywords: Spatiotemporal data fusion, High spatial and temporal resolution, Weighted integration

©2019. Japan Geoscience Union. All Right Reserved.

[E] Poster | S (Solid Earth Sciences)：S-SS Seismology

Sun. May 26, 2019 3:30 PM - 5:00 PM JST | Sun. May 26, 2019 6:30 AM - 8:00 AM UTC | Poster Hall International Exhibition Hall8, Makuhari Messe_13

[S-SS04] New methods for seismicity characterization

convener:Francesco Grigoli(ETH-Zurich, Swiss Seismological Service), Aitaro Kato(Earthquake Research Institute, the University of Tokyo), Yosuke Aoki(Earthquake Research Institute, University of Tokyo), Claudio Satriano(Institut de Physique du Globe de Paris)

In the last two decades the number of high quality seismic instruments being installed around the world has grown exponentially and probably will continue to grow in the coming decades. This data explosion has shown the limits of the current standard routine seismic analysis, often performed manually by seismologists. Exploiting the massive amount of data is a challenge that can be overcome by using new generation, fully automated and noise robust seismic processing techniques. In the last years waveform-based detection and location methods have grown in popularity and their application have dramatically improved seismic monitoring capability. More recently, Machine Learning techniques, which are a perfect playground for data-intensive applications, are showing promising results in seismicity characterization applications opening new horizons for the development of innovative, fully automated and noise robust seismic analysis methods. Such techniques are particularly useful when working with datasets characterised by a massive number of weak events with low signal-to-noise ratio, such as those collected in induced seismicity and volcanic monitoring operations. This session aims to bring to light new methods that can be applied to large datasets, either retro-actively or in near-real time, to characterize seismicity (i.e. detection, location, magnitude and source mechanisms estimation) at different scales and in different environments. We thus encourage contributions that demonstrate how the proposed methods helps improve our understanding of earthquake and/or volcanic processes.

[SSS04-P01] Constraint of focal mechanisms of induced seismicity by using misfit angles based on known *in-situ* stress

*Yusuke Mukuhira[1], Makoto Naoi[2], Michael C Fehler[3], Hirokazu Moriya[5], Takatoshi Ito[1], Hiroshi Asanuma[4], Markus O Häring[6] (1.Institute of Fluid Science, Tohoku University, 2.Disaster Prevention Research Institute, Kyoto University, 3.Earth Resources Laboratory, MIT, 4.FREA, AIST, 5.School of Engineering, Tohoku University, 6.Häring GeoProject)

[SSS04-P02] Kinematic slip imaging of the Mw 3.3 earthquake in the St. Gallen 2013 geothermal reservoir, Switzerland, using an isochrone back projection approach

*Claudio Satriano[1], Eszter Király-Proag[2], Pascal Bernard[1], Stefan Wiemer[2] (1.Institut de Physique du Globe de Paris, France, 2.ETH Swiss Federal Institute of Technology Zurich, Switzerland)

[SSS04-P03] Monitoring induced seismicity with a single seismic station by combining coda wave interferometry with distance geometry solvers

*Francesco Grigoli[1], Simone Cesca[2], Alessandro Vuan[3], Filippo Broggini[1], John Clinton[1], Stefan Wiemer[1] (1.ETH-Zurich, Switzerland, 2.GFZ-Potsdam, Germany, 3.OGS-Trieste, Italy)

[SSS04-P04] Automatic Earthquake Locating by Stacking Characteristic Functions in a Source Scanning Method

★Invited Papers

*Hilary Chang[1], Alison Malcolm[1], Frédérick Massin[2], Francesco Grigoli[2] (1.Memorial University of Newfoundland, Earth Sciences, Canada, 2. ETH Zurich, Department of Earth Sciences, Zürich, Switzerland)

[SSS04-P05] Earthquake nowcasting: further development and application to Japan

*Kazuyoshi Nanjo[1], John B. Rundle[2], Tetsuo Sakurada[3] (1.University of Shizuoka, 2.University of California at Davis, 3.SAKURADA&Company)

Constraint of focal mechanisms of induced seismicity by using misfit angles based on known *in-situ* stress

*Yusuke Mukuhira[1], Makoto Naoi[2], Michael C Fehler[3], Hirokazu Moriya[5], Takatoshi Ito[1], Hiroshi Asanuma[4], Markus O Häring[6]

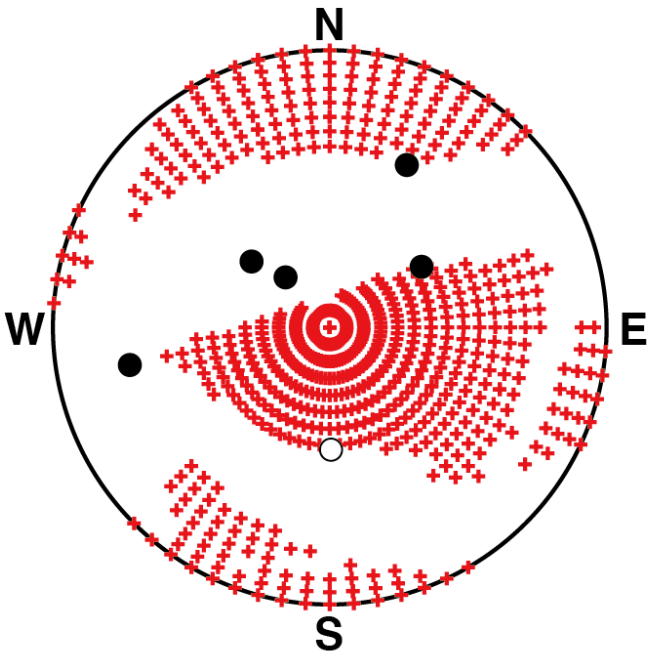
1. Institute of Fluid Science, Tohoku University, 2. Disaster Prevention Research Institute, Kyoto University, 3. Earth Resources Laboratory, MIT, 4. FREA, AIST, 5. School of Engineering, Tohoku University, 6. Häring GeoProject

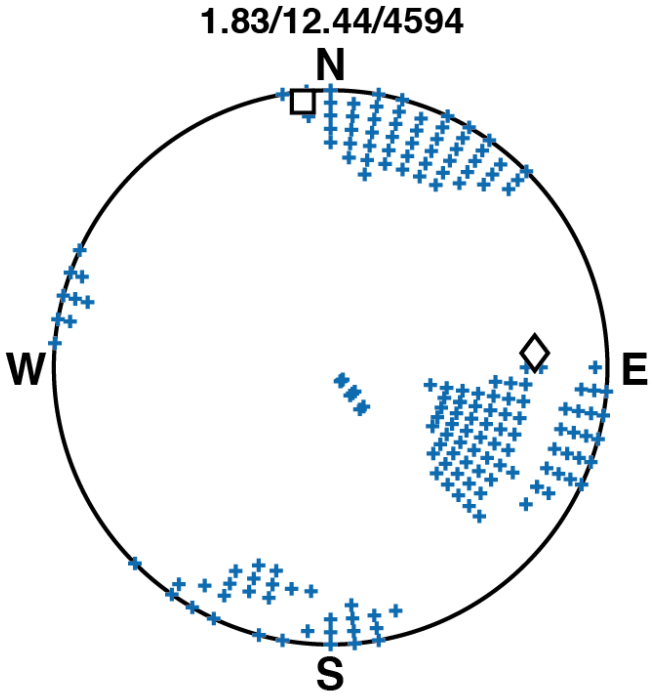
Microseismic monitoring is essential for successful hydraulic stimulation/fracking in unconventional oil/gas development, engineered geothermal system development and carbon capture and sequestration. In addition to the hypocenter location of the microseismicity, knowledge of the geometry of the fracture is also crucial for better understanding of fractured reservoir, fluid flow, and design of the energy extraction. Geofluid flows in the fracture and its permeability are correlated with the relation of the geometry of the fracture and in-situ stress. Fracture orientation can be estimated by the seismological method such as moment tensor inversion or focal mechanism analysis, only when the waveforms of the events are well recorded by a number of well-distributed stations. However, in realistic microseismic monitoring situations, it is often difficult to constrain the focal mechanism of microseismicity from first motion information due to the small number of stations.

We proposed a method to improve the estimates of focal mechanisms by introducing in-situ stress information from borehole logging information. We eliminate candidate focal mechanisms that are consistent with first motion data but cannot have shear slip under a given stress state and pore pressure increase. In this study, we also check the consistency between the shear slip vector estimated from the stress state and the rakes. We compare the shear slip vector and the slip vector from the rake. Then we reject the fault if the difference in the two vectors is significantly large. With this process, we reject the fault planes and auxiliary planes which are not consistent with stress state. We apply this method to induced seismicity dataset from Basel, Switzerland, where we already have well-constrained focal mechanisms estimated by many surface stations over a large region. We use these focal mechanisms as references to check whether our method can constrain the range of focal mechanisms using a small number of nearby stations. We find that the consistency check between two vectors significantly and reliably limits the range of focal mechanisms. Furthermore, we combine the constrained range of focal mechanism by this method and that by stability analysis to have more constraint of focal mechanisms satisfying the conditions of the geomechanical problem.

Keywords: Induced seismicity, Focal mechanism, In-situ stress

©2019. Japan Geoscience Union. All Right Reserved.





©2019. Japan Geoscience Union. All Right Reserved.

Kinematic slip imaging of the Mw 3.3 earthquake in the St. Gallen 2013 geothermal reservoir, Switzerland, using an isochrone back projection approach

*Claudio Satriano[1], Eszter Király-Proag[2], Pascal Bernard[1], Stefan Wiemer[2]

1. Institut de Physique du Globe de Paris, France, 2. ETH Swiss Federal Institute of Technology Zurich, Switzerland

In most models and analyses, small earthquakes (i.e., M<4) are considered either point sources or "penny-shaped" solid surfaces with homogeneous or isotropic source properties. While these assumptions may be valid, details of individual earthquakes are more complex. Due to the insufficient resolution of most monitoring networks, micro-earthquakes (M<2) must be still approximated as dislocation on penny-shaped surfaces. But in case of larger events (M>3) recorded on well-distributed local seismic stations, detailed space-time slip pattern within the rupture area can be imaged.

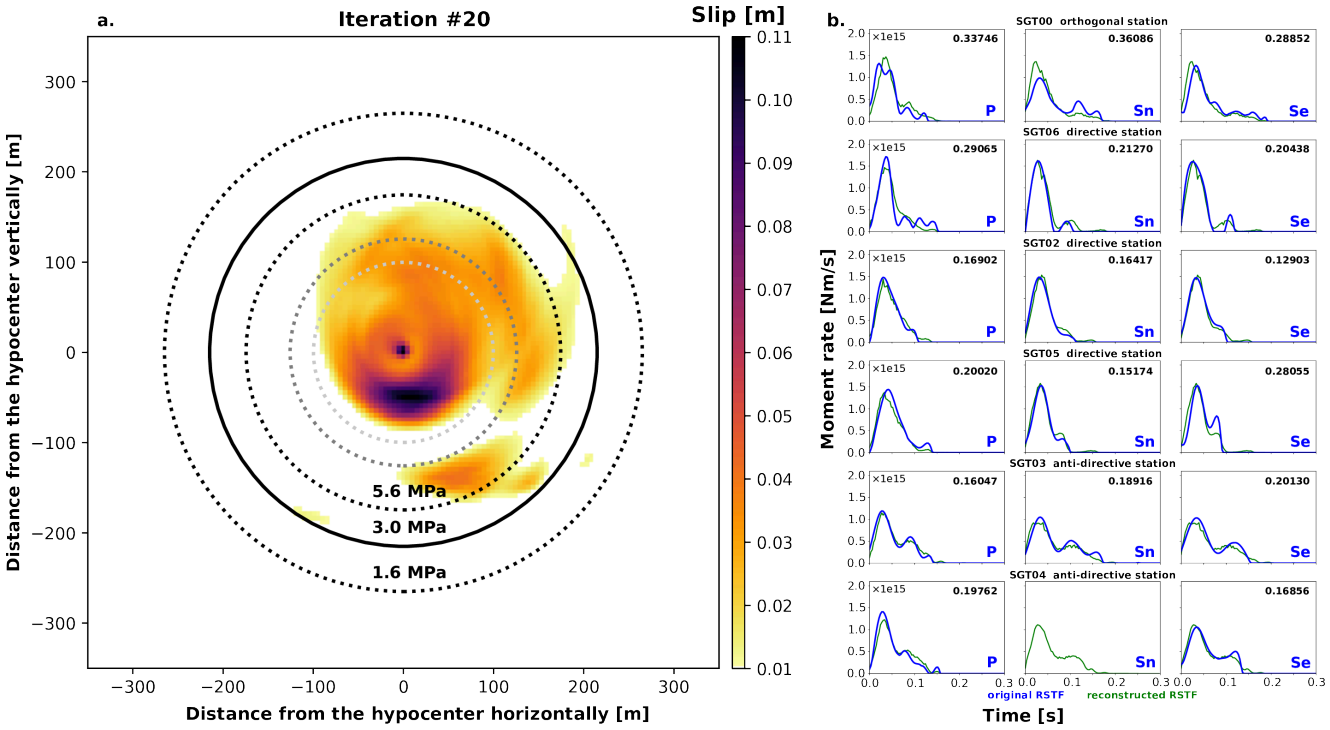
Here, we analyze slip distribution and rupture kinematics of a moderate induced event (ML 3.5) occurred in the St. Gallen geothermal reservoir (NE Switzerland) in 2013. To image the slip of such a small magnitude earthquake, we carry out a two-step procedure: (1) we deconvolve the propagation effects from the seismograms using an empirical Green's function resulting in relative source time functions (RSTF) at all seismic stations; (2) the RSTFs are back-projected to the fault plane using the position of equal time delays, i.e., isochrones.

Results reveal that the mainshock rupture propagates towards NNE from the hypocenter with an average velocity of about 2000 m/s. Spatio-temporal organization of fore- and aftershocks suggests that the mainshock released a previously less active portion of the fault and that the sequence is mainly stress-driven.

Applying this method in an operational environment could enable to quickly map seismic slip allowing assessment of fault asperities and structures involved in the reservoir creation process.

Keywords: Earthquake Source, Earthquake Kinematics, Back Projection, Induced Seismicity

©2019. Japan Geoscience Union. All Right Reserved.



©2019. Japan Geoscience Union. All Right Reserved.

Monitoring induced seismicity with a single seismic station by combining coda wave interferometry with distance geometry solvers

*Francesco Grigoli[1], Simone Cesca[2], Alessandro Vuan[3], Filippo Broggini[1], John Clinton[1], Stefan Wiemer[1]

1. ETH-Zurich, Switzerland, 2. GFZ-Potsdam, Germany, 3. OGS-Trieste, Italy

Microseismic monitoring networks are nowadays extensively used, in combination with risk analysis tools, to ensure the safety of the industrial operations which may trigger or induce earthquakes. However, in many cases the lack of dense enough microseismic monitoring networks affects the performance of the routine data analysis procedures limiting the application of adequate risk mitigation strategies. In this work we propose a novel approach based on the combination of Coda Wave Interferometry (CWI) and Distance Geometry Solvers (DGS) that allow to locate microseismic events by using a single seismic station. The use of CWI allows to determine, for pairs of earthquakes characterized by high similarity of waveforms (i.e. with similar location and focal mechanism), the absolute inter-event distance of each pair (Snieder and Vrijlandt, 2005), while DGS allow to determine their location based only on the given values of the distances between member pairs. Microseismic events can be classified in different families by combining a waveform correlation analysis and a clustering technique. Clustered events are characterized by a high similarity of waveforms, which implies a similarity in both source mechanism and location. In these conditions, the analysis of seismic coda recorded at a single receiver can be used to infer a measure of the spatial separation between two seismic sources. Coda waves are radiated in all directions with a radiation pattern determined by the source mechanism and a small change in the source position affects the interference pattern of the scattered waves that constitute the coda. This change in the coda waves is used to constrain the inter-event distance for each events pair. Absolute locations can be then retrieved by using DGS and considering all inter-event distances, a procedure which requires at least four reference locations. In order to show the potential of this approach we firstly validated the method with a synthetic dataset, then we applied it to the September-October 2013 induced seismicity sequence associated to the underground gas storage operations performed in the offshore Spain. The largest event of the sequence, a magnitude Mw 4.3 earthquake occurred on 2013 October 4th, was preceded by about 1000 seismic events, mostly with magnitude below 2. However, the poor monitoring network in the area (the closest seismic station was located at about ~20 km distance from the platform) did not allow to properly locate these small events. In this work we relocate these low magnitude events, showing that our approach provides better results than those obtained by using standard location methods, making this method particularly useful in poorly monitored areas where only a limited number of stations is available.

References:

Snieder, R., and Vrijlandt, M., 2005. Constraining the source separation with coda wave interferometry: Theory and application to earthquake doublets in the Hayward fault, California, J. Geophys. Res., doi:10.1029/2004JB003317

Keywords: Coda Wave Interferometry, Microseismicity, Induced Seismicity

©2019. Japan Geoscience Union. All Right Reserved.

Automatic Earthquake Locating by Stacking Characteristic Functions in a Source Scanning Method

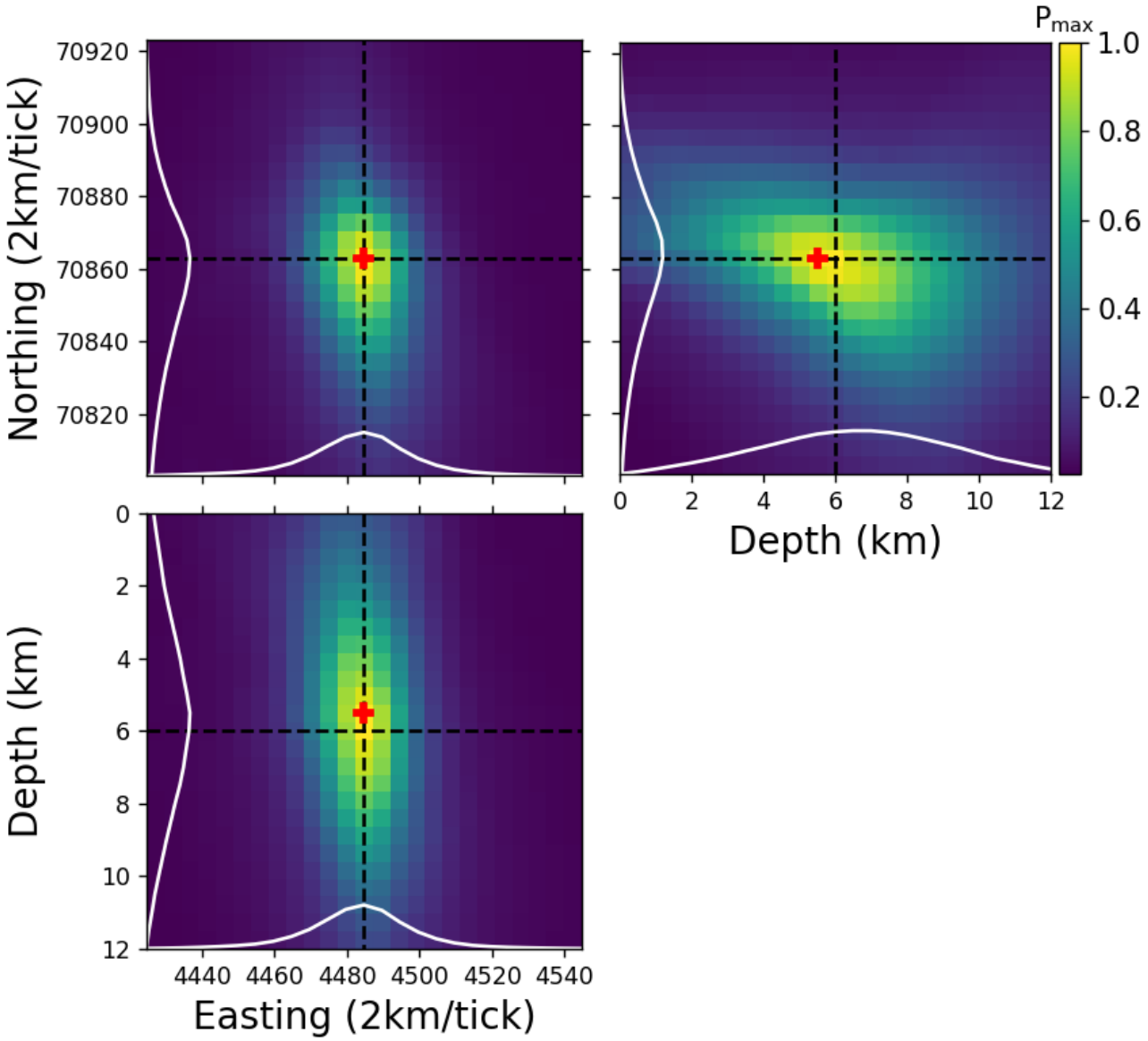
*Hilary Chang[1], Alison Malcolm[1], Frédérick Massin[2], Francesco Grigoli[2]

1. Memorial University of Newfoundland, Earth Sciences, Canada, 2. ETH Zurich, Department of Earth Sciences, Zürich, Switzerland

Exact source locating for microseismic events helps us understand subsurface structures, monitor volcanic activities and assess earthquake hazards. Conventionally, the locating problem can be solved by picking phase arrivals. However, for microseismicity which contains large numbers of low-magnitude events, phase picking is often difficult and time-consuming. In this research, we use an improved waveform-based method to locate microseismic events without phase picking. We use the Source Scanning Algorithm (SSA) to stack the Characteristic Functions (CFs) in time and space, where the maximum stack gives the best estimate of the event origin time and source location. This approach allows us to locate the event automatically by evaluating waveform coherency in terms of changes in amplitude and polarization. We conduct synthetic test using the geometry of the SIL network in Reykjane Peninsula, SW Iceland. The results show that we can locate the synthetic source with error <1km, <0.1s when the noise amplitude is less than the amplitude of the target phase. In addition, stacking CFs that evaluate changes in amplitudes gives more stable results at all noise level, while stacking CFs that consider changes in polarization gives more stable results when the noise varies with frequency. We also conduct field data test using 215 microseismic events (M<2) occurred during Aug 2010 and Mar 2011 recorded by the same network. Our results show that stacking CFs that considers changes in amplitudes gives the closest results to the manually picking method, while stacking a combined version of CF rejects more outliers. In summary, stacking CFs in the SSA provides us with the ability to consider different waveform characteristics and improved noise-robustness in source locating problems. This improved automatic waveform-based procedure offers reliable solutions to large data set with low SNR and helps reduce human intervention.

Keywords: earthquake location, source scanning algorithm, waveform characteristics

©2019. Japan Geoscience Union. All Right Reserved.



©2019. Japan Geoscience Union. All Right Reserved.

Earthquake nowcasting: further development and application to Japan

*Kazuyoshi Nanjo[1], John B. Rundle[2], Tetsuo Sakurada[3]

1. University of Shizuoka, 2. University of California at Davis, 3. SAKURADA&Company

We adopted and further developed the earthquake nowcasting method (Rundle et al., 2016). This method determines the current state of the fault system in a predefined region and its current level of progress through the earthquake cycle, using only empirical data: magnitudes (M) and times of earthquakes in the region. The characteristic is that the method does not involve any model other than the idea of an earthquake cycle. We performed a case study from southern Kanto, using the earthquake catalog maintained by Japan Meteorological Agency (JMA). Two earthquake magnitudes are selected, one large ($M \geqq M_L$), and one small ($M \geqq M_S$), where $M_L > M_S$. The method utilizes the number of small earthquakes that occurs between pairs of large earthquakes. The cumulative probability distribution of these values is obtained. The earthquake potential score (EPS), an index of the current level of the progress through the earthquake cycle, is defined by the “natural time”, the number of small earthquakes that has occurred since the last large earthquake, the point where this number falls on the cumulative probability distribution. For southern Kanto, we used earthquakes since 1926 with depths shallower than 150 km and set M_L=6.0 and M_S=4.2. The obtained result as of December 20, 2018 is EPS of 8%. This is interpreted as an indication that if a large (M6+) earthquake occurred on this date, the recurrence interval would be relatively short. Errors that arise from statistics-based estimation such as this must be considered so that we introduced the calculation of uncertainties to the earthquake nowcasting, using a bootstrap approach. Taking into account the contribution of these errors to the EPS calculations, we conclude that the earthquake nowcasting generates stable estimates of EPS for southern Kanto (Nanjo, 2018). To check the stability estimation for other regions, we computed EPS and its uncertainty for selected regions in Japan. We also discuss a technique of spatial mapping of EPS over the Japan’s mainlands. This technique allows us to move towards a full description of current EPS as a function of space, providing possible usability for ranking locations on the earthquake hazard.

Keywords: nowcasting, earthquake, natural time

©2019. Japan Geoscience Union. All Right Reserved.

[E] Poster | S (Solid Earth Sciences)：S-SS Seismology

Sun. May 26, 2019 5:15 PM - 6:30 PM JST | Sun. May 26, 2019 8:15 AM - 9:30 AM UTC | Poster Hall International Exhibition Hall8, Makuhari Messe_24

[S-SS04] New methods for seismicity characterization

convener:Francesco Grigoli(ETH-Zurich, Swiss Seismological Service), Aitaro Kato(Earthquake Research Institute, the University of Tokyo), Yosuke Aoki(Earthquake Research Institute, University of Tokyo), Claudio Satriano(Institut de Physique du Globe de Paris)

In the last two decades the number of high quality seismic instruments being installed around the world has grown exponentially and probably will continue to grow in the coming decades. This data explosion has shown the limits of the current standard routine seismic analysis, often performed manually by seismologists. Exploiting the massive amount of data is a challenge that can be overcome by using new generation, fully automated and noise robust seismic processing techniques. In the last years waveform-based detection and location methods have grown in popularity and their application have dramatically improved seismic monitoring capability. More recently, Machine Learning techniques, which are a perfect playground for data-intensive applications, are showing promising results in seismicity characterization applications opening new horizons for the development of innovative, fully automated and noise robust seismic analysis methods. Such techniques are particularly useful when working with datasets characterised by a massive number of weak events with low signal-to-noise ratio, such as those collected in induced seismicity and volcanic monitoring operations. This session aims to bring to light new methods that can be applied to large datasets, either retro-actively or in near-real time, to characterize seismicity (i.e. detection, location, magnitude and source mechanisms estimation) at different scales and in different environments. We thus encourage contributions that demonstrate how the proposed methods helps improve our understanding of earthquake and/or volcanic processes.

[SSS04-P01] Constraint of focal mechanisms of induced seismicity by using misfit angles based on known *in-situ* stress

*Yusuke Mukuhira[1], Makoto Naoi[2], Michael C Fehler[3], Hirokazu Moriya[5], Takatoshi Ito[1], Hiroshi Asanuma[4], Markus O Häring[6] (1.Institute of Fluid Science, Tohoku University, 2.Disaster Prevention Research Institute, Kyoto University, 3.Earth Resources Laboratory, MIT, 4.FREA, AIST, 5.School of Engineering, Tohoku University, 6.Häring GeoProject)

[SSS04-P02] Kinematic slip imaging of the Mw 3.3 earthquake in the St. Gallen 2013 geothermal reservoir, Switzerland, using an isochrone back projection approach

*Claudio Satriano[1], Eszter Király-Proag[2], Pascal Bernard[1], Stefan Wiemer[2] (1.Institut de Physique du Globe de Paris, France, 2.ETH Swiss Federal Institute of Technology Zurich, Switzerland)

[SSS04-P03] Monitoring induced seismicity with a single seismic station by combining coda wave interferometry with distance geometry solvers

*Francesco Grigoli[1], Simone Cesca[2], Alessandro Vuan[3], Filippo Broggini[1], John Clinton[1], Stefan Wiemer[1] (1.ETH-Zurich, Switzerland, 2.GFZ-Potsdam, Germany, 3.OGS-Trieste, Italy)

[SSS04-P04] Automatic Earthquake Locating by Stacking Characteristic Functions in a Source Scanning Method

★Invited Papers

*Hilary Chang[1], Alison Malcolm[1], Frédérick Massin[2], Francesco Grigoli[2] (1.Memorial University of Newfoundland, Earth Sciences, Canada, 2. ETH Zurich, Department of Earth Sciences, Zürich, Switzerland)

[SSS04-P05] Earthquake nowcasting: further development and application to Japan

*Kazuyoshi Nanjo[1], John B. Rundle[2], Tetsuo Sakurada[3] (1.University of Shizuoka, 2.University of California at Davis, 3.SAKURADA&Company)

Constraint of focal mechanisms of induced seismicity by using misfit angles based on known *in-situ* stress

*Yusuke Mukuhira[1], Makoto Naoi[2], Michael C Fehler[3], Hirokazu Moriya[5], Takatoshi Ito[1], Hiroshi Asanuma[4], Markus O Häring[6]

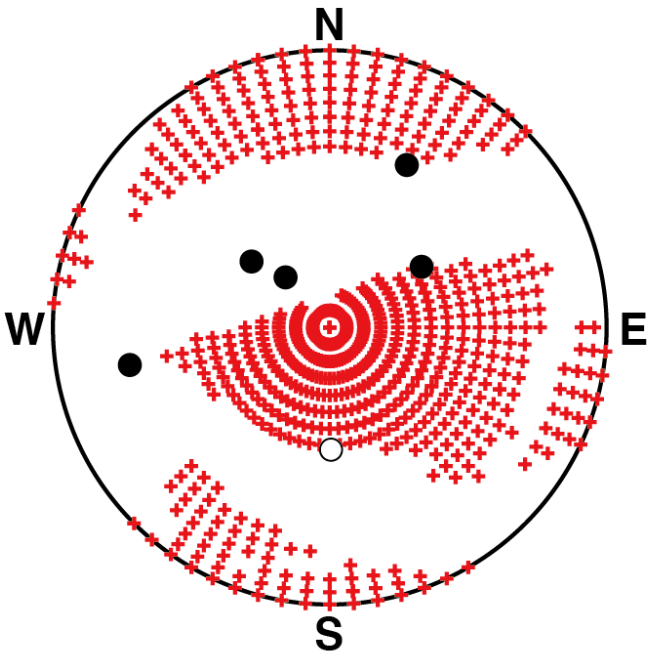
1. Institute of Fluid Science, Tohoku University, 2. Disaster Prevention Research Institute, Kyoto University, 3. Earth Resources Laboratory, MIT, 4. FREA, AIST, 5. School of Engineering, Tohoku University, 6. Häring GeoProject

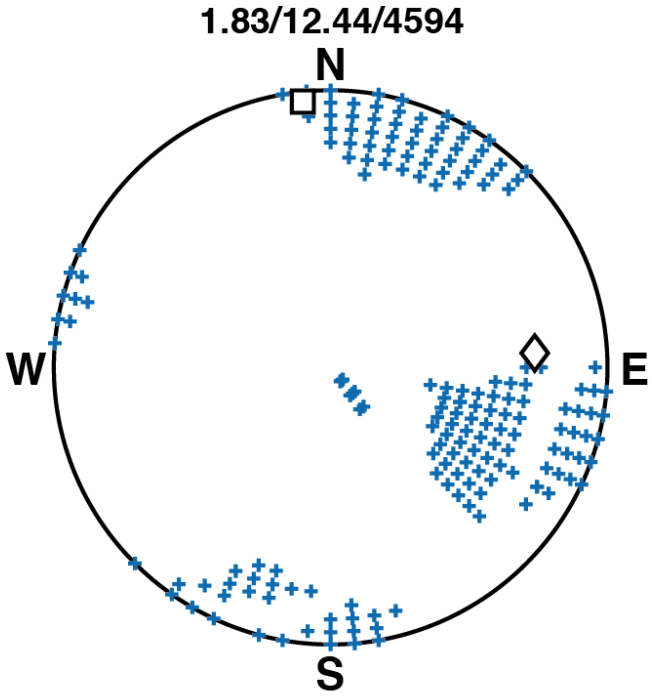
Microseismic monitoring is essential for successful hydraulic stimulation/fracking in unconventional oil/gas development, engineered geothermal system development and carbon capture and sequestration. In addition to the hypocenter location of the microseismicity, knowledge of the geometry of the fracture is also crucial for better understanding of fractured reservoir, fluid flow, and design of the energy extraction. Geofluid flows in the fracture and its permeability are correlated with the relation of the geometry of the fracture and in-situ stress. Fracture orientation can be estimated by the seismological method such as moment tensor inversion or focal mechanism analysis, only when the waveforms of the events are well recorded by a number of well-distributed stations. However, in realistic microseismic monitoring situations, it is often difficult to constrain the focal mechanism of microseismicity from first motion information due to the small number of stations.

We proposed a method to improve the estimates of focal mechanisms by introducing in-situ stress information from borehole logging information. We eliminate candidate focal mechanisms that are consistent with first motion data but cannot have shear slip under a given stress state and pore pressure increase. In this study, we also check the consistency between the shear slip vector estimated from the stress state and the rakes. We compare the shear slip vector and the slip vector from the rake. Then we reject the fault if the difference in the two vectors is significantly large. With this process, we reject the fault planes and auxiliary planes which are not consistent with stress state. We apply this method to induced seismicity dataset from Basel, Switzerland, where we already have well-constrained focal mechanisms estimated by many surface stations over a large region. We use these focal mechanisms as references to check whether our method can constrain the range of focal mechanisms using a small number of nearby stations. We find that the consistency check between two vectors significantly and reliably limits the range of focal mechanisms. Furthermore, we combine the constrained range of focal mechanism by this method and that by stability analysis to have more constraint of focal mechanisms satisfying the conditions of the geomechanical problem.

Keywords: Induced seismicity, Focal mechanism, In-situ stress

©2019. Japan Geoscience Union. All Right Reserved.





©2019. Japan Geoscience Union. All Right Reserved.

Kinematic slip imaging of the Mw 3.3 earthquake in the St. Gallen 2013 geothermal reservoir, Switzerland, using an isochrone back projection approach

*Claudio Satriano[1], Eszter Király-Proag[2], Pascal Bernard[1], Stefan Wiemer[2]

1. Institut de Physique du Globe de Paris, France, 2. ETH Swiss Federal Institute of Technology Zurich, Switzerland

In most models and analyses, small earthquakes (i.e., M<4) are considered either point sources or "penny-shaped" solid surfaces with homogeneous or isotropic source properties. While these assumptions may be valid, details of individual earthquakes are more complex. Due to the insufficient resolution of most monitoring networks, micro-earthquakes (M<2) must be still approximated as dislocation on penny-shaped surfaces. But in case of larger events (M>3) recorded on well-distributed local seismic stations, detailed space-time slip pattern within the rupture area can be imaged.

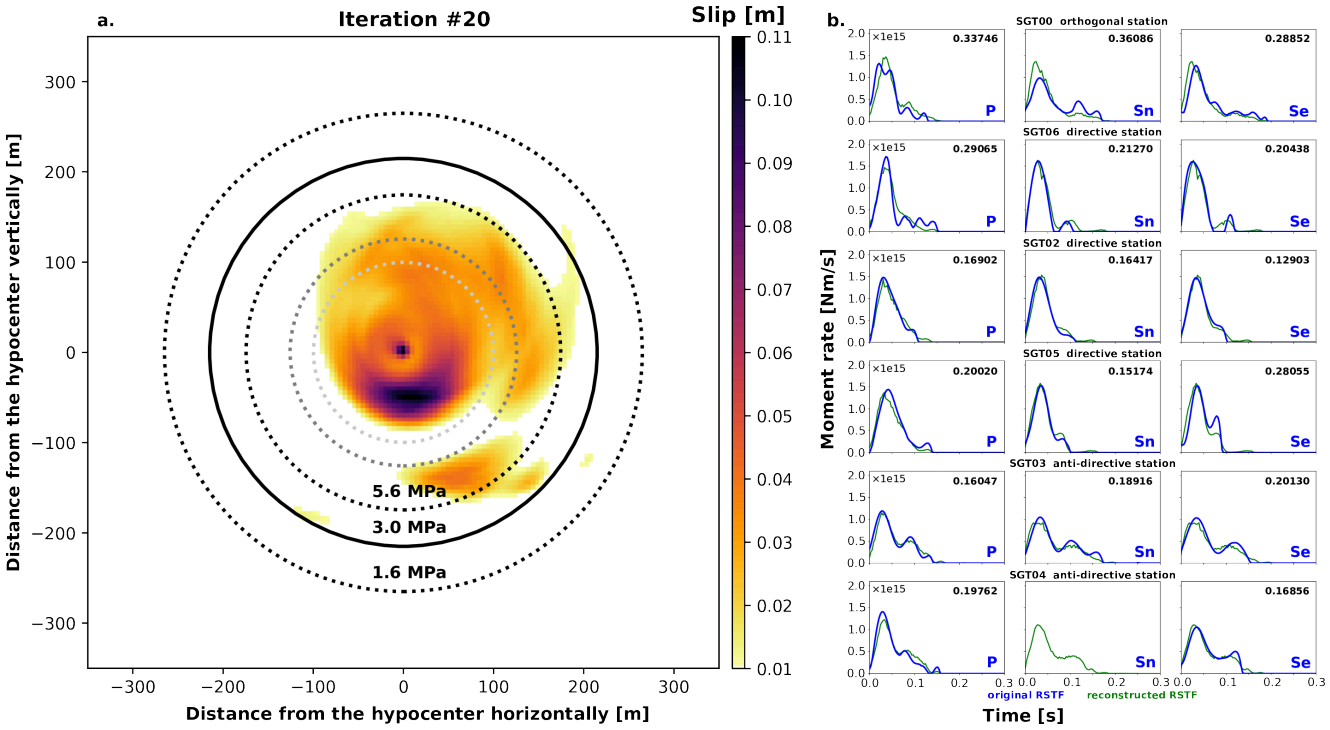
Here, we analyze slip distribution and rupture kinematics of a moderate induced event (ML 3.5) occurred in the St. Gallen geothermal reservoir (NE Switzerland) in 2013. To image the slip of such a small magnitude earthquake, we carry out a two-step procedure: (1) we deconvolve the propagation effects from the seismograms using an empirical Green's function resulting in relative source time functions (RSTF) at all seismic stations; (2) the RSTFs are back-projected to the fault plane using the position of equal time delays, i.e., isochrones.

Results reveal that the mainshock rupture propagates towards NNE from the hypocenter with an average velocity of about 2000 m/s. Spatio-temporal organization of fore- and aftershocks suggests that the mainshock released a previously less active portion of the fault and that the sequence is mainly stress-driven.

Applying this method in an operational environment could enable to quickly map seismic slip allowing assessment of fault asperities and structures involved in the reservoir creation process.

Keywords: Earthquake Source, Earthquake Kinematics, Back Projection, Induced Seismicity

©2019. Japan Geoscience Union. All Right Reserved.



©2019. Japan Geoscience Union. All Right Reserved.

Monitoring induced seismicity with a single seismic station by combining coda wave interferometry with distance geometry solvers

*Francesco Grigoli[1], Simone Cesca[2], Alessandro Vuan[3], Filippo Broggini[1], John Clinton[1], Stefan Wiemer[1]

1. ETH-Zurich, Switzerland, 2. GFZ-Potsdam, Germany, 3. OGS-Trieste, Italy

Microseismic monitoring networks are nowadays extensively used, in combination with risk analysis tools, to ensure the safety of the industrial operations which may trigger or induce earthquakes. However, in many cases the lack of dense enough microseismic monitoring networks affects the performance of the routine data analysis procedures limiting the application of adequate risk mitigation strategies. In this work we propose a novel approach based on the combination of Coda Wave Interferometry (CWI) and Distance Geometry Solvers (DGS) that allow to locate microseismic events by using a single seismic station. The use of CWI allows to determine, for pairs of earthquakes characterized by high similarity of waveforms (i.e. with similar location and focal mechanism), the absolute inter-event distance of each pair (Snieder and Vrijlandt, 2005), while DGS allow to determine their location based only on the given values of the distances between member pairs. Microseismic events can be classified in different families by combining a waveform correlation analysis and a clustering technique. Clustered events are characterized by a high similarity of waveforms, which implies a similarity in both source mechanism and location. In these conditions, the analysis of seismic coda recorded at a single receiver can be used to infer a measure of the spatial separation between two seismic sources. Coda waves are radiated in all directions with a radiation pattern determined by the source mechanism and a small change in the source position affects the interference pattern of the scattered waves that constitute the coda. This change in the coda waves is used to constrain the inter-event distance for each events pair. Absolute locations can be then retrieved by using DGS and considering all inter-event distances, a procedure which requires at least four reference locations. In order to show the potential of this approach we firstly validated the method with a synthetic dataset, then we applied it to the September-October 2013 induced seismicity sequence associated to the underground gas storage operations performed in the offshore Spain. The largest event of the sequence, a magnitude Mw 4.3 earthquake occurred on 2013 October 4th, was preceded by about 1000 seismic events, mostly with magnitude below 2. However, the poor monitoring network in the area (the closest seismic station was located at about ~20 km distance from the platform) did not allow to properly locate these small events. In this work we relocate these low magnitude events, showing that our approach provides better results than those obtained by using standard location methods, making this method particularly useful in poorly monitored areas where only a limited number of stations is available.

References:

Snieder, R., and Vrijlandt, M., 2005. Constraining the source separation with coda wave interferometry: Theory and application to earthquake doublets in the Hayward fault, California, J. Geophys. Res., doi:10.1029/2004JB003317

Keywords: Coda Wave Interferometry, Microseismicity, Induced Seismicity

©2019. Japan Geoscience Union. All Right Reserved.

Automatic Earthquake Locating by Stacking Characteristic Functions in a Source Scanning Method

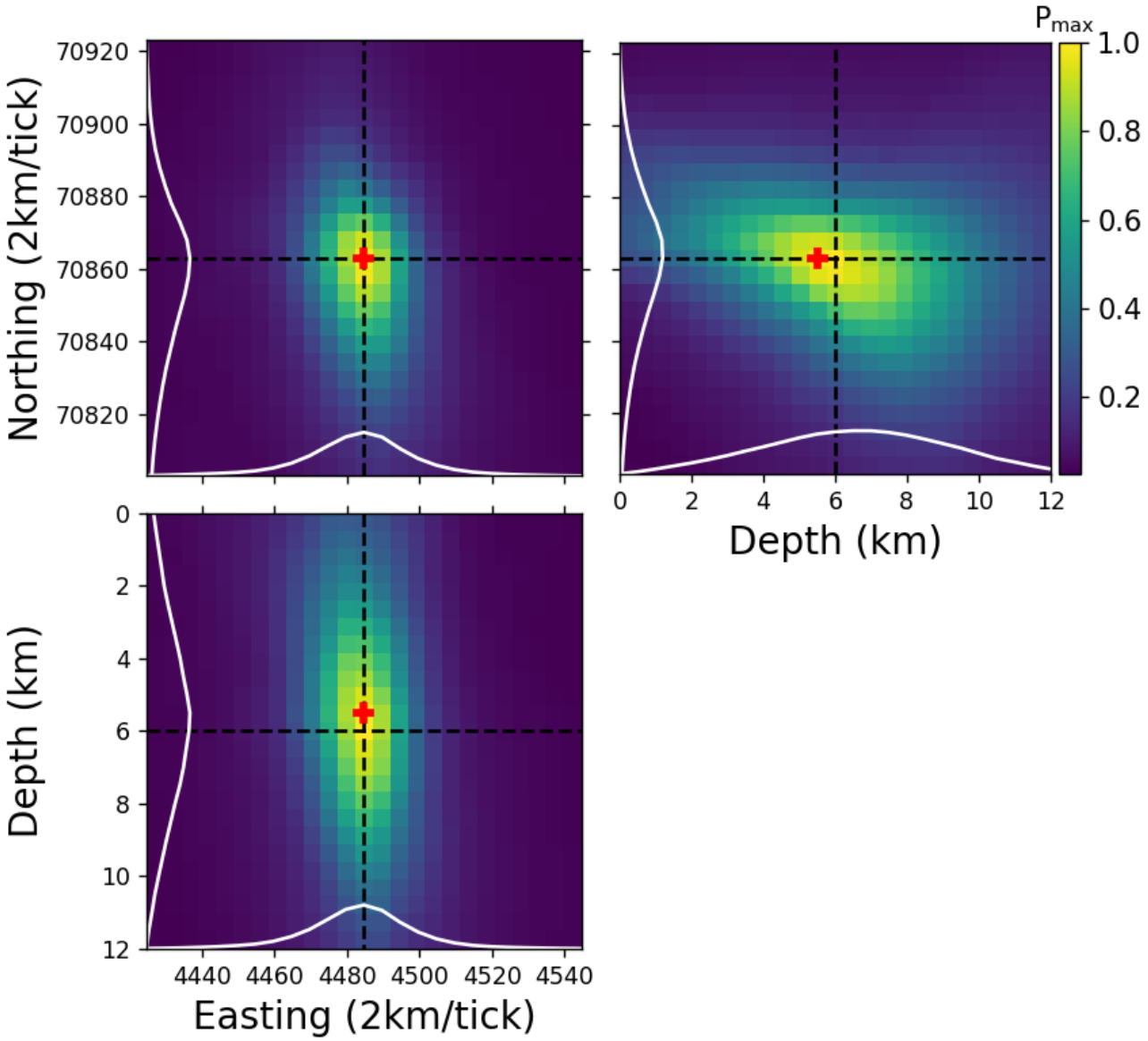
*Hilary Chang[1], Alison Malcolm[1], Frédérick Massin[2], Francesco Grigoli[2]

1. Memorial University of Newfoundland, Earth Sciences, Canada, 2. ETH Zurich, Department of Earth Sciences, Zürich, Switzerland

Exact source locating for microseismic events helps us understand subsurface structures, monitor volcanic activities and assess earthquake hazards. Conventionally, the locating problem can be solved by picking phase arrivals. However, for microseismicity which contains large numbers of low-magnitude events, phase picking is often difficult and time-consuming. In this research, we use an improved waveform-based method to locate microseismic events without phase picking. We use the Source Scanning Algorithm (SSA) to stack the Characteristic Functions (CFs) in time and space, where the maximum stack gives the best estimate of the event origin time and source location. This approach allows us to locate the event automatically by evaluating waveform coherency in terms of changes in amplitude and polarization. We conduct synthetic test using the geometry of the SIL network in Reykjane Peninsula, SW Iceland. The results show that we can locate the synthetic source with error <1km, <0.1s when the noise amplitude is less than the amplitude of the target phase. In addition, stacking CFs that evaluate changes in amplitudes gives more stable results at all noise level, while stacking CFs that consider changes in polarization gives more stable results when the noise varies with frequency. We also conduct field data test using 215 microseismic events (M<2) occurred during Aug 2010 and Mar 2011 recorded by the same network. Our results show that stacking CFs that considers changes in amplitudes gives the closest results to the manually picking method, while stacking a combined version of CF rejects more outliers. In summary, stacking CFs in the SSA provides us with the ability to consider different waveform characteristics and improved noise-robustness in source locating problems. This improved automatic waveform-based procedure offers reliable solutions to large data set with low SNR and helps reduce human intervention.

Keywords: earthquake location, source scanning algorithm, waveform characteristics

©2019. Japan Geoscience Union. All Right Reserved.



©2019. Japan Geoscience Union. All Right Reserved.

Earthquake nowcasting: further development and application to Japan

*Kazuyoshi Nanjo[1], John B. Rundle[2], Tetsuo Sakurada[3]

1. University of Shizuoka, 2. University of California at Davis, 3. SAKURADA&Company

We adopted and further developed the earthquake nowcasting method (Rundle et al., 2016). This method determines the current state of the fault system in a predefined region and its current level of progress through the earthquake cycle, using only empirical data: magnitudes (M) and times of earthquakes in the region. The characteristic is that the method does not involve any model other than the idea of an earthquake cycle. We performed a case study from southern Kanto, using the earthquake catalog maintained by Japan Meteorological Agency (JMA). Two earthquake magnitudes are selected, one large ($M \geqq M_L$), and one small ($M \geqq M_S$), where $M_L > M_S$. The method utilizes the number of small earthquakes that occurs between pairs of large earthquakes. The cumulative probability distribution of these values is obtained. The earthquake potential score (EPS), an index of the current level of the progress through the earthquake cycle, is defined by the “natural time”, the number of small earthquakes that has occurred since the last large earthquake, the point where this number falls on the cumulative probability distribution. For southern Kanto, we used earthquakes since 1926 with depths shallower than 150 km and set M_L=6.0 and M_S=4.2. The obtained result as of December 20, 2018 is EPS of 8%. This is interpreted as an indication that if a large (M6+) earthquake occurred on this date, the recurrence interval would be relatively short. Errors that arise from statistics-based estimation such as this must be considered so that we introduced the calculation of uncertainties to the earthquake nowcasting, using a bootstrap approach. Taking into account the contribution of these errors to the EPS calculations, we conclude that the earthquake nowcasting generates stable estimates of EPS for southern Kanto (Nanjo, 2018). To check the stability estimation for other regions, we computed EPS and its uncertainty for selected regions in Japan. We also discuss a technique of spatial mapping of EPS over the Japan’s mainlands. This technique allows us to move towards a full description of current EPS as a function of space, providing possible usability for ranking locations on the earthquake hazard.

Keywords: nowcasting, earthquake, natural time

©2019. Japan Geoscience Union. All Right Reserved.

[E] Poster | S (Solid Earth Sciences)：S-SS Seismology

Sun. May 26, 2019 10:45 AM - 12:15 PM JST | Sun. May 26, 2019 1:45 AM - 3:15 AM UTC | Poster Hall International Exhibition Hall8, Makuhari Messe_6

[S-SS05] Induced and triggered seismicity: case-studies, monitoring and modeling techniques

convener:Luca Urpi(Swiss Seismological Service - ETH Zurich), Bogdan Enescu(Department of Geophysics, Kyoto University), Yosuke Aoki(Earthquake Research Institute, University of Tokyo), Francesco Grigoli(ETH-Zurich, Swiss Seismological Service)

Induced and triggered seismicity occurs in conjunction with human activities such as reservoir impoundments, mining operations, conventional and non-conventional hydrocarbon production, geothermal energy exploitation, wastewater disposal, CO2 sequestration and gas storage operations as well as volcanic and hydrogeological processes. The stability of faults is affected by external solicitations such as pore-pressure diffusion, relaxation effects as well as stress field perturbations related to mass and/or volume changes, dike intrusions and earthquake-earthquake interactions. A better understanding of the physical processes governing induced and triggered seismicity is important for the assess the risk of current and future industrial activities, including the geological disposal of nuclear waste.

The study of Induced and triggered seismicity is inherently an interdisciplinary problem, which requires the combination of seismological, hydrogeological, geodetic data and a wide range of modeling approaches. This session welcome contributions covering the analysis and modeling of induced and triggered seismicity at different spatial scales and environments.

Relevant topics to be presented include but are not limited to case-studies of induced and triggered seismicity, spatio-temporal variations of physical parameters (including stress, pressure and temperature changes), spatio-temporal patterns of seismicity, modeling and risk mitigation strategies.

The goal of the session is to cover both theoretical and experimental aspects of these topics.

[SSS05-P01] Harmonic seismic waves excited by far-field earthquakes

*Osamu Murakami[1] (1.Tono Rearch Institute of Earthquake Science, Association for the Development of Earthquake Prediction)

[SSS05-P02] **Dynamic triggering of microseismicity around Yunnan following the 2004 Sumatra and 2012 Indian Ocean Earthquakes**

*Lu Li[1], Baoshan Wang[1,4], Zhigang Peng[2], Danning Li[3] (1.Institute of Geophysics, CEA, 2.Georgia Tech, 3.Yunnan Earthquake Agency, 4.USTC)

[SSS05-P03] Megathrust-inducing azimuthal seismic anisotropy in local and regional crusts

*Tae-Kyung Hong[1], Junhyung Lee[1], Ilgoo Kim[1], Seongjun Park[1] (1.Department of Earth System Sciences, Yonsei University)

[SSS05-P04] **A Novel Method to Estimate Fracture Permeability: Combining microseismic observational data and reservoir engineering model**

*Meihua Yang[1,2], Yusuke Mukuhira[2], Takatoshi Ito[2] (1.State Key Laboratory of Oil and Gas Geology and Exploitation, Chendu University of Technology (China) , 2.Institute of Fluid Science, Tohoku University (Japan))

[SSS05-P05] Doublet Earthquake Triggering for the April 2014 Events in the Solomon Islands

*Calvin Luiramo Qwana[1], Masatoshi Miyazawa[2], James Mori[2] (1.Graduate School of Science, Kyoto University, 2.DPRI, Kyoto Univ.)

[SSS05-P06] Thermal pressurization in a deep geological repository as a possible mechanism for fault reactivation

*Luca Urpi[1], Antonio Pio Rinaldi[1], Jonny Rutqvist[2], Stefan Wiemer[1] (1.Swiss Seismological Service, ETH Zurich, Switzerland, 2.Energy Geosceinces Division, LBNL, USA)

Harmonic seismic waves excited by far-field earthquakes

*Osamu Murakami[1]

1. Tono Rearch Institute of Earthquake Science, Association for the Development of Earthquake Prediction

It was observed the very harmonic seismic waves with a period of 17 s after 09:30 (UT) on Nov. 11 in 2018, at the mostly seismic stations in the global broadband seismograph network. It is assumed that the hypocenter of the harmonic waves was off Mayotte Island in the northern Mozambique channels between the continent of Africa and Madagascar Island. The physical cause of these waves remains unclear.

In order to understand such characteristic seismic waves, I firstly calculated the running spectra from Nov. 1 to Nov. 20 in 2018, using the observed seismograms at the station, ABPO, operated by IRIS/IDA. This station is the nearest station from the assumed hypocenter among the stations of the global seismograph network. From these running spectra, I found that the harmonic waves excited by the near- and far-field earthquakes. There were 10 far-field earthquakes whose magnitudes were larger than 6, in this period. Because the depths of 3 earthquakes in these 10 earthquakes were deeper than 100 km, I considered the remaining 7 shallow earthquakes. I investigated 2 larger earthquakes than others. The first one occurred in Jan Mayen Island region on Nov. 9 in 2018 (Mw6.7, hereafter EQ-J2018), and the second one occurred in South Sandwich Islands region on Nov. 15 in 2018 (Mw6.4, EQ-S2018). There was another earthquake near EQ-J2018. It occurred on Aug. 20 in 2012 (Mw6.7, EQ-J2012). There were two similar earthquakes near EQ-S2018, occurred on Dec. 8 in 2010 (Mw6.3, EQ-S2010) and on May 10 in 2017 (Mw6.5, EQ-S2017). From the comparison of the observed seismic waves between the similar hypocenter earthquakes, I found that the amplitudes of the surface waves in the earthquakes in 2018 (EQ-J2018, EQ-S2018) were several times as much as the ones in the previous earthquakes (EQ-J2012, EQ-S2010, EQ-S2017), at some stations.

In this study, I will show the features of these harmonic waves and to discuss the possible mechanisms.

Keywords: harmonic seismic waves, Mayotte Island, surface waves

©2019. Japan Geoscience Union. All Right Reserved.

Dynamic triggering of microseismicity around Yunnan following the 2004 Sumatra and 2012 Indian Ocean Earthquakes

*Lu Li[1], Baoshan Wang[1,4], Zhigang Peng[2], Danning Li[3]

1. Institute of Geophysics, CEA, 2. Georgia Tech, 3. Yunnan Earthquake Agency, 4. USTC

We conduct a systematic detection of microseismicity around Yunnan following the 2004 Mw9.1 Sumatra and 2012 Mw8.6 Indian Ocean earthquakes to better understand the physical mechanism of dynamic triggering. Based on seismicity analysis on China Earthquake Network Center (CENC) catalog and spectral analysis of continuous waveforms, we find clear evidence of triggered seismicity in Yunnan immediately after the 2004 mainshock and a lack of instantaneous triggering following the 2012 mainshock. We further apply a matched filter technique to detect microearthquakes in Tengchong volcanic region 15 days before and 15 days after the 2012 mainshock. The seismicity rate remains stable immediately after the 2012 mainshock, and increases in the next few days, indicating a possible delayed triggering. In addition, we find possible evidence of remote triggering near the city of Yibin in Southern Sichuan Province, near the sites with ongoing shale gas development. We also examine other magnitude > 8 earthquakes from the Sumatra region and do not find any additional evidence of dynamic triggering around Yunnan. We suggest that the absolute value of dynamic stress change is the most important factor to explain why the 2004 Sumatra event triggered a widespread seismicity rate increase around Yunnan, while other great events around Sumatra did not.

Keywords: dynamic triggering, dynamic stress changes, Yunnan region

©2019. Japan Geoscience Union. All Right Reserved.

Megathrust-inducing azimuthal seismic anisotropy in local and regional crusts

*Tae-Kyung Hong[1], Junhyung Lee[1], Ilgoo Kim[1], Seongjun Park[1]

1. Department of Earth System Sciences, Yonsei University

Megathrust earthquakes produce large coseismic and postseismic lithospheric displacements. The 2011 M9.0 Tohoku-Oki megathrust earthquakes produced large displacements up to regional distances. The lithospheric displacements directing to the epicenter on the convergent plate boundary developed transient uniaxial tension field over the backarc lithospheres. The Vp/Vs changes display characteristic 2 theta azimuthal variations in the upper crust of the Japanese islands, ranging between -0.0458 and 0.0422. Large lateral variations in Vp/Vs changes suggest medium-dependent perturbation. The lower crust of the Korean Peninsula in distances of ~1300 km displayed coseismic velocity changes of 3 % after the megathrust earthquake. The Vp/Vsratios and seismic velocities recovered gradually over time. Peak Vp/Vs and seismic velocity changes were observed along paths subparallel or subperpendicular to the directions toward the megathrust earthquake. The azimuthal seismic anisotropy may have developed from preferential crack orientation and azimuthal lithostatic stress changes. It appears that recovery of the medium properties may take decades. A series of moderate-sized earthquakes occurred as a consequence of medium response to the temporal evolution of stress field in the Korean Peninsula.

Keywords: megathrust earthquake, crustal deformation, induced seismicity

©2019. Japan Geoscience Union. All Right Reserved.

A Novel Method to Estimate Fracture Permeability: Combining microseismic observational data and reservoir engineering model

*Meihua Yang[1,2], Yusuke Mukuhira[2], Takatoshi Ito[2]

1. State Key Laboratory of Oil and Gas Geology and Exploitation, Chendu University of Technology (China) , 2. Institute of Fluid Science, Tohoku University (Japan)

Effective utilization of geothermal resources is crucial to realize a sustainable society. Geothermal resources are widely present in Japan and the western United States, and the usage of geothermal resources are gradually increasing with many efforts. Meanwhile, the exploration and exploitation of geothermal resources in China has gradually developed. One of the challenges in conventional/next generation geothermal development (Enhanced/Engineered Geothermal System: EGS) is to understand the hydraulic properties of the geothermal reservoir. We often attempt to measure the hydraulic property (permeability or diffusivity) by wellbore tests or by using indicators such as migration of microseismicity. However, these quantities are often interpreted as representative value of hydraulic property for entire reservoir. Meanwhile, geothermal fluid circulates or flows in the existing/nucleated fracture system where permeability varies depending on condition of each fractures. Geothermal fluid is extracted from those permeable fractures very locally throughout production well drilled into the specific part of reservoir. Therefore, we need to have the best estimates of permeability for each fracture (local permeability) beyond representative permeability (global permeability). In addition, it is important to consider how the hydraulic properties can be affected by changes in the state of stress in the subsurface. This information is beneficial for design of geothermal energy extraction system and understanding of hydrology in the reservoir.

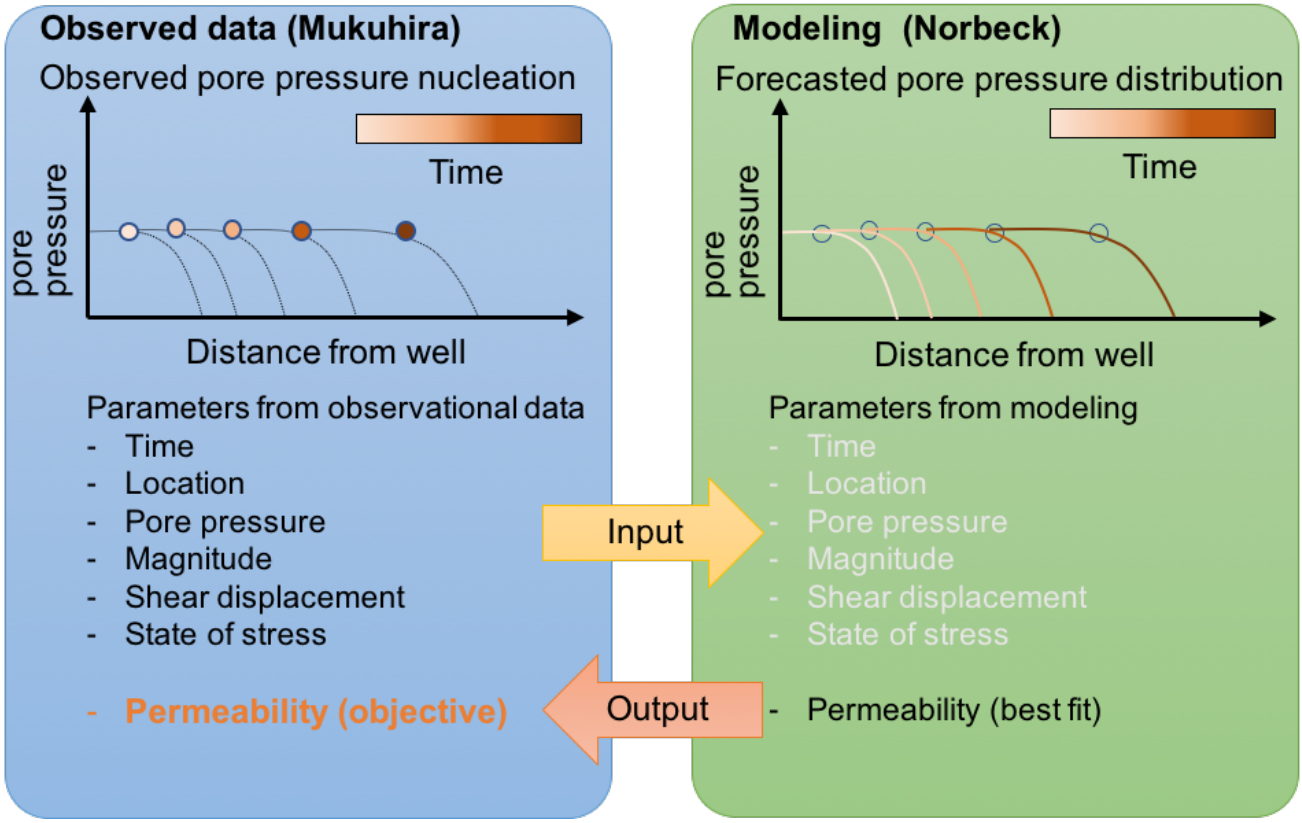
In this paper, we propose a novel method to estimate permeability of each individual fractures which experience shear slip at hydraulic stimulation. The spatiotemporal distribution of reservoir fluid pressure will be estimated using microseismic data. Using a hydromechanical fractured reservoir model, we will invert for the shear-dilation enhanced permeability change that controls the evolution of pressure along fractures and faults.

The first step is to estimate pore pressure distribution with microseismic data from real EGS field and observe how pore pressure migrated within single fracture (Figure 1 left: coloured circles). Meanwhile, using the hydromechanical fractured reservoir numerical model, we simulate pore pressure distribution within one fracture of given permeability and evaluate the evolution of hydraulic properties during a stimulation treatment (Figure 1 right: coloured sold lines). Therefore, we can use parameters from observational data as input parameters into hydromechanical model and estimate the best permeability which explain observed pore pressure distribution. We will also simulate all microseismic clusters and estimate permeability of each fractures. Then analyse the fracture permeability distribution (permeability mapping) in the study area.

In this research, it is the first attempt to estimate local permeability for each fracture. So far, only global permeability can be estimated by wellbore test or microseismic data and this permeability is not effective for each fracture in subsurface. Information of local permeability is quite valuable for designing a sustainable energy extraction system. Local permeability information also brings the way to model the flow of geothermal fluid in the reservoir, which is important for long-term management of geothermal resources.

©2019. Japan Geoscience Union. All Right Reserved.

Keywords: Permeability, Microseismic, Reservoir engineering model



©2019. Japan Geoscience Union. All Right Reserved.

Doublet Earthquake Triggering for the April 2014 Events in the Solomon Islands

*Calvin Luiramo Qwana[1], Masatoshi Miyazawa[2], James Mori[2]

1. Graduate School of Science, Kyoto University, 2. DPRI, Kyoto Univ.

In 2014 at 20:14 (UTC) on April 12th and 12:36 on April 13th, a doublet earthquake with moment magnitudes of M7.6 and M7.4, respectively occurred near Makira Island (San Cristobal) in the Solomon Islands. The depths of the events were 27 km and 37 km, respectively (GCMT). To understand the interrelation between the first (M7.6) and second (M7.4) events , we check the role of Coulomb stress triggering on aftershocks that follow the M7.6 main shock and the coulomb failure stress changes on both of the focal mechanism nodal planes for the second event. To understand if the coulomb stress triggering played a role in the evolution of the triggered event M7.4 earthquake, we evaluate the transient aftershocks from the M7.6 to see if it promoted failure on the rupture plane for the second event (M7.4). We evaluate the doublet source process of the events and recover the slip distribution on each of the faults. We use an iterative inversion method by Kikuchi and Kanamori (1991) for the teleseismic P waveforms recorded from more than 20 stations of the Global Seismographic Network in a distance range of 30˚ to 90˚. A fault plane with fixed strike and dip is placed in the region of the earthquake hypocenter and divided into subfaults, and a constant rupture velocity of 2.5 km/s is assumed. Synthetic waveforms are calculated at the teleseismic stations for dislocations at each subfault. Using the synthetic Green’ s functions, the observed seismograms are inverted to determine the fault plane and obtain the distribution of slips for the two events. The results show that the mechanism for the Mw7.6 first event is left-lateral strike-slip faulting for a plane of strike 116, dip 74 , and rake 24. The other NW-SE oriented nodal plane is almost parallel to Australian and Pacific plate boundary. Results for the mechanism of the Mw7.4 event indicates thrust faulting on fault plane oriented WNW –ESE with two possible nodal planes. The first plane (NP1) has strike 279, dip 46, rake 86 and the second (NP2)has strike 104, dip 44 and rake 94. The possibility for triggering the second event (M7.4) as influence by the main shock was examined in terms of the Coulomb failure stress function. The components of strain tensor were calculated by using the program DC3D (Okada, 1992). We calculated the changes in normal and shear stress and obtained a value for the Coulomb failure stress function of +148.5 kPa and +88.5 kPa at the hypocenter for NP1 and NP2, respectively. Both cases show increase of stress which encourages the likelihood of triggering on the recipient fault.

Keywords: Earthquake doublet , Triggering, Aftershock, Solomon Islands

©2019. Japan Geoscience Union. All Right Reserved.

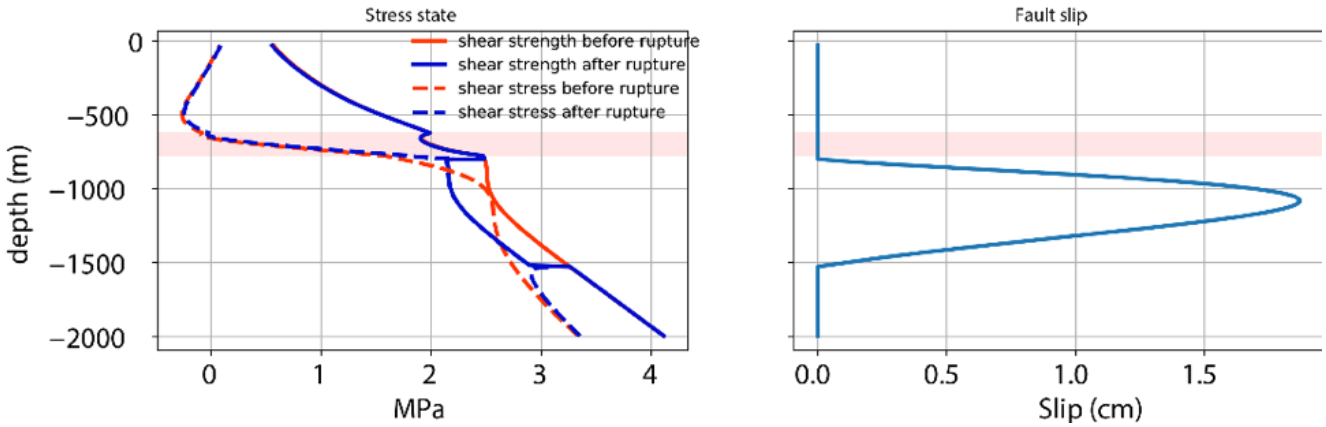
Thermal pressurization in a deep geological repository as a possible mechanism for fault reactivation

*Luca Urpi[1], Antonio Pio Rinaldi[1], Jonny Rutqvist[2], Stefan Wiemer[1]

1. Swiss Seismological Service, ETH Zurich, Switzerland, 2. Energy Geosceinces Division, LBNL, USA

A safe geological disposal site of radioactive waste requires identification of a rock formation that guarantees isolation to prevent unacceptable concentrations of radionuclides from migrating to the accessible environment. A common design for spent nuclear fuel disposal is the emplacement of specifically engineered canisters containing vitrified high-level radioactive waste (HLW) in a clay formation. The increase of temperature of a low permeability, fluid-saturated, media may trigger significant thermal pressurization, where the expansion of pore fluid cannot be accommodated by the thermal expansion of the pore space. With the aid of a coupled thermo-hydro-mechanical numerical simulator, we investigate the possible impact of thermal pressurization during the life of a deep geological repository on the stability of a nearby plane of weakness, assuming that the clay formation mantains its sealing properties. In our model, we represent the fault as a planar structure embedded in a thermo-poro-elastic material and shear activation evaluated by a strain-softening Mohr-Coulomb failure criterion. The results show that stress changes caused by temperature and thermal pressurization of a rock mass volume around the emplacement tunnels may trigger a slip event on a fault plane in proximity of the disposal site, with rupture nucleating at depth, hundreds of meter below the repository itself. We found that stress transfer plays an important role, while a direct hydraulic connection between the repository and the nucleation zone is not necessary in order to reach failure conditions. With a critical stress state (low horizontal to vertical stress ratio) the occurrence of slip may happen for a fault at a distance of up to 600m from the outermost tunnel. Intrinsic properties of the fault dictates the occurrence of seismic or aseismic slip, which may vary with depth. These results stress the need of investigating hydromechanical properties and local stress conditions to guarantee safe operations and predictable behavior of the HLW disposal site.

Keywords: Fault reactivation, thermal pressurization, stress transfer, deep geological repository high level storage, Rupture nucleation, Geomechanics



©2019. Japan Geoscience Union. All Right Reserved.

[E] Poster | S (Solid Earth Sciences)：S-SS Seismology

Sun. May 26, 2019 5:15 PM - 6:30 PM JST | Sun. May 26, 2019 8:15 AM - 9:30 AM UTC | Poster Hall International Exhibition Hall8, Makuhari Messe_25

[S-SS05] Induced and triggered seismicity: case-studies, monitoring and modeling techniques

convener:Luca Urpi(Swiss Seismological Service - ETH Zurich), Bogdan Enescu(Department of Geophysics, Kyoto University), Yosuke Aoki(Earthquake Research Institute, University of Tokyo), Francesco Grigoli(ETH-Zurich, Swiss Seismological Service)

Induced and triggered seismicity occurs in conjunction with human activities such as reservoir impoundments, mining operations, conventional and non-conventional hydrocarbon production, geothermal energy exploitation, wastewater disposal, CO2 sequestration and gas storage operations as well as volcanic and hydrogeological processes. The stability of faults is affected by external solicitations such as pore-pressure diffusion, relaxation effects as well as stress field perturbations related to mass and/or volume changes, dike intrusions and earthquake-earthquake interactions. A better understanding of the physical processes governing induced and triggered seismicity is important for the assess the risk of current and future industrial activities, including the geological disposal of nuclear waste.

The study of Induced and triggered seismicity is inherently an interdisciplinary problem, which requires the combination of seismological, hydrogeological, geodetic data and a wide range of modeling approaches. This session welcome contributions covering the analysis and modeling of induced and triggered seismicity at different spatial scales and environments.

Relevant topics to be presented include but are not limited to case-studies of induced and triggered seismicity, spatio-temporal variations of physical parameters (including stress, pressure and temperature changes), spatio-temporal patterns of seismicity, modeling and risk mitigation strategies.

The goal of the session is to cover both theoretical and experimental aspects of these topics.

[SSS05-P01] Harmonic seismic waves excited by far-field earthquakes

*Osamu Murakami[1] (1.Tono Rearch Institute of Earthquake Science, Association for the Development of Earthquake Prediction)

[SSS05-P02] **Dynamic triggering of microseismicity around Yunnan following the 2004 Sumatra and 2012 Indian Ocean Earthquakes**

*Lu Li[1], Baoshan Wang[1,4], Zhigang Peng[2], Danning Li[3] (1.Institute of Geophysics, CEA, 2.Georgia Tech, 3.Yunnan Earthquake Agency, 4.USTC)

[SSS05-P03] Megathrust-inducing azimuthal seismic anisotropy in local and regional crusts

*Tae-Kyung Hong[1], Junhyung Lee[1], Ilgoo Kim[1], Seongjun Park[1] (1.Department of Earth System Sciences, Yonsei University)

[SSS05-P04] **A Novel Method to Estimate Fracture Permeability: Combining microseismic observational data and reservoir engineering model**

*Meihua Yang[1,2], Yusuke Mukuhira[2], Takatoshi Ito[2] (1.State Key Laboratory of Oil and Gas Geology and Exploitation, Chendu University of Technology (China) , 2.Institute of Fluid Science, Tohoku University (Japan))

[SSS05-P05] Doublet Earthquake Triggering for the April 2014 Events in the Solomon Islands

*Calvin Luiramo Qwana[1], Masatoshi Miyazawa[2], James Mori[2] (1.Graduate School of Science, Kyoto University, 2.DPRI, Kyoto Univ.)

[SSS05-P06] Thermal pressurization in a deep geological repository as a possible mechanism for fault reactivation

*Luca Urpi[1], Antonio Pio Rinaldi[1], Jonny Rutqvist[2], Stefan Wiemer[1] (1.Swiss Seismological Service, ETH Zurich, Switzerland, 2.Energy Geosceinces Division, LBNL, USA)

Harmonic seismic waves excited by far-field earthquakes

*Osamu Murakami[1]

1. Tono Rearch Institute of Earthquake Science, Association for the Development of Earthquake Prediction

It was observed the very harmonic seismic waves with a period of 17 s after 09:30 (UT) on Nov. 11 in 2018, at the mostly seismic stations in the global broadband seismograph network. It is assumed that the hypocenter of the harmonic waves was off Mayotte Island in the northern Mozambique channels between the continent of Africa and Madagascar Island. The physical cause of these waves remains unclear.

In order to understand such characteristic seismic waves, I firstly calculated the running spectra from Nov. 1 to Nov. 20 in 2018, using the observed seismograms at the station, ABPO, operated by IRIS/IDA. This station is the nearest station from the assumed hypocenter among the stations of the global seismograph network. From these running spectra, I found that the harmonic waves excited by the near- and far-field earthquakes. There were 10 far-field earthquakes whose magnitudes were larger than 6, in this period. Because the depths of 3 earthquakes in these 10 earthquakes were deeper than 100 km, I considered the remaining 7 shallow earthquakes. I investigated 2 larger earthquakes than others. The first one occurred in Jan Mayen Island region on Nov. 9 in 2018 (Mw6.7, hereafter EQ-J2018), and the second one occurred in South Sandwich Islands region on Nov. 15 in 2018 (Mw6.4, EQ-S2018). There was another earthquake near EQ-J2018. It occurred on Aug. 20 in 2012 (Mw6.7, EQ-J2012). There were two similar earthquakes near EQ-S2018, occurred on Dec. 8 in 2010 (Mw6.3, EQ-S2010) and on May 10 in 2017 (Mw6.5, EQ-S2017). From the comparison of the observed seismic waves between the similar hypocenter earthquakes, I found that the amplitudes of the surface waves in the earthquakes in 2018 (EQ-J2018, EQ-S2018) were several times as much as the ones in the previous earthquakes (EQ-J2012, EQ-S2010, EQ-S2017), at some stations.

In this study, I will show the features of these harmonic waves and to discuss the possible mechanisms.

Keywords: harmonic seismic waves, Mayotte Island, surface waves

©2019. Japan Geoscience Union. All Right Reserved.

Dynamic triggering of microseismicity around Yunnan following the 2004 Sumatra and 2012 Indian Ocean Earthquakes

*Lu Li[1], Baoshan Wang[1,4], Zhigang Peng[2], Danning Li[3]

1. Institute of Geophysics, CEA, 2. Georgia Tech, 3. Yunnan Earthquake Agency, 4. USTC

We conduct a systematic detection of microseismicity around Yunnan following the 2004 Mw9.1 Sumatra and 2012 Mw8.6 Indian Ocean earthquakes to better understand the physical mechanism of dynamic triggering. Based on seismicity analysis on China Earthquake Network Center (CENC) catalog and spectral analysis of continuous waveforms, we find clear evidence of triggered seismicity in Yunnan immediately after the 2004 mainshock and a lack of instantaneous triggering following the 2012 mainshock. We further apply a matched filter technique to detect microearthquakes in Tengchong volcanic region 15 days before and 15 days after the 2012 mainshock. The seismicity rate remains stable immediately after the 2012 mainshock, and increases in the next few days, indicating a possible delayed triggering. In addition, we find possible evidence of remote triggering near the city of Yibin in Southern Sichuan Province, near the sites with ongoing shale gas development. We also examine other magnitude > 8 earthquakes from the Sumatra region and do not find any additional evidence of dynamic triggering around Yunnan. We suggest that the absolute value of dynamic stress change is the most important factor to explain why the 2004 Sumatra event triggered a widespread seismicity rate increase around Yunnan, while other great events around Sumatra did not.

Keywords: dynamic triggering, dynamic stress changes, Yunnan region

©2019. Japan Geoscience Union. All Right Reserved.

Megathrust-inducing azimuthal seismic anisotropy in local and regional crusts

*Tae-Kyung Hong[1], Junhyung Lee[1], Ilgoo Kim[1], Seongjun Park[1]

1. Department of Earth System Sciences, Yonsei University

Megathrust earthquakes produce large coseismic and postseismic lithospheric displacements. The 2011 M9.0 Tohoku-Oki megathrust earthquakes produced large displacements up to regional distances. The lithospheric displacements directing to the epicenter on the convergent plate boundary developed transient uniaxial tension field over the backarc lithospheres. The Vp/Vs changes display characteristic 2 theta azimuthal variations in the upper crust of the Japanese islands, ranging between -0.0458 and 0.0422. Large lateral variations in Vp/Vs changes suggest medium-dependent perturbation. The lower crust of the Korean Peninsula in distances of ~1300 km displayed coseismic velocity changes of 3 % after the megathrust earthquake. The Vp/Vsratios and seismic velocities recovered gradually over time. Peak Vp/Vs and seismic velocity changes were observed along paths subparallel or subperpendicular to the directions toward the megathrust earthquake. The azimuthal seismic anisotropy may have developed from preferential crack orientation and azimuthal lithostatic stress changes. It appears that recovery of the medium properties may take decades. A series of moderate-sized earthquakes occurred as a consequence of medium response to the temporal evolution of stress field in the Korean Peninsula.

Keywords: megathrust earthquake, crustal deformation, induced seismicity

©2019. Japan Geoscience Union. All Right Reserved.

A Novel Method to Estimate Fracture Permeability: Combining microseismic observational data and reservoir engineering model

*Meihua Yang[1,2], Yusuke Mukuhira[2], Takatoshi Ito[2]

1. State Key Laboratory of Oil and Gas Geology and Exploitation, Chendu University of Technology (China) , 2. Institute of Fluid Science, Tohoku University (Japan)

Effective utilization of geothermal resources is crucial to realize a sustainable society. Geothermal resources are widely present in Japan and the western United States, and the usage of geothermal resources are gradually increasing with many efforts. Meanwhile, the exploration and exploitation of geothermal resources in China has gradually developed. One of the challenges in conventional/next generation geothermal development (Enhanced/Engineered Geothermal System: EGS) is to understand the hydraulic properties of the geothermal reservoir. We often attempt to measure the hydraulic property (permeability or diffusivity) by wellbore tests or by using indicators such as migration of microseismicity. However, these quantities are often interpreted as representative value of hydraulic property for entire reservoir. Meanwhile, geothermal fluid circulates or flows in the existing/nucleated fracture system where permeability varies depending on condition of each fractures. Geothermal fluid is extracted from those permeable fractures very locally throughout production well drilled into the specific part of reservoir. Therefore, we need to have the best estimates of permeability for each fracture (local permeability) beyond representative permeability (global permeability). In addition, it is important to consider how the hydraulic properties can be affected by changes in the state of stress in the subsurface. This information is beneficial for design of geothermal energy extraction system and understanding of hydrology in the reservoir.

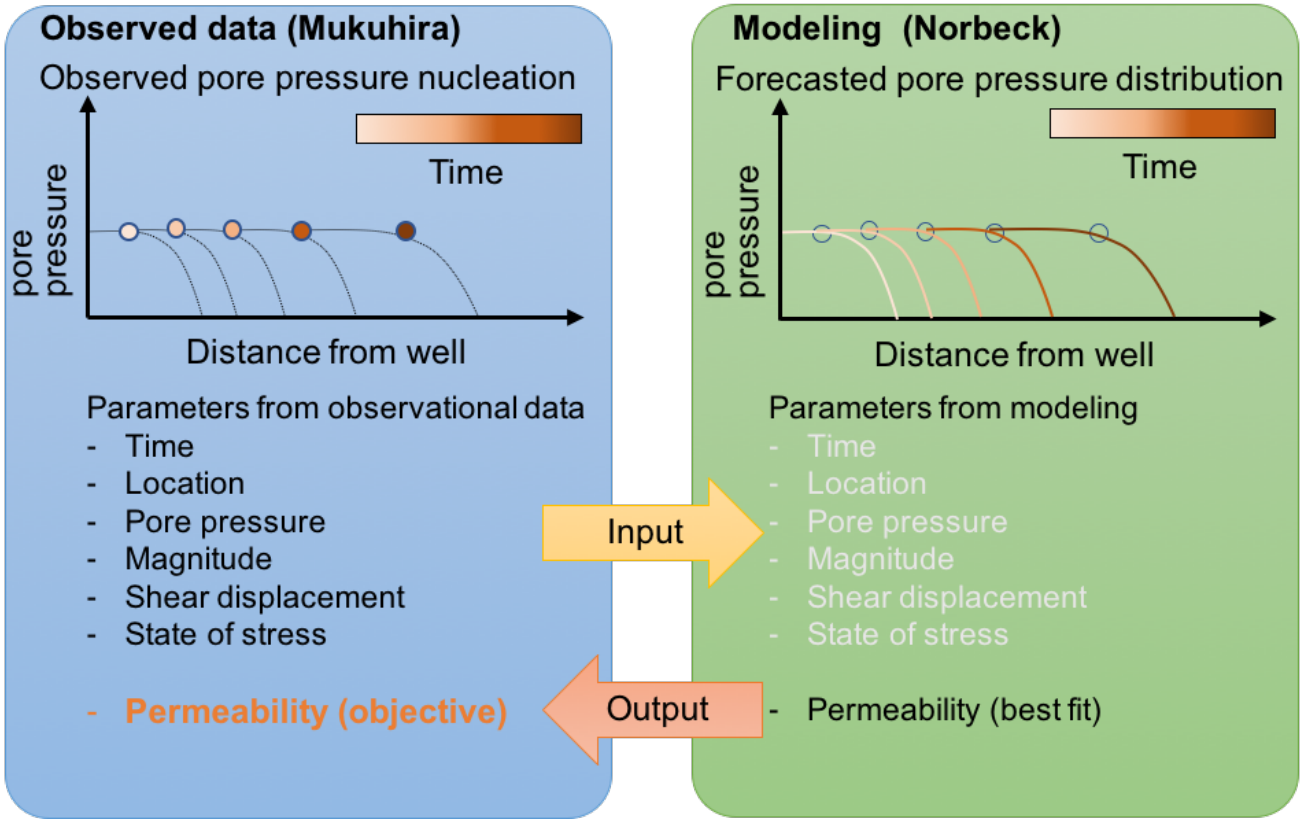
In this paper, we propose a novel method to estimate permeability of each individual fractures which experience shear slip at hydraulic stimulation. The spatiotemporal distribution of reservoir fluid pressure will be estimated using microseismic data. Using a hydromechanical fractured reservoir model, we will invert for the shear-dilation enhanced permeability change that controls the evolution of pressure along fractures and faults.

The first step is to estimate pore pressure distribution with microseismic data from real EGS field and observe how pore pressure migrated within single fracture (Figure 1 left: coloured circles). Meanwhile, using the hydromechanical fractured reservoir numerical model, we simulate pore pressure distribution within one fracture of given permeability and evaluate the evolution of hydraulic properties during a stimulation treatment (Figure 1 right: coloured sold lines). Therefore, we can use parameters from observational data as input parameters into hydromechanical model and estimate the best permeability which explain observed pore pressure distribution. We will also simulate all microseismic clusters and estimate permeability of each fractures. Then analyse the fracture permeability distribution (permeability mapping) in the study area.

In this research, it is the first attempt to estimate local permeability for each fracture. So far, only global permeability can be estimated by wellbore test or microseismic data and this permeability is not effective for each fracture in subsurface. Information of local permeability is quite valuable for designing a sustainable energy extraction system. Local permeability information also brings the way to model the flow of geothermal fluid in the reservoir, which is important for long-term management of geothermal resources.

©2019. Japan Geoscience Union. All Right Reserved.

Keywords: Permeability, Microseismic, Reservoir engineering model



©2019. Japan Geoscience Union. All Right Reserved.

Doublet Earthquake Triggering for the April 2014 Events in the Solomon Islands

*Calvin Luiramo Qwana[1], Masatoshi Miyazawa[2], James Mori[2]

1. Graduate School of Science, Kyoto University, 2. DPRI, Kyoto Univ.

In 2014 at 20:14 (UTC) on April 12th and 12:36 on April 13th, a doublet earthquake with moment magnitudes of M7.6 and M7.4, respectively occurred near Makira Island (San Cristobal) in the Solomon Islands. The depths of the events were 27 km and 37 km, respectively (GCMT). To understand the interrelation between the first (M7.6) and second (M7.4) events , we check the role of Coulomb stress triggering on aftershocks that follow the M7.6 main shock and the coulomb failure stress changes on both of the focal mechanism nodal planes for the second event. To understand if the coulomb stress triggering played a role in the evolution of the triggered event M7.4 earthquake, we evaluate the transient aftershocks from the M7.6 to see if it promoted failure on the rupture plane for the second event (M7.4). We evaluate the doublet source process of the events and recover the slip distribution on each of the faults. We use an iterative inversion method by Kikuchi and Kanamori (1991) for the teleseismic P waveforms recorded from more than 20 stations of the Global Seismographic Network in a distance range of 30˚ to 90˚. A fault plane with fixed strike and dip is placed in the region of the earthquake hypocenter and divided into subfaults, and a constant rupture velocity of 2.5 km/s is assumed. Synthetic waveforms are calculated at the teleseismic stations for dislocations at each subfault. Using the synthetic Green’ s functions, the observed seismograms are inverted to determine the fault plane and obtain the distribution of slips for the two events. The results show that the mechanism for the Mw7.6 first event is left-lateral strike-slip faulting for a plane of strike 116, dip 74 , and rake 24. The other NW-SE oriented nodal plane is almost parallel to Australian and Pacific plate boundary. Results for the mechanism of the Mw7.4 event indicates thrust faulting on fault plane oriented WNW –ESE with two possible nodal planes. The first plane (NP1) has strike 279, dip 46, rake 86 and the second (NP2)has strike 104, dip 44 and rake 94. The possibility for triggering the second event (M7.4) as influence by the main shock was examined in terms of the Coulomb failure stress function. The components of strain tensor were calculated by using the program DC3D (Okada, 1992). We calculated the changes in normal and shear stress and obtained a value for the Coulomb failure stress function of +148.5 kPa and +88.5 kPa at the hypocenter for NP1 and NP2, respectively. Both cases show increase of stress which encourages the likelihood of triggering on the recipient fault.

Keywords: Earthquake doublet , Triggering, Aftershock, Solomon Islands

©2019. Japan Geoscience Union. All Right Reserved.

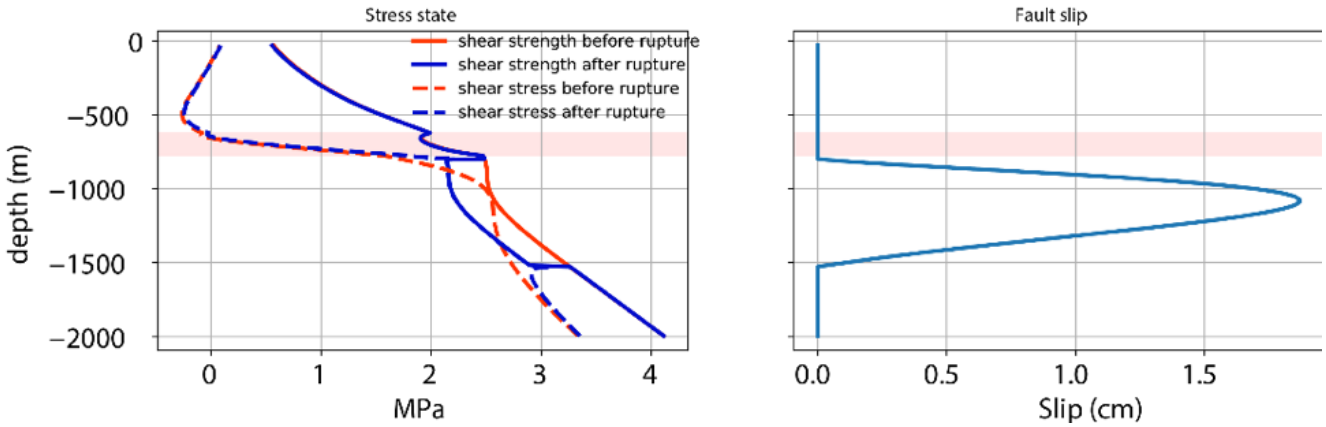
Thermal pressurization in a deep geological repository as a possible mechanism for fault reactivation

*Luca Urpi[1], Antonio Pio Rinaldi[1], Jonny Rutqvist[2], Stefan Wiemer[1]

1. Swiss Seismological Service, ETH Zurich, Switzerland, 2. Energy Geosceinces Division, LBNL, USA

A safe geological disposal site of radioactive waste requires identification of a rock formation that guarantees isolation to prevent unacceptable concentrations of radionuclides from migrating to the accessible environment. A common design for spent nuclear fuel disposal is the emplacement of specifically engineered canisters containing vitrified high-level radioactive waste (HLW) in a clay formation. The increase of temperature of a low permeability, fluid-saturated, media may trigger significant thermal pressurization, where the expansion of pore fluid cannot be accommodated by the thermal expansion of the pore space. With the aid of a coupled thermo-hydro-mechanical numerical simulator, we investigate the possible impact of thermal pressurization during the life of a deep geological repository on the stability of a nearby plane of weakness, assuming that the clay formation mantains its sealing properties. In our model, we represent the fault as a planar structure embedded in a thermo-poro-elastic material and shear activation evaluated by a strain-softening Mohr-Coulomb failure criterion. The results show that stress changes caused by temperature and thermal pressurization of a rock mass volume around the emplacement tunnels may trigger a slip event on a fault plane in proximity of the disposal site, with rupture nucleating at depth, hundreds of meter below the repository itself. We found that stress transfer plays an important role, while a direct hydraulic connection between the repository and the nucleation zone is not necessary in order to reach failure conditions. With a critical stress state (low horizontal to vertical stress ratio) the occurrence of slip may happen for a fault at a distance of up to 600m from the outermost tunnel. Intrinsic properties of the fault dictates the occurrence of seismic or aseismic slip, which may vary with depth. These results stress the need of investigating hydromechanical properties and local stress conditions to guarantee safe operations and predictable behavior of the HLW disposal site.

Keywords: Fault reactivation, thermal pressurization, stress transfer, deep geological repository high level storage, Rupture nucleation, Geomechanics



©2019. Japan Geoscience Union. All Right Reserved.

[E] Poster | S (Solid Earth Sciences)：S-IT Science of the Earth's Interior & Techtonophysics

Sun. May 26, 2019 3:30 PM - 5:00 PM JST | Sun. May 26, 2019 6:30 AM - 8:00 AM UTC | Poster Hall International Exhibition Hall8, Makuhari Messe_16

[S-IT20] Property and role of liquids inside terrestrial planets

convener:Tatsuya Sakamaki(Department of Earth Science, Tohoku University), Yoichi Nakajima(Kumamoto University, Priority Organization for Innovation and Excellence)

Liquids of silicates and metals inside of terrestrial planets play important role in the physical, chemical, and thermal evolutions of planets. This session aims at understanding the physical and chemical properties of liquids from shallower to deep parts of terrestrial planets, which are strongly related to the long history of those planets from the planetary accretion to the present-day dynamics. In addition, we call for presentations by researchers from various backgrounds of geochemical, experimental, theoretical/computational, and seismic/geodynamical ones, who investigate the physical and chemical properties of liquids and the behaviors and roles inside of terrestrial planets. Relevant topics include, but are not limited to, partial melting and melt extraction, liquid-solid partitioning, high pressure experiments on melts, and seismic detections of mantle melts and outer core anomaly.

[SIT20-P01] Melting relations in the Fe-P system at high pressures

*Yoichi Nakajima[1,2], Haruki Obata[2], Daisuke Kinoshita[2], Shigehiko Tateno[3], Kei Hirose[3,4], Naohisa Hirao[5], Saori I. Kawaguchi[5], Yasuo Ohishi[5] (1.Priority Organization for Innovation and Excellence, Kumamoto University, 2.Department of Phsyics, Kumamoto University,, 3.Earth-Life Science Institue, Tokyo Institute of Technology, 4.Department of Earth and Planertary Science, The University of Tokyo, 5.JASRI)

[SIT20-P02] Elastic property and structure of pyrope glass at high pressure

*Naoki Hisano[1], Tatsuya Sakamaki[1], Tomonori Ohashi[1], Ken-ichi Funakoshi[2], Yuji Higo[3], Yuki Shibazaki[4], Akio Suzuki[1] (1.Department of Earth Science, Graduate School of Science, Tohoku University, 2.Neutron Science & Technology Center, Comprehensive Research Organization for Science and Society (CROSS), 3.Japan Synchrotron Radiation Research Institute, 4.International Center for Young Scientists, National Institute for Materials Science)

[SIT20-P03] The effect of water and redox state on melting at the top of the lower mantle

*Ayano Nakajima[1], Tatsuya Sakamaki[1], Akio Suzuki[1] (1.Tohoku University)

[SIT20-P04] Sound velocity measurements on liquid Fe-P alloy up to 80 GPa

*Daisuke Kinoshita[1], Yoichi Nakajima[1,2], Yasuhiro Kuwayama[2,3], Kei Hirose[3], Daisuke Ishikawa[2,4], Baron Q.R. Alfred[2] (1.Kumamoto University, 2.RIKEN MDL, 3.Tokyo University, 4.JASRI)

[SIT20-P05] High-pressure structural investigations for hydrous sodium silicate melts

*Tomonori Ohashi[1], Tatsuya Sakamaki[1], Ken-ichi Funakoshi[2], Miki Muranushi[1], Chikara Shito[1], Yuki Shibazaki[3], Akio Suzuki[1] (1.Department of Earth Science, Tohoku University, 2.Neutron Science and Technology Center, Comprehensive Research Organization for Science and Society (CROSS), 3.National Institute for Materials Science (NIMS))

[SIT20-P06] Inelastic X-ray scattering measurements of liquid Fe-N alloy under high pressure

*Asaki Iwamoto[1], Yoichi Nakajima[1,2], Daisuke Kinoshita[1], Yasuhiro Kuwayama[2,3], Kei Hirose[3], Daisuke Ishikawa[2,4], Alfred Q.R. Baron[2] (1.Kumamoto University, 2.RIKEN MDL, 3.The University of Tokyo, 4.JASRI)

[SIT20-P07] Formation of highly pure anorthite crust on the low-volatile astral bodies by low-viscous magma ocean

*Tatsuya Sakamaki[1], Yoshio Kono[2] (1.Graduate School of Science, Tohoku University, 2.Geodynamics Research Center, Ehime University)

Melting relations in the Fe-P system at high pressures

*Yoichi Nakajima[1,2], Haruki Obata[2], Daisuke Kinoshita[2], Shigehiko Tateno[3], Kei Hirose[3,4], Naohisa Hirao[5], Saori I. Kawaguchi[5], Yasuo Ohishi[5]

1. Priority Organization for Innovation and Excellence, Kumamoto University, 2. Department of Phsyics, Kumamoto University,, 3. Earth-Life Science Institue, Tokyo Institute of Technology, 4. Department of Earth and Planertary Science, The University of Tokyo, 5. JASRI

The present-day temperature profile of the Earth's core is key to understanding of the thermal history and dynamics of the core. The temperature in the outer core region is over the melting temperature of the core material and crossovers it at the inner-outer core boundary. Thus, the melting temperature of the core material under relevant high-pressure conditions is crucial to constrain the core temperature. It is well known that the core is composed mainly of Fe, but including 10% lighter elements [1], though the nature of the light elements is still unclear. Phosphorous is also one of the candidates for the core light elements because it is found in iron-meteorites [2] and depleted in the silicate mantle relative to chondrites [3]. In this study, we performed melting experiments on Fe_3P up to 80 GPa by using a laser-heated diamond anvil cell.

The melting relation was determined from in-situ X-ray diffraction measurements at the beamline BL10XU of the SPring-8 synchrotron facility. During heating, we observed a peritectic melting of Fe_3P to liquid + Fe_2P and complete melting up to 60 GPa. The onset and complete melting of the sample were judged from the intensity of diffuse scattering signals from the liquid. This melting phase relation was also confirmed from the chemical analysis on some recovered samples. Above 60 GPa, we observed the change in diffraction pattern of the Fe_3P sample at subsolidus temperature conditions, which might be the decomposition to iron-rich and Fe_2P phases. For this two-phase mixture, we also determined the solidus and liquidus temperatures. In the present experimental pressure conditions, the peritectic (or solidus) and liquidus temperatures of the Fe_3P composition are ~700 K and ~200-300 K lower, respectively, relative to the melting temperature of Fe [4]. These indicate that phosphorous reduces strongly the melting temperature of Fe.

References

[1] Birch, *J. Geophys. Res.*, **57**, 227 (1952).

[2] Skála and Císařova, *Phys. Chem. Mine.*, **31**, 721 (2005)

[3] McDonough, *Treatise on Geochem.,* **Vol.2**, 547 (2003)

[4] Anzellini et al., *Science*, **340**, 464 (2013).

Keywords: Earth's core, Core light element, Melting relations, High pressure

©2019. Japan Geoscience Union. All Right Reserved.

Elastic property and structure of pyrope glass at high pressure

*Naoki Hisano[1], Tatsuya Sakamaki[1], Tomonori Ohashi[1], Ken-ichi Funakoshi[2], Yuji Higo[3], Yuki Shibazaki[4], Akio Suzuki[1]

1. Department of Earth Science, Graduate School of Science, Tohoku University, 2. Neutron Science & Technology Center, Comprehensive Research Organization for Science and Society (CROSS), 3. Japan Synchrotron Radiation Research Institute, 4. International Center for Young Scientists, National Institute for Materials Science

Structural properties of magma are closely correlated to their physical, chemical, and thermal properties. One of approaches for obtaining insights of magmas is an examination of silicate glasses. Aluminum is one of the major elements in the Earth and an important element for controlling the silicate network in melts and glasses because Al^{3+} behaves as an intermediate species in the silicate melts. Aluminum cation can act as either a network former or a modifier, depending on the composition. In the case of a fully-polymerized melt, such as jadeite and albite composition, all TO_4 tetrahedra (where T represents cations, such as Si, Al, etc.) are interconnected via oxygen anions, forming a three-dimensional network structure. Compositional differences are generally considered in terms of variety of alkaline (e.g., Na^{+}) and alkaline-earth (e.g., Mg^{2+}, Ca^{2+}) cations in the melts. These cations are called network modifiers and tend to cut Si-O-Si bonds between a SiO_4 tetrahedron and the adjacent ones. In addition to aluminum cation, other network modifiers also affect the melt behavior. A Mg-aluminosilicate, pyrope ($Mg_3Al_2Si_3O_{12}$) is an important mineral of mantle because of its abundance in the Earth's upper mantle. Change in the slope of melting curve of pyrope around 7-10 GPa has been reported, and pressure-induced Al-coordination change was suggested. Although investigations of structure and elasticity of Mg-aluminosilicate glasses and pyrope-composition glasses have been conducted at ambient pressure, those observations at high pressures are still poor.

Here, we have measured sound velocities of pyrope glass at pressures up to 12.9 GPa using ultrasonic technique at BL04B1 of SPring-8. Longitudinal and transverse wave velocities decreased up to 5.6 GPa, and then the velocities started to increase with pressure. Pressure dependence of elastic moduli and Poisson's ratio of the glass also changed around 7-8 GPa. The structural determination of the glass was conducted based on the energy-dispersive X-ray diffraction method at beamline NE5C of PF-AR in order to understand the mechanism of changes in microscopic physical properties in terms of macroscopic structural evolution. The characteristic shrinkage of the intermediate-range ordering in silicate network was observed around 7 GPa. We could find some correlation between elastic properties and structure. Detailed discussion will be shown in the meeting.

Keywords: silicate glass, elastic wave velocity, X-ray diffraction, structure, ultrasonic measurement

©2019. Japan Geoscience Union. All Right Reserved.

The effect of water and redox state on melting at the top of the lower mantle

*Ayano Nakajima[1], Tatsuya Sakamaki[1], Akio Suzuki[1]

1. Tohoku University

There are various igneous activities in the Earth. On the surface of the Earth, for example, igneous activities occur in island arcs, mid-ocean ridges, hot spots and petit spots. However, not only on the surface, but also in the interior, melting phenomena are also suggested at the top of the asthenosphere [e.g., Barazangi & Isacks, 1971 *JGR*; Schmerr, 2012 *Science*] and the bottom of the upper mantle [e.g., Bercovici & Karato, 2003 *Nature*; Song *et al.*, 2004 *Nature*]. In this study, we focused on the melting of hydrous peridotite at the top of the lower mantle because seismological observation indicates the low velocity anomaly [Schmandt *et al.*, 2014 *Scienc*e; Liu *et al.*, 2016 *GRL*; Liu *et al.*, 2018 *EPSL*]. The low-velocity region is expected to be caused by mantle melting due to dehydration decomposition of ringwoodite to bridgmanite and ferro-periclase with a downward flow.

Here, we performed melting experiments of peridotite with 2.0 wt. % H_2O at 26 GPa and 1600 ˚C - 2000 ˚C. As a starting material, two peridotite samples were synthesized: one was Fe_2O_3-bearing sample and the other was FeO-bearing. The samples were sealed by gold capsules. Recovered product of reductive sample (= FeO-bearing) from 2000 ˚C and 26 GPa showed a partial melting texture. This indicates that mantle melting can be occurred under this experimental condition. On the other hand, there are no melting texture of recovered sample of Fe_2O_3 system from 2000 ˚C and 26 GPa. In short, the materials constituting the lower mantle melts in the reduced state but not in the oxidized state. It is reported that ferric iron occupies a majority in the redox state at the top of the lower mantle [McCammon, 1997 *Nature* ; Frost *et al.*, 2004 *Nature*]. Thus, it is considered that melting phenomenon may or may not occur due to the regional difference of redox state. At 2000 ˚C, compared to bridgmanite in this study, the composition of melt was SiO_2- and Al_2O_3-poor and MgO- and CaO-rich. Although the FeO component concentrated in the melt, this behavior is closer to the tendency of the anhydrous melting experiments (2400 ˚C or more) [Ito & Takahashi, 1987 *Nature*; Trønnes & Frost, 2002 *EPSL*] than the hydrous system (~1400 ˚C) [Kawamoto, 2004 *PEPI*] because of the small amount of water. We calculated the density and compressibility of the magma based on the obtained melt composition. Comparing with seismological model, this melt is lighter than the lower mantle rock. This implies that a small amount of water (2.0 wt. %) can cause a light melt at the top of lower mantle and form the seismological low velocity zone.

Keywords: dehydration melting, lower mantle, hydrous magma, redox state

©2019. Japan Geoscience Union. All Right Reserved.

Sound velocity measurements on liquid Fe-P alloy up to 80 GPa

*Daisuke Kinoshita[1], Yoichi Nakajima[1,2], Yasuhiro Kuwayama[2,3], Kei Hirose[3], Daisuke Ishikawa[2,4], Baron Q.R. Alfred[2]

1. Kumamoto University, 2. RIKEN MDL, 3. Tokyo University, 4. JASRI

The Earth’ s liquid outer core is composed mainly of iron, alloying with 5% nickel and 10% lighter elements [1]. The core composition is important to understand the environment and mechanism of the core formation process and the present-day magnetic field. The sound velocity of liquid iron alloys under relevant high-pressure and -temperature conditions in the core is key to constraining the core composition because the direct observations for the core is seismologic wave passing through the core only. Phosphorous is one of the candidates for light elements in the core because it is found in iron-meteorites [2] and depleted in the silicate mantle relative to chondrites [3]. In this study, we determined the P-wave velocity of liquid $Fe_{75}P_{25}$ up to 80 GPa using a laser-heated diamond-anvil cell in combination with an inelastic X-ray scattering (IXS) spectroscopy. We performed IXS measurements at a beamline BL43LXU [4] of the RIKEN SPring-8 Center in Japan. The P-wave velocity of liquid $Fe_{75}P_{25}$ were obtained based on the observed acoustic phonon dispersion. The present results exhibit that the influence of phosphorus on liquid iron sound velocity is almost negligible under the present experimental conditions. On the other hands, the density of liquid Fe can be reduced by phosphorous.

References

[1] Stevenson, 1981 Science. Vol.214, 611-619
[2] Skála and Císařova, 2005 Physics and Chemistry of Minerals. Vol.31, 721-732
[3] McDonough, 2003 Treatise on Geochem. Vol.2, 547-568
[4] Baron, 2010 SPring-8 Inf. Newsl. Vol.15, No.1 14-19

Keywords: outer core, sound velocity, high pressure

©2019. Japan Geoscience Union. All Right Reserved.

High-pressure structural investigations for hydrous sodium silicate melts

*Tomonori Ohashi[1], Tatsuya Sakamaki[1], Ken-ichi Funakoshi[2], Miki Muranushi[1], Chikara Shito[1], Yuki Shibazaki[3], Akio Suzuki[1]

1. Department of Earth Science, Tohoku University, 2. Neutron Science and Technology Center, Comprehensive Research Organization for Science and Society (CROSS), 3. National Institute for Materials Science (NIMS)

The behaviors of high-pressure silicate melts, which is controlled by their physico-chemical properties, are important to understand the magma activity in the deep Earth. Particularly, the H_2O content significantly affects the properties, such as density (e.g., Sakamaki et al., 2006) and viscosity (e.g., Suzuki et al., 2011; Poe et al., 2006). Since such macroscopic properties are known to be largely determined by the microscopic structure, there are considerable interests in revealing how the structure changes with increasing pressure.

Here, structures of hydrous Na_2O-8/3SiO_2 melts with 5 wt% (NS8/3_H5) and with 9 wt% H_2O (NS8/3_H9) were determined under high pressure and temperature by the in-situ X-ray diffraction (XRD). The in-situ XRD study was carried out using a cubic-type multi-anvil apparatus MAX80, which is installed at the AR-NE5C beamline of PF-AR at Tsukuba, Japan. The experimental *P*-*T* conditions were about 1.5–3.0 GPa and 550–970 ˚C, respectively.

The obtained total structure factors, $S(Q)$ of both liquids show that the position of the first sharp diffraction peaks (FSDP) shift to higher-Q with pressure. This positional shift indicates the intermediate-range order structure of present melts become compact. The reduced radial distribution functions, $G(r)$ indicate different pressure evolutions in the average Si-O bond lengths ($r_{Si\text{-}O}$) depending on their water contents. The $r_{Si\text{-}O}$ in the NS8/3_H9 melt shows the monotonic decrease with increasing pressure, however, the $r_{Si\text{-}O}$ of the NS8/3_H5 melt hardly changes after its contraction below 1.6 GPa. The structure of the NS8/3_H9 melt is assumed to be slightly more depolymerized than the NS8/3_H5 melt at ambient pressure (Zotov and Keppler, 1998). This difference might be due to a phenomenon that the number of strongly hydrogen-bonded SiOH groups, which are favored in sodium silicate glasses and melts (Xue and Kanzaki, 2004), increase more significantly during pressure-induced depolymerization in the NS8/3_H9 melt than in the NS8/3_H5 melt. This raises Si(-NBO)/Si(-BO) (NBO: non-bridging oxygen, BO: bridging oxygen) ratio, and hence, the $r_{Si\text{-}O}$ becomes shorter.

Keywords: hydrous silicate melt, effect of water, amorphous structure, high pressure and temperature

©2019. Japan Geoscience Union. All Right Reserved.

Inelastic X-ray scattering measurements of liquid Fe-N alloy under high pressure

*Asaki Iwamoto[1], Yoichi Nakajima[1,2], Daisuke Kinoshita[1], Yasuhiro Kuwayama[2,3], Kei Hirose[3], Daisuke Ishikawa[2,4], Alfred Q.R. Baron[2]

1. Kumamoto University, 2. RIKEN MDL, 3. The University of Tokyo, 4. JASRI

The Earth’ s liquid outer core is composed mainly of iron, alloying with ~5% nickel and ~10% some light elements [1]. Nitrogen is one of candidates for the light elements. The abundance of nitrogen in the silicate mantle relative to that in primordial meteorites is less than those of similar volatile components such as H_2O, C and Ar, so that large portion of nitrogen in bulk Earth can be stored in the core [2,3]. In order to examine the possibility of nitrogen in the core, it is benefit to compare the sound velocity of liquid Fe-N alloy under high-pressure and -temperature relevant to the core conditions with the seismological observations. In this study, we performed inelastic X-ray scattering (IXS) measurements on liquid Fe-N alloy and determined its longitudinal velocity of the liquid Fe-N alloy under high pressure and temperature.

We carried out high-pressure and -temperature IXS measurements using a laser-heated diamond-anvil cell (LH-DAC) at the beamline BL43LXU of SPring-8 [4]. We used an Fe_4N foil (hereafter called $Fe_{80}N_{20}$) as a starting sample and single crystal Al_2O_3 discs as a thermal insulator. We judged the sample melting based on X-ray diffraction measurements during heating and then measured IXS of the liquid sample. The longitudinal sound wave (P-wave) velocity of liquid $Fe_{80}N_{20}$ was determined from the dispersion relation of the longitudinal acoustic phonon mode of the sample. We obtained the velocity of liquid $Fe_{80}N_{20}$ up to 76 GPa and 2200 K. We found that the P-wave velocity of liquid $Fe_{80}N_{20}$ is slightly faster by c.a. 4% than that of liquid Fe [5]. The P-wave velocity of liquid outer core is faster by 4% than liquid Fe [5]. Therefore, the present results give the upper limit of 5.9 wt.% (20 at.%) for the nitrogen content in the outer core.

[1] Stevenson, Science **214**, 611-619 (1981).

[2] Marty, Earth Planet. Sci. Lett. **313-314**, 56-66 (2012).

[3] Li et al., Earth Planet. Sci. Lett. **377-378**, 311-323 (2013).

[4] Baron, SPring-8 Inf. Newsl. **15**(1), 14-19 (2010).

[5] Anderson and Ahrens, J. Geophys. Res. **99**(B3), 4273-4284 (1994)

Keywords: Earth's liquid outer core, Light element, P-wave velocity, High pressure

©2019. Japan Geoscience Union. All Right Reserved.

Formation of highly pure anorthite crust on the low-volatile astral bodies by low-viscous magma ocean

*Tatsuya Sakamaki[1], Yoshio Kono[2]

1. Graduate School of Science, Tohoku University, 2. Geodynamics Research Center, Ehime University

Anorthite ($CaAl_2Si_2O_8$) is a Ca-endmember of plagioclase, and it is a main component of a crust on the astral bodies, such as Moon and 4 Vesta, Thick anorthite-rich crust has been formed through a process of magma ocean. Here we conduct high-pressure and high-temperature experiments and *in-situ* X-ray analysis to simultaneously assess the viscosity and structure of anorthite magmas under pressures of up to 6.6 GPa. We find contrasting behavior in the viscosity between liquid anorthite and albite ($NaAlSi_3O_8$), which is Na-endmember of plagioclase. The big difference in viscosity between anorthite and albite melts has important implications for planetary differentiation. Na-poor astral bodies (Moon, 4 Vesta, etc.) have been dominated by low-viscous magma ocean and, eventually caused an efficient differentiation between crystal and magma. This process prevented the melt from trapping in the grain boundaries of floating anorthites. This makes the highly pure anorthite crust on the Moon observed by the remote sensing.

Keywords: anorthite melt, viscosity, structure, high pressure, high temperature, lunar magma ocean

©2019. Japan Geoscience Union. All Right Reserved.

[E] Poster | S (Solid Earth Sciences)：S-IT Science of the Earth's Interior & Techtonophysics

Sun. May 26, 2019 5:15 PM - 6:30 PM JST | Sun. May 26, 2019 8:15 AM - 9:30 AM UTC | Poster Hall International Exhibition Hall8, Makuhari Messe_28

[S-IT20] Property and role of liquids inside terrestrial planets

convener:Tatsuya Sakamaki(Department of Earth Science, Tohoku University), Yoichi Nakajima(Kumamoto University, Priority Organization for Innovation and Excellence)

Liquids of silicates and metals inside of terrestrial planets play important role in the physical, chemical, and thermal evolutions of planets. This session aims at understanding the physical and chemical properties of liquids from shallower to deep parts of terrestrial planets, which are strongly related to the long history of those planets from the planetary accretion to the present-day dynamics. In addition, we call for presentations by researchers from various backgrounds of geochemical, experimental, theoretical/computational, and seismic/geodynamical ones, who investigate the physical and chemical properties of liquids and the behaviors and roles inside of terrestrial planets. Relevant topics include, but are not limited to, partial melting and melt extraction, liquid-solid partitioning, high pressure experiments on melts, and seismic detections of mantle melts and outer core anomaly.

[SIT20-P01] Melting relations in the Fe-P system at high pressures

*Yoichi Nakajima[1,2], Haruki Obata[2], Daisuke Kinoshita[2], Shigehiko Tateno[3], Kei Hirose[3,4], Naohisa Hirao[5], Saori I. Kawaguchi[5], Yasuo Ohishi[5] (1.Priority Organization for Innovation and Excellence, Kumamoto University, 2.Department of Phsyics, Kumamoto University,, 3.Earth-Life Science Institue, Tokyo Institute of Technology, 4.Department of Earth and Planertary Science, The University of Tokyo, 5.JASRI)

[SIT20-P02] Elastic property and structure of pyrope glass at high pressure

*Naoki Hisano[1], Tatsuya Sakamaki[1], Tomonori Ohashi[1], Ken-ichi Funakoshi[2], Yuji Higo[3], Yuki Shibazaki[4], Akio Suzuki[1] (1.Department of Earth Science, Graduate School of Science, Tohoku University, 2.Neutron Science & Technology Center, Comprehensive Research Organization for Science and Society (CROSS), 3.Japan Synchrotron Radiation Research Institute, 4.International Center for Young Scientists, National Institute for Materials Science)

[SIT20-P03] The effect of water and redox state on melting at the top of the lower mantle

*Ayano Nakajima[1], Tatsuya Sakamaki[1], Akio Suzuki[1] (1.Tohoku University)

[SIT20-P04] Sound velocity measurements on liquid Fe-P alloy up to 80 GPa

*Daisuke Kinoshita[1], Yoichi Nakajima[1,2], Yasuhiro Kuwayama[2,3], Kei Hirose[3], Daisuke Ishikawa[2,4], Baron Q.R. Alfred[2] (1.Kumamoto University, 2.RIKEN MDL, 3.Tokyo University, 4.JASRI)

[SIT20-P05] High-pressure structural investigations for hydrous sodium silicate melts

*Tomonori Ohashi[1], Tatsuya Sakamaki[1], Ken-ichi Funakoshi[2], Miki Muranushi[1], Chikara Shito[1], Yuki Shibazaki[3], Akio Suzuki[1] (1.Department of Earth Science, Tohoku University, 2.Neutron Science and Technology Center, Comprehensive Research Organization for Science and Society (CROSS), 3.National Institute for Materials Science (NIMS))

[SIT20-P06] Inelastic X-ray scattering measurements of liquid Fe-N alloy under high pressure

*Asaki Iwamoto[1], Yoichi Nakajima[1,2], Daisuke Kinoshita[1], Yasuhiro Kuwayama[2,3], Kei Hirose[3], Daisuke Ishikawa[2,4], Alfred Q.R. Baron[2] (1.Kumamoto University, 2.RIKEN MDL, 3.The University of Tokyo, 4.JASRI)

[SIT20-P07] Formation of highly pure anorthite crust on the low-volatile astral bodies by low-viscous magma ocean

*Tatsuya Sakamaki[1], Yoshio Kono[2] (1.Graduate School of Science, Tohoku University, 2.Geodynamics Research Center, Ehime University)

Melting relations in the Fe-P system at high pressures

*Yoichi Nakajima[1,2], Haruki Obata[2], Daisuke Kinoshita[2], Shigehiko Tateno[3], Kei Hirose[3,4], Naohisa Hirao[5], Saori I. Kawaguchi[5], Yasuo Ohishi[5]

1. Priority Organization for Innovation and Excellence, Kumamoto University, 2. Department of Phsyics, Kumamoto University,, 3. Earth-Life Science Institue, Tokyo Institute of Technology, 4. Department of Earth and Planertary Science, The University of Tokyo, 5. JASRI

The present-day temperature profile of the Earth's core is key to understanding of the thermal history and dynamics of the core. The temperature in the outer core region is over the melting temperature of the core material and crossovers it at the inner-outer core boundary. Thus, the melting temperature of the core material under relevant high-pressure conditions is crucial to constrain the core temperature. It is well known that the core is composed mainly of Fe, but including 10% lighter elements [1], though the nature of the light elements is still unclear. Phosphorous is also one of the candidates for the core light elements because it is found in iron-meteorites [2] and depleted in the silicate mantle relative to chondrites [3]. In this study, we performed melting experiments on Fe_3P up to 80 GPa by using a laser-heated diamond anvil cell.

The melting relation was determined from in-situ X-ray diffraction measurements at the beamline BL10XU of the SPring-8 synchrotron facility. During heating, we observed a peritectic melting of Fe_3P to liquid + Fe_2P and complete melting up to 60 GPa. The onset and complete melting of the sample were judged from the intensity of diffuse scattering signals from the liquid. This melting phase relation was also confirmed from the chemical analysis on some recovered samples. Above 60 GPa, we observed the change in diffraction pattern of the Fe_3P sample at subsolidus temperature conditions, which might be the decomposition to iron-rich and Fe_2P phases. For this two-phase mixture, we also determined the solidus and liquidus temperatures. In the present experimental pressure conditions, the peritectic (or solidus) and liquidus temperatures of the Fe_3P composition are ~700 K and ~200-300 K lower, respectively, relative to the melting temperature of Fe [4]. These indicate that phosphorous reduces strongly the melting temperature of Fe.

References

[1] Birch, *J. Geophys. Res.*, **57**, 227 (1952).

[2] Skála and Císařova, *Phys. Chem. Mine.*, **31**, 721 (2005)

[3] McDonough, *Treatise on Geochem.,* **Vol.2**, 547 (2003)

[4] Anzellini et al., *Science*, **340**, 464 (2013).

Keywords: Earth's core, Core light element, Melting relations, High pressure

©2019. Japan Geoscience Union. All Right Reserved.

Elastic property and structure of pyrope glass at high pressure

*Naoki Hisano[1], Tatsuya Sakamaki[1], Tomonori Ohashi[1], Ken-ichi Funakoshi[2], Yuji Higo[3], Yuki Shibazaki[4], Akio Suzuki[1]

1. Department of Earth Science, Graduate School of Science, Tohoku University, 2. Neutron Science & Technology Center, Comprehensive Research Organization for Science and Society (CROSS), 3. Japan Synchrotron Radiation Research Institute, 4. International Center for Young Scientists, National Institute for Materials Science

Structural properties of magma are closely correlated to their physical, chemical, and thermal properties. One of approaches for obtaining insights of magmas is an examination of silicate glasses. Aluminum is one of the major elements in the Earth and an important element for controlling the silicate network in melts and glasses because Al^{3+} behaves as an intermediate species in the silicate melts. Aluminum cation can act as either a network former or a modifier, depending on the composition. In the case of a fully-polymerized melt, such as jadeite and albite composition, all TO_4 tetrahedra (where T represents cations, such as Si, Al, etc.) are interconnected via oxygen anions, forming a three-dimensional network structure. Compositional differences are generally considered in terms of variety of alkaline (e.g., Na^{+}) and alkaline-earth (e.g., Mg^{2+}, Ca^{2+}) cations in the melts. These cations are called network modifiers and tend to cut Si-O-Si bonds between a SiO_4 tetrahedron and the adjacent ones. In addition to aluminum cation, other network modifiers also affect the melt behavior. A Mg-aluminosilicate, pyrope ($Mg_3Al_2Si_3O_{12}$) is an important mineral of mantle because of its abundance in the Earth's upper mantle. Change in the slope of melting curve of pyrope around 7-10 GPa has been reported, and pressure-induced Al-coordination change was suggested. Although investigations of structure and elasticity of Mg-aluminosilicate glasses and pyrope-composition glasses have been conducted at ambient pressure, those observations at high pressures are still poor.

Here, we have measured sound velocities of pyrope glass at pressures up to 12.9 GPa using ultrasonic technique at BL04B1 of SPring-8. Longitudinal and transverse wave velocities decreased up to 5.6 GPa, and then the velocities started to increase with pressure. Pressure dependence of elastic moduli and Poisson's ratio of the glass also changed around 7-8 GPa. The structural determination of the glass was conducted based on the energy-dispersive X-ray diffraction method at beamline NE5C of PF-AR in order to understand the mechanism of changes in microscopic physical properties in terms of macroscopic structural evolution. The characteristic shrinkage of the intermediate-range ordering in silicate network was observed around 7 GPa. We could find some correlation between elastic properties and structure. Detailed discussion will be shown in the meeting.

Keywords: silicate glass, elastic wave velocity, X-ray diffraction, structure, ultrasonic measurement

©2019. Japan Geoscience Union. All Right Reserved.

The effect of water and redox state on melting at the top of the lower mantle

*Ayano Nakajima[1], Tatsuya Sakamaki[1], Akio Suzuki[1]

1. Tohoku University

There are various igneous activities in the Earth. On the surface of the Earth, for example, igneous activities occur in island arcs, mid-ocean ridges, hot spots and petit spots. However, not only on the surface, but also in the interior, melting phenomena are also suggested at the top of the asthenosphere [e.g., Barazangi & Isacks, 1971 *JGR*; Schmerr, 2012 *Science*] and the bottom of the upper mantle [e.g., Bercovici & Karato, 2003 *Nature*; Song *et al.*, 2004 *Nature*]. In this study, we focused on the melting of hydrous peridotite at the top of the lower mantle because seismological observation indicates the low velocity anomaly [Schmandt *et al.*, 2014 *Scienc*e; Liu *et al.*, 2016 *GRL*; Liu *et al.*, 2018 *EPSL*]. The low-velocity region is expected to be caused by mantle melting due to dehydration decomposition of ringwoodite to bridgmanite and ferro-periclase with a downward flow.

Here, we performed melting experiments of peridotite with 2.0 wt. % H_2O at 26 GPa and 1600 ˚C - 2000 ˚C. As a starting material, two peridotite samples were synthesized: one was Fe_2O_3-bearing sample and the other was FeO-bearing. The samples were sealed by gold capsules. Recovered product of reductive sample (= FeO-bearing) from 2000 ˚C and 26 GPa showed a partial melting texture. This indicates that mantle melting can be occurred under this experimental condition. On the other hand, there are no melting texture of recovered sample of Fe_2O_3 system from 2000 ˚C and 26 GPa. In short, the materials constituting the lower mantle melts in the reduced state but not in the oxidized state. It is reported that ferric iron occupies a majority in the redox state at the top of the lower mantle [McCammon, 1997 *Nature* ; Frost *et al.*, 2004 *Nature*]. Thus, it is considered that melting phenomenon may or may not occur due to the regional difference of redox state. At 2000 ˚C, compared to bridgmanite in this study, the composition of melt was SiO_2- and Al_2O_3-poor and MgO- and CaO-rich. Although the FeO component concentrated in the melt, this behavior is closer to the tendency of the anhydrous melting experiments (2400 ˚C or more) [Ito & Takahashi, 1987 *Nature*; Trønnes & Frost, 2002 *EPSL*] than the hydrous system (~1400 ˚C) [Kawamoto, 2004 *PEPI*] because of the small amount of water. We calculated the density and compressibility of the magma based on the obtained melt composition. Comparing with seismological model, this melt is lighter than the lower mantle rock. This implies that a small amount of water (2.0 wt. %) can cause a light melt at the top of lower mantle and form the seismological low velocity zone.

Keywords: dehydration melting, lower mantle, hydrous magma, redox state

©2019. Japan Geoscience Union. All Right Reserved.

Sound velocity measurements on liquid Fe-P alloy up to 80 GPa

*Daisuke Kinoshita[1], Yoichi Nakajima[1,2], Yasuhiro Kuwayama[2,3], Kei Hirose[3], Daisuke Ishikawa[2,4], Baron Q.R. Alfred[2]

1. Kumamoto University, 2. RIKEN MDL, 3. Tokyo University, 4. JASRI

The Earth’ s liquid outer core is composed mainly of iron, alloying with 5% nickel and 10% lighter elements [1]. The core composition is important to understand the environment and mechanism of the core formation process and the present-day magnetic field. The sound velocity of liquid iron alloys under relevant high-pressure and -temperature conditions in the core is key to constraining the core composition because the direct observations for the core is seismologic wave passing through the core only. Phosphorous is one of the candidates for light elements in the core because it is found in iron-meteorites [2] and depleted in the silicate mantle relative to chondrites [3]. In this study, we determined the P-wave velocity of liquid $Fe_{75}P_{25}$ up to 80 GPa using a laser-heated diamond-anvil cell in combination with an inelastic X-ray scattering (IXS) spectroscopy. We performed IXS measurements at a beamline BL43LXU [4] of the RIKEN SPring-8 Center in Japan. The P-wave velocity of liquid $Fe_{75}P_{25}$ were obtained based on the observed acoustic phonon dispersion. The present results exhibit that the influence of phosphorus on liquid iron sound velocity is almost negligible under the present experimental conditions. On the other hands, the density of liquid Fe can be reduced by phosphorous.

References

[1] Stevenson, 1981 Science. Vol.214, 611-619
[2] Skála and Císařova, 2005 Physics and Chemistry of Minerals. Vol.31, 721-732
[3] McDonough, 2003 Treatise on Geochem. Vol.2, 547-568
[4] Baron, 2010 SPring-8 Inf. Newsl. Vol.15, No.1 14-19

Keywords: outer core, sound velocity, high pressure

©2019. Japan Geoscience Union. All Right Reserved.

High-pressure structural investigations for hydrous sodium silicate melts

*Tomonori Ohashi[1], Tatsuya Sakamaki[1], Ken-ichi Funakoshi[2], Miki Muranushi[1], Chikara Shito[1], Yuki Shibazaki[3], Akio Suzuki[1]

1. Department of Earth Science, Tohoku University, 2. Neutron Science and Technology Center, Comprehensive Research Organization for Science and Society (CROSS), 3. National Institute for Materials Science (NIMS)

The behaviors of high-pressure silicate melts, which is controlled by their physico-chemical properties, are important to understand the magma activity in the deep Earth. Particularly, the H_2O content significantly affects the properties, such as density (e.g., Sakamaki et al., 2006) and viscosity (e.g., Suzuki et al., 2011; Poe et al., 2006). Since such macroscopic properties are known to be largely determined by the microscopic structure, there are considerable interests in revealing how the structure changes with increasing pressure.

Here, structures of hydrous Na_2O-8/3SiO_2 melts with 5 wt% (NS8/3_H5) and with 9 wt% H_2O (NS8/3_H9) were determined under high pressure and temperature by the in-situ X-ray diffraction (XRD). The in-situ XRD study was carried out using a cubic-type multi-anvil apparatus MAX80, which is installed at the AR-NE5C beamline of PF-AR at Tsukuba, Japan. The experimental *P*-*T* conditions were about 1.5–3.0 GPa and 550–970 ˚C, respectively.

The obtained total structure factors, $S(Q)$ of both liquids show that the position of the first sharp diffraction peaks (FSDP) shift to higher-Q with pressure. This positional shift indicates the intermediate-range order structure of present melts become compact. The reduced radial distribution functions, $G(r)$ indicate different pressure evolutions in the average Si-O bond lengths ($r_{Si\text{-}O}$) depending on their water contents. The $r_{Si\text{-}O}$ in the NS8/3_H9 melt shows the monotonic decrease with increasing pressure, however, the $r_{Si\text{-}O}$ of the NS8/3_H5 melt hardly changes after its contraction below 1.6 GPa. The structure of the NS8/3_H9 melt is assumed to be slightly more depolymerized than the NS8/3_H5 melt at ambient pressure (Zotov and Keppler, 1998). This difference might be due to a phenomenon that the number of strongly hydrogen-bonded SiOH groups, which are favored in sodium silicate glasses and melts (Xue and Kanzaki, 2004), increase more significantly during pressure-induced depolymerization in the NS8/3_H9 melt than in the NS8/3_H5 melt. This raises Si(-NBO)/Si(-BO) (NBO: non-bridging oxygen, BO: bridging oxygen) ratio, and hence, the $r_{Si\text{-}O}$ becomes shorter.

Keywords: hydrous silicate melt, effect of water, amorphous structure, high pressure and temperature

©2019. Japan Geoscience Union. All Right Reserved.

Inelastic X-ray scattering measurements of liquid Fe-N alloy under high pressure

*Asaki Iwamoto[1], Yoichi Nakajima[1,2], Daisuke Kinoshita[1], Yasuhiro Kuwayama[2,3], Kei Hirose[3], Daisuke Ishikawa[2,4], Alfred Q.R. Baron[2]

1. Kumamoto University, 2. RIKEN MDL, 3. The University of Tokyo, 4. JASRI

The Earth’ s liquid outer core is composed mainly of iron, alloying with ~5% nickel and ~10% some light elements [1]. Nitrogen is one of candidates for the light elements. The abundance of nitrogen in the silicate mantle relative to that in primordial meteorites is less than those of similar volatile components such as H_2O, C and Ar, so that large portion of nitrogen in bulk Earth can be stored in the core [2,3]. In order to examine the possibility of nitrogen in the core, it is benefit to compare the sound velocity of liquid Fe-N alloy under high-pressure and -temperature relevant to the core conditions with the seismological observations. In this study, we performed inelastic X-ray scattering (IXS) measurements on liquid Fe-N alloy and determined its longitudinal velocity of the liquid Fe-N alloy under high pressure and temperature.

We carried out high-pressure and -temperature IXS measurements using a laser-heated diamond-anvil cell (LH-DAC) at the beamline BL43LXU of SPring-8 [4]. We used an Fe_4N foil (hereafter called $Fe_{80}N_{20}$) as a starting sample and single crystal Al_2O_3 discs as a thermal insulator. We judged the sample melting based on X-ray diffraction measurements during heating and then measured IXS of the liquid sample. The longitudinal sound wave (P-wave) velocity of liquid $Fe_{80}N_{20}$ was determined from the dispersion relation of the longitudinal acoustic phonon mode of the sample. We obtained the velocity of liquid $Fe_{80}N_{20}$ up to 76 GPa and 2200 K. We found that the P-wave velocity of liquid $Fe_{80}N_{20}$ is slightly faster by c.a. 4% than that of liquid Fe [5]. The P-wave velocity of liquid outer core is faster by 4% than liquid Fe [5]. Therefore, the present results give the upper limit of 5.9 wt.% (20 at.%) for the nitrogen content in the outer core.

[1] Stevenson, Science **214**, 611-619 (1981).

[2] Marty, Earth Planet. Sci. Lett. **313-314**, 56-66 (2012).

[3] Li et al., Earth Planet. Sci. Lett. **377-378**, 311-323 (2013).

[4] Baron, SPring-8 Inf. Newsl. **15**(1), 14-19 (2010).

[5] Anderson and Ahrens, J. Geophys. Res. **99**(B3), 4273-4284 (1994)

Keywords: Earth's liquid outer core, Light element, P-wave velocity, High pressure

©2019. Japan Geoscience Union. All Right Reserved.

Formation of highly pure anorthite crust on the low-volatile astral bodies by low-viscous magma ocean

*Tatsuya Sakamaki[1], Yoshio Kono[2]

1. Graduate School of Science, Tohoku University, 2. Geodynamics Research Center, Ehime University

Anorthite ($CaAl_2Si_2O_8$) is a Ca-endmember of plagioclase, and it is a main component of a crust on the astral bodies, such as Moon and 4 Vesta, Thick anorthite-rich crust has been formed through a process of magma ocean. Here we conduct high-pressure and high-temperature experiments and *in-situ* X-ray analysis to simultaneously assess the viscosity and structure of anorthite magmas under pressures of up to 6.6 GPa. We find contrasting behavior in the viscosity between liquid anorthite and albite ($NaAlSi_3O_8$), which is Na-endmember of plagioclase. The big difference in viscosity between anorthite and albite melts has important implications for planetary differentiation. Na-poor astral bodies (Moon, 4 Vesta, etc.) have been dominated by low-viscous magma ocean and, eventually caused an efficient differentiation between crystal and magma. This process prevented the melt from trapping in the grain boundaries of floating anorthites. This makes the highly pure anorthite crust on the Moon observed by the remote sensing.

Keywords: anorthite melt, viscosity, structure, high pressure, high temperature, lunar magma ocean

©2019. Japan Geoscience Union. All Right Reserved.

[E] Poster | S (Solid Earth Sciences)：S-IT Science of the Earth's Interior & Techtonophysics

Sun. May 26, 2019 10:45 AM - 12:15 PM JST | Sun. May 26, 2019 1:45 AM - 3:15 AM UTC | Poster Hall International Exhibition Hall8, Makuhari Messe_7

[S-IT23] Structure and Dynamics of Earth and Planetary Mantles

convener:Takashi Nakagawa(Department of Earth Sciences, The University of Hong Kong), Takashi Yoshino(Institute for Planetary Materials, Okayama University), Dapeng Zhao(Department of Geophysics, Tohoku University)

Interdisciplinary approach can lead to a better understanding of dynamics and evolution of the deep interiors of the Earth and planets. We welcome any submissions of recent results in observational, theoretical and experimental studies on seismology, geomagnetism, mineral physics, dynamics of deep interiors, and any other relevant fields from researchers in many countries. Integration of such results is also welcome. In particular, we encourage any contributions focusing on "plate and mantle dynamics in Earth and terrestrial planets". We also encourage papers stimulating an interdisciplinary collaboration relating to establishment of the Japan-SEDI community.

[SIT23-P01] Interaction between volcanisms inland and the spreading center: example of Galápagos archipelago

*Walid Ben Mansour[1], Guust Nolet[2], Mario Ruiz[3], Juan Carlos Afonso[1] (1.Department of Earth and Planetary Sciences, Macquarie University, Sydney (Australia), 2.Geoazur, Université Cote d'Azur, Sophia Antipolis (France), 3.Instituto Geofisco, Escuela Politecnica Nacional, Quito (Ecuador))

[SIT23-P02] **Effect of iron content on thermal conductivity of olivine with implications for cooling history of rocky planets**

*Youyue Zhang[1], Takashi Yoshino[1], Akira Yoneda[1], Masahiro Osako[2] (1.Institute for Planetary Materials, Okayama University, 2.Division of Physical Sciences, National Museum of Nature and Science)

[SIT23-P03] **The distribution of Cenozoic conglomerates and its sedimentological constraint on the uplift of the South Tianshan, NW China**

*SUN HAITAO[1] (1.China University of Petroluem-Beijing)

[SIT23-P04] **Electrical conductivity of diaspore, δ-AlOOH and ε-FeOOH**

*Ran Wang[1] (1.Institute for Planetary Materials, Okayama University)

[SIT23-P05] Multi-mode surface wave tomography for azimuthal anisotropy in the Australasian upper mantle

*Yuka Nishimura[1], Kazunori Yoshizawa[2] (1. Graduate School of Science, Hokkaido University, 2.Faculty of Science, Hokkaido University)

[SIT23-P06] Mapping multi-mode surface wave phase speeds in North America using mode-branch waveforms decomposed by linear Radon transform

*Hitoshi Matsuzawa[1], Kazunori Yoshizawa[2] (1.Graduate School of Science, Hokkaido University, 2.Faculty of Science, Hokkaido University)

[SIT23-P07] Radial anisotropy in the upper mantle using multi-mode surface waves incorporating the η_k parameter: Application to the Pacific and Australian regions

Shuya Okuyama[1], *Kazunori Yoshizawa[1,2], Hitoshi Kawakatsu[3], Takehi Isse[3] (1.Graduate School of Science, Hokkaido University, 2.Faculty of Science, Hokkaido University, 3.Earthquake Research Institute, University of Tokyo)

[SIT23-P08] Pure to impure and dry to wet olivine rheology based on high temperature dependency of diffusion creep

*Kosuke Yabe[1], Takehiko Hiraga[1] (1.School of Science, The University of Tokyo)

[SIT23-P09] Finite frequency S wave tomography model beneath the Ontong Java Plateau using data recorded by broadband ocean bottom seismographs

*Misaki Horiuchi[3], Hiroko Sugioka[3], Masayuki Obayashi[1], Daisuke Suetsugu[1], Hajime Shiobara[2], Aki Ito[1], Yasushi Ishihara[1], Satoru Tanaka[1], Takehi Isse[2], Takashi Tonegawa[1], Junko Yoshimitsu[1], Takumi Kobayashi[3] (1.Japan Agency for Marine-Earth Science and Technology, Yokosuka, Japan, 2.Earthquake Research Institute, The University of Tokyo, Tokyo, Japan, 3.The University of Kobe, Hyogo, Japan)

[SIT23-P10] Shear wave structure of the upper mantle beneath the Ontong Java Plateau

*Takehi Isse[1], Daisuke Suetsugu[2], Hajime Shiobara[1], Hiroko Sugioka[3], Aki Ito[2], Yasushi Ishihara[2], Satoru Tanaka[2], Masayuki Obayashi[2], Takashi Tonegawa[2], Junko Yoshimitsu[2], Takumi Kobayashi[3], Kazunori Yoshizawa[4] (1.Earthquake Research Institute University of Tokyo, 2.Japan Agency for Marine-Earth Science and Technology, 3.Kobe University, 4.Faculty of Science, Hokkaido University)

[SIT23-P11] Effect of impurity on post-post-perovskite transition of $MgSiO_3$ by first principles

*Koichiro Umemoto[1] (1.Earth-Life Science Institute, Tokyo Institute of Technology)

[SIT23-P12] Unsusual high-Ti corundum recovered from the Horoman peridotites, Hokkaido, Japan

*oosawa takumi[1], Shinji Yamamoto[1] (1.yokohama national university)

[SIT23-P13] Deformation experiments on akimotoite

*Longli Guan[1], Daisuke Yamazaki[1], Noriyoshi Tsujino[1] (1.Institute for Planetary Materials, Okayama University, Misasa, Japan)

[SIT23-P14] Fate of water in subducted hydrous sediments deduced from stability fields of FeOOH and AlOOH up to 20 GPa

*Takashi Yoshino[1], Edward Baker[2], Kyle Duffey[3] (1.Institute for Planetary Materials, Okayama University, 2.Department of Earth Sciences, University of Oxford, 3.Department of Geosciences, Princeton University)

Interaction between volcanisms inland and the spreading center: example of Galápagos archipelago

*Walid Ben Mansour[1], Guust Nolet[2], Mario Ruiz[3], Juan Carlos Afonso[1]

1. Department of Earth and Planetary Sciences, Macquarie University, Sydney (Australia), 2. Geoazur, Université Cote d'Azur, Sophia Antipolis (France), 3. Instituto Geofisco, Escuela Politecnica Nacional, Quito (Ecuador)

The Galápagos archipelago, located west of Ecuador, is a good example where a mantle plume interacts with a spreading center and modifies physical and chemical properties of the oceanic lithosphere. The Galápagos Spreading Center (GSC) and the Galápagos hotspot interact over more than 1,000 km with unusual features for a hot spot region (large number of historical active volcanoes, large range of lavas composition, alignment of volcanic centers and seamounts). To bring new information on the physical and chemical properties of this region, we are constructing a new P-wave velocity model of this region by combining data from 10 seismic broadband stations and from 9 MERMAIDS (Mobile Earthquake Recorder in Marine Areas by Independent Divers) deployed in this region between 2014 and 2016. We focus on Pn head waves to better constraint the Moho depth in this region and image the interaction between the hot spot and the GSC. We selected150 seismic events between May 2014 and September 2016, with epicentral distance between 3°and 35° and picked more than 2,500 Pn phases that we will invert in a probabilistic tomography inversion in a second step. In this presentation, we will show examples and statistics of Pn data. We will discuss the benefits of developing a multi-observable thermochemical tomography in this region to better image the intricate interaction of a hot spot with the overlying oceanic lithosphere and evaluate current physio-chemical evolutionary models.

Keywords: Pn tomography, mantle plume, thermochemical structure

©2019. Japan Geoscience Union. All Right Reserved.

Effect of iron content on thermal conductivity of olivine with implications for cooling history of rocky planets

*Youyue Zhang[1], Takashi Yoshino[1], Akira Yoneda[1], Masahiro Osako[2]

1. Institute for Planetary Materials, Okayama University, 2. Division of Physical Sciences, National Museum of Nature and Science

Knowledge of thermal transport properties of mantle materials is essential for understanding the thermal state and dynamics of the Earth and planetary interiors. Previous studies have suggested that temperature and pressure dependences of thermal conductivity can affect mantle convection and plate tectonics involving subduction dynamics. Olivine is the most abundant mineral in the Earth's upper mantle and chemical composition of olivine in the Earth's upper mantle is characterized by high forsterite content around Fo_{90}. For other terrestrial planets, Mercury is believed to have a FeO-poor mantle along with end member silicates, whereas olivine in the Martian mantle would be more Fe-rich, speculated to be Fo_{67}. Recent studies suggested that surface of some asteroids is dominated by olivine of composition from Fo_{49} to Fo_{70}. Hence, the effect of Fe content in olivine on thermal conductivity could be significant for understanding the thermal structure and cooling history of these terrestrial planets and asteroids.

In this study, thermal conductivity and diffusivity of olivine were determined simultaneously by combining multi-anvil high pressure experimental technique and pulse heating method. Thermal properties of olivine with six different Fe contents (Fo, Fo_{90}, Fo_{70}, Fo_{50}, Fo_{31}, Fo_{0}) were measured under the Earth's upper mantle condition in a 5000-ton Kawai type multi-anvil press. The minimum λ was found to be at composition near Fo_{31}; the absolute λ value of Fo_{31} is about 65% lower than that of Fo. Small amounts of minor elements can strongly reduce the thermal conductivity at low temperature; λ value of Fo90 is about 50% of Fo at room temperature. As temperature increases, the difference in λ among olivine samples with various Fe contents tends to become smaller. Thermal conductivities of polycrystalline olivine have smaller absolute values and weak pressure and temperature dependences, compared with those of natural single crystal olivine determined by previous studies. Heat capacity of olivine calculated from λ and κ is independent of pressure and is controlled by nearly constant thermal expansion coefficient of Fo_{70} and Fo_{50} with increasing temperature. Smaller λ of olivine aggregate with high Fe content would produce thicker crust in the Fe-rich Mars, while heat in the Fe-poor Mercury can escape faster than the other terrestrial planets. Olivine-dominant asteroids with high Fe concentration could have longer cooling history and lower thermal inertia on the surface.

Keywords: Thermal conductivity, Olivine, Heat capacity, High pressure, Mantle

©2019. Japan Geoscience Union. All Right Reserved.

The distribution of Cenozoic conglomerates and its sedimentological constraint on the uplift of the South Tianshan, NW China

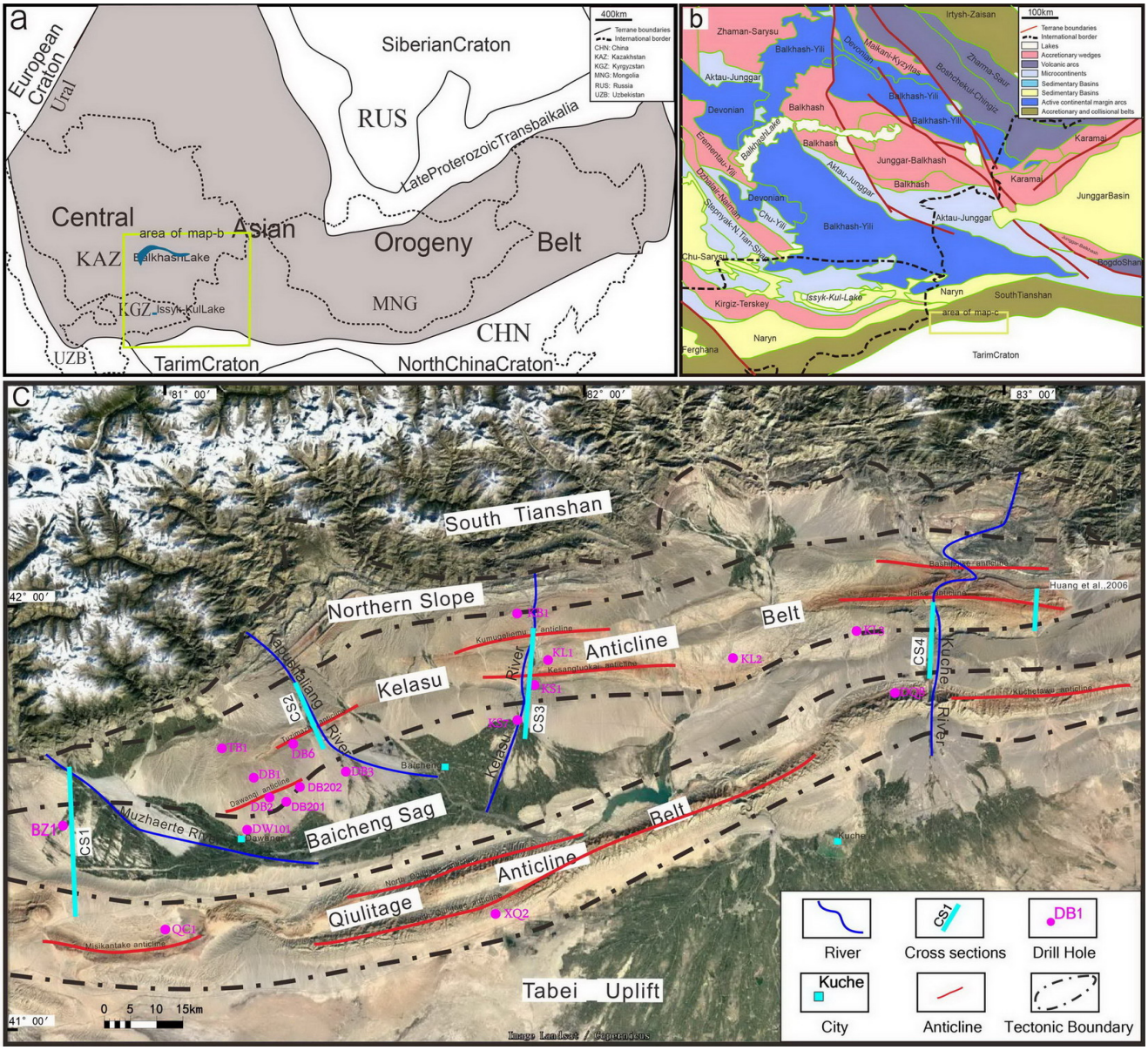
*SUN HAITAO[1]

1. China University of Petroluem-Beijing

The Cenozoic alluvial fan deposits in the Kuqa Depression of Tarim Basin, likely in response to a tectonic event, can provide critical evidence for constraining the timing of the South Tianshan uplift and reconstructing the paleotectonic evolution of the Central Asian Orogenic Belt. The sedimentological analysis shows that the conglomerates were deposited in alluvial fan environment. The initial uplift stage was started from the Jidike Formation at ~23Ma, resulting only small but angular gravels. Then the rapid uplift was since 15.97 Ma leading to the deposition of Kangcun conglomerate layers. And the next rapid and intensely uplift was started at ~4 Ma of the deposition of Kuqa Formation, according to ~2000m thick alluvial fan conglomerates. After a short quiescence, the most remarkable uplift of South Tianshan regenerated and caused the most extensive alluvial fan conglomerates of Xiyu Formation since 2.58 Ma and continuing to the present.

Keywords: Cenozoic, Central Asian Orogenic Belt, Conglomerate

©2019. Japan Geoscience Union. All Right Reserved.



©2019. Japan Geoscience Union. All Right Reserved.

Electrical conductivity of diaspore, δ-AlOOH and ε-FeOOH

*Ran Wang[1]

1. Institute for Planetary Materials, Okayama University

FeOOH and AlOOH are dominant hydrous phases in sedimentary rocks deposited in the sea or lake basins which were considered to be possibly related to the deep water cycle by slab subduction. Therefore, understanding of the electrical conductivity behaviors of these phases are essential to explore the nature and dynamic process of the Earth's interior. In this study, electrical conductivity of diaspore (α-AlOOH), δ-AlOOH and ε-FeOOH was measured by impedance spectroscopy with a frequency range from 10^{-1} to 10^{6} Hz at pressures up to 15, 20 and 12 GPa and temperatures of 1200, 1200 and 1000 K well below the dehydration temperatures of these phases under the relevant pressures. For diaspore at 8, 10, and 12 GPa, the relationship between electrical conductivity and reciprocal temperature could be well fitted by the Arrhenius formula: $\sigma = \sigma_0 \exp[-(\Delta E+P\Delta V)/kT]$ and shows the pre-exponential factor (σ_0), activation energy (ΔE) and activation volume (ΔV) of 55.94 ±1.16 S/m, 0.547 ±0.016 eV and 1.683 ±0.123 cm^3/mol, respectively. However, data of diaspore obtained below 6 GPa could not be fitted by the Arrhenius formula, which was thought to be due to the remnant of free water in the sample caused by heating to insufficient temperature to proceed dehydration of interstitial water. Thus, it is quite difficult to measure the electrical conductivity of diaspore at low pressures. The electrical conductivity of diaspore increased with pressures ranging from 8 to 12 GPa by half order of magnitude and then the conductivity change with pressures from 12 to 15 GPa became negligibly small. The dominant conduction mechanism of diaspore is regarded as proton conduction. δ-AlOOH and ε-FeOOH show one and two orders of magnitude higher electrical conductivity than diaspore. Due to isostructural $CaCl_2$-type hydroxide structure, δ-AlOOH and ε-FeOOH display the nearly identical activation enthalpy (0.384 ±0.007 eV, 0.330 ±0.048 eV) which is relatively lower than that of diaspore.

Keywords: Electrical conductivity, Diaspore, δ-AlOOH, ε-FeOOH

©2019. Japan Geoscience Union. All Right Reserved.

Multi-mode surface wave tomography for azimuthal anisotropy in the Australasian upper mantle

*Yuka Nishimura[1], Kazunori Yoshizawa[2]

1. Graduate School of Science, Hokkaido University, 2. Faculty of Science, Hokkaido University

Azimuthal anisotropy in the upper mantle derived from seismic surface waves provides us with the information of mantle dynamics, such as the present-day mantle flow and the remnant of past deformation in the lithosphere and asthenosphere.The Australian plate is currently the fastest-moving tectonic plate including a large continent, encompassed by the intensive seismicity, particularly in its north (Indonesia) and east (Tonga-Kermadec to New Zealand). Thus, the entire continent can be covered by dense ray paths utilizing broad-band seismic stations deployed throughout the continent. This unique tectonic setting of Australian plate allows us to reconstruct high-resolution tomography models in the Australian region (e.g., Fishwick et al., 2008, Tectonics; Yoshizawa, 2014, PEPI).

In this study, we construct new phase speed maps in and around the Australian continent incorporating azimuthal anisotropy for both multi-mode Love and Rayleigh waves using the method developed by Yoshizawa & Kennett (2004, JGR). We employ the data base of path-specific multi-mode phase speeds for the fundamental mode and up to the fourth-higher modes by Yoshizawa (2014, PEPI), which has been measured by using the non-linear waveform fitting method (Yoshizawa & Ekstrom, 2010, GJI). We have performed checkerboard resolution tests as well as jackknife resampling tests, which suggest that our current phase speed data set can provide us with the robust estimation of azimuthally anisotropic phase speed maps in the Australasian region.

The multi-mode phase speed models indicate that the fastest directions of azimuthal anisotropy estimated from the different modes are consistent each other as far as they have the maximum sensitivity at the common depth. Comparisons between the direction of absolute plate motion (HS2-NUVEL-1) by Gripp & Gordon (1990, GRL) and the fastest direction of azimuthal anisotropy suggests that they agree well particularly at around the depth of 100km under the ocean area (Coral and Taman Seas) off the east-coast of the Australian continent and 300km under the continental area of Australia. These results are likely to reflect the differences in the depth of asthenosphere where the effects of the lattice preferred orientation of mantle materials due to the present-day mantle flow can be more significant.

Keywords: Azimuthal anisotropy, Surface wave tomography, Australia

©2019. Japan Geoscience Union. All Right Reserved.

Mapping multi-mode surface wave phase speeds in North America using mode-branch waveforms decomposed by linear Radon transform

*Hitoshi Matsuzawa[1], Kazunori Yoshizawa[2]

1. Graduate School of Science, Hokkaido University, 2. Faculty of Science, Hokkaido University

The use of higher-mode surface waves is inevitable for further enhancement of vertical resolution of tomography model since they are much more sensitive to the deep structure of the Earth’ s upper mantle than the fundamental modes. However, measuring the multi-mode phase speeds is not a straightforward issue since wavetrains of different modes overlap each other in a seismogram.

We have developed the two-step array-based method for higher-mode analysis, which consists of (1) multi-mode phase speed measurements based of a classical *f-k* analysis using a long-range linear array with several-thousand kilometers (e.g., Nolet, 1975, GRL) and (2) modal waveform decomposition for the centroid location of the linear array using the linear Radon transform (e.g. Luo *et al*., 2015, GJI).

We have previously applied the method to a large data set of seismograms observed at Transportable Array stations of USArray and employed the average phase speeds of linear array to map phase speed distributions in North America (Matsuzawa and Yoshizawa, SSJ Fall Meeting 2018; AGU Fall Meeting 2018). We could obtain phase speed maps of the fundamental-mode and the first four higher-mode surface waves. Although the large-scale anomalies (i.e., fast phase speeds in cratons in the stable eastern U.S., slow phase speeds in the tectonically-active western U.S.) can be identified, the lateral resolution of the phase speed maps were insufficient compared to inter-station/array based tomography models. This suggests that the small-scale tectonic features have been blurred and averaged out due to the direct use of long linear array (2000–4000 km) with relatively large measurement errors.

In this study, we apply the inter-station dispersion analysis with nonlinear waveform fitting (Hamada and Yoshizawa, 2015, GJI) to the decomposed modal waveforms of the fundamental-mode surface waves derived from method using the centroids of the linear array as imaginary stations.The lateral resolution of resultant phase speed maps has been improved up to about 2.0 degrees owing to the relatively shorter inter-station (inter-centroid) distances used in the inversions.We can find typical small-scale tectonic features in the inland region of eastern and central US. Average phase speeds along each short ray path (several-hundred kilometers) have been measured stably without interference by overtones, which is likely to be of help in improving the accuracy of the resultant tomography maps.

The decomposed modal waveforms of the higher modes as well as the fundamental mode can be applied to the secondary dispersion analyses such as the inter-station dispersion measurements as done in this study and/or a 2-D beamforming analysis, which can be expected to enhance both the lateral and vertical resolutions of surface wave tomography models.

Keywords: Surface wave, Higher mode, Array-based analysis, Tomography, North America

©2019. Japan Geoscience Union. All Right Reserved.

Radial anisotropy in the upper mantle using multi-mode surface waves incorporating the η_κ parameter: Application to the Pacific and Australian regions

Shuya Okuyama[1], *Kazunori Yoshizawa[1,2], Hitoshi Kawakatsu[3], Takehi Isse[3]

1. Graduate School of Science, Hokkaido University, 2. Faculty of Science, Hokkaido University, 3. Earthquake Research Institute, University of Tokyo

Radial anisotropy can be described by five elastic parameters; four parameters related to seismic wave speeds (β_v, β_h, α_h, α_v) and an additional fifth anisotropic parameter (η). One of the anisotropic parameters, η, was originally defined by Anderson (1961), but its physical proprieties have been rather unclear compared with other four parameters related to elastic velocity.

The re-defined fifth anisotropic parameter η_κ by Kawakatsu et al. (2015) makes it easier to understand its physical proprieties compared with conventional η. The introduction of η_κ affects the shape of sensitivity kernels of Rayleigh wave phase speeds with respect to η_κ, PH-wave speeds α_h and PV-wave speeds α_v (Kawakatsu, 2016b). Since the sensitivity of Rayleigh wave phase speeds to η_κ becomes greater than that to η, we can expect a possibility of resolving the η_κ parameter. However, since the inverse correlation between the sensitivity kernels of SV-wave speed β_v and η_κ becomes rather stronger, the trade-off between β_v and may easily occur. Therefore, the independent determination of η_κ parameter from the inversions of surface-wave dispersion curves is not a straightforward issue.

In this study, incorporating η_κ, we performed inversions for five elastic parameters in the upper mantle, employing a classical iterativenonlinear least-squares inversion method (Tarantola and Valette, 1982). We used multi-mode dispersion data sets of surface waves in the Australian region (Yoshizawa, 2014, PEPI) and Pacific (Isse et al., 2019, EPSL) to reconstruct 3-D radially anisotropic model. In these inversions, we used isotropic PREM as a starting model to avoid the influence of reference anisotropy model.

The retrieved spatial distribution of the η_κ parameter can be mostly explained by trade-offs with SV wave speed β_v at many locations in Australia and Pacific. Still, we can find structural features in our 3-D β_v and η_κ models, particularly in some major structural boundaries such as ridges and the Tasman Line in eastern Australia, which cannot simply be attributed to the trade-off between β_v and η_κ, indicating possible intrinsic character of η_κ in the upper mantle.

Keywords: radial anisotropy, surface waves, inversion

©2019. Japan Geoscience Union. All Right Reserved.

Pure to impure and dry to wet olivine rheology based on high temperature dependency of diffusion creep

*Kosuke Yabe[1], Takehiko Hiraga[1]

1. School of Science, The University of Tokyo

There has been a large discrepancy in creep properties of olivine aggregates in dry diffusion creep regime between Minnesota group (Hirth and Kohlstedt, 1995) and ANU group (Faul and Jackson, 2007). Our recent deformation experiments on undoped and doped olivine aggregate synthesized by a new method different from previous studies demonstrate (i) the activation energy of grain boundary diffusion creep of undoped olivine is 465 kJ/mol, (ii) the creep rate is enhanced by doping of Ca and Al above ~1200 C with very high temperature sensitivity well represented by activation energy of ~700 kJ/mol, and (iii) presence of melt phase had little contribution to the change in the creep strength. Such observations are consistent with Yamauchi and Takei (2016) which attributed the observation to pre-melting at near solidus.

In this study, we compile all rheological data of olivine diffusion creep based on solidus which changes with the chemical compositions and amount of water. The solidi of dry samples are estimated from experiments and/or phase diagrams. The solidi of wet samples are calculated by cryoscopic approach following Hirshmann et al. (2009). We demonstrate that not only dry but also wet data are well explained by the operation of grain boundary diffusion creep with activation energy of 465 kJ/mol at <~0.93 × solidus and 700 kJ/mol at >~0.93 ×solidus. The controversy on the effect of water on grain boundary diffusion by Mei and Kohlstedt (2000) and Fei et al. (2016) is explained by the experimental temperatures with respect to the solidus of their systems. The viscosity depth profile in the upper mantle based on our new diffusion creep model will be presented.

Keywords: mantle rheology, olivine aggregates, diffusion creep

©2019. Japan Geoscience Union. All Right Reserved.

Finite frequency S wave tomography model beneath the Ontong Java Plateau using data recorded by broadband ocean bottom seismographs

*Misaki Horiuchi[3], Hiroko Sugioka[3], Masayuki Obayashi[1], Daisuke Suetsugu[1], Hajime Shiobara[2], Aki Ito[1], Yasushi Ishihara[1], Satoru Tanaka[1], Takehi Isse[2], Takashi Tonegawa[1], Junko Yoshimitsu[1], Takumi Kobayashi[3]

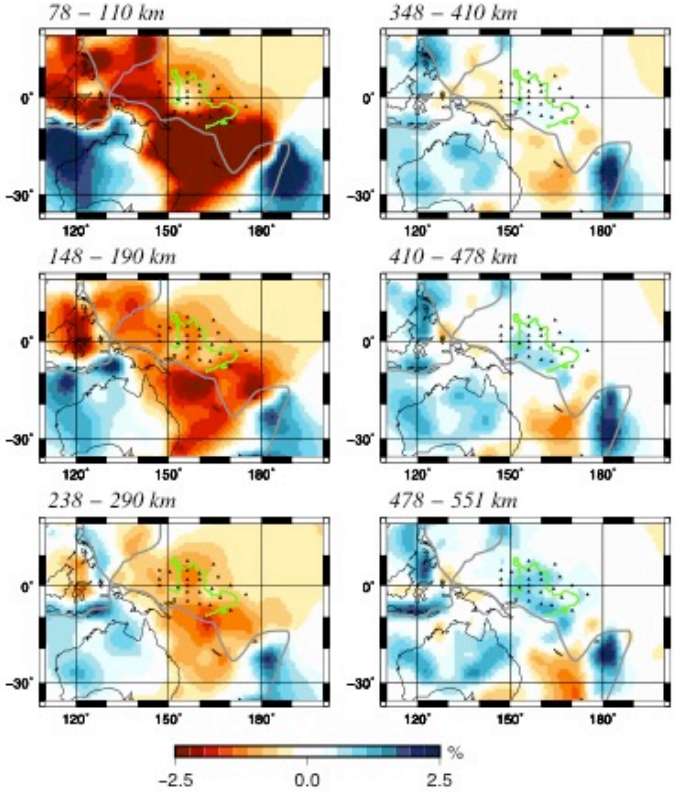
1. Japan Agency for Marine-Earth Science and Technology, Yokosuka, Japan, 2. Earthquake Research Institute, The University of Tokyo, Tokyo, Japan, 3. The University of Kobe, Hyogo, Japan

We determined three-dimensional S wave model beneath the Ontong Java Plateau (OJP) by finite frequency tomography using data recorded by broadband seismographs deployed at ocean bottom covered the OJP and at neighbor islands (Suetsugu *et al.*, 2018). Our dataset contains absolute and period-depended differential travel time data. The former consists of ~1,100,000 direct S-wave onset times reported by International Seismological Centre (ISC) and ~400 direct S-wave onset times picked up on broadband waveform records around the OJP and the latter is composed of ~3,000 differential traveltimes between two different stations around the OJP measured by waveform cross correlation at 7 different passband of which center periods varies from 5.3 sec to 42 sec. We used adaptive stacking method (Rawlinson and Kennett, 2004) to measure absolute travel time data near the OJP. These data were inverted based on the infinite frequency travel time tomography method for the absolute travel time data (Inoue *et al.*, 1990; Fukao *et al.*, 1992; Obayashi *et al.*, 2013) and the finite frequency travel time method for the relative travel time data (Dahlen *et al.*, 2000; Obayashi *et al.*, 2013). We obtained a well resolved S wave velocity model beneath the OJP. It shows significant high velocity anomalies in the mantle transition zone, which are considered as stagnant Pacific slabs related to the trench retreating as well as seafloor spreading in the Santa Cruz Basin and Melanesia Basin during the Eocene and Oligocene. It also reveals that S wave velocity just below the OJP is a little higher than the surrounding strong slow anomalies in the mantle shallower than 200 km. We will discuss these remarkable features beneath the OJP in comparison with P wave tomographic model (Obayashi *et al.*, 2018) in this presentation.

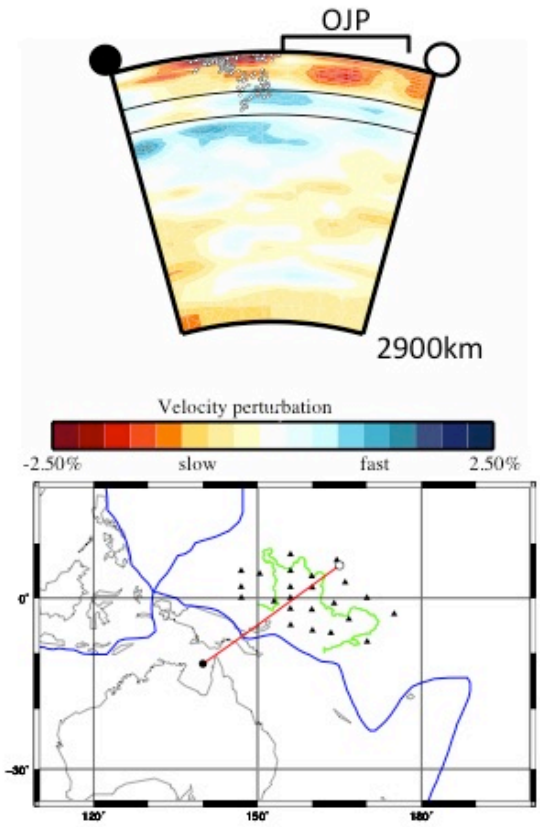
Keywords: finite frequency tomography, S wave velocity structure

©2019. Japan Geoscience Union. All Right Reserved.

(a)



(b)



©2019. Japan Geoscience Union. All Right Reserved.

Shear wave structure of the upper mantle beneath the Ontong Java Plateau

*Takehi Isse[1], Daisuke Suetsugu[2], Hajime Shiobara[1], Hiroko Sugioka[3], Aki Ito[2], Yasushi Ishihara[2], Satoru Tanaka[2], Masayuki Obayashi[2], Takashi Tonegawa[2], Junko Yoshimitsu[2], Takumi Kobayashi[3], Kazunori Yoshizawa[4]

1. Earthquake Research Institute University of Tokyo, 2. Japan Agency for Marine-Earth Science and Technology, 3. Kobe University, 4. Faculty of Science, Hokkaido University

Ontong Java Plateau (OJP) is the vastest Large Igneous Provinces (LIPs) in the oceanic region of the Earth. The OJP was emplaced at 122 and 90 Ma by massive volcanism, but the origin of this volcanism is still under discussion.
Richardson et al. (2000) obtained a large low-velocity root of the OJP extending as deep as 300km, though its existence and cause are still in debating.
One reason for poor understanding of the OJP is the insufficient information about the crust and mantle structure beneath the OJP because of the lack of long-term seafloor observation. Between 2014 and 2017, we conducted the first seismological and electromagnetic observations on the seafloor and islands in the OJP, named "OJP array", to clarify the origin of the OJP.
Using the broadband data from the OJP array as well as those from stations on land and seafloor in the western Pacific Ocean, we constructed three-dimensional shear wave speed structure beneath the OJP by surface wave tomography. using phase speed dispersions of Love and Rayleigh waves up to the 4th higher modes. Checkerboard resolution tests suggests that the spatial resolution of the obtained model is ~300km, which is higher than previous studies.

Obtained shear wave speed structure down to the depth of 300 km shows the following new features:
(1) In the center of the OJP at depths between 70–150 km, about 2% fast anomalies exists;
(2) No strong slow anomaly is found beneath the OJP at depths down to 300 km;
(3) Beneath the Caroline Islands, in the north of the OJP, 2 % slow anomalies exist, which may be associated with the Caroline hotspot activity.

These newly found features suggest that further investigation to reveal the origin of the OJP is necessary.

Keywords: upper mantle structure, Ontong Java, surface wave tomography, BBOBS

©2019. Japan Geoscience Union. All Right Reserved.

Effect of impurity on post-post-perovskite transition of $MgSiO_3$ by first principles

*Koichiro Umemoto[1]

1. Earth-Life Science Institute, Tokyo Institute of Technology

Several computational studies have predicted post-post-perovskite transitions in MgSiO3 at ultrahigh pressures and temperatures which can occur at deep interiors of super-Earths: $MgSiO_3$ --> Mg_2SiO_4+ $MgSi_2O_5$ --> Mg_2SiO_4+ SiO_2 --> MgO + SiO_2) and recombination (MgO + $MgSiO_3$ --> Mg_2SiO_4 or SiO_2 + $MgSiO_3$ --> $MgSi_2O_5$) [1-5]. As demonstrated in a very recent numerical simulation, these transitions are crucially important in modeling interiors of super-Earths up to 20 times Earth’ s mass [6]. However, in the previous studies, these post-post-perovskite transitions were considered only for pure Mg-Si-O. In actual super-Earths, impurities, Fe, Al, or so forth, should exist. Here we will investigate effects of impurities on post-post-perovskite transitions: transition pressures, local atomic structures, and equation of states.

[1] K. Umemoto, R. M. Wentzcovitch, P. B. Allen, Science **311**, 983 (2006).

[2] K. Umemoto and R. M. Wentzcovitch, Earth Plent. Sci. Lett. **311**, 225 (2011).

[3] S. Q. Wu et al., J. Phys.: Condens. Matter, **26**, 035402 (2014).

[4] H. Niu et al., Scientic Reports **5**, 18347 (2015).

[5] K. Umemoto et al., Earth Planet. Sci. Lett. 478, 40-45(2017).

[6] A. P. van den Berg et al., Icarus 317, 412-426(2019).

Keywords: super-Earth, post-post-perovskite transition, first principles

©2019. Japan Geoscience Union. All Right Reserved.

Unsusual high-Ti corundum recovered from the Horoman peridotites, Hokkaido, Japan

*oosawa takumi[1], Shinji Yamamoto[1]

1. yokohama national university

Oceanic and continental crust are recycled into the mantle due to subduction of oceanic plate in the mantle, and the crustal materials are thought to be mixed in the mantle through mantle convection (W.Xu et al., 2008). However, the mode and process of crustal mixing in peridotites are unknown, and constraints using recycled crust minerals are needed for elucidating the mantle-crust circulations. Horoman peridotites, located in the Hidaka Mountains of Hokkaido, is known as a fresh peridotite that is less serpentinized. By the metasomatism of the melt-mantle reaction, the harzburgite-lherzolite shows a remarkable stratigraphic structure. Recently, the occurrence of crustal minerals has been reported by Li et al., (2017) from the Horoman peridotites, such as zircon, rutile, diamond with a low carbon isotopic ratio, suggesting that these crustal minerals in the Horoman peridotites have recycled origin due to the past subduction and mixing in the mantle. However, the origin of crustal minerals in the Horoman peridotitare unclear, and few recovered cases. To better understand the origin of crustal minerals in the Horoman peridotites. we improve the mineral separation techniques and recovered unusual Ti-rich corundum from the Horoman peridotite. describe the separated minerals in details.

In this study, peridotite samples collected from the quarry of Toho Olivine Industry Co., Ltd., were employed for the heavy mineral separations. Each peridotite samples, 764 kg of harzburgite and 954 kg of lherzolite, were cut to a plate shape and transported to the Yokohama National University. Using a jaw crusher and a continuous crusher, it was crushed to 0,1 mm in size and then subjected to sieving, gravity, and magnetic separations, and finally hand picking the remaining minerals, which embedded in epoxy resin and polished. Six zircons, one rutile (TiO_2) were recovered from within the lherzolite. On the other hand, grains recovered from nonmagnetic fraction harzburgitewere embedded for mineral exploration using EPMA , and as a result, twelve corundum (Al_2O_3) grains were discovered. Inclusions and attached minerals coexisted in corundum were observed under the stereoscopic microscope. SEM-EDS analysis of six corundum grains confirmed that inclusions and attatched phase consisting of (1) Si-Al-K rich silicate, (2)Ti-Zr oxide,aand (3) Si-Ti alloy.

Morishita et al., (1998; 2000) previously reported the corundum xenocryst containing a trace amount of Cr from the gabbro boulder in the Ponsanushibetsu river in Samani town. This corundum is interpreted as a metamorphic product of gabbro protolith or xenocrust from the Hidaka crust. The characteristics of corundum obtained in this study is (1) almost no Cr, (2) unusual high-Ti content (maximum 2.3 wt% of TiO_2), (3) unique inclusions such as Ti-Zr oxide and Si-Ti alloys. Therefore, it is thought that a corundum recovered from the Horoman peridotite have different origin from that of Morishita et al. (1998; 2000). In another case, corundum with high TiO_2 concentration and specific inclusion (Ti-Zr oxide, Ti-Si alloy) has been reported from xenocrysts related from alkaline basalts of Israel Mt.Carmel (Griffine et al., 2016; 2018). Origin of Mt. Carmel corundum is still unclear, but tentatively proposed to be crystallized from mafic to ultramafic melt near the crust-mantle boundary under the highly reducing conditions (Griffine et al., 2018) The discovery of unusual high-Ti corundum from the Horoman peridotites will shed light on significant petrological issue on peridotite studies.

©2019. Japan Geoscience Union. All Right Reserved.

Reference

Griffin1,William L. (2016) “Deep-earth methane and mantle dynamics: insights from northern Israel, southern Tibet and Kamchatka,” JOURNAL & PROCEEDINGS OF THE ROYAL SOCIETY OF NEW SOUTH WALES, VOL. 149,PARTS 1 & 2, 2016, PP. 17-33
Yibing Li. AGU. FALL MEETING 2017. AGU Contact Technical Support AGU Privacy Policy. https://agu.confex.com/agu/fm17/meetingapp.cgi/Paper/222963 [2019/02/19].
Morishita, T., 1998, ” finding of corundum-bearing gabbro boulder possibly derived from the Horoman Peridotitie complex, Hokkaido, northern Japan, ” JOURNAL OF MINERALOGY, PETROLOGY AND ECONOMIC GEOLOGY, 93(2), 52-63.

Keywords: mantle peridotite , recycle, corundum, Titanium

©2019. Japan Geoscience Union. All Right Reserved.

Deformation experiments on akimotoite

*Longli Guan[1], Daisuke Yamazaki[1], Noriyoshi Tsujino[1]

1. Institute for Planetary Materials, Okayama University, Misasa, Japan

The ilmenite structure of $MgSiO_3$, known as akimotoite, is inferred to occur in cold subducting slabs in the bottom of Earth’ s mantle transition zone and the uppermost lower mantle along a low-temperature geotherm (Akaogi et al., 2002). Akimotoite is thought to be the most anisotropic mineral in the Earth’ s mantle transition zone (Zhang et al., 2005; Weidner & Ito,1985). The elastic anisotropy caused by the lattice preferred orientation of akimotoite due to slab-induced deformation may be used plausibly to interpret the significant seismic anisotropy observed in mid-mantle (depths 410-670km) (Nowacki et ali.,2015; Foley & Long, 2011). However, previous studies did not determine the slip plane or the dominant slip system precisely (Shiraishi et al., 2008). In this study, therefore, we conducted deformation experiment on akimotoite aggregates to investigate precise and detailed microstructures. For the preparation of starting material of akimotoite aggregates for deformation experiment, high pressure experiments using $MgSiO_3$ glass as starting material have been performed at 20-22GPa and 1400 ℃, in the Kawai-type multi anvil apparatus. The recovered samples were investigated by X-ray diffraction, electron probe microanalysis and scanning electron microscopy to identify phase, measure chemical composition and observe microstructure, respectively, showing that samples were well-sintered and no-crack akimotoite aggregates with grain size of 2-8 μm. These akimotoite aggregates were suitable as a starting material for deformation experiments. We subsequently conducted pure shear deformation experiment on such akimotoite aggregates at ~21 GPa and 1200 ˚C by using high pressure deformation apparatus, so called D-111 type apparatus, installed at Institute for Planetary Materials, Okayama University. The relationship between displacement and load of D-rams may suggest the mechanism change from elastic to plastic deformation with the progress of deformation. As a result, we observed the plastic deformation on the recovered sample and the strain and average strain rate were estimated to be ~0.12 and ~1.6×10^{-5} s^{-1}, respectively. It is considered that the strain of ~0.12 is sufficient to form the lattice preferred orientation which can be analyzed by electron backscattered diffraction technique.

Keywords: akimotoite, lattice preferred orientation, deformation at high pressure, anisotropy , mantle

©2019. Japan Geoscience Union. All Right Reserved.

Fate of water in subducted hydrous sediments deduced from stability fields of FeOOH and AlOOH up to 20 GPa

*Takashi Yoshino[1], Edward Baker[2], Kyle Duffey[3]

1. Institute for Planetary Materials, Okayama University, 2. Department of Earth Sciences, University of Oxford, 3. Department of Geosciences, Princeton University

Fe- and Al-hydroxides (FeOOH and AlOOH) in sedimentary rocks form the top part of the subducted oceanic lithosphere and are known to be stable along a normal geotherm in the lower mantle. Banded Iron Formations (BIFs) and bauxite ore deposits formed in the Earth’s oceans can transport significant amount of water into the Earth’s deep interior by subduction of FeOOH and AlOOH and may occasionally serve water to the core. However, stabilities of these hydrous phases have not been well constrained in upper mantle conditions. We determined dehydration curves for FeOOH and AlOOH in upper mantle and mantle transition zone conditions (5–20 GPa, 673–1573K)by quench and *in situ*X-ray diffraction to constrain their capability of water transport to the deep mantle. Dehydration temperatures of these minerals increase with increasing pressure. Comparison between our results and geothermal gradients of subducting slab surfaces demonstrates dehydration of FeOOH in early subduction stage (around 2 GPa). In most cases, diaspore (AlOOH) also dehydrates in early subduction. Despite the implications of the stability of these phases at high pressure, our results show that the sediments located at the slab surface are unlikely candidates for transporting water to the deep mantle.

Keywords: water, sediment, dehydration, hydrous minerals, subduction

©2019. Japan Geoscience Union. All Right Reserved.

[E] Poster | S (Solid Earth Sciences)：S-IT Science of the Earth's Interior & Techtonophysics

Sun. May 26, 2019 5:15 PM - 6:30 PM JST | Sun. May 26, 2019 8:15 AM - 9:30 AM UTC | Poster Hall International Exhibition Hall8, Makuhari Messe_29

[S-IT23] Structure and Dynamics of Earth and Planetary Mantles

convener:Takashi Nakagawa(Department of Earth Sciences, The University of Hong Kong), Takashi Yoshino(Institute for Planetary Materials, Okayama University), Dapeng Zhao(Department of Geophysics, Tohoku University)

Interdisciplinary approach can lead to a better understanding of dynamics and evolution of the deep interiors of the Earth and planets. We welcome any submissions of recent results in observational, theoretical and experimental studies on seismology, geomagnetism, mineral physics, dynamics of deep interiors, and any other relevant fields from researchers in many countries. Integration of such results is also welcome. In particular, we encourage any contributions focusing on "plate and mantle dynamics in Earth and terrestrial planets". We also encourage papers stimulating an interdisciplinary collaboration relating to establishment of the Japan-SEDI community.

[SIT23-P01] Interaction between volcanisms inland and the spreading center: example of Galápagos archipelago

*Walid Ben Mansour[1], Guust Nolet[2], Mario Ruiz[3], Juan Carlos Afonso[1] (1.Department of Earth and Planetary Sciences, Macquarie University, Sydney (Australia), 2.Geoazur, Université Cote d'Azur, Sophia Antipolis (France), 3.Instituto Geofisco, Escuela Politecnica Nacional, Quito (Ecuador))

[SIT23-P02] **Effect of iron content on thermal conductivity of olivine with implications for cooling history of rocky planets**

*Youyue Zhang[1], Takashi Yoshino[1], Akira Yoneda[1], Masahiro Osako[2] (1.Institute for Planetary Materials, Okayama University, 2.Division of Physical Sciences, National Museum of Nature and Science)

[SIT23-P03] **The distribution of Cenozoic conglomerates and its sedimentological constraint on the uplift of the South Tianshan, NW China**

*SUN HAITAO[1] (1.China University of Petroluem-Beijing)

[SIT23-P04] **Electrical conductivity of diaspore, δ-AlOOH and ε-FeOOH**

*Ran Wang[1] (1.Institute for Planetary Materials, Okayama University)

[SIT23-P05] Multi-mode surface wave tomography for azimuthal anisotropy in the Australasian upper mantle

*Yuka Nishimura[1], Kazunori Yoshizawa[2] (1. Graduate School of Science, Hokkaido University, 2.Faculty of Science, Hokkaido University)

[SIT23-P06] Mapping multi-mode surface wave phase speeds in North America using mode-branch waveforms decomposed by linear Radon transform

*Hitoshi Matsuzawa[1], Kazunori Yoshizawa[2] (1.Graduate School of Science, Hokkaido University, 2.Faculty of Science, Hokkaido University)

[SIT23-P07] Radial anisotropy in the upper mantle using multi-mode surface waves incorporating the η_k parameter: Application to the Pacific and Australian regions

Shuya Okuyama[1], *Kazunori Yoshizawa[1,2], Hitoshi Kawakatsu[3], Takehi Isse[3] (1.Graduate School of Science, Hokkaido University, 2.Faculty of Science, Hokkaido University, 3.Earthquake Research Institute, University of Tokyo)

[SIT23-P08] Pure to impure and dry to wet olivine rheology based on high temperature dependency of diffusion creep

*Kosuke Yabe[1], Takehiko Hiraga[1] (1.School of Science, The University of Tokyo)

[SIT23-P09] Finite frequency S wave tomography model beneath the Ontong Java Plateau using data recorded by broadband ocean bottom seismographs

*Misaki Horiuchi[3], Hiroko Sugioka[3], Masayuki Obayashi[1], Daisuke Suetsugu[1], Hajime Shiobara[2], Aki Ito[1], Yasushi Ishihara[1], Satoru Tanaka[1], Takehi Isse[2], Takashi Tonegawa[1], Junko Yoshimitsu[1], Takumi Kobayashi[3] (1.Japan Agency for Marine-Earth Science and Technology, Yokosuka, Japan, 2.Earthquake Research Institute, The University of Tokyo, Tokyo, Japan, 3.The University of Kobe, Hyogo, Japan)

[SIT23-P10] Shear wave structure of the upper mantle beneath the Ontong Java Plateau

*Takehi Isse[1], Daisuke Suetsugu[2], Hajime Shiobara[1], Hiroko Sugioka[3], Aki Ito[2], Yasushi Ishihara[2], Satoru Tanaka[2], Masayuki Obayashi[2], Takashi Tonegawa[2], Junko Yoshimitsu[2], Takumi Kobayashi[3], Kazunori Yoshizawa[4] (1.Earthquake Research Institute University of Tokyo, 2.Japan Agency for Marine-Earth Science and Technology, 3.Kobe University, 4.Faculty of Science, Hokkaido University)

[SIT23-P11] Effect of impurity on post-post-perovskite transition of $MgSiO_3$ by first principles

*Koichiro Umemoto[1] (1.Earth-Life Science Institute, Tokyo Institute of Technology)

[SIT23-P12] Unsusual high-Ti corundum recovered from the Horoman peridotites, Hokkaido, Japan

*oosawa takumi[1], Shinji Yamamoto[1] (1.yokohama national university)

[SIT23-P13] Deformation experiments on akimotoite

*Longli Guan[1], Daisuke Yamazaki[1], Noriyoshi Tsujino[1] (1.Institute for Planetary Materials, Okayama University, Misasa, Japan)

[SIT23-P14] Fate of water in subducted hydrous sediments deduced from stability fields of FeOOH and AlOOH up to 20 GPa

*Takashi Yoshino[1], Edward Baker[2], Kyle Duffey[3] (1.Institute for Planetary Materials, Okayama University, 2.Department of Earth Sciences, University of Oxford, 3.Department of Geosciences, Princeton University)

Interaction between volcanisms inland and the spreading center: example of Galápagos archipelago

*Walid Ben Mansour[1], Guust Nolet[2], Mario Ruiz[3], Juan Carlos Afonso[1]

1. Department of Earth and Planetary Sciences, Macquarie University, Sydney (Australia), 2. Geoazur, Université Cote d'Azur, Sophia Antipolis (France), 3. Instituto Geofisco, Escuela Politecnica Nacional, Quito (Ecuador)

The Galápagos archipelago, located west of Ecuador, is a good example where a mantle plume interacts with a spreading center and modifies physical and chemical properties of the oceanic lithosphere. The Galápagos Spreading Center (GSC) and the Galápagos hotspot interact over more than 1,000 km with unusual features for a hot spot region (large number of historical active volcanoes, large range of lavas composition, alignment of volcanic centers and seamounts). To bring new information on the physical and chemical properties of this region, we are constructing a new P-wave velocity model of this region by combining data from 10 seismic broadband stations and from 9 MERMAIDS (Mobile Earthquake Recorder in Marine Areas by Independent Divers) deployed in this region between 2014 and 2016. We focus on Pn head waves to better constraint the Moho depth in this region and image the interaction between the hot spot and the GSC. We selected150 seismic events between May 2014 and September 2016, with epicentral distance between 3°and 35° and picked more than 2,500 Pn phases that we will invert in a probabilistic tomography inversion in a second step. In this presentation, we will show examples and statistics of Pn data. We will discuss the benefits of developing a multi-observable thermochemical tomography in this region to better image the intricate interaction of a hot spot with the overlying oceanic lithosphere and evaluate current physio-chemical evolutionary models.

Keywords: Pn tomography, mantle plume, thermochemical structure

©2019. Japan Geoscience Union. All Right Reserved.

Effect of iron content on thermal conductivity of olivine with implications for cooling history of rocky planets

*Youyue Zhang[1], Takashi Yoshino[1], Akira Yoneda[1], Masahiro Osako[2]

1. Institute for Planetary Materials, Okayama University, 2. Division of Physical Sciences, National Museum of Nature and Science

Knowledge of thermal transport properties of mantle materials is essential for understanding the thermal state and dynamics of the Earth and planetary interiors. Previous studies have suggested that temperature and pressure dependences of thermal conductivity can affect mantle convection and plate tectonics involving subduction dynamics. Olivine is the most abundant mineral in the Earth's upper mantle and chemical composition of olivine in the Earth's upper mantle is characterized by high forsterite content around Fo_{90}. For other terrestrial planets, Mercury is believed to have a FeO-poor mantle along with end member silicates, whereas olivine in the Martian mantle would be more Fe-rich, speculated to be Fo_{67}. Recent studies suggested that surface of some asteroids is dominated by olivine of composition from Fo_{49} to Fo_{70}. Hence, the effect of Fe content in olivine on thermal conductivity could be significant for understanding the thermal structure and cooling history of these terrestrial planets and asteroids.

In this study, thermal conductivity and diffusivity of olivine were determined simultaneously by combining multi-anvil high pressure experimental technique and pulse heating method. Thermal properties of olivine with six different Fe contents (Fo, Fo_{90}, Fo_{70}, Fo_{50}, Fo_{31}, Fo_{0}) were measured under the Earth's upper mantle condition in a 5000-ton Kawai type multi-anvil press. The minimum λ was found to be at composition near Fo_{31}; the absolute λ value of Fo_{31} is about 65% lower than that of Fo. Small amounts of minor elements can strongly reduce the thermal conductivity at low temperature; λ value of Fo90 is about 50% of Fo at room temperature. As temperature increases, the difference in λ among olivine samples with various Fe contents tends to become smaller. Thermal conductivities of polycrystalline olivine have smaller absolute values and weak pressure and temperature dependences, compared with those of natural single crystal olivine determined by previous studies. Heat capacity of olivine calculated from λ and κ is independent of pressure and is controlled by nearly constant thermal expansion coefficient of Fo_{70} and Fo_{50} with increasing temperature. Smaller λ of olivine aggregate with high Fe content would produce thicker crust in the Fe-rich Mars, while heat in the Fe-poor Mercury can escape faster than the other terrestrial planets. Olivine-dominant asteroids with high Fe concentration could have longer cooling history and lower thermal inertia on the surface.

Keywords: Thermal conductivity, Olivine, Heat capacity, High pressure, Mantle

©2019. Japan Geoscience Union. All Right Reserved.

The distribution of Cenozoic conglomerates and its sedimentological constraint on the uplift of the South Tianshan, NW China

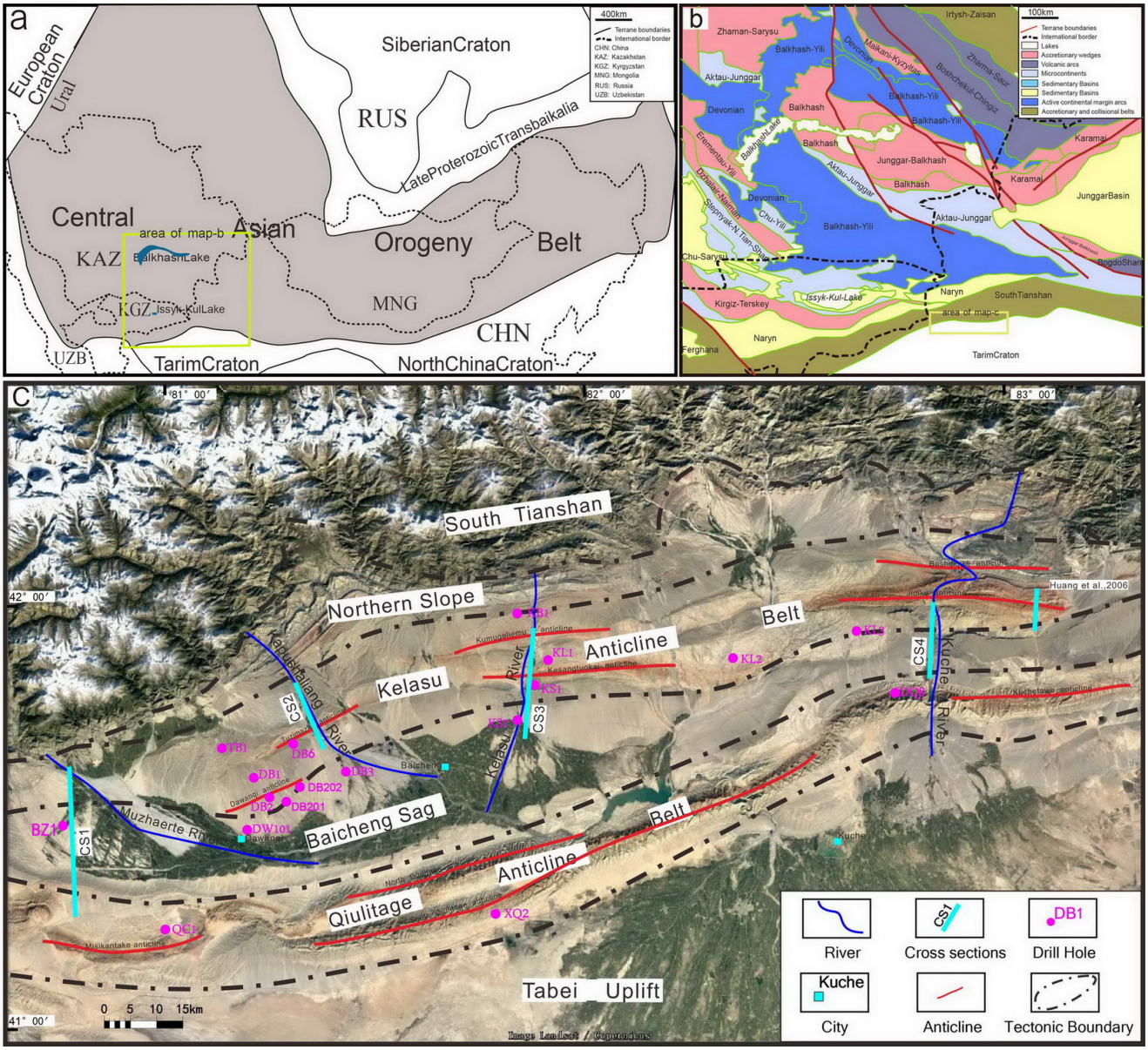
*SUN HAITAO[1]

1. China University of Petroluem-Beijing

The Cenozoic alluvial fan deposits in the Kuqa Depression of Tarim Basin, likely in response to a tectonic event, can provide critical evidence for constraining the timing of the South Tianshan uplift and reconstructing the paleotectonic evolution of the Central Asian Orogenic Belt. The sedimentological analysis shows that the conglomerates were deposited in alluvial fan environment. The initial uplift stage was started from the Jidike Formation at ~23Ma, resulting only small but angular gravels. Then the rapid uplift was since 15.97 Ma leading to the deposition of Kangcun conglomerate layers. And the next rapid and intensely uplift was started at ~4 Ma of the deposition of Kuqa Formation, according to ~2000m thick alluvial fan conglomerates. After a short quiescence, the most remarkable uplift of South Tianshan regenerated and caused the most extensive alluvial fan conglomerates of Xiyu Formation since 2.58 Ma and continuing to the present.

Keywords: Cenozoic, Central Asian Orogenic Belt, Conglomerate

©2019. Japan Geoscience Union. All Right Reserved.



©2019. Japan Geoscience Union. All Right Reserved.

Electrical conductivity of diaspore, δ-AlOOH and ε-FeOOH

*Ran Wang[1]

1. Institute for Planetary Materials, Okayama University

FeOOH and AlOOH are dominant hydrous phases in sedimentary rocks deposited in the sea or lake basins which were considered to be possibly related to the deep water cycle by slab subduction. Therefore, understanding of the electrical conductivity behaviors of these phases are essential to explore the nature and dynamic process of the Earth's interior. In this study, electrical conductivity of diaspore (α-AlOOH), δ-AlOOH and ε-FeOOH was measured by impedance spectroscopy with a frequency range from 10^{-1} to 10^{6} Hz at pressures up to 15, 20 and 12 GPa and temperatures of 1200, 1200 and 1000 K well below the dehydration temperatures of these phases under the relevant pressures. For diaspore at 8, 10, and 12 GPa, the relationship between electrical conductivity and reciprocal temperature could be well fitted by the Arrhenius formula: $\sigma = \sigma_0 \exp[-(\Delta E+P\Delta V)/kT]$ and shows the pre-exponential factor (σ_0), activation energy (ΔE) and activation volume (ΔV) of 55.94 ±1.16 S/m, 0.547 ±0.016 eV and 1.683 ±0.123 cm^3/mol, respectively. However, data of diaspore obtained below 6 GPa could not be fitted by the Arrhenius formula, which was thought to be due to the remnant of free water in the sample caused by heating to insufficient temperature to proceed dehydration of interstitial water. Thus, it is quite difficult to measure the electrical conductivity of diaspore at low pressures. The electrical conductivity of diaspore increased with pressures ranging from 8 to 12 GPa by half order of magnitude and then the conductivity change with pressures from 12 to 15 GPa became negligibly small. The dominant conduction mechanism of diaspore is regarded as proton conduction. δ-AlOOH and ε-FeOOH show one and two orders of magnitude higher electrical conductivity than diaspore. Due to isostructural $CaCl_2$-type hydroxide structure, δ-AlOOH and ε-FeOOH display the nearly identical activation enthalpy (0.384 ±0.007 eV, 0.330 ±0.048 eV) which is relatively lower than that of diaspore.

Keywords: Electrical conductivity, Diaspore, δ-AlOOH, ε-FeOOH

©2019. Japan Geoscience Union. All Right Reserved.

Multi-mode surface wave tomography for azimuthal anisotropy in the Australasian upper mantle

*Yuka Nishimura[1], Kazunori Yoshizawa[2]

1. Graduate School of Science, Hokkaido University, 2. Faculty of Science, Hokkaido University

Azimuthal anisotropy in the upper mantle derived from seismic surface waves provides us with the information of mantle dynamics, such as the present-day mantle flow and the remnant of past deformation in the lithosphere and asthenosphere.The Australian plate is currently the fastest-moving tectonic plate including a large continent, encompassed by the intensive seismicity, particularly in its north (Indonesia) and east (Tonga-Kermadec to New Zealand). Thus, the entire continent can be covered by dense ray paths utilizing broad-band seismic stations deployed throughout the continent. This unique tectonic setting of Australian plate allows us to reconstruct high-resolution tomography models in the Australian region (e.g., Fishwick et al., 2008, Tectonics; Yoshizawa, 2014, PEPI).

In this study, we construct new phase speed maps in and around the Australian continent incorporating azimuthal anisotropy for both multi-mode Love and Rayleigh waves using the method developed by Yoshizawa & Kennett (2004, JGR). We employ the data base of path-specific multi-mode phase speeds for the fundamental mode and up to the fourth-higher modes by Yoshizawa (2014, PEPI), which has been measured by using the non-linear waveform fitting method (Yoshizawa & Ekstrom, 2010, GJI). We have performed checkerboard resolution tests as well as jackknife resampling tests, which suggest that our current phase speed data set can provide us with the robust estimation of azimuthally anisotropic phase speed maps in the Australasian region.

The multi-mode phase speed models indicate that the fastest directions of azimuthal anisotropy estimated from the different modes are consistent each other as far as they have the maximum sensitivity at the common depth. Comparisons between the direction of absolute plate motion (HS2-NUVEL-1) by Gripp & Gordon (1990, GRL) and the fastest direction of azimuthal anisotropy suggests that they agree well particularly at around the depth of 100km under the ocean area (Coral and Taman Seas) off the east-coast of the Australian continent and 300km under the continental area of Australia. These results are likely to reflect the differences in the depth of asthenosphere where the effects of the lattice preferred orientation of mantle materials due to the present-day mantle flow can be more significant.

Keywords: Azimuthal anisotropy, Surface wave tomography, Australia

©2019. Japan Geoscience Union. All Right Reserved.

Mapping multi-mode surface wave phase speeds in North America using mode-branch waveforms decomposed by linear Radon transform

*Hitoshi Matsuzawa[1], Kazunori Yoshizawa[2]

1. Graduate School of Science, Hokkaido University, 2. Faculty of Science, Hokkaido University

The use of higher-mode surface waves is inevitable for further enhancement of vertical resolution of tomography model since they are much more sensitive to the deep structure of the Earth’ s upper mantle than the fundamental modes. However, measuring the multi-mode phase speeds is not a straightforward issue since wavetrains of different modes overlap each other in a seismogram.

We have developed the two-step array-based method for higher-mode analysis, which consists of (1) multi-mode phase speed measurements based of a classical *f-k* analysis using a long-range linear array with several-thousand kilometers (e.g., Nolet, 1975, GRL) and (2) modal waveform decomposition for the centroid location of the linear array using the linear Radon transform (e.g. Luo *et al*., 2015, GJI).

We have previously applied the method to a large data set of seismograms observed at Transportable Array stations of USArray and employed the average phase speeds of linear array to map phase speed distributions in North America (Matsuzawa and Yoshizawa, SSJ Fall Meeting 2018; AGU Fall Meeting 2018). We could obtain phase speed maps of the fundamental-mode and the first four higher-mode surface waves. Although the large-scale anomalies (i.e., fast phase speeds in cratons in the stable eastern U.S., slow phase speeds in the tectonically-active western U.S.) can be identified, the lateral resolution of the phase speed maps were insufficient compared to inter-station/array based tomography models. This suggests that the small-scale tectonic features have been blurred and averaged out due to the direct use of long linear array (2000–4000 km) with relatively large measurement errors.

In this study, we apply the inter-station dispersion analysis with nonlinear waveform fitting (Hamada and Yoshizawa, 2015, GJI) to the decomposed modal waveforms of the fundamental-mode surface waves derived from method using the centroids of the linear array as imaginary stations.The lateral resolution of resultant phase speed maps has been improved up to about 2.0 degrees owing to the relatively shorter inter-station (inter-centroid) distances used in the inversions.We can find typical small-scale tectonic features in the inland region of eastern and central US. Average phase speeds along each short ray path (several-hundred kilometers) have been measured stably without interference by overtones, which is likely to be of help in improving the accuracy of the resultant tomography maps.

The decomposed modal waveforms of the higher modes as well as the fundamental mode can be applied to the secondary dispersion analyses such as the inter-station dispersion measurements as done in this study and/or a 2-D beamforming analysis, which can be expected to enhance both the lateral and vertical resolutions of surface wave tomography models.

Keywords: Surface wave, Higher mode, Array-based analysis, Tomography, North America

©2019. Japan Geoscience Union. All Right Reserved.

Radial anisotropy in the upper mantle using multi-mode surface waves incorporating the η_κ parameter: Application to the Pacific and Australian regions

Shuya Okuyama[1], *Kazunori Yoshizawa[1,2], Hitoshi Kawakatsu[3], Takehi Isse[3]

1. Graduate School of Science, Hokkaido University, 2. Faculty of Science, Hokkaido University, 3. Earthquake Research Institute, University of Tokyo

Radial anisotropy can be described by five elastic parameters; four parameters related to seismic wave speeds (β_v, β_h, α_h, α_v) and an additional fifth anisotropic parameter (η). One of the anisotropic parameters, η, was originally defined by Anderson (1961), but its physical proprieties have been rather unclear compared with other four parameters related to elastic velocity.

The re-defined fifth anisotropic parameter η_κ by Kawakatsu et al. (2015) makes it easier to understand its physical proprieties compared with conventional η. The introduction of η_κ affects the shape of sensitivity kernels of Rayleigh wave phase speeds with respect to η_κ, PH-wave speeds α_h and PV-wave speeds α_v (Kawakatsu, 2016b). Since the sensitivity of Rayleigh wave phase speeds to η_κ becomes greater than that to η, we can expect a possibility of resolving the η_κ parameter. However, since the inverse correlation between the sensitivity kernels of SV-wave speed β_v and η_κ becomes rather stronger, the trade-off between β_v and may easily occur. Therefore, the independent determination of η_κ parameter from the inversions of surface-wave dispersion curves is not a straightforward issue.

In this study, incorporating η_κ, we performed inversions for five elastic parameters in the upper mantle, employing a classical iterativenonlinear least-squares inversion method (Tarantola and Valette, 1982). We used multi-mode dispersion data sets of surface waves in the Australian region (Yoshizawa, 2014, PEPI) and Pacific (Isse et al., 2019, EPSL) to reconstruct 3-D radially anisotropic model. In these inversions, we used isotropic PREM as a starting model to avoid the influence of reference anisotropy model.

The retrieved spatial distribution of the η_κ parameter can be mostly explained by trade-offs with SV wave speed β_v at many locations in Australia and Pacific. Still, we can find structural features in our 3-D β_v and η_κ models, particularly in some major structural boundaries such as ridges and the Tasman Line in eastern Australia, which cannot simply be attributed to the trade-off between β_v and η_κ, indicating possible intrinsic character of η_κ in the upper mantle.

Keywords: radial anisotropy, surface waves, inversion

©2019. Japan Geoscience Union. All Right Reserved.

Pure to impure and dry to wet olivine rheology based on high temperature dependency of diffusion creep

*Kosuke Yabe[1], Takehiko Hiraga[1]

1. School of Science, The University of Tokyo

There has been a large discrepancy in creep properties of olivine aggregates in dry diffusion creep regime between Minnesota group (Hirth and Kohlstedt, 1995) and ANU group (Faul and Jackson, 2007). Our recent deformation experiments on undoped and doped olivine aggregate synthesized by a new method different from previous studies demonstrate (i) the activation energy of grain boundary diffusion creep of undoped olivine is 465 kJ/mol, (ii) the creep rate is enhanced by doping of Ca and Al above ~1200 C with very high temperature sensitivity well represented by activation energy of ~700 kJ/mol, and (iii) presence of melt phase had little contribution to the change in the creep strength. Such observations are consistent with Yamauchi and Takei (2016) which attributed the observation to pre-melting at near solidus.

In this study, we compile all rheological data of olivine diffusion creep based on solidus which changes with the chemical compositions and amount of water. The solidi of dry samples are estimated from experiments and/or phase diagrams. The solidi of wet samples are calculated by cryoscopic approach following Hirshmann et al. (2009). We demonstrate that not only dry but also wet data are well explained by the operation of grain boundary diffusion creep with activation energy of 465 kJ/mol at <~0.93 × solidus and 700 kJ/mol at >~0.93 ×solidus. The controversy on the effect of water on grain boundary diffusion by Mei and Kohlstedt (2000) and Fei et al. (2016) is explained by the experimental temperatures with respect to the solidus of their systems. The viscosity depth profile in the upper mantle based on our new diffusion creep model will be presented.

Keywords: mantle rheology, olivine aggregates, diffusion creep

©2019. Japan Geoscience Union. All Right Reserved.

Finite frequency S wave tomography model beneath the Ontong Java Plateau using data recorded by broadband ocean bottom seismographs

*Misaki Horiuchi[3], Hiroko Sugioka[3], Masayuki Obayashi[1], Daisuke Suetsugu[1], Hajime Shiobara[2], Aki Ito[1], Yasushi Ishihara[1], Satoru Tanaka[1], Takehi Isse[2], Takashi Tonegawa[1], Junko Yoshimitsu[1], Takumi Kobayashi[3]

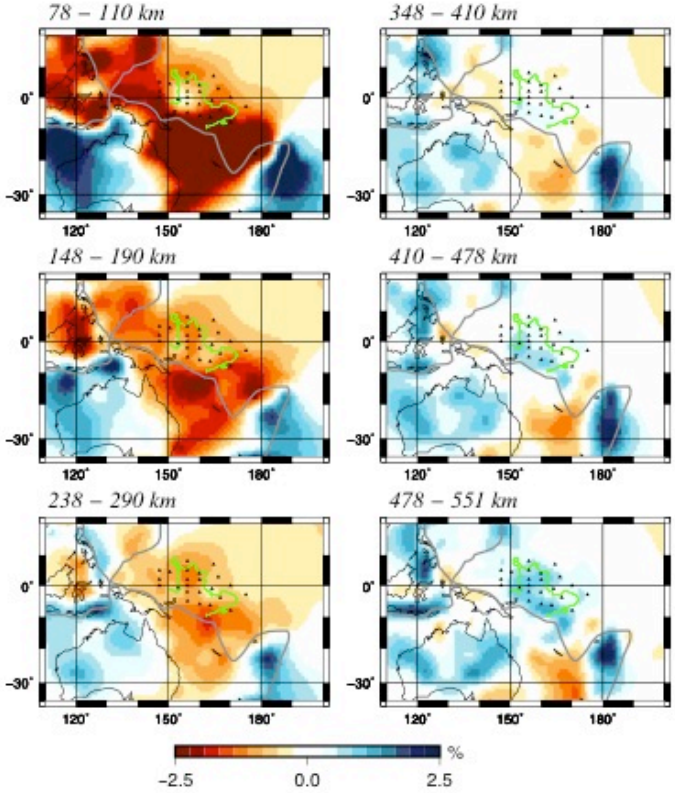
1. Japan Agency for Marine-Earth Science and Technology, Yokosuka, Japan, 2. Earthquake Research Institute, The University of Tokyo, Tokyo, Japan, 3. The University of Kobe, Hyogo, Japan

We determined three-dimensional S wave model beneath the Ontong Java Plateau (OJP) by finite frequency tomography using data recorded by broadband seismographs deployed at ocean bottom covered the OJP and at neighbor islands (Suetsugu *et al.*, 2018). Our dataset contains absolute and period-depended differential travel time data. The former consists of ~1,100,000 direct S-wave onset times reported by International Seismological Centre (ISC) and ~400 direct S-wave onset times picked up on broadband waveform records around the OJP and the latter is composed of ~3,000 differential traveltimes between two different stations around the OJP measured by waveform cross correlation at 7 different passband of which center periods varies from 5.3 sec to 42 sec. We used adaptive stacking method (Rawlinson and Kennett, 2004) to measure absolute travel time data near the OJP. These data were inverted based on the infinite frequency travel time tomography method for the absolute travel time data (Inoue *et al.*, 1990; Fukao *et al.*, 1992; Obayashi *et al.*, 2013) and the finite frequency travel time method for the relative travel time data (Dahlen *et al.*, 2000; Obayashi *et al.*, 2013). We obtained a well resolved S wave velocity model beneath the OJP. It shows significant high velocity anomalies in the mantle transition zone, which are considered as stagnant Pacific slabs related to the trench retreating as well as seafloor spreading in the Santa Cruz Basin and Melanesia Basin during the Eocene and Oligocene. It also reveals that S wave velocity just below the OJP is a little higher than the surrounding strong slow anomalies in the mantle shallower than 200 km. We will discuss these remarkable features beneath the OJP in comparison with P wave tomographic model (Obayashi *et al.*, 2018) in this presentation.

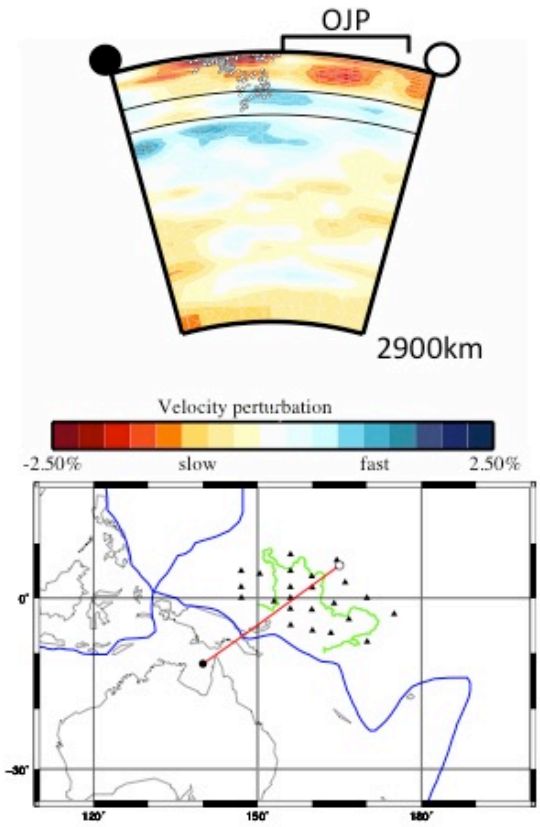
Keywords: finite frequency tomography, S wave velocity structure

©2019. Japan Geoscience Union. All Right Reserved.

(a)



(b)



©2019. Japan Geoscience Union. All Right Reserved.

Shear wave structure of the upper mantle beneath the Ontong Java Plateau

*Takehi Isse[1], Daisuke Suetsugu[2], Hajime Shiobara[1], Hiroko Sugioka[3], Aki Ito[2], Yasushi Ishihara[2], Satoru Tanaka[2], Masayuki Obayashi[2], Takashi Tonegawa[2], Junko Yoshimitsu[2], Takumi Kobayashi[3], Kazunori Yoshizawa[4]

1. Earthquake Research Institute University of Tokyo, 2. Japan Agency for Marine-Earth Science and Technology, 3. Kobe University, 4. Faculty of Science, Hokkaido University

Ontong Java Plateau (OJP) is the vastest Large Igneous Provinces (LIPs) in the oceanic region of the Earth. The OJP was emplaced at 122 and 90 Ma by massive volcanism, but the origin of this volcanism is still under discussion.
Richardson et al. (2000) obtained a large low-velocity root of the OJP extending as deep as 300km, though its existence and cause are still in debating.
One reason for poor understanding of the OJP is the insufficient information about the crust and mantle structure beneath the OJP because of the lack of long-term seafloor observation. Between 2014 and 2017, we conducted the first seismological and electromagnetic observations on the seafloor and islands in the OJP, named "OJP array", to clarify the origin of the OJP.
Using the broadband data from the OJP array as well as those from stations on land and seafloor in the western Pacific Ocean, we constructed three-dimensional shear wave speed structure beneath the OJP by surface wave tomography. using phase speed dispersions of Love and Rayleigh waves up to the 4th higher modes. Checkerboard resolution tests suggests that the spatial resolution of the obtained model is ~300km, which is higher than previous studies.

Obtained shear wave speed structure down to the depth of 300 km shows the following new features:
(1) In the center of the OJP at depths between 70–150 km, about 2% fast anomalies exists;
(2) No strong slow anomaly is found beneath the OJP at depths down to 300 km;
(3) Beneath the Caroline Islands, in the north of the OJP, 2 % slow anomalies exist, which may be associated with the Caroline hotspot activity.

These newly found features suggest that further investigation to reveal the origin of the OJP is necessary.

Keywords: upper mantle structure, Ontong Java, surface wave tomography, BBOBS

©2019. Japan Geoscience Union. All Right Reserved.

Effect of impurity on post-post-perovskite transition of $MgSiO_3$ by first principles

*Koichiro Umemoto[1]

1. Earth-Life Science Institute, Tokyo Institute of Technology

Several computational studies have predicted post-post-perovskite transitions in MgSiO3 at ultrahigh pressures and temperatures which can occur at deep interiors of super-Earths: $MgSiO_3$ --> Mg_2SiO_4+ $MgSi_2O_5$ --> Mg_2SiO_4+ SiO_2 --> MgO + SiO_2) and recombination (MgO + $MgSiO_3$ --> Mg_2SiO_4 or SiO_2 + $MgSiO_3$ --> $MgSi_2O_5$) [1-5]. As demonstrated in a very recent numerical simulation, these transitions are crucially important in modeling interiors of super-Earths up to 20 times Earth’ s mass [6]. However, in the previous studies, these post-post-perovskite transitions were considered only for pure Mg-Si-O. In actual super-Earths, impurities, Fe, Al, or so forth, should exist. Here we will investigate effects of impurities on post-post-perovskite transitions: transition pressures, local atomic structures, and equation of states.

[1] K. Umemoto, R. M. Wentzcovitch, P. B. Allen, Science **311**, 983 (2006).

[2] K. Umemoto and R. M. Wentzcovitch, Earth Plent. Sci. Lett. **311**, 225 (2011).

[3] S. Q. Wu et al., J. Phys.: Condens. Matter, **26**, 035402 (2014).

[4] H. Niu et al., Scientic Reports **5**, 18347 (2015).

[5] K. Umemoto et al., Earth Planet. Sci. Lett. 478, 40-45(2017).

[6] A. P. van den Berg et al., Icarus 317, 412-426(2019).

Keywords: super-Earth, post-post-perovskite transition, first principles

©2019. Japan Geoscience Union. All Right Reserved.

Unsusual high-Ti corundum recovered from the Horoman peridotites, Hokkaido, Japan

*oosawa takumi[1], Shinji Yamamoto[1]

1. yokohama national university

Oceanic and continental crust are recycled into the mantle due to subduction of oceanic plate in the mantle, and the crustal materials are thought to be mixed in the mantle through mantle convection (W.Xu et al., 2008). However, the mode and process of crustal mixing in peridotites are unknown, and constraints using recycled crust minerals are needed for elucidating the mantle-crust circulations. Horoman peridotites, located in the Hidaka Mountains of Hokkaido, is known as a fresh peridotite that is less serpentinized. By the metasomatism of the melt-mantle reaction, the harzburgite-lherzolite shows a remarkable stratigraphic structure. Recently, the occurrence of crustal minerals has been reported by Li et al., (2017) from the Horoman peridotites, such as zircon, rutile, diamond with a low carbon isotopic ratio, suggesting that these crustal minerals in the Horoman peridotites have recycled origin due to the past subduction and mixing in the mantle. However, the origin of crustal minerals in the Horoman peridotitare unclear, and few recovered cases. To better understand the origin of crustal minerals in the Horoman peridotites. we improve the mineral separation techniques and recovered unusual Ti-rich corundum from the Horoman peridotite. describe the separated minerals in details.

In this study, peridotite samples collected from the quarry of Toho Olivine Industry Co., Ltd., were employed for the heavy mineral separations. Each peridotite samples, 764 kg of harzburgite and 954 kg of lherzolite, were cut to a plate shape and transported to the Yokohama National University. Using a jaw crusher and a continuous crusher, it was crushed to 0,1 mm in size and then subjected to sieving, gravity, and magnetic separations, and finally hand picking the remaining minerals, which embedded in epoxy resin and polished. Six zircons, one rutile (TiO_2) were recovered from within the lherzolite. On the other hand, grains recovered from nonmagnetic fraction harzburgitewere embedded for mineral exploration using EPMA , and as a result, twelve corundum (Al_2O_3) grains were discovered. Inclusions and attached minerals coexisted in corundum were observed under the stereoscopic microscope. SEM-EDS analysis of six corundum grains confirmed that inclusions and attatched phase consisting of (1) Si-Al-K rich silicate, (2)Ti-Zr oxide,aand (3) Si-Ti alloy.

Morishita et al., (1998; 2000) previously reported the corundum xenocryst containing a trace amount of Cr from the gabbro boulder in the Ponsanushibetsu river in Samani town. This corundum is interpreted as a metamorphic product of gabbro protolith or xenocrust from the Hidaka crust. The characteristics of corundum obtained in this study is (1) almost no Cr, (2) unusual high-Ti content (maximum 2.3 wt% of TiO_2), (3) unique inclusions such as Ti-Zr oxide and Si-Ti alloys. Therefore, it is thought that a corundum recovered from the Horoman peridotite have different origin from that of Morishita et al. (1998; 2000). In another case, corundum with high TiO_2 concentration and specific inclusion (Ti-Zr oxide, Ti-Si alloy) has been reported from xenocrysts related from alkaline basalts of Israel Mt.Carmel (Griffine et al., 2016; 2018). Origin of Mt. Carmel corundum is still unclear, but tentatively proposed to be crystallized from mafic to ultramafic melt near the crust-mantle boundary under the highly reducing conditions (Griffine et al., 2018) The discovery of unusual high-Ti corundum from the Horoman peridotites will shed light on significant petrological issue on peridotite studies.

©2019. Japan Geoscience Union. All Right Reserved.

Reference

Griffin1,William L. (2016) “Deep-earth methane and mantle dynamics: insights from northern Israel, southern Tibet and Kamchatka,” JOURNAL & PROCEEDINGS OF THE ROYAL SOCIETY OF NEW SOUTH WALES, VOL. 149,PARTS 1 & 2, 2016, PP. 17-33
Yibing Li. AGU. FALL MEETING 2017. AGU Contact Technical Support AGU Privacy Policy. https://agu.confex.com/agu/fm17/meetingapp.cgi/Paper/222963 [2019/02/19].
Morishita, T., 1998, ” finding of corundum-bearing gabbro boulder possibly derived from the Horoman Peridotitie complex, Hokkaido, northern Japan, ” JOURNAL OF MINERALOGY, PETROLOGY AND ECONOMIC GEOLOGY, 93(2), 52-63.

Keywords: mantle peridotite , recycle, corundum, Titanium

©2019. Japan Geoscience Union. All Right Reserved.

Deformation experiments on akimotoite

*Longli Guan[1], Daisuke Yamazaki[1], Noriyoshi Tsujino[1]

1. Institute for Planetary Materials, Okayama University, Misasa, Japan

The ilmenite structure of $MgSiO_3$, known as akimotoite, is inferred to occur in cold subducting slabs in the bottom of Earth’ s mantle transition zone and the uppermost lower mantle along a low-temperature geotherm (Akaogi et al., 2002). Akimotoite is thought to be the most anisotropic mineral in the Earth’ s mantle transition zone (Zhang et al., 2005; Weidner & Ito,1985). The elastic anisotropy caused by the lattice preferred orientation of akimotoite due to slab-induced deformation may be used plausibly to interpret the significant seismic anisotropy observed in mid-mantle (depths 410-670km) (Nowacki et ali.,2015; Foley & Long, 2011). However, previous studies did not determine the slip plane or the dominant slip system precisely (Shiraishi et al., 2008). In this study, therefore, we conducted deformation experiment on akimotoite aggregates to investigate precise and detailed microstructures. For the preparation of starting material of akimotoite aggregates for deformation experiment, high pressure experiments using $MgSiO_3$ glass as starting material have been performed at 20-22GPa and 1400 ℃, in the Kawai-type multi anvil apparatus. The recovered samples were investigated by X-ray diffraction, electron probe microanalysis and scanning electron microscopy to identify phase, measure chemical composition and observe microstructure, respectively, showing that samples were well-sintered and no-crack akimotoite aggregates with grain size of 2-8 μm. These akimotoite aggregates were suitable as a starting material for deformation experiments. We subsequently conducted pure shear deformation experiment on such akimotoite aggregates at ~21 GPa and 1200 ˚C by using high pressure deformation apparatus, so called D-111 type apparatus, installed at Institute for Planetary Materials, Okayama University. The relationship between displacement and load of D-rams may suggest the mechanism change from elastic to plastic deformation with the progress of deformation. As a result, we observed the plastic deformation on the recovered sample and the strain and average strain rate were estimated to be ~0.12 and ~1.6×10^{-5} s^{-1}, respectively. It is considered that the strain of ~0.12 is sufficient to form the lattice preferred orientation which can be analyzed by electron backscattered diffraction technique.

Keywords: akimotoite, lattice preferred orientation, deformation at high pressure, anisotropy , mantle

©2019. Japan Geoscience Union. All Right Reserved.

Fate of water in subducted hydrous sediments deduced from stability fields of FeOOH and AlOOH up to 20 GPa

*Takashi Yoshino[1], Edward Baker[2], Kyle Duffey[3]

1. Institute for Planetary Materials, Okayama University, 2. Department of Earth Sciences, University of Oxford, 3. Department of Geosciences, Princeton University

Fe- and Al-hydroxides (FeOOH and AlOOH) in sedimentary rocks form the top part of the subducted oceanic lithosphere and are known to be stable along a normal geotherm in the lower mantle. Banded Iron Formations (BIFs) and bauxite ore deposits formed in the Earth’s oceans can transport significant amount of water into the Earth’s deep interior by subduction of FeOOH and AlOOH and may occasionally serve water to the core. However, stabilities of these hydrous phases have not been well constrained in upper mantle conditions. We determined dehydration curves for FeOOH and AlOOH in upper mantle and mantle transition zone conditions (5–20 GPa, 673–1573K)by quench and *in situ*X-ray diffraction to constrain their capability of water transport to the deep mantle. Dehydration temperatures of these minerals increase with increasing pressure. Comparison between our results and geothermal gradients of subducting slab surfaces demonstrates dehydration of FeOOH in early subduction stage (around 2 GPa). In most cases, diaspore (AlOOH) also dehydrates in early subduction. Despite the implications of the stability of these phases at high pressure, our results show that the sediments located at the slab surface are unlikely candidates for transporting water to the deep mantle.

Keywords: water, sediment, dehydration, hydrous minerals, subduction

©2019. Japan Geoscience Union. All Right Reserved.

[E] Poster | S (Solid Earth Sciences)：S-IT Science of the Earth's Interior & Techtonophysics

Sun. May 26, 2019 3:30 PM - 5:00 PM JST | Sun. May 26, 2019 6:30 AM - 8:00 AM UTC | Poster Hall International Exhibition Hall8, Makuhari Messe_17

[S-IT24] Attenuation from crust to core: in situ experiments, observaions and implications

convener:Konishi Kensuke(Institute of Earth Sciences, Academia Sinica), Ikuo Katayama(Department of Earth and Planetary Systems Science, Hiroshima University), Takashi Yoshino(Institute for Planetary Materials, Okayama University), Alexandre Schubnel(CNRS)

Most tomographic studies have been focused upon drawing maps of seismic velocity (SV) structures based on seismic data, with the ultimate goal of learning more about the structure and the composition of the mantle. Another key physical property that is accessible from seismic data is seismic attenuation (SA). Due to complications in isolating its intrinsic causes - e.g. local physical changes - and its extrinsic contributions - mainly scattering and other wave-propagation effects - SA has been underutilized. Yet, advances in waveform inversion have in association with recent enhancements of data permitted for a finer, more comprehensive determination of SA, opening the way to structural interpretations.
Difficulties in classifying and modelling the possible causes of intrinsic SA - e.g. temperature, melt, volatiles, and grain size - have also been raised. Increasingly, theoretical and experimental mineral physics have come to document the relationship between the behavior of SA and an assortment of other phenomena - most particularly, partial melt. These results can subsequently be used interpret seismological observations.
Seismic attenuation is critically implicated in structure, composition, and in fine mantle dynamics at the local, regional, and global scales. It may be used to constrain the existence of water in the transition zone; the presence of melt in various regions - for instance around subduction zones; and in the temperature field of the deep mantle - which would, in turn, help to resolve the chemical contribution to SV observed in this region.
In this session, we would like to discuss aspects of mantle attenuation, with the aim of sharing the current state of all relevant fields of study. We welcome contributions from different fields - in particular, from seismology, mineral physics, and geodynamics, as these may advance our mutual comprehension of SA and its implications; and lay the groundwork for future research and applications thereof.

[SIT24-P01] Attenuation of seismic wave in water-saturated granite during triaxial deformation

*Ikuo Katayama[1], Keiya Yamada[1], Kanta Zaima[1] (1.Department of Earth and Planetary Systems Science, Hiroshima University)

[SIT24-P02] Waveform inversion for the radial elastic and anelastic structure of the lowermost mantle beneath Central America and the Caribbean

*Anselme F. E. Borgeaud[1,2], Frederic Deschamps[1], Kensuke Konishi[1], Kenji Kawai[2], Robert J. Geller[2] (1.Institute of Earth Sciences, Academia Sinica, 2.Department of Earth and Planetary Science, Graduate School of Science, University of Tokyo)

[SIT24-P03] 3-D elastic and anelastic structure of the lowermost mantle beneath the western Pacific from finite-frequency tomography

*Konishi Kensuke[1], Nobuaki Fuji[2], Frederic Deschamps[1] (1.Institute of Earth Sciences, Academia Sinica, 2.Institut de Physique du Globe de Paris)

[SIT24-P04] Inferring the lowermost mantle thermo-chemical structure beneath the Western Pacific with seismic attenuation and shear-wave speed anomalies

*Frederic Deschamps[1], Kensuke Konishi[1], Nobuaki Fuji[2], Laura J Cobden[3] (1.Academia Sinica, 2.Institut de Physique du Globe de Paris, 3.Utrecht University)

[SIT24-P05] Intrinsic attenuation factor Q of partially molten Fe–S–O system

*Chao Liu[1], Takashi Yoshino[1] (1.Institute for Planetary Materials, Okayama University)

[SIT24-P06] Effect of pore pressure on attenuation of seismic waves in thermally cracked granite

*Keiya Yamada[1], Kazuki Sawayama[2], Ikuo Katayama[1] (1.Hiroshima University, 2.Kyushu University)

Attenuation of seismic wave in water-saturated granite during triaxial deformation

*Ikuo Katayama[1], Keiya Yamada[1], Kanta Zaima[1]

1. Department of Earth and Planetary Systems Science, Hiroshima University

Rock microfracturing significantly affects attenuation of seismic wave as well as seismic velocity. In this study, seismic wave attenuation in fluid-saturated granite was estimated during triaxial deformation experiments, with particular attention focused on how microfracturing affects the attenuation.
Fine-grained Aji granite was used for experiments, with 40 mm long and 20 mm in diameter. Triaxial experiments were carried at a constant strain-rate of ~10^{-6} s^{-1} under confining pressure of 20 MPa and pore pressure of 10 MPa. During deformation, elastic wave was monitored by a pulse transmission method using both P and S wave transducers with a resonant frequency of 2 MHz. In the early stage of deformation, amplitudes of both P and S waves increase slightly due to closure of preexisting cracks and then decrease due to nucleation and growth of microcracks as the sample approaches failure, with agreement of changes in seismic velocity. Change in amplitude of shear wave tends to be larger than compressional wave, similar to those observed in fluid-saturated sandstone, suggesting that inter-crack fluid flow acts as a main source of energy dissipation. We use these wavelets to estimate attenuation (quality factor) using the spectral ratio method described by Toksoz et al. (1979); the results will be presented during the meeting.

©2019. Japan Geoscience Union. All Right Reserved.

Waveform inversion for the radial elastic and anelastic structure of the lowermost mantle beneath Central America and the Caribbean

*Anselme F. E. Borgeaud[1,2], Frederic Deschamps[1], Kensuke Konishi[1], Kenji Kawai[2], Robert J. Geller[2]

1. Institute of Earth Sciences, Academia Sinica, 2. Department of Earth and Planetary Science, Graduate School of Science, University of Tokyo

The origin of velocity anomalies in the lowermost mantle, e.g., thermal, chemical, or due to phase transition, is still debated. Intrinsic seismic attenuation (Q) strongly depends on temperature, thus could provide additional constraints on the thermal contribution to seismic anomalies in the lowermost mantle. In this study, we investigate the radial (1-D) elastic (Vs) and anelastic (Q) structure of the lowermost mantle beneath Central America and the Caribbean using waveform inversion. We use ~50 intermediate and deep focus earthquakes in South America recorded at the USArray and other small networks between 2004–2015. Waveforms are filtered between 12.5–200 s and cut ~20 s before the arrival of the direct S phase, and ~60 s after the arrival of the ScS phase. We use the S phase as a reference phase to correct for the effects of the structure near the events and receivers on the travel-time and amplitude of ScS waveforms (Konishi et al., 2017). Synthetic tests show that we can resolve the 1-D Q and Vs structures of the lowermost mantle, with some amount of tradeoff between them. In an attempt to reduce the tradeoff between the Vs and Q structure, we perform iterative inversion inferring in a first step the Vs structure only, and in a second step the Vs and Q structures simultaneously.

Keywords: Seismic attenuation, Waveform inversion, Lowermost mantle

©2019. Japan Geoscience Union. All Right Reserved.

3-D elastic and anelastic structure of the lowermost mantle beneath the western Pacific from finite-frequency tomography

*Konishi Kensuke[1], Nobuaki Fuji[2], Frederic Deschamps[1]

1. Institute of Earth Sciences, Academia Sinica, 2. Institut de Physique du Globe de Paris

We introduce a finite-frequency tomography method as to simultaneously obtain 3-D shear velocity (V_S) and seismic attenuation (described as quality factor Q) structures using travel time and amplitude data. We apply this method to the mapping of V_S and Q structure in the lowermost mantle beneath the western Pacific, at an edge of the Pacific large low shear velocity province (LLSVP). We used S and ScS waves of seismograms for 31 earthquakes which occurred around the region of Tonga and Fiji. Our dataset consists of the transverse components of 1341 traces obtained from the F-net Japanese seismic station network. The waveform data is rendered to a bandpass filter of a range of 12.5–200 s, corresponding to 0.005–0.08 Hz. Both shear velocity and attenuation (Q) have lower values than PREM at the center of the bottom depth range. This feature is robust per a variety of inversions in different inversion configurations. Based upon the obtained shear velocity and attenuation (Q), we also predict possible temperature anomalies in this region. Discrepancy between the temperature anomalies predicted by the two data sets suggests that shear velocity anomalies result not only from temperature anomalies but chemical anomalis. Assuming that Q-anomalies are a good proxy for temperature, and that compositional anomalies primarily consist of an excess in iron oxide and depletion, we propose a possible thermal and compositional structure for this region. Revisions to fundamental analytical software have been effected such that more varieties of waveform analysis may be performed, utilizing progressively larger datasets. The design of packages for the computation of forward propagation has been refined to greater efficiency. The purpose, for the present, is to enable the Montecarlo inversion of waveforms. We will present the current version of the software, and demonstrate preliminary attempts to perform the Montecarlo inversion.

Keywords: attenuation, lowermost mantle, waveform inversion

©2019. Japan Geoscience Union. All Right Reserved.

Inferring the lowermost mantle thermo-chemical structure beneath the Western Pacific with seismic attenuation and shear-wave speed anomalies

*Frederic Deschamps[1], Kensuke Konishi[1], Nobuaki Fuji[2], Laura J Cobden[3]

1. Academia Sinica, 2. Institut de Physique du Globe de Paris, 3. Utrecht University

The Earth’ s deep mantle seismic structure is dominated by two large low shear-wave velocity provinces (LLSVPs) located beneath Africa and the Pacific. These structures have been observed by many studies and data sets, but their nature, purely thermal or thermo-chemical, is still debated. Due to trade-off between temperature and composition, maps of shear-wave velocity anomalies (d$\ln V_S$) alone are unable to discriminate between purely thermal and thermo-chemical hypotheses. Seismic shear-wave attenuation, measured by the quality factor Q_S, strongly depends on temperature and may bring additional information on this parameter, allowing to resolve the trade-off between temperature and composition. Here, we invert seismic waveform data jointly for radial models of d$\ln V_S$, and Q_S at two different locations beneath the Pacific, and from a depth of 2000 km down to the core-mantle boundary (CMB). At the Northern Pacific (NP) location, sampling a region around 50º N latitude and 180º E longitude, around V_S and Q_S remain close to the PREM values, representing the horizontal average mantle, throughout the investigated depth-range, with d$\ln V_S$ ~ -0.1% and Q_S ~ 300 (compared to Q_{PREM} = 312). At the Western Pacific (WP) location, sampling the western tip of the Pacific LLSVP and the Caroline plume, both V_S and Q_S are substantially lower than PREM. Importantly, d$\ln V_S$ and Q_S sharply decrease in the lowermost 500 km, from -0.6 % and 255 at 2500 km, to -2.5% and 215 close to the CMB. We then show that WP models cannot be explained by thermal anomalies alone, but require excess in iron of 3.5 to 4.5 % from the CMB up to 2600 km, and about 0.4 to 1.0 % at shallower depths. This later enrichment may be due to the entrainment of small amounts of the Pacific LLSVP material by the Caroline plume. The values of Q_S we observe give an estimate of the temperature anomalies, around 300-400 K close to the CMB, and 150 K at shallower depths. By contrast, NP models may have a purely thermal origin and can be explained by a temperature excess of about 50 K.

Keywords: Seismic waveform, Seismic attenuation, Mantle structure, LLSVP

©2019. Japan Geoscience Union. All Right Reserved.

Intrinsic attenuation factor Q of partially molten Fe–S–O system

*Chao Liu[1], Takashi Yoshino[1]

1. Institute for Planetary Materials, Okayama University

Heterogeneous seismic structures have been found at the top of the Earth’ s inner core in terms of attenuation and velocity (Iritani et al., 2014; Souriau and Romanowicz, 1997; Tanaka, 2012). The outermost part of the inner core with approximately 30 km thickness shows low attenuation, then attenuation increases beneath this layer (Cao and Romanowicz, 2004; Ibourichene and Romanowicz, 2018; Waszek and Deuss, 2013). The positive and negative correlations between velocity and attenuation were observed from the uppermost inner core in different areas: Pacific center in the inner core has negative correlation and the rest area has positive correlation (Attanayake et al., 2014; Godwin et al., 2018). In this study, experiments on attenuation of partially molten Fe–S–O system were performed to explain the possibility that could cause seismic anomalies.

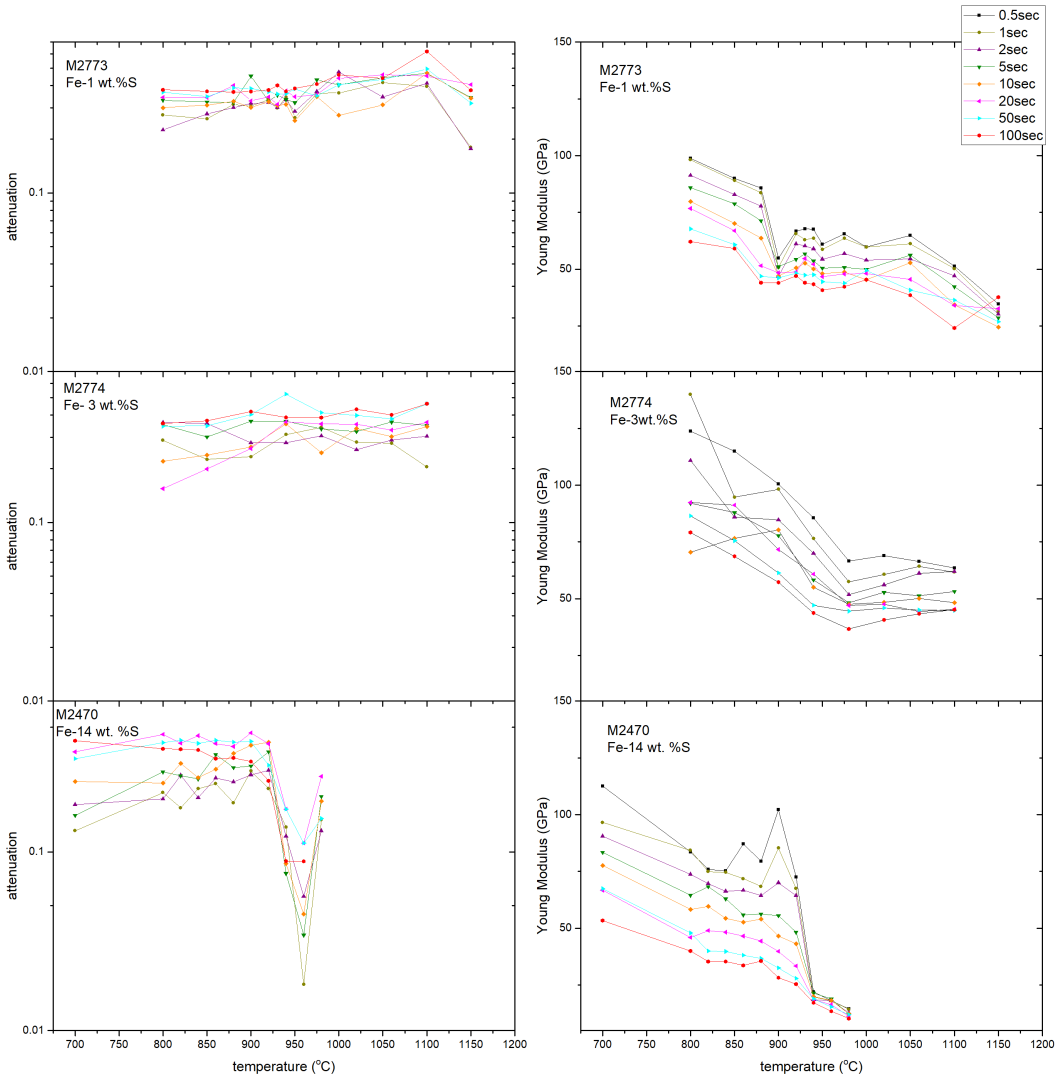
We investigated Fe-S-O system. Sulfur and oxygen are regarded as the representative light element in the Earth’ s core. Fe samples with 1, 3 and 14 wt. % S were synthesized in piston cylinder apparatus at 900° C and 1 GPa. a small amount of oxygen was included accidentally. In-situ X-ray radiographic observations were performed at the bending magnet beam line BL04B1 at SPring-8. Deformation-DIA press with a facility of cyclic loading was used. This system could produce sinusoidal displacement in a wide range of oscillation periods from 0.2 to 100 s and generating variable amplitudes (Yoshino et al., 2016). Q value characterizing intrinsic attenuation was determined by phase lag of sample strain against the reference material at 1 GPa and up to 1200°C.

The experimental results show that frequency dependence of attenuation is not remarkable except for a fine grained-sample, whereas decrease of attenuation was found at 1100 and 920°C for Fe- 1 wt. %S and Fe- 14 wt. %S samples, respectively. The attenuation drop would occur with increasing melt fraction. Experiments of Fe-14 wt. %S sample along heating and cooling paths were done to check the influence of grain growth during experiments. Data obtained from both heating and cooling paths show that abrupt change of the attenuation occurred at around 925°C. The Young’ s modulus calculated from the strain ratio of sample and reference shows strong temperature dependence. An obvious drop occurred between 900 and 980°C in association with the occurrence of partial melting. Relationship between velocity and attenuation anomalies of the Fe–S–O system shows a positive correlation when melt fraction reaches a certain value.

Partial melting could decrease Q^{-1}, which could explain the relative low attenuation on uppermost 30 km layer throughout the top of the inner core. Combing with the positive correlation between attenuation and velocity, a large amount of partial melting could occur on the uppermost 30 km layer of the rest area except the Pacific hemisphere in the inner core.

Keywords: attenuation, partially melting, Young Modulus, inner core

©2019. Japan Geoscience Union. All Right Reserved.



©2019. Japan Geoscience Union. All Right Reserved.

Effect of pore pressure on attenuation of seismic waves in thermally cracked granite

*Keiya Yamada[1], Kazuki Sawayama[2], Ikuo Katayama[1]

1. Hiroshima University, 2. Kyushu University

Elastic wave attenuation is one of important physical properties to estimate the subsurface structure by geophysical explorations, and it is very sensitive to the existence of cracks and pore fluid. Especially, pore pressure is essential parameter that is closely related to geothermal fluid productions and earthquakes. To quantify pore pressure or observe its change over years may lead to the precise evaluation of the geothermal fluid reservoir and prediction of earthquakes. Therefore, it is needed to understand the quantitative relationship between elastic wave attenuation and pore pressure. Previous experimental studies have measured elastic wave attenuation, in those experiments pore pressure is constant and confining pressure is increased. However, there are few studies that measured elastic wave attenuation focusing on the change of pore pressure. In this study, We carried out hydrostatic tests using thermally cracked granite and investing the effect of pore pressure on elastic wave attenuation.
The material we used throughout this study is Aji granite. Specimens were cored from the same block and shape into cylindrical (20 mm in a diameter, 40 mm in a length). Thermal cracking was introduced by slowly heating and cooling specimens up to 200, 400, 600℃ and thereby porosity (initial 0.6%) increases to 0.8, 0.9, 2.8% respectively. Hydrostatic tests were performed under dry and wet (water fully saturated) condition, at room temperature, using intra-vessel deformation and fluid-flow apparatus at Hiroshima University. Under dry condition, confining pressure was increased to 60 MPa. Under wet condition, confining pressure remained a constant value of 60 MPa and pore pressure was decreased from 50 MPa to the atmosphere. Elastic wave was measured by the pulse transmission method and transducers were glued to both sides of specimens. We calculated elastic wave velocity (Vp, Vs) from waveforms recorded in the oscilloscope, and estimated elastic wave attenuation (Qp^{-1}, Qs^{-1}) using Fourier spectral ratio method. As a result, Vp and Vs increase with confining pressure under dry condition whereas they decrease with increasing pore pressure under wet condition. In terms of the attenuation, $Qp^{-1}$and Qs^{-1}decrease as confining pressure increases under dry condition while they increase with pore pressure under wet condition. As confining pressure is increased, attenuation by friction decreased due to the closing and locking of crack contacts. In the experiment of specimen which was heated to 600℃, $Qp^{-1}$is much smaller than Qs^{-1}under wet condition, and the trend is differ from that under dry condition. Under wet condition, attenuation by fluid flow must have a greater effect on Qs^{-1}than Qp^{-1}. Our results indicate that the response to pore pressure is different between velocity and attenuation: as pore pressure increases, Vp/Vs increases but Qp^{-1}/Qs^{-1}decreased. Because attenuation changes more greatly than velocity and is more sensitive to the change of pore pressure, elastic wave attenuation could be useful to observe the change of pore pressure under the ground.

Keywords: Elastic wave attenuation, Pore pressure, Elastic wave velocity, Aji granite, Thermal cracking

©2019. Japan Geoscience Union. All Right Reserved.

[E] Poster | S (Solid Earth Sciences)：S-IT Science of the Earth's Interior & Techtonophysics

Sun. May 26, 2019 5:15 PM - 6:30 PM JST | Sun. May 26, 2019 8:15 AM - 9:30 AM UTC | Poster Hall International Exhibition Hall8, Makuhari Messe_30

[S-IT24] Attenuation from crust to core: in situ experiments, observaions and implications

convener:Konishi Kensuke(Institute of Earth Sciences, Academia Sinica), Ikuo Katayama(Department of Earth and Planetary Systems Science, Hiroshima University), Takashi Yoshino(Institute for Planetary Materials, Okayama University), Alexandre Schubnel(CNRS)

Most tomographic studies have been focused upon drawing maps of seismic velocity (SV) structures based on seismic data, with the ultimate goal of learning more about the structure and the composition of the mantle. Another key physical property that is accessible from seismic data is seismic attenuation (SA). Due to complications in isolating its intrinsic causes - e.g. local physical changes - and its extrinsic contributions - mainly scattering and other wave-propagation effects - SA has been underutilized. Yet, advances in waveform inversion have in association with recent enhancements of data permitted for a finer, more comprehensive determination of SA, opening the way to structural interpretations.
Difficulties in classifying and modelling the possible causes of intrinsic SA - e.g. temperature, melt, volatiles, and grain size - have also been raised. Increasingly, theoretical and experimental mineral physics have come to document the relationship between the behavior of SA and an assortment of other phenomena - most particularly, partial melt. These results can subsequently be used interpret seismological observations.
Seismic attenuation is critically implicated in structure, composition, and in fine mantle dynamics at the local, regional, and global scales. It may be used to constrain the existence of water in the transition zone; the presence of melt in various regions - for instance around subduction zones; and in the temperature field of the deep mantle - which would, in turn, help to resolve the chemical contribution to SV observed in this region.
In this session, we would like to discuss aspects of mantle attenuation, with the aim of sharing the current state of all relevant fields of study. We welcome contributions from different fields - in particular, from seismology, mineral physics, and geodynamics, as these may advance our mutual comprehension of SA and its implications; and lay the groundwork for future research and applications thereof.

[SIT24-P01] Attenuation of seismic wave in water-saturated granite during triaxial deformation

*Ikuo Katayama[1], Keiya Yamada[1], Kanta Zaima[1] (1.Department of Earth and Planetary Systems Science, Hiroshima University)

[SIT24-P02] Waveform inversion for the radial elastic and anelastic structure of the lowermost mantle beneath Central America and the Caribbean

*Anselme F. E. Borgeaud[1,2], Frederic Deschamps[1], Kensuke Konishi[1], Kenji Kawai[2], Robert J. Geller[2] (1.Institute of Earth Sciences, Academia Sinica, 2.Department of Earth and Planetary Science, Graduate School of Science, University of Tokyo)

[SIT24-P03] 3-D elastic and anelastic structure of the lowermost mantle beneath the western Pacific from finite-frequency tomography

*Konishi Kensuke[1], Nobuaki Fuji[2], Frederic Deschamps[1] (1.Institute of Earth Sciences, Academia Sinica, 2.Institut de Physique du Globe de Paris)

[SIT24-P04] Inferring the lowermost mantle thermo-chemical structure beneath the Western Pacific with seismic attenuation and shear-wave speed anomalies

*Frederic Deschamps[1], Kensuke Konishi[1], Nobuaki Fuji[2], Laura J Cobden[3] (1.Academia Sinica, 2.Institut de Physique du Globe de Paris, 3.Utrecht University)

[SIT24-P05] Intrinsic attenuation factor Q of partially molten Fe–S–O system

*Chao Liu[1], Takashi Yoshino[1] (1.Institute for Planetary Materials, Okayama University)

[SIT24-P06] Effect of pore pressure on attenuation of seismic waves in thermally cracked granite

*Keiya Yamada[1], Kazuki Sawayama[2], Ikuo Katayama[1] (1.Hiroshima University, 2.Kyushu University)

Attenuation of seismic wave in water-saturated granite during triaxial deformation

*Ikuo Katayama[1], Keiya Yamada[1], Kanta Zaima[1]

1. Department of Earth and Planetary Systems Science, Hiroshima University

Rock microfracturing significantly affects attenuation of seismic wave as well as seismic velocity. In this study, seismic wave attenuation in fluid-saturated granite was estimated during triaxial deformation experiments, with particular attention focused on how microfracturing affects the attenuation.
Fine-grained Aji granite was used for experiments, with 40 mm long and 20 mm in diameter. Triaxial experiments were carried at a constant strain-rate of ~10^{-6} s^{-1} under confining pressure of 20 MPa and pore pressure of 10 MPa. During deformation, elastic wave was monitored by a pulse transmission method using both P and S wave transducers with a resonant frequency of 2 MHz. In the early stage of deformation, amplitudes of both P and S waves increase slightly due to closure of preexisting cracks and then decrease due to nucleation and growth of microcracks as the sample approaches failure, with agreement of changes in seismic velocity. Change in amplitude of shear wave tends to be larger than compressional wave, similar to those observed in fluid-saturated sandstone, suggesting that inter-crack fluid flow acts as a main source of energy dissipation. We use these wavelets to estimate attenuation (quality factor) using the spectral ratio method described by Toksoz et al. (1979); the results will be presented during the meeting.

©2019. Japan Geoscience Union. All Right Reserved.

Waveform inversion for the radial elastic and anelastic structure of the lowermost mantle beneath Central America and the Caribbean

*Anselme F. E. Borgeaud[1,2], Frederic Deschamps[1], Kensuke Konishi[1], Kenji Kawai[2], Robert J. Geller[2]

1. Institute of Earth Sciences, Academia Sinica, 2. Department of Earth and Planetary Science, Graduate School of Science, University of Tokyo

The origin of velocity anomalies in the lowermost mantle, e.g., thermal, chemical, or due to phase transition, is still debated. Intrinsic seismic attenuation (Q) strongly depends on temperature, thus could provide additional constraints on the thermal contribution to seismic anomalies in the lowermost mantle. In this study, we investigate the radial (1-D) elastic (Vs) and anelastic (Q) structure of the lowermost mantle beneath Central America and the Caribbean using waveform inversion. We use ~50 intermediate and deep focus earthquakes in South America recorded at the USArray and other small networks between 2004–2015. Waveforms are filtered between 12.5–200 s and cut ~20 s before the arrival of the direct S phase, and ~60 s after the arrival of the ScS phase. We use the S phase as a reference phase to correct for the effects of the structure near the events and receivers on the travel-time and amplitude of ScS waveforms (Konishi et al., 2017). Synthetic tests show that we can resolve the 1-D Q and Vs structures of the lowermost mantle, with some amount of tradeoff between them. In an attempt to reduce the tradeoff between the Vs and Q structure, we perform iterative inversion inferring in a first step the Vs structure only, and in a second step the Vs and Q structures simultaneously.

Keywords: Seismic attenuation, Waveform inversion, Lowermost mantle

©2019. Japan Geoscience Union. All Right Reserved.

3-D elastic and anelastic structure of the lowermost mantle beneath the western Pacific from finite-frequency tomography

*Konishi Kensuke[1], Nobuaki Fuji[2], Frederic Deschamps[1]

1. Institute of Earth Sciences, Academia Sinica, 2. Institut de Physique du Globe de Paris

We introduce a finite-frequency tomography method as to simultaneously obtain 3-D shear velocity (V_S) and seismic attenuation (described as quality factor Q) structures using travel time and amplitude data. We apply this method to the mapping of V_S and Q structure in the lowermost mantle beneath the western Pacific, at an edge of the Pacific large low shear velocity province (LLSVP). We used S and ScS waves of seismograms for 31 earthquakes which occurred around the region of Tonga and Fiji. Our dataset consists of the transverse components of 1341 traces obtained from the F-net Japanese seismic station network. The waveform data is rendered to a bandpass filter of a range of 12.5–200 s, corresponding to 0.005–0.08 Hz. Both shear velocity and attenuation (Q) have lower values than PREM at the center of the bottom depth range. This feature is robust per a variety of inversions in different inversion configurations. Based upon the obtained shear velocity and attenuation (Q), we also predict possible temperature anomalies in this region. Discrepancy between the temperature anomalies predicted by the two data sets suggests that shear velocity anomalies result not only from temperature anomalies but chemical anomalis. Assuming that Q-anomalies are a good proxy for temperature, and that compositional anomalies primarily consist of an excess in iron oxide and depletion, we propose a possible thermal and compositional structure for this region. Revisions to fundamental analytical software have been effected such that more varieties of waveform analysis may be performed, utilizing progressively larger datasets. The design of packages for the computation of forward propagation has been refined to greater efficiency. The purpose, for the present, is to enable the Montecarlo inversion of waveforms. We will present the current version of the software, and demonstrate preliminary attempts to perform the Montecarlo inversion.

Keywords: attenuation, lowermost mantle, waveform inversion

©2019. Japan Geoscience Union. All Right Reserved.

Inferring the lowermost mantle thermo-chemical structure beneath the Western Pacific with seismic attenuation and shear-wave speed anomalies

*Frederic Deschamps[1], Kensuke Konishi[1], Nobuaki Fuji[2], Laura J Cobden[3]

1. Academia Sinica, 2. Institut de Physique du Globe de Paris, 3. Utrecht University

The Earth’ s deep mantle seismic structure is dominated by two large low shear-wave velocity provinces (LLSVPs) located beneath Africa and the Pacific. These structures have been observed by many studies and data sets, but their nature, purely thermal or thermo-chemical, is still debated. Due to trade-off between temperature and composition, maps of shear-wave velocity anomalies (d$\ln V_S$) alone are unable to discriminate between purely thermal and thermo-chemical hypotheses. Seismic shear-wave attenuation, measured by the quality factor Q_S, strongly depends on temperature and may bring additional information on this parameter, allowing to resolve the trade-off between temperature and composition. Here, we invert seismic waveform data jointly for radial models of d$\ln V_S$, and Q_S at two different locations beneath the Pacific, and from a depth of 2000 km down to the core-mantle boundary (CMB). At the Northern Pacific (NP) location, sampling a region around 50º N latitude and 180º E longitude, around V_S and Q_S remain close to the PREM values, representing the horizontal average mantle, throughout the investigated depth-range, with d$\ln V_S$ ~ -0.1% and Q_S ~ 300 (compared to Q_{PREM} = 312). At the Western Pacific (WP) location, sampling the western tip of the Pacific LLSVP and the Caroline plume, both V_S and Q_S are substantially lower than PREM. Importantly, d$\ln V_S$ and Q_S sharply decrease in the lowermost 500 km, from -0.6 % and 255 at 2500 km, to -2.5% and 215 close to the CMB. We then show that WP models cannot be explained by thermal anomalies alone, but require excess in iron of 3.5 to 4.5 % from the CMB up to 2600 km, and about 0.4 to 1.0 % at shallower depths. This later enrichment may be due to the entrainment of small amounts of the Pacific LLSVP material by the Caroline plume. The values of Q_S we observe give an estimate of the temperature anomalies, around 300-400 K close to the CMB, and 150 K at shallower depths. By contrast, NP models may have a purely thermal origin and can be explained by a temperature excess of about 50 K.

Keywords: Seismic waveform, Seismic attenuation, Mantle structure, LLSVP

©2019. Japan Geoscience Union. All Right Reserved.

Intrinsic attenuation factor Q of partially molten Fe–S–O system

*Chao Liu[1], Takashi Yoshino[1]

1. Institute for Planetary Materials, Okayama University

Heterogeneous seismic structures have been found at the top of the Earth’ s inner core in terms of attenuation and velocity (Iritani et al., 2014; Souriau and Romanowicz, 1997; Tanaka, 2012). The outermost part of the inner core with approximately 30 km thickness shows low attenuation, then attenuation increases beneath this layer (Cao and Romanowicz, 2004; Ibourichene and Romanowicz, 2018; Waszek and Deuss, 2013). The positive and negative correlations between velocity and attenuation were observed from the uppermost inner core in different areas: Pacific center in the inner core has negative correlation and the rest area has positive correlation (Attanayake et al., 2014; Godwin et al., 2018). In this study, experiments on attenuation of partially molten Fe–S–O system were performed to explain the possibility that could cause seismic anomalies.

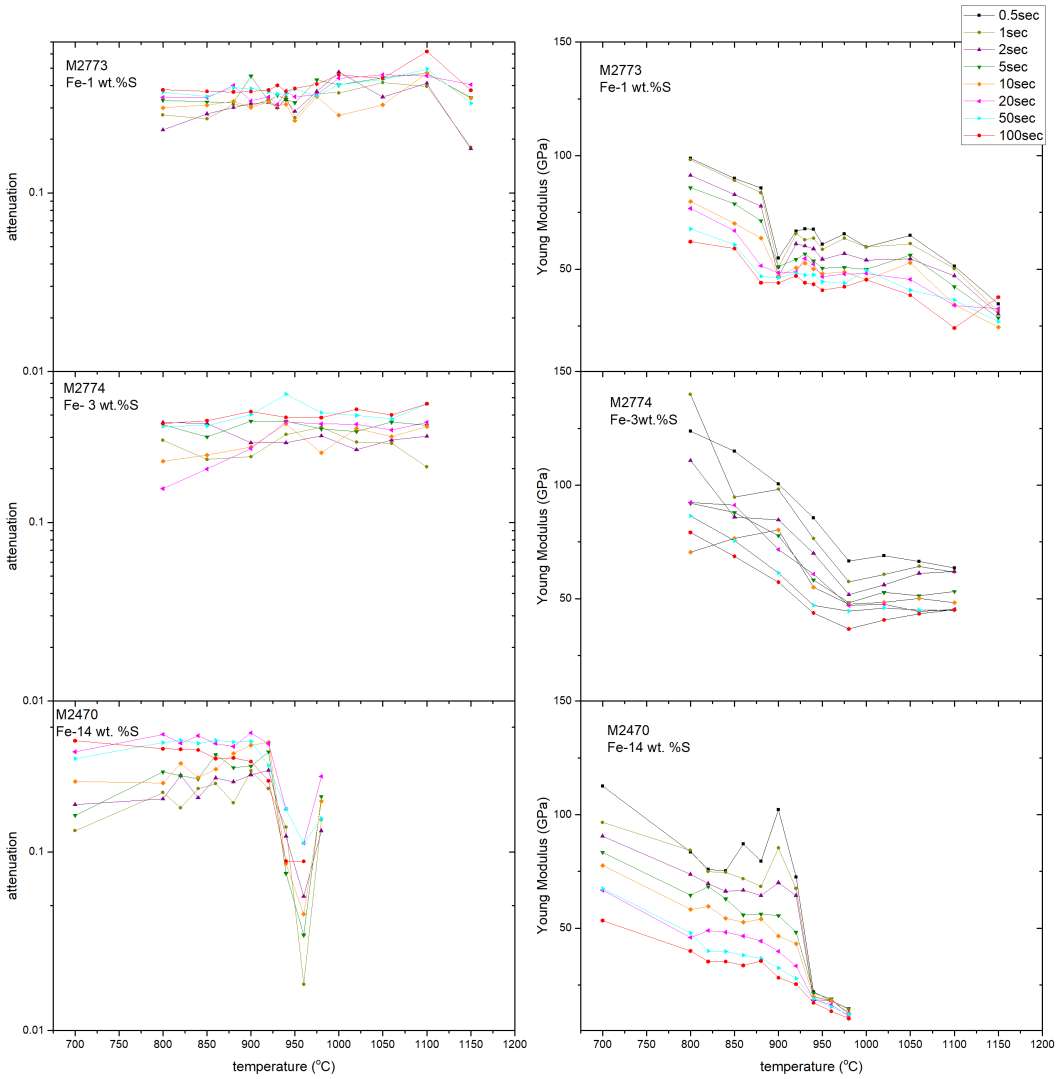
We investigated Fe-S-O system. Sulfur and oxygen are regarded as the representative light element in the Earth’ s core. Fe samples with 1, 3 and 14 wt. % S were synthesized in piston cylinder apparatus at 900° C and 1 GPa. a small amount of oxygen was included accidentally. In-situ X-ray radiographic observations were performed at the bending magnet beam line BL04B1 at SPring-8. Deformation-DIA press with a facility of cyclic loading was used. This system could produce sinusoidal displacement in a wide range of oscillation periods from 0.2 to 100 s and generating variable amplitudes (Yoshino et al., 2016). Q value characterizing intrinsic attenuation was determined by phase lag of sample strain against the reference material at 1 GPa and up to 1200°C.

The experimental results show that frequency dependence of attenuation is not remarkable except for a fine grained-sample, whereas decrease of attenuation was found at 1100 and 920°C for Fe- 1 wt. %S and Fe- 14 wt. %S samples, respectively. The attenuation drop would occur with increasing melt fraction. Experiments of Fe-14 wt. %S sample along heating and cooling paths were done to check the influence of grain growth during experiments. Data obtained from both heating and cooling paths show that abrupt change of the attenuation occurred at around 925°C. The Young’ s modulus calculated from the strain ratio of sample and reference shows strong temperature dependence. An obvious drop occurred between 900 and 980°C in association with the occurrence of partial melting. Relationship between velocity and attenuation anomalies of the Fe–S–O system shows a positive correlation when melt fraction reaches a certain value.

Partial melting could decrease Q^{-1}, which could explain the relative low attenuation on uppermost 30 km layer throughout the top of the inner core. Combing with the positive correlation between attenuation and velocity, a large amount of partial melting could occur on the uppermost 30 km layer of the rest area except the Pacific hemisphere in the inner core.

Keywords: attenuation, partially melting, Young Modulus, inner core

©2019. Japan Geoscience Union. All Right Reserved.



©2019. Japan Geoscience Union. All Right Reserved.

Effect of pore pressure on attenuation of seismic waves in thermally cracked granite

*Keiya Yamada[1], Kazuki Sawayama[2], Ikuo Katayama[1]

1. Hiroshima University, 2. Kyushu University

Elastic wave attenuation is one of important physical properties to estimate the subsurface structure by geophysical explorations, and it is very sensitive to the existence of cracks and pore fluid. Especially, pore pressure is essential parameter that is closely related to geothermal fluid productions and earthquakes. To quantify pore pressure or observe its change over years may lead to the precise evaluation of the geothermal fluid reservoir and prediction of earthquakes. Therefore, it is needed to understand the quantitative relationship between elastic wave attenuation and pore pressure. Previous experimental studies have measured elastic wave attenuation, in those experiments pore pressure is constant and confining pressure is increased. However, there are few studies that measured elastic wave attenuation focusing on the change of pore pressure. In this study, We carried out hydrostatic tests using thermally cracked granite and investing the effect of pore pressure on elastic wave attenuation.
The material we used throughout this study is Aji granite. Specimens were cored from the same block and shape into cylindrical (20 mm in a diameter, 40 mm in a length). Thermal cracking was introduced by slowly heating and cooling specimens up to 200, 400, 600℃ and thereby porosity (initial 0.6%) increases to 0.8, 0.9, 2.8% respectively. Hydrostatic tests were performed under dry and wet (water fully saturated) condition, at room temperature, using intra-vessel deformation and fluid-flow apparatus at Hiroshima University. Under dry condition, confining pressure was increased to 60 MPa. Under wet condition, confining pressure remained a constant value of 60 MPa and pore pressure was decreased from 50 MPa to the atmosphere. Elastic wave was measured by the pulse transmission method and transducers were glued to both sides of specimens. We calculated elastic wave velocity (Vp, Vs) from waveforms recorded in the oscilloscope, and estimated elastic wave attenuation (Qp^{-1}, Qs^{-1}) using Fourier spectral ratio method. As a result, Vp and Vs increase with confining pressure under dry condition whereas they decrease with increasing pore pressure under wet condition. In terms of the attenuation, $Qp^{-1}$and Qs^{-1}decrease as confining pressure increases under dry condition while they increase with pore pressure under wet condition. As confining pressure is increased, attenuation by friction decreased due to the closing and locking of crack contacts. In the experiment of specimen which was heated to 600℃, $Qp^{-1}$is much smaller than Qs^{-1}under wet condition, and the trend is differ from that under dry condition. Under wet condition, attenuation by fluid flow must have a greater effect on Qs^{-1}than Qp^{-1}. Our results indicate that the response to pore pressure is different between velocity and attenuation: as pore pressure increases, Vp/Vs increases but Qp^{-1}/Qs^{-1}decreased. Because attenuation changes more greatly than velocity and is more sensitive to the change of pore pressure, elastic wave attenuation could be useful to observe the change of pore pressure under the ground.

Keywords: Elastic wave attenuation, Pore pressure, Elastic wave velocity, Aji granite, Thermal cracking

©2019. Japan Geoscience Union. All Right Reserved.

[E] Poster | S (Solid Earth Sciences)：S-TT Technology & Techniques

Sun. May 26, 2019 3:30 PM - 5:00 PM JST | Sun. May 26, 2019 6:30 AM - 8:00 AM UTC | Poster Hall International Exhibition Hall8, Makuhari Messe_19

[S-TT42] Recent Advances in Exploration Geophysics 2019

convener:Hitoshi Mikada(Kyoto University), Yoshihisa Iio(Disater Prevention Research Institute, Kyoto University), Nobukazu Seama(Department of Planetology, Graduate School of Science, Kobe University), Junichi Takekawa(Graduate School of Science, Kyoto University)

Geophysical exploration methods are widely used to estimate physical or chemical properties of media that are located in the environment where it is difficult for human beings to access. We would welcome presentations and discussions on theories, applications, case studies in which geophysical exploration schemes are applied for using artificial/natural signals or potentials. A proceeding paper within 4 A4 pages for each submission is to be asked to prepare after the acceptance based on the quality of the abstract of the submission and will be published electronically with doi on EarthDoc (http://earthdoc.eage.org/publication/eventoverview?p=78) under MoU with the European Association of Geoscientists and Engineers.

[STT42-P01] DISCRIMINATION OF HYDRATE BEARING MARINE SEDIMENTS BY USING FREQUENCY BASED ATTENUATION

*Nisar Ahmed[1], Mubasher Ahmad[1], Perveiz Khalid[1] (1.Institute of Geology, University of the Punjab, Lahore 54590, Pakistan)

[STT42-P02] Evaluation of methane hydrate based on attenuation parameter in seismic exploration

*Mizuki Kawabe[1], Hitoshi Mikada[1], Junichi Takekawa[1] (1.Kyoto Unibercity)

[STT42-P03] Estimating the earthquake source mechanism using full waveform inversion

*Jang Iktae[1], Hitoshi Mikada[1], Junichi Takekawa[1] (1.Kyoto University)

[STT42-P04] A quantitative analysis of the passive seismic emission tomography using the lattice Boltzmann method

*Sakemi Yuichi[1], Hitoshi Mikada[1], Junichi Takekawa[1] (1.Kyoto University)

[STT42-P05] A feasibility study for supercritical geothermal energy in enhanced geothermal system

*Tatsuki Ueda[1], Hitoshi Mikada[1], Junichi Takekawa[1] (1.Kyoto University)

DISCRIMINATION OF HYDRATE BEARING MARINE SEDIMENTS BY USING FREQUENCY BASED ATTENUATION

*Nisar Ahmed[1], Mubasher Ahmad[1], Perveiz Khalid[1]

1. Institute of Geology, University of the Punjab, Lahore 54590, Pakistan

We have examined the seismic wave attenuation and dispersion effects due to wave-induced fluid flow (WIFF) in heterogeneous porous marine sediments at mesoscopic scale of heterogeneity. The mesoscopic is the scale
larger as compared to the reservoir rock pore size but smaller than the seismic the wavelength and considered most significant scale for fluid related P wave attenuation and velocity dispersion. White’ s model
has been used for the current study which calculates a relaxation mechanism, because of pressure equilibrium, attenuation-dispersion of seismic waves occurred. Gas hydrates-bearing marine sediments of the Makran offshore, Pakistan are considered as numerical example for this study. The numerical results show that the seismic wave attenuation and velocity dispersion can be used as a good indicator to identify gas hydrates and both attenuation-dispersion increases with the increase of saturation of gas hydrates. The
maximum P wave attenuation is observed at 64 % gas hydrate saturation. However, in the case of free gas in the
marine sediments, low gas saturation level causes of high attenuation and velocity dispersion.

Keywords: Seismic attenuation, Velocity dispersion, Marine sediments, Gas hydrates, White model, Elastic wave theory

©2019. Japan Geoscience Union. All Right Reserved.

Evaluation of methane hydrate based on attenuation parameter in seismic exploration

*Mizuki Kawabe[1], Hitoshi Mikada[1], Junichi Takekawa[1]

1. Kyoto Unibercity

In recent years, methane hydrate (MH) has drawn attention as a new domestic energy resource in Japan. Although field production experiments have been conducted in real fields, some MH samples collected in real fields revealed the difficulty to evaluate the amount of MH based quantitative only with the evaluation of bottom simulating reflector (BSR). For efficient development of MH reservoirs, it is therefore important to estimate the thickness of MH concentrated zones accurately. Since MH layer has high attenuation that takes place as a function of propagation path through the attenuating medium, the evaluation of MH using seismic exploration could be an effective approach. However, the previous studies indicated that it is difficult to estimate attenuation structure even if the full-waveform information is utilized. On the other hand, the amplitude of seismic waves passing through MH layer must be affected by its high attenuation, but the approach of full waveform inversion (FWI) has been reported ineffective due to its back-propagation process. In the present study, we hypothesize that additional constraint enables us to estimate attenuation parameter of MH layer without any back propagation of residual wavefield. We assume that the layer structure in the subsurface is known, and the physical properties of MH layer are unknown. Based on the above assumption, we conducted numerical experiments to investigate the effectiveness of inversion based on utilization of full-waveform to provide information on estimation of the amount of MH resources based on the linearized general inverse theory.
In our numerical model, the seismic source and receivers are put in the sea water and on the sea bed, respectively. Synthetic waveforms are created by solving the visco-elastic equation using the finite-difference method. Our numerical experiments revealed that simultaneous inversion of the Lame’ s parameter and attenuation parameter of P-wave (Qp) is difficult. To overcome this, we proposed a kind of the relaxation method, i.e. we separately solve the Lame’ s parameters (and) and Qp in our inversion process. The proposed method can obtain the true value not only the Lame’ s parameters but also Qp with sufficient accuracy. Our numerical results indicate that the seismic exploration can provide valuable information on MH layer by estimating physical properties including the attenuation parameter.

Keywords: methane hydrate, seismic exploration, numerical experiment, finite-difference method

©2019. Japan Geoscience Union. All Right Reserved.

Estimating the earthquake source mechanism using full waveform inversion

*Jang Iktae[1], Hitoshi Mikada[1], Junichi Takekawa[1]

1. Kyoto University

An immediate understanding of the source mechanism of an earthquake after the occurrence is an important task for disaster mitigation to realize a safe society. One of the most important tasks for considering the mechanism of an earthquake is estimating the earthquake source mechanism. Due to the lack of seismic data and computational requirements, the centroid-moment tensor (CMT) solution has been widely used to estimate the focal mechanism until recent years. However, long term observation of the spatial distribution of aftershocks is required to identify the nodal plane that caused the fault motion. Since the earthquake waveform caused by a nodal plane becomes different from that caused by the other conjugate nodal plane, the analysis of full-waveform could be utilized to identify which nodal plane has caused the fault motion so that the focal mechanism of the earthquake could be estimated before the observation of aftershocks. Although some numerical experiments revealed that the possibility of FWI to inversion of earthquake source mechanism, the sensitivity of each fault parameter to full-waveforms has not been fully investigated yet.

In this study, we investigate the applicability of full-waveform inversion (FWI) to determine focal mechanism using numerical experiments. In FWI, L2-norm error function is often used as an objective function to be minimized. We evaluate the effect of some fault parameters (strike, dip, and rake) on the difference of recorded waveforms.

We make a three-dimensional numerical model with an earthquake source, and simulate elastic wave propagation using the finite-difference method. The seismic waves are recorded by receivers located on the ground surface. Subsequently, we slightly change the fault parameters, and then, simulate elastic wave propagation. We calculate the residuals between two recorded waveforms. This procedure enables us to investigate the sensitivity of the parameters on the L2-norm error function. Our numerical results indicate that rake has poor sensitivity whereas the change of strike and dip has a large effect on the recorded waveforms.

Keywords: Full-Waveform Inversion (FWI), Earthquake Source Mechanism, Numerical Experiment

©2019. Japan Geoscience Union. All Right Reserved.

A quantitative analysis of the passive seismic emission tomography using the lattice Boltzmann method

*Sakemi Yuichi[1], Hitoshi Mikada[1], Junichi Takekawa[1]

1. Kyoto University

In recent years, monitoring seismic emission caused by subsurface fluid motion has been widely used in development of hydrocarbon reservoirs. Although this technique can provide the position and the depth of fluid flow in the reservoir, it is difficult to obtain further kinematic information such as flow velocity, fluid viscosity, or pore shape. Previous studies suggested that utilizing waveform analysis of seismic emission would make it possible to image the location of fluid flow, but the mechanism of such seismic emission has not been well revealed. Recently we proposed a model of seismic emission due to fluid flow but found our method has a problem that needs to be worked out, i.e. the utilization of inappropriate sound velocity to reduce the cost of calculation in Lattice Boltzmann method (LBM). In LBM, the incorrect fluid properties are often used since the correct properties induce a numerical instability. This means that it is difficult to evaluate our results in a quantitative manner. In the present study, we focused on this problem and set two types of models to tackle the problem of sound velocity in fluid; one is normal LBM model and the other one has the real sound velocity. We conducted numerical experiments using these models. We have found that the result calculated by the normal model can be modified to fit the results with the real properties by using an appropriate correction coefficient. Therefore, we have concluded that the normal LBM calculation could be adopted to reduce the cost of numerical simulation, and therefore, it is possible to quantitatively evaluate their experimental reuslts.

Keywords: Passive seismic, Fluid flow, Lattice Boltzmann method

©2019. Japan Geoscience Union. All Right Reserved.

A feasibility study for supercritical geothermal energy in enhanced geothermal system

*Tatsuki Ueda[1], Hitoshi Mikada[1], Junichi Takekawa[1]

1. Kyoto University

Japan has many volcanoes and large potential of geothermal energies. However, since 1996, the construction of large-scale geothermal plants in Japan has been stopped, and the amount of electricity generated by the geothermal plants decreased by about 30 percent compared to the peak time in 1997. Existing geothermal energy development has mainly targeted shallow geothermal resources. However, shallow geothermal resources are eccentrically located so we can generate power at narrow area and obtain the limited amount of energy. On the other hand, geothermal power generation using supercritical water is expected to increase power output with one power plant than the conventional geothermal power plants. Moreover, by constructing artificial reservoir, it becomes possible to introduce it in wide area and it is expected to contribute to reduction of development and attenuation risk. However, the feasibility of the geothermal power plants using supercritical water has not been fully investigated yet. In this research, we focus on artificial geothermal reservoir under supercritical environment, and quantitatively investigate its feasibility using numerical simulations. Specifically, artificial supercritical geothermal power generation with a downhole coaxial heat exchanger and a single U-shaped pipe method are considered as the heat exchanger method. We solve the unsteady thermal conduction problem using the finite-difference method with various flow rate and injection pressure conditions. As the result of numerical simulation, it was confirmed that in the case of both the double pipe system and the single U-shaped pipe, it is possible to extract supercritical water. Moreover, it was also found that high-performance heat insulating tubes are required for the inner pipe or the production well in either the double pipe type or the single U-shaped pipe type.

Keywords: supercritical geothermal power generation, numerical simulation, finite-difference method

©2019. Japan Geoscience Union. All Right Reserved.

[E] Poster | S (Solid Earth Sciences)：S-TT Technology & Techniques

Sun. May 26, 2019 5:15 PM - 6:30 PM JST | Sun. May 26, 2019 8:15 AM - 9:30 AM UTC | Poster Hall International Exhibition Hall8, Makuhari Messe_32

[S-TT42] Recent Advances in Exploration Geophysics 2019

convener:Hitoshi Mikada(Kyoto University), Yoshihisa Iio(Disater Prevention Research Institute, Kyoto University), Nobukazu Seama(Department of Planetology, Graduate School of Science, Kobe University), Junichi Takekawa(Graduate School of Science, Kyoto University)

Geophysical exploration methods are widely used to estimate physical or chemical properties of media that are located in the environment where it is difficult for human beings to access. We would welcome presentations and discussions on theories, applications, case studies in which geophysical exploration schemes are applied for using artificial/natural signals or potentials. A proceeding paper within 4 A4 pages for each submission is to be asked to prepare after the acceptance based on the quality of the abstract of the submission and will be published electronically with doi on EarthDoc (http://earthdoc.eage.org/publication/eventoverview?p=78) under MoU with the European Association of Geoscientists and Engineers.

[STT42-P01] DISCRIMINATION OF HYDRATE BEARING MARINE SEDIMENTS BY USING FREQUENCY BASED ATTENUATION

*Nisar Ahmed[1], Mubasher Ahmad[1], Perveiz Khalid[1] (1.Institute of Geology, University of the Punjab, Lahore 54590, Pakistan)

[STT42-P02] Evaluation of methane hydrate based on attenuation parameter in seismic exploration

*Mizuki Kawabe[1], Hitoshi Mikada[1], Junichi Takekawa[1] (1.Kyoto Unibercity)

[STT42-P03] Estimating the earthquake source mechanism using full waveform inversion

*Jang Iktae[1], Hitoshi Mikada[1], Junichi Takekawa[1] (1.Kyoto University)

[STT42-P04] A quantitative analysis of the passive seismic emission tomography using the lattice Boltzmann method

*Sakemi Yuichi[1], Hitoshi Mikada[1], Junichi Takekawa[1] (1.Kyoto University)

[STT42-P05] A feasibility study for supercritical geothermal energy in enhanced geothermal system

*Tatsuki Ueda[1], Hitoshi Mikada[1], Junichi Takekawa[1] (1.Kyoto University)

DISCRIMINATION OF HYDRATE BEARING MARINE SEDIMENTS BY USING FREQUENCY BASED ATTENUATION

*Nisar Ahmed[1], Mubasher Ahmad[1], Perveiz Khalid[1]

1. Institute of Geology, University of the Punjab, Lahore 54590, Pakistan

We have examined the seismic wave attenuation and dispersion effects due to wave-induced fluid flow (WIFF) in heterogeneous porous marine sediments at mesoscopic scale of heterogeneity. The mesoscopic is the scale
larger as compared to the reservoir rock pore size but smaller than the seismic the wavelength and considered most significant scale for fluid related P wave attenuation and velocity dispersion. White’ s model
has been used for the current study which calculates a relaxation mechanism, because of pressure equilibrium, attenuation-dispersion of seismic waves occurred. Gas hydrates-bearing marine sediments of the Makran offshore, Pakistan are considered as numerical example for this study. The numerical results show that the seismic wave attenuation and velocity dispersion can be used as a good indicator to identify gas hydrates and both attenuation-dispersion increases with the increase of saturation of gas hydrates. The
maximum P wave attenuation is observed at 64 % gas hydrate saturation. However, in the case of free gas in the
marine sediments, low gas saturation level causes of high attenuation and velocity dispersion.

Keywords: Seismic attenuation, Velocity dispersion, Marine sediments, Gas hydrates, White model, Elastic wave theory

©2019. Japan Geoscience Union. All Right Reserved.

Evaluation of methane hydrate based on attenuation parameter in seismic exploration

*Mizuki Kawabe[1], Hitoshi Mikada[1], Junichi Takekawa[1]

1. Kyoto Unibercity

In recent years, methane hydrate (MH) has drawn attention as a new domestic energy resource in Japan. Although field production experiments have been conducted in real fields, some MH samples collected in real fields revealed the difficulty to evaluate the amount of MH based quantitative only with the evaluation of bottom simulating reflector (BSR). For efficient development of MH reservoirs, it is therefore important to estimate the thickness of MH concentrated zones accurately. Since MH layer has high attenuation that takes place as a function of propagation path through the attenuating medium, the evaluation of MH using seismic exploration could be an effective approach. However, the previous studies indicated that it is difficult to estimate attenuation structure even if the full-waveform information is utilized. On the other hand, the amplitude of seismic waves passing through MH layer must be affected by its high attenuation, but the approach of full waveform inversion (FWI) has been reported ineffective due to its back-propagation process. In the present study, we hypothesize that additional constraint enables us to estimate attenuation parameter of MH layer without any back propagation of residual wavefield. We assume that the layer structure in the subsurface is known, and the physical properties of MH layer are unknown. Based on the above assumption, we conducted numerical experiments to investigate the effectiveness of inversion based on utilization of full-waveform to provide information on estimation of the amount of MH resources based on the linearized general inverse theory.
In our numerical model, the seismic source and receivers are put in the sea water and on the sea bed, respectively. Synthetic waveforms are created by solving the visco-elastic equation using the finite-difference method. Our numerical experiments revealed that simultaneous inversion of the Lame’ s parameter and attenuation parameter of P-wave (Qp) is difficult. To overcome this, we proposed a kind of the relaxation method, i.e. we separately solve the Lame’ s parameters (and) and Qp in our inversion process. The proposed method can obtain the true value not only the Lame’ s parameters but also Qp with sufficient accuracy. Our numerical results indicate that the seismic exploration can provide valuable information on MH layer by estimating physical properties including the attenuation parameter.

Keywords: methane hydrate, seismic exploration, numerical experiment, finite-difference method

©2019. Japan Geoscience Union. All Right Reserved.

Estimating the earthquake source mechanism using full waveform inversion

*Jang Iktae[1], Hitoshi Mikada[1], Junichi Takekawa[1]

1. Kyoto University

An immediate understanding of the source mechanism of an earthquake after the occurrence is an important task for disaster mitigation to realize a safe society. One of the most important tasks for considering the mechanism of an earthquake is estimating the earthquake source mechanism. Due to the lack of seismic data and computational requirements, the centroid-moment tensor (CMT) solution has been widely used to estimate the focal mechanism until recent years. However, long term observation of the spatial distribution of aftershocks is required to identify the nodal plane that caused the fault motion. Since the earthquake waveform caused by a nodal plane becomes different from that caused by the other conjugate nodal plane, the analysis of full-waveform could be utilized to identify which nodal plane has caused the fault motion so that the focal mechanism of the earthquake could be estimated before the observation of aftershocks. Although some numerical experiments revealed that the possibility of FWI to inversion of earthquake source mechanism, the sensitivity of each fault parameter to full-waveforms has not been fully investigated yet.

In this study, we investigate the applicability of full-waveform inversion (FWI) to determine focal mechanism using numerical experiments. In FWI, L2-norm error function is often used as an objective function to be minimized. We evaluate the effect of some fault parameters (strike, dip, and rake) on the difference of recorded waveforms.

We make a three-dimensional numerical model with an earthquake source, and simulate elastic wave propagation using the finite-difference method. The seismic waves are recorded by receivers located on the ground surface. Subsequently, we slightly change the fault parameters, and then, simulate elastic wave propagation. We calculate the residuals between two recorded waveforms. This procedure enables us to investigate the sensitivity of the parameters on the L2-norm error function. Our numerical results indicate that rake has poor sensitivity whereas the change of strike and dip has a large effect on the recorded waveforms.

Keywords: Full-Waveform Inversion (FWI), Earthquake Source Mechanism, Numerical Experiment

©2019. Japan Geoscience Union. All Right Reserved.

A quantitative analysis of the passive seismic emission tomography using the lattice Boltzmann method

*Sakemi Yuichi[1], Hitoshi Mikada[1], Junichi Takekawa[1]

1. Kyoto University

In recent years, monitoring seismic emission caused by subsurface fluid motion has been widely used in development of hydrocarbon reservoirs. Although this technique can provide the position and the depth of fluid flow in the reservoir, it is difficult to obtain further kinematic information such as flow velocity, fluid viscosity, or pore shape. Previous studies suggested that utilizing waveform analysis of seismic emission would make it possible to image the location of fluid flow, but the mechanism of such seismic emission has not been well revealed. Recently we proposed a model of seismic emission due to fluid flow but found our method has a problem that needs to be worked out, i.e. the utilization of inappropriate sound velocity to reduce the cost of calculation in Lattice Boltzmann method (LBM). In LBM, the incorrect fluid properties are often used since the correct properties induce a numerical instability. This means that it is difficult to evaluate our results in a quantitative manner. In the present study, we focused on this problem and set two types of models to tackle the problem of sound velocity in fluid; one is normal LBM model and the other one has the real sound velocity. We conducted numerical experiments using these models. We have found that the result calculated by the normal model can be modified to fit the results with the real properties by using an appropriate correction coefficient. Therefore, we have concluded that the normal LBM calculation could be adopted to reduce the cost of numerical simulation, and therefore, it is possible to quantitatively evaluate their experimental reuslts.

Keywords: Passive seismic, Fluid flow, Lattice Boltzmann method

©2019. Japan Geoscience Union. All Right Reserved.

A feasibility study for supercritical geothermal energy in enhanced geothermal system

*Tatsuki Ueda[1], Hitoshi Mikada[1], Junichi Takekawa[1]

1. Kyoto University

Japan has many volcanoes and large potential of geothermal energies. However, since 1996, the construction of large-scale geothermal plants in Japan has been stopped, and the amount of electricity generated by the geothermal plants decreased by about 30 percent compared to the peak time in 1997. Existing geothermal energy development has mainly targeted shallow geothermal resources. However, shallow geothermal resources are eccentrically located so we can generate power at narrow area and obtain the limited amount of energy. On the other hand, geothermal power generation using supercritical water is expected to increase power output with one power plant than the conventional geothermal power plants. Moreover, by constructing artificial reservoir, it becomes possible to introduce it in wide area and it is expected to contribute to reduction of development and attenuation risk. However, the feasibility of the geothermal power plants using supercritical water has not been fully investigated yet. In this research, we focus on artificial geothermal reservoir under supercritical environment, and quantitatively investigate its feasibility using numerical simulations. Specifically, artificial supercritical geothermal power generation with a downhole coaxial heat exchanger and a single U-shaped pipe method are considered as the heat exchanger method. We solve the unsteady thermal conduction problem using the finite-difference method with various flow rate and injection pressure conditions. As the result of numerical simulation, it was confirmed that in the case of both the double pipe system and the single U-shaped pipe, it is possible to extract supercritical water. Moreover, it was also found that high-performance heat insulating tubes are required for the inner pipe or the production well in either the double pipe type or the single U-shaped pipe type.

Keywords: supercritical geothermal power generation, numerical simulation, finite-difference method

©2019. Japan Geoscience Union. All Right Reserved.

[E] Poster | B (Biogeosciences)：B-PT Paleontology

Sun. May 26, 2019 3:30 PM - 5:00 PM JST | Sun. May 26, 2019 6:30 AM - 8:00 AM UTC | Poster Hall International Exhibition Hall8, Makuhari Messe_22

[B-PT04] Biomineralization and the Geochemistry of Proxies

convener:Takashi Toyofuku(Japan Agency for Marine-Earth Science and Technology (JAMSTEC)), Hiroshi Kitazato(Tokyo University of Marine Science and Technology (TUMSAT)), Jelle Bijma(Alfred-Wegener-Institut Helmholtz-Zentrum f?r Polar- und Meeresforschung), Kotaro Hirose(Faculty of Science & Engineering, Waseda University)

Biomineralization and the Geochemistry of Proxies - Biology, laboratory culture-experiments and their applications to the paleo-research -
In order to reconstruct the Earth climate system, marine paleoclimatologists resort to transfer functions or geochemical proxies, which are produced or affected by organisms. The relationships used for reconstructions are generally based on field calibrations or derived from laboratory experiments. The danger of these so-called empirical relationships is that they may be valid only within the restricted parameter space of their calibration. Application of proxy relationships to very different environmental settings (e.g. high vs. low latitude or glacial vs. interglacial) requires a mechanistic understanding of these relationships. Much progress can be expected by a better understanding of the biomineralization mechanisms and the incorporation of proxy signals.
In this session we facilitate contributions related to the biomineralization, calibration and validation of marine proxies from field study, laboratory culture experiment and paleo-environmental reconstruction.

[BPT04-P01] Living (stained) benthic foraminifera in the West-Gironde mud patch (Bay of Biscay, France): An ongoing survey for the European Community.

*Christophe Fontanier[1,2], Bruno Deflandre[1], Sylvain Rigaud[3], Sabine Schmidt[1], Bastien Lamarque[1], Pascal Lebleu[1], Dominique Poirier[1], Antoine Grémare[1] (1. Bordeaux University, EPOC Laboratory, UMR CNRS 5805 OASU, F-33615 Pessac, FRANCE, 2.FORAM Research Group, F-49140 Villevêque, FRANCE, 3.Nîmes University, GIS Laboratory, EA 7352 CHROME, F-30035 Nïmes, FRANCE)

[BPT04-P02] Biomonitoring in the Cassidaigne Canyon (NW Mediterranean): the resilience and recovery of deep-sea benthic foraminifera at a bauxite industrial waste site

*Pauline Duros[1], Christophe Fontanier[1,2,3], Briony Mamo[4,5], Deborah Mille[6], Olivier Herlory[6] (1.FORAM Research Group, F-49140 Villevêque, FRANCE, 2.Bordeaux University, EPOC Laboratory, UMR CNRS 5805 OASU, F-33615 Pessac, FRANCE, 3.Angers University, 4 boulevard Lavoisier, F-49000 Angers, FRANCE., 4.School of Biological Sciences, University of Hong Kong, Pokfulam Road Sai Wan, Hong Kong SAR, CHINA. , 5.Department of Biology, Macquarie University, North Ryde, NSW, 2109, AUSTRALIA., 6.CREOCEAN, Agence PACA Corse, 230 Avenue de Rome, Valparc-Bât B, F-83500 La Seyne sur Mer, FRANCE.)

[BPT04-P03] Comparison between assemblages of diatom fossil and biomarkers in surface sediments from Seto Inland Sea

*Kotaro Hirose[1], Hideto Nakamura[2], Takuto Ando[4], Satoshi Asaoka[3], Ken Sawada[5] (1.Faculty of Science & Engineering, Waseda University, 2.Faculty of Science, Osaka City University, 3.Research Center for Inland Seas & Department of Planetology, Kobe University, 4.Arctic Research Center, Hokkaido University, 5.Department of Earth & Planetary Science, Faculty of Science, Hokkaido University)

[BPT04-P04] Combined impacts of ocean acidification and desalination: culture experiments on the coastal species *Ammonia* sp. and *Elphidium crispum*

*Laurie Marie Charrieau[1], Helena L. Filipsson[2], Yukiko Nagai[1], Sachiko Kawada[1], Karl Ljung[2], Emma Kritzberg[3], Takashi Toyofuku[1,4] (1.Japan Agency for Marine-Earth Science and Technology, 2.Department of Geology, Lund University, Sweden, 3.Department of Biology, Lund University, Sweden, 4.Tokyo University of Marine Science and Technology (TUMSAT), Japan)

[BPT04-P05] Effects on larger benthic foraminiferal shell density under global warming

*Shunichi Kinoshita[1], Azumi Kuroyanagi[2], Hiroshi Nishi[2], Osamu Sasaki[2], Kazuhiko Fujita[3], Atsushi Suzuki[4], Hodaka Kawahata[5] (1.Graduate School of Science, Tohoku University, 2.The Tohoku University Museum, The Center for Academic Resources and Archives, Tohoku Univerity, 3.Department of Physics and Earth Sciences, Faculty of Science and Tropical Biosphere Research Center, University of the Ryukyus, 4.Geological Survey of Japan National Institute of Advanced Industrial Science and Technology, 5.Atmosphere and Ocean Research Institute, the University of Tokyo)

[BPT04-P06] Estimation of the calcification rate of foraminifera -exceptionally fast extending of the shell-

*Yukiko Nagai[1,2], Katsuyuki Uematsu[3], Takashi Toyofuku[2,4] (1.National Museum of Nature and Science of Tokyo, 2.Japan Agency for Marine-Earth Science and Technology, 3.Marine Works Japan Enterprise, 4.Tokyo university of Marine Science and Technology)

[BPT04-P07] Estimation of foraminiferal calcification process from live imaging and FIB-SEM approach

*Takashi Toyofuku[1,2], Yukiko Nagai[1,3] (1.Japan Agency for Marine-Earth Science and Technology (JAMSTEC), 2.Tokyo University of Marine Science and Technology, 3.National Museum of Nature and Science,Tokyo)

[BPT04-P08] Toward a better understanding of planktic foraminiferal proxies: Are they photosymbiotic or not?

*Haruka TAKAGI[1], Katsunori KIMOTO[2], Tetsuichi FUJIKI[2], Kazuyoshi MORIYA[3], Hiroaki SAITO[1] (1.Atmosphere and Ocean Research Institute, The University of Tokyo, 2.Japan Agency for Marine-Earth Science and Technology, 3.School of Education, Waseda University)

[BPT04-P09] Evaluation of geochemistry in hypercalcified demosponges as a paleoceanographic proxy

*Ryuji Asami[1], Tohru Naruse[2], Masaru Mizuyama[3], Ryu Uemura[3], Ryuichi Shinjo[3], Yuji Ise[4], Yoshihisa Fujita[5], Takashi Sakamaki[6] (1.Graduate School of Science, Tohoku University, 2.Tropical Biosphere Research Center, University of the Ryukyus, 3.Faculty of Science, University of the Ryukyus, 4.Centre for Marine and Coastal Studies, Universiti Sains Malaysis, 5.Okinawa Prefectural University of Arts, 6.Graduate School of Engineering, Tohoku University)

Living (stained) benthic foraminifera in the West-Gironde mud patch (Bay of Biscay, France): An ongoing survey for the European Community.

*Christophe Fontanier[1,2], Bruno Deflandre[1], Sylvain Rigaud[3], Sabine Schmidt[1], Bastien Lamarque[1], Pascal Lebleu[1], Dominique Poirier[1], Antoine Grémare[1]

1. Bordeaux University, EPOC Laboratory, UMR CNRS 5805 OASU, F-33615 Pessac, FRANCE, 2. FORAM Research Group, F-49140 Villevêque, FRANCE, 3. Nîmes University, GIS Laboratory, EA 7352 CHROME, F-30035 Nïmes, FRANCE

During an environmental survey performed in summer 2017 (JERICObent-2 Cruise), living (stained) benthic foraminiferal faunas were investigated at 7 stations sampled within the West-Gironde mud patch, a mud belt located on the marine shelf in front of the Gironde River (Bay of Biscay, France). This study area is really strategic for local fisheries since substantial marine resources (demersal fishes, shrimps...) are easily accessible for coastal fishermen. Moreover, the mud belt is considered an important hotspot for marine biodiversity as far as food (i.e. sedimentary organic matter), which is naturally abundant there, could sustain an assumedly enhanced heterogeneity of benthic habitats for various taxon. In the framework of the European project JERICONext (ID 654410), we have been studying biological (prokaryotes, benthic meiofauna and macrofauna), sedimentary and geochemical patterns of mud-flat ecosystems in order to better understand how both spatial and temporal variability of riverine regime and coastal hydrodynamics impact the dynamics of the benthic life, especially foraminifera. Stations investigated in this presentation are located between 39 and 69 m water depth from the inner shelf to the mid-shelf. At most sites, surface sediment is characterized by clay-silt facies more or less enriched in organic matter. Oxygen penetration depth within the sediment is less than 7±3 mm. Foraminiferal simple diversity (S) presents relatively moderate values ranging between 15 and 35 taxa. According to Shannon Index H' and Rarefaction Index ES(100), foraminiferal diversity tends to slightly increase with water depth. This trend is supported by *Eggerelloides scabrus;* its contribution decreases from the shallower stations (~50%) of the proximal mud patch (<55 m depth) to the deeper stations (<30%) of the distal mud patch (>55 m depth). This agglutinated species is generally considered a reliable bio-indicator of organic-matter enriched sediment in front of river mouths. It is noteworthy that the shallowest station (station 1, 39 m) is also characterised by the exclusive contribution of *Quinqueloculina lata/laevigata* and *Ammonia beccarii,* which are both typical of inner-shelf environments. There, surface sediment is made of fine sand. The deeper stations (>55 m depth) located in the distal mud patch are characterised by a remarkable contribution (~30%) of *Pseudoeponides falsobeccarii* and Buliminids (~30% respectively). They are accompanied by *Rectuvigerina phlegeri* and *Nonion fabum*, which are typical of mid- and outer-shelf ecosystems. The contribution of Buliminids underline the gradual increase of sedimentary organic content (>1.2% DW) with water depth.

Keywords: Living Benthic Foraminifera, Mud Belt, Environmental Spatial Variability, Sedimentary Organic Matter, Oxygenation Level

©2019. Japan Geoscience Union. All Right Reserved.

Biomonitoring in the Cassidaigne Canyon (NW Mediterranean): the resilience and recovery of deep-sea benthic foraminifera at a bauxite industrial waste site

*Pauline Duros[1], Christophe Fontanier[1,2,3], Briony Mamo[4,5], Deborah Mille[6], Olivier Herlory[6]

1. FORAM Research Group, F-49140 Villevêque, FRANCE, 2. Bordeaux University, EPOC Laboratory, UMR CNRS 5805 OASU, F-33615 Pessac, FRANCE, 3. Angers University, 4 boulevard Lavoisier, F-49000 Angers, FRANCE., 4. School of Biological Sciences, University of Hong Kong, Pokfulam Road Sai Wan, Hong Kong SAR, CHINA. , 5. Department of Biology, Macquarie University, North Ryde, NSW, 2109, AUSTRALIA., 6. CREOCEAN, Agence PACA Corse, 230 Avenue de Rome, Valparc-Bât B, F-83500 La Seyne sur Mer, FRANCE.

During an environmental survey performed in autumn 2016, living (stained) benthic foraminiferal faunas were investigated at 16 stations sampled within the Cassidaigne Canyon (NW Mediterranean Sea) and surrounding area. For many decades, industrial bauxite residues of red mud have drained into the canyon via a submarine pipe, causing physical disturbance and chemical contamination. In January 2016, solid waste disposal ceased and was replaced with the dumping of a low-density liquid effluent. Stations investigated in this paper are located between 265–2500 m water depth from the shelf break to the deeper basin and from a distance between 4–70 km from the pipe outlet. At many sites, surface sediment is characterized by historical deposits of red mud and their geochemical imprints. Our ecological observations at the 725 m-depth station closest to the Cassidaigne Canyon submarine pipe show the highest concentration of the opportunistic and stress-tolerant species *Bulimina marginata* d' Orbigny, 1826, commonly identified as a recolonizer of disturbed areas. At the other fifteen stations, foraminiferal standing stocks and simple diversity (S) decrease with decreasing food input to the seafloor and increasing water depth. There, foraminiferal composition is characterized by a minor contribution of stress-tolerant species and echoes the overall meso-oligotrophic patterns of a relatively stable ecosystem. Our study clearly shows that in September 2016, 10 months after a historical shift in discharged industrial wastes (from dense red mud to liquid effluent), foraminiferal diversity close to the pipe outlet in the Cassidaigne Canyon remains altered, but appears to be slowly recovering.

Keywords: Benthic foraminifera, Bauxite residues, Cassidaigne Canyon, Resilience

©2019. Japan Geoscience Union. All Right Reserved.

Comparison between assemblages of diatom fossil and biomarkers in surface sediments from Seto Inland Sea

*Kotaro Hirose[1], Hideto Nakamura[2], Takuto Ando[4], Satoshi Asaoka[3], Ken Sawada[5]

1. Faculty of Science & Engineering, Waseda University, 2. Faculty of Science, Osaka City University, 3. Research Center for Inland Seas & Department of Planetology, Kobe University, 4. Arctic Research Center, Hokkaido University, 5. Department of Earth & Planetary Science, Faculty of Science, Hokkaido University

We investigate the fossil diatom abundances and biomarker concentrations in marine sediment to assess their relationships. 14 sample of surface (uppermost 5 cm of sea bottom) sediments are taken in 5 areas (Aki-nada Bay, Hiuchi-nada Bay, Harimanada-Bay, Osaka Bay and Kii Strait) of Seto Inland Seas in July 2015. Additional 8 samples are taken in Harimanada-Bay in October 2015. Although the precise age of the core has not been determined yet, it could be deposited within 10 years, according to the sedimentation rates by previous study (Yasuhara et al., 2007).
Diatom species such as small *Thalassiosira*spp., *skeletonema costatum*, resting spore of *Chaetoceros* spp. and *Neodelphyneis pelagica*, which were reported by previous study (Hirose et al., 2008), are observed as the dominant taxa in all samples. *Rhizosolenia* spp. and *Pleurosigma* spp., known HBI producers, were occurred in low proportions. As specific diatom biomarkers, we identified C25 di- and tri-unsaturated highly branched isoprenoids (HBIs), along with relatively minor amount of C25 and C35 cyclic HBIs. Total abundances of diatom valves and HBIs were generally correlated, probably reflecting variations of diatom production. Meanwhile, Aki-bay and some samples of Harima-nada Bay were characterized with relatively low abundance of HBIs relative to valves. In these area, focused analysis on the minor diatom taxa would be needed to provide quantitative dataset to discuss further relation of HBIs and produces and their spatial distribution.

Keywords: diatom assemblage, diatom biomarkers, HBIs, surface sediment, Seto Inland Seas

©2019. Japan Geoscience Union. All Right Reserved.

Combined impacts of ocean acidification and desalination: culture experiments on the coastal species *Ammonia* sp. and *Elphidium crispum*

*Laurie Marie Charrieau[1], Helena L. Filipsson[2], Yukiko Nagai[1], Sachiko Kawada[1], Karl Ljung[2], Emma Kritzberg[3], Takashi Toyofuku[1,4]

1. Japan Agency for Marine-Earth Science and Technology, 2. Department of Geology, Lund University, Sweden, 3. Department of Biology, Lund University, Sweden, 4. Tokyo University of Marine Science and Technology (TUMSAT), Japan

Coastal areas display natural large environmental variability such as frequent changes in salinity, pH, and carbonate chemistry. Anthropogenic impacts –especially ocean acidification –increase this variability, which may affect the living conditions of coastal species, particularly, calcifiers, such as foraminifera.

The purpose of this study was to evaluate the combined effect of two typical environmental stressors on the coast - salinity and pH –on calcifying organisms. We performed culture experiments on living benthic foraminifera to study the combined effects of lowered pH and salinity on the calcification abilities and survival of the coastal, calcitic species Ammonia sp. and *Elphidium crispum*.

We found that these two species could tolerate low pH and low salinity, which reflects the environmental variations in their natural habitats. However, in open ocean conditions (salinity ~35) and lower pH treatment, the species displayed resistance to test dissolution for a longer time than in brackish conditions (salinity ~5 to 20). Moreover, the response of foraminifera to the different treatments was species-specific, and *Ammonia* sp. appeared more resistant than *E. crispum* when placed in the same conditions of pH and salinity. We also observed living dissolved specimens of juveniles *Ammonia* sp. under the combined effect of low pH and very low salinity, and we showed that desalination is one cause for the decalcification. However, they were not able to recalcify when returned to higher salinities, probably due to a sensitive balance in environmental parameters. Finally, we highlight the ability of foraminifera to survive under $\Omega calc < 1$, and that high salinity and $[Ca^{2+}]$ as building blocks are crucial for the foraminiferal calcification process.

We conclude that coastal benthic foraminifera will not immediately be affected by ocean acidification, but rather by a combination of decreasing salinity and lowered pH.

Keywords: Coastal ocean acidification, Desalination, Culture experiment, Benthic foraminifera, Calcification process

©2019. Japan Geoscience Union. All Right Reserved.

Effects on larger benthic foraminiferal shell density under global warming

*Shunichi Kinoshita[1], Azumi Kuroyanagi[2], Hiroshi Nishi[2], Osamu Sasaki[2], Kazuhiko Fujita[3], Atsushi Suzuki[4], Hodaka Kawahata[5]

1. Graduate School of Science, Tohoku University, 2. The Tohoku University Museum, The Center for Academic Resources and Archives, Tohoku Univerity, 3. Department of Physics and Earth Sciences, Faculty of Science and Tropical Biosphere Research Center, University of the Ryukyus, 4. Geological Survey of Japan National Institute of Advanced Industrial Science and Technology, 5. Atmosphere and Ocean Research Institute, the University of Tokyo

On the recent ocean environment, due to progresses of global warming and ocean acidification, it is concerned that calcifying organisms will be seriously affected from these environmental changes. Larger benthic foraminifers (LBFs) build calcium carbonate shells. Their carbonate productivity is the third highest rate in coral reef area next to reef corals and calcareous algae. Therefore, it is important to clarify the relationship between ocean environmental changes and the response of LBFs for predicting future ocean environment including carbon cycle. Based upon test diameter and shell weight, previous studies expected how foraminifers react to sea water conditions where they are living. However, in those reports, it is still not clear whether the changing of shell weight is due to changing of shell thickness (shell volume) or shell density, also whether that changing is depending sea water temperature or acidity. Thus, this study was performed for clarifying the relationships between water temperature and LBFs shell parameters with laboratory experiments and means of micro computed tomography (CT).

In this study, we cultured the LBF *Sorites orbiculus* in filtered sea water until reproduction. Soon after *S. orbiculus* reproduced, clonal individuals from same mother individual were picked and separated into seven groups. One group was selected as initial stage sample, and other six groups were provided for culture experiments. We cultured each groups under six different temperature conditions (19, 21, 23, 25, 27 and 29 ˚C). Because clonal specimens were reproduced asexually from same individual, it was expected the genetic factors were kept to a minimum. We used micro CT to investigate mean CT number (proxy of density), shell volume, test diameter and chamber number of every clonal specimen after culturing. The results show the high correlation of mean CT number with temperature in contrast to the correlation of shell volume and temperature. This suggests changing in temperature of sea water causes shell density difference, furthermore, LBFs build the higher density shell in the higher temperature as long as they lives in 19 to 29 C˚ environment.

Keywords: Larger benthic foraminifer, shell density, micro CT, laboratory experiments, global warming

©2019. Japan Geoscience Union. All Right Reserved.

Estimation of the calcification rate of foraminifera -exceptionally fast extending of the shell-

*Yukiko Nagai[1,2], Katsuyuki Uematsu[3], Takashi Toyofuku[2,4]

1. National Museum of Nature and Science of Tokyo, 2. Japan Agency for Marine-Earth Science and Technology, 3. Marine Works Japan Enterprise, 4. Tokyo university of Marine Science and Technology

The process of biomineralization of foraminiferal test is essential for its characteristic morphogenesis and the composition of element and isotope to be taken in is used also as paleo environmental proxy, numerous studies have been approched to reveal the mechanism of shell formation. However, how fast the foraminifera calicification and how much calcium carbonate deposits depends on the species, which is not well understood in most species.
The foraminifera *Spirillina vivipara* does not form a chamber, but elongate a tubular test spirally with their cytoplasmic growth. *Spirillina vivipara* is also known to be rapidly changing generations that can be reproduced in a several days after division of mother cells (Myers, 1936). From our current observations, it was also found that the shell formation is repeatedly carried out in the day, and the elongation rate of the shell is very fast. Therefore, in this study, Spirillina vivipara was used to estimate calcification rate.
In this presentation, we report on the fastest shell extending rate in foraminifera.

Keywords: Calcification, foraminifera, FIB-SEM

©2019. Japan Geoscience Union. All Right Reserved.

Estimation of foraminiferal calcification process from live imaging and FIB-SEM approach

*Takashi Toyofuku[1,2], Yukiko Nagai[1,3]

1. Japan Agency for Marine-Earth Science and Technology (JAMSTEC), 2. Tokyo University of Marine Science and Technology, 3. National Museum of Nature and Science,Tokyo

Calcareous foraminifera have been thought a major carbonate producer in ocean. Their tests (shells) are fundamental tools as paleo-environmental indicators in various studies because their calcareous tests have been archived as numerous fossils in sediment for geologic time and various environmental information are brought by faunal structure, shell morphology and geochemical compsitions of calccitic test. The other hand, the calcification process itself is interested for us. Pseudopodia sticking out into sea water build organic templates in the form of chamber. Calcium carbonate is precipitated on the both side of template within several hours. Calcium and carbonate are fixed at there by foraminiferal biological process. The newly added chamber wall was flexible in a first day, the chamber solidified in a few days and became a solid test. It is very interesting to record this process in video. Our studies showed the variable change of pH and Ca during the biomineralization of foraminifera by the application of fluorescent indicators (e.g. Toyofuku et al., 2017). Recently, we also apply the method to clear cut the site of calcification under SEM by focused ion beam (FIB-SEM)(Nagai et al., 2018). The nano-scale fine structures have been revealed the distribution of soft orgnic structures (i.e. pseudopodia) and hard tissue (precipitated calium carbonate)by this observation.

Keywords: calcification, foraminifera, imaging

©2019. Japan Geoscience Union. All Right Reserved.

Toward a better understanding of planktic foraminiferal proxies: Are they photosymbiotic or not?

*Haruka TAKAGI[1], Katsunori KIMOTO[2], Tetsuichi FUJIKI[2], Kazuyoshi MORIYA[3], Hiroaki SAITO[1]

1. Atmosphere and Ocean Research Institute, The University of Tokyo, 2. Japan Agency for Marine-Earth Science and Technology, 3. School of Education, Waseda University

Geochemistry of planktic foraminiferal tests is an important archive to understand paleoenvironment. However, many biotic factors can affect the geochemical composition and thus may lead misinterpretation of the proxy signals. Photosymbiosis (endosymbiosis with autotrophic algae) is thought to give specific effects on foraminiferal test geochemistry such as $\delta^{13}C$ due to photosynthetic activity of the symbionts. This is because photosynthesis can alter the geochemical condition of the vicinity of the foraminiferal test where calcification takes place, and eventually elevate the $\delta^{13}C$ of the test. Therefore, whether foraminiferal species have photosymbiotic ecology or not, and how active the photosynthesis is are important information for precise paleoenvironmental reconstructions. However, photosymbiotic information of planktic foraminifers is still limited even for extant species which are often utilized to generate proxy records.
In this study, we investigated 30 species of modern planktic foraminifers covering four families; Globigerinidae, Hastigerinidae, Globorotaliidae, and Candeinidae, using active chlorophyll fluorometry (fast repetition rate fluorometry; FRRF). FRRF performs non-destructive and non-invasive measurements of algal physiology based on real-time variable fluorescence profiles. When it is applied to symbiotic consortia of planktic foraminifers, it enables us to quantify chlorophyll content of a specimen, and to qualify of photophysiological features that are useful diagnostics of symbiont photosynthetic fitness. It can provide us with convincing information on individual-based photosymbiosis.
Specimens were collected from various oceanic settings; from tropical to subpolar region, encompassing Pacific to Atlantic. We have sampled across much of the northern hemisphere tropical-subtropical gradient to get the endemic species and to replicate for the others. The detection rate of photosymbiosis in each species, the biomass of symbionts (indicated by chlorophyll content), and the state of symbionts (indicated by photophysiological parameters) were investigated. Using principal component analysis, species were ranked by their “strength” of photosymbiosis. This thorough investigation will provide a more systematic understanding of photosymbiosis in modern planktic foraminifers and will help us to choose which species to use to reconstruct paleoenvironment.

Keywords: planktic foraminifers, photosymbiosis

©2019. Japan Geoscience Union. All Right Reserved.

Evaluation of geochemistry in hypercalcified demosponges as a paleoceanographic proxy

*Ryuji Asami[1], Tohru Naruse[2], Masaru Mizuyama[3], Ryu Uemura[3], Ryuichi Shinjo[3], Yuji Ise[4], Yoshihisa Fujita[5], Takashi Sakamaki[6]

1. Graduate School of Science, Tohoku University, 2. Tropical Biosphere Research Center, University of the Ryukyus, 3. Faculty of Science, University of the Ryukyus, 4. Centre for Marine and Coastal Studies, Universiti Sains Malaysis, 5. Okinawa Prefectural University of Arts, 6. Graduate School of Engineering, Tohoku University

Hypercalcified sponges (hereafter, “sclerosponges”), living in dark environments of tropical to subtropical shallow oceans, precipitate calcium carbonate skeleton with growth bands. They grow slowly at an approximate rate of <1 mm/year unlike corals (ca. 1 cm/year) but can be so long-lived for several decades to hundred years like corals (e.g., Benavides and Druffel, 1986 Coral Reefs). Skeletal oxygen isotopic ratios in sclerosponges can reflect variations in sea surface temperature and seawater with the latter being potentially related to salinity reflecting the precipitation–evaporation balance at the sea surface and changes in water mass transport (e.g., Grottoli et al., 2010 J. Geophys. Res.). In contrast to zooxanthellate corals, which occasionally show positive correlations between skeletal oxygen and carbon isotopic ratios, it is considered that there do not exist vital effects in the secretion of sclerosponge skeleton. Previous studies showed significant decrease trends in the carbon isotope records toward the present, which is probably a result of isotopically-light carbon dioxide added into the atmosphere/ocean from fossil fuel burning (e.g., Swart et al., 2010 Geophys. Res. Lett.). Therefore, sclerosponges are shown to provide annually resolved time series of proxy records of ocean environments since the Industrial Revolution. However, few evaluation studies on the environmental proxy of sclerosponges are reported, and temporally longer (>100 year-continuous-long) records from sclerosponges were derived only from the Atlantic Ocean.

Here we present stable oxygen and carbon isotope ratios and trace elements (Mg, Ca, Sr, Ba, Pb and U) from sclerosponges (*Astrosclera willeyana* and *Acanthochaetetes wellsi*) collected from Kume-jima, Okinawa-jima and Miyako-jima, Ryukyu Islands in the North Pacific. In order to evaluate the utility of sclerosponge as an environmental proxy, within-skeleton and intraspecific variations in stable isotopic and trace elemental records of 37 samples were investigated. Soft X-ray images of large-size sclerosponges showed highly developed skeletal growth bands with >100 high/low density layers. The secular changes in radiocarbon-dated time series of the sclerosponge carbon records were consistent with previously reported data from Atlantic and Pacific corals and sclerosponges. The long-term oxygen isotopic trends of the samples are characterized by slight depletions throughout their living periods, indicative of an overall trend toward warmer ocean environment around the Ryukyu Islands. Our sclerosponge-based estimates of sea surface temperature and salinity may document thermal and hydrologic variations in the Ryukyu Islands, furthering a better understanding of northwestern tropical-subtropical Pacific climate change for the last several centuries in conjunction with coral-based long proxy records.

Keywords: sclerosponge, oxygen isotope, carbon isotope, trace element, paleoceanogrpahy, Okinawa

©2019. Japan Geoscience Union. All Right Reserved.

[E] Poster | B (Biogeosciences)：B-PT Paleontology

Sun. May 26, 2019 5:15 PM - 6:30 PM JST | Sun. May 26, 2019 8:15 AM - 9:30 AM UTC | Poster Hall International Exhibition Hall8, Makuhari Messe_36

[B-PT04] Biomineralization and the Geochemistry of Proxies

convener:Takashi Toyofuku(Japan Agency for Marine-Earth Science and Technology (JAMSTEC)), Hiroshi Kitazato(Tokyo University of Marine Science and Technology (TUMSAT)), Jelle Bijma(Alfred-Wegener-Institut Helmholtz-Zentrum f?r Polar- und Meeresforschung), Kotaro Hirose(Faculty of Science & Engineering, Waseda University)

Biomineralization and the Geochemistry of Proxies - Biology, laboratory culture-experiments and their applications to the paleo-research -
In order to reconstruct the Earth climate system, marine paleoclimatologists resort to transfer functions or geochemical proxies, which are produced or affected by organisms. The relationships used for reconstructions are generally based on field calibrations or derived from laboratory experiments. The danger of these so-called empirical relationships is that they may be valid only within the restricted parameter space of their calibration. Application of proxy relationships to very different environmental settings (e.g. high vs. low latitude or glacial vs. interglacial) requires a mechanistic understanding of these relationships. Much progress can be expected by a better understanding of the biomineralization mechanisms and the incorporation of proxy signals.
In this session we facilitate contributions related to the biomineralization, calibration and validation of marine proxies from field study, laboratory culture experiment and paleo-environmental reconstruction.

[BPT04-P01] Living (stained) benthic foraminifera in the West-Gironde mud patch (Bay of Biscay, France): An ongoing survey for the European Community.

*Christophe Fontanier[1,2], Bruno Deflandre[1], Sylvain Rigaud[3], Sabine Schmidt[1], Bastien Lamarque[1], Pascal Lebleu[1], Dominique Poirier[1], Antoine Grémare[1] (1. Bordeaux University, EPOC Laboratory, UMR CNRS 5805 OASU, F-33615 Pessac, FRANCE, 2.FORAM Research Group, F-49140 Villevêque, FRANCE, 3.Nîmes University, GIS Laboratory, EA 7352 CHROME, F-30035 Nïmes, FRANCE)

[BPT04-P02] Biomonitoring in the Cassidaigne Canyon (NW Mediterranean): the resilience and recovery of deep-sea benthic foraminifera at a bauxite industrial waste site

*Pauline Duros[1], Christophe Fontanier[1,2,3], Briony Mamo[4,5], Deborah Mille[6], Olivier Herlory[6] (1.FORAM Research Group, F-49140 Villevêque, FRANCE, 2.Bordeaux University, EPOC Laboratory, UMR CNRS 5805 OASU, F-33615 Pessac, FRANCE, 3.Angers University, 4 boulevard Lavoisier, F-49000 Angers, FRANCE., 4.School of Biological Sciences, University of Hong Kong, Pokfulam Road Sai Wan, Hong Kong SAR, CHINA. , 5.Department of Biology, Macquarie University, North Ryde, NSW, 2109, AUSTRALIA., 6.CREOCEAN, Agence PACA Corse, 230 Avenue de Rome, Valparc-Bât B, F-83500 La Seyne sur Mer, FRANCE.)

[BPT04-P03] Comparison between assemblages of diatom fossil and biomarkers in surface sediments from Seto Inland Sea

*Kotaro Hirose[1], Hideto Nakamura[2], Takuto Ando[4], Satoshi Asaoka[3], Ken Sawada[5] (1.Faculty of Science & Engineering, Waseda University, 2.Faculty of Science, Osaka City University, 3.Research Center for Inland Seas & Department of Planetology, Kobe University, 4.Arctic Research Center, Hokkaido University, 5.Department of Earth & Planetary Science, Faculty of Science, Hokkaido University)

[BPT04-P04] Combined impacts of ocean acidification and desalination: culture experiments on the coastal species *Ammonia* sp. and *Elphidium crispum*

*Laurie Marie Charrieau[1], Helena L. Filipsson[2], Yukiko Nagai[1], Sachiko Kawada[1], Karl Ljung[2], Emma Kritzberg[3], Takashi Toyofuku[1,4] (1.Japan Agency for Marine-Earth Science and Technology, 2.Department of Geology, Lund University, Sweden, 3.Department of Biology, Lund University, Sweden, 4.Tokyo University of Marine Science and Technology (TUMSAT), Japan)

[BPT04-P05] Effects on larger benthic foraminiferal shell density under global warming

*Shunichi Kinoshita[1], Azumi Kuroyanagi[2], Hiroshi Nishi[2], Osamu Sasaki[2], Kazuhiko Fujita[3], Atsushi Suzuki[4], Hodaka Kawahata[5] (1.Graduate School of Science, Tohoku University, 2.The Tohoku University Museum, The Center for Academic Resources and Archives, Tohoku Univerity, 3.Department of Physics and Earth Sciences, Faculty of Science and Tropical Biosphere Research Center, University of the Ryukyus, 4.Geological Survey of Japan National Institute of Advanced Industrial Science and Technology, 5.Atmosphere and Ocean Research Institute, the University of Tokyo)

[BPT04-P06] Estimation of the calcification rate of foraminifera -exceptionally fast extending of the shell-

*Yukiko Nagai[1,2], Katsuyuki Uematsu[3], Takashi Toyofuku[2,4] (1.National Museum of Nature and Science of Tokyo, 2.Japan Agency for Marine-Earth Science and Technology, 3.Marine Works Japan Enterprise, 4.Tokyo university of Marine Science and Technology)

[BPT04-P07] Estimation of foraminiferal calcification process from live imaging and FIB-SEM approach

*Takashi Toyofuku[1,2], Yukiko Nagai[1,3] (1.Japan Agency for Marine-Earth Science and Technology (JAMSTEC), 2.Tokyo University of Marine Science and Technology, 3.National Museum of Nature and Science,Tokyo)

[BPT04-P08] Toward a better understanding of planktic foraminiferal proxies: Are they photosymbiotic or not?

*Haruka TAKAGI[1], Katsunori KIMOTO[2], Tetsuichi FUJIKI[2], Kazuyoshi MORIYA[3], Hiroaki SAITO[1] (1.Atmosphere and Ocean Research Institute, The University of Tokyo, 2.Japan Agency for Marine-Earth Science and Technology, 3.School of Education, Waseda University)

[BPT04-P09] Evaluation of geochemistry in hypercalcified demosponges as a paleoceanographic proxy

*Ryuji Asami[1], Tohru Naruse[2], Masaru Mizuyama[3], Ryu Uemura[3], Ryuichi Shinjo[3], Yuji Ise[4], Yoshihisa Fujita[5], Takashi Sakamaki[6] (1.Graduate School of Science, Tohoku University, 2.Tropical Biosphere Research Center, University of the Ryukyus, 3.Faculty of Science, University of the Ryukyus, 4.Centre for Marine and Coastal Studies, Universiti Sains Malaysis, 5.Okinawa Prefectural University of Arts, 6.Graduate School of Engineering, Tohoku University)

Living (stained) benthic foraminifera in the West-Gironde mud patch (Bay of Biscay, France): An ongoing survey for the European Community.

*Christophe Fontanier[1,2], Bruno Deflandre[1], Sylvain Rigaud[3], Sabine Schmidt[1], Bastien Lamarque[1], Pascal Lebleu[1], Dominique Poirier[1], Antoine Grémare[1]

1. Bordeaux University, EPOC Laboratory, UMR CNRS 5805 OASU, F-33615 Pessac, FRANCE, 2. FORAM Research Group, F-49140 Villevêque, FRANCE, 3. Nîmes University, GIS Laboratory, EA 7352 CHROME, F-30035 Nïmes, FRANCE

During an environmental survey performed in summer 2017 (JERICObent-2 Cruise), living (stained) benthic foraminiferal faunas were investigated at 7 stations sampled within the West-Gironde mud patch, a mud belt located on the marine shelf in front of the Gironde River (Bay of Biscay, France). This study area is really strategic for local fisheries since substantial marine resources (demersal fishes, shrimps...) are easily accessible for coastal fishermen. Moreover, the mud belt is considered an important hotspot for marine biodiversity as far as food (i.e. sedimentary organic matter), which is naturally abundant there, could sustain an assumedly enhanced heterogeneity of benthic habitats for various taxon. In the framework of the European project JERICONext (ID 654410), we have been studying biological (prokaryotes, benthic meiofauna and macrofauna), sedimentary and geochemical patterns of mud-flat ecosystems in order to better understand how both spatial and temporal variability of riverine regime and coastal hydrodynamics impact the dynamics of the benthic life, especially foraminifera. Stations investigated in this presentation are located between 39 and 69 m water depth from the inner shelf to the mid-shelf. At most sites, surface sediment is characterized by clay-silt facies more or less enriched in organic matter. Oxygen penetration depth within the sediment is less than 7±3 mm. Foraminiferal simple diversity (S) presents relatively moderate values ranging between 15 and 35 taxa. According to Shannon Index H' and Rarefaction Index ES(100), foraminiferal diversity tends to slightly increase with water depth. This trend is supported by *Eggerelloides scabrus;* its contribution decreases from the shallower stations (~50%) of the proximal mud patch (<55 m depth) to the deeper stations (<30%) of the distal mud patch (>55 m depth). This agglutinated species is generally considered a reliable bio-indicator of organic-matter enriched sediment in front of river mouths. It is noteworthy that the shallowest station (station 1, 39 m) is also characterised by the exclusive contribution of *Quinqueloculina lata/laevigata* and *Ammonia beccarii,* which are both typical of inner-shelf environments. There, surface sediment is made of fine sand. The deeper stations (>55 m depth) located in the distal mud patch are characterised by a remarkable contribution (~30%) of *Pseudoeponides falsobeccarii* and Buliminids (~30% respectively). They are accompanied by *Rectuvigerina phlegeri* and *Nonion fabum*, which are typical of mid- and outer-shelf ecosystems. The contribution of Buliminids underline the gradual increase of sedimentary organic content (>1.2% DW) with water depth.

Keywords: Living Benthic Foraminifera, Mud Belt, Environmental Spatial Variability, Sedimentary Organic Matter, Oxygenation Level

©2019. Japan Geoscience Union. All Right Reserved.

Biomonitoring in the Cassidaigne Canyon (NW Mediterranean): the resilience and recovery of deep-sea benthic foraminifera at a bauxite industrial waste site

*Pauline Duros[1], Christophe Fontanier[1,2,3], Briony Mamo[4,5], Deborah Mille[6], Olivier Herlory[6]

1. FORAM Research Group, F-49140 Villevêque, FRANCE, 2. Bordeaux University, EPOC Laboratory, UMR CNRS 5805 OASU, F-33615 Pessac, FRANCE, 3. Angers University, 4 boulevard Lavoisier, F-49000 Angers, FRANCE., 4. School of Biological Sciences, University of Hong Kong, Pokfulam Road Sai Wan, Hong Kong SAR, CHINA. , 5. Department of Biology, Macquarie University, North Ryde, NSW, 2109, AUSTRALIA., 6. CREOCEAN, Agence PACA Corse, 230 Avenue de Rome, Valparc-Bât B, F-83500 La Seyne sur Mer, FRANCE.

During an environmental survey performed in autumn 2016, living (stained) benthic foraminiferal faunas were investigated at 16 stations sampled within the Cassidaigne Canyon (NW Mediterranean Sea) and surrounding area. For many decades, industrial bauxite residues of red mud have drained into the canyon via a submarine pipe, causing physical disturbance and chemical contamination. In January 2016, solid waste disposal ceased and was replaced with the dumping of a low-density liquid effluent. Stations investigated in this paper are located between 265–2500 m water depth from the shelf break to the deeper basin and from a distance between 4–70 km from the pipe outlet. At many sites, surface sediment is characterized by historical deposits of red mud and their geochemical imprints. Our ecological observations at the 725 m-depth station closest to the Cassidaigne Canyon submarine pipe show the highest concentration of the opportunistic and stress-tolerant species *Bulimina marginata* d' Orbigny, 1826, commonly identified as a recolonizer of disturbed areas. At the other fifteen stations, foraminiferal standing stocks and simple diversity (S) decrease with decreasing food input to the seafloor and increasing water depth. There, foraminiferal composition is characterized by a minor contribution of stress-tolerant species and echoes the overall meso-oligotrophic patterns of a relatively stable ecosystem. Our study clearly shows that in September 2016, 10 months after a historical shift in discharged industrial wastes (from dense red mud to liquid effluent), foraminiferal diversity close to the pipe outlet in the Cassidaigne Canyon remains altered, but appears to be slowly recovering.

Keywords: Benthic foraminifera, Bauxite residues, Cassidaigne Canyon, Resilience

©2019. Japan Geoscience Union. All Right Reserved.

Comparison between assemblages of diatom fossil and biomarkers in surface sediments from Seto Inland Sea

*Kotaro Hirose[1], Hideto Nakamura[2], Takuto Ando[4], Satoshi Asaoka[3], Ken Sawada[5]

1. Faculty of Science & Engineering, Waseda University, 2. Faculty of Science, Osaka City University, 3. Research Center for Inland Seas & Department of Planetology, Kobe University, 4. Arctic Research Center, Hokkaido University, 5. Department of Earth & Planetary Science, Faculty of Science, Hokkaido University

We investigate the fossil diatom abundances and biomarker concentrations in marine sediment to assess their relationships. 14 sample of surface (uppermost 5 cm of sea bottom) sediments are taken in 5 areas (Aki-nada Bay, Hiuchi-nada Bay, Harimanada-Bay, Osaka Bay and Kii Strait) of Seto Inland Seas in July 2015. Additional 8 samples are taken in Harimanada-Bay in October 2015. Although the precise age of the core has not been determined yet, it could be deposited within 10 years, according to the sedimentation rates by previous study (Yasuhara et al., 2007).
Diatom species such as small *Thalassiosira*spp., *skeletonema costatum*, resting spore of *Chaetoceros* spp. and *Neodelphyneis pelagica*, which were reported by previous study (Hirose et al., 2008), are observed as the dominant taxa in all samples. *Rhizosolenia* spp. and *Pleurosigma* spp., known HBI producers, were occurred in low proportions. As specific diatom biomarkers, we identified C25 di- and tri-unsaturated highly branched isoprenoids (HBIs), along with relatively minor amount of C25 and C35 cyclic HBIs. Total abundances of diatom valves and HBIs were generally correlated, probably reflecting variations of diatom production. Meanwhile, Aki-bay and some samples of Harima-nada Bay were characterized with relatively low abundance of HBIs relative to valves. In these area, focused analysis on the minor diatom taxa would be needed to provide quantitative dataset to discuss further relation of HBIs and produces and their spatial distribution.

Keywords: diatom assemblage, diatom biomarkers, HBIs, surface sediment, Seto Inland Seas

©2019. Japan Geoscience Union. All Right Reserved.

Combined impacts of ocean acidification and desalination: culture experiments on the coastal species *Ammonia* sp. and *Elphidium crispum*

*Laurie Marie Charrieau[1], Helena L. Filipsson[2], Yukiko Nagai[1], Sachiko Kawada[1], Karl Ljung[2], Emma Kritzberg[3], Takashi Toyofuku[1,4]

1. Japan Agency for Marine-Earth Science and Technology, 2. Department of Geology, Lund University, Sweden, 3. Department of Biology, Lund University, Sweden, 4. Tokyo University of Marine Science and Technology (TUMSAT), Japan

Coastal areas display natural large environmental variability such as frequent changes in salinity, pH, and carbonate chemistry. Anthropogenic impacts –especially ocean acidification –increase this variability, which may affect the living conditions of coastal species, particularly, calcifiers, such as foraminifera.

The purpose of this study was to evaluate the combined effect of two typical environmental stressors on the coast - salinity and pH –on calcifying organisms. We performed culture experiments on living benthic foraminifera to study the combined effects of lowered pH and salinity on the calcification abilities and survival of the coastal, calcitic species Ammonia sp. and *Elphidium crispum*.

We found that these two species could tolerate low pH and low salinity, which reflects the environmental variations in their natural habitats. However, in open ocean conditions (salinity ~35) and lower pH treatment, the species displayed resistance to test dissolution for a longer time than in brackish conditions (salinity ~5 to 20). Moreover, the response of foraminifera to the different treatments was species-specific, and *Ammonia* sp. appeared more resistant than *E. crispum* when placed in the same conditions of pH and salinity. We also observed living dissolved specimens of juveniles *Ammonia* sp. under the combined effect of low pH and very low salinity, and we showed that desalination is one cause for the decalcification. However, they were not able to recalcify when returned to higher salinities, probably due to a sensitive balance in environmental parameters. Finally, we highlight the ability of foraminifera to survive under $\Omega calc < 1$, and that high salinity and $[Ca^{2+}]$ as building blocks are crucial for the foraminiferal calcification process.

We conclude that coastal benthic foraminifera will not immediately be affected by ocean acidification, but rather by a combination of decreasing salinity and lowered pH.

Keywords: Coastal ocean acidification, Desalination, Culture experiment, Benthic foraminifera, Calcification process

©2019. Japan Geoscience Union. All Right Reserved.

Effects on larger benthic foraminiferal shell density under global warming

*Shunichi Kinoshita[1], Azumi Kuroyanagi[2], Hiroshi Nishi[2], Osamu Sasaki[2], Kazuhiko Fujita[3], Atsushi Suzuki[4], Hodaka Kawahata[5]

1. Graduate School of Science, Tohoku University, 2. The Tohoku University Museum, The Center for Academic Resources and Archives, Tohoku Univerity, 3. Department of Physics and Earth Sciences, Faculty of Science and Tropical Biosphere Research Center, University of the Ryukyus, 4. Geological Survey of Japan National Institute of Advanced Industrial Science and Technology, 5. Atmosphere and Ocean Research Institute, the University of Tokyo

On the recent ocean environment, due to progresses of global warming and ocean acidification, it is concerned that calcifying organisms will be seriously affected from these environmental changes. Larger benthic foraminifers (LBFs) build calcium carbonate shells. Their carbonate productivity is the third highest rate in coral reef area next to reef corals and calcareous algae. Therefore, it is important to clarify the relationship between ocean environmental changes and the response of LBFs for predicting future ocean environment including carbon cycle. Based upon test diameter and shell weight, previous studies expected how foraminifers react to sea water conditions where they are living. However, in those reports, it is still not clear whether the changing of shell weight is due to changing of shell thickness (shell volume) or shell density, also whether that changing is depending sea water temperature or acidity. Thus, this study was performed for clarifying the relationships between water temperature and LBFs shell parameters with laboratory experiments and means of micro computed tomography (CT).

In this study, we cultured the LBF *Sorites orbiculus* in filtered sea water until reproduction. Soon after *S. orbiculus* reproduced, clonal individuals from same mother individual were picked and separated into seven groups. One group was selected as initial stage sample, and other six groups were provided for culture experiments. We cultured each groups under six different temperature conditions (19, 21, 23, 25, 27 and 29 ˚C). Because clonal specimens were reproduced asexually from same individual, it was expected the genetic factors were kept to a minimum. We used micro CT to investigate mean CT number (proxy of density), shell volume, test diameter and chamber number of every clonal specimen after culturing. The results show the high correlation of mean CT number with temperature in contrast to the correlation of shell volume and temperature. This suggests changing in temperature of sea water causes shell density difference, furthermore, LBFs build the higher density shell in the higher temperature as long as they lives in 19 to 29 C˚ environment.

Keywords: Larger benthic foraminifer, shell density, micro CT, laboratory experiments, global warming

©2019. Japan Geoscience Union. All Right Reserved.

Estimation of the calcification rate of foraminifera -exceptionally fast extending of the shell-

*Yukiko Nagai[1,2], Katsuyuki Uematsu[3], Takashi Toyofuku[2,4]

1. National Museum of Nature and Science of Tokyo, 2. Japan Agency for Marine-Earth Science and Technology, 3. Marine Works Japan Enterprise, 4. Tokyo university of Marine Science and Technology

The process of biomineralization of foraminiferal test is essential for its characteristic morphogenesis and the composition of element and isotope to be taken in is used also as paleo environmental proxy, numerous studies have been approched to reveal the mechanism of shell formation. However, how fast the foraminifera calicification and how much calcium carbonate deposits depends on the species, which is not well understood in most species.
The foraminifera *Spirillina vivipara* does not form a chamber, but elongate a tubular test spirally with their cytoplasmic growth. *Spirillina vivipara* is also known to be rapidly changing generations that can be reproduced in a several days after division of mother cells (Myers, 1936). From our current observations, it was also found that the shell formation is repeatedly carried out in the day, and the elongation rate of the shell is very fast. Therefore, in this study, Spirillina vivipara was used to estimate calcification rate.
In this presentation, we report on the fastest shell extending rate in foraminifera.

Keywords: Calcification, foraminifera, FIB-SEM

©2019. Japan Geoscience Union. All Right Reserved.

Estimation of foraminiferal calcification process from live imaging and FIB-SEM approach

*Takashi Toyofuku[1,2], Yukiko Nagai[1,3]

1. Japan Agency for Marine-Earth Science and Technology (JAMSTEC), 2. Tokyo University of Marine Science and Technology, 3. National Museum of Nature and Science,Tokyo

Calcareous foraminifera have been thought a major carbonate producer in ocean. Their tests (shells) are fundamental tools as paleo-environmental indicators in various studies because their calcareous tests have been archived as numerous fossils in sediment for geologic time and various environmental information are brought by faunal structure, shell morphology and geochemical compsitions of calccitic test. The other hand, the calcification process itself is interested for us. Pseudopodia sticking out into sea water build organic templates in the form of chamber. Calcium carbonate is precipitated on the both side of template within several hours. Calcium and carbonate are fixed at there by foraminiferal biological process. The newly added chamber wall was flexible in a first day, the chamber solidified in a few days and became a solid test. It is very interesting to record this process in video. Our studies showed the variable change of pH and Ca during the biomineralization of foraminifera by the application of fluorescent indicators (e.g. Toyofuku et al., 2017). Recently, we also apply the method to clear cut the site of calcification under SEM by focused ion beam (FIB-SEM)(Nagai et al., 2018). The nano-scale fine structures have been revealed the distribution of soft orgnic structures (i.e. pseudopodia) and hard tissue (precipitated calium carbonate)by this observation.

Keywords: calcification, foraminifera, imaging

©2019. Japan Geoscience Union. All Right Reserved.

Toward a better understanding of planktic foraminiferal proxies: Are they photosymbiotic or not?

*Haruka TAKAGI[1], Katsunori KIMOTO[2], Tetsuichi FUJIKI[2], Kazuyoshi MORIYA[3], Hiroaki SAITO[1]

1. Atmosphere and Ocean Research Institute, The University of Tokyo, 2. Japan Agency for Marine-Earth Science and Technology, 3. School of Education, Waseda University

Geochemistry of planktic foraminiferal tests is an important archive to understand paleoenvironment. However, many biotic factors can affect the geochemical composition and thus may lead misinterpretation of the proxy signals. Photosymbiosis (endosymbiosis with autotrophic algae) is thought to give specific effects on foraminiferal test geochemistry such as $\delta^{13}C$ due to photosynthetic activity of the symbionts. This is because photosynthesis can alter the geochemical condition of the vicinity of the foraminiferal test where calcification takes place, and eventually elevate the $\delta^{13}C$ of the test. Therefore, whether foraminiferal species have photosymbiotic ecology or not, and how active the photosynthesis is are important information for precise paleoenvironmental reconstructions. However, photosymbiotic information of planktic foraminifers is still limited even for extant species which are often utilized to generate proxy records.
In this study, we investigated 30 species of modern planktic foraminifers covering four families; Globigerinidae, Hastigerinidae, Globorotaliidae, and Candeinidae, using active chlorophyll fluorometry (fast repetition rate fluorometry; FRRF). FRRF performs non-destructive and non-invasive measurements of algal physiology based on real-time variable fluorescence profiles. When it is applied to symbiotic consortia of planktic foraminifers, it enables us to quantify chlorophyll content of a specimen, and to qualify of photophysiological features that are useful diagnostics of symbiont photosynthetic fitness. It can provide us with convincing information on individual-based photosymbiosis.
Specimens were collected from various oceanic settings; from tropical to subpolar region, encompassing Pacific to Atlantic. We have sampled across much of the northern hemisphere tropical-subtropical gradient to get the endemic species and to replicate for the others. The detection rate of photosymbiosis in each species, the biomass of symbionts (indicated by chlorophyll content), and the state of symbionts (indicated by photophysiological parameters) were investigated. Using principal component analysis, species were ranked by their “strength” of photosymbiosis. This thorough investigation will provide a more systematic understanding of photosymbiosis in modern planktic foraminifers and will help us to choose which species to use to reconstruct paleoenvironment.

Keywords: planktic foraminifers, photosymbiosis

©2019. Japan Geoscience Union. All Right Reserved.

Evaluation of geochemistry in hypercalcified demosponges as a paleoceanographic proxy

*Ryuji Asami[1], Tohru Naruse[2], Masaru Mizuyama[3], Ryu Uemura[3], Ryuichi Shinjo[3], Yuji Ise[4], Yoshihisa Fujita[5], Takashi Sakamaki[6]

1. Graduate School of Science, Tohoku University, 2. Tropical Biosphere Research Center, University of the Ryukyus, 3. Faculty of Science, University of the Ryukyus, 4. Centre for Marine and Coastal Studies, Universiti Sains Malaysis, 5. Okinawa Prefectural University of Arts, 6. Graduate School of Engineering, Tohoku University

Hypercalcified sponges (hereafter, “sclerosponges”), living in dark environments of tropical to subtropical shallow oceans, precipitate calcium carbonate skeleton with growth bands. They grow slowly at an approximate rate of <1 mm/year unlike corals (ca. 1 cm/year) but can be so long-lived for several decades to hundred years like corals (e.g., Benavides and Druffel, 1986 Coral Reefs). Skeletal oxygen isotopic ratios in sclerosponges can reflect variations in sea surface temperature and seawater with the latter being potentially related to salinity reflecting the precipitation–evaporation balance at the sea surface and changes in water mass transport (e.g., Grottoli et al., 2010 J. Geophys. Res.). In contrast to zooxanthellate corals, which occasionally show positive correlations between skeletal oxygen and carbon isotopic ratios, it is considered that there do not exist vital effects in the secretion of sclerosponge skeleton. Previous studies showed significant decrease trends in the carbon isotope records toward the present, which is probably a result of isotopically-light carbon dioxide added into the atmosphere/ocean from fossil fuel burning (e.g., Swart et al., 2010 Geophys. Res. Lett.). Therefore, sclerosponges are shown to provide annually resolved time series of proxy records of ocean environments since the Industrial Revolution. However, few evaluation studies on the environmental proxy of sclerosponges are reported, and temporally longer (>100 year-continuous-long) records from sclerosponges were derived only from the Atlantic Ocean.

Here we present stable oxygen and carbon isotope ratios and trace elements (Mg, Ca, Sr, Ba, Pb and U) from sclerosponges (*Astrosclera willeyana* and *Acanthochaetetes wellsi*) collected from Kume-jima, Okinawa-jima and Miyako-jima, Ryukyu Islands in the North Pacific. In order to evaluate the utility of sclerosponge as an environmental proxy, within-skeleton and intraspecific variations in stable isotopic and trace elemental records of 37 samples were investigated. Soft X-ray images of large-size sclerosponges showed highly developed skeletal growth bands with >100 high/low density layers. The secular changes in radiocarbon-dated time series of the sclerosponge carbon records were consistent with previously reported data from Atlantic and Pacific corals and sclerosponges. The long-term oxygen isotopic trends of the samples are characterized by slight depletions throughout their living periods, indicative of an overall trend toward warmer ocean environment around the Ryukyu Islands. Our sclerosponge-based estimates of sea surface temperature and salinity may document thermal and hydrologic variations in the Ryukyu Islands, furthering a better understanding of northwestern tropical-subtropical Pacific climate change for the last several centuries in conjunction with coral-based long proxy records.

Keywords: sclerosponge, oxygen isotope, carbon isotope, trace element, paleoceanogrpahy, Okinawa

©2019. Japan Geoscience Union. All Right Reserved.

[E] Poster | M (Multidisciplinary and Interdisciplinary) : M-IS Intersection

Sun. May 26, 2019 10:45 AM - 12:15 PM JST | Sun. May 26, 2019 1:45 AM - 3:15 AM UTC | Poster Hall International Exhibition Hall8, Makuhari Messe_9

[M-IS01] Environmental, socio-economic and climatic changes in Northern Eurasia

convener:Pavel Groisman(NC State University Research Scholar at NOAA National Centers for Environmental Information, Asheville, North Carolina, USA), Shamil Maksyutov(National Institute for Environmental Studies), Evgeny P Gordov(Institute of Monitoring of Climatic and Ecological Systems SB RAS), Dmitry A Streletskiy(George Washington University)

We invite presentations on the biogeochemical cycles, the surface energy budget and water cycle, and climate and ecosystem interactions in Northern Eurasia (land-cover and land-use change, atmospheric aerosols, soil, and permafrost changes that affect and are being affected by climate and ecosystem change), human dimension, and tools to address the Northern Eurasia studies. In environmental studies, our Session foci are on the carbon cycle of Northern Eurasia and on the permafrost changes in Siberia, Asian Mountains, and the Arctic coastal regions.
In the regional water cycle studies, our Session foci are on the changing distribution of precipitation intensity, frequency, especially, in the cold/shoulder season transition periods when surface air temperature is close to 0 deg.C, and on the pattern and seasonal cycle changes of runoff.
In the human dimension studies, our Session foci are on assessments of impact of the ongoing environmental changes in Northern Eurasia on the human well-being and on mitigation strategies development in response to harmful consequences of these changes
The particular foci of this Session will be the studies of changes that impacts regional sustainable development in the Dry Latitudinal Belt of Northern Eurasia that expands through the continent from Pannonian Steppes in the west to the drylands of northern China in the east.
We invite also early career scientists associated with (or interested in) the Northern Eurasia Earth Science Partnership Initiative and its continuation, Northern Eurasia Future Initiative (http://nefi-neespi.org/NEFI-WhitePaper.pdf).

Conveners:
Pavel Groisman, NC State University, USA (pasha.groisman@noaa.gov)
Shamil Maksyutov, National Institute for Environmental JAPAN (shamil@nies.go.jp)
Evgeny Gordov, Siberian Center for Environmental Research and Training, RUSSIA (gordov@scert.ru)
Yizhao Chen, Nanjing Forestry University, CHINA (chenyzvest@gmail.com)

[MIS01-P01] Effects of clear-cutting on carbon dioxide fluxes in a boreal forest ecosystem - results of numerical experiments with a three-dimensional turbulent exchange model

Yulia Mukhartova[3], Maria Dyachenko[3], Polina Mangura[3], Alexander Krupenko[3], *Alexander Olchev[1,2] (1.Faculty of Geography, Lomonosov Moscow State University, 2.A.N. Severtsov Institute of Ecology and Evolution, Russian Academy of Sciences, 3.Faculty of Physics, Lomonosov Moscow State University)

[MIS01-P02] Retrieving the forest species composition from remote sensing data using a three-dimensional radiative transfer model

*Alexander Olchev[1,2], Natalia Levashova[3], Dmitry Lukyanenko[3] (1.Faculty of Geography, Lomonosov Moscow State University , 2.Severtsov Institute of Ecology and Evolution, Russian Academy of Science, 3.Faculty of Physics, Lomonosov Moscow State University)

[MIS01-P03] Satellite-derived Burned Area for Siberia (1979 – 2000)

*Amber Jeanine Soja[1], Brian J. Stocks[2], Stefano Potter[3], Brendan Rogers[3], Donald R. Cahoon[4], Natasha Jurko[5], Susan G. Conard[6], William 'Bill' deGroot[5], Nadezhda Tchebakova[7] (1.National Iinstitute of Aerospace / NASA Langley Research Center, 2.B.J. Stocks Wildfire Investigations Ltd., 3.Woods Hole Research Center , 4.Terra Systems Research, 5.Canadian Forest Service/Service canadien des forêts, 6.George Mason University,Fairfax, VA, 7.Sukachev Institute of Forestry, Siberian Branch of the Russian Academy of Sciences)

[MIS01-P04] Analysis and prediction of hazardous hydrometeorological phenomena in the coastal areas of the Arctic

*Irina Repina[1,2] (1.A.M.Obukhov Institute of Atmospheric Physics RAS, 2.Lomonosov Moscow State University)

[MIS01-P05] **Recent baric and climatic conditions over East Europe with a focus on Belarus**

*Irina Danilovich[1], Vladimir Loginov[1], Pavel Groisman[2] (1. Institute for Nature Management National Academy of Science, Minsk, Belarus, 2. NC State University at NOAA National Centers for Environmental Information, Asheville, USA)

[MIS01-P06] **Assessment of climatic and environmental conditions along the track of projected Kyzyl-Kuragino railway line (the Western Sayan Mountains)**

★Invited Papers

*Aleksandra Alekseevna Mikheeva[1], Margarita Syromyatina[1], Yurii Kurochkin[1] (1.Institute of Earth Sciences, Saint Petersburg State University, Russia)

[MIS01-P07] **Assessment of interlinkages among industrialization, climate change, and forest fire activity: Thematic study of the Republic of Sakha (Yakutia), Russia**

*Kiunnei Kirillina[1], Wanglin Yan[1] (1.Graduate School of Media and Governance, Keio University SFC)

[MIS01-P08] Quantitative Evaluation of Winter Daily Precipitation over Northern Japan

*Minami Masuda[1], Akiyo Yatagai[1], Toshiyuki Nakaegawa[2], Kenji Kamiguchi[3] (1.Graduate School of Science and Technology, Hirosaki University, 2.Meteorological Research Institute/Japan Meteorological Agency, 3.Japan Meteorological Agency)

[MIS01-P09] Seasonal variation of wetland carbon dioxide and methane fluxes measured by automatic chambers at the Bakchar bog, West Siberia

*Shamil Maksyutov[1], Alexandre Fofonov[2], Denis Davydov[2], Oleg Krasnov[2], Tadanobu Nakayama[1], Mikhail Glagolev[3] (1.National Institute for Environmental Studies, 2.V.E. Zuev Institute of Atmospheric Optics, 3.M.V. Lomonosov Moscow State University)

[MIS01-P10] Climatic distances between origin and labor locations for migrants in a changing climate in Siberia by the end of the 21st century

*Elena I. Parfenova[1], Nadezhda M. Tchebakova[1] (1.V.N.Sukachev Institute of Forest SB RAS, FRC SB RAS)

Effects of clear-cutting on carbon dioxide fluxes in a boreal forest ecosystem - results of numerical experiments with a three-dimensional turbulent exchange model

Yulia Mukhartova[3], Maria Dyachenko[3], Polina Mangura[3], Alexander Krupenko[3], *Alexander Olchev[1,2]

1. Faculty of Geography, Lomonosov Moscow State University, 2. A.N. Severtsov Institute of Ecology and Evolution, Russian Academy of Sciences, 3. Faculty of Physics, Lomonosov Moscow State University

To estimate the possible effects of clear-cutting on the air flow disturbances within the atmospheric surface layer as well as on the spatial patterns of vertical carbon dioxide (CO2) fluxes and horizontal advection terms within and around the clear-cut area a process-based three-dimensional (3D) hydrodynamic momentum, energy and CO2 exchange model was developed. Clear-cutting is one of the most widespread logging practice, which can substantially transform the energy, water vapor and CO2 exchange between forest ecosystems and atmosphere and affect the climate system at multiple scales. Developed 3D hydrodynamic model is based on a 1.5-order closure scheme and uses a system of averaged Navier-Stokes and continuity equations for the mean wind speed components, as well as the reaction-advection-diffusion equation for CO2 transfer within the atmospheric surface layer (Mukhartova et al. 2015). The model applies Reynolds's decomposition and expresses the wind speed and concentrations of CO2 as sums of their mean values and deviations. The 1.5-closure scheme assumes that the turbulent fluxes can be expressed using the turbulent exchange coefficients (that depend on turbulent kinetic energy and its dissipation rate) and the gradients of corresponding functions (wind speed components and CO2 concentrations).
The clear-cut area selected for the study is situated in the south-western part of Valdai Hills in European Russia. The area of the clear-cut is about 4.5 ha and it is surrounded by a mixed forest stand represented mainly by Norway spruce, White birch and Eurasian aspen species with tree heights ranged between 18 and 22 m (Mamkin et al. 2016, 2019). The vegetation at the clear-cut area is mainly represented by herbaceous species and a small number of juvenile aspen trees.
Results of numerical experiments with the developed 3D model showed that clear-cutting has significant effect on spatial distributions of wind speed components as well as atmospheric momentum and CO2 fluxes. Spatial flux heterogeneity is also enhanced by complex shape of the clear-cut boundary. The largest effect of the clear-cut on the air flows is mainly appeared along the windward forest edge whereas at the leeward forest edge this effect is less pronounced. The leeward part of the clear-cut is characterized by prevailed downward air flows (with negative values of vertical wind component) whereas the upward air flows (with prevailed positive values of vertical wind component) are appeared at its windward part. It is very important to point out that the horizontal gradients of vertical and horizontal wind velocities at the lowest part of the atmospheric surface layer (up to the height 3-4 m above the ground surface) as well as horizontal turbulent and non-turbulent CO2 advection terms in the central part of the clear-cut is relatively small that can be used as important criteria indicating sufficient reestablishing of the air flow in this part of the clear-cut after its disturbance at the leeward forest edge.

Reference

Mamkin V., Kurbatova J., Avilov V., Mukhartova Yu, Krupenko A., Ivanov D., Levashova N., Olchev A. Changes in net ecosystem exchange of CO2, latent and sensible heat fluxes in a recently clear-cut spruce forest in western Russia: results from an experimental and modeling analysis. 2016. Environmental

©2019. Japan Geoscience Union. All Right Reserved.

Research Letters. 11(12). 125012
Mamkin V., Kurbatova J., Avilov V., Ivanov D., Kuricheva O., Varlagin A., Yaseneva I., Olchev A. 2019 Energy and CO2 exchange in an undisturbed spruce forest and clear-cut in the Southern Taiga. Agricultural and Forest Meteorology, 265, 252-268
Mukhartova Yu. V., Levashova N. T., Olchev A. V., Shapkina N. E. 2015 Application of a 2D model for describing the turbulent transfer of CO2 in a spatially heterogeneous vegetation cover. Moscow University Physics Bulletin 70(1), 14-21

Keywords: turbulent exchange model, clear-cut, momentum fluxes, CO2 fluxes

©2019. Japan Geoscience Union. All Right Reserved.

Retrieving the forest species composition from remote sensing data using a three-dimensional radiative transfer model

*Alexander Olchev[1,2], Natalia Levashova[3], Dmitry Lukyanenko[3]

1. Faculty of Geography, Lomonosov Moscow State University , 2. Severtsov Institute of Ecology and Evolution, Russian Academy of Science, 3. Faculty of Physics, Lomonosov Moscow State University

A three-dimensional model was developed to derive the reflection, absorption and transmission of photosynthetically active radiation (PAR) by a non-uniform forest canopy with a multi-species structure (Levashova et al., 2018). The model algorithm describing solar radiation transfer through a forest canopy considers direct and diffuse radiation penetrating through gaps in the canopy, transmitted by leaves and reflected from leaves, bark and soil surface. To estimate the canopy the reflection, absorption and transmission the model uses external data about 3D structure of each tree species in the forest stand, about the spectral properties of photosynthesizing and non-photosynthesizing parts of the different trees species, and about spectral reflectance of soil surface. Moreover it uses also information about incoming solar radiation, sun elevation, the ratio of incoming direct and diffuse solar radiation, and surface topography. The model is based on steady-state transport equations initially suggested by Ross (Ross, 1981) and further developed and described by Myneni and Knyazikhin (Myneni et al., 1990; Knyazikhin et al., 2005). Calculation of the direct solar radiation fluxes within the canopy is based on estimation of the probability that a ray of light passing through the foliage reaches a given location within the canopy without interception. Diffuse solar radiation is calculated taking into account both diffuse solar radiation from the sky penetrating through foliage gaps and direct and diffuse radiation scattered by canopy foliage and woody components. The numerical scheme for solving the integro-differential equations is based on the discrete ordinates method.
The model was used to describe the spatial patterns of solar radiation reflection and transmission by non-uniform mixed forest canopy and to develop an algorithm that allows to retrieve the proportion of different tree species in a mixed forest stand from measured canopy reflection coefficients for blue, green, red and near-infrared spectral bands (obtained from e.g. the Landsat satellite imagery). This approach allowed us to quantify the proportion of different tree species (both coniferous and deciduous) in a forest stand in case if their spectral reflection properties of the leaves are not the same. The accuracy of assessing the proportion of vegetation species using this method depended on the number of reflection measurements under various solar conditions (e.g. different sun elevations) that can reached by several measurements during the growing seasons. An increase of the input data volume (determined by the number of the measurements) resulted in higher accuracies for prediction of the proportions of different tree species.

References

Knyazikhin Y., Marshak A., Myneni R.B. Three dimensional radiative transfer in vegetation canopies. In: Three Dimensional Radiative Transfer in the Cloudy Atmosphere, Marshak, A., Davis, A.B., Eds., Springer Verlag: Berlin, Heidelberg, 2005, 617-652.
Levashova N., Lukyanenko D., Mukhartova Y., Olchev A. Application of a three-dimensional radiative transfer model to retrieve the species composition of a mixed forest stand from canopy reflected radiation. Remote Sensing, 2018, 10 (10), 1661.
Myneni R.B., Asrar G., Gerstl S.A.W. Radiative transfer in three dimensional leaf canopies. Transport Theory and Statistical Physics, 1990, 19, 205–250.
Ross J. The radiation regime and architecture of plant stands; Dr. W. Junk Publishers: The Hague,

©2019. Japan Geoscience Union. All Right Reserved.

Netherlands, 1981, 390 p.

Keywords: radiative transfer, three-dimensional model, mixed forest, canopy reflection, inverse problem

©2019. Japan Geoscience Union. All Right Reserved.

Satellite-derived Burned Area for Siberia (1979 –2000)

*Amber Jeanine Soja[1], Brian J. Stocks[2], Stefano Potter[3], Brendan Rogers[3], Donald R. Cahoon[4], Natasha Jurko[5], Susan G. Conard[6], William 'Bill' deGroot[5], Nadezhda Tchebakova[7]

1. National Iinstitute of Aerospace / NASA Langley Research Center, 2. B.J. Stocks Wildfire Investigations Ltd., 3. Woods Hole Research Center , 4. Terra Systems Research, 5. Canadian Forest Service/Service canadien des forêts, 6. George Mason University,Fairfax, VA, 7. Sukachev Institute of Forestry, Siberian Branch of the Russian Academy of Sciences

Siberia is a distinct and crucial region because it has the physical size necessary to effect regional and global climate. The circumboreal zone contains the largest stock of terrestrial carbon on Earth, and Russia holds roughly two-thirds of that carbon pool. Fire is the primary natural disturbance in boreal forest, which acts to cycle carbon and maintain ecosystem diversity in sync with the climate. Under current climate change scenarios, the Russian boreal is expected to experience temperature increases that exceed the global mean. We have developed a long-term burned area database that will enable novel analyses on the multi-decadal time scale that is ultimately required for robust assessments, including those focused on carbon cycling, fire emissions, and importantly the links between fire regimes, fire weather, ecosystems, and climate.

In this presentation, we present a long-term burned area database that has been developed using Advanced Very High Resolution Radiometer (AVHRR) Global Area Coverage (GAC) data from 1979-2000. Burned area has been verified using Total Ozone Mapping Spectrometer data and validated using available Landsat imagery (160 scenes thus far representing 5.6 Mha of burned area, 219 fire events, and 11% of the total area burned in the AVHRR database). Visually the burned scar data compare well. Validation is in ongoing, though initial analyses show an intersection of 42% with commission and omission errors of 31% and 25%, respectively. Most commission and omission errors are related to spatial inconsistencies using imagery with significantly different spatial resolutions. Of the fire events missed by AVHRR (i.e., omissions), 86% are related to fires <10,000 ha (~ 6 AVHRR pixels) and 44% are related to fires <3,000ha (~ 2 AVHRR pixels). Total burned area compares well, with the AVHRR database under-representing burned area by 10% compared to the Landsat data analyzed. Correlation in burned scar area between the AVHRR and Landsat data is 0.98 for all fires and 0.68 for fires that are < 0.1 Mha.

Keywords: Wildland Fire, Remote Sensing, Biomass Burning, Russia

©2019. Japan Geoscience Union. All Right Reserved.

Analysis and prediction of hazardous hydrometeorological phenomena in the coastal areas of the Arctic

*Irina Repina[1,2]

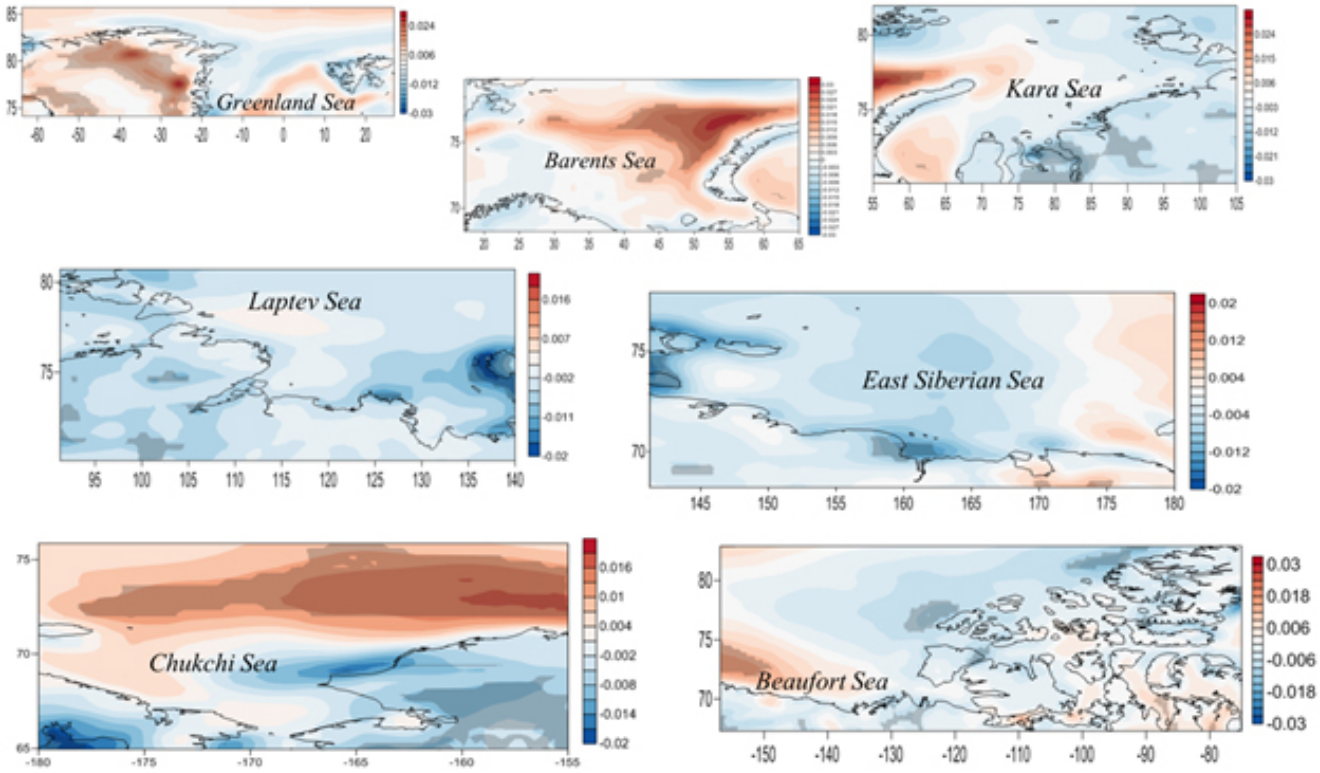
1. A.M.Obukhov Institute of Atmospheric Physics RAS, 2. Lomonosov Moscow State University

Currently, the Arctic is attracting increased attention not only as a region with the most noticeable climate change, but also as a world mineral storage, whose development prospects are being actively discussed. For Russia, which owns the bulk of the Arctic shelf, the Arctic is also a promising trade and transport artery, as in recent decades new opportunities for using the Northern Sea Route have been discovered. But climate change can lead to less favorable consequences. The increase in the ice-free sea surface enhances the role of wind waves in the Arctic basin, which threatens platforms for the extraction of hydrocarbons on the continental shelf, vessels navigating the Northern Sea Route or its sections, as well as onshore structures, including by increasing the rate of erosion shore. Reducing the duration of the ice season activates the dynamics of ice, increasing its hummocking, and, as a result, the effect of drifting formations drifting to the ice in the ice fields increases. The development of important economic sectors in the difficult climatic conditions of the Arctic is impossible without the development of reliable systems for forecasting regional changes in weather and climate. The main objective of the work is to analyze changes in wind-wave conditions and mesoscale atmospheric processes in the coastal regions of the Russian Arctic in recent decades and forecast their dynamics under conditions of a decrease in the ice extent of the Arctic Ocean. Unique archives of satellite and hydrometeorological data, reanalysis data, climatic, regional and wind-wave models are used. The main goal of the work is to improve the accuracy of regional forecasts of hazardous hydrometeorological phenomena in the polar regions based on the development of integrated monitoring technology for mesoscale atmospheric processes in the coastal zones of the Arctic seas of the Russian Federation based on a joint analysis of ground and satellite observations and mathematical modeling results. Most of the work's tasks - namely, the development of forecasting systems for leeward storms, mesoscale cyclones, assessment of the risks of their occurrence in the context of modern climate changes, are being solved for the first time.Currently, the Arctic is attracting increased attention not only as a region with the most noticeable climate change, but also as a world mineral storage, whose development prospects are being actively discussed. For Russia, which owns the bulk of the Arctic shelf, the Arctic is also a promising trade and transport artery, as in recent decades new opportunities for using the Northern Sea Route have been discovered.
But climate change can lead to less favorable consequences. The increase in the ice-free sea surface enhances the role of wind waves in the Arctic basin, which threatens platforms for the extraction of hydrocarbons on the continental shelf, vessels navigating the Northern Sea Route or its sections, as well as onshore structures, including by increasing the rate of erosion shore. Reducing the duration of the ice season activates the dynamics of ice, increasing its hummocking, and, as a result, the effect of drifting formations drifting to the ice in the ice fields increases. The development of important economic sectors in the difficult climatic conditions of the Arctic is impossible without the development of reliable systems for forecasting regional changes in weather and climate. The main objective of the work is to analyze changes in wind-wave conditions and mesoscale atmospheric processes in the coastal regions of the Russian Arctic in recent decades and forecast their dynamics under conditions of a decrease in the ice extent of the Arctic Ocean. Unique archives of satellite and hydrometeorological data, reanalysis data, climatic, regional and wind-wave models are used. The main goal of the work is to improve the accuracy of regional forecasts of hazardous hydrometeorological phenomena in the polar regions based on the development of integrated monitoring technology for mesoscale atmospheric processes in the coastal

©2019. Japan Geoscience Union. All Right Reserved.

zones of the Arctic seas of the Russian Federation based on a joint analysis of ground and satellite observations and mathematical modeling results. Most of the work's tasks - namely, the development of forecasting systems for leeward storms, mesoscale cyclones, assessment of the risks of their occurrence in the context of modern climate changes, are being solved for the first time.
The figure shows the linear trend of the average for December-February wind speed (m / s / year) in different regions of the Arctic according to the CFSR data from 1979 to 2017. Gray indicates significant trends.

Keywords: Arctic climate, wind-wave-ice interaction, polar low



©2019. Japan Geoscience Union. All Right Reserved.

Recent baric and climatic conditions over East Europe with a focus on Belarus

*Irina Danilovich[1], Vladimir Loginov[1], Pavel Groisman[2]

1. Institute for Nature Management National Academy of Science, Minsk, Belarus, 2. NC State University at NOAA National Centers for Environmental Information, Asheville, USA

The global and regional climate changes are the object of intent monitoring and research works. The results of climatic investigations are highly demanded and taken into account in projecting of any kinds of economic and social activities. At the same time the reasons of climate changes still remain as a point of scientific discussion. Despite the heightened attention to the anthropogenic contribution to the climate change, the natural factors still lead in the climatic system fluctuations. In this connection the aim of the present study is an analysis of current peculiarities of the atmospheric circulation as a main natural climatic driver, estimation of the prevailing cyclonic passes over East Europe region and its climatology.

The hypothesis of the research work is that climatic changes observed in the study region in the recent decades (increase of air temperature, especially in winter season, regional changes of the moistening pattern, number and spatial distribution of extreme events) are caused by changes in the frequency of cyclones of different origin which led to various hydrometeorological conditions on their passes. According to the pattern of cyclones movement over the Atlantic-European region, we analyzed cyclonic activity by approaching cyclone selection in groups by their origin: (a) cyclones originated in the North Atlantic and sampled by two sub-groups: the West (with zonal west-east pass from Atlantic to the continent) and the Scandinavian (with meridian pass from the Scandinavia to the south); (b) cyclones that originate in the Mediterranean Sea, the Balkan Peninsula, and the Black Sea and are moving in the northward direction. The frequency of occurrence, radius, duration, and atmospheric pressure in the cyclone center (cyclone depth) have been studied for all types of cyclones.

The input information for the study is presented as two data-sets of cyclone tracks derived with the algorithms developed by different groups of authors: (1) the P.P. Shirshov Institute of Oceanology of the Russian Academy of Sciences and (2) the A.M. Obukhov Institute of Atmospheric Physics of the Russian Academy of Sciences. Both algorithms were applied to the ECMWF Era-Interim reanalysis. The study period is 1979-2016 (37 years). The cyclonic data-sets presented as coordinates and sea level pressure in the cyclone center during their life. The correspondent meteorological phenomena are used to investigate the long-term climatological anomalies in the study region such as invasions of warm and cold air masses, severe droughts, intensive precipitation, etc.

In our previous study (Partasenok *et al* 2014), we established some peculiarities of cyclone tracks change in the Atlantic-European region in winter season and in this connection the streamflow freshet formation in Belarus. The main feature of the study was an increase of the West cyclones number in the Atlantic-European region and detection the third sub-group of the Atlantic cyclones named the North cyclones. The increase this type of cyclones and its shift to the northward led to the precipitation growth in the northern part of Belarus in winter and formation the special hydrometeorological conditions for smaller than average snow-melting floods in the country during recent decades. The present study is a continuation of this research work with spreading calculations to all seasons of the year and emphasizing on the long-living climatological anomalies and extreme events connected with cyclones of the different origin.

©2019. Japan Geoscience Union. All Right Reserved.

Reference: Partasenok (Danilovich) I.S., P. Ya. Groisman, R.S. Chekan, and V. I. Melnik, 2014: Winter cyclone frequency and following freshet streamflow formation on the rivers in Belarus. *Environ. Res. Lett.*, **9,** 09005 (13 pp). doi:10.1088/1748-9326/9/9/095005 *Environ. Res. Lett.* **9** (2014) 109602 (2 pp) doi:10.1088/1748-9326/9/10/109602

Keywords: East Europe, regional climatic change, regional changes in atmospheric circulation, Belarus

©2019. Japan Geoscience Union. All Right Reserved.

Assessment of climatic and environmental conditions along the track of projected Kyzyl-Kuragino railway line (the Western Sayan Mountains)

*Aleksandra Alekseevna Mikheeva[1], Margarita Syromyatina[1], Yurii Kurochkin[1]

1. Institute of Earth Sciences, Saint Petersburg State University, Russia

Currently there is a large investment project of the Kyzyl-Kuragino railway line construction mostly along the mountainous territory of Tuva and Krasnoyarsk Krai. The main relevance of the project is the possibility of more active involvement of the Tuva coal complex in commercial operation, which means economic development of the region. At the same time it is planned also to extend the road to Mongolia with the prospect to reach China thereby take into account international interests.

Despite the positive economic and social effects there are significant difficulties in the realization of the project due to the natural and climatic conditions. The projected railway track is mostly located in the Western Sayan Mountains and is characterized by complex environmental conditions, in particular geological and geomorphological, as well as extreme climatic characteristics, permafrost etc. The main goal of this research was to conduct an independent scientific expertise of assessment of the environmental conditions during the implementation of one the largest transport projects in Siberian region.

The natural conditions were assessed according to the following indicators: extreme values of air temperature and precipitation, strong winds, snow cover thickness, avalanche danger, seismicity and some slope processes. Analysis was made using various map documents, statistical data, results of expert interviews with the representatives of regional ministries of transport and ministries of economic development, universities and research institutes. For the analysis of extreme climatic characteristics data from weather stations of the study region were used. The entire area of projected road construction was divided into several sections, where it is necessary to take into account certain parameters mainly extreme natural phenomena. As a result the assessment of the potential natural risks during the construction and further operation of the railway was made.

Keywords: natural conditions, railway line construction, mountains, Tuva and Krasnoyarsk Krai

©2019. Japan Geoscience Union. All Right Reserved.

Assessment of interlinkages among industrialization, climate change, and forest fire activity: Thematic study of the Republic of Sakha (Yakutia), Russia

*Kiunnei Kirillina[1], Wanglin Yan[1]

1. Graduate School of Media and Governance, Keio University SFC

Forest fires play a critical role in shaping the ecosystem and atmospheric patterns. In turn, fire regimes are highly influenced by climate and human activities. Natural cycles, human activities like land-use changes and fire exclusion, and human-caused climate change can also influence the likelihood of fires. This study aimed to identify the causes underlying the increase of fire activity in one of the most fire-hazardous regions of Russia, the Republic of Sakha (Yakutia). The forest in this republic is performing the important function of permafrost protection. Deforestation might cause a catastrophic permafrost degradation, as the decrease of forests there mainly occurs due to fires.

To understand the patterns of historical fire activity, we analyzed the past history of fire events in the Sakha Republic through a newly developed approach for historical fire regimes characterization. Then, to identify the exact cause of intensification of fire activity was constructed an analytical approach for the assessment of interlinkages among industrialization, climate change, and forest fire activity. The study found that the main contributor to the increased historical fire activity in the republic was climate warming documented there since the 1960s, especially in spring season, which affected the overall duration of the fire season. As one main cause of recent expansion of fires, this research identified as significant the socioeconomic and land use changes undergone on the territory of the republic since the 2000s, which have resulted in extensive use of forest and forested land, and increased number of anthropogenic fires and related atmospheric changes.

Keywords: forest fires and climate change, land use changes, anthropogenic fires, GHG emissions

©2019. Japan Geoscience Union. All Right Reserved.

Quantitative Evaluation of Winter Daily Precipitation over Northern Japan

*Minami Masuda[1], Akiyo Yatagai[1], Toshiyuki Nakaegawa[2], Kenji Kamiguchi[3]

1. Graduate School of Science and Technology, Hirosaki University, 2. Meteorological Research Institute/Japan Meteorological Agency, 3. Japan Meteorological Agency

Snowfall is an important parameter for water resources. An accurate, quantitative evaluation is needed to clarify the impact of global warming on snowfall and vice versa. For that evaluation, a gridded precipitation data set based on rain-gauges is suitable, because rain-gauges measure precipitation directly. However, rain-gauge data include systematic biases due to interpolation and observation biases. For example, the long-term average, daily gridded precipitation data from APHRO_JP (P) underestimates by 30% the sum of evapotranspiration (E) and inflow (R) from dam catchments located in Northern Japan. We know this because if APHRO_JP was accurate, P should be equal to $R+E$ and it is not. It was reported that the annual mean precipitation of Japan was well simulated in the non-hydrostatic regional climate model (NHRCM, spatial resolutions 5 km/2 km) produced by the Meteorological Research Institute (MRI). From the above, we validated the interpolation bias of APHRO_JP using precipitation from the NHRCM to quantitatively evaluate winter precipitation over Northern Japan. The bias in the water balance from the dam catchments was reduced to 1% after adjusting for three systematic biases.

First, we validated and adjusted the interpolation bias. We created daily precipitation gridded data based on the distribution of the Automated Meteorological Data Acquisition System (AMeDAS) using hourly precipitation from the NHRCM (spatial distribution 2 km) and we compared it with precipitation from the NHRCM. We found that precipitation from the Mesh precipitation climatology which is used in APHRO_JP underestimated precipitation over mountain areas where rain-gauges were not set up. Because of this, APHRO_JP underestimated winter precipitation over mountain areas by approximately 3 mm/day. This daily precipitation bias over mountain areas was halved when we used climatology based on precipitation from the NHRCM instead of Mesh precipitation climatology.

Even with this adjustment, precipitation over mountain areas was still underestimated. This stemmed from the interpolation method used to predict rainfall, because the climatology indicate that the ratio of precipitation increases seasonally with elevation over mountain areas. This underestimation was controlled by an adjustment to the interpolation bias from the precipitation pattern detected by an Empirical Orthogonal Function (EOF) analysis.

On the basis of these validation results, we created daily precipitation gridded data based on the AMeDAS rain-gauge. We then applied the three adjustments from the climatology, precipitation pattern and precipitation undercatch and evaluated their contribution. We found that the annual precipitation over Japan was 2054 mm/year, which was an 18% increase on APHRO_JP. Furthermore, at the four dam catchments in Northern Japan, this adjusted precipitation explained 99% of the precipitation estimated by inflow from the dam catchments and evapotranspiration.

Finally, we measured the contribution of the systematic bias in winter precipitation in Northern Japan (138.5–141˚E, 36.8–38.8˚N). Precipitation was increased 11% by changing the climatology and increased 12% by adjusting for precipitation undercatch. The impact of the precipitation pattern adjustment was small. For extreme events, the adjustment effect was different. On average, in the four dam catchments,

©2019. Japan Geoscience Union. All Right Reserved.

precipitation was increased 18% by the change of climatology 7% by adjustment for precipitation undercatch. However, these ratios were different at each dam, and in dams where the catchments were in high mountain regions, there was a much greater effect from a change in the climatology. Because there are few rain-gauges in high mountain regions, it important to change climatology used in APHRO_JP. Furthermore, our results indicate uncertainty in precipitation from internal variability when the precipitation pattern adjustment was not used. Our application of these adjustments to APHRO_JP reduced systematic bias and improved precipitation measurements.

Keywords: APHRO_JP, winter precipitation, water resource

©2019. Japan Geoscience Union. All Right Reserved.

Seasonal variation of wetland carbon dioxide and methane fluxes measured by automatic chambers at the Bakchar bog, West Siberia

*Shamil Maksyutov[1], Alexandre Fofonov[2], Denis Davydov[2], Oleg Krasnov[2], Tadanobu Nakayama[1], Mikhail Glagolev[3]

1. National Institute for Environmental Studies, 2. V.E. Zuev Institute of Atmospheric Optics, 3. M.V. Lomonosov Moscow State University

Wetland CO_2 and CH_4 fluxes were observed at the Bakchar bog (N56˚, E82˚), West Siberia. Measurements were performed by two solar powered automated systems, each consisting of NDIR Li-820 CO_2 analyzer, an SnO_2-based methane sensor, six static chambers installed along transects, the air drying and distribution unit, and a datalogger. Observations were made during the May to October period in 2014 to 2017 at two types of open wetlands: mesotrophic open bog and patterned wetland with forested ridges, flat hollows and water pool. Each chamber is automatically opened and closed with pneumatic actuator. Water level is measured in the wetland and surrounding forest locations. Net uptake of CO_2 is observed from the beginning of June through the end of August with a maximum from mid-June through the end of July. Seasonal pattern of methane fluxes showed that CH_4 emission increases at the beginning of June, then weakens gradually in autumn. Seasonal variation of the emissions correlates well with the soil temperature at 5-10 cm depth. Carbon dioxide and methane fluxes correlate spatially; higher methane emissions are observed at wet mesotrophic locations with higher photosynthesis/respiration rates. Lower CH_4 emissions were observed on oligotrophic patterned wetland.

Keywords: methane emissions, wetland, Siberia, CO2 fluxes

©2019. Japan Geoscience Union. All Right Reserved.

Climatic distances between origin and labor locations for migrants in a changing climate in Siberia by the end of the 21st century

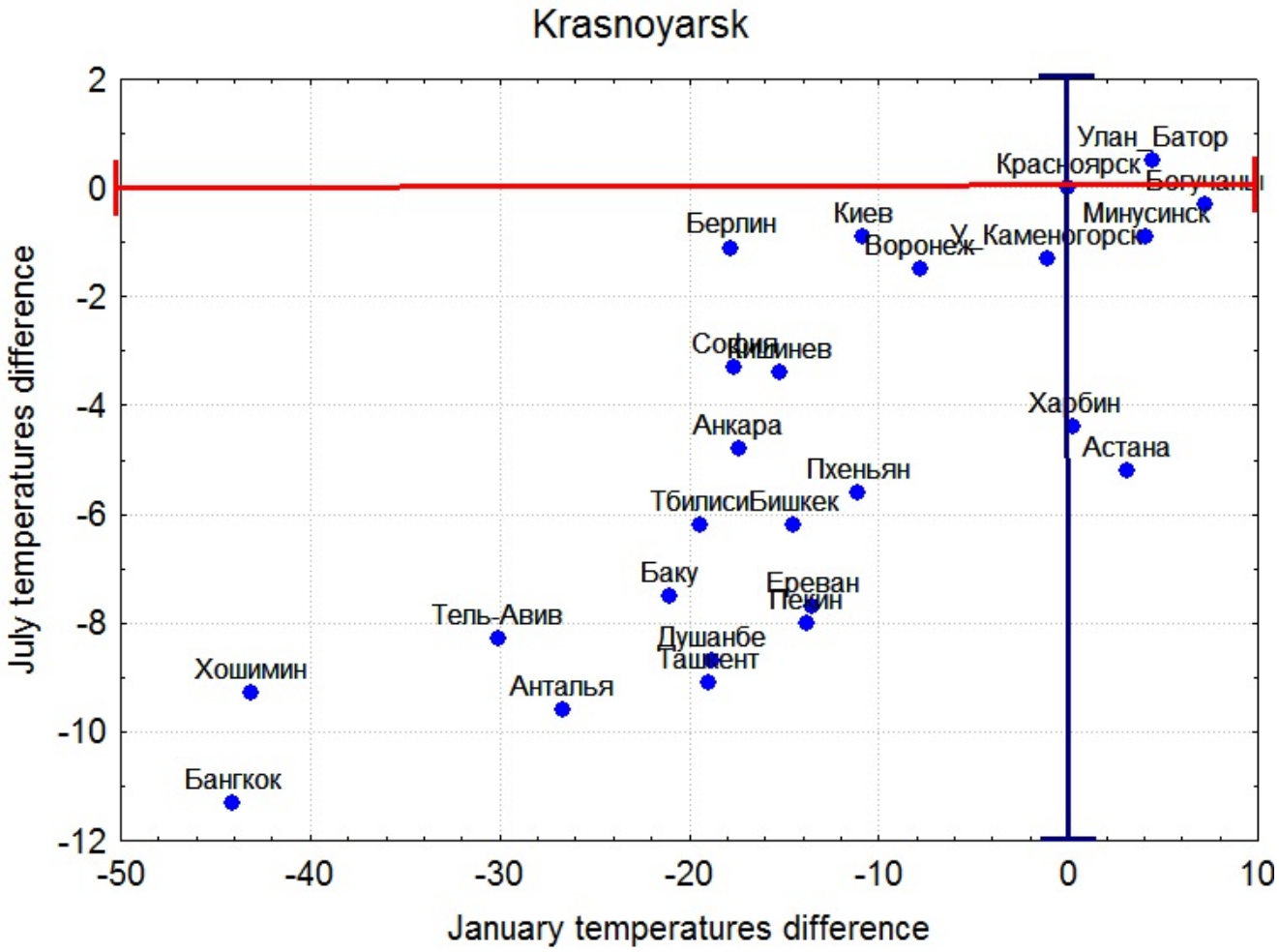
*Elena I. Parfenova[1], Nadezhda M. Tchebakova[1]

1. V.N.Sukachev Institute of Forest SB RAS, FRC SB RAS

The goals of our work were to evaluate climatic distances between climates from which potential migrants originate and climates of various regions over Siberia for which they migrate; and evaluate Siberian regions from view points of comfort-discomfort for migrants in current and future climates by the end of the century. We have completed this research from the example of the Krasnoyarsk Territory that is located in the center of Siberia and stretches from the south to north at a distance 2,000 km. Statistics on migrations show that migrants arrive to the Krasnoyarsk Territory from the European Russia and far abroad: Northern Korea, China, Vietnam. We studied four large industrial regions of the Territory for labor migrations. We used two climate variables that reflect winter and summer conditions: mean January and July temperatures. In total, 30 cities were ordinated in the axes of the differences in these temperatures between migrants' origins and migration locations. To characterize the future climates by the end of the century we used January and July temperature departure means from the ensemble of twenty general circulation models from the CMIP5. Two scenarios were used to characterize the range of climate change: a mild RCP 2.6 and a sharp RCP 8.5 climate scenarios. In total, 12 portraits of potential labor migrations were outlined in current and future climates. The "null" point in each portrait showed conditions for the natives of a particular region and the distance from the null to a country of origin showed physiological and psychological discrepancy that migrants should overcome to live in new climate.

Keywords: migration, climate change, transfer function, Siberia, January and July temperatures

©2019. Japan Geoscience Union. All Right Reserved.



©2019. Japan Geoscience Union. All Right Reserved.

[E] Poster | M (Multidisciplinary and Interdisciplinary)：M-IS Intersection

Sun. May 26, 2019 5:15 PM - 6:30 PM JST | Sun. May 26, 2019 8:15 AM - 9:30 AM UTC | Poster Hall International Exhibition Hall8, Makuhari Messe_40

[M-IS01] Environmental, socio-economic and climatic changes in Northern Eurasia

convener:Pavel Groisman(NC State University Research Scholar at NOAA National Centers for Environmental Information, Asheville, North Carolina, USA), Shamil Maksyutov(National Institute for Environmental Studies), Evgeny P Gordov(Institute of Monitoring of Climatic and Ecological Systems SB RAS), Dmitry A Streletskiy(George Washington University)

We invite presentations on the biogeochemical cycles, the surface energy budget and water cycle, and climate and ecosystem interactions in Northern Eurasia (land-cover and land-use change, atmospheric aerosols, soil, and permafrost changes that affect and are being affected by climate and ecosystem change), human dimension, and tools to address the Northern Eurasia studies. In environmental studies, our Session foci are on the carbon cycle of Northern Eurasia and on the permafrost changes in Siberia, Asian Mountains, and the Arctic coastal regions.
In the regional water cycle studies, our Session foci are on the changing distribution of precipitation intensity, frequency, especially, in the cold/shoulder season transition periods when surface air temperature is close to 0 deg.C, and on the pattern and seasonal cycle changes of runoff.
In the human dimension studies, our Session foci are on assessments of impact of the ongoing environmental changes in Northern Eurasia on the human well-being and on mitigation strategies development in response to harmful consequences of these changes
The particular foci of this Session will be the studies of changes that impacts regional sustainable development in the Dry Latitudinal Belt of Northern Eurasia that expands through the continent from Pannonian Steppes in the west to the drylands of northern China in the east.
We invite also early career scientists associated with (or interested in) the Northern Eurasia Earth Science Partnership Initiative and its continuation, Northern Eurasia Future Initiative (http://nefi-neespi.org/NEFI-WhitePaper.pdf).

Conveners:
Pavel Groisman, NC State University, USA (pasha.groisman@noaa.gov)
Shamil Maksyutov, National Institute for Environmental JAPAN (shamil@nies.go.jp)
Evgeny Gordov, Siberian Center for Environmental Research and Training, RUSSIA (gordov@scert.ru)
Yizhao Chen, Nanjing Forestry University, CHINA (chenyzvest@gmail.com)

[MIS01-P01] Effects of clear-cutting on carbon dioxide fluxes in a boreal forest ecosystem - results of numerical experiments with a three-dimensional turbulent exchange model

Yulia Mukhartova[3], Maria Dyachenko[3], Polina Mangura[3], Alexander Krupenko[3], *Alexander Olchev[1,2] (1.Faculty of Geography, Lomonosov Moscow State University, 2.A.N. Severtsov Institute of Ecology and Evolution, Russian Academy of Sciences, 3.Faculty of Physics, Lomonosov Moscow State University)

[MIS01-P02] Retrieving the forest species composition from remote sensing data using a three-dimensional radiative transfer model

*Alexander Olchev[1,2], Natalia Levashova[3], Dmitry Lukyanenko[3] (1.Faculty of Geography, Lomonosov Moscow State University , 2.Severtsov Institute of Ecology and Evolution, Russian Academy of Science, 3.Faculty of Physics, Lomonosov Moscow State University)

[MIS01-P03] Satellite-derived Burned Area for Siberia (1979 – 2000)

*Amber Jeanine Soja[1], Brian J. Stocks[2], Stefano Potter[3], Brendan Rogers[3], Donald R. Cahoon[4], Natasha Jurko[5], Susan G. Conard[6], William 'Bill' deGroot[5], Nadezhda Tchebakova[7] (1.National Iinstitute of Aerospace / NASA Langley Research Center, 2.B.J. Stocks Wildfire Investigations Ltd., 3.Woods Hole Research Center , 4.Terra Systems Research, 5.Canadian Forest Service/Service canadien des forêts, 6.George Mason University,Fairfax, VA, 7.Sukachev Institute of Forestry, Siberian Branch of the Russian Academy of Sciences)

[MIS01-P04] Analysis and prediction of hazardous hydrometeorological phenomena in the coastal areas of the Arctic

*Irina Repina[1,2] (1.A.M.Obukhov Institute of Atmospheric Physics RAS, 2.Lomonosov Moscow State University)

[MIS01-P05] **Recent baric and climatic conditions over East Europe with a focus on Belarus**

*Irina Danilovich[1], Vladimir Loginov[1], Pavel Groisman[2] (1. Institute for Nature Management National Academy of Science, Minsk, Belarus, 2. NC State University at NOAA National Centers for Environmental Information, Asheville, USA)

[MIS01-P06] **Assessment of climatic and environmental conditions along the track of projected Kyzyl-Kuragino railway line (the Western Sayan Mountains)**

★Invited Papers

*Aleksandra Alekseevna Mikheeva[1], Margarita Syromyatina[1], Yurii Kurochkin[1] (1.Institute of Earth Sciences, Saint Petersburg State University, Russia)

[MIS01-P07] **Assessment of interlinkages among industrialization, climate change, and forest fire activity: Thematic study of the Republic of Sakha (Yakutia), Russia**

*Kiunnei Kirillina[1], Wanglin Yan[1] (1.Graduate School of Media and Governance, Keio University SFC)

[MIS01-P08] Quantitative Evaluation of Winter Daily Precipitation over Northern Japan

*Minami Masuda[1], Akiyo Yatagai[1], Toshiyuki Nakaegawa[2], Kenji Kamiguchi[3] (1.Graduate School of Science and Technology, Hirosaki University, 2.Meteorological Research Institute/Japan Meteorological Agency, 3.Japan Meteorological Agency)

[MIS01-P09] Seasonal variation of wetland carbon dioxide and methane fluxes measured by automatic chambers at the Bakchar bog, West Siberia

*Shamil Maksyutov[1], Alexandre Fofonov[2], Denis Davydov[2], Oleg Krasnov[2], Tadanobu Nakayama[1], Mikhail Glagolev[3] (1.National Institute for Environmental Studies, 2.V.E. Zuev Institute of Atmospheric Optics, 3.M.V. Lomonosov Moscow State University)

[MIS01-P10] Climatic distances between origin and labor locations for migrants in a changing climate in Siberia by the end of the 21st century

*Elena I. Parfenova[1], Nadezhda M. Tchebakova[1] (1.V.N.Sukachev Institute of Forest SB RAS, FRC SB RAS)

Effects of clear-cutting on carbon dioxide fluxes in a boreal forest ecosystem - results of numerical experiments with a three-dimensional turbulent exchange model

Yulia Mukhartova[3], Maria Dyachenko[3], Polina Mangura[3], Alexander Krupenko[3], *Alexander Olchev[1,2]

1. Faculty of Geography, Lomonosov Moscow State University, 2. A.N. Severtsov Institute of Ecology and Evolution, Russian Academy of Sciences, 3. Faculty of Physics, Lomonosov Moscow State University

To estimate the possible effects of clear-cutting on the air flow disturbances within the atmospheric surface layer as well as on the spatial patterns of vertical carbon dioxide (CO2) fluxes and horizontal advection terms within and around the clear-cut area a process-based three-dimensional (3D) hydrodynamic momentum, energy and CO2 exchange model was developed. Clear-cutting is one of the most widespread logging practice, which can substantially transform the energy, water vapor and CO2 exchange between forest ecosystems and atmosphere and affect the climate system at multiple scales. Developed 3D hydrodynamic model is based on a 1.5-order closure scheme and uses a system of averaged Navier-Stokes and continuity equations for the mean wind speed components, as well as the reaction-advection-diffusion equation for CO2 transfer within the atmospheric surface layer (Mukhartova et al. 2015). The model applies Reynolds's decomposition and expresses the wind speed and concentrations of CO2 as sums of their mean values and deviations. The 1.5-closure scheme assumes that the turbulent fluxes can be expressed using the turbulent exchange coefficients (that depend on turbulent kinetic energy and its dissipation rate) and the gradients of corresponding functions (wind speed components and CO2 concentrations).
The clear-cut area selected for the study is situated in the south-western part of Valdai Hills in European Russia. The area of the clear-cut is about 4.5 ha and it is surrounded by a mixed forest stand represented mainly by Norway spruce, White birch and Eurasian aspen species with tree heights ranged between 18 and 22 m (Mamkin et al. 2016, 2019). The vegetation at the clear-cut area is mainly represented by herbaceous species and a small number of juvenile aspen trees.
Results of numerical experiments with the developed 3D model showed that clear-cutting has significant effect on spatial distributions of wind speed components as well as atmospheric momentum and CO2 fluxes. Spatial flux heterogeneity is also enhanced by complex shape of the clear-cut boundary. The largest effect of the clear-cut on the air flows is mainly appeared along the windward forest edge whereas at the leeward forest edge this effect is less pronounced. The leeward part of the clear-cut is characterized by prevailed downward air flows (with negative values of vertical wind component) whereas the upward air flows (with prevailed positive values of vertical wind component) are appeared at its windward part. It is very important to point out that the horizontal gradients of vertical and horizontal wind velocities at the lowest part of the atmospheric surface layer (up to the height 3-4 m above the ground surface) as well as horizontal turbulent and non-turbulent CO2 advection terms in the central part of the clear-cut is relatively small that can be used as important criteria indicating sufficient reestablishing of the air flow in this part of the clear-cut after its disturbance at the leeward forest edge.

Reference

Mamkin V., Kurbatova J., Avilov V., Mukhartova Yu, Krupenko A., Ivanov D., Levashova N., Olchev A. Changes in net ecosystem exchange of CO2, latent and sensible heat fluxes in a recently clear-cut spruce forest in western Russia: results from an experimental and modeling analysis. 2016. Environmental

©2019. Japan Geoscience Union. All Right Reserved.

Research Letters. 11(12). 125012
Mamkin V., Kurbatova J., Avilov V., Ivanov D., Kuricheva O., Varlagin A., Yaseneva I., Olchev A. 2019 Energy and CO2 exchange in an undisturbed spruce forest and clear-cut in the Southern Taiga. Agricultural and Forest Meteorology, 265, 252-268
Mukhartova Yu. V., Levashova N. T., Olchev A. V., Shapkina N. E. 2015 Application of a 2D model for describing the turbulent transfer of CO2 in a spatially heterogeneous vegetation cover. Moscow University Physics Bulletin 70(1), 14-21

Keywords: turbulent exchange model, clear-cut, momentum fluxes, CO2 fluxes

©2019. Japan Geoscience Union. All Right Reserved.

Retrieving the forest species composition from remote sensing data using a three-dimensional radiative transfer model

*Alexander Olchev[1,2], Natalia Levashova[3], Dmitry Lukyanenko[3]

1. Faculty of Geography, Lomonosov Moscow State University , 2. Severtsov Institute of Ecology and Evolution, Russian Academy of Science, 3. Faculty of Physics, Lomonosov Moscow State University

A three-dimensional model was developed to derive the reflection, absorption and transmission of photosynthetically active radiation (PAR) by a non-uniform forest canopy with a multi-species structure (Levashova et al., 2018). The model algorithm describing solar radiation transfer through a forest canopy considers direct and diffuse radiation penetrating through gaps in the canopy, transmitted by leaves and reflected from leaves, bark and soil surface. To estimate the canopy the reflection, absorption and transmission the model uses external data about 3D structure of each tree species in the forest stand, about the spectral properties of photosynthesizing and non-photosynthesizing parts of the different trees species, and about spectral reflectance of soil surface. Moreover it uses also information about incoming solar radiation, sun elevation, the ratio of incoming direct and diffuse solar radiation, and surface topography. The model is based on steady-state transport equations initially suggested by Ross (Ross, 1981) and further developed and described by Myneni and Knyazikhin (Myneni et al., 1990; Knyazikhin et al., 2005). Calculation of the direct solar radiation fluxes within the canopy is based on estimation of the probability that a ray of light passing through the foliage reaches a given location within the canopy without interception. Diffuse solar radiation is calculated taking into account both diffuse solar radiation from the sky penetrating through foliage gaps and direct and diffuse radiation scattered by canopy foliage and woody components. The numerical scheme for solving the integro-differential equations is based on the discrete ordinates method.
The model was used to describe the spatial patterns of solar radiation reflection and transmission by non-uniform mixed forest canopy and to develop an algorithm that allows to retrieve the proportion of different tree species in a mixed forest stand from measured canopy reflection coefficients for blue, green, red and near-infrared spectral bands (obtained from e.g. the Landsat satellite imagery). This approach allowed us to quantify the proportion of different tree species (both coniferous and deciduous) in a forest stand in case if their spectral reflection properties of the leaves are not the same. The accuracy of assessing the proportion of vegetation species using this method depended on the number of reflection measurements under various solar conditions (e.g. different sun elevations) that can reached by several measurements during the growing seasons. An increase of the input data volume (determined by the number of the measurements) resulted in higher accuracies for prediction of the proportions of different tree species.

References

Knyazikhin Y., Marshak A., Myneni R.B. Three dimensional radiative transfer in vegetation canopies. In: Three Dimensional Radiative Transfer in the Cloudy Atmosphere, Marshak, A., Davis, A.B., Eds., Springer Verlag: Berlin, Heidelberg, 2005, 617-652.
Levashova N., Lukyanenko D., Mukhartova Y., Olchev A. Application of a three-dimensional radiative transfer model to retrieve the species composition of a mixed forest stand from canopy reflected radiation. Remote Sensing, 2018, 10 (10), 1661.
Myneni R.B., Asrar G., Gerstl S.A.W. Radiative transfer in three dimensional leaf canopies. Transport Theory and Statistical Physics, 1990, 19, 205–250.
Ross J. The radiation regime and architecture of plant stands; Dr. W. Junk Publishers: The Hague,

©2019. Japan Geoscience Union. All Right Reserved.

Netherlands, 1981, 390 p.

Keywords: radiative transfer, three-dimensional model, mixed forest, canopy reflection, inverse problem

©2019. Japan Geoscience Union. All Right Reserved.

Satellite-derived Burned Area for Siberia (1979 –2000)

*Amber Jeanine Soja[1], Brian J. Stocks[2], Stefano Potter[3], Brendan Rogers[3], Donald R. Cahoon[4], Natasha Jurko[5], Susan G. Conard[6], William 'Bill' deGroot[5], Nadezhda Tchebakova[7]

1. National Iinstitute of Aerospace / NASA Langley Research Center, 2. B.J. Stocks Wildfire Investigations Ltd., 3. Woods Hole Research Center , 4. Terra Systems Research, 5. Canadian Forest Service/Service canadien des forêts, 6. George Mason University,Fairfax, VA, 7. Sukachev Institute of Forestry, Siberian Branch of the Russian Academy of Sciences

Siberia is a distinct and crucial region because it has the physical size necessary to effect regional and global climate. The circumboreal zone contains the largest stock of terrestrial carbon on Earth, and Russia holds roughly two-thirds of that carbon pool. Fire is the primary natural disturbance in boreal forest, which acts to cycle carbon and maintain ecosystem diversity in sync with the climate. Under current climate change scenarios, the Russian boreal is expected to experience temperature increases that exceed the global mean. We have developed a long-term burned area database that will enable novel analyses on the multi-decadal time scale that is ultimately required for robust assessments, including those focused on carbon cycling, fire emissions, and importantly the links between fire regimes, fire weather, ecosystems, and climate.

In this presentation, we present a long-term burned area database that has been developed using Advanced Very High Resolution Radiometer (AVHRR) Global Area Coverage (GAC) data from 1979-2000. Burned area has been verified using Total Ozone Mapping Spectrometer data and validated using available Landsat imagery (160 scenes thus far representing 5.6 Mha of burned area, 219 fire events, and 11% of the total area burned in the AVHRR database). Visually the burned scar data compare well. Validation is in ongoing, though initial analyses show an intersection of 42% with commission and omission errors of 31% and 25%, respectively. Most commission and omission errors are related to spatial inconsistencies using imagery with significantly different spatial resolutions. Of the fire events missed by AVHRR (i.e., omissions), 86% are related to fires <10,000 ha (~ 6 AVHRR pixels) and 44% are related to fires <3,000ha (~ 2 AVHRR pixels). Total burned area compares well, with the AVHRR database under-representing burned area by 10% compared to the Landsat data analyzed. Correlation in burned scar area between the AVHRR and Landsat data is 0.98 for all fires and 0.68 for fires that are < 0.1 Mha.

Keywords: Wildland Fire, Remote Sensing, Biomass Burning, Russia

©2019. Japan Geoscience Union. All Right Reserved.

Analysis and prediction of hazardous hydrometeorological phenomena in the coastal areas of the Arctic

*Irina Repina[1,2]

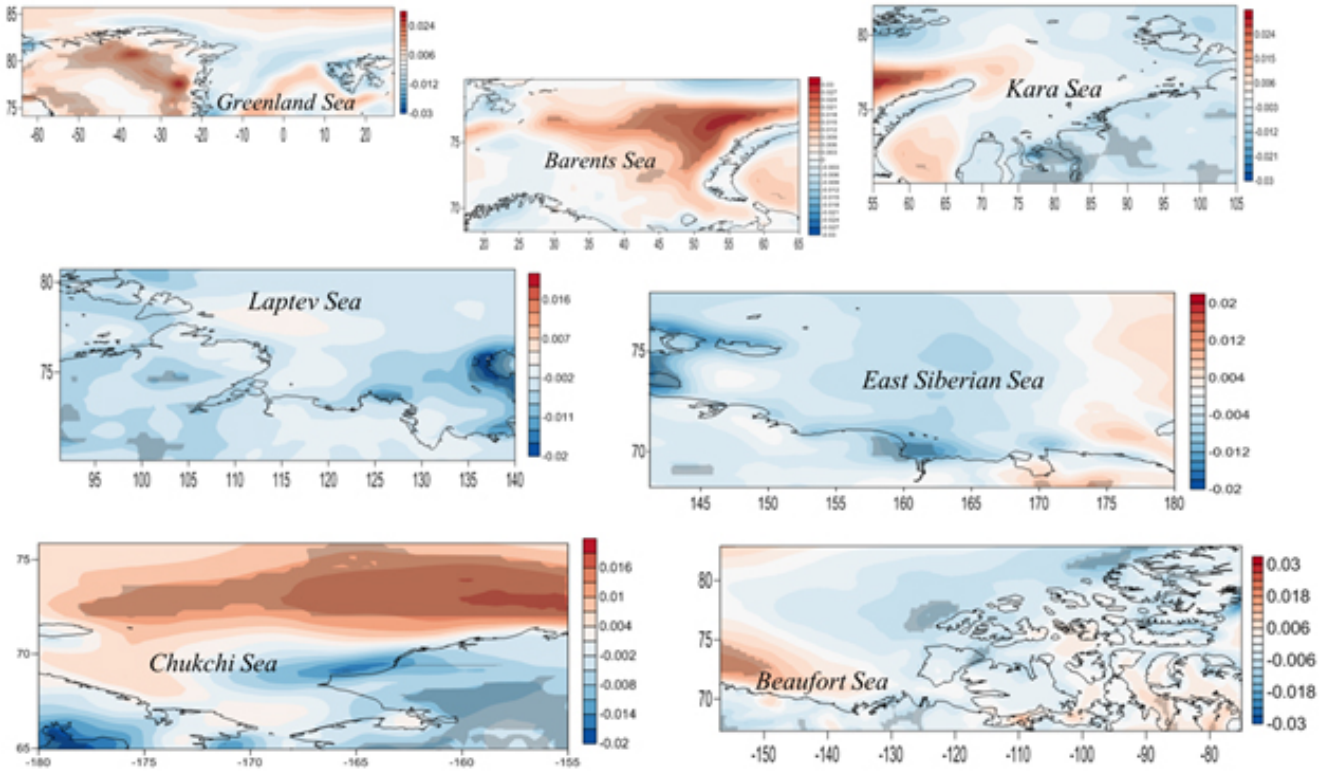
1. A.M.Obukhov Institute of Atmospheric Physics RAS, 2. Lomonosov Moscow State University

Currently, the Arctic is attracting increased attention not only as a region with the most noticeable climate change, but also as a world mineral storage, whose development prospects are being actively discussed. For Russia, which owns the bulk of the Arctic shelf, the Arctic is also a promising trade and transport artery, as in recent decades new opportunities for using the Northern Sea Route have been discovered. But climate change can lead to less favorable consequences. The increase in the ice-free sea surface enhances the role of wind waves in the Arctic basin, which threatens platforms for the extraction of hydrocarbons on the continental shelf, vessels navigating the Northern Sea Route or its sections, as well as onshore structures, including by increasing the rate of erosion shore. Reducing the duration of the ice season activates the dynamics of ice, increasing its hummocking, and, as a result, the effect of drifting formations drifting to the ice in the ice fields increases. The development of important economic sectors in the difficult climatic conditions of the Arctic is impossible without the development of reliable systems for forecasting regional changes in weather and climate. The main objective of the work is to analyze changes in wind-wave conditions and mesoscale atmospheric processes in the coastal regions of the Russian Arctic in recent decades and forecast their dynamics under conditions of a decrease in the ice extent of the Arctic Ocean. Unique archives of satellite and hydrometeorological data, reanalysis data, climatic, regional and wind-wave models are used. The main goal of the work is to improve the accuracy of regional forecasts of hazardous hydrometeorological phenomena in the polar regions based on the development of integrated monitoring technology for mesoscale atmospheric processes in the coastal zones of the Arctic seas of the Russian Federation based on a joint analysis of ground and satellite observations and mathematical modeling results. Most of the work's tasks - namely, the development of forecasting systems for leeward storms, mesoscale cyclones, assessment of the risks of their occurrence in the context of modern climate changes, are being solved for the first time.Currently, the Arctic is attracting increased attention not only as a region with the most noticeable climate change, but also as a world mineral storage, whose development prospects are being actively discussed. For Russia, which owns the bulk of the Arctic shelf, the Arctic is also a promising trade and transport artery, as in recent decades new opportunities for using the Northern Sea Route have been discovered.
But climate change can lead to less favorable consequences. The increase in the ice-free sea surface enhances the role of wind waves in the Arctic basin, which threatens platforms for the extraction of hydrocarbons on the continental shelf, vessels navigating the Northern Sea Route or its sections, as well as onshore structures, including by increasing the rate of erosion shore. Reducing the duration of the ice season activates the dynamics of ice, increasing its hummocking, and, as a result, the effect of drifting formations drifting to the ice in the ice fields increases. The development of important economic sectors in the difficult climatic conditions of the Arctic is impossible without the development of reliable systems for forecasting regional changes in weather and climate. The main objective of the work is to analyze changes in wind-wave conditions and mesoscale atmospheric processes in the coastal regions of the Russian Arctic in recent decades and forecast their dynamics under conditions of a decrease in the ice extent of the Arctic Ocean. Unique archives of satellite and hydrometeorological data, reanalysis data, climatic, regional and wind-wave models are used. The main goal of the work is to improve the accuracy of regional forecasts of hazardous hydrometeorological phenomena in the polar regions based on the development of integrated monitoring technology for mesoscale atmospheric processes in the coastal

©2019. Japan Geoscience Union. All Right Reserved.

zones of the Arctic seas of the Russian Federation based on a joint analysis of ground and satellite observations and mathematical modeling results. Most of the work's tasks - namely, the development of forecasting systems for leeward storms, mesoscale cyclones, assessment of the risks of their occurrence in the context of modern climate changes, are being solved for the first time.
The figure shows the linear trend of the average for December-February wind speed (m / s / year) in different regions of the Arctic according to the CFSR data from 1979 to 2017. Gray indicates significant trends.

Keywords: Arctic climate, wind-wave-ice interaction, polar low



©2019. Japan Geoscience Union. All Right Reserved.

Recent baric and climatic conditions over East Europe with a focus on Belarus

*Irina Danilovich[1], Vladimir Loginov[1], Pavel Groisman[2]

1. Institute for Nature Management National Academy of Science, Minsk, Belarus, 2. NC State University at NOAA National Centers for Environmental Information, Asheville, USA

The global and regional climate changes are the object of intent monitoring and research works. The results of climatic investigations are highly demanded and taken into account in projecting of any kinds of economic and social activities. At the same time the reasons of climate changes still remain as a point of scientific discussion. Despite the heightened attention to the anthropogenic contribution to the climate change, the natural factors still lead in the climatic system fluctuations. In this connection the aim of the present study is an analysis of current peculiarities of the atmospheric circulation as a main natural climatic driver, estimation of the prevailing cyclonic passes over East Europe region and its climatology.

The hypothesis of the research work is that climatic changes observed in the study region in the recent decades (increase of air temperature, especially in winter season, regional changes of the moistening pattern, number and spatial distribution of extreme events) are caused by changes in the frequency of cyclones of different origin which led to various hydrometeorological conditions on their passes. According to the pattern of cyclones movement over the Atlantic-European region, we analyzed cyclonic activity by approaching cyclone selection in groups by their origin: (a) cyclones originated in the North Atlantic and sampled by two sub-groups: the West (with zonal west-east pass from Atlantic to the continent) and the Scandinavian (with meridian pass from the Scandinavia to the south); (b) cyclones that originate in the Mediterranean Sea, the Balkan Peninsula, and the Black Sea and are moving in the northward direction. The frequency of occurrence, radius, duration, and atmospheric pressure in the cyclone center (cyclone depth) have been studied for all types of cyclones.

The input information for the study is presented as two data-sets of cyclone tracks derived with the algorithms developed by different groups of authors: (1) the P.P. Shirshov Institute of Oceanology of the Russian Academy of Sciences and (2) the A.M. Obukhov Institute of Atmospheric Physics of the Russian Academy of Sciences. Both algorithms were applied to the ECMWF Era-Interim reanalysis. The study period is 1979-2016 (37 years). The cyclonic data-sets presented as coordinates and sea level pressure in the cyclone center during their life. The correspondent meteorological phenomena are used to investigate the long-term climatological anomalies in the study region such as invasions of warm and cold air masses, severe droughts, intensive precipitation, etc.

In our previous study (Partasenok *et al* 2014), we established some peculiarities of cyclone tracks change in the Atlantic-European region in winter season and in this connection the streamflow freshet formation in Belarus. The main feature of the study was an increase of the West cyclones number in the Atlantic-European region and detection the third sub-group of the Atlantic cyclones named the North cyclones. The increase this type of cyclones and its shift to the northward led to the precipitation growth in the northern part of Belarus in winter and formation the special hydrometeorological conditions for smaller than average snow-melting floods in the country during recent decades. The present study is a continuation of this research work with spreading calculations to all seasons of the year and emphasizing on the long-living climatological anomalies and extreme events connected with cyclones of the different origin.

©2019. Japan Geoscience Union. All Right Reserved.

Reference: Partasenok (Danilovich) I.S., P. Ya. Groisman, R.S. Chekan, and V. I. Melnik, 2014: Winter cyclone frequency and following freshet streamflow formation on the rivers in Belarus. *Environ. Res. Lett.*, **9,** 09005 (13 pp). doi:10.1088/1748-9326/9/9/095005 *Environ. Res. Lett.* **9** (2014) 109602 (2 pp) doi:10.1088/1748-9326/9/10/109602

Keywords: East Europe, regional climatic change, regional changes in atmospheric circulation, Belarus

©2019. Japan Geoscience Union. All Right Reserved.

Assessment of climatic and environmental conditions along the track of projected Kyzyl-Kuragino railway line (the Western Sayan Mountains)

*Aleksandra Alekseevna Mikheeva[1], Margarita Syromyatina[1], Yurii Kurochkin[1]

1. Institute of Earth Sciences, Saint Petersburg State University, Russia

Currently there is a large investment project of the Kyzyl-Kuragino railway line construction mostly along the mountainous territory of Tuva and Krasnoyarsk Krai. The main relevance of the project is the possibility of more active involvement of the Tuva coal complex in commercial operation, which means economic development of the region. At the same time it is planned also to extend the road to Mongolia with the prospect to reach China thereby take into account international interests.

Despite the positive economic and social effects there are significant difficulties in the realization of the project due to the natural and climatic conditions. The projected railway track is mostly located in the Western Sayan Mountains and is characterized by complex environmental conditions, in particular geological and geomorphological, as well as extreme climatic characteristics, permafrost etc. The main goal of this research was to conduct an independent scientific expertise of assessment of the environmental conditions during the implementation of one the largest transport projects in Siberian region.

The natural conditions were assessed according to the following indicators: extreme values of air temperature and precipitation, strong winds, snow cover thickness, avalanche danger, seismicity and some slope processes. Analysis was made using various map documents, statistical data, results of expert interviews with the representatives of regional ministries of transport and ministries of economic development, universities and research institutes. For the analysis of extreme climatic characteristics data from weather stations of the study region were used. The entire area of projected road construction was divided into several sections, where it is necessary to take into account certain parameters mainly extreme natural phenomena. As a result the assessment of the potential natural risks during the construction and further operation of the railway was made.

Keywords: natural conditions, railway line construction, mountains, Tuva and Krasnoyarsk Krai

©2019. Japan Geoscience Union. All Right Reserved.

Assessment of interlinkages among industrialization, climate change, and forest fire activity: Thematic study of the Republic of Sakha (Yakutia), Russia

*Kiunnei Kirillina[1], Wanglin Yan[1]

1. Graduate School of Media and Governance, Keio University SFC

Forest fires play a critical role in shaping the ecosystem and atmospheric patterns. In turn, fire regimes are highly influenced by climate and human activities. Natural cycles, human activities like land-use changes and fire exclusion, and human-caused climate change can also influence the likelihood of fires. This study aimed to identify the causes underlying the increase of fire activity in one of the most fire-hazardous regions of Russia, the Republic of Sakha (Yakutia). The forest in this republic is performing the important function of permafrost protection. Deforestation might cause a catastrophic permafrost degradation, as the decrease of forests there mainly occurs due to fires.

To understand the patterns of historical fire activity, we analyzed the past history of fire events in the Sakha Republic through a newly developed approach for historical fire regimes characterization. Then, to identify the exact cause of intensification of fire activity was constructed an analytical approach for the assessment of interlinkages among industrialization, climate change, and forest fire activity. The study found that the main contributor to the increased historical fire activity in the republic was climate warming documented there since the 1960s, especially in spring season, which affected the overall duration of the fire season. As one main cause of recent expansion of fires, this research identified as significant the socioeconomic and land use changes undergone on the territory of the republic since the 2000s, which have resulted in extensive use of forest and forested land, and increased number of anthropogenic fires and related atmospheric changes.

Keywords: forest fires and climate change, land use changes, anthropogenic fires, GHG emissions

©2019. Japan Geoscience Union. All Right Reserved.

Quantitative Evaluation of Winter Daily Precipitation over Northern Japan

*Minami Masuda[1], Akiyo Yatagai[1], Toshiyuki Nakaegawa[2], Kenji Kamiguchi[3]

1. Graduate School of Science and Technology, Hirosaki University, 2. Meteorological Research Institute/Japan Meteorological Agency, 3. Japan Meteorological Agency

Snowfall is an important parameter for water resources. An accurate, quantitative evaluation is needed to clarify the impact of global warming on snowfall and vice versa. For that evaluation, a gridded precipitation data set based on rain-gauges is suitable, because rain-gauges measure precipitation directly. However, rain-gauge data include systematic biases due to interpolation and observation biases. For example, the long-term average, daily gridded precipitation data from APHRO_JP (P) underestimates by 30% the sum of evapotranspiration (E) and inflow (R) from dam catchments located in Northern Japan. We know this because if APHRO_JP was accurate, P should be equal to $R+E$ and it is not. It was reported that the annual mean precipitation of Japan was well simulated in the non-hydrostatic regional climate model (NHRCM, spatial resolutions 5 km/2 km) produced by the Meteorological Research Institute (MRI). From the above, we validated the interpolation bias of APHRO_JP using precipitation from the NHRCM to quantitatively evaluate winter precipitation over Northern Japan. The bias in the water balance from the dam catchments was reduced to 1% after adjusting for three systematic biases.

First, we validated and adjusted the interpolation bias. We created daily precipitation gridded data based on the distribution of the Automated Meteorological Data Acquisition System (AMeDAS) using hourly precipitation from the NHRCM (spatial distribution 2 km) and we compared it with precipitation from the NHRCM. We found that precipitation from the Mesh precipitation climatology which is used in APHRO_JP underestimated precipitation over mountain areas where rain-gauges were not set up. Because of this, APHRO_JP underestimated winter precipitation over mountain areas by approximately 3 mm/day. This daily precipitation bias over mountain areas was halved when we used climatology based on precipitation from the NHRCM instead of Mesh precipitation climatology.

Even with this adjustment, precipitation over mountain areas was still underestimated. This stemmed from the interpolation method used to predict rainfall, because the climatology indicate that the ratio of precipitation increases seasonally with elevation over mountain areas. This underestimation was controlled by an adjustment to the interpolation bias from the precipitation pattern detected by an Empirical Orthogonal Function (EOF) analysis.

On the basis of these validation results, we created daily precipitation gridded data based on the AMeDAS rain-gauge. We then applied the three adjustments from the climatology, precipitation pattern and precipitation undercatch and evaluated their contribution. We found that the annual precipitation over Japan was 2054 mm/year, which was an 18% increase on APHRO_JP. Furthermore, at the four dam catchments in Northern Japan, this adjusted precipitation explained 99% of the precipitation estimated by inflow from the dam catchments and evapotranspiration.

Finally, we measured the contribution of the systematic bias in winter precipitation in Northern Japan (138.5–141˚E, 36.8–38.8˚N). Precipitation was increased 11% by changing the climatology and increased 12% by adjusting for precipitation undercatch. The impact of the precipitation pattern adjustment was small. For extreme events, the adjustment effect was different. On average, in the four dam catchments,

©2019. Japan Geoscience Union. All Right Reserved.

precipitation was increased 18% by the change of climatology 7% by adjustment for precipitation undercatch. However, these ratios were different at each dam, and in dams where the catchments were in high mountain regions, there was a much greater effect from a change in the climatology. Because there are few rain-gauges in high mountain regions, it important to change climatology used in APHRO_JP. Furthermore, our results indicate uncertainty in precipitation from internal variability when the precipitation pattern adjustment was not used. Our application of these adjustments to APHRO_JP reduced systematic bias and improved precipitation measurements.

Keywords: APHRO_JP, winter precipitation, water resource

©2019. Japan Geoscience Union. All Right Reserved.

Seasonal variation of wetland carbon dioxide and methane fluxes measured by automatic chambers at the Bakchar bog, West Siberia

*Shamil Maksyutov[1], Alexandre Fofonov[2], Denis Davydov[2], Oleg Krasnov[2], Tadanobu Nakayama[1], Mikhail Glagolev[3]

1. National Institute for Environmental Studies, 2. V.E. Zuev Institute of Atmospheric Optics, 3. M.V. Lomonosov Moscow State University

Wetland CO_2 and CH_4 fluxes were observed at the Bakchar bog (N56˚, E82˚), West Siberia. Measurements were performed by two solar powered automated systems, each consisting of NDIR Li-820 CO_2 analyzer, an SnO_2-based methane sensor, six static chambers installed along transects, the air drying and distribution unit, and a datalogger. Observations were made during the May to October period in 2014 to 2017 at two types of open wetlands: mesotrophic open bog and patterned wetland with forested ridges, flat hollows and water pool. Each chamber is automatically opened and closed with pneumatic actuator. Water level is measured in the wetland and surrounding forest locations. Net uptake of CO_2 is observed from the beginning of June through the end of August with a maximum from mid-June through the end of July. Seasonal pattern of methane fluxes showed that CH_4 emission increases at the beginning of June, then weakens gradually in autumn. Seasonal variation of the emissions correlates well with the soil temperature at 5-10 cm depth. Carbon dioxide and methane fluxes correlate spatially; higher methane emissions are observed at wet mesotrophic locations with higher photosynthesis/respiration rates. Lower CH_4 emissions were observed on oligotrophic patterned wetland.

Keywords: methane emissions, wetland, Siberia, CO2 fluxes

©2019. Japan Geoscience Union. All Right Reserved.

Climatic distances between origin and labor locations for migrants in a changing climate in Siberia by the end of the 21st century

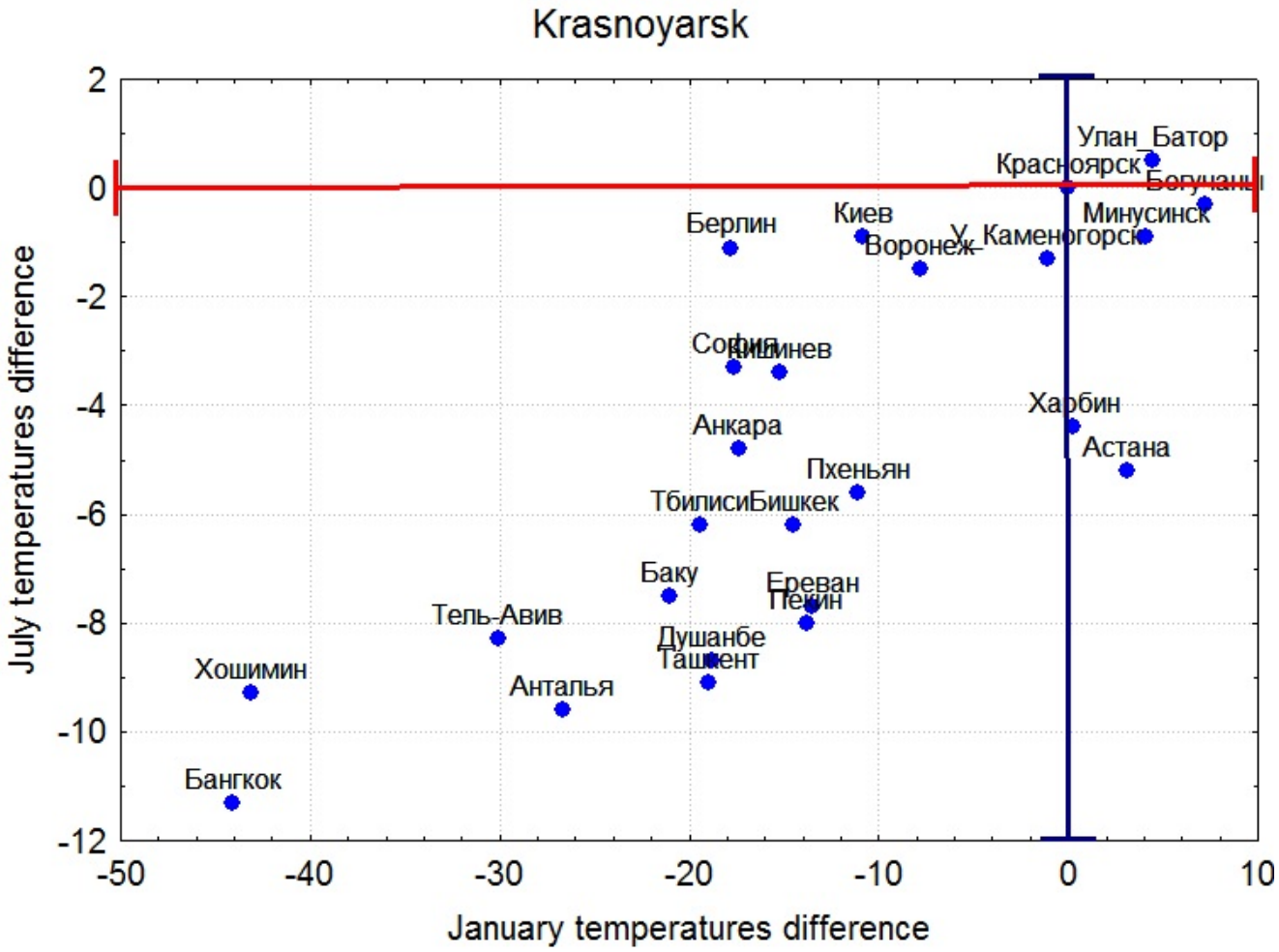
*Elena I. Parfenova[1], Nadezhda M. Tchebakova[1]

1. V.N.Sukachev Institute of Forest SB RAS, FRC SB RAS

The goals of our work were to evaluate climatic distances between climates from which potential migrants originate and climates of various regions over Siberia for which they migrate; and evaluate Siberian regions from view points of comfort-discomfort for migrants in current and future climates by the end of the century. We have completed this research from the example of the Krasnoyarsk Territory that is located in the center of Siberia and stretches from the south to north at a distance 2,000 km. Statistics on migrations show that migrants arrive to the Krasnoyarsk Territory from the European Russia and far abroad: Northern Korea, China, Vietnam. We studied four large industrial regions of the Territory for labor migrations. We used two climate variables that reflect winter and summer conditions: mean January and July temperatures. In total, 30 cities were ordinated in the axes of the differences in these temperatures between migrants' origins and migration locations. To characterize the future climates by the end of the century we used January and July temperature departure means from the ensemble of twenty general circulation models from the CMIP5. Two scenarios were used to characterize the range of climate change: a mild RCP 2.6 and a sharp RCP 8.5 climate scenarios. In total, 12 portraits of potential labor migrations were outlined in current and future climates. The "null" point in each portrait showed conditions for the natives of a particular region and the distance from the null to a country of origin showed physiological and psychological discrepancy that migrants should overcome to live in new climate.

Keywords: migration, climate change, transfer function, Siberia, January and July temperatures

©2019. Japan Geoscience Union. All Right Reserved.



©2019. Japan Geoscience Union. All Right Reserved.

[E] Poster | M (Multidisciplinary and Interdisciplinary)：M-GI General Geosciences, Information Geosciences & Simulations

Sun. May 26, 2019 1:45 PM - 3:15 PM JST | Sun. May 26, 2019 4:45 AM - 6:15 AM UTC | Poster Hall International Exhibition Hall8, Makuhari Messe_7

[M-GI31] Open Science in Action: Research Data Sharing, Infrastructure, Transparency, and International Cooperation

convener:Yasuhiro Murayama(Strategic Program Produce Office, National Institute of Information and Communications Technology), Yasuhisa Kondo(Research Institute for Humanity and Nature), Shelley Stall(American Geophysical Union), Baptiste Cecconi(LESIA, Observatoire de Paris, CNRS, PSL Research University)

Open Science is growing up as a new research paradigm to accelerate scientific innovation. Deployed by ICSU-WDS (2008), G8 Open Data Charter (2013), deployment of Research Data Alliance (2013), OECD Global Science Forum's research projects (2016), and G7 Science Ministers' Communique (2017), it commonly refers to the top-down policies to make results of publicly-funded research freely available and accessible. On the other hand, this term also refers to the participatory bottom-up approaches such as citizen science, crowdfunding, and transdisciplinary research (Kitamoto 2016). It is noted that both approaches envision the transformation of research process to more findable, accessible, interoperable, and reusable one (Wilkinson et al. 2016).
After the JpGU-AGU Great Debate "Role of open data and open science in Geoscience" in JpGU Annual Meeting 2018 and a follow-up session in the AGU Fall Meeting 2018, this session reviews the current broad spectrum of Open Science in an international context. The session welcomes a wide range of papers and posters covering (but not limited to) open research data, open source licenses, data papers and journals, data repository, data sharing infrastructures and platforms, citizen science, crowdsourcing, crowdfunding, transdisciplinary research, capacity building, international networking, and deployment in earth and planetary sciences.

[MGI31-P01] Open Science, Community Science, and AGU’s Thriving Earth Exchange.

*Shelley Stall[1], Raj Pandya[1] (1.American Geophysical Union)

[MGI31-P02] RDUF (Research Data Utilization Forum): an arena for community discussion of international and regional research data sharing and management

Hideaki Takeda[2], *Yasuhiro Murayama[1], RDUF secretary office[3] (1.Strategic Program Produce Office, National Institute of Information and Communications Technology, 2.National Institute of Informatics, 3.Japan Science and Technology Agency)

[MGI31-P03] Query string-controlled web service for sharable and reproducible data visualization of earth, planetary and space sciences

*Koji Imai[1], Yasuhiro Murayama[1] (1.National Institute of Information and Communications Technology)

[MGI31-P04] Development of ground pipeline system for high-level scientific data products of the Hisaki satellite mission and its application to planetary space weather

*Tomoki Kimura[1], Atsushi Yamazaki[2], Kazuo Yoshioka[3], Go Murakami[2], Fuminori Tsuchiya[4], Hajime Kita[2], Chihiro Tao[5], Ichiro Yoshikawa[3], Atsushi Kumamoto[6], Yamauchi Chisato[7] (1.Frontier Research Institute for Interdisciplinary Sciences, Tohoku University, 2.Institute of Space and Astronautical Science, Japan Aerospace Exploration Agency, 3.Department of Complexity Science and Engineering, University of Tokyo, 4.Planetary Plasma and Atmospheric Research Center, Tohoku University, 5.National Institute of Information and Communications Technology, 6.Space and Terrestrial Plasma Physics Laboratory, Tohoku University, 7.Misato Observatory)

[MGI31-P05] Recent activities of the IUGONET for accelerating the integrated solar terrestrial science

*Shuji Abe[1], Yoshimasa Tanaka[2], Norio Umemura[3], Atsuki Shinbori[3], Satoru UeNo[4], Masahito Nose[3] (1.International Center for Space Weather Science and Education, Japan, 2.National Institute of Polar

Research, 3.Institute for Space-Earth Environmental Research, Nagoya University, 4.Kwasan & Hida Observatories, School of Science, Kyoto University)

[MGI31-P06] Attempt for Research Data Sharing and Citation in context of Open Science - Sharing Atmospheric MF Radar Observation Database as a Case Study

*Isoda Fusako[1], Yasuhiro Murayama[1], Koji Imai[1] (1.National Institute of Information and Communications Technology)

[MGI31-P07] A case example of sharing meteor radio observational data by small laboratory

*Yukinobu Koyama[1], Yusuke Miyanari[1] (1.National Institute of Technology, Oita College)

[MGI31-P08] Promotion of an Open-Science Activity of the Earth Science - Coordinated Observations and Data Analyses of meteor-associated Low-Frequency Radio Emission and Anomalous Hearing

*Takashi Watanabe[1] (1.ISC World Data System International Programme Office)

[MGI31-P09] Current status of minting DOIs for research data in JAMSTEC

*Kazuyo Fukuda[1], Hajime Kawakami[1], Tomoki Sasaki[1], Hiroki Horikawa[1], Hideaki Saito[1], Chizuru Saito[1], Sonoda Akira[1] (1.Japan Agency for Marine-Earth Science and Technology)

[MGI31-P10] Application of Web and GIS Technology to Develop Military's Differential Action Information Platform

*Chien Hao Chang[1], Ch Yu Liu[1], Chun Ta Wei[1] (1.Department of Computer Science and Information Engineering,CCIT)

Open Science, Community Science, and AGU’s Thriving Earth Exchange.

*Shelley Stall[1], Raj Pandya[1]

1. American Geophysical Union

Climate change, environmental degradation, and increased vulnerability to natural hazards place humanity, and the planet, in a precarious position. Science is necessary, but not sufficient, to addresses these challenges and chart a course to a sustainable future. Traditional models of scientific research need be augmented with new models of engagement and application that are more open, more transparent, and better connect scientific evidence, data, and ways of thinking to civic action.

One such model of engagement is community science, in which scientist and community leaders design and carry out scientific activities to advance community priorities. Thriving Earth Exchange, a five-year old program of the AGU, contributes to open science by advancing Community Science. Thriving Earth Exchange has launched over 90 community science projects all over the United States and world. Projects include working with community leaders to improve the carbon inventories so that cities can identify and mitigate emissions by sector or region and working with neighborhood residents to design rain gardens that prevent local flooding and sequester carbon. AGU is seeking to expand Thriving Earth Exchange internationally and advance the practice of community science around the world.

Drawing on experience in Thriving Earth Exchange, this poster will document the practices of successful community science projects. Successful projects involve partnership and shared decision making at every stage of the scientific process—from defining scientific questions, to deciding how and what data to collect, to applying new understanding to local issues. The most successful projects put scientific knowledge in a larger context and offer science with awareness of and respect for local decision processes. Community science, therefor, appreciates other ways of knowing and deciding, and never insists on the superiority of scientific perspectives. Finally, successful community science projects advance equity by providing a way for communities—especially communities who have been historically neglected, marginalized or oppressed—to help guide and use science to advance their priorities.
This poster will offer also offer scientists tips for doing community science- tips gleaned from AGU’s experience with the Thriving Earth Exchange. These tips involve practicing humility, being willing to balance research and application, attending to equity and power, and respecting local and community knowledge. Community science also requires a willingness to work across disciplines, to get comfortable with messy problems, and to apply systems perspectives. Some of the things that scientists bring to this work, in addition to the deep expertise, are their ability to frame problems, their ability to find and access scientific knowledge and data, and the professional and personal networks that come with being part of privileged institutions.

Keywords: Community Science, Open Science

©2019. Japan Geoscience Union. All Right Reserved.

RDUF (Research Data Utilization Forum): an arena for community discussion of international and regional research data sharing and management

Hideaki Takeda[2], *Yasuhiro Murayama[1], RDUF secretary office[3]

1. Strategic Program Produce Office, National Institute of Information and Communications Technology, 2. National Institute of Informatics, 3. Japan Science and Technology Agency

Open Science and Research Data Sharing have been hot topics in international experts' discussions like in G8, OECD and AGU. Research Data Alliance (RDA) is the major arena for these topics and RDUF (Research Data Utilization Forum) has been set up inside Japan to make a local forum of Japanese experts and stakeholders. RDUF's individual membership is free of charge. We welcome your active participation in RDUF for research data discussions.

Keywords: research data management, open science

©2019. Japan Geoscience Union. All Right Reserved.

Query string-controlled web service for sharable and reproducible data visualization of earth, planetary and space sciences

*Koji Imai[1], Yasuhiro Murayama[1]

1. National Institute of Information and Communications Technology

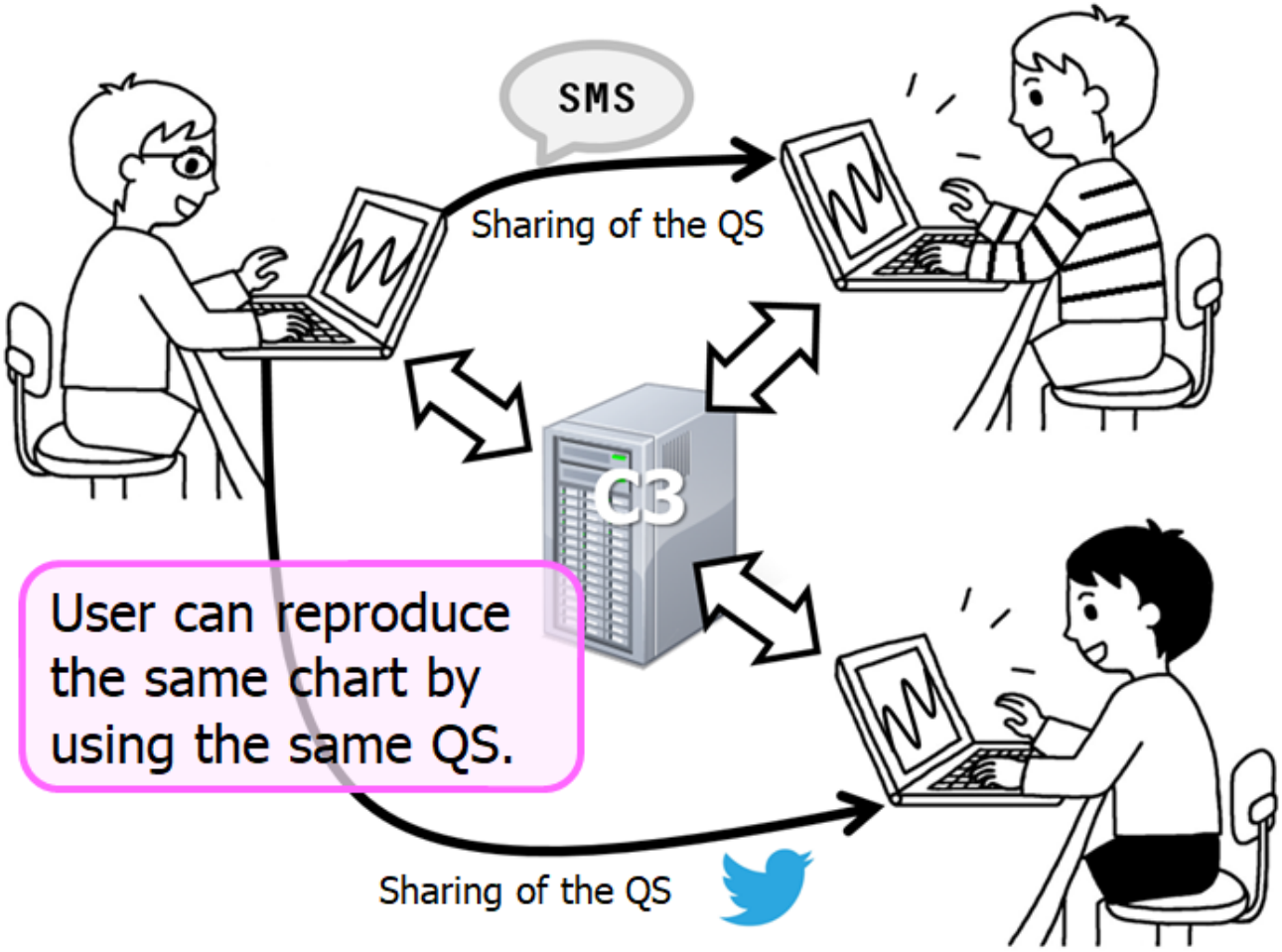
We propose a new method for sharable and reproducible data visualization on a web browser. Reproducibility is one of the foundations of the scientific method. Reproducible evidence is imperative to build new scientific knowledge. Most natural scientists use figures, graphs, plots or diagrams to understand a phenomenon in detail. Therefore, information and communication technology for reproducible charts needs to promote scientific development. However, it is not easy especially for studies dealing with scientific data of different fields, because each data set is usually stored in a different place and a different format. For this reason, we have been building a web service, Cross-Cutting Comparisons (C3; Imai et al., 2018; doi/10.20637/JAXA-RR-17-009/0001; https://www.darts.isas.jaxa.jp/C3/).
One of the features of C3 is the interactive interface. By the inductive entry form, it is easy to make flexible charts of earth, planetary and space sciences on a web browser. C3 also has a query string (QS)-controllable system which includes information of data handling procedures in the QS in an orderly manner as follow:

(URL of CGI program)?(header)+(data selection)+(data extraction)+(option).

The QS consists of four parts separated by plusses (+): header, data selection, data extraction, and option. The information of data set and figure type is described in the data selection part. The information of data extraction is in the data extraction part. By explicitly showing the inputted setting in an orderly manner in the URL, it is easy to understand how the charts are made. User can make the charts by directly enter the QS in an address bar and also share the QS with text-based communication tools.

Keywords: open science, data visualization, sharable, reproducible, web service, query string

©2019. Japan Geoscience Union. All Right Reserved.



©2019. Japan Geoscience Union. All Right Reserved.

Development of ground pipeline system for high-level scientific data products of the Hisaki satellite mission and its application to planetary space weather

*Tomoki Kimura[1], Atsushi Yamazaki[2], Kazuo Yoshioka[3], Go Murakami[2], Fuminori Tsuchiya[4], Hajime Kita[2], Chihiro Tao[5], Ichiro Yoshikawa[3], Atsushi Kumamoto[6], Yamauchi Chisato[7]

1. Frontier Research Institute for Interdisciplinary Sciences, Tohoku University, 2. Institute of Space and Astronautical Science, Japan Aerospace Exploration Agency, 3. Department of Complexity Science and Engineering, University of Tokyo, 4. Planetary Plasma and Atmospheric Research Center, Tohoku University, 5. National Institute of Information and Communications Technology, 6. Space and Terrestrial Plasma Physics Laboratory, Tohoku University, 7. Misato Observatory

The Hisaki satellite is the first-ever space telescope mission that is dedicated to planetary sciences. Atmospheres and magnetospheres of our solar system planets are continuously monitored by the extreme ultraviolet (EUV) spectrometer onboard Hisaki. Here we describe a data pipeline system developed for processing high-level scientific and ancillary data products of the Hisaki mission. The telemetry data downlinked from the satellite is stored in a ground telemetry database, processed to imaging spectral data with a 1-min temporal resolution and ancillary data products in the pipeline, and archived in a public database. The imaging spectra are further reduced to higher-level data products for practical scientific use. For example, light curves of the power emitted from Jupiter’ s aurora and plasma torus with a temporal resolution of 10 minutes are reduced from the imaging spectral data. The reduced light curve revealed transport process of energy and mass in Jupiter’ s magnetosphere and associated interplanetary solar wind conditions. The continuous monitoring with Hisaki largely contributes to understanding of space weather the planets in our solar system.

Keywords: Planetary Space Weather, Hisaki

©2019. Japan Geoscience Union. All Right Reserved.

Recent activities of the IUGONET for accelerating the integrated solar terrestrial science

*Shuji Abe[1], Yoshimasa Tanaka[2], Norio Umemura[3], Atsuki Shinbori[3], Satoru UeNo[4], Masahito Nose[3]

1. International Center for Space Weather Science and Education, Japan, 2. National Institute of Polar Research, 3. Institute for Space-Earth Environmental Research, Nagoya University, 4. Kwasan & Hida Observatories, School of Science, Kyoto University

The Inter-university Upper atmosphere Global Observation NETwork (IUGONET) is a scientific community by many Japanese institutes conducting observational research for upper atmosphere with 80km altitude and more. This region is a complex research field affected by both upper, for example solar radiations, and lower, for example atmospheric waves. Therefore, accelerating our science is not possible without data sharing infrastructures and platform for cross-sectional research. For the above reason, five Japanese institutes established IUGONET at 2009. IUGONET released many results for promoting the multidisciplinary research by using various kinds of data in the solar terrestrial science. IUGONET Type-A is a one-stop web service to provide data information (metadata) and visualization (quick look images and plots). Users can analysis data and make plots as you see on IUGONET Type-A by performing the indicated process on the analysis software, introduced below. UDAS (iUgonet Data Analysis Software) is a data analysis software written in Interactive Data Language (IDL). It works under SPEDAS (Space Physics Environment Data Analysis Software) as a plug-in. In addition, we developed program templates, called as UDAS egg (UDAS Easy Guide to Generate your load routines), for easily reading various kinds of data on SPEDAS. Users can easily load, analyze and visualize the data owned by each researcher by replacing a few codes (about 10 lines in total) marked on the template according to the instructions. This function is equipped to the latest version of the SPEDAS executables for users who do not own IDL licenses. It allows users to utilize data for interdisciplinary study, and supports the development of integrated solar terrestrial science. We also consider that it is one of our essential task for the future and development of the research field to develop both Japanese and foreign young researchers who can handle data easily. It is so difficult to accomplish it by only one project. Therefore, we holds many data analysis workshops each year in Japan and overseas countries in collaboration with other programs related to scientific research and data, for example ISELION, ISELLI, VarSITI, and WDS, etc. IUGONET developers join workshops and have lecture courses on these, and participants can practically learn how to get and analyze data. In last fiscal year, we held two times domestic lecture courses in Japan, and four international lecture courses in Malaysia, India, China, and Indonesia. The effects of this activity are very clear from the increase of scientific papers by using IUGONET products. In conclusion, Open Data activities of IUGONET mainly intend at the development of solar-terrestrial science, and make many scientific and educational results in our domain. We hope our activity will be helpful for other fields.

©2019. Japan Geoscience Union. All Right Reserved.

Attempt for Research Data Sharing and Citation in context of Open Science - Sharing Atmospheric MF Radar Observation Database as a Case Study

*Isoda Fusako[1], Yasuhiro Murayama[1], Koji Imai[1]

1. National Institute of Information and Communications Technology

Research Data Sharing is one element that constitutes Open Science. In recent discussion, it is said that scientists should share data that they collect and/or generate, to allow free and open access [1)].

Scientific data sharing are often carried out for responding to requests by funding agencies to open research data, for raising the transparency and fairness of research, for validation of research results, for increasing new research opportunities using shared data from multi-domains and interdisciplinary fields, and for increasing recognition of and rewarding achievement of scientists and experts of data management and publication [2)].

It is being promoted to cite research data like citing other articles in a research paper[3)]. When the data is cited, the DOI (Digital Object Identifier) is becoming to be used widely[4)]. Minting DOIs to a research paper or document is prevailing already. In the examples of data citations, the data is increasingly often cited with its DOI in the acknowledgement or the reference of a paper[5)]. It is expected that recognition of data creators, providers, curators, and managers will increase with help of data DOI through automatic surveillance of cited data DOIs on Internet [6)].

We are preparing sharing on a Web site of the neutral wind data observed with MF (Medium Frequency) radars at Wakkanai (45.36N, 141.81E) and Yamawaga (31.20N, 130.62E) of Japan. The 30 min. averaged data will be provided which is useful with increased confidence to analyze atmospheric dynamical phenomena (Original time interval of the observation are 3-4 min.). Currently FAIR data principle (Findable, Accessible, Interoperable and Re-usable) [7)] is being discussed to be a preferable condition for research data sharing. We are trying to increase FAIR-principle compliance level of the MF Radar data. Currently the data is: described in ASCII text format (difficult to lose readability if a human reads the data file), including the simple description in each data field in the file (although technical terms need to be improved since some are not very intelligible like "AVERAGED VELOCITY" "DATA COUNT” are to be , simpler HTML page having static URLs (dynamic data/web page generation can be a barrier for citability of online data objects). Minting the DOI is being planned.

In future, of open science activity, it is thought that research data sharing will become an important "building block" for researchers and stakeholders. This experiment in the present paper is a case study of simple data sharing, which is expected to lead to a case study for helping development of a research data sharing framework, our target is that what we will learn from this study will contribute to knowledge and techniques more universally adaptable to other data sharing practices in future.

Keywords: Research Data Sharing, Digital Object Identifier, Mesosphere and Lower Thermosphere

©2019. Japan Geoscience Union. All Right Reserved.

A case example of sharing meteor radio observational data by small laboratory

*Yukinobu Koyama[1], Yusuke Miyanari[1]

1. National Institute of Technology, Oita College

As a result of being ionized by the meteor, the ionospheric electrical conductivity increases so much as to reflect the 50MHz radio waves which penetrates the ionosphere usually. We have been observing it in Oita of Japan for two years. However, there is not much information on the ionosphere obtained from one observatory. How to share data with other groups become the key in order to construct multipoint observation network to investigate the ionosphere in detail. In this presentation, we show a case example of data sharing, aware of FAIR principles, by using Google Drive with Google Apps Scripts.

Keywords: Meteor radio observation, Data sharing, Metadata, Image processing, Deep learning

©2019. Japan Geoscience Union. All Right Reserved.

Promotion of an Open-Science Activity of the Earth Science - Coordinated Observations and Data Analyses of meteor-associated Low-Frequency Radio Emission and Anomalous Hearing

*Takashi Watanabe[1]

1. ISC World Data System International Programme Office

In the Open Science era, collaborations between researchers and citizens are strongly endorsed, but selection of a “good” project will be essential to involve many citizen scientists. Simultaneously audible “sounds” associated with the flight of very bright meteors (fireballs) have been reported by many people including citizens and researchers in many years, even in the modern science era. Keay (1980, 1992) proposed that the anomalous hearing is caused by the very strong radio emission from fireball at very low frequencies, mainly in the ELF/VLF region. Although the mechanism of the proposed strong radio emission is sensed as “sound” is unknown, the detection of very low-frequency radio noise from fireballs will be a challenging research objective in the field of earth science because many fireballs are observed in the lower ionosphere at the altitudes between 80 to 120 km. The first detection of the meteor-associated VLF radio emission was reported by Watanabe et al. (1988) for a -6 mag Perseid fireball appeared at about 03:53:41 (JST), 13 August 1981, as a burst-like VLF emission with peculiar spectral characteristics. Since the discovery, several papers on observations of meteor-associated VLF radio emission in the period of prominent meteoric showers but one-to-one connections with individual meteors were not made and distinction from ordinal spherices (e.g. radio pulses caused by lightning activity) were not clearly examined. We are planning to perform a research program between researchers and citizen scientists in Japan involving optical, radio, and Video observers for prominent meteoric showers. The Perseid appearing every year in the mid of August will be the best target because many observational groups of universities and high schools and Video observers will be involved to this project. We will collaborate with members of Japan Meteor Society to assemble and archive observational data. We will also to correct reports of anomalous hearing of meteoric sound from observes. This project will be organized by T. Watanabe (WDS-IPO, NICT), H. Oya (Chiba Univ.), K. Shiokawa (ISEE, Nagoya Univ.), Y. Kato (ISEE, Nagoya Univ.) and K. Suzuki (Nippon Meteor Sciety).

Keay C. S. L., Anomalous Sounds from the Entry of Meteor Fireballs, Science, Vol. 210, 11-15, 1980.

Watanabe T., Okada T. and Suzuki K., Meteors and Radio Waves, HAM Journal, No. 54, 109-115, 1988.

Keay, C. S. L., Asteroids, Comets, Meteors 1991, Lunar and Planetary Institute, Houston, 297 300, 1992

Keywords: Open Science, Meteoric Radio Emission, Meteoric Anomalous Hereing

©2019. Japan Geoscience Union. All Right Reserved.

Current status of minting DOIs for research data in JAMSTEC

*Kazuyo Fukuda[1], Hajime Kawakami[1], Tomoki Sasaki[1], Hiroki Horikawa[1], Hideaki Saito[1], Chizuru Saito[1], Sonoda Akira[1]

1. Japan Agency for Marine-Earth Science and Technology

Japan Agency for Marine-Earth Science and Technology (JAMSTEC) has collected information of several precedent examples to clarify effective data Digital Object Identifier (DOI) workflow since 2015, and started to assign DOI to an oceanographic research data in 2017. In JpGU2018, we introduced development of the Data DOI Management System to manage DOI metadata and generate landing pages. We will report the current status including following topics in this presentation.

- Functional enhancement for related database
The Data and Sample Research System for Whole Cruise Information (DARWIN) disseminates information of research cruise, dive, observation data and samples obtained by JAMSTEC's research vessels and submersibles. DARWIN has been enhanced to allow linkage of DOI metadata with the Data DOI Management System via Web API to achieve effective DOI maintenance for a large amount of content.

- Survey of DOI for research data
A wide variety of databases depending on the disciplines, research project, and types of data are disseminated by several departments and groups within JAMSTEC. Therefore, a survey of minting DOI for research data is being conducted to grasp data creators' needs. We extracted the target databases from catalog metadata published in JAMSTEC data catalog. The questions in this survey ask about ownership of data, conditions for data usage, granularity of DOI assignment, and continuity of database services.

The first edition of guidelines for minting DOIs for research data in JAMSTEC will be developed based on the practical operation of systems and the survey results by the end of the year 2019.

Related URLs
JAMSTEC Data DOI, http://www.jamstec.go.jp/datadoi/doi/10.17596/e/about.html
DARWIN, http://www.godac.jamstec.go.jp/darwin/e
JAMSTEC data catalog, http://www.godac.jamstec.go.jp/catalog/data_catalog/e/

Keywords: open science, open research data, DOI

©2019. Japan Geoscience Union. All Right Reserved.

Application of Web and GIS Technology to Develop Military's Differential Action Information Platform

*Chien Hao Chang[1], Ch Yu Liu[1], Chun Ta Wei[1]

1. Department of Computer Science and Information Engineering,CCIT

Taiwan is located in a special environment where geographical location and plate transfer, rainfall and earthquakes occur frequently, geological disasters are diverse and complex, and disaster prevention is an important issue that cannot be evaded by the whole people. In the face of such frequent natural disasters, the government’ s disaster prevention and relief work is particularly important.
On July 13, 1999, the Legislative Yuan officially read the "Disaster Prevention Act" [1] sub-amendment amendment, which not only allowed the Fire Department to transform into a disaster prevention and rescue department, but also assigned the national army to prevent disasters. Source of law. In keeping with the "disaster relief as a warfare" attitude, the National Army can, in response to each exercise and drill, be able to give full play to the rapid relief efforts of the national army in the golden rescue moment of major disasters, and avoid the national social disaster caused by environmental safety issues. The National Army has followed the policy guidance of "advance deployment, pre-set strength, and always-time rescue" for disaster relief, and is on standby to carry out disaster prevention and rescue missions such as preventive evacuation to protect the lives and property of the people.
To construct a multi-disaster information platform from the forward-looking command post to the users of the various levels of command posts at the back-end, to provide real-time information on the disaster relief center, to facilitate the disaster, and to control and issue orders through the information platform. For the officers and men, the mission is smooth and the delivery time is shortened. After the National Army has been refined, the number of people has been greatly reduced. In the future, in the implementation of disaster prevention, it is necessary to integrate and properly use the resources of the entire army to meet the needs of the people.

Keywords: disaster relief, military, information platform

©2019. Japan Geoscience Union. All Right Reserved.

[E] Poster | M (Multidisciplinary and Interdisciplinary)：M-GI General Geosciences, Information Geosciences & Simulations

Sun. May 26, 2019 5:15 PM - 6:30 PM JST | Sun. May 26, 2019 8:15 AM - 9:30 AM UTC | Poster Hall International Exhibition Hall8, Makuhari Messe_43

[M-GI31] Open Science in Action: Research Data Sharing, Infrastructure, Transparency, and International Cooperation

convener:Yasuhiro Murayama(Strategic Program Produce Office, National Institute of Information and Communications Technology), Yasuhisa Kondo(Research Institute for Humanity and Nature), Shelley Stall(American Geophysical Union), Baptiste Cecconi(LESIA, Observatoire de Paris, CNRS, PSL Research University)

Open Science is growing up as a new research paradigm to accelerate scientific innovation. Deployed by ICSU-WDS (2008), G8 Open Data Charter (2013), deployment of Research Data Alliance (2013), OECD Global Science Forum's research projects (2016), and G7 Science Ministers' Communique (2017), it commonly refers to the top-down policies to make results of publicly-funded research freely available and accessible. On the other hand, this term also refers to the participatory bottom-up approaches such as citizen science, crowdfunding, and transdisciplinary research (Kitamoto 2016). It is noted that both approaches envision the transformation of research process to more findable, accessible, interoperable, and reusable one (Wilkinson et al. 2016).
After the JpGU-AGU Great Debate "Role of open data and open science in Geoscience" in JpGU Annual Meeting 2018 and a follow-up session in the AGU Fall Meeting 2018, this session reviews the current broad spectrum of Open Science in an international context. The session welcomes a wide range of papers and posters covering (but not limited to) open research data, open source licenses, data papers and journals, data repository, data sharing infrastructures and platforms, citizen science, crowdsourcing, crowdfunding, transdisciplinary research, capacity building, international networking, and deployment in earth and planetary sciences.

[MGI31-P01] Open Science, Community Science, and AGU’s Thriving Earth Exchange.

*Shelley Stall[1], Raj Pandya[1] (1.American Geophysical Union)

[MGI31-P02] RDUF (Research Data Utilization Forum): an arena for community discussion of international and regional research data sharing and management

Hideaki Takeda[2], *Yasuhiro Murayama[1], RDUF secretary office[3] (1.Strategic Program Produce Office, National Institute of Information and Communications Technology, 2.National Institute of Informatics, 3.Japan Science and Technology Agency)

[MGI31-P03] Query string-controlled web service for sharable and reproducible data visualization of earth, planetary and space sciences

*Koji Imai[1], Yasuhiro Murayama[1] (1.National Institute of Information and Communications Technology)

[MGI31-P04] Development of ground pipeline system for high-level scientific data products of the Hisaki satellite mission and its application to planetary space weather

*Tomoki Kimura[1], Atsushi Yamazaki[2], Kazuo Yoshioka[3], Go Murakami[2], Fuminori Tsuchiya[4], Hajime Kita[2], Chihiro Tao[5], Ichiro Yoshikawa[3], Atsushi Kumamoto[6], Yamauchi Chisato[7] (1.Frontier Research Institute for Interdisciplinary Sciences, Tohoku University, 2.Institute of Space and Astronautical Science, Japan Aerospace Exploration Agency, 3.Department of Complexity Science and Engineering, University of Tokyo, 4.Planetary Plasma and Atmospheric Research Center, Tohoku University, 5.National Institute of Information and Communications Technology, 6.Space and Terrestrial Plasma Physics Laboratory, Tohoku University, 7.Misato Observatory)

[MGI31-P05] Recent activities of the IUGONET for accelerating the integrated solar terrestrial science

*Shuji Abe[1], Yoshimasa Tanaka[2], Norio Umemura[3], Atsuki Shinbori[3], Satoru UeNo[4], Masahito Nose[3] (1.International Center for Space Weather Science and Education, Japan, 2.National Institute of Polar

Research, 3.Institute for Space-Earth Environmental Research, Nagoya University, 4.Kwasan & Hida Observatories, School of Science, Kyoto University)

[MGI31-P06] Attempt for Research Data Sharing and Citation in context of Open Science - Sharing Atmospheric MF Radar Observation Database as a Case Study

*Isoda Fusako[1], Yasuhiro Murayama[1], Koji Imai[1] (1.National Institute of Information and Communications Technology)

[MGI31-P07] A case example of sharing meteor radio observational data by small laboratory

*Yukinobu Koyama[1], Yusuke Miyanari[1] (1.National Institute of Technology, Oita College)

[MGI31-P08] Promotion of an Open-Science Activity of the Earth Science - Coordinated Observations and Data Analyses of meteor-associated Low-Frequency Radio Emission and Anomalous Hearing

*Takashi Watanabe[1] (1.ISC World Data System International Programme Office)

[MGI31-P09] Current status of minting DOIs for research data in JAMSTEC

*Kazuyo Fukuda[1], Hajime Kawakami[1], Tomoki Sasaki[1], Hiroki Horikawa[1], Hideaki Saito[1], Chizuru Saito[1], Sonoda Akira[1] (1.Japan Agency for Marine-Earth Science and Technology)

[MGI31-P10] Application of Web and GIS Technology to Develop Military's Differential Action Information Platform

*Chien Hao Chang[1], Ch Yu Liu[1], Chun Ta Wei[1] (1.Department of Computer Science and Information Engineering,CCIT)

Open Science, Community Science, and AGU’s Thriving Earth Exchange.

*Shelley Stall[1], Raj Pandya[1]

1. American Geophysical Union

Climate change, environmental degradation, and increased vulnerability to natural hazards place humanity, and the planet, in a precarious position. Science is necessary, but not sufficient, to addresses these challenges and chart a course to a sustainable future. Traditional models of scientific research need be augmented with new models of engagement and application that are more open, more transparent, and better connect scientific evidence, data, and ways of thinking to civic action.

One such model of engagement is community science, in which scientist and community leaders design and carry out scientific activities to advance community priorities. Thriving Earth Exchange, a five-year old program of the AGU, contributes to open science by advancing Community Science. Thriving Earth Exchange has launched over 90 community science projects all over the United States and world. Projects include working with community leaders to improve the carbon inventories so that cities can identify and mitigate emissions by sector or region and working with neighborhood residents to design rain gardens that prevent local flooding and sequester carbon. AGU is seeking to expand Thriving Earth Exchange internationally and advance the practice of community science around the world.

Drawing on experience in Thriving Earth Exchange, this poster will document the practices of successful community science projects. Successful projects involve partnership and shared decision making at every stage of the scientific process—from defining scientific questions, to deciding how and what data to collect, to applying new understanding to local issues. The most successful projects put scientific knowledge in a larger context and offer science with awareness of and respect for local decision processes. Community science, therefor, appreciates other ways of knowing and deciding, and never insists on the superiority of scientific perspectives. Finally, successful community science projects advance equity by providing a way for communities—especially communities who have been historically neglected, marginalized or oppressed—to help guide and use science to advance their priorities.
This poster will offer also offer scientists tips for doing community science- tips gleaned from AGU’s experience with the Thriving Earth Exchange. These tips involve practicing humility, being willing to balance research and application, attending to equity and power, and respecting local and community knowledge. Community science also requires a willingness to work across disciplines, to get comfortable with messy problems, and to apply systems perspectives. Some of the things that scientists bring to this work, in addition to the deep expertise, are their ability to frame problems, their ability to find and access scientific knowledge and data, and the professional and personal networks that come with being part of privileged institutions.

Keywords: Community Science, Open Science

©2019. Japan Geoscience Union. All Right Reserved.

RDUF (Research Data Utilization Forum): an arena for community discussion of international and regional research data sharing and management

Hideaki Takeda[2], *Yasuhiro Murayama[1], RDUF secretary office[3]

1. Strategic Program Produce Office, National Institute of Information and Communications Technology, 2. National Institute of Informatics, 3. Japan Science and Technology Agency

Open Science and Research Data Sharing have been hot topics in international experts' discussions like in G8, OECD and AGU. Research Data Alliance (RDA) is the major arena for these topics and RDUF (Research Data Utilization Forum) has been set up inside Japan to make a local forum of Japanese experts and stakeholders. RDUF's individual membership is free of charge. We welcome your active participation in RDUF for research data discussions.

Keywords: research data management, open science

©2019. Japan Geoscience Union. All Right Reserved.

Query string-controlled web service for sharable and reproducible data visualization of earth, planetary and space sciences

*Koji Imai[1], Yasuhiro Murayama[1]

1. National Institute of Information and Communications Technology

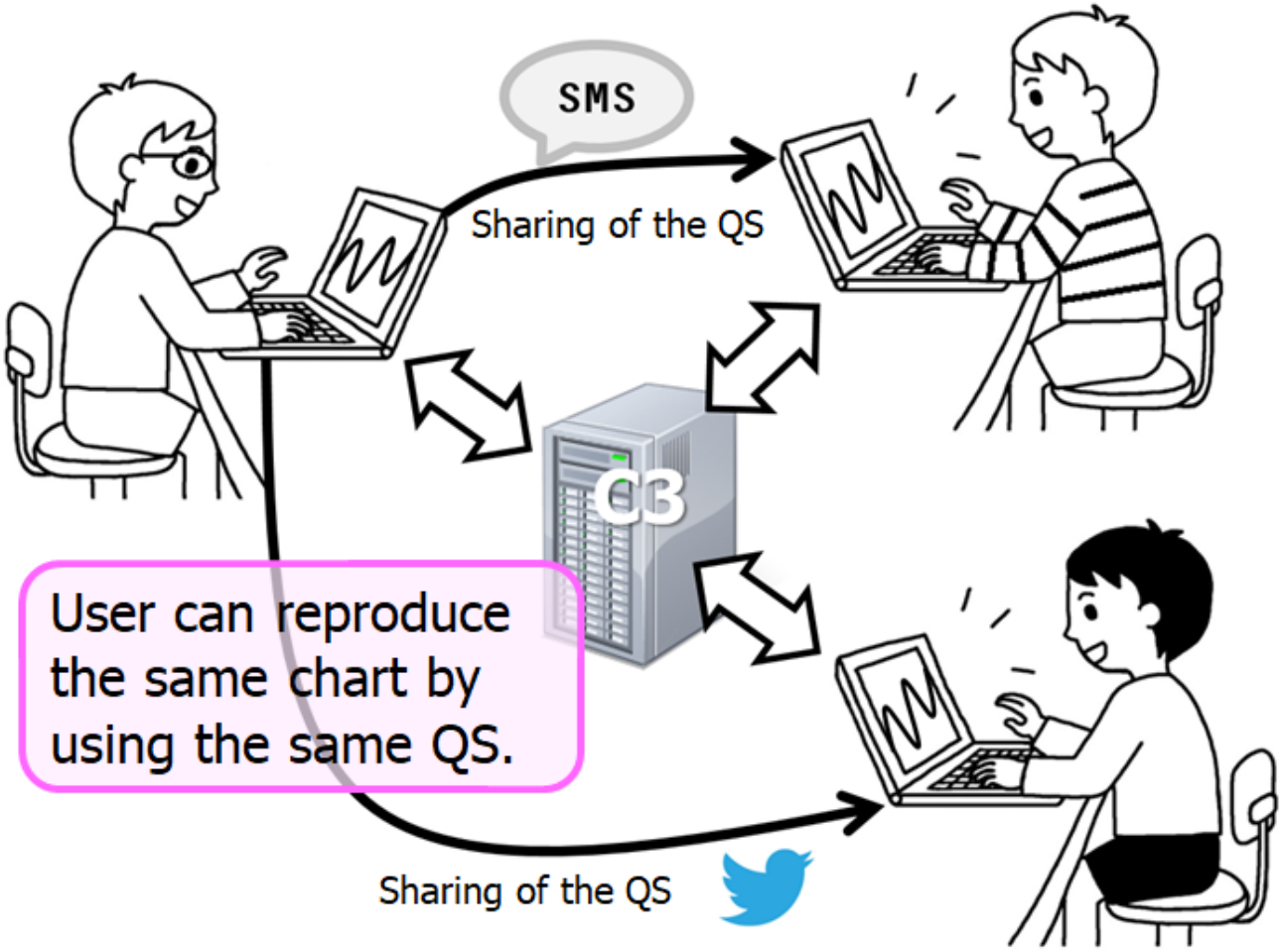
We propose a new method for sharable and reproducible data visualization on a web browser. Reproducibility is one of the foundations of the scientific method. Reproducible evidence is imperative to build new scientific knowledge. Most natural scientists use figures, graphs, plots or diagrams to understand a phenomenon in detail. Therefore, information and communication technology for reproducible charts needs to promote scientific development. However, it is not easy especially for studies dealing with scientific data of different fields, because each data set is usually stored in a different place and a different format. For this reason, we have been building a web service, Cross-Cutting Comparisons (C3; Imai et al., 2018; doi/10.20637/JAXA-RR-17-009/0001; https://www.darts.isas.jaxa.jp/C3/).
One of the features of C3 is the interactive interface. By the inductive entry form, it is easy to make flexible charts of earth, planetary and space sciences on a web browser. C3 also has a query string (QS)-controllable system which includes information of data handling procedures in the QS in an orderly manner as follow:

(URL of CGI program)?(header)+(data selection)+(data extraction)+(option).

The QS consists of four parts separated by plusses (+): header, data selection, data extraction, and option. The information of data set and figure type is described in the data selection part. The information of data extraction is in the data extraction part. By explicitly showing the inputted setting in an orderly manner in the URL, it is easy to understand how the charts are made. User can make the charts by directly enter the QS in an address bar and also share the QS with text-based communication tools.

Keywords: open science, data visualization, sharable, reproducible, web service, query string

©2019. Japan Geoscience Union. All Right Reserved.



©2019. Japan Geoscience Union. All Right Reserved.

Development of ground pipeline system for high-level scientific data products of the Hisaki satellite mission and its application to planetary space weather

*Tomoki Kimura[1], Atsushi Yamazaki[2], Kazuo Yoshioka[3], Go Murakami[2], Fuminori Tsuchiya[4], Hajime Kita[2], Chihiro Tao[5], Ichiro Yoshikawa[3], Atsushi Kumamoto[6], Yamauchi Chisato[7]

1. Frontier Research Institute for Interdisciplinary Sciences, Tohoku University, 2. Institute of Space and Astronautical Science, Japan Aerospace Exploration Agency, 3. Department of Complexity Science and Engineering, University of Tokyo, 4. Planetary Plasma and Atmospheric Research Center, Tohoku University, 5. National Institute of Information and Communications Technology, 6. Space and Terrestrial Plasma Physics Laboratory, Tohoku University, 7. Misato Observatory

The Hisaki satellite is the first-ever space telescope mission that is dedicated to planetary sciences. Atmospheres and magnetospheres of our solar system planets are continuously monitored by the extreme ultraviolet (EUV) spectrometer onboard Hisaki. Here we describe a data pipeline system developed for processing high-level scientific and ancillary data products of the Hisaki mission. The telemetry data downlinked from the satellite is stored in a ground telemetry database, processed to imaging spectral data with a 1-min temporal resolution and ancillary data products in the pipeline, and archived in a public database. The imaging spectra are further reduced to higher-level data products for practical scientific use. For example, light curves of the power emitted from Jupiter’ s aurora and plasma torus with a temporal resolution of 10 minutes are reduced from the imaging spectral data. The reduced light curve revealed transport process of energy and mass in Jupiter’ s magnetosphere and associated interplanetary solar wind conditions. The continuous monitoring with Hisaki largely contributes to understanding of space weather the planets in our solar system.

Keywords: Planetary Space Weather, Hisaki

©2019. Japan Geoscience Union. All Right Reserved.

Recent activities of the IUGONET for accelerating the integrated solar terrestrial science

*Shuji Abe[1], Yoshimasa Tanaka[2], Norio Umemura[3], Atsuki Shinbori[3], Satoru UeNo[4], Masahito Nose[3]

1. International Center for Space Weather Science and Education, Japan, 2. National Institute of Polar Research, 3. Institute for Space-Earth Environmental Research, Nagoya University, 4. Kwasan & Hida Observatories, School of Science, Kyoto University

The Inter-university Upper atmosphere Global Observation NETwork (IUGONET) is a scientific community by many Japanese institutes conducting observational research for upper atmosphere with 80km altitude and more. This region is a complex research field affected by both upper, for example solar radiations, and lower, for example atmospheric waves. Therefore, accelerating our science is not possible without data sharing infrastructures and platform for cross-sectional research. For the above reason, five Japanese institutes established IUGONET at 2009. IUGONET released many results for promoting the multidisciplinary research by using various kinds of data in the solar terrestrial science. IUGONET Type-A is a one-stop web service to provide data information (metadata) and visualization (quick look images and plots). Users can analysis data and make plots as you see on IUGONET Type-A by performing the indicated process on the analysis software, introduced below. UDAS (iUgonet Data Analysis Software) is a data analysis software written in Interactive Data Language (IDL). It works under SPEDAS (Space Physics Environment Data Analysis Software) as a plug-in. In addition, we developed program templates, called as UDAS egg (UDAS Easy Guide to Generate your load routines), for easily reading various kinds of data on SPEDAS. Users can easily load, analyze and visualize the data owned by each researcher by replacing a few codes (about 10 lines in total) marked on the template according to the instructions. This function is equipped to the latest version of the SPEDAS executables for users who do not own IDL licenses. It allows users to utilize data for interdisciplinary study, and supports the development of integrated solar terrestrial science. We also consider that it is one of our essential task for the future and development of the research field to develop both Japanese and foreign young researchers who can handle data easily. It is so difficult to accomplish it by only one project. Therefore, we holds many data analysis workshops each year in Japan and overseas countries in collaboration with other programs related to scientific research and data, for example ISELION, ISELLI, VarSITI, and WDS, etc. IUGONET developers join workshops and have lecture courses on these, and participants can practically learn how to get and analyze data. In last fiscal year, we held two times domestic lecture courses in Japan, and four international lecture courses in Malaysia, India, China, and Indonesia. The effects of this activity are very clear from the increase of scientific papers by using IUGONET products. In conclusion, Open Data activities of IUGONET mainly intend at the development of solar-terrestrial science, and make many scientific and educational results in our domain. We hope our activity will be helpful for other fields.

©2019. Japan Geoscience Union. All Right Reserved.

Attempt for Research Data Sharing and Citation in context of Open Science - Sharing Atmospheric MF Radar Observation Database as a Case Study

*Isoda Fusako[1], Yasuhiro Murayama[1], Koji Imai[1]

1. National Institute of Information and Communications Technology

Research Data Sharing is one element that constitutes Open Science. In recent discussion, it is said that scientists should share data that they collect and/or generate, to allow free and open access [1)].

Scientific data sharing are often carried out for responding to requests by funding agencies to open research data, for raising the transparency and fairness of research, for validation of research results, for increasing new research opportunities using shared data from multi-domains and interdisciplinary fields, and for increasing recognition of and rewarding achievement of scientists and experts of data management and publication [2)].

It is being promoted to cite research data like citing other articles in a research paper[3)]. When the data is cited, the DOI (Digital Object Identifier) is becoming to be used widely[4)]. Minting DOIs to a research paper or document is prevailing already. In the examples of data citations, the data is increasingly often cited with its DOI in the acknowledgement or the reference of a paper[5)]. It is expected that recognition of data creators, providers, curators, and managers will increase with help of data DOI through automatic surveillance of cited data DOIs on Internet [6)].

We are preparing sharing on a Web site of the neutral wind data observed with MF (Medium Frequency) radars at Wakkanai (45.36N, 141.81E) and Yamawaga (31.20N, 130.62E) of Japan. The 30 min. averaged data will be provided which is useful with increased confidence to analyze atmospheric dynamical phenomena (Original time interval of the observation are 3-4 min.). Currently FAIR data principle (Findable, Accessible, Interoperable and Re-usable) [7)] is being discussed to be a preferable condition for research data sharing. We are trying to increase FAIR-principle compliance level of the MF Radar data. Currently the data is: described in ASCII text format (difficult to lose readability if a human reads the data file), including the simple description in each data field in the file (although technical terms need to be improved since some are not very intelligible like "AVERAGED VELOCITY" "DATA COUNT" are to be , simpler HTML page having static URLs (dynamic data/web page generation can be a barrier for citability of online data objects). Minting the DOI is being planned.

In future, of open science activity, it is thought that research data sharing will become an important "building block" for researchers and stakeholders. This experiment in the present paper is a case study of simple data sharing, which is expected to lead to a case study for helping development of a research data sharing framework, our target is that what we will learn from this study will contribute to knowledge and techniques more universally adaptable to other data sharing practices in future.

Keywords: Research Data Sharing, Digital Object Identifier, Mesosphere and Lower Thermosphere

©2019. Japan Geoscience Union. All Right Reserved.

A case example of sharing meteor radio observational data by small laboratory

*Yukinobu Koyama[1], Yusuke Miyanari[1]

1. National Institute of Technology, Oita College

As a result of being ionized by the meteor, the ionospheric electrical conductivity increases so much as to reflect the 50MHz radio waves which penetrates the ionosphere usually. We have been observing it in Oita of Japan for two years. However, there is not much information on the ionosphere obtained from one observatory. How to share data with other groups become the key in order to construct multipoint observation network to investigate the ionosphere in detail. In this presentation, we show a case example of data sharing, aware of FAIR principles, by using Google Drive with Google Apps Scripts.

Keywords: Meteor radio observation, Data sharing, Metadata, Image processing, Deep learning

©2019. Japan Geoscience Union. All Right Reserved.

Promotion of an Open-Science Activity of the Earth Science - Coordinated Observations and Data Analyses of meteor-associated Low-Frequency Radio Emission and Anomalous Hearing

*Takashi Watanabe[1]

1. ISC World Data System International Programme Office

In the Open Science era, collaborations between researchers and citizens are strongly endorsed, but selection of a “good” project will be essential to involve many citizen scientists. Simultaneously audible “sounds” associated with the flight of very bright meteors (fireballs) have been reported by many people including citizens and researchers in many years, even in the modern science era. Keay (1980, 1992) proposed that the anomalous hearing is caused by the very strong radio emission from fireball at very low frequencies, mainly in the ELF/VLF region. Although the mechanism of the proposed strong radio emission is sensed as “sound” is unknown, the detection of very low-frequency radio noise from fireballs will be a challenging research objective in the field of earth science because many fireballs are observed in the lower ionosphere at the altitudes between 80 to 120 km. The first detection of the meteor-associated VLF radio emission was reported by Watanabe et al. (1988) for a -6 mag Perseid fireball appeared at about 03:53:41 (JST), 13 August 1981, as a burst-like VLF emission with peculiar spectral characteristics. Since the discovery, several papers on observations of meteor-associated VLF radio emission in the period of prominent meteoric showers but one-to-one connections with individual meteors were not made and distinction from ordinal spherices (e.g. radio pulses caused by lightning activity) were not clearly examined. We are planning to perform a research program between researchers and citizen scientists in Japan involving optical, radio, and Video observers for prominent meteoric showers. The Perseid appearing every year in the mid of August will be the best target because many observational groups of universities and high schools and Video observers will be involved to this project. We will collaborate with members of Japan Meteor Society to assemble and archive observational data. We will also to correct reports of anomalous hearing of meteoric sound from observes. This project will be organized by T. Watanabe (WDS-IPO, NICT), H. Oya (Chiba Univ.), K. Shiokawa (ISEE, Nagoya Univ.), Y. Kato (ISEE, Nagoya Univ.) and K. Suzuki (Nippon Meteor Sciety).

Keay C. S. L., Anomalous Sounds from the Entry of Meteor Fireballs, Science, Vol. 210, 11-15, 1980.

Watanabe T., Okada T. and Suzuki K., Meteors and Radio Waves, HAM Journal, No. 54, 109-115, 1988.

Keay, C. S. L., Asteroids, Comets, Meteors 1991, Lunar and Planetary Institute, Houston, 297 300, 1992

Keywords: Open Science, Meteoric Radio Emission, Meteoric Anomalous Hereing

©2019. Japan Geoscience Union. All Right Reserved.

Current status of minting DOIs for research data in JAMSTEC

*Kazuyo Fukuda[1], Hajime Kawakami[1], Tomoki Sasaki[1], Hiroki Horikawa[1], Hideaki Saito[1], Chizuru Saito[1], Sonoda Akira[1]

1. Japan Agency for Marine-Earth Science and Technology

Japan Agency for Marine-Earth Science and Technology (JAMSTEC) has collected information of several precedent examples to clarify effective data Digital Object Identifier (DOI) workflow since 2015, and started to assign DOI to an oceanographic research data in 2017. In JpGU2018, we introduced development of the Data DOI Management System to manage DOI metadata and generate landing pages. We will report the current status including following topics in this presentation.

- Functional enhancement for related database
The Data and Sample Research System for Whole Cruise Information (DARWIN) disseminates information of research cruise, dive, observation data and samples obtained by JAMSTEC's research vessels and submersibles. DARWIN has been enhanced to allow linkage of DOI metadata with the Data DOI Management System via Web API to achieve effective DOI maintenance for a large amount of content.

- Survey of DOI for research data
A wide variety of databases depending on the disciplines, research project, and types of data are disseminated by several departments and groups within JAMSTEC. Therefore, a survey of minting DOI for research data is being conducted to grasp data creators' needs. We extracted the target databases from catalog metadata published in JAMSTEC data catalog. The questions in this survey ask about ownership of data, conditions for data usage, granularity of DOI assignment, and continuity of database services.

The first edition of guidelines for minting DOIs for research data in JAMSTEC will be developed based on the practical operation of systems and the survey results by the end of the year 2019.

Related URLs
JAMSTEC Data DOI, http://www.jamstec.go.jp/datadoi/doi/10.17596/e/about.html
DARWIN, http://www.godac.jamstec.go.jp/darwin/e
JAMSTEC data catalog, http://www.godac.jamstec.go.jp/catalog/data_catalog/e/

Keywords: open science, open research data, DOI

©2019. Japan Geoscience Union. All Right Reserved.

Application of Web and GIS Technology to Develop Military's Differential Action Information Platform

*Chien Hao Chang[1], Ch Yu Liu[1], Chun Ta Wei[1]

1. Department of Computer Science and Information Engineering,CCIT

Taiwan is located in a special environment where geographical location and plate transfer, rainfall and earthquakes occur frequently, geological disasters are diverse and complex, and disaster prevention is an important issue that cannot be evaded by the whole people. In the face of such frequent natural disasters, the government’ s disaster prevention and relief work is particularly important.
On July 13, 1999, the Legislative Yuan officially read the "Disaster Prevention Act" [1] sub-amendment amendment, which not only allowed the Fire Department to transform into a disaster prevention and rescue department, but also assigned the national army to prevent disasters. Source of law. In keeping with the "disaster relief as a warfare" attitude, the National Army can, in response to each exercise and drill, be able to give full play to the rapid relief efforts of the national army in the golden rescue moment of major disasters, and avoid the national social disaster caused by environmental safety issues. The National Army has followed the policy guidance of "advance deployment, pre-set strength, and always-time rescue" for disaster relief, and is on standby to carry out disaster prevention and rescue missions such as preventive evacuation to protect the lives and property of the people.
To construct a multi-disaster information platform from the forward-looking command post to the users of the various levels of command posts at the back-end, to provide real-time information on the disaster relief center, to facilitate the disaster, and to control and issue orders through the information platform. For the officers and men, the mission is smooth and the delivery time is shortened. After the National Army has been refined, the number of people has been greatly reduced. In the future, in the implementation of disaster prevention, it is necessary to integrate and properly use the resources of the entire army to meet the needs of the people.

Keywords: disaster relief, military, information platform

©2019. Japan Geoscience Union. All Right Reserved.

[E] Poster | M (Multidisciplinary and Interdisciplinary)：M-SD Space Development & Earth Observation from Space

Sun. May 26, 2019 1:45 PM - 3:15 PM JST | Sun. May 26, 2019 4:45 AM - 6:15 AM UTC | Poster Hall International Exhibition Hall8, Makuhari Messe_8

[M-SD42] A new era of international space collaboration using microsatellites

convener:Junichi Kurihara(Graduate School of Science, Hokkaido University), Joel Joseph Jr Marciano(Advanced Science and Technology Institute, Department of Science and Technology, Philippines), Huy Xuan Le(Vietnam National Space Center)

Microsatellites have great potential as remote sensing platforms, because of the cost-effective implementation of satellite constellations, which increase their overall temporal resolution and ground coverage for Earth observation. However, it is difficult for one single university or institution to maintain a satellite constellation composed of many microsatellites. Recently, the Asian Microsatellite Consortium (AMC) comprising 16 space agencies and universities from nine Asian nations has been created to develop microsatellite technologies and use collected data relating to the environment and natural disasters, etc. This international framework is the first step to share remote sensing data from the microsatellites by the members of the consortium, instead of making a satellite constellation by a single owner. The microsatellites such as the DIWATA-2 (Philippines), MicroDragon (Vietnam), and RISESAT (Japan) developed by the AMC members will be launched in the last quarter of 2018. This session is a unique opportunity to discuss microsatellite development and utilization in terms of international collaboration and data sharing. This session welcomes presentations on microsatellite remote sensing including satellite development and operation, sensor development and calibration, data analysis and utilization. We also seek presentations on ground and information systems, international collaborations, and educational programs using microsatellites.

[MSD42-P01] A high spatial resolution multispectral remote sensing by the RISESAT microsatellite

*Junichi Kurihara[1], Toshinori Kuwahara[2], Shinya Fujita[2], Yuji Sakamoto[2], Yukihiro Takahashi[1] (1.Graduate School of Science, Hokkaido University, 2.Graduate School of Engineering)

[MSD42-P02] Initial check out and experiment plan of Very Small Optical Transmitter (VSOTA) on board a micro satellite RISESAT for Space-Ground Optical Communication

*Hiroo Kunimori[1], Hideki Takenaka[1], Toshinori Kuwahara[2], Yuji Sakamoto[2], Shinya Fujita[2], Hannah Tomio[2], MOROKOT SAKAL[2], Junichi Kurihara[3] (1.National Institute of Information and Communications Technology, 2.Tohoku Univ., 3.Hokkaido Univ.)

[MSD42-P03] Ten years history of Tohoku University ground station and operation system for micro and nano satellites

*Yuji Sakamoto[1], Toshinori Kuwahara[1], Shinya Fujita[1] (1.Tohoku University)

[MSD42-P04] Development of Thermal Infrared Sensor Camera on board LAPAN-A4 for Thunderstorm Cloud Observation

*Purwadi Purwadi[1,2], Yukihiro Takahashi[1], Junichi Kurihara[1], M. Arif Saifudin[3] (1.Department of Cosmosciences, Hokkaido University, Sapporo 0600810, Japan, 2.Agency for Assessment and Application of Technology (BPPT), Jakarta 10340, Indonesia, 3.Indonesian National Institute of Aeronautics and Space (LAPAN), Jawa Barat, 16310, Indonesia)

A high spatial resolution multispectral remote sensing by the RISESAT microsatellite

*Junichi Kurihara[1], Toshinori Kuwahara[2], Shinya Fujita[2], Yuji Sakamoto[2], Yukihiro Takahashi[1]

1. Graduate School of Science, Hokkaido University, 2. Graduate School of Engineering

Microsatellites for Earth observation have been developed jointly by Hokkaido and Tohoku Universities in Japan. The High-Precision Telescope (HPT), which is a high (3-5 m) spatial resolution multispectral sensor, was developed by Hokkaido University. The HPT has been installed on the RISING-2 (launched in 2014), DIWATA-1 (2016), and DIWATA-2 (2018) microsatellites developed mainly by Tohoku University. However, the HPT installed on the RISESAT microsatellite using the liquid crystal tunable filter (LCTF) technology for wavelength scanning in the visible (420–700 nm) and the near-infrared region (650–1050 nm) is the greatest in terms of number of spectral bands. The advantages offered by the LCTF technology are reductions in the size, weight, and power consumption of the sensor, the flexibility of the spectral bands and data volume, and compatibility with off-nadir pointing. The central wavelength of the spectral bands is electrically tunable for every image acquisition; hence, the data volume could be reduced by choosing appropriate spectral bands for specific purposes. This flexibility allows a single multispectral sensor on a nano/microsatellite to be applied to various remote sensing fields, making it comparable with hyperspectral sensors.

The RISESAT microsatellite was successfully launched by the Epsilon-4 launch vehicle on 18 January 2019 from Uchinoura Space Center, Kagoshima, Japan. The satellite was injected into a Sun-synchronous, low Earth orbit at about 500 km. In this paper, we present preliminary results of multispectral imaging by the HPT and review its performance evaluation. We also discuss the scientific collaboration with other microsatellites and the possible contribution to the Asian Microsatellite Consortium.

Keywords: Earth observation, microsatellite, multispectral sensor, remote sensing

©2019. Japan Geoscience Union. All Right Reserved.

Initial check out and experiment plan of Very Small Optical Transmitter (VSOTA) on board a micro satellite RISESAT for Space-Ground Optical Communication

*Hiroo Kunimori[1], Hideki Takenaka[1], Toshinori Kuwahara[2], Yuji Sakamoto[2], Shinya Fujita[2], Hannah Tomio[2], MOROKOT SAKAL[2], Junichi Kurihara[3]

1. National Institute of Information and Communications Technology, 2. Tohoku Univ., 3. Hokkaido Univ.

A 1 kg class optical transmitter on board a 50 kg class satellite Rapid International Scientific Experiment Satellite (RISESAT) launched by Epsilon rocket #4 in January 18, 2019. The transmitter named Very Small Optical Transmitter (VSOTA) has heritage from NICT space optical communication development over 2 decades and most recently the Small Optical Transponder (SOTA) equipped on board a micro satellite SOCRATES which NICT conducted demonstration from 2014 to 2016 between satellite and optical ground station in Japan and international partners.
VSOTA has 2 wavelengths laser diodes for optical downlink with no gimbal tracking function. The communication speed can be selected in the range from 10 kbps to a 6 Mbps. A retro reflector is located to assist satellite pointing and orbit prediction as well.
It is the most compact and lightweight optical communication device onboard for satellite developed in Japan so far. It narrowed down its function to the simplest form to adapt limited resource on satellite in size, weight and power consumption, aiming to expand its downlink capability for micro sat at the same time with lower cost. The goal of the mission is to acquire optical communication technology in micro satellites to apply an on-demand type remote sensing with featuring the high attitude control system such as target pointing needed as well for the optical communication to target ground station.
The orientation to the ground is based on satellite attitude control. It has a function of performing the guide beam for laser ranging from the ground using a camera for science such as High Precision Telescope (HPT) on board.
On January 21 and February 13, we confirmed that the electrical parts including Laser Diode (LD) was turned on and it operated normally by checking telemetry of power and temperature sensors built in LD circuit board.
We describe the features of communication and ranging experiment plan and initial check out result for the satellite as well as for the ground station.

Keywords: Micro satellite, Optical Space Communication, Satellite Laser Ranging

©2019. Japan Geoscience Union. All Right Reserved.

Ten years history of Tohoku University ground station and operation system for micro and nano satellites

*Yuji Sakamoto[1], Toshinori Kuwahara[1], Shinya Fujita[1]

1. Tohoku University

Tohoku University and collaboration companies have developed three satellites, DIWATA-2, RISESAT, and ALE-1, which were launched on Oct. 2018 and Jan. 2019. The ground station with 2.4-m diameter parabola dish and U/S/X band antennas is being managed in the university, and three satellites are now being operated every day. In this presentation, the hardware and software system included in this ground station are described, which were being maintained and extended since 2009. Also, ground station network with our collaboration universities and companies are introduced, which are located in Philippines, Sweden, Hakodate and Fukui.

Ground station in Tohoku University, called CRESST, was refurbished for our 1st satellite SPRITE-SAT in 2009. In these 10 years, the station used for total 6 microsatellites and 4 cubesats. Low earth orbit satellites are flying over the station for 9 to 12 minutes per opportunity, and the antennas and transceiver frequencies are controlled by calculating the satellite orbits. By only setting the target satellite names, the station is automatically woken up, controlled properly, and suspended again. Operations are not necessary to manage the antennas, and can concentrate on the communication with satellites.

Currently, more 3 satellites, DIWATA-1, RISING-2, and SPRITE-SAT are also tracked and communicated as well as latest 3 satellites. The satellites compatible to this station are registered as JCUBE-B group satellites in International Telecommunication Union. Several satellite are planned to use this station in a few years. The register to ITU will spend the time more than 1 year, and this can make a trouble in project schedule. A satellite can be completed in 1 to 1.5 years in short-term project, and radio license can be a matter. By using this station and compatible radio specifications, it will promote a new satellite project and expand the collaborative partners.

Keywords: microsatellite, satellite operation, ground station

©2019. Japan Geoscience Union. All Right Reserved.

Development of Thermal Infrared Sensor Camera on board LAPAN-A4 for Thunderstorm Cloud Observation

*Purwadi Purwadi[1,2], Yukihiro Takahashi[1], Junichi Kurihara[1], M. Arif Saifudin[3]

1. Department of Cosmosciences, Hokkaido University, Sapporo 0600810, Japan, 2. Agency for Assessment and Application of Technology (BPPT), Jakarta 10340, Indonesia, 3. Indonesian National Institute of Aeronautics and Space (LAPAN), Jawa Barat, 16310, Indonesia

Thunderstorm cloud, which growth vertically, has potential disaster risk like heavy rainfall, hail, micro-burst, and lightning. Cloud top altitude, volume, and growth speeds of thunderstorm cloud could be the parameter to predict its potential hazard. In this session, we will show our methodology to observe thunderstorm cloud using thermal infrared sensors camera which will be installed in the LAPAN-A4. This micro-satellite will be launched in 2020 FSY in the altitude ~ 500 kilometer with sun-synchronous polar orbit and inclination 97°. So, thermal infrared sensor camera will provide a temperature distribution with a resolution of ~ 180 meters and a field of view of ~ 56.3 x 42.2 kilometers. Using this high resolution thermal infrared sensor camera, the cloud top altitude can be estimated, assuming a temperature profile of the ambient atmosphere. By making such observation at some time interval, the developing speed of the thunderstorm cloud can be calculated in 3D.

Acknowledgement: This work was supported by Japan Society for the Promotion of Science (JSPS), Core-to-Core Program, B. Asia-Africa Science Platforms, by Japan Science and Technology Agency(JST) together with Technology and Higher Education(RISTEKDIKTI) of the of Indonesia under the e-ASIA Joint Research Program, and by Japan International Cooperation Agency (JICA) and JST, SATREPS.

Keywords: Thunderstorm cloud, thermal infrared sensor camera, LAPAN-A4

©2019. Japan Geoscience Union. All Right Reserved.

[E] Poster | M (Multidisciplinary and Interdisciplinary)：M-SD Space Development & Earth Observation from Space

Sun. May 26, 2019 5:15 PM - 6:30 PM JST | Sun. May 26, 2019 8:15 AM - 9:30 AM UTC | Poster Hall International Exhibition Hall8, Makuhari Messe_47

[M-SD42] A new era of international space collaboration using microsatellites

convener:Junichi Kurihara(Graduate School of Science, Hokkaido University), Joel Joseph Jr Marciano(Advanced Science and Technology Institute, Department of Science and Technology, Philippines), Huy Xuan Le(Vietnam National Space Center)

Microsatellites have great potential as remote sensing platforms, because of the cost-effective implementation of satellite constellations, which increase their overall temporal resolution and ground coverage for Earth observation. However, it is difficult for one single university or institution to maintain a satellite constellation composed of many microsatellites. Recently, the Asian Microsatellite Consortium (AMC) comprising 16 space agencies and universities from nine Asian nations has been created to develop microsatellite technologies and use collected data relating to the environment and natural disasters, etc. This international framework is the first step to share remote sensing data from the microsatellites by the members of the consortium, instead of making a satellite constellation by a single owner. The microsatellites such as the DIWATA-2 (Philippines), MicroDragon (Vietnam), and RISESAT (Japan) developed by the AMC members will be launched in the last quarter of 2018. This session is a unique opportunity to discuss microsatellite development and utilization in terms of international collaboration and data sharing. This session welcomes presentations on microsatellite remote sensing including satellite development and operation, sensor development and calibration, data analysis and utilization. We also seek presentations on ground and information systems, international collaborations, and educational programs using microsatellites.

[MSD42-P01] A high spatial resolution multispectral remote sensing by the RISESAT microsatellite

*Junichi Kurihara[1], Toshinori Kuwahara[2], Shinya Fujita[2], Yuji Sakamoto[2], Yukihiro Takahashi[1] (1.Graduate School of Science, Hokkaido University, 2.Graduate School of Engineering)

[MSD42-P02] Initial check out and experiment plan of Very Small Optical Transmitter (VSOTA) on board a micro satellite RISESAT for Space-Ground Optical Communication

*Hiroo Kunimori[1], Hideki Takenaka[1], Toshinori Kuwahara[2], Yuji Sakamoto[2], Shinya Fujita[2], Hannah Tomio[2], MOROKOT SAKAL[2], Junichi Kurihara[3] (1.National Institute of Information and Communications Technology, 2.Tohoku Univ., 3.Hokkaido Univ.)

[MSD42-P03] Ten years history of Tohoku University ground station and operation system for micro and nano satellites

*Yuji Sakamoto[1], Toshinori Kuwahara[1], Shinya Fujita[1] (1.Tohoku University)

[MSD42-P04] Development of Thermal Infrared Sensor Camera on board LAPAN-A4 for Thunderstorm Cloud Observation

*Purwadi Purwadi[1,2], Yukihiro Takahashi[1], Junichi Kurihara[1], M. Arif Saifudin[3] (1.Department of Cosmosciences, Hokkaido University, Sapporo 0600810, Japan, 2.Agency for Assessment and Application of Technology (BPPT), Jakarta 10340, Indonesia, 3.Indonesian National Institute of Aeronautics and Space (LAPAN), Jawa Barat, 16310, Indonesia)

A high spatial resolution multispectral remote sensing by the RISESAT microsatellite

*Junichi Kurihara[1], Toshinori Kuwahara[2], Shinya Fujita[2], Yuji Sakamoto[2], Yukihiro Takahashi[1]

1. Graduate School of Science, Hokkaido University, 2. Graduate School of Engineering

Microsatellites for Earth observation have been developed jointly by Hokkaido and Tohoku Universities in Japan. The High-Precision Telescope (HPT), which is a high (3-5 m) spatial resolution multispectral sensor, was developed by Hokkaido University. The HPT has been installed on the RISING-2 (launched in 2014), DIWATA-1 (2016), and DIWATA-2 (2018) microsatellites developed mainly by Tohoku University. However, the HPT installed on the RISESAT microsatellite using the liquid crystal tunable filter (LCTF) technology for wavelength scanning in the visible (420–700 nm) and the near-infrared region (650–1050 nm) is the greatest in terms of number of spectral bands. The advantages offered by the LCTF technology are reductions in the size, weight, and power consumption of the sensor, the flexibility of the spectral bands and data volume, and compatibility with off-nadir pointing. The central wavelength of the spectral bands is electrically tunable for every image acquisition; hence, the data volume could be reduced by choosing appropriate spectral bands for specific purposes. This flexibility allows a single multispectral sensor on a nano/microsatellite to be applied to various remote sensing fields, making it comparable with hyperspectral sensors.

The RISESAT microsatellite was successfully launched by the Epsilon-4 launch vehicle on 18 January 2019 from Uchinoura Space Center, Kagoshima, Japan. The satellite was injected into a Sun-synchronous, low Earth orbit at about 500 km. In this paper, we present preliminary results of multispectral imaging by the HPT and review its performance evaluation. We also discuss the scientific collaboration with other microsatellites and the possible contribution to the Asian Microsatellite Consortium.

Keywords: Earth observation, microsatellite, multispectral sensor, remote sensing

©2019. Japan Geoscience Union. All Right Reserved.

Initial check out and experiment plan of Very Small Optical Transmitter (VSOTA) on board a micro satellite RISESAT for Space-Ground Optical Communication

*Hiroo Kunimori[1], Hideki Takenaka[1], Toshinori Kuwahara[2], Yuji Sakamoto[2], Shinya Fujita[2], Hannah Tomio[2], MOROKOT SAKAL[2], Junichi Kurihara[3]

1. National Institute of Information and Communications Technology, 2. Tohoku Univ., 3. Hokkaido Univ.

A 1 kg class optical transmitter on board a 50 kg class satellite Rapid International Scientific Experiment Satellite (RISESAT) launched by Epsilon rocket #4 in January 18, 2019. The transmitter named Very Small Optical Transmitter (VSOTA) has heritage from NICT space optical communication development over 2 decades and most recently the Small Optical Transponder (SOTA) equipped on board a micro satellite SOCRATES which NICT conducted demonstration from 2014 to 2016 between satellite and optical ground station in Japan and international partners.
VSOTA has 2 wavelengths laser diodes for optical downlink with no gimbal tracking function. The communication speed can be selected in the range from 10 kbps to a 6 Mbps. A retro reflector is located to assist satellite pointing and orbit prediction as well.
It is the most compact and lightweight optical communication device onboard for satellite developed in Japan so far. It narrowed down its function to the simplest form to adapt limited resource on satellite in size, weight and power consumption, aiming to expand its downlink capability for micro sat at the same time with lower cost. The goal of the mission is to acquire optical communication technology in micro satellites to apply an on-demand type remote sensing with featuring the high attitude control system such as target pointing needed as well for the optical communication to target ground station.
The orientation to the ground is based on satellite attitude control. It has a function of performing the guide beam for laser ranging from the ground using a camera for science such as High Precision Telescope (HPT) on board.
On January 21 and February 13, we confirmed that the electrical parts including Laser Diode (LD) was turned on and it operated normally by checking telemetry of power and temperature sensors built in LD circuit board.
We describe the features of communication and ranging experiment plan and initial check out result for the satellite as well as for the ground station.

Keywords: Micro satellite, Optical Space Communication, Satellite Laser Ranging

©2019. Japan Geoscience Union. All Right Reserved.

Ten years history of Tohoku University ground station and operation system for micro and nano satellites

*Yuji Sakamoto[1], Toshinori Kuwahara[1], Shinya Fujita[1]

1. Tohoku University

Tohoku University and collaboration companies have developed three satellites, DIWATA-2, RISESAT, and ALE-1, which were launched on Oct. 2018 and Jan. 2019. The ground station with 2.4-m diameter parabola dish and U/S/X band antennas is being managed in the university, and three satellites are now being operated every day. In this presentation, the hardware and software system included in this ground station are described, which were being maintained and extended since 2009. Also, ground station network with our collaboration universities and companies are introduced, which are located in Philippines, Sweden, Hakodate and Fukui.

Ground station in Tohoku University, called CRESST, was refurbished for our 1st satellite SPRITE-SAT in 2009. In these 10 years, the station used for total 6 microsatellites and 4 cubesats. Low earth orbit satellites are flying over the station for 9 to 12 minutes per opportunity, and the antennas and transceiver frequencies are controlled by calculating the satellite orbits. By only setting the target satellite names, the station is automatically woken up, controlled properly, and suspended again. Operations are not necessary to manage the antennas, and can concentrate on the communication with satellites.

Currently, more 3 satellites, DIWATA-1, RISING-2, and SPRITE-SAT are also tracked and communicated as well as latest 3 satellites. The satellites compatible to this station are registered as JCUBE-B group satellites in International Telecommunication Union. Several satellite are planned to use this station in a few years. The register to ITU will spend the time more than 1 year, and this can make a trouble in project schedule. A satellite can be completed in 1 to 1.5 years in short-term project, and radio license can be a matter. By using this station and compatible radio specifications, it will promote a new satellite project and expand the collaborative partners.

Keywords: microsatellite, satellite operation, ground station

©2019. Japan Geoscience Union. All Right Reserved.

Development of Thermal Infrared Sensor Camera on board LAPAN-A4 for Thunderstorm Cloud Observation

*Purwadi Purwadi[1,2], Yukihiro Takahashi[1], Junichi Kurihara[1], M. Arif Saifudin[3]

1. Department of Cosmosciences, Hokkaido University, Sapporo 0600810, Japan, 2. Agency for Assessment and Application of Technology (BPPT), Jakarta 10340, Indonesia, 3. Indonesian National Institute of Aeronautics and Space (LAPAN), Jawa Barat, 16310, Indonesia

Thunderstorm cloud, which growth vertically, has potential disaster risk like heavy rainfall, hail, micro-burst, and lightning. Cloud top altitude, volume, and growth speeds of thunderstorm cloud could be the parameter to predict its potential hazard. In this session, we will show our methodology to observe thunderstorm cloud using thermal infrared sensors camera which will be installed in the LAPAN-A4. This micro-satellite will be launched in 2020 FSY in the altitude ~ 500 kilometer with sun-synchronous polar orbit and inclination 97°. So, thermal infrared sensor camera will provide a temperature distribution with a resolution of ~ 180 meters and a field of view of ~ 56.3 x 42.2 kilometers. Using this high resolution thermal infrared sensor camera, the cloud top altitude can be estimated, assuming a temperature profile of the ambient atmosphere. By making such observation at some time interval, the developing speed of the thunderstorm cloud can be calculated in 3D.

Acknowledgement: This work was supported by Japan Society for the Promotion of Science (JSPS), Core-to-Core Program, B. Asia-Africa Science Platforms, by Japan Science and Technology Agency(JST) together with Technology and Higher Education(RISTEKDIKTI) of the of Indonesia under the e-ASIA Joint Research Program, and by Japan International Cooperation Agency (JICA) and JST, SATREPS.

Keywords: Thunderstorm cloud, thermal infrared sensor camera, LAPAN-A4

©2019. Japan Geoscience Union. All Right Reserved.

[E] Poster | P (Space and Planetary Sciences)：P-PS Planetary Sciences

Mon. May 27, 2019 3:30 PM - 5:00 PM JST | Mon. May 27, 2019 6:30 AM - 8:00 AM UTC | Poster Hall International Exhibition Hall8, Makuhari Messe_1

[P-PS05] Recent advances of Venus science

convener:Takehiko Satoh(Institute of Space and Astronautical Science, Japan Aerospace Exploration Agency), Takeshi Horinouchi(Faculty of Environmental Earth Science, Hokkaido University), Masaru Yamamoto(Research Institute for Applied Mechanics, Kyushu University), Kevin McGouldrick(University of Colorado Boulder)

Akatsuki, being in Venus orbit since December 2015, has acquired a volume of high-quality data, unveiled many new phenomena and is allowing researchers to investigate the underlying mechanisms. As the data accumulate, numerical models and theories are being advanced as well. We are no doubt living in the new golden era of Venus studies. This session invites papers of the new scientific results with Akatsuki data and the latest results of theoretical and numerical works. We expect participants of this session share the latest research results through presentations and discussion.

[PPS05-P01] New thermal infrared camera for fine horizontal brightness temperature structures at the cloud-top level of Venus

*Tetsuya Fukuhara[1], Makoto Taguchi[1], Takeshi Imamura[2], Sanjay S Limaye[3] (1.Rikkyo University, 2.The University of Tokyo, 3.University of Wisconsin)

[PPS05-P02] Temperature and wind variations in Venusian mesosphere and lower thermosphere by mid-infrared heterodyne spectrometer in 2018

*Kosuke Takami[1], Hiromu Nakagawa[1], Hideo Sagawa[2], Isao Murata[1], Yasumasa Kasaba[1] (1.Graduate School of Science, Tohoku University, 2.Division of Science, Kyoto Sangyo University)

[PPS05-P03] Local time dependence of limb darkening seen in the thermal infrared Venus disk

*Masahiro Akiba[1] (1.Rikkyo University)

[PPS05-P04] Stationary wavy features and Banded structures at Venusian cloud top extracted by averaging multiple LIR images

*Kiichi Fukuya[1], Takeshi Imamura[1], Makoto Taguchi[2], Tetsuya Fukuhara[2], Toru Kouyama[3] (1.Univ. of Tokyo, 2.Rikkyo Univ., 3.AIST)

[PPS05-P05] Akatsuki's IR2 Nightside Photometry Restoration by Deconvolution

*Choon Wei Vun[1], Takehiko Satoh[2,1], Kevin McGouldrick[3], Takeshi Horinouchi[4], Takao M. Sato[5] (1.SOKENDAI, 2.ISAS/JAXA, 3.University of Colorado Boulder, 4.Hokkaido University, 5.Hokkaido Information University)

[PPS05-P06] Enormous cloud cover as seen by Akatsuki/IR2 on the night-side disk of Venus

*Takehiko Satoh[1,2], Choon Wei Vun[2], Takao M. Sato[3], Takeshi Horinouchi[4], George HASHIMOTO[5], Kevin McGouldrick[6] (1.Institute of Space and Astronautical Science, Japan Aerospace Exploration Agency, 2.Department of Space Science, SOKENDAI, 3.Department of Business and Information Systems, Hokkaido Information University, 4.Faculty of Environmental Earth Science, Hokkaido University, 5.Department of Earth Science, Okayama University, 6.LASP, University of Colorado Boulder)

[PPS05-P07] The global variation of Venus cloud obtained from IR1 camera onboard AKATSUKI

*Seiko Takagi[1], Naomoto Iwagami, Yukihiro Takahashi[1], Mitsuteru Sato[1] (1.Hokkaido University, Graduate School of Science)

[PPS05-P08] Development of a Venus' cloud formation scheme for a convection resolving model

*Ko-ichiro SUGIYAMA[1], Nozomu Fukuhara[1], Masatsugu Odaka[2], Kensuke Nakajima[3], Masaki Ishiwatari[2], Takeshi Imamura[4], Yoshi-Yuki Hayashi[5] (1.National Institute of Technology, Matsue College, 2.Department of Cosmoscience, Graduate School of Science, Hokkaido University, 3.Department of Earth and Planetary Sciences,Flculty of Sciences,Kyushu University, 4.Graduate School of Frontier Sciences, The University of Tokyo, 5.Department of Planetology, Graduate School of Science, Kobe University / Center for Planetary Science (CPS))

[PPS05-P09] Zonal mean structure of Venus atmosphere observed in a Venus general circulation model with explicit radiative transfer

★Invited Papers

*Yoshi-Yuki Hayashi[1], Chisato Shiojiri[1], Hiroki Kashimura[1], Yoshiyuki O. Takahashi[1] (1.Department of Planetology/CPS, Graduate School of Science, Kobe University)

[PPS05-P10] Gravity wave packets detected in radio occultation temperature profiles of the Venus atmosphere

*Ryota Mori[1], Takeshi Imamura[1], Javier Peralta[2] (1.The University of Tokyo, 2.Japan Aerospace Exploration Agency)

[PPS05-P11] **Status of lightning hunt in Venus with Akatsuki/LAC and Pirka telescope**

*Yukihiro Takahashi[1,2], Mitsuteru Sato[1,2], Masataka Imai[3], Ralph Lorenz[4], Seiko Takagi[1,2], Ono Tatsuharu[1] (1.Graduate School of Science, Hokkaido University, 2.Faculty of Science, Hokkaido University, 3.National Institute of Advanced Industrial Science and Technology,, 4.Applied Physics Laboratory, Johns Hopkins University)

[PPS05-P12] **Possibility of electric discharge in the Venusian atmosphere due to the super-rotation of clouds**

*Adhithiyan Neduncheran[1], Ugur Guven[1,2], Ananyo Bhattacharya[3] (1.University of Petroleum and Energy Studies, India, 2.United Nations Centre for Space Science and Technology Education in Asia and the Pacific, 3.Sardar Vallabhbhai National Institute of Technology,India)

New thermal infrared camera for fine horizontal brightness temperature structures at the cloud-top level of Venus

*Tetsuya Fukuhara[1], Makoto Taguchi[1], Takeshi Imamura[2], Sanjay S Limaye[3]

1. Rikkyo University, 2. The University of Tokyo, 3. University of Wisconsin

The Longwave Infrared Camera (LIR), which is an uncooled microbolometer camera, is currently acquiring thermal infrared images (8-12 μm) of Venus and depicting the cloud-top brightness temperatures from Akatsuki orbiter around Venus since December 2015. The outstanding result of LIR has been the discovery of an interhemispheric bow-shaped structure meridionally stretching 10,000 km across the equator at the Venus cloud-top. Over several days of observations, the bow-shaped structure remains relatively fixed in position above the highland on the slowly rotating surface, despite the background atmospheric super rotation at ~100 m/s. We infer that the bow-shaped structure is the result of an atmospheric gravity wave generated in the lower atmosphere by mountain topography that then propagated upwards [1]. This indicates that the horizontal temperature distribution seen at the cloud-top level represents not only direct physical property at the cloud-top but also influence of dynamics in the lower atmosphere. In fact, preliminary observation of LIR has detected fine structure (~100 km) in temperature distribution from close-up observations near the periapsis. We suggest that this may be caused by the upward propagation of a gravity wave, which is generated by the convection layer at ~40 km altitude. However, the spatial resolution of LIR seems insufficient to understand the origins of such a fine structure. We need better observations at higher spatial resolution than possible from LIR in Akatsuki's orbit.

We propose that a future Venus orbiter carries an updated version of the uncooled microbolometer camera (BOL) with 1024x768 pixels and angular resolution of ~0.01 deg/pixel to detect fine temperature structure on the cloud-tops. When the orbiter is typically injected to a high-inclined elliptical orbit with altitude of 500-50,000 km, BOL provides a spatial resolution of 8.5 km at apoapsis and 0.08 km at periapsis, respectively. It will be enough to observe the fine temperature structure at the cloud-top. Further, BOL will capture the fine temperature structure at polar region near the "eye" of the hemispheric vortex situated over the poles, where the horizontal temperature varies drastically near the Venus cloud-tops. VIRTIS instrument on Venus Express orbiter showed complex structures at near infrared wavelengths [2]. Akatsuki from its near equatorial elliptical orbit cannot observe the fine structure in polar regions.

During 2012-2014, we developed an uncooled micro-bolometer array (UMBA) camera for the 50 kg class Earth observing satellite based on the experience of LIR development [3]. The camera with the pixel size of 640 ×480 was launched in 2014 and successfully detect a small wildfire which was main observation target for the mission. The results showed that its performance was better than expected. Furthermore, the newest UMBA camera with the pixel size increased to 1024 ×768 has been developed for the next wildfire mission to take finer spatial resolution image with ~0.01 deg/pixel. Unfortunately, this camera has lost the launch opportunity. However, the flight-model has been assembled and has passed function tests. Since BOL does not need heavy cryogenic systems, its mass and size are less than ~1 kg and 100 mm x 100 mm x 120 mm, respectively; it would be a relatively small mass increment for the future Venus mission.

References

[1] Fukuhara, T., et al., 2017, Large stationary gravity wave in the atmosphere of Venus, Nature Geoscience, Vol. 10, 85–88.

©2019. Japan Geoscience Union. All Right Reserved.

[2] Garate-Lopez, I., et al., 2015, Atmospheric dynamics at the southern pole of Venus: Three-dimensional winds, temperature and vorticity, AGU Fall Meeting Abstracts, 23.
[3] Fukuhara, T., et al., 2017, Detection of small wildfire by thermal infrared camera with the uncooled microbolometer array for 50 kg class satellite, IEEE Transactions on Geoscience and Remote Sensing, 2017, Vol. 55, No. 8, 4314-4324

Keywords: Venus, atmosphere, Akatsuki

©2019. Japan Geoscience Union. All Right Reserved.

Temperature and wind variations in Venusian mesosphere and lower thermosphere by mid-infrared heterodyne spectrometer in 2018

*Kosuke Takami[1], Hiromu Nakagawa[1], Hideo Sagawa[2], Isao Murata[1], Yasumasa Kasaba[1]

1. Graduate School of Science, Tohoku University, 2. Division of Science, Kyoto Sangyo University

The most extensive observations of Venusian mesosphere have been performed by Venus Express (VEX) up to 2014 (e.g., Patzold et al., 2007; Mahieux et al., 2015). These observations have found the highly spatial and temporal variations in the thermal structure. The temperature discrepancies between observations by VEX/SOIR and general circulation models in the altitude of 80 - 100 km have not been properly interpreted (Bougher et al., 2015; Gilli et al., 2017). In addition, the mesospheric dynamics located between retrograde superrotational zonal wind (cloud deck) and subsolar-to-antisolar flow (above 120 km altitude) have not been well understood due to lack of observations. On the other hand, the lower thermosphere has been observed by mid-infrared heterodyne spectrometer (MIR-HS). Temperature in this region varied extensively between 140 K and 240 K, and wind velocity changed intensely from 130 m/s to 190 m/s for a terrestrial day (Sornig et al., 2013; Krause et al., 2018). Temperature and wind variations such as periodicity and locality in Venusian mesosphere and lower thermosphere have not been comprehended. The purpose of our observations is to solve it with continuous observations by MIR-HS.
Our Mid-Infrared Laser Heterodyne Instrument (MILAHI) have been inserted to Tohoku 60 cm telescope located the summit of Mt. Haleakala in Maui, Hawaii (Nakagawa et al., 2016). MILAHI has 10 um CO_2 laser as local oscillator. The field of view is 4 arcsec with 60 cm telescope and in the wavelength of 10 um. MIR-HS can retrieve temperature and wind in different altitude between dayside observations and nightside observations. CO_2 emerge non-local thermodynamic equilibrium emission from 100 –120 km altitude in dayside (Lopez-Valverde et al., 2011). Temperature and wind are derived from Doppler width and Doppler shift of the emission spectra, respectively. In nightside, CO_2 in the mesosphere absorbs background radiation from the cloud deck. Temperature profile and wind are retrieved from this absorption spectra with radiative transfer equation and inverse method of AMATERASU developed in National Institute of Information and Communications Technology.
Dayside observations were conducted between 24th and 27th in June, 2018. Apparent diameter was 15 arcsec and apparent dayside was half of the disk in this term. Observed points were North, South, disk center, and equator with integration times of 30 - 55 minutes. Each observed point gave different temperature variation feature. Temperature variation range was 170 - 220 K in agreement with Sonnabend et al. (2010). Temperature distribution showed both latitudinal dependence in 25th and convergence at 200 K in 26th.
Nightside observations were conducted from 11th to 13th, 19th, and 20th in November, 2018. Apparent diameter of Venus changed between 55.4 and 49.4 arcsec after inferior conjunction. We observed equator with three days, north 33 degree and south 33 degree for diurnal and latitudinal variations with integration times of 80 - 130 minutes. The observed spectra in the unit of relative intensity are under conversion because the retrieval with AMATERASU is necessary to use absolute radiation. We will show retrieved temperature profile and wind velocity at this presentation.

Keywords: Venus, Mesosphere, mid-infrared spectroscopy

©2019. Japan Geoscience Union. All Right Reserved.

Local time dependence of limb darkening seen in the thermal infrared Venus disk

*Masahiro Akiba[1]

1. Rikkyo University

Brightness temperature of the Venus disk obtained by Longwave Infrared Camera (LIR) onboard Akatuski shows clear limb darkening in the low and middle latitudes. Limb darkening is an apparent temperature decrease from the center to the limb of the Venus disk. It is caused by thermal and radiative characteristics that the sensing altitude of LIR increases as an emission angle, which is a zenith angle of direction of emission from the Venus atmosphere to the sensor, increases and that the atmospheric temperature monotonically decreases with altitude. In higher latitudes limb brightening is observed, because an inversion layer exists at the cloud-top altitudes in higher latitudes. In other word a profile of the limb darkening reflects vertical distributions of atmospheric temperature and optical thickness of cloud particles. Taylor et al. [1980] presented local time dependence of limb darkening using brightness temperature data obtained by the Pioneer Venus orbiter, but did not mention its physical mechanism. In this study brightness temperature distributions obtained by LIR when Akatsuki was in the altitude range from 60,000 to 100,000 km during the period from October 19, 2016 to July 17, 2018 were analyzed to investigate temperature and cloud particle property at the cloud-tops. Each brightness temperature image with 328 x 248 pixels was divided into 3280 x 2480 sub-pixels, and 32 successive images were accumulated after precise adjustment of the Venus disk position to improve S/N. Brightness temperature profiles as a function of the emission angle were derived for 24 local time zones and 9 zonal belts with a latitudinal width of 10˚ within ±45˚. A degree of limb darkening and a brightness temperature at the disk center were determined by least-square function fitting. As a result, the degree of limb darkening shows a clear semi-diurnal variation, and is the strongest at 11h and 22h and the weakest at 7h and 18h in local time. The amplitude of semi-diurnal variation peaks at the equator, whereas its phase seems constant in all latitudes. The temperature at the disk center also shows a semi-diurnal variation with a phase shift of approximately two hours earlier than the phase of the degree of limb darkening and a slight diurnal variation in higher latitudes. These semi-diurnal and diurnal components observed by LIR are consistent with the past observation of thermal tides in the Venus atmosphere by VENERA 15 [Zasova et al., 2007]. The physical mechanism of the semi-diurnal and diurnal thermal tide components seen in the degree of limb darkening and cloud-top temperature will be discussed.

©2019. Japan Geoscience Union. All Right Reserved.

Local time dependence of limb darkening seen in the thermal infrared Venus disk

Masahiro Akiba, Tetsuya Fukuhara, and Makoto Taguchi
Rikkyo University

Brightness temperature of the Venus disk obtained by Longwave Infrared Camera (LIR) onboard Akatuski shows clear limb darkening in the low and middle latitudes. Limb darkening is an apparent temperature decrease from the center to the limb of the Venus disk. It is caused by thermal and radiative characteristics that the sensing altitude of LIR increases as an emission angle, which is a zenith angle of direction of emission from the Venus atmosphere to the sensor, increases and that the atmospheric temperature monotonically decreases with altitude. In higher latitudes limb brightening is observed, because an inversion layer exists at the cloud-top altitudes in higher latitudes. In other word a profile of the limb darkening reflects vertical distributions of atmospheric temperature and optical thickness of cloud particles. Taylor et al. [1980] presented local time dependence of limb darkening using brightness temperature data obtained by the Pioneer Venus orbiter, but did not mention its physical mechanism. In this study brightness temperature distributions obtained by LIR when Akatsuki was in the altitude range from 60,000 to 100,000 km during the period from October 19, 2016 to July 17, 2018 were analyzed to investigate temperature and cloud particle property at the cloud-tops. Each brightness temperature image with 328 x 248 pixels was divided into 3280 x 2480 sub-pixels, and 32 successive images were accumulated after precise adjustment of the Venus disk position to improve S/N. Brightness temperature profiles as a function of the emission angle were derived for 24 local time zones and 9 zonal belts with a latitudinal width of 10° within ±45°. A degree of limb darkening and a brightness temperature at the disk center were determined by least-square function fitting. As a result, the degree of limb darkening shows a clear semi-diurnal variation, and is the strongest at 11h and 22h and the weakest at 7h and 18h in local time. The amplitude of semi-diurnal variation peaks at the equator, whereas its phase seems constant in all latitudes. The temperature at the disk center also shows a semi-diurnal variation with a phase shift of approximately two hours earlier than the phase of the degree of limb darkening and a slight diurnal variation in higher latitudes. These semi-diurnal and diurnal components observed by LIR are consistent with the past observation of thermal tides in the Venus atmosphere by VENERA 15 [Zasova et al., 2007]. The physical mechanism of the semi-diurnal and diurnal thermal tide components seen in the degree of limb darkening and cloud-top temperature will be discussed.

©2019. Japan Geoscience Union. All Right Reserved.

Stationary wavy features and Banded structures at Venusian cloud top extracted by averaging multiple LIR images

*Kiichi Fukuya[1], Takeshi Imamura[1], Makoto Taguchi[2], Tetsuya Fukuhara[2], Toru Kouyama[3]

1. Univ. of Tokyo, 2. Rikkyo Univ., 3. AIST

Venus' cloud-top temperature distribution is now continuously mapped by LIR (Long-wave Infrared camera) mounted on the Venus orbiter Akatsuki. Fukuhara et al. (2017) analyzed LIR data and reported the existence of bow-shaped structures extending over 10,000 km in the north-south direction. The features are fixed in position without flowing with the super-rotation and appear above highlands with altitudes higher than 3 km. It was suggested based on a comparison with numerical simulations that the features are gravity waves generated by near-surface flows impinging on mountains. Kouyama et al. (2017) observed stationary features over 4 Venus days and revealed that the features tend to occur in the local afternoon. Gravity waves, whose restoring force is buoyancy, transport horizontal momentum in the vertical direction and accelerate or decelerate the background wind when they dissipate. Therefore, stationary gravity waves influence the general circulation of the atmosphere. In order to estimate the influence, it is essential to reveal the spatial and temporal distributions of gravity waves.
In the previous studies using LIR data, only planetary-scale stationary features have been investigated. On the other hand, Peralta et al. (2017) analyzed the data taken by VIRTIS onboard Venus Express, and reported the existence of many small-scale stationary features; however, VIRTIS can observe the night side only, and the observations were confined to the high latitude of the southern hemisphere because of the geometry of the orbit. Therefore, we intend to investigate with a new analysis method the topographical and local time dependency of small-scale, weak stationary features by using LIR data, which can observe all latitude regions at any local time. Though the S/N ratio of LIR is lower than VIRTIS, averaging of multiple images can suppress noises and at the same time emphasize stationary patterns. By using this method, small-scale, stationary wave trains were newly found above relatively-low topographic rises with altitudes of 1-3 km. In addition to stationary features, zonally-elongated banded structures were also found in averaged LIR images. Such structures have once been detected in LIR images taken during Akatsuki's Venus flyby in 2010 (Taguchi et al., 2012); the new analysis confirmed that banded structures are ubiquitous at the cloud top. The orientations of the banded structures are different from those of dark streaks found in ultraviolet images.

Keywords: Stationary gravity waves, Venus, Akatsuki

©2019. Japan Geoscience Union. All Right Reserved.

Akatsuki's IR2 Nightside Photometry Restoration by Deconvolution

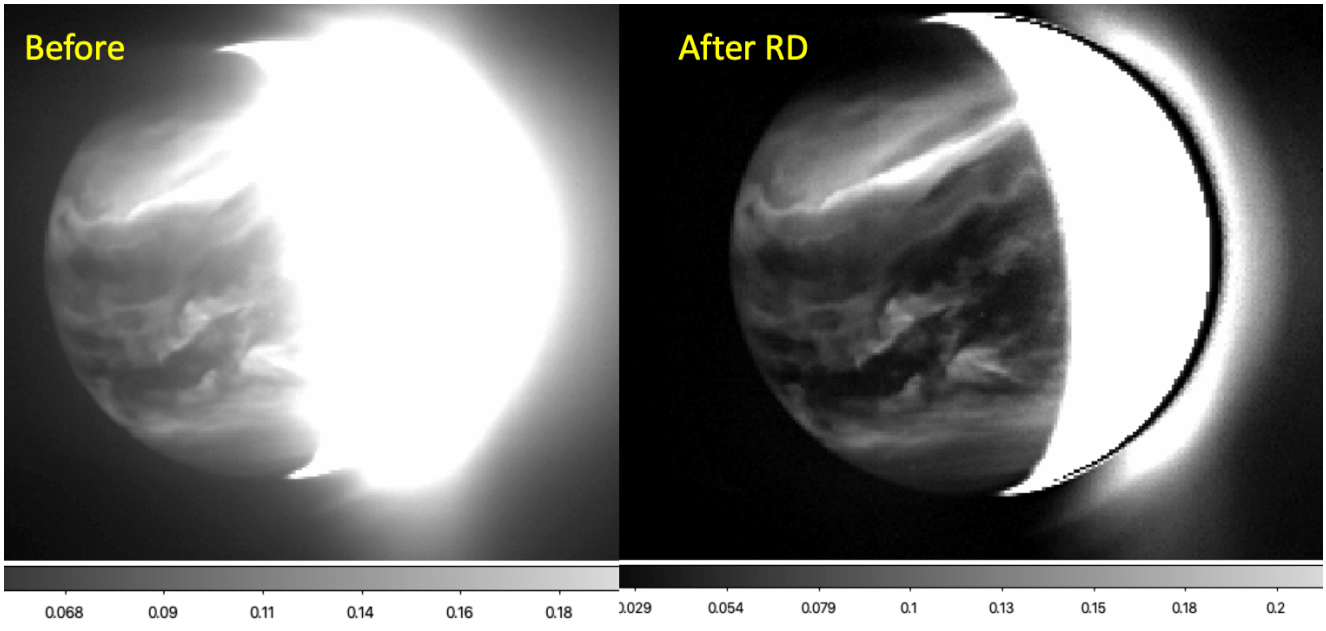
*Choon Wei Vun[1], Takehiko Satoh[2,1], Kevin McGouldrick[3], Takeshi Horinouchi[4], Takao M. Sato[5]

1. SOKENDAI, 2. ISAS/JAXA, 3. University of Colorado Boulder, 4. Hokkaido University, 5. Hokkaido Information University

Akatsuki’s IR2 camera captures images of Venus at different filters: 1.735um, 2.26um, and 2.32um. At near-dawn/dusk views (phase angles ~90 to 115 degree) of these images, the nightside photometry is contaminated by the intense dayside reflectance. As the potential well of a pixel is overfilled with incoming generated photoelectrons, the pixel is saturated and hence no longer contain information. This saturation can occur in the dayside and nightside near the terminator.
Owing to the saturation problem, main task of the restoration process is thus to simulate both day and night sides to replace the information loss in saturation. Point spread function (PSF) of the IR2 camera was modeled using Moffat function with observation of experimental image taken of point source street light before launch. Then, deconvolution by model-PSF can restore the nightside photometry of unsaturated pixels. Dayside reflectance was modeled with Lambert’s law, where its distribution is multiplied by an F factor (W m^{-2} sr^{-1} um^{-1}). Methods of finding the F factor will be shown.
We present our Restoration by Deconvolution (RD) results of the selected dates. The restored images were limb darkening corrected. Efficiency of RD can be restored to ~0.005 sigma in standard deviation accuracy when performed on synthetic image with known answer image.
Correlation plot of unsaturated nightside radiances between two filters (2.26mm and 1.735mm) were produced to extract possible ‘branch’ phenomena. The branching in the correlation plot indicates the differences in optical depths of different particle size modes [1].
Restoration of nightside pixels also opens up the opportunity to study the cloud dynamics transiting from the dayside into the nightside. Moreover, interesting cloud features such as vortices, instabilities, and streaks are more distinct in recovered images. This in overall opens up new window to understanding the evolution of cloud motion in the middle layer.
References: [1] Carlson R.W. et al. (1993) *Planet. Space Sci., 41,* No. 7, 477-485. [2] Grinspoon D.H. et al. (1993) *Planet. Spce Sci, 41,* No. 7, 515-542. [3] Nakamura M. et al. (2011)*Earth, Planets and Space, 63,* 443-457. [4] Satoh T. et al. (2016) *Earth, Planets and Space 68:74*. [5] Satoh T. et al. (2017) *Earth, Planets and Space 69:154.* [6] Wilson C.F. et al. (2008) *JGR, 113,* E00B13

Keywords: Venus, atmosphere, image restoration, infrared

©2019. Japan Geoscience Union. All Right Reserved.



©2019. Japan Geoscience Union. All Right Reserved.

Enormous cloud cover as seen by Akatsuki/IR2 on the night-side disk of Venus

*Takehiko Satoh[1,2], Choon Wei Vun[2], Takao M. Sato[3], Takeshi Horinouchi[4], George HASHIMOTO[5], Kevin McGouldrick[6]

1. Institute of Space and Astronautical Science, Japan Aerospace Exploration Agency, 2. Department of Space Science, SOKENDAI, 3. Department of Business and Information Systems, Hokkaido Information University, 4. Faculty of Environmental Earth Science, Hokkaido University, 5. Department of Earth Science, Okayama University, 6. LASP, University of Colorado Boulder

Night-side observations in transparency windows of CO_2 atmosphere of Venus allow visualizing inhomogeneous clouds in ~50 to ~60 km altitudes. The IR2 camera on board Akatsuki captured such images at 1.735, 2.26, and 2.32 um wavelengths. In the IR2 night-side data, an enormous cloud of greater opacity and very sharp edge in the front (western end) is seen repeatedly. This feature seems to encircle the planet with a period of ~4.5 days (Peralta).
Although interesting, property of particles in this feature was not studied before due to difficulty of photometric measurements in IR2 night-side data. This difficulty comes from a combination of the intense day crescent and extended tail of IR2 point-spread function (multiple reflection in the detector is the cause). We have developed a technique to restore the contrast of the night-side data by deconvolution so that the photometric studies can be done with IR2 night-side data.
The data acquired on 18th and 27th August 2016 are analyzed. We have performed a series of radiative transfer computations to reproduce both 1.735- and 2.26-um opacities in this enormous cloud. Properties of the cloud partices will be presented and possible mechanism of this remarkable phenomenon will be discussed.

Keywords: Akatsuki IR2, Venus night-side, Cloud opacity

©2019. Japan Geoscience Union. All Right Reserved.

The global variation of Venus cloud obtained from IR1 camera onboard AKATSUKI

*Seiko Takagi[1], Naomoto Iwagami, Yukihiro Takahashi[1], Mitsuteru Sato[1]

1. Hokkaido University, Graduate School of Science

Venus is our nearest neighbor, and has a size very similar to the Earth's. However, previous observations discovered an extremely dense (92 bar at the surface) and CO_2-rich atmosphere, with H_2SO_4 thick clouds. The Venus cloud consists of H_2SO_4 main cloud deck at 47 −70 km, with thinner hazes above and below. The upper haze on Venus lies above the main cloud surrounding the planet, ranging from the top of the cloud (70 km) up to as high as 90 km. Near infrared (0.986 um) dayside image of Venus has taken by solid state imaging (SSI) of the Galileo spacecraft (NASA). It appears almost flat, there are some small scale features with a contrast of 3 %[Belton et al., 1991]. In Takagi and Iwagami. (2011), it may be calculated that the source of the contrast of the order of 3 % in near infrared Venus dayside image is due to variation in the cloud optical thickness. On December 7, 2015, AKATSUKI (JAXA) approached Venus and the Venus orbit insertion was successful. After the Venus orbit insertion, many 0.90 um Venus dayside images were taken by the 1 um near infrared camera (IR1) onboard AKATSUKI. In this study, Venus cloud variations are investigated from 0.90 um Venus dayside images taken by IR1 camera globally. Further, meteorological some changes that contribute to cloud variation are examined in using radiative transfer calculation with high altitude cloud model obtained from Venus Express/SOIR observation. Furthermore, I will introduce observation plan with PIRKA telescope of Hokkaido University.

Keywords: Venus, cloud, near infrared

©2019. Japan Geoscience Union. All Right Reserved.

Development of a Venus' cloud formation scheme for a convection resolving model

*Ko-ichiro SUGIYAMA[1], Nozomu Fukuhara[1], Masatsugu Odaka[2], Kensuke Nakajima[3], Masaki Ishiwatari[2], Takeshi Imamura[4], Yoshi-Yuki Hayashi[5]

1. National Institute of Technology, Matsue College, 2. Department of Cosmoscience, Graduate School of Science, Hokkaido University, 3. Department of Earth and Planetary Sciences,FIculty of Sciences,Kyushu University, 4. Graduate School of Frontier Sciences, The University of Tokyo, 5. Department of Planetology, Graduate School of Science, Kobe University / Center for Planetary Science (CPS)

Although convection has been suggested to occur in the lower part of Venus' cloud layer by some observational evidences, its structure remains to be clarified. In the previous studies, Baker et al. (1998, 2000), Imamura et al. (2014), and Lefevre et al. (2017) try to simulate Venus' cloud-level convection, but their models they utilized do not consider cloud formation process. Our purpose is to develop new cloud formation scheme and to perform numerical simulation using the scheme in order to investigate a possible structure of Venus' cloud-level convection and clouds distribution.

Our cloud formation scheme is based on Imamura and Hashimoto (1998). The number densities of sulfuric acid (H2SO4) and water (H2O) in the gas and liquid phases are calculated. Sedimentation of H2SO4-H2O solution droplets and chemical reactions of sulfuric acid are also considered. The scheme is implemented into our convection resolving model developed by Sugiyama et al. (2009). The model is based on the quasi-compressible system (Klemp and Wilhelmson, 1978), and is used in the simulations of the atmospheric convections of Jupiter (Sugiyama et al., 2011, 2014) and Mars (Yamashita et al. 2017).

In our poster, we will show the details of our cloud formation scheme and demonstrate some results of our calculation using similar settings of Imamura et al. (2014).

Keywords: Venus atmosphere, convection, cloud formation, numerical modeling

©2019. Japan Geoscience Union. All Right Reserved.

Zonal mean structure of Venus atmosphere observed in a Venus general circulation model with explicit radiative transfer

*Yoshi-Yuki Hayashi[1], Chisato Shiojiri[1], Hiroki Kashimura[1], Yoshiyuki O. Takahashi[1]

1. Department of Planetology/CPS, Graduate School of Science, Kobe University

Zonal mean zonal wind in Venus atmosphere is different from those in other planetary atmospheres. It is a strong prograde wind in all latitudinal ranges and is referred to as super-rotation. This unique zonal wind has been investigated by a lot of previous researchers with numerical simulations as well as ground-based and spacecraft observations. Among the studies with numerical simulations, in 2010s, Lebonnois et al. (2010) and Ikeda (2010) performed general circulation model simulations with an explicit radiative transfer model and successfully represented strong prograde zonal wind. These studies overcome a shortcoming of previous studies, in which models use Newtonian cooling as a radiative forcing.

In our group, we have been developing a general circulation model for planetary atmospheres. In addition, we have just developed a Venus radiation model, which can be used in a general circulation model. In this study, by implementing the radiation model into our general circulation model, we try to perform general circulation model simulations of Venus atmosphere and investigate the zonal mean structure of Venus atmosphere and evaluate differences between previous studies.

The general circulation model used in this study is DCPAM (http://www.gfd-dennou.org/library/dcpam/). The model is based on primitive equation system and the equation system is solved by a spectral transform method. The DCPAM includes physical processes of radiation and turbulent mixing processes. In addition, heat diffusion in soil is considered to evaluate surface temperature. The radiation model implemented into the DCPAM has also been developed in our group, and is based on a correlated k-distribution method. Radiative fluxes calculated by this radiation model are compared well with observed ones. By the use of the model, we performed two experiments with and without surface orographic variation. Resolution of experiments is T15L52, in which the model has 48 (longitude) times 24 (latitude) grids in horizontal direction and 52 layers in vertical direction. Initial conditions for those experiments are the same, and are
motionless atmospheres with horizontally uniform temperature distribution based on VIRA. With this initial condition, the model is integrated for 150000 Earth days with diurnal variation and with no seasonal variation, i.e. zero
obliquity.

Statistically steady states are achieved after about 100000 Earth days from the start of integrations. In steady state, prograde zonal winds with velocity of about 50 m/s in low and middle latitude are maintained at cloud layer in both experiments with and without orographic variation, although the velocity is about a half of that observed in Venus
atmosphere.

Meridional circulation observed in the model has large direct cells in both hemispheres. The direct cells in the experiment without surface orography have vertical extent from the ground up to top of the model, except for low latitude region just above the ground where indirect cells form. However, in the experiment with surface orography, the cells are split in the vertical direction at bottom of cloud layer. In addition to direct cells, several indirect cells are also observed in the experiments. One of those is indirect cell at

©2019. Japan Geoscience Union. All Right Reserved.

cloud layer in high latitude. Other ones are several indirect cells which extends from the ground up to bottom of cloud layer in the experiment with surface orography. These indicate that the effects of surface orography can be observed below the cloud layer, clearly.

In the presentation, results of analysis on zonal mean structure observed in the model, such as angular momentum, will also be presented.

Keywords: Venus, planetary atmosphere, general circulation model, explicit calculation of radiative transfer

©2019. Japan Geoscience Union. All Right Reserved.

Gravity wave packets detected in radio occultation temperature profiles of the Venus atmosphere

*Ryota Mori[1], Takeshi Imamura[1], Javier Peralta[2]

1. The University of Tokyo, 2. Japan Aerospace Exploration Agency

Temperature profiles has been obtained from 2016 by the radio occultation experiment in the Venus orbiter mission Akatsuki. The radio occultation experiment is a method that measures the change of the atmospheric refractive index as a change of the frequency of the signal received on the ground. At the opportunity when the radio wave transmitted from Akatsuki toward the Earth pass through the planetary atmosphere, the wave is refracted and then reaches the receiving station. We can retrieve the vertical profiles of the pressure and the temperature from each refractive index profiles. In the temperature profile obtained in this way, variations due to various atmospheric disturbances are observed. We focus on gravity waves which are thought to play an import role in driving the general atmosphere circulation.

Gravity waves are small-scale waves with the restoring force being the buoyancy in the atmosphere. Gravity waves play a role in carrying the momentum in the vertical direction. So, it results in acceleration or deceleration of the mean wind by passing momentum on the background atmosphere while dissipating. This process should affect the global structure of the high-speed zonal wind. However, since gravity waves have properties that the spatial scale is small and the wave period is relatively short, it is difficult to capture the spatial structure by observation. The latitudinal profile of the amplitude of short vertical-scale temperature disturbances, which are thought to be associated with gravity waves, has been investigated; however, the dominant wavelength and the typical vertical extent have not been studied.

In this study, we applied wavelet analysis to the temperature profiles and extracted spatially localized temperature disturbances. Though there have been studies that apply Fourier transform to the temperature data, Fourier transform assumes infinitely lasting waves and it is not suitable for extracting spatially localized wave packets. Wavelet analysis is an effective way of obtaining the periods and the amplitudes of waves in such finite intervals. In this presentation, we report the result of wavelet analysis applied to the temperature data obtained with high vertical resolution by radio holographic method. From the obtained results, we also report the relationship between the length and the packet length of gravity wave in the atmosphere.

Keywords: Akatsuki, Gravity wave in the atmosphere, The radio occultation experiment

©2019. Japan Geoscience Union. All Right Reserved.

Status of lightning hunt in Venus with Akatsuki/LAC and Pirka telescope

*Yukihiro Takahashi[1,2], Mitsuteru Sato[1,2], Masataka Imai[3], Ralph Lorenz[4], Seiko Takagi[1,2], Ono Tatsuharu[1]

1. Graduate School of Science, Hokkaido University, 2. Faculty of Science, Hokkaido University, 3. National Institute of Advanced Industrial Science and Technology,, 4. Applied Physics Laboratory, Johns Hopkins University

The existence of lightning discharge in Venus has been controversial for three decades, which might be attributed to the luck of conclusive observational evidence. There had been no satellite payload intentionally designed for the detection of lightning phenomena using radio wave or optical sensor. LAC, lightning and airglow camera, on board Akatsuki spacecraft, is the first sensor optimized for the lightning optical flash measurement in planets other than the Earth. It is expected that LAC could conclude this 30-year discussion on the existence of lightning in Venus. Unique performance of LAC compared to other equipment used in the previous exploration of Venus is the high-speed sampling rate at 20 kHz with 32 pixels of Avalanche Photo Diode (APD) matrix, enabling us to distinguish the natural optical lightning flash from other pulsing noises, including artificial electrical noise and cosmic rays. We selected OI 777 nm line for lightning detection, which is expected to be the most prominent emission in CO2-dominant atmosphere based on the laboratory experiments.

The triggering parameter was set so as to optimize for the light curve similar to the normal lightning in the Earth and data obtained totally for about 4 hours were examined. However, we couldn’ t find any lightning signals. Adding to this triggering parameter set, we added one more parameter set, optimized for sprite type emission with duration of up to 10s of ms. Furthermore, in order to investigate fainter emissions, we are now conducting successive force triggering recordings without any threshold, achieving 5 times better sensitivity than the intensity of 1 digital unit at best.

The total coverage of the LAC lightning hunt became 81.6 [million km2-hr], meaning 81 percent detectability of previous results with ground-based telescope by Hansell et al. (1995). Here we report the detailed strategy and the latest status of the LAC observation in 2018, and discuss the future observation plan.

Also we will make ground observation with a high-speed photometer installed at Pirka telescope, a 1.6-m reflector deployed by Hokkaido University. Here we report the initial results of lightning flash observation with it.

Keywords: lightning, Venus, Akatsuki, Pirka telescope

©2019. Japan Geoscience Union. All Right Reserved.

Possibility of electric discharge in the Venusian atmosphere due to the super-rotation of clouds

*Adhithiyan Neduncheran[1], Ugur Guven[1,2], Ananyo Bhattacharya[3]

1. University of Petroleum and Energy Studies, India, 2. United Nations Centre for Space Science and Technology Education in Asia and the Pacific, 3. Sardar Vallabhbhai National Institute of Technology,India

Several evidences of electromagnetic bursts were measured by various landers and orbiters studying Venus atmosphere (Venera landers, Venus Express and the Pioneer Venus Orbiter). The electromagnetic bursts that are taking place in the cloud region in the form of lightning or fluorescence might be a result of momentum transfer, solar convection and charge dispersion in the clouds of Venus. While the lightning in Earth takes place mostly in the equatorial region, in case of Venus it is possible for lightning to occur in the polar regions, considering the kinetic energy transfer and the formation of dipoles in both hemispheres of Venus. The meridional and zonal flows can interact and cause the charge separation which possibly lead to electromagnetic bursts in different spectrum and in different regions in Venus. In labs, it is observed that SO2 emissions in UV region cause fluorescence which is one of the major phenomena taking place in the cloud tops. Based on the photochemical model published by *Krasnopolsky 2011(*doi:10.1016/j.icarus.2011.11.012) and the principle of refraction, we present the possibility of lightning/fluorescence phenomena being caused by the super-rotation of the clouds in the Venusian atmosphere.

Keywords: Venus , Super-rotation, lightning, electric discharge, atmosphere

©2019. Japan Geoscience Union. All Right Reserved.

[E] Poster | P (Space and Planetary Sciences)：P-PS Planetary Sciences

Mon. May 27, 2019 5:15 PM - 6:30 PM JST | Mon. May 27, 2019 8:15 AM - 9:30 AM UTC | Poster Hall International Exhibition Hall8, Makuhari Messe_2

[P-PS05] Recent advances of Venus science

convener:Takehiko Satoh(Institute of Space and Astronautical Science, Japan Aerospace Exploration Agency), Takeshi Horinouchi(Faculty of Environmental Earth Science, Hokkaido University), Masaru Yamamoto(Research Institute for Applied Mechanics, Kyushu University), Kevin McGouldrick(University of Colorado Boulder)

Akatsuki, being in Venus orbit since December 2015, has acquired a volume of high-quality data, unveiled many new phenomena and is allowing researchers to investigate the underlying mechanisms. As the data accumulate, numerical models and theories are being advanced as well. We are no doubt living in the new golden era of Venus studies. This session invites papers of the new scientific results with Akatsuki data and the latest results of theoretical and numerical works. We expect participants of this session share the latest research results through presentations and discussion.

[PPS05-P01] New thermal infrared camera for fine horizontal brightness temperature structures at the cloud-top level of Venus

*Tetsuya Fukuhara[1], Makoto Taguchi[1], Takeshi Imamura[2], Sanjay S Limaye[3] (1.Rikkyo University, 2.The University of Tokyo, 3.University of Wisconsin)

[PPS05-P02] Temperature and wind variations in Venusian mesosphere and lower thermosphere by mid-infrared heterodyne spectrometer in 2018

*Kosuke Takami[1], Hiromu Nakagawa[1], Hideo Sagawa[2], Isao Murata[1], Yasumasa Kasaba[1] (1.Graduate School of Science, Tohoku University, 2.Division of Science, Kyoto Sangyo University)

[PPS05-P03] Local time dependence of limb darkening seen in the thermal infrared Venus disk

*Masahiro Akiba[1] (1.Rikkyo University)

[PPS05-P04] Stationary wavy features and Banded structures at Venusian cloud top extracted by averaging multiple LIR images

*Kiichi Fukuya[1], Takeshi Imamura[1], Makoto Taguchi[2], Tetsuya Fukuhara[2], Toru Kouyama[3] (1.Univ. of Tokyo, 2.Rikkyo Univ., 3.AIST)

[PPS05-P05] Akatsuki's IR2 Nightside Photometry Restoration by Deconvolution

*Choon Wei Vun[1], Takehiko Satoh[2,1], Kevin McGouldrick[3], Takeshi Horinouchi[4], Takao M. Sato[5] (1.SOKENDAI, 2.ISAS/JAXA, 3.University of Colorado Boulder, 4.Hokkaido University, 5.Hokkaido Information University)

[PPS05-P06] Enormous cloud cover as seen by Akatsuki/IR2 on the night-side disk of Venus

*Takehiko Satoh[1,2], Choon Wei Vun[2], Takao M. Sato[3], Takeshi Horinouchi[4], George HASHIMOTO[5], Kevin McGouldrick[6] (1.Institute of Space and Astronautical Science, Japan Aerospace Exploration Agency, 2.Department of Space Science, SOKENDAI, 3.Department of Business and Information Systems, Hokkaido Information University, 4.Faculty of Environmental Earth Science, Hokkaido University, 5.Department of Earth Science, Okayama University, 6.LASP, University of Colorado Boulder)

[PPS05-P07] The global variation of Venus cloud obtained from IR1 camera onboard AKATSUKI

*Seiko Takagi[1], Naomoto Iwagami, Yukihiro Takahashi[1], Mitsuteru Sato[1] (1.Hokkaido University, Graduate School of Science)

[PPS05-P08] Development of a Venus' cloud formation scheme for a convection resolving model

*Ko-ichiro SUGIYAMA[1], Nozomu Fukuhara[1], Masatsugu Odaka[2], Kensuke Nakajima[3], Masaki Ishiwatari[2], Takeshi Imamura[4], Yoshi-Yuki Hayashi[5] (1.National Institute of Technology, Matsue College, 2.Department of Cosmoscience, Graduate School of Science, Hokkaido University, 3.Department of Earth and Planetary Sciences,Flculty of Sciences,Kyushu University, 4.Graduate School of Frontier Sciences, The University of Tokyo, 5.Department of Planetology, Graduate School of Science, Kobe University / Center for Planetary Science (CPS))

[PPS05-P09] Zonal mean structure of Venus atmosphere observed in a Venus general circulation model with explicit radiative transfer

★Invited Papers

*Yoshi-Yuki Hayashi[1], Chisato Shiojiri[1], Hiroki Kashimura[1], Yoshiyuki O. Takahashi[1] (1.Department of Planetology/CPS, Graduate School of Science, Kobe University)

[PPS05-P10] Gravity wave packets detected in radio occultation temperature profiles of the Venus atmosphere

*Ryota Mori[1], Takeshi Imamura[1], Javier Peralta[2] (1.The University of Tokyo, 2.Japan Aerospace Exploration Agency)

[PPS05-P11] **Status of lightning hunt in Venus with Akatsuki/LAC and Pirka telescope**

*Yukihiro Takahashi[1,2], Mitsuteru Sato[1,2], Masataka Imai[3], Ralph Lorenz[4], Seiko Takagi[1,2], Ono Tatsuharu[1] (1.Graduate School of Science, Hokkaido University, 2.Faculty of Science, Hokkaido University, 3.National Institute of Advanced Industrial Science and Technology,, 4.Applied Physics Laboratory, Johns Hopkins University)

[PPS05-P12] **Possibility of electric discharge in the Venusian atmosphere due to the super-rotation of clouds**

*Adhithiyan Neduncheran[1], Ugur Guven[1,2], Ananyo Bhattacharya[3] (1.University of Petroleum and Energy Studies, India, 2.United Nations Centre for Space Science and Technology Education in Asia and the Pacific, 3.Sardar Vallabhbhai National Institute of Technology,India)

New thermal infrared camera for fine horizontal brightness temperature structures at the cloud-top level of Venus

*Tetsuya Fukuhara[1], Makoto Taguchi[1], Takeshi Imamura[2], Sanjay S Limaye[3]

1. Rikkyo University, 2. The University of Tokyo, 3. University of Wisconsin

The Longwave Infrared Camera (LIR), which is an uncooled microbolometer camera, is currently acquiring thermal infrared images (8-12 μm) of Venus and depicting the cloud-top brightness temperatures from Akatsuki orbiter around Venus since December 2015. The outstanding result of LIR has been the discovery of an interhemispheric bow-shaped structure meridionally stretching 10,000 km across the equator at the Venus cloud-top. Over several days of observations, the bow-shaped structure remains relatively fixed in position above the highland on the slowly rotating surface, despite the background atmospheric super rotation at ~100 m/s. We infer that the bow-shaped structure is the result of an atmospheric gravity wave generated in the lower atmosphere by mountain topography that then propagated upwards [1]. This indicates that the horizontal temperature distribution seen at the cloud-top level represents not only direct physical property at the cloud-top but also influence of dynamics in the lower atmosphere. In fact, preliminary observation of LIR has detected fine structure (~100 km) in temperature distribution from close-up observations near the periapsis. We suggest that this may be caused by the upward propagation of a gravity wave, which is generated by the convection layer at ~40 km altitude. However, the spatial resolution of LIR seems insufficient to understand the origins of such a fine structure. We need better observations at higher spatial resolution than possible from LIR in Akatsuki's orbit.

We propose that a future Venus orbiter carries an updated version of the uncooled microbolometer camera (BOL) with 1024x768 pixels and angular resolution of ~0.01 deg/pixel to detect fine temperature structure on the cloud-tops. When the orbiter is typically injected to a high-inclined elliptical orbit with altitude of 500-50,000 km, BOL provides a spatial resolution of 8.5 km at apoapsis and 0.08 km at periapsis, respectively. It will be enough to observe the fine temperature structure at the cloud-top. Further, BOL will capture the fine temperature structure at polar region near the "eye" of the hemispheric vortex situated over the poles, where the horizontal temperature varies drastically near the Venus cloud-tops. VIRTIS instrument on Venus Express orbiter showed complex structures at near infrared wavelengths [2]. Akatsuki from its near equatorial elliptical orbit cannot observe the fine structure in polar regions.

During 2012-2014, we developed an uncooled micro-bolometer array (UMBA) camera for the 50 kg class Earth observing satellite based on the experience of LIR development [3]. The camera with the pixel size of 640 ×480 was launched in 2014 and successfully detect a small wildfire which was main observation target for the mission. The results showed that its performance was better than expected. Furthermore, the newest UMBA camera with the pixel size increased to 1024 ×768 has been developed for the next wildfire mission to take finer spatial resolution image with ~0.01 deg/pixel. Unfortunately, this camera has lost the launch opportunity. However, the flight-model has been assembled and has passed function tests. Since BOL does not need heavy cryogenic systems, its mass and size are less than ~1 kg and 100 mm x 100 mm x 120 mm, respectively; it would be a relatively small mass increment for the future Venus mission.

References

[1] Fukuhara, T., et al., 2017, Large stationary gravity wave in the atmosphere of Venus, Nature Geoscience, Vol. 10, 85–88.

©2019. Japan Geoscience Union. All Right Reserved.

[2] Garate-Lopez, I., et al., 2015, Atmospheric dynamics at the southern pole of Venus: Three-dimensional winds, temperature and vorticity, AGU Fall Meeting Abstracts, 23.
[3] Fukuhara, T., et al., 2017, Detection of small wildfire by thermal infrared camera with the uncooled microbolometer array for 50 kg class satellite, IEEE Transactions on Geoscience and Remote Sensing, 2017, Vol. 55, No. 8, 4314-4324

Keywords: Venus, atmosphere, Akatsuki

©2019. Japan Geoscience Union. All Right Reserved.

Temperature and wind variations in Venusian mesosphere and lower thermosphere by mid-infrared heterodyne spectrometer in 2018

*Kosuke Takami[1], Hiromu Nakagawa[1], Hideo Sagawa[2], Isao Murata[1], Yasumasa Kasaba[1]

1. Graduate School of Science, Tohoku University, 2. Division of Science, Kyoto Sangyo University

The most extensive observations of Venusian mesosphere have been performed by Venus Express (VEX) up to 2014 (e.g., Patzold et al., 2007; Mahieux et al., 2015). These observations have found the highly spatial and temporal variations in the thermal structure. The temperature discrepancies between observations by VEX/SOIR and general circulation models in the altitude of 80 - 100 km have not been properly interpreted (Bougher et al., 2015; Gilli et al., 2017). In addition, the mesospheric dynamics located between retrograde superrotational zonal wind (cloud deck) and subsolar-to-antisolar flow (above 120 km altitude) have not been well understood due to lack of observations. On the other hand, the lower thermosphere has been observed by mid-infrared heterodyne spectrometer (MIR-HS). Temperature in this region varied extensively between 140 K and 240 K, and wind velocity changed intensely from 130 m/s to 190 m/s for a terrestrial day (Sornig et al., 2013; Krause et al., 2018). Temperature and wind variations such as periodicity and locality in Venusian mesosphere and lower thermosphere have not been comprehended. The purpose of our observations is to solve it with continuous observations by MIR-HS.
Our Mid-Infrared Laser Heterodyne Instrument (MILAHI) have been inserted to Tohoku 60 cm telescope located the summit of Mt. Haleakala in Maui, Hawaii (Nakagawa et al., 2016). MILAHI has 10 um CO_2 laser as local oscillator. The field of view is 4 arcsec with 60 cm telescope and in the wavelength of 10 um. MIR-HS can retrieve temperature and wind in different altitude between dayside observations and nightside observations. CO_2 emerge non-local thermodynamic equilibrium emission from 100 –120 km altitude in dayside (Lopez-Valverde et al., 2011). Temperature and wind are derived from Doppler width and Doppler shift of the emission spectra, respectively. In nightside, CO_2 in the mesosphere absorbs background radiation from the cloud deck. Temperature profile and wind are retrieved from this absorption spectra with radiative transfer equation and inverse method of AMATERASU developed in National Institute of Information and Communications Technology.
Dayside observations were conducted between 24th and 27th in June, 2018. Apparent diameter was 15 arcsec and apparent dayside was half of the disk in this term. Observed points were North, South, disk center, and equator with integration times of 30 - 55 minutes. Each observed point gave different temperature variation feature. Temperature variation range was 170 - 220 K in agreement with Sonnabend et al. (2010). Temperature distribution showed both latitudinal dependence in 25th and convergence at 200 K in 26th.
Nightside observations were conducted from 11th to 13th, 19th, and 20th in November, 2018. Apparent diameter of Venus changed between 55.4 and 49.4 arcsec after inferior conjunction. We observed equator with three days, north 33 degree and south 33 degree for diurnal and latitudinal variations with integration times of 80 - 130 minutes. The observed spectra in the unit of relative intensity are under conversion because the retrieval with AMATERASU is necessary to use absolute radiation. We will show retrieved temperature profile and wind velocity at this presentation.

Keywords: Venus, Mesosphere, mid-infrared spectroscopy

©2019. Japan Geoscience Union. All Right Reserved.

Local time dependence of limb darkening seen in the thermal infrared Venus disk

*Masahiro Akiba[1]

1. Rikkyo University

Brightness temperature of the Venus disk obtained by Longwave Infrared Camera (LIR) onboard Akatuski shows clear limb darkening in the low and middle latitudes. Limb darkening is an apparent temperature decrease from the center to the limb of the Venus disk. It is caused by thermal and radiative characteristics that the sensing altitude of LIR increases as an emission angle, which is a zenith angle of direction of emission from the Venus atmosphere to the sensor, increases and that the atmospheric temperature monotonically decreases with altitude. In higher latitudes limb brightening is observed, because an inversion layer exists at the cloud-top altitudes in higher latitudes. In other word a profile of the limb darkening reflects vertical distributions of atmospheric temperature and optical thickness of cloud particles. Taylor et al. [1980] presented local time dependence of limb darkening using brightness temperature data obtained by the Pioneer Venus orbiter, but did not mention its physical mechanism. In this study brightness temperature distributions obtained by LIR when Akatsuki was in the altitude range from 60,000 to 100,000 km during the period from October 19, 2016 to July 17, 2018 were analyzed to investigate temperature and cloud particle property at the cloud-tops. Each brightness temperature image with 328 x 248 pixels was divided into 3280 x 2480 sub-pixels, and 32 successive images were accumulated after precise adjustment of the Venus disk position to improve S/N. Brightness temperature profiles as a function of the emission angle were derived for 24 local time zones and 9 zonal belts with a latitudinal width of 10˚ within ±45˚. A degree of limb darkening and a brightness temperature at the disk center were determined by least-square function fitting. As a result, the degree of limb darkening shows a clear semi-diurnal variation, and is the strongest at 11h and 22h and the weakest at 7h and 18h in local time. The amplitude of semi-diurnal variation peaks at the equator, whereas its phase seems constant in all latitudes. The temperature at the disk center also shows a semi-diurnal variation with a phase shift of approximately two hours earlier than the phase of the degree of limb darkening and a slight diurnal variation in higher latitudes. These semi-diurnal and diurnal components observed by LIR are consistent with the past observation of thermal tides in the Venus atmosphere by VENERA 15 [Zasova et al., 2007]. The physical mechanism of the semi-diurnal and diurnal thermal tide components seen in the degree of limb darkening and cloud-top temperature will be discussed.

©2019. Japan Geoscience Union. All Right Reserved.

Local time dependence of limb darkening seen in the thermal infrared Venus disk

Masahiro Akiba, Tetsuya Fukuhara, and Makoto Taguchi
Rikkyo University

Brightness temperature of the Venus disk obtained by Longwave Infrared Camera (LIR) onboard Akatuski shows clear limb darkening in the low and middle latitudes. Limb darkening is an apparent temperature decrease from the center to the limb of the Venus disk. It is caused by thermal and radiative characteristics that the sensing altitude of LIR increases as an emission angle, which is a zenith angle of direction of emission from the Venus atmosphere to the sensor, increases and that the atmospheric temperature monotonically decreases with altitude. In higher latitudes limb brightening is observed, because an inversion layer exists at the cloud-top altitudes in higher latitudes. In other word a profile of the limb darkening reflects vertical distributions of atmospheric temperature and optical thickness of cloud particles. Taylor et al. [1980] presented local time dependence of limb darkening using brightness temperature data obtained by the Pioneer Venus orbiter, but did not mention its physical mechanism. In this study brightness temperature distributions obtained by LIR when Akatsuki was in the altitude range from 60,000 to 100,000 km during the period from October 19, 2016 to July 17, 2018 were analyzed to investigate temperature and cloud particle property at the cloud-tops. Each brightness temperature image with 328 x 248 pixels was divided into 3280 x 2480 sub-pixels, and 32 successive images were accumulated after precise adjustment of the Venus disk position to improve S/N. Brightness temperature profiles as a function of the emission angle were derived for 24 local time zones and 9 zonal belts with a latitudinal width of 10° within ±45°. A degree of limb darkening and a brightness temperature at the disk center were determined by least-square function fitting. As a result, the degree of limb darkening shows a clear semi-diurnal variation, and is the strongest at 11h and 22h and the weakest at 7h and 18h in local time. The amplitude of semi-diurnal variation peaks at the equator, whereas its phase seems constant in all latitudes. The temperature at the disk center also shows a semi-diurnal variation with a phase shift of approximately two hours earlier than the phase of the degree of limb darkening and a slight diurnal variation in higher latitudes. These semi-diurnal and diurnal components observed by LIR are consistent with the past observation of thermal tides in the Venus atmosphere by VENERA 15 [Zasova et al., 2007]. The physical mechanism of the semi-diurnal and diurnal thermal tide components seen in the degree of limb darkening and cloud-top temperature will be discussed.

©2019. Japan Geoscience Union. All Right Reserved.

Stationary wavy features and Banded structures at Venusian cloud top extracted by averaging multiple LIR images

*Kiichi Fukuya[1], Takeshi Imamura[1], Makoto Taguchi[2], Tetsuya Fukuhara[2], Toru Kouyama[3]

1. Univ. of Tokyo, 2. Rikkyo Univ., 3. AIST

Venus' cloud-top temperature distribution is now continuously mapped by LIR (Long-wave Infrared camera) mounted on the Venus orbiter Akatsuki. Fukuhara et al. (2017) analyzed LIR data and reported the existence of bow-shaped structures extending over 10,000 km in the north-south direction. The features are fixed in position without flowing with the super-rotation and appear above highlands with altitudes higher than 3 km. It was suggested based on a comparison with numerical simulations that the features are gravity waves generated by near-surface flows impinging on mountains. Kouyama et al. (2017) observed stationary features over 4 Venus days and revealed that the features tend to occur in the local afternoon. Gravity waves, whose restoring force is buoyancy, transport horizontal momentum in the vertical direction and accelerate or decelerate the background wind when they dissipate. Therefore, stationary gravity waves influence the general circulation of the atmosphere. In order to estimate the influence, it is essential to reveal the spatial and temporal distributions of gravity waves.
In the previous studies using LIR data, only planetary-scale stationary features have been investigated. On the other hand, Peralta et al. (2017) analyzed the data taken by VIRTIS onboard Venus Express, and reported the existence of many small-scale stationary features; however, VIRTIS can observe the night side only, and the observations were confined to the high latitude of the southern hemisphere because of the geometry of the orbit. Therefore, we intend to investigate with a new analysis method the topographical and local time dependency of small-scale, weak stationary features by using LIR data, which can observe all latitude regions at any local time. Though the S/N ratio of LIR is lower than VIRTIS, averaging of multiple images can suppress noises and at the same time emphasize stationary patterns. By using this method, small-scale, stationary wave trains were newly found above relatively-low topographic rises with altitudes of 1-3 km. In addition to stationary features, zonally-elongated banded structures were also found in averaged LIR images. Such structures have once been detected in LIR images taken during Akatsuki's Venus flyby in 2010 (Taguchi et al., 2012); the new analysis confirmed that banded structures are ubiquitous at the cloud top. The orientations of the banded structures are different from those of dark streaks found in ultraviolet images.

Keywords: Stationary gravity waves, Venus, Akatsuki

©2019. Japan Geoscience Union. All Right Reserved.

Akatsuki's IR2 Nightside Photometry Restoration by Deconvolution

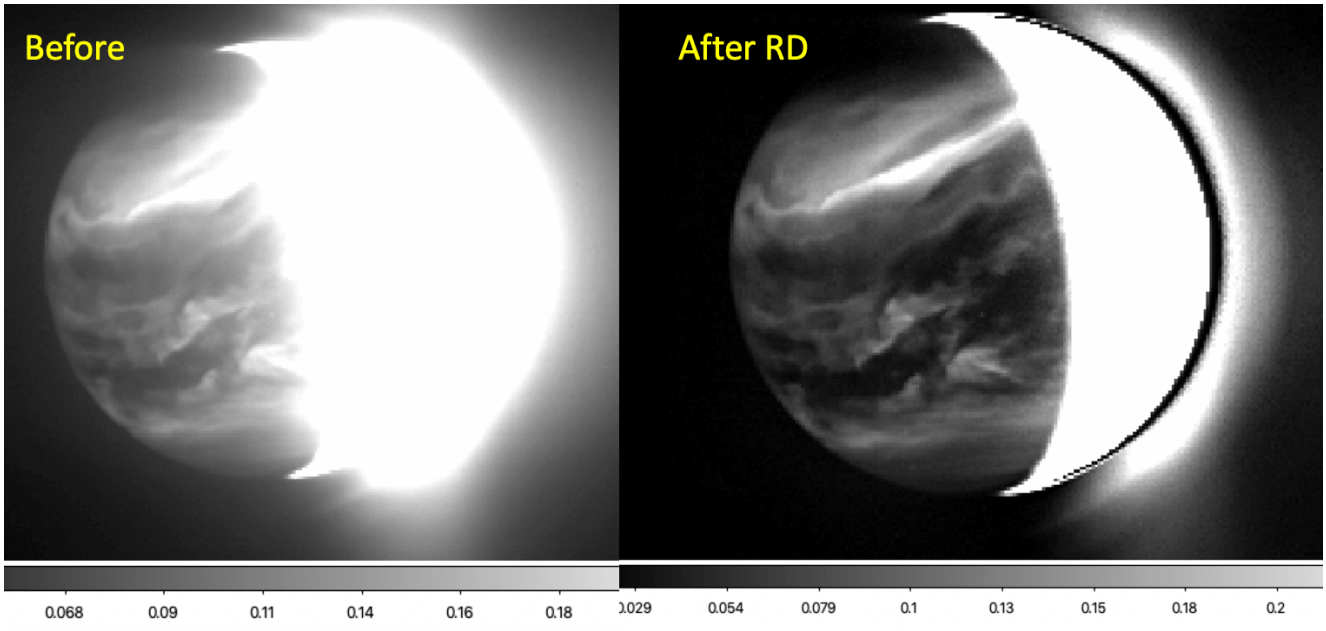
*Choon Wei Vun[1], Takehiko Satoh[2,1], Kevin McGouldrick[3], Takeshi Horinouchi[4], Takao M. Sato[5]

1. SOKENDAI, 2. ISAS/JAXA, 3. University of Colorado Boulder, 4. Hokkaido University, 5. Hokkaido Information University

Akatsuki’s IR2 camera captures images of Venus at different filters: 1.735um, 2.26um, and 2.32um. At near-dawn/dusk views (phase angles ~90 to 115 degree) of these images, the nightside photometry is contaminated by the intense dayside reflectance. As the potential well of a pixel is overfilled with incoming generated photoelectrons, the pixel is saturated and hence no longer contain information. This saturation can occur in the dayside and nightside near the terminator.
Owing to the saturation problem, main task of the restoration process is thus to simulate both day and night sides to replace the information loss in saturation. Point spread function (PSF) of the IR2 camera was modeled using Moffat function with observation of experimental image taken of point source street light before launch. Then, deconvolution by model-PSF can restore the nightside photometry of unsaturated pixels. Dayside reflectance was modeled with Lambert’s law, where its distribution is multiplied by an F factor (W m^{-2} sr^{-1} um^{-1}). Methods of finding the F factor will be shown.
We present our Restoration by Deconvolution (RD) results of the selected dates. The restored images were limb darkening corrected. Efficiency of RD can be restored to ~0.005 sigma in standard deviation accuracy when performed on synthetic image with known answer image.
Correlation plot of unsaturated nightside radiances between two filters (2.26mm and 1.735mm) were produced to extract possible ‘branch’ phenomena. The branching in the correlation plot indicates the differences in optical depths of different particle size modes [1].
Restoration of nightside pixels also opens up the opportunity to study the cloud dynamics transiting from the dayside into the nightside. Moreover, interesting cloud features such as vortices, instabilities, and streaks are more distinct in recovered images. This in overall opens up new window to understanding the evolution of cloud motion in the middle layer.
References: [1] Carlson R.W. et al. (1993) *Planet. Space Sci., 41,* No. 7, 477-485. [2] Grinspoon D.H. et al. (1993) *Planet. Spce Sci, 41,* No. 7, 515-542. [3] Nakamura M. et al. (2011)*Earth, Planets and Space, 63,* 443-457. [4] Satoh T. et al. (2016) *Earth, Planets and Space 68:74*. [5] Satoh T. et al. (2017) *Earth, Planets and Space 69:154.* [6] Wilson C.F. et al. (2008) *JGR, 113,* E00B13

Keywords: Venus, atmosphere, image restoration, infrared

©2019. Japan Geoscience Union. All Right Reserved.



©2019. Japan Geoscience Union. All Right Reserved.

Enormous cloud cover as seen by Akatsuki/IR2 on the night-side disk of Venus

*Takehiko Satoh[1,2], Choon Wei Vun[2], Takao M. Sato[3], Takeshi Horinouchi[4], George HASHIMOTO[5], Kevin McGouldrick[6]

1. Institute of Space and Astronautical Science, Japan Aerospace Exploration Agency, 2. Department of Space Science, SOKENDAI, 3. Department of Business and Information Systems, Hokkaido Information University, 4. Faculty of Environmental Earth Science, Hokkaido University, 5. Department of Earth Science, Okayama University, 6. LASP, University of Colorado Boulder

Night-side observations in transparency windows of CO_2 atmosphere of Venus allow visualizing inhomogeneous clouds in ~50 to ~60 km altitudes. The IR2 camera on board Akatsuki captured such images at 1.735, 2.26, and 2.32 um wavelengths. In the IR2 night-side data, an enormous cloud of greater opacity and very sharp edge in the front (western end) is seen repeatedly. This feature seems to encircle the planet with a period of ~4.5 days (Peralta).
Although interesting, property of particles in this feature was not studied before due to difficulty of photometric measurements in IR2 night-side data. This difficulty comes from a combination of the intense day crescent and extended tail of IR2 point-spread function (multiple reflection in the detector is the cause). We have developed a technique to restore the contrast of the night-side data by deconvolution so that the photometric studies can be done with IR2 night-side data.
The data acquired on 18th and 27th August 2016 are analyzed. We have performed a series of radiative transfer computations to reproduce both 1.735- and 2.26-um opacities in this enormous cloud. Properties of the cloud partices will be presented and possible mechanism of this remarkable phenomenon will be discussed.

Keywords: Akatsuki IR2, Venus night-side, Cloud opacity

©2019. Japan Geoscience Union. All Right Reserved.

The global variation of Venus cloud obtained from IR1 camera onboard AKATSUKI

*Seiko Takagi[1], Naomoto Iwagami, Yukihiro Takahashi[1], Mitsuteru Sato[1]

1. Hokkaido University, Graduate School of Science

Venus is our nearest neighbor, and has a size very similar to the Earth's. However, previous observations discovered an extremely dense (92 bar at the surface) and CO_2-rich atmosphere, with H_2SO_4 thick clouds. The Venus cloud consists of H_2SO_4 main cloud deck at 47 −70 km, with thinner hazes above and below. The upper haze on Venus lies above the main cloud surrounding the planet, ranging from the top of the cloud (70 km) up to as high as 90 km. Near infrared (0.986 um) dayside image of Venus has taken by solid state imaging (SSI) of the Galileo spacecraft (NASA). It appears almost flat, there are some small scale features with a contrast of 3 %[Belton et al., 1991]. In Takagi and Iwagami. (2011), it may be calculated that the source of the contrast of the order of 3 % in near infrared Venus dayside image is due to variation in the cloud optical thickness. On December 7, 2015, AKATSUKI (JAXA) approached Venus and the Venus orbit insertion was successful. After the Venus orbit insertion, many 0.90 um Venus dayside images were taken by the 1 um near infrared camera (IR1) onboard AKATSUKI. In this study, Venus cloud variations are investigated from 0.90 um Venus dayside images taken by IR1 camera globally. Further, meteorological some changes that contribute to cloud variation are examined in using radiative transfer calculation with high altitude cloud model obtained from Venus Express/SOIR observation. Furthermore, I will introduce observation plan with PIRKA telescope of Hokkaido University.

Keywords: Venus, cloud, near infrared

©2019. Japan Geoscience Union. All Right Reserved.

Development of a Venus' cloud formation scheme for a convection resolving model

*Ko-ichiro SUGIYAMA[1], Nozomu Fukuhara[1], Masatsugu Odaka[2], Kensuke Nakajima[3], Masaki Ishiwatari[2], Takeshi Imamura[4], Yoshi-Yuki Hayashi[5]

1. National Institute of Technology, Matsue College, 2. Department of Cosmoscience, Graduate School of Science, Hokkaido University, 3. Department of Earth and Planetary Sciences,FIculty of Sciences,Kyushu University, 4. Graduate School of Frontier Sciences, The University of Tokyo, 5. Department of Planetology, Graduate School of Science, Kobe University / Center for Planetary Science (CPS)

Although convection has been suggested to occur in the lower part of Venus' cloud layer by some observational evidences, its structure remains to be clarified. In the previous studies, Baker et al. (1998, 2000), Imamura et al. (2014), and Lefevre et al. (2017) try to simulate Venus' cloud-level convection, but their models they utilized do not consider cloud formation process. Our purpose is to develop new cloud formation scheme and to perform numerical simulation using the scheme in order to investigate a possible structure of Venus' cloud-level convection and clouds distribution.

Our cloud formation scheme is based on Imamura and Hashimoto (1998). The number densities of sulfuric acid (H2SO4) and water (H2O) in the gas and liquid phases are calculated. Sedimentation of H2SO4-H2O solution droplets and chemical reactions of sulfuric acid are also considered. The scheme is implemented into our convection resolving model developed by Sugiyama et al. (2009). The model is based on the quasi-compressible system (Klemp and Wilhelmson, 1978), and is used in the simulations of the atmospheric convections of Jupiter (Sugiyama et al., 2011, 2014) and Mars (Yamashita et al. 2017).

In our poster, we will show the details of our cloud formation scheme and demonstrate some results of our calculation using similar settings of Imamura et al. (2014).

Keywords: Venus atmosphere, convection, cloud formation, numerical modeling

©2019. Japan Geoscience Union. All Right Reserved.

Zonal mean structure of Venus atmosphere observed in a Venus general circulation model with explicit radiative transfer

*Yoshi-Yuki Hayashi[1], Chisato Shiojiri[1], Hiroki Kashimura[1], Yoshiyuki O. Takahashi[1]

1. Department of Planetology/CPS, Graduate School of Science, Kobe University

Zonal mean zonal wind in Venus atmosphere is different from those in other planetary atmospheres. It is a strong prograde wind in all latitudinal ranges and is referred to as super-rotation. This unique zonal wind has been investigated by a lot of previous researchers with numerical simulations as well as ground-based and spacecraft observations. Among the studies with numerical simulations, in 2010s, Lebonnois et al. (2010) and Ikeda (2010) performed general circulation model simulations with an explicit radiative transfer model and successfully represented strong prograde zonal wind. These studies overcome a shortcoming of previous studies, in which models use Newtonian cooling as a radiative forcing.

In our group, we have been developing a general circulation model for planetary atmospheres. In addition, we have just developed a Venus radiation model, which can be used in a general circulation model. In this study, by implementing the radiation model into our general circulation model, we try to perform general circulation model simulations of Venus atmosphere and investigate the zonal mean structure of Venus atmosphere and evaluate differences between previous studies.

The general circulation model used in this study is DCPAM (http://www.gfd-dennou.org/library/dcpam/). The model is based on primitive equation system and the equation system is solved by a spectral transform method. The DCPAM includes physical processes of radiation and turbulent mixing processes. In addition, heat diffusion in soil is considered to evaluate surface temperature. The radiation model implemented into the DCPAM has also been developed in our group, and is based on a correlated k-distribution method. Radiative fluxes calculated by this radiation model are compared well with observed ones. By the use of the model, we performed two experiments with and without surface orographic variation. Resolution of experiments is T15L52, in which the model has 48 (longitude) times 24 (latitude) grids in horizontal direction and 52 layers in vertical direction. Initial conditions for those experiments are the same, and are
motionless atmospheres with horizontally uniform temperature distribution based on VIRA. With this initial condition, the model is integrated for 150000 Earth days with diurnal variation and with no seasonal variation, i.e. zero
obliquity.

Statistically steady states are achieved after about 100000 Earth days from the start of integrations. In steady state, prograde zonal winds with velocity of about 50 m/s in low and middle latitude are maintained at cloud layer in both experiments with and without orographic variation, although the velocity is about a half of that observed in Venus
atmosphere.

Meridional circulation observed in the model has large direct cells in both hemispheres. The direct cells in the experiment without surface orography have vertical extent from the ground up to top of the model, except for low latitude region just above the ground where indirect cells form. However, in the experiment with surface orography, the cells are split in the vertical direction at bottom of cloud layer. In addition to direct cells, several indirect cells are also observed in the experiments. One of those is indirect cell at

©2019. Japan Geoscience Union. All Right Reserved.

cloud layer in high latitude. Other ones are several indirect cells which extends from the ground up to bottom of cloud layer in the experiment with surface orography. These indicate that the effects of surface orography can be observed below the cloud layer, clearly.

In the presentation, results of analysis on zonal mean structure observed in the model, such as angular momentum, will also be presented.

Keywords: Venus, planetary atmosphere, general circulation model, explicit calculation of radiative transfer

©2019. Japan Geoscience Union. All Right Reserved.

Gravity wave packets detected in radio occultation temperature profiles of the Venus atmosphere

*Ryota Mori[1], Takeshi Imamura[1], Javier Peralta[2]

1. The University of Tokyo, 2. Japan Aerospace Exploration Agency

Temperature profiles has been obtained from 2016 by the radio occultation experiment in the Venus orbiter mission Akatsuki. The radio occultation experiment is a method that measures the change of the atmospheric refractive index as a change of the frequency of the signal received on the ground. At the opportunity when the radio wave transmitted from Akatsuki toward the Earth pass through the planetary atmosphere, the wave is refracted and then reaches the receiving station. We can retrieve the vertical profiles of the pressure and the temperature from each refractive index profiles. In the temperature profile obtained in this way, variations due to various atmospheric disturbances are observed. We focus on gravity waves which are thought to play an import role in driving the general atmosphere circulation.

Gravity waves are small-scale waves with the restoring force being the buoyancy in the atmosphere. Gravity waves play a role in carrying the momentum in the vertical direction. So, it results in acceleration or deceleration of the mean wind by passing momentum on the background atmosphere while dissipating. This process should affect the global structure of the high-speed zonal wind. However, since gravity waves have properties that the spatial scale is small and the wave period is relatively short, it is difficult to capture the spatial structure by observation. The latitudinal profile of the amplitude of short vertical-scale temperature disturbances, which are thought to be associated with gravity waves, has been investigated; however, the dominant wavelength and the typical vertical extent have not been studied.

In this study, we applied wavelet analysis to the temperature profiles and extracted spatially localized temperature disturbances. Though there have been studies that apply Fourier transform to the temperature data, Fourier transform assumes infinitely lasting waves and it is not suitable for extracting spatially localized wave packets. Wavelet analysis is an effective way of obtaining the periods and the amplitudes of waves in such finite intervals. In this presentation, we report the result of wavelet analysis applied to the temperature data obtained with high vertical resolution by radio holographic method. From the obtained results, we also report the relationship between the length and the packet length of gravity wave in the atmosphere.

Keywords: Akatsuki, Gravity wave in the atmosphere, The radio occultation experiment

©2019. Japan Geoscience Union. All Right Reserved.

Status of lightning hunt in Venus with Akatsuki/LAC and Pirka telescope

*Yukihiro Takahashi[1,2], Mitsuteru Sato[1,2], Masataka Imai[3], Ralph Lorenz[4], Seiko Takagi[1,2], Ono Tatsuharu[1]

1. Graduate School of Science, Hokkaido University, 2. Faculty of Science, Hokkaido University, 3. National Institute of Advanced Industrial Science and Technology,, 4. Applied Physics Laboratory, Johns Hopkins University

The existence of lightning discharge in Venus has been controversial for three decades, which might be attributed to the luck of conclusive observational evidence. There had been no satellite payload intentionally designed for the detection of lightning phenomena using radio wave or optical sensor. LAC, lightning and airglow camera, on board Akatsuki spacecraft, is the first sensor optimized for the lightning optical flash measurement in planets other than the Earth. It is expected that LAC could conclude this 30-year discussion on the existence of lightning in Venus. Unique performance of LAC compared to other equipment used in the previous exploration of Venus is the high-speed sampling rate at 20 kHz with 32 pixels of Avalanche Photo Diode (APD) matrix, enabling us to distinguish the natural optical lightning flash from other pulsing noises, including artificial electrical noise and cosmic rays. We selected OI 777 nm line for lightning detection, which is expected to be the most prominent emission in CO2-dominant atmosphere based on the laboratory experiments.

The triggering parameter was set so as to optimize for the light curve similar to the normal lightning in the Earth and data obtained totally for about 4 hours were examined. However, we couldn’ t find any lightning signals. Adding to this triggering parameter set, we added one more parameter set, optimized for sprite type emission with duration of up to 10s of ms. Furthermore, in order to investigate fainter emissions, we are now conducting successive force triggering recordings without any threshold, achieving 5 times better sensitivity than the intensity of 1 digital unit at best.

The total coverage of the LAC lightning hunt became 81.6 [million km2-hr], meaning 81 percent detectability of previous results with ground-based telescope by Hansell et al. (1995). Here we report the detailed strategy and the latest status of the LAC observation in 2018, and discuss the future observation plan.

Also we will make ground observation with a high-speed photometer installed at Pirka telescope, a 1.6-m reflector deployed by Hokkaido University. Here we report the initial results of lightning flash observation with it.

Keywords: lightning, Venus, Akatsuki, Pirka telescope

©2019. Japan Geoscience Union. All Right Reserved.

Possibility of electric discharge in the Venusian atmosphere due to the super-rotation of clouds

*Adhithiyan Neduncheran[1], Ugur Guven[1,2], Ananyo Bhattacharya[3]

1. University of Petroleum and Energy Studies, India, 2. United Nations Centre for Space Science and Technology Education in Asia and the Pacific, 3. Sardar Vallabhbhai National Institute of Technology,India

Several evidences of electromagnetic bursts were measured by various landers and orbiters studying Venus atmosphere (Venera landers, Venus Express and the Pioneer Venus Orbiter). The electromagnetic bursts that are taking place in the cloud region in the form of lightning or fluorescence might be a result of momentum transfer, solar convection and charge dispersion in the clouds of Venus. While the lightning in Earth takes place mostly in the equatorial region, in case of Venus it is possible for lightning to occur in the polar regions, considering the kinetic energy transfer and the formation of dipoles in both hemispheres of Venus. The meridional and zonal flows can interact and cause the charge separation which possibly lead to electromagnetic bursts in different spectrum and in different regions in Venus. In labs, it is observed that SO2 emissions in UV region cause fluorescence which is one of the major phenomena taking place in the cloud tops. Based on the photochemical model published by *Krasnopolsky 2011(*doi:10.1016/j.icarus.2011.11.012) and the principle of refraction, we present the possibility of lightning/fluorescence phenomena being caused by the super-rotation of the clouds in the Venusian atmosphere.

Keywords: Venus , Super-rotation, lightning, electric discharge, atmosphere

©2019. Japan Geoscience Union. All Right Reserved.

[E] Poster | P (Space and Planetary Sciences)：P-EM Solar-Terrestrial Sciences, Space Electromagnetism & Space Environment

Mon. May 27, 2019 1:45 PM - 3:15 PM JST | Mon. May 27, 2019 4:45 AM - 6:15 AM UTC | Poster Hall International Exhibition Hall8, Makuhari Messe_1

[P-EM10] Multi-scale Coupling in the Magnetosphere-Ionosphere-Thermosphere System

convener:Yue Deng(University of Texas at Arlington), Toshi Nishimura(Boston University), Huixin Liu(Earth and Planetary Science Division, Kyushu University SERC, Kyushu University), Yanshi Huang(Harbin Institute of Technology, Shenzhen)

Determining the effects of energy deposition and transport, and momentum exchange across different spatial and temporal scales is an important objective in the M-I-T system, due to the clear evidence of multi-scale forcing. Coupling over multiple scales is also a critical challenge since observational and modeling methodologies for bridging different scales do not presently exist. This session solicits presentations on a wide range of coupling processes in the high-latitude M-I-T system from global to small-scale processes and related solar wind forcing. Relevant topics include (but are not limited to) (1) density structures and temperature gradients (polar cap, cusp, plume, trough, irregularities); (2) convection (flow channels, SAPS) and FAC; (3) energy transfer and deposition by precipitation and ULF waves, conductivity, aurora, and heating; and (4) coupling and feedback into the magnetosphere. Discussions of relevant multi-scale observations by means of multiple instruments, including space and ground-based, modeling and data science are encouraged.

[PEM10-P01] Atmospheric responses in both hemispheres to relativistic electron precipitation

*Yoshimasa Tanaka[1,13,14], Takanori Nishiyama[1,14], Akira Kadokura[1,13,14], Mitsunori Ozaki[2], Yoshizumi Miyoshi[3], Shin-ichiro Oyama[3,15], Ryuho Kataoka[1,14], Masaki Tsutsumi[1,14], Koji Nishimura[1,13,14], Kaoru Sato[4], Yoshiya Kasahara[2], Atsushi Kumamoto[5], Fuminori Tsuchiya[5], Mizuki Fukizawa[5], Mitsuru Hikishima[6], Shoya Matsuda[6], Ayako Matsuoka[6], Iku Shinohara[6], Masahito Nose[3], Tsutomu Nagatsuma[7], Manabu Shinohara[8], Akiko Fujimoto[9], Mariko Teramoto[3], Reiko Nomura[10], Akira Sessai Yukimatu[1,14], Keisuke Hosokawa[11], Masafumi Shoji[3], Ralph Latteck[12] (1.National Institute of Polar Research, 2.Institute of Science and Engineering, Kanazawa University, 3.Institute for Space-Earth Environmental Research, Nagoya University, 4.Graduate School of Science, The University of Tokyo, 5.Graduate School of Science, Tohoku University, 6.Japan aerospace exploration agency, Institute of space and astronautical science, 7.National Institute of Information and Communications Technology, 8.Kagoshima National College of Technology, 9.Kyushu Institute of Technology, 10.National Observatory of Japan, 11.Department of Communication Engineering and Informatics, University of Electro-Communications, 12.Leibniz-Institute of Atmospheric Physics e.V. at the University Rostock, Germany, 13.Polar Environment Data Science Center, Joint-Support Center for Data Science Research, Research Organization of Information and Systems, 14.The Graduate University for Advanced Studies (SOKENDAI), 15.University of Oulu, Finland)

[PEM10-P02] Comparison of precipitating particle energy of proton aurora at geomagnetic conjugate points

*Makoto Taguchi[1], Tatsuki Nishijima[1], Akira Kadokura[2] (1.Rikkyo University, 2.Research Organization of Information and Systems)

[PEM10-P03] A regularized deep convolutional general adversarial network (R-DCGAN) for total electron content map completion

*Mingwu Jin[1], Zhou Chen[2,3], Yue Deng[1], Yang Pan[1], Jin-Song Wang[2] (1.University of Texas at Arlington, 2.Institute of Space Science and Technology, Nanchang University, Nanchang, China, 3.Key Laboratory of Space Weather, National Center for Space Weather, China Meteorological Administration, Beijing, China)

[PEM10-P04] A long-lasting auroral bright spot around magnetic north pole: Is it the evidence of stable magnetic reconnection?

*Qing-He Zhang[1], Guo-Cheng Shen[1], Yong-Liang Zhang[2], Kjellmar Oksavik[3], Michael Lockwood[4], Zan-Yang Xing[1], Yu-Zhang Ma[1] (1.Institute of Space Sciences, Shandong University, Weihai, China, 2.The Johns Hopkins University Applied Physics Laboratory, Laurel, Maryland, USA, 3.Birkeland Centre for Space

Science, University of Bergen, Bergen, Norway, 4.Department of Meteorology, University of Reading, Earley Gate, Post Office Box 243, RG6 6BB, UK.)

[PEM10-P05] Statistical study of the relationship between ion upflow and field-aligned current in the topside ionosphere for both hemispheres during disturbed and quiet times

Shan-Yu Zhou[1], *Qing-He Zhang[1], P. T. Jayachandran[2], Kjellmar Oksavik[3], Larry Lyons[4], Zan-Yang Xing[1], Yu-Zhang Ma[1], Marc Hairston[5], Yong Wang[1] (1.Institute of Space Sciences, Shandong University, Weihai, China, 2.Physics Department, University of New Brunswick, Fredericton, New Brunswick, Canada, 3.Birkeland Centre for Space Science, University of Bergen, Bergen, Norway, 4.Department of Atmospheric and Oceanic Sciences, University of California, Los Angeles, California, USA, 5.William B. Hanson Center for Space Sciences, University of Texas at Dallas, Richardson, Texas, USA)

[PEM10-P06] SAPS in the 2013 March 17 Storm Event: Initial Results from the Coupled Magnetosphere-Ionosphere-Thermosphere Model

*Dong Lin[1,2], Wenbin Wang[2], Wayne Scales[1], Kevin Pham[2], Jing Liu[2], Binzheng Zhang[2], Viacheslav Merkin[3], Xueling Shi[1] (1.Virginia Tech, 2.High Altitude Observatory, NCAR, 3.APL, John Hopkins Univ.)

[PEM10-P07] **Westward turning motions of nighttime medium-scale traveling ionospheric disturbances (MSTIDs) at the equatorward side of the dusk side auroral oval associated with auroral brightening**

*Sneha Yadav[1,2], Kazuo Shiokawa[1], Shin-ichiro Oyama[1,3,4], Yuichi Otsuka[1] (1.ISEE, Nagoya University, Nagoya, Japan, 2.SPL, VSSC, India, 3.Ionosphere Research Unit, University of Oulu, Oulu, Finland, 4.NIPR, Tachikawa, Japan)

Atmospheric responses in both hemispheres to relativistic electron precipitation

*Yoshimasa Tanaka[1,13,14], Takanori Nishiyama[1,14], Akira Kadokura[1,13,14], Mitsunori Ozaki[2], Yoshizumi Miyoshi[3], Shin-ichiro Oyama[3,15], Ryuho Kataoka[1,14], Masaki Tsutsumi[1,14], Koji Nishimura[1,13,14], Kaoru Sato[4], Yoshiya Kasahara[2], Atsushi Kumamoto[5], Fuminori Tsuchiya[5], Mizuki Fukizawa[5], Mitsuru Hikishima[6], Shoya Matsuda[6], Ayako Matsuoka[6], Iku Shinohara[6], Masahito Nose[3], Tsutomu Nagatsuma[7], Manabu Shinohara[8], Akiko Fujimoto[9], Mariko Teramoto[3], Reiko Nomura[10], Akira Sessai Yukimatu[1,14], Keisuke Hosokawa[11], Masafumi Shoji[3], Ralph Latteck[12]

1. National Institute of Polar Research, 2. Institute of Science and Engineering, Kanazawa University, 3. Institute for Space-Earth Environmental Research, Nagoya University, 4. Graduate School of Science, The University of Tokyo, 5. Graduate School of Science, Tohoku University, 6. Japan aerospace exploration agency, Institute of space and astronautical science, 7. National Institute of Information and Communications Technology, 8. Kagoshima National College of Technology, 9. Kyushu Institute of Technology, 10. National Observatory of Japan, 11. Department of Communication Engineering and Informatics, University of Electro-Communications, 12. Leibniz-Institute of Atmospheric Physics e.V. at the University Rostock, Germany, 13. Polar Environment Data Science Center, Joint-Support Center for Data Science Research, Research Organization of Information and Systems, 14. The Graduate University for Advanced Studies (SOKENDAI), 15. University of Oulu, Finland

Relativistic electron precipitation (REP) in the polar atmosphere has been paid attention to because it changes atmospheric composition, causing ozone depletion after migrating to the lower altitude during polar winter. A plausible mechanism for REP is the interaction with magnetospheric plasma waves, such as electromagnetic ion cyclotron (EMIC) waves and whistler-mode chorus waves. Previous studies have already shown that EMIC waves can effectively drive REP, however, observational evidence that chorus waves can drive REP was lacking. In this study we present direct comparison between magnetospheric plasma waves and polar mesosphere winter echoes (PMWE) simultaneously observed with the Arase satellite and high-power Mesosphere, Stratosphere and Troposphere (MST) radars in both hemispheres, PANSY and MAARSY. PMWE can be related to the ionization in the mesosphere due to REP. The PMWE were observed at 03-07 UT on March 21, 2017 during the passage of corotating interaction region (CIR), during which the Arase footprints were close to Syowa Station (SYO; −69.00S, 39.58E), Antarctica, and Husafell (HUS; 65.67N, −21.03E), Iceland.
The observational results are summarized as follows. (1) EMIC waves and whistler-mode chorus waves were observed by Arase near the equatorial magnetosphere during 02:30-04:45 UT and 04:45-07:00 UT, respectively. (2) PMWE were detected with both the MAARSY radar at Andøya (AND; 69.30N, 16.04E), Norway, and the PANSY radar at SYO, Antarctica, during 04:45-07:00 UT, which was the recovery phase of an isolated substorm. We believe this is the first time PMWE have been observed in both hemispheres at exactly the same time. (3) During 04:45-07:00 UT, the temporal variation of the chorus wave power was similar to those of the PMWE power in the both hemispheres. (4) The PMWE observed at SYO during 03:00-04:00 UT before the substorm onset was consistent with the occurrence of the EMIC waves. The item (2) shows direct evidence that chorus waves during the substorm recovery phase cause REP. We estimated the resonance energy of electrons interacting with the observed LBC waves, however, the estimated energy was too low to cause PMWE at an altitude lower than 70 km. However, we found that the resonance energy becomes greater than 1 MeV, if LBC waves propagate to the magnetic latitude greater than 30 degrees and resonate with energetic electrons there. As for item (4), the PMWE observed at SYO during 03:00-04:00 can be related to wave-particle interaction with EMIC waves, which may be generated inside the plasmapause by ring-current hot ions with temperature anisotropy. This anisotropy

©2019. Japan Geoscience Union. All Right Reserved.

was caused by magnetospheric compression due to increasing solar wind dynamic pressure during 01:00–06:00 UT just after the arrival of the CIR. Since CIRs are main sources of geomagnetic disturbances during the declining phase of the solar cycle and solar minimum, this event is not rare but rather a common atmospheric response caused by interaction between recurrent large-scale solar wind structures and geospace.

Keywords: Polar Mesosphere Winter Echoes, Arase satellite, PANSY radar, MAARSY radar, relativistic electron precipitation, magnetospheric plasma waves

©2019. Japan Geoscience Union. All Right Reserved.

Comparison of precipitating particle energy of proton aurora at geomagnetic conjugate points

*Makoto Taguchi[1], Tatsuki Nishijima[1], Akira Kadokura[2]

1. Rikkyo University, 2. Research Organization of Information and Systems

It is expected that mirror images of aurora are observed at geomagnetic conjugate points in the northern and southern auroral zones connected by a geomagnetic field line. However, geomagnetic conjugate auroras often show non-conjugacy, which reflects north-south asymmetry of the solar wind, the magnetosphere and the ionospheres. In other words acceleration mechanism of auroral particles may be studied by comparing aurora simultaneously occurring at geomagnetic conjugate points. A hydrogen Balmer beta emission at the wavelength of 486.1 nm which is the brightest among the proton auroral lines was observed at a pair of geomagnetic conjugate points to compare precipitating particle energy. Two identical Proton Auroral Specrographs (PASs) which obtain auroral spectra along a geomagnetic meridian at a rate of 1 image/min were installed at Tjornes in Iceland and Syowa Station in Antarctica. Data obtained during a period from September 4, 2018 to October 9, 2018 were analyzed to derive an average kinetic energy of precipitating protons along a local geomagnetic field line from a Doppler shift of the H beta line. As a result we are succeeded in simultaneous observations of proton auroras at both conjugate points in 5 nights on September 4, 5, 6, 7 , and 10. The average energies of precipitating protons range from 0 keV to 7 keV, and sometimes show a periodical variation with a period of 4 - 5 min. Conjugacy of precipitating particle energy will be discussed in the presentation.

©2019. Japan Geoscience Union. All Right Reserved.

A regularized deep convolutional general adversarial network (R-DCGAN) for total electron content map completion

*Mingwu Jin[1], Zhou Chen[2,3], Yue Deng[1], Yang Pan[1], Jin-Song Wang[2]

1. University of Texas at Arlington, 2. Institute of Space Science and Technology, Nanchang University, Nanchang, China, 3. Key Laboratory of Space Weather, National Center for Space Weather, China Meteorological Administration, Beijing, China

Observations with a complete global coverage are important for space physics research and applications. However, due to the technical limitations and costs, such a complete global coverage is often unavailable. Thus, data filling algorithms are often pursued to fill missing data gaps to create a global map from the incomplete data. In this work, a novel deep learning algorithm, regularized deep convolutional generative adversarial network (R-DCGAN), is developed by adding an extra discriminator to the conventional DCGAN to fill the missing data of total electron content (TEC) map images. R-DCGAN incorporates the knowledge from reference TEC maps of the International Global Navigation Satellite Systems Service Ionosphere Working Group to achieve much better TEC map completion performance than the conventional DCGAN as demonstrated by both synthetic and real data. The R-DCGAN framework can be extended to other fields of space sciences to address the missing observation data issues.

Keywords: Deep learning method, TEC , map completion

©2019. Japan Geoscience Union. All Right Reserved.

A long-lasting auroral bright spot around magnetic north pole: Is it the evidence of stable magnetic reconnection?

*Qing-He Zhang[1], Guo-Cheng Shen[1], Yong-Liang Zhang[2], Kjellmar Oksavik[3], Michael Lockwood[4], Zan-Yang Xing[1], Yu-Zhang Ma[1]

1. Institute of Space Sciences, Shandong University, Weihai, China, 2. The Johns Hopkins University Applied Physics Laboratory, Laurel, Maryland, USA, 3. Birkeland Centre for Space Science, University of Bergen, Bergen, Norway, 4. Department of Meteorology, University of Reading, Earley Gate, Post Office Box 243, RG6 6BB, UK.

An intense and large auroral bright spot appears around the magnetic north pole observed by the Special Sensor Ultraviolet Spectrographic Imager (SSUSI) on board four different Defense Meteorological Satellite Program (DMSP) satellites during long time northward IMF conditions. The bright spot is even brighter than aurora in the auroral oval which is about 5-10° magnetic latitude equatorward of the bright spot. The bright spot is lasting about 8 hours, and sometimes appears as a cyclone-shape with a clockwise rotation. The DMSP in situ plasma observations suggest that the bright spot is clear associated with electron invert-V acceleration with 10s keV energy electron precipitations around the center regions and 1s keV energy electron precipitations around the egde regions. There are also strong flow shears between the two sides of the bright spot: strong sunward flows on the duskside and antisunward flows on the dawnside. These types of plasma should come from the high-latitude lobe region of the magnetotail due to the high-latitude lobe magnetic reconnections. Is it the evidence of stable lobe reconnection during long time northward IMF conditions? The detail and further analysis should be pursued in the following studies.

Keywords: Auroral bright spot, Magnetosphere-ionosphere coupling, High-latitude lobe magnetic reconnection, Stable reconnection

©2019. Japan Geoscience Union. All Right Reserved.

Statistical study of the relationship between ion upflow and field-aligned current in the topside ionosphere for both hemispheres during disturbed and quiet times

Shan-Yu Zhou[1], *Qing-He Zhang[1], P. T. Jayachandran[2], Kjellmar Oksavik[3], Larry Lyons[4], Zan-Yang Xing[1], Yu-Zhang Ma[1], Marc Hairston[5], Yong Wang[1]

1. Institute of Space Sciences, Shandong University, Weihai, China, 2. Physics Department, University of New Brunswick, Fredericton, New Brunswick, Canada, 3. Birkeland Centre for Space Science, University of Bergen, Bergen, Norway, 4. Department of Atmospheric and Oceanic Sciences, University of California, Los Angeles, California, USA, 5. William B. Hanson Center for Space Sciences, University of Texas at Dallas, Richardson, Texas, USA

A statistical study of ion upflow and field-aligned currents (FACs) has been performed in the topside ionosphere of both hemispheres for magnetic quiet and disturbed times by using DMSP satellite observations from 2010-2013. Distributions in MLT/MLAT reveal that ion upflow shows a dawn-dusk asymmetry distribution that corresponds well with the region 1 field-aligned currents. In addition, there are highest occurrence regions near noon and within the near midnight auroral disturbance area. These correspond to cusp and nightside dynamical processes, respectively. Both the ion upflow occurrence and FAC regions expand equatorward to a wider area during disturbed times.

Keywords: Ion upflows, Field-aligned current, Magnetosphere-ionosphere coupling

©2019. Japan Geoscience Union. All Right Reserved.

SAPS in the 2013 March 17 Storm Event: Initial Results from the Coupled Magnetosphere-Ionosphere-Thermosphere Model

*Dong Lin[1,2], Wenbin Wang[2], Wayne Scales[1], Kevin Pham[2], Jing Liu[2], Binzheng Zhang[2], Viacheslav Merkin[3], Xueling Shi[1]

1. Virginia Tech, 2. High Altitude Observatory, NCAR, 3. APL, John Hopkins Univ.

Subauroral polarization stream (SAPS) are latitudinally narrow flow channels of large westward plasma drifts in the subauroral ionosphere. In this study, the global structure and dynamic evolution of SAPS are investigated by using the National Center for Atmospheric Research (NCAR) Coupled Magnetosphere-Ionosphere-Thermosphere (CMIT) model with Ring Current extension, namely the LFM-TIEGCM-RCM (LTR) model, to simulate the 2013 St. Patrick's Day storm event. This is the first time that the global distribution and temporal evolution of SAPS are investigated using first-principle models. The model shows a strong westward ion drift channel formed equatorward of the auroral electron precipitation boundary on the duskside, which is identified as the SAPS structure. The simulated ion drift velocity and auroral electron precipitation sampled along the trajectory of the DMSP F18 satellite are in good agreement with the satellite measurements. SAPS initiate in the pre-dusk sector when the interplanetary magnetic field (IMF) turns southward. SAPS latitude generally decreases with magnetic local time (MLT) from dusk to midnight. The SAPS channel shows wedge, inverse wedge, and crescent morphologies during the storm, and becomes discontinuous when the IMF is weakly southward. The SAPS mean latitude has a correlation coefficient of 0.77 with the Dst index. The mean latitude moves equatorward and the flow channel broadens in the storm main phase. The simulation results are consistent with observational studies. They also illustrate the global distributions and highly dynamic behaviors of SAPS that are not readily apparent from observation data.

Keywords: SAPS, Magnetosphere-Ionosphere-Thermosphere coupling, LFM-TIEGCM-RCM

©2019. Japan Geoscience Union. All Right Reserved.

Westward turning motions of nighttime medium-scale traveling ionospheric disturbances (MSTIDs) at the equatorward side of the dusk side auroral oval associated with auroral brightening

*Sneha Yadav[1,2], Kazuo Shiokawa[1], Shin-ichiro Oyama[1,3,4], Yuichi Otsuka[1]

1. ISEE, Nagoya University, Nagoya, Japan, 2. SPL, VSSC, India, 3. Ionosphere Research Unit, University of Oulu, Oulu, Finland, 4. NIPR, Tachikawa, Japan

The characteristics of high-latitude nighttime medium-scale traveling ionospheric disturbances (MSTIDs) have not been well investigated using all-sky imagers because of the hindrance caused by the bright aurora. The limited results on the propagation characteristics of MSTIDs over high-latitudes hindered the progress in our understanding on these dynamical structure. In a case study carried out by Shiokawa et al. (JGR, 2012), an event of oscillating MSTIDs was reported over Tromsø (69.6˚N, 19.2˚E; corrected geomagnetic latitude: 66.6˚N), which was observed to be associated with auroral brightening. However, after this case study, which comprised of only one event, no observations showing oscillating motion of MSTIDs have been reported till date. In this study, for the first time, the comprehensive investigation on the westward turning of the MSTIDs in the equatorward side of the dusk side auroral oval has been performed. The all-sky imaging data of 630.0 nm airglow emissions during 2010-2018 are used to study the motions of MSTIDs over Tromsø. The results indicate that the nighttime MSTIDs primarily exhibit eastward motion under quiet magnetic conditions but turned in the westward direction during the active geomagnetic conditions. The turning of MSTIDs in the westward direction were invariably associated with the auroral brightening observed at the poleward edge of the all-sky image and localized magnetic field perturbations observed by ground-based magnetometers at Tromsø. The interesting aspect of the observations is the fact that these westward moving MSTIDs again turned in the eastward direction when the geomagnetic disturbance ceases. The SuperDARN (Super Dual Auroral Radar Network) convection maps revealed that the location of Tromsø was inside/outside the convection cell region during the time of appearance of westward/eastward moving MSTIDs. The Doppler shift measurement of the 630-nm airglow by a Fabry-Perot interferometer at Tromsø showed that northeastward winds were predominant during the appearance of eastward moving MSTIDs. The cause of the observed MSTIDs remains in question as they might either be triggered by atmospheric gravity waves or by Perkins instability. These experimental evidences suggest that the MSTIDs tend to move eastward in accordance with the background F-region dynamo electric field, but show westward motion under the influence of electric field associated with auroral activities in the dusk side of two-cell convection pattern.

Keywords: MSTIDs, Auroral oval, Airglow

©2019. Japan Geoscience Union. All Right Reserved.

[E] Poster | P (Space and Planetary Sciences)：P-EM Solar-Terrestrial Sciences, Space Electromagnetism & Space Environment

Mon. May 27, 2019 5:15 PM - 6:30 PM JST | Mon. May 27, 2019 8:15 AM - 9:30 AM UTC | Poster Hall International Exhibition Hall8, Makuhari Messe_4

[P-EM10] Multi-scale Coupling in the Magnetosphere-Ionosphere-Thermosphere System

convener:Yue Deng(University of Texas at Arlington), Toshi Nishimura(Boston University), Huixin Liu(Earth and Planetary Science Division, Kyushu University SERC, Kyushu University), Yanshi Huang(Harbin Institute of Technology, Shenzhen)

Determining the effects of energy deposition and transport, and momentum exchange across different spatial and temporal scales is an important objective in the M-I-T system, due to the clear evidence of multi-scale forcing. Coupling over multiple scales is also a critical challenge since observational and modeling methodologies for bridging different scales do not presently exist. This session solicits presentations on a wide range of coupling processes in the high-latitude M-I-T system from global to small-scale processes and related solar wind forcing. Relevant topics include (but are not limited to) (1) density structures and temperature gradients (polar cap, cusp, plume, trough, irregularities); (2) convection (flow channels, SAPS) and FAC; (3) energy transfer and deposition by precipitation and ULF waves, conductivity, aurora, and heating; and (4) coupling and feedback into the magnetosphere. Discussions of relevant multi-scale observations by means of multiple instruments, including space and ground-based, modeling and data science are encouraged.

[PEM10-P01] Atmospheric responses in both hemispheres to relativistic electron precipitation

*Yoshimasa Tanaka[1,13,14], Takanori Nishiyama[1,14], Akira Kadokura[1,13,14], Mitsunori Ozaki[2], Yoshizumi Miyoshi[3], Shin-ichiro Oyama[3,15], Ryuho Kataoka[1,14], Masaki Tsutsumi[1,14], Koji Nishimura[1,13,14], Kaoru Sato[4], Yoshiya Kasahara[2], Atsushi Kumamoto[5], Fuminori Tsuchiya[5], Mizuki Fukizawa[5], Mitsuru Hikishima[6], Shoya Matsuda[6], Ayako Matsuoka[6], Iku Shinohara[6], Masahito Nose[3], Tsutomu Nagatsuma[7], Manabu Shinohara[8], Akiko Fujimoto[9], Mariko Teramoto[3], Reiko Nomura[10], Akira Sessai Yukimatu[1,14], Keisuke Hosokawa[11], Masafumi Shoji[3], Ralph Latteck[12] (1.National Institute of Polar Research, 2.Institute of Science and Engineering, Kanazawa University, 3.Institute for Space-Earth Environmental Research, Nagoya University, 4.Graduate School of Science, The University of Tokyo, 5.Graduate School of Science, Tohoku University, 6.Japan aerospace exploration agency, Institute of space and astronautical science, 7.National Institute of Information and Communications Technology, 8.Kagoshima National College of Technology, 9.Kyushu Institute of Technology, 10.National Observatory of Japan, 11.Department of Communication Engineering and Informatics, University of Electro-Communications, 12.Leibniz-Institute of Atmospheric Physics e.V. at the University Rostock, Germany, 13.Polar Environment Data Science Center, Joint-Support Center for Data Science Research, Research Organization of Information and Systems, 14.The Graduate University for Advanced Studies (SOKENDAI), 15.University of Oulu, Finland)

[PEM10-P02] Comparison of precipitating particle energy of proton aurora at geomagnetic conjugate points

*Makoto Taguchi[1], Tatsuki Nishijima[1], Akira Kadokura[2] (1.Rikkyo University, 2.Research Organization of Information and Systems)

[PEM10-P03] A regularized deep convolutional general adversarial network (R-DCGAN) for total electron content map completion

*Mingwu Jin[1], Zhou Chen[2,3], Yue Deng[1], Yang Pan[1], Jin-Song Wang[2] (1.University of Texas at Arlington, 2.Institute of Space Science and Technology, Nanchang University, Nanchang, China, 3.Key Laboratory of Space Weather, National Center for Space Weather, China Meteorological Administration, Beijing, China)

[PEM10-P04] A long-lasting auroral bright spot around magnetic north pole: Is it the evidence of stable magnetic reconnection?

*Qing-He Zhang[1], Guo-Cheng Shen[1], Yong-Liang Zhang[2], Kjellmar Oksavik[3], Michael Lockwood[4], Zan-Yang Xing[1], Yu-Zhang Ma[1] (1.Institute of Space Sciences, Shandong University, Weihai, China, 2.The Johns Hopkins University Applied Physics Laboratory, Laurel, Maryland, USA, 3.Birkeland Centre for Space

Science, University of Bergen, Bergen, Norway, 4.Department of Meteorology, University of Reading, Earley Gate, Post Office Box 243, RG6 6BB, UK.)

[PEM10-P05] Statistical study of the relationship between ion upflow and field-aligned current in the topside ionosphere for both hemispheres during disturbed and quiet times

Shan-Yu Zhou[1], *Qing-He Zhang[1], P. T. Jayachandran[2], Kjellmar Oksavik[3], Larry Lyons[4], Zan-Yang Xing[1], Yu-Zhang Ma[1], Marc Hairston[5], Yong Wang[1] (1.Institute of Space Sciences, Shandong University, Weihai, China, 2.Physics Department, University of New Brunswick, Fredericton, New Brunswick, Canada, 3.Birkeland Centre for Space Science, University of Bergen, Bergen, Norway, 4.Department of Atmospheric and Oceanic Sciences, University of California, Los Angeles, California, USA, 5.William B. Hanson Center for Space Sciences, University of Texas at Dallas, Richardson, Texas, USA)

[PEM10-P06] SAPS in the 2013 March 17 Storm Event: Initial Results from the Coupled Magnetosphere-Ionosphere-Thermosphere Model

*Dong Lin[1,2], Wenbin Wang[2], Wayne Scales[1], Kevin Pham[2], Jing Liu[2], Binzheng Zhang[2], Viacheslav Merkin[3], Xueling Shi[1] (1.Virginia Tech, 2.High Altitude Observatory, NCAR, 3.APL, John Hopkins Univ.)

[PEM10-P07] **Westward turning motions of nighttime medium-scale traveling ionospheric disturbances (MSTIDs) at the equatorward side of the dusk side auroral oval associated with auroral brightening**

*Sneha Yadav[1,2], Kazuo Shiokawa[1], Shin-ichiro Oyama[1,3,4], Yuichi Otsuka[1] (1.ISEE, Nagoya University, Nagoya, Japan, 2.SPL, VSSC, India, 3.Ionosphere Research Unit, University of Oulu, Oulu, Finland, 4.NIPR, Tachikawa, Japan)

Atmospheric responses in both hemispheres to relativistic electron precipitation

*Yoshimasa Tanaka[1,13,14], Takanori Nishiyama[1,14], Akira Kadokura[1,13,14], Mitsunori Ozaki[2], Yoshizumi Miyoshi[3], Shin-ichiro Oyama[3,15], Ryuho Kataoka[1,14], Masaki Tsutsumi[1,14], Koji Nishimura[1,13,14], Kaoru Sato[4], Yoshiya Kasahara[2], Atsushi Kumamoto[5], Fuminori Tsuchiya[5], Mizuki Fukizawa[5], Mitsuru Hikishima[6], Shoya Matsuda[6], Ayako Matsuoka[6], Iku Shinohara[6], Masahito Nose[3], Tsutomu Nagatsuma[7], Manabu Shinohara[8], Akiko Fujimoto[9], Mariko Teramoto[3], Reiko Nomura[10], Akira Sessai Yukimatu[1,14], Keisuke Hosokawa[11], Masafumi Shoji[3], Ralph Latteck[12]

1. National Institute of Polar Research, 2. Institute of Science and Engineering, Kanazawa University, 3. Institute for Space-Earth Environmental Research, Nagoya University, 4. Graduate School of Science, The University of Tokyo, 5. Graduate School of Science, Tohoku University, 6. Japan aerospace exploration agency, Institute of space and astronautical science, 7. National Institute of Information and Communications Technology, 8. Kagoshima National College of Technology, 9. Kyushu Institute of Technology, 10. National Observatory of Japan, 11. Department of Communication Engineering and Informatics, University of Electro-Communications, 12. Leibniz-Institute of Atmospheric Physics e.V. at the University Rostock, Germany, 13. Polar Environment Data Science Center, Joint-Support Center for Data Science Research, Research Organization of Information and Systems, 14. The Graduate University for Advanced Studies (SOKENDAI), 15. University of Oulu, Finland

Relativistic electron precipitation (REP) in the polar atmosphere has been paid attention to because it changes atmospheric composition, causing ozone depletion after migrating to the lower altitude during polar winter. A plausible mechanism for REP is the interaction with magnetospheric plasma waves, such as electromagnetic ion cyclotron (EMIC) waves and whistler-mode chorus waves. Previous studies have already shown that EMIC waves can effectively drive REP, however, observational evidence that chorus waves can drive REP was lacking. In this study we present direct comparison between magnetospheric plasma waves and polar mesosphere winter echoes (PMWE) simultaneously observed with the Arase satellite and high-power Mesosphere, Stratosphere and Troposphere (MST) radars in both hemispheres, PANSY and MAARSY. PMWE can be related to the ionization in the mesosphere due to REP. The PMWE were observed at 03-07 UT on March 21, 2017 during the passage of corotating interaction region (CIR), during which the Arase footprints were close to Syowa Station (SYO; −69.00S, 39.58E), Antarctica, and Husafell (HUS; 65.67N, −21.03E), Iceland.
The observational results are summarized as follows. (1) EMIC waves and whistler-mode chorus waves were observed by Arase near the equatorial magnetosphere during 02:30-04:45 UT and 04:45-07:00 UT, respectively. (2) PMWE were detected with both the MAARSY radar at Andøya (AND; 69.30N, 16.04E), Norway, and the PANSY radar at SYO, Antarctica, during 04:45-07:00 UT, which was the recovery phase of an isolated substorm. We believe this is the first time PMWE have been observed in both hemispheres at exactly the same time. (3) During 04:45-07:00 UT, the temporal variation of the chorus wave power was similar to those of the PMWE power in the both hemispheres. (4) The PMWE observed at SYO during 03:00-04:00 UT before the substorm onset was consistent with the occurrence of the EMIC waves. The item (2) shows direct evidence that chorus waves during the substorm recovery phase cause REP. We estimated the resonance energy of electrons interacting with the observed LBC waves, however, the estimated energy was too low to cause PMWE at an altitude lower than 70 km. However, we found that the resonance energy becomes greater than 1 MeV, if LBC waves propagate to the magnetic latitude greater than 30 degrees and resonate with energetic electrons there. As for item (4), the PMWE observed at SYO during 03:00-04:00 can be related to wave-particle interaction with EMIC waves, which may be generated inside the plasmapause by ring-current hot ions with temperature anisotropy. This anisotropy

©2019. Japan Geoscience Union. All Right Reserved.

was caused by magnetospheric compression due to increasing solar wind dynamic pressure during 01:00–06:00 UT just after the arrival of the CIR. Since CIRs are main sources of geomagnetic disturbances during the declining phase of the solar cycle and solar minimum, this event is not rare but rather a common atmospheric response caused by interaction between recurrent large-scale solar wind structures and geospace.

Keywords: Polar Mesosphere Winter Echoes, Arase satellite, PANSY radar, MAARSY radar, relativistic electron precipitation, magnetospheric plasma waves

©2019. Japan Geoscience Union. All Right Reserved.

Comparison of precipitating particle energy of proton aurora at geomagnetic conjugate points

*Makoto Taguchi[1], Tatsuki Nishijima[1], Akira Kadokura[2]

1. Rikkyo University, 2. Research Organization of Information and Systems

It is expected that mirror images of aurora are observed at geomagnetic conjugate points in the northern and southern auroral zones connected by a geomagnetic field line. However, geomagnetic conjugate auroras often show non-conjugacy, which reflects north-south asymmetry of the solar wind, the magnetosphere and the ionospheres. In other words acceleration mechanism of auroral particles may be studied by comparing aurora simultaneously occurring at geomagnetic conjugate points. A hydrogen Balmer beta emission at the wavelength of 486.1 nm which is the brightest among the proton auroral lines was observed at a pair of geomagnetic conjugate points to compare precipitating particle energy. Two identical Proton Auroral Specrographs (PASs) which obtain auroral spectra along a geomagnetic meridian at a rate of 1 image/min were installed at Tjornes in Iceland and Syowa Station in Antarctica. Data obtained during a period from September 4, 2018 to October 9, 2018 were analyzed to derive an average kinetic energy of precipitating protons along a local geomagnetic field line from a Doppler shift of the H beta line. As a result we are succeeded in simultaneous observations of proton auroras at both conjugate points in 5 nights on September 4, 5, 6, 7 , and 10. The average energies of precipitating protons range from 0 keV to 7 keV, and sometimes show a periodical variation with a period of 4 - 5 min. Conjugacy of precipitating particle energy will be discussed in the presentation.

©2019. Japan Geoscience Union. All Right Reserved.

A regularized deep convolutional general adversarial network (R-DCGAN) for total electron content map completion

*Mingwu Jin[1], Zhou Chen[2,3], Yue Deng[1], Yang Pan[1], Jin-Song Wang[2]

1. University of Texas at Arlington, 2. Institute of Space Science and Technology, Nanchang University, Nanchang, China, 3. Key Laboratory of Space Weather, National Center for Space Weather, China Meteorological Administration, Beijing, China

Observations with a complete global coverage are important for space physics research and applications. However, due to the technical limitations and costs, such a complete global coverage is often unavailable. Thus, data filling algorithms are often pursued to fill missing data gaps to create a global map from the incomplete data. In this work, a novel deep learning algorithm, regularized deep convolutional generative adversarial network (R-DCGAN), is developed by adding an extra discriminator to the conventional DCGAN to fill the missing data of total electron content (TEC) map images. R-DCGAN incorporates the knowledge from reference TEC maps of the International Global Navigation Satellite Systems Service Ionosphere Working Group to achieve much better TEC map completion performance than the conventional DCGAN as demonstrated by both synthetic and real data. The R-DCGAN framework can be extended to other fields of space sciences to address the missing observation data issues.

Keywords: Deep learning method, TEC , map completion

©2019. Japan Geoscience Union. All Right Reserved.

A long-lasting auroral bright spot around magnetic north pole: Is it the evidence of stable magnetic reconnection?

*Qing-He Zhang[1], Guo-Cheng Shen[1], Yong-Liang Zhang[2], Kjellmar Oksavik[3], Michael Lockwood[4], Zan-Yang Xing[1], Yu-Zhang Ma[1]

1. Institute of Space Sciences, Shandong University, Weihai, China, 2. The Johns Hopkins University Applied Physics Laboratory, Laurel, Maryland, USA, 3. Birkeland Centre for Space Science, University of Bergen, Bergen, Norway, 4. Department of Meteorology, University of Reading, Earley Gate, Post Office Box 243, RG6 6BB, UK.

An intense and large auroral bright spot appears around the magnetic north pole observed by the Special Sensor Ultraviolet Spectrographic Imager (SSUSI) on board four different Defense Meteorological Satellite Program (DMSP) satellites during long time northward IMF conditions. The bright spot is even brighter than aurora in the auroral oval which is about 5-10° magnetic latitude equatorward of the bright spot. The bright spot is lasting about 8 hours, and sometimes appears as a cyclone-shape with a clockwise rotation. The DMSP in situ plasma observations suggest that the bright spot is clear associated with electron invert-V acceleration with 10s keV energy electron precipitations around the center regions and 1s keV energy electron precipitations around the egde regions. There are also strong flow shears between the two sides of the bright spot: strong sunward flows on the duskside and antisunward flows on the dawnside. These types of plasma should come from the high-latitude lobe region of the magnetotail due to the high-latitude lobe magnetic reconnections. Is it the evidence of stable lobe reconnection during long time northward IMF conditions? The detail and further analysis should be pursued in the following studies.

Keywords: Auroral bright spot, Magnetosphere-ionosphere coupling, High-latitude lobe magnetic reconnection, Stable reconnection

©2019. Japan Geoscience Union. All Right Reserved.

Statistical study of the relationship between ion upflow and field-aligned current in the topside ionosphere for both hemispheres during disturbed and quiet times

Shan-Yu Zhou[1], *Qing-He Zhang[1], P. T. Jayachandran[2], Kjellmar Oksavik[3], Larry Lyons[4], Zan-Yang Xing[1], Yu-Zhang Ma[1], Marc Hairston[5], Yong Wang[1]

1. Institute of Space Sciences, Shandong University, Weihai, China, 2. Physics Department, University of New Brunswick, Fredericton, New Brunswick, Canada, 3. Birkeland Centre for Space Science, University of Bergen, Bergen, Norway, 4. Department of Atmospheric and Oceanic Sciences, University of California, Los Angeles, California, USA, 5. William B. Hanson Center for Space Sciences, University of Texas at Dallas, Richardson, Texas, USA

A statistical study of ion upflow and field-aligned currents (FACs) has been performed in the topside ionosphere of both hemispheres for magnetic quiet and disturbed times by using DMSP satellite observations from 2010-2013. Distributions in MLT/MLAT reveal that ion upflow shows a dawn-dusk asymmetry distribution that corresponds well with the region 1 field-aligned currents. In addition, there are highest occurrence regions near noon and within the near midnight auroral disturbance area. These correspond to cusp and nightside dynamical processes, respectively. Both the ion upflow occurrence and FAC regions expand equatorward to a wider area during disturbed times.

Keywords: Ion upflows, Field-aligned current, Magnetosphere-ionosphere coupling

©2019. Japan Geoscience Union. All Right Reserved.

SAPS in the 2013 March 17 Storm Event: Initial Results from the Coupled Magnetosphere-Ionosphere-Thermosphere Model

*Dong Lin[1,2], Wenbin Wang[2], Wayne Scales[1], Kevin Pham[2], Jing Liu[2], Binzheng Zhang[2], Viacheslav Merkin[3], Xueling Shi[1]

1. Virginia Tech, 2. High Altitude Observatory, NCAR, 3. APL, John Hopkins Univ.

Subauroral polarization stream (SAPS) are latitudinally narrow flow channels of large westward plasma drifts in the subauroral ionosphere. In this study, the global structure and dynamic evolution of SAPS are investigated by using the National Center for Atmospheric Research (NCAR) Coupled Magnetosphere-Ionosphere-Thermosphere (CMIT) model with Ring Current extension, namely the LFM-TIEGCM-RCM (LTR) model, to simulate the 2013 St. Patrick's Day storm event. This is the first time that the global distribution and temporal evolution of SAPS are investigated using first-principle models. The model shows a strong westward ion drift channel formed equatorward of the auroral electron precipitation boundary on the duskside, which is identified as the SAPS structure. The simulated ion drift velocity and auroral electron precipitation sampled along the trajectory of the DMSP F18 satellite are in good agreement with the satellite measurements. SAPS initiate in the pre-dusk sector when the interplanetary magnetic field (IMF) turns southward. SAPS latitude generally decreases with magnetic local time (MLT) from dusk to midnight. The SAPS channel shows wedge, inverse wedge, and crescent morphologies during the storm, and becomes discontinuous when the IMF is weakly southward. The SAPS mean latitude has a correlation coefficient of 0.77 with the Dst index. The mean latitude moves equatorward and the flow channel broadens in the storm main phase. The simulation results are consistent with observational studies. They also illustrate the global distributions and highly dynamic behaviors of SAPS that are not readily apparent from observation data.

Keywords: SAPS, Magnetosphere-Ionosphere-Thermosphere coupling, LFM-TIEGCM-RCM

©2019. Japan Geoscience Union. All Right Reserved.

Westward turning motions of nighttime medium-scale traveling ionospheric disturbances (MSTIDs) at the equatorward side of the dusk side auroral oval associated with auroral brightening

*Sneha Yadav[1,2], Kazuo Shiokawa[1], Shin-ichiro Oyama[1,3,4], Yuichi Otsuka[1]

1. ISEE, Nagoya University, Nagoya, Japan, 2. SPL, VSSC, India, 3. Ionosphere Research Unit, University of Oulu, Oulu, Finland, 4. NIPR, Tachikawa, Japan

The characteristics of high-latitude nighttime medium-scale traveling ionospheric disturbances (MSTIDs) have not been well investigated using all-sky imagers because of the hindrance caused by the bright aurora. The limited results on the propagation characteristics of MSTIDs over high-latitudes hindered the progress in our understanding on these dynamical structure. In a case study carried out by Shiokawa et al. (JGR, 2012), an event of oscillating MSTIDs was reported over Tromsø (69.6˚N, 19.2˚E; corrected geomagnetic latitude: 66.6˚N), which was observed to be associated with auroral brightening. However, after this case study, which comprised of only one event, no observations showing oscillating motion of MSTIDs have been reported till date. In this study, for the first time, the comprehensive investigation on the westward turning of the MSTIDs in the equatorward side of the dusk side auroral oval has been performed. The all-sky imaging data of 630.0 nm airglow emissions during 2010-2018 are used to study the motions of MSTIDs over Tromsø. The results indicate that the nighttime MSTIDs primarily exhibit eastward motion under quiet magnetic conditions but turned in the westward direction during the active geomagnetic conditions. The turning of MSTIDs in the westward direction were invariably associated with the auroral brightening observed at the poleward edge of the all-sky image and localized magnetic field perturbations observed by ground-based magnetometers at Tromsø. The interesting aspect of the observations is the fact that these westward moving MSTIDs again turned in the eastward direction when the geomagnetic disturbance ceases. The SuperDARN (Super Dual Auroral Radar Network) convection maps revealed that the location of Tromsø was inside/outside the convection cell region during the time of appearance of westward/eastward moving MSTIDs. The Doppler shift measurement of the 630-nm airglow by a Fabry-Perot interferometer at Tromsø showed that northeastward winds were predominant during the appearance of eastward moving MSTIDs. The cause of the observed MSTIDs remains in question as they might either be triggered by atmospheric gravity waves or by Perkins instability. These experimental evidences suggest that the MSTIDs tend to move eastward in accordance with the background F-region dynamo electric field, but show westward motion under the influence of electric field associated with auroral activities in the dusk side of two-cell convection pattern.

Keywords: MSTIDs, Auroral oval, Airglow

©2019. Japan Geoscience Union. All Right Reserved.

[E] Poster | A (Atmospheric and Hydrospheric Sciences)：A-OS Ocean Sciences & Ocean Environment

Mon. May 27, 2019 3:30 PM - 5:00 PM JST | Mon. May 27, 2019 6:30 AM - 8:00 AM UTC | Poster Hall International Exhibition Hall8, Makuhari Messe_3

[A-OS12] Marine ecosystems and biogeochemical cycles: theory, observation and modeling

convener:Shin-ichi Ito(Atmosphere and Ocean Research Institute, The University of Tokyo), Takafumi Hirata(Faculty of Environmental Earth Science, Hokkaido University), Enrique N Curchitser(Rutgers University New Brunswick), Eileen E Hofmann(Old Dominion University)

The ocean accounts for about 50% of global net primary production. This production is significant for carbon cycling and ecosystem functioning, and is related directly or indirectly to a variety of climatic and ecological phenomena. The responses to natural and anthropogenic environmental stressors that influence marine production and diversity can cause perturbations to marine ecosystems that alter trophic dependencies and interactions among organisms at a range of space and time scales. Quantification of the principal mechanisms driving spatio-temporal variability of marine ecosystem remains to be done, especially in terms of evaluation of uncertainty in responses. As a result, evaluating vulnerability of marine ecosystems to environmental change requires systematic and holistic approaches that integrate physics to ecology and are based in observations and modelling. In addition, expectations to deliver these science to public society is raising. This session aims to provide a venue for not only discussing recent advances in understanding marine biogeochemical cycles, ecosystems and their interactions, but also networking with a variety of people to seed new ideas in marine ecological research. Observational, modeling and conceptual studies, including technological development and operational applications, that consider linkages among biogeochemical and ecosystem processes, biodiversity, and the effects of multiple stressors from molecular to planetary scales are encouraged.

[AOS12-P01] Impact of the nutrient transport through the Tsushima Strait on the ecosystem in the Japan Sea

*Ryota Shibano[1], Akihiko Morimoto[1], Katsumi Takayama[2], Tetsutaro Takikawa[3], Masashi Ito[4] (1.Center for Marine Environmental Studies, Ehime University, 2.Research Institute for Applied Mechanics, Kyushu University, 3.Graduate School of Fisheries and Environmental Sciences, Nagasaki University, 4.Fisheries Oceanography Department, Japan Sea National Fisheries Research Institute)

[AOS12-P02] Revisiting vertical variations in stoichiometry during oceanic organic matter decomposition

*Masahito Shigemitsu[1], Michio Aoyama[1], Toshimasa Doi[1], Taichi Yokokawa[1], Akihiko Murata[1] (1.Japan Agency for Marine-Earth Science and Technology)

[AOS12-P03] Reproduction of iron-rich intermediate water in the Sea of Okhotsk by high resolution biogeochemical model.

*Hatsumi Nishikawa[1], Humio Mitsudera[1], Hiroshi Yoshinari[2], Takuya Nakanowatari[3], Tomohiro Nakamura[1], Keisuke Uchimoto[4], Hiroyasu Hasumi[5] (1.Institute of Low Temperature Science, Hokkaido University, 2.National Institute for Environmental Studies, 3.Tohoku National Fisheries Research Institute, Japan Fisheries Research and Education Agency, 4.Research Institute of Innovative Technology for the Earth, 5.Atmosphere and Ocean Research Institute, University of Tokyo)

[AOS12-P04] The global oceanic iron distribution estimated by data assimilation approach

*Doi Toshimasa[1], Satoshi Osafune[1], Shuhei Masuda[1], Hajime Obata[2], Kazuhiro Misumi[3], Jun Nishioka[4] (1.Japan Agency for Marine-Earth Science and Technology, 2.The University of Tokyo, 3.Central Research Institute of Electric Power Industry, 4.Hokkaido University)

[AOS12-P05] A high-resolution multi-purpose particle tracking framework for coastal areas near Japan

*Yoshimasa Matsumura[1], Shota Katsura[1], Masao Kurogi[2], Hideyuki Nakano[3], Takateru Yamagishi[4] (1.Atmosphere and Ocean Research Institute, University of Tokyo, 2.Japan Agency for Marine-Earth Science and Technology, 3.Meteorological Research Institute, Japan Meteorological Agency , 4.Research organization for Information Science and Technology)

[AOS12-P06] Numerical study on seasonality of ocean litters collected at the Dongsha Island in the northern South China Sea

*Yi-Chia Hsin[1], Chia-Ying Ko[2], Ming-Shiou Jeng[3] (1.Research Center for Environmental Changes, Academia Sinica, 2.Institute of Fisheries Science, National Taiwan University, 3.Biodiversity Research Center, Academia Sinica)

[AOS12-P07] A key spot and timing to monitor chlorophyll-a in the Kuroshio western boundary current

*Takafumi Hirata[1] (1.Faculty of Environmental Earth Science, Hokkaido University)

[AOS12-P08] **Impacts of cyclonic eddies on phytoplankton biomass and phenology in the Kuroshio Extension region**

*Eko Siswanto[1], Yoshikazu Sasai[1] (1.Japan Agency for Marine-Earth Science and Technology)

[AOS12-P09] Diagnostic estimation and uncertainties of nutrient limitation of phytoplankton growth in Michaelis-Menten functional form

*Taketo Hashioka[1], Maki Noguchi Aita[1] (1.Japan Agency for Marine-Science and Technology)

[AOS12-P10] Modeling productivity in lower trophic levels in Otsuchi Bay, northeast of Japan, using a nested OGCM with a biogeochemical component

*Takashi T Sakamoto[1], L. Shogo Urakawa[2], Sachihiko Itoh[1], Hiroyasu Hasumi[1], Kiyoshi Tanaka[1] (1.Atmosphere and Ocean Research Institute, the University of Tokyo, 2.Meteorological Research Institute, Japan Meteorologica Agancy)

[AOS12-P11] Change in lower trophic level ecosystems to decadal scale variation of climate system in the North Pacific Ocean

*Maki Noguchi Aita[1], Kazuaki Tadokoro[2], Yoshiki Komuro[3], Taketo Hashioka[1], Naomi Harada[1] (1.Research and Development Center for Global Change, Japan Agency for Marine-Earth Science and Technology, 2.Tohoku National Fisheries Research Institute, Japan Fisheries Research and Education Agency, 3.Institute of Arctic Climate and Environment Research, Japan Agency for Marine-Earth Science and Technology)

[AOS12-P12] Estimation of experienced environment of jack mackerel in the East China Sea

*Tomihiko Higuchi[1], Motomitsu Takahashi[2], Kotaro Shirai[1], Shin-ichi Ito[1] (1.Atmosphere and Ocean Research Institute, The University of Tokyo, 2.Seikai National Fisheries Research Institute,FRA)

Impact of the nutrient transport through the Tsushima Strait on the ecosystem in the Japan Sea

*Ryota Shibano[1], Akihiko Morimoto[1], Katsumi Takayama[2], Tetsutaro Takikawa[3], Masashi Ito[4]

1. Center for Marine Environmental Studies, Ehime University, 2. Research Institute for Applied Mechanics, Kyushu University, 3. Graduate School of Fisheries and Environmental Sciences, Nagasaki University, 4. Fisheries Oceanography Department, Japan Sea National Fisheries Research Institute

The Japan Sea is a semi-closed sea with narrow and shallow straits such as the Tsushima/Korea Strait. The nutrient transports through the Tsushima Strait have an impact the ecosystem around the coast of Japan. The nutrient transports are originated in the sources from the sea, Kuroshio (Pacific), Taiwan Strait, and Yellow Sea, and the sources from the land, Changjiang river, Yellow river, and dusts. We investigated the ship cruise data in the strait from 2005 to 2017 to reveal the interannual variations in the volume transport, nutrient concentration, and nutrient transport. The nutrient transport in the strait has large interannual variations of ±50% compared to the average transport.

The recently studies indicated the contribution ratio in the nutrient transports on the sources from the Kuroshio and the rivers also change, when the yearly nutrient transport changes (e.g. Morimoto et al., 2012).

We developed a coupled ocean circulation and ecosystem model, in which the lateral boundary condition is applied based on observation data, and investigated the biogeochemical responses in the Japan Sea and the East China Sea to the interannual variations in the nutrient flux through the Tsushima Strait. We discussed about the contribution ratio in the nutrient flux on the 6 sources from Kuroshio, Taiwan Strait, Changjiang river, Yellow river, the dust, and the bottom (Yellow Sea).

Keywords: Tsushima Warm Current, nutrient transport, the Sea of Japan

©2019. Japan Geoscience Union. All Right Reserved.

Revisiting vertical variations in stoichiometry during oceanic organic matter decomposition

*Masahito Shigemitsu[1], Michio Aoyama[1], Toshimasa Doi[1], Taichi Yokokawa[1], Akihiko Murata[1]

1. Japan Agency for Marine-Earth Science and Technology

Using the new global nutrient data set, we re-evaluate basin-wide stoichiometric ratios of remineralization estimated by Anderson and Sarmiento (1994) (hereinafter, AS94). For the same latitudinal ranges of the Atlantic, Indian and Pacific Oceans as in AS94, we construct one or two end-member mixing models on 14 neutral surfaces and estimate the stoichiometric ratios with a probabilistic approach. Unlike the results of AS94, significant vertical variations in the stoichiometry are found in the Atlantic and Pacific, while relatively constant stoichiometry with depth is found in the Indian Ocean, similar to AS94. The decreases in the C/P and $-O_2$/P ratios with depth in the Atlantic could be caused via dark DIC fixation by chemoautotrophs in the deep waters. In the Pacific, changes in organic matter composition with depth would be the most important factor in the increases in stoichiometry with depth. In all the basins, the N/P ratios are probably affected by benthic denitrification, as in AS94. The P/C/-O_2ratios (mean and $5^{th}$to 95^{th} percentile) are estimated to be 1/111(97 to 129)/155(149 to 163) in the depths below 2000 m of the Indian and Pacific Oceans, where DIC fixation and vertical change in organic matter composition have little influence on the stoichiometry estimates. We suggest that chemoautotrophic DIC fixation and the effect of change in organic matter composition with depth on the stoichiometry in waters above 2000 m should be considered for large-scale biogeochemical modeling and estimation of oceanic uptake of anthropogenic carbon from observational data.

Keywords: nutrients, stoichiometric ratios, remineralization of organic matter

©2019. Japan Geoscience Union. All Right Reserved.

Reproduction of iron-rich intermediate water in the Sea of Okhotsk by high resolution biogeochemical model.

*Hatsumi Nishikawa[1], Humio Mitsudera[1], Hiroshi Yoshinari[2], Takuya Nakanowatari[3], Tomohiro Nakamura[1], Keisuke Uchimoto[4], Hiroyasu Hasumi[5]

1. Institute of Low Temperature Science, Hokkaido University, 2. National Institute for Environmental Studies, 3. Tohoku National Fisheries Research Institute, Japan Fisheries Research and Education Agency, 4. Research Institute of Innovative Technology for the Earth, 5. Atmosphere and Ocean Research Institute, University of Tokyo

Recent observation studies suggest that iron supply from sediment on the northwest continental shelf the Okhotsk Sea plays an important role for the subarctic primary production (e.g. Nishioka et al., 2013). Dense shelf water (DSW) takes up iron from sediment, thereby transporting iron into the Okhotsk Sea intermediate water. However, observational data is still limited.

To clarify detailed structure of iron circulation in the North Pacific, we develop the high-resolution biogeochemical model. However, our model did not reproduce high iron concentration in the intermediate water the Sea of Okhotsk. We use biogeochemical model developed by Parekh et al. (2005). They set the value of total ligand concentration to constant value in all place. Recent observations, however, suggest that ligand concentration varies with sea area and depth. Then, we conducted a new experiment with the ligand concentration changed in the vertical direction. The iron concentration intermediate water of the new experiment becaame higher than before.

Keywords: High-resolution modeling, Iron-rich intermediate water, Ligand concentration

©2019. Japan Geoscience Union. All Right Reserved.

The global oceanic iron distribution estimated by data assimilation approach

*Doi Toshimasa[1], Satoshi Osafune[1], Shuhei Masuda[1], Hajime Obata[2], Kazuhiro Misumi[3], Jun Nishioka[4]

1. Japan Agency for Marine-Earth Science and Technology, 2. The University of Tokyo, 3. Central Research Institute of Electric Power Industry, 4. Hokkaido University

Since distribution of oceanic iron is considered as one of the restriction factors of phytoplankton activity, it is necessary for a pelagic lower trophic level ecosystem model to take into account the effect of iron. In this study, we constructed a three dimensional gridded data of oceanic iron concentration by using both available in situ observation and simple iron cycle model. For the physical process of iron transport, the advection/diffusion model was used along with the flow field of ESTOC (Estimated State of Global Ocean for Climate Research). The falling atmospheric dust in the sea-surface and flux from the sediment at sea floor of the coast were set as the input of the iron. The scavenging or desorption by particulate matter in the water column were employed as the control variables and we constructed the simple iron cycle model. The optimized set of control parameters was obtained based on a Green's function approach by using available in situ iron concentration observations. The results showed that the iron concentration in the southern hemisphere is lower than northern hemisphere, and the low iron regions were well reproduced around the regions of high nutrient / low chlorophyll. Moreover, it is suggested that the Atlantic Ocean is more affected by the atmospheric dust compared with the Pacific Ocean.

Keywords: oceanic iron, data assimilation

©2019. Japan Geoscience Union. All Right Reserved.

A high-resolution multi-purpose particle tracking framework for coastal areas near Japan

*Yoshimasa Matsumura[1], Shota Katsura[1], Masao Kurogi[2], Hideyuki Nakano[3], Takateru Yamagishi[4]

1. Atmosphere and Ocean Research Institute, University of Tokyo, 2. Japan Agency for Marine-Earth Science and Technology, 3. Meteorological Research Institute, Japan Meteorological Agency , 4. Research organization for Information Science and Technology

A comprehensive and multi-purpose particle tracking framework using latest high resolution velocity field in the coastal regions near Japan is developed.
The particle tracking system uses accurate fourth order Runge-Kutta method and implements random-walk based diffusivity, and is built-in the recent versions of MRI.com (an OGCM developed in Meteorological Research Institute, Japan Meteorological Agency) and kinaco (a non-hydrostatic ocean model developed in Atmosphere and Ocean Research Institute, University of Tokyo) for *on-line* use. Each particle is able to store up to seven arbitrary properties (such as size, age, exposed temperature, orientation, mass and buoyancy, etc.) and record the history of them.

The code is effectively parallelized (using MPI and OpenMP hybrid technique) and allows ~O(10^{10}) particles on modern massive-parallel supercomputers, and is also ported to GPU architecture using CUDA language.

This particle tracking framework has no particular target in a priori, and can be applied to various purposes for both physical oceanography (from large scale tracking of water masses to small scale modeling of suspended sediment matter or frazil ice crystals) and ocean biogeochemistry (tracking of trace elements, Laglangian modeling of plankton and detritus, individual based modeling of fishes and marine resources), only by defining appropriate properties and inserting a few lines of code that manipulats them corresponding to the particular target use.

In the presentation, we will introduce an application of this framework to the tracking of passive particles scattered in the coastal areas near Japan using velocity field provided by the latest very high resolution ocean modeling (~300 m mesh). Each model particle records its trajectory and the history of exposed environment, and can be interpreted as eggs or larvae (before acquiring swimming ability) of species of corresponding spawning areas and seasons as well as the tracers for small scale water mass exchanges.

Keywords: Particle tracking system

©2019. Japan Geoscience Union. All Right Reserved.

Numerical study on seasonality of ocean litters collected at the Dongsha Island in the northern South China Sea

*Yi-Chia Hsin[1], Chia-Ying Ko[2], Ming-Shiou Jeng[3]

1. Research Center for Environmental Changes, Academia Sinica, 2. Institute of Fisheries Science, National Taiwan University, 3. Biodiversity Research Center, Academia Sinica

Distribution of ocean litters collected at the Dongsha Island, an isolated island in the northern South China Sea, shows a significant seasonal change. More litters were accumulated in the northern (southern) part of the island in winter (summer). By means of backward-tracking simulation by considering the effect of both ocean currents and winds (i.e., windage), a series of numerical experiments are carried out to clarify the possible source and mechanisms for the observational seasonal change of litters. Results exhibit that, in winter, low-windage litters are mainly from the western Philippine Sea via the Luzon Strait while the high-windage ones are contributed from the Taiwan Strait. In summer, litters from the southwestern South China Sea, i.e. east of Vietnam, could be a major origin.

Keywords: ocean litters, numercial study, South China Sea

©2019. Japan Geoscience Union. All Right Reserved.

A key spot and timing to monitor chlorophyll-a in the Kuroshio western boundary current

*Takafumi Hirata[1]

1. Faculty of Environmental Earth Science, Hokkaido University

The Kuroshio western boundary current originates from the subtropics in the Western Pacific and carries a thermal energy and oceanic water mass towards the north, including the south coasts and offshore islands of Japan. In spite of the oligotrophy of the origin water that the Kuroshio carries, the Kuroshio water is known for spawning and feeding grounds of commercial/non-commercial fish larvae, explaining a higher fisheries production in the region. Thus, it puzzles an oceanographic and ecological relationships among nutrient fields, standing stock and productivity of organisms. In order to understand the complex Kuroshio ecosystems, phytoplankton dynamics is investigated using remote sensing data, namely phytoplankton pigment or chlorophyll-a observed by Advanced Himawari Imager (AHI) onboard Himawari-8. The area-integrated, and the area average of, Kuroshio chlorophyll-a was found predictable from a chlorophyll-a measurement in the 134-136 ˚E, where the Kuroshio current direction is most stable between 130-150 ˚E . An analysis of short term variability (< 1 year) of the Kuroshio chlorophyll-a concentration revealed that a cumulative, and monthly average of, chlorophyll-a over a month in the Kuroshio surface water could be estimated from a chlorophyll-a measurement at a single day in the month. These results suggest that there is a key spot and timing to monitor the phytoplankton activities in the Kuroshio current.

Keywords: Kuroshio, Chlorophyll, Remote Sensing

©2019. Japan Geoscience Union. All Right Reserved.

Impacts of cyclonic eddies on phytoplankton biomass and phenology in the Kuroshio Extension region

*Eko Siswanto[1], Yoshikazu Sasai[1]

1. Japan Agency for Marine-Earth Science and Technology

Two-decade ocean color chlorophyll-a concentration (CHL, a metric of phytoplankton biomass) data from 1997 to 2017 were used to comprehend the impact of cyclonic eddies on phytoplankton biomass and phenology in the Kuroshio Extension region (KE) of the western North Pacific Ocean. The CHL data have 4-km and 8-day spatiotemporal resolution and were acquired from the ESA Ocean Colour-Climate Change Initiative (http://www.esa-oceancolour-cci.org/). Prior to defining spring bloom onset, spatiotemporal gaps in CHL data were filled by applying empirical orthogonal function-based interpolation. The analysis was mainly focused on the winter season (January-March) as oceanographic conditions during the winter largely control phytoplankton spring bloom in terms of both magnitude and onset. Based on winter sea surface height anomaly (SSHa), cyclonic eddies (negative SSHa) were dominant mainly within the periods from 1998 to 2001 and from 2005 to 2009, whereas anti-cyclonic eddies (positive SSHa) were dominant mainly within the periods from 2002 to 2004 and from 2011 to 2015. Based on datasets from all seasons, the concurrences of negative SSHa and positive phytoplankton chlorophyll anomaly (CHLa) were observed, albeit not always. This indicates an eddy-induced upwelling supplies nutrients to the near-surface layer. Upwelled nutrients eventually promote phytoplankton growth. Such a concurrence of low SSHa and high CHLa was less obvious during the winter indicating that another factor (such as intense winter vertical mixing) also non-trivially controlled nutrient input to the surface layer, and hence CHLa variability. Overall temporal mean indeed showed that the active cyclonic eddy area (approximately south of the Kuroshio Current main axis) was characterized by high CHLa, low SSHa, and shoaled mixed layer. In this study, a Cumulative Sum method was applied to find phytoplankton spring bloom onset. Correlation between SSHa and spring bloom onset time was investigated, and it was found that approximately over the active cyclonic eddy area, positive correlation between winter/late winter SSHa and time of spring bloom onset was observed. Such a positive correlation indicates that cyclonic eddies during the winter likely tended to advance phytoplankton spring bloom onset.

Keywords: Ocean color, Phytoplankton, Bloom onset, Upwelling

©2019. Japan Geoscience Union. All Right Reserved.

Diagnostic estimation and uncertainties of nutrient limitation of phytoplankton growth in Michaelis-Menten functional form

*Taketo Hashioka[1], Maki Noguchi Aita[1]

1. Japan Agency for Marine-Science and Technology

Michaelis-Menten functional form (MM) is most widely used relationship of nutrient limitation of phytoplankton growth in large-scale ecosystem models. In MM functional form, the choice of parameter value of a half-saturation constant is a key point for controlling the strength of nutrient limitation. In general, the half-saturation constant increase with the size of the phytoplankton cell depending on the surface-to-volume ratio by diffusive hypothesis, and wide ranges of values are reported from observational studies. On the other hand, the most of Plankton Functional Types (PFT) models represent a phytoplankton type as one representative PFT with one global parameter. The parameter value is chosen in the observed range as a most reasonable value that could reproduce observed chl-a or nutrient concentration in each model. As a result, there are uncertainties of the global pattern of nutrient limitation among models. In this study, we diagnostically estimated the nutrient limitation using various parameter set of different global PFT models form CMIP5 together with the observation based nutrient concentrations (World Ocean Atlas for macro nutrient and multi-model median for dissolved iron and ammonium concentration). Then we show uncertainties and robustness of estimation of nutrient limitation in the current PFT models with MM functional form.

Keywords: Plankton Functional Types model, Michaelis-Menten functional form

©2019. Japan Geoscience Union. All Right Reserved.

Modeling productivity in lower trophic levels in Otsuchi Bay, northeast of Japan, using a nested OGCM with a biogeochemical component

*Takashi T Sakamoto[1], L. Shogo Urakawa[2], Sachihiko Itoh[1], Hiroyasu Hasumi[1], Kiyoshi Tanaka[1]

1. Atmosphere and Ocean Research Institute, the University of Tokyo, 2. Meteorological Research Institute, Japan Meteorologica Agancy

Otsuchi Bay is located on the northeast coast of Honshu Island, Japan, where was extensively damaged by the huge tsunamis caused by the 2011 off the Pacific coast of Tohoku Earthquake. Motivated by how the biogeochemical circumstance and fishery resource recover, some observations have been conducted in the bay, but those have not been enough because of several restrictions and human resources. Aimed at filling the observational shortage and the acquirement of some information about physical and low trophic fields, a modeling approach has been discussed. Using a triply-nested OGCM and a downscaling method, the authors succeeded to reproduce seasonal variability of the circulation in the bay, and also showed a seasonality of the water exchange mechanism between the bay and the open ocean (Sakamoto et al. 2017). In order to know the low trophic processes in the bay, a numerical simulation using a nested OGCM with a NPZD model is conducted. The OGCM is an improved version of Sakamoto et al’ s (2017) model, and the NPZD one is based on Nagata and Hasumi (2014). In this poster, our modeling strategy and some results will be presented. The final goal of this study is to perform hindcasting simulations of the bay with realistic boundary conditions, that are the river runoff, the atmospheric forcings, and the open ocean states.

Keywords: downscaling, nest-modeling, NPZD model

©2019. Japan Geoscience Union. All Right Reserved.

Change in lower trophic level ecosystems to decadal scale variation of climate system in the North Pacific Ocean

*Maki Noguchi Aita[1], Kazuaki Tadokoro[2], Yoshiki Komuro[3], Taketo Hashioka[1], Naomi Harada[1]

1. Research and Development Center for Global Change, Japan Agency for Marine-Earth Science and Technology, 2. Tohoku National Fisheries Research Institute, Japan Fisheries Research and Education Agency, 3. Institute of Arctic Climate and Environment Research, Japan Agency for Marine-Earth Science and Technology

The changes related to interdecadal climate variations, such as the Pacific Decadal Oscillation and the 18.6-y tidal cycle, have been discussed in many marine ecosystem studies. By analyzing data from observation of nutrient concentrations, decreasing and increasing trends of nutrients in the surface and subsurface layers, have been reported in many studies. Changes have also been observed in the biomass of phytoplankton and zooplankton. To clarify variability of lower trophic level productivity and its controlling factor, we simulated changes in the marine ecosystem caused by interdecadal climate variability, using the JRA55-do (Japanese 55-year atmospheric reanalysis) dataset from 1958 to 2017 to drive an ecosystem model, NEMURO, embedded in a global three-dimensional physical-biological coupled model, ‘COCO-NEMURO’. We compared and verified ecosystem model results with observations of phytoplankton and zooplankton species composition data collected by the Tohoku National Fisheries Research Institute, Japan Fisheries Research and Education Agency (FRA). Our model results showed that changes in biomass and nutrient concentration greatly differ depending on the region. According to our model results, sea surface temperature (SST) was very low during mid 1960s to mid 1970s, then SST increased after the mid 1970s to the end of 1990s in the western subarctic North Pacific. Changes in phytoplankton biomass was follow to this. However, the change in SST and phytoplankton and zooplankton biomass were contrary to this in the western subtropical North Pacific. We also checked decadal time series of annual mean sea ice concentration, SST, and phytoplankton biomass in the eastern Bering Sea and the western Arctic. The simulated sea ice concentration in the eastern Bering Sea decreased from the late 1970s to the early 1980s, while it was higher in the early 1990s and the late 2000s. The SST had its peaks in the late 1970s and the early 2000s. The phytoplankton biomass was inversely correlated with the sea ice concentration. In the western Arctic, the simulated sea ice concentration (SST) showed negative (positive) trends on the decadal timescale. The phytoplankton biomass has also been increasing, but its trend was not so simple. To elucidate the mechanism that sustains marine ecosystems, we will also analyze focusing on primary producers and zooplankton to key link to higher trophic levels.

Keywords: Climate change, decadal change, lower trophic marine ecosystem, marine ecosystem model 'NEMURO'

©2019. Japan Geoscience Union. All Right Reserved.

Estimation of experienced environment of jack mackerel in the East China Sea

*Tomihiko Higuchi[1], Motomitsu Takahashi[2], Kotaro Shirai[1], Shin-ichi Ito[1]

1. Atmosphere and Ocean Research Institute, The University of Tokyo, 2. Seikai National Fisheries Research Institute,FRA

Jack mackerel *Trachurus japonicus* is distributed on the continental shelf waters along the subtropical Kuroshio Current and the Tsushima Warm Current in the western North Pacific. The East China Sea (ECS) is one of major region for jack mackerel and understanding the recruitment processes of jack mackerel into the fishing grounds in the ECS is important. However, marine environment such as water temperature that jack mackerel actually experiences is not directly observed yet. In this study, oxygen ($\delta^{18}O$) and carbon ($\delta^{13}C$) stable isotope of jack mackerel otolith were analyzed and the experienced environment was estimated. When we compared $\delta^{18}O$ of otolith caught in between three different station with different temperature, average of $\delta^{18}O$ varied and was negatively correlated with water temperature of sampling station. Most of individual indicated that $\delta^{13}C$ relatively increased from core part to edge in otolith. Thus, these results suggest that otolith of jack mackerel recorded experienced environment. However, because jack mackerel migrate vertically, it needs to consider vertical profile of seawater temperature and other parameters such as salinity and prey availability. A combination with fish distribution information and ecological modeling may help the improvement of estimation for detail experienced environment.

Keywords: fish otolith, isotope analysis, experienced environment, fish migration

©2019. Japan Geoscience Union. All Right Reserved.

[E] Poster | A (Atmospheric and Hydrospheric Sciences)：A-OS Ocean Sciences & Ocean Environment

Mon. May 27, 2019 5:15 PM - 6:30 PM JST | Mon. May 27, 2019 8:15 AM - 9:30 AM UTC | Poster Hall International Exhibition Hall8, Makuhari Messe_5

[A-OS12] Marine ecosystems and biogeochemical cycles: theory, observation and modeling

convener:Shin-ichi Ito(Atmosphere and Ocean Research Institute, The University of Tokyo), Takafumi Hirata(Faculty of Environmental Earth Science, Hokkaido University), Enrique N Curchitser(Rutgers University New Brunswick), Eileen E Hofmann(Old Dominion University)

The ocean accounts for about 50% of global net primary production. This production is significant for carbon cycling and ecosystem functioning, and is related directly or indirectly to a variety of climatic and ecological phenomena. The responses to natural and anthropogenic environmental stressors that influence marine production and diversity can cause perturbations to marine ecosystems that alter trophic dependencies and interactions among organisms at a range of space and time scales. Quantification of the principal mechanisms driving spatio-temporal variability of marine ecosystem remains to be done, especially in terms of evaluation of uncertainty in responses. As a result, evaluating vulnerability of marine ecosystems to environmental change requires systematic and holistic approaches that integrate physics to ecology and are based in observations and modelling. In addition, expectations to deliver these science to public society is raising. This session aims to provide a venue for not only discussing recent advances in understanding marine biogeochemical cycles, ecosystems and their interactions, but also networking with a variety of people to seed new ideas in marine ecological research. Observational, modeling and conceptual studies, including technological development and operational applications, that consider linkages among biogeochemical and ecosystem processes, biodiversity, and the effects of multiple stressors from molecular to planetary scales are encouraged.

[AOS12-P01] Impact of the nutrient transport through the Tsushima Strait on the ecosystem in the Japan Sea

*Ryota Shibano[1], Akihiko Morimoto[1], Katsumi Takayama[2], Tetsutaro Takikawa[3], Masashi Ito[4] (1.Center for Marine Environmental Studies, Ehime University, 2.Research Institute for Applied Mechanics, Kyushu University, 3.Graduate School of Fisheries and Environmental Sciences, Nagasaki University, 4.Fisheries Oceanography Department, Japan Sea National Fisheries Research Institute)

[AOS12-P02] Revisiting vertical variations in stoichiometry during oceanic organic matter decomposition

*Masahito Shigemitsu[1], Michio Aoyama[1], Toshimasa Doi[1], Taichi Yokokawa[1], Akihiko Murata[1] (1.Japan Agency for Marine-Earth Science and Technology)

[AOS12-P03] Reproduction of iron-rich intermediate water in the Sea of Okhotsk by high resolution biogeochemical model.

*Hatsumi Nishikawa[1], Humio Mitsudera[1], Hiroshi Yoshinari[2], Takuya Nakanowatari[3], Tomohiro Nakamura[1], Keisuke Uchimoto[4], Hiroyasu Hasumi[5] (1.Institute of Low Temperature Science, Hokkaido University, 2.National Institute for Environmental Studies, 3.Tohoku National Fisheries Research Institute, Japan Fisheries Research and Education Agency, 4.Research Institute of Innovative Technology for the Earth, 5.Atmosphere and Ocean Research Institute, University of Tokyo)

[AOS12-P04] The global oceanic iron distribution estimated by data assimilation approach

*Doi Toshimasa[1], Satoshi Osafune[1], Shuhei Masuda[1], Hajime Obata[2], Kazuhiro Misumi[3], Jun Nishioka[4] (1.Japan Agency for Marine-Earth Science and Technology, 2.The University of Tokyo, 3.Central Research Institute of Electric Power Industry, 4.Hokkaido University)

[AOS12-P05] A high-resolution multi-purpose particle tracking framework for coastal areas near Japan

*Yoshimasa Matsumura[1], Shota Katsura[1], Masao Kurogi[2], Hideyuki Nakano[3], Takateru Yamagishi[4] (1.Atmosphere and Ocean Research Institute, University of Tokyo, 2.Japan Agency for Marine-Earth Science and Technology, 3.Meteorological Research Institute, Japan Meteorological Agency , 4.Research organization for Information Science and Technology)

[AOS12-P06] Numerical study on seasonality of ocean litters collected at the Dongsha Island in the northern South China Sea

*Yi-Chia Hsin[1], Chia-Ying Ko[2], Ming-Shiou Jeng[3] (1.Research Center for Environmental Changes, Academia Sinica, 2.Institute of Fisheries Science, National Taiwan University, 3.Biodiversity Research Center, Academia Sinica)

[AOS12-P07] A key spot and timing to monitor chlorophyll-a in the Kuroshio western boundary current

*Takafumi Hirata[1] (1.Faculty of Environmental Earth Science, Hokkaido University)

[AOS12-P08] **Impacts of cyclonic eddies on phytoplankton biomass and phenology in the Kuroshio Extension region**

*Eko Siswanto[1], Yoshikazu Sasai[1] (1.Japan Agency for Marine-Earth Science and Technology)

[AOS12-P09] Diagnostic estimation and uncertainties of nutrient limitation of phytoplankton growth in Michaelis-Menten functional form

*Taketo Hashioka[1], Maki Noguchi Aita[1] (1.Japan Agency for Marine-Science and Technology)

[AOS12-P10] Modeling productivity in lower trophic levels in Otsuchi Bay, northeast of Japan, using a nested OGCM with a biogeochemical component

*Takashi T Sakamoto[1], L. Shogo Urakawa[2], Sachihiko Itoh[1], Hiroyasu Hasumi[1], Kiyoshi Tanaka[1] (1.Atmosphere and Ocean Research Institute, the University of Tokyo, 2.Meteorological Research Institute, Japan Meteorologica Agancy)

[AOS12-P11] Change in lower trophic level ecosystems to decadal scale variation of climate system in the North Pacific Ocean

*Maki Noguchi Aita[1], Kazuaki Tadokoro[2], Yoshiki Komuro[3], Taketo Hashioka[1], Naomi Harada[1] (1.Research and Development Center for Global Change, Japan Agency for Marine-Earth Science and Technology, 2.Tohoku National Fisheries Research Institute, Japan Fisheries Research and Education Agency, 3.Institute of Arctic Climate and Environment Research, Japan Agency for Marine-Earth Science and Technology)

[AOS12-P12] Estimation of experienced environment of jack mackerel in the East China Sea

*Tomihiko Higuchi[1], Motomitsu Takahashi[2], Kotaro Shirai[1], Shin-ichi Ito[1] (1.Atmosphere and Ocean Research Institute, The University of Tokyo, 2.Seikai National Fisheries Research Institute,FRA)

Impact of the nutrient transport through the Tsushima Strait on the ecosystem in the Japan Sea

*Ryota Shibano[1], Akihiko Morimoto[1], Katsumi Takayama[2], Tetsutaro Takikawa[3], Masashi Ito[4]

1. Center for Marine Environmental Studies, Ehime University, 2. Research Institute for Applied Mechanics, Kyushu University, 3. Graduate School of Fisheries and Environmental Sciences, Nagasaki University, 4. Fisheries Oceanography Department, Japan Sea National Fisheries Research Institute

The Japan Sea is a semi-closed sea with narrow and shallow straits such as the Tsushima/Korea Strait. The nutrient transports through the Tsushima Strait have an impact the ecosystem around the coast of Japan. The nutrient transports are originated in the sources from the sea, Kuroshio (Pacific), Taiwan Strait, and Yellow Sea, and the sources from the land, Changjiang river, Yellow river, and dusts. We investigated the ship cruise data in the strait from 2005 to 2017 to reveal the interannual variations in the volume transport, nutrient concentration, and nutrient transport. The nutrient transport in the strait has large interannual variations of ±50% compared to the average transport.

The recently studies indicated the contribution ratio in the nutrient transports on the sources from the Kuroshio and the rivers also change, when the yearly nutrient transport changes (e.g. Morimoto et al., 2012).

We developed a coupled ocean circulation and ecosystem model, in which the lateral boundary condition is applied based on observation data, and investigated the biogeochemical responses in the Japan Sea and the East China Sea to the interannual variations in the nutrient flux through the Tsushima Strait. We discussed about the contribution ratio in the nutrient flux on the 6 sources from Kuroshio, Taiwan Strait, Changjiang river, Yellow river, the dust, and the bottom (Yellow Sea).

Keywords: Tsushima Warm Current, nutrient transport, the Sea of Japan

©2019. Japan Geoscience Union. All Right Reserved.

Revisiting vertical variations in stoichiometry during oceanic organic matter decomposition

*Masahito Shigemitsu[1], Michio Aoyama[1], Toshimasa Doi[1], Taichi Yokokawa[1], Akihiko Murata[1]

1. Japan Agency for Marine-Earth Science and Technology

Using the new global nutrient data set, we re-evaluate basin-wide stoichiometric ratios of remineralization estimated by Anderson and Sarmiento (1994) (hereinafter, AS94). For the same latitudinal ranges of the Atlantic, Indian and Pacific Oceans as in AS94, we construct one or two end-member mixing models on 14 neutral surfaces and estimate the stoichiometric ratios with a probabilistic approach. Unlike the results of AS94, significant vertical variations in the stoichiometry are found in the Atlantic and Pacific, while relatively constant stoichiometry with depth is found in the Indian Ocean, similar to AS94. The decreases in the C/P and $-O_2$/P ratios with depth in the Atlantic could be caused via dark DIC fixation by chemoautotrophs in the deep waters. In the Pacific, changes in organic matter composition with depth would be the most important factor in the increases in stoichiometry with depth. In all the basins, the N/P ratios are probably affected by benthic denitrification, as in AS94. The P/C/-O_2ratios (mean and $5^{th}$to 95^{th} percentile) are estimated to be 1/111(97 to 129)/155(149 to 163) in the depths below 2000 m of the Indian and Pacific Oceans, where DIC fixation and vertical change in organic matter composition have little influence on the stoichiometry estimates. We suggest that chemoautotrophic DIC fixation and the effect of change in organic matter composition with depth on the stoichiometry in waters above 2000 m should be considered for large-scale biogeochemical modeling and estimation of oceanic uptake of anthropogenic carbon from observational data.

Keywords: nutrients, stoichiometric ratios, remineralization of organic matter

©2019. Japan Geoscience Union. All Right Reserved.

Reproduction of iron-rich intermediate water in the Sea of Okhotsk by high resolution biogeochemical model.

*Hatsumi Nishikawa[1], Humio Mitsudera[1], Hiroshi Yoshinari[2], Takuya Nakanowatari[3], Tomohiro Nakamura[1], Keisuke Uchimoto[4], Hiroyasu Hasumi[5]

1. Institute of Low Temperature Science, Hokkaido University, 2. National Institute for Environmental Studies, 3. Tohoku National Fisheries Research Institute, Japan Fisheries Research and Education Agency, 4. Research Institute of Innovative Technology for the Earth, 5. Atmosphere and Ocean Research Institute, University of Tokyo

Recent observation studies suggest that iron supply from sediment on the northwest continental shelf the Okhotsk Sea plays an important role for the subarctic primary production (e.g. Nishioka et al., 2013). Dense shelf water (DSW) takes up iron from sediment, thereby transporting iron into the Okhotsk Sea intermediate water. However, observational data is still limited.

To clarify detailed structure of iron circulation in the North Pacific, we develop the high-resolution biogeochemical model. However, our model did not reproduce high iron concentration in the intermediate water the Sea of Okhotsk. We use biogeochemical model developed by Parekh et al. (2005). They set the value of total ligand concentration to constant value in all place. Recent observations, however, suggest that ligand concentration varies with sea area and depth. Then, we conducted a new experiment with the ligand concentration changed in the vertical direction. The iron concentration intermediate water of the new experiment becaame higher than before.

Keywords: High-resolution modeling, Iron-rich intermediate water, Ligand concentration

©2019. Japan Geoscience Union. All Right Reserved.

The global oceanic iron distribution estimated by data assimilation approach

*Doi Toshimasa[1], Satoshi Osafune[1], Shuhei Masuda[1], Hajime Obata[2], Kazuhiro Misumi[3], Jun Nishioka[4]

1. Japan Agency for Marine-Earth Science and Technology, 2. The University of Tokyo, 3. Central Research Institute of Electric Power Industry, 4. Hokkaido University

Since distribution of oceanic iron is considered as one of the restriction factors of phytoplankton activity, it is necessary for a pelagic lower trophic level ecosystem model to take into account the effect of iron. In this study, we constructed a three dimensional gridded data of oceanic iron concentration by using both available in situ observation and simple iron cycle model. For the physical process of iron transport, the advection/diffusion model was used along with the flow field of ESTOC (Estimated State of Global Ocean for Climate Research). The falling atmospheric dust in the sea-surface and flux from the sediment at sea floor of the coast were set as the input of the iron. The scavenging or desorption by particulate matter in the water column were employed as the control variables and we constructed the simple iron cycle model. The optimized set of control parameters was obtained based on a Green's function approach by using available in situ iron concentration observations. The results showed that the iron concentration in the southern hemisphere is lower than northern hemisphere, and the low iron regions were well reproduced around the regions of high nutrient / low chlorophyll. Moreover, it is suggested that the Atlantic Ocean is more affected by the atmospheric dust compared with the Pacific Ocean.

Keywords: oceanic iron, data assimilation

©2019. Japan Geoscience Union. All Right Reserved.

A high-resolution multi-purpose particle tracking framework for coastal areas near Japan

*Yoshimasa Matsumura[1], Shota Katsura[1], Masao Kurogi[2], Hideyuki Nakano[3], Takateru Yamagishi[4]

1. Atmosphere and Ocean Research Institute, University of Tokyo, 2. Japan Agency for Marine-Earth Science and Technology, 3. Meteorological Research Institute, Japan Meteorological Agency , 4. Research organization for Information Science and Technology

A comprehensive and multi-purpose particle tracking framework using latest high resolution velocity field in the coastal regions near Japan is developed.
The particle tracking system uses accurate fourth order Runge-Kutta method and implements random-walk based diffusivity, and is built-in the recent versions of MRI.com (an OGCM developed in Meteorological Research Institute, Japan Meteorological Agency) and kinaco (a non-hydrostatic ocean model developed in Atmosphere and Ocean Research Institute, University of Tokyo) for *on-line* use. Each particle is able to store up to seven arbitrary properties (such as size, age, exposed temperature, orientation, mass and buoyancy, etc.) and record the history of them.

The code is effectively parallelized (using MPI and OpenMP hybrid technique) and allows ~O(10^{10}) particles on modern massive-parallel supercomputers, and is also ported to GPU architecture using CUDA language.

This particle tracking framework has no particular target in a priori, and can be applied to various purposes for both physical oceanography (from large scale tracking of water masses to small scale modeling of suspended sediment matter or frazil ice crystals) and ocean biogeochemistry (tracking of trace elements, Laglangian modeling of plankton and detritus, individual based modeling of fishes and marine resources), only by defining appropriate properties and inserting a few lines of code that manipulats them corresponding to the particular target use.

In the presentation, we will introduce an application of this framework to the tracking of passive particles scattered in the coastal areas near Japan using velocity field provided by the latest very high resolution ocean modeling (~300 m mesh). Each model particle records its trajectory and the history of exposed environment, and can be interpreted as eggs or larvae (before acquiring swimming ability) of species of corresponding spawning areas and seasons as well as the tracers for small scale water mass exchanges.

Keywords: Particle tracking system

©2019. Japan Geoscience Union. All Right Reserved.

Numerical study on seasonality of ocean litters collected at the Dongsha Island in the northern South China Sea

*Yi-Chia Hsin[1], Chia-Ying Ko[2], Ming-Shiou Jeng[3]

1. Research Center for Environmental Changes, Academia Sinica, 2. Institute of Fisheries Science, National Taiwan University, 3. Biodiversity Research Center, Academia Sinica

Distribution of ocean litters collected at the Dongsha Island, an isolated island in the northern South China Sea, shows a significant seasonal change. More litters were accumulated in the northern (southern) part of the island in winter (summer). By means of backward-tracking simulation by considering the effect of both ocean currents and winds (i.e., windage), a series of numerical experiments are carried out to clarify the possible source and mechanisms for the observational seasonal change of litters. Results exhibit that, in winter, low-windage litters are mainly from the western Philippine Sea via the Luzon Strait while the high-windage ones are contributed from the Taiwan Strait. In summer, litters from the southwestern South China Sea, i.e. east of Vietnam, could be a major origin.

Keywords: ocean litters, numercial study, South China Sea

©2019. Japan Geoscience Union. All Right Reserved.

A key spot and timing to monitor chlorophyll-a in the Kuroshio western boundary current

*Takafumi Hirata[1]

1. Faculty of Environmental Earth Science, Hokkaido University

The Kuroshio western boundary current originates from the subtropics in the Western Pacific and carries a thermal energy and oceanic water mass towards the north, including the south coasts and offshore islands of Japan. In spite of the oligotrophy of the origin water that the Kuroshio carries, the Kuroshio water is known for spawning and feeding grounds of commercial/non-commercial fish larvae, explaining a higher fisheries production in the region. Thus, it puzzles an oceanographic and ecological relationships among nutrient fields, standing stock and productivity of organisms. In order to understand the complex Kuroshio ecosystems, phytoplankton dynamics is investigated using remote sensing data, namely phytoplankton pigment or chlorophyll-a observed by Advanced Himawari Imager (AHI) onboard Himawari-8. The area-integrated, and the area average of, Kuroshio chlorophyll-a was found predictable from a chlorophyll-a measurement in the 134-136 ˚E, where the Kuroshio current direction is most stable between 130-150 ˚E . An analysis of short term variability (< 1 year) of the Kuroshio chlorophyll-a concentration revealed that a cumulative, and monthly average of, chlorophyll-a over a month in the Kuroshio surface water could be estimated from a chlorophyll-a measurement at a single day in the month. These results suggest that there is a key spot and timing to monitor the phytoplankton activities in the Kuroshio current.

Keywords: Kuroshio, Chlorophyll, Remote Sensing

©2019. Japan Geoscience Union. All Right Reserved.

Impacts of cyclonic eddies on phytoplankton biomass and phenology in the Kuroshio Extension region

*Eko Siswanto[1], Yoshikazu Sasai[1]

1. Japan Agency for Marine-Earth Science and Technology

Two-decade ocean color chlorophyll-a concentration (CHL, a metric of phytoplankton biomass) data from 1997 to 2017 were used to comprehend the impact of cyclonic eddies on phytoplankton biomass and phenology in the Kuroshio Extension region (KE) of the western North Pacific Ocean. The CHL data have 4-km and 8-day spatiotemporal resolution and were acquired from the ESA Ocean Colour-Climate Change Initiative (http://www.esa-oceancolour-cci.org/). Prior to defining spring bloom onset, spatiotemporal gaps in CHL data were filled by applying empirical orthogonal function-based interpolation. The analysis was mainly focused on the winter season (January-March) as oceanographic conditions during the winter largely control phytoplankton spring bloom in terms of both magnitude and onset. Based on winter sea surface height anomaly (SSHa), cyclonic eddies (negative SSHa) were dominant mainly within the periods from 1998 to 2001 and from 2005 to 2009, whereas anti-cyclonic eddies (positive SSHa) were dominant mainly within the periods from 2002 to 2004 and from 2011 to 2015. Based on datasets from all seasons, the concurrences of negative SSHa and positive phytoplankton chlorophyll anomaly (CHLa) were observed, albeit not always. This indicates an eddy-induced upwelling supplies nutrients to the near-surface layer. Upwelled nutrients eventually promote phytoplankton growth. Such a concurrence of low SSHa and high CHLa was less obvious during the winter indicating that another factor (such as intense winter vertical mixing) also non-trivially controlled nutrient input to the surface layer, and hence CHLa variability. Overall temporal mean indeed showed that the active cyclonic eddy area (approximately south of the Kuroshio Current main axis) was characterized by high CHLa, low SSHa, and shoaled mixed layer. In this study, a Cumulative Sum method was applied to find phytoplankton spring bloom onset. Correlation between SSHa and spring bloom onset time was investigated, and it was found that approximately over the active cyclonic eddy area, positive correlation between winter/late winter SSHa and time of spring bloom onset was observed. Such a positive correlation indicates that cyclonic eddies during the winter likely tended to advance phytoplankton spring bloom onset.

Keywords: Ocean color, Phytoplankton, Bloom onset, Upwelling

©2019. Japan Geoscience Union. All Right Reserved.

Diagnostic estimation and uncertainties of nutrient limitation of phytoplankton growth in Michaelis-Menten functional form

*Taketo Hashioka[1], Maki Noguchi Aita[1]

1. Japan Agency for Marine-Science and Technology

Michaelis-Menten functional form (MM) is most widely used relationship of nutrient limitation of phytoplankton growth in large-scale ecosystem models. In MM functional form, the choice of parameter value of a half-saturation constant is a key point for controlling the strength of nutrient limitation. In general, the half-saturation constant increase with the size of the phytoplankton cell depending on the surface-to-volume ratio by diffusive hypothesis, and wide ranges of values are reported from observational studies. On the other hand, the most of Plankton Functional Types (PFT) models represent a phytoplankton type as one representative PFT with one global parameter. The parameter value is chosen in the observed range as a most reasonable value that could reproduce observed chl-a or nutrient concentration in each model. As a result, there are uncertainties of the global pattern of nutrient limitation among models. In this study, we diagnostically estimated the nutrient limitation using various parameter set of different global PFT models form CMIP5 together with the observation based nutrient concentrations (World Ocean Atlas for macro nutrient and multi-model median for dissolved iron and ammonium concentration). Then we show uncertainties and robustness of estimation of nutrient limitation in the current PFT models with MM functional form.

Keywords: Plankton Functional Types model, Michaelis-Menten functional form

©2019. Japan Geoscience Union. All Right Reserved.

Modeling productivity in lower trophic levels in Otsuchi Bay, northeast of Japan, using a nested OGCM with a biogeochemical component

*Takashi T Sakamoto[1], L. Shogo Urakawa[2], Sachihiko Itoh[1], Hiroyasu Hasumi[1], Kiyoshi Tanaka[1]

1. Atmosphere and Ocean Research Institute, the University of Tokyo, 2. Meteorological Research Institute, Japan Meteorologica Agancy

Otsuchi Bay is located on the northeast coast of Honshu Island, Japan, where was extensively damaged by the huge tsunamis caused by the 2011 off the Pacific coast of Tohoku Earthquake. Motivated by how the biogeochemical circumstance and fishery resource recover, some observations have been conducted in the bay, but those have not been enough because of several restrictions and human resources. Aimed at filling the observational shortage and the acquirement of some information about physical and low trophic fields, a modeling approach has been discussed. Using a triply-nested OGCM and a downscaling method, the authors succeeded to reproduce seasonal variability of the circulation in the bay, and also showed a seasonality of the water exchange mechanism between the bay and the open ocean (Sakamoto et al. 2017). In order to know the low trophic processes in the bay, a numerical simulation using a nested OGCM with a NPZD model is conducted. The OGCM is an improved version of Sakamoto et al’ s (2017) model, and the NPZD one is based on Nagata and Hasumi (2014). In this poster, our modeling strategy and some results will be presented. The final goal of this study is to perform hindcasting simulations of the bay with realistic boundary conditions, that are the river runoff, the atmospheric forcings, and the open ocean states.

Keywords: downscaling, nest-modeling, NPZD model

©2019. Japan Geoscience Union. All Right Reserved.

Change in lower trophic level ecosystems to decadal scale variation of climate system in the North Pacific Ocean

*Maki Noguchi Aita[1], Kazuaki Tadokoro[2], Yoshiki Komuro[3], Taketo Hashioka[1], Naomi Harada[1]

1. Research and Development Center for Global Change, Japan Agency for Marine-Earth Science and Technology, 2. Tohoku National Fisheries Research Institute, Japan Fisheries Research and Education Agency, 3. Institute of Arctic Climate and Environment Research, Japan Agency for Marine-Earth Science and Technology

The changes related to interdecadal climate variations, such as the Pacific Decadal Oscillation and the 18.6-y tidal cycle, have been discussed in many marine ecosystem studies. By analyzing data from observation of nutrient concentrations, decreasing and increasing trends of nutrients in the surface and subsurface layers, have been reported in many studies. Changes have also been observed in the biomass of phytoplankton and zooplankton. To clarify variability of lower trophic level productivity and its controlling factor, we simulated changes in the marine ecosystem caused by interdecadal climate variability, using the JRA55-do (Japanese 55-year atmospheric reanalysis) dataset from 1958 to 2017 to drive an ecosystem model, NEMURO, embedded in a global three-dimensional physical-biological coupled model, ‘COCO-NEMURO’. We compared and verified ecosystem model results with observations of phytoplankton and zooplankton species composition data collected by the Tohoku National Fisheries Research Institute, Japan Fisheries Research and Education Agency (FRA). Our model results showed that changes in biomass and nutrient concentration greatly differ depending on the region. According to our model results, sea surface temperature (SST) was very low during mid 1960s to mid 1970s, then SST increased after the mid 1970s to the end of 1990s in the western subarctic North Pacific. Changes in phytoplankton biomass was follow to this. However, the change in SST and phytoplankton and zooplankton biomass were contrary to this in the western subtropical North Pacific. We also checked decadal time series of annual mean sea ice concentration, SST, and phytoplankton biomass in the eastern Bering Sea and the western Arctic. The simulated sea ice concentration in the eastern Bering Sea decreased from the late 1970s to the early 1980s, while it was higher in the early 1990s and the late 2000s. The SST had its peaks in the late 1970s and the early 2000s. The phytoplankton biomass was inversely correlated with the sea ice concentration. In the western Arctic, the simulated sea ice concentration (SST) showed negative (positive) trends on the decadal timescale. The phytoplankton biomass has also been increasing, but its trend was not so simple. To elucidate the mechanism that sustains marine ecosystems, we will also analyze focusing on primary producers and zooplankton to key link to higher trophic levels.

Keywords: Climate change, decadal change, lower trophic marine ecosystem, marine ecosystem model 'NEMURO'

©2019. Japan Geoscience Union. All Right Reserved.

Estimation of experienced environment of jack mackerel in the East China Sea

*Tomihiko Higuchi[1], Motomitsu Takahashi[2], Kotaro Shirai[1], Shin-ichi Ito[1]

1. Atmosphere and Ocean Research Institute, The University of Tokyo, 2. Seikai National Fisheries Research Institute,FRA

Jack mackerel *Trachurus japonicus* is distributed on the continental shelf waters along the subtropical Kuroshio Current and the Tsushima Warm Current in the western North Pacific. The East China Sea (ECS) is one of major region for jack mackerel and understanding the recruitment processes of jack mackerel into the fishing grounds in the ECS is important. However, marine environment such as water temperature that jack mackerel actually experiences is not directly observed yet. In this study, oxygen ($\delta^{18}O$) and carbon ($\delta^{13}C$) stable isotope of jack mackerel otolith were analyzed and the experienced environment was estimated. When we compared $\delta^{18}O$ of otolith caught in between three different station with different temperature, average of $\delta^{18}O$ varied and was negatively correlated with water temperature of sampling station. Most of individual indicated that $\delta^{13}C$ relatively increased from core part to edge in otolith. Thus, these results suggest that otolith of jack mackerel recorded experienced environment. However, because jack mackerel migrate vertically, it needs to consider vertical profile of seawater temperature and other parameters such as salinity and prey availability. A combination with fish distribution information and ecological modeling may help the improvement of estimation for detail experienced environment.

Keywords: fish otolith, isotope analysis, experienced environment, fish migration

©2019. Japan Geoscience Union. All Right Reserved.

[E] Poster | H (Human Geosciences)：H-DS Disaster geosciences

Mon. May 27, 2019 1:45 PM - 3:15 PM JST | Mon. May 27, 2019 4:45 AM - 6:15 AM UTC | Poster Hall International Exhibition Hall8, Makuhari Messe_3

[H-DS11] Subaqueous Landslides and Their Anthropogenic Impact for Coastal Regions

convener:Yujin Kitamura(Department of Earth and Environmental Sciences, Graduate School of Science and Engineering, Kagoshima University), Yasuhiro Yamada(Japan Agency for Marine-Earth Science and Technology (JAMSTEC), R&D Center for Ocean Drilling Science (ODS))

A large number of people inhabit coastal areas around the world that are susceptible to natural catastrophes and subaqueous landslides are one of such hazards as demostrated recently. The risk associated with the occurrence of subaqueous landslides is not only constrained to passive margins or subduction zones but any of water areas is also susceptible to their occurrence since subaqueous failures can be triggered at very low slope angles. This realization poses a significant challenge that requires the collection of vast amounts of information and data to unravel the true nature of these events and their potential risk to coastal communities. Despite these challenges, recent technical and engineering advances in the acquisition and processing of sea floor and shallow subsurface data are encouraging. There has also been a concerted effort by scientists from different earth-science disciplines to increase interdisciplinary cooperation at an international level to advance our collective understanding of subaqueous landslides and their consequences.
This session calls for technical contributions covering all aspects of subaqueous landslide research including but not limited to: physical properties of deformed sediments (pre- and post- deformation), role of interstitial fluids in subaqueous landslide development, slope stability and risk assessments, geomorphological and sedimentological/stratigraphic descriptions, tsunamigenic risk and modeling, description of ancient subaqueous landslides, sand-box models and numerical simulations of subaqueous landslides. Case studies from lacustrine landslides and subaerial coastal landslides transitioning into the marine realm are also welcome. Case studies associated with the broader topic of subaqueous gravity-driven flows (e.g.: turbidites and transitional flows) and their relationship with seafloor faulting are also of interest to this session. Participants of IUGS project S4SLIDE IGCP-640 sponsor this session.

[HDS11-P01] Deformed sediment gravity flow deposits associated with bypassing slides:an example from the Miocene Ushikiri Formation, Southwest Japan

*Miki Kobayashi[1], Tetsuya Sakai[2] (1.Nippon Koei, 2.Shimane University)

[HDS11-P02] Submarine Landslide and Resulting Tsunami on the Continental Shelf Slope off Shikoku

*Youdai Gon[1], Toshitaka Baba[1], Tetsuo Matsuno, Mitsuru Hayashi, Hiroshi Ichihara (1.Tokushima University graduate school)

[HDS11-P03] Sedimentary environment estimated from physical properties of sediment core collected during the cruise of Hakuho-maru KH-18-3 in the South Yatsushiro sea, western Kyushu.

*Koki Hori[1], Yujin Kitamura[2], Hakuho-maru KH-18-3 Scientists (1.Department of Earth and Planetary Sciences, Graduate School of Science, Kyushu University , 2.Department of Earth and Environmental Sciences, Graduate School of Science and Engineering , Kagoshima University)

[HDS11-P04] Variation in vane shear strength and magnetic susceptibility in the cores recovered by Hakuho-maru KH-18-3 cruise in Yatsushiro sea

*Yujin Kitamura[1], Haruka Kageyama[2], Kaede Yamasaki[2], Ryoya Goto[2], Koki Hori[2], Yuta Ikebata[2], Kuniyo Kawabata[1], Daiki Oyama[2], Hakuho-maru KH-18-3 Scientists (1.Department of Earth and Environmental Sciences, Graduate School of Science and Engineering, Kagoshima University, 2.Department of Earth and Environmental Sciences, Faculty of Science, Kagoshima University)

[HDS11-P05] Identification of turbidites in the Yatsushiro Sea surface sediment core samples from non-destructive measurements: Hakuho-maru KH-18-3 Cruise, Yatsushiro Sea, Western

Kyushu, Japan

*Ryoya Goto[1], Yujin Kitamura[2], Hakuho-maru KH-18-3 Cruise Scientist (1.Atmosphere and Ocean Research Institute, The University of Tokyo, 2.Department of Earth and Environmental Sciences, Graduate School of Science, Kagoshima University)

[HDS11-P06] Revised columnar section based on grain size distribution analysis of samples from Hakuho-maru KH-18-3 in Yatsushiro sea

*Yuta Ikebata[1], Yujin Kitamura[2], Hakuho-maru KH-18-3 Scientists Family (1.Kyusyu University Graduate School Of Science Earth and Planetary Science, 2.Graduate school of science, Kagoshima University)

Deformed sediment gravity flow deposits associated with bypassing slides: an example from the Miocene Ushikiri Formation, Southwest Japan

*Miki Kobayashi[1], Tetsuya Sakai[2]

1. Nippon Koei, 2. Shimane University

The Middle Miocene Ushikiri Formation in Shimane Peninsula, southwest Japan, is interpreted to have been deposited on the shelf margin to the middle continental shelf, and is known to contain unique sediment gravity flow deposits, similar to hybrid sediment gravity flow deposits (turbidite + debrite). Intensely deformed mud clasts have been described from this formation. However, their formation has not been focused on previous studies. The present study aims to characterize the deformation of sandstone beds and mud clasts contained within the sediment gravity flow deposits and to discuss of the deformation process of the sediments.

Many of the sandstone beds in the upper Ushikiri Formation (averaging 0.6 m thick) are bipartite, with lower parts showing characteristics similar to Ta or Ta-b turbidites with rich mud clasts. The upper parts of the sandstone beds are represented by poorly-sorted muddy sand with scattered mud clasts having debrite-like features. The small mud clasts in the lower part show features different from those in ordinary turbidites: some are subject to injection of surrounding sand and some scattered in sands show jigsaw-puzzle patterns, suggesting in situ mud clast fragmentation. Some mud clasts are intensely stretched. The beds also host large mud clasts (maximum length: ca 3 m), in which deformation structures, such as slump folds, are well developed. Mud clast shapes are not consistent with internal deformation structures and the most of them have sharp margins. The sand around some large mud clasts shows local liquefaction. Local grading is also found above the large mud clasts and does not continue beyond the edge of the mud clasts.

The injection of sand into mud clasts and their in situ fragmentation into jigsaw-puzzle patterns can be explained by liquefaction of beds with overburden pressure. A possible pressure source is slides that passed over a freshly deposited turbidite bed. When a slide bypassed the sand bed, the bed once deposited as turbidite easily liquefied under the moving slide mass, having led overburden pressure in the bed that caused injection and in situ fragmentation. On the contrary, the large mud clasts may have been fragments ripped from a major sliding body that bypassed the studied locality. Local liquefaction around large mud clasts indicates they sank or were forced into the bed from above. The presence of local grading above the mud clasts can be explained by local resuspension of sand around the mud clasts when they sank into the sand. The above mentioned sediment deformation process is supported by beds with a slide deposit above a sandy part having similar mud clast deformation.
The bypassing of the slide may have been due to hydroplaning of the slide mass. The slide deposits are represented by up to 2 m thick of large mud block rich sediments with variety of deformation structures, which grades from an underlying debrite-like bed that consists of poorly-sorted muddy sand with rich mud clasts with injection of surrounding muddy sand. Some mud clasts in the muddy sandstone beds are intensely stretched, implying that shear stress exerted within the beds. The poorly-sorted muddy sand is thus interpreted as a fluid layer, which has been existed below the moving landslide mass, having triggered the hydroplaning.

©2019. Japan Geoscience Union. All Right Reserved.

Keywords: submarine landslide deposit, bypassing of landslide mass, Shamane

©2019. Japan Geoscience Union. All Right Reserved.

Submarine Landslide and Resulting Tsunami on the Continental Shelf Slope off Shikoku

*Youdai Gon[1], Toshitaka Baba[1], Tetsuo Matsuno, Mitsuru Hayashi, Hiroshi Ichihara

1. Tokushima University graduate school

Submarine landslide occurs mainly due to earthquake shaking damaging marine infrastructure such as submarine communication and causing tsunami. The bathymetry in the Nankai Trough has traces of numerous submarine landslides. One of them is located on the continental shelf 24 km off the Shikoku coast. The submarine landslide off Shikoku would have a potential causing tsunami. Therefore, in this study, with the purpose revealing the topographical features of the submarine landslide off Shikoku in detail, multi-narrow beam surveys were conducted. We also discuss the tsunami potential of the submarine landslide from numerical simulations.

The multi-narrow beam surveys were conducted once in 2017 and twice in 2018 covering an area 30 km x 20 km by a training ship, Kobe University Graduate School of Maritime Sciences Attachment Practice Ship Fukae Maru. The acquired bathymetric map indicated four head scarps neighboring to each other (hereafter scarp A, B, C, D from the west). Sediment deposition was confirmed below scarp A. The scarp A seems to be younger than the other scarps. The slopes collapsed multiple times implying occurrence of a new collapse in the future.

Tsunami calculations were carried out for slump A, B and C. But, from the topographic features, slump B and C were assumed to be a simultaneous collapse. We also assumed new two submarine landslides (slump E and F) to the east of slump D with the same size of sump A. In the calculation results, the tsunamis arrive at about 15 min. after the initiation of slump A and the simultaneous slump B and C. For slump E and F, tsunami arrives at about 20 min. The maximum tsunami heights were estimated to be about 2 m, 2 m, 4.5 m and 5 m for slump A, B-C, E and F, respectively. We are going to conduct more simulations to evaluate risk of tsunami caused by the submarine landslide tsunamis in the study area.

Keywords: The submarine landslide off Shikoku, Tsunami simulation

©2019. Japan Geoscience Union. All Right Reserved.

Sedimentary environment estimated from physical properties of sediment core collected during the cruise of Hakuho-maru KH-18-3 in the South Yatsushiro sea, western Kyushu.

*Koki Hori[1], Yujin Kitamura[2], Hakuho-maru KH-18-3 Scientists

1. Department of Earth and Planetary Sciences, Graduate School of Science, Kyushu University , 2. Department of Earth and Environmental Sciences, Graduate School of Science and Engineering , Kagoshima University

The research cruise KH-18-3 was carried out in the South Yatsushiro sea from 27th to 30th July 2018. The purpose of this cruise is to clarify the occurrence history of the submarine landslides in the Yatsushiro sea. In this survey, bottom surface sediment samples were collected by using Piston corer which is 6 meters long.
The study on physical properties of event sediment using core samples are conducted in ocean areas around the world. For example, Prior et al. (1984) reported that Mass transport deposits (MTD) commonly have a higher density than surrounding, sediments that are not submarine landslide origin. Therefore, in this study, the physical properties that serve as the basic information of the core samples were measured. In addition, we estimated the sedimentary environment in the survey area by applying tidal current, sedimentation rate, and bottom surface muddy rate in the south Yatsushiro sea (Rifardi et al.,1998) and conventional radiocarbon ages of piston core samples recovered in the same area reported by Inoue et al. (2011).

Core samples were collected from 11 sites (core name:PC01 to PC11) in the south Yatsushiro sea where the Taura-Tsunagi Oki fault group and Minamata Oki fault group are distributed.
All analyses other than the grain size distribution analysis were conducted at the Center for Advanced Marine Core Research, Kochi University. Initially, GRA density, Magnetic susceptibility and fractional porosity were measured using Whole round multi sensor core logger (MSCL-W). After the analysis, core samples were divided vertically and visual observation and color measurement of them were performed. Subsequently, a vane shear test and sub-samples which were used for MAD measurements and grain size distribution analysis collecting were performed at approximately 50 cm intervals, respectively, and the test and two sampling location were the same points.

Area 1 is under condition of rather stagnant water masses or rather weak tidal current system and is characterized fine-grained sediments. We estimated age of core samples by comparing physical properties reported by Inoue et al. (2011) because sampling point in this area matched with piston coring points of Inoue et al. (2011) and the behaviors of both physical properties were similar. As a result, a gap of more than 7000 years of sediment age is estimated at depth of 2 to 3 meters in area 1a (PC01 to PC03) and it is presumed that sediments indicating the age of about 10,000 years BP exist at depth of several tens of centimeters from the seabed surface in area 1b (PC06, PC07). In addition, K-Ah volcanic ash layer (7.3ka) could not be confirmed from sediments in both sea areas. From this, it is assumed that there was an event such as a submarine landslide or erosion with the lower part of the tephra as a sliding or eroding surface.
Since we could not obtain an index to estimate the age of the PC 08 to PC 11, we estimated the sedimentary environment using only the physical properties of sediments. PC08 and PC10 (Area 2) is located near the strait of Goshoura-jima and sisi-jima island, under influence of strong tidal and bottom currents, and is characterized by coarse sediments. Especially, upward grain refinement was observed and

©2019. Japan Geoscience Union. All Right Reserved.

the tendency that the porosity decreases within each monolayer is repeated in PC10. From this, it is assumed that the upper sediment functions as an impermeable layer against the lower sediment, and the drainage is difficult to proceed. PC 09 and PC 11 (Area 3) are relatively close to supply sources such as Minamata River and Komenotsu River, and are characterized as relatively coarse sediments. From the depth of 60 cm of PC09, and from the outermost surface layer in PC 11, the porosity does not decrease almost from around 60%. From this, it is estimated that the new sediment has been recently cleared recently.

Keywords: Piston coring, Yatsushiro sea

©2019. Japan Geoscience Union. All Right Reserved.

Variation in vane shear strength and magnetic susceptibility in the cores recovered by Hakuho-maru KH-18-3 cruise in Yatsushiro sea

*Yujin Kitamura[1], Haruka Kageyama[2], Kaede Yamasaki[2], Ryoya Goto[2], Koki Hori[2], Yuta Ikebata[2], Kuniyo Kawabata[1], Daiki Oyama[2], Hakuho-maru KH-18-3 Scientists

1. Department of Earth and Environmental Sciences, Graduate School of Science and Engineering, Kagoshima University, 2. Department of Earth and Environmental Sciences, Faculty of Science, Kagoshima University

Introduction

The 2016 Kumamoto Earthquake was sourced from a part of active faults of the Futagawa-Hinagu fault zones. The southwestern part of Hinagu fault zone forms the Yatsushiro section as a group of submarine active faults. Earthquake shaking occasionally triggers submarine landslide, however, any record of submarine landslide in this area has not been reported. We therefore conducted research cruise with R/V Hakuho-maru and recovered sediment cores in Yatsushiro sea. As it is known that the shear strength decreases at the bottom of mass transport deposits, we conducted vane shear test with the cores. We also referred the variation of magnetic susceptibility to establish core correlation with previous works.

Method

Here we conducted four-days research cruise with R/V Hakuho-maru (KH-18-3) in July, 2018 to reveal submarine landslide records and benthic environment in Yatsushiro sea. We used six-meters-long piston corers and cored at 11 sites and recovered cores were cut into 6 sections onboard. Cores were analyzed at Kochi Kore Center using X-ray CT scanner, multi-sensor core logger (gamma ray density: GRD; and magnetic susceptibility: MS), core imaging apparatus, visual core description, color spectroscope, X-ray fluorescence core scanner (Itrax). Vane shear apparatus is used with split core section and tested every about 50 cm.

Results and Discussion

Sediments are dominated by matrices of olive gray to black sand or mud. CT value, MS and GRD generally increase with depth. As MS shows cyclic fluctuation, we classified into several MS units by defining units with each broad peak. Our MS units was correlated with previous studies of high resolution seismic profile by Yagi et al. (2016) and piston cores by Inoue et al. (2011). MS units was in good agreement with Yagi's seismic profile. It is inferred that our samples include the sediments during Late Glacial Maximum to Jomon Transgression below hiatus. MS data by Inoue et al. (2011) and this study are in accordance with each other. The event layers Inoue suggested are discriminable in our cores which are characterized as local maximum of MS. Iron shows high concentration around the event layers so that the iron is a candidate for indicator for searching the events. We assume that this iron anomaly is caused by the rapid deposition during eventic turbidites.

The results of vane shear test showed that the strength increases with depth with a change in its rate at assumed hiatus. This shows that the sediments below hiatus was further deeply buried and compacted. At sites PC04 to PC06, the strength is low at their surface, indicating that the hiatus at these sites are very shallow and thus the recent surface erosion is assumed.

©2019. Japan Geoscience Union. All Right Reserved.

Keywords: turbidites, shallow marine deposits, 2016 Kumamoto earthquake

©2019. Japan Geoscience Union. All Right Reserved.

Identification of turbidites in the Yatsushiro Sea surface sediment core samples from non-destructive measurements: Hakuho-maru KH-18-3 Cruise, Yatsushiro Sea, Western Kyushu, Japan

*Ryoya Goto[1], Yujin Kitamura[2], Hakuho-maru KH-18-3 Cruise Scientist

1. Atmosphere and Ocean Research Institute, The University of Tokyo, 2. Department of Earth and Environmental Sciences, Graduate School of Science, Kagoshima University

Submarine active faults in Yatsusiro Sea, western Kyushu, Japan, constitute the Yatsushiro section of Hinagu fault zone in its southwest end (AIST et al., 2011). The 2016 Kumamoto Earthquake was sourced from a part of active faults of the Futagawa-Hinagu fault zones (JMA, 2018), and survey has hardly conducted in the sea area after the earthquake occurrence. Earthquake shaking occasionally triggers turbidity currents by submarine landslides and resuspension of unconsolidated sediments on the seafloor (Ikehara et al., 2018). In recent years, the study of earthquake occurrence history using earthquake turbidites formed by turbidity currents is being conducted throughout the world. As earthquake-origin turbidity currents can take place in very gentle slope (e.g. the Mississippi-Delta 0.01°: D. B. Prior et al., 1978), its occurrence is sufficiently thought even in Yatsushiro Sea. However, any record of earthquake turbidites in this area has not been reported. In this study, identification of turbidites in the Yatsushiro Sea surface sediment core samples from non-destructive measurements.

Here we conducted four-days research cruise Hakuho-maru KH-18-3 in July, 2018. We conducted sub-bottom profiling on eight lines, piston coring at 11 sites in Yatsushiro Sea, western Kyushu, Japan. Recovered cores are analyzed by X-ray CT scanner, multi-sensor core logger, core imaging apparatus, visual core description, color spectroscope and X-ray fluorescence core scanner (Itrax) in the Center for Advanced Marine Core Research, Kochi University. With reference to the previous studies (Iwai et al., 2014, JGS abstract; Isabel Rodríguez-Germade et al, 2015; Okutsu et al., 2017, JGS abstract), the behavior of Ca/Ti and Fe/Ti where the peak was observed at the base of turbidites, and the behavior of Fe/Ti and Zr/Ti where the peak was observed at the base of volcaniclastics turbidites.

Our results revealed turbidites and volcaniclastics turbidites in six piston coring sites (PC01 to PC06). As all of sites are located in the Taura-Tsunagioki fault group or Minamataoki fault group, turbidites were considered to be present in all of sites. However, turbidites were identified from PC01 to PC06, but not identified from PC07 to PC11. According to Rifardi et al. (1998), PC01 to PC06 are located in the sea area where the deposition rate is high, and PC07 to PC11 are located in the sea area where the deposition rate is slow.

As turbidite is formed by various factors besides earthquakes, it is necessary to consider whether the turbidites identified in this study are earthquake turbidites. In addition, to investigate the history of earthquakes, it is also a future task to conduct individual sample measurements (such as grain size distribution analysis) and dating.

Hakuho-maru KH-18-3 Cruise Scientists: Takashi Tomiyasu, Hitoshi Kodamatani, Kuniyo Kawabata, Daiki Oyama, Haruka Kageyama, Kaede Yamasaki (Kagoshima Univ.), Yuta Ikebata, Koki Hori (Kyushu Univ.), Asuka Yamaguchi, Fumiaki Tsunomori, Kameo Katsura, Tsubasa Miki, Natsumi Okutsu, Hiroaki Koge,

©2019. Japan Geoscience Union. All Right Reserved.

Kotaro Fujita, Ayaka Nakazawa, Yuichi Okuma, Genki Kobayashi, Rina Fukuchi (Tokyo Univ.), Jun Kameda, Tomonori Morisaki (Hokkaido Univ.)

Keywords: submarine landslides, turbidites, shallow sea deposits, Yatsushiro Sea, 2016 Kumamoto Earthquake

©2019. Japan Geoscience Union. All Right Reserved.

Revised columnar section based on grain size distribution analysis of samples from Hakuho-maru KH-18-3 in Yatsushiro sea

*Yuta Ikebata[1], Yujin Kitamura[2], Hakuho-maru KH-18-3 Scientists Family

1. Kyusyu University Graduate School Of Science Earth and Planetary Science, 2. Graduate school of science, Kagoshima University

Hakuho-maru KH-18-3 was held in the Yatsushiro Sea from 27th to 30th July 2018 for clarifying history of occurrence of submarine landslides. Earthquake is a one of big trigger of submarine landslides, and submarine landslides occurs in an very easy slope. Kumamoto earthquake occurred at April, 2016 and a lot of surveys in the land area were conducted but survey in the sea area weren't conducted much. In the Yatsushiro sea, the occurrence of submarine landslides caused by earthquake of the Futagawa-Hinagu fault zones can be considered sufficiently. Therefore, in this study, the creation of the columnar section which is the basic information of the submarine landslide accreditation was made based on the grain size distribution analysis.

In the Expedition, eleven piston cores(6m) from PC01 to PC11 were collected in the southern part of Yatsushiro sea, and the obtained core was subjected to non-destructive measurement and individual sample measurement at the Kochi Core Center. For non-destructive measurement, CT images and core continuous images were taken, and for individual sample measurement, Density, Magnetic susceptibility, porosity, vane shear strength, color, concentration change of major elements were examined. Grain size distribution analysis was conducted at Kagoshima University. Samples used for grain size distribution analysis were collected every 50 cm and analyzed with a laser diffraction type grain size distribution analyzer. Since it is difficult to judge the stratum boundary only with the result of grain size distribution measurement at intervals of 50 cm, it was judged by using γ ray density, magnetic susceptibility and color measurement result which are continuous data.

Grain size distribution analysis revealed PC01 to PC07 are muddy cores and PC08 to PC11 contains much sand. Grain size of PC01, PC04, PC06, PC07, PC09, PC11 are very different in Grain size distribution analysis and visual core description. Based on the results of the grain size distribution analysis, the stratum boundary was determined from the change commonly seen in the γ ray density, magnetic susceptibility and color, and a columnar section was prepared. In Rifardi et al.(1998), the distribution of mud content in the Yatsushiro Sea has been surveyed. As a result of comparing the columnar map of this study with its distribution for each sampling point, cores excluding PC08 corresponded well. It is thought that it is influenced by the supply of sediment by river and stagnant water mass, tide current as in previous research. Also, in Inoue et al.(2011), which was a reference for determining the core harvest point, dating is done in the same area. At Hori(2019MS), we compare the data with Inoue et al.(2011) and estimate the core age of this research. We also compare the columnar section made in this study with the columnar section of Inoue et al.(2011), using the comparative categories determined at the time of estimating the age. As a result, PC01 and PC02 were in good agreement, PC06 and PC07 had different stratum in the surface layer. This is probably because the sampling site of PC06 is actually about 150 m far from Inoue et al.(2011) and the sampling site of PC07 is actually about 111 m far from Inoue et al.(2011), and the sedimentary environment is slightly different. Also, in the grain size distribution analysis of this study, there is a possibility that coarse grains may be selectively left out when putting the sample into the machine, and it may be doubtful in accuracy.

©2019. Japan Geoscience Union. All Right Reserved.

Keywords: Submarine landslide

©2019. Japan Geoscience Union. All Right Reserved.

[E] Poster | H (Human Geosciences)：H-DS Disaster geosciences

Mon. May 27, 2019 5:15 PM - 6:30 PM JST | Mon. May 27, 2019 8:15 AM - 9:30 AM UTC | Poster Hall International Exhibition Hall8, Makuhari Messe_13

[H-DS11] Subaqueous Landslides and Their Anthropogenic Impact for Coastal Regions

convener:Yujin Kitamura(Department of Earth and Environmental Sciences, Graduate School of Science and Engineering, Kagoshima University), Yasuhiro Yamada(Japan Agency for Marine-Earth Science and Technology (JAMSTEC), R&D Center for Ocean Drilling Science (ODS))

A large number of people inhabit coastal areas around the world that are susceptible to natural catastrophes and subaqueous landslides are one of such hazards as demostrated recently. The risk associated with the occurrence of subaqueous landslides is not only constrained to passive margins or subduction zones but any of water areas is also susceptible to their occurrence since subaqueous failures can be triggered at very low slope angles. This realization poses a significant challenge that requires the collection of vast amounts of information and data to unravel the true nature of these events and their potential risk to coastal communities. Despite these challenges, recent technical and engineering advances in the acquisition and processing of sea floor and shallow subsurface data are encouraging. There has also been a concerted effort by scientists from different earth-science disciplines to increase interdisciplinary cooperation at an international level to advance our collective understanding of subaqueous landslides and their consequences.
This session calls for technical contributions covering all aspects of subaqueous landslide research including but not limited to: physical properties of deformed sediments (pre- and post- deformation), role of interstitial fluids in subaqueous landslide development, slope stability and risk assessments, geomorphological and sedimentological/stratigraphic descriptions, tsunamigenic risk and modeling, description of ancient subaqueous landslides, sand-box models and numerical simulations of subaqueous landslides. Case studies from lacustrine landslides and subaerial coastal landslides transitioning into the marine realm are also welcome. Case studies associated with the broader topic of subaqueous gravity-driven flows (e.g.: turbidites and transitional flows) and their relationship with seafloor faulting are also of interest to this session. Participants of IUGS project S4SLIDE IGCP-640 sponsor this session.

[HDS11-P01] Deformed sediment gravity flow deposits associated with bypassing slides:an example from the Miocene Ushikiri Formation, Southwest Japan

*Miki Kobayashi[1], Tetsuya Sakai[2] (1.Nippon Koei, 2.Shimane University)

[HDS11-P02] Submarine Landslide and Resulting Tsunami on the Continental Shelf Slope off Shikoku

*Youdai Gon[1], Toshitaka Baba[1], Tetsuo Matsuno, Mitsuru Hayashi, Hiroshi Ichihara (1.Tokushima University graduate school)

[HDS11-P03] Sedimentary environment estimated from physical properties of sediment core collected during the cruise of Hakuho-maru KH-18-3 in the South Yatsushiro sea, western Kyushu.

*Koki Hori[1], Yujin Kitamura[2], Hakuho-maru KH-18-3 Scientists (1.Department of Earth and Planetary Sciences, Graduate School of Science, Kyushu University , 2.Department of Earth and Environmental Sciences, Graduate School of Science and Engineering , Kagoshima University)

[HDS11-P04] Variation in vane shear strength and magnetic susceptibility in the cores recovered by Hakuho-maru KH-18-3 cruise in Yatsushiro sea

*Yujin Kitamura[1], Haruka Kageyama[2], Kaede Yamasaki[2], Ryoya Goto[2], Koki Hori[2], Yuta Ikebata[2], Kuniyo Kawabata[1], Daiki Oyama[2], Hakuho-maru KH-18-3 Scientists (1.Department of Earth and Environmental Sciences, Graduate School of Science and Engineering, Kagoshima University, 2.Department of Earth and Environmental Sciences, Faculty of Science, Kagoshima University)

[HDS11-P05] Identification of turbidites in the Yatsushiro Sea surface sediment core samples from non-destructive measurements: Hakuho-maru KH-18-3 Cruise, Yatsushiro Sea, Western

Kyushu, Japan

*Ryoya Goto[1], Yujin Kitamura[2], Hakuho-maru KH-18-3 Cruise Scientist (1.Atmosphere and Ocean Research Institute, The University of Tokyo, 2.Department of Earth and Environmental Sciences, Graduate School of Science, Kagoshima University)

[HDS11-P06] Revised columnar section based on grain size distribution analysis of samples from Hakuho-maru KH-18-3 in Yatsushiro sea

*Yuta Ikebata[1], Yujin Kitamura[2], Hakuho-maru KH-18-3 Scientists Family (1.Kyusyu University Graduate School Of Science Earth and Planetary Science, 2.Graduate school of science, Kagoshima University)

Deformed sediment gravity flow deposits associated with bypassing slides: an example from the Miocene Ushikiri Formation, Southwest Japan

*Miki Kobayashi[1], Tetsuya Sakai[2]

1. Nippon Koei, 2. Shimane University

The Middle Miocene Ushikiri Formation in Shimane Peninsula, southwest Japan, is interpreted to have been deposited on the shelf margin to the middle continental shelf, and is known to contain unique sediment gravity flow deposits, similar to hybrid sediment gravity flow deposits (turbidite + debrite). Intensely deformed mud clasts have been described from this formation. However, their formation has not been focused on previous studies. The present study aims to characterize the deformation of sandstone beds and mud clasts contained within the sediment gravity flow deposits and to discuss of the deformation process of the sediments.

Many of the sandstone beds in the upper Ushikiri Formation (averaging 0.6 m thick) are bipartite, with lower parts showing characteristics similar to Ta or Ta-b turbidites with rich mud clasts. The upper parts of the sandstone beds are represented by poorly-sorted muddy sand with scattered mud clasts having debrite-like features. The small mud clasts in the lower part show features different from those in ordinary turbidites: some are subject to injection of surrounding sand and some scattered in sands show jigsaw-puzzle patterns, suggesting in situ mud clast fragmentation. Some mud clasts are intensely stretched. The beds also host large mud clasts (maximum length: ca 3 m), in which deformation structures, such as slump folds, are well developed. Mud clast shapes are not consistent with internal deformation structures and the most of them have sharp margins. The sand around some large mud clasts shows local liquefaction. Local grading is also found above the large mud clasts and does not continue beyond the edge of the mud clasts.

The injection of sand into mud clasts and their in situ fragmentation into jigsaw-puzzle patterns can be explained by liquefaction of beds with overburden pressure. A possible pressure source is slides that passed over a freshly deposited turbidite bed. When a slide bypassed the sand bed, the bed once deposited as turbidite easily liquefied under the moving slide mass, having led overburden pressure in the bed that caused injection and in situ fragmentation. On the contrary, the large mud clasts may have been fragments ripped from a major sliding body that bypassed the studied locality. Local liquefaction around large mud clasts indicates they sank or were forced into the bed from above. The presence of local grading above the mud clasts can be explained by local resuspension of sand around the mud clasts when they sank into the sand. The above mentioned sediment deformation process is supported by beds with a slide deposit above a sandy part having similar mud clast deformation.
The bypassing of the slide may have been due to hydroplaning of the slide mass. The slide deposits are represented by up to 2 m thick of large mud block rich sediments with variety of deformation structures, which grades from an underlying debrite-like bed that consists of poorly-sorted muddy sand with rich mud clasts with injection of surrounding muddy sand. Some mud clasts in the muddy sandstone beds are intensely stretched, implying that shear stress exerted within the beds. The poorly-sorted muddy sand is thus interpreted as a fluid layer, which has been existed below the moving landslide mass, having triggered the hydroplaning.

©2019. Japan Geoscience Union. All Right Reserved.

Keywords: submarine landslide deposit, bypassing of landslide mass, Shamane

©2019. Japan Geoscience Union. All Right Reserved.

Submarine Landslide and Resulting Tsunami on the Continental Shelf Slope off Shikoku

*Youdai Gon[1], Toshitaka Baba[1], Tetsuo Matsuno, Mitsuru Hayashi, Hiroshi Ichihara

1. Tokushima University graduate school

Submarine landslide occurs mainly due to earthquake shaking damaging marine infrastructure such as submarine communication and causing tsunami. The bathymetry in the Nankai Trough has traces of numerous submarine landslides. One of them is located on the continental shelf 24 km off the Shikoku coast. The submarine landslide off Shikoku would have a potential causing tsunami. Therefore, in this study, with the purpose revealing the topographical features of the submarine landslide off Shikoku in detail, multi-narrow beam surveys were conducted. We also discuss the tsunami potential of the submarine landslide from numerical simulations.

The multi-narrow beam surveys were conducted once in 2017 and twice in 2018 covering an area 30 km x 20 km by a training ship, Kobe University Graduate School of Maritime Sciences Attachment Practice Ship Fukae Maru. The acquired bathymetric map indicated four head scarps neighboring to each other (hereafter scarp A, B, C, D from the west). Sediment deposition was confirmed below scarp A. The scarp A seems to be younger than the other scarps. The slopes collapsed multiple times implying occurrence of a new collapse in the future.

Tsunami calculations were carried out for slump A, B and C. But, from the topographic features, slump B and C were assumed to be a simultaneous collapse. We also assumed new two submarine landslides (slump E and F) to the east of slump D with the same size of sump A. In the calculation results, the tsunamis arrive at about 15 min. after the initiation of slump A and the simultaneous slump B and C. For slump E and F, tsunami arrives at about 20 min. The maximum tsunami heights were estimated to be about 2 m, 2 m, 4.5 m and 5 m for slump A, B-C, E and F, respectively. We are going to conduct more simulations to evaluate risk of tsunami caused by the submarine landslide tsunamis in the study area.

Keywords: The submarine landslide off Shikoku, Tsunami simulation

©2019. Japan Geoscience Union. All Right Reserved.

Sedimentary environment estimated from physical properties of sediment core collected during the cruise of Hakuho-maru KH-18-3 in the South Yatsushiro sea, western Kyushu.

*Koki Hori[1], Yujin Kitamura[2], Hakuho-maru KH-18-3 Scientists

1. Department of Earth and Planetary Sciences, Graduate School of Science, Kyushu University , 2. Department of Earth and Environmental Sciences, Graduate School of Science and Engineering , Kagoshima University

The research cruise KH-18-3 was carried out in the South Yatsushiro sea from 27th to 30th July 2018. The purpose of this cruise is to clarify the occurrence history of the submarine landslides in the Yatsushiro sea. In this survey, bottom surface sediment samples were collected by using Piston corer which is 6 meters long.
The study on physical properties of event sediment using core samples are conducted in ocean areas around the world. For example, Prior et al. (1984) reported that Mass transport deposits (MTD) commonly have a higher density than surrounding, sediments that are not submarine landslide origin. Therefore, in this study, the physical properties that serve as the basic information of the core samples were measured. In addition, we estimated the sedimentary environment in the survey area by applying tidal current, sedimentation rate, and bottom surface muddy rate in the south Yatsushiro sea (Rifardi et al.,1998) and conventional radiocarbon ages of piston core samples recovered in the same area reported by Inoue et al. (2011).

Core samples were collected from 11 sites (core name:PC01 to PC11) in the south Yatsushiro sea where the Taura-Tsunagi Oki fault group and Minamata Oki fault group are distributed.
All analyses other than the grain size distribution analysis were conducted at the Center for Advanced Marine Core Research, Kochi University. Initially, GRA density, Magnetic susceptibility and fractional porosity were measured using Whole round multi sensor core logger (MSCL-W). After the analysis, core samples were divided vertically and visual observation and color measurement of them were performed. Subsequently, a vane shear test and sub-samples which were used for MAD measurements and grain size distribution analysis collecting were performed at approximately 50 cm intervals, respectively, and the test and two sampling location were the same points.

Area 1 is under condition of rather stagnant water masses or rather weak tidal current system and is characterized fine-grained sediments. We estimated age of core samples by comparing physical properties reported by Inoue et al. (2011) because sampling point in this area matched with piston coring points of Inoue et al. (2011) and the behaviors of both physical properties were similar. As a result, a gap of more than 7000 years of sediment age is estimated at depth of 2 to 3 meters in area 1a (PC01 to PC03) and it is presumed that sediments indicating the age of about 10,000 years BP exist at depth of several tens of centimeters from the seabed surface in area 1b (PC06, PC07). In addition, K-Ah volcanic ash layer (7.3ka) could not be confirmed from sediments in both sea areas. From this, it is assumed that there was an event such as a submarine landslide or erosion with the lower part of the tephra as a sliding or eroding surface.
Since we could not obtain an index to estimate the age of the PC 08 to PC 11, we estimated the sedimentary environment using only the physical properties of sediments. PC08 and PC10 (Area 2) is located near the strait of Goshoura-jima and sisi-jima island, under influence of strong tidal and bottom currents, and is characterized by coarse sediments. Especially, upward grain refinement was observed and

©2019. Japan Geoscience Union. All Right Reserved.

the tendency that the porosity decreases within each monolayer is repeated in PC10. From this, it is assumed that the upper sediment functions as an impermeable layer against the lower sediment, and the drainage is difficult to proceed. PC 09 and PC 11 (Area 3) are relatively close to supply sources such as Minamata River and Komenotsu River, and are characterized as relatively coarse sediments. From the depth of 60 cm of PC09, and from the outermost surface layer in PC 11, the porosity does not decrease almost from around 60%. From this, it is estimated that the new sediment has been recently cleared recently.

Keywords: Piston coring, Yatsushiro sea

©2019. Japan Geoscience Union. All Right Reserved.

Variation in vane shear strength and magnetic susceptibility in the cores recovered by Hakuho-maru KH-18-3 cruise in Yatsushiro sea

*Yujin Kitamura[1], Haruka Kageyama[2], Kaede Yamasaki[2], Ryoya Goto[2], Koki Hori[2], Yuta Ikebata[2], Kuniyo Kawabata[1], Daiki Oyama[2], Hakuho-maru KH-18-3 Scientists

1. Department of Earth and Environmental Sciences, Graduate School of Science and Engineering, Kagoshima University, 2. Department of Earth and Environmental Sciences, Faculty of Science, Kagoshima University

Introduction

The 2016 Kumamoto Earthquake was sourced from a part of active faults of the Futagawa-Hinagu fault zones. The southwestern part of Hinagu fault zone forms the Yatsushiro section as a group of submarine active faults. Earthquake shaking occasionally triggers submarine landslide, however, any record of submarine landslide in this area has not been reported. We therefore conducted research cruise with R/V Hakuho-maru and recovered sediment cores in Yatsushiro sea. As it is known that the shear strength decreases at the bottom of mass transport deposits, we conducted vane shear test with the cores. We also referred the variation of magnetic susceptibility to establish core correlation with previous works.

Method

Here we conducted four-days research cruise with R/V Hakuho-maru (KH-18-3) in July, 2018 to reveal submarine landslide records and benthic environment in Yatsushiro sea. We used six-meters-long piston corers and cored at 11 sites and recovered cores were cut into 6 sections onboard. Cores were analyzed at Kochi Kore Center using X-ray CT scanner, multi-sensor core logger (gamma ray density: GRD; and magnetic susceptibility: MS), core imaging apparatus, visual core description, color spectroscope, X-ray fluorescence core scanner (Itrax). Vane shear apparatus is used with split core section and tested every about 50 cm.

Results and Discussion

Sediments are dominated by matrices of olive gray to black sand or mud. CT value, MS and GRD generally increase with depth. As MS shows cyclic fluctuation, we classified into several MS units by defining units with each broad peak. Our MS units was correlated with previous studies of high resolution seismic profile by Yagi et al. (2016) and piston cores by Inoue et al. (2011). MS units was in good agreement with Yagi's seismic profile. It is inferred that our samples include the sediments during Late Glacial Maximum to Jomon Transgression below hiatus. MS data by Inoue et al. (2011) and this study are in accordance with each other. The event layers Inoue suggested are discriminable in our cores which are characterized as local maximum of MS. Iron shows high concentration around the event layers so that the iron is a candidate for indicator for searching the events. We assume that this iron anomaly is caused by the rapid deposition during eventic turbidites.

The results of vane shear test showed that the strength increases with depth with a change in its rate at assumed hiatus. This shows that the sediments below hiatus was further deeply buried and compacted. At sites PC04 to PC06, the strength is low at their surface, indicating that the hiatus at these sites are very shallow and thus the recent surface erosion is assumed.

©2019. Japan Geoscience Union. All Right Reserved.

Keywords: turbidites, shallow marine deposits, 2016 Kumamoto earthquake

©2019. Japan Geoscience Union. All Right Reserved.

Identification of turbidites in the Yatsushiro Sea surface sediment core samples from non-destructive measurements: Hakuho-maru KH-18-3 Cruise, Yatsushiro Sea, Western Kyushu, Japan

*Ryoya Goto[1], Yujin Kitamura[2], Hakuho-maru KH-18-3 Cruise Scientist

1. Atmosphere and Ocean Research Institute, The University of Tokyo, 2. Department of Earth and Environmental Sciences, Graduate School of Science, Kagoshima University

Submarine active faults in Yatsusiro Sea, western Kyushu, Japan, constitute the Yatsushiro section of Hinagu fault zone in its southwest end (AIST et al., 2011). The 2016 Kumamoto Earthquake was sourced from a part of active faults of the Futagawa-Hinagu fault zones (JMA, 2018), and survey has hardly conducted in the sea area after the earthquake occurrence. Earthquake shaking occasionally triggers turbidity currents by submarine landslides and resuspension of unconsolidated sediments on the seafloor (Ikehara et al., 2018). In recent years, the study of earthquake occurrence history using earthquake turbidites formed by turbidity currents is being conducted throughout the world. As earthquake-origin turbidity currents can take place in very gentle slope (e.g. the Mississippi-Delta 0.01°: D. B. Prior et al., 1978), its occurrence is sufficiently thought even in Yatsushiro Sea. However, any record of earthquake turbidites in this area has not been reported. In this study, identification of turbidites in the Yatsushiro Sea surface sediment core samples from non-destructive measurements.

Here we conducted four-days research cruise Hakuho-maru KH-18-3 in July, 2018. We conducted sub-bottom profiling on eight lines, piston coring at 11 sites in Yatsushiro Sea, western Kyushu, Japan. Recovered cores are analyzed by X-ray CT scanner, multi-sensor core logger, core imaging apparatus, visual core description, color spectroscope and X-ray fluorescence core scanner (Itrax) in the Center for Advanced Marine Core Research, Kochi University. With reference to the previous studies (Iwai et al., 2014, JGS abstract; Isabel Rodríguez-Germade et al, 2015; Okutsu et al., 2017, JGS abstract), the behavior of Ca/Ti and Fe/Ti where the peak was observed at the base of turbidites, and the behavior of Fe/Ti and Zr/Ti where the peak was observed at the base of volcaniclastics turbidites.

Our results revealed turbidites and volcaniclastics turbidites in six piston coring sites (PC01 to PC06). As all of sites are located in the Taura-Tsunagioki fault group or Minamataoki fault group, turbidites were considered to be present in all of sites. However, turbidites were identified from PC01 to PC06, but not identified from PC07 to PC11. According to Rifardi et al. (1998), PC01 to PC06 are located in the sea area where the deposition rate is high, and PC07 to PC11 are located in the sea area where the deposition rate is slow.

As turbidite is formed by various factors besides earthquakes, it is necessary to consider whether the turbidites identified in this study are earthquake turbidites. In addition, to investigate the history of earthquakes, it is also a future task to conduct individual sample measurements (such as grain size distribution analysis) and dating.

Hakuho-maru KH-18-3 Cruise Scientists: Takashi Tomiyasu, Hitoshi Kodamatani, Kuniyo Kawabata, Daiki Oyama, Haruka Kageyama, Kaede Yamasaki (Kagoshima Univ.), Yuta Ikebata, Koki Hori (Kyushu Univ.), Asuka Yamaguchi, Fumiaki Tsunomori, Kameo Katsura, Tsubasa Miki, Natsumi Okutsu, Hiroaki Koge,

©2019. Japan Geoscience Union. All Right Reserved.

Kotaro Fujita, Ayaka Nakazawa, Yuichi Okuma, Genki Kobayashi, Rina Fukuchi (Tokyo Univ.), Jun Kameda, Tomonori Morisaki (Hokkaido Univ.)

Keywords: submarine landslides, turbidites, shallow sea deposits, Yatsushiro Sea, 2016 Kumamoto Earthquake

©2019. Japan Geoscience Union. All Right Reserved.

Revised columnar section based on grain size distribution analysis of samples from Hakuho-maru KH-18-3 in Yatsushiro sea

*Yuta Ikebata[1], Yujin Kitamura[2], Hakuho-maru KH-18-3 Scientists Family

1. Kyusyu University Graduate School Of Science Earth and Planetary Science, 2. Graduate school of science, Kagoshima University

Hakuho-maru KH-18-3 was held in the Yatsushiro Sea from 27th to 30th July 2018 for clarifying history of occurrence of submarine landslides. Earthquake is a one of big trigger of submarine landslides, and submarine landslides occurs in an very easy slope. Kumamoto earthquake occurred at April, 2016 and a lot of surveys in the land area were conducted but survey in the sea area weren't conducted much. In the Yatsushiro sea, the occurrence of submarine landslides caused by earthquake of the Futagawa-Hinagu fault zones can be considered sufficiently. Therefore, in this study, the creation of the columnar section which is the basic information of the submarine landslide accreditation was made based on the grain size distribution analysis.

In the Expedition, eleven piston cores(6m) from PC01 to PC11 were collected in the southern part of Yatsushiro sea, and the obtained core was subjected to non-destructive measurement and individual sample measurement at the Kochi Core Center. For non-destructive measurement, CT images and core continuous images were taken, and for individual sample measurement, Density, Magnetic susceptibility, porosity, vane shear strength, color, concentration change of major elements were examined. Grain size distribution analysis was conducted at Kagoshima University. Samples used for grain size distribution analysis were collected every 50 cm and analyzed with a laser diffraction type grain size distribution analyzer. Since it is difficult to judge the stratum boundary only with the result of grain size distribution measurement at intervals of 50 cm, it was judged by using γ ray density, magnetic susceptibility and color measurement result which are continuous data.

Grain size distribution analysis revealed PC01 to PC07 are muddy cores and PC08 to PC11 contains much sand. Grain size of PC01, PC04, PC06, PC07, PC09, PC11 are very different in Grain size distribution analysis and visual core description. Based on the results of the grain size distribution analysis, the stratum boundary was determined from the change commonly seen in the γ ray density, magnetic susceptibility and color, and a columnar section was prepared. In Rifardi et al.(1998), the distribution of mud content in the Yatsushiro Sea has been surveyed. As a result of comparing the columnar map of this study with its distribution for each sampling point, cores excluding PC08 corresponded well. It is thought that it is influenced by the supply of sediment by river and stagnant water mass, tide current as in previous research. Also, in Inoue et al.(2011), which was a reference for determining the core harvest point, dating is done in the same area. At Hori(2019MS), we compare the data with Inoue et al.(2011) and estimate the core age of this research. We also compare the columnar section made in this study with the columnar section of Inoue et al.(2011), using the comparative categories determined at the time of estimating the age. As a result, PC01 and PC02 were in good agreement, PC06 and PC07 had different stratum in the surface layer. This is probably because the sampling site of PC06 is actually about 150 m far from Inoue et al.(2011) and the sampling site of PC07 is actually about 111 m far from Inoue et al.(2011), and the sedimentary environment is slightly different. Also, in the grain size distribution analysis of this study, there is a possibility that coarse grains may be selectively left out when putting the sample into the machine, and it may be doubtful in accuracy.

©2019. Japan Geoscience Union. All Right Reserved.

Keywords: Submarine landslide

©2019. Japan Geoscience Union. All Right Reserved.

[E] Poster | H (Human Geosciences)：H-DS Disaster geosciences

Mon. May 27, 2019 1:45 PM - 3:15 PM JST | Mon. May 27, 2019 4:45 AM - 6:15 AM UTC | Poster Hall International Exhibition Hall8, Makuhari Messe_4

[H-DS12] Advanced Remote Sensing toward Mega-Disaster Response

convener:Young-Joo Kwak(ICHARM-UNESCO: International Centre for Water Hazard And Risk Management), Wataru Takeuchi(Institute of Industrial Science, The University of Tokyo)

Natural disaster under climate change is a serious threat to sustainable development, and in recent years natural disasters, i.e., hydro-geo-meteorological hazards and risks, have been frequently experienced in many countries by both developing and developed countries.
To achieve Sustainable Development Goals (SDGs), this session introduces papers focused on both principles and applications of remote sensing to promote investment in disaster risk reduction using integrated GIS and space infra data. Advanced remote sensing with Earth observation (EO) data appears to be the way forward in reducing damages and the death toll or affected people at local, national, regional and global levels.
We encourage the presentation of new research findings and novel approaches on land surface dynamics due to mega disasters between near-real time observation and long-term trends with water/hydrological cycle, such as floods, tropical cyclones (typhoons), storm surges, earthquakes, tsunamis, landslides, and wildfires.

[HDS12-P01] Satellite-based assessment of electricity restoration efforts in Puerto Rico after Hurricane Maria

*Miguel O Roman[1], Eleanor Stokes[2,3], Zhuosen Wang[2,3], Virginia Kalb[3], Ranjay Shrestha[4,3] (1.Earth from Space Institute, Universities Space Research Association, 2.Earth System Science Interdisciplinary Center, University of Maryland, 3.NASA Goddard Space Flight Center, 4.Science Systems and Applications, Inc)

[HDS12-P02] Flood inundation forecasting coupled with in-situ water level and satellite data

*Young-Joo Kwak[1], Jonggeol Park[2], Wataru Takeuchi[3] (1.ICHARM-UNESCO: International Centre for Water Hazard And Risk Management, 2.Tokyo University of Information and Sciences, 3.University of Tokyo)

[HDS12-P03] Long term monitoring of flood damage in the coastal area of Bangladesh

★Invited Papers

*Park Jonggeol[1], Young-Joo Kwak[2] (1.Tokyo University of Information Sciences, 2.ICHARM-UNESCO)

[HDS12-P04] Automatic shoreline detection and coastal change detection using multiple satellite data in Bangladesh

*Young-Joo Kwak[1] (1.ICHARM-UNESCO: International Centre for Water Hazard And Risk Management)

Satellite-based assessment of electricity restoration efforts in Puerto Rico after Hurricane Maria

*Miguel O Roman[1], Eleanor Stokes[2,3], Zhuosen Wang[2,3], Virginia Kalb[3], Ranjay Shrestha[4,3]

1. Earth from Space Institute, Universities Space Research Association, 2. Earth System Science Interdisciplinary Center, University of Maryland, 3. NASA Goddard Space Flight Center, 4. Science Systems and Applications, Inc

Understanding the distribution and duration of power outages after a disaster is a precursor to minimizing their harmful consequences, especially to vulnerable communities. Here, we use satellite-derived daily estimates of lights to monitor electricity restoration efforts in Puerto Rico following Hurricane Maria, which caused the longest blackout in US history. Within all settlements, we track how long it took to restore electricity, and assess the characteristics of communities that shouldered the most extended outages. Our results show an 80% decrease in lights, in total, immediately after Hurricane Maria. During the recovery, a disproportionate share of long-duration power failures (> 120 days) occurred in rural municipalities (41% of rural municipalities vs. 29% of urban municipalities), and in the northern and eastern districts. Unexpectedly, we also identify significant disparities in electricity recovery within municipalities. Land use, proximity to highways, and the structure and density of the built environment were all factors that influenced restoration times. For many urban municipalities, poor residents lived in less dense, detached housing—where power restoration lagged. The results demonstrate the capability of nighttime satellite imagery to monitor power availability at a high spatial resolution, linking monitoring efforts to neighborhood-scale demographic data. They also identify the unintended consequences of current density-based power restoration protocols. Through the integration of in-situ, satellite, and socioeconomic data products, disaster responses to long-term events can become more strategic to minimize harm, incorporating adaptive community capacity as an additional variable to determine where power should be restored.

Keywords: VIIRS DNB, Black Marble, nighttime lights, power outage detection, energy access, disaster risk reduction

©2019. Japan Geoscience Union. All Right Reserved.

Flood inundation forecasting coupled with in-situ water level and satellite data

*Young-Joo Kwak[1], Jonggeol Park[2], Wataru Takeuchi[3]

1. ICHARM-UNESCO: International Centre for Water Hazard And Risk Management, 2. Tokyo University of Information and Sciences, 3. University of Tokyo

With extreme weather events, catastrophic floods occur as one of the major disasters in the world. With the development of spaceborne optical and SAR (synthetic aperture radar) sensors, flood detection algorithms should be progressively developed to produce more accurate flood maps

Despite very limited satellite-based data, this study introduces good examples of snapshot flood detection and flood inundation forecasting focusing on short-term flood extent change using a new index-based flood algorithm with a synchronized floodwater index ($SfWI^2$). MODIS (MODerate resolution Imaging Spectroradiometer, NASA-USGS) time series data were mainly employed to detect the annual and potential flood extent of 2017. The pilot study was selected in the mega deltas over vast low-lying areas of Bangladesh and India (i.e., the 2017 flood in the basins of the Ganges, Brahmaputra and Magna rivers) As preliminary results, the resultant maps represented the dynamics of flood extent and flood propagation process. This approach shows a methodological possibility for instant and comprehensive flood mapping at the international river-basin level. For application to a global flood mapping, reliable satellite-derived flood maps will contribute flood risk management. In order to improve the accuracy of rapid flood mapping, we should solve many ambiguities in particular, surface complexity, i.e., urbanized mega-delta floodplains.

Keywords: Flood detection, Inundation forecasting, MODIS

©2019. Japan Geoscience Union. All Right Reserved.

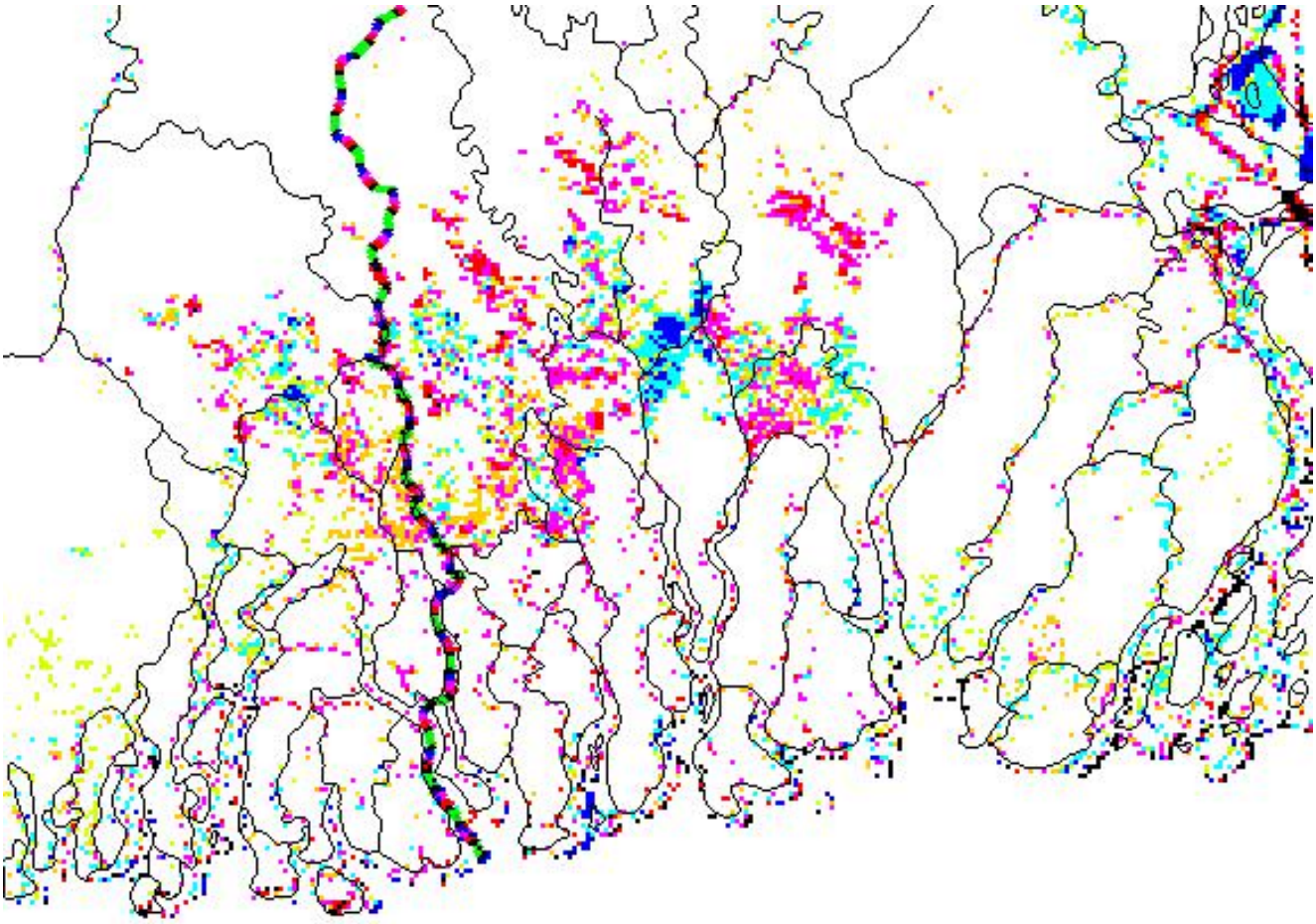
Long term monitoring of flood damage in the coastal area of Bangladesh

*Park Jonggeol[1], Young-Joo Kwak[2]

1. Tokyo University of Information Sciences, 2. ICHARM-UNESCO

The major natural hazards which Bangladesh has to confront regularly include floods, cyclones and accompanying storm surge. Flooding from river waters overflowing the banks, particularly during monsoon, is an annual phenomenon. On average, one-third of the country goes under water every year. In this study, we investigated the flooding area of Bangladesh using time series MOD13A2 data of 15 years. Discriminant analysis using both NDVI and MDWI is more effective than extracting water bodies using existing NDWI only. The flash flood was from the Indian plateau bordering the northern part of Bangladesh to flow from April to May and a wide wetland was formed and the longest flooding period in Bangladesh was revealed as it is as it is the rainy season.

Keywords: Flood, MODIS, NDWI



©2019. Japan Geoscience Union. All Right Reserved.

Automatic shoreline detection and coastal change detection using multiple satellite data in Bangladesh

*Young-Joo Kwak[1]

1. ICHARM-UNESCO: International Centre for Water Hazard And Risk Management

The Bangladesh government has been faced with the risk of coastal erosion as one of the urgent issues in land use planning and coastal management. As a preliminary investigation, an automated algorithm was proposed focusing on shoreline detection using multiple satellite data. The selected study site is located in the estuary of the Meghna River around the Gulf of Bengal in Bangladesh.

We employed Landsat-7, -8 data (90m and 30m spatial resolution, respectively) and ALOS, ALOS-2 (12.5m and 25m spatial resolution, respectively) to detect accurate coastal lines during the similar snapshot period.

As a result of automatic shoreline detection and coastal change detection by the interpretation and classification, the average rate of coastal line change was 0.5km (eroded) per year for the period between 2010 and 2019 in case of Meghna River along Noahkali (Noler Char). In addition, the resultant coastal change line was also verified by ground truth and field survey data using a small unmanned aerial vehicle (sUAV: Quadcopter with a flight control system, ©DJI Technology Co. Ltd., China) for comprehensive validation.

This feasibility study will continually investigate the characteristics of short-term and long-term changes with the relationship between hydrological parameters such as precipitation, river discharge, wave, and tidal effect.

Keywords: Shoreline detection, Coastal change

©2019. Japan Geoscience Union. All Right Reserved.

[E] Poster | H (Human Geosciences)：H-DS Disaster geosciences

Mon. May 27, 2019 5:15 PM - 6:30 PM JST | Mon. May 27, 2019 8:15 AM - 9:30 AM UTC | Poster Hall International Exhibition Hall8, Makuhari Messe_14

[H-DS12] Advanced Remote Sensing toward Mega-Disaster Response

convener:Young-Joo Kwak(ICHARM-UNESCO: International Centre for Water Hazard And Risk Management), Wataru Takeuchi(Institute of Industrial Science, The University of Tokyo)

Natural disaster under climate change is a serious threat to sustainable development, and in recent years natural disasters, i.e., hydro-geo-meteorological hazards and risks, have been frequently experienced in many countries by both developing and developed countries.
To achieve Sustainable Development Goals (SDGs), this session introduces papers focused on both principles and applications of remote sensing to promote investment in disaster risk reduction using integrated GIS and space infra data. Advanced remote sensing with Earth observation (EO) data appears to be the way forward in reducing damages and the death toll or affected people at local, national, regional and global levels.
We encourage the presentation of new research findings and novel approaches on land surface dynamics due to mega disasters between near-real time observation and long-term trends with water/hydrological cycle, such as floods, tropical cyclones (typhoons), storm surges, earthquakes, tsunamis, landslides, and wildfires.

[HDS12-P01] Satellite-based assessment of electricity restoration efforts in Puerto Rico after Hurricane Maria

*Miguel O Roman[1], Eleanor Stokes[2,3], Zhuosen Wang[2,3], Virginia Kalb[3], Ranjay Shrestha[4,3] (1.Earth from Space Institute, Universities Space Research Association, 2.Earth System Science Interdisciplinary Center, University of Maryland, 3.NASA Goddard Space Flight Center, 4.Science Systems and Applications, Inc)

[HDS12-P02] **Flood inundation forecasting coupled with in-situ water level and satellite data**

*Young-Joo Kwak[1], Jonggeol Park[2], Wataru Takeuchi[3] (1.ICHARM-UNESCO: International Centre for Water Hazard And Risk Management, 2.Tokyo University of Information and Sciences, 3.University of Tokyo)

[HDS12-P03] Long term monitoring of flood damage in the coastal area of Bangladesh

★Invited Papers

*Park Jonggeol[1], Young-Joo Kwak[2] (1.Tokyo University of Information Sciences, 2.ICHARM-UNESCO)

[HDS12-P04] Automatic shoreline detection and coastal change detection using multiple satellite data in Bangladesh

*Young-Joo Kwak[1] (1.ICHARM-UNESCO: International Centre for Water Hazard And Risk Management)

Satellite-based assessment of electricity restoration efforts in Puerto Rico after Hurricane Maria

*Miguel O Roman[1], Eleanor Stokes[2,3], Zhuosen Wang[2,3], Virginia Kalb[3], Ranjay Shrestha[4,3]

1. Earth from Space Institute, Universities Space Research Association, 2. Earth System Science Interdisciplinary Center, University of Maryland, 3. NASA Goddard Space Flight Center, 4. Science Systems and Applications, Inc

Understanding the distribution and duration of power outages after a disaster is a precursor to minimizing their harmful consequences, especially to vulnerable communities. Here, we use satellite-derived daily estimates of lights to monitor electricity restoration efforts in Puerto Rico following Hurricane Maria, which caused the longest blackout in US history. Within all settlements, we track how long it took to restore electricity, and assess the characteristics of communities that shouldered the most extended outages. Our results show an 80% decrease in lights, in total, immediately after Hurricane Maria. During the recovery, a disproportionate share of long-duration power failures (> 120 days) occurred in rural municipalities (41% of rural municipalities vs. 29% of urban municipalities), and in the northern and eastern districts. Unexpectedly, we also identify significant disparities in electricity recovery within municipalities. Land use, proximity to highways, and the structure and density of the built environment were all factors that influenced restoration times. For many urban municipalities, poor residents lived in less dense, detached housing—where power restoration lagged. The results demonstrate the capability of nighttime satellite imagery to monitor power availability at a high spatial resolution, linking monitoring efforts to neighborhood-scale demographic data. They also identify the unintended consequences of current density-based power restoration protocols. Through the integration of in-situ, satellite, and socioeconomic data products, disaster responses to long-term events can become more strategic to minimize harm, incorporating adaptive community capacity as an additional variable to determine where power should be restored.

Keywords: VIIRS DNB, Black Marble, nighttime lights, power outage detection, energy access, disaster risk reduction

©2019. Japan Geoscience Union. All Right Reserved.

Flood inundation forecasting coupled with in-situ water level and satellite data

*Young-Joo Kwak[1], Jonggeol Park[2], Wataru Takeuchi[3]

1. ICHARM-UNESCO: International Centre for Water Hazard And Risk Management, 2. Tokyo University of Information and Sciences, 3. University of Tokyo

With extreme weather events, catastrophic floods occur as one of the major disasters in the world. With the development of spaceborne optical and SAR (synthetic aperture radar) sensors, flood detection algorithms should be progressively developed to produce more accurate flood maps

Despite very limited satellite-based data, this study introduces good examples of snapshot flood detection and flood inundation forecasting focusing on short-term flood extent change using a new index-based flood algorithm with a synchronized floodwater index ($SfWI^2$). MODIS (MODerate resolution Imaging Spectroradiometer, NASA-USGS) time series data were mainly employed to detect the annual and potential flood extent of 2017. The pilot study was selected in the mega deltas over vast low-lying areas of Bangladesh and India (i.e., the 2017 flood in the basins of the Ganges, Brahmaputra and Magna rivers) As preliminary results, the resultant maps represented the dynamics of flood extent and flood propagation process. This approach shows a methodological possibility for instant and comprehensive flood mapping at the international river-basin level. For application to a global flood mapping, reliable satellite-derived flood maps will contribute flood risk management. In order to improve the accuracy of rapid flood mapping, we should solve many ambiguities in particular, surface complexity, i.e., urbanized mega-delta floodplains.

Keywords: Flood detection, Inundation forecasting, MODIS

©2019. Japan Geoscience Union. All Right Reserved.

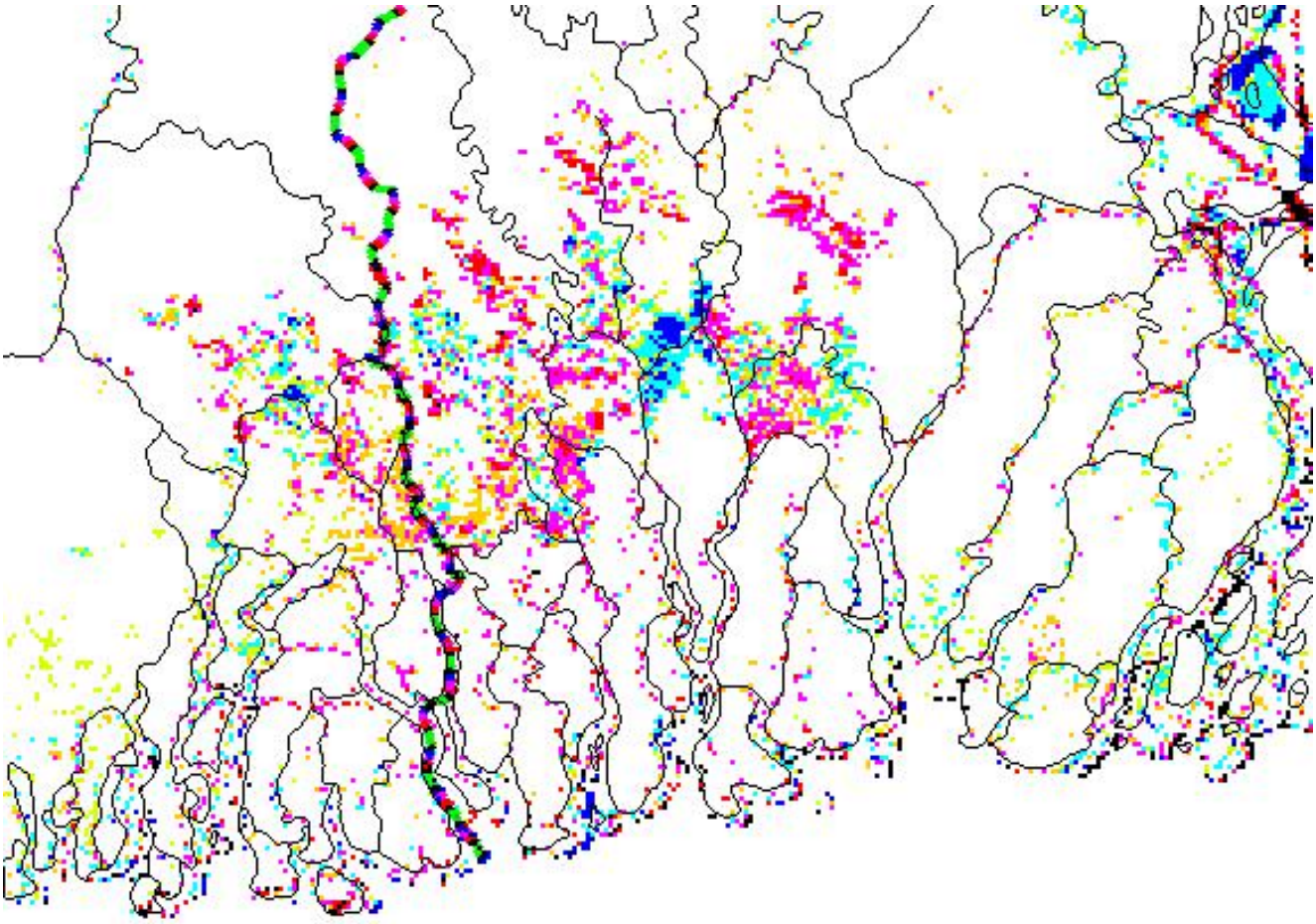
Long term monitoring of flood damage in the coastal area of Bangladesh

*Park Jonggeol[1], Young-Joo Kwak[2]

1. Tokyo University of Information Sciences, 2. ICHARM-UNESCO

The major natural hazards which Bangladesh has to confront regularly include floods, cyclones and accompanying storm surge. Flooding from river waters overflowing the banks, particularly during monsoon, is an annual phenomenon. On average, one-third of the country goes under water every year. In this study, we investigated the flooding area of Bangladesh using time series MOD13A2 data of 15 years. Discriminant analysis using both NDVI and MDWI is more effective than extracting water bodies using existing NDWI only. The flash flood was from the Indian plateau bordering the northern part of Bangladesh to flow from April to May and a wide wetland was formed and the longest flooding period in Bangladesh was revealed as it is as it is the rainy season.

Keywords: Flood, MODIS, NDWI



©2019. Japan Geoscience Union. All Right Reserved.

Automatic shoreline detection and coastal change detection using multiple satellite data in Bangladesh

*Young-Joo Kwak[1]

1. ICHARM-UNESCO: International Centre for Water Hazard And Risk Management

The Bangladesh government has been faced with the risk of coastal erosion as one of the urgent issues in land use planning and coastal management. As a preliminary investigation, an automated algorithm was proposed focusing on shoreline detection using multiple satellite data. The selected study site is located in the estuary of the Meghna River around the Gulf of Bengal in Bangladesh.

We employed Landsat-7, -8 data (90m and 30m spatial resolution, respectively) and ALOS, ALOS-2 (12.5m and 25m spatial resolution, respectively) to detect accurate coastal lines during the similar snapshot period.

As a result of automatic shoreline detection and coastal change detection by the interpretation and classification, the average rate of coastal line change was 0.5km (eroded) per year for the period between 2010 and 2019 in case of Meghna River along Noahkali (Noler Char). In addition, the resultant coastal change line was also verified by ground truth and field survey data using a small unmanned aerial vehicle (sUAV: Quadcopter with a flight control system, ©DJI Technology Co. Ltd., China) for comprehensive validation.

This feasibility study will continually investigate the characteristics of short-term and long-term changes with the relationship between hydrological parameters such as precipitation, river discharge, wave, and tidal effect.

Keywords: Shoreline detection, Coastal change

©2019. Japan Geoscience Union. All Right Reserved.

[E] Poster | H (Human Geosciences)：H-CG Complex & General

Mon. May 27, 2019 3:30 PM - 5:00 PM JST | Mon. May 27, 2019 6:30 AM - 8:00 AM UTC | Poster Hall International Exhibition Hall8, Makuhari Messe_9

[H-CG26] Deltas and estuaries: multidisciplinary analyses of complex river-mouth systems

convener:Yoshiki Saito(Estuary Research Center, Shimane University), Guan-Hong Lee(Inha University), David L Dettman(University of Arizona), Kazuaki Hori(Department of Geography, Graduate School of Environmental Studies, Nagoya University)

This session has foci on morphodynamics, material cycling, and sustainability in deltas and estuaries. We invite contributions that advance research on deltas and estuaries as complex river-mouth systems from modern and ancient examples, and that develop integrated frameworks for delta & estuary dynamics modeling on a broad range of temporal and spatial scales: from studies of coastal evolution over the Quaternary to small-scale sediment/material transport processes. We also invite physical processes studies based on field observations, numerical simulation and flume experiments. Finally, the conveners encourage contributions that promote data collection and sharing for both advancing science and local problem solving, that consider policy and governance issues linked to the sustainable development of deltas and estuaries, and that use in-situ and satellite data for modeling and risk assessment.

[HCG26-P01] Deltafront Clinoform of Abandoned Yellow River Delta in Jiangsu Province, China

*LIANGYONG ZHOU[1] (1.Qingdao Institute of Marine Geology China Geological Survey)

[HCG26-P02] Holocene evolution and Anthropocene destruction of the Krishna delta, east coast of India: delta lobe shifts, human impact, and sea-level history

Kakani Nageswara Rao[2], *Yoshiki Saito[1], K.Ch.V. Nagakumar[4], Sumiko Kubo[3], Shilpa Pandey[5], Zhen Li[6], G. Demudu[2], A.S. Rajawat[7] (1.Estuary Research Center, Shimane University, 2.Andhra University, 3.Waseda University, 4.Centre for Water Resources and Management, 5.Birbal Sahni Institute of Palaeosciences, 6.University of Victoria, 7.Space Applications Centre)

[HCG26-P03] Offset in radiocarbon ages between marine bioclast and terrestrial plant pairs in the Holocene sediments around Japan

*Nakanishi Toshimichi[1,2], Futoshi Nanayama[3,4], Atsushi Urabe[5], Kazuaki Hori[6], Wan Hong[7] (1.Kyoto Univ., 2.JAEA, 3.AIST, 4.Kumamoto Univ., 5.Niigata Univ., 6.Nagoya Univ., 7.KIGAM)

[HCG26-P04] Assessment of MEIS for Marine Spatial Planning in the Nakdong River Estuary, Busan Metropolitan City, South Korea

*Jun-Ho Lee[1], Han Jun Woo[1], Hoi-Soo Jung[1], Chan Mi Park[1] (1.Korea Institute of Ocean Science and Technology)

[HCG26-P05] Tidal changes at Asian deltas in response to future sea-level rise

*Katsuto Uehara[1] (1.Kyushu University)

[HCG26-P06] **A governing equation of non-deltaic transgressive profile: 2D numerical simulation and flume experiments**

*Junhui Wang[1,2,3], Tetsuji Muto[3] (1.China University of Petroleum (Beijing), 2.State Key Laboratory of Petroleum Resources and Prospecting, China, 3.Nagasaki University)

Deltafront Clinoform of Abandoned Yellow River Delta in Jiangsu Province, China

*LIANGYONG ZHOU[1]

1. Qingdao Institute of Marine Geology China Geological Survey

The abandoned Yellow River delta in Jiangsu province is a major sediment supplier to the South Yellow Sea and East China Sea. In this study, comparison of historical maps, two cores and three seismic profiles were used to examine its deltafront clinoform (nearshore clinoform). The original historical maps and nautical charts since AD 1750s were collected and compared after calibration, showing the accretion of the shoreline before 1855, when the Yellow River shifted to the Bohai Sea. Near Sheyang River mouth, two 20m-long cores onshore (1 m above present sea level) and offshore (6 m bellow present sea level) were on a line normal to the shoreline. Samples og both cores were dated using AMS ^{14}C and OSL(Optical Stimulated Luminescence) dating technologies. Ages in bottoms of the cores are 43000 to 44000 cal yr BP. At approximate 17.5m bellow present sea level in both cores, yellow and younger (younger than 5000 yr BP) silt sediment occurs. Several young ages in upper part of two cores were obtained, and these show a clear clinoform pattern. Furthermore, seismic profiles across the offshore core show the deltafront clinoform. The upper part weak reflector or transparent part in seismic profiles become thinner seaward and the lower part is strong reflectors. Sea bottom nearshore show a convex shape, but the seaward low gradient part show erosional gullies. The evolution of the deltafront clinoform was revealed in profiles and in plan view.

Keywords: Abandoned Yellow River Delta, Deltafront clinoform, C-14 ages, OSL ages

©2019. Japan Geoscience Union. All Right Reserved.

Holocene evolution and Anthropocene destruction of the Krishna delta, east coast of India: delta lobe shifts, human impact, and sea-level history

Kakani Nageswara Rao[2], *Yoshiki Saito[1], K.Ch.V. Nagakumar[4], Sumiko Kubo[3], Shilpa Pandey[5], Zhen Li[6], G. Demudu[2], A.S. Rajawat[7]

1. Estuary Research Center, Shimane University, 2. Andhra University, 3. Waseda University, 4. Centre for Water Resources and Management, 5. Birbal Sahni Institute of Palaeosciences, 6. University of Victoria, 7. Space Applications Centre

Holocene evolution of the Krishna delta was inferred using landform characteristics and 11 sediment cores with 59 Accelerator Mass Spectrometry ^{14}C dates. Landform assemblage in 5880 km^2area of the Krishna delta indicated the upper river-built fluvial plain and the lower marine-built beach-ridge delta plain with the maximum landwardbeach ridge located at˜30 km from the shoreline separating the two plains. Sedimentary facies and their ages showed the Holocene marine sediment overlying the Pleistocene basement and progressively thickened seaward from <10 m to 25 m below the present sea level. The basal mangrove peat layers indicated that the sea level rose from −9 m to −3 m during 8.3–6.3 cal ky BP before stabilizing at the present level around 5 cal ky BP.
Considering the spatiotemporal variations of sediment facies and sediment accumulation rates and the configuration of the palaeo beach ridges (former shorelines), we surmised five major stages in the growth of 3539 km^2area of the Krishna delta beach-ridge plain during the last 6 cal ky BP with distinct lateral and seaward migration of delta lobes (depocentre shifts). Delta progradation was accelerated in the last 500 years, forming an out-building lobate delta. However, predominant erosion along the sediment-starved Krishna delta front coast during the past 50 years, due to impoundment of the riverine inputs at the burgeoning upstream dams pushed the Krishna delta into a persistent a destruction phase after ˜6,000 years of delta progradation.

Keywords: Beach-ridge plain, Sedimentary facies, Delta lobes, Coastal erosion

©2019. Japan Geoscience Union. All Right Reserved.

Offset in radiocarbon ages between marine bioclast and terrestrial plant pairs in the Holocene sediments around Japan

*Nakanishi Toshimichi[1,2], Futoshi Nanayama[3,4], Atsushi Urabe[5], Kazuaki Hori[6], Wan Hong[7]

1. Kyoto Univ., 2. JAEA, 3. AIST, 4. Kumamoto Univ., 5. Niigata Univ., 6. Nagoya Univ., 7. KIGAM

To identify chronological and spatial changes in the radiocarbon (^{14}C) marine reservoir effects, the ^{14}C ages of eight pairs of marine bioclasts and terrestrial plants were measured from the same horizons of one core of Holocene sediments around Japan (Nakanishi et al. 2013, 2015, 2017abc). The reservoir ages ranged from 60 to 1100 years, scattered over the period 100-10,200 cal BP, which were significantly larger than the values from “prebomb” samples of known age, before AD 1955 in this area. These results indicate that the information on reservoir effects is indispensable for chronological control not only from prebomb samples but also from geological and archaeological samples. Moreover, the effects also reflects the influence of complex river-mouth systems such as deltas and estuaries. To determine the direct chronological changes of the marine reservoir effect between the Kuroshio and Tsushima Currents, radiocarbon ages from pairs of marine bioclasts and terrestrial plants were measured from the same stratigraphic horizons within three cores of Holocene sediments beneath the Sukumo Plain, Miyazaki Plain, and Oki Islands, in west Japan. Subsequently, the results were compared with values from the Oita Plain and Hakata Bay on the northern coast of Kyushu (Nakanishi et al. 2017ac), as well as the Korean Peninsula (Nakanishi et al. 2013, 2015, 2017b). The study was partially funded by the Japan Society for the Promotion of Science Kakenhi grant number 18H01310.

References

Nakanishi T, Hong W, Sung KS, Lim J. 2013. Radiocarbon reservoir effect from shell and plant pair in Holocene sediments around the Yeongsan River in Korea. *Nuclear Instruments and Methods in Physics Research B* 294: 444–51.

Nakanishi T, Hong W, Sung KS, Sung KH, Nakashima R. 2015. Offsets in radiocarbon ages between plants and shells from same horizons of coastal sediments in Korea. *Nuclear Instruments and Methods in Physics Research B* 361: 670–9.

Nakanishi T, Hong W, Shimoyama S, Sato S, Park G, Lee JG. 2017a. Radiocarbon age offset between shell and plant pairs in the Holocene sediments under the Hakata Bay, western Japan. *Radiocarbon* 59 (2): 423–34.

Nakanishi T, Hong W, Sung KS, Nakashima R, Nahm WH, Lim J, Katsuki K. 2017b. Offset in radiocarbon age between plant and shell pairs in Holocene sediment around the Mae-ho Lagoon on the eastern coast of Korea. *Quaternary International* 447: 3–12.

Nakanishi T, Takemura K, Matsuyama H, Shimoyama S, Hong W, Okuno M. 2017c. Activity of the Funai fault and radiocarbon age offsets of shell and plant pairs from the latest Pleistocene to Holocene sediments beneath the Oita Plain, western Japan. *Radiocarbon* 59(6): 1737–48.

Keywords: Radiocarbon age, Marine reservoir effect, Holocene, Kuroshio Current

©2019. Japan Geoscience Union. All Right Reserved.

Assessment of MEIS for Marine Spatial Planning in the Nakdong River Estuary, Busan Metropolitan City, South Korea

*Jun-Ho Lee[1], Han Jun Woo[1], Hoi-Soo Jung[1], Chan Mi Park[1]

1. Korea Institute of Ocean Science and Technology

The Nakdong River has a length of nearly 510 km, with a drainage basin of around 23,400 km^2 in South Korea. The Nakdong River Estuary (NRE) in Busan city is a typical example of an estuary in which the throughput is manipulated artificially. The Noksan barrage, built in 1934, blocks the flow of the West Nakdong River, and the NRE barrage was completed between 1983 and 1987 to regulate the flow of the East Nakdong River. With the construction of several huge industrial complexes on reclaimed land near the NRE barrage in the last 65 years, the hydraulic circulation in the NRE has undergone dramatic changes in river discharge and geomorphic configuration, such as the formation of a series of barrier islands. In this study, marine environmental information system (MEIS) data collected after May 2015 were applied to support marine spatial planning (MSP) in the brackish water zone of NRE. The MEIS data in NRE consists of landscape classification of sub-environments, surface sediment distributions, characteristics of suspended sediment, short-term sedimentation, stratification index analysis in channels, closed circuit television (CCTV) using 4G long term evolution (LTE), automatic weather stations (AWS) in real time, calculated residual flow (R_f), net suspended sediment loads (Q_S), and net suspended sediment flux (F_S) in main stream inlet using mooring station, *etc*. The NRE could be divided into areas continuously managed by government, marine protected areas, areas for the development of marine attractions, areas conserved for research education, and coastal areas subject to safety management, e*tc*. For MSP, it was possible to use comparative data of the characteristics of environmental changes in the estuarine watershed to prepare the NRE for the partial opening or drainage extension in 2019 to 2021. This study aims to discuss how to predict environmental change after partial or full opening in NRE barrage and use ecological-based environmental maps in the process of MSP. The development of marine spatial planning mapping in NRE is much necessary for the nation at a time when the diversity of marine use and the demand for policies regarding marine space rapidly increase.

Keywords: Barrage, Busan, Estuary, Marine Environmental Information System, Marine Spatial Planning, Nakdong River Estuary

©2019. Japan Geoscience Union. All Right Reserved.

Assessment of MEIS for Marine Spatial Planning in the Nakdong River Estuary, Busan Metropolitan City, South Korea

Jun-Ho Lee[1] · Han Jun Woo[1] · Hoi-Soo Jung[1] · Chan Mi Park[1]

[1]Korean Seas Geosystem Research Unit, Korea Institute of Ocean Science & Technology, 385 Yeongdo, Busan 49111, Republic of Korea

The Nakdong River has a length of nearly 510 km, with a drainage basin of around 23,400 km^2 in South Korea. The Nakdong River Estuary (NRE) in Busan city is a typical example of an estuary in which the throughput is manipulated artificially. The Noksan barrage, built in 1934, blocks the flow of the West Nakdong River, and the NRE barrage was completed between 1983 and 1987 to regulate the flow of the East Nakdong River. With the construction of several huge industrial complexes on reclaimed land near the NRE barrage in the last 65 years, the hydraulic circulation in the NRE has undergone dramatic changes in river discharge and geomorphic configuration, such as the formation of a series of barrier islands. In this study, marine environmental information system (MEIS) data collected after May 2015 were applied to support marine spatial planning (MSP) in the brackish water zone of NRE. The MEIS data in NRE consists of landscape classification of sub-environments, surface sediment distributions, characteristics of suspended sediment, short-term sedimentation, stratification index analysis in channels, closed circuit television (CCTV) using 4G long term evolution (LTE), automatic weather stations (AWS) in real time, calculated residual flow (R_f), net suspended sediment loads (Q_S), and net suspended sediment flux (F_S) in main stream inlet using mooring station, *etc*. The NRE could be divided into areas continuously managed by government, marine protected areas, areas for the development of marine attractions, areas conserved for research education, and coastal areas subject to safety management, *etc*. For MSP, it was possible to use comparative data of the characteristics of environmental changes in the estuarine watershed to prepare the NRE for the partial opening or drainage extension in 2019 to 2021. This study aims to discuss how to predict environmental change after partial or full opening in NRE barrage and use ecological-based environmental maps in the process of MSP. The development of marine spatial planning mapping in NRE is much necessary for the nation at a time when the diversity of marine use and the demand for policies regarding marine space rapidly increase.

©2019. Japan Geoscience Union. All Right Reserved.

Tidal changes at Asian deltas in response to future sea-level rise

*Katsuto Uehara[1]

1. Kyushu University

A numerical model has been employed to assess the impact of sea level rise on tidal regimes in the East China Sea and the South China Sea with a special interest on tidal changes at around the deltaic region where the elevation is low and coasts are vulnerable to changes in water levels. The model covers the East and South China seas as a whole with a spatial resolution of 2 minutes (approx. 3 km). A preliminary result for the East China Sea suggests recognizable changes in the amplitude of M2 tides and M2 tidal currents at region such as Hangzhou Bay, the Changjiang Estuary and Haizhou Bay when the sea-level was raised by 1 m. Off the Changjiang Estuary, for example, tidal velocity increased for more than 10 cm/s at deep channels while decreased by about 5 cm/s on shoals. These results indicate that the sea-level rise may alter equilibrium among water currents and seafloor and modify the bottom topography of large estuaries and subaquatic deltas through the induced changes in tides and tidal currents.

Keywords: tides, china sea, sea level rise

©2019. Japan Geoscience Union. All Right Reserved.

A governing equation of non-deltaic transgressive profile: 2D numerical simulation and flume experiments

*Junhui Wang[1,2,3], Tetsuji Muto[3]

1. China University of Petroleum (Beijing), 2. State Key Laboratory of Petroleum Resources and Prospecting, China, 3. Nagasaki University

An alluvial river subject to relative sea level rise has a critical length (L_{crt}), beyond which the river can no longer sustain deltaic sedimentation but behaves to develop an estuarine environment. In such cases, there occurs non-deltaic rapid transgression. It is not difficult to imagine that non-deltaic transgression is pervasive in geological records, since most of the world large rivers would have “over-extended” to as far as the shelf edges during glacial or lowstand sea level periods. The configuration of non-deltaic transgressive profiles deserves a study because (1) it would provide a criterion for identifying non-deltaic transgression in the past and thus the fact of over-extension of the feeder alluvial river, and (2) it would constrain arguments on sediment transportation to the deep-water depositional systems.

Suppose that a river has an over-extended alluvial length of L ($>>L_{crt}$). During non-deltaic transgression, all the sediment fed by the river is consumed for alluvial aggradation and thus allocated in the subaerial realm. On the assumption that the supplied sediment is evenly distributed along the river profile which is approximately regarded as linear and has an averaged slope of α, the local transgressive slope Ψcan be expressed as:

$$\Psi = \alpha L / [L - \Lambda_{2D}(1+\alpha^2)^{0.5}] \quad (1)$$

We set an x–z coordinate system (x: basinward horizontal, z: vertical) that originates from the intersection of the initial horizontal line and the hinterland profile. Let x to be positive downstream and z to be positive upward. Equation 1 can be rewritten as:

$$\Psi_{x,z} = \alpha(\gamma x+z) / [(\gamma x+z) - \Lambda_{2D}(\gamma-\alpha)] \quad (2)$$

where $\gamma$is the averaged hinterland slope.

Equation 2 can be regarded as the derivative function of the governing equation of the non-deltaic transgressive profile, which can be expressed as:

$$\partial \eta_{x,z} / \partial x = \alpha(\gamma x+z) / [(\gamma x+z) - \Lambda_{2D}(\gamma-\alpha)] \quad (3)$$

where $\eta_{x,z}$ denotes the non-deltaic transgressive profile expressed as the pathway of shoreline. Note that sediment compaction is not considered.

Equation 3 can hardly be solved analytically but by numerical simulation. The solutions that we have obtained indicate that $\eta_{x,z}$ takes a concave-upward geometry with upstream-increasing gradient.

To test our numerical model, a series of 2D physical experiments was performed at Nagasaki University. The experiments were conducted using a 4 m-long and 2.0 cm-wide, open flume, from the upstream end of which sediment and water were fed at constant rates. Before each experimental run, we built a sufficiently long river profile inside the flume, to model the initial over-extended alluvial river ($L >> L_{crt}$). The initial river lengths were different by runs (L_0, ranging from 120–350 cm) and were set to be within a range of 0.139–0.158 (α). The hinterland slope was set as a constant value of 0.612 (γ). In each run, there occurred non-deltaic transgression as soon as base level started to rise.

©2019. Japan Geoscience Union. All Right Reserved.

Any of the resulting profiles of non-deltaic transgression shows a concave-upward geometry. The downstream end of the profile was tangent to the initial river profile (thus $\alpha \sim \Psi$). To the upstream, Ψ gradually increased, and approached a value as large as γ when the alluvial river was sufficiently shortened. The non-deltaic transgressive profiles generated in the experiments match well with the numerical model, implying that equation 3 can account for the non-deltaic transgressive profile in nature.

Keywords: Autostratigraphy, Non-deltaic transgressive profile, Numerical simulation, Flume experiments

©2019. Japan Geoscience Union. All Right Reserved.

[E] Poster | H (Human Geosciences)：H-CG Complex & General

Mon. May 27, 2019 5:15 PM - 6:30 PM JST | Mon. May 27, 2019 8:15 AM - 9:30 AM UTC | Poster Hall International Exhibition Hall8, Makuhari Messe_16

[H-CG26] Deltas and estuaries: multidisciplinary analyses of complex river-mouth systems

convener:Yoshiki Saito(Estuary Research Center, Shimane University), Guan-Hong Lee(Inha University), David L Dettman(University of Arizona), Kazuaki Hori(Department of Geography, Graduate School of Environmental Studies, Nagoya University)

This session has foci on morphodynamics, material cycling, and sustainability in deltas and estuaries. We invite contributions that advance research on deltas and estuaries as complex river-mouth systems from modern and ancient examples, and that develop integrated frameworks for delta & estuary dynamics modeling on a broad range of temporal and spatial scales: from studies of coastal evolution over the Quaternary to small-scale sediment/material transport processes. We also invite physical processes studies based on field observations, numerical simulation and flume experiments. Finally, the conveners encourage contributions that promote data collection and sharing for both advancing science and local problem solving, that consider policy and governance issues linked to the sustainable development of deltas and estuaries, and that use in-situ and satellite data for modeling and risk assessment.

[HCG26-P01] Deltafront Clinoform of Abandoned Yellow River Delta in Jiangsu Province, China

*LIANGYONG ZHOU[1] (1.Qingdao Institute of Marine Geology China Geological Survey)

[HCG26-P02] Holocene evolution and Anthropocene destruction of the Krishna delta, east coast of India: delta lobe shifts, human impact, and sea-level history

Kakani Nageswara Rao[2], *Yoshiki Saito[1], K.Ch.V. Nagakumar[4], Sumiko Kubo[3], Shilpa Pandey[5], Zhen Li[6], G. Demudu[2], A.S. Rajawat[7] (1.Estuary Research Center, Shimane University, 2.Andhra University, 3.Waseda University, 4.Centre for Water Resources and Management, 5.Birbal Sahni Institute of Palaeosciences, 6.University of Victoria, 7.Space Applications Centre)

[HCG26-P03] Offset in radiocarbon ages between marine bioclast and terrestrial plant pairs in the Holocene sediments around Japan

*Nakanishi Toshimichi[1,2], Futoshi Nanayama[3,4], Atsushi Urabe[5], Kazuaki Hori[6], Wan Hong[7] (1.Kyoto Univ., 2.JAEA, 3.AIST, 4.Kumamoto Univ., 5.Niigata Univ., 6.Nagoya Univ., 7.KIGAM)

[HCG26-P04] Assessment of MEIS for Marine Spatial Planning in the Nakdong River Estuary, Busan Metropolitan City, South Korea

*Jun-Ho Lee[1], Han Jun Woo[1], Hoi-Soo Jung[1], Chan Mi Park[1] (1.Korea Institute of Ocean Science and Technology)

[HCG26-P05] Tidal changes at Asian deltas in response to future sea-level rise

*Katsuto Uehara[1] (1.Kyushu University)

[HCG26-P06] **A governing equation of non-deltaic transgressive profile: 2D numerical simulation and flume experiments**

*Junhui Wang[1,2,3], Tetsuji Muto[3] (1.China University of Petroleum (Beijing), 2.State Key Laboratory of Petroleum Resources and Prospecting, China, 3.Nagasaki University)

Deltafront Clinoform of Abandoned Yellow River Delta in Jiangsu Province, China

*LIANGYONG ZHOU[1]

1. Qingdao Institute of Marine Geology China Geological Survey

The abandoned Yellow River delta in Jiangsu province is a major sediment supplier to the South Yellow Sea and East China Sea. In this study, comparison of historical maps, two cores and three seismic profiles were used to examine its deltafront clinoform (nearshore clinoform). The original historical maps and nautical charts since AD 1750s were collected and compared after calibration, showing the accretion of the shoreline before 1855, when the Yellow River shifted to the Bohai Sea. Near Sheyang River mouth, two 20m-long cores onshore (1 m above present sea level) and offshore (6 m bellow present sea level) were on a line normal to the shoreline. Samples og both cores were dated using AMS ^{14}C and OSL(Optical Stimulated Luminescence) dating technologies. Ages in bottoms of the cores are 43000 to 44000 cal yr BP. At approximate 17.5m bellow present sea level in both cores, yellow and younger (younger than 5000 yr BP) silt sediment occurs. Several young ages in upper part of two cores were obtained, and these show a clear clinoform pattern. Furthermore, seismic profiles across the offshore core show the deltafront clinoform. The upper part weak reflector or transparent part in seismic profiles become thinner seaward and the lower part is strong reflectors. Sea bottom nearshore show a convex shape, but the seaward low gradient part show erosional gullies. The evolution of the deltafront clinoform was revealed in profiles and in plan view.

Keywords: Abandoned Yellow River Delta, Deltafront clinoform, C-14 ages, OSL ages

©2019. Japan Geoscience Union. All Right Reserved.

Holocene evolution and Anthropocene destruction of the Krishna delta, east coast of India: delta lobe shifts, human impact, and sea-level history

Kakani Nageswara Rao[2], *Yoshiki Saito[1], K.Ch.V. Nagakumar[4], Sumiko Kubo[3], Shilpa Pandey[5], Zhen Li[6], G. Demudu[2], A.S. Rajawat[7]

1. Estuary Research Center, Shimane University, 2. Andhra University, 3. Waseda University, 4. Centre for Water Resources and Management, 5. Birbal Sahni Institute of Palaeosciences, 6. University of Victoria, 7. Space Applications Centre

Holocene evolution of the Krishna delta was inferred using landform characteristics and 11 sediment cores with 59 Accelerator Mass Spectrometry ^{14}C dates. Landform assemblage in 5880 km^2area of the Krishna delta indicated the upper river-built fluvial plain and the lower marine-built beach-ridge delta plain with the maximum landwardbeach ridge located at˜30 km from the shoreline separating the two plains. Sedimentary facies and their ages showed the Holocene marine sediment overlying the Pleistocene basement and progressively thickened seaward from <10 m to 25 m below the present sea level. The basal mangrove peat layers indicated that the sea level rose from −9 m to −3 m during 8.3–6.3 cal ky BP before stabilizing at the present level around 5 cal ky BP.
Considering the spatiotemporal variations of sediment facies and sediment accumulation rates and the configuration of the palaeo beach ridges (former shorelines), we surmised five major stages in the growth of 3539 km^2area of the Krishna delta beach-ridge plain during the last 6 cal ky BP with distinct lateral and seaward migration of delta lobes (depocentre shifts). Delta progradation was accelerated in the last 500 years, forming an out-building lobate delta. However, predominant erosion along the sediment-starved Krishna delta front coast during the past 50 years, due to impoundment of the riverine inputs at the burgeoning upstream dams pushed the Krishna delta into a persistent a destruction phase after ˜6,000 years of delta progradation.

Keywords: Beach-ridge plain, Sedimentary facies, Delta lobes, Coastal erosion

©2019. Japan Geoscience Union. All Right Reserved.

Offset in radiocarbon ages between marine bioclast and terrestrial plant pairs in the Holocene sediments around Japan

*Nakanishi Toshimichi[1,2], Futoshi Nanayama[3,4], Atsushi Urabe[5], Kazuaki Hori[6], Wan Hong[7]

1. Kyoto Univ., 2. JAEA, 3. AIST, 4. Kumamoto Univ., 5. Niigata Univ., 6. Nagoya Univ., 7. KIGAM

To identify chronological and spatial changes in the radiocarbon (^{14}C) marine reservoir effects, the ^{14}C ages of eight pairs of marine bioclasts and terrestrial plants were measured from the same horizons of one core of Holocene sediments around Japan (Nakanishi et al. 2013, 2015, 2017abc). The reservoir ages ranged from 60 to 1100 years, scattered over the period 100-10,200 cal BP, which were significantly larger than the values from “prebomb” samples of known age, before AD 1955 in this area. These results indicate that the information on reservoir effects is indispensable for chronological control not only from prebomb samples but also from geological and archaeological samples. Moreover, the effects also reflects the influence of complex river-mouth systems such as deltas and estuaries. To determine the direct chronological changes of the marine reservoir effect between the Kuroshio and Tsushima Currents, radiocarbon ages from pairs of marine bioclasts and terrestrial plants were measured from the same stratigraphic horizons within three cores of Holocene sediments beneath the Sukumo Plain, Miyazaki Plain, and Oki Islands, in west Japan. Subsequently, the results were compared with values from the Oita Plain and Hakata Bay on the northern coast of Kyushu (Nakanishi et al. 2017ac), as well as the Korean Peninsula (Nakanishi et al. 2013, 2015, 2017b). The study was partially funded by the Japan Society for the Promotion of Science Kakenhi grant number 18H01310.

References

Nakanishi T, Hong W, Sung KS, Lim J. 2013. Radiocarbon reservoir effect from shell and plant pair in Holocene sediments around the Yeongsan River in Korea. *Nuclear Instruments and Methods in Physics Research B* 294: 444–51.

Nakanishi T, Hong W, Sung KS, Sung KH, Nakashima R. 2015. Offsets in radiocarbon ages between plants and shells from same horizons of coastal sediments in Korea. *Nuclear Instruments and Methods in Physics Research B* 361: 670–9.

Nakanishi T, Hong W, Shimoyama S, Sato S, Park G, Lee JG. 2017a. Radiocarbon age offset between shell and plant pairs in the Holocene sediments under the Hakata Bay, western Japan. *Radiocarbon* 59 (2): 423–34.

Nakanishi T, Hong W, Sung KS, Nakashima R, Nahm WH, Lim J, Katsuki K. 2017b. Offset in radiocarbon age between plant and shell pairs in Holocene sediment around the Mae-ho Lagoon on the eastern coast of Korea. *Quaternary International* 447: 3–12.

Nakanishi T, Takemura K, Matsuyama H, Shimoyama S, Hong W, Okuno M. 2017c. Activity of the Funai fault and radiocarbon age offsets of shell and plant pairs from the latest Pleistocene to Holocene sediments beneath the Oita Plain, western Japan. *Radiocarbon* 59(6): 1737–48.

Keywords: Radiocarbon age, Marine reservoir effect, Holocene, Kuroshio Current

©2019. Japan Geoscience Union. All Right Reserved.

Assessment of MEIS for Marine Spatial Planning in the Nakdong River Estuary, Busan Metropolitan City, South Korea

*Jun-Ho Lee[1], Han Jun Woo[1], Hoi-Soo Jung[1], Chan Mi Park[1]

1. Korea Institute of Ocean Science and Technology

The Nakdong River has a length of nearly 510 km, with a drainage basin of around 23,400 km^2 in South Korea. The Nakdong River Estuary (NRE) in Busan city is a typical example of an estuary in which the throughput is manipulated artificially. The Noksan barrage, built in 1934, blocks the flow of the West Nakdong River, and the NRE barrage was completed between 1983 and 1987 to regulate the flow of the East Nakdong River. With the construction of several huge industrial complexes on reclaimed land near the NRE barrage in the last 65 years, the hydraulic circulation in the NRE has undergone dramatic changes in river discharge and geomorphic configuration, such as the formation of a series of barrier islands. In this study, marine environmental information system (MEIS) data collected after May 2015 were applied to support marine spatial planning (MSP) in the brackish water zone of NRE. The MEIS data in NRE consists of landscape classification of sub-environments, surface sediment distributions, characteristics of suspended sediment, short-term sedimentation, stratification index analysis in channels, closed circuit television (CCTV) using 4G long term evolution (LTE), automatic weather stations (AWS) in real time, calculated residual flow (R_f), net suspended sediment loads (Q_S), and net suspended sediment flux (F_S) in main stream inlet using mooring station, *etc*. The NRE could be divided into areas continuously managed by government, marine protected areas, areas for the development of marine attractions, areas conserved for research education, and coastal areas subject to safety management, e*tc*. For MSP, it was possible to use comparative data of the characteristics of environmental changes in the estuarine watershed to prepare the NRE for the partial opening or drainage extension in 2019 to 2021. This study aims to discuss how to predict environmental change after partial or full opening in NRE barrage and use ecological-based environmental maps in the process of MSP. The development of marine spatial planning mapping in NRE is much necessary for the nation at a time when the diversity of marine use and the demand for policies regarding marine space rapidly increase.

Keywords: Barrage, Busan, Estuary, Marine Environmental Information System, Marine Spatial Planning, Nakdong River Estuary

©2019. Japan Geoscience Union. All Right Reserved.

Assessment of MEIS for Marine Spatial Planning in the Nakdong River Estuary, Busan Metropolitan City, South Korea

Jun-Ho Lee[1] · Han Jun Woo[1] · Hoi-Soo Jung[1] · Chan Mi Park[1]

[1]Korean Seas Geosystem Research Unit, Korea Institute of Ocean Science & Technology, 385 Yeongdo, Busan 49111, Republic of Korea

The Nakdong River has a length of nearly 510 km, with a drainage basin of around 23,400 km^2 in South Korea. The Nakdong River Estuary (NRE) in Busan city is a typical example of an estuary in which the throughput is manipulated artificially. The Noksan barrage, built in 1934, blocks the flow of the West Nakdong River, and the NRE barrage was completed between 1983 and 1987 to regulate the flow of the East Nakdong River. With the construction of several huge industrial complexes on reclaimed land near the NRE barrage in the last 65 years, the hydraulic circulation in the NRE has undergone dramatic changes in river discharge and geomorphic configuration, such as the formation of a series of barrier islands. In this study, marine environmental information system (MEIS) data collected after May 2015 were applied to support marine spatial planning (MSP) in the brackish water zone of NRE. The MEIS data in NRE consists of landscape classification of sub-environments, surface sediment distributions, characteristics of suspended sediment, short-term sedimentation, stratification index analysis in channels, closed circuit television (CCTV) using 4G long term evolution (LTE), automatic weather stations (AWS) in real time, calculated residual flow (R_f), net suspended sediment loads (Q_S), and net suspended sediment flux (F_S) in main stream inlet using mooring station, *etc*. The NRE could be divided into areas continuously managed by government, marine protected areas, areas for the development of marine attractions, areas conserved for research education, and coastal areas subject to safety management, *etc*. For MSP, it was possible to use comparative data of the characteristics of environmental changes in the estuarine watershed to prepare the NRE for the partial opening or drainage extension in 2019 to 2021. This study aims to discuss how to predict environmental change after partial or full opening in NRE barrage and use ecological-based environmental maps in the process of MSP. The development of marine spatial planning mapping in NRE is much necessary for the nation at a time when the diversity of marine use and the demand for policies regarding marine space rapidly increase.

©2019. Japan Geoscience Union. All Right Reserved.

Tidal changes at Asian deltas in response to future sea-level rise

*Katsuto Uehara[1]

1. Kyushu University

A numerical model has been employed to assess the impact of sea level rise on tidal regimes in the East China Sea and the South China Sea with a special interest on tidal changes at around the deltaic region where the elevation is low and coasts are vulnerable to changes in water levels. The model covers the East and South China seas as a whole with a spatial resolution of 2 minutes (approx. 3 km). A preliminary result for the East China Sea suggests recognizable changes in the amplitude of M2 tides and M2 tidal currents at region such as Hangzhou Bay, the Changjiang Estuary and Haizhou Bay when the sea-level was raised by 1 m. Off the Changjiang Estuary, for example, tidal velocity increased for more than 10 cm/s at deep channels while decreased by about 5 cm/s on shoals. These results indicate that the sea-level rise may alter equilibrium among water currents and seafloor and modify the bottom topography of large estuaries and subaquatic deltas through the induced changes in tides and tidal currents.

Keywords: tides, china sea, sea level rise

©2019. Japan Geoscience Union. All Right Reserved.

A governing equation of non-deltaic transgressive profile: 2D numerical simulation and flume experiments

*Junhui Wang[1,2,3], Tetsuji Muto[3]

1. China University of Petroleum (Beijing), 2. State Key Laboratory of Petroleum Resources and Prospecting, China, 3. Nagasaki University

An alluvial river subject to relative sea level rise has a critical length (L_{crt}), beyond which the river can no longer sustain deltaic sedimentation but behaves to develop an estuarine environment. In such cases, there occurs non-deltaic rapid transgression. It is not difficult to imagine that non-deltaic transgression is pervasive in geological records, since most of the world large rivers would have “over-extended” to as far as the shelf edges during glacial or lowstand sea level periods. The configuration of non-deltaic transgressive profiles deserves a study because (1) it would provide a criterion for identifying non-deltaic transgression in the past and thus the fact of over-extension of the feeder alluvial river, and (2) it would constrain arguments on sediment transportation to the deep-water depositional systems.

Suppose that a river has an over-extended alluvial length of L ($>>L_{crt}$). During non-deltaic transgression, all the sediment fed by the river is consumed for alluvial aggradation and thus allocated in the subaerial realm. On the assumption that the supplied sediment is evenly distributed along the river profile which is approximately regarded as linear and has an averaged slope of α, the local transgressive slope Ψcan be expressed as:

$$\Psi = \alpha L / [L - \Lambda_{2D}(1+\alpha^2)^{0.5}] \quad (1)$$

We set an x–z coordinate system (x: basinward horizontal, z: vertical) that originates from the intersection of the initial horizontal line and the hinterland profile. Let x to be positive downstream and z to be positive upward. Equation 1 can be rewritten as:

$$\Psi_{x,z} = \alpha(\gamma x+z) / [(\gamma x+z) - \Lambda_{2D}(\gamma-\alpha)] \quad (2)$$

where $\gamma$is the averaged hinterland slope.

Equation 2 can be regarded as the derivative function of the governing equation of the non-deltaic transgressive profile, which can be expressed as:

$$\partial \eta_{x,z} / \partial x = \alpha(\gamma x+z) / [(\gamma x+z) - \Lambda_{2D}(\gamma-\alpha)] \quad (3)$$

where $\eta_{x,z}$ denotes the non-deltaic transgressive profile expressed as the pathway of shoreline. Note that sediment compaction is not considered.

Equation 3 can hardly be solved analytically but by numerical simulation. The solutions that we have obtained indicate that $\eta_{x,z}$ takes a concave-upward geometry with upstream-increasing gradient.

To test our numerical model, a series of 2D physical experiments was performed at Nagasaki University. The experiments were conducted using a 4 m-long and 2.0 cm-wide, open flume, from the upstream end of which sediment and water were fed at constant rates. Before each experimental run, we built a sufficiently long river profile inside the flume, to model the initial over-extended alluvial river ($L >> L_{crt}$). The initial river lengths were different by runs (L_0, ranging from 120–350 cm) and were set to be within a range of 0.139–0.158 (α). The hinterland slope was set as a constant value of 0.612 (γ). In each run, there occurred non-deltaic transgression as soon as base level started to rise.

©2019. Japan Geoscience Union. All Right Reserved.

Any of the resulting profiles of non-deltaic transgression shows a concave-upward geometry. The downstream end of the profile was tangent to the initial river profile (thus $\alpha \sim \Psi$). To the upstream, Ψ gradually increased, and approached a value as large as γ when the alluvial river was sufficiently shortened. The non-deltaic transgressive profiles generated in the experiments match well with the numerical model, implying that equation 3 can account for the non-deltaic transgressive profile in nature.

Keywords: Autostratigraphy, Non-deltaic transgressive profile, Numerical simulation, Flume experiments

©2019. Japan Geoscience Union. All Right Reserved.

[E] Poster | S (Solid Earth Sciences)：S-SS Seismology

Mon. May 27, 2019 1:45 PM - 3:15 PM JST | Mon. May 27, 2019 4:45 AM - 6:15 AM UTC | Poster Hall International Exhibition Hall8, Makuhari Messe_5

[S-SS07] Rigorous Seismicity Modelling and Hypothesis Testing

convener:Jiancang Zhuang(Institute of Statistical Mathematics), Danijel Schorlemmer(GFZ German Research Centre for Geosciences), Matt Gerstenberger(GNS Science), Hiroshi Tsuruoka(Earthquake Research Institute, Tokyo Univ.)

Probabilistic models have been developed for describing, analyzing, and forecasting seismicity since more than 100 years and, with the advent of large-scale digital networks, in high resolution during the last 30 years. These models include recurrence and stress-release models for long-term earthquake hazard assessment, and short-term models describing earthquake clustering, e.g. the ETAS model. Some models have become standard tools in seismic hazard assessment. However, the overall probabilities remain on the low end and the uncertainties of the forecasts are not well described. Rigorous data-based development and testing of models will help further improving forecasting power and accuracy of these models. Similarly, new hypotheses shall be evaluated rigorously using some existing model as the null hypothesis model or in dedicated tests addressing the hypothesis directly. In this context, the Collaboratory for the Study of Earthquake Predictability and its Japan branch provides the necessary testing capabilities for rigorous and unbiased evaluation of models and hypotheses. This session focuses on research that increases information on seismicity, being with respect to a reference model or as an independent hypothesis. We solicit contributions of model developments and hypothesis formulation based on the increased understanding of the physical process of earthquakes, such as the preparation and rupture processes of the earthquake source and the interaction between earthquakes and tectonic environments. We also welcome development and implementation of improved statistical methods for testing and validating physical hypotheses based on observed data. In particular, we welcome contributions about model- or hypothesis-test experiments that could be implemented in the Japan testing center.

[SSS07-P01] Development of Physics-based Ground Motion Simulation in A Hybrid Approach and Applications to Seismic Hazard Assessment in Taiwan

*Ming-Che Hsieh[1], Yin-Tung Yen[1], Kuo-Fong Ma[2,3] (1.Disaster Prevention Technology Research Center, Sinotech Engineering Consultants (Inc.), Taiwan, 2.Department of Earth Sciences, National Central University, Taiwan, 3.Earthquake-Disaster & Risk Evaluation and Management Center, National Central University, Taiwan)

[SSS07-P02] Increasing Earthquake Forecast Testability - CSEP Future Developments

*Danijel Schorlemmer[1], Naoshi Hirata[2], Fabrice Cotton[1], Matt Gerstenberger[3], Thomas Jordan[7], Warner Marzocchi[4], William Savran[7], Maximilian Werner[5], Stefan Wiemer[6], Thomas Beutin[1], David D Jackson[8], Philip Maechling[7], Sum Mak[1], Kazuyoshi Nanjo[9], Yosihiko Ogata[10], David Rhoades[3], Hiroshi Tsuruoka[2], Graeme Weatherill[1], Jiancang Zhuang[10] (1.GFZ German Research Centre for Geosciences, 2.Earthquake Research Institute, University of Tokyo, Japan, 3.GNS Science, Lower Hutt, New Zealand, 4.University of Naples, Naples, Italy, 5.University of Bristol, Bristol, United Kingdom, 6.ETH Zurich, Zurich, Switzerland, 7.University of Southern California, Los Angeles, USA, 8.University of California Los Angeles, Los Angeles, USA, 9.University of Shizuoka, Shizuoka, Japan, 10.Institute of Statistical Mathematics, Tachikawa, Japan)

[SSS07-P03] Precision versus uncertainty in regional seismic hazard mapping

*Matt Gerstenberger[1], Danijel Schorlemmer[2] (1.GNS Science, 2.GFZ-Potsdam)

[SSS07-P04] An extreme value analysis of seismograms designed for early forecast of aftershocks

*Kaoru Sawazaki[1] (1.National Research Institute for Earth Science and Disaster Resilience)

[SSS07-P05] **Spatio-temporal clustering of successive earthquakes: data analyses of global data.**

*THYSTERE MATONDO BANTIDI[1], Takeshi Nishimura[1] (1.Tohoku University)

[SSS07-P06] Kanto 3 month testing class results of CSEP Japan

*Hiroshi Tsuruoka[1], Naoshi Hirata[1] (1.Earthquake Research Institute, Tokyo Univ.)

[SSS07-P07] Long-term earthquake risk in North China estimated from a modern catalogue

Ziyao Xiong[2], *Jiancang Zhuang[1], Shiyong Zhou[2] (1.Institute of Statistical Mathematics, 2.Peking University)

[SSS07-P08] **Distributions of focal mechanisms in background seismicity and earthquake clusters in Japan**

*Jiancang Zhuang[1,2], Eri Maita[2] (1.Institute of Statistical Mathematics, 2.Graduate University for Advanced Studies)

[SSS07-P09] New Ground Motion Prediction Equations for Western Saudi Arabia

*Ryota Kiuchi[1,2], Walter Mooney[1], Hani Zahran[3] (1.U.S. Geological Survey, 2.Disaster Prevenetion Research Institute, Kyoto University, 3.Saudi Geological Survey)

[SSS07-P10] Study on the spatial and temporal change of velocity structure before and after 2003 Chengkung earthquake, Taiwan

*TING YA LIANG[1], Wen-Yen Chang[1,2,3], Strong Wen[4] (1.National DONG HWA University, 2.Eastern Taiwan Earthquake Research Center, 3.National Center for Research on Earthquake Engineering, 4.National Chung Cheng University)

Development of Physics-based Ground Motion Simulation in A Hybrid Approach and Applications to Seismic Hazard Assessment in Taiwan

*Ming-Che Hsieh[1], Yin-Tung Yen[1], Kuo-Fong Ma[2,3]

1. Disaster Prevention Technology Research Center, Sinotech Engineering Consultants (Inc.), Taiwan, 2. Department of Earth Sciences, National Central University, Taiwan, 3. Earthquake-Disaster & Risk Evaluation and Management Center, National Central University, Taiwan

Damages to engineering structures by an earthquake depend on the entire time history of the ground motion, which is affected by a number of factors including source-rupture process, seismic-wave velocity structure, topographic relief, and local site condition. To quantitatively assess these effects to ground motion, physics-based ground motion simulation is a powerful tool which enables rigorous modeling of each effect and their coupling. In this study, we present a recent-developed physics-based ground motion simulator in generating broadband seismograms for seismic hazard assessment. The simulator is essentially based on a hybrid approach in which long-period synthetics are calculated by the efficient 3-D strain Green’ s tensor (SGT) and short-period synthetics are modeled by the stochastic method. Physical effects of (1) source slip distribution, (2) seismic wave propagation, (3) surface topography and (4) site amplification are taken into account. This hybrid approach has been validated by the 2016 M_W6.6 Meinong earthquake in southern Taiwan and reveals good potential for engineering applications. We also carried out simulations to model rupture scenarios of seismogenic structure and subduction zone sources. Output full waveform and ground motion parameters, e.g. peak ground acceleration (PGA) and 1.0-s-period spectral acceleration (SA1.0), have been further implemented to risk estimation, and even earthquake drill. Our result shows the ground motion simulator has the potential for earthquake scenario modeling and hazard assessment.

Keywords: Ground motion simulation, Seismic hazard assessment, Strain Green’ s tensor, Stochastic method

©2019. Japan Geoscience Union. All Right Reserved.

Increasing Earthquake Forecast Testability - CSEP Future Developments

*Danijel Schorlemmer[1], Naoshi Hirata[2], Fabrice Cotton[1], Matt Gerstenberger[3], Thomas Jordan[7], Warner Marzocchi[4], William Savran[7], Maximilian Werner[5], Stefan Wiemer[6], Thomas Beutin[1], David D Jackson[8], Philip Maechling[7], Sum Mak[1], Kazuyoshi Nanjo[9], Yosihiko Ogata[10], David Rhoades[3], Hiroshi Tsuruoka[2], Graeme Weatherill[1], Jiancang Zhuang[10]

1. GFZ German Research Centre for Geosciences, 2. Earthquake Research Institute, University of Tokyo, Japan, 3. GNS Science, Lower Hutt, New Zealand, 4. University of Naples, Naples, Italy, 5. University of Bristol, Bristol, United Kingdom, 6. ETH Zurich, Zurich, Switzerland, 7. University of Southern California, Los Angeles, USA, 8. University of California Los Angeles, Los Angeles, USA, 9. University of Shizuoka, Shizuoka, Japan, 10. Institute of Statistical Mathematics, Tachikawa, Japan

The Collaboratory for the Study of Earthquake Predictability (CSEP) has expanded over the years to many different testing areas hosted at multiple testing centers. Hundreds of earthquake forecast models have been submitted to CSEP and are being tested. New testing metrics were developed and implemented and a lot of progress was made to establish CSEP as an institution that cannot be ignored when issuing earthquake forecasts. Its rigor and independence became the standard in evaluating earthquake forecasts and in reporting on the results.

In the framework of the testing activities of the Global Earthquake Model, one line of expanding the capabilities of CSEP was developed at GFZ Potsdam. The group there applied the mechanisms that CSEP introduced to earthquake forecast models to the area of intensity prediction equations (IPEs) and ground-motion prediction equations (GMPEs). The first truly prospective tests were carried out on IPEs for Italy and also on GMPEs for Japan and New Zealand. This new set of tests helped CSEP move into the hazard domain and increase the relevance of its results to the hazard community. Finally, the group at GFZ Potsdam has also conducted the first prospective test of the US national seismic hazard maps.

Although these tests have been successful and well-received, they have also shown the limitations of the CSEP approach. Many aspects of seismic hazard or earthquake forecasting remain inherently untestable if only the model forecasts are tested and not the model ingredients. We propose to continue along the lines of the GFZ Potsdam developments and create new areas of activity for CSEP, namely targeted experiments that cannot be conducted with the current CSEP software system. As part of the eGSIM (European Ground Shaking Intensity Models) service, we will introduce permanent testing of IPEs and GMPEs to the testing center to establish strong performance records to be used in hazard models. Further targeted experiments include the predictive power of b-values, discrimination of foreshocks for short-term forecasting, as well as a deeper look into precursory
phenomena applying CSEP-style rigorous testing. We support including testability in future hazard models or their components to move to better testable seismic hazard models. Finally, to expand into the risk domain, we will test exposure models against new and independent data.

Keywords: Seismicity, Forecasting, Testing

©2019. Japan Geoscience Union. All Right Reserved.

Precision versus uncertainty in regional seismic hazard mapping

*Matt Gerstenberger[1], Danijel Schorlemmer[2]

1. GNS Science, 2. GFZ-Potsdam

Regional and national seismic hazard mapping efforts have increasingly pursued more detailed and precise models and outputs, particularly in terms of source characterisation and modelling. With increasing precision comes increasing uncertainty. In recent years much attention has been paid to modelling uncertainty in ground-motion models and including this in seismic hazard modelling. However, much less effort has been made to quantify and model uncertainty in seismic source characterisation. This raises two questions: 1) is increasing precision appropriate when uncertainty remains poorly quantified? 2) what is the optimal balance between precision and uncertainty? Ultimately the answer to this depends on the end-uses of the models and the implications of increasing uncertainty with increasing precision. Here we explore some of the main sources of uncertainty in seismic source characterisation such as incomplete and limited records of earthquake occurrence in paleoseismic data and earthquake catalogues, non-stationarity of seismicity and the poisson assumption, fault source characterisation and so-called moment balancing. We pay particular focus to uncertainties in estimating hazard in less seismically active regions and the implications for building design guidance.

Keywords: Seismic hazard, PSHA, uncertainty

©2019. Japan Geoscience Union. All Right Reserved.

An extreme value analysis of seismograms designed for early forecast of aftershocks

*Kaoru Sawazaki[1]

1. National Research Institute for Earth Science and Disaster Resilience

Conventional aftershock forecasting has been operated through applying the Gutenberg-Richter and Omori-Utsu laws to an earthquake catalog. However, catalog's quality is influenced by detectability of earthquake signals (P or S waves), which causes degradation of the catalog in the early stage after a large earthquake and at regions which are sparsely covered by seismograph network. This eventually causes the catalog's nonuniformity and limitation of the forecasting performance.

In this study, we propose a new approach designed for high-performance early aftershock forecasting without using earthquake catalog. Instead, we use a continuous seismogram recorded at each station. First, we pick the maximum amplitude of the seismogram obtained in every assigned time interval (e.g., 1 minute). This picking process can be completely automated and is rarely affected by overlap of multiple seismic signals occurring in approximately the same time. We empirically derive a probability distribution (PD) that accounts for the frequency of the maximum amplitudes. This PD is essentially a non-stationary extreme value distribution derived from the generalized Pareto distribution (GPD) and the Omori-Utsu type temporal decay. We optimize three parameters that control the PD shape (K_a: parameter that controls whole aftershock activity, p_a: parameter that controls temporal decay of the aftershock frequency, m: parameter that controls power-law decay of the maximum amplitude) by applying the maximum likelihood estimation to the observed maximum amplitudes. By extrapolating the optimized PD, we estimate the number of maximum amplitudes that will exceed a threshold value within arbitral time interval in the future. The proposed approach provides forecast of peak ground motion at each station rather than magnitude, which is directly desired for public use. Moreover, the forecasted peak ground motion may automatically incorporate many factors that cannot be described by a simple ground motion attenuation model (e.g., site amplification, radiation pattern, rupture directivity, and so on).

We apply the proposed method to 25 Hi-net seismograms recorded the 2016 Kumamoto earthquakes in Japan. We set the learning periods every one hour after the mainshock (Mj7.3), and set the forecasting period within 24 hours after the end of each learning period. We find that parameters K_a and m become temporally stable within a few hours after the mainshock at many stations. On the other hand, the parameter p_a temporally varies more probably because the induced seismicity at northeast area (Aso and Oita regions) strongly affects the apparent temporal decay rate of the amplitudes. Within 3 hours after the mainshock, the forecasted number of the maximum amplitudes exceeding 10^{-4} m/s is within 0.5 to 2.0 times the actual observation for about 80 % of the used stations. For the threshold amplitude of 10^{-3} m/s, on the other hand, the forecasted number tends to overestimate, probably due to saturation of seismograms by both artificial and physical reasons.

Keywords: extreme value analysis, aftershock forecasting, peak ground motion

©2019. Japan Geoscience Union. All Right Reserved.

Spatio-temporal clustering of successive earthquakes: data analyses of global data.

*THYSTERE MATONDO BANTIDI[1], Takeshi Nishimura[1]

1. Tohoku University

Spatio-temporal clustering of seismicity is an interesting phenomenon in the earthquake generation process. We investigate the earthquakes closely occurring in space and time, which have been sometimes observed at various regions. A recent example is *Mw*6.5 earthquake at Hinagu active fault on April 14, 2016, followed by a *Mw*7.3 at Futagawa active fault on April 16. The present study analyzes moderate and large earthquakes to clarify characteristics of such successive occurrence of earthquakes.

We use the Global Centroid Moment Tensor catalog for the period from 1976 to 2016. Earthquakes with moment magnitudes (*Mw*) of larger or equal to 5.0 and with depths less than or equal to 70 km are analyzed. The earthquakes that occur within some horizontal distance ranges (Δd*:* from 10 to 500 km*)*, and lapse times (Δt=30, 180 and 365 days*)* from the occurrence of each target earthquake is grouped in a cluster, and the number of clusters are counted.

The results show that cumulative numbers of clusters almost constantly increase in the logarithmic scale with increasing Δt, and the number of clusters increases constantly in general with increasing Δd. For example, for the *Mw* 5.0 –5.5, the cumulative number of clusters at Δd*=100* km are 3177, 4525 and 4808, respectively, for Δt of 30, 180 and 365 days.

To examine whether or not these successive earthquakes occur randomly, in other words, whether or not these successive earthquakes occur under some physical conditions, we compare the observed results with simulations in which earthquakes are set to randomly occur in time. The results show that the observed cumulative numbers of clusters are larger than those of simulation in short distance ranges. The former gradually approach to the latter with increasing the horizontal distance, and merge into a same number at a distance, which is defined as “triggering distance” in the present study. As Δt increases, the occurrence probability decreases and approaches to the normal condition in which the occurrence time intervals of earthquakes obey a Poisson distribution. For example, the triggering distances of Mw5.0-5.5 are 420 km and 66 km, respectively, for Δt*=30* days and *365* days. The results obtained by changing the parameters related to the spatial and temporal distributions of aftershock show no significant difference in the number of clusters and triggering distances.

Keywords: Clustering, Successive earthquakes, Triggering distance

©2019. Japan Geoscience Union. All Right Reserved.

Kanto 3 month testing class results of CSEP Japan

*Hiroshi Tsuruoka[1], Naoshi Hirata[1]

1. Earthquake Research Institute, Tokyo Univ.

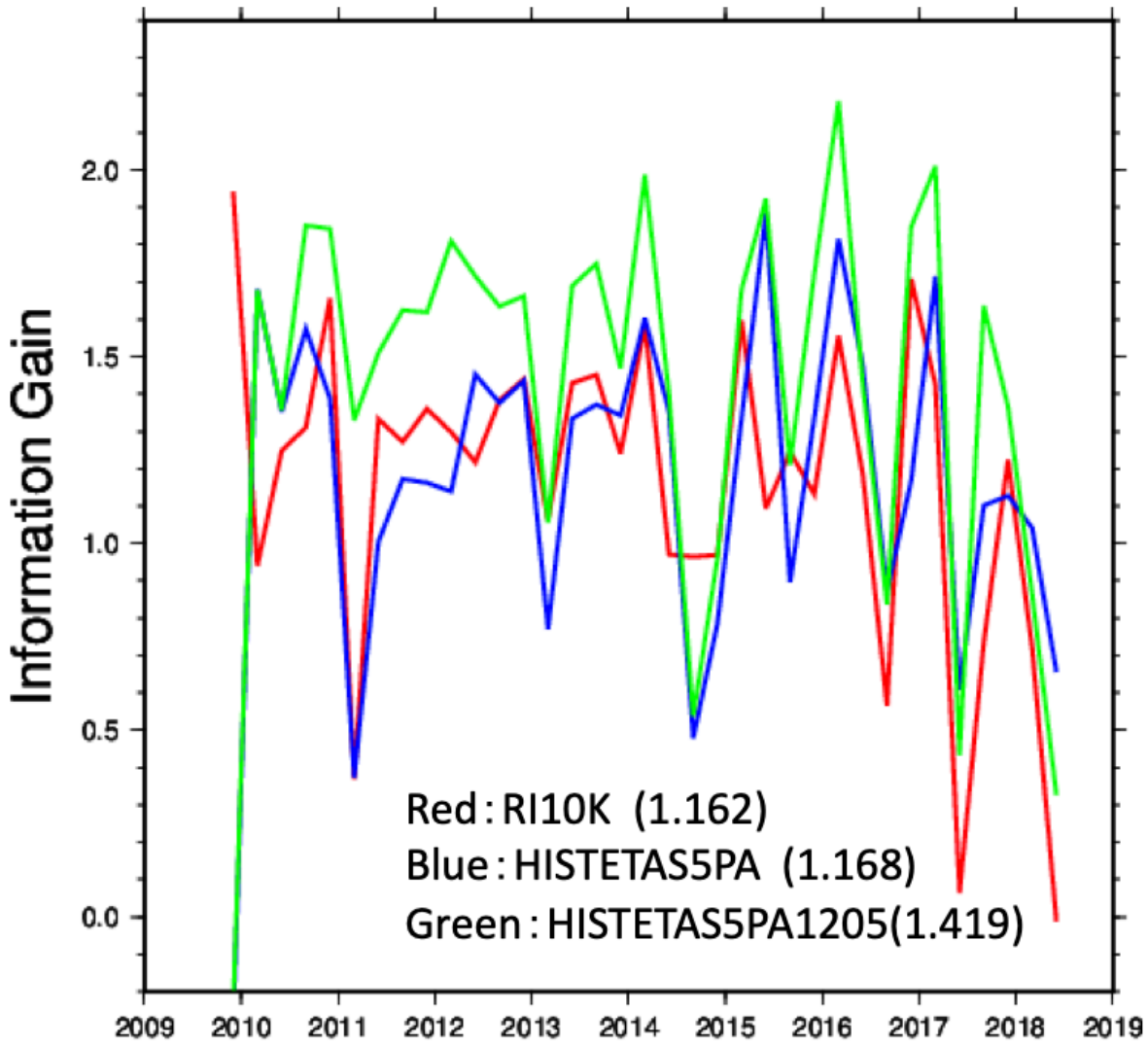
We report about 3 month testing class results of Kanto test region of CSEP Japan. We show the results of three models: RI10K, HISTETAS5PA and HISTETAS5PA1205. HISTETAS5 PA1205 is a model submitted to the Japan test center after the Tohoku-oki earthquake. The test results are about 40 rounds evaluated from 1 November 2009.

From the standard test results of CSEP, RI10K did not pass the S-test in the round of 2017/5 / 1-8 / 1. In addition, there were some rounds that did not pass N-Test in all models when the number of observed earthquakes was relatively small. Calculating the average of information gain values per earthquake for each model in all rounds was 1.419, 1.168, 1.162 for HISTETAS5PA1205, HISTETAS5PA, and RI10K respectively. Regarding the forecast of the number of earthquakes, HISTETA5PA1205 predicts the number of observation earthquakes well.

From the results of multiple rounds, forecast number of earthquakes improvement directly leads to improvement of an earthquake forecast model. Moreover, a model characteristic can be showed well by evaluating the spatial forecast performance and the performance of forecast number of earthquakes.

Keywords: Earthquake Predictability, CSEP

©2019. Japan Geoscience Union. All Right Reserved.



©2019. Japan Geoscience Union. All Right Reserved.

Long-term earthquake risk in North China estimated from a modern catalogue

Ziyao Xiong[2], *Jiancang Zhuang[1], Shiyong Zhou[2]

1. Institute of Statistical Mathematics, 2. Peking University

In this study, to obtain optimal estimates of the earthquake hazard in North China based on the modern earthquake catalogue, we used two variable kernel function estimation methods and two spatial tessellation methods to calculate the total and background seismic spatial occurrence rates for the study area.

The first problem of this study is to derive the best estimate of the long-term earthquake risk in North China. To address the first problem, we use the kernel function estimation methods of Stock and Smith (2002) and Zhuang et al. (2002), the Bayesian Delaunay-Tessellation Smoothing Method used by Ogata (ODTB) (2003, 2004), and ICVT to estimate the total earthquake hazard for North China. The results were compared and analyzed through the cross-validation method, to ensure accurate reflection of the seismic activity in North China. The sophisticated ODTB method is more stable than the others, but is relatively expensive, in terms of computation demands, while Zhuang et al.’ s kernel estimate and the new ICVT method are able to provide reasonable estimates and easier to implement.

For the second problem, of b-value, we use Ogata’ s method (2004, 2015) based on free nodes, to calculate the *b*-value spatial distribution. We expect that the obtained results of the spatial distribution of seismic risk and *b*-value provide a reference for the evaluation and prediction of large earthquakes and stress distribution in the study area.

For the third problem, we use two methods to estimate background seismic rates, and compare the results. The first method uses the result of the background seismic event probability, calculated by the epidemic-type aftershock sequence (ETAS) model (Zhuang et al., 2002; Zhuang, 2011), to simulate the background seismic risk distribution. The second method is to calculate the spatial distribution of earthquake hazard by using the HIST-ETAS model (Ogata, 2004).

Using comparative analyses and simulation experiments, we show that all of methods give similar spatial patterns of seismic occurrences.

Keywords: seismic risk, tessellation, background seismicity, ETAS model

©2019. Japan Geoscience Union. All Right Reserved.

Distributions of focal mechanisms in background seismicity and earthquake clusters in Japan

*Jiancang Zhuang[1,2], Eri Maita[2]

1. Institute of Statistical Mathematics, 2. Graduate University for Advanced Studies

This study tries to find the probability distributions of focal mechanisms in background seismicity and earthquake clusters in Japan by analyzing F-net data. To describe the probability distribution, each focal mechanism is discomposed as the result of a rotation about a particular pole starting from a reference focal mechanism. In this study, DC4 symmetry is considered, i.e., either nodal-plane can be the fault plane and the two sides of the fault plane are distinguishable.

To separate the background and clustering seismicity, we fit the space-time ETAS model (e.g., Zhuang et al, 2011) to the earthquakes with magnitude 4.2+ from 1997 to 2017 in the F-net catalog, and use the stochastic declustering method to estimate the background probabilities that each event is a background event and the triggered probabilities that each event is triggered by other events.

For the background events, the reference focal mechanism is taken as the average focal mechanism in each area, calculated by the method in Kagan (2014). The ration angles between a background event and the mean focal mechanisms at *(x, y)* is reconstructed by

$\zeta(\Delta) \propto \sum_j \phi_j I$(Rotation angle betwen *j* and the mean focal mechanism is within $(\Delta - \delta, \Delta + \delta)$),

where *j* runs over all background events near *x,y,* δ is a small number, and ϕj is the background probability estimated from fitting the space-time ETAS model. For the triggered events, the reference focal mechanism is naturally taken the focal mechanism of the event which triggers it. The rotation angles between the parent event and its direct offspring are reconstructed by

$\xi(\Delta) \propto \sum_{i,j} \rho_{i,j} I$(Rotation angle betwen *i* and *j* is within $(\Delta - \delta, \Delta + \delta)$) .

where *i* and *j* run over all the event pairs in the catalog, ρij is the probability that event *j* is triggered by event *i* estimated based on the ETAS model.

We find that the rotation poles are almost uniformly distributed. The reconstructed results for the rotation angles are shown in Figure 1.

Figure 1 (a) mean focal mechanisms of background seismicity in Japan. (b) Reconstructed distribution of rotation angles for focal mechanisms in the background seismicity and triggered seismicity.

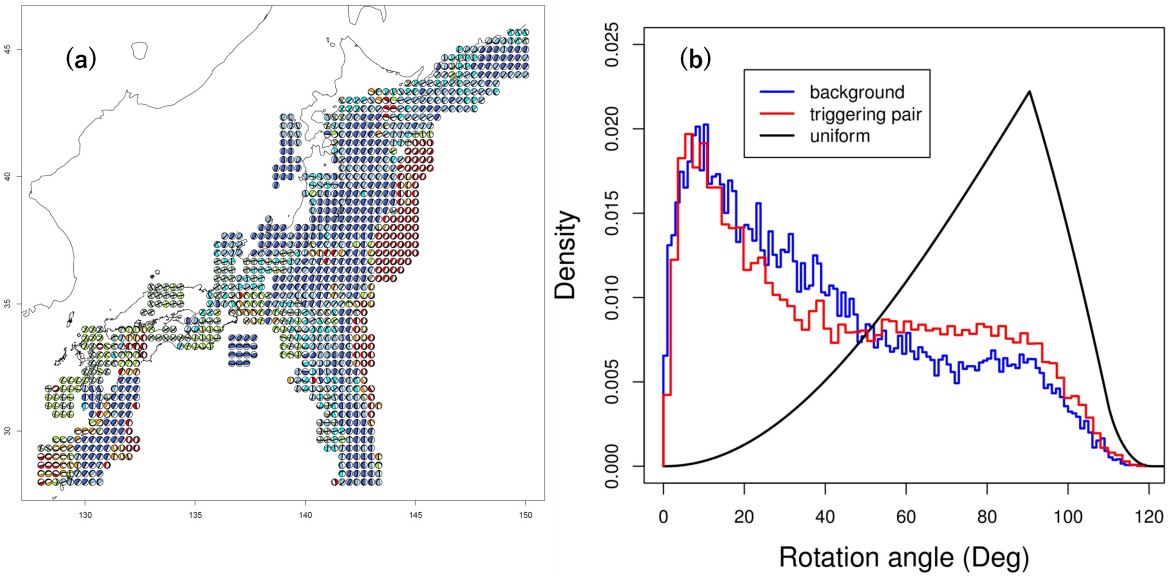
References:

Zhuang J., (2011) , *Next-day earthquake forecasts for the Japan region generated by the ETAS model*. **Earth Planets Space**, 63, 207-216. doi:10.5047/eps.2010.12.010.

Kagan Y.Y. and Jackson D. D. (2014) Statistical earthquake focal mechanism forecasts. **Geophys. J. Int.** 197, 620–629. doi: 10.1093/gji/ggu015.

©2019. Japan Geoscience Union. All Right Reserved.

Keywords: earthquake focal mechanism, probability distribution, earthquake cluster, background seismcity, ETAS model



©2019. Japan Geoscience Union. All Right Reserved.

New Ground Motion Prediction Equations for Western Saudi Arabia

*Ryota Kiuchi[1,2], Walter Mooney[1], Hani Zahran[3]

1. U.S. Geological Survey, 2. Disaster Prevenetion Research Institute, Kyoto University, 3. Saudi Geological Survey

We developed Ground Motion Prediction Equations (GMPEs) for western Saudi Arabia using 2770 selected records of PGA and PGV from 177 earthquakes of magnitude 3.0 –5.4, recorded at 58 stations in the distance range from 1 km to 400 km. Our GMPEs are developed based on one of the NGA-West2 Project GMPEs (Boore et al., 2014) by employing a mixed effects regression model.

Saudi Arabia is surrounded by several active tectonic regions, including an extension in the Red Sea and left-lateral strike-slip motion in the Gulf of Aqaba and along the Dead Sea Transform Fault (DSTF). In this area, multiple seismic swarms in and around volcanic fields, also known as harrats, have been detected over the past several decades (El-Isa and Shanti, 1989). The most recent large earthquake swarm in the region, which included more than 30,000 earthquakes, occurred from April to June 2009 beneath the volcanic field of Harrat Lunayyir in northwestern Saudi Arabia. The strongest seismic activity occurred May 13-19, 2009 and consisted of events M > 4 (Pallister et al., 2010). The largest earthquake occurred on May 19th, ML 5.4 as estimated by the SGS (Saudi Geological Survey) and Mw 5.7 by the USGS.

The NGA-West2 project used as a reference model mainly consists of shallow crustal earthquakes in active tectonic regions, rather than extensional earthquakes, such as those observed in Saudi Arabia. This deficiency is corrected by calculating a magnitude scaling of the new Saudi Arabia GMPEs compared to those of Boore et al. (2014). Furthermore, there is a clear difference in distance scaling for the Arabian GMPEs in comparison with the NGA-West2 GMPEs. This difference is especially significant at large distances and is mainly due to lower anelastic attenuation in the crystalline crust of western Saudi Arabia. Our empirical data demonstrate that the GMPEs presented here are in good agreement with observed earthquake ground motions in western Saudi Arabia.

Keywords: GMPE, Saudi Arabia, Seismic Hazard

©2019. Japan Geoscience Union. All Right Reserved.

Study on the spatial and temporal change of velocity structure before and after 2003 Chengkung earthquake, Taiwan

*TING YA LIANG[1], Wen-Yen Chang[1,2,3], Strong Wen[4]

1. National DONG HWA University, 2. Eastern Taiwan Earthquake Research Center, 3. National Center for Research on Earthquake Engineering, 4. National Chung Cheng University

Taiwan is located in the plate converge zone, in which the Longitudinal Valley(LV) is the suture zone between the Eurasian Plate and Philippine Sea Plate. The collision process yields two nearly parallel major fault systems: the Central Range fault (CRF) and the Longitudinal Valley fault(LVF). The Chihshang fault is a creeping thrust fault, which is located in the southern section of the LVF in eastern Taiwan. According to geodetic survey, this fault moves to northwest at a rate approximately 2–3 cm/yr. There were two significant earthquakes occurred nearby the Chihshang fault, the 1951 M7.1 Hualien-Taitung earthquake and the 2003 M6.4 Chengkung earthquake. In this study, the spatial and temporal variations of velocity structure before and after 2003 Chengkung earthquake were obtained through the tomography inversion beneath the southern segment of the Longitudinal Valley. The damping least-square technique and 3D ray tracing scheme were adopted to calculate the most appropriate solution and obtain the velocity structures. The results showed that the Vp values exhibit less significant variations than the parameters Vs and Vp/Vs ratio. But the Vs structures show larger variation after the 2003 mainshock. These results imply that Vp/Vs ratios began to increase before the mainshock, at the hanging wall of the Chihshang fault, which may be related to the increasing density of microcracks and fluid. Previous studies has shown that high Vp/Vs ratio may lead to cracks generating and fluid migration, which can result in changing rock volume and produce partial compensation. Therefore, our results not only give better understanding the seismogenic structures in the ES Taiwan, but also allow us to detect variations of physical parameters caused by crack propagating in stratum during the strong earthquake sequence. Hence, this study shows that the results from temporal and spatial variation of Vp/Vs values in the southern segment of the LVF could allow us to assess the seismic hazard potential in this area, and further explore the relationship between the seismicity and the rheology of fault plane. Finally, long-term monitoring of fault activities will contribute to the research of future earthquake early warning.

Keywords: spatial and temporal variations, Vp/Vs ratio

©2019. Japan Geoscience Union. All Right Reserved.

[E] Poster | S (Solid Earth Sciences)：S-SS Seismology

Mon. May 27, 2019 5:15 PM - 6:30 PM JST | Mon. May 27, 2019 8:15 AM - 9:30 AM UTC | Poster Hall International Exhibition Hall8, Makuhari Messe_19

[S-SS07] Rigorous Seismicity Modelling and Hypothesis Testing

convener:Jiancang Zhuang(Institute of Statistical Mathematics), Danijel Schorlemmer(GFZ German Research Centre for Geosciences), Matt Gerstenberger(GNS Science), Hiroshi Tsuruoka(Earthquake Research Institute, Tokyo Univ.)

Probabilistic models have been developed for describing, analyzing, and forecasting seismicity since more than 100 years and, with the advent of large-scale digital networks, in high resolution during the last 30 years. These models include recurrence and stress-release models for long-term earthquake hazard assessment, and short-term models describing earthquake clustering, e.g. the ETAS model. Some models have become standard tools in seismic hazard assessment. However, the overall probabilities remain on the low end and the uncertainties of the forecasts are not well described. Rigorous data-based development and testing of models will help further improving forecasting power and accuracy of these models. Similarly, new hypotheses shall be evaluated rigorously using some existing model as the null hypothesis model or in dedicated tests addressing the hypothesis directly. In this context, the Collaboratory for the Study of Earthquake Predictability and its Japan branch provides the necessary testing capabilities for rigorous and unbiased evaluation of models and hypotheses. This session focuses on research that increases information on seismicity, being with respect to a reference model or as an independent hypothesis. We solicit contributions of model developments and hypothesis formulation based on the increased understanding of the physical process of earthquakes, such as the preparation and rupture processes of the earthquake source and the interaction between earthquakes and tectonic environments. We also welcome development and implementation of improved statistical methods for testing and validating physical hypotheses based on observed data. In particular, we welcome contributions about model- or hypothesis-test experiments that could be implemented in the Japan testing center.

[SSS07-P01] Development of Physics-based Ground Motion Simulation in A Hybrid Approach and Applications to Seismic Hazard Assessment in Taiwan

*Ming-Che Hsieh[1], Yin-Tung Yen[1], Kuo-Fong Ma[2,3] (1.Disaster Prevention Technology Research Center, Sinotech Engineering Consultants (Inc.), Taiwan, 2.Department of Earth Sciences, National Central University, Taiwan, 3.Earthquake-Disaster & Risk Evaluation and Management Center, National Central University, Taiwan)

[SSS07-P02] Increasing Earthquake Forecast Testability - CSEP Future Developments

*Danijel Schorlemmer[1], Naoshi Hirata[2], Fabrice Cotton[1], Matt Gerstenberger[3], Thomas Jordan[7], Warner Marzocchi[4], William Savran[7], Maximilian Werner[5], Stefan Wiemer[6], Thomas Beutin[1], David D Jackson[8], Philip Maechling[7], Sum Mak[1], Kazuyoshi Nanjo[9], Yosihiko Ogata[10], David Rhoades[3], Hiroshi Tsuruoka[2], Graeme Weatherill[1], Jiancang Zhuang[10] (1.GFZ German Research Centre for Geosciences, 2.Earthquake Research Institute, University of Tokyo, Japan, 3.GNS Science, Lower Hutt, New Zealand, 4.University of Naples, Naples, Italy, 5.University of Bristol, Bristol, United Kingdom, 6.ETH Zurich, Zurich, Switzerland, 7.University of Southern California, Los Angeles, USA, 8.University of California Los Angeles, Los Angeles, USA, 9.University of Shizuoka, Shizuoka, Japan, 10.Institute of Statistical Mathematics, Tachikawa, Japan)

[SSS07-P03] Precision versus uncertainty in regional seismic hazard mapping

*Matt Gerstenberger[1], Danijel Schorlemmer[2] (1.GNS Science, 2.GFZ-Potsdam)

[SSS07-P04] An extreme value analysis of seismograms designed for early forecast of aftershocks

*Kaoru Sawazaki[1] (1.National Research Institute for Earth Science and Disaster Resilience)

[SSS07-P05] **Spatio-temporal clustering of successive earthquakes: data analyses of global data.**

*THYSTERE MATONDO BANTIDI[1], Takeshi Nishimura[1] (1.Tohoku University)

[SSS07-P06] Kanto 3 month testing class results of CSEP Japan

*Hiroshi Tsuruoka[1], Naoshi Hirata[1] (1.Earthquake Research Institute, Tokyo Univ.)

[SSS07-P07] Long-term earthquake risk in North China estimated from a modern catalogue

Ziyao Xiong[2], *Jiancang Zhuang[1], Shiyong Zhou[2] (1.Institute of Statistical Mathematics, 2.Peking University)

[SSS07-P08] **Distributions of focal mechanisms in background seismicity and earthquake clusters in Japan**

*Jiancang Zhuang[1,2], Eri Maita[2] (1.Institute of Statistical Mathematics, 2.Graduate University for Advanced Studies)

[SSS07-P09] New Ground Motion Prediction Equations for Western Saudi Arabia

*Ryota Kiuchi[1,2], Walter Mooney[1], Hani Zahran[3] (1.U.S. Geological Survey, 2.Disaster Prevenetion Research Institute, Kyoto University, 3.Saudi Geological Survey)

[SSS07-P10] Study on the spatial and temporal change of velocity structure before and after 2003 Chengkung earthquake, Taiwan

*TING YA LIANG[1], Wen-Yen Chang[1,2,3], Strong Wen[4] (1.National DONG HWA University, 2.Eastern Taiwan Earthquake Research Center, 3.National Center for Research on Earthquake Engineering, 4.National Chung Cheng University)

Development of Physics-based Ground Motion Simulation in A Hybrid Approach and Applications to Seismic Hazard Assessment in Taiwan

*Ming-Che Hsieh[1], Yin-Tung Yen[1], Kuo-Fong Ma[2,3]

1. Disaster Prevention Technology Research Center, Sinotech Engineering Consultants (Inc.), Taiwan, 2. Department of Earth Sciences, National Central University, Taiwan, 3. Earthquake-Disaster & Risk Evaluation and Management Center, National Central University, Taiwan

Damages to engineering structures by an earthquake depend on the entire time history of the ground motion, which is affected by a number of factors including source-rupture process, seismic-wave velocity structure, topographic relief, and local site condition. To quantitatively assess these effects to ground motion, physics-based ground motion simulation is a powerful tool which enables rigorous modeling of each effect and their coupling. In this study, we present a recent-developed physics-based ground motion simulator in generating broadband seismograms for seismic hazard assessment. The simulator is essentially based on a hybrid approach in which long-period synthetics are calculated by the efficient 3-D strain Green’ s tensor (SGT) and short-period synthetics are modeled by the stochastic method. Physical effects of (1) source slip distribution, (2) seismic wave propagation, (3) surface topography and (4) site amplification are taken into account. This hybrid approach has been validated by the 2016 M_W6.6 Meinong earthquake in southern Taiwan and reveals good potential for engineering applications. We also carried out simulations to model rupture scenarios of seismogenic structure and subduction zone sources. Output full waveform and ground motion parameters, e.g. peak ground acceleration (PGA) and 1.0-s-period spectral acceleration (SA1.0), have been further implemented to risk estimation, and even earthquake drill. Our result shows the ground motion simulator has the potential for earthquake scenario modeling and hazard assessment.

Keywords: Ground motion simulation, Seismic hazard assessment, Strain Green’ s tensor, Stochastic method

©2019. Japan Geoscience Union. All Right Reserved.

Increasing Earthquake Forecast Testability - CSEP Future Developments

*Danijel Schorlemmer[1], Naoshi Hirata[2], Fabrice Cotton[1], Matt Gerstenberger[3], Thomas Jordan[7], Warner Marzocchi[4], William Savran[7], Maximilian Werner[5], Stefan Wiemer[6], Thomas Beutin[1], David D Jackson[8], Philip Maechling[7], Sum Mak[1], Kazuyoshi Nanjo[9], Yosihiko Ogata[10], David Rhoades[3], Hiroshi Tsuruoka[2], Graeme Weatherill[1], Jiancang Zhuang[10]

1. GFZ German Research Centre for Geosciences, 2. Earthquake Research Institute, University of Tokyo, Japan, 3. GNS Science, Lower Hutt, New Zealand, 4. University of Naples, Naples, Italy, 5. University of Bristol, Bristol, United Kingdom, 6. ETH Zurich, Zurich, Switzerland, 7. University of Southern California, Los Angeles, USA, 8. University of California Los Angeles, Los Angeles, USA, 9. University of Shizuoka, Shizuoka, Japan, 10. Institute of Statistical Mathematics, Tachikawa, Japan

The Collaboratory for the Study of Earthquake Predictability (CSEP) has expanded over the years to many different testing areas hosted at multiple testing centers. Hundreds of earthquake forecast models have been submitted to CSEP and are being tested. New testing metrics were developed and implemented and a lot of progress was made to establish CSEP as an institution that cannot be ignored when issuing earthquake forecasts. Its rigor and independence became the standard in evaluating earthquake forecasts and in reporting on the results.

In the framework of the testing activities of the Global Earthquake Model, one line of expanding the capabilities of CSEP was developed at GFZ Potsdam. The group there applied the mechanisms that CSEP introduced to earthquake forecast models to the area of intensity prediction equations (IPEs) and ground-motion prediction equations (GMPEs). The first truly prospective tests were carried out on IPEs for Italy and also on GMPEs for Japan and New Zealand. This new set of tests helped CSEP move into the hazard domain and increase the relevance of its results to the hazard community. Finally, the group at GFZ Potsdam has also conducted the first prospective test of the US national seismic hazard maps.

Although these tests have been successful and well-received, they have also shown the limitations of the CSEP approach. Many aspects of seismic hazard or earthquake forecasting remain inherently untestable if only the model forecasts are tested and not the model ingredients. We propose to continue along the lines of the GFZ Potsdam developments and create new areas of activity for CSEP, namely targeted experiments that cannot be conducted with the current CSEP software system. As part of the eGSIM (European Ground Shaking Intensity Models) service, we will introduce permanent testing of IPEs and GMPEs to the testing center to establish strong performance records to be used in hazard models. Further targeted experiments include the predictive power of b-values, discrimination of foreshocks for short-term forecasting, as well as a deeper look into precursory
phenomena applying CSEP-style rigorous testing. We support including testability in future hazard models or their components to move to better testable seismic hazard models. Finally, to expand into the risk domain, we will test exposure models against new and independent data.

Keywords: Seismicity, Forecasting, Testing

©2019. Japan Geoscience Union. All Right Reserved.

Precision versus uncertainty in regional seismic hazard mapping

*Matt Gerstenberger[1], Danijel Schorlemmer[2]

1. GNS Science, 2. GFZ-Potsdam

Regional and national seismic hazard mapping efforts have increasingly pursued more detailed and precise models and outputs, particularly in terms of source characterisation and modelling. With increasing precision comes increasing uncertainty. In recent years much attention has been paid to modelling uncertainty in ground-motion models and including this in seismic hazard modelling. However, much less effort has been made to quantify and model uncertainty in seismic source characterisation. This raises two questions: 1) is increasing precision appropriate when uncertainty remains poorly quantified? 2) what is the optimal balance between precision and uncertainty? Ultimately the answer to this depends on the end-uses of the models and the implications of increasing uncertainty with increasing precision. Here we explore some of the main sources of uncertainty in seismic source characterisation such as incomplete and limited records of earthquake occurrence in paleoseismic data and earthquake catalogues, non-stationarity of seismicity and the poisson assumption, fault source characterisation and so-called moment balancing. We pay particular focus to uncertainties in estimating hazard in less seismically active regions and the implications for building design guidance.

Keywords: Seismic hazard, PSHA, uncertainty

©2019. Japan Geoscience Union. All Right Reserved.

An extreme value analysis of seismograms designed for early forecast of aftershocks

*Kaoru Sawazaki[1]

1. National Research Institute for Earth Science and Disaster Resilience

Conventional aftershock forecasting has been operated through applying the Gutenberg-Richter and Omori-Utsu laws to an earthquake catalog. However, catalog's quality is influenced by detectability of earthquake signals (P or S waves), which causes degradation of the catalog in the early stage after a large earthquake and at regions which are sparsely covered by seismograph network. This eventually causes the catalog's nonuniformity and limitation of the forecasting performance.

In this study, we propose a new approach designed for high-performance early aftershock forecasting without using earthquake catalog. Instead, we use a continuous seismogram recorded at each station. First, we pick the maximum amplitude of the seismogram obtained in every assigned time interval (e.g., 1 minute). This picking process can be completely automated and is rarely affected by overlap of multiple seismic signals occurring in approximately the same time. We empirically derive a probability distribution (PD) that accounts for the frequency of the maximum amplitudes. This PD is essentially a non-stationary extreme value distribution derived from the generalized Pareto distribution (GPD) and the Omori-Utsu type temporal decay. We optimize three parameters that control the PD shape (K_a: parameter that controls whole aftershock activity, p_a: parameter that controls temporal decay of the aftershock frequency, m: parameter that controls power-law decay of the maximum amplitude) by applying the maximum likelihood estimation to the observed maximum amplitudes. By extrapolating the optimized PD, we estimate the number of maximum amplitudes that will exceed a threshold value within arbitral time interval in the future. The proposed approach provides forecast of peak ground motion at each station rather than magnitude, which is directly desired for public use. Moreover, the forecasted peak ground motion may automatically incorporate many factors that cannot be described by a simple ground motion attenuation model (e.g., site amplification, radiation pattern, rupture directivity, and so on).

We apply the proposed method to 25 Hi-net seismograms recorded the 2016 Kumamoto earthquakes in Japan. We set the learning periods every one hour after the mainshock (Mj7.3), and set the forecasting period within 24 hours after the end of each learning period. We find that parameters K_a and m become temporally stable within a few hours after the mainshock at many stations. On the other hand, the parameter p_a temporally varies more probably because the induced seismicity at northeast area (Aso and Oita regions) strongly affects the apparent temporal decay rate of the amplitudes. Within 3 hours after the mainshock, the forecasted number of the maximum amplitudes exceeding 10^{-4} m/s is within 0.5 to 2.0 times the actual observation for about 80 % of the used stations. For the threshold amplitude of 10^{-3} m/s, on the other hand, the forecasted number tends to overestimate, probably due to saturation of seismograms by both artificial and physical reasons.

Keywords: extreme value analysis, aftershock forecasting, peak ground motion

©2019. Japan Geoscience Union. All Right Reserved.

Spatio-temporal clustering of successive earthquakes: data analyses of global data.

*THYSTERE MATONDO BANTIDI[1], Takeshi Nishimura[1]

1. Tohoku University

Spatio-temporal clustering of seismicity is an interesting phenomenon in the earthquake generation process. We investigate the earthquakes closely occurring in space and time, which have been sometimes observed at various regions. A recent example is *Mw*6.5 earthquake at Hinagu active fault on April 14, 2016, followed by a *Mw*7.3 at Futagawa active fault on April 16. The present study analyzes moderate and large earthquakes to clarify characteristics of such successive occurrence of earthquakes.

We use the Global Centroid Moment Tensor catalog for the period from 1976 to 2016. Earthquakes with moment magnitudes (*Mw*) of larger or equal to 5.0 and with depths less than or equal to 70 km are analyzed. The earthquakes that occur within some horizontal distance ranges (Δd*:* from 10 to 500 km*)*, and lapse times (Δt=30, 180 and 365 days*)* from the occurrence of each target earthquake is grouped in a cluster, and the number of clusters are counted.

The results show that cumulative numbers of clusters almost constantly increase in the logarithmic scale with increasing Δt, and the number of clusters increases constantly in general with increasing Δd. For example, for the *Mw* 5.0 –5.5, the cumulative number of clusters at Δd*=100* km are 3177, 4525 and 4808, respectively, for Δt of 30, 180 and 365 days.

To examine whether or not these successive earthquakes occur randomly, in other words, whether or not these successive earthquakes occur under some physical conditions, we compare the observed results with simulations in which earthquakes are set to randomly occur in time. The results show that the observed cumulative numbers of clusters are larger than those of simulation in short distance ranges. The former gradually approach to the latter with increasing the horizontal distance, and merge into a same number at a distance, which is defined as “triggering distance” in the present study. As Δt increases, the occurrence probability decreases and approaches to the normal condition in which the occurrence time intervals of earthquakes obey a Poisson distribution. For example, the triggering distances of Mw5.0-5.5 are 420 km and 66 km, respectively, for Δt*=30* days and *365* days. The results obtained by changing the parameters related to the spatial and temporal distributions of aftershock show no significant difference in the number of clusters and triggering distances.

Keywords: Clustering, Successive earthquakes, Triggering distance

©2019. Japan Geoscience Union. All Right Reserved.

Kanto 3 month testing class results of CSEP Japan

*Hiroshi Tsuruoka[1], Naoshi Hirata[1]

1. Earthquake Research Institute, Tokyo Univ.

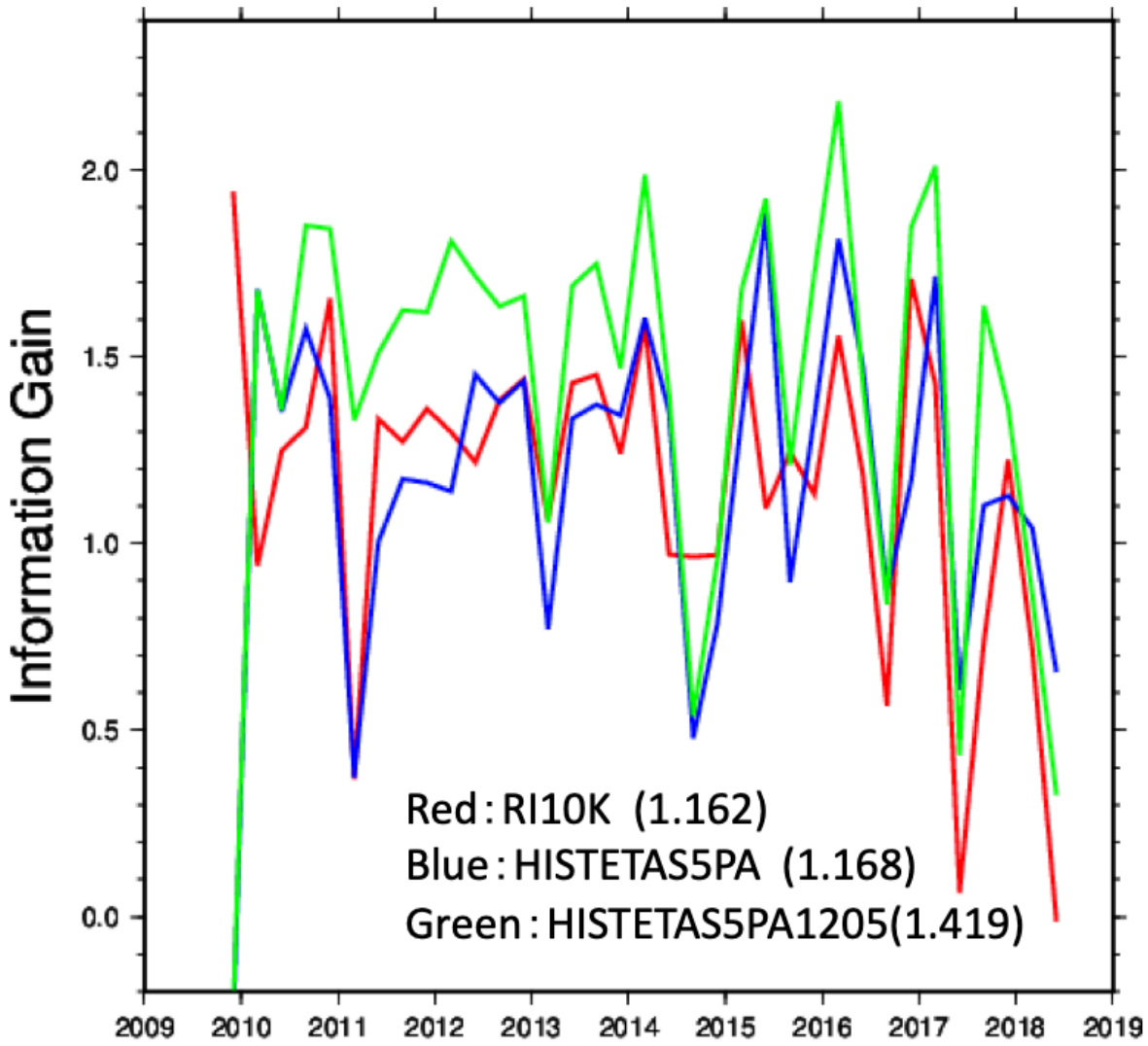
We report about 3 month testing class results of Kanto test region of CSEP Japan. We show the results of three models: RI10K, HISTETAS5PA and HISTETAS5PA1205. HISTETAS5 PA1205 is a model submitted to the Japan test center after the Tohoku-oki earthquake. The test results are about 40 rounds evaluated from 1 November 2009.

From the standard test results of CSEP, RI10K did not pass the S-test in the round of 2017/5 / 1-8 / 1. In addition, there were some rounds that did not pass N-Test in all models when the number of observed earthquakes was relatively small. Calculating the average of information gain values per earthquake for each model in all rounds was 1.419, 1.168, 1.162 for HISTETAS5PA1205, HISTETAS5PA, and RI10K respectively. Regarding the forecast of the number of earthquakes, HISTETA5PA1205 predicts the number of observation earthquakes well.

From the results of multiple rounds, forecast number of earthquakes improvement directly leads to improvement of an earthquake forecast model. Moreover, a model characteristic can be showed well by evaluating the spatial forecast performance and the performance of forecast number of earthquakes.

Keywords: Earthquake Predictability, CSEP

©2019. Japan Geoscience Union. All Right Reserved.



©2019. Japan Geoscience Union. All Right Reserved.

Long-term earthquake risk in North China estimated from a modern catalogue

Ziyao Xiong[2], *Jiancang Zhuang[1], Shiyong Zhou[2]

1. Institute of Statistical Mathematics, 2. Peking University

In this study, to obtain optimal estimates of the earthquake hazard in North China based on the modern earthquake catalogue, we used two variable kernel function estimation methods and two spatial tessellation methods to calculate the total and background seismic spatial occurrence rates for the study area.

The first problem of this study is to derive the best estimate of the long-term earthquake risk in North China. To address the first problem, we use the kernel function estimation methods of Stock and Smith (2002) and Zhuang et al. (2002), the Bayesian Delaunay-Tessellation Smoothing Method used by Ogata (ODTB) (2003, 2004), and ICVT to estimate the total earthquake hazard for North China. The results were compared and analyzed through the cross-validation method, to ensure accurate reflection of the seismic activity in North China. The sophisticated ODTB method is more stable than the others, but is relatively expensive, in terms of computation demands, while Zhuang et al.’ s kernel estimate and the new ICVT method are able to provide reasonable estimates and easier to implement.

For the second problem, of b-value, we use Ogata’ s method (2004, 2015) based on free nodes, to calculate the *b*-value spatial distribution. We expect that the obtained results of the spatial distribution of seismic risk and *b*-value provide a reference for the evaluation and prediction of large earthquakes and stress distribution in the study area.

For the third problem, we use two methods to estimate background seismic rates, and compare the results. The first method uses the result of the background seismic event probability, calculated by the epidemic-type aftershock sequence (ETAS) model (Zhuang et al., 2002; Zhuang, 2011), to simulate the background seismic risk distribution. The second method is to calculate the spatial distribution of earthquake hazard by using the HIST-ETAS model (Ogata, 2004).

Using comparative analyses and simulation experiments, we show that all of methods give similar spatial patterns of seismic occurrences.

Keywords: seismic risk, tessellation, background seismicity, ETAS model

©2019. Japan Geoscience Union. All Right Reserved.

Distributions of focal mechanisms in background seismicity and earthquake clusters in Japan

*Jiancang Zhuang[1,2], Eri Maita[2]

1. Institute of Statistical Mathematics, 2. Graduate University for Advanced Studies

This study tries to find the probability distributions of focal mechanisms in background seismicity and earthquake clusters in Japan by analyzing F-net data. To describe the probability distribution, each focal mechanism is discomposed as the result of a rotation about a particular pole starting from a reference focal mechanism. In this study, DC4 symmetry is considered, i.e., either nodal-plane can be the fault plane and the two sides of the fault plane are distinguishable.

To separate the background and clustering seismicity, we fit the space-time ETAS model (e.g., Zhuang et al, 2011) to the earthquakes with magnitude 4.2+ from 1997 to 2017 in the F-net catalog, and use the stochastic declustering method to estimate the background probabilities that each event is a background event and the triggered probabilities that each event is triggered by other events.

For the background events, the reference focal mechanism is taken as the average focal mechanism in each area, calculated by the method in Kagan (2014). The ration angles between a background event and the mean focal mechanisms at *(x, y)* is reconstructed by

$\zeta(\Delta) \propto \sum_j \phi_j I$(Rotation angle betwen *j* and the mean focal mechanism is within $(\Delta - \delta, \Delta + \delta)$),

where *j* runs over all background events near *x,y,* δ is a small number, and ϕj is the background probability estimated from fitting the space-time ETAS model. For the triggered events, the reference focal mechanism is naturally taken the focal mechanism of the event which triggers it. The rotation angles between the parent event and its direct offspring are reconstructed by

$\xi(\Delta) \propto \sum_{i,j} \rho_{i,j} I$(Rotation angle betwen *i* and *j* is within $(\Delta - \delta, \Delta + \delta)$) .

where *i* and *j* run over all the event pairs in the catalog, ρij is the probability that event *j* is triggered by event *i* estimated based on the ETAS model.

We find that the rotation poles are almost uniformly distributed. The reconstructed results for the rotation angles are shown in Figure 1.

Figure 1 (a) mean focal mechanisms of background seismicity in Japan. (b) Reconstructed distribution of rotation angles for focal mechanisms in the background seismicity and triggered seismicity.

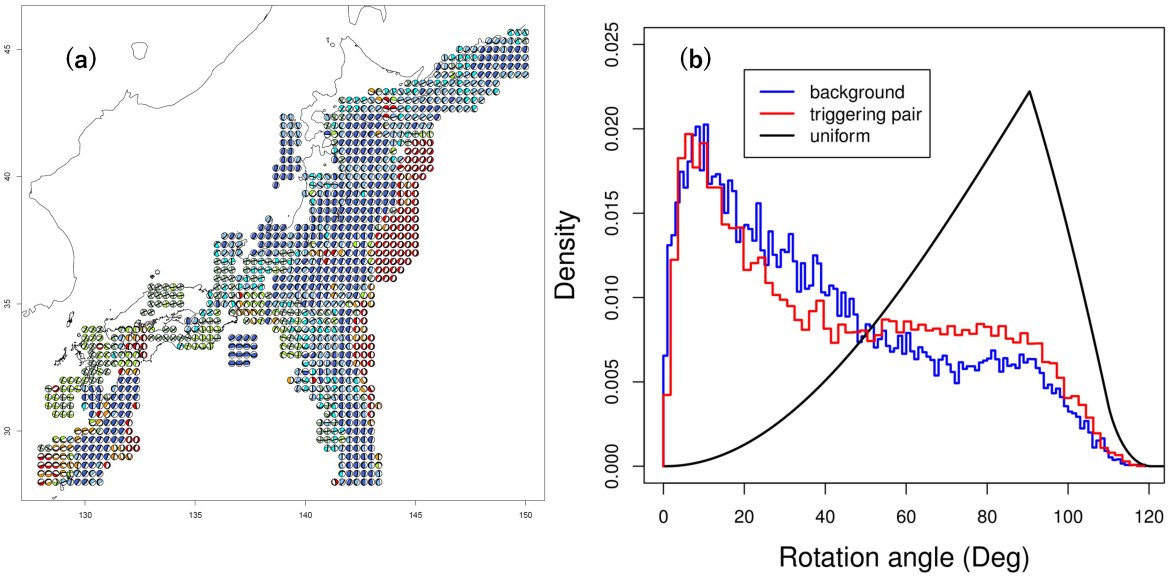
References:

Zhuang J., (2011) , *Next-day earthquake forecasts for the Japan region generated by the ETAS model*. **Earth Planets Space**, 63, 207-216. doi:10.5047/eps.2010.12.010.

Kagan Y.Y. and Jackson D. D. (2014) Statistical earthquake focal mechanism forecasts. **Geophys. J. Int.** 197, 620–629. doi: 10.1093/gji/ggu015.

©2019. Japan Geoscience Union. All Right Reserved.

Keywords: earthquake focal mechanism, probability distribution, earthquake cluster, background seismcity, ETAS model



©2019. Japan Geoscience Union. All Right Reserved.

New Ground Motion Prediction Equations for Western Saudi Arabia

*Ryota Kiuchi[1,2], Walter Mooney[1], Hani Zahran[3]

1. U.S. Geological Survey, 2. Disaster Prevenetion Research Institute, Kyoto University, 3. Saudi Geological Survey

We developed Ground Motion Prediction Equations (GMPEs) for western Saudi Arabia using 2770 selected records of PGA and PGV from 177 earthquakes of magnitude 3.0 –5.4, recorded at 58 stations in the distance range from 1 km to 400 km. Our GMPEs are developed based on one of the NGA-West2 Project GMPEs (Boore et al., 2014) by employing a mixed effects regression model.

Saudi Arabia is surrounded by several active tectonic regions, including an extension in the Red Sea and left-lateral strike-slip motion in the Gulf of Aqaba and along the Dead Sea Transform Fault (DSTF). In this area, multiple seismic swarms in and around volcanic fields, also known as harrats, have been detected over the past several decades (El-Isa and Shanti, 1989). The most recent large earthquake swarm in the region, which included more than 30,000 earthquakes, occurred from April to June 2009 beneath the volcanic field of Harrat Lunayyir in northwestern Saudi Arabia. The strongest seismic activity occurred May 13-19, 2009 and consisted of events M > 4 (Pallister et al., 2010). The largest earthquake occurred on May 19th, ML 5.4 as estimated by the SGS (Saudi Geological Survey) and Mw 5.7 by the USGS.

The NGA-West2 project used as a reference model mainly consists of shallow crustal earthquakes in active tectonic regions, rather than extensional earthquakes, such as those observed in Saudi Arabia. This deficiency is corrected by calculating a magnitude scaling of the new Saudi Arabia GMPEs compared to those of Boore et al. (2014). Furthermore, there is a clear difference in distance scaling for the Arabian GMPEs in comparison with the NGA-West2 GMPEs. This difference is especially significant at large distances and is mainly due to lower anelastic attenuation in the crystalline crust of western Saudi Arabia. Our empirical data demonstrate that the GMPEs presented here are in good agreement with observed earthquake ground motions in western Saudi Arabia.

Keywords: GMPE, Saudi Arabia, Seismic Hazard

©2019. Japan Geoscience Union. All Right Reserved.

Study on the spatial and temporal change of velocity structure before and after 2003 Chengkung earthquake, Taiwan

*TING YA LIANG[1], Wen-Yen Chang[1,2,3], Strong Wen[4]

1. National DONG HWA University, 2. Eastern Taiwan Earthquake Research Center, 3. National Center for Research on Earthquake Engineering, 4. National Chung Cheng University

Taiwan is located in the plate converge zone, in which the Longitudinal Valley(LV) is the suture zone between the Eurasian Plate and Philippine Sea Plate. The collision process yields two nearly parallel major fault systems: the Central Range fault (CRF) and the Longitudinal Valley fault(LVF). The Chihshang fault is a creeping thrust fault, which is located in the southern section of the LVF in eastern Taiwan. According to geodetic survey, this fault moves to northwest at a rate approximately 2–3 cm/yr. There were two significant earthquakes occurred nearby the Chihshang fault, the 1951 M7.1 Hualien-Taitung earthquake and the 2003 M6.4 Chengkung earthquake. In this study, the spatial and temporal variations of velocity structure before and after 2003 Chengkung earthquake were obtained through the tomography inversion beneath the southern segment of the Longitudinal Valley. The damping least-square technique and 3D ray tracing scheme were adopted to calculate the most appropriate solution and obtain the velocity structures. The results showed that the Vp values exhibit less significant variations than the parameters Vs and Vp/Vs ratio. But the Vs structures show larger variation after the 2003 mainshock. These results imply that Vp/Vs ratios began to increase before the mainshock, at the hanging wall of the Chihshang fault, which may be related to the increasing density of microcracks and fluid. Previous studies has shown that high Vp/Vs ratio may lead to cracks generating and fluid migration, which can result in changing rock volume and produce partial compensation. Therefore, our results not only give better understanding the seismogenic structures in the ES Taiwan, but also allow us to detect variations of physical parameters caused by crack propagating in stratum during the strong earthquake sequence. Hence, this study shows that the results from temporal and spatial variation of Vp/Vs values in the southern segment of the LVF could allow us to assess the seismic hazard potential in this area, and further explore the relationship between the seismicity and the rheology of fault plane. Finally, long-term monitoring of fault activities will contribute to the research of future earthquake early warning.

Keywords: spatial and temporal variations, Vp/Vs ratio

©2019. Japan Geoscience Union. All Right Reserved.

[E] Poster | S (Solid Earth Sciences)：S-IT Science of the Earth's Interior & Techtonophysics

Mon. May 27, 2019 3:30 PM - 5:00 PM JST | Mon. May 27, 2019 6:30 AM - 8:00 AM UTC | Poster Hall International Exhibition Hall8, Makuhari Messe_12

[S-IT21] Interaction and Coevolution of the Core and Mantle in the Earth and Planets

convener:Kenji Kawai(Department of Earth and Planetary Science, School of Science, University of Tokyo), Tsuyoshi Iizuka(University of Tokyo), Kenji Ohta(Department of Earth and Planetary Sciences, Tokyo Institute of Technology), Taku Tsuchiya(Geodynamics Research Center, Ehime University)

Recent observational and experimental investigations have significantly advanced our understanding of the structure and constituent materials of the deep Earth. Yet, even fundamental properties intimately linked with formation and evolution of the planet, such as details of the chemical heterogeneity in the mantle and light elements dissolved in the core, remained unclear. Seismological evidence has suggested a vigorous convection in the lower mantle, whereas geochemistry has suggested the presence of stable regions there that hold ancient chemical signatures. The amounts of radioactive isotopes that act as heat sources and drive dynamic behaviors of the deep Earth are also still largely unknown. We provide an opportunity to exchange the achievements and ideas, and encourage persons who try to elucidate these unsolved issues of the core-mantle evolution using various methods, including high-pressure and high-temperature experiments, high-precision geochemical and paleomagnetic analyses, high-resolution geophysical observations, geo-neutrino observations, and large-scale numerical simulations. Papers stimulating an interdisciplinary collaboration relating to establishment of the Japan-SEDI community are also welcomed.

[SIT21-P01] Sample-scale compositional variation of the Inada granite, Ibaraki, Japan -toward the reduction of geoneutrino flux estimation errors from the Japanese crust-

★Invited Papers

*Kenta Ueki[1], Minami Kazuki[2], Tsuyoshi Iizuka[3], Sanshiro Enomoto[4], Hiroyuki Tanaka[2] (1.Japan Agency for Marine-Earth Science and Technology, 2.Earthquake Research Institute, University of Tokyo, 3.Department of Earth and Planetary Science, University of Tokyo, 4.Center for Experimental Nuclear Physics and Astrophysics, University of Washington)

[SIT21-P02] Towards a better estimation of the temperature distribution beneath the Japanese Islands

*Akiko Tanaka[1], Makoto Yamano[2], Hideki Hamamoto[3], Shusaku Goto[4], Takumi Matsumoto[5] (1.Geological Survey of Japan, National Institute of Advanced Industrial Science and Technology, 2.Earthquake Research Institute, The University of Tokyo, 3.Center for Environmental Science in Saitama, 4.Institute for Geo-Resources and Environment National Institute of Advanced Industrial Science and Technology, 5.National Research Institute for Earth Science and Disaster Resilience)

[SIT21-P03] The estimation of the neutrino flux from the crust of the Japanese islands using the geochemical database

*Satoru Haraguchi[1], Kenta Ueki[1], Hikaru Iwamori[1,2,3] (1.Japan Agency for Marine-Earth Science and Technology, 2.Earthquake Research Institute, the University of Tokyo, 3.Tokyo Institute of Technology)

[SIT21-P04] Viscosity of potassium titanosilicate melt at high pressure

*Akio Suzuki[1] (1.Department of Earth Science, Graduate School of Science, Tohoku University)

[SIT21-P05] Lattice thermal conductivity of wadsleyite and ringwoodite at the mantle transition zone pressures

*seiji kimura[1], Kenji Ohta[6], Takaaki Kawazoe[2], Kei Hirose[3], Hiroyuki Kagi[4], Takashi Yagi[5] (1.Department of Earth and Planetary Sciences Tokyo Institute of Technology, 2.Department of Earth and Planetary Systems Science, Hiroshima University, 3.Earth-Life Science Institute, Tokyo Institute of Technology, 4.Geochemical Research Center, Graduate School of Science, University of Tokyo, 5.National Institute of Advanced Industrial Science and Technology, 6.Department of Earth and Planetary Sciences, Tokyo Institute of Technology)

[SIT21-P06] In-situ X-ray observations of the olivine-spinel transformation under shear deformation: preliminary results on the reaction-induced weakening

*Tomoaki Kubo[1], Moriyama Kazuya[1], Yuichiro Mori[1], Masahiro Imamura[1], Sanae Koizumi[2], Yu Nishihara[3], Akio Suzuki[4], Yuji Higo[5] (1.Kyushu Univ., 2.ERI, 3.GRC Ehime Univ., 4.Tohoku Univ., 5.JASRI)

[SIT21-P07] Internally resistive heated diamond anvil cell experiments with metal encapsulated minerals

*YAMAMOTO TOMONARI[1], Kenji Ohta[1], Sho Suehiro[1], Hayato Inoue[1] (1.Tokyo Institute of Technology)

[SIT21-P08] Shear deformation on post-spinel

*Daisuke Yamazaki[1], Noriyoshi Tsujino[1], Yu Nishihara[2] (1.Institute for Planetary Materials, Okayama University, 2.GRC, Ehime University)

[SIT21-P09] **Lattice thermal conductivity of $CaSiO_3$ perovskite at high pressures and high temperatures**

*Kotaro Onga[1], Kenji Ohta[1], Akira Hasegawa[1,2], Takashi Yagi[2], Kei Hirose[3,4], Yasuo Ohishi[5] (1.Department of Earth and Planetary Sciences, Tokyo Institute of Technology, 2.National Institute of Advanced Industrial Science and Technology, 3.Earth-Life Science Institute, Tokyo Institute of Technology, 4.Department of Earth and Planetary Science, The University of Tokyo, 5.Japan Synchrotron Radiation Research Institute)

[SIT21-P10] **Polycrystalline diamond sintered from ultradispersed nanodiamonds**

*Masayuki Nishi[1,2], Koichiro Yamamoto[1], Youmo Zhou[1], Tetsuo Irifune[2,1] (1.Geodynamics Research Center, Ehime University, 2.Earth-Life Science Institute, Tokyo Institute of Technology)

[SIT21-P11] Thermal conductivity measurements on iron and MgO periclase at high pressure and high temperature similar to the Earth's mid-lower mantle conditions

*Akira Hasegawa[1,2], Kenji Ohta[2], Takashi Yagi[1], Kei Hirose[3,4] (1.National Institute of Advanced Industrial Science and Technology, 2.Tokyo Institude of Technology, 3.Earth-Life Science Institute, Tokyo Institude of Technology, 4.The University of Tokyo)

[SIT21-P12] Azimuthal anisotropy in the lowermost mantle beneath Philippine from ScS-S times

*Satoru Tanaka[1] (1.Department of Deep Earth Structure and Dynamics Research Japan Agency for Marine-Earth Science and Technology)

[SIT21-P13] Detailed 3-D S-velocity structure within D" at the western Pacific LLSVP margin: smaller scale plumes and paleoslabs

*Yuki Suzuki[1], Kenji Kawai[1], Robert J. Geller[1], Satoru Tanaka[2], Weerachai Siripuvaraporn[3], Songkhun Boonchaisuku[3], Noisagool Sutthipong[3], Yasushi Ishihara[2], Taweoon Kim, Koji MIYAKAWA[4], Nozomu Takeuchi[4] (1.The University of Tokyo, 2.Japan Agency for Marine-Earth Science and Technology, 3.Mahidol University, 4.Earthquake Research Institute, The University of Tokyo)

[SIT21-P14] Possible interaction between the core and mantle inferred from a core surface flow model

*Masaki Matsushima[1] (1.Department of Earth and Planetary Sciences, School of Science, Tokyo Institute of Technology)

[SIT21-P15] Determination of the noble gas partition coefficients between metal-silicate melts under high-pressure and high-temperature conditions

*Tomotaka Tanaka[1], Hideharu Kuwahara[2], Satoshi Kishi[1], Ryuichi Nomura[3], Kenji Mibe[5], Hiroyuki Kagi[4], Shigehiko Tateno[6], Hirochika Sumino[1] (1.Department of Basic Science, Graduate School of Arts and

Sciences, The University of Tokyo , 2.Geodynamics Research Center, Ehime University, 3.Kyoto University, 4.Geochemical Research Center, Graduate School of Science, University of Tokyo, 5.Earthquake Research Institute, University of Tokyo, 6.Earth-Life Science Institute, Tokyo Institute of Technology)

[SIT21-P16] **Measurement of T-dependent electrical resistivity of solid and liquid Fe and Pt at fixed P**

*Innocent Ezenwa[1], Takashi Yoshino[1] (1.Institute for Planetary Materials, Okayama University)

[SIT21-P17] Ancient, highly depleted mantle constrained by Re-Os isotope and highly-siderophile element compositions of French Polynesian xenoliths

*Norikatsu Akizawa[1], Akira Ishikawa[2], Katsuhiko Suzuki[3], Tetsu Kogiso[4] (1.Atmosphere and Ocean Research Institute, The University of Tokyo, 2.Department of Earth and Planetary Sciences, Tokyo Institute of Technology, 3.Research and Development Center for Submarine Resources, Japan Agency for Marine-Earth Science and Technology (JAMSTEC), 4.Graduate School of Human and Environmental Studies, Kyoto University)

[SIT21-P18] First-principles prediction of hydrogen partitioning between the core and mantle

*Atsuroh Ohba[1], Taku Tsuchiya[1] (1.Ehime University Geodynamics Research Center)

[SIT21-P19] Microvolume stable isotope measuremetns and its applicaiton for high-pressure high-temperature experimental run products

*Madhusoodhan Satish-Kumar[1], Shinnosuke Aoyama[1] (1.Department of Geology, Faculty of Science, Niigata University)

[SIT21-P20] Electrical resistivity of hcp Fe-Si alloys at high pressure and temperature

*Hayato Inoue[1], Sho Suehiro[1], Kenji Ohta[1], Kei Hirose[2,3], Yasuo Ohishi[4] (1.Department of Earth and Planetary Sciences, Tokyo Institute of Technology, 2.Earth-Life Science Institute, Tokyo Institute of Technology, 3.Department of Earth and Planetary Science, The University of Tokyo, 4.Japan Synchrotron Radiation Research Institute)

[SIT21-P21] Electrical resistivity and thermal conductivity of fcc Fe: Implications for the Mercury's core

★Invited Papers

*Hitoshi Gomi[1], Takashi Yoshino[1] (1.Okayama University)

[SIT21-P22] Lateral heterogeneity in the lowermost outer core (F layer) of the Earth revealed by seismic analyses

*Toshiki Ohtaki[1], Satoshi Kaneshima[2], Taku Tsuchiya[3] (1.Geological Survey of Japan, National Institute of Advanced Industrial Science and Technology (AIST), 2.Department of Earth and Planetary Sciences, Kyushu University, 3.Geodynamics Research Center, Ehime University)

[SIT21-P23] Flows and light element distribution in the outer core associated with heterogeneous growth of the inner core of the Earth

*Shin-ichi Takehiro[1], Youhei SASAKI[2] (1.Research Institute for Mathematical Sciences, Kyoto University, 2.Department of Mathematics, Kyoto University)

[SIT21-P24] Sharpness of the hemispherical boundary in the inner core beneath the northern Pacific

*Ryohei Iritani[1], Hitoshi Kawakatsu[1], Nozomu Takeuchi[1] (1.Earthquake Research Institute, Univ. of Tokyo)

[SIT21-P25] Stable carbon isotope fractionation in Fe-C system from first principles

*Haruhiko Dekura[1], Taku Tsuchiya[1] (1.Geodynamics Research Center, Ehime University)

Sample-scale compositional variation of the Inada granite, Ibaraki, Japan -toward the reduction of geoneutrino flux estimation errors from the Japanese crust-

*Kenta Ueki[1], Minami Kazuki[2], Tsuyoshi Iizuka[3], Sanshiro Enomoto[4], Hiroyuki Tanaka[2]

1. Japan Agency for Marine-Earth Science and Technology, 2. Earthquake Research Institute, University of Tokyo, 3. Department of Earth and Planetary Science, University of Tokyo, 4. Center for Experimental Nuclear Physics and Astrophysics, University of Washington

Geoneutrio observed at anti-neutrino observatory "KamLAND" in Kamioka (Hida City, Gifu Prefecture), enables us to directly observe the abundance of radiogenic elements in the deep earth. As crustal rocks exhibit a high concentration of geoneutrino producing radiogenic elements (Uranium and Thorium) than mantle rocks, we have to subtract the contribution of geoneutrino from the Japanese crust from the observation value in Kamioka to estimate geoneutrino flux from core and mantle. For the purpose, we estimated the 3D distribution of uranium and thorium in the Japanese crust by the stochastic modeling using the seismic velocity structure, geological information and geochemical database for the Japanese crustal rock. Geoneutrino flux calculated using the compositional map exhibits a very large error (up to 80%) at present.
We found that information on the compositional heterogeneity (spatial correlation) of various length scale, such as of the single rock suite scale (km to m scale), and sample scale (cm to mm scale) are essential to reduce the estimation error of crustal geoneutrino flux as small as the observation error of the geoneutrino on KamLAND. Therefore, we conducted a grid sampling of the granite of Inada, Ibaraki prefecture, to obtain quantitative knowledge on the small scale compositional heterogeneity. Samples (about 500g) were divided into several centimeter scale split (about 25g). Based on the compositional variations between small splits from one sample, we discuss the small scale sample wise compositional variation. Whole rock chemical composition of each small split was analyzed using XRF. Also, we conducted surface analysis using an ED-XRF to evaluate the spatial distribution of elements in each split. As a result, even within a single sample (about 500g), a compositional variation of about several% at maximum was observed. This result indicates that when conducting the analysis based on the rock chemical composition considering the spatial context, it is necessary to properly evaluate the sample scale heterogeneity, in addition to the tectonic scale, the rock suite scale, and microscopic scale.Also, this result will contribute to the reduction of the estimation error of geoneutrino from the Japanese crust.

Keywords: Geoneutrino, Granite, Rock chemical composition

©2019. Japan Geoscience Union. All Right Reserved.

Towards a better estimation of the temperature distribution beneath the Japanese Islands

*Akiko Tanaka[1], Makoto Yamano[2], Hideki Hamamoto[3], Shusaku Goto[4], Takumi Matsumoto[5]

1. Geological Survey of Japan, National Institute of Advanced Industrial Science and Technology, 2. Earthquake Research Institute, The University of Tokyo, 3. Center for Environmental Science in Saitama, 4. Institute for Geo-Resources and Environment National Institute of Advanced Industrial Science and Technology, 5. National Research Institute for Earth Science and Disaster Resilience

To improve our understanding of the thermal evolution and structure of the deep Earth, it is necessary to know the shallow part of them. Surface heat flow provides important constraint on it. However, the number of heat flow data is limited and spatially very inhomogeneous and even in regions with measurements the data quality varies. For this reason, we have been working on compiling a comprehensive database of heat flow, thermal conductivity, and geothermal gradient. In 2004, Geological Survey of Japan published a digital geoscience map entitled "Geothermal Gradient and Heat Flow Data in and around Japan", which contains heat flow data in the northwestern Pacific area (from 0 to 60°N and from 120 to 160°E) and geothermal gradient data in and around Japan. In 2019, we will be releasing database entitled "Thermal Data Collection in and around Japan", which contains continuously updated of geothermal gradient and heat flow data and adds thermal conductivity data in and around Japan. Thermal conductivity data were compiled from published data and site-specific reports, and measured using the archived cores. This database offers considerable improvements over the previous version released in 2004, and will be published and available at https://www.gsj.jp/en/database/db-portal/index.html. It presents an opportunity to revisit the thermal state of the lithosphere along with other geophysical/geochemical constraints on heat flow extrapolation.

Keywords: heat flow, thermal conductivity, geothermal gradient

©2019. Japan Geoscience Union. All Right Reserved.

The estimation of the neutrino flux from the crust of the Japanese islands using the geochemical database

*Satoru Haraguchi[1], Kenta Ueki[1], Hikaru Iwamori[1,2,3]

1. Japan Agency for Marine-Earth Science and Technology, 2. Earthquake Research Institute, the University of Tokyo, 3. Tokyo Institute of Technology

Geoneutrino observed at the anti-neutrino observatory "KamLAND" at Kamioka allows us to obtain information on the amount and distribution of radiogenic elements (uranium and thorium) in the deep mantle and crust.. It is necessary to divide the contribution from Japanese from the observed neutrino flux on closely to precisely estimate the quantity of U, Th of the earth deep earth because such radiogenic elements exhibit high concentration in the crust. Previous estimation of the crust origin geoneutrino was estimated based on the relatively simple chemical assumption on the compositional variation and spatial distribution. However, the radioactive elements of the Japanese crustal rock are distributed with very wide compositional range with complex spatial distribution. Therefore, it is necessary to estimate spatial distribution of radioactive element in the Japanese crust for the precisely measurement of geoneutrino from Japanese crust. In addition, petrogical and geochemical structure of the Japanese crust of are fundamental information for understanding seismic activity, volcanic activity and tectonism. The analysis of the spatial variation of the chemical composition of the Japanese Islands crust is important in discussing about the evolution history of the Japanese Islands and the chemical evolution in the subduction zone.

In this study, we utilize DODAI to improve the estimation error of geoneutrino from the Japanese crust (Takeuchi et al., 2019). We published the database “DODAI” which compiled geochemical data published by the Japanese domestic journals and bulletins in the journal of the Geological Society of Japan (Haraguchi et al., 2018). This database incorporates the precise sampling position of individual geochemical data using an electronic map. Resolution of the positional information were improved drastically.
The "DODAI" database covers whole area of Japanese Islands with highly precise positional information is useful for data analysis and modeling. The geochemistry database with highly precise positional information is useful for modeling of the geochemical structure of the solid earth. In this study, we present the potential of the DODAI database and geoneutrion in the analysis of the geochemical structures of Japanese crust, as well as the deep earth.

Keywords: neutrino, geochemical database, geochemical structure of crust and mantle

©2019. Japan Geoscience Union. All Right Reserved.

Viscosity of potassium titanosilicate melt at high pressure

*Akio Suzuki[1]

1. Department of Earth Science, Graduate School of Science, Tohoku University

Viscosity of silicate melt is a fundamental property, which controls volcanic processes, including rates of melt extraction, ascent, and magma mixing. Titanium oxide is contained less than 10 wt% in terrestrial magmatic liquids, however, some lunar magmas contains it over 10 wt%. The addition of titanium to silicate melt affects on the properties such as viscosity, density, and compressibility. Especially the pressure dependence of viscosity is of great interest, because magma is generated in the planetary interiors. The aim of this study is to measure the viscosity of K2TiSi4O11 melt at high pressures to estimate the influence of the pressure-induced structural change of melt.
We performed in situ falling sphere viscometry in the pressure range from 1.3 to 7.4 GPa, by using the MAX-III high pressure apparatus at BL14C2 and NE7A beamlines at Photon Factory in KEK, Tsukuba, Japan. A falling platinum sphere in the melt was monitored by using an X-ray CCD camera with a YAG:Ce fluorescence screen. We observed that the viscosity of KTS4 melt decreased up to 3.3 GPa. In contrast, the pressure dependence in viscosity was not observed above 3.3 GPa. Based on XANES spectra of K2TiSi4O11 glasses quenched under high pressure, Paris et al. (1994) showed that the coordination number of titanium increased with increasing pressure. The present study suggests that the melt becomes depolymerized by the coordination change of titanium under high pressure.

Keywords: magma, viscosity, high pressure

©2019. Japan Geoscience Union. All Right Reserved.

Lattice thermal conductivity of wadsleyite and ringwoodite at the mantle transition zone pressures

*seiji kimura[1], Kenji Ohta[6], Takaaki Kawazoe[2], Kei Hirose[3], Hiroyuki Kagi[4], Takashi Yagi[5]

1. Department of Earth and Planetary Sciences Tokyo Institute of Technology, 2. Department of Earth and Planetary Systems Science, Hiroshima University, 3. Earth-Life Science Institute, Tokyo Institute of Technology, 4. Geochemical Research Center, Graduate School of Science, University of Tokyo, 5. National Institute of Advanced Industrial Science and Technology, 6. Department of Earth and Planetary Sciences, Tokyo Institute of Technology

The lattice thermal conductivities of wadsleyite (Wd) and ringwoodite (Rw), which predominantly occupy the Earth's mantle transition zone, are important transport properties to understand the dynamics and thermal structure of the mantle. In particular, the temperature in the subducting slab is mainly controlled by the thermal conduction of Wd and Rw. Wd and Rw are both thought to preserve a large amount of hydrogen ions, thus should play an important role as the main water reservoir in the Earth. Furthermore, it has been reported that the hydration affects the physical properties of minerals including thermal conductivity, and it is necessary to measure the lattice thermal conductivity of Wd and Rw considering their water content. However, so far, the reported lattice thermal conductivities of Wd and Rw has not been considered their water content (Xu et al., 2004). Here we measured the room temperature lattice thermal conductivity of $(Mg_{0.89}Fe_{0.11})_2SiO_4$ Wd and $(Mg_{0.91}Fe_{0.09})_2SiO_4$ Rw up to 27 GPa, respectively, to clarify their hydration dependence using the pulsed light heating thermoreflectance technique in a diamond anvil cell.The obtained results show similar pressure dependence of the lattice thermal conductivity to the previous study (Xu et al., 2004). However, the absolute values of the thermal conductivity are different; the lattice conductivities of hydrous Wd and Rd are ~52% and ~40% lower than the results of Xu et al. (2004), respectively. Our results suggest strong water content dependence of lattice thermal conductivities of Wd and Rw, implying that the water content in the mantle minerals is key factor for calculating the thermal structure in a subducting slab, mantle dynamics.

Keywords: wadsleyite, ringwoodite, mantle transition zone, hydrous minerals, thermal conductivity

©2019. Japan Geoscience Union. All Right Reserved.

In-situ X-ray observations of the olivine-spinel transformation under shear deformation: preliminary results on the reaction-induced weakening

*Tomoaki Kubo[1], Moriyama Kazuya[1], Yuichiro Mori[1], Masahiro Imamura[1], Sanae Koizumi[2], Yu Nishihara[3], Akio Suzuki[4], Yuji Higo[5]

1. Kyushu Univ., 2. ERI, 3. GRC Ehime Univ., 4. Tohoku Univ., 5. JASRI

It has been suggested that high-pressure transformations cause rheological weakening and large deformation of subducting slabs in mantle transition zone (MTZ) . However, there have been few direct experimental evidences so far largely because of the difficulties in quantitative deformation experiments under such conitions. Here we report preliminary results on the olivine-spinel transformation experiments under shear deformation upto MTZ pressures. D-111 (DT-cup) type high-pressure deformation apparatus was newly used for this purpose combined with high-energy synchrotron mono X-rays (50-60 keV) at Photon Factory (PFAR NE7 beamline), which enables in-situ observations of interactions between transformation and creep behaviors. Sintered Mg_2SiO_4 forsterite was first deformed at 15-25 GPa at 600˚C in shear, and subsequently heated to higher temperatures (~0.2˚C/s) to cause the olivine-spinel transformation under shear deformation. The transformation started at much lower temperatures under shear deformation (~900-1100˚C depending on the overpressure from the phase boundary) compared to that without deformation (~1400˚C), suggesting that the shear deformation enhances the olivine-spinel transition rate. The shear strain rate in the sample monitored by X-ray radiography was ~3-4 x 10^{-6} (s^{-1}) at 600˚C, and increased up to ~2-3 x 10^{-4} (s^{-1}) with ramping temperatures even keeping the anvil displacement rate constant (200 micron/h). We observed that the shear weakening does not occur at the same temperature, but reflects on the initiation of the olivine transition. Also, the weakening effects become significant at larger overpressures (and low T). This implies that the weakening of the shear zone induced by the grain-size reduction due to the olivine-spinel transition, however further evidences from microstructural observations are necessary. We plan to install 8-ch acoustic emission measurement system attached with D-111 apparatus to capture the transformation-induced shear instabitiy. Results of D-DIA shear deformation study on the olivine-spinel transition in Fe_2SiO_4 will also be presented and compared with those of the D-111 study in Mg_2SiO_4 .

©2019. Japan Geoscience Union. All Right Reserved.

Internally resistive heated diamond anvil cell experiments with metal encapsulated minerals

*YAMAMOTO TOMONARI[1], Kenji Ohta[1], Sho Suehiro[1], Hayato Inoue[1]

1. Tokyo Institute of Technology

Heating technique is crucial for *in-situ* high pressure-temperature (*P-T*) studies into the physical and chemical properties of minerals in the diamond anvil cell (DAC) under deep Earth's conditions. External resistive heating methods that use resistive heaters such as AlChrom-O wire and graphite surrounding the DAC or just the diamonds (Dubrovinskaia and Dubrovinsky, 2003; Du et al., 2013). This approach creates a homogeneous temperature field in the sample chamber but limits the maximum temperature of about 1200℃ due to graphitization of diamond anvils. Double-sided laser heating with a DAC generates the *P-T* conditions corresponding to the center of the Earth's (Tateno et al., 2010). However, tightly focused laser beams, instabilities in output laser power and misalignment of the focused beams on the sample surface result in significant temperature variation within the sample in the DAC. Internally resistive heated DAC is an effective heating method to overcome the temperature limitation of external heated DAC and the significant temperature gradients experienced in conventional laser-heated DAC (e.g., Zha and Bassett, 2003). However, the internally resistive heated DAC is mostly applied to metal sample to study the properties of the planetary metallic core despite this technique could be applicable to an insulating mineral.

In this study, we modified the internally resistive heated DAC technique for nonmetallic material. We developed a microfabrication technique for total metal encapsulation of the nonmetallic sample. The sample encapsulated by platinum was loaded in DAC with thermal insulator and connected with two electrical leads to make electrical circuit for resistive heating. We confirmed very stable and homogeneous heating for insulating sample at 30 GPa to 2450 K in the modified internally resistive heated DAC. The highest temperature which this method can generate depends on the metal heater encapsulating the sample. This method offers a larger heating volume with more stable and uniform temperature than laser heating and at temperatures much greater than those that can be generated by external resistive heating methods.

References

Dubrovinskaia, N., & Dubrovinsky, L. (2003). Whole-cell heater for the diamond anvil cell. *Review of Scientific Instruments*, *74*(7), 3433-3437.

Du, Z., Miyagi, L., Amulele, G., & Lee, K. K. (2013). Efficient graphite ring heater suitable for diamond-anvil cells to 1300 K. *Review of Scientific Instruments*, *84*(2), 024502.

Tateno, S., Hirose, K., Ohishi, Y., & Tatsumi, Y. (2010). The structure of iron in Earth's inner core. *Science*, *330*(6002), 359-361.

Zha, C. S., & Bassett, W. A. (2003). Internal resistive heating in diamond anvil cell for in situ X-ray diffraction and Raman scattering. *Review of scientific instruments*, *74*(3), 1255-1262.

©2019. Japan Geoscience Union. All Right Reserved.

Keywords: Internally resistive heated diamond anvil cell, high pressure-temperature experiments

©2019. Japan Geoscience Union. All Right Reserved.

Shear deformation on post-spinel

*Daisuke Yamazaki[1], Noriyoshi Tsujino[1], Yu Nishihara[2]

1. Institute for Planetary Materials, Okayama University, 2. GRC, Ehime University

Earth’ s lower mantle is mainly composed of ferro-periclase and bridgmanite. The viscosity of ferro-periclase is considered to be 2-3 orders of magnitude lower than that of bridgmanite. Such large discrepancy in viscosity may cause the significant effect of microstructure of the aggregate of bridgmanite and ferro-periclase on bulk viscosity. For example, bulk viscosity is low when the interconnected weak layer structure is formed, whereas bulk viscosity is as high as the viscosity of bridgmanite when the load bearing framework structure is formed [1].

Microstructural evolution from the load bearing framework structure to the interconnected weak layer structure in post-spinel phase (mixture of bridgmanite and ferro-periclase) during deformation was previously reported based on the rotational Drickamer apparatus [2]. This results suggests the important viscosity reduction during deformation in the lower mantle. We therefore considered that more detailed and precise experiments are necessary to discuss the lower mantle rheology quantitatively.

Deformation experiments under the lower mantle conditions can be conducted by using D111-type deformation Kawai-type high pressure apparatus. This apparatus was previously installed at UCL followed by PF-AR and Misasa. In this study, we use these apparatus for the deformation on post-spinel phase.

Starting material for deformation experiment was well-sintered aggregate of bridgmanite and ferro-periclase synthesized at 24 GPa and 1873 K. For the simple shear deformation, we used 45 degree cut design. In in-situ X-ray experiments at PF-AR, we used tapered and coned anvils for X-ray paths. On the other hand, in “quench” experiments at Misasa, we used a simple cubic anvils (TEL=2.0 mm). All deformation experiments were performed with constant D-rams displacement rate.
We deformed sample up to shear strain of ~0.8 with the 0.4 mm displacements of D-rams. SEM observation on the recovered sample by SEM shows that there is no significant evolution in microstructure, indicating that viscosity reduction is not expected with shear deformation to gamma~1. [1] D. Yamazaki, S. Karato: Am. Mineral., **86**, 385 (2001). [2] J. Girard et al.: Science, **351**, 144 (2016).

©2019. Japan Geoscience Union. All Right Reserved.

Lattice thermal conductivity of $CaSiO_3$ perovskite at high pressures and high temperatures

*Kotaro Onga[1], Kenji Ohta[1], Akira Hasegawa[1,2], Takashi Yagi[2], Kei Hirose[3,4], Yasuo Ohishi[5]

1. Department of Earth and Planetary Sciences, Tokyo Institute of Technology, 2. National Institute of Advanced Industrial Science and Technology, 3. Earth-Life Science Institute, Tokyo Institute of Technology, 4. Department of Earth and Planetary Science, The University of Tokyo, 5. Japan Synchrotron Radiation Research Institute

Laboratory measurements of thermal conductivity of deep Earth materials provide important information on the dynamics and thermal evolution of the mantle and the core. $CaSiO_3$ perovskite (CaPv) is a constituent of pyrolitic lower mantle and of the subducting oceanic crust at depth greater than 560 km. In recent years, there are many reports of the laboratory-based lower mantle thermal conductivity profiles, but the thermal conductivity of CaPv has never been measured and included in the models [1,2,3,4,5] . CaPv is an unquenchable high-pressure phase at ambient conditions, and temperature-induced structure change from tetragonal to cubic occurs at around 500 K [6]. Therefore, *in-situ* high pressure and temperature X-ray diffraction (XRD) and thermal conductivity measurements are required to determine the thermal conductivity of CaPv in the Earth’ s deep interior.
In this study, we determined the thermal conductivity of CaPv at about 50 GPa and high temperature to 1950 K by a combination of synchrotron XRD measurements and the pulsed light heating thermoreflectance technique. Based on our experimental results, we consider the effect of the presence of CaPv on the thermal conductivity of the pyrolitic lower mantle and the subducting oceanic crust.

Reference: [1] Manthilake, G. et al., *Proc National Acad Sci.* **108,** 17901–17904 (2011). [2] Ohta, K. et al., *Earth Planet Sc. Lett.* **349,**109–115 (2012). [3] Ohta, K. et al., *Earth Planet Sc. Lett.* **465,** 29–37 (2017). [4] Okuda, Y. et al., *Earth Planet Sc. Lett.* **474,** 25–31 (2017). [5] Hsieh, W.-P. et al., J. Geophys. Res. Solid Earth 122, 4900-4917 (2017). [6] Komabayashi, T. et al., *Earth Planet Sc. Lett.* **260,** 564–569 (2007).

Keywords: CaPv, thermal conductivity, lower mantle

©2019. Japan Geoscience Union. All Right Reserved.

Polycrystalline diamond sintered from ultradispersed nanodiamonds

*Masayuki Nishi[1,2], Koichiro Yamamoto[1], Youmo Zhou[1], Tetsuo Irifune[2,1]

1. Geodynamics Research Center, Ehime University, 2. Earth-Life Science Institute, Tokyo Institute of Technology

NPD is a binder-less nanodiamond aggregate (~50 nm) synthesized by direct conversion of graphite under high pressure and temperature [1]. Although NPD has extremely high hardness exceeding that of single-crystalline diamond, it is difficult to obtain the large size of the NPD above 1 cm^3, because extreme high pressure conditions are required. Here we show nanodiamond polyclystalline sintered from ultradispersive nanodiamond under relatively moderate pressure and temperature conditions.

We used a multi-anvil apparatus to sinter the nanodiamonds at 8-15 GPa and 1600-2300˚C, where the diamond is thermodynamically stabilized. The starting materials were enclosed in metal capsules. The microstructures and chemical compositions of the recovered samples were examined using a field-emission scanning electron microscope with energy-dispersive X-ray spectroscopy. Well-sintered polycrystalline were subjected to the Knoop indentation test to evaluate its hardness.

We succeeded in recovering the well-sintered polycrystalline diamonds with grain size of ~10-30 nm in some runs (Figure 1). Full width at half maximum of XRD peaks decreased with increasing temperature due to the grain growth of diamond particles. The color, hardness, and grain size of the sintered polycrystalline changed depending on the capsule materials as well as the pressure and temperature conditions. These features might be affected by the porosity, the grain size, and the impurities. Further studies are required to synthesize the polycrystalline with high hardness comparable to NPD.

References: [1] T. Irifune, A. Kurio, S. Sakamoto, T. Inoue, H. Sumiya., *Nature*, **421**, 599 (2003).

Keywords: multianvil apparatus, nanodiamond, NPD

©2019. Japan Geoscience Union. All Right Reserved.

Thermal conductivity measurements on iron and MgO periclase at high pressure and high temperature similar to the Earth’s mid-lower mantle conditions

*Akira Hasegawa[1,2], Kenji Ohta[2], Takashi Yagi[1], Kei Hirose[3,4]

1. National Institute of Advanced Industrial Science and Technology, 2. Tokyo Institude of Technology, 3. Earth-Life Science Institute, Tokyo Institude of Technology, 4. The University of Tokyo

The thermal transport properties of the Earth’s constituents are important information to constrain the thermal evolution and the heat budget of the Earth. In particular, the thermal conductivity of the core, the largest heat source of the Earth, and the lower mantle, occupying more than half the volume of the whole Earth, are indispensable.

In recent years, thermal conductivity measurement on the sample inside the diamond anvil cell has been carried out utilizing the thermoreflectance phenomenon, the reflectance of metal changes slightly due to the temperature perturbation of several kelvin (e.g. Hsieh et al., 2009 Phys Rev B; Yagi et al., 2011 Meas Sci Technol). However, the reported temperature condition is far from that in Earth’s interior.

In this study, we combined the pulsed light heating thermoreflectance method with high power CW laser heating to obtain the thermal conductivity of material *in-situ* at high pressures and temperatures. As a result of test measurement for Pt, we obtained thermal conductivities of Pt up to 60 GPa and 2000 K, which is in good agreement with the measured values using flash heating method in a laser heated diamond anvil cell (McWilliams et al., 2015 Phys Earth Planet In).

The thermal conductivities of iron and MgO periclase were measured up to 60 GPa and 1700 K with this developed system. We found that the obtained thermal conductivities of iron and MgO have negative temperature dependence, and are consistent with the literatures (Fe: Konôpková et al., 2016 Nature; Ohta et al., 2016 Nature, MgO; Manthilake et al., 2011 Proc National Acad Sci; Dekura and Tsuchiya, 2017 Phys Rev B). The newly developed system here would be a powerful tool to examine the thermal conductivity of Earth’s deep interior.

Keywords: thermal conductivity, laser heated diamond anvil cell, pulsed light heating thermoreflectance method, lower mantle, core

©2019. Japan Geoscience Union. All Right Reserved.

Azimuthal anisotropy in the lowermost mantle beneath Philippine from ScS-S times

*Satoru Tanaka[1]

1. Department of Deep Earth Structure and Dynamics Research Japan Agency for Marine-Earth Science and Technology

Introduction: Seismic anisotropy in the lowermost mantle has been detected by splitting of diffracted S and ScS phases, the discrepancy of shear wave splitting of SKS and SKKS, to date. In many cases, the propagation direction of such seismic waves is restricted due to the combination of sources and receivers. Thus, the azimuthal anisotropy using ray paths passing in multi-directions has been rarely discussed. Now, seismic networks and large-scale seismic arrays have been increasing especially in the eastern Asia where there are also many earthquakes. It is a good opportunity to examine an azimuthal variation of travel times passing through the outside of the Pacific Large Low Shear Velocity Province, where the existence of anisotropy in the lowermost mantle is expected.

Data and Method: I used the seismograms of earthquakes occurred in Mariana, east China, Indonesia, and Vanuatu that are record with the seismic stations belonging to IRIS GSN and PASSCAL, Thai Metrological Department, F-net, JISNET, NECESSArray. This geometry gives a good condition that the mid-points of seismic ray paths are located near Philippine with various azimuths.I measured ScS–S differential travel times using a waveform cross-correlation method, which can effectively cancel the heterogeneity in the crust and upper mantle and the uncertainty of hypocenters. The differential travel times are compared with theoretical travel times by PREM with correction of physical dispersion due to anelasticity for the typical period of 10 s, that for ellipticity of the Earth, finally I obtained about 500 residuals. Even though I used the differential travel times, the ScS–S residuals show the large scattering and the correlation with the residuals of S travel times are much larger than that of ScS phases. This means that the raw ScS–S residuals are affected by heterogeneity in the upper part of the lower mantle where only S waves are propagated. Thus, we applied the further corrections using 3D mantle heterogeneity models.

Results and Discussion: We used S-wave 3D models of S16U6L8, S4BL16, S40RTS, SEMUCB-WM, and a P-wave 3D model of GAP-P4 with conversion rate dlnVs/dlnVp=1.7. I found that the scatter of the ScS–S residuals are much improved and that the correlation coefficient between the residuals of ScS–S and ScS are increased and that between ScS–S and S are much reduced when the GAP-P4 model are used for the correction, probably due to its high spatial resolution in the upper lower mantle. As a result, only the ScS–S residuals corrected with the modified GAP-P4 can be used to infer seismic anisotropy in the lowermost mantle.

Then I fitted cos 2qand cos 4qcurves with least square to obtain the characteristics of the azimuthal variation of the ScS–S residuals, clearly indicating that cos 2qcomponent is significant with the fastest direction (the minimum ScS–S) is along ESE-WNW (N110˚E). This can be explained if [100] axis of post-perovskite is oriented vertically and the direction of [001] axis is ESE-WNW for the incident angle of 45˚. The S-wave fastest direction is nearly parallel to the plate motion directions of the Philippine Sea plate and Sunda block. The amplitude of the azimuthal variation in the ScS–S residual is ±1.1 s, which corresponds to 1.7 % anisotropy if we assume the D” thickness of 300 km based on the previous studies on the D” discontinuity.

©2019. Japan Geoscience Union. All Right Reserved.

Keywords: lowermost mantle, seismic anisotropy

©2019. Japan Geoscience Union. All Right Reserved.

Detailed 3-D S-velocity structure within D" at the western Pacific LLSVP margin: smaller scale plumes and paleoslabs

*Yuki Suzuki[1], Kenji Kawai[1], Robert J. Geller[1], Satoru Tanaka[2], Weerachai Siripuvaraporn[3], Songkhun Boonchaisuku[3], Noisagool Sutthipong[3], Yasushi Ishihara[2], Taweoon Kim, Koji MIYAKAWA[4], Nozomu Takeuchi[4]

1. The University of Tokyo, 2. Japan Agency for Marine-Earth Science and Technology, 3. Mahidol University, 4. Earthquake Research Institute, The University of Tokyo

Global tomographic models of shear velocity have shown two large-scale low shear velocity provinces (LLSVPs) in D″ beneath the Pacific and Africa. It has been controversial whether these LLSVPs are due to thermal effects, chemical effects, or their combination. The nature and origin of the LLSVPs are of fundamental importance since each of the proposed geodynamical scenarios carries different implications for the thermal, chemical and dynamical evolution of the Earth. Previous seismological studies based on travel-time analysis or forward modeling inferred a sharp-sided velocity contrast of the Pacific LLSVP beneath the western Pacific and suggested that the LLSVP is chemically distinct, although the suggested structures of the western edge of the Pacific LLSVP different from each other. To better understand the origin of LLSVPs, it is essential to infer the detailed three-dimensional (3-D) velocity structure within LLSVP beneath the western Pacific. We recently deployed a seismic array stations in Thailand (Thai Seismic Array—TSAR). We assemble waveforms recorded by TSAR as well as other networks such as TM, AU, MM, and MY, allowing us to sample a wider region than previous studies. We conducted waveform inversion using ~5,300 transverse component records of this dataset for the detailed 3-D shear velocity structure in the lowermost 400 km of the mantle beneath the western Pacific. The inferred model shows a low-velocity anomaly immediately above the core-mantle boundary (CMB) and high-velocity anomalies extending vertically from 400 km to the CMB. Taken into account the previous geodynamical simulation studies, the size of the inferred low velocity anomaly suggests a thermal plume rather than a chemical anomaly. The location of the high velocity anomaly in D″ is consistent with the paleo-Izanagi plate subduction boundary about 200 Ma. This implies that a cold paleo-slab produces the strong lateral velocity contrast at the western edge of the western Pacific LLSVP. Hence, we conclude that the western margin of the Pacific LLSVP and its sharp velocity boundary can be explained mainly by thermal effects, and this implies that the lowermost mantle would be well-mixed and the Pacific LLSVP would not be geochemical reservoir.

Keywords: D" region, Pacific LLSVP, Waveform Inversion, Thai Seismic Array (TSAR)

©2019. Japan Geoscience Union. All Right Reserved.

Possible interaction between the core and mantle inferred from a core surface flow model

*Masaki Matsushima[1]

1. Department of Earth and Planetary Sciences, School of Science, Tokyo Institute of Technology

Fluid flow in the Earth's liquid outer core is responsible for the dynamo action by which the geomagnetic field is generated and maintained. The fluid flow can be estimated from geomagnetic field data, such as spatial distribution of geomagnetic field and its temporal change referred to as secular variations. This implies that spatial and temporal variations of fluid flow in the core provide information on any interaction between the core and mantle. To investigate possible core-mantle interaction, a core surface flow model is obtained from a geomagnetic field model, COV-OBS.x1 (Gillet et al., 2015) using the method of Matsushima (2015). That is, inside a viscous boundary layer at the core-mantle boundary (CMB), magnetic diffusion is assumed to significantly contribute to temporal change of geomagnetic field, and the radial dependence of core flow is expressed in terms of a spiral similar to the Ekman spiral. Below the boundary layer, magnetic diffusion is neglected as in the frozen-flux approximation, and the tangentially magnetostrophic constraint is imposed on the flow.

Any inhomogeneous structure, such as temperature or heat flux, at the CMB is likely to have a strong effect on the core flow. The inhomogeneity successively influences the flow pattern. Therefore, average of fluid flow is expected to show possible core-mantle interaction. Hence, fluid flows inside and below the boundary layer are averaged over the time from 1840 to 2015 covered by the COV-OBS.x1 model. However, mean amplitudes of upwelling and downwelling flows as well as mean horizontal flows are found to be smaller than those at respective times. This result suggests that possible thermal heterogeneity due to the lowermost mantle structure has little effect on the core surface flow; that is, compositional convection is dominant in the Earth's outer core. It should be noted, however, that there is a noticeable upwelling flow corresponding to a counterclockwise vortex beneath the south of Africa, and that the location is just outside the tangent cylinder, an imaginary cylinder parallel to the rotational axis and attached to the equator of the inner core. This may indicate that the vortex corresponds to an edge of columnar convective motion, although the other edge in the northern hemisphere is unclear.

Keywords: core-mantle interaction, core surface flow

©2019. Japan Geoscience Union. All Right Reserved.

Determination of the noble gas partition coefficients between metal-silicate melts under high-pressure and high-temperature conditions

*Tomotaka Tanaka[1], Hideharu Kuwahara[2], Satoshi Kishi[1], Ryuichi Nomura[3], Kenji Mibe[5], Hiroyuki Kagi[4], Shigehiko Tateno[6], Hirochika Sumino[1]

1. Department of Basic Science, Graduate School of Arts and Sciences, The University of Tokyo , 2. Geodynamics Research Center, Ehime University, 3. Kyoto University, 4. Geochemical Research Center, Graduate School of Science, University of Tokyo, 5. Earthquake Research Institute, University of Tokyo, 6. Earth-Life Science Institute, Tokyo Institute of Technology

Analyses of ocean island basalts reveal a geochemical reservoir characterized by unradiogenic, “primordial” noble gas signatures (e.g., high $^{3}He/^{4}He$ and low $^{40}Ar/^{36}Ar$ ratios), likely residing in the deep mantle. There has been much debate about the area holding the “primordial” noble gases deep in the Earth (Porcelli & Ballentine, 2002), including that the “primordial” noble gasses have been retained in the deepest region of the mantle since 4.4 Ga (Mukhopadhyay, 2012), or in the core since the core-mantle separation (Trieloff & Kunz, 2005; Bouhifd et al., 2013). However, the validity of latter strongly depends on the quantity of noble gases the core incorporates during accretion and can hold in the present day.

In order to investigate noble gas partitioning behavior between the core and mantle, noble gases were dissolved into metal-silicate melts under high temperature and pressure conditions, and then the samples were quenched, recovered, and analyzed for noble gas concentrations. Sample synthesis was performed at the Geodynamics Research Center, Ehime University. Noble-gas doped silicate glass and iron were melted and equilibrated under high pressure and temperature (3-6 GPa, 1700 and 1800 ˚C) using a multianvil apparatus. The sample capsule was cut and the polished surface of the section was investigated with scanning electron microscope and Raman spectroscopy. The chemical compositions of silicate and metal phases were determined with electron microprobe. And then, the noble gases in the silicate phase were extracted by an ultraviolet laser ablation apparatus and analyzed using a noble gas mass spectrometer at the University of Tokyo.

From the Raman spectra, it was found that crystallization (clinopyroxene) had occurred in samples synthesized at pressures of 6 GPa or higher, indicating that the sample quenching was not enough rapid. There is a possibility that noble gas may not be contained much in the crystallized part because a previous study showed that noble gas content in pyroxene crystal is smaller than those in glass (melt) by about 10^{-4} (Heber *et al.*, 2007). The noble gas concentrations in silicate glass phase are fairly homogeneous, even where a crack is formed during quenching. In future we will measure the noble gases in the iron part and determine the partition coefficient of the noble gases.

References: Bouhifd et al, *Nature Geoscience*. **6**, 982-986, 2013; Mukhopadhyay, *Nature* **486**, 101-104, 2012; Porcelli & Ballentine, *Rev. Mineral. Geochem.* **47**, 411-480, 2002; Trieloff & Kunz, *Phys. Earth Planet. Inter.* **148**, 13-38, 2005; Herber *et al*, *Geochim. Cosmochim. Acta*. **71**, 1041-1061, 2007

©2019. Japan Geoscience Union. All Right Reserved.

Measurement of T-dependent electrical resistivity of solid and liquid Fe and Pt at fixed P

*Innocent Ezenwa[1], Takashi Yoshino[1]

1. Institute for Planetary Materials, Okayama University

Knowledge of the thermal and electrical conductivity of solid and liquid Fe and its relevant alloys at P and T conditions is essential for understanding the cooling history of planetary cores and modelling their dynamo. The general understanding of the electrical transport properties of the transition metals at lower P will perhaps give insight in understanding Fe behavior at the inaccessible planetary core conditions. Theoretical investigation has suggested that the electrical and thermal conductivity of solid and liquid Fe at Earth’ s core conditions are similar in value (Wagle and Steinle-Neumann, (2017). At ambient T, experimental investigation showed that hcp ε -phase of Fe becomes paramagnetic at ~18GPa while Pt is paramagnetic and crystalize fcc at ambient conditions. Since Fe and Pt have an unfilled *d*-band electronic structure and at high P both exhibits closed packed crystal structures, experimental determination of the transport properties of molten Pt at lower P conditions is important for understanding the behavior of molten Fe preceding ε -phase at ~80 GPa. We develop a technique and cell design for the investigation of the electrical resistivity of metals that keeps it free from contamination using multianvil press. And, we report measurements on Fe and Pt. The sample was kept pure by making the electrodes and the sample the same composition while the thermocouple (TC) is placed close to the sample and taking through the gasket. The major challenge of TC breakage during compression and/or heating was overcome by shielding the TC with a cylindrical hollow coiling ring made of the same composition as the TC leads. The use of current polarity reversal to eliminate biased voltage as deployed in previous studies was adopted. On Fe and Pt, resistivity increases and decreases with T and P respectively, was observed. On melting, Fe result at 3 GPa agrees with very recent data by Silber et al. (2018) which showed an increasing difference in the resistivity value of solid and liquid with increasing P. While, Pt resistivity at 3 GPa appears constant comparable to its 1 atm value.

Keywords: Electrical resistivity, Thermal Conductivity, Iron Fe

©2019. Japan Geoscience Union. All Right Reserved.

Ancient, highly depleted mantle constrained by Re-Os isotope and highly-siderophile element compositions of French Polynesian xenoliths

*Norikatsu Akizawa[1], Akira Ishikawa[2], Katsuhiko Suzuki[3], Tetsu Kogiso[4]

1. Atmosphere and Ocean Research Institute, The University of Tokyo, 2. Department of Earth and Planetary Sciences, Tokyo Institute of Technology, 3. Research and Development Center for Submarine Resources, Japan Agency for Marine-Earth Science and Technology (JAMSTEC), 4. Graduate School of Human and Environmental Studies, Kyoto University

Mantle xenoliths, which are fragmented mantle material trapped by ascending magma, can provide lithological and geochemical information of the inaccessible mantle. In order to better understand the lithological and geochemical characteristics of the mantle, we conducted extensive sampling of mantle xenoliths throughout French Polynesia archipelago: Tahiti, Moorea, and Rurutu islands. We collected a total of 42 mantle xenoliths: 1 lherzolite, 14 harzburgites, 22 dunites, 3 wehrlites, and 2 orthopyroxenites. Here, we present whole-rock rhenium-osmium isotope and highly-siderophile element (Os, Ir, Ru, Pt, Pd, and Re) compositions in addition to whole-rock major-element compositions. Osmium isotope ratio ($^{187}Os/^{188}Os$) of the mantle xenoliths ranges from 0.1172 to 0.1464, where the harzburgites show a statistical bimodal distribution with unradiogenic ($^{187}Os/^{188}Os < 0.125$) and radiogenic ($^{187}Os/^{188}Os > 0.125$) compositions. The harzburgites with unradiogenic $^{187}Os/^{188}Os$ are depleted with regards to whole-rock major-element compositions (< 1.22 wt% Al_2O_3), and chondrite-normalized patterns of highly-siderophile elements. Considering the lithological variation of the mantle xenoliths used herein, the mantle is considerably heterogeneous beneath French Polynesia archipelago. In particular, the contrasting isotopic compositions of the harzburgites suggest different mantle reservoirs with unradiogenic and radiogenic $^{187}Os/^{188}Os$ compositions. We propose a possibility that the harzburgites with unradiogenic $^{187}Os/^{188}Os$ are impinged mantle material beneath normal oceanic lithosphere due probably to ascending plumes.

Keywords: Harzburgite, Dunite, PGE, TIMS, ICP-MS, Whole-rock chemical composition

©2019. Japan Geoscience Union. All Right Reserved.

First-principles prediction of hydrogen partitioning between the core and mantle

*Atsuroh Ohba[1], Taku Tsuchiya[1]

1. Ehime University Geodynamics Research Center

Some recent studies have reported high-P,T hydrous minerals which are stable at the core mantle boundary (CMB) pressure (Sano et al., 2008; Ohhira et al., 2016; Nishi et al., 2017). In order to elucidate the water circulation in the Earth's interior, experiments on the reaction between iron and hydrous minerals or water were also conducted (Iizuka-Oku et al., 2016; Mao et al., 2018; Clesi et al., 2018). However, the partition of hydrogen reported is different in different studies. In this study, we try estimating hydrogen partitioning between molten silicate and liquid iron under the CMB conditions based on the first principles calculation method combined with thermodynamic integration similar to our previous study (Xiong et al., 2018). Here, we assume following the exchange reaction of water between liquid iron and molten silicate is expressed as follows
(16MgSiO3+H2O) + 50Fe ⇔16MgSiO3 + (50Fe+H2O)
as a first example with ensuring the charge neutrality. Here, reaction free energy is calculated by the thermodynamic integration molecular dynamics method (Taniuchi & Tsuchiya, 2018). In the moment, simulations suggest that water prefer liquid iron. Now, additional computations are ongoing for improving numerical accuracy. The mechanism dissolving water into liquid iron is also investigated.

©2019. Japan Geoscience Union. All Right Reserved.

Microvolume stable isotope measuremetns and its applicaiton for high-pressure high-temperature experimental run products

*Madhusoodhan Satish-Kumar[1], Shinnosuke Aoyama[1]

1. Department of Geology, Faculty of Science, Niigata University

Light elements are very important in deep earth processes. Its composition in the lower mantle and core is still not well constrained. Stable isotope composition can be effectively used as an independent proxy. Although isotope fractionation in the deep earth occur in a narrow range, the volume of light element content in the mantle and core are extremely high, which can effectively cause significant natural isotopic compositional variations. It is necessary to accurately measure the isotope composition accurately in micro to nanomole scales, because the high-pressure experimental run products are small in volume. Recent studies have predicted the presence of isotope fractionation even at lower mantle and core *P-T* conditions, especially in magma ocean environment and during the core segregation. Despite the necessity of the micro-volume stable isotope measurement, there is always a tradeoff between the accuracy and the sample size.

At Niigata University, a MAT-253 mass spectrometer (Thermo Fisher Scientific) was installed through the MEXT Grant-in-Aid for Scientific Research on Innovative Areas. Carbon and oxygen isotopic compositions are measured using $CO_2$and multiple sulfur isotopic composition are measured using SF_6gas. A new micro-volume inlet system was installed and fundamental parameters such as pressure effect and capillary flow effect were tested. Using the micro-volume inlet system the minimum volume required for analysis is 1 micro-mole sample gas, and the precession for carbon and oxygen isotopic composition are better than 0.1‰. The precession for sulfur isotopes is ±0.3‰ and ±0.01‰ (1s) for $\delta^{34}S$ and $D^{33}S$, respectively, based on the repeated analyses of standard Ag_2S (IAEA S-1).Multiple sulfur isotope measurement system consists of 1) curie point pyrolyzer for rapid conversion of small volume samples to SF_6gas, 2) vacuum line system for pumping out non-condensable gasses, 3) gas chromatograph for purifying the SF_6gas and 4) micro-volume inlet system for introduction of sample gas to ionization chamber.
Multiple sulfur isotope ratios experimental run products were measured using the new system. Metal phases were separated and sulfur was extracted using Cr(II) reduction method [6]. Preliminary results indicate that S isotope fractionations occur in the pressure range of 3–5 GPa, under high-temperature conditions corresponding to the magma ocean environment. The negative $\delta^{34}S$ of mantle, can hence be explained by sulfur isotope fractionation in a magma ocean environment. Sulfur isotope measurements were also carried out on granitoid samples from the Archean with sulfide sulfur showing positive $\delta^{34}S$ values. Mass independent isotope fractionation, expressed as $\Delta^{33}S$, was also observed, suggesting that sulfur in the mantle alone cannot explain these variations. The incorporation of surface sulfur from sedimentary rocks and seawater is proposed.

Keywords: HPHT experiments, Micro-volume stable isotope measurements, Sulfur isotopes

©2019. Japan Geoscience Union. All Right Reserved.

Electrical resistivity of hcp Fe-Si alloys at high pressure and temperature

*Hayato Inoue[1], Sho Suehiro[1], Kenji Ohta[1], Kei Hirose[2,3], Yasuo Ohishi[4]

1. Department of Earth and Planetary Sciences, Tokyo Institute of Technology, 2. Earth-Life Science Institute, Tokyo Institute of Technology, 3. Department of Earth and Planetary Science, The University of Tokyo, 4. Japan Synchrotron Radiation Research Institute

Silicon (Si) has been repeatedly suggested to be the major light element in the Earth’ s core that mainly consists of iron [1]. Alloying the light element(s) affects a variety of physical properties of iron. Electrical and thermal conductivities strongly constrain the dynamics and thermal evolution of Earth’ s core and these parameters are linked by the Wiedemann-Franz law ($\kappa = \sigma LT$; κ : thermal conductivity, σ : electrical conductivity, L: Lorenz number, T: absolute temperature). However, measurements of electrical and thermal conductivities under static condition at extremely high pressures (P) and temperature (T) are limited for pure iron [2], [3]. The estimates of the core conductivity considering the effect of light element(s) have been done based on the resistivity saturation model, but the validity of the model at the core condition is unclear [4], [5].
In this study, we examined electrical resistivity (the reciprocal of electrical conductivity) of Fe-2, 4 and 6.5 wt.%Si at high P-T conditions in an internally-heated diamond anvil cell (IHDAC) up to 99 GPa and 2910 K. Our results of electrical resistivity of hcp Fe-Si alloys showed its nonlinear temperature dependence, indicating the occurrence of the resistivity saturation. The resistivity saturation in Fe-Si alloys observed in this study supports the notion of high core conductivity and resulting molten lowermost mantle and young inner core.

References: [1] Poirier: *Phys. Earth Planet. Inter.* **85**, 319-337 (1994).;[2] Ohta et al.: *Nature* **534**, 95–98 (2016).;[3] Konôpková et al.: *Nature* **534**, 99–101 (2016).;[4] Gomi et al.: *Phys. Earth Planet. Inter.* **224**, 88–103 (2013).;[5] Gomi et al.: *Earth Planet. Sci. Lett.* **451**, 51–61 (2016).

Keywords: Electrical conductivity, Thermal conductivity, Earth's core

©2019. Japan Geoscience Union. All Right Reserved.

Electrical resistivity and thermal conductivity of fcc Fe: Implications for the Mercury's core

*Hitoshi Gomi[1], Takashi Yoshino[1]

1. Okayama University

The Mercury's magnetic field may be sustained by the geodynamo motion in the liquid Fe core. However, its strength is about 1% of that of Earth. This weak magnetic field may implies a partly stratified core. Gomi et al. (2013) pointed out that the geometry of the thermal stratification depends critically on the depth dependency of the thermal conductivity. In this study, we conducted first-principles calculations on the face-centered cubic (fcc) Fe to constrain the electrical resistivity and the thermal conductivity of the Mercury's core.

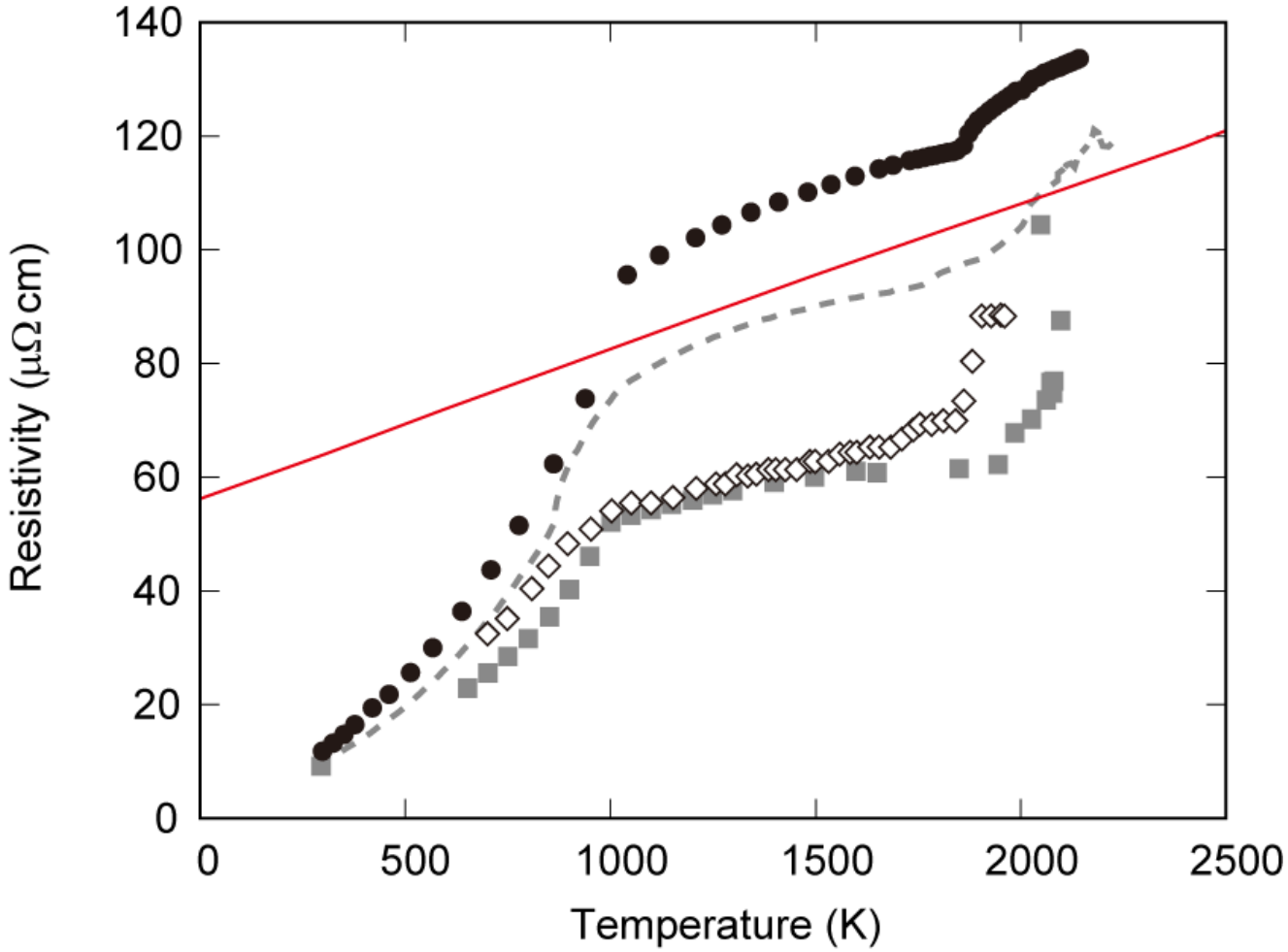
We calculated the electrical resistivity and the thermal conductivity of fcc Fe by means of the Korringa-Kohn-Rostoker method combined with the coherent potential approximation (KKR-CPA) (Akai, 1989). The CPA was adopted to treat the disorder effects due to the atomic vibrations and the magnetic fluctuations on the electronic band structure (Glasbrenner et al., 2014; Ebert et al., 2015; Kou and Akai, 2018). Within the alloy analogy model, the thermal atomic displacements were represented by a discrete set of N_v displacement vectors $\Delta R_v(T)$, where $|\Delta R_v(T)|=\sqrt{<u^2>}$ is the root mean square displacement of atoms, which is based on the Debye model without zero point vibration. The lattice parameter and the Debye temperature are obtained from the equation of state of fcc Fe (Tsujino et al., 2013). In addition to the non-magnetic state, the magnetic disorder was simulated by the local magnetic disorder (LMD) approach. The conductivity was calculated by the Kubo-Greenwood formula with the vertex correction.

The calculated electrical resistivities and thermal conductivities with LMD state are consistent with the literature data at 0 GPa (Ho et al., 1972; 1983), whereas the non-magnetic results show smaller resistivity and larger thermal conductivity. This suggests the importance of the magnetic scattering at low pressures. However, our calculation predicts that the magnetic contribution banishes at higher pressures than 20 GPa. Figure 1 compares the present results and previous experiments (gray broken line; Secco and Scholoessin, 1989, gray square; Deng et al., 2013, open diamond; Pommier, 2018, black circle; Silber et al., 2018) on the electrical resistivity at ~5 GPa. Note that, within the fcc stability field, previous measurements have a large variation. Our calculated resistivity values are between Secco and Scholoessin (1989) and Silber et al. (2018).

We further calculated the electrical resistivity and the thermal conductivity of fcc Fe up to 50 GPa and 3000 K. The thermal conductivity increases with increasing pressure and temperature. This means that, if the inner core is absent, the thermal stratification starts from the bottom, and, after the onset of the inner core, a thick thermal stratified layer may develop at the top of the fluid core (Gomi et al., 2013).

Keywords: electrical resistivity, thermal conductivity, Mercury, core, thermal stratification

©2019. Japan Geoscience Union. All Right Reserved.



©2019. Japan Geoscience Union. All Right Reserved.

Lateral heterogeneity in the lowermost outer core (F layer) of the Earth revealed by seismic analyses

*Toshiki Ohtaki[1], Satoshi Kaneshima[2], Taku Tsuchiya[3]

1. Geological Survey of Japan, National Institute of Advanced Industrial Science and Technology (AIST), 2. Department of Earth and Planetary Sciences, Kyushu University, 3. Geodynamics Research Center, Ehime University

We have determined seismic velocity structures of the lowermost outer core (F layer) beneath Northeast Pacific and Australia (Ohtaki and Kaneshima, 2015; Ohtaki et al., 2018), and found that the F layer is seismologically heterogeneous. These structures were obtained using a combination of two observations. First one is differential traveltimes between waves that reflect at the inner core boundary (ICB) and that graze the boundary; the second is dispersion (frequency dependence of velocity) of the grazing wave.

Our results show a somewhat strange velocity profile in the F layer beneath Australia, which has a lower-velocity-gradient layer than that of the Preliminary Reference Earth Model (PREM; Dziewonski and Anderson, 1981) on the ICB, and a higher-gradient layer just above the layer. Recent advance in high pressure research enables seismologists to translate lateral seismic velocity variation to relative chemical abundance in the outer core condition. Based on the results of Ichikawa and Tsuchiya (e.g., 2018), we showed light-element enrichment there. This result suggests that lighter fluid exists beneath Australia in the lowermost part of the liquid core, although the outer core is low-viscosity fluid.

The solid inner core of the Earth has quasi-hemispherical structure (e.g., Tanaka and Hamaguchi, 1997). As the origin of this hemispherical structure, uneven growth of the inner core has been proposed (e.g., Aubert et al., 2008; Alboussière et al., 2010; Monnereau et al., 2010). When the liquid in the outer core solidifies at the inner core surface, excess light element is partitioned to residue because the solid inner core is poorer in light elements compared with the liquid outer core. Thus, the uneven growth of the inner core is tied with an uneven release of the light elements to the F layer, which may be related to our results of the heterogeneous F layer. Then, a question arises: this heterogeneity has hemispherical structure like the inner core or local one?

We have not answered it yet because the survey areas of the above studies are restricted. Furthermore, other studies focusing F-layer velocity are not so many. Souriau (2015) determined lateral variations of velocity in the lower outer core using traveltimes of waves that turn there, and suggested that heterogeneity in F has degree-one feature. We also determined the seismic structure of the F layer beneath Antarctica using amplitude ratios between waves that turn just above the inner core and that get into the inner core. Although the resolution and reliability of structure obtained using amplitude ratios is lower than those using the method of our recent papers, the structure beneath Antarctica has a much lower velocity gradient in the F layer compared with PREM. Such a lower gradient is close to the model beneath Australia.

In this paper, we will show the summary of the heterogeneous F-layer structures of velocity and chemical abundance at this stage.

References

Alboussière, T., R. Deguen, and M. Melzani (2010), *Nature*, *466*, 744–747, doi:10.1038/nature09257.

©2019. Japan Geoscience Union. All Right Reserved.

Aubert, J., H. Amit, G. Hulot, and P. Olson (2008), *Nature*, *454*, 758–761, doi:10.1038/nature07109.
Dziewonski, A. M., and D. L. Anderson (1981), *Phys. Earth Planet. Inter.*, 25, 297–356, doi:10.1016/0031-9201(81)90046-7.
Monnereau, M., M. Calvet, L. Margerin, and A. Souriau (2010), *Science*, *328*, 1014–1017, doi:10.1126/science.1186212.
Ichikawa, H., and T. Tsuchiya (2018), J. Geography, 127, 631-646 (in Japanese with English abstract).
Ohtaki, T., S. Kaneshima, and K. Kanjo (2012), *J. Geophys. Res.*, 117, B03312, doi:10.1029/2011JB008717.
Ohtaki, T., and S. Kaneshima (2015), *J. Geophys. Res. Solid Earth*, 120, 7572–7586, doi:10.1002/2015JB012140.
Ohtaki, T., S. Kaneshima, H. Ichikawa, and T. Tsuchiya (2018), *J. Geophys. Res. Solid Earth*, doi:10.1029/2018JB015857.
Tanaka, S., and H. Hamaguchi (1997), *J. Geophys. Res.*, *102*, 2925–2938, doi:10.1029/96JB03187.

Keywords: F layer, lowermost outer core, Heterogeneity of the outer core, Light element concentration in the F layer beneath Australia

©2019. Japan Geoscience Union. All Right Reserved.

Flows and light element distribution in the outer core associated with heterogeneous growth of the inner core of the Earth

*Shin-ichi Takehiro[1], Youhei SASAKI[2]

1. Research Institute for Mathematical Sciences, Kyoto University, 2. Department of Mathematics, Kyoto University

Recent seismological observations suggest longitudinal heterogeneity of seismological wave velocity of the inner core of the Earth, which stimulates a discussion that phase change at the inner core boundary (ICB) does not occur uniformly in the horizontal directions. It is simply supposed from this suggestion that temperature is lower and concentration of light element is higher just above the solidification hemisphere at ICB, and vice versa. The heterogeneous structure of the inner core and thermodynamic properties just above ICB in the outer core is expected to be correlated, however, more recent analysis shows that distribution of seismological wave velocity anomaly does not correspond to longitudinal heterogeneity of the inner core.

There are two kinds of mechanisms explaining heterogeneous growth of the inner core. One of the mechanisms is that the heterogeneous thermal condition at the core mantle boundary (CMB) drives horizontal thermal convection which induces non-uniform temperature distribution at ICB. However, since this study uses co-density, which combines density variations by temperature and light element concentration, it cannot find distribution of the light elements just above ICB. Another mechanism is that hydrodynamic instability of the inner core surrounded by the phase boundary causes translational motion inside the inner core. However, since the theory assumes homogeneous light element distribution in the outer core, it is not clear this mechanism can explain the light element distribution above ICB.

In this study, by using a rotating spherical shell model in which temperature and light element concentration are independent variables, we perform numerical experiments of thermal and compositional convection related to two kinds of mechanisms. Obtained distributions of light element concentration are compared with the distribution of seismological wave velocity anomaly, and plausible dynamical regimes of thermal and compositional convection in the outer core are discussed.

Keywords: Heterogeneity, Inner core, Core-mantle boundary

©2019. Japan Geoscience Union. All Right Reserved.

Sharpness of the hemispherical boundary in the inner core beneath the northern Pacific

*Ryohei Iritani[1], Hitoshi Kawakatsu[1], Nozomu Takeuchi[1]

1. Earthquake Research Institute, Univ. of Tokyo

The hemispherical heterogeneity in the topmost of the Earth’ s inner core, faster velocity and higher attenuation in the eastern hemisphere and slower velocity and weaker attenuation in the western hemisphere, has been revealed by seismological studies. However, how the transition structure between two hemispheres looks like has not been known because of the difficulty to analyze complex core-sensitive data and the limitation of earthquake and seismic array distribution. In this study, we apply the array-based waveform inversion (Iritani et al., 2014) to core phase data that propagate beneath the northern Pacific, and investigate the nature of the transition structure in this region.Dataset used in this study consists of two directional event-station pairs, seismograms observed by the permanent European stations for events at Fiji-Tonga region, and USArray for events near Indonesia. We analyze the broadband vertical component of core phase data containing PKIKP and PKP phases (i.e. the epicentral distance between 145 –155 degree). Resultant analyzed waveforms for EU stations and USArray are 2,108 and 1,172 traces respectively.
In the analysis, waveform inversion approach is employed for each event data to measure traveltime and attenuation in the inner core. As a result, traveltime anomalies observed by EU stations show obvious positive anomaly suggesting mainly propagating the eastern hemisphere, while traveltimes observed by USAray show relatively smaller (or no) anomalies suggesting effects from both of hemispheres. On the other hand, attenuation parameters for both arrays show similar trend that suggests high attenuation corresponding to the eastern hemisphere. To investigate a hemispherical transition boundary in the sampled region, we conduct a ray theory based forward modeling of traveltimes by changing a shape of boundary from meridian boundary to eyeball shaped boundary, and its position. We compute root-mean-square (RMS) of residual between observations and theoretical traveltimes computed with each boundary model. Then, an eyeball shaped boundary, that is located at longitude of 158°W on the equatorial line and latitude of 80°N at the northernmost point, obtained as the preferred boundary model. Finally, we investigate a sharpness of the boundary by varying a width of hemispherical transition. We assume linear variation from the eastern and western hemisphere in a given width and compute RMS. As a result, a width of 600 km at the surface of the inner core shows smaller RMS than sharp boundary. Geophysical significance of this finding will be further discussed.

Keywords: Inner core, Waveform inversion

©2019. Japan Geoscience Union. All Right Reserved.

Stable carbon isotope fractionation in Fe-C system from first principles

*Haruhiko Dekura[1], Taku Tsuchiya[1]

1. Geodynamics Research Center, Ehime University

Carbon is the fourth most abundant element in the solar system and likely one of the constituent light elements in the Earth’s core. Determination of its equilibrium isotope fractionation factor (α) under high pressure (P) and temperature (T) is a key for understanding chemical evolution such as the whole Earth carbon distributions and the amount in the Earth’s core (e.g., Kumar et al., 2011). Because experimental measurement of the isotope fractionation remains technically challenging at the deep mantle condition, attempts to evaluate the α among mantle minerals by first-principles calculations have been made in recent years (e.g., Huang et al., 2014). Recently, our group initiated the theoretical determination of the α in the Fe-C system in the Earth’s deep interior with a full ab initio approach based on the density-functional theory. We performed ab initio lattice dynamics calculations for diamond and iron-carbide (hexagonal Fe7C3) having the two stable carbon isotopes (12C and 13C). The α between the two phases were then determined by using the Gibbs free energies calculated at P ~300 GPa and T ~2000-6000 K. The obtained $10^3 \ln \alpha$ dia-Fe7C3 is found to vary with T from ~+8‰ (2000 K) to ~+5‰ (6000 K). This result indicates that the Fe7C3 is enriched in the heavier isotope (13C) compared with diamond. This trend is qualitatively consistent with low-pressure experimental observations (Kumar et al., 2011).

Keywords: Isotope fractionation, First-principles calculation

©2019. Japan Geoscience Union. All Right Reserved.

[E] Poster | S (Solid Earth Sciences)：S-IT Science of the Earth's Interior & Techtonophysics

Mon. May 27, 2019 5:15 PM - 6:30 PM JST | Mon. May 27, 2019 8:15 AM - 9:30 AM UTC | Poster Hall International Exhibition Hall8, Makuhari Messe_22

[S-IT21] Interaction and Coevolution of the Core and Mantle in the Earth and Planets

convener:Kenji Kawai(Department of Earth and Planetary Science, School of Science, University of Tokyo), Tsuyoshi Iizuka(University of Tokyo), Kenji Ohta(Department of Earth and Planetary Sciences, Tokyo Institute of Technology), Taku Tsuchiya(Geodynamics Research Center, Ehime University)

Recent observational and experimental investigations have significantly advanced our understanding of the structure and constituent materials of the deep Earth. Yet, even fundamental properties intimately linked with formation and evolution of the planet, such as details of the chemical heterogeneity in the mantle and light elements dissolved in the core, remained unclear. Seismological evidence has suggested a vigorous convection in the lower mantle, whereas geochemistry has suggested the presence of stable regions there that hold ancient chemical signatures. The amounts of radioactive isotopes that act as heat sources and drive dynamic behaviors of the deep Earth are also still largely unknown. We provide an opportunity to exchange the achievements and ideas, and encourage persons who try to elucidate these unsolved issues of the core-mantle evolution using various methods, including high-pressure and high-temperature experiments, high-precision geochemical and paleomagnetic analyses, high-resolution geophysical observations, geo-neutrino observations, and large-scale numerical simulations. Papers stimulating an interdisciplinary collaboration relating to establishment of the Japan-SEDI community are also welcomed.

[SIT21-P01] Sample-scale compositional variation of the Inada granite, Ibaraki, Japan -toward the reduction of geoneutrino flux estimation errors from the Japanese crust-

★Invited Papers

*Kenta Ueki[1], Minami Kazuki[2], Tsuyoshi Iizuka[3], Sanshiro Enomoto[4], Hiroyuki Tanaka[2] (1.Japan Agency for Marine-Earth Science and Technology, 2.Earthquake Research Institute, University of Tokyo, 3.Department of Earth and Planetary Science, University of Tokyo, 4.Center for Experimental Nuclear Physics and Astrophysics, University of Washington)

[SIT21-P02] Towards a better estimation of the temperature distribution beneath the Japanese Islands

*Akiko Tanaka[1], Makoto Yamano[2], Hideki Hamamoto[3], Shusaku Goto[4], Takumi Matsumoto[5] (1.Geological Survey of Japan, National Institute of Advanced Industrial Science and Technology, 2.Earthquake Research Institute, The University of Tokyo, 3.Center for Environmental Science in Saitama, 4.Institute for Geo-Resources and Environment National Institute of Advanced Industrial Science and Technology, 5.National Research Institute for Earth Science and Disaster Resilience)

[SIT21-P03] The estimation of the neutrino flux from the crust of the Japanese islands using the geochemical database

*Satoru Haraguchi[1], Kenta Ueki[1], Hikaru Iwamori[1,2,3] (1.Japan Agency for Marine-Earth Science and Technology, 2.Earthquake Research Institute, the University of Tokyo, 3.Tokyo Institute of Technology)

[SIT21-P04] Viscosity of potassium titanosilicate melt at high pressure

*Akio Suzuki[1] (1.Department of Earth Science, Graduate School of Science, Tohoku University)

[SIT21-P05] Lattice thermal conductivity of wadsleyite and ringwoodite at the mantle transition zone pressures

*seiji kimura[1], Kenji Ohta[6], Takaaki Kawazoe[2], Kei Hirose[3], Hiroyuki Kagi[4], Takashi Yagi[5] (1.Department of Earth and Planetary Sciences Tokyo Institute of Technology, 2.Department of Earth and Planetary Systems Science, Hiroshima University, 3.Earth-Life Science Institute, Tokyo Institute of Technology, 4.Geochemical Research Center, Graduate School of Science, University of Tokyo, 5.National Institute of Advanced Industrial Science and Technology, 6.Department of Earth and Planetary Sciences, Tokyo Institute of Technology)

[SIT21-P06] In-situ X-ray observations of the olivine-spinel transformation under shear deformation: preliminary results on the reaction-induced weakening

*Tomoaki Kubo[1], Moriyama Kazuya[1], Yuichiro Mori[1], Masahiro Imamura[1], Sanae Koizumi[2], Yu Nishihara[3], Akio Suzuki[4], Yuji Higo[5] (1.Kyushu Univ., 2.ERI, 3.GRC Ehime Univ., 4.Tohoku Univ., 5.JASRI)

[SIT21-P07] Internally resistive heated diamond anvil cell experiments with metal encapsulated minerals

*YAMAMOTO TOMONARI[1], Kenji Ohta[1], Sho Suehiro[1], Hayato Inoue[1] (1.Tokyo Institute of Technology)

[SIT21-P08] Shear deformation on post-spinel

*Daisuke Yamazaki[1], Noriyoshi Tsujino[1], Yu Nishihara[2] (1.Institute for Planetary Materials, Okayama University, 2.GRC, Ehime University)

[SIT21-P09] **Lattice thermal conductivity of $CaSiO_3$ perovskite at high pressures and high temperatures**

*Kotaro Onga[1], Kenji Ohta[1], Akira Hasegawa[1,2], Takashi Yagi[2], Kei Hirose[3,4], Yasuo Ohishi[5] (1.Department of Earth and Planetary Sciences, Tokyo Institute of Technology, 2.National Institute of Advanced Industrial Science and Technology, 3.Earth-Life Science Institute, Tokyo Institute of Technology, 4.Department of Earth and Planetary Science, The University of Tokyo, 5.Japan Synchrotron Radiation Research Institute)

[SIT21-P10] **Polycrystalline diamond sintered from ultradispersed nanodiamonds**

*Masayuki Nishi[1,2], Koichiro Yamamoto[1], Youmo Zhou[1], Tetsuo Irifune[2,1] (1.Geodynamics Research Center, Ehime University, 2.Earth-Life Science Institute, Tokyo Institute of Technology)

[SIT21-P11] Thermal conductivity measurements on iron and MgO periclase at high pressure and high temperature similar to the Earth's mid-lower mantle conditions

*Akira Hasegawa[1,2], Kenji Ohta[2], Takashi Yagi[1], Kei Hirose[3,4] (1.National Institute of Advanced Industrial Science and Technology, 2.Tokyo Institude of Technology, 3.Earth-Life Science Institute, Tokyo Institude of Technology, 4.The University of Tokyo)

[SIT21-P12] Azimuthal anisotropy in the lowermost mantle beneath Philippine from ScS-S times

*Satoru Tanaka[1] (1.Department of Deep Earth Structure and Dynamics Research Japan Agency for Marine-Earth Science and Technology)

[SIT21-P13] Detailed 3-D S-velocity structure within D" at the western Pacific LLSVP margin: smaller scale plumes and paleoslabs

*Yuki Suzuki[1], Kenji Kawai[1], Robert J. Geller[1], Satoru Tanaka[2], Weerachai Siripuvaraporn[3], Songkhun Boonchaisuku[3], Noisagool Sutthipong[3], Yasushi Ishihara[2], Taweoon Kim, Koji MIYAKAWA[4], Nozomu Takeuchi[4] (1.The University of Tokyo, 2.Japan Agency for Marine-Earth Science and Technology, 3.Mahidol University, 4.Earthquake Research Institute, The University of Tokyo)

[SIT21-P14] Possible interaction between the core and mantle inferred from a core surface flow model

*Masaki Matsushima[1] (1.Department of Earth and Planetary Sciences, School of Science, Tokyo Institute of Technology)

[SIT21-P15] Determination of the noble gas partition coefficients between metal-silicate melts under high-pressure and high-temperature conditions

*Tomotaka Tanaka[1], Hideharu Kuwahara[2], Satoshi Kishi[1], Ryuichi Nomura[3], Kenji Mibe[5], Hiroyuki Kagi[4], Shigehiko Tateno[6], Hirochika Sumino[1] (1.Department of Basic Science, Graduate School of Arts and

Sciences, The University of Tokyo , 2.Geodynamics Research Center, Ehime University, 3.Kyoto University, 4.Geochemical Research Center, Graduate School of Science, University of Tokyo, 5.Earthquake Research Institute, University of Tokyo, 6.Earth-Life Science Institute, Tokyo Institute of Technology)

[SIT21-P16] **Measurement of T-dependent electrical resistivity of solid and liquid Fe and Pt at fixed P**

*Innocent Ezenwa[1], Takashi Yoshino[1] (1.Institute for Planetary Materials, Okayama University)

[SIT21-P17] Ancient, highly depleted mantle constrained by Re-Os isotope and highly-siderophile element compositions of French Polynesian xenoliths

*Norikatsu Akizawa[1], Akira Ishikawa[2], Katsuhiko Suzuki[3], Tetsu Kogiso[4] (1.Atmosphere and Ocean Research Institute, The University of Tokyo, 2.Department of Earth and Planetary Sciences, Tokyo Institute of Technology, 3.Research and Development Center for Submarine Resources, Japan Agency for Marine-Earth Science and Technology (JAMSTEC), 4.Graduate School of Human and Environmental Studies, Kyoto University)

[SIT21-P18] First-principles prediction of hydrogen partitioning between the core and mantle

*Atsuroh Ohba[1], Taku Tsuchiya[1] (1.Ehime University Geodynamics Research Center)

[SIT21-P19] Microvolume stable isotope measuremetns and its applicaiton for high-pressure high-temperature experimental run products

*Madhusoodhan Satish-Kumar[1], Shinnosuke Aoyama[1] (1.Department of Geology, Faculty of Science, Niigata University)

[SIT21-P20] Electrical resistivity of hcp Fe-Si alloys at high pressure and temperature

*Hayato Inoue[1], Sho Suehiro[1], Kenji Ohta[1], Kei Hirose[2,3], Yasuo Ohishi[4] (1.Department of Earth and Planetary Sciences, Tokyo Institute of Technology, 2.Earth-Life Science Institute, Tokyo Institute of Technology, 3.Department of Earth and Planetary Science, The University of Tokyo, 4.Japan Synchrotron Radiation Research Institute)

[SIT21-P21] Electrical resistivity and thermal conductivity of fcc Fe: Implications for the Mercury's core

★Invited Papers

*Hitoshi Gomi[1], Takashi Yoshino[1] (1.Okayama University)

[SIT21-P22] Lateral heterogeneity in the lowermost outer core (F layer) of the Earth revealed by seismic analyses

*Toshiki Ohtaki[1], Satoshi Kaneshima[2], Taku Tsuchiya[3] (1.Geological Survey of Japan, National Institute of Advanced Industrial Science and Technology (AIST), 2.Department of Earth and Planetary Sciences, Kyushu University, 3.Geodynamics Research Center, Ehime University)

[SIT21-P23] Flows and light element distribution in the outer core associated with heterogeneous growth of the inner core of the Earth

*Shin-ichi Takehiro[1], Youhei SASAKI[2] (1.Research Institute for Mathematical Sciences, Kyoto University, 2.Department of Mathematics, Kyoto University)

[SIT21-P24] Sharpness of the hemispherical boundary in the inner core beneath the northern Pacific

*Ryohei Iritani[1], Hitoshi Kawakatsu[1], Nozomu Takeuchi[1] (1.Earthquake Research Institute, Univ. of Tokyo)

[SIT21-P25] Stable carbon isotope fractionation in Fe-C system from first principles

*Haruhiko Dekura[1], Taku Tsuchiya[1] (1.Geodynamics Research Center, Ehime University)

Sample-scale compositional variation of the Inada granite, Ibaraki, Japan -toward the reduction of geoneutrino flux estimation errors from the Japanese crust-

*Kenta Ueki[1], Minami Kazuki[2], Tsuyoshi Iizuka[3], Sanshiro Enomoto[4], Hiroyuki Tanaka[2]

1. Japan Agency for Marine-Earth Science and Technology, 2. Earthquake Research Institute, University of Tokyo, 3. Department of Earth and Planetary Science, University of Tokyo, 4. Center for Experimental Nuclear Physics and Astrophysics, University of Washington

Geoneutrio observed at anti-neutrino observatory "KamLAND" in Kamioka (Hida City, Gifu Prefecture), enables us to directly observe the abundance of radiogenic elements in the deep earth. As crustal rocks exhibit a high concentration of geoneutrino producing radiogenic elements (Uranium and Thorium) than mantle rocks, we have to subtract the contribution of geoneutrino from the Japanese crust from the observation value in Kamioka to estimate geoneutrino flux from core and mantle. For the purpose, we estimated the 3D distribution of uranium and thorium in the Japanese crust by the stochastic modeling using the seismic velocity structure, geological information and geochemical database for the Japanese crustal rock. Geoneutrino flux calculated using the compositional map exhibits a very large error (up to 80%) at present.
We found that information on the compositional heterogeneity (spatial correlation) of various length scale, such as of the single rock suite scale (km to m scale), and sample scale (cm to mm scale) are essential to reduce the estimation error of crustal geoneutrino flux as small as the observation error of the geoneutrino on KamLAND. Therefore, we conducted a grid sampling of the granite of Inada, Ibaraki prefecture, to obtain quantitative knowledge on the small scale compositional heterogeneity. Samples (about 500g) were divided into several centimeter scale split (about 25g). Based on the compositional variations between small splits from one sample, we discuss the small scale sample wise compositional variation. Whole rock chemical composition of each small split was analyzed using XRF. Also, we conducted surface analysis using an ED-XRF to evaluate the spatial distribution of elements in each split. As a result, even within a single sample (about 500g), a compositional variation of about several% at maximum was observed. This result indicates that when conducting the analysis based on the rock chemical composition considering the spatial context, it is necessary to properly evaluate the sample scale heterogeneity, in addition to the tectonic scale, the rock suite scale, and microscopic scale.Also, this result will contribute to the reduction of the estimation error of geoneutrino from the Japanese crust.

Keywords: Geoneutrino, Granite, Rock chemical composition

©2019. Japan Geoscience Union. All Right Reserved.

Towards a better estimation of the temperature distribution beneath the Japanese Islands

*Akiko Tanaka[1], Makoto Yamano[2], Hideki Hamamoto[3], Shusaku Goto[4], Takumi Matsumoto[5]

1. Geological Survey of Japan, National Institute of Advanced Industrial Science and Technology, 2. Earthquake Research Institute, The University of Tokyo, 3. Center for Environmental Science in Saitama, 4. Institute for Geo-Resources and Environment National Institute of Advanced Industrial Science and Technology, 5. National Research Institute for Earth Science and Disaster Resilience

To improve our understanding of the thermal evolution and structure of the deep Earth, it is necessary to know the shallow part of them. Surface heat flow provides important constraint on it. However, the number of heat flow data is limited and spatially very inhomogeneous and even in regions with measurements the data quality varies. For this reason, we have been working on compiling a comprehensive database of heat flow, thermal conductivity, and geothermal gradient. In 2004, Geological Survey of Japan published a digital geoscience map entitled "Geothermal Gradient and Heat Flow Data in and around Japan", which contains heat flow data in the northwestern Pacific area (from 0 to 60°N and from 120 to 160°E) and geothermal gradient data in and around Japan. In 2019, we will be releasing database entitled "Thermal Data Collection in and around Japan", which contains continuously updated of geothermal gradient and heat flow data and adds thermal conductivity data in and around Japan. Thermal conductivity data were compiled from published data and site-specific reports, and measured using the archived cores. This database offers considerable improvements over the previous version released in 2004, and will be published and available at https://www.gsj.jp/en/database/db-portal/index.html. It presents an opportunity to revisit the thermal state of the lithosphere along with other geophysical/geochemical constraints on heat flow extrapolation.

Keywords: heat flow, thermal conductivity, geothermal gradient

©2019. Japan Geoscience Union. All Right Reserved.

The estimation of the neutrino flux from the crust of the Japanese islands using the geochemical database

*Satoru Haraguchi[1], Kenta Ueki[1], Hikaru Iwamori[1,2,3]

1. Japan Agency for Marine-Earth Science and Technology, 2. Earthquake Research Institute, the University of Tokyo, 3. Tokyo Institute of Technology

Geoneutrino observed at the anti-neutrino observatory "KamLAND" at Kamioka allows us to obtain information on the amount and distribution of radiogenic elements (uranium and thorium) in the deep mantle and crust.. It is necessary to divide the contribution from Japanese from the observed neutrino flux on closely to precisely estimate the quantity of U, Th of the earth deep earth because such radiogenic elements exhibit high concentration in the crust. Previous estimation of the crust origin geoneutrino was estimated based on the relatively simple chemical assumption on the compositional variation and spatial distribution. However, the radioactive elements of the Japanese crustal rock are distributed with very wide compositional range with complex spatial distribution. Therefore, it is necessary to estimate spatial distribution of radioactive element in the Japanese crust for the precisely measurement of geoneutrino from Japanese crust. In addition, petrogical and geochemical structure of the Japanese crust of are fundamental information for understanding seismic activity, volcanic activity and tectonism. The analysis of the spatial variation of the chemical composition of the Japanese Islands crust is important in discussing about the evolution history of the Japanese Islands and the chemical evolution in the subduction zone.

In this study, we utilize DODAI to improve the estimation error of geoneutrino from the Japanese crust (Takeuchi et al., 2019). We published the database “DODAI” which compiled geochemical data published by the Japanese domestic journals and bulletins in the journal of the Geological Society of Japan (Haraguchi et al., 2018). This database incorporates the precise sampling position of individual geochemical data using an electronic map. Resolution of the positional information were improved drastically.
The "DODAI" database covers whole area of Japanese Islands with highly precise positional information is useful for data analysis and modeling. The geochemistry database with highly precise positional information is useful for modeling of the geochemical structure of the solid earth. In this study, we present the potential of the DODAI database and geoneutrion in the analysis of the geochemical structures of Japanese crust, as well as the deep earth.

Keywords: neutrino, geochemical database, geochemical structure of crust and mantle

©2019. Japan Geoscience Union. All Right Reserved.

Viscosity of potassium titanosilicate melt at high pressure

*Akio Suzuki[1]

1. Department of Earth Science, Graduate School of Science, Tohoku University

Viscosity of silicate melt is a fundamental property, which controls volcanic processes, including rates of melt extraction, ascent, and magma mixing. Titanium oxide is contained less than 10 wt% in terrestrial magmatic liquids, however, some lunar magmas contains it over 10 wt%. The addition of titanium to silicate melt affects on the properties such as viscosity, density, and compressibility. Especially the pressure dependence of viscosity is of great interest, because magma is generated in the planetary interiors. The aim of this study is to measure the viscosity of K2TiSi4O11 melt at high pressures to estimate the influence of the pressure-induced structural change of melt.
We performed in situ falling sphere viscometry in the pressure range from 1.3 to 7.4 GPa, by using the MAX-III high pressure apparatus at BL14C2 and NE7A beamlines at Photon Factory in KEK, Tsukuba, Japan. A falling platinum sphere in the melt was monitored by using an X-ray CCD camera with a YAG:Ce fluorescence screen. We observed that the viscosity of KTS4 melt decreased up to 3.3 GPa. In contrast, the pressure dependence in viscosity was not observed above 3.3 GPa. Based on XANES spectra of K2TiSi4O11 glasses quenched under high pressure, Paris et al. (1994) showed that the coordination number of titanium increased with increasing pressure. The present study suggests that the melt becomes depolymerized by the coordination change of titanium under high pressure.

Keywords: magma, viscosity, high pressure

©2019. Japan Geoscience Union. All Right Reserved.

Lattice thermal conductivity of wadsleyite and ringwoodite at the mantle transition zone pressures

*seiji kimura[1], Kenji Ohta[6], Takaaki Kawazoe[2], Kei Hirose[3], Hiroyuki Kagi[4], Takashi Yagi[5]

1. Department of Earth and Planetary Sciences Tokyo Institute of Technology, 2. Department of Earth and Planetary Systems Science, Hiroshima University, 3. Earth-Life Science Institute, Tokyo Institute of Technology, 4. Geochemical Research Center, Graduate School of Science, University of Tokyo, 5. National Institute of Advanced Industrial Science and Technology, 6. Department of Earth and Planetary Sciences, Tokyo Institute of Technology

The lattice thermal conductivities of wadsleyite (Wd) and ringwoodite (Rw), which predominantly occupy the Earth's mantle transition zone, are important transport properties to understand the dynamics and thermal structure of the mantle. In particular, the temperature in the subducting slab is mainly controlled by the thermal conduction of Wd and Rw. Wd and Rw are both thought to preserve a large amount of hydrogen ions, thus should play an important role as the main water reservoir in the Earth. Furthermore, it has been reported that the hydration affects the physical properties of minerals including thermal conductivity, and it is necessary to measure the lattice thermal conductivity of Wd and Rw considering their water content. However, so far, the reported lattice thermal conductivities of Wd and Rw has not been considered their water content (Xu et al., 2004). Here we measured the room temperature lattice thermal conductivity of $(Mg_{0.89}Fe_{0.11})_2SiO_4$ Wd and $(Mg_{0.91}Fe_{0.09})_2SiO_4$ Rw up to 27 GPa, respectively, to clarify their hydration dependence using the pulsed light heating thermoreflectance technique in a diamond anvil cell.The obtained results show similar pressure dependence of the lattice thermal conductivity to the previous study (Xu et al., 2004). However, the absolute values of the thermal conductivity are different; the lattice conductivities of hydrous Wd and Rd are ~52% and ~40% lower than the results of Xu et al. (2004), respectively. Our results suggest strong water content dependence of lattice thermal conductivities of Wd and Rw, implying that the water content in the mantle minerals is key factor for calculating the thermal structure in a subducting slab, mantle dynamics.

Keywords: wadsleyite, ringwoodite, mantle transition zone, hydrous minerals, thermal conductivity

©2019. Japan Geoscience Union. All Right Reserved.

In-situ X-ray observations of the olivine-spinel transformation under shear deformation: preliminary results on the reaction-induced weakening

*Tomoaki Kubo[1], Moriyama Kazuya[1], Yuichiro Mori[1], Masahiro Imamura[1], Sanae Koizumi[2], Yu Nishihara[3], Akio Suzuki[4], Yuji Higo[5]

1. Kyushu Univ., 2. ERI, 3. GRC Ehime Univ., 4. Tohoku Univ., 5. JASRI

It has been suggested that high-pressure transformations cause rheological weakening and large deformation of subducting slabs in mantle transition zone (MTZ) . However, there have been few direct experimental evidences so far largely because of the difficulties in quantitative deformation experiments under such conitions. Here we report preliminary results on the olivine-spinel transformation experiments under shear deformation upto MTZ pressures. D-111 (DT-cup) type high-pressure deformation apparatus was newly used for this purpose combined with high-energy synchrotron mono X-rays (50-60 keV) at Photon Factory (PFAR NE7 beamline), which enables in-situ observations of interactions between transformation and creep behaviors. Sintered Mg_2SiO_4 forsterite was first deformed at 15-25 GPa at 600˚C in shear, and subsequently heated to higher temperatures (~0.2˚C/s) to cause the olivine-spinel transformation under shear deformation. The transformation started at much lower temperatures under shear deformation (~900-1100˚C depending on the overpressure from the phase boundary) compared to that without deformation (~1400˚C), suggesting that the shear deformation enhances the olivine-spinel transition rate. The shear strain rate in the sample monitored by X-ray radiography was ~3-4 x 10^{-6} (s^{-1}) at 600˚C, and increased up to ~2-3 x 10^{-4} (s^{-1}) with ramping temperatures even keeping the anvil displacement rate constant (200 micron/h). We observed that the shear weakening does not occur at the same temperature, but reflects on the initiation of the olivine transition. Also, the weakening effects become significant at larger overpressures (and low T). This implies that the weakening of the shear zone induced by the grain-size reduction due to the olivine-spinel transition, however further evidences from microstructural observations are necessary. We plan to install 8-ch acoustic emission measurement system attached with D-111 apparatus to capture the transformation-induced shear instabitiy. Results of D-DIA shear deformation study on the olivine-spinel transition in Fe_2SiO_4 will also be presented and compared with those of the D-111 study in Mg_2SiO_4 .

©2019. Japan Geoscience Union. All Right Reserved.

Internally resistive heated diamond anvil cell experiments with metal encapsulated minerals

*YAMAMOTO TOMONARI[1], Kenji Ohta[1], Sho Suehiro[1], Hayato Inoue[1]

1. Tokyo Institute of Technology

Heating technique is crucial for *in-situ* high pressure-temperature (*P-T*) studies into the physical and chemical properties of minerals in the diamond anvil cell (DAC) under deep Earth's conditions. External resistive heating methods that use resistive heaters such as AlChrom-O wire and graphite surrounding the DAC or just the diamonds (Dubrovinskaia and Dubrovinsky, 2003; Du et al., 2013). This approach creates a homogeneous temperature field in the sample chamber but limits the maximum temperature of about 1200℃ due to graphitization of diamond anvils. Double-sided laser heating with a DAC generates the *P-T* conditions corresponding to the center of the Earth's (Tateno et al., 2010). However, tightly focused laser beams, instabilities in output laser power and misalignment of the focused beams on the sample surface result in significant temperature variation within the sample in the DAC. Internally resistive heated DAC is an effective heating method to overcome the temperature limitation of external heated DAC and the significant temperature gradients experienced in conventional laser-heated DAC (e.g., Zha and Bassett, 2003). However, the internally resistive heated DAC is mostly applied to metal sample to study the properties of the planetary metallic core despite this technique could be applicable to an insulating mineral.

In this study, we modified the internally resistive heated DAC technique for nonmetallic material. We developed a microfabrication technique for total metal encapsulation of the nonmetallic sample. The sample encapsulated by platinum was loaded in DAC with thermal insulator and connected with two electrical leads to make electrical circuit for resistive heating. We confirmed very stable and homogeneous heating for insulating sample at 30 GPa to 2450 K in the modified internally resistive heated DAC. The highest temperature which this method can generate depends on the metal heater encapsulating the sample. This method offers a larger heating volume with more stable and uniform temperature than laser heating and at temperatures much greater than those that can be generated by external resistive heating methods.

References

Dubrovinskaia, N., & Dubrovinsky, L. (2003). Whole-cell heater for the diamond anvil cell. *Review of Scientific Instruments*, *74*(7), 3433-3437.

Du, Z., Miyagi, L., Amulele, G., & Lee, K. K. (2013). Efficient graphite ring heater suitable for diamond-anvil cells to 1300 K. *Review of Scientific Instruments*, *84*(2), 024502.

Tateno, S., Hirose, K., Ohishi, Y., & Tatsumi, Y. (2010). The structure of iron in Earth's inner core. *Science*, *330*(6002), 359-361.

Zha, C. S., & Bassett, W. A. (2003). Internal resistive heating in diamond anvil cell for in situ X-ray diffraction and Raman scattering. *Review of scientific instruments*, *74*(3), 1255-1262.

©2019. Japan Geoscience Union. All Right Reserved.

Keywords: Internally resistive heated diamond anvil cell, high pressure-temperature experiments

©2019. Japan Geoscience Union. All Right Reserved.

Shear deformation on post-spinel

*Daisuke Yamazaki[1], Noriyoshi Tsujino[1], Yu Nishihara[2]

1. Institute for Planetary Materials, Okayama University, 2. GRC, Ehime University

Earth’ s lower mantle is mainly composed of ferro-periclase and bridgmanite. The viscosity of ferro-periclase is considered to be 2-3 orders of magnitude lower than that of bridgmanite. Such large discrepancy in viscosity may cause the significant effect of microstructure of the aggregate of bridgmanite and ferro-periclase on bulk viscosity. For example, bulk viscosity is low when the interconnected weak layer structure is formed, whereas bulk viscosity is as high as the viscosity of bridgmanite when the load bearing framework structure is formed [1].

Microstructural evolution from the load bearing framework structure to the interconnected weak layer structure in post-spinel phase (mixture of bridgmanite and ferro-periclase) during deformation was previously reported based on the rotational Drickamer apparatus [2]. This results suggests the important viscosity reduction during deformation in the lower mantle. We therefore considered that more detailed and precise experiments are necessary to discuss the lower mantle rheology quantitatively.

Deformation experiments under the lower mantle conditions can be conducted by using D111-type deformation Kawai-type high pressure apparatus. This apparatus was previously installed at UCL followed by PF-AR and Misasa. In this study, we use these apparatus for the deformation on post-spinel phase.

Starting material for deformation experiment was well-sintered aggregate of bridgmanite and ferro-periclase synthesized at 24 GPa and 1873 K. For the simple shear deformation, we used 45 degree cut design. In in-situ X-ray experiments at PF-AR, we used tapered and coned anvils for X-ray paths. On the other hand, in “quench” experiments at Misasa, we used a simple cubic anvils (TEL=2.0 mm). All deformation experiments were performed with constant D-rams displacement rate.
We deformed sample up to shear strain of ~0.8 with the 0.4 mm displacements of D-rams. SEM observation on the recovered sample by SEM shows that there is no significant evolution in microstructure, indicating that viscosity reduction is not expected with shear deformation to gamma~1. [1] D. Yamazaki, S. Karato: Am. Mineral., **86**, 385 (2001). [2] J. Girard et al.: Science, **351**, 144 (2016).

©2019. Japan Geoscience Union. All Right Reserved.

Lattice thermal conductivity of $CaSiO_3$ perovskite at high pressures and high temperatures

*Kotaro Onga[1], Kenji Ohta[1], Akira Hasegawa[1,2], Takashi Yagi[2], Kei Hirose[3,4], Yasuo Ohishi[5]

1. Department of Earth and Planetary Sciences, Tokyo Institute of Technology, 2. National Institute of Advanced Industrial Science and Technology, 3. Earth-Life Science Institute, Tokyo Institute of Technology, 4. Department of Earth and Planetary Science, The University of Tokyo, 5. Japan Synchrotron Radiation Research Institute

Laboratory measurements of thermal conductivity of deep Earth materials provide important information on the dynamics and thermal evolution of the mantle and the core. $CaSiO_3$ perovskite (CaPv) is a constituent of pyrolitic lower mantle and of the subducting oceanic crust at depth greater than 560 km. In recent years, there are many reports of the laboratory-based lower mantle thermal conductivity profiles, but the thermal conductivity of CaPv has never been measured and included in the models [1,2,3,4,5] . CaPv is an unquenchable high-pressure phase at ambient conditions, and temperature-induced structure change from tetragonal to cubic occurs at around 500 K [6]. Therefore, *in-situ* high pressure and temperature X-ray diffraction (XRD) and thermal conductivity measurements are required to determine the thermal conductivity of CaPv in the Earth’ s deep interior.
In this study, we determined the thermal conductivity of CaPv at about 50 GPa and high temperature to 1950 K by a combination of synchrotron XRD measurements and the pulsed light heating thermoreflectance technique. Based on our experimental results, we consider the effect of the presence of CaPv on the thermal conductivity of the pyrolitic lower mantle and the subducting oceanic crust.

Reference: [1] Manthilake, G. et al., *Proc National Acad Sci.* **108,** 17901–17904 (2011). [2] Ohta, K. et al., *Earth Planet Sc. Lett.* **349,**109–115 (2012). [3] Ohta, K. et al., *Earth Planet Sc. Lett.* **465,** 29–37 (2017). [4] Okuda, Y. et al., *Earth Planet Sc. Lett.* **474,** 25–31 (2017). [5] Hsieh, W.-P. et al., J. Geophys. Res. Solid Earth 122, 4900-4917 (2017). [6] Komabayashi, T. et al., *Earth Planet Sc. Lett.* **260,** 564–569 (2007).

Keywords: CaPv, thermal conductivity, lower mantle

©2019. Japan Geoscience Union. All Right Reserved.

Polycrystalline diamond sintered from ultradispersed nanodiamonds

*Masayuki Nishi[1,2], Koichiro Yamamoto[1], Youmo Zhou[1], Tetsuo Irifune[2,1]

1. Geodynamics Research Center, Ehime University, 2. Earth-Life Science Institute, Tokyo Institute of Technology

NPD is a binder-less nanodiamond aggregate (~50 nm) synthesized by direct conversion of graphite under high pressure and temperature [1]. Although NPD has extremely high hardness exceeding that of single-crystalline diamond, it is difficult to obtain the large size of the NPD above 1 cm^3, because extreme high pressure conditions are required. Here we show nanodiamond polyclystalline sintered from ultradispersive nanodiamond under relatively moderate pressure and temperature conditions.

We used a multi-anvil apparatus to sinter the nanodiamonds at 8-15 GPa and 1600-2300˚C, where the diamond is thermodynamically stabilized. The starting materials were enclosed in metal capsules. The microstructures and chemical compositions of the recovered samples were examined using a field-emission scanning electron microscope with energy-dispersive X-ray spectroscopy. Well-sintered polycrystalline were subjected to the Knoop indentation test to evaluate its hardness.

We succeeded in recovering the well-sintered polycrystalline diamonds with grain size of ~10-30 nm in some runs (Figure 1). Full width at half maximum of XRD peaks decreased with increasing temperature due to the grain growth of diamond particles. The color, hardness, and grain size of the sintered polycrystalline changed depending on the capsule materials as well as the pressure and temperature conditions. These features might be affected by the porosity, the grain size, and the impurities. Further studies are required to synthesize the polycrystalline with high hardness comparable to NPD.

References: [1] T. Irifune, A. Kurio, S. Sakamoto, T. Inoue, H. Sumiya., *Nature*, **421**, 599 (2003).

Keywords: multianvil apparatus, nanodiamond, NPD

©2019. Japan Geoscience Union. All Right Reserved.

Thermal conductivity measurements on iron and MgO periclase at high pressure and high temperature similar to the Earth’s mid-lower mantle conditions

*Akira Hasegawa[1,2], Kenji Ohta[2], Takashi Yagi[1], Kei Hirose[3,4]

1. National Institute of Advanced Industrial Science and Technology, 2. Tokyo Institude of Technology, 3. Earth-Life Science Institute, Tokyo Institude of Technology, 4. The University of Tokyo

The thermal transport properties of the Earth’s constituents are important information to constrain the thermal evolution and the heat budget of the Earth. In particular, the thermal conductivity of the core, the largest heat source of the Earth, and the lower mantle, occupying more than half the volume of the whole Earth, are indispensable.

In recent years, thermal conductivity measurement on the sample inside the diamond anvil cell has been carried out utilizing the thermoreflectance phenomenon, the reflectance of metal changes slightly due to the temperature perturbation of several kelvin (e.g. Hsieh et al., 2009 Phys Rev B; Yagi et al., 2011 Meas Sci Technol). However, the reported temperature condition is far from that in Earth’s interior.

In this study, we combined the pulsed light heating thermoreflectance method with high power CW laser heating to obtain the thermal conductivity of material *in-situ* at high pressures and temperatures. As a result of test measurement for Pt, we obtained thermal conductivities of Pt up to 60 GPa and 2000 K, which is in good agreement with the measured values using flash heating method in a laser heated diamond anvil cell (McWilliams et al., 2015 Phys Earth Planet In).

The thermal conductivities of iron and MgO periclase were measured up to 60 GPa and 1700 K with this developed system. We found that the obtained thermal conductivities of iron and MgO have negative temperature dependence, and are consistent with the literatures (Fe: Konôpková et al., 2016 Nature; Ohta et al., 2016 Nature, MgO; Manthilake et al., 2011 Proc National Acad Sci; Dekura and Tsuchiya, 2017 Phys Rev B). The newly developed system here would be a powerful tool to examine the thermal conductivity of Earth’s deep interior.

Keywords: thermal conductivity, laser heated diamond anvil cell, pulsed light heating thermoreflectance method, lower mantle, core

©2019. Japan Geoscience Union. All Right Reserved.

Azimuthal anisotropy in the lowermost mantle beneath Philippine from ScS-S times

*Satoru Tanaka[1]

1. Department of Deep Earth Structure and Dynamics Research Japan Agency for Marine-Earth Science and Technology

Introduction: Seismic anisotropy in the lowermost mantle has been detected by splitting of diffracted S and ScS phases, the discrepancy of shear wave splitting of SKS and SKKS, to date. In many cases, the propagation direction of such seismic waves is restricted due to the combination of sources and receivers. Thus, the azimuthal anisotropy using ray paths passing in multi-directions has been rarely discussed. Now, seismic networks and large-scale seismic arrays have been increasing especially in the eastern Asia where there are also many earthquakes. It is a good opportunity to examine an azimuthal variation of travel times passing through the outside of the Pacific Large Low Shear Velocity Province, where the existence of anisotropy in the lowermost mantle is expected.

Data and Method: I used the seismograms of earthquakes occurred in Mariana, east China, Indonesia, and Vanuatu that are record with the seismic stations belonging to IRIS GSN and PASSCAL, Thai Metrological Department, F-net, JISNET, NECESSArray. This geometry gives a good condition that the mid-points of seismic ray paths are located near Philippine with various azimuths.I measured ScS–S differential travel times using a waveform cross-correlation method, which can effectively cancel the heterogeneity in the crust and upper mantle and the uncertainty of hypocenters. The differential travel times are compared with theoretical travel times by PREM with correction of physical dispersion due to anelasticity for the typical period of 10 s, that for ellipticity of the Earth, finally I obtained about 500 residuals. Even though I used the differential travel times, the ScS–S residuals show the large scattering and the correlation with the residuals of S travel times are much larger than that of ScS phases. This means that the raw ScS–S residuals are affected by heterogeneity in the upper part of the lower mantle where only S waves are propagated. Thus, we applied the further corrections using 3D mantle heterogeneity models.

Results and Discussion: We used S-wave 3D models of S16U6L8, S4BL16, S40RTS, SEMUCB-WM, and a P-wave 3D model of GAP-P4 with conversion rate dlnVs/dlnVp=1.7. I found that the scatter of the ScS–S residuals are much improved and that the correlation coefficient between the residuals of ScS–S and ScS are increased and that between ScS–S and S are much reduced when the GAP-P4 model are used for the correction, probably due to its high spatial resolution in the upper lower mantle. As a result, only the ScS–S residuals corrected with the modified GAP-P4 can be used to infer seismic anisotropy in the lowermost mantle.

Then I fitted cos 2qand cos 4qcurves with least square to obtain the characteristics of the azimuthal variation of the ScS–S residuals, clearly indicating that cos 2qcomponent is significant with the fastest direction (the minimum ScS–S) is along ESE-WNW (N110˚E). This can be explained if [100] axis of post-perovskite is oriented vertically and the direction of [001] axis is ESE-WNW for the incident angle of 45˚. The S-wave fastest direction is nearly parallel to the plate motion directions of the Philippine Sea plate and Sunda block. The amplitude of the azimuthal variation in the ScS–S residual is ±1.1 s, which corresponds to 1.7 % anisotropy if we assume the D” thickness of 300 km based on the previous studies on the D” discontinuity.

©2019. Japan Geoscience Union. All Right Reserved.

Keywords: lowermost mantle, seismic anisotropy

©2019. Japan Geoscience Union. All Right Reserved.

Detailed 3-D S-velocity structure within D" at the western Pacific LLSVP margin: smaller scale plumes and paleoslabs

*Yuki Suzuki[1], Kenji Kawai[1], Robert J. Geller[1], Satoru Tanaka[2], Weerachai Siripuvaraporn[3], Songkhun Boonchaisuku[3], Noisagool Sutthipong[3], Yasushi Ishihara[2], Taweoon Kim, Koji MIYAKAWA[4], Nozomu Takeuchi[4]

1. The University of Tokyo, 2. Japan Agency for Marine-Earth Science and Technology, 3. Mahidol University, 4. Earthquake Research Institute, The University of Tokyo

Global tomographic models of shear velocity have shown two large-scale low shear velocity provinces (LLSVPs) in D″ beneath the Pacific and Africa. It has been controversial whether these LLSVPs are due to thermal effects, chemical effects, or their combination. The nature and origin of the LLSVPs are of fundamental importance since each of the proposed geodynamical scenarios carries different implications for the thermal, chemical and dynamical evolution of the Earth. Previous seismological studies based on travel-time analysis or forward modeling inferred a sharp-sided velocity contrast of the Pacific LLSVP beneath the western Pacific and suggested that the LLSVP is chemically distinct, although the suggested structures of the western edge of the Pacific LLSVP different from each other. To better understand the origin of LLSVPs, it is essential to infer the detailed three-dimensional (3-D) velocity structure within LLSVP beneath the western Pacific. We recently deployed a seismic array stations in Thailand (Thai Seismic Array—TSAR). We assemble waveforms recorded by TSAR as well as other networks such as TM, AU, MM, and MY, allowing us to sample a wider region than previous studies. We conducted waveform inversion using ~5,300 transverse component records of this dataset for the detailed 3-D shear velocity structure in the lowermost 400 km of the mantle beneath the western Pacific. The inferred model shows a low-velocity anomaly immediately above the core-mantle boundary (CMB) and high-velocity anomalies extending vertically from 400 km to the CMB. Taken into account the previous geodynamical simulation studies, the size of the inferred low velocity anomaly suggests a thermal plume rather than a chemical anomaly. The location of the high velocity anomaly in D″ is consistent with the paleo-Izanagi plate subduction boundary about 200 Ma. This implies that a cold paleo-slab produces the strong lateral velocity contrast at the western edge of the western Pacific LLSVP. Hence, we conclude that the western margin of the Pacific LLSVP and its sharp velocity boundary can be explained mainly by thermal effects, and this implies that the lowermost mantle would be well-mixed and the Pacific LLSVP would not be geochemical reservoir.

Keywords: D" region, Pacific LLSVP, Waveform Inversion, Thai Seismic Array (TSAR)

©2019. Japan Geoscience Union. All Right Reserved.

Possible interaction between the core and mantle inferred from a core surface flow model

*Masaki Matsushima[1]

1. Department of Earth and Planetary Sciences, School of Science, Tokyo Institute of Technology

Fluid flow in the Earth's liquid outer core is responsible for the dynamo action by which the geomagnetic field is generated and maintained. The fluid flow can be estimated from geomagnetic field data, such as spatial distribution of geomagnetic field and its temporal change referred to as secular variations. This implies that spatial and temporal variations of fluid flow in the core provide information on any interaction between the core and mantle. To investigate possible core-mantle interaction, a core surface flow model is obtained from a geomagnetic field model, COV-OBS.x1 (Gillet et al., 2015) using the method of Matsushima (2015). That is, inside a viscous boundary layer at the core-mantle boundary (CMB), magnetic diffusion is assumed to significantly contribute to temporal change of geomagnetic field, and the radial dependence of core flow is expressed in terms of a spiral similar to the Ekman spiral. Below the boundary layer, magnetic diffusion is neglected as in the frozen-flux approximation, and the tangentially magnetostrophic constraint is imposed on the flow.

Any inhomogeneous structure, such as temperature or heat flux, at the CMB is likely to have a strong effect on the core flow. The inhomogeneity successively influences the flow pattern. Therefore, average of fluid flow is expected to show possible core-mantle interaction. Hence, fluid flows inside and below the boundary layer are averaged over the time from 1840 to 2015 covered by the COV-OBS.x1 model. However, mean amplitudes of upwelling and downwelling flows as well as mean horizontal flows are found to be smaller than those at respective times. This result suggests that possible thermal heterogeneity due to the lowermost mantle structure has little effect on the core surface flow; that is, compositional convection is dominant in the Earth's outer core. It should be noted, however, that there is a noticeable upwelling flow corresponding to a counterclockwise vortex beneath the south of Africa, and that the location is just outside the tangent cylinder, an imaginary cylinder parallel to the rotational axis and attached to the equator of the inner core. This may indicate that the vortex corresponds to an edge of columnar convective motion, although the other edge in the northern hemisphere is unclear.

Keywords: core-mantle interaction, core surface flow

©2019. Japan Geoscience Union. All Right Reserved.

Determination of the noble gas partition coefficients between metal-silicate melts under high-pressure and high-temperature conditions

*Tomotaka Tanaka[1], Hideharu Kuwahara[2], Satoshi Kishi[1], Ryuichi Nomura[3], Kenji Mibe[5], Hiroyuki Kagi[4], Shigehiko Tateno[6], Hirochika Sumino[1]

1. Department of Basic Science, Graduate School of Arts and Sciences, The University of Tokyo , 2. Geodynamics Research Center, Ehime University, 3. Kyoto University, 4. Geochemical Research Center, Graduate School of Science, University of Tokyo, 5. Earthquake Research Institute, University of Tokyo, 6. Earth-Life Science Institute, Tokyo Institute of Technology

Analyses of ocean island basalts reveal a geochemical reservoir characterized by unradiogenic, “primordial” noble gas signatures (e.g., high $^{3}He/^{4}He$ and low $^{40}Ar/^{36}Ar$ ratios), likely residing in the deep mantle. There has been much debate about the area holding the “primordial” noble gases deep in the Earth (Porcelli & Ballentine, 2002), including that the “primordial” noble gasses have been retained in the deepest region of the mantle since 4.4 Ga (Mukhopadhyay, 2012), or in the core since the core-mantle separation (Trieloff & Kunz, 2005; Bouhifd et al., 2013). However, the validity of latter strongly depends on the quantity of noble gases the core incorporates during accretion and can hold in the present day.

In order to investigate noble gas partitioning behavior between the core and mantle, noble gases were dissolved into metal-silicate melts under high temperature and pressure conditions, and then the samples were quenched, recovered, and analyzed for noble gas concentrations. Sample synthesis was performed at the Geodynamics Research Center, Ehime University. Noble-gas doped silicate glass and iron were melted and equilibrated under high pressure and temperature (3-6 GPa, 1700 and 1800 ˚C) using a multianvil apparatus. The sample capsule was cut and the polished surface of the section was investigated with scanning electron microscope and Raman spectroscopy. The chemical compositions of silicate and metal phases were determined with electron microprobe. And then, the noble gases in the silicate phase were extracted by an ultraviolet laser ablation apparatus and analyzed using a noble gas mass spectrometer at the University of Tokyo.

From the Raman spectra, it was found that crystallization (clinopyroxene) had occurred in samples synthesized at pressures of 6 GPa or higher, indicating that the sample quenching was not enough rapid. There is a possibility that noble gas may not be contained much in the crystallized part because a previous study showed that noble gas content in pyroxene crystal is smaller than those in glass (melt) by about 10^{-4} (Heber *et al.*, 2007). The noble gas concentrations in silicate glass phase are fairly homogeneous, even where a crack is formed during quenching. In future we will measure the noble gases in the iron part and determine the partition coefficient of the noble gases.

References: Bouhifd et al, *Nature Geoscience*. **6**, 982-986, 2013; Mukhopadhyay, *Nature* **486**, 101-104, 2012; Porcelli & Ballentine, *Rev. Mineral. Geochem.* **47**, 411-480, 2002; Trieloff & Kunz, *Phys. Earth Planet. Inter.* **148**, 13-38, 2005; Herber *et al*, *Geochim. Cosmochim. Acta*. **71**, 1041-1061, 2007

©2019. Japan Geoscience Union. All Right Reserved.

Measurement of T-dependent electrical resistivity of solid and liquid Fe and Pt at fixed P

*Innocent Ezenwa[1], Takashi Yoshino[1]

1. Institute for Planetary Materials, Okayama University

Knowledge of the thermal and electrical conductivity of solid and liquid Fe and its relevant alloys at P and T conditions is essential for understanding the cooling history of planetary cores and modelling their dynamo. The general understanding of the electrical transport properties of the transition metals at lower P will perhaps give insight in understanding Fe behavior at the inaccessible planetary core conditions. Theoretical investigation has suggested that the electrical and thermal conductivity of solid and liquid Fe at Earth’ s core conditions are similar in value (Wagle and Steinle-Neumann, (2017). At ambient T, experimental investigation showed that hcp ε -phase of Fe becomes paramagnetic at ~18GPa while Pt is paramagnetic and crystalize fcc at ambient conditions. Since Fe and Pt have an unfilled *d*-band electronic structure and at high P both exhibits closed packed crystal structures, experimental determination of the transport properties of molten Pt at lower P conditions is important for understanding the behavior of molten Fe preceding ε -phase at ~80 GPa. We develop a technique and cell design for the investigation of the electrical resistivity of metals that keeps it free from contamination using multianvil press. And, we report measurements on Fe and Pt. The sample was kept pure by making the electrodes and the sample the same composition while the thermocouple (TC) is placed close to the sample and taking through the gasket. The major challenge of TC breakage during compression and/or heating was overcome by shielding the TC with a cylindrical hollow coiling ring made of the same composition as the TC leads. The use of current polarity reversal to eliminate biased voltage as deployed in previous studies was adopted. On Fe and Pt, resistivity increases and decreases with T and P respectively, was observed. On melting, Fe result at 3 GPa agrees with very recent data by Silber et al. (2018) which showed an increasing difference in the resistivity value of solid and liquid with increasing P. While, Pt resistivity at 3 GPa appears constant comparable to its 1 atm value.

Keywords: Electrical resistivity, Thermal Conductivity, Iron Fe

©2019. Japan Geoscience Union. All Right Reserved.

Ancient, highly depleted mantle constrained by Re-Os isotope and highly-siderophile element compositions of French Polynesian xenoliths

*Norikatsu Akizawa[1], Akira Ishikawa[2], Katsuhiko Suzuki[3], Tetsu Kogiso[4]

1. Atmosphere and Ocean Research Institute, The University of Tokyo, 2. Department of Earth and Planetary Sciences, Tokyo Institute of Technology, 3. Research and Development Center for Submarine Resources, Japan Agency for Marine-Earth Science and Technology (JAMSTEC), 4. Graduate School of Human and Environmental Studies, Kyoto University

Mantle xenoliths, which are fragmented mantle material trapped by ascending magma, can provide lithological and geochemical information of the inaccessible mantle. In order to better understand the lithological and geochemical characteristics of the mantle, we conducted extensive sampling of mantle xenoliths throughout French Polynesia archipelago: Tahiti, Moorea, and Rurutu islands. We collected a total of 42 mantle xenoliths: 1 lherzolite, 14 harzburgites, 22 dunites, 3 wehrlites, and 2 orthopyroxenites. Here, we present whole-rock rhenium-osmium isotope and highly-siderophile element (Os, Ir, Ru, Pt, Pd, and Re) compositions in addition to whole-rock major-element compositions. Osmium isotope ratio ($^{187}Os/^{188}Os$) of the mantle xenoliths ranges from 0.1172 to 0.1464, where the harzburgites show a statistical bimodal distribution with unradiogenic ($^{187}Os/^{188}Os < 0.125$) and radiogenic ($^{187}Os/^{188}Os > 0.125$) compositions. The harzburgites with unradiogenic $^{187}Os/^{188}Os$ are depleted with regards to whole-rock major-element compositions (< 1.22 wt% Al_2O_3), and chondrite-normalized patterns of highly-siderophile elements. Considering the lithological variation of the mantle xenoliths used herein, the mantle is considerably heterogeneous beneath French Polynesia archipelago. In particular, the contrasting isotopic compositions of the harzburgites suggest different mantle reservoirs with unradiogenic and radiogenic $^{187}Os/^{188}Os$ compositions. We propose a possibility that the harzburgites with unradiogenic $^{187}Os/^{188}Os$ are impinged mantle material beneath normal oceanic lithosphere due probably to ascending plumes.

Keywords: Harzburgite, Dunite, PGE, TIMS, ICP-MS, Whole-rock chemical composition

©2019. Japan Geoscience Union. All Right Reserved.

First-principles prediction of hydrogen partitioning between the core and mantle

*Atsuroh Ohba[1], Taku Tsuchiya[1]

1. Ehime University Geodynamics Research Center

Some recent studies have reported high-P,T hydrous minerals which are stable at the core mantle boundary (CMB) pressure (Sano et al., 2008; Ohhira et al., 2016; Nishi et al., 2017). In order to elucidate the water circulation in the Earth's interior, experiments on the reaction between iron and hydrous minerals or water were also conducted (Iizuka-Oku et al., 2016; Mao et al., 2018; Clesi et al., 2018). However, the partition of hydrogen reported is different in different studies. In this study, we try estimating hydrogen partitioning between molten silicate and liquid iron under the CMB conditions based on the first principles calculation method combined with thermodynamic integration similar to our previous study (Xiong et al., 2018). Here, we assume following the exchange reaction of water between liquid iron and molten silicate is expressed as follows
(16MgSiO3+H2O) + 50Fe ⇔16MgSiO3 + (50Fe+H2O)
as a first example with ensuring the charge neutrality. Here, reaction free energy is calculated by the thermodynamic integration molecular dynamics method (Taniuchi & Tsuchiya, 2018). In the moment, simulations suggest that water prefer liquid iron. Now, additional computations are ongoing for improving numerical accuracy. The mechanism dissolving water into liquid iron is also investigated.

©2019. Japan Geoscience Union. All Right Reserved.

Microvolume stable isotope measuremetns and its applicaiton for high-pressure high-temperature experimental run products

*Madhusoodhan Satish-Kumar[1], Shinnosuke Aoyama[1]

1. Department of Geology, Faculty of Science, Niigata University

Light elements are very important in deep earth processes. Its composition in the lower mantle and core is still not well constrained. Stable isotope composition can be effectively used as an independent proxy. Although isotope fractionation in the deep earth occur in a narrow range, the volume of light element content in the mantle and core are extremely high, which can effectively cause significant natural isotopic compositional variations. It is necessary to accurately measure the isotope composition accurately in micro to nanomole scales, because the high-pressure experimental run products are small in volume. Recent studies have predicted the presence of isotope fractionation even at lower mantle and core *P-T* conditions, especially in magma ocean environment and during the core segregation. Despite the necessity of the micro-volume stable isotope measurement, there is always a tradeoff between the accuracy and the sample size.

At Niigata University, a MAT-253 mass spectrometer (Thermo Fisher Scientific) was installed through the MEXT Grant-in-Aid for Scientific Research on Innovative Areas. Carbon and oxygen isotopic compositions are measured using $CO_2$and multiple sulfur isotopic composition are measured using SF_6gas. A new micro-volume inlet system was installed and fundamental parameters such as pressure effect and capillary flow effect were tested. Using the micro-volume inlet system the minimum volume required for analysis is 1 micro-mole sample gas, and the precession for carbon and oxygen isotopic composition are better than 0.1‰. The precession for sulfur isotopes is ±0.3‰ and ±0.01‰ (1s) for $\delta^{34}S$ and $D^{33}S$, respectively, based on the repeated analyses of standard Ag_2S (IAEA S-1).Multiple sulfur isotope measurement system consists of 1) curie point pyrolyzer for rapid conversion of small volume samples to SF_6gas, 2) vacuum line system for pumping out non-condensable gasses, 3) gas chromatograph for purifying the SF_6gas and 4) micro-volume inlet system for introduction of sample gas to ionization chamber.
Multiple sulfur isotope ratios experimental run products were measured using the new system. Metal phases were separated and sulfur was extracted using Cr(II) reduction method [6]. Preliminary results indicate that S isotope fractionations occur in the pressure range of 3–5 GPa, under high-temperature conditions corresponding to the magma ocean environment. The negative $\delta^{34}S$ of mantle, can hence be explained by sulfur isotope fractionation in a magma ocean environment. Sulfur isotope measurements were also carried out on granitoid samples from the Archean with sulfide sulfur showing positive $\delta^{34}S$ values. Mass independent isotope fractionation, expressed as $\Delta^{33}S$, was also observed, suggesting that sulfur in the mantle alone cannot explain these variations. The incorporation of surface sulfur from sedimentary rocks and seawater is proposed.

Keywords: HPHT experiments, Micro-volume stable isotope measurements, Sulfur isotopes

©2019. Japan Geoscience Union. All Right Reserved.

Electrical resistivity of hcp Fe-Si alloys at high pressure and temperature

*Hayato Inoue[1], Sho Suehiro[1], Kenji Ohta[1], Kei Hirose[2,3], Yasuo Ohishi[4]

1. Department of Earth and Planetary Sciences, Tokyo Institute of Technology, 2. Earth-Life Science Institute, Tokyo Institute of Technology, 3. Department of Earth and Planetary Science, The University of Tokyo, 4. Japan Synchrotron Radiation Research Institute

Silicon (Si) has been repeatedly suggested to be the major light element in the Earth’ s core that mainly consists of iron [1]. Alloying the light element(s) affects a variety of physical properties of iron. Electrical and thermal conductivities strongly constrain the dynamics and thermal evolution of Earth’ s core and these parameters are linked by the Wiedemann-Franz law ($\kappa = \sigma LT$; κ : thermal conductivity, σ : electrical conductivity, L: Lorenz number, T: absolute temperature). However, measurements of electrical and thermal conductivities under static condition at extremely high pressures (P) and temperature (T) are limited for pure iron [2], [3]. The estimates of the core conductivity considering the effect of light element(s) have been done based on the resistivity saturation model, but the validity of the model at the core condition is unclear [4], [5].
In this study, we examined electrical resistivity (the reciprocal of electrical conductivity) of Fe-2, 4 and 6.5 wt.%Si at high P-T conditions in an internally-heated diamond anvil cell (IHDAC) up to 99 GPa and 2910 K. Our results of electrical resistivity of hcp Fe-Si alloys showed its nonlinear temperature dependence, indicating the occurrence of the resistivity saturation. The resistivity saturation in Fe-Si alloys observed in this study supports the notion of high core conductivity and resulting molten lowermost mantle and young inner core.

References: [1] Poirier: *Phys. Earth Planet. Inter.* **85**, 319-337 (1994).;[2] Ohta et al.: *Nature* **534**, 95–98 (2016).;[3] Konôpková et al.: *Nature* **534**, 99–101 (2016).;[4] Gomi et al.: *Phys. Earth Planet. Inter.* **224**, 88–103 (2013).;[5] Gomi et al.: *Earth Planet. Sci. Lett.* **451**, 51–61 (2016).

Keywords: Electrical conductivity, Thermal conductivity, Earth's core

©2019. Japan Geoscience Union. All Right Reserved.

Electrical resistivity and thermal conductivity of fcc Fe: Implications for the Mercury's core

*Hitoshi Gomi[1], Takashi Yoshino[1]

1. Okayama University

The Mercury's magnetic field may be sustained by the geodynamo motion in the liquid Fe core. However, its strength is about 1% of that of Earth. This weak magnetic field may implies a partly stratified core. Gomi et al. (2013) pointed out that the geometry of the thermal stratification depends critically on the depth dependency of the thermal conductivity. In this study, we conducted first-principles calculations on the face-centered cubic (fcc) Fe to constrain the electrical resistivity and the thermal conductivity of the Mercury's core.

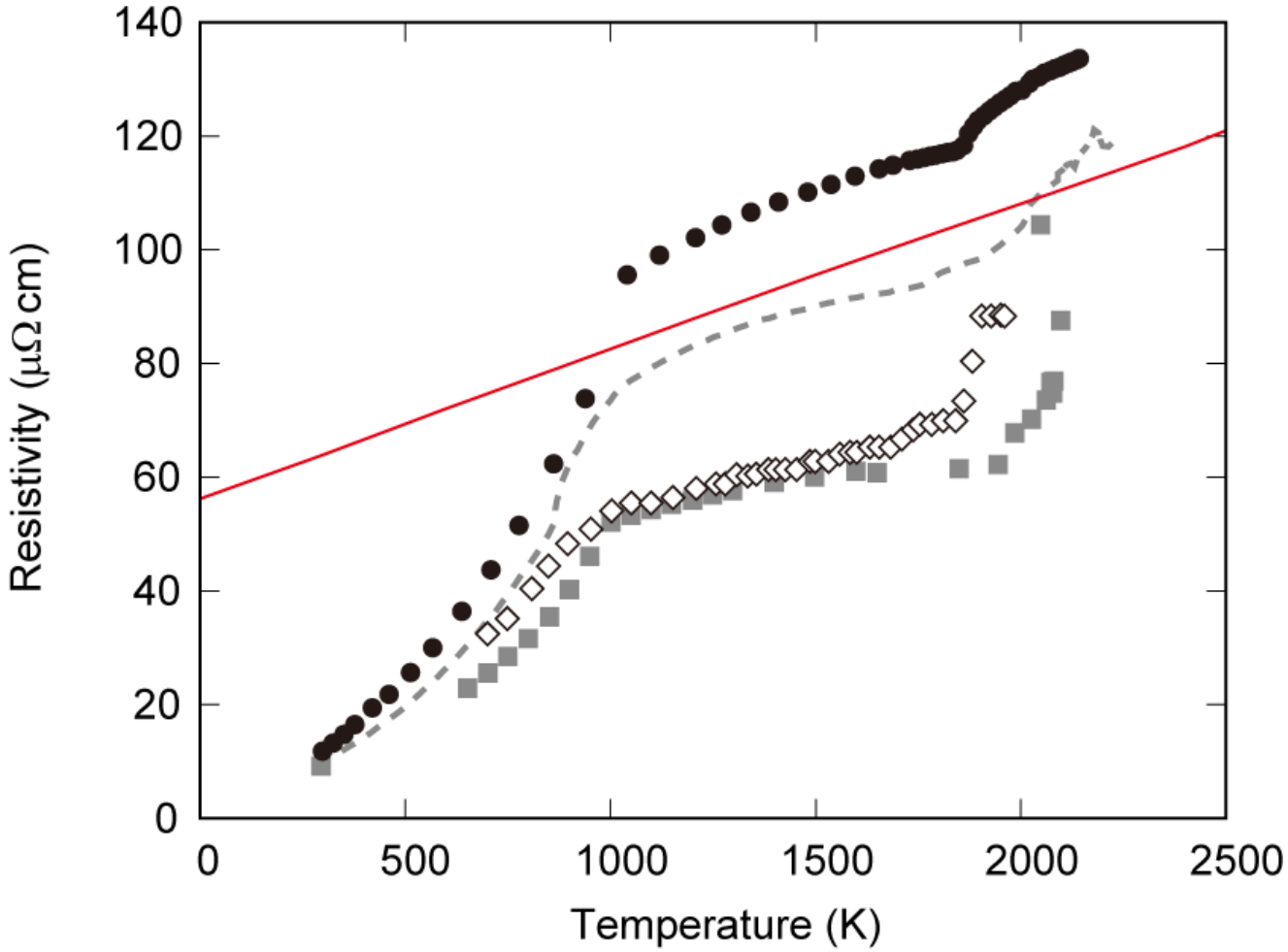
We calculated the electrical resistivity and the thermal conductivity of fcc Fe by means of the Korringa-Kohn-Rostoker method combined with the coherent potential approximation (KKR-CPA) (Akai, 1989). The CPA was adopted to treat the disorder effects due to the atomic vibrations and the magnetic fluctuations on the electronic band structure (Glasbrenner et al., 2014; Ebert et al., 2015; Kou and Akai, 2018). Within the alloy analogy model, the thermal atomic displacements were represented by a discrete set of N_v displacement vectors $\Delta R_v(T)$, where $|\Delta R_v(T)|=\sqrt{<u^2>}$ is the root mean square displacement of atoms, which is based on the Debye model without zero point vibration. The lattice parameter and the Debye temperature are obtained from the equation of state of fcc Fe (Tsujino et al., 2013). In addition to the non-magnetic state, the magnetic disorder was simulated by the local magnetic disorder (LMD) approach. The conductivity was calculated by the Kubo-Greenwood formula with the vertex correction.

The calculated electrical resistivities and thermal conductivities with LMD state are consistent with the literature data at 0 GPa (Ho et al., 1972; 1983), whereas the non-magnetic results show smaller resistivity and larger thermal conductivity. This suggests the importance of the magnetic scattering at low pressures. However, our calculation predicts that the magnetic contribution banishes at higher pressures than 20 GPa. Figure 1 compares the present results and previous experiments (gray broken line; Secco and Scholoessin, 1989, gray square; Deng et al., 2013, open diamond; Pommier, 2018, black circle; Silber et al., 2018) on the electrical resistivity at ~5 GPa. Note that, within the fcc stability field, previous measurements have a large variation. Our calculated resistivity values are between Secco and Scholoessin (1989) and Silber et al. (2018).

We further calculated the electrical resistivity and the thermal conductivity of fcc Fe up to 50 GPa and 3000 K. The thermal conductivity increases with increasing pressure and temperature. This means that, if the inner core is absent, the thermal stratification starts from the bottom, and, after the onset of the inner core, a thick thermal stratified layer may develop at the top of the fluid core (Gomi et al., 2013).

Keywords: electrical resistivity, thermal conductivity, Mercury, core, thermal stratification

©2019. Japan Geoscience Union. All Right Reserved.



©2019. Japan Geoscience Union. All Right Reserved.

Lateral heterogeneity in the lowermost outer core (F layer) of the Earth revealed by seismic analyses

*Toshiki Ohtaki[1], Satoshi Kaneshima[2], Taku Tsuchiya[3]

1. Geological Survey of Japan, National Institute of Advanced Industrial Science and Technology (AIST), 2. Department of Earth and Planetary Sciences, Kyushu University, 3. Geodynamics Research Center, Ehime University

We have determined seismic velocity structures of the lowermost outer core (F layer) beneath Northeast Pacific and Australia (Ohtaki and Kaneshima, 2015; Ohtaki et al., 2018), and found that the F layer is seismologically heterogeneous. These structures were obtained using a combination of two observations. First one is differential traveltimes between waves that reflect at the inner core boundary (ICB) and that graze the boundary; the second is dispersion (frequency dependence of velocity) of the grazing wave.

Our results show a somewhat strange velocity profile in the F layer beneath Australia, which has a lower-velocity-gradient layer than that of the Preliminary Reference Earth Model (PREM; Dziewonski and Anderson, 1981) on the ICB, and a higher-gradient layer just above the layer. Recent advance in high pressure research enables seismologists to translate lateral seismic velocity variation to relative chemical abundance in the outer core condition. Based on the results of Ichikawa and Tsuchiya (e.g., 2018), we showed light-element enrichment there. This result suggests that lighter fluid exists beneath Australia in the lowermost part of the liquid core, although the outer core is low-viscosity fluid.

The solid inner core of the Earth has quasi-hemispherical structure (e.g., Tanaka and Hamaguchi, 1997). As the origin of this hemispherical structure, uneven growth of the inner core has been proposed (e.g., Aubert et al., 2008; Alboussière et al., 2010; Monnereau et al., 2010). When the liquid in the outer core solidifies at the inner core surface, excess light element is partitioned to residue because the solid inner core is poorer in light elements compared with the liquid outer core. Thus, the uneven growth of the inner core is tied with an uneven release of the light elements to the F layer, which may be related to our results of the heterogeneous F layer. Then, a question arises: this heterogeneity has hemispherical structure like the inner core or local one?

We have not answered it yet because the survey areas of the above studies are restricted. Furthermore, other studies focusing F-layer velocity are not so many. Souriau (2015) determined lateral variations of velocity in the lower outer core using traveltimes of waves that turn there, and suggested that heterogeneity in F has degree-one feature. We also determined the seismic structure of the F layer beneath Antarctica using amplitude ratios between waves that turn just above the inner core and that get into the inner core. Although the resolution and reliability of structure obtained using amplitude ratios is lower than those using the method of our recent papers, the structure beneath Antarctica has a much lower velocity gradient in the F layer compared with PREM. Such a lower gradient is close to the model beneath Australia.

In this paper, we will show the summary of the heterogeneous F-layer structures of velocity and chemical abundance at this stage.

References

Alboussière, T., R. Deguen, and M. Melzani (2010), *Nature*, *466*, 744–747, doi:10.1038/nature09257.

©2019. Japan Geoscience Union. All Right Reserved.

Aubert, J., H. Amit, G. Hulot, and P. Olson (2008), *Nature*, *454*, 758–761, doi:10.1038/nature07109.
Dziewonski, A. M., and D. L. Anderson (1981), *Phys. Earth Planet. Inter.*, 25, 297–356, doi:10.1016/0031-9201(81)90046-7.
Monnereau, M., M. Calvet, L. Margerin, and A. Souriau (2010), *Science*, *328*, 1014–1017, doi:10.1126/science.1186212.
Ichikawa, H., and T. Tsuchiya (2018), J. Geography, 127, 631-646 (in Japanese with English abstract).
Ohtaki, T., S. Kaneshima, and K. Kanjo (2012), *J. Geophys. Res.*, 117, B03312, doi:10.1029/2011JB008717.
Ohtaki, T., and S. Kaneshima (2015), *J. Geophys. Res. Solid Earth*, 120, 7572–7586, doi:10.1002/2015JB012140.
Ohtaki, T., S. Kaneshima, H. Ichikawa, and T. Tsuchiya (2018), *J. Geophys. Res. Solid Earth*, doi:10.1029/2018JB015857.
Tanaka, S., and H. Hamaguchi (1997), *J. Geophys. Res.*, *102*, 2925–2938, doi:10.1029/96JB03187.

Keywords: F layer, lowermost outer core, Heterogeneity of the outer core, Light element concentration in the F layer beneath Australia

©2019. Japan Geoscience Union. All Right Reserved.

Flows and light element distribution in the outer core associated with heterogeneous growth of the inner core of the Earth

*Shin-ichi Takehiro[1], Youhei SASAKI[2]

1. Research Institute for Mathematical Sciences, Kyoto University, 2. Department of Mathematics, Kyoto University

Recent seismological observations suggest longitudinal heterogeneity of seismological wave velocity of the inner core of the Earth, which stimulates a discussion that phase change at the inner core boundary (ICB) does not occur uniformly in the horizontal directions. It is simply supposed from this suggestion that temperature is lower and concentration of light element is higher just above the solidification hemisphere at ICB, and vice versa. The heterogeneous structure of the inner core and thermodynamic properties just above ICB in the outer core is expected to be correlated, however, more recent analysis shows that distribution of seismological wave velocity anomaly does not correspond to longitudinal heterogeneity of the inner core.

There are two kinds of mechanisms explaining heterogeneous growth of the inner core. One of the mechanisms is that the heterogeneous thermal condition at the core mantle boundary (CMB) drives horizontal thermal convection which induces non-uniform temperature distribution at ICB. However, since this study uses co-density, which combines density variations by temperature and light element concentration, it cannot find distribution of the light elements just above ICB. Another mechanism is that hydrodynamic instability of the inner core surrounded by the phase boundary causes translational motion inside the inner core. However, since the theory assumes homogeneous light element distribution in the outer core, it is not clear this mechanism can explain the light element distribution above ICB.

In this study, by using a rotating spherical shell model in which temperature and light element concentration are independent variables, we perform numerical experiments of thermal and compositional convection related to two kinds of mechanisms. Obtained distributions of light element concentration are compared with the distribution of seismological wave velocity anomaly, and plausible dynamical regimes of thermal and compositional convection in the outer core are discussed.

Keywords: Heterogeneity, Inner core, Core-mantle boundary

©2019. Japan Geoscience Union. All Right Reserved.

Sharpness of the hemispherical boundary in the inner core beneath the northern Pacific

*Ryohei Iritani[1], Hitoshi Kawakatsu[1], Nozomu Takeuchi[1]

1. Earthquake Research Institute, Univ. of Tokyo

The hemispherical heterogeneity in the topmost of the Earth’ s inner core, faster velocity and higher attenuation in the eastern hemisphere and slower velocity and weaker attenuation in the western hemisphere, has been revealed by seismological studies. However, how the transition structure between two hemispheres looks like has not been known because of the difficulty to analyze complex core-sensitive data and the limitation of earthquake and seismic array distribution. In this study, we apply the array-based waveform inversion (Iritani et al., 2014) to core phase data that propagate beneath the northern Pacific, and investigate the nature of the transition structure in this region.Dataset used in this study consists of two directional event-station pairs, seismograms observed by the permanent European stations for events at Fiji-Tonga region, and USArray for events near Indonesia. We analyze the broadband vertical component of core phase data containing PKIKP and PKP phases (i.e. the epicentral distance between 145 –155 degree). Resultant analyzed waveforms for EU stations and USArray are 2,108 and 1,172 traces respectively.
In the analysis, waveform inversion approach is employed for each event data to measure traveltime and attenuation in the inner core. As a result, traveltime anomalies observed by EU stations show obvious positive anomaly suggesting mainly propagating the eastern hemisphere, while traveltimes observed by USAray show relatively smaller (or no) anomalies suggesting effects from both of hemispheres. On the other hand, attenuation parameters for both arrays show similar trend that suggests high attenuation corresponding to the eastern hemisphere. To investigate a hemispherical transition boundary in the sampled region, we conduct a ray theory based forward modeling of traveltimes by changing a shape of boundary from meridian boundary to eyeball shaped boundary, and its position. We compute root-mean-square (RMS) of residual between observations and theoretical traveltimes computed with each boundary model. Then, an eyeball shaped boundary, that is located at longitude of 158°W on the equatorial line and latitude of 80°N at the northernmost point, obtained as the preferred boundary model. Finally, we investigate a sharpness of the boundary by varying a width of hemispherical transition. We assume linear variation from the eastern and western hemisphere in a given width and compute RMS. As a result, a width of 600 km at the surface of the inner core shows smaller RMS than sharp boundary. Geophysical significance of this finding will be further discussed.

Keywords: Inner core, Waveform inversion

©2019. Japan Geoscience Union. All Right Reserved.

Stable carbon isotope fractionation in Fe-C system from first principles

*Haruhiko Dekura[1], Taku Tsuchiya[1]

1. Geodynamics Research Center, Ehime University

Carbon is the fourth most abundant element in the solar system and likely one of the constituent light elements in the Earth’s core. Determination of its equilibrium isotope fractionation factor (α) under high pressure (P) and temperature (T) is a key for understanding chemical evolution such as the whole Earth carbon distributions and the amount in the Earth’s core (e.g., Kumar et al., 2011). Because experimental measurement of the isotope fractionation remains technically challenging at the deep mantle condition, attempts to evaluate the α among mantle minerals by first-principles calculations have been made in recent years (e.g., Huang et al., 2014). Recently, our group initiated the theoretical determination of the α in the Fe-C system in the Earth’s deep interior with a full ab initio approach based on the density-functional theory. We performed ab initio lattice dynamics calculations for diamond and iron-carbide (hexagonal Fe7C3) having the two stable carbon isotopes (12C and 13C). The α between the two phases were then determined by using the Gibbs free energies calculated at P ~300 GPa and T ~2000-6000 K. The obtained $10^3 \ln \alpha$ dia-Fe7C3 is found to vary with T from ~+8‰ (2000 K) to ~+5‰ (6000 K). This result indicates that the Fe7C3 is enriched in the heavier isotope (13C) compared with diamond. This trend is qualitatively consistent with low-pressure experimental observations (Kumar et al., 2011).

Keywords: Isotope fractionation, First-principles calculation

©2019. Japan Geoscience Union. All Right Reserved.

[E] Poster | B (Biogeosciences)：B-BG Biogeosciences & Geosphere-Biosphere Interactions

Mon. May 27, 2019 1:45 PM - 3:15 PM JST | Mon. May 27, 2019 4:45 AM - 6:15 AM UTC | Poster Hall International Exhibition Hall8, Makuhari Messe_6

[B-BG01] Elemental cycling in terrestrial and coastal ecosystems- Carbon and Nitrogen perspectives

convener:Punyasloke Bhadury(Indian Institute of Science Education and Research Kolkata)

Biogeochemical cycling of carbon and nitrogen hold the key to cropping cycle, monsoonal patterns and climate globally. Biological communities that make up the biosphere are essential for cycling of carbon and nitrogen and their functions are regulated by numerous factors including redox conditions, trace metal availability, and energy sources. At the same time temporal and spatial variability of biological communities such as those observed in microbes strongly affect the rate of carbon and nitrogen cycling in various environments including land and marine systems. In this session, submissions are welcomed from scientists including early career scientists working on various aspects of carbon and nitrogen cycling across terrestrial, coastal and oceanic environments. Submissions are also encouraged addressing challenges related to estimation of carbon and nitrogen budgets representing local, regional and global scales.

[BBG01-P01] Forest-CEW: A Forest Ecosystems Model for Carbon-Energy-Water Processes.

*Zhenghong Tan[1] (1.Hainan University China)

[BBG01-P02] **Interdependent Dynamics of LAI-ET across Roofing Landscapes: the Mongolian and Tibetan Plateaus**

*Li Tian[1] (1.Institute of Geographic Sciences and Natural Resources Research, Chinese Academy of Sciences)

[BBG01-P03] **Particle Phase Organic compounds (PAHs and VOCs) at Two Big Cities (Dhaka and Rajshahi) in Bangladesh**

*Islam Nazrul nazrulislam6727@gmail.com[1], Tanzina Tul Karim[1], Rasheda Nahida[1], Nusrat Mousume[1], Farha Jeba[1], Abdus Salam[1] (1.Department of Chemistry, University of Dhaka, Dhaka-1000, Bangladesh)

[BBG01-P04] **Diversity and activity of diazotrophs in the coastal waters of Southeastern Arabian Sea (SEAS)**

*JABIR THAJUDEEN[1], Mohamed Hatha Abdullah (1.Cochin University of Science and Technology India)

[BBG01-P05] **Bloom of *Palmerina hardmaniana*, a marine centric planktonic diatom in a coastal mangrove ecosystem- implication for coastal carbon cycling**

*Punyasloke Bhadury[1] (1.Centre for Climate and Environmental Studies and Department of Biological Sciences, Indian Institute of Science Education and Research Kolkata)

[BBG01-P06] Dynamics of Carbon and Nitrogen influx in large river system: Isotopic study from river Ganga, India

*Anurag Kumar[1], Prasanta Sanyal[1,2], Punyasloke Bhadury[3,2] (1.Department of Earth Sciences, Indian Institute of Science Education and Research Kolkata, Mohanpur 741246, India, 2.Centre for Climate and Environmental studies, Indian Institute of Science Education and Research Kolkata, Mohanpur 741246, India, 3.Department of Biological Sciences, Indian Institute of Science Education and Research Kolkata, Mohanpur 741246, India)

Forest-CEW: A Forest Ecosystems Model for Carbon-Energy-Water Processes.

*Zhenghong Tan[1]

1. Hainan University China

Forest ecosystem models (FEM) are essential tools for studying the forest carbon budget, which is an important subject in the global climate change studies. Although using FEM has a long history and there exist many types of FEM, new models are still being developed for special uses. This presentation introduces Forest-CEW, a forest ecosystems model for carbon-energy-water processes. The model is aimed at having a structure that can be configured flexibly for different forest ecosystems, a graphic interface for inexperienced users, and a command execution mode for experts. The time scale of the model is at the hourly level. Model validation using the data from Tomakomai flux research site (asiaflux.net/index.php?page_id=113) shows that the model can well reconstruct major ecosystem variables including net ecosystem exchange, soil temperature and water content. We also compared Forest-CEW with those include in the TDE ecosystem model intercomparison (cdiac.ess-dive.lbl.gov/epubs/tdemodel/models.html) and the results show that its performance is among the best of the 13 models.

Keywords: Model, Forest Ecosystem, Carbon, Water, Energy

©2019. Japan Geoscience Union. All Right Reserved.

Interdependent Dynamics of LAI-ET across Roofing Landscapes: the Mongolian and Tibetan Plateaus

*Li Tian[1]

1. Institute of Geographic Sciences and Natural Resources Research, Chinese Academy of Sciences

The Mongolian and Tibetan Plateaus have experienced higher-than-global average warming in recent decades, resulting in many significant changes in ecosystem structure and function. Among them are Leaf area index (LAI) and evapotranspiration (ET) that play a fundamental role in shaping many causes and consequences of land surface processes and climate. Here, we focused on the spatiotemporal changes of the LAI, ET and their relationships on these two roofing landscapes. Based on the MODIS products from 2000 through 2014. We found that there existed a general positive relationship between LAI and ET on the Mongolia Plateau (MP), while there was not synergy on the Tibetan Plateau (TP).

Overall, 49.38% (50.62%) of land areas on the TP experienced significant increased (decreased) in LAI, while 94.92% (5.09%) on the MP. For the ET, the increased land area was 21.70% (124.10×10^3 km^2) on the TP and 88.01% (341.60×10^3 km^2) on the MP. More importantly, the relationships varied substantially across the space and over time, with mismatches found in some parts of the landscapes. Substantial additional efforts with observational and/or experimental investigations are need to explore the relationships, including the influences of vegetation characteristics and disturbances.

Keywords: ET, LAI, Eurasian continent, alpine, land surface process

©2019. Japan Geoscience Union. All Right Reserved.

Particle Phase Organic compounds (PAHs and VOCs) at Two Big Cities (Dhaka and Rajshahi) in Bangladesh

*Islam Nazrul nazrulislam6727@gmail.com[1], Tanzina Tul Karim[1], Rasheda Nahida[1], Nusrat Mousume[1], Farha Jeba[1], Abdus Salam[1]

1. Department of Chemistry, University of Dhaka, Dhaka-1000, Bangladesh

Particle Phase Organic compounds (PAHs and VOCs) at Two Big Cities (Dhaka and Rajshahi) in Bangladesh

Md. Nazrul Islam[1*], Tanzina Tul Karim, Rasheda Nahida, Nusrut Mousume, Farha Jeba, and Abdus Salam[2*]

Department of Chemistry, University of Dhaka, Dhaka 1000, Bangladesh

Corresponding Author: [1] nazrulislam6727@gmail.com, Tel: +8801717672748; [2*] asalam@gmail.com, Tel: +880117061160

Atmospheric pollution has a significant impact on human health, climate change, agriculture, and ecosystem. Air quality and the climate change is the top most concern of the World Health Organization (WHO, 2019). Bangladesh is a rapidly developing country with kinds of environmental problems. It became the top most country in the world for the human deaths due to environmental pollution, which was accounted about 27% of the total death (Lancet, 207). Only air pollution caused two thirds of these deaths (Lancet, 2017). Dhaka along with Narayanganj and Gazipur are the top ranking cities in the World for the air pollution (WHO, 2014). Volatile organic compounds (VOCs) and poly aromatic hydrocarbons (PAHs) are the major organic pollutants in the atmosphere. Until now there is no information of VOCs and PAHs regarding their occurrences, sources, seasonal variation and health impact in Bangladesh. In this study we have collected particulate matters samples on quartz filters with a low volume sampler at two big cities in Bangladesh (Capital Dhaka and North West City Rajshahi) from January 2015 to February 2019. Individual organic compounds were extracted with acetone and n-hexane from the particulate matter loaded filters. The chemical analysis was done with Gas Chromatography (GC)-Mass spectrometry (MS). The analyzed organic compounds were naphthalene, anthracene, diazinon, deltramethrin, pyrabenxoime, pyrazosulfuran, prophenophos butachlor, propiconazole, cymoxanil, cypermethrin, lamda cyhalothrin, dimethoate, chloropyriphos, carbofuran, metalaxyl, pentane, hexane, propene, isobutene, 1,3-butadiene, dichloroflouromethane, ethanol, benzene, toluene, ethylbenzene, xylene, styrene, 1,2,3trimethylbenzene, isoprene, cyclopentane, and cyclohexane. Positive matrix factorization (PMF) and air mass trajectory analysis were done for source characterization. Health risk assessment and life time cancer risk (LCR)

©2019. Japan Geoscience Union. All Right Reserved.

were determined with US EPA based model. The elevated concentrations of the determined compounds at both Dhaka and Rajshahi were observed; Dhaka values were slightly higher than Rajshahi. The concentrations of determined compounds were higher during the winter months basically December to February and lower during the monsoon period in the month of July. PMF model revealed that the sources of organic compounds in Bangladesh were diesel exhaust, coal and biomass burning, industry and gasoline exhaust. Ethyl benzene, dichlorouflouromethane, 1,2,3-trimethylbenzene have the potential carcinogenic impact.

Key words: Particle Phase Organics, PAHs, VOCs, PMF, Health Risk Assessment

Keywords: Particle Phase Organics, PAHs and VOCs, PMF and Health Risk Assessment

©2019. Japan Geoscience Union. All Right Reserved.

Diversity and activity of diazotrophs in the coastal waters of Southeastern Arabian Sea (SEAS)

*JABIR THAJUDEEN[1], Mohamed Hatha Abdullah

1. Cochin University of Science and Technology India

In marine environments availability of nitrogen (N2) limits the primary productivity. Nitrogen fixing bacteria (diazotrophs) could convert atmospheric nitrogen to ammonium thereby providing significant input of new nitrogen into the ocean. The knowledge about their diversity, distribution and physiological activity are limited in tropical coastal marine environments. In this study, we determined diversity of nitrogen fixing bacteria and the nitrogen fixation rate through *nifH* based clone library analysis and 15N2 bubble method respectively. We encountered *Trichodesmium*bloom and diatom diazotrophic associations along the coastal environments of SEAS. Nitrogen fixation rate in the coastal waters were varied from 0.15 to 1.02 nmolN/L/h. *Trichodesmium*bloom in the Arabian Sea during pre-monsoon season showed higher nitrogen fixation rate of 3.6 nmolN/L/h. Clone library analysis revealed that 19 Operational Taxonomic Units (OTUs) of nitrogen fixing bacteria were observed from the coastal waters SEAS. The OTUs were related to 7 OTUs of cyanobacteria and 12 OTUs of heterotrophic diazotrophs. Major cyanobacterial OTUs are closely similar to *Trichodesmium*sp., *Richelia*sp., *Synechocystis*sp.. Major heterotrophic diazotrophs belonged to alpha-, beta-, gamma-, epislon-, proteobacteria and firmicutes. Gamma proteobacterial clones were dominating among heterotrophic diazotrophs in the coastal water column of south eastern Arabian Sea. Nitrogen fixation rate in the water column were significantly correlated with dissolved Fe (R^2= 0.66, p= 0.05) and phosphorous (R^2= 0.49, p= 0.05), which revealed these are the major factors controlling nitrogen fixation process in the coastal environments of SEAS.

Keywords: Nitrogen fixation , diazotrophs, Fe, SEAS

©2019. Japan Geoscience Union. All Right Reserved.

Bloom of *Palmerina hardmaniana*, a marine centric planktonic diatom in a coastal mangrove ecosystem- implication for coastal carbon cycling

*Punyasloke Bhadury[1]

1. Centre for Climate and Environmental Studies and Department of Biological Sciences, Indian Institute of Science Education and Research Kolkata

Large celled diatoms play an important role in export of carbon in coastal ecosystems. In the Sundarbans mangrove ecosystem located on the delta of Ganga-Brahmaputra-Meghna riverine systems and facing the coastal Bay of Bengal, a bloom of *Palmerina hardmaniana* (Greville) Hasle was tracked in 2015. The bloom of this centric diatom species was tracked from April- July, 2015 in Sundarbans Biological Observatory Time Series (SBOTS) site of Sundarbans. During pre-bloom (April) dissolved oxygen (DO) concentration was 6.82 mg/L while during bloom (May-June) DO concentration decreased to 3.83 mg/L. This also coincided with Chlorophyll-a concentration which ranged from 0.22-6.28 mg/L during the study period, with highest concentration of 6.28 mg/L in bloom period and overwhelmingly dominated by cells belonging to *Palmerina hardmaniana* (40.8 X 10^4 cells/L). In total 72 phytoplankton species were observed from April-July, 2015 in SBOTS site. The frustules of *Palmerina hardmaniana* ranged from 291-358 μm in length and from 195 to 260 μm in width. Based on *rbc*L phylogeny of RuBISCO, the dominance of *P. hardmaniana* was also confirmed. Increased air and surface water temperatures in SBOTS site showed significant correlation with observed cell abundance of *P. hardmaniana* with the onset of bloom. This is the first report of *P. hardmaniana* bloom in the coastal Sundarbans mangrove ecosystem. Therefore, understanding the physiological success of this centric diatom species in relation to dynamic environmental conditions has consequences for tracking export of carbon by centric diatoms in coastal water and resulting implications for coastal carbon cycling.

Keywords: diatom, phytoplankton bloom, mangrove, carbon cycling

©2019. Japan Geoscience Union. All Right Reserved.

Dynamics of Carbon and Nitrogen influx in large river system: Isotopic study from river Ganga, India

*Anurag Kumar[1], Prasanta Sanyal[1,2], Punyasloke Bhadury[3,2]

1. Department of Earth Sciences, Indian Institute of Science Education and Research Kolkata, Mohanpur 741246, India, 2. Centre for Climate and Environmental studies, Indian Institute of Science Education and Research Kolkata, Mohanpur 741246, India, 3. Department of Biological Sciences, Indian Institute of Science Education and Research Kolkata, Mohanpur 741246, India

Freshwater flux transport large amount of carbon (dissolved and particulate, organic and inorganic) and nitrogen (Dissolved) from continent into the ocean, contributing significantly to the global carbon and nitrogen cycle. The present sources and sinks of naturally as well as anthropogenically produced C and N compounds in the global carbon and nitrogen cycle remains enigmatic. Among the carbon sources in the river ecosystem, the dissolved inorganic carbon (DIC) constitute major component of carbon influx from land to ocean. These fluxes are significantly influenced by the terrestrial and estuary processes. The isotopic composition of DIC can be used to understand the sources and cycling of carbon in rivers and estuaries. In this study, $d^{13}C$ of DIC in river water of Ganga has been used to understand the dissolved inorganic carbon sources into the river. The river Ganga (2500 km) is the largest river of the Indian subcontinent which originates from the Gangotri glacier and drains into Bay of Bengal through its vast delta in the Sunderban. The $d^{13}C_{DIC}$ of river water were measured from source (Gomukh) to sink (Bay of Bengal) of the river Ganga for pre and post-monsoon period. The seasonal variation in the $d^{13}C_{DIC}$ shows enriched isotopic values in pre-monsoon compared to post-monsoon samples, indicating increased biological activities in the riverine system during pre-monsoon. A varied enrichment factor in the $d^{13}C_{DIC}$ values were observed for upper, middle and lower stretch of the river Ganga which might be indicating different sources contributing water in different stretch of the river Ganga. The $d^{18}O$ value of river water, ground water and rain water were used to delineate the different sources of water into the river Ganga. The water budget of the river Ganga shows high glacier melt in the upper stretch, high ground water influx in middle stretch and high rain water input in lower stretch of the river Ganga.

On similar note, the dissolved form of nitrogen in river water (NO_3^-) also significantly impacts the riverine as well as costal ecosystem. The increased influx of nitrate changes the competition between species causing disruption in the biological diversity. The lower stretch of the river Ganga receives maximum rain water input; therefore the region becomes prone to pollutant as result of surface runoff from the catchment areas. The isotopic composition of dissolved nitrate in water can be used to delineate the sources of NO_3^- into the riverine system. The $d^{15}N$ and $d^{18}O$ of the dissolved nitrate in river water from the lower stretch (Kolkata) of the river Ganga indicates the input of anthropogenic activities (pollutant) to river water. The data indicates manure from septic pipe lines as major source of dissolved nitrate present in the river Ganga.

Keywords: DIC, Ganga river, nitrate isotope, India

©2019. Japan Geoscience Union. All Right Reserved.

[E] Poster | B (Biogeosciences)：B-BG Biogeosciences & Geosphere-Biosphere Interactions

Mon. May 27, 2019 5:15 PM - 6:30 PM JST | Mon. May 27, 2019 8:15 AM - 9:30 AM UTC | Poster Hall International Exhibition Hall8, Makuhari Messe_31

[B-BG01] Elemental cycling in terrestrial and coastal ecosystems- Carbon and Nitrogen perspectives

convener:Punyasloke Bhadury(Indian Institute of Science Education and Research Kolkata)

Biogeochemical cycling of carbon and nitrogen hold the key to cropping cycle, monsoonal patterns and climate globally. Biological communities that make up the biosphere are essential for cycling of carbon and nitrogen and their functions are regulated by numerous factors including redox conditions, trace metal availability, and energy sources. At the same time temporal and spatial variability of biological communities such as those observed in microbes strongly affect the rate of carbon and nitrogen cycling in various environments including land and marine systems. In this session, submissions are welcomed from scientists including early career scientists working on various aspects of carbon and nitrogen cycling across terrestrial, coastal and oceanic environments. Submissions are also encouraged addressing challenges related to estimation of carbon and nitrogen budgets representing local, regional and global scales.

[BBG01-P01] Forest-CEW: A Forest Ecosystems Model for Carbon-Energy-Water Processes.

*Zhenghong Tan[1] (1.Hainan University China)

[BBG01-P02] **Interdependent Dynamics of LAI-ET across Roofing Landscapes: the Mongolian and Tibetan Plateaus**

*Li Tian[1] (1.Institute of Geographic Sciences and Natural Resources Research, Chinese Academy of Sciences)

[BBG01-P03] **Particle Phase Organic compounds (PAHs and VOCs) at Two Big Cities (Dhaka and Rajshahi) in Bangladesh**

*Islam Nazrul nazrulislam6727@gmail.com[1], Tanzina Tul Karim[1], Rasheda Nahida[1], Nusrat Mousume[1], Farha Jeba[1], Abdus Salam[1] (1.Department of Chemistry, University of Dhaka, Dhaka-1000, Bangladesh)

[BBG01-P04] **Diversity and activity of diazotrophs in the coastal waters of Southeastern Arabian Sea (SEAS)**

*JABIR THAJUDEEN[1], Mohamed Hatha Abdullah (1.Cochin University of Science and Technology India)

[BBG01-P05] **Bloom of *Palmerina hardmaniana*, a marine centric planktonic diatom in a coastal mangrove ecosystem- implication for coastal carbon cycling**

*Punyasloke Bhadury[1] (1.Centre for Climate and Environmental Studies and Department of Biological Sciences, Indian Institute of Science Education and Research Kolkata)

[BBG01-P06] Dynamics of Carbon and Nitrogen influx in large river system: Isotopic study from river Ganga, India

*Anurag Kumar[1], Prasanta Sanyal[1,2], Punyasloke Bhadury[3,2] (1.Department of Earth Sciences, Indian Institute of Science Education and Research Kolkata, Mohanpur 741246, India, 2.Centre for Climate and Environmental studies, Indian Institute of Science Education and Research Kolkata, Mohanpur 741246, India, 3.Department of Biological Sciences, Indian Institute of Science Education and Research Kolkata, Mohanpur 741246, India)

Forest-CEW: A Forest Ecosystems Model for Carbon-Energy-Water Processes.

*Zhenghong Tan[1]

1. Hainan University China

Forest ecosystem models (FEM) are essential tools for studying the forest carbon budget, which is an important subject in the global climate change studies. Although using FEM has a long history and there exist many types of FEM, new models are still being developed for special uses. This presentation introduces Forest-CEW, a forest ecosystems model for carbon-energy-water processes. The model is aimed at having a structure that can be configured flexibly for different forest ecosystems, a graphic interface for inexperienced users, and a command execution mode for experts. The time scale of the model is at the hourly level. Model validation using the data from Tomakomai flux research site (asiaflux.net/index.php?page_id=113) shows that the model can well reconstruct major ecosystem variables including net ecosystem exchange, soil temperature and water content. We also compared Forest-CEW with those include in the TDE ecosystem model intercomparison (cdiac.ess-dive.lbl.gov/epubs/tdemodel/models.html) and the results show that its performance is among the best of the 13 models.

Keywords: Model, Forest Ecosystem, Carbon, Water, Energy

©2019. Japan Geoscience Union. All Right Reserved.

Interdependent Dynamics of LAI-ET across Roofing Landscapes: the Mongolian and Tibetan Plateaus

*Li Tian[1]

1. Institute of Geographic Sciences and Natural Resources Research, Chinese Academy of Sciences

The Mongolian and Tibetan Plateaus have experienced higher-than-global average warming in recent decades, resulting in many significant changes in ecosystem structure and function. Among them are Leaf area index (LAI) and evapotranspiration (ET) that play a fundamental role in shaping many causes and consequences of land surface processes and climate. Here, we focused on the spatiotemporal changes of the LAI, ET and their relationships on these two roofing landscapes. Based on the MODIS products from 2000 through 2014. We found that there existed a general positive relationship between LAI and ET on the Mongolia Plateau (MP), while there was not synergy on the Tibetan Plateau (TP).

Overall, 49.38% (50.62%) of land areas on the TP experienced significant increased (decreased) in LAI, while 94.92% (5.09%) on the MP. For the ET, the increased land area was 21.70% (124.10×10^3 km^2) on the TP and 88.01% (341.60×10^3 km^2) on the MP. More importantly, the relationships varied substantially across the space and over time, with mismatches found in some parts of the landscapes. Substantial additional efforts with observational and/or experimental investigations are need to explore the relationships, including the influences of vegetation characteristics and disturbances.

Keywords: ET, LAI, Eurasian continent, alpine, land surface process

©2019. Japan Geoscience Union. All Right Reserved.

Particle Phase Organic compounds (PAHs and VOCs) at Two Big Cities (Dhaka and Rajshahi) in Bangladesh

*Islam Nazrul nazrulislam6727@gmail.com[1], Tanzina Tul Karim[1], Rasheda Nahida[1], Nusrat Mousume[1], Farha Jeba[1], Abdus Salam[1]

1. Department of Chemistry, University of Dhaka, Dhaka-1000, Bangladesh

Particle Phase Organic compounds (PAHs and VOCs) at Two Big Cities (Dhaka and Rajshahi) in Bangladesh

Md. Nazrul Islam[1*], Tanzina Tul Karim, Rasheda Nahida, Nusrut Mousume, Farha Jeba, and Abdus Salam[2*]

Department of Chemistry, University of Dhaka, Dhaka 1000, Bangladesh

Corresponding Author: [1] nazrulislam6727@gmail.com, Tel: +8801717672748; [2*] asalam@gmail.com, Tel: +880117061160

Atmospheric pollution has a significant impact on human health, climate change, agriculture, and ecosystem. Air quality and the climate change is the top most concern of the World Health Organization (WHO, 2019). Bangladesh is a rapidly developing country with kinds of environmental problems. It became the top most country in the world for the human deaths due to environmental pollution, which was accounted about 27% of the total death (Lancet, 207). Only air pollution caused two thirds of these deaths (Lancet, 2017). Dhaka along with Narayanganj and Gazipur are the top ranking cities in the World for the air pollution (WHO, 2014). Volatile organic compounds (VOCs) and poly aromatic hydrocarbons (PAHs) are the major organic pollutants in the atmosphere. Until now there is no information of VOCs and PAHs regarding their occurrences, sources, seasonal variation and health impact in Bangladesh. In this study we have collected particulate matters samples on quartz filters with a low volume sampler at two big cities in Bangladesh (Capital Dhaka and North West City Rajshahi) from January 2015 to February 2019. Individual organic compounds were extracted with acetone and n-hexane from the particulate matter loaded filters. The chemical analysis was done with Gas Chromatography (GC)-Mass spectrometry (MS). The analyzed organic compounds were naphthalene, anthracene, diazinon, deltramethrin, pyrabenxoime, pyrazosulfuran, prophenophos butachlor, propiconazole, cymoxanil, cypermethrin, lamda cyhalothrin, dimethoate, chloropyriphos, carbofuran, metalaxyl, pentane, hexane, propene, isobutene, 1,3-butadiene, dichloroflouromethane, ethanol, benzene, toluene, ethylbenzene, xylene, styrene, 1,2,3trimethylbenzene, isoprene, cyclopentane, and cyclohexane. Positive matrix factorization (PMF) and air mass trajectory analysis were done for source characterization. Health risk assessment and life time cancer risk (LCR)

©2019. Japan Geoscience Union. All Right Reserved.

were determined with US EPA based model. The elevated concentrations of the determined compounds at both Dhaka and Rajshahi were observed; Dhaka values were slightly higher than Rajshahi. The concentrations of determined compounds were higher during the winter months basically December to February and lower during the monsoon period in the month of July. PMF model revealed that the sources of organic compounds in Bangladesh were diesel exhaust, coal and biomass burning, industry and gasoline exhaust. Ethyl benzene, dichlorouflouromethane, 1,2,3-trimethylbenzene have the potential carcinogenic impact.

Key words: Particle Phase Organics, PAHs, VOCs, PMF, Health Risk Assessment

Keywords: Particle Phase Organics, PAHs and VOCs, PMF and Health Risk Assessment

©2019. Japan Geoscience Union. All Right Reserved.

Diversity and activity of diazotrophs in the coastal waters of Southeastern Arabian Sea (SEAS)

*JABIR THAJUDEEN[1], Mohamed Hatha Abdullah

1. Cochin University of Science and Technology India

In marine environments availability of nitrogen (N2) limits the primary productivity. Nitrogen fixing bacteria (diazotrophs) could convert atmospheric nitrogen to ammonium thereby providing significant input of new nitrogen into the ocean. The knowledge about their diversity, distribution and physiological activity are limited in tropical coastal marine environments. In this study, we determined diversity of nitrogen fixing bacteria and the nitrogen fixation rate through *nifH* based clone library analysis and 15N2 bubble method respectively. We encountered *Trichodesmium*bloom and diatom diazotrophic associations along the coastal environments of SEAS. Nitrogen fixation rate in the coastal waters were varied from 0.15 to 1.02 nmolN/L/h. *Trichodesmium*bloom in the Arabian Sea during pre-monsoon season showed higher nitrogen fixation rate of 3.6 nmolN/L/h. Clone library analysis revealed that 19 Operational Taxonomic Units (OTUs) of nitrogen fixing bacteria were observed from the coastal waters SEAS. The OTUs were related to 7 OTUs of cyanobacteria and 12 OTUs of heterotrophic diazotrophs. Major cyanobacterial OTUs are closely similar to *Trichodesmium*sp., *Richelia*sp., *Synechocystis*sp.. Major heterotrophic diazotrophs belonged to alpha-, beta-, gamma-, epislon-, proteobacteria and firmicutes. Gamma proteobacterial clones were dominating among heterotrophic diazotrophs in the coastal water column of south eastern Arabian Sea. Nitrogen fixation rate in the water column were significantly correlated with dissolved Fe (R^2= 0.66, p= 0.05) and phosphorous (R^2= 0.49, p= 0.05), which revealed these are the major factors controlling nitrogen fixation process in the coastal environments of SEAS.

Keywords: Nitrogen fixation , diazotrophs, Fe, SEAS

©2019. Japan Geoscience Union. All Right Reserved.

Bloom of *Palmerina hardmaniana*, a marine centric planktonic diatom in a coastal mangrove ecosystem- implication for coastal carbon cycling

*Punyasloke Bhadury[1]

1. Centre for Climate and Environmental Studies and Department of Biological Sciences, Indian Institute of Science Education and Research Kolkata

Large celled diatoms play an important role in export of carbon in coastal ecosystems. In the Sundarbans mangrove ecosystem located on the delta of Ganga-Brahmaputra-Meghna riverine systems and facing the coastal Bay of Bengal, a bloom of *Palmerina hardmaniana* (Greville) Hasle was tracked in 2015. The bloom of this centric diatom species was tracked from April- July, 2015 in Sundarbans Biological Observatory Time Series (SBOTS) site of Sundarbans. During pre-bloom (April) dissolved oxygen (DO) concentration was 6.82 mg/L while during bloom (May-June) DO concentration decreased to 3.83 mg/L. This also coincided with Chlorophyll-a concentration which ranged from 0.22-6.28 mg/L during the study period, with highest concentration of 6.28 mg/L in bloom period and overwhelmingly dominated by cells belonging to *Palmerina hardmaniana* (40.8 X 10^4 cells/L). In total 72 phytoplankton species were observed from April-July, 2015 in SBOTS site. The frustules of *Palmerina hardmaniana* ranged from 291-358 μm in length and from 195 to 260 μm in width. Based on *rbc*L phylogeny of RuBISCO, the dominance of *P. hardmaniana* was also confirmed. Increased air and surface water temperatures in SBOTS site showed significant correlation with observed cell abundance of *P. hardmaniana* with the onset of bloom. This is the first report of *P. hardmaniana* bloom in the coastal Sundarbans mangrove ecosystem. Therefore, understanding the physiological success of this centric diatom species in relation to dynamic environmental conditions has consequences for tracking export of carbon by centric diatoms in coastal water and resulting implications for coastal carbon cycling.

Keywords: diatom, phytoplankton bloom, mangrove, carbon cycling

©2019. Japan Geoscience Union. All Right Reserved.

Dynamics of Carbon and Nitrogen influx in large river system: Isotopic study from river Ganga, India

*Anurag Kumar[1], Prasanta Sanyal[1,2], Punyasloke Bhadury[3,2]

1. Department of Earth Sciences, Indian Institute of Science Education and Research Kolkata, Mohanpur 741246, India, 2. Centre for Climate and Environmental studies, Indian Institute of Science Education and Research Kolkata, Mohanpur 741246, India, 3. Department of Biological Sciences, Indian Institute of Science Education and Research Kolkata, Mohanpur 741246, India

Freshwater flux transport large amount of carbon (dissolved and particulate, organic and inorganic) and nitrogen (Dissolved) from continent into the ocean, contributing significantly to the global carbon and nitrogen cycle. The present sources and sinks of naturally as well as anthropogenically produced C and N compounds in the global carbon and nitrogen cycle remains enigmatic. Among the carbon sources in the river ecosystem, the dissolved inorganic carbon (DIC) constitute major component of carbon influx from land to ocean. These fluxes are significantly influenced by the terrestrial and estuary processes. The isotopic composition of DIC can be used to understand the sources and cycling of carbon in rivers and estuaries. In this study, $d^{13}C$ of DIC in river water of Ganga has been used to understand the dissolved inorganic carbon sources into the river. The river Ganga (2500 km) is the largest river of the Indian subcontinent which originates from the Gangotri glacier and drains into Bay of Bengal through its vast delta in the Sunderban. The $d^{13}C_{DIC}$ of river water were measured from source (Gomukh) to sink (Bay of Bengal) of the river Ganga for pre and post-monsoon period. The seasonal variation in the $d^{13}C_{DIC}$ shows enriched isotopic values in pre-monsoon compared to post-monsoon samples, indicating increased biological activities in the riverine system during pre-monsoon. A varied enrichment factor in the $d^{13}C_{DIC}$ values were observed for upper, middle and lower stretch of the river Ganga which might be indicating different sources contributing water in different stretch of the river Ganga. The $d^{18}O$ value of river water, ground water and rain water were used to delineate the different sources of water into the river Ganga. The water budget of the river Ganga shows high glacier melt in the upper stretch, high ground water influx in middle stretch and high rain water input in lower stretch of the river Ganga.

On similar note, the dissolved form of nitrogen in river water (NO_3^-) also significantly impacts the riverine as well as costal ecosystem. The increased influx of nitrate changes the competition between species causing disruption in the biological diversity. The lower stretch of the river Ganga receives maximum rain water input; therefore the region becomes prone to pollutant as result of surface runoff from the catchment areas. The isotopic composition of dissolved nitrate in water can be used to delineate the sources of NO_3^- into the riverine system. The $d^{15}N$ and $d^{18}O$ of the dissolved nitrate in river water from the lower stretch (Kolkata) of the river Ganga indicates the input of anthropogenic activities (pollutant) to river water. The data indicates manure from septic pipe lines as major source of dissolved nitrate present in the river Ganga.

Keywords: DIC, Ganga river, nitrate isotope, India

©2019. Japan Geoscience Union. All Right Reserved.

[E] Poster | M (Multidisciplinary and Interdisciplinary)：M-IS Intersection

Mon. May 27, 2019 3:30 PM - 5:00 PM JST | Mon. May 27, 2019 6:30 AM - 8:00 AM UTC | Poster Hall International Exhibition Hall8, Makuhari Messe_19

[M-IS02] Drilling Earth Science

convener:Yasuhiro Yamada(Japan Agency for Marine-Earth Science and Technology (JAMSTEC), R&D Center for Ocean Drilling Science (ODS)), Yumiko Harigane(Geological Survey of Japan, National Institute of Advanced Industrial Science and Technology (AIST)), Azumi Kuroyanagi(Tohoku University Museum, The Center for Academic Resources and Archives, Tohoku University), Kosei E. Yamaguchi(Toho University and NASA Astrobiology Institute)

"Earth Drilling Science" session aims to exchange the latest information and scientific achievements in Ocean/Continental drilling projects and to promote the interdisciplinary science. The session covers a wide range of drilling sciences, earth dynamics, environments, and the drilling-related technologies. The overview of the recent IODP cruises as well as future projects of any types of scientific drilling will be reported.

[MIS02-P01] Utilization and curation of frozen core samples in IODP and implementation of the Nagoya Protocol in ocean drilling science

*Nan XIAO[1] (1.Japan Agency for Marine Earthe Science and Technology)

[MIS02-P02] In-situ rock strength calculated from drilling parameters. Comparison of results from various sites.

*Adam Wspanialy[1], Yasuhiro Yamada[1], Saneatsu Saito[1], KYAW MOE[1] (1.Japan Agency for Marine-Earth Science and Technology)

[MIS02-P03] Interaction between submarine landslides and subseafloor sedimentary microbiome: Chikyu SCORE Expedition 910 off Cape Erimo

*Tatsuhiko Hoshino[1], Go-Ichiro Uramoto[2], Satoshi Tonai[2], Yuki Morono[1], Akira Ijiri[1], Shino Suzuki[1], Yusuke Kubo[1], Fumio Inagaki[1], Chikyu SCORE Exp. 910 Scientists . (1.Japan Agency for Marine-Earth Science and Technology, 2.Kochi University)

[MIS02-P04] High-resolution continuous records of the chemical composition of the marine sediment off Cape Erimo, Hokkaido, Japan

*Masafumi MURAYAMA[1], Shinsuke Yagyu[3], Satoshi Tonai[2], Go-Ichiro Uramoto[3], Yasuhiro Yamada[4], Fumio Inagaki[4], Yusuke Kubo[5] (1.Faculty of Agriculture and Marine Science, Kochi University, 2.Faculty of Science and Technology, Kochi University, 3.Center for Advanced Marine Core Research, Kochi University, 4.Research and Development Center for Ocean Drilling Science, JAMSTEC, 5.Center for Deep Earth Exploration, JAMSTEC)

[MIS02-P05] Thermal property measurements of core samples retrieved from Futagawa fault drilling

*Terasu Sano[1], Weiren Lin[1], Susumu Shibutani[1,2], Nana Kamiya[1], Tatsuhiro Sugimoto[1], Kazuya Ishitsuka[1], Aiming Lin[3] (1.Graduate School of Engineering, Kyoto University, 2.Chi-ken Sogo Consultants Co., Ltd.,, 3.Graduate School of Science, Kyoto University)

[MIS02-P06] Results of geotechnical tests on shallow sediment cores recovered from Lord Howe Rise, off eastern Australia: Implications for future Lord Howe Rise riser drilling

*Takamitsu Sugihara[1], Kan Aoike[1], Saneatsu Saito[2], Tatsuya Murayama[1], Kentaro Takeda[1], Takuya Onodera[3], Ayumi Sumikawa[3], Yukari Kido[1], Yoshinori Sanada[1] (1.Center for deep earth exploration, Japan Agency for Marine-Science and Technology, 2.Research and development center for ocean drilling science, Japan Agency for Marine-Science and Technology, 3.Nippon Marine Enterprises, Ltd.)

[MIS02-P07] ICDP DSeis 4: Drilling, core logging, and in-hole geophysical logging of ICDP DSeis drilling into the M5.5 aftershock zones in a South African gold mines.

*Shunsuke YOSHIDA[1], Tadokoro Ryogo[1], Kosuke Sugimura[1], Kanematsu Makoto[1], Mitsuya Higashi[1], Benni Liebenberg[2], Esterhuizen van Heerden[2], Stephen Tau[3], Siyanda Mngadi[3], Ray Durrheim[3], Martin Ziegler[4], Yusuke Mukuhira[5], Ronald Conze[6], Yasuo Yabe[7], Shunya Kaneki[8], Yuki Yokoyama[9], Nomqhele Nkosi[10], Dave Roberts[10], Sifiso Buccio[11], Hiroshi Ogasawara[1] (1.Graduate school of science and engineering, Ritsumeikan , 2.Moab Khotsong mine, Vijoenskroon, 3.Univ. Witwatersrand, School of Geoscience, 4.ETH, Zurich Dep. Earth Sciences, 5.Inst. Fluid Science, Tohoku Univ., 6.GFZ, Potzdam, 7.Graduate School of Science, Tohoku Univ., 8.Disaster Prevention Research Inst., Kyoto Univ., 9.Graduate School of Science,Osaka Univ., 10.Mandela Mining Precinct, CSIR, 11.Council for Geoscience)

[MIS02-P08] ICDP DSeis 5: Diametrical Core Deformation Analysis of the M5.5 aftershock zone core - stress concentration at reflective intrusives and transition in stress regimes.

*Kosuke Sugimura[1], Shunsuke YOSHIDA[1], Ryogo Tadokoro[1], Hiroshi Ogasawara[2], Akimasa Ishida, Yasuo Yabe[3], Takatoshi Ito[4], Akio Funato[5], Siyanda Mngadi[6], Ray Durrheim[6] (1.Graduate school of science and engineering, Ritsumeikan, 2.College of Science and Engineering, Ritsumeikan Univ., 3.Graduate School of Science, Tohoku Univ., 4.Inst. Fluid Science, Tohoku Univ., 5.Fukada Geological Institute, 6.Univ. Witwatersrand, School of Geoscience)

[MIS02-P09] ICDP DSeis 6: Deformation Rate Analysis of the M5.5 aftershock zone core - stress concentration at reflective intrusives

*Kanematsu Makoto[1], Mitsuya Higashi[1], Yasuo Yabe[2], Shuhei Abe[2], Bryan Watson[3], Ray Durrheim[3], Hiroshi Ogasawara[1] (1.Ritsumeikan Univ., 2.Tohoku Univ., 3.Univ. Witwatersrand)

[MIS02-P10] ICDP DSeis 7: compilation of stress information and comparison with calculated stresses in the M5.5 aftershock zones

*Mitsuya Higashi[1], Yasuo Yabe[2], Kosuke Sugimura[1], Akimasa Ishida, Makoto Kanematsu[1], Shunsuke YOSHIDA[1], Ryogo Tadokoro[1], Takatoshi Ito[4], Akio Funato[5], Hiroshi Ogasawara[3] (1.Graduate School of Science and Engineering, Ritsumeikan Univ., 2.Research Center for Prediction of Earthquakes and Volcanic Eruptions, Graduate School of Science, Tohoku University, 3.College of Science and Engineering, Ritsumeikan Univ., 4.Inst. Fluid Science, Tohoku Univ., 5.Fukada Geological Institute)

[MIS02-P11] ICDP DSeis 8: the M5.5 fault structure and reflective intrusives in legacy 3D seismic reflection data

*Noda Taku[1], Musa Manzi[2], Hiroyuki Ogasawara[1], Lindsay Linzer[2], Stephanie Enslin[2], Ray Durrheim[2], Hiroshi Ogasawara[1] (1.Ritsumeikan Univ., 2.Univ. Witwatersrand)

[MIS02-P12] ICDP DSeis 9: are streaks in the M5.5 aftershocks potentially located on highly stressed intrusive?

*Ryogo Tadokoro[1], Katsuya Ishibashi[2], Horiuchi Shigeki[3], Hiroshi Ogasawara[4] (1.Graduate School of Science and Engineering, Ritsumeikan Univ., 2.School of Science and Engineering, Ritsumeikan Univ., 3.Homeseismo ltd., 4.College of Science and Engineering, Ritsumeikan Univ.)

Utilization and curation of frozen core samples in IODP and implementation of the Nagoya Protocol in ocean drilling science

*Nan XIAO[1]

1. Japan Agency for Marine Earthe Science and Technology

Deep biosphere research has become one of the major scientific focuses in ocean drilling science. How to access to core samples with sufficient quality has been a changes for scientists. Currently there are two methods of accessing to deep biosphere samples which are participating in drilling expeditions and requesting samples from core repositories. The Kochi Core Center has curated deep biosphere samples that were processed aseptically and stored at deep frozen (-80 degree C) condition from more than 10 drilling expeditions. Increased scientific attention to microbiological research of the subseafloor envrionment raises the complications and concerns related to adherence to the Nagoya Protocol of the Convention on Biological Diversity (CBD). The Nagoya Protocol is an international agreement that aims to guide countries in developing standart protocols and protections for accessing biological materials, and sharing benefits derived from their utilization. Since its commencement, the Nagoya Protocol has placed international biological research, especially fieldwork, under greater political scrutiny and increased its complexity due to the variation in implementation between nations. We present the central points of the Nagoya Protocol on access and benefit-sharing (ABS) and discuss their relationship to ocean drilling research. In addition, we address the challenges faced by ocean drilling in complying with this internation convention.

Keywords: ocean drilling program, frozen core sample, Nagoya Protocol, convention on biological diversity

©2019. Japan Geoscience Union. All Right Reserved.

In-situ rock strength calculated from drilling parameters. Comparison of results from various sites.

*Adam Wspanialy[1], Yasuhiro Yamada[1], Saneatsu Saito[1], KYAW MOE[1]

1. Japan Agency for Marine-Earth Science and Technology

Drilling parameters are excellent datasets to understand in-situ physical properties of the rock. Continuous core samples along with parameters such as Torque, RPM, WOB and ROP have been collected during drilling operations. The borehole data acquisition was complemented with full LWD/MWD and wireline logging. After core delivery to surface core scratch tests have been carried out to measure Unconfined Compressive Strength (UCS). Our comprehensive approach enabled us to integrate all data and conduct detailed analysis of the in-situ subsurface physical and mechanical properties of a rock cut by a drill bit.

Here we present some results from offshore and onshore drilling experiments carried out in Japan, Oman and Australia. Methods such as Specific Energy (SE) and Equivalent Strength (EST) have been used to estimate in-situ rock properties, namely UCS and analyse drilling process.

Our results demonstrate that the calculated in-situ rock strength based on SE/EST methods correlates well with sonic derived UCS and core scratch derived UCS. Utilised methods also successfully detect fractures in the formation, show developing drilling dysfunctions such as vibration, and bit balling.

Keywords: rock strength, drilling parameters, Specific Energy

©2019. Japan Geoscience Union. All Right Reserved.

Interaction between submarine landslides and subseafloor sedimentary microbiome: Chikyu SCORE Expedition 910 off Cape Erimo

*Tatsuhiko Hoshino[1], Go-Ichiro Uramoto[2], Satoshi Tonai[2], Yuki Morono[1], Akira Ijiri[1], Shino Suzuki[1], Yusuke Kubo[1], Fumio Inagaki[1], Chikyu SCORE Exp. 910 Scientists .

1. Japan Agency for Marine-Earth Science and Technology, 2. Kochi University

During the past decades, scientific ocean drilling has explored the subseafloor sedimentary biosphere down to over 2 kilometers below seafloor (Inagaki et al., 2015). The total biomass and diversity of microbial community in the subseafloor biosphere are comparable to those in the hydrosphere (Kallmeyer et al., 2012). Taxonomic composition of subseafloor microbial communities are distinct from those of other habitats on Earth’ s surface, such as ocean and soil, inferring that adaptive evolution of microbial community to the energy-limited deep sedimentary habitats have occurred. In a previous study of bioturbated layers in surface marine sediments, it has been reported that seawater-migration by macrofauna activity during the initial depositional stage notably affected microbial community structures (Chen et al. 2017). Similarly, it can be hypothesized that submarine landslides have introduced easily degradable fresh organic matter and dissolved electron acceptors (e.g., oxygen, sulfate) to the sedimentary habitats, and consequently caused a shift of microbial communities and its function.

In 2017, we conducted the Chikyu’ s first SCORE Expedition 910 at the Hidaka Trough off Cap Erimo and obtained sediment cores down to 100 meters below the seafloor. In the core column, four intervals of deformed sediments were identified, indicating the occurrences of multiple submarine landslides in this area. In those deformed sediment intervals, we observed no clear anomaly in the profile of cell abundance, which decrease with sediment depth as generally seen in the other subserfloor sediments. In addition, pore water chemistry data do not show clear anomaly either, indicating recovery of sediment geochemistry from the turbation caused by landslides. While both profiles of microbial cell abundance and pore water geochemistry did not show anomaly in the deformed sediment intervals, the DNA-based analyses, showed some unusual appearances of microbial taxa relative to the depth, suggesting the potential migration of microbes from the upper horizons by submarine landslides.

Reference

Inagaki F, et al (2015). Science 349: 420-424; Kallmeyer J, et al (2012). Proc Natl Acad Sci U S A 109: 16213-16216; Chen X, et al (2017). Sci Rep 7: 2400.

Keywords: Chikyu SCORE, Deep biosphere, Mass transport deposit

©2019. Japan Geoscience Union. All Right Reserved.

High-resolution continuous records of the chemical composition of the marine sediment off Cape Erimo, Hokkaido, Japan

*Masafumi MURAYAMA[1], Shinsuke Yagyu[3], Satoshi Tonai[2], Go-Ichiro Uramoto[3], Yasuhiro Yamada[4], Fumio Inagaki[4], Yusuke Kubo[5]

1. Faculty of Agriculture and Marine Science, Kochi University, 2. Faculty of Science and Technology, Kochi University, 3. Center for Advanced Marine Core Research, Kochi University, 4. Research and Development Center for Ocean Drilling Science, JAMSTEC, 5. Center for Deep Earth Exploration, JAMSTEC

About 100 m sediment cores were taken from off Cape Erimo, Hokkaido, Japan on the Shallow Core Program (SCORE) by D/V Chikyu in 2017. The sedimentary sequence is intercalated with mass transport deposits caused by earthquake-triggered submarine landslides and/or climate changes. Here we report a result of high-resolution continuous geochemical composition of these cores using XRF core scanning technique.

Keywords: sediment core off Cape Erimo, XRF core scanner (ITARX), Shallow Core Program (SCORE), D/V Chikyu

©2019. Japan Geoscience Union. All Right Reserved.

Thermal property measurements of core samples retrieved from Futagawa fault drilling

*Terasu Sano[1], Weiren Lin[1], Susumu Shibutani[1,2], Nana Kamiya[1], Tatsuhiro Sugimoto[1], Kazuya Ishitsuka[1], Aiming Lin[3]

1. Graduate School of Engineering, Kyoto University, 2. Chi-ken Sogo Consultants Co., Ltd.,, 3. Graduate School of Science, Kyoto University

In 2017~2018, to retrieve rock samples from the Futagawa fault ruptured during the 2016 Kumamoto earthquake in Japan, a borehole was drilled down to 700 m depth through the fault in Mashikimachi, Kumamoto prefecture located in the southwest of the Aso volcano. In this borehole, temperature depth profile was measured from ~50 m to ~650 m below the surface (Lin et al., 2019 JpGU). As a preliminary result, an anomaly of temperature, about 1 ℃/km geothermal gradient, was found in the depth range of 310 - 430 m (Lin et al., 2019 JpGU). To examine if this this temperature anomaly comes from thermal conductivity change of the ricks, we collected rock core samples from the borehole and measured their thermal properties.

We measured density, porosity and three thermal transport properties (thermal conductivities, thermal diffusivities, specific heat capacities) of 20 cores drilled from the borehole in the depth range from 300 m to 700 m. I selected typical rock cores to cover not only the depth intervals and also all the main rock types. The rock types of cores are basal sedimentary rocks in 300 m - 353 m , andesite in 353 m - 514 m, sandstone and/or conglomerate in 514 m - 562 m, and tuff in 562 m - 700 m. Measured wet densities and porosities are 1.57 g/cm^3 - 2.02 g/cm^3, 40.0% - 47.8% for basal sedimentary rocks, 2.31 g/cm^3 - 2.95 g/cm^3, 3.1% - 25.5% for andesite, 2.29 g/cm^3 - 2.41 g/cm^3, 21.6% - 29.4% for sandstone and/or conglomerate, 1.99 g/cm^3 - 2.29 g/cm^3, 9.4 % - 35.8% for tuff. Measured thermal conductivities are 0.88 W/(mK) - 1.10 W/(mK) for basal sedimentary rocks, 1.00 W/(mK) - 1.81 W/(mK) for andesite, 1.26 W/(mK) - 1.31 W/(mK) for sandstone and/or conglomerate, 0.96 W/(mK) - 1.27 W/(mK) for tuff. And measured thermal diffusivities and specific heat capacities are 0.85 J/(g･K) - 3.46 J/(g･K) for alluvium, 0.48 m^2/s - 0.91 m^2/s, 1.36 J/(g･K) - 2.60 J/(g･K) for andesite, 0.49 m^2/s - 0.66 m^2/s, 1.95 J/(g･K) - 2.70 J/(g･K) for sandstone and/or conglomerate, 0.40 m^2/s - 0.99 m^2/s, 1.40 J/(g･K) - 2.93 J/(g･K) for tuff. From data of measured temperature of borehole and thermal conductivities of the cores, we calculated heat flow of in the borehole. Using this heat flow and thermal conductivities, we reconstructed the temperature profile in the borehole.

In this estimation, we couldn't reproduce the anomaly of measured temperature. So we conclude that the anomaly of measured temperature is not caused by the significant change of the thermal conductivity in 310 m - 430 m depth.

Keywords: Drilling, thermal properties, Temperature

©2019. Japan Geoscience Union. All Right Reserved.

Results of geotechnical tests on shallow sediment cores recovered from Lord Howe Rise, off eastern Australia: Implications for future Lord Howe Rise riser drilling

*Takamitsu Sugihara[1], Kan Aoike[1], Saneatsu Saito[2], Tatsuya Murayama[1], Kentaro Takeda[1], Takuya Onodera[3], Ayumi Sumikawa[3], Yukari Kido[1], Yoshinori Sanada[1]

1. Center for deep earth exploration, Japan Agency for Marine-Science and Technology, 2. Research and development center for ocean drilling science, Japan Agency for Marine-Science and Technology, 3. Nippon Marine Enterprises, Ltd.

Lord Howe Rise (LHR) Drilling Project (871-CPP2) is an accepted IODP drilling proposal to reconstruct Cretaceous tectonic history of northern Zealandia, designated as a Chikyu riser drilling project. In order to plan a riser drilling operation, it is important to evaluate mechanical strength and physical properties of shallow sediment (0 to 100 or 200 meters below sea floor, mbsf) for setting Blow-out Prevention (BOP) system and riser with heavy weight on the seafloor. Geotechnical core test (e.g., triaxial compressive test and consolidation test) is an essential work to directly measure rock strength and physical properties of geological materials. Therefore, the geotechnical core tests are usually conducted for the surface sediment to evaluate their mechanical and physical properties. In the LHR region, calcareous sediment is broadly and predominantly distributed, and clayey sediment is not observed in shallow sediments. In general, deep seafloor is composed of clayey sediment, and their mechanical and physical properties are well understood. However, mechanical and physical properties of calcareous sediment in both ambient and confined pressure conditions are not well known.

In this study, results of geotechnical test for shallow cores taken in the LHR region are presented, and characteristics of mechanical and physical properties (especially shear strength and permeability) are discussed.

Shallow cores for geotechnical test were taken by R/V Kairei with a gravity piston corer in KR17-15C and by D/V JOIDES Resolution with a rotary core barrel (RCB) in Expedition 371. The gravity piston coring by R/V Kairei was conducted at the proposed riser drilling sites DLHR-5A and -3A, and two cores with approximately 7 m length were taken at each site. The RCB coring by D/V JOIDES Resolution was conducted at Site U1506 in Expedition 371. A whole-round sample with 40 cm length was taken from U1506A-13R for our investigation, and depth of the whole-round sample is 116.5 mbsf. In order to measure physical and mechanical properties for the core samples, geotechnical tests of Penetrometer test, Bulk density, Grain density, Liquid limit, Plastic limit, Grain size distribution, Constant rate of strain consolidation test (CRSC test), and Triaxial compressive strength test with pore pressure measurement (Consolidated-Undrained conditions) were carried out.

Most of the tests except penetrometer test were carried out by OYO Co. Procedures of those measurements and tests were based on the regulations established by Japanese Geotechnical Society (JGS) and Japanese Industrial Standards (JIS). Those are almost the same as their regulations in the ASTM.

All of core samples are composed of calcareous ooze, and grain size distribution of the core samples shows clay size fraction (less than 5 micro meters) is dominant (more than 80 %).

©2019. Japan Geoscience Union. All Right Reserved.

Based on the bulk density data, overburden stresses were calculated and consolidation pressures corresponding to depth of 10 to 240 mbsf for the triaxial test were estimated assuming k0 compaction (k0 factor = 0.5). The result of the triaxial test show shear strength profile gradually increases with depth and is almost identical to those of clayey sediment from Kumano Basin and Nankai Trough. However, the result of the penetrometer test indicates that shear strength of calcareous ooze under ambient condition is quite lower than those of clayey sediment. This observation suggests mechanical strength of calcareous ooze is easily released with depressurizing of sediment.

Based on the result of the CRSC test, it is indicated that calcareous ooze shows no obvious preconsolidation stress, and this result is in good agreement with the result of the triaxial test mentioned above. Permeability of calcareous ooze calculated from the CRSC test results is similar to sandy sediment and the results indicate calcareous ooze is more permeable as compared with clayey sediment.

Those results will be dedicated to analysis for the riser operation in the LHR area.

Keywords: Lord Howe Rise, Riser drilling, Rock strength test, Shear strength, Permeability

©2019. Japan Geoscience Union. All Right Reserved.

ICDP DSeis 4: Drilling, core logging, and in-hole geophysical logging of ICDP DSeis drilling into the M5.5 aftershock zones in a South African gold mines.

*Shunsuke YOSHIDA[1], Tadokoro Ryogo[1], Kosuke Sugimura[1], Kanematsu Makoto[1], Mitsuya Higashi[1], Benni Liebenberg[2], Esterhuizen van Heerden[2], Stephen Tau[3], Siyanda Mngadi[3], Ray Durrheim[3], Martin Ziegler[4], Yusuke Mukuhira[5], Ronald Conze[6], Yasuo Yabe[7], Shunya Kaneki[8], Yuki Yokoyama[9], Nomqhele Nkosi[10], Dave Roberts[10], Sifiso Buccio[11], Hiroshi Ogasawara[1]

1. Graduate school of science and engineering, Ritsumeikan , 2. Moab Khotsong mine, Vijoenskroon, 3. Univ. Witwatersrand, School of Geoscience, 4. ETH, Zurich Dep. Earth Sciences, 5. Inst. Fluid Science, Tohoku Univ., 6. GFZ, Potzdam, 7. Graduate School of Science, Tohoku Univ., 8. Disaster Prevention Research Inst., Kyoto Univ., 9. Graduate School of Science,Osaka Univ., 10. Mandela Mining Precinct, CSIR, 11. Council for Geoscience

ICDP drilling into the aftershock zone of the 2014 M5.5 earthquake near Orkney, South Africa commenced on 2017 and was completed in 2018. This M5.5 earthquake started from a depth about 5 km and ruptured West Rand Group below mining horizon on unknown geological structure in a deep gold mine. The mechanism of left-lateral slip of this M5.5 earthquake contradicted normal-faulting mechanisms of typical mining-induced earthquakes on mining horizons. The upper fringe of the aftershock zone was several hundreds of meters from the deepest level of the mine. Two NQ holes were collared at a depth of 2.9 km (95 level) below surface at a deep gold mine. Hole A (817m) deviated too much to intersect the M5.5 fault but Hole B (700m) intersected the M5.5 fault. A 3-m double-tube couldn't recover the fault material much, while a 1.5m triple-tube could recover the fault material more in Hole C branched from 544 m in Hole B. Geophysical logging, core logging, and water/gas monitoring followed drilling. All the core was transported to Mandela Mining Precinct, CSIR, Johannesburg and systematically described and scanned by the ICDP DMT scanner. Some of the core were selected for core stress measurements.

In JpGU 2019 meeting, nine papers (ICDP DSeis 1-9) report on the outcomes. This poster (ICDP DSeis 4) compiles drilling, core logging, and in-hole geophysical logging of ICDP DSeis drilling into the M5.5 aftershock zones in a South African gold mines. A core orientation tool was used during drilling but not 100% reliable because there was a case that a bottom line in a core run was different by more than 90 degrees from the bottom line in the next core run. We elaborated to compare OTV image with core to carefully check the core orientation. The modified core orientation allowed us to modify the maximum stress direction that Ishida et al. (2018) measured. We could confirm good consistency with borehole breakout analysis (Richenbacher 2018; ETH master thesis). We will report on other associated outcomes. Refer other papers (ICDP DSeis 1-3, 5-9) for other related outcomes.

Acknowledgement: The DSeis team includes co-authors of the papers ICDP DSeis 2-9 and members shown at https://www.icdp-online.org/projects/world/africa/orkney-s-africa/details/. We thank Harmony Gold, Anglogold Ashanthi, Lesedi, Digital Surveying, OHMS, Seismogen, 3D Geoscience. ICDP, JSPS, SA NRF, MEXT Japan, US NSF, German DRF, and Ritsumeikan Univ. financially support the project.

©2019. Japan Geoscience Union. All Right Reserved.

©2019. Japan Geoscience Union. All Right Reserved.

ICDP DSeis 5: Diametrical Core Deformation Analysis of the M5.5 aftershock zone core - stress concentration at reflective intrusives and transition in stress regimes.

*Kosuke Sugimura[1], Shunsuke YOSHIDA[1], Ryogo Tadokoro[1], Hiroshi Ogasawara[2], Akimasa Ishida, Yasuo Yabe[3], Takatoshi Ito[4], Akio Funato[5], Siyanda Mngadi[6], Ray Durrheim[6]

1. Graduate school of science and engineering, Ritsumeikan, 2. College of Science and Engineering, Ritsumeikan Univ., 3. Graduate School of Science, Tohoku Univ., 4. Inst. Fluid Science, Tohoku Univ., 5. Fukada Geological Institute, 6. Univ. Witwatersrand, School of Geoscience

ICDP drilling into the aftershock zone of the 2014 M5.5 earthquake near Orkney, South Africa commenced on 2017 and was completed in 2018. Drilling was designed to minimize damage on core and borehole, being able to maximize core recovery. Hole A (817m) was drilled in 2017. It unfortunately didn't intersect the M5.5 fault, running eventually sub-parallel and roughly 100m from the aftershock zone. As the hole was stable we could recover almost 100% of core from the area traversing the periphery of the M5.5 aftershock zone for a distance of several hundreds of meters. Ishida et al. (2018) carried out Diametrical Core Diameter Analysis (Ito and Funato, 2017). This analysis measures the change in core diameter with roll angle around the core axis, which was caused by a relief of anisotropic stress during drilling. We used this analysis because (1) the expected stress was too high for hydrofracturing method, (2) uncertainty in stress magnitude is unavoidable in damage interpretations, (3) DSeis hole were too long for overcoring technique, and (4) DCDA is non-destructive and very easy to make if core is recovered. Ishida et al. (2018) measured 186 pieces of core from Hole A (817m collared at 2.9km depth) that were recovered near the M5.5 aftershock zone. They successfully illustrated spatial variation in differential stress in a plane perpendicular to Hole A axis. They found stress concentration at intrusives with one located at the depth of the upper fringe of the M5.5 aftershock zone. We carried out additional measurement for the remaining part of Hole A and Hole B. With additional data measured at adjacent locations, we could confirm that the stress concentration Ishida et al (2018) found at intrusives was not an outlier. We will report how Hole B that intersected the M5.5 fault differ from Hole A stress.

This is one of nine ICDP DSeis papers (ICDP DSeis 1-9) presented in JpGU 2019. Refer other papers for other topic on drilling, logging, other stress measurement, fault materials, comparison with calculated stress, legacy 3D seismic reflection data, and relocated aftershocks.

©2019. Japan Geoscience Union. All Right Reserved.

ICDP DSeis 6: Deformation Rate Analysis of the M5.5 aftershock zone core - stress concentration at reflective intrusives

*Kanematsu Makoto[1], Mitsuya Higashi[1], Yasuo Yabe[2], Shuhei Abe[2], Bryan Watson[3], Ray Durrheim[3], Hiroshi Ogasawara[1]

1. Ritsumeikan Univ., 2. Tohoku Univ., 3. Univ. Witwatersrand

ICDP drilling into the aftershock zone of the 2014 M5.5 earthquake near Orkney, South Africa commenced on 2017 and was completed in 2018. Ishida et al. (2018) and Sugimura et al. (2019; ICDP DSeis 5) report on spatial variation of differential stress in a plane perpendicular to the borehole axis. It is ideal to have different stress component especially at critical location where significant characteristics were found. Deformation Rate Analysis (Yamamoto, 2009) can measure stress in any direction although the method takes time and the specimen are not reusable for other test. So, we planned to selected samples where characteristic spatial variation was found by DCDA method (Ishida et al. 2018 and Sugimura et al. 2019). It was confirmed also in normal stress component along the borehole axis that stress was concentrated at the intrusive at about 400m.

This is one of nine ICDP DSeis papers (ICDP DSeis 1-9) presented in JpGU 2019. Refer other papers for other topics on drilling, logging, other stress measurement, fault materials, comparison with calculated stress, legacy 3D seismic reflection data, and relocated aftershocks.

Acknowledgement: The DSeis team includes co-authors of the papers ICDP DSeis 2-9 and members shown at https://www.icdp-online.org/projects/world/africa/orkney-s-africa/details/. We thank Harmony Gold, Anglogold Ashanthi, Lesedi, Digital Surveying, OHMS, Seismogen, 3D Geoscience. ICDP, JSPS, SA NRF, MEXT Japan, US NSF, German DRF, and Ritsumeikan Univ. financially support the project.

Keywords: Seismogenic zone, Stress Measurement, DRA

©2019. Japan Geoscience Union. All Right Reserved.

ICDP DSeis 7: compilation of stress information and comparison with calculated stresses in the M5.5 aftershock zones

*Mitsuya Higashi[1], Yasuo Yabe[2], Kosuke Sugimura[1], Akimasa Ishida, Makoto Kanematsu[1], Shunsuke YOSHIDA[1], Ryogo Tadokoro[1], Takatoshi Ito[4], Akio Funato[5], Hiroshi Ogasawara[3]

1. Graduate School of Science and Engineering, Ritsumeikan Univ., 2. Research Center for Prediction of Earthquakes and Volcanic Eruptions, Graduate School of Science, Tohoku University, 3. College of Science and Engineering, Ritsumeikan Univ., 4. Inst. Fluid Science, Tohoku Univ., 5. Fukada Geological Institute

ICDP drilling into the aftershock zone of the 2014 M5.5 earthquake near Orkney, South Africa commenced on 2017 and was completed in 2018. Spatial variation in stress was measured by Ishida et al. (2018) and Sugimura et al. (2019; ICDP DSeis 5) by DCDA method (Funato and Ito, 2017) and Kanematsu et al. (2019; ICDP DSeis 6). This poster reports on compilation of stress information including the other information sources and compares with calculated stress.

We first compared with a 3D stress state that Ogasawara et al. (2012) measured in 2011 at 98L (3.0 km depth from surface). We assume zero stress on surface, the measured 3D stress (normal faulting stress regime) at 3.0 km, and stress linearly increasing with depth. The calculated stress was consistent with DCDA results measured in the initial 100m section in Hole A, while inconsistent in deeper section. The calculated direction of maximum stress in a plane perpendicular to the borehole axis was also inconsistent with the measured stress information (Yoshida et al. 2019 JpGU; ICDP DSeis 5). Except for the stress concentration measured at intrusives, the measured DCDA results were systematically lower than the calculated stress. In a stress regime that caused the left-lateral horizontal slip on the M5.5 fault, horizontal stress should be larger, which will increase horizontal stress component in a plane perpendicular to the Hole A axis. This increase should decrease difference in stress in the plane perpendicular to the Hole A axis. By JpGU 2019, we will make additional effort to interpret more from the comparison between the measured and calculated stress.

This is one of nine papers (ICDP DSeis 1-9). Refer other papers for other topic on drilling, logging, other stress measurement, fault materials, legacy 3D seismic reflection data, and relocated aftershocks.

Acknowledgement: The DSeis team includes co-authors of the papers ICDP DSeis 2-9 and members shown at https://www.icdp-online.org/projects/world/africa/orkney-s-africa/details/. We thank Harmony Gold, Anglogold Ashanthi, Lesedi, Digital Surveying, OHMS, Seismogen, 3D Geoscience. ICDP, JSPS, SA NRF, MEXT Japan, US NSF, German DRF, and Ritsumeikan Univ. financially support the project.

©2019. Japan Geoscience Union. All Right Reserved.

ICDP DSeis 8: the M5.5 fault structure and reflective intrusives in legacy 3D seismic reflection data

*Noda Taku[1], Musa Manzi[2], Hiroyuki Ogasawara[1], Lindsay Linzer[2], Stephanie Enslin[2], Ray Durrheim[2], Hiroshi Ogasawara[1]

1. Ritsumeikan Univ., 2. Univ. Witwatersrand

ICDP drilling into the aftershock zone of the 2014 M5.5 earthquake near Orkney, South Africa commenced on 2017 and was completed in 2018. Hiroyuki et al. (2017 AGU) reported on legacy seismic reflection to analyze geological structures in the southern most area of the M5.5 aftershock zones. They found vertical structures in four 2-D lines that were potentially responsible for the M5.5 earthquake and illustrated cross-cutting relations of the M5.5 structure and other known faults that dislocated gold reefs more than several hundreds of meters both horizontally and vertically. Another legacy seismic reflection data which was recorded in 1996 and covered much wider area of the M5.5 aftershock zone was found. We calibrated velocity structure by tying with borehole data including DSeis Holes A and B, we found some of intrusives (sills) that Hole A and B were strong reflectors in the legacy 3D seismic reflection data.

Aftershocks located by in-mine 46 geophones are dense at the southern upper fringe, with a sharp cut-off dipping about 20 degrees to the south; some clear stripes of aftershocks are also seen, in parallel to the upper fringe (Tadokoro et al., JpGU2019, ICDP DSeis 9). It is interesting to note that the reflector (sills) are also in parallel to the upper fringe of the aftershock zone and the aftershock stripes. It is also notable that stress concentration is reported at the intrusives by Sugimura et al. (JpGU2019; ICDP DSeis 5) and Kanematsu et al. (JpGU2019; ICDP DSeis 6). Some mechanism that controls the extent of the aftershocks should exist.

This paper is one of nine papers (ICDP DSeis 1-9). Refer other papers for other topics, e.g. on drilling, logging, stress measurements and evaluation, fault materials, and relocated aftershocks.

Acknowledgement: The DSeis team includes co-authors of the papers ICDP DSeis 2-9 and members shown at https://www.icdp-online.org/projects/world/africa/orkney-s-africa/details/. We thank Harmony Gold, Anglogold Ashanthi, Lesedi, Digital Surveying, OHMS, Seismogen, 3D Geoscience. ICDP, JSPS, SA NRF, MEXT Japan, US NSF, German DRF, and Ritsumeikan Univ. financially support the project.

Keywords: ICDP DSeis, The M5.5 seismogenic zone, Seismic reflection

©2019. Japan Geoscience Union. All Right Reserved.

ICDP DSeis 9: are streaks in the M5.5 aftershocks potentially located on highly stressed intrusive?

*Ryogo Tadokoro[1], Katsuya Ishibashi[2], Horiuchi Shigeki[3], Hiroshi Ogasawara[4]

1. Graduate School of Science and Engineering, Ritsumeikan Univ., 2. School of Science and Engineering, Ritsumeikan Univ., 3. Homeseismo ltd., 4. College of Science and Engineering, Ritsumeikan Univ.

ICDP drilling into the aftershock zone of the 2014 M5.5 earthquake near Orkney, South Africa commenced on 2017 and was completed in 2018. Aftershocks located by in-mine 46 geophones are dense at the southern upper fringe, with a sharp cut-off dipping about 20 degrees to the south. Some clear stripes of aftershocks are also seen, in parallel to the upper fringe. It is interesting to note that the reflector (sills) are also in parallel to the upper fringe of the aftershock zone and the aftershock stripes. It is also notable that stress concentration is reported at the intrusives by Sugimura et al. (JpGU2019; ICDP DSeis 5) and Kanematsu et al. (JpGU2019; ICDP DSeis 6). Some mechanism that controls the extent of the aftershocks should exist.

In order to discuss further, we relocated aftershocks with the Double-Difference method (Waldhouser and Ellsworth, 2004). At the moment, we could relocate only 60 events at the upper fringe of the aftershocks. We used in-mine seismic network data of Anglogold Ashanti. P- and S- arrival times that the algorithm of Horiuchi et al. (2011) was used. A sharper alignment of aftershocks is successfully illustrated. By JpGU 2019, we will make additional efforts to extend the area of relocation to discuss more.

Acknowledgement: The DSeis team includes co-authors of the papers ICDP DSeis 2-9 and members shown at https://www.icdp-online.org/projects/world/africa/orkney-s-africa/details/. We thank Harmony Gold, Anglogold Ashanthi, Lesedi, Digital Surveying, OHMS, Seismogen, 3D Geoscience. ICDP, JSPS, SA NRF, MEXT Japan, US NSF, German DRF, and Ritsumeikan Univ. financially support the project.

©2019. Japan Geoscience Union. All Right Reserved.

[E] Poster | M (Multidisciplinary and Interdisciplinary)：M-IS Intersection

Mon. May 27, 2019 5:15 PM - 6:30 PM JST | Mon. May 27, 2019 8:15 AM - 9:30 AM UTC | Poster Hall International Exhibition Hall8, Makuhari Messe_32

[M-IS02] Drilling Earth Science

convener:Yasuhiro Yamada(Japan Agency for Marine-Earth Science and Technology (JAMSTEC), R&D Center for Ocean Drilling Science (ODS)), Yumiko Harigane(Geological Survey of Japan, National Institute of Advanced Industrial Science and Technology (AIST)), Azumi Kuroyanagi(Tohoku University Museum, The Center for Academic Resources and Archives, Tohoku University), Kosei E. Yamaguchi(Toho University and NASA Astrobiology Institute)

"Earth Drilling Science" session aims to exchange the latest information and scientific achievements in Ocean/Continental drilling projects and to promote the interdisciplinary science. The session covers a wide range of drilling sciences, earth dynamics, environments, and the drilling-related technologies. The overview of the recent IODP cruises as well as future projects of any types of scientific drilling will be reported.

[MIS02-P01] Utilization and curation of frozen core samples in IODP and implementation of the Nagoya Protocol in ocean drilling science

*Nan XIAO[1] (1.Japan Agency for Marine Earthe Science and Technology)

[MIS02-P02] In-situ rock strength calculated from drilling parameters. Comparison of results from various sites.

*Adam Wspanialy[1], Yasuhiro Yamada[1], Saneatsu Saito[1], KYAW MOE[1] (1.Japan Agency for Marine-Earth Science and Technology)

[MIS02-P03] Interaction between submarine landslides and subseafloor sedimentary microbiome: Chikyu SCORE Expedition 910 off Cape Erimo

*Tatsuhiko Hoshino[1], Go-Ichiro Uramoto[2], Satoshi Tonai[2], Yuki Morono[1], Akira Ijiri[1], Shino Suzuki[1], Yusuke Kubo[1], Fumio Inagaki[1], Chikyu SCORE Exp. 910 Scientists . (1.Japan Agency for Marine-Earth Science and Technology, 2.Kochi University)

[MIS02-P04] High-resolution continuous records of the chemical composition of the marine sediment off Cape Erimo, Hokkaido, Japan

*Masafumi MURAYAMA[1], Shinsuke Yagyu[3], Satoshi Tonai[2], Go-Ichiro Uramoto[3], Yasuhiro Yamada[4], Fumio Inagaki[4], Yusuke Kubo[5] (1.Faculty of Agriculture and Marine Science, Kochi University, 2.Faculty of Science and Technology, Kochi University, 3.Center for Advanced Marine Core Research, Kochi University, 4.Research and Development Center for Ocean Drilling Science, JAMSTEC, 5.Center for Deep Earth Exploration, JAMSTEC)

[MIS02-P05] Thermal property measurements of core samples retrieved from Futagawa fault drilling

*Terasu Sano[1], Weiren Lin[1], Susumu Shibutani[1,2], Nana Kamiya[1], Tatsuhiro Sugimoto[1], Kazuya Ishitsuka[1], Aiming Lin[3] (1.Graduate School of Engineering, Kyoto University, 2.Chi-ken Sogo Consultants Co., Ltd.,, 3.Graduate School of Science, Kyoto University)

[MIS02-P06] Results of geotechnical tests on shallow sediment cores recovered from Lord Howe Rise, off eastern Australia: Implications for future Lord Howe Rise riser drilling

*Takamitsu Sugihara[1], Kan Aoike[1], Saneatsu Saito[2], Tatsuya Murayama[1], Kentaro Takeda[1], Takuya Onodera[3], Ayumi Sumikawa[3], Yukari Kido[1], Yoshinori Sanada[1] (1.Center for deep earth exploration, Japan Agency for Marine-Science and Technology, 2.Research and development center for ocean drilling science, Japan Agency for Marine-Science and Technology, 3.Nippon Marine Enterprises, Ltd.)

[MIS02-P07] ICDP DSeis 4: Drilling, core logging, and in-hole geophysical logging of ICDP DSeis drilling into the M5.5 aftershock zones in a South African gold mines.

*Shunsuke YOSHIDA[1], Tadokoro Ryogo[1], Kosuke Sugimura[1], Kanematsu Makoto[1], Mitsuya Higashi[1], Benni Liebenberg[2], Esterhuizen van Heerden[2], Stephen Tau[3], Siyanda Mngadi[3], Ray Durrheim[3], Martin Ziegler[4], Yusuke Mukuhira[5], Ronald Conze[6], Yasuo Yabe[7], Shunya Kaneki[8], Yuki Yokoyama[9], Nomqhele Nkosi[10], Dave Roberts[10], Sifiso Buccio[11], Hiroshi Ogasawara[1] (1.Graduate school of science and engineering, Ritsumeikan , 2.Moab Khotsong mine, Vijoenskroon, 3.Univ. Witwatersrand, School of Geoscience, 4.ETH, Zurich Dep. Earth Sciences, 5.Inst. Fluid Science, Tohoku Univ., 6.GFZ, Potzdam, 7.Graduate School of Science, Tohoku Univ., 8.Disaster Prevention Research Inst., Kyoto Univ., 9.Graduate School of Science,Osaka Univ., 10.Mandela Mining Precinct, CSIR, 11.Council for Geoscience)

[MIS02-P08] ICDP DSeis 5: Diametrical Core Deformation Analysis of the M5.5 aftershock zone core - stress concentration at reflective intrusives and transition in stress regimes.

*Kosuke Sugimura[1], Shunsuke YOSHIDA[1], Ryogo Tadokoro[1], Hiroshi Ogasawara[2], Akimasa Ishida, Yasuo Yabe[3], Takatoshi Ito[4], Akio Funato[5], Siyanda Mngadi[6], Ray Durrheim[6] (1.Graduate school of science and engineering, Ritsumeikan, 2.College of Science and Engineering, Ritsumeikan Univ., 3.Graduate School of Science, Tohoku Univ., 4.Inst. Fluid Science, Tohoku Univ., 5.Fukada Geological Institute, 6.Univ. Witwatersrand, School of Geoscience)

[MIS02-P09] ICDP DSeis 6: Deformation Rate Analysis of the M5.5 aftershock zone core - stress concentration at reflective intrusives

*Kanematsu Makoto[1], Mitsuya Higashi[1], Yasuo Yabe[2], Shuhei Abe[2], Bryan Watson[3], Ray Durrheim[3], Hiroshi Ogasawara[1] (1.Ritsumeikan Univ., 2.Tohoku Univ., 3.Univ. Witwatersrand)

[MIS02-P10] ICDP DSeis 7: compilation of stress information and comparison with calculated stresses in the M5.5 aftershock zones

*Mitsuya Higashi[1], Yasuo Yabe[2], Kosuke Sugimura[1], Akimasa Ishida, Makoto Kanematsu[1], Shunsuke YOSHIDA[1], Ryogo Tadokoro[1], Takatoshi Ito[4], Akio Funato[5], Hiroshi Ogasawara[3] (1.Graduate School of Science and Engineering, Ritsumeikan Univ., 2.Research Center for Prediction of Earthquakes and Volcanic Eruptions, Graduate School of Science, Tohoku University, 3.College of Science and Engineering, Ritsumeikan Univ., 4.Inst. Fluid Science, Tohoku Univ., 5.Fukada Geological Institute)

[MIS02-P11] ICDP DSeis 8: the M5.5 fault structure and reflective intrusives in legacy 3D seismic reflection data

*Noda Taku[1], Musa Manzi[2], Hiroyuki Ogasawara[1], Lindsay Linzer[2], Stephanie Enslin[2], Ray Durrheim[2], Hiroshi Ogasawara[1] (1.Ritsumeikan Univ., 2.Univ. Witwatersrand)

[MIS02-P12] ICDP DSeis 9: are streaks in the M5.5 aftershocks potentially located on highly stressed intrusive?

*Ryogo Tadokoro[1], Katsuya Ishibashi[2], Horiuchi Shigeki[3], Hiroshi Ogasawara[4] (1.Graduate School of Science and Engineering, Ritsumeikan Univ., 2.School of Science and Engineering, Ritsumeikan Univ., 3.Homeseismo ltd., 4.College of Science and Engineering, Ritsumeikan Univ.)

Utilization and curation of frozen core samples in IODP and implementation of the Nagoya Protocol in ocean drilling science

*Nan XIAO[1]

1. Japan Agency for Marine Earthe Science and Technology

Deep biosphere research has become one of the major scientific focuses in ocean drilling science. How to access to core samples with sufficient quality has been a changes for scientists. Currently there are two methods of accessing to deep biosphere samples which are participating in drilling expeditions and requesting samples from core repositories. The Kochi Core Center has curated deep biosphere samples that were processed aseptically and stored at deep frozen (-80 degree C) condition from more than 10 drilling expeditions. Increased scientific attention to microbiological research of the subseafloor envrionment raises the complications and concerns related to adherence to the Nagoya Protocol of the Convention on Biological Diversity (CBD). The Nagoya Protocol is an international agreement that aims to guide countries in developing standart protocols and protections for accessing biological materials, and sharing benefits derived from their utilization. Since its commencement, the Nagoya Protocol has placed international biological research, especially fieldwork, under greater political scrutiny and increased its complexity due to the variation in implementation between nations. We present the central points of the Nagoya Protocol on access and benefit-sharing (ABS) and discuss their relationship to ocean drilling research. In addition, we address the challenges faced by ocean drilling in complying with this internation convention.

Keywords: ocean drilling program, frozen core sample, Nagoya Protocol, convention on biological diversity

©2019. Japan Geoscience Union. All Right Reserved.

In-situ rock strength calculated from drilling parameters. Comparison of results from various sites.

*Adam Wspanialy[1], Yasuhiro Yamada[1], Saneatsu Saito[1], KYAW MOE[1]

1. Japan Agency for Marine-Earth Science and Technology

Drilling parameters are excellent datasets to understand in-situ physical properties of the rock. Continuous core samples along with parameters such as Torque, RPM, WOB and ROP have been collected during drilling operations. The borehole data acquisition was complemented with full LWD/MWD and wireline logging. After core delivery to surface core scratch tests have been carried out to measure Unconfined Compressive Strength (UCS). Our comprehensive approach enabled us to integrate all data and conduct detailed analysis of the in-situ subsurface physical and mechanical properties of a rock cut by a drill bit.

Here we present some results from offshore and onshore drilling experiments carried out in Japan, Oman and Australia. Methods such as Specific Energy (SE) and Equivalent Strength (EST) have been used to estimate in-situ rock properties, namely UCS and analyse drilling process.

Our results demonstrate that the calculated in-situ rock strength based on SE/EST methods correlates well with sonic derived UCS and core scratch derived UCS. Utilised methods also successfully detect fractures in the formation, show developing drilling dysfunctions such as vibration, and bit balling.

Keywords: rock strength, drilling parameters, Specific Energy

©2019. Japan Geoscience Union. All Right Reserved.

Interaction between submarine landslides and subseafloor sedimentary microbiome: Chikyu SCORE Expedition 910 off Cape Erimo

*Tatsuhiko Hoshino[1], Go-Ichiro Uramoto[2], Satoshi Tonai[2], Yuki Morono[1], Akira Ijiri[1], Shino Suzuki[1], Yusuke Kubo[1], Fumio Inagaki[1], Chikyu SCORE Exp. 910 Scientists .

1. Japan Agency for Marine-Earth Science and Technology, 2. Kochi University

During the past decades, scientific ocean drilling has explored the subseafloor sedimentary biosphere down to over 2 kilometers below seafloor (Inagaki et al., 2015). The total biomass and diversity of microbial community in the subseafloor biosphere are comparable to those in the hydrosphere (Kallmeyer et al., 2012). Taxonomic composition of subseafloor microbial communities are distinct from those of other habitats on Earth’ s surface, such as ocean and soil, inferring that adaptive evolution of microbial community to the energy-limited deep sedimentary habitats have occurred. In a previous study of bioturbated layers in surface marine sediments, it has been reported that seawater-migration by macrofauna activity during the initial depositional stage notably affected microbial community structures (Chen et al. 2017). Similarly, it can be hypothesized that submarine landslides have introduced easily degradable fresh organic matter and dissolved electron acceptors (e.g., oxygen, sulfate) to the sedimentary habitats, and consequently caused a shift of microbial communities and its function.

In 2017, we conducted the Chikyu’ s first SCORE Expedition 910 at the Hidaka Trough off Cap Erimo and obtained sediment cores down to 100 meters below the seafloor. In the core column, four intervals of deformed sediments were identified, indicating the occurrences of multiple submarine landslides in this area. In those deformed sediment intervals, we observed no clear anomaly in the profile of cell abundance, which decrease with sediment depth as generally seen in the other subserfloor sediments. In addition, pore water chemistry data do not show clear anomaly either, indicating recovery of sediment geochemistry from the turbation caused by landslides. While both profiles of microbial cell abundance and pore water geochemistry did not show anomaly in the deformed sediment intervals, the DNA-based analyses, showed some unusual appearances of microbial taxa relative to the depth, suggesting the potential migration of microbes from the upper horizons by submarine landslides.

Reference

Inagaki F, et al (2015). Science 349: 420-424; Kallmeyer J, et al (2012). Proc Natl Acad Sci U S A 109: 16213-16216; Chen X, et al (2017). Sci Rep 7: 2400.

Keywords: Chikyu SCORE, Deep biosphere, Mass transport deposit

©2019. Japan Geoscience Union. All Right Reserved.

High-resolution continuous records of the chemical composition of the marine sediment off Cape Erimo, Hokkaido, Japan

*Masafumi MURAYAMA[1], Shinsuke Yagyu[3], Satoshi Tonai[2], Go-Ichiro Uramoto[3], Yasuhiro Yamada[4], Fumio Inagaki[4], Yusuke Kubo[5]

1. Faculty of Agriculture and Marine Science, Kochi University, 2. Faculty of Science and Technology, Kochi University, 3. Center for Advanced Marine Core Research, Kochi University, 4. Research and Development Center for Ocean Drilling Science, JAMSTEC, 5. Center for Deep Earth Exploration, JAMSTEC

About 100 m sediment cores were taken from off Cape Erimo, Hokkaido, Japan on the Shallow Core Program (SCORE) by D/V Chikyu in 2017. The sedimentary sequence is intercalated with mass transport deposits caused by earthquake-triggered submarine landslides and/or climate changes. Here we report a result of high-resolution continuous geochemical composition of these cores using XRF core scanning technique.

Keywords: sediment core off Cape Erimo, XRF core scanner (ITARX), Shallow Core Program (SCORE), D/V Chikyu

©2019. Japan Geoscience Union. All Right Reserved.

Thermal property measurements of core samples retrieved from Futagawa fault drilling

*Terasu Sano[1], Weiren Lin[1], Susumu Shibutani[1,2], Nana Kamiya[1], Tatsuhiro Sugimoto[1], Kazuya Ishitsuka[1], Aiming Lin[3]

1. Graduate School of Engineering, Kyoto University, 2. Chi-ken Sogo Consultants Co., Ltd.,, 3. Graduate School of Science, Kyoto University

In 2017~2018, to retrieve rock samples from the Futagawa fault ruptured during the 2016 Kumamoto earthquake in Japan, a borehole was drilled down to 700 m depth through the fault in Mashikimachi, Kumamoto prefecture located in the southwest of the Aso volcano. In this borehole, temperature depth profile was measured from ~50 m to ~650 m below the surface (Lin et al., 2019 JpGU). As a preliminary result, an anomaly of temperature, about 1 ℃/km geothermal gradient, was found in the depth range of 310 - 430 m (Lin et al., 2019 JpGU). To examine if this this temperature anomaly comes from thermal conductivity change of the ricks, we collected rock core samples from the borehole and measured their thermal properties.

We measured density, porosity and three thermal transport properties (thermal conductivities, thermal diffusivities, specific heat capacities) of 20 cores drilled from the borehole in the depth range from 300 m to 700 m. I selected typical rock cores to cover not only the depth intervals and also all the main rock types. The rock types of cores are basal sedimentary rocks in 300 m - 353 m , andesite in 353 m - 514 m, sandstone and/or conglomerate in 514 m - 562 m, and tuff in 562 m - 700 m. Measured wet densities and porosities are 1.57 g/cm^3 - 2.02 g/cm^3, 40.0% - 47.8% for basal sedimentary rocks, 2.31 g/cm^3 - 2.95 g/cm^3, 3.1% - 25.5% for andesite, 2.29 g/cm^3 - 2.41 g/cm^3, 21.6% - 29.4% for sandstone and/or conglomerate, 1.99 g/cm^3 - 2.29 g/cm^3, 9.4 % - 35.8% for tuff. Measured thermal conductivities are 0.88 W/(mK) - 1.10 W/(mK) for basal sedimentary rocks, 1.00 W/(mK) - 1.81 W/(mK) for andesite, 1.26 W/(mK) - 1.31 W/(mK) for sandstone and/or conglomerate, 0.96 W/(mK) - 1.27 W/(mK) for tuff. And measured thermal diffusivities and specific heat capacities are 0.85 J/(g･K) - 3.46 J/(g･K) for alluvium, 0.48 m^2/s - 0.91 m^2/s, 1.36 J/(g･K) - 2.60 J/(g･K) for andesite, 0.49 m^2/s - 0.66 m^2/s, 1.95 J/(g･K) - 2.70 J/(g･K) for sandstone and/or conglomerate, 0.40 m^2/s - 0.99 m^2/s, 1.40 J/(g･K) - 2.93 J/(g･K) for tuff. From data of measured temperature of borehole and thermal conductivities of the cores, we calculated heat flow of in the borehole. Using this heat flow and thermal conductivities, we reconstructed the temperature profile in the borehole.

In this estimation, we couldn't reproduce the anomaly of measured temperature. So we conclude that the anomaly of measured temperature is not caused by the significant change of the thermal conductivity in 310 m - 430 m depth.

Keywords: Drilling, thermal properties, Temperature

©2019. Japan Geoscience Union. All Right Reserved.

Results of geotechnical tests on shallow sediment cores recovered from Lord Howe Rise, off eastern Australia: Implications for future Lord Howe Rise riser drilling

*Takamitsu Sugihara[1], Kan Aoike[1], Saneatsu Saito[2], Tatsuya Murayama[1], Kentaro Takeda[1], Takuya Onodera[3], Ayumi Sumikawa[3], Yukari Kido[1], Yoshinori Sanada[1]

1. Center for deep earth exploration, Japan Agency for Marine-Science and Technology, 2. Research and development center for ocean drilling science, Japan Agency for Marine-Science and Technology, 3. Nippon Marine Enterprises, Ltd.

Lord Howe Rise (LHR) Drilling Project (871-CPP2) is an accepted IODP drilling proposal to reconstruct Cretaceous tectonic history of northern Zealandia, designated as a Chikyu riser drilling project. In order to plan a riser drilling operation, it is important to evaluate mechanical strength and physical properties of shallow sediment (0 to 100 or 200 meters below sea floor, mbsf) for setting Blow-out Prevention (BOP) system and riser with heavy weight on the seafloor. Geotechnical core test (e.g., triaxial compressive test and consolidation test) is an essential work to directly measure rock strength and physical properties of geological materials. Therefore, the geotechnical core tests are usually conducted for the surface sediment to evaluate their mechanical and physical properties. In the LHR region, calcareous sediment is broadly and predominantly distributed, and clayey sediment is not observed in shallow sediments. In general, deep seafloor is composed of clayey sediment, and their mechanical and physical properties are well understood. However, mechanical and physical properties of calcareous sediment in both ambient and confined pressure conditions are not well known.

In this study, results of geotechnical test for shallow cores taken in the LHR region are presented, and characteristics of mechanical and physical properties (especially shear strength and permeability) are discussed.

Shallow cores for geotechnical test were taken by R/V Kairei with a gravity piston corer in KR17-15C and by D/V JOIDES Resolution with a rotary core barrel (RCB) in Expedition 371. The gravity piston coring by R/V Kairei was conducted at the proposed riser drilling sites DLHR-5A and -3A, and two cores with approximately 7 m length were taken at each site. The RCB coring by D/V JOIDES Resolution was conducted at Site U1506 in Expedition 371. A whole-round sample with 40 cm length was taken from U1506A-13R for our investigation, and depth of the whole-round sample is 116.5 mbsf. In order to measure physical and mechanical properties for the core samples, geotechnical tests of Penetrometer test, Bulk density, Grain density, Liquid limit, Plastic limit, Grain size distribution, Constant rate of strain consolidation test (CRSC test), and Triaxial compressive strength test with pore pressure measurement (Consolidated-Undrained conditions) were carried out.

Most of the tests except penetrometer test were carried out by OYO Co. Procedures of those measurements and tests were based on the regulations established by Japanese Geotechnical Society (JGS) and Japanese Industrial Standards (JIS). Those are almost the same as their regulations in the ASTM.

All of core samples are composed of calcareous ooze, and grain size distribution of the core samples shows clay size fraction (less than 5 micro meters) is dominant (more than 80 %).

©2019. Japan Geoscience Union. All Right Reserved.

Based on the bulk density data, overburden stresses were calculated and consolidation pressures corresponding to depth of 10 to 240 mbsf for the triaxial test were estimated assuming k0 compaction (k0 factor = 0.5). The result of the triaxial test show shear strength profile gradually increases with depth and is almost identical to those of clayey sediment from Kumano Basin and Nankai Trough. However, the result of the penetrometer test indicates that shear strength of calcareous ooze under ambient condition is quite lower than those of clayey sediment. This observation suggests mechanical strength of calcareous ooze is easily released with depressurizing of sediment.

Based on the result of the CRSC test, it is indicated that calcareous ooze shows no obvious preconsolidation stress, and this result is in good agreement with the result of the triaxial test mentioned above. Permeability of calcareous ooze calculated from the CRSC test results is similar to sandy sediment and the results indicate calcareous ooze is more permeable as compared with clayey sediment.

Those results will be dedicated to analysis for the riser operation in the LHR area.

Keywords: Lord Howe Rise, Riser drilling, Rock strength test, Shear strength, Permeability

©2019. Japan Geoscience Union. All Right Reserved.

ICDP DSeis 4: Drilling, core logging, and in-hole geophysical logging of ICDP DSeis drilling into the M5.5 aftershock zones in a South African gold mines.

*Shunsuke YOSHIDA[1], Tadokoro Ryogo[1], Kosuke Sugimura[1], Kanematsu Makoto[1], Mitsuya Higashi[1], Benni Liebenberg[2], Esterhuizen van Heerden[2], Stephen Tau[3], Siyanda Mngadi[3], Ray Durrheim[3], Martin Ziegler[4], Yusuke Mukuhira[5], Ronald Conze[6], Yasuo Yabe[7], Shunya Kaneki[8], Yuki Yokoyama[9], Nomqhele Nkosi[10], Dave Roberts[10], Sifiso Buccio[11], Hiroshi Ogasawara[1]

1. Graduate school of science and engineering, Ritsumeikan , 2. Moab Khotsong mine, Vijoenskroon, 3. Univ. Witwatersrand, School of Geoscience, 4. ETH, Zurich Dep. Earth Sciences, 5. Inst. Fluid Science, Tohoku Univ., 6. GFZ, Potzdam, 7. Graduate School of Science, Tohoku Univ., 8. Disaster Prevention Research Inst., Kyoto Univ., 9. Graduate School of Science,Osaka Univ., 10. Mandela Mining Precinct, CSIR, 11. Council for Geoscience

ICDP drilling into the aftershock zone of the 2014 M5.5 earthquake near Orkney, South Africa commenced on 2017 and was completed in 2018. This M5.5 earthquake started from a depth about 5 km and ruptured West Rand Group below mining horizon on unknown geological structure in a deep gold mine. The mechanism of left-lateral slip of this M5.5 earthquake contradicted normal-faulting mechanisms of typical mining-induced earthquakes on mining horizons. The upper fringe of the aftershock zone was several hundreds of meters from the deepest level of the mine. Two NQ holes were collared at a depth of 2.9 km (95 level) below surface at a deep gold mine. Hole A (817m) deviated too much to intersect the M5.5 fault but Hole B (700m) intersected the M5.5 fault. A 3-m double-tube couldn't recover the fault material much, while a 1.5m triple-tube could recover the fault material more in Hole C branched from 544 m in Hole B. Geophysical logging, core logging, and water/gas monitoring followed drilling. All the core was transported to Mandela Mining Precinct, CSIR, Johannesburg and systematically described and scanned by the ICDP DMT scanner. Some of the core were selected for core stress measurements.

In JpGU 2019 meeting, nine papers (ICDP DSeis 1-9) report on the outcomes. This poster (ICDP DSeis 4) compiles drilling, core logging, and in-hole geophysical logging of ICDP DSeis drilling into the M5.5 aftershock zones in a South African gold mines. A core orientation tool was used during drilling but not 100% reliable because there was a case that a bottom line in a core run was different by more than 90 degrees from the bottom line in the next core run. We elaborated to compare OTV image with core to carefully check the core orientation. The modified core orientation allowed us to modify the maximum stress direction that Ishida et al. (2018) measured. We could confirm good consistency with borehole breakout analysis (Richenbacher 2018; ETH master thesis). We will report on other associated outcomes. Refer other papers (ICDP DSeis 1-3, 5-9) for other related outcomes.

Acknowledgement: The DSeis team includes co-authors of the papers ICDP DSeis 2-9 and members shown at https://www.icdp-online.org/projects/world/africa/orkney-s-africa/details/. We thank Harmony Gold, Anglogold Ashanthi, Lesedi, Digital Surveying, OHMS, Seismogen, 3D Geoscience. ICDP, JSPS, SA NRF, MEXT Japan, US NSF, German DRF, and Ritsumeikan Univ. financially support the project.

©2019. Japan Geoscience Union. All Right Reserved.

©2019. Japan Geoscience Union. All Right Reserved.

ICDP DSeis 5: Diametrical Core Deformation Analysis of the M5.5 aftershock zone core - stress concentration at reflective intrusives and transition in stress regimes.

*Kosuke Sugimura[1], Shunsuke YOSHIDA[1], Ryogo Tadokoro[1], Hiroshi Ogasawara[2], Akimasa Ishida, Yasuo Yabe[3], Takatoshi Ito[4], Akio Funato[5], Siyanda Mngadi[6], Ray Durrheim[6]

1. Graduate school of science and engineering, Ritsumeikan, 2. College of Science and Engineering, Ritsumeikan Univ., 3. Graduate School of Science, Tohoku Univ., 4. Inst. Fluid Science, Tohoku Univ., 5. Fukada Geological Institute, 6. Univ. Witwatersrand, School of Geoscience

ICDP drilling into the aftershock zone of the 2014 M5.5 earthquake near Orkney, South Africa commenced on 2017 and was completed in 2018. Drilling was designed to minimize damage on core and borehole, being able to maximize core recovery. Hole A (817m) was drilled in 2017. It unfortunately didn't intersect the M5.5 fault, running eventually sub-parallel and roughly 100m from the aftershock zone. As the hole was stable we could recover almost 100% of core from the area traversing the periphery of the M5.5 aftershock zone for a distance of several hundreds of meters. Ishida et al. (2018) carried out Diametrical Core Diameter Analysis (Ito and Funato, 2017). This analysis measures the change in core diameter with roll angle around the core axis, which was caused by a relief of anisotropic stress during drilling. We used this analysis because (1) the expected stress was too high for hydrofracturing method, (2) uncertainty in stress magnitude is unavoidable in damage interpretations, (3) DSeis hole were too long for overcoring technique, and (4) DCDA is non-destructive and very easy to make if core is recovered. Ishida et al. (2018) measured 186 pieces of core from Hole A (817m collared at 2.9km depth) that were recovered near the M5.5 aftershock zone. They successfully illustrated spatial variation in differential stress in a plane perpendicular to Hole A axis. They found stress concentration at intrusives with one located at the depth of the upper fringe of the M5.5 aftershock zone. We carried out additional measurement for the remaining part of Hole A and Hole B. With additional data measured at adjacent locations, we could confirm that the stress concentration Ishida et al (2018) found at intrusives was not an outlier. We will report how Hole B that intersected the M5.5 fault differ from Hole A stress.

This is one of nine ICDP DSeis papers (ICDP DSeis 1-9) presented in JpGU 2019. Refer other papers for other topic on drilling, logging, other stress measurement, fault materials, comparison with calculated stress, legacy 3D seismic reflection data, and relocated aftershocks.

©2019. Japan Geoscience Union. All Right Reserved.

ICDP DSeis 6: Deformation Rate Analysis of the M5.5 aftershock zone core - stress concentration at reflective intrusives

*Kanematsu Makoto[1], Mitsuya Higashi[1], Yasuo Yabe[2], Shuhei Abe[2], Bryan Watson[3], Ray Durrheim[3], Hiroshi Ogasawara[1]

1. Ritsumeikan Univ., 2. Tohoku Univ., 3. Univ. Witwatersrand

ICDP drilling into the aftershock zone of the 2014 M5.5 earthquake near Orkney, South Africa commenced on 2017 and was completed in 2018. Ishida et al. (2018) and Sugimura et al. (2019; ICDP DSeis 5) report on spatial variation of differential stress in a plane perpendicular to the borehole axis. It is ideal to have different stress component especially at critical location where significant characteristics were found. Deformation Rate Analysis (Yamamoto, 2009) can measure stress in any direction although the method takes time and the specimen are not reusable for other test. So, we planned to selected samples where characteristic spatial variation was found by DCDA method (Ishida et al. 2018 and Sugimura et al. 2019). It was confirmed also in normal stress component along the borehole axis that stress was concentrated at the intrusive at about 400m.

This is one of nine ICDP DSeis papers (ICDP DSeis 1-9) presented in JpGU 2019. Refer other papers for other topics on drilling, logging, other stress measurement, fault materials, comparison with calculated stress, legacy 3D seismic reflection data, and relocated aftershocks.

Acknowledgement: The DSeis team includes co-authors of the papers ICDP DSeis 2-9 and members shown at https://www.icdp-online.org/projects/world/africa/orkney-s-africa/details/. We thank Harmony Gold, Anglogold Ashanthi, Lesedi, Digital Surveying, OHMS, Seismogen, 3D Geoscience. ICDP, JSPS, SA NRF, MEXT Japan, US NSF, German DRF, and Ritsumeikan Univ. financially support the project.

Keywords: Seismogenic zone, Stress Measurement, DRA

©2019. Japan Geoscience Union. All Right Reserved.

ICDP DSeis 7: compilation of stress information and comparison with calculated stresses in the M5.5 aftershock zones

*Mitsuya Higashi[1], Yasuo Yabe[2], Kosuke Sugimura[1], Akimasa Ishida, Makoto Kanematsu[1], Shunsuke YOSHIDA[1], Ryogo Tadokoro[1], Takatoshi Ito[4], Akio Funato[5], Hiroshi Ogasawara[3]

1. Graduate School of Science and Engineering, Ritsumeikan Univ., 2. Research Center for Prediction of Earthquakes and Volcanic Eruptions, Graduate School of Science, Tohoku University, 3. College of Science and Engineering, Ritsumeikan Univ., 4. Inst. Fluid Science, Tohoku Univ., 5. Fukada Geological Institute

ICDP drilling into the aftershock zone of the 2014 M5.5 earthquake near Orkney, South Africa commenced on 2017 and was completed in 2018. Spatial variation in stress was measured by Ishida et al. (2018) and Sugimura et al. (2019; ICDP DSeis 5) by DCDA method (Funato and Ito, 2017) and Kanematsu et al. (2019; ICDP DSeis 6). This poster reports on compilation of stress information including the other information sources and compares with calculated stress.

We first compared with a 3D stress state that Ogasawara et al. (2012) measured in 2011 at 98L (3.0 km depth from surface). We assume zero stress on surface, the measured 3D stress (normal faulting stress regime) at 3.0 km, and stress linearly increasing with depth. The calculated stress was consistent with DCDA results measured in the initial 100m section in Hole A, while inconsistent in deeper section. The calculated direction of maximum stress in a plane perpendicular to the borehole axis was also inconsistent with the measured stress information (Yoshida et al. 2019 JpGU; ICDP DSeis 5). Except for the stress concentration measured at intrusives, the measured DCDA results were systematically lower than the calculated stress. In a stress regime that caused the left-lateral horizontal slip on the M5.5 fault, horizontal stress should be larger, which will increase horizontal stress component in a plane perpendicular to the Hole A axis. This increase should decrease difference in stress in the plane perpendicular to the Hole A axis. By JpGU 2019, we will make additional effort to interpret more from the comparison between the measured and calculated stress.

This is one of nine papers (ICDP DSeis 1-9). Refer other papers for other topic on drilling, logging, other stress measurement, fault materials, legacy 3D seismic reflection data, and relocated aftershocks.

Acknowledgement: The DSeis team includes co-authors of the papers ICDP DSeis 2-9 and members shown at https://www.icdp-online.org/projects/world/africa/orkney-s-africa/details/. We thank Harmony Gold, Anglogold Ashanthi, Lesedi, Digital Surveying, OHMS, Seismogen, 3D Geoscience. ICDP, JSPS, SA NRF, MEXT Japan, US NSF, German DRF, and Ritsumeikan Univ. financially support the project.

©2019. Japan Geoscience Union. All Right Reserved.

ICDP DSeis 8: the M5.5 fault structure and reflective intrusives in legacy 3D seismic reflection data

*Noda Taku[1], Musa Manzi[2], Hiroyuki Ogasawara[1], Lindsay Linzer[2], Stephanie Enslin[2], Ray Durrheim[2], Hiroshi Ogasawara[1]

1. Ritsumeikan Univ., 2. Univ. Witwatersrand

ICDP drilling into the aftershock zone of the 2014 M5.5 earthquake near Orkney, South Africa commenced on 2017 and was completed in 2018. Hiroyuki et al. (2017 AGU) reported on legacy seismic reflection to analyze geological structures in the southern most area of the M5.5 aftershock zones. They found vertical structures in four 2-D lines that were potentially responsible for the M5.5 earthquake and illustrated cross-cutting relations of the M5.5 structure and other known faults that dislocated gold reefs more than several hundreds of meters both horizontally and vertically. Another legacy seismic reflection data which was recorded in 1996 and covered much wider area of the M5.5 aftershock zone was found. We calibrated velocity structure by tying with borehole data including DSeis Holes A and B, we found some of intrusives (sills) that Hole A and B were strong reflectors in the legacy 3D seismic reflection data.

Aftershocks located by in-mine 46 geophones are dense at the southern upper fringe, with a sharp cut-off dipping about 20 degrees to the south; some clear stripes of aftershocks are also seen, in parallel to the upper fringe (Tadokoro et al., JpGU2019, ICDP DSeis 9). It is interesting to note that the reflector (sills) are also in parallel to the upper fringe of the aftershock zone and the aftershock stripes. It is also notable that stress concentration is reported at the intrusives by Sugimura et al. (JpGU2019; ICDP DSeis 5) and Kanematsu et al. (JpGU2019; ICDP DSeis 6). Some mechanism that controls the extent of the aftershocks should exist.

This paper is one of nine papers (ICDP DSeis 1-9). Refer other papers for other topics, e.g. on drilling, logging, stress measurements and evaluation, fault materials, and relocated aftershocks.

Acknowledgement: The DSeis team includes co-authors of the papers ICDP DSeis 2-9 and members shown at https://www.icdp-online.org/projects/world/africa/orkney-s-africa/details/. We thank Harmony Gold, Anglogold Ashanthi, Lesedi, Digital Surveying, OHMS, Seismogen, 3D Geoscience. ICDP, JSPS, SA NRF, MEXT Japan, US NSF, German DRF, and Ritsumeikan Univ. financially support the project.

Keywords: ICDP DSeis, The M5.5 seismogenic zone, Seismic reflection

©2019. Japan Geoscience Union. All Right Reserved.

ICDP DSeis 9: are streaks in the M5.5 aftershocks potentially located on highly stressed intrusive?

*Ryogo Tadokoro[1], Katsuya Ishibashi[2], Horiuchi Shigeki[3], Hiroshi Ogasawara[4]

1. Graduate School of Science and Engineering, Ritsumeikan Univ., 2. School of Science and Engineering, Ritsumeikan Univ., 3. Homeseismo ltd., 4. College of Science and Engineering, Ritsumeikan Univ.

ICDP drilling into the aftershock zone of the 2014 M5.5 earthquake near Orkney, South Africa commenced on 2017 and was completed in 2018. Aftershocks located by in-mine 46 geophones are dense at the southern upper fringe, with a sharp cut-off dipping about 20 degrees to the south. Some clear stripes of aftershocks are also seen, in parallel to the upper fringe. It is interesting to note that the reflector (sills) are also in parallel to the upper fringe of the aftershock zone and the aftershock stripes. It is also notable that stress concentration is reported at the intrusives by Sugimura et al. (JpGU2019; ICDP DSeis 5) and Kanematsu et al. (JpGU2019; ICDP DSeis 6). Some mechanism that controls the extent of the aftershocks should exist.

In order to discuss further, we relocated aftershocks with the Double-Difference method (Waldhouser and Ellsworth, 2004). At the moment, we could relocate only 60 events at the upper fringe of the aftershocks. We used in-mine seismic network data of Anglogold Ashanti. P- and S- arrival times that the algorithm of Horiuchi et al. (2011) was used. A sharper alignment of aftershocks is successfully illustrated. By JpGU 2019, we will make additional efforts to extend the area of relocation to discuss more.

Acknowledgement: The DSeis team includes co-authors of the papers ICDP DSeis 2-9 and members shown at https://www.icdp-online.org/projects/world/africa/orkney-s-africa/details/. We thank Harmony Gold, Anglogold Ashanthi, Lesedi, Digital Surveying, OHMS, Seismogen, 3D Geoscience. ICDP, JSPS, SA NRF, MEXT Japan, US NSF, German DRF, and Ritsumeikan Univ. financially support the project.

©2019. Japan Geoscience Union. All Right Reserved.

[E] Poster | M (Multidisciplinary and Interdisciplinary)：M-TT Technology & Techniques

Mon. May 27, 2019 1:45 PM - 3:15 PM JST | Mon. May 27, 2019 4:45 AM - 6:15 AM UTC | Poster Hall International Exhibition Hall8, Makuhari Messe_10

[M-TT46] New phase of GPS/GNSS application as an integrated earth observation system

convener:Yoshinori Shoji(The Second Laboratory of Meteorological Satellite and Observation System Research Department, Meteorological Research Institute), Kaoru Ichikawa(Research Institute for Applied Mechanics, Kyushu University), Yusaku Ohta(Research Center for Prediction of Earthquakes and Volcanic Eruptions, Graduate School of Science, Tohoku University), Takuya Tsugawa(National Institute of Information and Communications Technology)

GNSS has become a fundamental tool for studies on atmosphere, ionosphere, and solid earth. Ground and space-based GNSS measurements have operationally contributed to improve global and regional NWP since 2006. In recent years, studies utilizing reflected GNSS signals to derive altimetric height, surface roughness, soil moisture, snow depth, humidity or vegetation index have been evolving. Ocean-platform GNSS observations have been demonstrating their capability of real-time monitoring of maritime water vapor as well as sea level. Increasing observations provided through Multi-GNSS (GPS, GLONASS, BEIDOU, GALILEO, QZSS etc.) enhances capability of the GNSS as an integrated earth observation system.
The purpose of this session is to share the latest development of GNSS researches on monitoring the earth system and to stimulate synergetic interdisciplinary studies. Contributions on atmosphere (troposphere and ionosphere) studies, reflectometry (GNSS-R), and integrations of different observation techniques like GNSS-Acoustic measurement to monitor ocean floor positioning are welcome.

[MTT46-P01] Continuous acoustic ranging from a GNSS buoy for the new method of seafloor crustal deformation measurements

*Keiichi Tadokoro[1], Natsuki Kinugasa[1], Teruyuki Kato[2], Yukihiro Terada[3], Akira Futamura[4], Kenjiro Matsuhiro[1] (1.Research Center for Seismology, Volcanology and Earthquake and Volcano Research Center, Nagoya University, 2.Hot Springs Research Institute of Kanagawa Prefecture, 3.Kochi National College of Technology, 4.National Institute of Technology, Yuge College)

[MTT46-P02] Accuracy and precision assessment of the real-time kinematic GNSS time series for moored buoy using three-axis programable moving table

*Yusaku Ohta[1], Misae Imano[1], Motoyuki Kido[2] (1.Research Center for Prediction of Earthquakes and Volcanic Eruptions, Graduate School of Science, Tohoku University, 2.IRIDeS, Tohoku University)

[MTT46-P03] GNSS-R altimetry using a Geostationary Satellite

*Kaoru Ichikawa[1], Tatsuki Okumura[2], Masanori Konda[3], Yasuyuki Baba[4] (1.Res. Inst. Appl. Mech., Kyushu Univ., 2.Dept. ESST, Interdicipl. Grad. School Eng. Sc., Kyushu Univ., 3.Graduate School of Science, Kyoto Univ., 4.Disaster Prevention Res. Inst., Kyoto Univ.)

[MTT46-P04] Estimation of typhoon wind speed using CYGNSS observations: A case study of Typhoon Lan in 2017

*Kako Shinichiro[1], Hiroyuki Tomita[2], Kaoru Ichikawa[3] (1.Graduate School of Science and Engineering, Kagoshima University, 2.Institute for Space-Earth Environment, Nagoya University, 3.Research institute for Applied Mechanics, Kyushu University)

[MTT46-P05] Ionospheric and seismic effects caused by the North Korea nuclear tests realized on 2006-2017

Nataliia Perevalova[2], *Nikolai Shestakov[1], Anna Dobrynina[3,4], Dmitry Kostylev[7], Meng Guojie[5], Wei-Wei Wu[5,6] (1.Institute for Applied Mathematics FEB RAS, Vladivostok, Russia; Far Eastern Federal University, Vladivostok, Russia, 2.Institute of Solar-Terrestrial Physics SB RAS, Irkutsk, Russia, 3.Institute of the Earth's Crust SB RAS, Irkutsk, Russia , 4.Geological institute SB RAS, Ulan-Ude, Russia , 5.Institute of Earthquake Forecasting, China Earthquake Administration, Beijing, China, 6.College of Surveying and

Geo-informatics, Tongji University, Shanghai, China, 7.Sakhalin Branch of Federal Research Center Geophysical Survey RAS, Yuzhno_Sakhalinsk, Russia)

[MTT46-P06] Relationships between Water Vapor Concentration Index derived from GNSS and Surface Wind Convergence during Localized Heavy Rainfall in Tokyo in Summer

*Yoshihito Seto[1], Yoshinori Shoji[2], Nobumitsu Tsunematsu[3], Hideo Takahashi[1] (1.Department of Geography, Graduate School of Urban Environmental Sciences, Tokyo Metropolitan University, 2.Meteorological Research Institute, 3.Tokyo Metropolitan Research Institute for Environmental Protection)

[MTT46-P07] Development of novel ground-based microwave radiometer for earth science - preliminary report-

*Ryuichi Ichikawa[1], Hideki Ujihara[1], Shinsuke Satoh[1], Jun Amagai[1], Yusaku Ohta[2], Basara Miyahara[3], Hiroshi Munekane[3], Taketo Nagasaki[4], Osamu Tajima[5], Kentaro Araki[6], Takuya Tajiri[6], Hiroshi Takiguchi[7], Takeshi Matsushima[8], Nobuo Matsushima[9], Tatsuya Momotani[10], Kenji Utsunomiya[10] (1.National Institute of Information and Communications Technology, 2.Tohoku University, 3.Geospatial Information Authority of Japan, 4.High Energy Accelerator Research Organization, 5.Kyoto University, 6.Meteorological Research Institute, JMA, 7.Japan Aerospace eXploration Agency, 8.Kyushu University, 9.National Institute of Advanced Industrial Science and Technology, 10.Japan Weather Association)

[MTT46-P08] Refractivity Distributions over the Kanto Plain Obtained by Dual-polarization Radar

*Hiromu Seko[1], Eiichi Sato[1], Hiroshi Yamauchi[2] (1.Meteorological Research Institute, 2.Japan Meteorological Agency)

[MTT46-P09] Spatial and temporal distribution of tropospheric water vapor observed by a Raman lidar and a GNSS receiver network over Shigaraki, Japan

*Masanori Yabuki[1], Toshitaka Tsuda[1], Yuya Kawano[2], Yusaku Tottori[2], Makoto Tsukamoto[2], Eiji Takeuchi[2] (1.Research Institute for Sustainable Humanosphere, Kyoto University, 2.EKO Instruments Co., Ltd.)

[MTT46-P10] **Study of the Mechanisms of Severe Thunderstorm in Tokyo Metropolitan Area using High Frequent Assimilation of GNSS and Other Ground-based Observations**

*Yoshinori Shoji[1], Tetsu Sakai[2], Ahoro Adachi[1], Satoru Yoshida[2], Tomohiro Nagai[2] (1.The Second Laboratory of Meteorological Satellite and Observation System Research Department, Meteorological Research Institute, 2.The Third Laboratory of Meteorological Satellite and Observation System Research Department, Meteorological Research Institute)

Continuous acoustic ranging from a GNSS buoy for the new method of seafloor crustal deformation measurements

*Keiichi Tadokoro[1], Natsuki Kinugasa[1], Teruyuki Kato[2], Yukihiro Terada[3], Akira Futamura[4], Kenjiro Matsuhiro[1]

1. Research Center for Seismology, Volcanology and Earthquake and Volcano Research Center, Nagoya University, 2. Hot Springs Research Institute of Kanagawa Prefecture, 3. Kochi National College of Technology, 4. National Institute of Technology, Yuge College

Our research group has been testing a measurement system for the continuous seafloor crustal deformation at a moored buoysite operated by Kochi prefecture, located 32 km off Cape Ashizuri, Japan.An acoustic transducer was fixed at about 1.7 m beneath the sea surface with a pole mounted on the buoy body.Three ocean bottom acoustic transponders had been installed around the moored point of the buoy. The acoustic signals are sequentially transmitted to these three transponders every three minutes. The recorded data on the buoy are planned to transmitted to a ground base station through a commercial communication satellite operated by Thuraya Telecommunications Company.
We performed a test for the continuous acoustic ranging between the buoy and the ocean bottom transponders from March 28 to 31 and from June 2 to July 12 (1st period), and from November 16to December 17 (2nd period) in 2018. The acoustic ranging was continuously possible throughout the above periods when power was supplied whereas it was unexpectedly terminated because of power failure during the winter season. The acoustic signals were transmitted 27,856 times in total, and the buoy-mounted acoustic ranging unit received 23,342 signals from the ocean bottom transponders. However, the acoustic data sent to the ground base station was only 12 % because of some trouble of the satellite communication modem.
The reflected signals from the buoy body and/or the seafloor sometimes contaminated the received acoustic signals; also multiple reflections inside of an anti-reflection cover attached to the buoy-mounted transducer, whose purpose is to cut off the reflection from the sea surface, were remarkable during the 1st period. The multiple reflections caused the misidentification of the direct wave from the sea-bottom units. We, therefore, removed the anti-reflection cover during the 2nd period, which remarkably reduced the confused reflections.
We coded a program for detecting the arrival time of direct acoustic wave automatically on the basis of thresholds of cross-correlation coefficient and energy ratio (the ratio of the squared amplitudes preceding and following a test point) to reduce the capacity of data transferred via satellite communication using the acoustic waveform recorded during the 1st period. The program successfully picked the correct direct wave onset for more than 99 % of the waveforms recorded during the 2nd period.

©2019. Japan Geoscience Union. All Right Reserved.

Accuracy and precision assessment of the real-time kinematic GNSS time series for moored buoy using three-axis programable moving table

*Yusaku Ohta[1], Misae Imano[1], Motoyuki Kido[2]

1. Research Center for Prediction of Earthquakes and Volcanic Eruptions, Graduate School of Science, Tohoku University, 2. IRIDeS, Tohoku University

Rapid understanding of the magnitude of large earthquakes and their associated fault dimensions are extremely important. Especially, capture of the coseismic deformation in the offshore region will be key information to understand the fault dimensions for the large interplate earthquake. Based on this background, Tohoku University and JAMSTEC are jointly developing the on-demand crustal deformation monitoring system using moored buoy system. The buoy can measure the sea-floor horizontal crustal deformation by GNSS/Acoustic technique and vertical deformation using ocean bottom pressure sensor. One of the key technology in our developed system is the real-time kinematic GNSS which can measure three-dimensional position of the buoy in real-time. In contrast, it is difficult to understand quantitatively the precision and accuracy of estimated buoy position because no reference for the position. Thus, we assess the precision and accuracy of real-time kinematic GNSS time series using programable three-axis movable table.

We have developed the single-axis precise programable movable table (Ohta et al., 2016). We expanded this developed system to three-axis. For the real-time kinematic analysis, we adopted Trimble CenterPoint RTX (hereafter, RTX) with 10Hz sampling interval. The correction message for the analysis was received via a stationary satellite. We also estimated the GNSS antenna position using very short-baseline kinematic analysis as reference solution. The developed movable table can operate single axis horizontal displacement, rotational movement, and tilt deformation. To simulate the actual buoy movement, we gave the motion to the movable table based on the actual buoy movement. We conducted the experiment in 24 hours duration.

We calculated the residual time series between obtain time series by RTX and short-baseline kinematic solution. The difference between averaged absolute position was quite good in the horizontal components which was less than 10mm. In contrast, the vertical component shows the clear discrepancy between them. RTX time series shows systemically higher than the baseline analysis which reached approximately 230mm. In contrast, the precision of the calculated residual time series was good in both of the components. Calculated standard deviations were 10-11mm and 28mm in horizontal components and vertical component, respectively. We will show the more detailed results from our experiment and discuss the ability of the real-time kinematic analysis in our developed buoy.

©2019. Japan Geoscience Union. All Right Reserved.

GNSS-R altimetry using a Geostationary Satellite

*Kaoru Ichikawa[1], Tatsuki Okumura[2], Masanori Konda[3], Yasuyuki Baba[4]

1. Res. Inst. Appl. Mech., Kyushu Univ., 2. Dept. ESST, Interdicipl. Grad. School Eng. Sc., Kyushu Univ., 3. Graduate School of Science, Kyoto Univ., 4. Disaster Prevention Res. Inst., Kyoto Univ.

The GNSS reflectometry (GNSS-R) uses GNSS signals reflected at the sea surface, which are usually eliminated as the multipath error. The reflected GNSS path received at an antenna is always longer than the direct path, so that the height of the antenna from the sea surface is geometrically determined from the excess path length. The excess path length can be either directly determined by measuring the temporal delay of the reflected signals, or indirectly estimated from interferometric cyclic modulations of the received power (often referred as signal-to-noise ratio; SNR) induced by phase differences between the direct and reflected GNSS signals. In the latter method, as the elevation angle of an earth orbiting GNSS satellite changes in time, the geometric reflection point on the sea surface temporally displaces, which results in interferometric changes of the path length during a period while the satellite is in sight. Meanwhile, for a geostationary satellite in BeiDou constellations that are always in sight, the path length changes not by the movement of the satellite but the elevation of the reflection surface, *i.e.* the sea level rise. In this study, we used the three-month time series (2016/09-11) of the 1Hz SNR of the geostationary BeiDou #02 satellite observed by a GNSS-R system deployed to the Shirahama Oceanographic Observatory Tower owned by Kyoto University (33deg, 42’ 32’’ N, 135deg, 19’ 58’’ E) at the height of ~20m. The geostationary GNSS-R altimetry observed significant flood tides when the wind speed is stably low; the 0.6m sea level rise was successfully determined by the SNR interferometry with 0.05m rms difference. However, significant interferometric SNR changes by tides were not recorded at high or low tides since at least 0.25m sea level change is required for the interferometry cycle. Consequently, the cyclic periods of the geostationary GNSS-R altimetry for tides become long (1-4 hours for 0.25m change in Shirahama), the interferometric variations were usually contaminated by SNR changes induced by the other factors such as winds. On the contrary, faster sea level changes by wave motions could be recognized by the geostationary GNSS-R altimetry, although the temporal sampling intervals of the present data were not adequate.

Keywords: GNSS-R , altimetry, BeiDou geostationary GNSS satellite

©2019. Japan Geoscience Union. All Right Reserved.

Estimation of typhoon wind speed using CYGNSS observations: A case study of Typhoon Lan in 2017

*Kako Shinichiro[1], Hiroyuki Tomita[2], Kaoru Ichikawa[3]

1. Graduate School of Science and Engineering, Kagoshima University, 2. Institute for Space-Earth Environment, Nagoya University, 3. Research institute for Applied Mechanics, Kyushu University

We conducted a case study of Typhoon Lan, which occurred in 2017, to investigate the impact of the Cyclone Global Navigation Satellite System (CYGNSS) on the estimation of extremely high wind speeds, such as those occurring during typhoons. We studied CYGNSS because it is expected to be capable of observing wind speeds in regions with extremely high wind speeds and heavy rains (i.e., typhoons) where it is difficult to perform measurements using the current microwave instrument. Firstly, we compared CYGNSS-derived wind speeds produced by NASA with those derived from AMSR2 produced by the Japan Aerospace Exploration Agency. CYGNSS was found to underestimate the wind speeds around Typhoon Lan compared with AMSR2. We then attempted to estimate the wind speeds using the leading edge slope (LES) and mean square slope (MSS) derived from the CYGNSS observations. Although the relationship between the MSS and wind speed differs depending on the wave age (Zhao and Tobe, 2003), it is difficult to estimate the wave age because this estimation is required the wind and wave speeds. We used the wave period as a substitute for the wave age since the wave period is expected to be similar to the wave age. We therefore first computed the fourth power of the wave period (T4) in line with Wang and Ichikawa (2016). Next, we classified the ocean into three regions based on T4 to investigate the relationship between the MSS and the wind speed observed by AMSR2 in each region. Finally, we approximated the curves relating the MSS to the wind speed using exponential functions in the three regions and estimated the wind speed using these curves. The comparison between the wind speeds produced by NASA and those estimated in this study demonstrated that our method can estimate high wind speeds more accurate than the CYGNSS wind speeds produced by NASA.

Keywords: CYGNSS, AMSR2, tyhoon

©2019. Japan Geoscience Union. All Right Reserved.

Ionospheric and seismic effects caused by the North Korea nuclear tests realized on 2006-2017

Nataliia Perevalova[2], *Nikolai Shestakov[1], Anna Dobrynina[3,4], Dmitry Kostylev[7], Meng Guojie[5], Wei-Wei Wu[5,6]

1. Institute for Applied Mathematics FEB RAS, Vladivostok, Russia; Far Eastern Federal University, Vladivostok, Russia, 2. Institute of Solar-Terrestrial Physics SB RAS, Irkutsk, Russia, 3. Institute of the Earth's Crust SB RAS, Irkutsk, Russia , 4. Geological institute SB RAS, Ulan-Ude, Russia , 5. Institute of Earthquake Forecasting, China Earthquake Administration, Beijing, China, 6. College of Surveying and Geo-informatics, Tongji University, Shanghai, China, 7. Sakhalin Branch of Federal Research Center Geophysical Survey RAS, Yuzhno_Sakhalinsk, Russia

Using data from GPS/GLONASS receivers and seismic networks, we studied the ionospheric and lithospheric effects caused by six underground nuclear tests realized in North Korea on 2006-2017.
To investigate the ionospheric disturbances, we analyzed data from several continuous GNSS-networks (GPS and GLONASS) operating in Asia - Western Pacific region: IGS, GEONET, FEB RAS and FEFU complex geodynamic network, a set of stations belonging to China and South Korea GNSS-networks. Sites close to the Korean Peninsula were selected for the analysis. Series of total electron content (TEC) in the ionosphere were calculated on the base of dual-frequency phase measurements of GNSS receivers. To detect disturbances caused by the nuclear tests, TEC series were filtered in the range of periods from 1 to 10 minutes. Despite the small magnitudes of seismic events associated with the nuclear tests, we were able to identify ionospheric disturbances which were most likely generated by these explosions. Such disturbances were detected for 4 out of 6 nuclear tests. The main parameters of the disturbances were determined. From our analysis we concluded that characteristics of ionospheric disturbances caused by the underground nuclear tests differed significantly from the parameters of disturbances that are usually observed after earthquakes.
For seismic analysis, we used data from the broadband seismic station networks located at distances up to 23 degrees from the Korean Peninsula: II, IC, IU, TW, JP, G, KS, and KG given by IRIS, and regional seismic network BY. The frequency content of P and surface Rayleigh waves registered by 46 broadband stations was analyzed. For some events, the P-wave frequency content showed the prevalence of low frequencies in spectra (~0.45 Hz). The peak frequencies of the surface Rayleigh waves was in the 0.05-0.45 Hz range. Preliminary analysis of the peak frequencies spatial distribution showed that the continental massive area is characterized by the relatively high frequencies (0.14-0.50 Hz) while for the areas adjacent to marginal seas the low values of peak frequencies are observed (from 0.13 Hz and less).
Acknowledgments. We are deeply indebted to Scripps Orbit and Permanent Array Center (SOPAC) for the IGS-network data, to Geospatial Information Authority of Japan for GEONET network data, to Korea Astronomy & Space Science Institute for access to GNSS data on the Korean Peninsula, CCU CC FEB RAS for access to data from the FEB RAS and FEFU complex geodynamic network; Institute of Earthquake Forecasting, China Earthquake Administration for access to GNSS data in China. The facilities of the IRIS Data Management System, and specifically the IRIS Data Management Center, and Baikal Regional Seismological Center and Sakhalin Branch of Federal Research Center Geophysical Survey RAS were used to get waveform and metadata required in this study. This work was performed with budgetary funding of Basic Research program II.16 and was also partially supported by RFBR grants 17-45-388072_p_a, 17-45-388049_ p_a, 17-55-53110_GFEN_a, 19-05-00889_a.

Keywords: North Korea nuclear tests, ionospheric and lithospheric effects, GPS/GLONASS-observations

©2019. Japan Geoscience Union. All Right Reserved.

©2019. Japan Geoscience Union. All Right Reserved.

Relationships between Water Vapor Concentration Index derived from GNSS and Surface Wind Convergence during Localized Heavy Rainfall in Tokyo in Summer

*Yoshihito Seto[1], Yoshinori Shoji[2], Nobumitsu Tsunematsu[3], Hideo Takahashi[1]

1. Department of Geography, Graduate School of Urban Environmental Sciences, Tokyo Metropolitan University, 2. Meteorological Research Institute, 3. Tokyo Metropolitan Research Institute for Environmental Protection

In recent years, short-term heavy-rainfall events that have caused severe damages such as flooding have frequently occurred in the Tokyo Metropolitan area in summer. In view of the development process of cumulonimbus clouds, the convergence of surface winds and the spatial concentration of water vapor are supposed to have taken place prior to the occurrence of heavy rainfall. This study aims to clarify the evolutionary process of short-term heavy rainfall as a contribution to short-range forecasting of heavy rainfall that occurs locally.

The relationships between the occurrence of heavy rainfall and the convergence of surface winds and water vapor concentration for heavy-rainfall cases were examined using data from July to September obtained from high-density meteorological observations in Tokyo, Japan. We used the water vapor concentration (WVC) index derived from the global navigation satellite system (GNSS) analysis as indices for the degree of divergence and convergence of water vapor in the lower troposphere (Shoji 2013).

Corresponding to heavy-rainfall areas, the convergence of surface winds tended to increase for several tens of minutes prior to the heavy rainfall. The peak time of wind convergence was observed 10–30 min before the heavy-rainfall occurrence, and the convergence continued to increase for approximately 30 min until the convergence peak time (Seto et al. 2018). Around the heavy-rainfall area, the increase in the WVC index coincided with the increase in convergence. On the other hand, it was considered that the temporal and spatial scales of the WVC index are larger than those of wind convergence. From these results, by monitoring the temporal variations and distributions of these parameters using a high-density observation network, it should be possible to predict the occurrence of heavy rainfall rapidly and accurately.

References

Seto, Y., Yokoyama, H., Nakatani, T., Ando, H., Tsunematsu, N., Shoji, Y., Kusunoki, K., Nakayama, M., Saitoh, Y. and Takahashi, H. 2018. Relationships among rainfall distribution, surface wind, and precipitable water vapor during heavy rainfall in central Tokyo in summer. J. Meteor. Soc. Japan, 96A, 35–49.

Shoji, Y. 2013. Retrieval of water vapor inhomogeneity using the Japanese nationwide GPS array and its potential for prediction of convective precipitation. J. Meteor. Soc. Japan, 91, 43–62.

Keywords: localized heavy rainfall, wind convergence, water vapor, high-density observation

©2019. Japan Geoscience Union. All Right Reserved.

Development of novel ground-based microwave radiometer for earth science -preliminary report-

*Ryuichi Ichikawa[1], Hideki Ujihara[1], Shinsuke Satoh[1], Jun Amagai[1], Yusaku Ohta[2], Basara Miyahara[3], Hiroshi Munekane[3], Taketo Nagasaki[4], Osamu Tajima[5], Kentaro Araki[6], Takuya Tajiri[6], Hiroshi Takiguchi[7], Takeshi Matsushima[8], Nobuo Matsushima[9], Tatsuya Momotani[10], Kenji Utsunomiya[10]

1. National Institute of Information and Communications Technology, 2. Tohoku University, 3. Geospatial Information Authority of Japan, 4. High Energy Accelerator Research Organization, 5. Kyoto University, 6. Meteorological Research Institute, JMA, 7. Japan Aerospace eXploration Agency, 8. Kyushu University, 9. National Institute of Advanced Industrial Science and Technology, 10. Japan Weather Association

We have started to develop a next-generation microwave radiometer to be used in millimeter-wave spectroscopy for the high-resolution and high-precision monitoring of water vapor behavior. The new radiometer will be suitable for not only space geodetic techniques such as VLBI and GNSS, but also field measurements such as monitoring volcanic activities and cumulonimbus cloud generation. The basic design concept of the new radiometer follows the previous version named KUMODeS (KEK Universal Moisture and Oxygen Detection System) developed by the High Energy Accelerator Research Organization (KEK). The KUMODeS can measure spectra using two receivers with frequency bands of 20–30 GHz and 50–60 GHz. The low-noise amplifier (LNA) of the first KUMODeS receiver and a cold calibration source are implemented in a cryostat, which is maintained at 10 K to improve the sensitivity of detecting the characteristic broad peak of water vapor at approximately 22 GHz. The second receiver is used to measure the absorption peaks of oxygen (60 GHz). We have carried out comparative measurements of precipitable water vapor (PWV) to investigate the potential of KUMODeS/PWV measurements. The preliminary results of PWV comparisons imply that KUMODeS technology will be useful for retrieving the accurate behavior of water vapor with high temporal resolution. We will implement a wide bandwidth feed of 20–60 GHz into the new system on the basis of a previous comparison study. A signal is separated into two linear orthogonal polarized signals from the feed, one is in the 20–30 GHz feed and the other in the 50–60 GHz feed, using an orthomode transducer (OMT). The wideband feed, OMT, and the LNA for each signal are cooled at 77 K using a Stirling cryocooler to improve signal-to-noise ratio. The development of a new front-end module will be completed at the end of 2019, and we are planning to implement the module in an existing dish antenna to perform validation measurements.

Keywords: GNSS, microwave radiometer, water vapor

©2019. Japan Geoscience Union. All Right Reserved.

Refractivity Distributions over the Kanto Plain Obtained by Dual-polarization Radar

*Hiromu Seko[1], Eiichi Sato[1], Hiroshi Yamauchi[2]

1. Meteorological Research Institute, 2. Japan Meteorological Agency

Temperature and water vapor near the surface play crucial roles for the generation of convection cells. However, their variations just before the generations of convection cells still are not understood completely. In this study the temporal variations of refractivity index were obtained by MRI dual-polarization Doppler radar. The features of temperature and water vapor including generation period of convection cells will be shown in this presentation. On 19th August 2017, the sea breeze invaded from Kashima-Nada and the refractivity increased along the front of the sea breeze. The scattered weak echoes that appeared around the front seem to be related with the increase of refractivity. These are the features near the surface. The comparison with other data such as GNSS PWV will be also presented.

Keywords: Observation method, Doppler radar, Refractivity index

©2019. Japan Geoscience Union. All Right Reserved.

Spatial and temporal distribution of tropospheric water vapor observed by a Raman lidar and a GNSS receiver network over Shigaraki, Japan

*Masanori Yabuki[1], Toshitaka Tsuda[1], Yuya Kawano[2], Yusaku Tottori[2], Makoto Tsukamoto[2], Eiji Takeuchi[2]

1. Research Institute for Sustainable Humanosphere, Kyoto University, 2. EKO Instruments Co., Ltd.

Understanding the spatial and temporal distributions of water vapor in the atmosphere is critical for unveiling the fundamental mechanisms of localized extreme weather events. Besides, it is highly beneficial for improving the accuracy of weather forecasts by mesoscale numerical weather prediction models. To achieve the continuous monitoring of water vapor distributions, we performed simultaneous measurements by Raman lidar in the UV-C region and a dense Global Navigation Satellite System (GNSS) network. The former is a novel technology that can be utilized for profiling the vertical distribution of the water vapor mixing ratio for twenty-four hours, while the latter can be used for detecting the horizontal distribution of precipitable water vapor. The Raman lidar employs a laser at a wavelength of 266 nm and detects the light separated into an elastic backscatter signal and vibrational Raman signals of oxygen, nitrogen, and water vapor at wavelengths of 266, 277, 284, and 295 nm, respectively. The use of these wavelengths is convenient because of the low background noise during daytime, since most of the solar radiation in the ultraviolet range below 300 nm is absorbed by the ozone layer in the stratosphere. The lidar was encased in a temperature-controlled compact container, resistant to a variety of environmental conditions. Continuous observation of water vapor profiles by lidar has been conducted at the Shigaraki MU radar observatory (34˚51’ N, 136˚06’ E, 385 m a.s.l.) since November 2017. The dense GNSS receiver network consisted of 10 dual-frequency GNSS stations which were installed with a horizontal spacing of 3-4 km near the observatory on July 2017. In this study, we present our water vapor monitoring system as well as the preliminary results on the spatio-temporal water vapor distributions in 2018.

Acknowledgements
A part of this study is supported by JSPS KAKENHI Grant Number 15H03724.

Keywords: water vapor, Raman lidar, dense GNSS network

©2019. Japan Geoscience Union. All Right Reserved.

Study of the Mechanisms of Severe Thunderstorm in Tokyo Metropolitan Area using High Frequent Assimilation of GNSS and Other Ground-based Observations

*Yoshinori Shoji[1], Tetsu Sakai[2], Ahoro Adachi[1], Satoru Yoshida[2], Tomohiro Nagai[2]

1. The Second Laboratory of Meteorological Satellite and Observation System Research Department, Meteorological Research Institute, 2. The Third Laboratory of Meteorological Satellite and Observation System Research Department, Meteorological Research Institute

Highly urbanized Tokyo metropolitan area is vulnerable to severe storms such as local torrential rainfall, thunder lightning and tornado. Recently, the number of days with thunderstorms has been increasing in Tokyo. Elucidation of the mechanism of extreme weather in Tokyo is urgent matter (Nakatani et al. 2013). To study the rolls of water vapor and wind for the rapid life-cycle (initiation, development and dissipation) of hazardous cumulus convection, we installed a mobile Raman-lidar (Sakai et al. 2018), a wind profiler, and five GNSS stations in and around Tokyo.

Using 3DVAR capability of WRF data assimilation system (WRFDA)(Barker et al. 2012) , three-dimensional atmospheric fields with 1 km horizontal resolution were produced at every 10min throughout the August 2017 and 2018. Background fields were produced by JMA nonhydrostatic model (NHM)(Saito et al. 2007). In addition to the observed data at these campaign observation instruments, Japan Meteorological Agency’ s operational surface meteorological stations, wind-profiler stations and GNSS PWV derived at dense GNSS network of Geospatial Information Authority of Japan are assimilated. We confirmed that the reproduced atmospheric fields (Temperature, humidity, and wind) showed better agreement with observations of radiosonde, lidar derived water vapor mixing ratio, and wind-profiler than background fields at altitudes lower than 2 km. Assimilation of surface meteorological observations (atmospheric pressure, temperature, humidity and wind) introduced better agreement mainly at altitude lower than 0.5 km. Inclusion of GNSS derived PWV resulted better agreement of humidity at altitude higher than 0.5 km and inclusion of wind field from wind-profiler led better agreement of wind field.

We have investigated roles of water vapor for several local heavy rainfall events occurred in Tokyo in August 2017 and 2018 and found that convergence of water vapor flux at 0.5 km altitude had intensified prior to the occurrence of torrential precipitation. Statistical and quantitative results will be discussed at the symposium.

This study is supported by JSPS KAKENHI Grants 17H00852.

Keywords: Water vapor, Data assimilation, Localized heavy rainfall

©2019. Japan Geoscience Union. All Right Reserved.

[E] Poster | M (Multidisciplinary and Interdisciplinary)：M-TT Technology & Techniques

Mon. May 27, 2019 5:15 PM - 6:30 PM JST | Mon. May 27, 2019 8:15 AM - 9:30 AM UTC | Poster Hall International Exhibition Hall8, Makuhari Messe_43

[M-TT46] New phase of GPS/GNSS application as an integrated earth observation system

convener:Yoshinori Shoji(The Second Laboratory of Meteorological Satellite and Observation System Research Department, Meteorological Research Institute), Kaoru Ichikawa(Research Institute for Applied Mechanics, Kyushu University), Yusaku Ohta(Research Center for Prediction of Earthquakes and Volcanic Eruptions, Graduate School of Science, Tohoku University), Takuya Tsugawa(National Institute of Information and Communications Technology)

GNSS has become a fundamental tool for studies on atmosphere, ionosphere, and solid earth. Ground and space-based GNSS measurements have operationally contributed to improve global and regional NWP since 2006. In recent years, studies utilizing reflected GNSS signals to derive altimetric height, surface roughness, soil moisture, snow depth, humidity or vegetation index have been evolving. Ocean-platform GNSS observations have been demonstrating their capability of real-time monitoring of maritime water vapor as well as sea level. Increasing observations provided through Multi-GNSS (GPS, GLONASS, BEIDOU, GALILEO, QZSS etc.) enhances capability of the GNSS as an integrated earth observation system.
The purpose of this session is to share the latest development of GNSS researches on monitoring the earth system and to stimulate synergetic interdisciplinary studies. Contributions on atmosphere (troposphere and ionosphere) studies, reflectometry (GNSS-R), and integrations of different observation techniques like GNSS-Acoustic measurement to monitor ocean floor positioning are welcome.

[MTT46-P01] Continuous acoustic ranging from a GNSS buoy for the new method of seafloor crustal deformation measurements

*Keiichi Tadokoro[1], Natsuki Kinugasa[1], Teruyuki Kato[2], Yukihiro Terada[3], Akira Futamura[4], Kenjiro Matsuhiro[1] (1.Research Center for Seismology, Volcanology and Earthquake and Volcano Research Center, Nagoya University, 2.Hot Springs Research Institute of Kanagawa Prefecture, 3.Kochi National College of Technology, 4.National Institute of Technology, Yuge College)

[MTT46-P02] Accuracy and precision assessment of the real-time kinematic GNSS time series for moored buoy using three-axis programable moving table

*Yusaku Ohta[1], Misae Imano[1], Motoyuki Kido[2] (1.Research Center for Prediction of Earthquakes and Volcanic Eruptions, Graduate School of Science, Tohoku University, 2.IRIDeS, Tohoku University)

[MTT46-P03] GNSS-R altimetry using a Geostationary Satellite

*Kaoru Ichikawa[1], Tatsuki Okumura[2], Masanori Konda[3], Yasuyuki Baba[4] (1.Res. Inst. Appl. Mech., Kyushu Univ., 2.Dept. ESST, Interdicipl. Grad. School Eng. Sc., Kyushu Univ., 3.Graduate School of Science, Kyoto Univ., 4.Disaster Prevention Res. Inst., Kyoto Univ.)

[MTT46-P04] Estimation of typhoon wind speed using CYGNSS observations: A case study of Typhoon Lan in 2017

*Kako Shinichiro[1], Hiroyuki Tomita[2], Kaoru Ichikawa[3] (1.Graduate School of Science and Engineering, Kagoshima University, 2.Institute for Space-Earth Environment, Nagoya University, 3.Research institute for Applied Mechanics, Kyushu University)

[MTT46-P05] Ionospheric and seismic effects caused by the North Korea nuclear tests realized on 2006-2017

Nataliia Perevalova[2], *Nikolai Shestakov[1], Anna Dobrynina[3,4], Dmitry Kostylev[7], Meng Guojie[5], Wei-Wei Wu[5,6] (1.Institute for Applied Mathematics FEB RAS, Vladivostok, Russia; Far Eastern Federal University, Vladivostok, Russia, 2.Institute of Solar-Terrestrial Physics SB RAS, Irkutsk, Russia, 3.Institute of the Earth's Crust SB RAS, Irkutsk, Russia , 4.Geological institute SB RAS, Ulan-Ude, Russia , 5.Institute of Earthquake Forecasting, China Earthquake Administration, Beijing, China, 6.College of Surveying and

Geo-informatics, Tongji University, Shanghai, China, 7.Sakhalin Branch of Federal Research Center Geophysical Survey RAS, Yuzhno_Sakhalinsk, Russia)

[MTT46-P06] Relationships between Water Vapor Concentration Index derived from GNSS and Surface Wind Convergence during Localized Heavy Rainfall in Tokyo in Summer

*Yoshihito Seto[1], Yoshinori Shoji[2], Nobumitsu Tsunematsu[3], Hideo Takahashi[1] (1.Department of Geography, Graduate School of Urban Environmental Sciences, Tokyo Metropolitan University, 2.Meteorological Research Institute, 3.Tokyo Metropolitan Research Institute for Environmental Protection)

[MTT46-P07] Development of novel ground-based microwave radiometer for earth science - preliminary report-

*Ryuichi Ichikawa[1], Hideki Ujihara[1], Shinsuke Satoh[1], Jun Amagai[1], Yusaku Ohta[2], Basara Miyahara[3], Hiroshi Munekane[3], Taketo Nagasaki[4], Osamu Tajima[5], Kentaro Araki[6], Takuya Tajiri[6], Hiroshi Takiguchi[7], Takeshi Matsushima[8], Nobuo Matsushima[9], Tatsuya Momotani[10], Kenji Utsunomiya[10] (1.National Institute of Information and Communications Technology, 2.Tohoku University, 3.Geospatial Information Authority of Japan, 4.High Energy Accelerator Research Organization, 5.Kyoto University, 6.Meteorological Research Institute, JMA, 7.Japan Aerospace eXploration Agency, 8.Kyushu University, 9.National Institute of Advanced Industrial Science and Technology, 10.Japan Weather Association)

[MTT46-P08] Refractivity Distributions over the Kanto Plain Obtained by Dual-polarization Radar

*Hiromu Seko[1], Eiichi Sato[1], Hiroshi Yamauchi[2] (1.Meteorological Research Institute, 2.Japan Meteorological Agency)

[MTT46-P09] Spatial and temporal distribution of tropospheric water vapor observed by a Raman lidar and a GNSS receiver network over Shigaraki, Japan

*Masanori Yabuki[1], Toshitaka Tsuda[1], Yuya Kawano[2], Yusaku Tottori[2], Makoto Tsukamoto[2], Eiji Takeuchi[2] (1.Research Institute for Sustainable Humanosphere, Kyoto University, 2.EKO Instruments Co., Ltd.)

[MTT46-P10] **Study of the Mechanisms of Severe Thunderstorm in Tokyo Metropolitan Area using High Frequent Assimilation of GNSS and Other Ground-based Observations**

*Yoshinori Shoji[1], Tetsu Sakai[2], Ahoro Adachi[1], Satoru Yoshida[2], Tomohiro Nagai[2] (1.The Second Laboratory of Meteorological Satellite and Observation System Research Department, Meteorological Research Institute, 2.The Third Laboratory of Meteorological Satellite and Observation System Research Department, Meteorological Research Institute)

Continuous acoustic ranging from a GNSS buoy for the new method of seafloor crustal deformation measurements

*Keiichi Tadokoro[1], Natsuki Kinugasa[1], Teruyuki Kato[2], Yukihiro Terada[3], Akira Futamura[4], Kenjiro Matsuhiro[1]

1. Research Center for Seismology, Volcanology and Earthquake and Volcano Research Center, Nagoya University, 2. Hot Springs Research Institute of Kanagawa Prefecture, 3. Kochi National College of Technology, 4. National Institute of Technology, Yuge College

Our research group has been testing a measurement system for the continuous seafloor crustal deformation at a moored buoysite operated by Kochi prefecture, located 32 km off Cape Ashizuri, Japan.An acoustic transducer was fixed at about 1.7 m beneath the sea surface with a pole mounted on the buoy body.Three ocean bottom acoustic transponders had been installed around the moored point of the buoy. The acoustic signals are sequentially transmitted to these three transponders every three minutes. The recorded data on the buoy are planned to transmitted to a ground base station through a commercial communication satellite operated by Thuraya Telecommunications Company.
We performed a test for the continuous acoustic ranging between the buoy and the ocean bottom transponders from March 28 to 31 and from June 2 to July 12 (1st period), and from November 16to December 17 (2nd period) in 2018. The acoustic ranging was continuously possible throughout the above periods when power was supplied whereas it was unexpectedly terminated because of power failure during the winter season. The acoustic signals were transmitted 27,856 times in total, and the buoy-mounted acoustic ranging unit received 23,342 signals from the ocean bottom transponders. However, the acoustic data sent to the ground base station was only 12 % because of some trouble of the satellite communication modem.
The reflected signals from the buoy body and/or the seafloor sometimes contaminated the received acoustic signals; also multiple reflections inside of an anti-reflection cover attached to the buoy-mounted transducer, whose purpose is to cut off the reflection from the sea surface, were remarkable during the 1st period. The multiple reflections caused the misidentification of the direct wave from the sea-bottom units. We, therefore, removed the anti-reflection cover during the 2nd period, which remarkably reduced the confused reflections.
We coded a program for detecting the arrival time of direct acoustic wave automatically on the basis of thresholds of cross-correlation coefficient and energy ratio (the ratio of the squared amplitudes preceding and following a test point) to reduce the capacity of data transferred via satellite communication using the acoustic waveform recorded during the 1st period. The program successfully picked the correct direct wave onset for more than 99 % of the waveforms recorded during the 2nd period.

©2019. Japan Geoscience Union. All Right Reserved.

Accuracy and precision assessment of the real-time kinematic GNSS time series for moored buoy using three-axis programable moving table

*Yusaku Ohta[1], Misae Imano[1], Motoyuki Kido[2]

1. Research Center for Prediction of Earthquakes and Volcanic Eruptions, Graduate School of Science, Tohoku University, 2. IRIDeS, Tohoku University

Rapid understanding of the magnitude of large earthquakes and their associated fault dimensions are extremely important. Especially, capture of the coseismic deformation in the offshore region will be key information to understand the fault dimensions for the large interplate earthquake. Based on this background, Tohoku University and JAMSTEC are jointly developing the on-demand crustal deformation monitoring system using moored buoy system. The buoy can measure the sea-floor horizontal crustal deformation by GNSS/Acoustic technique and vertical deformation using ocean bottom pressure sensor. One of the key technology in our developed system is the real-time kinematic GNSS which can measure three-dimensional position of the buoy in real-time. In contrast, it is difficult to understand quantitatively the precision and accuracy of estimated buoy position because no reference for the position. Thus, we assess the precision and accuracy of real-time kinematic GNSS time series using programable three-axis movable table.

We have developed the single-axis precise programable movable table (Ohta et al., 2016). We expanded this developed system to three-axis. For the real-time kinematic analysis, we adopted Trimble CenterPoint RTX (hereafter, RTX) with 10Hz sampling interval. The correction message for the analysis was received via a stationary satellite. We also estimated the GNSS antenna position using very short-baseline kinematic analysis as reference solution. The developed movable table can operate single axis horizontal displacement, rotational movement, and tilt deformation. To simulate the actual buoy movement, we gave the motion to the movable table based on the actual buoy movement. We conducted the experiment in 24 hours duration.

We calculated the residual time series between obtain time series by RTX and short-baseline kinematic solution. The difference between averaged absolute position was quite good in the horizontal components which was less than 10mm. In contrast, the vertical component shows the clear discrepancy between them. RTX time series shows systemically higher than the baseline analysis which reached approximately 230mm. In contrast, the precision of the calculated residual time series was good in both of the components. Calculated standard deviations were 10-11mm and 28mm in horizontal components and vertical component, respectively. We will show the more detailed results from our experiment and discuss the ability of the real-time kinematic analysis in our developed buoy.

©2019. Japan Geoscience Union. All Right Reserved.

GNSS-R altimetry using a Geostationary Satellite

*Kaoru Ichikawa[1], Tatsuki Okumura[2], Masanori Konda[3], Yasuyuki Baba[4]

1. Res. Inst. Appl. Mech., Kyushu Univ., 2. Dept. ESST, Interdicipl. Grad. School Eng. Sc., Kyushu Univ., 3. Graduate School of Science, Kyoto Univ., 4. Disaster Prevention Res. Inst., Kyoto Univ.

The GNSS reflectometry (GNSS-R) uses GNSS signals reflected at the sea surface, which are usually eliminated as the multipath error. The reflected GNSS path received at an antenna is always longer than the direct path, so that the height of the antenna from the sea surface is geometrically determined from the excess path length. The excess path length can be either directly determined by measuring the temporal delay of the reflected signals, or indirectly estimated from interferometric cyclic modulations of the received power (often referred as signal-to-noise ratio; SNR) induced by phase differences between the direct and reflected GNSS signals. In the latter method, as the elevation angle of an earth orbiting GNSS satellite changes in time, the geometric reflection point on the sea surface temporally displaces, which results in interferometric changes of the path length during a period while the satellite is in sight. Meanwhile, for a geostationary satellite in BeiDou constellations that are always in sight, the path length changes not by the movement of the satellite but the elevation of the reflection surface, *i.e.* the sea level rise. In this study, we used the three-month time series (2016/09-11) of the 1Hz SNR of the geostationary BeiDou #02 satellite observed by a GNSS-R system deployed to the Shirahama Oceanographic Observatory Tower owned by Kyoto University (33deg, 42’ 32’’ N, 135deg, 19’ 58’’ E) at the height of ~20m. The geostationary GNSS-R altimetry observed significant flood tides when the wind speed is stably low; the 0.6m sea level rise was successfully determined by the SNR interferometry with 0.05m rms difference. However, significant interferometric SNR changes by tides were not recorded at high or low tides since at least 0.25m sea level change is required for the interferometry cycle. Consequently, the cyclic periods of the geostationary GNSS-R altimetry for tides become long (1-4 hours for 0.25m change in Shirahama), the interferometric variations were usually contaminated by SNR changes induced by the other factors such as winds. On the contrary, faster sea level changes by wave motions could be recognized by the geostationary GNSS-R altimetry, although the temporal sampling intervals of the present data were not adequate.

Keywords: GNSS-R , altimetry, BeiDou geostationary GNSS satellite

©2019. Japan Geoscience Union. All Right Reserved.

Estimation of typhoon wind speed using CYGNSS observations: A case study of Typhoon Lan in 2017

*Kako Shinichiro[1], Hiroyuki Tomita[2], Kaoru Ichikawa[3]

1. Graduate School of Science and Engineering, Kagoshima University, 2. Institute for Space-Earth Environment, Nagoya University, 3. Research institute for Applied Mechanics, Kyushu University

We conducted a case study of Typhoon Lan, which occurred in 2017, to investigate the impact of the Cyclone Global Navigation Satellite System (CYGNSS) on the estimation of extremely high wind speeds, such as those occurring during typhoons. We studied CYGNSS because it is expected to be capable of observing wind speeds in regions with extremely high wind speeds and heavy rains (i.e., typhoons) where it is difficult to perform measurements using the current microwave instrument. Firstly, we compared CYGNSS-derived wind speeds produced by NASA with those derived from AMSR2 produced by the Japan Aerospace Exploration Agency. CYGNSS was found to underestimate the wind speeds around Typhoon Lan compared with AMSR2. We then attempted to estimate the wind speeds using the leading edge slope (LES) and mean square slope (MSS) derived from the CYGNSS observations. Although the relationship between the MSS and wind speed differs depending on the wave age (Zhao and Tobe, 2003), it is difficult to estimate the wave age because this estimation is required the wind and wave speeds. We used the wave period as a substitute for the wave age since the wave period is expected to be similar to the wave age. We therefore first computed the fourth power of the wave period (T4) in line with Wang and Ichikawa (2016). Next, we classified the ocean into three regions based on T4 to investigate the relationship between the MSS and the wind speed observed by AMSR2 in each region. Finally, we approximated the curves relating the MSS to the wind speed using exponential functions in the three regions and estimated the wind speed using these curves. The comparison between the wind speeds produced by NASA and those estimated in this study demonstrated that our method can estimate high wind speeds more accurate than the CYGNSS wind speeds produced by NASA.

Keywords: CYGNSS, AMSR2, tyhoon

©2019. Japan Geoscience Union. All Right Reserved.

Ionospheric and seismic effects caused by the North Korea nuclear tests realized on 2006-2017

Nataliia Perevalova[2], *Nikolai Shestakov[1], Anna Dobrynina[3,4], Dmitry Kostylev[7], Meng Guojie[5], Wei-Wei Wu[5,6]

1. Institute for Applied Mathematics FEB RAS, Vladivostok, Russia; Far Eastern Federal University, Vladivostok, Russia, 2. Institute of Solar-Terrestrial Physics SB RAS, Irkutsk, Russia, 3. Institute of the Earth's Crust SB RAS, Irkutsk, Russia , 4. Geological institute SB RAS, Ulan-Ude, Russia , 5. Institute of Earthquake Forecasting, China Earthquake Administration, Beijing, China, 6. College of Surveying and Geo-informatics, Tongji University, Shanghai, China, 7. Sakhalin Branch of Federal Research Center Geophysical Survey RAS, Yuzhno_Sakhalinsk, Russia

Using data from GPS/GLONASS receivers and seismic networks, we studied the ionospheric and lithospheric effects caused by six underground nuclear tests realized in North Korea on 2006-2017.
To investigate the ionospheric disturbances, we analyzed data from several continuous GNSS-networks (GPS and GLONASS) operating in Asia - Western Pacific region: IGS, GEONET, FEB RAS and FEFU complex geodynamic network, a set of stations belonging to China and South Korea GNSS-networks. Sites close to the Korean Peninsula were selected for the analysis. Series of total electron content (TEC) in the ionosphere were calculated on the base of dual-frequency phase measurements of GNSS receivers. To detect disturbances caused by the nuclear tests, TEC series were filtered in the range of periods from 1 to 10 minutes. Despite the small magnitudes of seismic events associated with the nuclear tests, we were able to identify ionospheric disturbances which were most likely generated by these explosions. Such disturbances were detected for 4 out of 6 nuclear tests. The main parameters of the disturbances were determined. From our analysis we concluded that characteristics of ionospheric disturbances caused by the underground nuclear tests differed significantly from the parameters of disturbances that are usually observed after earthquakes.
For seismic analysis, we used data from the broadband seismic station networks located at distances up to 23 degrees from the Korean Peninsula: II, IC, IU, TW, JP, G, KS, and KG given by IRIS, and regional seismic network BY. The frequency content of P and surface Rayleigh waves registered by 46 broadband stations was analyzed. For some events, the P-wave frequency content showed the prevalence of low frequencies in spectra (~0.45 Hz). The peak frequencies of the surface Rayleigh waves was in the 0.05-0.45 Hz range. Preliminary analysis of the peak frequencies spatial distribution showed that the continental massive area is characterized by the relatively high frequencies (0.14-0.50 Hz) while for the areas adjacent to marginal seas the low values of peak frequencies are observed (from 0.13 Hz and less).
Acknowledgments. We are deeply indebted to Scripps Orbit and Permanent Array Center (SOPAC) for the IGS-network data, to Geospatial Information Authority of Japan for GEONET network data, to Korea Astronomy & Space Science Institute for access to GNSS data on the Korean Peninsula, CCU CC FEB RAS for access to data from the FEB RAS and FEFU complex geodynamic network; Institute of Earthquake Forecasting, China Earthquake Administration for access to GNSS data in China. The facilities of the IRIS Data Management System, and specifically the IRIS Data Management Center, and Baikal Regional Seismological Center and Sakhalin Branch of Federal Research Center Geophysical Survey RAS were used to get waveform and metadata required in this study. This work was performed with budgetary funding of Basic Research program II.16 and was also partially supported by RFBR grants 17-45-388072_p_a, 17-45-388049_ p_a, 17-55-53110_GFEN_a, 19-05-00889_a.

Keywords: North Korea nuclear tests, ionospheric and lithospheric effects, GPS/GLONASS-observations

©2019. Japan Geoscience Union. All Right Reserved.

©2019. Japan Geoscience Union. All Right Reserved.

Relationships between Water Vapor Concentration Index derived from GNSS and Surface Wind Convergence during Localized Heavy Rainfall in Tokyo in Summer

*Yoshihito Seto[1], Yoshinori Shoji[2], Nobumitsu Tsunematsu[3], Hideo Takahashi[1]

1. Department of Geography, Graduate School of Urban Environmental Sciences, Tokyo Metropolitan University, 2. Meteorological Research Institute, 3. Tokyo Metropolitan Research Institute for Environmental Protection

In recent years, short-term heavy-rainfall events that have caused severe damages such as flooding have frequently occurred in the Tokyo Metropolitan area in summer. In view of the development process of cumulonimbus clouds, the convergence of surface winds and the spatial concentration of water vapor are supposed to have taken place prior to the occurrence of heavy rainfall. This study aims to clarify the evolutionary process of short-term heavy rainfall as a contribution to short-range forecasting of heavy rainfall that occurs locally.

The relationships between the occurrence of heavy rainfall and the convergence of surface winds and water vapor concentration for heavy-rainfall cases were examined using data from July to September obtained from high-density meteorological observations in Tokyo, Japan. We used the water vapor concentration (WVC) index derived from the global navigation satellite system (GNSS) analysis as indices for the degree of divergence and convergence of water vapor in the lower troposphere (Shoji 2013).

Corresponding to heavy-rainfall areas, the convergence of surface winds tended to increase for several tens of minutes prior to the heavy rainfall. The peak time of wind convergence was observed 10–30 min before the heavy-rainfall occurrence, and the convergence continued to increase for approximately 30 min until the convergence peak time (Seto et al. 2018). Around the heavy-rainfall area, the increase in the WVC index coincided with the increase in convergence. On the other hand, it was considered that the temporal and spatial scales of the WVC index are larger than those of wind convergence. From these results, by monitoring the temporal variations and distributions of these parameters using a high-density observation network, it should be possible to predict the occurrence of heavy rainfall rapidly and accurately.

References

Seto, Y., Yokoyama, H., Nakatani, T., Ando, H., Tsunematsu, N., Shoji, Y., Kusunoki, K., Nakayama, M., Saitoh, Y. and Takahashi, H. 2018. Relationships among rainfall distribution, surface wind, and precipitable water vapor during heavy rainfall in central Tokyo in summer. J. Meteor. Soc. Japan, 96A, 35–49.

Shoji, Y. 2013. Retrieval of water vapor inhomogeneity using the Japanese nationwide GPS array and its potential for prediction of convective precipitation. J. Meteor. Soc. Japan, 91, 43–62.

Keywords: localized heavy rainfall, wind convergence, water vapor, high-density observation

©2019. Japan Geoscience Union. All Right Reserved.

Development of novel ground-based microwave radiometer for earth science -preliminary report-

*Ryuichi Ichikawa[1], Hideki Ujihara[1], Shinsuke Satoh[1], Jun Amagai[1], Yusaku Ohta[2], Basara Miyahara[3], Hiroshi Munekane[3], Taketo Nagasaki[4], Osamu Tajima[5], Kentaro Araki[6], Takuya Tajiri[6], Hiroshi Takiguchi[7], Takeshi Matsushima[8], Nobuo Matsushima[9], Tatsuya Momotani[10], Kenji Utsunomiya[10]

1. National Institute of Information and Communications Technology, 2. Tohoku University, 3. Geospatial Information Authority of Japan, 4. High Energy Accelerator Research Organization, 5. Kyoto University, 6. Meteorological Research Institute, JMA, 7. Japan Aerospace eXploration Agency, 8. Kyushu University, 9. National Institute of Advanced Industrial Science and Technology, 10. Japan Weather Association

We have started to develop a next-generation microwave radiometer to be used in millimeter-wave spectroscopy for the high-resolution and high-precision monitoring of water vapor behavior. The new radiometer will be suitable for not only space geodetic techniques such as VLBI and GNSS, but also field measurements such as monitoring volcanic activities and cumulonimbus cloud generation. The basic design concept of the new radiometer follows the previous version named KUMODeS (KEK Universal Moisture and Oxygen Detection System) developed by the High Energy Accelerator Research Organization (KEK). The KUMODeS can measure spectra using two receivers with frequency bands of 20–30 GHz and 50–60 GHz. The low-noise amplifier (LNA) of the first KUMODeS receiver and a cold calibration source are implemented in a cryostat, which is maintained at 10 K to improve the sensitivity of detecting the characteristic broad peak of water vapor at approximately 22 GHz. The second receiver is used to measure the absorption peaks of oxygen (60 GHz). We have carried out comparative measurements of precipitable water vapor (PWV) to investigate the potential of KUMODeS/PWV measurements. The preliminary results of PWV comparisons imply that KUMODeS technology will be useful for retrieving the accurate behavior of water vapor with high temporal resolution. We will implement a wide bandwidth feed of 20–60 GHz into the new system on the basis of a previous comparison study. A signal is separated into two linear orthogonal polarized signals from the feed, one is in the 20–30 GHz feed and the other in the 50–60 GHz feed, using an orthomode transducer (OMT). The wideband feed, OMT, and the LNA for each signal are cooled at 77 K using a Stirling cryocooler to improve signal-to-noise ratio. The development of a new front-end module will be completed at the end of 2019, and we are planning to implement the module in an existing dish antenna to perform validation measurements.

Keywords: GNSS, microwave radiometer, water vapor

©2019. Japan Geoscience Union. All Right Reserved.

Refractivity Distributions over the Kanto Plain Obtained by Dual-polarization Radar

*Hiromu Seko[1], Eiichi Sato[1], Hiroshi Yamauchi[2]

1. Meteorological Research Institute, 2. Japan Meteorological Agency

Temperature and water vapor near the surface play crucial roles for the generation of convection cells. However, their variations just before the generations of convection cells still are not understood completely. In this study the temporal variations of refractivity index were obtained by MRI dual-polarization Doppler radar. The features of temperature and water vapor including generation period of convection cells will be shown in this presentation. On 19th August 2017, the sea breeze invaded from Kashima-Nada and the refractivity increased along the front of the sea breeze. The scattered weak echoes that appeared around the front seem to be related with the increase of refractivity. These are the features near the surface. The comparison with other data such as GNSS PWV will be also presented.

Keywords: Observation method, Doppler radar, Refractivity index

©2019. Japan Geoscience Union. All Right Reserved.

Spatial and temporal distribution of tropospheric water vapor observed by a Raman lidar and a GNSS receiver network over Shigaraki, Japan

*Masanori Yabuki[1], Toshitaka Tsuda[1], Yuya Kawano[2], Yusaku Tottori[2], Makoto Tsukamoto[2], Eiji Takeuchi[2]

1. Research Institute for Sustainable Humanosphere, Kyoto University, 2. EKO Instruments Co., Ltd.

Understanding the spatial and temporal distributions of water vapor in the atmosphere is critical for unveiling the fundamental mechanisms of localized extreme weather events. Besides, it is highly beneficial for improving the accuracy of weather forecasts by mesoscale numerical weather prediction models. To achieve the continuous monitoring of water vapor distributions, we performed simultaneous measurements by Raman lidar in the UV-C region and a dense Global Navigation Satellite System (GNSS) network. The former is a novel technology that can be utilized for profiling the vertical distribution of the water vapor mixing ratio for twenty-four hours, while the latter can be used for detecting the horizontal distribution of precipitable water vapor. The Raman lidar employs a laser at a wavelength of 266 nm and detects the light separated into an elastic backscatter signal and vibrational Raman signals of oxygen, nitrogen, and water vapor at wavelengths of 266, 277, 284, and 295 nm, respectively. The use of these wavelengths is convenient because of the low background noise during daytime, since most of the solar radiation in the ultraviolet range below 300 nm is absorbed by the ozone layer in the stratosphere. The lidar was encased in a temperature-controlled compact container, resistant to a variety of environmental conditions. Continuous observation of water vapor profiles by lidar has been conducted at the Shigaraki MU radar observatory (34˚51’ N, 136˚06’ E, 385 m a.s.l.) since November 2017. The dense GNSS receiver network consisted of 10 dual-frequency GNSS stations which were installed with a horizontal spacing of 3-4 km near the observatory on July 2017. In this study, we present our water vapor monitoring system as well as the preliminary results on the spatio-temporal water vapor distributions in 2018.

Acknowledgements
A part of this study is supported by JSPS KAKENHI Grant Number 15H03724.

Keywords: water vapor, Raman lidar, dense GNSS network

©2019. Japan Geoscience Union. All Right Reserved.

Study of the Mechanisms of Severe Thunderstorm in Tokyo Metropolitan Area using High Frequent Assimilation of GNSS and Other Ground-based Observations

*Yoshinori Shoji[1], Tetsu Sakai[2], Ahoro Adachi[1], Satoru Yoshida[2], Tomohiro Nagai[2]

1. The Second Laboratory of Meteorological Satellite and Observation System Research Department, Meteorological Research Institute, 2. The Third Laboratory of Meteorological Satellite and Observation System Research Department, Meteorological Research Institute

Highly urbanized Tokyo metropolitan area is vulnerable to severe storms such as local torrential rainfall, thunder lightning and tornado. Recently, the number of days with thunderstorms has been increasing in Tokyo. Elucidation of the mechanism of extreme weather in Tokyo is urgent matter (Nakatani et al. 2013). To study the rolls of water vapor and wind for the rapid life-cycle (initiation, development and dissipation) of hazardous cumulus convection, we installed a mobile Raman-lidar (Sakai et al. 2018), a wind profiler, and five GNSS stations in and around Tokyo.

Using 3DVAR capability of WRF data assimilation system (WRFDA)(Barker et al. 2012) , three-dimensional atmospheric fields with 1 km horizontal resolution were produced at every 10min throughout the August 2017 and 2018. Background fields were produced by JMA nonhydrostatic model (NHM)(Saito et al. 2007). In addition to the observed data at these campaign observation instruments, Japan Meteorological Agency’ s operational surface meteorological stations, wind-profiler stations and GNSS PWV derived at dense GNSS network of Geospatial Information Authority of Japan are assimilated. We confirmed that the reproduced atmospheric fields (Temperature, humidity, and wind) showed better agreement with observations of radiosonde, lidar derived water vapor mixing ratio, and wind-profiler than background fields at altitudes lower than 2 km. Assimilation of surface meteorological observations (atmospheric pressure, temperature, humidity and wind) introduced better agreement mainly at altitude lower than 0.5 km. Inclusion of GNSS derived PWV resulted better agreement of humidity at altitude higher than 0.5 km and inclusion of wind field from wind-profiler led better agreement of wind field.

We have investigated roles of water vapor for several local heavy rainfall events occurred in Tokyo in August 2017 and 2018 and found that convergence of water vapor flux at 0.5 km altitude had intensified prior to the occurrence of torrential precipitation. Statistical and quantitative results will be discussed at the symposium.

This study is supported by JSPS KAKENHI Grants 17H00852.

Keywords: Water vapor, Data assimilation, Localized heavy rainfall

©2019. Japan Geoscience Union. All Right Reserved.

[E] Poster | M (Multidisciplinary and Interdisciplinary)：M-TT Technology & Techniques

Mon. May 27, 2019 1:45 PM - 3:15 PM JST | Mon. May 27, 2019 4:45 AM - 6:15 AM UTC | Poster Hall International Exhibition Hall8, Makuhari Messe_11

[M-TT47] GEOSCIENTIFIC APPLICATIONS OF HIGH-DEFINITION TOPOGRAPHY AND GEOPHYSICAL DATA IN THE ANTHROPOCENE

convener:Yuichi S. Hayakawa(Faculty of Environmental Earth Science, Hokkaido University), Shigekazu Kusumoto(Graduate School of Science and Engineering for Research, University of Toyama), Christopher A Gomez(Kobe University Faculty of Maritime Sciences Volcanic Risk at Sea Research Group)

Recent technical developments of high-definition topographic and geophysical data acquisition have enabled us to further investigate geoscientific issues including land surface processes, subsurface structures, submarine and aerial environments, geo-ecological interactions, and disaster mitigation. Such high-definition or high-resolution data are particularly useful for studies in short-term temporal scales, and future predictions such as numerical modelings. In this session, we expect submissions on topics challenging such issues in the Anthropocene, the most recent geological era of the Earth. A range of topics would fit the session framework, including theoretical work, improvements in data acquisition, extensive data preservation and archiving, pre- and post-processing, statistical analysis, modeling, and simulation for geoscientific research and geohazard assessments in the Anthropocene. The methodological approaches may include, but not limited to, laser scanning, SfM-MVS photogrammetry, GNSS precise positioning, SAR interferometry, multi-beam sonar, and electromagnetic sensors, based on terrestrial (fixed or mobile) and aerial (UAV or manned airborne) platforms.

[MTT47-P01] High-definition topography monitoring after riverbed cultivation in the Echi River, central Japan

*Takuro Ogura[1,2], Satoshi Asano[3], Toshiaki Mizuno[3], Yoshihiro Azuma[3], Takeshi Kitai[4], Yuichi S Hayakawa[5,6], Kotaro Iizuka[6] (1.Graduate School of Frontier Sciences, The University of Tokyo, 2.Graduate School of Environmental Science, Hokkaido University, 3.Lake Biwa Environmental Research Institute , 4.Lake Biwa Museum, 5.Faculty of Environmental Earth Science, Hokkaido University, 6.Center for Spatial information Science, The University of Tokyo)

[MTT47-P02] Spatial distribution of land surface displacements in the crater of Tateyama Midagahara Volcano using high-definition topographic data

*Yuichi S. Hayakawa[1], Shigekazu Kusumoto[2], Takuro Ogura[3,4] (1.Faculty of Environmental Earth Science, Hokkaido University, 2.Graduate School of Science and Engineering for Research, University of Toyama, 3.Graduate School of Frontier Science, The University of Tokyo, 4.Graduate School of Environmental Science, Hokkaido University)

[MTT47-P03] Study on a simplified measurement of water depth and reconstruction of the riverbed form by using SfM and MVS.

*OSAWA KOTA[1], Tadafumi Niizato [2], Katsuaki Mitachi[3], Makoto Kawamura[1], Masahiro Ohkawa[1] (1.Mitsubishi Materials Techno corporation , 2.Japan Atomic Energy Agency, 3.ATOM TRANSPORT SERVICE CO., LTD)

[MTT47-P04] Ground Penetrating Radar Imaging of Moisture and Water movement in volcanic soil

*Christopher A Gomez[1] (1.Kobe University Faculty of Maritime Sciences Volcanic Risk at Sea Research Group)

[MTT47-P05] Estimating Eruptive Volumes of Mud Volcano Southwestern Taiwan by Using UAV and SfM-MVS Photogrammetry

*CHIA-YING LIU [1], Ray Y Chuang[1], Horng-Yue Chen [2] (1.Department of Geography, National Taiwan University, 2.Academia Sinica, Institute of Earth Sciences)

[MTT47-P06] Increasing temporal depth of urban Land-Use Regression Models by wind-data driven dynamic buffer generation

*Tilman Leo Hohenberger[1], King Wai Leung[1] (1.Division of Environment and Sustainability, Hong Kong University of Science and Technology)

High-definition topography monitoring after riverbed cultivation in the Echi River, central Japan

*Takuro Ogura[1,2], Satoshi Asano[3], Toshiaki Mizuno[3], Yoshihiro Azuma[3], Takeshi Kitai[4], Yuichi S Hayakawa[5,6], Kotaro Iizuka[6]

1. Graduate School of Frontier Sciences, The University of Tokyo, 2. Graduate School of Environmental Science, Hokkaido University, 3. Lake Biwa Environmental Research Institute , 4. Lake Biwa Museum, 5. Faculty of Environmental Earth Science, Hokkaido University, 6. Center for Spatial information Science, The University of Tokyo

Natural processes of erosion and deposition on riverbeds are generally limited in Japan due to large-scale public constructions including dams and banks. As a result of the construction of dams, sediment transport may dramatically decrease in the downstream area are, and the river ecosystem can also be affected. To make sediment move more vigorously, we cultivated the armored gravel riverbed with heavy machinery. We then explore the effects of riverbed cultivating by monitoring the topographic changes with high-frequency and high-definition measurements (HF-HD measurements), whereas conventional measurement technologies do not compensate spatial resolution and temporal resolution to capture the topographic change. Using UAS (Unmanned Aerial Vehicle) and SfM-MVS (Structure-from-Motion –Multi-view Stereo) photogrammetry, we found the transportation of the fixed gravels were occurring after cultivating the riverbed in 2017. The temporal and spatial resolutions of the HF-HD topographic data was approximately 2 months and 10 cm, respectively. In July 2018, water flow at 130 m^3/s was discharged from the upstream dam, and we confirmed that a part of the gravels in the cultivated area was eroded and replaced with new sediments (Fig. 1). These observations indicate that riverbed monitoring using UAV and SfM - MVS can be a practical tool for proper management of riverbeds. Applying this result, we will further clarify the relationships between the water quantity discharged from the dam and the riverbed topographic changes.

Keywords: High-definition topographic data, riverbed cultivation, UAV, SfM-MVS photogrammetry, Echi river

©2019. Japan Geoscience Union. All Right Reserved.

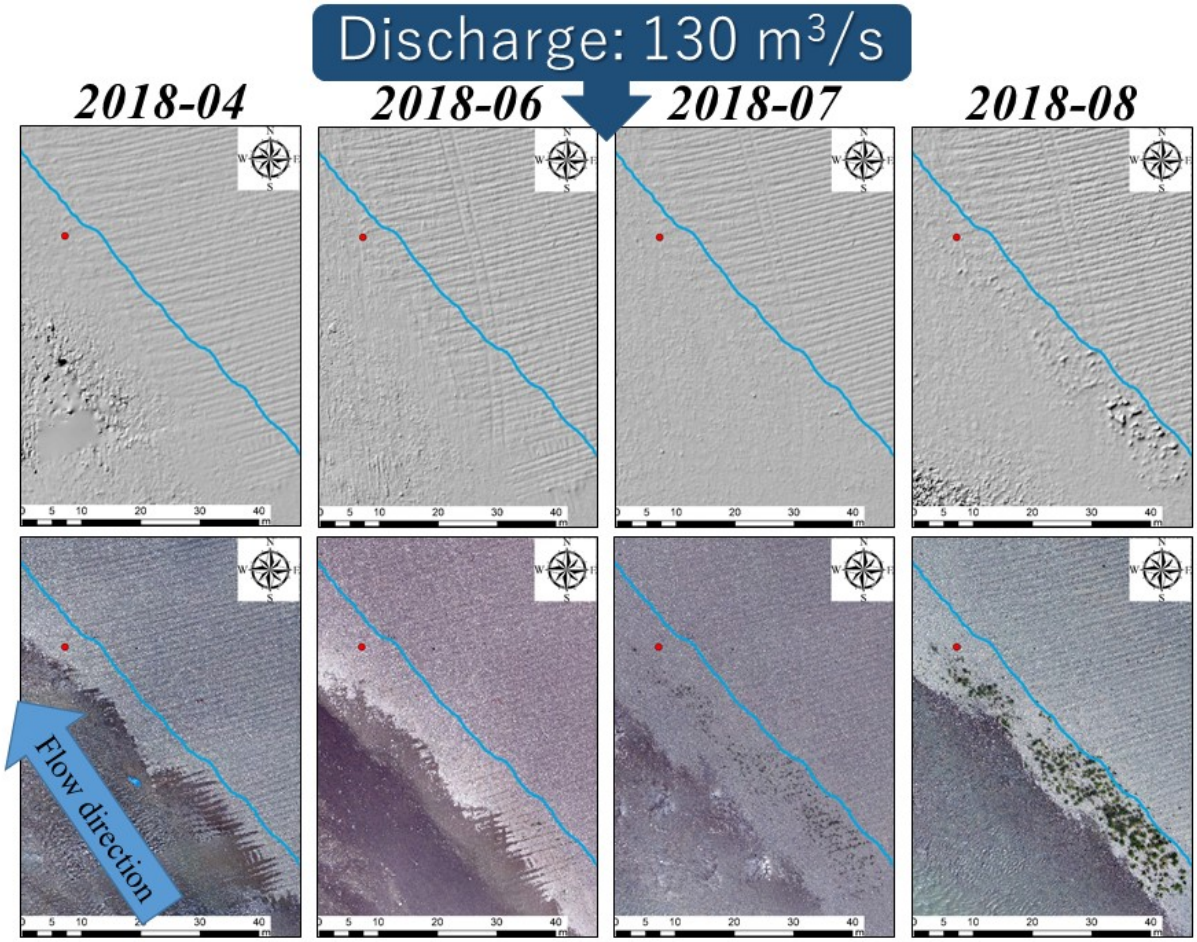


Fig.1. Hillshade images and ortho images of cultivated area.

©2019. Japan Geoscience Union. All Right Reserved.

Spatial distribution of land surface displacements in the crater of Tateyama Midagahara Volcano using high-definition topographic data

*Yuichi S. Hayakawa[1], Shigekazu Kusumoto[2], Takuro Ogura[3,4]

1. Faculty of Environmental Earth Science, Hokkaido University, 2. Graduate School of Science and Engineering for Research, University of Toyama, 3. Graduate School of Frontier Science, The University of Tokyo, 4. Graduate School of Environmental Science, Hokkaido University

Detailed monitoring of land surface displacements is crucial for the assessment of activities of a volcano, especially in its crater area. Close-range remote sensing of high-definition topographic data is advantageous in the detection of centimeter-scale ground-surface displacements in a wide spacial extent, whereas the conventional leveling method is capable of detecting millimeter-scale displacements along a measurement line. We investigated the spatial distribution of land surface displacements in the Jigoku-Dani crater area of Mt. Tateyama Midagahara Volcano in Toyama Prefecture, central Japan by high-definition topographic measurements including terrestrial laser scanning and unmanned aerial vehicle-based structure-from-motion photogrammetry. The annual measurements were performed for three years (2015 to 2017). The range of uplift detected by terrestrial laser scanning corresponds with that by leveling. Together with the analytical results of the leveling data, the spatial pattern of the uplift suggests the extent of an underground pressured zone to cause the exhumation. For the prediction of the volcanic activities, further monitoring is required to reveal the spatiotemporal patterns of the displacements.

Keywords: terrestrial laser scanning, unmanned aerial system structure-from-motion, point cloud

©2019. Japan Geoscience Union. All Right Reserved.

Study on a simplified measurement of water depth and reconstruction of the riverbed form by using SfM and MVS.

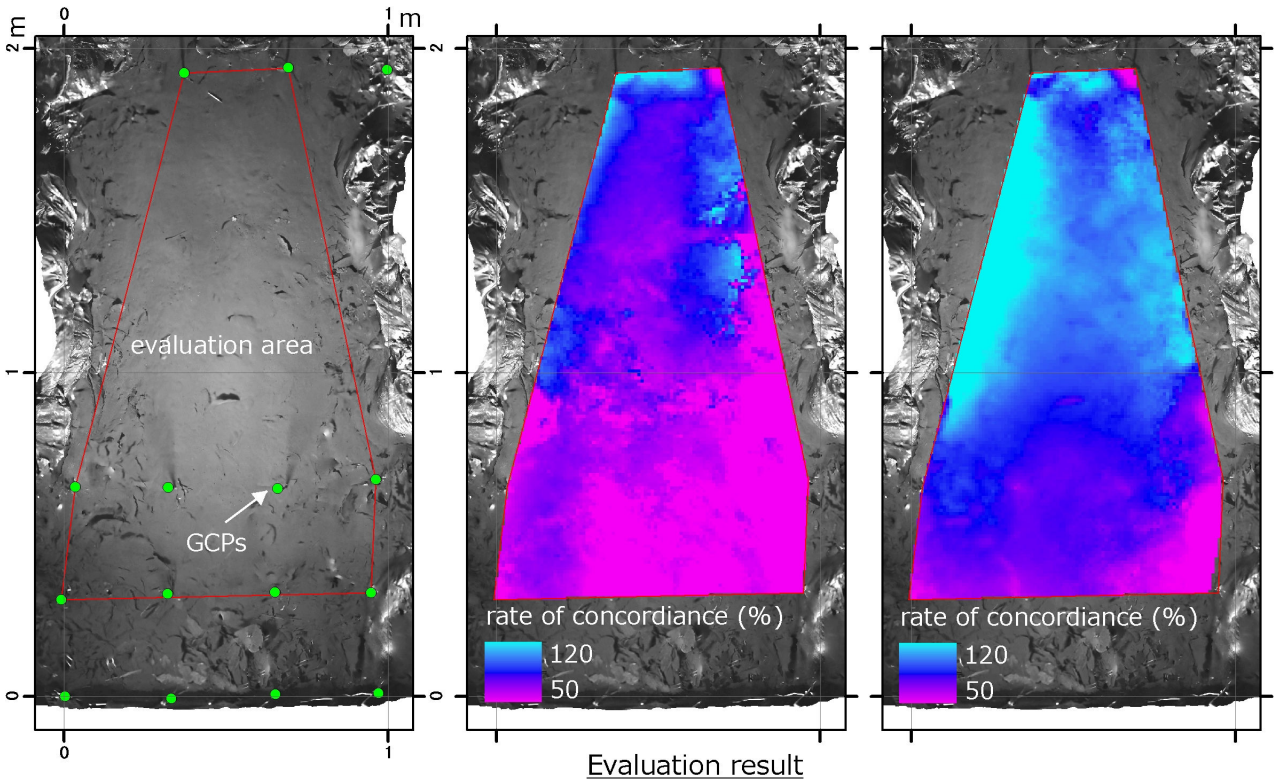
*OSAWA KOTA[1], Tadafumi Niizato [2], Katsuaki Mitachi[3], Makoto Kawamura[1], Masahiro Ohkawa[1]

1. Mitsubishi Materials Techno corporation , 2. Japan Atomic Energy Agency, 3. ATOM TRANSPORT SERVICE CO., LTD

Primary outflow process of radiocesium, which is released by the TEPCO’ s Fukushima Dai-ichi Nuclear Power Plant accident, from a forested hillslope to a mountain stream is a particulate-bond state transport. A detailed estimation of the riverbed form and sediment volume changing with time is a key issue to assess the radiocesium distribution in the forested environment. Changes in the sediment volume can be calculated from the water depth and the difference between measured water surface and reference water surface levels setting up at the initial. Conventional method for a water depth determination is a direct measurement of the stream water depth by using a scale. But it requires a lot of time and labor to evaluate the change of riverbed form and water depth in detail.
In this study, we attempted an accurate and labor-effective method to evaluate the water depth and three-dimensional (3D) structure of underwater riverbed form by applying the SfM (Structure from Motion) /MVS (Multi View Stereo) techniques and the optical image data collected on consumer-grade-camera. These images were photographed beside of the small stream located at southern part of the Abukuma Mountains, Fukushima. Light propagation properties such as attenuation or reflection influence precise reconstruction of 3D model using underwater images. This was done to reduce influence of light propagation in two steps: 1) to reduce the influence of reflection, photographing at the time of twilight using LED light and Circular PL filter. 2) to reduce the influence of attenuation, installing blue colored film on the LED light and omitting band R, G for SfM/MVS analysis. And we also photographed at the day time and reconstructed 3D model (Day Model: DM) to compare and confirm the model applying two steps (Twilight Model: TM). As a criterion for evaluation of these models, we carried out the direct measurement of water depth. Rate of estimation concordance was calculated by dividing analytical water depth by the direct measurement depth, then convert to percentage.
Discrepancy between measured and analytical results increased with depth, the rate of estimation concordances were 46 % (DM) and 73 % (TM) in the water depth of 20-25 cm, and 62 % (DM) and 93 % (TM) in 10-15 cm, respectively (Figure). Next step is an improvement of the correction and image-capturing methods to reduce the estimation errors by elimination of the light refraction on the stream water surface.

Keywords: SfM/MVS, measurement of water depth, riverbed form

©2019. Japan Geoscience Union. All Right Reserved.



Evaluation result

Left: Orthographic Image, Evaluation area (red polygon) and location of GCPs (green dot),
Center: Discrepancy between measured and analysis (DM),
Right: Discrepancy between measured and analysis (TM)

©2019. Japan Geoscience Union. All Right Reserved.

Ground Penetrating Radar Imaging of Moisture and Water movement in volcanic soil

*Christopher A Gomez[1]

1. Kobe University Faculty of Maritime Sciences Volcanic Risk at Sea Research Group

Ground Penetrating Radar is a non-invasive subsurface method that provides results on the dielectric properties of the ground between 0 and 30 m on average in sediments. Working from sediments from Mt Unzen in Japan, tests over the moisture content and the air content change were conducted on the material in order to infer further data during field measurement. The GPR used in the survey is a Ramac Mala mounted with an antenna of 800 Mhz and a stack signal over time. The data were processed using Matlab using data filtering and time-depth conversion, and calculation of the dielectric properties variations. The signal analysis shows that the velocity does change over time depending on the moisture content and the change in air/void ratio. For a given homogeneous material, like at volcanoes, multiplying such analysis is a step forward the development of relatable tables for various environments.

Keywords: Ground Penetrating Radar, Soil moisture content, Volcanic material

©2019. Japan Geoscience Union. All Right Reserved.

Estimating Eruptive Volumes of Mud Volcano Southwestern Taiwan by Using UAV and SfM-MVS Photogrammetry

*CHIA-YING LIU[1], Ray Y Chuang[1], Horng-Yue Chen[2]

1. Department of Geography, National Taiwan University, 2. Academia Sinica, Institute of Earth Sciences

Mud volcanoes are special geologic features occurred in tectonic areas with horizontal compression. Complete research for mud volcanos can help us to understand the interaction of the crust and surface. In Taiwan, mud volcanoes are present on-land and off-shore southwestern Taiwan around the transitional area from subduction to orogeny. Among all mud volcanoes in Taiwan, the Wandan mud volcano erupts sporadically with significantly large amount of effluent mud. However, the mechanism of the eruption remains unclear because we lack fundamental information such as eruptive volumes, duration of mud eruption, impact factors and recurrence intervals. Therefore, it is important to estimate the eruptive volumes and further to examine the spatiotemporal pattern of the Wandan mud volcano eruption. We first compile literature and newspapers for historic eruption events to estimate two groups of recurrence interval: 150-180 days for highly active period and 300-600 days for less active period.

Since the sporadic eruption make different for rapid survey by using traditional methods, we take advantage of unmanned aerial vehicles (UAV) to design a survey network specifically. Therefore, we estimate the eruptive volumes of recent eruptions for the Wandan mud volcano by using aerial images taken from UAV, and 3D models derived from the structure-from-motion (SfM) photogrammetry technique. We use RTK-GPS and leveling for horizontal and vertical measurements of ground control point, respectively. We use the SfM software to generate DSMs, point clouds, and orthophotos with cm-level accuracy. We estimate the eruptive volume by subtracting the pre-eruption DSM from the post-eruption DSM. Our results show that for the event on 15 May, 2018, the eruptive area is 12,761 m^2 and the volume is 13,106.3625 ±13.0105m^3.

Keywords: UAS, GNSS, digital surface modeling, control survey

©2019. Japan Geoscience Union. All Right Reserved.

Increasing temporal depth of urban Land-Use Regression Models by wind-data driven dynamic buffer generation

*Tilman Leo Hohenberger[1], King Wai Leung[1]

1. Division of Environment and Sustainability, Hong Kong University of Science and Technology

Land-use regression (LUR) models are commonly used as an inexpensive and easy to set-up way to predict spatial variability in air-pollution. They are successfully applied to regional and, more and more, urban settings, making use of spatial predictors such as land-use, vegetation, morphology and geography. New approaches include an improved use of wind-data for buffer-creation and predictor calculation.

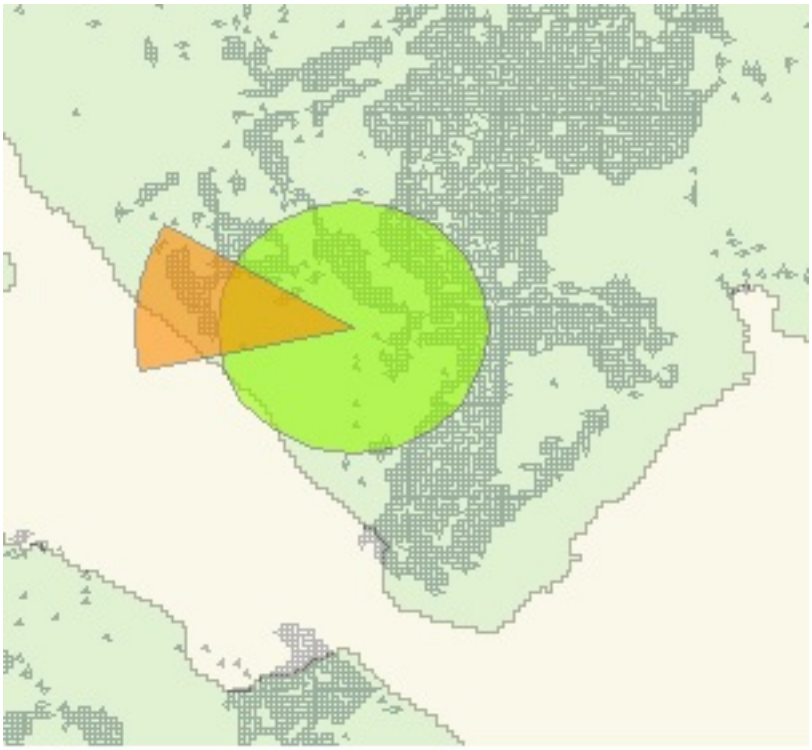
Traditionally, LUR models are used to generate annual or seasonal concentration averages and are not able cover deeper temporal variability. We aim at increasing temporal depth by using a novel approach in generating dynamic buffers for predictor calculation using both monthly wind-speed and wind-direction averages. The traditional circular buffers are replaced by wedges, whose orientation and radius are bound to these meteorological variables.

Here, Hong Kong’ s diverse territory is taken as a study site, and our model is trained with 5 years data from 16 government air quality monitoring stations and deployed portable sensors network. We compare our novel approach to both traditional LUR models and a sophisticated urban chemical transport model (ADMS-Urban).

Results will highlight the opportunities in using LUR models for monthly air-quality pollution concentration as an alternative to chemical transport modelling.

Keywords: Wind, Land Use Regression, Spatial Data, Meteorology

©2019. Japan Geoscience Union. All Right Reserved.



Dynamic and circular LUR buffer in Hong Kong's urban environment

©2019. Japan Geoscience Union. All Right Reserved.

[E] Poster | M (Multidisciplinary and Interdisciplinary)：M-TT Technology & Techniques

Mon. May 27, 2019 5:15 PM - 6:30 PM JST | Mon. May 27, 2019 8:15 AM - 9:30 AM UTC | Poster Hall International Exhibition Hall8, Makuhari Messe_44

[M-TT47] GEOSCIENTIFIC APPLICATIONS OF HIGH-DEFINITION TOPOGRAPHY AND GEOPHYSICAL DATA IN THE ANTHROPOCENE

convener:Yuichi S. Hayakawa(Faculty of Environmental Earth Science, Hokkaido University), Shigekazu Kusumoto(Graduate School of Science and Engineering for Research, University of Toyama), Christopher A Gomez(Kobe University Faculty of Maritime Sciences Volcanic Risk at Sea Research Group)

Recent technical developments of high-definition topographic and geophysical data acquisition have enabled us to further investigate geoscientific issues including land surface processes, subsurface structures, submarine and aerial environments, geo-ecological interactions, and disaster mitigation. Such high-definition or high-resolution data are particularly useful for studies in short-term temporal scales, and future predictions such as numerical modelings. In this session, we expect submissions on topics challenging such issues in the Anthropocene, the most recent geological era of the Earth. A range of topics would fit the session framework, including theoretical work, improvements in data acquisition, extensive data preservation and archiving, pre- and post-processing, statistical analysis, modeling, and simulation for geoscientific research and geohazard assessments in the Anthropocene. The methodological approaches may include, but not limited to, laser scanning, SfM-MVS photogrammetry, GNSS precise positioning, SAR interferometry, multi-beam sonar, and electromagnetic sensors, based on terrestrial (fixed or mobile) and aerial (UAV or manned airborne) platforms.

[MTT47-P01] High-definition topography monitoring after riverbed cultivation in the Echi River, central Japan

*Takuro Ogura[1,2], Satoshi Asano[3], Toshiaki Mizuno[3], Yoshihiro Azuma[3], Takeshi Kitai[4], Yuichi S Hayakawa[5,6], Kotaro Iizuka[6] (1.Graduate School of Frontier Sciences, The University of Tokyo, 2.Graduate School of Environmental Science, Hokkaido University, 3.Lake Biwa Environmental Research Institute , 4.Lake Biwa Museum, 5.Faculty of Environmental Earth Science, Hokkaido University, 6.Center for Spatial information Science, The University of Tokyo)

[MTT47-P02] Spatial distribution of land surface displacements in the crater of Tateyama Midagahara Volcano using high-definition topographic data

*Yuichi S. Hayakawa[1], Shigekazu Kusumoto[2], Takuro Ogura[3,4] (1.Faculty of Environmental Earth Science, Hokkaido University, 2.Graduate School of Science and Engineering for Research, University of Toyama, 3.Graduate School of Frontier Science, The University of Tokyo, 4.Graduate School of Environmental Science, Hokkaido University)

[MTT47-P03] Study on a simplified measurement of water depth and reconstruction of the riverbed form by using SfM and MVS.

*OSAWA KOTA[1], Tadafumi Niizato [2], Katsuaki Mitachi[3], Makoto Kawamura[1], Masahiro Ohkawa[1] (1.Mitsubishi Materials Techno corporation , 2.Japan Atomic Energy Agency, 3.ATOM TRANSPORT SERVICE CO., LTD)

[MTT47-P04] Ground Penetrating Radar Imaging of Moisture and Water movement in volcanic soil

*Christopher A Gomez[1] (1.Kobe University Faculty of Maritime Sciences Volcanic Risk at Sea Research Group)

[MTT47-P05] Estimating Eruptive Volumes of Mud Volcano Southwestern Taiwan by Using UAV and SfM-MVS Photogrammetry

*CHIA-YING LIU [1], Ray Y Chuang[1], Horng-Yue Chen [2] (1.Department of Geography, National Taiwan University, 2.Academia Sinica, Institute of Earth Sciences)

[MTT47-P06] Increasing temporal depth of urban Land-Use Regression Models by wind-data driven dynamic buffer generation

*Tilman Leo Hohenberger[1], King Wai Leung[1] (1.Division of Environment and Sustainability, Hong Kong University of Science and Technology)

High-definition topography monitoring after riverbed cultivation in the Echi River, central Japan

*Takuro Ogura[1,2], Satoshi Asano[3], Toshiaki Mizuno[3], Yoshihiro Azuma[3], Takeshi Kitai[4], Yuichi S Hayakawa[5,6], Kotaro Iizuka[6]

1. Graduate School of Frontier Sciences, The University of Tokyo, 2. Graduate School of Environmental Science, Hokkaido University, 3. Lake Biwa Environmental Research Institute , 4. Lake Biwa Museum, 5. Faculty of Environmental Earth Science, Hokkaido University, 6. Center for Spatial information Science, The University of Tokyo

Natural processes of erosion and deposition on riverbeds are generally limited in Japan due to large-scale public constructions including dams and banks. As a result of the construction of dams, sediment transport may dramatically decrease in the downstream area are, and the river ecosystem can also be affected. To make sediment move more vigorously, we cultivated the armored gravel riverbed with heavy machinery. We then explore the effects of riverbed cultivating by monitoring the topographic changes with high-frequency and high-definition measurements (HF-HD measurements), whereas conventional measurement technologies do not compensate spatial resolution and temporal resolution to capture the topographic change. Using UAS (Unmanned Aerial Vehicle) and SfM-MVS (Structure-from-Motion –Multi-view Stereo) photogrammetry, we found the transportation of the fixed gravels were occurring after cultivating the riverbed in 2017. The temporal and spatial resolutions of the HF-HD topographic data was approximately 2 months and 10 cm, respectively. In July 2018, water flow at 130 m^3/s was discharged from the upstream dam, and we confirmed that a part of the gravels in the cultivated area was eroded and replaced with new sediments (Fig. 1). These observations indicate that riverbed monitoring using UAV and SfM - MVS can be a practical tool for proper management of riverbeds. Applying this result, we will further clarify the relationships between the water quantity discharged from the dam and the riverbed topographic changes.

Keywords: High-definition topographic data, riverbed cultivation, UAV, SfM-MVS photogrammetry, Echi river

©2019. Japan Geoscience Union. All Right Reserved.

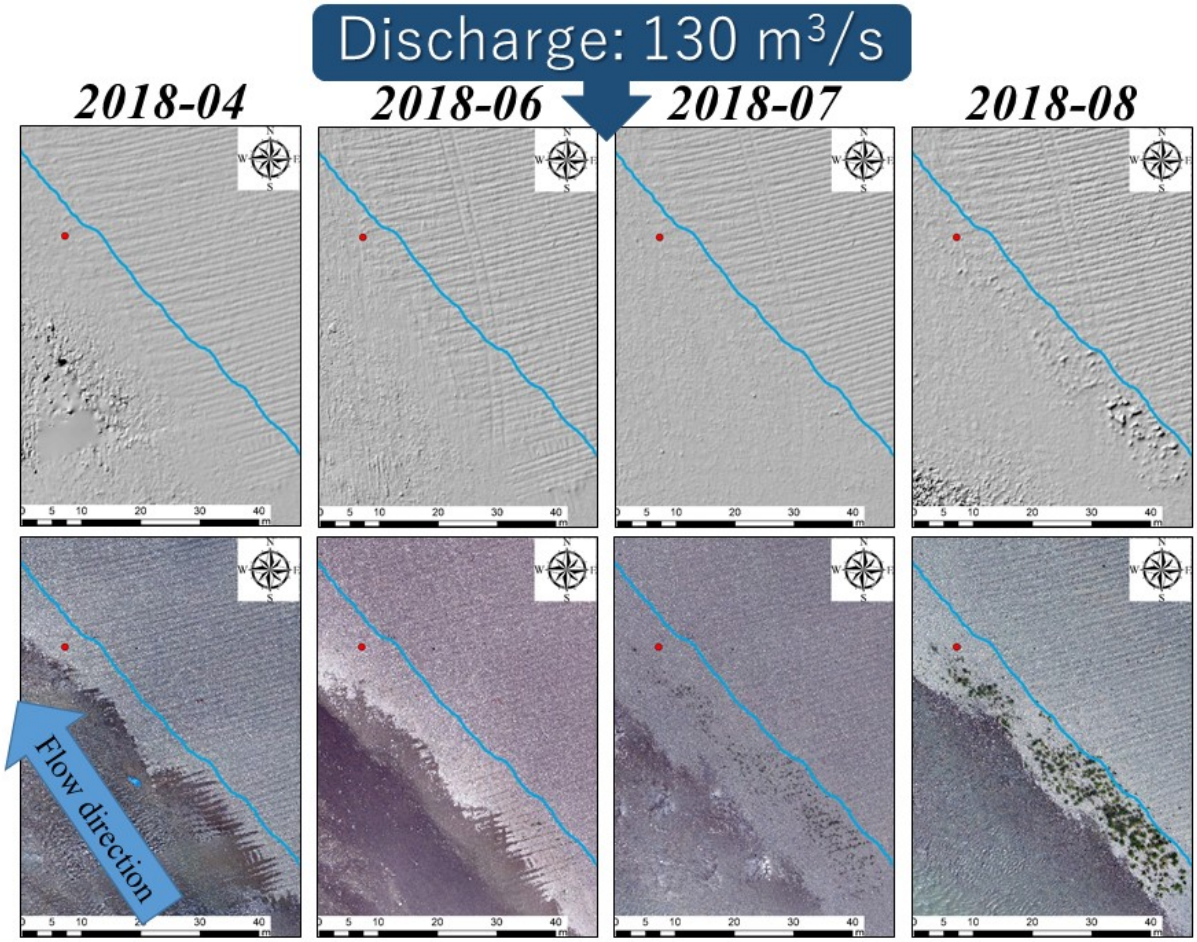


Fig.1. Hillshade images and ortho images of cultivated area.

©2019. Japan Geoscience Union. All Right Reserved.

Spatial distribution of land surface displacements in the crater of Tateyama Midagahara Volcano using high-definition topographic data

*Yuichi S. Hayakawa[1], Shigekazu Kusumoto[2], Takuro Ogura[3,4]

1. Faculty of Environmental Earth Science, Hokkaido University, 2. Graduate School of Science and Engineering for Research, University of Toyama, 3. Graduate School of Frontier Science, The University of Tokyo, 4. Graduate School of Environmental Science, Hokkaido University

Detailed monitoring of land surface displacements is crucial for the assessment of activities of a volcano, especially in its crater area. Close-range remote sensing of high-definition topographic data is advantageous in the detection of centimeter-scale ground-surface displacements in a wide spacial extent, whereas the conventional leveling method is capable of detecting millimeter-scale displacements along a measurement line. We investigated the spatial distribution of land surface displacements in the Jigoku-Dani crater area of Mt. Tateyama Midagahara Volcano in Toyama Prefecture, central Japan by high-definition topographic measurements including terrestrial laser scanning and unmanned aerial vehicle-based structure-from-motion photogrammetry. The annual measurements were performed for three years (2015 to 2017). The range of uplift detected by terrestrial laser scanning corresponds with that by leveling. Together with the analytical results of the leveling data, the spatial pattern of the uplift suggests the extent of an underground pressured zone to cause the exhumation. For the prediction of the volcanic activities, further monitoring is required to reveal the spatiotemporal patterns of the displacements.

Keywords: terrestrial laser scanning, unmanned aerial system structure-from-motion, point cloud

©2019. Japan Geoscience Union. All Right Reserved.

Study on a simplified measurement of water depth and reconstruction of the riverbed form by using SfM and MVS.

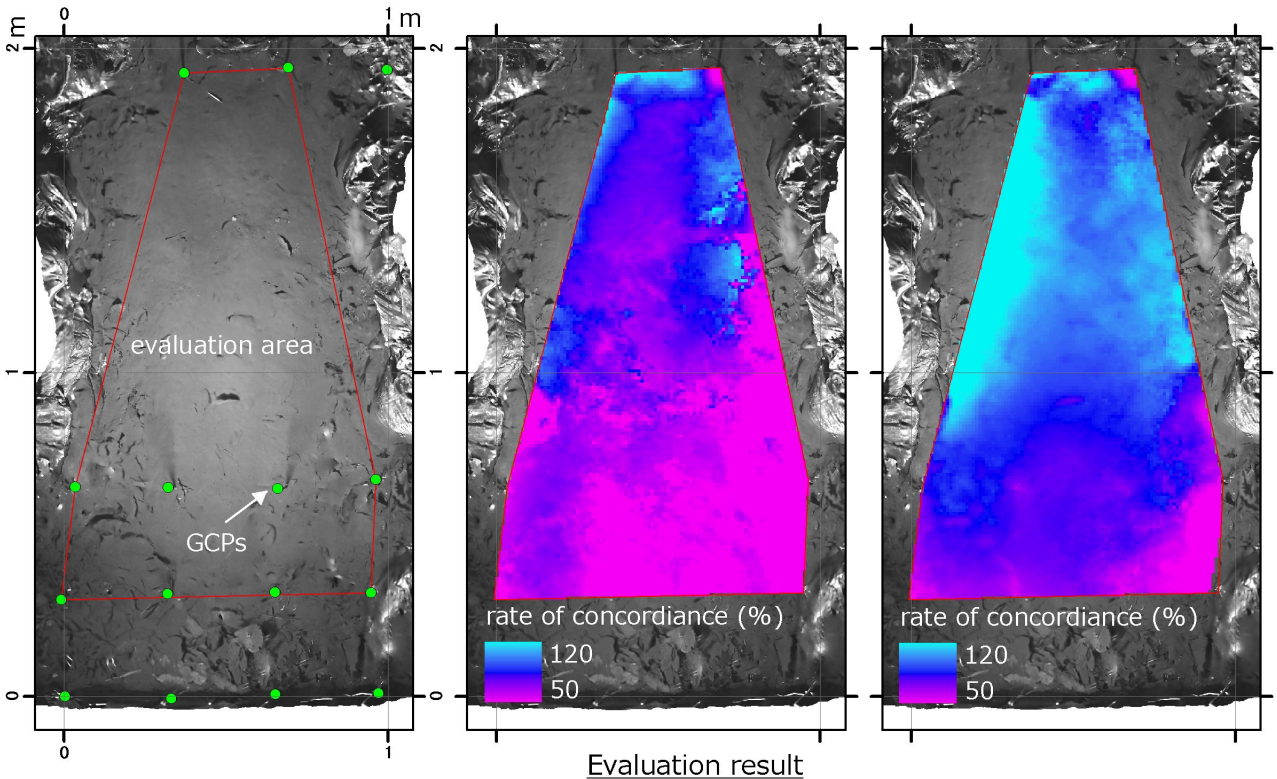
*OSAWA KOTA[1], Tadafumi Niizato [2], Katsuaki Mitachi[3], Makoto Kawamura[1], Masahiro Ohkawa[1]

1. Mitsubishi Materials Techno corporation , 2. Japan Atomic Energy Agency, 3. ATOM TRANSPORT SERVICE CO., LTD

Primary outflow process of radiocesium, which is released by the TEPCO’ s Fukushima Dai-ichi Nuclear Power Plant accident, from a forested hillslope to a mountain stream is a particulate-bond state transport. A detailed estimation of the riverbed form and sediment volume changing with time is a key issue to assess the radiocesium distribution in the forested environment. Changes in the sediment volume can be calculated from the water depth and the difference between measured water surface and reference water surface levels setting up at the initial. Conventional method for a water depth determination is a direct measurement of the stream water depth by using a scale. But it requires a lot of time and labor to evaluate the change of riverbed form and water depth in detail.
In this study, we attempted an accurate and labor-effective method to evaluate the water depth and three-dimensional (3D) structure of underwater riverbed form by applying the SfM (Structure from Motion) /MVS (Multi View Stereo) techniques and the optical image data collected on consumer-grade-camera. These images were photographed beside of the small stream located at southern part of the Abukuma Mountains, Fukushima. Light propagation properties such as attenuation or reflection influence precise reconstruction of 3D model using underwater images. This was done to reduce influence of light propagation in two steps: 1) to reduce the influence of reflection, photographing at the time of twilight using LED light and Circular PL filter. 2) to reduce the influence of attenuation, installing blue colored film on the LED light and omitting band R, G for SfM/MVS analysis. And we also photographed at the day time and reconstructed 3D model (Day Model: DM) to compare and confirm the model applying two steps (Twilight Model: TM). As a criterion for evaluation of these models, we carried out the direct measurement of water depth. Rate of estimation concordance was calculated by dividing analytical water depth by the direct measurement depth, then convert to percentage.
Discrepancy between measured and analytical results increased with depth, the rate of estimation concordances were 46 % (DM) and 73 % (TM) in the water depth of 20-25 cm, and 62 % (DM) and 93 % (TM) in 10-15 cm, respectively (Figure). Next step is an improvement of the correction and image-capturing methods to reduce the estimation errors by elimination of the light refraction on the stream water surface.

Keywords: SfM/MVS, measurement of water depth, riverbed form

©2019. Japan Geoscience Union. All Right Reserved.



Evaluation result

Left: Orthographic Image, Evaluation area (red polygon) and location of GCPs (green dot),
Center: Discrepancy between measured and analysis (DM),
Right: Discrepancy between measured and analysis (TM)

©2019. Japan Geoscience Union. All Right Reserved.

Ground Penetrating Radar Imaging of Moisture and Water movement in volcanic soil

*Christopher A Gomez[1]

1. Kobe University Faculty of Maritime Sciences Volcanic Risk at Sea Research Group

Ground Penetrating Radar is a non-invasive subsurface method that provides results on the dielectric properties of the ground between 0 and 30 m on average in sediments. Working from sediments from Mt Unzen in Japan, tests over the moisture content and the air content change were conducted on the material in order to infer further data during field measurement. The GPR used in the survey is a Ramac Mala mounted with an antenna of 800 Mhz and a stack signal over time. The data were processed using Matlab using data filtering and time-depth conversion, and calculation of the dielectric properties variations. The signal analysis shows that the velocity does change over time depending on the moisture content and the change in air/void ratio. For a given homogeneous material, like at volcanoes, multiplying such analysis is a step forward the development of relatable tables for various environments.

Keywords: Ground Penetrating Radar, Soil moisture content, Volcanic material

©2019. Japan Geoscience Union. All Right Reserved.

Estimating Eruptive Volumes of Mud Volcano Southwestern Taiwan by Using UAV and SfM-MVS Photogrammetry

*CHIA-YING LIU[1], Ray Y Chuang[1], Horng-Yue Chen[2]

1. Department of Geography, National Taiwan University, 2. Academia Sinica, Institute of Earth Sciences

Mud volcanoes are special geologic features occurred in tectonic areas with horizontal compression. Complete research for mud volcanos can help us to understand the interaction of the crust and surface. In Taiwan, mud volcanoes are present on-land and off-shore southwestern Taiwan around the transitional area from subduction to orogeny. Among all mud volcanoes in Taiwan, the Wandan mud volcano erupts sporadically with significantly large amount of effluent mud. However, the mechanism of the eruption remains unclear because we lack fundamental information such as eruptive volumes, duration of mud eruption, impact factors and recurrence intervals. Therefore, it is important to estimate the eruptive volumes and further to examine the spatiotemporal pattern of the Wandan mud volcano eruption. We first compile literature and newspapers for historic eruption events to estimate two groups of recurrence interval: 150-180 days for highly active period and 300-600 days for less active period.

Since the sporadic eruption make different for rapid survey by using traditional methods, we take advantage of unmanned aerial vehicles (UAV) to design a survey network specifically. Therefore, we estimate the eruptive volumes of recent eruptions for the Wandan mud volcano by using aerial images taken from UAV, and 3D models derived from the structure-from-motion (SfM) photogrammetry technique. We use RTK-GPS and leveling for horizontal and vertical measurements of ground control point, respectively. We use the SfM software to generate DSMs, point clouds, and orthophotos with cm-level accuracy. We estimate the eruptive volume by subtracting the pre-eruption DSM from the post-eruption DSM. Our results show that for the event on 15 May, 2018, the eruptive area is 12,761 m^2 and the volume is 13,106.3625 ±13.0105m^3.

Keywords: UAS, GNSS, digital surface modeling, control survey

©2019. Japan Geoscience Union. All Right Reserved.

Increasing temporal depth of urban Land-Use Regression Models by wind-data driven dynamic buffer generation

*Tilman Leo Hohenberger[1], King Wai Leung[1]

1. Division of Environment and Sustainability, Hong Kong University of Science and Technology

Land-use regression (LUR) models are commonly used as an inexpensive and easy to set-up way to predict spatial variability in air-pollution. They are successfully applied to regional and, more and more, urban settings, making use of spatial predictors such as land-use, vegetation, morphology and geography. New approaches include an improved use of wind-data for buffer-creation and predictor calculation.

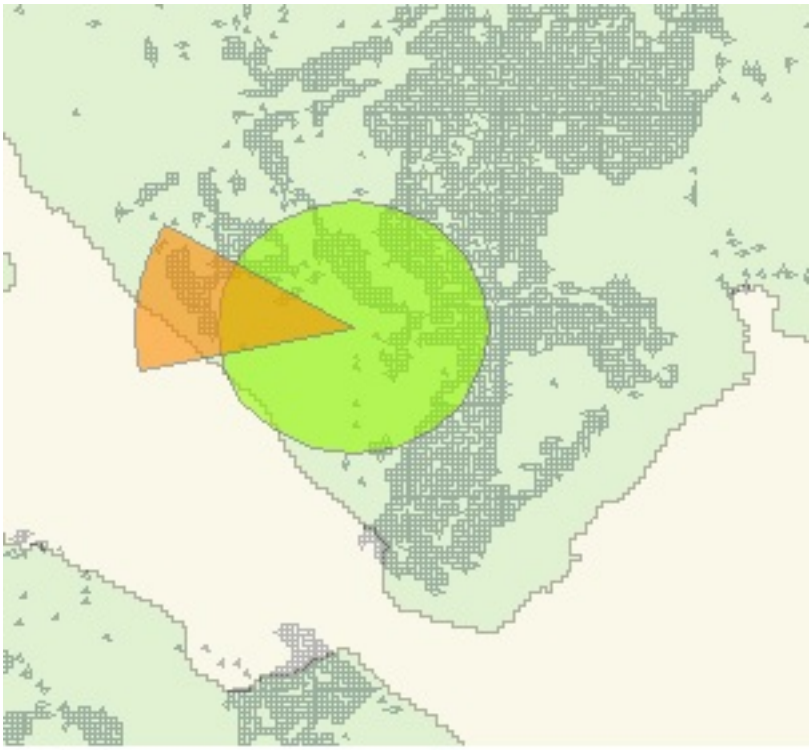
Traditionally, LUR models are used to generate annual or seasonal concentration averages and are not able cover deeper temporal variability. We aim at increasing temporal depth by using a novel approach in generating dynamic buffers for predictor calculation using both monthly wind-speed and wind-direction averages. The traditional circular buffers are replaced by wedges, whose orientation and radius are bound to these meteorological variables.

Here, Hong Kong’ s diverse territory is taken as a study site, and our model is trained with 5 years data from 16 government air quality monitoring stations and deployed portable sensors network. We compare our novel approach to both traditional LUR models and a sophisticated urban chemical transport model (ADMS-Urban).

Results will highlight the opportunities in using LUR models for monthly air-quality pollution concentration as an alternative to chemical transport modelling.

Keywords: Wind, Land Use Regression, Spatial Data, Meteorology

©2019. Japan Geoscience Union. All Right Reserved.



Dynamic and circular LUR buffer in Hong Kong's urban environment

©2019. Japan Geoscience Union. All Right Reserved.

[E] Poster | P (Space and Planetary Sciences)：P-PS Planetary Sciences

Tue. May 28, 2019 3:30 PM - 5:00 PM JST | Tue. May 28, 2019 6:30 AM - 8:00 AM UTC | Poster Hall International Exhibition Hall8, Makuhari Messe_1

[P-PS01] Outer Solar System Exploration Today, and Tomorrow

convener:Jun Kimura(Osaka University), Yasumasa Kasaba(Planetary Plasma and Atmospheric Research Center, Tohoku University), Kunio M. Sayanagi(Hampton University)

The giant planets provide many keys to understanding planetary processes. They play an important role in shaping our solar system, and the physical and chemical processes they harbor also provide a unique opportunity to study the phenomena relevant for studying Earth and other planets, including exoplanetary systems. In this session, we discuss a wide range of topics encompassing the giant planets and their moons, including their origins, interiors, atmospheres, compositions, surface features, and electromagnetic fields. To advocate for current and future outer planets exploration (Cassini, Juno, New Horizons, JUICE, and beyond), we also call for discussions on future missions to explore giant planet systems, including how to develop better international cooperation. Discussion in this latter category will include progress in developing a solar sail mission concept for observing the Jupiter system and its trojan asteroids.

[PPS01-P01] Critical Role of Entry Probes in Giant Planet Exploration

*Sushil K Atreya[1], Olivier Mousis[2] (1.University of Michigan Ann Arbor, 2.Laboratoire d'Astrophysique de Marseille)

[PPS01-P02] OKEANOS – Jupiter Trojan Asteroid Rendezvous and Landing Experiments Using a Solar Power Sail

*Tatsuaki Okada[1,2], Takahiro Iwata[1], Yoko Kebukawa[3], Motoo Ito[4], Jun Aoki[5], Yosuke Kawai[5], Shoichiro Yokota[5], Yoshifumi Saito[1], Kentaro Terada[5], Michisato Toyoda[5], Hikaru Yabuta[6], Hisayoshi Yurimoto[1,7], Shuji Matsuura[8], Kohji Tsumura[9], Daisuke Yonetoku[10], Tatehiro Mihara[11], Ayako Matsuoka[1], Reiko Nomura[12], Hajime Yano[1], Takayuki Hirai[13], Atsushi Kumamoto[9], Ryosuke Nakamura[14], Stephan Ulamec[15], Ralf Jaumann[15], Jean-Pierre Bibring[16], Noel Grand[17], Cyril Szopa[18], Ernesto Palomba[19], Jorn Helbert[15], Alain Herique[20], Matthias Grott[15], Hans-Ulrich Auster[21], Goester Klingelhoefer[22], Fumi Yoshida[13], Makoto Yoshikawa[1], Jun Matsumoto[1], Toshihiro Chujo[1], Masanori Matsushita[1], Takanao Saiki[1], Hideki Kato[1], Osamu Mori[1], Junichiro Kawaguchi[1] (1.Japan Aerospace Exploration Agency, 2.University of Tokyo, 3.Yokohama National University, 4.Japan Agency for Marine-Earth Science and Technology, 5.Osaka University, 6.Hiroshima University, 7.Hokkaido University, 8.Kwansei Gakuin University, 9.Tohoku University, 10.Kanazawa University, 11.RIKEN, 12.National Astronomical Observatory of Japan, 13.Chiba Institute of Technology, 14.National Institute of Advanced Industrial Science and Technology, 15.German Aerospace Center, 16.Institut d'Astrophysique Spatiale, 17.LISA, 18.LATMOS, 19.INAF-IAPS, 20.IPAG, 21.TU Braunschweig, 22.Leibniz Universität Hannover)

[PPS01-P03] Magnetic field model of Jovian magnetosphere

*Naoya Momoki[1], Hiroaki TOH[1] (1.Division of Earth and Planetary Sciences, Graduate School of Science, Kyoto University)

[PPS01-P04] Enhancement of the Jovian thermospheric temperature above the Great Red Spot based on the infrared spectroscopic data obtained with IRTF/iSHELL

*Ayumu Kambara[1], Hajime Kita[2], Takeshi Sakanoi[1], Yasumasa Kasaba[1], Masato Kagitani[1], Haruna Watanabe[1] (1.Planetary Plasma and Atmospheric Research Center, Graduate School of Science, Tohoku University, 2.Institute of Space and Astronautical Science, Japan Aerospace Exploration Agency)

[PPS01-P05] Pulsation-like variation of Jovian infrared polar emission observed by Subaru 8-m: H3+ and methane emissions

*Yasumasa Kasaba[1], Haruna Watanabe[1], Hajime Kita[2], Chihiro Tao[3], Takeshi Sakanoi[1], Masato Kagitani[1], Orton Glenn[1,4], James Sinclair[4] (1.Planetary Plasma and Atmospheric Research Center, 2.ISAS/JAXA,

3.NICT, 4.NASA/JPL)

[PPS01-P06] Structure of Io plasma torus observed with the Tohoku 60-cm telescope

*Masato Kagitani[1], Fuminori Tsuchiya[1], Kazuo Yoshioka[2], Go Murakami[3], Tomoki Kimura[1], Ryoichi Koga[1], Reina Hikida[4], Takeshi Sakanoi[1] (1.Graduate School of Science, Tohoku University, 2.Graduate School of frontier Science, The University of Tokyo, 3.Institute of Space and Astronautical Science, Japan Aerospace Exploration Agency, 4.Department of Earth and Planetary Science, Graduate School of Science, Tokyo University)

[PPS01-P07] Ion Scale Height Variability in Hisaki Io Torus Observations

*Nicholas McCord Schneider[1], Carl Schmidt[2], Masato Kagitani[3], Yasumasa Kasaba[3], Tomoki Kimura[3], Go Murakami[4], Fuminori Tsuchiya[3], Hajime Kita[3], Reina Hikida[5], Ichiro Yoshikawa[5], Kazuo Yoshioka[5] (1.LASP, University of Colorado Boulder, 2.Boston University, 3.Tohoku University, 4.ISAS/JAXA, 5.University of Tokyo)

[PPS01-P08] Size of the Smallest Particles in Saturn's Rings

*Keiji Ohtsuki[1], Hiroshi Kawamura[1], Naoyuki Hirata[1], Hiroshi Daisaka[2], Hiroshi Kimura[3] (1.Graduate School of Science, Kobe University, 2.Graduate School of Commerce and Management, Hitotsubashi University, 3.Planetary Exploration Research Center, Chiba Institute of Technology)

[PPS01-P09] The Radio & Plasma Wave Investigation (RPWI) for JUICE for the investigation of Jupiter and Icy Moons System: Contributions from Japan

*Yasumasa Kasaba[1], Hiroaki Misawa[1], Fuminori Tsuchiya[1], Atsushi Kumamoto[2], Yuto Katoh[2], Tomoki Kimura[2], Hajime Kita[3], J.-E. Wahlund[4] (1.Planetary Plasma and Atmospheric Research Center, Tohoku University, 2.Department of Geophysics, Tohoku University, 3.ISAS/JAXA, 4.IRF Uppsala, Sweden)

[PPS01-P10] Magnetic field experiment at Jupiter icy moons (JUICE J-MAG) and in-flight alignment calibration

*Ayako Matsuoka[1], Michele Karen Dougherty[2], Patrick Brown[2], Futoshi Takahashi[3], Hisayoshi Shimizu[4], Masaki Matsushima[5] (1.Research Division for Space Plasma, Institute of Space and Astronautical Science, Japan Aerospace Exploration Agency, 2.Imperial College London, 3.Kyushu University, 4.University of Tokyo, 5.Tokyo Institute of Technology)

[PPS01-P11] Science targets of the GAnymede Laser Altimeter (GALA) for the JUICE mission

*Jun Kimura[1], Shunichi Kamata[2], Koji Matsumoto[3], Noriyuki Namiki[3], Keigo Enya[4], Masanori Kobayashi[5], Hiroshi Araki[3], Hirotomo Noda[3], Ko Ishibashi[5], Hauke Hussmann[6], Kay Lingenauber[6] (1.Osaka University, 2.Hokkaido University, 3.National Astronomical Observatory Japan, 4.ISAS/JAXA, 5.Chiba Institute of Technology, 6.German Aerospace Center (DLR), Berlin)

[PPS01-P12] Current status of the antenna developments, the data processing, scientific target for JUICE/SWI JAPAN.

*YASUKO KASAI[1], JUICE SWI Japanese Team (1.National Institute of Information and Communications Technology (NICT))

Critical Role of Entry Probes in Giant Planet Exploration

*Sushil K Atreya[1], Olivier Mousis[2]

1. University of Michigan Ann Arbor, 2. Laboratoire d'Astrophysique de Marseille

Flyby and orbiting spacecraft have explored the giant planets since the early 1970’s. In situ measurements in the troposphere are essential, however, for constraining the models of formation, evolution and interior processes of the giant planets. The models employ abundances and isotopic ratios of key elements, in particular C,N, S, O, He, Ne, Ar, Kr, Xe and D/H, derived from the measurement of their (bulk) reservoir species. That was the scientific rationale for the 1995 Galileo Probe at Jupiter and a Saturn Probe in NASA’s New Frontiers list of candidate missions. Considering that the icy giant planets are distinct from the gas giants, they represent the missing pieces of the puzzle of the formation of the outer solar system, besides being the closest analog for nearly half of the confirmed exoplanets. Thus, their comprehensive exploration with an orbiter-probe spacecraft is essential. The principal focus of this talk is the science, feasibility and implementation strategy of in situ measurements with entry probes at the icy giant planets, Uranus and Neptune, guided by thermochemical models and lessons learned from the Galileo Probe and the ongoing Juno Orbiter. [www.umich.edu/~atreya]

Keywords: Icy Giants, Origin and Evolution, Uranus, Neptune, Entry Probes, Exoplanets

©2019. Japan Geoscience Union. All Right Reserved.

OKEANOS –Jupiter Trojan Asteroid Rendezvous and Landing Experiments Using a Solar Power Sail

*Tatsuaki Okada[1,2], Takahiro Iwata[1], Yoko Kebukawa[3], Motoo Ito[4], Jun Aoki[5], Yosuke Kawai[5], Shoichiro Yokota[5], Yoshifumi Saito[1], Kentaro Terada[5], Michisato Toyoda[5], Hikaru Yabuta[6], Hisayoshi Yurimoto[1,7], Shuji Matsuura[8], Kohji Tsumura[9], Daisuke Yonetoku[10], Tatehiro Mihara[11], Ayako Matsuoka[1], Reiko Nomura[12], Hajime Yano[1], Takayuki Hirai[13], Atsushi Kumamoto[9], Ryosuke Nakamura[14], Stephan Ulamec[15], Ralf Jaumann[15], Jean-Pierre Bibring[16], Noel Grand[17], Cyril Szopa[18], Ernesto Palomba[19], Jorn Helbert[15], Alain Herique[20], Matthias Grott[15], Hans-Ulrich Auster[21], Goester Klingelhoefer[22], Fumi Yoshida[13], Makoto Yoshikawa[1], Jun Matsumoto[1], Toshihiro Chujo[1], Masanori Matsushita[1], Takanao Saiki[1], Hideki Kato[1], Osamu Mori[1], Junichiro Kawaguchi[1]

1. Japan Aerospace Exploration Agency, 2. University of Tokyo, 3. Yokohama National University, 4. Japan Agency for Marine-Earth Science and Technology, 5. Osaka University, 6. Hiroshima University, 7. Hokkaido University, 8. Kwansei Gakuin University, 9. Tohoku University, 10. Kanazawa University, 11. RIKEN, 12. National Astronomical Observatory of Japan, 13. Chiba Institute of Technology, 14. National Institute of Advanced Industrial Science and Technology, 15. German Aerospace Center, 16. Institut d’ Astrophysique Spatiale, 17. LISA, 18. LATMOS, 19. INAF-IAPS, 20. IPAG, 21. TU Braunschweig, 22. Leibniz Universität Hannover

The OKEANOS (Oversize Kite-craft for Exploration and AstroNautics in the Outer Solar system) is a mission under study to rendezvous with and land on a Jupiter Trojan asteroid [1]. The target is a Jupiter Trojan but will be the Saturnian system in the future. It is an engineering mission to demonstrate advanced technologies such as the hybrid thrusting with the enhanced ion engine powered by a 40 x 40 m class large area solar cells to explore the outer solar system cost-effectively. With the new technology, the mission will conduct in-depth scientific measurements for understanding the origin and evolution of the solar system and life. The concept is complementary to NASA Lucy mission [2], multi-flybys to six Jupiter Trojans for understanding the variation of Jupiter Trojans.

Jupiter Trojans are D/P-types enriched in volatiles. They might have experienced almost no or only a low degree of alteration. Their origin and evolution, as well as chemical and physical state still remain unknown. Jupiter Trojans should be a missing link of materials that originate from the inner or the outer solar system by gravity scattering due to migration of giant planets [3]. They are key targets to understand the evolution of astromaterials and the radial distribution of elements and isotopes in the early solar system.

The OKEANOS has been downscaled from the previous proposal [4] due to the severe cost cap. The spacecraft of 1400 kg including a 40 kg lander will be launched in 2027 or later, assisted by gravity of Earth and Jupiter. It will arrive at the target asteroid after a 13-year cruise. 30 kg is allocated for science, 12 kg of which is reserved for international collaboration. Bus instruments such as the optical navigation cameras (ONC-T and -W), LIDAR, and radio science are used for scientific purposes. The lander is like Mascot with uprighting capability on the asteroid surface and 12 kg is allocated for science mission.

During the cruise, science experiments will be carried out from the “deep-space platform”. Measurements of IDPs and magnetic fields will continuously monitor their radial distribution in the solar system and sudden events. The gamma-ray polarimeter will be used for precise positioning of gamma-ray bursts using a very long baseline. Visible to near-infrared telescope will map the zodiacal lights and observe the deep sky under a dust-free condition from outside of the asteroid main belt.

©2019. Japan Geoscience Union. All Right Reserved.

After arrival, global mapping is carried out to characterize the asteroid and select the landing site. The asteroid shape, size, rotation state, and geologic features are imaged by ONC. Gravity is measured by radio tracking and LIDAR. Near-infrared spectroscopy characterizes red or less red patterns, the degree of hydration, mineralogy, and abundance of ices, organics, and brines. Thermal infrared multi-bands inform on thermophysical properties, mineralogy and amorphous phases. A radar probes the surface physical state and also contributes to altimetry. *In situ* experiments with the lander will characterize the footprint and surrounding area by imaging and spectroscopy, followed by measurements of mineralogical, elemental, and organic composition as well as physical, thermal, and magnetic properties at the site. The asteroid surface sample is collected to conduct high-resolution mass spectroscopy (HRMS) based on MULTUM system (infi-TOF type mass spectrometer [5]), especially to determine the isotopic ratios of δD and δ^{15}N and the volatile species contained in the sample. Details will be decided during the critical joint study in 2019. Those experiences will be inherited to future missions.

References: [1] Mori O. et al. (2018) Trans. JSASS Aerospace Tech. Japan, 16, 328-333. [2] Levison H.F. et al. (2016) Lunar Planet. Sci. Conf., 47, #2061. [3] Morbidelli A. et al. (2005) *Nature 435*, 462-466. [4] Okada T. et al. (2018) Planet. Space Sci. 161, 99-106. [6] Toyoda M. et al. (2003) J. Mass Spectrom. 38, 1125-1142.

Keywords: Solar Sail, Trojan, Landing

©2019. Japan Geoscience Union. All Right Reserved.

Magnetic field model of Jovian magnetosphere

*Naoya Momoki[1], Hiroaki TOH[1]

1. Division of Earth and Planetary Sciences, Graduate School of Science, Kyoto University

Europa, Ganymede, Callisto are the Jovian icy satellites called Galilean moons, and are possibly with internal oceans each. While ice is almost an insulator electrically, water including ions has high electrical conductivity, and existence of internal oceans can be verified using electromagnetic (EM) induction methods. In this study, we updated the necessary model of the external magnetic field to the icy satellites for the EM induction studies. Namely, parameters of the Euler potential model of the Jovian magnetosphere (Khurana, 1997) were renewed by adding magnetic data from both Galileo and JUNO spacecrafts.

The configuration of the Jovian current sheet was modeled by Khurana [1992] using three parameters, while the Jovian magnetospheric magnetic field modeled by Khurana [1997] was characterized by 14 parameters. We applied a non-linear optimization technique, i.e., the steepest descent method, to the parameters by newly adding magnetic data from Galileo and Juno spacecrafts. We minimized the root mean squared between the model and the data by exploring the parameter space around several initial sets of the parameters.

As a result, time-varying model parameters for each spacecraft orbit were obtained. Their temporal variation may reflect that of both magnetic field and electric current system in the Jovian magnetosphere.The changes of the parameters can be attributed to the interaction between the Jovian magnetosphere and the solar wind. It, therefore, preferable that the temporal variation of the model parameters is incorporated when the updated magnetic field model of the Jovian magnetosphere is applied to the EM induction studies in search for the internal oceans of the icy satellites.

Keywords: Jupiter, Magnetosphere

©2019. Japan Geoscience Union. All Right Reserved.

Enhancement of the Jovian thermospheric temperature above the Great Red Spot based on the infrared spectroscopic data obtained with IRTF/iSHELL

*Ayumu Kambara[1], Hajime Kita[2], Takeshi Sakanoi[1], Yasumasa Kasaba[1], Masato Kagitani[1], Haruna Watanabe[1]

1. Planetary Plasma and Atmospheric Research Center, Graduate School of Science, Tohoku University, 2. Institute of Space and Astronautical Science, Japan Aerospace Exploration Agency

It is known that the thermospheric temperature of all giant planets including Jupiter is several hundred kelvins higher than that expected from solar heating. At mid- to low-latitudes, although the direct atmospheric heating caused by precipitating particles and the energy transportation from high-latitude auroral region have been considered, it is not enough to explain. Another candidate for the heating is energy transportation by atmospheric waves from the lower atmosphere. Recently, O'Donoghue *et al.* [2016] revealed the heating in the thermosphere above the Great red spot from the intensity ratio of two emission lines (3.383um/3.454um) of the vibrational-rotational spectrum of thermospheic H_3^+ taken by IRTF /SpeX (R~2500) in December 2012. They estimated that the temperature above the Great red spot is 1644±161K, and that on surrounding mid- to low-latitude region is 900±42K. They considered that the reason was the energy transport from the lower atmosphere in the Great red spot region, that is, the propagation of atmospheric gravity waves and acousitic waves generated in the Great red spot, the tropospheric anticyclonic storm, to the thermosphere. However, the infrared spectrum observed SpeX might be contaminated by CH_4 line due to its low-resolution capability.
In this study, we carried out the thermosphere temperature observation in the Jovian mid-latitude region near the Great red spot by IRTF/iSHELL on January 11, 2017. This observation was performed with the iSHELL's Lp1-mode (3.265-3.657um), and the data reduction was performed with NASA's data reduction tool Spextool ver. 5.0.1. Similar to the past study by O'Donoghue *et al.* [2016], we adopted the intensity ratio of two emission lines of H_3^+ (3.3839um/3.4548um), and estimated the temperature precisely distinguished from CH_4 line by iSHELL’s higher wavelength resolution (R~75000). As a result, we estimated the thermospheric temperature above the Great red spot to be 910±132K, and that in the surrounding region to be 583±30K, showing about 300K increase on Great red spot. The estimated temperature was lower than that in O’Donoghue *et al.* [2016], there is possibility that the thermosphere temperature varies in time. However, we confirmed the temperature above Great red spot is higher than that in the surrounding region. This suggests the existence of energy transport from the lower to the upper atmosphere in the Great red spot. In the presentation, we report the result of carefully reduction.

Keywords: Jupiter, Great red spot, Thermosphere

©2019. Japan Geoscience Union. All Right Reserved.

Pulsation-like variation of Jovian infrared polar emission observed by Subaru 8-m: H3+ and methane emissions

*Yasumasa Kasaba[1], Haruna Watanabe[1], Hajime Kita[2], Chihiro Tao[3], Takeshi Sakanoi[1], Masato Kagitani[1], Orton Glenn[1,4], James Sinclair[4]

1. Planetary Plasma and Atmospheric Research Center, 2. ISAS/JAXA, 3. NICT, 4. NASA/JPL

In the Jovian high-latitude region, there are emissions with various wavelengths ranges, morphologies, and time variations. They are important tracers of energy injection carried by auroral particles that precipitate from the magnetosphere. The polar IR emissions excited in the Jovian upper atmosphere, which include the H_3^+ aurora and thermal emissions of hydrocarbons, reflect not only the abundance of emission sources but also the thermal structures. Both are affected by auroral precipitation into the source region. It is known that, in the polar region inner than the auroral oval, the flux of auroral precipitation can have time variations over various scales from years to seconds.

The H_3^+ aurora observed in near infrared is emitted in thermosphere / ionosphere from thermally excited H_3^+ ions above the CH_4 homopause. Auroral precipitation ionized H_2 and produce H_3^+ ions through ion chemistries. In previous observational studies, the shortest timescale of H_3^+ auroral intensity change was ~30 min, but detected by ~16-min step imaging. We performed the temporal imaging observation of the Jovian H_3^+ IR aurora with Subaru/IRCS and the H_3^+ narrow-band filter on 31 January 2015 and 25 May 2016. The adaptive optics enabled us to see the target with high spatial resolution (~0.2 arcsec). From the images obtained with time resolution of ~150 s on 25 May 2016, we detected a patch-like auroral feature pulsating with a period of ~10 min in noon sector of northern polar region. On the other hand, we could not find any periodic variations from the data obtained on 31 January 2015, which was obtained as slit-viewer image for the other study, and whose time intervals of ~10–30 min every several images was not optimized to this research. In addition, the location where the patch-like emissions observed with high intensities on 25 May 2016 were not so bright on 31 January 2015. The patch-like auroral feature that was pulsating during our observation period on 25 May 2016 have been sometimes observed in UV, but not always. Previous UV observations reported some pulsating auroral features with the periods of ~2–11 min in the northern polar region. However, the locations of them are not consistent with the patch-like feature in this study. The pulsation period of the X-ray aurora, which has a hot spot coinciding with our patch-like IR aurora, is 40–50 min. This region is estimated to connect magnetically to out of the magnetopause, and auroral precipitation there can be caused by dayside reconnection between the Jovian magnetospheric field and interplanetary field.

On the other hand, the hydrocarbon polar emission observed in mid-infrared is emitted from the whole stratosphere. From their locations and morphologies, it is estimated to be related with auroral particles penetrating under the homopause. However, the mechanisms of this link (composition change and/or heating by particle precipitations) are not well understood. Previous studies found the intensity time variation of polar CH_4 emission over days and months. We tried to detect the time variation of CH_4 emission intensity by continuous imaging observations of the northern polar region over several tens of minutes on 31 March, 24 and 25 May 2018 with Subaru/COMICS. We obtained the images using the 7.8 μm filter, which is sensitive to the CH_4 thermal emissions occurring in the pressure range of 20–0.5 mbar and 1 μbar in the Jovian upper stratosphere, with time resolution of ~1 min. On all observation days, the polar region was not bright in 7.8 μm. In addition, we could not find clear time variations of polar CH_4 emission intensity during our observation periods, 25, 50 and 60 min on 31 March, 24 and 25 May 2018.

©2019. Japan Geoscience Union. All Right Reserved.

This observation result is consistent to the model estimation by *Kuroda et al.* [2014], which suggested the relaxation time of hydrocarbon thermal emissions in the Jovian upper stratosphere, where is a possible source region of polar CH_4 emission, is at least ~10^5 s (~28 h).

Keywords: Jupiter, polar emission, H3+, CH4, short time variations

©2019. Japan Geoscience Union. All Right Reserved.

Structure of Io plasma torus observed with the Tohoku 60-cm telescope

*Masato Kagitani[1], Fuminori Tsuchiya[1], Kazuo Yoshioka[2], Go Murakami[3], Tomoki Kimura[1], Ryoichi Koga[1], Reina Hikida[4], Takeshi Sakanoi[1]

1. Graduate School of Science, Tohoku University, 2. Graduate School of frontier Science, The University of Tokyo, 3. Institute of Space and Astronautical Science, Japan Aerospace Exploration Agency, 4. Department of Earth and Planetary Science, Graduate School of Science, Tokyo University

Volcanic gases (mainly composed of SO_2, SO and S) originated from jovian satellite Io are ionized by interaction with magnetospheric plasma and then form a donut-shaped region called Io plasma torus. Ion pickup is the most significant energy source on the plasma torus though, distribution of pick-up region and its variability is still unclear. Density profiles of ions along the magnetic field line are determined under condition of diffusive equilibrium. Based on the equilibrium, plasma equator is close to the centrifugal equator though, higher ion anisotropy moves the plasma equator toward the magnetic equator. Measuring ion distribution with enough spatial resolution enables us to derive ion anisotropy which is tightly related to the amount of fresh pickup ion. On this study, we focus on variability of latitudinal structure of Io plasma torus as well as its radial structure using ground-based observation over six month period in 2018. The ground-based observation of sulfur ion emission, [SII] 671.6nm and 673.1nm was made at Haleakala observatory in Hawaii during March through August 2018 using the Tohoku 60-cm telescope (T60). A monochromatic imager with coronagraph attached onto the Cassegrain focus of T60 enables to measure distribution of S^+ with spatial resolution of 0.03 jovian radii (R_J). A digital micro-mirror device DMD was employed to block light from Jupiter disk and Galilean moons. Typical integration time of each frame was 20 minutes and total number of reduced image is 480. We also made observation of neutral sodium cloud extending up to several hundred of R_J as a proxy of supply of neutral particles from Io (Yoneda et al., 2015). Based on observation over the six month, [SII] brightness increases from DOY 80 through 140, then gradually decreases though DOY 230 in 2018. The data reduction of iogenic neutral sodium cloud is still undergoing though, neutral sodium cloud seems to increase from DOY 50 through 135, as [SII] brightness increases. The result suggests that increased volcanic activity from DOY 50-135 caused increase of S+ and brightening of [SII] emission. As for variability of shorter duration, we find [SII] brightening event within a short period (< 2 days) at around 28 through 30 July over a small region (< 30 degrees in longitude). [SII] 671.6 and 673.1 nm emissions are sensitive to cold electron (1-10eV) rather than hot electron (>100eV). Thus, increase of cold electron temperature explains the observed [SII] brightening well as the EUV space telescope Hisaki observed brightening of Io plasma torus associated with injection of hot electron. We also find variation of latitudinal structure of Io plasma torus. Longitudinal peak of S^+ emission at the same system III longitude 279 degree are -0.73, -0.80 and -0.79 R_J on 26, 29 July 7 and August, respectively. The shift of S^+ density peak toward magnetic equator implies higher anisotropy 29 on July and 7 August compared with 26 July. One of the possible explanation of the latitudinal shift of S^+ plasma is an increase of flesh pickup ion which makes higher anisotropy. Further study using Colorado Io Plasma Torus Emission Package (CITEP) will be presented on the presentation to take into account for line-of-sight integration effect of the ground-based observation.

Keywords: Io plasma torus

©2019. Japan Geoscience Union. All Right Reserved.

Ion Scale Height Variability in Hisaki Io Torus Observations

*Nicholas McCord Schneider[1], Carl Schmidt[2], Masato Kagitani[3], Yasumasa Kasaba[3], Tomoki Kimura[3], Go Murakami[4], Fuminori Tsuchiya[3], Hajime Kita[3], Reina Hikida[5], Ichiro Yoshikawa[5], Kazuo Yoshioka[5]

1. LASP, University of Colorado Boulder, 2. Boston University, 3. Tohoku University, 4. ISAS/JAXA, 5. University of Tokyo

Ion temperature is a critical variable in Io plasma torus energetics, but is difficult to derive from remote sensing measurements. The relative importance of hot ions vs. hot electrons in powering the torus emissions remains an open question. Torus brightenings, whether caused by episodic changes in the volcanic supply to the torus or periodic System III/IV enhancements, offer the best chance to search for driving variations in hot electrons or ions. Much attention has been paid to hot electron populations, derivable from detailed spectral modeling, but less work has been done on ion temperature. Ground-based studies have successfully derived $T_{\perp}$ from very high resolution spectra, and $T_{||}$ from scale height measurements in images, both over limited datasets. Schneider et al. 1997 found strong longitudinal variations in $T_{||}$ during a week-long dataset, and anti-correlated System III brightness, but more extended followup datasets have not previously been available.

The Hisaki dataset presents the possibility of an unparalleled opportunity to study long-term and short-term variations in ion temperatures. The instrument is not designed to take images of specific emissions, but its large entrance slit accepts the full height and width of the torus. In the ideal case, each spectral emission feature would appear as an image of the torus at its appropriate position in the spectrum, creating an “overlapogram” (as did the Cassini UVIS instrument). In reality, the emissions are blurred due to instrumental resolution and aberrations, and multiple spectral feature overlap. Furthermore, the changing opening angle of the rotating torus adds a spurious apparent scale height variation which must be removed, with special attention to asymmetries introduced by Jupiter's changing tilt. With allowances for all these effects, we will report on our search for ion temperature variations during the first two years of Hisaki observations, and compare our results to a previous independent study by M. Shishido (M.S. thesis, U. Tohoku).

Keywords: Jupiter, Io, plasma torus, magnetosphere , hisaki, ultraviolet

©2019. Japan Geoscience Union. All Right Reserved.

Size of the Smallest Particles in Saturn's Rings

*Keiji Ohtsuki[1], Hiroshi Kawamura[1], Naoyuki Hirata[1], Hiroshi Daisaka[2], Hiroshi Kimura[3]

1. Graduate School of Science, Kobe University, 2. Graduate School of Commerce and Management, Hitotsubashi University, 3. Planetary Exploration Research Center, Chiba Institute of Technology

Spacecraft and ground-based observations have shown that particles in Saturn's main rings have a power-law distribution roughly between centimeter and ten meters, but sub-centimeter particles appear to be lacking. Recent studies based on Cassini observations suggest that the size of the smallest particles is on the order of millimeters. Cohesive force between particles has been proposed to explain the paucity of sub-centimeter particles, but its strength depends on impact velocity. In order to better understand recent Cassini observations about small ring particles, we examine impact velocity between ring particles using N-body simulation including size distribution. We find that most collisions take place at velocities lower than 0.1 cm per second; even in dense rings where particles' velocity dispersion is enhanced by gravitational wakes, they collide at such low velocities because particles tend to move coherently in the wakes. This velocity is too low to detach sub-centimeter particles that are attached to the surface of large ones due to the cohesive force, explaining their paucity in the main rings. On the other hand, more infrequent high-velocity impacts can release millimeter-sized particles strongly attached to the surface of large ones, explaining the observed free millimeter-sized particles with relatively low abundance. We will discuss implications of our results for the observed size of the smallest particles in Saturn's main rings.

Keywords: Saturn, rings, Cassini

©2019. Japan Geoscience Union. All Right Reserved.

The Radio & Plasma Wave Investigation (RPWI) for JUICE for the investigation of Jupiter and Icy Moons System: Contributions from Japan

*Yasumasa Kasaba[1], Hiroaki Misawa[1], Fuminori Tsuchiya[1], Atsushi Kumamoto[2], Yuto Katoh[2], Tomoki Kimura[2], Hajime Kita[3], J.-E. Wahlund[4]

1. Planetary Plasma and Atmospheric Research Center, Tohoku University, 2. Department of Geophysics, Tohoku University, 3. ISAS/JAXA, 4. IRF Uppsala, Sweden

The Radio & Plasma Wave Investigation (RPWI) for the ESA JUICE mission (launch: 2022, Observations: 2030s) provides an elaborate suite of electromagnetic fields and plasma instruments. RPWI focuses on cold plasma studies and will investigate how the transfer of momentum and energy in the Jovian huge magnetosphere and the electrodynamic coupling with the icy Galilean moons. Remote sensing and direction finding of the Jovian radio emissions will be carried out. This capability is also devoted to the ices and the deep interiors of the icy moons. Investigations of the ice shells will be performed by means of a novel passive ground penetrating radar technique, which utilizes Jovian strong radio emissions as the transmitted signal. On the Ganymede orbit, continuous measurements of the electric field with the JUICE Magnetometer (JMAG) measurements will determine the electric coupling between any ocean, the ionosphere, and the magnetosphere, and provide the constraints on the physical characteristics of the subsurface ocean of Ganymede.
For those objectives, RPWI sensors consist of 4 Langmuir probes (LP-PWI) for determination of the vector electric field up to 1.6 MHz and cold plasma properties (including active measurements by LP sweeps and mutual impedance sounding) up to 1.6 MHz, a tri-axial search coil magnetometer (SCM) for determination of the vector magnetic field up to 20 kHz, and a tri-dipole antenna system (RWI) for monitoring of radio emissions (80 kHz - 45 MHz). From Japan, the RWI preamp and its High Frequency receiver with the onboard software will be provided, based on the modifications from the BepiColombo PWI and Arase PWE developments. Since Arase already shows the good performance in the radiation hard environment around Earth, we have enough confidence for the possible functions and performance on the Jovian hard environment. We will also provide Software Wave-Particle Interaction Analyzer (SWPIA) function to RPWI DPU, for the onboard quantitative detection of electromagnetic field - ion interactions, modifying from the Arase SWPIA which is also activating on the space now.
HF reciever will provide the first highly-resolved information of Jovian radio emissions emitted from Jovian multiple regions including lightning activity and icy moons, by the 3-ch receiver system manufactured by Japan and Sweden connected to the 3-elements 1.25-m E-filed dipole antenna system manufactured by Poland and Japan. Highly matured onboard and ground data processing will also be provided by France and Japan. As a byproduct, reflected Jovian emission can also be expected from the boundary of icy crust and conductive liquid subsurface ocean. Such reflection components could be observed as the Lunar surface reflection of terrestrial auroral kilometric radiation (AKR) seen by Kaguya Lunar Radar Sounder. JUICE has the RIME (Radar for Icy Moons Exploration) instrument, an active radar which emits 9 MHz pulse from 16 m tip-to-tip antenna and tries to detect the ocean under ~10 km icy crust. Since the frequency of Jovian radiation is wider (several 100 kHz to several 10s MHz), RPWI will provide complementary information, including the vertical distributions of conductivity and permittivity in the icy crust.
In the srping 2019, we are manufacturing and testing the Flight Models (FM) which will be shipped in June - July 2019 to Europe. The long road are connected to the first Jupiter and outer planet tour of the

©2019. Japan Geoscience Union. All Right Reserved.

hardware from Japan.

Keywords: Jupiter, JUICE, Radio waves

©2019. Japan Geoscience Union. All Right Reserved.

Magnetic field experiment at Jupiter icy moons (JUICE J-MAG) and in-flight alignment calibration

*Ayako Matsuoka[1], Michele Karen Dougherty[2], Patrick Brown[2], Futoshi Takahashi[3], Hisayoshi Shimizu[4], Masaki Matsushima[5]

1. Research Division for Space Plasma, Institute of Space and Astronautical Science, Japan Aerospace Exploration Agency, 2. Imperial College London, 3. Kyushu University, 4. University of Tokyo, 5. Tokyo Institute of Technology

The magnetometer instrument (J-MAG) is one of the core instruments on the JUICE spacecraft and is critical for resolving prime science objectives of the mission. The importance of a magnetometer instrument on JUICE can be described under following themes. Firstly, the magnetic field drives the plasma processes occurring within the Jupiter system. Understanding such observations allows for a better understanding of dynamical plasma processes, of the generation of aurora and of the various current systems which arise within this rapidly rotating magnetosphere. Secondary, the magnetometer science which is unique to JUICE lies in being able to gain an understanding of the interior structure of the icy moons of Jupiter, specifically those of Ganymede, Callisto and Europa. Of particular interest are knowledge of the depth at which the liquid oceans reside beneath their icy surfaces, the strength of any internal magnetic fields such as at Ganymede and the strength of any induced magnetic fields arising within these oceans.

J-MAG science requirements result in a requirement on the spacecraft to determine accurate knowledge of the orientation of the fluxgate sensors (MAGIBS and MAGOB). Due to the long MAG boom it is not possible to meet J-MAG’ s alignment requirement by mechanical stability alone, therefore the spacecraft includes two orthogonal coils mounted around its body. The coils can be driven with a current which produces a measurable magnetic field vector at the fluxgate sensors. This signal can then be used by the fluxgates to track the variation in the sensor alignment. This technical note describes the results of an analysis using an alignment recovery technique that was developed for the Kaguya mission, applied to the specific case of JUICE, considering the relative positions of the fluxgate sensors with respect to the JACS coils.

We derived equations to calculate the directions of the measurement axes in the frame fixed to the spacecraft, namely alignment angles, from the measurement results of reference magnetic fields generated by JACS. The errors of the alignment angle estimation and their dependence on measurement noise as well as inaccuracy of the coil current intensity are examined. Based on the quantitative results, the requirements to the JACS design and operation to satisfy the requests to the alignment accuracy are determined.

Keywords: Jupiter, Jovian moons, magnetometer

©2019. Japan Geoscience Union. All Right Reserved.

Science targets of the GAnymede Laser Altimeter (GALA) for the JUICE mission

*Jun Kimura[1], Shunichi Kamata[2], Koji Matsumoto[3], Noriyuki Namiki[3], Keigo Enya[4], Masanori Kobayashi[5], Hiroshi Araki[3], Hirotomo Noda[3], Ko Ishibashi[5], Hauke Hussmann[6], Kay Lingenauber[6]

1. Osaka University, 2. Hokkaido University, 3. National Astronomical Observatory Japan, 4. ISAS/JAXA, 5. Chiba Institute of Technology, 6. German Aerospace Center (DLR), Berlin

The JUpiter Icy Moons Explorer (JUICE), led by European Space Agency, has started development toward launch in 2022 (arrival at Jupiter in 2029, and Ganymede orbit insertion in 2032), and we are now developing the GALA instrument onboard JUICE spacecraft collaborating with German Aerospace Center (DLR) and other institutions in Europe. GALA will acquire the key information for understanding the evolution of Jovian icy moons and to play an essential role in the JUICE's purpose: exploration of deep habitat.

Jovian icy moon Ganymede, which is the largest moon in the Solar System and the primary target of the JUICE, can be said to be one of the typical solid bodies along with terrestrial planets in terms of its size and the intrinsic magnetic field originated from the metallic core. However, current knowledge provided by previous explorations is extremely limited since it comes from only several fly-bys. The JUICE will unveil the whole picture of Ganymede by the first orbiting in the history around extra-terrestrial moon. Expected new big picture of the origin and evolution of Ganymede will not only be a key to unveil the origin of diversity among the Solar System bodies, but also contribute to an understanding of exoplanets with a wide diversity.

The GALA will measure a distance between the spacecraft and the surface of icy moons and acquire the topography data (globally for Ganymede, and fly-by region for Europa and Callisto). It will be a first-ever laser altimetry for the icy object. Such information makes surface geologies clear and tremendously improves our understanding of the icy tectonics. By comparing their tectonic styles on the rocky planets/moons, GALA data leads to reconsider the Earth's plate tectonics. In addition, the GALA will confirm a presence/absence of the subsurface ocean by measuring tidal and rotational response, and the gravitational information reflecting the interior structure will be greatly improved. Furthermore, strength and waveform of reflected laser pulse have an information about surface reflectance at the laser wavelength and small-scale roughness. Finally we can see degrees of erosion and space weathering without being affected by illumination condition through GALA measurements.

In order to interpret and understand such measurements, accumulated studies for the Earth over the years will be effectively utilized: e.g., the data for surface topography, roughness and albedo will lead to describe the icy tectonics through the knowledge from terrestrial glaciology and experiments on impact and deformation process. The tidal measurements by GALA will also be a window to see its interior based on our knowledge and experiences cultivated through the past geodetic observations, e.g., the SELENE mission for the terrestrial Moon.

Characterization of the icy moons will be achieved not only from the GALA measurements but also synergy of other scientific instruments onboard JUICE spacecraft, for examples, surface images taken by optical camera (JANUS) will confirm the position of GALA laser footprint to complement the GALA "point" data for precise topographic mapping. A radar sounder (RIME) and a radio science experiment (3GM) probe

©2019. Japan Geoscience Union. All Right Reserved.

the interior structure, especially interior of the icy crust to figure out an occurrence of tectonic features. A visible and infrared imaging spectrometer (MAJIS), an ultraviolet imaging spectrograph (UVS) and a sub-millimeter wave instrument (SWI) will acquire a surface and atmosphere compositional data. A magnetometer (J-MAG) monitors moons' inductive response to the Jovian magnetic field and probes the subsurface ocean with the help of a particle environment package (PEP) and a radio and plasma wave investigation (RPWI). The GALA works closely together with these instruments and plays a leading and a supporting role to clarify the whole picture of Ganymede and other icy moons.

Keywords: Jupiter, Icy moons, Laser altimetry

©2019. Japan Geoscience Union. All Right Reserved.

Current status of the antenna developments, the data processing, scientific target for JUICE/SWI JAPAN.

*YASUKO KASAI[1], [Group] JUICE SWI Japanese Team

1. National Institute of Information and Communications Technology (NICT)

The Submillimetre-Wave Instrument (SWI) is one of the 10 scientific payloads on the JUpiter ICy moon Explorer (JUICE). The main scientific objectives of SWI is to investigate the structure, compositions and dynamics of the middle atmosphere of Jupiter and exosphere of its moons, as well as thermophysical properties if the satellite surfaces. SWI observations will provide pioneering direct measurements of atmospheric compositions in Jupiter system. SWI will performed limb and nadir observations in the frequency region 530-600 and 1075-1275 GHz. Japanese contribution is the development of main- and sub- reflectors, actuators for the instruments, feasibility studies, data processing, and scientific contributions. We present Current status of the antenna developments, the data processing, scientific target for JUICE/SWI JAPAN.

Keywords: Jupiter, Jovian moons, submm instrument, JUICE, SWI

©2019. Japan Geoscience Union. All Right Reserved.

[E] Poster | P (Space and Planetary Sciences)：P-PS Planetary Sciences

Tue. May 28, 2019 5:15 PM - 6:30 PM JST | Tue. May 28, 2019 8:15 AM - 9:30 AM UTC | Poster Hall International Exhibition Hall8, Makuhari Messe_1

[P-PS01] Outer Solar System Exploration Today, and Tomorrow

convener:Jun Kimura(Osaka University), Yasumasa Kasaba(Planetary Plasma and Atmospheric Research Center, Tohoku University), Kunio M. Sayanagi(Hampton University)

The giant planets provide many keys to understanding planetary processes. They play an important role in shaping our solar system, and the physical and chemical processes they harbor also provide a unique opportunity to study the phenomena relevant for studying Earth and other planets, including exoplanetary systems. In this session, we discuss a wide range of topics encompassing the giant planets and their moons, including their origins, interiors, atmospheres, compositions, surface features, and electromagnetic fields. To advocate for current and future outer planets exploration (Cassini, Juno, New Horizons, JUICE, and beyond), we also call for discussions on future missions to explore giant planet systems, including how to develop better international cooperation. Discussion in this latter category will include progress in developing a solar sail mission concept for observing the Jupiter system and its trojan asteroids.

[PPS01-P01] Critical Role of Entry Probes in Giant Planet Exploration

*Sushil K Atreya[1], Olivier Mousis[2] (1.University of Michigan Ann Arbor, 2.Laboratoire d'Astrophysique de Marseille)

[PPS01-P02] OKEANOS – Jupiter Trojan Asteroid Rendezvous and Landing Experiments Using a Solar Power Sail

*Tatsuaki Okada[1,2], Takahiro Iwata[1], Yoko Kebukawa[3], Motoo Ito[4], Jun Aoki[5], Yosuke Kawai[5], Shoichiro Yokota[5], Yoshifumi Saito[1], Kentaro Terada[5], Michisato Toyoda[5], Hikaru Yabuta[6], Hisayoshi Yurimoto[1,7], Shuji Matsuura[8], Kohji Tsumura[9], Daisuke Yonetoku[10], Tatehiro Mihara[11], Ayako Matsuoka[1], Reiko Nomura[12], Hajime Yano[1], Takayuki Hirai[13], Atsushi Kumamoto[9], Ryosuke Nakamura[14], Stephan Ulamec[15], Ralf Jaumann[15], Jean-Pierre Bibring[16], Noel Grand[17], Cyril Szopa[18], Ernesto Palomba[19], Jorn Helbert[15], Alain Herique[20], Matthias Grott[15], Hans-Ulrich Auster[21], Goester Klingelhoefer[22], Fumi Yoshida[13], Makoto Yoshikawa[1], Jun Matsumoto[1], Toshihiro Chujo[1], Masanori Matsushita[1], Takanao Saiki[1], Hideki Kato[1], Osamu Mori[1], Junichiro Kawaguchi[1] (1.Japan Aerospace Exploration Agency, 2.University of Tokyo, 3.Yokohama National University, 4.Japan Agency for Marine-Earth Science and Technology, 5.Osaka University, 6.Hiroshima University, 7.Hokkaido University, 8.Kwansei Gakuin University, 9.Tohoku University, 10.Kanazawa University, 11.RIKEN, 12.National Astronomical Observatory of Japan, 13.Chiba Institute of Technology, 14.National Institute of Advanced Industrial Science and Technology, 15.German Aerospace Center, 16.Institut d'Astrophysique Spatiale, 17.LISA, 18.LATMOS, 19.INAF-IAPS, 20.IPAG, 21.TU Braunschweig, 22.Leibniz Universität Hannover)

[PPS01-P03] Magnetic field model of Jovian magnetosphere

*Naoya Momoki[1], Hiroaki TOH[1] (1.Division of Earth and Planetary Sciences, Graduate School of Science, Kyoto University)

[PPS01-P04] Enhancement of the Jovian thermospheric temperature above the Great Red Spot based on the infrared spectroscopic data obtained with IRTF/iSHELL

*Ayumu Kambara[1], Hajime Kita[2], Takeshi Sakanoi[1], Yasumasa Kasaba[1], Masato Kagitani[1], Haruna Watanabe[1] (1.Planetary Plasma and Atmospheric Research Center, Graduate School of Science, Tohoku University, 2.Institute of Space and Astronautical Science, Japan Aerospace Exploration Agency)

[PPS01-P05] Pulsation-like variation of Jovian infrared polar emission observed by Subaru 8-m: H3+ and methane emissions

*Yasumasa Kasaba[1], Haruna Watanabe[1], Hajime Kita[2], Chihiro Tao[3], Takeshi Sakanoi[1], Masato Kagitani[1], Orton Glenn[1,4], James Sinclair[4] (1.Planetary Plasma and Atmospheric Research Center, 2.ISAS/JAXA,

3.NICT, 4.NASA/JPL)

[PPS01-P06] Structure of Io plasma torus observed with the Tohoku 60-cm telescope

*Masato Kagitani[1], Fuminori Tsuchiya[1], Kazuo Yoshioka[2], Go Murakami[3], Tomoki Kimura[1], Ryoichi Koga[1], Reina Hikida[4], Takeshi Sakanoi[1] (1.Graduate School of Science, Tohoku University, 2.Graduate School of frontier Science, The University of Tokyo, 3.Institute of Space and Astronautical Science, Japan Aerospace Exploration Agency, 4.Department of Earth and Planetary Science, Graduate School of Science, Tokyo University)

[PPS01-P07] Ion Scale Height Variability in Hisaki Io Torus Observations

*Nicholas McCord Schneider[1], Carl Schmidt[2], Masato Kagitani[3], Yasumasa Kasaba[3], Tomoki Kimura[3], Go Murakami[4], Fuminori Tsuchiya[3], Hajime Kita[3], Reina Hikida[5], Ichiro Yoshikawa[5], Kazuo Yoshioka[5] (1.LASP, University of Colorado Boulder, 2.Boston University, 3.Tohoku University, 4.ISAS/JAXA, 5.University of Tokyo)

[PPS01-P08] Size of the Smallest Particles in Saturn's Rings

*Keiji Ohtsuki[1], Hiroshi Kawamura[1], Naoyuki Hirata[1], Hiroshi Daisaka[2], Hiroshi Kimura[3] (1.Graduate School of Science, Kobe University, 2.Graduate School of Commerce and Management, Hitotsubashi University, 3.Planetary Exploration Research Center, Chiba Institute of Technology)

[PPS01-P09] The Radio & Plasma Wave Investigation (RPWI) for JUICE for the investigation of Jupiter and Icy Moons System: Contributions from Japan

*Yasumasa Kasaba[1], Hiroaki Misawa[1], Fuminori Tsuchiya[1], Atsushi Kumamoto[2], Yuto Katoh[2], Tomoki Kimura[2], Hajime Kita[3], J.-E. Wahlund[4] (1.Planetary Plasma and Atmospheric Research Center, Tohoku University, 2.Department of Geophysics, Tohoku University, 3.ISAS/JAXA, 4.IRF Uppsala, Sweden)

[PPS01-P10] Magnetic field experiment at Jupiter icy moons (JUICE J-MAG) and in-flight alignment calibration

*Ayako Matsuoka[1], Michele Karen Dougherty[2], Patrick Brown[2], Futoshi Takahashi[3], Hisayoshi Shimizu[4], Masaki Matsushima[5] (1.Research Division for Space Plasma, Institute of Space and Astronautical Science, Japan Aerospace Exploration Agency, 2.Imperial College London, 3.Kyushu University, 4.University of Tokyo, 5.Tokyo Institute of Technology)

[PPS01-P11] Science targets of the GAnymede Laser Altimeter (GALA) for the JUICE mission

*Jun Kimura[1], Shunichi Kamata[2], Koji Matsumoto[3], Noriyuki Namiki[3], Keigo Enya[4], Masanori Kobayashi[5], Hiroshi Araki[3], Hirotomo Noda[3], Ko Ishibashi[5], Hauke Hussmann[6], Kay Lingenauber[6] (1.Osaka University, 2.Hokkaido University, 3.National Astronomical Observatory Japan, 4.ISAS/JAXA, 5.Chiba Institute of Technology, 6.German Aerospace Center (DLR), Berlin)

[PPS01-P12] Current status of the antenna developments, the data processing, scientific target for JUICE/SWI JAPAN.

*YASUKO KASAI[1], JUICE SWI Japanese Team (1.National Institute of Information and Communications Technology (NICT))

Critical Role of Entry Probes in Giant Planet Exploration

*Sushil K Atreya[1], Olivier Mousis[2]

1. University of Michigan Ann Arbor, 2. Laboratoire d'Astrophysique de Marseille

Flyby and orbiting spacecraft have explored the giant planets since the early 1970’s. In situ measurements in the troposphere are essential, however, for constraining the models of formation, evolution and interior processes of the giant planets. The models employ abundances and isotopic ratios of key elements, in particular C,N, S, O, He, Ne, Ar, Kr, Xe and D/H, derived from the measurement of their (bulk) reservoir species. That was the scientific rationale for the 1995 Galileo Probe at Jupiter and a Saturn Probe in NASA’s New Frontiers list of candidate missions. Considering that the icy giant planets are distinct from the gas giants, they represent the missing pieces of the puzzle of the formation of the outer solar system, besides being the closest analog for nearly half of the confirmed exoplanets. Thus, their comprehensive exploration with an orbiter-probe spacecraft is essential. The principal focus of this talk is the science, feasibility and implementation strategy of in situ measurements with entry probes at the icy giant planets, Uranus and Neptune, guided by thermochemical models and lessons learned from the Galileo Probe and the ongoing Juno Orbiter. [www.umich.edu/~atreya]

Keywords: Icy Giants, Origin and Evolution, Uranus, Neptune, Entry Probes, Exoplanets

©2019. Japan Geoscience Union. All Right Reserved.

OKEANOS –Jupiter Trojan Asteroid Rendezvous and Landing Experiments Using a Solar Power Sail

*Tatsuaki Okada[1,2], Takahiro Iwata[1], Yoko Kebukawa[3], Motoo Ito[4], Jun Aoki[5], Yosuke Kawai[5], Shoichiro Yokota[5], Yoshifumi Saito[1], Kentaro Terada[5], Michisato Toyoda[5], Hikaru Yabuta[6], Hisayoshi Yurimoto[1,7], Shuji Matsuura[8], Kohji Tsumura[9], Daisuke Yonetoku[10], Tatehiro Mihara[11], Ayako Matsuoka[1], Reiko Nomura[12], Hajime Yano[1], Takayuki Hirai[13], Atsushi Kumamoto[9], Ryosuke Nakamura[14], Stephan Ulamec[15], Ralf Jaumann[15], Jean-Pierre Bibring[16], Noel Grand[17], Cyril Szopa[18], Ernesto Palomba[19], Jorn Helbert[15], Alain Herique[20], Matthias Grott[15], Hans-Ulrich Auster[21], Goester Klingelhoefer[22], Fumi Yoshida[13], Makoto Yoshikawa[1], Jun Matsumoto[1], Toshihiro Chujo[1], Masanori Matsushita[1], Takanao Saiki[1], Hideki Kato[1], Osamu Mori[1], Junichiro Kawaguchi[1]

1. Japan Aerospace Exploration Agency, 2. University of Tokyo, 3. Yokohama National University, 4. Japan Agency for Marine-Earth Science and Technology, 5. Osaka University, 6. Hiroshima University, 7. Hokkaido University, 8. Kwansei Gakuin University, 9. Tohoku University, 10. Kanazawa University, 11. RIKEN, 12. National Astronomical Observatory of Japan, 13. Chiba Institute of Technology, 14. National Institute of Advanced Industrial Science and Technology, 15. German Aerospace Center, 16. Institut d’ Astrophysique Spatiale, 17. LISA, 18. LATMOS, 19. INAF-IAPS, 20. IPAG, 21. TU Braunschweig, 22. Leibniz Universität Hannover

The OKEANOS (Oversize Kite-craft for Exploration and AstroNautics in the Outer Solar system) is a mission under study to rendezvous with and land on a Jupiter Trojan asteroid [1]. The target is a Jupiter Trojan but will be the Saturnian system in the future. It is an engineering mission to demonstrate advanced technologies such as the hybrid thrusting with the enhanced ion engine powered by a 40 x 40 m class large area solar cells to explore the outer solar system cost-effectively. With the new technology, the mission will conduct in-depth scientific measurements for understanding the origin and evolution of the solar system and life. The concept is complementary to NASA Lucy mission [2], multi-flybys to six Jupiter Trojans for understanding the variation of Jupiter Trojans.

Jupiter Trojans are D/P-types enriched in volatiles. They might have experienced almost no or only a low degree of alteration. Their origin and evolution, as well as chemical and physical state still remain unknown. Jupiter Trojans should be a missing link of materials that originate from the inner or the outer solar system by gravity scattering due to migration of giant planets [3]. They are key targets to understand the evolution of astromaterials and the radial distribution of elements and isotopes in the early solar system.

The OKEANOS has been downscaled from the previous proposal [4] due to the severe cost cap. The spacecraft of 1400 kg including a 40 kg lander will be launched in 2027 or later, assisted by gravity of Earth and Jupiter. It will arrive at the target asteroid after a 13-year cruise. 30 kg is allocated for science, 12 kg of which is reserved for international collaboration. Bus instruments such as the optical navigation cameras (ONC-T and -W), LIDAR, and radio science are used for scientific purposes. The lander is like Mascot with uprighting capability on the asteroid surface and 12 kg is allocated for science mission.

During the cruise, science experiments will be carried out from the “deep-space platform”. Measurements of IDPs and magnetic fields will continuously monitor their radial distribution in the solar system and sudden events. The gamma-ray polarimeter will be used for precise positioning of gamma-ray bursts using a very long baseline. Visible to near-infrared telescope will map the zodiacal lights and observe the deep sky under a dust-free condition from outside of the asteroid main belt.

©2019. Japan Geoscience Union. All Right Reserved.

After arrival, global mapping is carried out to characterize the asteroid and select the landing site. The asteroid shape, size, rotation state, and geologic features are imaged by ONC. Gravity is measured by radio tracking and LIDAR. Near-infrared spectroscopy characterizes red or less red patterns, the degree of hydration, mineralogy, and abundance of ices, organics, and brines. Thermal infrared multi-bands inform on thermophysical properties, mineralogy and amorphous phases. A radar probes the surface physical state and also contributes to altimetry. *In situ* experiments with the lander will characterize the footprint and surrounding area by imaging and spectroscopy, followed by measurements of mineralogical, elemental, and organic composition as well as physical, thermal, and magnetic properties at the site. The asteroid surface sample is collected to conduct high-resolution mass spectroscopy (HRMS) based on MULTUM system (infi-TOF type mass spectrometer [5]), especially to determine the isotopic ratios of δD and δ^{15}N and the volatile species contained in the sample. Details will be decided during the critical joint study in 2019. Those experiences will be inherited to future missions.

References: [1] Mori O. et al. (2018) Trans. JSASS Aerospace Tech. Japan, 16, 328-333. [2] Levison H.F. et al. (2016) Lunar Planet. Sci. Conf., 47, #2061. [3] Morbidelli A. et al. (2005) *Nature 435*, 462-466. [4] Okada T. et al. (2018) Planet. Space Sci. 161, 99-106. [6] Toyoda M. et al. (2003) J. Mass Spectrom. 38, 1125-1142.

Keywords: Solar Sail, Trojan, Landing

©2019. Japan Geoscience Union. All Right Reserved.

Magnetic field model of Jovian magnetosphere

*Naoya Momoki[1], Hiroaki TOH[1]

1. Division of Earth and Planetary Sciences, Graduate School of Science, Kyoto University

Europa, Ganymede, Callisto are the Jovian icy satellites called Galilean moons, and are possibly with internal oceans each. While ice is almost an insulator electrically, water including ions has high electrical conductivity, and existence of internal oceans can be verified using electromagnetic (EM) induction methods. In this study, we updated the necessary model of the external magnetic field to the icy satellites for the EM induction studies. Namely, parameters of the Euler potential model of the Jovian magnetosphere (Khurana, 1997) were renewed by adding magnetic data from both Galileo and JUNO spacecrafts.

The configuration of the Jovian current sheet was modeled by Khurana [1992] using three parameters, while the Jovian magnetospheric magnetic field modeled by Khurana [1997] was characterized by 14 parameters. We applied a non-linear optimization technique, i.e., the steepest descent method, to the parameters by newly adding magnetic data from Galileo and Juno spacecrafts. We minimized the root mean squared between the model and the data by exploring the parameter space around several initial sets of the parameters.

As a result, time-varying model parameters for each spacecraft orbit were obtained. Their temporal variation may reflect that of both magnetic field and electric current system in the Jovian magnetosphere.The changes of the parameters can be attributed to the interaction between the Jovian magnetosphere and the solar wind. It, therefore, preferable that the temporal variation of the model parameters is incorporated when the updated magnetic field model of the Jovian magnetosphere is applied to the EM induction studies in search for the internal oceans of the icy satellites.

Keywords: Jupiter, Magnetosphere

©2019. Japan Geoscience Union. All Right Reserved.

Enhancement of the Jovian thermospheric temperature above the Great Red Spot based on the infrared spectroscopic data obtained with IRTF/iSHELL

*Ayumu Kambara[1], Hajime Kita[2], Takeshi Sakanoi[1], Yasumasa Kasaba[1], Masato Kagitani[1], Haruna Watanabe[1]

1. Planetary Plasma and Atmospheric Research Center, Graduate School of Science, Tohoku University, 2. Institute of Space and Astronautical Science, Japan Aerospace Exploration Agency

It is known that the thermospheric temperature of all giant planets including Jupiter is several hundred kelvins higher than that expected from solar heating. At mid- to low-latitudes, although the direct atmospheric heating caused by precipitating particles and the energy transportation from high-latitude auroral region have been considered, it is not enough to explain. Another candidate for the heating is energy transportation by atmospheric waves from the lower atmosphere. Recently, O'Donoghue *et al.* [2016] revealed the heating in the thermosphere above the Great red spot from the intensity ratio of two emission lines (3.383um/3.454um) of the vibrational-rotational spectrum of thermospheic H_3^+ taken by IRTF /SpeX (R~2500) in December 2012. They estimated that the temperature above the Great red spot is 1644±161K, and that on surrounding mid- to low-latitude region is 900±42K. They considered that the reason was the energy transport from the lower atmosphere in the Great red spot region, that is, the propagation of atmospheric gravity waves and acousitic waves generated in the Great red spot, the tropospheric anticyclonic storm, to the thermosphere. However, the infrared spectrum observed SpeX might be contaminated by CH_4 line due to its low-resolution capability.
In this study, we carried out the thermosphere temperature observation in the Jovian mid-latitude region near the Great red spot by IRTF/iSHELL on January 11, 2017. This observation was performed with the iSHELL's Lp1-mode (3.265-3.657um), and the data reduction was performed with NASA's data reduction tool Spextool ver. 5.0.1. Similar to the past study by O'Donoghue *et al.* [2016], we adopted the intensity ratio of two emission lines of H_3^+ (3.3839um/3.4548um), and estimated the temperature precisely distinguished from CH_4 line by iSHELL’s higher wavelength resolution (R~75000). As a result, we estimated the thermospheric temperature above the Great red spot to be 910±132K, and that in the surrounding region to be 583±30K, showing about 300K increase on Great red spot. The estimated temperature was lower than that in O’Donoghue *et al.* [2016], there is possibility that the thermosphere temperature varies in time. However, we confirmed the temperature above Great red spot is higher than that in the surrounding region. This suggests the existence of energy transport from the lower to the upper atmosphere in the Great red spot. In the presentation, we report the result of carefully reduction.

Keywords: Jupiter, Great red spot, Thermosphere

©2019. Japan Geoscience Union. All Right Reserved.

Pulsation-like variation of Jovian infrared polar emission observed by Subaru 8-m: H3+ and methane emissions

*Yasumasa Kasaba[1], Haruna Watanabe[1], Hajime Kita[2], Chihiro Tao[3], Takeshi Sakanoi[1], Masato Kagitani[1], Orton Glenn[1,4], James Sinclair[4]

1. Planetary Plasma and Atmospheric Research Center, 2. ISAS/JAXA, 3. NICT, 4. NASA/JPL

In the Jovian high-latitude region, there are emissions with various wavelengths ranges, morphologies, and time variations. They are important tracers of energy injection carried by auroral particles that precipitate from the magnetosphere. The polar IR emissions excited in the Jovian upper atmosphere, which include the H_3^+ aurora and thermal emissions of hydrocarbons, reflect not only the abundance of emission sources but also the thermal structures. Both are affected by auroral precipitation into the source region. It is known that, in the polar region inner than the auroral oval, the flux of auroral precipitation can have time variations over various scales from years to seconds.

The H_3^+ aurora observed in near infrared is emitted in thermosphere / ionosphere from thermally excited H_3^+ ions above the CH_4 homopause. Auroral precipitation ionized H_2 and produce H_3^+ ions through ion chemistries. In previous observational studies, the shortest timescale of H_3^+ auroral intensity change was ~30 min, but detected by ~16-min step imaging. We performed the temporal imaging observation of the Jovian H_3^+ IR aurora with Subaru/IRCS and the H_3^+ narrow-band filter on 31 January 2015 and 25 May 2016. The adaptive optics enabled us to see the target with high spatial resolution (~0.2 arcsec). From the images obtained with time resolution of ~150 s on 25 May 2016, we detected a patch-like auroral feature pulsating with a period of ~10 min in noon sector of northern polar region. On the other hand, we could not find any periodic variations from the data obtained on 31 January 2015, which was obtained as slit-viewer image for the other study, and whose time intervals of ~10–30 min every several images was not optimized to this research. In addition, the location where the patch-like emissions observed with high intensities on 25 May 2016 were not so bright on 31 January 2015. The patch-like auroral feature that was pulsating during our observation period on 25 May 2016 have been sometimes observed in UV, but not always. Previous UV observations reported some pulsating auroral features with the periods of ~2–11 min in the northern polar region. However, the locations of them are not consistent with the patch-like feature in this study. The pulsation period of the X-ray aurora, which has a hot spot coinciding with our patch-like IR aurora, is 40–50 min. This region is estimated to connect magnetically to out of the magnetopause, and auroral precipitation there can be caused by dayside reconnection between the Jovian magnetospheric field and interplanetary field.

On the other hand, the hydrocarbon polar emission observed in mid-infrared is emitted from the whole stratosphere. From their locations and morphologies, it is estimated to be related with auroral particles penetrating under the homopause. However, the mechanisms of this link (composition change and/or heating by particle precipitations) are not well understood. Previous studies found the intensity time variation of polar CH_4 emission over days and months. We tried to detect the time variation of CH_4 emission intensity by continuous imaging observations of the northern polar region over several tens of minutes on 31 March, 24 and 25 May 2018 with Subaru/COMICS. We obtained the images using the 7.8 μm filter, which is sensitive to the CH_4 thermal emissions occurring in the pressure range of 20–0.5 mbar and 1 μbar in the Jovian upper stratosphere, with time resolution of ~1 min. On all observation days, the polar region was not bright in 7.8 μm. In addition, we could not find clear time variations of polar CH_4 emission intensity during our observation periods, 25, 50 and 60 min on 31 March, 24 and 25 May 2018.

©2019. Japan Geoscience Union. All Right Reserved.

This observation result is consistent to the model estimation by *Kuroda et al.* [2014], which suggested the relaxation time of hydrocarbon thermal emissions in the Jovian upper stratosphere, where is a possible source region of polar CH_4 emission, is at least ~10^5 s (~28 h).

Keywords: Jupiter, polar emission, H3+, CH4, short time variations

©2019. Japan Geoscience Union. All Right Reserved.

Structure of Io plasma torus observed with the Tohoku 60-cm telescope

*Masato Kagitani[1], Fuminori Tsuchiya[1], Kazuo Yoshioka[2], Go Murakami[3], Tomoki Kimura[1], Ryoichi Koga[1], Reina Hikida[4], Takeshi Sakanoi[1]

1. Graduate School of Science, Tohoku University, 2. Graduate School of frontier Science, The University of Tokyo, 3. Institute of Space and Astronautical Science, Japan Aerospace Exploration Agency, 4. Department of Earth and Planetary Science, Graduate School of Science, Tokyo University

Volcanic gases (mainly composed of SO_2, SO and S) originated from jovian satellite Io are ionized by interaction with magnetospheric plasma and then form a donut-shaped region called Io plasma torus. Ion pickup is the most significant energy source on the plasma torus though, distribution of pick-up region and its variability is still unclear. Density profiles of ions along the magnetic field line are determined under condition of diffusive equilibrium. Based on the equilibrium, plasma equator is close to the centrifugal equator though, higher ion anisotropy moves the plasma equator toward the magnetic equator. Measuring ion distribution with enough spatial resolution enables us to derive ion anisotropy which is tightly related to the amount of fresh pickup ion. On this study, we focus on variability of latitudinal structure of Io plasma torus as well as its radial structure using ground-based observation over six month period in 2018. The ground-based observation of sulfur ion emission, [SII] 671.6nm and 673.1nm was made at Haleakala observatory in Hawaii during March through August 2018 using the Tohoku 60-cm telescope (T60). A monochromatic imager with coronagraph attached onto the Cassegrain focus of T60 enables to measure distribution of S^+ with spatial resolution of 0.03 jovian radii (R_J). A digital micro-mirror device DMD was employed to block light from Jupiter disk and Galilean moons. Typical integration time of each frame was 20 minutes and total number of reduced image is 480. We also made observation of neutral sodium cloud extending up to several hundred of R_J as a proxy of supply of neutral particles from Io (Yoneda et al., 2015). Based on observation over the six month, [SII] brightness increases from DOY 80 through 140, then gradually decreases though DOY 230 in 2018. The data reduction of iogenic neutral sodium cloud is still undergoing though, neutral sodium cloud seems to increase from DOY 50 through 135, as [SII] brightness increases. The result suggests that increased volcanic activity from DOY 50-135 caused increase of S+ and brightening of [SII] emission. As for variability of shorter duration, we find [SII] brightening event within a short period (< 2 days) at around 28 through 30 July over a small region (< 30 degrees in longitude). [SII] 671.6 and 673.1 nm emissions are sensitive to cold electron (1-10eV) rather than hot electron (>100eV). Thus, increase of cold electron temperature explains the observed [SII] brightening well as the EUV space telescope Hisaki observed brightening of Io plasma torus associated with injection of hot electron. We also find variation of latitudinal structure of Io plasma torus. Longitudinal peak of S^+ emission at the same system III longitude 279 degree are -0.73, -0.80 and -0.79 R_J on 26, 29 July 7 and August, respectively. The shift of S^+ density peak toward magnetic equator implies higher anisotropy 29 on July and 7 August compared with 26 July. One of the possible explanation of the latitudinal shift of S^+ plasma is an increase of flesh pickup ion which makes higher anisotropy. Further study using Colorado Io Plasma Torus Emission Package (CITEP) will be presented on the presentation to take into account for line-of-sight integration effect of the ground-based observation.

Keywords: Io plasma torus

©2019. Japan Geoscience Union. All Right Reserved.

Ion Scale Height Variability in Hisaki Io Torus Observations

*Nicholas McCord Schneider[1], Carl Schmidt[2], Masato Kagitani[3], Yasumasa Kasaba[3], Tomoki Kimura[3], Go Murakami[4], Fuminori Tsuchiya[3], Hajime Kita[3], Reina Hikida[5], Ichiro Yoshikawa[5], Kazuo Yoshioka[5]

1. LASP, University of Colorado Boulder, 2. Boston University, 3. Tohoku University, 4. ISAS/JAXA, 5. University of Tokyo

Ion temperature is a critical variable in Io plasma torus energetics, but is difficult to derive from remote sensing measurements. The relative importance of hot ions vs. hot electrons in powering the torus emissions remains an open question. Torus brightenings, whether caused by episodic changes in the volcanic supply to the torus or periodic System III/IV enhancements, offer the best chance to search for driving variations in hot electrons or ions. Much attention has been paid to hot electron populations, derivable from detailed spectral modeling, but less work has been done on ion temperature. Ground-based studies have successfully derived $T_{\perp}$ from very high resolution spectra, and $T_{||}$ from scale height measurements in images, both over limited datasets. Schneider et al. 1997 found strong longitudinal variations in $T_{||}$ during a week-long dataset, and anti-correlated System III brightness, but more extended followup datasets have not previously been available.

The Hisaki dataset presents the possibility of an unparalleled opportunity to study long-term and short-term variations in ion temperatures. The instrument is not designed to take images of specific emissions, but its large entrance slit accepts the full height and width of the torus. In the ideal case, each spectral emission feature would appear as an image of the torus at its appropriate position in the spectrum, creating an “overlapogram” (as did the Cassini UVIS instrument). In reality, the emissions are blurred due to instrumental resolution and aberrations, and multiple spectral feature overlap. Furthermore, the changing opening angle of the rotating torus adds a spurious apparent scale height variation which must be removed, with special attention to asymmetries introduced by Jupiter's changing tilt. With allowances for all these effects, we will report on our search for ion temperature variations during the first two years of Hisaki observations, and compare our results to a previous independent study by M. Shishido (M.S. thesis, U. Tohoku).

Keywords: Jupiter, Io, plasma torus, magnetosphere , hisaki, ultraviolet

©2019. Japan Geoscience Union. All Right Reserved.

Size of the Smallest Particles in Saturn's Rings

*Keiji Ohtsuki[1], Hiroshi Kawamura[1], Naoyuki Hirata[1], Hiroshi Daisaka[2], Hiroshi Kimura[3]

1. Graduate School of Science, Kobe University, 2. Graduate School of Commerce and Management, Hitotsubashi University, 3. Planetary Exploration Research Center, Chiba Institute of Technology

Spacecraft and ground-based observations have shown that particles in Saturn's main rings have a power-law distribution roughly between centimeter and ten meters, but sub-centimeter particles appear to be lacking. Recent studies based on Cassini observations suggest that the size of the smallest particles is on the order of millimeters. Cohesive force between particles has been proposed to explain the paucity of sub-centimeter particles, but its strength depends on impact velocity. In order to better understand recent Cassini observations about small ring particles, we examine impact velocity between ring particles using N-body simulation including size distribution. We find that most collisions take place at velocities lower than 0.1 cm per second; even in dense rings where particles' velocity dispersion is enhanced by gravitational wakes, they collide at such low velocities because particles tend to move coherently in the wakes. This velocity is too low to detach sub-centimeter particles that are attached to the surface of large ones due to the cohesive force, explaining their paucity in the main rings. On the other hand, more infrequent high-velocity impacts can release millimeter-sized particles strongly attached to the surface of large ones, explaining the observed free millimeter-sized particles with relatively low abundance. We will discuss implications of our results for the observed size of the smallest particles in Saturn's main rings.

Keywords: Saturn, rings, Cassini

©2019. Japan Geoscience Union. All Right Reserved.

The Radio & Plasma Wave Investigation (RPWI) for JUICE for the investigation of Jupiter and Icy Moons System: Contributions from Japan

*Yasumasa Kasaba[1], Hiroaki Misawa[1], Fuminori Tsuchiya[1], Atsushi Kumamoto[2], Yuto Katoh[2], Tomoki Kimura[2], Hajime Kita[3], J.-E. Wahlund[4]

1. Planetary Plasma and Atmospheric Research Center, Tohoku University, 2. Department of Geophysics, Tohoku University, 3. ISAS/JAXA, 4. IRF Uppsala, Sweden

The Radio & Plasma Wave Investigation (RPWI) for the ESA JUICE mission (launch: 2022, Observations: 2030s) provides an elaborate suite of electromagnetic fields and plasma instruments. RPWI focuses on cold plasma studies and will investigate how the transfer of momentum and energy in the Jovian huge magnetosphere and the electrodynamic coupling with the icy Galilean moons. Remote sensing and direction finding of the Jovian radio emissions will be carried out. This capability is also devoted to the ices and the deep interiors of the icy moons. Investigations of the ice shells will be performed by means of a novel passive ground penetrating radar technique, which utilizes Jovian strong radio emissions as the transmitted signal. On the Ganymede orbit, continuous measurements of the electric field with the JUICE Magnetometer (JMAG) measurements will determine the electric coupling between any ocean, the ionosphere, and the magnetosphere, and provide the constraints on the physical characteristics of the subsurface ocean of Ganymede.
For those objectives, RPWI sensors consist of 4 Langmuir probes (LP-PWI) for determination of the vector electric field up to 1.6 MHz and cold plasma properties (including active measurements by LP sweeps and mutual impedance sounding) up to 1.6 MHz, a tri-axial search coil magnetometer (SCM) for determination of the vector magnetic field up to 20 kHz, and a tri-dipole antenna system (RWI) for monitoring of radio emissions (80 kHz - 45 MHz). From Japan, the RWI preamp and its High Frequency receiver with the onboard software will be provided, based on the modifications from the BepiColombo PWI and Arase PWE developments. Since Arase already shows the good performance in the radiation hard environment around Earth, we have enough confidence for the possible functions and performance on the Jovian hard environment. We will also provide Software Wave-Particle Interaction Analyzer (SWPIA) function to RPWI DPU, for the onboard quantitative detection of electromagnetic field - ion interactions, modifying from the Arase SWPIA which is also activating on the space now.
HF reciever will provide the first highly-resolved information of Jovian radio emissions emitted from Jovian multiple regions including lightning activity and icy moons, by the 3-ch receiver system manufactured by Japan and Sweden connected to the 3-elements 1.25-m E-filed dipole antenna system manufactured by Poland and Japan. Highly matured onboard and ground data processing will also be provided by France and Japan. As a byproduct, reflected Jovian emission can also be expected from the boundary of icy crust and conductive liquid subsurface ocean. Such reflection components could be observed as the Lunar surface reflection of terrestrial auroral kilometric radiation (AKR) seen by Kaguya Lunar Radar Sounder. JUICE has the RIME (Radar for Icy Moons Exploration) instrument, an active radar which emits 9 MHz pulse from 16 m tip-to-tip antenna and tries to detect the ocean under ~10 km icy crust. Since the frequency of Jovian radiation is wider (several 100 kHz to several 10s MHz), RPWI will provide complementary information, including the vertical distributions of conductivity and permittivity in the icy crust.
In the srping 2019, we are manufacturing and testing the Flight Models (FM) which will be shipped in June - July 2019 to Europe. The long road are connected to the first Jupiter and outer planet tour of the

©2019. Japan Geoscience Union. All Right Reserved.

hardware from Japan.

Keywords: Jupiter, JUICE, Radio waves

©2019. Japan Geoscience Union. All Right Reserved.

Magnetic field experiment at Jupiter icy moons (JUICE J-MAG) and in-flight alignment calibration

*Ayako Matsuoka[1], Michele Karen Dougherty[2], Patrick Brown[2], Futoshi Takahashi[3], Hisayoshi Shimizu[4], Masaki Matsushima[5]

1. Research Division for Space Plasma, Institute of Space and Astronautical Science, Japan Aerospace Exploration Agency, 2. Imperial College London, 3. Kyushu University, 4. University of Tokyo, 5. Tokyo Institute of Technology

The magnetometer instrument (J-MAG) is one of the core instruments on the JUICE spacecraft and is critical for resolving prime science objectives of the mission. The importance of a magnetometer instrument on JUICE can be described under following themes. Firstly, the magnetic field drives the plasma processes occurring within the Jupiter system. Understanding such observations allows for a better understanding of dynamical plasma processes, of the generation of aurora and of the various current systems which arise within this rapidly rotating magnetosphere. Secondary, the magnetometer science which is unique to JUICE lies in being able to gain an understanding of the interior structure of the icy moons of Jupiter, specifically those of Ganymede, Callisto and Europa. Of particular interest are knowledge of the depth at which the liquid oceans reside beneath their icy surfaces, the strength of any internal magnetic fields such as at Ganymede and the strength of any induced magnetic fields arising within these oceans.

J-MAG science requirements result in a requirement on the spacecraft to determine accurate knowledge of the orientation of the fluxgate sensors (MAGIBS and MAGOB). Due to the long MAG boom it is not possible to meet J-MAG’ s alignment requirement by mechanical stability alone, therefore the spacecraft includes two orthogonal coils mounted around its body. The coils can be driven with a current which produces a measurable magnetic field vector at the fluxgate sensors. This signal can then be used by the fluxgates to track the variation in the sensor alignment. This technical note describes the results of an analysis using an alignment recovery technique that was developed for the Kaguya mission, applied to the specific case of JUICE, considering the relative positions of the fluxgate sensors with respect to the JACS coils.

We derived equations to calculate the directions of the measurement axes in the frame fixed to the spacecraft, namely alignment angles, from the measurement results of reference magnetic fields generated by JACS. The errors of the alignment angle estimation and their dependence on measurement noise as well as inaccuracy of the coil current intensity are examined. Based on the quantitative results, the requirements to the JACS design and operation to satisfy the requests to the alignment accuracy are determined.

Keywords: Jupiter, Jovian moons, magnetometer

©2019. Japan Geoscience Union. All Right Reserved.

Science targets of the GAnymede Laser Altimeter (GALA) for the JUICE mission

*Jun Kimura[1], Shunichi Kamata[2], Koji Matsumoto[3], Noriyuki Namiki[3], Keigo Enya[4], Masanori Kobayashi[5], Hiroshi Araki[3], Hirotomo Noda[3], Ko Ishibashi[5], Hauke Hussmann[6], Kay Lingenauber[6]

1. Osaka University, 2. Hokkaido University, 3. National Astronomical Observatory Japan, 4. ISAS/JAXA, 5. Chiba Institute of Technology, 6. German Aerospace Center (DLR), Berlin

The JUpiter Icy Moons Explorer (JUICE), led by European Space Agency, has started development toward launch in 2022 (arrival at Jupiter in 2029, and Ganymede orbit insertion in 2032), and we are now developing the GALA instrument onboard JUICE spacecraft collaborating with German Aerospace Center (DLR) and other institutions in Europe. GALA will acquire the key information for understanding the evolution of Jovian icy moons and to play an essential role in the JUICE's purpose: exploration of deep habitat.

Jovian icy moon Ganymede, which is the largest moon in the Solar System and the primary target of the JUICE, can be said to be one of the typical solid bodies along with terrestrial planets in terms of its size and the intrinsic magnetic field originated from the metallic core. However, current knowledge provided by previous explorations is extremely limited since it comes from only several fly-bys. The JUICE will unveil the whole picture of Ganymede by the first orbiting in the history around extra-terrestrial moon. Expected new big picture of the origin and evolution of Ganymede will not only be a key to unveil the origin of diversity among the Solar System bodies, but also contribute to an understanding of exoplanets with a wide diversity.

The GALA will measure a distance between the spacecraft and the surface of icy moons and acquire the topography data (globally for Ganymede, and fly-by region for Europa and Callisto). It will be a first-ever laser altimetry for the icy object. Such information makes surface geologies clear and tremendously improves our understanding of the icy tectonics. By comparing their tectonic styles on the rocky planets/moons, GALA data leads to reconsider the Earth's plate tectonics. In addition, the GALA will confirm a presence/absence of the subsurface ocean by measuring tidal and rotational response, and the gravitational information reflecting the interior structure will be greatly improved. Furthermore, strength and waveform of reflected laser pulse have an information about surface reflectance at the laser wavelength and small-scale roughness. Finally we can see degrees of erosion and space weathering without being affected by illumination condition through GALA measurements.

In order to interpret and understand such measurements, accumulated studies for the Earth over the years will be effectively utilized: e.g., the data for surface topography, roughness and albedo will lead to describe the icy tectonics through the knowledge from terrestrial glaciology and experiments on impact and deformation process. The tidal measurements by GALA will also be a window to see its interior based on our knowledge and experiences cultivated through the past geodetic observations, e.g., the SELENE mission for the terrestrial Moon.

Characterization of the icy moons will be achieved not only from the GALA measurements but also synergy of other scientific instruments onboard JUICE spacecraft, for examples, surface images taken by optical camera (JANUS) will confirm the position of GALA laser footprint to complement the GALA "point" data for precise topographic mapping. A radar sounder (RIME) and a radio science experiment (3GM) probe

©2019. Japan Geoscience Union. All Right Reserved.

the interior structure, especially interior of the icy crust to figure out an occurrence of tectonic features. A visible and infrared imaging spectrometer (MAJIS), an ultraviolet imaging spectrograph (UVS) and a sub-millimeter wave instrument (SWI) will acquire a surface and atmosphere compositional data. A magnetometer (J-MAG) monitors moons' inductive response to the Jovian magnetic field and probes the subsurface ocean with the help of a particle environment package (PEP) and a radio and plasma wave investigation (RPWI). The GALA works closely together with these instruments and plays a leading and a supporting role to clarify the whole picture of Ganymede and other icy moons.

Keywords: Jupiter, Icy moons, Laser altimetry

©2019. Japan Geoscience Union. All Right Reserved.

Current status of the antenna developments, the data processing, scientific target for JUICE/SWI JAPAN.

*YASUKO KASAI[1], [Group] JUICE SWI Japanese Team

1. National Institute of Information and Communications Technology (NICT)

The Submillimetre-Wave Instrument (SWI) is one of the 10 scientific payloads on the JUpiter ICy moon Explorer (JUICE). The main scientific objectives of SWI is to investigate the structure, compositions and dynamics of the middle atmosphere of Jupiter and exosphere of its moons, as well as thermophysical properties if the satellite surfaces. SWI observations will provide pioneering direct measurements of atmospheric compositions in Jupiter system. SWI will performed limb and nadir observations in the frequency region 530-600 and 1075-1275 GHz. Japanese contribution is the development of main- and sub- reflectors, actuators for the instruments, feasibility studies, data processing, and scientific contributions. We present Current status of the antenna developments, the data processing, scientific target for JUICE/SWI JAPAN.

Keywords: Jupiter, Jovian moons, submm instrument, JUICE, SWI

©2019. Japan Geoscience Union. All Right Reserved.

[E] Poster | P (Space and Planetary Sciences)：P-EM Solar-Terrestrial Sciences, Space Electromagnetism & Space Environment

Tue. May 28, 2019 3:30 PM - 5:00 PM JST | Tue. May 28, 2019 6:30 AM - 8:00 AM UTC | Poster Hall International Exhibition Hall8, Makuhari Messe_3

[P-EM12] Space Weather and Space Climate

convener:Ryuho Kataoka(National Institute of Polar Research), Antti A Pulkkinen(NASA Goddard Space Flight Center), Kanya Kusano(Institute for Space-Earth Environmental Research, Nagoya University), Kaori Sakaguchi(National Institute of Information and Communications Technology)

We share the latest scientific papers to understand how the solar-terrestrial environment changes in various time scales, and to discuss how we will react via international and interdisciplinary collaborations. More specifically, welcomed papers include space climate studies to reconstruct long-term variations from radio isotopes; cutting-edge observational and modeling studies of the ionosphere, geospace, heliosphere and the sun; simulation and statistical studies to predict the future space weather and space climate; applied science such as operational space weather forecast and mitigation of the social impact due to extreme space hazards.

[PEM12-P01] Reconnection signatures in solar magnetograms during the solar storms of 4-10 September 2017

*Robert Dean Loper[1,2] (1.Air Force Institute of Technology, Department of Engineering Physics, 2.National Center for Atmospheric Research, High Altitude Observatory)

[PEM12-P02] Statistical Relation between Solar Flares and Coronal Mass Ejections with Respect to Sigmoidal Structures in Active Regions

*Yusuke Kawabata[1,2], Yusuke Iida[3], Takafumi Doi, Sachiko Akiyama[4], Seiji Yashiro[4], Toshifumi Shimizu[2] (1.Earth and Planetary Science, The University of Tokyo, 2.Institute of Space and Astronautical Science, JAXA, 3.Kwansei Gakuin University, 4.The Catholic University of America)

[PEM12-P03] Multi-wavelength Observations of Pre-flare Quasi-periodic Pulsation in the C2.2 Flare on 2012 October 15

*Yung-Chi Yang[1], Ya-Hui Yang[1], Baolin Tan[2], Chengming Tan[2], Y.H. Yan[2] (1.Graduate Institute of Space Science National Central University, 2.Key Laboratory of Solar Activities, National Astronomical Observatories)

[PEM12-P04] Investigation of pre-flare type III solar radio bursts and their potential solar origins

*Shao-Fu Hsieh[1], Ya-Hui Yang[1], Baolin Tan[2], Chengming Tan[2], Y.H. Yan[2] (1.Graduate Institute of Space Science National Central University, 2.Key Laboratory of Solar Activities, National Astronomical Observatories, Chinese Academy of Sciences)

[PEM12-P05] Statistical and observational research of solar flare for constructing total emission spectra prediction model

*Shohei Nishimoto[1], kyoko Watanabe[1], Shinsuke Imada[2], Tomoko Kawate[3], Kyoung-Sun Lee[4] (1.National Defense Academy, 2.Institute for Space-Earth Environmental Research, Nagoya University, 3.Institute Of Space And Astronautical Science, Japan Aerospace Exploration Agency, 4.National Astronomical Observatory of Japan)

[PEM12-P06] Modeling of solar active regions using local linear force-free fields to estimate magnetic twist

*Kento Nakatani[1], Kanya Kusano[1], Sung-Hong Park[1], Leka KD[2] (1.Institute for space-Earth Environmental Research, Nagoya University, 2.North West Reserch Associates)

[PEM12-P07] Magnetohydrodynamic Simulation of an Erupting Magnetic Flux Rope on February 13 2009: Journey to Coronal Mass Ejection

*Satoshi Inoue[1], Antonia Savcheva[2] (1.Institute for Space-Earth Environmental Research, Nagoya University, 2.Harvard-Smithsonian Center for Astrophysics)

[PEM12-P08] Investigation of flow structures in the solar interior through the surface magnetic elements' tracking

*Yusuke Iida[1] (1.Kwansei Gakuin University)

[PEM12-P09] High-precision measurement of carbon-14 in tree rings around the onset of the Maunder Minimum

*Hiroko Miyahara[1], Fuyuki Tokanai[2], Toru Moriya[2], Hideyuki Hotta[3] (1.Musashino Art University, 2.Yamagata University, 3.Chiba University)

[PEM12-P10] Examination of ^{10}Be in travertine sediment as a possible tool to reconstruct past solar activity

*Hongyang Xu[1,2], Hiroko Miyahara[2], Kazuho Horiuchi[3], Hiroyuki Matsuzaki[4], Hailong Sun[5], Weijun Luo[5], Xiangmin Zheng[1], Yusuke Suganuma[6,7], Shijie Wang[5], Limin Zhou[1] (1.East China Normal University, 2.Musashino Art University, 3.Hirosaki University, 4.University of Tokyo, 5.Chinese Academy of Sciences, 6.National Institute of Polar Research, 7.The Graduate University for Advanced Studies (SOKENDAI))

[PEM12-P11] Examination of ^{10}Be in travertine sediment as a possible tool to reconstruct past solar activity II

*Hongyang Xu[1,2], Hiroko Miyahara[2], Kazuho Horiuchi[3], Hiroyuki Matsuzaki[4], Hailong Sun[5], Weijun Luo[5], Xiangmin Zheng[1], Yusuke Suganuma[6,7], Shijie Wang[5], Limin Zhou[1] (1.East China Normal University, 2.Musashino Art University, 3.Hirosaki University, 4.University of Tokyo, 5.Chinese Academy of Sciences, 6.National Institute of Polar Research, 7.The Graduate University for Advanced Studies (SOKENDAI))

[PEM12-P12] 1 year of CR observation at Syowa Station in the Antarctic.

*Chihiro Kato[1], Kazuoki Munakata[1], Akira Kadokura[2], Ryuho Kataoka[2], Paul Evenson[3] (1.Shinshu University, 2.National Institute of Polar Research, 3.University of Delaware)

[PEM12-P13] Space weather forecast archives at NICT: handwritten solar activity charts

*Kaori Sakaguchi[1], Daikou Shiota[1], Kaori Fukunaga[1], Katsuhide Marubashi[1], Hiromitsu Ishibashi[1], Yuki Kubo[1], Mamoru Ishii[1] (1.National Institute of Information and Communications Technology)

[PEM12-P14] IMF dependence on solar wind parameters

*Tohru Araki, Yuki Harada[1] (1.Kyoto University)

[PEM12-P15] **Dipole Tilt Effect of Geomagnetic Activity from Low- to High-latitudes**

*Nowada Motoharu[1] (1.Shandong University at Weihai)

[PEM12-P16] A New Prediction Model for Solar Wind-Triggered Magnetospheric Disturbances Based on Potential Learning (Neural Network)

*Ryozo Kitajima[1], Motoharu Nowada[2], Ryotaro Kamimura[3] (1.Seikei University, 2.Shandong University at Weihai, 3.Tokai University)

[PEM12-P17] Real-time magnetosphere simulator for space weather using REProduce Plasma Universe code

*Yasubumi Kubota[1], Aoi Nakamizo[1], Kaori Sakaguchi[1], Mitsue Den[1], Yuki Kubo[1], Tsutomu Nagatsuma[1], Takashi Tanaka[1,2] (1.National Institute of Information and Communications Technology, 2.Kyushu University)

[PEM12-P18] **Simulation of GIC flowing through the power transmission network (187 kV-500 kV) in Japan**

*Nishida Yuichiro[1,6], Yusuke Ebihara[1], Satoko Nakamura[1], Shinichi Watari[2], Kumiko Hashimoto[3], Kentaro Kitamura[4], Takashi Kikuchi[5] (1.Kyoto University Reserch Institute for Sustainable Humanosphere, 2.National Institute of Information and Communications Technology, 3.Kibi International University, 4.National Insutitute of Technology, Tokuyama College, 5.Nagoya University, 6.Kyoto University Department of Electrical Engineering)

[PEM12-P19] Climatological features of the upper atmosphere reproduced by a revised version of a whole atmosphere-ionosphere coupled model GAIA

*Hidekatsu Jin[1], Yasunobu Miyoshi[2], Chihiro Tao[1], Hiroyuki Shinagawa[1], Hitoshi Fujiwara[3] (1.National Institude of Information and Communications Technology, 2.Kyushu University, 3.Seikei University)

[PEM12-P20] Investigation of the thermospheric mass density variations below 200 km

*Hitoshi Fujiwara[1], Yasunobu Miyoshi[2], Masayoshi Utashima[1], Huixin Liu[2] (1.Faculty of Science and Technology, Seikei University, 2.Department of Earth and Planetary Sciences, Faculty of Sciences, Kyushu University)

[PEM12-P21] Low-latitude HF Doppler observations of magnetospheric electric fields during space weather disturbances

*Kumiko K. Hashimoto[1], Takashi Kikuchi[2], Ichiro Tomizawa[3], Keisuke Hosokawa[3], Jaroslav Chum[4] (1.Kibi International University, 2.Nagoya University, 3.University of Electro-Commnunications, 4.Institute of Atmospheric Physics, Prague)

[PEM12-P22] Stratospheric ionization during magnetic storms

*Ryuho Kataoka[1] (1.National Institute of Polar Research)

[PEM12-P23] Calculating propagation time of HF radio wave using ray-tracing method and simple comparison with the observation.

*Ryo Nakao[1], Hiroyuki Nakata[1], Hiroyo Ohya[1], Toshiaki Takano[1], Kornyanat Hozumi[2], Takuya Tsugawa[2], Susumu Saito[3], Mamoru Ishii[2] (1.Graduate School of Engineering, Chiba University, 2.National Institute of imformation and Communications Technology, 3.Electronic Navigation Research Institute)

[PEM12-P24] Why do some probabilistic forecasts lack reliability?

*Yuki Kubo[1] (1.National Institute of Information and Communications Technology)

[PEM12-P25] An estimation method of GEO spacecraft surface charging for a real-time spacecraft risk assessment

*Masao Nakamura[1], Ryota Kawachi[1], Go Takahashi[1], Tsutomu Nagatsuma[2], Mamoru Ishii[2] (1.Osaka Prefecture University, 2.NICT)

[PEM12-P26] A network of HF Doppler sounding systems in Japan

*Keisuke Hosokawa[1], Hiroyuki Nakata[2], Kumiko K. Hashimoto[3], Ichiro Tomizawa[1], Jun Sakai[1], Takashi Kikuchi[4] (1.University of Electro-Communications, 2.Chiba University, 3.Kibi International University, 4.ISEE, Nagoya University)

Reconnection signatures in solar magnetograms during the solar storms of 4-10 September 2017

*Robert Dean Loper[1,2]

1. Air Force Institute of Technology, Department of Engineering Physics, 2. National Center for Atmospheric Research, High Altitude Observatory

Solar flare forecasting is limited to active region classification and historical correlation, due largely to our lack of understanding of magnetic reconnection as a driving mechanism for solar flares and coronal mass ejections. Photospheric observations indicate magnetic field changes during solar flares, brought about during magnetic reconnection and related to magnetic field helicity on the solar surface. While the neutral point of the reconnection event associated with a flare usually occurs in the solar corona, some signs of the magnetic field changes should manifest as low as the photosphere. This study utilizes data from SDO HMI and Space-Weather HMI Active Regions Patches (SHARPS) to analyze full vector field component data in the photospheric magnetic field during several magnetic reconnection events during the space weather events of 4-10 September 2017.

Keywords: solar atmosphere, sunspots, magnetogram, solar flares

©2019. Japan Geoscience Union. All Right Reserved.

Statistical Relation between Solar Flares and Coronal Mass Ejections with Respect to Sigmoidal Structures in Active Regions

*Yusuke Kawabata[1,2], Yusuke Iida[3], Takafumi Doi, Sachiko Akiyama[4], Seiji Yashiro[4], Toshifumi Shimizu[2]

1. Earth and Planetary Science, The University of Tokyo, 2. Institute of Space and Astronautical Science, JAXA, 3. Kwansei Gakuin University, 4. The Catholic University of America

We will report statistical dependences among features of coronal mass ejections (CMEs), solar flares, and sigmoidal structures in soft-X-ray images (Kawabata et al. 2018). We applied analysis methods to all the features in the same way in order to investigate the reproducibility of the correlations among them, which may be found from previous statistical studies. Samples of 211 M-class and X-class flares, observed between 2006 and 2015 by the Hinode/X-ray telescope, Solar and Heliospheric Observatory/Large Angle and Spectrometric Coronagraph, and Geostationary Operational Environmental Satellite, were examined statistically. Five kinds of analysis were performed: Occurrence rate analysis, linear-correlation analysis, association analysis, the Kolmogorov–Smirnov test, and the Anderson–Darling test. These give three main results. First, the sigmoidal structure and long-duration events (LDEs) have a stronger dependence on CME occurrence than large X-ray-class events in on-disk events. Second, for the limb events, a significant dependence exists between LDEs and CME occurrence, and between X-ray-class events and CME occurrence. Third, 32.4% of on-disk flare events have sigmoidal structure and are not accompanied by CMEs. However, the occurrence probability of CMEs without sigmoidal structure is very small, 8.8%, in on-disk events. While the first and second results are consistent with previous studies, we provide for the first time a difference between the on-disk and limb events. The third result, that non-sigmoidal regions produce fewer eruptive events, is also different from previous results. We suggest that sigmoidal structures in soft X-ray images will be a helpful feature for CME prediction in on-disk flare events.

Keywords: Sun, Solar flares, Coronal mass ejections, Sigmoid

©2019. Japan Geoscience Union. All Right Reserved.

Multi-wavelength Observations of Pre-flare Quasi-periodic Pulsation in the C2.2 Flare on 2012 October 15

*Yung-Chi Yang[1], Ya-Hui Yang[1], Baolin Tan[2], Chengming Tan[2], Y.H. Yan[2]

1. Graduate Institute of Space Science National Central University, 2. Key Laboratory of Solar Activities, National Astronomical Observatories

Quasi-periodic pulsation (QPP) is thought to be the nature of solar flares, which can be observed during and before flares in various wavelengths, such as the radio, microwave, SXR, and EUV. In this study, we analyze a pre-flare QPP event on 2012 October 15 and its association with the following C2.2 flare based on the radio data in the ranges of 2.81-2.85 GHz and 2.91-2.95 GHz from Solar Broadband Radio Spectrometer (SBRS), EUV images from AIA multi-wavelength observations, and wavelet analysis. Our result show that the main period of the radio QPP is ~800 s which is similar to the period of ~13.5 min obtained in SXR by Tan et al. (2016). Moreover, we analyze several localized areas in the flare-eruptive AR 11593 to search for the possible regions responsible for the occurrence of pre-flare QPP. We find that the footpoints of brightening loops in 211 Åshow the quasi-periodic behavior of ~850 s. It is thus suggested that the pre-flare QPP with a period of 13-15 min can be manifested in both of the thermal (SXR, EUV) and nonthermal (radio) radiation processes. The relationship between the pre-flare QPP and the subsequent C2.2 flare will also be discussed.

Keywords: sun, solar flares, solar oscillation

©2019. Japan Geoscience Union. All Right Reserved.

Investigation of pre-flare type III solar radio bursts and their potential solar origins

*Shao-Fu Hsieh[1], Ya-Hui Yang[1], Baolin Tan[2], Chengming Tan[2], Y.H. Yan[2]

1. Graduate Institute of Space Science National Central University, 2. Key Laboratory of Solar Activities, National Astronomical Observatories, Chinese Academy of Sciences

Type III solar radio bursts are characterized as the fast-drifting radio emissions in a dynamic spectrogram, which is believed to be produced by the propagating electron beams and often accompanied with the solar flares or magnetic reconnection. Studying the type III radio bursts in high-frequency range before flares would be important for understanding the trigger of energy release although it is rarely reported previously. Here we present two pre-flare type III burst events found in the range of 2.6-3.8 GHz at Solar Broadband Radio Spectrometer (SBRS). By comparing with the SDO/AIA multi-wavelength observations in flare active regions, the pre-flare type III radio bursts have good temporal correlations with the increases of EUV emissions. Furthermore, we find that one event is related to the EUV brightening with 1-min delay, implying the existence of plasma heating before energy release. The other event has a simultaneous EUV jet with a speed of ~700 km/s indicating the occurrence of magnetic reconnection. We suppose both pre-flare events are associated with small-scale energy release via magnetic reconnection.

Keywords: sun, solar flares, solar radio bursts

©2019. Japan Geoscience Union. All Right Reserved.

Statistical and observational research of solar flare for constructing total emission spectra prediction model

*Shohei Nishimoto[1], kyoko Watanabe[1], Shinsuke Imada[2], Tomoko Kawate[3], Kyoung-Sun Lee[4]

1. National Defense Academy, 2. Institute for Space-Earth Environmental Research, Nagoya University, 3. Institute Of Space And Astronautical Science, Japan Aerospace Exploration Agency, 4. National Astronomical Observatory of Japan

Impulsive energy release phenomena such as solar flares, sometimes affect to the solar-terrestrial environment. Usually, we use soft X-ray flux (GOES class) as the index of flare scale. However, the magnitude of effect to the solar-terrestrial environment is not proportional to this scale. Therefore, it is considered that the GOES class is not optimal parameter for predicting the Sudden Ionospheric Disturbance (SID). To identify the relationship between solar flare phenomena and influence to the solar-terrestrial environment, we need to understand the full spectra of solar flares in detail.
There is the solar flare irradiance model named the Flare Irradiance Spectral Model (FISM) (Chamberlin et al., 2006, 2007, 2008). FISM is the most used model, and can estimate solar flare spectra with high wavelength and temporal resolution. However, this model can not express the time evolution of emitted plasma during the solar flare, and has low accuracy on short wavelength that might strongly affect to the total flare spectra. Therefore, individual SID phenomenon can not be reproduced.
In this work, in order to solve the problems of FISM, we performed statistical analysis on observational data during the solar flares. From This study, we tried to find the parameters that control the solar flare emission spectra. We selected solar flare events larger than M-class from the Hinode flare catalogue (Watanabe et al., 2012). First, we focused on the EUV emission observed by the SDO/EVE. We examined the intensities and time evolutions of five EUV lines (Fe XX, Fe XVIII, Fe XVI, Fe VIII, and He II) for 54 flare events. As a result, we found positive correlation between the “GOES class” and the “EUV peak flux” for all Fe lines. Moreover, we found that hotter lines peaked earlier than cooler lines. On the other hand, He II line data have poor correlation with GOES X-ray data. Furthermore, we considered that the geometrical features of solar flares effect to those time evolutions. We measured flare ribbon length for 33 flare events observed by SDO/AIA, and found positive correlation between the “flare duration” and the “ribbon length”. From the statistical research of these observational data, we found that the time evolution of EUV emission can be explained by the X-ray emission.
Then, we tried to identify parameters that determine the solar flare spectra by comparing the flare emissions derived from physical based numerical model of solar flare with the actual observational data. Consequently, we used numerical simulation same as Imada et al.(2015). This numerical model can reproduce the movement and ionization of the plasma in the flare loop.
In this presentation, we will show some results of numerical simulation, and discuss the parameters for total solar flare emission spectra by comparing of simulation results, observational data and FISM.

Keywords: Space Weather, Solar Flare

©2019. Japan Geoscience Union. All Right Reserved.

Modeling of solar active regions using local linear force-free fields to estimate magnetic twist

*Kento Nakatani[1], Kanya Kusano[1], Sung-Hong Park[1], Leka KD[2]

1. Institute for space-Earth Environmental Research, Nagoya University, 2. North West Reserch Associates

The prediction of solar flares is an important issue for space weather forecasting. Although solar flares are believed to be caused by the magnetohydrodynamic (MHD) instability in solar active regions, the method for accurately evaluating the stability of solar magnetic field is not yet established. Recently, Ishiguro & Kusano (2017) proposed that a new instability called the Double Arc Instability (DAI) plays a role of initial driver of solar flares and the critical parameter for this instability can be used to evaluate the stability of active regions. The parameter can be derived by the integration of the magnetic twist as the function of magnetic flux. One way for it is given by the nonlinear force-free field (NLFFF) extrapolation using the photospheric vector magnetic field data. However, the NLFFF extrapolation demands heavy computation and it sometimes cannot well work as a model of solar coronal magnetic field because the force-free condition is limited on the photosphere. Therefore, in order to improve the efficiency and applicability of the flare prediction using , it may be required to develop a method to approximately but much quickly capture the overall features of magnetic field in solar active regions, especially in the flare triggering region. From this point of view, we try to develop a method to extract the characteristic feature of magnetic field in solar active regions using the linear force-free field (LFFF) model. For this objective, we compare the several methods to accurately capture the structure of using LFFF. In this study, we report the result of the analysis for the solar active region NOAA 11429.

Keywords: Space weather, solar , twist, force-free, photosphere, active region

©2019. Japan Geoscience Union. All Right Reserved.

Magnetohydrodynamic Simulation of an Erupting Magnetic Flux Rope on February 13 2009: Journey to Coronal Mass Ejection

*Satoshi Inoue[1], Antonia Savcheva[2]

1. Institute for Space-Earth Environmental Research, Nagoya University, 2. Harvard-Smithsonian Center for Astrophysics

We performed a magnetohydrodynamic (MHD) simulation of a solar eruption launched from solar active region 11012 on February 13, 2009. We in particular concentrated on the evolution of the magnetic flux rope (MFR) leading a coronal mass ejection. We first extrapolated the pre-eruptive magnetic flux ropes using a flux insertion method, in which the MFRs can be extrapolated from the normal component of the magnetic field (Bz) observed by SOHO/MDI and Extreme-Ultra Violet (EUV) images observed by the STEREO satellite. The extrapolated magnetic field reproduced the sigmoidal magnetic structure observed in EUV image well. Next we performed the MHD simulation using the extrapolated magnetic field.

The resulting simulation showed the dramatic eruption of the magnetic flux rope under which the current sheet and the post-flare loops are formed. This is well explained by the standard CSHKP flare model. The evolution of the MFR did not show simple dynamics, rather it showed very complicated dynamics through a magnetic reconnection. We found, during the eruption, that the coherent MFR is created through the reconnection of multiple pre-existing MFRs. Magnetic reconnection plays a role in producing the coherent, erupting MFR and supplying further twist into it. Furthermore we found that the footpoints of the erupting MFR moves along or away from the polarity inversion line, as seen in two-ribbon flares. The locations of both the footpoints of the MFR correspond to those of dimming regions observed in EUV images. Since the location and shape of the post-flare loops obtained from the simulation is reproduced in the observations, we can confirm the reliability of our simulation.

Keywords: Solar Flare, Solar Eruption, Magnetohydrodynamics

©2019. Japan Geoscience Union. All Right Reserved.

Investigation of flow structures in the solar interior through the surface magnetic elements' tracking

*Yusuke Iida[1]

1. Kwansei Gakuin University

We investigate the correlation of meridional flow and rotation velocity in the solar interior by tracking huge number of the surface magnetic elements.

As reported in JpGU2017 meeting, we found that the meridional flow velocity from the magnetic elements' tracking depends positively on their flux and size. We discussed that it may come from that the larger magnetic elements are rooted in the deeper solar interior. We further investigate this issue by correlating the meridional flow velocity and rotation velocity.

We use line-of-sight magnetograms obtained by SDO/HMI in July 2016. Time cadence is 45 seconds, in which the travel distance of magnetic element is smaller than 1 pixel. The magnetograms are transposed from the Earth-view coordinate to the Stonyhurst coordinate. We use the data within 75 degree from the disk center. Magnetic field strength is converted with an assumption that magnetic field is vertical to the surface and interpolated with a cubic spline interpolation.

We detected approximately 8,000 elements in each magnetogram and 4.5x108 displacements in our data set. The meridional flow and rotation velocity on magnetic flux are investigated. The rotation velocity shows negative dependence on the flux at the latitude within 45 degree while it shows weekly positive dependence at the latitude higher than 45 degree. This result is consistent with the depth dependence of rotation velocity obtained by previous helioseismology researches.

Keywords: Sun, Bigdata, Turbulence

©2019. Japan Geoscience Union. All Right Reserved.

High-precision measurement of carbon-14 in tree rings around the onset of the Maunder Minimum

*Hiroko Miyahara[1], Fuyuki Tokanai[2], Toru Moriya[2], Hideyuki Hotta[3]

1. Musashino Art University, 2. Yamagata University, 3. Chiba University

It is well known that the Sun indicates long-term variations at time scales of a few hundred years to a few millennia. It sometimes brings the grand minima, at which period the sunspots disappear for more than several decades. The detailed process of such long-lasting disappearance of sunspots, however, remains unclear. We therefore have been trying to reconstruct solar cycles around the onset of grand minima based on high-precision measurement of carbon-14 in tree rings. In this paper, we report on our preliminary result on the measurement of carbon-14 around the onset of the Maunder Minimum.

Keywords: solar cycle, grand minima, cosmogenic nuclide

©2019. Japan Geoscience Union. All Right Reserved.

Examination of ^{10}Be in travertine sediment as a possible tool to reconstruct past solar activity

*Hongyang Xu[1,2], Hiroko Miyahara[2], Kazuho Horiuchi[3], Hiroyuki Matsuzaki[4], Hailong Sun[5], Weijun Luo[5], Xiangmin Zheng[1], Yusuke Suganuma[6,7], Shijie Wang[5], Limin Zhou[1]

1. East China Normal University, 2. Musashino Art University, 3. Hirosaki University, 4. University of Tokyo, 5. Chinese Academy of Sciences, 6. National Institute of Polar Research, 7. The Graduate University for Advanced Studies (SOKENDAI)

In this study, we explore the possibility of using travertine sediment for reconstructing the past solar activity. We obtained an annual ^{10}Be record from travertine deposit from the modern period and compared with the neutron monitor data. We discuss a possible methodology to calibrate the climatological impact on ^{10}Be deposition and to obtain the signal of past solar and cosmic-ray variations.

Keywords: Beryllium-10, cosmogenic nuclide, solar activity, endogenic travertine

©2019. Japan Geoscience Union. All Right Reserved.

Examination of ^{10}Be in travertine sediment as a possible tool to reconstruct past solar activity II

*Hongyang Xu[1,2], Hiroko Miyahara[2], Kazuho Horiuchi[3], Hiroyuki Matsuzaki[4], Hailong Sun[5], Weijun Luo[5], Xiangmin Zheng[1], Yusuke Suganuma[6,7], Shijie Wang[5], Limin Zhou[1]

1. East China Normal University, 2. Musashino Art University, 3. Hirosaki University, 4. University of Tokyo, 5. Chinese Academy of Sciences, 6. National Institute of Polar Research, 7. The Graduate University for Advanced Studies (SOKENDAI)

We have been examining the potential of ^{10}Be in travertine sediment as a tool to reconstruct past solar and cosmic-ray variations. In this paper, we compare the ^{10}Be profile in the travertine layers from the rainy and dry seasons, and discuss the nature of ^{10}Be deposition at the two seasons.

Keywords: Beryllium-10, cosmogenic nuclide, solar activity, endogenic travertine

©2019. Japan Geoscience Union. All Right Reserved.

1 year of CR observation at Syowa Station in the Antarctic.

*Chihiro Kato[1], Kazuoki Munakata[1], Akira Kadokura[2], Ryuho Kataoka[2], Paul Evenson[3]

1. Shinshu University, 2. National Institute of Polar Research, 3. University of Delaware

CR observation has been carried out for 1 year at Syowa Station in the Antarctic. There was no serious unavailability of data during the whole year. It is now concluded that this station can contribute to a space weather study as one of the CR monitoring station of Global Muon Detector Network (GMDN). We report observed data and its stability as GMDN.

Keywords: Cosmic Rays, Space Weather

©2019. Japan Geoscience Union. All Right Reserved.

Space weather forecast archives at NICT: handwritten solar activity charts

*Kaori Sakaguchi[1], Daikou Shiota[1], Kaori Fukunaga[1], Katsuhide Marubashi[1], Hiromitsu Ishibashi[1], Yuki Kubo[1], Mamoru Ishii[1]

1. National Institute of Information and Communications Technology

About 40 years ago from 1978 to 1999, at Hiraiso Branch, Radio Research Laboratory; present Space Environment Laboratory of National Institute for Information and Communication Technology (NICT) in Japan, space environment data had been recorded in "solar activity chart" by hand for the operation of the radio wave warning service. The charts were created based on URSIgram codes, which were developed to facilitate the rapid exchange of information by telex in periods when internet was not available. Based on the exchanged codes, sunspots transitions and solar flare occurrences on the solar surface, these effects on shortwave propagation, geomagnetic disturbance, and cosmic ray flux over Japan were written in the solar activity charts together with comments and sketch by recorders. One chart was created for each Bertel’ s solar rotation number between No. 1974 and No. 2254, corresponding to sunspot cycles 21 and 22. We realized that the data exchange is almost only once a day from each observation point and charts was accumulation of the available data in real-time at that time.It might be quite difficult to decide future forecast from such a limited real-time data set. Currently, we are digitizing the solar activities charts and the data shown there. In this poster, we present examples of solar activity charts and possible real-time data set and time delay, as well as the verifying result of the solar flare / geomagnetism storm forecast at the time.

Keywords: Space Weather Archive, URSIgram

©2019. Japan Geoscience Union. All Right Reserved.

IMF dependence on solar wind parameters

*Tohru Araki, Yuki Harada[1]

1. Kyoto University

We studied IMF dependence upon solar wind parameters using OMNI hourly values.

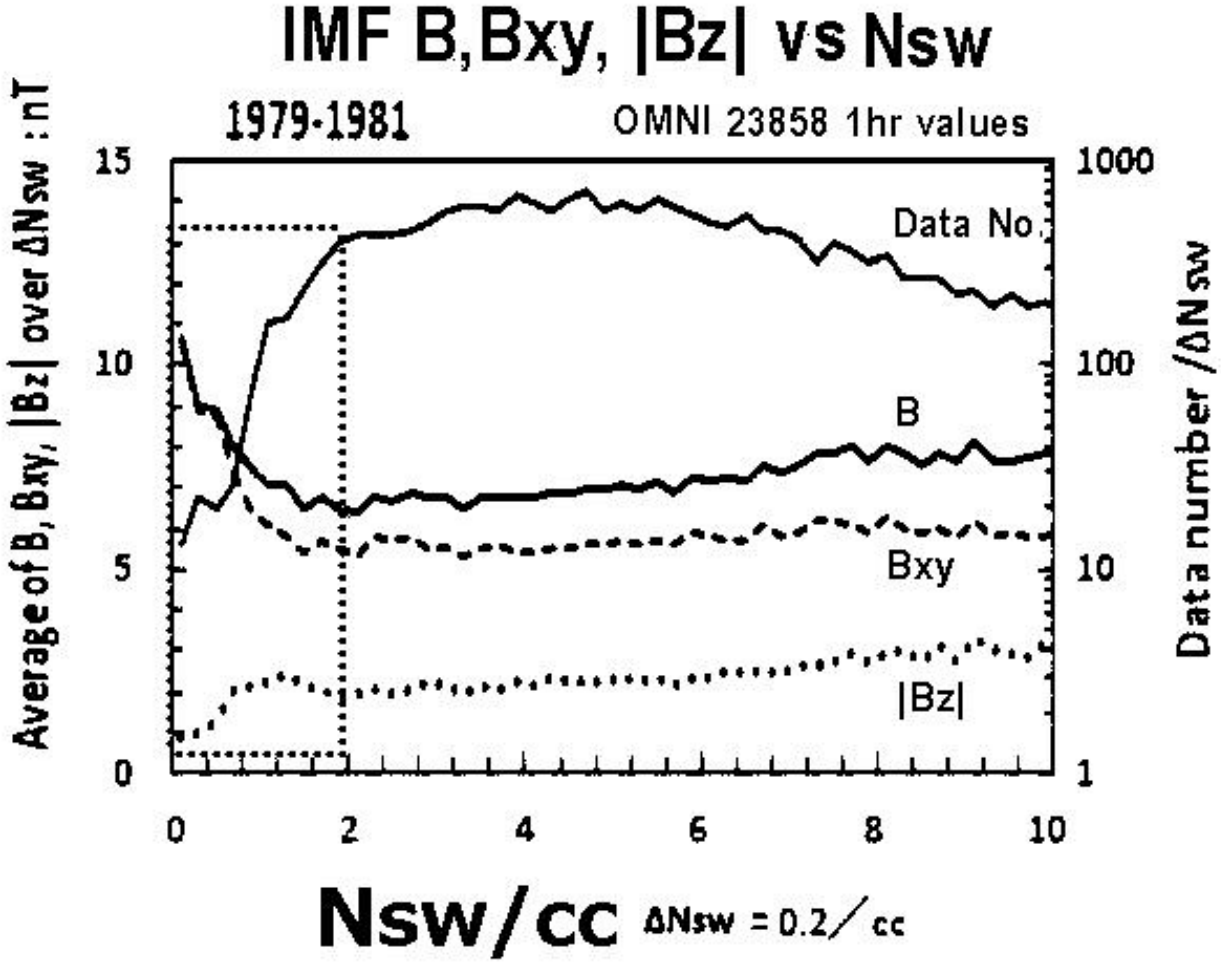
Figure below is a plot of the total force (B), horizontal component (Bxy) in the ecliptic plane and vertical component (Bz) of IMF versus the solar wind density (Nsw). The IMF is averaged over 0.2/cc bin of Nsw. Data number in each bin is also plotted. The data period here is 1979-1981 (maximum SSN phase).

The figure shows (1) that B, Bxy and Bz slowly decrease with decreasing Nsw and (2) that when Nsw approaches further to zero. B and Bxy begin to increase and converges to the same finite value (about 10 nT here) while Bz converges to zero. The property (2) suggests that IMF converges to a typical spiral pattern when solar wind density converges to zero.

Two other data periods, 1999-2001 (SSN maximum) and 2007-2009 (SSN minimum) are examined. IMF observed by MAVEN orbiting Mars is also studied for the period, 2014-2018. The results of the analysis are roughly consistent with the description above. We also checked IMF dependence on solar wind velocity

Keywords: IMF, solar wind density, solar wind melocity

©2019. Japan Geoscience Union. All Right Reserved.



©2019. Japan Geoscience Union. All Right Reserved.

Dipole Tilt Effect of Geomagnetic Activity from Low- to High-latitudes

*Nowada Motoharu[1]

1. Shandong University at Weihai

Geomagnetic activity is dominantly impacted by the orientation of the Interplanetary Magnetic Field (IMF). However, when trying to address why the variations of geomagnetic activity are “semi-annual”, and are greater at equinoxes than at solstices, only IMF control of geomagnetic activity is not enough. This is because these variations are strongly dependent on the Earth’s dipole tilt; the dipole tilt is smaller at the equinoxes than at the solstices. Primitive studies assumed that magnetic reconnection occurs only at the subsolar point of dayside magnetopause. In their studies, the dipole tilt effect was not considered, but only the magnetic field direction between the IMF and the magnetosphere at the subsolar point was discussed in their studies. After them, geomagnetic variations where both dipole tilt effect and IMF direction are taken into account have been investigated. Based on a large database of IMF and AL/AU, we examined the relationship between the IMF clock angle and AL/AU at various dipole tilts. For both positive and negative dipole tilts, geomagnetic activity decrease as the clock angle moves away from 180˚. The AL/AU indices also tend to become smaller for larger dipole tilts. This dipole tilt dependence enhances the semi-annual variation of high-latitude geomagnetic activity.
It also remains unclear how degree energy input rate from solar wind to ring current (dD_{st}^{*}/dt) depends on dipole tilt under various interplanetary magnetic field (IMF) orientation and whether or not ring current development also follows this dipole tilt dependence. We tried to statistically investigate the dependence of dipole tilt and IMF clock angles on low- and middle-latitude geomagnetic activity (D_{st}^{*}), which is a proxy of ring current development, and solar wind energy input rate to ring current (dD_{st}^{*}/dt) over one solar cycle (1978 - 1988). D_{st}^{*} was calculated with the solar wind dynamic pressure and original D_{st} index, and the dipole tilt angle was defined as function of the day of year and universal time. The (dD_{st}^{*}/dt) values were obtained based on the solar wind electric field under the southward IMF conditions. Under positive and negative dipole tilts, the (dD_{st}^{*}/dt) values under low dipole tilt are negatively larger than those in case of high dipole tilt. Further peaks at 180˚ of the IMF clock angle are seen in most of the dipole tilt cases. However, the D_{st}^{*} index shows neither a peak at 180˚ of the IMF clock angle nor particular dipole tilt dependence in case of negative dipole tilt angles. This result suggests that low- and middle latitude geomagnetic activity (ring current development) does not necessarily show dipole tilt dependence and a one-to-one correlation with solar wind energy input rate to ring current (dD_{st}^{*}/dt).

Keywords: Geomagnetic activity (Dst*), Solar wind energy input rate to ring current (dDst*/dt), Semiannual variation , Dipole tilt effect, Interplanetary magnetic field and clock angel, Magnetic reconnection

©2019. Japan Geoscience Union. All Right Reserved.

A New Prediction Model for Solar Wind-Triggered Magnetospheric Disturbances Based on Potential Learning (Neural Network)

*Ryozo Kitajima[1], Motoharu Nowada[2], Ryotaro Kamimura[3]

1. Seikei University, 2. Shandong University at Weihai, 3. Tokai University

Nowadays, it becomes so important in saving our economic activity, and preventing the disasters caused by terrestrial electromagnetic effects to predict a scale and the duration of the geomagnetic disturbances based on in-situ solar wind observations. Recently, one of the notable techniques for the predictions of the magnetospheric disturbances is Neural Network (NN). However, most of these studies are focused on the reproduction of the behaviors of the index values, which represent the geomagnetic disturbances (e.g, D_{st} and AE), by inputting the solar wind parameters measured by the satellites. In our study, we apply a novel neural network model of ‘Potential Learning (PL)’.
Basically, Neural Networks (NNs) are models which imitate the information processing in the nervous system of brain. The nerve is made of cells as referred to as “neurons”, which specializes the information processing. NNs consist of “artificial” neurons, and can process information by learning. Therefore, using NNs, we can obtain some characteristics of the data inputted. The PL is a new kind of the NNs. A feature of the PL is to make a network that can understand the input variables based on learning by “input potentialities”, which are indices as calculated with the variances derived from the input variables. If using this PL, we can specify what input variable(s) is (are) potentially important and influential for a phenomenon.
In this study, introducing the PL technique, we try to specify which solar wind parameter plays an essential role in causing the geomagnetic disturbances. Although the conventional PL, where we used, had automatically selected the variables of interest, we develop a “improved” PL in this study so that the variables can manually be selected. We benchmark this new algorithm using the 4 polar magnetic storm cases occurred under the southward Interplanetary Magnetic Field (IMF)-B_z conditions, and advisedly set the maximum potentiality for the IMF-B_z, so that the IMF-B_z component is the most possible solar wind parameter to cause the geomagnetic disturbances. We note “second” solar wind parameter(s) to possibly cause the magnetospheric disturbances, following the IMF-B_z component. After testing our new technique to actual storm events, we might distinguish the magnetospheric disturbances into two different types, that is, the geomagnetic disturbances driven by “IMF-dominant” and “combination of IMF with solar wind plasma (dynamic pressure)”. The advantages to adopt this new algorithm to space weather, and more detailed results will be discussed in this presentation.

Keywords: Predictions of Geomagnetic Activity, Neural Network Considered Potential Learning, Development of Space Weather

©2019. Japan Geoscience Union. All Right Reserved.

Real-time magnetosphere simulator for space weather using REProduce Plasma Universe code

*Yasubumi Kubota[1], Aoi Nakamizo[1], Kaori Sakaguchi[1], Mitsue Den[1], Yuki Kubo[1], Tsutomu Nagatsuma[1], Takashi Tanaka[1,2]

1. National Institute of Information and Communications Technology, 2. Kyushu University

Surface charging of artificial satellite is one of risks caused by dynamical variations of space environment. It occurs when a satellite exposes high energy electrons around 10 keV created by plasma injection accompanied with substorm. Therefore we want to predict timing and electron energy of plasma injection using magnetosphere-ionosphere coupling global MHD simulation. Now we are developing a real-time numerical simulator for space weather forecast using magnetosphere-ionosphere coupling global MHD simulation called REPPU (REProduce Plasma Universe) code. The feature of the simulation code is highly robust to extreme solar wind parameters because the unstructured grid system has no singular point and is able to calculate in the uniform accuracy over the whole region. We use the real-time solar wind data formatted in the GSM coordinate system observed by DSCOVR spacecraft. Magnetic-dipole axis is fixed to z-direction in our simulation. Therefore daily variation of magnetic-dipole axis is not reproduced. Instead, we convert the input direction of the solar wind velocity and magnetic field into that which tilts including daily variation of magnetic dipole axis in x-z plane. In the method the solar wind structure is not exact. However we can relatively reproduce the magnetosphere response including daily variation of the magnetic-dipole axis against solar wind. The resolution is 7682 grids in the horizontal direction and 240 grids in the radial direction.
In this presentation, we compare the simulation results with the CPCP, AE index, and plasma variations observed by geostationary orbit satellites. Density and temperature of plasma injection derived from MHD simulation tends to estimate larger and smaller values than observation respectively because the MHD simulation does not include kinetic heating effects. We have to interpret MHD simulation results for prediction of electron density and temperature. We will discuss how to interpret electron density and temperature between observation and MHD simulation.

Keywords: global MHD simulation, surface charging

©2019. Japan Geoscience Union. All Right Reserved.

Simulation of GIC flowing through the power transmission network (187 kV-500 kV) in Japan

*Nishida Yuichiro[1,6], Yusuke Ebihara[1], Satoko Nakamura[1], Shinichi Watari[2], Kumiko Hashimoto[3], Kentaro Kitamura[4], Takashi Kikuchi[5]

1. Kyoto University Reserch Institute for Sustainable Humanosphere, 2. National Institute of Information and Communications Technology, 3. Kibi International University, 4. National Insutitute of Technology, Tokuyama College, 5. Nagoya University, 6. Kyoto University Department of Electrical Engineering

The energy released from the sun can enhance electric currents in Earth’ s magnetosphere, which induces an electric field on the ground surface. This electric field, called a geomagnetically induced electric field (GIE), gives rise to geomagnetically induced current (GIC) flowing in a transmission line. Japan is situated at geomagnetically low latitudes, but the potential risk is probably non-zero because a large-amplitude of GIC, as high as 129 A, was recorded in the Japanese power grid during the Halloween storm in October 2003. To evaluate the potential risk of the Japanese power grid properly, we modeled the Japanese power grid with high voltage class over 187 kV on the basis of publicly available data. The model consists of 602 nodes and 763 paths. The uniform GIE imposed on Japan was estimated on the basis of the geoelectric field observed in April 2018 at Kakioka Magnetic Observatory. We applied the uniform GIE on the model. The calculated GIC is roughly in agreement with that measured at 4 substations in Japan. For the westmost substation, a disagreement was found when we considered only the highest class of the power grid (500 kV), which may imply that the lower voltage class of the grid (<500 kV) may have some contribution to the GIC in Japan. We discuss the general tendency of the GIC flowing in the Japanese power grid, and prediction capability of the currently available model.

©2019. Japan Geoscience Union. All Right Reserved.

Simulation of GIC flowing through the power transmission network (187 kV-500 kV) in Japan

Yuichiro Nishida
Yusuke Ebihara
Satoko Nakamura
Shin-Ichi Watari
Kumiko Hashimoto
Kentaro Kitamura
Takashi Kikuchi

Abstract

The energy released from the sun can enhance electric currents in Earth's magnetosphere, which induces an electric field on the ground surface. This electric field, called a geomagnetically induced electric field (GIE), gives rise to geomagnetically induced current (GIC) flowing in a transmission line. Japan is situated at geomagnetically low latitudes, but the potential risk is probably non-zero because a large-amplitude of GIC, as high as 129 A, was recorded in the Japanese power grid during the Halloween storm in October 2003. To evaluate the potential risk of the Japanese power grid properly, we modeled the Japanese power grid with high voltage class over 187 kV on the basis of publicly available data. The model consists of 602 nodes and 763 paths. The uniform GIE imposed on Japan was estimated on the basis of the geoelectric field observed in April 2018 at Kakioka Magnetic Observatory. We applied the uniform GIE on the model. The calculated GIC is roughly in agreement with that measured at 4 substations in Japan. For the westmost substation, a disagreement was found when we considered only the highest class of the power grid (500 kV), which may imply that the lower voltage class of the grid (<500 kV) may have some contribution to the GIC in Japan. We discuss the general tendency of the GIC flowing in the Japanese power grid, and prediction capability of the currently available model.

©2019. Japan Geoscience Union. All Right Reserved.

Climatological features of the upper atmosphere reproduced by a revised version of a whole atmosphere-ionosphere coupled model GAIA

*Hidekatsu Jin[1], Yasunobu Miyoshi[2], Chihiro Tao[1], Hiroyuki Shinagawa[1], Hitoshi Fujiwara[3]

1. National Institude of Information and Communications Technology, 2. Kyushu University, 3. Seikei University

Temporal and spatial variations in the ionospheric electron density and thermospheric mass density could have significant impacts on radio communications between ground and space, and particle and atmospheric drag environments around satellites. Origins of such upper atmospheric variations are not only in the solar atmosphere through the emissions of solar radiation, high-speed plasma gas and high-energy particles, but also in the Earth’ s lower atmosphere, where meteorological phenomena could give rise to atmospheric waves propagating upward. In order to nowcast and forecast the upper atmospheric variations and disturbances, a whole atmospheric model, GAIA, has been developed, which combines a whole atmospheric GCM, an ionospheric model and an electrodynamics model in a self-consistent manner.

So far, for the purpose of its validation, we have compared climatological features of thermosphere and ionosphere reproduced by GAIA with those from ionospheric observation and observation-based empirical models. The comparison indicates that the model and observations are generally in good agreements, but in some condition such as at solar maximum there are significant disagreements in the ionospheric electron density distribution. In order to improve the accuracy of the model, we have made several updates such as ion chemical processes, energetics, parameterization, and so on. We also have introduced magnetospheric effects into the model, such as electrodynamics coupling with magnetosphere and particle precipitation. In this presentation, we discuss how the upper atmospheric model can improve its accuracy and how they can be validated.

Keywords: space weather, whole atmosphere, ionosphere, simulation, thermosphere, assimilation

©2019. Japan Geoscience Union. All Right Reserved.

Investigation of the thermospheric mass density variations below 200 km

*Hitoshi Fujiwara[1], Yasunobu Miyoshi[2], Masayoshi Utashima[1], Huixin Liu[2]

1. Faculty of Science and Technology, Seikei University, 2. Department of Earth and Planetary Sciences, Faculty of Sciences, Kyushu University

Since both the effects from the lower atmosphere and in-situ forcing are significant in the thermospheric region between 100 and 200 km altitude, the thermosphere in the region shows complex variations depending on various conditions. In addition, observations of the thermosphere (neutral atmosphere) between 100 and 200 km are very few compared to the upper thermosphere (above 300 km) and the ionosphere. These make it difficult to improve reliability of empirical and numerical models. Observations from Low Earth Orbit (LOE) satellites would be essential for building up available data sets in the thermospheric region between 100 and 200 km altitude. We will introduce our research project to investigate the thermospheric mass density variations in the 100-200 km altitude region with the LOE satellite, e.g., Tsubame (SLATS), data and a whole atmosphere GCM.

Keywords: thermosphere, mass density, Low Earth Orbit (LOE) satellite, GCM

©2019. Japan Geoscience Union. All Right Reserved.

Low-latitude HF Doppler observations of magnetospheric electric fields during space weather disturbances

*Kumiko K. Hashimoto[1], Takashi Kikuchi[2], Ichiro Tomizawa[3], Keisuke Hosokawa[3], Jaroslav Chum[4]

1. Kibi International University, 2. Nagoya University, 3. University of Electro-Commnunications, 4. Institute of Atmospheric Physics, Prague

Ionospheric electric fields penetrated from the magnetosphere to the low latitude ionosphere have been observed as geomagnetic disturbances caused by ionospheric currents, such as the equatorial electrojet (EEJ) at the dayside equator. The ionospheric currents are too weak to be a detector of the electric field at low latitudes on the dayside and even at the equator on the nightside. The HF Doppler (HFD) sounder is another powerful tool for observations of the electric filed at low latitudes on both the day- and night-sides. We have shown that the electric fields of the geomagnetic sudden commencements (SC) are composed of the preliminary impulse followed by the main impulse, of which directions are opposite to each other and both electric fields are opposite on the day- to night-sides (Kikuchi et al. 2016 JGR). We have also shown that the substorm electric fields are composed of the growth phase followed by expansion phase overshielding electric fields, of which directions are opposite to each other (Hashimoto et al., 2017). In this paper, we show that the HFD sounder is capable of detecting stormtime electric fields and that the electric fields are found to decay rather rapidly over one hour during the main phase with the time scale of a few hours. Combining with the equatorial magnetometer data, we would be able to estimate the decaying rate of the HFD electric fields, which helps obtain the stormtime electric fields quantitatively from the HFD data. We discuss advantages of widely separated HFD sounder operations and cooperations with SuperDARN as well as with magnetometer networks.

Keywords: HF Doppler observation, ionosphere electric field, magnetospheric electric field, geomagnetic storm, equatorial electrojet

©2019. Japan Geoscience Union. All Right Reserved.

Stratospheric ionization during magnetic storms

*Ryuho Kataoka[1]

1. National Institute of Polar Research

Transient mesospheric ionization was detected at an altitude of 65-70 km during the auroral breakup that occurred from 2220 to 2226 UT on June 30, 2017. During this event, the footprint of the Arase satellite was located within the field of view of the all-sky imagers at Syowa Station in the Antarctic. Auroral observations at Syowa Station revealed the dominant precipitation of relatively soft electrons during the auroral breakup. A corresponding spike in cosmic noise absorption was also observed at Syowa Station, while the Arase satellite observed a flux enhancement of >100 keV electrons and a broadband noise without detecting chorus waves or electromagnetic ion cyclotron waves. A general-purpose Monte Carlo particle transport simulation code was used to quantitatively evaluate the ionization in the middle atmosphere. Results of this study indicate that the precipitation of energetic electrons of >100 keV, rather than X-rays from the auroral electrons, played a dominant role in the transient and deep (65-70 km) mesospheric ionization during the observed auroral breakup. Based on the above results of Kataoka et al. (2019), we further discuss a possible role of X-rays to ionize the stratosphere during magnetic storms.

Reference:
Kataoka et al. (2019), Earth, Planets and Space, 71, 9, https://doi.org/10.1186/s40623-019-0989-7

©2019. Japan Geoscience Union. All Right Reserved.

Calculating propagation time of HF radio wave using ray-tracing method and simple comparison with the observation.

*Ryo Nakao[1], Hiroyuki Nakata[1], Hiroyo Ohya[1], Toshiaki Takano[1], Kornyanat Hozumi[2], Takuya Tsugawa[2], Susumu Saito[3], Mamoru Ishii[2]

1. Graduate School of Engineering, Chiba University, 2. National Institute of imformation and Communications Technology, 3. Electronic Navigation Research Institute

To provide the information of nowcast of radio propagation, we have started a project, HF-START (HF simulator Targeting for All user's Regional Telecommunications). In this project, a simulator that is able to predict propagation of HF radio waves is constructed by ray-tracing calculation.
Using this simulator, we have examined whether HF radio wave travels between any two points. In this calculation, the electron density, which is necessary to calculate reflection index is determined by International Reference Ionosphere (IRI).In this project, HF receivers have been installed at Chiba University (Chiba, 35.62N, 140.10E), Sarobetu (Hokkaido, 45.16N, 141.74E), Numata (Gunma, 36.62N, 139.02E), Yamagawa (Kagoshima, 31.20N, 130.61), Ogimi (Okinawa, 26.68, 128.15E) for observing HF radio wave transmitted from radioNIKKEI (Nagara, Chiba, 35.46N, 140.20E) to confirm the results of the ray-tracing calculation. In the ray-tracing calculation, therefore, we set the same locations of the transmitter and receivers as the observatories of HF-START. As a result of simple comparison between the ray-tracing results and the observation, it is found that there was a difference of the propagation time between the ray-tracing results and the observations. It is possible that the radio wave propagation between radioNIKKEI and Ciba University is not ground wave but sky wave that is reflected by ionosphere. As for further calculation, we plan to use the electron density distributions determined by GAIA and GNSS tomography in the ray-tracing calculation.

©2019. Japan Geoscience Union. All Right Reserved.

Why do some probabilistic forecasts lack reliability?

*Yuki Kubo[1]

1. National Institute of Information and Communications Technology

One of the important attributes to be satisfied for the probabilistic forecast system is reliability. However, some probabilistic forecast systems lack reliability. Why do some probabilistic forecasts lack reliability? We investigate a condition for a probabilistic binary forecast to be reliable in this work. We mathematically prove that a necessary, but not sufficient, condition for achieving a reliable probabilistic forecast is maximizing the Peirce skill score (PSS) at the threshold probability of the climatological base rate. The condition is confirmed by using artificially synthesized forecast-outcome pair data and previously published probabilistic solar flare forecast models. The condition gives a partial answer as to why some probabilistic forecast systems lack reliability, because the system, which does not satisfy the proved condition, can never be reliable. The result implies that those who want to develop a reliable probabilistic forecast system must adjust or train the system so as to maximize PSS near the threshold probability of the climatological base rate.

Keywords: Probabilistic forecast, Reliability

©2019. Japan Geoscience Union. All Right Reserved.

An estimation method of GEO spacecraft surface charging for a real-time spacecraft risk assessment

*Masao Nakamura[1], Ryota Kawachi[1], Go Takahashi[1], Tsutomu Nagatsuma[2], Mamoru Ishii[2]

1. Osaka Prefecture University, 2. NICT

Spacecraft anomalies are often induced by electrostatic discharges due to surface charging. Some spacecraft charging simulation software is developed by space agencies and research institutes and used for spacecraft designs and charging analysis. However these simulations cannot be used for a real-time estimation because they need hours or days to calculate the surface potential for a given plasma environment. Therefore we develop a quick estimation method of GEO spacecraft surface charging for the Space Environment Customized Risk Estimation for Spacecraft (SECURES) of the space weather forecast Project for Solar-Terrestrial Environment Prediction (PSTEP). We estimate the surface potentials by interpolation using lookup tables of the pre-simulated surface potentials for combinations of plasma temperatures and densities. We study fitting functions used in the interpolation and how to make the lookup tables for the good estimation. Then we can real-time estimate the surface potentials of the target GEO spacecraft when the on-orbit plasma environment is predicted or observed. The spacecraft risk assessment can be accomplished by additional information about the experimental discharging differential potential of the surface materials.

Keywords: Spacecraft surface charging, Space weather, Spacecraft risk assessment

©2019. Japan Geoscience Union. All Right Reserved.

A network of HF Doppler sounding systems in Japan

*Keisuke Hosokawa[1], Hiroyuki Nakata[2], Kumiko K. Hashimoto[3], Ichiro Tomizawa[1], Jun Sakai[1], Takashi Kikuchi[4]

1. University of Electro-Communications, 2. Chiba University, 3. Kibi International University, 4. ISEE, Nagoya University

Since 2003, a network observation of HF Doppler sounding has been conducted in Japan for remote-sensing the atmospheric, ionospheric and magnetospheric processes. Currently, 1 transmitting station (Tx) and 7 receiving stations (Rx) are operative by a collaborative effort of four difference universities. The main transmitting station is located at Chofu, Tokyo, Japan in the Campus of University of Electro-Communications (JG2XA). JG2XA transmits continuous waves at 5006 kHz and 8006 kHz with a transmitting power of 200 W. By receiving this JG2XA signal at 7 Rx stations (Sugadaira, Oarai, Kure, Kashima, Iitate, Fujisawa and Sugito) we derive the Doppler shift imposed during the propagation and reflection in the ionosphere. In particular, the Doppler shift data can be used to detect vertical motion of the ionospheric F region with a temporal resolution of 10 s. At some stations, we also have observed signals from Radio Nikkei 1 (JOZ at 3925 kHz, JOZ2 at 6055 kHz, and JOZ3 at 9595 kHz) transmitted from Nagara, Chiba, Japan, which allows us to observe the vertical motion of the ionosphere at several altitude levels. The data obtained from this experiment since 2003 are all available at http://gwave.cei.uec.ac.jp/~hfd. Not only quick-look plots but also several types of digital data (raw wave form and Doppler shift data) can be retrieved from this database. The experiment covers various ionospheric phenomena in the Magnetosphere-Ionospheric (M-I) coupling system, such as sporadic E-layer (Es), medium-scale traveling ionospheric disturbances (MSTIDs), large-scale traveling ionospheric disturbances (LSTIDs), global-scale electric field variation, geomagnetic pulsations, and sudden commencement (SC). The data can also be used for the studies of vertical coupling between the lower atmosphere and ionosphere, for example, observations of ionospheric variation after large earthquakes, volcanic eruptions and typhoons. To facilitate analyses of the phenomena listed above, it is desired to observe a wider area in latitude and longitude. For this purpose we plan to extend the network covering the entire ionosphere over Japan in the near future. In the presentation, we will give a brief introduction to the experiments and online database, and then discuss the future direction of the studies of atmosphere, ionosphere and magnetosphere using the HF Doppler sounding in a framework of international collaborations.

Keywords: HF Doppler experiment, Ionosphere

©2019. Japan Geoscience Union. All Right Reserved.

[E] Poster | P (Space and Planetary Sciences)：P-EM Solar-Terrestrial Sciences, Space Electromagnetism & Space Environment

Tue. May 28, 2019 5:15 PM - 6:30 PM JST | Tue. May 28, 2019 8:15 AM - 9:30 AM UTC | Poster Hall International Exhibition Hall8, Makuhari Messe_3

[P-EM12] Space Weather and Space Climate

convener:Ryuho Kataoka(National Institute of Polar Research), Antti A Pulkkinen(NASA Goddard Space Flight Center), Kanya Kusano(Institute for Space-Earth Environmental Research, Nagoya University), Kaori Sakaguchi(National Institute of Information and Communications Technology)

We share the latest scientific papers to understand how the solar-terrestrial environment changes in various time scales, and to discuss how we will react via international and interdisciplinary collaborations. More specifically, welcomed papers include space climate studies to reconstruct long-term variations from radio isotopes; cutting-edge observational and modeling studies of the ionosphere, geospace, heliosphere and the sun; simulation and statistical studies to predict the future space weather and space climate; applied science such as operational space weather forecast and mitigation of the social impact due to extreme space hazards.

[PEM12-P01] Reconnection signatures in solar magnetograms during the solar storms of 4-10 September 2017

*Robert Dean Loper[1,2] (1.Air Force Institute of Technology, Department of Engineering Physics, 2.National Center for Atmospheric Research, High Altitude Observatory)

[PEM12-P02] Statistical Relation between Solar Flares and Coronal Mass Ejections with Respect to Sigmoidal Structures in Active Regions

*Yusuke Kawabata[1,2], Yusuke Iida[3], Takafumi Doi, Sachiko Akiyama[4], Seiji Yashiro[4], Toshifumi Shimizu[2] (1.Earth and Planetary Science, The University of Tokyo, 2.Institute of Space and Astronautical Science, JAXA, 3.Kwansei Gakuin University, 4.The Catholic University of America)

[PEM12-P03] Multi-wavelength Observations of Pre-flare Quasi-periodic Pulsation in the C2.2 Flare on 2012 October 15

*Yung-Chi Yang[1], Ya-Hui Yang[1], Baolin Tan[2], Chengming Tan[2], Y.H. Yan[2] (1.Graduate Institute of Space Science National Central University, 2.Key Laboratory of Solar Activities, National Astronomical Observatories)

[PEM12-P04] Investigation of pre-flare type III solar radio bursts and their potential solar origins

*Shao-Fu Hsieh[1], Ya-Hui Yang[1], Baolin Tan[2], Chengming Tan[2], Y.H. Yan[2] (1.Graduate Institute of Space Science National Central University, 2.Key Laboratory of Solar Activities, National Astronomical Observatories, Chinese Academy of Sciences)

[PEM12-P05] Statistical and observational research of solar flare for constructing total emission spectra prediction model

*Shohei Nishimoto[1], kyoko Watanabe[1], Shinsuke Imada[2], Tomoko Kawate[3], Kyoung-Sun Lee[4] (1.National Defense Academy, 2.Institute for Space-Earth Environmental Research, Nagoya University, 3.Institute Of Space And Astronautical Science, Japan Aerospace Exploration Agency, 4.National Astronomical Observatory of Japan)

[PEM12-P06] Modeling of solar active regions using local linear force-free fields to estimate magnetic twist

*Kento Nakatani[1], Kanya Kusano[1], Sung-Hong Park[1], Leka KD[2] (1.Institute for space-Earth Environmental Research, Nagoya University, 2.North West Reserch Associates)

[PEM12-P07] Magnetohydrodynamic Simulation of an Erupting Magnetic Flux Rope on February 13 2009: Journey to Coronal Mass Ejection

*Satoshi Inoue[1], Antonia Savcheva[2] (1.Institute for Space-Earth Environmental Research, Nagoya University, 2.Harvard-Smithsonian Center for Astrophysics)

[PEM12-P08] Investigation of flow structures in the solar interior through the surface magnetic elements' tracking

*Yusuke Iida[1] (1.Kwansei Gakuin University)

[PEM12-P09] High-precision measurement of carbon-14 in tree rings around the onset of the Maunder Minimum

*Hiroko Miyahara[1], Fuyuki Tokanai[2], Toru Moriya[2], Hideyuki Hotta[3] (1.Musashino Art University, 2.Yamagata University, 3.Chiba University)

[PEM12-P10] Examination of ^{10}Be in travertine sediment as a possible tool to reconstruct past solar activity

*Hongyang Xu[1,2], Hiroko Miyahara[2], Kazuho Horiuchi[3], Hiroyuki Matsuzaki[4], Hailong Sun[5], Weijun Luo[5], Xiangmin Zheng[1], Yusuke Suganuma[6,7], Shijie Wang[5], Limin Zhou[1] (1.East China Normal University, 2.Musashino Art University, 3.Hirosaki University, 4.University of Tokyo, 5.Chinese Academy of Sciences, 6.National Institute of Polar Research, 7.The Graduate University for Advanced Studies (SOKENDAI))

[PEM12-P11] Examination of ^{10}Be in travertine sediment as a possible tool to reconstruct past solar activity II

*Hongyang Xu[1,2], Hiroko Miyahara[2], Kazuho Horiuchi[3], Hiroyuki Matsuzaki[4], Hailong Sun[5], Weijun Luo[5], Xiangmin Zheng[1], Yusuke Suganuma[6,7], Shijie Wang[5], Limin Zhou[1] (1.East China Normal University, 2.Musashino Art University, 3.Hirosaki University, 4.University of Tokyo, 5.Chinese Academy of Sciences, 6.National Institute of Polar Research, 7.The Graduate University for Advanced Studies (SOKENDAI))

[PEM12-P12] 1 year of CR observation at Syowa Station in the Antarctic.

*Chihiro Kato[1], Kazuoki Munakata[1], Akira Kadokura[2], Ryuho Kataoka[2], Paul Evenson[3] (1.Shinshu University, 2.National Institute of Polar Research, 3.University of Delaware)

[PEM12-P13] Space weather forecast archives at NICT: handwritten solar activity charts

*Kaori Sakaguchi[1], Daikou Shiota[1], Kaori Fukunaga[1], Katsuhide Marubashi[1], Hiromitsu Ishibashi[1], Yuki Kubo[1], Mamoru Ishii[1] (1.National Institute of Information and Communications Technology)

[PEM12-P14] IMF dependence on solar wind parameters

*Tohru Araki, Yuki Harada[1] (1.Kyoto University)

[PEM12-P15] **Dipole Tilt Effect of Geomagnetic Activity from Low- to High-latitudes**

*Nowada Motoharu[1] (1.Shandong University at Weihai)

[PEM12-P16] A New Prediction Model for Solar Wind-Triggered Magnetospheric Disturbances Based on Potential Learning (Neural Network)

*Ryozo Kitajima[1], Motoharu Nowada[2], Ryotaro Kamimura[3] (1.Seikei University, 2.Shandong University at Weihai, 3.Tokai University)

[PEM12-P17] Real-time magnetosphere simulator for space weather using REProduce Plasma Universe code

*Yasubumi Kubota[1], Aoi Nakamizo[1], Kaori Sakaguchi[1], Mitsue Den[1], Yuki Kubo[1], Tsutomu Nagatsuma[1], Takashi Tanaka[1,2] (1.National Institute of Information and Communications Technology, 2.Kyushu University)

[PEM12-P18] **Simulation of GIC flowing through the power transmission network (187 kV-500 kV) in Japan**

*Nishida Yuichiro[1,6], Yusuke Ebihara[1], Satoko Nakamura[1], Shinichi Watari[2], Kumiko Hashimoto[3], Kentaro Kitamura[4], Takashi Kikuchi[5] (1.Kyoto University Reserch Institute for Sustainable Humanosphere, 2.National Institute of Information and Communications Technology, 3.Kibi International University, 4.National Insutitute of Technology, Tokuyama College, 5.Nagoya University, 6.Kyoto University Department of Electrical Engineering)

[PEM12-P19] Climatological features of the upper atmosphere reproduced by a revised version of a whole atmosphere-ionosphere coupled model GAIA

*Hidekatsu Jin[1], Yasunobu Miyoshi[2], Chihiro Tao[1], Hiroyuki Shinagawa[1], Hitoshi Fujiwara[3] (1.National Institude of Information and Communications Technology, 2.Kyushu University, 3.Seikei University)

[PEM12-P20] Investigation of the thermospheric mass density variations below 200 km

*Hitoshi Fujiwara[1], Yasunobu Miyoshi[2], Masayoshi Utashima[1], Huixin Liu[2] (1.Faculty of Science and Technology, Seikei University, 2.Department of Earth and Planetary Sciences, Faculty of Sciences, Kyushu University)

[PEM12-P21] Low-latitude HF Doppler observations of magnetospheric electric fields during space weather disturbances

*Kumiko K. Hashimoto[1], Takashi Kikuchi[2], Ichiro Tomizawa[3], Keisuke Hosokawa[3], Jaroslav Chum[4] (1.Kibi International University, 2.Nagoya University, 3.University of Electro-Commnunications, 4.Institute of Atmospheric Physics, Prague)

[PEM12-P22] Stratospheric ionization during magnetic storms

*Ryuho Kataoka[1] (1.National Institute of Polar Research)

[PEM12-P23] Calculating propagation time of HF radio wave using ray-tracing method and simple comparison with the observation.

*Ryo Nakao[1], Hiroyuki Nakata[1], Hiroyo Ohya[1], Toshiaki Takano[1], Kornyanat Hozumi[2], Takuya Tsugawa[2], Susumu Saito[3], Mamoru Ishii[2] (1.Graduate School of Engineering, Chiba University, 2.National Institute of imformation and Communications Technology, 3.Electronic Navigation Research Institute)

[PEM12-P24] Why do some probabilistic forecasts lack reliability?

*Yuki Kubo[1] (1.National Institute of Information and Communications Technology)

[PEM12-P25] An estimation method of GEO spacecraft surface charging for a real-time spacecraft risk assessment

*Masao Nakamura[1], Ryota Kawachi[1], Go Takahashi[1], Tsutomu Nagatsuma[2], Mamoru Ishii[2] (1.Osaka Prefecture University, 2.NICT)

[PEM12-P26] A network of HF Doppler sounding systems in Japan

*Keisuke Hosokawa[1], Hiroyuki Nakata[2], Kumiko K. Hashimoto[3], Ichiro Tomizawa[1], Jun Sakai[1], Takashi Kikuchi[4] (1.University of Electro-Communications, 2.Chiba University, 3.Kibi International University, 4.ISEE, Nagoya University)

Reconnection signatures in solar magnetograms during the solar storms of 4-10 September 2017

*Robert Dean Loper[1,2]

1. Air Force Institute of Technology, Department of Engineering Physics, 2. National Center for Atmospheric Research, High Altitude Observatory

Solar flare forecasting is limited to active region classification and historical correlation, due largely to our lack of understanding of magnetic reconnection as a driving mechanism for solar flares and coronal mass ejections. Photospheric observations indicate magnetic field changes during solar flares, brought about during magnetic reconnection and related to magnetic field helicity on the solar surface. While the neutral point of the reconnection event associated with a flare usually occurs in the solar corona, some signs of the magnetic field changes should manifest as low as the photosphere. This study utilizes data from SDO HMI and Space-Weather HMI Active Regions Patches (SHARPS) to analyze full vector field component data in the photospheric magnetic field during several magnetic reconnection events during the space weather events of 4-10 September 2017.

Keywords: solar atmosphere, sunspots, magnetogram, solar flares

©2019. Japan Geoscience Union. All Right Reserved.

Statistical Relation between Solar Flares and Coronal Mass Ejections with Respect to Sigmoidal Structures in Active Regions

*Yusuke Kawabata[1,2], Yusuke Iida[3], Takafumi Doi, Sachiko Akiyama[4], Seiji Yashiro[4], Toshifumi Shimizu[2]

1. Earth and Planetary Science, The University of Tokyo, 2. Institute of Space and Astronautical Science, JAXA, 3. Kwansei Gakuin University, 4. The Catholic University of America

We will report statistical dependences among features of coronal mass ejections (CMEs), solar flares, and sigmoidal structures in soft-X-ray images (Kawabata et al. 2018). We applied analysis methods to all the features in the same way in order to investigate the reproducibility of the correlations among them, which may be found from previous statistical studies. Samples of 211 M-class and X-class flares, observed between 2006 and 2015 by the Hinode/X-ray telescope, Solar and Heliospheric Observatory/Large Angle and Spectrometric Coronagraph, and Geostationary Operational Environmental Satellite, were examined statistically. Five kinds of analysis were performed: Occurrence rate analysis, linear-correlation analysis, association analysis, the Kolmogorov–Smirnov test, and the Anderson–Darling test. These give three main results. First, the sigmoidal structure and long-duration events (LDEs) have a stronger dependence on CME occurrence than large X-ray-class events in on-disk events. Second, for the limb events, a significant dependence exists between LDEs and CME occurrence, and between X-ray-class events and CME occurrence. Third, 32.4% of on-disk flare events have sigmoidal structure and are not accompanied by CMEs. However, the occurrence probability of CMEs without sigmoidal structure is very small, 8.8%, in on-disk events. While the first and second results are consistent with previous studies, we provide for the first time a difference between the on-disk and limb events. The third result, that non-sigmoidal regions produce fewer eruptive events, is also different from previous results. We suggest that sigmoidal structures in soft X-ray images will be a helpful feature for CME prediction in on-disk flare events.

Keywords: Sun, Solar flares, Coronal mass ejections, Sigmoid

©2019. Japan Geoscience Union. All Right Reserved.

Multi-wavelength Observations of Pre-flare Quasi-periodic Pulsation in the C2.2 Flare on 2012 October 15

*Yung-Chi Yang[1], Ya-Hui Yang[1], Baolin Tan[2], Chengming Tan[2], Y.H. Yan[2]

1. Graduate Institute of Space Science National Central University, 2. Key Laboratory of Solar Activities, National Astronomical Observatories

Quasi-periodic pulsation (QPP) is thought to be the nature of solar flares, which can be observed during and before flares in various wavelengths, such as the radio, microwave, SXR, and EUV. In this study, we analyze a pre-flare QPP event on 2012 October 15 and its association with the following C2.2 flare based on the radio data in the ranges of 2.81-2.85 GHz and 2.91-2.95 GHz from Solar Broadband Radio Spectrometer (SBRS), EUV images from AIA multi-wavelength observations, and wavelet analysis. Our result show that the main period of the radio QPP is ~800 s which is similar to the period of ~13.5 min obtained in SXR by Tan et al. (2016). Moreover, we analyze several localized areas in the flare-eruptive AR 11593 to search for the possible regions responsible for the occurrence of pre-flare QPP. We find that the footpoints of brightening loops in 211 Åshow the quasi-periodic behavior of ~850 s. It is thus suggested that the pre-flare QPP with a period of 13-15 min can be manifested in both of the thermal (SXR, EUV) and nonthermal (radio) radiation processes. The relationship between the pre-flare QPP and the subsequent C2.2 flare will also be discussed.

Keywords: sun, solar flares, solar oscillation

©2019. Japan Geoscience Union. All Right Reserved.

Investigation of pre-flare type III solar radio bursts and their potential solar origins

*Shao-Fu Hsieh[1], Ya-Hui Yang[1], Baolin Tan[2], Chengming Tan[2], Y.H. Yan[2]

1. Graduate Institute of Space Science National Central University, 2. Key Laboratory of Solar Activities, National Astronomical Observatories, Chinese Academy of Sciences

Type III solar radio bursts are characterized as the fast-drifting radio emissions in a dynamic spectrogram, which is believed to be produced by the propagating electron beams and often accompanied with the solar flares or magnetic reconnection. Studying the type III radio bursts in high-frequency range before flares would be important for understanding the trigger of energy release although it is rarely reported previously. Here we present two pre-flare type III burst events found in the range of 2.6-3.8 GHz at Solar Broadband Radio Spectrometer (SBRS). By comparing with the SDO/AIA multi-wavelength observations in flare active regions, the pre-flare type III radio bursts have good temporal correlations with the increases of EUV emissions. Furthermore, we find that one event is related to the EUV brightening with 1-min delay, implying the existence of plasma heating before energy release. The other event has a simultaneous EUV jet with a speed of ~700 km/s indicating the occurrence of magnetic reconnection. We suppose both pre-flare events are associated with small-scale energy release via magnetic reconnection.

Keywords: sun, solar flares, solar radio bursts

©2019. Japan Geoscience Union. All Right Reserved.

Statistical and observational research of solar flare for constructing total emission spectra prediction model

*Shohei Nishimoto[1], kyoko Watanabe[1], Shinsuke Imada[2], Tomoko Kawate[3], Kyoung-Sun Lee[4]

1. National Defense Academy, 2. Institute for Space-Earth Environmental Research, Nagoya University, 3. Institute Of Space And Astronautical Science, Japan Aerospace Exploration Agency, 4. National Astronomical Observatory of Japan

Impulsive energy release phenomena such as solar flares, sometimes affect to the solar-terrestrial environment. Usually, we use soft X-ray flux (GOES class) as the index of flare scale. However, the magnitude of effect to the solar-terrestrial environment is not proportional to this scale. Therefore, it is considered that the GOES class is not optimal parameter for predicting the Sudden Ionospheric Disturbance (SID). To identify the relationship between solar flare phenomena and influence to the solar-terrestrial environment, we need to understand the full spectra of solar flares in detail.
There is the solar flare irradiance model named the Flare Irradiance Spectral Model (FISM) (Chamberlin et al., 2006, 2007, 2008). FISM is the most used model, and can estimate solar flare spectra with high wavelength and temporal resolution. However, this model can not express the time evolution of emitted plasma during the solar flare, and has low accuracy on short wavelength that might strongly affect to the total flare spectra. Therefore, individual SID phenomenon can not be reproduced.
In this work, in order to solve the problems of FISM, we performed statistical analysis on observational data during the solar flares. From This study, we tried to find the parameters that control the solar flare emission spectra. We selected solar flare events larger than M-class from the Hinode flare catalogue (Watanabe et al., 2012). First, we focused on the EUV emission observed by the SDO/EVE. We examined the intensities and time evolutions of five EUV lines (Fe XX, Fe XVIII, Fe XVI, Fe VIII, and He II) for 54 flare events. As a result, we found positive correlation between the “GOES class” and the “EUV peak flux” for all Fe lines. Moreover, we found that hotter lines peaked earlier than cooler lines. On the other hand, He II line data have poor correlation with GOES X-ray data. Furthermore, we considered that the geometrical features of solar flares effect to those time evolutions. We measured flare ribbon length for 33 flare events observed by SDO/AIA, and found positive correlation between the “flare duration” and the “ribbon length”. From the statistical research of these observational data, we found that the time evolution of EUV emission can be explained by the X-ray emission.
Then, we tried to identify parameters that determine the solar flare spectra by comparing the flare emissions derived from physical based numerical model of solar flare with the actual observational data. Consequently, we used numerical simulation same as Imada et al.(2015). This numerical model can reproduce the movement and ionization of the plasma in the flare loop.
In this presentation, we will show some results of numerical simulation, and discuss the parameters for total solar flare emission spectra by comparing of simulation results, observational data and FISM.

Keywords: Space Weather, Solar Flare

©2019. Japan Geoscience Union. All Right Reserved.

Modeling of solar active regions using local linear force-free fields to estimate magnetic twist

*Kento Nakatani[1], Kanya Kusano[1], Sung-Hong Park[1], Leka KD[2]

1. Institute for space-Earth Environmental Research, Nagoya University, 2. North West Reserch Associates

The prediction of solar flares is an important issue for space weather forecasting. Although solar flares are believed to be caused by the magnetohydrodynamic (MHD) instability in solar active regions, the method for accurately evaluating the stability of solar magnetic field is not yet established. Recently, Ishiguro & Kusano (2017) proposed that a new instability called the Double Arc Instability (DAI) plays a role of initial driver of solar flares and the critical parameter for this instability can be used to evaluate the stability of active regions. The parameter can be derived by the integration of the magnetic twist as the function of magnetic flux. One way for it is given by the nonlinear force-free field (NLFFF) extrapolation using the photospheric vector magnetic field data. However, the NLFFF extrapolation demands heavy computation and it sometimes cannot well work as a model of solar coronal magnetic field because the force-free condition is limited on the photosphere. Therefore, in order to improve the efficiency and applicability of the flare prediction using , it may be required to develop a method to approximately but much quickly capture the overall features of magnetic field in solar active regions, especially in the flare triggering region. From this point of view, we try to develop a method to extract the characteristic feature of magnetic field in solar active regions using the linear force-free field (LFFF) model. For this objective, we compare the several methods to accurately capture the structure of using LFFF. In this study, we report the result of the analysis for the solar active region NOAA 11429.

Keywords: Space weather, solar , twist, force-free, photosphere, active region

©2019. Japan Geoscience Union. All Right Reserved.

Magnetohydrodynamic Simulation of an Erupting Magnetic Flux Rope on February 13 2009: Journey to Coronal Mass Ejection

*Satoshi Inoue[1], Antonia Savcheva[2]

1. Institute for Space-Earth Environmental Research, Nagoya University, 2. Harvard-Smithsonian Center for Astrophysics

We performed a magnetohydrodynamic (MHD) simulation of a solar eruption launched from solar active region 11012 on February 13, 2009. We in particular concentrated on the evolution of the magnetic flux rope (MFR) leading a coronal mass ejection. We first extrapolated the pre-eruptive magnetic flux ropes using a flux insertion method, in which the MFRs can be extrapolated from the normal component of the magnetic field (Bz) observed by SOHO/MDI and Extreme-Ultra Violet (EUV) images observed by the STEREO satellite. The extrapolated magnetic field reproduced the sigmoidal magnetic structure observed in EUV image well. Next we performed the MHD simulation using the extrapolated magnetic field.

The resulting simulation showed the dramatic eruption of the magnetic flux rope under which the current sheet and the post-flare loops are formed. This is well explained by the standard CSHKP flare model. The evolution of the MFR did not show simple dynamics, rather it showed very complicated dynamics through a magnetic reconnection. We found, during the eruption, that the coherent MFR is created through the reconnection of multiple pre-existing MFRs. Magnetic reconnection plays a role in producing the coherent, erupting MFR and supplying further twist into it. Furthermore we found that the footpoints of the erupting MFR moves along or away from the polarity inversion line, as seen in two-ribbon flares. The locations of both the footpoints of the MFR correspond to those of dimming regions observed in EUV images. Since the location and shape of the post-flare loops obtained from the simulation is reproduced in the observations, we can confirm the reliability of our simulation.

Keywords: Solar Flare, Solar Eruption, Magnetohydrodynamics

©2019. Japan Geoscience Union. All Right Reserved.

Investigation of flow structures in the solar interior through the surface magnetic elements' tracking

*Yusuke Iida[1]

1. Kwansei Gakuin University

We investigate the correlation of meridional flow and rotation velocity in the solar interior by tracking huge number of the surface magnetic elements.

As reported in JpGU2017 meeting, we found that the meridional flow velocity from the magnetic elements' tracking depends positively on their flux and size. We discussed that it may come from that the larger magnetic elements are rooted in the deeper solar interior. We further investigate this issue by correlating the meridional flow velocity and rotation velocity.

We use line-of-sight magnetograms obtained by SDO/HMI in July 2016. Time cadence is 45 seconds, in which the travel distance of magnetic element is smaller than 1 pixel. The magnetograms are transposed from the Earth-view coordinate to the Stonyhurst coordinate. We use the data within 75 degree from the disk center. Magnetic field strength is converted with an assumption that magnetic field is vertical to the surface and interpolated with a cubic spline interpolation.

We detected approximately 8,000 elements in each magnetogram and 4.5x108 displacements in our data set. The meridional flow and rotation velocity on magnetic flux are investigated. The rotation velocity shows negative dependence on the flux at the latitude within 45 degree while it shows weekly positive dependence at the latitude higher than 45 degree. This result is consistent with the depth dependence of rotation velocity obtained by previous helioseismology researches.

Keywords: Sun, Bigdata, Turbulence

©2019. Japan Geoscience Union. All Right Reserved.

High-precision measurement of carbon-14 in tree rings around the onset of the Maunder Minimum

*Hiroko Miyahara[1], Fuyuki Tokanai[2], Toru Moriya[2], Hideyuki Hotta[3]

1. Musashino Art University, 2. Yamagata University, 3. Chiba University

It is well known that the Sun indicates long-term variations at time scales of a few hundred years to a few millennia. It sometimes brings the grand minima, at which period the sunspots disappear for more than several decades. The detailed process of such long-lasting disappearance of sunspots, however, remains unclear. We therefore have been trying to reconstruct solar cycles around the onset of grand minima based on high-precision measurement of carbon-14 in tree rings. In this paper, we report on our preliminary result on the measurement of carbon-14 around the onset of the Maunder Minimum.

Keywords: solar cycle, grand minima, cosmogenic nuclide

©2019. Japan Geoscience Union. All Right Reserved.

Examination of ^{10}Be in travertine sediment as a possible tool to reconstruct past solar activity

*Hongyang Xu[1,2], Hiroko Miyahara[2], Kazuho Horiuchi[3], Hiroyuki Matsuzaki[4], Hailong Sun[5], Weijun Luo[5], Xiangmin Zheng[1], Yusuke Suganuma[6,7], Shijie Wang[5], Limin Zhou[1]

1. East China Normal University, 2. Musashino Art University, 3. Hirosaki University, 4. University of Tokyo, 5. Chinese Academy of Sciences, 6. National Institute of Polar Research, 7. The Graduate University for Advanced Studies (SOKENDAI)

In this study, we explore the possibility of using travertine sediment for reconstructing the past solar activity. We obtained an annual ^{10}Be record from travertine deposit from the modern period and compared with the neutron monitor data. We discuss a possible methodology to calibrate the climatological impact on ^{10}Be deposition and to obtain the signal of past solar and cosmic-ray variations.

Keywords: Beryllium-10, cosmogenic nuclide, solar activity, endogenic travertine

©2019. Japan Geoscience Union. All Right Reserved.

Examination of ^{10}Be in travertine sediment as a possible tool to reconstruct past solar activity II

*Hongyang Xu[1,2], Hiroko Miyahara[2], Kazuho Horiuchi[3], Hiroyuki Matsuzaki[4], Hailong Sun[5], Weijun Luo[5], Xiangmin Zheng[1], Yusuke Suganuma[6,7], Shijie Wang[5], Limin Zhou[1]

1. East China Normal University, 2. Musashino Art University, 3. Hirosaki University, 4. University of Tokyo, 5. Chinese Academy of Sciences, 6. National Institute of Polar Research, 7. The Graduate University for Advanced Studies (SOKENDAI)

We have been examining the potential of ^{10}Be in travertine sediment as a tool to reconstruct past solar and cosmic-ray variations. In this paper, we compare the ^{10}Be profile in the travertine layers from the rainy and dry seasons, and discuss the nature of ^{10}Be deposition at the two seasons.

Keywords: Beryllium-10, cosmogenic nuclide, solar activity, endogenic travertine

©2019. Japan Geoscience Union. All Right Reserved.

1 year of CR observation at Syowa Station in the Antarctic.

*Chihiro Kato[1], Kazuoki Munakata[1], Akira Kadokura[2], Ryuho Kataoka[2], Paul Evenson[3]

1. Shinshu University, 2. National Institute of Polar Research, 3. University of Delaware

CR observation has been carried out for 1 year at Syowa Station in the Antarctic. There was no serious unavailability of data during the whole year. It is now concluded that this station can contribute to a space weather study as one of the CR monitoring station of Global Muon Detector Network (GMDN). We report observed data and its stability as GMDN.

Keywords: Cosmic Rays, Space Weather

©2019. Japan Geoscience Union. All Right Reserved.

Space weather forecast archives at NICT: handwritten solar activity charts

*Kaori Sakaguchi[1], Daikou Shiota[1], Kaori Fukunaga[1], Katsuhide Marubashi[1], Hiromitsu Ishibashi[1], Yuki Kubo[1], Mamoru Ishii[1]

1. National Institute of Information and Communications Technology

About 40 years ago from 1978 to 1999, at Hiraiso Branch, Radio Research Laboratory; present Space Environment Laboratory of National Institute for Information and Communication Technology (NICT) in Japan, space environment data had been recorded in "solar activity chart" by hand for the operation of the radio wave warning service. The charts were created based on URSIgram codes, which were developed to facilitate the rapid exchange of information by telex in periods when internet was not available. Based on the exchanged codes, sunspots transitions and solar flare occurrences on the solar surface, these effects on shortwave propagation, geomagnetic disturbance, and cosmic ray flux over Japan were written in the solar activity charts together with comments and sketch by recorders. One chart was created for each Bertel’ s solar rotation number between No. 1974 and No. 2254, corresponding to sunspot cycles 21 and 22. We realized that the data exchange is almost only once a day from each observation point and charts was accumulation of the available data in real-time at that time.It might be quite difficult to decide future forecast from such a limited real-time data set. Currently, we are digitizing the solar activities charts and the data shown there. In this poster, we present examples of solar activity charts and possible real-time data set and time delay, as well as the verifying result of the solar flare / geomagnetism storm forecast at the time.

Keywords: Space Weather Archive, URSIgram

©2019. Japan Geoscience Union. All Right Reserved.

IMF dependence on solar wind parameters

*Tohru Araki, Yuki Harada[1]

1. Kyoto University

We studied IMF dependence upon solar wind parameters using OMNI hourly values.

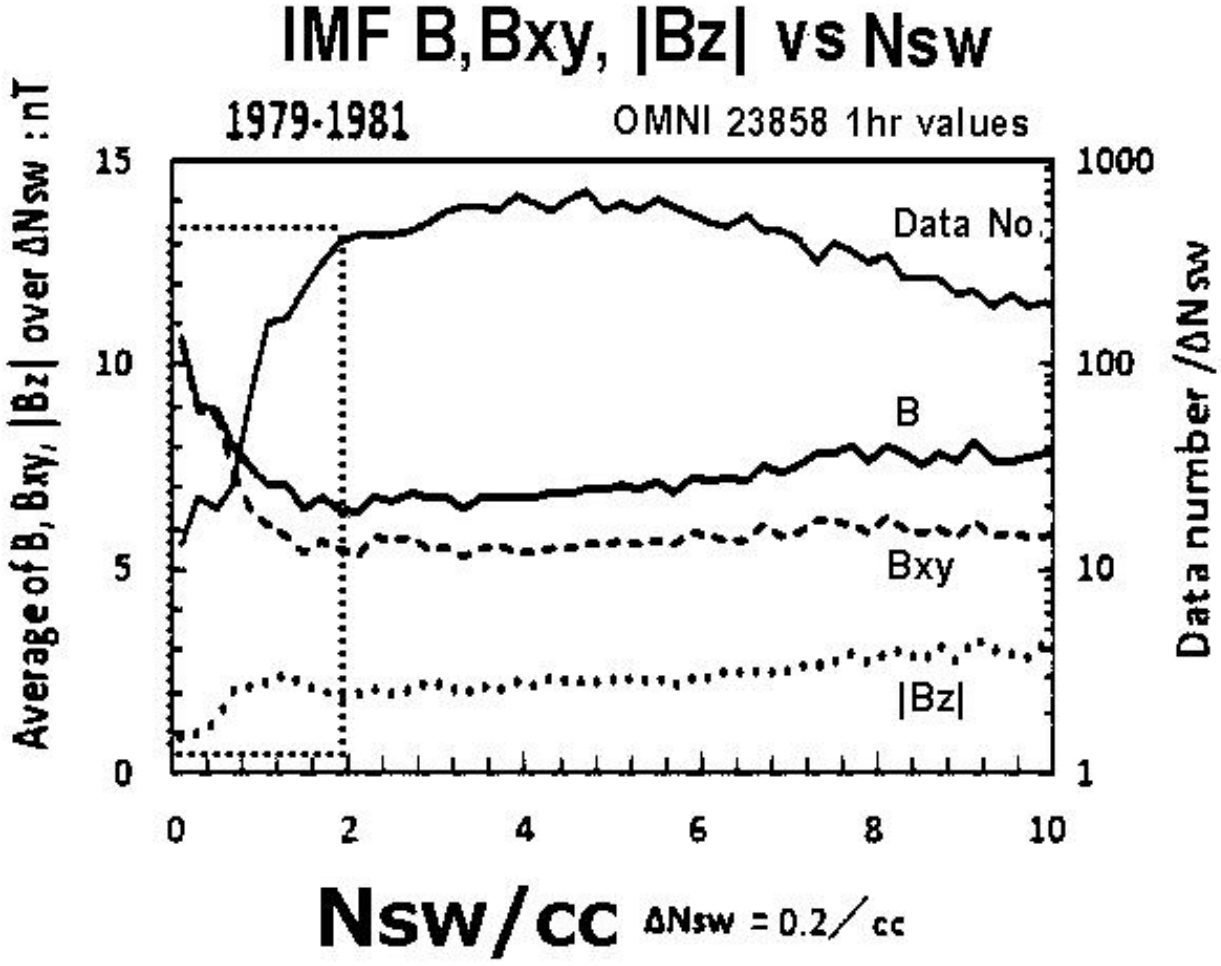
Figure below is a plot of the total force (B), horizontal component (Bxy) in the ecliptic plane and vertical component (Bz) of IMF versus the solar wind density (Nsw). The IMF is averaged over 0.2/cc bin of Nsw. Data number in each bin is also plotted. The data period here is 1979-1981 (maximum SSN phase).

The figure shows (1) that B, Bxy and Bz slowly decrease with decreasing Nsw and (2) that when Nsw approaches further to zero. B and Bxy begin to increase and converges to the same finite value (about 10 nT here) while Bz converges to zero. The property (2) suggests that IMF converges to a typical spiral pattern when solar wind density converges to zero.

Two other data periods, 1999-2001 (SSN maximum) and 2007-2009 (SSN minimum) are examined. IMF observed by MAVEN orbiting Mars is also studied for the period, 2014-2018. The results of the analysis are roughly consistent with the description above. We also checked IMF dependence on solar wind velocity

Keywords: IMF, solar wind density, solar wind melocity

©2019. Japan Geoscience Union. All Right Reserved.



©2019. Japan Geoscience Union. All Right Reserved.

Dipole Tilt Effect of Geomagnetic Activity from Low- to High-latitudes

*Nowada Motoharu[1]

1. Shandong University at Weihai

Geomagnetic activity is dominantly impacted by the orientation of the Interplanetary Magnetic Field (IMF). However, when trying to address why the variations of geomagnetic activity are “semi-annual”, and are greater at equinoxes than at solstices, only IMF control of geomagnetic activity is not enough. This is because these variations are strongly dependent on the Earth’s dipole tilt; the dipole tilt is smaller at the equinoxes than at the solstices. Primitive studies assumed that magnetic reconnection occurs only at the subsolar point of dayside magnetopause. In their studies, the dipole tilt effect was not considered, but only the magnetic field direction between the IMF and the magnetosphere at the subsolar point was discussed in their studies. After them, geomagnetic variations where both dipole tilt effect and IMF direction are taken into account have been investigated. Based on a large database of IMF and AL/AU, we examined the relationship between the IMF clock angle and AL/AU at various dipole tilts. For both positive and negative dipole tilts, geomagnetic activity decrease as the clock angle moves away from 180˚. The AL/AU indices also tend to become smaller for larger dipole tilts. This dipole tilt dependence enhances the semi-annual variation of high-latitude geomagnetic activity.
It also remains unclear how degree energy input rate from solar wind to ring current (dD_{st}^{*}/dt) depends on dipole tilt under various interplanetary magnetic field (IMF) orientation and whether or not ring current development also follows this dipole tilt dependence. We tried to statistically investigate the dependence of dipole tilt and IMF clock angles on low- and middle-latitude geomagnetic activity (D_{st}^{*}), which is a proxy of ring current development, and solar wind energy input rate to ring current (dD_{st}^{*}/dt) over one solar cycle (1978 - 1988). D_{st}^{*} was calculated with the solar wind dynamic pressure and original D_{st} index, and the dipole tilt angle was defined as function of the day of year and universal time. The (dD_{st}^{*}/dt) values were obtained based on the solar wind electric field under the southward IMF conditions. Under positive and negative dipole tilts, the (dD_{st}^{*}/dt) values under low dipole tilt are negatively larger than those in case of high dipole tilt. Further peaks at 180˚ of the IMF clock angle are seen in most of the dipole tilt cases. However, the D_{st}^{*} index shows neither a peak at 180˚ of the IMF clock angle nor particular dipole tilt dependence in case of negative dipole tilt angles. This result suggests that low- and middle latitude geomagnetic activity (ring current development) does not necessarily show dipole tilt dependence and a one-to-one correlation with solar wind energy input rate to ring current (dD_{st}^{*}/dt).

Keywords: Geomagnetic activity (Dst*), Solar wind energy input rate to ring current (dDst*/dt), Semiannual variation , Dipole tilt effect, Interplanetary magnetic field and clock angel, Magnetic reconnection

©2019. Japan Geoscience Union. All Right Reserved.

A New Prediction Model for Solar Wind-Triggered Magnetospheric Disturbances Based on Potential Learning (Neural Network)

*Ryozo Kitajima[1], Motoharu Nowada[2], Ryotaro Kamimura[3]

1. Seikei University, 2. Shandong University at Weihai, 3. Tokai University

Nowadays, it becomes so important in saving our economic activity, and preventing the disasters caused by terrestrial electromagnetic effects to predict a scale and the duration of the geomagnetic disturbances based on in-situ solar wind observations. Recently, one of the notable techniques for the predictions of the magnetospheric disturbances is Neural Network (NN). However, most of these studies are focused on the reproduction of the behaviors of the index values, which represent the geomagnetic disturbances (e.g, D_{st} and AE), by inputting the solar wind parameters measured by the satellites. In our study, we apply a novel neural network model of ‘Potential Learning (PL)’.
Basically, Neural Networks (NNs) are models which imitate the information processing in the nervous system of brain. The nerve is made of cells as referred to as “neurons”, which specializes the information processing. NNs consist of “artificial” neurons, and can process information by learning. Therefore, using NNs, we can obtain some characteristics of the data inputted. The PL is a new kind of the NNs. A feature of the PL is to make a network that can understand the input variables based on learning by “input potentialities”, which are indices as calculated with the variances derived from the input variables. If using this PL, we can specify what input variable(s) is (are) potentially important and influential for a phenomenon.
In this study, introducing the PL technique, we try to specify which solar wind parameter plays an essential role in causing the geomagnetic disturbances. Although the conventional PL, where we used, had automatically selected the variables of interest, we develop a “improved” PL in this study so that the variables can manually be selected. We benchmark this new algorithm using the 4 polar magnetic storm cases occurred under the southward Interplanetary Magnetic Field (IMF)-B_z conditions, and advisedly set the maximum potentiality for the IMF-B_z, so that the IMF-B_z component is the most possible solar wind parameter to cause the geomagnetic disturbances. We note “second” solar wind parameter(s) to possibly cause the magnetospheric disturbances, following the IMF-B_z component. After testing our new technique to actual storm events, we might distinguish the magnetospheric disturbances into two different types, that is, the geomagnetic disturbances driven by “IMF-dominant” and “combination of IMF with solar wind plasma (dynamic pressure)”. The advantages to adopt this new algorithm to space weather, and more detailed results will be discussed in this presentation.

Keywords: Predictions of Geomagnetic Activity, Neural Network Considered Potential Learning, Development of Space Weather

©2019. Japan Geoscience Union. All Right Reserved.

Real-time magnetosphere simulator for space weather using REProduce Plasma Universe code

*Yasubumi Kubota[1], Aoi Nakamizo[1], Kaori Sakaguchi[1], Mitsue Den[1], Yuki Kubo[1], Tsutomu Nagatsuma[1], Takashi Tanaka[1,2]

1. National Institute of Information and Communications Technology, 2. Kyushu University

Surface charging of artificial satellite is one of risks caused by dynamical variations of space environment. It occurs when a satellite exposes high energy electrons around 10 keV created by plasma injection accompanied with substorm. Therefore we want to predict timing and electron energy of plasma injection using magnetosphere-ionosphere coupling global MHD simulation. Now we are developing a real-time numerical simulator for space weather forecast using magnetosphere-ionosphere coupling global MHD simulation called REPPU (REProduce Plasma Universe) code. The feature of the simulation code is highly robust to extreme solar wind parameters because the unstructured grid system has no singular point and is able to calculate in the uniform accuracy over the whole region. We use the real-time solar wind data formatted in the GSM coordinate system observed by DSCOVR spacecraft. Magnetic-dipole axis is fixed to z-direction in our simulation. Therefore daily variation of magnetic-dipole axis is not reproduced. Instead, we convert the input direction of the solar wind velocity and magnetic field into that which tilts including daily variation of magnetic dipole axis in x-z plane. In the method the solar wind structure is not exact. However we can relatively reproduce the magnetosphere response including daily variation of the magnetic-dipole axis against solar wind. The resolution is 7682 grids in the horizontal direction and 240 grids in the radial direction.
In this presentation, we compare the simulation results with the CPCP, AE index, and plasma variations observed by geostationary orbit satellites. Density and temperature of plasma injection derived from MHD simulation tends to estimate larger and smaller values than observation respectively because the MHD simulation does not include kinetic heating effects. We have to interpret MHD simulation results for prediction of electron density and temperature. We will discuss how to interpret electron density and temperature between observation and MHD simulation.

Keywords: global MHD simulation, surface charging

©2019. Japan Geoscience Union. All Right Reserved.

Simulation of GIC flowing through the power transmission network (187 kV-500 kV) in Japan

*Nishida Yuichiro[1,6], Yusuke Ebihara[1], Satoko Nakamura[1], Shinichi Watari[2], Kumiko Hashimoto[3], Kentaro Kitamura[4], Takashi Kikuchi[5]

1. Kyoto University Reserch Institute for Sustainable Humanosphere, 2. National Institute of Information and Communications Technology, 3. Kibi International University, 4. National Insutitute of Technology, Tokuyama College, 5. Nagoya University, 6. Kyoto University Department of Electrical Engineering

The energy released from the sun can enhance electric currents in Earth’ s magnetosphere, which induces an electric field on the ground surface. This electric field, called a geomagnetically induced electric field (GIE), gives rise to geomagnetically induced current (GIC) flowing in a transmission line. Japan is situated at geomagnetically low latitudes, but the potential risk is probably non-zero because a large-amplitude of GIC, as high as 129 A, was recorded in the Japanese power grid during the Halloween storm in October 2003. To evaluate the potential risk of the Japanese power grid properly, we modeled the Japanese power grid with high voltage class over 187 kV on the basis of publicly available data. The model consists of 602 nodes and 763 paths. The uniform GIE imposed on Japan was estimated on the basis of the geoelectric field observed in April 2018 at Kakioka Magnetic Observatory. We applied the uniform GIE on the model. The calculated GIC is roughly in agreement with that measured at 4 substations in Japan. For the westmost substation, a disagreement was found when we considered only the highest class of the power grid (500 kV), which may imply that the lower voltage class of the grid (<500 kV) may have some contribution to the GIC in Japan. We discuss the general tendency of the GIC flowing in the Japanese power grid, and prediction capability of the currently available model.

©2019. Japan Geoscience Union. All Right Reserved.

Simulation of GIC flowing through the power transmission network (187 kV-500 kV) in Japan

Yuichiro Nishida
Yusuke Ebihara
Satoko Nakamura
Shin-Ichi Watari
Kumiko Hashimoto
Kentaro Kitamura
Takashi Kikuchi

Abstract

The energy released from the sun can enhance electric currents in Earth's magnetosphere, which induces an electric field on the ground surface. This electric field, called a geomagnetically induced electric field (GIE), gives rise to geomagnetically induced current (GIC) flowing in a transmission line. Japan is situated at geomagnetically low latitudes, but the potential risk is probably non-zero because a large-amplitude of GIC, as high as 129 A, was recorded in the Japanese power grid during the Halloween storm in October 2003. To evaluate the potential risk of the Japanese power grid properly, we modeled the Japanese power grid with high voltage class over 187 kV on the basis of publicly available data. The model consists of 602 nodes and 763 paths. The uniform GIE imposed on Japan was estimated on the basis of the geoelectric field observed in April 2018 at Kakioka Magnetic Observatory. We applied the uniform GIE on the model. The calculated GIC is roughly in agreement with that measured at 4 substations in Japan. For the westmost substation, a disagreement was found when we considered only the highest class of the power grid (500 kV), which may imply that the lower voltage class of the grid (<500 kV) may have some contribution to the GIC in Japan. We discuss the general tendency of the GIC flowing in the Japanese power grid, and prediction capability of the currently available model.

©2019. Japan Geoscience Union. All Right Reserved.

Climatological features of the upper atmosphere reproduced by a revised version of a whole atmosphere-ionosphere coupled model GAIA

*Hidekatsu Jin[1], Yasunobu Miyoshi[2], Chihiro Tao[1], Hiroyuki Shinagawa[1], Hitoshi Fujiwara[3]

1. National Institude of Information and Communications Technology, 2. Kyushu University, 3. Seikei University

Temporal and spatial variations in the ionospheric electron density and thermospheric mass density could have significant impacts on radio communications between ground and space, and particle and atmospheric drag environments around satellites. Origins of such upper atmospheric variations are not only in the solar atmosphere through the emissions of solar radiation, high-speed plasma gas and high-energy particles, but also in the Earth’ s lower atmosphere, where meteorological phenomena could give rise to atmospheric waves propagating upward. In order to nowcast and forecast the upper atmospheric variations and disturbances, a whole atmospheric model, GAIA, has been developed, which combines a whole atmospheric GCM, an ionospheric model and an electrodynamics model in a self-consistent manner.

So far, for the purpose of its validation, we have compared climatological features of thermosphere and ionosphere reproduced by GAIA with those from ionospheric observation and observation-based empirical models. The comparison indicates that the model and observations are generally in good agreements, but in some condition such as at solar maximum there are significant disagreements in the ionospheric electron density distribution. In order to improve the accuracy of the model, we have made several updates such as ion chemical processes, energetics, parameterization, and so on. We also have introduced magnetospheric effects into the model, such as electrodynamics coupling with magnetosphere and particle precipitation. In this presentation, we discuss how the upper atmospheric model can improve its accuracy and how they can be validated.

Keywords: space weather, whole atmosphere, ionosphere, simulation, thermosphere, assimilation

©2019. Japan Geoscience Union. All Right Reserved.

Investigation of the thermospheric mass density variations below 200 km

*Hitoshi Fujiwara[1], Yasunobu Miyoshi[2], Masayoshi Utashima[1], Huixin Liu[2]

1. Faculty of Science and Technology, Seikei University, 2. Department of Earth and Planetary Sciences, Faculty of Sciences, Kyushu University

Since both the effects from the lower atmosphere and in-situ forcing are significant in the thermospheric region between 100 and 200 km altitude, the thermosphere in the region shows complex variations depending on various conditions. In addition, observations of the thermosphere (neutral atmosphere) between 100 and 200 km are very few compared to the upper thermosphere (above 300 km) and the ionosphere. These make it difficult to improve reliability of empirical and numerical models. Observations from Low Earth Orbit (LOE) satellites would be essential for building up available data sets in the thermospheric region between 100 and 200 km altitude. We will introduce our research project to investigate the thermospheric mass density variations in the 100-200 km altitude region with the LOE satellite, e.g., Tsubame (SLATS), data and a whole atmosphere GCM.

Keywords: thermosphere, mass density, Low Earth Orbit (LOE) satellite, GCM

©2019. Japan Geoscience Union. All Right Reserved.

Low-latitude HF Doppler observations of magnetospheric electric fields during space weather disturbances

*Kumiko K. Hashimoto[1], Takashi Kikuchi[2], Ichiro Tomizawa[3], Keisuke Hosokawa[3], Jaroslav Chum[4]

1. Kibi International University, 2. Nagoya University, 3. University of Electro-Commnunications, 4. Institute of Atmospheric Physics, Prague

Ionospheric electric fields penetrated from the magnetosphere to the low latitude ionosphere have been observed as geomagnetic disturbances caused by ionospheric currents, such as the equatorial electrojet (EEJ) at the dayside equator. The ionospheric currents are too weak to be a detector of the electric field at low latitudes on the dayside and even at the equator on the nightside. The HF Doppler (HFD) sounder is another powerful tool for observations of the electric filed at low latitudes on both the day- and night-sides. We have shown that the electric fields of the geomagnetic sudden commencements (SC) are composed of the preliminary impulse followed by the main impulse, of which directions are opposite to each other and both electric fields are opposite on the day- to night-sides (Kikuchi et al. 2016 JGR). We have also shown that the substorm electric fields are composed of the growth phase followed by expansion phase overshielding electric fields, of which directions are opposite to each other (Hashimoto et al., 2017). In this paper, we show that the HFD sounder is capable of detecting stormtime electric fields and that the electric fields are found to decay rather rapidly over one hour during the main phase with the time scale of a few hours. Combining with the equatorial magnetometer data, we would be able to estimate the decaying rate of the HFD electric fields, which helps obtain the stormtime electric fields quantitatively from the HFD data. We discuss advantages of widely separated HFD sounder operations and cooperations with SuperDARN as well as with magnetometer networks.

Keywords: HF Doppler observation, ionosphere electric field, magnetospheric electric field, geomagnetic storm, equatorial electrojet

©2019. Japan Geoscience Union. All Right Reserved.

Stratospheric ionization during magnetic storms

*Ryuho Kataoka[1]

1. National Institute of Polar Research

Transient mesospheric ionization was detected at an altitude of 65-70 km during the auroral breakup that occurred from 2220 to 2226 UT on June 30, 2017. During this event, the footprint of the Arase satellite was located within the field of view of the all-sky imagers at Syowa Station in the Antarctic. Auroral observations at Syowa Station revealed the dominant precipitation of relatively soft electrons during the auroral breakup. A corresponding spike in cosmic noise absorption was also observed at Syowa Station, while the Arase satellite observed a flux enhancement of >100 keV electrons and a broadband noise without detecting chorus waves or electromagnetic ion cyclotron waves. A general-purpose Monte Carlo particle transport simulation code was used to quantitatively evaluate the ionization in the middle atmosphere. Results of this study indicate that the precipitation of energetic electrons of >100 keV, rather than X-rays from the auroral electrons, played a dominant role in the transient and deep (65-70 km) mesospheric ionization during the observed auroral breakup. Based on the above results of Kataoka et al. (2019), we further discuss a possible role of X-rays to ionize the stratosphere during magnetic storms.

Reference:
Kataoka et al. (2019), Earth, Planets and Space, 71, 9, https://doi.org/10.1186/s40623-019-0989-7

©2019. Japan Geoscience Union. All Right Reserved.

Calculating propagation time of HF radio wave using ray-tracing method and simple comparison with the observation.

*Ryo Nakao[1], Hiroyuki Nakata[1], Hiroyo Ohya[1], Toshiaki Takano[1], Kornyanat Hozumi[2], Takuya Tsugawa[2], Susumu Saito[3], Mamoru Ishii[2]

1. Graduate School of Engineering, Chiba University, 2. National Institute of imformation and Communications Technology, 3. Electronic Navigation Research Institute

To provide the information of nowcast of radio propagation, we have started a project, HF-START (HF simulator Targeting for All user's Regional Telecommunications). In this project, a simulator that is able to predict propagation of HF radio waves is constructed by ray-tracing calculation.
Using this simulator, we have examined whether HF radio wave travels between any two points. In this calculation, the electron density, which is necessary to calculate reflection index is determined by International Reference Ionosphere (IRI).In this project, HF receivers have been installed at Chiba University (Chiba, 35.62N, 140.10E), Sarobetu (Hokkaido, 45.16N, 141.74E), Numata (Gunma, 36.62N, 139.02E), Yamagawa (Kagoshima, 31.20N, 130.61), Ogimi (Okinawa, 26.68, 128.15E) for observing HF radio wave transmitted from radioNIKKEI (Nagara, Chiba, 35.46N, 140.20E) to confirm the results of the ray-tracing calculation. In the ray-tracing calculation, therefore, we set the same locations of the transmitter and receivers as the observatories of HF-START. As a result of simple comparison between the ray-tracing results and the observation, it is found that there was a difference of the propagation time between the ray-tracing results and the observations. It is possible that the radio wave propagation between radioNIKKEI and Ciba University is not ground wave but sky wave that is reflected by ionosphere. As for further calculation, we plan to use the electron density distributions determined by GAIA and GNSS tomography in the ray-tracing calculation.

©2019. Japan Geoscience Union. All Right Reserved.

Why do some probabilistic forecasts lack reliability?

*Yuki Kubo[1]

1. National Institute of Information and Communications Technology

One of the important attributes to be satisfied for the probabilistic forecast system is reliability. However, some probabilistic forecast systems lack reliability. Why do some probabilistic forecasts lack reliability? We investigate a condition for a probabilistic binary forecast to be reliable in this work. We mathematically prove that a necessary, but not sufficient, condition for achieving a reliable probabilistic forecast is maximizing the Peirce skill score (PSS) at the threshold probability of the climatological base rate. The condition is confirmed by using artificially synthesized forecast-outcome pair data and previously published probabilistic solar flare forecast models. The condition gives a partial answer as to why some probabilistic forecast systems lack reliability, because the system, which does not satisfy the proved condition, can never be reliable. The result implies that those who want to develop a reliable probabilistic forecast system must adjust or train the system so as to maximize PSS near the threshold probability of the climatological base rate.

Keywords: Probabilistic forecast, Reliability

©2019. Japan Geoscience Union. All Right Reserved.

An estimation method of GEO spacecraft surface charging for a real-time spacecraft risk assessment

*Masao Nakamura[1], Ryota Kawachi[1], Go Takahashi[1], Tsutomu Nagatsuma[2], Mamoru Ishii[2]

1. Osaka Prefecture University, 2. NICT

Spacecraft anomalies are often induced by electrostatic discharges due to surface charging. Some spacecraft charging simulation software is developed by space agencies and research institutes and used for spacecraft designs and charging analysis. However these simulations cannot be used for a real-time estimation because they need hours or days to calculate the surface potential for a given plasma environment. Therefore we develop a quick estimation method of GEO spacecraft surface charging for the Space Environment Customized Risk Estimation for Spacecraft (SECURES) of the space weather forecast Project for Solar-Terrestrial Environment Prediction (PSTEP). We estimate the surface potentials by interpolation using lookup tables of the pre-simulated surface potentials for combinations of plasma temperatures and densities. We study fitting functions used in the interpolation and how to make the lookup tables for the good estimation. Then we can real-time estimate the surface potentials of the target GEO spacecraft when the on-orbit plasma environment is predicted or observed. The spacecraft risk assessment can be accomplished by additional information about the experimental discharging differential potential of the surface materials.

Keywords: Spacecraft surface charging, Space weather, Spacecraft risk assessment

©2019. Japan Geoscience Union. All Right Reserved.

A network of HF Doppler sounding systems in Japan

*Keisuke Hosokawa[1], Hiroyuki Nakata[2], Kumiko K. Hashimoto[3], Ichiro Tomizawa[1], Jun Sakai[1], Takashi Kikuchi[4]

1. University of Electro-Communications, 2. Chiba University, 3. Kibi International University, 4. ISEE, Nagoya University

Since 2003, a network observation of HF Doppler sounding has been conducted in Japan for remote-sensing the atmospheric, ionospheric and magnetospheric processes. Currently, 1 transmitting station (Tx) and 7 receiving stations (Rx) are operative by a collaborative effort of four difference universities. The main transmitting station is located at Chofu, Tokyo, Japan in the Campus of University of Electro-Communications (JG2XA). JG2XA transmits continuous waves at 5006 kHz and 8006 kHz with a transmitting power of 200 W. By receiving this JG2XA signal at 7 Rx stations (Sugadaira, Oarai, Kure, Kashima, Iitate, Fujisawa and Sugito) we derive the Doppler shift imposed during the propagation and reflection in the ionosphere. In particular, the Doppler shift data can be used to detect vertical motion of the ionospheric F region with a temporal resolution of 10 s. At some stations, we also have observed signals from Radio Nikkei 1 (JOZ at 3925 kHz, JOZ2 at 6055 kHz, and JOZ3 at 9595 kHz) transmitted from Nagara, Chiba, Japan, which allows us to observe the vertical motion of the ionosphere at several altitude levels. The data obtained from this experiment since 2003 are all available at http://gwave.cei.uec.ac.jp/~hfd. Not only quick-look plots but also several types of digital data (raw wave form and Doppler shift data) can be retrieved from this database. The experiment covers various ionospheric phenomena in the Magnetosphere-Ionospheric (M-I) coupling system, such as sporadic E-layer (Es), medium-scale traveling ionospheric disturbances (MSTIDs), large-scale traveling ionospheric disturbances (LSTIDs), global-scale electric field variation, geomagnetic pulsations, and sudden commencement (SC). The data can also be used for the studies of vertical coupling between the lower atmosphere and ionosphere, for example, observations of ionospheric variation after large earthquakes, volcanic eruptions and typhoons. To facilitate analyses of the phenomena listed above, it is desired to observe a wider area in latitude and longitude. For this purpose we plan to extend the network covering the entire ionosphere over Japan in the near future. In the presentation, we will give a brief introduction to the experiments and online database, and then discuss the future direction of the studies of atmosphere, ionosphere and magnetosphere using the HF Doppler sounding in a framework of international collaborations.

Keywords: HF Doppler experiment, Ionosphere

©2019. Japan Geoscience Union. All Right Reserved.

[E] Poster | P (Space and Planetary Sciences)：P-CG Complex & General

Tue. May 28, 2019 10:45 AM - 12:15 PM JST | Tue. May 28, 2019 1:45 AM - 3:15 AM UTC | Poster Hall International Exhibition Hall8, Makuhari Messe_1

[P-CG22] Shock responses of planetary materials elucidated from meteorites and dynamic compression experiments

convener:Toshimori Sekine(Center for High Pressure Science and Technology Advanced Research), Takuo Okuchi(Institute for Planetary Materials, Okayama University)

Impact phenomena had played essential roles in the process of planetary evolution. Recent analytical and experimental developments reveal a new prospective on the effects of shock-compression process for planetary materials. For deeper understanding of such shock effects, it is necessary to evaluate the detailed shock conditions from the observations of naturally-shocked planetary materials, and to compare them with the results on the planetary materials experienced a wide range of known shock conditions. Several metastable phases, that have not been known before, have recently been identified in shocked meteorites. They suggest that the shock state is often not in equilibrium and that it is more complicated process than ever thought. Experimental techniques including laser-driven shock compression and x-ray free electron laser diagnostics have been progressed to successfully simulate a wide range of shock conditions. The recent results indicate that shocked grains are fractured and rotated at relatively low pressures, and that they are subsequently transformed into denser phases or melts, or their mixtures at pressures of a few 100s GPa. Understanding of such shock dynamics requires another prospect, which is qualitatively different from the static high pressure and high temperature consensus. Therefore, it is timely to have an international symposium on dynamics of planetary materials.

[PCG22-P01] discussion

*Takuo Okuchi[1], Toshimori Sekine[2] (1.Institute for Planetary Materials, Okayama University, 2.Center for High Pressure Science and Technology Advanced Research)

[PCG22-P02] Shock-compressed behavior of quartz by XFEL

*Tomoko Sato[1], Yoshinori Tange[2], Yusuke Seto[3], Toshimori Sekine[4,5], Norimasa Ozaki[4], Toyohito Nishikawa[4], Kohei Miyanishi[4], Kensuke Matsuoka[4], Ryosuke Kodama[4], Tadashi Togashi[2], Yuichi Inubushi[2], Toshinori Yabuuchi[6], Makina Yabashi[6] (1.Hiroshima University, 2.Japan Synchrotron Radiation Research Institute, 3.Kobe University, 4.Osaka University, 5.Center for High Pressure Science &Technology Advanced Research, 6.RIKEN)

[PCG22-P04] Laser-shock experiments of dense polymorphs of Mg_2SiO_4: technical developments using synthetic single crystals

*Narangoo Purevjav[1], Takuo Okuchi[1], Norimasa Ozaki[2], Takayoshi Sano[3], Yuhei Umeda[2], Shintaro Morioka[2], Nobuki Kamimura[2] (1.Institute for Planetary Materials, Okayama University, 2.Graduate School of Engineering, Osaka University, 3.Institute of Laser Engineering, Osaka University)

[PCG22-P05] Richtmyer-Meshkov instability in inhomogeneous density materials and its application to planetary science

*Takayoshi Sano[1] (1.Institute of Laser Engineering, Osaka University)

[PCG22-P06] Impact-induced dehydration reactions of Fe- and Al-hydrates as potential storage, carrier and source of water

*Tsubasa Tobase[1], Toshimori Sekine[1], Ginga Kitahara[2], Makoto Tokuda[2], Akira Yoshiasa[2], Makoto Takafuji[2], Tsutomu Mashimo[2], Nobuaki Kawai[2] (1.HPSTAR, 2.Graduate School of Science and Technology, Kumamoto University)

[PCG22-P07] Crystallization of amorphous $MgSiO_3$ by shock compression

*Akane Arasuna[1], Masayuki Okuno[1], Nobuaki Kawai[2] (1.Kanazawa University, 2.Kumamoto University)

[PCG22-P08] First-principle study of the structural and electronic properties of N-doped $MgAl_2O_4$ spinel

*Chi Pui Tang[1], Pak Kin Leong[1], Toshimori Sekine[2,3] (1.State Key Laboratory of Lunar and Planetary Sciences, Macau University of Science and Technology, 2.Center for High Pressure Science and Technology Advanced Research (HPSTAR) Shanghai Laboratory of HPSTAR, Shanghai, P.R. China, 3.Graduate School of Engineering, Osaka University)

[PCG22-P09] Transparency of shock-compressed single crystal diamond

*Kento Katagiri[1], Norimasa Ozaki[1,2], Kohei Miyanishi[2], Yuhei Umeda[1], Shintaro Morioka[1], Takayoshi Sano[2], Ryosuke Kodama[1,2] (1.Osaka University, 2.Institute of Laser Engineering, Osaka Unversity)

[PCG22-P10] Pb-Pb dating of the NWA 7203 angrite and relationship to its shock metamorphism

*Hideyuki Hayashi[1], Takashi Mikouchi[1], Yuji Sano[1], Martin Bizzarro[2] (1.The university of Tokyo, 2.University of Copenhagen)

[PCG22-P11] Shock recovery of high-pressure phase of SiO_2 using high-power laser

*Tadashi Kondo[1], Hiromoto Kengo[1], Tatsuhiro Sakaiya[1], Hidenori Terasaki[1], Keisuke Shigemori[2], Youichiro Hironaka[2] (1.Department of Earth and Space Science, Graduate School of Science Osaka University, 2.Institute of Laser Engineering, Osaka University)

[PCG22-P12] Hugoniot measurement of calcite under meteorite collision condition

*Fukui Keiya[1], Norimasa Ozaki[1,2], Yuhei Umeda[1], Kohei Miyanishi[3], Kento Katagiri[1], Shintaro Morioka[1], Takayoshi Sano[3], Ryosuke Kodama[1,2,3] (1.Graduate School of Engineering,Osaka univ., 2.PPC, Osaka Univ., 3.ILE, Osaka Univ.)

[PCG22-P13] Direct observation of the transformation toughening of tetragonal stabilized zirconia under shock deformation condition by ns time-resolved XRD.

*Sota Takagi[1,2], Kouhei Ichiyanagi[2,3], Nobuaki Kawai[4], Ryo Fukaya[2], Shunsuke Nozawa[2], Atsushi Kyono[1], Nobumasa Funamori[2], Shin-ichi Adachi[2] (1.University of Tsukuba, 2.KEK PF, 3.Jichi Medical University, 4.Kumamoto University)

discussion

*Takuo Okuchi[1], Toshimori Sekine[2]

1. Institute for Planetary Materials, Okayama University, 2. Center for High Pressure Science and Technology Advanced Research

We discuss natural and experimendal evidences on impact phenomena, which had played essential roles in the process of early planetary evolution. Recent analytical and experimenotal developments reveal a new prospective on the effects of shock-compression process of planetary materials. For deeper understanding of such shock effects, it is necessary to evaluate the detailed shock conditions from the observations of naturally-shocked planetary materials, as well as to compare them with the results of shock-compression experiments of these materials obtained at laboratory conditions.

Keywords: discussion

©2019. Japan Geoscience Union. All Right Reserved.

Shock-compressed behavior of quartz by XFEL

*Tomoko Sato[1], Yoshinori Tange[2], Yusuke Seto[3], Toshimori Sekine[4,5], Norimasa Ozaki[4], Toyohito Nishikawa[4], Kohei Miyanishi[4], Kensuke Matsuoka[4], Ryosuke Kodama[4], Tadashi Togashi[2], Yuichi Inubushi[2], Toshinori Yabuuchi[6], Makina Yabashi[6]

1. Hiroshima University, 2. Japan Synchrotron Radiation Research Institute, 3. Kobe University, 4. Osaka University, 5. Center for High Pressure Science &Technology Advanced Research, 6. RIKEN

We have conducted x-ray diffraction measurement (XRD) with femtosecond x-ray pulses generated by the x-ray free electron laser (XFEL) to observe lattice dynamics and phase transformation of single-crystal quartz under high strain-rate shock compression (~10^9 s^{-1}) and high pressure. Single-crystal quartz samples were shock-compressed by high-power short- and long-pulse lasers. In the short-pulse experiments, the lattice was reduced to 15% and 1.5% in the direction parallel and perpendicular to the compression axis, respectively. The sample was uniaxially compressed over its known Hugoniot elastic limit. In the long-pulse experiments, three different states were observed. Polycrystalline stishovite appeared at first, and elastically compressed state and a topotaxially transformed new phase were observed successively.

Keywords: Shock compression, in-situ X-ray diffraction, quartz

©2019. Japan Geoscience Union. All Right Reserved.

Laser-shock experiments of dense polymorphs of Mg_2SiO_4: technical developments using synthetic single crystals

*Narangoo Purevjav[1], Takuo Okuchi[1], Norimasa Ozaki[2], Takayoshi Sano[3], Yuhei Umeda[2], Shintaro Morioka[2], Nobuki Kamimura[2]

1. Institute for Planetary Materials, Okayama University, 2. Graduate School of Engineering, Osaka University, 3. Institute of Laser Engineering, Osaka University

Mg_2SiO_4 polymorphs (α-phase as forsterite, β-phase as wadsleyite, and γ-phase as ringwoodite) are the major constituents of our Earth's mantle and also for Earth-like planets. Thus studying these polymorphs at extreme pressure and temperature conditions will lead to understanding their changes of chemical and physical properties at extremely high pressure and temperature conditions, such as those occurring during the giant impacts phenomena of such planets at their final stage of accretion. Shock compression of forsterite has been studied up to ~ 1000 GPa by using polycrystalline and single crystal samples [1-3]. The studies have reported contradicting results for the shock compression of forsterite. Sekine et al (2016) reported that there are several phase transformations in the liquid state of Mg_2SiO_4 at > 270 GPa, while other two studies were reported no phase transformation [1, 3]. Thus it is interesting to see how the Hugonoit relations of Mg_2SiO_4 polymorphs will come up at different pressure and temperature conditions. However, Hugoniot relations of wadsleyite and ringwoodite have not been studied well. Especially, there is any data on the densest polymorph ringwoodite. Shock compression of wadsleyite was carried out up to 200 GPa by using polycrystalline samples [4]. In addition, there are no studies by using single crystal samples for both wadsleyite and ringwoodite. To newly conduct such studies, the denser polymorph of Mg_2SiO_4 are needed to be synthesized and grown at their relevant conditions of deep mantle corresponding to the 15 –21 GPa and 1000 –1500 ˚C in the laboratory. Most importantly, the synthesized minerals must be chemically, physically and optically homogenous and should have suitable sizes for the laser-shock experiments. Here, by utilizing the results of our previous efforts for growing such quality of single crystals, we made possible to obtain Hugoniot relation of wadsleyite and ringwoodite by laser-shock compression. Their crystals were synthesized and grown by using a scaled-up Kawai-type cell by together with applying our pre-established a slow-cooling method at their relevant conditions [5]. Recovered crystals were up to 1 mm in sizes and confirmed to be chemically homogenous and free from twinning, cracks, and inclusions. The crystals were then doubly polished separately down to 100 mm in thickness and with an area of > 500 mm. They were assembled to form targets which are optimized for the laser-shock experiments. laser-shock experiments at GEKKO XII were conducted at Institute of Laser Engineering, Osaka University. The crystals are optical to give very clean VISAR (Velocity Interferometer System for Any Reflector) images. The details of our technical developments will be discussed on the poster.

[1] Root, T., Townsend, J. L., Davies, E., Lemke, R. W., Bliss, D. E., Fratanduono, D. E., et al. (2018). *Geophys. Res. Lett.*, **45**:3865. [2] Sekine, T., Ozaki, N., Miyanishi, K., Asaumi, Y., Kimura, T., Albertazzi, B. et al. (2016). *Sci. Adv.*, **2**:e1600157. [3] Bolis, R. M., Morard, G., Vinci, T., Ravasio, A., Bambrink, E. et al. (2016). *Geophys. Res. Lett.*, **43**:9475. [4] Mosenfelder, J. L., Asimow, P. D. and Ahrens, T. J. (2007). *J. Geophys. Res.*, **112**:B06208. [5] Okuchi, T., Purevjav, N., Tomioka, N., Lin, J. F., Kuribayashi, T. et al. (2015). *Am. Mineral.*, **100**:1483.

Keywords: laser-shock compression, Mg2SiO4 polymorphs

©2019. Japan Geoscience Union. All Right Reserved.

©2019. Japan Geoscience Union. All Right Reserved.

Richtmyer-Meshkov instability in inhomogeneous density materials and its application to planetary science

*Takayoshi Sano[1]

1. Institute of Laser Engineering, Osaka University

Richtmyer-Meshkov instability (RMI) is a hydrodynamic interfacial instability, which occurs by the interaction between a shock wave and corrugated density jump. Because of the corrugation of the interface, the surface profiles of the transmitted and reflected shocks are also rippled. The RMI is driven by the vorticity left by these rippled shocks at the interface and in the fluid. In this study, we consider shock propagation in inhomogeneous density materials (e.g., uniform density materials with small round voids) and the turbulent growth of the interface. For these cases, the vorticity distribution and turbulent motion are much more complicated than the standard RMI cases. Then the spatial fluctuation of pressure or temperature could be significantly large after the shock passage. Using two-dimensional hydrodynamic simulations, we will examine the dependence of the pressure fluctuation on the density inhomogeneity. As the application of this numerical study, we will discuss about the shock propagation in meteorites with large density fluctuation.

Keywords: shock waves, Richtmyer-Meshkov instability

©2019. Japan Geoscience Union. All Right Reserved.

Impact-induced dehydration reactions of Fe- and Al-hydrates as potential storage, carrier and source of water

*Tsubasa Tobase[1], Toshimori Sekine[1], Ginga Kitahara[2], Makoto Tokuda[2], Akira Yoshiasa[2], Makoto Takafuji[2], Tsutomu Mashimo[2], Nobuaki Kawai[2]

1. HPSTAR, 2. Graduate School of Science and Technology, Kumamoto University

Hydrous minerals have been known to play an important role to preserve and carry water because a mechanism is required for water to reach the inner planets such as Earth far beyond the snow line that defines the boundary between water ice and vapor. In order to understand the detailes, we need to know the stability at high temperature and high pressure and impact resistance for possible hydrous minerals. Fe- and Al-hydrates (FeOOH and AlOOH) have been reported to be stable under static high temperature and static high pressure. In addition, they are observed in some meteorites and the surface on Mars. Although there are some data available on clay minerals and serpentine, those Fe- and Al-hydrates are considered to be present in the Earth’ s deep lower mantle according to the recent studies.

We have investigated the impact resistibility through shock recovery techniques. Our peak shock pressures are 24 GPa and 31 GPa for the recovered Fe- and Al-hydrates, respectively, where they displayed significant dehydration. We set various range of sample porosity and peak shock pressure to investing the dehydration reaction. These impact conditions correspond to impact velocities of 2.6 km/s and 4.9 km/s if we assume face to face impacts between carbonaceous chondrite such as Murchison. These are within a range of velocity for possible meteoritic collisions, and we need to know the relationship between impact condition and degree of dehydration. Using TG/DTA analyses of samples we estimated the relationship. The phase changes by impact dehydration are investigated by XRD, XAFS and Raman spectroscopy. We also try to understand dynamical void formation process by dehydration that can occur during adiabatic quenching through observation of void distribution in the recovered samples.

In our previous research for shock recovery experiments of hydrous minerals, we observed heterogenous temperature rise in dehydration process. We tried to confirm whether heterogeneous temperature rise occurs even in Fe- and Al-hydrates by comparison with the results between previously reported hydrous minerals. We will be able to select most possible candidate by comparing the thermal stability and impact resistibility among them.

Keywords: Shock recovered experiments, hydrous mineral, dynamic water loss, Powder x-ray diffraction

©2019. Japan Geoscience Union. All Right Reserved.

Crystallization of amorphous $MgSiO_3$ by shock compression

*Akane Arasuna[1], Masayuki Okuno[1], Nobuaki Kawai[2]

1. Kanazawa University, 2. Kumamoto University

Structural change of synthesized amorphous $MgSiO_3$ by shock compression up to 22.2 GPa has been investigated using XRD and IR analyses. The obtained result provides information for elucidating of the collision behavior of $MgSiO_3$ contained in cosmic dust.

Amorphous $MgSiO_3$ sample was prepared by an aqueous solution of TEOS, Magnesium Nitrate Hexahydrate, and ethanol with ammonia as a catalyst. As-prepared sample was heated at 700 C˚ to dehydrate excess water. TG curve of this sample indicated that the sample contained about 8.8 wt% of water molecules and hydroxyl groups.

A powdered heated (original) sample was put in an aluminum tubes and pressed at 20 kN for 10 minutes to obtain samples for shock compression experiment. These samples were compressed at 13.6, 17.2, and 22.2 GPa using a single-stage propellant gun at Kumamoto University.

XRD pattern of the pressed sample showed no crystalline peak as same as the original sample. However, the XRD pattern of thesample compressed at 13.6 GPa showed the weak crystalline peaks at around 2θ = 28, 31, 35-36˚. These peaks became intense with increasing shock pressure. Crystalline peaks observed in the XRD pattern for the sample of 22.2 GPa were attributed to those of enstatite. However, some peaks was due to the formation of Mg_2SiO_4. IR spectra for the compressed samples showed the similar trend as the result of XRD analysis. But IR analysis indicated that the sample contains water molecules even after the shock compression at 22.2 GPa. Water molecules probably present in the remaining amorphous part. Crystallization of sample by shock compression has not been reported in shock experiments for other crystalline and non-crystalline silicates. The crystallization of our samples at low pressure may be due to the simple chain structure of enstatite. Also, high shock temperature which generated by friction due to the porosity of the sample may promote this crystallization.

Keywords: MgSiO3, amorphous , shock compression, enstatite

©2019. Japan Geoscience Union. All Right Reserved.

First-principle study of the structural and electronic properties of N-doped $MgAl_2O_4$ spinel

*Chi Pui Tang[1], Pak Kin Leong[1], Toshimori Sekine[2,3]

1. State Key Laboratory of Lunar and Planetary Sciences, Macau University of Science and Technology, 2. Center for High Pressure Science and Technology Advanced Research (HPSTAR) Shanghai Laboratory of HPSTAR, Shanghai, P.R. China, 3. Graduate School of Engineering, Osaka University

On basis of the first principle calculation, we report a possible nitrogen doped structure of $MgAl_2O_4$ spinel. The structural and electronic properties (include the band structure, density of states and phonon) of spinel ($MgAl_2O_4$) and N-doped spinel ($MgAl_2O_{3.5}N_{0.5}$) compounds are performed using density functional theory (DFT). The density and space group of two crystal cells are 3.47 g/cm^3 (Fd3m) for $MgAl_2O_4$ and 3.38 g/cm^3 (R3m) for $MgAl_2O_{3.5}N_{0.5}$, respectively. The calculated direct band gaps at the Γ-point are about 5.13 eV for $MgAl_2O_4$ and 4.24 eV for $MgAl_2O_{3.5}N_{0.5}$, respectively. The projected density of states (PDOS) shows that the tops of the valence bands are built up from ~93% of *p*(O) states and ~60% of *p*(N) + ~32% of *p*(O) states (for $MgAl_2O_4$ and $MgAl_2O_{3.5}N_{0.5}$, respectively). In the phonon analysis, the lowest frequency of $MgAl_2O_{3.5}N_{0.5}$ is redshifted to 36.6 cm^{-1} ($MgAl_2O_4$ is 39.8 cm^{-1}) caused by the N-doped. We also calculate their cohesive energy in the pressure range of 0-150 GPa. We found that the cohesive energy of $MgAl_2O_{3.5}N_{0.5}$ is lower than $MgAl_2O_4$ at the pressure higher than ~115 GPa, it implies that $MgAl_2O_{3.5}N_{0.5}$ is more stable than $MgAl_2O_4$ at high pressure. Finally, we suggest that nitrogen atom would replace the oxygen of spinel in the depths of the earth. The results imply the deep mantle may storage a considerable amount of nitrogen.

Keywords: First principle calculation, Density functional theory, Spinel

©2019. Japan Geoscience Union. All Right Reserved.

Transparency of shock-compressed single crystal diamond

*Kento Katagiri[1], Norimasa Ozaki[1,2], Kohei Miyanishi[2], Yuhei Umeda[1], Shintaro Morioka[1], Takayoshi Sano[2], Ryosuke Kodama[1,2]

1. Osaka University, 2. Institute of Laser Engineering, Osaka Unversity

Carbon is one of the most prominent elements in nature and it is abundant in the Earth and many other planets. Diamond, a metastable phase of carbon, is naturally synthesized in deep inside of the Earth where substances are isotropically pressured. Diamond is known for its many unique properties such as high hardness, low compressibility, small thermal expansion coefficient, and transparency. Since it is important to understand how substances behave under high pressure, properties of compressed diamond have been measured in a wide range of pressures up to 5 TPa. However, the transparency of diamond under pressure has not been fully elucidated. Here, we report the measurment of the pressure dependency of the absorption coefficient of laser shock compressed single crystalline diamond. A high-intensity laser was utilized to shock compress the diamond sample along its <100> direction, and velocity interferometer systems for any reflector (VISARs) were used to determine the absorption coefficient and pressure. It was found that single crystalline diamond remains largely transparent to the probe laser for VISAR (λ =532 nm) up to 140 GPa. The pressure dependence of the refractive index will also be discussed.

This experiment was conducted under the joint research of the Institute of Laser Engineering, Osaka University. This work was supported in part by JSPS KAKENHI grant No. 16H02246 and No. 16H01119. The part of work was also supported by Genesis Research Institute, Inc. (Konpon-ken, TOYOTA).

Keywords: Shock-compression, High intensity laser, Diamond, Transparency, Refractive index

©2019. Japan Geoscience Union. All Right Reserved.

Pb-Pb dating of the NWA 7203 angrite and relationship to its shock metamorphism

*Hideyuki Hayashi[1], Takashi Mikouchi[1], Yuji Sano[1], Martin Bizzarro[2]

1. The university of Tokyo, 2. University of Copenhagen

Introduction: Angrite is one of the oldest basaltic achondrites in the early solar system which is depleted in volatile elements and enriched in refractory elements (e.g., Keil, 2012). Almost all angrites show either a quenched or slowly-cooled texture. The crystallization ages of quenched angrites are older (ca. 4564 Ma) than those of slowly-cooled samples (ca. 4558 Ma). One of the most striking mineralogical characteristics about angrites is the lack of shock metamorphism. Thus, quenched angrites can be good time anchors to connect absolute and relative ages, because the age differences between two systems can be ignored due to fast cooling and furthermore there is no chronological reset by shock metamorphism. However, NWA 1670 and NWA 7203 are known to show evidence for shock (Mikouchi et al., 2003; Hayashi et al., 2018), and especially we found that NWA 7203 exhibited remarkable shock metamorphic textures. The Pb-Pb dating of angrites has been done only for angrites without shock textures, indicating the obtained ages are crystallization ages. Pb-Pb age is relatively easy to be reset by shock heating. Therefore, Pb-Pb age of NWA 1670 or especially NWA 7203 may be reset by shock heating. However, there is no study which measured Pb-Pb dating of NWA 1670 or NWA 7203. In this study, we measured Pb isotopic ratios of silico-apatite in NWA 7203 by Nano-SIMS, and discussed the Pb-Pb age of NWA 7203.

Sample: We used NWA 7203 for this study. NWA 7203 is an angrite meteorite showing a quenched texture. NWA 7203 consists of a dendritic texture of olivine and anorthite, and pyroxene fills gaps of the dendrites. Grain size exhibits large variations from fine grains (~1 μm) to coarse grains (>100 μm). This is not a typical characteristic of quenched angrites. NWA 7203 is composed mainly of olivine, pyroxene and anorthite, and the accessory minerals are troilite, ulvospinel and silico-apatite.

Methods: Observation was carried out on thin sections by optical microscope and BSE images of FE-EPMA. Mineral phases were identified by micro-Raman spectroscopic analysis. Pb-Pb dating of NWA 7203 was carried out by measuring Pb isotope ratios of silico-apatites using Nano-SIMS at AORI, Univ. of Tokyo. Measurement conditions were 300 pA for primary ions and $^{16}O^-$ for ion sources. Pre-sputtering was performed for 8 minutes in the range of 10 x 10 μm. In the SIMS measurement, raster diameter of 3 x 3 μm and analysis time of 60 seconds were applied for two magnetic fields, respectively, and repeated for 30 cycles. For the standard, NIST SRM 610 was used.

Result and discussion: Pb isotopic ratios of silico-apatite in the NWA 7203 angrite were obtained. We obtained a weighted approximate straight line for each plot and found the Pb-Pb age to be 4551 ±17 Ma. These plots are relatively variable. This is probably because Pb isotopic ratios were disturbed by shock metamorphism. In fact, the Pb-Pb age of silico-apatite grains that are at least 200 μm away from the shock veins was found to be 4560 ±16 Ma. It is considered that the Pb isotopic ratios of these silico-apatite grains are relatively undisturbed as they are linearly aligned. This age coincides with the crystallization age of other quenched angrites within the error range. Takenouchi et al. (2019) measured the Ar-Ar ages of NWA 7203 and found that it has two plateau ages of 3800 ±440 Ma and 2300 ±140 Ma, and concluded that the shock metamorphism of NWA 7203 occurred at 2300 ±140 Ma. From this result, it is considered that the Pb-Pb age of NWA 7203 is not completely reset, but slightly disturbed.

©2019. Japan Geoscience Union. All Right Reserved.

Keywords: NWA 7203, Angrite, Pb-Pb dating, Shock metamorphism, Parent body

©2019. Japan Geoscience Union. All Right Reserved.

Shock recovery of high-pressure phase of SiO_2 using high-power laser

*Tadashi Kondo[1], Hiromoto Kengo[1], Tatsuhiro Sakaiya[1], Hidenori Terasaki[1], Keisuke Shigemori[2], Youichiro Hironaka[2]

1. Department of Earth and Space Science, Graduate School of Science Osaka University, 2. Institute of Laser Engineering, Osaka University

High-pressure phases in meteorites provide us the important information of shock history in natural materials. Experimental approach to reproduce such high-pressure phase have been studied intensively mainly by light-gas gun so far, though shock condition with impact velocity beyond 10km/s is difficult. Recent technical progress of high-intensity laser as a tool of shock experiment realize the recovery of samples with shock condition above 10km/s(Nagaki et al.,2016). However, the limited shock duration time of about 10 nsec has been too short to drive structural conversion to high-pressure form in single crystal sample. In this study, we explored recovery condition of high-pressure phase of SiO_2 using finely ground samples of quartz, cristobalite and fused silica as starting materials. Laser shock experiments were performed using GXII hyper laser at Institute of Laser Engineering, Osaka University. The whole sample retaining relative locations in the recovered box made of aluminum was quenched without significant scattering in each run. The sectioned sample at shocked center were examined by optical microscope, micro-focused X-ray diffraction and SEM-EDS. We will report the characteristic feature of top portion of sample, which shows layered structure with different metamorphism, and distribution of grass and stishovite phase found in the samples shocked above 100GPa, which have still a residual stress to 10GPa in the ambient condition. We will discuss the dependence of the initial state of crystal to recover the high-pressure phase in shocked samples in nsec.

Keywords: shocked quartz, high-intensity laser, recovery experiments

©2019. Japan Geoscience Union. All Right Reserved.

Hugoniot measurement of calcite under meteorite collision condition

*Fukui Keiya[1], Norimasa Ozaki[1,2], Yuhei Umeda[1], Kohei Miyanishi[3], Kento Katagiri[1], Shintaro Morioka[1], Takayoshi Sano[3], Ryosuke Kodama[1,2,3]

1. Graduate School of Engineering,Osaka univ., 2. PPC, Osaka Univ., 3. ILE, Osaka Univ.

Volatile substances inside planetary materialsare generated and released as gas under the extreme condition caused by collision phenomenon that is thought to contribute greatly to the formation of the planetary atmosphere [1]. Particularly the degassing reaction of carbonate, may generate CO or CO_2as greenhouse gas and affect the temperature of the planetary surface. A typical planetary mineral as carbonate of calcite ($CaCO_3$) is expected degassing above 3300 K at pressure of 150 GPa along the Hugoniot[2].
In the previous study, the experimental investigations for the shock-degassing reaction were carried out only below the impact pressure of 100 GPa. Also, we have not understood when the degassing reaction of calcite occur on a compressed state or a released state [3]
In natural, typical meteorite impacts exceed 10 km/s in impact velocity, and can generate at the pressure above 150 GPa. The purpose of this research is to understand the impact compression characteristics of calcite under the meteorite collision condition.

This experiment was conducted in Shock Drive Laser (Gekko XII) atInstitute for Laser Engineering, Osaka University. The target consists of polypropylene as an ablator aluminum as a piston, quartz as a standard material, and calcite as a sample from laser side. The impact pressures and temperatures were estimated by the measured shock wave velocity using Velocity interferometer system for any reflector (VISAR) and self-emission intensity using radiance thermometer (SOP).
As a result of this experiments, we obtained the Hugoniot date at the puressure from 200 GPa to 1 Tpa at the temperature above 5000 K. The detailed results will be shown as this presentation.
Acknowledgements

This experiment was conducted on the joint research of the Institute of Laser Engineering, Osaka University. This work was supported in part by JSPS KAKENHI grant No. 16H02246 and No. 16H01119. The part of work was also supported by Genesis Research Institute, Inc. (Konpon-ken, TOYOTA).

REFERENCES

[1] T. Matsui and Y.Abe: Nature, 319, 303 - 319 (1986).

[2] B.Ivanov and A. Deutsch: Physics of the Earth and Planetary Interiors, 129, 131-143 (2002).

[3] K.Kawaragi et al.: Earth and Planetary Science Letters, 282, 56 - 64 (2009).

Keywords: Laser-Shock-compression, hugoniot, calcite, degassing

©2019. Japan Geoscience Union. All Right Reserved.

Direct observation of the transformation toughening of tetragonal stabilized zirconia under shock deformation condition by ns time-resolved XRD.

*Sota Takagi[1,2], Kouhei Ichiyanagi[2,3], Nobuaki Kawai[4], Ryo Fukaya[2], Shunsuke Nozawa[2], Atsushi Kyono[1], Nobumasa Funamori[2], Shin-ichi Adachi[2]

1. University of Tsukuba, 2. KEK PF, 3. Jichi Medical University, 4. Kumamoto University

The enhancement of strength and toughness was found in oxide-doped tetragonal stabilized zirconia, with the suggestion that the absorption of energy during the martensitic transformation contribute to the increment [Gravie et al., 1975; Gupta et al., 1977]. Using transmission electron microscopy (TEM), in recovery sample, it was observed that the stress-induced transformation from stabilized tetragonal phase to monoclinic phase can be occurred around the crack tip [Porter et al., 1977], and the transformation-toughening model were devised [McMeeking et al., 1982; Hannink et al., 2000]. In high-pressure experiments, the phase transformation behavior of tetragonal stabilized zirconia has not been clarified in both static and shock compression because a lack of in-situ observation [Ohtaka et al., 1988; Grady et al., 1992]. We tried to observe the behavior of tetragonal stabilized zirconia under shock compression condition using time-resolved XRD method.We performed the experiments at NW14A beamline at PF-AR (Photon Factory Advanced Ring), High Energy Accelerator Research Organization (KEK), Japan. Nd:glass laser with the wavelength of 1064 nm, pulse energy of 16 J, pulse width of 12 ns was used for shock-driving source. The laser beam was focused by optical lens to the size of 500 μm × 500 μm on the sample surface. For TR-XRD experiments, the synchrotron X-ray pulse of PF-AR was used as a probe source. The energy, the pulse width, and the size on the sample were 15.68 keV, about 100 ps, and 450 μm (H) ×250 μm (W), respectively. The irradiation timing between laser pulse and X-ray pulse on the sample surface were controlled by delay generator at ns time scale. The targets consisted of an 25 um PET film ablator with Al coated on the surface and 50 um polycrystalline 3 mol% yttria doped tetragonal stabilized zirconia.
The XRD change were observed up to 35 ns after shock compression started. Before shock, the (101), (002), (110), (102), (112), (200) diffraction of tetragonal phase were observed. 6.5 ns after shock, the diffraction from compression region appeared with maximum compression of 6%. No phase transition occurred at compression states. At release states (~11.4 ns), on the other hand, the (-111), (111), (022), (-221) diffraction peaks of monoclinic phase were appeared. We will discuss the detail of the experimental results and the transformation toughening mechanism.

Keywords: Synchrotron X-ray, Time-resolved XRD, Laser-induced shock wave, Tetragonal stabilized zirconia

©2019. Japan Geoscience Union. All Right Reserved.

[E] Poster | P (Space and Planetary Sciences)：P-CG Complex & General

Tue. May 28, 2019 5:15 PM - 6:30 PM JST | Tue. May 28, 2019 8:15 AM - 9:30 AM UTC | Poster Hall International Exhibition Hall8, Makuhari Messe_4

[P-CG22] Shock responses of planetary materials elucidated from meteorites and dynamic compression experiments

convener:Toshimori Sekine(Center for High Pressure Science and Technology Advanced Research), Takuo Okuchi(Institute for Planetary Materials, Okayama University)

Impact phenomena had played essential roles in the process of planetary evolution. Recent analytical and experimental developments reveal a new prospective on the effects of shock-compression process for planetary materials. For deeper understanding of such shock effects, it is necessary to evaluate the detailed shock conditions from the observations of naturally-shocked planetary materials, and to compare them with the results on the planetary materials experienced a wide range of known shock conditions. Several metastable phases, that have not been known before, have recently been identified in shocked meteorites. They suggest that the shock state is often not in equilibrium and that it is more complicated process than ever thought. Experimental techniques including laser-driven shock compression and x-ray free electron laser diagnostics have been progressed to successfully simulate a wide range of shock conditions. The recent results indicate that shocked grains are fractured and rotated at relatively low pressures, and that they are subsequently transformed into denser phases or melts, or their mixtures at pressures of a few 100s GPa. Understanding of such shock dynamics requires another prospect, which is qualitatively different from the static high pressure and high temperature consensus. Therefore, it is timely to have an international symposium on dynamics of planetary materials.

[PCG22-P01] discussion

*Takuo Okuchi[1], Toshimori Sekine[2] (1.Institute for Planetary Materials, Okayama University, 2.Center for High Pressure Science and Technology Advanced Research)

[PCG22-P02] Shock-compressed behavior of quartz by XFEL

*Tomoko Sato[1], Yoshinori Tange[2], Yusuke Seto[3], Toshimori Sekine[4,5], Norimasa Ozaki[4], Toyohito Nishikawa[4], Kohei Miyanishi[4], Kensuke Matsuoka[4], Ryosuke Kodama[4], Tadashi Togashi[2], Yuichi Inubushi[2], Toshinori Yabuuchi[6], Makina Yabashi[6] (1.Hiroshima University, 2.Japan Synchrotron Radiation Research Institute, 3.Kobe University, 4.Osaka University, 5.Center for High Pressure Science &Technology Advanced Research, 6.RIKEN)

[PCG22-P04] Laser-shock experiments of dense polymorphs of Mg_2SiO_4: technical developments using synthetic single crystals

*Narangoo Purevjav[1], Takuo Okuchi[1], Norimasa Ozaki[2], Takayoshi Sano[3], Yuhei Umeda[2], Shintaro Morioka[2], Nobuki Kamimura[2] (1.Institute for Planetary Materials, Okayama University, 2.Graduate School of Engineering, Osaka University, 3.Institute of Laser Engineering, Osaka University)

[PCG22-P05] Richtmyer-Meshkov instability in inhomogeneous density materials and its application to planetary science

*Takayoshi Sano[1] (1.Institute of Laser Engineering, Osaka University)

[PCG22-P06] Impact-induced dehydration reactions of Fe- and Al-hydrates as potential storage, carrier and source of water

*Tsubasa Tobase[1], Toshimori Sekine[1], Ginga Kitahara[2], Makoto Tokuda[2], Akira Yoshiasa[2], Makoto Takafuji[2], Tsutomu Mashimo[2], Nobuaki Kawai[2] (1.HPSTAR, 2.Graduate School of Science and Technology, Kumamoto University)

[PCG22-P07] Crystallization of amorphous $MgSiO_3$ by shock compression

*Akane Arasuna[1], Masayuki Okuno[1], Nobuaki Kawai[2] (1.Kanazawa University, 2.Kumamoto University)

[PCG22-P08] First-principle study of the structural and electronic properties of N-doped $MgAl_2O_4$ spinel

*Chi Pui Tang[1], Pak Kin Leong[1], Toshimori Sekine[2,3] (1.State Key Laboratory of Lunar and Planetary Sciences, Macau University of Science and Technology, 2.Center for High Pressure Science and Technology Advanced Research (HPSTAR) Shanghai Laboratory of HPSTAR, Shanghai, P.R. China, 3.Graduate School of Engineering, Osaka University)

[PCG22-P09] Transparency of shock-compressed single crystal diamond

*Kento Katagiri[1], Norimasa Ozaki[1,2], Kohei Miyanishi[2], Yuhei Umeda[1], Shintaro Morioka[1], Takayoshi Sano[2], Ryosuke Kodama[1,2] (1.Osaka University, 2.Institute of Laser Engineering, Osaka Unversity)

[PCG22-P10] Pb-Pb dating of the NWA 7203 angrite and relationship to its shock metamorphism

*Hideyuki Hayashi[1], Takashi Mikouchi[1], Yuji Sano[1], Martin Bizzarro[2] (1.The university of Tokyo, 2.University of Copenhagen)

[PCG22-P11] Shock recovery of high-pressure phase of SiO_2 using high-power laser

*Tadashi Kondo[1], Hiromoto Kengo[1], Tatsuhiro Sakaiya[1], Hidenori Terasaki[1], Keisuke Shigemori[2], Youichiro Hironaka[2] (1.Department of Earth and Space Science, Graduate School of Science Osaka University, 2.Institute of Laser Engineering, Osaka University)

[PCG22-P12] Hugoniot measurement of calcite under meteorite collision condition

*Fukui Keiya[1], Norimasa Ozaki[1,2], Yuhei Umeda[1], Kohei Miyanishi[3], Kento Katagiri[1], Shintaro Morioka[1], Takayoshi Sano[3], Ryosuke Kodama[1,2,3] (1.Graduate School of Engineering,Osaka univ., 2.PPC, Osaka Univ., 3.ILE, Osaka Univ.)

[PCG22-P13] Direct observation of the transformation toughening of tetragonal stabilized zirconia under shock deformation condition by ns time-resolved XRD.

*Sota Takagi[1,2], Kouhei Ichiyanagi[2,3], Nobuaki Kawai[4], Ryo Fukaya[2], Shunsuke Nozawa[2], Atsushi Kyono[1], Nobumasa Funamori[2], Shin-ichi Adachi[2] (1.University of Tsukuba, 2.KEK PF, 3.Jichi Medical University, 4.Kumamoto University)

discussion

*Takuo Okuchi[1], Toshimori Sekine[2]

1. Institute for Planetary Materials, Okayama University, 2. Center for High Pressure Science and Technology Advanced Research

We discuss natural and experimendal evidences on impact phenomena, which had played essential roles in the process of early planetary evolution. Recent analytical and experimenotal developments reveal a new prospective on the effects of shock-compression process of planetary materials. For deeper understanding of such shock effects, it is necessary to evaluate the detailed shock conditions from the observations of naturally-shocked planetary materials, as well as to compare them with the results of shock-compression experiments of these materials obtained at laboratory conditions.

Keywords: discussion

©2019. Japan Geoscience Union. All Right Reserved.

Shock-compressed behavior of quartz by XFEL

*Tomoko Sato[1], Yoshinori Tange[2], Yusuke Seto[3], Toshimori Sekine[4,5], Norimasa Ozaki[4], Toyohito Nishikawa[4], Kohei Miyanishi[4], Kensuke Matsuoka[4], Ryosuke Kodama[4], Tadashi Togashi[2], Yuichi Inubushi[2], Toshinori Yabuuchi[6], Makina Yabashi[6]

1. Hiroshima University, 2. Japan Synchrotron Radiation Research Institute, 3. Kobe University, 4. Osaka University, 5. Center for High Pressure Science &Technology Advanced Research, 6. RIKEN

We have conducted x-ray diffraction measurement (XRD) with femtosecond x-ray pulses generated by the x-ray free electron laser (XFEL) to observe lattice dynamics and phase transformation of single-crystal quartz under high strain-rate shock compression (~10^9 s^{-1}) and high pressure. Single-crystal quartz samples were shock-compressed by high-power short- and long-pulse lasers. In the short-pulse experiments, the lattice was reduced to 15% and 1.5% in the direction parallel and perpendicular to the compression axis, respectively. The sample was uniaxially compressed over its known Hugoniot elastic limit. In the long-pulse experiments, three different states were observed. Polycrystalline stishovite appeared at first, and elastically compressed state and a topotaxially transformed new phase were observed successively.

Keywords: Shock compression, in-situ X-ray diffraction, quartz

©2019. Japan Geoscience Union. All Right Reserved.

Laser-shock experiments of dense polymorphs of Mg_2SiO_4: technical developments using synthetic single crystals

*Narangoo Purevjav[1], Takuo Okuchi[1], Norimasa Ozaki[2], Takayoshi Sano[3], Yuhei Umeda[2], Shintaro Morioka[2], Nobuki Kamimura[2]

1. Institute for Planetary Materials, Okayama University, 2. Graduate School of Engineering, Osaka University, 3. Institute of Laser Engineering, Osaka University

Mg_2SiO_4 polymorphs (α-phase as forsterite, β-phase as wadsleyite, and γ-phase as ringwoodite) are the major constituents of our Earth's mantle and also for Earth-like planets. Thus studying these polymorphs at extreme pressure and temperature conditions will lead to understanding their changes of chemical and physical properties at extremely high pressure and temperature conditions, such as those occurring during the giant impacts phenomena of such planets at their final stage of accretion. Shock compression of forsterite has been studied up to ~ 1000 GPa by using polycrystalline and single crystal samples [1-3]. The studies have reported contradicting results for the shock compression of forsterite. Sekine et al (2016) reported that there are several phase transformations in the liquid state of Mg_2SiO_4 at > 270 GPa, while other two studies were reported no phase transformation [1, 3]. Thus it is interesting to see how the Hugonoit relations of Mg_2SiO_4 polymorphs will come up at different pressure and temperature conditions. However, Hugoniot relations of wadsleyite and ringwoodite have not been studied well. Especially, there is any data on the densest polymorph ringwoodite. Shock compression of wadsleyite was carried out up to 200 GPa by using polycrystalline samples [4]. In addition, there are no studies by using single crystal samples for both wadsleyite and ringwoodite. To newly conduct such studies, the denser polymorph of Mg_2SiO_4 are needed to be synthesized and grown at their relevant conditions of deep mantle corresponding to the 15 –21 GPa and 1000 –1500 ˚C in the laboratory. Most importantly, the synthesized minerals must be chemically, physically and optically homogenous and should have suitable sizes for the laser-shock experiments. Here, by utilizing the results of our previous efforts for growing such quality of single crystals, we made possible to obtain Hugoniot relation of wadsleyite and ringwoodite by laser-shock compression. Their crystals were synthesized and grown by using a scaled-up Kawai-type cell by together with applying our pre-established a slow-cooling method at their relevant conditions [5]. Recovered crystals were up to 1 mm in sizes and confirmed to be chemically homogenous and free from twinning, cracks, and inclusions. The crystals were then doubly polished separately down to 100 mm in thickness and with an area of > 500 mm. They were assembled to form targets which are optimized for the laser-shock experiments. laser-shock experiments at GEKKO XII were conducted at Institute of Laser Engineering, Osaka University. The crystals are optical to give very clean VISAR (Velocity Interferometer System for Any Reflector) images. The details of our technical developments will be discussed on the poster.

[1] Root, T., Townsend, J. L., Davies, E., Lemke, R. W., Bliss, D. E., Fratanduono, D. E., et al. (2018). *Geophys. Res. Lett.*, **45**:3865. [2] Sekine, T., Ozaki, N., Miyanishi, K., Asaumi, Y., Kimura, T., Albertazzi, B. et al. (2016). *Sci. Adv.*, **2**:e1600157. [3] Bolis, R. M., Morard, G., Vinci, T., Ravasio, A., Bambrink, E. et al. (2016). *Geophys. Res. Lett.*, **43**:9475. [4] Mosenfelder, J. L., Asimow, P. D. and Ahrens, T. J. (2007). *J. Geophys. Res.*, **112**:B06208. [5] Okuchi, T., Purevjav, N., Tomioka, N., Lin, J. F., Kuribayashi, T. et al. (2015). *Am. Mineral.*, **100**:1483.

Keywords: laser-shock compression, Mg2SiO4 polymorphs

©2019. Japan Geoscience Union. All Right Reserved.

©2019. Japan Geoscience Union. All Right Reserved.

Richtmyer-Meshkov instability in inhomogeneous density materials and its application to planetary science

*Takayoshi Sano[1]

1. Institute of Laser Engineering, Osaka University

Richtmyer-Meshkov instability (RMI) is a hydrodynamic interfacial instability, which occurs by the interaction between a shock wave and corrugated density jump. Because of the corrugation of the interface, the surface profiles of the transmitted and reflected shocks are also rippled. The RMI is driven by the vorticity left by these rippled shocks at the interface and in the fluid. In this study, we consider shock propagation in inhomogeneous density materials (e.g., uniform density materials with small round voids) and the turbulent growth of the interface. For these cases, the vorticity distribution and turbulent motion are much more complicated than the standard RMI cases. Then the spatial fluctuation of pressure or temperature could be significantly large after the shock passage. Using two-dimensional hydrodynamic simulations, we will examine the dependence of the pressure fluctuation on the density inhomogeneity. As the application of this numerical study, we will discuss about the shock propagation in meteorites with large density fluctuation.

Keywords: shock waves, Richtmyer-Meshkov instability

©2019. Japan Geoscience Union. All Right Reserved.

Impact-induced dehydration reactions of Fe- and Al-hydrates as potential storage, carrier and source of water

*Tsubasa Tobase[1], Toshimori Sekine[1], Ginga Kitahara[2], Makoto Tokuda[2], Akira Yoshiasa[2], Makoto Takafuji[2], Tsutomu Mashimo[2], Nobuaki Kawai[2]

1. HPSTAR, 2. Graduate School of Science and Technology, Kumamoto University

Hydrous minerals have been known to play an important role to preserve and carry water because a mechanism is required for water to reach the inner planets such as Earth far beyond the snow line that defines the boundary between water ice and vapor. In order to understand the detailes, we need to know the stability at high temperature and high pressure and impact resistance for possible hydrous minerals. Fe- and Al-hydrates (FeOOH and AlOOH) have been reported to be stable under static high temperature and static high pressure. In addition, they are observed in some meteorites and the surface on Mars. Although there are some data available on clay minerals and serpentine, those Fe- and Al-hydrates are considered to be present in the Earth’ s deep lower mantle according to the recent studies.

We have investigated the impact resistibility through shock recovery techniques. Our peak shock pressures are 24 GPa and 31 GPa for the recovered Fe- and Al-hydrates, respectively, where they displayed significant dehydration. We set various range of sample porosity and peak shock pressure to investing the dehydration reaction. These impact conditions correspond to impact velocities of 2.6 km/s and 4.9 km/s if we assume face to face impacts between carbonaceous chondrite such as Murchison. These are within a range of velocity for possible meteoritic collisions, and we need to know the relationship between impact condition and degree of dehydration. Using TG/DTA analyses of samples we estimated the relationship. The phase changes by impact dehydration are investigated by XRD, XAFS and Raman spectroscopy. We also try to understand dynamical void formation process by dehydration that can occur during adiabatic quenching through observation of void distribution in the recovered samples.

In our previous research for shock recovery experiments of hydrous minerals, we observed heterogenous temperature rise in dehydration process. We tried to confirm whether heterogeneous temperature rise occurs even in Fe- and Al-hydrates by comparison with the results between previously reported hydrous minerals. We will be able to select most possible candidate by comparing the thermal stability and impact resistibility among them.

Keywords: Shock recovered experiments, hydrous mineral, dynamic water loss, Powder x-ray diffraction

©2019. Japan Geoscience Union. All Right Reserved.

Crystallization of amorphous $MgSiO_3$ by shock compression

*Akane Arasuna[1], Masayuki Okuno[1], Nobuaki Kawai[2]

1. Kanazawa University, 2. Kumamoto University

Structural change of synthesized amorphous $MgSiO_3$ by shock compression up to 22.2 GPa has been investigated using XRD and IR analyses. The obtained result provides information for elucidating of the collision behavior of $MgSiO_3$ contained in cosmic dust.

Amorphous $MgSiO_3$ sample was prepared by an aqueous solution of TEOS, Magnesium Nitrate Hexahydrate, and ethanol with ammonia as a catalyst. As-prepared sample was heated at 700 C˚ to dehydrate excess water. TG curve of this sample indicated that the sample contained about 8.8 wt% of water molecules and hydroxyl groups.

A powdered heated (original) sample was put in an aluminum tubes and pressed at 20 kN for 10 minutes to obtain samples for shock compression experiment. These samples were compressed at 13.6, 17.2, and 22.2 GPa using a single-stage propellant gun at Kumamoto University.

XRD pattern of the pressed sample showed no crystalline peak as same as the original sample. However, the XRD pattern of thesample compressed at 13.6 GPa showed the weak crystalline peaks at around 2θ = 28, 31, 35-36˚. These peaks became intense with increasing shock pressure. Crystalline peaks observed in the XRD pattern for the sample of 22.2 GPa were attributed to those of enstatite. However, some peaks was due to the formation of Mg_2SiO_4. IR spectra for the compressed samples showed the similar trend as the result of XRD analysis. But IR analysis indicated that the sample contains water molecules even after the shock compression at 22.2 GPa. Water molecules probably present in the remaining amorphous part. Crystallization of sample by shock compression has not been reported in shock experiments for other crystalline and non-crystalline silicates. The crystallization of our samples at low pressure may be due to the simple chain structure of enstatite. Also, high shock temperature which generated by friction due to the porosity of the sample may promote this crystallization.

Keywords: MgSiO3, amorphous , shock compression, enstatite

©2019. Japan Geoscience Union. All Right Reserved.

First-principle study of the structural and electronic properties of N-doped $MgAl_2O_4$ spinel

*Chi Pui Tang[1], Pak Kin Leong[1], Toshimori Sekine[2,3]

1. State Key Laboratory of Lunar and Planetary Sciences, Macau University of Science and Technology, 2. Center for High Pressure Science and Technology Advanced Research (HPSTAR) Shanghai Laboratory of HPSTAR, Shanghai, P.R. China, 3. Graduate School of Engineering, Osaka University

On basis of the first principle calculation, we report a possible nitrogen doped structure of $MgAl_2O_4$ spinel. The structural and electronic properties (include the band structure, density of states and phonon) of spinel ($MgAl_2O_4$) and N-doped spinel ($MgAl_2O_{3.5}N_{0.5}$) compounds are performed using density functional theory (DFT). The density and space group of two crystal cells are 3.47 g/cm^3 (Fd3m) for $MgAl_2O_4$ and 3.38 g/cm^3 (R3m) for $MgAl_2O_{3.5}N_{0.5}$, respectively. The calculated direct band gaps at the Γ-point are about 5.13 eV for $MgAl_2O_4$ and 4.24 eV for $MgAl_2O_{3.5}N_{0.5}$, respectively. The projected density of states (PDOS) shows that the tops of the valence bands are built up from ~93% of *p*(O) states and ~60% of *p*(N) + ~32% of *p*(O) states (for $MgAl_2O_4$ and $MgAl_2O_{3.5}N_{0.5}$, respectively). In the phonon analysis, the lowest frequency of $MgAl_2O_{3.5}N_{0.5}$ is redshifted to 36.6 cm^{-1} ($MgAl_2O_4$ is 39.8 cm^{-1}) caused by the N-doped. We also calculate their cohesive energy in the pressure range of 0-150 GPa. We found that the cohesive energy of $MgAl_2O_{3.5}N_{0.5}$ is lower than $MgAl_2O_4$ at the pressure higher than ~115 GPa, it implies that $MgAl_2O_{3.5}N_{0.5}$ is more stable than $MgAl_2O_4$ at high pressure. Finally, we suggest that nitrogen atom would replace the oxygen of spinel in the depths of the earth. The results imply the deep mantle may storage a considerable amount of nitrogen.

Keywords: First principle calculation, Density functional theory, Spinel

©2019. Japan Geoscience Union. All Right Reserved.

Transparency of shock-compressed single crystal diamond

*Kento Katagiri[1], Norimasa Ozaki[1,2], Kohei Miyanishi[2], Yuhei Umeda[1], Shintaro Morioka[1], Takayoshi Sano[2], Ryosuke Kodama[1,2]

1. Osaka University, 2. Institute of Laser Engineering, Osaka Unversity

Carbon is one of the most prominent elements in nature and it is abundant in the Earth and many other planets. Diamond, a metastable phase of carbon, is naturally synthesized in deep inside of the Earth where substances are isotropically pressured. Diamond is known for its many unique properties such as high hardness, low compressibility, small thermal expansion coefficient, and transparency. Since it is important to understand how substances behave under high pressure, properties of compressed diamond have been measured in a wide range of pressures up to 5 TPa. However, the transparency of diamond under pressure has not been fully elucidated. Here, we report the measurment of the pressure dependency of the absorption coefficient of laser shock compressed single crystalline diamond. A high-intensity laser was utilized to shock compress the diamond sample along its <100> direction, and velocity interferometer systems for any reflector (VISARs) were used to determine the absorption coefficient and pressure. It was found that single crystalline diamond remains largely transparent to the probe laser for VISAR (λ =532 nm) up to 140 GPa. The pressure dependence of the refractive index will also be discussed.

This experiment was conducted under the joint research of the Institute of Laser Engineering, Osaka University. This work was supported in part by JSPS KAKENHI grant No. 16H02246 and No. 16H01119. The part of work was also supported by Genesis Research Institute, Inc. (Konpon-ken, TOYOTA).

Keywords: Shock-compression, High intensity laser, Diamond, Transparency, Refractive index

©2019. Japan Geoscience Union. All Right Reserved.

Pb-Pb dating of the NWA 7203 angrite and relationship to its shock metamorphism

*Hideyuki Hayashi[1], Takashi Mikouchi[1], Yuji Sano[1], Martin Bizzarro[2]

1. The university of Tokyo, 2. University of Copenhagen

Introduction: Angrite is one of the oldest basaltic achondrites in the early solar system which is depleted in volatile elements and enriched in refractory elements (e.g., Keil, 2012). Almost all angrites show either a quenched or slowly-cooled texture. The crystallization ages of quenched angrites are older (ca. 4564 Ma) than those of slowly-cooled samples (ca. 4558 Ma). One of the most striking mineralogical characteristics about angrites is the lack of shock metamorphism. Thus, quenched angrites can be good time anchors to connect absolute and relative ages, because the age differences between two systems can be ignored due to fast cooling and furthermore there is no chronological reset by shock metamorphism. However, NWA 1670 and NWA 7203 are known to show evidence for shock (Mikouchi et al., 2003; Hayashi et al., 2018), and especially we found that NWA 7203 exhibited remarkable shock metamorphic textures. The Pb-Pb dating of angrites has been done only for angrites without shock textures, indicating the obtained ages are crystallization ages. Pb-Pb age is relatively easy to be reset by shock heating. Therefore, Pb-Pb age of NWA 1670 or especially NWA 7203 may be reset by shock heating. However, there is no study which measured Pb-Pb dating of NWA 1670 or NWA 7203. In this study, we measured Pb isotopic ratios of silico-apatite in NWA 7203 by Nano-SIMS, and discussed the Pb-Pb age of NWA 7203.

Sample: We used NWA 7203 for this study. NWA 7203 is an angrite meteorite showing a quenched texture. NWA 7203 consists of a dendritic texture of olivine and anorthite, and pyroxene fills gaps of the dendrites. Grain size exhibits large variations from fine grains (~1 μm) to coarse grains (>100 μm). This is not a typical characteristic of quenched angrites. NWA 7203 is composed mainly of olivine, pyroxene and anorthite, and the accessory minerals are troilite, ulvospinel and silico-apatite.

Methods: Observation was carried out on thin sections by optical microscope and BSE images of FE-EPMA. Mineral phases were identified by micro-Raman spectroscopic analysis. Pb-Pb dating of NWA 7203 was carried out by measuring Pb isotope ratios of silico-apatites using Nano-SIMS at AORI, Univ. of Tokyo. Measurement conditions were 300 pA for primary ions and $^{16}O^-$ for ion sources. Pre-sputtering was performed for 8 minutes in the range of 10 x 10 μm. In the SIMS measurement, raster diameter of 3 x 3 μm and analysis time of 60 seconds were applied for two magnetic fields, respectively, and repeated for 30 cycles. For the standard, NIST SRM 610 was used.

Result and discussion: Pb isotopic ratios of silico-apatite in the NWA 7203 angrite were obtained. We obtained a weighted approximate straight line for each plot and found the Pb-Pb age to be 4551 ±17 Ma. These plots are relatively variable. This is probably because Pb isotopic ratios were disturbed by shock metamorphism. In fact, the Pb-Pb age of silico-apatite grains that are at least 200 μm away from the shock veins was found to be 4560 ±16 Ma. It is considered that the Pb isotopic ratios of these silico-apatite grains are relatively undisturbed as they are linearly aligned. This age coincides with the crystallization age of other quenched angrites within the error range. Takenouchi et al. (2019) measured the Ar-Ar ages of NWA 7203 and found that it has two plateau ages of 3800 ±440 Ma and 2300 ±140 Ma, and concluded that the shock metamorphism of NWA 7203 occurred at 2300 ±140 Ma. From this result, it is considered that the Pb-Pb age of NWA 7203 is not completely reset, but slightly disturbed.

©2019. Japan Geoscience Union. All Right Reserved.

Keywords: NWA 7203, Angrite, Pb-Pb dating, Shock metamorphism, Parent body

©2019. Japan Geoscience Union. All Right Reserved.

Shock recovery of high-pressure phase of SiO_2 using high-power laser

*Tadashi Kondo[1], Hiromoto Kengo[1], Tatsuhiro Sakaiya[1], Hidenori Terasaki[1], Keisuke Shigemori[2], Youichiro Hironaka[2]

1. Department of Earth and Space Science, Graduate School of Science Osaka University, 2. Institute of Laser Engineering, Osaka University

High-pressure phases in meteorites provide us the important information of shock history in natural materials. Experimental approach to reproduce such high-pressure phase have been studied intensively mainly by light-gas gun so far, though shock condition with impact velocity beyond 10km/s is difficult. Recent technical progress of high-intensity laser as a tool of shock experiment realize the recovery of samples with shock condition above 10km/s(Nagaki et al.,2016). However, the limited shock duration time of about 10 nsec has been too short to drive structural conversion to high-pressure form in single crystal sample. In this study, we explored recovery condition of high-pressure phase of SiO_2 using finely ground samples of quartz, cristobalite and fused silica as starting materials. Laser shock experiments were performed using GXII hyper laser at Institute of Laser Engineering, Osaka University. The whole sample retaining relative locations in the recovered box made of aluminum was quenched without significant scattering in each run. The sectioned sample at shocked center were examined by optical microscope, micro-focused X-ray diffraction and SEM-EDS. We will report the characteristic feature of top portion of sample, which shows layered structure with different metamorphism, and distribution of grass and stishovite phase found in the samples shocked above 100GPa, which have still a residual stress to 10GPa in the ambient condition. We will discuss the dependence of the initial state of crystal to recover the high-pressure phase in shocked samples in nsec.

Keywords: shocked quartz, high-intensity laser, recovery experiments

©2019. Japan Geoscience Union. All Right Reserved.

Hugoniot measurement of calcite under meteorite collision condition

*Fukui Keiya[1], Norimasa Ozaki[1,2], Yuhei Umeda[1], Kohei Miyanishi[3], Kento Katagiri[1], Shintaro Morioka[1], Takayoshi Sano[3], Ryosuke Kodama[1,2,3]

1. Graduate School of Engineering,Osaka univ., 2. PPC, Osaka Univ., 3. ILE, Osaka Univ.

Volatile substances inside planetary materialsare generated and released as gas under the extreme condition caused by collision phenomenon that is thought to contribute greatly to the formation of the planetary atmosphere [1]. Particularly the degassing reaction of carbonate, may generate CO or CO_2as greenhouse gas and affect the temperature of the planetary surface. A typical planetary mineral as carbonate of calcite ($CaCO_3$) is expected degassing above 3300 K at pressure of 150 GPa along the Hugoniot[2].
In the previous study, the experimental investigations for the shock-degassing reaction were carried out only below the impact pressure of 100 GPa. Also, we have not understood when the degassing reaction of calcite occur on a compressed state or a released state [3]
In natural, typical meteorite impacts exceed 10 km/s in impact velocity, and can generate at the pressure above 150 GPa. The purpose of this research is to understand the impact compression characteristics of calcite under the meteorite collision condition.

This experiment was conducted in Shock Drive Laser (Gekko XII) atInstitute for Laser Engineering, Osaka University. The target consists of polypropylene as an ablator aluminum as a piston, quartz as a standard material, and calcite as a sample from laser side. The impact pressures and temperatures were estimated by the measured shock wave velocity using Velocity interferometer system for any reflector (VISAR) and self-emission intensity using radiance thermometer (SOP).
As a result of this experiments, we obtained the Hugoniot date at the puressure from 200 GPa to 1 Tpa at the temperature above 5000 K. The detailed results will be shown as this presentation.
Acknowledgements

This experiment was conducted on the joint research of the Institute of Laser Engineering, Osaka University. This work was supported in part by JSPS KAKENHI grant No. 16H02246 and No. 16H01119. The part of work was also supported by Genesis Research Institute, Inc. (Konpon-ken, TOYOTA).

REFERENCES

[1] T. Matsui and Y.Abe: Nature, 319, 303 - 319 (1986).

[2] B.Ivanov and A. Deutsch: Physics of the Earth and Planetary Interiors, 129, 131-143 (2002).

[3] K.Kawaragi et al.: Earth and Planetary Science Letters, 282, 56 - 64 (2009).

Keywords: Laser-Shock-compression, hugoniot, calcite, degassing

©2019. Japan Geoscience Union. All Right Reserved.

Direct observation of the transformation toughening of tetragonal stabilized zirconia under shock deformation condition by ns time-resolved XRD.

*Sota Takagi[1,2], Kouhei Ichiyanagi[2,3], Nobuaki Kawai[4], Ryo Fukaya[2], Shunsuke Nozawa[2], Atsushi Kyono[1], Nobumasa Funamori[2], Shin-ichi Adachi[2]

1. University of Tsukuba, 2. KEK PF, 3. Jichi Medical University, 4. Kumamoto University

The enhancement of strength and toughness was found in oxide-doped tetragonal stabilized zirconia, with the suggestion that the absorption of energy during the martensitic transformation contribute to the increment [Gravie et al., 1975; Gupta et al., 1977]. Using transmission electron microscopy (TEM), in recovery sample, it was observed that the stress-induced transformation from stabilized tetragonal phase to monoclinic phase can be occurred around the crack tip [Porter et al., 1977], and the transformation-toughening model were devised [McMeeking et al., 1982; Hannink et al., 2000]. In high-pressure experiments, the phase transformation behavior of tetragonal stabilized zirconia has not been clarified in both static and shock compression because a lack of in-situ observation [Ohtaka et al., 1988; Grady et al., 1992]. We tried to observe the behavior of tetragonal stabilized zirconia under shock compression condition using time-resolved XRD method.We performed the experiments at NW14A beamline at PF-AR (Photon Factory Advanced Ring), High Energy Accelerator Research Organization (KEK), Japan. Nd:glass laser with the wavelength of 1064 nm, pulse energy of 16 J, pulse width of 12 ns was used for shock-driving source. The laser beam was focused by optical lens to the size of 500 μm × 500 μm on the sample surface. For TR-XRD experiments, the synchrotron X-ray pulse of PF-AR was used as a probe source. The energy, the pulse width, and the size on the sample were 15.68 keV, about 100 ps, and 450 μm (H) ×250 μm (W), respectively. The irradiation timing between laser pulse and X-ray pulse on the sample surface were controlled by delay generator at ns time scale. The targets consisted of an 25 um PET film ablator with Al coated on the surface and 50 um polycrystalline 3 mol% yttria doped tetragonal stabilized zirconia.
The XRD change were observed up to 35 ns after shock compression started. Before shock, the (101), (002), (110), (102), (112), (200) diffraction of tetragonal phase were observed. 6.5 ns after shock, the diffraction from compression region appeared with maximum compression of 6%. No phase transition occurred at compression states. At release states (~11.4 ns), on the other hand, the (-111), (111), (022), (-221) diffraction peaks of monoclinic phase were appeared. We will discuss the detail of the experimental results and the transformation toughening mechanism.

Keywords: Synchrotron X-ray, Time-resolved XRD, Laser-induced shock wave, Tetragonal stabilized zirconia

©2019. Japan Geoscience Union. All Right Reserved.

[E] Poster | A (Atmospheric and Hydrospheric Sciences)：A-AS Atmospheric Sciences, Meteorology & Atmospheric Environment

Tue. May 28, 2019 10:45 AM - 12:15 PM JST | Tue. May 28, 2019 1:45 AM - 3:15 AM UTC | Poster Hall International Exhibition Hall8, Makuhari Messe_2

[A-AS03] Large-scale moisture and organized cloud systems

convener:Hiroaki Miura(The University of Tokyo), Atsushi Hamada(University of Toyama), Satoru Yokoi(Japan Agency for Marine-Earth Science and Technology), Masaki Satoh(Atmosphere and Ocean Research Institute, The University of Tokyo)

Water vapor plays a significant role in regulating the global atmospheric circulation, especially in the troposphere. The overturning circulation is directly driven by the longwave radiative cooling of water vapor and the latent heating/cooling through microphysical processes to balance it. This global circulation is composed of diverse atmospheric phenomena with various spatial and temporal scales. Developments of some significant turbulent motions such as 3D isotropic turbulence in clouds, stratocumulus and cumulus convection, squall lines and tropical cyclones, and the Madden-Julian oscillation, are essentially associated with moisture anomaly in each scale. Moisture is accumulated relatively slowly in larger horizontal scales, but is consumed relatively quickly in smaller ones. This significant scale gaps between the accumulation and consumption may be one of the causes of the long-lasting difficulty in developing the theory of the moist atmosphere. The aim of this session is to share the recent researches about the relationships between moisture and organized cloud systems in wider spatial and temporal scales to enhance collaborations between modeling, observational, and theoretical approaches in tackling this challenging task. Research results relating to the Years of the Maritime Continent (YMC) and Radiative-Convective Equilibrium Model Intercomparison Project (RCEMPI) are welcome.

[AAS03-P01] Numerical investigation on the shape, terminal velocity, and drag coefficient of a small raindrop by the improved immersed boundary method

*Ong Chia Rui[1], Hiroaki Miura[1] (1.The University of Tokyo)

[AAS03-P02] **A diagnostic study of water vapor during an extreme precipitation event in Yili river valleyA diagnostic study of water vapor during an extreme precipitation event in Yili river valley**

*Jing LiU[1], Yushu Zhou[2], Lianmei Yang[1] (1.Institute of Desert Meteorology,CMA, 2.Institute of Atmospheric Physics,CAS)

[AAS03-P03] **The Study on the Characteristics of Weather and Cloud Types in the Summer and Winter Seasons of the South China Sea**

*Jou Ping Hou[1], Bo-Shiou Wei[1], Li-Zhen Su[1] (1.Chung Cheng Institute of Technology)

[AAS03-P04] **Linkages between the South and East Asian Monsoon water vapor transport during boreal summer**

*Yong Liu[1] (1.Institute of Atmospheric Physics, Beijing , China)

[AAS03-P05] Interannual Modulation of the Local Hadley Circulation on Clouds, Radiation and Diagnostic Fields over the Western North Pacific

*Xinyue Wang[1], Hironobu Iwabuchi[1] (1.Tohoku Univ.)

[AAS03-P06] Seasonal and Regional Variation of Diurnal Cycle of Rainfall over Java Island and the Surrounding Area

*Madam Taqiyya Maulana[1], Takeshi Yamazaki[1] (1.Tohoku University)

[AAS03-P07] **Study on atmospheric circulation characteristics of precipitation anomalies in arid region of Central Asia**

*Lianmei Yang[1], Xuefeng Guan[1] (1.Institute of Desert Meteorology, China Meteorological Administration,)

[AAS03-P08] Mechanisms for northward propagation of boreal summer intraseasonal oscillation

*Kanta Nakae[1], Masaki Satoh[1], Daisuke Takasuka[1] (1.Atmosphere and Ocean Research Institute, The University of Tokyo)

[AAS03-P09] Fractality in the perimeter of tropical clouds observed by Himawari-8 or simulated by a high-resolution model

*Takuya Jinno[1] (1.Graduate School of Science, The University of Tokyo)

[AAS03-P10] **Large-scale deformation of tropical cloud band in the ITCZ detected in NICAM simulations**

*Noriyuki Nishi[1], Atsushi Hamada[4], Yohei Yamada[2], Tomoe Nasuno[2], Reona Satoh[5], Masaki Satoh[3] (1.Faculty of Science, Fukuoka Universtiy, 2.JAMSTEC, 3.AORI, University of Tokyo, 4.Graduate School of Science and Engineering for Education, University of Toyama, 5.Graduate School of Science, Fukuoka University)

[AAS03-P11] **Improvement of single-moment bulk microphysics for super-cooled water clouds over the Southern Ocean in NICAM using Joint simulator and double-moment microphysics**

*Woosub Roh[1], Tatsuya Seiki[2], Masaki Satoh[1], Tempei Hashino[3] (1.AORI, the university of Tokyo, 2.JAMSTEC, 3.Kochi university of technology)

[AAS03-P12] High-cloud property responses to SST change: sensitivity study using a global nonhydrostatic model

*Tomoki Ohno[1], Masaki Satoh[2] (1.Japan Agency for Marine-Earth Science and Technology, 2.Atmosphere and Ocean Research Institute, The University of Tokyo)

[AAS03-P13] Effects of different cloud overlapping parameters on simulated total cloud fraction over the globe and East Asian region

*bo hai Wang[1], hua Zhang[2] (1.Institute of Atmospheric Physics, Chinese Academy of Sciences, 2.State Key Laboratory of Severe Weather, Chinese Academy of Meteorological Sciences)

Numerical investigation on the shape, terminal velocity, and drag coefficient of a small raindrop by the improved immersed boundary method

*Ong Chia Rui[1], Hiroaki Miura[1]

1. The University of Tokyo

The cloud microphysical processes play a crucial part in controlling the water cycle, cloud formation, and radiation transfer in the atmosphere. These process are parameterized in a numerical weather prediction model by empirical formulae. In particular, empirical formulae for the prediction of the terminal velocity, drag coefficient, and shape of a free-falling water droplet are used widely in the parameterizations. Despite that the model accuracy is sensitive to the microphysics parameterizations to a considerable extent, these formulae are only verified by experiments which are conducted at room temperature and standard atmospheric pressure or linear theories in an ideal condition. The validity of the parameterizations is therefore questionable under general conditions and the accuracy of the numerical prediction may be affected.
In this work, a new numerical tool, the immersed boundary method, is proposed as an alternative way to investigate the terminal velocity, drag coefficient, and shape of an axisymmetric free-falling raindrop. This improved immersed boundary method for water droplet simulations is applied to verify those commonly used empirical formulae under different conditions. The largest size of the free-falling raindrop in this work is 0.5 mm. To first verify the reliability and robustness of this new method the terminal velocity and drag coefficient obtained from axisymmetric raindrop simulations at standard pressure and temperature fit well with the experimental data. Further simulation results of an axisymmetric free-falling raindrop of diameters of 0.025, 0.01, and 0.5 mm at different altitudes assuming a fixed lapse rate show that the variation of the shape of the raindrop is negligibly small, and there is a significant discrepancy between the numerical results and some of the widely used empirical formulae. The discrepancy is larger at higher altitudes for small raindrops. This is because of the assumption of the fixed drag coefficient in the derivation of those empirical formulae. A new parameterization with better accuracy for terminal velocity aloft of raindrops with diameter smaller than 0.5 mm is proposed. A further sensitivity test of a 0.5 mm free-falling axisymmetric raindrop with different surface tension coefficients are performed and the numerical results suggest that the change in the shape and terminal velocity is negligible with respect to aerosols.

Keywords: Cloud Microphysis, Immersed boundary method, Terminal velocity

©2019. Japan Geoscience Union. All Right Reserved.

A diagnostic study of water vapor during an extreme precipitation event in Yili river valleyA diagnostic study of water vapor during an extreme precipitation event in Yili river valley

*Jing LiU[1], Yushu Zhou[2], Lianmei Yang[1]

1. Institute of Desert Meteorology,CMA, 2. Institute of Atmospheric Physics,CAS

An extreme precipitation events was happened during 31 July to 1 August, 2016 at Yili river valley which multi-stations breakthrough extreme precipitation’ s value. Based on calculation of water vapor transport stream function and the non-divergent (rotational) components, potential function and divergent (irrotational) components, the water vapor transport budget and water vapor transport trajectories for the Yili river valley using the conventional detection,1° x 1° NCEP/NCAR reanalysis, HYSPLIT model based on Lagrangian method, Ground-based GPS observation precipitable water vapor data(GPS-PWV) , the large-scale water vapor transport and convergence characteristics were analyzed during the heavy rainfall period. The results showed that: (1) The Indian, the Pacific and the Atlantic ocean all contributed to the water supply during the heavy rain period, and Indian summer monsoon circulation, the south China sea summer monsoon circulation at low latitudes and Atlantic ocean’ s east airflow at mid-latitude were constituted the water vapor transmission channel, which the Indian Ocean southwest water vapor transport mainly concentrated in the lower troposphere, and middle troposphere water vapor transport was given priority to the west flow of the Atlantic ocean and low trough itself; the valley was in the convergence area of water vapor flux during the heavy rain, and the convergence and uplift of the terrain to the West opening caused vertical motion development provided a favorable dynamic convergence mechanism for the occurrence of local heavy rain.(2) The 3000 m water vapor transmission trajectory included the westward and eastward path at bottom layer and the northward path at middle troposphere as complement of water vapor for the lower troposphere through the vertical motion, the southward path at lower troposphere which water vapor come from the Arabian sea,and the mid-latitude water vapor transport of the westward path was the most powerful ; The 5000 m water vapor transmission trajectory was dominated by the westward path and the low trough itself;(3) During the precipitation period, the water vapor was concentrated in the lower troposphere which transported to the upper level through vertical movement, and the water vapor was positive at the middle and upper layers contrasted with negative at the lower layer. south boundary of water vapor inflow was rapidly increasing at the lower layer while the middle and higher layer water vapor inflow derived from the western boundary during the heavy rainfall period;(4)Yili river valley GPS-PWV jumped caused by the southwest airflow front of low trough before the rainfall happened and steadily maintain the high value influenced by India southwest monsoon during the heavy rainfall period. The large-scale water vapor transport convergence enhancement corresponding local GPS-PWV increased, suggested that the water vapor supply in local heavy rain event was at least associated with the water vapor transport and convergence of hemisphere scale.

Keywords: torrential rain, transfer of water vapor, lagrange trajectory, ground-based GPS

©2019. Japan Geoscience Union. All Right Reserved.

The Study on the Characteristics of Weather and Cloud Types in the Summer and Winter Seasons of the South China Sea

*Jou Ping Hou[1], Bo-Shiou Wei[1], Li-Zhen Su[1]

1. Chung Cheng Institute of Technology

The South China Sea is vast with a tropical maritime climate near the equator and a subtropical climate in the north. Therefore, although it is winter, there are still deep convective and strong precipitation systems in the South China Sea. In summer, thermal convection is strong, sometimes typhoons pass; Dongsha Island and Taiping Island are located in the north and south of the South China Sea. The weather in the region is bound to be significantly affected by various weather systems in the South China Sea. We selected the winter of December 2017 and the summer of June 2018 to study it. The Dongsha Island and Taiping Island areas were subjected to research on the northeast monsoon and tropical convection. The dual island observation and satellite data were combined with numerical models to analyze the mutual interaction between the thermal and dynamic processes in the South China Sea. To enhance the understanding of the weather evolution mechanism in the South China Sea, in order to further clarify the various cloud-phase characteristics of the monsoon circulation and thermal convection in the South China Sea. The results show that the change of northeast monsoon intensity obviously affects the interaction of air-sea in the South China Sea, enhances the intensity of precipitation, and changes the amount and height of the stratus cumulus in the sea. In addition, the northeast monsoon circulation may interact with the surrounding terrain of the South China Sea, thus induces local deep convection. In the summer, the southwest monsoon will be enhanced and thermal convection is very strong. The intensity and life cycle of the typhoon can be maintained when it passes this area.

Keywords: Dongsha Island, Taiping Island, Air-Sea interaction, Deep Convection

©2019. Japan Geoscience Union. All Right Reserved.

Linkages between the South and East Asian Monsoon water vapor transport during boreal summer

*Yong Liu[1]

1. Institute of Atmospheric Physics, Beijing , China

This study provides a water vapor transport (WVT) perspective on the linkages between the South and East Asian summer monsoons (SASM and EASM) and indicates two robustly coupled modes of the vertical integrated WVT (VIWVT) over the two monsoons that accounts for above 90% of the total squared covariance fraction. The first coupled mode (SVD1 mode) depicts a meridional linkage between the meridional dipole VIWVT anomalies over both the SASM and EASM. While the second coupled mode (SVD2 mode) illustrates a zonal connection of an anomalous cyclonic/anticyclone VIWVT over the SASM and a zonal wave-like VIWVT over the EASM. The SVD1 mode is linked through the anomalous subtropical High over the western North Pacific (WNPSH) and primarily associated with the transition phase of El Niñ o/La Niña (ENSO) and simultaneous Indian Ocean Basin mode (IOBM) SST warming/cooling. The meridional connection of the VIWVT in the SVD1 mode experienced a clear intensification since the late-1970s that may be attributed to the strengthened impacts of the ENSO/IOBM on the EASM and SASM after the late-1970s. The SVD2 mode is connected by the Circumglobal teleconnection (CGT) pattern and related to the developing phase of ENSO and summer north Atlantic tripole (NAT) SST anomalies. The zonal VIWVT connection in SVD2 mode is strongly modulated by the SASM-CGT connections and reveals significant weakening since the late-1970s but re-intensifies after the early-1990s. This may be associated with the weakened ENSO-SASM relationship after the late-1970s and interdecadal decreasing of the all Indian summer rainfall since the early-1990s.

Keywords: Water vapor transport, South and East Asian summer monsoon, linkage, interdecadal change

©2019. Japan Geoscience Union. All Right Reserved.

Interannual Modulation of the Local Hadley Circulation on Clouds, Radiation and Diagnostic Fields over the Western North Pacific

*Xinyue Wang[1], Hironobu Iwabuchi[1]

1. Tohoku Univ.

Variation of the local Hadley cell (HC) northern boundary over the western North Pacific, and its interannual imprints on the tropospheric clouds and atmospheric fields are examined with observation and reanalysis data for the winter season from December 1982 to February 2016. The poleward shift of the local HC subsiding edge is marked by anomalous rising motion, large-scale decreased static stability, and corresponding increases of the midlevel cloud amount over the climatological sinking zone around 30N. These responses primarily locate over the continental and coastal areas instead of the open oceans. Concomitant with the increasing cloud fraction, a net negative top-of-atmosphere radiation anomaly is identified, and the main contributor is suggested to be the cumulus congestus, whose top pressures are in a range of 440–680 hPa, and optical thicknesses in a range of 23–60. Interactions between this specific cloud type and the vertical moist instability, and their constrains on the precipitation field is further discussed.

Keywords: Regional Hadley cell, Cloud and radiation, Precipitation pattern

©2019. Japan Geoscience Union. All Right Reserved.

Seasonal and Regional Variation of Diurnal Cycle of Rainfall over Java Island and the Surrounding Area

*Madam Taqiyya Maulana[1], Takeshi Yamazaki[1]

1. Tohoku University

The seasonality and regional variability of diurnal cycle of rainfall (DCR) over Java Island and the surrounding area (coastal region of the Java Sea and the Indian Ocean) are analyzed through satellite observations. This study focus on the area where the studies of the seasonality of DCR over Indonesian Maritime Continent (IMC) are still limited. The DCR is a prominent phenomenon over IMC which is important for aviation industry and related to heavy precipitation events that cause hydro-meteorological disasters.

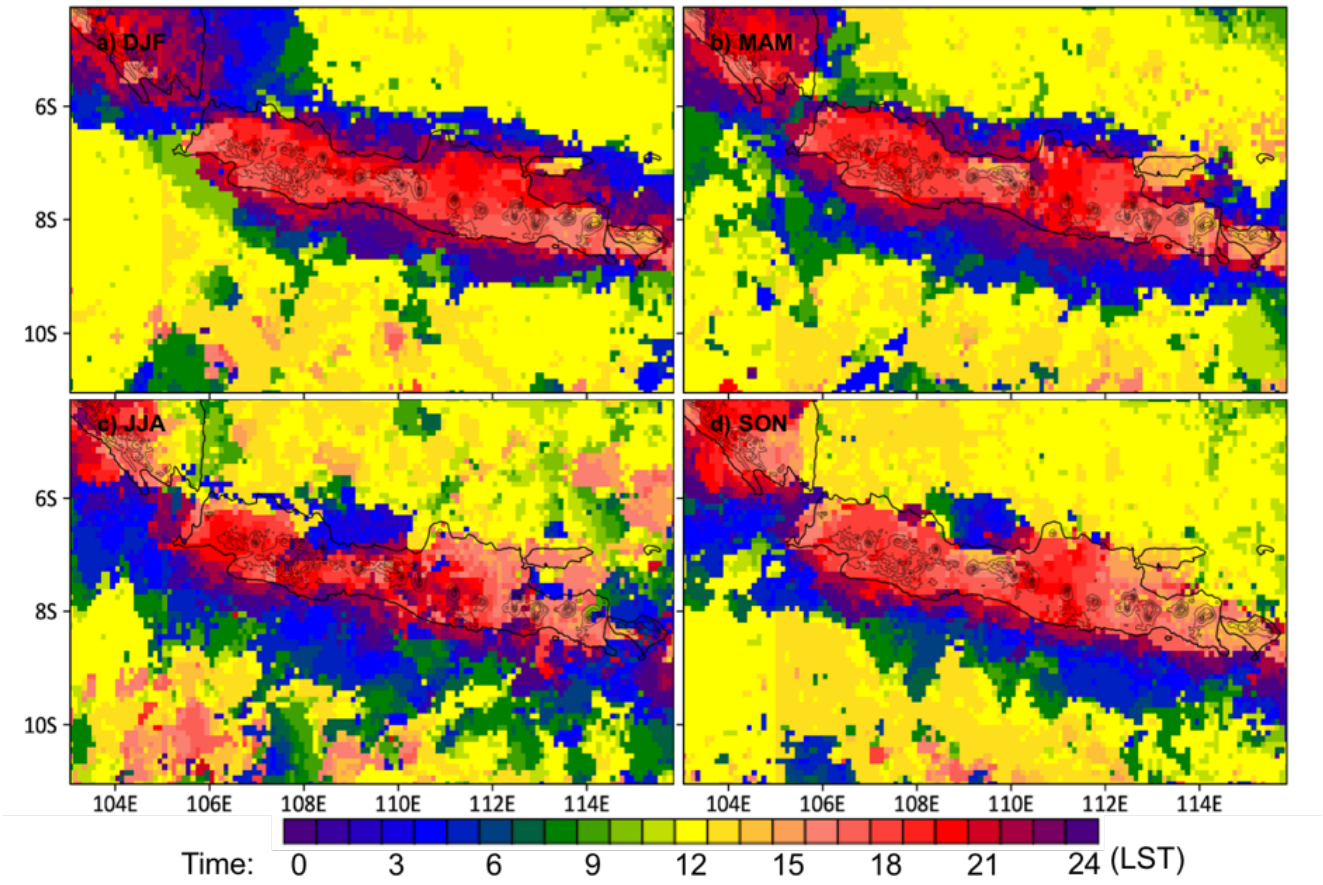
In this study, **we investigate seasonal and regional variation of DCR (the phase and the amplitude)** through satellite observations. High resolution (spatial and temporal) rainfall estimate is needed to capture feature of DCR over the study area which is difficult to obtain from ground observation. We **mainly employ the high-resolution dataset of Global Satellite Mapping of Precipitation (GSMaP) reanalysis (GSMaP_RNL) and near real time (GSMaP_NRT).** The analysis of DCR seasonal variability is based on investigation throughout boreal winter (December-January-February), boreal spring (March-April-May), boreal summer (June-July-August), and boreal autumn (September-October-November) from 2008-2018 (GSMaP_NRT) and 2009-2014 (GSMaP_RNL).

The results show that hourly data of GSMaP_RNL and GSMaP_NRT with 0.1˚ spatial resolution are able to depict the detailed features of the seasonality and regional variability of DCRover Java Island and surrounding areas. **The comparison between GSMaP_RNL and GSMaP_NRT shows that GSMaP_NRT represents significant time lag of DCR phase over off shore region. GSMaP_NRT shows that the offshore region of the Java Sea is dominated by noon-afternoon rainfall while GSMaP_RNL shows morning rainfall.** However, both of GSMaP_RNL and GSMaP_NRT show similar pattern on phase and amplitude of DCR. Phase of DCR indicates the time when maximum rainfall occurs, while amplitudes indicates the magnitude of DCR. In general, both of GSMaP_RNL and GSMaP_NRT composites, show that the land region with wider landmass area (West Java and western part of East Java) is dominated by evening phase while narrow landmass area (Central Java and eastern part of Java Island) is dominated by late afternoon phase. A large magnitude of the DCR is concentrated inland. The Java Sea has a higher amplitude of DCR compared to the Indian Ocean and the coastal region. The amplitude over the coastal region of the Indian Ocean is higher than over the Indian Ocean and the coastal area of the Java Sea.

Both of rainfall estimates capture inhomogeneous seasonal shifting phase of DCR over this region. The remarkable seasonal shifting phase occurs along the coastal area of the Java Sea. Though, phase shifting over inland of a wide landmass area and the coastal region of the Indian Ocean is not significant. Inhomogeneous seasonal shifting phase of DCR indicated interactions between local circulations, which affected by the topography (e.g. terrain and shape of the coastline), and large circulations (background wind, synoptic conditions, etc.). The analysis of wind profile from reanalysis data confirms the seasonal change of interactions between large and small circulations that caused seasonal shifting phase of DCR.

Keywords: Diurnal cycle of rainfall (DCR), Seasonal variability, Regional variability, Shifting Phase, GSMaP

©2019. Japan Geoscience Union. All Right Reserved.



©2019. Japan Geoscience Union. All Right Reserved.

Study on atmospheric circulation characteristics of precipitation anomalies in arid region of Central Asia

*Lianmei Yang[1], Xuefeng Guan[1]

1. Institute of Desert Meteorology, China Meteorological Administration,

As climate transition zone between Mediterranean climate region and East Asian monsoon region, arid region of Central Asia (including five Central Asian countries and Xinjiang province of China) which is influenced by high, middle and low latitude circulations has different synoptic-climatic characteristics from that of Europe and East Asia while its climate characteristics also varies greatly within the region. Central Asia has unique and complicated topography and ecosystem patterns like deserts, oasis, glaciers and basins, forming a highly representative meteorological disaster-breeding environment under the influence of multiple-background, multiple-factor and multiple-scale. This area has abundant solar-heat energy, large evaporation and dramatic temperature changes. Besides, its precipitation is scarce and has extremely uneven distribution with high value in the western and middle parts of Tianshan Mountains. Over the last one hundred years, Central Asia has experienced a warm and wet trend. Central Asia low value system together with the high, middle and low latitude circulation systems linked by West Asia westerly jet stream have contributed to the interdecadal and interannual variations of precipitation in Xinjiang. However, due to the insufficient construction of integrated meteorological observation network, the studies concerning regional featured circulation system, regularity and mechanism of disastrous weathers, high resolution regional numerical model, impacts of land-atmosphere interaction on regional weather and climate change prediction are still inadequate. Correspondingly, to carry out those studies has essential scientific significance and strategic value for the sustainable social and economic development in Silk Road Economic Belt.

Keywords: Arid region of Central Asia, synoptic-climatic characteristics, precipitation anomaly, atmospheric circulation, water vapor

©2019. Japan Geoscience Union. All Right Reserved.

Mechanisms for northward propagation of boreal summer intraseasonal oscillation

*Kanta Nakae[1], Masaki Satoh[1], Daisuke Takasuka[1]

1. Atmosphere and Ocean Research Institute, The University of Tokyo

The 20-90-day Intraseasonal Oscillation (ISO) is one of the dominant modes of tropical variability. In boreal summer northward propagation (NP), which occurs on ISO time scales, originates near the equator and extends to India and western North Pacific Ocean. Understanding the NP of the boreal summer ISO (BSISO) is of vital importance to extended-range weather prediction. Hence, several mechanisms of the NP have been examined. However, they are still incompletely understood. The purpose of this study is to investigate the importance of vertical shear and sea surface temperature (SST) for the NP of the BSISO. In order to obtain a basic structure of the BSISO, we have conducted JJA-perpetual experiments using the Non-hydrostatic Icosahedral Atmospheric Model (NICAM) with a 56-km horizontal mesh.
Although the perpetual experiment has strong Indian monsoon over Arabian sea due to the bias of surface temperature on land, it is found that the NP of the BSISO from Indian Ocean (IO) has two abovementioned mechanisms. One warm SST anomaly north of convection destabilize the lower troposphere, while another tilted vertical shear can generate positive barotropic vorticity to the north of convection. In order to assess the effect of the former mechanism, we made an experiment using fix SST (SSTFIX) obtained from CTL experiment. SSTFIX experiment reproduces the NP of the BSISO from IO, although the amplitude became lower. Therefore, it suggests that the NP of the BSISO from IO doesn’t need warm SST anomaly. To Improve the bias related to basic state like vertical shear, we conducted an experiment using nudging method for surface temperature on land (LNDADJ). In LNDADJ experiment the NP of the BSISO from IO isn’t reproduced due to reduction of column water vapor over Bay of Bengal. Thus, tilted vertical shear can just begin the NP. On the other hand, it is suggested that the NP needs SST and column water vapor to maintain its strength.

Keywords: Boreal summer intraseasonal oscillation, Asian monsoon, Northward propagation

©2019. Japan Geoscience Union. All Right Reserved.

Fractality in the perimeter of tropical clouds observed by Himawari-8 or simulated by a high-resolution model

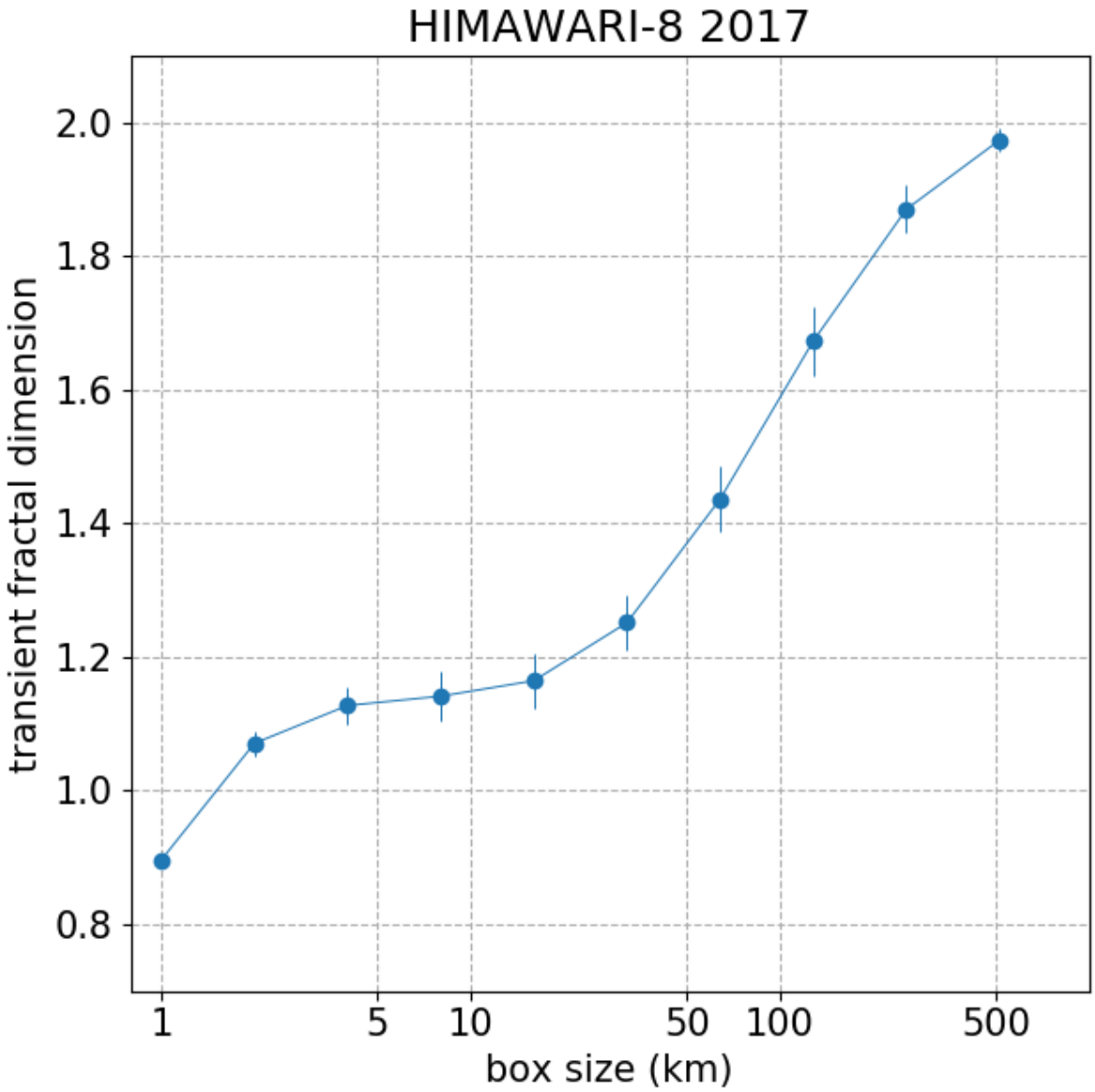
*Takuya Jinno[1]

1. Graduate School of Science, The University of Tokyo

Cloud clusters show a wide variety of shape and size, and their spatial pattern is often taken up as a typical example of fractal. However, the methods of studying fractal are in an early stage of development. In this study, we conducted fractal analysis on the perimeter of tropical clouds using satellite observation and cloud-resolving simulation of sub-kilometer resolution. We evaluated fractal dimension as a function of spatial scale (transient fractal dimension) and quantified the characteristic spatial scale of the pattern from the scale where self-similarity breaks down. From the observational data from HIMAWARI-8, It is shown that the self-similarity of the cloud perimeter persists only in the spatial scale range from 2 km up to 30 km. The limit of the self-similarity is suggested to be the characteristic scale of the pattern formation of tropical clouds. The cloud-resolving simulation data with NICAM also shows finite-size self-similarity. However, the profile of the transient fractal dimension changed with integration time far more rapidly than HIMAWARI-8 observation, and it lost its self-similarity at the end of the 48-hour simulation. This process is suggested to reflect the increase of stratiform cloud in the upper-troposphere as an adjustment to the transition of spatial resolution.

Keywords: fractal, HIMAWARI-8, cloud-resolving model

©2019. Japan Geoscience Union. All Right Reserved.



©2019. Japan Geoscience Union. All Right Reserved.

Large-scale deformation of tropical cloud band in the ITCZ detected in NICAM simulations

*Noriyuki Nishi[1], Atsushi Hamada[4], Yohei Yamada[2], Tomoe Nasuno[2], Reona Satoh[5], Masaki Satoh[3]

1. Faculty of Science, Fukuoka Universtiy, 2. JAMSTEC, 3. AORI, University of Tokyo, 4. Graduate School of Science and Engineering for Education, University of Toyama, 5. Graduate School of Science, Fukuoka University

Over the central/eastern tropical Pacific, the Inter Tropical Convergence Zone (ITCZ) is detected in the northern side of the equator. In the ITCZ, we can sometimes observe drastic deformation of the cloud bands elongated zonally with several thousand-kilometer scale. The initial stage of the band, which is composed of deep convective systems, expands meridionally and separates into two or three parallel cirrus bands that keep alive one or two days (Hamada et al., 2013, JMSJ). These separation events cannot be well described in the objective analysis datasets, probably due to lack of the observations over the open ocean; investigation of their mechanism with the analysis data is difficult. In order to study their mechanism, we attempted to use the numerical simulation results of global cloud system resolving model NICAM (Satoh et al. 2014, Progress in Earth and Planetary Science) to find similar events in them. If we can find separation events in the results, we can examine the mechanism with many physical parameters including wind, various kinds of hydrometeors. We have already analyzed several numerical experiment results for different periods, resolution and physical schemes.

We found a similar separation event in an output of the simulation for one year from June 2004 and horizontal resolution 3.5 km. We examined the life cycle of the cirrus bands after separation. One interesting point is on the height of the cirrus clouds in the separated bands. The simulated cirrus clouds in the bands lie in the 13-14 km height level, while the height of the maximum meridional wind that contributes to the meridional movement of the cirrus bands is about 12 km. This difference of the heights means that the cirrus clouds were not just advected by meridional wind but were possibly developed in the course of the separation.

The trigger of zonally simultaneous separation of a long band is another our interest. Inertial instability may be a candidate since vertical exchange of zonal momentum by deep convection would occur in an original band and result in the large meridional shear of the zonal wind in the upper troposphere. We tried to confirm necessary condition for inertial instability by calculating geostrophic vorticity, following the general procedure. However, the position of the bands is too close to the equator (3-7N) to establish geostrophic relationship, and the spatial pattern of the geostrophic vorticity is too noisy to analyze. Therefore, we instead calculate simple absolute vorticity. We found that the absolute vorticity around the separated bands was almost negative. It suggests the possibility of the inertial (or similar kind of) instability.

We are now analyzing another numerical experiment including four kinds of runs using a cloud scheme with different cloud parameter settings. In the real atmosphere, a separation event occurred on 16-17 June 2008 at the just east of the date line. The event can be simulated in all of four runs at 36 hours from the initial time. It suggests that the basic mechanism of the separation is not sensitive to the detail of cloud systems. By analyzing the dynamical fields of these outputs, we are trying to find the key mechanisms to trigger the meridional separation of the cloud bands.

©2019. Japan Geoscience Union. All Right Reserved.

Keywords: tropics, ITCZ, cirrus

©2019. Japan Geoscience Union. All Right Reserved.

Improvement of single-moment bulk microphysics for super-cooled water clouds over the Southern Ocean in NICAM using Joint simulator and double-moment microphysics

*Woosub Roh[1], Tatsuya Seiki[2], Masaki Satoh[1], Tempei Hashino[3]

1. AORI, the university of Tokyo, 2. JAMSTEC, 3. Kochi university of technology

It is important to evaluate and improve the cloud properties in global non-hydrostatic models like a Nonhydrostatic ICosahedral Atmospheric Model (NICAM, Satoh et al. 2014) using observation data. One of the methods is a radiance-based evaluation using satellite data and a satellite simulator (here Joint simulator, Hashino et al. 2013), which avoids making different settings of the microphysics between retrieval algorithms and NICAM.

One of the challenging issues is an evaluation of mixed-phase clouds, which consist of water vapor, ice particles, and supercooled water droplets. It is known one of the main reasons why climate models reveal large errors about the reflection of solar radiation over the Southern Ocean and Arctic.

This study is an evaluation and improvement of mixed-phase clouds over the Southern Ocean in NICAM using a Cloud-Aerosol Lidar and Infrared Pathfinder Satellite Observation (CALIPSO) and a satellite simulator. We evaluated thermodynamics phase of mixed phases clouds over the Southern Ocean in a regional version of NICAM between 45˚S to 65˚S and 170˚E to 170˚W following Yoshida et al. (2010) method. We found underestimation of supercooled water clouds in our single moment scheme. We improved the single moment microphysics scheme using a double moment microphysics and a single column model. We also investigate the impact of microphysics scheme on moisture distributions and the size of cloud systems.

Keywords: microphysics, CALIPSO, Satellite simulator

©2019. Japan Geoscience Union. All Right Reserved.

High-cloud property responses to SST change: sensitivity study using a global nonhydrostatic model

*Tomoki Ohno[1], Masaki Satoh[2]

1. Japan Agency for Marine-Earth Science and Technology, 2. Atmosphere and Ocean Research Institute, The University of Tokyo

Since it has been recognized that the uncertainty of cloud feedback is one of main contributors to the intermodel spread of climate sensitivity, the reduction of the uncertainties associated with cloud response to global warming has been one of central issues for robust projections and predictions of climate variability and change. High clouds have large impacts on the Earth’ s radiative energy budget, and the uncertainty of their response to climate change is known as one of large sources of the climate sensitivity spread although several possible hypotheses to predict the response have been proposed. As the radiation-cloud interaction plays a crucial role in the determination of life time of high clouds, the improvement of the understanding of cloud property responses to global warming helps the reduction of climate-sensitivity variability associated with the high-clouds feedback.

In order to investigate the cloud-property response to climate change, we conducted simulations with RCE configurations using a high-resolution nonhydrostatic global circulation model (the Nonhydrostatic Icosahedral Atmospheric Model; NICAM) with the earth-like sphere for simplifying the problem. Sea surface temperatures (SSTs) are fixed at 300K and 304K and a double-moment bulk scheme are used without cumulus parameterization scheme.

We found that high cloud amount increases with SST increase, as consistent with the previous NICAM studies. It was also determined that the change in particularly optically thin clouds whose optical thicknesses were <3 was dominant, and such thin clouds tended to have large particle sizes. These suggests that the slow evaporative property of ice phase clouds and their representability can play one of key roles in the uncertainty of the high-cloud amount change in global warming.

Keywords: cloud property responses, cloud feedback, climate change

©2019. Japan Geoscience Union. All Right Reserved.

Effects of different cloud overlapping parameters on simulated total cloud fraction over the globe and East Asian region

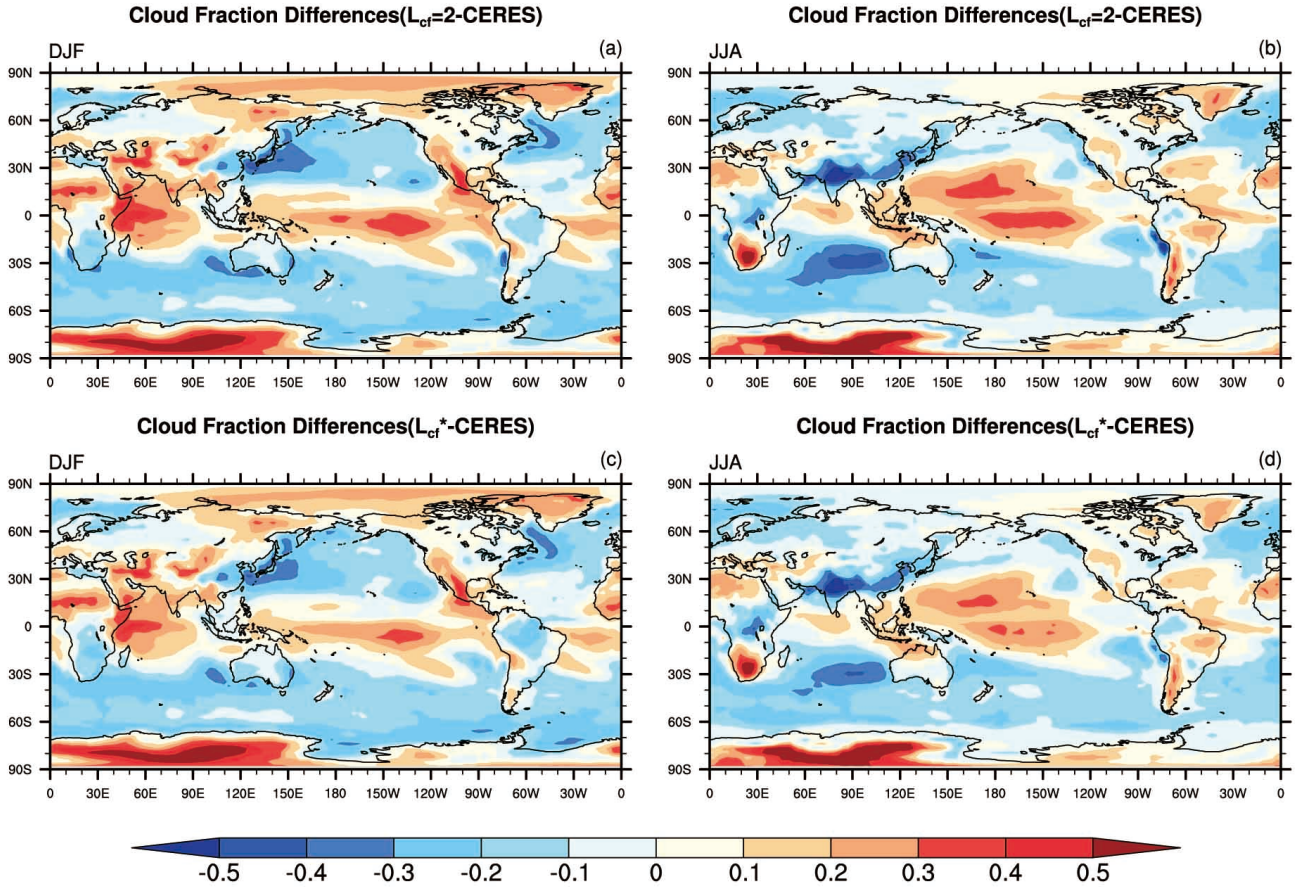
*bo hai Wang[1], hua Zhang[2]

1. Institute of Atmospheric Physics, Chinese Academy of Sciences, 2. State Key Laboratory of Severe Weather, Chinese Academy of Meteorological Sciences

The cloud overlapping parameter (vertical decorrelation length, L_{cf}) from CloudSat/CALIPSO is implemented in Beijing Climate Center’ s GCM (BCC_AGCM2.0) to reduce the uncertainly in radiation field. Comparing the climate simulation results obtained by using the constant L_{cf} of 2 km with those using the above retrieved L_{cf}, it is found that the total cloud fraction simulation has been obviously improved by using the satellite-based L_{cf}. The error of global mean total cloud fraction between simulations and CERES (Clouds and the Earth's Radiant Energy System) satellite data is decreased by 1.6% in both the winter and summer, of which the positive deviation of total cloud amount at tropical convection area and the negative deviation in subtropical region both are significantly reduced. These improvements are helpful for better simulation of energy budget differences between different regions. In East Asia, using the satellite-based L_{cf} can decrease the error of average total cloud fraction (compared to the CERES) by 1.8% (1.4%) in the winter (summer).Overall, using L_{cf} from CloudSat/CALIPSO satellite data can improve the simulation of total cloud fraction and thus obtain more accurate simulation of radiation field.

Keywords: Cloud overlapping parameter, Vertical decorrelation length, Total cloud fraction

©2019. Japan Geoscience Union. All Right Reserved.



©2019. Japan Geoscience Union. All Right Reserved.

[E] Poster | A (Atmospheric and Hydrospheric Sciences)：A-AS Atmospheric Sciences, Meteorology & Atmospheric Environment

Tue. May 28, 2019 5:15 PM - 6:30 PM JST | Tue. May 28, 2019 8:15 AM - 9:30 AM UTC | Poster Hall International Exhibition Hall8, Makuhari Messe_6

[A-AS03] Large-scale moisture and organized cloud systems

convener:Hiroaki Miura(The University of Tokyo), Atsushi Hamada(University of Toyama), Satoru Yokoi(Japan Agency for Marine-Earth Science and Technology), Masaki Satoh(Atmosphere and Ocean Research Institute, The University of Tokyo)

Water vapor plays a significant role in regulating the global atmospheric circulation, especially in the troposphere. The overturning circulation is directly driven by the longwave radiative cooling of water vapor and the latent heating/cooling through microphysical processes to balance it. This global circulation is composed of diverse atmospheric phenomena with various spatial and temporal scales. Developments of some significant turbulent motions such as 3D isotropic turbulence in clouds, stratocumulus and cumulus convection, squall lines and tropical cyclones, and the Madden-Julian oscillation, are essentially associated with moisture anomaly in each scale. Moisture is accumulated relatively slowly in larger horizontal scales, but is consumed relatively quickly in smaller ones. This significant scale gaps between the accumulation and consumption may be one of the causes of the long-lasting difficulty in developing the theory of the moist atmosphere. The aim of this session is to share the recent researches about the relationships between moisture and organized cloud systems in wider spatial and temporal scales to enhance collaborations between modeling, observational, and theoretical approaches in tackling this challenging task. Research results relating to the Years of the Maritime Continent (YMC) and Radiative-Convective Equilibrium Model Intercomparison Project (RCEMPI) are welcome.

[AAS03-P01] Numerical investigation on the shape, terminal velocity, and drag coefficient of a small raindrop by the improved immersed boundary method

*Ong Chia Rui[1], Hiroaki Miura[1] (1.The University of Tokyo)

[AAS03-P02] **A diagnostic study of water vapor during an extreme precipitation event in Yili river valleyA diagnostic study of water vapor during an extreme precipitation event in Yili river valley**

*Jing LiU[1], Yushu Zhou[2], Lianmei Yang[1] (1.Institute of Desert Meteorology,CMA, 2.Institute of Atmospheric Physics,CAS)

[AAS03-P03] **The Study on the Characteristics of Weather and Cloud Types in the Summer and Winter Seasons of the South China Sea**

*Jou Ping Hou[1], Bo-Shiou Wei[1], Li-Zhen Su[1] (1.Chung Cheng Institute of Technology)

[AAS03-P04] **Linkages between the South and East Asian Monsoon water vapor transport during boreal summer**

*Yong Liu[1] (1.Institute of Atmospheric Physics, Beijing , China)

[AAS03-P05] Interannual Modulation of the Local Hadley Circulation on Clouds, Radiation and Diagnostic Fields over the Western North Pacific

*Xinyue Wang[1], Hironobu Iwabuchi[1] (1.Tohoku Univ.)

[AAS03-P06] Seasonal and Regional Variation of Diurnal Cycle of Rainfall over Java Island and the Surrounding Area

*Madam Taqiyya Maulana[1], Takeshi Yamazaki[1] (1.Tohoku University)

[AAS03-P07] **Study on atmospheric circulation characteristics of precipitation anomalies in arid region of Central Asia**

*Lianmei Yang[1], Xuefeng Guan[1] (1.Institute of Desert Meteorology, China Meteorological Administration,)

[AAS03-P08] Mechanisms for northward propagation of boreal summer intraseasonal oscillation

*Kanta Nakae[1], Masaki Satoh[1], Daisuke Takasuka[1] (1.Atmosphere and Ocean Research Institute, The University of Tokyo)

[AAS03-P09] Fractality in the perimeter of tropical clouds observed by Himawari-8 or simulated by a high-resolution model

*Takuya Jinno[1] (1.Graduate School of Science, The University of Tokyo)

[AAS03-P10] **Large-scale deformation of tropical cloud band in the ITCZ detected in NICAM simulations**

*Noriyuki Nishi[1], Atsushi Hamada[4], Yohei Yamada[2], Tomoe Nasuno[2], Reona Satoh[5], Masaki Satoh[3] (1.Faculty of Science, Fukuoka Universtiy, 2.JAMSTEC, 3.AORI, University of Tokyo, 4.Graduate School of Science and Engineering for Education, University of Toyama, 5.Graduate School of Science, Fukuoka University)

[AAS03-P11] **Improvement of single-moment bulk microphysics for super-cooled water clouds over the Southern Ocean in NICAM using Joint simulator and double-moment microphysics**

*Woosub Roh[1], Tatsuya Seiki[2], Masaki Satoh[1], Tempei Hashino[3] (1.AORI, the university of Tokyo, 2.JAMSTEC, 3.Kochi university of technology)

[AAS03-P12] High-cloud property responses to SST change: sensitivity study using a global nonhydrostatic model

*Tomoki Ohno[1], Masaki Satoh[2] (1.Japan Agency for Marine-Earth Science and Technology, 2.Atmosphere and Ocean Research Institute, The University of Tokyo)

[AAS03-P13] Effects of different cloud overlapping parameters on simulated total cloud fraction over the globe and East Asian region

*bo hai Wang[1], hua Zhang[2] (1.Institute of Atmospheric Physics, Chinese Academy of Sciences, 2.State Key Laboratory of Severe Weather, Chinese Academy of Meteorological Sciences)

Numerical investigation on the shape, terminal velocity, and drag coefficient of a small raindrop by the improved immersed boundary method

*Ong Chia Rui[1], Hiroaki Miura[1]

1. The University of Tokyo

The cloud microphysical processes play a crucial part in controlling the water cycle, cloud formation, and radiation transfer in the atmosphere. These process are parameterized in a numerical weather prediction model by empirical formulae. In particular, empirical formulae for the prediction of the terminal velocity, drag coefficient, and shape of a free-falling water droplet are used widely in the parameterizations. Despite that the model accuracy is sensitive to the microphysics parameterizations to a considerable extent, these formulae are only verified by experiments which are conducted at room temperature and standard atmospheric pressure or linear theories in an ideal condition. The validity of the parameterizations is therefore questionable under general conditions and the accuracy of the numerical prediction may be affected.
In this work, a new numerical tool, the immersed boundary method, is proposed as an alternative way to investigate the terminal velocity, drag coefficient, and shape of an axisymmetric free-falling raindrop. This improved immersed boundary method for water droplet simulations is applied to verify those commonly used empirical formulae under different conditions. The largest size of the free-falling raindrop in this work is 0.5 mm. To first verify the reliability and robustness of this new method the terminal velocity and drag coefficient obtained from axisymmetric raindrop simulations at standard pressure and temperature fit well with the experimental data. Further simulation results of an axisymmetric free-falling raindrop of diameters of 0.025, 0.01, and 0.5 mm at different altitudes assuming a fixed lapse rate show that the variation of the shape of the raindrop is negligibly small, and there is a significant discrepancy between the numerical results and some of the widely used empirical formulae. The discrepancy is larger at higher altitudes for small raindrops. This is because of the assumption of the fixed drag coefficient in the derivation of those empirical formulae. A new parameterization with better accuracy for terminal velocity aloft of raindrops with diameter smaller than 0.5 mm is proposed. A further sensitivity test of a 0.5 mm free-falling axisymmetric raindrop with different surface tension coefficients are performed and the numerical results suggest that the change in the shape and terminal velocity is negligible with respect to aerosols.

Keywords: Cloud Microphysis, Immersed boundary method, Terminal velocity

©2019. Japan Geoscience Union. All Right Reserved.

A diagnostic study of water vapor during an extreme precipitation event in Yili river valleyA diagnostic study of water vapor during an extreme precipitation event in Yili river valley

*Jing LiU[1], Yushu Zhou[2], Lianmei Yang[1]

1. Institute of Desert Meteorology,CMA, 2. Institute of Atmospheric Physics,CAS

An extreme precipitation events was happened during 31 July to 1 August, 2016 at Yili river valley which multi-stations breakthrough extreme precipitation’ s value. Based on calculation of water vapor transport stream function and the non-divergent (rotational) components, potential function and divergent (irrotational) components, the water vapor transport budget and water vapor transport trajectories for the Yili river valley using the conventional detection,1° x 1° NCEP/NCAR reanalysis, HYSPLIT model based on Lagrangian method, Ground-based GPS observation precipitable water vapor data(GPS-PWV) , the large-scale water vapor transport and convergence characteristics were analyzed during the heavy rainfall period. The results showed that: (1) The Indian, the Pacific and the Atlantic ocean all contributed to the water supply during the heavy rain period, and Indian summer monsoon circulation, the south China sea summer monsoon circulation at low latitudes and Atlantic ocean’ s east airflow at mid-latitude were constituted the water vapor transmission channel, which the Indian Ocean southwest water vapor transport mainly concentrated in the lower troposphere, and middle troposphere water vapor transport was given priority to the west flow of the Atlantic ocean and low trough itself; the valley was in the convergence area of water vapor flux during the heavy rain, and the convergence and uplift of the terrain to the West opening caused vertical motion development provided a favorable dynamic convergence mechanism for the occurrence of local heavy rain.(2) The 3000 m water vapor transmission trajectory included the westward and eastward path at bottom layer and the northward path at middle troposphere as complement of water vapor for the lower troposphere through the vertical motion, the southward path at lower troposphere which water vapor come from the Arabian sea,and the mid-latitude water vapor transport of the westward path was the most powerful ; The 5000 m water vapor transmission trajectory was dominated by the westward path and the low trough itself;(3) During the precipitation period, the water vapor was concentrated in the lower troposphere which transported to the upper level through vertical movement, and the water vapor was positive at the middle and upper layers contrasted with negative at the lower layer. south boundary of water vapor inflow was rapidly increasing at the lower layer while the middle and higher layer water vapor inflow derived from the western boundary during the heavy rainfall period;(4)Yili river valley GPS-PWV jumped caused by the southwest airflow front of low trough before the rainfall happened and steadily maintain the high value influenced by India southwest monsoon during the heavy rainfall period. The large-scale water vapor transport convergence enhancement corresponding local GPS-PWV increased, suggested that the water vapor supply in local heavy rain event was at least associated with the water vapor transport and convergence of hemisphere scale.

Keywords: torrential rain, transfer of water vapor, lagrange trajectory, ground-based GPS

©2019. Japan Geoscience Union. All Right Reserved.

The Study on the Characteristics of Weather and Cloud Types in the Summer and Winter Seasons of the South China Sea

*Jou Ping Hou[1], Bo-Shiou Wei[1], Li-Zhen Su[1]

1. Chung Cheng Institute of Technology

The South China Sea is vast with a tropical maritime climate near the equator and a subtropical climate in the north. Therefore, although it is winter, there are still deep convective and strong precipitation systems in the South China Sea. In summer, thermal convection is strong, sometimes typhoons pass; Dongsha Island and Taiping Island are located in the north and south of the South China Sea. The weather in the region is bound to be significantly affected by various weather systems in the South China Sea. We selected the winter of December 2017 and the summer of June 2018 to study it. The Dongsha Island and Taiping Island areas were subjected to research on the northeast monsoon and tropical convection. The dual island observation and satellite data were combined with numerical models to analyze the mutual interaction between the thermal and dynamic processes in the South China Sea. To enhance the understanding of the weather evolution mechanism in the South China Sea, in order to further clarify the various cloud-phase characteristics of the monsoon circulation and thermal convection in the South China Sea. The results show that the change of northeast monsoon intensity obviously affects the interaction of air-sea in the South China Sea, enhances the intensity of precipitation, and changes the amount and height of the stratus cumulus in the sea. In addition, the northeast monsoon circulation may interact with the surrounding terrain of the South China Sea, thus induces local deep convection. In the summer, the southwest monsoon will be enhanced and thermal convection is very strong. The intensity and life cycle of the typhoon can be maintained when it passes this area.

Keywords: Dongsha Island, Taiping Island, Air-Sea interaction, Deep Convection

©2019. Japan Geoscience Union. All Right Reserved.

Linkages between the South and East Asian Monsoon water vapor transport during boreal summer

*Yong Liu[1]

1. Institute of Atmospheric Physics, Beijing , China

This study provides a water vapor transport (WVT) perspective on the linkages between the South and East Asian summer monsoons (SASM and EASM) and indicates two robustly coupled modes of the vertical integrated WVT (VIWVT) over the two monsoons that accounts for above 90% of the total squared covariance fraction. The first coupled mode (SVD1 mode) depicts a meridional linkage between the meridional dipole VIWVT anomalies over both the SASM and EASM. While the second coupled mode (SVD2 mode) illustrates a zonal connection of an anomalous cyclonic/anticyclone VIWVT over the SASM and a zonal wave-like VIWVT over the EASM. The SVD1 mode is linked through the anomalous subtropical High over the western North Pacific (WNPSH) and primarily associated with the transition phase of El Niñ o/La Niña (ENSO) and simultaneous Indian Ocean Basin mode (IOBM) SST warming/cooling. The meridional connection of the VIWVT in the SVD1 mode experienced a clear intensification since the late-1970s that may be attributed to the strengthened impacts of the ENSO/IOBM on the EASM and SASM after the late-1970s. The SVD2 mode is connected by the Circumglobal teleconnection (CGT) pattern and related to the developing phase of ENSO and summer north Atlantic tripole (NAT) SST anomalies. The zonal VIWVT connection in SVD2 mode is strongly modulated by the SASM-CGT connections and reveals significant weakening since the late-1970s but re-intensifies after the early-1990s. This may be associated with the weakened ENSO-SASM relationship after the late-1970s and interdecadal decreasing of the all Indian summer rainfall since the early-1990s.

Keywords: Water vapor transport, South and East Asian summer monsoon, linkage, interdecadal change

©2019. Japan Geoscience Union. All Right Reserved.

Interannual Modulation of the Local Hadley Circulation on Clouds, Radiation and Diagnostic Fields over the Western North Pacific

*Xinyue Wang[1], Hironobu Iwabuchi[1]

1. Tohoku Univ.

Variation of the local Hadley cell (HC) northern boundary over the western North Pacific, and its interannual imprints on the tropospheric clouds and atmospheric fields are examined with observation and reanalysis data for the winter season from December 1982 to February 2016. The poleward shift of the local HC subsiding edge is marked by anomalous rising motion, large-scale decreased static stability, and corresponding increases of the midlevel cloud amount over the climatological sinking zone around 30N. These responses primarily locate over the continental and coastal areas instead of the open oceans. Concomitant with the increasing cloud fraction, a net negative top-of-atmosphere radiation anomaly is identified, and the main contributor is suggested to be the cumulus congestus, whose top pressures are in a range of 440–680 hPa, and optical thicknesses in a range of 23–60. Interactions between this specific cloud type and the vertical moist instability, and their constrains on the precipitation field is further discussed.

Keywords: Regional Hadley cell, Cloud and radiation, Precipitation pattern

©2019. Japan Geoscience Union. All Right Reserved.

Seasonal and Regional Variation of Diurnal Cycle of Rainfall over Java Island and the Surrounding Area

*Madam Taqiyya Maulana[1], Takeshi Yamazaki[1]

1. Tohoku University

The seasonality and regional variability of diurnal cycle of rainfall (DCR) over Java Island and the surrounding area (coastal region of the Java Sea and the Indian Ocean) are analyzed through satellite observations. This study focus on the area where the studies of the seasonality of DCR over Indonesian Maritime Continent (IMC) are still limited. The DCR is a prominent phenomenon over IMC which is important for aviation industry and related to heavy precipitation events that cause hydro-meteorological disasters.

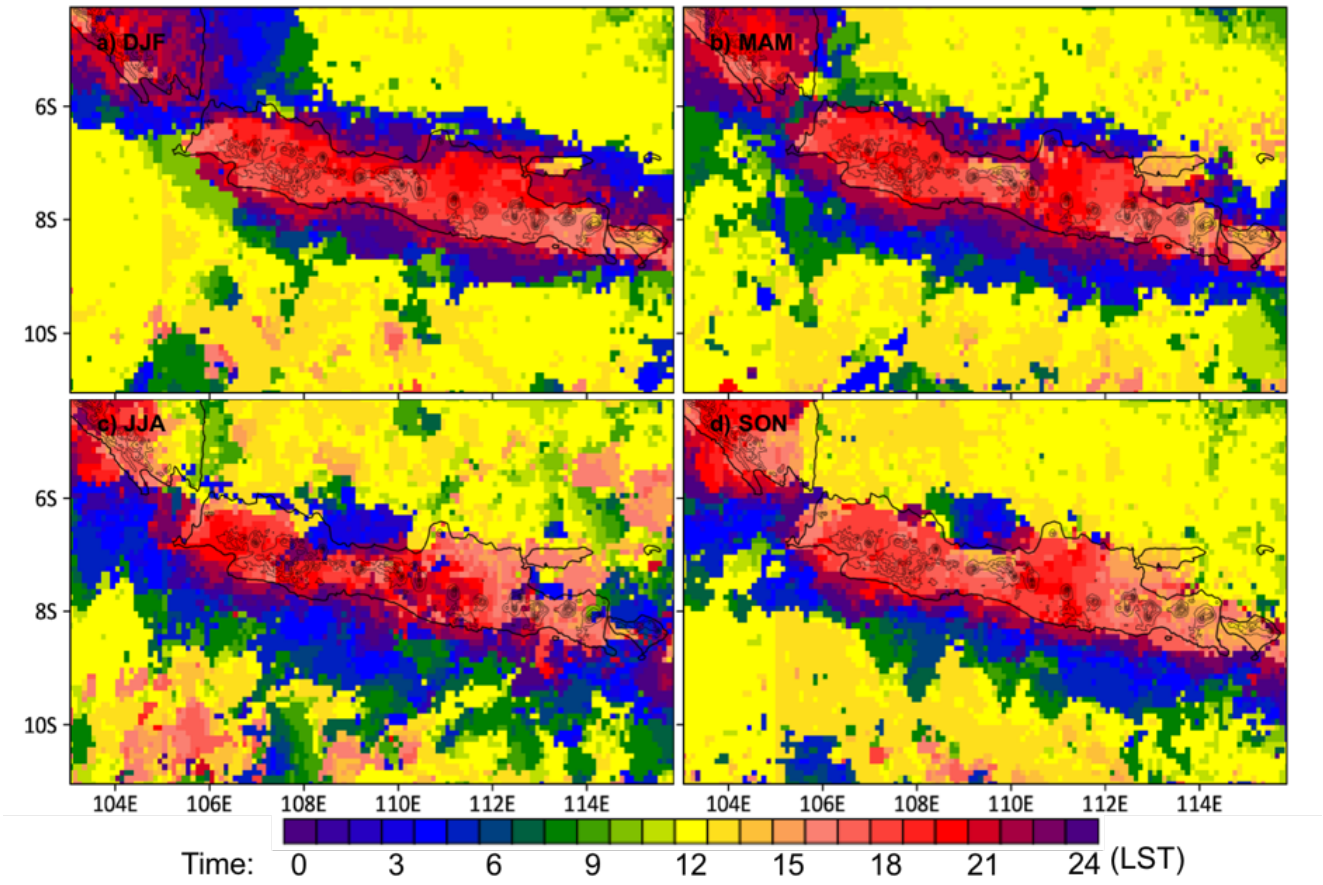
In this study, **we investigate seasonal and regional variation of DCR (the phase and the amplitude)** through satellite observations. High resolution (spatial and temporal) rainfall estimate is needed to capture feature of DCR over the study area which is difficult to obtain from ground observation. We **mainly employ the high-resolution dataset of Global Satellite Mapping of Precipitation (GSMaP) reanalysis (GSMaP_RNL) and near real time (GSMaP_NRT).** The analysis of DCR seasonal variability is based on investigation throughout boreal winter (December-January-February), boreal spring (March-April-May), boreal summer (June-July-August), and boreal autumn (September-October-November) from 2008-2018 (GSMaP_NRT) and 2009-2014 (GSMaP_RNL).

The results show that hourly data of GSMaP_RNL and GSMaP_NRT with 0.1˚ spatial resolution are able to depict the detailed features of the seasonality and regional variability of DCRover Java Island and surrounding areas. **The comparison between GSMaP_RNL and GSMaP_NRT shows that GSMaP_NRT represents significant time lag of DCR phase over off shore region. GSMaP_NRT shows that the offshore region of the Java Sea is dominated by noon-afternoon rainfall while GSMaP_RNL shows morning rainfall.** However, both of GSMaP_RNL and GSMaP_NRT show similar pattern on phase and amplitude of DCR. Phase of DCR indicates the time when maximum rainfall occurs, while amplitudes indicates the magnitude of DCR. In general, both of GSMaP_RNL and GSMaP_NRT composites, show that the land region with wider landmass area (West Java and western part of East Java) is dominated by evening phase while narrow landmass area (Central Java and eastern part of Java Island) is dominated by late afternoon phase. A large magnitude of the DCR is concentrated inland. The Java Sea has a higher amplitude of DCR compared to the Indian Ocean and the coastal region. The amplitude over the coastal region of the Indian Ocean is higher than over the Indian Ocean and the coastal area of the Java Sea.

Both of rainfall estimates capture inhomogeneous seasonal shifting phase of DCR over this region. The remarkable seasonal shifting phase occurs along the coastal area of the Java Sea. Though, phase shifting over inland of a wide landmass area and the coastal region of the Indian Ocean is not significant. Inhomogeneous seasonal shifting phase of DCR indicated interactions between local circulations, which affected by the topography (e.g. terrain and shape of the coastline), and large circulations (background wind, synoptic conditions, etc.). The analysis of wind profile from reanalysis data confirms the seasonal change of interactions between large and small circulations that caused seasonal shifting phase of DCR.

Keywords: Diurnal cycle of rainfall (DCR), Seasonal variability, Regional variability, Shifting Phase, GSMaP

©2019. Japan Geoscience Union. All Right Reserved.



©2019. Japan Geoscience Union. All Right Reserved.

Study on atmospheric circulation characteristics of precipitation anomalies in arid region of Central Asia

*Lianmei Yang[1], Xuefeng Guan[1]

1. Institute of Desert Meteorology, China Meteorological Administration,

As climate transition zone between Mediterranean climate region and East Asian monsoon region, arid region of Central Asia (including five Central Asian countries and Xinjiang province of China) which is influenced by high, middle and low latitude circulations has different synoptic-climatic characteristics from that of Europe and East Asia while its climate characteristics also varies greatly within the region. Central Asia has unique and complicated topography and ecosystem patterns like deserts, oasis, glaciers and basins, forming a highly representative meteorological disaster-breeding environment under the influence of multiple-background, multiple-factor and multiple-scale. This area has abundant solar-heat energy, large evaporation and dramatic temperature changes. Besides, its precipitation is scarce and has extremely uneven distribution with high value in the western and middle parts of Tianshan Mountains. Over the last one hundred years, Central Asia has experienced a warm and wet trend. Central Asia low value system together with the high, middle and low latitude circulation systems linked by West Asia westerly jet stream have contributed to the interdecadal and interannual variations of precipitation in Xinjiang. However, due to the insufficient construction of integrated meteorological observation network, the studies concerning regional featured circulation system, regularity and mechanism of disastrous weathers, high resolution regional numerical model, impacts of land-atmosphere interaction on regional weather and climate change prediction are still inadequate. Correspondingly, to carry out those studies has essential scientific significance and strategic value for the sustainable social and economic development in Silk Road Economic Belt.

Keywords: Arid region of Central Asia, synoptic-climatic characteristics, precipitation anomaly, atmospheric circulation, water vapor

©2019. Japan Geoscience Union. All Right Reserved.

Mechanisms for northward propagation of boreal summer intraseasonal oscillation

*Kanta Nakae[1], Masaki Satoh[1], Daisuke Takasuka[1]

1. Atmosphere and Ocean Research Institute, The University of Tokyo

The 20-90-day Intraseasonal Oscillation (ISO) is one of the dominant modes of tropical variability. In boreal summer northward propagation (NP), which occurs on ISO time scales, originates near the equator and extends to India and western North Pacific Ocean. Understanding the NP of the boreal summer ISO (BSISO) is of vital importance to extended-range weather prediction. Hence, several mechanisms of the NP have been examined. However, they are still incompletely understood. The purpose of this study is to investigate the importance of vertical shear and sea surface temperature (SST) for the NP of the BSISO. In order to obtain a basic structure of the BSISO, we have conducted JJA-perpetual experiments using the Non-hydrostatic Icosahedral Atmospheric Model (NICAM) with a 56-km horizontal mesh.
Although the perpetual experiment has strong Indian monsoon over Arabian sea due to the bias of surface temperature on land, it is found that the NP of the BSISO from Indian Ocean (IO) has two abovementioned mechanisms. One warm SST anomaly north of convection destabilize the lower troposphere, while another tilted vertical shear can generate positive barotropic vorticity to the north of convection. In order to assess the effect of the former mechanism, we made an experiment using fix SST (SSTFIX) obtained from CTL experiment. SSTFIX experiment reproduces the NP of the BSISO from IO, although the amplitude became lower. Therefore, it suggests that the NP of the BSISO from IO doesn’t need warm SST anomaly. To Improve the bias related to basic state like vertical shear, we conducted an experiment using nudging method for surface temperature on land (LNDADJ). In LNDADJ experiment the NP of the BSISO from IO isn’t reproduced due to reduction of column water vapor over Bay of Bengal. Thus, tilted vertical shear can just begin the NP. On the other hand, it is suggested that the NP needs SST and column water vapor to maintain its strength.

Keywords: Boreal summer intraseasonal oscillation, Asian monsoon, Northward propagation

©2019. Japan Geoscience Union. All Right Reserved.

Fractality in the perimeter of tropical clouds observed by Himawari-8 or simulated by a high-resolution model

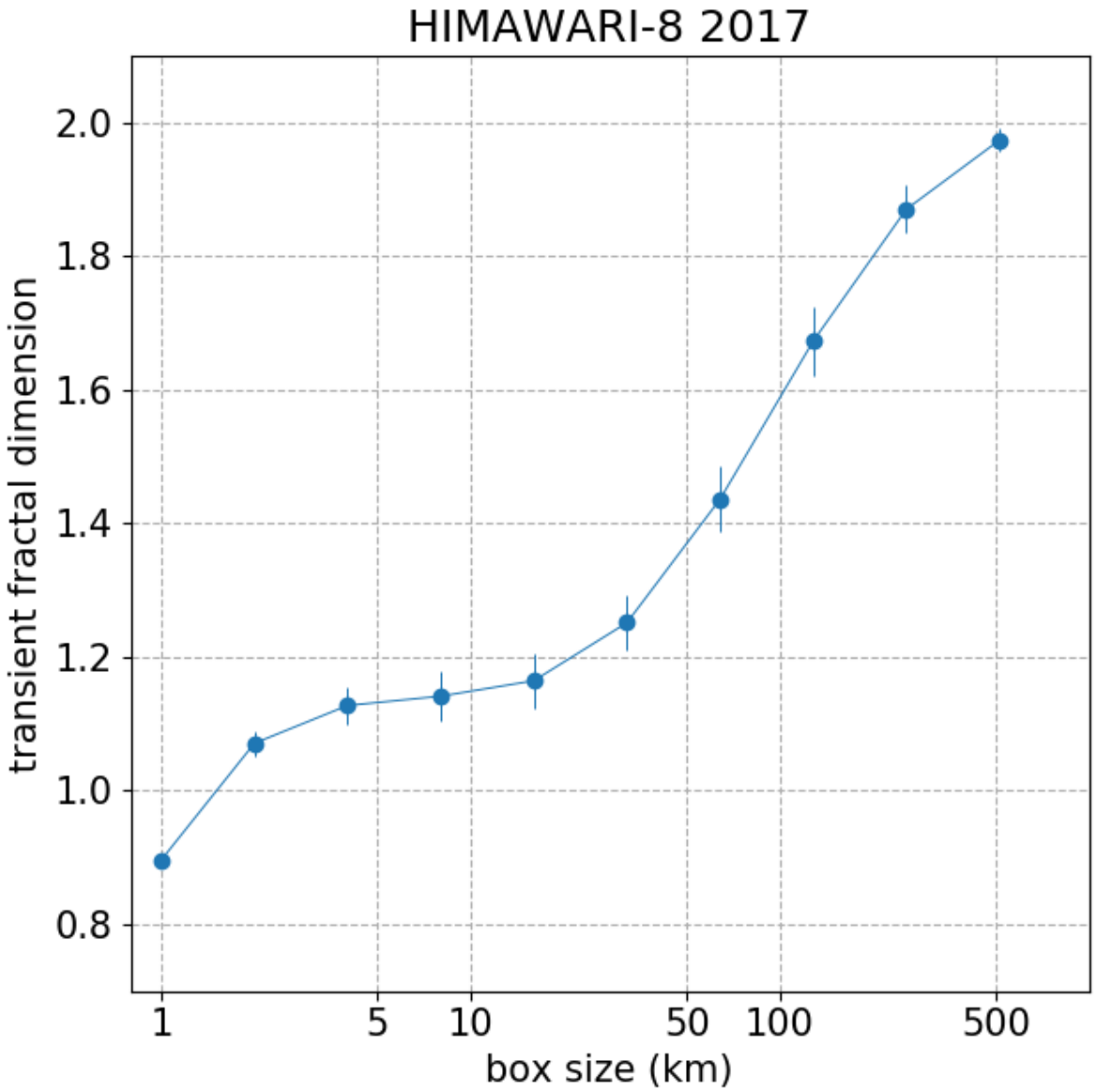
*Takuya Jinno[1]

1. Graduate School of Science, The University of Tokyo

Cloud clusters show a wide variety of shape and size, and their spatial pattern is often taken up as a typical example of fractal. However, the methods of studying fractal are in an early stage of development. In this study, we conducted fractal analysis on the perimeter of tropical clouds using satellite observation and cloud-resolving simulation of sub-kilometer resolution. We evaluated fractal dimension as a function of spatial scale (transient fractal dimension) and quantified the characteristic spatial scale of the pattern from the scale where self-similarity breaks down. From the observational data from HIMAWARI-8, It is shown that the self-similarity of the cloud perimeter persists only in the spatial scale range from 2 km up to 30 km. The limit of the self-similarity is suggested to be the characteristic scale of the pattern formation of tropical clouds. The cloud-resolving simulation data with NICAM also shows finite-size self-similarity. However, the profile of the transient fractal dimension changed with integration time far more rapidly than HIMAWARI-8 observation, and it lost its self-similarity at the end of the 48-hour simulation. This process is suggested to reflect the increase of stratiform cloud in the upper-troposphere as an adjustment to the transition of spatial resolution.

Keywords: fractal, HIMAWARI-8, cloud-resolving model

©2019. Japan Geoscience Union. All Right Reserved.



©2019. Japan Geoscience Union. All Right Reserved.

Large-scale deformation of tropical cloud band in the ITCZ detected in NICAM simulations

*Noriyuki Nishi[1], Atsushi Hamada[4], Yohei Yamada[2], Tomoe Nasuno[2], Reona Satoh[5], Masaki Satoh[3]

1. Faculty of Science, Fukuoka Universtiy, 2. JAMSTEC, 3. AORI, University of Tokyo, 4. Graduate School of Science and Engineering for Education, University of Toyama, 5. Graduate School of Science, Fukuoka University

Over the central/eastern tropical Pacific, the Inter Tropical Convergence Zone (ITCZ) is detected in the northern side of the equator. In the ITCZ, we can sometimes observe drastic deformation of the cloud bands elongated zonally with several thousand-kilometer scale. The initial stage of the band, which is composed of deep convective systems, expands meridionally and separates into two or three parallel cirrus bands that keep alive one or two days (Hamada et al., 2013, JMSJ). These separation events cannot be well described in the objective analysis datasets, probably due to lack of the observations over the open ocean; investigation of their mechanism with the analysis data is difficult. In order to study their mechanism, we attempted to use the numerical simulation results of global cloud system resolving model NICAM (Satoh et al. 2014, Progress in Earth and Planetary Science) to find similar events in them. If we can find separation events in the results, we can examine the mechanism with many physical parameters including wind, various kinds of hydrometeors. We have already analyzed several numerical experiment results for different periods, resolution and physical schemes.

We found a similar separation event in an output of the simulation for one year from June 2004 and horizontal resolution 3.5 km. We examined the life cycle of the cirrus bands after separation. One interesting point is on the height of the cirrus clouds in the separated bands. The simulated cirrus clouds in the bands lie in the 13-14 km height level, while the height of the maximum meridional wind that contributes to the meridional movement of the cirrus bands is about 12 km. This difference of the heights means that the cirrus clouds were not just advected by meridional wind but were possibly developed in the course of the separation.

The trigger of zonally simultaneous separation of a long band is another our interest. Inertial instability may be a candidate since vertical exchange of zonal momentum by deep convection would occur in an original band and result in the large meridional shear of the zonal wind in the upper troposphere. We tried to confirm necessary condition for inertial instability by calculating geostrophic vorticity, following the general procedure. However, the position of the bands is too close to the equator (3-7N) to establish geostrophic relationship, and the spatial pattern of the geostrophic vorticity is too noisy to analyze. Therefore, we instead calculate simple absolute vorticity. We found that the absolute vorticity around the separated bands was almost negative. It suggests the possibility of the inertial (or similar kind of) instability.

We are now analyzing another numerical experiment including four kinds of runs using a cloud scheme with different cloud parameter settings. In the real atmosphere, a separation event occurred on 16-17 June 2008 at the just east of the date line. The event can be simulated in all of four runs at 36 hours from the initial time. It suggests that the basic mechanism of the separation is not sensitive to the detail of cloud systems. By analyzing the dynamical fields of these outputs, we are trying to find the key mechanisms to trigger the meridional separation of the cloud bands.

©2019. Japan Geoscience Union. All Right Reserved.

Keywords: tropics, ITCZ, cirrus

©2019. Japan Geoscience Union. All Right Reserved.

Improvement of single-moment bulk microphysics for super-cooled water clouds over the Southern Ocean in NICAM using Joint simulator and double-moment microphysics

*Woosub Roh[1], Tatsuya Seiki[2], Masaki Satoh[1], Tempei Hashino[3]

1. AORI, the university of Tokyo, 2. JAMSTEC, 3. Kochi university of technology

It is important to evaluate and improve the cloud properties in global non-hydrostatic models like a Nonhydrostatic ICosahedral Atmospheric Model (NICAM, Satoh et al. 2014) using observation data. One of the methods is a radiance-based evaluation using satellite data and a satellite simulator (here Joint simulator, Hashino et al. 2013), which avoids making different settings of the microphysics between retrieval algorithms and NICAM.

One of the challenging issues is an evaluation of mixed-phase clouds, which consist of water vapor, ice particles, and supercooled water droplets. It is known one of the main reasons why climate models reveal large errors about the reflection of solar radiation over the Southern Ocean and Arctic.

This study is an evaluation and improvement of mixed-phase clouds over the Southern Ocean in NICAM using a Cloud-Aerosol Lidar and Infrared Pathfinder Satellite Observation (CALIPSO) and a satellite simulator. We evaluated thermodynamics phase of mixed phases clouds over the Southern Ocean in a regional version of NICAM between 45˚S to 65˚S and 170˚E to 170˚W following Yoshida et al. (2010) method. We found underestimation of supercooled water clouds in our single moment scheme. We improved the single moment microphysics scheme using a double moment microphysics and a single column model. We also investigate the impact of microphysics scheme on moisture distributions and the size of cloud systems.

Keywords: microphysics, CALIPSO, Satellite simulator

©2019. Japan Geoscience Union. All Right Reserved.

High-cloud property responses to SST change: sensitivity study using a global nonhydrostatic model

*Tomoki Ohno[1], Masaki Satoh[2]

1. Japan Agency for Marine-Earth Science and Technology, 2. Atmosphere and Ocean Research Institute, The University of Tokyo

Since it has been recognized that the uncertainty of cloud feedback is one of main contributors to the intermodel spread of climate sensitivity, the reduction of the uncertainties associated with cloud response to global warming has been one of central issues for robust projections and predictions of climate variability and change. High clouds have large impacts on the Earth’ s radiative energy budget, and the uncertainty of their response to climate change is known as one of large sources of the climate sensitivity spread although several possible hypotheses to predict the response have been proposed. As the radiation-cloud interaction plays a crucial role in the determination of life time of high clouds, the improvement of the understanding of cloud property responses to global warming helps the reduction of climate-sensitivity variability associated with the high-clouds feedback.

In order to investigate the cloud-property response to climate change, we conducted simulations with RCE configurations using a high-resolution nonhydrostatic global circulation model (the Nonhydrostatic Icosahedral Atmospheric Model; NICAM) with the earth-like sphere for simplifying the problem. Sea surface temperatures (SSTs) are fixed at 300K and 304K and a double-moment bulk scheme are used without cumulus parameterization scheme.

We found that high cloud amount increases with SST increase, as consistent with the previous NICAM studies. It was also determined that the change in particularly optically thin clouds whose optical thicknesses were <3 was dominant, and such thin clouds tended to have large particle sizes. These suggests that the slow evaporative property of ice phase clouds and their representability can play one of key roles in the uncertainty of the high-cloud amount change in global warming.

Keywords: cloud property responses, cloud feedback, climate change

©2019. Japan Geoscience Union. All Right Reserved.

Effects of different cloud overlapping parameters on simulated total cloud fraction over the globe and East Asian region

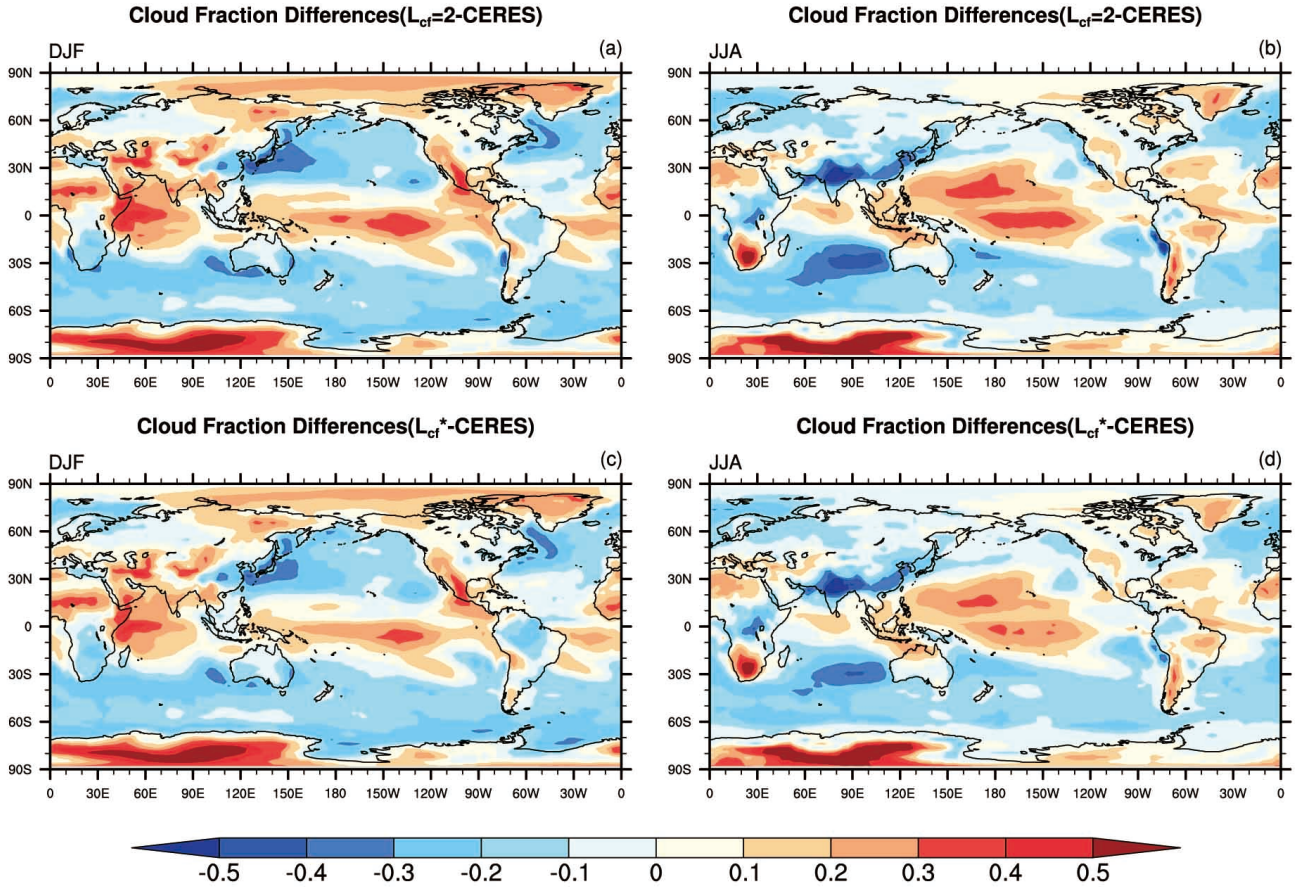
*bo hai Wang[1], hua Zhang[2]

1. Institute of Atmospheric Physics, Chinese Academy of Sciences, 2. State Key Laboratory of Severe Weather, Chinese Academy of Meteorological Sciences

The cloud overlapping parameter (vertical decorrelation length, L_{cf}) from CloudSat/CALIPSO is implemented in Beijing Climate Center’ s GCM (BCC_AGCM2.0) to reduce the uncertainly in radiation field. Comparing the climate simulation results obtained by using the constant L_{cf} of 2 km with those using the above retrieved L_{cf}, it is found that the total cloud fraction simulation has been obviously improved by using the satellite-based L_{cf}. The error of global mean total cloud fraction between simulations and CERES (Clouds and the Earth's Radiant Energy System) satellite data is decreased by 1.6% in both the winter and summer, of which the positive deviation of total cloud amount at tropical convection area and the negative deviation in subtropical region both are significantly reduced. These improvements are helpful for better simulation of energy budget differences between different regions. In East Asia, using the satellite-based L_{cf} can decrease the error of average total cloud fraction (compared to the CERES) by 1.8% (1.4%) in the winter (summer).Overall, using L_{cf} from CloudSat/CALIPSO satellite data can improve the simulation of total cloud fraction and thus obtain more accurate simulation of radiation field.

Keywords: Cloud overlapping parameter, Vertical decorrelation length, Total cloud fraction

©2019. Japan Geoscience Union. All Right Reserved.



©2019. Japan Geoscience Union. All Right Reserved.

[E] Poster | A (Atmospheric and Hydrospheric Sciences)：A-CG Complex & General

Tue. May 28, 2019 10:45 AM - 12:15 PM JST | Tue. May 28, 2019 1:45 AM - 3:15 AM UTC | Poster Hall International Exhibition Hall8, Makuhari Messe_3

[A-CG32] Global Carbon Cycle Observation and Analysis

convener:Kazuhito Ichii(Chiba University), Prabir Patra(Research Institute for Global Change, JAMSTEC), Forrest M. Hoffman(Oak Ridge National Laboratory), Makoto Saito(National Institute of Environmental Studies)

The landmark Paris Agreement under the United Nations Framework Convention on Climate Change (UNFCCC) aims at reduction of greenhouse gases (GHGs) emission to keep the global warming below 2 degC. As per the agreement the nationally determined commitments (NDCs) and their progresses should be carefully monitored and verified by international bodies. The emission verification will be based on observation of the time evolution of greenhouse gases and model-based estimations of emissions from time to time.

In recent years, the number of observations and new techniques to monitor GHGs budget have been increasing. The improvements includes observational platforms for monitoring atmospheric GHGs, national or regional emission inventories, top-down models (e.g. atmospheric inverse models), and bottom-up models (e.g. process-based models). However, due to uncertainties in modeling and sparse observation network, high uncertainty exists in GHGs sources/sinks estimations at global and regional scales. These uncertainties lead to large variations in future projection of GHG budgets and climate changes.

The purpose of the session is to discuss state-of-the-art techniques for estimations of GHGs (e.g. CO2, CH4, N2O) budget at global and regional scales. The topic includes natural and anthropogenic processes, various methodologies (e.g. in-situ observation, aircraft monitoring, remote sensing, modeling), and various targets (e.g. atmosphere, terrestrial, and ocean), various spatial and temporal coverage (e.g. regional to global scales and past-present-future). Improved estimates of emissions from land use change, forest fires, and other anthropogenic sources (urban developments and thermal power station etc.) are also of interest. We also welcome discussions for designs and plans for future studies targeting city and country scale emission estimations using sophisticated modeling tools.

[ACG32-P01] Regional budgets of 3 major greenhouse gases using inverse modelling of atmospheric data

*Prabir Patra[1], Naveen Chandra[1], Jagat Bisht[1] (1.Japan Agency for Marine-Earth Science and Technology (JAMSTEC))

[ACG32-P02] Analysis of hot summer in 2018

*Kazutaka Murakami[1], Kazuhito Ichii[1,2], Yukio Yoshida[1], Haruki Oshio[1], Makoto Saito[1] (1.National Institute for Environmental Studies, 2.Chiba University)

[ACG32-P03] Updated Data-Driven GPP and NEE Estimation Using Machine Learning Algorithms with Remote Sensing and Flux Data

*Zhiyan Liu[1], Kazuhito Ichii[1], Yusuke Hayasi[1], Riku Kawase[1], Masahito Ueyama[2], Yuji Kominami[3] (1.Chiba University, 2.Osaka Prefecture University, 3.Forest Research and Management Organization)

[ACG32-P04] Response of a Bornean Rainforest to the Climatic Changes imposed by ENSO during 2009-2016

*Julie Karine Michelon[1], Tomo'omi Kumagai[2,3], Tetsuya Hiyama[3], Hatsuki Fujinami[3], Kazuho Matsumoto[4], Tomonori Kume[5], Takami Saito[6] (1.Graduate School of Environmental Studies, Nagoya University, 2.Graduate School of Agricultural and Life Sciences, The University of Tokyo, 3.Institute for Space-Earth Environmental Research, Nagoya University, 4.Faculty of Agriculture, University of the Ryukyus, 5.Faculty of Agriculture, Kyushu University, 6.Forest Research and Management Organization)

[ACG32-P05] Monitoring and Evaluating CO2 Flux in the Grassland Areas of Mongolia

*Qinxue Wang[1], Tomohiro Okadera[1], Deni Eer[1], Masataka Watanabe[2], Tomohiro Shishime[2], Akihiro Oba[2], Ochirbat Batkhishig[3] (1.National Institute for Environmental Studies, 2.Research and Development Initiative, Chuo University, 3.Institute of Geography and Geoecology, Mongolian Academy of Sciences)

[ACG32-P06] Data-driven monitoring of terrestrial carbon cycle in Mongolia

*ZAYA MART[1], Zhiyan Liu[1], Riku Kawase[1], Kazuhito Ichii[1] (1.Chiba University)

Regional budgets of 3 major greenhouse gases using inverse modelling of atmospheric data

*Prabir Patra[1], Naveen Chandra[1], Jagat Bisht[1]

1. Japan Agency for Marine-Earth Science and Technology (JAMSTEC)

Atmospheric observations of greenhouse gases provide accurate record the changes in their abundance in the Earth's environments, and it has now been well established that the increase in greenhouse gases concentrations is causing the rise in the mean surface air temperature. Using atmospheric chemistry-transport models (ACTM), along with the concentration measurements, we can estimate the sources and sinks of the chemical species. Using MIROC4-ACTM at JAMSTEC, we estimated regional sources and sinks of carbon dioxide (CO2), methane (CH4) and nitrous oxide (N2O) over the period of 1996 to 2016. This will help global stocktake every 5 years, as a independent estimate, when the coutries report their progress on nationally determined contributions (NDCs) under the Paris Agreement and their ammendments, overseen by the UNFCCC.

Keywords: Inverse modelling, Greenhouse gases sources and sinks, Paris Agreement and NDCs

©2019. Japan Geoscience Union. All Right Reserved.

Analysis of hot summer in 2018

*Kazutaka Murakami[1], Kazuhito Ichii[1,2], Yukio Yoshida[1], Haruki Oshio[1], Makoto Saito[1]

1. National Institute for Environmental Studies, 2. Chiba University

Global averaged temperature in 2018 was considerably higher than normal year. Probably it is the fourth highest in the past. Especially, it was memorable that East Asia, Europe, and the southwestern part of the United States were hit by record heat waves in this summer. It is important for the ecological resilience to investigate how much such extreme weather damages the terrestrial ecosystem and how will it change after that. In this study, we analyzed the effect of this extremely high temperature on terrestrial vegetation using satellite remote sensing data. First, we investigated the high temperature area using MODIS land surface temperature (LST) product. Then, focusing on these high LST areas, we analyzed the impact to satellite observed Solar Induced Fluorescence (SIF) that closely related to a photosynthetic activity. As a result, it was found that the LST of 2018 in the East Asia (Japan, Korea and North Korea) was the highest during 2002 - 2018 years. And it also indicated abnormal high LST regions from Germany to northern Europe. Analysis of SIF data showed a positive decline in Europe but did not show a clear trend in Asia. In addition, similar trends were seen from other satellite vegetation indices, and it was found that the terrestrial vegetation shows different responses in both areas affected by the same hot summer.

Keywords: 2018 summer, heat wave, satellite observation, SIF

©2019. Japan Geoscience Union. All Right Reserved.

Updated Data-Driven GPP and NEE Estimation Using Machine Learning Algorithms with Remote Sensing and Flux Data

*Zhiyan Liu[1], Kazuhito Ichii[1], Yusuke Hayasi[1], Riku Kawase[1], Masahito Ueyama[2], Yuji Kominami[3]

1. Chiba University, 2. Osaka Prefecture University, 3. Forest Research and Management Organization

Abstract

Data-driven approach is effective for understanding and up-scaling observation network data of terrestrial carbon fluxes. Recently, the expansion of observation network, the improvement of remote sensing products and more application of machine learning on natural science make it more possible. In this study, we estimated two important parameters of terrestrial ecosystem, terrestrial gross primary productivity (GPP) and net ecosystem exchange (NEE) through re-assessment of previous approaches [Ichii et al. 2017; Kondo et al. 2015]. We tested multiple combinations of input parameters with lagged effect, additional new input parameters and the updated MODIS datasets (Collection C6). Besides, we selected 3 typical machine learning methods (Random Forest, RF; Support Vector Regression, SVR; Artificial Neural Network, ANN) as data-driven method and compare the estimation from 3 different types of machine learning model. The site-level analysis shows that use of the new version data and the time-lagged improved the model performance. Finally, we compared our new estimation of GPP and NEE with several terrestrial models output and other available datasets and we found our new results show better consistency with them. This shows our estimation provides a good benchmark for understanding spatio-temporal variability in terrestrial GPP and NEE.

Acknowledgement

This research was financially supported by the Environment Research and Technology Development Fund (2-1701) of the Environmental Restoration and Conservation Agency of Japan.

Keywords: Terrestrial Carbon Cycle, MODIS Collection6, Data-driven, time-lag effect

©2019. Japan Geoscience Union. All Right Reserved.

Response of a Bornean Rainforest to the Climatic Changes imposed by ENSO during 2009-2016

*Julie Karine Michelon[1], Tomo'omi Kumagai[2,3], Tetsuya Hiyama[3], Hatsuki Fujinami[3], Kazuho Matsumoto[4], Tomonori Kume[5], Takami Saito[6]

1. Graduate School of Environmental Studies, Nagoya University, 2. Graduate School of Agricultural and Life Sciences, The University of Tokyo, 3. Institute for Space-Earth Environmental Research, Nagoya University, 4. Faculty of Agriculture, University of the Ryukyus, 5. Faculty of Agriculture, Kyushu University, 6. Forest Research and Management Organization

Tropical rainforests belong to the most important biomes, as they are one of the largest terrestrial carbon sink and also a consequent source of latent energy. Furthermore, they will be among the first ecosystems to undergo climatic changes in the near future. Understanding how they will response to those changes is essential. El Niño-Southern Oscillation (ENSO) is an opportunity to study ecosystem response under real climatic change conditions.

Transpiration (Tr), net ecosystem exchange (NEE) and heat fluxes were measured with an eddy covariance system in a natural rainforest in Sarawak, Malaysia. Meteorological and soil moisture observations were also conducted. This region does not have phase-locked dry periods, and seasonal variations of both air temperature and solar radiation are small. However, it is directly impacted by ENSO events. During the study period, from November 2009 to December 2016, two events were selected : La Niña 2010-2011 and El Niño 2014-2016. Normal conditions were assumed as a third "neutral" period. Comparisons of measured flux and meteorological drivers between the three periods were carried out, and analysis of environmental controls, as canopy conductance (g_c) were made.

Precipitation and air temperature were significantly different between the three periods. While the water cycle (latent heat flux, Tr, g_c) responded immediately to the changes imposed by La Niña, the enhancement of the ecosystem respiration balanced the gross primary production gain, resulting into a NEE similar to neutral conditions. Conversely, the NEE during El Niño was significantly smaller than during neutral, when the water cycle seemed not impacted. However, further observations of this late rainforest response evolution showed that, during the first part of El Niño, Tr and g_c increased while CO_2 flux reduced. Then, during the second part, the trend reversed : CO_2 flux increased and Tr, as well as g_c, reduced. This may indicate a time lag between the meteorological drivers (precipitation and air temperature) changes imposed by El Niño and the ecosystem response (H_2O and CO_2 fluxes). The response delay may be caused by the rainforest tendency to poorly regulate its water use, being a particular moist environment. As for the response itself, it may be triggered by the depletion of the soil water content.

Those results imply that considering the length of El Niño and the ecosystem response trigger are important to understand and model bornean rainforest fluxes under future climatic scenario.

Keywords: Borneo, Rainforest, ENSO, NEE, Transpiration

©2019. Japan Geoscience Union. All Right Reserved.

Monitoring and Evaluating CO2 Flux in the Grassland Areas of Mongolia

*Qinxue Wang[1], Tomohiro Okadera[1], Deni Eer[1], Masataka Watanabe[2], Tomohiro Shishime[2], Akihiro Oba[2], Ochirbat Batkhishig[3]

1. National Institute for Environmental Studies, 2. Research and Development Initiative, Chuo University, 3. Institute of Geography and Geoecology, Mongolian Academy of Sciences

For verification of data products of the Greenhouse Gas Observing Satellite (GOSAT), in this study, we monitored and evaluated CO2 flux, that is, the absorption and emission of CO2 by ecosystems in the grasslands of Mongolia by the eddy correlation method. Two flux towers were established in 2015 at the Nalaikh site near Ulaanbaatar City and the Hustai site with less influence of cities, respectively. The CO2 analyzers installed on the towers were calibrated every year by using the standard gas imported from Japan. Up to now, about 4-year monitoring data have been accumulated since 2015. The data analysis shows that the CO2 absorption was larger than emissions at both sites, which indicated that the ecosystem at both sites are carbon sinks. The annual mean value of the CO2 absorption at the Nalaikh site was about 2.66 μmol m^{-2} s^{-1} and the emission was about 1.53 μmol m^{-2} s^{-1}, but the absorption at the Hustai site was about 2.11 μmol m^{-2} s^{-1}, and the emission was about 1.37 μmol m^{-2} s^{-1} (Figure 1). Generally, the net CO2 absorption at the Nalaikh site (0.76 μmol m^{-2} s^{-1}) was found to be larger than that at the Hustai site (0.36 μmol m^{-2} s^{-1}).

To compare the GOSAT L4B data with the ground observation at both sites, we extracted the monthly mean value of CO2 absorption/emission from the grid data of GOSAT during 2009-2015 and compared with the observed data. We found that although the seasonal changing pattern and fluctuation range are similar, the CO2 emission derived by GOSAT were larger than absorption, which suggested that the steppe ecosystems at both sites are the carbon sources. However, the ground observations showed that the CO2 absorption at both sites was larger than emission, which suggested that the grassland ecosystems at both sites are carbon sinks (Figure 2). It is essential for us to find the reasons of this difference in the future.

Finally, to evaluate the spatiotemporal distribution of carbon absorption and emission in the whole country, we have developed a carbon budget model considering the influence of grazing density. The primary simulation results showed that the percentage of carbon loss by grazing (CLG) accounted for 19-38% of the net ecosystem production (NEP) in the Nalaikh area around the city of Ulaanbaatar, where the grazing density was 1.5-2.3 sheep/ha during 2012-2016. On the other hand, CLG accounted for only 7-20% of NEP in the Hustai area away from the city, where the grazing density was only 0.4-0.6 sheep/ha (Figure 3). The result implied that the carbon budget was greatly influenced by animal husbandry near cities, where the grazing density is large. The monitoring cameras installed at both sites show that the biomass inside and outside the fence was greatly influenced by the ingestion of livestock.

This study was funded by “the Project to implement MRV and related technological improvements contributing to the Joint Crediting Mechanism (JCM) in Mongolia”, Ministry of the Environment, Japan.

Keywords: Carbon flux, Grassland ecosystem, The Greenhouse Gases Observing Satellite (GOSAT)

©2019. Japan Geoscience Union. All Right Reserved.

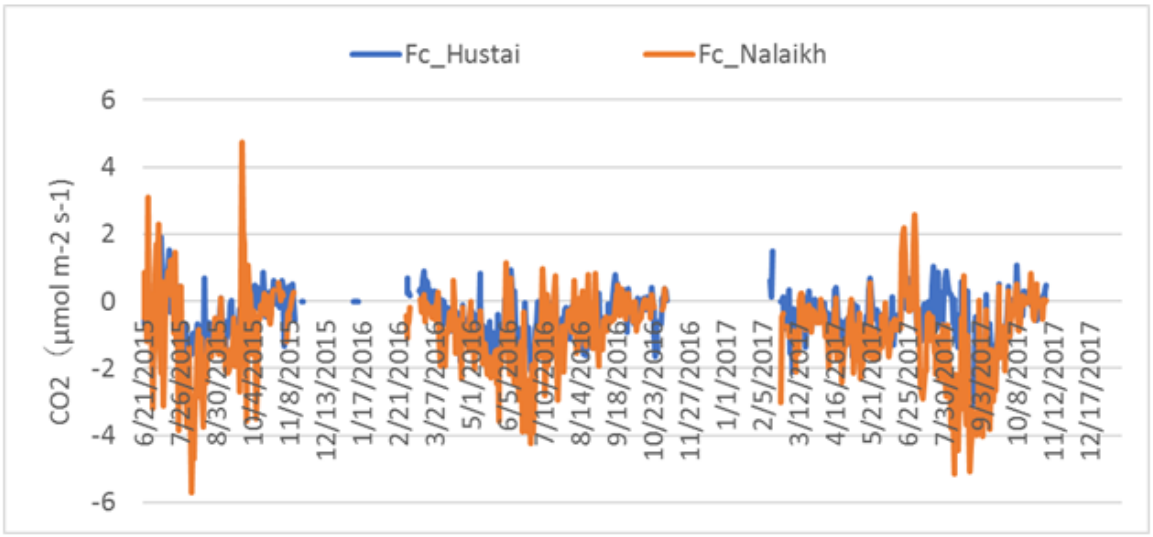


Figure 1 Comparison of CO2 flux observed at Nalaikh Site and Hustai Site

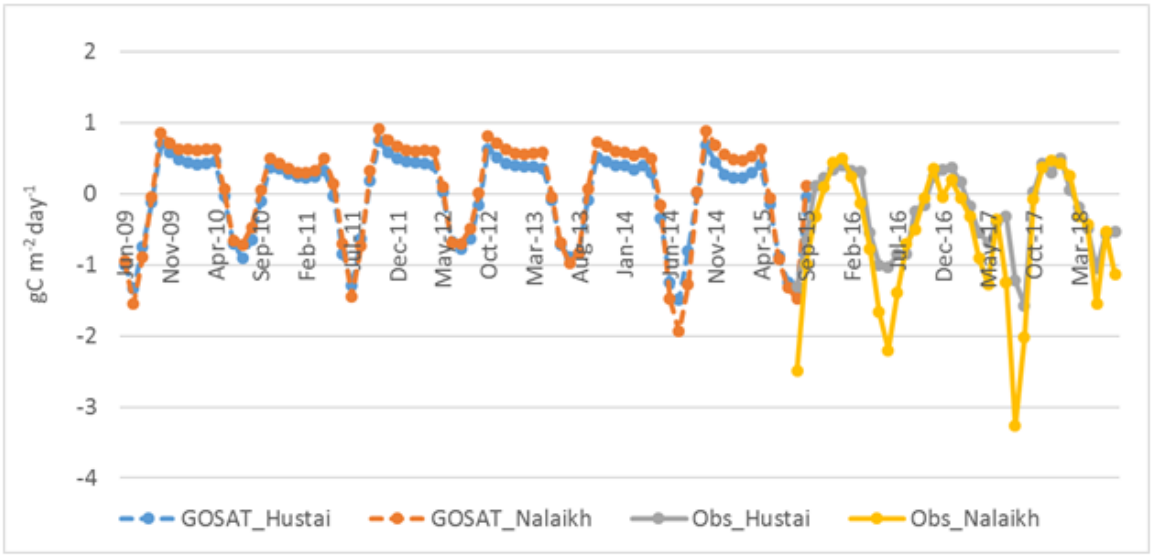


Figure 2 Comparison of GOSAT L4B and observations at Nalaikh Site and Hustai Site

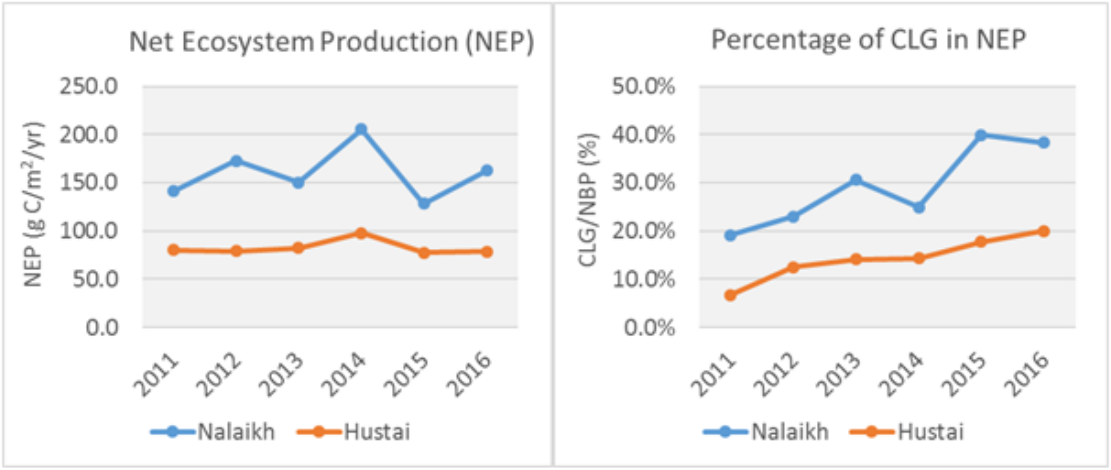


Figure 3 Impact of livestock grazing on NEP at Nalaikh Site and Hustai Site

©2019. Japan Geoscience Union. All Right Reserved.

Data-driven monitoring of terrestrial carbon cycle in Mongolia

*ZAYA MART[1], Zhiyan Liu[1], Riku Kawase[1], Kazuhito Ichii[1]

1. Chiba University

Mongolia has been experiencing both climate changes and anthropogenic environmental changes. Therefore, it is important to monitor environmental changes. In particular, more and more observation-based data sets are available, and synthesis analysis using these multiple observation-based data sets are essential.

We analyzed changes in the terrestrial environmental environment in Mongolia from the 1980s to 2010s. We focused on two different temporal periods, the 1980s to 2010s and 2000 to 2015. As for the first period (1980s to 2010s), we used NOAA AVHRR data sets, observed climate data sets for the analysis. As for the second period (1980s to 2010s), we used multiple remote sensing data sets (e.g. Terra MODIS), empirically upscaled CO2 flux products, and outputs from terrestrial ecosystem models. We will show and discuss the estimated terrestrial environmental changes in Mongolia at the conference.

Keywords: climate change, terrestrial environments, carbon cycle

©2019. Japan Geoscience Union. All Right Reserved.

[E] Poster | A (Atmospheric and Hydrospheric Sciences)：A-CG Complex & General

Tue. May 28, 2019 5:15 PM - 6:30 PM JST | Tue. May 28, 2019 8:15 AM - 9:30 AM UTC | Poster Hall International Exhibition Hall8, Makuhari Messe_13

[A-CG32] Global Carbon Cycle Observation and Analysis

convener:Kazuhito Ichii(Chiba University), Prabir Patra(Research Institute for Global Change, JAMSTEC), Forrest M. Hoffman(Oak Ridge National Laboratory), Makoto Saito(National Institute of Environmental Studies)

The landmark Paris Agreement under the United Nations Framework Convention on Climate Change (UNFCCC) aims at reduction of greenhouse gases (GHGs) emission to keep the global warming below 2 degC. As per the agreement the nationally determined commitments (NDCs) and their progresses should be carefully monitored and verified by international bodies. The emission verification will be based on observation of the time evolution of greenhouse gases and model-based estimations of emissions from time to time.

In recent years, the number of observations and new techniques to monitor GHGs budget have been increasing. The improvements includes observational platforms for monitoring atmospheric GHGs, national or regional emission inventories, top-down models (e.g. atmospheric inverse models), and bottom-up models (e.g. process-based models). However, due to uncertainties in modeling and sparse observation network, high uncertainty exists in GHGs sources/sinks estimations at global and regional scales. These uncertainties lead to large variations in future projection of GHG budgets and climate changes.

The purpose of the session is to discuss state-of-the-art techniques for estimations of GHGs (e.g. CO2, CH4, N2O) budget at global and regional scales. The topic includes natural and anthropogenic processes, various methodologies (e.g. in-situ observation, aircraft monitoring, remote sensing, modeling), and various targets (e.g. atmosphere, terrestrial, and ocean), various spatial and temporal coverage (e.g. regional to global scales and past-present-future). Improved estimates of emissions from land use change, forest fires, and other anthropogenic sources (urban developments and thermal power station etc.) are also of interest. We also welcome discussions for designs and plans for future studies targeting city and country scale emission estimations using sophisticated modeling tools.

[ACG32-P01] Regional budgets of 3 major greenhouse gases using inverse modelling of atmospheric data

*Prabir Patra[1], Naveen Chandra[1], Jagat Bisht[1] (1.Japan Agency for Marine-Earth Science and Technology (JAMSTEC))

[ACG32-P02] Analysis of hot summer in 2018

*Kazutaka Murakami[1], Kazuhito Ichii[1,2], Yukio Yoshida[1], Haruki Oshio[1], Makoto Saito[1] (1.National Institute for Environmental Studies, 2.Chiba University)

[ACG32-P03] Updated Data-Driven GPP and NEE Estimation Using Machine Learning Algorithms with Remote Sensing and Flux Data

*Zhiyan Liu[1], Kazuhito Ichii[1], Yusuke Hayasi[1], Riku Kawase[1], Masahito Ueyama[2], Yuji Kominami[3] (1.Chiba University, 2.Osaka Prefecture University, 3.Forest Research and Management Organization)

[ACG32-P04] Response of a Bornean Rainforest to the Climatic Changes imposed by ENSO during 2009-2016

*Julie Karine Michelon[1], Tomo'omi Kumagai[2,3], Tetsuya Hiyama[3], Hatsuki Fujinami[3], Kazuho Matsumoto[4], Tomonori Kume[5], Takami Saito[6] (1.Graduate School of Environmental Studies, Nagoya University, 2.Graduate School of Agricultural and Life Sciences, The University of Tokyo, 3.Institute for Space-Earth Environmental Research, Nagoya University, 4.Faculty of Agriculture, University of the Ryukyus, 5.Faculty of Agriculture, Kyushu University, 6.Forest Research and Management Organization)

[ACG32-P05] Monitoring and Evaluating CO2 Flux in the Grassland Areas of Mongolia

*Qinxue Wang[1], Tomohiro Okadera[1], Deni Eer[1], Masataka Watanabe[2], Tomohiro Shishime[2], Akihiro Oba[2], Ochirbat Batkhishig[3] (1.National Institute for Environmental Studies, 2.Research and Development Initiative, Chuo University, 3.Institute of Geography and Geoecology, Mongolian Academy of Sciences)

[ACG32-P06] Data-driven monitoring of terrestrial carbon cycle in Mongolia

*ZAYA MART[1], Zhiyan Liu[1], Riku Kawase[1], Kazuhito Ichii[1] (1.Chiba University)

Regional budgets of 3 major greenhouse gases using inverse modelling of atmospheric data

*Prabir Patra[1], Naveen Chandra[1], Jagat Bisht[1]

1. Japan Agency for Marine-Earth Science and Technology (JAMSTEC)

Atmospheric observations of greenhouse gases provide accurate record the changes in their abundance in the Earth's environments, and it has now been well established that the increase in greenhouse gases concentrations is causing the rise in the mean surface air temperature. Using atmospheric chemistry-transport models (ACTM), along with the concentration measurements, we can estimate the sources and sinks of the chemical species. Using MIROC4-ACTM at JAMSTEC, we estimated regional sources and sinks of carbon dioxide (CO2), methane (CH4) and nitrous oxide (N2O) over the period of 1996 to 2016. This will help global stocktake every 5 years, as a independent estimate, when the coutries report their progress on nationally determined contributions (NDCs) under the Paris Agreement and their ammendments, overseen by the UNFCCC.

Keywords: Inverse modelling, Greenhouse gases sources and sinks, Paris Agreement and NDCs

©2019. Japan Geoscience Union. All Right Reserved.

Analysis of hot summer in 2018

*Kazutaka Murakami[1], Kazuhito Ichii[1,2], Yukio Yoshida[1], Haruki Oshio[1], Makoto Saito[1]

1. National Institute for Environmental Studies, 2. Chiba University

Global averaged temperature in 2018 was considerably higher than normal year. Probably it is the fourth highest in the past. Especially, it was memorable that East Asia, Europe, and the southwestern part of the United States were hit by record heat waves in this summer. It is important for the ecological resilience to investigate how much such extreme weather damages the terrestrial ecosystem and how will it change after that. In this study, we analyzed the effect of this extremely high temperature on terrestrial vegetation using satellite remote sensing data. First, we investigated the high temperature area using MODIS land surface temperature (LST) product. Then, focusing on these high LST areas, we analyzed the impact to satellite observed Solar Induced Fluorescence (SIF) that closely related to a photosynthetic activity. As a result, it was found that the LST of 2018 in the East Asia (Japan, Korea and North Korea) was the highest during 2002 - 2018 years. And it also indicated abnormal high LST regions from Germany to northern Europe. Analysis of SIF data showed a positive decline in Europe but did not show a clear trend in Asia. In addition, similar trends were seen from other satellite vegetation indices, and it was found that the terrestrial vegetation shows different responses in both areas affected by the same hot summer.

Keywords: 2018 summer, heat wave, satellite observation, SIF

©2019. Japan Geoscience Union. All Right Reserved.

Updated Data-Driven GPP and NEE Estimation Using Machine Learning Algorithms with Remote Sensing and Flux Data

*Zhiyan Liu[1], Kazuhito Ichii[1], Yusuke Hayasi[1], Riku Kawase[1], Masahito Ueyama[2], Yuji Kominami[3]

1. Chiba University, 2. Osaka Prefecture University, 3. Forest Research and Management Organization

Abstract

Data-driven approach is effective for understanding and up-scaling observation network data of terrestrial carbon fluxes. Recently, the expansion of observation network, the improvement of remote sensing products and more application of machine learning on natural science make it more possible. In this study, we estimated two important parameters of terrestrial ecosystem, terrestrial gross primary productivity (GPP) and net ecosystem exchange (NEE) through re-assessment of previous approaches [Ichii et al. 2017; Kondo et al. 2015]. We tested multiple combinations of input parameters with lagged effect, additional new input parameters and the updated MODIS datasets (Collection C6). Besides, we selected 3 typical machine learning methods (Random Forest, RF; Support Vector Regression, SVR; Artificial Neural Network, ANN) as data-driven method and compare the estimation from 3 different types of machine learning model. The site-level analysis shows that use of the new version data and the time-lagged improved the model performance. Finally, we compared our new estimation of GPP and NEE with several terrestrial models output and other available datasets and we found our new results show better consistency with them. This shows our estimation provides a good benchmark for understanding spatio-temporal variability in terrestrial GPP and NEE.

Acknowledgement

This research was financially supported by the Environment Research and Technology Development Fund (2-1701) of the Environmental Restoration and Conservation Agency of Japan.

Keywords: Terrestrial Carbon Cycle, MODIS Collection6, Data-driven, time-lag effect

©2019. Japan Geoscience Union. All Right Reserved.

Response of a Bornean Rainforest to the Climatic Changes imposed by ENSO during 2009-2016

*Julie Karine Michelon[1], Tomo'omi Kumagai[2,3], Tetsuya Hiyama[3], Hatsuki Fujinami[3], Kazuho Matsumoto[4], Tomonori Kume[5], Takami Saito[6]

1. Graduate School of Environmental Studies, Nagoya University, 2. Graduate School of Agricultural and Life Sciences, The University of Tokyo, 3. Institute for Space-Earth Environmental Research, Nagoya University, 4. Faculty of Agriculture, University of the Ryukyus, 5. Faculty of Agriculture, Kyushu University, 6. Forest Research and Management Organization

Tropical rainforests belong to the most important biomes, as they are one of the largest terrestrial carbon sink and also a consequent source of latent energy. Furthermore, they will be among the first ecosystems to undergo climatic changes in the near future. Understanding how they will response to those changes is essential. El Niño-Southern Oscillation (ENSO) is an opportunity to study ecosystem response under real climatic change conditions.

Transpiration (Tr), net ecosystem exchange (NEE) and heat fluxes were measured with an eddy covariance system in a natural rainforest in Sarawak, Malaysia. Meteorological and soil moisture observations were also conducted. This region does not have phase-locked dry periods, and seasonal variations of both air temperature and solar radiation are small. However, it is directly impacted by ENSO events. During the study period, from November 2009 to December 2016, two events were selected : La Niña 2010-2011 and El Niño 2014-2016. Normal conditions were assumed as a third "neutral" period. Comparisons of measured flux and meteorological drivers between the three periods were carried out, and analysis of environmental controls, as canopy conductance (g_c) were made.

Precipitation and air temperature were significantly different between the three periods. While the water cycle (latent heat flux, Tr, g_c) responded immediately to the changes imposed by La Niña, the enhancement of the ecosystem respiration balanced the gross primary production gain, resulting into a NEE similar to neutral conditions. Conversely, the NEE during El Niño was significantly smaller than during neutral, when the water cycle seemed not impacted. However, further observations of this late rainforest response evolution showed that, during the first part of El Niño, Tr and g_c increased while CO_2 flux reduced. Then, during the second part, the trend reversed : CO_2 flux increased and Tr, as well as g_c, reduced. This may indicate a time lag between the meteorological drivers (precipitation and air temperature) changes imposed by El Niño and the ecosystem response (H_2O and CO_2 fluxes). The response delay may be caused by the rainforest tendency to poorly regulate its water use, being a particular moist environment. As for the response itself, it may be triggered by the depletion of the soil water content.

Those results imply that considering the length of El Niño and the ecosystem response trigger are important to understand and model bornean rainforest fluxes under future climatic scenario.

Keywords: Borneo, Rainforest, ENSO, NEE, Transpiration

©2019. Japan Geoscience Union. All Right Reserved.

Monitoring and Evaluating CO2 Flux in the Grassland Areas of Mongolia

*Qinxue Wang[1], Tomohiro Okadera[1], Deni Eer[1], Masataka Watanabe[2], Tomohiro Shishime[2], Akihiro Oba[2], Ochirbat Batkhishig[3]

1. National Institute for Environmental Studies, 2. Research and Development Initiative, Chuo University, 3. Institute of Geography and Geoecology, Mongolian Academy of Sciences

For verification of data products of the Greenhouse Gas Observing Satellite (GOSAT), in this study, we monitored and evaluated CO2 flux, that is, the absorption and emission of CO2 by ecosystems in the grasslands of Mongolia by the eddy correlation method. Two flux towers were established in 2015 at the Nalaikh site near Ulaanbaatar City and the Hustai site with less influence of cities, respectively. The CO2 analyzers installed on the towers were calibrated every year by using the standard gas imported from Japan. Up to now, about 4-year monitoring data have been accumulated since 2015. The data analysis shows that the CO2 absorption was larger than emissions at both sites, which indicated that the ecosystem at both sites are carbon sinks. The annual mean value of the CO2 absorption at the Nalaikh site was about 2.66 μmol m^{-2} s^{-1} and the emission was about 1.53 μmol m^{-2} s^{-1}, but the absorption at the Hustai site was about 2.11 μmol m^{-2} s^{-1}, and the emission was about 1.37 μmol m^{-2} s^{-1} (Figure 1). Generally, the net CO2 absorption at the Nalaikh site (0.76 μmol m^{-2} s^{-1}) was found to be larger than that at the Hustai site (0.36 μmol m^{-2} s^{-1}).

To compare the GOSAT L4B data with the ground observation at both sites, we extracted the monthly mean value of CO2 absorption/emission from the grid data of GOSAT during 2009-2015 and compared with the observed data. We found that although the seasonal changing pattern and fluctuation range are similar, the CO2 emission derived by GOSAT were larger than absorption, which suggested that the steppe ecosystems at both sites are the carbon sources. However, the ground observations showed that the CO2 absorption at both sites was larger than emission, which suggested that the grassland ecosystems at both sites are carbon sinks (Figure 2). It is essential for us to find the reasons of this difference in the future.

Finally, to evaluate the spatiotemporal distribution of carbon absorption and emission in the whole country, we have developed a carbon budget model considering the influence of grazing density. The primary simulation results showed that the percentage of carbon loss by grazing (CLG) accounted for 19-38% of the net ecosystem production (NEP) in the Nalaikh area around the city of Ulaanbaatar, where the grazing density was 1.5-2.3 sheep/ha during 2012-2016. On the other hand, CLG accounted for only 7-20% of NEP in the Hustai area away from the city, where the grazing density was only 0.4-0.6 sheep/ha (Figure 3). The result implied that the carbon budget was greatly influenced by animal husbandry near cities, where the grazing density is large. The monitoring cameras installed at both sites show that the biomass inside and outside the fence was greatly influenced by the ingestion of livestock.

This study was funded by “the Project to implement MRV and related technological improvements contributing to the Joint Crediting Mechanism (JCM) in Mongolia”, Ministry of the Environment, Japan.

Keywords: Carbon flux, Grassland ecosystem, The Greenhouse Gases Observing Satellite (GOSAT)

©2019. Japan Geoscience Union. All Right Reserved.

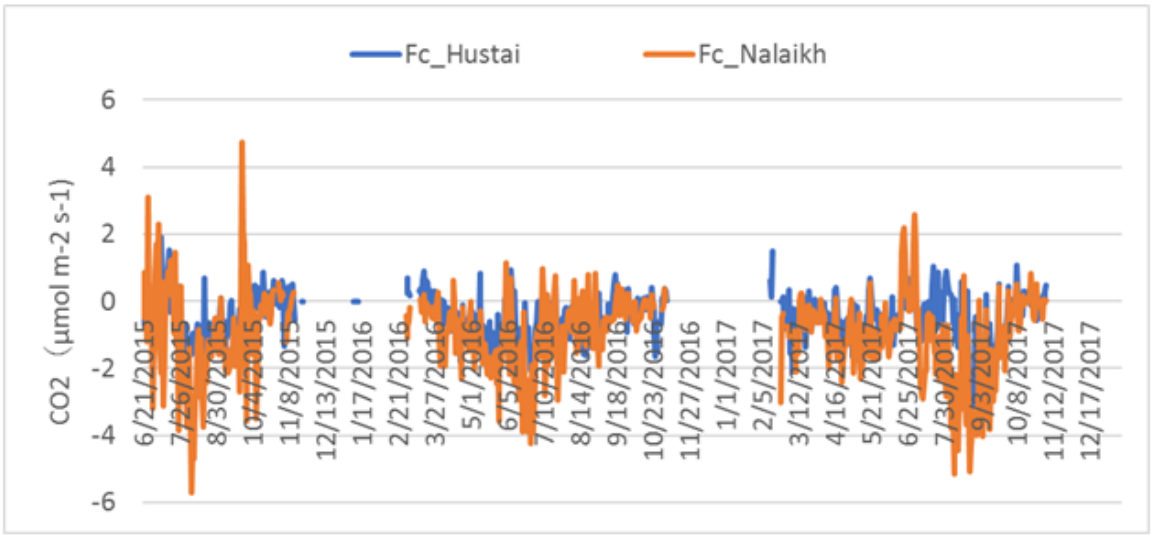


Figure 1 Comparison of CO2 flux observed at Nalaikh Site and Hustai Site

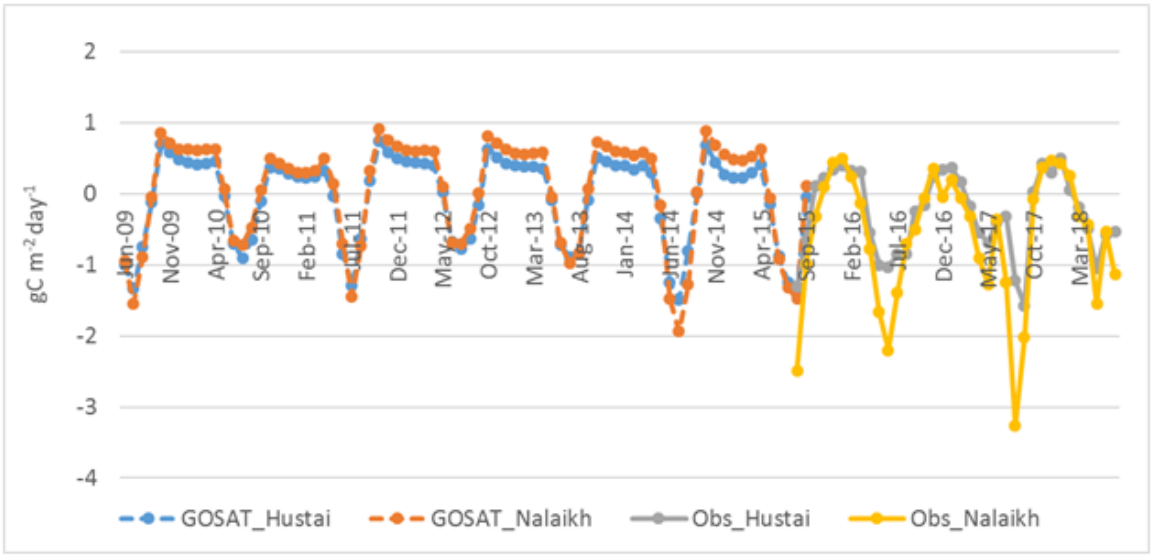


Figure 2 Comparison of GOSAT L4B and observations at Nalaikh Site and Hustai Site

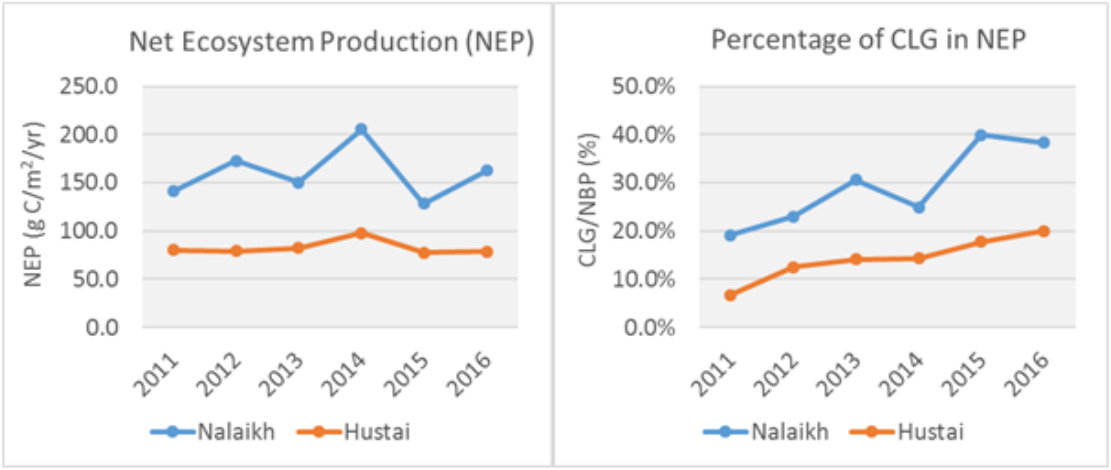


Figure 3 Impact of livestock grazing on NEP at Nalaikh Site and Hustai Site

©2019. Japan Geoscience Union. All Right Reserved.

Data-driven monitoring of terrestrial carbon cycle in Mongolia

*ZAYA MART[1], Zhiyan Liu[1], Riku Kawase[1], Kazuhito Ichii[1]

1. Chiba University

Mongolia has been experiencing both climate changes and anthropogenic environmental changes. Therefore, it is important to monitor environmental changes. In particular, more and more observation-based data sets are available, and synthesis analysis using these multiple observation-based data sets are essential.

We analyzed changes in the terrestrial environmental environment in Mongolia from the 1980s to 2010s. We focused on two different temporal periods, the 1980s to 2010s and 2000 to 2015. As for the first period (1980s to 2010s), we used NOAA AVHRR data sets, observed climate data sets for the analysis. As for the second period (1980s to 2010s), we used multiple remote sensing data sets (e.g. Terra MODIS), empirically upscaled CO2 flux products, and outputs from terrestrial ecosystem models. We will show and discuss the estimated terrestrial environmental changes in Mongolia at the conference.

Keywords: climate change, terrestrial environments, carbon cycle

©2019. Japan Geoscience Union. All Right Reserved.

[E] Poster | H (Human Geosciences)：H-DS Disaster geosciences

Tue. May 28, 2019 3:30 PM - 5:00 PM JST | Tue. May 28, 2019 6:30 AM - 8:00 AM UTC | Poster Hall International Exhibition Hall8, Makuhari Messe_12

[H-DS09] Landslides and related phenomena

convener:Masahiro Chigira(Disaster Prevention Research Institute, Kyoto University), Gonghui Wang(Disaster Prevention Research Institute, Kyoto University), Fumitoshi Imaizumi(Faculty of Agriculture, Shizuoka University)

Mass movements, such as landslides, rockfalls, and debris flows, have been occurring extensively in a large number of countries, causing heavy damage. In order to understand them and mitigate induced disasters, we invite contributions that report and discuss on mass movements and related phenomena, focusing on improved understanding of their characteristics; new insights into landslide mechanisms; the development of new approaches to monitoring; novel approaches to behavior forecasting and prediction; studies of successful landslide management; and the development of methods for hazard and risk evaluation. In particular, papers about recent landslide hazards, induced by 2017 northern Kyushu rainstorm, 2018 Osaka earthquake, 2018 western Japan rainstorm, and 2018 Hokkaido earthquake are welcome.

[HDS09-P01] **Fluidized landslides triggered by the liquefaction of subsurface volcanic deposits during the 2018 Iburi–Tobu earthquake, Hokkaido**

*Jun Kameda[1], Hiro Kamiya[2], Hirokazu Masumoto[1], Tomonori Morisaki[1], Toru Hiratsuka[2], Chisaki Inaoi (1.Department of Natural History Sciences, Graduate School of Science, Hokkaido University, 2.Department of Earth and Planetary Sciences, School of Science, Hokkaido University)

[HDS09-P02] A comparison between the acoustic signals and seismic signals generated during a dam-break test

★Invited Papers

*Zheng-yi Feng[1], Hao-yang Huang[1], Chia-Ming Chuang[1] (1.Department of Soil and Water Conservation, National Chung Hsing University, Taichung, Taiwan)

[HDS09-P03] Evaluation of factors of safety and landslide risk for a watershed by Scoops3D

*Zheng-yi Feng[1], Chia-Ming Chuang[1], Hao-yang Huang[1] (1.Department of Soil and Water Conservation, National Chung Hsing University, Taichung, Taiwan)

[HDS09-P04] **Fuzzy Clustering Algorithms for Establishing Landslide Susceptibility Map**

*Pei-hsun Tsai[1], Syuan-yi Wang[1], Jie-shin Cheng[1] (1.Chaoyang University of Technology)

[HDS09-P05] **A Study on Landslides and Debris Flows Susceptibility Mapping Using Unmanned Aerial Vehicles**

*Sheng-Jia Liu[1] (1.qwepoi13@gmail.com)

[HDS09-P06] Largescale landslide induced by AD1586 Tensho-Earthquake in Gifu Prefecture, central Japan

*Takahiro Kurimoto[1], Yoshihiko Kariya[2], Kuniyasu Mokudai[3], Ryuji Yamada[4], Takashi Kimura[4] (1.Undergraduate Senshu University, 2.Department of Geography, Senshu University, 3.Japan Geoservice Incorporated, 4.National Research Institute for Earth Science and Disaster Resilience)

[HDS09-P07] Failure Probability of Lushan Landslide, Taiwan

*Wei-Ting Lin[1], Kuang-Tsung Chang[1] (1.National Chung Hsing University)

[HDS09-P08] Interpretation of landslide surface deformation in Kali Gandaki River watershed, Nepal using ALOS-2/PALSAR-2 InSAR image

*Hiroshi, P. Sato[1] (1.College of Humanities and Sciences, Nihon University)

[HDS09-P09] A depth-integrated model for granular flows on the transition of different bed conditions

*Ling-Yi Hsu[1], Chi-Yao Hung[1] (1.National Chung Hsing University)

[HDS09-P10] A viscous granular flow experiment with new refractive index matching material

*Tsai-Jung Lin[1], Chi-Yao Hung[1] (1.National Chung Hsing University)

[HDS09-P11] Sandbox experiments of submarine landslide caused by water film in low permeability layer

*Shogo Kawakita[1], Daisuke Asahina[2], Keiji Kitajima[3], Mitsukazu Nakanishi[3] (1.Graduate School of Science & Technology, Nihon Univ., 2.National Institute of Advanced Industrial Science and Technology, 3.College of Science & Technology, Nihon Univ.)

[HDS09-P12] **Study on Creep Properties of Sand and Cemented Sand**

*JIN-YI YU[1], KUANG-TSUNG CHANG[1] (1.National Chung Hsing University)

[HDS09-P13] The effects of seepage force and the Poisson’s ratio on slope stability

*Hirokazu Fukui[1], Tomomi Terajima[2] (1.Graduate school of Science, Kyoto University, 2.Disaster Prevention Research Institute, Kyoto University)

[HDS09-P14] Study on the factors of seepage erosion

*Szu-Wei Fu[1], Kuang-Tsung Chang[1] (1.National Chung Hsing University)

[HDS09-P15] Deformation of slope models with different orientations of weak planes

*taeyuan tseng[1], Kuang-Tsung Chang[1] (1.National Chung Hsing University)

Fluidized landslides triggered by the liquefaction of subsurface volcanic deposits during the 2018 Iburi–Tobu earthquake, Hokkaido

*Jun Kameda[1], Hiro Kamiya[2], Hirokazu Masumoto[1], Tomonori Morisaki[1], Toru Hiratsuka[2], Chisaki Inaoi

1. Department of Natural History Sciences, Graduate School of Science, Hokkaido University, 2. Department of Earth and Planetary Sciences, School of Science, Hokkaido University

The Iburi–Tobu earthquake of M_w = 6.7 occurred at 3:07 AM (local time) on 6 September 2018, in southern Hokkaido, Japan. The earthquake caused power cuts and destroyed distribution networks across Hokkaido, creating widespread disruption. A total of 41 people were killed during the earthquake, with most of these (36 people) perishing in landslides near the epicenter. The hills in southwestern Hokkaido are widely covered by volcanic deposits, derived from the repeated eruptions of nearby volcanoes such as Tarumai, Eniwa, and Shikotsu (e.g., Nakagawa et al., 2018). On 4 September, Typhoon Jebi caused heavy rainfall in this area, which likely soaked and weakened the volcanic soils. Subsequent earthquake ground motion (with a maximum intensity of 7 on the intensity scale of Japan Meteorology Agency; Japan Meteorology Agency, 2018) may have triggered sudden whole-slope failures. The total number of the present landslides was ~6000 (Yamagishi and Yamazaki, 2018), and most of the recorded landslides are shallow and show features characteristic of fluidized landslides, such as long runouts of debris on a flat depositional area.
To investigate the mechanism generating the landslides triggered by the Iburi–Tobu earthquake, we conducted a field survey at a typical landslide in the Tomisato area of Atsuma, and we found a distinctive occurrence of liquefaction in the field, which could be a precursive condition for the generation of the fluidized landslides triggered by the earthquake. In the scarp of the landslide, an altered halloysite-bearing volcanic layer is observed at a level almost coincident with the sliding surface. The layer is intensely undulating and can be divided into an upper clay-rich layer and a lower pumice-rich layer, suggesting that the altered layer had liquefied as a result of the strong coseismic ground motion. The layer had been soaked by heavy rainfall just one day before the earthquake and could have liquefied by interstitial fluid pressurization, producing a weak and slippery plane, resulting in the catastrophic landslides in this area.

Keywords: fluidized landslide, 2018 Iburi–Tobu earthquake, halloysite

©2019. Japan Geoscience Union. All Right Reserved.

A comparison between the acoustic signals and seismic signals generated during a dam-break test

*Zheng-yi Feng[1], Hao-yang Huang[1], Chia-Ming Chuang[1]

1. Department of Soil and Water Conservation, National Chung Hsing University, Taichung, Taiwan

Natural events, such as landslide, sediment transport, flooding, etc., usually release energy to produce acoustic waves and seismic waves. Acoustic wave is transmitted through air and seismic wave is transmitted through geologic structure. Therefore, the characteristics of acoustic waves and the seismic waves induced by these events should be different. This study focus on the differences in the acoustic signals and seismic signals during a dam-break test performed by the authors. We built a model dam and slope in a creek for the test. We filled the dam with water and caused it to overflow. The overflow water caused the downward erosion of the dam. The flood due to the dam-break eroded the toe of the model slope causing the slope to collapse locally. We set up microphones to collect acoustic signals and installed accelerometers to collect vertical seismic signals generated by the flood and collapse events during the test. During the test we also used unmanned aerial vehicle (UAV) to continuously take photos for the collapsed areas for making the digital surface model (DSM) of the slope to analyze the volumes of the collapsed materials. We used Hilbert-Huang Transform (HHT) to obtain the time-frequency spectra for the acoustic signals and seismic signals. From the spectra, we compared the energy and frequency content of the two kinds of signals and their differences. The results show that the acoustic signal showing earlier indication of overtopping than that of the seismic signal. In addition, the acoustic and seismic signals generated during the flood can correspond to each other. The collapse events of the slope during the flood can be investigated also by examining the time-frequency spectrum of the seismic signal. Usually the signals of the collapse events can be distinguished from the flooding signals.

Keywords: dam break, landslide, slope, acoustic signal, seismic signal, flood

©2019. Japan Geoscience Union. All Right Reserved.

Evaluation of factors of safety and landslide risk for a watershed by Scoops3D

*Zheng-yi Feng[1], Chia-Ming Chuang[1], Hao-yang Huang[1]

1. Department of Soil and Water Conservation, National Chung Hsing University, Taichung, Taiwan

In this study, the Scoops3D code (USGS, 2015) is used to analyze the three-dimensional stability of the slopes in a watershed in Taiwan. To perform Scoops3D it requires the inputs such as digital elevation model (DEM), geological materials, groundwater level, earthquake, etc. The code calculates the minimum factor of safety (F.S.) and the associated potential failure volumes by using three-dimensional limit equilibrium method. We performed a comprehensive analysis of slope stability for the research areas using the Scoops3D code. The ArcMap software was used to present the F.S. that are less than unity as a 2D contoured map. We can observe this contoured map to understand the overall slope stability of the studied watershed. We perform a parametrical study by set three different sizes of sliding volume, “large”, “medium” and “small”, for evaluating the risk of landslide for the three different volume sizes.

Keywords: Landslide, Scoops3D, Factor of safety, Risk

©2019. Japan Geoscience Union. All Right Reserved.

Fuzzy Clustering Algorithms for Establishing Landslide Susceptibility Map

*Pei-hsun Tsai[1], Syuan-yi Wang[1], Jie-shin Cheng[1]

1. Chaoyang University of Technology

In recent years, the rainfall distribution is not uniform because of extreme weather events, the occurrence frequency of heavy rain increases. Coupled with steep terrain and complicated geological condition, so that the slope often occurred landslide when typhoon or heavy rain. Landslide susceptibility map delineates the potential zones for landslide occurrence. To develop the landslide model, we used several independent data layers that are recognized as effective factors in landslide occurrence, including slope, aspect, shear strength of rock or soil, dip and dip direction of stratum, and distance to road. All data layers were converted to raster layers with a 30 m ×30 m cell size. A total of 231336 cells were derived in study area. For assessing landslide susceptibility spatially, this study used fuzzy c-means clustering algorithm to classify the aforementioned data set in the study area into six clusters. Each cluster has similar natural environmental conditions and collapse situation. It is helpful to establish the monitoring management system and it can be applied to an early warning system in the landslide. Results of validation show that this model can accurately predict the occurrence of new landslides.

Keywords: Landslide susceptibility map, Fuzzy c-means , Clustering algorithm

©2019. Japan Geoscience Union. All Right Reserved.

A Study on Landslides and Debris Flows Susceptibility Mapping Using Unmanned Aerial Vehicles

*Sheng-Jia Liu[1]

1. qwepoi13@gmail.com

The geology of Taiwan is generally vulnerable due to the natural adverse conditions such as younger strata, steep topography, active orogeny, frequent seismic activity, weathering and erosion, frequent typhoons, high rainfall, etc. Furthermore, the human factors like immature law and regulations, the weak execution, and improper land use and development also play an important role in reducing the slope stability. These factors to some degree worsen the slope conditions, lead to a more frequent natural disaster and cause the loss of life and property.

In order to effectively evaluate the landslide susceptibility and map the high risk areas, the Soil and Water Conservation Bureau of Taiwan Executive Yuan (SWCB) provides an assessment method for assessing the risk level of landslide susceptibility by selecting the combinations of impact factors that may trigger landslides. However, the accuracy and efficiency of data acquisitions, in a conventional way, for the assessment method are still limited.
With the advantages of UAVs, the digital image with high resolutions for a wider area without terrain restrictions can be obtained efficiently. Its applications have become more widespread, from battlefield detections and communications to forest management and mapping. This study utilizes the latest Dynamic Post-Processing Motion (PPK) positioning system to capture high-resolution image data from a chosen site in the northern part of Taiwan. The terrain information was extracted from aerial images using Pix4Dmapper with aerial triangulation techniques, thus the external direction of each image and the camera's internal direction parameters can be obtained, the point cloud data can be matched automatically, and a digital surface mode can be established. Further, a three-dimensional model with topographic map and landslide susceptibility evaluations can be established and performed by comparing with historical data and monitoring the slope conditions. A modified assessment method is proposed using the three factors (slope, the volume of soil and rock accumulations, and rainfall) to assess the landslide susceptibility of the study area. The evaluations made by the proposed method are in agreement with the SWCB method. The results from this study can be used in slope management and precaution, and rescue and recovery.

Keywords: UAVs, landslides, debris flows, susceptibility evaluation

©2019. Japan Geoscience Union. All Right Reserved.

Largescale landslide induced by AD1586 Tensho-Earthquake in Gifu Prefecture, central Japan

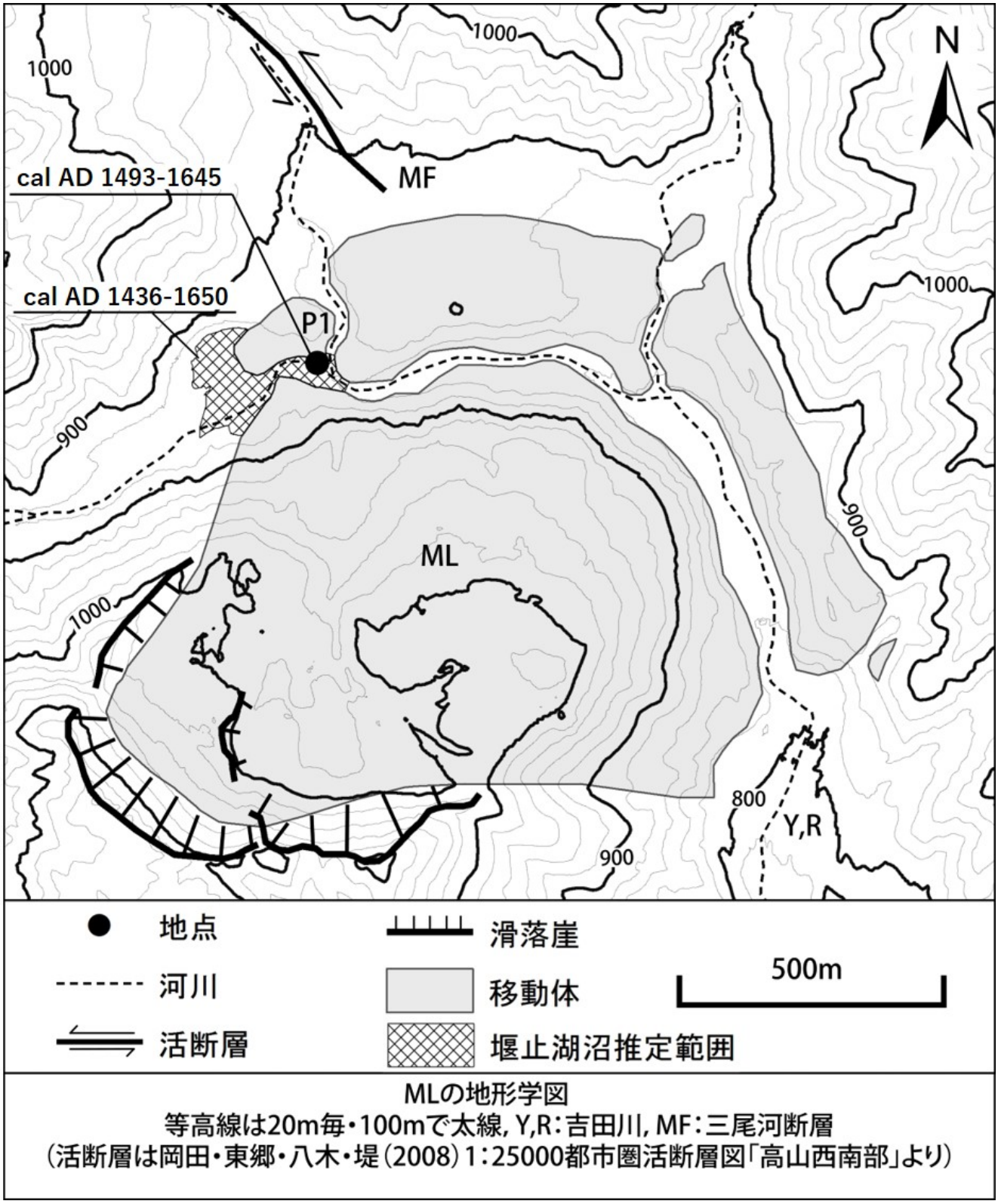
*Takahiro Kurimoto[1], Yoshihiko Kariya[2], Kuniyasu Mokudai[3], Ryuji Yamada[4], Takashi Kimura[4]

1. Undergraduate Senshu University, 2. Department of Geography, Senshu University, 3. Japan Geoservice Incorporated, 4. National Research Institute for Earth Science and Disaster Resilience

On the basis of field investigation and topographic analysis by using GIS, we clarified the geological and geomorphological features of a large-scale landslide (V=2.2×10^7 m^3) called Mizore Landslide (ML) in Gujo City of Gifu Prefecture, central Japan. According to old documents, it is thought to ML was caused by AD1586 Tensho earthquake (generated from the Shokawa fault zone close to the ML and estimated M=7 to 8). However, there are few studies on geomorphological and geological basis. The main results are as follows: a) The ML holds a set of three head scarps and three landslide bodies both showing multiple activities of slope movement; b) The ML shows unique sedimentological and geomorphological characteristics such as a jigsaw crack structure in landslide deposits and hummocks and depressions upon the ground surface of the landslide bodies; c) Both involved buried soils in the landslide deposits and fossil wood logs in the dammed lake deposits enable us to date the landslide events; d) According to those ^{14}C dates of soils and logs, the latest landslide event is thought to occur in the period from cal AD1436 to 1650; e) The latest landslide event would be triggered by AD1586 Tensho earthquake. AD1596 Keicho-Fushimi earthquake occurred around Kyoto is a candidate event for further consideration.

Keywords: AD1586 Tensho-earthquake, Large-scale landslide, Shokawa fault zone, Dammed lake

©2019. Japan Geoscience Union. All Right Reserved.



MLの地形学図
等高線は20m毎・100mで太線, Y,R:吉田川, MF:三尾河断層
(活断層は岡田・東郷・八木・堤(2008)1:25000都市圏活断層図「高山西南部」より)

©2019. Japan Geoscience Union. All Right Reserved.

Failure Probability of Lushan Landslide, Taiwan

*Wei-Ting Lin[1], Kuang-Tsung Chang[1]

1. National Chung Hsing University

The Lushan landslide located in the middle of Taiwan, has slid and damaged the road due to typhoons or heavy rainfalls for recent decades. It’ s seriously affecting the safety of life and property of the Lushan Hot Spring Tourist Area and local residents in the lower slope. In order to understand the probability of failure (Pf) of Lushan landslide, we built a numerical model by Plaxis2D, which is validated by the monitoring data of the 2009 typhoon Morakot. However, due to the lack of complete parameter data, uncertainties exist and may affect the simulation result of the collapse. With the back calculated friction angle (∅) and cohesion (c) from Plaxis2D, we used the Monte Carlo Simulation (MCS) to consider the friction angle and the cohesion of sliding body as random variables with uncertainty. The results are statistically analyzed to obtain the Probability Density Function (PDF) of the two parameters. Based on the parameter settings above, with the designed rainfall events at 24hr, 48hr and 72hr rainfall duration and 10, 25, 50, 100 and 200 years of recurrence interval, we calculate the factor of safety (SF) of the Lushan landslide in these 18 simulated rainfall events. Finally, we can obtain the distribution of factor of safety (SF) and probability of failure (Pf) of the Lushan landslide in different rainfall durations and recurrence intervals.

Keywords: probability of failure, Monte Carlo Simulation, uncertainty

©2019. Japan Geoscience Union. All Right Reserved.

Interpretation of landslide surface deformation in Kali Gandaki River watershed, Nepal using ALOS-2/PALSAR-2 InSAR image

*Hiroshi, P. Sato[1]

1. College of Humanities and Sciences, Nihon University

Previous studies have revealed and mapped glacial landform, fluvial terraces, and landslide landform in Thakkohla-Muktinath region, between Kagbeni and Ghasa along Kali Gandaki River, Nepal. And many attentions were paid to detect landslides that brock channels in the region, especially after Gorkha earthquake (25 Apr 2015; Mw7.8). Therefore, I tried to interpret landslide surface deformation on mountain slopes in Kali Gandaki River watershed after the earthquake, using Synthetic Aperture Radar interferometry (InSAR) image. The number of produced InSAR images was six, which is master image/slave image in order from ALOS-2/PALSAR-2 data, 08Oct2015/17Dec2015, 08Oct2015/30Nov2017, 25Feb2016/06Oct2016, 30Nov2017/24Jan2019, 08Mar2018/24Jan2019 and 31May2018/24Jan2019. In these InSAR images clear precursory landslide surface deformation was not interpreted on mountain slopes facing main stream of Kali Gandaki River. However, whose tributary watershed; i.e., Myagdi River watershed gave some landslide surface deformations (e.g., in 83.3983E, 28.4842N) clearly interpreted in the InSAR image of 08Oct2015/17Dec2015, which was relatively better coherence than the rest five images.

Keywords: SAR, earthquake, landslide, interpretation

©2019. Japan Geoscience Union. All Right Reserved.

A depth-integrated model for granular flows on the transition of different bed conditions

*Ling-Yi Hsu[1], Chi-Yao Hung[1]

1. National Chung Hsing University

The different basal boundary conditions profoundly affected the flow behavior of debris flow. However, it is hard to have a general and straightforward model to describe the flow profile switching from different bed conditions. In this study, we purpose a new depth-averaged model to simulate the dense granular flow transition between the rigid and mobile bed. The model is based on mass conservation, momentum conservation, and kinetic energy conservation. We apply the linearized mu(I) rheology to describe granular deformation and assume Coulomb friction along the sidewalls. By incorporating the basal shear rate term into the equations, the theory can balance the extra force from rigid bed friction force. To check the model approach, we conducted an equilibrium and non-equilibrium heap flow experiments using the narrow see-saw channel, which can be tilted to different angles between runs or during flows. To compare the experimental results with the theory, the flow fields are monitored using high-speed video and particle-tracking velocimetry.

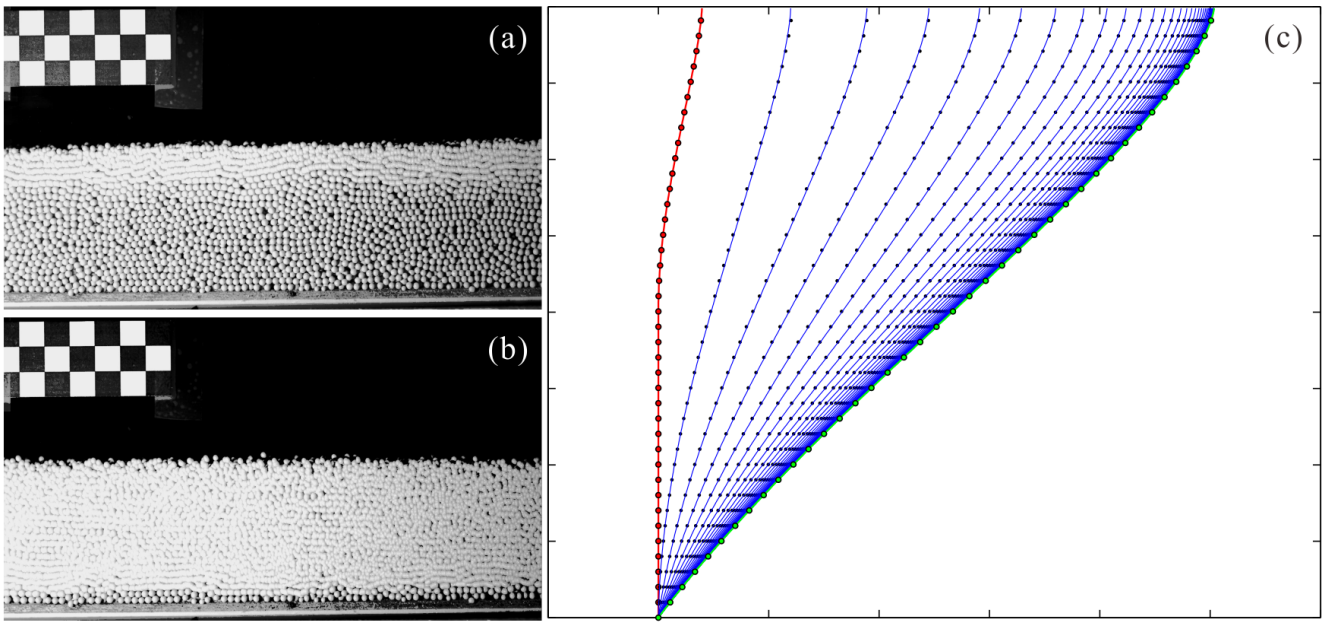


Fig.1 Experimental longexpousre image (a) over deposition bed; (b) over rigid bed; and (c) the transition velocity profile of theory prediction.

©2019. Japan Geoscience Union. All Right Reserved.

A viscous granular flow experiment with new refractive index matching material

*Tsai-Jung Lin[1], Chi-Yao Hung[1]

1. National Chung Hsing University

Entrainment rate at base controls how far the debris flow can travel and how large the debris flow becomes. Flow rheology of Refractive Index Matching (RIM) material are generally limited by the mono-particle properties (such as polymethyl methacrylate/liquid para-cymene etc.). In this study, a new RIM material (polyacrylamide polymer/18% Methanol solution) having a wide range of particle size distribution and viscosity (Fig. 1L) are purposed to visualize and measure the erosion process of mobile bed dam break experiments. Various rheology models may be formed by the different ratio of particle size. To improve the contrast between the particle phase and the liquid phase, a dye is used to make the particles bright under laser illumination. By varying the dye concentration, the entraining/detraining processes are easily distinguished (Fig. 1R). Granular motion is captured through a high-speed camera and Particle Tracking Velocimetry (PTV) method. Finally, an empirical relationship between the rheology and the entraining/ detraining process is developed.

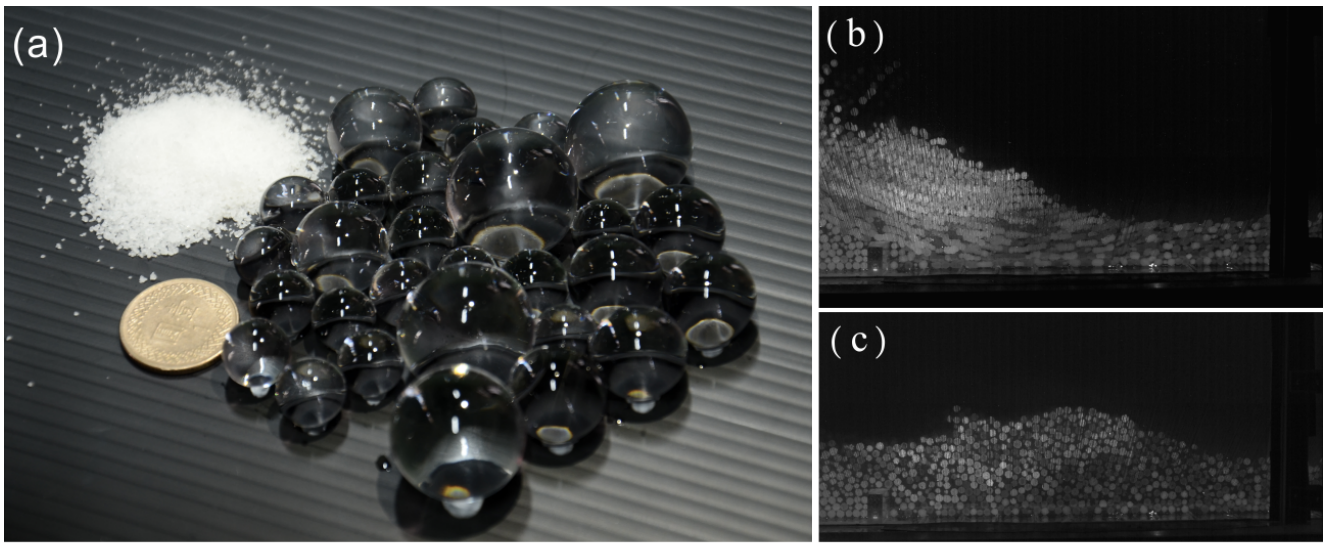


Fig.1 Experimental image (a)wide range of particle size; (b)longexposure image of dam break occurrence; (c)particles with different concentration of dye.

©2019. Japan Geoscience Union. All Right Reserved.

Sandbox experiments of submarine landslide caused by water film in low permeability layer

*Shogo Kawakita[1], Daisuke Asahina[2], Keiji Kitajima[3], Mitsukazu Nakanishi[3]

1. Graduate School of Science & Technology, Nihon Univ., 2. National Institute of Advanced Industrial Science and Technology, 3. College of Science & Technology, Nihon Univ.

Submarine landslides can be serious geohazards since they potentially cause tsunamis and damage seafloor infrastructure. Submarine landslides can be larger in scale than landslides on land. Direct measurements/observations of submarine landslides at deep seafloor still remain a challenging task. Kokusho et al. (2000) proposed a water film effect and its mechanism on lateral flow with less frictional resistance to explain a driving force of large-scale submarine landslides

In this study, we conducted laboratory experiments to understand the relationship between sand liquefaction and lateral flow by water film, and investigate the influence of water film formation on lateral flow of upper layer. In general, it is difficult to observe the formations of liquefaction and lateral flow at the same time. This is because sand particles of sloping layer model start to move when vibration is applied, and inclination disappears before liquefaction. To solve this problem, we devised a mechanism to prevent the flow of the lower layer by providing a weir plate in inside the soil tank. This mechanism enables to distinguish and observe the movement of sand by the liquefaction and the lateral flow by the water film.

The results obtained in this study clearly show three stages: first, the lower layer was liquefied; then pore water was stored below the low permeability layer; and finally, the lateral flow was occurred by the water film effect. The experimental results show that there was no clear correlation between the increase in the angle of sloping layer and the travel distance or the maximum flow velocity. We also discuss the relationship between the layer angle and the location of sand boil. The location where sand soiling occurred moved to the upper side of the slope as the layer angle become larger.

[Reference]

Kokusho, T.: Mechanism for water film generation and lateral flow in liquefied sand layer, Soils and Foundations, Vol.40, No.5, p 99-111, 2000.

Keywords: Submarine Landslides, Pore Water Pressure, Water Film, Lateral Flow

©2019. Japan Geoscience Union. All Right Reserved.

Study on Creep Properties of Sand and Cemented Sand

*JIN-YI YU[1], KUANG-TSUNG CHANG[1]

1. National Chung Hsing University

In this study, we investigated the effects of creep on sand and cemented sand, using triaxial test. Sand represents a non-cohesive material, while cemented sand represents a brittle material. Before the failure of specimens, the deviator stress was fixed and the cyclic mean stress was applied to study the influence of creep on the materials. According to the test results, the axial strain accumulation of sand caused by creep is less, and the peak strength is larger than that of the monotonic loading when the axial loading is resumed. For cemented sand, creep causes microcracks inside the specimens, gradually forming a failure surface. When the axial strain accumulation is large enough, the reapplication of the axial loading shows a reduction of peak strength. We conclude that the influence of creep on non-cohesive material (sand) is limited, whereas creep can reduce the strength of the brittle material (cemented sand) and even cause failure.

Keywords: creep, triaxial test, sand, cemented sand, strength, failure

©2019. Japan Geoscience Union. All Right Reserved.

The effects of seepage force and the Poisson’ s ratio on slope stability

*Hirokazu Fukui[1], Tomomi Terajima[2]

1. Graduate school of Science, Kyoto University, 2. Disaster Prevention Research Institute, Kyoto University

To predict accurately the timing of shallow landslide occurrence, we need to consider the direction and magnitude of seepage force and earth pressure. A model sandy slope (L: 9m, W:1m, H:4m) was used to measure the hydraulic gradient and seepage force with the tensiometers under the artificial rainfall of 80mm/h. We incorporated not only the seepage force but also the Poisson’ s ratio into conventional slope stability analysis by the limit equilibrium method. As a result, the calculated timing of shallow landslide occurrence was almost agree with the timing of that in the experiment and also more accurate than the timing calculated by the Spenser method which took into account the magnitude and moment equilibrium of the force. These results imply that, based on both monitoring at fields and conducting more experiments by a real-size model slope, we need to verify the effects of seepage force and earth pressure as the important factors causing rainfall-induced slope instability.

Keywords: process-based model, Seepage force, the Poisson's ratio, Shallow landslide, Sandy model slope

©2019. Japan Geoscience Union. All Right Reserved.

Study on the factors of seepage erosion

*Szu-Wei Fu[1], Kuang-Tsung Chang[1]

1. National Chung Hsing University

The causes of many slope disasters are often related to the seepage behaviors of soil. For instance, groundwater seepage may cause internal erosion of the soil. The soil particles are taken away by seepage water to form void or pipe. In addition , the earth pressure leads to the collapse of the overlying soil.

In this study, we designed a set of apparatus that can add confining pressure to the outside of the specimen. In order to simulate the situation of sand in slopes, we investigated the critical seepage velocity of sands caused by seepage erosion failure under different confining pressure, with different particle size distributions, sizes of outflow, etc. Then a failure criterion for seepage erosion is developed based on the drag equation in fluid dynamics and confirm with experimental data.

The results show that the critical seepage velocity at failure is affected by the particle size distributions, sizes of outflow and the confining pressure. The theoretical results are compared well to the experimental data.

Keywords: seepage erosion, Drag equation

©2019. Japan Geoscience Union. All Right Reserved.

Deformation of slope models with different orientations of weak planes

*taeyuan tseng[1], Kuang-Tsung Chang[1]

1. National Chung Hsing University

Weak planes influence failure and deformation of slopes. We conducted experiments to simulate slopes of different orientations of weak planes, including cataclinal and analcinal slopes with 30˚ and 60˚ inclination angles of weak planes. We stacked artificial bricks to make small-sized slope models. The artificial bricks were made of gypsum, sand, cement and water with different weight proportion. In view of the scaling law, the artificial bricks were made less strength than natural rocks. The slope models were weakened under rainfall, resulting in deformation and final collapse. The slope deformation processes were photographed by a camera, and the displacement vector fields were analyzed using the Particle Image Velocimetry (PIV). The deformation and accumulated displacements were compared between slopes of different orientations of weak planes.

Keywords: cataclinal slope, analcinal slopes, rainfall, Particle Image Velocimetry (PIV), weak planes, deformation

©2019. Japan Geoscience Union. All Right Reserved.

[E] Poster | H (Human Geosciences)：H-DS Disaster geosciences

Tue. May 28, 2019 5:15 PM - 6:30 PM JST | Tue. May 28, 2019 8:15 AM - 9:30 AM UTC | Poster Hall International Exhibition Hall8, Makuhari Messe_20

[H-DS09] Landslides and related phenomena

convener:Masahiro Chigira(Disaster Prevention Research Institute, Kyoto University), Gonghui Wang(Disaster Prevention Research Institute, Kyoto University), Fumitoshi Imaizumi(Faculty of Agriculture, Shizuoka University)

Mass movements, such as landslides, rockfalls, and debris flows, have been occurring extensively in a large number of countries, causing heavy damage. In order to understand them and mitigate induced disasters, we invite contributions that report and discuss on mass movements and related phenomena, focusing on improved understanding of their characteristics; new insights into landslide mechanisms; the development of new approaches to monitoring; novel approaches to behavior forecasting and prediction; studies of successful landslide management; and the development of methods for hazard and risk evaluation. In particular, papers about recent landslide hazards, induced by 2017 northern Kyushu rainstorm, 2018 Osaka earthquake, 2018 western Japan rainstorm, and 2018 Hokkaido earthquake are welcome.

[HDS09-P01] **Fluidized landslides triggered by the liquefaction of subsurface volcanic deposits during the 2018 Iburi–Tobu earthquake, Hokkaido**

*Jun Kameda[1], Hiro Kamiya[2], Hirokazu Masumoto[1], Tomonori Morisaki[1], Toru Hiratsuka[2], Chisaki Inaoi (1.Department of Natural History Sciences, Graduate School of Science, Hokkaido University, 2.Department of Earth and Planetary Sciences, School of Science, Hokkaido University)

[HDS09-P02] A comparison between the acoustic signals and seismic signals generated during a dam-break test

★Invited Papers

*Zheng-yi Feng[1], Hao-yang Huang[1], Chia-Ming Chuang[1] (1.Department of Soil and Water Conservation, National Chung Hsing University, Taichung, Taiwan)

[HDS09-P03] Evaluation of factors of safety and landslide risk for a watershed by Scoops3D

*Zheng-yi Feng[1], Chia-Ming Chuang[1], Hao-yang Huang[1] (1.Department of Soil and Water Conservation, National Chung Hsing University, Taichung, Taiwan)

[HDS09-P04] **Fuzzy Clustering Algorithms for Establishing Landslide Susceptibility Map**

*Pei-hsun Tsai[1], Syuan-yi Wang[1], Jie-shin Cheng[1] (1.Chaoyang University of Technology)

[HDS09-P05] **A Study on Landslides and Debris Flows Susceptibility Mapping Using Unmanned Aerial Vehicles**

*Sheng-Jia Liu[1] (1.qwepoi13@gmail.com)

[HDS09-P06] Largescale landslide induced by AD1586 Tensho-Earthquake in Gifu Prefecture, central Japan

*Takahiro Kurimoto[1], Yoshihiko Kariya[2], Kuniyasu Mokudai[3], Ryuji Yamada[4], Takashi Kimura[4] (1.Undergraduate Senshu University, 2.Department of Geography, Senshu University, 3.Japan Geoservice Incorporated, 4.National Research Institute for Earth Science and Disaster Resilience)

[HDS09-P07] Failure Probability of Lushan Landslide, Taiwan

*Wei-Ting Lin[1], Kuang-Tsung Chang[1] (1.National Chung Hsing University)

[HDS09-P08] Interpretation of landslide surface deformation in Kali Gandaki River watershed, Nepal using ALOS-2/PALSAR-2 InSAR image

*Hiroshi, P. Sato[1] (1.College of Humanities and Sciences, Nihon University)

[HDS09-P09] A depth-integrated model for granular flows on the transition of different bed conditions

*Ling-Yi Hsu[1], Chi-Yao Hung[1] (1.National Chung Hsing University)

[HDS09-P10] A viscous granular flow experiment with new refractive index matching material

*Tsai-Jung Lin[1], Chi-Yao Hung[1] (1.National Chung Hsing University)

[HDS09-P11] Sandbox experiments of submarine landslide caused by water film in low permeability layer

*Shogo Kawakita[1], Daisuke Asahina[2], Keiji Kitajima[3], Mitsukazu Nakanishi[3] (1.Graduate School of Science & Technology, Nihon Univ., 2.National Institute of Advanced Industrial Science and Technology, 3.College of Science & Technology, Nihon Univ.)

[HDS09-P12] **Study on Creep Properties of Sand and Cemented Sand**

*JIN-YI YU[1], KUANG-TSUNG CHANG[1] (1.National Chung Hsing University)

[HDS09-P13] The effects of seepage force and the Poisson’s ratio on slope stability

*Hirokazu Fukui[1], Tomomi Terajima[2] (1.Graduate school of Science, Kyoto University, 2.Disaster Prevention Research Institute, Kyoto University)

[HDS09-P14] Study on the factors of seepage erosion

*Szu-Wei Fu[1], Kuang-Tsung Chang[1] (1.National Chung Hsing University)

[HDS09-P15] Deformation of slope models with different orientations of weak planes

*taeyuan tseng[1], Kuang-Tsung Chang[1] (1.National Chung Hsing University)

Fluidized landslides triggered by the liquefaction of subsurface volcanic deposits during the 2018 Iburi–Tobu earthquake, Hokkaido

*Jun Kameda[1], Hiro Kamiya[2], Hirokazu Masumoto[1], Tomonori Morisaki[1], Toru Hiratsuka[2], Chisaki Inaoi

1. Department of Natural History Sciences, Graduate School of Science, Hokkaido University, 2. Department of Earth and Planetary Sciences, School of Science, Hokkaido University

The Iburi–Tobu earthquake of M_w = 6.7 occurred at 3:07 AM (local time) on 6 September 2018, in southern Hokkaido, Japan. The earthquake caused power cuts and destroyed distribution networks across Hokkaido, creating widespread disruption. A total of 41 people were killed during the earthquake, with most of these (36 people) perishing in landslides near the epicenter. The hills in southwestern Hokkaido are widely covered by volcanic deposits, derived from the repeated eruptions of nearby volcanoes such as Tarumai, Eniwa, and Shikotsu (e.g., Nakagawa et al., 2018). On 4 September, Typhoon Jebi caused heavy rainfall in this area, which likely soaked and weakened the volcanic soils. Subsequent earthquake ground motion (with a maximum intensity of 7 on the intensity scale of Japan Meteorology Agency; Japan Meteorology Agency, 2018) may have triggered sudden whole-slope failures. The total number of the present landslides was ~6000 (Yamagishi and Yamazaki, 2018), and most of the recorded landslides are shallow and show features characteristic of fluidized landslides, such as long runouts of debris on a flat depositional area.
To investigate the mechanism generating the landslides triggered by the Iburi–Tobu earthquake, we conducted a field survey at a typical landslide in the Tomisato area of Atsuma, and we found a distinctive occurrence of liquefaction in the field, which could be a precursive condition for the generation of the fluidized landslides triggered by the earthquake. In the scarp of the landslide, an altered halloysite-bearing volcanic layer is observed at a level almost coincident with the sliding surface. The layer is intensely undulating and can be divided into an upper clay-rich layer and a lower pumice-rich layer, suggesting that the altered layer had liquefied as a result of the strong coseismic ground motion. The layer had been soaked by heavy rainfall just one day before the earthquake and could have liquefied by interstitial fluid pressurization, producing a weak and slippery plane, resulting in the catastrophic landslides in this area.

Keywords: fluidized landslide, 2018 Iburi–Tobu earthquake, halloysite

©2019. Japan Geoscience Union. All Right Reserved.

A comparison between the acoustic signals and seismic signals generated during a dam-break test

*Zheng-yi Feng[1], Hao-yang Huang[1], Chia-Ming Chuang[1]

1. Department of Soil and Water Conservation, National Chung Hsing University, Taichung, Taiwan

Natural events, such as landslide, sediment transport, flooding, etc., usually release energy to produce acoustic waves and seismic waves. Acoustic wave is transmitted through air and seismic wave is transmitted through geologic structure. Therefore, the characteristics of acoustic waves and the seismic waves induced by these events should be different. This study focus on the differences in the acoustic signals and seismic signals during a dam-break test performed by the authors. We built a model dam and slope in a creek for the test. We filled the dam with water and caused it to overflow. The overflow water caused the downward erosion of the dam. The flood due to the dam-break eroded the toe of the model slope causing the slope to collapse locally. We set up microphones to collect acoustic signals and installed accelerometers to collect vertical seismic signals generated by the flood and collapse events during the test. During the test we also used unmanned aerial vehicle (UAV) to continuously take photos for the collapsed areas for making the digital surface model (DSM) of the slope to analyze the volumes of the collapsed materials. We used Hilbert-Huang Transform (HHT) to obtain the time-frequency spectra for the acoustic signals and seismic signals. From the spectra, we compared the energy and frequency content of the two kinds of signals and their differences. The results show that the acoustic signal showing earlier indication of overtopping than that of the seismic signal. In addition, the acoustic and seismic signals generated during the flood can correspond to each other. The collapse events of the slope during the flood can be investigated also by examining the time-frequency spectrum of the seismic signal. Usually the signals of the collapse events can be distinguished from the flooding signals.

Keywords: dam break, landslide, slope, acoustic signal, seismic signal, flood

©2019. Japan Geoscience Union. All Right Reserved.

Evaluation of factors of safety and landslide risk for a watershed by Scoops3D

*Zheng-yi Feng[1], Chia-Ming Chuang[1], Hao-yang Huang[1]

1. Department of Soil and Water Conservation, National Chung Hsing University, Taichung, Taiwan

In this study, the Scoops3D code (USGS, 2015) is used to analyze the three-dimensional stability of the slopes in a watershed in Taiwan. To perform Scoops3D it requires the inputs such as digital elevation model (DEM), geological materials, groundwater level, earthquake, etc. The code calculates the minimum factor of safety (F.S.) and the associated potential failure volumes by using three-dimensional limit equilibrium method. We performed a comprehensive analysis of slope stability for the research areas using the Scoops3D code. The ArcMap software was used to present the F.S. that are less than unity as a 2D contoured map. We can observe this contoured map to understand the overall slope stability of the studied watershed. We perform a parametrical study by set three different sizes of sliding volume, “large”, “medium” and “small”, for evaluating the risk of landslide for the three different volume sizes.

Keywords: Landslide, Scoops3D, Factor of safety, Risk

©2019. Japan Geoscience Union. All Right Reserved.

Fuzzy Clustering Algorithms for Establishing Landslide Susceptibility Map

*Pei-hsun Tsai[1], Syuan-yi Wang[1], Jie-shin Cheng[1]

1. Chaoyang University of Technology

In recent years, the rainfall distribution is not uniform because of extreme weather events, the occurrence frequency of heavy rain increases. Coupled with steep terrain and complicated geological condition, so that the slope often occurred landslide when typhoon or heavy rain. Landslide susceptibility map delineates the potential zones for landslide occurrence. To develop the landslide model, we used several independent data layers that are recognized as effective factors in landslide occurrence, including slope, aspect, shear strength of rock or soil, dip and dip direction of stratum, and distance to road. All data layers were converted to raster layers with a 30 m ×30 m cell size. A total of 231336 cells were derived in study area. For assessing landslide susceptibility spatially, this study used fuzzy c-means clustering algorithm to classify the aforementioned data set in the study area into six clusters. Each cluster has similar natural environmental conditions and collapse situation. It is helpful to establish the monitoring management system and it can be applied to an early warning system in the landslide. Results of validation show that this model can accurately predict the occurrence of new landslides.

Keywords: Landslide susceptibility map, Fuzzy c-means , Clustering algorithm

©2019. Japan Geoscience Union. All Right Reserved.

A Study on Landslides and Debris Flows Susceptibility Mapping Using Unmanned Aerial Vehicles

*Sheng-Jia Liu[1]

1. qwepoi13@gmail.com

The geology of Taiwan is generally vulnerable due to the natural adverse conditions such as younger strata, steep topography, active orogeny, frequent seismic activity, weathering and erosion, frequent typhoons, high rainfall, etc. Furthermore, the human factors like immature law and regulations, the weak execution, and improper land use and development also play an important role in reducing the slope stability. These factors to some degree worsen the slope conditions, lead to a more frequent natural disaster and cause the loss of life and property.

In order to effectively evaluate the landslide susceptibility and map the high risk areas, the Soil and Water Conservation Bureau of Taiwan Executive Yuan (SWCB) provides an assessment method for assessing the risk level of landslide susceptibility by selecting the combinations of impact factors that may trigger landslides. However, the accuracy and efficiency of data acquisitions, in a conventional way, for the assessment method are still limited.
With the advantages of UAVs, the digital image with high resolutions for a wider area without terrain restrictions can be obtained efficiently. Its applications have become more widespread, from battlefield detections and communications to forest management and mapping. This study utilizes the latest Dynamic Post-Processing Motion (PPK) positioning system to capture high-resolution image data from a chosen site in the northern part of Taiwan. The terrain information was extracted from aerial images using Pix4Dmapper with aerial triangulation techniques, thus the external direction of each image and the camera's internal direction parameters can be obtained, the point cloud data can be matched automatically, and a digital surface mode can be established. Further, a three-dimensional model with topographic map and landslide susceptibility evaluations can be established and performed by comparing with historical data and monitoring the slope conditions. A modified assessment method is proposed using the three factors (slope, the volume of soil and rock accumulations, and rainfall) to assess the landslide susceptibility of the study area. The evaluations made by the proposed method are in agreement with the SWCB method. The results from this study can be used in slope management and precaution, and rescue and recovery.

Keywords: UAVs, landslides, debris flows, susceptibility evaluation

©2019. Japan Geoscience Union. All Right Reserved.

Largescale landslide induced by AD1586 Tensho-Earthquake in Gifu Prefecture, central Japan

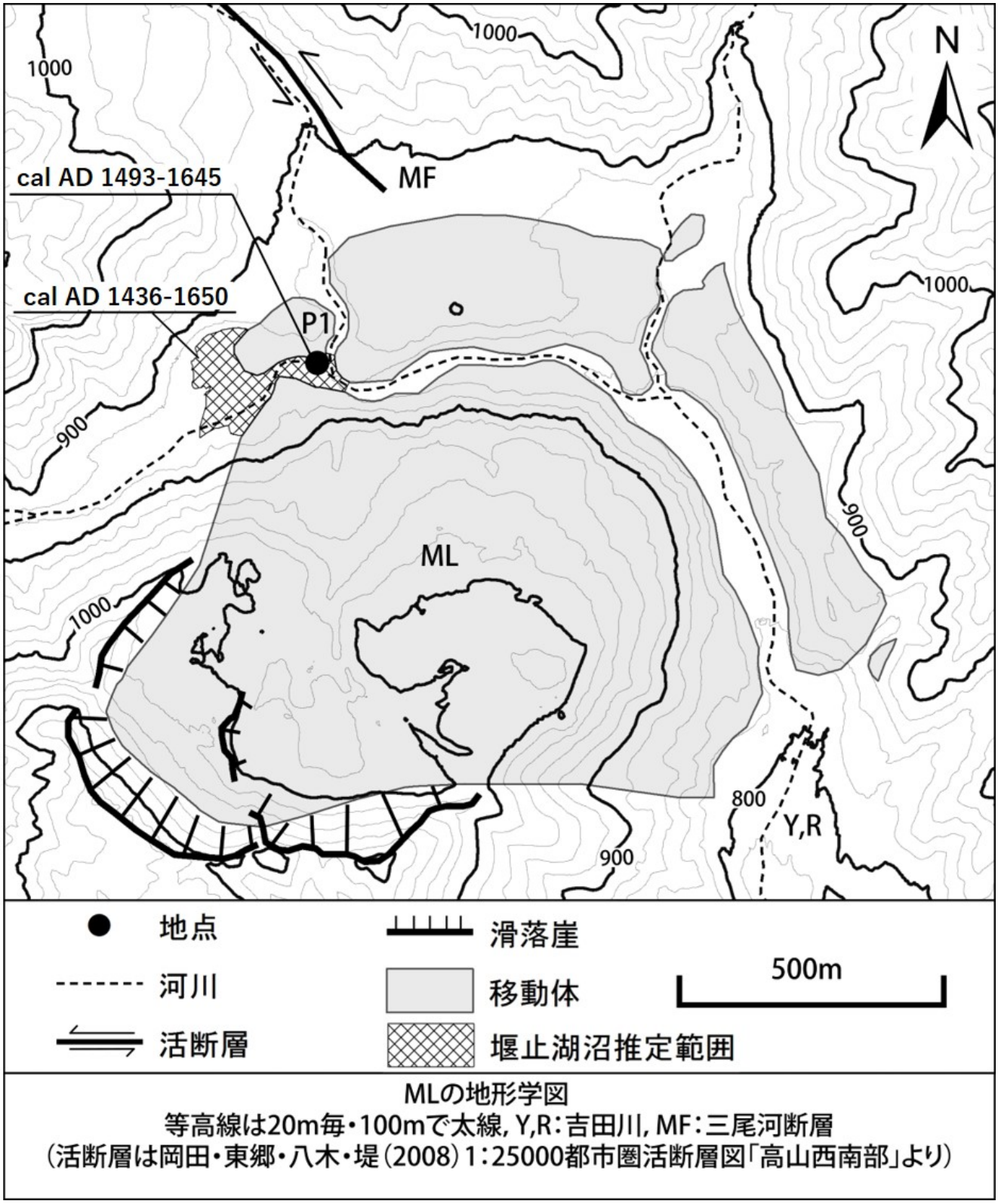
*Takahiro Kurimoto[1], Yoshihiko Kariya[2], Kuniyasu Mokudai[3], Ryuji Yamada[4], Takashi Kimura[4]

1. Undergraduate Senshu University, 2. Department of Geography, Senshu University, 3. Japan Geoservice Incorporated, 4. National Research Institute for Earth Science and Disaster Resilience

On the basis of field investigation and topographic analysis by using GIS, we clarified the geological and geomorphological features of a large-scale landslide (V=2.2×10^7 m^3) called Mizore Landslide (ML) in Gujo City of Gifu Prefecture, central Japan. According to old documents, it is thought to ML was caused by AD1586 Tensho earthquake (generated from the Shokawa fault zone close to the ML and estimated M=7 to 8). However, there are few studies on geomorphological and geological basis. The main results are as follows: a) The ML holds a set of three head scarps and three landslide bodies both showing multiple activities of slope movement; b) The ML shows unique sedimentological and geomorphological characteristics such as a jigsaw crack structure in landslide deposits and hummocks and depressions upon the ground surface of the landslide bodies; c) Both involved buried soils in the landslide deposits and fossil wood logs in the dammed lake deposits enable us to date the landslide events; d) According to those ^{14}C dates of soils and logs, the latest landslide event is thought to occur in the period from cal AD1436 to 1650; e) The latest landslide event would be triggered by AD1586 Tensho earthquake. AD1596 Keicho-Fushimi earthquake occurred around Kyoto is a candidate event for further consideration.

Keywords: AD1586 Tensho-earthquake, Large-scale landslide, Shokawa fault zone, Dammed lake

©2019. Japan Geoscience Union. All Right Reserved.



MLの地形学図
等高線は20m毎・100mで太線, Y,R:吉田川, MF:三尾河断層
(活断層は岡田・東郷・八木・堤(2008)1:25000都市圏活断層図「高山西南部」より)

©2019. Japan Geoscience Union. All Right Reserved.

Failure Probability of Lushan Landslide, Taiwan

*Wei-Ting Lin[1], Kuang-Tsung Chang[1]

1. National Chung Hsing University

The Lushan landslide located in the middle of Taiwan, has slid and damaged the road due to typhoons or heavy rainfalls for recent decades. It’ s seriously affecting the safety of life and property of the Lushan Hot Spring Tourist Area and local residents in the lower slope. In order to understand the probability of failure (Pf) of Lushan landslide, we built a numerical model by Plaxis2D, which is validated by the monitoring data of the 2009 typhoon Morakot. However, due to the lack of complete parameter data, uncertainties exist and may affect the simulation result of the collapse. With the back calculated friction angle (∅) and cohesion (c) from Plaxis2D, we used the Monte Carlo Simulation (MCS) to consider the friction angle and the cohesion of sliding body as random variables with uncertainty. The results are statistically analyzed to obtain the Probability Density Function (PDF) of the two parameters. Based on the parameter settings above, with the designed rainfall events at 24hr, 48hr and 72hr rainfall duration and 10, 25, 50, 100 and 200 years of recurrence interval, we calculate the factor of safety (SF) of the Lushan landslide in these 18 simulated rainfall events. Finally, we can obtain the distribution of factor of safety (SF) and probability of failure (Pf) of the Lushan landslide in different rainfall durations and recurrence intervals.

Keywords: probability of failure, Monte Carlo Simulation, uncertainty

©2019. Japan Geoscience Union. All Right Reserved.

Interpretation of landslide surface deformation in Kali Gandaki River watershed, Nepal using ALOS-2/PALSAR-2 InSAR image

*Hiroshi, P. Sato[1]

1. College of Humanities and Sciences, Nihon University

Previous studies have revealed and mapped glacial landform, fluvial terraces, and landslide landform in Thakkohla-Muktinath region, between Kagbeni and Ghasa along Kali Gandaki River, Nepal. And many attentions were paid to detect landslides that brock channels in the region, especially after Gorkha earthquake (25 Apr 2015; Mw7.8). Therefore, I tried to interpret landslide surface deformation on mountain slopes in Kali Gandaki River watershed after the earthquake, using Synthetic Aperture Radar interferometry (InSAR) image. The number of produced InSAR images was six, which is master image/slave image in order from ALOS-2/PALSAR-2 data, 08Oct2015/17Dec2015, 08Oct2015/30Nov2017, 25Feb2016/06Oct2016, 30Nov2017/24Jan2019, 08Mar2018/24Jan2019 and 31May2018/24Jan2019. In these InSAR images clear precursory landslide surface deformation was not interpreted on mountain slopes facing main stream of Kali Gandaki River. However, whose tributary watershed; i.e., Myagdi River watershed gave some landslide surface deformations (e.g., in 83.3983E, 28.4842N) clearly interpreted in the InSAR image of 08Oct2015/17Dec2015, which was relatively better coherence than the rest five images.

Keywords: SAR, earthquake, landslide, interpretation

©2019. Japan Geoscience Union. All Right Reserved.

A depth-integrated model for granular flows on the transition of different bed conditions

*Ling-Yi Hsu[1], Chi-Yao Hung[1]

1. National Chung Hsing University

The different basal boundary conditions profoundly affected the flow behavior of debris flow. However, it is hard to have a general and straightforward model to describe the flow profile switching from different bed conditions. In this study, we purpose a new depth-averaged model to simulate the dense granular flow transition between the rigid and mobile bed. The model is based on mass conservation, momentum conservation, and kinetic energy conservation. We apply the linearized mu(I) rheology to describe granular deformation and assume Coulomb friction along the sidewalls. By incorporating the basal shear rate term into the equations, the theory can balance the extra force from rigid bed friction force. To check the model approach, we conducted an equilibrium and non-equilibrium heap flow experiments using the narrow see-saw channel, which can be tilted to different angles between runs or during flows. To compare the experimental results with the theory, the flow fields are monitored using high-speed video and particle-tracking velocimetry.

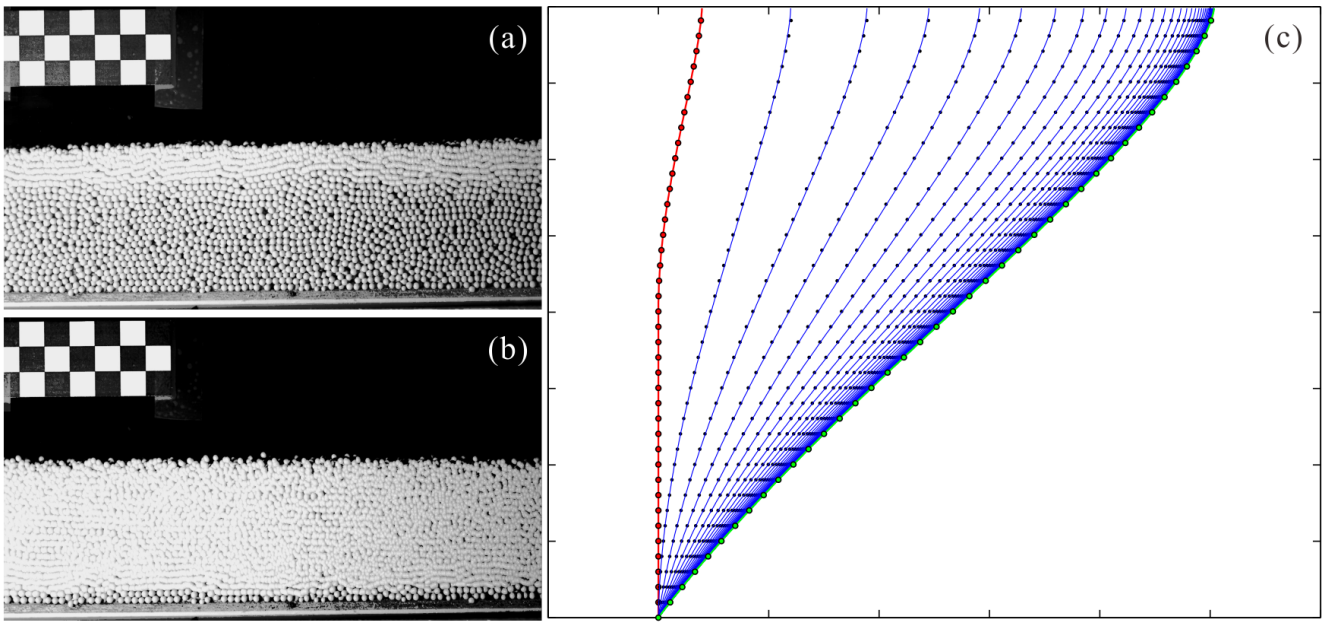


Fig.1 Experimental longexpousre image (a) over deposition bed; (b) over rigid bed; and (c) the transition velocity profile of theory prediction.

©2019. Japan Geoscience Union. All Right Reserved.

A viscous granular flow experiment with new refractive index matching material

*Tsai-Jung Lin[1], Chi-Yao Hung[1]

1. National Chung Hsing University

Entrainment rate at base controls how far the debris flow can travel and how large the debris flow becomes. Flow rheology of Refractive Index Matching (RIM) material are generally limited by the mono-particle properties (such as polymethyl methacrylate/liquid para-cymene etc.). In this study, a new RIM material (polyacrylamide polymer/18% Methanol solution) having a wide range of particle size distribution and viscosity (Fig. 1L) are purposed to visualize and measure the erosion process of mobile bed dam break experiments. Various rheology models may be formed by the different ratio of particle size. To improve the contrast between the particle phase and the liquid phase, a dye is used to make the particles bright under laser illumination. By varying the dye concentration, the entraining/detraining processes are easily distinguished (Fig. 1R). Granular motion is captured through a high-speed camera and Particle Tracking Velocimetry (PTV) method. Finally, an empirical relationship between the rheology and the entraining/ detraining process is developed.

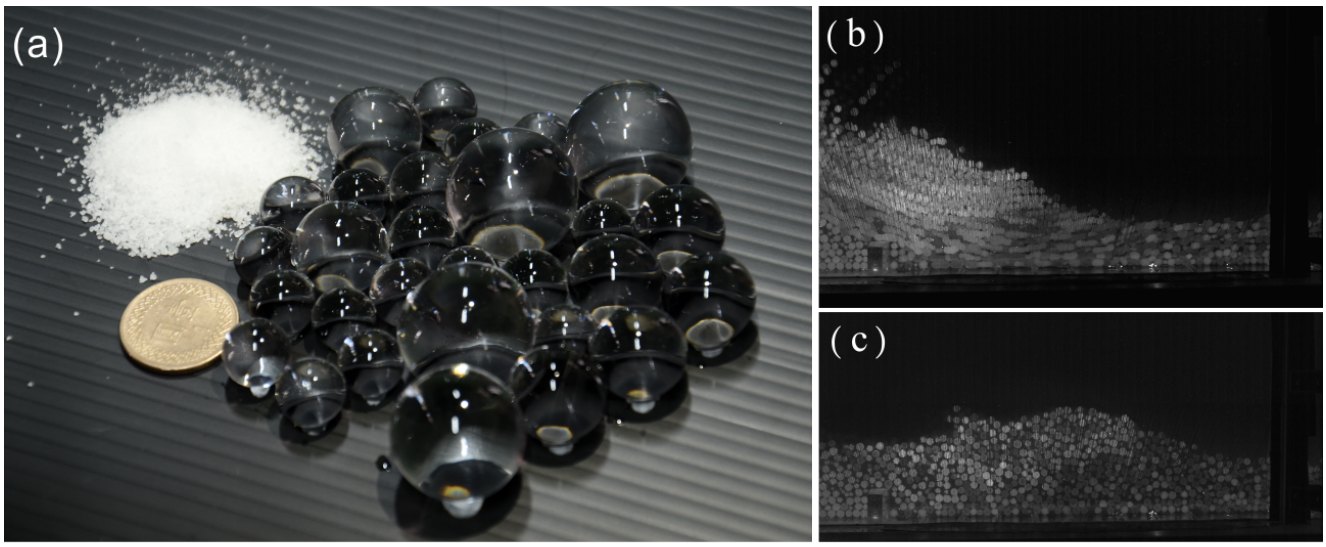


Fig.1 Experimental image (a)wide range of particle size; (b)longexposure image of dam break occurrence; (c)particles with different concentration of dye.

©2019. Japan Geoscience Union. All Right Reserved.

Sandbox experiments of submarine landslide caused by water film in low permeability layer

*Shogo Kawakita[1], Daisuke Asahina[2], Keiji Kitajima[3], Mitsukazu Nakanishi[3]

1. Graduate School of Science & Technology, Nihon Univ., 2. National Institute of Advanced Industrial Science and Technology, 3. College of Science & Technology, Nihon Univ.

Submarine landslides can be serious geohazards since they potentially cause tsunamis and damage seafloor infrastructure. Submarine landslides can be larger in scale than landslides on land. Direct measurements/observations of submarine landslides at deep seafloor still remain a challenging task. Kokusho et al. (2000) proposed a water film effect and its mechanism on lateral flow with less frictional resistance to explain a driving force of large-scale submarine landslides

In this study, we conducted laboratory experiments to understand the relationship between sand liquefaction and lateral flow by water film, and investigate the influence of water film formation on lateral flow of upper layer. In general, it is difficult to observe the formations of liquefaction and lateral flow at the same time. This is because sand particles of sloping layer model start to move when vibration is applied, and inclination disappears before liquefaction. To solve this problem, we devised a mechanism to prevent the flow of the lower layer by providing a weir plate in inside the soil tank. This mechanism enables to distinguish and observe the movement of sand by the liquefaction and the lateral flow by the water film.

The results obtained in this study clearly show three stages: first, the lower layer was liquefied; then pore water was stored below the low permeability layer; and finally, the lateral flow was occurred by the water film effect. The experimental results show that there was no clear correlation between the increase in the angle of sloping layer and the travel distance or the maximum flow velocity. We also discuss the relationship between the layer angle and the location of sand boil. The location where sand soiling occurred moved to the upper side of the slope as the layer angle become larger.

[Reference]

Kokusho, T.: Mechanism for water film generation and lateral flow in liquefied sand layer, Soils and Foundations, Vol.40, No.5, p 99-111, 2000.

Keywords: Submarine Landslides, Pore Water Pressure, Water Film, Lateral Flow

©2019. Japan Geoscience Union. All Right Reserved.

Study on Creep Properties of Sand and Cemented Sand

*JIN-YI YU[1], KUANG-TSUNG CHANG[1]

1. National Chung Hsing University

In this study, we investigated the effects of creep on sand and cemented sand, using triaxial test. Sand represents a non-cohesive material, while cemented sand represents a brittle material. Before the failure of specimens, the deviator stress was fixed and the cyclic mean stress was applied to study the influence of creep on the materials. According to the test results, the axial strain accumulation of sand caused by creep is less, and the peak strength is larger than that of the monotonic loading when the axial loading is resumed. For cemented sand, creep causes microcracks inside the specimens, gradually forming a failure surface. When the axial strain accumulation is large enough, the reapplication of the axial loading shows a reduction of peak strength. We conclude that the influence of creep on non-cohesive material (sand) is limited, whereas creep can reduce the strength of the brittle material (cemented sand) and even cause failure.

Keywords: creep, triaxial test, sand, cemented sand, strength, failure

©2019. Japan Geoscience Union. All Right Reserved.

The effects of seepage force and the Poisson’ s ratio on slope stability

*Hirokazu Fukui[1], Tomomi Terajima[2]

1. Graduate school of Science, Kyoto University, 2. Disaster Prevention Research Institute, Kyoto University

To predict accurately the timing of shallow landslide occurrence, we need to consider the direction and magnitude of seepage force and earth pressure. A model sandy slope (L: 9m, W:1m, H:4m) was used to measure the hydraulic gradient and seepage force with the tensiometers under the artificial rainfall of 80mm/h. We incorporated not only the seepage force but also the Poisson’ s ratio into conventional slope stability analysis by the limit equilibrium method. As a result, the calculated timing of shallow landslide occurrence was almost agree with the timing of that in the experiment and also more accurate than the timing calculated by the Spenser method which took into account the magnitude and moment equilibrium of the force. These results imply that, based on both monitoring at fields and conducting more experiments by a real-size model slope, we need to verify the effects of seepage force and earth pressure as the important factors causing rainfall-induced slope instability.

Keywords: process-based model, Seepage force, the Poisson's ratio, Shallow landslide, Sandy model slope

©2019. Japan Geoscience Union. All Right Reserved.

Study on the factors of seepage erosion

*Szu-Wei Fu[1], Kuang-Tsung Chang[1]

1. National Chung Hsing University

The causes of many slope disasters are often related to the seepage behaviors of soil. For instance, groundwater seepage may cause internal erosion of the soil. The soil particles are taken away by seepage water to form void or pipe. In addition , the earth pressure leads to the collapse of the overlying soil.

In this study, we designed a set of apparatus that can add confining pressure to the outside of the specimen. In order to simulate the situation of sand in slopes, we investigated the critical seepage velocity of sands caused by seepage erosion failure under different confining pressure, with different particle size distributions, sizes of outflow, etc. Then a failure criterion for seepage erosion is developed based on the drag equation in fluid dynamics and confirm with experimental data.

The results show that the critical seepage velocity at failure is affected by the particle size distributions, sizes of outflow and the confining pressure. The theoretical results are compared well to the experimental data.

Keywords: seepage erosion, Drag equation

©2019. Japan Geoscience Union. All Right Reserved.

Deformation of slope models with different orientations of weak planes

*taeyuan tseng[1], Kuang-Tsung Chang[1]

1. National Chung Hsing University

Weak planes influence failure and deformation of slopes. We conducted experiments to simulate slopes of different orientations of weak planes, including cataclinal and analcinal slopes with 30˚ and 60˚ inclination angles of weak planes. We stacked artificial bricks to make small-sized slope models. The artificial bricks were made of gypsum, sand, cement and water with different weight proportion. In view of the scaling law, the artificial bricks were made less strength than natural rocks. The slope models were weakened under rainfall, resulting in deformation and final collapse. The slope deformation processes were photographed by a camera, and the displacement vector fields were analyzed using the Particle Image Velocimetry (PIV). The deformation and accumulated displacements were compared between slopes of different orientations of weak planes.

Keywords: cataclinal slope, analcinal slopes, rainfall, Particle Image Velocimetry (PIV), weak planes, deformation

©2019. Japan Geoscience Union. All Right Reserved.

[E] Poster | H (Human Geosciences)：H-TT Technology & Techniques

Tue. May 28, 2019 3:30 PM - 5:00 PM JST | Tue. May 28, 2019 6:30 AM - 8:00 AM UTC | Poster Hall International Exhibition Hall8, Makuhari Messe_13

[H-TT18] Development and application of environmental traceability methods

convener:Ichiro Tayasu(Research Institute for Humanity and Nature), Nobuhito Ohte(Department of Social Informatics, Graduate School of Informatics, Kyoto University), Gabriel J Bowen(University of Utah)

Modern society uses almost all the elements present in the natural world. Although there have long been calls for the sustainable use of the resources that provide these elements and the building of human societies that are in harmony with the environment, the survival of the human race is increasingly at risk as a result of qualitative changes to the environment as a whole. Implementation by the society of methodologies for diagnosing and tracking these various elements of the natural environment and their relationships with humans are now required.
Elements cycle within and among the Earth system spheres, human society and the human body. Information on the concentrations and stable isotopes of elements is powerful tool for tracing this cycling and has been applied in studies of atmosphere-hydrosphere circulation, ecological systems, and the life, health and history of humans. We propose a session to discuss development and applications of environmental traceability methods toward the goal of establishing traceability in natural and human systems.
We encourage the presentation of research integrating isotopic information in various disciplines, such as geochemistry, hydrology, ecology, geology, mineralogy, anthropology, food science, and forensics. Studies applying "Isoscapes", maps of spatial isotopic variation, in addition to traditional database-based approaches, are strongly encouraged.

[HTT18-P01] Isotopic study on seasonal nitrogen dynamics at Lake Biwa

*Takaaki Ishibashi[1], Ken'ichi Osaka[1], Keisuke Koba[2], Takashi Nakamura[3], Kei Nishida[3] (1.Department of ecosystem study, University of Shiga Prefecture, 2.Center for Ecological Research, Kyoto University, 3.International Research Center for River Basin Environment, University of YAMANASHI)

[HTT18-P02] Relationship between residence time, water quality, and stable isotopes of spring water and groundwater in coastal area of Fukushima prefecture

*Shiho Yabusaki[1], Kazuyoshi Asai[2] (1. Research Institute for Humanity and Nature・Faculty of Symbiotic Systems Science, Fukushima University, 2.Geo Science Laboratory)

[HTT18-P03] Applicability evaluation of CIA due to river and lake

*yusuke hataya[1], SEIKI KAWAGOE[1], Shiho Yabusaki[2], KEN Suzuki[1] (1.fukushima university, 2.Research Institute for Humanity and Nature)

[HTT18-P04] Chemical property analysis of short time scale to determine snowfall source

*Suzuki hiromichi[1], SEIKI KAWAGOE[1], SHO ADACHI[1], Shiho Yabusaki[2] (1.Fukushima University, 2.Research Institute for Humanity and Nature)

[HTT18-P05] Analyzing the origin of surface water in the Saijo Plain, Japan, based on the antimony concentration in the water

*Minoru TOKUMASU[1,2], Ki-Cheol SHIN[3], Yoshihiro YAMADA[4] (1.The United Graduate School of Agricultural Sciences, Ehime University, 2.Saijo City, 3.The Research Institute for Humanity and Nature (RIHN) , 4.Kagawa University, Faculty of Agriculture)

[HTT18-P06] Basic kinetic study on stable isotope ratios of nitrogen compounds: a case study for groundwater in the Kathmandu Valley, Nepal

*Ken Yokozawa[1,2], Kei Nishida[1,3], Takashi Nakamura[1,3], Ken'ichi Osaka[4] (1.University of Yamanashi, 2.Special Graduate Program on River Basin Environmental Science,, 3.ICRE, 4.Department of ecosystem study Univercity of Shiga prefecture)

[HTT18-P07] Usefulness of strontium isotope composition for determining the geographical origin of wasabi and potato

*Takafumi Kamitani[1], Ki-Cheol Shin[2], Sachiko Nakamura[1], Rika Koda[1], Tomoya Oka[1], Noriaki Fushimi[1], Yasuhide Muranaka[1] (1.Shizuoka Institute of Environment and Hygiene, 2.Research Institute for Humanity and Nature)

[HTT18-P08] Reconstruction of sea surface temperature and salinity for the Medieval Climatic Anomaly using a long-lived fossil coral collected at Ishigaki Island, southwestern Japan

*Osamu Abe[1], Maki Morimoto[2], Ryuji Asami[3], Takeshi Nakatsuka[1,4] (1.Graduate School of Environmental Studies, Nagoya University, 2.School of Education, Gifu University, 3.Graduate School of Science, Tohoku University, 4.Research Institute for Humanity and Nature)

[HTT18-P09] Development of the analytical method for sulfur isotope in SO_2 gas

*Masaaki Takahashi[1], Hiroyuki Sase[1], Tsuyoshi Ohizumi[1] (1.Asia Center for Air Pollution Research)

[HTT18-P10] Zinc isotope analysis on human tooth enamel samples to reconstruct diet of the Jomon period.

*Soichiro Kusaka[1], Ki-Cheol Shin[2] (1.Tokai Univ., 2.Research Institute for Humanity and Nature)

[HTT18-P11] Zinc stable isotope analysis of environmental reference materials

*Ki-Cheol Shin[1] (1.Research Institute for Humanity and Nature)

Isotopic study on seasonal nitrogen dynamics at Lake Biwa

*Takaaki Ishibashi[1], Ken'ichi Osaka[1], Keisuke Koba[2], Takashi Nakamura[3], Kei Nishida[3]

1. Department of ecosystem study, University of Shiga Prefecture, 2. Center for Ecological Research, Kyoto University, 3. International Research Center for River Basin Environment, University of YAMANASHI

To clarify nitrogen dynamics in Lake Biwa, we measured the concentrations of nitrogen compounds and their nitrogen stable isotopic ratios in 14 depths in north basin of Lake Biwa. In the lake, particulate nitrogen (PN), such as phytoplankton, is generally decomposed to dissolved nitrogen (DN); in order of dissolved organic nitrogen (DON), ammonia nitrogen (NH_4^+) and nitrate nitrogen (NO_3^-). These dissolved nitrogen compounds are taken up by phytoplankton again, and the nitrogen circulation in the lake is established. To predict the water quality in future, it is necessary to understand the nitrogen cycle in the lake, as well as nutrient load to the lake.

In this study, we collected lake water sample at 14 depths in north basin of Lake Biwa (water depth is 90 m) in 1-2 months interval. The lake waster sample was analyzed for the concentration of PN, PC, DN, NO_3^-, NO_2^- and NH_4^+, $d^{15}N$ of PN, DN and NO_3^-.

NO_3^- concentration was lower in the surface layer (0-20m), and higher in the deep layer (20-90m) during the stratification period, whereas NO_3^- concentration was constant in all layers during the circulation period. PN concentration also increased in the surface layer from April to June, decreased sharply in July. These indicate that phytoplankton which grew on the surface layer from April to June used NO_3^-, thereafter, NO_3^- was depleted after June, then, phytoplankton decreased after July respectively. On the other hand, NO_3^- concentration is considered to be increased by decomposition of the precipitated PN from surface layer. It is considered that the NO_3^- concentration became constant in all layers because of mixing of deep layer and the surface layer.

The weighted average $d^{15}N_{DN}$, $d^{15}N_{NO3}$ in the unit water columns decreased about 3‰ in the circulation period, in the circulation period, then, increased during the stratification period. The decrease of $d^{15}N_{DN}$, $d^{15}N_{NO3}$ at the water column during circulation period can not be explained by mixing of deep layer and the surface layer. We will discuss the mechanisms of $d^{15}N_{DN}$, $d^{15}N_{NO3}$ decrease during circulation period in the presentation.

Keywords: nitrogen dynamics, nitrogen isotope, seasonality

©2019. Japan Geoscience Union. All Right Reserved.

Relationship between residence time, water quality, and stable isotopes of spring water and groundwater in coastal area of Fukushima prefecture

*Shiho Yabusaki[1], Kazuyoshi Asai[2]

1. Research Institute for Humanity and Nature・Faculty of Symbiotic Systems Science, Fukushima University, 2. Geo Science Laboratory

After the Great East Japan Earthquake occurred, the investigation near the coast area in northern part of Fukushima prefecture has been carried out to clarify the groundwater flow and residence time in this area. The measuring of EC, pH, water temperature, ORP and sampling of groundwater, spring water and river water have been carried out several times at Shinchi town, Soma city, Minamisoma city, Namie town, Okuma town, Iitate village and Date city since September in 2012. The inorganic ions, stable isotopes of oxygen and hydrogen, trace elements were analyzed for all samples by using the IC (ICS-3000), CRDS (Picarro L2130-i) and ICP-MS (Agilent 7500cx). For estimating the residence time, tritium concentration, CFCs and SF_6 measurements were made in several samples.

The water quality of river water and shallow groundwater indicates mainly Ca-HCO_3 type. In the part of the flooded area by a tsunami, the water quality of shallow groundwater and spring water is Na-Cl type. The Ca-SO_4 type and mixed type were also confirmed in some sites. In the case of deep groundwater, the water quality shows the Na-HCO_3 type and Ca-HCO_3 type. The concentration of Fe, Mn and Al were relatively high in some parts of deep groundwater. It is considered that the origin of these trace elements is soil.

The stable isotopes of oxygen and hydrogen ($\delta^{18}O$ and δD) in river water of Niida river, Mano river and Kamimano river indicate altitude effect. Because the stable isotopes in deep groundwater is relatively low, it is anticipated the recharge are of deep groundwater is about 300 m higher than that of shallow groundwater. It is expected that the recharge area of deep groundwater is around the Abukuma Mountains.

The average residence time of deep groundwater and spring water which indicate the Na-HCO_3 type is about 60 to 70 years. On the other hand, the average residence time of shallow groundwater which indicate the Ca-HCO_3 type is less than 10 years.

The information of groundwater flow is useful for considering the groundwater use with revival of the coastal area. We will continue the investigation of coastal area and make clear the groundwater flow system.

Keywords: Minamisoma city, Fukushima prefecture, CFCs・SF6, residence time, water quality, stable isotopes, groundwater flow

©2019. Japan Geoscience Union. All Right Reserved.

Applicability evaluation of CIA due to river and lake

*yusuke hataya[1], SEIKI KAWAGOE[1], Shiho Yabusaki[2], KEN Suzuki[1]

1. fukushima university, 2. Research Institute for Humanity and Nature

Water resources management must be further attention because extreme weather condition generate to predict climate change. However, a water area have the various regional characteristics. Therefore a universal way may not also be able to indicate the effect management. If categorized basin tool is developing to obtain characteristic, it is possible to choose suitable management technique in water areas. We tried to develop database to manage basin as chemical and geographical information. In this research, Water factors (Chemical condition, land use condition, soil condition and geological condition) between basins (rivers and reservoirs) were compared to develop data base. Especially, we applied to Chemical Index of Alteration (CIA) as chemical condition factor. As results, It was possible to obtain the basin area scale to apply CIA.

Keywords: CIA, water resource, Numerical geographic information

©2019. Japan Geoscience Union. All Right Reserved.

Chemical property analysis of short time scale to determine snowfall source

*Suzuki hiromichi[1], SEIKI KAWAGOE[1], SHO ADACHI[1], Shiho Yabusaki[2]

1. Fukushima University, 2. Research Institute for Humanity and Nature

Occurrence of the strange weather phenomenon is predicted from the current state depending on climate change. To ask this influence, we have to advance the match which raises the future predictability. And, we have to mark a phenomenon of the current state detail. This study targets to obtain chemically snow environment. The aim of this study was to analyse and predict the stable water isotopic composition of the snow cover at specific basin (Agano river). In addition, the dependence of short time step isotopic composition of the entire snow cover was analysed. Snow in 3 catchments was sampled at the end of the accumulation period from December 2016 to April 2018. The observed variability of short time step isotopic composition of the snow cover was analysed chemical verification. Especially, basin The Inawashiro-Lake north side of the northern upstream region indicated the low chemical feature (Suzuki et al 2018). I'm working on the investigation analysis to grasp the chemical special quality of the snow event of the short time scale at present based on this result (2016-2018). It was that a chemical analysis makes the sample which sampled and acquired it by each day the time of a snowfall at Fukushima, Hibara and Yonezawa located in an upstream region in a basin, and we tried to follow up a snowfall origin of the short time scale.

As results, a strong pressure pattern of southern high and northern low could admit January 22nd-the 25th, the result obtained from the result of analysis also reacted to the weather situation sensitively. And influence of a characteristic snowfall origin was admitted at 3 spots. The difference in the spatial time lags was done clearly.

Keywords: d-excess value, isotope, short time scale

©2019. Japan Geoscience Union. All Right Reserved.

Analyzing the origin of surface water in the Saijo Plain, Japan, based on the antimony concentration in the water

*Minoru TOKUMASU[1,2], Ki-Cheol SHIN[3], Yoshihiro YAMADA[4]

1. The United Graduate School of Agricultural Sciences, Ehime University, 2. Saijo City, 3. The Research Institute for Humanity and Nature (RIHN) , 4. Kagawa University, Faculty of Agriculture

1. Introduction

The flow of river water in many medium and small rivers is managed for water use and flood control. However, it is almost impossible to understand how the water taken from the rivers circulates throughout a basin. The source of water in the Saijo Plain in Ehime Prefecture is from the Kamo River surface water flow, shallow groundwater (unconfined ground water), and deep groundwater (confined ground water). Therefore, it is necessary to quantitatively clarify the source of water for sustainable water use. In this study, we tried to quantify the origin of river water in the plain based on the concentration of some chemical elements. In particular, antimony (Sb) was used as the main trace element because of large differences in its concentration between the water sources.

2. Materials and Methods

On November 25 and 26, 2017, during the non-irrigation period and on the 27th and 28th of July, 2018, during the irrigation period, surface water was collected at a total of 43 sites on small and medium rivers and waterways in the Saijo Plain. Multi-element analysis was carried out on the collected water using ICP-MS 7500 cx.

3. Results and Discussion

There was a large difference in the concentration of Sb among the sites. The highest concentration was found in the water from the Ichino River (Stn. 2) at 113 (2017) and 158 μg/L (2018). There was once an antimony mine in the Ichino River basin, so high concentrations of the element in the river water can be regarded as reflecting the influence of the geology. In the main stream of the Kamo River before joining the Ichinose River (Stn. 1), the Sb concentration was as low as 0.2 μg/L, and after the junction of the two rivers (Stn. 3), the concentration increased to 4.3 (2017) and 7.2 μg/L (2018). The concentration was 4.2 (2017) and 7.2 μg/L (2018) at Stn. 4 of the Kamo River, 11.6 (2017) and 11.7 μg/L (2018) in the unconfined ground water (average of Stns. 13, 14, 15), and 0.4 (2017) and 0.5 μg/L (2018) in the confined ground water (average of Stns. 28, 29, 40, 41, 43). The concentration of Si was 2.7 (2017) and 3.2 mg/L (2018) at Stn. 4 of the Kamo River, 3.4 (2017) and 2.9 mg/L (2018) in the unconfined ground water (average of Stns. 13, 14, 15), and 4.1 (2017) and 3.9 mg/L (2018) in the confined ground water (average of Stns. 28, 29, 40, 41, 43).
The ratio of water origin at each survey site was estimated using the above three sources as end members. In the upstream area, the irrigation water taken from the Kamo River occupied most of the surface water. In the middlestream area, the ratio of water taken from the rivers was smaller, and the contribution of

©2019. Japan Geoscience Union. All Right Reserved.

unconfined ground water exceeded 80%. In the downstream area, the confined ground water contribution exceeded 40% at many sites. In the Saijo Plain, the water origins are different in the upstream, middlestream, and downstream areas, where the contribution of irrigation water is small overall, and the contribution of the confined ground water is large.

©2019. Japan Geoscience Union. All Right Reserved.

Basic kinetic study on stable isotope ratios of nitrogen compounds: a case study for groundwater in the Kathmandu Valley, Nepal

*Ken Yokozawa[1,2], Kei Nishida[1,3], Takashi Nakamura[1,3], Ken'ichi Osaka[4]

1. University of Yamanashi, 2. Special Graduate Program on River Basin Environmental Science,, 3. ICRE, 4. Department of ecosystem study Univercity of Shiga prefecture

Groundwater is a valuable source of water in developing countries where water demand is increasing with population increase. At the same time, nitrogen contamination by industrial wastewater, domestic wastewater and agricultural activities has been reported. In underground environments, it is not unusual to identify sources of contamination since the forms and the concentrations of nitrogen compounds vary at different water flow or microbial metabolism. Stable isotopic analysis is one of the effective methods to detail the variations. However, the isotope value is also greatly affected by environmental conditions, and the theoretical enforcement for describing the variation of the isotope value is needed. In this study, we aimed to quantitatively understand and identify the factors of mixing and isotopic fractionation that determine the stable isotope ratio with a case study on groundwater contamination in the Kathmandu Valley, Nepal.

The data used for the analysis was obtained from the groundwater survey of the Kathmandu Valley conducted from September 2014 to August 2018. Based on the stable isotope ratios of nitrogen and oxygen of nitrate, the contamination patterns were roughly categorized. The mixing line and the denitrification line were prepared based on the dynamic fractionation for the stable isotope ratios of nitrate nitrogen, and the spatial distribution of denitrification-related samples was examined on the map. In addition, assuming that the reactants exist sufficiently and homogeneously in the system, an equilibrium fractionation model was formulated by combining nitrification and denitrification for oxygen stable isotope ratios of nitrate and water. The range of the model parameters were determined by using the measured data from the filed survey, the influence of each process on the stable oxygen isotope ratio of nitrate was quantified.

The result showed that the nitrate in shallow groundwater partially originated from the atmospheric source through infiltration of rainwater. A characteristic of denitrification was observed, which was initiated and proceeded over the valley. Additionally, the correspondent isotopic fractionation differed at the location and the season, particularly controlled by ammonia oxidation, nitrite reduction and oxygen exchange between nitrite and water.

Keywords: groundwater , nitrogen and oxygen stable isotope ratios, nitrification, denitrification, mixing, fractionation

©2019. Japan Geoscience Union. All Right Reserved.

Usefulness of strontium isotope composition for determining the geographical origin of wasabi and potato

*Takafumi Kamitani[1], Ki-Cheol Shin[2], Sachiko Nakamura[1], Rika Koda[1], Tomoya Oka[1], Noriaki Fushimi[1], Yasuhide Muranaka[1]

1. Shizuoka Institute of Environment and Hygiene, 2. Research Institute for Humanity and Nature

Originally, the use of strontium isotope ratios ($^{87}Sr/^{86}Sr$) was restricted to geology and petrology, but they have been used as a particularly effective tracer of geographical food origin, as plants reflect the strontium isotope composition of the regionally based rock, soil, and water. This study aims to evaluate the usefulness of $^{87}Sr/^{86}Sr$ for determining the geographical origin of wasabi (Japanese horseradish) and potato, which are specialty crops in Shizuoka Prefecture, Japan.

Wasabi is cultivated in springs and streams located at the top of rivers, where dissolved element and isotopic compositions in water would reflect the geological characteristics without the effects of atmospheric deposition and human activity. We collected wasabi and water samples from 40 locations of major production areas in Japan: Shizuoka, Iwate, Nagano, Tokyo, and Shimane. These samples were subjected to trace elements and $^{87}Sr/^{86}Sr$ analyses. The $^{87}Sr/^{86}Sr$ values differed, based on the geological characteristics of their site locations, and the value of wasabi was well accorded with that of water in the same location. The wasabi samples collected from Izu Peninsula and Mt. Fuji regions in Shizuoka, where young volcanic rocks such as Quaternary basalts are distributed, had low $^{87}Sr/^{86}Sr$ (below 0.7040), whereas those from Nagano and Tokyo, where older rocks such as Mesozoic granites and accretionary complex are distributed, showed higher ratios (over 0.7095). We conclude that $^{87}Sr/^{86}Sr$ value of wasabi allowed us to distinguish the production area clearly.

On the other hand, the $^{87}Sr/^{86}Sr$ values of crops cultivated in the field are considered to be partly affected by precipitation and fertilizer. Therefore we conducted field survey and planter test for potato in Shizuoka. Field survey was conducted at Mishima, in eastern part of Shizuoka prefecture, and at Mikatahara, in western part of it, and $^{87}Sr/^{86}Sr$ of potato and soil exchangeable fraction were compared. As a result, there was a correlation between potato and soil in $^{87}Sr/^{86}Sr$, although the effects of precipitation and fertilizer were observed. The planter test suggests that the influence of fertilizer on $^{87}Sr/^{86}Sr$ varies depending on the amount of exchangeable Sr contained in the original soil.

Keywords: geographical origin, strontium isotope ratio, wasabi, potato, Shizuoka

©2019. Japan Geoscience Union. All Right Reserved.

Reconstruction of sea surface temperature and salinity for the Medieval Climatic Anomaly using a long-lived fossil coral collected at Ishigaki Island, southwestern Japan

*Osamu Abe[1], Maki Morimoto[2], Ryuji Asami[3], Takeshi Nakatsuka[1,4]

1. Graduate School of Environmental Studies, Nagoya University, 2. School of Education, Gifu University, 3. Graduate School of Science, Tohoku University, 4. Research Institute for Humanity and Nature

The period between 950 and 1250CE is called as the Medieval Climate Anomaly (MCA; Masson-Delmotte et al., 2013), at the time when the warmer climate seemed dominant globally (Bradley et al., 2003). Recent investigations based on the proxy record such as tree-ring widths, speleothems, ice cores, and historical documents indicated that a significant climate change occurred during the latter half of the 10th century. Mann et al. (2009) found that an increase of the average air temperature in the northern hemisphere at the late 10c. coincided with an increase of sea surface temperature at northern subpolar oceans. Yan et al. (2011) indicated that atmospheric environments in the equatorial Pacific shifted from the La Nina like condition to the El Nino like condition around 1000CE. In East Asia, Zhang et al. (2008) and Ge et al. (2013) described that the activity of East Asian Summer Monsoon (EASM) had been enhanced during the late 10c., then the climate in China shifted to warmer and wetter. Whereas Lie et al. (2014) showed that the EASM had been weakened during the 11th century. In addition, the climate in southern China was reported as relatively dry (Chen et al., 2015).

These studies demonstrated that a large climatic shift occurred around 1000CE, however, most of them have relied on records collected on land. There is little long-term high-resolution marine record during the MCA.

We reconstructed sea surface temperature (SST) and salinity with a temporal resolution of one month for 300 years using a long-lived fossil coral collected at Ishigaki Island, southwestern Japan. Based on the U/Th dating in the youngest part of the coral skeletons as well as the band counting, this coral sample had lived between 845 and 1130CE, largely covered the MCA period. Skeletal Sr/Ca and oxygen isotopic composition were analyzed for about 4,000 samples.

The empirical equations between Sr/Ca and water temperature; between oxygen isotopic composition of coral skeleton and seawater, and water temperature, were established using the present coral records, observed water temperature and oxygen isotopic composition of seawater. With these equations and the relationship between seawater salinity and oxygen isotopic composition, proposed by Abe et al. (2009), SST and seawater salinity from 845 to 1130CE were reconstructed from the fossil coral Sr/Ca and oxygen isotopic composition.

Through the entire period, average summer and winter SSTs were 2 and 1 deg. C higher than the present, respectively. In addition, SST increased significantly after 1040CE; 0.9 for the annual average, 0.7 for summer and 1.1 for winter. Salinity also increased after 990CE; 0.8 all for the annual average, summer and winter. Salinity was significantly higher through the entire period than the present, however, its absolute value seems unconfirmed yet.

©2019. Japan Geoscience Union. All Right Reserved.

Increasing SST and salinity found in this study during ca. 1000 and 1130CE were consistent with the weakening of EASM during the 11th and 12th centuries shown by Liu et al. (2014). They argued the weakening occurred as a consequence of weakening of the solar activity and the decrease of SST at the western Pacific warm pool. In this study region, the decrease of precipitation during the Baiu period induced the increase of salinity as well as local SST increase due to the decrease of the cloud cover. Our results were also consistent with the warming of China in the late 10c. (Ge et al., 2013), and a drier condition in southern China (Chen et al., 2015).

The periodicity of SST and salinity based on the spectral analysis will be discussed in the presentation.

Keywords: Coral annual bands, Medieval Climate Anomaly

©2019. Japan Geoscience Union. All Right Reserved.

Development of the analytical method for sulfur isotope in SO_2 gas

*Masaaki Takahashi[1], Hiroyuki Sase[1], Tsuyoshi Ohizumi[1]

1. Asia Center for Air Pollution Research

1. Introduction

Sulfur is a major source of acid deposition. Usually sulfur is emitted as SO_2 and it is oxidized to SO_4^{2-} in atmosphere. S isotopic analysis of water and particulate samples were conducted in many studies. But gaseous SO_2 was rarely used for isotopic study. Isotopic ratio of SO_2 is strongly influenced by emission source near the sampling point. Because most of SO_2 emitted far from sampling point is oxidized to SO_4^{2-} during transportation. It is possible to distinguish domestic emission from transboundary emission. Moreover, dry deposition processes of SO_2 and particulate SO_4^{2-} and their interactions with tree canopy could be discussed more precisely. Isotopic analysis of SO_2 is considered as a powerful method to investigate the behavior of S in the atmosphere and ecosystems. We studied about the analytical method for S isotope in SO_2.

2. Method

(1) Equipment

SO_2 concentration in Japan is very low (e.g. annual 0.02ppb at Sado). We need to collect air sample at least $1m^3$ that is the amount we can obtain 1.2mg of $BaSO_4$ precipitation enough for isotopic analysis. High volume air sampler is generally used to collect around $1m^3$ of air sample. It uses filter, so we examined filter collection of SO_2 by K_2CO_3 filter generally used to collect SO_2 in filter-pack method.

(2) Filters

We used quarts filter for particulate SO_4^{2-} and K_2CO_3 filter for gaseous SO_2 next to it. K_2CO_3 filter is made on the basis of EANET manual. But to get enough flow rate for high volume air sampler, the size of K_2CO_3 filter is larger (20×26 cm, same size with quarts filter) than the manual and already dried before sampling.

(3) Flow rate/leak test

Under flow rate 100~400 L/min in this system, we confirmed weather sampling can be carried out stably. And we checked leak using two K_2CO_3 filters.

(4) Sample treatment

©2019. Japan Geoscience Union. All Right Reserved.

On the basis of EANET manual, the sample was extracted with 0.05% H_2O_2aq and filtered. Then 2N HCl was added and concentrated to remove CO_3^{2-}. Next 1%(w/w)$BaCl_2$ was added. We filtered forming $BaSO_4$ precipitation. We examined the method to get $BaSO_4$ precipitation and to remove the components from K_2CO_3 filter.

3. Results

(1) Sampling and sample treatment

Sampling could be conducted under flow rate 100~400 L/min. Sampling efficiency was about 80%..

Several conditions to get $BaSO_4$ precipitation ware examined, it could be gotten by the method as below.

Filter was cut and ultrasonic extracted with 0.05% H_2O_2aq 30 minutes and filtered. 2.5 ml of 2N HCl was added and concentrated to around 10 ml. Then 1 ml of heated 1 %(w/w) $BaCl_2$ was added under pH 4~6. Next evaporated all solvent and added 10 ml of water. $BaSO_4$ precipitation was observed. After put for one night, the precipitation was separated by centrifuge 3,600 rpm for 10 minutes and we removed the solvent. The precipitation was washed twice by 10 ml of water and filtered. At last the filter was ashed for four hours in muffle furnace in 800 ℃ .

(2) Actual analysis

We used two K_2CO_3 filters and collected 2160.2 m^3 of air sample under flow rate 300 L/min. 3.80 mg of particular SO_4^{2-} and 0.89 mg (first) and 0.14 mg (second) of SO_4^{2-} from SO_2 were obtained. $\delta^{34}S$ of particular SO_4^{2-} was 8.64 ‰and that of SO_2 from the first filter was -1.54 ‰. The amount of precipitation from second filter was not enough for isotopic analysis. This difference was caused by effect of sea salt mainly. But nss- $\delta^{34}S$ of particular SO_4^{2-} was 4.78 ‰. It was still higher than SO_2. It suggested that nss- SO_4^{2-} contains both transboundary SO_4^{2-} and domestic SO_4^{2-}. According to the relevant literature, domestic SO_2 may have negative isotopic values because of imported oil from Middle East. Considering that this sampling was carried out in January, possible effect of transboundary SO_2 with higher isotopic values should also be taken into account for source identification of the collected SO_2.
We would like to discuss at the conference with the latest data.

Keywords: sulfur isotope, SO2 gas

©2019. Japan Geoscience Union. All Right Reserved.

Zinc isotope analysis on human tooth enamel samples to reconstruct diet of the Jomon period.

*Soichiro Kusaka[1], Ki-Cheol Shin[2]

1. Tokai Univ., 2. Research Institute for Humanity and Nature

This study investigates zinc isotope ratios in tooth enamels of human skeletal remains of the Jomon period in Japan. Carbon and nitrogen isotope analysis on bone collagen were traditionary used to reconstruct diet and trophic levels on prehistoric people. The progress of isotope measurements using MC-ICP-MS enables us to analyze isotope ratios of zinc and other metals. Some researches report that the zinc isotope ratios of animals reflect dietary sources and vary according to trophic levels. This study newly develops zinc isotope analysis on human tooth enamels. The zinc isotope analysis has great potential to reconstruct dietary information from inorganic materials of archaeological bones or fossils.

The material used in this study is SRM1400 (bone ash), six samples of human tooth enamels from the Yoshigo and Inariyama shell mounds of Aichi prefecture, and faunal remains (six deer enamels, three boar enamels, six marine fish bones, and six modern plant leaves). Zinc was purified from these samples using anion exchange resin. Zinc isotope ratios were measured by MC-ICP-MS with the zinc standard solution of AA-ETH. The mass bias was corrected with Cu standard solution added to all standards and samples. The zinc isotope ratios of SRM1400 showed similar value with the value previously reported. The difference of zinc isotope ratios between washed and unwashed samples with acetic acids were very small, suggesting no significant diagenetic alteration. The deer and marine fish samples showed the value expected from their dietary ecology. The zinc isotope ratios of Jomon skeletal remains was higher than those of plants, but lower than deer and marine fish. This result indicates that sources of zinc for humans were terrestrial and marine meat as well as terrestrial plants.

Keywords: Zinc Isotope, Jomon period, Human skeletal remains

©2019. Japan Geoscience Union. All Right Reserved.

Zinc stable isotope analysis of environmental reference materials

*Ki-Cheol Shin[1]

1. Research Institute for Humanity and Nature

Zinc has atomic number 30 and atomic mass 65.39. It is a trace element of terrestrial rocks and widely distributed throughout the lithosphere and biosphere. It is chalcophile features and has rich coordination chemistry, participates in a large number of important biological compounds and reactions. The zinc plays an important role as an essential trace metal in all living systems from bacteria to humans. Zn has five stable isotopes ^{64}Zn, ^{66}Zn, ^{67}Zn, ^{68}Zn, and ^{70}Zn. Their isotopic fractionation could provide valuable information about environmental processes, especially in biological processes.

With the advent of multi-collector ICP-MS, it is possible to measure the precise value of ^{66}Zn/^{64}Zn in Zn solution. To promote the environmental stable isotope traceability, RIHN is desired to determine the isotope ratios of zinc for environmental reference materials with high precision and accuracy, rapidness, and convenience.

Here, I report a simple and efficient method for zinc isotope analysis. The various environmental samples over 20 types were used for the study. All samples have purified with an anion exchange resin to separated Zn and Fe at a time. Zinc isotope ratios were measured by MC-ICP-MS (NEPTUNE plus) with AA-ETH, which is a new zinc isotopic standard solution reported by Archer et al. (2017). The mass bias correction conducted with Cu standard solution (NIST SRM 976).

Keywords: stable isotope , Zinc, environmental reference materials

©2019. Japan Geoscience Union. All Right Reserved.

[E] Poster | H (Human Geosciences)：H-TT Technology & Techniques

Tue. May 28, 2019 5:15 PM - 6:30 PM JST | Tue. May 28, 2019 8:15 AM - 9:30 AM UTC | Poster Hall International Exhibition Hall8, Makuhari Messe_23

[H-TT18] Development and application of environmental traceability methods

convener:Ichiro Tayasu(Research Institute for Humanity and Nature), Nobuhito Ohte(Department of Social Informatics, Graduate School of Informatics, Kyoto University), Gabriel J Bowen(University of Utah)

Modern society uses almost all the elements present in the natural world. Although there have long been calls for the sustainable use of the resources that provide these elements and the building of human societies that are in harmony with the environment, the survival of the human race is increasingly at risk as a result of qualitative changes to the environment as a whole. Implementation by the society of methodologies for diagnosing and tracking these various elements of the natural environment and their relationships with humans are now required.
Elements cycle within and among the Earth system spheres, human society and the human body. Information on the concentrations and stable isotopes of elements is powerful tool for tracing this cycling and has been applied in studies of atmosphere-hydrosphere circulation, ecological systems, and the life, health and history of humans. We propose a session to discuss development and applications of environmental traceability methods toward the goal of establishing traceability in natural and human systems.
We encourage the presentation of research integrating isotopic information in various disciplines, such as geochemistry, hydrology, ecology, geology, mineralogy, anthropology, food science, and forensics. Studies applying "Isoscapes", maps of spatial isotopic variation, in addition to traditional database-based approaches, are strongly encouraged.

[HTT18-P01] Isotopic study on seasonal nitrogen dynamics at Lake Biwa

*Takaaki Ishibashi[1], Ken'ichi Osaka[1], Keisuke Koba[2], Takashi Nakamura[3], Kei Nishida[3] (1.Department of ecosystem study, University of Shiga Prefecture, 2.Center for Ecological Research, Kyoto University, 3.International Research Center for River Basin Environment, University of YAMANASHI)

[HTT18-P02] Relationship between residence time, water quality, and stable isotopes of spring water and groundwater in coastal area of Fukushima prefecture

*Shiho Yabusaki[1], Kazuyoshi Asai[2] (1. Research Institute for Humanity and Nature・Faculty of Symbiotic Systems Science, Fukushima University, 2.Geo Science Laboratory)

[HTT18-P03] Applicability evaluation of CIA due to river and lake

*yusuke hataya[1], SEIKI KAWAGOE[1], Shiho Yabusaki[2], KEN Suzuki[1] (1.fukushima university, 2.Research Institute for Humanity and Nature)

[HTT18-P04] Chemical property analysis of short time scale to determine snowfall source

*Suzuki hiromichi[1], SEIKI KAWAGOE[1], SHO ADACHI[1], Shiho Yabusaki[2] (1.Fukushima University, 2.Research Institute for Humanity and Nature)

[HTT18-P05] Analyzing the origin of surface water in the Saijo Plain, Japan, based on the antimony concentration in the water

*Minoru TOKUMASU[1,2], Ki-Cheol SHIN[3], Yoshihiro YAMADA[4] (1.The United Graduate School of Agricultural Sciences, Ehime University, 2.Saijo City, 3.The Research Institute for Humanity and Nature (RIHN) , 4.Kagawa University, Faculty of Agriculture)

[HTT18-P06] Basic kinetic study on stable isotope ratios of nitrogen compounds: a case study for groundwater in the Kathmandu Valley, Nepal

*Ken Yokozawa[1,2], Kei Nishida[1,3], Takashi Nakamura[1,3], Ken'ichi Osaka[4] (1.University of Yamanashi, 2.Special Graduate Program on River Basin Environmental Science,, 3.ICRE, 4.Department of ecosystem study Univercity of Shiga prefecture)

[HTT18-P07] Usefulness of strontium isotope composition for determining the geographical origin of wasabi and potato

*Takafumi Kamitani[1], Ki-Cheol Shin[2], Sachiko Nakamura[1], Rika Koda[1], Tomoya Oka[1], Noriaki Fushimi[1], Yasuhide Muranaka[1] (1.Shizuoka Institute of Environment and Hygiene, 2.Research Institute for Humanity and Nature)

[HTT18-P08] Reconstruction of sea surface temperature and salinity for the Medieval Climatic Anomaly using a long-lived fossil coral collected at Ishigaki Island, southwestern Japan

*Osamu Abe[1], Maki Morimoto[2], Ryuji Asami[3], Takeshi Nakatsuka[1,4] (1.Graduate School of Environmental Studies, Nagoya University, 2.School of Education, Gifu University, 3.Graduate School of Science, Tohoku University, 4.Research Institute for Humanity and Nature)

[HTT18-P09] Development of the analytical method for sulfur isotope in SO_2 gas

*Masaaki Takahashi[1], Hiroyuki Sase[1], Tsuyoshi Ohizumi[1] (1.Asia Center for Air Pollution Research)

[HTT18-P10] Zinc isotope analysis on human tooth enamel samples to reconstruct diet of the Jomon period.

*Soichiro Kusaka[1], Ki-Cheol Shin[2] (1.Tokai Univ., 2.Research Institute for Humanity and Nature)

[HTT18-P11] Zinc stable isotope analysis of environmental reference materials

*Ki-Cheol Shin[1] (1.Research Institute for Humanity and Nature)

Isotopic study on seasonal nitrogen dynamics at Lake Biwa

*Takaaki Ishibashi[1], Ken'ichi Osaka[1], Keisuke Koba[2], Takashi Nakamura[3], Kei Nishida[3]

1. Department of ecosystem study, University of Shiga Prefecture, 2. Center for Ecological Research, Kyoto University, 3. International Research Center for River Basin Environment, University of YAMANASHI

To clarify nitrogen dynamics in Lake Biwa, we measured the concentrations of nitrogen compounds and their nitrogen stable isotopic ratios in 14 depths in north basin of Lake Biwa. In the lake, particulate nitrogen (PN), such as phytoplankton, is generally decomposed to dissolved nitrogen (DN); in order of dissolved organic nitrogen (DON), ammonia nitrogen (NH_4^+) and nitrate nitrogen (NO_3^-). These dissolved nitrogen compounds are taken up by phytoplankton again, and the nitrogen circulation in the lake is established. To predict the water quality in future, it is necessary to understand the nitrogen cycle in the lake, as well as nutrient load to the lake.

In this study, we collected lake water sample at 14 depths in north basin of Lake Biwa (water depth is 90 m) in 1-2 months interval. The lake waster sample was analyzed for the concentration of PN, PC, DN, NO_3^-, NO_2^- and NH_4^+, $d^{15}N$ of PN, DN and NO_3^-.

NO_3^- concentration was lower in the surface layer (0-20m), and higher in the deep layer (20-90m) during the stratification period, whereas NO_3^- concentration was constant in all layers during the circulation period. PN concentration also increased in the surface layer from April to June, decreased sharply in July. These indicate that phytoplankton which grew on the surface layer from April to June used NO_3^-, thereafter, NO_3^- was depleted after June, then, phytoplankton decreased after July respectively. On the other hand, NO_3^- concentration is considered to be increased by decomposition of the precipitated PN from surface layer. It is considered that the NO_3^- concentration became constant in all layers because of mixing of deep layer and the surface layer.

The weighted average $d^{15}N_{DN}$, $d^{15}N_{NO3}$ in the unit water columns decreased about 3‰ in the circulation period, in the circulation period, then, increased during the stratification period. The decrease of $d^{15}N_{DN}$, $d^{15}N_{NO3}$ at the water column during circulation period can not be explained by mixing of deep layer and the surface layer. We will discuss the mechanisms of $d^{15}N_{DN}$, $d^{15}N_{NO3}$ decrease during circulation period in the presentation.

Keywords: nitrogen dynamics, nitrogen isotope, seasonality

©2019. Japan Geoscience Union. All Right Reserved.

Relationship between residence time, water quality, and stable isotopes of spring water and groundwater in coastal area of Fukushima prefecture

*Shiho Yabusaki[1], Kazuyoshi Asai[2]

1. Research Institute for Humanity and Nature・Faculty of Symbiotic Systems Science, Fukushima University, 2. Geo Science Laboratory

After the Great East Japan Earthquake occurred, the investigation near the coast area in northern part of Fukushima prefecture has been carried out to clarify the groundwater flow and residence time in this area. The measuring of EC, pH, water temperature, ORP and sampling of groundwater, spring water and river water have been carried out several times at Shinchi town, Soma city, Minamisoma city, Namie town, Okuma town, Iitate village and Date city since September in 2012. The inorganic ions, stable isotopes of oxygen and hydrogen, trace elements were analyzed for all samples by using the IC (ICS-3000), CRDS (Picarro L2130-i) and ICP-MS (Agilent 7500cx). For estimating the residence time, tritium concentration, CFCs and SF_6 measurements were made in several samples.

The water quality of river water and shallow groundwater indicates mainly Ca-HCO_3 type. In the part of the flooded area by a tsunami, the water quality of shallow groundwater and spring water is Na-Cl type. The Ca-SO_4 type and mixed type were also confirmed in some sites. In the case of deep groundwater, the water quality shows the Na-HCO_3 type and Ca-HCO_3 type. The concentration of Fe, Mn and Al were relatively high in some parts of deep groundwater. It is considered that the origin of these trace elements is soil.

The stable isotopes of oxygen and hydrogen ($\delta^{18}O$ and δD) in river water of Niida river, Mano river and Kamimano river indicate altitude effect. Because the stable isotopes in deep groundwater is relatively low, it is anticipated the recharge are of deep groundwater is about 300 m higher than that of shallow groundwater. It is expected that the recharge area of deep groundwater is around the Abukuma Mountains.

The average residence time of deep groundwater and spring water which indicate the Na-HCO_3 type is about 60 to 70 years. On the other hand, the average residence time of shallow groundwater which indicate the Ca-HCO_3 type is less than 10 years.

The information of groundwater flow is useful for considering the groundwater use with revival of the coastal area. We will continue the investigation of coastal area and make clear the groundwater flow system.

Keywords: Minamisoma city, Fukushima prefecture, CFCs・SF6, residence time, water quality, stable isotopes, groundwater flow

©2019. Japan Geoscience Union. All Right Reserved.

Applicability evaluation of CIA due to river and lake

*yusuke hataya[1], SEIKI KAWAGOE[1], Shiho Yabusaki[2], KEN Suzuki[1]

1. fukushima university, 2. Research Institute for Humanity and Nature

Water resources management must be further attention because extreme weather condition generate to predict climate change. However, a water area have the various regional characteristics. Therefore a universal way may not also be able to indicate the effect management. If categorized basin tool is developing to obtain characteristic, it is possible to choose suitable management technique in water areas. We tried to develop database to manage basin as chemical and geographical information. In this research, Water factors (Chemical condition, land use condition, soil condition and geological condition) between basins (rivers and reservoirs) were compared to develop data base. Especially, we applied to Chemical Index of Alteration (CIA) as chemical condition factor. As results, It was possible to obtain the basin area scale to apply CIA.

Keywords: CIA, water resource, Numerical geographic information

©2019. Japan Geoscience Union. All Right Reserved.

Chemical property analysis of short time scale to determine snowfall source

*Suzuki hiromichi[1], SEIKI KAWAGOE[1], SHO ADACHI[1], Shiho Yabusaki[2]

1. Fukushima University, 2. Research Institute for Humanity and Nature

Occurrence of the strange weather phenomenon is predicted from the current state depending on climate change. To ask this influence, we have to advance the match which raises the future predictability. And, we have to mark a phenomenon of the current state detail. This study targets to obtain chemically snow environment. The aim of this study was to analyse and predict the stable water isotopic composition of the snow cover at specific basin (Agano river). In addition, the dependence of short time step isotopic composition of the entire snow cover was analysed. Snow in 3 catchments was sampled at the end of the accumulation period from December 2016 to April 2018. The observed variability of short time step isotopic composition of the snow cover was analysed chemical verification. Especially, basin The Inawashiro-Lake north side of the northern upstream region indicated the low chemical feature (Suzuki et al 2018). I'm working on the investigation analysis to grasp the chemical special quality of the snow event of the short time scale at present based on this result (2016-2018). It was that a chemical analysis makes the sample which sampled and acquired it by each day the time of a snowfall at Fukushima, Hibara and Yonezawa located in an upstream region in a basin, and we tried to follow up a snowfall origin of the short time scale.

As results, a strong pressure pattern of southern high and northern low could admit January 22nd-the 25th, the result obtained from the result of analysis also reacted to the weather situation sensitively. And influence of a characteristic snowfall origin was admitted at 3 spots. The difference in the spatial time lags was done clearly.

Keywords: d-excess value, isotope, short time scale

©2019. Japan Geoscience Union. All Right Reserved.

Analyzing the origin of surface water in the Saijo Plain, Japan, based on the antimony concentration in the water

*Minoru TOKUMASU[1,2], Ki-Cheol SHIN[3], Yoshihiro YAMADA[4]

1. The United Graduate School of Agricultural Sciences, Ehime University, 2. Saijo City, 3. The Research Institute for Humanity and Nature (RIHN) , 4. Kagawa University, Faculty of Agriculture

1. Introduction

The flow of river water in many medium and small rivers is managed for water use and flood control. However, it is almost impossible to understand how the water taken from the rivers circulates throughout a basin. The source of water in the Saijo Plain in Ehime Prefecture is from the Kamo River surface water flow, shallow groundwater (unconfined ground water), and deep groundwater (confined ground water). Therefore, it is necessary to quantitatively clarify the source of water for sustainable water use. In this study, we tried to quantify the origin of river water in the plain based on the concentration of some chemical elements. In particular, antimony (Sb) was used as the main trace element because of large differences in its concentration between the water sources.

2. Materials and Methods

On November 25 and 26, 2017, during the non-irrigation period and on the 27th and 28th of July, 2018, during the irrigation period, surface water was collected at a total of 43 sites on small and medium rivers and waterways in the Saijo Plain. Multi-element analysis was carried out on the collected water using ICP-MS 7500 cx.

3. Results and Discussion

There was a large difference in the concentration of Sb among the sites. The highest concentration was found in the water from the Ichino River (Stn. 2) at 113 (2017) and 158 μg/L (2018). There was once an antimony mine in the Ichino River basin, so high concentrations of the element in the river water can be regarded as reflecting the influence of the geology. In the main stream of the Kamo River before joining the Ichinose River (Stn. 1), the Sb concentration was as low as 0.2 μg/L, and after the junction of the two rivers (Stn. 3), the concentration increased to 4.3 (2017) and 7.2 μg/L (2018). The concentration was 4.2 (2017) and 7.2 μg/L (2018) at Stn. 4 of the Kamo River, 11.6 (2017) and 11.7 μg/L (2018) in the unconfined ground water (average of Stns. 13, 14, 15), and 0.4 (2017) and 0.5 μg/L (2018) in the confined ground water (average of Stns. 28, 29, 40, 41, 43). The concentration of Si was 2.7 (2017) and 3.2 mg/L (2018) at Stn. 4 of the Kamo River, 3.4 (2017) and 2.9 mg/L (2018) in the unconfined ground water (average of Stns. 13, 14, 15), and 4.1 (2017) and 3.9 mg/L (2018) in the confined ground water (average of Stns. 28, 29, 40, 41, 43).
The ratio of water origin at each survey site was estimated using the above three sources as end members. In the upstream area, the irrigation water taken from the Kamo River occupied most of the surface water. In the middlestream area, the ratio of water taken from the rivers was smaller, and the contribution of

©2019. Japan Geoscience Union. All Right Reserved.

unconfined ground water exceeded 80%. In the downstream area, the confined ground water contribution exceeded 40% at many sites. In the Saijo Plain, the water origins are different in the upstream, middlestream, and downstream areas, where the contribution of irrigation water is small overall, and the contribution of the confined ground water is large.

©2019. Japan Geoscience Union. All Right Reserved.

Basic kinetic study on stable isotope ratios of nitrogen compounds: a case study for groundwater in the Kathmandu Valley, Nepal

*Ken Yokozawa[1,2], Kei Nishida[1,3], Takashi Nakamura[1,3], Ken'ichi Osaka[4]

1. University of Yamanashi, 2. Special Graduate Program on River Basin Environmental Science,, 3. ICRE, 4. Department of ecosystem study Univercity of Shiga prefecture

Groundwater is a valuable source of water in developing countries where water demand is increasing with population increase. At the same time, nitrogen contamination by industrial wastewater, domestic wastewater and agricultural activities has been reported. In underground environments, it is not unusual to identify sources of contamination since the forms and the concentrations of nitrogen compounds vary at different water flow or microbial metabolism. Stable isotopic analysis is one of the effective methods to detail the variations. However, the isotope value is also greatly affected by environmental conditions, and the theoretical enforcement for describing the variation of the isotope value is needed. In this study, we aimed to quantitatively understand and identify the factors of mixing and isotopic fractionation that determine the stable isotope ratio with a case study on groundwater contamination in the Kathmandu Valley, Nepal.

The data used for the analysis was obtained from the groundwater survey of the Kathmandu Valley conducted from September 2014 to August 2018. Based on the stable isotope ratios of nitrogen and oxygen of nitrate, the contamination patterns were roughly categorized. The mixing line and the denitrification line were prepared based on the dynamic fractionation for the stable isotope ratios of nitrate nitrogen, and the spatial distribution of denitrification-related samples was examined on the map. In addition, assuming that the reactants exist sufficiently and homogeneously in the system, an equilibrium fractionation model was formulated by combining nitrification and denitrification for oxygen stable isotope ratios of nitrate and water. The range of the model parameters were determined by using the measured data from the filed survey, the influence of each process on the stable oxygen isotope ratio of nitrate was quantified.

The result showed that the nitrate in shallow groundwater partially originated from the atmospheric source through infiltration of rainwater. A characteristic of denitrification was observed, which was initiated and proceeded over the valley. Additionally, the correspondent isotopic fractionation differed at the location and the season, particularly controlled by ammonia oxidation, nitrite reduction and oxygen exchange between nitrite and water.

Keywords: groundwater , nitrogen and oxygen stable isotope ratios, nitrification, denitrification, mixing, fractionation

©2019. Japan Geoscience Union. All Right Reserved.

Usefulness of strontium isotope composition for determining the geographical origin of wasabi and potato

*Takafumi Kamitani[1], Ki-Cheol Shin[2], Sachiko Nakamura[1], Rika Koda[1], Tomoya Oka[1], Noriaki Fushimi[1], Yasuhide Muranaka[1]

1. Shizuoka Institute of Environment and Hygiene, 2. Research Institute for Humanity and Nature

Originally, the use of strontium isotope ratios ($^{87}Sr/^{86}Sr$) was restricted to geology and petrology, but they have been used as a particularly effective tracer of geographical food origin, as plants reflect the strontium isotope composition of the regionally based rock, soil, and water. This study aims to evaluate the usefulness of $^{87}Sr/^{86}Sr$ for determining the geographical origin of wasabi (Japanese horseradish) and potato, which are specialty crops in Shizuoka Prefecture, Japan.

Wasabi is cultivated in springs and streams located at the top of rivers, where dissolved element and isotopic compositions in water would reflect the geological characteristics without the effects of atmospheric deposition and human activity. We collected wasabi and water samples from 40 locations of major production areas in Japan: Shizuoka, Iwate, Nagano, Tokyo, and Shimane. These samples were subjected to trace elements and $^{87}Sr/^{86}Sr$ analyses. The $^{87}Sr/^{86}Sr$ values differed, based on the geological characteristics of their site locations, and the value of wasabi was well accorded with that of water in the same location. The wasabi samples collected from Izu Peninsula and Mt. Fuji regions in Shizuoka, where young volcanic rocks such as Quaternary basalts are distributed, had low $^{87}Sr/^{86}Sr$ (below 0.7040), whereas those from Nagano and Tokyo, where older rocks such as Mesozoic granites and accretionary complex are distributed, showed higher ratios (over 0.7095). We conclude that $^{87}Sr/^{86}Sr$ value of wasabi allowed us to distinguish the production area clearly.

On the other hand, the $^{87}Sr/^{86}Sr$ values of crops cultivated in the field are considered to be partly affected by precipitation and fertilizer. Therefore we conducted field survey and planter test for potato in Shizuoka. Field survey was conducted at Mishima, in eastern part of Shizuoka prefecture, and at Mikatahara, in western part of it, and $^{87}Sr/^{86}Sr$ of potato and soil exchangeable fraction were compared. As a result, there was a correlation between potato and soil in $^{87}Sr/^{86}Sr$, although the effects of precipitation and fertilizer were observed. The planter test suggests that the influence of fertilizer on $^{87}Sr/^{86}Sr$ varies depending on the amount of exchangeable Sr contained in the original soil.

Keywords: geographical origin, strontium isotope ratio, wasabi, potato, Shizuoka

©2019. Japan Geoscience Union. All Right Reserved.

Reconstruction of sea surface temperature and salinity for the Medieval Climatic Anomaly using a long-lived fossil coral collected at Ishigaki Island, southwestern Japan

*Osamu Abe[1], Maki Morimoto[2], Ryuji Asami[3], Takeshi Nakatsuka[1,4]

1. Graduate School of Environmental Studies, Nagoya University, 2. School of Education, Gifu University, 3. Graduate School of Science, Tohoku University, 4. Research Institute for Humanity and Nature

The period between 950 and 1250CE is called as the Medieval Climate Anomaly (MCA; Masson-Delmotte et al., 2013), at the time when the warmer climate seemed dominant globally (Bradley et al., 2003). Recent investigations based on the proxy record such as tree-ring widths, speleothems, ice cores, and historical documents indicated that a significant climate change occurred during the latter half of the 10th century. Mann et al. (2009) found that an increase of the average air temperature in the northern hemisphere at the late 10c. coincided with an increase of sea surface temperature at northern subpolar oceans. Yan et al. (2011) indicated that atmospheric environments in the equatorial Pacific shifted from the La Nina like condition to the El Nino like condition around 1000CE. In East Asia, Zhang et al. (2008) and Ge et al. (2013) described that the activity of East Asian Summer Monsoon (EASM) had been enhanced during the late 10c., then the climate in China shifted to warmer and wetter. Whereas Lie et al. (2014) showed that the EASM had been weakened during the 11th century. In addition, the climate in southern China was reported as relatively dry (Chen et al., 2015).

These studies demonstrated that a large climatic shift occurred around 1000CE, however, most of them have relied on records collected on land. There is little long-term high-resolution marine record during the MCA.

We reconstructed sea surface temperature (SST) and salinity with a temporal resolution of one month for 300 years using a long-lived fossil coral collected at Ishigaki Island, southwestern Japan. Based on the U/Th dating in the youngest part of the coral skeletons as well as the band counting, this coral sample had lived between 845 and 1130CE, largely covered the MCA period. Skeletal Sr/Ca and oxygen isotopic composition were analyzed for about 4,000 samples.

The empirical equations between Sr/Ca and water temperature; between oxygen isotopic composition of coral skeleton and seawater, and water temperature, were established using the present coral records, observed water temperature and oxygen isotopic composition of seawater. With these equations and the relationship between seawater salinity and oxygen isotopic composition, proposed by Abe et al. (2009), SST and seawater salinity from 845 to 1130CE were reconstructed from the fossil coral Sr/Ca and oxygen isotopic composition.

Through the entire period, average summer and winter SSTs were 2 and 1 deg. C higher than the present, respectively. In addition, SST increased significantly after 1040CE; 0.9 for the annual average, 0.7 for summer and 1.1 for winter. Salinity also increased after 990CE; 0.8 all for the annual average, summer and winter. Salinity was significantly higher through the entire period than the present, however, its absolute value seems unconfirmed yet.

©2019. Japan Geoscience Union. All Right Reserved.

Increasing SST and salinity found in this study during ca. 1000 and 1130CE were consistent with the weakening of EASM during the 11th and 12th centuries shown by Liu et al. (2014). They argued the weakening occurred as a consequence of weakening of the solar activity and the decrease of SST at the western Pacific warm pool. In this study region, the decrease of precipitation during the Baiu period induced the increase of salinity as well as local SST increase due to the decrease of the cloud cover. Our results were also consistent with the warming of China in the late 10c. (Ge et al., 2013), and a drier condition in southern China (Chen et al., 2015).

The periodicity of SST and salinity based on the spectral analysis will be discussed in the presentation.

Keywords: Coral annual bands, Medieval Climate Anomaly

©2019. Japan Geoscience Union. All Right Reserved.

Development of the analytical method for sulfur isotope in SO_2 gas

*Masaaki Takahashi[1], Hiroyuki Sase[1], Tsuyoshi Ohizumi[1]

1. Asia Center for Air Pollution Research

1. Introduction

Sulfur is a major source of acid deposition. Usually sulfur is emitted as SO_2 and it is oxidized to SO_4^{2-} in atmosphere. S isotopic analysis of water and particulate samples were conducted in many studies. But gaseous SO_2 was rarely used for isotopic study. Isotopic ratio of SO_2 is strongly influenced by emission source near the sampling point. Because most of SO_2 emitted far from sampling point is oxidized to SO_4^{2-} during transportation. It is possible to distinguish domestic emission from transboundary emission. Moreover, dry deposition processes of SO_2 and particulate SO_4^{2-} and their interactions with tree canopy could be discussed more precisely. Isotopic analysis of SO_2 is considered as a powerful method to investigate the behavior of S in the atmosphere and ecosystems. We studied about the analytical method for S isotope in SO_2.

2. Method

(1) Equipment

SO_2 concentration in Japan is very low (e.g. annual 0.02ppb at Sado). We need to collect air sample at least $1m^3$ that is the amount we can obtain 1.2mg of $BaSO_4$ precipitation enough for isotopic analysis. High volume air sampler is generally used to collect around $1m^3$ of air sample. It uses filter, so we examined filter collection of SO_2 by K_2CO_3 filter generally used to collect SO_2 in filter-pack method.

(2) Filters

We used quarts filter for particulate SO_4^{2-} and K_2CO_3 filter for gaseous SO_2 next to it. K_2CO_3 filter is made on the basis of EANET manual. But to get enough flow rate for high volume air sampler, the size of K_2CO_3 filter is larger (20×26 cm, same size with quarts filter) than the manual and already dried before sampling.

(3) Flow rate/leak test

Under flow rate 100~400 L/min in this system, we confirmed weather sampling can be carried out stably. And we checked leak using two K_2CO_3 filters.

(4) Sample treatment

©2019. Japan Geoscience Union. All Right Reserved.

On the basis of EANET manual, the sample was extracted with 0.05% H_2O_2aq and filtered. Then 2N HCl was added and concentrated to remove CO_3^{2-}. Next 1%(w/w)$BaCl_2$ was added. We filtered forming $BaSO_4$ precipitation. We examined the method to get $BaSO_4$ precipitation and to remove the components from K_2CO_3 filter.

3. Results

(1) Sampling and sample treatment

Sampling could be conducted under flow rate 100~400 L/min. Sampling efficiency was about 80%..

Several conditions to get $BaSO_4$ precipitation ware examined, it could be gotten by the method as below.

Filter was cut and ultrasonic extracted with 0.05% H_2O_2aq 30 minutes and filtered. 2.5 ml of 2N HCl was added and concentrated to around 10 ml. Then 1 ml of heated 1 %(w/w) $BaCl_2$ was added under pH 4~6. Next evaporated all solvent and added 10 ml of water. $BaSO_4$ precipitation was observed. After put for one night, the precipitation was separated by centrifuge 3,600 rpm for 10 minutes and we removed the solvent. The precipitation was washed twice by 10 ml of water and filtered. At last the filter was ashed for four hours in muffle furnace in 800 ℃ .

(2) Actual analysis

We used two K_2CO_3 filters and collected 2160.2 m^3 of air sample under flow rate 300 L/min. 3.80 mg of particular SO_4^{2-} and 0.89 mg (first) and 0.14 mg (second) of SO_4^{2-} from SO_2 were obtained. $\delta^{34}S$ of particular SO_4^{2-} was 8.64 ‰and that of SO_2 from the first filter was -1.54 ‰. The amount of precipitation from second filter was not enough for isotopic analysis. This difference was caused by effect of sea salt mainly. But nss- $\delta^{34}S$ of particular SO_4^{2-} was 4.78 ‰. It was still higher than SO_2. It suggested that nss- SO_4^{2-} contains both transboundary SO_4^{2-} and domestic SO_4^{2-}. According to the relevant literature, domestic SO_2 may have negative isotopic values because of imported oil from Middle East. Considering that this sampling was carried out in January, possible effect of transboundary SO_2 with higher isotopic values should also be taken into account for source identification of the collected SO_2.
We would like to discuss at the conference with the latest data.

Keywords: sulfur isotope, SO2 gas

©2019. Japan Geoscience Union. All Right Reserved.

Zinc isotope analysis on human tooth enamel samples to reconstruct diet of the Jomon period.

*Soichiro Kusaka[1], Ki-Cheol Shin[2]

1. Tokai Univ., 2. Research Institute for Humanity and Nature

This study investigates zinc isotope ratios in tooth enamels of human skeletal remains of the Jomon period in Japan. Carbon and nitrogen isotope analysis on bone collagen were traditionary used to reconstruct diet and trophic levels on prehistoric people. The progress of isotope measurements using MC-ICP-MS enables us to analyze isotope ratios of zinc and other metals. Some researches report that the zinc isotope ratios of animals reflect dietary sources and vary according to trophic levels. This study newly develops zinc isotope analysis on human tooth enamels. The zinc isotope analysis has great potential to reconstruct dietary information from inorganic materials of archaeological bones or fossils.

The material used in this study is SRM1400 (bone ash), six samples of human tooth enamels from the Yoshigo and Inariyama shell mounds of Aichi prefecture, and faunal remains (six deer enamels, three boar enamels, six marine fish bones, and six modern plant leaves). Zinc was purified from these samples using anion exchange resin. Zinc isotope ratios were measured by MC-ICP-MS with the zinc standard solution of AA-ETH. The mass bias was corrected with Cu standard solution added to all standards and samples. The zinc isotope ratios of SRM1400 showed similar value with the value previously reported. The difference of zinc isotope ratios between washed and unwashed samples with acetic acids were very small, suggesting no significant diagenetic alteration. The deer and marine fish samples showed the value expected from their dietary ecology. The zinc isotope ratios of Jomon skeletal remains was higher than those of plants, but lower than deer and marine fish. This result indicates that sources of zinc for humans were terrestrial and marine meat as well as terrestrial plants.

Keywords: Zinc Isotope, Jomon period, Human skeletal remains

©2019. Japan Geoscience Union. All Right Reserved.

Zinc stable isotope analysis of environmental reference materials

*Ki-Cheol Shin[1]

1. Research Institute for Humanity and Nature

Zinc has atomic number 30 and atomic mass 65.39. It is a trace element of terrestrial rocks and widely distributed throughout the lithosphere and biosphere. It is chalcophile features and has rich coordination chemistry, participates in a large number of important biological compounds and reactions. The zinc plays an important role as an essential trace metal in all living systems from bacteria to humans. Zn has five stable isotopes ^{64}Zn, ^{66}Zn, ^{67}Zn, ^{68}Zn, and ^{70}Zn. Their isotopic fractionation could provide valuable information about environmental processes, especially in biological processes.

With the advent of multi-collector ICP-MS, it is possible to measure the precise value of ^{66}Zn/^{64}Zn in Zn solution. To promote the environmental stable isotope traceability, RIHN is desired to determine the isotope ratios of zinc for environmental reference materials with high precision and accuracy, rapidness, and convenience.

Here, I report a simple and efficient method for zinc isotope analysis. The various environmental samples over 20 types were used for the study. All samples have purified with an anion exchange resin to separated Zn and Fe at a time. Zinc isotope ratios were measured by MC-ICP-MS (NEPTUNE plus) with AA-ETH, which is a new zinc isotopic standard solution reported by Archer et al. (2017). The mass bias correction conducted with Cu standard solution (NIST SRM 976).

Keywords: stable isotope , Zinc, environmental reference materials

©2019. Japan Geoscience Union. All Right Reserved.

[E] Poster | H (Human Geosciences)：H-CG Complex & General

Tue. May 28, 2019 1:45 PM - 3:15 PM JST | Tue. May 28, 2019 4:45 AM - 6:15 AM UTC | Poster Hall International Exhibition Hall8, Makuhari Messe_6

[H-CG28] Implementing Integrated Research for Sustainable Future

convener:Yukio Himiyama(Emeritus Professor, Hokkaido University of Education), Akihiko Kondoh(Center for Environmental Remote Sensing, Chiba University), Takeshi Sakurai(Graduate School of Agricultural and Life Sciences, The University of Tokyo), Kenichi Abe(Research Institute for Humanity and Nature)

The world global environmental studies are being re-organized in the framework of Future Earth, which is considered to be an important driver to achieve the Sustainable Development Goals (SDGs) set by UN in 2015. Geoscience, which has traditionally been concerned about the dynamic nature and phenomena of the Earth, including lithosphere, hydrosphere, atmosphere and biosphere, is now increasingly committed to human sphere and human dimensions of global change, assuming unique roles in Future Earth and the SDGs. The session is intended to discuss the crucial issues related with them, particularly in reference to such SDGs as good health and well-being, quality education, clean water and sanitation, sustainable cities and communities, climate action, life below water and life on land. Those interested in Future Earth, SDGs, and ESD (Education for Sustainable Development) particularly those who have already started or are about to start related projects, or are interested in Future Earth Knowledge-Action Networks (KANs), such as Ocean, Food-Water-Energy Nexus, Health, Disasters, Cities, Natural Assets, will find this Session an ideal place to present his/her research results, to exchange information and ideas, and to seek new collaborative relations with other research groups and even with partners in the society.

[HCG28-P01] Ground Motion Instrumentation Network and Earthquake Early Warning System for Uttarakhand

*Pankaj Kumar[1,2], Ashok - Kumar[1,2], Ajay - Gairola[1,2] (1.Indian Institute of Technology Roorkee, India, 2.Earthquake Early Warning Laboratory, Centre of Excellence in Disaster Mitigation & Management, IIT Roorkee)

[HCG28-P02] Linking Socioeconomic and Geographical Model to Analyze Land Use Changes in the Jakarta - Bandung Mega Urban Regions

*Didit Okta Pribadi[1,2] (1.Center for Regional Systems Analysis, Planning and Development (CrestPent) - IPB University, 2.Research Center for Plant Conservation and Botanic Gardens - Indonesian Institute of Sciences)

[HCG28-P03] Development of an Integrated Model for Evaluation of Pasture Carrying Capacity and its Vulnerability based on Water Resources in Arid and Semi-arid Regions-----A Case Study in Mongolia

★Invited Papers

*Qinxue Wang[1], Tomohiro Okadera[1], Tadanobu Nakayama[1], Deni Eer[1], Ochirbat Batkhishig[2], Dorjgotov Battogtokh[2], Uudus Bayasaikhan[3] (1.National Institute for Environmental Studies, 2.Institute of Geography and Geoecology, Mongolian Academy of Sciences, 3.School of Arts and Sciences, National University of Mongolia)

[HCG28-P04] Influence of land use histories on vegetation and ecosystem services of restored wetlands in Tumen River basin, China

*CAO GUANGLAN[1], Kazuaki Tsuchiya[1], Weihong Zhu[2], OKURO TOSHIYA[1] (1.The University of Tokyo, 2.Yanbian University)

[HCG28-P05] The spatial flow of freshwater ecosystem services: A case study of Tumen River watershed

*JIAN ZHANG[1], Shizuka hashimoto[1], Kazuaki Tsuchiya[1], Weihong Zhu[2], OKURO TOSHIYA[1] (1.The University of Tokyo, 2.Yanbian University)

Ground Motion Instrumentation Network and Earthquake Early Warning System for Uttarakhand

*Pankaj Kumar[1,2], Ashok - Kumar[1,2], Ajay - Gairola[1,2]

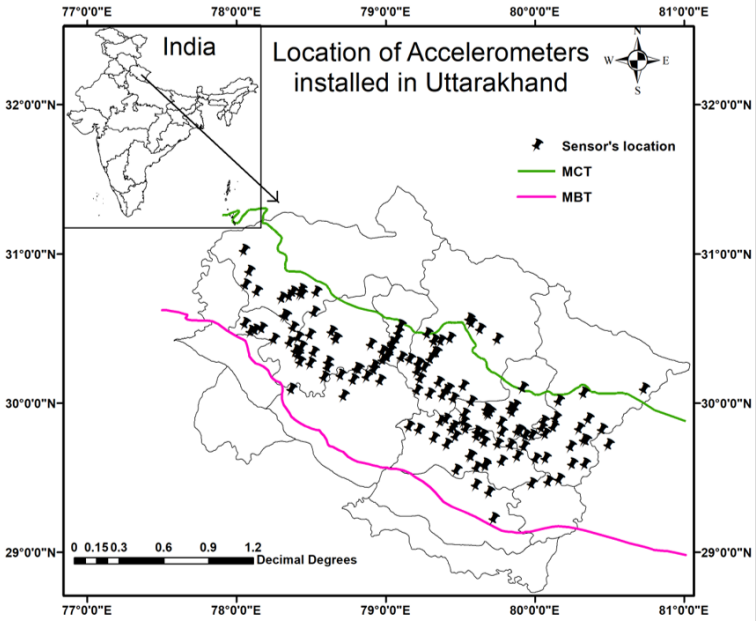
1. Indian Institute of Technology Roorkee, India, 2. Earthquake Early Warning Laboratory, Centre of Excellence in Disaster Mitigation & Management, IIT Roorkee

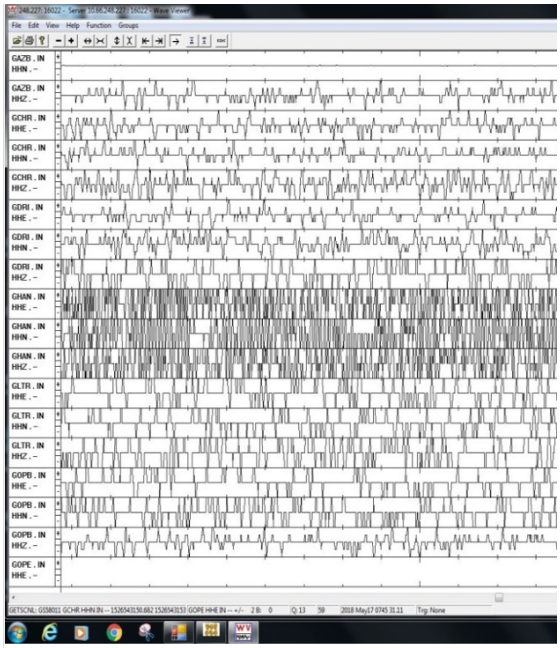
An Earthquake Early Warning System (EEWS) has been developed by Indian institute of Technology Roorkee (IIT Roorkee) for Uttarakhand, a Himalayan province of India. The region behind to set up first EEWS in India for Uttarakhand is that the main central thrust (MCT) and main boundary thrust (MBT) passes through it and central seismic gap exists in its region and seismologist envisaged a big earthquake will hit this region in near future. Under this project, 155 accelerometers have been installed in 53,483 km^2 area in the Himalayan part of Uttarakhand. These accelerometers are installed on the ground floor of government owned offices of Bharat Sanchar Nigam Limited (BSNL) mobile towers and State Wide Area Network (SWAN) available in the province. The average station to station distance is kept between 10 to 20 km which ensure the triggering of more than 6 accelerometers if an earthquake of magnitude greater than 6 triggers in the region. The data is streamed at the central server located in Earthquake Early Warning Laboratory at Centre of Excellence in Disaster Mitigation & Management in IIT Roorkee through private network of BSNL and SWAN on 24 ×7 basis. The location of installed accelerometers and their streaming at the Earthquake Early Warning Laboratory is shown in figure 1. Whole system is automatic and the early warning parameter is peak displacement (Pd). When an earthquake of magnitude greater than 6 will strike in the instrumented region an earthquake warning will be issued to public through the sirens. The early warning sirens are installed in the public offices, government buildings, schools, colleges of the two major cities, Dehradun and Haldwani, and all 13 district emergency operation center of the province. After hearing, earthquake alarm, people can take necessary precautionary measures. This paper presents the details of instrumentation and working of the EEWS.

Fig 1. Installed accelerometers are shown in Uttarakhand’ s map. MCT and MBT passes through the Himalayan province. Streaming of the data from accelerometer to central server at EEW laboratory is shown in the snapshot.

Keywords: Instrumentation, Accelerometers, Seismic gap, EEWS, Sirens

©2019. Japan Geoscience Union. All Right Reserved.





©2019. Japan Geoscience Union. All Right Reserved.

Linking Socioeconomic and Geographical Model to Analyze Land Use Changes in the Jakarta - Bandung Mega Urban Regions

*Didit Okta Pribadi[1,2]

1. Center for Regional Systems Analysis, Planning and Development (CrestPent) - IPB University, 2. Research Center for Plant Conservation and Botanic Gardens - Indonesian Institute of Sciences

Continuing rapid urbanization has led to escalating socio-economic and physical interaction between two adjacent megacities in Indonesia namely Jakarta and Bandung megacity. Physically, enhancing the connection over time has formed urban corridors that stimulate rapid land use changes as well as the expansion of urban-rural land use mixture in the vast area between the two big cities. As land use composition is essential to achieve urban sustainability, modelling land use changes is required as a tool for decision makers to assess the sustainability of different urban form. Nowadays, land use changes model has been rapidly developed owing to increasing computation capacity which is capable of incorporating previous trend of land use changes (e.g. Markov Chain), spatial correlation (e.g. Cellular Automata), and related driving factors (e.g. Logistic Regression or Neural Network) within the model. However, this model is too focused on geographical aspect, while lacking to consider socio-economic factors which spatially might have distinctive properties such as spatial heterogeneity, spatial network, and spatial multiplier effect. This paper aims to combine socioeconomic and geographical factors to analyze complex and dynamic land use systems as found in Jakarta-Bandung Megacity corridors. Land Change Modeler (LCM) from Idrisi Tersset software as a combination of Neural Network and CA-Markov model would be enhanced by incorporating socioeconomic aspects analyzed by GWR (Geographical Weighted Regression) for detecting spatial heterogeneity, gravity model for analyzing spatial network, and spatial autocorrelation model (SAM) for defining spatial multiplier effect. This model would be compared to the results of LCM as a single approach. A new model is suggested as an enhanced approach to understand multiple factors that influence land use changes in Jakarta-Bandung megacity corridors, thus more comprehensive policies can be formulated.

Keywords: Urbanization, Socioeconomic model, Geographical Model, Land Use Changes, Jakarta-Bandung Mega Urban Regions

©2019. Japan Geoscience Union. All Right Reserved.

Development of an Integrated Model for Evaluation of Pasture Carrying Capacity and its Vulnerability based on Water Resources in Arid and Semi-arid Regions------A Case Study in Mongolia

*Qinxue Wang[1], Tomohiro Okadera[1], Tadanobu Nakayama[1], Deni Eer[1], Ochirbat Batkhishig[2], Dorjgotov Battogtokh[2], Uudus Bayasaikhan[3]

1. National Institute for Environmental Studies, 2. Institute of Geography and Geoecology, Mongolian Academy of Sciences, 3. School of Arts and Sciences, National University of Mongolia

Arid and semi-arid regions cover 41% of the global land area and near 2 billion people (34.7%) live there, where fragile environment is getting more vulnerable due to climate change and human activities. Pasture carrying capacity and its vulnerability can be recognized as the integrated indicators for SDGs in arid and semi-arid regions. Our previous study revealed that climate change in past few decades caused the obvious degradation of permafrost, the water deficit of land-surface, and then the decrease of pasture productivity and carrying capacity. However, beside climate change, land use/cover changes caused by human activities such as urbanization, cultivation and mining industry may also have a large influence on pasture carrying capacity. In such regions, it is essential for us to develop some indicators to be used for sustainable management of pasture ecosystems.

In this study, we have developed an integrated model based on water resources to evaluate the pasture Carrying Capacity (CC), Grazing Pressure (GP) and Vulnerability Index (VI) under the influences of both climate change and land use/cover changes, such as urbanization, cultivation and mining & so on (Figure 1). The input data include the pasture net primary production, land use, gradient of slope and grazing density, etc. In order to evaluate the impact of land use/cover changes, we applied the model to four target areas: urban area (Ulaanbaatar City) and steppe area (Altanbulag Soum) in semi-arid regions of northern Mongolia and mining area (Khanbogd Soum) and desert (Manlai Soum) in arid regions of southern Mongolia, and the estimated result was shown in Figure 2, which indicates:

Carrying Capacity (CC): steppe area > urban area > desert area > mining area
Grazing Pressure (GP): urban area > steppe area > mining area > desert area
Vulnerability Index (VI): urban area > mining area > desert area > steppe area

We also applied the model to the Soum level in Mongolia and found that the areas with high vulnerability expanded rapidly, especially in central Mongolia in last decades. We are now trying to use the model to do sensitivity analysis to parameters, such as water accessibility, harvest index and so on, to be able to evaluate the efficiency of adaptation strategies, such as well construction for enhancing groundwater usage, forage plantation for enhancing harvest index and so on.

Keywords: Pasture Carrying Capacity, Environmental Vulnerability, Arid and Semi-arid Regions, Water Resources

©2019. Japan Geoscience Union. All Right Reserved.

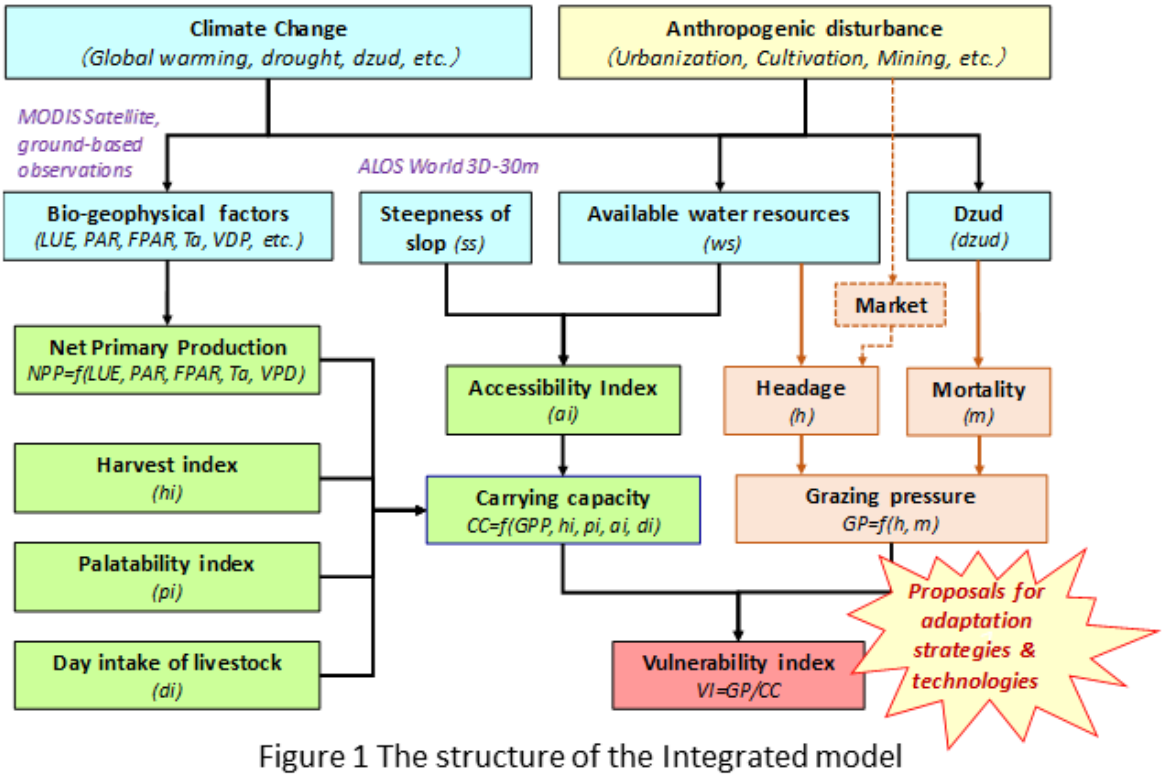


Figure 1 The structure of the Integrated model

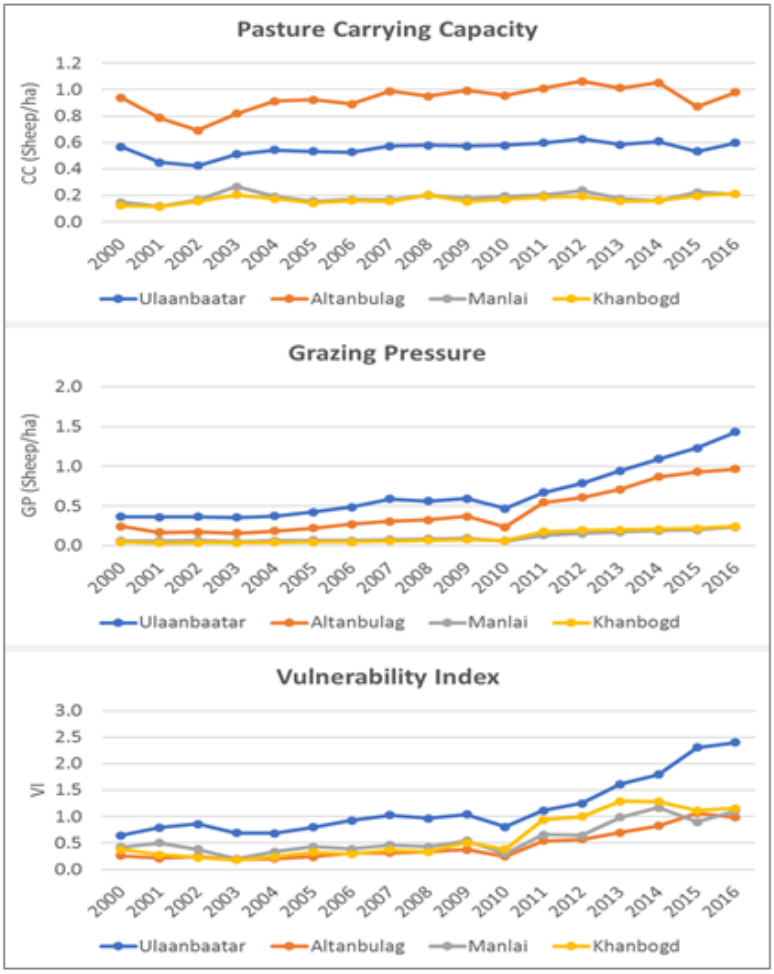


Figure 2 Evaluated pasture CC and VI in four target areas

©2019. Japan Geoscience Union. All Right Reserved.

Influence of land use histories on vegetation and ecosystem services of restored wetlands in Tumen River basin, China

*CAO GUANGLAN[1], Kazuaki Tsuchiya[1], Weihong Zhu[2], OKURO TOSHIYA[1]

1. The University of Tokyo, 2. Yanbian University

Wetlands are among the world’ s most productive and valuable ecosystems. They are important habitats for a variety of flora and fauna, and are vital ecosystems that provide diverse services. They not only are essential for ecological functions such as maintaining biodiversity, controlling floods, and removing pollutants, but also serve necessary economic functions in rice and fish production, transport, and hydropower energy. Despite this, they have suffered a loss of 54%–57% of their area worldwide, which continues under pressures from agriculture, urban expansion, industrialization, and resource extraction. Conservation and restoration of wetland ecosystems is important issues for conservation biodiversity and sustainable use of ecosystem services. In this study, we focus on the lower of Tumen River, Northeast China where the wetlands decreased dramatically because of reclamation. Our objective was to determine the influence of land use and management histories on vegetation structure and ecosystem services and future analyse their associations with environmental factors. The results of this study are of great significance to the impact of management measures on wetland ecosystems, as well as the analysis and evaluation of vegetation restoration.

Keywords: land use histories, vegetation dynamics, wetland restoration, ecosystem services

©2019. Japan Geoscience Union. All Right Reserved.

The spatial flow of freshwater ecosystem services: A case study of Tumen River watershed

*JIAN ZHANG[1], Shizuka hashimoto[1], Kazuaki Tsuchiya[1], Weihong Zhu[2], OKURO TOSHIYA[1]

1. The University of Tokyo, 2. Yanbian University

Freshwater is widely regarded as the most essential natural resource underpinning the well-being of human society, and while scientists translate it into ecosystem services' valuable processes, the supply of clean freshwater has the highest value among various provisioning services. However, due to the land-use intensification and projected warming climate, an increasing likelihood of persistent drought condition, and inadequate conservation, freshwater scarcity issues continue to gain urgency in science and policies. The fusion of the concept of ecosystem services with natural resources management nowadays represents a new conservation paradigm, but still faces notable limitations. Some scientists, noticing the occurrence of spatial mismatch between the supply and demand of ecosystem services, put forward the concept of ecosystem services flow to deal with the problem. Ecosystem services flow research brings out a spatio-temporal connection between the supply and demand, and an deepened understanding about when ,where, and how those benefits were enjoyed. Many papers also suggested that studies at landscape scale may offer a better understanding of ecosystem processes, ecosystem functions, ecosystem services and link them from one to another, as landscape patterns have long been discussed as tools for explaining numerous ecological consequences. In 2017, the annual meeting of IALE in USA as well emphasized the pressing need of integrating landscape patterns to ecosystem services. Thus the study attempt to conduct an analysis of freshwater ecosystem services flow in an intact watershed with the combination of landscape ecology theories. The conceptual framework and progress of this study will be introduced.

Keywords: freshwater ecosystem services, services flow, andscape pattern, watershed

©2019. Japan Geoscience Union. All Right Reserved.

[E] Poster | H (Human Geosciences)：H-CG Complex & General

Tue. May 28, 2019 5:15 PM - 6:30 PM JST | Tue. May 28, 2019 8:15 AM - 9:30 AM UTC | Poster Hall International Exhibition Hall8, Makuhari Messe_25

[H-CG28] Implementing Integrated Research for Sustainable Future

convener:Yukio Himiyama(Emeritus Professor, Hokkaido University of Education), Akihiko Kondoh(Center for Environmental Remote Sensing, Chiba University), Takeshi Sakurai(Graduate School of Agricultural and Life Sciences, The University of Tokyo), Kenichi Abe(Research Institute for Humanity and Nature)

The world global environmental studies are being re-organized in the framework of Future Earth, which is considered to be an important driver to achieve the Sustainable Development Goals (SDGs) set by UN in 2015. Geoscience, which has traditionally been concerned about the dynamic nature and phenomena of the Earth, including lithosphere, hydrosphere, atmosphere and biosphere, is now increasingly committed to human sphere and human dimensions of global change, assuming unique roles in Future Earth and the SDGs. The session is intended to discuss the crucial issues related with them, particularly in reference to such SDGs as good health and well-being, quality education, clean water and sanitation, sustainable cities and communities, climate action, life below water and life on land. Those interested in Future Earth, SDGs, and ESD (Education for Sustainable Development) particularly those who have already started or are about to start related projects, or are interested in Future Earth Knowledge-Action Networks (KANs), such as Ocean, Food-Water-Energy Nexus, Health, Disasters, Cities, Natural Assets, will find this Session an ideal place to present his/her research results, to exchange information and ideas, and to seek new collaborative relations with other research groups and even with partners in the society.

[HCG28-P01] Ground Motion Instrumentation Network and Earthquake Early Warning System for Uttarakhand

*Pankaj Kumar[1,2], Ashok - Kumar[1,2], Ajay - Gairola[1,2] (1.Indian Institute of Technology Roorkee, India, 2.Earthquake Early Warning Laboratory, Centre of Excellence in Disaster Mitigation & Management, IIT Roorkee)

[HCG28-P02] Linking Socioeconomic and Geographical Model to Analyze Land Use Changes in the Jakarta - Bandung Mega Urban Regions

*Didit Okta Pribadi[1,2] (1.Center for Regional Systems Analysis, Planning and Development (CrestPent) - IPB University, 2.Research Center for Plant Conservation and Botanic Gardens - Indonesian Institute of Sciences)

[HCG28-P03] Development of an Integrated Model for Evaluation of Pasture Carrying Capacity and its Vulnerability based on Water Resources in Arid and Semi-arid Regions-----A Case Study in Mongolia

★Invited Papers

*Qinxue Wang[1], Tomohiro Okadera[1], Tadanobu Nakayama[1], Deni Eer[1], Ochirbat Batkhishig[2], Dorjgotov Battogtokh[2], Uudus Bayasaikhan[3] (1.National Institute for Environmental Studies, 2.Institute of Geography and Geoecology, Mongolian Academy of Sciences, 3.School of Arts and Sciences, National University of Mongolia)

[HCG28-P04] Influence of land use histories on vegetation and ecosystem services of restored wetlands in Tumen River basin, China

*CAO GUANGLAN[1], Kazuaki Tsuchiya[1], Weihong Zhu[2], OKURO TOSHIYA[1] (1.The University of Tokyo, 2.Yanbian University)

[HCG28-P05] The spatial flow of freshwater ecosystem services: A case study of Tumen River watershed

*JIAN ZHANG[1], Shizuka hashimoto[1], Kazuaki Tsuchiya[1], Weihong Zhu[2], OKURO TOSHIYA[1] (1.The University of Tokyo, 2.Yanbian University)

Ground Motion Instrumentation Network and Earthquake Early Warning System for Uttarakhand

*Pankaj Kumar[1,2], Ashok - Kumar[1,2], Ajay - Gairola[1,2]

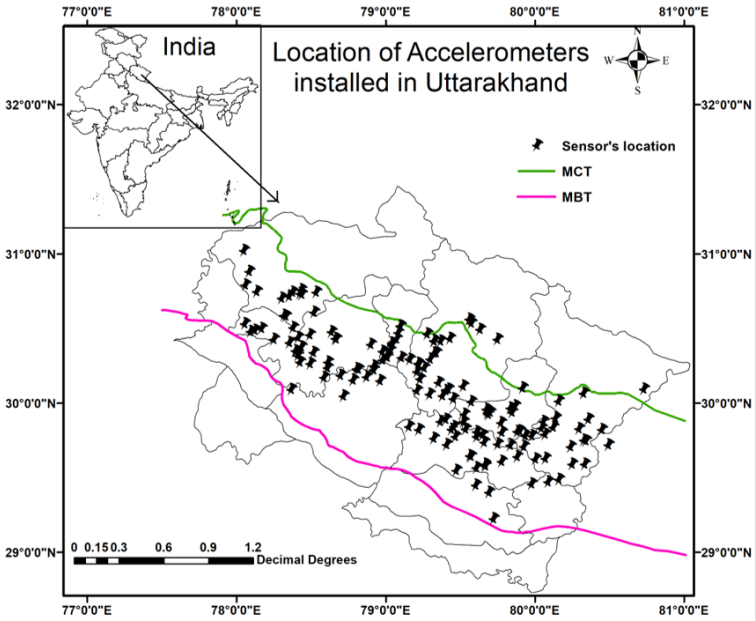
1. Indian Institute of Technology Roorkee, India, 2. Earthquake Early Warning Laboratory, Centre of Excellence in Disaster Mitigation & Management, IIT Roorkee

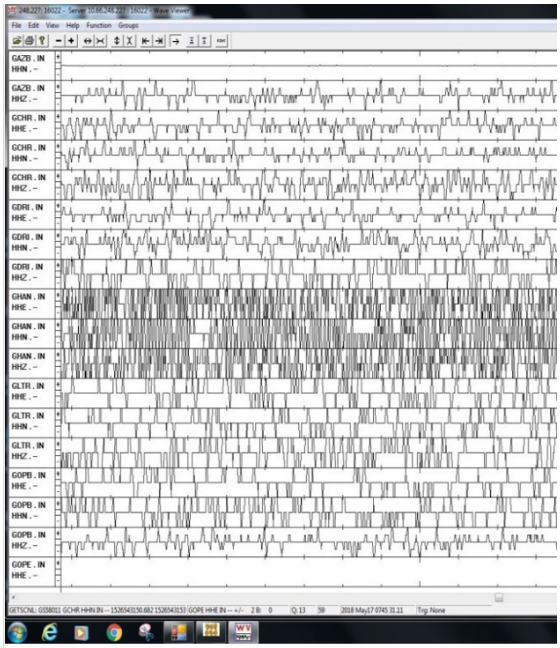
An Earthquake Early Warning System (EEWS) has been developed by Indian institute of Technology Roorkee (IIT Roorkee) for Uttarakhand, a Himalayan province of India. The region behind to set up first EEWS in India for Uttarakhand is that the main central thrust (MCT) and main boundary thrust (MBT) passes through it and central seismic gap exists in its region and seismologist envisaged a big earthquake will hit this region in near future. Under this project, 155 accelerometers have been installed in 53,483 km^2 area in the Himalayan part of Uttarakhand. These accelerometers are installed on the ground floor of government owned offices of Bharat Sanchar Nigam Limited (BSNL) mobile towers and State Wide Area Network (SWAN) available in the province. The average station to station distance is kept between 10 to 20 km which ensure the triggering of more than 6 accelerometers if an earthquake of magnitude greater than 6 triggers in the region. The data is streamed at the central server located in Earthquake Early Warning Laboratory at Centre of Excellence in Disaster Mitigation & Management in IIT Roorkee through private network of BSNL and SWAN on 24 ×7 basis. The location of installed accelerometers and their streaming at the Earthquake Early Warning Laboratory is shown in figure 1. Whole system is automatic and the early warning parameter is peak displacement (Pd). When an earthquake of magnitude greater than 6 will strike in the instrumented region an earthquake warning will be issued to public through the sirens. The early warning sirens are installed in the public offices, government buildings, schools, colleges of the two major cities, Dehradun and Haldwani, and all 13 district emergency operation center of the province. After hearing, earthquake alarm, people can take necessary precautionary measures. This paper presents the details of instrumentation and working of the EEWS.

Fig 1. Installed accelerometers are shown in Uttarakhand’ s map. MCT and MBT passes through the Himalayan province. Streaming of the data from accelerometer to central server at EEW laboratory is shown in the snapshot.

Keywords: Instrumentation, Accelerometers, Seismic gap, EEWS, Sirens

©2019. Japan Geoscience Union. All Right Reserved.





©2019. Japan Geoscience Union. All Right Reserved.

Linking Socioeconomic and Geographical Model to Analyze Land Use Changes in the Jakarta - Bandung Mega Urban Regions

*Didit Okta Pribadi[1,2]

1. Center for Regional Systems Analysis, Planning and Development (CrestPent) - IPB University, 2. Research Center for Plant Conservation and Botanic Gardens - Indonesian Institute of Sciences

Continuing rapid urbanization has led to escalating socio-economic and physical interaction between two adjacent megacities in Indonesia namely Jakarta and Bandung megacity. Physically, enhancing the connection over time has formed urban corridors that stimulate rapid land use changes as well as the expansion of urban-rural land use mixture in the vast area between the two big cities. As land use composition is essential to achieve urban sustainability, modelling land use changes is required as a tool for decision makers to assess the sustainability of different urban form. Nowadays, land use changes model has been rapidly developed owing to increasing computation capacity which is capable of incorporating previous trend of land use changes (e.g. Markov Chain), spatial correlation (e.g. Cellular Automata), and related driving factors (e.g. Logistic Regression or Neural Network) within the model. However, this model is too focused on geographical aspect, while lacking to consider socio-economic factors which spatially might have distinctive properties such as spatial heterogeneity, spatial network, and spatial multiplier effect. This paper aims to combine socioeconomic and geographical factors to analyze complex and dynamic land use systems as found in Jakarta-Bandung Megacity corridors. Land Change Modeler (LCM) from Idrisi Tersset software as a combination of Neural Network and CA-Markov model would be enhanced by incorporating socioeconomic aspects analyzed by GWR (Geographical Weighted Regression) for detecting spatial heterogeneity, gravity model for analyzing spatial network, and spatial autocorrelation model (SAM) for defining spatial multiplier effect. This model would be compared to the results of LCM as a single approach. A new model is suggested as an enhanced approach to understand multiple factors that influence land use changes in Jakarta-Bandung megacity corridors, thus more comprehensive policies can be formulated.

Keywords: Urbanization, Socioeconomic model, Geographical Model, Land Use Changes, Jakarta-Bandung Mega Urban Regions

©2019. Japan Geoscience Union. All Right Reserved.

Development of an Integrated Model for Evaluation of Pasture Carrying Capacity and its Vulnerability based on Water Resources in Arid and Semi-arid Regions------A Case Study in Mongolia

*Qinxue Wang[1], Tomohiro Okadera[1], Tadanobu Nakayama[1], Deni Eer[1], Ochirbat Batkhishig[2], Dorjgotov Battogtokh[2], Uudus Bayasaikhan[3]

1. National Institute for Environmental Studies, 2. Institute of Geography and Geoecology, Mongolian Academy of Sciences, 3. School of Arts and Sciences, National University of Mongolia

Arid and semi-arid regions cover 41% of the global land area and near 2 billion people (34.7%) live there, where fragile environment is getting more vulnerable due to climate change and human activities. Pasture carrying capacity and its vulnerability can be recognized as the integrated indicators for SDGs in arid and semi-arid regions. Our previous study revealed that climate change in past few decades caused the obvious degradation of permafrost, the water deficit of land-surface, and then the decrease of pasture productivity and carrying capacity. However, beside climate change, land use/cover changes caused by human activities such as urbanization, cultivation and mining industry may also have a large influence on pasture carrying capacity. In such regions, it is essential for us to develop some indicators to be used for sustainable management of pasture ecosystems.

In this study, we have developed an integrated model based on water resources to evaluate the pasture Carrying Capacity (CC), Grazing Pressure (GP) and Vulnerability Index (VI) under the influences of both climate change and land use/cover changes, such as urbanization, cultivation and mining & so on (Figure 1). The input data include the pasture net primary production, land use, gradient of slope and grazing density, etc. In order to evaluate the impact of land use/cover changes, we applied the model to four target areas: urban area (Ulaanbaatar City) and steppe area (Altanbulag Soum) in semi-arid regions of northern Mongolia and mining area (Khanbogd Soum) and desert (Manlai Soum) in arid regions of southern Mongolia, and the estimated result was shown in Figure 2, which indicates:

Carrying Capacity (CC): steppe area > urban area > desert area > mining area
Grazing Pressure (GP): urban area > steppe area > mining area > desert area
Vulnerability Index (VI): urban area > mining area > desert area > steppe area

We also applied the model to the Soum level in Mongolia and found that the areas with high vulnerability expanded rapidly, especially in central Mongolia in last decades. We are now trying to use the model to do sensitivity analysis to parameters, such as water accessibility, harvest index and so on, to be able to evaluate the efficiency of adaptation strategies, such as well construction for enhancing groundwater usage, forage plantation for enhancing harvest index and so on.

Keywords: Pasture Carrying Capacity, Environmental Vulnerability, Arid and Semi-arid Regions, Water Resources

©2019. Japan Geoscience Union. All Right Reserved.

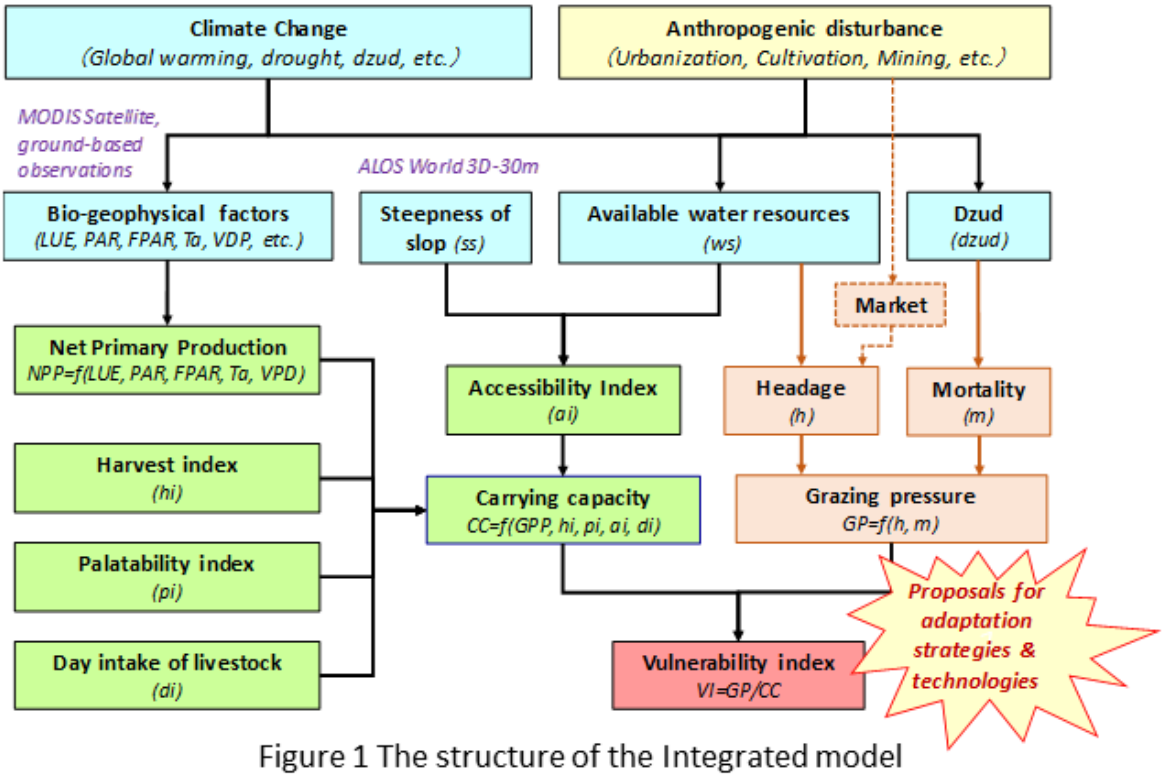


Figure 1 The structure of the Integrated model

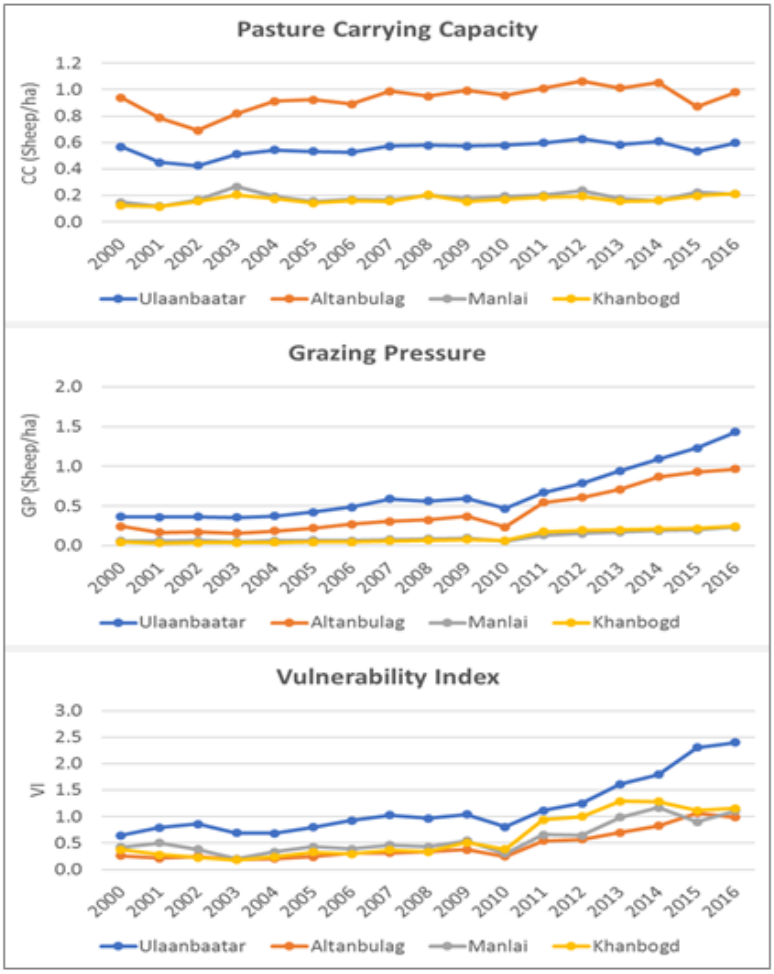


Figure 2 Evaluated pasture CC and VI in four target areas

©2019. Japan Geoscience Union. All Right Reserved.

Influence of land use histories on vegetation and ecosystem services of restored wetlands in Tumen River basin, China

*CAO GUANGLAN[1], Kazuaki Tsuchiya[1], Weihong Zhu[2], OKURO TOSHIYA[1]

1. The University of Tokyo, 2. Yanbian University

Wetlands are among the world’ s most productive and valuable ecosystems. They are important habitats for a variety of flora and fauna, and are vital ecosystems that provide diverse services. They not only are essential for ecological functions such as maintaining biodiversity, controlling floods, and removing pollutants, but also serve necessary economic functions in rice and fish production, transport, and hydropower energy. Despite this, they have suffered a loss of 54%–57% of their area worldwide, which continues under pressures from agriculture, urban expansion, industrialization, and resource extraction. Conservation and restoration of wetland ecosystems is important issues for conservation biodiversity and sustainable use of ecosystem services. In this study, we focus on the lower of Tumen River, Northeast China where the wetlands decreased dramatically because of reclamation. Our objective was to determine the influence of land use and management histories on vegetation structure and ecosystem services and future analyse their associations with environmental factors. The results of this study are of great significance to the impact of management measures on wetland ecosystems, as well as the analysis and evaluation of vegetation restoration.

Keywords: land use histories, vegetation dynamics, wetland restoration, ecosystem services

©2019. Japan Geoscience Union. All Right Reserved.

The spatial flow of freshwater ecosystem services: A case study of Tumen River watershed

*JIAN ZHANG[1], Shizuka hashimoto[1], Kazuaki Tsuchiya[1], Weihong Zhu[2], OKURO TOSHIYA[1]

1. The University of Tokyo, 2. Yanbian University

Freshwater is widely regarded as the most essential natural resource underpinning the well-being of human society, and while scientists translate it into ecosystem services' valuable processes, the supply of clean freshwater has the highest value among various provisioning services. However, due to the land-use intensification and projected warming climate, an increasing likelihood of persistent drought condition, and inadequate conservation, freshwater scarcity issues continue to gain urgency in science and policies. The fusion of the concept of ecosystem services with natural resources management nowadays represents a new conservation paradigm, but still faces notable limitations. Some scientists, noticing the occurrence of spatial mismatch between the supply and demand of ecosystem services, put forward the concept of ecosystem services flow to deal with the problem. Ecosystem services flow research brings out a spatio-temporal connection between the supply and demand, and an deepened understanding about when ,where, and how those benefits were enjoyed. Many papers also suggested that studies at landscape scale may offer a better understanding of ecosystem processes, ecosystem functions, ecosystem services and link them from one to another, as landscape patterns have long been discussed as tools for explaining numerous ecological consequences. In 2017, the annual meeting of IALE in USA as well emphasized the pressing need of integrating landscape patterns to ecosystem services. Thus the study attempt to conduct an analysis of freshwater ecosystem services flow in an intact watershed with the combination of landscape ecology theories. The conceptual framework and progress of this study will be introduced.

Keywords: freshwater ecosystem services, services flow, andscape pattern, watershed

©2019. Japan Geoscience Union. All Right Reserved.

[E] Poster | S (Solid Earth Sciences)：S-SS Seismology

Tue. May 28, 2019 3:30 PM - 5:00 PM JST | Tue. May 28, 2019 6:30 AM - 8:00 AM UTC | Poster Hall International Exhibition Hall8, Makuhari Messe_16

[S-SS06] Nankai Trough Seismogenic Zone Experiment: Logging and sampling the seismogenic megathrust

convener:Kyuichi Kanagawa(Graduate School of Science, Chiba University), Demian M Saffer(Pennsylvania State University), Masataka Kinoshita(Earthquake Research Institute, University of Tokyo)

The Nankai Trough Seismogenic Zone Experiment (NanTroSEIZE) is a multidisciplinary investigation of fault mechanics and seismogenesis along the megathrust at the Nankai Trough subduction zone, and includes reflection and refraction seismic imaging, direct sampling by drilling, in situ measurements, and long-term monitoring in conjunction with laboratory and numerical modeling studies. During the past 12 IODP expeditions off Kii Peninsula since 2007, 15 sites have been drilled by D/V "Chikyu" down to depths from 100s of meters to more than 3000 meters below seafloor, where the inner and outer wedge of the Nankai margin has been logged and sampled extensively, and three state-of-the-art real-time downhole observatories are now in operation. The final NanTroSEIZE expedition aiming to log and sample the seismogenic megathrust at ~5200 meters below seafloor is now ongoing from October, 2018 to March, 2019.
In this session, we expect presentations not only on scientific outcomes from the past NanTroSEIZE expeditions, but also on the exciting preliminary results of the final NanTroSEIZE expedition. We welcome presentations on, but are not limited to, seismic imaging, borehole logging and monitoring, chemical analyses of pore water and mud gas, lithology, structures, physical properties and laboratory experiments of cuttings and core samples, and theoretical and numerical modeling.

[SSS06-P01] Crustal structure in the Nankai Trough seismogenic zone based on renewed depth images and seismic attribute analysis

*Kazuya Shiraishi[1], Yasuhiro Yamada[1], Masataka Kinoshita[2], Gaku Kimura[3] (1.Japan Agency for Marine-Earth Science and Technology, 2.Earthquake Research Institute, The University of Tokyo, 3.Tokyo University of Marine Science and Technology)

[SSS06-P02] Along-strike variations in protothrust zone characteristics at the Nankai Trough subduction margin

*Hannah Tilley[1], Gregory F Moore[1], Mikiya Yamashita[2], Shuichi Kodaira[2] (1.University of Hawaii at Manoa, 2.JAMSTEC)

[SSS06-P03] Temporal change in seismic velocity in the Nankai subduction zone from cross-correlation analysis of ambient noise

*Tatsunori Ikeda[1], Takeshi Tsuji[1] (1.Kyushu University)

[SSS06-P04] Strength profile of the Nankai accretionary prism evaluated from drilling parameters

★Invited Papers

*Yohei Hamada[1], Manami Kitamura[2], Takehiro Hirose[1], Yasuhiro Yamada[1], Yoshinori Sanada[1], Takamitsu Sugihara[1], Saneatsu Saito[1], KYAW MOE[1] (1.Japan Agency for Marine-Earth Science and Technology, 2.National Institute of Advanced Industrial Science andTechnology)

[SSS06-P05] Paleotemperature anomalies deduced from thermal-maturity parameters within the décollement, off Cape of Muroto, Japan

*Nana Kamiya[1,2], Takehiro Hirose[2], Yuzuru Yamamoto[2], Yohei Hamada[2], Stephen A Bowden[3], Man-Yin Tsang[4], Kiho Yang[5], Satoshi Tonai[6], Weiren Lin[1,2] (1.Graduate School of Engineering, Kyoto University, 2.JAMSTEC, 3.University of Aberdeen, 4.University of Toronto, 5.Yonsei University, 6.Kochi University)

[SSS06-P06] Modelling thermal maturity of an accretionary wedge

Utsav Mannu[2], *Masataka Kinoshita[1], Taras Gerya[3] (1.Earthquake Research Institute, University of Tokyo, 2.Department of Earth and Climate Science, IISER Pune, 3.Institute of Geophysics, ETH Zürich)

Crustal structure in the Nankai Trough seismogenic zone based on renewed depth images and seismic attribute analysis

*Kazuya Shiraishi[1], Yasuhiro Yamada[1], Masataka Kinoshita[2], Gaku Kimura[3]

1. Japan Agency for Marine-Earth Science and Technology, 2. Earthquake Research Institute, The University of Tokyo, 3. Tokyo University of Marine Science and Technology

To better understand geological structure in the Nankai Trough seismogenic zone, we investigate deformations in the accretionary prism based on renewed depth images and seismic attribute analyses. We reprocessed subareas of the Kumano-nada 3D MCS data acquired in 2006: 25 km x 12 km area including IODP C0002 site in Phase 1 (2015-2016) and 20 km x 12 km area including IODP C0006 site in Phase 2 (2017-2018). We also reprocessed 2D MCS data along a 50-km line crossing C0002 site in NW-SE direction, which was selected from a 2D survey ODKM03 in 2003 with a longer streamer cable (6 km) than streamer cables of the 3D survey (4.5 km). Quality improvement of reflection signals was achieved by applying recent broadband processing and advanced process to attenuate noise and multiple reflections. Depth domain reflection images were obtained after applying new pre-stack depth migration methods. Then, we calculated several seismic attributes from the 3D reflection image volumes, such as coherence and structure dips which are useful to interpret structural features.
As a result of our investigation, deformed structure within the inner accreted sediments and its relation with the megathrust fault are clearer than before. Anticlines are identified just below the Kumano forearc basin and fragmented reflections can be seen below the anticlines. Characteristic patterns of folds can be recognized on the horizontal section of the coherence cube, which are corresponding to the anticlines on the vertical sections. These reflection features imply development of fold structures due to thrust faults with branched minor faults. In the reprocessed 2D section, curved reflectors with stepwise displacement are imaged in the region of 4 - 6 km depth. These reflectors may represent multiple thrust faults with back-thrusts, and the thrust faults are consistent with the structural features in the 3D images. The detachments of the thrust faults seem to converge to wavy points on the megathrust fault surface. Furthermore, details of deformation and fracture in the outer accretionary prism are imaged clearer than the previous images. Lithological boundaries with displacement along imbricated thrusts can be traced beyond the fault, and conjugate faults due to horizontal compression which cut the in-sequence thrusts are recognized on the horizontal section from superimposed view of the coherence and dip angles. Reflectors within underthrusted sediments beneath the imbricated thrust layer are clearly imaged. Some of the reflectors can be identified as parts of detachment of the thrust faults. The topographic relief of the oceanic crust should be considered when the deformed structures in the overburden sediments and distribution of décollement are revisited.

Acknowledgements:
This research is supported by JSPS KAKENHI (JP15H05717).

Keywords: Nankai Trough seismogenic zone, crustal structure, reflection seismic, seismic attribute

©2019. Japan Geoscience Union. All Right Reserved.

Along-strike variations in protothrust zone characteristics at the Nankai Trough subduction margin

*Hannah Tilley[1], Gregory F Moore[1], Mikiya Yamashita[2], Shuichi Kodaira[2]

1. University of Hawaii at Manoa, 2. JAMSTEC

Protothrust zones (PTZs) are assumed to control the development of new frontal thrusts at subduction zones. PTZs are areas of incipient thrust faulting between the deformation front and the frontal thrust. However, limited resolution of previous seismic studies has hindered the study of their role in subduction accretion. New high-resolution seismic reflection surveys enabled detailed analysis of the PTZ along the Nankai Trough, SE Japan. Seventeen multichannel seismic reflection lines were collected perpendicular to the trench axis between Cape Ashizuri and Cape Muroto using a 1200m long, 192 channel hydrophone cable and a 380 in^3 (5.24L) cluster airgun array. These lines were processed using pre-stack depth migration. PTZs only existed where a turbidite sequence was present beneath the trench wedge. The PTZs consisted of closely spaced, sub-parallel protothrusts that decreased in spacing and increased in length landward. Where the turbidites were truncated by basement topography, there was a transitional PTZ heterogeneous protothrusts and small displacement thrust faults. We hypothesize that elevated pore pressures due to the low permeability hemipelagic sediment inhibit the formation of PTZs and favor small displacement thrusts in a narrow trench wedge. Conversely, turbidite layers within the hemipelagic sediment allow drainage and reduce the pore pressure. This increases the effective stress and shear strength on faults, resulting in strain localizing protothrusts. This implies that the changes in pore pressure imposed by differences in the sediment permeability control the style of deformation in the trench wedge and consequently, the geometry of the accretionary wedge.

Keywords: Nankai Trough, Protothrust Zone, Subduction zone

©2019. Japan Geoscience Union. All Right Reserved.

Temporal change in seismic velocity in the Nankai subduction zone from cross-correlation analysis of ambient noise

*Tatsunori Ikeda[1], Takeshi Tsuji[1]

1. Kyushu University

To investigate the temporal variation of stress or strain in the Nankai subduction zone, we estimated the temporal variation of seismic velocity by using cross-correlations of ambient noise in the frequency range 0.7–2.0 Hz, which was dominated by ACR waves, recorded by the DONET offshore seismic network from 1 October 2014 to 30 November 2017. The 1 April 2016 Off-Mie earthquake (M_W 5.9) and its aftershocks occurred beneath the seismic network.

Our results document a clear decrease in seismic velocity at the time of the earthquake. These coseismic velocity drops were correlated with peak ground velocities at each station, suggesting that dynamic stress changes due to strong ground motions are a primary factor in coseismic velocity variations. Differences in the sensitivity of seismic velocity changes to peak ground velocity may reflect subsurface conditions at each station, such as geological structures and effective pressure conditions. We also observed a long-term increase in seismic velocities, independent of the 2016 earthquake, that may reflect tectonic strain accumulation around the Nankai subduction zone. After removing the long-term trend, we found that the coseismic velocity drops had not completely recovered by the end of the observation period, possibly indicating nonlinear effects of the 2016 earthquake. Our results suggest that ambient noise cross-correlation might be used to monitor the stress state in the Nankai accretionary prism in offshore environments, which would contribute to a better understanding of earthquake processes.

Keywords: Nankai Trough, 2016 Off-Mie earthquake, monitoring, ambient noise, seismic interferometry

©2019. Japan Geoscience Union. All Right Reserved.

Strength profile of the Nankai accretionary prism evaluated from drilling parameters

*Yohei Hamada[1], Manami Kitamura[2], Takehiro Hirose[1], Yasuhiro Yamada[1], Yoshinori Sanada[1], Takamitsu Sugihara[1], Saneatsu Saito[1], KYAW MOE[1]

1. Japan Agency for Marine-Earth Science and Technology, 2. National Institute of Advanced Industrial Science andTechnology

In-situ rock strength with depth under the ground/seafloor is a critical parameter for various studies in geology and seismology. The measurements on rock/core samples, however, hardly have been done with success due to lack of drilled cores and sufficient knowledge about the in situ conditions. We proposed a new indicator of the strength, equivalent strength (EST) developing previous mechanical parameter (Mechanical specific energy: Teal, 1964) from the oil industry, which is converted only from drilling performance parameters such as drillstring rotational torque, bit depth and drillstring rotational per minute. The data processing was applied to the data taken from International Ocean Discovery Program (IODP) expeditions in the Nankai Trough (sites C0002 and C0023). The depth profiles of the EST at Site C0002 are drawn from 0 to 3000 meter-below-seafloor (mbsf), across the forearc basin and the accretionary prism, and the values of the calculated EST are consistent with compressive strength measured on core samples under estimated in situ stress conditions in laboratory. The high (~20 MPa) EST in the forearc basin sediments corresponds to the high $CaCO_3$ content indicating the carbonate is cementing the shallow formation. The EST did not show a significant increase at the forearc basin–accretionary prism boundary, however clearly increased within the prism, ca. below 1500 mbsf. This result may indicate that even the shallow accretionary prism has been strengthened by horizontal compression derived from plate subduction. At the site C0023, where the toe of the accretionary prism area off Cape Muroto, the EST trend increases with depth and suddenly changes between 600–650 mbsf, 840–870 mbsf, and 1120 ~ mbsf, corresponding to tuff0rich zone, top of the subducting sediments and the basement igneous rocks, respectively. This EST trend shows good agreement with P-wave velocity curve measured on core samples. The EST decreases from ~20 MPa to 5 MPa below the frontal decollement with sharp negative peak. This low-EST zone probably indicate the existence of excess fluid pressure.

Keywords: The Nankai Trough, Equivalent strength, Nankai Trough SeismogenicZone Experiment, T-Limit of the Deep Biosphere off Muroto

©2019. Japan Geoscience Union. All Right Reserved.

Paleotemperature anomalies deduced from thermal-maturity parameters within the décollement, off Cape of Muroto, Japan

*Nana Kamiya[1,2], Takehiro Hirose[2], Yuzuru Yamamoto[2], Yohei Hamada[2], Stephen A Bowden[3], Man-Yin Tsang[4], Kiho Yang[5], Satoshi Tonai[6], Weiren Lin[1,2]

1. Graduate School of Engineering, Kyoto University, 2. JAMSTEC, 3. University of Aberdeen, 4. University of Toronto, 5. Yonsei University, 6. Kochi University

Heat flow is characteristically high at the toe of the Nankai accretionary prism, off cape Muroto, and this is considered to be a consequence of the subduction of a hot and active ridge (e.g. Yamano et al., 2003). Despite present-day heat flow being known, how heat has changed over time in this area remains uncertain and is poorly constrained. To address this question, we have investigated palaeotemperatures using thermal maturity parameters measured on cores collected during IODP Expedition 370. Paleotemperature data were evaluated within the context of present-day heat flow and expected changes in temperature with respect to depth; e.g., numerical constraint whether present-day temperatures are too hot or cold to explain thermal maturity measurements, and whether there are anomalies with respect to depth. This is particularly important for Expedition 370 (T-limits) which selected the Muroto-site (Site C0023) because of its high heat flow and the chance this offers to investigate the habitability of the deep biosphere with respect to the temperature. Site C0023 is located 120 km from Cape Muroto, and is in the protothrust-zone of the Nankai accretionary prism. The hole encountered the décollement at 758-795 mbsf, and present-day temperatures were measured down to ~350 mbsf. Vitrinite reflectance was used to estimate maximum paleotemperatures and to look for thermal anomalies. The vitrinite reflectance increases with depth from 0.2 to 0.6 % from 200 to 700 mbsf, typical of conventional burial metamorphism, but changes little from 700 to 1000 mbsf (values stay about 0.6 %). There is a notable high value at 1090 mbsf (about 1%). There are anomalously high values of both vitrinite reflectance and sterane and hopane biomarker data at about 800 mbsf. For heating durations of 400, 4000, 40000 and 400000 years, and assuming thermal maturation using the EasyVit model of Burnham and Sweeny (1990), temperatures of 40~140 ℃ can explain data between 200 to 750 mbsf. To match measurements of vitrinite reflectance at 750 mbsf, a maximum paleotemperature of 140 ℃ is required. At 1090 mbsf, temperatures as high as ~200 ℃ could be needed. The difference between the paleo- and present-day temperatures is the notably the greatest at the décollement, strongly suggesting an elevated heat flow at some time. A heating duration of 400 years, an elevated a heat flow of 130 ±90 mW/m^2 and a temperature > 150 ℃ can explain the observations on the vitrinite reflectance. Considering the scales of space and time of thermal advection, a high-temperature fluid along the décollement zone is our currently preferred explanation.

Keywords: Muroto, Décollement, Paleotemperature anomalies

©2019. Japan Geoscience Union. All Right Reserved.

Modelling thermal maturity of an accretionary wedge

Utsav Mannu[2], *Masataka Kinoshita[1], Taras Gerya[3]

1. Earthquake Research Institute, University of Tokyo, 2. Department of Earth and Climate Science, IISER Pune, 3. Institute of Geophysics, ETH Zürich

In accretionary margins, the estimation of peak heating through the thermal maturity of organic material reveals differentiated deformational pathways in the adjoining sections of the wedge. As the thermal maturity of the deformed structures is a function of both the geothermal gradient and the duration of time it has been exposed to different gradients, the distribution of vitrinite reflectance (the measure of thermal maturity) in the wedge does not necessarily reveal the temporal deformational pathway of the individual pockets. As a result, the different portions of the accretionary wedge exhibit different correlations between the thermal maturity and a unique deformational pathway. These different correlations can be explored through the means of geodynamic modelling which can then be used in the field to ascertain a more holistic picture of deformation in an accretionary wedge. Therefore, in this study, we use a 2D plate subduction thermomechanical model, to simulate formation of accretionary wedge and the track the evolution of the vitrinite reflectance in the accretionary wedge.

Keywords: thermal maturity, accretionary wedge, numerical simulation

©2019. Japan Geoscience Union. All Right Reserved.

[E] Poster | S (Solid Earth Sciences)：S-SS Seismology

Tue. May 28, 2019 5:15 PM - 6:30 PM JST | Tue. May 28, 2019 8:15 AM - 9:30 AM UTC | Poster Hall International Exhibition Hall8, Makuhari Messe_28

[S-SS06] Nankai Trough Seismogenic Zone Experiment: Logging and sampling the seismogenic megathrust

convener:Kyuichi Kanagawa(Graduate School of Science, Chiba University), Demian M Saffer(Pennsylvania State University), Masataka Kinoshita(Earthquake Research Institute, University of Tokyo)

The Nankai Trough Seismogenic Zone Experiment (NanTroSEIZE) is a multidisciplinary investigation of fault mechanics and seismogenesis along the megathrust at the Nankai Trough subduction zone, and includes reflection and refraction seismic imaging, direct sampling by drilling, in situ measurements, and long-term monitoring in conjunction with laboratory and numerical modeling studies. During the past 12 IODP expeditions off Kii Peninsula since 2007, 15 sites have been drilled by D/V "Chikyu" down to depths from 100s of meters to more than 3000 meters below seafloor, where the inner and outer wedge of the Nankai margin has been logged and sampled extensively, and three state-of-the-art real-time downhole observatories are now in operation. The final NanTroSEIZE expedition aiming to log and sample the seismogenic megathrust at ~5200 meters below seafloor is now ongoing from October, 2018 to March, 2019.
In this session, we expect presentations not only on scientific outcomes from the past NanTroSEIZE expeditions, but also on the exciting preliminary results of the final NanTroSEIZE expedition. We welcome presentations on, but are not limited to, seismic imaging, borehole logging and monitoring, chemical analyses of pore water and mud gas, lithology, structures, physical properties and laboratory experiments of cuttings and core samples, and theoretical and numerical modeling.

[SSS06-P01] Crustal structure in the Nankai Trough seismogenic zone based on renewed depth images and seismic attribute analysis

*Kazuya Shiraishi[1], Yasuhiro Yamada[1], Masataka Kinoshita[2], Gaku Kimura[3] (1.Japan Agency for Marine-Earth Science and Technology, 2.Earthquake Research Institute, The University of Tokyo, 3.Tokyo University of Marine Science and Technology)

[SSS06-P02] Along-strike variations in protothrust zone characteristics at the Nankai Trough subduction margin

*Hannah Tilley[1], Gregory F Moore[1], Mikiya Yamashita[2], Shuichi Kodaira[2] (1.University of Hawaii at Manoa, 2.JAMSTEC)

[SSS06-P03] Temporal change in seismic velocity in the Nankai subduction zone from cross-correlation analysis of ambient noise

*Tatsunori Ikeda[1], Takeshi Tsuji[1] (1.Kyushu University)

[SSS06-P04] Strength profile of the Nankai accretionary prism evaluated from drilling parameters

★Invited Papers

*Yohei Hamada[1], Manami Kitamura[2], Takehiro Hirose[1], Yasuhiro Yamada[1], Yoshinori Sanada[1], Takamitsu Sugihara[1], Saneatsu Saito[1], KYAW MOE[1] (1.Japan Agency for Marine-Earth Science and Technology, 2.National Institute of Advanced Industrial Science andTechnology)

[SSS06-P05] Paleotemperature anomalies deduced from thermal-maturity parameters within the décollement, off Cape of Muroto, Japan

*Nana Kamiya[1,2], Takehiro Hirose[2], Yuzuru Yamamoto[2], Yohei Hamada[2], Stephen A Bowden[3], Man-Yin Tsang[4], Kiho Yang[5], Satoshi Tonai[6], Weiren Lin[1,2] (1.Graduate School of Engineering, Kyoto University, 2.JAMSTEC, 3.University of Aberdeen, 4.University of Toronto, 5.Yonsei University, 6.Kochi University)

[SSS06-P06] Modelling thermal maturity of an accretionary wedge

Utsav Mannu[2], *Masataka Kinoshita[1], Taras Gerya[3] (1.Earthquake Research Institute, University of Tokyo, 2.Department of Earth and Climate Science, IISER Pune, 3.Institute of Geophysics, ETH Zürich)

Crustal structure in the Nankai Trough seismogenic zone based on renewed depth images and seismic attribute analysis

*Kazuya Shiraishi[1], Yasuhiro Yamada[1], Masataka Kinoshita[2], Gaku Kimura[3]

1. Japan Agency for Marine-Earth Science and Technology, 2. Earthquake Research Institute, The University of Tokyo, 3. Tokyo University of Marine Science and Technology

To better understand geological structure in the Nankai Trough seismogenic zone, we investigate deformations in the accretionary prism based on renewed depth images and seismic attribute analyses. We reprocessed subareas of the Kumano-nada 3D MCS data acquired in 2006: 25 km x 12 km area including IODP C0002 site in Phase 1 (2015-2016) and 20 km x 12 km area including IODP C0006 site in Phase 2 (2017-2018). We also reprocessed 2D MCS data along a 50-km line crossing C0002 site in NW-SE direction, which was selected from a 2D survey ODKM03 in 2003 with a longer streamer cable (6 km) than streamer cables of the 3D survey (4.5 km). Quality improvement of reflection signals was achieved by applying recent broadband processing and advanced process to attenuate noise and multiple reflections. Depth domain reflection images were obtained after applying new pre-stack depth migration methods. Then, we calculated several seismic attributes from the 3D reflection image volumes, such as coherence and structure dips which are useful to interpret structural features.
As a result of our investigation, deformed structure within the inner accreted sediments and its relation with the megathrust fault are clearer than before. Anticlines are identified just below the Kumano forearc basin and fragmented reflections can be seen below the anticlines. Characteristic patterns of folds can be recognized on the horizontal section of the coherence cube, which are corresponding to the anticlines on the vertical sections. These reflection features imply development of fold structures due to thrust faults with branched minor faults. In the reprocessed 2D section, curved reflectors with stepwise displacement are imaged in the region of 4 - 6 km depth. These reflectors may represent multiple thrust faults with back-thrusts, and the thrust faults are consistent with the structural features in the 3D images. The detachments of the thrust faults seem to converge to wavy points on the megathrust fault surface. Furthermore, details of deformation and fracture in the outer accretionary prism are imaged clearer than the previous images. Lithological boundaries with displacement along imbricated thrusts can be traced beyond the fault, and conjugate faults due to horizontal compression which cut the in-sequence thrusts are recognized on the horizontal section from superimposed view of the coherence and dip angles. Reflectors within underthrusted sediments beneath the imbricated thrust layer are clearly imaged. Some of the reflectors can be identified as parts of detachment of the thrust faults. The topographic relief of the oceanic crust should be considered when the deformed structures in the overburden sediments and distribution of décollement are revisited.

Acknowledgements:
This research is supported by JSPS KAKENHI (JP15H05717).

Keywords: Nankai Trough seismogenic zone, crustal structure, reflection seismic, seismic attribute

©2019. Japan Geoscience Union. All Right Reserved.

Along-strike variations in protothrust zone characteristics at the Nankai Trough subduction margin

*Hannah Tilley[1], Gregory F Moore[1], Mikiya Yamashita[2], Shuichi Kodaira[2]

1. University of Hawaii at Manoa, 2. JAMSTEC

Protothrust zones (PTZs) are assumed to control the development of new frontal thrusts at subduction zones. PTZs are areas of incipient thrust faulting between the deformation front and the frontal thrust. However, limited resolution of previous seismic studies has hindered the study of their role in subduction accretion. New high-resolution seismic reflection surveys enabled detailed analysis of the PTZ along the Nankai Trough, SE Japan. Seventeen multichannel seismic reflection lines were collected perpendicular to the trench axis between Cape Ashizuri and Cape Muroto using a 1200m long, 192 channel hydrophone cable and a 380 in^3 (5.24L) cluster airgun array. These lines were processed using pre-stack depth migration. PTZs only existed where a turbidite sequence was present beneath the trench wedge. The PTZs consisted of closely spaced, sub-parallel protothrusts that decreased in spacing and increased in length landward. Where the turbidites were truncated by basement topography, there was a transitional PTZ heterogeneous protothrusts and small displacement thrust faults. We hypothesize that elevated pore pressures due to the low permeability hemipelagic sediment inhibit the formation of PTZs and favor small displacement thrusts in a narrow trench wedge. Conversely, turbidite layers within the hemipelagic sediment allow drainage and reduce the pore pressure. This increases the effective stress and shear strength on faults, resulting in strain localizing protothrusts. This implies that the changes in pore pressure imposed by differences in the sediment permeability control the style of deformation in the trench wedge and consequently, the geometry of the accretionary wedge.

Keywords: Nankai Trough, Protothrust Zone, Subduction zone

©2019. Japan Geoscience Union. All Right Reserved.

Temporal change in seismic velocity in the Nankai subduction zone from cross-correlation analysis of ambient noise

*Tatsunori Ikeda[1], Takeshi Tsuji[1]

1. Kyushu University

To investigate the temporal variation of stress or strain in the Nankai subduction zone, we estimated the temporal variation of seismic velocity by using cross-correlations of ambient noise in the frequency range 0.7–2.0 Hz, which was dominated by ACR waves, recorded by the DONET offshore seismic network from 1 October 2014 to 30 November 2017. The 1 April 2016 Off-Mie earthquake (M_W 5.9) and its aftershocks occurred beneath the seismic network.

Our results document a clear decrease in seismic velocity at the time of the earthquake. These coseismic velocity drops were correlated with peak ground velocities at each station, suggesting that dynamic stress changes due to strong ground motions are a primary factor in coseismic velocity variations. Differences in the sensitivity of seismic velocity changes to peak ground velocity may reflect subsurface conditions at each station, such as geological structures and effective pressure conditions. We also observed a long-term increase in seismic velocities, independent of the 2016 earthquake, that may reflect tectonic strain accumulation around the Nankai subduction zone. After removing the long-term trend, we found that the coseismic velocity drops had not completely recovered by the end of the observation period, possibly indicating nonlinear effects of the 2016 earthquake. Our results suggest that ambient noise cross-correlation might be used to monitor the stress state in the Nankai accretionary prism in offshore environments, which would contribute to a better understanding of earthquake processes.

Keywords: Nankai Trough, 2016 Off-Mie earthquake, monitoring, ambient noise, seismic interferometry

©2019. Japan Geoscience Union. All Right Reserved.

Strength profile of the Nankai accretionary prism evaluated from drilling parameters

*Yohei Hamada[1], Manami Kitamura[2], Takehiro Hirose[1], Yasuhiro Yamada[1], Yoshinori Sanada[1], Takamitsu Sugihara[1], Saneatsu Saito[1], KYAW MOE[1]

1. Japan Agency for Marine-Earth Science and Technology, 2. National Institute of Advanced Industrial Science andTechnology

In-situ rock strength with depth under the ground/seafloor is a critical parameter for various studies in geology and seismology. The measurements on rock/core samples, however, hardly have been done with success due to lack of drilled cores and sufficient knowledge about the in situ conditions. We proposed a new indicator of the strength, equivalent strength (EST) developing previous mechanical parameter (Mechanical specific energy: Teal, 1964) from the oil industry, which is converted only from drilling performance parameters such as drillstring rotational torque, bit depth and drillstring rotational per minute. The data processing was applied to the data taken from International Ocean Discovery Program (IODP) expeditions in the Nankai Trough (sites C0002 and C0023). The depth profiles of the EST at Site C0002 are drawn from 0 to 3000 meter-below-seafloor (mbsf), across the forearc basin and the accretionary prism, and the values of the calculated EST are consistent with compressive strength measured on core samples under estimated in situ stress conditions in laboratory. The high (~20 MPa) EST in the forearc basin sediments corresponds to the high $CaCO_3$ content indicating the carbonate is cementing the shallow formation. The EST did not show a significant increase at the forearc basin–accretionary prism boundary, however clearly increased within the prism, ca. below 1500 mbsf. This result may indicate that even the shallow accretionary prism has been strengthened by horizontal compression derived from plate subduction. At the site C0023, where the toe of the accretionary prism area off Cape Muroto, the EST trend increases with depth and suddenly changes between 600–650 mbsf, 840–870 mbsf, and 1120 ~ mbsf, corresponding to tuff0rich zone, top of the subducting sediments and the basement igneous rocks, respectively. This EST trend shows good agreement with P-wave velocity curve measured on core samples. The EST decreases from ~20 MPa to 5 MPa below the frontal decollement with sharp negative peak. This low-EST zone probably indicate the existence of excess fluid pressure.

Keywords: The Nankai Trough, Equivalent strength, Nankai Trough SeismogenicZone Experiment, T-Limit of the Deep Biosphere off Muroto

©2019. Japan Geoscience Union. All Right Reserved.

Paleotemperature anomalies deduced from thermal-maturity parameters within the décollement, off Cape of Muroto, Japan

*Nana Kamiya[1,2], Takehiro Hirose[2], Yuzuru Yamamoto[2], Yohei Hamada[2], Stephen A Bowden[3], Man-Yin Tsang[4], Kiho Yang[5], Satoshi Tonai[6], Weiren Lin[1,2]

1. Graduate School of Engineering, Kyoto University, 2. JAMSTEC, 3. University of Aberdeen, 4. University of Toronto, 5. Yonsei University, 6. Kochi University

Heat flow is characteristically high at the toe of the Nankai accretionary prism, off cape Muroto, and this is considered to be a consequence of the subduction of a hot and active ridge (e.g. Yamano et al., 2003). Despite present-day heat flow being known, how heat has changed over time in this area remains uncertain and is poorly constrained. To address this question, we have investigated palaeotemperatures using thermal maturity parameters measured on cores collected during IODP Expedition 370. Paleotemperature data were evaluated within the context of present-day heat flow and expected changes in temperature with respect to depth; e.g., numerical constraint whether present-day temperatures are too hot or cold to explain thermal maturity measurements, and whether there are anomalies with respect to depth. This is particularly important for Expedition 370 (T-limits) which selected the Muroto-site (Site C0023) because of its high heat flow and the chance this offers to investigate the habitability of the deep biosphere with respect to the temperature. Site C0023 is located 120 km from Cape Muroto, and is in the protothrust-zone of the Nankai accretionary prism. The hole encountered the décollement at 758-795 mbsf, and present-day temperatures were measured down to ~350 mbsf. Vitrinite reflectance was used to estimate maximum paleotemperatures and to look for thermal anomalies. The vitrinite reflectance increases with depth from 0.2 to 0.6 % from 200 to 700 mbsf, typical of conventional burial metamorphism, but changes little from 700 to 1000 mbsf (values stay about 0.6 %). There is a notable high value at 1090 mbsf (about 1%). There are anomalously high values of both vitrinite reflectance and sterane and hopane biomarker data at about 800 mbsf. For heating durations of 400, 4000, 40000 and 400000 years, and assuming thermal maturation using the EasyVit model of Burnham and Sweeny (1990), temperatures of 40~140 ℃ can explain data between 200 to 750 mbsf. To match measurements of vitrinite reflectance at 750 mbsf, a maximum paleotemperature of 140 ℃ is required. At 1090 mbsf, temperatures as high as ~200 ℃ could be needed. The difference between the paleo- and present-day temperatures is the notably the greatest at the décollement, strongly suggesting an elevated heat flow at some time. A heating duration of 400 years, an elevated a heat flow of 130 ±90 mW/m^2 and a temperature > 150 ℃ can explain the observations on the vitrinite reflectance. Considering the scales of space and time of thermal advection, a high-temperature fluid along the décollement zone is our currently preferred explanation.

Keywords: Muroto, Décollement, Paleotemperature anomalies

©2019. Japan Geoscience Union. All Right Reserved.

Modelling thermal maturity of an accretionary wedge

Utsav Mannu[2], *Masataka Kinoshita[1], Taras Gerya[3]

1. Earthquake Research Institute, University of Tokyo, 2. Department of Earth and Climate Science, IISER Pune, 3. Institute of Geophysics, ETH Zürich

In accretionary margins, the estimation of peak heating through the thermal maturity of organic material reveals differentiated deformational pathways in the adjoining sections of the wedge. As the thermal maturity of the deformed structures is a function of both the geothermal gradient and the duration of time it has been exposed to different gradients, the distribution of vitrinite reflectance (the measure of thermal maturity) in the wedge does not necessarily reveal the temporal deformational pathway of the individual pockets. As a result, the different portions of the accretionary wedge exhibit different correlations between the thermal maturity and a unique deformational pathway. These different correlations can be explored through the means of geodynamic modelling which can then be used in the field to ascertain a more holistic picture of deformation in an accretionary wedge. Therefore, in this study, we use a 2D plate subduction thermomechanical model, to simulate formation of accretionary wedge and the track the evolution of the vitrinite reflectance in the accretionary wedge.

Keywords: thermal maturity, accretionary wedge, numerical simulation

©2019. Japan Geoscience Union. All Right Reserved.

[E] Poster | S (Solid Earth Sciences)：S-MP Mineralogy & Petrology

Tue. May 28, 2019 10:45 AM - 12:15 PM JST | Tue. May 28, 2019 1:45 AM - 3:15 AM UTC | Poster Hall International Exhibition Hall8, Makuhari Messe_7

[S-MP29] Oceanic and Continental Subduction Processes

convener:REHMAN Ur Hafiz(Department of Earth and Environmental Sciences, Graduate School of Science and Engineering, Kagoshima University), Tatsuki Tsujimori(Tohoku University), Chin-Ho Tsai(Department of Natural Resources and Environmental Studies, National Dong Hwa University), Kazuaki Okamoto(Faculty of Education, Saitama University)

This JpGU-AGU joint session aims at bringing earth scientists from Japan and overseas to present their research related to the processes of oceanic and continent subduction, continent-continent collisions, metamorphism of crustal rocks, formation of the oceanic/continental arcs, and accretion/ tectonic erosion of material along subduction boundaries.

Topics such as role of the fore- and back-arcs in the subduction zones, process of accretion of volcaniclastic and terrigenous sediments along the subduction/collision boundaries, deformation and metamorphism of subducted crust, and exhumation will be the main focus of the session.

In addition to the above mentioned topics, our focus for the10th anniversary of this international session will be towards our understanding and progress on the ultrahigh-pressure/temperature metamorphic terranes in the world.

Exchange of ideas among geoscientists applying different approaches on problems related to the theme of the session are most welcome.

[SMP29-P01] Zircon U-Pb ages of metasedimentary rocks in the Hakogase (Hida Marginal) area, Fukui Prefecture.

*Atsushi MIYASHITA[1], Tatsuki Tsujimori[2], Daniel Pastor-Galán[3], Yi Keewook[4] (1.Seikei University, 2.Tohoku University, 3.Salamanca University, 4.Korea Basic Science Institue)

[SMP29-P02] Late Permian to Early Triassic back-arc type volcanism in the southern Mongolia volcano-plutonic belt of the Central Asian Orogenic Belt: Implication for timing of the final closure of the Palaeo-Asian Ocean

*Takeshi Imayama[1], Yoichiro Koh[2], Kazumasa Aoki[3], Mototaka Saneyoshi[4], Koshi Yagi[5], Shogo Aoki[4], Yoshihiro Sawada[6], Chiaki Ikawa[5], Tomoya Terada[4], Shinobu Ishigaki[4], Shin Toyoda[3], Khishigjav Tsogtbaatar[7], Buuvei Mainbayar[7] (1.Research Institute of Natural Sciences, Okayama University of Science, 2.Graduate School of Environmental Science, Hokkaido University, 3.Faculty of Science, Okayama University of Science, 4.Faculty of Biosphere - Geosphere Science, Okayama University of Science, 5.Hiruzen Institute for Geology and Chronology, 6.Emeritus Professor of Shimane University, 7.Institute of Paleontology and Geology, Mongolian Academy of Sciences)

[SMP29-P03] Mantle dynamics of slab breakoff constrained from the temporal change of the melting depth estimated from the Cumulate Member of the Ordovician Hayachine-Miyamori Ophiolite

*Takafumi Kimura[1], Kazuhito Ozawa[1] (1.Department of Earth and Planetary Science, The University of Tokyo)

[SMP29-P04] **Evidence of HIMU seamount on the Farallon Plate: Application of *in-situ* Sr-Pb isotope analysis to Franciscan lawsonite-bearing metagreywacke**

*Tomomi Hara[1], Tatsuki Tsujimori[1], Jun-Ichi Kimura[2] (1.Tohoku University, 2.Japan Agency for Marine-Earth Science and Technology)

[SMP29-P05] Boron isotope variations of antigorite serpentinites associated with high-pressure metamorphic rocks: A case study in the Itoigawa–Omi area of the Hida-Gaien Belt, Japan

*Chinatsu Yamada[1], Tatsuki Tsujimori[1], King Chang[2], Jun-Ichi Kimura[2] (1.Tohoku University, 2.Japan Aegency for Marine-Earth Science and Technology)

[SMP29-P06] **Study of zircons structures from the Miocene Shibi-san Granodiorite, Kagoshima Prefecture, Japan**

*Nakabayashi Marimo[1], REHMAN Ur Hafiz[1] (1.Kagoshima University)

[SMP29-P07] **Experimental modeling of eclogite and C-O-H fluid interaction in the subduction zones**

*Nadezda Chertkova[1], Shigeru Yamashita[2], Hiroaki Ohfuji[1], Tetsuo Irifune[1], Hirokazu Kadobayashi[1], Yoshitaka Yamamoto[3] (1.Ehime University, Geodynamics Research Center, 2.Okayama University, Institute for Planetary Materials, 3.National Institute of Advanced Industrial Science and Technology)

[SMP29-P08] Microfabrics of omphacite and garnet in eclogite from the Lanterman Range, northern Victoria Land, Antarctica

*Daeyeong Kim[1], Taehwan Kim[2], Jungmin Kim[3] (1.Division of Polar-Earth Sciences, Korea Polar Research Institute, 2.School of Earth and Environmental Sciences, Seoul National University, 3.Earth and Environmental Sciences, Korea University)

[SMP29-P09] Primordial Apatite from Ophiolite in Taiwan

*Nobuaki Niitsuma[1], Reishi Takashima[2], Yuan Hsi Lee[3] (1.Institute of Geosciences,Shizuoka University, 2.Tohoku University Museum, 3.National Chung-Cheng University, Taiwan)

[SMP29-P10] The evolution of the Cretaceous Jinan Basin in South Korea and the age and tectonic setting for the volcanic rocks in it

*Seung Hwan LEE[1], Chang Whan Oh[1] (1.Department of earth and environmental sciences Chonbuk national university)

[SMP29-P11] GEOCHORONOLOGY AND PETROCHEMISTREY OF LATE PALEOZOIC MAGMATIC ROCKS OF THE MANDAKH AREA, SOUTHEAST MONGOLIA

*Undarmaa Batsaikhan[1], Noriyoshi Tsuchiya[1], Masaoki Uno[1], Yukio Isozaki[2], Uyanga Bold[2], Hikaru Sawada[2] (1.Graduate School of Environmental Studies, Tohoku University, 2.Graduate School of Arts and Sciences The University of Tokyo)

[SMP29-P12] Feedbacks Offshore the Cascadia Margin

*Joan S Gomberg[1] (1.USGS Earthquake Science Center)

Zircon U-Pb ages of metasedimentary rocks in the Hakogase (Hida Marginal) area, Fukui Prefecture.

*Atsushi MIYASHITA[1], Tatsuki Tsujimori[2], Daniel Pastor-Galán[3], Yi Keewook[4]

1. Seikei University, 2. Tohoku University, 3. Salamanca University, 4. Korea Basic Science Institue

Combined chronological study using detrital zircon U-Pb dating and phengite K-Ar dating enables to understand the tectonic evolution of the high *P/T* metamorphic belt. The youngest age of detrital zircon U-Pb ages of psamites in the Hida marginal metamorphic rocks (HMMR = Renge belt) approximate its depositional ages (Tsutsumi et al., 2009). The closure temperature of the phengite K-Ar ages are controlled by deformation and recrystallization during exhumation of the metamorphic rocks(Itaya and Tsujimori, 2015). Therefore, the gap between the youngest age of detrital zircons and phengite K-Ar ages are the age difference between subuduction and uplift of metamorphics.
The Hakogase (Nigure-gawa, Kuzuryu, Fukui Prefecture) metamorphic rocks belong to HMMR member as the olistolith in the Cretaceous Tedori Group. It consists mainly pelites with small amount of basites and mables. The main index mineral assemblage of metasediments are garnet + chlorite, and the phenigite K-Ar ages are 287.8 - 283.6 Ma (Kunugiza et al., 2004). Relic Lawsonite was also found in the basaites and psamites (Miyakawa, 1982).
The detrital Zircons U-Pb ages in the two pelites are obtained by the SHRIMP II of KBSI. The youngest U-Pb ages of detrital zircons are 307Ma. The gap of the sedimentation between uplift of the Hakogase metamorphics is estimated 20 Ma. This value means the migration speed of the HMMR metamorphic rocks are 1/10 of plate motion. This rapid migration speed is common for the high *P/T* metamorphic rocks.

Keywords: high P/T metamorphic rocks, Zircon U-Pb ages, Phengite K-Ar ages

©2019. Japan Geoscience Union. All Right Reserved.

Late Permian to Early Triassic back-arc type volcanism in the southern Mongolia volcano-plutonic belt of the Central Asian Orogenic Belt: Implication for timing of the final closure of the Palaeo-Asian Ocean

*Takeshi Imayama[1], Yoichiro Koh[2], Kazumasa Aoki[3], Mototaka Saneyoshi[4], Koshi Yagi[5], Shogo Aoki[4], Yoshihiro Sawada[6], Chiaki Ikawa[5], Tomoya Terada[4], Shinobu Ishigaki[4], Shin Toyoda[3], Khishigjav Tsogtbaatar[7], Buuvei Mainbayar[7]

1. Research Institute of Natural Sciences, Okayama University of Science, 2. Graduate School of Environmental Science, Hokkaido University, 3. Faculty of Science, Okayama University of Science, 4. Faculty of Biosphere - Geosphere Science, Okayama University of Science, 5. Hiruzen Institute for Geology and Chronology, 6. Emeritus Professor of Shimane University, 7. Institute of Paleontology and Geology, Mongolian Academy of Sciences

The timing of final subduction and closure of the Palaeo-Asian Ocean is still controversial in the eastern segments of the Central Asian Orogenic Belt (CAOB). A more detailed understanding is needed with respect to the formation of volcanic rocks and sediments associated with the final closure of the Palaeo-Asian Ocean in southern Mongolia. We investigated alkali series volcanic rocks newly discovered in the southern Mongolia volcano-plutonic belt of the CAOB and classified as basalt, basaltic trachyandesite, andesite, trachyandesite, and trachyte, mainly showing andesitic-dacitic compositions. In Harker diagrams, the TiO_2, FeO, MnO, Al_2O_3, CaO, and MgO contents generally decrease with increasing SiO_2, representing a series of differentiated volcanic rocks. The primitive mantle-normalized trace element spider diagram is characterized by incompatible element-rich patterns and negative Nb anomalies. The tectonic discrimination diagrams show that the volcanic rocks were formed by arc-related volcanism rather than within-plate volcanism. K-Ar dating of feldspars from six volcanic rocks yields ages ranging from 270 to 239 Ma, indicating that andesitic and dacitic magmatism occurred during this period. These geochemical and geochronological data indicate that the differentiated volcanic rocks intruding middle to late Palaeozoic volcanic sediments were formed by back-arc type subduction ca. 270–240 Ma. Based on detrital zircon U-Pb ages, the terrigenous sandstones underlain by the volcanic sediments record a maximum depositional age of Late Triassic (ca. 220–200 Ma) and include a main cluster of Early Devonian ages (ca. 410–390 Ma), possibly derived from the Devonian-Carboniferous arc complex observed surrounding this study area. These results from the volcanic and sedimentary rocks in this study, combined with investigations in previous studies, imply that subduction beneath the eastern segments of the CAOB to consume the Palaeo-Asian Ocean continued until Late Permian to Early Triassic.

Keywords: Palaeo-Asian Ocean, southern Mongolia, Central Asian Orogenic Belt, back-arc type volcanism

©2019. Japan Geoscience Union. All Right Reserved.

Mantle dynamics of slab breakoff constrained from the temporal change of the melting depth estimated from the Cumulate Member of the Ordovician Hayachine-Miyamori Ophiolite

*Takafumi Kimura[1], Kazuhito Ozawa[1]

1. Department of Earth and Planetary Science, The University of Tokyo

Slab breakoff, detachment of oceanic lithosphere highly expected during arc-continent collision, is one of the important mechanisms inducing passive upwelling of the asthenosphere and magma generation in arc environments [1]. In order to better understand the mantle dynamics of slab breakoff, we need to use continuous geological record with high time resolution. In this study, we have extracted a record of temporal change of the magma generation depth from cumulates in an Ordovician arc ophiolite at a time resolution of several tens of million years.
The Hayachine-Miyamori Ophiolite, northern Japan, is one of the Ordovician ophiolite formed in an arc environment [2]. The ultramafic member was built up by three main magmatic stages, which are recorded in three rock units: Tectonite Member, Cumulate Member, and ultramafic dikes, in the order of formation ages. The last two units in the entire evolution of the ophiolite is explained by decompressional melting of sub-slab mantle triggered by slab breakoff [2][3]. The melting depth of an ultramafic magma solidified as dikes in the Cumulate Member is estimated to be ~170km [3]. Our recent field study clarified a large-scale stratification characterized by alternation of wehrlite-dominant and dunite-dominant layers in the Cumulate Member. Each layer has a thickness from several meters to ~1 km and, the total thickness attains ~3km. Moreover, we succeeded in specifying the strike and plunge of the gravity field to be ~N48°E and ~20°NE during the cumulate formation from field information and westward stratigraphic younging [4].
We estimated the temporal change of generation depth of parent magmas of the Cumulate Member by garnet signature in heavy rare earth elements (HREEs) as depth proxy. The information may constrain the mantle dynamics during the slab breakoff. We examined stratigraphic variation of HREE ratio at the core of clinopyroxenes over the thickness of ~2km in the Cumulate Member. The obtained variation of the Dy/Lu increases from ~12.9 to ~16.5 with increasing the stratigraphic height. We estimated the extent of melting in the garnet stability field increasing from ~50 to ~90% of the total melting by applying an open-system fractional melting model to reproduce the Dy/Lu variation.
We also estimated the time scale of formation of the Cumulate Member by using cm –10cm scale heterogeneity recorded in contact zone of intruded magma and the host. The profile of Mg# of olivine in xenoliths of the Tectonite Member occurring at the bottom of the Cumulate Member shows that the cooling time is less than several tens of million years [5]. The dunite of the Cumulate Member contacting the ultramafic dike shows a systematic decrease of Mg# from 90 to 86.8 over the distance of 54 mm towards the contact. We calculated the time scale of subsolidus diffusional exchange between the dunite and dike and obtained several tens of million years at ~1000℃. The host was kept at a high temperature when the dikes intruded because of the absence of chilled margin. We thus estimated time scale of formation of the Cumulate Member to be < several tens of million years.
We propose the following tectonic model in the Ordovician northern Japan on the basis of the above result. The slab breakoff took place at the depth slightly deeper than the boundary of spinel and garnet stability fields (~80 km) and induced counter flow and adiabatic melting of the sub-slab mantle. The melting depth deepened down to ~170 km on the time scale of several tens of million years, which corresponds to the time scale to complete the slab breakoff. The sinking velocity of the slab is more than

©2019. Japan Geoscience Union. All Right Reserved.

a few millimeters per year.

[1]: Davies et al., 1995. [2]: Ozawa et al., 2015. [3],[4]: Kimura et al., 2017, 2018, JpGU abstract. [5]: Ozawa, 1983.

Keywords: slab breakoff, arc ophiolite, cumulate

©2019. Japan Geoscience Union. All Right Reserved.

Evidence of HIMU seamount on the Farallon Plate: Application of *in-situ* Sr-Pb isotope analysis to Franciscan lawsonite-bearing metagreywacke

*Tomomi Hara[1], Tatsuki Tsujimori[1], Jun-Ichi Kimura[2]

1. Tohoku University, 2. Japan Agency for Marine-Earth Science and Technology

Since bulk isotopic composition of oceanic basalt is susceptible to element remobilization during alteration process, there is a risk of causing misread of geochemical signatures from bulk metabasaltic rocks in subduction complex. As Hara et al. (2018) demonstrated, however, *in-situ* Sr-Pb isotope analysis of lawsonite in high-pressure metabasaltic rocks has a great potential for tracing the geochemical signatures reflecting the igneous protolith. In this study, we have applied the method to lawsonite in metasedimentary rocks to explore clastic components of a trench-fill sediment. A jadeite-bearing Franciscan metagreywacke from Pacheco Pass area, east-central Diablo Range, California Coast Ranges was selected for geochemical reconnaissance.

Lawsonites in the Franciscan metagreywacke record a high initial Pb isotope ratios ($^{206}Pb/^{204}Pb$ = 18.74–19.66, $^{207}Pb/^{204}Pb$ = 15.58–15.70 and $^{208}Pb/^{204}Pb$ = 38.41–39.34). This Pb-isotope signature suggests that a protolith of the metagreywacke have contained a debris derived from a HIMU-type basalt. Considering the maximum depositional age of the metagreywacke at ~102 Ma, the underflow of the Farallon Plate beneath continental crust of the North American Plate would have carried a HIMU seamount to a Franciscan trench.

Our study has demonstrated the potential application of 'lawsonitology' as sedimentary provenance analyses for metamorphosed accretionary complex. Moreover, the results would manifest that Pb isotopic signature of ancient oceanic basalt can be detectable from Ca-Al silicate mineral, such as lawsonite, epidote and pumpellyite, in metamorphic rocks.

Keywords: Lawsonite, Sr-Pb isotope, LA-MC-ICPMS, HIMU, Metasediment

©2019. Japan Geoscience Union. All Right Reserved.

Boron isotope variations of antigorite serpentinites associated with high-pressure metamorphic rocks: A case study in the Itoigawa–Omi area of the Hida-Gaien Belt, Japan

*Chinatsu Yamada[1], Tatsuki Tsujimori[1], King Chang[2], Jun-Ichi Kimura[2]

1. Tohoku University, 2. Japan Aegency for Marine-Earth Science and Technology

Boron isotope study of serpentinites in the Franciscan Complex using an ablation volume correction (AVC) LA-MC-ICPMS discriminates two groups (Yamada et al., 2018 JpGU abstr.; Yamada et al. 2019, in press). Serpentinites associated with blueschists are characterized by lighter boron isotope than serpentinites without blueschist-facies rocks. The lighter boron isotope signature (< ~10 ‰) of blueschist-bearing serpentinites results from interaction with forearc slab fluids with low δ^{11}B in deeper depth. In order to evaluate the versatility of B isotopes and composition of high-pressure metamorphosed serpentinites, we investigated antigorite serpentinites associated with three different type of high-pressure metamorphic rocks in the Itoigawa–Omi area.

The investigated serpentinites can be grouped into two types based on the B isotopes. Antigorite serpentinite with blueschist- and eclogite-facies metamorphic rocks in the Yunotani Valley is characterized by moderate boron (12.5–48.4 $\mu g \cdot g^{-1}$) and lower δ^{11}B (+6.6 to +12.3‰ [mostly smaller than +8‰]; n= 10); Brucite-bearing antigorite serpentinite with barroisite-bearing mafic schist in the Kotaki-gawa River is characterized by very high boron (37.5 –302 $\mu g \cdot g^{-1}$) and lower δ^{11}B (+5.8 to +10.7‰ [mostly smaller than +8‰]; n= 10). In contrast, antigorite serpentinite with garnet amphibolite in the Omi-gawa River is characterized by a wide range of boron (9.1–145 $\mu g \cdot g^{-1}$) and relatively high δ^{11}B (+11.5 to + 14.8 ‰; n= 10).

Our preliminary reconnaissance shows significantly lower δ^{11}B (smaller than +8‰) in antigorite serpentinites of the 'Eclogite Unit' proposed by Tsujimori (2002). This trend is consistent with our earlier study in the Franciscan Complex. The antigorite serpentinites in the 'Eclogite Unit' might have been affected by a deep forearc slab fluids.

Keywords: Serpentinite, boron isotope, subduction zone

©2019. Japan Geoscience Union. All Right Reserved.

Study of zircons structures from the Miocene Shibi-san Granodiorite, Kagoshima Prefecture, Japan

*Nakabayashi Marimo[1], REHMAN Ur Hafiz[1]

1. Kagoshima University

The Miocene granodiorite body (zircon fission track age by Miyachi, 1985) of the Mount Shibi, Kagoshima prefecture is a lenticular stock that intrudes the Cretaceous sedimentary rocks of the Shimanto belt. Previous studies subdivided the granodiorite body into the Kusu-bae (core facies) and Hira-bae (marginal facies) types based on the changes in litho-facies and distinct chemical composition of biotite and amphibole (Yamamoto et al., 1988). We conducted field survey in the study area and found no clear contrasts to sub-divide the body, instead it represents a single pluton with local chemical variation along the marginal portions. Based on detailed petrography, the entire body appears as homogeneous stock exhibiting identical mineral assemblage with no clear evidence that can mark the boundary between Kusu-bae and Hira-bae types. Moreover, to understand the processes of magmatic crystallization we investigated more than 600 zircon grains from about 8 samples for external (applying the zircon morphology method of Pupin, 1980) and internal morphology using the Cathodoluminescence imaging. Based on the Pupin’ s method, the deduced temperature range for the zircon crystallization was between 750 and 850℃. In addition, internal structures of zircon (CL images) showed oscillatory zoning with continuous growth domains and abundant apatite inclusions, suggesting the magma was fluid-rich and have been crystallized under relatively higher temperature. We also investigated zircons from the surrounding hornfels (Shimanto belt rocks) that were affected thermally due to the contact metamorphism. Zircons from the hornfels are completely different and rounded with different internal structures. Zircons from the so-called Kusu-bae and Hira-bae types are identical and suggest their crystallization from a single parental magma hence the pluton cannot be sub divisible.

References
Miyachi M. (1985). Fission track ages of some granitic rocks in Outer Zone ofKyushu, Japan. Journal of Mineralogical and Petrological Sciences 80, 406-409.
Pupin J. P. (1980). Zircon and granite petrology. Contribution to Mineralogy and Petrology 73, 207-220.
Yamamoto M., Oniwa N., Toyota K. (1988). Compositional Variation of the Shibi-san Granodioraite Body, Kagoshima Prefecture, Japan. Bulletin of the Kagoshima University Science Faculty 21, 35-49.

Keywords: zircon, granodiorite, crystal shape

©2019. Japan Geoscience Union. All Right Reserved.

Experimental modeling of eclogite and C-O-H fluid interaction in the subduction zones

*Nadezda Chertkova[1], Shigeru Yamashita[2], Hiroaki Ohfuji[1], Tetsuo Irifune[1], Hirokazu Kadobayashi[1], Yoshitaka Yamamoto[3]

1. Ehime University, Geodynamics Research Center, 2. Okayama University, Institute for Planetary Materials, 3. National Institute of Advanced Industrial Science and Technology

The presence of volatile components controls melting relationships in the subducting oceanic plate and the overlying mantle wedge, affecting their physical properties and seismic observables. The major volatile species in the mantle low oxygen fugacity environment are considered to be H_2O and CH_4, as estimated for mantle xenoliths and C-O-H fluid speciation in equilibrium with diamond [1,2]. Experimental studies with the direct monitoring of phase assemblages and melting relationships in the silicate systems with C-O-H components can shed light on the processes, which take place in the subduction zones, and provide important data for interpretation of observed physical parameters.
In this study, we employed *in situ* spectroscopic methods in combination with the diamond anvil cell (DAC) technique for investigation of C-O-H fluid behavior and its influence on phase relationships in the eclogite–$5.75H_2O$–CH_4 system at temperatures up to 1000 degree C and pressures exceeding 5 GPa. We designed a new cell assembly for Mao-type symmetric diamond anvil cell with large optical access to the sample in order to make it suitable for infrared and Raman measurements directly at high-pressure and high-temperature conditions. Mineral phase assemblages, observed during experiments, are consistent with those described in the dry system of the similar basaltic composition [3]. At the same time, miscibility between aqueous and carbonaceous components in the fluid phase coexisting with silicate minerals was confirmed at temperatures above 800 degree C and pressures above 3.2 GPa.

References

[1] Shirey, S.B., Cartigny, P., Frost, D.J., Keshav, S., Nestola, F., Nimis, P., Pearson, D.G., Sobolev, N.V. and Walter, M.J. (2013) *Rev. Mineral. Geochem.*, **75**, 355-421.
[2] Belonoshko, A. and Saxena, S. (1992) *Geochim. Cosmochim. Acta*, **56**, 3611-3626.
[3] Yasuda, A., Fujii, T. and Kurita, K. (1994) *J. Geophys. Res.: Solid Earth*, **99**, 9401-9414.

©2019. Japan Geoscience Union. All Right Reserved.

Microfabrics of omphacite and garnet in eclogite from the Lanterman Range, northern Victoria Land, Antarctica

*Daeyeong Kim[1], Taehwan Kim[2], Jungmin Kim[3]

1. Division of Polar-Earth Sciences, Korea Polar Research Institute, 2. School of Earth and Environmental Sciences, Seoul National University, 3. Earth and Environmental Sciences, Korea University

Layered structures in metamorphic rocks are sometimes crucial to occur strain localization then affect to seismic properties. We conducted microstructural analyses omphacite and garnet in foliated eclogite from the Lanterman Range, northern Victoria Land, Antarctica, to determine the influence of the layered structure on seismic observations in subduction zone. The analyzed eclogite, composed of layered garnet-rich and omphacite-rich layers, shows the low aspect ratios, similar angular distribution of long axes relative to the foliation, uniform grain size distribution, near-random crystallographic preferred orientations (CPOs), and misorientation angle distributions of garnet and opposite characteristics of omphacite in both layers. The results of fabric analyses are consistent with strain localization into omphacite or omphacite-rich layers rather than garnet or garnet-rich layers. Our results therefore demonstrate the importance of the layered structure in strain localization and in the development of the seismic anisotropies of subducting oceanic crust.

Keywords: Eclogite, EBSD, Layered structure

©2019. Japan Geoscience Union. All Right Reserved.

Primordial Apatite from Ophiolite in Taiwan

*Nobuaki Niitsuma[1], Reishi Takashima[2], Yuan Hsi Lee[3]

1. Institute of Geosciences,Shizuoka University, 2. Tohoku University Museum, 3. National Chung-Cheng University, Taiwan

Apatite is a common accessory mineral in igneous rocks. Because apatite has a wide range of trace element compositions as well as strong resistance to diagenetic alteration, the trace element composition of apatite has been used for tracing petrogenetic processes of plutonic bodies as well as the tephrochronology of Paleozoic tephras and Quaternary volcaniclastic deposits.

We studied trace element compositions of apatites from Ophiolite in Taiwan. The Ophiolite with mafic-ulatramafic rocks (150811-14) expose along the anticlinal axes of the metamorphic belts in Backbone Range of Taiwan, and exotic gabbro block (MA-15B) in chaotic deposits of Lichi Melange, in the southern end of Longitudinal Valley, in East Taiwan.

Lee (2015 JpGU; Chen et al., 2017 Tectonics) reported that zircon ages of Ophiolites in Taiwan are concentrated to 15 Ma, which should relate with termination of spreading in South China Sea and Shikoku & Parece Vela Basin just before Japan Sea Opening, and large scale igneous activities in the Outer Zone of Southwest Japan just after Japan Sea Opening (Niitsuma & Lee, 2018 JpGU).

Fifteen and twelve apatite phenocrysts from samples of MA-15B and 150811-14 were analyzed for major and minor elements using a JEOL 8530F wavelength dispersive Electron Probe Micro Analyzer (Takashima et al., 2017 Quaternary Geochronology) in weight % as follow;
__major elements: P=17.956 +/-0.100, 17.926 +/-0.129
_____Ca=38.362 +/-0.329, 38.128 +/-0.273
_____F=1.082+/-0.151, 0.445+/-0.046
__trace elements: Cl<0.01, 0.04 Mg<0.01, 0.01 Mn<0.04, 0.05
_____Fe<0.03, 0.17 Ce<0.09, 0.05 Y<0.13, 0.04

The contents of trace elements are extremely low and we concluded the apatite might be primordial without any contaminations and petrogenetic effect, and crystallized directly in the magma above rifted mantle along the northwestern margin of West Philippine Basin just before Japan Sea Opening.

Keywords: Apatite, trace element , Ophiolite, Taiwan, Opening of Japan Sea

©2019. Japan Geoscience Union. All Right Reserved.

The evolution of the Cretaceous Jinan Basin in South Korea and the age and tectonic setting for the volcanic rocks in it

*Seung Hwan LEE[1], Chang Whan Oh[1]

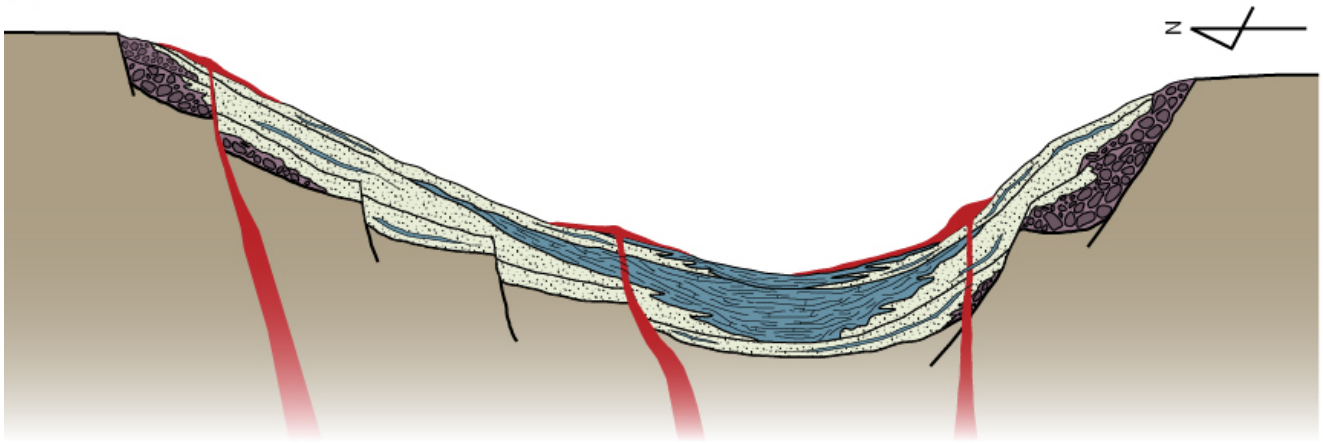
1. Department of earth and environmental sciences Chonbuk national university

The Jinan Basin is one of the Cretaceous pull-apart basins in the South Korea. It locates along the Yongdong-Gwangju fault system and consists of non-marine sediments with volcanic and pyroclastic rocks. The sinistral strike slip movement which formed the Cretaceous pull apart basins was occurred by the collision between Siberian and Manchuria blocks at ca. 130~100Ma. LA-MC-ICPMS age dating on the zircons from sedimentary and igneous rocks indicates followings. The sedimentation in the Jinan Basin had started at least from 97.7Ma and continued until 89.47Ma. During the sedimentation, basaltic andesite extruded at 90-92 Ma and later rhyolitc and andesitic magma intruded the Jinan Basin at 90-89 Ma and 85-84 Ma respectively. Later the Jinan Basin uplifted to form Noryeong mountain range due to the compression which was related with dextral strike slip fault movement. This fault movement is expected to be caused by the collision between Indian plate and Eurasian plate at ca. 55~25Ma. AFT(Apatite Fission Track) age from sediments in the Jinan Basin is approximately 68Ma. Due to the formation of Noryeong mountain range, the *Coreoleuciscus splendidus* was differentiated into two species, these two species of *Coreoleuciscus splendidus* have the same ancestors at around 38Ma. These data indicate that the Noryeong mountain range including the Jinan Basin are expected to have uplifted at around 68-38Ma. Rhyolitic volcanic rocks in and around the Jinan Basin are plotted on the VAG (Volcanic Arc Granite) field and basaltic to intermediated volcanic rocks are plotted on the CAB (Calc-Alkaline Basalt) and WPB (WIthin Plate Basalt) fields in the tectonic discrimination diagrams. There was a roll back of subduction zone toward Pacific ocean at ca. 100 Ma. These data suggest that the igneous rocks in the Jinan Basin formed by the mantle upwelling due to extension caused by the roll back of subduction zone. The upwelling asthenospheric mantle supplied heat which caused the felsic magma by the melting of the lithospheric mantle and crust which had been contaminated by crustal material supplied from subducting sediment or ocean before roll back of the subduction zone. The upwelling asthenospheric mantle was also melted to form basaltic magma. The deep faults formed by sinistral strike slip movement around the Jinan Basin at the Cretaceous, gave the path toward surface for the magma at deep depth.

Keywords: Jinan Basin, pull-apart basin, Igneous rock, Cretaceous

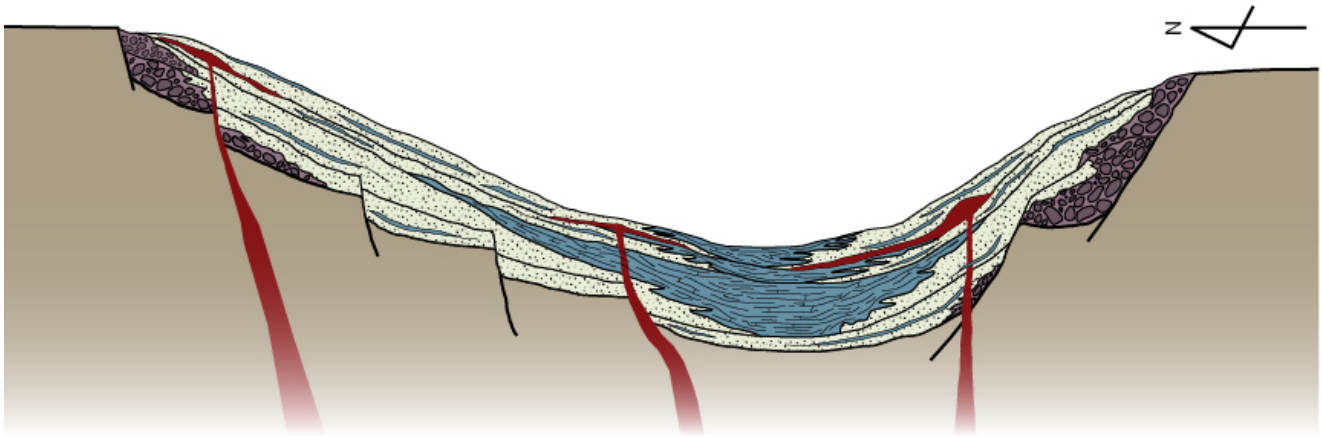
©2019. Japan Geoscience Union. All Right Reserved.

(a) ca. 97 ~90 Ma.



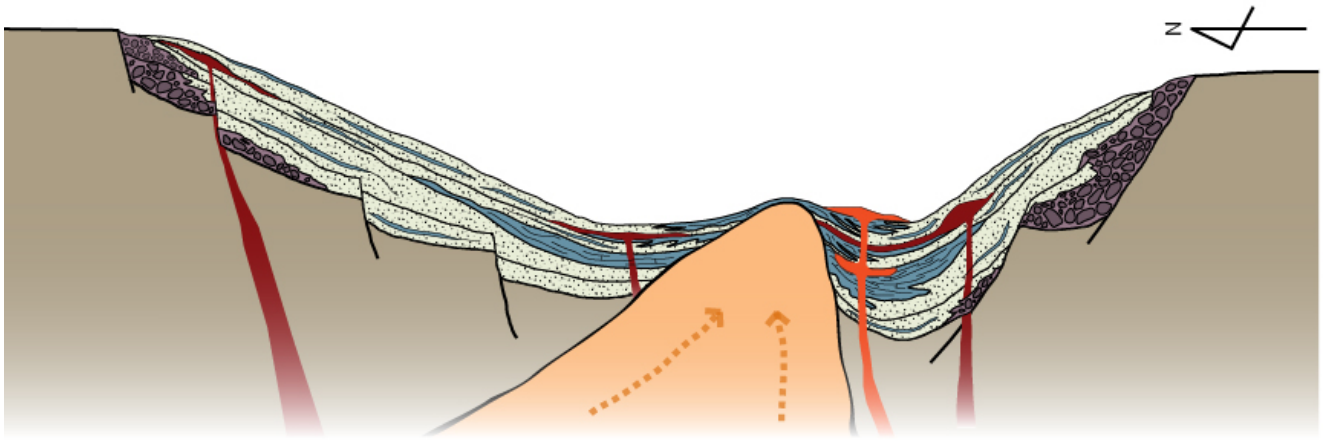
Deposition of lower part sedimentary rocks in the Jinan Basin(97~92 Ma) with extrusion of basaltic andesite(92~90 Ma)

(b) ca. 90 ~89 Ma.



Deposition of upper part sedimentary rocks on the lower part sedimentary rocks and basaltic andesite extrusive volcanic rocks

(c) ca. 89 ~84 Ma.



Intrusion and extrusion of rhyolite(ca. 89Ma) with late intrusion of andesitic volcanic rocks(ca. 84Ma)

Intrusive andesitic volcanic rocks
Rhyolite
Basalt and basaltic andesite
Conglomerate
Sandstone
Shale or mudstone

©2019. Japan Geoscience Union. All Right Reserved.

©2019. Japan Geoscience Union. All Right Reserved.

GEOCHORONOLOGY AND PETROCHEMISTREY OF LATE PALEOZOIC MAGMATIC ROCKS OF THE MANDAKH AREA, SOUTHEAST MONGOLIA

*Undarmaa Batsaikhan[1], Noriyoshi Tsuchiya[1], Masaoki Uno[1], Yukio Isozaki[2], Uyanga Bold[2], Hikaru Sawada[2]

1. Graduate School of Environmental Studies, Tohoku University, 2. Graduate School of Arts and Sciences The University of Tokyo

The southeast Mongolia has become a major survey area for unraveling the Paleozoic tectonic evolution because Mongolia occupies the central part of the CAOB which is enormous and composed of a multiplicity of terranes including ancient island and continental arcs, ophiolites, passive continental margins, Precambrian continental blocks and high-T/low-P metamorphic zones and where porphyry Cu deposits occur. The late Paleozoic magmatic rocks are widely distributed in the Mandakh area which is located in the Curvansaikhan and Manlai terrains, in the southeast Mongolia. We will discuss petrochemical features, mineral assemblage and new geochronological constrain of magmatic rocks in the Mandakh area. Furthermore, we compared petrochemical characteristics of the Mandakh area with Tampakan deposit (Philippines), Cerro Colorado deposit (Chili) and negative criteria of Cu deposits (Japan) in order to characterize potential of the porphyry copper deposit in Mandakh area.

The Mandakh area’ s igneous rocks the geochemical features are calc-alkaline, magnetite-series, I type and similar to adakite type. The Devonian intrusive rocks comprised of syenite and syenogranite, while the Carboniferous intrusive rocks consist of granodiorite, monzodiorite, quartz-monzonite and hornblende granite. Devonian magmatic rocks are more alkali in composition. Although Devonian and Carboniferous igneous rocks in the Mandakh area are a little different each other, these igneous rocks are possibility copper deposits as suggested by petrochemical comparisions with bonanza copper deposits in the world.

Keywords: Petrochemistry, Geochoronology, Southeastern Mongolia, Porphyry Copper deposits

©2019. Japan Geoscience Union. All Right Reserved.

Feedbacks Offshore the Cascadia Margin

*Joan S Gomberg[1]

1. USGS Earthquake Science Center

A growing body of evidence from the Cascadia subduction zone in the U.S. Pacific Northwest suggests that there are significant feedbacks among the offshore upper-plate material properties, geologic and geomorphic structures, seismic shaking, sediment redistribution, and mega-thrust slip behaviors. Analyses of seafloor seismic data show that the thick accretionary wedge sediments amplify and prolong shaking by low-frequency seismic waves and attenuate high frequencies (Gomberg, 2018). This strong contrast in shaking feeds back into reshaping the sediments, by controlling where they are likely to be destabilized and redistributed by shaking. Analyses of submarine landslide morphology and numerical modeling of slope strength suggest that different feedbacks, perhaps related to shaking-induced sediment compaction, may actually make sediments stronger (ten Brink et al., 2016; Scholz et al., 2016). Understanding of these contrasting influences in turn feeds into interpretations of turbidites as proxies for paleo-earthquakes, and hazard assessments based on earthquake recurrence models derived from them; for example, regions with greater numbers of turbidites may reflect permanent features of the shaking that are more suitable to trigger failure, but may be interpreted as indicative of a greater rate of earthquakes. Abrupt strike-perpendicular changes in shaking characteristics, apparent along most of the length of the margin, coincide with sharp gradients in topography and structure along the edge of the continental shelf. This same apparent boundary along the shelf-edge also coincides with concentrations of methane bubble plumes, with gas characteristics indicative of origins within the accretionary prism. One explanation is that the shelf is bounded by faults that connect with the megathrust and act as conduits for gas extrusion, some of which may connect with the megathrust directly or indirectly. This suggests another feedback, as structural changes promote or are caused by faulting, which itself permits pore pressure changes that modify the potential for additional faulting. Taken together, the aforementioned correlations and others observed between areas of non-volcanic tremor with gravity lows, crustal faulting patterns, and marginal basins, imply feedbacks between processes along the megathrust and upper plate structure (Wells et al., 2017). To reduce the degree of speculation about some of these feedbacks, several major experiments are planned and underway. These experiments, to be summarized in this presentation, will image the margin structure with sufficient resolution to identify and characterize faults, map changes in material properties, and more, along nearly the entire length of the Cascadia margin.

Gomberg, J. (2018). Cascadia onshore- offshore site response, submarine sediment mobilization, and earthquake recurrence. Journal of Geophysical Research: Solid Earth, 123, 1381–1404. https://doi.org/10.1002/2017JB014985
Johnson, H. P., Miller, U. K., Salmi, M. S., & Solomon, E. A. (2015). Analysis of bubble plume distributions to evaluate methane hydrate decomposition on the continental slope. Geochemistry, Geophysics, Geosystems, 16, 3825–3839. https://doi.org/10.1002/2015GC005955
Scholz, N. A., Riedel, M., Urlaub, M., Spence, G. D., & Hyndman, R. D. (2016). Submarine landslides offshore Vancouver Island along the northern Cascadia margin, British Columbia: Why preconditioning is likely required to trigger slope failure. Geo-Marine Letters, 36(5), 323–337. https://doi.org/10.1007/s00367-016-0452-8
ten Brink, U. S., Andrews, B. D., & Miller, N. C. (2016). Seismicity and sedimentation rate effects on submarine slope stability. Geology, 44(7), 563–566. https://doi.org/10.1130/G37866.1
Wells, R.E., R.J. Blakely, A.G. Wech, P.A. McCrory, and A. Michael (2017). Cascadia subduction tremor

©2019. Japan Geoscience Union. All Right Reserved.

muted by crustal faults, Geology, 45(6), 515-518, doi:10.1130/G38835.1

©2019. Japan Geoscience Union. All Right Reserved.

[E] Poster | S (Solid Earth Sciences)：S-MP Mineralogy & Petrology

Tue. May 28, 2019 5:15 PM - 6:30 PM JST | Tue. May 28, 2019 8:15 AM - 9:30 AM UTC | Poster Hall International Exhibition Hall8, Makuhari Messe_32

[S-MP29] Oceanic and Continental Subduction Processes

convener:REHMAN Ur Hafiz(Department of Earth and Environmental Sciences, Graduate School of Science and Engineering, Kagoshima University), Tatsuki Tsujimori(Tohoku University), Chin-Ho Tsai(Department of Natural Resources and Environmental Studies, National Dong Hwa University), Kazuaki Okamoto(Faculty of Education, Saitama University)

This JpGU-AGU joint session aims at bringing earth scientists from Japan and overseas to present their research related to the processes of oceanic and continent subduction, continent-continent collisions, metamorphism of crustal rocks, formation of the oceanic/continental arcs, and accretion/ tectonic erosion of material along subduction boundaries.

Topics such as role of the fore- and back-arcs in the subduction zones, process of accretion of volcaniclastic and terrigenous sediments along the subduction/collision boundaries, deformation and metamorphism of subducted crust, and exhumation will be the main focus of the session.

In addition to the above mentioned topics, our focus for the10th anniversary of this international session will be towards our understanding and progress on the ultrahigh-pressure/temperature metamorphic terranes in the world.

Exchange of ideas among geoscientists applying different approaches on problems related to the theme of the session are most welcome.

[SMP29-P01] Zircon U-Pb ages of metasedimentary rocks in the Hakogase (Hida Marginal) area, Fukui Prefecture.

*Atsushi MIYASHITA[1], Tatsuki Tsujimori[2], Daniel Pastor-Galán[3], Yi Keewook[4] (1.Seikei University, 2.Tohoku University, 3.Salamanca University, 4.Korea Basic Science Institue)

[SMP29-P02] Late Permian to Early Triassic back-arc type volcanism in the southern Mongolia volcano-plutonic belt of the Central Asian Orogenic Belt: Implication for timing of the final closure of the Palaeo-Asian Ocean

*Takeshi Imayama[1], Yoichiro Koh[2], Kazumasa Aoki[3], Mototaka Saneyoshi[4], Koshi Yagi[5], Shogo Aoki[4], Yoshihiro Sawada[6], Chiaki Ikawa[5], Tomoya Terada[4], Shinobu Ishigaki[4], Shin Toyoda[3], Khishigjav Tsogtbaatar[7], Buuvei Mainbayar[7] (1.Research Institute of Natural Sciences, Okayama University of Science, 2.Graduate School of Environmental Science, Hokkaido University, 3.Faculty of Science, Okayama University of Science, 4.Faculty of Biosphere - Geosphere Science, Okayama University of Science, 5.Hiruzen Institute for Geology and Chronology, 6.Emeritus Professor of Shimane University, 7.Institute of Paleontology and Geology, Mongolian Academy of Sciences)

[SMP29-P03] Mantle dynamics of slab breakoff constrained from the temporal change of the melting depth estimated from the Cumulate Member of the Ordovician Hayachine-Miyamori Ophiolite

*Takafumi Kimura[1], Kazuhito Ozawa[1] (1.Department of Earth and Planetary Science, The University of Tokyo)

[SMP29-P04] **Evidence of HIMU seamount on the Farallon Plate: Application of *in-situ* Sr-Pb isotope analysis to Franciscan lawsonite-bearing metagreywacke**

*Tomomi Hara[1], Tatsuki Tsujimori[1], Jun-Ichi Kimura[2] (1.Tohoku University, 2.Japan Agency for Marine-Earth Science and Technology)

[SMP29-P05] Boron isotope variations of antigorite serpentinites associated with high-pressure metamorphic rocks: A case study in the Itoigawa–Omi area of the Hida-Gaien Belt, Japan

*Chinatsu Yamada[1], Tatsuki Tsujimori[1], King Chang[2], Jun-Ichi Kimura[2] (1.Tohoku University, 2.Japan Aegency for Marine-Earth Science and Technology)

[SMP29-P06] **Study of zircons structures from the Miocene Shibi-san Granodiorite, Kagoshima Prefecture, Japan**

*Nakabayashi Marimo[1], REHMAN Ur Hafiz[1] (1.Kagoshima University)

[SMP29-P07] **Experimental modeling of eclogite and C-O-H fluid interaction in the subduction zones**

*Nadezda Chertkova[1], Shigeru Yamashita[2], Hiroaki Ohfuji[1], Tetsuo Irifune[1], Hirokazu Kadobayashi[1], Yoshitaka Yamamoto[3] (1.Ehime University, Geodynamics Research Center, 2.Okayama University, Institute for Planetary Materials, 3.National Institute of Advanced Industrial Science and Technology)

[SMP29-P08] Microfabrics of omphacite and garnet in eclogite from the Lanterman Range, northern Victoria Land, Antarctica

*Daeyeong Kim[1], Taehwan Kim[2], Jungmin Kim[3] (1.Division of Polar-Earth Sciences, Korea Polar Research Institute, 2.School of Earth and Environmental Sciences, Seoul National University, 3.Earth and Environmental Sciences, Korea University)

[SMP29-P09] Primordial Apatite from Ophiolite in Taiwan

*Nobuaki Niitsuma[1], Reishi Takashima[2], Yuan Hsi Lee[3] (1.Institute of Geosciences,Shizuoka University, 2.Tohoku University Museum, 3.National Chung-Cheng University, Taiwan)

[SMP29-P10] The evolution of the Cretaceous Jinan Basin in South Korea and the age and tectonic setting for the volcanic rocks in it

*Seung Hwan LEE[1], Chang Whan Oh[1] (1.Department of earth and environmental sciences Chonbuk national university)

[SMP29-P11] GEOCHORONOLOGY AND PETROCHEMISTREY OF LATE PALEOZOIC MAGMATIC ROCKS OF THE MANDAKH AREA, SOUTHEAST MONGOLIA

*Undarmaa Batsaikhan[1], Noriyoshi Tsuchiya[1], Masaoki Uno[1], Yukio Isozaki[2], Uyanga Bold[2], Hikaru Sawada[2] (1.Graduate School of Environmental Studies, Tohoku University, 2.Graduate School of Arts and Sciences The University of Tokyo)

[SMP29-P12] Feedbacks Offshore the Cascadia Margin

*Joan S Gomberg[1] (1.USGS Earthquake Science Center)

Zircon U-Pb ages of metasedimentary rocks in the Hakogase (Hida Marginal) area, Fukui Prefecture.

*Atsushi MIYASHITA[1], Tatsuki Tsujimori[2], Daniel Pastor-Galán[3], Yi Keewook[4]

1. Seikei University, 2. Tohoku University, 3. Salamanca University, 4. Korea Basic Science Institue

Combined chronological study using detrital zircon U-Pb dating and phengite K-Ar dating enables to understand the tectonic evolution of the high *P/T* metamorphic belt. The youngest age of detrital zircon U-Pb ages of psamites in the Hida marginal metamorphic rocks (HMMR = Renge belt) approximate its depositional ages (Tsutsumi et al., 2009). The closure temperature of the phengite K-Ar ages are controlled by deformation and recrystallization during exhumation of the metamorphic rocks(Itaya and Tsujimori, 2015). Therefore, the gap between the youngest age of detrital zircons and phengite K-Ar ages are the age difference between subuduction and uplift of metamorphics.
The Hakogase (Nigure-gawa, Kuzuryu, Fukui Prefecture) metamorphic rocks belong to HMMR member as the olistolith in the Cretaceous Tedori Group. It consists mainly pelites with small amount of basites and mables. The main index mineral assemblage of metasediments are garnet + chlorite, and the phenigite K-Ar ages are 287.8 - 283.6 Ma (Kunugiza et al., 2004). Relic Lawsonite was also found in the basaites and psamites (Miyakawa, 1982).
The detrital Zircons U-Pb ages in the two pelites are obtained by the SHRIMP II of KBSI. The youngest U-Pb ages of detrital zircons are 307Ma. The gap of the sedimentation between uplift of the Hakogase metamorphics is estimated 20 Ma. This value means the migration speed of the HMMR metamorphic rocks are 1/10 of plate motion. This rapid migration speed is common for the high *P/T* metamorphic rocks.

Keywords: high P/T metamorphic rocks, Zircon U-Pb ages, Phengite K-Ar ages

©2019. Japan Geoscience Union. All Right Reserved.

Late Permian to Early Triassic back-arc type volcanism in the southern Mongolia volcano-plutonic belt of the Central Asian Orogenic Belt: Implication for timing of the final closure of the Palaeo-Asian Ocean

*Takeshi Imayama[1], Yoichiro Koh[2], Kazumasa Aoki[3], Mototaka Saneyoshi[4], Koshi Yagi[5], Shogo Aoki[4], Yoshihiro Sawada[6], Chiaki Ikawa[5], Tomoya Terada[4], Shinobu Ishigaki[4], Shin Toyoda[3], Khishigjav Tsogtbaatar[7], Buuvei Mainbayar[7]

1. Research Institute of Natural Sciences, Okayama University of Science, 2. Graduate School of Environmental Science, Hokkaido University, 3. Faculty of Science, Okayama University of Science, 4. Faculty of Biosphere - Geosphere Science, Okayama University of Science, 5. Hiruzen Institute for Geology and Chronology, 6. Emeritus Professor of Shimane University, 7. Institute of Paleontology and Geology, Mongolian Academy of Sciences

The timing of final subduction and closure of the Palaeo-Asian Ocean is still controversial in the eastern segments of the Central Asian Orogenic Belt (CAOB). A more detailed understanding is needed with respect to the formation of volcanic rocks and sediments associated with the final closure of the Palaeo-Asian Ocean in southern Mongolia. We investigated alkali series volcanic rocks newly discovered in the southern Mongolia volcano-plutonic belt of the CAOB and classified as basalt, basaltic trachyandesite, andesite, trachyandesite, and trachyte, mainly showing andesitic-dacitic compositions. In Harker diagrams, the TiO_2, FeO, MnO, Al_2O_3, CaO, and MgO contents generally decrease with increasing SiO_2, representing a series of differentiated volcanic rocks. The primitive mantle-normalized trace element spider diagram is characterized by incompatible element-rich patterns and negative Nb anomalies. The tectonic discrimination diagrams show that the volcanic rocks were formed by arc-related volcanism rather than within-plate volcanism. K-Ar dating of feldspars from six volcanic rocks yields ages ranging from 270 to 239 Ma, indicating that andesitic and dacitic magmatism occurred during this period. These geochemical and geochronological data indicate that the differentiated volcanic rocks intruding middle to late Palaeozoic volcanic sediments were formed by back-arc type subduction ca. 270–240 Ma. Based on detrital zircon U-Pb ages, the terrigenous sandstones underlain by the volcanic sediments record a maximum depositional age of Late Triassic (ca. 220–200 Ma) and include a main cluster of Early Devonian ages (ca. 410–390 Ma), possibly derived from the Devonian-Carboniferous arc complex observed surrounding this study area. These results from the volcanic and sedimentary rocks in this study, combined with investigations in previous studies, imply that subduction beneath the eastern segments of the CAOB to consume the Palaeo-Asian Ocean continued until Late Permian to Early Triassic.

Keywords: Palaeo-Asian Ocean, southern Mongolia, Central Asian Orogenic Belt, back-arc type volcanism

©2019. Japan Geoscience Union. All Right Reserved.

Mantle dynamics of slab breakoff constrained from the temporal change of the melting depth estimated from the Cumulate Member of the Ordovician Hayachine-Miyamori Ophiolite

*Takafumi Kimura[1], Kazuhito Ozawa[1]

1. Department of Earth and Planetary Science, The University of Tokyo

Slab breakoff, detachment of oceanic lithosphere highly expected during arc-continent collision, is one of the important mechanisms inducing passive upwelling of the asthenosphere and magma generation in arc environments [1]. In order to better understand the mantle dynamics of slab breakoff, we need to use continuous geological record with high time resolution. In this study, we have extracted a record of temporal change of the magma generation depth from cumulates in an Ordovician arc ophiolite at a time resolution of several tens of million years.
The Hayachine-Miyamori Ophiolite, northern Japan, is one of the Ordovician ophiolite formed in an arc environment [2]. The ultramafic member was built up by three main magmatic stages, which are recorded in three rock units: Tectonite Member, Cumulate Member, and ultramafic dikes, in the order of formation ages. The last two units in the entire evolution of the ophiolite is explained by decompressional melting of sub-slab mantle triggered by slab breakoff [2][3]. The melting depth of an ultramafic magma solidified as dikes in the Cumulate Member is estimated to be ~170km [3]. Our recent field study clarified a large-scale stratification characterized by alternation of wehrlite-dominant and dunite-dominant layers in the Cumulate Member. Each layer has a thickness from several meters to ~1 km and, the total thickness attains ~3km. Moreover, we succeeded in specifying the strike and plunge of the gravity field to be ~N48°E and ~20°NE during the cumulate formation from field information and westward stratigraphic younging [4].
We estimated the temporal change of generation depth of parent magmas of the Cumulate Member by garnet signature in heavy rare earth elements (HREEs) as depth proxy. The information may constrain the mantle dynamics during the slab breakoff. We examined stratigraphic variation of HREE ratio at the core of clinopyroxenes over the thickness of ~2km in the Cumulate Member. The obtained variation of the Dy/Lu increases from ~12.9 to ~16.5 with increasing the stratigraphic height. We estimated the extent of melting in the garnet stability field increasing from ~50 to ~90% of the total melting by applying an open-system fractional melting model to reproduce the Dy/Lu variation.
We also estimated the time scale of formation of the Cumulate Member by using cm –10cm scale heterogeneity recorded in contact zone of intruded magma and the host. The profile of Mg# of olivine in xenoliths of the Tectonite Member occurring at the bottom of the Cumulate Member shows that the cooling time is less than several tens of million years [5]. The dunite of the Cumulate Member contacting the ultramafic dike shows a systematic decrease of Mg# from 90 to 86.8 over the distance of 54 mm towards the contact. We calculated the time scale of subsolidus diffusional exchange between the dunite and dike and obtained several tens of million years at ~1000℃. The host was kept at a high temperature when the dikes intruded because of the absence of chilled margin. We thus estimated time scale of formation of the Cumulate Member to be < several tens of million years.
We propose the following tectonic model in the Ordovician northern Japan on the basis of the above result. The slab breakoff took place at the depth slightly deeper than the boundary of spinel and garnet stability fields (~80 km) and induced counter flow and adiabatic melting of the sub-slab mantle. The melting depth deepened down to ~170 km on the time scale of several tens of million years, which corresponds to the time scale to complete the slab breakoff. The sinking velocity of the slab is more than

©2019. Japan Geoscience Union. All Right Reserved.

a few millimeters per year.

[1]: Davies et al., 1995. [2]: Ozawa et al., 2015. [3],[4]: Kimura et al., 2017, 2018, JpGU abstract. [5]: Ozawa, 1983.

Keywords: slab breakoff, arc ophiolite, cumulate

©2019. Japan Geoscience Union. All Right Reserved.

Evidence of HIMU seamount on the Farallon Plate: Application of *in-situ* Sr-Pb isotope analysis to Franciscan lawsonite-bearing metagreywacke

*Tomomi Hara[1], Tatsuki Tsujimori[1], Jun-Ichi Kimura[2]

1. Tohoku University, 2. Japan Agency for Marine-Earth Science and Technology

Since bulk isotopic composition of oceanic basalt is susceptible to element remobilization during alteration process, there is a risk of causing misread of geochemical signatures from bulk metabasaltic rocks in subduction complex. As Hara et al. (2018) demonstrated, however, *in-situ* Sr-Pb isotope analysis of lawsonite in high-pressure metabasaltic rocks has a great potential for tracing the geochemical signatures reflecting the igneous protolith. In this study, we have applied the method to lawsonite in metasedimentary rocks to explore clastic components of a trench-fill sediment. A jadeite-bearing Franciscan metagreywacke from Pacheco Pass area, east-central Diablo Range, California Coast Ranges was selected for geochemical reconnaissance.

Lawsonites in the Franciscan metagreywacke record a high initial Pb isotope ratios ($^{206}Pb/^{204}Pb$ = 18.74–19.66, $^{207}Pb/^{204}Pb$ = 15.58–15.70 and $^{208}Pb/^{204}Pb$ = 38.41–39.34). This Pb-isotope signature suggests that a protolith of the metagreywacke have contained a debris derived from a HIMU-type basalt. Considering the maximum depositional age of the metagreywacke at ~102 Ma, the underflow of the Farallon Plate beneath continental crust of the North American Plate would have carried a HIMU seamount to a Franciscan trench.

Our study has demonstrated the potential application of 'lawsonitology' as sedimentary provenance analyses for metamorphosed accretionary complex. Moreover, the results would manifest that Pb isotopic signature of ancient oceanic basalt can be detectable from Ca-Al silicate mineral, such as lawsonite, epidote and pumpellyite, in metamorphic rocks.

Keywords: Lawsonite, Sr-Pb isotope, LA-MC-ICPMS, HIMU, Metasediment

©2019. Japan Geoscience Union. All Right Reserved.

Boron isotope variations of antigorite serpentinites associated with high-pressure metamorphic rocks: A case study in the Itoigawa–Omi area of the Hida-Gaien Belt, Japan

*Chinatsu Yamada[1], Tatsuki Tsujimori[1], King Chang[2], Jun-Ichi Kimura[2]

1. Tohoku University, 2. Japan Aegency for Marine-Earth Science and Technology

Boron isotope study of serpentinites in the Franciscan Complex using an ablation volume correction (AVC) LA-MC-ICPMS discriminates two groups (Yamada et al., 2018 JpGU abstr.; Yamada et al. 2019, in press). Serpentinites associated with blueschists are characterized by lighter boron isotope than serpentinites without blueschist-facies rocks. The lighter boron isotope signature (< ~10 ‰) of blueschist-bearing serpentinites results from interaction with forearc slab fluids with low δ^{11}B in deeper depth. In order to evaluate the versatility of B isotopes and composition of high-pressure metamorphosed serpentinites, we investigated antigorite serpentinites associated with three different type of high-pressure metamorphic rocks in the Itoigawa–Omi area.

The investigated serpentinites can be grouped into two types based on the B isotopes. Antigorite serpentinite with blueschist- and eclogite-facies metamorphic rocks in the Yunotani Valley is characterized by moderate boron (12.5–48.4 $\mu g \cdot g^{-1}$) and lower δ^{11}B (+6.6 to +12.3‰ [mostly smaller than +8‰]; n= 10); Brucite-bearing antigorite serpentinite with barroisite-bearing mafic schist in the Kotaki-gawa River is characterized by very high boron (37.5 –302 $\mu g \cdot g^{-1}$) and lower δ^{11}B (+5.8 to +10.7‰ [mostly smaller than +8‰]; n= 10). In contrast, antigorite serpentinite with garnet amphibolite in the Omi-gawa River is characterized by a wide range of boron (9.1–145 $\mu g \cdot g^{-1}$) and relatively high δ^{11}B (+11.5 to + 14.8 ‰; n= 10).

Our preliminary reconnaissance shows significantly lower δ^{11}B (smaller than +8‰) in antigorite serpentinites of the 'Eclogite Unit' proposed by Tsujimori (2002). This trend is consistent with our earlier study in the Franciscan Complex. The antigorite serpentinites in the 'Eclogite Unit' might have been affected by a deep forearc slab fluids.

Keywords: Serpentinite, boron isotope, subduction zone

©2019. Japan Geoscience Union. All Right Reserved.

Study of zircons structures from the Miocene Shibi-san Granodiorite, Kagoshima Prefecture, Japan

*Nakabayashi Marimo[1], REHMAN Ur Hafiz[1]

1. Kagoshima University

The Miocene granodiorite body (zircon fission track age by Miyachi, 1985) of the Mount Shibi, Kagoshima prefecture is a lenticular stock that intrudes the Cretaceous sedimentary rocks of the Shimanto belt. Previous studies subdivided the granodiorite body into the Kusu-bae (core facies) and Hira-bae (marginal facies) types based on the changes in litho-facies and distinct chemical composition of biotite and amphibole (Yamamoto et al., 1988). We conducted field survey in the study area and found no clear contrasts to sub-divide the body, instead it represents a single pluton with local chemical variation along the marginal portions. Based on detailed petrography, the entire body appears as homogeneous stock exhibiting identical mineral assemblage with no clear evidence that can mark the boundary between Kusu-bae and Hira-bae types. Moreover, to understand the processes of magmatic crystallization we investigated more than 600 zircon grains from about 8 samples for external (applying the zircon morphology method of Pupin, 1980) and internal morphology using the Cathodoluminescence imaging. Based on the Pupin’ s method, the deduced temperature range for the zircon crystallization was between 750 and 850℃. In addition, internal structures of zircon (CL images) showed oscillatory zoning with continuous growth domains and abundant apatite inclusions, suggesting the magma was fluid-rich and have been crystallized under relatively higher temperature. We also investigated zircons from the surrounding hornfels (Shimanto belt rocks) that were affected thermally due to the contact metamorphism. Zircons from the hornfels are completely different and rounded with different internal structures. Zircons from the so-called Kusu-bae and Hira-bae types are identical and suggest their crystallization from a single parental magma hence the pluton cannot be sub divisible.

References
Miyachi M. (1985). Fission track ages of some granitic rocks in Outer Zone ofKyushu, Japan. Journal of Mineralogical and Petrological Sciences 80, 406-409.
Pupin J. P. (1980). Zircon and granite petrology. Contribution to Mineralogy and Petrology 73, 207-220.
Yamamoto M., Oniwa N., Toyota K. (1988). Compositional Variation of the Shibi-san Granodioraite Body, Kagoshima Prefecture, Japan. Bulletin of the Kagoshima University Science Faculty 21, 35-49.

Keywords: zircon, granodiorite, crystal shape

©2019. Japan Geoscience Union. All Right Reserved.

Experimental modeling of eclogite and C-O-H fluid interaction in the subduction zones

*Nadezda Chertkova[1], Shigeru Yamashita[2], Hiroaki Ohfuji[1], Tetsuo Irifune[1], Hirokazu Kadobayashi[1], Yoshitaka Yamamoto[3]

1. Ehime University, Geodynamics Research Center, 2. Okayama University, Institute for Planetary Materials, 3. National Institute of Advanced Industrial Science and Technology

The presence of volatile components controls melting relationships in the subducting oceanic plate and the overlying mantle wedge, affecting their physical properties and seismic observables. The major volatile species in the mantle low oxygen fugacity environment are considered to be H_2O and CH_4, as estimated for mantle xenoliths and C-O-H fluid speciation in equilibrium with diamond [1,2]. Experimental studies with the direct monitoring of phase assemblages and melting relationships in the silicate systems with C-O-H components can shed light on the processes, which take place in the subduction zones, and provide important data for interpretation of observed physical parameters.
In this study, we employed *in situ* spectroscopic methods in combination with the diamond anvil cell (DAC) technique for investigation of C-O-H fluid behavior and its influence on phase relationships in the eclogite–$5.75H_2O$–CH_4 system at temperatures up to 1000 degree C and pressures exceeding 5 GPa. We designed a new cell assembly for Mao-type symmetric diamond anvil cell with large optical access to the sample in order to make it suitable for infrared and Raman measurements directly at high-pressure and high-temperature conditions. Mineral phase assemblages, observed during experiments, are consistent with those described in the dry system of the similar basaltic composition [3]. At the same time, miscibility between aqueous and carbonaceous components in the fluid phase coexisting with silicate minerals was confirmed at temperatures above 800 degree C and pressures above 3.2 GPa.

References

[1] Shirey, S.B., Cartigny, P., Frost, D.J., Keshav, S., Nestola, F., Nimis, P., Pearson, D.G., Sobolev, N.V. and Walter, M.J. (2013) *Rev. Mineral. Geochem.*, **75**, 355-421.
[2] Belonoshko, A. and Saxena, S. (1992) *Geochim. Cosmochim. Acta*, **56**, 3611-3626.
[3] Yasuda, A., Fujii, T. and Kurita, K. (1994) *J. Geophys. Res.: Solid Earth*, **99**, 9401-9414.

©2019. Japan Geoscience Union. All Right Reserved.

Microfabrics of omphacite and garnet in eclogite from the Lanterman Range, northern Victoria Land, Antarctica

*Daeyeong Kim[1], Taehwan Kim[2], Jungmin Kim[3]

1. Division of Polar-Earth Sciences, Korea Polar Research Institute, 2. School of Earth and Environmental Sciences, Seoul National University, 3. Earth and Environmental Sciences, Korea University

Layered structures in metamorphic rocks are sometimes crucial to occur strain localization then affect to seismic properties. We conducted microstructural analyses omphacite and garnet in foliated eclogite from the Lanterman Range, northern Victoria Land, Antarctica, to determine the influence of the layered structure on seismic observations in subduction zone. The analyzed eclogite, composed of layered garnet-rich and omphacite-rich layers, shows the low aspect ratios, similar angular distribution of long axes relative to the foliation, uniform grain size distribution, near-random crystallographic preferred orientations (CPOs), and misorientation angle distributions of garnet and opposite characteristics of omphacite in both layers. The results of fabric analyses are consistent with strain localization into omphacite or omphacite-rich layers rather than garnet or garnet-rich layers. Our results therefore demonstrate the importance of the layered structure in strain localization and in the development of the seismic anisotropies of subducting oceanic crust.

Keywords: Eclogite, EBSD, Layered structure

©2019. Japan Geoscience Union. All Right Reserved.

Primordial Apatite from Ophiolite in Taiwan

*Nobuaki Niitsuma[1], Reishi Takashima[2], Yuan Hsi Lee[3]

1. Institute of Geosciences,Shizuoka University, 2. Tohoku University Museum, 3. National Chung-Cheng University, Taiwan

Apatite is a common accessory mineral in igneous rocks. Because apatite has a wide range of trace element compositions as well as strong resistance to diagenetic alteration, the trace element composition of apatite has been used for tracing petrogenetic processes of plutonic bodies as well as the tephrochronology of Paleozoic tephras and Quaternary volcaniclastic deposits.

We studied trace element compositions of apatites from Ophiolite in Taiwan. The Ophiolite with mafic-ulatramafic rocks (150811-14) expose along the anticlinal axes of the metamorphic belts in Backbone Range of Taiwan, and exotic gabbro block (MA-15B) in chaotic deposits of Lichi Melange, in the southern end of Longitudinal Valley, in East Taiwan.

Lee (2015 JpGU; Chen et al., 2017 Tectonics) reported that zircon ages of Ophiolites in Taiwan are concentrated to 15 Ma, which should relate with termination of spreading in South China Sea and Shikoku & Parece Vela Basin just before Japan Sea Opening, and large scale igneous activities in the Outer Zone of Southwest Japan just after Japan Sea Opening (Niitsuma & Lee, 2018 JpGU).

Fifteen and twelve apatite phenocrysts from samples of MA-15B and 150811-14 were analyzed for major and minor elements using a JEOL 8530F wavelength dispersive Electron Probe Micro Analyzer (Takashima et al., 2017 Quaternary Geochronology) in weight % as follow;
__major elements: P=17.956 +/-0.100, 17.926 +/-0.129
_____Ca=38.362 +/-0.329, 38.128 +/-0.273
_____F=1.082+/-0.151, 0.445+/-0.046
__trace elements: Cl<0.01, 0.04 Mg<0.01, 0.01 Mn<0.04, 0.05
_____Fe<0.03, 0.17 Ce<0.09, 0.05 Y<0.13, 0.04

The contents of trace elements are extremely low and we concluded the apatite might be primordial without any contaminations and petrogenetic effect, and crystallized directly in the magma above rifted mantle along the northwestern margin of West Philippine Basin just before Japan Sea Opening.

Keywords: Apatite, trace element , Ophiolite, Taiwan, Opening of Japan Sea

©2019. Japan Geoscience Union. All Right Reserved.

The evolution of the Cretaceous Jinan Basin in South Korea and the age and tectonic setting for the volcanic rocks in it

*Seung Hwan LEE[1], Chang Whan Oh[1]

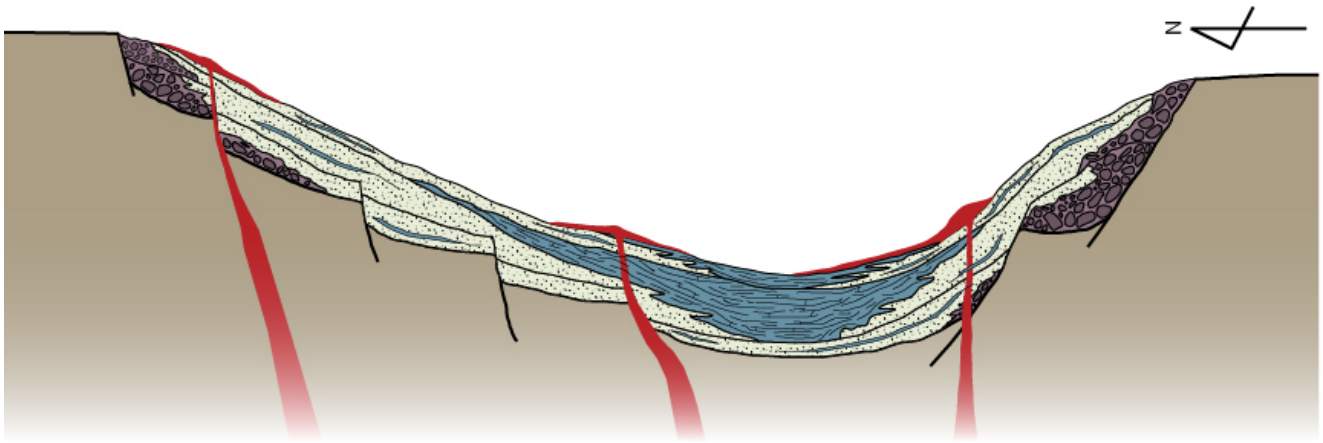
1. Department of earth and environmental sciences Chonbuk national university

The Jinan Basin is one of the Cretaceous pull-apart basins in the South Korea. It locates along the Yongdong-Gwangju fault system and consists of non-marine sediments with volcanic and pyroclastic rocks. The sinistral strike slip movement which formed the Cretaceous pull apart basins was occurred by the collision between Siberian and Manchuria blocks at ca. 130~100Ma. LA-MC-ICPMS age dating on the zircons from sedimentary and igneous rocks indicates followings. The sedimentation in the Jinan Basin had started at least from 97.7Ma and continued until 89.47Ma. During the sedimentation, basaltic andesite extruded at 90-92 Ma and later rhyolitc and andesitic magma intruded the Jinan Basin at 90-89 Ma and 85-84 Ma respectively. Later the Jinan Basin uplifted to form Noryeong mountain range due to the compression which was related with dextral strike slip fault movement. This fault movement is expected to be caused by the collision between Indian plate and Eurasian plate at ca. 55~25Ma. AFT(Apatite Fission Track) age from sediments in the Jinan Basin is approximately 68Ma. Due to the formation of Noryeong mountain range, the *Coreoleuciscus splendidus* was differentiated into two species, these two species of *Coreoleuciscus splendidus* have the same ancestors at around 38Ma. These data indicate that the Noryeong mountain range including the Jinan Basin are expected to have uplifted at around 68-38Ma. Rhyolitic volcanic rocks in and around the Jinan Basin are plotted on the VAG (Volcanic Arc Granite) field and basaltic to intermediated volcanic rocks are plotted on the CAB (Calc-Alkaline Basalt) and WPB (WIthin Plate Basalt) fields in the tectonic discrimination diagrams. There was a roll back of subduction zone toward Pacific ocean at ca. 100 Ma. These data suggest that the igneous rocks in the Jinan Basin formed by the mantle upwelling due to extension caused by the roll back of subduction zone. The upwelling asthenospheric mantle supplied heat which caused the felsic magma by the melting of the lithospheric mantle and crust which had been contaminated by crustal material supplied from subducting sediment or ocean before roll back of the subduction zone. The upwelling asthenospheric mantle was also melted to form basaltic magma. The deep faults formed by sinistral strike slip movement around the Jinan Basin at the Cretaceous, gave the path toward surface for the magma at deep depth.

Keywords: Jinan Basin, pull-apart basin, Igneous rock, Cretaceous

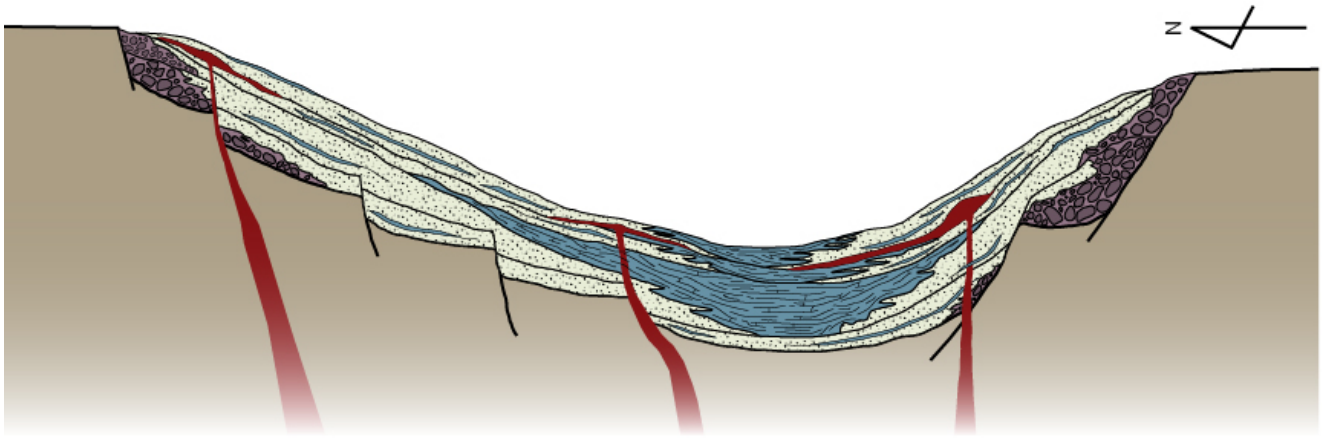
©2019. Japan Geoscience Union. All Right Reserved.

(a) ca. 97 ~90 Ma.



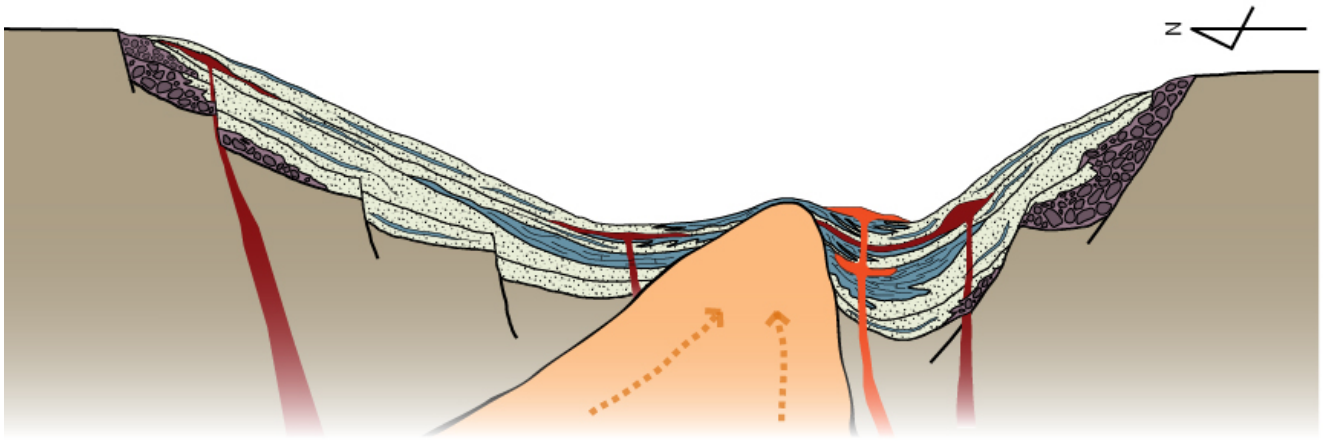
Deposition of lower part sedimentary rocks in the Jinan Basin(97~92 Ma) with extrusion of basaltic andesite(92~90 Ma)

(b) ca. 90 ~89 Ma.



Deposition of upper part sedimentary rocks on the lower part sedimentary rocks and basaltic andesite extrusive volcanic rocks

(c) ca. 89 ~84 Ma.



Intrusion and extrusion of rhyolite(ca. 89Ma) with late intrusion of andesitic volcanic rocks(ca. 84Ma)

Intrusive andesitic volcanic rocks
Rhyolite
Basalt and basaltic andesite
Conglomerate
Sandstone
Shale or mudstone

©2019. Japan Geoscience Union. All Right Reserved.

©2019. Japan Geoscience Union. All Right Reserved.

GEOCHORONOLOGY AND PETROCHEMISTREY OF LATE PALEOZOIC MAGMATIC ROCKS OF THE MANDAKH AREA, SOUTHEAST MONGOLIA

*Undarmaa Batsaikhan[1], Noriyoshi Tsuchiya[1], Masaoki Uno[1], Yukio Isozaki[2], Uyanga Bold[2], Hikaru Sawada[2]

1. Graduate School of Environmental Studies, Tohoku University, 2. Graduate School of Arts and Sciences The University of Tokyo

The southeast Mongolia has become a major survey area for unraveling the Paleozoic tectonic evolution because Mongolia occupies the central part of the CAOB which is enormous and composed of a multiplicity of terranes including ancient island and continental arcs, ophiolites, passive continental margins, Precambrian continental blocks and high-T/low-P metamorphic zones and where porphyry Cu deposits occur. The late Paleozoic magmatic rocks are widely distributed in the Mandakh area which is located in the Curvansaikhan and Manlai terrains, in the southeast Mongolia. We will discuss petrochemical features, mineral assemblage and new geochronological constrain of magmatic rocks in the Mandakh area. Furthermore, we compared petrochemical characteristics of the Mandakh area with Tampakan deposit (Philippines), Cerro Colorado deposit (Chili) and negative criteria of Cu deposits (Japan) in order to characterize potential of the porphyry copper deposit in Mandakh area.

The Mandakh area’ s igneous rocks the geochemical features are calc-alkaline, magnetite-series, I type and similar to adakite type. The Devonian intrusive rocks comprised of syenite and syenogranite, while the Carboniferous intrusive rocks consist of granodiorite, monzodiorite, quartz-monzonite and hornblende granite. Devonian magmatic rocks are more alkali in composition. Although Devonian and Carboniferous igneous rocks in the Mandakh area are a little different each other, these igneous rocks are possibility copper deposits as suggested by petrochemical comparisions with bonanza copper deposits in the world.

Keywords: Petrochemistry, Geochoronology, Southeastern Mongolia, Porphyry Copper deposits

©2019. Japan Geoscience Union. All Right Reserved.

Feedbacks Offshore the Cascadia Margin

*Joan S Gomberg[1]

1. USGS Earthquake Science Center

A growing body of evidence from the Cascadia subduction zone in the U.S. Pacific Northwest suggests that there are significant feedbacks among the offshore upper-plate material properties, geologic and geomorphic structures, seismic shaking, sediment redistribution, and mega-thrust slip behaviors. Analyses of seafloor seismic data show that the thick accretionary wedge sediments amplify and prolong shaking by low-frequency seismic waves and attenuate high frequencies (Gomberg, 2018). This strong contrast in shaking feeds back into reshaping the sediments, by controlling where they are likely to be destabilized and redistributed by shaking. Analyses of submarine landslide morphology and numerical modeling of slope strength suggest that different feedbacks, perhaps related to shaking-induced sediment compaction, may actually make sediments stronger (ten Brink et al., 2016; Scholz et al., 2016). Understanding of these contrasting influences in turn feeds into interpretations of turbidites as proxies for paleo-earthquakes, and hazard assessments based on earthquake recurrence models derived from them; for example, regions with greater numbers of turbidites may reflect permanent features of the shaking that are more suitable to trigger failure, but may be interpreted as indicative of a greater rate of earthquakes. Abrupt strike-perpendicular changes in shaking characteristics, apparent along most of the length of the margin, coincide with sharp gradients in topography and structure along the edge of the continental shelf. This same apparent boundary along the shelf-edge also coincides with concentrations of methane bubble plumes, with gas characteristics indicative of origins within the accretionary prism. One explanation is that the shelf is bounded by faults that connect with the megathrust and act as conduits for gas extrusion, some of which may connect with the megathrust directly or indirectly. This suggests another feedback, as structural changes promote or are caused by faulting, which itself permits pore pressure changes that modify the potential for additional faulting. Taken together, the aforementioned correlations and others observed between areas of non-volcanic tremor with gravity lows, crustal faulting patterns, and marginal basins, imply feedbacks between processes along the megathrust and upper plate structure (Wells et al., 2017). To reduce the degree of speculation about some of these feedbacks, several major experiments are planned and underway. These experiments, to be summarized in this presentation, will image the margin structure with sufficient resolution to identify and characterize faults, map changes in material properties, and more, along nearly the entire length of the Cascadia margin.

Gomberg, J. (2018). Cascadia onshore- offshore site response, submarine sediment mobilization, and earthquake recurrence. Journal of Geophysical Research: Solid Earth, 123, 1381–1404. https://doi.org/10.1002/2017JB014985
Johnson, H. P., Miller, U. K., Salmi, M. S., & Solomon, E. A. (2015). Analysis of bubble plume distributions to evaluate methane hydrate decomposition on the continental slope. Geochemistry, Geophysics, Geosystems, 16, 3825–3839. https://doi.org/10.1002/2015GC005955
Scholz, N. A., Riedel, M., Urlaub, M., Spence, G. D., & Hyndman, R. D. (2016). Submarine landslides offshore Vancouver Island along the northern Cascadia margin, British Columbia: Why preconditioning is likely required to trigger slope failure. Geo-Marine Letters, 36(5), 323–337. https://doi.org/10.1007/s00367-016-0452-8
ten Brink, U. S., Andrews, B. D., & Miller, N. C. (2016). Seismicity and sedimentation rate effects on submarine slope stability. Geology, 44(7), 563–566. https://doi.org/10.1130/G37866.1
Wells, R.E., R.J. Blakely, A.G. Wech, P.A. McCrory, and A. Michael (2017). Cascadia subduction tremor

©2019. Japan Geoscience Union. All Right Reserved.

muted by crustal faults, Geology, 45(6), 515-518, doi:10.1130/G38835.1

©2019. Japan Geoscience Union. All Right Reserved.

[E] Poster | S (Solid Earth Sciences)：S-MP Mineralogy & Petrology

Tue. May 28, 2019 10:45 AM - 12:15 PM JST | Tue. May 28, 2019 1:45 AM - 3:15 AM UTC | Poster Hall International Exhibition Hall8, Makuhari Messe_8

[S-MP30] Crust-Mantle Connections

convener:Yoshihiko Tamura(Research Institute for Marine Geodynamics, Japan Agency for Maine-Earth Science and Technology), Osamu Ishizuka(Geological Survey of Japan, AIST), Chris Conway(Geological Survey of Japan)

A paradigm of the solid Earth geochemical cycles is that the Earth's crust forms by melting of the Earth's upper peridotitic mantle. How divers is the spectrum of primary melts and which factors may contribute to its variations? What is the influence of crustal processing vs. primary magma diversity in creating the diversity of the Earth's crust? The session seeks to explore the crust-mantle connections at divergent and convergent plate boundaries, and oceanic island settings based on volcanology, petrology, geochemistry, geophysics, geochronology, and geodynamics studies.

[SMP30-P01] Secular evolution of proto-Izu-Bonin-Mariana arc volcanism: Constraints from statistical analysis of melt inclusion compositions

*Morihisa Hamada[1], Hikaru Iwamori[1,2], Philipp A. Brandl[3], Takayuki Ushikubo[4], Kenji Shimizu[4], Motoo Ito[4], He Li[5], Ivan P. Savov[6] (1.Department of Solid Earth Geochemistry, Japan Agency for Marine-Earth Science and Technology, 2.Earthquake Research Institute, University of Tokyo, 3.GEOMAR Helmholtz Centre for Ocean Research Kiel, 4.Kochi Institute for Core Sample Research, Japan Agency for Marine-Earth Science and Technology, 5.Institute of Oceanology, Chinese Academy of Sciences, 6.School of Earth and Environment, University of Leeds)

[SMP30-P02] The Jurassic magmatism of protoliths of Mikabu greenstones in SW Japan: zircon U-Pb dating and trace element analysis

*Hikaru Sawada[1], Yukio Isozaki[1], Shogo Aoki[3], Shuhei Sakata[2], Ryo Hasegawa[1], Yasuo Nakamura[1] (1.Department of General Systems Studies, the University of Tokyo, 2.Department of Chemistry, Gakushuin Universtiy, 3.Department of Applied Science, Okayama University of Science)

[SMP30-P03] Origin of variable CaO/Al_2O_3 in olivine-hosted melt inclusions from Kibblewhite Volcano, Kermadec Arc

*Yasuhiro Hirai[1], Yoshihiko Tamura[2], Kaj Hoernle[3], Christian Timm[4], Folkmar Hauff[3], Reinhard Werner[3], Takeshi Hanyu[2], Bogdan Vaglarov[2], Qing Chang[2], Takashi Miyazaki[2], Jun-Ichi Kimura[2] (1.Graduate School of Natural Science and Technology, Kanazawa University, Japan, 2.Japan Agency for Marine-Earth Science and Technology (JAMSTEC), Yokosuka, Kanagawa, Japan, 3.GEOMAR Helmholtz Centre for Ocean Research, Kiel, Germany, 4.GNS Science, Lower Hutt, New Zealand)

[SMP30-P04] Ankaramite from Doyo seamount in the Izu-Ogasawara arc: A precursor of continents?

*Yoshihiko Tamura[1], Tomoki Sato[1], Osamu Ishizuka[1,2], Takashi Miyazaki[1], Yasuhiro Hirai[1,3], Mami Takehara[4], Eri Sakamoto[5] (1.JAMSTEC, 2.AIST, 3.Kanazawa Univ., 4.NIPR, 5.NME)

[SMP30-P05] Different Moho reflections adjacent to Minami-Tori Shima and their petrologic origins

*Yoshihiko Tamura[1], Kentaro Kaneda[2], Gou Fujie[1], Akane Ohira[1], Eiichi TAKAZAWA[3], Georges Ceuleneer[4], Katsuyoshi Michibayashi[5], Tomoki Sato[1], Shuichi Kodaira[1], Seiichi Miura[1] (1.Japan Agency for Maine-Earth Science and Technology, 2.Japan Coast Guard, 3.Niigata University, 4.Universite de Toulouse, 5.Nagoya University)

[SMP30-P06] Melt-rock interaction in plagioclase peridotites from the southern Palawan Ophiolite, Philippines

*FLORENCE ANNETTE CRUSPERO LABIS[1], BETCHAIDA D PAYOT[1], GABRIEL THEOPHILUS V VALERA[1], JULIUS A PASCO[1], JESLEY MEI A DYCOCO[1] (1.UNIVERSITY OF THE PHILIPPINES)

[SMP30-P07] Intra-oceanic arc magma genesis: a case study from Havre volcano, Kermadec arc

*Chris Conway[1], Kenichiro Tani[2] (1.Geological Survey of Japan, 2.National Museum of Nature and Science)

Secular evolution of proto-Izu-Bonin-Mariana arc volcanism: Constraints from statistical analysis of melt inclusion compositions

*Morihisa Hamada[1], Hikaru Iwamori[1,2], Philipp A. Brandl[3], Takayuki Ushikubo[4], Kenji Shimizu[4], Motoo Ito[4], He Li[5], Ivan P. Savov[6]

1. Department of Solid Earth Geochemistry, Japan Agency for Marine-Earth Science and Technology, 2. Earthquake Research Institute, University of Tokyo, 3. GEOMAR Helmholtz Centre for Ocean Research Kiel, 4. Kochi Institute for Core Sample Research, Japan Agency for Marine-Earth Science and Technology, 5. Institute of Oceanology, Chinese Academy of Sciences, 6. School of Earth and Environment, University of Leeds

International Ocean Discovery Program (IODP) Expedition 351 'Izu–Bonin–Mariana (IBM) Arc Origins' drilled Site U1438, situated in the north-western margin of the Philippine Sea, into volcaniclastic sediments of the proto-IBM arc. Brandl *et al.* (2017, *Earth and Planetary Science Letters*) have analysed the major, trace and volatile elements of 304 melt inclusions hosted in fresh silicate minerals to unveil the magmatic evolution of the proto-IBM arc between 30 and 40 Ma, when the arc volcanism matured following subduction initiation at 52 Ma. Brandl *et al.* (2017) concluded that: (1) volcanism of the proto-IBM arc shifted from calc-alkaline affinity to tholeiitic affinity over time; and (2) such compositional shift is linked to both the volcanic productivity and the maturation of an evolving island arc. To better integrate the composition of melt inclusions with the magmatic evolution of the proto-IBM arc, this study extends the dataset of Brandl *et al.* (2017) by: (1) additional analysis of volatiles (H_2O, S, F and Cl) and P_2O_5 for 47 carefully selected melt inclusions by Secondary Ion Mass Spectrometry (SIMS); and (2) statistical analysis on the composition of 237 representative melt inclusions covering the full time range (30–40 Ma) of the dataset. Based on statistical analysis of the melt inclusion compositions and by considering trace element compositions and volatile concentrations, we can confidently distinguish five main clusters of melt inclusion compositions which can be further separated into a total of nine sub-clusters. Among the nine sub-clusters, we identified three major magma types: (1) medium-K enriched magmas which form a tholeiitic trend (30–38 Ma); (2) less-depleted medium-K melts which form a calc-alkaline trend (35–39 Ma); and (3) low-K depleted magmas which form a calc-alkaline trend (35–40 Ma). We demonstrate that: (1) volcanism of calc-alkaline depleted magmas lasted until 35 Ma; (2) the volcanism of calc-alkaline depleted magmas and that of more enriched normal arc magmas (tholeiitic and calc-alkaline affinities) overlap between 35 and 38–39 Ma and; (iii) the volcanism of normal arc magmas became predominant thereafter at the proto-IBM arc. Such identification of three major magma types is distinct from that of Brandl *et al.* (2017), in which less-depleted medium-K calc-alkaline magmas amd depleted low-K calc-alkaline gammas were not distinguished. We infer that depleted source mantle had been replaced by enriched mantle due to mantle convection beneath the proto-IBM arc from >40 Ma to 35 Ma. Statistical analysis is a useful tool to partition a mixture of multivariable dataset, such as datasets of melt inclusion compositions, into several distinct groups and potentially reconstruct their geological evolution.

Keywords: Amami Sankaku Basin, International Ocean Discovery Ptrogram, Izu-Bonin-Mariana arc, Melt inclusion, Statistical analysis, Volatiles

©2019. Japan Geoscience Union. All Right Reserved.

The Jurassic magmatism of protoliths of Mikabu greenstones in SW Japan: zircon U-Pb dating and trace element analysis

*Hikaru Sawada[1], Yukio Isozaki[1], Shogo Aoki[3], Shuhei Sakata[2], Ryo Hasegawa[1], Yasuo Nakamura[1]

1. Department of General Systems Studies, the University of Tokyo, 2. Department of Chemistry, Gakushuin Universtiy, 3. Department of Applied Science, Okayama University of Science

The Mikabu greenstones, incorporated with the Cretaceous high P/T-type Sanbagawa metamorphic belt in SW Japan, are accreted fragments of an oceanic plateau. We identified a Late Jurassic igneous age for the protoliths of the Mikabu greenstones in the eastern Kii Peninsula, by measuring U-Pb age and trace element composition (REE, Y, Sc, Nb, Ta, Hf, U, Th) of zircon grains with an Agilent 8800 single-collector triple quadrupole ICPMS coupled to a NWR-213 laser-ablation system. The U-Pb ages have a weighted average of 154.6 ±1.6 Ma (the Kimmeridgian, Late Jurassic) with an overlap within 2-sigma error. The igneous age is slightly younger than the previously reported radiolarian ages (Middle Jurassic) of deep-sea pelagic chert associated with the Mikabu greenstones. The age difference between them suggests that mafic magmas intruded pelagic deep-sea sediments on the pre-existing oceanic lithosphere. Trace element composition further indicates that the dated zircon grains are more similar to those in oceanic crusts than in granitic continental crusts, and the host mafic magma of the zircon grains was derived from depleted mantle like the mid-oceanic ridge-type source, rather than fertile mantle sources like Hawaii and Iceland. As rocks from the Shatsky Rise in the modern NW Pacific Ocean have similar age and compositional characteristics, this study concluded that the protoliths of the Mikabu greenstones had formed a part of an oceanic plateau, which was generated by the Late Jurassic intra-oceanic plate mafic magmatism in the ancient Pacific Ocean.

Keywords: Mikabu greenstones, zircon, Jurassic, oceanic plateau, U-Pb age, trace element

©2019. Japan Geoscience Union. All Right Reserved.

Origin of variable CaO/Al_2O_3 in olivine-hosted melt inclusions from Kibblewhite Volcano, Kermadec Arc

*Yasuhiro Hirai[1], Yoshihiko Tamura[2], Kaj Hoernle[3], Christian Timm[4], Folkmar Hauff[3], Reinhard Werner[3], Takeshi Hanyu[2], Bogdan Vaglarov[2], Qing Chang[2], Takashi Miyazaki[2], Jun-Ichi Kimura[2]

1. Graduate School of Natural Science and Technology, Kanazawa University, Japan, 2. Japan Agency for Marine-Earth Science and Technology (JAMSTEC), Yokosuka, Kanagawa, Japan, 3. GEOMAR Helmholtz Centre for Ocean Research, Kiel, Germany, 4. GNS Science, Lower Hutt, New Zealand

During R/V SONNE expedition SO-255 mafic basaltic to magnesian andesitic lavas containing melt inclusion hosting forsteritic olivines ($Fo_{90.3–92.4}$) were recovered from Kibblewhite Volcano, southern Kermadec Arc. The re-homogenized melt inclusions have compositions similar to primitive basalt (49.6–52.0 wt.% SiO_2; 12.7–15.9 wt.% MgO). Their CaO/Al_2O_3 values, however, range from 0.9 to 1.6, which cannot be explained by melting of lherzolite. Moreover, CaO/Al_2O_3 values in the melt inclusions correlate negatively with Ni contents of their host olivines suggesting that the high CaO/Al_2O_3 values result from interaction between mafic melts and subarc lithospheric mantle. Prior to the interaction the mafic magma must have had high Ni contents and low CaO/Al_2O_3 values, thus they crystallized high Ni olivines trapping low CaO/Al_2O_3 melt inclusions. During the interaction the olivines crystallized from the mafic magmas and its latent heat assimilated pyroxenes from the surrounding lithospheric mantle. This assimilation of pyroxenes allowed the Ni content of the melt to decrease and CaO/Al_2O_3 to increase while buffering the the Mg-number of the mafic magmas during the ascent. Thus, magmas during and after the interaction could crystallize low Ni olivines bearing high CaO/Al_2O_3 melt inclusions.

Keywords: Subduction zone, Kermadec Arc, Kibblewhite Volcano, SO-255, Olivine-hosted melt inclusion

©2019. Japan Geoscience Union. All Right Reserved.

Ankaramite from Doyo seamount in the Izu-Ogasawara arc: A precursor of continents?

*Yoshihiko Tamura[1], Tomoki Sato[1], Osamu Ishizuka[1,2], Takashi Miyazaki[1], Yasuhiro Hirai[1,3], Mami Takehara[4], Eri Sakamoto[5]

1. JAMSTEC, 2. AIST, 3. Kanazawa Univ., 4. NIPR, 5. NME

Izu-Ogasawara-Mariana (IOM) system of arcs (also known as the Izu-Bonin-Mariana arc system) is a typical oceanic arc produced by subduction of the Pacific Plate beneath the Philippine Sea Plate. Volcanoes along the southern segment of the Izu-Ogasawara arc are underlain by thin crust (10-20 km). According to the hypothesis presented by Tamura *et al.* (2016), rising mantle diapirs stall near the base of the oceanic crust at depths controlled by the thickness of the overlying crust. Where the crust is thin, melting occurs at relatively low pressures in the mantle wedge producing andesitic magmas. Andesites erupted from Nishinoshima that were produced in the recent history of the volcano have been generated by olivine fractionation of primary andesitic magmas (Tamura *et al.*, 2019).

To further examine this hypothesis, we have dived Doyo Seamount by using manned submersible SHINKAI 6500 to sample primitive magmas from the volcano, which is located about 50 km north of Nishinoshima and is underlain by thinner curst (15 km) compared to Nishinoshima. Doyo Seamount is located approximately 900 km south of Tokyo at 27˚41’ N, 140˚48’ E in the Ogasawara Arc. The seamount attained an elevation of ~400 m below sea level (mbsl) and its submarine flanks extend to the depth of 3,200 mbsl. The basal dimeter of the volcano is about 30 km. The deeper parts of this large submarine edifice have yet to be explored. Primitive lavas tend to erupt in the deeper parts of submarine volcanoes at the depth of ~2,000 m. Deeper satellite vents are expected to erupt more primitive magmas compared to the main summit vents because primitive magmas could bypass the shallow magma chambers where crystal fractionation and magma mixing happen.

There is a small satellite cone about 11 km east of the summit of Doyo Seamount at the depth of ~3,000 m. A ridge extends on the flank of the volcano from the summit in the ENE direction to the depth of ~2,400 m. Thus, we tried to sample this satellite cone and the deeper part of the ridge. Interestingly, 13 samples out of all 21 samples, which we have recovered during this dive 6K#1519, are olivine-clinopyroxene basalts containing 20-40 % of very coarse clinopyroxene phenocrysts, which could be called ankaramite (Figure 1). Ankaramites are strongly vesiculated and their blocks have rough and rugged surface, which are different from smooth surface of basaltic pillow lavas. Some of ankaramite magmas might have had explosive eruptions at the depth of 2,000~3,000 m, which have resulted in volcaniclastic cones or brecciated lava flows.

Similar primitive and phenocryst-rich ankaramitic basalts were recovered from the old submarine knolls near Nishinoshima (Tamura et al., 2019). We suggested that lithospheric mantle was thicker before the development of Nishinoshima volcano (Figure 2). Primary basaltic magmas could have been generated at depth beneath the thicker lithospheric lid, and these magmas might have interacted with the lithospheric uppermost mantle during their ascent and have resulted in the unique ankaramite magmas (Figure 1). The temperature of the upper part of the mantle wedge increases with frequent passage of magmas through it, and continuous subduction beneath it will drench the whole mantle wedge, thus, the thickness of the lithosphere will decrease and approach the thickness of the curst in mature arcs. Doyo Seamount could represent the early stage of Nishinoshima volcano, and thus, ankaramite magma is deemed to be a

©2019. Japan Geoscience Union. All Right Reserved.

precursor of andesitic magmas.

References

Tamura et al. (2016). Advent of continents: A new hypothesis. *Scientific Reports* **6,** 33517.
Tamura et al. (2019). Nishinoshima volcano in the Ogasawara Arc: New continent from the ocean? *Island Arc* **28,** e12285.

Keywords: ankaramite, andesite, continent, oceanic arc, lithosphere, mantle wedge

©2019. Japan Geoscience Union. All Right Reserved.

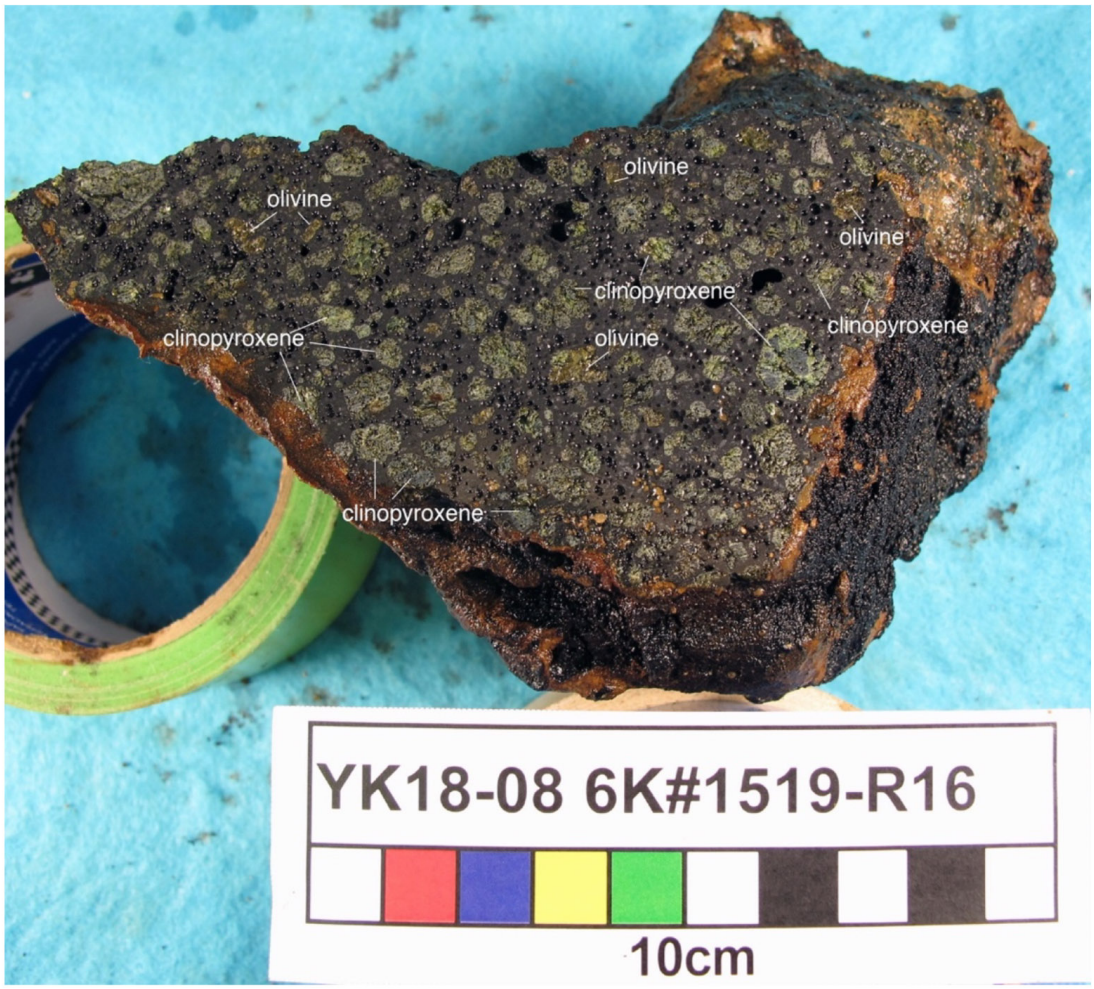


Figure 1. Ankaramite recovered from Doyo Seamount.

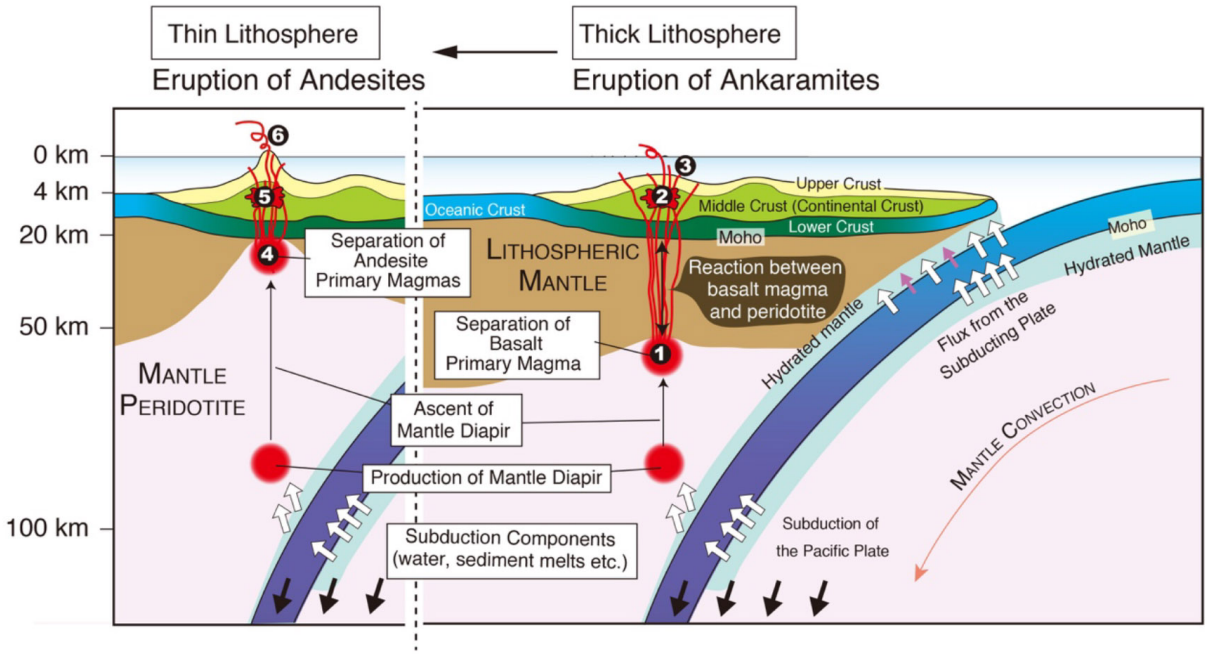


Figure 2. Schematic diagrams showing the genesis of andesite and ankaramite magmas in the Ogasawara arc.

©2019. Japan Geoscience Union. All Right Reserved.

Different Moho reflections adjacent to Minami-Tori Shima and their petrologic origins

*Yoshihiko Tamura[1], Kentaro Kaneda[2], Gou Fujie[1], Akane Ohira[1], Eiichi TAKAZAWA[3], Georges Ceuleneer[4], Katsuyoshi Michibayashi[5], Tomoki Sato[1], Shuichi Kodaira[1], Seiichi Miura[1]

1. Japan Agency for Maine-Earth Science and Technology, 2. Japan Coast Guard, 3. Niigata University, 4. Universite de Toulouse, 5. Nagoya University

It is the common knowledge that Moho is the boundary between the crust and mantle, which was discovered by and named after Croatian seismologist Mohorovičić. We have shown that Moho is not the crust-mantle boundary and presented a new hypothesis about the origin of Moho based on seismological and petrological observations (Tamura et al., EGU2018-11069-2; JpGU2018 SMP36-05; AGCC2018 abstract volume590; Tamura et al., in preparation). Direct drilling and sampling of Moho could be the best scenario to examine the hypothesis. However, IODP drillings of basaltic crust could estimate the petrologic origins of the crust-mantle boundary far below the seafloor, which could be useful to examine the hypothesis of formation of Moho.

Kaneda et al. (2010) conducted seismic surveys across the Marcus-Wake seamount chain near Minami-Tori Shima, which is the Japanese easternmost and one and only island on the Pacific Plate. They found contrasting seafloor in the north and south of the seamount chain, which were referred to the northern and southern basins (Figure 1). Average water depths in the northern and southern basins are about 5900 m and 5700 m, respectively. Magnetic anomalies suggest Jurassic ages of M32 (159 Ma) and M42 (167 Ma) for the northern and southern basins, respectively. The southern basin has the clear Moho reflections, which are characteristically sharp, single, flat, and continuous, and of large amplitude, but in the northern basin, Moho reflections are extremely weak or even absent. Interestingly, the crust of the southern basin has a constant thickness of 7.5-8.0 km, but the crust of the northern basin shows a constant thickness of 6 km, 1.5-2 km thinner than that of the northern basin.The correlation between Moho reflections and crustal thicknesses have been generally observed in other seismic profiles (e.g. Ohira et al., 2017).

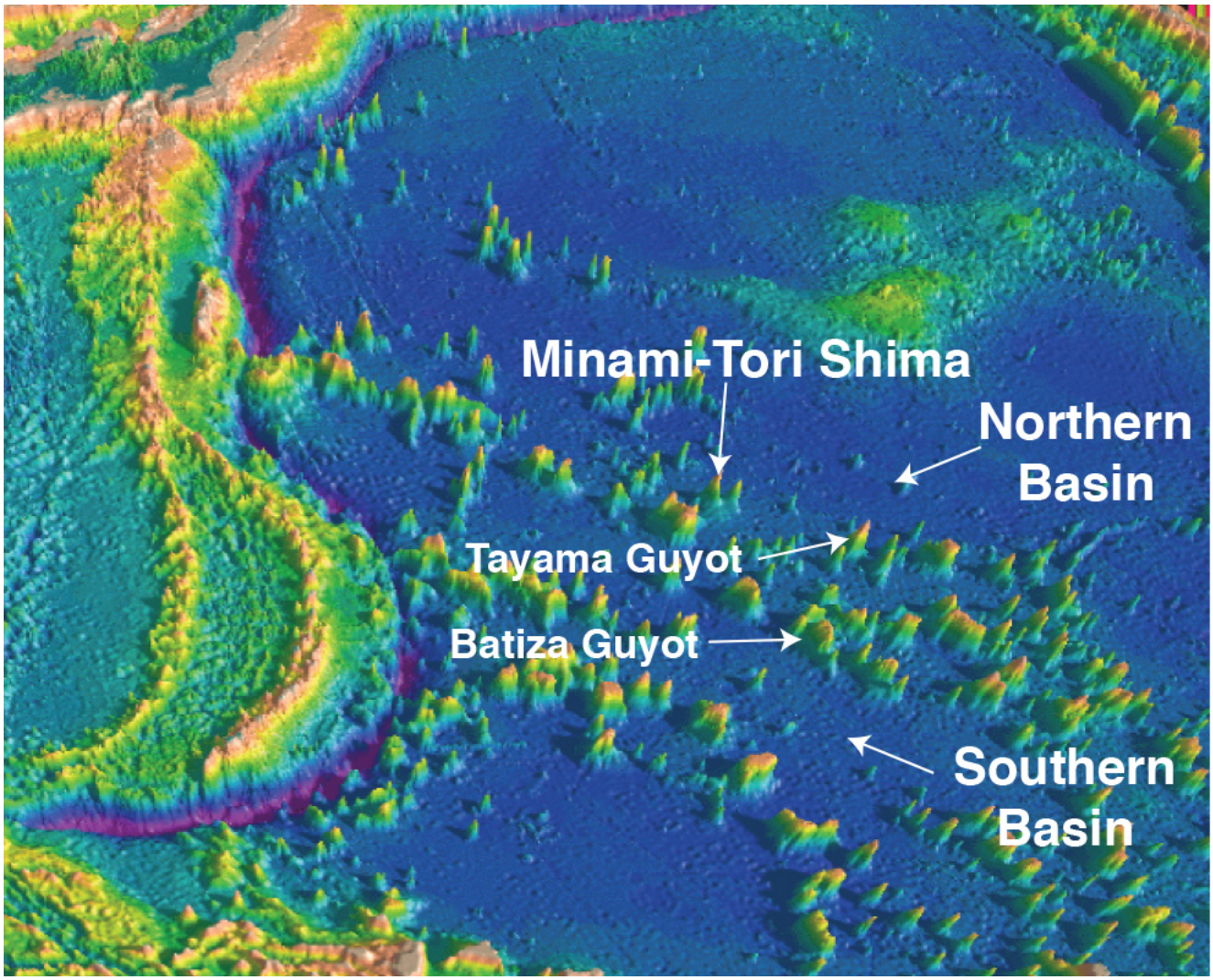
The boundary between mantle peridotite and layered gabbro from the lower oceanic crust in the Oman ophiolite consists of a dunitic transition zone (DTZ), mostly made of olivine + scattered Cr-spinel. The thickness of DTZ ranges from a few meters to a few hundred meters. When mantle melts under hydrous conditions, the liquidus field of forsterite expands relative to that of enstatite and enstatite melts incongruently to produce dunites and andesitic melts.

We present here a new hypothesis that (1) accidental influx of seawater at the mid-ocean ridges results in hydrous melting of mantle peridotite just beneath the crust and produces thick dunite at the crust-mantle boundaries, (2) the thick dunite represents reflective Moho, and (3) this additional hydrous melting of shallowest mantle increases the thickness of oceanic crust.

Although the andesitic melts, which are the outgrowth of dunites, would be mixed with dominant basaltic melts extracted from the deeper parts of melting column of MORB, there must be systematic and significant differences between crustal materials with Moho and those without Moho. Comparative drillings of oceanic crust in the northern and southern basins for future IODP expeditions will reveal the differences of basalts and examine the models for Moho.

©2019. Japan Geoscience Union. All Right Reserved.

Keywords: Moho, Minami-Tori Shima, dunite, mantle, crust, basalt



©2019. Japan Geoscience Union. All Right Reserved.

Melt-rock interaction in plagioclase peridotites from the southern Palawan Ophiolite, Philippines

*FLORENCE ANNETTE CRUSPERO LABIS[1], BETCHAIDA D PAYOT[1], GABRIEL THEOPHILUS V VALERA[1], JULIUS A PASCO[1], JESLEY MEI A DYCOCO[1]

1. UNIVERSITY OF THE PHILIPPINES

This work presents new petrographic and geochemical data on the plagioclase peridotites and the spinel harzburgites of the mantle section of the southern Palawan Ophiolite. The plagioclase peridotites show peculiar textures evident of melt-rock interaction as indicated by: (1) interstitial clinopyroxene and subhedral orthopyroxene around plagioclase, and (2) plagioclase blebs within the peridotite matrix. The spinel harzburgites display protogranular to porphyroclastic textures and dominantly composed of olivine, orthopyroxene, and small amounts of clinopyroxene and spinel. These minerals show kink banding and bent lamellae which are indicative of plastic deformation. Major element geochemistry of the spinel harzburgites reveals high Cr# (0.53-0.78) and Mg# (0.40-0.51) in spinel, and high NiO wt.% (0.40-0.43) and Fo contents (89.9-90.5) in olivine reflecting residual origin. Their geochemical composition is comparable to the residual peridotites in arc settings. Consequently, the plagioclase peridotites have lower Mg# (0.23-0.34) and relatively high Cr# (0.60-0.61) in spinel, as well as lower Fo (83.3-85.9) contents in olivine. Spinel and clinopyroxene in the plagioclase peridotites have higher TiO_2 contents compared with those of the spinel harzburgites. Clinopyroxene in plagioclase peridotites are marked by strong depletion in LREE and flat MREE to HREE with significant negative Eu and Sr anomalies. In contrast, the spinel harzburgites have lower REE abundances which suggest higher degrees of partial melting. We propose that the spinel harzburgites of the southern Palawan Ophiolite are residual peridotites formed by high degrees of partial melting above a subduction zone and were subsequently infiltrated by melts leading to the formation of the plagioclase peridotites.

Keywords: Palawan Ophiolite, plagioclase peridotites, melt-rock interaction

©2019. Japan Geoscience Union. All Right Reserved.

Intra-oceanic arc magma genesis: a case study from Havre volcano, Kermadec arc

*Chris Conway[1], Kenichiro Tani[2]

1. Geological Survey of Japan, 2. National Museum of Nature and Science

The Kermadec intra-oceanic arc comprises 33 active arc front volcanoes along its ~1200 km length, which represent key targets for studying the formation of Earth’ s crust. The discovery of numerous submarine caldera volcanoes and dacitic to rhyolitic pumice deposits from this setting has prompted new models for the genesis of intra-oceanic silicic arc magmas. A detailed investigation of the 2012 eruption of rhyolite pumice and lava at Havre volcano has provided a valuable opportunity to test these models. Moreover, the retrieval of older volcanic deposits from the edifice has given critical context for studying magma genesis throughout the lifetime of the volcano. Here we present whole-rock, mineral and glass major and trace element data for volcanic rock samples collected from Havre volcano. The samples, which span a compositional range from basalt to rhyolite, display several key features that support arguments against the derivation of silicic magmas primarily through crustal anatexis: (1) the range of sample compositions fit along coherent crystal fractionation trends; (2) low-MgO aphyric andesites fill the gap within the general bimodality of eruptive products from the Kermadec arc; and (3) there is a scarcity of tonalitic xenoliths. These features favour crystal fractionation over crustal anatexis as the dominant process for generating the compositional diversity seen at Havre volcano.

Keywords: rhyolite, magma genesis, Havre volcano

©2019. Japan Geoscience Union. All Right Reserved.

[E] Poster | S (Solid Earth Sciences)：S-MP Mineralogy & Petrology

Tue. May 28, 2019 5:15 PM - 6:30 PM JST | Tue. May 28, 2019 8:15 AM - 9:30 AM UTC | Poster Hall International Exhibition Hall8, Makuhari Messe_33

[S-MP30] Crust-Mantle Connections

convener:Yoshihiko Tamura(Research Institute for Marine Geodynamics, Japan Agency for Maine-Earth Science and Technology), Osamu Ishizuka(Geological Survey of Japan, AIST), Chris Conway(Geological Survey of Japan)

A paradigm of the solid Earth geochemical cycles is that the Earth's crust forms by melting of the Earth's upper peridotitic mantle. How divers is the spectrum of primary melts and which factors may contribute to its variations? What is the influence of crustal processing vs. primary magma diversity in creating the diversity of the Earth's crust? The session seeks to explore the crust-mantle connections at divergent and convergent plate boundaries, and oceanic island settings based on volcanology, petrology, geochemistry, geophysics, geochronology, and geodynamics studies.

[SMP30-P01] Secular evolution of proto-Izu-Bonin-Mariana arc volcanism: Constraints from statistical analysis of melt inclusion compositions

*Morihisa Hamada[1], Hikaru Iwamori[1,2], Philipp A. Brandl[3], Takayuki Ushikubo[4], Kenji Shimizu[4], Motoo Ito[4], He Li[5], Ivan P. Savov[6] (1.Department of Solid Earth Geochemistry, Japan Agency for Marine-Earth Science and Technology, 2.Earthquake Research Institute, University of Tokyo, 3.GEOMAR Helmholtz Centre for Ocean Research Kiel, 4.Kochi Institute for Core Sample Research, Japan Agency for Marine-Earth Science and Technology, 5.Institute of Oceanology, Chinese Academy of Sciences, 6.School of Earth and Environment, University of Leeds)

[SMP30-P02] The Jurassic magmatism of protoliths of Mikabu greenstones in SW Japan: zircon U-Pb dating and trace element analysis

*Hikaru Sawada[1], Yukio Isozaki[1], Shogo Aoki[3], Shuhei Sakata[2], Ryo Hasegawa[1], Yasuo Nakamura[1] (1.Department of General Systems Studies, the University of Tokyo, 2.Department of Chemistry, Gakushuin Universtiy, 3.Department of Applied Science, Okayama University of Science)

[SMP30-P03] Origin of variable CaO/Al_2O_3 in olivine-hosted melt inclusions from Kibblewhite Volcano, Kermadec Arc

*Yasuhiro Hirai[1], Yoshihiko Tamura[2], Kaj Hoernle[3], Christian Timm[4], Folkmar Hauff[3], Reinhard Werner[3], Takeshi Hanyu[2], Bogdan Vaglarov[2], Qing Chang[2], Takashi Miyazaki[2], Jun-Ichi Kimura[2] (1.Graduate School of Natural Science and Technology, Kanazawa University, Japan, 2.Japan Agency for Marine-Earth Science and Technology (JAMSTEC), Yokosuka, Kanagawa, Japan, 3.GEOMAR Helmholtz Centre for Ocean Research, Kiel, Germany, 4.GNS Science, Lower Hutt, New Zealand)

[SMP30-P04] Ankaramite from Doyo seamount in the Izu-Ogasawara arc: A precursor of continents?

*Yoshihiko Tamura[1], Tomoki Sato[1], Osamu Ishizuka[1,2], Takashi Miyazaki[1], Yasuhiro Hirai[1,3], Mami Takehara[4], Eri Sakamoto[5] (1.JAMSTEC, 2.AIST, 3.Kanazawa Univ., 4.NIPR, 5.NME)

[SMP30-P05] Different Moho reflections adjacent to Minami-Tori Shima and their petrologic origins

*Yoshihiko Tamura[1], Kentaro Kaneda[2], Gou Fujie[1], Akane Ohira[1], Eiichi TAKAZAWA[3], Georges Ceuleneer[4], Katsuyoshi Michibayashi[5], Tomoki Sato[1], Shuichi Kodaira[1], Seiichi Miura[1] (1.Japan Agency for Maine-Earth Science and Technology, 2.Japan Coast Guard, 3.Niigata University, 4.Universite de Toulouse, 5.Nagoya University)

[SMP30-P06] Melt-rock interaction in plagioclase peridotites from the southern Palawan Ophiolite, Philippines

*FLORENCE ANNETTE CRUSPERO LABIS[1], BETCHAIDA D PAYOT[1], GABRIEL THEOPHILUS V VALERA[1], JULIUS A PASCO[1], JESLEY MEI A DYCOCO[1] (1.UNIVERSITY OF THE PHILIPPINES)

[SMP30-P07] Intra-oceanic arc magma genesis: a case study from Havre volcano, Kermadec arc

*Chris Conway[1], Kenichiro Tani[2] (1.Geological Survey of Japan, 2.National Museum of Nature and Science)

Secular evolution of proto-Izu-Bonin-Mariana arc volcanism: Constraints from statistical analysis of melt inclusion compositions

*Morihisa Hamada[1], Hikaru Iwamori[1,2], Philipp A. Brandl[3], Takayuki Ushikubo[4], Kenji Shimizu[4], Motoo Ito[4], He Li[5], Ivan P. Savov[6]

1. Department of Solid Earth Geochemistry, Japan Agency for Marine-Earth Science and Technology, 2. Earthquake Research Institute, University of Tokyo, 3. GEOMAR Helmholtz Centre for Ocean Research Kiel, 4. Kochi Institute for Core Sample Research, Japan Agency for Marine-Earth Science and Technology, 5. Institute of Oceanology, Chinese Academy of Sciences, 6. School of Earth and Environment, University of Leeds

International Ocean Discovery Program (IODP) Expedition 351 'Izu–Bonin–Mariana (IBM) Arc Origins' drilled Site U1438, situated in the north-western margin of the Philippine Sea, into volcaniclastic sediments of the proto-IBM arc. Brandl *et al.* (2017, *Earth and Planetary Science Letters*) have analysed the major, trace and volatile elements of 304 melt inclusions hosted in fresh silicate minerals to unveil the magmatic evolution of the proto-IBM arc between 30 and 40 Ma, when the arc volcanism matured following subduction initiation at 52 Ma. Brandl *et al.* (2017) concluded that: (1) volcanism of the proto-IBM arc shifted from calc-alkaline affinity to tholeiitic affinity over time; and (2) such compositional shift is linked to both the volcanic productivity and the maturation of an evolving island arc. To better integrate the composition of melt inclusions with the magmatic evolution of the proto-IBM arc, this study extends the dataset of Brandl *et al.* (2017) by: (1) additional analysis of volatiles (H_2O, S, F and Cl) and P_2O_5 for 47 carefully selected melt inclusions by Secondary Ion Mass Spectrometry (SIMS); and (2) statistical analysis on the composition of 237 representative melt inclusions covering the full time range (30–40 Ma) of the dataset. Based on statistical analysis of the melt inclusion compositions and by considering trace element compositions and volatile concentrations, we can confidently distinguish five main clusters of melt inclusion compositions which can be further separated into a total of nine sub-clusters. Among the nine sub-clusters, we identified three major magma types: (1) medium-K enriched magmas which form a tholeiitic trend (30–38 Ma); (2) less-depleted medium-K melts which form a calc-alkaline trend (35–39 Ma); and (3) low-K depleted magmas which form a calc-alkaline trend (35–40 Ma). We demonstrate that: (1) volcanism of calc-alkaline depleted magmas lasted until 35 Ma; (2) the volcanism of calc-alkaline depleted magmas and that of more enriched normal arc magmas (tholeiitic and calc-alkaline affinities) overlap between 35 and 38–39 Ma and; (iii) the volcanism of normal arc magmas became predominant thereafter at the proto-IBM arc. Such identification of three major magma types is distinct from that of Brandl *et al.* (2017), in which less-depleted medium-K calc-alkaline magmas amd depleted low-K calc-alkaline gammas were not distinguished. We infer that depleted source mantle had been replaced by enriched mantle due to mantle convection beneath the proto-IBM arc from >40 Ma to 35 Ma. Statistical analysis is a useful tool to partition a mixture of multivariable dataset, such as datasets of melt inclusion compositions, into several distinct groups and potentially reconstruct their geological evolution.

Keywords: Amami Sankaku Basin, International Ocean Discovery Ptrogram, Izu-Bonin-Mariana arc, Melt inclusion, Statistical analysis, Volatiles

©2019. Japan Geoscience Union. All Right Reserved.

The Jurassic magmatism of protoliths of Mikabu greenstones in SW Japan: zircon U-Pb dating and trace element analysis

*Hikaru Sawada[1], Yukio Isozaki[1], Shogo Aoki[3], Shuhei Sakata[2], Ryo Hasegawa[1], Yasuo Nakamura[1]

1. Department of General Systems Studies, the University of Tokyo, 2. Department of Chemistry, Gakushuin Universtiy, 3. Department of Applied Science, Okayama University of Science

The Mikabu greenstones, incorporated with the Cretaceous high P/T-type Sanbagawa metamorphic belt in SW Japan, are accreted fragments of an oceanic plateau. We identified a Late Jurassic igneous age for the protoliths of the Mikabu greenstones in the eastern Kii Peninsula, by measuring U-Pb age and trace element composition (REE, Y, Sc, Nb, Ta, Hf, U, Th) of zircon grains with an Agilent 8800 single-collector triple quadrupole ICPMS coupled to a NWR-213 laser-ablation system. The U-Pb ages have a weighted average of 154.6 ±1.6 Ma (the Kimmeridgian, Late Jurassic) with an overlap within 2-sigma error. The igneous age is slightly younger than the previously reported radiolarian ages (Middle Jurassic) of deep-sea pelagic chert associated with the Mikabu greenstones. The age difference between them suggests that mafic magmas intruded pelagic deep-sea sediments on the pre-existing oceanic lithosphere. Trace element composition further indicates that the dated zircon grains are more similar to those in oceanic crusts than in granitic continental crusts, and the host mafic magma of the zircon grains was derived from depleted mantle like the mid-oceanic ridge-type source, rather than fertile mantle sources like Hawaii and Iceland. As rocks from the Shatsky Rise in the modern NW Pacific Ocean have similar age and compositional characteristics, this study concluded that the protoliths of the Mikabu greenstones had formed a part of an oceanic plateau, which was generated by the Late Jurassic intra-oceanic plate mafic magmatism in the ancient Pacific Ocean.

Keywords: Mikabu greenstones, zircon, Jurassic, oceanic plateau, U-Pb age, trace element

©2019. Japan Geoscience Union. All Right Reserved.

Origin of variable CaO/Al_2O_3 in olivine-hosted melt inclusions from Kibblewhite Volcano, Kermadec Arc

*Yasuhiro Hirai[1], Yoshihiko Tamura[2], Kaj Hoernle[3], Christian Timm[4], Folkmar Hauff[3], Reinhard Werner[3], Takeshi Hanyu[2], Bogdan Vaglarov[2], Qing Chang[2], Takashi Miyazaki[2], Jun-Ichi Kimura[2]

1. Graduate School of Natural Science and Technology, Kanazawa University, Japan, 2. Japan Agency for Marine-Earth Science and Technology (JAMSTEC), Yokosuka, Kanagawa, Japan, 3. GEOMAR Helmholtz Centre for Ocean Research, Kiel, Germany, 4. GNS Science, Lower Hutt, New Zealand

During R/V SONNE expedition SO-255 mafic basaltic to magnesian andesitic lavas containing melt inclusion hosting forsteritic olivines ($Fo_{90.3–92.4}$) were recovered from Kibblewhite Volcano, southern Kermadec Arc. The re-homogenized melt inclusions have compositions similar to primitive basalt (49.6–52.0 wt.% SiO_2; 12.7–15.9 wt.% MgO). Their CaO/Al_2O_3 values, however, range from 0.9 to 1.6, which cannot be explained by melting of lherzolite. Moreover, CaO/Al_2O_3 values in the melt inclusions correlate negatively with Ni contents of their host olivines suggesting that the high CaO/Al_2O_3 values result from interaction between mafic melts and subarc lithospheric mantle. Prior to the interaction the mafic magma must have had high Ni contents and low CaO/Al_2O_3 values, thus they crystallized high Ni olivines trapping low CaO/Al_2O_3 melt inclusions. During the interaction the olivines crystallized from the mafic magmas and its latent heat assimilated pyroxenes from the surrounding lithospheric mantle. This assimilation of pyroxenes allowed the Ni content of the melt to decrease and CaO/Al_2O_3 to increase while buffering the the Mg-number of the mafic magmas during the ascent. Thus, magmas during and after the interaction could crystallize low Ni olivines bearing high CaO/Al_2O_3 melt inclusions.

Keywords: Subduction zone, Kermadec Arc, Kibblewhite Volcano, SO-255, Olivine-hosted melt inclusion

©2019. Japan Geoscience Union. All Right Reserved.

Ankaramite from Doyo seamount in the Izu-Ogasawara arc: A precursor of continents?

*Yoshihiko Tamura[1], Tomoki Sato[1], Osamu Ishizuka[1,2], Takashi Miyazaki[1], Yasuhiro Hirai[1,3], Mami Takehara[4], Eri Sakamoto[5]

1. JAMSTEC, 2. AIST, 3. Kanazawa Univ., 4. NIPR, 5. NME

Izu-Ogasawara-Mariana (IOM) system of arcs (also known as the Izu-Bonin-Mariana arc system) is a typical oceanic arc produced by subduction of the Pacific Plate beneath the Philippine Sea Plate. Volcanoes along the southern segment of the Izu-Ogasawara arc are underlain by thin crust (10-20 km). According to the hypothesis presented by Tamura *et al.* (2016), rising mantle diapirs stall near the base of the oceanic crust at depths controlled by the thickness of the overlying crust. Where the crust is thin, melting occurs at relatively low pressures in the mantle wedge producing andesitic magmas. Andesites erupted from Nishinoshima that were produced in the recent history of the volcano have been generated by olivine fractionation of primary andesitic magmas (Tamura *et al.*, 2019).

To further examine this hypothesis, we have dived Doyo Seamount by using manned submersible SHINKAI 6500 to sample primitive magmas from the volcano, which is located about 50 km north of Nishinoshima and is underlain by thinner curst (15 km) compared to Nishinoshima. Doyo Seamount is located approximately 900 km south of Tokyo at 27˚41’ N, 140˚48’ E in the Ogasawara Arc. The seamount attained an elevation of ~400 m below sea level (mbsl) and its submarine flanks extend to the depth of 3,200 mbsl. The basal dimeter of the volcano is about 30 km. The deeper parts of this large submarine edifice have yet to be explored. Primitive lavas tend to erupt in the deeper parts of submarine volcanoes at the depth of ~2,000 m. Deeper satellite vents are expected to erupt more primitive magmas compared to the main summit vents because primitive magmas could bypass the shallow magma chambers where crystal fractionation and magma mixing happen.

There is a small satellite cone about 11 km east of the summit of Doyo Seamount at the depth of ~3,000 m. A ridge extends on the flank of the volcano from the summit in the ENE direction to the depth of ~2,400 m. Thus, we tried to sample this satellite cone and the deeper part of the ridge. Interestingly, 13 samples out of all 21 samples, which we have recovered during this dive 6K#1519, are olivine-clinopyroxene basalts containing 20-40 % of very coarse clinopyroxene phenocrysts, which could be called ankaramite (Figure 1). Ankaramites are strongly vesiculated and their blocks have rough and rugged surface, which are different from smooth surface of basaltic pillow lavas. Some of ankaramite magmas might have had explosive eruptions at the depth of 2,000~3,000 m, which have resulted in volcaniclastic cones or brecciated lava flows.

Similar primitive and phenocryst-rich ankaramitic basalts were recovered from the old submarine knolls near Nishinoshima (Tamura et al., 2019). We suggested that lithospheric mantle was thicker before the development of Nishinoshima volcano (Figure 2). Primary basaltic magmas could have been generated at depth beneath the thicker lithospheric lid, and these magmas might have interacted with the lithospheric uppermost mantle during their ascent and have resulted in the unique ankaramite magmas (Figure 1). The temperature of the upper part of the mantle wedge increases with frequent passage of magmas through it, and continuous subduction beneath it will drench the whole mantle wedge, thus, the thickness of the lithosphere will decrease and approach the thickness of the curst in mature arcs. Doyo Seamount could represent the early stage of Nishinoshima volcano, and thus, ankaramite magma is deemed to be a

©2019. Japan Geoscience Union. All Right Reserved.

precursor of andesitic magmas.

References

Tamura et al. (2016). Advent of continents: A new hypothesis. *Scientific Reports* **6,** 33517.
Tamura et al. (2019). Nishinoshima volcano in the Ogasawara Arc: New continent from the ocean? *Island Arc* **28,** e12285.

Keywords: ankaramite, andesite, continent, oceanic arc, lithosphere, mantle wedge

©2019. Japan Geoscience Union. All Right Reserved.

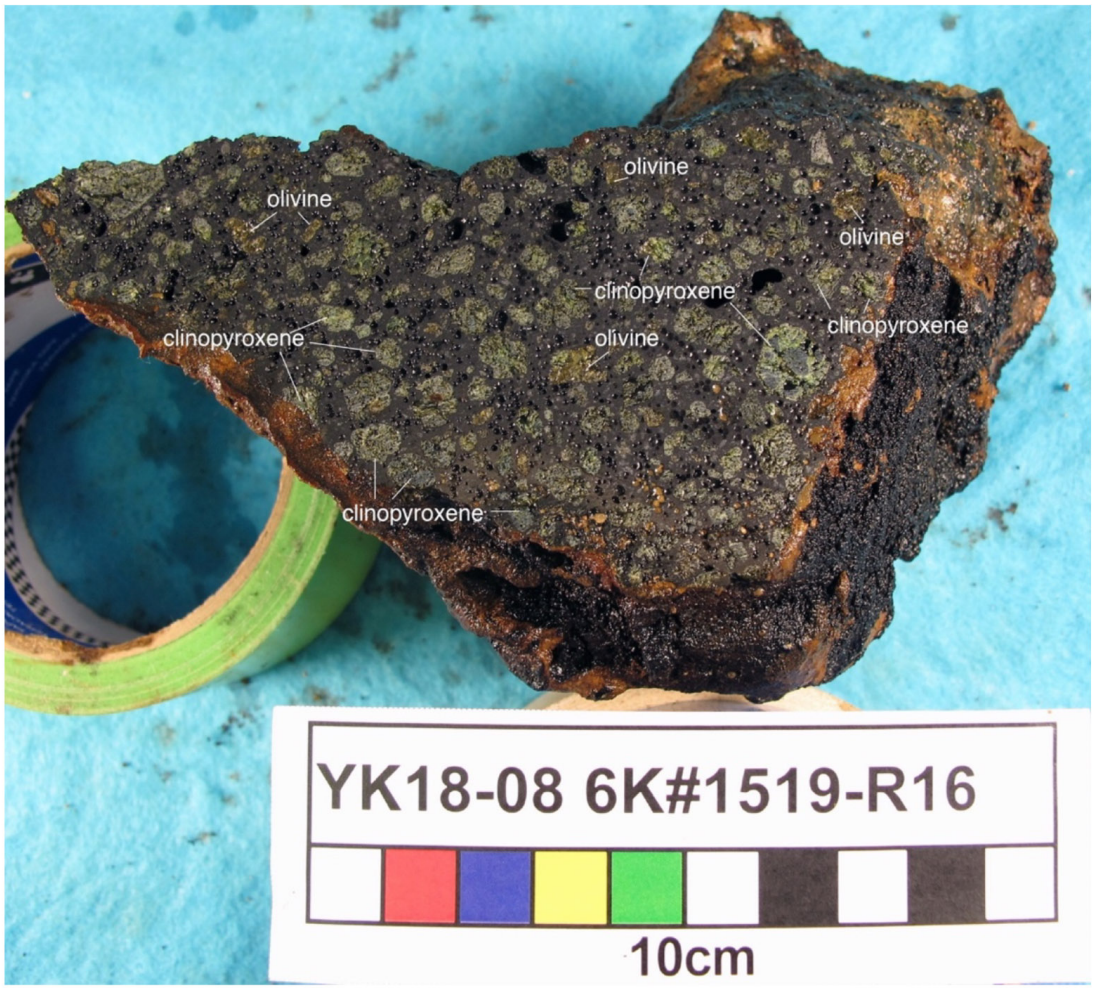


Figure 1. Ankaramite recovered from Doyo Seamount.

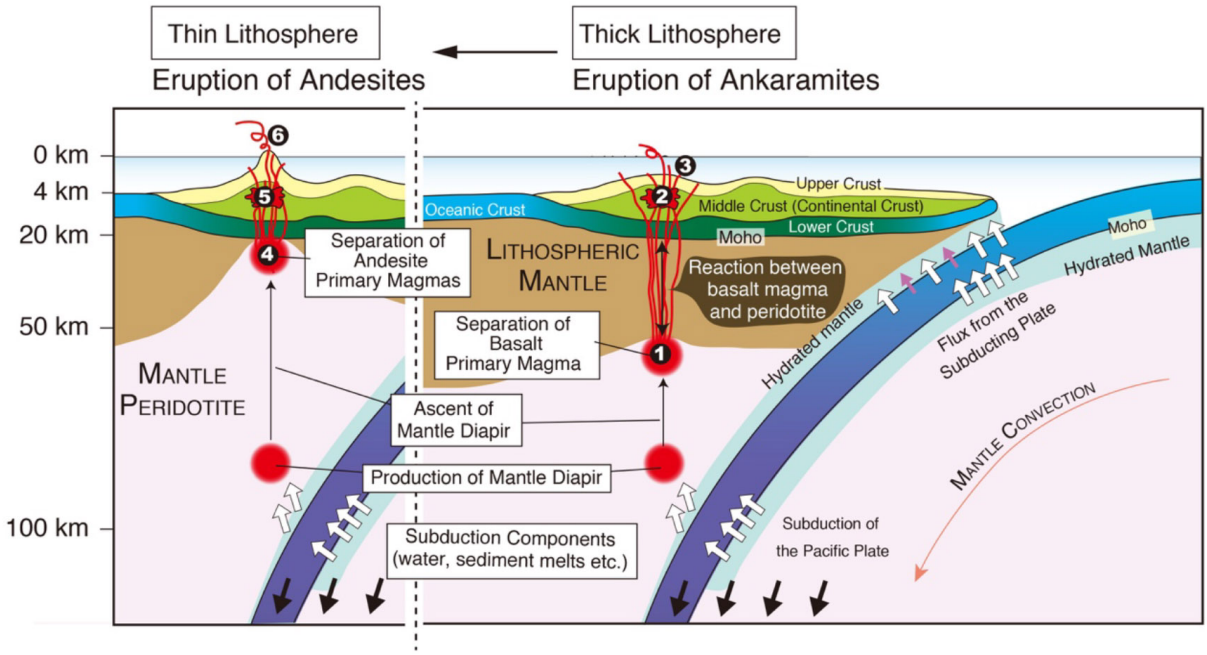


Figure 2. Schematic diagrams showing the genesis of andesite and ankaramite magmas in the Ogasawara arc.

©2019. Japan Geoscience Union. All Right Reserved.

Different Moho reflections adjacent to Minami-Tori Shima and their petrologic origins

*Yoshihiko Tamura[1], Kentaro Kaneda[2], Gou Fujie[1], Akane Ohira[1], Eiichi TAKAZAWA[3], Georges Ceuleneer[4], Katsuyoshi Michibayashi[5], Tomoki Sato[1], Shuichi Kodaira[1], Seiichi Miura[1]

1. Japan Agency for Maine-Earth Science and Technology, 2. Japan Coast Guard, 3. Niigata University, 4. Universite de Toulouse, 5. Nagoya University

It is the common knowledge that Moho is the boundary between the crust and mantle, which was discovered by and named after Croatian seismologist Mohorovičić. We have shown that Moho is not the crust-mantle boundary and presented a new hypothesis about the origin of Moho based on seismological and petrological observations (Tamura et al., EGU2018-11069-2; JpGU2018 SMP36-05; AGCC2018 abstract volume590; Tamura et al., in preparation). Direct drilling and sampling of Moho could be the best scenario to examine the hypothesis. However, IODP drillings of basaltic crust could estimate the petrologic origins of the crust-mantle boundary far below the seafloor, which could be useful to examine the hypothesis of formation of Moho.

Kaneda et al. (2010) conducted seismic surveys across the Marcus-Wake seamount chain near Minami-Tori Shima, which is the Japanese easternmost and one and only island on the Pacific Plate. They found contrasting seafloor in the north and south of the seamount chain, which were referred to the northern and southern basins (Figure 1). Average water depths in the northern and southern basins are about 5900 m and 5700 m, respectively. Magnetic anomalies suggest Jurassic ages of M32 (159 Ma) and M42 (167 Ma) for the northern and southern basins, respectively. The southern basin has the clear Moho reflections, which are characteristically sharp, single, flat, and continuous, and of large amplitude, but in the northern basin, Moho reflections are extremely weak or even absent. Interestingly, the crust of the southern basin has a constant thickness of 7.5-8.0 km, but the crust of the northern basin shows a constant thickness of 6 km, 1.5-2 km thinner than that of the northern basin.The correlation between Moho reflections and crustal thicknesses have been generally observed in other seismic profiles (e.g. Ohira et al., 2017).

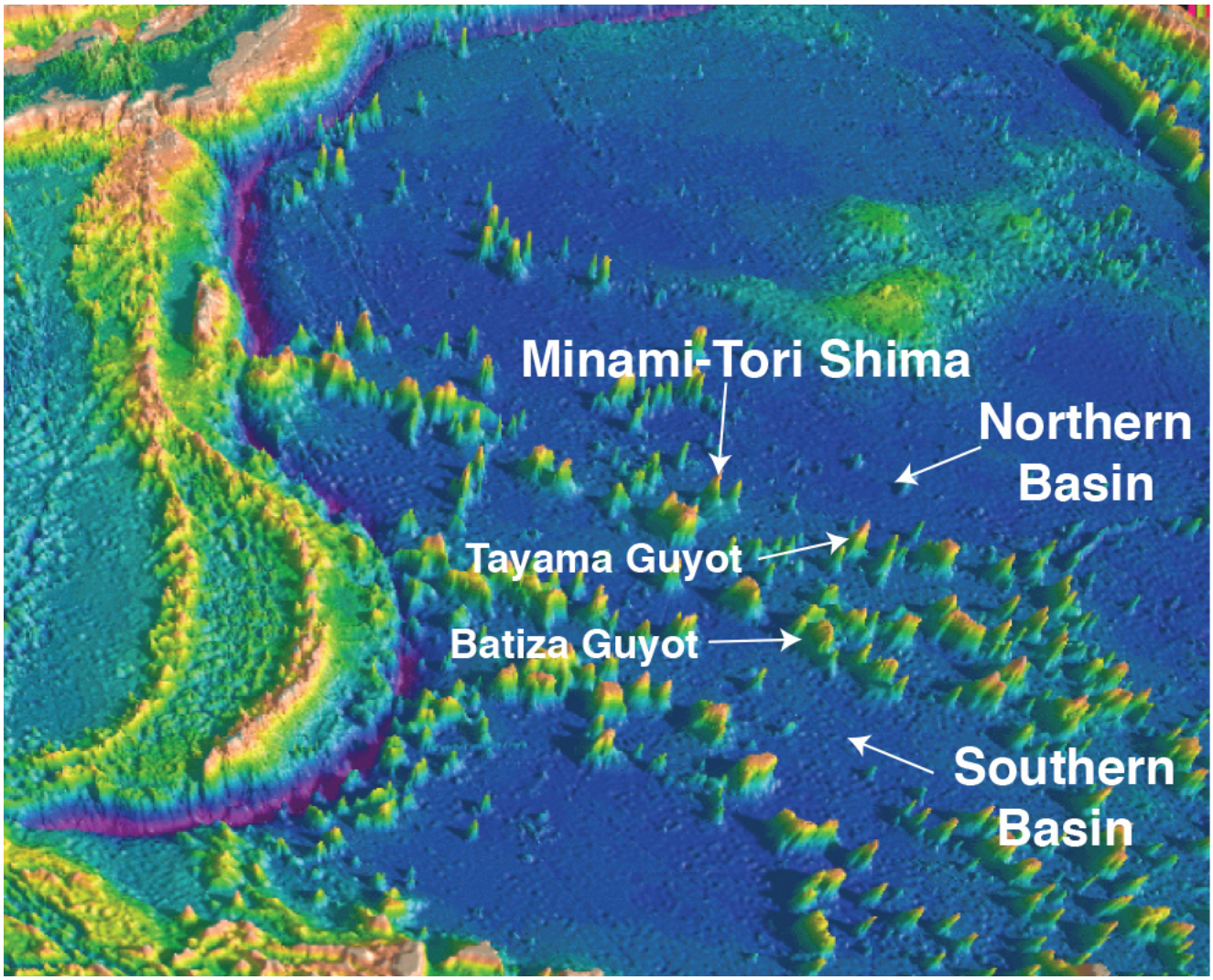
The boundary between mantle peridotite and layered gabbro from the lower oceanic crust in the Oman ophiolite consists of a dunitic transition zone (DTZ), mostly made of olivine + scattered Cr-spinel. The thickness of DTZ ranges from a few meters to a few hundred meters. When mantle melts under hydrous conditions, the liquidus field of forsterite expands relative to that of enstatite and enstatite melts incongruently to produce dunites and andesitic melts.

We present here a new hypothesis that (1) accidental influx of seawater at the mid-ocean ridges results in hydrous melting of mantle peridotite just beneath the crust and produces thick dunite at the crust-mantle boundaries, (2) the thick dunite represents reflective Moho, and (3) this additional hydrous melting of shallowest mantle increases the thickness of oceanic crust.

Although the andesitic melts, which are the outgrowth of dunites, would be mixed with dominant basaltic melts extracted from the deeper parts of melting column of MORB, there must be systematic and significant differences between crustal materials with Moho and those without Moho. Comparative drillings of oceanic crust in the northern and southern basins for future IODP expeditions will reveal the differences of basalts and examine the models for Moho.

©2019. Japan Geoscience Union. All Right Reserved.

Keywords: Moho, Minami-Tori Shima, dunite, mantle, crust, basalt



©2019. Japan Geoscience Union. All Right Reserved.

Melt-rock interaction in plagioclase peridotites from the southern Palawan Ophiolite, Philippines

*FLORENCE ANNETTE CRUSPERO LABIS[1], BETCHAIDA D PAYOT[1], GABRIEL THEOPHILUS V VALERA[1], JULIUS A PASCO[1], JESLEY MEI A DYCOCO[1]

1. UNIVERSITY OF THE PHILIPPINES

This work presents new petrographic and geochemical data on the plagioclase peridotites and the spinel harzburgites of the mantle section of the southern Palawan Ophiolite. The plagioclase peridotites show peculiar textures evident of melt-rock interaction as indicated by: (1) interstitial clinopyroxene and subhedral orthopyroxene around plagioclase, and (2) plagioclase blebs within the peridotite matrix. The spinel harzburgites display protogranular to porphyroclastic textures and dominantly composed of olivine, orthopyroxene, and small amounts of clinopyroxene and spinel. These minerals show kink banding and bent lamellae which are indicative of plastic deformation. Major element geochemistry of the spinel harzburgites reveals high Cr# (0.53-0.78) and Mg# (0.40-0.51) in spinel, and high NiO wt.% (0.40-0.43) and Fo contents (89.9-90.5) in olivine reflecting residual origin. Their geochemical composition is comparable to the residual peridotites in arc settings. Consequently, the plagioclase peridotites have lower Mg# (0.23-0.34) and relatively high Cr# (0.60-0.61) in spinel, as well as lower Fo (83.3-85.9) contents in olivine. Spinel and clinopyroxene in the plagioclase peridotites have higher TiO_2 contents compared with those of the spinel harzburgites. Clinopyroxene in plagioclase peridotites are marked by strong depletion in LREE and flat MREE to HREE with significant negative Eu and Sr anomalies. In contrast, the spinel harzburgites have lower REE abundances which suggest higher degrees of partial melting. We propose that the spinel harzburgites of the southern Palawan Ophiolite are residual peridotites formed by high degrees of partial melting above a subduction zone and were subsequently infiltrated by melts leading to the formation of the plagioclase peridotites.

Keywords: Palawan Ophiolite, plagioclase peridotites, melt-rock interaction

©2019. Japan Geoscience Union. All Right Reserved.

Intra-oceanic arc magma genesis: a case study from Havre volcano, Kermadec arc

*Chris Conway[1], Kenichiro Tani[2]

1. Geological Survey of Japan, 2. National Museum of Nature and Science

The Kermadec intra-oceanic arc comprises 33 active arc front volcanoes along its ~1200 km length, which represent key targets for studying the formation of Earth’ s crust. The discovery of numerous submarine caldera volcanoes and dacitic to rhyolitic pumice deposits from this setting has prompted new models for the genesis of intra-oceanic silicic arc magmas. A detailed investigation of the 2012 eruption of rhyolite pumice and lava at Havre volcano has provided a valuable opportunity to test these models. Moreover, the retrieval of older volcanic deposits from the edifice has given critical context for studying magma genesis throughout the lifetime of the volcano. Here we present whole-rock, mineral and glass major and trace element data for volcanic rock samples collected from Havre volcano. The samples, which span a compositional range from basalt to rhyolite, display several key features that support arguments against the derivation of silicic magmas primarily through crustal anatexis: (1) the range of sample compositions fit along coherent crystal fractionation trends; (2) low-MgO aphyric andesites fill the gap within the general bimodality of eruptive products from the Kermadec arc; and (3) there is a scarcity of tonalitic xenoliths. These features favour crystal fractionation over crustal anatexis as the dominant process for generating the compositional diversity seen at Havre volcano.

Keywords: rhyolite, magma genesis, Havre volcano

©2019. Japan Geoscience Union. All Right Reserved.

[E] Poster | S (Solid Earth Sciences)：S-MP Mineralogy & Petrology

Tue. May 28, 2019 3:30 PM - 5:00 PM JST | Tue. May 28, 2019 6:30 AM - 8:00 AM UTC | Poster Hall International Exhibition Hall8, Makuhari Messe_18

[S-MP31] Supercontinents and Crustal Evolution

convener:Madhusoodhan Satish-Kumar(Department of Geology, Faculty of Science, Niigata University), Tomokazu Hokada(National Institute of Polar Research), Krishnan Sajeev(Centre for Earth Sciences, Indian Institute of Science), Yasuhito Osanai(Division of Evolution of Earth Environments, Faculty of Social and Cultural Studies, Kyushu University)

Supercontinent formation and dispersion has been enigmatic in the Earth's history. Eurasia is one such current supercontinent and incredible progress in the understanding of its geological evolution has been achieved in the past decade. Earlier supercontinents in the Earth's history such as Gondwana (0.5 Ga), Rodinia (1.0 Ga), Columbia/Nuna (2.0 Ga), Kenorland (2.5 Ga) and Vaalbara (3.1 Ga), have been the focus of several studies, however limited information on older supercontinents has restricted an understanding of their tectonic evolution. In this session, we invite authors around the world to present new data as well as review existing results on the continental scale crustal processes and tectonic evolution that are associated with supercontinent formation and breakup events in the Earth's history. The well-studied Eurasia and Gondwana supercontinents are of particular focus. Topics of interest include, but not restricted to, extremes in metamorphism, P-T-d-t evolution, magmatism, and the role of fluids. We hope to provide a platform for scientific discussions that will enlighten our understanding of the physical and chemical processes in the continental crust that records episodes of orogenesis that contributed to the formation and evolution of supercontinents.

[SMP31-P01] Re-examination of metamorphic and geochronologic events in Rayner Complex and Western Rayner Complex in Antarctica

*Tomokazu Hokada[1,2], Sotaro Baba[3], Atsushi Kamei[4], Ippei Kitano[5], Kenji Horie[1,2], Yoshikuni Hiroi[1,6], Yoichi Motoyoshi[1,2], Mami Takehara[1], Kazuyuki Shiraishi[1] (1.National Institute of Polar Research, 2.The Graduate University for Advanced Studies (SOKENDAI), 3.University of the Ryukyus, 4.Shimane University, 5.Kyushu University, 6.Chiba University)

[SMP31-P02] Composition of constituent minerals in corona-bearing and -free mafic gneisses from the Lützow-Holm Complex at Skallen, East Antarctica

*Yuki Mori[1], Takeshi Ikeda[2] (1.Department of Earth and Planetary Sciences, Graduate School of Sciences, Kyushu University, 2.Department of Earth and Planetary Sciences, Faculty of Sciences, Kyushu University)

[SMP31-P03] “Pseudo-concordance” of U-Pb system in zircon at Harvey Nunatak, Napier Complex, East Antarctica

*Mami Takehara[1] (1.National Institute of Polar Research)

[SMP31-P04] Rapid UHT metamorphism and exhumation of the Lützow-Holm Complex in Antarctica

*Yoshikuni Hiroi[1], Tomokazu Hokada[2], Tatsuro Adachi[3], Yasuhito Osanai[3], Yoichi Motoyoshi[2], Kazuyuki Shiraishi[2] (1.Chiba Univ, 2.National Institute of Polar Research, 3.Kyushu University)

[SMP31-P05] Tectonic History of Hiroo Complex and its implication inpaleo-Kuril Arc evolution

*Sreehari Lakshmanan[1], Tsuyoshi Toyoshima[2], Futoshi Nanayama[3] (1.Graduate School of Science and Technology, Niigata University, Niigata, Japan, 2.Department of Geology, Faculty of Science, Niigata Univ. , 3.Geological Survey of Japan, AIST)

[SMP31-P06] Behaviour of C, O, Sr, Nd and Pb isotopes in high-grade metacarbonate rocks

*Madhusoodhan Satish-Kumar[1], Akari Imura[1], Momoko Shirakawa[2], Gen Shimoda[3], Kosuke T. Goto[3], M A Sanjeewa P K Malaviarachchi[4] (1.Department of Geology, Faculty of Science, Niigata University, 2.Graduate School of Science and Technology, Niigata University, 3.Geological Survey of Japan, 4.University of Peradeniya, Sri Lanka)

Re-examination of metamorphic and geochronologic events in Rayner Complex and Western Rayner Complex in Antarctica

*Tomokazu Hokada[1,2], Sotaro Baba[3], Atsushi Kamei[4], Ippei Kitano[5], Kenji Horie[1,2], Yoshikuni Hiroi[1,6], Yoichi Motoyoshi[1,2], Mami Takehara[1], Kazuyuki Shiraishi[1]

1. National Institute of Polar Research, 2. The Graduate University for Advanced Studies (SOKENDAI), 3. University of the Ryukyus, 4. Shimane University, 5. Kyushu University, 6. Chiba University

Enderby Land in Antarctica comprises of Neoproterozoic-Cambrian (c.650-500 Ma) high-grade metamorphic terranes that constituting Gondwana supercontinent (e.g., Shiraishi et al., 2008). Easternmost part is “Western Rayner Complex” of which granulite-facies and partly UHT metamorphism (Motoyoshi et al., 1994, 1995) and 2400-1000 Ma protolith and 540-520 Ma metamorphic ages were reported (Shiraishi et al., 1997). Neighboring “Rayner Complex” is characterized by >2500-1000 Ma protolith and 980-910 Ma granulite-facies metamorphic ages. Boundary between the Rayner and the Western Rayner Complex has been not clearly defined until when Horie et al. (2016) obtained 934-894 Ma SHIRMP zircon U-Pb ages from Mt. Lira, Condon Hills and Mt. Yuzhnaya regions with minor 590-570 Ma zircons from Mt. Yuzhnaya. Hiroi (unpublished data) also demonstrated contrasting metamorphic P-T evolution among the Mt. Lira, Condon Hills and Mt. Yuzhnaya regions.

JARE-58 (2016-2017) geology team made a short visit and sampling at a small nunatak of west of Mt. Yuzhnaya, a small nunatak of east of Forefinger Point, and Point Widdows in order to assess the relationship between the Rayner and the Western Rayner Complexes. We will report and discuss the update of the characteristic features of the Rayner and the Western Rayner Complexes.

Keywords: Antarctica, Gondwana, Supercontinent, metamorphism, geochronology

©2019. Japan Geoscience Union. All Right Reserved.

Composition of constituent minerals in corona-bearing and -free mafic gneisses from the Lützow-Holm Complex at Skallen, East Antarctica

*Yuki Mori[1], Takeshi Ikeda[2]

1. Department of Earth and Planetary Sciences, Graduate School of Sciences, Kyushu University, 2. Department of Earth and Planetary Sciences, Faculty of Sciences, Kyushu University

Corona is one of the non-equilibrium microstructures and has been employed to infer pressure-temperature path of the metamorphic rocks. The corona around garnet is common in mafic to ultramafic gneisses in the Lützow-Holm Complex (LHC) of East Antarctica (e.g., Hiroi et al., 1991). However, not every garnet in mafic to ultramafic gneisses accompanies the corona. In our ongoing study to reveal the controlling factors of presence and absence of the corona, we compare the composition of garnet and hornblende of the corona-bearing (no. I-223) and -free (no. I-232) mafic gneisses from Skallen.

The metamorphic grade of the complex increases progressively from the upper amphibolite facies to granulite facies toward the southwest, and the LHC is divided into three zones referred to as the amphibolite-facies zone, transitional zone, and granulite-facies zone (Hiroi et al., 1991). Recent studies have revealed that both transitional and granulite-facies zones had undergone high temperatures that exceed 800 ˚C (e.g., Iwamura et al, 2013; Kawakami et al., 2016). Skallen is an exposure located in the granulite-facies zone.

The constituent minerals in the matrix of the studied samples are almost same (garnet, hornblende, plagioclase with minor amounts of clinopyroxene and orthopyroxene), but I-223 further contains biotite. The microstructure and chemical composition of I-223 is as follows. The garnet grain is coarse (15 mm in diameter) and surrounded by a symplectitic corona composed of orthopyroxene and plagioclase. Garnet is clearly divided into two domains of Ca-rich core (Xgrs=0.23) and Ca-poor rim (Xgrs=0.18). X_{Mg} [=Mg/(Mg+Fe)] increases toward rim from 0.22 to 0.27, and that in the outer part of the rim decreases toward the boundary between the garnet and the corona from 0.27 to 0.22. The Ca-poor rim of the garnet includes irregular-shaped nanogranite composed of quartz, biotite, plagioclase, and K-feldspar. Hornblende is brown to brownish-green and polygonal. The X_{Mg} of the hornblende is 0.46-0.50. Matrix plagioclase often shows antiperthite intergrowing An50 plagioclase with Or96 K-feldspar. The coronal plagioclase has higher anorthite content (An80) than that in the matrix (An50). The microstructure and chemical composition of I-232 is as follows. The garnet grain is coarse (10 mm long) and elongated. The garnet and the hornblende define foliation of the rock. The hornblende is brown to pale brown. The composition of garnet gradually changes from core (Alm52Prp31Grs14Sps3) to rim (Alm52Prp28Grs17Sps3). The X_{Mg} in the hornblende varies from 0.60-0.70, and the composition is heterogeneous even in one grain. Most part of plagioclase is An45, and some parts of rim of the plagioclase have higher anorthite content of 70.

The garnet and hornblende in the corona-bearing gneiss have lower X_{Mg} than those in the corona-free gneiss. In addition, calcium content of the garnet and matrix plagioclase in the corona-bearing gneiss is higher than that in the corona-free gneiss. Therefore, we consider that bulk composition is one of the factors controlling the corona formation. The presence of nanogranite in the garnet surrounded by the corona suggests that partial melting and transport of the melt would cause the change of bulk composition in part.

©2019. Japan Geoscience Union. All Right Reserved.

Keywords: corona, garnet, nanogranite, Lützow-Holm Complex, Antarctica

©2019. Japan Geoscience Union. All Right Reserved.

“Pseudo-concordance” of U-Pb system in zircon at Harvey Nunatak, Napier Complex, East Antarctica

*Mami Takehara[1]

1. National Institute of Polar Research

U-Pb zircon dating has played a pivotal role in geochronology due to zircon’s high durability and high closure temperature. In addition, the paired decay scheme of two U isotopes allows us to verify the determined U-Pb zircon age. The Napier Complex in East Antarctica is well known because it preserves both of evidence of ultrahigh-temperature (UHT) metamorphism (e.g., Sheraton et al., 1987; Harley & Hensen 1990) and long Archaean crustal history from 3800 Ma to 2500 Ma (e.g., Harley & Black 1997). Previous researchers also reported the possibilities of the early Archean crust in the Napier Complex (e.g., Compston and Williams, 1982). Some previous researchers pointed out discordant U-Pb data including reverse discordance which was derived from the redistribution of radiogenic Pb isotopes in zircon in the Napier Complex samples (e.g., Kusiak et al., 2013). The some discordant U-Pb data looks concordant but actually reflect the Pb redistribution, namely “pseudo-concordance.” They suggest the redistribution of the radiogenic Pb isotopes in zircons was associated with the UHT metamorphism based on the Pb isotope mapping of the zircons. This report is critical for accurate U-Pb zircon geochronology in the UHT metamorphic region, such as the Napier Complex. Therefore, in this study, the zircons from the rock sample of the Napier Complex were characterized on the basis of the observation and trace-element contents, and the information was utilized for interpretation of the U-Pb data.
Zircons collected from a tonalitic gneiss (170223-2A-09) were first analyzed using sensitive high resolution ion-microprobes (SHRIMP IIe and SHRIMP IIe/AMC) at the National Institute of Polar Research, Japan. The sample was collected at the Harvey Nunatak, which is located close to Mt. Sones. The geochronological data from the Harvey Nunatak had never been reported. The sample was crushed by a high-voltage pulse power fragmentation device (Selfrag Lab) to preserve the external morphology of zircons and prevent contamination (Takehara et al., 2018). After pulverizing, the zircon grains were concentrated using conventional mineral separation techniques, including heavy liquid separation with methylene iodide and magnetic separation.
The zircon grains include fractures and slightly mineral inclusion based on the observation of transmitted light images by an optical microscope. BSE images show that some zircon grains have darker BSE-response domains, which suggests depletion of contents of Zr and Si during hydrothermal alteration of zircon. The zircons show typically high U contents (average is ~2500 ppm), and the U-Pb age from the high U zircons was corrected for the matrix effect derived from the high U contents according to the method by Williams & Hergt (2000) and White & Ireland (2012). It seems that the unaltered zircons show concordant data from about 2450 Ma to 2540 Ma with discordance (Disc.(%) = 1 −(206Pb/238U age)/(207Pb/206Pb age)} ×100 (e.g, Song et al., 1996)) ranges from -5 to +9%. On the other hand, trace element geochemistry of zircons does not support detritus protolith. In this presentation, the information of trace-element contents in zircons was utilized for the interpretation of U-Pb data and “pseudo-concordance.”

©2019. Japan Geoscience Union. All Right Reserved.

Rapid UHT metamorphism and exhumation of the Lützow-Holm Complex in Antarctica

*Yoshikuni Hiroi[1], Tomokazu Hokada[2], Tatsuro Adachi[3], Yasuhito Osanai[3], Yoichi Motoyoshi[2], Kazuyuki Shiraishi[2]

1. Chiba Univ, 2. National Institute of Polar Research, 3. Kyushu University

The Lützow-Holm Complex in Antarctica is a part of Neoproterozoic-Cambrian (c.650-500 Ma) collisional orogen to form Gondwana supercontinent. It is characterized by progressive metamorphism from upper amphibolite facies in the eastern part of the Prince Olav Coast to upper granulite facies in the southern Sô ya Coast (e.g., Hiroi et al., 1991). UHT metamorphism is evidenced by such diagnostic mineral assemblages as Opx + Sil + Grt + Rt + Qz and Spr + Qz in Mg-Al-rich pelitic granulites in Rundvågshetta. Intimate intergrowths of Ky + Spr + Grt and Sil + Spr + Grt as well as andalusite-bearing falsite-nanogranite inclusions are included in the same porphyroblastic garnet, which is compositionally zoned, with Mg-rich core, Fe–Mn-rich rim, and core-to-rim oscillation of Ca. Integration of these new data with those previously documented leads to the inference of a rapid change in pressure–temperature conditions during regional UHT metamorphism in this part of the late Neoproterozoic to early Paleozoic ‘large and hot orogen’. Several lines of evidence indicate that partial melting and melt extraction took place even in mafic granulites of fragmented gabbro origin.

Keywords: Antarctica, Gondwana, Supercontinent, UHT metamorphism

©2019. Japan Geoscience Union. All Right Reserved.

Tectonic History of Hiroo Complex and its implication inpaleo-Kuril Arc evolution

*Sreehari Lakshmanan[1], Tsuyoshi Toyoshima[2], Futoshi Nanayama[3]

1. Graduate School of Science and Technology, Niigata University, Niigata, Japan, 2. Department of Geology, Faculty of Science, Niigata Univ. , 3. Geological Survey of Japan, AIST

Melanges records information about deformation history and tectonic events in plate margins and orogens and hence they are important in evolution of accretionary complexes [1]. Mélange facies rocks and brocken formations distributed in Nakanogawa Group of Hidaak Belt in Central Hokkaido is known as Hiroo Complex. We carried out detailed field mapping and structural studies on melange facies rocks distributed around Tachiiwa, Kamitoyoni and Daimaruyama region of Hiroo Complex. Four different deformation processes (D1,D2,D3 and D4) are identified from field to micro-scale observations. D1 event shear zones are wide and considerd as penitrative but D2, D3 and D4 shear zones observed in narrow deformation zones and considerd as less penitrative local events. D1 shearzones are identified as scaly fabric in mudstone and asymmetrically sheared sandstone clast distributed in it. This is similar to 'block in matrix' structure, typical of tectonic melange devoloped in accretionary complexes. D1 foliation trends in N-NNW direction. Tectonic evolution of theses rocks confirmed by pressure solution cleavage, composite planar fabrics (P-Y-R shear), asymmetrical folds and dip-parallel streching lineation. P-Y-R shear relation and other asymmetrical structures in both field and microscale observation shows east-side-up sense of movement. This shear sense suggest that major penetrative deformatoin phase in melange was connected to accretionary complex devolopment in paleo-Kuril-Arc region, where initial subduction was directed in N-S direction and later it rotated clockwise and attained its present position. D2, D3 and D4 events were recognized as dextral strike-slip movement, sinistral-strike-slip to oblique-slip movement and west-side-down movement sense respectively . Mega-micro scale observation of D2 and D3 events show the properties of cataclastic deformation and D4 event is that of fault gouge. Based on this D2, D3 and D4 events are considered as upper crustal or local deformation processes. We consider these are linked to post-melange deformation processes and related to final stages of devolopment of Hidaka Metamorphic Belt (HMB). Recent geochemical studies from Daimaruyama region and geochronological studies from Nakanogawa Group region points that Hiroo Complex was part of initiallly northward subducting Paleo-Kuril Arc region [2]. Through detailed strucural analysis, this study also confirms that Hiroo Complex was devoloped in accretionary complex of paleo- Kuril-Arc by an offscrapping mode of evolution. Later Hiroo Complex became part of Nakanogawa Group through a series of deformation processes asocciated with arc-arc colission between paleo-Kuril Arc and paleo-Japan Arc.
[1]A. Festa et al., 2012. Tectonophysics, 568, 7-24 [2] T.Yamasaki, F. Nanayama, 2018. Lithos. 302, 224-241

Keywords: Hiroo Complex, Paleo Kuri lArc, Mélange tectonics, Accretionary Complex, Nakanogawa Group

©2019. Japan Geoscience Union. All Right Reserved.

Behaviour of C, O, Sr, Nd and Pb isotopes in high-grade metacarbonate rocks

*Madhusoodhan Satish-Kumar[1], Akari Imura[1], Momoko Shirakawa[2], Gen Shimoda[3], Kosuke T. Goto[3], M A Sanjeewa P K Malaviarachchi[4]

1. Department of Geology, Faculty of Science, Niigata University, 2. Graduate School of Science and Technology, Niigata University, 3. Geological Survey of Japan, 4. University of Peradeniya, Sri Lanka

Tectonic environment of metasedimentary sequences deposit in orogenic belts is of importance in understanding the formation and evolution of supercontinents. In particular, chemically deposited carbonate rocks are supposed to hold key information of extinct paleo-oceans, since they are directly precipitated from seawater. In this study, we carried out a comprehensive trace and rare earth element analysis, carbon, oxygen, strontium, neodymium and lead isotope measurements in metacarbonate rocks from the Highland Complex, Sri Lanka. The isotopic systems studied have distinct residence and mixing time in seawater, and are also controlled by the input from surrounding continents. We present here the behaviour of each isotopic system with respect to different processes right from the deposition of carbonate from the seawater through diagenesis and then prograde and retrograde metamorphism. TheProterozoic basement of Sri Lanka is subdivided into four lithotectonic units, namely, the Highland Complex (HC), the Wanni Complex (WC), the Vijayan Complex (VC), and the Kadugannawa Complex (KC), based on Nd isotope model ages. The HC is mainly composed of metasedimentary rocks (granulite facies metaquartzites, metapelitic gneisses and metacarbonate rocks), whereas exposures of the WC and the VC are mainly metaigneous rocks. The metacarbonate rocks in the HC generally occur as layers parallel with other metasedimentary lithological units, and show a NE trend.

We measured oxygen and carbon isotope ratios to understand the effect of diagenetic to metamorphic alterations, which can be recognized in negative isotope shifts. In general, the metacarbonate rocks have positive oxygen isotopic composition comparable with the Proterozoic unmetamorphosed carbonates, suggesting that these rocks were not affected by external fluids during digenesis, dolomitization or metamorphism. However, some of the rock units have been affected by later fluid infiltration as seen in major shifts in oxygen isotopic composition. Negative shifts in both carbon and oxygen isotopes correspond to the metamorphic decarbonation reactions being prominent. Strontium isotope chemostratigraphy was applied for the selected samples with least signatures of alteration. The depositional ages show a younging direction of sedimentation from the Wanni-side to the Vijayan-side. In the case of Nd isotopes, the values correspond to variable mixing of continent derived and oceanic crust derived components during carbonate deposition. This is clearly depicted in the ε Sr vs. ε Nd cross-plots where typical seawater-rock mixing relationship in metacarbonate rocks associated with continents and oceanic crusts can be deduced.Pb isotopic composition of the metacarbonate rocks in Sri Lanka indicated significant differences within the HC; the Vijayan side is more radiogenic than that of Wanni side. This might be due to the difference of initial composition, as well as the relationship to depositional basin and seawater composition. We also observed very low U/Pb ratios, which are considered to have occurred due to the U-loss during metamorphic recrystallization.Thus, the Sr-Nd-Pb isotopic composition in metacarbonate rocks suggests interaction between the oceanic crust and carbonate rocks on the Wanni side whereas on the Vijayan side, carbonate sedimentation was accompanied by interaction with cratonic continental crust.Thus, by applying a multi-element isotope geochemical approach on metacarbonate rocks collected from continental collisional zones, and by comparing the data with basement rocks from various neighbouring Gondwana continents, regional affinities could be established.

©2019. Japan Geoscience Union. All Right Reserved.

Sr, Nd and Pb isotopic compositions provide important information about the depositional settings of sedimentary rocks and provide key information about the surrounding terrains of oceanic and continental affinities during the time of deposition. This can lead to a better understanding of paleo-tectonic settings of crustal fragments that assemble to form supercontinents.

Keywords: metacarbonates, Sr-Nd-Pb isotopes, Sri Lanka

©2019. Japan Geoscience Union. All Right Reserved.

[E] Poster | S (Solid Earth Sciences)：S-MP Mineralogy & Petrology

Tue. May 28, 2019 5:15 PM - 6:30 PM JST | Tue. May 28, 2019 8:15 AM - 9:30 AM UTC | Poster Hall International Exhibition Hall8, Makuhari Messe_34

[S-MP31] Supercontinents and Crustal Evolution

convener:Madhusoodhan Satish-Kumar(Department of Geology, Faculty of Science, Niigata University), Tomokazu Hokada(National Institute of Polar Research), Krishnan Sajeev(Centre for Earth Sciences, Indian Institute of Science), Yasuhito Osanai(Division of Evolution of Earth Environments, Faculty of Social and Cultural Studies, Kyushu University)

Supercontinent formation and dispersion has been enigmatic in the Earth's history. Eurasia is one such current supercontinent and incredible progress in the understanding of its geological evolution has been achieved in the past decade. Earlier supercontinents in the Earth's history such as Gondwana (0.5 Ga), Rodinia (1.0 Ga), Columbia/Nuna (2.0 Ga), Kenorland (2.5 Ga) and Vaalbara (3.1 Ga), have been the focus of several studies, however limited information on older supercontinents has restricted an understanding of their tectonic evolution. In this session, we invite authors around the world to present new data as well as review existing results on the continental scale crustal processes and tectonic evolution that are associated with supercontinent formation and breakup events in the Earth's history. The well-studied Eurasia and Gondwana supercontinents are of particular focus. Topics of interest include, but not restricted to, extremes in metamorphism, P-T-d-t evolution, magmatism, and the role of fluids. We hope to provide a platform for scientific discussions that will enlighten our understanding of the physical and chemical processes in the continental crust that records episodes of orogenesis that contributed to the formation and evolution of supercontinents.

[SMP31-P01] Re-examination of metamorphic and geochronologic events in Rayner Complex and Western Rayner Complex in Antarctica

*Tomokazu Hokada[1,2], Sotaro Baba[3], Atsushi Kamei[4], Ippei Kitano[5], Kenji Horie[1,2], Yoshikuni Hiroi[1,6], Yoichi Motoyoshi[1,2], Mami Takehara[1], Kazuyuki Shiraishi[1] (1.National Institute of Polar Research, 2.The Graduate University for Advanced Studies (SOKENDAI), 3.University of the Ryukyus, 4.Shimane University, 5.Kyushu University, 6.Chiba University)

[SMP31-P02] Composition of constituent minerals in corona-bearing and -free mafic gneisses from the Lützow-Holm Complex at Skallen, East Antarctica

*Yuki Mori[1], Takeshi Ikeda[2] (1.Department of Earth and Planetary Sciences, Graduate School of Sciences, Kyushu University, 2.Department of Earth and Planetary Sciences, Faculty of Sciences, Kyushu University)

[SMP31-P03] “Pseudo-concordance” of U-Pb system in zircon at Harvey Nunatak, Napier Complex, East Antarctica

*Mami Takehara[1] (1.National Institute of Polar Research)

[SMP31-P04] Rapid UHT metamorphism and exhumation of the Lützow-Holm Complex in Antarctica

*Yoshikuni Hiroi[1], Tomokazu Hokada[2], Tatsuro Adachi[3], Yasuhito Osanai[3], Yoichi Motoyoshi[2], Kazuyuki Shiraishi[2] (1.Chiba Univ, 2.National Institute of Polar Research, 3.Kyushu University)

[SMP31-P05] Tectonic History of Hiroo Complex and its implication inpaleo-Kuril Arc evolution

*Sreehari Lakshmanan[1], Tsuyoshi Toyoshima[2], Futoshi Nanayama[3] (1.Graduate School of Science and Technology, Niigata University, Niigata, Japan, 2.Department of Geology, Faculty of Science, Niigata Univ. , 3.Geological Survey of Japan, AIST)

[SMP31-P06] Behaviour of C, O, Sr, Nd and Pb isotopes in high-grade metacarbonate rocks

*Madhusoodhan Satish-Kumar[1], Akari Imura[1], Momoko Shirakawa[2], Gen Shimoda[3], Kosuke T. Goto[3], M A Sanjeewa P K Malaviarachchi[4] (1.Department of Geology, Faculty of Science, Niigata University, 2.Graduate School of Science and Technology, Niigata University, 3.Geological Survey of Japan, 4.University of Peradeniya, Sri Lanka)

Re-examination of metamorphic and geochronologic events in Rayner Complex and Western Rayner Complex in Antarctica

*Tomokazu Hokada[1,2], Sotaro Baba[3], Atsushi Kamei[4], Ippei Kitano[5], Kenji Horie[1,2], Yoshikuni Hiroi[1,6], Yoichi Motoyoshi[1,2], Mami Takehara[1], Kazuyuki Shiraishi[1]

1. National Institute of Polar Research, 2. The Graduate University for Advanced Studies (SOKENDAI), 3. University of the Ryukyus, 4. Shimane University, 5. Kyushu University, 6. Chiba University

Enderby Land in Antarctica comprises of Neoproterozoic-Cambrian (c.650-500 Ma) high-grade metamorphic terranes that constituting Gondwana supercontinent (e.g., Shiraishi et al., 2008). Easternmost part is “Western Rayner Complex” of which granulite-facies and partly UHT metamorphism (Motoyoshi et al., 1994, 1995) and 2400-1000 Ma protolith and 540-520 Ma metamorphic ages were reported (Shiraishi et al., 1997). Neighboring “Rayner Complex” is characterized by >2500-1000 Ma protolith and 980-910 Ma granulite-facies metamorphic ages. Boundary between the Rayner and the Western Rayner Complex has been not clearly defined until when Horie et al. (2016) obtained 934-894 Ma SHIRMP zircon U-Pb ages from Mt. Lira, Condon Hills and Mt. Yuzhnaya regions with minor 590-570 Ma zircons from Mt. Yuzhnaya. Hiroi (unpublished data) also demonstrated contrasting metamorphic P-T evolution among the Mt. Lira, Condon Hills and Mt. Yuzhnaya regions.

JARE-58 (2016-2017) geology team made a short visit and sampling at a small nunatak of west of Mt. Yuzhnaya, a small nunatak of east of Forefinger Point, and Point Widdows in order to assess the relationship between the Rayner and the Western Rayner Complexes. We will report and discuss the update of the characteristic features of the Rayner and the Western Rayner Complexes.

Keywords: Antarctica, Gondwana, Supercontinent, metamorphism, geochronology

©2019. Japan Geoscience Union. All Right Reserved.

Composition of constituent minerals in corona-bearing and -free mafic gneisses from the Lützow-Holm Complex at Skallen, East Antarctica

*Yuki Mori[1], Takeshi Ikeda[2]

1. Department of Earth and Planetary Sciences, Graduate School of Sciences, Kyushu University, 2. Department of Earth and Planetary Sciences, Faculty of Sciences, Kyushu University

Corona is one of the non-equilibrium microstructures and has been employed to infer pressure-temperature path of the metamorphic rocks. The corona around garnet is common in mafic to ultramafic gneisses in the Lützow-Holm Complex (LHC) of East Antarctica (e.g., Hiroi et al., 1991). However, not every garnet in mafic to ultramafic gneisses accompanies the corona. In our ongoing study to reveal the controlling factors of presence and absence of the corona, we compare the composition of garnet and hornblende of the corona-bearing (no. I-223) and -free (no. I-232) mafic gneisses from Skallen.

The metamorphic grade of the complex increases progressively from the upper amphibolite facies to granulite facies toward the southwest, and the LHC is divided into three zones referred to as the amphibolite-facies zone, transitional zone, and granulite-facies zone (Hiroi et al., 1991). Recent studies have revealed that both transitional and granulite-facies zones had undergone high temperatures that exceed 800 ˚C (e.g., Iwamura et al, 2013; Kawakami et al., 2016). Skallen is an exposure located in the granulite-facies zone.

The constituent minerals in the matrix of the studied samples are almost same (garnet, hornblende, plagioclase with minor amounts of clinopyroxene and orthopyroxene), but I-223 further contains biotite. The microstructure and chemical composition of I-223 is as follows. The garnet grain is coarse (15 mm in diameter) and surrounded by a symplectitic corona composed of orthopyroxene and plagioclase. Garnet is clearly divided into two domains of Ca-rich core (Xgrs=0.23) and Ca-poor rim (Xgrs=0.18). X_{Mg} [=Mg/(Mg+Fe)] increases toward rim from 0.22 to 0.27, and that in the outer part of the rim decreases toward the boundary between the garnet and the corona from 0.27 to 0.22. The Ca-poor rim of the garnet includes irregular-shaped nanogranite composed of quartz, biotite, plagioclase, and K-feldspar. Hornblende is brown to brownish-green and polygonal. The X_{Mg} of the hornblende is 0.46-0.50. Matrix plagioclase often shows antiperthite intergrowing An50 plagioclase with Or96 K-feldspar. The coronal plagioclase has higher anorthite content (An80) than that in the matrix (An50). The microstructure and chemical composition of I-232 is as follows. The garnet grain is coarse (10 mm long) and elongated. The garnet and the hornblende define foliation of the rock. The hornblende is brown to pale brown. The composition of garnet gradually changes from core (Alm52Prp31Grs14Sps3) to rim (Alm52Prp28Grs17Sps3). The X_{Mg} in the hornblende varies from 0.60-0.70, and the composition is heterogeneous even in one grain. Most part of plagioclase is An45, and some parts of rim of the plagioclase have higher anorthite content of 70.

The garnet and hornblende in the corona-bearing gneiss have lower X_{Mg} than those in the corona-free gneiss. In addition, calcium content of the garnet and matrix plagioclase in the corona-bearing gneiss is higher than that in the corona-free gneiss. Therefore, we consider that bulk composition is one of the factors controlling the corona formation. The presence of nanogranite in the garnet surrounded by the corona suggests that partial melting and transport of the melt would cause the change of bulk composition in part.

©2019. Japan Geoscience Union. All Right Reserved.

Keywords: corona, garnet, nanogranite, Lützow-Holm Complex, Antarctica

©2019. Japan Geoscience Union. All Right Reserved.

“Pseudo-concordance” of U-Pb system in zircon at Harvey Nunatak, Napier Complex, East Antarctica

*Mami Takehara[1]

1. National Institute of Polar Research

U-Pb zircon dating has played a pivotal role in geochronology due to zircon’s high durability and high closure temperature. In addition, the paired decay scheme of two U isotopes allows us to verify the determined U-Pb zircon age. The Napier Complex in East Antarctica is well known because it preserves both of evidence of ultrahigh-temperature (UHT) metamorphism (e.g., Sheraton et al., 1987; Harley & Hensen 1990) and long Archaean crustal history from 3800 Ma to 2500 Ma (e.g., Harley & Black 1997). Previous researchers also reported the possibilities of the early Archean crust in the Napier Complex (e.g., Compston and Williams, 1982). Some previous researchers pointed out discordant U-Pb data including reverse discordance which was derived from the redistribution of radiogenic Pb isotopes in zircon in the Napier Complex samples (e.g., Kusiak et al., 2013). The some discordant U-Pb data looks concordant but actually reflect the Pb redistribution, namely “pseudo-concordance.” They suggest the redistribution of the radiogenic Pb isotopes in zircons was associated with the UHT metamorphism based on the Pb isotope mapping of the zircons. This report is critical for accurate U-Pb zircon geochronology in the UHT metamorphic region, such as the Napier Complex. Therefore, in this study, the zircons from the rock sample of the Napier Complex were characterized on the basis of the observation and trace-element contents, and the information was utilized for interpretation of the U-Pb data.
Zircons collected from a tonalitic gneiss (170223-2A-09) were first analyzed using sensitive high resolution ion-microprobes (SHRIMP IIe and SHRIMP IIe/AMC) at the National Institute of Polar Research, Japan. The sample was collected at the Harvey Nunatak, which is located close to Mt. Sones. The geochronological data from the Harvey Nunatak had never been reported. The sample was crushed by a high-voltage pulse power fragmentation device (Selfrag Lab) to preserve the external morphology of zircons and prevent contamination (Takehara et al., 2018). After pulverizing, the zircon grains were concentrated using conventional mineral separation techniques, including heavy liquid separation with methylene iodide and magnetic separation.
The zircon grains include fractures and slightly mineral inclusion based on the observation of transmitted light images by an optical microscope. BSE images show that some zircon grains have darker BSE-response domains, which suggests depletion of contents of Zr and Si during hydrothermal alteration of zircon. The zircons show typically high U contents (average is ~2500 ppm), and the U-Pb age from the high U zircons was corrected for the matrix effect derived from the high U contents according to the method by Williams & Hergt (2000) and White & Ireland (2012). It seems that the unaltered zircons show concordant data from about 2450 Ma to 2540 Ma with discordance (Disc.(%) = 1 −(206Pb/238U age)/(207Pb/206Pb age)} ×100 (e.g, Song et al., 1996)) ranges from -5 to +9%. On the other hand, trace element geochemistry of zircons does not support detritus protolith. In this presentation, the information of trace-element contents in zircons was utilized for the interpretation of U-Pb data and “pseudo-concordance.”

©2019. Japan Geoscience Union. All Right Reserved.

Rapid UHT metamorphism and exhumation of the Lützow-Holm Complex in Antarctica

*Yoshikuni Hiroi[1], Tomokazu Hokada[2], Tatsuro Adachi[3], Yasuhito Osanai[3], Yoichi Motoyoshi[2], Kazuyuki Shiraishi[2]

1. Chiba Univ, 2. National Institute of Polar Research, 3. Kyushu University

The Lützow-Holm Complex in Antarctica is a part of Neoproterozoic-Cambrian (c.650-500 Ma) collisional orogen to form Gondwana supercontinent. It is characterized by progressive metamorphism from upper amphibolite facies in the eastern part of the Prince Olav Coast to upper granulite facies in the southern Sô ya Coast (e.g., Hiroi et al., 1991). UHT metamorphism is evidenced by such diagnostic mineral assemblages as Opx + Sil + Grt + Rt + Qz and Spr + Qz in Mg-Al-rich pelitic granulites in Rundvågshetta. Intimate intergrowths of Ky + Spr + Grt and Sil + Spr + Grt as well as andalusite-bearing falsite-nanogranite inclusions are included in the same porphyroblastic garnet, which is compositionally zoned, with Mg-rich core, Fe–Mn-rich rim, and core-to-rim oscillation of Ca. Integration of these new data with those previously documented leads to the inference of a rapid change in pressure–temperature conditions during regional UHT metamorphism in this part of the late Neoproterozoic to early Paleozoic ‘large and hot orogen’. Several lines of evidence indicate that partial melting and melt extraction took place even in mafic granulites of fragmented gabbro origin.

Keywords: Antarctica, Gondwana, Supercontinent, UHT metamorphism

©2019. Japan Geoscience Union. All Right Reserved.

Tectonic History of Hiroo Complex and its implication inpaleo-Kuril Arc evolution

*Sreehari Lakshmanan[1], Tsuyoshi Toyoshima[2], Futoshi Nanayama[3]

1. Graduate School of Science and Technology, Niigata University, Niigata, Japan, 2. Department of Geology, Faculty of Science, Niigata Univ. , 3. Geological Survey of Japan, AIST

Melanges records information about deformation history and tectonic events in plate margins and orogens and hence they are important in evolution of accretionary complexes [1]. Mélange facies rocks and brocken formations distributed in Nakanogawa Group of Hidaak Belt in Central Hokkaido is known as Hiroo Complex. We carried out detailed field mapping and structural studies on melange facies rocks distributed around Tachiiwa, Kamitoyoni and Daimaruyama region of Hiroo Complex. Four different deformation processes (D1,D2,D3 and D4) are identified from field to micro-scale observations. D1 event shear zones are wide and considerd as penitrative but D2, D3 and D4 shear zones observed in narrow deformation zones and considerd as less penitrative local events. D1 shearzones are identified as scaly fabric in mudstone and asymmetrically sheared sandstone clast distributed in it. This is similar to 'block in matrix' structure, typical of tectonic melange devoloped in accretionary complexes. D1 foliation trends in N-NNW direction. Tectonic evolution of theses rocks confirmed by pressure solution cleavage, composite planar fabrics (P-Y-R shear), asymmetrical folds and dip-parallel streching lineation. P-Y-R shear relation and other asymmetrical structures in both field and microscale observation shows east-side-up sense of movement. This shear sense suggest that major penetrative deformatoin phase in melange was connected to accretionary complex devolopment in paleo-Kuril-Arc region, where initial subduction was directed in N-S direction and later it rotated clockwise and attained its present position. D2, D3 and D4 events were recognized as dextral strike-slip movement, sinistral-strike-slip to oblique-slip movement and west-side-down movement sense respectively . Mega-micro scale observation of D2 and D3 events show the properties of cataclastic deformation and D4 event is that of fault gouge. Based on this D2, D3 and D4 events are considered as upper crustal or local deformation processes. We consider these are linked to post-melange deformation processes and related to final stages of devolopment of Hidaka Metamorphic Belt (HMB). Recent geochemical studies from Daimaruyama region and geochronological studies from Nakanogawa Group region points that Hiroo Complex was part of initiallly northward subducting Paleo-Kuril Arc region [2]. Through detailed strucural analysis, this study also confirms that Hiroo Complex was devoloped in accretionary complex of paleo- Kuril-Arc by an offscrapping mode of evolution. Later Hiroo Complex became part of Nakanogawa Group through a series of deformation processes asocciated with arc-arc colission between paleo-Kuril Arc and paleo-Japan Arc.
[1]A. Festa et al., 2012. Tectonophysics, 568, 7-24 [2] T.Yamasaki, F. Nanayama, 2018. Lithos. 302, 224-241

Keywords: Hiroo Complex, Paleo Kuri lArc, Mélange tectonics, Accretionary Complex, Nakanogawa Group

©2019. Japan Geoscience Union. All Right Reserved.

Behaviour of C, O, Sr, Nd and Pb isotopes in high-grade metacarbonate rocks

*Madhusoodhan Satish-Kumar[1], Akari Imura[1], Momoko Shirakawa[2], Gen Shimoda[3], Kosuke T. Goto[3], M A Sanjeewa P K Malaviarachchi[4]

1. Department of Geology, Faculty of Science, Niigata University, 2. Graduate School of Science and Technology, Niigata University, 3. Geological Survey of Japan, 4. University of Peradeniya, Sri Lanka

Tectonic environment of metasedimentary sequences deposit in orogenic belts is of importance in understanding the formation and evolution of supercontinents. In particular, chemically deposited carbonate rocks are supposed to hold key information of extinct paleo-oceans, since they are directly precipitated from seawater. In this study, we carried out a comprehensive trace and rare earth element analysis, carbon, oxygen, strontium, neodymium and lead isotope measurements in metacarbonate rocks from the Highland Complex, Sri Lanka. The isotopic systems studied have distinct residence and mixing time in seawater, and are also controlled by the input from surrounding continents. We present here the behaviour of each isotopic system with respect to different processes right from the deposition of carbonate from the seawater through diagenesis and then prograde and retrograde metamorphism. TheProterozoic basement of Sri Lanka is subdivided into four lithotectonic units, namely, the Highland Complex (HC), the Wanni Complex (WC), the Vijayan Complex (VC), and the Kadugannawa Complex (KC), based on Nd isotope model ages. The HC is mainly composed of metasedimentary rocks (granulite facies metaquartzites, metapelitic gneisses and metacarbonate rocks), whereas exposures of the WC and the VC are mainly metaigneous rocks. The metacarbonate rocks in the HC generally occur as layers parallel with other metasedimentary lithological units, and show a NE trend.

We measured oxygen and carbon isotope ratios to understand the effect of diagenetic to metamorphic alterations, which can be recognized in negative isotope shifts. In general, the metacarbonate rocks have positive oxygen isotopic composition comparable with the Proterozoic unmetamorphosed carbonates, suggesting that these rocks were not affected by external fluids during digenesis, dolomitization or metamorphism. However, some of the rock units have been affected by later fluid infiltration as seen in major shifts in oxygen isotopic composition. Negative shifts in both carbon and oxygen isotopes correspond to the metamorphic decarbonation reactions being prominent. Strontium isotope chemostratigraphy was applied for the selected samples with least signatures of alteration. The depositional ages show a younging direction of sedimentation from the Wanni-side to the Vijayan-side. In the case of Nd isotopes, the values correspond to variable mixing of continent derived and oceanic crust derived components during carbonate deposition. This is clearly depicted in the ε Sr vs. ε Nd cross-plots where typical seawater-rock mixing relationship in metacarbonate rocks associated with continents and oceanic crusts can be deduced.Pb isotopic composition of the metacarbonate rocks in Sri Lanka indicated significant differences within the HC; the Vijayan side is more radiogenic than that of Wanni side. This might be due to the difference of initial composition, as well as the relationship to depositional basin and seawater composition. We also observed very low U/Pb ratios, which are considered to have occurred due to the U-loss during metamorphic recrystallization.Thus, the Sr-Nd-Pb isotopic composition in metacarbonate rocks suggests interaction between the oceanic crust and carbonate rocks on the Wanni side whereas on the Vijayan side, carbonate sedimentation was accompanied by interaction with cratonic continental crust.Thus, by applying a multi-element isotope geochemical approach on metacarbonate rocks collected from continental collisional zones, and by comparing the data with basement rocks from various neighbouring Gondwana continents, regional affinities could be established.

©2019. Japan Geoscience Union. All Right Reserved.

Sr, Nd and Pb isotopic compositions provide important information about the depositional settings of sedimentary rocks and provide key information about the surrounding terrains of oceanic and continental affinities during the time of deposition. This can lead to a better understanding of paleo-tectonic settings of crustal fragments that assemble to form supercontinents.

Keywords: metacarbonates, Sr-Nd-Pb isotopes, Sri Lanka

©2019. Japan Geoscience Union. All Right Reserved.

[E] Poster | S (Solid Earth Sciences)：S-CG Complex & General

Tue. May 28, 2019 3:30 PM - 5:00 PM JST | Tue. May 28, 2019 6:30 AM - 8:00 AM UTC | Poster Hall International Exhibition Hall8, Makuhari Messe_19

[S-CG49] Hard-Rock Drilling Science: From Continental to Deep Sea Drilling, and Oman Project

convener:Katsuyoshi Michibayashi(Department of Earth and Planetary Sciences, Nagoya University), Eiichi TAKAZAWA(Department of Geology, Faculty of Science, Niigata University), Norikatsu Akizawa(Department of Ocean Floor Geoscience, Atmosphere and Ocean Research Institute, The University of Tokyo)

The Oman Drilling Project (OmDP) has completed to drill numerous hard-rock cores within ancient oceanic lithosphere and the underlying subduction zone of the Samail ophiolite in Oman, with support from ICDP, IODP, Japan Society for the Promotion of Science, the Sloan Foundation's Deep Carbon Observatory, US, and European research agencies. Moreover, a number of IODP expeditions have focused on hard-rock drilling over the last several years including Expedition 352 in 2014, which drilled the volcanic sequence associated with subduction initiation in the Bonin fore-arc, Expedition 357, which drilled the Lost City hydrothermal field, Expedition 360, which drilled the lithosphere associated with ultraslow-spreading at the Southwest Indian Ridge in 2016, and Expedition 366, which drilled the serpentinite seamounts in the Mariana fore-arc. In this session, we invite presentations on the scientific results of hard-rock drilling at these and other sites. We also invite related presentations on oceanic lithosphere, island arc formation, and any other significant issue that could be addressed by future hard-rock drilling. This includes marine studies of oceanic lithosphere and on-land geological investigations of ophiolites, accreted arcs, and subduction complexes. The session is intended to be interdisciplinary, including the fields of geophysics, geochemistry, petrology, engineering, and biology.

[SCG49-P01] Permeability profile in the Oman Drilling Project inferred from resistivity measurements

*Ikuo Katayama[1], Keishi Okazaki[2], Natsue Abe[2], Ole Ivar Ulven[3], Gilbert Hong[4], Wenlu Zhu[5], Benoit Cordonnier[3], Kohei Hatakeyama[1], Yuya Akamatsu[1], Katsuyoshi Michibayashi[6], Marguerite Godard[7], Peter Kelemen[8], Science Party The Oman Drilling Project Phase 2 (1.Hiroshima University, 2.JAMSTEC, 3.University of Oslo, 4.Seoul National University, 5.University of Maryland, 6.Nagoya University, 7.Universitè Montpellier, 8.Columbia University)

[SCG49-P02] Relationship between alteration intensity and elastic wave velocity of gabbroic rocks from ICDP Hole CM1A, Oman Drilling Project Phase II

*Kosuke Kimura[1], Ikuo Katayama[1], Kohei Hatakeyama[1], Yuya Akamatsu[1], Natsue Abe[2], Keishi Okazaki[2], The Oman Drilling Project Phase II Science Party (1.Hiroshima University, 2.JAMSTEC)

[SCG49-P03] Physical property of the fossilized crust-mantle transition zone from ICDP Oman Drilling Project Hole CM1A and CM2B measured onboard D/V Chikyu

*Keishi Okazaki[1], Natsue Abe[1], Kohei Hatakeyama[2], Yuya Akamatsu[2], Ikuo Katayama[2], Eiichi TAKAZAWA[3], Damon A H Teagle[4], Peter B Kelemen[5], Jude Coggon[4], The Oman Drilling Project Phase 2 Science Party (1.Japan Agency for Marine-Earth Science and Technology, 2.Hiroshima University, 3.Niigata University, 4.University of Southampton, 5.Columbia University)

[SCG49-P04] Microstructures of lower crust gabbros from the Oman Ophiolite: Analyses of the drilled cores of the Oman Drilling Project

*Koki Iida[1], Takahiro Fudai[1], Susumu Umino[1], Yuki Kusano[2] (1.Kanazawa University, 2.Geological Survey of Japan)

[SCG49-P05] Olivine fabric and mineral compositions in the Maqsad area of the Samail massif, the southern Oman ophiolite

*Kaho Takahashi[1], Eiichi TAKAZAWA[2,3], Katsuyoshi Michibayashi[4], Kakihata Yuki[4], Ryoko Senda[5] (1.Graduate School of Science and Technology, Niigata University, 2.Department of Geology, Faculty of

Science, Niigata University, 3.JAMSTEC, 4.Nagoya University, 5.Kyushu University)

[SCG49-P06] The evolution of melt inclusions in podiform chromitite in Oman

*Yuan YAO[1], Eiichi TAKAZAWA[2,3], Oman Drilling Project Phase 2 Science Party (1.Graduate School of Sciences& Technology, Niigata University, Japan, 2.Department of Geology, Faculty of Science, Niigata University, Japan, 3.Research and Development Center for Ocean Drilling Science, JAMSTEC, Japan)

[SCG49-P07] Melt/fluid - rock reaction inferred from the Wadi Tayin mantle section in the southern Oman ophiolite

*Keisuke ISHII[1], Eiichi TAKAZAWA[2], Akihiro kuriyama[2], Kyouka Someya[2], Yoshihiko Tamura[3] (1.Graduate School of Science and Technology, Niigata University, 2.Department of Geology, Faculty of Science, Niigata University , 3.R&D Center for Ocean Drilling Science, Japan Agency for Marine-Earth Science and Technology)

[SCG49-P08] Numerical simulations for reaction-induced fracture formation of layered gabbro during hydration process

*Kazuki Yoshida[1], Hiroyuki Shimizu[2], Noriyoshi Tsuchiya[1], Atsushi Okamoto[1], Phase 2 Science Party Oman Drilling Project[3] (1.Tohoku university, 2.Geotechnical Analysis Group, Advanced Analysis Department, Civil Engineering Design Division, Kajima Corporation, 3.Oman Drilling Project Phase 2 Science Party)

[SCG49-P09] X-ray CT images of oceanic lithologies obtained on Oman Drilling Project drillcores during ChikyuOman 2017 and 2018

*Katsuyoshi Michibayashi[1], Peter B Kelemen[2], Margurette Godard[3], Eiichi TAKAZAWA[4], Damon A H Teagle[5], The Oman Drilling Project Science Party[6] (1.Department of Earth and Planetary Sciences, Nagoya University, 2.Columbia University, 3.Université Montpellier, 4.Niigata University, 5.Southampton University, 6.ICDP)

[SCG49-P10] Re-examination of the crystallization process of clinopyroxene oikocrysts in layered gabbros at Hess Deep Rift, EPR

*Akane Yasui[1], Takashi Hoshide[1] (1.Graduate School of International Resource Sciences, Akita University)

[SCG49-P11] Structural petrology of peridotites from the Kalaymyo ophiolite

*Kouhei Asano[1,2], Katsuyoshi Michibayashi[1], Jung-Woo Park[3] (1.Graduate School of Environmental Studies, Nagoya University, 2.Shizuoka University, 3.Seoul National University)

[SCG49-P12] Reevaluation of the origin of mafic layers in the Upper Zone of the Horoman Peridotite

*Yumeto KOGURE[1], Eiichi TAKAZAWA[1] (1.Department of Geology, Faculty of Science, Niigata University)

[SCG49-P13] A structural and petrological study of "Shibukawa ultramafic body" in the Sanbagawa belt, western Shizuoka, Japan

*Hikaru Shioya[1,2], Katsuyoshi Michibayashi[1], Ken-ichi Hirauchi[2] (1.Graduate School of Environmental Studies, Nagoya University, 2.Institute of Geosciences, Shizuoka University)

Permeability profile in the Oman Drilling Project inferred from resistivity measurements

*Ikuo Katayama[1], Keishi Okazaki[2], Natsue Abe[2], Ole Ivar Ulven[3], Gilbert Hong[4], Wenlu Zhu[5], Benoit Cordonnier[3], Kohei Hatakeyama[1], Yuya Akamatsu[1], Katsuyoshi Michibayashi[6], Marguerite Godard[7], Peter Kelemen[8], Science Party The Oman Drilling Project Phase 2

1. Hiroshima University, 2. JAMSTEC, 3. University of Oslo, 4. Seoul National University, 5. University of Maryland, 6. Nagoya University, 7. Universitè Montpellier, 8. Columbia University

Permeability is a key property that controls heat and chemical exchange in the oceanic lithosphere as well as microbial activity in the sub-seafloor. Although direct measurements of permeability were not made on board D/V Chikyu during analysis of cores from the Oman Drilling Project, we estimated permeability profiles based on onboard measurements of electrical resistivity. For each core sample, we measure its resistivity at nominally dry conditions to obtain the dry resistivity. We then saturate the sample with NaCl solution (3.5g/L) and repeat the resistivity measurements at brine-saturated conditions to obtain the wet resistivity. Owing to the conductive brine in the pore space, the wet resistivity is systematically lower than dry resistivity. Because the difference between dry and wet resistivity is predominantly controlled by the movement of dissolved ions in the brine that occupied the pore space, we can use the resistivity data to infer the volume fraction of pores that contribute to electrical transport (termed “transport porosity”). We apply the Hashin-Shtrikman upper bound to estimate transport porosity. The estimated transport porosity shows a positive correlation with bulk porosity measured on board (MAD analysis), but is approximately one order of magnitude lower. Using an empirical cubic law between transport porosity and permeability, we produce estimated permeability profiles for the crust-mantle transition zone and the serpentinized mantle sections in the Hole CM1A, BA1B, BA3A and BA4A. The results indicate, (1) the gabbro sequence exhibits a markedly lower permeability than the underlying mantle sequence, (2) serpentinized dunites have higher permeability compared to serpentinized harzburgites, and (3) the general variation of discrete sample permeability is correlated with fault zone and intervals with abundant fractures. These permeability structures are most likely modified by alteration and juxtapositions, and do not represent the in-situ profile of the oceanic lithosphere; but this technique can be applicable to infer on-board permeability in future hard rock drilling.

©2019. Japan Geoscience Union. All Right Reserved.

Relationship between alteration intensity and elastic wave velocity of gabbroic rocks from ICDP Hole CM1A, Oman Drilling Project Phase II

*Kosuke Kimura[1], Ikuo Katayama[1], Kohei Hatakeyama[1], Yuya Akamatsu[1], Natsue Abe[2], Keishi Okazaki[2], The Oman Drilling Project Phase II Science Party

1. Hiroshima University, 2. JAMSTEC

The mafic to ultramafic rocks suffer metamorphism and metasomatism by the seafloor hydrothermal activities. These alterations can influence the elastic wave velocity due to the change of mineral assemblages during the ocean floor metamorphism. However, most previous studies have measured the elastic wave velocity of relatively unaltered samples. In this study, we measured elastic wave velocity of the altered gabbro from the Semail ophiolite collected from the Oman Drilling Project Phase II in order to estimate the effect of ocean floor metamorphism on the elastic wave velocity.

Gabbro samples were collected from CM1A site that is reported to be a layered gabbro sequence. Total seven samples those have different alteration intensity were measured. We use intra-vessel deformation and fluid flow apparatus at Hiroshima University to measure elastic wave velocity under confining pressure up to 200 MPa. Elastic wave velocity was measured by the pulse transmission method, with the amplitude and the frequency of a trigger wave of 5 V and 2 MHz, respectively. After measurements under dry condition, measurements under wet conditions injecting pore water were performed (P_P = 10 MPa). Alteration intensity is recognized by the relative abundances of the secondary minerals.

On the basis of the petrography, alteration group could be divided into four types. First type is almost fresh, olivine altered to serpentine and chlorite partially with less green minerals present. Second type has saussuritized plagioclase dominantly and also some sample shows alteration of clinopyroxene to amphibole. In the third type amphibolitization of clinopyroxene is dominant, and also saussuritization of plagioclase occur. Fourth type is the most altered sample showing alteration halo along the veins. Almost of the minerals are changed to prehnite except a few relict clinopyroxene. This type has higher porosity than other types.

Sample density ranges from 2.77-3.08 g/cm^3, and porosity ranges from 0.02-0.22% except ca. 1% from halo alteration sample. Data from these samples show a trend that elastic wave velocities (V_P and V_S) increase with increasing the confining pressure from 20 to 200 MPa. V_P increases from 5.68-6.80 to 6.16-6.91 km/s, V_S slightly increases from 3.65-3.97 to 3.69-3.99 km/s and V_P/V_S is almost constant ranging between 1.56-1.86 to 1.64-1.88 under dry condition, and on the other hand, V_P increases from 6.08-6.82 to 6.31-6.93 km/s, V_S slightly increases from 3.64-3.98 to 3.69-4.00 km/s and V_P/V_S is almost constant 1.67-1.86 to 1.68-1.87 under fluid-saturated condition, respectively. This result is mostly consistent with the layered gabbro occur in a normal oceanic crust (e.g. White et al., 1992; Shinohara et al., 2008).

At 200 MPa and under dry condition, V_P moderately decreases with increase in alteration intensity. About 0.75 km/s decreases in response to the increase in alteration intensity from 10 to 80 %. Comparing dV_P (difference in calculated and measured values) from the back-calculated original mineral assemblages of gabbro and peridotite reveled that the decrease in dV_P for the former is less than the latter. Moreover, both the curves of V_P and impedance change cross-over each other for gabbro and peridotite after nearly 50% of alteration.

©2019. Japan Geoscience Union. All Right Reserved.

From the above results, we suggest that if both gabbro and peridotite suffer more than 50% alteration, reversal of seismic velocity and impedance occurs, which effectively would affect the determination of geophysical Moho.

Reference: White et al. (1992) J. Geophys. Res. 97, 19,683-19,715. Shinohara et al. (2008) Phys. Earth Plan. Inter., 170, 95-106. Christensen (2004) Inter. Geol. Rev., 46, 795-816.

Keywords: Oman ophiolite, Gabbroic rocks, Elastic Wave Velocity, alteration

©2019. Japan Geoscience Union. All Right Reserved.

Physical property of the fossilized crust-mantle transition zone from ICDP Oman Drilling Project Hole CM1A and CM2B measured onboard D/V Chikyu

*Keishi Okazaki[1], Natsue Abe[1], Kohei Hatakeyama[2], Yuya Akamatsu[2], Ikuo Katayama[2], Eiichi TAKAZAWA[3], Damon A H Teagle[4], Peter B Kelemen[5], Jude Coggon[4], The Oman Drilling Project Phase 2 Science Party

1. Japan Agency for Marine-Earth Science and Technology, 2. Hiroshima University, 3. Niigata University, 4. University of Southampton, 5. Columbia University

To understand physical properties of the oceanic crust and the mantle is fundamentally important to reveal the dynamics of plate tectonics, and the global circulations of H_2O and CO_2 fluids. We report results on physical property measurements of core samples from Oman Drilling Project (OmanDP) Holes CM1A and CM2B, which drilled from the lower igneous crust into the upper mantle in the Samail Ophiolite, Sultanate of Oman.

X-ray CT, bulk/grain density, porosity, magnetic susceptibility, P-wave velocity, electrical resistivity and thermal conductivity were measured onboard D/V Chikyu using whole-round cores and discrete samples for core sections from CM1A and CM2B.

The paleo-Moho in CM1A may not preserve the original structure due to minor faulting, possibly during obduction. The gabbro-dunite transition (paleo-Moho) in Hole CM1A is characterized by a sharp change in physical property data. For example, P-wave velocity decreases from ~6.7 km/s in the layered gabbro sequence to ~4.9 km/s in the MTZ. Low P-wave velocity and density (~2.6 g/cm^3) in serpentinized dunites reflect the fact that olivine in the dunites is almost completely serpentinized. Serpentinization could have occurred during hydrothermal alteration near the spreading ridge axis, during subduction of 100’s of km of oceanic crust and sediment beneath the ophiolite, during obduction onto the Arabian continental margin, and/or during present-day weathering. In contrast to the paleo-Moho, the boundary between the Crust-Mantle Transition (CMT) sequences (i.e., dunites and dunites with gabbro lenses) and the underlying, residual mantle harzburgites is somewhat gradual. P-wave velocity gradually increases from ~4.9 km/s for dunite in the CMT to ~5.5 km/s for harzburgite in the mantle sequence. The thickness of the CMT is 50–70 m in Holes CM1A and CM2B. We also report on correlations between physical properties, especially electrical conductivity and magnetic susceptibility, and the fault intensity and alteration intensity from the core descriptions.

Keywords: ophiolite, mantle, oceanic crust, moho

©2019. Japan Geoscience Union. All Right Reserved.

Microstructures of lower crust gabbros from the Oman Ophiolite: Analyses of the drilled cores of the Oman Drilling Project

*Koki Iida[1], Takahiro Fudai[1], Susumu Umino[1], Yuki Kusano[2]

1. Kanazawa University, 2. Geological Survey of Japan

Oman Drilling Project in 2016 to 2017 recovered 400 m long cores of layered gabbros at Site GT1 in the Wadi Tayin Massif of the Oman Ophiolilte. The purpose of this research is to describe microstructures of the layered gabbro core samples and to discuss the conditions of magmatic and hypersolidus deformation that operated in the lower crust beneath the Oman paleoridge.

Core samples were cut into slabs parallel to foliation and slabs normal to foliation and parallel to lineation, which were made into thin sections for microscopic observations. Structural fabrics and the relationships between crystal shapes and alliginment were described to identify magmatic and hypersolidus deformation structures.

Cored samples are predominantly olivine gabbros consisting of anhedral olivine, anhedral to subhedral clinopyroxene and subhedral to euhedral plagioclase. Grain size ranges from 0.5 mm to a few millimeters irrespective of mineral species.

The structures shown by the gabbros are classified into three regimes by temperature or the amount of melt present: Regime I, magmatic conditions without or minimal plastic deformation; regime Ⅱ, plastic deformation assisted by interstitial melt (Dunn, 2000); regime Ⅲ, near solidus deformation. Regime Ⅱ is identified by ameboid grain boundaries with no intracrystalline deformation and equigranular textures, resulted from decreasing internal strain energy by at high temperatures. The presence of melt is evidenced by the clear euhedral plagioclase rims with resorbed turbid cores as discussed below.

Regime I. Magmatic structures are identified as modal layering due to changes in mineral mode, no preferred orientation or shape-preferred orientation of clinopyroxene and plagioclase, poikilitic texture of olivine enclosing plagioclase laths and ophitic texture of clinopyroxene including plagioclase laths.

Regime II. The hypersolidus deformation structures overprint igneous structures: ameboid olivine with or without strain in the crystal, elongated olivine, and lenticular aggregates of olivine grains with an asymmetric quarter structure. Single clinopyroxene crystals show an asymmetric quarter structure like olivine aggregates. Ophitic clinopyroxenes consist of subgrains with slightly different orientations <10˚. Plagioclase shows deformation twin and undulose extinction. Equigranular fine-grained plagioclase with grain boundaries intersecting at 120˚ are common. Large plagioclases have a resorbed core with a wavy outline and are surrounded by euhedral rim.

Regime III. Subsolidus recrystallization includes buldging and grain boundary migration resulted in ameoboid grain boundaries of clinopyroxene. Undulose extinction and kinked twinning of plagioclase are observed.

It is well known that mid-ocean ridge basalt magma commonly crystallizes in the order of olivine, plagioclase and clinopyroxene, which is also true for the gabbros of the Oman Ophiolite (Adachi and Miyashita, 2003). Nevertheless, only plagioclase shows euhedral to subhedral shapes in the observed

©2019. Japan Geoscience Union. All Right Reserved.

layered gabbro core samples. Deformed olivine aggregates and clinopyroxene with quarter structures are embedded in plagioclase with equilibrium granoblastic textures and large euhedral plagioclases with resorbed turbid cores. Considering these textures combined with the mechanical strength of the three constituent minerals, these gabbros suffered deformation under the presence of melt, which assisted complete recovery of strain through recrystallization of fine-grained plagioclase and overgrowth of euhedral rims around magmatic plagioclase cores. Poikilitic olivine occurs through the hole, whereas ophitic Cpx occurs at 73 m and 220 m in depth. Most deformation structures of regime II are present irrespective to depth. The asymmetric structures of olivine and clinopyroxene were used to determine the relative sense of shear. Both dextral and sinistral sense of shear are observed within the same samples.

Keywords: Oman ophiolite, Oman Drilling Project , Layered gabbro , Foliated gabbro , Microstructures , Lower crust

©2019. Japan Geoscience Union. All Right Reserved.

Olivine fabric and mineral compositions in the Maqsad area of the Samail massif, the southern Oman ophiolite

*Kaho Takahashi[1], Eiichi TAKAZAWA[2,3], Katsuyoshi Michibayashi[4], Kakihata Yuki[4], Ryoko Senda[5]

1. Graduate School of Science and Technology, Niigata University, 2. Department of Geology, Faculty of Science, Niigata University, 3. JAMSTEC, 4. Nagoya University, 5. Kyushu University

In this study, we conducted structural and chemical analysis of oriented samples of 17 harzburgites and 4 dunites collected from the Maqsad area of Samail massif in the southern Oman ophiolite. We investigated the degree of partial melting and the mantle-melt reaction with relation to mantle diapir structure.

The crystallographic preferred orientation (CPO) of olivine grains were measured in highly polished XZ thin sections using a scanning electron microscope equipped with an electron-back scatter diffraction system at Shizuoka University. After plotting the results in the Vp Flinn plot expanded for olivine fabric types [1,2], the fabric type of peridotites in this study are summarized as follows. The distribution of A type is limited in the southeastern part where the diapir structure has been identified [3], whereas D type is dominant in the peripheral part of the diapir. Minor amounts of AG type and E type are also observed in the peripheral part. From these, the olivine in the southeastern part (diapir area) of this study area is likely to have been deformed under high temperature whereas the peripheral part was deformed at slightly lower temperature. The CPOs of olivine in both areas do not show any influence from the presence of H2O except for only one sample with E type CPO. Moreover, strong alignment of [100] to the vertical orientation was observed in the southeastern part (diapir area) of this study area. Since vertical mantle flow has been estimated in this diapir area, our results are consistent with the previous study [3,4].

The Cr# (=Cr/[Cr+Al] atomic ratio) of spinel in the harzburgites and dunites are as high as 0.55-0.58 in the central part of the southeastern part (diapir area) and along the paleo-ridge axis running in the NW - SE direction [3,4]. On the other hand, the Cr# of spinel in the peripheral part is 0.41-0.55 indicating slightly less depleted than in the central part. In addition, the REE abundance of clinopyroxenes in the central part of the diapir area is lower than in the peripheral part being consistent with the distribution of spinel Cr#.

We consider that the upwelling rate in the southeastern part (diapir area) may have been greater than the peripheral part possibly due to higher temperature in the focused vertical mantle flow. This model is consistent with the distribution of the Cr# of spinel: the degree of melting was greater in the diapir area where Cr# of spinel are higher than the peripheral part. The strongly focused pipe-like model for axis location [3,5] is well fitted by our observations in this study.

[1] Karato et al., 2008, Ann. Rev. Earth Planet. Sci., 36, 59-95. [2] Michibayashi, 2015, J. Geography, 124, 397-409. [3] Jousselin et al., 1998, JGR, 103, 18153-18170. [4] Nicolas et al., 2000, Marine Geophys. Res., 21, 147-179. [5] Nicolas and Boudier, 1995, JGR, 100, 6179-6197.

Keywords: Oman ophiolite, crystalographic preferred orientation, olivine, fabric, peridotite, mantle flow

©2019. Japan Geoscience Union. All Right Reserved.

The evolution of melt inclusions in podiform chromitite in Oman

*Yuan YAO[1], Eiichi TAKAZAWA[2,3], Oman Drilling Project Phase 2 Science Party

1. Graduate School of Sciences& Technology, Niigata University, Japan, 2. Department of Geology, Faculty of Science, Niigata University, Japan, 3. Research and Development Center for Ocean Drilling Science, JAMSTEC, Japan

Melt inclusions are tiny inclusions which trapped in the host magmatic minerals. After trapping, the host mineral can be considered as a closed and isolated system (Roedder, 1984). Thus, melt inclusions behave as time capsules, which record the liquid line of descent of magmatic systems (Frezzotti, 2001). Therefore, melt inclusions can provide important information of the primary melts (Kent, 2008).

We studied the melt inclusions in chromite from a chromitite deposit mine in the north of Maqsad and the core sample from the Oman drilling project phase 2. The silicate inclusions range in diameter from 5 μm to 200 μm, contain pargasite, tremolite, aspidolite, high Cr# (=Cr/[Cr+Al] atomic ratio) chromite, diopside, enstatite, forsterite, grossular, albite, titanite, pentlandite, apatite, chlorite, wollastonite and serpentine. We found the high Cr# chromite occurs as lining of the inclusion, moreover the daughter minerals precipitated in the high Cr# chromite lining. Those phenomenon can be explained by the crystallization of chromite on the wall of inclusion. In addition, this is the first report about the necking down of melt inclusion in chromitite. The necking down of inclusions is an originally large, liquid-filled inclusion divided into smaller inclusions. If the necking down happens after the phase change of inclusion, the compositions of smaller inclusions probably are inhomogeneity. Last year, we conducted the high temperature homogenized experiments, the result showed that the homogenized quenching glass are heterogeneous. We consider the inhomogeneity of inclusions perhaps caused by the necking down. Based above all, we suggest the composition of homogenized inclusion can not represent the parental melt.

To summarize, we suggest before analysis and experiment of inclusions in chromite, the origin and the evolution of inclusions should be carefully studied.

Reference

Frezzotti, M. (2001). "Silicate-melt inclusions in magmatic rocks: applications to petrology." Lithos **55** (1-4): 273-299.
Kent, A. J. R. (2008). "Melt Inclusions in Basaltic and Related Volcanic Rocks." Reviews in Mineralogy and Geochemistry **69** (1): 273-331.
Roedder, E. (1984). Fluid inclusions, Walter de Gruyter GmbH & Co KG.

Keywords: melt inclusion, Oman, chromitite

©2019. Japan Geoscience Union. All Right Reserved.

Melt/fluid - rock reaction inferred from the Wadi Tayin mantle section in the southern Oman ophiolite

*Keisuke ISHII[1], Eiichi TAKAZAWA[2], Akihiro kuriyama[2], Kyouka Someya[2], Yoshihiko Tamura[3]

1. Graduate School of Science and Technology, Niigata University, 2. Department of Geology, Faculty of Science, Niigata University , 3. R&D Center for Ocean Drilling Science, Japan Agency for Marine-Earth Science and Technology

We report the petrology and the mineral compositions of peridotites from the Wadi Tayin massif in the southern Oman ophiolite [1-3] to investigate the influence of arc related magmatism during oceanic thrusting of the ophiolite. Harzburgites, dunites and a small number of lherzolite were systematically corrected along wadis to cover the mantle section from the boundary between lower crust and uppermost mantle namely “Moho” to the basal thrust. Spinel Cr# [=Cr/(Cr+Al) atomic ratio] of harzburgite varies from 0.22 to 0.58 similar to the range in abyssal peridotites [4]. Moreover, it gradually increases from the basal part to the Moho indicating the compositional variation expected for the residual mantle column formed at a mid ocean ridge. On the other hand, the spinel Cr# of dunite often exceeds 0.6 in the NW-SE striking shear zone in the middle part of the study area. The chondrite-normalized rare earth element (REE) patterns of clinopyroxenes in peridotites from the shear zone show a linear pattern that monotonously decreases from heavy REE to light REE (LREE). Calculated melt compositions in equilibrium with these clinopyroxenes are equivalent with the V2 (Type2) lava reported in the northern Oman ophiolite [5-6].

The plots in Cr# of spinel versus Ce/Yb ratio of clinopyroxenes show a linear trend with a positive correlation. It indicates that the LREE enrichment of clinopyroxene is associated with an increase in the degree of melting. Clinopyroxenes in the dunite from the shear zone are most significantly enriched in LREE to middle REE and have REE abundances being in equilibrium with the V2 lava. We consider that harzburgites were suffered from a flux melting by infiltration of H2O-rich fluid producing V2 lava. Comparing to the results from the northern massifs the linear trend in the diagram of Cr# of spinel versus Ce/Yb ratio of clinopyroxenes in the southern massif is obviously shifted toward lower in Cr#. It suggests that the infiltration of H2O-rich fluid may have started at early stage of melting in the Wadi Tayin massif relative to the northern massifs.

[1] Kelemen et al., 1995, Nature, 375, 747-753, [2] Godard al., 2000, EPSL, 180, 133-148, [3] HanghØj et al., 2010, J. Petrol., 51, 201-227, [4] Dick and Bullen, 1984, CMP, 86, 54-76, [5] Godard et al., 2003, G-cubed, 4, 8609, [6] Kusano et al., 2016, Chem. Geol., 449, 206-225.

Keywords: Oman ophiolite, Mantle section, Peridotite, Melt/rock reaction

©2019. Japan Geoscience Union. All Right Reserved.

Numerical simulations for reaction-induced fracture formation of layered gabbro during hydration process

*Kazuki Yoshida[1], Hiroyuki Shimizu[2], Noriyoshi Tsuchiya[1], Atsushi Okamoto[1], Phase 2 Science Party Oman Drilling Project[3]

1. Tohoku university, 2. Geotechnical Analysis Group, Advanced Analysis Department, Civil Engineering Design Division, Kajima Corporation, 3. Oman Drilling Project Phase 2 Science Party

Serpentinization of oceanic lithosphere is important for various geological processes, including magmatism and earthquake at subduction zone, and generation of hydrogen and hydrocarbon at seafloor. For understanding the extent of the water infiltration into mantle within the oceanic lithosphere, permeability of the lower crust is an important factor, since gabbro has low permeability at high confining pressure (Katayama et al., 2012). In natural olivine-bearing gabbro, serpentinization of olivine grains produced radial fractures within the plagioclase matrix, which can potentially enhance the permeability (Jamtveit et al., 2008). Based on the numerical simulations using discrete element method (DEM), Jamtveit et al. (2008) shows that fracture network is produced by the volume expansion of olivine grains during hydration. However, their model dos not treat the advective fluid flow explicitly, it is not clear how permeability evolves during such processes. In this study, inspired by the natural textures of olivine gabbro taken from CM1A-7A (Wazi Zeeb, Oman Drilling Project), we conducted the DEM simulation for understanding the feedback of the fluid flow –olivine hydration –fracturing to the layered gabbro, which consists of olivine-rich layer and olivine-poor layer alternately. In particular, we focus on the contrasting fracture patterns between olivine and plagioclase, the evolution and anisotropy of permeability produced by the reaction-induced fracturing within the layered gabbro.

We conducted the two-dimensional DEM model, and the details of the model follows Okamoto and Shimizu (2015) and Shimizu and Okamoto (2016). We consider a simple volume increasing hydration reaction (A + H_2O →B; 50% volume increase), and the reaction rate is defined as a linear function of fluid pressure. In the model, advective fluid flow occurs through apertures between particles, in response to difference of fluid pressure of individual domains. The rock model is consist of reactive part (it can change from olivine to sperneitne) and non-reactive part (e.g., plagioclase and clnopyronene). The reaction rate constant and aperture width of matrix and fracture are defined based on the non-dimensional numbers based on Shimizu and Okamoto (2016).

Firstly, we conducted the simulations for the model in which a single olivine exists in non-reactive matrix. When fluid is supplied through matrix, hydration of olivine starts, which produces the mesh-like textures inside the olivine grain and radial cracks within the unreactive matrix, which is consistent with those observed in the gabbro sample from CM1A. Second, we conducted a case where several olivine grains exist in matrix. In this case, we found the formation of fracture network that connects among the olivine grains, and positive relationship between the reaction rate and permeability. Finally, we tested the case of the layered structure that consists of olivine-rich layer and olivine-absent layer, and that fluid flows in direction perpendicular to the layers. The results of the simulations reveals that the development of vertical fractures in both olivine-rich and non-reactive layers, whereas the horizontal fractures are only developed in the olivine-rich layers. These features of fracture orientation are consistent with the natural observations and indicate that he reaction-induced fracturing could significantly enhance the fluid infiltration through layered gabbro.

©2019. Japan Geoscience Union. All Right Reserved.

References

Katayama I, Terada T, Okazaki K, Tanikawa W (2012) Nat Geosci 5:731–734.

Jamtveit B., Malthe-Sørenssen A., Kostenko O., 2008. Earth Planet. Sci. Lett., 267, pp. 620-627

Okamoto,A.,Shimizu,H., 2015. Earth and Planetary Science Letters 415, 9–18.

Shimizu, H., Okamoto, A., 2016. Contributions to Mineralogy and Petrology, 171, 73.

Keywords: Oman Drilling Project, layered gabbro, permeability, Discrete Element Method, serpentinization

©2019. Japan Geoscience Union. All Right Reserved.

X-ray CT images of oceanic lithologies obtained on Oman Drilling Project drillcores during ChikyuOman 2017 and 2018

*Katsuyoshi Michibayashi[1], Peter B Kelemen[2], Margurette Godard[3], Eiichi TAKAZAWA[4], Damon A H Teagle[5], The Oman Drilling Project Science Party[6]

1. Department of Earth and Planetary Sciences, Nagoya University, 2. Columbia University, 3. Université Montpellier, 4. Niigata University, 5. Southampton University, 6. ICDP

The Oman Drilling Project (OmanDP) has drilled >3,200 meters of the Oman ophiolite during Phases 1 and 2 in Holes GT1A, GT2A, GT3A, BT1B, CM1A, CM2B, BA1B, BA3A and BA4A. All cores have been described on board D/V Chikyu during the summers of 2017 and 2018. X-ray computed tomography (X-ray CT) images were obtained on all cores as a routine part of the IODP measurement protocol onboard D/V Chikyu.

The X-ray CT scanner (Discovery CT 750HD, GE Medical Systems) scans and reconstructs an image of a 1.4 m section in 10 minutes and produces a series of scan images, each 0.625 mm thick. The X-ray source and detector are installed inside of the gantry opposite each other. The excitation voltage and current for X-ray tube are 140 kV and 100 mA, respectively. Core samples are scanned in the gantry with a scanning rate of 20 mm/sec. The distribution of attenuation values mapped to an individual slice comprises the raw data that are used for subsequent image processing. Successive two-dimensional (2D) slices of 512 x 512 pixels yield a representation of attenuation values in three-dimensional (3D) voxels of 512 x 512 by ~1600 in length. Data generated for each core consist of core-axis-normal planes (XY planes) of X-ray attenuation values with dimensions of 512 ×512 pixels in 9 cm ×9 cm cross-section, with a resolution of 0.176 mm/pixel.

As a consequence, we have >3,200 meters length of X-ray CT images from the dyke/gabbro transition zone to the gabbroic sequence to the mantle sequence to the basal thrust of the ophiolite. All X-ray CT images have been processed to match with individual photo images of the archive halves of the cores. The data are useful for assessing sample locations and quality. X-ray CT images can be used for 3D fabric analyses even after core has been cut in half and subsampled for other analyses.

Keywords: OmanDP, XCT, image

©2019. Japan Geoscience Union. All Right Reserved.

Re-examination of the crystallization process of clinopyroxene oikocrysts in layered gabbros at Hess Deep Rift, EPR

*Akane Yasui[1], Takashi Hoshide[1]

1. Graduate School of International Resource Sciences, Akita University

In the Hess Deep Rift, located about 60km east of the East Pacific Rise, the lower crustal gabbros which have been formed at the fast-spreading ridge are exposed. In the IODP Exp. 345, primitive layered gabbros were collected from the lower crust as mainly three drill cores (U1415 I, J, P; Gillis et al., 2014). From the U1415J, unique gabbroic rocks (troctolites) with poikilitic clinopyroxenes (oikocrysts) including many small plagioclase laths have been found (Maeda and Kaise, 2015, Abstracts of the Geological Society of Japan).

Recently, on the origins of clinopyroxene-oikocryst-bearing gabbroic rocks, the different hypotheses have been proposed by Leuthold et al. (2018) and Maeda and Kaise (2015).
Leuthold et al. (2018) proposed that initial olivine gabbros had been partially molten by the intrusion of a primitive melt and then clinopyroxene oikocrysts had crystallized from clinopyroxene-rich basaltic melts formed by the mixing between the partial melt and the primitive magma.
On the other hands, Maeda and Kaise (2015) proposed that clinopyroxenes have first crystallized from a primitive magma and after molten by the encounter with another primitive magma they have continued to grow further and then, the clinopyroxene rim has simultaneously crystallized with matrix olivine and plagioclase. Several hypotheses other than those above (e.g.,Tegner et al., 1995; Nicolas and Boudier., 2011) have been also proposed for the origin of the clinopyroxene oikocrysts in gabbroic rocks. The question is still open to discussion.
Therefore, I re-examine the process of clinopyroxene-oikocryst formation through the textural observation and chemical analysis of the constituent minerals for 8 samples of clinopyroxene-oikocryst-bearing gabbros from 3R, 5R, 7G, 8R and 15G of the U1415J core collected at the IODP Exp. 345.

The matrix part is troctolite consisting mainly of olivine (about 0.5 mm - 2 mm in size, amoeboidal, Fo85~) and plagioclase (about 1 mm in size, An#77-82). Spherical to ellipsoidal clinopyroxene oikocrysts (5-10 mm in size, Mg#85 to 88) is distributed in the matrix troctolite. In addition, clinopyroxene oikocrysts exhibit the following characteristics:

(1) Clinopyroxene oikocrysts basically do not contain any olivine crystals. Rarely, they contain aggregates of plagioclase and olivine.
(2) Orthopyroxene rims (about 100 μm thick, film-like, Mg#85-87) are observed only in matrix olivines (Fo85~) near the rim of the clinopyroxene oikocryst. The olivine crystals rimmed by orthopyroxene are shrinked.
(3) The decreases in Al and Cr contents towards the plagioclase chadacrysts are observed in clinopyroxene oikocrysts.
(4) In the core of the clinopyroxene oikocrysts, we can find parts with Mg# higher than the values which can be in the Fe/Mg equilibrium with olivine in the matrix troctolite.

The facts of (1) and (2) indicate that the assemblage of olivine and plagioclase had already existed when the clinopyroxene oikocrysts crystallized from the melt. In additions, these facts suggest that the melt which formed clinopyroxene oikocryst was in a reaction relationship with olivine. These interpretations

©2019. Japan Geoscience Union. All Right Reserved.

are consistent with the hypothesis of Leuthold et al. (2018).

Keywords: clinopyroxene oikocrysts, Hess Deep, troctolite, Magma mixing, MORB

©2019. Japan Geoscience Union. All Right Reserved.

Structural petrology of peridotites from the Kalaymyo ophiolite

*Kouhei Asano[1,2], Katsuyoshi Michibayashi[1], Jung-Woo Park[3]

1. Graduate School of Environmental Studies, Nagoya University, 2. Shizuoka University, 3. Seoul National University

The Kalaymyo ophiolite is located at Myanmar. The Kalaymyo ophiolite includes large peridotite massifs, where peridotites are commonly well preserved. In recent years, petrologic and geochemical studies have been carried out on the Kalaymyo peridotites. These results suggest that the Kalaymyo peridotites have been undergone melt-rock interactions. In this study, we used fourteen samples from outcrops and drill cores, and carried out analyses of crystal preferred orientations (CPOs) of olivine and of major elements of olivine and spinel. The samples show coarse-grained equigranular textures. The mineral compositions in spinel Cr# and olivine Mg# plot in the field of OSMA (olivine-spinel mantle array) indicate that these samples represent residual upper mantle rocks after partial melting. Spinel grains with Cr# higher than 0.3 have relatively high TiO_2 contents (0.10-0.20 wt.%). Because Ti is incompatible element, high spinel TiO_2 content suggests that these peridotites have experienced melt-rock interaction. There is a positive correlation between J-index and spinel Cr# in the samples. The correlation also has two trends: high and low positive relationships between J-index and spinel Cr#, respectively. Samples experienced melt-rock interaction belong to the low positive trend. It suggests that melt percolation by melt-rock interaction could have an impact on deformation, in particular on CPO development. We propose that melt-rock interaction was synchronous with deformation. It is noted that peridotites experienced melt-rock interaction are intensely located on a narrow range with respect to the elevation, indicating that the occurrence of melt-rock interaction was localized within the Kalaymyo ophiolite.

Keywords: Kalaymyo ophiolite, peridotite, melt-rock interaction, J-index

©2019. Japan Geoscience Union. All Right Reserved.

Reevaluation of the origin of mafic layers in the Upper Zone of the Horoman Peridotite

*Yumeto KOGURE[1], Eiichi TAKAZAWA[1]

1. Department of Geology, Faculty of Science, Niigata University

Horoman peridotite is situated at the southern tip of the Hidaka mountain range, spreads 8 km east-west, 10 km north-south, and has a layer thickness of 3,000 m. We reevaluated the origin of the mafic layer in the Upper Zone of the Horoman Peridotite. We studied Fumo section in the Upper Zone. This section has total thickness of 263 m and consists of plagioclase lherzolite, harzburgite and mafic layer. In the Fumo section, the mafic layer is only interlayered in the plagioclase lherzolite. In the Al2O3, CaO, and Na2O vs. MgO diagrams of whole rock compositions, the mafic layer is plotted on the extension of the linear composition trend indicated by plagioclase lherzolite and harzburgite. There are two types of mafic layer, one plotted in the vicinity of N-MORB and the other plotted in the vicinity of plagioclase lherzolite. The plagioclase lherzolites which have higher Al2O3, CaO, and Na2O and lower MgO contents than the Depleted MORB Mantle (DMM) [1] contain amphiboles whereas the other plagioclase lherzolite which has lower Al2O3, CaO, and Na2O contents and higher MgO content than the DMM do not contain amphibole. Chondrite-normalized whole rock rare earth element (REE) patterns of plagioclase lherzolites are flat from heavy REE to middle REE and show convex upward pattern with depletion in light REE. The mafic layers also show the similar pattern although the abundances of REE is much lower than N-MORB.

From these results, the mafic layers in the Fumo section do not have the composition of primary melt and is considered to be cumulate [2,3]. Also, in the whole rock FeO, TiO2 vs. MgO diagrams, the compositional trends suddenly bend at the most fertile plagioclase lherzolite and becomes depleted in FeO, TiO2 toward the thin mafic layers. On the extension of this bent trends reach to the composition of Cpx and plagioclase. The mafic layer in the Fumo section suggests the possibility that Cpx and plagioclase were crystallized from a melt penetrated into plagioclase lherzolite in a relatively low pressure where the combination of Cpx and plagioclase was stable.

[1] Workman and Hart, 2005, EPSL, 231, 53-72. [2] Shiotani and Niida, 1997, Memoir. Geol. Soc. Japan, 47, 123–137. [3] Takazawa et al., 1999, J. Petrol., 40, 1827-1851.

Keywords: Horoman Peridotite, mantle, mafic layer, orogenic lherzolite, Hidaka Metamorphic Belt

©2019. Japan Geoscience Union. All Right Reserved.

A structural and petrological study of "Shibukawa ultramafic body" in the Sanbagawa belt, western Shizuoka, Japan

*Hikaru Shioya[1,2], Katsuyoshi Michibayashi[1], Ken-ichi Hirauchi[2]

1. Graduate School of Environmental Studies, Nagoya University, 2. Institute of Geosciences, Shizuoka University

We studied an ultramafic body, which is named "Shibukawa ultramafic body" in this study, in the Sanbagawa belt located to the western Shizuoka, focusing on their primary mineral olivine to reveal its petrogenesis. Shibukawa ultramafic body is composed of dunites and wehlites, although the body was heavily weathered due to serpentinization. Yet, most of samples still contain olivine, spinel and a few amounts of clinopyroxene. The olivine crystal preferred orientations (CPOs) of this body were divided into two types: D type and single maxima type. The CPO intensities were relatively high in the north area, whereas those in the south area were relatively low. Considering the grain size distribution of olivine in the samples, the samples in the south area was weakly deformed as they preserve porphyroclastic olivine grains in the fine-grained matrix. In contrast, grain size reduction due to deformation has been completed in the north area. Olivine CPO patterns and major elements composition of both olivine and spinel indicate that the origin of this ultramafic body could be cumulate such as the Mikabu belt and is different from those of Shikoku mountains in the Sanbagawa belt.

Keywords: Sanbagawa belt, Mikabu belt, Cumulate, Ultramafic, Olivine fabrics, Dunite

©2019. Japan Geoscience Union. All Right Reserved.

[E] Poster | S (Solid Earth Sciences)：S-CG Complex & General

Tue. May 28, 2019 5:15 PM - 6:30 PM JST | Tue. May 28, 2019 8:15 AM - 9:30 AM UTC | Poster Hall International Exhibition Hall8, Makuhari Messe_35

[S-CG49] Hard-Rock Drilling Science: From Continental to Deep Sea Drilling, and Oman Project

convener:Katsuyoshi Michibayashi(Department of Earth and Planetary Sciences, Nagoya University), Eiichi TAKAZAWA(Department of Geology, Faculty of Science, Niigata University), Norikatsu Akizawa(Department of Ocean Floor Geoscience, Atmosphere and Ocean Research Institute, The University of Tokyo)

The Oman Drilling Project (OmDP) has completed to drill numerous hard-rock cores within ancient oceanic lithosphere and the underlying subduction zone of the Samail ophiolite in Oman, with support from ICDP, IODP, Japan Society for the Promotion of Science, the Sloan Foundation's Deep Carbon Observatory, US, and European research agencies. Moreover, a number of IODP expeditions have focused on hard-rock drilling over the last several years including Expedition 352 in 2014, which drilled the volcanic sequence associated with subduction initiation in the Bonin fore-arc, Expedition 357, which drilled the Lost City hydrothermal field, Expedition 360, which drilled the lithosphere associated with ultraslow-spreading at the Southwest Indian Ridge in 2016, and Expedition 366, which drilled the serpentinite seamounts in the Mariana fore-arc. In this session, we invite presentations on the scientific results of hard-rock drilling at these and other sites. We also invite related presentations on oceanic lithosphere, island arc formation, and any other significant issue that could be addressed by future hard-rock drilling. This includes marine studies of oceanic lithosphere and on-land geological investigations of ophiolites, accreted arcs, and subduction complexes. The session is intended to be interdisciplinary, including the fields of geophysics, geochemistry, petrology, engineering, and biology.

[SCG49-P01] Permeability profile in the Oman Drilling Project inferred from resistivity measurements

*Ikuo Katayama[1], Keishi Okazaki[2], Natsue Abe[2], Ole Ivar Ulven[3], Gilbert Hong[4], Wenlu Zhu[5], Benoit Cordonnier[3], Kohei Hatakeyama[1], Yuya Akamatsu[1], Katsuyoshi Michibayashi[6], Marguerite Godard[7], Peter Kelemen[8], Science Party The Oman Drilling Project Phase 2 (1.Hiroshima University, 2.JAMSTEC, 3.University of Oslo, 4.Seoul National University, 5.University of Maryland, 6.Nagoya University, 7.Universitè Montpellier, 8.Columbia University)

[SCG49-P02] Relationship between alteration intensity and elastic wave velocity of gabbroic rocks from ICDP Hole CM1A, Oman Drilling Project Phase II

*Kosuke Kimura[1], Ikuo Katayama[1], Kohei Hatakeyama[1], Yuya Akamatsu[1], Natsue Abe[2], Keishi Okazaki[2], The Oman Drilling Project Phase II Science Party (1.Hiroshima University, 2.JAMSTEC)

[SCG49-P03] Physical property of the fossilized crust-mantle transition zone from ICDP Oman Drilling Project Hole CM1A and CM2B measured onboard D/V Chikyu

*Keishi Okazaki[1], Natsue Abe[1], Kohei Hatakeyama[2], Yuya Akamatsu[2], Ikuo Katayama[2], Eiichi TAKAZAWA[3], Damon A H Teagle[4], Peter B Kelemen[5], Jude Coggon[4], The Oman Drilling Project Phase 2 Science Party (1.Japan Agency for Marine-Earth Science and Technology, 2.Hiroshima University, 3.Niigata University, 4.University of Southampton, 5.Columbia University)

[SCG49-P04] Microstructures of lower crust gabbros from the Oman Ophiolite: Analyses of the drilled cores of the Oman Drilling Project

*Koki Iida[1], Takahiro Fudai[1], Susumu Umino[1], Yuki Kusano[2] (1.Kanazawa University, 2.Geological Survey of Japan)

[SCG49-P05] Olivine fabric and mineral compositions in the Maqsad area of the Samail massif, the southern Oman ophiolite

*Kaho Takahashi[1], Eiichi TAKAZAWA[2,3], Katsuyoshi Michibayashi[4], Kakihata Yuki[4], Ryoko Senda[5] (1.Graduate School of Science and Technology, Niigata University, 2.Department of Geology, Faculty of

Science, Niigata University, 3.JAMSTEC, 4.Nagoya University, 5.Kyushu University)

[SCG49-P06] The evolution of melt inclusions in podiform chromitite in Oman

*Yuan YAO[1], Eiichi TAKAZAWA[2,3], Oman Drilling Project Phase 2 Science Party (1.Graduate School of Sciences& Technology, Niigata University, Japan, 2.Department of Geology, Faculty of Science, Niigata University, Japan, 3.Research and Development Center for Ocean Drilling Science, JAMSTEC, Japan)

[SCG49-P07] Melt/fluid - rock reaction inferred from the Wadi Tayin mantle section in the southern Oman ophiolite

*Keisuke ISHII[1], Eiichi TAKAZAWA[2], Akihiro kuriyama[2], Kyouka Someya[2], Yoshihiko Tamura[3] (1.Graduate School of Science and Technology, Niigata University, 2.Department of Geology, Faculty of Science, Niigata University , 3.R&D Center for Ocean Drilling Science, Japan Agency for Marine-Earth Science and Technology)

[SCG49-P08] Numerical simulations for reaction-induced fracture formation of layered gabbro during hydration process

*Kazuki Yoshida[1], Hiroyuki Shimizu[2], Noriyoshi Tsuchiya[1], Atsushi Okamoto[1], Phase 2 Science Party Oman Drilling Project[3] (1.Tohoku university, 2.Geotechnical Analysis Group, Advanced Analysis Department, Civil Engineering Design Division, Kajima Corporation, 3.Oman Drilling Project Phase 2 Science Party)

[SCG49-P09] X-ray CT images of oceanic lithologies obtained on Oman Drilling Project drillcores during ChikyuOman 2017 and 2018

*Katsuyoshi Michibayashi[1], Peter B Kelemen[2], Margurette Godard[3], Eiichi TAKAZAWA[4], Damon A H Teagle[5], The Oman Drilling Project Science Party[6] (1.Department of Earth and Planetary Sciences, Nagoya University, 2.Columbia University, 3.Université Montpellier, 4.Niigata University, 5.Southampton University, 6.ICDP)

[SCG49-P10] Re-examination of the crystallization process of clinopyroxene oikocrysts in layered gabbros at Hess Deep Rift, EPR

*Akane Yasui[1], Takashi Hoshide[1] (1.Graduate School of International Resource Sciences, Akita University)

[SCG49-P11] Structural petrology of peridotites from the Kalaymyo ophiolite

*Kouhei Asano[1,2], Katsuyoshi Michibayashi[1], Jung-Woo Park[3] (1.Graduate School of Environmental Studies, Nagoya University, 2.Shizuoka University, 3.Seoul National University)

[SCG49-P12] Reevaluation of the origin of mafic layers in the Upper Zone of the Horoman Peridotite

*Yumeto KOGURE[1], Eiichi TAKAZAWA[1] (1.Department of Geology, Faculty of Science, Niigata University)

[SCG49-P13] A structural and petrological study of "Shibukawa ultramafic body" in the Sanbagawa belt, western Shizuoka, Japan

*Hikaru Shioya[1,2], Katsuyoshi Michibayashi[1], Ken-ichi Hirauchi[2] (1.Graduate School of Environmental Studies, Nagoya University, 2.Institute of Geosciences, Shizuoka University)

Permeability profile in the Oman Drilling Project inferred from resistivity measurements

*Ikuo Katayama[1], Keishi Okazaki[2], Natsue Abe[2], Ole Ivar Ulven[3], Gilbert Hong[4], Wenlu Zhu[5], Benoit Cordonnier[3], Kohei Hatakeyama[1], Yuya Akamatsu[1], Katsuyoshi Michibayashi[6], Marguerite Godard[7], Peter Kelemen[8], Science Party The Oman Drilling Project Phase 2

1. Hiroshima University, 2. JAMSTEC, 3. University of Oslo, 4. Seoul National University, 5. University of Maryland, 6. Nagoya University, 7. Universitè Montpellier, 8. Columbia University

Permeability is a key property that controls heat and chemical exchange in the oceanic lithosphere as well as microbial activity in the sub-seafloor. Although direct measurements of permeability were not made on board D/V Chikyu during analysis of cores from the Oman Drilling Project, we estimated permeability profiles based on onboard measurements of electrical resistivity. For each core sample, we measure its resistivity at nominally dry conditions to obtain the dry resistivity. We then saturate the sample with NaCl solution (3.5g/L) and repeat the resistivity measurements at brine-saturated conditions to obtain the wet resistivity. Owing to the conductive brine in the pore space, the wet resistivity is systematically lower than dry resistivity. Because the difference between dry and wet resistivity is predominantly controlled by the movement of dissolved ions in the brine that occupied the pore space, we can use the resistivity data to infer the volume fraction of pores that contribute to electrical transport (termed “transport porosity”). We apply the Hashin-Shtrikman upper bound to estimate transport porosity. The estimated transport porosity shows a positive correlation with bulk porosity measured on board (MAD analysis), but is approximately one order of magnitude lower. Using an empirical cubic law between transport porosity and permeability, we produce estimated permeability profiles for the crust-mantle transition zone and the serpentinized mantle sections in the Hole CM1A, BA1B, BA3A and BA4A. The results indicate, (1) the gabbro sequence exhibits a markedly lower permeability than the underlying mantle sequence, (2) serpentinized dunites have higher permeability compared to serpentinized harzburgites, and (3) the general variation of discrete sample permeability is correlated with fault zone and intervals with abundant fractures. These permeability structures are most likely modified by alteration and juxtapositions, and do not represent the in-situ profile of the oceanic lithosphere; but this technique can be applicable to infer on-board permeability in future hard rock drilling.

©2019. Japan Geoscience Union. All Right Reserved.

Relationship between alteration intensity and elastic wave velocity of gabbroic rocks from ICDP Hole CM1A, Oman Drilling Project Phase II

*Kosuke Kimura[1], Ikuo Katayama[1], Kohei Hatakeyama[1], Yuya Akamatsu[1], Natsue Abe[2], Keishi Okazaki[2], The Oman Drilling Project Phase II Science Party

1. Hiroshima University, 2. JAMSTEC

The mafic to ultramafic rocks suffer metamorphism and metasomatism by the seafloor hydrothermal activities. These alterations can influence the elastic wave velocity due to the change of mineral assemblages during the ocean floor metamorphism. However, most previous studies have measured the elastic wave velocity of relatively unaltered samples. In this study, we measured elastic wave velocity of the altered gabbro from the Semail ophiolite collected from the Oman Drilling Project Phase II in order to estimate the effect of ocean floor metamorphism on the elastic wave velocity.

Gabbro samples were collected from CM1A site that is reported to be a layered gabbro sequence. Total seven samples those have different alteration intensity were measured. We use intra-vessel deformation and fluid flow apparatus at Hiroshima University to measure elastic wave velocity under confining pressure up to 200 MPa. Elastic wave velocity was measured by the pulse transmission method, with the amplitude and the frequency of a trigger wave of 5 V and 2 MHz, respectively. After measurements under dry condition, measurements under wet conditions injecting pore water were performed (P_P = 10 MPa). Alteration intensity is recognized by the relative abundances of the secondary minerals.

On the basis of the petrography, alteration group could be divided into four types. First type is almost fresh, olivine altered to serpentine and chlorite partially with less green minerals present. Second type has saussuritized plagioclase dominantly and also some sample shows alteration of clinopyroxene to amphibole. In the third type amphibolitization of clinopyroxene is dominant, and also saussuritization of plagioclase occur. Fourth type is the most altered sample showing alteration halo along the veins. Almost of the minerals are changed to prehnite except a few relict clinopyroxene. This type has higher porosity than other types.

Sample density ranges from 2.77-3.08 g/cm^3, and porosity ranges from 0.02-0.22% except ca. 1% from halo alteration sample. Data from these samples show a trend that elastic wave velocities (V_P and V_S) increase with increasing the confining pressure from 20 to 200 MPa. V_P increases from 5.68-6.80 to 6.16-6.91 km/s, V_S slightly increases from 3.65-3.97 to 3.69-3.99 km/s and V_P/V_S is almost constant ranging between 1.56-1.86 to 1.64-1.88 under dry condition, and on the other hand, V_P increases from 6.08-6.82 to 6.31-6.93 km/s, V_S slightly increases from 3.64-3.98 to 3.69-4.00 km/s and V_P/V_S is almost constant 1.67-1.86 to 1.68-1.87 under fluid-saturated condition, respectively. This result is mostly consistent with the layered gabbro occur in a normal oceanic crust (e.g. White et al., 1992; Shinohara et al., 2008).

At 200 MPa and under dry condition, V_P moderately decreases with increase in alteration intensity. About 0.75 km/s decreases in response to the increase in alteration intensity from 10 to 80 %. Comparing dV_P (difference in calculated and measured values) from the back-calculated original mineral assemblages of gabbro and peridotite reveled that the decrease in dV_P for the former is less than the latter. Moreover, both the curves of V_P and impedance change cross-over each other for gabbro and peridotite after nearly 50% of alteration.

©2019. Japan Geoscience Union. All Right Reserved.

From the above results, we suggest that if both gabbro and peridotite suffer more than 50% alteration, reversal of seismic velocity and impedance occurs, which effectively would affect the determination of geophysical Moho.

Reference: White et al. (1992) J. Geophys. Res. 97, 19,683-19,715. Shinohara et al. (2008) Phys. Earth Plan. Inter., 170, 95-106. Christensen (2004) Inter. Geol. Rev., 46, 795-816.

Keywords: Oman ophiolite, Gabbroic rocks, Elastic Wave Velocity, alteration

©2019. Japan Geoscience Union. All Right Reserved.

Physical property of the fossilized crust-mantle transition zone from ICDP Oman Drilling Project Hole CM1A and CM2B measured onboard D/V Chikyu

*Keishi Okazaki[1], Natsue Abe[1], Kohei Hatakeyama[2], Yuya Akamatsu[2], Ikuo Katayama[2], Eiichi TAKAZAWA[3], Damon A H Teagle[4], Peter B Kelemen[5], Jude Coggon[4], The Oman Drilling Project Phase 2 Science Party

1. Japan Agency for Marine-Earth Science and Technology, 2. Hiroshima University, 3. Niigata University, 4. University of Southampton, 5. Columbia University

To understand physical properties of the oceanic crust and the mantle is fundamentally important to reveal the dynamics of plate tectonics, and the global circulations of H_2O and CO_2 fluids. We report results on physical property measurements of core samples from Oman Drilling Project (OmanDP) Holes CM1A and CM2B, which drilled from the lower igneous crust into the upper mantle in the Samail Ophiolite, Sultanate of Oman.

X-ray CT, bulk/grain density, porosity, magnetic susceptibility, P-wave velocity, electrical resistivity and thermal conductivity were measured onboard D/V Chikyu using whole-round cores and discrete samples for core sections from CM1A and CM2B.

The paleo-Moho in CM1A may not preserve the original structure due to minor faulting, possibly during obduction. The gabbro-dunite transition (paleo-Moho) in Hole CM1A is characterized by a sharp change in physical property data. For example, P-wave velocity decreases from ~6.7 km/s in the layered gabbro sequence to ~4.9 km/s in the MTZ. Low P-wave velocity and density (~2.6 g/cm^3) in serpentinized dunites reflect the fact that olivine in the dunites is almost completely serpentinized. Serpentinization could have occurred during hydrothermal alteration near the spreading ridge axis, during subduction of 100’s of km of oceanic crust and sediment beneath the ophiolite, during obduction onto the Arabian continental margin, and/or during present-day weathering. In contrast to the paleo-Moho, the boundary between the Crust-Mantle Transition (CMT) sequences (i.e., dunites and dunites with gabbro lenses) and the underlying, residual mantle harzburgites is somewhat gradual. P-wave velocity gradually increases from ~4.9 km/s for dunite in the CMT to ~5.5 km/s for harzburgite in the mantle sequence. The thickness of the CMT is 50–70 m in Holes CM1A and CM2B. We also report on correlations between physical properties, especially electrical conductivity and magnetic susceptibility, and the fault intensity and alteration intensity from the core descriptions.

Keywords: ophiolite, mantle, oceanic crust, moho

©2019. Japan Geoscience Union. All Right Reserved.

Microstructures of lower crust gabbros from the Oman Ophiolite: Analyses of the drilled cores of the Oman Drilling Project

*Koki Iida[1], Takahiro Fudai[1], Susumu Umino[1], Yuki Kusano[2]

1. Kanazawa University, 2. Geological Survey of Japan

Oman Drilling Project in 2016 to 2017 recovered 400 m long cores of layered gabbros at Site GT1 in the Wadi Tayin Massif of the Oman Ophiolilte. The purpose of this research is to describe microstructures of the layered gabbro core samples and to discuss the conditions of magmatic and hypersolidus deformation that operated in the lower crust beneath the Oman paleoridge.

Core samples were cut into slabs parallel to foliation and slabs normal to foliation and parallel to lineation, which were made into thin sections for microscopic observations. Structural fabrics and the relationships between crystal shapes and alliginment were described to identify magmatic and hypersolidus deformation structures.

Cored samples are predominantly olivine gabbros consisting of anhedral olivine, anhedral to subhedral clinopyroxene and subhedral to euhedral plagioclase. Grain size ranges from 0.5 mm to a few millimeters irrespective of mineral species.

The structures shown by the gabbros are classified into three regimes by temperature or the amount of melt present: Regime I, magmatic conditions without or minimal plastic deformation; regime Ⅱ, plastic deformation assisted by interstitial melt (Dunn, 2000); regime Ⅲ, near solidus deformation. Regime Ⅱ is identified by ameboid grain boundaries with no intracrystalline deformation and equigranular textures, resulted from decreasing internal strain energy by at high temperatures. The presence of melt is evidenced by the clear euhedral plagioclase rims with resorbed turbid cores as discussed below.

Regime I. Magmatic structures are identified as modal layering due to changes in mineral mode, no preferred orientation or shape-preferred orientation of clinopyroxene and plagioclase, poikilitic texture of olivine enclosing plagioclase laths and ophitic texture of clinopyroxene including plagioclase laths.

Regime II. The hypersolidus deformation structures overprint igneous structures: ameboid olivine with or without strain in the crystal, elongated olivine, and lenticular aggregates of olivine grains with an asymmetric quarter structure. Single clinopyroxene crystals show an asymmetric quarter structure like olivine aggregates. Ophitic clinopyroxenes consist of subgrains with slightly different orientations <10˚. Plagioclase shows deformation twin and undulose extinction. Equigranular fine-grained plagioclase with grain boundaries intersecting at 120˚ are common. Large plagioclases have a resorbed core with a wavy outline and are surrounded by euhedral rim.

Regime III. Subsolidus recrystallization includes buldging and grain boundary migration resulted in ameoboid grain boundaries of clinopyroxene. Undulose extinction and kinked twinning of plagioclase are observed.

It is well known that mid-ocean ridge basalt magma commonly crystallizes in the order of olivine, plagioclase and clinopyroxene, which is also true for the gabbros of the Oman Ophiolite (Adachi and Miyashita, 2003). Nevertheless, only plagioclase shows euhedral to subhedral shapes in the observed

©2019. Japan Geoscience Union. All Right Reserved.

layered gabbro core samples. Deformed olivine aggregates and clinopyroxene with quarter structures are embedded in plagioclase with equilibrium granoblastic textures and large euhedral plagioclases with resorbed turbid cores. Considering these textures combined with the mechanical strength of the three constituent minerals, these gabbros suffered deformation under the presence of melt, which assisted complete recovery of strain through recrystallization of fine-grained plagioclase and overgrowth of euhedral rims around magmatic plagioclase cores. Poikilitic olivine occurs through the hole, whereas ophitic Cpx occurs at 73 m and 220 m in depth. Most deformation structures of regime II are present irrespective to depth. The asymmetric structures of olivine and clinopyroxene were used to determine the relative sense of shear. Both dextral and sinistral sense of shear are observed within the same samples.

Keywords: Oman ophiolite, Oman Drilling Project , Layered gabbro , Foliated gabbro , Microstructures , Lower crust

©2019. Japan Geoscience Union. All Right Reserved.

Olivine fabric and mineral compositions in the Maqsad area of the Samail massif, the southern Oman ophiolite

*Kaho Takahashi[1], Eiichi TAKAZAWA[2,3], Katsuyoshi Michibayashi[4], Kakihata Yuki[4], Ryoko Senda[5]

1. Graduate School of Science and Technology, Niigata University, 2. Department of Geology, Faculty of Science, Niigata University, 3. JAMSTEC, 4. Nagoya University, 5. Kyushu University

In this study, we conducted structural and chemical analysis of oriented samples of 17 harzburgites and 4 dunites collected from the Maqsad area of Samail massif in the southern Oman ophiolite. We investigated the degree of partial melting and the mantle-melt reaction with relation to mantle diapir structure.

The crystallographic preferred orientation (CPO) of olivine grains were measured in highly polished XZ thin sections using a scanning electron microscope equipped with an electron-back scatter diffraction system at Shizuoka University. After plotting the results in the Vp Flinn plot expanded for olivine fabric types [1,2], the fabric type of peridotites in this study are summarized as follows. The distribution of A type is limited in the southeastern part where the diapir structure has been identified [3], whereas D type is dominant in the peripheral part of the diapir. Minor amounts of AG type and E type are also observed in the peripheral part. From these, the olivine in the southeastern part (diapir area) of this study area is likely to have been deformed under high temperature whereas the peripheral part was deformed at slightly lower temperature. The CPOs of olivine in both areas do not show any influence from the presence of H2O except for only one sample with E type CPO. Moreover, strong alignment of [100] to the vertical orientation was observed in the southeastern part (diapir area) of this study area. Since vertical mantle flow has been estimated in this diapir area, our results are consistent with the previous study [3,4].

The Cr# (=Cr/[Cr+Al] atomic ratio) of spinel in the harzburgites and dunites are as high as 0.55-0.58 in the central part of the southeastern part (diapir area) and along the paleo-ridge axis running in the NW - SE direction [3,4]. On the other hand, the Cr# of spinel in the peripheral part is 0.41-0.55 indicating slightly less depleted than in the central part. In addition, the REE abundance of clinopyroxenes in the central part of the diapir area is lower than in the peripheral part being consistent with the distribution of spinel Cr#.

We consider that the upwelling rate in the southeastern part (diapir area) may have been greater than the peripheral part possibly due to higher temperature in the focused vertical mantle flow. This model is consistent with the distribution of the Cr# of spinel: the degree of melting was greater in the diapir area where Cr# of spinel are higher than the peripheral part. The strongly focused pipe-like model for axis location [3,5] is well fitted by our observations in this study.

[1] Karato et al., 2008, Ann. Rev. Earth Planet. Sci., 36, 59-95. [2] Michibayashi, 2015, J. Geography, 124, 397-409. [3] Jousselin et al., 1998, JGR, 103, 18153-18170. [4] Nicolas et al., 2000, Marine Geophys. Res., 21, 147-179. [5] Nicolas and Boudier, 1995, JGR, 100, 6179-6197.

Keywords: Oman ophiolite, crystalographic preferred orientation, olivine, fabric, peridotite, mantle flow

©2019. Japan Geoscience Union. All Right Reserved.

The evolution of melt inclusions in podiform chromitite in Oman

*Yuan YAO[1], Eiichi TAKAZAWA[2,3], Oman Drilling Project Phase 2 Science Party

1. Graduate School of Sciences& Technology, Niigata University, Japan, 2. Department of Geology, Faculty of Science, Niigata University, Japan, 3. Research and Development Center for Ocean Drilling Science, JAMSTEC, Japan

Melt inclusions are tiny inclusions which trapped in the host magmatic minerals. After trapping, the host mineral can be considered as a closed and isolated system (Roedder, 1984). Thus, melt inclusions behave as time capsules, which record the liquid line of descent of magmatic systems (Frezzotti, 2001). Therefore, melt inclusions can provide important information of the primary melts (Kent, 2008).

We studied the melt inclusions in chromite from a chromitite deposit mine in the north of Maqsad and the core sample from the Oman drilling project phase 2. The silicate inclusions range in diameter from 5 μm to 200 μm, contain pargasite, tremolite, aspidolite, high Cr# (=Cr/[Cr+Al] atomic ratio) chromite, diopside, enstatite, forsterite, grossular, albite, titanite, pentlandite, apatite, chlorite, wollastonite and serpentine. We found the high Cr# chromite occurs as lining of the inclusion, moreover the daughter minerals precipitated in the high Cr# chromite lining. Those phenomenon can be explained by the crystallization of chromite on the wall of inclusion. In addition, this is the first report about the necking down of melt inclusion in chromitite. The necking down of inclusions is an originally large, liquid-filled inclusion divided into smaller inclusions. If the necking down happens after the phase change of inclusion, the compositions of smaller inclusions probably are inhomogeneity. Last year, we conducted the high temperature homogenized experiments, the result showed that the homogenized quenching glass are heterogeneous. We consider the inhomogeneity of inclusions perhaps caused by the necking down. Based above all, we suggest the composition of homogenized inclusion can not represent the parental melt.

To summarize, we suggest before analysis and experiment of inclusions in chromite, the origin and the evolution of inclusions should be carefully studied.

Reference

Frezzotti, M. (2001). "Silicate-melt inclusions in magmatic rocks: applications to petrology." Lithos **55** (1-4): 273-299.
Kent, A. J. R. (2008). "Melt Inclusions in Basaltic and Related Volcanic Rocks." Reviews in Mineralogy and Geochemistry **69** (1): 273-331.
Roedder, E. (1984). Fluid inclusions, Walter de Gruyter GmbH & Co KG.

Keywords: melt inclusion, Oman, chromitite

©2019. Japan Geoscience Union. All Right Reserved.

Melt/fluid - rock reaction inferred from the Wadi Tayin mantle section in the southern Oman ophiolite

*Keisuke ISHII[1], Eiichi TAKAZAWA[2], Akihiro kuriyama[2], Kyouka Someya[2], Yoshihiko Tamura[3]

1. Graduate School of Science and Technology, Niigata University, 2. Department of Geology, Faculty of Science, Niigata University , 3. R&D Center for Ocean Drilling Science, Japan Agency for Marine-Earth Science and Technology

We report the petrology and the mineral compositions of peridotites from the Wadi Tayin massif in the southern Oman ophiolite [1-3] to investigate the influence of arc related magmatism during oceanic thrusting of the ophiolite. Harzburgites, dunites and a small number of lherzolite were systematically corrected along wadis to cover the mantle section from the boundary between lower crust and uppermost mantle namely “Moho” to the basal thrust. Spinel Cr# [=Cr/(Cr+Al) atomic ratio] of harzburgite varies from 0.22 to 0.58 similar to the range in abyssal peridotites [4]. Moreover, it gradually increases from the basal part to the Moho indicating the compositional variation expected for the residual mantle column formed at a mid ocean ridge. On the other hand, the spinel Cr# of dunite often exceeds 0.6 in the NW-SE striking shear zone in the middle part of the study area. The chondrite-normalized rare earth element (REE) patterns of clinopyroxenes in peridotites from the shear zone show a linear pattern that monotonously decreases from heavy REE to light REE (LREE). Calculated melt compositions in equilibrium with these clinopyroxenes are equivalent with the V2 (Type2) lava reported in the northern Oman ophiolite [5-6].

The plots in Cr# of spinel versus Ce/Yb ratio of clinopyroxenes show a linear trend with a positive correlation. It indicates that the LREE enrichment of clinopyroxene is associated with an increase in the degree of melting. Clinopyroxenes in the dunite from the shear zone are most significantly enriched in LREE to middle REE and have REE abundances being in equilibrium with the V2 lava. We consider that harzburgites were suffered from a flux melting by infiltration of H2O-rich fluid producing V2 lava. Comparing to the results from the northern massifs the linear trend in the diagram of Cr# of spinel versus Ce/Yb ratio of clinopyroxenes in the southern massif is obviously shifted toward lower in Cr#. It suggests that the infiltration of H2O-rich fluid may have started at early stage of melting in the Wadi Tayin massif relative to the northern massifs.

[1] Kelemen et al., 1995, Nature, 375, 747-753, [2] Godard al., 2000, EPSL, 180, 133-148, [3] HanghØj et al., 2010, J. Petrol., 51, 201-227, [4] Dick and Bullen, 1984, CMP, 86, 54-76, [5] Godard et al., 2003, G-cubed, 4, 8609, [6] Kusano et al., 2016, Chem. Geol., 449, 206-225.

Keywords: Oman ophiolite, Mantle section, Peridotite, Melt/rock reaction

©2019. Japan Geoscience Union. All Right Reserved.

Numerical simulations for reaction-induced fracture formation of layered gabbro during hydration process

*Kazuki Yoshida[1], Hiroyuki Shimizu[2], Noriyoshi Tsuchiya[1], Atsushi Okamoto[1], Phase 2 Science Party Oman Drilling Project[3]

1. Tohoku university, 2. Geotechnical Analysis Group, Advanced Analysis Department, Civil Engineering Design Division, Kajima Corporation, 3. Oman Drilling Project Phase 2 Science Party

Serpentinization of oceanic lithosphere is important for various geological processes, including magmatism and earthquake at subduction zone, and generation of hydrogen and hydrocarbon at seafloor. For understanding the extent of the water infiltration into mantle within the oceanic lithosphere, permeability of the lower crust is an important factor, since gabbro has low permeability at high confining pressure (Katayama et al., 2012). In natural olivine-bearing gabbro, serpentinization of olivine grains produced radial fractures within the plagioclase matrix, which can potentially enhance the permeability (Jamtveit et al., 2008). Based on the numerical simulations using discrete element method (DEM), Jamtveit et al. (2008) shows that fracture network is produced by the volume expansion of olivine grains during hydration. However, their model dos not treat the advective fluid flow explicitly, it is not clear how permeability evolves during such processes. In this study, inspired by the natural textures of olivine gabbro taken from CM1A-7A (Wazi Zeeb, Oman Drilling Project), we conducted the DEM simulation for understanding the feedback of the fluid flow –olivine hydration –fracturing to the layered gabbro, which consists of olivine-rich layer and olivine-poor layer alternately. In particular, we focus on the contrasting fracture patterns between olivine and plagioclase, the evolution and anisotropy of permeability produced by the reaction-induced fracturing within the layered gabbro.

We conducted the two-dimensional DEM model, and the details of the model follows Okamoto and Shimizu (2015) and Shimizu and Okamoto (2016). We consider a simple volume increasing hydration reaction (A + H_2O →B; 50% volume increase), and the reaction rate is defined as a linear function of fluid pressure. In the model, advective fluid flow occurs through apertures between particles, in response to difference of fluid pressure of individual domains. The rock model is consist of reactive part (it can change from olivine to sperneitne) and non-reactive part (e.g., plagioclase and clnopyronene). The reaction rate constant and aperture width of matrix and fracture are defined based on the non-dimensional numbers based on Shimizu and Okamoto (2016).

Firstly, we conducted the simulations for the model in which a single olivine exists in non-reactive matrix. When fluid is supplied through matrix, hydration of olivine starts, which produces the mesh-like textures inside the olivine grain and radial cracks within the unreactive matrix, which is consistent with those observed in the gabbro sample from CM1A. Second, we conducted a case where several olivine grains exist in matrix. In this case, we found the formation of fracture network that connects among the olivine grains, and positive relationship between the reaction rate and permeability. Finally, we tested the case of the layered structure that consists of olivine-rich layer and olivine-absent layer, and that fluid flows in direction perpendicular to the layers. The results of the simulations reveals that the development of vertical fractures in both olivine-rich and non-reactive layers, whereas the horizontal fractures are only developed in the olivine-rich layers. These features of fracture orientation are consistent with the natural observations and indicate that he reaction-induced fracturing could significantly enhance the fluid infiltration through layered gabbro.

©2019. Japan Geoscience Union. All Right Reserved.

References

Katayama I, Terada T, Okazaki K, Tanikawa W (2012) Nat Geosci 5:731–734.

Jamtveit B., Malthe-Sørenssen A., Kostenko O., 2008. Earth Planet. Sci. Lett., 267, pp. 620-627

Okamoto,A.,Shimizu,H., 2015. Earth and Planetary Science Letters 415, 9–18.

Shimizu, H., Okamoto, A., 2016. Contributions to Mineralogy and Petrology, 171, 73.

Keywords: Oman Drilling Project, layered gabbro, permeability, Discrete Element Method, serpentinization

©2019. Japan Geoscience Union. All Right Reserved.

X-ray CT images of oceanic lithologies obtained on Oman Drilling Project drillcores during ChikyuOman 2017 and 2018

*Katsuyoshi Michibayashi[1], Peter B Kelemen[2], Margurette Godard[3], Eiichi TAKAZAWA[4], Damon A H Teagle[5], The Oman Drilling Project Science Party[6]

1. Department of Earth and Planetary Sciences, Nagoya University, 2. Columbia University, 3. Université Montpellier, 4. Niigata University, 5. Southampton University, 6. ICDP

The Oman Drilling Project (OmanDP) has drilled >3,200 meters of the Oman ophiolite during Phases 1 and 2 in Holes GT1A, GT2A, GT3A, BT1B, CM1A, CM2B, BA1B, BA3A and BA4A. All cores have been described on board D/V Chikyu during the summers of 2017 and 2018. X-ray computed tomography (X-ray CT) images were obtained on all cores as a routine part of the IODP measurement protocol onboard D/V Chikyu.

The X-ray CT scanner (Discovery CT 750HD, GE Medical Systems) scans and reconstructs an image of a 1.4 m section in 10 minutes and produces a series of scan images, each 0.625 mm thick. The X-ray source and detector are installed inside of the gantry opposite each other. The excitation voltage and current for X-ray tube are 140 kV and 100 mA, respectively. Core samples are scanned in the gantry with a scanning rate of 20 mm/sec. The distribution of attenuation values mapped to an individual slice comprises the raw data that are used for subsequent image processing. Successive two-dimensional (2D) slices of 512 x 512 pixels yield a representation of attenuation values in three-dimensional (3D) voxels of 512 x 512 by ~1600 in length. Data generated for each core consist of core-axis-normal planes (XY planes) of X-ray attenuation values with dimensions of 512 ×512 pixels in 9 cm ×9 cm cross-section, with a resolution of 0.176 mm/pixel.

As a consequence, we have >3,200 meters length of X-ray CT images from the dyke/gabbro transition zone to the gabbroic sequence to the mantle sequence to the basal thrust of the ophiolite. All X-ray CT images have been processed to match with individual photo images of the archive halves of the cores. The data are useful for assessing sample locations and quality. X-ray CT images can be used for 3D fabric analyses even after core has been cut in half and subsampled for other analyses.

Keywords: OmanDP, XCT, image

©2019. Japan Geoscience Union. All Right Reserved.

Re-examination of the crystallization process of clinopyroxene oikocrysts in layered gabbros at Hess Deep Rift, EPR

*Akane Yasui[1], Takashi Hoshide[1]

1. Graduate School of International Resource Sciences, Akita University

In the Hess Deep Rift, located about 60km east of the East Pacific Rise, the lower crustal gabbros which have been formed at the fast-spreading ridge are exposed. In the IODP Exp. 345, primitive layered gabbros were collected from the lower crust as mainly three drill cores (U1415 I, J, P; Gillis et al., 2014). From the U1415J, unique gabbroic rocks (troctolites) with poikilitic clinopyroxenes (oikocrysts) including many small plagioclase laths have been found (Maeda and Kaise, 2015, Abstracts of the Geological Society of Japan).

Recently, on the origins of clinopyroxene-oikocryst-bearing gabbroic rocks, the different hypotheses have been proposed by Leuthold et al. (2018) and Maeda and Kaise (2015).
Leuthold et al. (2018) proposed that initial olivine gabbros had been partially molten by the intrusion of a primitive melt and then clinopyroxene oikocrysts had crystallized from clinopyroxene-rich basaltic melts formed by the mixing between the partial melt and the primitive magma.
On the other hands, Maeda and Kaise (2015) proposed that clinopyroxenes have first crystallized from a primitive magma and after molten by the encounter with another primitive magma they have continued to grow further and then, the clinopyroxene rim has simultaneously crystallized with matrix olivine and plagioclase. Several hypotheses other than those above (e.g.,Tegner et al., 1995; Nicolas and Boudier., 2011) have been also proposed for the origin of the clinopyroxene oikocrysts in gabbroic rocks. The question is still open to discussion.
Therefore, I re-examine the process of clinopyroxene-oikocryst formation through the textural observation and chemical analysis of the constituent minerals for 8 samples of clinopyroxene-oikocryst-bearing gabbros from 3R, 5R, 7G, 8R and 15G of the U1415J core collected at the IODP Exp. 345.

The matrix part is troctolite consisting mainly of olivine (about 0.5 mm - 2 mm in size, amoeboidal, Fo85~) and plagioclase (about 1 mm in size, An#77-82). Spherical to ellipsoidal clinopyroxene oikocrysts (5-10 mm in size, Mg#85 to 88) is distributed in the matrix troctolite. In addition, clinopyroxene oikocrysts exhibit the following characteristics:

(1) Clinopyroxene oikocrysts basically do not contain any olivine crystals. Rarely, they contain aggregates of plagioclase and olivine.
(2) Orthopyroxene rims (about 100 μm thick, film-like, Mg#85-87) are observed only in matrix olivines (Fo85~) near the rim of the clinopyroxene oikocryst. The olivine crystals rimmed by orthopyroxene are shrinked.
(3) The decreases in Al and Cr contents towards the plagioclase chadacrysts are observed in clinopyroxene oikocrysts.
(4) In the core of the clinopyroxene oikocrysts, we can find parts with Mg# higher than the values which can be in the Fe/Mg equilibrium with olivine in the matrix troctolite.

The facts of (1) and (2) indicate that the assemblage of olivine and plagioclase had already existed when the clinopyroxene oikocrysts crystallized from the melt. In additions, these facts suggest that the melt which formed clinopyroxene oikocryst was in a reaction relationship with olivine. These interpretations

©2019. Japan Geoscience Union. All Right Reserved.

are consistent with the hypothesis of Leuthold et al. (2018).

Keywords: clinopyroxene oikocrysts, Hess Deep, troctolite, Magma mixing, MORB

©2019. Japan Geoscience Union. All Right Reserved.

Structural petrology of peridotites from the Kalaymyo ophiolite

*Kouhei Asano[1,2], Katsuyoshi Michibayashi[1], Jung-Woo Park[3]

1. Graduate School of Environmental Studies, Nagoya University, 2. Shizuoka University, 3. Seoul National University

The Kalaymyo ophiolite is located at Myanmar. The Kalaymyo ophiolite includes large peridotite massifs, where peridotites are commonly well preserved. In recent years, petrologic and geochemical studies have been carried out on the Kalaymyo peridotites. These results suggest that the Kalaymyo peridotites have been undergone melt-rock interactions. In this study, we used fourteen samples from outcrops and drill cores, and carried out analyses of crystal preferred orientations (CPOs) of olivine and of major elements of olivine and spinel. The samples show coarse-grained equigranular textures. The mineral compositions in spinel Cr# and olivine Mg# plot in the field of OSMA (olivine-spinel mantle array) indicate that these samples represent residual upper mantle rocks after partial melting. Spinel grains with Cr# higher than 0.3 have relatively high TiO_2 contents (0.10-0.20 wt.%). Because Ti is incompatible element, high spinel TiO_2 content suggests that these peridotites have experienced melt-rock interaction. There is a positive correlation between J-index and spinel Cr# in the samples. The correlation also has two trends: high and low positive relationships between J-index and spinel Cr#, respectively. Samples experienced melt-rock interaction belong to the low positive trend. It suggests that melt percolation by melt-rock interaction could have an impact on deformation, in particular on CPO development. We propose that melt-rock interaction was synchronous with deformation. It is noted that peridotites experienced melt-rock interaction are intensely located on a narrow range with respect to the elevation, indicating that the occurrence of melt-rock interaction was localized within the Kalaymyo ophiolite.

Keywords: Kalaymyo ophiolite, peridotite, melt-rock interaction, J-index

©2019. Japan Geoscience Union. All Right Reserved.

Reevaluation of the origin of mafic layers in the Upper Zone of the Horoman Peridotite

*Yumeto KOGURE[1], Eiichi TAKAZAWA[1]

1. Department of Geology, Faculty of Science, Niigata University

Horoman peridotite is situated at the southern tip of the Hidaka mountain range, spreads 8 km east-west, 10 km north-south, and has a layer thickness of 3,000 m. We reevaluated the origin of the mafic layer in the Upper Zone of the Horoman Peridotite. We studied Fumo section in the Upper Zone. This section has total thickness of 263 m and consists of plagioclase lherzolite, harzburgite and mafic layer. In the Fumo section, the mafic layer is only interlayered in the plagioclase lherzolite. In the Al2O3, CaO, and Na2O vs. MgO diagrams of whole rock compositions, the mafic layer is plotted on the extension of the linear composition trend indicated by plagioclase lherzolite and harzburgite. There are two types of mafic layer, one plotted in the vicinity of N-MORB and the other plotted in the vicinity of plagioclase lherzolite. The plagioclase lherzolites which have higher Al2O3, CaO, and Na2O and lower MgO contents than the Depleted MORB Mantle (DMM) [1] contain amphiboles whereas the other plagioclase lherzolite which has lower Al2O3, CaO, and Na2O contents and higher MgO content than the DMM do not contain amphibole. Chondrite-normalized whole rock rare earth element (REE) patterns of plagioclase lherzolites are flat from heavy REE to middle REE and show convex upward pattern with depletion in light REE. The mafic layers also show the similar pattern although the abundances of REE is much lower than N-MORB.

From these results, the mafic layers in the Fumo section do not have the composition of primary melt and is considered to be cumulate [2,3]. Also, in the whole rock FeO, TiO2 vs. MgO diagrams, the compositional trends suddenly bend at the most fertile plagioclase lherzolite and becomes depleted in FeO, TiO2 toward the thin mafic layers. On the extension of this bent trends reach to the composition of Cpx and plagioclase. The mafic layer in the Fumo section suggests the possibility that Cpx and plagioclase were crystallized from a melt penetrated into plagioclase lherzolite in a relatively low pressure where the combination of Cpx and plagioclase was stable.

[1] Workman and Hart, 2005, EPSL, 231, 53-72. [2] Shiotani and Niida, 1997, Memoir. Geol. Soc. Japan, 47, 123–137. [3] Takazawa et al., 1999, J. Petrol., 40, 1827-1851.

Keywords: Horoman Peridotite, mantle, mafic layer, orogenic lherzolite, Hidaka Metamorphic Belt

©2019. Japan Geoscience Union. All Right Reserved.

A structural and petrological study of "Shibukawa ultramafic body" in the Sanbagawa belt, western Shizuoka, Japan

*Hikaru Shioya[1,2], Katsuyoshi Michibayashi[1], Ken-ichi Hirauchi[2]

1. Graduate School of Environmental Studies, Nagoya University, 2. Institute of Geosciences, Shizuoka University

We studied an ultramafic body, which is named "Shibukawa ultramafic body" in this study, in the Sanbagawa belt located to the western Shizuoka, focusing on their primary mineral olivine to reveal its petrogenesis. Shibukawa ultramafic body is composed of dunites and wehlites, although the body was heavily weathered due to serpentinization. Yet, most of samples still contain olivine, spinel and a few amounts of clinopyroxene. The olivine crystal preferred orientations (CPOs) of this body were divided into two types: D type and single maxima type. The CPO intensities were relatively high in the north area, whereas those in the south area were relatively low. Considering the grain size distribution of olivine in the samples, the samples in the south area was weakly deformed as they preserve porphyroclastic olivine grains in the fine-grained matrix. In contrast, grain size reduction due to deformation has been completed in the north area. Olivine CPO patterns and major elements composition of both olivine and spinel indicate that the origin of this ultramafic body could be cumulate such as the Mikabu belt and is different from those of Shikoku mountains in the Sanbagawa belt.

Keywords: Sanbagawa belt, Mikabu belt, Cumulate, Ultramafic, Olivine fabrics, Dunite

©2019. Japan Geoscience Union. All Right Reserved.

[E] Poster | B (Biogeosciences)：B-CG Complex & General

Tue. May 28, 2019 3:30 PM - 5:00 PM JST | Tue. May 28, 2019 6:30 AM - 8:00 AM UTC | Poster Hall International Exhibition Hall8, Makuhari Messe_22

[B-CG06] Earth and Planetary Science Frontiers for Life and Global Environment

convener:Yoshinori Takano(Japan Agency for Marine-Earth Science and Technology (JAMSTEC)), Yohey Suzuki(Graduate School of Science, The University of Tokyo), Shingo Kato(RIKEN), Keisuke Fukushi(Institute of Nature & Environmental Technology, Kanazawa University)

Earth and planetary science is currently capable of sampling from four frontiers: space, polar regions, deep ocean and deep underground for the study of the origin and evolution of life. Next generation sequencing technology of nucleic acids and nanotechnology-driven innovation of solid characterizations are very powerful to expand our understanding of many fields of earth and planetary sciences. It is also important for us to be aware of global warming and climate change that dramatically affect biodiversity, biological activities and elemental cycling. The aim of this session is to cross the border of science sections to explore the frontiers of earth and planetary science.

[BCG06-P01] Dynamisms and characteristics of dissolved organic matter (DOM) in deep aquifer: A scope for deep biosphere

*Atsushi Urai[1,2], Yoshinori Takano[2], Naohiko Ohkouchi[2] (1.Department of Science and Technology, Graduate School of Medicine, Science and Technology, Shinshu University, 2.Department of Biogeochemistry, Japan Agency for Marine-Earth Science and Technology)

[BCG06-P02] Correlations of magnetosome-related genes in Nitrospirae genomes to magnetosome geometry and redox stratification in deep-sea environments

*Shinsaku Nakano[1], Shingo Kato[2], Mariko Kouduka[1], Toshitsugu Yamazaki[3], Yohey Suzuki[1] (1.Graduate School of Science, The University of Tokyo, 2.RIKEN, 3.Atmosphere and Ocean Research Institute, The University of Tokyo)

[BCG06-P03] Reconstruction of key ecological responses leading to the most recent dead zone formations in Japan Sea through ancient DNA metabarcodring

*Mariko Kouduka[1], Yohey Suzuki[1] (1.Department of Earth and Planetary Science, The University of Tokyo, 7-3-1 Hongo, Bunkyo-ku, Tokyo, Japan.)

[BCG06-P04] Search for microbial CH_4 production processes in lake sediments and surface water associated with cyanobacterial bloom

*Makoto Matsushita[1], Yoshinori Takano[1], Hiroyuki Imachi[1], Atsushi Urai[2], Ho-Dong Park[3], Hiroki Iwata[3], Naohiko Ohkouchi[1] (1.Japan Agency for Marine-Earth Science and Technology, 2.Department of Science and Technology, Graduate School of Medicine, Science and Technology, Shinshu University, 3.Department of Environmental Sciences, Faculty of Science, Shinshu University)

[BCG06-P05] Did life emerge in a deep-sea metal sulfide chimney? New insights from an archaeal genome and a nanoscale microbe-silicate assemblage

*Hinako Takamiya[1], Hiroki Mukai[2], Mariko Kouduka[1], Shingo Kato[4], Motoo Ito[3], Yohey Suzuki[1] (1.Earth and Planetary Science Graduate School of Science, The University of Tokyo , 2.National Institute of Advanced Industrial Science and Technology, 3.Kochi Institute for Core Sample Research JAMSTEC, 4.RIKEN)

[BCG06-P06] X-ray computed nano-tomography for visualizing microbial cells and their surrounding environments

*Yuki Morono[1], Go-Ichiro Uramoto[2,1], Kentaro Uesugi[3], Nobuhisa Takeuchi[3], Masayuki Uesugi[3], Kengo Kubota[4], Tatsuhiko Hoshino[1], Fumio Inagaki[1] (1.Japan Agency for Marine-Earth Science and Technology, 2.Kochi University, 3.Japan Synchrotron Radiation Research Institute, 4.Tohoku University)

[BCG06-P07] **Carbon signatures in amino acids during deep-sea anoxic methanotrophy**

*Yoshinori Takano[1] (1.Japan Agency for Marine-Earth Science and Technology (JAMSTEC))

Dynamisms and characteristics of dissolved organic matter (DOM) in deep aquifer: A scope for deep biosphere

*Atsushi Urai[1,2], Yoshinori Takano[2], Naohiko Ohkouchi[2]

1. Department of Science and Technology, Graduate School of Medicine, Science and Technology, Shinshu University, 2. Department of Biogeochemistry, Japan Agency for Marine-Earth Science and Technology

Dissolved organic matter (DOM) is generally derived from multiple sources and affected by complicated transformation and degradation reactions. In a general geochemical description of marine environments, high-molecular-weight DOM (HMW-DOM; >1 kDa) particularly represents a unique organic carbon pool, which is accompanied by considerable difference in the molecular and stable isotopic compositions from other organic components such as particulate organic matter (POM) and low-molecular-weight DOM (LMW-DOM; <1 kDa) (e.g., Benner et al., 1997).

To date, formation of DOM fraction and potential microbial interaction in deep aquifer have been particularly poorly understood on the context of prokaryotic ecology. We investigated the molecular composition of DOM fraction including LMW and HMW by an improved method (Urai et al., 2018). The filtered samples are tentatively defined by conventional size scales; macromolecular scale (100 mm >> 40 mm), POM (40 mm >> 0.6 mm), HMW-DOM(0.6 mm>>1kDa), and total-DOM (<0.6 mm). We also have a validation to distinguish the molecular signature between phototrophic primary producers (i.e., fossil molecules) and presently living benthic prokaryotes (i.e., modern molecules; cf. biological methanogenesis, Kaneko et al., 2014). We report a preliminary result of the feasibility study and discuss a perspective from the view of deep biosphere.

References:

Benner et al. Abundance, size distribution, and stable carbon and nitrogen isotopic compositions of marine organic matter isolated by tangential-flow ultrafiltration. Marine Chemistry 57, 243-263 (1997).

Kaneko et al. Quantitative analysis of coenzyme F430 in environmental samples: a new diagnostic tool for methanogenesis and anaerobic methane oxidation. Analytical Chemistry 86, 3633-3638 (2014).

Urai et al. Algal-derived 24-ethylcholesta-5, 22-dien-3β-ol (stigmasterol) is frequently found in high-molecular-weight dissolved organic matter (HMW-DOM) during summer in freshwater and brackish lakes. Geochemical Journal 52, e15-e20 (2018).

Keywords: HMW-DOM, sterol, carbon and hydrogen isotopic compositions, deep aquifer, methanogenesis

©2019. Japan Geoscience Union. All Right Reserved.

Correlations of magnetosome-related genes in Nitrospirae genomes to magnetosome geometry and redox stratification in deep-sea environments

*Shinsaku Nakano[1], Shingo Kato[2], Mariko Kouduka[1], Toshitsugu Yamazaki[3], Yohey Suzuki[1]

1. Graduate School of Science, The University of Tokyo, 2. RIKEN, 3. Atmosphere and Ocean Research Institute, The University of Tokyo

Biogenic magnetic particles are ubiquitously found in deep-sea sediments and important carriers of rock magnetism for reconstructing the Earth’ s past regarding sediment age and geomagnetic field. However, microorganisms responsible for the formation of magnetic particles are largely unknown in the deep-sea environment, because of the difficulty in sampling, cultivation, and magnetic separation of magnetotactic cells for single-cell genomics. In this study, deep-sea sediments from Japan Sea and a metal sulfide chimney from South Mariana Trough were subjected to magnetic separation and subsequent electron microscopic observations. Although teardrop-shaped magnetite (Fe_3O_4) particles without microbial cells and 16S rRNA gene sequences related to magnetotactic Nitrospirae species were previously obtained from Japan Sea sediments with a redox zonation enriched with dissolved Fe(II) (the iron boundary), no magnetotactic cells were observed after the magnetic separation. From the metal sulfide chimney, magnetotactic cells were observed with teardrop-shaped magnetite particles. Metagenomic analysis of the chimney sample revealed that contig sequences encoding genes involved in the formation of magnetosome, membrane-bound magnetic particles, were mostly affiliated within Nitrospirae based on sequence similarity. Previous studies have reported that magnetosome-related genes are clustered together as the magnetosome island (MAI) in known magnetotactic bacteria. However, those genes were scattered in a near-complete Nitrospirae genome reconstructed from the chimney sample. Although magnetotactic bacteria are generally considered to align magnetic particles into a chain for efficiently moving in a vertical redox zonation by orienting the cell along the geomagnetic filed, Nitrospirae-affiliated genes involved in chain formation were not found in the near-complete Nitrospirae genome from the chimney with a horizontal redox zonation. Comparative analysis of near-complete Nitrospirae genomes available from public databases revealed that the chain-related genes were found in the genomes from terrestrial deep aquifers and deep-sea sediments with a vertical redox zonation. As the Nitrospirae species associated with teardrop magnetite and the iron boundary in Japan Sea was closely related to Nitrospirae species with the chain-related genes, the presence of the chain-related genes appears to be correlated with a vertical redox zonation. In addition, our results suggest that the Nitrospirae species without MAI are responsible for the production of teardrop magnetite in deep-sea environment, and that teardrop magnetite is a paleoredox indicator especially for the iron boundary.

Keywords: magnetotactic bacteria, metal sulfide chimney, magnetofossil, remnant magnetization

©2019. Japan Geoscience Union. All Right Reserved.

Reconstruction of key ecological responses leading to the most recent dead zone formations in Japan Sea through ancient DNA metabarcodring

*Mariko Kouduka[1], Yohey Suzuki[1]

1. Department of Earth and Planetary Science, The University of Tokyo, 7-3-1 Hongo, Bunkyo-ku, Tokyo, Japan.

Semi-closed ocean basins are very sensitive to climate changes as recorded in frequent formations of sediments with clearly laminated layers, which was caused by the lack of O_2 available to benthic organisms. This is so-called “dead zone formation” and caused by water stagnation after channel closure and/or nutrient inflow through upwelling and channel opening. In contrast to the hydrologic causes, it remains poorly understood about organismal causes such as enhanced primary production and heterotrophic consumption of O_2. We investigated ancient eukaryotic DNA obtained from a thinly laminated layer deposited in the Japan Sea across the most recent global warming event after Younger Dryas (TL-1). Metabarcoding of 18S rRNA gene sequences clarified that across the transition from oxygenated to anoxic bottom water conditions, dominant protist populations shifted through five stages:

Stage1: Under oxygenated bottom conditions, the most dominant taxonomic group was Marine Stramenopiles Group 9 (MAST-9). MAST-9 encompasses diverse uncharacterized planktonic species, 18S rRNA gene sequences of which were detected from both anoxic and oxic water bodies in Pacific and Atlantic Oceans, Mediterranean Sea and South China Sea.

Stage 2: Before the onset of dead zone formation, the sharp decline of MAST-9 was accompanied with the expansion of marine diatom species of the genus Skeletonema, many members of which are known to be a cause of red tide around the world.

Stage 3: The dead zone formation was synchronized with the expansion of marine radiolarians of the order Chaunacanthida, the members of which are encrusted within $SrSO_4$.

Stage 4: Stages 2 was repeated, whereas the expansion of the Chaunacanthida radiolarians was not evident.

Stage 5: The uncharacterized MAST-9 that was dominant before the dead zone formation was gradually recovered towards oxygenated bottom conditions.

From these results, it is suspected that the expansion of Radiolaria species encrusted with $SrSO_4$ triggered dead zone formation by the accelerated downward transport of dead cells and subsequent heterotrophic consumption of O_2. From bioturbated sediment samples from a maximum depth of 31 mbsf with a depositional age of 100 ka, the Chaunacanthida sequences closely related to that from the laminated sediments have been previously detected.It is therefore suggested the record of the Chaunacanthida species can be reconstructed from sediments with great depth and age.

Keywords: global warming paleo-analogue, hypoxemia expansion, molecular paleoecologcail dynamics, biogeochemical cycling

©2019. Japan Geoscience Union. All Right Reserved.

©2019. Japan Geoscience Union. All Right Reserved.

Search for microbial CH_4 production processes in lake sediments and surface water associated with cyanobacterial bloom

*Makoto Matsushita[1], Yoshinori Takano[1], Hiroyuki Imachi[1], Atsushi Urai[2], Ho-Dong Park[3], Hiroki Iwata[3], Naohiko Ohkouchi[1]

1. Japan Agency for Marine-Earth Science and Technology, 2. Department of Science and Technology, Graduate School of Medicine, Science and Technology, Shinshu University, 3. Department of Environmental Sciences, Faculty of Science, Shinshu University

Methane (CH_4) is an important greenhouse gas and contributes substantial budget to global warming. Freshwater lakes are identified as one of the main CH_4 sources, as it is estimated that they contribute to 6-16% of natural CH_4 emissions [1]. The main part of CH_4 released from lakes is considered to be produced by methanogenic archaea in anoxic sediments as terminal step in the degradation of organic matter. The microbial CH_4 production in lake sediments has been mainly investigated by microbiological studies using culture-dependent methods and molecular analysis.

Microbial CH_4 production is still regarded by many as a process limited to anoxic environments. Nevertheless, over the past few decades, increasing evidence of CH_4 accumulation in oxygen-saturated lake and marine surface water has emerged [2]. To explain the enigmatic issues, it has been proposed that CH_4 production by methanogenic archaea takes place in anoxic microenvironments such as detritus and animals' gut. Alternatively, recent studies suggest that some bacteria break down methylphosphonate (MPn) or dimethylsulfoniopropionate (DMSP) and release CH_4 as a biogenic byproduct. These novel microbial CH_4 production processes may play a potential contribution to the total atmospheric carbon cycle.

Oxic CH_4 peaks have been found to be closely associated with phytoplankton dynamics across multiple lakes. Grossart *et al*. [3] found potentially methanogenic archaea associated with cyanobacteria such as *Aphanizomenon* and *Microcystis* in oxygenated surface water. Additionally, Berg *et al*. [4] showed that hydrogen produced during nitrogen fixation by cyanobacteria can be consumed by methanogenic archaea. These studies suggest the presence of a CH_4 production process by methanogenic archaea associated with cyanobacteria in lake surface water. However, it is unclear whether the CH_4 production is taking place in actual environments.

In this study, we investigated microbial CH_4 production in sediments and surface water of Lake Suwa in Nagano Prefecture, Japan, a typical hypertrophic shallow lake, using culture-independent methods. Especially, we focused on cyanobacterial bloom and tried to identify a CH_4 production process by methanogenic archaea associated with cyanobacteria. 16S rRNA gene analyses revealed the presence of methanogenic archaea closely related to the order *Methanobacteriales*, *Methanomicrobiales*, and *Methanosarcinales* in sediment core samples from 30 cm depth. On the other hand, 16S rRNA genes and *mcrA* genes of methanogenic archaea were not detected in bulk DNA from cyanobacterial bloom sample (mainly *Microcystis*)[5]. In order to estimate the potential for methanogenic archaea, we extracted Coenzyme F430, a biomarker for methanogenic archaea, from sediment and bloom samples and determined by using HPLC [6]. F430 was detected from sediment samples, but that from bloom sample was currently below detection limit (<1 pmol).

These results suggest that methanogenic archaea actively produce CH_4 in the sediments of Lake Suwa,

©2019. Japan Geoscience Union. All Right Reserved.

however, its contribution in oxygenated surface water seems to be small. We are currently conducting a more sensitive analysis of F430 using LC-MS/MS [6] with the pre-treatment procedure [7]. The analysis may identify the CH_4 production process by methanogenic archaea associated with cyanobacteria in the surface water. Although this study did not cover other CH_4 production processes such as MPn and DMSP decomposition, our results may also be applicable to estimate the *in situ* contribution of these novel CH_4 source.

Refs.
[1] Bastviken *et al.*, *Global Biogeochem. Cycles*, 18, GB4009 (2004). [2] Tang *et al.*, *Environ. Sci. Technol. Lett.*, 3, 227-233 (2016). [3] Grossart *et al. PNAS*, 108, 19657-19661 (2011). [4] Berg *et al. World J. Microbiol. Biotechnol.*, 30, 539-545 (2014). [5] Park *et al., Environ. Toxicol. Water Qual.*, 13, 61-72 (1998). [6] Kaneko *et al.*, *Anal. Chem.*, 86, 3633-3638 (2014). [7] Kaneko *et al., Geochem. J.,* 50, 453-460 (2016).

Keywords: Microbial methane production, Methane paradox, Freshwater lake, Methanogenic archaea, Cyanobacterial bloom

©2019. Japan Geoscience Union. All Right Reserved.

Did life emerge in a deep-sea metal sulfide chimney? New insights from an archaeal genome and a nanoscale microbe-silicate assemblage

*Hinako Takamiya[1], Hiroki Mukai[2], Mariko Kouduka[1], Shingo Kato[4], Motoo Ito[3], Yohey Suzuki[1]

1. Earth and Planetary Science Graduate School of Science, The University of Tokyo , 2. National Institute of Advanced Industrial Science and Technology, 3. Kochi Institute for Core Sample Research JAMSTEC, 4. RIKEN

Deep-sea hydrothermal activities have continued for 3.8 billion years on Earth. After the formation of metal sulfide chimneys from high-temperature fluid, their low-temperature interactions with ambient seawater potentially provide the cold, stable habitat for microbial life. In such a challenging habitat with metal toxicity, 16S rRNA gene sequences formerly affiliated within Deep-Sea Hydrothermal Vent Euryarchaeota Subtype 6 (DHVE6) and recently reclassified as Pacearchaeota are dominantly detected by 16S rRNA gene sequence analysis. However, the distribution and metabolic activities of Pacearchaeota in metal sulfide chimneys are largely unknown. In this study, a metal sulfide chimney collected from a deep-sea hydrothermal field in South Mariana Trough was subjected to genome-resolved metagenomics analysis. It was revealed that a near-complete Pacearchaeota genome has carbon metabolism genes involved in glycolysis and pentose phosphate pathway linked to nucleotide salvage pathway with light-independent CO_2incorporating ribulose bisphosphate carboxylase/oxygenase (RubisCO). By comparative analysis of Pacearchaeota genomes from deep-sea metal sulfide deposits and terrestrial subsurface aquifers, the carbon metabolism was commonly found with genes annotated for Cu detoxification. Based on the NanoSIMS ion imaging analysis, we found an evidence of a dense microbial colonization inside the chimney where the surface of chalcopyrite ($CuFeS_2$) was overlayered with a silica-bearing material enriched in CN, S and P. Our results explain the geographically and physicochemically diverse distributions of Pacearchaeota indicated by 16S rRNA gene sequence analysis as well as the predominance of Pacearchaeota in the metal sulfide chimney where energy sources from photosynthesis and hydrothermal fluid are limited. The carbon metabolism operated by Pacearchaeota in one of candidate environments for the origin of life could be relevant to that operated by primitive life on early Earth.

Keywords: hydrothermal vent, metagenomic analysis, extremophile ecology, origin of life, microbial carbon metabolism, Rock life detection

©2019. Japan Geoscience Union. All Right Reserved.

X-ray computed nano-tomography for visualizing microbial cells and their surrounding environments

*Yuki Morono[1], Go-Ichiro Uramoto[2,1], Kentaro Uesugi[3], Nobuhisa Takeuchi[3], Masayuki Uesugi[3], Kengo Kubota[4], Tatsuhiko Hoshino[1], Fumio Inagaki[1]

1. Japan Agency for Marine-Earth Science and Technology, 2. Kochi University, 3. Japan Synchrotron Radiation Research Institute, 4. Tohoku University

Recent developments of the X-ray computed tomography (CT) reaches to the spatial resolution of down to few tens of nanometers scale, which is enough to visualize single microbial cells, together with those distributions as well as its surrounding environments. In this study, we tried to visualize microbial cells in the environmental samples by using nanometer-scale X-ray CT.
We used anaerobic granular sludge and subseafloor sediments for the test samples. The X-ray CT analyses were conducted at beamlines of BL20XU and BL47XU in synchrotron radiation facility of Spring-8. The soft samples were either freeze-dried or embedded in the epoxy resin for the analysis. Since the high-spatial resolution observation of the X-ray CT analysis requires a higher density of X-ray per field, the samples often deformed during the analysis, which results in the failure of the 3D reconstruction of the data. Optimization of the resin, its polymerization condition, together with the stain of the cells by osmium tetroxide to put heavy element onto the microbial cells, we could successfully visualize single microbial cells in the samples. Also, the observations of the sample at the pre- and post-edge energies of the element (such as Os) enabled specific signal enhancement of osmium-stained cells.
The investigations of subseafloor biosphere have often based on destructive measurements. Although these analyses revealed the large-scale distribution of microbes along the chemical gradients, no previous attempt explored the spatial distribution of microbial cells at their size range. The visualization of microbes with its surrounding environments will give basic but critical information to understand the microbial in-situ ecophysiology.

Keywords: X-ray Computed Tomography, Subseafloor biosphere

©2019. Japan Geoscience Union. All Right Reserved.

Carbon signatures in amino acids during deep-sea anoxic methanotrophy

*Yoshinori Takano[1]

1. Japan Agency for Marine-Earth Science and Technology (JAMSTEC)

Microorganisms play a central role in both methane production and consumption in the global carbon cycle. Oceanic methane from global deep-sea sediment is largely consumed through microbially mediated sulfate-coupled oxidation, resulting in 13C-depleted cell biomass of anaerobic methanotrophic archaea (ANME). The general ecological importance of subseafloor ANME has been well recognized in the last two decades. However, the crucial biochemical pathways for the overall anaerobic oxidation of methane (AOM) still remain enigmatic. In the present study, methanotrophic pathways were analyzed to trace 13C-depleted amino acid biosynthesis in two clades of ANME (ANME-1 and ANME-2) from the Black Sea. Compound-specific analysis of ANME-dominated microbial mats showed a significant 13C-depletion trend in association with increasing carbon numbers in protein-derived amino acid families within the pyruvate family in the order of alanine, valine, isoleucine and leucine down to -114‰. This result indicates a stepwise elongation of 13C-depleted carbon during amino acid biosynthesis. The overall results suggest that intracellular protein amino acids and the most 13C-depleted signature of leucine, which has a specific branched-chain structure, are potentially propagated as isoprenoid precursor molecules into archaeal biosynthesis, resulting in the extremely 13C- and 14C-depleted nature of ANME cells in the deep microbial oasis.

References:
Takano, Y., Chikaraishi, Y., Imachi, H., Miyairi, Y., Ogawa, N.O., Kaneko, M., Yokoyama, Y., Kruger, M. and Ohkouchi, N. (2018) Insight into anaerobic methanotrophy from 13C/12C- amino acids and 14C/12C-ANME cells in seafloor microbial ecology. Scientific Reports, 8:14070, doi: 10.1038/s41598-018-31004-5.

Supplementary Information:
https://www.nature.com/articles/s41598-018-31004-5#article-info

Acknowledgments:
We thank Dr. R. Seifert and Prof. Dr. W. Michaelis (Univ. Hamburg) and the shipboard party of the R/V Meteor cruise (M72/1: Geochemical cycling and microbial life at active gas seeps). We also thank Y. Saito, Y. Sasaki (JAMSTEC) for technical support and Dr. Y. Takaki (JAMSTEC) for the discussion of genomic sequence. The study was supported in part by the Japan Society for the Promotion of Science (JSPS) and the Submarine Resources Research Project in JAMSTEC.

Keywords: Carbon signatures in ANMEs, Organic molecules, Anoxic methanotrophy

©2019. Japan Geoscience Union. All Right Reserved.

[E] Poster | B (Biogeosciences)：B-CG Complex & General

Tue. May 28, 2019 5:15 PM - 6:30 PM JST | Tue. May 28, 2019 8:15 AM - 9:30 AM UTC | Poster Hall International Exhibition Hall8, Makuhari Messe_40

[B-CG06] Earth and Planetary Science Frontiers for Life and Global Environment

convener:Yoshinori Takano(Japan Agency for Marine-Earth Science and Technology (JAMSTEC)), Yohey Suzuki(Graduate School of Science, The University of Tokyo), Shingo Kato(RIKEN), Keisuke Fukushi(Institute of Nature & Environmental Technology, Kanazawa University)

Earth and planetary science is currently capable of sampling from four frontiers: space, polar regions, deep ocean and deep underground for the study of the origin and evolution of life. Next generation sequencing technology of nucleic acids and nanotechnology-driven innovation of solid characterizations are very powerful to expand our understanding of many fields of earth and planetary sciences. It is also important for us to be aware of global warming and climate change that dramatically affect biodiversity, biological activities and elemental cycling. The aim of this session is to cross the border of science sections to explore the frontiers of earth and planetary science.

[BCG06-P01] Dynamisms and characteristics of dissolved organic matter (DOM) in deep aquifer: A scope for deep biosphere

*Atsushi Urai[1,2], Yoshinori Takano[2], Naohiko Ohkouchi[2] (1.Department of Science and Technology, Graduate School of Medicine, Science and Technology, Shinshu University, 2.Department of Biogeochemistry, Japan Agency for Marine-Earth Science and Technology)

[BCG06-P02] Correlations of magnetosome-related genes in Nitrospirae genomes to magnetosome geometry and redox stratification in deep-sea environments

*Shinsaku Nakano[1], Shingo Kato[2], Mariko Kouduka[1], Toshitsugu Yamazaki[3], Yohey Suzuki[1] (1.Graduate School of Science, The University of Tokyo, 2.RIKEN, 3.Atmosphere and Ocean Research Institute, The University of Tokyo)

[BCG06-P03] Reconstruction of key ecological responses leading to the most recent dead zone formations in Japan Sea through ancient DNA metabarcodring

*Mariko Kouduka[1], Yohey Suzuki[1] (1.Department of Earth and Planetary Science, The University of Tokyo, 7-3-1 Hongo, Bunkyo-ku, Tokyo, Japan.)

[BCG06-P04] Search for microbial CH_4 production processes in lake sediments and surface water associated with cyanobacterial bloom

*Makoto Matsushita[1], Yoshinori Takano[1], Hiroyuki Imachi[1], Atsushi Urai[2], Ho-Dong Park[3], Hiroki Iwata[3], Naohiko Ohkouchi[1] (1.Japan Agency for Marine-Earth Science and Technology, 2.Department of Science and Technology, Graduate School of Medicine, Science and Technology, Shinshu University, 3.Department of Environmental Sciences, Faculty of Science, Shinshu University)

[BCG06-P05] Did life emerge in a deep-sea metal sulfide chimney? New insights from an archaeal genome and a nanoscale microbe-silicate assemblage

*Hinako Takamiya[1], Hiroki Mukai[2], Mariko Kouduka[1], Shingo Kato[4], Motoo Ito[3], Yohey Suzuki[1] (1.Earth and Planetary Science Graduate School of Science, The University of Tokyo , 2.National Institute of Advanced Industrial Science and Technology, 3.Kochi Institute for Core Sample Research JAMSTEC, 4.RIKEN)

[BCG06-P06] X-ray computed nano-tomography for visualizing microbial cells and their surrounding environments

*Yuki Morono[1], Go-Ichiro Uramoto[2,1], Kentaro Uesugi[3], Nobuhisa Takeuchi[3], Masayuki Uesugi[3], Kengo Kubota[4], Tatsuhiko Hoshino[1], Fumio Inagaki[1] (1.Japan Agency for Marine-Earth Science and Technology, 2.Kochi University, 3.Japan Synchrotron Radiation Research Institute, 4.Tohoku University)

[BCG06-P07] **Carbon signatures in amino acids during deep-sea anoxic methanotrophy**

*Yoshinori Takano[1] (1.Japan Agency for Marine-Earth Science and Technology (JAMSTEC))

Dynamisms and characteristics of dissolved organic matter (DOM) in deep aquifer: A scope for deep biosphere

*Atsushi Urai[1,2], Yoshinori Takano[2], Naohiko Ohkouchi[2]

1. Department of Science and Technology, Graduate School of Medicine, Science and Technology, Shinshu University, 2. Department of Biogeochemistry, Japan Agency for Marine-Earth Science and Technology

Dissolved organic matter (DOM) is generally derived from multiple sources and affected by complicated transformation and degradation reactions. In a general geochemical description of marine environments, high-molecular-weight DOM (HMW-DOM; >1 kDa) particularly represents a unique organic carbon pool, which is accompanied by considerable difference in the molecular and stable isotopic compositions from other organic components such as particulate organic matter (POM) and low-molecular-weight DOM (LMW-DOM; <1 kDa) (e.g., Benner et al., 1997).

To date, formation of DOM fraction and potential microbial interaction in deep aquifer have been particularly poorly understood on the context of prokaryotic ecology. We investigated the molecular composition of DOM fraction including LMW and HMW by an improved method (Urai et al., 2018). The filtered samples are tentatively defined by conventional size scales; macromolecular scale (100 mm >> 40 mm), POM (40 mm >> 0.6 mm), HMW-DOM(0.6 mm>>1kDa), and total-DOM (<0.6 mm). We also have a validation to distinguish the molecular signature between phototrophic primary producers (i.e., fossil molecules) and presently living benthic prokaryotes (i.e., modern molecules; cf. biological methanogenesis, Kaneko et al., 2014). We report a preliminary result of the feasibility study and discuss a perspective from the view of deep biosphere.

References:

Benner et al. Abundance, size distribution, and stable carbon and nitrogen isotopic compositions of marine organic matter isolated by tangential-flow ultrafiltration. Marine Chemistry 57, 243-263 (1997).

Kaneko et al. Quantitative analysis of coenzyme F430 in environmental samples: a new diagnostic tool for methanogenesis and anaerobic methane oxidation. Analytical Chemistry 86, 3633-3638 (2014).

Urai et al. Algal-derived 24-ethylcholesta-5, 22-dien-3β-ol (stigmasterol) is frequently found in high-molecular-weight dissolved organic matter (HMW-DOM) during summer in freshwater and brackish lakes. Geochemical Journal 52, e15-e20 (2018).

Keywords: HMW-DOM, sterol, carbon and hydrogen isotopic compositions, deep aquifer, methanogenesis

©2019. Japan Geoscience Union. All Right Reserved.

Correlations of magnetosome-related genes in Nitrospirae genomes to magnetosome geometry and redox stratification in deep-sea environments

*Shinsaku Nakano[1], Shingo Kato[2], Mariko Kouduka[1], Toshitsugu Yamazaki[3], Yohey Suzuki[1]

1. Graduate School of Science, The University of Tokyo, 2. RIKEN, 3. Atmosphere and Ocean Research Institute, The University of Tokyo

Biogenic magnetic particles are ubiquitously found in deep-sea sediments and important carriers of rock magnetism for reconstructing the Earth’ s past regarding sediment age and geomagnetic field. However, microorganisms responsible for the formation of magnetic particles are largely unknown in the deep-sea environment, because of the difficulty in sampling, cultivation, and magnetic separation of magnetotactic cells for single-cell genomics. In this study, deep-sea sediments from Japan Sea and a metal sulfide chimney from South Mariana Trough were subjected to magnetic separation and subsequent electron microscopic observations. Although teardrop-shaped magnetite (Fe_3O_4) particles without microbial cells and 16S rRNA gene sequences related to magnetotactic Nitrospirae species were previously obtained from Japan Sea sediments with a redox zonation enriched with dissolved Fe(II) (the iron boundary), no magnetotactic cells were observed after the magnetic separation. From the metal sulfide chimney, magnetotactic cells were observed with teardrop-shaped magnetite particles. Metagenomic analysis of the chimney sample revealed that contig sequences encoding genes involved in the formation of magnetosome, membrane-bound magnetic particles, were mostly affiliated within Nitrospirae based on sequence similarity. Previous studies have reported that magnetosome-related genes are clustered together as the magnetosome island (MAI) in known magnetotactic bacteria. However, those genes were scattered in a near-complete Nitrospirae genome reconstructed from the chimney sample. Although magnetotactic bacteria are generally considered to align magnetic particles into a chain for efficiently moving in a vertical redox zonation by orienting the cell along the geomagnetic filed, Nitrospirae-affiliated genes involved in chain formation were not found in the near-complete Nitrospirae genome from the chimney with a horizontal redox zonation. Comparative analysis of near-complete Nitrospirae genomes available from public databases revealed that the chain-related genes were found in the genomes from terrestrial deep aquifers and deep-sea sediments with a vertical redox zonation. As the Nitrospirae species associated with teardrop magnetite and the iron boundary in Japan Sea was closely related to Nitrospirae species with the chain-related genes, the presence of the chain-related genes appears to be correlated with a vertical redox zonation. In addition, our results suggest that the Nitrospirae species without MAI are responsible for the production of teardrop magnetite in deep-sea environment, and that teardrop magnetite is a paleoredox indicator especially for the iron boundary.

Keywords: magnetotactic bacteria, metal sulfide chimney, magnetofossil, remnant magnetization

©2019. Japan Geoscience Union. All Right Reserved.

Reconstruction of key ecological responses leading to the most recent dead zone formations in Japan Sea through ancient DNA metabarcodring

*Mariko Kouduka[1], Yohey Suzuki[1]

1. Department of Earth and Planetary Science, The University of Tokyo, 7-3-1 Hongo, Bunkyo-ku, Tokyo, Japan.

Semi-closed ocean basins are very sensitive to climate changes as recorded in frequent formations of sediments with clearly laminated layers, which was caused by the lack of O_2 available to benthic organisms. This is so-called “dead zone formation” and caused by water stagnation after channel closure and/or nutrient inflow through upwelling and channel opening. In contrast to the hydrologic causes, it remains poorly understood about organismal causes such as enhanced primary production and heterotrophic consumption of O_2. We investigated ancient eukaryotic DNA obtained from a thinly laminated layer deposited in the Japan Sea across the most recent global warming event after Younger Dryas (TL-1). Metabarcoding of 18S rRNA gene sequences clarified that across the transition from oxygenated to anoxic bottom water conditions, dominant protist populations shifted through five stages:

Stage1: Under oxygenated bottom conditions, the most dominant taxonomic group was Marine Stramenopiles Group 9 (MAST-9). MAST-9 encompasses diverse uncharacterized planktonic species, 18S rRNA gene sequences of which were detected from both anoxic and oxic water bodies in Pacific and Atlantic Oceans, Mediterranean Sea and South China Sea.

Stage 2: Before the onset of dead zone formation, the sharp decline of MAST-9 was accompanied with the expansion of marine diatom species of the genus Skeletonema, many members of which are known to be a cause of red tide around the world.

Stage 3: The dead zone formation was synchronized with the expansion of marine radiolarians of the order Chaunacanthida, the members of which are encrusted within $SrSO_4$.

Stage 4: Stages 2 was repeated, whereas the expansion of the Chaunacanthida radiolarians was not evident.

Stage 5: The uncharacterized MAST-9 that was dominant before the dead zone formation was gradually recovered towards oxygenated bottom conditions.

From these results, it is suspected that the expansion of Radiolaria species encrusted with $SrSO_4$ triggered dead zone formation by the accelerated downward transport of dead cells and subsequent heterotrophic consumption of O_2. From bioturbated sediment samples from a maximum depth of 31 mbsf with a depositional age of 100 ka, the Chaunacanthida sequences closely related to that from the laminated sediments have been previously detected.It is therefore suggested the record of the Chaunacanthida species can be reconstructed from sediments with great depth and age.

Keywords: global warming paleo-analogue, hypoxemia expansion, molecular paleoecologcail dynamics, biogeochemical cycling

©2019. Japan Geoscience Union. All Right Reserved.

©2019. Japan Geoscience Union. All Right Reserved.

Search for microbial CH_4 production processes in lake sediments and surface water associated with cyanobacterial bloom

*Makoto Matsushita[1], Yoshinori Takano[1], Hiroyuki Imachi[1], Atsushi Urai[2], Ho-Dong Park[3], Hiroki Iwata[3], Naohiko Ohkouchi[1]

1. Japan Agency for Marine-Earth Science and Technology, 2. Department of Science and Technology, Graduate School of Medicine, Science and Technology, Shinshu University, 3. Department of Environmental Sciences, Faculty of Science, Shinshu University

Methane (CH_4) is an important greenhouse gas and contributes substantial budget to global warming. Freshwater lakes are identified as one of the main CH_4 sources, as it is estimated that they contribute to 6-16% of natural CH_4 emissions [1]. The main part of CH_4 released from lakes is considered to be produced by methanogenic archaea in anoxic sediments as terminal step in the degradation of organic matter. The microbial CH_4 production in lake sediments has been mainly investigated by microbiological studies using culture-dependent methods and molecular analysis.

Microbial CH_4 production is still regarded by many as a process limited to anoxic environments. Nevertheless, over the past few decades, increasing evidence of CH_4 accumulation in oxygen-saturated lake and marine surface water has emerged [2]. To explain the enigmatic issues, it has been proposed that CH_4 production by methanogenic archaea takes place in anoxic microenvironments such as detritus and animals' gut. Alternatively, recent studies suggest that some bacteria break down methylphosphonate (MPn) or dimethylsulfoniopropionate (DMSP) and release CH_4 as a biogenic byproduct. These novel microbial CH_4 production processes may play a potential contribution to the total atmospheric carbon cycle.

Oxic CH_4 peaks have been found to be closely associated with phytoplankton dynamics across multiple lakes. Grossart *et al*. [3] found potentially methanogenic archaea associated with cyanobacteria such as *Aphanizomenon* and *Microcystis* in oxygenated surface water. Additionally, Berg *et al*. [4] showed that hydrogen produced during nitrogen fixation by cyanobacteria can be consumed by methanogenic archaea. These studies suggest the presence of a CH_4 production process by methanogenic archaea associated with cyanobacteria in lake surface water. However, it is unclear whether the CH_4 production is taking place in actual environments.

In this study, we investigated microbial CH_4 production in sediments and surface water of Lake Suwa in Nagano Prefecture, Japan, a typical hypertrophic shallow lake, using culture-independent methods. Especially, we focused on cyanobacterial bloom and tried to identify a CH_4 production process by methanogenic archaea associated with cyanobacteria. 16S rRNA gene analyses revealed the presence of methanogenic archaea closely related to the order *Methanobacteriales*, *Methanomicrobiales*, and *Methanosarcinales* in sediment core samples from 30 cm depth. On the other hand, 16S rRNA genes and *mcrA* genes of methanogenic archaea were not detected in bulk DNA from cyanobacterial bloom sample (mainly *Microcystis*)[5]. In order to estimate the potential for methanogenic archaea, we extracted Coenzyme F430, a biomarker for methanogenic archaea, from sediment and bloom samples and determined by using HPLC [6]. F430 was detected from sediment samples, but that from bloom sample was currently below detection limit (<1 pmol).

These results suggest that methanogenic archaea actively produce CH_4 in the sediments of Lake Suwa,

©2019. Japan Geoscience Union. All Right Reserved.

however, its contribution in oxygenated surface water seems to be small. We are currently conducting a more sensitive analysis of F430 using LC-MS/MS [6] with the pre-treatment procedure [7]. The analysis may identify the CH_4 production process by methanogenic archaea associated with cyanobacteria in the surface water. Although this study did not cover other CH_4 production processes such as MPn and DMSP decomposition, our results may also be applicable to estimate the *in situ* contribution of these novel CH_4 source.

Refs.
[1] Bastviken *et al.*, *Global Biogeochem. Cycles*, 18, GB4009 (2004). [2] Tang *et al.*, *Environ. Sci. Technol. Lett.*, 3, 227-233 (2016). [3] Grossart *et al. PNAS*, 108, 19657-19661 (2011). [4] Berg *et al. World J. Microbiol. Biotechnol.*, 30, 539-545 (2014). [5] Park *et al., Environ. Toxicol. Water Qual.*, 13, 61-72 (1998). [6] Kaneko *et al.*, *Anal. Chem.*, 86, 3633-3638 (2014). [7] Kaneko *et al., Geochem. J.,* 50, 453-460 (2016).

Keywords: Microbial methane production, Methane paradox, Freshwater lake, Methanogenic archaea, Cyanobacterial bloom

©2019. Japan Geoscience Union. All Right Reserved.

Did life emerge in a deep-sea metal sulfide chimney? New insights from an archaeal genome and a nanoscale microbe-silicate assemblage

*Hinako Takamiya[1], Hiroki Mukai[2], Mariko Kouduka[1], Shingo Kato[4], Motoo Ito[3], Yohey Suzuki[1]

1. Earth and Planetary Science Graduate School of Science, The University of Tokyo , 2. National Institute of Advanced Industrial Science and Technology, 3. Kochi Institute for Core Sample Research JAMSTEC, 4. RIKEN

Deep-sea hydrothermal activities have continued for 3.8 billion years on Earth. After the formation of metal sulfide chimneys from high-temperature fluid, their low-temperature interactions with ambient seawater potentially provide the cold, stable habitat for microbial life. In such a challenging habitat with metal toxicity, 16S rRNA gene sequences formerly affiliated within Deep-Sea Hydrothermal Vent Euryarchaeota Subtype 6 (DHVE6) and recently reclassified as Pacearchaeota are dominantly detected by 16S rRNA gene sequence analysis. However, the distribution and metabolic activities of Pacearchaeota in metal sulfide chimneys are largely unknown. In this study, a metal sulfide chimney collected from a deep-sea hydrothermal field in South Mariana Trough was subjected to genome-resolved metagenomics analysis. It was revealed that a near-complete Pacearchaeota genome has carbon metabolism genes involved in glycolysis and pentose phosphate pathway linked to nucleotide salvage pathway with light-independent CO_2incorporating ribulose bisphosphate carboxylase/oxygenase (RubisCO). By comparative analysis of Pacearchaeota genomes from deep-sea metal sulfide deposits and terrestrial subsurface aquifers, the carbon metabolism was commonly found with genes annotated for Cu detoxification. Based on the NanoSIMS ion imaging analysis, we found an evidence of a dense microbial colonization inside the chimney where the surface of chalcopyrite ($CuFeS_2$) was overlayered with a silica-bearing material enriched in CN, S and P. Our results explain the geographically and physicochemically diverse distributions of Pacearchaeota indicated by 16S rRNA gene sequence analysis as well as the predominance of Pacearchaeota in the metal sulfide chimney where energy sources from photosynthesis and hydrothermal fluid are limited. The carbon metabolism operated by Pacearchaeota in one of candidate environments for the origin of life could be relevant to that operated by primitive life on early Earth.

Keywords: hydrothermal vent, metagenomic analysis, extremophile ecology, origin of life, microbial carbon metabolism, Rock life detection

©2019. Japan Geoscience Union. All Right Reserved.

X-ray computed nano-tomography for visualizing microbial cells and their surrounding environments

*Yuki Morono[1], Go-Ichiro Uramoto[2,1], Kentaro Uesugi[3], Nobuhisa Takeuchi[3], Masayuki Uesugi[3], Kengo Kubota[4], Tatsuhiko Hoshino[1], Fumio Inagaki[1]

1. Japan Agency for Marine-Earth Science and Technology, 2. Kochi University, 3. Japan Synchrotron Radiation Research Institute, 4. Tohoku University

Recent developments of the X-ray computed tomography (CT) reaches to the spatial resolution of down to few tens of nanometers scale, which is enough to visualize single microbial cells, together with those distributions as well as its surrounding environments. In this study, we tried to visualize microbial cells in the environmental samples by using nanometer-scale X-ray CT.
We used anaerobic granular sludge and subseafloor sediments for the test samples. The X-ray CT analyses were conducted at beamlines of BL20XU and BL47XU in synchrotron radiation facility of Spring-8. The soft samples were either freeze-dried or embedded in the epoxy resin for the analysis. Since the high-spatial resolution observation of the X-ray CT analysis requires a higher density of X-ray per field, the samples often deformed during the analysis, which results in the failure of the 3D reconstruction of the data. Optimization of the resin, its polymerization condition, together with the stain of the cells by osmium tetroxide to put heavy element onto the microbial cells, we could successfully visualize single microbial cells in the samples. Also, the observations of the sample at the pre- and post-edge energies of the element (such as Os) enabled specific signal enhancement of osmium-stained cells.
The investigations of subseafloor biosphere have often based on destructive measurements. Although these analyses revealed the large-scale distribution of microbes along the chemical gradients, no previous attempt explored the spatial distribution of microbial cells at their size range. The visualization of microbes with its surrounding environments will give basic but critical information to understand the microbial in-situ ecophysiology.

Keywords: X-ray Computed Tomography, Subseafloor biosphere

©2019. Japan Geoscience Union. All Right Reserved.

Carbon signatures in amino acids during deep-sea anoxic methanotrophy

*Yoshinori Takano[1]

1. Japan Agency for Marine-Earth Science and Technology (JAMSTEC)

Microorganisms play a central role in both methane production and consumption in the global carbon cycle. Oceanic methane from global deep-sea sediment is largely consumed through microbially mediated sulfate-coupled oxidation, resulting in 13C-depleted cell biomass of anaerobic methanotrophic archaea (ANME). The general ecological importance of subseafloor ANME has been well recognized in the last two decades. However, the crucial biochemical pathways for the overall anaerobic oxidation of methane (AOM) still remain enigmatic. In the present study, methanotrophic pathways were analyzed to trace 13C-depleted amino acid biosynthesis in two clades of ANME (ANME-1 and ANME-2) from the Black Sea. Compound-specific analysis of ANME-dominated microbial mats showed a significant 13C-depletion trend in association with increasing carbon numbers in protein-derived amino acid families within the pyruvate family in the order of alanine, valine, isoleucine and leucine down to -114‰. This result indicates a stepwise elongation of 13C-depleted carbon during amino acid biosynthesis. The overall results suggest that intracellular protein amino acids and the most 13C-depleted signature of leucine, which has a specific branched-chain structure, are potentially propagated as isoprenoid precursor molecules into archaeal biosynthesis, resulting in the extremely 13C- and 14C-depleted nature of ANME cells in the deep microbial oasis.

References:
Takano, Y., Chikaraishi, Y., Imachi, H., Miyairi, Y., Ogawa, N.O., Kaneko, M., Yokoyama, Y., Kruger, M. and Ohkouchi, N. (2018) Insight into anaerobic methanotrophy from 13C/12C- amino acids and 14C/12C-ANME cells in seafloor microbial ecology. Scientific Reports, 8:14070, doi: 10.1038/s41598-018-31004-5.

Supplementary Information:
https://www.nature.com/articles/s41598-018-31004-5#article-info

Acknowledgments:
We thank Dr. R. Seifert and Prof. Dr. W. Michaelis (Univ. Hamburg) and the shipboard party of the R/V Meteor cruise (M72/1: Geochemical cycling and microbial life at active gas seeps). We also thank Y. Saito, Y. Sasaki (JAMSTEC) for technical support and Dr. Y. Takaki (JAMSTEC) for the discussion of genomic sequence. The study was supported in part by the Japan Society for the Promotion of Science (JSPS) and the Submarine Resources Research Project in JAMSTEC.

Keywords: Carbon signatures in ANMEs, Organic molecules, Anoxic methanotrophy

©2019. Japan Geoscience Union. All Right Reserved.

[E] Poster | M (Multidisciplinary and Interdisciplinary) : M-IS Intersection

Tue. May 28, 2019 10:45 AM - 12:15 PM JST | Tue. May 28, 2019 1:45 AM - 3:15 AM UTC | Poster Hall International Exhibition Hall8, Makuhari Messe_10

[M-IS05] New technologies to monitor thunderstorm and severe weather activities

convener:Mitsuteru Sato(Department of Cosmoscience, Hokkaido University), Yukihiro Takahashi(Department of Cosmosciences, Graduate School of Science, Hokkaido University), Hisayuki Kubota(Hokkaido University), Kozo Yamashita(Ashikaga University, Department of Engineering.)

In order to predict the intensity development of severe weather, lightning and thunderstorm are markers of severe weather, often accompanied by precipitation, hail and strong winds that can create significant natural hazards, especially in disaster-prone area. Lightning is also a strong indicator of convection, and it becomes a key parameter to predict the intensity development of tropical cyclones (typhoons and hurricanes). As the climate warms in the first decades of the 21st century, the intensity and frequency of thunderstorms is projected to increase. The need for detecting and monitoring the development of thunderstorms and lightning activities on global, local, and regional scales is therefore clear and urgent.
This session seeks topics presenting new technologies to monitor thunderstorm and severe weather activities. In addition, observational and theoretical contributions on thunderstorm microphysics and dynamics, convective systems and tropical storms are welcome. Present patterns and distributions of lightning and extreme weather events derived from the ground-based networks and satellites, as well as forecasts of future trends, are also of interest. Lightning detecting and monitoring system performance and validation, and early-warning schemes are requested, either in operational or planning phase. The session will also highlight regional and global lightning and atmospheric electricity networks and invite contributions on technological innovations in this field.

[MIS05-P01] Study on monitoring of thunderstorm activity based on multiple electrostatic measurement

*Kozo Yamashita[1], Kakeru Kanno[1], Mitsuteru Sato[2], Yukihiro Takahashi[2] (1.Ashikaga Univ., 2.Hokkaido Univ.)

[MIS05-P02] Contribution of Rainfall and Lightning Activities to the Fair Weather Electric Field Evaluated by 3D GEC Model

*Kittanapat Bandholnopparat[1], Mitsuteru Sato[2], Yukihiro Takahashi[2], Toru Adachi[3], Masashi Kamogawa[5], Yasuhiro Minamoto[5], Akira Kadokura[6], Tomoo Ushio[4] (1.Department of Cosmosciences, Hokkaido University, Sapporo, Japan, 2.Faculty of Science, Hokkaido University, Sapporo, Japan, 3.Meteorological Research Institute, Tsukuba, Japan, 4.Department of Aerospace Engineering, Tokyo Metropolitan University, Hino, Japan, 5.Tokyo Gakugei University, Tokyo, Japan, 6.National Institute of Polar Research, Tokyo, Japan)

[MIS05-P03] A method for locating lightning discharges using tweek atmospherics

*Masafumi Kanno[1], Hiroyo Ohya[2], Kazuo Shiokawa[3], Hiroyuki Nakata[2], Toshiaki Takano[2] (1.Graduate School of Science and Engineering, Chiba University, 2.Graduate School of Engineering, Chiba University, 3.Institute for Space-Earth Environmental Research, Nagoya University)

[MIS05-P04] Monitoring for lightning activities and thunder cloud development over the Tokyo metropolitan area during the 2018 summer

*Jun-Ichi Hamada[1], Jun Matsumoto[1], Kozo Yamashita[2], Masashi Kamogawa[3], Yukihiro Takahashi[4] (1.Faculty of Urban Environmental Sciences, Tokyo Metropolitan University, 2.Department of Engineering, Ashikaga University, 3.Department of Physics, Tokyo Gakugei University, 4.Department of Cosmosciences, Graduate School of Science, Hokkaido University)

Study on monitoring of thunderstorm activity based on multiple electrostatic measurement

*Kozo Yamashita[1], Kakeru Kanno[1], Mitsuteru Sato[2], Yukihiro Takahashi[2]

1. Ashikaga Univ., 2. Hokkaido Univ.

Quantitative evaluation of thundercloud activity is essential for early detection and short-term forecast of severe weather events such as heavy rainfall, lightning stroke, downburst, and so on. In previous researches, lightning observation based on electromagnetic measurement has been focused on as an effective tool for nowcast of thunderstorm activity. Advanced lightning sensors have high sensitivity and makes it possible to detect whole lightning activity. Lightning discharge occurs as a result of vertical atmospheric convection which causes thunderstorm. Preceding studies pointed that lighting occurrence could be an indicator of vertical deep convection in storm region and severe thunderstorm intensity.

Ground-based measurement of electrostatic field has been also considered as an efficient way to detect electrification in thundercloud and monitor development of severe storm. In preceding studies, multiple electrostatic measurement has been examined to estimate charge amount in cloud. One of the difficulties for those studies is to understand correlation between electrostatic field on ground and charges in horizontally extended thunderstorm. In this study, methodology for quantitative evaluation of charge amount in cloud is developed. We newly construct multipoint electrostatic sensor network in Tochigi, Japan. In this region, isolated thunderstorm whose horizontal scale is about 10 km occurs. By analyzing Isolated thunderstorm, we can simplify the correlation between ground-based electrostatic field and charge in cloud. In this presentation, initial result of electrostatic measurement with multiple sensors is summarized.

Keywords: thunderstorm, electrostatic field, sensor network

©2019. Japan Geoscience Union. All Right Reserved.

Contribution of Rainfall and Lightning Activities to the Fair Weather Electric Field Evaluated by 3D GEC Model

*Kittanapat Bandholnopparat[1], Mitsuteru Sato[2], Yukihiro Takahashi[2], Toru Adachi[3], Masashi Kamogawa[5], Yasuhiro Minamoto[5], Akira Kadokura[6], Tomoo Ushio[4]

1. Department of Cosmosciences, Hokkaido University, Sapporo, Japan, 2. Faculty of Science, Hokkaido University, Sapporo, Japan, 3. Meteorological Research Institute, Tsukuba, Japan, 4. Department of Aerospace Engineering, Tokyo Metropolitan University, Hino, Japan, 5. Tokyo Gakugei University, Tokyo, Japan, 6. National Institute of Polar Research, Tokyo, Japan

Lightning and precipitation are the main current sources in the global atmospheric electric circuit (GEC). The lightning and precipitation currents maintain the electrical potential gap of ~250 kV between the ionosphere and the Earth’ s surface. However, the contribution of lightning current to the GEC is not well understood due to the difficulty of estimating the global occurrence number of intracloud (IC) discharges. In addition, it is difficult to quantitatively estimate the contribution of the global precipitation current to the GEC due to the difficulty of identifying the rain volume and its global distribution. The purposes of this study are to estimate the global occurrence number of IC discharges and to investigate the contribution of lightning and precipitation currents to the GEC. Firstly, the global Z-value map obtained by the JEM-GLIMS spaced-based mission and the cloud-to-ground (CG) lightning data obtained by the WWLLN were combined to estimate the occurrence number of the global IC discharges with the time resolution of 5 minutes and with the spatial resolution of 0.2º×0.2º. Then, the estimated occurrence number of the global IC and CG discharges and the precipitation data provided by the global precipitation measurement (GPM) project were used as the input parameters in a 3-dimensional model of the GEC, which we have newly developed. In this model, the average column resistance including the influence of the cloud coverage was assumed. Using this model, we estimated the total GEC current and the fair weather electric field at the Syowa station on March 16, July 20, and September 29, 2014. It is found that the average lightning and precipitation currents in the GEC were ~70 A and ~ 670 A, respectively. It is also found that the average fair weather electric field at the Syowa station is ~ 70 V/m. The absolute value of the estimated fair weather electric field is almost consistent with the observational data. From these results, the role of lightning current in the GEC is quantitatively evaluated, and we found that the upward current from thunderclouds to the ionosphere generated by lightning discharges is only 9% while that induced by the precipitation is ~91%.

©2019. Japan Geoscience Union. All Right Reserved.

A method for locating lightning discharges using tweek atmospherics

*Masafumi Kanno[1], Hiroyo Ohya[2], Kazuo Shiokawa[3], Hiroyuki Nakata[2], Toshiaki Takano[2]

1. Graduate School of Science and Engineering, Chiba University, 2. Graduate School of Engineering, Chiba University, 3. Institute for Space-Earth Environmental Research, Nagoya University

Locating accuracy for lightning discharges of world-wide lightning location (WWLLN) is high to be less than 10 km [Rodger et al., 2005], although the accuracy of horizontal propagation distance for tweek atmospherics is low to be ~60 km [Santolik and Kolmasova, 2017]. Tweek atmospherics are very low frequency (VLF)/extremely low frequency (ELF) waves radiated from lightning discharges, and propagate between the Earth surface and the bottom of the ionosphere for a long distance (several thousand kilometers). In this study, we improve the estimation method for the tweek propagation distance, and compare between the lightning location estimated from tweek propagation distance by intersection method with those from the WWLLN data and cloud images derived by the MTSAT-2 satellite. We used two wideband VLF data observed at Kagoshima (31.48˚N, 130.72˚E) and Moshiri (44.37˚N, 142.27˚E), Japan, at 12:20-12:22 UT, on 23 August, 2013. The main point of the improvement was modification for the width of window on dynamic spectra drawn by maximum entropy method. The accuracy of the estimation became higher and the error for the propagation distance became the half of the original estimation, by using narrow window for the beginning, and wide window for the end of the tweek signals. We estimated the lightning location by both automatic and manual methods. In the manual method, the estimated location of lightning for the two-minute data was in good agreement with thick clouds observed by the MTSAT-2 satellite. However, in the automatic method, the location of the lightning was in disagreement with cloud images, because the accuracy of triggered times were not sufficient due to overlapping tweeks or noises such like short pulses just before the tweeks. In the presentation, we discuss the estimation method for the lightning location in detail.

©2019. Japan Geoscience Union. All Right Reserved.

Monitoring for lightning activities and thunder cloud development over the Tokyo metropolitan area during the 2018 summer

*Jun-Ichi Hamada[1], Jun Matsumoto[1], Kozo Yamashita[2], Masashi Kamogawa[3], Yukihiro Takahashi[4]

1. Faculty of Urban Environmental Sciences, Tokyo Metropolitan University, 2. Department of Engineering, Ashikaga University, 3. Department of Physics, Tokyo Gakugei University, 4. Department of Cosmosciences, Graduate School of Science, Hokkaido University

In order to monitor lightning activities and development of thunder cloud, we have established an observational network with electromagnetic and electrostatic field measurements over the Tokyo metropolitan area since 2016. In the summer season of 2018, we observed atmospheric electrostatic field with the electric field monitor (BOLTEK ELF-100) at Hachioji campus of Tokyo Metropolitan University and the surrounding area. Lightning activities were measured with ELV-VLF band radio observation system at a few sites in the area. We also used the worldwide lightning location network (WWLLN) data to indicate temporal and spatial variations of lightning and the climatological characteristics over the area. Lightning observations showed clear intra-seasonal variations of lightning activities over the area during the summer. Significant lightning events at around Hachioji were observed in 6th, 13th, and 27th of August as a synoptic frontal system located in the north from Kanto area. The electrostatic field measurement at Hachioji detected frequent lightning events and developing/approaching of thunder cloud near the site in these days. At the presentation, we will introduce more detail observation results on thunder cloud developments based on the XRAIN (eXtended RAdar Information Network) observation data.

This work was partly supported by Japan Science and Technology Agency (JST) and Japan International Cooperation Agency (JICA) under SATREPS.

Keywords: Lightning, Heavy rainfall

©2019. Japan Geoscience Union. All Right Reserved.

[E] Poster | M (Multidisciplinary and Interdisciplinary) : M-IS Intersection

Tue. May 28, 2019 5:15 PM - 6:30 PM JST | Tue. May 28, 2019 8:15 AM - 9:30 AM UTC | Poster Hall International Exhibition Hall8, Makuhari Messe_42

[M-IS05] New technologies to monitor thunderstorm and severe weather activities

convener:Mitsuteru Sato(Department of Cosmoscience, Hokkaido University), Yukihiro Takahashi(Department of Cosmosciences, Graduate School of Science, Hokkaido University), Hisayuki Kubota(Hokkaido University), Kozo Yamashita(Ashikaga University, Department of Engineering.)

In order to predict the intensity development of severe weather, lightning and thunderstorm are markers of severe weather, often accompanied by precipitation, hail and strong winds that can create significant natural hazards, especially in disaster-prone area. Lightning is also a strong indicator of convection, and it becomes a key parameter to predict the intensity development of tropical cyclones (typhoons and hurricanes). As the climate warms in the first decades of the 21st century, the intensity and frequency of thunderstorms is projected to increase. The need for detecting and monitoring the development of thunderstorms and lightning activities on global, local, and regional scales is therefore clear and urgent.
This session seeks topics presenting new technologies to monitor thunderstorm and severe weather activities. In addition, observational and theoretical contributions on thunderstorm microphysics and dynamics, convective systems and tropical storms are welcome. Present patterns and distributions of lightning and extreme weather events derived from the ground-based networks and satellites, as well as forecasts of future trends, are also of interest. Lightning detecting and monitoring system performance and validation, and early-warning schemes are requested, either in operational or planning phase. The session will also highlight regional and global lightning and atmospheric electricity networks and invite contributions on technological innovations in this field.

[MIS05-P01] Study on monitoring of thunderstorm activity based on multiple electrostatic measurement

*Kozo Yamashita[1], Kakeru Kanno[1], Mitsuteru Sato[2], Yukihiro Takahashi[2] (1.Ashikaga Univ., 2.Hokkaido Univ.)

[MIS05-P02] Contribution of Rainfall and Lightning Activities to the Fair Weather Electric Field Evaluated by 3D GEC Model

*Kittanapat Bandholnopparat[1], Mitsuteru Sato[2], Yukihiro Takahashi[2], Toru Adachi[3], Masashi Kamogawa[5], Yasuhiro Minamoto[5], Akira Kadokura[6], Tomoo Ushio[4] (1.Department of Cosmosciences, Hokkaido University, Sapporo, Japan, 2.Faculty of Science, Hokkaido University, Sapporo, Japan, 3.Meteorological Research Institute, Tsukuba, Japan, 4.Department of Aerospace Engineering, Tokyo Metropolitan University, Hino, Japan, 5.Tokyo Gakugei University, Tokyo, Japan, 6.National Institute of Polar Research, Tokyo, Japan)

[MIS05-P03] A method for locating lightning discharges using tweek atmospherics

*Masafumi Kanno[1], Hiroyo Ohya[2], Kazuo Shiokawa[3], Hiroyuki Nakata[2], Toshiaki Takano[2] (1.Graduate School of Science and Engineering, Chiba University, 2.Graduate School of Engineering, Chiba University, 3.Institute for Space-Earth Environmental Research, Nagoya University)

[MIS05-P04] Monitoring for lightning activities and thunder cloud development over the Tokyo metropolitan area during the 2018 summer

*Jun-Ichi Hamada[1], Jun Matsumoto[1], Kozo Yamashita[2], Masashi Kamogawa[3], Yukihiro Takahashi[4] (1.Faculty of Urban Environmental Sciences, Tokyo Metropolitan University, 2.Department of Engineering, Ashikaga University, 3.Department of Physics, Tokyo Gakugei University, 4.Department of Cosmosciences, Graduate School of Science, Hokkaido University)

Study on monitoring of thunderstorm activity based on multiple electrostatic measurement

*Kozo Yamashita[1], Kakeru Kanno[1], Mitsuteru Sato[2], Yukihiro Takahashi[2]

1. Ashikaga Univ., 2. Hokkaido Univ.

Quantitative evaluation of thundercloud activity is essential for early detection and short-term forecast of severe weather events such as heavy rainfall, lightning stroke, downburst, and so on. In previous researches, lightning observation based on electromagnetic measurement has been focused on as an effective tool for nowcast of thunderstorm activity. Advanced lightning sensors have high sensitivity and makes it possible to detect whole lightning activity. Lightning discharge occurs as a result of vertical atmospheric convection which causes thunderstorm. Preceding studies pointed that lighting occurrence could be an indicator of vertical deep convection in storm region and severe thunderstorm intensity.

Ground-based measurement of electrostatic field has been also considered as an efficient way to detect electrification in thundercloud and monitor development of severe storm. In preceding studies, multiple electrostatic measurement has been examined to estimate charge amount in cloud. One of the difficulties for those studies is to understand correlation between electrostatic field on ground and charges in horizontally extended thunderstorm. In this study, methodology for quantitative evaluation of charge amount in cloud is developed. We newly construct multipoint electrostatic sensor network in Tochigi, Japan. In this region, isolated thunderstorm whose horizontal scale is about 10 km occurs. By analyzing Isolated thunderstorm, we can simplify the correlation between ground-based electrostatic field and charge in cloud. In this presentation, initial result of electrostatic measurement with multiple sensors is summarized.

Keywords: thunderstorm, electrostatic field, sensor network

©2019. Japan Geoscience Union. All Right Reserved.

Contribution of Rainfall and Lightning Activities to the Fair Weather Electric Field Evaluated by 3D GEC Model

*Kittanapat Bandholnopparat[1], Mitsuteru Sato[2], Yukihiro Takahashi[2], Toru Adachi[3], Masashi Kamogawa[5], Yasuhiro Minamoto[5], Akira Kadokura[6], Tomoo Ushio[4]

1. Department of Cosmosciences, Hokkaido University, Sapporo, Japan, 2. Faculty of Science, Hokkaido University, Sapporo, Japan, 3. Meteorological Research Institute, Tsukuba, Japan, 4. Department of Aerospace Engineering, Tokyo Metropolitan University, Hino, Japan, 5. Tokyo Gakugei University, Tokyo, Japan, 6. National Institute of Polar Research, Tokyo, Japan

Lightning and precipitation are the main current sources in the global atmospheric electric circuit (GEC). The lightning and precipitation currents maintain the electrical potential gap of ~250 kV between the ionosphere and the Earth’ s surface. However, the contribution of lightning current to the GEC is not well understood due to the difficulty of estimating the global occurrence number of intracloud (IC) discharges. In addition, it is difficult to quantitatively estimate the contribution of the global precipitation current to the GEC due to the difficulty of identifying the rain volume and its global distribution. The purposes of this study are to estimate the global occurrence number of IC discharges and to investigate the contribution of lightning and precipitation currents to the GEC. Firstly, the global Z-value map obtained by the JEM-GLIMS spaced-based mission and the cloud-to-ground (CG) lightning data obtained by the WWLLN were combined to estimate the occurrence number of the global IC discharges with the time resolution of 5 minutes and with the spatial resolution of 0.2º×0.2º. Then, the estimated occurrence number of the global IC and CG discharges and the precipitation data provided by the global precipitation measurement (GPM) project were used as the input parameters in a 3-dimensional model of the GEC, which we have newly developed. In this model, the average column resistance including the influence of the cloud coverage was assumed. Using this model, we estimated the total GEC current and the fair weather electric field at the Syowa station on March 16, July 20, and September 29, 2014. It is found that the average lightning and precipitation currents in the GEC were ~70 A and ~ 670 A, respectively. It is also found that the average fair weather electric field at the Syowa station is ~ 70 V/m. The absolute value of the estimated fair weather electric field is almost consistent with the observational data. From these results, the role of lightning current in the GEC is quantitatively evaluated, and we found that the upward current from thunderclouds to the ionosphere generated by lightning discharges is only 9% while that induced by the precipitation is ~91%.

©2019. Japan Geoscience Union. All Right Reserved.

A method for locating lightning discharges using tweek atmospherics

*Masafumi Kanno[1], Hiroyo Ohya[2], Kazuo Shiokawa[3], Hiroyuki Nakata[2], Toshiaki Takano[2]

1. Graduate School of Science and Engineering, Chiba University, 2. Graduate School of Engineering, Chiba University, 3. Institute for Space-Earth Environmental Research, Nagoya University

Locating accuracy for lightning discharges of world-wide lightning location (WWLLN) is high to be less than 10 km [Rodger et al., 2005], although the accuracy of horizontal propagation distance for tweek atmospherics is low to be ~60 km [Santolik and Kolmasova, 2017]. Tweek atmospherics are very low frequency (VLF)/extremely low frequency (ELF) waves radiated from lightning discharges, and propagate between the Earth surface and the bottom of the ionosphere for a long distance (several thousand kilometers). In this study, we improve the estimation method for the tweek propagation distance, and compare between the lightning location estimated from tweek propagation distance by intersection method with those from the WWLLN data and cloud images derived by the MTSAT-2 satellite. We used two wideband VLF data observed at Kagoshima (31.48˚N, 130.72˚E) and Moshiri (44.37˚N, 142.27˚E), Japan, at 12:20-12:22 UT, on 23 August, 2013. The main point of the improvement was modification for the width of window on dynamic spectra drawn by maximum entropy method. The accuracy of the estimation became higher and the error for the propagation distance became the half of the original estimation, by using narrow window for the beginning, and wide window for the end of the tweek signals. We estimated the lightning location by both automatic and manual methods. In the manual method, the estimated location of lightning for the two-minute data was in good agreement with thick clouds observed by the MTSAT-2 satellite. However, in the automatic method, the location of the lightning was in disagreement with cloud images, because the accuracy of triggered times were not sufficient due to overlapping tweeks or noises such like short pulses just before the tweeks. In the presentation, we discuss the estimation method for the lightning location in detail.

©2019. Japan Geoscience Union. All Right Reserved.

Monitoring for lightning activities and thunder cloud development over the Tokyo metropolitan area during the 2018 summer

*Jun-Ichi Hamada[1], Jun Matsumoto[1], Kozo Yamashita[2], Masashi Kamogawa[3], Yukihiro Takahashi[4]

1. Faculty of Urban Environmental Sciences, Tokyo Metropolitan University, 2. Department of Engineering, Ashikaga University, 3. Department of Physics, Tokyo Gakugei University, 4. Department of Cosmosciences, Graduate School of Science, Hokkaido University

In order to monitor lightning activities and development of thunder cloud, we have established an observational network with electromagnetic and electrostatic field measurements over the Tokyo metropolitan area since 2016. In the summer season of 2018, we observed atmospheric electrostatic field with the electric field monitor (BOLTEK ELF-100) at Hachioji campus of Tokyo Metropolitan University and the surrounding area. Lightning activities were measured with ELV-VLF band radio observation system at a few sites in the area. We also used the worldwide lightning location network (WWLLN) data to indicate temporal and spatial variations of lightning and the climatological characteristics over the area. Lightning observations showed clear intra-seasonal variations of lightning activities over the area during the summer. Significant lightning events at around Hachioji were observed in 6th, 13th, and 27th of August as a synoptic frontal system located in the north from Kanto area. The electrostatic field measurement at Hachioji detected frequent lightning events and developing/approaching of thunder cloud near the site in these days. At the presentation, we will introduce more detail observation results on thunder cloud developments based on the XRAIN (eXtended RAdar Information Network) observation data.

This work was partly supported by Japan Science and Technology Agency (JST) and Japan International Cooperation Agency (JICA) under SATREPS.

Keywords: Lightning, Heavy rainfall

©2019. Japan Geoscience Union. All Right Reserved.

[E] Poster | M (Multidisciplinary and Interdisciplinary)：M-GI General Geosciences, Information Geosciences & Simulations

Tue. May 28, 2019 3:30 PM - 5:00 PM JST | Tue. May 28, 2019 6:30 AM - 8:00 AM UTC | Poster Hall International Exhibition Hall8, Makuhari Messe_28

[M-GI29] Near Surface Investigation and Modeling for Groundwater Resources Assessment and Conservation

convener:Jui-Pin Tsai(National Cheng Kung University, Taiwan), Hwa-Lung Yu(National Taiwan University), Ching-Chung Cheng(National Chiao Tung University Taiwan), Jing-Sen Cai(China University of Geosciences)

Groundwater resources serve as a vital source for regional water supply under the climate change condition. However, improper use of the available groundwater resources leads to serious environmental disasters such as land subsidence or seawater intrusion. Therefore, groundwater management is a key issue for groundwater resources conservation. Before applying any management practice, it is essential to accurately assess the groundwater system in multi-scales. In this session, we focus on the issues associated with the application of near-surface investigation and modeling on groundwater resources assessment. We welcome studies related to numerical modeling, spatiotemporal modeling, data fusion, and field investigation using hydrogeological approaches, geophysical approaches, geochemical approaches, and remote sensing. We also welcome the studies associated with groundwater contamination transport and remediation, geothermal energy exchange, groundwater microorganisms, hot spring, volcanic hydrology, and environmental disasters evaluation and prevention. We especially encourage the pilot groundwater management studies that solve multi-scale and interdisciplinary problems.

[MGI29-P01] Modelling of self-potential signals associated with groundwater flows

*ayaka ishikawa[1], Katsumi Hattori[1] (1.chiba university)

[MGI29-P02] Estimating the Hydraulic Conductivity and Heat Capacity of the Aquifer between the River and Well Site Using Joint Inversion Approach

*Jui-Pin Tsai[1], Chin-Tsai Hsiao[4], Liang-Cheng Chang[2], You-Cheng Chen[2], Chun-Hung Chen[3], Yun-Ta Cheng[3], Jen-Hung Yu[3] (1.National Cheng Kung University, Taiwan , 2.National Chiao Tung University, Taiwan , 3.Water Resources Planning Institute, Water Resources Agency, Taiwan, 4.Department of Information Management, Chung Chou University of Science and Technology)

[MGI29-P03] Evaluation on Soil Permeability Using Electrical Resistant Tomography

*CHIHPING KUO[1], BONIAN SHEN[1], CHIHWEI HUANG[1], YUCHIAO LEE[1], SHENXIANG HUANG[1], YENLIN CHEN[1] (1.Department and Institute of Civil Engineering and Environmental Informatics, Minghsin University of Science and Technology)

[MGI29-P04] The Potential Study of Open Loop System Geothermal Heat Pump in Gifu City, Japan

*Randa Permanda[1], Tomoyuki Ohtani[2] (1.Department of Civil and Environmental Engineering, Gifu University, 2.Department of Civil Engineering, Gifu University)

[MGI29-P05] Application of TL-CHERT Smart Characterization Method to Investigate a Groundwater Contaminated Site

*Tzu-Pin Wang[1,2,5], Yao-Tsung Chen[3], Tien-Hsing Tung[3], Chih-Hung Cheng[2], Jie Wang[4] (1.NCU TW, 2.Geophysical Technology and Engineering Co.,Ltd. R.O.C, 3.Apollo Technology Co.,Ltd. R.O.C., 4.Department of Civil Engineering, Chien Hsin University of Science and Technology, Taoyuan City, Taiwan, 5.Disaster Reduction Research Center, Chien Hsin University of Science and Technology, Taoyuan City, Taiwan)

[MGI29-P06] Data Assimilation in Hydraulic Conductivity Identification using Bayesian Statistical Method

*Shih-Yang Cheng[1], Kuo-Chin Hsu[1] (1.National Cheng Kung Univ.)

[MGI29-P07] Groundwater recharge estimation by using empirical orthogonal function method

Hua-Ting Zeng [1], *Hwa-Lung Yu[1] (1. National Taiwan University)

[MGI29-P08] The Application of Drought Early Warning Index for Regional Hydrological Circumstance Analysis

*Chih Chao Ho[1], Ta Wei Chen[2] (1.Construction and Disaster Prevention Research Center, Feng Chia Univ., 2.Taiwan Hsin-Chu Irrigation Association)

Modelling of self-potential signals associated with groundwater flows

*ayaka ishikawa[1], Katsumi Hattori[1]

1. chiba university

Landslides triggered by rainfall are one of the most dangerous natural disasters which give the loss of lives and properties. Although the importance of the short-term forecast of landslides is widely accepted, it is not achieved. In this research, we pay attention to electro-magnetic approach for monitoring ground water condition under the slope. That is, we understand the processes of the landslide and develop the system for forecast to detect precursory signal through the electromagnetic changes. In this study, we apply the self-potential approach, which is related on electro-kinetic effects or streaming potential. We have conducted several flume tests and sandbox experiments and the results showed the repeatability of the phenomena or correlation between self-potential and ground water condition. Therefore, we will report the model and numerical computation for the sandbox experiment on injection in this presentation.

SP signals measured in the sandbox during pumping experiment are considered to be due to the electro-kinetic effects. The total current density j is $j=sE-l\mathrm{d}h/\mathrm{d}x_i$, where s (in S m^{-1}) is the electrical conductivity, E (in Vm^{-1}) is the electric field, l (in A Pa^{-1} m^{-1}) is the current coupling coefficient, and h (in m) is the hydraulic head. The variation of SP signals of the sandbox gives quasi-instantaneous information on changes of the hydraulic head. Therefore we consider this problem with quasi-static limit condition i.e. div j = 0. It leads $\mathrm{div}(s\,\mathrm{grad}\,phi)=-\mathrm{div}(l\,\mathrm{grad}\,h)$.Where phi (in V) is electric potential. In addition, we assume that s and l are uniform through the sandbox because we assume saturated condition. Finally, the solved equation is $s\mathrm{d}^2phi/dx_i^2=-l\mathrm{d}^2h/dx_i^2$. We simulated distribution of hydraulic head during pumping test using finite element method. Then, we modeled the SP generation.

Consequently, the variation of SP modeled and observed are generally consistent with each other. Therefore, we found that groundwater flows control the occurrence of SP in the sandbox experiment. However, in the detail of time variation, modeled SP differ from those of observed partly. We consider that heterogeneity of soil or necessary of 3D modeling could cause these discordances. Details will be shown in our presentation.

Keywords: self-potential, ground water flow, modelling

©2019. Japan Geoscience Union. All Right Reserved.

Estimating the Hydraulic Conductivity and Heat Capacity of the Aquifer between the River and Well Site Using Joint Inversion Approach

*Jui-Pin Tsai[1], Chin-Tsai Hsiao[4], Liang-Cheng Chang[2], You-Cheng Chen[2], Chun-Hung Chen[3], Yun-Ta Cheng[3], Jen-Hung Yu[3]

1. National Cheng Kung University, Taiwan , 2. National Chiao Tung University, Taiwan , 3. Water Resources Planning Institute, Water Resources Agency, Taiwan, 4. Department of Information Management, Chung Chou University of Science and Technology

This study continued to measure the water temperature and pressure at the riverbed, agricultural waterway, and groundwater monitoring well from Oct. to Nov. 2018. These observations were then used to estimate the hydraulic conductivity (K) and flux between the river and the aquifer of the well site. The water pressure data reveal that the correlation coefficient between river and groundwater level reaches 0.9 and that between the agricultural waterway and groundwater level is almost 0. This reveals that the groundwater head variation mainly affected by the river stage of the nearby river. The temperature data show that the groundwater temperature is correlated to the temperature of the river water and is uncorrelated to the air temperature. Accordingly, the temperature and head data of the groundwater and river water were used to estimate K and heat capacity of the aquifer between the river and well site using a joint inversion approach. The results show that the estimated K and heat capacity are 67.53 m ⁄ day and 4485000 J ⁄ (m^3–℃), respectively.

Keywords: Hydraulic conductivity, Soil heat capactiy , Joint inversion, Temperature, Groundwater head , Interaction between groundwater and river water

©2019. Japan Geoscience Union. All Right Reserved.

Evaluation on Soil Permeability Using Electrical Resistant Tomography

*CHIHPING KUO[1], BONIAN SHEN[1], CHIHWEI HUANG[1], YUCHIAO LEE[1], SHENXIANG HUANG[1], YENLIN CHEN[1]

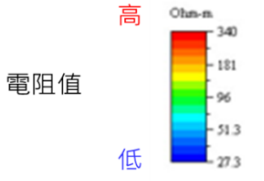
1. Department and Institute of Civil Engineering and Environmental Informatics, Minghsin University of Science and Technology

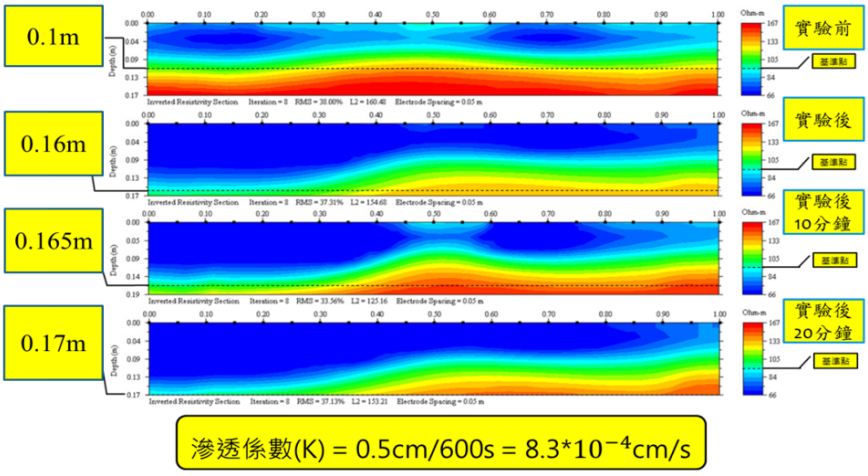
The permeability of soil is used to adapt field constant head permeability test or variable head permeability test. The former test is suitable for soil with higher permeability like sand and gravels; the later test is suitable for soil with lower permeability like silt and clays. Both tests need in-situ drilling holes. The required operating time is usually about couple of hours. A widely used geophysical method, Electrical Resistant Tomography (ERT), is adapted here to evaluate the soil permeability. Two types of soil with different permeability were performed, and the results were compared with the result of same samples using traditional permeability test. The result showed that they were very close. The operating time of ERT for one soil was only less than one hour. The idea of evaluating soil permeability using ERT is proposed in this study.

Keywords: Soil Permeability, Electrical Resistant Tomography



主機設定 (107.10.31 攝於明學樓噴水池旁)





©2019. Japan Geoscience Union. All Right Reserved.

The Potential Study of Open Loop System Geothermal Heat Pump in Gifu City, Japan

*Randa Permanda[1], Tomoyuki Ohtani[2]

1. Department of Civil and Environmental Engineering, Gifu University, 2. Department of Civil Engineering, Gifu University

Geothermal heat pumps (GHPs) are considered to be one of the most energy efficient and environmentally friendly air-conditioning systems for temperate zones. In Japan, the expansive use of GHPs technology is finite, because of insufficient information on the advantages offered by the system and high installation cost. Therefore, the prediction of potential energy of GHPs at the first stage of installation is desirable. Open-loop system is one of GHPs types system which mostly depends on geological and hydrogeological parameter. This system interacts directly with ground and groundwater factor, because it uses groundwater as direct heat transfer medium through extraction and injection wells. Accordingly, groundwater flow with heat transfer is the most important factor that could affect the performance of open-loop GHPs system. Therefore groundwater flow system as well as distribution of subsurface temperature must be comprehended in detail. The aim of this study is to understand the distribution of groundwater flow and heat transport in study area from the simulation study using the program, FEFLOW. FEFLOW is a finite element code which can numerically simulate groundwater flow and heat transport. As the final result, the simulation model can be used to understand of open loop GHPs system in specified area.

The study area is an alluvial fan of the Nagara River, Gifu city, Japan. It is bounded by mountain ranges from north to northeast side and plain area remains. The Nagara River flows in the center of the plain. This alluvial fan is composed of sands and gravels and often intercalate thin fine sand and silt layers. Groundwater flow occur mainly in the Quaternary deposits, which are sand and gravel layers. Alluvial fans are recharge areas of groundwater and rapid groundwater flow are expected. The underground temperature in alluvial fan is affected by rapid groundwater flow recharged from a river. For assessment of potential energy of open loop GHPs, 3D model of groundwater flow with heat transport in Gifu city was developed using FEFLOW program. Model is constructed first by geological and hydrogeological data. The pre-existing geological columns and profile of study area were collected, which consisted of borehole and cross section data. Furthermore, pre-existing hydrogeological data which consist of groundwater table, underground temperature, and temperature of river water data in study area are also compiled to construct the simulation model. Boundary condition of groundwater flow system is defined by water table distribution. Bottom of the model is basement rock, treated as impermeable boundary and lateral sides are set as no flow boundaries. For boundary conditions of heat transport, top and bottom of the model are fixed by constant temperature boundaries, and lateral sides are as insulated. Based on constructed model, the simulation on groundwater flow with heat transport is performed. The effectiveness of heat transport and fluid flow are affected by material properties. Material properties were determined on the basis of formation types. Groundwater temperature were matched against observed temperatures, using the result of groundwater flow simulation. The observed underground temperatures in study area are fluctuated not only near surface but also in aquifer. This temperature change is resulted from lateral flow of the recharged groundwater. The calculated groundwater temperature will be adjusted until simulation result agreed with observed data from field. So that model can represent the groundwater flow system in alluvial fan of the Nagara River, Gifu city, Japan. For future plan, simulation model is used to investigate potential open loop GHPs system resulted from presence flowing groundwater in study area. This

©2019. Japan Geoscience Union. All Right Reserved.

simulation model is effective to predict the natural change of underground temperature, one main factor that affecting heat pumps efficiency.

Keywords: Geothermal heat pump, Groundwater flow, Heat transport, Open loop system, FEFLOW

©2019. Japan Geoscience Union. All Right Reserved.

Application of TL-CHERT Smart Characterization Method to Investigate a Groundwater Contaminated Site

*Tzu-Pin Wang[1,2,5], Yao-Tsung Chen[3], Tien-Hsing Tung[3], Chih-Hung Cheng[2], Jie Wang[4]

1. NCU TW, 2. Geophysical Technology and Engineering Co.,Ltd. R.O.C, 3. Apollo Technology Co.,Ltd. R.O.C., 4. Department of Civil Engineering, Chien Hsin University of Science and Technology, Taoyuan City, Taiwan, 5. Disaster Reduction Research Center, Chien Hsin University of Science and Technology, Taoyuan City, Taiwan

The Environmental Protection Administration in Taiwan effectively integrates Cross-Hole Electrical Resistivity Tomography (CHERT) into remediation planning in the anticipatory improvement project of sites with no polluter. During the reagent injection, Time-lapse Cross-Hole Electrical Resistivity (TL-CHERT) data are collected continuously. After data preprocessing and inversion algorithm, the ERT results are presented in images. 4D images could depict the main transmission range of reagent during the reagent injection, and further adjust or revise the second stage of remediation design. Therefore, CHERT could not only improve the remediation of complex groundwater contaminated sites, but also achieve the goal of precise surgical remediation. Besides, setting geophysical exploration equipment together with monitoring wells could greatly increase the use efficiency of the wells. Because groundwater contamination is usually a severe problem, a cross-professional cooperation is necessary. It is expected that this study will provide a worth case study for the survey application of similar contaminated site.

Keywords: CHERT, groundwater, pollution, resistiviy, geophysics, SCM

©2019. Japan Geoscience Union. All Right Reserved.

Data Assimilation in Hydraulic Conductivity Identification using Bayesian Statistical Method

*Shih-Yang Cheng[1], Kuo-Chin Hsu[1]

1. National Cheng Kung Univ.

Characterizing spatially heterogeneous hydraulic conductivity plays a crucial role in groundwater resources management and subsurface contaminant remediation. Since the direct measurements of hydraulic conductivity are sparse, the uncertainty is inherent in the estimated parameters. We propose decreasing the uncertainty by assimilating auxiliary data (electrical resistivity) with the direct data (hydraulic conductivity) using Bayesian statistical method. Different from classical geostatistical methods, both linear and nonlinear relations between the direct and auxiliary data can be considered in Bayesian statistical method. A synthetic example is designed to evaluate the method. Results show that the accuracy of hydraulic conductivity is improved through the Bayesian statistical method. Moreover, the effectiveness of auxiliary data in estimation error decrease is more significant when high correlation exists. However, the relation type has little influence on the accuracy. The estimation uncertainty quantified by variance is also compared. The uncertainty is inversely proportional to the amounts of auxiliary data and the correlation in both linear and nonlinear cases. The usefulness of auxiliary data in variance reduction is more obvious in linear cases. A systemic discussion of the sampling strategies of auxiliary data for improving hydraulic conductivity identification is also proposed.

Keywords: Data assimilation, Bayesian statistical method, Hydraulic conductivity, Nonlinear

©2019. Japan Geoscience Union. All Right Reserved.

Groundwater recharge estimation by using empirical orthogonal function method

Hua-Ting Zeng [1], *Hwa-Lung Yu[1]

1. National Taiwan University

Groundwater recharge estimation has been challenging due to the limited knowledge of the hyogeological heterogeneity. This issue is particularly important in the areas with high dependence on groundwater resources. This study proposed a data-driven approach along with a simple ODE model to estimate the groundwater recharge in our study area, Cho-shui river aquifer which is one of the most water-abundant aquifers in Taiwan; however, is suffered from the water overdraft. We analyzed the daily groundwater level observations during 2004-2010 from all wells across the entire study area. Based upon our proposed method, we identified two major recharge areas, i.e., proximal fan of the aquifer and Min-Chu basin at its upstream. The two areas obtained about 181.9 million and 78.8million tons of recharge water annually, resectively, in which about 131 million tons of water flowing from Min-Chu basin into Cho-shui aquifer annually. In summary, this study proposed a novel method for the groundwater recharge estimation.

Keywords: Groundwater, Recharge, EOF

©2019. Japan Geoscience Union. All Right Reserved.

The Application of Drought Early Warning Index for Regional Hydrological Circumstance Analysis

*Chih Chao Ho[1], Ta Wei Chen[2]

1. Construction and Disaster Prevention Research Center, Feng Chia Univ., 2. Taiwan Hsin-Chu Irrigation Association

Recently, rainfall become more unevenly both in special and temporal distribution caused by global climate change. The frequency of drought decrease from once every 17 years to once every 9 years. How to define warning signs of a drought and propose adaptive strategies is one of the key topic for water resources management. The drought can be divided into meteorological drought, agricultural drought and hydrological drought. The study tries to introduces difference Drought Early Warning Index, such as Standardized Precipitation Index, Standardized Groundwater Index, Normalized Difference Vegetation Index etc., to predict drought circumstance. The result can be a reference for development of drought early warning system.

Keywords: Standardized Precipitation Index, Standardized Groundwater Index, Normalized Difference Vegetation Index

©2019. Japan Geoscience Union. All Right Reserved.

[E] Poster | M (Multidisciplinary and Interdisciplinary)：M-GI General Geosciences, Information Geosciences & Simulations

Tue. May 28, 2019 5:15 PM - 6:30 PM JST | Tue. May 28, 2019 8:15 AM - 9:30 AM UTC | Poster Hall International Exhibition Hall8, Makuhari Messe_47

[M-GI29] Near Surface Investigation and Modeling for Groundwater Resources Assessment and Conservation

convener:Jui-Pin Tsai(National Cheng Kung University, Taiwan), Hwa-Lung Yu(National Taiwan University), Ching-Chung Cheng(National Chiao Tung University Taiwan), Jing-Sen Cai(China University of Geosciences)

Groundwater resources serve as a vital source for regional water supply under the climate change condition. However, improper use of the available groundwater resources leads to serious environmental disasters such as land subsidence or seawater intrusion. Therefore, groundwater management is a key issue for groundwater resources conservation. Before applying any management practice, it is essential to accurately assess the groundwater system in multi-scales. In this session, we focus on the issues associated with the application of near-surface investigation and modeling on groundwater resources assessment. We welcome studies related to numerical modeling, spatiotemporal modeling, data fusion, and field investigation using hydrogeological approaches, geophysical approaches, geochemical approaches, and remote sensing. We also welcome the studies associated with groundwater contamination transport and remediation, geothermal energy exchange, groundwater microorganisms, hot spring, volcanic hydrology, and environmental disasters evaluation and prevention. We especially encourage the pilot groundwater management studies that solve multi-scale and interdisciplinary problems.

[MGI29-P01] Modelling of self-potential signals associated with groundwater flows

*ayaka ishikawa[1], Katsumi Hattori[1] (1.chiba university)

[MGI29-P02] Estimating the Hydraulic Conductivity and Heat Capacity of the Aquifer between the River and Well Site Using Joint Inversion Approach

*Jui-Pin Tsai[1], Chin-Tsai Hsiao[4], Liang-Cheng Chang[2], You-Cheng Chen[2], Chun-Hung Chen[3], Yun-Ta Cheng[3], Jen-Hung Yu[3] (1.National Cheng Kung University, Taiwan , 2.National Chiao Tung University, Taiwan , 3.Water Resources Planning Institute, Water Resources Agency, Taiwan, 4.Department of Information Management, Chung Chou University of Science and Technology)

[MGI29-P03] Evaluation on Soil Permeability Using Electrical Resistant Tomography

*CHIHPING KUO[1], BONIAN SHEN[1], CHIHWEI HUANG[1], YUCHIAO LEE[1], SHENXIANG HUANG[1], YENLIN CHEN[1] (1.Department and Institute of Civil Engineering and Environmental Informatics, Minghsin University of Science and Technology)

[MGI29-P04] The Potential Study of Open Loop System Geothermal Heat Pump in Gifu City, Japan

*Randa Permanda[1], Tomoyuki Ohtani[2] (1.Department of Civil and Environmental Engineering, Gifu University, 2.Department of Civil Engineering, Gifu University)

[MGI29-P05] Application of TL-CHERT Smart Characterization Method to Investigate a Groundwater Contaminated Site

*Tzu-Pin Wang[1,2,5], Yao-Tsung Chen[3], Tien-Hsing Tung[3], Chih-Hung Cheng[2], Jie Wang[4] (1.NCU TW, 2.Geophysical Technology and Engineering Co.,Ltd. R.O.C, 3.Apollo Technology Co.,Ltd. R.O.C., 4.Department of Civil Engineering, Chien Hsin University of Science and Technology, Taoyuan City, Taiwan, 5.Disaster Reduction Research Center, Chien Hsin University of Science and Technology, Taoyuan City, Taiwan)

[MGI29-P06] Data Assimilation in Hydraulic Conductivity Identification using Bayesian Statistical Method

*Shih-Yang Cheng[1], Kuo-Chin Hsu[1] (1.National Cheng Kung Univ.)

[MGI29-P07] Groundwater recharge estimation by using empirical orthogonal function method

Hua-Ting Zeng [1], *Hwa-Lung Yu[1] (1. National Taiwan University)

[MGI29-P08] The Application of Drought Early Warning Index for Regional Hydrological Circumstance Analysis

*Chih Chao Ho[1], Ta Wei Chen[2] (1.Construction and Disaster Prevention Research Center, Feng Chia Univ., 2.Taiwan Hsin-Chu Irrigation Association)

Modelling of self-potential signals associated with groundwater flows

*ayaka ishikawa[1], Katsumi Hattori[1]

1. chiba university

Landslides triggered by rainfall are one of the most dangerous natural disasters which give the loss of lives and properties. Although the importance of the short-term forecast of landslides is widely accepted, it is not achieved. In this research, we pay attention to electro-magnetic approach for monitoring ground water condition under the slope. That is, we understand the processes of the landslide and develop the system for forecast to detect precursory signal through the electromagnetic changes. In this study, we apply the self-potential approach, which is related on electro-kinetic effects or streaming potential. We have conducted several flume tests and sandbox experiments and the results showed the repeatability of the phenomena or correlation between self-potential and ground water condition. Therefore, we will report the model and numerical computation for the sandbox experiment on injection in this presentation.

SP signals measured in the sandbox during pumping experiment are considered to be due to the electro-kinetic effects. The total current density j is $j=sE-l\mathrm{d}h/\mathrm{d}x_i$, where s (in S m^{-1}) is the electrical conductivity, E (in Vm^{-1}) is the electric field, l (in A Pa^{-1} m^{-1}) is the current coupling coefficient, and h (in m) is the hydraulic head. The variation of SP signals of the sandbox gives quasi-instantaneous information on changes of the hydraulic head. Therefore we consider this problem with quasi-static limit condition i.e. div j = 0. It leads $\mathrm{div}(s\,\mathrm{grad}\,phi)=-\mathrm{div}(l\,\mathrm{grad}\,h)$.Where phi (in V) is electric potential. In addition, we assume that s and l are uniform through the sandbox because we assume saturated condition. Finally, the solved equation is $s\mathrm{d}^2phi/dx_i^2=-l\mathrm{d}^2h/dx_i^2$. We simulated distribution of hydraulic head during pumping test using finite element method. Then, we modeled the SP generation.

Consequently, the variation of SP modeled and observed are generally consistent with each other. Therefore, we found that groundwater flows control the occurrence of SP in the sandbox experiment. However, in the detail of time variation, modeled SP differ from those of observed partly. We consider that heterogeneity of soil or necessary of 3D modeling could cause these discordances. Details will be shown in our presentation.

Keywords: self-potential, ground water flow, modelling

©2019. Japan Geoscience Union. All Right Reserved.

Estimating the Hydraulic Conductivity and Heat Capacity of the Aquifer between the River and Well Site Using Joint Inversion Approach

*Jui-Pin Tsai[1], Chin-Tsai Hsiao[4], Liang-Cheng Chang[2], You-Cheng Chen[2], Chun-Hung Chen[3], Yun-Ta Cheng[3], Jen-Hung Yu[3]

1. National Cheng Kung University, Taiwan , 2. National Chiao Tung University, Taiwan , 3. Water Resources Planning Institute, Water Resources Agency, Taiwan, 4. Department of Information Management, Chung Chou University of Science and Technology

This study continued to measure the water temperature and pressure at the riverbed, agricultural waterway, and groundwater monitoring well from Oct. to Nov. 2018. These observations were then used to estimate the hydraulic conductivity (K) and flux between the river and the aquifer of the well site. The water pressure data reveal that the correlation coefficient between river and groundwater level reaches 0.9 and that between the agricultural waterway and groundwater level is almost 0. This reveals that the groundwater head variation mainly affected by the river stage of the nearby river. The temperature data show that the groundwater temperature is correlated to the temperature of the river water and is uncorrelated to the air temperature. Accordingly, the temperature and head data of the groundwater and river water were used to estimate K and heat capacity of the aquifer between the river and well site using a joint inversion approach. The results show that the estimated K and heat capacity are 67.53 m ⁄ day and 4485000 J ⁄ (m^3–℃), respectively.

Keywords: Hydraulic conductivity, Soil heat capactiy , Joint inversion, Temperature, Groundwater head , Interaction between groundwater and river water

©2019. Japan Geoscience Union. All Right Reserved.

Evaluation on Soil Permeability Using Electrical Resistant Tomography

*CHIHPING KUO[1], BONIAN SHEN[1], CHIHWEI HUANG[1], YUCHIAO LEE[1], SHENXIANG HUANG[1], YENLIN CHEN[1]

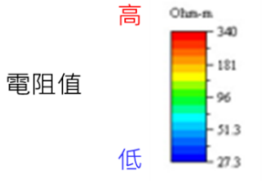
1. Department and Institute of Civil Engineering and Environmental Informatics, Minghsin University of Science and Technology

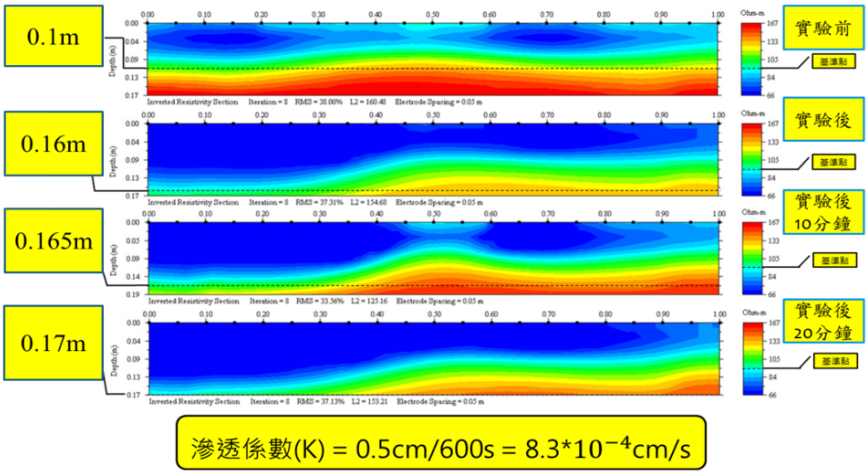
The permeability of soil is used to adapt field constant head permeability test or variable head permeability test. The former test is suitable for soil with higher permeability like sand and gravels; the later test is suitable for soil with lower permeability like silt and clays. Both tests need in-situ drilling holes. The required operating time is usually about couple of hours. A widely used geophysical method, Electrical Resistant Tomography (ERT), is adapted here to evaluate the soil permeability. Two types of soil with different permeability were performed, and the results were compared with the result of same samples using traditional permeability test. The result showed that they were very close. The operating time of ERT for one soil was only less than one hour. The idea of evaluating soil permeability using ERT is proposed in this study.

Keywords: Soil Permeability, Electrical Resistant Tomography



主機設定 (107.10.31 攝於明學樓噴水池旁)





©2019. Japan Geoscience Union. All Right Reserved.

The Potential Study of Open Loop System Geothermal Heat Pump in Gifu City, Japan

*Randa Permanda[1], Tomoyuki Ohtani[2]

1. Department of Civil and Environmental Engineering, Gifu University, 2. Department of Civil Engineering, Gifu University

Geothermal heat pumps (GHPs) are considered to be one of the most energy efficient and environmentally friendly air-conditioning systems for temperate zones. In Japan, the expansive use of GHPs technology is finite, because of insufficient information on the advantages offered by the system and high installation cost. Therefore, the prediction of potential energy of GHPs at the first stage of installation is desirable. Open-loop system is one of GHPs types system which mostly depends on geological and hydrogeological parameter. This system interacts directly with ground and groundwater factor, because it uses groundwater as direct heat transfer medium through extraction and injection wells. Accordingly, groundwater flow with heat transfer is the most important factor that could affect the performance of open-loop GHPs system. Therefore groundwater flow system as well as distribution of subsurface temperature must be comprehended in detail. The aim of this study is to understand the distribution of groundwater flow and heat transport in study area from the simulation study using the program, FEFLOW. FEFLOW is a finite element code which can numerically simulate groundwater flow and heat transport. As the final result, the simulation model can be used to understand of open loop GHPs system in specified area.

The study area is an alluvial fan of the Nagara River, Gifu city, Japan. It is bounded by mountain ranges from north to northeast side and plain area remains. The Nagara River flows in the center of the plain. This alluvial fan is composed of sands and gravels and often intercalate thin fine sand and silt layers. Groundwater flow occur mainly in the Quaternary deposits, which are sand and gravel layers. Alluvial fans are recharge areas of groundwater and rapid groundwater flow are expected. The underground temperature in alluvial fan is affected by rapid groundwater flow recharged from a river. For assessment of potential energy of open loop GHPs, 3D model of groundwater flow with heat transport in Gifu city was developed using FEFLOW program. Model is constructed first by geological and hydrogeological data. The pre-existing geological columns and profile of study area were collected, which consisted of borehole and cross section data. Furthermore, pre-existing hydrogeological data which consist of groundwater table, underground temperature, and temperature of river water data in study area are also compiled to construct the simulation model. Boundary condition of groundwater flow system is defined by water table distribution. Bottom of the model is basement rock, treated as impermeable boundary and lateral sides are set as no flow boundaries. For boundary conditions of heat transport, top and bottom of the model are fixed by constant temperature boundaries, and lateral sides are as insulated. Based on constructed model, the simulation on groundwater flow with heat transport is performed. The effectiveness of heat transport and fluid flow are affected by material properties. Material properties were determined on the basis of formation types. Groundwater temperature were matched against observed temperatures, using the result of groundwater flow simulation. The observed underground temperatures in study area are fluctuated not only near surface but also in aquifer. This temperature change is resulted from lateral flow of the recharged groundwater. The calculated groundwater temperature will be adjusted until simulation result agreed with observed data from field. So that model can represent the groundwater flow system in alluvial fan of the Nagara River, Gifu city, Japan. For future plan, simulation model is used to investigate potential open loop GHPs system resulted from presence flowing groundwater in study area. This

©2019. Japan Geoscience Union. All Right Reserved.

simulation model is effective to predict the natural change of underground temperature, one main factor that affecting heat pumps efficiency.

Keywords: Geothermal heat pump, Groundwater flow, Heat transport, Open loop system, FEFLOW

©2019. Japan Geoscience Union. All Right Reserved.

Application of TL-CHERT Smart Characterization Method to Investigate a Groundwater Contaminated Site

*Tzu-Pin Wang[1,2,5], Yao-Tsung Chen[3], Tien-Hsing Tung[3], Chih-Hung Cheng[2], Jie Wang[4]

1. NCU TW, 2. Geophysical Technology and Engineering Co.,Ltd. R.O.C, 3. Apollo Technology Co.,Ltd. R.O.C., 4. Department of Civil Engineering, Chien Hsin University of Science and Technology, Taoyuan City, Taiwan, 5. Disaster Reduction Research Center, Chien Hsin University of Science and Technology, Taoyuan City, Taiwan

The Environmental Protection Administration in Taiwan effectively integrates Cross-Hole Electrical Resistivity Tomography (CHERT) into remediation planning in the anticipatory improvement project of sites with no polluter. During the reagent injection, Time-lapse Cross-Hole Electrical Resistivity (TL-CHERT) data are collected continuously. After data preprocessing and inversion algorithm, the ERT results are presented in images. 4D images could depict the main transmission range of reagent during the reagent injection, and further adjust or revise the second stage of remediation design. Therefore, CHERT could not only improve the remediation of complex groundwater contaminated sites, but also achieve the goal of precise surgical remediation. Besides, setting geophysical exploration equipment together with monitoring wells could greatly increase the use efficiency of the wells. Because groundwater contamination is usually a severe problem, a cross-professional cooperation is necessary. It is expected that this study will provide a worth case study for the survey application of similar contaminated site.

Keywords: CHERT, groundwater, pollution, resistiviy, geophysics, SCM

©2019. Japan Geoscience Union. All Right Reserved.

Data Assimilation in Hydraulic Conductivity Identification using Bayesian Statistical Method

*Shih-Yang Cheng[1], Kuo-Chin Hsu[1]

1. National Cheng Kung Univ.

Characterizing spatially heterogeneous hydraulic conductivity plays a crucial role in groundwater resources management and subsurface contaminant remediation. Since the direct measurements of hydraulic conductivity are sparse, the uncertainty is inherent in the estimated parameters. We propose decreasing the uncertainty by assimilating auxiliary data (electrical resistivity) with the direct data (hydraulic conductivity) using Bayesian statistical method. Different from classical geostatistical methods, both linear and nonlinear relations between the direct and auxiliary data can be considered in Bayesian statistical method. A synthetic example is designed to evaluate the method. Results show that the accuracy of hydraulic conductivity is improved through the Bayesian statistical method. Moreover, the effectiveness of auxiliary data in estimation error decrease is more significant when high correlation exists. However, the relation type has little influence on the accuracy. The estimation uncertainty quantified by variance is also compared. The uncertainty is inversely proportional to the amounts of auxiliary data and the correlation in both linear and nonlinear cases. The usefulness of auxiliary data in variance reduction is more obvious in linear cases. A systemic discussion of the sampling strategies of auxiliary data for improving hydraulic conductivity identification is also proposed.

Keywords: Data assimilation, Bayesian statistical method, Hydraulic conductivity, Nonlinear

©2019. Japan Geoscience Union. All Right Reserved.

Groundwater recharge estimation by using empirical orthogonal function method

Hua-Ting Zeng [1], *Hwa-Lung Yu[1]

1. National Taiwan University

Groundwater recharge estimation has been challenging due to the limited knowledge of the hyogeological heterogeneity. This issue is particularly important in the areas with high dependence on groundwater resources. This study proposed a data-driven approach along with a simple ODE model to estimate the groundwater recharge in our study area, Cho-shui river aquifer which is one of the most water-abundant aquifers in Taiwan; however, is suffered from the water overdraft. We analyzed the daily groundwater level observations during 2004-2010 from all wells across the entire study area. Based upon our proposed method, we identified two major recharge areas, i.e., proximal fan of the aquifer and Min-Chu basin at its upstream. The two areas obtained about 181.9 million and 78.8million tons of recharge water annually, resectively, in which about 131 million tons of water flowing from Min-Chu basin into Cho-shui aquifer annually. In summary, this study proposed a novel method for the groundwater recharge estimation.

Keywords: Groundwater, Recharge, EOF

©2019. Japan Geoscience Union. All Right Reserved.

The Application of Drought Early Warning Index for Regional Hydrological Circumstance Analysis

*Chih Chao Ho[1], Ta Wei Chen[2]

1. Construction and Disaster Prevention Research Center, Feng Chia Univ., 2. Taiwan Hsin-Chu Irrigation Association

Recently, rainfall become more unevenly both in special and temporal distribution caused by global climate change. The frequency of drought decrease from once every 17 years to once every 9 years. How to define warning signs of a drought and propose adaptive strategies is one of the key topic for water resources management. The drought can be divided into meteorological drought, agricultural drought and hydrological drought. The study tries to introduces difference Drought Early Warning Index, such as Standardized Precipitation Index, Standardized Groundwater Index, Normalized Difference Vegetation Index etc., to predict drought circumstance. The result can be a reference for development of drought early warning system.

Keywords: Standardized Precipitation Index, Standardized Groundwater Index, Normalized Difference Vegetation Index

©2019. Japan Geoscience Union. All Right Reserved.

[E] Poster | M (Multidisciplinary and Interdisciplinary) : M-ZZ Others

Tue. May 28, 2019 1:45 PM - 3:15 PM JST | Tue. May 28, 2019 4:45 AM - 6:15 AM UTC | Poster Hall International Exhibition Hall8, Makuhari Messe_10

[M-ZZ50] Governance for Trans-boundary Volcanic Disaster

convener:Mayumi Sakamoto(Graduate School of Disaster Resilience and Governance, University of Hyogo), Haruhisa Nakamichi(Sakurajima Volcano Research Center, Disaster Prevention Research Institute, Kyoto University), MASARU ARAKIDA(Asian Disaster Reduction Center)

Volcanic monitoring systems are developed and managed for the purpose to observe a specific volcanic activity in each country based on its own regulation. However, the experience of Icelandic volcano Eyjafjallajokull eruption in 2010 caused huge air traffic disturbances, and left large economic and social impact to international community. In order to reduce possible financial, environmental, health or social damages caused by trans-boundary volcanic disaster, it is important to develop international cooperative system to monitor and share the information of emission, dispersion or deposition of volcanic products. In this session, we discuss trans-boundary effect of volcanic eruption, and how to establish international collaborative mechanism from different research disciplines such as disaster management, volcanology, environmental politics or international law.

[MZZ50-P01] Governance for Trans-boundary Volcanic Disaster -a case of 2010 Eyjafjallajökull Eruption-

*Mayumi Sakamoto[1] (1.Graduate School of Disaster Resilience and Governance, University of Hyogo)

[MZZ50-P02] Regional Cooperation against Cross-border Disasters

*MASARU ARAKIDA[1] (1.Asian Disaster Reduction Center)

[MZZ50-P03] Issues of Japan's volcanic disaster prevention system as viewed from overseas alert systems

*Erika Ishimizu[1], Mayumi Sakamoto[1] (1.Graduate School of Disaster Resilience and Governance University of Hyogo)

Governance for Trans-boundary Volcanic Disaster -a case of 2010 Eyjafjallajökull Eruption-

*Mayumi Sakamoto[1]

1. Graduate School of Disaster Resilience and Governance, University of Hyogo

The volcanic eruption occurred in one country can trigger different effect in other country. The experience of 2010 Icelandic volcano Eyjafjallajökull eruption demonstrated the necessity of international governance for trans-boundary effect caused by eruption. In Iceland, national disaster response was effective to evacuate people from hazardous area and there were no humanitarian damages caused by eruption. However, the estimation of volcanic ash plumes and its dispersion caused huge international air traffic disruption or airport closure, and left large international economic and industrial impact. Followings are problems found through the 2010 eruption.
First, the necessity of international collaboration for observing atmospheric dispersion of volcanic ash. As for 2010 eruption, Icelandic Meteorological Agency (IMO) informed London Volcanic Ash Advisory Center (VAAC) which observes Iceland, about the plume height, ash content and other data. Based on the provided data, London VAAC predicted ash dispersion over Europe. However, there was no detailed discussion between IMO and London VAAC when and how often they communicate prior to eruption. It is important to update forecast using satellite imagery or observation of ashfalls in other countries.
Second, the necessity of immediate information sharing with both local and international medias. During the eruption, there was a huge need for information from international medias. A communication team, composed by professional communicator from various institutions gathered at the National Crisis Coordination and Command Center (NCCCC). Press conference were held and status reports were prepared and distributed. Such an international information sharing system should be discussed prior to disaster.
Disaster management systems are generally developed to respond hazard activity in each country based on its own regulation. However, 2010 experience showed there is no international agreement or regime to respond such a trans-boundary effect. Immediate crisis communication among hazard origin country, international institute and possibly affective country is required to reduce secondary effect, which shows importance or precautionary approaches for trans-boundary volcanic disaster.

Keywords: trans-boudary disaster, volcano, governance, Eyjafjallajökull

©2019. Japan Geoscience Union. All Right Reserved.

Regional Cooperation against Cross-border Disasters

*MASARU ARAKIDA[1]

1. Asian Disaster Reduction Center

Since affected area by disasters such as floods on international scale river, haize by forest fire, and volcanic ejectaare are recognized as no boundaries, there are many benefits of working together through regional cooperation. These include the sharing of best practices for handling major disasters, responding together on search and rescue efforts, and understanding and improving DRR through early warnings, the mutual exchange of information, joint education and training exercises, and joint assistance on disaster response.

Keywords: cross-border disaster, regional cooperation

©2019. Japan Geoscience Union. All Right Reserved.

Issues of Japan's volcanic disaster prevention system as viewed from overseas alert systems

*Erika Ishimizu[1], Mayumi Sakamoto[1]

1. Graduate School of Disaster Resilience and Governance University of Hyogo

Volcanic alert levels was introduced in Japan in 2007. Thereafter, the level was raised or lowered for several volcanoes, some volcanoes erupted and residents evacuated. Among them, the problem of exploiting volcanic alert levels for evacuation has become clear. In this research, by comparing Japan's warning system with overseas (the United States, Indonesia, New Zealand), we will examine the issues of Japanese volcanic disaster prevention system and future disaster prevention system.
In Japan, several institutions, such as universities and Japan Meteorological Agency (JMA), are conducting observations of volcanic activity. In the volcano where volcanic alert levels is introduced, JMA announces five levels of volcanic alert levels according to the activity of the volcano. Each municipality carries out basic disaster response such as issuance of evacuation information.
In the United States, the United States Geological Survey (USGS) will unite from the observation of a volcano to the announcement of an alarm (4 stages). Basic disaster response is handled by municipalities and counties. If requested, the state government responds, and if it is still difficult, FEMA is asked.
In Indonesia, the Center of Volcanology and Geological Hazard Mitigation (PVMBG) classify active volcanoes into three stages, ranging from A to C class, and is conducting observations. When the volcano becomes active, they present four levels of warning level. The basic disaster response such as the issuance of evacuation information is taken by the Regional Disaster Management Agency in Indonesia (BPBD), and the National Agency for Disaster Countermeasure (BNPB) supports this. If evacuation accompanied with level rise but the eruption does not occur, BNPB bears the expenses.
In New Zealand, GNS Science Corporation conducts observation of volcanic activity and issuance of alarm (6 stages).An evacuation information issuance is made by CDEM which is a collaboration body of local public bodies.
This presentation discusses issues of volcanic disaster prevention system in Japan and future disaster prevention system by comparing systems of each country.

Keywords: volcano, volcanic disaster prevention system , volcanic alert level

©2019. Japan Geoscience Union. All Right Reserved.

[E] Poster | M (Multidisciplinary and Interdisciplinary)：M-ZZ Others

Tue. May 28, 2019 5:15 PM - 6:30 PM JST | Tue. May 28, 2019 8:15 AM - 9:30 AM UTC | Poster Hall International Exhibition Hall8, Makuhari Messe_50

[M-ZZ50] Governance for Trans-boundary Volcanic Disaster

convener:Mayumi Sakamoto(Graduate School of Disaster Resilience and Governance, University of Hyogo), Haruhisa Nakamichi(Sakurajima Volcano Research Center, Disaster Prevention Research Institute, Kyoto University), MASARU ARAKIDA(Asian Disaster Reduction Center)

Volcanic monitoring systems are developed and managed for the purpose to observe a specific volcanic activity in each country based on its own regulation. However, the experience of Icelandic volcano Eyjafjallajokull eruption in 2010 caused huge air traffic disturbances, and left large economic and social impact to international community. In order to reduce possible financial, environmental, health or social damages caused by trans-boundary volcanic disaster, it is important to develop international cooperative system to monitor and share the information of emission, dispersion or deposition of volcanic products. In this session, we discuss trans-boundary effect of volcanic eruption, and how to establish international collaborative mechanism from different research disciplines such as disaster management, volcanology, environmental politics or international law.

[MZZ50-P01] Governance for Trans-boundary Volcanic Disaster -a case of 2010 Eyjafjallajökull Eruption-

*Mayumi Sakamoto[1] (1.Graduate School of Disaster Resilience and Governance, University of Hyogo)

[MZZ50-P02] Regional Cooperation against Cross-border Disasters

*MASARU ARAKIDA[1] (1.Asian Disaster Reduction Center)

[MZZ50-P03] Issues of Japan's volcanic disaster prevention system as viewed from overseas alert systems

*Erika Ishimizu[1], Mayumi Sakamoto[1] (1.Graduate School of Disaster Resilience and Governance University of Hyogo)

Governance for Trans-boundary Volcanic Disaster -a case of 2010 Eyjafjallajökull Eruption-

*Mayumi Sakamoto[1]

1. Graduate School of Disaster Resilience and Governance, University of Hyogo

The volcanic eruption occurred in one country can trigger different effect in other country. The experience of 2010 Icelandic volcano Eyjafjallajökull eruption demonstrated the necessity of international governance for trans-boundary effect caused by eruption. In Iceland, national disaster response was effective to evacuate people from hazardous area and there were no humanitarian damages caused by eruption. However, the estimation of volcanic ash plumes and its dispersion caused huge international air traffic disruption or airport closure, and left large international economic and industrial impact. Followings are problems found through the 2010 eruption.
First, the necessity of international collaboration for observing atmospheric dispersion of volcanic ash. As for 2010 eruption, Icelandic Meteorological Agency (IMO) informed London Volcanic Ash Advisory Center (VAAC) which observes Iceland, about the plume height, ash content and other data. Based on the provided data, London VAAC predicted ash dispersion over Europe. However, there was no detailed discussion between IMO and London VAAC when and how often they communicate prior to eruption. It is important to update forecast using satellite imagery or observation of ashfalls in other countries.
Second, the necessity of immediate information sharing with both local and international medias. During the eruption, there was a huge need for information from international medias. A communication team, composed by professional communicator from various institutions gathered at the National Crisis Coordination and Command Center (NCCCC). Press conference were held and status reports were prepared and distributed. Such an international information sharing system should be discussed prior to disaster.
Disaster management systems are generally developed to respond hazard activity in each country based on its own regulation. However, 2010 experience showed there is no international agreement or regime to respond such a trans-boundary effect. Immediate crisis communication among hazard origin country, international institute and possibly affective country is required to reduce secondary effect, which shows importance or precautionary approaches for trans-boundary volcanic disaster.

Keywords: trans-boudary disaster, volcano, governance, Eyjafjallajökull

©2019. Japan Geoscience Union. All Right Reserved.

Regional Cooperation against Cross-border Disasters

*MASARU ARAKIDA[1]

1. Asian Disaster Reduction Center

Since affected area by disasters such as floods on international scale river, haize by forest fire, and volcanic ejectaare are recognized as no boundaries, there are many benefits of working together through regional cooperation. These include the sharing of best practices for handling major disasters, responding together on search and rescue efforts, and understanding and improving DRR through early warnings, the mutual exchange of information, joint education and training exercises, and joint assistance on disaster response.

Keywords: cross-border disaster, regional cooperation

©2019. Japan Geoscience Union. All Right Reserved.

Issues of Japan's volcanic disaster prevention system as viewed from overseas alert systems

*Erika Ishimizu[1], Mayumi Sakamoto[1]

1. Graduate School of Disaster Resilience and Governance University of Hyogo

Volcanic alert levels was introduced in Japan in 2007. Thereafter, the level was raised or lowered for several volcanoes, some volcanoes erupted and residents evacuated. Among them, the problem of exploiting volcanic alert levels for evacuation has become clear. In this research, by comparing Japan's warning system with overseas (the United States, Indonesia, New Zealand), we will examine the issues of Japanese volcanic disaster prevention system and future disaster prevention system.
In Japan, several institutions, such as universities and Japan Meteorological Agency (JMA), are conducting observations of volcanic activity. In the volcano where volcanic alert levels is introduced, JMA announces five levels of volcanic alert levels according to the activity of the volcano. Each municipality carries out basic disaster response such as issuance of evacuation information.
In the United States, the United States Geological Survey (USGS) will unite from the observation of a volcano to the announcement of an alarm (4 stages). Basic disaster response is handled by municipalities and counties. If requested, the state government responds, and if it is still difficult, FEMA is asked.
In Indonesia, the Center of Volcanology and Geological Hazard Mitigation (PVMBG) classify active volcanoes into three stages, ranging from A to C class, and is conducting observations. When the volcano becomes active, they present four levels of warning level. The basic disaster response such as the issuance of evacuation information is taken by the Regional Disaster Management Agency in Indonesia (BPBD), and the National Agency for Disaster Countermeasure (BNPB) supports this. If evacuation accompanied with level rise but the eruption does not occur, BNPB bears the expenses.
In New Zealand, GNS Science Corporation conducts observation of volcanic activity and issuance of alarm (6 stages).An evacuation information issuance is made by CDEM which is a collaboration body of local public bodies.
This presentation discusses issues of volcanic disaster prevention system in Japan and future disaster prevention system by comparing systems of each country.

Keywords: volcano, volcanic disaster prevention system , volcanic alert level

©2019. Japan Geoscience Union. All Right Reserved.

[E] Poster | P (Space and Planetary Sciences)：P-PS Planetary Sciences

Wed. May 29, 2019 10:45 AM - 12:15 PM JST | Wed. May 29, 2019 1:45 AM - 3:15 AM UTC | Poster Hall International Exhibition Hall8, Makuhari Messe_2

[P-PS02] Regolith Science

convener:Koji Wada(Planetary Exploration Research Center, Chiba Institute of Technology), Akiko Nakamura(Graduate School of Science, Kobe University), Patrick Michel(Observatoire De La Cote D'Azur), Kevin John Walsh(Southwest Research Institute Boulder)

Recent planetary explorations have revealed that almost all solid bodies in the solar system are covered with small particles, called regolith. The surface geology, especially regolith behavior on the surfaces of solid bodies, becomes increasingly more important as represented by Hayabusa mission and other on-going and planned sample-return missions such as Hayabusa2, OSIRIS-REx, and MMX.

For fully understanding the regolith science, it is required to know and compare the regolith conditions on various celestial bodies, from asteroids to planets, with various methods.

Therefore, this session welcomes broad topics related to regolith on various celestial bodies, such as asteroids, comets, the Moon, the martian moons, Mars, etc. Papers on the formation, evolution, and alteration processes of regolith particles and regolith systems on the surface of planetary bodies, remote and in-situ observational results and techniques, analyses and results of returned samples, and laboratory, numerical, and theoretical studies on the fundamental physical and chemical processes are all welcome.

Note that what we call regolith is not just fine grains: all kinds of materials (more or less loose) that lie on the surface, from cobbles to finer grains, are our targets.

[PPS02-P01] Abrasion experiments of mineral and meteorite grains: Dependence of particle size and vibration rate on abrasion rate and its application to Itokawa and lunar regolith particles.

*Hirotaka Yamaguchi[1], Akira Tsuchiyama[1], Akiko Nakamura[2] (1.National University Corporation, Kyoto University, 2.National University Corporation,Kobe University)

[PPS02-P02] Measurements of adhesive force of meteorite powders using centrifugal method

*Yuuya Nagaashi[1], Akiko Nakamura[1] (1.Kobe University)

[PPS02-P03] Laboratory impact penetration experiments conducted at simulated reduced gravity

*Akiko Nakamura[1], Kana Morizono[2], Yuuya Nagaashi[1] (1.Graduate School of Science, Kobe University, 2.Faculty of Science, Kobe University)

[PPS02-P04] MARAUDERS: Using instrumented nano-impactors to probe the icy properties of Lunar permanently shadowed regions

*Ronald Ballouz[1], Sarah T Crites[2], Naoya Ozaki[2], Shun Arahata[3], Nicola Baresi[2], Ralf Bolden, Onur Celik[4,2], Yu Himeno[3], Lucie Riu[2], Kevin J Walsh[5] (1.Lunar and Planetary Lab, University of Arizona, Tucson, AZ, USA, 2.Institute of Space and Astronautical Science, Sagamihara, Japan, 3.University of Tokyo, Tokyo, Japan, 4.Sokendai Graduate University, Japan, 5.Southwest Research Institute, Boulder, CO, USA)

[PPS02-P05] Surface size-frequency distribution of accumulating boulders using discrete element simulations of spherical particles in 3D

*Hiroshi Kikuchi[1], Hideaki Miyamoto[1] (1.The University of Tokyo)

[PPS02-P06] Experimental Study to Determine the Best Compression Ratio of High-Resolution Images of Small Bodies for the Martian Moons eXploration (MMX) Mission

*Yuta Shimizu[1], Hiroaki Kamiyoshihara[1], Takafumi Niihara[1], Hideaki Miyamoto[1] (1.University of Tokyo)

Abrasion experiments of mineral and meteorite grains: Dependence of particle size and vibration rate on abrasion rate and its application to Itokawa and lunar regolith particles.

*Hirotaka Yamaguchi[1], Akira Tsuchiyama[1], Akiko Nakamura[2]

1. National University Corporation, Kyoto University, 2. National University Corporation,Kobe University

Rounded edges were found in some regolith particles collected from asteroid Itokawa [1] and Moon [2]. These particles should be formed by mechanical abrasion [1]. Seismic-induced grain motion by micrometeoroid impacts [1] and YORP effect [3] were proposed for the abrasion process on Itokawa. However, it is not clear how these processes actually work on the surfaces of the airless celestial bodies.

In order to understand detailed process of the abrasion, our research group have carried out abrasion experiments using mineral, rock and meteorite grains (grain size: 1-2 mm) [4]. Samples used were quartz, olivine, corundum, marble, L5 chondrite meteorite (Sayh al Uhaymir 001) and CM chondrite meteorite (Murchison). These particles were put into a vessel of 10 mL with the filling ratio of ~50 % and the sample was vibrated with the rate from 1000 to 3000 rpm using a multi-beads-shocker (YASUIKIKAI Co.). The proportion of powder (<250 μm) produced by vibration at first 1 min., ΔP_1, was adopted as the measure of abrasion and its dependence of the vibration rate and the sample strength was examined. However, the particle size used in the experiments (1-2 mm) is larger than Itokawa particles (< a few hundred μm). In addition, the vibration rates used in the experiments are larger than those estimated for Itokawa(~100 rpm) and Moon (~700 rpm) by considering the maximum seismic acceleration due to micrometeoroidimpacts onto their surface [5]. In the present study, therefore, we conducted new experiments with different parameters such as particle size and vibration rate using the same experimental procedure as [4]. In the present experiments, we used quartz grains for examining the effect of packing ratio in the vessel (Exp-1), particle size (Exp-2), mixing ratio of large and small particles (Exp-3). The effect of lower vibration rate (100 - 1000 rpm) was examined using olivine and basalt as well as quartz (Exp-4). Experiments using basalt at higher vibration rates were also made.

We obtained following results. Exp-1: $\Delta P_1$was constant in a wide range of the filling rate except for the filling rate of 2/3, where ΔP_1showed a peak value. Exp-2: $\Delta P_1$is proportional to the particle size. Exp-3: When the proportion of large particles is larger than 25%, $\Delta P_1$is almost constant and the same as $\Delta P_1$for the large particles. Exp-4: In the previous experiments, ΔP_1increases with the vibration rate with the power of 1.1-2.9 for large vibration rates (>~1000 rpm) [4] while the power becomes smaller (0.67-0.77) for smaller vibration rates (<~1000 rpm). This result shows that the abrasion mode changed at ~1000 rpm. In order to understand abrasion modes, SEM observation of powder particles produced in the abrasion experiments were also made. It was found that chipping of particle edges occurred at low vibration rate (~100 rpm) and the proportion of gradual wearing on the whole particle surface gradually increased as the vibration rate increased.

We estimated the amount of abrasion of Itokawa and lunar regolith particles in a regolith layer by impact based on the present experiments. ΔP_1values of basalt at 100 and 700 rpm, which corresponding to Itokawa and Moon [4], are ~0.1 %and ~1 %, respectively (Exp-4). If we consider the size of Itokawa and Moon particle (~100 μm), ΔP_1on Itokawa and Moon should be ~0.01%and ~0.1%, respectively(Exp-2). These values are larger than those estimated from the previous experiments [4] by the order of about 1.

©2019. Japan Geoscience Union. All Right Reserved.

The present results suggest that abrasion is possible on the Moon and may occur on Itokawa as well.

[1] Tsuchiyama et al. 2011. Science, 333, 1125-1128.

[2] Sakurama et al. 2016. JpGU, Abstract, PPS03-13.

[3] Connolly et al. 2015. Earth Planet and Space, 67: 12.

[4] Tsuchiyama et al. 2018. LPSC, Abstract 1844.

[5] Yasui et al. 2015. Icarus, 260: 320-331.

©2019. Japan Geoscience Union. All Right Reserved.

Measurements of adhesive force of meteorite powders using centrifugal method

*Yuuya Nagaashi[1], Akiko Nakamura[1]

1. Kobe University

Introduction: Layer of fine particles in the laboratory shows fluffy structure owing to interparticle force (e.g., Kiuchi and Nakamura, 2014). On small bodies, interparticle forces are thought to be dominant compared to gravitational force for small particles. Fast rotators spin in excess of what gravity alone could hold together were shown to be explained by cohesive force between constituent particles (Sánchez & Scheeres, 2016). Measurements of cohesive force between micron-size spherical silica particles using an atomic force microscope cantilever (Heim et al., 1999) showed that the results agree with predictions of the JKR model (Johnson et al., 1971). On the other hand, measurements of cohesive force between 50 or 100 μm glass beads and a glass plate using centrifugal method showed that the results are by several orders of magnitude smaller than predictions of the JKR theory (Nagaashi et al., 2018). In addition, it was also shown that ~ 70 μm irregularly-shaped silica and alumina grains have the range of adhesive force similar to the glass beads, indicating that the adhesive force of the spherical and the irregular particles used in the measurement is dependent not on the macroscopic shape but on the microscopic surface roughness. However, it is not clear whether the adhesive force of the particles that actually form the asteroids is similar to those of silica grains. Measurements of adhesive force of meteorite powders will bring important knowledge of adhesive force of the asteroid-forming particles for understanding physical processes occurring on asteroids.

Experimental method: In this study, we used centrifugal method as in our previous study (Nagaashi et al., 2018) in order to measure cohesive or adhesive force between a particle and a plate. This method can directly measure the cohesive or adhesive force of many particles at the same time, which enables us to statistically analyze the results. Additionally, it can also deal with irregularly shaped particles. The measurements were conducted for carbonaceous chondrite (CV3: Allende, CM2: Murchison), ordinary chondrite (LL3.5: NWA 539, LL5: NWA 1794, LL6: NWA 542), and Eucrite (Millbillillie) powders of median diameter ~ 50 μm. We discretely increased the centrifugal acceleration from 10g to 5000g (g: the Earth's gravitational acceleration) and took optical microscope images of the same location of the plate before and after applying centrifugal force at each centrifugal acceleration. We determined the range of centrifugal acceleration within which the particle separated from the plate based on the microscope images and estimated the cohesive or adhesive force between the particle and the plate. More detail description of the procedure is described in Nagaashi et al. (2018).

Results: As compared with the JKR adhesion force $F_{ad} = 3\pi\gamma R$ (γ: surface energy, R: reduced radius of particle) for a spherical particle of silica composition, we calculated the effective surface energy of particles which reproduces the measurement value, and compared the results of each type of meteorite powders. Similar to the previous results described in the above (Nagaashi et al., 2018), the measurements of meteorite powders showed a wide range of adhesive force distributions over several orders of magnitude for all measured meteorite types. In addition, we found that the effective surface energy of Allende and Murchison meteorite particles were several times smaller than those for the particles of the other meteorite types. There is no difference in the axial ratio of each type of meteorite powders, and therefore this is likely due to differences in material composition or micro-topography of the particles.

©2019. Japan Geoscience Union. All Right Reserved.

©2019. Japan Geoscience Union. All Right Reserved.

Laboratory impact penetration experiments conducted at simulated reduced gravity

*Akiko Nakamura[1], Kana Morizono[2], Yuuya Nagaashi[1]

1. Graduate School of Science, Kobe University, 2. Faculty of Science, Kobe University

Small bodies are covered with a layer of regolith made up of particles of various sizes. It is important to understand the interactions that occur with surface regolith when a spacecraft lands on or when a block secondarily collide with the regolith layer at low velocity. Penetration depth of an impactor in granular layer was investigated under Earth’ s gravity and an empirical relationship between the drop height and penetration depth was shown to reproduce the experimental results for various granular materials (Uehara et al., 2013). Deceleration of spherical impactor in granular layer was experimentally and theoretically investigated and deceleration formulae were proposed (Katsuragi and Durian 2007, Nakamura et al., 2013; Katsuragi and Durian 2013). On the other hand, interactions of spheres with simulated regolith have been studied at reduced gravity and micro-gravity conditions (Murdoch et al., 2016; Brisset et al., 2018). However, more data of penetration depth of impactor are required to establish quantitative understanding of the penetration process in regolith under low gravity.

We conducted laboratory low-velocity impact experiments of a sphere into granular layer at reduced gravity. Impactor was a glass sphere with a diameter of 16.7 mm and granular layer consisted of glass beads with a diameter of 1 mm. The glass beads were packed in a bucket having a diameter of 15 cm and a depth of 15 cm. The bucket was hung with three constant load springs. The bucket was fixed with two electromagnets, and when the electromagnet was switched off, it dropped vertically downward with the gravity reduced. The simulated reduced gravity level was monitored by an accelerometer placed in a bucket and found to be on average 0.26 G. A plastic straw with horizontal line drawing was glued to the glass sphere. The glass sphere collided with the glass bead layer at a relative velocity between 2 and 4 ms $^{-1}$. The penetration process of the glass sphere with the straw was imaged at 240 fps by a camera attached to the bucket. The final depth of the glass sphere was found to be systematically deeper than the depth found in the experiment conducted at 1 G.

Keywords: regolith, low gravity, impact

©2019. Japan Geoscience Union. All Right Reserved.

MARAUDERS: Using instrumented nano-impactors to probe the icy properties of Lunar permanently shadowed regions

*Ronald Ballouz[1], Sarah T Crites[2], Naoya Ozaki[2], Shun Arahata[3], Nicola Baresi[2], Ralf Bolden, Onur Celik[4,2], Yu Himeno[3], Lucie Riu[2], Kevin J Walsh[5]

1. Lunar and Planetary Lab, University of Arizona, Tucson, AZ, USA, 2. Institute of Space and Astronautical Science, Sagamihara, Japan, 3. University of Tokyo, Tokyo, Japan, 4. Sokendai Graduate University, Japan, 5. Southwest Research Institute, Boulder, CO, USA

The Mini lAndeRs And boUncers Deployed for Exploration and Regolith Science (MARAUDERS) is a small satellite concept that aims to characterize the surface and volatile properties of regolith in permanently shadowed regions (PSRs) around the Moon’s poles. Large PSRs are cold enough to trap scientifically and economically valuable volatiles such as water ice. However, despite ongoing studies, the distribution, abundance, and physical phase of volatiles at the Moon’s poles remains elusive [1]. *In-situ* measurements are required to conclusively determine the geotechnical and physical properties of lunar polar volatiles. To address these needs, the MARAUDERS team is currently developing a technique using instrumented nano-impactors to determine the mechanical properties of regolith at the impact point.

Small spacecraft equipped with penetrators or inertial measurement units (IMU) can characterize the strength and structure of the planetary surface that they impact. Early space exploration used penetrometers to determine the surface properties of the Moon and Mars before the arrival of astronauts and rovers. In recent decades, spacecraft equipped with IMUs characterized the surface of Titan [1], and determined the sub-surface stratification of ice and rock on the comet 67P/C-G [2]. While this technique is unable to relay the detailed mineralogical and elemental composition at the impact point, it obtains a first-order structural knowledge of potentially hazardous surfaces and sub-surfaces that cannot be obtained through remote sensing. This is highly relevant for PSRs due to extreme environmental conditions such as the lack of solar illumination, cold temperatures, and challenging communications.

Here, we present preliminary analysis on the instrument capabilities based on the potential deployment scenarios to PSRs, and the possible mechanical properties of the regolith found within these regions (Fig. 1). We present a computational study of the varying response of an instrumented impactor impacting regolith with variable i) water ice content (0-10%), ii) impactor speeds (50-250 m/s], and iii) impact angles (45-90˚), using a discrete element method code [4]. Furthermore, we analyse the ejecta properties and resulting crater morphology in order to gain a better understanding of impact processes on icy bodies. Our next steps will be to conduct laboratory impact experiments using prototypes of our instrumented impactors to calibrate the impact response on lunar simulant with variable water-ice content.

References:

1. Lorenz, R. et al. (1994) Meas. Sci. Technol. 5, 1033-1041

2. Biele, J. et al. (2016), Science, 349, 6247.

3. Holsapple, K.A. (1994) LPSC 25, 559.

©2019. Japan Geoscience Union. All Right Reserved.

4. Richardson, D.C. et al. (2011) Icarus, 212, 427–437.

Acknowledgements:

This material is based upon work supported by ISAS/JAXA’s start-up fund for international collaborations, the Aerospace Project Research Associate Program, and the International Top Young Fellow Program.

Keywords: Moon, Permanently Shadowed Regions, Volatiles, Regolith Characterization

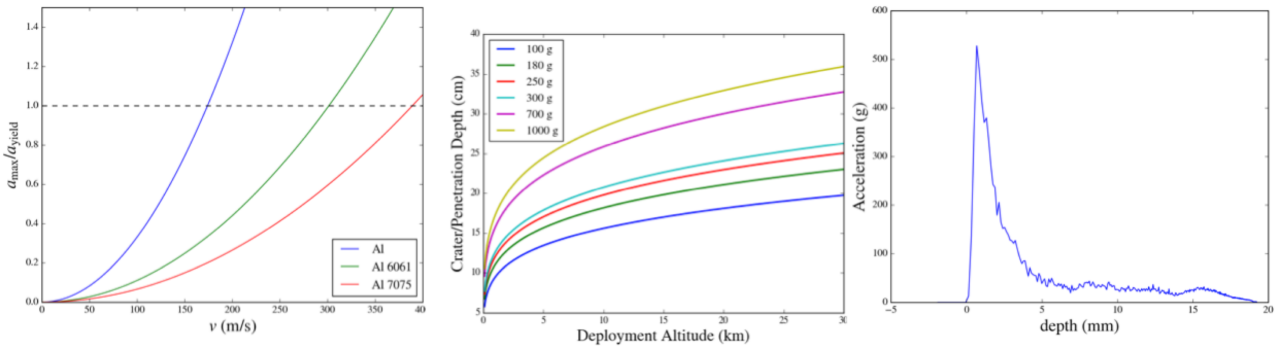


Fig. 1. Preliminary analysis showing shock tolerance, penetration depth, and instrument response for different instrument designs and impact speeds. Left: Maximum shock tolerance before material failure for three different aluminum alloy instrument housings. An Al-7075 housing can withstand impact speeds greater than 350 m/s. Middle: Penetrations depths for a 250 m/s impact for different impactor masses (100 - 1000 grams). For a nominal impactor mass of 180 g, a deployment from 15 km from the lunar surface results in a penetration depth of < 20 cm (based on [3]). Right: Simulated response of a 180 g impactor using a particle dynamics simulation.

©2019. Japan Geoscience Union. All Right Reserved.

Surface size-frequency distribution of accumulating boulders using discrete element simulations of spherical particles in 3D

*Hiroshi Kikuchi[1], Hideaki Miyamoto[1]

1. The University of Tokyo

Several spacecraft have revealed new detail about small bodies such as asteroids, comets, and small satellites. Images from Hayabusa, Hayabusa2, and OSIRIS-REx showed more boulders on the surfaces than originally expected. Owing to the high resolution at which images were taken, a number of boulders could often be observed in clusters. In future explorations, because we expect to observe more cases of boulder-rich surfaces, the characterization of the size-frequency distribution (SFD) will be important especially for the missions involving a lander such as MMX. Basically, measuring the SFD of boulders on a surface is expected to represent that of the interior. However, considering that surface boulders can hide the underlying boulder, it is not clear that the SFD in a volume can adequately be represented by its surface. Therefore, in this work, we focus on how accumulating boulders with a known SFD appear from above.
In order to compare the SFD on a surface with that of a volume, the initial SFD has to be known. For the initial study, numerical simulations are convenient, because they can easily prepare the suitable conditions. In the previous studies, spherical boulders were randomly distributed in three-dimensional space, and only those on the surface were automatically extracted and measured (Tancredi et al., 2015). It was found that the particle distribution on the surface well reproduces the overall particle distribution. We consider that there is room for improvement in the arrangement of particles and the measurement of particles. Thus, we implement a three-dimensional discrete element method using rigid spherical particles to simulate the accumulation of a boulder-rich regolith. We then measure particles one by one manually when viewed from above the surface. For initial conditions, we set the size and the number of boulders randomly as specified by the power law index of -3. During a simulation, particles are not initially adjacent to each other and are instead dropped from the height of 30 m above the 54 x 54 m planar surface. The total number of particles is changed from 3000 to 7000 in 1000 increments. After the simulation, the size and number of the particles are measured manually when viewing the surface from the vertical direction. Then we refer to Clauset et al. (2009) for fitting and evaluating the data using the p-value metric.
We find that the power law index of the SFD is low when the number of particles is 3000. This may be because the larger particles are not buried in the smaller particles, resulting in only the number of smaller particles being reduced when viewed from above. When the total number is 4000 or more in a volume and p-value is high, the surface power law index from the multiple simulations is consistent with the specified value of -3 for some cases.
The SFD observed on the surface corresponds to the SFD in the interior of the body for the following conditions: the thickness of the deposited particles is larger than the largest particle and the p-value is high. For more detailed analyses, investigating the effects of the number of simulations, the complicated shapes of boulders, and parameter studies are needed. In addition, for a deeper understanding of the problem, experiments in a similar condition to the airless bodies using simulated regolith particles such as UTPS-TB and UTPS-IB (Miyamoto et al., 2018) are also required.

Keywords: Discrete element method, Boulder size-frequency distribution, Interior of small bodies

©2019. Japan Geoscience Union. All Right Reserved.

Experimental Study to Determine the Best Compression Ratio of High-Resolution Images of Small Bodies for the Martian Moons eXploration (MMX) Mission

*Yuta Shimizu[1], Hiroaki Kamiyoshihara[1], Takafumi Niihara[1], Hideaki Miyamoto[1]

1. University of Tokyo

Data transmission rate becomes one of the biggest limiting factors in space explorations; technological advance in increasing pixel numbers of camera images dominates the improvement of the data transmission rate. Yet, high demand exists for high-resolution images especially in geological studies, and thus there is a tradeoff between the spatial resolutions (or pixel numbers) and the number of images to be transmitted to Earth. The telecommunications issue is critical for Martian Moons eXploration (MMX) mission that explore either/both Phobos and Deimos and return samples. Especially, timely transmission of high-resolution images is required for the selection of sampling site both in terms of scientific impacts and of the landing safety. The highest image resolution of the current camera configuration is as good as several tens of centimeters per pixel and the size of image is 3296 x 2472 pixels, which means 7 color (3 bands) images can be up to 1 GB if no compression is considered. During the landing phase, such large data have to be sent at the limited bitrate (< 32 kbps) to select landing and sampling sites, while the landing duration is about 4 hours. Thus, considering the best compression scheme of images is a big issue for landing operation. Lossy compression can significantly reduce the sizes of images, though images can be scientifically worthless when compressed too much. The best compression ratio should make the sizes of images as small as possible without losing scientific importance.

Here, we develop a method of rapidly determining the best compression ratio of high-resolution images of the surface of small bodies. For preparing the image studied in this research, we take an experimental scheme, where we develop a simulated Phobos surface by using a high-quality simulant of Phobos regolith (UTPS-TB) and take simulated images of the surface of Phobos in somehow similar condition with the camera of the MMX mission. The images are compressed by JPEG2000, which is planned to be used in MMX mission, and the influence of the compression is analyzed by objective methods such as Structural SIMilarity (SSIM) and entropy of image. The results shows that they are able to rapidly detect the exact ratio, in which the quality of the images started to be diminished.

Moreover, by defining scientific value of images as detectability of rock gravel on the surface of celestial bodies and showing that the loss of scientific value can be expressed by the change in the value of slope of Cumulative Size-Frequency Distribution (CSFD) of gravel, we carefully confirm whether the decrease in the image quality is truly connected with the loss of scientific information such as for landing operations and conclude that those objective methods can determine the best compression ratio. By using those methods, the spacecraft can autonomously complete the process of finding the best compression ratio, compressing images and sending it to the ground within a few minutes even if it has only a limited transmission rate.

Keywords: the best compression ratio, Cumulative Size-Frequency Distribution (CSFD), Martian Moons eXploration (MMX)

©2019. Japan Geoscience Union. All Right Reserved.

[E] Poster | P (Space and Planetary Sciences)：P-PS Planetary Sciences

Wed. May 29, 2019 5:15 PM - 6:30 PM JST | Wed. May 29, 2019 8:15 AM - 9:30 AM UTC | Poster Hall International Exhibition Hall8, Makuhari Messe_2

[P-PS02] Regolith Science

convener:Koji Wada(Planetary Exploration Research Center, Chiba Institute of Technology), Akiko Nakamura(Graduate School of Science, Kobe University), Patrick Michel(Observatoire De La Cote D'Azur), Kevin John Walsh(Southwest Research Institute Boulder)

Recent planetary explorations have revealed that almost all solid bodies in the solar system are covered with small particles, called regolith. The surface geology, especially regolith behavior on the surfaces of solid bodies, becomes increasingly more important as represented by Hayabusa mission and other on-going and planned sample-return missions such as Hayabusa2, OSIRIS-REx, and MMX.

For fully understanding the regolith science, it is required to know and compare the regolith conditions on various celestial bodies, from asteroids to planets, with various methods.

Therefore, this session welcomes broad topics related to regolith on various celestial bodies, such as asteroids, comets, the Moon, the martian moons, Mars, etc. Papers on the formation, evolution, and alteration processes of regolith particles and regolith systems on the surface of planetary bodies, remote and in-situ observational results and techniques, analyses and results of returned samples, and laboratory, numerical, and theoretical studies on the fundamental physical and chemical processes are all welcome.

Note that what we call regolith is not just fine grains: all kinds of materials (more or less loose) that lie on the surface, from cobbles to finer grains, are our targets.

[PPS02-P01] Abrasion experiments of mineral and meteorite grains: Dependence of particle size and vibration rate on abrasion rate and its application to Itokawa and lunar regolith particles.

*Hirotaka Yamaguchi[1], Akira Tsuchiyama[1], Akiko Nakamura[2] (1.National University Corporation, Kyoto University, 2.National University Corporation,Kobe University)

[PPS02-P02] Measurements of adhesive force of meteorite powders using centrifugal method

*Yuuya Nagaashi[1], Akiko Nakamura[1] (1.Kobe University)

[PPS02-P03] Laboratory impact penetration experiments conducted at simulated reduced gravity

*Akiko Nakamura[1], Kana Morizono[2], Yuuya Nagaashi[1] (1.Graduate School of Science, Kobe University, 2.Faculty of Science, Kobe University)

[PPS02-P04] MARAUDERS: Using instrumented nano-impactors to probe the icy properties of Lunar permanently shadowed regions

*Ronald Ballouz[1], Sarah T Crites[2], Naoya Ozaki[2], Shun Arahata[3], Nicola Baresi[2], Ralf Bolden, Onur Celik[4,2], Yu Himeno[3], Lucie Riu[2], Kevin J Walsh[5] (1.Lunar and Planetary Lab, University of Arizona, Tucson, AZ, USA, 2.Institute of Space and Astronautical Science, Sagamihara, Japan, 3.University of Tokyo, Tokyo, Japan, 4.Sokendai Graduate University, Japan, 5.Southwest Research Institute, Boulder, CO, USA)

[PPS02-P05] Surface size-frequency distribution of accumulating boulders using discrete element simulations of spherical particles in 3D

*Hiroshi Kikuchi[1], Hideaki Miyamoto[1] (1.The University of Tokyo)

[PPS02-P06] Experimental Study to Determine the Best Compression Ratio of High-Resolution Images of Small Bodies for the Martian Moons eXploration (MMX) Mission

*Yuta Shimizu[1], Hiroaki Kamiyoshihara[1], Takafumi Niihara[1], Hideaki Miyamoto[1] (1.University of Tokyo)

Abrasion experiments of mineral and meteorite grains: Dependence of particle size and vibration rate on abrasion rate and its application to Itokawa and lunar regolith particles.

*Hirotaka Yamaguchi[1], Akira Tsuchiyama[1], Akiko Nakamura[2]

1. National University Corporation, Kyoto University, 2. National University Corporation,Kobe University

Rounded edges were found in some regolith particles collected from asteroid Itokawa [1] and Moon [2]. These particles should be formed by mechanical abrasion [1]. Seismic-induced grain motion by micrometeoroid impacts [1] and YORP effect [3] were proposed for the abrasion process on Itokawa. However, it is not clear how these processes actually work on the surfaces of the airless celestial bodies.

In order to understand detailed process of the abrasion, our research group have carried out abrasion experiments using mineral, rock and meteorite grains (grain size: 1-2 mm) [4]. Samples used were quartz, olivine, corundum, marble, L5 chondrite meteorite (Sayh al Uhaymir 001) and CM chondrite meteorite (Murchison). These particles were put into a vessel of 10 mL with the filling ratio of ~50 % and the sample was vibrated with the rate from 1000 to 3000 rpm using a multi-beads-shocker (YASUIKIKAI Co.). The proportion of powder (<250 μm) produced by vibration at first 1 min., ΔP_1, was adopted as the measure of abrasion and its dependence of the vibration rate and the sample strength was examined. However, the particle size used in the experiments (1-2 mm) is larger than Itokawa particles (< a few hundred μm). In addition, the vibration rates used in the experiments are larger than those estimated for Itokawa(~100 rpm) and Moon (~700 rpm) by considering the maximum seismic acceleration due to micrometeoroidimpacts onto their surface [5]. In the present study, therefore, we conducted new experiments with different parameters such as particle size and vibration rate using the same experimental procedure as [4]. In the present experiments, we used quartz grains for examining the effect of packing ratio in the vessel (Exp-1), particle size (Exp-2), mixing ratio of large and small particles (Exp-3). The effect of lower vibration rate (100 - 1000 rpm) was examined using olivine and basalt as well as quartz (Exp-4). Experiments using basalt at higher vibration rates were also made.

We obtained following results. Exp-1: $\Delta P_1$was constant in a wide range of the filling rate except for the filling rate of 2/3, where ΔP_1showed a peak value. Exp-2: $\Delta P_1$is proportional to the particle size. Exp-3: When the proportion of large particles is larger than 25%, $\Delta P_1$is almost constant and the same as $\Delta P_1$for the large particles. Exp-4: In the previous experiments, ΔP_1increases with the vibration rate with the power of 1.1-2.9 for large vibration rates (>~1000 rpm) [4] while the power becomes smaller (0.67-0.77) for smaller vibration rates (<~1000 rpm). This result shows that the abrasion mode changed at ~1000 rpm. In order to understand abrasion modes, SEM observation of powder particles produced in the abrasion experiments were also made. It was found that chipping of particle edges occurred at low vibration rate (~100 rpm) and the proportion of gradual wearing on the whole particle surface gradually increased as the vibration rate increased.

We estimated the amount of abrasion of Itokawa and lunar regolith particles in a regolith layer by impact based on the present experiments. ΔP_1values of basalt at 100 and 700 rpm, which corresponding to Itokawa and Moon [4], are ~0.1 %and ~1 %, respectively (Exp-4). If we consider the size of Itokawa and Moon particle (~100 μm), ΔP_1on Itokawa and Moon should be ~0.01%and ~0.1%, respectively(Exp-2). These values are larger than those estimated from the previous experiments [4] by the order of about 1.

©2019. Japan Geoscience Union. All Right Reserved.

The present results suggest that abrasion is possible on the Moon and may occur on Itokawa as well.

[1] Tsuchiyama et al. 2011. Science, 333, 1125-1128.

[2] Sakurama et al. 2016. JpGU, Abstract, PPS03-13.

[3] Connolly et al. 2015. Earth Planet and Space, 67: 12.

[4] Tsuchiyama et al. 2018. LPSC, Abstract 1844.

[5] Yasui et al. 2015. Icarus, 260: 320-331.

©2019. Japan Geoscience Union. All Right Reserved.

Measurements of adhesive force of meteorite powders using centrifugal method

*Yuuya Nagaashi[1], Akiko Nakamura[1]

1. Kobe University

Introduction: Layer of fine particles in the laboratory shows fluffy structure owing to interparticle force (e.g., Kiuchi and Nakamura, 2014). On small bodies, interparticle forces are thought to be dominant compared to gravitational force for small particles. Fast rotators spin in excess of what gravity alone could hold together were shown to be explained by cohesive force between constituent particles (Sánchez & Scheeres, 2016). Measurements of cohesive force between micron-size spherical silica particles using an atomic force microscope cantilever (Heim et al., 1999) showed that the results agree with predictions of the JKR model (Johnson et al., 1971). On the other hand, measurements of cohesive force between 50 or 100 μm glass beads and a glass plate using centrifugal method showed that the results are by several orders of magnitude smaller than predictions of the JKR theory (Nagaashi et al., 2018). In addition, it was also shown that ~ 70 μm irregularly-shaped silica and alumina grains have the range of adhesive force similar to the glass beads, indicating that the adhesive force of the spherical and the irregular particles used in the measurement is dependent not on the macroscopic shape but on the microscopic surface roughness. However, it is not clear whether the adhesive force of the particles that actually form the asteroids is similar to those of silica grains. Measurements of adhesive force of meteorite powders will bring important knowledge of adhesive force of the asteroid-forming particles for understanding physical processes occurring on asteroids.

Experimental method: In this study, we used centrifugal method as in our previous study (Nagaashi et al., 2018) in order to measure cohesive or adhesive force between a particle and a plate. This method can directly measure the cohesive or adhesive force of many particles at the same time, which enables us to statistically analyze the results. Additionally, it can also deal with irregularly shaped particles. The measurements were conducted for carbonaceous chondrite (CV3: Allende, CM2: Murchison), ordinary chondrite (LL3.5: NWA 539, LL5: NWA 1794, LL6: NWA 542), and Eucrite (Millbillillie) powders of median diameter ~ 50 μm. We discretely increased the centrifugal acceleration from 10g to 5000g (g: the Earth's gravitational acceleration) and took optical microscope images of the same location of the plate before and after applying centrifugal force at each centrifugal acceleration. We determined the range of centrifugal acceleration within which the particle separated from the plate based on the microscope images and estimated the cohesive or adhesive force between the particle and the plate. More detail description of the procedure is described in Nagaashi et al. (2018).

Results: As compared with the JKR adhesion force $F_{ad} = 3\pi\gamma R$ (γ: surface energy, R: reduced radius of particle) for a spherical particle of silica composition, we calculated the effective surface energy of particles which reproduces the measurement value, and compared the results of each type of meteorite powders. Similar to the previous results described in the above (Nagaashi et al., 2018), the measurements of meteorite powders showed a wide range of adhesive force distributions over several orders of magnitude for all measured meteorite types. In addition, we found that the effective surface energy of Allende and Murchison meteorite particles were several times smaller than those for the particles of the other meteorite types. There is no difference in the axial ratio of each type of meteorite powders, and therefore this is likely due to differences in material composition or micro-topography of the particles.

©2019. Japan Geoscience Union. All Right Reserved.

©2019. Japan Geoscience Union. All Right Reserved.

Laboratory impact penetration experiments conducted at simulated reduced gravity

*Akiko Nakamura[1], Kana Morizono[2], Yuuya Nagaashi[1]

1. Graduate School of Science, Kobe University, 2. Faculty of Science, Kobe University

Small bodies are covered with a layer of regolith made up of particles of various sizes. It is important to understand the interactions that occur with surface regolith when a spacecraft lands on or when a block secondarily collide with the regolith layer at low velocity. Penetration depth of an impactor in granular layer was investigated under Earth’ s gravity and an empirical relationship between the drop height and penetration depth was shown to reproduce the experimental results for various granular materials (Uehara et al., 2013). Deceleration of spherical impactor in granular layer was experimentally and theoretically investigated and deceleration formulae were proposed (Katsuragi and Durian 2007, Nakamura et al., 2013; Katsuragi and Durian 2013). On the other hand, interactions of spheres with simulated regolith have been studied at reduced gravity and micro-gravity conditions (Murdoch et al., 2016; Brisset et al., 2018). However, more data of penetration depth of impactor are required to establish quantitative understanding of the penetration process in regolith under low gravity.

We conducted laboratory low-velocity impact experiments of a sphere into granular layer at reduced gravity. Impactor was a glass sphere with a diameter of 16.7 mm and granular layer consisted of glass beads with a diameter of 1 mm. The glass beads were packed in a bucket having a diameter of 15 cm and a depth of 15 cm. The bucket was hung with three constant load springs. The bucket was fixed with two electromagnets, and when the electromagnet was switched off, it dropped vertically downward with the gravity reduced. The simulated reduced gravity level was monitored by an accelerometer placed in a bucket and found to be on average 0.26 G. A plastic straw with horizontal line drawing was glued to the glass sphere. The glass sphere collided with the glass bead layer at a relative velocity between 2 and 4 ms $^{-1}$. The penetration process of the glass sphere with the straw was imaged at 240 fps by a camera attached to the bucket. The final depth of the glass sphere was found to be systematically deeper than the depth found in the experiment conducted at 1 G.

Keywords: regolith, low gravity, impact

©2019. Japan Geoscience Union. All Right Reserved.

MARAUDERS: Using instrumented nano-impactors to probe the icy properties of Lunar permanently shadowed regions

*Ronald Ballouz[1], Sarah T Crites[2], Naoya Ozaki[2], Shun Arahata[3], Nicola Baresi[2], Ralf Bolden, Onur Celik[4,2], Yu Himeno[3], Lucie Riu[2], Kevin J Walsh[5]

1. Lunar and Planetary Lab, University of Arizona, Tucson, AZ, USA, 2. Institute of Space and Astronautical Science, Sagamihara, Japan, 3. University of Tokyo, Tokyo, Japan, 4. Sokendai Graduate University, Japan, 5. Southwest Research Institute, Boulder, CO, USA

The Mini lAndeRs And boUncers Deployed for Exploration and Regolith Science (MARAUDERS) is a small satellite concept that aims to characterize the surface and volatile properties of regolith in permanently shadowed regions (PSRs) around the Moon’s poles. Large PSRs are cold enough to trap scientifically and economically valuable volatiles such as water ice. However, despite ongoing studies, the distribution, abundance, and physical phase of volatiles at the Moon’s poles remains elusive [1]. *In-situ* measurements are required to conclusively determine the geotechnical and physical properties of lunar polar volatiles. To address these needs, the MARAUDERS team is currently developing a technique using instrumented nano-impactors to determine the mechanical properties of regolith at the impact point.

Small spacecraft equipped with penetrators or inertial measurement units (IMU) can characterize the strength and structure of the planetary surface that they impact. Early space exploration used penetrometers to determine the surface properties of the Moon and Mars before the arrival of astronauts and rovers. In recent decades, spacecraft equipped with IMUs characterized the surface of Titan [1], and determined the sub-surface stratification of ice and rock on the comet 67P/C-G [2]. While this technique is unable to relay the detailed mineralogical and elemental composition at the impact point, it obtains a first-order structural knowledge of potentially hazardous surfaces and sub-surfaces that cannot be obtained through remote sensing. This is highly relevant for PSRs due to extreme environmental conditions such as the lack of solar illumination, cold temperatures, and challenging communications.

Here, we present preliminary analysis on the instrument capabilities based on the potential deployment scenarios to PSRs, and the possible mechanical properties of the regolith found within these regions (Fig. 1). We present a computational study of the varying response of an instrumented impactor impacting regolith with variable i) water ice content (0-10%), ii) impactor speeds (50-250 m/s], and iii) impact angles (45-90˚), using a discrete element method code [4]. Furthermore, we analyse the ejecta properties and resulting crater morphology in order to gain a better understanding of impact processes on icy bodies. Our next steps will be to conduct laboratory impact experiments using prototypes of our instrumented impactors to calibrate the impact response on lunar simulant with variable water-ice content.

References:

1. Lorenz, R. et al. (1994) Meas. Sci. Technol. 5, 1033-1041

2. Biele, J. et al. (2016), Science, 349, 6247.

3. Holsapple, K.A. (1994) LPSC 25, 559.

©2019. Japan Geoscience Union. All Right Reserved.

4. Richardson, D.C. et al. (2011) Icarus, 212, 427–437.

Acknowledgements:

This material is based upon work supported by ISAS/JAXA’s start-up fund for international collaborations, the Aerospace Project Research Associate Program, and the International Top Young Fellow Program.

Keywords: Moon, Permanently Shadowed Regions, Volatiles, Regolith Characterization

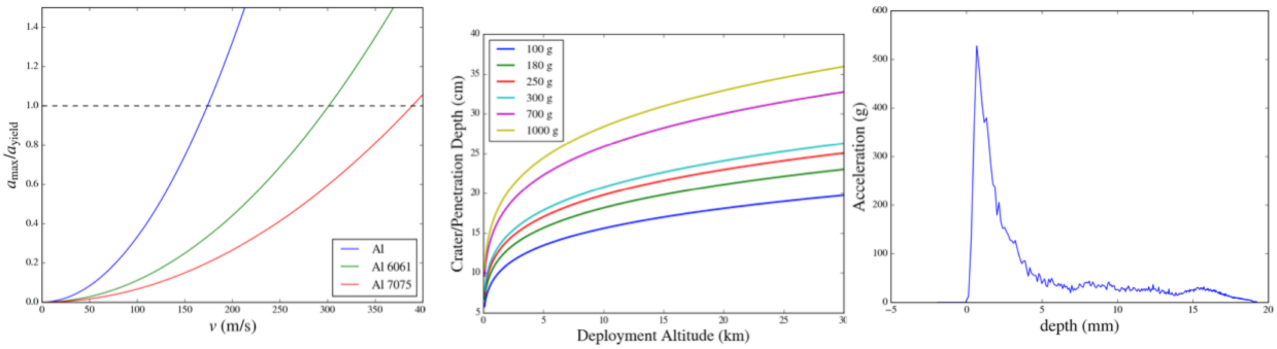


Fig. 1. Preliminary analysis showing shock tolerance, penetration depth, and instrument response for different instrument designs and impact speeds. Left: Maximum shock tolerance before material failure for three different aluminum alloy instrument housings. An Al-7075 housing can withstand impact speeds greater than 350 m/s. Middle: Penetrations depths for a 250 m/s impact for different impactor masses (100 - 1000 grams). For a nominal impactor mass of 180 g, a deployment from 15 km from the lunar surface results in a penetration depth of < 20 cm (based on [3]). Right: Simulated response of a 180 g impactor using a particle dynamics simulation.

©2019. Japan Geoscience Union. All Right Reserved.

Surface size-frequency distribution of accumulating boulders using discrete element simulations of spherical particles in 3D

*Hiroshi Kikuchi[1], Hideaki Miyamoto[1]

1. The University of Tokyo

Several spacecraft have revealed new detail about small bodies such as asteroids, comets, and small satellites. Images from Hayabusa, Hayabusa2, and OSIRIS-REx showed more boulders on the surfaces than originally expected. Owing to the high resolution at which images were taken, a number of boulders could often be observed in clusters. In future explorations, because we expect to observe more cases of boulder-rich surfaces, the characterization of the size-frequency distribution (SFD) will be important especially for the missions involving a lander such as MMX. Basically, measuring the SFD of boulders on a surface is expected to represent that of the interior. However, considering that surface boulders can hide the underlying boulder, it is not clear that the SFD in a volume can adequately be represented by its surface. Therefore, in this work, we focus on how accumulating boulders with a known SFD appear from above.
In order to compare the SFD on a surface with that of a volume, the initial SFD has to be known. For the initial study, numerical simulations are convenient, because they can easily prepare the suitable conditions. In the previous studies, spherical boulders were randomly distributed in three-dimensional space, and only those on the surface were automatically extracted and measured (Tancredi et al., 2015). It was found that the particle distribution on the surface well reproduces the overall particle distribution. We consider that there is room for improvement in the arrangement of particles and the measurement of particles. Thus, we implement a three-dimensional discrete element method using rigid spherical particles to simulate the accumulation of a boulder-rich regolith. We then measure particles one by one manually when viewed from above the surface. For initial conditions, we set the size and the number of boulders randomly as specified by the power law index of -3. During a simulation, particles are not initially adjacent to each other and are instead dropped from the height of 30 m above the 54 x 54 m planar surface. The total number of particles is changed from 3000 to 7000 in 1000 increments. After the simulation, the size and number of the particles are measured manually when viewing the surface from the vertical direction. Then we refer to Clauset et al. (2009) for fitting and evaluating the data using the p-value metric.
We find that the power law index of the SFD is low when the number of particles is 3000. This may be because the larger particles are not buried in the smaller particles, resulting in only the number of smaller particles being reduced when viewed from above. When the total number is 4000 or more in a volume and p-value is high, the surface power law index from the multiple simulations is consistent with the specified value of -3 for some cases.
The SFD observed on the surface corresponds to the SFD in the interior of the body for the following conditions: the thickness of the deposited particles is larger than the largest particle and the p-value is high. For more detailed analyses, investigating the effects of the number of simulations, the complicated shapes of boulders, and parameter studies are needed. In addition, for a deeper understanding of the problem, experiments in a similar condition to the airless bodies using simulated regolith particles such as UTPS-TB and UTPS-IB (Miyamoto et al., 2018) are also required.

Keywords: Discrete element method, Boulder size-frequency distribution, Interior of small bodies

©2019. Japan Geoscience Union. All Right Reserved.

Experimental Study to Determine the Best Compression Ratio of High-Resolution Images of Small Bodies for the Martian Moons eXploration (MMX) Mission

*Yuta Shimizu[1], Hiroaki Kamiyoshihara[1], Takafumi Niihara[1], Hideaki Miyamoto[1]

1. University of Tokyo

Data transmission rate becomes one of the biggest limiting factors in space explorations; technological advance in increasing pixel numbers of camera images dominates the improvement of the data transmission rate. Yet, high demand exists for high-resolution images especially in geological studies, and thus there is a tradeoff between the spatial resolutions (or pixel numbers) and the number of images to be transmitted to Earth. The telecommunications issue is critical for Martian Moons eXploration (MMX) mission that explore either/both Phobos and Deimos and return samples. Especially, timely transmission of high-resolution images is required for the selection of sampling site both in terms of scientific impacts and of the landing safety. The highest image resolution of the current camera configuration is as good as several tens of centimeters per pixel and the size of image is 3296 x 2472 pixels, which means 7 color (3 bands) images can be up to 1 GB if no compression is considered. During the landing phase, such large data have to be sent at the limited bitrate (< 32 kbps) to select landing and sampling sites, while the landing duration is about 4 hours. Thus, considering the best compression scheme of images is a big issue for landing operation. Lossy compression can significantly reduce the sizes of images, though images can be scientifically worthless when compressed too much. The best compression ratio should make the sizes of images as small as possible without losing scientific importance.

Here, we develop a method of rapidly determining the best compression ratio of high-resolution images of the surface of small bodies. For preparing the image studied in this research, we take an experimental scheme, where we develop a simulated Phobos surface by using a high-quality simulant of Phobos regolith (UTPS-TB) and take simulated images of the surface of Phobos in somehow similar condition with the camera of the MMX mission. The images are compressed by JPEG2000, which is planned to be used in MMX mission, and the influence of the compression is analyzed by objective methods such as Structural SIMilarity (SSIM) and entropy of image. The results shows that they are able to rapidly detect the exact ratio, in which the quality of the images started to be diminished.

Moreover, by defining scientific value of images as detectability of rock gravel on the surface of celestial bodies and showing that the loss of scientific value can be expressed by the change in the value of slope of Cumulative Size-Frequency Distribution (CSFD) of gravel, we carefully confirm whether the decrease in the image quality is truly connected with the loss of scientific information such as for landing operations and conclude that those objective methods can determine the best compression ratio. By using those methods, the spacecraft can autonomously complete the process of finding the best compression ratio, compressing images and sending it to the ground within a few minutes even if it has only a limited transmission rate.

Keywords: the best compression ratio, Cumulative Size-Frequency Distribution (CSFD), Martian Moons eXploration (MMX)

©2019. Japan Geoscience Union. All Right Reserved.

[E] Poster | P (Space and Planetary Sciences)：P-PS Planetary Sciences

Wed. May 29, 2019 3:30 PM - 5:00 PM JST | Wed. May 29, 2019 6:30 AM - 8:00 AM UTC | Poster Hall International Exhibition Hall8, Makuhari Messe_1

[P-PS03] Solar System Small Bodies: A New Frontier Arising Hayabusa 2, OSIRIS-REx and Other Projects

convener:Masateru Ishiguro(Department of Physics and Astronomy, Seoul National University), Taishi Nakamoto(Tokyo Institute of Technology), Masanao Abe(Institute of Space and Astronautical Science, Japan Aerospace Exploration Agency), Olivier S Barnouin(Johns Hopkins University Applied Physics Laboratory)

In June 2018, the Hayabusa 2 spacecraft arrived at the target asteroid Ryugu after three and half years journey. In addition, another spacecraft, OSIRIS-REx will soon arrive at its destination Bennu. With these arrivals, the solar system research is about to enter a new era. We have organized this small bodies session since 2012 and had a broad range of discussions from viewpoints of laboratory experiments, observations, space explorations, theoretical modeling, and sample analyses. In particular, this time, we aim to hold this session to bring the latest research on solar system small bodies, focusing on the initial results of Hayabusa 2 and OSIRIS-REx. Presentations in the related fields other than these two asteroidal missions are also welcomed.

[PPS03-P01] Impact experiments on low strength coarse-grained regolith simulating surface materials on asteroid Ryugu

*Yuya Yamamoto[1], Masahiko Arakawa[1], Minami Yasui[1], Sunao Hasegawa[2], Ryo Sugimura[1] (1.Graduate School of Science, Kobe University, 2.ISAS, JAXA)

[PPS03-P02] Reflectance estimation of asteroid Ryugu using MASCOT

*Marika Ishida[1], Koto Amano[1], Keiichi Moroi[1], ERI TATSUMI[2], Tra-Mi Ho[10], Shingo Kameda[1], Seiji Sugita[2], Rie Honda[3], Tomokatsu Morota[4], yokota yasuhiro[5], Toru Kouyama[6], Hidehiko Suzuki[7], Manabu Yamada[8], Naoya Sakatani[5], Chikatoshi Honda[9], Masahiko Hayakawa[5], Kazuo Yoshioka[2], Moe Matsuoka[5], Yuichiro Cho[2], Hirotaka Sawada[5] (1.Rikkyo Univ., 2.Univ. of Tokyo, 3.Kochi Univ., 4.Nagoya Univ., 5.JAXA/ISAS, 6.AIST, 7.Meiji Univ., 8.Chiba Inst. Tech, 9.Univ. of Aizu, 10.DLR)

[PPS03-P03] Flyby observation of Asteroid (3200) Phaethon by DESTINY$^+$ onboard cameras

*Ko Ishibashi[1], Shingo Kameda[2], Masato Kagitani[3], Peng Hong[1], Manabu Yamada[1], Osamu Okudaira[1], Tomoko Arai[1], Fumi Yoshida[1], Shunsuke Sato[4], Takahiro Ishimaru[4], Takaya Okamoto[4], Takahiro Iwata[4], Tatsuaki Okada[4], Takeshi Takashima[4] (1.Chiba Institute of Technology, 2.Rikkyo University, 3.Tohoku Universtiy, 4.Japan Aerospace Exploration Agency)

[PPS03-P04] Polarimetric Study of Asteroids in Comet-Like Orbits (ACOs)

*Jooyeon Geem[1], Masateru Ishiguro[1], Yoonsoo P. Bach[1], Daisuke Kuroda[2], Hiroyuki Naito[3], Hidekazu Hanayama[4], yoonyoung kim[10], Yuna G. Kwon[1], Sunho Jin[1], Tomohiko Sekiguchi[5], Ryo Okazaki[5], Jeremie J. Vaubaillon[6], Masataka Imai[7], Tatsuharu Oono[8], Yuki Futamuts[8], Seiko Takagi[8], Mitsuteru Sato[8], Kiyoshi Kuramoto[8], Makoto Watanabe[9] (1.Astronomy program, Dept of Physics and Astronomy, Seoul National University, 2.Okayama Observatory, Kyoto University, 3.Nayoro Observatory, 4.Ishigakijima Astronomical Observatory, National Astronomical Observatory of Japan, 5.Hokkaido University of Education, 6.Observatoire de Paris, I.M.C.C.E., 7.National Institute of Advanced Industrial Science and Technology, 8.Department of Cosmosciences, Graduate School of Science, Hokkaido University, 9.Department of Applied Physics, Okayama University of Science, 10.Max Planck Institute for Solar System Research)

[PPS03-P05] Dynamical lifetime of the Oort Cloud new comets under planetary perturbation

*Ito Takashi[1], Arika Higuchi[1] (1.National Astronomical Observatory of Japan)

[PPS03-P06] Thermal Infrared Imaging of C-type Asteroid 162173 Ryugu with Porous Surfaces

*Tatsuaki Okada[1,2], Tetsuya Fukuhara[3], Satoshi Tanaka[1], Makoto Taguchi[3], Takehiko Arai[4], Naoya Sakatani[1], Yuri Shimaki[1], Hiroki Senshu[5], Yoshiko Ogawa[6], Hirohide Demura[6], Kentaro Suko[6], Kohei Kitazato[6], Toru Kouyama[7], Tomohiko Sekiguchi[8], Jun Takita[9], Sunao Hasegawa[1], Tsuneo Matsunaga[10], Takehiko Wada[1], Takeshi Imamura[2], Jorn Helbert[11], Thomas G. Mueller[12], Axel Hagermann[13], Jens Biele[11], Matthias Grott[11], Maximiliam Hamm[11], Marco Delbo[14], Yukio Yamamoto[1], Naru Hirata[6], Naoyuki Hirata[15], Fuyuto Terui[1], Takanao Saiki[1], Satoru Nakazawa[1], Makoto Yoshikawa[1], Sei-ichiro WATANABE[1,16], Yuichi Tuda[1] (1.Institute of Space and Astronautical Science, Japan Aerospace Exploration Agency, 2.University of Tokyo, 3.Rikkyo University, 4.Ashikaga University, 5.Chiba Institute of Technology, 6.University of Aizu, 7.National Institute of Advanced Industrial Science and Technology, 8.Hokkaido University of Education, 9.Hokkaido Kitami-Hokuto High School, 10.National Institute for Environmental Studies, 11.German Aerospace Center, 12.Max-Planck Institute for Extraterrestrial Physics, 13.University of Stirling, 14.Observatoire de la Côte d'Azur, 15.Kobe University, 16.Nagoya University)

[PPS03-P07] Data Release of Asteroid 162173 Ryugu by Observation of Thermal Infrared Imager onboard Hayabusa2

*Takehiko Arai[1], Hirohide Demura[2], Toru Kouyama[7], Naoya Sakatani[3], Kentaro Suko[2], Yuri Shimaki[3], Hiroki Senshu[5], Tomohiko Sekiguchi[6], Yoshiko Ogawa[2], Sunao Hasegawa[3], Takehiko Wada[3], Takeshi Imamura[10], Tsuneo Matsunaga[9], Jun Takita[8], Kohei Kitazato[2], Makoto Taguchi[4], Tetsuya Fukuhara[4], Satoshi Tanaka[3], Tatsuaki Okada[3] (1.Ashikaga University, 2.The University of Aizu, 3.Japan Aerospace Exploration Agency (JAXA), 4.Rikkyo University, 5.Chiba Institute of Technology, 6.Hokkaido University of Education, 7.National Institute of Advanced Industrial Science and Technology (AIST), 8.Hokkaido Kitami Hokuto High School, 9.National Institute for Environmental Studies (NIES), 10.The University of Tokyo)

[PPS03-P08] Multi-mission capability of HARMONICS

*Shintaro Tsunoda[1], Hirohide Demura[1], Naru Hirata[1] (1.The University of Aizu)

[PPS03-P09] New interface of verification for calibration and conversion in HEAT : Hayabusa2 Exploration Assistant for TIR

*Tatsuro Kobayashi[1], Kentaro Suko[1], Hirohide Demura[1], Yoshiko Ogawa[1], Takehiko Arai[2], Naoya Sakatani[3], Tatsuaki Okada[3], Satoshi Tanaka[3], Tetsuya Fukuhara[4] (1.The University of Aizu, 2.Ashikaga University, 3.Institute of Space and Astronautical Science, Japan Aerospace Exploration Agency, 4.Rikkyo University)

[PPS03-P10] **Dust particle evolution of a near-Earth object 252P/LINEAR from near-infrared polarimetric observations in 2016**

*Yuna G Kwon[1], Masateru Ishiguro[1], Jungmi Kwon[2], Daisuke Kuroda[3], Myungshin Im[1], Changsu Choi[1], Motohide Tamura[4], Takahiro Nagayama[5], Nobuyuki Kawai[6], Jun-ichi Watanabe[7] (1.Seoul National Univ., 2.ISAS/Japan Aerospace Exploration Agency, 3.Okayama Astrophysical Observatory, 4.The Univ. of Tokyo, 5.Kagoshima Univ., 6.Tokyo Institute of Technology, 7.National Astronomical Observatory of Japan)

[PPS03-P11] **Performance Evaluation of TRIPOL on the 61-cm Telescope at Seoul National University for Polarimetric Observations of Solar System Small Bodies**

*Sunho Jin[1], Masateru Ishiguro[1], Yuna G Kwon[1], Jooyeon Geem[1], Yoonsoo P. Bach[1], Jinguk Seo[1], Hiroshi Sasago[2], Shuji Sato[3] (1.Seoul National University, 2.Sasago Co.,Ltd, 3.Nagoya University)

[PPS03-P12] Smart Interface of HEAT: Hayabusa2 Exploration Assistant for TIR

*Kentaro Suko[1], Tatsuro Kobayashi[1], Hirohide Demura[1], Takehiko Arai[2], Naoya Sakatani[3], Tatsuaki Okada[3], Satoshi Tanaka[3], Tetsuya Fukuhara[4] (1.The University of Aizu, 2.Ashikaga University, 3.Institute of Space and Astronautical Science, Japan Aerospace Exploration Agency, 4.Rikkyo University)

[PPS03-P13] Experimental Study on Collision Crater Formed on Bulge Geography

*Yusaku Yokota[1], Yuya Yamamoto[2], Minami Yasui[2], Masahiko Arakawa[2] (1.Faculty of Science, Kobe University, 2.Graduate School of Science, Kobe University)

[PPS03-P14] Initial analysis plan of soluble organic compounds for the Hayabusa2 sample from asteroid Ryugu

*Hiroshi Naraoka[1], Yoshinori Takano[2], Jason P. Dworkin[3], SOM Analysis Team (1.Department of Earth and Planetary Sciences, Research Center for Planetary Trace Organic Compounds, Kyushu University, 2.Japan Agency for Marine-Earth Science and Technology, 3.Astrochemistry Laboratory NASA Goddard Space Flight Center, Greenbelt, MD 20771 USA)

[PPS03-P15] Radar and optical simultaneous observations of faint meteors with MU radar and Tomo-e Gozen

*Ryou Ohsawa[1], Akira Hirota[2], Shinsuke Abe[2], Daniel Kastinen[3], Kero Johan[3], yasunori Fujiwara[4], Takuji Nakamura[5], Shigeyuki Sako[1], Yuto Kojima[1], Jun-ichi Watanabe[6] (1.Institute of Astronomy, Graduate School of Science, The University of Tokyo, 2.Department of Aerospace Engineering, College of Science & Technology, Nihon University, 3.Swedish Institute of Space Physics, 4.SOKENDAI (The Graduate University for Advanced Studies), 5.National Institute of Polar Research, 6.National Astronomical Observatory of Japan)

[PPS03-P16] Global distribution and spectral characteristics of bright spots on asteroid Ryugu

*Masanori Suemitsu[1], Tomokatsu Morota[1], Rie Honda[2], Singo Kameda[15], Eri Tatsumi[3], Manabu Yamada[4], Naoya Sakatani[5], Toru Kouyama[6], Yokota Yasuhiro[7], Yuichiro Cho[8], Hidehiko Suzuki[9], Masahiko Hayakawa[10], Moe Matsuoka[10], Chikatoshi Honda[11], Tatsuhiro Michikami[12], Kazuo Yoshioka[13], Kazunori Ogawa[14], Hirotaka Sawada[5], Seiji Sugita[3] (1.Graduate School of Environmental Studies, Nagoya University, 2.Department of Science and Technology, System of Natural Science, Kochi Unicversity, 3.Graduate School of Earth and Planetary Science, Tokyo Unicversity, 4.Planetary Exploration Reserch Center, Chiba Institute of Technology, 5.Institute of Space and Astoronautical Science, Japan Aerospace Exploration Agency, 6.National Institute of Advanced Industrial Science and Technology, 7.Kochi University, 8.Department of Earth and Planetary Science, Tokyo University, 9.Depertment of physics, Meiji University , 10.Department of Solar System Science, Institute of Space and Astoronautical Science, Japan Aerospace Exploration Agency, 11.Aizu University, 12.Faculty of Engineering, Kindai University, 13.Graduate School of frontier Science, Tokyo University, 14.Kobe University, 15.Rikkyo University)

[PPS03-P17] Polarimetry of (155140) 2005 UD: the Dynamical Association with (3200) Phaethon

*Masateru Ishiguro[1], Jooyeon Geem[1], Hiroyuki Naito[2], Yoonsoo P. Bach[1], Daisuke Kuroda[3], Tatsuharu Ono[4], Seiko Takagi[4], Mitsuteru Sato[4], Kiyoshi Kuramoto[4], Tomohiko Sekiguchi[5], Masataka Imai[6], Makoto Watanabe[7], Katsuhito Ohtsuka[8], Sunao Hasegawa[9], Takashi Ito[10], Fumi Yoshida[11], Tomoko Arai[11] (1.Department of Physics and Astronomy, Seoul National University, 2.Nayoro Observatory, 3.Okayama Observatory, Kyoto University, 4.Department of Cosmosciences, Graduate School of Science, Hokkaido University, 5.Hokkaido University of Education, 6.National Institute of Advanced Industrial Science and Technology, 7.Department of Applied Physics, Okayama University of Science, 8.Tokyo Meteor Network, 9.Japan Aerospace Exploration Agency, 10.National Astronomical Observatory of Japan, 11.Planetary Exploration Research Center, Chiba Institute of Technology)

[PPS03-P18] **Follow-up observations for AKARI/IRC near-infrared asteroid spectroscopic survey (AcuA-spec)**

*Sunao Hasegawa[1], Daisuke KURODA[2], Kenshi YANAGISAWA[3], Fumihiko Usui[4] (1.Japan Aerospace Exploration Agency, 2.Kyoto University, 3.National Astronomical Observatory of Japan, 4.Kobe University)

[PPS03-P19] Amino acids on witness coupons collected from the ISAS/JAXA curation facility for the assessment and quality control of the Hayabusa2 sampling procedure

*Haruna Sugahara[1,2], Yoshinori Takano[1], Yuzuru Karouji[3], Kazuya Kumagai[4], Toru Yada[3], Naohiko Ohkouchi[1], Masanao Abe[3], Hayabusa2 project team (1.Japan Agency for Marine-Earth Science and Technology (JAMSTEC), 2. Institut de Chimie de Nice, Universite Cote dAzur, 3.Japan Aerospace Exploration Agency (JAXA), 4.Marine Works Japan Ltd.)

[PPS03-P20] Hayabusa2 orbit determination using c5++ software

*Keiko Yamamoto[1], Toshimichi Otsubo[2], Koji Matsumoto[1], Hirotomo Noda[1], Noriyuki Namiki[1], Hiroki Senshu[3], Takahide Mizuno[4], Naoko Ogawa[4], Go Ono[4], Yuya Mimasu[4], Kent Yoshikawa[4], Tadateru Takahashi[4], Yuto Takei[4], Atsushi Fujii[4], Fuyuto Terui[4], Takanao Saiki[4], Satoru Nakazawa[4], Makoto Yoshikawa[4], Yuichi Tsuda[4] (1.National Astronomical Observatory of Japan, 2.Hitotsubashi University, 3.Chiba Institute of Technology, 4.Japan Aerospace Exploration Agency)

[PPS03-P21] **Landing Site Selection for Hayabusa2: Scientific Evaluation of the Candidate Sites on Asteroid (162173) Ryugu**

*Hikaru Yabuta[1], Sei-ichiro WATANABE[2], Tomoki Nakamura[3], Naru Hirata[4], Seiji Sugita[5], Tatsuaki Okada[6], Kohei Kitazato[4], Yoshiaki Ishihara[7], Tomokatsu Morota[2], Naoya Sakatani[6], Koji Matsumoto[8], Koji Wada[9], Shogo Tachibana[5], Mutsumi Komatsu[10], ERI TATSUMI[5], Moe Matsuoka[6], Chikatoshi Honda[4], Takahiro Hiroi[11], Hiroki Senshu[9], Rie Honda[12], Yasuhiro Yokota[6], Rina Noguchi[6], Yuri Shimaki[6], Deborah Lorin Domingue[13], Lucille Le Corre[13], Antonella Barucci[14], Ernest Palomba[15], Shota Kikuchi[6], Akira Miura[6], Tomohiro Yamaguchi[6], Yukio Yamamoto[6], Takanao Saiki[6], Satoshi Tanaka[6], Makoto Yoshikawa[6], Yuichi Tsuda[6] (1.Hiroshima University, Department of Earth and Planetary Systems Science, 2.Nagoya University, 3.Tohoku University, 4.University of Aizu, 5.The University of Tokyo, 6.ISAS/JAXA, 7.NIES, 8.NAOJ, 9.Chiba Institute of Technology, Planetary Exploration Research Center (PERC), 10.Sokendai, 11.Brown University, 12.Kochi University, 13.Planetary Science Institute, USA, 14.Observatoire Paris-Site de Meudon, LESIA, France, 15.INAF-IAPS, Italy.)

[PPS03-P22] Visible Photometric, Spectroscopic and Polarimetric observations of an inactive comet, P/2016 BA14 with the 1.6m Pirka Telescope

*Ryo Yamagata[1], Tomohiko Sekiguchi[1], Ryo Okazaki[1], Kazuya Doi[1], Daisuke Kuroda[2], Masateru Ishiguro[3], Hiroyuki Naito[4] (1.Hokkaido University of Education, 2.Kyoto University, 3.Seoul National University, 4.Nayoro Observatory)

[PPS03-P23] **Polycyclic aromatic hydrocarbons and aliphatic hydrocarbons in Jbilet Winselwan carbonaceous chondrite : Attempt to evaluate the thermal metamorphism degree on the parent body**

Hiroki Kato[1], *Hikaru Yabuta[1] (1.Hiroshima University, Department of Earth and Planetary Systems Science)

[PPS03-P24] Disk-Resolved Photometry Analysis of the Asteroid Ryugu Images Obtained by Hayabusa2 Visible Camera ONC

*yokota yasuhiro[1,2], Rie Honda[1], ERI TATSUMI[3], Deborah Domingue[4], Stefanus E. Schroeder[5], Moe Matsuoka[2], Seiji Sugita[3], Tomokatsu Morota[6], Shingo Kameda[7], Toru Kouyama[8], Hidehiko Suzuki[9], Manabu Yamada[10], Naoya Sakatani[2], Chikatoshi Honda[11], Masahiko Hayakawa[2], Kazuo Yoshioka[3], Yuichiro Cho[3], Hirotaka Sawada[2] (1.Kochi University, 2.ISAS/JAXA, 3.Univ. of Tokyo, 4.Planetary Science Institute, 5.DLR, 6.Nagoya Univ., 7.Rikkyo Univ., 8.AIST, 9.Meiji Univ., 10.Chiba Institute od Technology, 11.Aizu Univ.)

Impact experiments on low strength coarse-grained regolith simulating surface materials on asteroid Ryugu

*Yuya Yamamoto[1], Masahiko Arakawa[1], Minami Yasui[1], Sunao Hasegawa[2], Ryo Sugimura[1]

1. Graduate School of Science, Kobe University, 2. ISAS, JAXA

Impact cratering is one of the most important physical processes, then we study crater scaling laws and impact induced seismic waves in order to elucidate various flow processes on asteroids caused by impacts. The conventional crater scaling laws are categorized into two regions according to the controlling physics for the crater growth: they are gravity and material strength. A crater formed on regolith layer is surely controlled by the gravity, however when the regolith layer was filled with coarse particles with low mechanical strength, then the several coarse grains might be disrupted to consume the Ek. Thus, the crater size could be affected by the disruptions of the coarse grains. We speculate that not only the gravity but also the grain strength could affect the final crater size. Then, we made cratering experiments by using the target made of weak particles, and studied the effects of the particle strength on the crater scaling law and the impact induced seismic wave.

Experiments: Cratering experiments were conducted by using a gas gun set at Kobe University and ISAS. Granular targets were prepared by using weathered tuff granules with the size of 1 to 4mm (small particle) and the size of 1 to 4cm (large particle). The crush strength of these tuff particles was measured to be about 60 kPa. A spherical projectile with the size of 3mm which is made of iron, zirconia, alumina, glass, and nylon) was lunched at the impact velocity from 40 to 200m/s, and a spherical Al projectile with the size of 2mm was impacted at the impact velocity from 1.2 to 4.5km/s, then these two types of the projectile were impacted on the target surface at the normal direction. Impact cratering process and ejecta curtain growth were observed by a high-speed camera at 10^3-10^5 fps, and the video images were used to analyze ejecta particles to reconstruct the trajectories. After the shot, the crater morphology was recorded and the diameter and the depth were measured. Impact induced seismic waves were measured by using 3 accelerometers (specific frequency is 30kHz) set at different positions from the impact point, and a data logger was used to record the seismic data through charge amplifiers (data acquisition rate is 100kHz) connecting to the accelerometer.

Results: The crater size was found to increase with the projectile kinetic energy (Ek) at lower than 0.14J and at higher than 0.63J, so that the crater size was almost constant among them, and more the crater size obtained at very high Ek was almost on the extrapolated line from the relationship given by the low Ek data. The pi-scaling law was used to construct the relationship between normalized radius (πR) and normalized gravity (π2), and πR at small π2 was found to be rather smaller than that obtained for sand and glass beads targets, and more πR at large π2 was found to be consistent with that for sand and glass beads. More detail analysis tells us that all the data separated into two trends with large offset according to the impact velocity and the projectile material. This offset might be caused by the disruption of several tuff particles. The ejection velocities of each tuff particle were so scattered, then the distinctive relationship between initial position of particle and the ejection velocity was not derived in the low velocity range. The propagation velocity of the impact induced seismic wave was about 30 m/s, and it is 1/3 of that for glass beads. Furthermore, we found that the relationship between the maximum acceleration and the distance from the impact point was about 1/10 of that obtained for glass beads: the seismic wave in the tuff granules attenuated so quickly compared to the glass beads. But, when the distance is normalized by the crater radius, these relationships almost consistent each other, so that the

©2019. Japan Geoscience Union. All Right Reserved.

normalized distance could be a good parameter for the scaling of the acceleration of seismic wave.

Keywords: impact cratering experiment, low strength, impact-induced seismic shaking, crater scaling law

©2019. Japan Geoscience Union. All Right Reserved.

Reflectance estimation of asteroid Ryugu using MASCOT

*Marika Ishida[1], Koto Amano[1], Keiichi Moroi[1], ERI TATSUMI[2], Tra-Mi Ho[10], Shingo Kameda[1], Seiji Sugita[2], Rie Honda[3], Tomokatsu Morota[4], yokota yasuhiro[5], Toru Kouyama[6], Hidehiko Suzuki[7], Manabu Yamada[8], Naoya Sakatani[5], Chikatoshi Honda[9], Masahiko Hayakawa[5], Kazuo Yoshioka[2], Moe Matsuoka[5], Yuichiro Cho[2], Hirotaka Sawada[5]

1. Rikkyo Univ., 2. Univ. of Tokyo, 3. Kochi Univ., 4. Nagoya Univ., 5. JAXA/ISAS, 6. AIST, 7. Meiji Univ., 8. Chiba Inst. Tech, 9. Univ. of Aizu, 10. DLR

Hayabusa2 is a sample-return mission for the C-type asteroid 162173 Ryugu. Hayabusa2 arrived at Ryugu on 27 June 2018, and various observations are still being conducted. Hayabusa2 performs multiband spectral observation by employing the optical navigation camera telescope (ONC-T)and can thereby obtain spectral map of Ryugu, which enables the study of material distribution and degree of space weathering of Ryugu. However, the sensitivity of ONC-T has been previously calibrated by incorporating the inflight data of stars with significant uncertainty. Hence, the authors aim to estimate the reflectance of Ryugu by employing Mobile Asteroid Surface Scout (MASCOT).
MASCOT comprises four instruments (MASCAM, MicrOmega, MARA, and MASMAG) that are employed for analyzing the soil of Ryugu. The upper side of the MASCOT landeris coated with white paint, and its spectral image was captured by ONC-T after its release from Hayabusa2 to Ryugu. The authors conducted on-ground reflectance measurement of a white plate whose white paint is identical to that of MASCOT. Hence, the primary objective of the proposed study is to estimate the reflectance of Ryugu by comparing MASCOT’ s white side’ s spectrum captured by ONC-T with the on-ground reflectance measurement of the white plate that has identical paint as MASCOT, and thus evaluate the validity.

Keywords: Hayabusa2, ONC-T, MASCOT

©2019. Japan Geoscience Union. All Right Reserved.

Flyby observation of Asteroid (3200) Phaethon by DESTINY$^+$ onboard cameras

*Ko Ishibashi[1], Shingo Kameda[2], Masato Kagitani[3], Peng Hong[1], Manabu Yamada[1], Osamu Okudaira[1], Tomoko Arai[1], Fumi Yoshida[1], Shunsuke Sato[4], Takahiro Ishimaru[4], Takaya Okamoto[4], Takahiro Iwata[4], Tatsuaki Okada[4], Takeshi Takashima[4]

1. Chiba Institute of Technology, 2. Rikkyo University, 3. Tohoku Universtiy, 4. Japan Aerospace Exploration Agency

DESTINY$^+$ (Demonstration and Experiment of Space Technology for INterplanetary voYage, Phaethon fLy-by and dUst Science) is a mission proposed for JAXA/ISAS Epsilon class small program, currently in the pre-project phase (Phase-A) with a launch targeted for 2023. DESTINY$^+$ is a joint mission of technology demonstration and scientific observation. The near-Earth asteroid (3200) Phaethon, the flyby target, is known as a parent body of the Geminid meteor shower, the size of which is approximately 5 to 6 km in diameter.

In this mission, spatially resolved images of Phaethon will be taken by two onboard cameras, the Telescopic CAmera for Phaethon (TCAP) and the Multiband CAmera for Phaethon (MCAP) during the flyby, in order to understand the nature of a meteor shower's parent body, which is one of the sources of interplanetary dust particles that are thought to be an important transport medium of organic matter to the Earth. The spacecraft flybys Phaethon with a relative speed of 30 to 40 km/s. Despite such a high flyby speed, the cameras are required to take un-blurred images of Phaethon.

The main purposes of the DESTINY$^+$ flyby observation of Phaethon is to understand the geology of a parent body of a meteor shower, and in particular constrain the dust ejection mechanisms from active (i.e., dust-ejecting) asteroids. The specific objectives of the camera observation are taking images for (1) obtaining the light curve of Phaethon in order to estimate the rotational period, (2) measuring the outline shape of Phaeton, (3) making a 3D shape model of Phaethon, (4) observing the surface geological features of Phaethon including dust ejection features, and (5) observing the surface material distribution of Phaethon. The observations (1) to (4) will be conducted by TCAP, and (5) by MCAP.

TCAP is a telescopic panchromatic camera for high spatial resolution imaging of the surface of Phaethon and have a rotational mirror for asteroid tracking during flyby. The rotational mirror can change the direction of the line of sight from 0 deg to 180 deg. This enables to observe Phaethon throughout the flyby with wide solar phase angles, which is extremely important to image and understand the surfaces of planetary bodies because the solar phase angle affects significantly the appearance of geological features in taken images.

MCAP is a multiband camera, the wavelengths of which are 400, 480, 550, 700, 850, and 950 nm (480 and 950 nm are optional bands) and has multiple optical systems and sensors in order to take all band images simultaneously. This is because there is not enough time to take each band image in turn with changing bandpass filters using such as a filter wheel in this high speed flyby mission. MCAP does not have a tracking mirror due to the weight limitation, and the line of sight of MCAP is fixed to the spacecraft with 40 deg off the relative velocity vector of the spacecraft.

We will explain the flyby imaging sequence of DESTINY$^+$, and show the conceptual designs of TCAP and MCAP.

©2019. Japan Geoscience Union. All Right Reserved.

Keywords: Phaethon, DESTINY+, Flyby, Camera

©2019. Japan Geoscience Union. All Right Reserved.

Polarimetric Study of Asteroids in Comet-Like Orbits (ACOs)

*Jooyeon Geem[1], Masateru Ishiguro[1], Yoonsoo P. Bach[1], Daisuke Kuroda[2], Hiroyuki Naito[3], Hidekazu Hanayama[4], yoonyoung kim[10], Yuna G. Kwon[1], Sunho Jin[1], Tomohiko Sekiguchi[5], Ryo Okazaki[5], Jeremie J. Vaubaillon[6], Masataka Imai[7], Tatsuharu Oono[8], Yuki Futamuts[8], Seiko Takagi[8], Mitsuteru Sato[8], Kiyoshi Kuramoto[8], Makoto Watanabe[9]

1. Astronomy program, Dept of Physics and Astronomy, Seoul National University, 2. Okayama Observatory, Kyoto University, 3. Nayoro Observatory, 4. Ishigakijima Astronomical Observatory, National Astronomical Observatory of Japan, 5. Hokkaido University of Education, 6. Observatoire de Paris, I.M.C.C.E., 7. National Institute of Advanced Industrial Science and Technology, 8. Department of Cosmosciences, Graduate School of Science, Hokkaido University, 9. Department of Applied Physics, Okayama University of Science, 10. Max Planck Institute for Solar System Research

It is important to determine the taxonomic types of small bodies in the solar system and further to study the spatial distribution of the planetary system. Among the small bodies, it is considered that there should be dormant comets that have lost a significant fraction of volatile materials in their subsurface layers. As a result, they are unable to produce any detectable coma and recognized as asteroids. It has been challenging to find out such dormant comet population from a list of known asteroids because of the asteroidal appearances. There are several attempts to find the dormant comet nuclei from asteroidal catalogs, for example, by using their reflectance spectra or orbital elements. However, little has been studied via polarimetry.
We conduct a polarimetric study of three candidates of dormant comet nuclei, (331471) 1984 QY1, (3552) Don Quixote and (944) Hidalgo, by using the 1.6-m Pirka Telescope at the Nayoro observatory (operated by Hokkaido University, Japan). We chose these asteroids in comet-like orbits (ACOs) based on the orbital elements (i.e., the Tisserand parameter with respect to Jupiter $T_J < 3$). We found that 1984 QY1 has a polarimetric albedo (geometric albedo determined via polarimetry) $p_V = 0.16 \pm 0.06$ while both Don Quixote and Hidalgo have Rc-band polarimetric albedo $p_R < 0.05$. Based on the polarimetric result together with a dynamical analysis, we conjectured that 1984 QY1 could be an S-type asteroid transported into the current orbit via 3:1 mean motion resonance with Jupiter. From the previous spectroscopic study, Don Quixote and Hidalgo are classified into D-type taxonomic group, which are typical of comet nuclei. In this presentation, we will introduce our polarimetric observations of ACOs and emphasize that polarimetry is a powerful tool for discriminating the asteroidal and cometary origins.

Keywords: Polarimetry, Asteroid

©2019. Japan Geoscience Union. All Right Reserved.

Dynamical lifetime of the Oort Cloud new comets under planetary perturbation

*Ito Takashi[1], Arika Higuchi[1]

1. National Astronomical Observatory of Japan

Nearly isotropic comets with very long orbital period are supposed to come from the Oort Cloud. Recent observational and theoretical studies have greatly revealed the dynamical nature of this cloud and its evolutionally history, but many issues are yet to be known. Our goal is to trace the dynamical evolution of the Oort Cloud new comets (OCNCs) produced by evolving comet cloud, hopefully estimating the fraction of OCNCs embedded in the current populations of the solar system small bodies. We combine two models to follow the dynamical evolution of OCNCs beginning from their production until their ejection out of the solar system, obtaining statistics of the dynamical lifetime of OCNCs: The first model is a semi-analytical one about the OCNC production in an evolving comet cloud under the perturbation of the galactic tide and stellar encounters. The second model numerically deals with planetary perturbation over OCNCs' dynamics in planetary region. The main results of the present study are: (1) Typical dynamical lifetime of OCNCs in our models turned out to be O(10^7) years. Once entering into the planetary region, most OCNCs stay there just for this timespan, then get ejected out of the solar system on hyperbolic orbits. (2) While averaged orbital inclination of OCNCs is small, the so-called "planet barrier" works rather effectively, preventing some OCNCs from penetrating into the terrestrial planetary region.

Keywords: Oort Cloud, comet, orbital dynamics

©2019. Japan Geoscience Union. All Right Reserved.

Thermal Infrared Imaging of C-type Asteroid 162173 Ryugu with Porous Surfaces

*Tatsuaki Okada[1,2], Tetsuya Fukuhara[3], Satoshi Tanaka[1], Makoto Taguchi[3], Takehiko Arai[4], Naoya Sakatani[1], Yuri Shimaki[1], Hiroki Senshu[5], Yoshiko Ogawa[6], Hirohide Demura[6], Kentaro Suko[6], Kohei Kitazato[6], Toru Kouyama[7], Tomohiko Sekiguchi[8], Jun Takita[9], Sunao Hasegawa[1], Tsuneo Matsunaga[10], Takehiko Wada[1], Takeshi Imamura[2], Jorn Helbert[11], Thomas G. Mueller[12], Axel Hagermann[13], Jens Biele[11], Matthias Grott[11], Maximiliam Hamm[11], Marco Delbo[14], Yukio Yamamoto[1], Naru Hirata[6], Naoyuki Hirata[15], Fuyuto Terui[1], Takanao Saiki[1], Satoru Nakazawa[1], Makoto Yoshikawa[1], Sei-ichiro WATANABE[1,16], Yuichi Tuda[1]

1. Institute of Space and Astronautical Science, Japan Aerospace Exploration Agency, 2. University of Tokyo, 3. Rikkyo University, 4. Ashikaga University, 5. Chiba Institute of Technology, 6. University of Aizu, 7. National Institute of Advanced Industrial Science and Technology, 8. Hokkaido University of Education, 9. Hokkaido Kitami-Hokuto High School, 10. National Institute for Environmental Studies, 11. German Aerospace Center, 12. Max-Planck Institute for Extraterrestrial Physics, 13. University of Stirling, 14. Observatoire de la Côte d'Azur, 15. Kobe University, 16. Nagoya University

Thermal images from global to close-up scales taken by the Thermal Infrared Imager TIR [1] on Hayabusa2 [2] have revealed thermophysical properties of the C-type Near-Earth Asteroid 162173 Ryugu. On 27 June 2018, Hayabusa2 arrived at Ryugu and started remote sensing to characterize the nature of the asteroid and find the proper landing sites. *In situ* surface experiments were conducted using the robotic landers Minerva-II and Mascot [3]. *In situ* radiometry was conducted by MARA on MASCOT during a day-night cycle to derive the thermal inertia of a single boulder [4]. Ground-based observations [5] have been informed that the averaged thermal inertia of the asteroid is from 150 to 300 [tiu = J m^{-2} $s^{-0.5}$ K^{-1}] [5,6], corresponding to the surface covered with cm-sized granules.

TIR is the same design as the LIR on Akatsuki Venus climate orbiter [6], with 8 to 12 μm wavelength range, 328 x 248 effective pixels, and the FOV and IFOV of 16.7˚ x 12.7˚ and 0.051˚ per pixel, respectively. The first image of Ryugu detected by TIR was a point source on 6 June 2018, as was previously predicted [7]. Disc-resolved thermal images of Ryugu was taken from the HP on 30 June. The surface temperature was measured at 300 to 370K at about 1AU from the Sun, and gradually decreased with the solar distance. Comparison of the results with modeling [8] shows that the surface of Ryugu is not like fine regolith nor base rocks. Most of large boulders on Ryugu show temperatures almost the same as the surrounding surfaces. Diurnal temperature profiles of Ryugu are rather flatter than expected for a smooth terrain. Apparent thermal inertia is ~300 tiu or larger, but probably lower than the value when the surface roughness is considered. All these facts are consistent with a very rough and porous surface with low porosity (~35 ±10 %) [9] and the surrounding surface is dominated by porous rocks larger than several centimeters. Macro porosity should be 30 to 50 % to account for the bulk density of Ryugu ~1200 kg m^{-3}.

During the descent operations for the release of landers and the touchdowns for sample collection, TIR has taken close-up thermal images of the local sites, continually from the altitude of 500 m until the start of final descent at 10 or 20 m altitude. Close-up thermal images show the surface physical state and a variety of boulders. Most of the boulders in close-up images have temperatures similar to the surroundings but with more variety. A small number of boulders are remarkably colder than the surroundings, indicating dense rocks with lower porosity.

©2019. Japan Geoscience Union. All Right Reserved.

These facts indicate that Ryugu is probably a rubble pile of loosely-bound porous rocks, which might originate from the outer layer of parent body where compaction did not occur effectively, while the dense boulders might originate the compacted center region of parent body or from the different parent body. A different composition (e.g., organic rich materials) cannot be ruled out so far to account for such a low thermal inertia (and low density) of Ryugu.

Acknowledgments: The authors appreciate all the members of the Hayabusa2 Project and supporting staff for their technical assistance and scientific discussions. This research is partly supported by the JSPS KAKENHI No. J26287108, No. J17H06459 (Aqua Planetology), and the Core-to-Core program “International Network of Planetary Sciences”. MDB acknowledges support from CNES.

References: [1] Okada T. et al. (2017) *SSR.,* 208, 255-286. [2] Tsuda Y. et al. (2013) *Acta. Astronautica, 91* , 356-362. [3] Ho T.M. et al. (2017) *SSR.,* 208, 255-286. [4] Grott, M. et al. (2019), submitted to Nature. [5] Mueller T.G. et al. (2016) Astronon. Astrophys., doi:10.1051/0004-6361/201629143. [6] Fukuhara T. et al. (2011) *EPS,* 63, 1009-1018. [7] Okada T. et al. (2018) *PSS., 158, 46-52.* [8] Takita J., et al. SSR, 2018, 287-315. [9] Okada T. (2016) *LPSC.*, 47, #1457.

Keywords: Hayabsua2, Thermal Infrared Imager, Thermal Inertia

©2019. Japan Geoscience Union. All Right Reserved.

Data Release of Asteroid 162173 Ryugu by Observation of Thermal Infrared Imager onboard Hayabusa2

*Takehiko Arai[1], Hirohide Demura[2], Toru Kouyama[7], Naoya Sakatani[3], Kentaro Suko[2], Yuri Shimaki[3], Hiroki Senshu[5], Tomohiko Sekiguchi[6], Yoshiko Ogawa[2], Sunao Hasegawa[3], Takehiko Wada[3], Takeshi Imamura[10], Tsuneo Matsunaga[9], Jun Takita[8], Kohei Kitazato[2], Makoto Taguchi[4], Tetsuya Fukuhara[4], Satoshi Tanaka[3], Tatsuaki Okada[3]

1. Ashikaga University, 2. The University of Aizu, 3. Japan Aerospace Exploration Agency (JAXA), 4. Rikkyo University, 5. Chiba Institute of Technology, 6. Hokkaido University of Education, 7. National Institute of Advanced Industrial Science and Technology (AIST), 8. Hokkaido Kitami Hokuto High School, 9. National Institute for Environmental Studies (NIES), 10. The University of Tokyo

The thermal infrared imager (TIR) onboard the Hayabusa2 spacecraft performed thermography of the asteroid 162173 Ryugu through in-situ observations from 2018 to 2019. The primary purpose of TIR is to determine the global thermophysical properties of the asteroid and to reveal the evolutional history such as physical properties of the coalesced bodies, orbital changes due to radiation force, and the thermal evolution. This study introduces observed data of TIR and public data for scientists. The data are released by JAXA data archives (DARTS) and NASA PDS.

Keywords: Hayabusa2, Thermal Infrared Imager, Asteroid Ryugu

©2019. Japan Geoscience Union. All Right Reserved.

Multi-mission capability of HARMONICS

*Shintaro Tsunoda[1], Hirohide Demura[1], Naru Hirata[1]

1. The University of Aizu

This research has updated HARMONICS from a viewpoint of multi-mission capability, such as the Martian satellite exploration mission MMX in 2020s. Newly additional function is Switching on the shape model interface.
Bird view and visualization of FOV is important in robotics control. This technology is also used for deep space explorer missions.
HARMONICS is visualization tool of FOV(Field Of View) of scientific instruments and spacecraft’s position for HAYABUSA mission. The software has been updated by University of Aizu students of the past. The original HARMONICS had been developed by Nemoto(2006). GUI of HARMONICS had been replaced GUI library from GKT to Qt and added new functions, such as interactive modification of input mission plan by Ueno+(2017). The software had been add FOV frustum function by Aoki(2017). HARMONICS has tried to manage data for each project based on preference file in 2018.
HARMONICS should improved scalability to be compatible for ongoing mission. HARMONICS had been used to decide shutter chance by Camera Science Team in the asteroid Itokawa rendezvous of HAYABUSA. This software has not used in the asteroid Ryugu rendezvous of HAYABUSA2. The proven software should be use for future ongoing missions other than HAYABUSA. This research is development to HARMONICS adapt to ongoing missions.
I separated the designation of the data set from the source code and clarified the part edited by the user and the part edited by the developer.
HARMONICS has the function to switch and display data of different missions by this research. When users extend HARMONICS for multiple missions, users don’t need edit source code. User needs only kernel and the shape model of spacecraft and target asteroid. User do not need tough coding. User can use easily HARMONICS by editing preference file and kernel.

Keywords: Hayabusa2, Ryugu, Software, visualization

©2019. Japan Geoscience Union. All Right Reserved.

New interface of verification for calibration and conversion in HEAT : Hayabusa2 Exploration Assistant for TIR

*Tatsuro Kobayashi[1], Kentaro Suko[1], Hirohide Demura[1], Yoshiko Ogawa[1], Takehiko Arai[2], Naoya Sakatani[3], Tatsuaki Okada[3], Satoshi Tanaka[3], Tetsuya Fukuhara[4]

1. The University of Aizu, 2. Ashikaga University, 3. Institute of Space and Astronautical Science, Japan Aerospace Exploration Agency, 4. Rikkyo University

Hayabusa2 is an ongoing mission for sample return from the asteroid Ryugu.
Candidates of sampling sites are selected based on surface mapping by optical instruments such as Thermal Camera (TIR). TIR observes surface infrared radiation from the asteroid. A software package peculiar to TIR is HEAT: Hayabusa2 Exploration Assistant for TIR. The software has four functions; Database for ground tests, calibration of flight data based on the ground tests, conversion from raw data to temperature one, and analysis for verifying the calibration and conversion. The converted data products are divided into some levels: Lv1 Raw data [DN], Lv2a Temperature [K], Lv2b is Brightness [W/m2], and higher thermal model with VTK format [K]. This research implements new interface of verification for calibration and conversion based on hearing and survey for requirements from TIR science team. The environment of implementation is following tool. OS: macOS Mojave 10.14.2. Computing language: C++, OpenGL. Frameworks: Qt5.4. Tools: Fits, Qt creator, SPICE toolkit, Visualization Toolkit, QcustomPlot, Xcode10.1.

Keywords: Hayabusa2, Software, Ryugu, Calibration

©2019. Japan Geoscience Union. All Right Reserved.

Dust particle evolution of a near-Earth object 252P/LINEAR from near-infrared polarimetric observations in 2016

*Yuna G Kwon[1], Masateru Ishiguro[1], Jungmi Kwon[2], Daisuke Kuroda[3], Myungshin Im[1], Changsu Choi[1], Motohide Tamura[4], Takahiro Nagayama[5], Nobuyuki Kawai[6], Jun-ichi Watanabe[7]

1. Seoul National Univ., 2. ISAS/Japan Aerospace Exploration Agency, 3. Okayama Astrophysical Observatory, 4. The Univ. of Tokyo, 5. Kagoshima Univ., 6. Tokyo Institute of Technology, 7. National Astronomical Observatory of Japan

Comets, one of the least-altered leftovers from the early solar system, have probably preserved the primitive structure inside, whereas their surfaces become differentiated from initial states after repetitive orbital revolutions around the sun. Resurfacing makes the surface drier and more consolidated than the bulk nuclei, creating inert refractory dust layer (so-called “dust mantle”). Near-Infrared (NIR) polarimetry is theoretically expected to maximize the contrast of the porosity between inner fresh and evolved dust particles, by harboring more dust constituents in the single wavelength than the optical, and thus intensifying electromagnetic interference in dust agglomerates. Despite the advantage, only few studies have been conducted in this approach at multiple observation epochs. Herein, we present our new multi-band NIR polarimetric (1.25—2.25 microns) study of near-Earth object 252P/LINEAR over 12 days near perihelion; alongside broadband optical photometric (0.48—0.80 microns) data over four months in 2016 and a subsidiary dynamical simulation over 1000 year backward in time. 252P/LINEAR drew attention due to (1) its close approach to the Earth (~0.036 au on 2016 March 16), (2) its possible pairing to a comet P/2016 BA14 (PanSTARRS), and (3) its very low activity level despite its relatively young dynamical age. In this study, we detected two discontinuous brightness enhancements of 252P/LINEAR, particularly, the former of which accompanied a significant increase of NIR polarization degree of the comet (by ~13 % at most) with unusual blue polarimetric color. We will discuss the most probable scenario of the observed results, together with the orbital evolution of the comet and a dynamical association with its pair.

Keywords: Comet, Near-earth object, Polarimetry, Dust

©2019. Japan Geoscience Union. All Right Reserved.

Performance Evaluation of TRIPOL on the 61-cm Telescope at Seoul National University for Polarimetric Observations of Solar System Small Bodies

*Sunho Jin[1], Masateru Ishiguro[1], Yuna G Kwon[1], Jooyeon Geem[1], Yoonsoo P. Bach[1], Jinguk Seo[1], Hiroshi Sasago[2], Shuji Sato[3]

1. Seoul National University, 2. Sasago Co.,Ltd, 3. Nagoya University

Polarimetry of solar system small bodies is a powerful technique for investigating their physical properties, such as albedos, particle sizes, and porosities of these bodies. Observational opportunities arise sometimes suddenly, that is, just after unforeseeable activations of comets and discoveries of near-miss asteroids. Here, we introduce our activity to install the polarimetric instrument, TRIPOL (Triple-Range Imager and POLarimeter) on the 61-cm telescope (a Ritchey-Chretien reflector with f/7.0) at the Center for Astronomy and Space Science, Seoul National University, and report an observational result of three comets. This combination provides an 8.0’ ´8.0’ field of view and pixel resolution of 0.94” pixel^{-1}. Throughout photometric observations, we determined the limiting magnitudes (defined as magnitudes for S/N=5) of 15.17±0.06 (g’-band), 15.68±0.01 (r’-band), 16.24±0.03 (I’-band), respectively, with total 240-seconds exposure (four 60-seconds exposure images, each was taken at different rotation angle for the half-wave plate). We also found that the instrumental polarizations are negligibly small, that is, -0.32±0.04% (g’-band), -0.36±0.05% (r’-band) and -0.21±0.04% (I’-band), while the polarization efficiencies are large enough to maximize the performance, that is, 97.52±0.03% (g’-band), 98.83±0.02% (r’-band) and 99.15±0.02% (I’-band).

With this instrument, we conducted polarimetric observations of three Jupiter-family comets, 21P/Giacobini-Zinner, 38P/Stephan-Oterma, and 46P/Wirtanen on a trial basis. It is known from a recent study that the polarization degrees of cometary dust particles are significantly influenced by gas emissions [1] With multiband data taken with TRIPOL, we eliminated an influence of gas contaminations and found that the dust polarization degrees of these three comets coincide with those of so-called ‘dust-rich comets’. From this result, we conjecture that the polarimetric property of Jupiter-family comets is broadly homogeneous, unlike asteroids. We plan to describe our future plan using the polarimetric system.

[1] Kwon, Y. G. et al. Astronomical Journal, 154, 4, 173, 2017

Keywords: Comet, Instrument, Polarimetry

©2019. Japan Geoscience Union. All Right Reserved.

Smart Interface of HEAT: Hayabusa2 Exploration Assistant for TIR

*Kentaro Suko[1], Tatsuro Kobayashi[1], Hirohide Demura[1], Takehiko Arai[2], Naoya Sakatani[3], Tatsuaki Okada[3], Satoshi Tanaka[3], Tetsuya Fukuhara[4]

1. The University of Aizu, 2. Ashikaga University, 3. Institute of Space and Astronautical Science, Japan Aerospace Exploration Agency, 4. Rikkyo University

The Hayabusa2 project is a sample return mission to the asteroid Ryugu. It was launched on Dec. 3, 2014, and it has been at Ryugu since June 27, 2018. Hayabusa2 has optical instrument called Thermal Infrared Imager (TIR). These main functions are to know natures of the asteroid and to select the candidate of safe landing sites for sampling based on thermos-physical properties of the surface. TIR records infrared radiation from the target as a digital number (DN). The infrared signal is affected by sensor-surrounding objects; lens, shutter, package, and case. TIR requires consideration about this effect when converts DN images to temperature one. This study improved conversion system to increase conversion efficiency.

Hayabusa2 TIR Science Team has developed an analysis supporting tool called Hayabusa2 Exploration Assistant for TIR (HEAT). HEAT is used to search TIR data interactively, display TIR images, and visualize thermal models. We receive TIR raw images (Product Level 1) from ISAS/JAXA and convert them to brightness temperature images (Level 2a) and radiance images (Level 2b) using HEAT at Univ. of Aizu. The converted images are provided to the Hayabusa2 project data server.

This part introduces a concept model. The spectral radiance emitted from a blackbody B(λ ,T) (W s r-1m-2) is given by the Planck function based on wavelength λ (m) and temperature T(K) as follows:

$$B(\lambda,T) = (2hc2/\lambda 5)* (1/(\exp(\lambda kBT)-1))$$

H = 6.63*1034 (m2 kg s-2 s-1) is the Planck constant, c=2.9972*108(ms-1) is the speed of light, and KB= 1.38*10-23 (m2 kg s-2K-1) is the Boltzmann constant. The observed radiance L(T) (W sr−1 m−2) is as follows:

$$L(T)= \varepsilon \int BR(\lambda)d\lambda$$

ε is the spectral thermal emissivity, and R(λ) is the response function such as the detection efficiency of the bolometer, the measured transmittance of optics including the band-pass filter and the germanium lens. The calibration formula with two regressed parameters A and B is written as follows:

$$DN=A * L(T) + B$$

The converted temperatures of the Moon were lower than expected because each pixel did not cover the sunlit area entirely or due to roughness effect of the cratered terrain. TIR has been observing Ryugu in approach and rendezvous phases. The altitudes of TIR observations during the rendezvous phase range from 20 km to less than 10 m. This study has processed about 3000 Ryugu images observed by TIR since June 2018.

©2019. Japan Geoscience Union. All Right Reserved.

This study improved conversion system. Previous conversion system converts a TIR image one by one, but current conversion system converts TIR images in selected directory at once.

Keywords: Hayabusa2, TIR, HEAT, Software

©2019. Japan Geoscience Union. All Right Reserved.

Experimental Study on Collision Crater Formed on Bulge Geography

*Yusaku Yokota[1], Yuya Yamamoto[2], Minami Yasui[2], Masahiko Arakawa[2]

1. Faculty of Science, Kobe University, 2. Graduate School of Science, Kobe University

An equatorial bulge was found on the surface of asteroid Ryugu and Bennu by recent spacecrafts of Hayabusa2 and OSIRIS-Rex, and ridge structures with various scales originated by geological activities have been recognized on icy satellites. Impact craters are dominant geological features on solid planets such as asteroids and satellites, and a crater rim are also recognized as a ridge or bulge with a circular shape. These bulges and ridges are shown to be erased with time because small scale impacts excavate and disrupt these topographies. It is well known that old craters gradually degraded by small impacts to get blurred and could be completely erased. We can expect the similar degradation process on large bulges and ridge structures, so that the life time of these structures by small impacts is a good indicator of the formation age of these structure by geologic activities. So far, the effect of small impacts on the degradation is estimated by using the results on the flat surface, but actually the surface of the bulge is curved and there is a summit on the bulge. Therefore, if we estimate the life time of the bulge structure, we should consider the effect of the topography such as a summit and curvature. Then, the impacts on the bulge structure was studied to clarify how the bulge structure affected the crater formation efficiency. In this study, we suppose the bulge made from regolith and boulders, such as an equatorial bulge of Ryugu and assume the crater formation process dominated by not the strength but the gravity.

We prepared a triangular prism target to simulate the bilge structure, and set it like that the base of this prism is rectangle, then it looks triangle when we look it at the horizontal direction, and we can look at the linear summit from the top view. Quartz sands with the size of 100μm was used to build the target and the angle of repose for this quartz sand is about 30 degree. The slope of the prism was measured from the base, and we set the angle from 20 to 30 degree. The quartz sands were filled into a transparent water tank with the depth of 20 cm to prepare the bulge structure. Impact experiments were conducted by using a vertical type gas gun, and the water tank was set in the chamber to evacuate below 1000 Pa. A alumina sphere projectile with the size of 3mm was launched at the velocity from 70 to 200 m/s, and it was impacted on the bulge in the vertical direction: the impact angle measured from the target surface was about 60 degree when the slope was 30 degree. The distance from the impact pint to the summit (deviation distance, d_d) was changed from 0 to 20mm.

We found that the crater shape strongly depended on the d_d, so the crater shape was an ellipsoid when the impact point was near the summit. Th major axis appeared along the linear summit and the minor axis appeared across the summit. The aspect ratio of the major axis to the minor axis gradually changed toward 1 with the increase of d_d. Moreover, the aspect ratio becomes large at the same d_d when the impact velocity increased. The major axis of the ellipsoid crater formed on the bulge was slightly larger than the crater diameter formed on the flat surface, and the slope angle might affect the size of the ellipsoid because we found that the crater formed on the slope of 30 degree was systematically larger than that formed on the slope of 20 degree. We also observed an asymmetric ejecta curtain from the impact point on the bulge, moreover the ejecta curtain was notice to be deformed so much at the impact point near the summit because of the effect of curvature of the bulge on the crater flow.

Angle of repose, Impact crater, Bulge and ridge structure, Ejecta curtain

©2019. Japan Geoscience Union. All Right Reserved.

©2019. Japan Geoscience Union. All Right Reserved.

Initial analysis plan of soluble organic compounds for the Hayabusa2 sample from asteroid Ryugu

*Hiroshi Naraoka[1], Yoshinori Takano[2], Jason P. Dworkin[3], SOM Analysis Team

1. Department of Earth and Planetary Sciences, Research Center for Planetary Trace Organic Compounds, Kyushu University, 2. Japan Agency for Marine-Earth Science and Technology, 3. Astrochemistry Laboratory NASA Goddard Space Flight Center, Greenbelt, MD 20771 USA

The spectra of asteroid 162173 Ryugu taken by Near-Infrared Spectrometer (NIRS3) onboard Hayabusa2 are nearly featureless and consistent with carbonaceous chondrites (Matsuoka et al., 2018). The Hayabusa2 spacecraft will collect surface samples of Ryugu and deliver to the Earth during late 2020. The initial analysis of the Ryugu samples will focus on (1) detailed chemical and mineralogical characterization of the samples and (2) understanding the history of Ryugu and the Solar System in order to maximize the scientific achievement of the project and (3) to prove the scientific potential of the samples to the community for the analytical opportunity (Tachibana et al., 2014). We have organized an international team, consisting of 24 members currently, for the initial analysis of soluble organic matter (SOM) for the returned samples.
The primitive asteroidal materials are expected to contain diverse and complex (e.g. elemental, structural, and optical) organic matter all at low concentrations. The occurrence of SOM will provide clues to the origins of organic compounds as well as prebiotic molecules of potential relevance to origins of life on Earth and possibly elsewhere in the Solar System. We propose the comprehensive SOM analyses to reveal the chemical evolution of Ryugu using high-sensitive and high-resolution analytical methods as follows:

1) High-resolution mass spectrometry (HRMS) of various solvent extracts with electrospray ionization (ESI) coupled with or without nano-liquid chromatography.
2) Enantiomerically resolved amino acid analysis using high-resolution column chromatography with high-sensitive fluorescence spectroscopy coupled with HRMS.
3) *In situ* organic compound analysis and molecular imaging using desorption electrospray ionization (DESI) and/or direct analysis in real time (DART) equipped with HRMS.
4) Spatial resolution imaging of organic compounds using time of flight-secondary ion mass spectrometry (ToF-SIMS; Naraoka et al., 2015).

In addition, if the sample is available, we will also perform the following additional analyses:

5) Compound-specific isotope analysis using gas chromatography/combustion or pyrolysis /isotope ratio mass spectrometry (GC/C or pyrolysis/IRMS).
6) Bulk chemical and isotopic analysis of organic matter (C, H, N and S) using nano-EA/IRMS system and laser-tunable FT-IR spectroscopy.

Depending to the sample size available to the initial analysis, we will perform preliminary analytical tests using 30 mg, 10 mg, and 1 mg samples of the Murchison meteorite (CM2, positive SOM-rich), Yamato 793321 meteorite (heated CM2, positive SOM-depleted), and baked serpentine (negative SOM-depleted) as well as procedural blank. The analytical protocol will be discussed in the meeting.

< References >
Tachibana, S. et al. (2014) Hayabusa2: Scientific importance of samples returned from C-type near-Earth

©2019. Japan Geoscience Union. All Right Reserved.

asteroid (162173) 1999 JU3. Geochemical Journal. 48. 571-581. 10.2343/geochemj.2.0350.
Matsuoka, M. et al. (2018) Spectral comparison between asteroid (162173) Ryugu and carbonaceous meteorites. American Astronomical Society, DPS meeting #50.
Naraoka, H. et al. (2015) ToF-SIMS analysis of carbonaceous particles in the sample catcher of the Hayabusa spacecraft. Earth, Planets and Space, 67:67. DOI 10.1186/s40623-015-0224-0.
Naraoka, H. and Hashiguchi, M. (2018) *In situ* organic compound analysis on a meteorite surface by desorption electrospray ionization coupled with an Orbitrap mass spectrometer. Rapid Commun. Mass Spectrom. 32, 959-964.

Keywords: Hayabusa2, Ryugu, Carbonaceous Asteroid, Soluble Organic Matter

©2019. Japan Geoscience Union. All Right Reserved.

Radar and optical simultaneous observations of faint meteors with MU radar and Tomo-e Gozen

*Ryou Ohsawa[1], Akira Hirota[2], Shinsuke Abe[2], Daniel Kastinen[3], Kero Johan[3], yasunori Fujiwara[4], Takuji Nakamura[5], Shigeyuki Sako[1], Yuto Kojima[1], Jun-ichi Watanabe[6]

1. Institute of Astronomy, Graduate School of Science, The University of Tokyo, 2. Department of Aerospace Engineering, College of Science & Technology, Nihon University, 3. Swedish Institute of Space Physics, 4. SOKENDAI (The Graduate University for Advanced Studies), 5. National Institute of Polar Research, 6. National Astronomical Observatory of Japan

The Earth is surrounded by small dust grains produced by comets and asteroids. Tons of such grains plunge into the Earth's atmosphere hourly. Part of their kinetic energy excites and ionizes the surrounding atmosphere, which is observed as a meteor phenomenon. A simultaneous radar and optical observation is promising to constrain the motion and mass of a meteor at a time. We launched a project to observe faint meteors with Middle and Upper Atmosphere Radar (MU radar) and a wide-field CMOS mosaic camera Tomo-e Gozen installed on the 105 cm Kiso Schmidt telescope. The observations were carried out in 18--21, April, 2018. From tons of the detected meteors, the simultaneous detections were extracted in terms of the times, loci, and directions of the meteors. Finally, we identified the 894 meteor events simultaneously detected in the both sites. The optical brightness of the simultaneous meteors ranged from about 3--11 mag. in the V-band, which is about 5 magnitude fainter than in previous studies. We confirmed a clear correlation between the meteor brightnesses and the radar cross sections.

Keywords: meteor, interplanetary dust

©2019. Japan Geoscience Union. All Right Reserved.

Global distribution and spectral characteristics of bright spots on asteroid Ryugu

*Masanori Suemitsu[1], Tomokatsu Morota[1], Rie Honda[2], Singo Kameda[15], Eri Tatsumi[3], Manabu Yamada[4], Naoya Sakatani[5], Toru Kouyama[6], Yokota Yasuhiro[7], Yuichiro Cho[8], Hidehiko Suzuki[9], Masahiko Hayakawa[10], Moe Matsuoka[10], Chikatoshi Honda[11], Tatsuhiro Michikami[12], Kazuo Yoshioka[13], Kazunori Ogawa[14], Hirotaka Sawada[5], Seiji Sugita[3]

1. Graduate School of Environmental Studies, Nagoya University, 2. Department of Science and Technology, System of Natural Science, Kochi Unicversity, 3. Graduate School of Earth and Planetary Science, Tokyo Unicversity, 4. Planetary Exploration Reserch Center, Chiba Institute of Technology, 5. Institute of Space and Astoronautical Science, Japan Aerospace Exploration Agency, 6. National Institute of Advanced Industrial Science and Technology, 7. Kochi University, 8. Department of Earth and Planetary Science, Tokyo University, 9. Depertment of physics, Meiji University , 10. Department of Solar System Science, Institute of Space and Astoronautical Science, Japan Aerospace Exploration Agency, 11. Aizu University, 12. Faculty of Engineering, Kindai University, 13. Graduate School of frontier Science, Tokyo University, 14. Kobe University, 15. Rikkyo University

On June 27, 2018, the asteroid explorer Hayabusa2 arrived at the target C-type asteroid 162173 Ryugu. The telescopic optical navigation camera (ONC-T) on-board Hayabusa2 has acquired the multiband image data for the entire surface of Ryugu with spatial resolutions better than 2 m/pixel. These data show that the Ryugu surface has the very low surface reflectance, flat spectra, and its spatial homogeneity [Sugita et al. 2019]. However, more detailed observations on Ryugu have revealed that many boulders exhibit different spectral properties and that a number of spots with distinctively brighter than the surroundings [Sugita et al. 2019]. Although larger boulders have been analyzed to show that they form two distinctive spectral trends, no substantial spectral analyses on bright spots have been conducted. Determining whether or not these bright spots are one of the materials that originate from the parent body of Ryugu is important to understand the differentiation and geologic processes on the parent body. In this study, in order to understand origins of the bright spots, we investigated spectral characteristics of the bright spots and compared those of the boulders on Ryugu. We used the ONC-T multiband images obtained in Box-A (20 km altitude) and mid-altitude (5 km altitude) operations.

We found seven meter-sized bright spots that have radiance factor 1.3 to 2.0 times higher than that of the surrounding area. The spectra of these bright spots were classified into two types, one being a flat spectrum type and another being a convex spectrum type. The former type has spectrum similar to but flatter and brighter than the mean spectra of the whole Ryugu and boulders, suggesting that the bright spots originate from parent body of Ryugu. The latter type has spectrum similar to those of S-type asteroids, suggesting their exogenous origin.

Keywords: asteroids, Ryugu, bright spot, spectrum, boulder

©2019. Japan Geoscience Union. All Right Reserved.

Polarimetry of (155140) 2005 UD: the Dynamical Association with (3200) Phaethon

*Masateru Ishiguro[1], Jooyeon Geem[1], Hiroyuki Naito[2], Yoonsoo P. Bach[1], Daisuke Kuroda[3], Tatsuharu Ono[4], Seiko Takagi[4], Mitsuteru Sato[4], Kiyoshi Kuramoto[4], Tomohiko Sekiguchi[5], Masataka Imai[6], Makoto Watanabe[7], Katsuhito Ohtsuka[8], Sunao Hasegawa[9], Takashi Ito[10], Fumi Yoshida[11], Tomoko Arai[11]

1. Department of Physics and Astronomy, Seoul National University, 2. Nayoro Observatory, 3. Okayama Observatory, Kyoto University, 4. Department of Cosmosciences, Graduate School of Science, Hokkaido University, 5. Hokkaido University of Education, 6. National Institute of Advanced Industrial Science and Technology, 7. Department of Applied Physics, Okayama University of Science, 8. Tokyo Meteor Network, 9. Japan Aerospace Exploration Agency, 10. National Astronomical Observatory of Japan, 11. Planetary Exploration Research Center, Chiba Institute of Technology

An Apollo-type near--Earth asteroid, (155140) 2005 UD, is considered as a possible fragment from (3200) Phaethon, suggesting that Phaethon precursor body might undergo a catastrophic disruption in the past. Here we present our new observational evidence for supporting these two are common origin. We thus conducted a polarimetric observation in 2018 September-October and found that 2005 UD exhibited a polarimetric property significantly different from those of major taxonomic classes of NEAs (i.e., S- and C-type) but similar to that of Phaethon at a wide range of the solar phase angles. Using the polarimetric data, we derived the geometric albedo of ~0.1. In addition, we made a photometric observation at the opposition (the zero phase angle), and determined the mean absolute magnitude of 17.2, the synodic rotational period 5.23 hr, and the effective diameter 1.5 km in combination with the derived geometric albedo. From these evidence, we found that the Phaethon precursor body might have lost more than a few percents of the mass via a disruption if 2005 UD was indeed ejected from the Phaethon precursor.

Keywords: Asteroids, Space Mission (Destiny+)

©2019. Japan Geoscience Union. All Right Reserved.

Follow-up observations for AKARI/IRC near-infrared asteroid spectroscopic survey (AcuA-spec)

*Sunao Hasegawa[1], Daisuke KURODA[2], Kenshi YANAGISAWA[3], Fumihiko Usui[4]

1. Japan Aerospace Exploration Agency, 2. Kyoto University, 3. National Astronomical Observatory of Japan, 4. Kobe University

In the range from 1 to 2.5 μm, we made the spectroscopic observations of the AcuA-spec asteroids (Hasegawa et al. 2017, PASJ, 69, 9), whose spectra were obtained in continuous covered between 2.5 and 5.0 μm by NIR/IRC/AKARI (Usui et al. 2019, PASJ, 71, 1). Candidates of AcuA-spec asteroids were selected from only main-belt asteroids classified based on visible spectrophotometric and spectroscopic observations (Tholen 1984, PhD thesis, Arizona University; Bus & Binzel 2002, Icarus, 158, 146; Lazzaro et al. 2004, Icarus, 172, 179). About 200 classified asteroids were raised as observational candidates. Spectroscopic observations for 65 AcuA-spec asteroids which were selected among the AcuA-spec candidate catalogue in taking account of signal-noise ratio and target opportunity by AKARI were executed.
Section work of the AcuA-spec candidate catalogue was done around 2005, yet there were not many spectroscopic observations of asteroids in the near-infrared wavelength range. As a result of survey of published paper for near-infrared spectroscopic observations of asteroids, howevwer, it was found that spectroscopic observations in the near-infrared region of 1–2.5 μm for most AcuA-spec asteroids are performed except for several asteroids.
If data in near-infrared wavelength range of the lacked AcuA-spec asteroids were acquired, all AcuA-spec asteroids will have 0.35–5 μm of data available. Obtaining continuous reflectance of asteroids is essential data to compare with those such as meteorites. Based on the Bus-DeMeo taxonomy (DeMeo et al. 2009, Icarus, 202, 160), we conducted classification of all AcuA-spec asteroids using published and our observational data.

Keywords: asteroids, spectroscopy

©2019. Japan Geoscience Union. All Right Reserved.

Amino acids on witness coupons collected from the ISAS/JAXA curation facility for the assessment and quality control of the Hayabusa2 sampling procedure

*Haruna Sugahara[1,2], Yoshinori Takano[1], Yuzuru Karouji[3], Kazuya Kumagai[4], Toru Yada[3], Naohiko Ohkouchi[1], Masanao Abe[3], Hayabusa2 project team

1. Japan Agency for Marine-Earth Science and Technology (JAMSTEC), 2. Institut de Chimie de Nice, Universite Cote dAzur, 3. Japan Aerospace Exploration Agency (JAXA), 4. Marine Works Japan Ltd.

The Hayabusa2 spacecraft is visiting a near-Earth carbonaceous type (C-type) asteroid, 162173 Ryugu, and planning to return the pristine samples to the Earth. C-type asteroids are considered to be related with carbonaceous chondrites that are enriched in organic and volatile materials. The one of the scientific goals of Hayabusa2 mission is to understand the origin and evolution of organic materials through interactions with water and minerals in the early solar system [e.g., 1]. Thus, the characterization of organic materials in the returned sample has great importance for this purpose. However, the analysis of small quantities of extraterrestrial organic materials in the returned samples requires a great care to avoid the introduction of terrestrial contaminants and any artifact materials to the pristine samples. Thus, the assessment of the degrees of the terrestrial contaminants to the samples as well as the comprehensive and specific managements to minimize the terrestrial contamination throughout the mission is essential.

The purpose of the study is to investigate the potential terrestrial organic contamination in a clean chamber for the Hayabusa2 returned samples in an Institute of Space and Astronautical Science/Japan Aerospace Exploration Agency (ISAS/JAXA) curation room [2-4]. As the indicator of the terrestrial organic contaminants, we selected amino acids that ubiquitously exist in the terrestrial environments and are also the target molecules in the Hayabusa2 mission. In the study, we used witness coupons made of aluminum foil to collect the contaminants in the clean chamber. The witness coupons were collected at different exposure times, ranging from 1 day to 1 month to examine the accumulation rate of the contaminants. After the collection, amino acids on the witness coupons were extracted in hot water, hydrolysed with HCl, and then converted to *N*-pivaloyl isopropyl (Pv/iPr) ester derivatives for gas chromatographic (GC) analysis [5].

On the witness coupons, eight terrestrially common amino acids (glycine, alanine, valine, leucine, isoleucine, proline, aspartic acid and glutamic acid) were detected and seven of them, except valine due to the under quantification limit, were quantified. Among them, glycine was the most abundant species with the highest concentration of 10 pmol/cm^2. A time-dependent profile of the four major amino acids (glycine, alanine, aspartic acid and glutamic acid) showed the increasing trend between 1 to 7 days. The average accumulation rates are 1.2 pmol/cm^2/day for glycine, 0.6 pmol/cm^2/day for alanine, 0.1 pmol/cm^2/day for aspartic acid and 0.2 pmol/cm^2/day for glutamic acid. The species and the concentrations of amino acids on our witness coupons are similar to those reported by the National Aeronautics and Space Administration/Johnson Space Center (NASA/JSC) OSIRIS-REx team [6]. Thus, the quality control against terrestrial contaminants in ISAS/JAXA curation facility is at the same quantitative level as in their facility. This inter-laboratory evaluation [7] about the terrestrial organic contamination will provide important information for the curation procedure of the Hayabusa2-returned samples.

©2019. Japan Geoscience Union. All Right Reserved.

References: [1] Tachibana S. et al. (2014) Geochem. J., 48, 571-587. doi: 10.2343/geochemj.2.0350. [2] Yada T. et al. (2014) Meteorit. Planet. Sci., 49, 135-153. doi: 10.1111/maps.12027. [3] Sawada H. et al. (2017) Space Sci. Rev. 208, 81–106. doi: 10.1007/s11214-017-0338-8. [4] Okazaki R. et al. (2017) Space Sci. Rev. 208, 107–124. doi: 10.1007/s11214-016-0289-5. [5] Chikaraishi Y. et al. (2010) in *Earth, Life, Isotopes*, Kyoto Univ. Press, pp.367-386. [6] Dworkin et al. (2018) Space Sci. Rev. 214, 9. doi: 10.1007/s11214-017-0439-4. [7] Sugahara et al. (2018) Earth, Planets Space, 70, 194. doi: 10.1186/s40623-018-0965-7.

Keywords: Amino acid, Hayabusa2, Curation, Witness coupons, Quality control

©2019. Japan Geoscience Union. All Right Reserved.

Hayabusa2 orbit determination using c5++ software

*Keiko Yamamoto[1], Toshimichi Otsubo[2], Koji Matsumoto[1], Hirotomo Noda[1], Noriyuki Namiki[1], Hiroki Senshu[3], Takahide Mizuno[4], Naoko Ogawa[4], Go Ono[4], Yuya Mimasu[4], Kent Yoshikawa[4], Tadateru Takahashi[4], Yuto Takei[4], Atsushi Fujii[4], Fuyuto Terui[4], Takanao Saiki[4], Satoru Nakazawa[4], Makoto Yoshikawa[4], Yuichi Tsuda[4]

1. National Astronomical Observatory of Japan, 2. Hitotsubashi University, 3. Chiba Institute of Technology, 4. Japan Aerospace Exploration Agency

Hayabusa2 arrived at the target asteroid Ryugu in June 2018 and is currently conducting remote sensing observations with various onboard instruments. So far, we have improved orbit determination software c5++, originally developed for the analysis of satellite laser ranging (SLR) data of the Earth, so that it can be used for the analysis of laser ranging data between Hayabusa2 and Ryugu obtained by Hayabusa2 LIDAR. Then we used it for the estimation of Hayabusa2 trajectory and the GM value of Ryugu. However, in the case of Hayabusa2, it is difficult to determine all of the 6 components of the initial state vector precisely if only LIDAR range data was used, and the simultaneously estimated GM value also had large uncertainty. To overcome this problem, in addition to LIDAR ranging data, we used Automated-Image-Tracking (AIT) data obtained by wide-angle optical navigation camera (ONC-W1) for the estimation of Hayabusa2 trajectory. In principle, LIDAR data gives information on the radial direction and AIT data give the ones on the across and along track directions. Thus, both data sets are complementary and help to improve the precision of the trajectory estimation. For this purpose, we improved c5 ++ so that it can deal with AIT data as observation data. In the presentation, we will show the results of trajectory and GM estimations using LIDAR and AIT data, and show how much the precision and accuracy are improved compared to the case using LIDAR data only.

Keywords: Hayabusa2, Orbit Determination, Ryugu

©2019. Japan Geoscience Union. All Right Reserved.

Landing Site Selection for Hayabusa2: Scientific Evaluation of the Candidate Sites on Asteroid (162173) Ryugu

*Hikaru Yabuta[1], Sei-ichiro WATANABE[2], Tomoki Nakamura[3], Naru Hirata[4], Seiji Sugita[5], Tatsuaki Okada[6], Kohei Kitazato[4], Yoshiaki Ishihara[7], Tomokatsu Morota[2], Naoya Sakatani[6], Koji Matsumoto[8], Koji Wada[9], Shogo Tachibana[5], Mutsumi Komatsu[10], ERI TATSUMI[5], Moe Matsuoka[6], Chikatoshi Honda[4], Takahiro Hiroi[11], Hiroki Senshu[9], Rie Honda[12], Yasuhiro Yokota[6], Rina Noguchi[6], Yuri Shimaki[6], Deborah Lorin Domingue[13], Lucille Le Corre[13], Antonella Barucci[14], Ernest Palomba[15], Shota Kikuchi[6], Akira Miura[6], Tomohiro Yamaguchi[6], Yukio Yamamoto[6], Takanao Saiki[6], Satoshi Tanaka[6], Makoto Yoshikawa[6], Yuichi Tsuda[6]

1. Hiroshima University, Department of Earth and Planetary Systems Science, 2. Nagoya University, 3. Tohoku University, 4. University of Aizu, 5. The University of Tokyo, 6. ISAS/JAXA, 7. NIES, 8. NAOJ, 9. Chiba Institute of Technology, Planetary Exploration Research Center (PERC), 10. Sokendai, 11. Brown University, 12. Kochi University, 13. Planetary Science Institute, USA, 14. Observatoire Paris-Site de Meudon, LESIA, France, 15. INAF-IAPS, Italy.

On June 27, 2018, JAXA’s Hayabusa2 spacecraft arrived at its target C-type asteroid Ryugu. Immediately after arrival, remote-sensing observations were carried out with the Optical Navigation Camera (ONC), the Near Infrared Spectrometer (NIRS3), the Thermal Infrared Imager (TIR), and the Laser Altimeter (LIDAR). Based on data from this suite of instruments, we carried out the landing site selection for the first touch-down (TD1). Since the mission aims to understand i) the origin and chemical evolution of the solar system and ii) the formation process and structure of the asteroid, we have set the most scientifically valuable TD1 site as the least altered region where water and/or carbon are potentially abundant.

Landing candidate sites were first selected by engineering evaluation for operational safety followed by scientific evaluations based on criteria such as science and samplability for the most interesting sites. The process was repeated using the observations from the altitudes of 20 km, 6 km, and 5 km.

Scientific evaluations of the landing site candidates were conducted based on the data products from ONC, NIRS3, TIR, and LIDAR. The shape modeling team produced two different shape models. ONC produced multiband images and reflectance spectra, as well as maps of spectral indices and X-means clustering analysis. Measurements of boulder size-frequency and Hapke parameters in the candidate landing areas were examined. NIRS3 produced four types of spectral feature maps. TIR provided maps of maximum temperature from the October 22, 2018 TD1 practice operations, apparent thermal inertia, and typical grain size determinations. LIDAR provided time series ranging data, topography, and corrected spacecraft trajectory.

Engineering evaluation: The possible landing site candidates were selected from the engineering safety score map evaluated based on the sub-Earth distance, local solar angle, local slope and elevation maximum difference. Thermal prediction results for TD1 were obtained by TIR. Temperatures of each site are < 350 K, confirming the safe conditions. The regions that satisfied all the conditions were, L05, L07, L08, L12, M01, M03 and M04.

Scientific evaluation:
1) Boulders. Based on the distribution of boulders with a diameter larger than 3 m for each potential landing site, regions L07, L08, and M04 show smaller percentages of boulder coverage than other areas, and are regarded as safer sites for landing.

©2019. Japan Geoscience Union. All Right Reserved.

2) Geology. Ryugu exhibits a variety of topographic features and geologic settings. From a scientific perspective, it is of interest to be able to study various materials representing the evolution of Ryugu.
3) Hydrous minerals. The NIR spectral properties are nearly homogeneous across Ryugu’s surface, especially between the candidate sites. The near-infrared reflectance spectra of Ryugu is similar to experimentally heated Murchison meteorite at 400˚C.
4) Carbon contents. It is likely that visible reflectance at 0.55 μm (R(0.55)) is influenced mostly by carbon content. R(0.55) is almost homogeneous across the surface with a low value, regardless of the candidate sites.
5) Secondary processes. Although the surface of Ryugu is almost homogeneous at the macro scale in the map of spectral slope from 0.48 to 0.86 μm, a slight heterogeneity is observed across the candidate regions. L-regions are relatively bluish and M-regions are reddish. Considering that spectral reddening is observed by laser irradiation of dehydrated carbonaceous chondrites, L regions are probably less altered and preferable for sampling.

In the total evaluation, L08, L07 and M04 were selected as the TD1 candidates on August 17, 2018. In September 2018, many boulders > 50 cm were additionally found for the sites during the rehearsal of TD1. Thus, the originally scheduled TD1 in October was postponed. Further search for a flat and safe site continued, and L08-E1 was determined as the TD1 site. The TD1 will be scheduled on Feb 22, 2019.

Keywords: Hayabusa2, Landing Site Selection

©2019. Japan Geoscience Union. All Right Reserved.

Visible Photometric, Spectroscopic and Polarimetric observations of an inactive comet, P/2016 BA14 with the 1.6m Pirka Telescope

*Ryo Yamagata[1], Tomohiko Sekiguchi[1], Ryo Okazaki[1], Kazuya Doi[1], Daisuke Kuroda[2], Masateru Ishiguro[3], Hiroyuki Naito[4]

1. Hokkaido University of Education, 2. Kyoto University, 3. Seoul National University, 4. Nayoro Observatory

We performed photometric, spectroscopic and polarimetric observations of an inactive comet, P/2016 BA14 with the 1.6m Pirka Telescope, Hokkaido.

P/2016 BA14 (a=3.02 au, e=0.67, i=18.9 deg.) was discovered as an unusual asteroid with a cometary orbit by the PANSTAARS on 2016 January 21.Since Knight et al. 2016 detected its cometary tail when the object close to sun(r=1.018au). It was classified into a Jupiter Family Comets. It can be regarded as a bare nucleus invisible coma because very weak comet activity that is different from general comet. There is a remarkable similarity between the orbits of 252P/LINEAR (a=3.05au, e=0.67, i=10.4deg) and P/2016 BA14. Jupiter Tisserand parameter is 252P/LINEAR and that of P/2016 BA14 are 2.82. P/2016 BA14 and 252P/LINEAR is division comet that is originally same comet (Jian-Yang.2017).

In this study, surface reflection properties of P/2016 BA14 classify D-type asteroids (Bus-DeMeo taxonomy) from result of visible spectroscopy (435-820nm). Color of surface is little red as D-type asteroid, but very blue as comet nucleus from result of BVRI photometry. The linear polarization Pr=10.46.±0.11% (α=46°) is in close accord with that of D-type asteroids and comet nucleus.

Keywords: P/2016 BA14, Photometric, Spectroscopic, Polarimetric, D-type

©2019. Japan Geoscience Union. All Right Reserved.

Polycyclic aromatic hydrocarbons and aliphatic hydrocarbons in Jbilet Winselwan carbonaceous chondrite : Attempt to evaluate the thermal metamorphism degree on the parent body

Hiroki Kato[1], *Hikaru Yabuta[1]

1. Hiroshima University, Department of Earth and Planetary Systems Science

Introduction: On June 27, 2018, Hayabusa2 spacecraft arrived at the C-type asteroid Ryugu. The surface of Ryugu has been thought to have experienced dehydration at least partially, according to the grand-based observation (Vilas et al. 2008; Hiroi et al. 1993). Therefore, it is important to investigate the chemical compositions of dehydrated carbonaceous CM chondrites for understanding the surface process of asteroid Ryugu. Although the extents of thermal metamorphism of CM chondrites have been evaluated by mineralogical compositions (e.g., Nakamura et al. 2006) and elemental and molecular compositions of insoluble organic matter (IOM) (e.g., Naraoka et al. 2004; Yabuta et al. 2005), the estimated temperature varies widely. On the other hand, soluble organic molecules from the dehydrated CM chondrites have not been quantified or below detection (e.g. Shimoyama et al. 1989), and there has been no study which evaluated thermal metamorphism based on the compositions of soluble organic molecules. Therefore, in this study, we analyzed aliphatic hydrocarbons and polycyclic aromatic hydrocarbons (PAHs) in Jbilet Winselwan CM chondrite, which is a dehydrated CM chondrite (Zolensky et al 2016) and show similar reflectance spectrum to that of asteroid Ryugu (Kameda et al. 2015), for precise evaluation of parent body thermal metamorphism. The relative abundances of the hydrocarbons were compared with those of Murray meteorite, which is a primitive CM chondrite.

Samples and Methods: Powdered samples of Jbilet Winselwan meteorite and Murray meteorite (0.2 - 0.4g) were extracted with dichloromethane/methanol (9:1) by sonication. The extracts were applied to a silica gel column. From the column, aliphatic hydrocarbons were eluated with hexane and then PAHs were eluated with dichloromethane. The hexane and dichloromethane eluates were concentrated to 100 μl individually under a nitrogen flow for analysis by a gas chromatography coupled with mass spectrometry (GC-MS). Identification and quantification of compounds were made by comparison of peak retention times on mass chromatograms and mass spectra, and peak areas, respectively, with those of standard compounds. For compounds without standard compounds, identification was made by comparison of mass spectra with library data.

Results and discussion: Total concentration of *n*-alkanes from Jbilet Winselwan meteorite (1.85 μg/g meteorite) was 40 times lower than those from Murray meteorite (80.7 μg/g meteorite). Relative abundances of short-chain *n*-alkanes (C_{15}-C_{16}) were dominant in Jbilet Winselwan meteorite, while those of long-chain *n*-alkanes (C_{17}-C_{21}) were dominant in Murray meteorite. This difference implies that short-chain *n*-alkanes were resulted from cracking of long-chain *n*-alkanes and/or IOM during thermal metamorphism of the parent body of Jbilet Winselwan meteorite. Total concentration of PAHs from Jbilet Winselwan meteorite (0.05 μg/ meteorite) was 1000 times lower than those from Murray meteorite (62.0 μg/g meteorite). Dimethylnaphthalene, fluorine, phenanthrene, pyrene, fluoranthene, methylbiphenyl (0.003-0.039 μg/g meteorite) were identified, while low molecular weight PAHs, such as naphthalene, methylnaphthalene, and acenaphthene, were not detected. The results suggest that PAHs with high volatility in Jbilet Winselwan meteorite were lost or involved in further aromatization during thermal metamorphism. Distributions of dimethylnaphthalene and methylbiphenyl isomers in Jbilet Winselwan

©2019. Japan Geoscience Union. All Right Reserved.

and Murray meteorites were similar, respectively, which indicates that the parent body of Jbilet Winselwan meteorite experienced relatively mild thermal metamorphism.

Keywords: Jbilet Winselwan meteorite, Soluble organic molecules, Dehydration

©2019. Japan Geoscience Union. All Right Reserved.

Disk-Resolved Photometry Analysis of the Asteroid Ryugu Images Obtained by Hayabusa2 Visible Camera ONC

*yokota yasuhiro[1,2], Rie Honda[1], ERI TATSUMI[3], Deborah Domingue[4], Stefanus E. Schroeder[5], Moe Matsuoka[2], Seiji Sugita[3], Tomokatsu Morota[6], Shingo Kameda[7], Toru Kouyama[8], Hidehiko Suzuki[9], Manabu Yamada[10], Naoya Sakatani[2], Chikatoshi Honda[11], Masahiko Hayakawa[2], Kazuo Yoshioka[3], Yuichiro Cho[3], Hirotaka Sawada[2]

1. Kochi University, 2. ISAS/JAXA, 3. Univ. of Tokyo, 4. Planetary Science Institute, 5. DLR, 6. Nagoya Univ., 7. Rikkyo Univ., 8. AIST, 9. Meiji Univ., 10. Chiba Institute od Technology, 11. Aizu Univ.

Since June 2018, the Optical Navigation Camera (ONC) onboard Hayabusa2, has observed the C-type asteroid 162173 Ryugu at a distance below 20 km. ONC-T and ONC-W1 are used for surface imaging operations, and their images allow us to investigate the disk-resolved photometric properties of the surface. A narrow-angle camera ONC-T has 7 broad-band filters ranging in wavelength from 0.39–0.95 μm. ONC-W1 is a wide-angle (> 65˚) pan-chromatic camera mainly used for optical navigation during cruise and low-altitude (< 20km) operations. We are proceeding the analysis of both dataset, ONC-T and ONC-W1.

Since Hayabusa2’s position is nominally fixed on the line connecting Ryugu and the Earth, the available solar phase angle range by ONC-T changes seasonally with the orbits of Earth and Ryugu around the sun. Therefore, we are collecting a large number of ONC-T images over a long period of time to cover a wide phase angle range.

ONC-W1 data has a strong point that it covers a wide phase angle range within a single frame during the descent operations, because of its wide field of view. One of our current challenges is deriving a precise viewing geometries (incidence angle, emission angle, and phase angle) at each pixel. Additionally, comparison of the absolute brightness value (radiance factor) with ONC-T is an ongoing issue.

Keywords: Asteroid, Photometry, Ryugu, Hayabusa2

©2019. Japan Geoscience Union. All Right Reserved.

[E] Poster | P (Space and Planetary Sciences)：P-PS Planetary Sciences

Wed. May 29, 2019 5:15 PM - 6:30 PM JST | Wed. May 29, 2019 8:15 AM - 9:30 AM UTC | Poster Hall International Exhibition Hall8, Makuhari Messe_3

[P-PS03] Solar System Small Bodies: A New Frontier Arising Hayabusa 2, OSIRIS-REx and Other Projects

convener:Masateru Ishiguro(Department of Physics and Astronomy, Seoul National University), Taishi Nakamoto(Tokyo Institute of Technology), Masanao Abe(Institute of Space and Astronautical Science, Japan Aerospace Exploration Agency), Olivier S Barnouin(Johns Hopkins University Applied Physics Laboratory)

In June 2018, the Hayabusa 2 spacecraft arrived at the target asteroid Ryugu after three and half years journey. In addition, another spacecraft, OSIRIS-REx will soon arrive at its destination Bennu. With these arrivals, the solar system research is about to enter a new era. We have organized this small bodies session since 2012 and had a broad range of discussions from viewpoints of laboratory experiments, observations, space explorations, theoretical modeling, and sample analyses. In particular, this time, we aim to hold this session to bring the latest research on solar system small bodies, focusing on the initial results of Hayabusa 2 and OSIRIS-REx. Presentations in the related fields other than these two asteroidal missions are also welcomed.

[PPS03-P01] Impact experiments on low strength coarse-grained regolith simulating surface materials on asteroid Ryugu

*Yuya Yamamoto[1], Masahiko Arakawa[1], Minami Yasui[1], Sunao Hasegawa[2], Ryo Sugimura[1] (1.Graduate School of Science, Kobe University, 2.ISAS, JAXA)

[PPS03-P02] Reflectance estimation of asteroid Ryugu using MASCOT

*Marika Ishida[1], Koto Amano[1], Keiichi Moroi[1], ERI TATSUMI[2], Tra-Mi Ho[10], Shingo Kameda[1], Seiji Sugita[2], Rie Honda[3], Tomokatsu Morota[4], yokota yasuhiro[5], Toru Kouyama[6], Hidehiko Suzuki[7], Manabu Yamada[8], Naoya Sakatani[5], Chikatoshi Honda[9], Masahiko Hayakawa[5], Kazuo Yoshioka[2], Moe Matsuoka[5], Yuichiro Cho[2], Hirotaka Sawada[5] (1.Rikkyo Univ., 2.Univ. of Tokyo, 3.Kochi Univ., 4.Nagoya Univ., 5.JAXA/ISAS, 6.AIST, 7.Meiji Univ., 8.Chiba Inst. Tech, 9.Univ. of Aizu, 10.DLR)

[PPS03-P03] Flyby observation of Asteroid (3200) Phaethon by DESTINY$^+$ onboard cameras

*Ko Ishibashi[1], Shingo Kameda[2], Masato Kagitani[3], Peng Hong[1], Manabu Yamada[1], Osamu Okudaira[1], Tomoko Arai[1], Fumi Yoshida[1], Shunsuke Sato[4], Takahiro Ishimaru[4], Takaya Okamoto[4], Takahiro Iwata[4], Tatsuaki Okada[4], Takeshi Takashima[4] (1.Chiba Institute of Technology, 2.Rikkyo University, 3.Tohoku Universtiy, 4.Japan Aerospace Exploration Agency)

[PPS03-P04] Polarimetric Study of Asteroids in Comet-Like Orbits (ACOs)

*Jooyeon Geem[1], Masateru Ishiguro[1], Yoonsoo P. Bach[1], Daisuke Kuroda[2], Hiroyuki Naito[3], Hidekazu Hanayama[4], yoonyoung kim[10], Yuna G. Kwon[1], Sunho Jin[1], Tomohiko Sekiguchi[5], Ryo Okazaki[5], Jeremie J. Vaubaillon[6], Masataka Imai[7], Tatsuharu Oono[8], Yuki Futamuts[8], Seiko Takagi[8], Mitsuteru Sato[8], Kiyoshi Kuramoto[8], Makoto Watanabe[9] (1.Astronomy program, Dept of Physics and Astronomy, Seoul National University, 2.Okayama Observatory, Kyoto University, 3.Nayoro Observatory, 4.Ishigakijima Astronomical Observatory, National Astronomical Observatory of Japan, 5.Hokkaido University of Education, 6.Observatoire de Paris, I.M.C.C.E., 7.National Institute of Advanced Industrial Science and Technology, 8.Department of Cosmosciences, Graduate School of Science, Hokkaido University, 9.Department of Applied Physics, Okayama University of Science, 10.Max Planck Institute for Solar System Research)

[PPS03-P05] Dynamical lifetime of the Oort Cloud new comets under planetary perturbation

*Ito Takashi[1], Arika Higuchi[1] (1.National Astronomical Observatory of Japan)

[PPS03-P06] Thermal Infrared Imaging of C-type Asteroid 162173 Ryugu with Porous Surfaces

*Tatsuaki Okada[1,2], Tetsuya Fukuhara[3], Satoshi Tanaka[1], Makoto Taguchi[3], Takehiko Arai[4], Naoya Sakatani[1], Yuri Shimaki[1], Hiroki Senshu[5], Yoshiko Ogawa[6], Hirohide Demura[6], Kentaro Suko[6], Kohei Kitazato[6], Toru Kouyama[7], Tomohiko Sekiguchi[8], Jun Takita[9], Sunao Hasegawa[1], Tsuneo Matsunaga[10], Takehiko Wada[1], Takeshi Imamura[2], Jorn Helbert[11], Thomas G. Mueller[12], Axel Hagermann[13], Jens Biele[11], Matthias Grott[11], Maximiliam Hamm[11], Marco Delbo[14], Yukio Yamamoto[1], Naru Hirata[6], Naoyuki Hirata[15], Fuyuto Terui[1], Takanao Saiki[1], Satoru Nakazawa[1], Makoto Yoshikawa[1], Sei-ichiro WATANABE[1,16], Yuichi Tuda[1] (1.Institute of Space and Astronautical Science, Japan Aerospace Exploration Agency, 2.University of Tokyo, 3.Rikkyo University, 4.Ashikaga University, 5.Chiba Institute of Technology, 6.University of Aizu, 7.National Institute of Advanced Industrial Science and Technology, 8.Hokkaido University of Education, 9.Hokkaido Kitami-Hokuto High School, 10.National Institute for Environmental Studies, 11.German Aerospace Center, 12.Max-Planck Institute for Extraterrestrial Physics, 13.University of Stirling, 14.Observatoire de la Côte d'Azur, 15.Kobe University, 16.Nagoya University)

[PPS03-P07] Data Release of Asteroid 162173 Ryugu by Observation of Thermal Infrared Imager onboard Hayabusa2

*Takehiko Arai[1], Hirohide Demura[2], Toru Kouyama[7], Naoya Sakatani[3], Kentaro Suko[2], Yuri Shimaki[3], Hiroki Senshu[5], Tomohiko Sekiguchi[6], Yoshiko Ogawa[2], Sunao Hasegawa[3], Takehiko Wada[3], Takeshi Imamura[10], Tsuneo Matsunaga[9], Jun Takita[8], Kohei Kitazato[2], Makoto Taguchi[4], Tetsuya Fukuhara[4], Satoshi Tanaka[3], Tatsuaki Okada[3] (1.Ashikaga University, 2.The University of Aizu, 3.Japan Aerospace Exploration Agency (JAXA), 4.Rikkyo University, 5.Chiba Institute of Technology, 6.Hokkaido University of Education, 7.National Institute of Advanced Industrial Science and Technology (AIST), 8.Hokkaido Kitami Hokuto High School, 9.National Institute for Environmental Studies (NIES), 10.The University of Tokyo)

[PPS03-P08] Multi-mission capability of HARMONICS

*Shintaro Tsunoda[1], Hirohide Demura[1], Naru Hirata[1] (1.The University of Aizu)

[PPS03-P09] New interface of verification for calibration and conversion in HEAT : Hayabusa2 Exploration Assistant for TIR

*Tatsuro Kobayashi[1], Kentaro Suko[1], Hirohide Demura[1], Yoshiko Ogawa[1], Takehiko Arai[2], Naoya Sakatani[3], Tatsuaki Okada[3], Satoshi Tanaka[3], Tetsuya Fukuhara[4] (1.The University of Aizu, 2.Ashikaga University, 3.Institute of Space and Astronautical Science, Japan Aerospace Exploration Agency, 4.Rikkyo University)

[PPS03-P10] **Dust particle evolution of a near-Earth object 252P/LINEAR from near-infrared polarimetric observations in 2016**

*Yuna G Kwon[1], Masateru Ishiguro[1], Jungmi Kwon[2], Daisuke Kuroda[3], Myungshin Im[1], Changsu Choi[1], Motohide Tamura[4], Takahiro Nagayama[5], Nobuyuki Kawai[6], Jun-ichi Watanabe[7] (1.Seoul National Univ., 2.ISAS/Japan Aerospace Exploration Agency, 3.Okayama Astrophysical Observatory, 4.The Univ. of Tokyo, 5.Kagoshima Univ., 6.Tokyo Institute of Technology, 7.National Astronomical Observatory of Japan)

[PPS03-P11] **Performance Evaluation of TRIPOL on the 61-cm Telescope at Seoul National University for Polarimetric Observations of Solar System Small Bodies**

*Sunho Jin[1], Masateru Ishiguro[1], Yuna G Kwon[1], Jooyeon Geem[1], Yoonsoo P. Bach[1], Jinguk Seo[1], Hiroshi Sasago[2], Shuji Sato[3] (1.Seoul National University, 2.Sasago Co.,Ltd, 3.Nagoya University)

[PPS03-P12] Smart Interface of HEAT: Hayabusa2 Exploration Assistant for TIR

*Kentaro Suko[1], Tatsuro Kobayashi[1], Hirohide Demura[1], Takehiko Arai[2], Naoya Sakatani[3], Tatsuaki Okada[3], Satoshi Tanaka[3], Tetsuya Fukuhara[4] (1.The University of Aizu, 2.Ashikaga University, 3.Institute of Space and Astronautical Science, Japan Aerospace Exploration Agency, 4.Rikkyo University)

[PPS03-P13] Experimental Study on Collision Crater Formed on Bulge Geography

*Yusaku Yokota[1], Yuya Yamamoto[2], Minami Yasui[2], Masahiko Arakawa[2] (1.Faculty of Science, Kobe University, 2.Graduate School of Science, Kobe University)

[PPS03-P14] Initial analysis plan of soluble organic compounds for the Hayabusa2 sample from asteroid Ryugu

*Hiroshi Naraoka[1], Yoshinori Takano[2], Jason P. Dworkin[3], SOM Analysis Team (1.Department of Earth and Planetary Sciences, Research Center for Planetary Trace Organic Compounds, Kyushu University, 2.Japan Agency for Marine-Earth Science and Technology, 3.Astrochemistry Laboratory NASA Goddard Space Flight Center, Greenbelt, MD 20771 USA)

[PPS03-P15] Radar and optical simultaneous observations of faint meteors with MU radar and Tomo-e Gozen

*Ryou Ohsawa[1], Akira Hirota[2], Shinsuke Abe[2], Daniel Kastinen[3], Kero Johan[3], yasunori Fujiwara[4], Takuji Nakamura[5], Shigeyuki Sako[1], Yuto Kojima[1], Jun-ichi Watanabe[6] (1.Institute of Astronomy, Graduate School of Science, The University of Tokyo, 2.Department of Aerospace Engineering, College of Science & Technology, Nihon University, 3.Swedish Institute of Space Physics, 4.SOKENDAI (The Graduate University for Advanced Studies), 5.National Institute of Polar Research, 6.National Astronomical Observatory of Japan)

[PPS03-P16] Global distribution and spectral characteristics of bright spots on asteroid Ryugu

*Masanori Suemitsu[1], Tomokatsu Morota[1], Rie Honda[2], Singo Kameda[15], Eri Tatsumi[3], Manabu Yamada[4], Naoya Sakatani[5], Toru Kouyama[6], Yokota Yasuhiro[7], Yuichiro Cho[8], Hidehiko Suzuki[9], Masahiko Hayakawa[10], Moe Matsuoka[10], Chikatoshi Honda[11], Tatsuhiro Michikami[12], Kazuo Yoshioka[13], Kazunori Ogawa[14], Hirotaka Sawada[5], Seiji Sugita[3] (1.Graduate School of Environmental Studies, Nagoya University, 2.Department of Science and Technology, System of Natural Science, Kochi Unicversity, 3.Graduate School of Earth and Planetary Science, Tokyo Unicversity, 4.Planetary Exploration Reserch Center, Chiba Institute of Technology, 5.Institute of Space and Astoronautical Science, Japan Aerospace Exploration Agency, 6.National Institute of Advanced Industrial Science and Technology, 7.Kochi University, 8.Department of Earth and Planetary Science, Tokyo University, 9.Depertment of physics, Meiji University , 10.Department of Solar System Science, Institute of Space and Astoronautical Science, Japan Aerospace Exploration Agency, 11.Aizu University, 12.Faculty of Engineering, Kindai University, 13.Graduate School of frontier Science, Tokyo University, 14.Kobe University, 15.Rikkyo University)

[PPS03-P17] Polarimetry of (155140) 2005 UD: the Dynamical Association with (3200) Phaethon

*Masateru Ishiguro[1], Jooyeon Geem[1], Hiroyuki Naito[2], Yoonsoo P. Bach[1], Daisuke Kuroda[3], Tatsuharu Ono[4], Seiko Takagi[4], Mitsuteru Sato[4], Kiyoshi Kuramoto[4], Tomohiko Sekiguchi[5], Masataka Imai[6], Makoto Watanabe[7], Katsuhito Ohtsuka[8], Sunao Hasegawa[9], Takashi Ito[10], Fumi Yoshida[11], Tomoko Arai[11] (1.Department of Physics and Astronomy, Seoul National University, 2.Nayoro Observatory, 3.Okayama Observatory, Kyoto University, 4.Department of Cosmosciences, Graduate School of Science, Hokkaido University, 5.Hokkaido University of Education, 6.National Institute of Advanced Industrial Science and Technology, 7.Department of Applied Physics, Okayama University of Science, 8.Tokyo Meteor Network, 9.Japan Aerospace Exploration Agency, 10.National Astronomical Observatory of Japan, 11.Planetary Exploration Research Center, Chiba Institute of Technology)

[PPS03-P18] **Follow-up observations for AKARI/IRC near-infrared asteroid spectroscopic survey (AcuA-spec)**

*Sunao Hasegawa[1], Daisuke KURODA[2], Kenshi YANAGISAWA[3], Fumihiko Usui[4] (1.Japan Aerospace Exploration Agency, 2.Kyoto University, 3.National Astronomical Observatory of Japan, 4.Kobe University)

[PPS03-P19] Amino acids on witness coupons collected from the ISAS/JAXA curation facility for the assessment and quality control of the Hayabusa2 sampling procedure

*Haruna Sugahara[1,2], Yoshinori Takano[1], Yuzuru Karouji[3], Kazuya Kumagai[4], Toru Yada[3], Naohiko Ohkouchi[1], Masanao Abe[3], Hayabusa2 project team (1.Japan Agency for Marine-Earth Science and Technology (JAMSTEC), 2. Institut de Chimie de Nice, Universite Cote dAzur, 3.Japan Aerospace Exploration Agency (JAXA), 4.Marine Works Japan Ltd.)

[PPS03-P20] Hayabusa2 orbit determination using c5++ software

*Keiko Yamamoto[1], Toshimichi Otsubo[2], Koji Matsumoto[1], Hirotomo Noda[1], Noriyuki Namiki[1], Hiroki Senshu[3], Takahide Mizuno[4], Naoko Ogawa[4], Go Ono[4], Yuya Mimasu[4], Kent Yoshikawa[4], Tadateru Takahashi[4], Yuto Takei[4], Atsushi Fujii[4], Fuyuto Terui[4], Takanao Saiki[4], Satoru Nakazawa[4], Makoto Yoshikawa[4], Yuichi Tsuda[4] (1.National Astronomical Observatory of Japan, 2.Hitotsubashi University, 3.Chiba Institute of Technology, 4.Japan Aerospace Exploration Agency)

[PPS03-P21] **Landing Site Selection for Hayabusa2: Scientific Evaluation of the Candidate Sites on Asteroid (162173) Ryugu**

*Hikaru Yabuta[1], Sei-ichiro WATANABE[2], Tomoki Nakamura[3], Naru Hirata[4], Seiji Sugita[5], Tatsuaki Okada[6], Kohei Kitazato[4], Yoshiaki Ishihara[7], Tomokatsu Morota[2], Naoya Sakatani[6], Koji Matsumoto[8], Koji Wada[9], Shogo Tachibana[5], Mutsumi Komatsu[10], ERI TATSUMI[5], Moe Matsuoka[6], Chikatoshi Honda[4], Takahiro Hiroi[11], Hiroki Senshu[9], Rie Honda[12], Yasuhiro Yokota[6], Rina Noguchi[6], Yuri Shimaki[6], Deborah Lorin Domingue[13], Lucille Le Corre[13], Antonella Barucci[14], Ernest Palomba[15], Shota Kikuchi[6], Akira Miura[6], Tomohiro Yamaguchi[6], Yukio Yamamoto[6], Takanao Saiki[6], Satoshi Tanaka[6], Makoto Yoshikawa[6], Yuichi Tsuda[6] (1.Hiroshima University, Department of Earth and Planetary Systems Science, 2.Nagoya University, 3.Tohoku University, 4.University of Aizu, 5.The University of Tokyo, 6.ISAS/JAXA, 7.NIES, 8.NAOJ, 9.Chiba Institute of Technology, Planetary Exploration Research Center (PERC), 10.Sokendai, 11.Brown University, 12.Kochi University, 13.Planetary Science Institute, USA, 14.Observatoire Paris-Site de Meudon, LESIA, France, 15.INAF-IAPS, Italy.)

[PPS03-P22] Visible Photometric, Spectroscopic and Polarimetric observations of an inactive comet, P/2016 BA14 with the 1.6m Pirka Telescope

*Ryo Yamagata[1], Tomohiko Sekiguchi[1], Ryo Okazaki[1], Kazuya Doi[1], Daisuke Kuroda[2], Masateru Ishiguro[3], Hiroyuki Naito[4] (1.Hokkaido University of Education, 2.Kyoto University, 3.Seoul National University, 4.Nayoro Observatory)

[PPS03-P23] **Polycyclic aromatic hydrocarbons and aliphatic hydrocarbons in Jbilet Winselwan carbonaceous chondrite : Attempt to evaluate the thermal metamorphism degree on the parent body**

Hiroki Kato[1], *Hikaru Yabuta[1] (1.Hiroshima University, Department of Earth and Planetary Systems Science)

[PPS03-P24] Disk-Resolved Photometry Analysis of the Asteroid Ryugu Images Obtained by Hayabusa2 Visible Camera ONC

*yokota yasuhiro[1,2], Rie Honda[1], ERI TATSUMI[3], Deborah Domingue[4], Stefanus E. Schroeder[5], Moe Matsuoka[2], Seiji Sugita[3], Tomokatsu Morota[6], Shingo Kameda[7], Toru Kouyama[8], Hidehiko Suzuki[9], Manabu Yamada[10], Naoya Sakatani[2], Chikatoshi Honda[11], Masahiko Hayakawa[2], Kazuo Yoshioka[3], Yuichiro Cho[3], Hirotaka Sawada[2] (1.Kochi University, 2.ISAS/JAXA, 3.Univ. of Tokyo, 4.Planetary Science Institute, 5.DLR, 6.Nagoya Univ., 7.Rikkyo Univ., 8.AIST, 9.Meiji Univ., 10.Chiba Institute od Technology, 11.Aizu Univ.)

Impact experiments on low strength coarse-grained regolith simulating surface materials on asteroid Ryugu

*Yuya Yamamoto[1], Masahiko Arakawa[1], Minami Yasui[1], Sunao Hasegawa[2], Ryo Sugimura[1]

1. Graduate School of Science, Kobe University, 2. ISAS, JAXA

Impact cratering is one of the most important physical processes, then we study crater scaling laws and impact induced seismic waves in order to elucidate various flow processes on asteroids caused by impacts. The conventional crater scaling laws are categorized into two regions according to the controlling physics for the crater growth: they are gravity and material strength. A crater formed on regolith layer is surely controlled by the gravity, however when the regolith layer was filled with coarse particles with low mechanical strength, then the several coarse grains might be disrupted to consume the Ek. Thus, the crater size could be affected by the disruptions of the coarse grains. We speculate that not only the gravity but also the grain strength could affect the final crater size. Then, we made cratering experiments by using the target made of weak particles, and studied the effects of the particle strength on the crater scaling law and the impact induced seismic wave.

Experiments: Cratering experiments were conducted by using a gas gun set at Kobe University and ISAS. Granular targets were prepared by using weathered tuff granules with the size of 1 to 4mm (small particle) and the size of 1 to 4cm (large particle). The crush strength of these tuff particles was measured to be about 60 kPa. A spherical projectile with the size of 3mm which is made of iron, zirconia, alumina, glass, and nylon) was lunched at the impact velocity from 40 to 200m/s, and a spherical Al projectile with the size of 2mm was impacted at the impact velocity from 1.2 to 4.5km/s, then these two types of the projectile were impacted on the target surface at the normal direction. Impact cratering process and ejecta curtain growth were observed by a high-speed camera at 10^3-10^5 fps, and the video images were used to analyze ejecta particles to reconstruct the trajectories. After the shot, the crater morphology was recorded and the diameter and the depth were measured. Impact induced seismic waves were measured by using 3 accelerometers (specific frequency is 30kHz) set at different positions from the impact point, and a data logger was used to record the seismic data through charge amplifiers (data acquisition rate is 100kHz) connecting to the accelerometer.

Results: The crater size was found to increase with the projectile kinetic energy (Ek) at lower than 0.14J and at higher than 0.63J, so that the crater size was almost constant among them, and more the crater size obtained at very high Ek was almost on the extrapolated line from the relationship given by the low Ek data. The pi-scaling law was used to construct the relationship between normalized radius (πR) and normalized gravity (π2), and πR at small π2 was found to be rather smaller than that obtained for sand and glass beads targets, and more πR at large π2 was found to be consistent with that for sand and glass beads. More detail analysis tells us that all the data separated into two trends with large offset according to the impact velocity and the projectile material. This offset might be caused by the disruption of several tuff particles. The ejection velocities of each tuff particle were so scattered, then the distinctive relationship between initial position of particle and the ejection velocity was not derived in the low velocity range. The propagation velocity of the impact induced seismic wave was about 30 m/s, and it is 1/3 of that for glass beads. Furthermore, we found that the relationship between the maximum acceleration and the distance from the impact point was about 1/10 of that obtained for glass beads: the seismic wave in the tuff granules attenuated so quickly compared to the glass beads. But, when the distance is normalized by the crater radius, these relationships almost consistent each other, so that the

©2019. Japan Geoscience Union. All Right Reserved.

normalized distance could be a good parameter for the scaling of the acceleration of seismic wave.

Keywords: impact cratering experiment, low strength, impact-induced seismic shaking, crater scaling law

©2019. Japan Geoscience Union. All Right Reserved.

Reflectance estimation of asteroid Ryugu using MASCOT

*Marika Ishida[1], Koto Amano[1], Keiichi Moroi[1], ERI TATSUMI[2], Tra-Mi Ho[10], Shingo Kameda[1], Seiji Sugita[2], Rie Honda[3], Tomokatsu Morota[4], yokota yasuhiro[5], Toru Kouyama[6], Hidehiko Suzuki[7], Manabu Yamada[8], Naoya Sakatani[5], Chikatoshi Honda[9], Masahiko Hayakawa[5], Kazuo Yoshioka[2], Moe Matsuoka[5], Yuichiro Cho[2], Hirotaka Sawada[5]

1. Rikkyo Univ., 2. Univ. of Tokyo, 3. Kochi Univ., 4. Nagoya Univ., 5. JAXA/ISAS, 6. AIST, 7. Meiji Univ., 8. Chiba Inst. Tech, 9. Univ. of Aizu, 10. DLR

Hayabusa2 is a sample-return mission for the C-type asteroid 162173 Ryugu. Hayabusa2 arrived at Ryugu on 27 June 2018, and various observations are still being conducted. Hayabusa2 performs multiband spectral observation by employing the optical navigation camera telescope (ONC-T)and can thereby obtain spectral map of Ryugu, which enables the study of material distribution and degree of space weathering of Ryugu. However, the sensitivity of ONC-T has been previously calibrated by incorporating the inflight data of stars with significant uncertainty. Hence, the authors aim to estimate the reflectance of Ryugu by employing Mobile Asteroid Surface Scout (MASCOT).
MASCOT comprises four instruments (MASCAM, MicrOmega, MARA, and MASMAG) that are employed for analyzing the soil of Ryugu. The upper side of the MASCOT landeris coated with white paint, and its spectral image was captured by ONC-T after its release from Hayabusa2 to Ryugu. The authors conducted on-ground reflectance measurement of a white plate whose white paint is identical to that of MASCOT. Hence, the primary objective of the proposed study is to estimate the reflectance of Ryugu by comparing MASCOT’ s white side’ s spectrum captured by ONC-T with the on-ground reflectance measurement of the white plate that has identical paint as MASCOT, and thus evaluate the validity.

Keywords: Hayabusa2, ONC-T, MASCOT

©2019. Japan Geoscience Union. All Right Reserved.

Flyby observation of Asteroid (3200) Phaethon by DESTINY$^+$ onboard cameras

*Ko Ishibashi[1], Shingo Kameda[2], Masato Kagitani[3], Peng Hong[1], Manabu Yamada[1], Osamu Okudaira[1], Tomoko Arai[1], Fumi Yoshida[1], Shunsuke Sato[4], Takahiro Ishimaru[4], Takaya Okamoto[4], Takahiro Iwata[4], Tatsuaki Okada[4], Takeshi Takashima[4]

1. Chiba Institute of Technology, 2. Rikkyo University, 3. Tohoku Universtiy, 4. Japan Aerospace Exploration Agency

DESTINY$^+$ (Demonstration and Experiment of Space Technology for INterplanetary voYage, Phaethon fLy-by and dUst Science) is a mission proposed for JAXA/ISAS Epsilon class small program, currently in the pre-project phase (Phase-A) with a launch targeted for 2023. DESTINY$^+$ is a joint mission of technology demonstration and scientific observation. The near-Earth asteroid (3200) Phaethon, the flyby target, is known as a parent body of the Geminid meteor shower, the size of which is approximately 5 to 6 km in diameter.

In this mission, spatially resolved images of Phaethon will be taken by two onboard cameras, the Telescopic CAmera for Phaethon (TCAP) and the Multiband CAmera for Phaethon (MCAP) during the flyby, in order to understand the nature of a meteor shower's parent body, which is one of the sources of interplanetary dust particles that are thought to be an important transport medium of organic matter to the Earth. The spacecraft flybys Phaethon with a relative speed of 30 to 40 km/s. Despite such a high flyby speed, the cameras are required to take un-blurred images of Phaethon.

The main purposes of the DESTINY$^+$ flyby observation of Phaethon is to understand the geology of a parent body of a meteor shower, and in particular constrain the dust ejection mechanisms from active (i.e., dust-ejecting) asteroids. The specific objectives of the camera observation are taking images for (1) obtaining the light curve of Phaethon in order to estimate the rotational period, (2) measuring the outline shape of Phaeton, (3) making a 3D shape model of Phaethon, (4) observing the surface geological features of Phaethon including dust ejection features, and (5) observing the surface material distribution of Phaethon. The observations (1) to (4) will be conducted by TCAP, and (5) by MCAP.

TCAP is a telescopic panchromatic camera for high spatial resolution imaging of the surface of Phaethon and have a rotational mirror for asteroid tracking during flyby. The rotational mirror can change the direction of the line of sight from 0 deg to 180 deg. This enables to observe Phaethon throughout the flyby with wide solar phase angles, which is extremely important to image and understand the surfaces of planetary bodies because the solar phase angle affects significantly the appearance of geological features in taken images.

MCAP is a multiband camera, the wavelengths of which are 400, 480, 550, 700, 850, and 950 nm (480 and 950 nm are optional bands) and has multiple optical systems and sensors in order to take all band images simultaneously. This is because there is not enough time to take each band image in turn with changing bandpass filters using such as a filter wheel in this high speed flyby mission. MCAP does not have a tracking mirror due to the weight limitation, and the line of sight of MCAP is fixed to the spacecraft with 40 deg off the relative velocity vector of the spacecraft.

We will explain the flyby imaging sequence of DESTINY$^+$, and show the conceptual designs of TCAP and MCAP.

©2019. Japan Geoscience Union. All Right Reserved.

Keywords: Phaethon, DESTINY+, Flyby, Camera

©2019. Japan Geoscience Union. All Right Reserved.

Polarimetric Study of Asteroids in Comet-Like Orbits (ACOs)

*Jooyeon Geem[1], Masateru Ishiguro[1], Yoonsoo P. Bach[1], Daisuke Kuroda[2], Hiroyuki Naito[3], Hidekazu Hanayama[4], yoonyoung kim[10], Yuna G. Kwon[1], Sunho Jin[1], Tomohiko Sekiguchi[5], Ryo Okazaki[5], Jeremie J. Vaubaillon[6], Masataka Imai[7], Tatsuharu Oono[8], Yuki Futamuts[8], Seiko Takagi[8], Mitsuteru Sato[8], Kiyoshi Kuramoto[8], Makoto Watanabe[9]

1. Astronomy program, Dept of Physics and Astronomy, Seoul National University, 2. Okayama Observatory, Kyoto University, 3. Nayoro Observatory, 4. Ishigakijima Astronomical Observatory, National Astronomical Observatory of Japan, 5. Hokkaido University of Education, 6. Observatoire de Paris, I.M.C.C.E., 7. National Institute of Advanced Industrial Science and Technology, 8. Department of Cosmosciences, Graduate School of Science, Hokkaido University, 9. Department of Applied Physics, Okayama University of Science, 10. Max Planck Institute for Solar System Research

It is important to determine the taxonomic types of small bodies in the solar system and further to study the spatial distribution of the planetary system. Among the small bodies, it is considered that there should be dormant comets that have lost a significant fraction of volatile materials in their subsurface layers. As a result, they are unable to produce any detectable coma and recognized as asteroids. It has been challenging to find out such dormant comet population from a list of known asteroids because of the asteroidal appearances. There are several attempts to find the dormant comet nuclei from asteroidal catalogs, for example, by using their reflectance spectra or orbital elements. However, little has been studied via polarimetry.
We conduct a polarimetric study of three candidates of dormant comet nuclei, (331471) 1984 QY1, (3552) Don Quixote and (944) Hidalgo, by using the 1.6-m Pirka Telescope at the Nayoro observatory (operated by Hokkaido University, Japan). We chose these asteroids in comet-like orbits (ACOs) based on the orbital elements (i.e., the Tisserand parameter with respect to Jupiter $T_J < 3$). We found that 1984 QY1 has a polarimetric albedo (geometric albedo determined via polarimetry) $p_V = 0.16 \pm 0.06$ while both Don Quixote and Hidalgo have Rc-band polarimetric albedo $p_R < 0.05$. Based on the polarimetric result together with a dynamical analysis, we conjectured that 1984 QY1 could be an S-type asteroid transported into the current orbit via 3:1 mean motion resonance with Jupiter. From the previous spectroscopic study, Don Quixote and Hidalgo are classified into D-type taxonomic group, which are typical of comet nuclei. In this presentation, we will introduce our polarimetric observations of ACOs and emphasize that polarimetry is a powerful tool for discriminating the asteroidal and cometary origins.

Keywords: Polarimetry, Asteroid

©2019. Japan Geoscience Union. All Right Reserved.

Dynamical lifetime of the Oort Cloud new comets under planetary perturbation

*Ito Takashi[1], Arika Higuchi[1]

1. National Astronomical Observatory of Japan

Nearly isotropic comets with very long orbital period are supposed to come from the Oort Cloud. Recent observational and theoretical studies have greatly revealed the dynamical nature of this cloud and its evolutionally history, but many issues are yet to be known. Our goal is to trace the dynamical evolution of the Oort Cloud new comets (OCNCs) produced by evolving comet cloud, hopefully estimating the fraction of OCNCs embedded in the current populations of the solar system small bodies. We combine two models to follow the dynamical evolution of OCNCs beginning from their production until their ejection out of the solar system, obtaining statistics of the dynamical lifetime of OCNCs: The first model is a semi-analytical one about the OCNC production in an evolving comet cloud under the perturbation of the galactic tide and stellar encounters. The second model numerically deals with planetary perturbation over OCNCs' dynamics in planetary region. The main results of the present study are: (1) Typical dynamical lifetime of OCNCs in our models turned out to be O(10^7) years. Once entering into the planetary region, most OCNCs stay there just for this timespan, then get ejected out of the solar system on hyperbolic orbits. (2) While averaged orbital inclination of OCNCs is small, the so-called "planet barrier" works rather effectively, preventing some OCNCs from penetrating into the terrestrial planetary region.

Keywords: Oort Cloud, comet, orbital dynamics

©2019. Japan Geoscience Union. All Right Reserved.

Thermal Infrared Imaging of C-type Asteroid 162173 Ryugu with Porous Surfaces

*Tatsuaki Okada[1,2], Tetsuya Fukuhara[3], Satoshi Tanaka[1], Makoto Taguchi[3], Takehiko Arai[4], Naoya Sakatani[1], Yuri Shimaki[1], Hiroki Senshu[5], Yoshiko Ogawa[6], Hirohide Demura[6], Kentaro Suko[6], Kohei Kitazato[6], Toru Kouyama[7], Tomohiko Sekiguchi[8], Jun Takita[9], Sunao Hasegawa[1], Tsuneo Matsunaga[10], Takehiko Wada[1], Takeshi Imamura[2], Jorn Helbert[11], Thomas G. Mueller[12], Axel Hagermann[13], Jens Biele[11], Matthias Grott[11], Maximiliam Hamm[11], Marco Delbo[14], Yukio Yamamoto[1], Naru Hirata[6], Naoyuki Hirata[15], Fuyuto Terui[1], Takanao Saiki[1], Satoru Nakazawa[1], Makoto Yoshikawa[1], Sei-ichiro WATANABE[1,16], Yuichi Tuda[1]

1. Institute of Space and Astronautical Science, Japan Aerospace Exploration Agency, 2. University of Tokyo, 3. Rikkyo University, 4. Ashikaga University, 5. Chiba Institute of Technology, 6. University of Aizu, 7. National Institute of Advanced Industrial Science and Technology, 8. Hokkaido University of Education, 9. Hokkaido Kitami-Hokuto High School, 10. National Institute for Environmental Studies, 11. German Aerospace Center, 12. Max-Planck Institute for Extraterrestrial Physics, 13. University of Stirling, 14. Observatoire de la Côte d'Azur, 15. Kobe University, 16. Nagoya University

Thermal images from global to close-up scales taken by the Thermal Infrared Imager TIR [1] on Hayabusa2 [2] have revealed thermophysical properties of the C-type Near-Earth Asteroid 162173 Ryugu. On 27 June 2018, Hayabusa2 arrived at Ryugu and started remote sensing to characterize the nature of the asteroid and find the proper landing sites. *In situ* surface experiments were conducted using the robotic landers Minerva-II and Mascot [3]. *In situ* radiometry was conducted by MARA on MASCOT during a day-night cycle to derive the thermal inertia of a single boulder [4]. Ground-based observations [5] have been informed that the averaged thermal inertia of the asteroid is from 150 to 300 [tiu = J m^{-2} $s^{-0.5}$ K^{-1}] [5,6], corresponding to the surface covered with cm-sized granules.

TIR is the same design as the LIR on Akatsuki Venus climate orbiter [6], with 8 to 12 μm wavelength range, 328 x 248 effective pixels, and the FOV and IFOV of 16.7˚ x 12.7˚ and 0.051˚ per pixel, respectively. The first image of Ryugu detected by TIR was a point source on 6 June 2018, as was previously predicted [7]. Disc-resolved thermal images of Ryugu was taken from the HP on 30 June. The surface temperature was measured at 300 to 370K at about 1AU from the Sun, and gradually decreased with the solar distance. Comparison of the results with modeling [8] shows that the surface of Ryugu is not like fine regolith nor base rocks. Most of large boulders on Ryugu show temperatures almost the same as the surrounding surfaces. Diurnal temperature profiles of Ryugu are rather flatter than expected for a smooth terrain. Apparent thermal inertia is ~300 tiu or larger, but probably lower than the value when the surface roughness is considered. All these facts are consistent with a very rough and porous surface with low porosity (~35 ±10 %) [9] and the surrounding surface is dominated by porous rocks larger than several centimeters. Macro porosity should be 30 to 50 % to account for the bulk density of Ryugu ~1200 kg m^{-3}.

During the descent operations for the release of landers and the touchdowns for sample collection, TIR has taken close-up thermal images of the local sites, continually from the altitude of 500 m until the start of final descent at 10 or 20 m altitude. Close-up thermal images show the surface physical state and a variety of boulders. Most of the boulders in close-up images have temperatures similar to the surroundings but with more variety. A small number of boulders are remarkably colder than the surroundings, indicating dense rocks with lower porosity.

©2019. Japan Geoscience Union. All Right Reserved.

These facts indicate that Ryugu is probably a rubble pile of loosely-bound porous rocks, which might originate from the outer layer of parent body where compaction did not occur effectively, while the dense boulders might originate the compacted center region of parent body or from the different parent body. A different composition (e.g., organic rich materials) cannot be ruled out so far to account for such a low thermal inertia (and low density) of Ryugu.

Acknowledgments: The authors appreciate all the members of the Hayabusa2 Project and supporting staff for their technical assistance and scientific discussions. This research is partly supported by the JSPS KAKENHI No. J26287108, No. J17H06459 (Aqua Planetology), and the Core-to-Core program “International Network of Planetary Sciences”. MDB acknowledges support from CNES.

References: [1] Okada T. et al. (2017) *SSR.,* 208, 255-286. [2] Tsuda Y. et al. (2013) *Acta. Astronautica, 91* , 356-362. [3] Ho T.M. et al. (2017) *SSR.,* 208, 255-286. [4] Grott, M. et al. (2019), submitted to Nature. [5] Mueller T.G. et al. (2016) Astronon. Astrophys., doi:10.1051/0004-6361/201629143. [6] Fukuhara T. et al. (2011) *EPS,* 63, 1009-1018. [7] Okada T. et al. (2018) *PSS., 158, 46-52.* [8] Takita J., et al. SSR, 2018, 287-315. [9] Okada T. (2016) *LPSC.*, 47, #1457.

Keywords: Hayabsua2, Thermal Infrared Imager, Thermal Inertia

©2019. Japan Geoscience Union. All Right Reserved.

Data Release of Asteroid 162173 Ryugu by Observation of Thermal Infrared Imager onboard Hayabusa2

*Takehiko Arai[1], Hirohide Demura[2], Toru Kouyama[7], Naoya Sakatani[3], Kentaro Suko[2], Yuri Shimaki[3], Hiroki Senshu[5], Tomohiko Sekiguchi[6], Yoshiko Ogawa[2], Sunao Hasegawa[3], Takehiko Wada[3], Takeshi Imamura[10], Tsuneo Matsunaga[9], Jun Takita[8], Kohei Kitazato[2], Makoto Taguchi[4], Tetsuya Fukuhara[4], Satoshi Tanaka[3], Tatsuaki Okada[3]

1. Ashikaga University, 2. The University of Aizu, 3. Japan Aerospace Exploration Agency (JAXA), 4. Rikkyo University, 5. Chiba Institute of Technology, 6. Hokkaido University of Education, 7. National Institute of Advanced Industrial Science and Technology (AIST), 8. Hokkaido Kitami Hokuto High School, 9. National Institute for Environmental Studies (NIES), 10. The University of Tokyo

The thermal infrared imager (TIR) onboard the Hayabusa2 spacecraft performed thermography of the asteroid 162173 Ryugu through in-situ observations from 2018 to 2019. The primary purpose of TIR is to determine the global thermophysical properties of the asteroid and to reveal the evolutional history such as physical properties of the coalesced bodies, orbital changes due to radiation force, and the thermal evolution. This study introduces observed data of TIR and public data for scientists. The data are released by JAXA data archives (DARTS) and NASA PDS.

Keywords: Hayabusa2, Thermal Infrared Imager, Asteroid Ryugu

©2019. Japan Geoscience Union. All Right Reserved.

Multi-mission capability of HARMONICS

*Shintaro Tsunoda[1], Hirohide Demura[1], Naru Hirata[1]

1. The University of Aizu

This research has updated HARMONICS from a viewpoint of multi-mission capability, such as the Martian satellite exploration mission MMX in 2020s. Newly additional function is Switching on the shape model interface.
Bird view and visualization of FOV is important in robotics control. This technology is also used for deep space explorer missions.
HARMONICS is visualization tool of FOV(Field Of View) of scientific instruments and spacecraft’s position for HAYABUSA mission. The software has been updated by University of Aizu students of the past. The original HARMONICS had been developed by Nemoto(2006). GUI of HARMONICS had been replaced GUI library from GKT to Qt and added new functions, such as interactive modification of input mission plan by Ueno+(2017). The software had been add FOV frustum function by Aoki(2017). HARMONICS has tried to manage data for each project based on preference file in 2018.
HARMONICS should improved scalability to be compatible for ongoing mission. HARMONICS had been used to decide shutter chance by Camera Science Team in the asteroid Itokawa rendezvous of HAYABUSA. This software has not used in the asteroid Ryugu rendezvous of HAYABUSA2. The proven software should be use for future ongoing missions other than HAYABUSA. This research is development to HARMONICS adapt to ongoing missions.
I separated the designation of the data set from the source code and clarified the part edited by the user and the part edited by the developer.
HARMONICS has the function to switch and display data of different missions by this research. When users extend HARMONICS for multiple missions, users don’t need edit source code. User needs only kernel and the shape model of spacecraft and target asteroid. User do not need tough coding. User can use easily HARMONICS by editing preference file and kernel.

Keywords: Hayabusa2, Ryugu, Software, visualization

©2019. Japan Geoscience Union. All Right Reserved.

New interface of verification for calibration and conversion in HEAT : Hayabusa2 Exploration Assistant for TIR

*Tatsuro Kobayashi[1], Kentaro Suko[1], Hirohide Demura[1], Yoshiko Ogawa[1], Takehiko Arai[2], Naoya Sakatani[3], Tatsuaki Okada[3], Satoshi Tanaka[3], Tetsuya Fukuhara[4]

1. The University of Aizu, 2. Ashikaga University, 3. Institute of Space and Astronautical Science, Japan Aerospace Exploration Agency, 4. Rikkyo University

Hayabusa2 is an ongoing mission for sample return from the asteroid Ryugu.
Candidates of sampling sites are selected based on surface mapping by optical instruments such as Thermal Camera (TIR). TIR observes surface infrared radiation from the asteroid. A software package peculiar to TIR is HEAT: Hayabusa2 Exploration Assistant for TIR. The software has four functions; Database for ground tests, calibration of flight data based on the ground tests, conversion from raw data to temperature one, and analysis for verifying the calibration and conversion. The converted data products are divided into some levels: Lv1 Raw data [DN], Lv2a Temperature [K], Lv2b is Brightness [W/m2], and higher thermal model with VTK format [K]. This research implements new interface of verification for calibration and conversion based on hearing and survey for requirements from TIR science team. The environment of implementation is following tool. OS: macOS Mojave 10.14.2. Computing language: C++, OpenGL. Frameworks: Qt5.4. Tools: Fits, Qt creator, SPICE toolkit, Visualization Toolkit, QcustomPlot, Xcode10.1.

Keywords: Hayabusa2, Software, Ryugu, Calibration

©2019. Japan Geoscience Union. All Right Reserved.

Dust particle evolution of a near-Earth object 252P/LINEAR from near-infrared polarimetric observations in 2016

*Yuna G Kwon[1], Masateru Ishiguro[1], Jungmi Kwon[2], Daisuke Kuroda[3], Myungshin Im[1], Changsu Choi[1], Motohide Tamura[4], Takahiro Nagayama[5], Nobuyuki Kawai[6], Jun-ichi Watanabe[7]

1. Seoul National Univ., 2. ISAS/Japan Aerospace Exploration Agency, 3. Okayama Astrophysical Observatory, 4. The Univ. of Tokyo, 5. Kagoshima Univ., 6. Tokyo Institute of Technology, 7. National Astronomical Observatory of Japan

Comets, one of the least-altered leftovers from the early solar system, have probably preserved the primitive structure inside, whereas their surfaces become differentiated from initial states after repetitive orbital revolutions around the sun. Resurfacing makes the surface drier and more consolidated than the bulk nuclei, creating inert refractory dust layer (so-called “dust mantle”). Near-Infrared (NIR) polarimetry is theoretically expected to maximize the contrast of the porosity between inner fresh and evolved dust particles, by harboring more dust constituents in the single wavelength than the optical, and thus intensifying electromagnetic interference in dust agglomerates. Despite the advantage, only few studies have been conducted in this approach at multiple observation epochs. Herein, we present our new multi-band NIR polarimetric (1.25—2.25 microns) study of near-Earth object 252P/LINEAR over 12 days near perihelion; alongside broadband optical photometric (0.48—0.80 microns) data over four months in 2016 and a subsidiary dynamical simulation over 1000 year backward in time. 252P/LINEAR drew attention due to (1) its close approach to the Earth (~0.036 au on 2016 March 16), (2) its possible pairing to a comet P/2016 BA14 (PanSTARRS), and (3) its very low activity level despite its relatively young dynamical age. In this study, we detected two discontinuous brightness enhancements of 252P/LINEAR, particularly, the former of which accompanied a significant increase of NIR polarization degree of the comet (by ~13 % at most) with unusual blue polarimetric color. We will discuss the most probable scenario of the observed results, together with the orbital evolution of the comet and a dynamical association with its pair.

Keywords: Comet, Near-earth object, Polarimetry, Dust

©2019. Japan Geoscience Union. All Right Reserved.

Performance Evaluation of TRIPOL on the 61-cm Telescope at Seoul National University for Polarimetric Observations of Solar System Small Bodies

*Sunho Jin[1], Masateru Ishiguro[1], Yuna G Kwon[1], Jooyeon Geem[1], Yoonsoo P. Bach[1], Jinguk Seo[1], Hiroshi Sasago[2], Shuji Sato[3]

1. Seoul National University, 2. Sasago Co.,Ltd, 3. Nagoya University

Polarimetry of solar system small bodies is a powerful technique for investigating their physical properties, such as albedos, particle sizes, and porosities of these bodies. Observational opportunities arise sometimes suddenly, that is, just after unforeseeable activations of comets and discoveries of near-miss asteroids. Here, we introduce our activity to install the polarimetric instrument, TRIPOL (Triple-Range Imager and POLarimeter) on the 61-cm telescope (a Ritchey-Chretien reflector with f/7.0) at the Center for Astronomy and Space Science, Seoul National University, and report an observational result of three comets. This combination provides an 8.0’ ´8.0’ field of view and pixel resolution of 0.94” pixel^{-1}. Throughout photometric observations, we determined the limiting magnitudes (defined as magnitudes for S/N=5) of 15.17±0.06 (g’-band), 15.68±0.01 (r’-band), 16.24±0.03 (I’-band), respectively, with total 240-seconds exposure (four 60-seconds exposure images, each was taken at different rotation angle for the half-wave plate). We also found that the instrumental polarizations are negligibly small, that is, -0.32±0.04% (g’-band), -0.36±0.05% (r’-band) and -0.21±0.04% (I’-band), while the polarization efficiencies are large enough to maximize the performance, that is, 97.52±0.03% (g’-band), 98.83±0.02% (r’-band) and 99.15±0.02% (I’-band).

With this instrument, we conducted polarimetric observations of three Jupiter-family comets, 21P/Giacobini-Zinner, 38P/Stephan-Oterma, and 46P/Wirtanen on a trial basis. It is known from a recent study that the polarization degrees of cometary dust particles are significantly influenced by gas emissions [1] With multiband data taken with TRIPOL, we eliminated an influence of gas contaminations and found that the dust polarization degrees of these three comets coincide with those of so-called ‘dust-rich comets’. From this result, we conjecture that the polarimetric property of Jupiter-family comets is broadly homogeneous, unlike asteroids. We plan to describe our future plan using the polarimetric system.

[1] Kwon, Y. G. et al. Astronomical Journal, 154, 4, 173, 2017

Keywords: Comet, Instrument, Polarimetry

©2019. Japan Geoscience Union. All Right Reserved.

Smart Interface of HEAT: Hayabusa2 Exploration Assistant for TIR

*Kentaro Suko[1], Tatsuro Kobayashi[1], Hirohide Demura[1], Takehiko Arai[2], Naoya Sakatani[3], Tatsuaki Okada[3], Satoshi Tanaka[3], Tetsuya Fukuhara[4]

1. The University of Aizu, 2. Ashikaga University, 3. Institute of Space and Astronautical Science, Japan Aerospace Exploration Agency, 4. Rikkyo University

The Hayabusa2 project is a sample return mission to the asteroid Ryugu. It was launched on Dec. 3, 2014, and it has been at Ryugu since June 27, 2018. Hayabusa2 has optical instrument called Thermal Infrared Imager (TIR). These main functions are to know natures of the asteroid and to select the candidate of safe landing sites for sampling based on thermos-physical properties of the surface. TIR records infrared radiation from the target as a digital number (DN). The infrared signal is affected by sensor-surrounding objects; lens, shutter, package, and case. TIR requires consideration about this effect when converts DN images to temperature one. This study improved conversion system to increase conversion efficiency.

Hayabusa2 TIR Science Team has developed an analysis supporting tool called Hayabusa2 Exploration Assistant for TIR (HEAT). HEAT is used to search TIR data interactively, display TIR images, and visualize thermal models. We receive TIR raw images (Product Level 1) from ISAS/JAXA and convert them to brightness temperature images (Level 2a) and radiance images (Level 2b) using HEAT at Univ. of Aizu. The converted images are provided to the Hayabusa2 project data server.

This part introduces a concept model. The spectral radiance emitted from a blackbody B(λ ,T) (W s r-1m-2) is given by the Planck function based on wavelength λ (m) and temperature T(K) as follows:

$$B(\lambda,T) = (2hc2/\lambda 5)* (1/(\exp(\lambda kBT)-1))$$

H = 6.63*1034 (m2 kg s-2 s-1) is the Planck constant, c=2.9972*108(ms-1) is the speed of light, and KB= 1.38*10-23 (m2 kg s-2K-1) is the Boltzmann constant. The observed radiance L(T) (W sr−1 m−2) is as follows:

$$L(T)= \varepsilon \int BR(\lambda)d\lambda$$

ε is the spectral thermal emissivity, and R(λ) is the response function such as the detection efficiency of the bolometer, the measured transmittance of optics including the band-pass filter and the germanium lens. The calibration formula with two regressed parameters A and B is written as follows:

$$DN=A * L(T) + B$$

The converted temperatures of the Moon were lower than expected because each pixel did not cover the sunlit area entirely or due to roughness effect of the cratered terrain. TIR has been observing Ryugu in approach and rendezvous phases. The altitudes of TIR observations during the rendezvous phase range from 20 km to less than 10 m. This study has processed about 3000 Ryugu images observed by TIR since June 2018.

©2019. Japan Geoscience Union. All Right Reserved.

This study improved conversion system. Previous conversion system converts a TIR image one by one, but current conversion system converts TIR images in selected directory at once.

Keywords: Hayabusa2, TIR, HEAT, Software

©2019. Japan Geoscience Union. All Right Reserved.

Experimental Study on Collision Crater Formed on Bulge Geography

*Yusaku Yokota[1], Yuya Yamamoto[2], Minami Yasui[2], Masahiko Arakawa[2]

1. Faculty of Science, Kobe University, 2. Graduate School of Science, Kobe University

An equatorial bulge was found on the surface of asteroid Ryugu and Bennu by recent spacecrafts of Hayabusa2 and OSIRIS-Rex, and ridge structures with various scales originated by geological activities have been recognized on icy satellites. Impact craters are dominant geological features on solid planets such as asteroids and satellites, and a crater rim are also recognized as a ridge or bulge with a circular shape. These bulges and ridges are shown to be erased with time because small scale impacts excavate and disrupt these topographies. It is well known that old craters gradually degraded by small impacts to get blurred and could be completely erased. We can expect the similar degradation process on large bulges and ridge structures, so that the life time of these structures by small impacts is a good indicator of the formation age of these structure by geologic activities. So far, the effect of small impacts on the degradation is estimated by using the results on the flat surface, but actually the surface of the bulge is curved and there is a summit on the bulge. Therefore, if we estimate the life time of the bulge structure, we should consider the effect of the topography such as a summit and curvature. Then, the impacts on the bulge structure was studied to clarify how the bulge structure affected the crater formation efficiency. In this study, we suppose the bulge made from regolith and boulders, such as an equatorial bulge of Ryugu and assume the crater formation process dominated by not the strength but the gravity.

We prepared a triangular prism target to simulate the bilge structure, and set it like that the base of this prism is rectangle, then it looks triangle when we look it at the horizontal direction, and we can look at the linear summit from the top view. Quartz sands with the size of 100μm was used to build the target and the angle of repose for this quartz sand is about 30 degree. The slope of the prism was measured from the base, and we set the angle from 20 to 30 degree. The quartz sands were filled into a transparent water tank with the depth of 20 cm to prepare the bulge structure. Impact experiments were conducted by using a vertical type gas gun, and the water tank was set in the chamber to evacuate below 1000 Pa. A alumina sphere projectile with the size of 3mm was launched at the velocity from 70 to 200 m/s, and it was impacted on the bulge in the vertical direction: the impact angle measured from the target surface was about 60 degree when the slope was 30 degree. The distance from the impact pint to the summit (deviation distance, d_d) was changed from 0 to 20mm.

We found that the crater shape strongly depended on the d_d, so the crater shape was an ellipsoid when the impact point was near the summit. Th major axis appeared along the linear summit and the minor axis appeared across the summit. The aspect ratio of the major axis to the minor axis gradually changed toward 1 with the increase of d_d. Moreover, the aspect ratio becomes large at the same d_d when the impact velocity increased. The major axis of the ellipsoid crater formed on the bulge was slightly larger than the crater diameter formed on the flat surface, and the slope angle might affect the size of the ellipsoid because we found that the crater formed on the slope of 30 degree was systematically larger than that formed on the slope of 20 degree. We also observed an asymmetric ejecta curtain from the impact point on the bulge, moreover the ejecta curtain was notice to be deformed so much at the impact point near the summit because of the effect of curvature of the bulge on the crater flow.

Angle of repose, Impact crater, Bulge and ridge structure, Ejecta curtain

©2019. Japan Geoscience Union. All Right Reserved.

©2019. Japan Geoscience Union. All Right Reserved.

Initial analysis plan of soluble organic compounds for the Hayabusa2 sample from asteroid Ryugu

*Hiroshi Naraoka[1], Yoshinori Takano[2], Jason P. Dworkin[3], SOM Analysis Team

1. Department of Earth and Planetary Sciences, Research Center for Planetary Trace Organic Compounds, Kyushu University, 2. Japan Agency for Marine-Earth Science and Technology, 3. Astrochemistry Laboratory NASA Goddard Space Flight Center, Greenbelt, MD 20771 USA

The spectra of asteroid 162173 Ryugu taken by Near-Infrared Spectrometer (NIRS3) onboard Hayabusa2 are nearly featureless and consistent with carbonaceous chondrites (Matsuoka et al., 2018). The Hayabusa2 spacecraft will collect surface samples of Ryugu and deliver to the Earth during late 2020. The initial analysis of the Ryugu samples will focus on (1) detailed chemical and mineralogical characterization of the samples and (2) understanding the history of Ryugu and the Solar System in order to maximize the scientific achievement of the project and (3) to prove the scientific potential of the samples to the community for the analytical opportunity (Tachibana et al., 2014). We have organized an international team, consisting of 24 members currently, for the initial analysis of soluble organic matter (SOM) for the returned samples.
The primitive asteroidal materials are expected to contain diverse and complex (e.g. elemental, structural, and optical) organic matter all at low concentrations. The occurrence of SOM will provide clues to the origins of organic compounds as well as prebiotic molecules of potential relevance to origins of life on Earth and possibly elsewhere in the Solar System. We propose the comprehensive SOM analyses to reveal the chemical evolution of Ryugu using high-sensitive and high-resolution analytical methods as follows:

1) High-resolution mass spectrometry (HRMS) of various solvent extracts with electrospray ionization (ESI) coupled with or without nano-liquid chromatography.
2) Enantiomerically resolved amino acid analysis using high-resolution column chromatography with high-sensitive fluorescence spectroscopy coupled with HRMS.
3) *In situ* organic compound analysis and molecular imaging using desorption electrospray ionization (DESI) and/or direct analysis in real time (DART) equipped with HRMS.
4) Spatial resolution imaging of organic compounds using time of flight-secondary ion mass spectrometry (ToF-SIMS; Naraoka et al., 2015).

In addition, if the sample is available, we will also perform the following additional analyses:

5) Compound-specific isotope analysis using gas chromatography/combustion or pyrolysis /isotope ratio mass spectrometry (GC/C or pyrolysis/IRMS).
6) Bulk chemical and isotopic analysis of organic matter (C, H, N and S) using nano-EA/IRMS system and laser-tunable FT-IR spectroscopy.

Depending to the sample size available to the initial analysis, we will perform preliminary analytical tests using 30 mg, 10 mg, and 1 mg samples of the Murchison meteorite (CM2, positive SOM-rich), Yamato 793321 meteorite (heated CM2, positive SOM-depleted), and baked serpentine (negative SOM-depleted) as well as procedural blank. The analytical protocol will be discussed in the meeting.

< References >
Tachibana, S. et al. (2014) Hayabusa2: Scientific importance of samples returned from C-type near-Earth

©2019. Japan Geoscience Union. All Right Reserved.

asteroid (162173) 1999 JU3. Geochemical Journal. 48. 571-581. 10.2343/geochemj.2.0350.
Matsuoka, M. et al. (2018) Spectral comparison between asteroid (162173) Ryugu and carbonaceous meteorites. American Astronomical Society, DPS meeting #50.
Naraoka, H. et al. (2015) ToF-SIMS analysis of carbonaceous particles in the sample catcher of the Hayabusa spacecraft. Earth, Planets and Space, 67:67. DOI 10.1186/s40623-015-0224-0.
Naraoka, H. and Hashiguchi, M. (2018) *In situ* organic compound analysis on a meteorite surface by desorption electrospray ionization coupled with an Orbitrap mass spectrometer. Rapid Commun. Mass Spectrom. 32, 959-964.

Keywords: Hayabusa2, Ryugu, Carbonaceous Asteroid, Soluble Organic Matter

©2019. Japan Geoscience Union. All Right Reserved.

Radar and optical simultaneous observations of faint meteors with MU radar and Tomo-e Gozen

*Ryou Ohsawa[1], Akira Hirota[2], Shinsuke Abe[2], Daniel Kastinen[3], Kero Johan[3], yasunori Fujiwara[4], Takuji Nakamura[5], Shigeyuki Sako[1], Yuto Kojima[1], Jun-ichi Watanabe[6]

1. Institute of Astronomy, Graduate School of Science, The University of Tokyo, 2. Department of Aerospace Engineering, College of Science & Technology, Nihon University, 3. Swedish Institute of Space Physics, 4. SOKENDAI (The Graduate University for Advanced Studies), 5. National Institute of Polar Research, 6. National Astronomical Observatory of Japan

The Earth is surrounded by small dust grains produced by comets and asteroids. Tons of such grains plunge into the Earth's atmosphere hourly. Part of their kinetic energy excites and ionizes the surrounding atmosphere, which is observed as a meteor phenomenon. A simultaneous radar and optical observation is promising to constrain the motion and mass of a meteor at a time. We launched a project to observe faint meteors with Middle and Upper Atmosphere Radar (MU radar) and a wide-field CMOS mosaic camera Tomo-e Gozen installed on the 105 cm Kiso Schmidt telescope. The observations were carried out in 18--21, April, 2018. From tons of the detected meteors, the simultaneous detections were extracted in terms of the times, loci, and directions of the meteors. Finally, we identified the 894 meteor events simultaneously detected in the both sites. The optical brightness of the simultaneous meteors ranged from about 3--11 mag. in the V-band, which is about 5 magnitude fainter than in previous studies. We confirmed a clear correlation between the meteor brightnesses and the radar cross sections.

Keywords: meteor, interplanetary dust

©2019. Japan Geoscience Union. All Right Reserved.

Global distribution and spectral characteristics of bright spots on asteroid Ryugu

*Masanori Suemitsu[1], Tomokatsu Morota[1], Rie Honda[2], Singo Kameda[15], Eri Tatsumi[3], Manabu Yamada[4], Naoya Sakatani[5], Toru Kouyama[6], Yokota Yasuhiro[7], Yuichiro Cho[8], Hidehiko Suzuki[9], Masahiko Hayakawa[10], Moe Matsuoka[10], Chikatoshi Honda[11], Tatsuhiro Michikami[12], Kazuo Yoshioka[13], Kazunori Ogawa[14], Hirotaka Sawada[5], Seiji Sugita[3]

1. Graduate School of Environmental Studies, Nagoya University, 2. Department of Science and Technology, System of Natural Science, Kochi Unicversity, 3. Graduate School of Earth and Planetary Science, Tokyo Unicversity, 4. Planetary Exploration Reserch Center, Chiba Institute of Technology, 5. Institute of Space and Astoronautical Science, Japan Aerospace Exploration Agency, 6. National Institute of Advanced Industrial Science and Technology, 7. Kochi University, 8. Department of Earth and Planetary Science, Tokyo University, 9. Depertment of physics, Meiji University , 10. Department of Solar System Science, Institute of Space and Astoronautical Science, Japan Aerospace Exploration Agency, 11. Aizu University, 12. Faculty of Engineering, Kindai University, 13. Graduate School of frontier Science, Tokyo University, 14. Kobe University, 15. Rikkyo University

On June 27, 2018, the asteroid explorer Hayabusa2 arrived at the target C-type asteroid 162173 Ryugu. The telescopic optical navigation camera (ONC-T) on-board Hayabusa2 has acquired the multiband image data for the entire surface of Ryugu with spatial resolutions better than 2 m/pixel. These data show that the Ryugu surface has the very low surface reflectance, flat spectra, and its spatial homogeneity [Sugita et al. 2019]. However, more detailed observations on Ryugu have revealed that many boulders exhibit different spectral properties and that a number of spots with distinctively brighter than the surroundings [Sugita et al. 2019]. Although larger boulders have been analyzed to show that they form two distinctive spectral trends, no substantial spectral analyses on bright spots have been conducted. Determining whether or not these bright spots are one of the materials that originate from the parent body of Ryugu is important to understand the differentiation and geologic processes on the parent body. In this study, in order to understand origins of the bright spots, we investigated spectral characteristics of the bright spots and compared those of the boulders on Ryugu. We used the ONC-T multiband images obtained in Box-A (20 km altitude) and mid-altitude (5 km altitude) operations.

We found seven meter-sized bright spots that have radiance factor 1.3 to 2.0 times higher than that of the surrounding area. The spectra of these bright spots were classified into two types, one being a flat spectrum type and another being a convex spectrum type. The former type has spectrum similar to but flatter and brighter than the mean spectra of the whole Ryugu and boulders, suggesting that the bright spots originate from parent body of Ryugu. The latter type has spectrum similar to those of S-type asteroids, suggesting their exogenous origin.

Keywords: asteroids, Ryugu, bright spot, spectrum, boulder

©2019. Japan Geoscience Union. All Right Reserved.

Polarimetry of (155140) 2005 UD: the Dynamical Association with (3200) Phaethon

*Masateru Ishiguro[1], Jooyeon Geem[1], Hiroyuki Naito[2], Yoonsoo P. Bach[1], Daisuke Kuroda[3], Tatsuharu Ono[4], Seiko Takagi[4], Mitsuteru Sato[4], Kiyoshi Kuramoto[4], Tomohiko Sekiguchi[5], Masataka Imai[6], Makoto Watanabe[7], Katsuhito Ohtsuka[8], Sunao Hasegawa[9], Takashi Ito[10], Fumi Yoshida[11], Tomoko Arai[11]

1. Department of Physics and Astronomy, Seoul National University, 2. Nayoro Observatory, 3. Okayama Observatory, Kyoto University, 4. Department of Cosmosciences, Graduate School of Science, Hokkaido University, 5. Hokkaido University of Education, 6. National Institute of Advanced Industrial Science and Technology, 7. Department of Applied Physics, Okayama University of Science, 8. Tokyo Meteor Network, 9. Japan Aerospace Exploration Agency, 10. National Astronomical Observatory of Japan, 11. Planetary Exploration Research Center, Chiba Institute of Technology

An Apollo-type near--Earth asteroid, (155140) 2005 UD, is considered as a possible fragment from (3200) Phaethon, suggesting that Phaethon precursor body might undergo a catastrophic disruption in the past. Here we present our new observational evidence for supporting these two are common origin. We thus conducted a polarimetric observation in 2018 September-October and found that 2005 UD exhibited a polarimetric property significantly different from those of major taxonomic classes of NEAs (i.e., S- and C-type) but similar to that of Phaethon at a wide range of the solar phase angles. Using the polarimetric data, we derived the geometric albedo of ~0.1. In addition, we made a photometric observation at the opposition (the zero phase angle), and determined the mean absolute magnitude of 17.2, the synodic rotational period 5.23 hr, and the effective diameter 1.5 km in combination with the derived geometric albedo. From these evidence, we found that the Phaethon precursor body might have lost more than a few percents of the mass via a disruption if 2005 UD was indeed ejected from the Phaethon precursor.

Keywords: Asteroids, Space Mission (Destiny+)

©2019. Japan Geoscience Union. All Right Reserved.

Follow-up observations for AKARI/IRC near-infrared asteroid spectroscopic survey (AcuA-spec)

*Sunao Hasegawa[1], Daisuke KURODA[2], Kenshi YANAGISAWA[3], Fumihiko Usui[4]

1. Japan Aerospace Exploration Agency, 2. Kyoto University, 3. National Astronomical Observatory of Japan, 4. Kobe University

In the range from 1 to 2.5 μm, we made the spectroscopic observations of the AcuA-spec asteroids (Hasegawa et al. 2017, PASJ, 69, 9), whose spectra were obtained in continuous covered between 2.5 and 5.0 μm by NIR/IRC/AKARI (Usui et al. 2019, PASJ, 71, 1). Candidates of AcuA-spec asteroids were selected from only main-belt asteroids classified based on visible spectrophotometric and spectroscopic observations (Tholen 1984, PhD thesis, Arizona University; Bus & Binzel 2002, Icarus, 158, 146; Lazzaro et al. 2004, Icarus, 172, 179). About 200 classified asteroids were raised as observational candidates. Spectroscopic observations for 65 AcuA-spec asteroids which were selected among the AcuA-spec candidate catalogue in taking account of signal-noise ratio and target opportunity by AKARI were executed.
Section work of the AcuA-spec candidate catalogue was done around 2005, yet there were not many spectroscopic observations of asteroids in the near-infrared wavelength range. As a result of survey of published paper for near-infrared spectroscopic observations of asteroids, howevwer, it was found that spectroscopic observations in the near-infrared region of 1–2.5 μm for most AcuA-spec asteroids are performed except for several asteroids.
If data in near-infrared wavelength range of the lacked AcuA-spec asteroids were acquired, all AcuA-spec asteroids will have 0.35–5 μm of data available. Obtaining continuous reflectance of asteroids is essential data to compare with those such as meteorites. Based on the Bus-DeMeo taxonomy (DeMeo et al. 2009, Icarus, 202, 160), we conducted classification of all AcuA-spec asteroids using published and our observational data.

Keywords: asteroids, spectroscopy

©2019. Japan Geoscience Union. All Right Reserved.

Amino acids on witness coupons collected from the ISAS/JAXA curation facility for the assessment and quality control of the Hayabusa2 sampling procedure

*Haruna Sugahara[1,2], Yoshinori Takano[1], Yuzuru Karouji[3], Kazuya Kumagai[4], Toru Yada[3], Naohiko Ohkouchi[1], Masanao Abe[3], Hayabusa2 project team

1. Japan Agency for Marine-Earth Science and Technology (JAMSTEC), 2. Institut de Chimie de Nice, Universite Cote dAzur, 3. Japan Aerospace Exploration Agency (JAXA), 4. Marine Works Japan Ltd.

The Hayabusa2 spacecraft is visiting a near-Earth carbonaceous type (C-type) asteroid, 162173 Ryugu, and planning to return the pristine samples to the Earth. C-type asteroids are considered to be related with carbonaceous chondrites that are enriched in organic and volatile materials. The one of the scientific goals of Hayabusa2 mission is to understand the origin and evolution of organic materials through interactions with water and minerals in the early solar system [e.g., 1]. Thus, the characterization of organic materials in the returned sample has great importance for this purpose. However, the analysis of small quantities of extraterrestrial organic materials in the returned samples requires a great care to avoid the introduction of terrestrial contaminants and any artifact materials to the pristine samples. Thus, the assessment of the degrees of the terrestrial contaminants to the samples as well as the comprehensive and specific managements to minimize the terrestrial contamination throughout the mission is essential.

The purpose of the study is to investigate the potential terrestrial organic contamination in a clean chamber for the Hayabusa2 returned samples in an Institute of Space and Astronautical Science/Japan Aerospace Exploration Agency (ISAS/JAXA) curation room [2-4]. As the indicator of the terrestrial organic contaminants, we selected amino acids that ubiquitously exist in the terrestrial environments and are also the target molecules in the Hayabusa2 mission. In the study, we used witness coupons made of aluminum foil to collect the contaminants in the clean chamber. The witness coupons were collected at different exposure times, ranging from 1 day to 1 month to examine the accumulation rate of the contaminants. After the collection, amino acids on the witness coupons were extracted in hot water, hydrolysed with HCl, and then converted to *N*-pivaloyl isopropyl (Pv/iPr) ester derivatives for gas chromatographic (GC) analysis [5].

On the witness coupons, eight terrestrially common amino acids (glycine, alanine, valine, leucine, isoleucine, proline, aspartic acid and glutamic acid) were detected and seven of them, except valine due to the under quantification limit, were quantified. Among them, glycine was the most abundant species with the highest concentration of 10 pmol/cm^2. A time-dependent profile of the four major amino acids (glycine, alanine, aspartic acid and glutamic acid) showed the increasing trend between 1 to 7 days. The average accumulation rates are 1.2 pmol/cm^2/day for glycine, 0.6 pmol/cm^2/day for alanine, 0.1 pmol/cm^2/day for aspartic acid and 0.2 pmol/cm^2/day for glutamic acid. The species and the concentrations of amino acids on our witness coupons are similar to those reported by the National Aeronautics and Space Administration/Johnson Space Center (NASA/JSC) OSIRIS-REx team [6]. Thus, the quality control against terrestrial contaminants in ISAS/JAXA curation facility is at the same quantitative level as in their facility. This inter-laboratory evaluation [7] about the terrestrial organic contamination will provide important information for the curation procedure of the Hayabusa2-returned samples.

©2019. Japan Geoscience Union. All Right Reserved.

References: [1] Tachibana S. et al. (2014) Geochem. J., 48, 571-587. doi: 10.2343/geochemj.2.0350. [2] Yada T. et al. (2014) Meteorit. Planet. Sci., 49, 135-153. doi: 10.1111/maps.12027. [3] Sawada H. et al. (2017) Space Sci. Rev. 208, 81–106. doi: 10.1007/s11214-017-0338-8. [4] Okazaki R. et al. (2017) Space Sci. Rev. 208, 107–124. doi: 10.1007/s11214-016-0289-5. [5] Chikaraishi Y. et al. (2010) in *Earth, Life, Isotopes*, Kyoto Univ. Press, pp.367-386. [6] Dworkin et al. (2018) Space Sci. Rev. 214, 9. doi: 10.1007/s11214-017-0439-4. [7] Sugahara et al. (2018) Earth, Planets Space, 70, 194. doi: 10.1186/s40623-018-0965-7.

Keywords: Amino acid, Hayabusa2, Curation, Witness coupons, Quality control

©2019. Japan Geoscience Union. All Right Reserved.

Hayabusa2 orbit determination using c5++ software

*Keiko Yamamoto[1], Toshimichi Otsubo[2], Koji Matsumoto[1], Hirotomo Noda[1], Noriyuki Namiki[1], Hiroki Senshu[3], Takahide Mizuno[4], Naoko Ogawa[4], Go Ono[4], Yuya Mimasu[4], Kent Yoshikawa[4], Tadateru Takahashi[4], Yuto Takei[4], Atsushi Fujii[4], Fuyuto Terui[4], Takanao Saiki[4], Satoru Nakazawa[4], Makoto Yoshikawa[4], Yuichi Tsuda[4]

1. National Astronomical Observatory of Japan, 2. Hitotsubashi University, 3. Chiba Institute of Technology, 4. Japan Aerospace Exploration Agency

Hayabusa2 arrived at the target asteroid Ryugu in June 2018 and is currently conducting remote sensing observations with various onboard instruments. So far, we have improved orbit determination software c5++, originally developed for the analysis of satellite laser ranging (SLR) data of the Earth, so that it can be used for the analysis of laser ranging data between Hayabusa2 and Ryugu obtained by Hayabusa2 LIDAR. Then we used it for the estimation of Hayabusa2 trajectory and the GM value of Ryugu. However, in the case of Hayabusa2, it is difficult to determine all of the 6 components of the initial state vector precisely if only LIDAR range data was used, and the simultaneously estimated GM value also had large uncertainty. To overcome this problem, in addition to LIDAR ranging data, we used Automated-Image-Tracking (AIT) data obtained by wide-angle optical navigation camera (ONC-W1) for the estimation of Hayabusa2 trajectory. In principle, LIDAR data gives information on the radial direction and AIT data give the ones on the across and along track directions. Thus, both data sets are complementary and help to improve the precision of the trajectory estimation. For this purpose, we improved c5 ++ so that it can deal with AIT data as observation data. In the presentation, we will show the results of trajectory and GM estimations using LIDAR and AIT data, and show how much the precision and accuracy are improved compared to the case using LIDAR data only.

Keywords: Hayabusa2, Orbit Determination, Ryugu

©2019. Japan Geoscience Union. All Right Reserved.

Landing Site Selection for Hayabusa2: Scientific Evaluation of the Candidate Sites on Asteroid (162173) Ryugu

*Hikaru Yabuta[1], Sei-ichiro WATANABE[2], Tomoki Nakamura[3], Naru Hirata[4], Seiji Sugita[5], Tatsuaki Okada[6], Kohei Kitazato[4], Yoshiaki Ishihara[7], Tomokatsu Morota[2], Naoya Sakatani[6], Koji Matsumoto[8], Koji Wada[9], Shogo Tachibana[5], Mutsumi Komatsu[10], ERI TATSUMI[5], Moe Matsuoka[6], Chikatoshi Honda[4], Takahiro Hiroi[11], Hiroki Senshu[9], Rie Honda[12], Yasuhiro Yokota[6], Rina Noguchi[6], Yuri Shimaki[6], Deborah Lorin Domingue[13], Lucille Le Corre[13], Antonella Barucci[14], Ernest Palomba[15], Shota Kikuchi[6], Akira Miura[6], Tomohiro Yamaguchi[6], Yukio Yamamoto[6], Takanao Saiki[6], Satoshi Tanaka[6], Makoto Yoshikawa[6], Yuichi Tsuda[6]

1. Hiroshima University, Department of Earth and Planetary Systems Science, 2. Nagoya University, 3. Tohoku University, 4. University of Aizu, 5. The University of Tokyo, 6. ISAS/JAXA, 7. NIES, 8. NAOJ, 9. Chiba Institute of Technology, Planetary Exploration Research Center (PERC), 10. Sokendai, 11. Brown University, 12. Kochi University, 13. Planetary Science Institute, USA, 14. Observatoire Paris-Site de Meudon, LESIA, France, 15. INAF-IAPS, Italy.

On June 27, 2018, JAXA’s Hayabusa2 spacecraft arrived at its target C-type asteroid Ryugu. Immediately after arrival, remote-sensing observations were carried out with the Optical Navigation Camera (ONC), the Near Infrared Spectrometer (NIRS3), the Thermal Infrared Imager (TIR), and the Laser Altimeter (LIDAR). Based on data from this suite of instruments, we carried out the landing site selection for the first touch-down (TD1). Since the mission aims to understand i) the origin and chemical evolution of the solar system and ii) the formation process and structure of the asteroid, we have set the most scientifically valuable TD1 site as the least altered region where water and/or carbon are potentially abundant.

Landing candidate sites were first selected by engineering evaluation for operational safety followed by scientific evaluations based on criteria such as science and samplability for the most interesting sites. The process was repeated using the observations from the altitudes of 20 km, 6 km, and 5 km.

Scientific evaluations of the landing site candidates were conducted based on the data products from ONC, NIRS3, TIR, and LIDAR. The shape modeling team produced two different shape models. ONC produced multiband images and reflectance spectra, as well as maps of spectral indices and X-means clustering analysis. Measurements of boulder size-frequency and Hapke parameters in the candidate landing areas were examined. NIRS3 produced four types of spectral feature maps. TIR provided maps of maximum temperature from the October 22, 2018 TD1 practice operations, apparent thermal inertia, and typical grain size determinations. LIDAR provided time series ranging data, topography, and corrected spacecraft trajectory.

Engineering evaluation: The possible landing site candidates were selected from the engineering safety score map evaluated based on the sub-Earth distance, local solar angle, local slope and elevation maximum difference. Thermal prediction results for TD1 were obtained by TIR. Temperatures of each site are < 350 K, confirming the safe conditions. The regions that satisfied all the conditions were, L05, L07, L08, L12, M01, M03 and M04.

Scientific evaluation:
1) Boulders. Based on the distribution of boulders with a diameter larger than 3 m for each potential landing site, regions L07, L08, and M04 show smaller percentages of boulder coverage than other areas, and are regarded as safer sites for landing.

©2019. Japan Geoscience Union. All Right Reserved.

2) Geology. Ryugu exhibits a variety of topographic features and geologic settings. From a scientific perspective, it is of interest to be able to study various materials representing the evolution of Ryugu.
3) Hydrous minerals. The NIR spectral properties are nearly homogeneous across Ryugu’s surface, especially between the candidate sites. The near-infrared reflectance spectra of Ryugu is similar to experimentally heated Murchison meteorite at 400˚C.
4) Carbon contents. It is likely that visible reflectance at 0.55 μm (R(0.55)) is influenced mostly by carbon content. R(0.55) is almost homogeneous across the surface with a low value, regardless of the candidate sites.
5) Secondary processes. Although the surface of Ryugu is almost homogeneous at the macro scale in the map of spectral slope from 0.48 to 0.86 μm, a slight heterogeneity is observed across the candidate regions. L-regions are relatively bluish and M-regions are reddish. Considering that spectral reddening is observed by laser irradiation of dehydrated carbonaceous chondrites, L regions are probably less altered and preferable for sampling.

In the total evaluation, L08, L07 and M04 were selected as the TD1 candidates on August 17, 2018. In September 2018, many boulders > 50 cm were additionally found for the sites during the rehearsal of TD1. Thus, the originally scheduled TD1 in October was postponed. Further search for a flat and safe site continued, and L08-E1 was determined as the TD1 site. The TD1 will be scheduled on Feb 22, 2019.

Keywords: Hayabusa2, Landing Site Selection

©2019. Japan Geoscience Union. All Right Reserved.

Visible Photometric, Spectroscopic and Polarimetric observations of an inactive comet, P/2016 BA14 with the 1.6m Pirka Telescope

*Ryo Yamagata[1], Tomohiko Sekiguchi[1], Ryo Okazaki[1], Kazuya Doi[1], Daisuke Kuroda[2], Masateru Ishiguro[3], Hiroyuki Naito[4]

1. Hokkaido University of Education, 2. Kyoto University, 3. Seoul National University, 4. Nayoro Observatory

We performed photometric, spectroscopic and polarimetric observations of an inactive comet, P/2016 BA14 with the 1.6m Pirka Telescope, Hokkaido.

P/2016 BA14 (a=3.02 au, e=0.67, i=18.9 deg.) was discovered as an unusual asteroid with a cometary orbit by the PANSTAARS on 2016 January 21.Since Knight et al. 2016 detected its cometary tail when the object close to sun(r=1.018au). It was classified into a Jupiter Family Comets. It can be regarded as a bare nucleus invisible coma because very weak comet activity that is different from general comet. There is a remarkable similarity between the orbits of 252P/LINEAR (a=3.05au, e=0.67, i=10.4deg) and P/2016 BA14. Jupiter Tisserand parameter is 252P/LINEAR and that of P/2016 BA14 are 2.82. P/2016 BA14 and 252P/LINEAR is division comet that is originally same comet (Jian-Yang.2017).

In this study, surface reflection properties of P/2016 BA14 classify D-type asteroids (Bus-DeMeo taxonomy) from result of visible spectroscopy (435-820nm). Color of surface is little red as D-type asteroid, but very blue as comet nucleus from result of BVRI photometry. The linear polarization Pr=10.46.±0.11% (α=46°) is in close accord with that of D-type asteroids and comet nucleus.

Keywords: P/2016 BA14, Photometric, Spectroscopic, Polarimetric, D-type

©2019. Japan Geoscience Union. All Right Reserved.

Polycyclic aromatic hydrocarbons and aliphatic hydrocarbons in Jbilet Winselwan carbonaceous chondrite : Attempt to evaluate the thermal metamorphism degree on the parent body

Hiroki Kato[1], *Hikaru Yabuta[1]

1. Hiroshima University, Department of Earth and Planetary Systems Science

Introduction: On June 27, 2018, Hayabusa2 spacecraft arrived at the C-type asteroid Ryugu. The surface of Ryugu has been thought to have experienced dehydration at least partially, according to the grand-based observation (Vilas et al. 2008; Hiroi et al. 1993). Therefore, it is important to investigate the chemical compositions of dehydrated carbonaceous CM chondrites for understanding the surface process of asteroid Ryugu. Although the extents of thermal metamorphism of CM chondrites have been evaluated by mineralogical compositions (e.g., Nakamura et al. 2006) and elemental and molecular compositions of insoluble organic matter (IOM) (e.g., Naraoka et al. 2004; Yabuta et al. 2005), the estimated temperature varies widely. On the other hand, soluble organic molecules from the dehydrated CM chondrites have not been quantified or below detection (e.g. Shimoyama et al. 1989), and there has been no study which evaluated thermal metamorphism based on the compositions of soluble organic molecules. Therefore, in this study, we analyzed aliphatic hydrocarbons and polycyclic aromatic hydrocarbons (PAHs) in Jbilet Winselwan CM chondrite, which is a dehydrated CM chondrite (Zolensky et al 2016) and show similar reflectance spectrum to that of asteroid Ryugu (Kameda et al. 2015), for precise evaluation of parent body thermal metamorphism. The relative abundances of the hydrocarbons were compared with those of Murray meteorite, which is a primitive CM chondrite.

Samples and Methods: Powdered samples of Jbilet Winselwan meteorite and Murray meteorite (0.2 - 0.4g) were extracted with dichloromethane/methanol (9:1) by sonication. The extracts were applied to a silica gel column. From the column, aliphatic hydrocarbons were eluated with hexane and then PAHs were eluated with dichloromethane. The hexane and dichloromethane eluates were concentrated to 100 μl individually under a nitrogen flow for analysis by a gas chromatography coupled with mass spectrometry (GC-MS). Identification and quantification of compounds were made by comparison of peak retention times on mass chromatograms and mass spectra, and peak areas, respectively, with those of standard compounds. For compounds without standard compounds, identification was made by comparison of mass spectra with library data.

Results and discussion: Total concentration of *n*-alkanes from Jbilet Winselwan meteorite (1.85 μg/g meteorite) was 40 times lower than those from Murray meteorite (80.7 μg/g meteorite). Relative abundances of short-chain *n*-alkanes (C_{15}-C_{16}) were dominant in Jbilet Winselwan meteorite, while those of long-chain *n*-alkanes (C_{17}-C_{21}) were dominant in Murray meteorite. This difference implies that short-chain *n*-alkanes were resulted from cracking of long-chain *n*-alkanes and/or IOM during thermal metamorphism of the parent body of Jbilet Winselwan meteorite. Total concentration of PAHs from Jbilet Winselwan meteorite (0.05 μg/ meteorite) was 1000 times lower than those from Murray meteorite (62.0 μg/g meteorite). Dimethylnaphthalene, fluorine, phenanthrene, pyrene, fluoranthene, methylbiphenyl (0.003-0.039 μg/g meteorite) were identified, while low molecular weight PAHs, such as naphthalene, methylnaphthalene, and acenaphthene, were not detected. The results suggest that PAHs with high volatility in Jbilet Winselwan meteorite were lost or involved in further aromatization during thermal metamorphism. Distributions of dimethylnaphthalene and methylbiphenyl isomers in Jbilet Winselwan

©2019. Japan Geoscience Union. All Right Reserved.

and Murray meteorites were similar, respectively, which indicates that the parent body of Jbilet Winselwan meteorite experienced relatively mild thermal metamorphism.

Keywords: Jbilet Winselwan meteorite, Soluble organic molecules, Dehydration

©2019. Japan Geoscience Union. All Right Reserved.

Disk-Resolved Photometry Analysis of the Asteroid Ryugu Images Obtained by Hayabusa2 Visible Camera ONC

*yokota yasuhiro[1,2], Rie Honda[1], ERI TATSUMI[3], Deborah Domingue[4], Stefanus E. Schroeder[5], Moe Matsuoka[2], Seiji Sugita[3], Tomokatsu Morota[6], Shingo Kameda[7], Toru Kouyama[8], Hidehiko Suzuki[9], Manabu Yamada[10], Naoya Sakatani[2], Chikatoshi Honda[11], Masahiko Hayakawa[2], Kazuo Yoshioka[3], Yuichiro Cho[3], Hirotaka Sawada[2]

1. Kochi University, 2. ISAS/JAXA, 3. Univ. of Tokyo, 4. Planetary Science Institute, 5. DLR, 6. Nagoya Univ., 7. Rikkyo Univ., 8. AIST, 9. Meiji Univ., 10. Chiba Institute od Technology, 11. Aizu Univ.

Since June 2018, the Optical Navigation Camera (ONC) onboard Hayabusa2, has observed the C-type asteroid 162173 Ryugu at a distance below 20 km. ONC-T and ONC-W1 are used for surface imaging operations, and their images allow us to investigate the disk-resolved photometric properties of the surface. A narrow-angle camera ONC-T has 7 broad-band filters ranging in wavelength from 0.39–0.95 μm. ONC-W1 is a wide-angle (> 65˚) pan-chromatic camera mainly used for optical navigation during cruise and low-altitude (< 20km) operations. We are proceeding the analysis of both dataset, ONC-T and ONC-W1.

Since Hayabusa2’s position is nominally fixed on the line connecting Ryugu and the Earth, the available solar phase angle range by ONC-T changes seasonally with the orbits of Earth and Ryugu around the sun. Therefore, we are collecting a large number of ONC-T images over a long period of time to cover a wide phase angle range.

ONC-W1 data has a strong point that it covers a wide phase angle range within a single frame during the descent operations, because of its wide field of view. One of our current challenges is deriving a precise viewing geometries (incidence angle, emission angle, and phase angle) at each pixel. Additionally, comparison of the absolute brightness value (radiance factor) with ONC-T is an ongoing issue.

Keywords: Asteroid, Photometry, Ryugu, Hayabusa2

©2019. Japan Geoscience Union. All Right Reserved.

[E] Poster | P (Space and Planetary Sciences)：P-EM Solar-Terrestrial Sciences, Space Electromagnetism & Space Environment

Wed. May 29, 2019 10:45 AM - 12:15 PM JST | Wed. May 29, 2019 1:45 AM - 3:15 AM UTC | Poster Hall International Exhibition Hall8, Makuhari Messe_3

[P-EM09] Vertical coupling in the atmosphere and Ionosphere

convener:Huixin Liu(Earth and Planetary Science Division, Kyushu University SERC, Kyushu University), Loren Chang(Institute of Space Science, National Central University), Yuichi Otsuka(Institute for Space-Earth Environmental Research, Nagoya University)

Vertical coupling mechanisms throughout the whole atmosphere are critical to understanding the near Earth space environment, as well as its sensitivity to the solar, geomagnetic, and atmospheric drivers. This international session focuses on physical/chemical processes occurring in the mesosphere, thermosphere, and ionosphere (MTI). Both quiet and disturbed states in response to lower atmospheric forcing or solar forcing are important for understanding the MTI system and its coupling to other regions. We invite presentations of observations and observational concepts with ground-based and/or space-borne instruments, theoretical studies, numerical simulations, and development of data analysis systems for various kinds of temporal and spatial variations in atmosphere-ionosphere coupled system.

[PEM09-P01] Local-time Variabilities of SABER CO_2 in the Mesosphere and Lower Thermosphere Region

*Cornelius Csar Jude Salinas[1], Loren Chang[1], Danie Liang[2], Jia Yue[3], Liying Qian[4], Quan Gan[5], James Russel III[3], Martin G Mlynczak[6] (1.Institute of Space Science, National Central University, 2.Institute of Earth Science, Academia Sinica, 3.Department of Atmospheric Sciences, Hampton University, 4.High Altitude Observatory, National Center for Atmospheric Research, 5.Department of Physics and Astronomy, Clemson University, 6.NASA Langley Research Center)

[PEM09-P02] Enhanced dynamo electric field as a possible cause of ionosphere disturbance before Large Earthquake

*Koichiro Oyama[1,2,3] (1.Institute of Plasma and Space Sciences,National Cheng Kung Univ., Taiwan, 2.International Ceneter for Space Weather Sudy and Education, Kyushu Univ.,, 3.CoLtd. Asia Space Environment Research Consortium, Japan)

[PEM09-P03] Morphology of E1 and E2 Kelvin waves from ECMWF reanalysis

*Chen-Jeih Pan[1], Wei-Sheng Chen[1], Uma Das[2] (1.Institute of Space Science, National Central University, 2.Department of Physics, Indian Institute of Information Technology, Kalyani, India)

[PEM09-P04] Impact of strong ENSO on TEC activity disturbed by ultra-fast Kelvin waves

*Wei-Sheng Chen[1], C.J. Pan[1], Uma Das[2], Chian-Chiau Lin[3] (1.Institute of Space Science, National Central University, Taiwan, 2.Department of Physics, Indian Institute of Information Technology, Kalyani, India, 3.Environmental Research and Information Center, Chang Jung Christian University, Taiwan)

[PEM09-P05] Observation and simulation of propagation of coseismic infrasound to the ionosphere

*Jaroslav Chum[1] (1.Institute of Atmospheric Physics of the Czech Academy of Sciences)

[PEM09-P06] Solar wind influence on tropical cyclones mediated by atmospheric gravity waves

*Paul Prikryl[1,2], Iurii Cherniak[3], Irina Zakharenkova[4,5], James M. Weygand[6], Bharat S. R. Kunduri[7] (1.Physics Department, University of New Brunswick, Fredericton, NB, Canada, 2.Geomagnetic Laboratory, Natural Resources Canada, Ottawa, ON, Canada, 3.COSMIC Program Office, University Corporation for Atmospheric Research, Boulder, CO, USA, 4.West Department of IZMIRAN, Kaliningrad, Russia, 5.University of Warmia and Mazury in Olsztyn, Poland, 6.Earth Planetary and Space Sciences, University of California, Los Angeles, CA, USA, 7.Bradley Dept. of Electrical and Computer Engineering, Virginia Tech, Blacksburg, VA, USA)

[PEM09-P07] VIPIR ionospheric observations in Japan

*Takuya Tsugawa[1], Hideo Maeno[1], Michi Nishioka[1], Takumi Kondo[1], Mamoru Ishii[1] (1.National Institute of Information and Communications Technology)

[PEM09-P08] Simulation Results and Performance Analysis of Phase Velocity Spectral Analysis Software (M-Transform) for Airglow Imaging Data

*Septi Perwitasari[1], Takuji Nakamura[2], Masaru Kogure[2], Yoshihiro Tomikawa[2], Mitsumu K. Ejiri[2] (1.LAPAN, 2.NIPR)

[PEM09-P09] Comparisons of Co-incident Ionospheric Plasma Observations Between FORMOSAT-5/AIP and Millstone Hill Incoherent Scatter Radar

*Yi-Wun Chen[1], Chi-Kuang Chao[1] (1.Graduate Institute of Space Science, National Central University, Taiwan)

[PEM09-P10] Sub-ionospheric effects of volcano eruptions using VLF/LF standard radio waves

*Kei Maruyama[1], Hiroyo Ohya[1], Fuminori Tsuchiya[2], Kenro Nozaki[5], Kozo Yamashita[3], Yukihiro Takahashi[4], Hiroyuki Nakata[1], Toshiaki Takano[1] (1.Chiba University, 2.Tohoku University, 3.Ashikaga University, 4.Hokkaido University, 5.National Institute of Information and Communications Technology)

[PEM09-P11] Observations of ionospheric and mesospheric wave structures by a low-cost airglow imaging system

*Keisuke Hosokawa[1], Nanami Kusuyama[1], Yuta Hozumi[1], Kohei Takami[1], Susumu Saito[2], Yasunobu Ogawa[3], Mamoru Ishii[4], Yuichi Otsuka[5], Takuya Tsugawa[4] (1.University of Electro-Communications, 2.ENRI, 3.NIPR, 4.NICT, 5.ISEE, Nagoya University)

[PEM09-P12] Analysis of characteristics of ionospheric parameters, Sq index and neutral winds over Taiwan

*Yu-Jung Chuo[1] (1.Department of Information Technology, Ling Tung University)

[PEM09-P13] Statistical study on daytime Es observed by ground-ionosonde and RO-COSMIC in magnetic Equator region in 2010

*Zheng Wang [1,2], Huixin Liu[1] (1.Department of Earth and Planetary Sciences, School of Science, Kyushu University, Japan. , 2.National Space Science Center, Chinese Academy of Sciences, China.)

[PEM09-P14] The statistical study of the growth rates of Medium-Scale Traveling Ionospheric Disturbances observed with GPS-TEC

*Takafumi Ikeda[1], Akinori Saito[1], Takuya Tsugawa[2], Hiroyuki Shinagawa[2] (1.Department of Geophysics, Graduate School of Science, Kyoto University, 2.National Institutes of Information and Communications Technology)

[PEM09-P15] Comparison of Gravity Wave Activity in the Mesosphere Observed by OH Airglow Imagers and MF Radars over the Antarctic (Syowa & Davis).

*Masaru Kogure[1], Takuji Nakamura[1,2], Yoshihiro Tomikawa[1,2], Mitsumu K. Ejiri[1,2], Takanori Nishiyama[2,1], Masaki Tsutsumi[1,2], Michael J. Taylor[3], Yucheng Zhao[3], P.-Dominique Pautet[3], Damian Murphy[4] (1.National Institute of Polar Research, 2.Department of Polar Science, Sokendai, 3.Physics Department, Utah State University, 4.Australian Antarctic Division)

Local-time Variabilities of SABER CO_2 in the Mesosphere and Lower Thermosphere Region

*Cornelius Csar Jude Salinas[1], Loren Chang[1], Danie Liang[2], Jia Yue[3], Liying Qian[4], Quan Gan[5], James Russel III[3], Martin G Mlynczak[6]

1. Institute of Space Science, National Central University, 2. Institute of Earth Science, Academia Sinica, 3. Department of Atmospheric Sciences, Hampton University, 4. High Altitude Observatory, National Center for Atmospheric Research, 5. Department of Physics and Astronomy, Clemson University, 6. NASA Langley Research Center

This work presents the local-time variabilities of CO_2 in the Mesosphere and Lower Thermosphere region (MLT region) as observed by the Sounding of the Atmosphere using Broadband Emission Radiometry (SABER) onboard the Thermosphere Ionosphere Mesosphere Energetics and Dynamics Satellite (TIMED Satellite). These are then compared to CO_2 as modeled by the Whole Atmosphere Community Climate Model –eXtended (WACCM-X). Also using WACCM-X, a tendency analysis using the continuity equation is done to explain the local-time variabilities of CO_2 in the MLT region. Finally, consequences of including a significant local-time variability in CO_2 when retrieving SABER temperature profiles are determined.

Keywords: Carbon Dioxide, Mesosphere and Lower Thermosphere Region, Tides

©2019. Japan Geoscience Union. All Right Reserved.

Enhanced dynamo electric field as a possible cause of ionosphere disturbance before Large Earthquake

*Koichiro Oyama[1,2,3]

1. Institute of Plasma and Space Sciences,National Cheng Kung Univ., Taiwan, 2. International Ceneter for Space Weather Sudy and Education, Kyushu Univ.,, 3. CoLtd. Asia Space Environment Research Consortium, Japan

Disturbance of ionosphere before large earthquakes has been very often reported. One of the possible disturbing drivers is electric field, which explains most of the ionosphere features we reported so far. However, the origin of the electric field is still in the darkness. One idea of electric field generation exists inside earth interior (Freund et a., 2006). We propose here that the electric field is dynamo field at the height of ≈100 km, which simply intensified before earthquake; intensified eastward (westward)electric field during daytime(nighttime). This idea explains satellite data (Oyama et al.,2008; Oyama et al.,2011; Ryu et al., 2014; Ryu et al., 2016; Oyama et al.,2016; Oyama et al., 2019).

Next question on the electric field generation is the mechanism which modifies the dynamo field. We speculate that modification of E field is a result of modification of neutral wind system, which is originally caused by internal gravity waves which propagate from below. Then again next question is on the origin of the internal gravity waves. The waves might be originally caused by the ground motion, and these waves which propagate upward might interact with planetary wave, and amplified. We show several side evidence of ground motions before earthquakes.

Keywords: Earthquake, Electric field, Ionosphere, Disturbance

©2019. Japan Geoscience Union. All Right Reserved.

Morphology of E1 and E2 Kelvin waves from ECMWF reanalysis

*Chen-Jeih Pan[1], Wei-Sheng Chen[1], Uma Das[2]

1. Institute of Space Science, National Central University, 2. Department of Physics, Indian Institute of Information Technology, Kalyani, India

Kelvin waves are planetary waves traveling eastwards and confined in the equatorial latitudes. The waves play an important role in middle atmosphere dynamics because they transfer energy and momentum from lower to higher altitudes, which contributes to the quasi-biennial oscillation (QBO) and further influences the global climate. Kelvin waves have been studied for many decades, and the most of studies were focused on the waves of wavenumber 1 (E1). On the other hand, the wavenumber-2 Kelvin waves (E2) are also an important part of Kelvin wave activities although their amplitude less than the E1. In this study, we analyzed the long-term European Centre for Medium-Range Weather Forecasts (ECMWF) reanalysis data and reported the morphology of E1 and E2 Kelvin waves in the stratospheric altitudes individually. The temperature from ECMWF reanalysis was used to extract the wave properties. Temperatures between latitudes of 10S and 10N were firstly gridded into the structure of day-altitude-longitude, and then subtract background (longitudinal means) to get equatorial temperature fluctuations. For each altitude, the two-dimensional fast Fourier transform was applied to each 96-day data segment and stepped forward in time by 1 day. The output spectra were then analyzed to get primary wave periods and amplitude variations. From spectra, the E1 amplitude is 1.5 to 2.0 times larger than the E2 in average. The E1 primary periods are 12 to 25 days and are restricted under the 20-km altitude. The periods of 8 to 14 days are the secondary group. They can propagate upward to the 40-km altitude. Regarding the E2, the primary periods are 7 to 12 days and are also restricted under the 20-km altitude. Its secondary group is the periods of 5 to 8 days, which also can propagate upward to the 40-km altitude. Furthermore, the altitude-time-amplitude variation show that the E2 waves are influenced strictly by the QBO westerly. Finally, the cross correlation between E1 and E2 show that the E1 and E2 have high correlation at altitudes close to the tropopause, which implies they are excited simultaneously.

Keywords: Kelvin waves, QBO

©2019. Japan Geoscience Union. All Right Reserved.

Impact of strong ENSO on TEC activity disturbed by ultra-fast Kelvin waves

*Wei-Sheng Chen[1], C.J. Pan[1], Uma Das[2], Chian-Chiau Lin[3]

1. Institute of Space Science, National Central University, Taiwan, 2. Department of Physics, Indian Institute of Information Technology, Kalyani, India, 3. Environmental Research and Information Center, Chang Jung Christian University, Taiwan

Ultra-fast Kelvin waves (UFKW) are a subclass of Kelvin waves that they have the shortest periods (2-5 days) and thus can propagate into the ionosphere. UFKW relate to ionospheric variations have been reported, which include ionospheric minimum virtual height (h'F), F2 maximum critical frequency (foF2), total electron content (TEC), S4 scintillations, etc. In the study, we analyzed the UFKW activities using SABER (Sounding of the Atmosphere using Broadband Emission Radiometry) temperatures and GIM (Global Ionospheric Maps) TEC from 2009 to 2011 to see how UFKW influence the ionosphere. The period 2009-2011 belongs to the strong ENSO period. Previous studies have shown that Kelvin waves were highly active in this period, especially in the early of 2010. Therefore, this study can implicitly reveal how the ionosphere responds to the ENSO. The wave signatures in SABER temperatures were extracted using the fast Fourier transform (FFT). Temperatures in the geographic equatorial latitudes were gridded into the day-altitude-longitude structure and then removed background to get temperature fluctuations. The two-dimensional FFT was applied to each 96-day data segment for each altitude and stepped forward in time by one day. Regarding TEC, the Lomb-Scargle periodogram was used to extract UFKW signatures. Because TEC has a strong local time variation and constrains by the geomagnetic configuration, TEC at 16 local time and low geomagnetic latitudes were selected. The background was removed firstly from the data and then fed TEC fluctuations into the Lomb-Scargle process, which also stepped forward in time by one day. The FFT and Lomb-Scargle process both outputted spectra, which revealed UFKW activities in the mesosphere and lower thermosphere (MLT) region (90-100 km) and the ionosphere (about 150-600 km). The results show that UFKW activities at two equatorial ionization anomalies (EIA) were almost identical, and both were higher than that at geomagnetic equator. Most of wave activities in the temperature field in the MLT region have corresponding activities in TEC. However, there are a lot of small amplitude activities only in TEC.

Keywords: ultra-fast Kelvin waves, ENSO, TEC

©2019. Japan Geoscience Union. All Right Reserved.

Observation and simulation of propagation of coseismic infrasound to the ionosphere

*Jaroslav Chum[1]

1. Institute of Atmospheric Physics of the Czech Academy of Sciences

Vertical motion of the ground surface caused by seismic waves generates acoustic waves that propagate nearly vertically upward owing to supersonic speed of seismic waves. As the air density decreases with height, the amplitude of acoustic waves increases to conserve the energy flux up to the altitudes where the air is so rarefied that it cannot sustain the propagation and the waves start dissipating. For distances up to about 1500 km from the epicenter of the strong earthquakes (M>7), the amplitude (oscillation velocity) of infrasound waves reaches significant values in the upper atmosphere. Consequently, the nonlinear phenomena start to play an important role. Spectral content of the wave packet is changed and the energy is transferred to lower frequencies, which can cause the formation of roughly bipolar N-shaped pulse. The simulation results are compared with observation for selected examples. It is also shown that only infrasound with periods larger than about 10 s (generated by long period seismic waves) can reach the ionospheric heights, namely the F layer where it can be easily detected.

Keywords: coseismic perturbation in the ionosphere, infrasound, nonlinear propagation

©2019. Japan Geoscience Union. All Right Reserved.

Solar wind influence on tropical cyclones mediated by atmospheric gravity waves

*Paul Prikryl[1,2], Iurii Cherniak[3], Irina Zakharenkova[4,5], James M. Weygand[6], Bharat S. R. Kunduri[7]

1. Physics Department, University of New Brunswick, Fredericton, NB, Canada, 2. Geomagnetic Laboratory, Natural Resources Canada, Ottawa, ON, Canada, 3. COSMIC Program Office, University Corporation for Atmospheric Research, Boulder, CO, USA, 4. West Department of IZMIRAN, Kaliningrad, Russia, 5. University of Warmia and Mazury in Olsztyn, Poland, 6. Earth Planetary and Space Sciences, University of California, Los Angeles, CA, USA, 7. Bradley Dept. of Electrical and Computer Engineering, Virginia Tech, Blacksburg, VA, USA

Solar wind coupling to the magnetosphere-ionosphere-atmosphere (MIA) system generates medium- and large-scale atmospheric gravity waves (AGWs) propagating globally from sources in the lower thermosphere at high latitudes. The AGWs propagate globally [1,2] upward and downward, are observed in the ionosphere as traveling ionospheric disturbances [3], can be ducted in lower atmosphere over long distances and reach troposphere. At the reflection point in the troposphere they can trigger moist instabilities to initiate convective bursts, with the latent heat release leading to intensification of storms [4]. In the follow-up studies [5,6,7] it was shown that explosive extratropical cyclones and rapid intensification of tropical cyclones tend to follow arrivals of solar wind high-speed streams (HSS) and/or interplanetary coronal mass ejections (ICMEs). The coupling of solar wind to MIA is most intense during the arrivals of co-rotating interaction regions (CIRs) and/or interplanetary shocks at the leading edges of HSSs and ICMEs when the amplitudes of aurorally-generated AGWs are largest. Ray tracing of AGWs in a model atmosphere show that they can reach tropical cyclones. Spiral gravity waves in typhoons were observed and simulated to propagate radially outward from the typhoon core [8]. The spectra of waves in surface pressure and surface wind measured by the Impacts of Typhoons on the Ocean in the Pacific (ITOP) buoy during the nearby passages of intense typhoons are similar to those of incoming aurorally-generated AGWs. It is suggested that the interaction of aurorally-generated gravity waves with the tropical cyclone vortex and the inner primary eyewall plays a role in the intensification process.

[1] Mayr H.G., et al., J. Geophys. Res., 89, 10929–10959, 1984.
[2] Prikryl P., et al., Ann. Geophys., 23, 401-417, 2005. doi:10.5194/angeo-23-401-2005
[3] Cherniak Iu., Zakharenkova I., Space Weather, 16, 2018. https://doi.org/10.1029/2018SW001869.
[4] Prikryl P., et al., Ann. Geophys. 27, 31–57, 2009. https://doi.org/10.5194/angeo-27-31-2009.
[5] Prikryl P., et al., J. Atmos. Sol.-Terr. Phys., 149, 219–231, 2016.
[6] Prikryl P., et al., J. Atmos. Sol.-Terr. Phys., 171, 94–110, 2018.
[7] Prikryl P., et al., J. Atmos. Sol.-Terr. Phys., 183, 36-60, https://doi.org/10.1016/j.jastp.2018.12.009.
[8] Nolan D.S., Zhang J.A., Geophys. Res. Lett., 44, 3924–3931, 2017. doi:10.1002/2017GL073572

Keywords: Solar wind-magnetosphere-ionosphere-atmosphere coupling, High-speed solar wind stream, Atmospheric gravity wave, Extratropical and tropical cyclones

©2019. Japan Geoscience Union. All Right Reserved.

VIPIR ionospheric observations in Japan

*Takuya Tsugawa[1], Hideo Maeno[1], Michi Nishioka[1], Takumi Kondo[1], Mamoru Ishii[1]

1. National Institute of Information and Communications Technology

National Institute of Information and Communications Technology (NICT) has observed ionosphere by ionosondes more than 70 years in Japan. At present, four ionosondes at Wakkanai (Sarobetsu), Kokubunji, Yamagawa, Okinawa (Ogimi) are automatically operated and controlled from Tokyo. Major ionospheric parameters such as foF2 and foEs are scaled from the ionograms automatically on a realtime basis and scaled manually for the final values. These scaled parameters are provided through our web site (http://wdc.nict.go.jp/IONO/). In 2017, we replaced the 10C ionosondes with Vertical Incidence Pulsed Ionospheric Radar 2 (VIPIR2) which can separate the O- and X-modes of ionospheric echoes which have improved the availability of automatic scaling of the ionogram. Our automatic scaling method has been improved using new O- and X-modes separated ionograms. As for future plans, we try to expand observation area by oblique sounding observations with VIPIRs in Japan and neighboring countries. We have also tried to detect arrival directions of ionospheric echo by using the 8ch receiving data as a interferometry. In this presentation, we will introduce current status and future plans of ionospheric observation in NICT.

Keywords: Ionosphere, Ionosonde, Space Weather

©2019. Japan Geoscience Union. All Right Reserved.

Simulation Results and Performance Analysis of Phase Velocity Spectral Analysis Software (M-Transform) for Airglow Imaging Data

*Septi Perwitasari[1], Takuji Nakamura[2], Masaru Kogure[2], Yoshihiro Tomikawa[2], Mitsumu K. Ejiri[2]

1. LAPAN, 2. NIPR

We have developed a user-friendly software based on *Matsuda et al.*, 2014's 3D-FFT method (M-Transform) for airglow data analysis as a function on Interactive Data Language (IDL). Input of this function is 3-D array of a time series of airglow image that have already been converted to geographical coordinate (*x*, *y*, *t*). The user can customize the wave parameters (e.g. horizontal wavelength (λ_h), wave period (τ), phase speed (*c*), image resolution in space (*dx*,*dy*) and time (*dt*)) in one-line command when executing the program, which depends on their analysis purpose. In order to exhibit this new function's performance and the characteristics/interpretation of the spectral analysis, we have run several test cases using artificial wave. The first case is artificial wave with constant speed (40 m/s) and different wave period (8, 15, 30 min) and horizontal wavelength. In second case, we applied Gaussian shape wave-packet with different FWHM (50, 100, 200 km). For the third test case, with a fixed wave packet size (100 km), we changed the wave packet duration (30, 60, 120 min). The results from the various simulations showed reasonable characteristics of the spectral analysis for different scenarios. We showed that the increase of wave period and horizontal wavelength lead to the wider spectrum with total power difference of ~10%. By changing the wave packet size, we showed that the bigger the wave packet size, the sharper and narrower the spectrum became with the total power increase 2x of the increase size of the wave packet. The result of changing the wave packet duration showed that the longer the duration of wave packet, the spectrum becomes sharper and the total power is proportional to the wave packet length. We also examined the aliasing and zero padding effect on the spectral analysis. In order to avoid the aliasing effect, it is recommended to set the period minimum to at least 2 x image interval (*dt*). More detailed analysis will be discussed during the presentation.

Keywords: Airglow, Gravity wave, Analysis software

©2019. Japan Geoscience Union. All Right Reserved.

Comparisons of Co-incident Ionospheric Plasma Observations Between FORMOSAT-5/AIP and Millstone Hill Incoherent Scatter Radar

*Yi-Wun Chen[1], Chi-Kuang Chao[1]

1. Graduate Institute of Space Science, National Central University, Taiwan

Advanced Ionospheric Probe (AIP) onboard FORMOSAT-5 satellite has routinely measured ionospheric plasma parameters, like ion concentration, velocity, and temperature in a sun-synchronous circular orbit at 720 km altitude along 2230 local-time sector since November 2017. AIP has found that the satellite has a much lower potential with respective to environmental plasma from measured current-voltage curves. A comparison study shall be performed to identify possible bias on the derived AIP parameters. Co-incident observations have been scheduled with Millstone Hill incoherent scatter radar during 30 January to 1 February 2019. In this poster, preliminary comparison results will be outlined and will be used to improve accuracy of the AIP measurement in the future.

Keywords: FORMOSAT-5, AIP, ionosphere

©2019. Japan Geoscience Union. All Right Reserved.

Sub-ionospheric effects of volcano eruptions using VLF/LF standard radio waves

*Kei Maruyama[1], Hiroyo Ohya[1], Fuminori Tsuchiya[2], Kenro Nozaki[5], Kozo Yamashita[3], Yukihiro Takahashi[4], Hiroyuki Nakata[1], Toshiaki Takano[1]

1. Chiba University, 2. Tohoku University, 3. Ashikaga University, 4. Hokkaido University, 5. National Institute of Information and Communications Technology

Several studies for the F-region ionosphere associated with volcano eruptions based on GPS-TEC data have been reported so far (e.g., Heki, 2006; Dautermann et al., 2009; Heki et al., 2010). These studies reported that acoustic waves excited by volcano eruptions reach up to the F-region ionosphere, and caused F-region perturbations. After eruption of the Kelud Volcano, Indonesia, in February 2014, acoustic resonance between the Earth’ s surface and lower thermosphere was reported based on TEC data and the seismic wave data (Nakashima et al., 2015). However, little studies on the D-region ionosphere associated with volcano eruptions have been reported. In this study, we investigate the D-region effects of eruptions of Sakurajima volcano (31.59N, 130.66E), Japan, at 04:11 UT on June 6, 2014, using intensity perturbation of VLF/LF transmitter signals. The VLF/LF propagation paths use in this study are JJY (JJY 60 kHz) - Tainan (TNN, Taiwan), and JJI (22.2 kHz) - TNN. Based on wavelet spectra, the perturbation of both transmitter signals had a frequency of 2-6 mHz during 04:12-04:30 UT after the eruptions (04:11 UT).We compared the perturbations with atmospheric pressure data obtained by an infrasonic meter observed by Sakurajima Volcano Research Center, Kyoto University, and seismic waves in the NIED F-net data (FUK, STM, and SBR) located close to the JJY-TNN path. The atmospheric pressure and vertical velocity of the seismic waves had the similar frequencies of 2-10 mHz during 04:12-04:47 UT. These similar frequencies suggest that the perturbations would be caused by acoustic resonance between the Earth's surface and lower thermosphere, or by acoustic and atmospheric gravity waves generated by volcanic eruptions. In the presentation, we will discuss the cause of the VLF/LF perturbations in more detail.

©2019. Japan Geoscience Union. All Right Reserved.

Observations of ionospheric and mesospheric wave structures by a low-cost airglow imaging system

*Keisuke Hosokawa[1], Nanami Kusuyama[1], Yuta Hozumi[1], Kohei Takami[1], Susumu Saito[2], Yasunobu Ogawa[3], Mamoru Ishii[4], Yuichi Otsuka[5], Takuya Tsugawa[4]

1. University of Electro-Communications, 2. ENRI, 3. NIPR, 4. NICT, 5. ISEE, Nagoya University

In the last two decades, all-sky airglow imagers with cooled CCD cameras have widely been used to observe large-scale wave structures in the F-region ionosphere, for example medium-scale traveling ionospheric disturbances (MSTIDs). Such wavy features are seen in the oxygen emission at 630.0 nm from altitudes slightly below the F-region peak. Similar optical observations of OH band emission have also enabled us to visualize atmospheric gravity waves at the mesospheric height. Deploying airglow imagers in multiple places is one of the cost-effective ways to visualize the large-scale structure of these wave structures at both the F-region ionosphere and mesosphere [e.g., Kubota et al., 2001; Suzuki et al., 2013]. However, ground-based airglow imagers equipped with a cooled CCD camera is still expensive; thus, it is rather difficult to deploy such systems in a wide area and carry out a network observation. To overcome this limitation, we recently developed a low-cost airglow imaging system (Low-Cost Airglow imaging System: LCAS) which consists of a small camera (WAT-910HX), fisheye lens and optical filter. We then confirmed its capability of imaging the spatial structure of polar cap patches and plasma bubble in the 630.0 nm emission from the F-region. But, still, it is unclarified if the system is also capable of detecting the two-dimensional structure of MSTIDs. On the night of May 12, 2018, we identified a weak wavy signature in the 630.0 nm airglow images from one of our LCAS stations in Ishigaki Island, Japan. The wave structure in the 630.0 nm images was smoothly connected to the structure of MSTIDs in the GPS-TEC data, which confirmed the ability of LCAS for detecting MSTIDs. We also identified smaller scale wave structures in the 630.0 nm images, showing characteristic concentric wave fronts. We speculate that gravity waves in the mesosphere were captured in the 630.0 nm images as a contamination of the OH airglow. This is mainly because we make use of an optical filter having 10 nm FWHM, which enables us to detect several spectral peaks of OH emission near the 630.0 nm oxygen emission. We have estimated the center of the concentric wave structures by using the curvature of the wave fronts, and then confirmed that active rain fall took place in a localized area close to the estimated center of the concentric waves. This result supports our hypothesis that the OH emission containing signatures of mesospheric gravity waves were detected in the 630.0 nm images. In summary, the 630.0 nm airglow observation of LCAS is able to observe MSTIDs and mesospheric gravity waves. This will allow us to monitor such wavy structures at two different altitudes by distributing the similar system in a wide area.

Keywords: Airglow, Traveling Ionospheric Disturbances

©2019. Japan Geoscience Union. All Right Reserved.

Analysis of characteristics of ionospheric parameters, Sq index and neutral winds over Taiwan

*Yu-Jung Chuo[1]

1. Department of Information Technology, Ling Tung University

In this paper, we examine the variation of thermospheric neutral winds and solar quiet (Sq) current of the geomagnetic fields for the equatorial ionospheric anomaly area (EIA) during the solar activity period in 1999. The thermospheric neutral winds are derived from the ionospheric F_2-layer peak height, hmF_2, by using the servo model method. The variability of the amplitude ofSq fields is derived from the ground geomagnetic fields in the components H and Z, respectively. Theresults of the current system show a same diurnal variation, which that peaks / valleys in the local noon time for Sq(H) / Sq(Z) in the low latitudes, respectively.The results also indicate a weak seasonal variation that peaks appear at the local summer of the Sq currents in H and Z components, respectively. The Sq current system is associated with the change of the equatorial electrojet (EEJ). Further, the variability is probably attributed to local thermospheric winds. The study also shows that the zonal and meridional components of the neutral winds at the EIA over Taiwan area. Furthermore, the study examines the variations of Sq(H), Sq(Z), neutral winds, and ionospheric parameters foE_s, NmF_2, and hmF_2during the disturbed geophysical conditions such as geomagnetic storm and earthquake. The result shows the variationsof ionospheric Sq(H), Sq(Z) and thermospheric neutral winds are different between the seismo-ionospheric and solar-terrestrial disturbed periods, even they lead the same decreasing electron density reaction in the ionosphere at the EIA over Taiwan area.

Keywords: Sq current, ionosphere, neutral winds

©2019. Japan Geoscience Union. All Right Reserved.

Statistical study on daytime Es observed by ground-ionosonde and RO-COSMIC in magnetic Equator region in 2010

*Zheng Wang [1,2], Huixin Liu[1]

1. Department of Earth and Planetary Sciences, School of Science, Kyushu University, Japan. , 2. National Space Science Center, Chinese Academy of Sciences, China.

Scintillations under 150 km height shown by radio occultation (RO) of COSMIC are considered to be associated with ionospheric sporadic E (Es) layer. In this paper, we make a Statistical study on daytime Es observed by ground-ionosonde at five stations in magnetic Equator region in 2010, and make a comparison with S4 index from RO-COSMIC within 6 degree of each station. The results show that: At each station the diurnal variation of foEs from ionosonde decrease a little around LT 0600 and then increase, having maximum around LT 1200, decrease around LT 1800 and then increase near LT 2000-2200; All the S4>=0.3 observations during daytime come from RO-COSMIC under 150 km height; The diurnal variation of S4 index under 150 km height from RO-COSMIC over each station has similar trend with that of foEs at the same station; S4 index over 150 km height from RO-COSMIC is only high during nighttime; For the stations at different longitudes, Es occurrences from ionosonde are positively associated with S4>=0.3 from RO-COSMIC. The comparison shows that the S4 index from RO-COSMIC could show some features of daytime Es layer in magnetic Equator region without the location limitation of ground stations.

Keywords: daytime ionospheric sporadic E, ground-ionosonde , radio occultation of COSMIC , magnetic Equator region

©2019. Japan Geoscience Union. All Right Reserved.

The statistical study of the growth rates of Medium-Scale Traveling Ionospheric Disturbances observed with GPS-TEC

*Takafumi Ikeda[1], Akinori Saito[1], Takuya Tsugawa[2], Hiroyuki Shinagawa[2]

1. Department of Geophysics, Graduate School of Science, Kyoto University, 2. National Institutes of Information and Communications Technology

We think two mechanism, E-F coupling and Perkins Instability, will relate to growth for nighttime-MSTID in mid-latitude [Tsunoda and Cosgrove., 2001 ; Perkins., 1973]. Linear growth rate of perturbation intensity of Pedersen conductivity expected from E-F coupling is around 15 minutes [Yokoyama et al., 2009], which is far shorter than one expected from Perkins Instability [Fukao and Kelley, 1991 ; Miller et al., 1997 ; Shiokawa et al., 2003]. However, Es layer’ s spatial and temporal scale is less than 100km and 15min [Maeda et al., 2013 ; S.Saito et al., 2007]. They are different from MSTID’ s ones, which are 200-400 km and around 2hours [Otsuka et al., 2011]. To decide which instability is responsible for growth of nighttime MSTID, the growth rate of MSTID was observationally determined with ground-based GPS network data.

We statistically investigated the growth rate of nighttime-MSTID in Japan in 2014 observed with GPS-TEC. The growth rate of nighttime -MSTID observed was 1.0 - 6.0 $\times 10^{-4}$ s^{-1} during 1800LT-2400LT in summer.Linear growth rate of Perkins instability in summer was 1.0 - 6.0 $\times 10^{-4}$ s^{-1} during 1800LT - 2400LT, so they were less than one of the E-F coupling instability. Also,Seasonal distribution of observed growth rate before midnight was similar to that of linear growth rate.U×B derived by GAIA model was high in spring - summer and seasonal distribution of U×B was similar to that of linear growth rate. Therefore, the growth of MSTID when propagating is not determined by E-F coupling instability but Perkins instability and neutral wind.

Keywords: MSTID, GPS-TEC, Ionosphere

©2019. Japan Geoscience Union. All Right Reserved.

Comparison of Gravity Wave Activity in the Mesosphere Observed by OH Airglow Imagers and MF Radars over the Antarctic (Syowa & Davis).

*Masaru Kogure[1], Takuji Nakamura[1,2], Yoshihiro Tomikawa[1,2], Mitsumu K. Ejiri[1,2], Takanori Nishiyama[2,1], Masaki Tsutsumi[1,2], Michael J. Taylor[3], Yucheng Zhao[3], P.-Dominique Pautet[3], Damian Murphy[4]

1. National Institute of Polar Research, 2. Department of Polar Science, Sokendai, 3. Physics Department, Utah State University, 4. Australian Antarctic Division

Gravity waves transport momentum and energy from the lower atmosphere to the upper atmosphere and drive the general circulation, which significantly changes the temperature in the middle atmosphere [Fritts and Alexander, 2003]. To understand this role quantitatively will improve the modern general circulation models [Garcia et al., 2017].

The polar night jet region is known to have high gravity-wave activity. However, sources of gravity waves, their propagation, and their spectra are poorly understood because of a lack of observations. In particular, little is known about the dependence of their characteristics on their spectra (i.e., wavenumber and frequency) and on interactions among waves with several wavenumbers and frequencies [Fritts and Alexander, 2003]. To understand these, our group has observed gravity waves at different sites over the Antarctic.

Observation techniques have limitations due to the breadth of the gravity wave spectrum and the target and physical parameter sensed by the observing system [Alexander et al., 1998]. In this study an OH imager and an MF radar are used. Both instruments cover the OH layer (~87 km altitude), but both cover quite different ranges of the wave spectrum. The OH imager can observe waves with shorter ground-based periods (8-60 min) and shorter horizontal wavelengths (2-100 km) [Matsuda et al., 2017]. On the other hand, the MF radar can observe waves with the longer ground-based periods (>~30 min). It also has a preference for the waves with longer horizontal wavelength because of its observational volume.

This study derives gravity-wave perturbations, over Syowa and Davis, from the OH imager data based on Matsuda et al. [2014] and the MF radar data based on Murphy et al. [2007], respectively. In this presentation, we would like to show the gravity wave activity, over Syowa and Davis, with the shorter horizontal wavelength (i.e., observed by the OH imagers) and with the longer horizontal wavelength (i.e., observed by the MF radars). The correlation and relationship between both wave activities will be discussed. Also, we would like to discuss the local variation of that relationship.

Keywords: Gravity Wave, Middle Atmosphere, OH Imager

©2019. Japan Geoscience Union. All Right Reserved.

[E] Poster | P (Space and Planetary Sciences)：P-EM Solar-Terrestrial Sciences, Space Electromagnetism & Space Environment

Wed. May 29, 2019 5:15 PM - 6:30 PM JST | Wed. May 29, 2019 8:15 AM - 9:30 AM UTC | Poster Hall International Exhibition Hall8, Makuhari Messe_4

[P-EM09] Vertical coupling in the atmosphere and Ionosphere

convener:Huixin Liu(Earth and Planetary Science Division, Kyushu University SERC, Kyushu University), Loren Chang(Institute of Space Science, National Central University), Yuichi Otsuka(Institute for Space-Earth Environmental Research, Nagoya University)

Vertical coupling mechanisms throughout the whole atmosphere are critical to understanding the near Earth space environment, as well as its sensitivity to the solar, geomagnetic, and atmospheric drivers. This international session focuses on physical/chemical processes occurring in the mesosphere, thermosphere, and ionosphere (MTI). Both quiet and disturbed states in response to lower atmospheric forcing or solar forcing are important for understanding the MTI system and its coupling to other regions. We invite presentations of observations and observational concepts with ground-based and/or space-borne instruments, theoretical studies, numerical simulations, and development of data analysis systems for various kinds of temporal and spatial variations in atmosphere-ionosphere coupled system.

[PEM09-P01] Local-time Variabilities of SABER CO_2 in the Mesosphere and Lower Thermosphere Region

*Cornelius Csar Jude Salinas[1], Loren Chang[1], Danie Liang[2], Jia Yue[3], Liying Qian[4], Quan Gan[5], James Russel III[3], Martin G Mlynczak[6] (1.Institute of Space Science, National Central University, 2.Institute of Earth Science, Academia Sinica, 3.Department of Atmospheric Sciences, Hampton University, 4.High Altitude Observatory, National Center for Atmospheric Research, 5.Department of Physics and Astronomy, Clemson University, 6.NASA Langley Research Center)

[PEM09-P02] Enhanced dynamo electric field as a possible cause of ionosphere disturbance before Large Earthquake

*Koichiro Oyama[1,2,3] (1.Institute of Plasma and Space Sciences,National Cheng Kung Univ., Taiwan, 2.International Ceneter for Space Weather Sudy and Education, Kyushu Univ.,, 3.CoLtd. Asia Space Environment Research Consortium, Japan)

[PEM09-P03] Morphology of E1 and E2 Kelvin waves from ECMWF reanalysis

*Chen-Jeih Pan[1], Wei-Sheng Chen[1], Uma Das[2] (1.Institute of Space Science, National Central University, 2.Department of Physics, Indian Institute of Information Technology, Kalyani, India)

[PEM09-P04] Impact of strong ENSO on TEC activity disturbed by ultra-fast Kelvin waves

*Wei-Sheng Chen[1], C.J. Pan[1], Uma Das[2], Chian-Chiau Lin[3] (1.Institute of Space Science, National Central University, Taiwan, 2.Department of Physics, Indian Institute of Information Technology, Kalyani, India, 3.Environmental Research and Information Center, Chang Jung Christian University, Taiwan)

[PEM09-P05] Observation and simulation of propagation of coseismic infrasound to the ionosphere

*Jaroslav Chum[1] (1.Institute of Atmospheric Physics of the Czech Academy of Sciences)

[PEM09-P06] Solar wind influence on tropical cyclones mediated by atmospheric gravity waves

*Paul Prikryl[1,2], Iurii Cherniak[3], Irina Zakharenkova[4,5], James M. Weygand[6], Bharat S. R. Kunduri[7] (1.Physics Department, University of New Brunswick, Fredericton, NB, Canada, 2.Geomagnetic Laboratory, Natural Resources Canada, Ottawa, ON, Canada, 3.COSMIC Program Office, University Corporation for Atmospheric Research, Boulder, CO, USA, 4.West Department of IZMIRAN, Kaliningrad, Russia, 5.University of Warmia and Mazury in Olsztyn, Poland, 6.Earth Planetary and Space Sciences, University of California, Los Angeles, CA, USA, 7.Bradley Dept. of Electrical and Computer Engineering, Virginia Tech, Blacksburg, VA, USA)

[PEM09-P07] VIPIR ionospheric observations in Japan

*Takuya Tsugawa[1], Hideo Maeno[1], Michi Nishioka[1], Takumi Kondo[1], Mamoru Ishii[1] (1.National Institute of Information and Communications Technology)

[PEM09-P08] Simulation Results and Performance Analysis of Phase Velocity Spectral Analysis Software (M-Transform) for Airglow Imaging Data

*Septi Perwitasari[1], Takuji Nakamura[2], Masaru Kogure[2], Yoshihiro Tomikawa[2], Mitsumu K. Ejiri[2] (1.LAPAN, 2.NIPR)

[PEM09-P09] Comparisons of Co-incident Ionospheric Plasma Observations Between FORMOSAT-5/AIP and Millstone Hill Incoherent Scatter Radar

*Yi-Wun Chen[1], Chi-Kuang Chao[1] (1.Graduate Institute of Space Science, National Central University, Taiwan)

[PEM09-P10] Sub-ionospheric effects of volcano eruptions using VLF/LF standard radio waves

*Kei Maruyama[1], Hiroyo Ohya[1], Fuminori Tsuchiya[2], Kenro Nozaki[5], Kozo Yamashita[3], Yukihiro Takahashi[4], Hiroyuki Nakata[1], Toshiaki Takano[1] (1.Chiba University, 2.Tohoku University, 3.Ashikaga University, 4.Hokkaido University, 5.National Institute of Information and Communications Technology)

[PEM09-P11] Observations of ionospheric and mesospheric wave structures by a low-cost airglow imaging system

*Keisuke Hosokawa[1], Nanami Kusuyama[1], Yuta Hozumi[1], Kohei Takami[1], Susumu Saito[2], Yasunobu Ogawa[3], Mamoru Ishii[4], Yuichi Otsuka[5], Takuya Tsugawa[4] (1.University of Electro-Communications, 2.ENRI, 3.NIPR, 4.NICT, 5.ISEE, Nagoya University)

[PEM09-P12] Analysis of characteristics of ionospheric parameters, Sq index and neutral winds over Taiwan

*Yu-Jung Chuo[1] (1.Department of Information Technology, Ling Tung University)

[PEM09-P13] Statistical study on daytime Es observed by ground-ionosonde and RO-COSMIC in magnetic Equator region in 2010

*Zheng Wang [1,2], Huixin Liu[1] (1.Department of Earth and Planetary Sciences, School of Science, Kyushu University, Japan. , 2.National Space Science Center, Chinese Academy of Sciences, China.)

[PEM09-P14] The statistical study of the growth rates of Medium-Scale Traveling Ionospheric Disturbances observed with GPS-TEC

*Takafumi Ikeda[1], Akinori Saito[1], Takuya Tsugawa[2], Hiroyuki Shinagawa[2] (1.Department of Geophysics, Graduate School of Science, Kyoto University, 2.National Institutes of Information and Communications Technology)

[PEM09-P15] Comparison of Gravity Wave Activity in the Mesosphere Observed by OH Airglow Imagers and MF Radars over the Antarctic (Syowa & Davis).

*Masaru Kogure[1], Takuji Nakamura[1,2], Yoshihiro Tomikawa[1,2], Mitsumu K. Ejiri[1,2], Takanori Nishiyama[2,1], Masaki Tsutsumi[1,2], Michael J. Taylor[3], Yucheng Zhao[3], P.-Dominique Pautet[3], Damian Murphy[4] (1.National Institute of Polar Research, 2.Department of Polar Science, Sokendai, 3.Physics Department, Utah State University, 4.Australian Antarctic Division)

Local-time Variabilities of SABER CO_2 in the Mesosphere and Lower Thermosphere Region

*Cornelius Csar Jude Salinas[1], Loren Chang[1], Danie Liang[2], Jia Yue[3], Liying Qian[4], Quan Gan[5], James Russel III[3], Martin G Mlynczak[6]

1. Institute of Space Science, National Central University, 2. Institute of Earth Science, Academia Sinica, 3. Department of Atmospheric Sciences, Hampton University, 4. High Altitude Observatory, National Center for Atmospheric Research, 5. Department of Physics and Astronomy, Clemson University, 6. NASA Langley Research Center

This work presents the local-time variabilities of CO_2 in the Mesosphere and Lower Thermosphere region (MLT region) as observed by the Sounding of the Atmosphere using Broadband Emission Radiometry (SABER) onboard the Thermosphere Ionosphere Mesosphere Energetics and Dynamics Satellite (TIMED Satellite). These are then compared to CO_2 as modeled by the Whole Atmosphere Community Climate Model –eXtended (WACCM-X). Also using WACCM-X, a tendency analysis using the continuity equation is done to explain the local-time variabilities of CO_2 in the MLT region. Finally, consequences of including a significant local-time variability in CO_2 when retrieving SABER temperature profiles are determined.

Keywords: Carbon Dioxide, Mesosphere and Lower Thermosphere Region, Tides

©2019. Japan Geoscience Union. All Right Reserved.

Enhanced dynamo electric field as a possible cause of ionosphere disturbance before Large Earthquake

*Koichiro Oyama[1,2,3]

1. Institute of Plasma and Space Sciences,National Cheng Kung Univ., Taiwan, 2. International Ceneter for Space Weather Sudy and Education, Kyushu Univ.,, 3. CoLtd. Asia Space Environment Research Consortium, Japan

Disturbance of ionosphere before large earthquakes has been very often reported. One of the possible disturbing drivers is electric field, which explains most of the ionosphere features we reported so far. However, the origin of the electric field is still in the darkness. One idea of electric field generation exists inside earth interior (Freund et a., 2006). We propose here that the electric field is dynamo field at the height of ≈100 km, which simply intensified before earthquake; intensified eastward (westward)electric field during daytime(nighttime). This idea explains satellite data (Oyama et al.,2008; Oyama et al.,2011; Ryu et al., 2014; Ryu et al., 2016; Oyama et al.,2016; Oyama et al., 2019).

Next question on the electric field generation is the mechanism which modifies the dynamo field. We speculate that modification of E field is a result of modification of neutral wind system, which is originally caused by internal gravity waves which propagate from below. Then again next question is on the origin of the internal gravity waves. The waves might be originally caused by the ground motion, and these waves which propagate upward might interact with planetary wave, and amplified. We show several side evidence of ground motions before earthquakes.

Keywords: Earthquake, Electric field, Ionosphere, Disturbance

©2019. Japan Geoscience Union. All Right Reserved.

Morphology of E1 and E2 Kelvin waves from ECMWF reanalysis

*Chen-Jeih Pan[1], Wei-Sheng Chen[1], Uma Das[2]

1. Institute of Space Science, National Central University, 2. Department of Physics, Indian Institute of Information Technology, Kalyani, India

Kelvin waves are planetary waves traveling eastwards and confined in the equatorial latitudes. The waves play an important role in middle atmosphere dynamics because they transfer energy and momentum from lower to higher altitudes, which contributes to the quasi-biennial oscillation (QBO) and further influences the global climate. Kelvin waves have been studied for many decades, and the most of studies were focused on the waves of wavenumber 1 (E1). On the other hand, the wavenumber-2 Kelvin waves (E2) are also an important part of Kelvin wave activities although their amplitude less than the E1. In this study, we analyzed the long-term European Centre for Medium-Range Weather Forecasts (ECMWF) reanalysis data and reported the morphology of E1 and E2 Kelvin waves in the stratospheric altitudes individually. The temperature from ECMWF reanalysis was used to extract the wave properties. Temperatures between latitudes of 10S and 10N were firstly gridded into the structure of day-altitude-longitude, and then subtract background (longitudinal means) to get equatorial temperature fluctuations. For each altitude, the two-dimensional fast Fourier transform was applied to each 96-day data segment and stepped forward in time by 1 day. The output spectra were then analyzed to get primary wave periods and amplitude variations. From spectra, the E1 amplitude is 1.5 to 2.0 times larger than the E2 in average. The E1 primary periods are 12 to 25 days and are restricted under the 20-km altitude. The periods of 8 to 14 days are the secondary group. They can propagate upward to the 40-km altitude. Regarding the E2, the primary periods are 7 to 12 days and are also restricted under the 20-km altitude. Its secondary group is the periods of 5 to 8 days, which also can propagate upward to the 40-km altitude. Furthermore, the altitude-time-amplitude variation show that the E2 waves are influenced strictly by the QBO westerly. Finally, the cross correlation between E1 and E2 show that the E1 and E2 have high correlation at altitudes close to the tropopause, which implies they are excited simultaneously.

Keywords: Kelvin waves, QBO

©2019. Japan Geoscience Union. All Right Reserved.

Impact of strong ENSO on TEC activity disturbed by ultra-fast Kelvin waves

*Wei-Sheng Chen[1], C.J. Pan[1], Uma Das[2], Chian-Chiau Lin[3]

1. Institute of Space Science, National Central University, Taiwan, 2. Department of Physics, Indian Institute of Information Technology, Kalyani, India, 3. Environmental Research and Information Center, Chang Jung Christian University, Taiwan

Ultra-fast Kelvin waves (UFKW) are a subclass of Kelvin waves that they have the shortest periods (2-5 days) and thus can propagate into the ionosphere. UFKW relate to ionospheric variations have been reported, which include ionospheric minimum virtual height (h'F), F2 maximum critical frequency (foF2), total electron content (TEC), S4 scintillations, etc. In the study, we analyzed the UFKW activities using SABER (Sounding of the Atmosphere using Broadband Emission Radiometry) temperatures and GIM (Global Ionospheric Maps) TEC from 2009 to 2011 to see how UFKW influence the ionosphere. The period 2009-2011 belongs to the strong ENSO period. Previous studies have shown that Kelvin waves were highly active in this period, especially in the early of 2010. Therefore, this study can implicitly reveal how the ionosphere responds to the ENSO. The wave signatures in SABER temperatures were extracted using the fast Fourier transform (FFT). Temperatures in the geographic equatorial latitudes were gridded into the day-altitude-longitude structure and then removed background to get temperature fluctuations. The two-dimensional FFT was applied to each 96-day data segment for each altitude and stepped forward in time by one day. Regarding TEC, the Lomb-Scargle periodogram was used to extract UFKW signatures. Because TEC has a strong local time variation and constrains by the geomagnetic configuration, TEC at 16 local time and low geomagnetic latitudes were selected. The background was removed firstly from the data and then fed TEC fluctuations into the Lomb-Scargle process, which also stepped forward in time by one day. The FFT and Lomb-Scargle process both outputted spectra, which revealed UFKW activities in the mesosphere and lower thermosphere (MLT) region (90-100 km) and the ionosphere (about 150-600 km). The results show that UFKW activities at two equatorial ionization anomalies (EIA) were almost identical, and both were higher than that at geomagnetic equator. Most of wave activities in the temperature field in the MLT region have corresponding activities in TEC. However, there are a lot of small amplitude activities only in TEC.

Keywords: ultra-fast Kelvin waves, ENSO, TEC

©2019. Japan Geoscience Union. All Right Reserved.

Observation and simulation of propagation of coseismic infrasound to the ionosphere

*Jaroslav Chum[1]

1. Institute of Atmospheric Physics of the Czech Academy of Sciences

Vertical motion of the ground surface caused by seismic waves generates acoustic waves that propagate nearly vertically upward owing to supersonic speed of seismic waves. As the air density decreases with height, the amplitude of acoustic waves increases to conserve the energy flux up to the altitudes where the air is so rarefied that it cannot sustain the propagation and the waves start dissipating. For distances up to about 1500 km from the epicenter of the strong earthquakes (M>7), the amplitude (oscillation velocity) of infrasound waves reaches significant values in the upper atmosphere. Consequently, the nonlinear phenomena start to play an important role. Spectral content of the wave packet is changed and the energy is transferred to lower frequencies, which can cause the formation of roughly bipolar N-shaped pulse. The simulation results are compared with observation for selected examples. It is also shown that only infrasound with periods larger than about 10 s (generated by long period seismic waves) can reach the ionospheric heights, namely the F layer where it can be easily detected.

Keywords: coseismic perturbation in the ionosphere, infrasound, nonlinear propagation

©2019. Japan Geoscience Union. All Right Reserved.

Solar wind influence on tropical cyclones mediated by atmospheric gravity waves

*Paul Prikryl[1,2], Iurii Cherniak[3], Irina Zakharenkova[4,5], James M. Weygand[6], Bharat S. R. Kunduri[7]

1. Physics Department, University of New Brunswick, Fredericton, NB, Canada, 2. Geomagnetic Laboratory, Natural Resources Canada, Ottawa, ON, Canada, 3. COSMIC Program Office, University Corporation for Atmospheric Research, Boulder, CO, USA, 4. West Department of IZMIRAN, Kaliningrad, Russia, 5. University of Warmia and Mazury in Olsztyn, Poland, 6. Earth Planetary and Space Sciences, University of California, Los Angeles, CA, USA, 7. Bradley Dept. of Electrical and Computer Engineering, Virginia Tech, Blacksburg, VA, USA

Solar wind coupling to the magnetosphere-ionosphere-atmosphere (MIA) system generates medium- and large-scale atmospheric gravity waves (AGWs) propagating globally from sources in the lower thermosphere at high latitudes. The AGWs propagate globally [1,2] upward and downward, are observed in the ionosphere as traveling ionospheric disturbances [3], can be ducted in lower atmosphere over long distances and reach troposphere. At the reflection point in the troposphere they can trigger moist instabilities to initiate convective bursts, with the latent heat release leading to intensification of storms [4]. In the follow-up studies [5,6,7] it was shown that explosive extratropical cyclones and rapid intensification of tropical cyclones tend to follow arrivals of solar wind high-speed streams (HSS) and/or interplanetary coronal mass ejections (ICMEs). The coupling of solar wind to MIA is most intense during the arrivals of co-rotating interaction regions (CIRs) and/or interplanetary shocks at the leading edges of HSSs and ICMEs when the amplitudes of aurorally-generated AGWs are largest. Ray tracing of AGWs in a model atmosphere show that they can reach tropical cyclones. Spiral gravity waves in typhoons were observed and simulated to propagate radially outward from the typhoon core [8]. The spectra of waves in surface pressure and surface wind measured by the Impacts of Typhoons on the Ocean in the Pacific (ITOP) buoy during the nearby passages of intense typhoons are similar to those of incoming aurorally-generated AGWs. It is suggested that the interaction of aurorally-generated gravity waves with the tropical cyclone vortex and the inner primary eyewall plays a role in the intensification process.

[1] Mayr H.G., et al., J. Geophys. Res., 89, 10929–10959, 1984.
[2] Prikryl P., et al., Ann. Geophys., 23, 401-417, 2005. doi:10.5194/angeo-23-401-2005
[3] Cherniak Iu., Zakharenkova I., Space Weather, 16, 2018. https://doi.org/10.1029/2018SW001869.
[4] Prikryl P., et al., Ann. Geophys. 27, 31–57, 2009. https://doi.org/10.5194/angeo-27-31-2009.
[5] Prikryl P., et al., J. Atmos. Sol.-Terr. Phys., 149, 219–231, 2016.
[6] Prikryl P., et al., J. Atmos. Sol.-Terr. Phys., 171, 94–110, 2018.
[7] Prikryl P., et al., J. Atmos. Sol.-Terr. Phys., 183, 36-60, https://doi.org/10.1016/j.jastp.2018.12.009.
[8] Nolan D.S., Zhang J.A., Geophys. Res. Lett., 44, 3924–3931, 2017. doi:10.1002/2017GL073572

Keywords: Solar wind-magnetosphere-ionosphere-atmosphere coupling, High-speed solar wind stream, Atmospheric gravity wave, Extratropical and tropical cyclones

©2019. Japan Geoscience Union. All Right Reserved.

VIPIR ionospheric observations in Japan

*Takuya Tsugawa[1], Hideo Maeno[1], Michi Nishioka[1], Takumi Kondo[1], Mamoru Ishii[1]

1. National Institute of Information and Communications Technology

National Institute of Information and Communications Technology (NICT) has observed ionosphere by ionosondes more than 70 years in Japan. At present, four ionosondes at Wakkanai (Sarobetsu), Kokubunji, Yamagawa, Okinawa (Ogimi) are automatically operated and controlled from Tokyo. Major ionospheric parameters such as foF2 and foEs are scaled from the ionograms automatically on a realtime basis and scaled manually for the final values. These scaled parameters are provided through our web site (http://wdc.nict.go.jp/IONO/). In 2017, we replaced the 10C ionosondes with Vertical Incidence Pulsed Ionospheric Radar 2 (VIPIR2) which can separate the O- and X-modes of ionospheric echoes which have improved the availability of automatic scaling of the ionogram. Our automatic scaling method has been improved using new O- and X-modes separated ionograms. As for future plans, we try to expand observation area by oblique sounding observations with VIPIRs in Japan and neighboring countries. We have also tried to detect arrival directions of ionospheric echo by using the 8ch receiving data as a interferometry. In this presentation, we will introduce current status and future plans of ionospheric observation in NICT.

Keywords: Ionosphere, Ionosonde, Space Weather

©2019. Japan Geoscience Union. All Right Reserved.

Simulation Results and Performance Analysis of Phase Velocity Spectral Analysis Software (M-Transform) for Airglow Imaging Data

*Septi Perwitasari[1], Takuji Nakamura[2], Masaru Kogure[2], Yoshihiro Tomikawa[2], Mitsumu K. Ejiri[2]

1. LAPAN, 2. NIPR

We have developed a user-friendly software based on *Matsuda et al.*, 2014's 3D-FFT method (M-Transform) for airglow data analysis as a function on Interactive Data Language (IDL). Input of this function is 3-D array of a time series of airglow image that have already been converted to geographical coordinate (*x*, *y*, *t*). The user can customize the wave parameters (e.g. horizontal wavelength (λ_h), wave period (τ), phase speed (*c*), image resolution in space (*dx*,*dy*) and time (*dt*)) in one-line command when executing the program, which depends on their analysis purpose. In order to exhibit this new function's performance and the characteristics/interpretation of the spectral analysis, we have run several test cases using artificial wave. The first case is artificial wave with constant speed (40 m/s) and different wave period (8, 15, 30 min) and horizontal wavelength. In second case, we applied Gaussian shape wave-packet with different FWHM (50, 100, 200 km). For the third test case, with a fixed wave packet size (100 km), we changed the wave packet duration (30, 60, 120 min). The results from the various simulations showed reasonable characteristics of the spectral analysis for different scenarios. We showed that the increase of wave period and horizontal wavelength lead to the wider spectrum with total power difference of ~10%. By changing the wave packet size, we showed that the bigger the wave packet size, the sharper and narrower the spectrum became with the total power increase 2x of the increase size of the wave packet. The result of changing the wave packet duration showed that the longer the duration of wave packet, the spectrum becomes sharper and the total power is proportional to the wave packet length. We also examined the aliasing and zero padding effect on the spectral analysis. In order to avoid the aliasing effect, it is recommended to set the period minimum to at least 2 x image interval (*dt*). More detailed analysis will be discussed during the presentation.

Keywords: Airglow, Gravity wave, Analysis software

©2019. Japan Geoscience Union. All Right Reserved.

Comparisons of Co-incident Ionospheric Plasma Observations Between FORMOSAT-5/AIP and Millstone Hill Incoherent Scatter Radar

*Yi-Wun Chen[1], Chi-Kuang Chao[1]

1. Graduate Institute of Space Science, National Central University, Taiwan

Advanced Ionospheric Probe (AIP) onboard FORMOSAT-5 satellite has routinely measured ionospheric plasma parameters, like ion concentration, velocity, and temperature in a sun-synchronous circular orbit at 720 km altitude along 2230 local-time sector since November 2017. AIP has found that the satellite has a much lower potential with respective to environmental plasma from measured current-voltage curves. A comparison study shall be performed to identify possible bias on the derived AIP parameters. Co-incident observations have been scheduled with Millstone Hill incoherent scatter radar during 30 January to 1 February 2019. In this poster, preliminary comparison results will be outlined and will be used to improve accuracy of the AIP measurement in the future.

Keywords: FORMOSAT-5, AIP, ionosphere

©2019. Japan Geoscience Union. All Right Reserved.

Sub-ionospheric effects of volcano eruptions using VLF/LF standard radio waves

*Kei Maruyama[1], Hiroyo Ohya[1], Fuminori Tsuchiya[2], Kenro Nozaki[5], Kozo Yamashita[3], Yukihiro Takahashi[4], Hiroyuki Nakata[1], Toshiaki Takano[1]

1. Chiba University, 2. Tohoku University, 3. Ashikaga University, 4. Hokkaido University, 5. National Institute of Information and Communications Technology

Several studies for the F-region ionosphere associated with volcano eruptions based on GPS-TEC data have been reported so far (e.g., Heki, 2006; Dautermann et al., 2009; Heki et al., 2010). These studies reported that acoustic waves excited by volcano eruptions reach up to the F-region ionosphere, and caused F-region perturbations. After eruption of the Kelud Volcano, Indonesia, in February 2014, acoustic resonance between the Earth’ s surface and lower thermosphere was reported based on TEC data and the seismic wave data (Nakashima et al., 2015). However, little studies on the D-region ionosphere associated with volcano eruptions have been reported. In this study, we investigate the D-region effects of eruptions of Sakurajima volcano (31.59N, 130.66E), Japan, at 04:11 UT on June 6, 2014, using intensity perturbation of VLF/LF transmitter signals. The VLF/LF propagation paths use in this study are JJY (JJY 60 kHz) - Tainan (TNN, Taiwan), and JJI (22.2 kHz) - TNN. Based on wavelet spectra, the perturbation of both transmitter signals had a frequency of 2-6 mHz during 04:12-04:30 UT after the eruptions (04:11 UT).We compared the perturbations with atmospheric pressure data obtained by an infrasonic meter observed by Sakurajima Volcano Research Center, Kyoto University, and seismic waves in the NIED F-net data (FUK, STM, and SBR) located close to the JJY-TNN path. The atmospheric pressure and vertical velocity of the seismic waves had the similar frequencies of 2-10 mHz during 04:12-04:47 UT. These similar frequencies suggest that the perturbations would be caused by acoustic resonance between the Earth's surface and lower thermosphere, or by acoustic and atmospheric gravity waves generated by volcanic eruptions. In the presentation, we will discuss the cause of the VLF/LF perturbations in more detail.

©2019. Japan Geoscience Union. All Right Reserved.

Observations of ionospheric and mesospheric wave structures by a low-cost airglow imaging system

*Keisuke Hosokawa[1], Nanami Kusuyama[1], Yuta Hozumi[1], Kohei Takami[1], Susumu Saito[2], Yasunobu Ogawa[3], Mamoru Ishii[4], Yuichi Otsuka[5], Takuya Tsugawa[4]

1. University of Electro-Communications, 2. ENRI, 3. NIPR, 4. NICT, 5. ISEE, Nagoya University

In the last two decades, all-sky airglow imagers with cooled CCD cameras have widely been used to observe large-scale wave structures in the F-region ionosphere, for example medium-scale traveling ionospheric disturbances (MSTIDs). Such wavy features are seen in the oxygen emission at 630.0 nm from altitudes slightly below the F-region peak. Similar optical observations of OH band emission have also enabled us to visualize atmospheric gravity waves at the mesospheric height. Deploying airglow imagers in multiple places is one of the cost-effective ways to visualize the large-scale structure of these wave structures at both the F-region ionosphere and mesosphere [e.g., Kubota et al., 2001; Suzuki et al., 2013]. However, ground-based airglow imagers equipped with a cooled CCD camera is still expensive; thus, it is rather difficult to deploy such systems in a wide area and carry out a network observation. To overcome this limitation, we recently developed a low-cost airglow imaging system (Low-Cost Airglow imaging System: LCAS) which consists of a small camera (WAT-910HX), fisheye lens and optical filter. We then confirmed its capability of imaging the spatial structure of polar cap patches and plasma bubble in the 630.0 nm emission from the F-region. But, still, it is unclarified if the system is also capable of detecting the two-dimensional structure of MSTIDs. On the night of May 12, 2018, we identified a weak wavy signature in the 630.0 nm airglow images from one of our LCAS stations in Ishigaki Island, Japan. The wave structure in the 630.0 nm images was smoothly connected to the structure of MSTIDs in the GPS-TEC data, which confirmed the ability of LCAS for detecting MSTIDs. We also identified smaller scale wave structures in the 630.0 nm images, showing characteristic concentric wave fronts. We speculate that gravity waves in the mesosphere were captured in the 630.0 nm images as a contamination of the OH airglow. This is mainly because we make use of an optical filter having 10 nm FWHM, which enables us to detect several spectral peaks of OH emission near the 630.0 nm oxygen emission. We have estimated the center of the concentric wave structures by using the curvature of the wave fronts, and then confirmed that active rain fall took place in a localized area close to the estimated center of the concentric waves. This result supports our hypothesis that the OH emission containing signatures of mesospheric gravity waves were detected in the 630.0 nm images. In summary, the 630.0 nm airglow observation of LCAS is able to observe MSTIDs and mesospheric gravity waves. This will allow us to monitor such wavy structures at two different altitudes by distributing the similar system in a wide area.

Keywords: Airglow, Traveling Ionospheric Disturbances

©2019. Japan Geoscience Union. All Right Reserved.

Analysis of characteristics of ionospheric parameters, Sq index and neutral winds over Taiwan

*Yu-Jung Chuo[1]

1. Department of Information Technology, Ling Tung University

In this paper, we examine the variation of thermospheric neutral winds and solar quiet (Sq) current of the geomagnetic fields for the equatorial ionospheric anomaly area (EIA) during the solar activity period in 1999. The thermospheric neutral winds are derived from the ionospheric F_2-layer peak height, hmF_2, by using the servo model method. The variability of the amplitude ofSq fields is derived from the ground geomagnetic fields in the components H and Z, respectively. Theresults of the current system show a same diurnal variation, which that peaks / valleys in the local noon time for Sq(H) / Sq(Z) in the low latitudes, respectively.The results also indicate a weak seasonal variation that peaks appear at the local summer of the Sq currents in H and Z components, respectively. The Sq current system is associated with the change of the equatorial electrojet (EEJ). Further, the variability is probably attributed to local thermospheric winds. The study also shows that the zonal and meridional components of the neutral winds at the EIA over Taiwan area. Furthermore, the study examines the variations of Sq(H), Sq(Z), neutral winds, and ionospheric parameters foE_s, NmF_2, and hmF_2during the disturbed geophysical conditions such as geomagnetic storm and earthquake. The result shows the variationsof ionospheric Sq(H), Sq(Z) and thermospheric neutral winds are different between the seismo-ionospheric and solar-terrestrial disturbed periods, even they lead the same decreasing electron density reaction in the ionosphere at the EIA over Taiwan area.

Keywords: Sq current, ionosphere, neutral winds

©2019. Japan Geoscience Union. All Right Reserved.

Statistical study on daytime Es observed by ground-ionosonde and RO-COSMIC in magnetic Equator region in 2010

*Zheng Wang [1,2], Huixin Liu[1]

1. Department of Earth and Planetary Sciences, School of Science, Kyushu University, Japan. , 2. National Space Science Center, Chinese Academy of Sciences, China.

Scintillations under 150 km height shown by radio occultation (RO) of COSMIC are considered to be associated with ionospheric sporadic E (Es) layer. In this paper, we make a Statistical study on daytime Es observed by ground-ionosonde at five stations in magnetic Equator region in 2010, and make a comparison with S4 index from RO-COSMIC within 6 degree of each station. The results show that: At each station the diurnal variation of foEs from ionosonde decrease a little around LT 0600 and then increase, having maximum around LT 1200, decrease around LT 1800 and then increase near LT 2000-2200; All the S4>=0.3 observations during daytime come from RO-COSMIC under 150 km height; The diurnal variation of S4 index under 150 km height from RO-COSMIC over each station has similar trend with that of foEs at the same station; S4 index over 150 km height from RO-COSMIC is only high during nighttime; For the stations at different longitudes, Es occurrences from ionosonde are positively associated with S4>=0.3 from RO-COSMIC. The comparison shows that the S4 index from RO-COSMIC could show some features of daytime Es layer in magnetic Equator region without the location limitation of ground stations.

Keywords: daytime ionospheric sporadic E, ground-ionosonde , radio occultation of COSMIC , magnetic Equator region

©2019. Japan Geoscience Union. All Right Reserved.

The statistical study of the growth rates of Medium-Scale Traveling Ionospheric Disturbances observed with GPS-TEC

*Takafumi Ikeda[1], Akinori Saito[1], Takuya Tsugawa[2], Hiroyuki Shinagawa[2]

1. Department of Geophysics, Graduate School of Science, Kyoto University, 2. National Institutes of Information and Communications Technology

We think two mechanism, E-F coupling and Perkins Instability, will relate to growth for nighttime-MSTID in mid-latitude [Tsunoda and Cosgrove., 2001 ; Perkins., 1973]. Linear growth rate of perturbation intensity of Pedersen conductivity expected from E-F coupling is around 15 minutes [Yokoyama et al., 2009], which is far shorter than one expected from Perkins Instability [Fukao and Kelley, 1991 ; Miller et al., 1997 ; Shiokawa et al., 2003]. However, Es layer’ s spatial and temporal scale is less than 100km and 15min [Maeda et al., 2013 ; S.Saito et al., 2007]. They are different from MSTID’ s ones, which are 200-400 km and around 2hours [Otsuka et al., 2011]. To decide which instability is responsible for growth of nighttime MSTID, the growth rate of MSTID was observationally determined with ground-based GPS network data.

We statistically investigated the growth rate of nighttime-MSTID in Japan in 2014 observed with GPS-TEC. The growth rate of nighttime -MSTID observed was 1.0 - 6.0 $\times 10^{-4}$ s^{-1} during 1800LT-2400LT in summer.Linear growth rate of Perkins instability in summer was 1.0 - 6.0 $\times 10^{-4}$ s^{-1} during 1800LT - 2400LT, so they were less than one of the E-F coupling instability. Also,Seasonal distribution of observed growth rate before midnight was similar to that of linear growth rate.U×B derived by GAIA model was high in spring - summer and seasonal distribution of U×B was similar to that of linear growth rate. Therefore, the growth of MSTID when propagating is not determined by E-F coupling instability but Perkins instability and neutral wind.

Keywords: MSTID, GPS-TEC, Ionosphere

©2019. Japan Geoscience Union. All Right Reserved.

Comparison of Gravity Wave Activity in the Mesosphere Observed by OH Airglow Imagers and MF Radars over the Antarctic (Syowa & Davis).

*Masaru Kogure[1], Takuji Nakamura[1,2], Yoshihiro Tomikawa[1,2], Mitsumu K. Ejiri[1,2], Takanori Nishiyama[2,1], Masaki Tsutsumi[1,2], Michael J. Taylor[3], Yucheng Zhao[3], P.-Dominique Pautet[3], Damian Murphy[4]

1. National Institute of Polar Research, 2. Department of Polar Science, Sokendai, 3. Physics Department, Utah State University, 4. Australian Antarctic Division

Gravity waves transport momentum and energy from the lower atmosphere to the upper atmosphere and drive the general circulation, which significantly changes the temperature in the middle atmosphere [Fritts and Alexander, 2003]. To understand this role quantitatively will improve the modern general circulation models [Garcia et al., 2017].

The polar night jet region is known to have high gravity-wave activity. However, sources of gravity waves, their propagation, and their spectra are poorly understood because of a lack of observations. In particular, little is known about the dependence of their characteristics on their spectra (i.e., wavenumber and frequency) and on interactions among waves with several wavenumbers and frequencies [Fritts and Alexander, 2003]. To understand these, our group has observed gravity waves at different sites over the Antarctic.

Observation techniques have limitations due to the breadth of the gravity wave spectrum and the target and physical parameter sensed by the observing system [Alexander et al., 1998]. In this study an OH imager and an MF radar are used. Both instruments cover the OH layer (~87 km altitude), but both cover quite different ranges of the wave spectrum. The OH imager can observe waves with shorter ground-based periods (8-60 min) and shorter horizontal wavelengths (2-100 km) [Matsuda et al., 2017]. On the other hand, the MF radar can observe waves with the longer ground-based periods (>~30 min). It also has a preference for the waves with longer horizontal wavelength because of its observational volume.

This study derives gravity-wave perturbations, over Syowa and Davis, from the OH imager data based on Matsuda et al. [2014] and the MF radar data based on Murphy et al. [2007], respectively. In this presentation, we would like to show the gravity wave activity, over Syowa and Davis, with the shorter horizontal wavelength (i.e., observed by the OH imagers) and with the longer horizontal wavelength (i.e., observed by the MF radars). The correlation and relationship between both wave activities will be discussed. Also, we would like to discuss the local variation of that relationship.

Keywords: Gravity Wave, Middle Atmosphere, OH Imager

©2019. Japan Geoscience Union. All Right Reserved.

[E] Poster | P (Space and Planetary Sciences)：P-EM Solar-Terrestrial Sciences, Space Electromagnetism & Space Environment

Wed. May 29, 2019 1:45 PM - 3:15 PM JST | Wed. May 29, 2019 4:45 AM - 6:15 AM UTC | Poster Hall International Exhibition Hall8, Makuhari Messe_1

[P-EM11] Dynamics of Magnetosphere and Ionosphere

convener:Aoi Nakamizo(Applied Electromagnetic Research Institute, National Institute of Information and Communications Technology), Mitsunori Ozaki(Faculty of Electrical and Computer Engineering, Institute of Science and Engineering, Kanazawa University), Akiko Fujimoto(Kyushu Institute of Technology), Tomoaki Hori(Institute for Space-Earth Environmental Research, Nagoya University)

This session provides an opportunity to present recent results from satellite and ground-based observations and theoretical and simulation studies on the magnetosphere, ionosphere, and their coupling processes. We invite talks and posters discussing various phenomena related to the magnetosphere-ionosphere system: solar wind-magnetosphere interaction, magnetosphere-ionosphere convection, field-aligned current, magnetic storms/substorms, neutral-plasma interaction, ionospheric ion inflow and outflow, aurora phenomena, and so forth. Discussions on planetary and satellite ionosphere and magnetospheres, future missions and instrument developments are also welcome.

[PEM11-P01] Effects of Inclination/Rotation of Earth's Magnetic Axis on Magnetosphere Simulated by Global MHD Model

*Aoi Nakamizo[1] (1.Applied Electromagnetic Research Institute, National Institute of Information and Communications Technology)

[PEM11-P02] Asymmetric deformation of the magnetosphere under low-density solar wind

*Masaki N Nishino[1,2], Yoshifumi Saito[2], Kazuo Shiokawa[1], Masaki Fujimoto[2] (1.Institute for Space-Earth Environmental Research, Nagoya University, 2.JAXA/ISAS)

[PEM11-P03] New perspectives on coupling processes in solar-terrestrial system obtained by comprehensive data analysis

*Yoshimasa Tanaka[1], Norio Umemura[2], Shuji Abe[3], Satoru UeNo[4], Masahito Nose[2], Yumi Nakagawa[5] (1.National Institute of Polar Research, 2.Institute for Space-Earth Environmental Research, Nagoya University, 3.International Center for Space Weather Science and Education, 4.Kwasan & Hida Observatories, School of Science, Kyoto University, 5.Ibaraki University)

[PEM11-P04] The interaction between the magnetosphere-ionosphere compound system and the magnetic field topology

*Shigeru Fujita[1], Takashi Tanaka[2], Masakazu Watanabe[2] (1.Meteorological College, Japan Meteorological Agency/ Nationa Institute of Polar Research, 2.Kyushu University)

[PEM11-P05] Effects of the dipole tilt and the interplanetary magnetic field Bx component on the dawn-dusk and interhemispheric asymmetries of the interchange convection cycle

*Masakazu Watanabe[1,2], Takashi Tanaka[2], Shigeru Fujita[3,4] (1.Graduate School of Science, Kyushu University, 2.International Center for Space Weather Science and Education, Kyushu University, 3.Meteorological College, 4.National Institute of Polar Research)

[PEM11-P06] Transient polar ionospheric convection response to negative dynamic pressure pulse

*Jianjun Liu[1] (1.Polar Research Institute of China)

[PEM11-P07] An active ionosphere: a new perspective of field line dipolarization

*Osuke Saka[1] (1.Office Geophysik)

[PEM11-P08] Toward the automatic identification of FLR signals in the SuperDARN data by using the gradient method

*Hideaki Kawano[1,2], Akira Sessai Yukimatu[3,4], Nozomu Nishitani[5], Yoshimasa Tanaka[3,4], Satoko Saita[6], Tomoaki Hori[5] (1.Dept. Earth Planet. Sci., Kyushu Univ., 2.ICSWSE, Kyushu University, 3.National Institute of Polar Research, 4.SOKENDAI, 5.ISEE, Nagoya University, 6.Kitakyushu College)

[PEM11-P09] A statistical study of Pi2 pulsations observed in the upper ionosphere using Swarm magnetic field data

*Park Jaehee[1], Khan-Hyuk Kim[1], Junga Hwang[2] (1.School of Space Research, Kyung Hee University, Gyeonggi, South Korea, 2.Korea Astronomy and Space Science Institute, Daejeon,South Korea)

[PEM11-P10] Study on the global distribution characteristics of Pc 1-2 geomagnetic pulsation with the 10Hz data of the MAGDAS system

*Taisei Kabasawa[1], Akimasa Yoshikawa[1], Teiji Uozumi[1], Akiko Fujimoto[1], Shuji Abe[1] (1.Kyushu University)

[PEM11-P11] In-situ Observations of Reconnection Separatrix Regions in the near-Earth Magnetotail

*Mizuho Araki[1], Masahiro Hoshino[1], Kunihiro Keika[1], Yoshifumi Saito[2] (1.Graduate School of Science, The University of Tokyo, 2.Institude of Space and Astronautical Science)

[PEM11-P12] Flow speed dependence of ion temperature, electron temperature, and their ratio in the near-Earth magnetotail reconnection region

*Kaori Watanabe[1], Masahiro Hoshino[1], Kunihiro Keika[1], Yoshifumi Saito[2], Naritoshi Kitamura[1] (1.Univ. of Tokyo, 2.ISAS/JAXA)

[PEM11-P13] **Examining Minimum Cyclotron Resonant Electron Energy of EMIC Waves with MMS**

*Si Liu[1] (1.Changsha University of Science and Technology)

[PEM11-P14] Small scale whistler mode waves near the magnetic field intensity minimum in the magnetosheath

*Naritoshi Kitamura[1], Takanobu Amano[1], Yoshiharu Omura[2], Satoko Nakamura[2], Chika Umegaki[1], Scott A Boardsen[3,4], Narges Ahmadi[5], Robert E Ergun[5], Olivier Le Contel[6], Per-Arne Lindqvist[7], Yoshifumi Saito[8], Shoichiro Yokota[9], Daniel J Gershman[3], Barbara L Giles[3], Thomas E Moore[3], William R Paterson[3], Craig J Pollock[10], Christopher T Russell[11], Robert J Strangeway[11], James L Burch[12] (1.Department of Earth and Planetary Science, Graduate School of Science, The University of Tokyo, 2.Research Institute for Sustainable Humanosphere, Kyoto University, 3.NASA Goddard Space Flight Center, 4.University of Maryland, 5.Laboratory for Atmospheric and Space Physics, University of Colorado, 6.Laboratoire de Physique des Plasmas, UMR7648 CNRS/Ecole Polytechnique/UPMC/Université Paris-Sud/Observatoire de Paris, 7.Royal Institute of Technology, 8.Institute of Space and Astronautical Science, Japan Aerospace Exploration Agency, 9.Department of Earth and Space Science, Graduate School of Science, Osaka University, 10.Denali Scientific, 11.Institute of Geophysics and Planetary Physics, University of California, Los Angeles, 12.Southwest Research Institute)

[PEM11-P15] Spatial characteristics of the internal modulation of pulsating aurora: multi-point high-speed optical observations in Scandinavia

*Yuki Kawamura[1], Keisuke Hosokawa[1], Shin-ichiro Oyama[2,3], Yoshizumi Miyoshi[2], Yasunobu Ogawa[3], Satoshi Kurita[2], Satoshi Ebukuro[1], Ryoichi Fujii[4] (1.Department of Communication Engineering and Informatics, University of Electro-Communications, 2.Institute for Space-Earth Environmental Research, Nagoya University, 3.National Institute of Polar Research, 4.Research Organization of Information and Systems)

[PEM11-P16] **Large-scale characteristics of pulsating aurora periodicities:multi-point high-speed optical observations in Scandinavia**

*Satoshi Ebukuro[1], Keisuke Hosokawa[1], Shin-ichiro Oyama[2,3,5], Yoshizumi Miyoshi[2], Yasunobu Ogawa[3], Satoshi Kurita[2], Yuki Kawamura[1], Ryoichi Fujii[4] (1.Department of Communication Engineering and Informatics, University of Electro-Communications, 2.Institute for Space-Earth Environmental Research, Nagoya University, 3.National Institute of Polar Research, 4.Research Organization of Information and Systems, 5.University of Oulu)

[PEM11-P17] Variations of cosmic noise absorption (CNA) by energetic electron precipitation (EEP) and changes of the auroral morphology

*Miyamoto Taishiro[1], Shin-ichiro Oyama[1,4,5], Yasunobu Ogawa[2], Keisuke Hosokawa[3], Satoshi Kurita[1], Yoshizumi Miyoshi[1], Ryuho Kataoka[2], Hiroshi Miyaoka[2], Tero Raita[4] (1. Institute for Space-Earth Environmental Research,Nagoya University, 2.National Institute of Polar Research, 3.Department of Communication Engineering and Informatics, University of Electro-Communications, 4.Sodankylä Geophysical Observatory, University of Oulu, 5.Ionosphere Research Unit, University of Oulu)

[PEM11-P18] Spatiotemporal characteristics on the source region of flash aurora using ray tracing analysis

*Tomohiro Inoue[1], Mitsunori Ozaki[1], Yoshitaka Goto[1], Satoshi Yagitani[1], Yoshiya Kasahara[1], Kazuo Shiokawa[2], Yoshizumi Miyoshi[2], Ryuho Kataoka[3], Yusuke Ebihara[4] (1.Kanazawa University , 2.Nagoya University, 3.National Institute of Polar Research, 4.Kyoto University)

[PEM11-P19] Molecular ion supply mechanisms from the low-altitude ionosphere to magnetosphere observed by EISCAT and Arase(ERG)

*Masayoshi Takada[1], Kanako Seki[1], Yasunobu Ogawa[2], Kunihiro Keika[3], Satoshi Kasahara[4], Shoichiro Yokota[5], Tomoaki Hori[7], Kazushi Asamura[6], Yoshizumi Miyoshi[7] (1.Graduate School of Science, Tokyo University, 2.National Institute of Polar Research, 3.Department of Earth and Planetary Science, Graduate School of Science, Tokyo University, 4.The University of Tokyo, 5.Graduate School of Science, Osaka University, 6.Institute of Space and Astronautical Science, Japan Aerospace Exploration Agency, 7.Institute for Space-Earth Environmental Research, Nagoya University)

[PEM11-P20] Optical and radar observation of the dynamic auroral forms

*Yunosuke Nagafusa[1], Tima Sergienko[2], Satoshi Taguchi[1], Urban Braendstroem[2], Masatoshi Yamauchi[2] (1.Graduate School of Science, Kyoto University, 2.Swedish Institute of Space Physics, Kiruna)

[PEM11-P21] Observations of MF/HF auroral radio emissions at three ground-based stations

*Yuka Sato[1], Atsushi Kumamoto[2], Yuto Katoh[2], Akira Kadokura[3,4], Yasunobu Ogawa[3,4], Atsuki Shinbori[5] (1.Nippon Institute of Technology (NIT), 2.Graduate School of Science, Tohoku University, 3.National Institute of Polar Research (NIPR), 4.The Graduate University for Advanced Studies, 5.Institute for Space-Earth Environmental Research (ISEE), Nagoya University)

[PEM11-P22] **Ionospheric F-region Drift Measurements Derived from DPS-4D at Zhongshan Station, Antarctic**

*Xiangcai Chen[1] (1.Polar Research Institute of China)

[PEM11-P23] PARM-HEP Observation of Precipitating High Energy Electrons over Pulsating Aurora

*Taku Namekawa[1], Takefumi Mitani[2], Kazushi Asamura[2], Yoshifumi Saito[2] (1.Department of Earth and Planetary Science, Graduate school of Science, The University of Tokyo, 2.Institute of Space and Astronautical Science, Japan Aerospace Exploration Agency)

[PEM11-P24] Development of the medium-energy electron detector with hemispherical field-of-view and the flight test in the PARM (Pulsating AuRora and Microburst) mission

*Shin Sugo[1], Oya Kawashima[1], Kazushi Asamura[2], Reiko Nomura[3], Yasunobu Ogawa[4], Keisuke Hosokawa[5], Yoshizumi Miyoshi[6], Takefumi Mitani[2], Taku Namekawa[1,2], Takeshi Sakanoi[7], Mizuki Fukizawa[7], Naoshi Yagi[7], Satoshi Kasahara[1] (1.The University of Tokyo, 2.Institute of Space and Astronautical Science, Japan Aerospace Exploration Agency, 3.National Astronomical Observatory of Japan, 4.National Institute of Polar Research, 5.The University of Electro-Communications, 6.Institute for Space-Earth Environmental Research, Nagoya University, 7.Tohoku University)

[PEM11-P25] Auroral substorm onset in satellite-based global images and ground-based all-sky images

*Akimasa Ieda[1], Kirsti Kauristie[2], Yukitoshi Nishimura[3], Yukinaga Miyashita[4], Harald U Frey[5], Liisa Juusola[2], Daniel Whiter[6], Masahito Nose[7], Matthew O Fillingim[5], Farideh Honary[8], Neil C Rogers[8], Yoshizumi Miyoshi[1], Shinobu Machida[1] (1.Institute for Space-Earth Environmental Research, Nagoya University, 2.Finnish Meteorological Institute, 3.Boston university, 4.Korea Astronomy and Space Science Institute, 5.University of California Berkeley, 6.University of Southampton, 7.Graduate School of Science, Kyoto University, 8.Lancaster University)

[PEM11-P26] Automatic Classification of Auroral images using optical flow feature

*Naoto Kashiwagi[1], Akiko Fujimoto[1], Terumasa Tokunaga[1], Yoshizumi Miyoshi[2], Yasunobu Ogawa[3], Keisuke Hosokawa[4] (1.Kyushu Institute of Technology, 2.Nagoya University, 3.National Institute of Polar Research, 4.The University of Electro-Communications)

[PEM11-P27] Fine-scale visualization of aurora in a wide area using color digital camera images from the International Space Station

*Sota Nanjo[1], Yuta Hozumi[1], Keisuke Hosokawa[1] (1.The University of Electro-Communications)

[PEM11-P28] Geospace Imaging via the soft X-ray imager: GEO-X mission

*Yoshizumi Miyoshi[1], Yuichiro Ezoe[2], Satoshi Kasahara[3], Yosuke Matsumoto[4], Kumi Ishikawa[5], Ryuho Kataoka[6], Hiroki Ito[1], Daiki Ishi[2], Masaki Numazawa[2], Atsushi Yamazaki[5], Hiroshi Hasegawa[5], Masaki Fujimoto[5], Kazuhisa Mitsuda[5] (1.Institute for Space-Earth Environmental Research, Nagoya University, 2.Tokyo Metropolitan University, 3.University of Tokyo, 4.Chiba University, 5.ISAS/JAXA, 6.NIPR)

Effects of Inclination/Rotation of Earth's Magnetic Axis on Magnetosphere Simulated by Global MHD Model

*Aoi Nakamizo[1]

1. Applied Electromagnetic Research Institute, National Institute of Information and Communications Technology

Recently, we have shown that the ionospheric Hall conductance distribution, owing to the polarization field generated by its nonuniformity, largely control the magnetospheric configuration and dynamics by using a global MHD model. The effects of the ionospheric conductance on the magnetosphere were also reported by previous studies based on other global models; for example, the current-voltage relationship in the solar wind-magnetosphere-ionosphere [Fedder and Lyon, 1987] and the plasma pressure distribution in the near-Earth region [Ridley et al., 2004]. These studies indicate that the ionospheric conductance is one of the most important settings in the global models to accurately simulate the magnetosphere.

On the other hand, in the development/improvement of the global MHD model in NICT, which was originally developed by Tanaka [1994] and Tanaka et al. [2010], introducing the inclination and rotation of Earth's magnetic axis with respect to the rotation axis has been remained as one of the most difficult problems. In other words, in the present model, the precession between the magnetic axis and the rotation axis is not included. This means that the simulated magnetosphere will show a different structure and temporal development than the actual magnetosphere.

We, for the first time, equivalently introduce the precession by rotating the background conductance distribution due to solar illumination (i.e., depending on the geographic coordinate) with respect to the geomagnetic coordinate. (Improvement of the conductance setting in the auroral region is the next challenge.) In this paper, we will show how the simulated magnetosphere is changed by this improvement, focusing on the near-Earth plasma environment.

Keywords: M-I Coupling, Global MHD Simulation, Ionospheric Effect

©2019. Japan Geoscience Union. All Right Reserved.

Asymmetric deformation of the magnetosphere under low-density solar wind

*Masaki N Nishino[1,2], Yoshifumi Saito[2], Kazuo Shiokawa[1], Masaki Fujimoto[2]

1. Institute for Space-Earth Environmental Research, Nagoya University, 2. JAXA/ISAS

The density of the solar wind around the Earth's magnetosphere sometimes decreases to only several percent of the usual value, and such density extrema results in a significant reduction of dynamic pressure and Alfvenic Mach number of the solar wind flow. While simple expansion of the Earth's magnetosphere by the low dynamic pressure was assumed in previous studies, a global-MHD simulation study predicted a remarkable dawn-dusk asymmetry of the magnetosphere in shape under low-density solar wind and Parker-spiral IMF configuration. Here we present evidence of asymmetric deformation of the magnetosphere under low-density solar wind and Parker-spiral IMF conditions, based on several events of GEOTAIL observations. As predicted by the global-MHD simulation, the magnetosphere on the dawnside expands much further than the magnetopause location of simple (symmetric) expansion, while no significant expansion is detected in the dusk tail flank. Fast ion beams detected at the flank magnetopause suggest that magnetic reconnection frequently occurs due to the low-beta environment of the magnetosheath.

Keywords: Low density solar wind, Magnetosphere, Plasma transport

©2019. Japan Geoscience Union. All Right Reserved.

New perspectives on coupling processes in solar-terrestrial system obtained by comprehensive data analysis

*Yoshimasa Tanaka[1], Norio Umemura[2], Shuji Abe[3], Satoru UeNo[4], Masahito Nose[2], Yumi Nakagawa[5]

1. National Institute of Polar Research, 2. Institute for Space-Earth Environmental Research, Nagoya University, 3. International Center for Space Weather Science and Education, 4. Kwasan & Hida Observatories, School of Science, Kyoto University, 5. Ibaraki University

In the Earth’ s upper atmosphere above 60 km, including magnetosphere and ionosphere, various phenomena are generated by energy inputs from solar radiation (including solar wind) and atmospheric waves propagating from the lower atmosphere. Thus, comprehensive analysis of various kinds of satellite and ground-based observational data using advanced methods is required to understand physical mechanism of the phenomena. For such interdisciplinary studies, it is important to share data distributed across many universities and institutes and use advanced tools, such as metadata database for cross-searching a variety of datasets and analysis software for analyzing various types of data in an integrated fashion. In fact, many scientific papers on the upper atmosphere have recently been obtained by comprehensive analysis of various data with such analysis tools.
We present some examples of scientific results achieved by comprehensively analyzing data from multiple regions. These examples include the effect of solar coronal holes on the Earth’ s geomagnetic activity and the interaction between solar wind, magnetosphere, ionosphere and neutral atmosphere. The former study investigated long-term trends of coronal boles, solar wind parameters, and Earth’ s geomagnetic indices during two solar cycles. It showed the possibility that the solar wind speed and geomagnetic activities may be controlled by the size and latitudinal distribution of coronal holes. The latter analyzed multi-instrument data simultaneously obtained from interplanetary space, magnetosphere, and ionosphere and mesosphere in both northern and southern hemispheres. They newly found that the polar mesosphere is affected by relativistic electron precipitation caused by the interaction with magnetospheric plasma waves during the high-speed solar wind stream. These studies demonstrate that sharing and comprehensive analysis of long-term, multiple-sphere, and multi-instrument data using sophisticated tools are very effective to produce scientific outcomes. At present there are data gap areas in the Asia and African regions. Therefore, we believe that filling in the data gap by international collaborations could be a breakthrough for unsolved issues in the upper atmosphere.

Keywords: upper atmosphere, coupling between multiple regions, comprehensive analysis, long-term observational data

©2019. Japan Geoscience Union. All Right Reserved.

The interaction between the magnetosphere-ionosphere compound system and the magnetic field topology

*Shigeru Fujita[1], Takashi Tanaka[2], Masakazu Watanabe[2]

1. Meteorological College, Japan Meteorological Agency/ Nationa Institute of Polar Research, 2. Kyushu University

The steady convection in the magnetosphere-ionosphere coupling system is composed of the following self-consistent elementary processes; dynamo in the cusp-mantle region, the field-perpendicular current system in the magnetosphere, the field-aligned current system connecting the ionosphere, the ionospheric electric field, the magnetospheric convection corresponding to the ionospheric electric field, and the high plasma pressure distribution in the cusp region [Tanaka, 2007].

The energy of the convection is transported from the solar wind across the magnetopause where the magnetic field configures the null-separator structure. Since the magnetic field configuration of the null-separator structure is originally derived from the superposition of two scalar fields [Stern, 1973], say, the dipole field and the uniform field, the magnetic field of the null-separator would not have free energy necessary for plasma acceleration. However, the simulation reveals that the magnetic field has a tension force near the null point. Therefore, we need a mechanism that transports the energy to this region.

It is revealed from the simulation that the bow shock supplies the energy. Indeed, the current from the bow shock deforms the magnetic field of the null-separator structure. In addition, it is noted that the Chapman-Ferraro current also deforms the magnetic field configuration in the magnetopause. This fact indicates that the convection system in the magnetosphere contributes to deformation of the null-separator structure. That is to say, energy transport from the solar wind to the magnetosphere-ionosphere compound system is affected by the physical processes in the convection. Therefore, as a result of the interaction between the magnetosphere-ionosphere convection and the null-separator structure, the magnetosphere-ionosphere compound system can be extended to the solar wind-magnetosphere-ionosphere compound system.

References

T. Tanaka (2007), Magnetosphere-Ionosphere Convection as a Compound System, Space Sci Rev, 133, 1-72, DOI 10.1007/s11214-007-9168-4.

Stern, D. P. (1973), A study of the electric field in an open magnetospheric model, J. Geophys. Res., 78(31), 7292-7305, doi:10.1029/JA078i031p07292.

Keywords: global MHD simulation, compound system

©2019. Japan Geoscience Union. All Right Reserved.

Effects of the dipole tilt and the interplanetary magnetic field Bx component on the dawn-dusk and interhemispheric asymmetries of the interchange convection cycle

*Masakazu Watanabe[1,2], Takashi Tanaka[2], Shigeru Fujita[3,4]

1. Graduate School of Science, Kyushu University, 2. International Center for Space Weather Science and Education, Kyushu University, 3. Meteorological College, 4. National Institute of Polar Research

The interchange cycle is a mode of magnetic flux circulation that appears for periods of northward interplanetary magnetic field (IMF). It is made up of IMF-to-open reconnection in one hemisphere and open-to-closed reconnection in the other hemisphere. The two reconnection processes have the same topological nature in that the roles of the two reconnecting field lines interchange at the time of reconnection. The interchange cycle is characterized by reciprocation of open magnetic flux between the two hemispheres. One observable signature of the interchange cycle is an appearance of a reverse cell circulating in the closed field line region of the ionosphere, which is named the “reciprocal cell.” The reciprocal cell appears in the open-to-closed reconnection hemisphere, whereas in the opposite IMF-to-open reconnection hemisphere, there appears a lobe cell circulating exclusively on open field lines. For given (1) IMF By, (2) IMF Bx, and (3) dipole tilt conditions, two interchange cycles concur, one on the dawnside and the other on the duskside. For an ideal case, one can easily expect the mode of the interchange cycles to occur. For example, for the case of due northward IMF with significant dipole tilt, the twin reverse cells in the summer hemisphere are both lobe cells, while in the winter hemisphere the twin reverse cells are both reciprocal cells. For the general case, however, one cannot predict the mode of the interchange cycles without quantitative modeling. The purpose of this study is to examine how the presence of dipole tilt or IMF Bx alters the dawn-dusk and north-south pattern of the twin reverse cells. For this purpose, we perform numerical magnetohydrodynamic simulations using the REPPU (Reproduce Plasma Universe) code developed by T. Tanaka. In the presentation, we discuss the dipole tilt and IMF Bx effects revealed by the numerical modeling.

Keywords: ionospheric convection, interchange reconnection, reciprocal cell

©2019. Japan Geoscience Union. All Right Reserved.

Transient polar ionospheric convection response to negative dynamic pressure pulse

*Jianjun Liu[1]

1. Polar Research Institute of China

The response of the high latitude ionospheric convection to a sudden decrease in solar wind dynamic pressure provides a unique opportunity to investigate how the solar wind couples to the dayside magnetosphere and ionosphere. Here, the event shows three IMF components do not have prominent changes, but the solar wind plasma went down to near zero magnitude, which leads to very weak solar wind driving during northward IMF. However, ionospheric convection observed by SuperDARN radars showed enhanced plasma flow speed in the central polar cap region just after the negative pressure pulse arrival to the magnetosphere. Simultaneous convection map generated by SuperDARN measurement presents enlarged convection cell with obvious equatorward moving Heppner-Maynard boundary. It is noted that cross polar cap potential enhanced instantly and this enhanced feature continued almost 10 min. The distribution of total electron content (TEC) exhibited typical auroral oval signature especially on dayside ionosphere, TEC density in auroral oval showed a noticeable decrease after the arrival of the negative pressure pulse. Both ionospheric convection and TEC distribution reveal that negative pressure pulse impacts the magnetosphere-ionosphere coupling system directly and dramatically. Moreover, the TIEGCM model also showed an enhanced polar potential pattern.

Keywords: Dynamic pressure, Ionospheric convection, Auroral oval

©2019. Japan Geoscience Union. All Right Reserved.

An active ionosphere: a new perspective of field line dipolarization

*Osuke Saka[1]

1. Office Geophysik

Transient westward electric fields from the magnetosphere generate equatorward plasma drifts of the order of kilometers per second in the auroral ionosphere. This flow channel extends in north-south directions and is produced in the initial pulse of Pi2 pulsations associated with the filed line dipolarization. Drifts in the ionosphere of the order of kilometers per second that accumulated plasmas at the low latitude end of the flow channel are of such large degree that possible vertical transport effects (including precipitation) along the field lines may be ignored. We suggest that plasma compression in the ionosphere implemented the ionosphere to be active. Active ionosphere generates field-aligned currents to satisfy the quasi-neutrality of the ionosphere, ion acoustic wave for ion outflows and the inverted-V type electron precipitations in the topside ionosphere, and poleward expansion of auroras due to a nonlinear evolution of the ionosphere. We will study auroral expansion in this acoustic regime.

Keywords: Substorm, Auroral substorm, Ionosphere

©2019. Japan Geoscience Union. All Right Reserved.

Toward the automatic identification of FLR signals in the SuperDARN data by using the gradient method

*Hideaki Kawano[1,2], Akira Sessai Yukimatu[3,4], Nozomu Nishitani[5], Yoshimasa Tanaka[3,4], Satoko Saita[6], Tomoaki Hori[5]

1. Dept. Earth Planet. Sci., Kyushu Univ., 2. ICSWSE, Kyushu University, 3. National Institute of Polar Research, 4. SOKENDAI, 5. ISEE, Nagoya University, 6. Kitakyushu College

The FLR (Field Line Resonance) takes place where the frequency of an incoming wave matches the eigen-frequency of magnetospheric magnetic field lines, and excites the eigen-oscillation of the field lines. The FLR can be identified by using the unique manner of change in the amplitude and the phase of thus excited eigen-oscillation across the resonant point. That is, the amplitude is maximum at the resonant point, and the phase changes the most steeply across the resonance point. The FLR-generated eigen-oscillations can be identified in the ground magnetic field data and the ionospheric plasma velocity data. From thus identified eigen-frequency ("FLR frequency" below) one can estimate the magnetospheric plasma density along the field line which passes through the ground/ionospheric observation point.

In this study we use the SuperDARN radar data to identify FLR: For each radar beam from each SuperDARN radar, the velocity of the ionospheric plasma flow along the line of sight (VLOS) of the beam is obtained; we use the VLOS data to identify the FLR and estimate the magnetospheric plasma density. Unlike the ground magnetometer data, the SuperDARN data is two-dimensional, enabling two-dimensional estimates of the magnetospheric equatorial plasma density and magnetospheric region identification.

To achieve that, it is important to identify as many FLR events as possible. Overwrapping of non-FLR waves/perturbations hides FLR events. As a countermeasure to this problem, the so-called gradient method has been applied to the ground magnetometer data; this method cancels out the overwrapping signals by dividing the data from a magnetometer by the data from another magnetometer having an adequate latitudinal distance from the other. The division yields the amplitude ratio and the phase difference. The gradient method is effective since the FLR frequency tends to depend on the latitude more strongly than the overwrapping signals.

The gradient method is also applicable to the SuperDARN VLOS data. The field of view of each beam is divided into Range Gates (RGs below) having the same length along the beam. The identification number of the RGs increases with increasing distance from the radar. The VLOS is obtained for each RG. Thus, each RG can be regarded as a "virtual observatory."

As an initial study, we have selected an FLR event which was identified in the VLOS data of a radar (at Hankasalmi) without the use of the gradient method, selected a beam, and selected a few pairs of RGs of the beam. We then have manually applied the gradient method to the VLOS data of the above-selected RG pairs, and successfully identified the FLR. In more detail, the identification has been successful only for two paired RGs whose RG numbers differs by two. This suggest that, since the length of the RG, mapped to the meridional plane, was about 40km for this event, about 80km distance was the best (with the resolution of 40km) for this event. This distance reflects the resonance width, which is an important quantity reflecting the diffusion and dissipation of the FLR energy.

©2019. Japan Geoscience Union. All Right Reserved.

In order to identify as many FLR events as possible, it is also important to automatically identify the FLR events, since visual identification is time-consuming. The gradient method enables automatic identification more easily than analyses of VLOS itself, since the gradient method yields peaks in both the amplitude ratio and the phase difference. We have started making a program for automatic identification by applying the gradient method to VLOS; the version at the time of this abstract has successfully identified FLRs for all of the above-stated pairs of RGs.

©2019. Japan Geoscience Union. All Right Reserved.

A statistical study of Pi2 pulsations observed in the upper ionosphere using Swarm magnetic field data

*Park Jaehee[1], Khan-Hyuk Kim[1], Junga Hwang[2]

1. School of Space Research, Kyung Hee University, Gyeonggi, South Korea, 2. Korea Astronomy and Space Science Institute, Daejeon,South Korea

The properties of Pi2 pulsations observed in the upper ionosphere are studied using magnetic field data acquired by the Swarm-A spacecraft in low Earth orbit (LEO) and at the low-latitude Bohyun ground station (BOH, L = 1,3) for January 2014-Jun 2015. From time intervals when Swarm-A was on the nightside (magnetic local time (MLT) = 1800-0600 hrs) and the BOH station was near midnight (MLT = 2100-0300 hrs), we identified 623 Pi2 events in the horizontal H component of the BOH data. For each event we examine the coherence between the horizontal H component on the ground and the B_x (radial) azimuthal B_y (azimuthal), or B_z (compressional) components at Swarm-A. Out of 623 events, the B_x-H high coherence (> 0.7) events are ~6%, the B_y-H high coherence events are ~4%, and the B_z-H high coherence events are ~25%. The ground-satellite high coherence events occurred when the spacecraft was located within a magnetic latitude range of ±50°. Using the ground-satellite high coherence events, we examined the latitudinal structure of the relative amplitude and phase of the ionospheric Pi2 pulsations detected at Swarm-A. Confirming previous observations at LEO, we found that the ionospheric Pi2 pulsations are characterized by symmetric odd mode standing oscillations in the north-south direction, having a node for B_x oscillation and an antinode for B_z oscillation, respectively, at the equator. This indicates that the source of ionospheric Pi2 pulsations is the plasmaspheric resonance.

Keywords: Pi2 pulsations

©2019. Japan Geoscience Union. All Right Reserved.

Study on the global distribution characteristics of Pc 1-2 geomagnetic pulsation with the 10Hz data of the MAGDAS system

*Taisei Kabasawa[1], Akimasa Yoshikawa[1], Teiji Uozumi[1], Akiko Fujimoto[1], Shuji Abe[1]

1. Kyushu University

The magnetic field observed on the ground is affected by the space weather phenomena such as magnetic storms and auroral storms.

The Pc1 geomagnetic pulsation (frequency range of 0.2-5.0 seconds) activated mainly around a high-latitude region is understood as a phenomenon accompanied by the excitation of EMIC waves to cause the particle acceleration in the equatorial region of the magnetosphere. Also, it is well known that Pc1 waves propagate horizontally in the ionospheric at the F layer. However, it is not clarified about the global occurrence and propagation properties of Pc1 geomagnetic pulsation on the ground. Moreover, although induction magnetometers are used to observe the high-frequency magnetic field disturbance phenomenon like Pc1 and Pc2 (frequency range of 5.0-10.0 seconds) geomagnetic pulsation, the global observation network with induction magnetometers covering from high-latitude to low-latitude area and equator domain does not exist at this stage. On the other hand, although it is common to use Fluxgate magnetometers for the observation of global space weather phenomenon, it is considered to be unsuitable for analysis of the high-frequency Pc1-2 geomagnetic pulsation because its time accuracy is usually one second value.

The ground multipoint magnetic field observation network which Kyushu University has developed (MAGDAS-9 magnetometer) acquire a 250Hz sampling and 10Hz mean data. Also, it is the only geomagnetic observation network that can investigate the global aspects of Pc1-2 geomagnetic pulsation.

In this study, we investigated the global distribution of Pc1-2 pulsation from polar region to equatorial region with magnetic field data provided by MAGDAS and Dst/AE index provided by the WDC for Geomagnetism, Kyoto. As a result, when the substorm have occurred during a magnetic storm time, generation of Pc1-2 pulsation from high-latitude to middle-and-low latitude region and further arrival of Pc2 pulsation to the dip-equator are identified. The elucidation of occurrence characteristic of the Pc1-2 pulsation on the ground with the EMIC waves excitation is very important not only for space weather application to be able to monitor particle energization process via EMIC excitation but also the elucidation of the super global coupling process from inner magnetosphere to the global ionosphere from polar to equatorial region. In this presentation, we will report the preliminary results of observational analysis of Pc1-2 pulsation by using MAGDAS network. We also discuss the comprehensive approach for understanding global coupling process among inner magnetosphere and high-middle-low latitude to the equatorial region by using FM-CW radar data, PWING induction magnetometer data, and the geo-space environment data from the ERG satellite.

Keywords: Pc1-2 pulsation, EMIC waves, global coupling

©2019. Japan Geoscience Union. All Right Reserved.

In-situ Observations of Reconnection Separatrix Regions in the near-Earth Magnetotail

*Mizuho Araki[1], Masahiro Hoshino[1], Kunihiro Keika[1], Yoshifumi Saito[2]

1. Graduate School of Science, The University of Tokyo, 2. Institude of Space and Astronautical Science

Magnetic reconnection which converts magnetic energy into thermal and kinetic energy of plasmas is an important physical mechanism of plasma heating and acceleration. Particularly in the Petschek-type reconnection, plasma acceleration and heating in the slow-mode shocks formed at the separatrices must be taken into consideration. The structure of the slow-mode shocks in the distant tail of the Earth’s magnetosphere was investigated with in-situ observations made by the GEOTAIL satellite (Saito et.al, 1995). It is observationally suggested that about 10% of the plasma sheet boundary layer (PSBL) is slow-mode shocks. It is, however, not fully understood what determines this percentage and what is the difference in the ion and electron temperature changes between slow-mode shocks and others separatrix regions.
In this study, we utilized multi-spacecraft in-situ observations of separatrix regions at magnetic reconnection in the near-Earth magnetotail (GSM-X is between ~13 and ~25RE). We used data obtained from FPI (Fast Plasma Investigation) and FGM (Fluxgate Magnetometer) on board the MMS satellite from June 1, 2017to August 31, 2017. We examined occurrence locations, ion flow directions and velocity of ion flow in downstream regions of observed events. We also examined changes in ion and electron temperatures and the ion-to-electron temperature ratio.

We classified their events into 2 types according to plasma beta in the in-flow regions: below 0.1 or around 1. We term them “lobe reconnection” and “plasma sheet reconnection”, respectively. In the former type, plasmas in the in-flow regions are cold and tenuous. In the latter type, plasmas in the in-flow regions are hot and dense. In both types, we observed increases in ion and electron temperatures increase, but their characteristics are different. In the lobe reconnection, ion temperatures increase from several hundred eV to several keV. In the plasma sheet reconnection, ion temperatures also increase from about 1 keV to several keV. The increase rate of the electron temperature is less than one order of magnitude for both types, smaller than that of the ion temperature; the electron temperature increases up to at most 1 keV. The ion-to-electron temperature ratio in the out-flow regions in both types is about 5 for both types. We then examined changes of the ion-to-electron temperature ratio and found that the changes are consistent with the result reported by Wang et al. (2012).

In this presentation, we will show the results of separatrix crossing events (both lobe and plasma sheet reconnection events) that occur in 2017 and 2018. We will identify whether each of the separatrices is a slow shock or not and how the separatrix conditions affect ion and electron heating. These characteristics will provide insights into heating mechanisms and energy conversion through separatrix regions.

Reference:

Yoshifumi Saito, Toshifumi Mukai, Toshio Terasawa, Atsuhiro Nishida, Shinobu Machida, Masafumi Hirahara, Kiyoshi Maezawa, Susumu Kokubun, and Tatsundo Yamamoto, Slow-mode shocks in the magneto, J. Geophys. Res., 100, A12, 23,567, 1995

©2019. Japan Geoscience Union. All Right Reserved.

Chih-Ping Wang, Matina Gkioulidou, Larry R. Lyons and Vassilis Angelopoulos, Spatial distributions of ion to electron temperature ratio in the magnetosheath and plasma sheet, J. Geophys. Res., 117, A08215, 2012

Keywords: Magnetic Reconnection, MMS satellite, Earth's Magnetotail

©2019. Japan Geoscience Union. All Right Reserved.

Flow speed dependence of ion temperature, electron temperature, and their ratio in the near-Earth magnetotail reconnection region

*Kaori Watanabe[1], Masahiro Hoshino[1], Kunihiro Keika[1], Yoshifumi Saito[2], Naritoshi Kitamura[1]

1. Univ. of Tokyo, 2. ISAS/JAXA

Plasma in the Earth's magnetotail are heated up to 1-10 keV and stored in the plasma sheet. One of the heating or acceleration mechanisms is the magnetic reconnection. Heated or accelerated plasma are transported both earthward and tailward as fast flow with a speed of several hundred kilometers per second. However, what determines the partition among ion and electron thermal energy and kinetic energy is an unresolved problem. It has been reported that ion temperature T_i, electron temperature T_e, and their ratio T_i/T_e vary spatially and depend on the conditions of fast flows [Wang et al., 2012, Runov et al., 2018] but there are few studies which focus on macroscopic profiles of them in reconnection regions in the magnetotail.

In this study, we examine the relation between flow speed and average profiles of T_i, T_e, and T_i/T_e in the magnetotail reconnection region by using data obtained from FPI and FGM on board the MMS spacecraft. We use the observations for a period from May to August 2017 and take out the data in the region of $X_{GSM} < -15$ Re, -10 Re $< Y_{GSM} < 10$ Re, and beta > 0.1. We then divide them into different groups according to flow speed normalized by alfven speed and show B_z/B_{lobe}– B_x/B_{lobe} maps of T_i, T_e, and T_i/T_e of each group. The results show that ion temperature increase with increasing flow speed while electron temperature decrease. Ion temperature are hotter around the X-point. The structure of inflow and outflow regions is pronounced in the profile of electron temperature. T_i/T_e in inflow region are greater than in outflow region, which means that ion and electron temperatures become comparable by passing through the diffusion region. The results suggest that electron get less energy when more energy is partitioned into plasma kinetic energy. We will discuss about the profiles of anisotropy of plasma temperatures to know more details about the heating mechanisms.

Keywords: temperature ratio, flow, MMS

©2019. Japan Geoscience Union. All Right Reserved.

Examining Minimum Cyclotron Resonant Electron Energy of EMIC Waves with MMS

*Si Liu[1]

1. Changsha University of Science and Technology

Electromagnetic ion cyclotron (EMIC) waves can be in cyclotron resonance with relativistic electrons, causing relativistic electron precipitation. The four ideal Magnetospheric Multiscale (MMS) spacecraft provide great opportunity to directly calculate the wave vector ***k*** of EMIC waves by phase differencing technique and hence estimate the minimum resonant energy by the resonance condition. Deriving a simplified analytic solution, we find that the phase differencing method can still provide an estimate of the dominant wave number when a finite wave number spread or a finite frequency spread is present. Numerical calculations indicate that quasi-antiparallel propagation dominates the EMIC event on 20 November 2015, which is consistent with the FFT spectral analysis results. We also find that obtained wave vectors, roughly agreeing with the validity of cold plasma theory, might significantly vary from wave packet to wave packet. Moreover, minimum resonant electron energies gradually increase from 0.5 MeV to tens of MeV with a decreasing parallel componet of ***k***. Current results provide evidence that EMIC waves can be in resonance with the electrons of energies down to hundreds of keV. It further demonstrates that EMIC waves in a narrow frequency band can effectively interact with the relativistic electrons with a broad energy range.

Keywords: EMIC waves, minimum resonant electron energy, wave vector, phase differencing

©2019. Japan Geoscience Union. All Right Reserved.

Small scale whistler mode waves near the magnetic field intensity minimum in the magnetosheath

*Naritoshi Kitamura[1], Takanobu Amano[1], Yoshiharu Omura[2], Satoko Nakamura[2], Chika Umegaki[1], Scott A Boardsen[3,4], Narges Ahmadi[5], Robert E Ergun[5], Olivier Le Contel[6], Per-Arne Lindqvist[7], Yoshifumi Saito[8], Shoichiro Yokota[9], Daniel J Gershman[3], Barbara L Giles[3], Thomas E Moore[3], William R Paterson[3], Craig J Pollock[10], Christopher T Russell[11], Robert J Strangeway[11], James L Burch[12]

1. Department of Earth and Planetary Science, Graduate School of Science, The University of Tokyo, 2. Research Institute for Sustainable Humanosphere, Kyoto University, 3. NASA Goddard Space Flight Center, 4. University of Maryland, 5. Laboratory for Atmospheric and Space Physics, University of Colorado, 6. Laboratoire de Physique des Plasmas, UMR7648 CNRS/Ecole Polytechnique/UPMC/Université Paris-Sud/Observatoire de Paris, 7. Royal Institute of Technology, 8. Institute of Space and Astronautical Science, Japan Aerospace Exploration Agency, 9. Department of Earth and Space Science, Graduate School of Science, Osaka University, 10. Denali Scientific, 11. Institute of Geophysics and Planetary Physics, University of California, Los Angeles, 12. Southwest Research Institute

Wave-particle interactions are thought to play a crucial role in energy transfer in collisionless space plasmas in which the motion of charged particles is controlled by electromagnetic fields. In the terrestrial magnetosheath, intense whistler mode waves, called 'Lion roars', are often detected by spacecraft around minima of semi-periodic fluctuations of magnetic field intensity due to mirror mode structures and motion of the structures. It is expected that whistler mode waves are efficiently generated near a local minimum of magnetic field intensity due to the smallest cyclotron resonance velocity. We report the detailed characteristics of such whistler mode waves using the data obtained by the four MMS (Magnetospheric Multiscale) spacecraft. Because reversals of field-aligned component of Poynting flux around minima in mirror mode structures correspond to reversals of gradient of magnetic field intensity along the magnetic field, whistler mode events with reversals of the field-aligned component of Poynting flux are good candidates of observations of effective wave generation regions along field lines. Even in such events, phase difference and change of amplitude of whistler mode waves observed by the four spacecraft do not have a clear correlation in cases of ~40 km separation, which is much smaller than the spatial scale of magnetic field depression due to mirror mode structures and is even smaller than the local thermal ion gyro scale. This result indicates that the coherent whistler wave generation in mirror mode structures has very limited spatial scale across field lines and is probably affected by any electron scale process. A plane wave approximation can be usable only in a very small scale. Because some events in cases of ~7 km separation showed good correlation among four spacecraft, the typical scale of coherent whistler wave across field lines can be at least an order of 10 km in mirror mode structures in the terrestrial magnetosheath. The whistler mode waves observed by a spacecraft in a mirror mode structure are a cluster of waves from multiple spatially small sources.

Keywords: Whistler mode wave, Plasma wave, MMS spacecraft, Wave-particle interaction

©2019. Japan Geoscience Union. All Right Reserved.

Spatial characteristics of the internal modulation of pulsating aurora: multi-point high-speed optical observations in Scandinavia

*Yuki Kawamura[1], Keisuke Hosokawa[1], Shin-ichiro Oyama[2,3], Yoshizumi Miyoshi[2], Yasunobu Ogawa[3], Satoshi Kurita[2], Satoshi Ebukuro[1], Ryoichi Fujii[4]

1. Department of Communication Engineering and Informatics, University of Electro-Communications, 2. Institute for Space-Earth Environmental Research, Nagoya University, 3. National Institute of Polar Research, 4. Research Organization of Information and Systems

Pulsating aurora (PsA) is a kind of diffuse aurora which almost always appears in the morning side during the recovery phase of auroral substorm. PsA typically has two characteristic temporal variations. One is so-called main pulsation whose period ranges from a few to a few tens of seconds. The other is a few Hz brightness modulation (internal modulation) which is often seen during the ON time of the main pulsation. Previous studies have suggested that the temporal variation of PsA is characterized by wave-particle interaction between whistler-mode chorus waves and high energy electrons in the magnetosphere. Especially, it has been indicated that there is one to one correspondence between the amplitude variation of chorus waves and the luminosity modulation of PsA.
Recent studies revealed the occurrence distribution of the frequency of the internal modulation. However, there have been no studies which analyzed the spatial distribution of the internal modulation.

To reveal the spatial characteristics of the internal modulation, we need to perform a frequency analysis of the internal modulation by using data from high speed optical instruments having wide spatial coverage. For this purpose, we make use of highly sensitive EMCCD cameras which have been operated in Sodankylä and Kevo in Finland, Tromsø in Norway, and Tjautjas in Sweden. In these observations, all-sky images are taken with a sampling rate of 100 Hz, which is sufficient to identify temporal variations of the internal modulation.

In the frequency analysis, we have employed all-sky images taken on March 15, 2018 (00:00 –01:30 UT) in Sodankylä, Kevo, Tromsø, and Tjautjas. We computed the average frequency of the internal modulation from each pixel of the EMCCD cameras and derived the spatial distribution of their dominant frequencies. Regardless of the latitude, each pulsating patch was fluctuating at a similar frequency. We also derived the frequency spectrum of several pulsating patches existing at different positions in the north-south direction and found that those frequency spectrums of pulsating patches have peaks at about 3 Hz. These results indicate that the frequency of the internal modulation does not depend on the magnetic latitude, and the frequency of the internal modulation is collimated on 3 Hz.
In the presentation, we discuss why the frequency of the internal modulation concentrate on 3 Hz by taking into account the time of flight of PsA electrons.

Keywords: Pulsating aurora, Internal modulation

©2019. Japan Geoscience Union. All Right Reserved.

Large-scale characteristics of pulsating aurora periodicities: multi-point high-speed optical observations in Scandinavia

*Satoshi Ebukuro[1], Keisuke Hosokawa[1], Shin-ichiro Oyama[2,3,5], Yoshizumi Miyoshi[2], Yasunobu Ogawa[3], Satoshi Kurita[2], Yuki Kawamura[1], Ryoichi Fujii[4]

1. Department of Communication Engineering and Informatics, University of Electro-Communications, 2. Institute for Space-Earth Environmental Research, Nagoya University, 3. National Institute of Polar Research, 4. Research Organization of Information and Systems, 5. University of Oulu

It has been known that most of diffuse aurorae in the morning side are composed of luminous patches whose brightness modulates quasi-periodically. Such aurorae are termed as pulsating aurora (PsA) and have been studied extensively in the last decade. PsA patches have a scale size of a few hundreds of km and are usually observed during the late recovery phase of substorms. The entire temporal variation of PsA consists of two individual modulations: main pulsation and internal modulation. The periodicity of the main pulsation ranges from a few to a few tens of seconds and the internal modulation, showing a few Hz scintillating luminosity changes, is often embedded within the ON time of the main pulsation. Previous studies using satellites indicated one-to-one correlation between PsA and chorus wave near the equatorial plane of the magnetosphere, suggesting that ground-based observations of PsA can be used for mapping the activity of chorus in the magnetosphere in 2D fashion. In the past, the spatial characteristics of chorus wave have not visualized in detail because satellite observations only cover a single point in the magnetosphere. To overcome this limitation, we derive the spatial distribution of chorus waves by using ground-based optical observations of PsA and discuss the ambient parameters which characterize the nature of chorus.
For this purpose, we have employed data from electron multiplying charge-coupled device (EMCCD) cameras deployed at multiple sites in Scandinavia to derive the large-scale characteristics of PsA. EMCCD cameras have been operative in Kevo and Sodankyla in Finland, Tromsoe in Norway, and Tjautjas in Sweden and their temporal resolution is 100 Hz. We conducted a frequency analysis for a PsA event on March 28, 2017 (23:30 to 24:10 UT). During the event studied, there existed three different regions of PsA, regions A, B and C, showing different modulation periods. It was also found that the boundaries between these three regions were sharp. We derived the 2D frequency map by using data from all the available stations. As a result, it became clear that the higher latitude region (region C) showed faster internal modulation than the lower latitude region (region A). In addition, region B, which was sandwiched by regions A and C, did not show any internal modulations (i.e., main pulsation without internal modulation). In the presentation, we discuss why the three regions showed different modulation periods with sharp boundaries. In particular, we address what ambient conditions can control the absence of internal modulation in region B. We also derived similar frequency maps of chorus waves by tracing the PsA modulation with the Tsyganenko 04 magnetic field model, which could be used to estimate the spatial extent of chorus wave generation region.

Keywords: Pulsating aurora, Chorus wave, Main pulsation, Internal modulation

©2019. Japan Geoscience Union. All Right Reserved.

Variations of cosmic noise absorption (CNA) by energetic electron precipitation (EEP) and changes of the auroral morphology

*Miyamoto Taishiro[1], Shin-ichiro Oyama[1,4,5], Yasunobu Ogawa[2], Keisuke Hosokawa[3], Satoshi Kurita[1], Yoshizumi Miyoshi[1], Ryuho Kataoka[2], Hiroshi Miyaoka[2], Tero Raita[4]

1. Institute for Space-Earth Environmental Research,Nagoya University, 2. National Institute of Polar Research, 3. Department of Communication Engineering and Informatics, University of Electro-Communications, 4. Sodankylä Geophysical Observatory, University of Oulu, 5. Ionosphere Research Unit, University of Oulu

Temporal and spatial variations of aurora morphology in association with substorm have been studied for more than half a century. Various types of aurora are known, such as discrete arc emitting at relatively high intensity and elongating along the zonal direction, and diffuse aurora with darker but more widely spreading in the sky. Pulsating aurora, which is characterized by quasi-periodic oscillations in the emission intensity at periods of a few to tens seconds, and auroral patches observed embedding in the pulsating aurora tend to appear at the recovery phase of substorm, especially from midnight to dawn. It is known that these types of aurora are accompanied by energetic electron precipitation exceeding several hundreds keV. Elucidation of the causality to produce pulsating aurora and energetic electron precipitation is an important theme to understand relationships between the radiation belt and upper-middle atmosphere of the earth. Analyzing measurements from satellite observations (e.g., Arase) and ground-based optical/radio technique observations, the generation mechanism is thought to be mainly attributed to wave particle interactions due to plasma wave and electrons in the magnetosphere. In this study, we focus on relationships between auroral morphological changes, in particular spatiotemporal evolutions to patches and coinciding precipitations of the energetic electron.

Some previous studies have presented changes in morphology from pulsating aurora to patch structures [e.g., Shiokawa et al., 2014] and temporal variations of energetic electron precipitation [e.g., Hosokawa and Ogawa, 2015]. As mentioned above, the wave-particle interaction has been widely accepted with experimental evidences to support generation of pulsating aurora and energetic electron precipitation. However, our understanding has not yet reached its maturity of presenting spatiotemporal evolutions of auroral morphology and associated electron precipitation. Oyama et al. [2017] presented enhancements of CNA (cosmic noise absorption) coinciding with appearance of the patch structure but with only two events. Furthermore, due to measurements with intensive diagnostic instruments, the result was based on information of a part of the auroral ionosphere. In this study, we conducted observations to capture simultaneously time evolutions and spatial distributions of auroral morphology and energetic electron precipitation by utilizing a network of EMCCD (Electron Multiplying Charge Coupled Device) cameras and riometers deployed in Northern Europe.

This study will present three events (February 19-20, 2018, March 6-7, 2017, and March 29-30, 2017). On the way of all events, after substorm onsets twice near Northern Europe, another onset occurred again at more west side (near Iceland or Greenland area) but at dawn in the Northern Europe. In this study, we have focused on the aurora and CNA associated with the latter onset, and at that time, the aurora spatially and temporally shifted from diffuse to pulsation and patch structures. This suggests that substorm activities occurred in the distance can induce these auroral morphological changes seen in the Northern Europe. CNA at that time is characterized by gradual variations with time scale of several hours. This trend cannot be seen at substorm onset near the Northern Europe. Moreover, in the latitude distribution, the feature was confirmed that CNA increases at the latitude where patch structure is seen, and CNA keeps

©2019. Japan Geoscience Union. All Right Reserved.

constant value at the latitude where patch structure is not seen. In the presentation, based on these observations, we will discuss physical mechanisms to cause changes in the auroral morphology and energetic electron precipitation, which can be seen as increases of CNA.

Keywords: Ionosphere, Aurora, Energetic Electron Precipitation (EEP)

©2019. Japan Geoscience Union. All Right Reserved.

Spatiotemporal characteristics on the source region of flash aurora using ray tracing analysis

*Tomohiro Inoue[1], Mitsunori Ozaki[1], Yoshitaka Goto[1], Satoshi Yagitani[1], Yoshiya Kasahara[1], Kazuo Shiokawa[2], Yoshizumi Miyoshi[2], Ryuho Kataoka[3], Yusuke Ebihara[4]

1. Kanazawa University , 2. Nagoya University, 3. National Institute of Polar Research, 4. Kyoto University

Whistler mode waves cause precipitation of high-energy electrons via wave-particle interactions in the magnetosphere. The scattered particles precipitate to the ground along the geomagnetic field line. Then, flush aurora, which is a rapid (less than 1 s) auroral phenomenon, is happened. Flash aurora is important for understanding the spatial evolution of wave-particle interaction region in the magnetosphere. We observed the mainly southward spread of flush aurora. In order to understand the spatial-time variation of wave-particle interaction region, we analyze the propagation effects of whistler mode waves near the magnetic equator region using ray tracing analysis. We calculated the ray paths of whistler mode waves (0.2 fce and 0.4 fce) near the magnetic equator (-10 to +10 degrees of geographic latitude), where fce is the electron cyclotron frequency at the magnetic equator. The initial ray paths put in the assumption of a spatial spread with the wave normal angles of tens of degrees along the magnetic field line at the magnetic equator (a point source). Then, we traced the magnetic field lines from the ray paths of whistler mode waves and estimated the precipitation area of electrons in the ionosphere using the IGRF model. The calculation results showed the precipitation area was not mainly spread southward, but evolved northward in the preliminary study.
In this presentation, we will present the spatiotemporal characteristics of flash aurora and the analysis results of ray tracing in detail.

Keywords: Flush aurora, Whistler mode wave, Ray tracing, Wave-particle interaction

©2019. Japan Geoscience Union. All Right Reserved.

Molecular ion supply mechanisms from the low-altitude ionosphere to magnetosphere observed by EISCAT and Arase(ERG)

*Masayoshi Takada[1], Kanako Seki[1], Yasunobu Ogawa[2], Kunihiro Keika[3], Satoshi Kasahara[4], Shoichiro Yokota[5], Tomoaki Hori[7], Kazushi Asamura[6], Yoshizumi Miyoshi[7]

1. Graduate School of Science, Tokyo University, 2. National Institute of Polar Research, 3. Department of Earth and Planetary Science, Graduate School of Science, Tokyo University, 4. The University of Tokyo, 5. Graduate School of Science, Osaka University, 6. Institute of Space and Astronautical Science, Japan Aerospace Exploration Agency, 7. Institute for Space-Earth Environmental Research, Nagoya University

Molecular ions (O_2^+/NO^+/N_2^+) in the magnetosphere have been observed during magnetic storms [Peterson et al., 1994; Klecker et al., 1986]. These molecular ions are considered to originate from the Earth’ s ionosphere. It is considered that they have been transported upward by some heating processes in the ionosphere. However, due to the larger mass than atomic ions (O^+), the molecular ions usually exist only in the low-altitude ionosphere below 300 km altitude. It is hence difficult to transport these molecular ions by overcoming loss by chemical reactions to the high-altitude ionosphere where the ion upflow and outflows usually take place [Peterson et al., 1994]. Therefore, it is necessary to reveal what mechanism causes molecular ion upflow during the magnetic storms. In this study, we aim at the observational assessments of the supply processes of the molecular ions from the low-altitude ionosphere to the magnetosphere based on conjugate observations by EISCAT radar and the Arase (ERG) satellite.

The EISCAT radar and the Arase (ERG) satellite have the conjunction event during the large magnetic storm with the minimum Dst of -124 nT on September 8, 2017. During the event, the Arase satellite was located in the dusk-side inner magnetosphere and observed molecular ions in the energy range of 12-180 keV/q. The EISCAT radar simultaneously observed the ion upflow (with the upward velocity of ~50-150 m/s) from the low-altitude ionosphere (~250-400 km) together with strong ion heating (>2000 K). The convective electric field was also enhanced by a factor of 2 in the same region. We estimated each term in the equation of motion for ions. The result indicates that the ion upflow reached stable equilibrium because the upward ion and electron pressure gradients are balanced with the downward gravitational force. It is suggested that the ion upflow can take place from the low-altitude ionosphere due to strong ion pressure gradient. We also estimated the flux decrease of molecular ions due to dissociative recombination. The flux decreased to ~1 % at 350 km compared with 280 km. The estimated upflow flux of molecular ions at 350 km is $>10^{10}$ m^{-2} s^{-1} . Comparison between distribution functions observed by Arase satellite and EISCAT radar suggests that acceleration by 3 orders of magnitudes is necessary during the outflow process. These results indicate that the strong ion frictional heating during magnetic storms enabled molecular ions to be transported upward from the low-altitude ionosphere and provide a source of molecular ion outflows into the magnetosphere.

Keywords: Molecular ion, EISCAT radar, Arase (ERG) satellite, Ion upflow, Ionospheric heating

©2019. Japan Geoscience Union. All Right Reserved.

Optical and radar observation of the dynamic auroral forms

*Yunosuke Nagafusa[1], Tima Sergienko[2], Satoshi Taguchi[1], Urban Braendstroem[2], Masatoshi Yamauchi[2]

1. Graduate School of Science, Kyoto University, 2. Swedish Institute of Space Physics, Kiruna

Ionosphere disturbances caused by the auroral electron precipitations are studied using auroral images taken by Auroral Large Imaging System (ALIS) and ionospheric parameters measured by EISCAT UHF radar that were conjugate with ALIS field-of-view. ALIS consists of several remote controlled stations located in northern Scandinavia, separated by approximately 50 km. Each station is equipped with a high-resolution CCD detector with 1024×1024 pixels, and a filter wheel with six positions for narrow-band interference filters. In this study we use the data obtained with the 557.7 nm filter, which show the auroral emission originated from the atomic oxygen. EISCAT UHF radar located in northern Norway near Tromsø operating in the BEATA program provides the ionospheric electron density, electron and ion temperatures, and ion velocity with the time resolution of 5 s and the spatial resolution of 1.5 km. The auroral images from the different ALIS stations were used for triangulation of the auroral forms in order to determine the aurora position in relation to the radar beam. For each auroral arc, the electron density, the electron and ion temperatures measured inside and in the vicinity of the auroral forms were analyzed with the aim of understanding the ionospheric response to the different types of auroral electron precipitations.

Keywords: aurora, ionospheric parameters, electron precipitations

©2019. Japan Geoscience Union. All Right Reserved.

Observations of MF/HF auroral radio emissions at three ground-based stations

*Yuka Sato[1], Atsushi Kumamoto[2], Yuto Katoh[2], Akira Kadokura[3,4], Yasunobu Ogawa[3,4], Atsuki Shinbori[5]

1. Nippon Institute of Technology (NIT), 2. Graduate School of Science, Tohoku University, 3. National Institute of Polar Research (NIPR), 4. The Graduate University for Advanced Studies, 5. Institute for Space-Earth Environmental Research (ISEE), Nagoya University

We started ground-based observations of MF/HF auroral radio emissions about 10 years ago at two stations (The Husafell Station, Iceland, September 2005; The Kjell Henriksen Observatory, Svalbard, September 2008) and found multiple unknown properties of MF/HF auroral radio emissions, e.g. polarization features [*Sato et al.*, 2008, 2015] and existence of a higher frequency component [*Sato et al.*, 2012]. To make a next siginificant step for a futher understanding of MF/HF auroral radio emissions, we installed a new dedicated instrumentation at the KAIRA (Kilpisjärvi Atmospheric Imaging Receiver Array) site in Kilpisjärvi, Finland (Latitude: 60.07 N, Longitude: 20.76 E) in the summer of 2018. It is a passive receiving system designed to realize a high-resolution spectral, interferometric and polarization measurements using 4 loop antennas and a software-defined radio (SDR) receiver. This SDR receiver can implement high-speed, flexible digital signal processing of RF signals and obtain high-resolution spectra pauselessly throughout the night in a wide frequency range up to 6 MHz. One of the main research subjects of this project is radio emission spontaneously emitted from aurora. There are long-known three types of MF/HF auroral radio emissions identified at ground level: auroral hiss, medium frequency burst (MFB), and auroral roar. Investigation into the generation of these emissions not only offers a tool of great promise for remote sensing of ionospheric plasma processes and parameters but also gives the foundation for understanding various radiation mechanisms that occur in planetary magnetospheres and plasma in space. In combination with the long-term continuous observations in Iceland and Svalbard and future EISCAT_3D experiments, observation with this new instrumentation will provide a first-time opportunity to reveal spatiotemporal variations of macro and fine structures of MF/HF auroral radio emissions associated with substorm evolution. In this presentation, we show detailed specification of this new instrumentation and some initial results.

Keywords: auroral phenomena, radio wave propagation, wave-particle interaction

©2019. Japan Geoscience Union. All Right Reserved.

Ionospheric F-region Drift Measurements Derived from DPS-4D at Zhongshan Station, Antarctic

*Xiangcai Chen[1]

1. Polar Research Institute of China

By means of high-frequency radio sounding, the ionospheric plasma drift can be measured by the Doppler frequency shift of signal. In this paper we analyze the ionospheric F-region plasma motion performed by Digisonde Portable Sounder (DPS-4D) at cusp latitude over Zhongshan Station in Antarctic. By restricting the echo arrival angle, and selecting the reflection height range at 175 –475 km, we present the variation of the F-region plasma drift measurements by setting limits on the Doppler frequency shift. Base on the 7.5 min interval Digisonde drift data from November 2011 to February 2012, we considered the variations of the plasma drift in F-region under the different geomagnetic activity (Kp) and magnetic local time, as well as it correlation with interplanetary magnetic field (IMF). The results indicate that properly restricting the Doppler frequency shift of the echo has a strong effect that contributes to the accurate and robust measurements of the ionospheric plasma drift. The mean value of horizontal drift mostly leveled off to about 600 m/s at altitude around of 230 km, while the field-aligned component of drift showed mean values of -25 m/s near pre-noon and +40 m/s during the night. These strong diurnal variations have dependence on the sign and strength of the IMF B_y and B_z components. It implies that the contraction and expansion of the polar cap with Kp and the convection in the proximity of the throat with different IMF conditions have a profound influence on the observed drift velocities.

Keywords: Digisonde DPS 4, Doppler frequency shift, remote sensing, polar ionosphere, plasma drift

©2019. Japan Geoscience Union. All Right Reserved.

PARM-HEP Observation of Precipitating High Energy Electrons over Pulsating Aurora

*Taku Namekawa[1], Takefumi Mitani[2], Kazushi Asamura[2], Yoshifumi Saito[2]

1. Department of Earth and Planetary Science, Graduate school of Science, The University of Tokyo, 2. Institute of Space and Astronautical Science, Japan Aerospace Exploration Agency

The phenomenon called microbursts that radiation belt particles precipitate to the Earth’ s atmosphere is thought to be largely related to the dissipation of high energy electrons in radiation belt. It is suggested that this phenomenon is caused by pitch angle scattering of the magnetospheric particles by plasma waves, which is a mechanism similar to the cause of the pulsating aurora observed in the Earth’ s polar region. There is a possibility that the origin of microburst can be clarified by proving simultaneous occurrence of microburst and pulsating aurora, but observational verification has not been made yet. For that purpose, we have developed a high-energy electron detector (HEP) for the observation of sub-relativistic - relativistic energy electrons that make up the microburst. HEP is designed to measure electrons between 300 keV and 2 MeV with energy resolution of 20% or less and with signal processing time of ~ 5 μs. Energy analysis is performed by the detection part of this instrument using SSD (Solid State Detector). Performance tests of this instrument are carried out using a sealed radiation source and a high energy electron beam line. This instrument is installed as one of the core instruments of the PARM instrument package developed for the simultaneous observation of the pulsating aurora and microburst by an international student sounding rocket experiment RockSat-XN and LAMP (Loss through Auroral Microburst Pulsation) sounding rocket experiment. We have succeeded in obtaining the flight data on 13 January 2019 from RockSat-XN sounding rocket experiment. In parallel, we are now preparing HEP analyzer for LAMP sounding rocket experiment. In this presentation, we will show the outline and observation results of RockSat-XN-HEP as well as the LAMP-HEP development status.

Keywords: Microburst, PARM, RockSat-XN, LAMP, Sounding rocket, Pulsating aurora

©2019. Japan Geoscience Union. All Right Reserved.

Development of the medium-energy electron detector with hemispherical field-of-view and the flight test in the PARM (Pulsating AuRora and Microburst) mission

*Shin Sugo[1], Oya Kawashima[1], Kazushi Asamura[2], Reiko Nomura[3], Yasunobu Ogawa[4], Keisuke Hosokawa[5], Yoshizumi Miyoshi[6], Takefumi Mitani[2], Taku Namekawa[1,2], Takeshi Sakanoi[7], Mizuki Fukizawa[7], Naoshi Yagi[7], Satoshi Kasahara[1]

1. The University of Tokyo, 2. Institute of Space and Astronautical Science, Japan Aerospace Exploration Agency, 3. National Astronomical Observatory of Japan, 4. National Institute of Polar Research, 5. The University of Electro-Communications, 6. Institute for Space-Earth Environmental Research, Nagoya University, 7. Tohoku University

Energetic electrons significantly affect ionospheric dynamics and the long-term evolution of surfaces and atmospheres of planets and moons. Since the energetic electron flux is not necessarily isotropic, it is important to cover the broad solid angle to quantitatively evaluate the effects on solar system bodies. With future planetary explorations in mind, we developed the medium-energy (20 - 100 keV) electron detector (MED) which can cover almost 2-pi steradian without the spacecraft spin. In order to test the performance of this analyzer in the relevant environment, we participated in the PARM mission, which aimed to measure electron precipitation using NASA’s sounding rocket RockSat-XN. In this presentation we report on MED observation results obtained through the flight on 13 January 2019.

©2019. Japan Geoscience Union. All Right Reserved.

Auroral substorm onset in satellite-based global images and ground-based all-sky images

*Akimasa Ieda[1], Kirsti Kauristie[2], Yukitoshi Nishimura[3], Yukinaga Miyashita[4], Harald U Frey[5], Liisa Juusola[2], Daniel Whiter[6], Masahito Nose[7], Matthew O Fillingim[5], Farideh Honary[8], Neil C Rogers[8], Yoshizumi Miyoshi[1], Shinobu Machida[1]

1. Institute for Space-Earth Environmental Research, Nagoya University, 2. Finnish Meteorological Institute, 3. Boston university, 4. Korea Astronomy and Space Science Institute, 5. University of California Berkeley, 6. University of Southampton, 7. Graduate School of Science, Kyoto University, 8. Lancaster University

Substorm onset has originally been defined as a longitudinally extended sudden auroral brightening (Akasofu initial brightening: AIB) followed a few minutes later by an auroral poleward expansion in ground-based all-sky images (ASIs). In contrast, such clearly marked two-stage development has not been evident in satellite-based global images (GIs). Instead, substorm onsets have been identified as localized sudden brightenings that expand immediately poleward.
To resolve these differences, optical substorm onset signatures in GIs and ASIs are compared in this study for a substorm that occurred on December 7, 1999. For this substorm, the Polar satellite ultraviolet global imager was operated with a fixed-filter (170 nm) mode, enabling a higher time resolution (37 s) than usual to resolve the possible two-stage development. These data were compared with 20-s resolution green-line (557.7 nm) ASIs at Muonio in Finland. The ASIs revealed the AIB at 2124:50 UT and the subsequent poleward expansion at 2127:50 UT, whereas the GIs revealed only an onset brightening that started at 2127:49 UT.
Thus, the onset in the GIs was delayed relative to the AIB and in fact agreed with the poleward expansion in the ASIs. The fact that the AIB was not evident in the GIs may be attributed to the limited spatial resolution of GIs for thin auroral arc brightenings. The implications of these results for the definition of substorm onset are discussed herein.

Keywords: substorm, auroral breakup, aurora

©2019. Japan Geoscience Union. All Right Reserved.

Original substorm onset (Akasofu 1964; 2010)

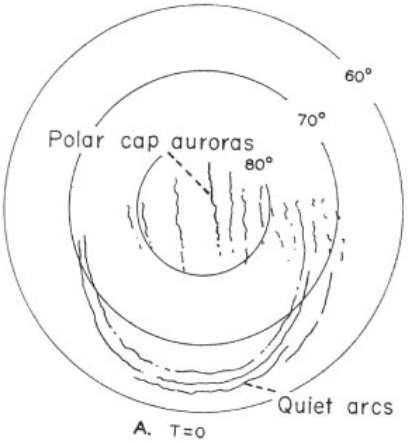


FIG. 2. THE DISTRIBUTION OF THE AURORAS DURING THE QUIET PHASE.

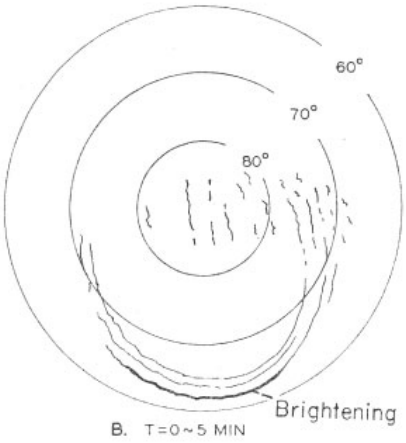


FIG. 3. AURORAS DURING THE EXPANSIVE PHASE (STAGE I).

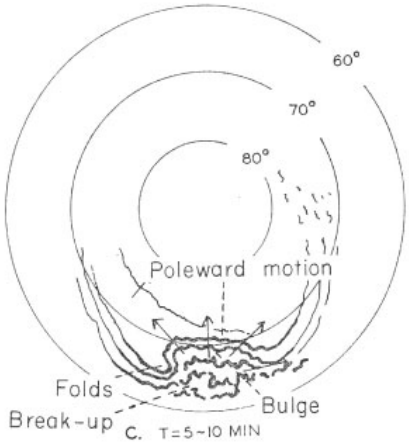


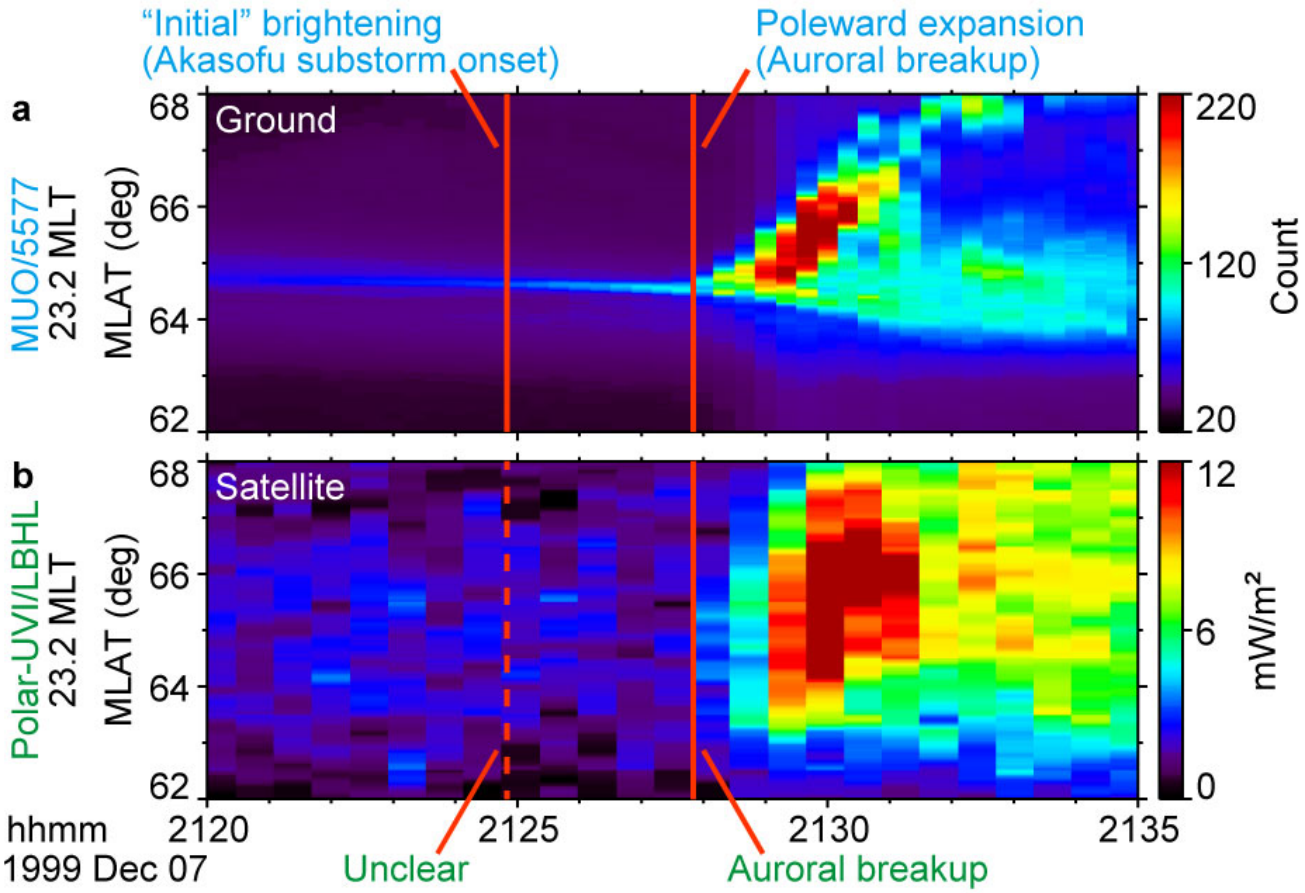
FIG. 4. AURORAS DURING THE EXPANSIVE PHASE (STAGE II).

a Time < 0
Before onset
Quiet arc

b T = 0 ~ 5 min
Expansion phase stage 1
Initial brightening
T = 0: Substorm onset

c T = 5 ~ 10 min
Expansion phase stage 2
Poleward expansion
(Auroral breakup)

Ground and satellite observations (Ieda et al. 2018: 10.1186/s40623-018-0843-3)



©2019. Japan Geoscience Union. All Right Reserved.

Automatic Classification of Auroral images using optical flow feature

*Naoto Kashiwagi[1], Akiko Fujimoto[1], Terumasa Tokunaga[1], Yoshizumi Miyoshi[2], Yasunobu Ogawa[3], Keisuke Hosokawa[4]

1. Kyushu Institute of Technology, 2. Nagoya University, 3. National Institute of Polar Research, 4. The University of Electro-Communications

The machine learning technique including the deep learning has been developed and the practical uses have increased on various field. On the study of auroral detection, the concern over the automatic image classification has risen using the approach of machine learning technique for the large statistical analysis of auroral images. The automatic auroral image classification has tried to use some techniques from computer vision, machine vision and pattern recognition. There are roughly two kinds of the selected feature: the color of image and the motion of aurora image sequences. The works based on the color feature of aurora image have been performed by Rao et al. (2014) and Tanaka et al. (2015). Rao et al. (2014) performed Support Vector Machines (SVM) classification with several local feature extraction techniques, and found that Scale Invariant Feature Transform (SIFT), OpponentSIFT, is the most effective feature for the automated classification of color aurora images. Tanaka et al. (2015) used the aurora area using the HSV model. They mentioned that it is difficult to classify the images including the diffuse aurora and cloud area. The color feature work well for the color auroral image, while the gray-scale (optically filtered) auroral images need other features on the automated classification. Blixt et al. (2006) applied the optical flow estimation to auroral image sequences. Their case study showed the useful tool for representing the motion of the aurora. In this study, we validate the optical flow estimation to extract the feature of auroral image, and automatically classify the large gray-scale auroral images using the machine learning with Convolution Neural Network (CNN). We use 63,486 gray-scale aurora images in total and use five categories for the preparation of supervised learning data, 1) aurora, 2) aurora and cloudy, 3) aurora and moon, 4) aurora, cloudy and moon, 5) noaurora. We perform the Hold-out and the Cross Validation to evaluate our classification performance. We obtained 98.58% of the classification accuracy based on Hold-out and 98.47% of the classification accuracy based on Cross Validation.

Keywords: Aurora, Optical flow, Convolution Neural Network

©2019. Japan Geoscience Union. All Right Reserved.

Fine-scale visualization of aurora in a wide area using color digital camera images from the International Space Station

*Sota Nanjo[1], Yuta Hozumi[1], Keisuke Hosokawa[1]

1. The University of Electro-Communications

Various ground-based and space-based imagers have been used to observe aurora borealis and australis. So far, however, it has been difficult to observe the detailed spatial structure of auroras in a wide area with sufficient spatial and temporal resolution. Since the photographs taken from the International Space Station (ISS) have sufficient spatial and temporal resolution, it is possible to visualize the fine-scale structures of aurora in a wide area. A calibration of imaging parameters of the photographs using star lights was proposed by a previous research. The accuracy in the timestamp was not guaranteed by the method based on the star lights because the position of the star lights in the image did not change with elapsed time. Thus, it is still difficult to use the mapped data for studying fast variations of aurora, for example pulsating aurora (PsA). Therefore, in this study, we calibrated the images from the ISS using city lights which change their apparent positions with elapsed time. In order to validate the calibration method using city light positions, we mapped two PsA events in the photographs to the geographical coordinate, and compared with those from ground-based all-sky imagers in Alaska and Canada. We found that the approximate shape of discrete aurora and the temporal variation of PsA derived from the ISS images are consistent with those from the ground-based observation. The accuracy in the timestamp is less than 0.5 sec and that in space in the direction perpendicular to the line of sight of the camera is within 5 km. In the presentation, we will also address how the mapped full-color images can be used for studies of PsA in the future work.

Keywords: aurora, ISS

©2019. Japan Geoscience Union. All Right Reserved.

PARM: Investigation of precipitating high-energy electrons into the auroral ionosphere with sounding rockets

*Kazushi Asamura[1], Yoshizumi Miyoshi[2], Keisuke Hosokawa[3], Takefumi Mitani[1], Taku Namekawa[1,5], Takeshi Sakanoi[4], Naoshi Yagi[4], Mizuki Fukizawa[4], Genki Ishizawa[4], Satoshi Kasahara[5], Shin Sugo[5], Oya Kawashima[5], Reiko Nomura[6], Masahito Nose[2], Mariko Teramoto[2], Yasunobu Ogawa[7], Shinji Saito[2], Ryoichi Fujii[8]

1. ISAS / JAXA, 2. ISEE, Nagoya University, 3. The University of Electro-Communications, 4. Tohoku University, 5. The University of Tokyo, 6. NAOJ / NINS, 7. NiPR / ROIS, 8. ROIS

Bursty precipitations of high-energy electrons into the polar ionopshere have been observed by low-altitude satellite, for example, SAMPEX and FIREBIRD II. These precipitations, called microburst, may contribute to the loss of the terrestrial radiation belt through the collisional energy loss with the dense, cold atmospheric particles. Recent numerical simulations successfully reproduce these microburst precipitations with a few Hz modulations by taking into account the pitch angle scattering with the whistler chorus elements at off-equator regions in the inner magnetosphere. Therefore, one can expect that the miscroburst precipitations have properties depending on auroral activities especially the pulsating auroras. In order to investigate the mechanisms of the microburst precipitations by in-situ observations, we are developing two instrument packages: PARM (Pulsating AuRora and Microbursts; already developed) and PARM-2 (being developed), both of which are designed suitable for sounding rocket experiments. PARM consists of four sensors; HEP (high-energy electron energy spectrometer), MED (medium-energy electron detector), AIC (auroral camera), and AFG (ASIC-based fluxgate magnetometer). PARM was onboard the NASA's RockSat-XN sounding rocket, and launched from Andoya, Norway at 09:13UT, Jan 13, 2019. On the other hand, PARM-2 is under development. It consists of HEP, two AICs, and MIM (magneto-impedance magnetometer). PARM-2 is to be onboard the NASA's LAMP sounding rocket which will fly from Poker Flat, Alaska in the period between the end of 2019 and the beginning of 2020.

We will present the overview of PARM missions including the initial results of RockSat-XN/PARM with ground-based observations and preparation status of LAMP/PARM-2.

Keywords: electron microburst precipitation, sounding rocket, pulsating aurora

©2019. Japan Geoscience Union. All Right Reserved.

[E] Poster | P (Space and Planetary Sciences)：P-EM Solar-Terrestrial Sciences, Space Electromagnetism & Space Environment

Wed. May 29, 2019 5:15 PM - 6:30 PM JST | Wed. May 29, 2019 8:15 AM - 9:30 AM UTC | Poster Hall International Exhibition Hall8, Makuhari Messe_5

[P-EM11] Dynamics of Magnetosphere and Ionosphere

convener:Aoi Nakamizo(Applied Electromagnetic Research Institute, National Institute of Information and Communications Technology), Mitsunori Ozaki(Faculty of Electrical and Computer Engineering, Institute of Science and Engineering, Kanazawa University), Akiko Fujimoto(Kyushu Institute of Technology), Tomoaki Hori(Institute for Space-Earth Environmental Research, Nagoya University)

This session provides an opportunity to present recent results from satellite and ground-based observations and theoretical and simulation studies on the magnetosphere, ionosphere, and their coupling processes. We invite talks and posters discussing various phenomena related to the magnetosphere-ionosphere system: solar wind-magnetosphere interaction, magnetosphere-ionosphere convection, field-aligned current, magnetic storms/substorms, neutral-plasma interaction, ionospheric ion inflow and outflow, aurora phenomena, and so forth. Discussions on planetary and satellite ionosphere and magnetospheres, future missions and instrument developments are also welcome.

[PEM11-P01] Effects of Inclination/Rotation of Earth's Magnetic Axis on Magnetosphere Simulated by Global MHD Model

*Aoi Nakamizo[1] (1.Applied Electromagnetic Research Institute, National Institute of Information and Communications Technology)

[PEM11-P02] Asymmetric deformation of the magnetosphere under low-density solar wind

*Masaki N Nishino[1,2], Yoshifumi Saito[2], Kazuo Shiokawa[1], Masaki Fujimoto[2] (1.Institute for Space-Earth Environmental Research, Nagoya University, 2.JAXA/ISAS)

[PEM11-P03] New perspectives on coupling processes in solar-terrestrial system obtained by comprehensive data analysis

*Yoshimasa Tanaka[1], Norio Umemura[2], Shuji Abe[3], Satoru UeNo[4], Masahito Nose[2], Yumi Nakagawa[5] (1.National Institute of Polar Research, 2.Institute for Space-Earth Environmental Research, Nagoya University, 3.International Center for Space Weather Science and Education, 4.Kwasan & Hida Observatories, School of Science, Kyoto University, 5.Ibaraki University)

[PEM11-P04] The interaction between the magnetosphere-ionosphere compound system and the magnetic field topology

*Shigeru Fujita[1], Takashi Tanaka[2], Masakazu Watanabe[2] (1.Meteorological College, Japan Meteorological Agency/ Nationa Institute of Polar Research, 2.Kyushu University)

[PEM11-P05] Effects of the dipole tilt and the interplanetary magnetic field Bx component on the dawn-dusk and interhemispheric asymmetries of the interchange convection cycle

*Masakazu Watanabe[1,2], Takashi Tanaka[2], Shigeru Fujita[3,4] (1.Graduate School of Science, Kyushu University, 2.International Center for Space Weather Science and Education, Kyushu University, 3.Meteorological College, 4.National Institute of Polar Research)

[PEM11-P06] Transient polar ionospheric convection response to negative dynamic pressure pulse

*Jianjun Liu[1] (1.Polar Research Institute of China)

[PEM11-P07] An active ionosphere: a new perspective of field line dipolarization

*Osuke Saka[1] (1.Office Geophysik)

[PEM11-P08] Toward the automatic identification of FLR signals in the SuperDARN data by using the gradient method

*Hideaki Kawano[1,2], Akira Sessai Yukimatu[3,4], Nozomu Nishitani[5], Yoshimasa Tanaka[3,4], Satoko Saita[6], Tomoaki Hori[5] (1.Dept. Earth Planet. Sci., Kyushu Univ., 2.ICSWSE, Kyushu University, 3.National Institute of Polar Research, 4.SOKENDAI, 5.ISEE, Nagoya University, 6.Kitakyushu College)

[PEM11-P09] A statistical study of Pi2 pulsations observed in the upper ionosphere using Swarm magnetic field data

*Park Jaehee[1], Khan-Hyuk Kim[1], Junga Hwang[2] (1.School of Space Research, Kyung Hee University, Gyeonggi, South Korea, 2.Korea Astronomy and Space Science Institute, Daejeon,South Korea)

[PEM11-P10] Study on the global distribution characteristics of Pc 1-2 geomagnetic pulsation with the 10Hz data of the MAGDAS system

*Taisei Kabasawa[1], Akimasa Yoshikawa[1], Teiji Uozumi[1], Akiko Fujimoto[1], Shuji Abe[1] (1.Kyushu University)

[PEM11-P11] In-situ Observations of Reconnection Separatrix Regions in the near-Earth Magnetotail

*Mizuho Araki[1], Masahiro Hoshino[1], Kunihiro Keika[1], Yoshifumi Saito[2] (1.Graduate School of Science, The University of Tokyo, 2.Institude of Space and Astronautical Science)

[PEM11-P12] Flow speed dependence of ion temperature, electron temperature, and their ratio in the near-Earth magnetotail reconnection region

*Kaori Watanabe[1], Masahiro Hoshino[1], Kunihiro Keika[1], Yoshifumi Saito[2], Naritoshi Kitamura[1] (1.Univ. of Tokyo, 2.ISAS/JAXA)

[PEM11-P13] **Examining Minimum Cyclotron Resonant Electron Energy of EMIC Waves with MMS**

*Si Liu[1] (1.Changsha University of Science and Technology)

[PEM11-P14] Small scale whistler mode waves near the magnetic field intensity minimum in the magnetosheath

*Naritoshi Kitamura[1], Takanobu Amano[1], Yoshiharu Omura[2], Satoko Nakamura[2], Chika Umegaki[1], Scott A Boardsen[3,4], Narges Ahmadi[5], Robert E Ergun[5], Olivier Le Contel[6], Per-Arne Lindqvist[7], Yoshifumi Saito[8], Shoichiro Yokota[9], Daniel J Gershman[3], Barbara L Giles[3], Thomas E Moore[3], William R Paterson[3], Craig J Pollock[10], Christopher T Russell[11], Robert J Strangeway[11], James L Burch[12] (1.Department of Earth and Planetary Science, Graduate School of Science, The University of Tokyo, 2.Research Institute for Sustainable Humanosphere, Kyoto University, 3.NASA Goddard Space Flight Center, 4.University of Maryland, 5.Laboratory for Atmospheric and Space Physics, University of Colorado, 6.Laboratoire de Physique des Plasmas, UMR7648 CNRS/Ecole Polytechnique/UPMC/Université Paris-Sud/Observatoire de Paris, 7.Royal Institute of Technology, 8.Institute of Space and Astronautical Science, Japan Aerospace Exploration Agency, 9.Department of Earth and Space Science, Graduate School of Science, Osaka University, 10.Denali Scientific, 11.Institute of Geophysics and Planetary Physics, University of California, Los Angeles, 12.Southwest Research Institute)

[PEM11-P15] Spatial characteristics of the internal modulation of pulsating aurora: multi-point high-speed optical observations in Scandinavia

*Yuki Kawamura[1], Keisuke Hosokawa[1], Shin-ichiro Oyama[2,3], Yoshizumi Miyoshi[2], Yasunobu Ogawa[3], Satoshi Kurita[2], Satoshi Ebukuro[1], Ryoichi Fujii[4] (1.Department of Communication Engineering and Informatics, University of Electro-Communications, 2.Institute for Space-Earth Environmental Research, Nagoya University, 3.National Institute of Polar Research, 4.Research Organization of Information and Systems)

[PEM11-P16] **Large-scale characteristics of pulsating aurora periodicities:multi-point high-speed optical observations in Scandinavia**

*Satoshi Ebukuro[1], Keisuke Hosokawa[1], Shin-ichiro Oyama[2,3,5], Yoshizumi Miyoshi[2], Yasunobu Ogawa[3], Satoshi Kurita[2], Yuki Kawamura[1], Ryoichi Fujii[4] (1.Department of Communication Engineering and Informatics, University of Electro-Communications, 2.Institute for Space-Earth Environmental Research, Nagoya University, 3.National Institute of Polar Research, 4.Research Organization of Information and Systems, 5.University of Oulu)

[PEM11-P17] Variations of cosmic noise absorption (CNA) by energetic electron precipitation (EEP) and changes of the auroral morphology

*Miyamoto Taishiro[1], Shin-ichiro Oyama[1,4,5], Yasunobu Ogawa[2], Keisuke Hosokawa[3], Satoshi Kurita[1], Yoshizumi Miyoshi[1], Ryuho Kataoka[2], Hiroshi Miyaoka[2], Tero Raita[4] (1. Institute for Space-Earth Environmental Research,Nagoya University, 2.National Institute of Polar Research, 3.Department of Communication Engineering and Informatics, University of Electro-Communications, 4.Sodankylä Geophysical Observatory, University of Oulu, 5.Ionosphere Research Unit, University of Oulu)

[PEM11-P18] Spatiotemporal characteristics on the source region of flash aurora using ray tracing analysis

*Tomohiro Inoue[1], Mitsunori Ozaki[1], Yoshitaka Goto[1], Satoshi Yagitani[1], Yoshiya Kasahara[1], Kazuo Shiokawa[2], Yoshizumi Miyoshi[2], Ryuho Kataoka[3], Yusuke Ebihara[4] (1.Kanazawa University , 2.Nagoya University, 3.National Institute of Polar Research, 4.Kyoto University)

[PEM11-P19] Molecular ion supply mechanisms from the low-altitude ionosphere to magnetosphere observed by EISCAT and Arase(ERG)

*Masayoshi Takada[1], Kanako Seki[1], Yasunobu Ogawa[2], Kunihiro Keika[3], Satoshi Kasahara[4], Shoichiro Yokota[5], Tomoaki Hori[7], Kazushi Asamura[6], Yoshizumi Miyoshi[7] (1.Graduate School of Science, Tokyo University, 2.National Institute of Polar Research, 3.Department of Earth and Planetary Science, Graduate School of Science, Tokyo University, 4.The University of Tokyo, 5.Graduate School of Science, Osaka University, 6.Institute of Space and Astronautical Science, Japan Aerospace Exploration Agency, 7.Institute for Space-Earth Environmental Research, Nagoya University)

[PEM11-P20] Optical and radar observation of the dynamic auroral forms

*Yunosuke Nagafusa[1], Tima Sergienko[2], Satoshi Taguchi[1], Urban Braendstroem[2], Masatoshi Yamauchi[2] (1.Graduate School of Science, Kyoto University, 2.Swedish Institute of Space Physics, Kiruna)

[PEM11-P21] Observations of MF/HF auroral radio emissions at three ground-based stations

*Yuka Sato[1], Atsushi Kumamoto[2], Yuto Katoh[2], Akira Kadokura[3,4], Yasunobu Ogawa[3,4], Atsuki Shinbori[5] (1.Nippon Institute of Technology (NIT), 2.Graduate School of Science, Tohoku University, 3.National Institute of Polar Research (NIPR), 4.The Graduate University for Advanced Studies, 5.Institute for Space-Earth Environmental Research (ISEE), Nagoya University)

[PEM11-P22] **Ionospheric F-region Drift Measurements Derived from DPS-4D at Zhongshan Station, Antarctic**

*Xiangcai Chen[1] (1.Polar Research Institute of China)

[PEM11-P23] PARM-HEP Observation of Precipitating High Energy Electrons over Pulsating Aurora

*Taku Namekawa[1], Takefumi Mitani[2], Kazushi Asamura[2], Yoshifumi Saito[2] (1.Department of Earth and Planetary Science, Graduate school of Science, The University of Tokyo, 2.Institute of Space and Astronautical Science, Japan Aerospace Exploration Agency)

[PEM11-P24] Development of the medium-energy electron detector with hemispherical field-of-view and the flight test in the PARM (Pulsating AuRora and Microburst) mission

*Shin Sugo[1], Oya Kawashima[1], Kazushi Asamura[2], Reiko Nomura[3], Yasunobu Ogawa[4], Keisuke Hosokawa[5], Yoshizumi Miyoshi[6], Takefumi Mitani[2], Taku Namekawa[1,2], Takeshi Sakanoi[7], Mizuki Fukizawa[7], Naoshi Yagi[7], Satoshi Kasahara[1] (1.The University of Tokyo, 2.Institute of Space and Astronautical Science, Japan Aerospace Exploration Agency, 3.National Astronomical Observatory of Japan, 4.National Institute of Polar Research, 5.The University of Electro-Communications, 6.Institute for Space-Earth Environmental Research, Nagoya University, 7.Tohoku University)

[PEM11-P25] Auroral substorm onset in satellite-based global images and ground-based all-sky images

*Akimasa Ieda[1], Kirsti Kauristie[2], Yukitoshi Nishimura[3], Yukinaga Miyashita[4], Harald U Frey[5], Liisa Juusola[2], Daniel Whiter[6], Masahito Nose[7], Matthew O Fillingim[5], Farideh Honary[8], Neil C Rogers[8], Yoshizumi Miyoshi[1], Shinobu Machida[1] (1.Institute for Space-Earth Environmental Research, Nagoya University, 2.Finnish Meteorological Institute, 3.Boston university, 4.Korea Astronomy and Space Science Institute, 5.University of California Berkeley, 6.University of Southampton, 7.Graduate School of Science, Kyoto University, 8.Lancaster University)

[PEM11-P26] Automatic Classification of Auroral images using optical flow feature

*Naoto Kashiwagi[1], Akiko Fujimoto[1], Terumasa Tokunaga[1], Yoshizumi Miyoshi[2], Yasunobu Ogawa[3], Keisuke Hosokawa[4] (1.Kyushu Institute of Technology, 2.Nagoya University, 3.National Institute of Polar Research, 4.The University of Electro-Communications)

[PEM11-P27] Fine-scale visualization of aurora in a wide area using color digital camera images from the International Space Station

*Sota Nanjo[1], Yuta Hozumi[1], Keisuke Hosokawa[1] (1.The University of Electro-Communications)

[PEM11-P28] Geospace Imaging via the soft X-ray imager: GEO-X mission

*Yoshizumi Miyoshi[1], Yuichiro Ezoe[2], Satoshi Kasahara[3], Yosuke Matsumoto[4], Kumi Ishikawa[5], Ryuho Kataoka[6], Hiroki Ito[1], Daiki Ishi[2], Masaki Numazawa[2], Atsushi Yamazaki[5], Hiroshi Hasegawa[5], Masaki Fujimoto[5], Kazuhisa Mitsuda[5] (1.Institute for Space-Earth Environmental Research, Nagoya University, 2.Tokyo Metropolitan University, 3.University of Tokyo, 4.Chiba University, 5.ISAS/JAXA, 6.NIPR)

Effects of Inclination/Rotation of Earth's Magnetic Axis on Magnetosphere Simulated by Global MHD Model

*Aoi Nakamizo[1]

1. Applied Electromagnetic Research Institute, National Institute of Information and Communications Technology

Recently, we have shown that the ionospheric Hall conductance distribution, owing to the polarization field generated by its nonuniformity, largely control the magnetospheric configuration and dynamics by using a global MHD model. The effects of the ionospheric conductance on the magnetosphere were also reported by previous studies based on other global models; for example, the current-voltage relationship in the solar wind-magnetosphere-ionosphere [Fedder and Lyon, 1987] and the plasma pressure distribution in the near-Earth region [Ridley et al., 2004]. These studies indicate that the ionospheric conductance is one of the most important settings in the global models to accurately simulate the magnetosphere.

On the other hand, in the development/improvement of the global MHD model in NICT, which was originally developed by Tanaka [1994] and Tanaka et al. [2010], introducing the inclination and rotation of Earth's magnetic axis with respect to the rotation axis has been remained as one of the most difficult problems. In other words, in the present model, the precession between the magnetic axis and the rotation axis is not included. This means that the simulated magnetosphere will show a different structure and temporal development than the actual magnetosphere.

We, for the first time, equivalently introduce the precession by rotating the background conductance distribution due to solar illumination (i.e., depending on the geographic coordinate) with respect to the geomagnetic coordinate. (Improvement of the conductance setting in the auroral region is the next challenge.) In this paper, we will show how the simulated magnetosphere is changed by this improvement, focusing on the near-Earth plasma environment.

Keywords: M-I Coupling, Global MHD Simulation, Ionospheric Effect

©2019. Japan Geoscience Union. All Right Reserved.

Asymmetric deformation of the magnetosphere under low-density solar wind

*Masaki N Nishino[1,2], Yoshifumi Saito[2], Kazuo Shiokawa[1], Masaki Fujimoto[2]

1. Institute for Space-Earth Environmental Research, Nagoya University, 2. JAXA/ISAS

The density of the solar wind around the Earth's magnetosphere sometimes decreases to only several percent of the usual value, and such density extrema results in a significant reduction of dynamic pressure and Alfvenic Mach number of the solar wind flow. While simple expansion of the Earth's magnetosphere by the low dynamic pressure was assumed in previous studies, a global-MHD simulation study predicted a remarkable dawn-dusk asymmetry of the magnetosphere in shape under low-density solar wind and Parker-spiral IMF configuration. Here we present evidence of asymmetric deformation of the magnetosphere under low-density solar wind and Parker-spiral IMF conditions, based on several events of GEOTAIL observations. As predicted by the global-MHD simulation, the magnetosphere on the dawnside expands much further than the magnetopause location of simple (symmetric) expansion, while no significant expansion is detected in the dusk tail flank. Fast ion beams detected at the flank magnetopause suggest that magnetic reconnection frequently occurs due to the low-beta environment of the magnetosheath.

Keywords: Low density solar wind, Magnetosphere, Plasma transport

©2019. Japan Geoscience Union. All Right Reserved.

New perspectives on coupling processes in solar-terrestrial system obtained by comprehensive data analysis

*Yoshimasa Tanaka[1], Norio Umemura[2], Shuji Abe[3], Satoru UeNo[4], Masahito Nose[2], Yumi Nakagawa[5]

1. National Institute of Polar Research, 2. Institute for Space-Earth Environmental Research, Nagoya University, 3. International Center for Space Weather Science and Education, 4. Kwasan & Hida Observatories, School of Science, Kyoto University, 5. Ibaraki University

In the Earth’ s upper atmosphere above 60 km, including magnetosphere and ionosphere, various phenomena are generated by energy inputs from solar radiation (including solar wind) and atmospheric waves propagating from the lower atmosphere. Thus, comprehensive analysis of various kinds of satellite and ground-based observational data using advanced methods is required to understand physical mechanism of the phenomena. For such interdisciplinary studies, it is important to share data distributed across many universities and institutes and use advanced tools, such as metadata database for cross-searching a variety of datasets and analysis software for analyzing various types of data in an integrated fashion. In fact, many scientific papers on the upper atmosphere have recently been obtained by comprehensive analysis of various data with such analysis tools.
We present some examples of scientific results achieved by comprehensively analyzing data from multiple regions. These examples include the effect of solar coronal holes on the Earth’ s geomagnetic activity and the interaction between solar wind, magnetosphere, ionosphere and neutral atmosphere. The former study investigated long-term trends of coronal boles, solar wind parameters, and Earth’ s geomagnetic indices during two solar cycles. It showed the possibility that the solar wind speed and geomagnetic activities may be controlled by the size and latitudinal distribution of coronal holes. The latter analyzed multi-instrument data simultaneously obtained from interplanetary space, magnetosphere, and ionosphere and mesosphere in both northern and southern hemispheres. They newly found that the polar mesosphere is affected by relativistic electron precipitation caused by the interaction with magnetospheric plasma waves during the high-speed solar wind stream. These studies demonstrate that sharing and comprehensive analysis of long-term, multiple-sphere, and multi-instrument data using sophisticated tools are very effective to produce scientific outcomes. At present there are data gap areas in the Asia and African regions. Therefore, we believe that filling in the data gap by international collaborations could be a breakthrough for unsolved issues in the upper atmosphere.

Keywords: upper atmosphere, coupling between multiple regions, comprehensive analysis, long-term observational data

©2019. Japan Geoscience Union. All Right Reserved.

The interaction between the magnetosphere-ionosphere compound system and the magnetic field topology

*Shigeru Fujita[1], Takashi Tanaka[2], Masakazu Watanabe[2]

1. Meteorological College, Japan Meteorological Agency/ Nationa Institute of Polar Research, 2. Kyushu University

The steady convection in the magnetosphere-ionosphere coupling system is composed of the following self-consistent elementary processes; dynamo in the cusp-mantle region, the field-perpendicular current system in the magnetosphere, the field-aligned current system connecting the ionosphere, the ionospheric electric field, the magnetospheric convection corresponding to the ionospheric electric field, and the high plasma pressure distribution in the cusp region [Tanaka, 2007].

The energy of the convection is transported from the solar wind across the magnetopause where the magnetic field configures the null-separator structure. Since the magnetic field configuration of the null-separator structure is originally derived from the superposition of two scalar fields [Stern, 1973], say, the dipole field and the uniform field, the magnetic field of the null-separator would not have free energy necessary for plasma acceleration. However, the simulation reveals that the magnetic field has a tension force near the null point. Therefore, we need a mechanism that transports the energy to this region.

It is revealed from the simulation that the bow shock supplies the energy. Indeed, the current from the bow shock deforms the magnetic field of the null-separator structure. In addition, it is noted that the Chapman-Ferraro current also deforms the magnetic field configuration in the magnetopause. This fact indicates that the convection system in the magnetosphere contributes to deformation of the null-separator structure. That is to say, energy transport from the solar wind to the magnetosphere-ionosphere compound system is affected by the physical processes in the convection. Therefore, as a result of the interaction between the magnetosphere-ionosphere convection and the null-separator structure, the magnetosphere-ionosphere compound system can be extended to the solar wind-magnetosphere-ionosphere compound system.

References

T. Tanaka (2007), Magnetosphere-Ionosphere Convection as a Compound System, Space Sci Rev, 133, 1-72, DOI 10.1007/s11214-007-9168-4.

Stern, D. P. (1973), A study of the electric field in an open magnetospheric model, J. Geophys. Res., 78(31), 7292-7305, doi:10.1029/JA078i031p07292.

Keywords: global MHD simulation, compound system

©2019. Japan Geoscience Union. All Right Reserved.

Effects of the dipole tilt and the interplanetary magnetic field Bx component on the dawn-dusk and interhemispheric asymmetries of the interchange convection cycle

*Masakazu Watanabe[1,2], Takashi Tanaka[2], Shigeru Fujita[3,4]

1. Graduate School of Science, Kyushu University, 2. International Center for Space Weather Science and Education, Kyushu University, 3. Meteorological College, 4. National Institute of Polar Research

The interchange cycle is a mode of magnetic flux circulation that appears for periods of northward interplanetary magnetic field (IMF). It is made up of IMF-to-open reconnection in one hemisphere and open-to-closed reconnection in the other hemisphere. The two reconnection processes have the same topological nature in that the roles of the two reconnecting field lines interchange at the time of reconnection. The interchange cycle is characterized by reciprocation of open magnetic flux between the two hemispheres. One observable signature of the interchange cycle is an appearance of a reverse cell circulating in the closed field line region of the ionosphere, which is named the “reciprocal cell.” The reciprocal cell appears in the open-to-closed reconnection hemisphere, whereas in the opposite IMF-to-open reconnection hemisphere, there appears a lobe cell circulating exclusively on open field lines. For given (1) IMF By, (2) IMF Bx, and (3) dipole tilt conditions, two interchange cycles concur, one on the dawnside and the other on the duskside. For an ideal case, one can easily expect the mode of the interchange cycles to occur. For example, for the case of due northward IMF with significant dipole tilt, the twin reverse cells in the summer hemisphere are both lobe cells, while in the winter hemisphere the twin reverse cells are both reciprocal cells. For the general case, however, one cannot predict the mode of the interchange cycles without quantitative modeling. The purpose of this study is to examine how the presence of dipole tilt or IMF Bx alters the dawn-dusk and north-south pattern of the twin reverse cells. For this purpose, we perform numerical magnetohydrodynamic simulations using the REPPU (Reproduce Plasma Universe) code developed by T. Tanaka. In the presentation, we discuss the dipole tilt and IMF Bx effects revealed by the numerical modeling.

Keywords: ionospheric convection, interchange reconnection, reciprocal cell

©2019. Japan Geoscience Union. All Right Reserved.

Transient polar ionospheric convection response to negative dynamic pressure pulse

*Jianjun Liu[1]

1. Polar Research Institute of China

The response of the high latitude ionospheric convection to a sudden decrease in solar wind dynamic pressure provides a unique opportunity to investigate how the solar wind couples to the dayside magnetosphere and ionosphere. Here, the event shows three IMF components do not have prominent changes, but the solar wind plasma went down to near zero magnitude, which leads to very weak solar wind driving during northward IMF. However, ionospheric convection observed by SuperDARN radars showed enhanced plasma flow speed in the central polar cap region just after the negative pressure pulse arrival to the magnetosphere. Simultaneous convection map generated by SuperDARN measurement presents enlarged convection cell with obvious equatorward moving Heppner-Maynard boundary. It is noted that cross polar cap potential enhanced instantly and this enhanced feature continued almost 10 min. The distribution of total electron content (TEC) exhibited typical auroral oval signature especially on dayside ionosphere, TEC density in auroral oval showed a noticeable decrease after the arrival of the negative pressure pulse. Both ionospheric convection and TEC distribution reveal that negative pressure pulse impacts the magnetosphere-ionosphere coupling system directly and dramatically. Moreover, the TIEGCM model also showed an enhanced polar potential pattern.

Keywords: Dynamic pressure, Ionospheric convection, Auroral oval

©2019. Japan Geoscience Union. All Right Reserved.

An active ionosphere: a new perspective of field line dipolarization

*Osuke Saka[1]

1. Office Geophysik

Transient westward electric fields from the magnetosphere generate equatorward plasma drifts of the order of kilometers per second in the auroral ionosphere. This flow channel extends in north-south directions and is produced in the initial pulse of Pi2 pulsations associated with the filed line dipolarization. Drifts in the ionosphere of the order of kilometers per second that accumulated plasmas at the low latitude end of the flow channel are of such large degree that possible vertical transport effects (including precipitation) along the field lines may be ignored. We suggest that plasma compression in the ionosphere implemented the ionosphere to be active. Active ionosphere generates field-aligned currents to satisfy the quasi-neutrality of the ionosphere, ion acoustic wave for ion outflows and the inverted-V type electron precipitations in the topside ionosphere, and poleward expansion of auroras due to a nonlinear evolution of the ionosphere. We will study auroral expansion in this acoustic regime.

Keywords: Substorm, Auroral substorm, Ionosphere

©2019. Japan Geoscience Union. All Right Reserved.

Toward the automatic identification of FLR signals in the SuperDARN data by using the gradient method

*Hideaki Kawano[1,2], Akira Sessai Yukimatu[3,4], Nozomu Nishitani[5], Yoshimasa Tanaka[3,4], Satoko Saita[6], Tomoaki Hori[5]

1. Dept. Earth Planet. Sci., Kyushu Univ., 2. ICSWSE, Kyushu University, 3. National Institute of Polar Research, 4. SOKENDAI, 5. ISEE, Nagoya University, 6. Kitakyushu College

The FLR (Field Line Resonance) takes place where the frequency of an incoming wave matches the eigen-frequency of magnetospheric magnetic field lines, and excites the eigen-oscillation of the field lines. The FLR can be identified by using the unique manner of change in the amplitude and the phase of thus excited eigen-oscillation across the resonant point. That is, the amplitude is maximum at the resonant point, and the phase changes the most steeply across the resonance point. The FLR-generated eigen-oscillations can be identified in the ground magnetic field data and the ionospheric plasma velocity data. From thus identified eigen-frequency ("FLR frequency" below) one can estimate the magnetospheric plasma density along the field line which passes through the ground/ionospheric observation point.

In this study we use the SuperDARN radar data to identify FLR: For each radar beam from each SuperDARN radar, the velocity of the ionospheric plasma flow along the line of sight (VLOS) of the beam is obtained; we use the VLOS data to identify the FLR and estimate the magnetospheric plasma density. Unlike the ground magnetometer data, the SuperDARN data is two-dimensional, enabling two-dimensional estimates of the magnetospheric equatorial plasma density and magnetospheric region identification.

To achieve that, it is important to identify as many FLR events as possible. Overwrapping of non-FLR waves/perturbations hides FLR events. As a countermeasure to this problem, the so-called gradient method has been applied to the ground magnetometer data; this method cancels out the overwrapping signals by dividing the data from a magnetometer by the data from another magnetometer having an adequate latitudinal distance from the other. The division yields the amplitude ratio and the phase difference. The gradient method is effective since the FLR frequency tends to depend on the latitude more strongly than the overwrapping signals.

The gradient method is also applicable to the SuperDARN VLOS data. The field of view of each beam is divided into Range Gates (RGs below) having the same length along the beam. The identification number of the RGs increases with increasing distance from the radar. The VLOS is obtained for each RG. Thus, each RG can be regarded as a "virtual observatory."

As an initial study, we have selected an FLR event which was identified in the VLOS data of a radar (at Hankasalmi) without the use of the gradient method, selected a beam, and selected a few pairs of RGs of the beam. We then have manually applied the gradient method to the VLOS data of the above-selected RG pairs, and successfully identified the FLR. In more detail, the identification has been successful only for two paired RGs whose RG numbers differs by two. This suggest that, since the length of the RG, mapped to the meridional plane, was about 40km for this event, about 80km distance was the best (with the resolution of 40km) for this event. This distance reflects the resonance width, which is an important quantity reflecting the diffusion and dissipation of the FLR energy.

©2019. Japan Geoscience Union. All Right Reserved.

In order to identify as many FLR events as possible, it is also important to automatically identify the FLR events, since visual identification is time-consuming. The gradient method enables automatic identification more easily than analyses of VLOS itself, since the gradient method yields peaks in both the amplitude ratio and the phase difference. We have started making a program for automatic identification by applying the gradient method to VLOS; the version at the time of this abstract has successfully identified FLRs for all of the above-stated pairs of RGs.

©2019. Japan Geoscience Union. All Right Reserved.

A statistical study of Pi2 pulsations observed in the upper ionosphere using Swarm magnetic field data

*Park Jaehee[1], Khan-Hyuk Kim[1], Junga Hwang[2]

1. School of Space Research, Kyung Hee University, Gyeonggi, South Korea, 2. Korea Astronomy and Space Science Institute, Daejeon,South Korea

The properties of Pi2 pulsations observed in the upper ionosphere are studied using magnetic field data acquired by the Swarm-A spacecraft in low Earth orbit (LEO) and at the low-latitude Bohyun ground station (BOH, L = 1,3) for January 2014-Jun 2015. From time intervals when Swarm-A was on the nightside (magnetic local time (MLT) = 1800-0600 hrs) and the BOH station was near midnight (MLT = 2100-0300 hrs), we identified 623 Pi2 events in the horizontal H component of the BOH data. For each event we examine the coherence between the horizontal H component on the ground and the B_x (radial) azimuthal B_y (azimuthal), or B_z (compressional) components at Swarm-A. Out of 623 events, the B_x-H high coherence (> 0.7) events are ~6%, the B_y-H high coherence events are ~4%, and the B_z-H high coherence events are ~25%. The ground-satellite high coherence events occurred when the spacecraft was located within a magnetic latitude range of ±50°. Using the ground-satellite high coherence events, we examined the latitudinal structure of the relative amplitude and phase of the ionospheric Pi2 pulsations detected at Swarm-A. Confirming previous observations at LEO, we found that the ionospheric Pi2 pulsations are characterized by symmetric odd mode standing oscillations in the north-south direction, having a node for B_x oscillation and an antinode for B_z oscillation, respectively, at the equator. This indicates that the source of ionospheric Pi2 pulsations is the plasmaspheric resonance.

Keywords: Pi2 pulsations

©2019. Japan Geoscience Union. All Right Reserved.

Study on the global distribution characteristics of Pc 1-2 geomagnetic pulsation with the 10Hz data of the MAGDAS system

*Taisei Kabasawa[1], Akimasa Yoshikawa[1], Teiji Uozumi[1], Akiko Fujimoto[1], Shuji Abe[1]

1. Kyushu University

The magnetic field observed on the ground is affected by the space weather phenomena such as magnetic storms and auroral storms.

The Pc1 geomagnetic pulsation (frequency range of 0.2-5.0 seconds) activated mainly around a high-latitude region is understood as a phenomenon accompanied by the excitation of EMIC waves to cause the particle acceleration in the equatorial region of the magnetosphere. Also, it is well known that Pc1 waves propagate horizontally in the ionospheric at the F layer. However, it is not clarified about the global occurrence and propagation properties of Pc1 geomagnetic pulsation on the ground. Moreover, although induction magnetometers are used to observe the high-frequency magnetic field disturbance phenomenon like Pc1 and Pc2 (frequency range of 5.0-10.0 seconds) geomagnetic pulsation, the global observation network with induction magnetometers covering from high-latitude to low-latitude area and equator domain does not exist at this stage. On the other hand, although it is common to use Fluxgate magnetometers for the observation of global space weather phenomenon, it is considered to be unsuitable for analysis of the high-frequency Pc1-2 geomagnetic pulsation because its time accuracy is usually one second value.

The ground multipoint magnetic field observation network which Kyushu University has developed (MAGDAS-9 magnetometer) acquire a 250Hz sampling and 10Hz mean data. Also, it is the only geomagnetic observation network that can investigate the global aspects of Pc1-2 geomagnetic pulsation.

In this study, we investigated the global distribution of Pc1-2 pulsation from polar region to equatorial region with magnetic field data provided by MAGDAS and Dst/AE index provided by the WDC for Geomagnetism, Kyoto. As a result, when the substorm have occurred during a magnetic storm time, generation of Pc1-2 pulsation from high-latitude to middle-and-low latitude region and further arrival of Pc2 pulsation to the dip-equator are identified. The elucidation of occurrence characteristic of the Pc1-2 pulsation on the ground with the EMIC waves excitation is very important not only for space weather application to be able to monitor particle energization process via EMIC excitation but also the elucidation of the super global coupling process from inner magnetosphere to the global ionosphere from polar to equatorial region. In this presentation, we will report the preliminary results of observational analysis of Pc1-2 pulsation by using MAGDAS network. We also discuss the comprehensive approach for understanding global coupling process among inner magnetosphere and high-middle-low latitude to the equatorial region by using FM-CW radar data, PWING induction magnetometer data, and the geo-space environment data from the ERG satellite.

Keywords: Pc1-2 pulsation, EMIC waves, global coupling

©2019. Japan Geoscience Union. All Right Reserved.

In-situ Observations of Reconnection Separatrix Regions in the near-Earth Magnetotail

*Mizuho Araki[1], Masahiro Hoshino[1], Kunihiro Keika[1], Yoshifumi Saito[2]

1. Graduate School of Science, The University of Tokyo, 2. Institude of Space and Astronautical Science

Magnetic reconnection which converts magnetic energy into thermal and kinetic energy of plasmas is an important physical mechanism of plasma heating and acceleration. Particularly in the Petschek-type reconnection, plasma acceleration and heating in the slow-mode shocks formed at the separatrices must be taken into consideration. The structure of the slow-mode shocks in the distant tail of the Earth’s magnetosphere was investigated with in-situ observations made by the GEOTAIL satellite (Saito et.al, 1995). It is observationally suggested that about 10% of the plasma sheet boundary layer (PSBL) is slow-mode shocks. It is, however, not fully understood what determines this percentage and what is the difference in the ion and electron temperature changes between slow-mode shocks and others separatrix regions.
In this study, we utilized multi-spacecraft in-situ observations of separatrix regions at magnetic reconnection in the near-Earth magnetotail (GSM-X is between ~13 and ~25RE). We used data obtained from FPI (Fast Plasma Investigation) and FGM (Fluxgate Magnetometer) on board the MMS satellite from June 1, 2017to August 31, 2017. We examined occurrence locations, ion flow directions and velocity of ion flow in downstream regions of observed events. We also examined changes in ion and electron temperatures and the ion-to-electron temperature ratio.

We classified their events into 2 types according to plasma beta in the in-flow regions: below 0.1 or around 1. We term them “lobe reconnection” and “plasma sheet reconnection”, respectively. In the former type, plasmas in the in-flow regions are cold and tenuous. In the latter type, plasmas in the in-flow regions are hot and dense. In both types, we observed increases in ion and electron temperatures increase, but their characteristics are different. In the lobe reconnection, ion temperatures increase from several hundred eV to several keV. In the plasma sheet reconnection, ion temperatures also increase from about 1 keV to several keV. The increase rate of the electron temperature is less than one order of magnitude for both types, smaller than that of the ion temperature; the electron temperature increases up to at most 1 keV. The ion-to-electron temperature ratio in the out-flow regions in both types is about 5 for both types. We then examined changes of the ion-to-electron temperature ratio and found that the changes are consistent with the result reported by Wang et al. (2012).

In this presentation, we will show the results of separatrix crossing events (both lobe and plasma sheet reconnection events) that occur in 2017 and 2018. We will identify whether each of the separatrices is a slow shock or not and how the separatrix conditions affect ion and electron heating. These characteristics will provide insights into heating mechanisms and energy conversion through separatrix regions.

Reference:

Yoshifumi Saito, Toshifumi Mukai, Toshio Terasawa, Atsuhiro Nishida, Shinobu Machida, Masafumi Hirahara, Kiyoshi Maezawa, Susumu Kokubun, and Tatsundo Yamamoto, Slow-mode shocks in the magneto, J. Geophys. Res., 100, A12, 23,567, 1995

©2019. Japan Geoscience Union. All Right Reserved.

Chih-Ping Wang, Matina Gkioulidou, Larry R. Lyons and Vassilis Angelopoulos, Spatial distributions of ion to electron temperature ratio in the magnetosheath and plasma sheet, J. Geophys. Res., 117, A08215, 2012

Keywords: Magnetic Reconnection, MMS satellite, Earth's Magnetotail

©2019. Japan Geoscience Union. All Right Reserved.

Flow speed dependence of ion temperature, electron temperature, and their ratio in the near-Earth magnetotail reconnection region

*Kaori Watanabe[1], Masahiro Hoshino[1], Kunihiro Keika[1], Yoshifumi Saito[2], Naritoshi Kitamura[1]

1. Univ. of Tokyo, 2. ISAS/JAXA

Plasma in the Earth's magnetotail are heated up to 1-10 keV and stored in the plasma sheet. One of the heating or acceleration mechanisms is the magnetic reconnection. Heated or accelerated plasma are transported both earthward and tailward as fast flow with a speed of several hundred kilometers per second. However, what determines the partition among ion and electron thermal energy and kinetic energy is an unresolved problem. It has been reported that ion temperature T_i, electron temperature T_e, and their ratio T_i/T_e vary spatially and depend on the conditions of fast flows [Wang et al., 2012, Runov et al., 2018] but there are few studies which focus on macroscopic profiles of them in reconnection regions in the magnetotail.

In this study, we examine the relation between flow speed and average profiles of T_i, T_e, and T_i/T_e in the magnetotail reconnection region by using data obtained from FPI and FGM on board the MMS spacecraft. We use the observations for a period from May to August 2017 and take out the data in the region of $X_{GSM} < -15$ Re, -10 Re $< Y_{GSM} < 10$ Re, and beta > 0.1. We then divide them into different groups according to flow speed normalized by alfven speed and show B_z/B_{lobe}– B_x/B_{lobe} maps of T_i, T_e, and T_i/T_e of each group. The results show that ion temperature increase with increasing flow speed while electron temperature decrease. Ion temperature are hotter around the X-point. The structure of inflow and outflow regions is pronounced in the profile of electron temperature. T_i/T_e in inflow region are greater than in outflow region, which means that ion and electron temperatures become comparable by passing through the diffusion region. The results suggest that electron get less energy when more energy is partitioned into plasma kinetic energy. We will discuss about the profiles of anisotropy of plasma temperatures to know more details about the heating mechanisms.

Keywords: temperature ratio, flow, MMS

©2019. Japan Geoscience Union. All Right Reserved.

Examining Minimum Cyclotron Resonant Electron Energy of EMIC Waves with MMS

*Si Liu[1]

1. Changsha University of Science and Technology

Electromagnetic ion cyclotron (EMIC) waves can be in cyclotron resonance with relativistic electrons, causing relativistic electron precipitation. The four ideal Magnetospheric Multiscale (MMS) spacecraft provide great opportunity to directly calculate the wave vector ***k*** of EMIC waves by phase differencing technique and hence estimate the minimum resonant energy by the resonance condition. Deriving a simplified analytic solution, we find that the phase differencing method can still provide an estimate of the dominant wave number when a finite wave number spread or a finite frequency spread is present. Numerical calculations indicate that quasi-antiparallel propagation dominates the EMIC event on 20 November 2015, which is consistent with the FFT spectral analysis results. We also find that obtained wave vectors, roughly agreeing with the validity of cold plasma theory, might significantly vary from wave packet to wave packet. Moreover, minimum resonant electron energies gradually increase from 0.5 MeV to tens of MeV with a decreasing parallel componet of ***k***. Current results provide evidence that EMIC waves can be in resonance with the electrons of energies down to hundreds of keV. It further demonstrates that EMIC waves in a narrow frequency band can effectively interact with the relativistic electrons with a broad energy range.

Keywords: EMIC waves, minimum resonant electron energy, wave vector, phase differencing

©2019. Japan Geoscience Union. All Right Reserved.

Small scale whistler mode waves near the magnetic field intensity minimum in the magnetosheath

*Naritoshi Kitamura[1], Takanobu Amano[1], Yoshiharu Omura[2], Satoko Nakamura[2], Chika Umegaki[1], Scott A Boardsen[3,4], Narges Ahmadi[5], Robert E Ergun[5], Olivier Le Contel[6], Per-Arne Lindqvist[7], Yoshifumi Saito[8], Shoichiro Yokota[9], Daniel J Gershman[3], Barbara L Giles[3], Thomas E Moore[3], William R Paterson[3], Craig J Pollock[10], Christopher T Russell[11], Robert J Strangeway[11], James L Burch[12]

1. Department of Earth and Planetary Science, Graduate School of Science, The University of Tokyo, 2. Research Institute for Sustainable Humanosphere, Kyoto University, 3. NASA Goddard Space Flight Center, 4. University of Maryland, 5. Laboratory for Atmospheric and Space Physics, University of Colorado, 6. Laboratoire de Physique des Plasmas, UMR7648 CNRS/Ecole Polytechnique/UPMC/Université Paris-Sud/Observatoire de Paris, 7. Royal Institute of Technology, 8. Institute of Space and Astronautical Science, Japan Aerospace Exploration Agency, 9. Department of Earth and Space Science, Graduate School of Science, Osaka University, 10. Denali Scientific, 11. Institute of Geophysics and Planetary Physics, University of California, Los Angeles, 12. Southwest Research Institute

Wave-particle interactions are thought to play a crucial role in energy transfer in collisionless space plasmas in which the motion of charged particles is controlled by electromagnetic fields. In the terrestrial magnetosheath, intense whistler mode waves, called 'Lion roars', are often detected by spacecraft around minima of semi-periodic fluctuations of magnetic field intensity due to mirror mode structures and motion of the structures. It is expected that whistler mode waves are efficiently generated near a local minimum of magnetic field intensity due to the smallest cyclotron resonance velocity. We report the detailed characteristics of such whistler mode waves using the data obtained by the four MMS (Magnetospheric Multiscale) spacecraft. Because reversals of field-aligned component of Poynting flux around minima in mirror mode structures correspond to reversals of gradient of magnetic field intensity along the magnetic field, whistler mode events with reversals of the field-aligned component of Poynting flux are good candidates of observations of effective wave generation regions along field lines. Even in such events, phase difference and change of amplitude of whistler mode waves observed by the four spacecraft do not have a clear correlation in cases of ~40 km separation, which is much smaller than the spatial scale of magnetic field depression due to mirror mode structures and is even smaller than the local thermal ion gyro scale. This result indicates that the coherent whistler wave generation in mirror mode structures has very limited spatial scale across field lines and is probably affected by any electron scale process. A plane wave approximation can be usable only in a very small scale. Because some events in cases of ~7 km separation showed good correlation among four spacecraft, the typical scale of coherent whistler wave across field lines can be at least an order of 10 km in mirror mode structures in the terrestrial magnetosheath. The whistler mode waves observed by a spacecraft in a mirror mode structure are a cluster of waves from multiple spatially small sources.

Keywords: Whistler mode wave, Plasma wave, MMS spacecraft, Wave-particle interaction

©2019. Japan Geoscience Union. All Right Reserved.

Spatial characteristics of the internal modulation of pulsating aurora: multi-point high-speed optical observations in Scandinavia

*Yuki Kawamura[1], Keisuke Hosokawa[1], Shin-ichiro Oyama[2,3], Yoshizumi Miyoshi[2], Yasunobu Ogawa[3], Satoshi Kurita[2], Satoshi Ebukuro[1], Ryoichi Fujii[4]

1. Department of Communication Engineering and Informatics, University of Electro-Communications, 2. Institute for Space-Earth Environmental Research, Nagoya University, 3. National Institute of Polar Research, 4. Research Organization of Information and Systems

Pulsating aurora (PsA) is a kind of diffuse aurora which almost always appears in the morning side during the recovery phase of auroral substorm. PsA typically has two characteristic temporal variations. One is so-called main pulsation whose period ranges from a few to a few tens of seconds. The other is a few Hz brightness modulation (internal modulation) which is often seen during the ON time of the main pulsation. Previous studies have suggested that the temporal variation of PsA is characterized by wave-particle interaction between whistler-mode chorus waves and high energy electrons in the magnetosphere. Especially, it has been indicated that there is one to one correspondence between the amplitude variation of chorus waves and the luminosity modulation of PsA.
Recent studies revealed the occurrence distribution of the frequency of the internal modulation. However, there have been no studies which analyzed the spatial distribution of the internal modulation.

To reveal the spatial characteristics of the internal modulation, we need to perform a frequency analysis of the internal modulation by using data from high speed optical instruments having wide spatial coverage. For this purpose, we make use of highly sensitive EMCCD cameras which have been operated in Sodankylä and Kevo in Finland, Tromsø in Norway, and Tjautjas in Sweden. In these observations, all-sky images are taken with a sampling rate of 100 Hz, which is sufficient to identify temporal variations of the internal modulation.

In the frequency analysis, we have employed all-sky images taken on March 15, 2018 (00:00 –01:30 UT) in Sodankylä, Kevo, Tromsø, and Tjautjas. We computed the average frequency of the internal modulation from each pixel of the EMCCD cameras and derived the spatial distribution of their dominant frequencies. Regardless of the latitude, each pulsating patch was fluctuating at a similar frequency. We also derived the frequency spectrum of several pulsating patches existing at different positions in the north-south direction and found that those frequency spectrums of pulsating patches have peaks at about 3 Hz. These results indicate that the frequency of the internal modulation does not depend on the magnetic latitude, and the frequency of the internal modulation is collimated on 3 Hz.
In the presentation, we discuss why the frequency of the internal modulation concentrate on 3 Hz by taking into account the time of flight of PsA electrons.

Keywords: Pulsating aurora, Internal modulation

©2019. Japan Geoscience Union. All Right Reserved.

Large-scale characteristics of pulsating aurora periodicities: multi-point high-speed optical observations in Scandinavia

*Satoshi Ebukuro[1], Keisuke Hosokawa[1], Shin-ichiro Oyama[2,3,5], Yoshizumi Miyoshi[2], Yasunobu Ogawa[3], Satoshi Kurita[2], Yuki Kawamura[1], Ryoichi Fujii[4]

1. Department of Communication Engineering and Informatics, University of Electro-Communications, 2. Institute for Space-Earth Environmental Research, Nagoya University, 3. National Institute of Polar Research, 4. Research Organization of Information and Systems, 5. University of Oulu

It has been known that most of diffuse aurorae in the morning side are composed of luminous patches whose brightness modulates quasi-periodically. Such aurorae are termed as pulsating aurora (PsA) and have been studied extensively in the last decade. PsA patches have a scale size of a few hundreds of km and are usually observed during the late recovery phase of substorms. The entire temporal variation of PsA consists of two individual modulations: main pulsation and internal modulation. The periodicity of the main pulsation ranges from a few to a few tens of seconds and the internal modulation, showing a few Hz scintillating luminosity changes, is often embedded within the ON time of the main pulsation. Previous studies using satellites indicated one-to-one correlation between PsA and chorus wave near the equatorial plane of the magnetosphere, suggesting that ground-based observations of PsA can be used for mapping the activity of chorus in the magnetosphere in 2D fashion. In the past, the spatial characteristics of chorus wave have not visualized in detail because satellite observations only cover a single point in the magnetosphere. To overcome this limitation, we derive the spatial distribution of chorus waves by using ground-based optical observations of PsA and discuss the ambient parameters which characterize the nature of chorus.
For this purpose, we have employed data from electron multiplying charge-coupled device (EMCCD) cameras deployed at multiple sites in Scandinavia to derive the large-scale characteristics of PsA. EMCCD cameras have been operative in Kevo and Sodankyla in Finland, Tromsoe in Norway, and Tjautjas in Sweden and their temporal resolution is 100 Hz. We conducted a frequency analysis for a PsA event on March 28, 2017 (23:30 to 24:10 UT). During the event studied, there existed three different regions of PsA, regions A, B and C, showing different modulation periods. It was also found that the boundaries between these three regions were sharp. We derived the 2D frequency map by using data from all the available stations. As a result, it became clear that the higher latitude region (region C) showed faster internal modulation than the lower latitude region (region A). In addition, region B, which was sandwiched by regions A and C, did not show any internal modulations (i.e., main pulsation without internal modulation). In the presentation, we discuss why the three regions showed different modulation periods with sharp boundaries. In particular, we address what ambient conditions can control the absence of internal modulation in region B. We also derived similar frequency maps of chorus waves by tracing the PsA modulation with the Tsyganenko 04 magnetic field model, which could be used to estimate the spatial extent of chorus wave generation region.

Keywords: Pulsating aurora, Chorus wave, Main pulsation, Internal modulation

©2019. Japan Geoscience Union. All Right Reserved.

Variations of cosmic noise absorption (CNA) by energetic electron precipitation (EEP) and changes of the auroral morphology

*Miyamoto Taishiro[1], Shin-ichiro Oyama[1,4,5], Yasunobu Ogawa[2], Keisuke Hosokawa[3], Satoshi Kurita[1], Yoshizumi Miyoshi[1], Ryuho Kataoka[2], Hiroshi Miyaoka[2], Tero Raita[4]

1. Institute for Space-Earth Environmental Research,Nagoya University, 2. National Institute of Polar Research, 3. Department of Communication Engineering and Informatics, University of Electro-Communications, 4. Sodankylä Geophysical Observatory, University of Oulu, 5. Ionosphere Research Unit, University of Oulu

Temporal and spatial variations of aurora morphology in association with substorm have been studied for more than half a century. Various types of aurora are known, such as discrete arc emitting at relatively high intensity and elongating along the zonal direction, and diffuse aurora with darker but more widely spreading in the sky. Pulsating aurora, which is characterized by quasi-periodic oscillations in the emission intensity at periods of a few to tens seconds, and auroral patches observed embedding in the pulsating aurora tend to appear at the recovery phase of substorm, especially from midnight to dawn. It is known that these types of aurora are accompanied by energetic electron precipitation exceeding several hundreds keV. Elucidation of the causality to produce pulsating aurora and energetic electron precipitation is an important theme to understand relationships between the radiation belt and upper-middle atmosphere of the earth. Analyzing measurements from satellite observations (e.g., Arase) and ground-based optical/radio technique observations, the generation mechanism is thought to be mainly attributed to wave particle interactions due to plasma wave and electrons in the magnetosphere. In this study, we focus on relationships between auroral morphological changes, in particular spatiotemporal evolutions to patches and coinciding precipitations of the energetic electron.

Some previous studies have presented changes in morphology from pulsating aurora to patch structures [e.g., Shiokawa et al., 2014] and temporal variations of energetic electron precipitation [e.g., Hosokawa and Ogawa, 2015]. As mentioned above, the wave-particle interaction has been widely accepted with experimental evidences to support generation of pulsating aurora and energetic electron precipitation. However, our understanding has not yet reached its maturity of presenting spatiotemporal evolutions of auroral morphology and associated electron precipitation. Oyama et al. [2017] presented enhancements of CNA (cosmic noise absorption) coinciding with appearance of the patch structure but with only two events. Furthermore, due to measurements with intensive diagnostic instruments, the result was based on information of a part of the auroral ionosphere. In this study, we conducted observations to capture simultaneously time evolutions and spatial distributions of auroral morphology and energetic electron precipitation by utilizing a network of EMCCD (Electron Multiplying Charge Coupled Device) cameras and riometers deployed in Northern Europe.

This study will present three events (February 19-20, 2018, March 6-7, 2017, and March 29-30, 2017). On the way of all events, after substorm onsets twice near Northern Europe, another onset occurred again at more west side (near Iceland or Greenland area) but at dawn in the Northern Europe. In this study, we have focused on the aurora and CNA associated with the latter onset, and at that time, the aurora spatially and temporally shifted from diffuse to pulsation and patch structures. This suggests that substorm activities occurred in the distance can induce these auroral morphological changes seen in the Northern Europe. CNA at that time is characterized by gradual variations with time scale of several hours. This trend cannot be seen at substorm onset near the Northern Europe. Moreover, in the latitude distribution, the feature was confirmed that CNA increases at the latitude where patch structure is seen, and CNA keeps

©2019. Japan Geoscience Union. All Right Reserved.

constant value at the latitude where patch structure is not seen. In the presentation, based on these observations, we will discuss physical mechanisms to cause changes in the auroral morphology and energetic electron precipitation, which can be seen as increases of CNA.

Keywords: Ionosphere, Aurora, Energetic Electron Precipitation (EEP)

©2019. Japan Geoscience Union. All Right Reserved.

Spatiotemporal characteristics on the source region of flash aurora using ray tracing analysis

*Tomohiro Inoue[1], Mitsunori Ozaki[1], Yoshitaka Goto[1], Satoshi Yagitani[1], Yoshiya Kasahara[1], Kazuo Shiokawa[2], Yoshizumi Miyoshi[2], Ryuho Kataoka[3], Yusuke Ebihara[4]

1. Kanazawa University , 2. Nagoya University, 3. National Institute of Polar Research, 4. Kyoto University

Whistler mode waves cause precipitation of high-energy electrons via wave-particle interactions in the magnetosphere. The scattered particles precipitate to the ground along the geomagnetic field line. Then, flush aurora, which is a rapid (less than 1 s) auroral phenomenon, is happened. Flash aurora is important for understanding the spatial evolution of wave-particle interaction region in the magnetosphere. We observed the mainly southward spread of flush aurora. In order to understand the spatial-time variation of wave-particle interaction region, we analyze the propagation effects of whistler mode waves near the magnetic equator region using ray tracing analysis. We calculated the ray paths of whistler mode waves (0.2 fce and 0.4 fce) near the magnetic equator (-10 to +10 degrees of geographic latitude), where fce is the electron cyclotron frequency at the magnetic equator. The initial ray paths put in the assumption of a spatial spread with the wave normal angles of tens of degrees along the magnetic field line at the magnetic equator (a point source). Then, we traced the magnetic field lines from the ray paths of whistler mode waves and estimated the precipitation area of electrons in the ionosphere using the IGRF model. The calculation results showed the precipitation area was not mainly spread southward, but evolved northward in the preliminary study.
In this presentation, we will present the spatiotemporal characteristics of flash aurora and the analysis results of ray tracing in detail.

Keywords: Flush aurora, Whistler mode wave, Ray tracing, Wave-particle interaction

©2019. Japan Geoscience Union. All Right Reserved.

Molecular ion supply mechanisms from the low-altitude ionosphere to magnetosphere observed by EISCAT and Arase(ERG)

*Masayoshi Takada[1], Kanako Seki[1], Yasunobu Ogawa[2], Kunihiro Keika[3], Satoshi Kasahara[4], Shoichiro Yokota[5], Tomoaki Hori[7], Kazushi Asamura[6], Yoshizumi Miyoshi[7]

1. Graduate School of Science, Tokyo University, 2. National Institute of Polar Research, 3. Department of Earth and Planetary Science, Graduate School of Science, Tokyo University, 4. The University of Tokyo, 5. Graduate School of Science, Osaka University, 6. Institute of Space and Astronautical Science, Japan Aerospace Exploration Agency, 7. Institute for Space-Earth Environmental Research, Nagoya University

Molecular ions (O_2^+/NO^+/N_2^+) in the magnetosphere have been observed during magnetic storms [Peterson et al., 1994; Klecker et al., 1986]. These molecular ions are considered to originate from the Earth’ s ionosphere. It is considered that they have been transported upward by some heating processes in the ionosphere. However, due to the larger mass than atomic ions (O^+), the molecular ions usually exist only in the low-altitude ionosphere below 300 km altitude. It is hence difficult to transport these molecular ions by overcoming loss by chemical reactions to the high-altitude ionosphere where the ion upflow and outflows usually take place [Peterson et al., 1994]. Therefore, it is necessary to reveal what mechanism causes molecular ion upflow during the magnetic storms. In this study, we aim at the observational assessments of the supply processes of the molecular ions from the low-altitude ionosphere to the magnetosphere based on conjugate observations by EISCAT radar and the Arase (ERG) satellite.

The EISCAT radar and the Arase (ERG) satellite have the conjunction event during the large magnetic storm with the minimum Dst of -124 nT on September 8, 2017. During the event, the Arase satellite was located in the dusk-side inner magnetosphere and observed molecular ions in the energy range of 12-180 keV/q. The EISCAT radar simultaneously observed the ion upflow (with the upward velocity of ~50-150 m/s) from the low-altitude ionosphere (~250-400 km) together with strong ion heating (>2000 K). The convective electric field was also enhanced by a factor of 2 in the same region. We estimated each term in the equation of motion for ions. The result indicates that the ion upflow reached stable equilibrium because the upward ion and electron pressure gradients are balanced with the downward gravitational force. It is suggested that the ion upflow can take place from the low-altitude ionosphere due to strong ion pressure gradient. We also estimated the flux decrease of molecular ions due to dissociative recombination. The flux decreased to ~1 % at 350 km compared with 280 km. The estimated upflow flux of molecular ions at 350 km is $>10^{10}$ m^{-2} s^{-1} . Comparison between distribution functions observed by Arase satellite and EISCAT radar suggests that acceleration by 3 orders of magnitudes is necessary during the outflow process. These results indicate that the strong ion frictional heating during magnetic storms enabled molecular ions to be transported upward from the low-altitude ionosphere and provide a source of molecular ion outflows into the magnetosphere.

Keywords: Molecular ion, EISCAT radar, Arase (ERG) satellite, Ion upflow, Ionospheric heating

©2019. Japan Geoscience Union. All Right Reserved.

Optical and radar observation of the dynamic auroral forms

*Yunosuke Nagafusa[1], Tima Sergienko[2], Satoshi Taguchi[1], Urban Braendstroem[2], Masatoshi Yamauchi[2]

1. Graduate School of Science, Kyoto University, 2. Swedish Institute of Space Physics, Kiruna

Ionosphere disturbances caused by the auroral electron precipitations are studied using auroral images taken by Auroral Large Imaging System (ALIS) and ionospheric parameters measured by EISCAT UHF radar that were conjugate with ALIS field-of-view. ALIS consists of several remote controlled stations located in northern Scandinavia, separated by approximately 50 km. Each station is equipped with a high-resolution CCD detector with 1024×1024 pixels, and a filter wheel with six positions for narrow-band interference filters. In this study we use the data obtained with the 557.7 nm filter, which show the auroral emission originated from the atomic oxygen. EISCAT UHF radar located in northern Norway near Tromsø operating in the BEATA program provides the ionospheric electron density, electron and ion temperatures, and ion velocity with the time resolution of 5 s and the spatial resolution of 1.5 km. The auroral images from the different ALIS stations were used for triangulation of the auroral forms in order to determine the aurora position in relation to the radar beam. For each auroral arc, the electron density, the electron and ion temperatures measured inside and in the vicinity of the auroral forms were analyzed with the aim of understanding the ionospheric response to the different types of auroral electron precipitations.

Keywords: aurora, ionospheric parameters, electron precipitations

©2019. Japan Geoscience Union. All Right Reserved.

Observations of MF/HF auroral radio emissions at three ground-based stations

*Yuka Sato[1], Atsushi Kumamoto[2], Yuto Katoh[2], Akira Kadokura[3,4], Yasunobu Ogawa[3,4], Atsuki Shinbori[5]

1. Nippon Institute of Technology (NIT), 2. Graduate School of Science, Tohoku University, 3. National Institute of Polar Research (NIPR), 4. The Graduate University for Advanced Studies, 5. Institute for Space-Earth Environmental Research (ISEE), Nagoya University

We started ground-based observations of MF/HF auroral radio emissions about 10 years ago at two stations (The Husafell Station, Iceland, September 2005; The Kjell Henriksen Observatory, Svalbard, September 2008) and found multiple unknown properties of MF/HF auroral radio emissions, e.g. polarization features [*Sato et al.*, 2008, 2015] and existence of a higher frequency component [*Sato et al.*, 2012]. To make a next siginificant step for a futher understanding of MF/HF auroral radio emissions, we installed a new dedicated instrumentation at the KAIRA (Kilpisjärvi Atmospheric Imaging Receiver Array) site in Kilpisjärvi, Finland (Latitude: 60.07 N, Longitude: 20.76 E) in the summer of 2018. It is a passive receiving system designed to realize a high-resolution spectral, interferometric and polarization measurements using 4 loop antennas and a software-defined radio (SDR) receiver. This SDR receiver can implement high-speed, flexible digital signal processing of RF signals and obtain high-resolution spectra pauselessly throughout the night in a wide frequency range up to 6 MHz. One of the main research subjects of this project is radio emission spontaneously emitted from aurora. There are long-known three types of MF/HF auroral radio emissions identified at ground level: auroral hiss, medium frequency burst (MFB), and auroral roar. Investigation into the generation of these emissions not only offers a tool of great promise for remote sensing of ionospheric plasma processes and parameters but also gives the foundation for understanding various radiation mechanisms that occur in planetary magnetospheres and plasma in space. In combination with the long-term continuous observations in Iceland and Svalbard and future EISCAT_3D experiments, observation with this new instrumentation will provide a first-time opportunity to reveal spatiotemporal variations of macro and fine structures of MF/HF auroral radio emissions associated with substorm evolution. In this presentation, we show detailed specification of this new instrumentation and some initial results.

Keywords: auroral phenomena, radio wave propagation, wave-particle interaction

©2019. Japan Geoscience Union. All Right Reserved.

Ionospheric F-region Drift Measurements Derived from DPS-4D at Zhongshan Station, Antarctic

*Xiangcai Chen[1]

1. Polar Research Institute of China

By means of high-frequency radio sounding, the ionospheric plasma drift can be measured by the Doppler frequency shift of signal. In this paper we analyze the ionospheric F-region plasma motion performed by Digisonde Portable Sounder (DPS-4D) at cusp latitude over Zhongshan Station in Antarctic. By restricting the echo arrival angle, and selecting the reflection height range at 175 –475 km, we present the variation of the F-region plasma drift measurements by setting limits on the Doppler frequency shift. Base on the 7.5 min interval Digisonde drift data from November 2011 to February 2012, we considered the variations of the plasma drift in F-region under the different geomagnetic activity (Kp) and magnetic local time, as well as it correlation with interplanetary magnetic field (IMF). The results indicate that properly restricting the Doppler frequency shift of the echo has a strong effect that contributes to the accurate and robust measurements of the ionospheric plasma drift. The mean value of horizontal drift mostly leveled off to about 600 m/s at altitude around of 230 km, while the field-aligned component of drift showed mean values of -25 m/s near pre-noon and +40 m/s during the night. These strong diurnal variations have dependence on the sign and strength of the IMF B_y and B_z components. It implies that the contraction and expansion of the polar cap with Kp and the convection in the proximity of the throat with different IMF conditions have a profound influence on the observed drift velocities.

Keywords: Digisonde DPS 4, Doppler frequency shift, remote sensing, polar ionosphere, plasma drift

©2019. Japan Geoscience Union. All Right Reserved.

PARM-HEP Observation of Precipitating High Energy Electrons over Pulsating Aurora

*Taku Namekawa[1], Takefumi Mitani[2], Kazushi Asamura[2], Yoshifumi Saito[2]

1. Department of Earth and Planetary Science, Graduate school of Science, The University of Tokyo, 2. Institute of Space and Astronautical Science, Japan Aerospace Exploration Agency

The phenomenon called microbursts that radiation belt particles precipitate to the Earth’ s atmosphere is thought to be largely related to the dissipation of high energy electrons in radiation belt. It is suggested that this phenomenon is caused by pitch angle scattering of the magnetospheric particles by plasma waves, which is a mechanism similar to the cause of the pulsating aurora observed in the Earth’ s polar region. There is a possibility that the origin of microburst can be clarified by proving simultaneous occurrence of microburst and pulsating aurora, but observational verification has not been made yet. For that purpose, we have developed a high-energy electron detector (HEP) for the observation of sub-relativistic - relativistic energy electrons that make up the microburst. HEP is designed to measure electrons between 300 keV and 2 MeV with energy resolution of 20% or less and with signal processing time of ~ 5 μs. Energy analysis is performed by the detection part of this instrument using SSD (Solid State Detector). Performance tests of this instrument are carried out using a sealed radiation source and a high energy electron beam line. This instrument is installed as one of the core instruments of the PARM instrument package developed for the simultaneous observation of the pulsating aurora and microburst by an international student sounding rocket experiment RockSat-XN and LAMP (Loss through Auroral Microburst Pulsation) sounding rocket experiment. We have succeeded in obtaining the flight data on 13 January 2019 from RockSat-XN sounding rocket experiment. In parallel, we are now preparing HEP analyzer for LAMP sounding rocket experiment. In this presentation, we will show the outline and observation results of RockSat-XN-HEP as well as the LAMP-HEP development status.

Keywords: Microburst, PARM, RockSat-XN, LAMP, Sounding rocket, Pulsating aurora

©2019. Japan Geoscience Union. All Right Reserved.

Development of the medium-energy electron detector with hemispherical field-of-view and the flight test in the PARM (Pulsating AuRora and Microburst) mission

*Shin Sugo[1], Oya Kawashima[1], Kazushi Asamura[2], Reiko Nomura[3], Yasunobu Ogawa[4], Keisuke Hosokawa[5], Yoshizumi Miyoshi[6], Takefumi Mitani[2], Taku Namekawa[1,2], Takeshi Sakanoi[7], Mizuki Fukizawa[7], Naoshi Yagi[7], Satoshi Kasahara[1]

1. The University of Tokyo, 2. Institute of Space and Astronautical Science, Japan Aerospace Exploration Agency, 3. National Astronomical Observatory of Japan, 4. National Institute of Polar Research, 5. The University of Electro-Communications, 6. Institute for Space-Earth Environmental Research, Nagoya University, 7. Tohoku University

Energetic electrons significantly affect ionospheric dynamics and the long-term evolution of surfaces and atmospheres of planets and moons. Since the energetic electron flux is not necessarily isotropic, it is important to cover the broad solid angle to quantitatively evaluate the effects on solar system bodies. With future planetary explorations in mind, we developed the medium-energy (20 - 100 keV) electron detector (MED) which can cover almost 2-pi steradian without the spacecraft spin. In order to test the performance of this analyzer in the relevant environment, we participated in the PARM mission, which aimed to measure electron precipitation using NASA’s sounding rocket RockSat-XN. In this presentation we report on MED observation results obtained through the flight on 13 January 2019.

©2019. Japan Geoscience Union. All Right Reserved.

Auroral substorm onset in satellite-based global images and ground-based all-sky images

*Akimasa Ieda[1], Kirsti Kauristie[2], Yukitoshi Nishimura[3], Yukinaga Miyashita[4], Harald U Frey[5], Liisa Juusola[2], Daniel Whiter[6], Masahito Nose[7], Matthew O Fillingim[5], Farideh Honary[8], Neil C Rogers[8], Yoshizumi Miyoshi[1], Shinobu Machida[1]

1. Institute for Space-Earth Environmental Research, Nagoya University, 2. Finnish Meteorological Institute, 3. Boston university, 4. Korea Astronomy and Space Science Institute, 5. University of California Berkeley, 6. University of Southampton, 7. Graduate School of Science, Kyoto University, 8. Lancaster University

Substorm onset has originally been defined as a longitudinally extended sudden auroral brightening (Akasofu initial brightening: AIB) followed a few minutes later by an auroral poleward expansion in ground-based all-sky images (ASIs). In contrast, such clearly marked two-stage development has not been evident in satellite-based global images (GIs). Instead, substorm onsets have been identified as localized sudden brightenings that expand immediately poleward.
To resolve these differences, optical substorm onset signatures in GIs and ASIs are compared in this study for a substorm that occurred on December 7, 1999. For this substorm, the Polar satellite ultraviolet global imager was operated with a fixed-filter (170 nm) mode, enabling a higher time resolution (37 s) than usual to resolve the possible two-stage development. These data were compared with 20-s resolution green-line (557.7 nm) ASIs at Muonio in Finland. The ASIs revealed the AIB at 2124:50 UT and the subsequent poleward expansion at 2127:50 UT, whereas the GIs revealed only an onset brightening that started at 2127:49 UT.
Thus, the onset in the GIs was delayed relative to the AIB and in fact agreed with the poleward expansion in the ASIs. The fact that the AIB was not evident in the GIs may be attributed to the limited spatial resolution of GIs for thin auroral arc brightenings. The implications of these results for the definition of substorm onset are discussed herein.

Keywords: substorm, auroral breakup, aurora

©2019. Japan Geoscience Union. All Right Reserved.

Original substorm onset (Akasofu 1964; 2010)

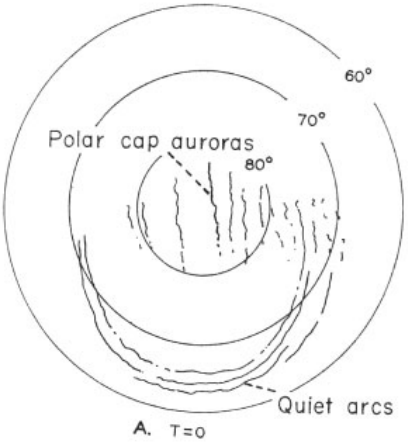


FIG. 2. THE DISTRIBUTION OF THE AURORAS DURING THE QUIET PHASE.

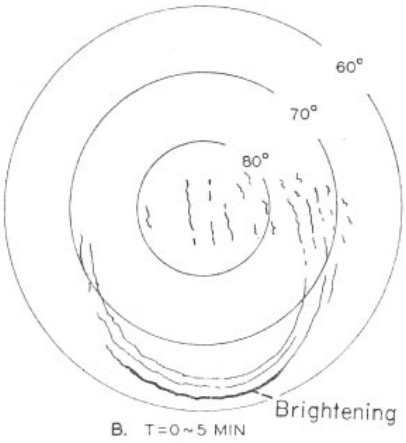


FIG. 3. AURORAS DURING THE EXPANSIVE PHASE (STAGE I).

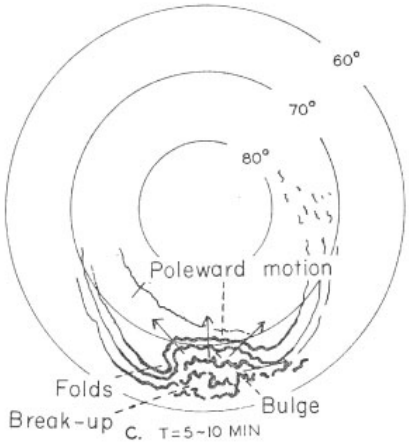


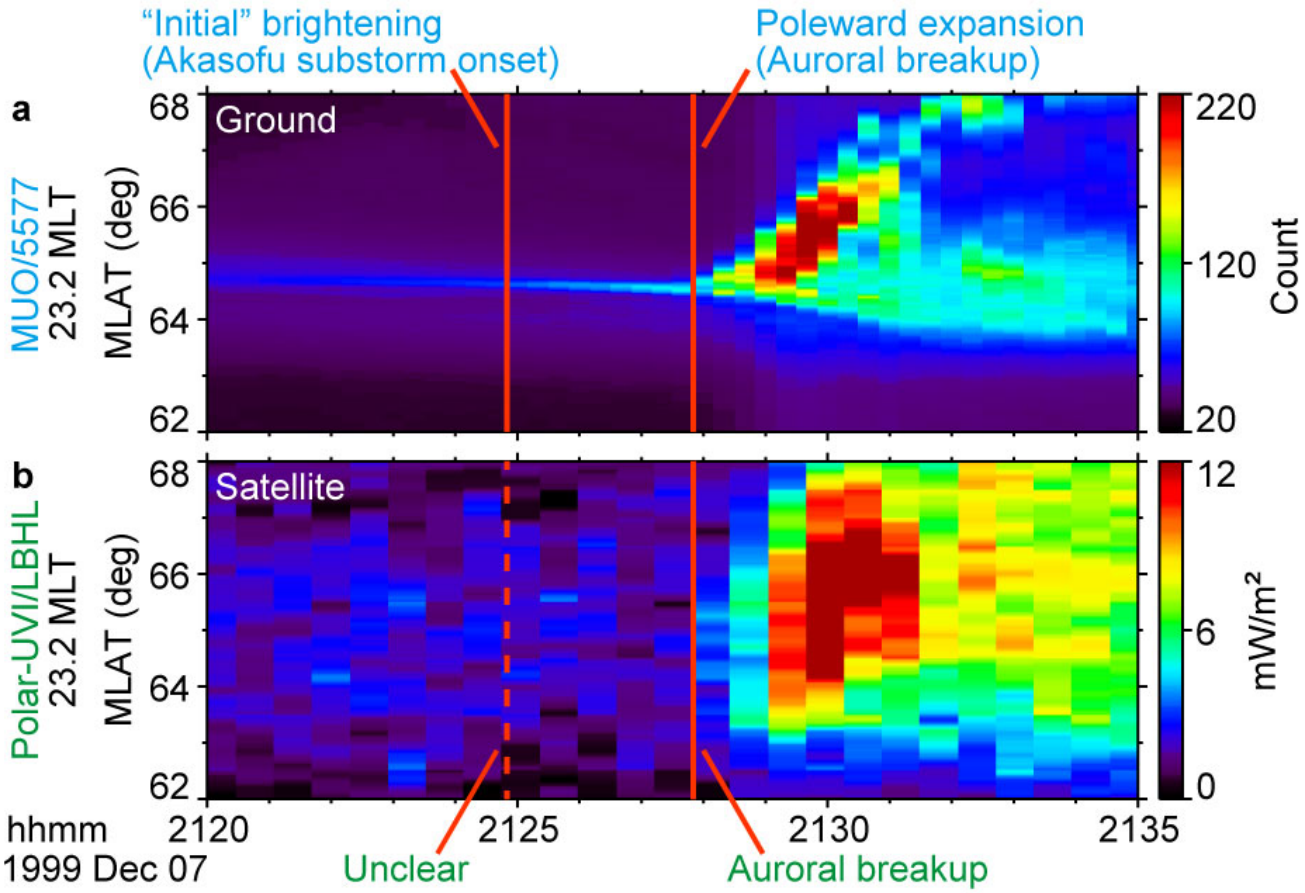
FIG. 4. AURORAS DURING THE EXPANSIVE PHASE (STAGE II).

a Time < 0
Before onset
Quiet arc

b T = 0 ~ 5 min
Expansion phase stage 1
Initial brightening
T = 0: Substorm onset

c T = 5 ~ 10 min
Expansion phase stage 2
Poleward expansion
(Auroral breakup)

Ground and satellite observations (Ieda et al. 2018: 10.1186/s40623-018-0843-3)



©2019. Japan Geoscience Union. All Right Reserved.

Automatic Classification of Auroral images using optical flow feature

*Naoto Kashiwagi[1], Akiko Fujimoto[1], Terumasa Tokunaga[1], Yoshizumi Miyoshi[2], Yasunobu Ogawa[3], Keisuke Hosokawa[4]

1. Kyushu Institute of Technology, 2. Nagoya University, 3. National Institute of Polar Research, 4. The University of Electro-Communications

The machine learning technique including the deep learning has been developed and the practical uses have increased on various field. On the study of auroral detection, the concern over the automatic image classification has risen using the approach of machine learning technique for the large statistical analysis of auroral images. The automatic auroral image classification has tried to use some techniques from computer vision, machine vision and pattern recognition. There are roughly two kinds of the selected feature: the color of image and the motion of aurora image sequences. The works based on the color feature of aurora image have been performed by Rao et al. (2014) and Tanaka et al. (2015). Rao et al. (2014) performed Support Vector Machines (SVM) classification with several local feature extraction techniques, and found that Scale Invariant Feature Transform (SIFT), OpponentSIFT, is the most effective feature for the automated classification of color aurora images. Tanaka et al. (2015) used the aurora area using the HSV model. They mentioned that it is difficult to classify the images including the diffuse aurora and cloud area. The color feature work well for the color auroral image, while the gray-scale (optically filtered) auroral images need other features on the automated classification. Blixt et al. (2006) applied the optical flow estimation to auroral image sequences. Their case study showed the useful tool for representing the motion of the aurora. In this study, we validate the optical flow estimation to extract the feature of auroral image, and automatically classify the large gray-scale auroral images using the machine learning with Convolution Neural Network (CNN). We use 63,486 gray-scale aurora images in total and use five categories for the preparation of supervised learning data, 1) aurora, 2) aurora and cloudy, 3) aurora and moon, 4) aurora, cloudy and moon, 5) noaurora. We perform the Hold-out and the Cross Validation to evaluate our classification performance. We obtained 98.58% of the classification accuracy based on Hold-out and 98.47% of the classification accuracy based on Cross Validation.

Keywords: Aurora, Optical flow, Convolution Neural Network

©2019. Japan Geoscience Union. All Right Reserved.

Fine-scale visualization of aurora in a wide area using color digital camera images from the International Space Station

*Sota Nanjo[1], Yuta Hozumi[1], Keisuke Hosokawa[1]

1. The University of Electro-Communications

Various ground-based and space-based imagers have been used to observe aurora borealis and australis. So far, however, it has been difficult to observe the detailed spatial structure of auroras in a wide area with sufficient spatial and temporal resolution. Since the photographs taken from the International Space Station (ISS) have sufficient spatial and temporal resolution, it is possible to visualize the fine-scale structures of aurora in a wide area. A calibration of imaging parameters of the photographs using star lights was proposed by a previous research. The accuracy in the timestamp was not guaranteed by the method based on the star lights because the position of the star lights in the image did not change with elapsed time. Thus, it is still difficult to use the mapped data for studying fast variations of aurora, for example pulsating aurora (PsA). Therefore, in this study, we calibrated the images from the ISS using city lights which change their apparent positions with elapsed time. In order to validate the calibration method using city light positions, we mapped two PsA events in the photographs to the geographical coordinate, and compared with those from ground-based all-sky imagers in Alaska and Canada. We found that the approximate shape of discrete aurora and the temporal variation of PsA derived from the ISS images are consistent with those from the ground-based observation. The accuracy in the timestamp is less than 0.5 sec and that in space in the direction perpendicular to the line of sight of the camera is within 5 km. In the presentation, we will also address how the mapped full-color images can be used for studies of PsA in the future work.

Keywords: aurora, ISS

©2019. Japan Geoscience Union. All Right Reserved.

PARM: Investigation of precipitating high-energy electrons into the auroral ionosphere with sounding rockets

*Kazushi Asamura[1], Yoshizumi Miyoshi[2], Keisuke Hosokawa[3], Takefumi Mitani[1], Taku Namekawa[1,5], Takeshi Sakanoi[4], Naoshi Yagi[4], Mizuki Fukizawa[4], Genki Ishizawa[4], Satoshi Kasahara[5], Shin Sugo[5], Oya Kawashima[5], Reiko Nomura[6], Masahito Nose[2], Mariko Teramoto[2], Yasunobu Ogawa[7], Shinji Saito[2], Ryoichi Fujii[8]

1. ISAS / JAXA, 2. ISEE, Nagoya University, 3. The University of Electro-Communications, 4. Tohoku University, 5. The University of Tokyo, 6. NAOJ / NINS, 7. NiPR / ROIS, 8. ROIS

Bursty precipitations of high-energy electrons into the polar ionopshere have been observed by low-altitude satellite, for example, SAMPEX and FIREBIRD II. These precipitations, called microburst, may contribute to the loss of the terrestrial radiation belt through the collisional energy loss with the dense, cold atmospheric particles. Recent numerical simulations successfully reproduce these microburst precipitations with a few Hz modulations by taking into account the pitch angle scattering with the whistler chorus elements at off-equator regions in the inner magnetosphere. Therefore, one can expect that the miscroburst precipitations have properties depending on auroral activities especially the pulsating auroras. In order to investigate the mechanisms of the microburst precipitations by in-situ observations, we are developing two instrument packages: PARM (Pulsating AuRora and Microbursts; already developed) and PARM-2 (being developed), both of which are designed suitable for sounding rocket experiments. PARM consists of four sensors; HEP (high-energy electron energy spectrometer), MED (medium-energy electron detector), AIC (auroral camera), and AFG (ASIC-based fluxgate magnetometer). PARM was onboard the NASA's RockSat-XN sounding rocket, and launched from Andoya, Norway at 09:13UT, Jan 13, 2019. On the other hand, PARM-2 is under development. It consists of HEP, two AICs, and MIM (magneto-impedance magnetometer). PARM-2 is to be onboard the NASA's LAMP sounding rocket which will fly from Poker Flat, Alaska in the period between the end of 2019 and the beginning of 2020.

We will present the overview of PARM missions including the initial results of RockSat-XN/PARM with ground-based observations and preparation status of LAMP/PARM-2.

Keywords: electron microburst precipitation, sounding rocket, pulsating aurora

©2019. Japan Geoscience Union. All Right Reserved.

[E] Poster | P (Space and Planetary Sciences)：P-EM Solar-Terrestrial Sciences, Space Electromagnetism & Space Environment

Wed. May 29, 2019 3:30 PM - 5:00 PM JST | Wed. May 29, 2019 6:30 AM - 8:00 AM UTC | Poster Hall International Exhibition Hall8, Makuhari Messe_2

[P-EM13] Inner magnetosphere: Recent understanding and new insights

convener:Yusuke Ebihara(Research Institute for Sustainable Humanosphere, Kyoto University), Danny Summers(Memorial University of Newfoundland), Yoshizumi Miyoshi(Institute for Space-Earth Environmental Research, Nagoya University), Shinji Saito(Graduate School of Science, Nagoya University)

The inner magnetosphere is characterized by the dominance of intrinsic dipolar Earth's magnetic field. The dipolar magnetic field traps charged particles, resulting in the formation of unique particle environment known as the plasmasphere, the ring current, and the radiation belt. The inner magnetosphere is always changing because of incoming energy from the outer magnetosphere and the ionosphere in the forms of particles and electromagnetic fields. In the inner magnetosphere, the particle energy is transferred to the field energy, and vice versa. The mutual coupling between particles and fields also makes the inner magnetosphere unique. The outgoing energy to these regions is also known to be significant, such as precipitation into the upper atmosphere and sub-auroral disturbances. A number of satellites (e.g., DMSP, NOAA, Geotail, Cluster, THEMIS, Van Allen Probes, MMS, and Arase), ground-based instruments (e.g., SuperDARN and EISCAT radars, magnetometers, and cameras), and numerical simulations (e.g., global particle simulation, PIC simulation, and hybrid simulation) have successfully surveyed the inner magnetosphere, which deepen our knowledge significantly. USAF DSX, UCLA Elfin and NASA CeRES will be launched soon, being expected to provide important information. We solicit papers describing recent results on the inner magnetosphere and/or its coupling with the other regions, including the ionosphere and the outer magnetosphere.

[PEM13-P01] Evaluation of wave normal and Poynting vector analyses for whistler mode waves observed by the waveform capture (WFC) on board the Arase

*Yoshiya Kasahara[1], Satoshi Ikarashi[1], Hiroyuki Nishizawa[1], Shoya Matsuda[2], Fuminori Tsuchiya[3], Atsushi Kumamoto[3], Yasumasa Kasaba[3], Mitsunori Ozaki[1], Ayako Matsuoka[2] (1.Kanazawa University, 2.ISAS/JAXA, 3.Tohoku University)

[PEM13-P02] Calibration of electric fields dedicated to the measurement of the S-WPIA of the Arase Satellite

*Miki Jumpei[1], Hirotsugu Kojima[2], Yuto Katoh[3], Shoya Matsuda[4], Yoshiya Kasahara[5], Mitsuru Hikishima[4], Satoshi Kurita[6], Masahiro Kitahara[3], Satoshi Kasahara[7], Yoshizumi Miyoshi[6], Atsushi Kumamoto[3], Ayako Matsuoka[4], Shoichiro Yokota[8], Tomoaki Hori[6], Kunihiro Keika[7] (1.Space Radio Engineering Laboratory, Division of Electrical Engineering, Kyoto University Graduated School, 2.Research Institute for Sustainable Humanosphere, Kyoto University, 3.Graduate School of Science and Faculty of Science, Tohoku University, 4.Institute of Space and Astronautical Science, JAXA, 5.Information Media Center, Kanazawa University, 6.Institute for Space-Earth Environmental Research, Nagoya University, 7.School of Science, The University of Tokyo, 8.School of Science, Osaka University)

[PEM13-P03] Enhancement of whistler-mode chorus in association with Pc 4-5 ULF waves and related variation of high energy electrons

*Atsuhiro Ono[1], Yuto Katoh[1], Atsushi Kumamoto[1], Fuminori Tsuchiya[1], Mariko Teramoto[2], Yoshiya Kasahara[3], Shoya Matsuda[4], Ayako Matsuoka[4], Takefumi Mitani[4], Tomoaki Hori[2], Satoshi Kasahara[5], Shoichiro Yokota[6], Kunihiro Keika[5], Yoshizumi Miyoshi[2], Iku Shinohara[4] (1.Tohoku University, 2.Nagoya University, 3.Kanazawa University, 4.ISAS/JAXA, 5.The University of Tokyo, 6.Osaka University)

[PEM13-P04] Sudden enhancements of electron cyclotron harmonic waves observed by the Arase satellite

*Shinjo Airi[1], Hirotsugu Kojima[1], Yoshiya Kasahara[2], Yoichi Kazama[3], Hideyuki Usui[4], Yoshizumi Miyoshi[5], Yasumasa Kasaba[6], Shoya Matsuda[7], Tomoaki Hori[5], S. -Y. Wang[8], Sunny W.Y. Tam[9], Atsushi

Kumamoto[10], Ayako Matsuoka[11] (1.Research institute for sustainable humanosphere, Kyoto University, 2.Information Media Center, Kanazawa University, 3.ASIAA, 4.Graduate school of system informatics Kobe University, 5.Institute for Space-Earth Environmental Research, Nagoya University, 6.Planetary Plasma and Atmospheric Research Center, Tohoku University, 7.Institute of Space and Astronautical Science/Japan Aerospace Exploration Agency, 8.ASIAA, Taiwan, 9.ISAPS, NCKU, Taiwan, 10.Department of Geophysics, Graduate School of Science, Tohoku University, 11.Research Division for Space Plasma, Institute of Space and Astronautical Science, Japan Aerospace Exploration Agency)

[PEM13-P05] Correlation between pulsating aurora and electrostatic electron cyclotron harmonic waves obtained from coordinated Arase and ground data

*Mizuki Fukizawa[1], Takeshi Sakanoi[1], Yoshizumi Miyoshi[2], Keisuke Hosokawa[3], Yoichi Kazama[4], Yoshiya Kasahara[5], Shoya Matsuda[6], Ayako Matsuoka[7], Wang Shiang-Yu[4], Sunny Wing-Yee Tam[8], Ryuho Kataoka[9] (1.Planetary Plasma and Atmospheric Research Center, Graduate School of Science, Tohoku University, 2.Institute for Space-Earth Environmental Research, Nagoya University, 3.Department of Communication Engineering and Informatics, University of Electro-Communications, 4.Academia Sinica Institute of Astronomy and Astrophysics, 5.Information Media Center, Kanazawa University, 6.Institute of Space and Astronautical Science/Japan Aerospace Exploration Agency, 7.Research Division for Space Plasma, Institute of Space and Astronautical Science, Japan Aerospace Exploration Agency, 8.Institute of Space and Plasma Sciences, College of Sciences, National Cheng Kung University , 9.National Institute of Polar Research)

[PEM13-P06] Automatic determination of Upper Hybrid Resonance Frequencies by Convolutional Neural Network.

*Shoya Matsuda[1], Tatsuhito Hasegawa[2], Atsushi Kumamoto[3], Fuminori Tsuchiya[3], Yoshiya Kasahara[4], Yoshizumi Miyoshi[5], Yasumasa Kasaba[3], Ayako Matsuoka[1] (1.Institute of Space and Astronautical Science/Japan Aerospace Exploration Agency, 2.University of Fukui, 3.Tohoku University, 4.Kanazawa University, 5.ISEE, Nagoya University)

[PEM13-P07] Amplitude dependence of whistler wave motion on electron scattering process

*Yoshiki Ito[1], Yoshizumi Miyoshi[1], Shinji Saito[1] (1.Nagoya University, ISEE)

[PEM13-P08] Two-dimensional simulation of whistler mode wave packets interacting with energetic electrons

*Takeshi Nogi[1], Yoshiharu Omura[1] (1.Reserch Institute for Sustainable Humanosphere, Kyoto University)

[PEM13-P09] Relativistic electron acceleration by whistler-mode chorus waves in 1D, 2D, and 3D magnetic field models.

*Keita Takahashi[1], Yoshiharu Omura[1], Yikai HSIEH[1], Danny Summers[2] (1.Research Institute for Sustainable Humanosphere, Kyoto University , 2.Department of Mathematics and Statistics, Memorial University of Newfoundland)

[PEM13-P10] Study of global spatio-temporal development of magnetospheric ELF/VLF waves for the 26-30 March 2017 storm based on ground and satellite observations and the RAM simulations

*Yuhei Takeshita[1], Kazuo Shiokawa[1], Yoshizumi Miyoshi[1], Mitsunori Ozaki[2], Yoshiya Kasahara[2], Martine Connors[3], Jyrki Manninen[4], Craig Kletzing[5], Vania Jordanova[6] (1.Nagoya University, Institute for Space-Earth Environmental Resarch, 2.Kanazawa University, 3.Athabasca University, 4.Sodankylä Geophysical Observatory, 5.The University of Iowa, 6.Los Alamos National Laboratory)

[PEM13-P11] Flux decrease of outer radiation belt electrons associated with solar wind pressure pulse: A Code coupling simulation of GEMSIS-RB and GEMSIS-GM

*Ito Hiroki[1], Yoshizumi Miyoshi[1], Shinji Saito[2], Yosuke Matsumoto[3], Takanobu Amano[4] (1.Institute for Space-Earth Environmental Research, Nagoya University, 2. Graduate School of Science, Nagoya

University, 3. Graduate School of Science, Chiba University, 4.Department of Earth and Planetary Science, University of Tokyo)

[PEM13-P12] Non-diffusive response of outer belt electrons on interplanetary shock

Takuma Toishi[1], *Yusuke Ebihara[1], Takashi Tanaka[2] (1.Research Institute for Sustainable Humanosphere, Kyoto University, 2.Kyushu University)

[PEM13-P13] PARM: Initial result of the auroral camera on the G-CHASER (RockSat-XN) rocket and status of the development of auroral cameras for the LAMP rocket experiment

*Naoshi Yagi[1], Takeshi Sakanoi[1], Fukizawa Mizuki[1], Kazushi Asamura[2], Yoshizumi Miyoshi[3], Keisuke Hosokawa[4], Genki Ishizawa[5] (1.Planetary Plasma and Atmospheric Research Center, Graduate School of Science, Tohoku University, 2.Institute of Space and Astronautical Science, Japan Aerospace Exploration Agency, 3.Institute for Space-Earth Environmental Research, Nagoya University, 4.Department of Communication Engineering and Informatics, University of Electro-Communications, 5.Space & terrestrial plasma pyhsics)

[PEM13-P14] First simultaneous observation of a SAR arc at subauroral latitudes using a ground all-sky camera and the Arase satellite in the inner magnetosphere

*Yudai Inaba[1], Kazuo Shiokawa[1], Shin-ichiro Oyama[1,8,9], Yuichi Otsuka[1], Atsuki Shinbori[1], Yoichi Kazama[2], Shiang-Yu Wang[2], Sunny W. Y. Tam[2], Shoichiro Yokota[3], Satoshi Kasahara[4], Kunihiro Keika[4], Tomoaki Hori[1], Ayako Matsuoka[5], Yoshiya Kasahara[6], Atsushi Kumamoto[7], Yasumasa Kasaba[7], Yoshizumi Miyoshi[1], Iku Shinohara[5], Arto Oksanen[10] (1.Institute for Space-Earth Environmental Research, 2.Academia Sinica, 3.Osaka Univ, 4.Tokyo Univ, 5.JAXA, 6.Kanazawa University, 7.Tohoku University, 8.University of Oulu, Finland, 9.National Institute of Polar Research, 10.Jyväskylän Sirius ry, Finland)

[PEM13-P15] Pi2 pulsations observed by the Arase satellite inside and outside the plasmapause

*Mariko Teramoto[1], Ayako Matsuoka[2], Reiko Nomura[5], Yoshiya Kasahara[3], Yasumasa Kasaba[4], Atsushi Kumamoto[4], Fuminori Tsuchiya[4], Shoya Matsuda[2], Masahito Nose[1], Masafumi Shoji[1], Yasunori Tsugawa[1], Shun Imajo[1], Yoshizumi Miyoshi[1], Iku Shinohara[2] (1.Institute for Space-Earth Environmental Research Nagoya University, 2.Institute of Space and Astronautical Science, Japan Aerospace eXploration Agency, 3.Kanazawa University, 4.Tohoku University, 5.National Astronomical Observatory of Japan)

[PEM13-P16] An extreme erosion of the plasmasphere during the 7–10 September 2017 storm

*Yuki Obana[1], Naomi Maruyama[2,3], Atsuki Shinbori[4], Kumiko K. Hashimoto[5], Mariangel Fedrizzi[2,3], Masahito Nose[4], Yuichi Otsuka[4], Nozomu Nishitani[4], Tomoaki Hori[4], Atsushi Kumamoto[6], Fuminori Tsuchiya[6], Shoya Matsuda[7], Ayako Matsuoka[7], Yoshiya Kasahara[8], Akimasa Yoshikawa[9], Yoshizumi Miyoshi[4], Iku Shinohara[7] (1.Osaka Electro-Communication University, 2.University of Colorado Boulder, 3.NOAA Space Weather Prediction Center, 4.Nagoya University, 5.Kibi International University, 6.Tohoku University, 7.Japan Aerospace Exploration Agency, 8.Kanazawa University, 9.Kyushu University)

[PEM13-P17] Relative contribution of ULF and chorus waves to the radiation belt variation: Comparison between multi-point observations and BATSRUS + CRCM simulation

*Naoko Takahashi[1], Kanako Seki[1], Mei-Ching Fok[2], Yihua Zheng[2], Yoshizumi Miyoshi[3], David Hartley[4], Ayako Matsuoka[5], Yoshiya Kasahara[6], Yasumasa Kasaba[7], Nana Higashio[8] (1.Graduate School of Science, University of Tokyo, 2.NASA Goddard Space Flight Center, 3.Institute for Space-Earth Environmental Research, Nagoya University, 4.Department of Physics and Astronomy, University of Iowa, 5.Institute of Space and Astronautical Science, Japan Aerospace Exploration Agency, 6.Information Media Center, Kanazawa University, 7.Planetary Plasma and Atmospheric Research Center, Tohoku University, 8.Japan Aerospace Exploration Agency)

[PEM13-P18] Modulation of the D-region ionosphere by Pc5 waves observed by VLF/LF standard radio waves

*Miyashita Takuya[1], Hiroyo Ohya[1], Fuminori Tsuchiya[2], Hiroyuki Nakata[1], Toshiaki Takano[1], Kazuo Shiokawa[3], Yoshizumi Miyoshi[3] (1.Chiba University, 2.Tohoku University, 3.Nagoya University)

[PEM13-P19] Oxygen-proton differences in ion energies dominating plasma pressure: Dependence on storm phases and solar wind drivers

*Kunihiro Keika[1], Satoshi Kasahara[1], Shoichiro Yokota[2], Masahiro Hoshino[1], Kanako Seki[1], Masahito Nose[3], Yoshizumi Miyoshi[3], Iku Shinohara[4] (1.Graduate School of Science, The University of Tokyo , 2.Graduate School of Science, Osaka University, 3.Institute for Space-Earth Environmental Research, Nagoya University, 4.Institute of Space and Astronautical Science, Japan Aerospace Exploration Agency)

[PEM13-P20] Mass dependence of penetration depth of multi-energy ions in the inner magnetosphere during magnetic storms: Arase observations

*Ryosuke Fujii[1], Yoshizumi Miyoshi[1], Masafumi Shoji[1], Kazushi Asamura[2], Lynn Kistler[1,8], Vania Jordanova[9], Tomoaki Hori[1], Satoshi Kurita[1], Mariko Teramoto[1], Yasunori Tsugawa[1], Yoshiya Kasahara[3], Yasumasa Kasaba[4], Atsushi Kumamoto[5], Fuminori Tsuchiya[4], Shoichiro Yokota[6], Kunihiro Keika[7], Ayako Matsuoka[2], Iku Shinohara[2] (1.Institute for Space-Earth Environmental Research, Nagoya University, 2.Institute of Space and Astronautical Science, Japan Aerospace Exploration Agency, 3.Information Media Center, Kanazawa University, 4.Planetary Plasma and Atmospheric Research Center, Tohoku University, 5.Department of Geophysics, Graduate School of Science, Tohoku University, 6.Graduate School of Science, Osaka University, 7.Department of Earth and Planetary Science, Graduate School of Science, The University of Tokyo, 8.University of New Hampshire, 9.Los Alamos National Laboratory)

[PEM13-P21] Relativistic Acceleration of Energetic Protons by Electromagnetic Ion Cyclotron Waves in the Jovian Magnetosphere

*Tomohiro Sekine[1], Yoshiharu Omura[1], Danny Summers[2], Yikai HSIEH[1], Satoko Nakamura[1] (1.Reserach Institute for Sustainable Humanosphere, Kyoto University, 2.Memorial University of Newfoundland)

[PEM13-P22] Statistical study of IPDP type EMIC wave-related electron precipitation at subauroral latitude

*Asuka Hirai[1], Fuminori Tsuchiya[1], Takahiro Obara[1], Yasumasa Kasaba[1], Yuto Katoh[2], Hiroaki Misawa[1], Kazuo Shiokawa[3], Yoshizumi Miyoshi[3], Satoshi Kurita[3], Martin G Connors[4] (1.Planetary Plasma and Atmospheric Research Center, Graduate School of Science, Tohoku Univ. , 2.Department of Geophysics, Graduate School of Science, Tohoku University, 3.Institute for Space-Earth Environmental Research, Nagoya University, 4.Athabasca University)

[PEM13-P23] Meridional distributions of proton plasma and pressure-driven currents in the nightside inner magnetosphere: Arase observations

*Shun Imajo[1], Masahito Nose[1], Satoshi Kasahara[2], Shoichiro Yokota[3], Ayako Matsuoka[4], Kunihiro Keika[2], Tomoaki Hori[1], Mariko Teramoto[1], Kazuhiro Yamamoto[5], Oimatsu Satoshi[5], Reiko Nomura[6], Akiko Fujimoto[7], Iku Shinohara[4], Yoshizumi Miyoshi[1] (1.Institute for Space-Earth Environmental Research, Nagoya University, 2.Graduate School of Science, The University of Tokyo, 3.Graduate School of Science, Osaka University, 4.Institute of Space and Astronautical Science, Japan Aerospace Exploration Agency, 5.Graduate School of Science, Kyoto University, 6.National Astronomical Observatory of Japan, 7.Kyushu Institute of Technology)

[PEM13-P24] Space Weather Effects on Energetic Proton Flux Response in South Atlantic Anomaly

*Kirolosse Mina GIRGIS[1,2], Tohru Hada[1], Shuichi Matsukiyo[1] (1.Earth System Science and Technology (ESST) Department, Interdisciplinary Graduate School of Engineering Sciences (IGSES), Kyushu University, Japan, 2.Aerospace Engineering Department, Faculty of Engineering, Cairo University, Egypt)

[PEM13-P25] Solar-cycle variations of >30 keV electron flux enhancements under the inner radiation belt

*ALLA SUVOROVA[1] (1.National Central University)

[PEM13-P26] Energy spectra variations of high energy electrons in the inner magnetosphere observed by HEP/XEP on ARASE and SEDA-e on HIMAWARI

*Takeshi Takashima[1], Takefumi Mitani[1], Nana Higashio[2], Tsutomu Nagatsuma[3] (1. ISAS/JAXA, 2.Research and Development Directorate/JAXA, 3.NiCT)

[PEM13-P27] Inter-channel calibration of the high-energy electron experiments (HEP) instrument onboard the Arase satellite

*Tomoaki Hori[1], Takefumi Mitani[2], Takeshi Takashima[2], Park Inchun[1], Satoshi Kurita[1], Mariko Teramoto[1], Nana Higashio[3], Satoshi Kasahara[4], Shoichiro Yokota[5], Yoshizumi Miyoshi[1], Iku Shinohara[2] (1.Institute for Space-Earth Environmental Research, Nagoya University, 2.Japan Aerospace Exploration Agency, Institute of Space and Astronautical Science, 3.Japan Aerospace Exploration Agency, 4.Graduate School of Science, The University of Tokyo, 5.Graduate School of Science, Osaka University)

[PEM13-P28] Particle simulation for calibrating the HEP data onboard the ARASE satellite

*PARK INCHUN[1], Yoshizumi Miyoshi[1], Takefumi Mitani[2], Tomoaki Hori[1], Satoshi Kurita[1], Mariko Teramoto[1], Takeshi Takashima[2], Nana Higashio[3], Iku Shinohara[2] (1.Nagoya University Institute for Space-Earth Environmental Research, 2.Japan Aerospace Exploration Agency Institute of Space and Astronautical Science , 3.Japan Aerospace Exploration Agency)

[PEM13-P29] Geant4 model calculation and energetic particle observation with HEP/Arase in the inner radiation belt

*Honoka Toda[1], Wataru Miyake[1], Takefumi Mitani[3], Takeshi Takashima[3], Yoshizumi Miyoshi[2], PARK INCHUN[2], Tomoaki Hori[2] (1.Tokai University, 2.ISEE/Nagoya University, 3.ISAS/JAXA)

[PEM13-P30] Validation of High-energy electron detector simulator for the HEP instruments onboard Arase

*Takefumi Mitani[1], PARK INCHUN[2], Tomoaki Hori[2], Taku Namekawa[1,3], Kazushi Asamura[1], Takeshi Takashima[1], Satoshi Kasahara[3], Satoshi Kurita[2], Mariko Teramoto[2], Nana Higashio[1], Yoshizumi Miyoshi[2], Iku Shinohara[1] (1.Japan Aerospace Exploration Agency, Institute of Space and Astronautical Science, 2.Institute for Space-Earth Environmental Research, Nagoya Univ., 3.The university of Tokyo)

Evaluation of wave normal and Poynting vector analyses for whistler mode waves observed by the waveform capture (WFC) on board the Arase

*Yoshiya Kasahara[1], Satoshi Ikarashi[1], Hiroyuki Nishizawa[1], Shoya Matsuda[2], Fuminori Tsuchiya[3], Atsushi Kumamoto[3], Yasumasa Kasaba[3], Mitsunori Ozaki[1], Ayako Matsuoka[2]

1. Kanazawa University, 2. ISAS/JAXA, 3. Tohoku University

The Plasma Wave Experiment (PWE) is one of scientific instruments on board the Arase (ERG) satellite to measure electric field from DC to 10 MHz and magnetic field from a few Hz to 100 kHz in the inner magnetosphere. It is well known that chorus wave, one of typical plasma waves in VLF range observed in the inner magnetosphere, is a plausible candidate that accelerates relativistic electrons in the radiation belt. Besides the chorus, the Arase has observed various kinds of plasma waves such as lightning whistlers and hiss waves. It is very important to study the propagation characteristics of these waves.

In the present paper, we developed a direction finding system applicable to whistler mode waves using the data from waveform capture (WFC), which is one of receivers covering the frequency range below 20kHz implemented in the PWE. The absolute directions of the wave normal and Poynting vectors were derived in the coordinate system referring the ambient magnetic field and geomagnetic meridian plane. We also estimated the Poynting vector theoretically using the derived wave normal vector, electron density and ambient magnetic field intensity to confirm the validity of the results from the observation data.

We demonstrated that the results were generally reliable, but further calibration is necessary for electric field to improve the accuracy of Poynting vector because the waveform of electric field is now calibrated under the assumptions of theoretical antenna capacitance in a vacuum and typical plasma impedance. In other words, we expect to be able to correct the calibration table for electric field measurements from the direction finding results.

In the presentation, we introduce some typical results which have been derived from the observation data of upper- and lower-band chorus, and lightning whistlers.

Keywords: Whistler mode wave, Waveform Capture, Direction finding, Plasma wave

©2019. Japan Geoscience Union. All Right Reserved.

Calibration of electric fields dedicated to the measurement of the S-WPIA of the Arase Satellite

*Miki Jumpei[1], Hirotsugu Kojima[2], Yuto Katoh[3], Shoya Matsuda[4], Yoshiya Kasahara[5], Mitsuru Hikishima[4], Satoshi Kurita[6], Masahiro Kitahara[3], Satoshi Kasahara[7], Yoshizumi Miyoshi[6], Atsushi Kumamoto[3], Ayako Matsuoka[4], Shoichiro Yokota[8], Tomoaki Hori[6], Kunihiro Keika[7]

1. Space Radio Engineering Laboratory, Division of Electrical Engineering, Kyoto University Graduated School, 2. Research Institute for Sustainable Humanosphere, Kyoto University, 3. Graduate School of Science and Faculty of Science, Tohoku University, 4. Institute of Space and Astronautical Science, JAXA, 5. Information Media Center, Kanazawa University, 6. Institute for Space-Earth Environmental Research, Nagoya University, 7. School of Science, The University of Tokyo, 8. School of Science, Osaka University

The outer radiation belt consists of high-energy electrons. They are strongly affected by geomagnetic activities in the relation to solar wind conditions. The important science target of the Arase mission is to clarify generation/loss mechanisms of relativistic electrons in the outer radiation belt. Wave-particle interactions are thought to be a plausible mechanism for generation/loss processes of relativistic electrons. S-WPIA (Software-type Wave-Particle Interaction Analyzer) is installed in the Arase satellite. The WPIA is a newly developed observation system that enables us to quantitatively understand the interaction between plasma waves and electrons. The WPIA has the capability to identify a relative phase angle of a plasma wave vector and a velocity vector of each detected particle. Since phase information of observed plasma waves is essential to the WPIA, precise calibrations of plasma wave data are important. While the calibration data for the magnetic field sensors are identical to those we obtained during the ground tests of the instruments, the calibration data for electric field sensors strongly depend on plasma parameters around the satellite. Furthermore, there are still unclear parameters at the inputs of preamplifiers relating to the connection with electric field sensors. The calibration for electric field data needs to be performed carefully consulting observation data after the launch.

The present paper focuses on the calibration of plasma wave data for the S-WPIA’s data processing. We picked up events including whistler-mode chorus emissions and lightning-whistler waves. They all are electromagnetic waves, so-called whistler mode waves. The amplitude ratios of their electric field and magnetic field components can be theoretically calculated referring to the Appleton-Hartlee equations. Poynting vectors of whistler mode waves can be also theoretically obtained. We compared the observation results of the picked up events with the theoretical ones. The results show the precise calibration for the magnetic field data have been made. On the other hand, the calibration for the electric field data should be further modified consulting plasma parameters and other uncertain parameters at the input of preamplifiers. In the present paper, we will discuss the improvement of the calibration for electric field data by correcting the calibration table to aim the precise S-WPIA data processing.

©2019. Japan Geoscience Union. All Right Reserved.

Enhancement of whistler-mode chorus in association with Pc 4-5 ULF waves and related variation of high energy electrons

*Atsuhiro Ono[1], Yuto Katoh[1], Atsushi Kumamoto[1], Fuminori Tsuchiya[1], Mariko Teramoto[2], Yoshiya Kasahara[3], Shoya Matsuda[4], Ayako Matsuoka[4], Takefumi Mitani[4], Tomoaki Hori[2], Satoshi Kasahara[5], Shoichiro Yokota[6], Kunihiro Keika[5], Yoshizumi Miyoshi[2], Iku Shinohara[4]

1. Tohoku University, 2. Nagoya University, 3. Kanazawa University, 4. ISAS/JAXA, 5. The University of Tokyo, 6. Osaka University

Whistler-mode chorus emissions play significant roles in the acceleration and loss of energetic electrons in the magnetosphere. One of the important factors which control periodic enhancement of chorus emissions is ULF (Ultra Low Frequency) waves. Previous studies reported that the compressional component of Pc4-5 ULF waves modulates the intensity of chorus waves [Li et al., 2011] and that the toroidal and poloidal components of Pc4-5 ULF waves as well [Jaynes et al., 2015]. Previous studies also suggested that enhancement of the temperature anisotropy of energetic electrons in the wave generation region should be required for the chorus generation. In order to understand the reported correspondence, in addition to the wave observation, we should examine simultaneously observed variations of the flux and the pitch angle distribution of energetic electrons.

In the present study, we investigate the relationship between chorus emissions and ULF waves using particle and electromagnetic field observations made by the Arase satellite. First, we analyze data observed by the Onboard Frequency Analyzer (OFA) of the Plasma Wave Experiment (PWE) and the Magnetic Field Experiment (MGF) during the campaign observation period of the Arase satellite with ground stations from March to April in 2017. As a result, we identified the simultaneous enhancement of chorus emissions and Pc4-5 ULF waves, which was dominated by the toroidal component, from 2130 to 2200 UT on March 27, 2017. The Arase satellite was located at the magnetic local time about 04:00, the magnetic latitude about -10 degrees, and the L-value about 6 during the event. We find that there is one-to-one correspondence between chorus emissions and the toroidal component of ULF waves; chorus emissions enhanced at the timings when the toroidal magnetic field component of ULF waves had a peak in the westward direction. The identified phase relationship is different from that reported by Jaynes et al. (2015), which isn't one-to-one correspondence. Next, we evaluate the resonance energy of the observed chorus emissions, using the ratio of the plasma frequency to the electron cyclotron frequency (f_p/f_{ce}) based on the upper-hybrid resonance frequency derived from the spectra observed by the High Frequency Analyzer (HFA) of PWE and the ambient magnetic field intensity observed by MGF. We find that f_p/f_{ce} is 3.3-3.4 during the event and that the resonance energy for whistler-mode waves in the frequency range of 0.1-0.2 f_{ce} is estimated to be about 100-400keV, which is larger than typical energies of resonating electrons observed in the inner magnetosphere. The estimated large resonant energy can be explained by the frequency range of the observed chorus emissions, approximately 0.1 - 0.2 f_{ce}, is relatively lower than that observed in typical cases.
We also analyze variations of the flux and the pitch angle distribution of energetic electrons during the event using data observed by the High-energy electron experiments (HEP) instrument onboard Arase. The result shows that both the flux and the pitch angle distribution of electrons in the kinetic energy range from 100 to 400 keV, which corresponds to the estimated resonance energy, did not fluctuate with the intensity variation of the chorus emissions and the ULF waves. In addition, we analyze the data observed by the Medium-energy particle experiments - electron analyzer (MEP-e) for energetic electrons in the energy range of 10-80 keV, lower than the estimated resonance energy. Then we identify the

©2019. Japan Geoscience Union. All Right Reserved.

corresponding variation of both the flux and the pitch angle distribution in the 40-60 keV energy range. One of the possible reasons why no significant variations were observed in the hundred keV range would be that the Arase satellite was located in the off-equatorial region during the event, and that the satellite was away from the wave generation region.

Keywords: ULF waves, chorus emissions

©2019. Japan Geoscience Union. All Right Reserved.

Sudden enhancements of electron cyclotron harmonic waves observed by the Arase satellite

*Shinjo Airi[1], Hirotsugu Kojima[1], Yoshiya Kasahara[2], Yoichi Kazama[3], Hideyuki Usui[4], Yoshizumi Miyoshi[5], Yasumasa Kasaba[6], Shoya Matsuda[7], Tomoaki Hori[5], S. -Y. Wang[8], Sunny W.Y. Tam[9], Atsushi Kumamoto[10], Ayako Matsuoka[11]

1. Research institute for sustainable humanosphere, Kyoto University, 2. Information Media Center, Kanazawa University, 3. ASIAA, 4. Graduate school of system informatics Kobe University, 5. Institute for Space-Earth Environmental Research, Nagoya University, 6. Planetary Plasma and Atmospheric Research Center, Tohoku University, 7. Institute of Space and Astronautical Science/Japan Aerospace Exploration Agency, 8. ASIAA, Taiwan, 9. ISAPS, NCKU, Taiwan, 10. Department of Geophysics, Graduate School of Science, Tohoku University, 11. Research Division for Space Plasma, Institute of Space and Astronautical Science, Japan Aerospace Exploration Agency

Electron cyclotron harmonic (ECH) waves are commonly observed in the low latitude region just outside the terrestrial plasmapause. They are purely electrostatic and their frequency spectra show harmonic structures. The harmonic structures are believed to depend on the temperature and density ratio between cold and hot background electrons. The Plasma Wave Experiment (PWE) onboard the Arase satellite has observed ECH waves since the start of its operation. The observed ECH waves are classified into two types. They are the diffuse ECH waves and the enhanced ECH waves. The diffuse ECH waves are weak and they appear as continuous emissions that last for more than a few minutes. The enhanced ECH waves are the sudden enhancements of the diffuse ECH in shorter periods. The present paper focuses on the enhanced ECH waves observed by the Arase satellite.

Kazama et al. (2018) introduced the event that the repeated enhancement of ECH waves is associated with density depletions near the plasmapause. They succeeded in revealing the good correlation of the enhancement of the ECH waves and the sudden decrease of the cold electrons with energies lower than the lowest energy limit of the particle detector. The observed electron features are clear in the relation to the enhancement of ECH waves, but the mechanism of the enhancement is still unclear. We searched for such events of the enhanced ECH waves and examined the correlation of wave intensities, spacecraft potentials and electron velocity distributions observed by the Arase satellite. Some of the events show the features similar to those of Kazama et al. (2018), but there are also many other events with no correlation between the enhancements of the ECH waves and the density depletions. In the present paper, we examine velocity distribution functions of electrons observed by the low-energy particle experiments-electron analyzer (LEPe) onboard Arase. Velocity distribution functions allow us to examine temperature anisotropies of electrons and calculate linear dispersion relations for the ECH waves. Once we get electron temperatures, resonance velocities are calculated. On the other hand, since the wavelength of the ECH waves is very short, the relation of the wavelength and the length of the Arase electric field sensors is also important in evaluating the time variations of the ECH wave intensity. We study the enhanced ECH waves in various viewpoints using wave and electron data observed by the Arase satellite and discuss the generation mechanism in the present paper.

©2019. Japan Geoscience Union. All Right Reserved.

Correlation between pulsating aurora and electrostatic electron cyclotron harmonic waves obtained from coordinated Arase and ground data

*Mizuki Fukizawa[1], Takeshi Sakanoi[1], Yoshizumi Miyoshi[2], Keisuke Hosokawa[3], Yoichi Kazama[4], Yoshiya Kasahara[5], Shoya Matsuda[6], Ayako Matsuoka[7], Wang Shiang-Yu[4], Sunny Wing-Yee Tam[8], Ryuho Kataoka[9]

1. Planetary Plasma and Atmospheric Research Center, Graduate School of Science, Tohoku University, 2. Institute for Space-Earth Environmental Research, Nagoya University, 3. Department of Communication Engineering and Informatics, University of Electro-Communications, 4. Academia Sinica Institute of Astronomy and Astrophysics, 5. Information Media Center, Kanazawa University, 6. Institute of Space and Astronautical Science/Japan Aerospace Exploration Agency, 7. Research Division for Space Plasma, Institute of Space and Astronautical Science, Japan Aerospace Exploration Agency, 8. Institute of Space and Plasma Sciences, College of Sciences, National Cheng Kung University , 9. National Institute of Polar Research

Pulsating auroras (PsAs) are thought to be generated by precipitating electrons scattered by lower-band chorus (LBC) waves near the magnetic equator through cyclotron resonance. Previous studies showed one-to-one correlation between LBC wave intensity observed by satellites near the magnetic equator and PsA intensity obtained by ground-based all-sky imager [e.g., Nishimura et al., Science, 2010, Nishimura et al., JGR, 2011]. In addition, electrostatic electron cyclotron harmonic (ECH) waves can also interact with magnetospheric electrons and scatter their pitch angle theoretically [e.g., Lyons, JGR, 1974]. However, characteristics of aurora caused by ECH are not understood. In our study, we report for the first time in the world that not only LBC but also ECH wave intensity has correlation with the PsA intensity using coordinated Arase and ground-based imager observations. The first campaign observations between the Arase satellite and ground-based optical imager were conducted in March 2017. A typical substorm occurred on 27 March 2017 and the ionospheric footprint of Arase traversed the field of view of all-sky imager at Sodankylä during 00:00–03:15 UT on 29 March 2017. Quasi-periodic LBC and ECH waves were observed by Arase near the magnetic equator and PsA was detected by the all-sky imager during 01:30–02:00 UT. We calculated the cross-correlation coefficients between auroral intensity and LBC or ECH wave intensity from 01:30 UT to 02:00 UT with a time window of every 2 minutes. The highest cross-correlation coefficient between auroral intensity and LBC wave intensity was 0.73 and that between auroral intensity and ECH wave intensity was 0.62 from 01:46 UT to 01:48 UT, and they were statistically significant. The period of auroral intensity which correlated with LBC intensity was shorter than 10 s and that correlated with ECH intensity was 10–20 s. We estimated the precipitating electron energy assuming that the time lag when the cross-correlation coefficient became the highest equals to the travel time of electrons from the modulated source region to the auroral emission height. We shifted the variation of auroral intensity against that of ECH or LBC wave intensity with a time step of 0.01 s using 100 Hz sampling image data taken by the all-sky imager. The estimated energy of precipitating electron interacted with LBC waves was ~20–67 keV and that interacted with ECH waves was ~3–4 keV. On the other hand, we independently estimated the cyclotron resonance energy of LBC and ECH waves from the Arase's observation data and geomagnetic field model by TS04 Model [Tsyganenko and Sitnov, JGR, 2005]. The estimated cyclotron resonance energy of LBC waves was ~30 keV. Although the cyclotron resonance energy of ECH waves could not be estimated because it was difficult to obtain the electron temperature and wave normal angle of ECH waves from Arase data, we suggest the cyclotron resonance energy of ECH waves to be a few keV with probable assumptions. From these results, we suggest that LBC waves interact with high energy electrons which cause auroral emission at lower altitudes, while ECH waves interact with

©2019. Japan Geoscience Union. All Right Reserved.

relatively low energy electrons which cause auroral emission at higher altitudes. These results were published in Fukizawa et al. [GRL, 2018].
To verify whether ECH waves indeed scatter the pitch angle of electrons, we compared ECH wave intensity with electron flux in the loss cone obtained with low-energy particle experiments-electron analyzer onboard Arase. We also give results of other coordinated observation events.

Keywords: pulsating aurora, ECH waves, wave-particle interaction

©2019. Japan Geoscience Union. All Right Reserved.

Automatic determination of Upper Hybrid Resonance Frequencies by Convolutional Neural Network.

*Shoya Matsuda[1], Tatsuhito Hasegawa[2], Atsushi Kumamoto[3], Fuminori Tsuchiya[3], Yoshiya Kasahara[4], Yoshizumi Miyoshi[5], Yasumasa Kasaba[3], Ayako Matsuoka[1]

1. Institute of Space and Astronautical Science/Japan Aerospace Exploration Agency, 2. University of Fukui, 3. Tohoku University, 4. Kanazawa University, 5. ISEE, Nagoya University

Electron number density is a key parameter for discussions of plasma wave generation/propagation, and wave-particle interaction in the inner magnetosphere. The High Frequency Analyzer (HFA) is a subsystem of Plasma Wave Experiment (PWE) aboard Arase [Kasahara et al. (2018), Kumamoto et al. (2018), Miyoshi et al. (2018)]. The HFA measures electric field spectra in a frequency range from 10 kHz to 10 MHz, which covers a typical frequency range of Upper Hybrid Resonance (UHR) frequency in the inner magnetosphere. Kumamoto et al. (2018) proposed the semiautomatic method for the identification of UHR frequency by computer and a human operator. However, it takes a enormous effort of a human operator.

We propose an automatic determination system of UHR frequency by machine learning. Machine learning is a technique in the field of artificial intelligence to give computers the ability to learn with data. In this study, we defined a task of UHR frequency determination as supervised regression that a computer estimates UHR frequencies using the dataset composed of electric field dynamic spectra with correct UHR frequency labels. We adopted Convolutional Neural Network (CNN) as a machine learning algorithm. In this study, we introduce our machine learning approach and initial results for determining UHR frequency from electric field spectra observed by PWE/HFA.

Keywords: Arase satellite, UHR frequency, Machine learning

©2019. Japan Geoscience Union. All Right Reserved.

Amplitude dependence of whistler wave motion on electron scattering process

*Yoshiki Ito[1], Yoshizumi Miyoshi[1], Shinji Saito[1]

1. Nagoya University, ISEE

Whistler mode chorus waves cause scattering and acceleration of energetic electrons in the inner magnetosphere. The interaction processes have been modeled as diffusive process. The pitch angle diffusion coefficients of the pitch angle scattering depend on the power of chorus waves, so that it is expected that the scattering rate also depends on the wave amplitude. On the other hand, several previous studies indicated that the Lorentz force by the wave magnetic field is larger than the mirror force if the wave amplitudes increase and the electron trajectories in the velocity space are different from the diffusive distributions. In this study, we investigate chorus wave amplitude dependence of electron scattering using the GEMSIS-RBW simulation code. The RBW simulation demonstrates generation of periodical rising-tone chorus waves propagating along a magnetic field line to higher latitudes, and calculates local pitch angle and energy change by the imposed waves on the field line. At small wave amplitudes, time variations of pitch angle and energy of electrons are similar to diffusive process. At large wave amplitudes, some electrons increase both pitch angle and energy at interaction with the first rising tone, and then they decrease these parameters at interaction with the second rising tone. The process in the first rising tone seems to be the phase trapping, while the process in the second rising tone seems to be dislocation. Therefore, nonlinear scattering processes, which are phase trapping and dislocations, occur during the interactions with periodical rising-tone chorus waves with large amplitudes, which are quite different from quasi-linear scattering process.

©2019. Japan Geoscience Union. All Right Reserved.

Two-dimensional simulation of whistler mode wave packets interacting with energetic electrons

*Takeshi Nogi[1], Yoshiharu Omura[1]

1. Reserch Institute for Sustainable Humanosphere, Kyoto University

We perform two-dimensional electromagnetic particle simulations to study basic characteristics of whistler-mode wave particle interaction involved in the generation and propagation processes of chorus emissions with wave normal angles oblique to the static magnetic field. We assume a simple periodic (x, y) system with the magnetic field taken in the x-direction. We find the linear phase of the instability is much affected by electrostatic thermal fluctuations. It is necessary to put many super-particles in a grid cell to suppress the thermal fluctuation. We next put an array of antennas perpendicular to the background magnetic field, and oscillate the antenna current to generate obliquely propagating waves. In addition to the nonlinear trapping of energetic electrons through the cyclotron resonance, another nonlinear trapping of electrons takes place through the Landau resonance. Structures of the nonlinear trapping potentials change with the varying frequency, affecting efficiency of energy transfer between the wave and energetic electrons. We study nonlinear evolution of the wave packet, and competing processes of both resonances in accelerating energetic electrons to higher energies.

©2019. Japan Geoscience Union. All Right Reserved.

Relativistic electron acceleration by whistler-mode chorus waves in 1D, 2D, and 3D magnetic field models.

*Keita Takahashi[1], Yoshiharu Omura[1], Yikai HSIEH[1], Danny Summers[2]

1. Research Institute for Sustainable Humanosphere, Kyoto University , 2. Department of Mathematics and Statistics, Memorial University of Newfoundland

We evaluate the acceleration efficiencies of relativistic electrons under a 1D, 2D, and 3D model magnetic fields. We perform test-particle simulations and analyze nonlinear trapping motions of resonant electrons in each model. As a chorus wave model, we assume that a chorus wave packet generated at the magnetic equator propagates along the magnetic field to higher latitudes. When we perform simulations with the whistler mode wave, the cyclotron resonance with energetic electrons occurs at the similar timing in each model. Although we find relativistic turning acceleration (RTA) [1] to take place in each model, acceleration efficiencies of resonant electrons are different in these models. In terms of the numerical Green’s function[2], we find a clear difference in time evolution of the distribution function in energy and equatorial pitch angle. The energy gap between resonant electrons and non-resonant electrons in the 1D model is slightly different from those in the 2D and 3D models. The energy gap in the 3D model is the largest among the three magnetic field models. This difference is due to additional oscillations in the velocity phase space, which only occur in the 2D and 3D models. These oscillations occur because the magnitude of the magnetic field changes during one period of relativistic cyclotron motion, affecting the nonlinear trapping conditions of resonant electrons.

References:

[1] Y. Omura, N. Furuya, D. Summers, Relativistic turning acceleration of resonant electrons by coherent whistler-mode waves in a dipole magnetic field, Journal Geophysical Research, Vol. 112, A06236, doi:10.1029/2006JA012243, 2007.

[2] Y. Omura, Y. Miyashita, M. Yoshikawa, D. Summers, M. Hikishima, Y. Ebihara, and Y. Kubota (2015), Formation process of relativistic electron flux through interaction with chorus emissions in the Earth’s inner magnetosphere, J. Geophys. Res. Space Physics, 120, 9545–9562, doi:10.1002/2015JA021563, 2015.

©2019. Japan Geoscience Union. All Right Reserved.

Study of global spatio-temporal development of magnetospheric ELF/VLF waves for the 26-30 March 2017 storm based on ground and satellite observations and the RAM simulations

*Yuhei Takeshita[1], Kazuo Shiokawa[1], Yoshizumi Miyoshi[1], Mitsunori Ozaki[2], Yoshiya Kasahara[2], Martine Connors[3], Jyrki Manninen[4], Craig Kletzing[5], Vania Jordanova[6]

1. Nagoya University, Institute for Space-Earth Environmental Resarch, 2. Kanazawa University, 3. Athabasca University, 4. Sodankylä Geophysical Observatory, 5. The University of Iowa, 6. Los Alamos National Laboratory

The magnetospheric ELF/VLF waves are plasma waves generated by energetic electrons from several keV to tens keV with temperature anisotropy at magnetospheric equatorial plane of the inner magnetosphere. These ELF/VLF waves with frequencies lower than local half gyro frequency (lower-band) can propagate to the ground along magnetic field line. It is also known that the ELF/VLF waves interact with electrons drifting longitudinally in the inner magnetosphere, and help accelerating them to relativistic energies. Takeshita et al. [SGEPSS, 2018] statistically investigated the longitudinal extent of the magnetospheric ELF/VLF waves using six ground-based stations for two months, and showed the average extent of the ELF/VLF waves as ~90 degrees in longitude. However, Jordanova et al. [JGR, 2010] investigated the global distribution of linear growth rate of whistler mode chorus waves using global ring current-atmosphere interactions model (RAM), and showed that the region of large linear growth rate can extend ~180 degrees in longitude during the geomagnetic storm of 22 April 2001.

In this study we investigate the spatio-temporal distibution of the source region of magnetospheric ELF/VLF waves based on ground and satellite observations during the geomagnetic storm period from 26-30 March 2017, and compare it with global distribution of non-linear waves proxy of whistler mode chorus waves obtained by the RAM simulation. In this preliminary simulation, the simple dipole field and the Volland-Stern electric field are used as ambient magnetic and electric fields. And we assumed simply the Maxwell distribution as an energy spectrum using the empirical model of Tsyganenko and Mukai [2003]. In order to evaluate the non-linear wave excitation, we have estimated the optimum amplitude and the threshold value indicated by Omura and Nunn [2011]. We investigated the existence of lower band chorus waves using ground based observations at Athabasca (ATH; 54.7N, 246.4E, MLAT: 61.3N), Kapuskasing (KAP; 49.4N, 277.8E, MLAT: 58.7N), Kannuslehto (KAN: 67.7N, 26.3E, MLAT: 64.5N) and satellite-based observations by ERG with an apogee in the pre-dawn sector and RBSP-A and RBSP-B with an apogees in the post-dusk sector. We found the magnetospheric ELF/VLF waves exist from 3 MLT to 12 MLT for most periods from main- to recovery-phases of the magnetic storm. However, the RAM simulation did not predict wave generation during recovery phase of the storm. We compare the simulation and the ground-satellite observation in detail, and calculate the over-estimate rate (the ratio of wave existence period on the simulation to no wave period on the observation) and under-estimate rate (the ratio of no wave period on the simulation to wave existence period on the observation). We found the over-estimate rate become high (0.2~0.9) and under-estimate rate become low (0~0.4) in the main phase of the storm. This indicates that the longitudinal size of chorus source region predicted by simulation is larger than the observed size at the main phase. We also found that the over-estimate rate becomes low (0~0.2) and under-estimate rate becomes high (~1) during the recovery phase of the storm. This indicates that the simulation does not reproduce the wave existence during the recovery phase of the storm. Looking into the MLT distribution, the simulation predicts the wave existence from dusk to the midnight sector, but the

©2019. Japan Geoscience Union. All Right Reserved.

waves were not observed in this local time sector during the main phase. In case of recovery phase, the simulation did not predict wave existence but the observation showed continuous wave existence from dawn to the noon sector.

Keywords: chorus, ERG satellite, ground based observation

©2019. Japan Geoscience Union. All Right Reserved.

Flux decrease of outer radiation belt electrons associated with solar wind pressure pulse: A Code coupling simulation of GEMSIS-RB and GEMSIS-GM

*Ito Hiroki[1], Yoshizumi Miyoshi[1], Shinji Saito[2], Yosuke Matsumoto[3], Takanobu Amano[4]

1. Institute for Space-Earth Environmental Research, Nagoya University, 2. Graduate School of Science, Nagoya University, 3. Graduate School of Science, Chiba University, 4. Department of Earth and Planetary Science, University of Tokyo

Relativistic electron flux of the outer radiation belt dynamically changes in response to solar wind variations. There exist several conditions to cause the flux drop-out of the outer belt electrons. The magnetopause shadowing (MPS) is one of the processes to cause the rapid loss of outer belt electrons (e.g.,Kim et al.,2008). In this study, we investigate how radiation belt electrons are lost through the MPS process with a code-coupling simulation using GEMSIS-RB test particle simulation code (Saito et al., 2010) and GEMSIS-GM global MHD magnetosphere simulation code (Matsumoto et al., 2010) by focusing the equatorial pitch angle and local time dependence. We calculate trajectories of electrons in electromagnetic fields calculated from GEMSIS-GM with initial L-shells from 6 to 11, initial energies from 1 MeV to 10 MeV, and initial pitch angles between 50 degrees and 90 degrees, using the relativistic guiding-center equation. The simulation consists of the following three phases associated with variations of the solar wind dynamic pressure; [i] The standoff distance of magnetopause at the subsolar point is 12 Re with the initial dynamic pressure of 1.0 nPa. [ii] The solar wind dynamic pressure becomes 2.5 nPa, and the magnetopause moves to 9 Re. [iii] The solar wind dynamic pressure decreases, so that the inflation of the magnetopause takes place and the standoff distance of the magnetopause is 10 Re. During phase [ii], the high-latitude reconnections occur at dawn-side firstly and many electrons escape from the magnetosphere to the interplanetary magnetic field along the field line in the dawn side. Subsequently, the high-latitude reconnections occur at the high-latitude in the dusk side. In phase [iii], the remained electrons in the magnetosphere escape into the interplanetary in both the dawn and dusk sides. The loss at the dusk-side is outward motion of the trapped electrons caused by the dawn-to-dusk electric fields associated with the inflation of the magnetosphere. The study showed detailed process of the electron escape into the interplanetary magnetic field and the electron escape occur in both enhancement/decrease of the dynamic pressure.

Keywords: Magnetopause Shadowing, global MHD magnetosphere simulation, test particle simulation

©2019. Japan Geoscience Union. All Right Reserved.

Non-diffusive response of outer belt electrons on interplanetary shock

Takuma Toishi[1], *Yusuke Ebihara[1], Takashi Tanaka[2]

1. Research Institute for Sustainable Humanosphere, Kyoto University, 2. Kyushu University

Test particle simulation is performed in the electric and magnetic fields given by a global magnetohydrodynamics (MHD) simulation. When an interplanetary shock strikes the magnetosphere, a compressional wave propagates tailward. Pre-existing relativistic electrons that are initially located at fixed radial distances are redistributed by the electric and magnetic fields associated with the compressional wave. When the electrons encounter the nightside, they undergo complicated paths under the complicated distribution of the electric and the magnetic fields. Consequently, a group of isolated electrons forms, suggesting non-diffusive response. We discuss the redistribution processes in terms of the magnetospheric processes.

Keywords: radiation belt, MHD simulation, Test particle simulation

©2019. Japan Geoscience Union. All Right Reserved.

PARM: Initial result of the auroral camera on the G-CHASER (RockSat-XN) rocket and status of the development of auroral cameras for the LAMP rocket experiment

*Naoshi Yagi[1], Takeshi Sakanoi[1], Fukizawa Mizuki[1], Kazushi Asamura[2], Yoshizumi Miyoshi[3], Keisuke Hosokawa[4], Genki Ishizawa[5]

1. Planetary Plasma and Atmospheric Research Center, Graduate School of Science, Tohoku University, 2. Institute of Space and Astronautical Science, Japan Aerospace Exploration Agency, 3. Institute for Space-Earth Environmental Research, Nagoya University, 4. Department of Communication Engineering and Informatics, University of Electro-Communications, 5. Space & terrestrial plasma pyhsics

We developed an Aurora Imaging Camera (AIC) for NASA’ s G-CHASER (RockSat-XN) sounding rocket launched on 13th January, 2019. In addition, LAMP sounding rocket scheduled to be launched from December 2019 to February 2020 to reveal the spatio-temporal relationship between PsA and relativistic electrons, namely microbursts. In this presentation, we report the development of AIC, the result f the G-CHASER (RockSat-XN) rocket, as well as the current status of LAMP rocket project.

On the G-CHASER rocket experiment, 7 scientific and educational instruments were provided from Japan, U.S., Norway and Puerto Rico. Japanese instrument, called PARM, consists of an intermediate energy (20 - 100 keV) electron detector MED, high energy (several hundred keV - 2 MeV) electron detector HEP, fluxgate magnetometer AFG, and auroral camera AIC. Concerning development of AIC, we carried out sensitivity calibration experiment, electrical function test, fabrications, focus adjustment and environmental (vibration, vacuum and thermal) tests from January to July 2018. AIC consists of detector unit AIC-S and power/data processing electric unit AIC-E. AIC-S consists of a CCD camera (Watec 910 HX), wide-angle lens (F-number: 1.6, focal length: 3.5 mm, field of view: 96.4˚x75˚) and a glass filter (RG665) that transmits light with a wavelength longer than 665 nm.

NASA decided to launch the G-CHASER rocket at 9:00UT on 13rd January 2019 from Andoya Space Center, Norway (69.3˚N, 16.0˚E in the geographic coordinate). At this time, the solar elevation was -4˚, hence twilight had been already started and the region above 15km was sunlit. AIC detected leak light from the rocket skirt until the separation of skirt at an altitude of 82.9km. From time variation of AIC data, rocket spin frequencies were estimated to be ~5Hz at ~20km altitude and ~1Hz at ~80km altitude. This is consistent with the modulation period of magnetic field data observed by AFG. Because AIC was designed to measure weak pulsating aurora with hundreds Rayleigh, the AIC data was saturated above 82.9km after separation of rocket in the sunlit region, and no aurora was observed.

We are also conducting the LAMP sounding rocket project whose PI is Dr. Sarah Jones in NASA/GSFC. This is scheduled to be launched at Poker Flat Research Range in Alaska in 2019 winter. Japanese PARM2 team will provide high energy (several hundred keV - 2 MeV) electron detector HEP, fluxgate magnetometer MIM, and auroral cameras AIC2. We concern AIC2 that consists of two cameras AIC2-S1/AIC2-S2 and power/data processing electric unit AIC2-E. AIC2-S1/S2 and AIC2-E will be installed on a despun platform to derotate rocket spin. AIC2-S1 measures N2 1stPG emission with a narrow FOV lens (F value: 0.95, focal length:17mm, field of view 27x27deg), and AIC-S2 measures OI 844.6nm emission with a wide-angle lens (F value:1.6, focal length:3.5 mm, diagonal field of view:120x120˚). AIC2-S1 will take fine structure of PsA in the region more than 100 x 100 km area around the magnetic footprint with a few kilometer resolution, while AIC2-S2 will obtain an altitude distribution of

©2019. Japan Geoscience Union. All Right Reserved.

PsA in the F-region as well as wide-range distribution of PsA. The characteristic energy of precipitating electron can be estimated from the ration of OI844.6 and N2 1stPG. The cameras are conducted by a single board computer NanoPi M4 via USB3.0 high speed interface. We confirmed to get frame sampling rate with approximately 10Hz with this system. Region-of-interest (ROI) of 3660 x 3660 pixel area is binned with 61x61pixels, and finally image data with 60 x 60 bin (16 bit/bin) is recorded at 10 Hz. The precise imaging and altitude distribution of PsA are obtained with AIC2 at two wavelengths with 10Hz sampling. The imaging data combined with precipitating electron data in the wide energy range enable us to investigate the relativistic electron precipitation in microbursts that is probably caused by chorus waves in the magnetosphere.

Keywords: auroral camera, rocket experiment

©2019. Japan Geoscience Union. All Right Reserved.

First simultaneous observation of a SAR arc at subauroral latitudes using a ground all-sky camera and the Arase satellite in the inner magnetosphere

*Yudai Inaba[1], Kazuo Shiokawa[1], Shin-ichiro Oyama[1,8,9], Yuichi Otsuka[1], Atsuki Shinbori[1], Yoichi Kazama[2], Shiang-Yu Wang[2], Sunny W. Y. Tam[2], Shoichiro Yokota[3], Satoshi Kasahara[4], Kunihiro Keika[4], Tomoaki Hori[1], Ayako Matsuoka[5], Yoshiya Kasahara[6], Atsushi Kumamoto[7], Yasumasa Kasaba[7], Yoshizumi Miyoshi[1], Iku Shinohara[5], Arto Oksanen[10]

1. Institute for Space-Earth Environmental Research, 2. Academia Sinica, 3. Osaka Univ, 4. Tokyo Univ, 5. JAXA, 6. Kanazawa University, 7. Tohoku University, 8. University of Oulu, Finland, 9. National Institute of Polar Research, 10. Jyväskylän Sirius ry, Finland

Stable Auroral Red (SAR) arc is characterized by a 630.0 nm emission observed at subauroral latitudes. The energy of precipitating electrons that cause the SAR arc emission is several electron volts (eV). Precipitation of low-energy electrons is expected to occur due to spatial overlap between the plasmasphere and the ring current, where high-energy (more than 10 keV) ring current ions heat low-energy (less than 1 eV) electrons in the plasmasphere. Simultaneous observations of SAR arcs using the ionospheric satellite and ground all-sky cameras have been already done [e.g., Foster et al., 1994]. However, there has been no reports on in-situ measurements of plasma and electromagnetic fields in the inner magnetosphere, where the plasmaspheric plasma is heated by the ring current. In this study, we report simultaneous observations of a SAR arc at 22:04 UT on March 28, 2017, by using an all-sky camera at Nyrola (62.34 N, 25.51 E, MLAT 59.4 N) at subauroral latitudes and the Arase satellite. We analyze the all-sky camera data and the satellite data of this event to investigate the generation mechanism of the SAR arc. We find interesting features in the electric field data and the energy flux of electrons observed by the electric field detector of the plasma wave experiment (EFD/PWE) and the low-energy particle experiments–electron analyzer (LEP-e), respectively, onboard the Arase satellite at the crossing of the SAR arc. A negative excursion of the Ez component of the electric field (GSE coordinate system) with an amplitude of ~2.4 mV/m was observed at the crossing time. The Bx component of the magnetic field (GSE coordinate system) was negative. Thus the direction of the E ×B drift is westward, which is consistent with the westward auroral motion observed in the SAR arc by the ground all-sky camera. At the SAR arc crossing, the energy flux of electrons below 100-eV electrons is slightly intensified. We will discuss these observations in relation to the proposed SAR-arc generation mechanisms.

Keywords: ERG, SAR arc, All-sky imager, Simultaneous observation

©2019. Japan Geoscience Union. All Right Reserved.

Pi2 pulsations observed by the Arase satellite inside and outside the plasmapause

*Mariko Teramoto[1], Ayako Matsuoka[2], Reiko Nomura[5], Yoshiya Kasahara[3], Yasumasa Kasaba[4], Atsushi Kumamoto[4], Fuminori Tsuchiya[4], Shoya Matsuda[2], Masahito Nose[1], Masafumi Shoji[1], Yasunori Tsugawa[1], Shun Imajo[1], Yoshizumi Miyoshi[1], Iku Shinohara[2]

1. Institute for Space-Earth Environmental Research Nagoya University, 2. Institute of Space and Astronautical Science, Japan Aerospace eXploration Agency, 3. Kanazawa University, 4. Tohoku University, 5. National Astronomical Observatory of Japan

The spatial structure of Pi2 pulsation relative to the plasmasphere has been studied using the magnetic and electric field observed from the equatorial orbiting satellite in the inner magnetosphere by Takahashi et al (2003; 1995). They showed that the nightside Pi2 pulsations in the inner magnetosphere, which have high coherence with those at low-latitude ground station, are dominated by the poloidal component (the radial and compressional components for the magnetic field and azimuthal component for the electric field). The amplitudes of the compressional magnetic field has maximum and azimuthal electric field and the compressional magnetic field have maximum and minimum in the vicinity of the plasmaspause, respectively. The phase of the azimuthal electric field relative to low-latitude Pi2 pulsations on ground is 90 degrees in the plasmasphere. Such radial profile of the amplitude and phase of Pi2 pulsations can be explained by a plasmaspheric cavity mode resonance. However, the latitudinal structure of Pi2 pulsations in the electric field has not been examined. We investigate the latitudinal characteristics of off-equatorial Pi2 pulsations on the nightside and their relation to the plasmapause using the magnetic field measured by the fluxgate magnetometer measured by the Magnetic Field Experiment (MGF), the electric field measured by the Electric field Detector (EFD), and electron density derived from the spectra measured by the High Frequency Analyzer (HFA) from the Arase satellite.

©2019. Japan Geoscience Union. All Right Reserved.

An extreme erosion of the plasmasphere during the 7–10 September 2017 storm

*Yuki Obana[1], Naomi Maruyama[2,3], Atsuki Shinbori[4], Kumiko K. Hashimoto[5], Mariangel Fedrizzi[2,3], Masahito Nose[4], Yuichi Otsuka[4], Nozomu Nishitani[4], Tomoaki Hori[4], Atsushi Kumamoto[6], Fuminori Tsuchiya[6], Shoya Matsuda[7], Ayako Matsuoka[7], Yoshiya Kasahara[8], Akimasa Yoshikawa[9], Yoshizumi Miyoshi[4], Iku Shinohara[7]

1. Osaka Electro-Communication University, 2. University of Colorado Boulder, 3. NOAA Space Weather Prediction Center, 4. Nagoya University, 5. Kibi International University, 6. Tohoku University, 7. Japan Aerospace Exploration Agency, 8. Kanazawa University, 9. Kyushu University

We report an extreme erosion of the plasmasphere arising from the September 2017 storm. The cold electron density is identified from the upper limit frequency of UHR waves observed by the HFA of the PWE instrument onboard the Arase spacecraft. The HFA provides the spectrograms of electric fields in a frequency range from 10 kHz to 10 MHz with an 8-sec time resolution (Kasahara et al., 2018; Kumamoto et al., 2018). Such wide frequency coverage allows observation of the UHR frequency even deep inside the plasmasphere.

The electron density profiles reveal that the plasmasphere was severely eroded during the recovery phase of the storm and the plasmapause was located at L~1.7 at 23 UT on 8 Sep 2017. This is the first report of such deep erosion of the plasmasphere (L_{PP}<2) with the in-situ observation of the electron density. The degree of the severity is much more than what is expected from the SYM-H minimum (−146 nT) of the event.

We further study absolute GNSS-TEC, ground-based magnetic field, the doppler velocity obtained from the SuperDARN Hokkaido Radars to investigate the location of the midlatitude ionospheric trough, the penetration of the convection electric field to the equator and middle latitudes, respectively. Our results suggest that the middle latitude electric field was penetrated from the high-latitude storm time convection for several hours. Futhermore, the Ionosphere-Plasmasphere-Electrodynamics (IPE) model (Sun et al., 2015; Maruyama et al., 2016) is used to understand the dynamics of the plasmasphere. The IPE results suggest that the middle latitude electric field penetrates from the high-latitude storm time convection that lasts for several hours can explain the degree of severity during the September 7-11 2017 storm.

Keywords: plasmasphere, innner magnetosphere, Magnetosphere-ionosphere coupling

©2019. Japan Geoscience Union. All Right Reserved.

Relative contribution of ULF and chorus waves to the radiation belt variation: Comparison between multi-point observations and BATSRUS + CRCM simulation

*Naoko Takahashi[1], Kanako Seki[1], Mei-Ching Fok[2], Yihua Zheng[2], Yoshizumi Miyoshi[3], David Hartley[4], Ayako Matsuoka[5], Yoshiya Kasahara[6], Yasumasa Kasaba[7], Nana Higashio[8]

1. Graduate School of Science, University of Tokyo, 2. NASA Goddard Space Flight Center, 3. Institute for Space-Earth Environmental Research, Nagoya University, 4. Department of Physics and Astronomy, University of Iowa, 5. Institute of Space and Astronautical Science, Japan Aerospace Exploration Agency, 6. Information Media Center, Kanazawa University, 7. Planetary Plasma and Atmospheric Research Center, Tohoku University, 8. Japan Aerospace Exploration Agency

Earth’ s radiation belt is the area where electrons with energies from hundreds of keV to several MeV are trapped. When, where, and how the radiation belt exhibits a dramatic variation during a magnetic storm is of global interest. The dynamic variation of the radiation belt is caused by various wave-particle interactions: (1) the radial diffusion of electrons driven by ultra-low-frequency (ULF) waves in Pc5 frequency ranges (1.6–6.7 mHz) and (2) the local acceleration caused by wave-particle interactions between whistler-mode chorus waves and radiation belt particles. Over the past decade, multi-point observations and numerical simulations have provided evidence to support above physical processes. However, it is debatable how much each wave contributes to the radiation belt variation during a magnetic storm. A few previous studies have quantitatively compared roles of local acceleration and radial transport by calculating diffusion coefficients, whereas the global context between the wave growth and the relativistic electron flux enhancement has not been extensively studied. To address these issues, the comprehensive study using multi-point observations and numerical simulations (not empirical models) makes essential and significant contributions.

We focus on the magnetic storm on 27-30 May 2017. This magnetic storm is triggered by coronal mass ejections and induces a clear interplanetary shock. Fortunately, several satellites are scattered in the inner magnetosphere and detect both ULF and chorus waves during this magnetic storm. Arase and Van Allen Probes also detect variations of relativistic electron fluxes associated with the Dst index variation. We examine L-value dependence of ULF and chorus wave powers and find the difference of wave activity during the recovery phase. The chorus wave activity is large during the early recovery phase, while the ULF wave activity is large during the late recovery phase. The difference of wave activity may contribute to the radial profile in the phase space density of relativistic electrons. To grasp the extent of individual wave contribution, we also perform the comprehensive ring current model (CRCM) coupled with Block-Adaptive-Tree Solar-Wind Roe-Type Upwind Scheme (BATSRUS) simulation. BATSRUS with CRCM well reproduces global characteristics of energetic electron fluxes and wave growth during this magnetic storm. We will further evaluate global distribution of simulated wave power comparing to the observation, and then discuss the temporal and spatial context between each wave growth and the radiation belt variation.

©2019. Japan Geoscience Union. All Right Reserved.

Modulation of the D-region ionosphere by Pc5 waves observed by VLF/LF standard radio waves

*Miyashita Takuya[1], Hiroyo Ohya[1], Fuminori Tsuchiya[2], Hiroyuki Nakata[1], Toshiaki Takano[1], Kazuo Shiokawa[3], Yoshizumi Miyoshi[3]

1. Chiba University, 2. Tohoku University, 3. Nagoya University

Ionospheric modulation due to ultra low frequency (ULF) Pc5 waves have been observed by GPS-total electron content (TEC), high frequency (HF) Doppler sounders, and SuperDARN HF radars [e.g., Pilipenko et al., 2014; Belakhovsky et al., 2016]. However, there are few reports for the modulation of the lower ionospheric associated with the ULF Pc5 waves using VLF/LF transmitter signals. In this study, we investigate the D-region signatures of the modulation due to the ULF Pc5 waves using a network of very low frequency (VLF)/low frequency (LF) standard radio waves. We show oscillations in intensities of the VLF/LF waves with a period of 4-6 minutes during substorms on 27 April, 2017. The transmitter signals from NAA (USA, 24.0 kHz, L = 2.88), NLK (USA, 24.8 kHz, L = 2.88), NDK (USA, 25.2 kHz, L = 2.98) and WWVB (USA, 60.0 kHz, L = 2.26) were observed by the receivers at ATH (Athabasca, L=4.31) and PKR (Poker Flat, L=5.95). The substorm occurred at 04:30 UT. Based on the wavelet analysis, we found that the intensities for the NDK-ATH and WWVB-ATH paths showed oscillations with a period of 4-6 minutes during the substorm growth phase (05:00-06:00 UT). Magnetic field variations observed by ground magnetometers around the NDK-ATH and WWVB-ATH paths also showed the same periodicity, which means that the variations in the VLF/LF intensities would be caused by Pc5 modulations. The magnetic field oscillations were observed in wide latitude range. The intensity of the oscillation was larger at high latitude magnetometers than those around the location of the NDK-ATH and WWVB-ATH path (mid-latitude). The Pc5 oscillations could be excited by solar wind because solar wind speed had similar period of the 4-6 minutes. In this presentation, we will discuss the cause of these VLF/LF oscillations.

Keywords: VLF/LF standard radio waves, Pc5, ULF

©2019. Japan Geoscience Union. All Right Reserved.

Oxygen-proton differences in ion energies dominating plasma pressure: Dependence on storm phases and solar wind drivers

*Kunihiro Keika[1], Satoshi Kasahara[1], Shoichiro Yokota[2], Masahiro Hoshino[1], Kanako Seki[1], Masahito Nose[3], Yoshizumi Miyoshi[3], Iku Shinohara[4]

1. Graduate School of Science, The University of Tokyo , 2. Graduate School of Science, Osaka University, 3. Institute for Space-Earth Environmental Research, Nagoya University, 4. Institute of Space and Astronautical Science, Japan Aerospace Exploration Agency

The ion pressure in the inner magnetosphere is generally dominated by protons with energies of a few to a few 100s keV. Oxygen ions of ionospheric origin, O+, can make a significant contribution to the ion pressure during geomagnetically active periods. Our previous study (Keika et al., 2018, GRL) examined the radial dependence of contributing energies, which we term an energy range that makes the dominant contribution to the plasma pressure, during the main phase of the six magnetic storms in Year 2017. We found clear oxygen-proton differences in the contributing energies in the outer part (L>5) of the ring current region. The contributing energies were higher for O+ than for H+. The results provided in situ evidence of the contribution from mass-dependent/selective acceleration processes to the energization of the outer part of the ring current.

The present study extends this analysis toward a larger database obtained from a longer period of magnetic storm times including the recovery phase. We also compare mass-dependent/selective energization between different solar wind drivers such as coronal mass ejections and corotational interaction regions. We primarily use data from the MEP-i (Medium-Energy Particle experiments - ion mass analyzer) on board the Arase spacecraft. MEP-i measures ions with energies of 10 to 180 keV/q and distinguishes between different ion species. Arase observed the nightside near-Earth magnetosphere (L<10) during 7 CME-driven and 7 CIR-driven storms with the Dst minimum of smaller than -50 nT in Years 2017 and 2018. The dependence on storm phases and solar wind drivers helps identify magnetospheric conditions favorable for mass-dependent/selective acceleration and in turn provides clues for understanding important physical mechanisms. Utilizing observations made by the MMS spacecraft in the near-Earth plasma sheet, we also compare oxygen-to-proton differences inside earthward bursty bulk flows with the Arase/MEP-i observations. The multi-spacecraft observations help better understand the temporal evolution of the mass-dependent/selective acceleration processes.

Keywords: Magnetic storms, Substorms, RIng current, Oxygen ions, Ion transport and acceleration

©2019. Japan Geoscience Union. All Right Reserved.

Mass dependence of penetration depth of multi-energy ions in the inner magnetosphere during magnetic storms: Arase observations

*Ryosuke Fujii[1], Yoshizumi Miyoshi[1], Masafumi Shoji[1], Kazushi Asamura[2], Lynn Kistler[1,8], Vania Jordanova[9], Tomoaki Hori[1], Satoshi Kurita[1], Mariko Teramoto[1], Yasunori Tsugawa[1], Yoshiya Kasahara[3], Yasumasa Kasaba[4], Atsushi Kumamoto[5], Fuminori Tsuchiya[4], Shoichiro Yokota[6], Kunihiro Keika[7], Ayako Matsuoka[2], Iku Shinohara[2]

1. Institute for Space-Earth Environmental Research, Nagoya University, 2. Institute of Space and Astronautical Science, Japan Aerospace Exploration Agency, 3. Information Media Center, Kanazawa University, 4. Planetary Plasma and Atmospheric Research Center, Tohoku University, 5. Department of Geophysics, Graduate School of Science, Tohoku University, 6. Graduate School of Science, Osaka University, 7. Department of Earth and Planetary Science, Graduate School of Science, The University of Tokyo, 8. University of New Hampshire, 9. Los Alamos National Laboratory

During magnetic storms, the ring current ions move toward the Earth, and the inner edge position of the ring current depends on the convection electric field. We investigate variations of the inner edge of the ring current ions, so-called, penetration depth, during magnetic storms using the ion measurements made by the Low-energy particle experiments-ion mass analyzer (LEP-i)/Medium-energy particle experiments-ion mass analyzer (MEP-i) instruments onboard the Arase satellite. The Arase satellite typically observes the earthward penetration of the ring current protons associated with the enhancement of the dawn-to-dusk electric field in the inner magnetosphere during the storm main phase. The plasmapause moves earthward during the main phase. On the other hand, the convection electric field decreases during the storm recovery phase in which the flux of ring current protons decreases. We identify that the penetration depth of protons depends on the minimum Dst index during the storms as well as the proton energy.

We also investigate the penetration depth of other ions, i.e., helium and oxygen ions. Because the life times of helium and oxygen ions due to charge exchange reaction for are longer than that of protons, it is expected that these ions can penetrate deeper than protons and temporal and spatial evolution can be observed clearly. We will also discuss the relation between the position of ring current inner edge and cross polar cap potential.

Keywords: The Arase satellite, Ring current, Ions

©2019. Japan Geoscience Union. All Right Reserved.

Relativistic Acceleration of Energetic Protons by Electromagnetic Ion Cyclotron Waves in the Jovian Magnetosphere

*Tomohiro Sekine[1], Yoshiharu Omura[1], Danny Summers[2], Yikai HSIEH[1], Satoko Nakamura[1]

1. Reserach Institute for Sustainable Humanosphere, Kyoto University, 2. Memorial University of Newfoundland

We perform test particle simulations of nonlinear interaction between energetic protons and EMIC waves. We assume a coherent EMIC waves that have a constant frequency and propagate parallel to the magnetic field. We find that protons can be trapped and accelerated by EMIC waves. We find a very efficient acceleration process of protons in which kinetic energy of protons increases while directions of parallel velocities reverses when we assume parameters in the Jovian magnetosphere. We notice that this phenomenon is very similar to the interaction process between relativistic electrons and whistler-mode waves, which is called Relativistic Turning Acceleration (RTA) [1]. In order to analyze the phenomena, we have developed nonlinear trapping theory of interaction between relativistic protons and EMIC waves. Next, we compare the theory and simulation results. We confirm that the results satisfy the conditions for RTA. Following the trajectories of many resonant protons, we obtain time evolution of the distribution function of relativistic protons as a function of energy and equatorial pitch angle based on the numerical Green’ s function method [2].

References:

[1] Y. Omura, N. Furuya, D. Summers, Relativistic turning acceleration of resonant electrons by coherent whistler-mode waves in a dipole magnetic field, Journal Geophysical Research, Vol. 112, A06236, doi:10.1029/2006JA012243, 2007.

[2] Y. Omura, Y. Miyashita, M. Yoshikawa, D. Summers, M. Hikishima, Y. Ebihara, and Y. Kubota (2015), Formation process of relativistic electron flux through interaction with chorus emissions in the Earth’ s inner magnetosphere, J. Geophys. Res. Space Physics, 120, 9545–9562, doi:10.1002/2015JA021563, 2015.

©2019. Japan Geoscience Union. All Right Reserved.

Statistical study of IPDP type EMIC wave-related electron precipitation at subauroral latitude

*Asuka Hirai[1], Fuminori Tsuchiya[1], Takahiro Obara[1], Yasumasa Kasaba[1], Yuto Katoh[2], Hiroaki Misawa[1], Kazuo Shiokawa[3], Yoshizumi Miyoshi[3], Satoshi Kurita[3], Martin G Connors[4]

1. Planetary Plasma and Atmospheric Research Center, Graduate School of Science, Tohoku Univ. , 2. Department of Geophysics, Graduate School of Science, Tohoku University, 3. Institute for Space-Earth Environmental Research, Nagoya University, 4. Athabasca University

The outer radiation belt electrons disappear during the main phase of geomagnetic storms. One of the loss mechanisms of electrons from the outer belt is precipitation into the atmosphere due to wave-particle interactions. Electromagnetic ion cyclotron (EMIC) waves are believed to be important plasma waves that contribute to the loss of the outer radiation belt due to pitch angle scattering. They can scatter relativistic and ultra-relativistic electrons. However, there are still questions left about the contribution of EMIC waves to the whole loss of radiation belt electrons and possible conditions favorable to pitch angle scattering.

EMIC waves mainly propagate along magnetic field lines and are observed on the ground as Pc1 geomagnetic pulsations. Intervals of pulsations of diminishing periods (IPDP) are Pc1/EMIC waves that are characterized by frequency rise from 0.1 to 1–2 Hz in a period of ~1 h, and often occur during substorms. Recent studies reported that IPDP are preferentially associated with relativistic electron precipitation. However, the statistical relation between IPDP waves and relativistic electron precipitation, and their physical mechanism, remain open issues.

We investigated differences in characteristics between IPDP and other types of Pc1 by using an induction magnetometer and VLF radio wave data that is a proxy of electron precipitations at subauroral latitude from 1 November 2016 to 30 June 2018. We used the induction magnetometer of PWING (study of dynamical variation of Particles and Waves in the INner magnetosphere using Ground-based network observations) at Athabasca, Canada (54.6˚N, 246.36˚E, L = 4.39). VLF radio waves propagate from transmitters to receivers in subionospheric waveguide. The modulations of VLF signals are detected as occurrence of sub-relativistic and relativistic electron (>100 keV) precipitation due to ionization changes in the lower ionosphere along the radio wave propagation path. VLF radio waves are transmitter from NDK, U.S. (46.367˚N, 261.467˚E, L =3.13) and NLK, U.S. (48.2˚N, 238.083˚E, L =2.84) and received at Athabasca. We selected EMIC wave events on the basis of the following criteria: (1) EMIC wave power is higher than 10^{-5} nT^2/Hz. (2) Duration of EMIC waves is longer than 20 min. (3) Interval between one EMIC wave event and the next one is longer than 30 min. Electron precipitation was identified as a decrease in amplitude of VLF signals from the quiet day curve (QDC). We counted as EMIC wave-driven electron precipitation if we detect temporal correspondence with EMIC waves. In this period, we found 950 EMIC wave events, and 87 of total EMIC wave events were IPDP events (9.2%). Local time dependence of EMIC waves shows that IPDP often occurs in the afternoon and evening sector, while other types of Pc1 occur in all local time range, but with a maximum in 12–16 MLT, which is consistent with previous studies. Simultaneous observation of the magnetometer and VLF radio waves were available for 286 days, and we found 163 EMIC wave events. 19 of 163 EMIC wave events were clearly associated with electron precipitation (12%). Among 19 electron precipitation events, 15 events were caused by IPDP (79%). Also, the electron precipitation events were observed in the evening sector with similar local time dependence to IPDP. This result suggests that IPDP is more likely to cause electron precipitation than other Pc1 wave types. In previous studies, IPDP occurs due to ion cyclotron instability of ring current ions in the evening sector, and favorable region for electron scattering by EMIC waves is high density duskside plasmapause

©2019. Japan Geoscience Union. All Right Reserved.

and plasmaspheric plume because dense plasma lowers minimum resonant energy of electrons. It is assumed that occurrence region of IPDP is coincident with the preferential region for MeV electron scattering by EMIC waves. For this reason, it is expected that IPDP type EMIC waves significantly cause relativistic electron precipitations in the duskside.

Keywords: EMIC waves, electron precipitation, subionospheric VLF radio waves

©2019. Japan Geoscience Union. All Right Reserved.

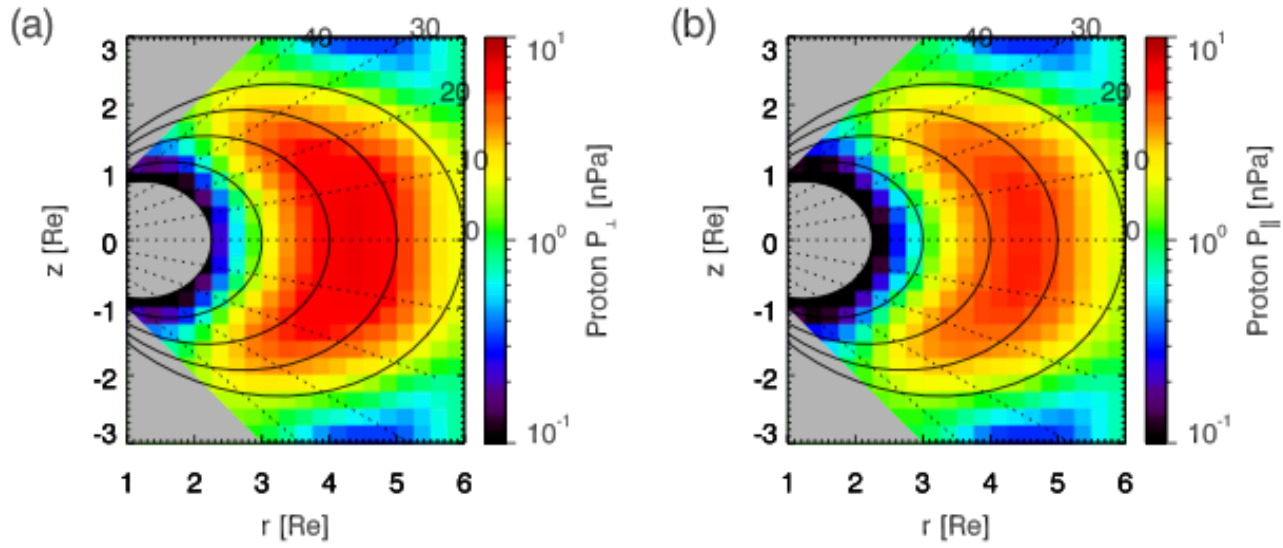
Meridional distributions of proton plasma and pressure-driven currents in the nightside inner magnetosphere: Arase observations

*Shun Imajo[1], Masahito Nose[1], Satoshi Kasahara[2], Shoichiro Yokota[3], Ayako Matsuoka[4], Kunihiro Keika[2], Tomoaki Hori[1], Mariko Teramoto[1], Kazuhiro Yamamoto[5], Oimatsu Satoshi[5], Reiko Nomura[6], Akiko Fujimoto[7], Iku Shinohara[4], Yoshizumi Miyoshi[1]

1. Institute for Space-Earth Environmental Research, Nagoya University, 2. Graduate School of Science, The University of Tokyo, 3. Graduate School of Science, Osaka University, 4. Institute of Space and Astronautical Science, Japan Aerospace Exploration Agency, 5. Graduate School of Science, Kyoto University, 6. National Astronomical Observatory of Japan, 7. Kyushu Institute of Technology

We examine the averaged meridional distributions of proton plasma parameters and pressure-driven currents in the nightside (20–04 h magnetic local time) ring current region during disturbed times (-80 < SYM-H* < -40 nT) using ion measurements covering energy range of 10–180 keV by the Arase satellite. Because the Arase satellite has a large inclination orbit of 31°, it covers the absolute value of magnetic latitude (|MLAT|) range of 0–40° and the radial distance of < 6 Re. We find that the plasma pressure decreases significantly with MLAT. The plasma pressure on the same L^* shell at 30°<|MLAT|<40° is about 10–60% of that at 0°<|MLAT|<10°, and the percentage of decrease is larger on lower L^* shells. The pressure anisotropy which is defined by the perpendicular pressure divided by the parallel pressure decreases with radial distance and shows a weak dependence on |MLAT|. The magnitude of the plasma beta at 30°<|MLAT|<40° is one or two order smaller than that at 0°<|MLAT|<10°. The relative plasma pressure distribution predicted from the magnetic strength and anisotropy is roughly consistent with the observed plasma pressure for L^*=3.5–5.5. The azimuthal pressure-gradient current derived from the plasma pressure distribution spreads over ~-20° |MLAT|, while the curvature current is limited in ~0–10° |MLAT|. We suggest that the latitudinal dependences should be taken into account when considering a temporal evolution of ring current particles from L distributions of successive orbits.

Keywords: meridional distributions, plasma pressure, pressure-driven currents, Arase satellite



©2019. Japan Geoscience Union. All Right Reserved.

Space Weather Effects on Energetic Proton Flux Response in South Atlantic Anomaly

*Kirolosse Mina GIRGIS[1,2], Tohru Hada[1], Shuichi Matsukiyo[1]

1. Earth System Science and Technology (ESST) Department, Interdisciplinary Graduate School of Engineering Sciences (IGSES), Kyushu University, Japan, 2. Aerospace Engineering Department, Faculty of Engineering, Cairo University, Egypt

In this research, energetic proton flux in the inner radiation belt, is studied inside the South Atlantic Anomaly (SAA) by performing test particle simulations, where the background time-varying magnetic field is provided by Tsyganenko model, according to *Dst* index and altitudes. The objective of this investigation, is to estimate and forecast the additional radiation dose, occurring on spacecraft and human bodies, due to their passage inside the anomaly, and precisely, during intense solar storms. It was found that within minutes, proton flux in the SAA, penetrated deeper downward by about 200 km, when the *Dst* index is decreased (< -210 nT), and a after few more minutes, it was significantly reduced at all the altitudes; the last conclusion was confirmed by satellite observations.

Keywords: South Atlantic Anomaly, Space Weather, Dst Index, Radiation Dose, Proton Flux

©2019. Japan Geoscience Union. All Right Reserved.

Solar-cycle variations of >30 keV electron flux enhancements under the inner radiation belt

*ALLA SUVOROVA[1]

1. National Central University

Intense fluxes of 30-300 electrons can arise in the equatorial ionosphere outside the South Atlantic Anomaly. It was established that the electrons were injected from the inner radiation belt probably due to a mechanism of fast radial transport in the crossed electric and magnetic fields. Continuous monitoring of energetic particles at low heights of ~850 km with the MEPED instrument onboard the NOAA/POES satellites allowed compiling large statistics of the >30 keV electron enhancements from 1998 to 2018. We studied particle flux variations with geomagnetic activity and solar cycle. We found that geomagnetic activity measured by Dst and AE indices are not key factors of occurrence rate increase for electron injections, but influence on intensity of particles. The occurrence rate is controlled by auroral conductivity on the dayside and significantly enhanced during northern summer. Descending phase of solar cycle plays a major role in the occurrence rate increase.

Keywords: magnetosphere-ionosphere, energetic electrons, low latitudes, solar cycle

©2019. Japan Geoscience Union. All Right Reserved.

Energy spectra variations of high energy electrons in the inner magnetosphere observed by HEP/XEP on ARASE and SEDA-e on HIMAWARI

*Takeshi Takashima[1], Takefumi Mitani[1], Nana Higashio[2], Tsutomu Nagatsuma[3]

1. ISAS/JAXA, 2. Research and Development Directorate/JAXA, 3. NiCT

The relativistic electrons in the outer radiation belt were disappeared/increased and their energy spectra were changed dynamically in some storms observed by XEP/HEP onboard the ARASE spacecraft. In the same time, SEDA-e with energy range 200keV-4.5MeV for electron on board the HIMAWARI-8, Japanese weather satellite on GEO, observed increase of relativistic electron in different local time.
When comparing the energy spectra, there are times when the spectrum matches or does not match. It is also observed that the change in the slope of the energy spectrum differs with time. These phenomena are observed even when there are two satellites at the same local time.
We will report on energy spectra variations of high energy electrons including calibrations of differential flux between XEP and HEP and discuss comparisons with energy spectra between ARAE and HIMAWARI that observed each storm in different local time.

Keywords: relativistic electron, inner magnetosphere, ARASE

©2019. Japan Geoscience Union. All Right Reserved.

Inter-channel calibration of the high-energy electron experiments (HEP) instrument onboard the Arase satellite

*Tomoaki Hori[1], Takefumi Mitani[2], Takeshi Takashima[2], Park Inchun[1], Satoshi Kurita[1], Mariko Teramoto[1], Nana Higashio[3], Satoshi Kasahara[4], Shoichiro Yokota[5], Yoshizumi Miyoshi[1], Iku Shinohara[2]

1. Institute for Space-Earth Environmental Research, Nagoya University, 2. Japan Aerospace Exploration Agency, Institute of Space and Astronautical Science, 3. Japan Aerospace Exploration Agency, 4. Graduate School of Science, The University of Tokyo, 5. Graduate School of Science, Osaka University

An inter-channel comparison of electron fluxes measured by the HEP instrument onboard the Arase satellite is conducted with a focus on the apparent non-uniformity in detection efficiency and relative offset of the background flux level between the channels, which was partly reported previously. We extend the data set to cover the entire two-year period since the start of the regular observations. The flux ratio of different channels is sorted by the electron flux level of much higher energies that was simultaneously measured by the extremely high-energy electron experiment (XEP) instrument onboard Arase. The result shows that the HEP flux of all azimuthal channels is more or less affected by MeV electrons which are most likely to have penetrated into the instrument box and directly hit the detectors. However, it is also revealed that the non-uniform count distribution over the channels still remains even when the penetrating electrons are absent. We conduct a set of Geant-4 simulations to trace electrons with various energies and incident angles to the detector plane in order to give a quantitative interpretation for the resultant count distributions, in terms of the effects of penetrating electrons and obliquely-colliding incident electrons.

Keywords: Arase satellite, particle instrument, calibration

©2019. Japan Geoscience Union. All Right Reserved.

Particle simulation for calibrating the HEP data onboard the ARASE satellite

*PARK INCHUN[1], Yoshizumi Miyoshi[1], Takefumi Mitani[2], Tomoaki Hori[1], Satoshi Kurita[1], Mariko Teramoto[1], Takeshi Takashima[2], Nana Higashio[3], Iku Shinohara[2]

1. Nagoya University Institute for Space-Earth Environmental Research, 2. Japan Aerospace Exploration Agency Institute of Space and Astronautical Science , 3. Japan Aerospace Exploration Agency

Understanding the detailed characteristics of the HEP (High-Energy electron Experiment) instrument onboard the Arase satellite is crucial for data calibration. Due to difficulties of reproducing the severe radiation environment of the inner magnetosphere on the ground, computer simulation is the best method to understand instrument responses to the ambient radiation environment. Through Monte-Carlo simulations using the Geant4 tool, we have reconstructed the geometry of the HEP instrument and modeled the high-energy particle environment. Using the developed model, we have studied the efficiency of the detectors, the angular resolution, and the g-factors, which depend on the particle energy and the sensor channels. While the previous studies were based on a uni-direction simulation with electron pencil beams, this study adopted all the detector channels and energy bends of HEP thus resulting in more advanced simulations. Based on the results, we have made a new calibration table depending on the angle of incident particles. We have also estimated the g-factor which depends on the incident particle energy. The updated calibration table and g-factors are important for calibrating the HEP data as well as inter-calibrations with other particle instruments' data.

Keywords: ARASE, Geant4, HEP

©2019. Japan Geoscience Union. All Right Reserved.

Geant4 model calculation and energetic particle observation with HEP/Arase in the inner radiation belt

*Honoka Toda[1], Wataru Miyake[1], Takefumi Mitani[3], Takeshi Takashima[3], Yoshizumi Miyoshi[2], PARK INCHUN[2], Tomoaki Hori[2]

1. Tokai University, 2. ISEE/Nagoya University, 3. ISAS/JAXA

The high-energy electron experiments (HEP) instrument installed on the Arase is designed to observe energetic electrons of 70 keV to 2 MeV. The HEP registers high electron counts for the MeV energy range, not only in the outer belt but also in the inner belt, in MeV energy range. On the contrary, Van Allen Probes have hardly detected MeV electrons in the inner radiation belt. A probable interpretation is that the counts of HEP are caused due to contamination of high-energy protons. In order to verify this idea, we have modeled the HEP instrument a Geant4 simulation to determine the energy of penetrating protons. The result clearly shows that high-energy protons, it has become clear that high-energy protons of a few to a few tens of MeV can contribute to the apparent high counts of HEP. No instrument for measuring protons in this energy range is installed on the satellite. We will discuss the possibility of research on the spatial distribution and time variation of high-energy protons in the inner belt based on observation data from the HEP instrument.

Keywords: Arase, Proton Radiation Belt, HEP

©2019. Japan Geoscience Union. All Right Reserved.

Validation of High-energy electron detector simulator for the HEP instruments onboard Arase

*Takefumi Mitani[1], PARK INCHUN[2], Tomoaki Hori[2], Taku Namekawa[1,3], Kazushi Asamura[1], Takeshi Takashima[1], Satoshi Kasahara[3], Satoshi Kurita[2], Mariko Teramoto[2], Nana Higashio[1], Yoshizumi Miyoshi[2], Iku Shinohara[1]

1. Japan Aerospace Exploration Agency, Institute of Space and Astronautical Science, 2. Institute for Space-Earth Environmental Research, Nagoya Univ., 3. The university of Tokyo

The high-energy electron experiments (HEP) onboard the Arase satellite detects 70 keV-2 MeV electrons and generates a three-dimensional velocity distribution for these electrons in every period of the satellite's rotation. Electrons are detected by two instruments, namely, HEP-L and HEP-H, which differ in their geometric factor (G-factor) and range of energies they detect. HEP-L detects 70 keV–1 MeV electrons and its G-factor is 9.3 $\times 10^{-4}$ cm^2 sr at maximum, while HEP-H observes 0.7 MeV–2 MeV electrons and its G-factor is 9.3 $\times 10^{-3}$ cm^2 sr at maximum. The instruments utilize silicon strip detectors and application-specific integrated circuits to readout the incident charge signal from each strip.

In order to deduce the distribution of incident electrons from the direction and energy detections in orbit, we have developed a detector simulator using the Geant4 toolkit. Especially contamination due to high energy particles must be considered quantitatively. We have also been working on electron beam experiments using HEP detector modules which are almost the same as the flight model in order to compare detailed simulations and experimental data.

We will present a comparison between results from the electron beam experiments and those from the detector simulator. And we will discuss its influence on the interpretation of the observational data obtained in orbit.

Keywords: high-energy electron, Arase, Geant4

©2019. Japan Geoscience Union. All Right Reserved.

[E] Poster | P (Space and Planetary Sciences)：P-EM Solar-Terrestrial Sciences, Space Electromagnetism & Space Environment

Wed. May 29, 2019 5:15 PM - 6:30 PM JST | Wed. May 29, 2019 8:15 AM - 9:30 AM UTC | Poster Hall International Exhibition Hall8, Makuhari Messe_6

[P-EM13] Inner magnetosphere: Recent understanding and new insights

convener:Yusuke Ebihara(Research Institute for Sustainable Humanosphere, Kyoto University), Danny Summers(Memorial University of Newfoundland), Yoshizumi Miyoshi(Institute for Space-Earth Environmental Research, Nagoya University), Shinji Saito(Graduate School of Science, Nagoya University)

The inner magnetosphere is characterized by the dominance of intrinsic dipolar Earth's magnetic field. The dipolar magnetic field traps charged particles, resulting in the formation of unique particle environment known as the plasmasphere, the ring current, and the radiation belt. The inner magnetosphere is always changing because of incoming energy from the outer magnetosphere and the ionosphere in the forms of particles and electromagnetic fields. In the inner magnetosphere, the particle energy is transferred to the field energy, and vice versa. The mutual coupling between particles and fields also makes the inner magnetosphere unique. The outgoing energy to these regions is also known to be significant, such as precipitation into the upper atmosphere and sub-auroral disturbances. A number of satellites (e.g., DMSP, NOAA, Geotail, Cluster, THEMIS, Van Allen Probes, MMS, and Arase), ground-based instruments (e.g., SuperDARN and EISCAT radars, magnetometers, and cameras), and numerical simulations (e.g., global particle simulation, PIC simulation, and hybrid simulation) have successfully surveyed the inner magnetosphere, which deepen our knowledge significantly. USAF DSX, UCLA Elfin and NASA CeRES will be launched soon, being expected to provide important information. We solicit papers describing recent results on the inner magnetosphere and/or its coupling with the other regions, including the ionosphere and the outer magnetosphere.

[PEM13-P01] Evaluation of wave normal and Poynting vector analyses for whistler mode waves observed by the waveform capture (WFC) on board the Arase

*Yoshiya Kasahara[1], Satoshi Ikarashi[1], Hiroyuki Nishizawa[1], Shoya Matsuda[2], Fuminori Tsuchiya[3], Atsushi Kumamoto[3], Yasumasa Kasaba[3], Mitsunori Ozaki[1], Ayako Matsuoka[2] (1.Kanazawa University, 2.ISAS/JAXA, 3.Tohoku University)

[PEM13-P02] Calibration of electric fields dedicated to the measurement of the S-WPIA of the Arase Satellite

*Miki Jumpei[1], Hirotsugu Kojima[2], Yuto Katoh[3], Shoya Matsuda[4], Yoshiya Kasahara[5], Mitsuru Hikishima[4], Satoshi Kurita[6], Masahiro Kitahara[3], Satoshi Kasahara[7], Yoshizumi Miyoshi[6], Atsushi Kumamoto[3], Ayako Matsuoka[4], Shoichiro Yokota[8], Tomoaki Hori[6], Kunihiro Keika[7] (1.Space Radio Engineering Laboratory, Division of Electrical Engineering, Kyoto University Graduated School, 2.Research Institute for Sustainable Humanosphere, Kyoto University, 3.Graduate School of Science and Faculty of Science, Tohoku University, 4.Institute of Space and Astronautical Science, JAXA, 5.Information Media Center, Kanazawa University, 6.Institute for Space-Earth Environmental Research, Nagoya University, 7.School of Science, The University of Tokyo, 8.School of Science, Osaka University)

[PEM13-P03] Enhancement of whistler-mode chorus in association with Pc 4-5 ULF waves and related variation of high energy electrons

*Atsuhiro Ono[1], Yuto Katoh[1], Atsushi Kumamoto[1], Fuminori Tsuchiya[1], Mariko Teramoto[2], Yoshiya Kasahara[3], Shoya Matsuda[4], Ayako Matsuoka[4], Takefumi Mitani[4], Tomoaki Hori[2], Satoshi Kasahara[5], Shoichiro Yokota[6], Kunihiro Keika[5], Yoshizumi Miyoshi[2], Iku Shinohara[4] (1.Tohoku University, 2.Nagoya University, 3.Kanazawa University, 4.ISAS/JAXA, 5.The University of Tokyo, 6.Osaka University)

[PEM13-P04] Sudden enhancements of electron cyclotron harmonic waves observed by the Arase satellite

*Shinjo Airi[1], Hirotsugu Kojima[1], Yoshiya Kasahara[2], Yoichi Kazama[3], Hideyuki Usui[4], Yoshizumi Miyoshi[5], Yasumasa Kasaba[6], Shoya Matsuda[7], Tomoaki Hori[5], S. -Y. Wang[8], Sunny W.Y. Tam[9], Atsushi

Kumamoto[10], Ayako Matsuoka[11] (1.Research institute for sustainable humanosphere, Kyoto University, 2.Information Media Center, Kanazawa University, 3.ASIAA, 4.Graduate school of system informatics Kobe University, 5.Institute for Space-Earth Environmental Research, Nagoya University, 6.Planetary Plasma and Atmospheric Research Center, Tohoku University, 7.Institute of Space and Astronautical Science/Japan Aerospace Exploration Agency, 8.ASIAA, Taiwan, 9.ISAPS, NCKU, Taiwan, 10.Department of Geophysics, Graduate School of Science, Tohoku University, 11.Research Division for Space Plasma, Institute of Space and Astronautical Science, Japan Aerospace Exploration Agency)

[PEM13-P05] Correlation between pulsating aurora and electrostatic electron cyclotron harmonic waves obtained from coordinated Arase and ground data

*Mizuki Fukizawa[1], Takeshi Sakanoi[1], Yoshizumi Miyoshi[2], Keisuke Hosokawa[3], Yoichi Kazama[4], Yoshiya Kasahara[5], Shoya Matsuda[6], Ayako Matsuoka[7], Wang Shiang-Yu[4], Sunny Wing-Yee Tam[8], Ryuho Kataoka[9] (1.Planetary Plasma and Atmospheric Research Center, Graduate School of Science, Tohoku University, 2.Institute for Space-Earth Environmental Research, Nagoya University, 3.Department of Communication Engineering and Informatics, University of Electro-Communications, 4.Academia Sinica Institute of Astronomy and Astrophysics, 5.Information Media Center, Kanazawa University, 6.Institute of Space and Astronautical Science/Japan Aerospace Exploration Agency, 7.Research Division for Space Plasma, Institute of Space and Astronautical Science, Japan Aerospace Exploration Agency, 8.Institute of Space and Plasma Sciences, College of Sciences, National Cheng Kung University , 9.National Institute of Polar Research)

[PEM13-P06] Automatic determination of Upper Hybrid Resonance Frequencies by Convolutional Neural Network.

*Shoya Matsuda[1], Tatsuhito Hasegawa[2], Atsushi Kumamoto[3], Fuminori Tsuchiya[3], Yoshiya Kasahara[4], Yoshizumi Miyoshi[5], Yasumasa Kasaba[3], Ayako Matsuoka[1] (1.Institute of Space and Astronautical Science/Japan Aerospace Exploration Agency, 2.University of Fukui, 3.Tohoku University, 4.Kanazawa University, 5.ISEE, Nagoya University)

[PEM13-P07] Amplitude dependence of whistler wave motion on electron scattering process

*Yoshiki Ito[1], Yoshizumi Miyoshi[1], Shinji Saito[1] (1.Nagoya University, ISEE)

[PEM13-P08] Two-dimensional simulation of whistler mode wave packets interacting with energetic electrons

*Takeshi Nogi[1], Yoshiharu Omura[1] (1.Reserch Institute for Sustainable Humanosphere, Kyoto University)

[PEM13-P09] Relativistic electron acceleration by whistler-mode chorus waves in 1D, 2D, and 3D magnetic field models.

*Keita Takahashi[1], Yoshiharu Omura[1], Yikai HSIEH[1], Danny Summers[2] (1.Research Institute for Sustainable Humanosphere, Kyoto University , 2.Department of Mathematics and Statistics, Memorial University of Newfoundland)

[PEM13-P10] Study of global spatio-temporal development of magnetospheric ELF/VLF waves for the 26-30 March 2017 storm based on ground and satellite observations and the RAM simulations

*Yuhei Takeshita[1], Kazuo Shiokawa[1], Yoshizumi Miyoshi[1], Mitsunori Ozaki[2], Yoshiya Kasahara[2], Martine Connors[3], Jyrki Manninen[4], Craig Kletzing[5], Vania Jordanova[6] (1.Nagoya University, Institute for Space-Earth Environmental Resarch, 2.Kanazawa University, 3.Athabasca University, 4.Sodankylä Geophysical Observatory, 5.The University of Iowa, 6.Los Alamos National Laboratory)

[PEM13-P11] Flux decrease of outer radiation belt electrons associated with solar wind pressure pulse: A Code coupling simulation of GEMSIS-RB and GEMSIS-GM

*Ito Hiroki[1], Yoshizumi Miyoshi[1], Shinji Saito[2], Yosuke Matsumoto[3], Takanobu Amano[4] (1.Institute for Space-Earth Environmental Research, Nagoya University, 2. Graduate School of Science, Nagoya

University, 3. Graduate School of Science, Chiba University, 4.Department of Earth and Planetary Science, University of Tokyo)

[PEM13-P12] Non-diffusive response of outer belt electrons on interplanetary shock

Takuma Toishi[1], *Yusuke Ebihara[1], Takashi Tanaka[2] (1.Research Institute for Sustainable Humanosphere, Kyoto University, 2.Kyushu University)

[PEM13-P13] PARM: Initial result of the auroral camera on the G-CHASER (RockSat-XN) rocket and status of the development of auroral cameras for the LAMP rocket experiment

*Naoshi Yagi[1], Takeshi Sakanoi[1], Fukizawa Mizuki[1], Kazushi Asamura[2], Yoshizumi Miyoshi[3], Keisuke Hosokawa[4], Genki Ishizawa[5] (1.Planetary Plasma and Atmospheric Research Center, Graduate School of Science, Tohoku University, 2.Institute of Space and Astronautical Science, Japan Aerospace Exploration Agency, 3.Institute for Space-Earth Environmental Research, Nagoya University, 4.Department of Communication Engineering and Informatics, University of Electro-Communications, 5.Space & terrestrial plasma pyhsics)

[PEM13-P14] First simultaneous observation of a SAR arc at subauroral latitudes using a ground all-sky camera and the Arase satellite in the inner magnetosphere

*Yudai Inaba[1], Kazuo Shiokawa[1], Shin-ichiro Oyama[1,8,9], Yuichi Otsuka[1], Atsuki Shinbori[1], Yoichi Kazama[2], Shiang-Yu Wang[2], Sunny W. Y. Tam[2], Shoichiro Yokota[3], Satoshi Kasahara[4], Kunihiro Keika[4], Tomoaki Hori[1], Ayako Matsuoka[5], Yoshiya Kasahara[6], Atsushi Kumamoto[7], Yasumasa Kasaba[7], Yoshizumi Miyoshi[1], Iku Shinohara[5], Arto Oksanen[10] (1.Institute for Space-Earth Environmental Research, 2.Academia Sinica, 3.Osaka Univ, 4.Tokyo Univ, 5.JAXA, 6.Kanazawa University, 7.Tohoku University, 8.University of Oulu, Finland, 9.National Institute of Polar Research, 10.Jyväskylän Sirius ry, Finland)

[PEM13-P15] Pi2 pulsations observed by the Arase satellite inside and outside the plasmapause

*Mariko Teramoto[1], Ayako Matsuoka[2], Reiko Nomura[5], Yoshiya Kasahara[3], Yasumasa Kasaba[4], Atsushi Kumamoto[4], Fuminori Tsuchiya[4], Shoya Matsuda[2], Masahito Nose[1], Masafumi Shoji[1], Yasunori Tsugawa[1], Shun Imajo[1], Yoshizumi Miyoshi[1], Iku Shinohara[2] (1.Institute for Space-Earth Environmental Research Nagoya University, 2.Institute of Space and Astronautical Science, Japan Aerospace eXploration Agency, 3.Kanazawa University, 4.Tohoku University, 5.National Astronomical Observatory of Japan)

[PEM13-P16] An extreme erosion of the plasmasphere during the 7–10 September 2017 storm

*Yuki Obana[1], Naomi Maruyama[2,3], Atsuki Shinbori[4], Kumiko K. Hashimoto[5], Mariangel Fedrizzi[2,3], Masahito Nose[4], Yuichi Otsuka[4], Nozomu Nishitani[4], Tomoaki Hori[4], Atsushi Kumamoto[6], Fuminori Tsuchiya[6], Shoya Matsuda[7], Ayako Matsuoka[7], Yoshiya Kasahara[8], Akimasa Yoshikawa[9], Yoshizumi Miyoshi[4], Iku Shinohara[7] (1.Osaka Electro-Communication University, 2.University of Colorado Boulder, 3.NOAA Space Weather Prediction Center, 4.Nagoya University, 5.Kibi International University, 6.Tohoku University, 7.Japan Aerospace Exploration Agency, 8.Kanazawa University, 9.Kyushu University)

[PEM13-P17] Relative contribution of ULF and chorus waves to the radiation belt variation: Comparison between multi-point observations and BATSRUS + CRCM simulation

*Naoko Takahashi[1], Kanako Seki[1], Mei-Ching Fok[2], Yihua Zheng[2], Yoshizumi Miyoshi[3], David Hartley[4], Ayako Matsuoka[5], Yoshiya Kasahara[6], Yasumasa Kasaba[7], Nana Higashio[8] (1.Graduate School of Science, University of Tokyo, 2.NASA Goddard Space Flight Center, 3.Institute for Space-Earth Environmental Research, Nagoya University, 4.Department of Physics and Astronomy, University of Iowa, 5.Institute of Space and Astronautical Science, Japan Aerospace Exploration Agency, 6.Information Media Center, Kanazawa University, 7.Planetary Plasma and Atmospheric Research Center, Tohoku University, 8.Japan Aerospace Exploration Agency)

[PEM13-P18] Modulation of the D-region ionosphere by Pc5 waves observed by VLF/LF standard radio waves

*Miyashita Takuya[1], Hiroyo Ohya[1], Fuminori Tsuchiya[2], Hiroyuki Nakata[1], Toshiaki Takano[1], Kazuo Shiokawa[3], Yoshizumi Miyoshi[3] (1.Chiba University, 2.Tohoku University, 3.Nagoya University)

[PEM13-P19] Oxygen-proton differences in ion energies dominating plasma pressure: Dependence on storm phases and solar wind drivers

*Kunihiro Keika[1], Satoshi Kasahara[1], Shoichiro Yokota[2], Masahiro Hoshino[1], Kanako Seki[1], Masahito Nose[3], Yoshizumi Miyoshi[3], Iku Shinohara[4] (1.Graduate School of Science, The University of Tokyo , 2.Graduate School of Science, Osaka University, 3.Institute for Space-Earth Environmental Research, Nagoya University, 4.Institute of Space and Astronautical Science, Japan Aerospace Exploration Agency)

[PEM13-P20] Mass dependence of penetration depth of multi-energy ions in the inner magnetosphere during magnetic storms: Arase observations

*Ryosuke Fujii[1], Yoshizumi Miyoshi[1], Masafumi Shoji[1], Kazushi Asamura[2], Lynn Kistler[1,8], Vania Jordanova[9], Tomoaki Hori[1], Satoshi Kurita[1], Mariko Teramoto[1], Yasunori Tsugawa[1], Yoshiya Kasahara[3], Yasumasa Kasaba[4], Atsushi Kumamoto[5], Fuminori Tsuchiya[4], Shoichiro Yokota[6], Kunihiro Keika[7], Ayako Matsuoka[2], Iku Shinohara[2] (1.Institute for Space-Earth Environmental Research, Nagoya University, 2.Institute of Space and Astronautical Science, Japan Aerospace Exploration Agency, 3.Information Media Center, Kanazawa University, 4.Planetary Plasma and Atmospheric Research Center, Tohoku University, 5.Department of Geophysics, Graduate School of Science, Tohoku University, 6.Graduate School of Science, Osaka University, 7.Department of Earth and Planetary Science, Graduate School of Science, The University of Tokyo, 8.University of New Hampshire, 9.Los Alamos National Laboratory)

[PEM13-P21] Relativistic Acceleration of Energetic Protons by Electromagnetic Ion Cyclotron Waves in the Jovian Magnetosphere

*Tomohiro Sekine[1], Yoshiharu Omura[1], Danny Summers[2], Yikai HSIEH[1], Satoko Nakamura[1] (1.Reserach Institute for Sustainable Humanosphere, Kyoto University, 2.Memorial University of Newfoundland)

[PEM13-P22] Statistical study of IPDP type EMIC wave-related electron precipitation at subauroral latitude

*Asuka Hirai[1], Fuminori Tsuchiya[1], Takahiro Obara[1], Yasumasa Kasaba[1], Yuto Katoh[2], Hiroaki Misawa[1], Kazuo Shiokawa[3], Yoshizumi Miyoshi[3], Satoshi Kurita[3], Martin G Connors[4] (1.Planetary Plasma and Atmospheric Research Center, Graduate School of Science, Tohoku Univ. , 2.Department of Geophysics, Graduate School of Science, Tohoku University, 3.Institute for Space-Earth Environmental Research, Nagoya University, 4.Athabasca University)

[PEM13-P23] Meridional distributions of proton plasma and pressure-driven currents in the nightside inner magnetosphere: Arase observations

*Shun Imajo[1], Masahito Nose[1], Satoshi Kasahara[2], Shoichiro Yokota[3], Ayako Matsuoka[4], Kunihiro Keika[2], Tomoaki Hori[1], Mariko Teramoto[1], Kazuhiro Yamamoto[5], Oimatsu Satoshi[5], Reiko Nomura[6], Akiko Fujimoto[7], Iku Shinohara[4], Yoshizumi Miyoshi[1] (1.Institute for Space-Earth Environmental Research, Nagoya University, 2.Graduate School of Science, The University of Tokyo, 3.Graduate School of Science, Osaka University, 4.Institute of Space and Astronautical Science, Japan Aerospace Exploration Agency, 5.Graduate School of Science, Kyoto University, 6.National Astronomical Observatory of Japan, 7.Kyushu Institute of Technology)

[PEM13-P24] Space Weather Effects on Energetic Proton Flux Response in South Atlantic Anomaly

*Kirolosse Mina GIRGIS[1,2], Tohru Hada[1], Shuichi Matsukiyo[1] (1.Earth System Science and Technology (ESST) Department, Interdisciplinary Graduate School of Engineering Sciences (IGSES), Kyushu University, Japan, 2.Aerospace Engineering Department, Faculty of Engineering, Cairo University, Egypt)

[PEM13-P25] Solar-cycle variations of >30 keV electron flux enhancements under the inner radiation belt

*ALLA SUVOROVA[1] (1.National Central University)

[PEM13-P26] Energy spectra variations of high energy electrons in the inner magnetosphere observed by HEP/XEP on ARASE and SEDA-e on HIMAWARI

*Takeshi Takashima[1], Takefumi Mitani[1], Nana Higashio[2], Tsutomu Nagatsuma[3] (1. ISAS/JAXA, 2.Research and Development Directorate/JAXA, 3.NiCT)

[PEM13-P27] Inter-channel calibration of the high-energy electron experiments (HEP) instrument onboard the Arase satellite

*Tomoaki Hori[1], Takefumi Mitani[2], Takeshi Takashima[2], Park Inchun[1], Satoshi Kurita[1], Mariko Teramoto[1], Nana Higashio[3], Satoshi Kasahara[4], Shoichiro Yokota[5], Yoshizumi Miyoshi[1], Iku Shinohara[2] (1.Institute for Space-Earth Environmental Research, Nagoya University, 2.Japan Aerospace Exploration Agency, Institute of Space and Astronautical Science, 3.Japan Aerospace Exploration Agency, 4.Graduate School of Science, The University of Tokyo, 5.Graduate School of Science, Osaka University)

[PEM13-P28] Particle simulation for calibrating the HEP data onboard the ARASE satellite

*PARK INCHUN[1], Yoshizumi Miyoshi[1], Takefumi Mitani[2], Tomoaki Hori[1], Satoshi Kurita[1], Mariko Teramoto[1], Takeshi Takashima[2], Nana Higashio[3], Iku Shinohara[2] (1.Nagoya University Institute for Space-Earth Environmental Research, 2.Japan Aerospace Exploration Agency Institute of Space and Astronautical Science , 3.Japan Aerospace Exploration Agency)

[PEM13-P29] Geant4 model calculation and energetic particle observation with HEP/Arase in the inner radiation belt

*Honoka Toda[1], Wataru Miyake[1], Takefumi Mitani[3], Takeshi Takashima[3], Yoshizumi Miyoshi[2], PARK INCHUN[2], Tomoaki Hori[2] (1.Tokai University, 2.ISEE/Nagoya University, 3.ISAS/JAXA)

[PEM13-P30] Validation of High-energy electron detector simulator for the HEP instruments onboard Arase

*Takefumi Mitani[1], PARK INCHUN[2], Tomoaki Hori[2], Taku Namekawa[1,3], Kazushi Asamura[1], Takeshi Takashima[1], Satoshi Kasahara[3], Satoshi Kurita[2], Mariko Teramoto[2], Nana Higashio[1], Yoshizumi Miyoshi[2], Iku Shinohara[1] (1.Japan Aerospace Exploration Agency, Institute of Space and Astronautical Science, 2.Institute for Space-Earth Environmental Research, Nagoya Univ., 3.The university of Tokyo)

Evaluation of wave normal and Poynting vector analyses for whistler mode waves observed by the waveform capture (WFC) on board the Arase

*Yoshiya Kasahara[1], Satoshi Ikarashi[1], Hiroyuki Nishizawa[1], Shoya Matsuda[2], Fuminori Tsuchiya[3], Atsushi Kumamoto[3], Yasumasa Kasaba[3], Mitsunori Ozaki[1], Ayako Matsuoka[2]

1. Kanazawa University, 2. ISAS/JAXA, 3. Tohoku University

The Plasma Wave Experiment (PWE) is one of scientific instruments on board the Arase (ERG) satellite to measure electric field from DC to 10 MHz and magnetic field from a few Hz to 100 kHz in the inner magnetosphere. It is well known that chorus wave, one of typical plasma waves in VLF range observed in the inner magnetosphere, is a plausible candidate that accelerates relativistic electrons in the radiation belt. Besides the chorus, the Arase has observed various kinds of plasma waves such as lightning whistlers and hiss waves. It is very important to study the propagation characteristics of these waves.

In the present paper, we developed a direction finding system applicable to whistler mode waves using the data from waveform capture (WFC), which is one of receivers covering the frequency range below 20kHz implemented in the PWE. The absolute directions of the wave normal and Poynting vectors were derived in the coordinate system referring the ambient magnetic field and geomagnetic meridian plane. We also estimated the Poynting vector theoretically using the derived wave normal vector, electron density and ambient magnetic field intensity to confirm the validity of the results from the observation data.

We demonstrated that the results were generally reliable, but further calibration is necessary for electric field to improve the accuracy of Poynting vector because the waveform of electric field is now calibrated under the assumptions of theoretical antenna capacitance in a vacuum and typical plasma impedance. In other words, we expect to be able to correct the calibration table for electric field measurements from the direction finding results.

In the presentation, we introduce some typical results which have been derived from the observation data of upper- and lower-band chorus, and lightning whistlers.

Keywords: Whistler mode wave, Waveform Capture, Direction finding, Plasma wave

©2019. Japan Geoscience Union. All Right Reserved.

Calibration of electric fields dedicated to the measurement of the S-WPIA of the Arase Satellite

*Miki Jumpei[1], Hirotsugu Kojima[2], Yuto Katoh[3], Shoya Matsuda[4], Yoshiya Kasahara[5], Mitsuru Hikishima[4], Satoshi Kurita[6], Masahiro Kitahara[3], Satoshi Kasahara[7], Yoshizumi Miyoshi[6], Atsushi Kumamoto[3], Ayako Matsuoka[4], Shoichiro Yokota[8], Tomoaki Hori[6], Kunihiro Keika[7]

1. Space Radio Engineering Laboratory, Division of Electrical Engineering, Kyoto University Graduated School, 2. Research Institute for Sustainable Humanosphere, Kyoto University, 3. Graduate School of Science and Faculty of Science, Tohoku University, 4. Institute of Space and Astronautical Science, JAXA, 5. Information Media Center, Kanazawa University, 6. Institute for Space-Earth Environmental Research, Nagoya University, 7. School of Science, The University of Tokyo, 8. School of Science, Osaka University

The outer radiation belt consists of high-energy electrons. They are strongly affected by geomagnetic activities in the relation to solar wind conditions. The important science target of the Arase mission is to clarify generation/loss mechanisms of relativistic electrons in the outer radiation belt. Wave-particle interactions are thought to be a plausible mechanism for generation/loss processes of relativistic electrons. S-WPIA (Software-type Wave-Particle Interaction Analyzer) is installed in the Arase satellite. The WPIA is a newly developed observation system that enables us to quantitatively understand the interaction between plasma waves and electrons. The WPIA has the capability to identify a relative phase angle of a plasma wave vector and a velocity vector of each detected particle. Since phase information of observed plasma waves is essential to the WPIA, precise calibrations of plasma wave data are important. While the calibration data for the magnetic field sensors are identical to those we obtained during the ground tests of the instruments, the calibration data for electric field sensors strongly depend on plasma parameters around the satellite. Furthermore, there are still unclear parameters at the inputs of preamplifiers relating to the connection with electric field sensors. The calibration for electric field data needs to be performed carefully consulting observation data after the launch.

The present paper focuses on the calibration of plasma wave data for the S-WPIA’s data processing. We picked up events including whistler-mode chorus emissions and lightning-whistler waves. They all are electromagnetic waves, so-called whistler mode waves. The amplitude ratios of their electric field and magnetic field components can be theoretically calculated referring to the Appleton-Hartlee equations. Poynting vectors of whistler mode waves can be also theoretically obtained. We compared the observation results of the picked up events with the theoretical ones. The results show the precise calibration for the magnetic field data have been made. On the other hand, the calibration for the electric field data should be further modified consulting plasma parameters and other uncertain parameters at the input of preamplifiers. In the present paper, we will discuss the improvement of the calibration for electric field data by correcting the calibration table to aim the precise S-WPIA data processing.

©2019. Japan Geoscience Union. All Right Reserved.

Enhancement of whistler-mode chorus in association with Pc 4-5 ULF waves and related variation of high energy electrons

*Atsuhiro Ono[1], Yuto Katoh[1], Atsushi Kumamoto[1], Fuminori Tsuchiya[1], Mariko Teramoto[2], Yoshiya Kasahara[3], Shoya Matsuda[4], Ayako Matsuoka[4], Takefumi Mitani[4], Tomoaki Hori[2], Satoshi Kasahara[5], Shoichiro Yokota[6], Kunihiro Keika[5], Yoshizumi Miyoshi[2], Iku Shinohara[4]

1. Tohoku University, 2. Nagoya University, 3. Kanazawa University, 4. ISAS/JAXA, 5. The University of Tokyo, 6. Osaka University

Whistler-mode chorus emissions play significant roles in the acceleration and loss of energetic electrons in the magnetosphere. One of the important factors which control periodic enhancement of chorus emissions is ULF (Ultra Low Frequency) waves. Previous studies reported that the compressional component of Pc4-5 ULF waves modulates the intensity of chorus waves [Li et al., 2011] and that the toroidal and poloidal components of Pc4-5 ULF waves as well [Jaynes et al., 2015]. Previous studies also suggested that enhancement of the temperature anisotropy of energetic electrons in the wave generation region should be required for the chorus generation. In order to understand the reported correspondence, in addition to the wave observation, we should examine simultaneously observed variations of the flux and the pitch angle distribution of energetic electrons.

In the present study, we investigate the relationship between chorus emissions and ULF waves using particle and electromagnetic field observations made by the Arase satellite. First, we analyze data observed by the Onboard Frequency Analyzer (OFA) of the Plasma Wave Experiment (PWE) and the Magnetic Field Experiment (MGF) during the campaign observation period of the Arase satellite with ground stations from March to April in 2017. As a result, we identified the simultaneous enhancement of chorus emissions and Pc4-5 ULF waves, which was dominated by the toroidal component, from 2130 to 2200 UT on March 27, 2017. The Arase satellite was located at the magnetic local time about 04:00, the magnetic latitude about -10 degrees, and the L-value about 6 during the event. We find that there is one-to-one correspondence between chorus emissions and the toroidal component of ULF waves; chorus emissions enhanced at the timings when the toroidal magnetic field component of ULF waves had a peak in the westward direction. The identified phase relationship is different from that reported by Jaynes et al. (2015), which isn't one-to-one correspondence. Next, we evaluate the resonance energy of the observed chorus emissions, using the ratio of the plasma frequency to the electron cyclotron frequency (f_p/f_{ce}) based on the upper-hybrid resonance frequency derived from the spectra observed by the High Frequency Analyzer (HFA) of PWE and the ambient magnetic field intensity observed by MGF. We find that f_p/f_{ce} is 3.3-3.4 during the event and that the resonance energy for whistler-mode waves in the frequency range of 0.1-0.2 f_{ce} is estimated to be about 100-400keV, which is larger than typical energies of resonating electrons observed in the inner magnetosphere. The estimated large resonant energy can be explained by the frequency range of the observed chorus emissions, approximately 0.1 - 0.2 f_{ce}, is relatively lower than that observed in typical cases.
We also analyze variations of the flux and the pitch angle distribution of energetic electrons during the event using data observed by the High-energy electron experiments (HEP) instrument onboard Arase. The result shows that both the flux and the pitch angle distribution of electrons in the kinetic energy range from 100 to 400 keV, which corresponds to the estimated resonance energy, did not fluctuate with the intensity variation of the chorus emissions and the ULF waves. In addition, we analyze the data observed by the Medium-energy particle experiments - electron analyzer (MEP-e) for energetic electrons in the energy range of 10-80 keV, lower than the estimated resonance energy. Then we identify the

©2019. Japan Geoscience Union. All Right Reserved.

corresponding variation of both the flux and the pitch angle distribution in the 40-60 keV energy range. One of the possible reasons why no significant variations were observed in the hundred keV range would be that the Arase satellite was located in the off-equatorial region during the event, and that the satellite was away from the wave generation region.

Keywords: ULF waves, chorus emissions

©2019. Japan Geoscience Union. All Right Reserved.

Sudden enhancements of electron cyclotron harmonic waves observed by the Arase satellite

*Shinjo Airi[1], Hirotsugu Kojima[1], Yoshiya Kasahara[2], Yoichi Kazama[3], Hideyuki Usui[4], Yoshizumi Miyoshi[5], Yasumasa Kasaba[6], Shoya Matsuda[7], Tomoaki Hori[5], S. -Y. Wang[8], Sunny W.Y. Tam[9], Atsushi Kumamoto[10], Ayako Matsuoka[11]

1. Research institute for sustainable humanosphere, Kyoto University, 2. Information Media Center, Kanazawa University, 3. ASIAA, 4. Graduate school of system informatics Kobe University, 5. Institute for Space-Earth Environmental Research, Nagoya University, 6. Planetary Plasma and Atmospheric Research Center, Tohoku University, 7. Institute of Space and Astronautical Science/Japan Aerospace Exploration Agency, 8. ASIAA, Taiwan, 9. ISAPS, NCKU, Taiwan, 10. Department of Geophysics, Graduate School of Science, Tohoku University, 11. Research Division for Space Plasma, Institute of Space and Astronautical Science, Japan Aerospace Exploration Agency

Electron cyclotron harmonic (ECH) waves are commonly observed in the low latitude region just outside the terrestrial plasmapause. They are purely electrostatic and their frequency spectra show harmonic structures. The harmonic structures are believed to depend on the temperature and density ratio between cold and hot background electrons. The Plasma Wave Experiment (PWE) onboard the Arase satellite has observed ECH waves since the start of its operation. The observed ECH waves are classified into two types. They are the diffuse ECH waves and the enhanced ECH waves. The diffuse ECH waves are weak and they appear as continuous emissions that last for more than a few minutes. The enhanced ECH waves are the sudden enhancements of the diffuse ECH in shorter periods. The present paper focuses on the enhanced ECH waves observed by the Arase satellite.

Kazama et al. (2018) introduced the event that the repeated enhancement of ECH waves is associated with density depletions near the plasmapause. They succeeded in revealing the good correlation of the enhancement of the ECH waves and the sudden decrease of the cold electrons with energies lower than the lowest energy limit of the particle detector. The observed electron features are clear in the relation to the enhancement of ECH waves, but the mechanism of the enhancement is still unclear. We searched for such events of the enhanced ECH waves and examined the correlation of wave intensities, spacecraft potentials and electron velocity distributions observed by the Arase satellite. Some of the events show the features similar to those of Kazama et al. (2018), but there are also many other events with no correlation between the enhancements of the ECH waves and the density depletions. In the present paper, we examine velocity distribution functions of electrons observed by the low-energy particle experiments-electron analyzer (LEPe) onboard Arase. Velocity distribution functions allow us to examine temperature anisotropies of electrons and calculate linear dispersion relations for the ECH waves. Once we get electron temperatures, resonance velocities are calculated. On the other hand, since the wavelength of the ECH waves is very short, the relation of the wavelength and the length of the Arase electric field sensors is also important in evaluating the time variations of the ECH wave intensity. We study the enhanced ECH waves in various viewpoints using wave and electron data observed by the Arase satellite and discuss the generation mechanism in the present paper.

©2019. Japan Geoscience Union. All Right Reserved.

Correlation between pulsating aurora and electrostatic electron cyclotron harmonic waves obtained from coordinated Arase and ground data

*Mizuki Fukizawa[1], Takeshi Sakanoi[1], Yoshizumi Miyoshi[2], Keisuke Hosokawa[3], Yoichi Kazama[4], Yoshiya Kasahara[5], Shoya Matsuda[6], Ayako Matsuoka[7], Wang Shiang-Yu[4], Sunny Wing-Yee Tam[8], Ryuho Kataoka[9]

1. Planetary Plasma and Atmospheric Research Center, Graduate School of Science, Tohoku University, 2. Institute for Space-Earth Environmental Research, Nagoya University, 3. Department of Communication Engineering and Informatics, University of Electro-Communications, 4. Academia Sinica Institute of Astronomy and Astrophysics, 5. Information Media Center, Kanazawa University, 6. Institute of Space and Astronautical Science/Japan Aerospace Exploration Agency, 7. Research Division for Space Plasma, Institute of Space and Astronautical Science, Japan Aerospace Exploration Agency, 8. Institute of Space and Plasma Sciences, College of Sciences, National Cheng Kung University , 9. National Institute of Polar Research

Pulsating auroras (PsAs) are thought to be generated by precipitating electrons scattered by lower-band chorus (LBC) waves near the magnetic equator through cyclotron resonance. Previous studies showed one-to-one correlation between LBC wave intensity observed by satellites near the magnetic equator and PsA intensity obtained by ground-based all-sky imager [e.g., Nishimura et al., Science, 2010, Nishimura et al., JGR, 2011]. In addition, electrostatic electron cyclotron harmonic (ECH) waves can also interact with magnetospheric electrons and scatter their pitch angle theoretically [e.g., Lyons, JGR, 1974]. However, characteristics of aurora caused by ECH are not understood. In our study, we report for the first time in the world that not only LBC but also ECH wave intensity has correlation with the PsA intensity using coordinated Arase and ground-based imager observations. The first campaign observations between the Arase satellite and ground-based optical imager were conducted in March 2017. A typical substorm occurred on 27 March 2017 and the ionospheric footprint of Arase traversed the field of view of all-sky imager at Sodankylä during 00:00–03:15 UT on 29 March 2017. Quasi-periodic LBC and ECH waves were observed by Arase near the magnetic equator and PsA was detected by the all-sky imager during 01:30–02:00 UT. We calculated the cross-correlation coefficients between auroral intensity and LBC or ECH wave intensity from 01:30 UT to 02:00 UT with a time window of every 2 minutes. The highest cross-correlation coefficient between auroral intensity and LBC wave intensity was 0.73 and that between auroral intensity and ECH wave intensity was 0.62 from 01:46 UT to 01:48 UT, and they were statistically significant. The period of auroral intensity which correlated with LBC intensity was shorter than 10 s and that correlated with ECH intensity was 10–20 s. We estimated the precipitating electron energy assuming that the time lag when the cross-correlation coefficient became the highest equals to the travel time of electrons from the modulated source region to the auroral emission height. We shifted the variation of auroral intensity against that of ECH or LBC wave intensity with a time step of 0.01 s using 100 Hz sampling image data taken by the all-sky imager. The estimated energy of precipitating electron interacted with LBC waves was ~20–67 keV and that interacted with ECH waves was ~3–4 keV. On the other hand, we independently estimated the cyclotron resonance energy of LBC and ECH waves from the Arase's observation data and geomagnetic field model by TS04 Model [Tsyganenko and Sitnov, JGR, 2005]. The estimated cyclotron resonance energy of LBC waves was ~30 keV. Although the cyclotron resonance energy of ECH waves could not be estimated because it was difficult to obtain the electron temperature and wave normal angle of ECH waves from Arase data, we suggest the cyclotron resonance energy of ECH waves to be a few keV with probable assumptions. From these results, we suggest that LBC waves interact with high energy electrons which cause auroral emission at lower altitudes, while ECH waves interact with

©2019. Japan Geoscience Union. All Right Reserved.

relatively low energy electrons which cause auroral emission at higher altitudes. These results were published in Fukizawa et al. [GRL, 2018].
To verify whether ECH waves indeed scatter the pitch angle of electrons, we compared ECH wave intensity with electron flux in the loss cone obtained with low-energy particle experiments-electron analyzer onboard Arase. We also give results of other coordinated observation events.

Keywords: pulsating aurora, ECH waves, wave-particle interaction

©2019. Japan Geoscience Union. All Right Reserved.

Automatic determination of Upper Hybrid Resonance Frequencies by Convolutional Neural Network.

*Shoya Matsuda[1], Tatsuhito Hasegawa[2], Atsushi Kumamoto[3], Fuminori Tsuchiya[3], Yoshiya Kasahara[4], Yoshizumi Miyoshi[5], Yasumasa Kasaba[3], Ayako Matsuoka[1]

1. Institute of Space and Astronautical Science/Japan Aerospace Exploration Agency, 2. University of Fukui, 3. Tohoku University, 4. Kanazawa University, 5. ISEE, Nagoya University

Electron number density is a key parameter for discussions of plasma wave generation/propagation, and wave-particle interaction in the inner magnetosphere. The High Frequency Analyzer (HFA) is a subsystem of Plasma Wave Experiment (PWE) aboard Arase [Kasahara et al. (2018), Kumamoto et al. (2018), Miyoshi et al. (2018)]. The HFA measures electric field spectra in a frequency range from 10 kHz to 10 MHz, which covers a typical frequency range of Upper Hybrid Resonance (UHR) frequency in the inner magnetosphere. Kumamoto et al. (2018) proposed the semiautomatic method for the identification of UHR frequency by computer and a human operator. However, it takes a enormous effort of a human operator.

We propose an automatic determination system of UHR frequency by machine learning. Machine learning is a technique in the field of artificial intelligence to give computers the ability to learn with data. In this study, we defined a task of UHR frequency determination as supervised regression that a computer estimates UHR frequencies using the dataset composed of electric field dynamic spectra with correct UHR frequency labels. We adopted Convolutional Neural Network (CNN) as a machine learning algorithm. In this study, we introduce our machine learning approach and initial results for determining UHR frequency from electric field spectra observed by PWE/HFA.

Keywords: Arase satellite, UHR frequency, Machine learning

©2019. Japan Geoscience Union. All Right Reserved.

Amplitude dependence of whistler wave motion on electron scattering process

*Yoshiki Ito[1], Yoshizumi Miyoshi[1], Shinji Saito[1]

1. Nagoya University, ISEE

Whistler mode chorus waves cause scattering and acceleration of energetic electrons in the inner magnetosphere. The interaction processes have been modeled as diffusive process. The pitch angle diffusion coefficients of the pitch angle scattering depend on the power of chorus waves, so that it is expected that the scattering rate also depends on the wave amplitude. On the other hand, several previous studies indicated that the Lorentz force by the wave magnetic field is larger than the mirror force if the wave amplitudes increase and the electron trajectories in the velocity space are different from the diffusive distributions. In this study, we investigate chorus wave amplitude dependence of electron scattering using the GEMSIS-RBW simulation code. The RBW simulation demonstrates generation of periodical rising-tone chorus waves propagating along a magnetic field line to higher latitudes, and calculates local pitch angle and energy change by the imposed waves on the field line. At small wave amplitudes, time variations of pitch angle and energy of electrons are similar to diffusive process. At large wave amplitudes, some electrons increase both pitch angle and energy at interaction with the first rising tone, and then they decrease these parameters at interaction with the second rising tone. The process in the first rising tone seems to be the phase trapping, while the process in the second rising tone seems to be dislocation. Therefore, nonlinear scattering processes, which are phase trapping and dislocations, occur during the interactions with periodical rising-tone chorus waves with large amplitudes, which are quite different from quasi-linear scattering process.

©2019. Japan Geoscience Union. All Right Reserved.

Two-dimensional simulation of whistler mode wave packets interacting with energetic electrons

*Takeshi Nogi[1], Yoshiharu Omura[1]

1. Reserch Institute for Sustainable Humanosphere, Kyoto University

We perform two-dimensional electromagnetic particle simulations to study basic characteristics of whistler-mode wave particle interaction involved in the generation and propagation processes of chorus emissions with wave normal angles oblique to the static magnetic field. We assume a simple periodic (x, y) system with the magnetic field taken in the x-direction. We find the linear phase of the instability is much affected by electrostatic thermal fluctuations. It is necessary to put many super-particles in a grid cell to suppress the thermal fluctuation. We next put an array of antennas perpendicular to the background magnetic field, and oscillate the antenna current to generate obliquely propagating waves. In addition to the nonlinear trapping of energetic electrons through the cyclotron resonance, another nonlinear trapping of electrons takes place through the Landau resonance. Structures of the nonlinear trapping potentials change with the varying frequency, affecting efficiency of energy transfer between the wave and energetic electrons. We study nonlinear evolution of the wave packet, and competing processes of both resonances in accelerating energetic electrons to higher energies.

©2019. Japan Geoscience Union. All Right Reserved.

Relativistic electron acceleration by whistler-mode chorus waves in 1D, 2D, and 3D magnetic field models.

*Keita Takahashi[1], Yoshiharu Omura[1], Yikai HSIEH[1], Danny Summers[2]

1. Research Institute for Sustainable Humanosphere, Kyoto University , 2. Department of Mathematics and Statistics, Memorial University of Newfoundland

We evaluate the acceleration efficiencies of relativistic electrons under a 1D, 2D, and 3D model magnetic fields. We perform test-particle simulations and analyze nonlinear trapping motions of resonant electrons in each model. As a chorus wave model, we assume that a chorus wave packet generated at the magnetic equator propagates along the magnetic field to higher latitudes. When we perform simulations with the whistler mode wave, the cyclotron resonance with energetic electrons occurs at the similar timing in each model. Although we find relativistic turning acceleration (RTA) [1] to take place in each model, acceleration efficiencies of resonant electrons are different in these models. In terms of the numerical Green’s function[2], we find a clear difference in time evolution of the distribution function in energy and equatorial pitch angle. The energy gap between resonant electrons and non-resonant electrons in the 1D model is slightly different from those in the 2D and 3D models. The energy gap in the 3D model is the largest among the three magnetic field models. This difference is due to additional oscillations in the velocity phase space, which only occur in the 2D and 3D models. These oscillations occur because the magnitude of the magnetic field changes during one period of relativistic cyclotron motion, affecting the nonlinear trapping conditions of resonant electrons.

References:

[1] Y. Omura, N. Furuya, D. Summers, Relativistic turning acceleration of resonant electrons by coherent whistler-mode waves in a dipole magnetic field, Journal Geophysical Research, Vol. 112, A06236, doi:10.1029/2006JA012243, 2007.

[2] Y. Omura, Y. Miyashita, M. Yoshikawa, D. Summers, M. Hikishima, Y. Ebihara, and Y. Kubota (2015), Formation process of relativistic electron flux through interaction with chorus emissions in the Earth’s inner magnetosphere, J. Geophys. Res. Space Physics, 120, 9545–9562, doi:10.1002/2015JA021563, 2015.

©2019. Japan Geoscience Union. All Right Reserved.

Study of global spatio-temporal development of magnetospheric ELF/VLF waves for the 26-30 March 2017 storm based on ground and satellite observations and the RAM simulations

*Yuhei Takeshita[1], Kazuo Shiokawa[1], Yoshizumi Miyoshi[1], Mitsunori Ozaki[2], Yoshiya Kasahara[2], Martine Connors[3], Jyrki Manninen[4], Craig Kletzing[5], Vania Jordanova[6]

1. Nagoya University, Institute for Space-Earth Environmental Resarch, 2. Kanazawa University, 3. Athabasca University, 4. Sodankylä Geophysical Observatory, 5. The University of Iowa, 6. Los Alamos National Laboratory

The magnetospheric ELF/VLF waves are plasma waves generated by energetic electrons from several keV to tens keV with temperature anisotropy at magnetospheric equatorial plane of the inner magnetosphere. These ELF/VLF waves with frequencies lower than local half gyro frequency (lower-band) can propagate to the ground along magnetic field line. It is also known that the ELF/VLF waves interact with electrons drifting longitudinally in the inner magnetosphere, and help accelerating them to relativistic energies. Takeshita et al. [SGEPSS, 2018] statistically investigated the longitudinal extent of the magnetospheric ELF/VLF waves using six ground-based stations for two months, and showed the average extent of the ELF/VLF waves as ~90 degrees in longitude. However, Jordanova et al. [JGR, 2010] investigated the global distribution of linear growth rate of whistler mode chorus waves using global ring current-atmosphere interactions model (RAM), and showed that the region of large linear growth rate can extend ~180 degrees in longitude during the geomagnetic storm of 22 April 2001.

In this study we investigate the spatio-temporal distibution of the source region of magnetospheric ELF/VLF waves based on ground and satellite observations during the geomagnetic storm period from 26-30 March 2017, and compare it with global distribution of non-linear waves proxy of whistler mode chorus waves obtained by the RAM simulation. In this preliminary simulation, the simple dipole field and the Volland-Stern electric field are used as ambient magnetic and electric fields. And we assumed simply the Maxwell distribution as an energy spectrum using the empirical model of Tsyganenko and Mukai [2003]. In order to evaluate the non-linear wave excitation, we have estimated the optimum amplitude and the threshold value indicated by Omura and Nunn [2011]. We investigated the existence of lower band chorus waves using ground based observations at Athabasca (ATH; 54.7N, 246.4E, MLAT: 61.3N), Kapuskasing (KAP; 49.4N, 277.8E, MLAT: 58.7N), Kannuslehto (KAN: 67.7N, 26.3E, MLAT: 64.5N) and satellite-based observations by ERG with an apogee in the pre-dawn sector and RBSP-A and RBSP-B with an apogees in the post-dusk sector. We found the magnetospheric ELF/VLF waves exist from 3 MLT to 12 MLT for most periods from main- to recovery-phases of the magnetic storm. However, the RAM simulation did not predict wave generation during recovery phase of the storm. We compare the simulation and the ground-satellite observation in detail, and calculate the over-estimate rate (the ratio of wave existence period on the simulation to no wave period on the observation) and under-estimate rate (the ratio of no wave period on the simulation to wave existence period on the observation). We found the over-estimate rate become high (0.2~0.9) and under-estimate rate become low (0~0.4) in the main phase of the storm. This indicates that the longitudinal size of chorus source region predicted by simulation is larger than the observed size at the main phase. We also found that the over-estimate rate becomes low (0~0.2) and under-estimate rate becomes high (~1) during the recovery phase of the storm. This indicates that the simulation does not reproduce the wave existence during the recovery phase of the storm. Looking into the MLT distribution, the simulation predicts the wave existence from dusk to the midnight sector, but the

©2019. Japan Geoscience Union. All Right Reserved.

waves were not observed in this local time sector during the main phase. In case of recovery phase, the simulation did not predict wave existence but the observation showed continuous wave existence from dawn to the noon sector.

Keywords: chorus, ERG satellite, ground based observation

©2019. Japan Geoscience Union. All Right Reserved.

Flux decrease of outer radiation belt electrons associated with solar wind pressure pulse: A Code coupling simulation of GEMSIS-RB and GEMSIS-GM

*Ito Hiroki[1], Yoshizumi Miyoshi[1], Shinji Saito[2], Yosuke Matsumoto[3], Takanobu Amano[4]

1. Institute for Space-Earth Environmental Research, Nagoya University, 2. Graduate School of Science, Nagoya University, 3. Graduate School of Science, Chiba University, 4. Department of Earth and Planetary Science, University of Tokyo

Relativistic electron flux of the outer radiation belt dynamically changes in response to solar wind variations. There exist several conditions to cause the flux drop-out of the outer belt electrons. The magnetopause shadowing (MPS) is one of the processes to cause the rapid loss of outer belt electrons (e.g.,Kim et al.,2008). In this study, we investigate how radiation belt electrons are lost through the MPS process with a code-coupling simulation using GEMSIS-RB test particle simulation code (Saito et al., 2010) and GEMSIS-GM global MHD magnetosphere simulation code (Matsumoto et al., 2010) by focusing the equatorial pitch angle and local time dependence. We calculate trajectories of electrons in electromagnetic fields calculated from GEMSIS-GM with initial L-shells from 6 to 11, initial energies from 1 MeV to 10 MeV, and initial pitch angles between 50 degrees and 90 degrees, using the relativistic guiding-center equation. The simulation consists of the following three phases associated with variations of the solar wind dynamic pressure; [i] The standoff distance of magnetopause at the subsolar point is 12 Re with the initial dynamic pressure of 1.0 nPa. [ii] The solar wind dynamic pressure becomes 2.5 nPa, and the magnetopause moves to 9 Re. [iii] The solar wind dynamic pressure decreases, so that the inflation of the magnetopause takes place and the standoff distance of the magnetopause is 10 Re. During phase [ii], the high-latitude reconnections occur at dawn-side firstly and many electrons escape from the magnetosphere to the interplanetary magnetic field along the field line in the dawn side. Subsequently, the high-latitude reconnections occur at the high-latitude in the dusk side. In phase [iii], the remained electrons in the magnetosphere escape into the interplanetary in both the dawn and dusk sides. The loss at the dusk-side is outward motion of the trapped electrons caused by the dawn-to-dusk electric fields associated with the inflation of the magnetosphere. The study showed detailed process of the electron escape into the interplanetary magnetic field and the electron escape occur in both enhancement/decrease of the dynamic pressure.

Keywords: Magnetopause Shadowing, global MHD magnetosphere simulation, test particle simulation

©2019. Japan Geoscience Union. All Right Reserved.

Non-diffusive response of outer belt electrons on interplanetary shock

Takuma Toishi[1], *Yusuke Ebihara[1], Takashi Tanaka[2]

1. Research Institute for Sustainable Humanosphere, Kyoto University, 2. Kyushu University

Test particle simulation is performed in the electric and magnetic fields given by a global magnetohydrodynamics (MHD) simulation. When an interplanetary shock strikes the magnetosphere, a compressional wave propagates tailward. Pre-existing relativistic electrons that are initially located at fixed radial distances are redistributed by the electric and magnetic fields associated with the compressional wave. When the electrons encounter the nightside, they undergo complicated paths under the complicated distribution of the electric and the magnetic fields. Consequently, a group of isolated electrons forms, suggesting non-diffusive response. We discuss the redistribution processes in terms of the magnetospheric processes.

Keywords: radiation belt, MHD simulation, Test particle simulation

©2019. Japan Geoscience Union. All Right Reserved.

PARM: Initial result of the auroral camera on the G-CHASER (RockSat-XN) rocket and status of the development of auroral cameras for the LAMP rocket experiment

*Naoshi Yagi[1], Takeshi Sakanoi[1], Fukizawa Mizuki[1], Kazushi Asamura[2], Yoshizumi Miyoshi[3], Keisuke Hosokawa[4], Genki Ishizawa[5]

1. Planetary Plasma and Atmospheric Research Center, Graduate School of Science, Tohoku University, 2. Institute of Space and Astronautical Science, Japan Aerospace Exploration Agency, 3. Institute for Space-Earth Environmental Research, Nagoya University, 4. Department of Communication Engineering and Informatics, University of Electro-Communications, 5. Space & terrestrial plasma pyhsics

We developed an Aurora Imaging Camera (AIC) for NASA’ s G-CHASER (RockSat-XN) sounding rocket launched on 13th January, 2019. In addition, LAMP sounding rocket scheduled to be launched from December 2019 to February 2020 to reveal the spatio-temporal relationship between PsA and relativistic electrons, namely microbursts. In this presentation, we report the development of AIC, the result f the G-CHASER (RockSat-XN) rocket, as well as the current status of LAMP rocket project.

On the G-CHASER rocket experiment, 7 scientific and educational instruments were provided from Japan, U.S., Norway and Puerto Rico. Japanese instrument, called PARM, consists of an intermediate energy (20 - 100 keV) electron detector MED, high energy (several hundred keV - 2 MeV) electron detector HEP, fluxgate magnetometer AFG, and auroral camera AIC. Concerning development of AIC, we carried out sensitivity calibration experiment, electrical function test, fabrications, focus adjustment and environmental (vibration, vacuum and thermal) tests from January to July 2018. AIC consists of detector unit AIC-S and power/data processing electric unit AIC-E. AIC-S consists of a CCD camera (Watec 910 HX), wide-angle lens (F-number: 1.6, focal length: 3.5 mm, field of view: 96.4˚x75˚) and a glass filter (RG665) that transmits light with a wavelength longer than 665 nm.

NASA decided to launch the G-CHASER rocket at 9:00UT on 13rd January 2019 from Andoya Space Center, Norway (69.3˚N, 16.0˚E in the geographic coordinate). At this time, the solar elevation was -4˚, hence twilight had been already started and the region above 15km was sunlit. AIC detected leak light from the rocket skirt until the separation of skirt at an altitude of 82.9km. From time variation of AIC data, rocket spin frequencies were estimated to be ~5Hz at ~20km altitude and ~1Hz at ~80km altitude. This is consistent with the modulation period of magnetic field data observed by AFG. Because AIC was designed to measure weak pulsating aurora with hundreds Rayleigh, the AIC data was saturated above 82.9km after separation of rocket in the sunlit region, and no aurora was observed.

We are also conducting the LAMP sounding rocket project whose PI is Dr. Sarah Jones in NASA/GSFC. This is scheduled to be launched at Poker Flat Research Range in Alaska in 2019 winter. Japanese PARM2 team will provide high energy (several hundred keV - 2 MeV) electron detector HEP, fluxgate magnetometer MIM, and auroral cameras AIC2. We concern AIC2 that consists of two cameras AIC2-S1/AIC2-S2 and power/data processing electric unit AIC2-E. AIC2-S1/S2 and AIC2-E will be installed on a despun platform to derotate rocket spin. AIC2-S1 measures N2 1stPG emission with a narrow FOV lens (F value: 0.95, focal length:17mm, field of view 27x27deg), and AIC-S2 measures OI 844.6nm emission with a wide-angle lens (F value:1.6, focal length:3.5 mm, diagonal field of view:120x120˚). AIC2-S1 will take fine structure of PsA in the region more than 100 x 100 km area around the magnetic footprint with a few kilometer resolution, while AIC2-S2 will obtain an altitude distribution of

©2019. Japan Geoscience Union. All Right Reserved.

PsA in the F-region as well as wide-range distribution of PsA. The characteristic energy of precipitating electron can be estimated from the ration of OI844.6 and N2 1stPG. The cameras are conducted by a single board computer NanoPi M4 via USB3.0 high speed interface. We confirmed to get frame sampling rate with approximately 10Hz with this system. Region-of-interest (ROI) of 3660 x 3660 pixel area is binned with 61x61pixels, and finally image data with 60 x 60 bin (16 bit/bin) is recorded at 10 Hz. The precise imaging and altitude distribution of PsA are obtained with AIC2 at two wavelengths with 10Hz sampling. The imaging data combined with precipitating electron data in the wide energy range enable us to investigate the relativistic electron precipitation in microbursts that is probably caused by chorus waves in the magnetosphere.

Keywords: auroral camera, rocket experiment

©2019. Japan Geoscience Union. All Right Reserved.

First simultaneous observation of a SAR arc at subauroral latitudes using a ground all-sky camera and the Arase satellite in the inner magnetosphere

*Yudai Inaba[1], Kazuo Shiokawa[1], Shin-ichiro Oyama[1,8,9], Yuichi Otsuka[1], Atsuki Shinbori[1], Yoichi Kazama[2], Shiang-Yu Wang[2], Sunny W. Y. Tam[2], Shoichiro Yokota[3], Satoshi Kasahara[4], Kunihiro Keika[4], Tomoaki Hori[1], Ayako Matsuoka[5], Yoshiya Kasahara[6], Atsushi Kumamoto[7], Yasumasa Kasaba[7], Yoshizumi Miyoshi[1], Iku Shinohara[5], Arto Oksanen[10]

1. Institute for Space-Earth Environmental Research, 2. Academia Sinica, 3. Osaka Univ, 4. Tokyo Univ, 5. JAXA, 6. Kanazawa University, 7. Tohoku University, 8. University of Oulu, Finland, 9. National Institute of Polar Research, 10. Jyväskylän Sirius ry, Finland

Stable Auroral Red (SAR) arc is characterized by a 630.0 nm emission observed at subauroral latitudes. The energy of precipitating electrons that cause the SAR arc emission is several electron volts (eV). Precipitation of low-energy electrons is expected to occur due to spatial overlap between the plasmasphere and the ring current, where high-energy (more than 10 keV) ring current ions heat low-energy (less than 1 eV) electrons in the plasmasphere. Simultaneous observations of SAR arcs using the ionospheric satellite and ground all-sky cameras have been already done [e.g., Foster et al., 1994]. However, there has been no reports on in-situ measurements of plasma and electromagnetic fields in the inner magnetosphere, where the plasmaspheric plasma is heated by the ring current. In this study, we report simultaneous observations of a SAR arc at 22:04 UT on March 28, 2017, by using an all-sky camera at Nyrola (62.34 N, 25.51 E, MLAT 59.4 N) at subauroral latitudes and the Arase satellite. We analyze the all-sky camera data and the satellite data of this event to investigate the generation mechanism of the SAR arc. We find interesting features in the electric field data and the energy flux of electrons observed by the electric field detector of the plasma wave experiment (EFD/PWE) and the low-energy particle experiments–electron analyzer (LEP-e), respectively, onboard the Arase satellite at the crossing of the SAR arc. A negative excursion of the Ez component of the electric field (GSE coordinate system) with an amplitude of ~2.4 mV/m was observed at the crossing time. The Bx component of the magnetic field (GSE coordinate system) was negative. Thus the direction of the E ×B drift is westward, which is consistent with the westward auroral motion observed in the SAR arc by the ground all-sky camera. At the SAR arc crossing, the energy flux of electrons below 100-eV electrons is slightly intensified. We will discuss these observations in relation to the proposed SAR-arc generation mechanisms.

Keywords: ERG, SAR arc, All-sky imager, Simultaneous observation

©2019. Japan Geoscience Union. All Right Reserved.

Pi2 pulsations observed by the Arase satellite inside and outside the plasmapause

*Mariko Teramoto[1], Ayako Matsuoka[2], Reiko Nomura[5], Yoshiya Kasahara[3], Yasumasa Kasaba[4], Atsushi Kumamoto[4], Fuminori Tsuchiya[4], Shoya Matsuda[2], Masahito Nose[1], Masafumi Shoji[1], Yasunori Tsugawa[1], Shun Imajo[1], Yoshizumi Miyoshi[1], Iku Shinohara[2]

1. Institute for Space-Earth Environmental Research Nagoya University, 2. Institute of Space and Astronautical Science, Japan Aerospace eXploration Agency, 3. Kanazawa University, 4. Tohoku University, 5. National Astronomical Observatory of Japan

The spatial structure of Pi2 pulsation relative to the plasmasphere has been studied using the magnetic and electric field observed from the equatorial orbiting satellite in the inner magnetosphere by Takahashi et al (2003; 1995). They showed that the nightside Pi2 pulsations in the inner magnetosphere, which have high coherence with those at low-latitude ground station, are dominated by the poloidal component (the radial and compressional components for the magnetic field and azimuthal component for the electric field). The amplitudes of the compressional magnetic field has maximum and azimuthal electric field and the compressional magnetic field have maximum and minimum in the vicinity of the plasmaspause, respectively. The phase of the azimuthal electric field relative to low-latitude Pi2 pulsations on ground is 90 degrees in the plasmasphere. Such radial profile of the amplitude and phase of Pi2 pulsations can be explained by a plasmaspheric cavity mode resonance. However, the latitudinal structure of Pi2 pulsations in the electric field has not been examined. We investigate the latitudinal characteristics of off-equatorial Pi2 pulsations on the nightside and their relation to the plasmapause using the magnetic field measured by the fluxgate magnetometer measured by the Magnetic Field Experiment (MGF), the electric field measured by the Electric field Detector (EFD), and electron density derived from the spectra measured by the High Frequency Analyzer (HFA) from the Arase satellite.

©2019. Japan Geoscience Union. All Right Reserved.

An extreme erosion of the plasmasphere during the 7–10 September 2017 storm

*Yuki Obana[1], Naomi Maruyama[2,3], Atsuki Shinbori[4], Kumiko K. Hashimoto[5], Mariangel Fedrizzi[2,3], Masahito Nose[4], Yuichi Otsuka[4], Nozomu Nishitani[4], Tomoaki Hori[4], Atsushi Kumamoto[6], Fuminori Tsuchiya[6], Shoya Matsuda[7], Ayako Matsuoka[7], Yoshiya Kasahara[8], Akimasa Yoshikawa[9], Yoshizumi Miyoshi[4], Iku Shinohara[7]

1. Osaka Electro-Communication University, 2. University of Colorado Boulder, 3. NOAA Space Weather Prediction Center, 4. Nagoya University, 5. Kibi International University, 6. Tohoku University, 7. Japan Aerospace Exploration Agency, 8. Kanazawa University, 9. Kyushu University

We report an extreme erosion of the plasmasphere arising from the September 2017 storm. The cold electron density is identified from the upper limit frequency of UHR waves observed by the HFA of the PWE instrument onboard the Arase spacecraft. The HFA provides the spectrograms of electric fields in a frequency range from 10 kHz to 10 MHz with an 8-sec time resolution (Kasahara et al., 2018; Kumamoto et al., 2018). Such wide frequency coverage allows observation of the UHR frequency even deep inside the plasmasphere.

The electron density profiles reveal that the plasmasphere was severely eroded during the recovery phase of the storm and the plasmapause was located at L~1.7 at 23 UT on 8 Sep 2017. This is the first report of such deep erosion of the plasmasphere (L_{PP}<2) with the in-situ observation of the electron density. The degree of the severity is much more than what is expected from the SYM-H minimum (−146 nT) of the event.

We further study absolute GNSS-TEC, ground-based magnetic field, the doppler velocity obtained from the SuperDARN Hokkaido Radars to investigate the location of the midlatitude ionospheric trough, the penetration of the convection electric field to the equator and middle latitudes, respectively. Our results suggest that the middle latitude electric field was penetrated from the high-latitude storm time convection for several hours. Futhermore, the Ionosphere-Plasmasphere-Electrodynamics (IPE) model (Sun et al., 2015; Maruyama et al., 2016) is used to understand the dynamics of the plasmasphere. The IPE results suggest that the middle latitude electric field penetrates from the high-latitude storm time convection that lasts for several hours can explain the degree of severity during the September 7-11 2017 storm.

Keywords: plasmasphere, innner magnetosphere, Magnetosphere-ionosphere coupling

©2019. Japan Geoscience Union. All Right Reserved.

Relative contribution of ULF and chorus waves to the radiation belt variation: Comparison between multi-point observations and BATSRUS + CRCM simulation

*Naoko Takahashi[1], Kanako Seki[1], Mei-Ching Fok[2], Yihua Zheng[2], Yoshizumi Miyoshi[3], David Hartley[4], Ayako Matsuoka[5], Yoshiya Kasahara[6], Yasumasa Kasaba[7], Nana Higashio[8]

1. Graduate School of Science, University of Tokyo, 2. NASA Goddard Space Flight Center, 3. Institute for Space-Earth Environmental Research, Nagoya University, 4. Department of Physics and Astronomy, University of Iowa, 5. Institute of Space and Astronautical Science, Japan Aerospace Exploration Agency, 6. Information Media Center, Kanazawa University, 7. Planetary Plasma and Atmospheric Research Center, Tohoku University, 8. Japan Aerospace Exploration Agency

Earth’ s radiation belt is the area where electrons with energies from hundreds of keV to several MeV are trapped. When, where, and how the radiation belt exhibits a dramatic variation during a magnetic storm is of global interest. The dynamic variation of the radiation belt is caused by various wave-particle interactions: (1) the radial diffusion of electrons driven by ultra-low-frequency (ULF) waves in Pc5 frequency ranges (1.6–6.7 mHz) and (2) the local acceleration caused by wave-particle interactions between whistler-mode chorus waves and radiation belt particles. Over the past decade, multi-point observations and numerical simulations have provided evidence to support above physical processes. However, it is debatable how much each wave contributes to the radiation belt variation during a magnetic storm. A few previous studies have quantitatively compared roles of local acceleration and radial transport by calculating diffusion coefficients, whereas the global context between the wave growth and the relativistic electron flux enhancement has not been extensively studied. To address these issues, the comprehensive study using multi-point observations and numerical simulations (not empirical models) makes essential and significant contributions.

We focus on the magnetic storm on 27-30 May 2017. This magnetic storm is triggered by coronal mass ejections and induces a clear interplanetary shock. Fortunately, several satellites are scattered in the inner magnetosphere and detect both ULF and chorus waves during this magnetic storm. Arase and Van Allen Probes also detect variations of relativistic electron fluxes associated with the Dst index variation. We examine L-value dependence of ULF and chorus wave powers and find the difference of wave activity during the recovery phase. The chorus wave activity is large during the early recovery phase, while the ULF wave activity is large during the late recovery phase. The difference of wave activity may contribute to the radial profile in the phase space density of relativistic electrons. To grasp the extent of individual wave contribution, we also perform the comprehensive ring current model (CRCM) coupled with Block-Adaptive-Tree Solar-Wind Roe-Type Upwind Scheme (BATSRUS) simulation. BATSRUS with CRCM well reproduces global characteristics of energetic electron fluxes and wave growth during this magnetic storm. We will further evaluate global distribution of simulated wave power comparing to the observation, and then discuss the temporal and spatial context between each wave growth and the radiation belt variation.

©2019. Japan Geoscience Union. All Right Reserved.

Modulation of the D-region ionosphere by Pc5 waves observed by VLF/LF standard radio waves

*Miyashita Takuya[1], Hiroyo Ohya[1], Fuminori Tsuchiya[2], Hiroyuki Nakata[1], Toshiaki Takano[1], Kazuo Shiokawa[3], Yoshizumi Miyoshi[3]

1. Chiba University, 2. Tohoku University, 3. Nagoya University

Ionospheric modulation due to ultra low frequency (ULF) Pc5 waves have been observed by GPS-total electron content (TEC), high frequency (HF) Doppler sounders, and SuperDARN HF radars [e.g., Pilipenko et al., 2014; Belakhovsky et al., 2016]. However, there are few reports for the modulation of the lower ionospheric associated with the ULF Pc5 waves using VLF/LF transmitter signals. In this study, we investigate the D-region signatures of the modulation due to the ULF Pc5 waves using a network of very low frequency (VLF)/low frequency (LF) standard radio waves. We show oscillations in intensities of the VLF/LF waves with a period of 4-6 minutes during substorms on 27 April, 2017. The transmitter signals from NAA (USA, 24.0 kHz, L = 2.88), NLK (USA, 24.8 kHz, L = 2.88), NDK (USA, 25.2 kHz, L = 2.98) and WWVB (USA, 60.0 kHz, L = 2.26) were observed by the receivers at ATH (Athabasca, L=4.31) and PKR (Poker Flat, L=5.95). The substorm occurred at 04:30 UT. Based on the wavelet analysis, we found that the intensities for the NDK-ATH and WWVB-ATH paths showed oscillations with a period of 4-6 minutes during the substorm growth phase (05:00-06:00 UT). Magnetic field variations observed by ground magnetometers around the NDK-ATH and WWVB-ATH paths also showed the same periodicity, which means that the variations in the VLF/LF intensities would be caused by Pc5 modulations. The magnetic field oscillations were observed in wide latitude range. The intensity of the oscillation was larger at high latitude magnetometers than those around the location of the NDK-ATH and WWVB-ATH path (mid-latitude). The Pc5 oscillations could be excited by solar wind because solar wind speed had similar period of the 4-6 minutes. In this presentation, we will discuss the cause of these VLF/LF oscillations.

Keywords: VLF/LF standard radio waves, Pc5, ULF

©2019. Japan Geoscience Union. All Right Reserved.

Oxygen-proton differences in ion energies dominating plasma pressure: Dependence on storm phases and solar wind drivers

*Kunihiro Keika[1], Satoshi Kasahara[1], Shoichiro Yokota[2], Masahiro Hoshino[1], Kanako Seki[1], Masahito Nose[3], Yoshizumi Miyoshi[3], Iku Shinohara[4]

1. Graduate School of Science, The University of Tokyo , 2. Graduate School of Science, Osaka University, 3. Institute for Space-Earth Environmental Research, Nagoya University, 4. Institute of Space and Astronautical Science, Japan Aerospace Exploration Agency

The ion pressure in the inner magnetosphere is generally dominated by protons with energies of a few to a few 100s keV. Oxygen ions of ionospheric origin, O+, can make a significant contribution to the ion pressure during geomagnetically active periods. Our previous study (Keika et al., 2018, GRL) examined the radial dependence of contributing energies, which we term an energy range that makes the dominant contribution to the plasma pressure, during the main phase of the six magnetic storms in Year 2017. We found clear oxygen-proton differences in the contributing energies in the outer part (L>5) of the ring current region. The contributing energies were higher for O+ than for H+. The results provided in situ evidence of the contribution from mass-dependent/selective acceleration processes to the energization of the outer part of the ring current.

The present study extends this analysis toward a larger database obtained from a longer period of magnetic storm times including the recovery phase. We also compare mass-dependent/selective energization between different solar wind drivers such as coronal mass ejections and corotational interaction regions. We primarily use data from the MEP-i (Medium-Energy Particle experiments - ion mass analyzer) on board the Arase spacecraft. MEP-i measures ions with energies of 10 to 180 keV/q and distinguishes between different ion species. Arase observed the nightside near-Earth magnetosphere (L<10) during 7 CME-driven and 7 CIR-driven storms with the Dst minimum of smaller than -50 nT in Years 2017 and 2018. The dependence on storm phases and solar wind drivers helps identify magnetospheric conditions favorable for mass-dependent/selective acceleration and in turn provides clues for understanding important physical mechanisms. Utilizing observations made by the MMS spacecraft in the near-Earth plasma sheet, we also compare oxygen-to-proton differences inside earthward bursty bulk flows with the Arase/MEP-i observations. The multi-spacecraft observations help better understand the temporal evolution of the mass-dependent/selective acceleration processes.

Keywords: Magnetic storms, Substorms, RIng current, Oxygen ions, Ion transport and acceleration

©2019. Japan Geoscience Union. All Right Reserved.

Mass dependence of penetration depth of multi-energy ions in the inner magnetosphere during magnetic storms: Arase observations

*Ryosuke Fujii[1], Yoshizumi Miyoshi[1], Masafumi Shoji[1], Kazushi Asamura[2], Lynn Kistler[1,8], Vania Jordanova[9], Tomoaki Hori[1], Satoshi Kurita[1], Mariko Teramoto[1], Yasunori Tsugawa[1], Yoshiya Kasahara[3], Yasumasa Kasaba[4], Atsushi Kumamoto[5], Fuminori Tsuchiya[4], Shoichiro Yokota[6], Kunihiro Keika[7], Ayako Matsuoka[2], Iku Shinohara[2]

1. Institute for Space-Earth Environmental Research, Nagoya University, 2. Institute of Space and Astronautical Science, Japan Aerospace Exploration Agency, 3. Information Media Center, Kanazawa University, 4. Planetary Plasma and Atmospheric Research Center, Tohoku University, 5. Department of Geophysics, Graduate School of Science, Tohoku University, 6. Graduate School of Science, Osaka University, 7. Department of Earth and Planetary Science, Graduate School of Science, The University of Tokyo, 8. University of New Hampshire, 9. Los Alamos National Laboratory

During magnetic storms, the ring current ions move toward the Earth, and the inner edge position of the ring current depends on the convection electric field. We investigate variations of the inner edge of the ring current ions, so-called, penetration depth, during magnetic storms using the ion measurements made by the Low-energy particle experiments-ion mass analyzer (LEP-i)/Medium-energy particle experiments-ion mass analyzer (MEP-i) instruments onboard the Arase satellite. The Arase satellite typically observes the earthward penetration of the ring current protons associated with the enhancement of the dawn-to-dusk electric field in the inner magnetosphere during the storm main phase. The plasmapause moves earthward during the main phase. On the other hand, the convection electric field decreases during the storm recovery phase in which the flux of ring current protons decreases. We identify that the penetration depth of protons depends on the minimum Dst index during the storms as well as the proton energy.

We also investigate the penetration depth of other ions, i.e., helium and oxygen ions. Because the life times of helium and oxygen ions due to charge exchange reaction for are longer than that of protons, it is expected that these ions can penetrate deeper than protons and temporal and spatial evolution can be observed clearly. We will also discuss the relation between the position of ring current inner edge and cross polar cap potential.

Keywords: The Arase satellite, Ring current, Ions

©2019. Japan Geoscience Union. All Right Reserved.

Relativistic Acceleration of Energetic Protons by Electromagnetic Ion Cyclotron Waves in the Jovian Magnetosphere

*Tomohiro Sekine[1], Yoshiharu Omura[1], Danny Summers[2], Yikai HSIEH[1], Satoko Nakamura[1]

1. Reserach Institute for Sustainable Humanosphere, Kyoto University, 2. Memorial University of Newfoundland

We perform test particle simulations of nonlinear interaction between energetic protons and EMIC waves. We assume a coherent EMIC waves that have a constant frequency and propagate parallel to the magnetic field. We find that protons can be trapped and accelerated by EMIC waves. We find a very efficient acceleration process of protons in which kinetic energy of protons increases while directions of parallel velocities reverses when we assume parameters in the Jovian magnetosphere. We notice that this phenomenon is very similar to the interaction process between relativistic electrons and whistler-mode waves, which is called Relativistic Turning Acceleration (RTA) [1]. In order to analyze the phenomena, we have developed nonlinear trapping theory of interaction between relativistic protons and EMIC waves. Next, we compare the theory and simulation results. We confirm that the results satisfy the conditions for RTA. Following the trajectories of many resonant protons, we obtain time evolution of the distribution function of relativistic protons as a function of energy and equatorial pitch angle based on the numerical Green’ s function method [2].

References:

[1] Y. Omura, N. Furuya, D. Summers, Relativistic turning acceleration of resonant electrons by coherent whistler-mode waves in a dipole magnetic field, Journal Geophysical Research, Vol. 112, A06236, doi:10.1029/2006JA012243, 2007.

[2] Y. Omura, Y. Miyashita, M. Yoshikawa, D. Summers, M. Hikishima, Y. Ebihara, and Y. Kubota (2015), Formation process of relativistic electron flux through interaction with chorus emissions in the Earth’ s inner magnetosphere, J. Geophys. Res. Space Physics, 120, 9545–9562, doi:10.1002/2015JA021563, 2015.

©2019. Japan Geoscience Union. All Right Reserved.

Statistical study of IPDP type EMIC wave-related electron precipitation at subauroral latitude

*Asuka Hirai[1], Fuminori Tsuchiya[1], Takahiro Obara[1], Yasumasa Kasaba[1], Yuto Katoh[2], Hiroaki Misawa[1], Kazuo Shiokawa[3], Yoshizumi Miyoshi[3], Satoshi Kurita[3], Martin G Connors[4]

1. Planetary Plasma and Atmospheric Research Center, Graduate School of Science, Tohoku Univ. , 2. Department of Geophysics, Graduate School of Science, Tohoku University, 3. Institute for Space-Earth Environmental Research, Nagoya University, 4. Athabasca University

The outer radiation belt electrons disappear during the main phase of geomagnetic storms. One of the loss mechanisms of electrons from the outer belt is precipitation into the atmosphere due to wave-particle interactions. Electromagnetic ion cyclotron (EMIC) waves are believed to be important plasma waves that contribute to the loss of the outer radiation belt due to pitch angle scattering. They can scatter relativistic and ultra-relativistic electrons. However, there are still questions left about the contribution of EMIC waves to the whole loss of radiation belt electrons and possible conditions favorable to pitch angle scattering.

EMIC waves mainly propagate along magnetic field lines and are observed on the ground as Pc1 geomagnetic pulsations. Intervals of pulsations of diminishing periods (IPDP) are Pc1/EMIC waves that are characterized by frequency rise from 0.1 to 1–2 Hz in a period of ~1 h, and often occur during substorms. Recent studies reported that IPDP are preferentially associated with relativistic electron precipitation. However, the statistical relation between IPDP waves and relativistic electron precipitation, and their physical mechanism, remain open issues.

We investigated differences in characteristics between IPDP and other types of Pc1 by using an induction magnetometer and VLF radio wave data that is a proxy of electron precipitations at subauroral latitude from 1 November 2016 to 30 June 2018. We used the induction magnetometer of PWING (study of dynamical variation of Particles and Waves in the INner magnetosphere using Ground-based network observations) at Athabasca, Canada (54.6˚N, 246.36˚E, L = 4.39). VLF radio waves propagate from transmitters to receivers in subionospheric waveguide. The modulations of VLF signals are detected as occurrence of sub-relativistic and relativistic electron (>100 keV) precipitation due to ionization changes in the lower ionosphere along the radio wave propagation path. VLF radio waves are transmitter from NDK, U.S. (46.367˚N, 261.467˚E, L =3.13) and NLK, U.S. (48.2˚N, 238.083˚E, L =2.84) and received at Athabasca. We selected EMIC wave events on the basis of the following criteria: (1) EMIC wave power is higher than 10^{-5} nT^2/Hz. (2) Duration of EMIC waves is longer than 20 min. (3) Interval between one EMIC wave event and the next one is longer than 30 min. Electron precipitation was identified as a decrease in amplitude of VLF signals from the quiet day curve (QDC). We counted as EMIC wave-driven electron precipitation if we detect temporal correspondence with EMIC waves. In this period, we found 950 EMIC wave events, and 87 of total EMIC wave events were IPDP events (9.2%). Local time dependence of EMIC waves shows that IPDP often occurs in the afternoon and evening sector, while other types of Pc1 occur in all local time range, but with a maximum in 12–16 MLT, which is consistent with previous studies. Simultaneous observation of the magnetometer and VLF radio waves were available for 286 days, and we found 163 EMIC wave events. 19 of 163 EMIC wave events were clearly associated with electron precipitation (12%). Among 19 electron precipitation events, 15 events were caused by IPDP (79%). Also, the electron precipitation events were observed in the evening sector with similar local time dependence to IPDP. This result suggests that IPDP is more likely to cause electron precipitation than other Pc1 wave types. In previous studies, IPDP occurs due to ion cyclotron instability of ring current ions in the evening sector, and favorable region for electron scattering by EMIC waves is high density duskside plasmapause

©2019. Japan Geoscience Union. All Right Reserved.

and plasmaspheric plume because dense plasma lowers minimum resonant energy of electrons. It is assumed that occurrence region of IPDP is coincident with the preferential region for MeV electron scattering by EMIC waves. For this reason, it is expected that IPDP type EMIC waves significantly cause relativistic electron precipitations in the duskside.

Keywords: EMIC waves, electron precipitation, subionospheric VLF radio waves

©2019. Japan Geoscience Union. All Right Reserved.

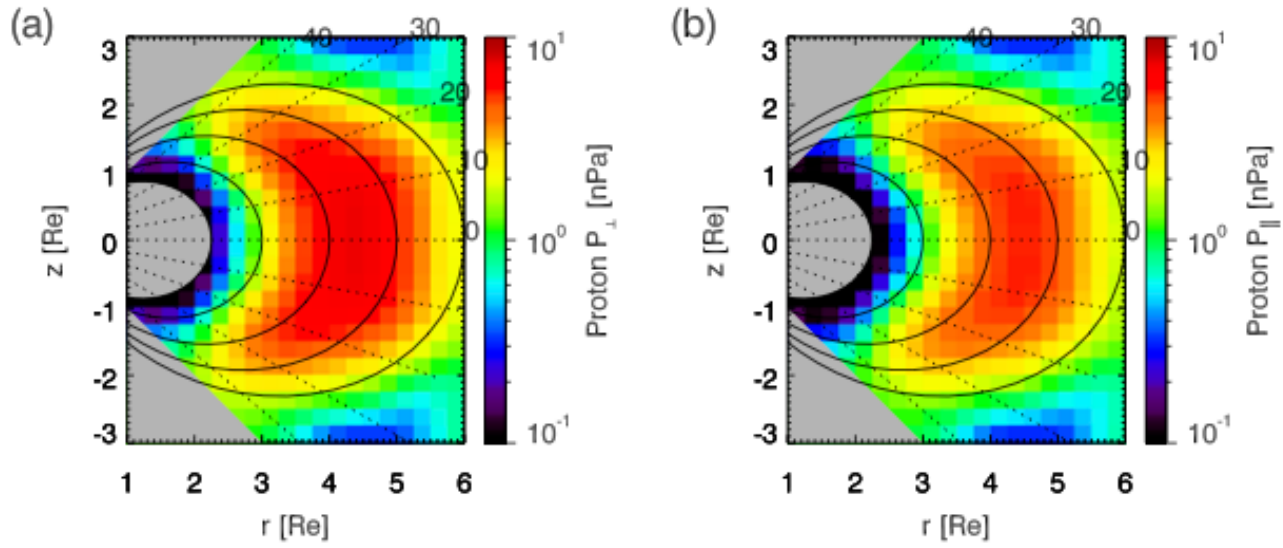
Meridional distributions of proton plasma and pressure-driven currents in the nightside inner magnetosphere: Arase observations

*Shun Imajo[1], Masahito Nose[1], Satoshi Kasahara[2], Shoichiro Yokota[3], Ayako Matsuoka[4], Kunihiro Keika[2], Tomoaki Hori[1], Mariko Teramoto[1], Kazuhiro Yamamoto[5], Oimatsu Satoshi[5], Reiko Nomura[6], Akiko Fujimoto[7], Iku Shinohara[4], Yoshizumi Miyoshi[1]

1. Institute for Space-Earth Environmental Research, Nagoya University, 2. Graduate School of Science, The University of Tokyo, 3. Graduate School of Science, Osaka University, 4. Institute of Space and Astronautical Science, Japan Aerospace Exploration Agency, 5. Graduate School of Science, Kyoto University, 6. National Astronomical Observatory of Japan, 7. Kyushu Institute of Technology

We examine the averaged meridional distributions of proton plasma parameters and pressure-driven currents in the nightside (20–04 h magnetic local time) ring current region during disturbed times (-80 < SYM-H* < -40 nT) using ion measurements covering energy range of 10–180 keV by the Arase satellite. Because the Arase satellite has a large inclination orbit of 31°, it covers the absolute value of magnetic latitude (|MLAT|) range of 0–40° and the radial distance of < 6 Re. We find that the plasma pressure decreases significantly with MLAT. The plasma pressure on the same L^* shell at 30°<|MLAT|<40° is about 10–60% of that at 0°<|MLAT|<10°, and the percentage of decrease is larger on lower L^* shells. The pressure anisotropy which is defined by the perpendicular pressure divided by the parallel pressure decreases with radial distance and shows a weak dependence on |MLAT|. The magnitude of the plasma beta at 30°<|MLAT|<40° is one or two order smaller than that at 0°<|MLAT|<10°. The relative plasma pressure distribution predicted from the magnetic strength and anisotropy is roughly consistent with the observed plasma pressure for L^*=3.5–5.5. The azimuthal pressure-gradient current derived from the plasma pressure distribution spreads over ~-20° |MLAT|, while the curvature current is limited in ~0–10° |MLAT|. We suggest that the latitudinal dependences should be taken into account when considering a temporal evolution of ring current particles from L distributions of successive orbits.

Keywords: meridional distributions, plasma pressure, pressure-driven currents, Arase satellite



©2019. Japan Geoscience Union. All Right Reserved.

Space Weather Effects on Energetic Proton Flux Response in South Atlantic Anomaly

*Kirolosse Mina GIRGIS[1,2], Tohru Hada[1], Shuichi Matsukiyo[1]

1. Earth System Science and Technology (ESST) Department, Interdisciplinary Graduate School of Engineering Sciences (IGSES), Kyushu University, Japan, 2. Aerospace Engineering Department, Faculty of Engineering, Cairo University, Egypt

In this research, energetic proton flux in the inner radiation belt, is studied inside the South Atlantic Anomaly (SAA) by performing test particle simulations, where the background time-varying magnetic field is provided by Tsyganenko model, according to *Dst* index and altitudes. The objective of this investigation, is to estimate and forecast the additional radiation dose, occurring on spacecraft and human bodies, due to their passage inside the anomaly, and precisely, during intense solar storms. It was found that within minutes, proton flux in the SAA, penetrated deeper downward by about 200 km, when the *Dst* index is decreased (< -210 nT), and a after few more minutes, it was significantly reduced at all the altitudes; the last conclusion was confirmed by satellite observations.

Keywords: South Atlantic Anomaly, Space Weather, Dst Index, Radiation Dose, Proton Flux

©2019. Japan Geoscience Union. All Right Reserved.

Solar-cycle variations of >30 keV electron flux enhancements under the inner radiation belt

*ALLA SUVOROVA[1]

1. National Central University

Intense fluxes of 30-300 electrons can arise in the equatorial ionosphere outside the South Atlantic Anomaly. It was established that the electrons were injected from the inner radiation belt probably due to a mechanism of fast radial transport in the crossed electric and magnetic fields. Continuous monitoring of energetic particles at low heights of ~850 km with the MEPED instrument onboard the NOAA/POES satellites allowed compiling large statistics of the >30 keV electron enhancements from 1998 to 2018. We studied particle flux variations with geomagnetic activity and solar cycle. We found that geomagnetic activity measured by Dst and AE indices are not key factors of occurrence rate increase for electron injections, but influence on intensity of particles. The occurrence rate is controlled by auroral conductivity on the dayside and significantly enhanced during northern summer. Descending phase of solar cycle plays a major role in the occurrence rate increase.

Keywords: magnetosphere-ionosphere, energetic electrons, low latitudes, solar cycle

©2019. Japan Geoscience Union. All Right Reserved.

Energy spectra variations of high energy electrons in the inner magnetosphere observed by HEP/XEP on ARASE and SEDA-e on HIMAWARI

*Takeshi Takashima[1], Takefumi Mitani[1], Nana Higashio[2], Tsutomu Nagatsuma[3]

1. ISAS/JAXA, 2. Research and Development Directorate/JAXA, 3. NiCT

The relativistic electrons in the outer radiation belt were disappeared/increased and their energy spectra were changed dynamically in some storms observed by XEP/HEP onboard the ARASE spacecraft. In the same time, SEDA-e with energy range 200keV-4.5MeV for electron on board the HIMAWARI-8, Japanese weather satellite on GEO, observed increase of relativistic electron in different local time.
When comparing the energy spectra, there are times when the spectrum matches or does not match. It is also observed that the change in the slope of the energy spectrum differs with time. These phenomena are observed even when there are two satellites at the same local time.
We will report on energy spectra variations of high energy electrons including calibrations of differential flux between XEP and HEP and discuss comparisons with energy spectra between ARAE and HIMAWARI that observed each storm in different local time.

Keywords: relativistic electron, inner magnetosphere, ARASE

©2019. Japan Geoscience Union. All Right Reserved.

Inter-channel calibration of the high-energy electron experiments (HEP) instrument onboard the Arase satellite

*Tomoaki Hori[1], Takefumi Mitani[2], Takeshi Takashima[2], Park Inchun[1], Satoshi Kurita[1], Mariko Teramoto[1], Nana Higashio[3], Satoshi Kasahara[4], Shoichiro Yokota[5], Yoshizumi Miyoshi[1], Iku Shinohara[2]

1. Institute for Space-Earth Environmental Research, Nagoya University, 2. Japan Aerospace Exploration Agency, Institute of Space and Astronautical Science, 3. Japan Aerospace Exploration Agency, 4. Graduate School of Science, The University of Tokyo, 5. Graduate School of Science, Osaka University

An inter-channel comparison of electron fluxes measured by the HEP instrument onboard the Arase satellite is conducted with a focus on the apparent non-uniformity in detection efficiency and relative offset of the background flux level between the channels, which was partly reported previously. We extend the data set to cover the entire two-year period since the start of the regular observations. The flux ratio of different channels is sorted by the electron flux level of much higher energies that was simultaneously measured by the extremely high-energy electron experiment (XEP) instrument onboard Arase. The result shows that the HEP flux of all azimuthal channels is more or less affected by MeV electrons which are most likely to have penetrated into the instrument box and directly hit the detectors. However, it is also revealed that the non-uniform count distribution over the channels still remains even when the penetrating electrons are absent. We conduct a set of Geant-4 simulations to trace electrons with various energies and incident angles to the detector plane in order to give a quantitative interpretation for the resultant count distributions, in terms of the effects of penetrating electrons and obliquely-colliding incident electrons.

Keywords: Arase satellite, particle instrument, calibration

©2019. Japan Geoscience Union. All Right Reserved.

Particle simulation for calibrating the HEP data onboard the ARASE satellite

*PARK INCHUN[1], Yoshizumi Miyoshi[1], Takefumi Mitani[2], Tomoaki Hori[1], Satoshi Kurita[1], Mariko Teramoto[1], Takeshi Takashima[2], Nana Higashio[3], Iku Shinohara[2]

1. Nagoya University Institute for Space-Earth Environmental Research, 2. Japan Aerospace Exploration Agency Institute of Space and Astronautical Science , 3. Japan Aerospace Exploration Agency

Understanding the detailed characteristics of the HEP (High-Energy electron Experiment) instrument onboard the Arase satellite is crucial for data calibration. Due to difficulties of reproducing the severe radiation environment of the inner magnetosphere on the ground, computer simulation is the best method to understand instrument responses to the ambient radiation environment. Through Monte-Carlo simulations using the Geant4 tool, we have reconstructed the geometry of the HEP instrument and modeled the high-energy particle environment. Using the developed model, we have studied the efficiency of the detectors, the angular resolution, and the g-factors, which depend on the particle energy and the sensor channels. While the previous studies were based on a uni-direction simulation with electron pencil beams, this study adopted all the detector channels and energy bends of HEP thus resulting in more advanced simulations. Based on the results, we have made a new calibration table depending on the angle of incident particles. We have also estimated the g-factor which depends on the incident particle energy. The updated calibration table and g-factors are important for calibrating the HEP data as well as inter-calibrations with other particle instruments' data.

Keywords: ARASE, Geant4, HEP

©2019. Japan Geoscience Union. All Right Reserved.

Geant4 model calculation and energetic particle observation with HEP/Arase in the inner radiation belt

*Honoka Toda[1], Wataru Miyake[1], Takefumi Mitani[3], Takeshi Takashima[3], Yoshizumi Miyoshi[2], PARK INCHUN[2], Tomoaki Hori[2]

1. Tokai University, 2. ISEE/Nagoya University, 3. ISAS/JAXA

The high-energy electron experiments (HEP) instrument installed on the Arase is designed to observe energetic electrons of 70 keV to 2 MeV. The HEP registers high electron counts for the MeV energy range, not only in the outer belt but also in the inner belt, in MeV energy range. On the contrary, Van Allen Probes have hardly detected MeV electrons in the inner radiation belt. A probable interpretation is that the counts of HEP are caused due to contamination of high-energy protons. In order to verify this idea, we have modeled the HEP instrument a Geant4 simulation to determine the energy of penetrating protons. The result clearly shows that high-energy protons, it has become clear that high-energy protons of a few to a few tens of MeV can contribute to the apparent high counts of HEP. No instrument for measuring protons in this energy range is installed on the satellite. We will discuss the possibility of research on the spatial distribution and time variation of high-energy protons in the inner belt based on observation data from the HEP instrument.

Keywords: Arase, Proton Radiation Belt, HEP

©2019. Japan Geoscience Union. All Right Reserved.

Validation of High-energy electron detector simulator for the HEP instruments onboard Arase

*Takefumi Mitani[1], PARK INCHUN[2], Tomoaki Hori[2], Taku Namekawa[1,3], Kazushi Asamura[1], Takeshi Takashima[1], Satoshi Kasahara[3], Satoshi Kurita[2], Mariko Teramoto[2], Nana Higashio[1], Yoshizumi Miyoshi[2], Iku Shinohara[1]

1. Japan Aerospace Exploration Agency, Institute of Space and Astronautical Science, 2. Institute for Space-Earth Environmental Research, Nagoya Univ., 3. The university of Tokyo

The high-energy electron experiments (HEP) onboard the Arase satellite detects 70 keV-2 MeV electrons and generates a three-dimensional velocity distribution for these electrons in every period of the satellite's rotation. Electrons are detected by two instruments, namely, HEP-L and HEP-H, which differ in their geometric factor (G-factor) and range of energies they detect. HEP-L detects 70 keV–1 MeV electrons and its G-factor is 9.3 $\times 10^{-4}$ cm^2 sr at maximum, while HEP-H observes 0.7 MeV–2 MeV electrons and its G-factor is 9.3 $\times 10^{-3}$ cm^2 sr at maximum. The instruments utilize silicon strip detectors and application-specific integrated circuits to readout the incident charge signal from each strip.

In order to deduce the distribution of incident electrons from the direction and energy detections in orbit, we have developed a detector simulator using the Geant4 toolkit. Especially contamination due to high energy particles must be considered quantitatively. We have also been working on electron beam experiments using HEP detector modules which are almost the same as the flight model in order to compare detailed simulations and experimental data.

We will present a comparison between results from the electron beam experiments and those from the detector simulator. And we will discuss its influence on the interpretation of the observational data obtained in orbit.

Keywords: high-energy electron, Arase, Geant4

©2019. Japan Geoscience Union. All Right Reserved.

[E] Poster | A (Atmospheric and Hydrospheric Sciences)：A-AS Atmospheric Sciences, Meteorology & Atmospheric Environment

Wed. May 29, 2019 3:30 PM - 5:00 PM JST | Wed. May 29, 2019 6:30 AM - 8:00 AM UTC | Poster Hall International Exhibition Hall8, Makuhari Messe_5

[A-AS01] High performance computing for next generation weather, climate, and environmental sc iences

convener:Hiromu Seko(Meteorological Research Institute), Takemasa Miyoshi(RIKEN), Chihiro Kodama(Japan Agency for Marine-Earth Science and Technology), Masayuki Takigawa(Japan Agency for Marine-Earth Science and Technology)

A lot of advanced simulation studies are being conducted by high performance supercomputers, such as K computer and Earth Simulator, in various fields including meteorology. The high performance supercomputers enable us to conduct numerical simulations and data assimilation of observation big-data (huge high-density and high-frequency data) with an order of magnitude higher resolutions and ensemble numbers than those with the previous supercomputers. In addition, the post-K computer will be available as a successor of K, and studies for the post-K computer are in progress. At this session, we comprehensively pick up the topics in the Atmospheric and Hydrospheric Sciences Sessions of the 2019 Union Meeting that comprise the atmospheric, oceanic and land sciences. This session aims to promote recent studies related to the issues on high performance computing in weather, climate, and environmental studies using the K computer and other supercomputers, and to enhance discussions on future directions of numerical simulations in meteorology.

[AAS01-P01] **Categorized correction forecast for accumulative precipitation of heavy rainfall processes based on optimal probability (OPPF) in medium-extended-range forecast time**

*Ruoyun Niu[1] (1.National Meteorological Center)

[AAS01-P02] **Characteristics of temporal and spatial distribution of regional rainstorm processes to the east of 95°E in China during 1981-2015**

*Ruoyun Niu[1], Couhua Liu[1] (1.National Meteorological Center)

[AAS01-P03] Near-real-time SCALE-LETKF forecasts of the record breaking rainfall in Japan in July 2018

*Takumi Honda[1], Guo-Yuan Lien[2,1], Takemasa Miyoshi[1] (1.RIKEN Center for Computational Science, 2.Central Weather Bureau)

[AAS01-P04] An objective Frontal Analysis Techniques and Application in Model Verification

*couhua liu[1] (1.National Meteorology Centre of China Meteorological Administration)

[AAS01-P05] Assimilating every 30-second phased array weather radar data in a torrential rainfall event on July 6, 2018 around Kobe city

*Yasumitsu Maejima[1], Shigenori Otsuka[1], Takemasa Miyoshi[1,2] (1.RIKEN Center for Computational Science, 2.University of Maryland, College Park)

[AAS01-P06] The impact of range sidelobes from phased array weather radar observations to short-range convective forecasts

*James David Taylor[1], Guo-Yuan Lien[1], Shinsuke Satoh[2], Takemasa Miyoshi[1] (1.RIKEN Research center for computational science, 2.NICT National Institute of Information and Communications Technology)

[AAS01-P07] Development of Hydro-debris 2D model for larger area

*Yosuke Alexandre Yamashiki[1], Tsutao OIZUMI[2], Bruno Ribeiro[1], Ryusuke Kuroki[1] (1.Earth & Planetary Water Resources Assessment Laboratory Graduate School of Advanced Integrated Studies in Human Survivability Kyoto University, 2.Japan Association of Marine-Earth Science and Tecnology)

[AAS01-P08] **Research on the application of an improved terrain-following vertical coordinates on GRAPES model**

*chao li[1] (1.NWPC.CMA)

[AAS01-P09] Development of a parallel spherical harmonic transform library: design and performance

*Fuyuki SAITO[1] (1.Japan Agency for Marine-Earth Science and Technology)

[AAS01-P10] Global data assimilation of multi-species satellite measurements for atmospheric chemistry analysis

*Takashi Sekiya[1], Kazuyuki Miyazaki[2,1], Koji Ogochi[1], Kengo Sudo[3,1], Masayuki Takigawa[1] (1.Japan Agency for Marine-Earth Science and Technology, 2.Jet Propulsion Laboratory/California Institute for Technology, 3.Graduate School of Environmental Studies, Nagoya University)

[AAS01-P11] The sensitivity to WRF shortwave radiation parameterizations in prediction of global horizontal irradiance for investigating interactions of atmosphere with croplands

*Ankur Srivastava[1], Sarita Kumari[1], Rajkumar Dhakar[2] (1.Indian Institute of Technology Delhi, 2.Indian Agriculture Research Institute)

[AAS01-P12] The development of an atmospheric aerosol/chemistry–climate model, BCC_AGCM_CUACE2.0, and simulated effective radiative forcing of nitrate aerosols

*QI AN[1,2,4], Hua Zhang[2], Zhili Wang[2], Yi Liu[1,4], Bing Xie[3], Qianxia Liu[3], Zaizhi Wang[3], Sunling Gong[2] (1.LAGEO, IAP, CAS, 2.LaSW, CAMS, 3.NCC,CMA, 4.UCAS)

[AAS01-P13] **Impacts of different types and intensities of El Niño events on winter aerosols over China**

*Xiaochao Yu[1,2], Zhili Wang[2,1], Hua Zhang[2], Shuyun Zhao[3] (1.Collaborative Innovation Center on Forecast and Evaluation of Meteorological Disasters, Nanjing University of Information Science and Technology, Nanjing, 210044, China, 2.State Key Laboratory of Severe Weather and Key Laboratory of Atmospheric Chemistry of CMA, Chinese Academy of Meteorological Sciences, Beijing, 100081, China., 3.National Climate Center, China Meteorological Administration, Beijing, 100081, China)

[AAS01-P14] High Cloud Annual Variation and Its Responses to Global Warming in the NICAM AMIP Experiment

*Ying-Wen Chen[1], Masaki Satoh[1,2], Chihiro Kodama[2], Akira Noda[2], Yohei Yamada[2] (1.Atmospheric and Ocean Research Institute, The University of Tokyo , 2.Japan Agency for Marine-Earth Science and Technology)

[AAS01-P15] Improvements in Simulating the Relationship between ENSO and East Asian Summer Rainfall in the CMIP5 Models

*Yuanhai FU[1], Riyu Lu[1] (1.IAP, CAS)

Categorized correction forecast for accumulative precipitation of heavy rainfall processes based on optimal probability (OPPF) in medium-extended-range forecast time

*Ruoyun Niu[1]

1. National Meteorological Center

By taking the ensemble prediction data from ECMWF and the intensive observations of precipitation in China, the technology of categorized correction forecast for accumulative precipitation of heavy rainfall processes based on optimal probability(OPPF) is developed, and 3 calculation schemes of OPPF are designed according to overall technical route. Then the reforecast test are carried for the accumulative precipitation of 67 heavy rainfall processes from May to September during 1981 to 2015 in China, and the forecast performance of the 3 OPPFs against that of ensemble mean (EMPF) and control number (CTPF) is evaluated and contrasted. The results show that:(1) In the medium-extended-range (096-360h) forecast time, the performance of the 3 OPPFs are better than that of EMPF and CTPF for heavy precipitation forecast and clear-rain forecast. the performance of OPPF1 and OPPF2 is close to that of EMPF for Moderate precipitation and larger precipitation. OPPF3 produces the best performance among the 3 OPPFs. (2) There are obvious regional differences in forecast performances. TS of OPPF3 in southern China are higher than in northern China, and the performance of OPPF3 for heavy precipitation is better than that of EMPF in southern China. During 096-240h forecast time, the performance of OPPF3 for heavy precipitation is also better than that of EMPF in eastern part of Northeast China.

Keywords: optimal probability, accumulative precipitation of heavy precipitation processes, categorized correction forecast, comparative evaluation of forecast performance

©2019. Japan Geoscience Union. All Right Reserved.

Characteristics of temporal and spatial distribution of regional rainstorm processes to the east of 95ºE in China during 1981-2015

*Ruoyun Niu[1], Couhua Liu[1]

1. National Meteorological Center

The events of the regional rainstorm processes (RRP) to the east of 95ºE in China over 1981-2015 are constructed based on intensive daily observations of precipitation in China and NCEP/NCAR reanalysis data by means of subjective and objective analyses. Temporal and spatial characteristic distribution of RRP in China are further investigated using the methods of wavelet power spectrum, nine-point binomial smoothing and Ward cluster analysis. The main conclusions are as follows. (1) The annual average number of RRP to the east of 95ºE in China is nearly 30. RRP in the Yangtze-Huaihe River valley occur most frequently among the six subareas with an annual average number of about 19, followed by that in South China and the eastern part of Southwest China with the annual average number of RRP 10.5 and 5.8 times respectively. Annual average number of RRP are only about 1-3 times in other subareas. (2) The inter-annual and inter-decadal variations of the annual number of RRP exhibit distinct fluctuation characteristics. The inter-annual and inter-decadal fluctuating variation in the Yangtze-Huaihe River valley is the most consistent with that to the east of 95E in China. Moreover, the fluctuating variations have a significant positive correlation between South China and eastern part of Southwest China, and also between Northeast China and North China. The annual number of RRP over the east of 95E in China and its subareas demonstrates a periodic variation of 2-4a, and also shows a periodic variation of 6-10a in the Yangtze-Huaihe River valley and South China and eastern part of Northwest China, while a 13-17a oscillation can be found in North China.(3) On the whole, the occurrence frequency of RRP to the east of 95E in China is the most in summer (especially in July), the least in winter, and higher in spring than in autumn. The months when RRP occur most frequently are June and July in the Yangtze-Huaihe River valley and eastern part of Southwest China, and May and June in South China. RRP mainly appear in July and August in other subareas.(4) The distribution patterns of RRP to the east of 95E in China are divided into 7 types. The heavy precipitation areas for pattern Ⅰ-Ⅳ migrate northward step by step from South China and southern part of Yangtze River valley to Huanghuai Basin and eastern part of Sichuan Basin.The heavy precipitation areas of pattern Ⅴ-Ⅶ all are located at the Coastal region of Southeast China.

Keywords: Regional rainstorm processes, Method for distinguishing, Temporal and spatial distribution, Patterns of extremely regional rainstorm processes

©2019. Japan Geoscience Union. All Right Reserved.

Near-real-time SCALE-LETKF forecasts of the record breaking rainfall in Japan in July 2018

*Takumi Honda[1], Guo-Yuan Lien[2,1], Takemasa Miyoshi[1]

1. RIKEN Center for Computational Science, 2. Central Weather Bureau

In July 2018, a stationary precipitation band associated with the Baiu front induced a record breaking rainfall and caused catastrophic destruction in Japan. This event was successfully captured by the near-real-time (NRT) SCALE-LETKF system (Lien et al. 2017) consisting of the Scalable Computing for Advanced Library and Environment-Regional Model (SCALE-RM, Nishizawa et al. 2015; Sato et al. 2015) and the Local Ensemble Transform Kalman Filter (LETKF, Hunt et al. 2007; Miyoshi and Yamane 2007). This system has been continuously operated since 2015 with an 18-km mesh model domain and the ensemble size of 50. In the NRT SCALE-LETKF system, only conventional observations are assimilated every 6 hours. By conducting a series of 50-member ensemble forecasts from the 6-hourly SCALE-LETKF analyses, this study aims to investigate predictability of this torrential rainfall event and important factors that contributed to the heavy precipitation. In general, the NRT SCALE-LETKF system provides skillful ensemble forecasts of the rainfall a few days in advance. Interestingly, the forecast skill exhibits sudden improvement due to assimilating conventional observations at a single location far southwest from the peak accumulated rainfall location. Forecast differences and ensemble correlations suggest that an extratropical cyclone over the Sea of Japan and a low-level trough near Taiwan play important roles in determining the front location.

Keywords: Data assimilation, Numerical Weather Prediction

©2019. Japan Geoscience Union. All Right Reserved.

An objective Frontal Analysis Techniques and Application in Model Verification

*Couhua Liu[1]

1. National Meteorology Centre of China Meteorological Administration

This paper presents an objective Frontal analysis method based on pressure field for east Asia. Comparing to methods based on thermo-dynamical elements such as temperature, the method developed in this paper can avoid the complex affection from sea-land and landform. The method will be used to identification of fronts in analysis and prediction of ECMWF model all over 2015, and then model error of predicted fronts will be verification. The verification result show that, comparing to analysis field, the moving speed of fronts in prediction field of ECMWF model is slower and strength is weaker.

Keywords: front, model, verification

©2019. Japan Geoscience Union. All Right Reserved.

Assimilating every 30-second phased array weather radar data in a torrential rainfall event on July 6, 2018 around Kobe city

*Yasumitsu Maejima[1], Shigenori Otsuka[1], Takemasa Miyoshi[1,2]

1. RIKEN Center for Computational Science, 2. University of Maryland, College Park

To investigate the impact of every 30-second phased array weather radar (PAWR; Yoshikawa et al. 2013, Ushio et al. 2014) observation on a simulation of a severe rainfall event occurred on July 6, 2018 around Kobe city, we perform 30-second-update 100-m-mesh data assimilation (DA) experiments using the Local Ensemble Transform Kalman Filter with the Scalable Computing for Advanced Library and Environment regional numerical weather prediction model. Two experiments were performed: the test experiment with every 30-second PAWR observation (TEST), and the other without observation (NO-DA).

The TEST analysis shows intense rainfalls with detailed structure of active convection, better matching with the PAWR observation compared to NO-DA analysis. In the forecast experiment, the forecast initialized by the ensemble mean analysis of TEST is skillful for 20 minutes compared with NO-DA, although the skill is decreased rapidly. The results suggest that the PAWR DA have a potential to improve the numerical simulation for this torrential rainfall event.

Keywords: Data assimilation, Heavy rainfall forecast, High performance computing

©2019. Japan Geoscience Union. All Right Reserved.

The impact of range sidelobes from phased array weather radar observations to short-range convective forecasts

*James David Taylor[1], Guo-Yuan Lien[1], Shinsuke Satoh[2], Takemasa Miyoshi[1]

1. RIKEN Research center for computational science, 2. NICT National Institute of Information and Communications Technology

Range sidelobes are an erroneous feature of radar observations that are generated by the pulse compression process used to improve the range resolution of target echoes in high resolution radar systems. Phased array weather radar (PAWR) is an advanced radar system providing very dense observations of reflectivity and Doppler radial velocity at 100m range resolution for over 100 elevation angles every 30 seconds. The use of pulse compression in PAWR to provide very high range resolution data makes it subject to these types of errors, which can result in false echoes observed at other ranges.

In this study we investigate the impact of assimilating range sidelobes from PAWR observations to short-range convective forecasts. This happens frequently in the current QC algorithm, although we plan to improve the QC in the future. We employ the use of the SCALE-LETKF system which couples the Local Ensemble Transform Kalman Filter (LETKF) with the Scalable Computing for Advanced Library and Environment (SCALE)-RM model. We focus on a convective rainfall event in August 2016 that brought heavy, intense rainfall over Osaka. PAWRs located in Suita, Osaka and in Kobe well-captured the convective system over its life cycle but featured prominent range sidelobes as part of their observations. Here, observations from both radars are first used to identify the range sidelobes before performing a series of 30-second update cycling experiments using observations from the Suita PAWR both with and without range sidelobes within a high-resolution 100-m mesh. As well as investigating their impact on short-range forecasts, we aim to show how we can further the usefulness of having two sets of PAWR observations to observe the same convective system by using them to identify and remove range sidelobes and improve short-range forecasts of severe convective events through the assimilation of this data.

Keywords: LETKF, Assimilation, Forecasts, Convection, Sidelobes

©2019. Japan Geoscience Union. All Right Reserved.

Development of Hydro-debris 2D model for larger area

*Yosuke Alexandre Yamashiki[1], Tsutao OIZUMI[2], Bruno Ribeiro[1], Ryusuke Kuroki[1]

1. Earth & Planetary Water Resources Assessment Laboratory Graduate School of Advanced Integrated Studies in Human Survivability Kyoto University, 2. Japan Association of Marine-Earth Science and Tecnology

The Hydro-debris 2D model has been developed and applied for both larger and limited zones in the Hiroshima debris-flow disasters that occurred both in 2014 & 2018. The model application for hindcast for wider and limited areas with the same scheme is tested in order to obtain better and precise hindcast as well as a future forecast of rainfall-induced debris flow disasters by improving the geological classification module for the initiation of the debris flow. A universal algorithm for predicting the debris flow disasters solely by the initial geological boundary conditions and forecasted rainfall distribution may contribute to improving early warnings in this field.

Keywords: Debris flow, Hindcast

©2019. Japan Geoscience Union. All Right Reserved.

Research on the application of an improved terrain-following vertical coordinates on GRAPES model

*chao li[1]

1. NWPC.CMA

Errors caused by topographic feathers of the coordinate planes can be reduced with the Smoothed-level terrain-following coordinate(T-F coordinate for short). On higher layors,coordinate planes of T-F coordinate based on trigonometric function of cos (COS coordinate for short)are horizontal with almost none errors. However,on the lower layers,thickness between planes is too small to keep the model stability.At the same time,it will bring larger calculating errors which result in bad performance of the model.Considering all above,an improved COS coordinate is designed to average the thickness of COS coordinate planes.
Ideal and real case tests are conducted with the GRAPES_Meso model using the improved COS coordinate.The results of the tests indicate that:compared with the COS coordinate, the improved COS coordinate ,on one hand ,keep the planes horizontal on the higher layers ,on the other hand, lead the distribute of the coordinate planes more uniformity , which greatly reduced the errors on the lower layers;The coordinate can reproduce in general the mountain induced gravity waves in comparison to the analytic solution. However, the shapes,vertical structures and intensity of the waves are better simulated by the improved COS coordinate, in the lower levels where the COS coordinate didn’ t behave so better. In the one-month real case tests, the improved COS coordinate gives the better results in terms of smaller forecast bias and root mean square error, and higher anomaly correlation coefficients than the COS coordinate. In conclusion, the improved COS coordinate solves the calculation problems of the COS coordinate ,and improves the prediction ability.

Keywords: GRAPES Model, Terrain-following coordinate, Dynamic Core, Numerical Modelling

©2019. Japan Geoscience Union. All Right Reserved.

Development of a parallel spherical harmonic transform library: design and performance

*Fuyuki SAITO[1]

1. Japan Agency for Marine-Earth Science and Technology

The spherical harmonic transform (SHT) is a typical method to describe the dynamical core in climate models (e.g. MIROC). SHT is a combination of two transformation: a Fourier transformation in longitude and an associate Legendre transformation in latitude. Therefore, a simple way to introduce SHT in parallel computing is to apply domain decomposition in latitudes only, involving a relocation in latitudes before/after the Legendre transformation. However, the number of maximum processors is limited by the size of latitude dimension, which is an obstacle to more efficient computing. Recently the `physics' routines in a climate model have become more and more complex and expensive, thus the heavy computation significantly suffers from the limitation. A new (yet-another) library, Flageolet, has been developed to help parallel processing of SHT in particular for climate models like MIROC, to support more flexible domain decomposition, following the approach adopted in several 3D FFT libraries and also some climate models. As a continuation of last-year's presentation, which reports the design and performance of FFT part, those of SHT part as well as transposition part between FFT and ALT are reported in this study for various sizes of domain around T213 etc, examined on the Earth simulator.

Keywords: spherical harmonic transform

©2019. Japan Geoscience Union. All Right Reserved.

Global data assimilation of multi-species satellite measurements for atmospheric chemistry analysis

*Takashi Sekiya[1], Kazuyuki Miyazaki[2,1], Koji Ogochi[1], Kengo Sudo[3,1], Masayuki Takigawa[1]

1. Japan Agency for Marine-Earth Science and Technology, 2. Jet Propulsion Laboratory/California Institute for Technology, 3. Graduate School of Environmental Studies, Nagoya University

Information on tropospheric ozone and its precursors are important for human health, ecosystem, and climate studies. The combined use of satellite measurements of ozone and its precursors has great potential to provide comprehensive information on the tropospheric chemistry system on various spatial scales. In this study, we present the results of global data assimilation of multi-species measurements (O_3, NO_2, CO, HNO_3, and SO_2) from multi-satellite sensors (OMI, GOME-2, SCIAMACHY, MOPITT, TES, and MLS) using the ensemble Kalman filter approach (Miyazaki et al., 2015). We demonstrated that increasing horizontal resolution from 2.8 to 0.56 degree is necessary for capturing high concentrations of NO_2 in the megacities, whereas 1.1-degree resolution is more suitable for optimizing tropospheric chemistry system on regional and global scales considering the current computational resources (computational cost was larger by a factor of 10 at 0.56-dgree resolution than at 1.1-degree resolution). Using the data assimilation system at 1.1-degree resolution, we constructed an updated version of tropospheric chemistry reanalysis (TCR-2; Miyazaki et al., in prep.) data for 2005—2017, which provide valuable information on decadal changes in air pollutant concentrations and emissions. The estimated NO_x emissions were strongly increased from 2005 to 2011 (+37%/decade) and decreased from 2011 to 2017 (-37%/decade) in China, while the emissions exhibited decreasing trends in Europe (-11%/decade) and the United States (-27%/decade) and an increasing trend in India (+23%/decade) during 2005—2017. A post peta-scale supercomputer such as post-K computer will facilitate the data assimilation calculation to produce tropospheric chemistry reanalysis data at 0.56-degree resolution for air pollutions on a megacity scale globally in a consistent way, which will benefit future study of atmospheric environment on various spatial scales.

Keywords: Data assimilation, Atmospheric chemistry, Atmospheric environment

©2019. Japan Geoscience Union. All Right Reserved.

The sensitivity to WRF shortwave radiation parameterizations in prediction of global horizontal irradiance for investigating interactions of atmosphere with croplands

*Ankur Srivastava[1], Sarita Kumari[1], Rajkumar Dhakar[2]

1. Indian Institute of Technology Delhi, 2. Indian Agriculture Research Institute

The present study intends to evaluate the Advanced Research Weather Research Forecating (ARW) model performance in representing the observed global horizontal irradiance (GHI) measurements while using different shortwave radiation (SWR) parameterization schemes. Two cases are considered, first case is ‘clear sky condition’ which includes model simulation of a clear/ cloudless day and second case is ‘all sky condition’ which includes model simulations of a cloudy and a rainy day. The above two cases are formulated on the basis that amount of incoming SWR will be different in each case owing to the differences in atmospheric conditions.
For the mentioned instances dates of 23rd February, 9th January and 12th March of 2016, which are clear, cloudy and rainy days respectively, are chosen for WRF model simulation. The shortwave radiation schemes that were evaluated are: Dudhia, Community Atmosphere Model (CAM), the updated Rapid Radiative Transfer Model (RRTMG), the updated Goddard and the
Goddard Fluid Dynamics Laboratory (GFDL) schemes. The model generated predictions are verified against the GHI measurements at weather station of Indian Agriculture Research Institute (IARI), New Delhi.
All schemes perform better under ‘clear sky condition’ i.e. for clear/cloudless day. For both the cases Dudhia scheme performs best with Mean Bias (MB) of 62.84 Wm^{-2} for clear day, 86.44 Wm^{-2} for cloudy day and 89.44 Wm^{-2} for rainy day. All-inclusive, the model derived predictions are over estimated in all the schemes.

Keywords: global horizontal irradiance , parameterization, shortwave radiation

©2019. Japan Geoscience Union. All Right Reserved.

The development of an atmospheric aerosol/chemistry–climate model, BCC_AGCM_CUACE2.0, and simulated effective radiative forcing of nitrate aerosols

*QI AN[1,2,4], Hua Zhang[2], Zhili Wang[2], Yi Liu[1,4], Bing Xie[3], Qianxia Liu[3], Zaizhi Wang[3], Sunling Gong[2]

1. LAGEO, IAP, CAS, 2. LaSW, CAMS, 3. NCC,CMA, 4. UCAS

As important components of total anthropogenic aerosols, nitrate aerosols have large impacts on aerosol radiative forcing and climate at regional and seasonal scales, but few current climate models coupled nitrate chemical modules online. This study developed a next-generation atmospheric aerosol/chemistry–climate model, the BCC_AGCM_CUACE2.0. Then, the performance of the model for nitrate was evaluated, and the direct radiative forcing (DRF) and effective radiative forcing (ERF) due to nitrate were simulated for the present day (2010), near future (2030) and middle future (2050) under the Representative Concentration Pathway (RCP) 4.5, 6.0, and 8.5 scenarios relative to the pre-industrial era (1850). The model reproduced the distributions and seasonal changes in nitrate loading well and simulated surface concentrations matched observations in Europe and North America. Current global mean annual loading of nitrates was predicted to increase by 1.12 mg m^{-2} relative to 1850, with the largest increases occurring in East Asia (3.89 mg m^{-2}), Europe (3.6 mg m^{-2}), and South Asia (1.86 mg m^{-2}). The current global mean annual ERF of nitrates was −0.21 W m^{-2} relative to 1850. Due to global reductions in pollutant emissions, the nitrate ERF values were predicted to decrease to −0.17 and −0.20 W m^{-2} in 2030, −0.07 and −0.18 W m^{-2} in 2050 for RCP4.5 and 6.0 relative to 1850, respectively. Under RCP8.5, nitrate ERF values were −0.24 and −0.19 W m^{-2} in 2030 and 2050, respectively. Although global mean nitrate values showed a declining trend, future nitrate loading remained high in East Asia and South Asia.

Keywords: Effective radiative forcing, Nitrate

©2019. Japan Geoscience Union. All Right Reserved.

Impacts of different types and intensities of El Niño events on winter aerosols over China

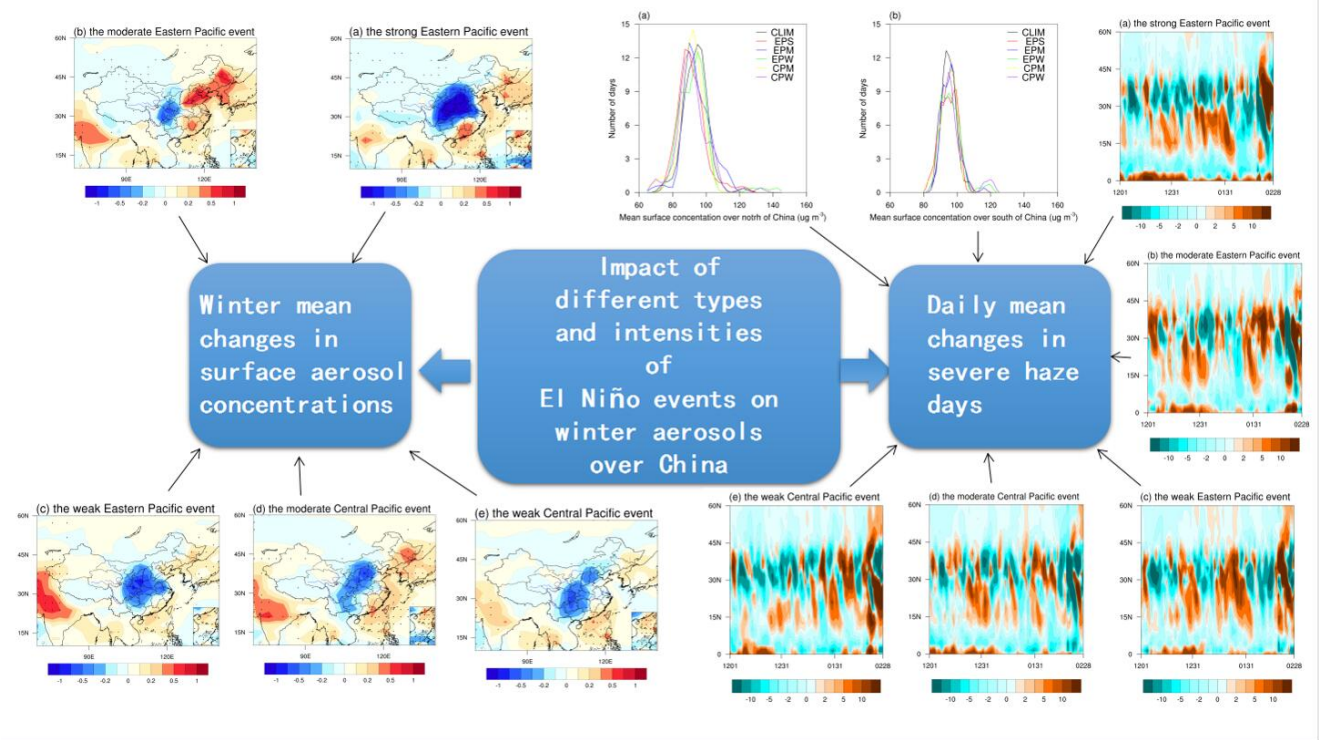
*Xiaochao Yu[1,2], Zhili Wang[2,1], Hua Zhang[2], Shuyun Zhao[3]

1. Collaborative Innovation Center on Forecast and Evaluation of Meteorological Disasters, Nanjing University of Information Science and Technology, Nanjing, 210044, China, 2. State Key Laboratory of Severe Weather and Key Laboratory of Atmospheric Chemistry of CMA, Chinese Academy of Meteorological Sciences, Beijing, 100081, China., 3. National Climate Center, China Meteorological Administration, Beijing, 100081, China

El Niño is a strong signal of interannual climate variability. The occurrence of an El Niño event may have an important impact on atmospheric pollutant concentrations in China through changes to the regional climate. This study quantitatively examines the differences among the effects of different types and intensities of El Niño events on winter mean aerosol concentration and severe haze days in China. It is found that Central Pacific (CP) El Niño events lead to larger increases in the aerosol burden over southern China relative to the same intensity of Eastern Pacific (EP) events. For El Niño events of the same type but with different intensities, moderate events induce large increases in surface aerosol concentrations over the entire eastern China, while strong and weak events lead to obvious decreases in the surface aerosol concentration over northern China. These differences are mainly attributed to changes in atmospheric circulation, with the resulting changes in aerosol mass transport occurring in response to the different types of El Niño event. Except for moderate CP events, all kinds of El Niño events lead to an increase in severe haze days in winter over northern China. Strong and weak EP El Niño events and weak CP El Niño events lead to an increase in severe haze days in winter over southern China. A change in the south-north transport of aerosols caused by El Niño events also play a dominate role in changing the occurrence of winter haze days in China.

Keywords: Eastern Pacific El Niño, Central Pacific El Niño, aerosol concentration, severe haze day

©2019. Japan Geoscience Union. All Right Reserved.



©2019. Japan Geoscience Union. All Right Reserved.

High Cloud Annual Variation and Its Responses to Global Warming in the NICAM AMIP Experiment

*Ying-Wen Chen[1], Masaki Satoh[1,2], Chihiro Kodama[2], Akira Noda[2], Yohei Yamada[2]

1. Atmospheric and Ocean Research Institute, The University of Tokyo , 2. Japan Agency for Marine-Earth Science and Technology

Uncertainties in climate sensitivity mainly come from the ambiguities in simulations of both high- and low-level clouds. The previous studies using NICAM’s short time simulation showed that the both the altitudes and amount of high clouds increase under the global warming condition, while other climate models show high cloud amount contrarily decreases.
Due to the progress in computer performance, long term climate simulation with $x < 20$ km becomes available. A pair of 25-year climate simulation (present and warming climate) with 14-km horizontal resolution (NICAM AMIP-like simulation, Kodama et al. 2015) has been performed by K computer. In this study, we analyze how the annual variation in high clouds is presented in the NICAM AMIP-like simulation. Satellite and in-situ data are used to investigate whether NICAM captures the observed responses of high clouds to the mean sea surface temperature (SST). Regressions between the high cloud amount variation and the SST variation is different with altitudes; positive regressions appear at altitudes above 100 hPa while negative regressions are found in altitudes below 100 hPa. The results are consistent with previous study based on observations (Zelinka and Hartmann 2011). Further analysis showed that the spatial pattern of high clouds is mainly associated with the El Nino response; as SST warmer, the high clouds shift in the eastern Pacific with higher. The increase of high clouds is associated with the increase of ice water content of cloud ice and snow. We argue that the response of high clouds to global warming is also explained by the change in the spatial distribution of the high clouds.

Keywords: Global Warming, Cloud-Resolving Model

©2019. Japan Geoscience Union. All Right Reserved.

Improvements in Simulating the Relationship between ENSO and East Asian Summer Rainfall in the CMIP5 Models

*Yuanhai FU[1], Riyu Lu[1]

1. IAP, CAS

There is a significant relationship between the preceding winter El Niño–Southern Oscillation (ENSO) and the subsequent East Asian summer rainfall (EASR), and this relationship is helpful for seasonal forecasting in East Asia. This study investigated the relationship between the preceding winter ENSO and EASR in the Coupled Model Intercomparison Project Phase 5 (CMIP5) models and compared the results with those from the CMIP3 models. In general, the CMIP5 models capture the ENSO–EASR relationship more realistically than the CMIP3 models. For instance, approximately two-thirds of the CMIP5 models capture the ENSO–EASR relationship, while less than one-third of the CMIP3 models capture the relationship. Further investigation suggests that the improvement could be attributed to simulating the physical processes of ENSO's impact on the EASR more realistically in the CMIP5 models, particularly the effect of ENSO on tropical Indian Ocean SST and the effect of Indian Ocean SST anomalies on the atmospheric convection over the Philippine Sea. However, there is large diversity in the ENSO–EASR relationship in the CMIP5 models, and most of the models underestimate the relationship. This underestimation comes from the underestimation of the physical processes, particularly from the underestimated impact of the atmospheric convection over the Philippine Sea on the EASR. The CMIP5 models that capture the ENSO–EASR relationship well/bad also show high/low skill in representing the physical processes.

Keywords: East Asian summer rainfall, ENSO, CMIP5 model

©2019. Japan Geoscience Union. All Right Reserved.

[E] Poster | A (Atmospheric and Hydrospheric Sciences)：A-AS Atmospheric Sciences, Meteorology & Atmospheric Environment

Wed. May 29, 2019 5:15 PM - 6:30 PM JST | Wed. May 29, 2019 8:15 AM - 9:30 AM UTC | Poster Hall International Exhibition Hall8, Makuhari Messe_9

[A-AS01] High performance computing for next generation weather, climate, and environmental sc iences

convener:Hiromu Seko(Meteorological Research Institute), Takemasa Miyoshi(RIKEN), Chihiro Kodama(Japan Agency for Marine-Earth Science and Technology), Masayuki Takigawa(Japan Agency for Marine-Earth Science and Technology)

A lot of advanced simulation studies are being conducted by high performance supercomputers, such as K computer and Earth Simulator, in various fields including meteorology. The high performance supercomputers enable us to conduct numerical simulations and data assimilation of observation big-data (huge high-density and high-frequency data) with an order of magnitude higher resolutions and ensemble numbers than those with the previous supercomputers. In addition, the post-K computer will be available as a successor of K, and studies for the post-K computer are in progress. At this session, we comprehensively pick up the topics in the Atmospheric and Hydrospheric Sciences Sessions of the 2019 Union Meeting that comprise the atmospheric, oceanic and land sciences. This session aims to promote recent studies related to the issues on high performance computing in weather, climate, and environmental studies using the K computer and other supercomputers, and to enhance discussions on future directions of numerical simulations in meteorology.

[AAS01-P01] **Categorized correction forecast for accumulative precipitation of heavy rainfall processes based on optimal probability (OPPF) in medium-extended-range forecast time**

*Ruoyun Niu[1] (1.National Meteorological Center)

[AAS01-P02] **Characteristics of temporal and spatial distribution of regional rainstorm processes to the east of 95°E in China during 1981-2015**

*Ruoyun Niu[1], Couhua Liu[1] (1.National Meteorological Center)

[AAS01-P03] Near-real-time SCALE-LETKF forecasts of the record breaking rainfall in Japan in July 2018

*Takumi Honda[1], Guo-Yuan Lien[2,1], Takemasa Miyoshi[1] (1.RIKEN Center for Computational Science, 2.Central Weather Bureau)

[AAS01-P04] An objective Frontal Analysis Techniques and Application in Model Verification

*couhua liu[1] (1.National Meteorology Centre of China Meteorological Administration)

[AAS01-P05] Assimilating every 30-second phased array weather radar data in a torrential rainfall event on July 6, 2018 around Kobe city

*Yasumitsu Maejima[1], Shigenori Otsuka[1], Takemasa Miyoshi[1,2] (1.RIKEN Center for Computational Science, 2.University of Maryland, College Park)

[AAS01-P06] The impact of range sidelobes from phased array weather radar observations to short-range convective forecasts

*James David Taylor[1], Guo-Yuan Lien[1], Shinsuke Satoh[2], Takemasa Miyoshi[1] (1.RIKEN Research center for computational science, 2.NICT National Institute of Information and Communications Technology)

[AAS01-P07] Development of Hydro-debris 2D model for larger area

*Yosuke Alexandre Yamashiki[1], Tsutao OIZUMI[2], Bruno Ribeiro[1], Ryusuke Kuroki[1] (1.Earth & Planetary Water Resources Assessment Laboratory Graduate School of Advanced Integrated Studies in Human Survivability Kyoto University, 2.Japan Association of Marine-Earth Science and Tecnology)

[AAS01-P08] **Research on the application of an improved terrain-following vertical coordinates on GRAPES model**

*chao li[1] (1.NWPC.CMA)

[AAS01-P09] Development of a parallel spherical harmonic transform library: design and performance

*Fuyuki SAITO[1] (1.Japan Agency for Marine-Earth Science and Technology)

[AAS01-P10] Global data assimilation of multi-species satellite measurements for atmospheric chemistry analysis

*Takashi Sekiya[1], Kazuyuki Miyazaki[2,1], Koji Ogochi[1], Kengo Sudo[3,1], Masayuki Takigawa[1] (1.Japan Agency for Marine-Earth Science and Technology, 2.Jet Propulsion Laboratory/California Institute for Technology, 3.Graduate School of Environmental Studies, Nagoya University)

[AAS01-P11] The sensitivity to WRF shortwave radiation parameterizations in prediction of global horizontal irradiance for investigating interactions of atmosphere with croplands

*Ankur Srivastava[1], Sarita Kumari[1], Rajkumar Dhakar[2] (1.Indian Institute of Technology Delhi, 2.Indian Agriculture Research Institute)

[AAS01-P12] The development of an atmospheric aerosol/chemistry–climate model, BCC_AGCM_CUACE2.0, and simulated effective radiative forcing of nitrate aerosols

*QI AN[1,2,4], Hua Zhang[2], Zhili Wang[2], Yi Liu[1,4], Bing Xie[3], Qianxia Liu[3], Zaizhi Wang[3], Sunling Gong[2] (1.LAGEO, IAP, CAS, 2.LaSW, CAMS, 3.NCC,CMA, 4.UCAS)

[AAS01-P13] **Impacts of different types and intensities of El Niño events on winter aerosols over China**

*Xiaochao Yu[1,2], Zhili Wang[2,1], Hua Zhang[2], Shuyun Zhao[3] (1.Collaborative Innovation Center on Forecast and Evaluation of Meteorological Disasters, Nanjing University of Information Science and Technology, Nanjing, 210044, China, 2.State Key Laboratory of Severe Weather and Key Laboratory of Atmospheric Chemistry of CMA, Chinese Academy of Meteorological Sciences, Beijing, 100081, China., 3.National Climate Center, China Meteorological Administration, Beijing, 100081, China)

[AAS01-P14] High Cloud Annual Variation and Its Responses to Global Warming in the NICAM AMIP Experiment

*Ying-Wen Chen[1], Masaki Satoh[1,2], Chihiro Kodama[2], Akira Noda[2], Yohei Yamada[2] (1.Atmospheric and Ocean Research Institute, The University of Tokyo , 2.Japan Agency for Marine-Earth Science and Technology)

[AAS01-P15] Improvements in Simulating the Relationship between ENSO and East Asian Summer Rainfall in the CMIP5 Models

*Yuanhai FU[1], Riyu Lu[1] (1.IAP, CAS)

Categorized correction forecast for accumulative precipitation of heavy rainfall processes based on optimal probability (OPPF) in medium-extended-range forecast time

*Ruoyun Niu[1]

1. National Meteorological Center

By taking the ensemble prediction data from ECMWF and the intensive observations of precipitation in China, the technology of categorized correction forecast for accumulative precipitation of heavy rainfall processes based on optimal probability(OPPF) is developed, and 3 calculation schemes of OPPF are designed according to overall technical route. Then the reforecast test are carried for the accumulative precipitation of 67 heavy rainfall processes from May to September during 1981 to 2015 in China, and the forecast performance of the 3 OPPFs against that of ensemble mean (EMPF) and control number (CTPF) is evaluated and contrasted. The results show that:(1) In the medium-extended-range (096-360h) forecast time, the performance of the 3 OPPFs are better than that of EMPF and CTPF for heavy precipitation forecast and clear-rain forecast. the performance of OPPF1 and OPPF2 is close to that of EMPF for Moderate precipitation and larger precipitation. OPPF3 produces the best performance among the 3 OPPFs. (2) There are obvious regional differences in forecast performances. TS of OPPF3 in southern China are higher than in northern China, and the performance of OPPF3 for heavy precipitation is better than that of EMPF in southern China. During 096-240h forecast time, the performance of OPPF3 for heavy precipitation is also better than that of EMPF in eastern part of Northeast China.

Keywords: optimal probability, accumulative precipitation of heavy precipitation processes, categorized correction forecast, comparative evaluation of forecast performance

©2019. Japan Geoscience Union. All Right Reserved.

Characteristics of temporal and spatial distribution of regional rainstorm processes to the east of 95ºE in China during 1981-2015

*Ruoyun Niu[1], Couhua Liu[1]

1. National Meteorological Center

The events of the regional rainstorm processes (RRP) to the east of 95ºE in China over 1981-2015 are constructed based on intensive daily observations of precipitation in China and NCEP/NCAR reanalysis data by means of subjective and objective analyses. Temporal and spatial characteristic distribution of RRP in China are further investigated using the methods of wavelet power spectrum, nine-point binomial smoothing and Ward cluster analysis. The main conclusions are as follows. (1) The annual average number of RRP to the east of 95ºE in China is nearly 30. RRP in the Yangtze-Huaihe River valley occur most frequently among the six subareas with an annual average number of about 19, followed by that in South China and the eastern part of Southwest China with the annual average number of RRP 10.5 and 5.8 times respectively. Annual average number of RRP are only about 1-3 times in other subareas. (2) The inter-annual and inter-decadal variations of the annual number of RRP exhibit distinct fluctuation characteristics. The inter-annual and inter-decadal fluctuating variation in the Yangtze-Huaihe River valley is the most consistent with that to the east of 95E in China. Moreover, the fluctuating variations have a significant positive correlation between South China and eastern part of Southwest China, and also between Northeast China and North China. The annual number of RRP over the east of 95E in China and its subareas demonstrates a periodic variation of 2-4a, and also shows a periodic variation of 6-10a in the Yangtze-Huaihe River valley and South China and eastern part of Northwest China, while a 13-17a oscillation can be found in North China.(3) On the whole, the occurrence frequency of RRP to the east of 95E in China is the most in summer (especially in July), the least in winter, and higher in spring than in autumn. The months when RRP occur most frequently are June and July in the Yangtze-Huaihe River valley and eastern part of Southwest China, and May and June in South China. RRP mainly appear in July and August in other subareas.(4) The distribution patterns of RRP to the east of 95E in China are divided into 7 types. The heavy precipitation areas for pattern Ⅰ-Ⅳ migrate northward step by step from South China and southern part of Yangtze River valley to Huanghuai Basin and eastern part of Sichuan Basin.The heavy precipitation areas of pattern Ⅴ-Ⅶ all are located at the Coastal region of Southeast China.

Keywords: Regional rainstorm processes, Method for distinguishing, Temporal and spatial distribution, Patterns of extremely regional rainstorm processes

©2019. Japan Geoscience Union. All Right Reserved.

Near-real-time SCALE-LETKF forecasts of the record breaking rainfall in Japan in July 2018

*Takumi Honda[1], Guo-Yuan Lien[2,1], Takemasa Miyoshi[1]

1. RIKEN Center for Computational Science, 2. Central Weather Bureau

In July 2018, a stationary precipitation band associated with the Baiu front induced a record breaking rainfall and caused catastrophic destruction in Japan. This event was successfully captured by the near-real-time (NRT) SCALE-LETKF system (Lien et al. 2017) consisting of the Scalable Computing for Advanced Library and Environment-Regional Model (SCALE-RM, Nishizawa et al. 2015; Sato et al. 2015) and the Local Ensemble Transform Kalman Filter (LETKF, Hunt et al. 2007; Miyoshi and Yamane 2007). This system has been continuously operated since 2015 with an 18-km mesh model domain and the ensemble size of 50. In the NRT SCALE-LETKF system, only conventional observations are assimilated every 6 hours. By conducting a series of 50-member ensemble forecasts from the 6-hourly SCALE-LETKF analyses, this study aims to investigate predictability of this torrential rainfall event and important factors that contributed to the heavy precipitation. In general, the NRT SCALE-LETKF system provides skillful ensemble forecasts of the rainfall a few days in advance. Interestingly, the forecast skill exhibits sudden improvement due to assimilating conventional observations at a single location far southwest from the peak accumulated rainfall location. Forecast differences and ensemble correlations suggest that an extratropical cyclone over the Sea of Japan and a low-level trough near Taiwan play important roles in determining the front location.

Keywords: Data assimilation, Numerical Weather Prediction

©2019. Japan Geoscience Union. All Right Reserved.

An objective Frontal Analysis Techniques and Application in Model Verification

*Couhua Liu[1]

1. National Meteorology Centre of China Meteorological Administration

This paper presents an objective Frontal analysis method based on pressure field for east Asia. Comparing to methods based on thermo-dynamical elements such as temperature, the method developed in this paper can avoid the complex affection from sea-land and landform. The method will be used to identification of fronts in analysis and prediction of ECMWF model all over 2015, and then model error of predicted fronts will be verification. The verification result show that, comparing to analysis field, the moving speed of fronts in prediction field of ECMWF model is slower and strength is weaker.

Keywords: front, model, verification

©2019. Japan Geoscience Union. All Right Reserved.

Assimilating every 30-second phased array weather radar data in a torrential rainfall event on July 6, 2018 around Kobe city

*Yasumitsu Maejima[1], Shigenori Otsuka[1], Takemasa Miyoshi[1,2]

1. RIKEN Center for Computational Science, 2. University of Maryland, College Park

To investigate the impact of every 30-second phased array weather radar (PAWR; Yoshikawa et al. 2013, Ushio et al. 2014) observation on a simulation of a severe rainfall event occurred on July 6, 2018 around Kobe city, we perform 30-second-update 100-m-mesh data assimilation (DA) experiments using the Local Ensemble Transform Kalman Filter with the Scalable Computing for Advanced Library and Environment regional numerical weather prediction model. Two experiments were performed: the test experiment with every 30-second PAWR observation (TEST), and the other without observation (NO-DA).

The TEST analysis shows intense rainfalls with detailed structure of active convection, better matching with the PAWR observation compared to NO-DA analysis. In the forecast experiment, the forecast initialized by the ensemble mean analysis of TEST is skillful for 20 minutes compared with NO-DA, although the skill is decreased rapidly. The results suggest that the PAWR DA have a potential to improve the numerical simulation for this torrential rainfall event.

Keywords: Data assimilation, Heavy rainfall forecast, High performance computing

©2019. Japan Geoscience Union. All Right Reserved.

The impact of range sidelobes from phased array weather radar observations to short-range convective forecasts

*James David Taylor[1], Guo-Yuan Lien[1], Shinsuke Satoh[2], Takemasa Miyoshi[1]

1. RIKEN Research center for computational science, 2. NICT National Institute of Information and Communications Technology

Range sidelobes are an erroneous feature of radar observations that are generated by the pulse compression process used to improve the range resolution of target echoes in high resolution radar systems. Phased array weather radar (PAWR) is an advanced radar system providing very dense observations of reflectivity and Doppler radial velocity at 100m range resolution for over 100 elevation angles every 30 seconds. The use of pulse compression in PAWR to provide very high range resolution data makes it subject to these types of errors, which can result in false echoes observed at other ranges.

In this study we investigate the impact of assimilating range sidelobes from PAWR observations to short-range convective forecasts. This happens frequently in the current QC algorithm, although we plan to improve the QC in the future. We employ the use of the SCALE-LETKF system which couples the Local Ensemble Transform Kalman Filter (LETKF) with the Scalable Computing for Advanced Library and Environment (SCALE)-RM model. We focus on a convective rainfall event in August 2016 that brought heavy, intense rainfall over Osaka. PAWRs located in Suita, Osaka and in Kobe well-captured the convective system over its life cycle but featured prominent range sidelobes as part of their observations. Here, observations from both radars are first used to identify the range sidelobes before performing a series of 30-second update cycling experiments using observations from the Suita PAWR both with and without range sidelobes within a high-resolution 100-m mesh. As well as investigating their impact on short-range forecasts, we aim to show how we can further the usefulness of having two sets of PAWR observations to observe the same convective system by using them to identify and remove range sidelobes and improve short-range forecasts of severe convective events through the assimilation of this data.

Keywords: LETKF, Assimilation, Forecasts, Convection, Sidelobes

©2019. Japan Geoscience Union. All Right Reserved.

Development of Hydro-debris 2D model for larger area

*Yosuke Alexandre Yamashiki[1], Tsutao OIZUMI[2], Bruno Ribeiro[1], Ryusuke Kuroki[1]

1. Earth & Planetary Water Resources Assessment Laboratory Graduate School of Advanced Integrated Studies in Human Survivability Kyoto University, 2. Japan Association of Marine-Earth Science and Tecnology

The Hydro-debris 2D model has been developed and applied for both larger and limited zones in the Hiroshima debris-flow disasters that occurred both in 2014 & 2018. The model application for hindcast for wider and limited areas with the same scheme is tested in order to obtain better and precise hindcast as well as a future forecast of rainfall-induced debris flow disasters by improving the geological classification module for the initiation of the debris flow. A universal algorithm for predicting the debris flow disasters solely by the initial geological boundary conditions and forecasted rainfall distribution may contribute to improving early warnings in this field.

Keywords: Debris flow, Hindcast

©2019. Japan Geoscience Union. All Right Reserved.

Research on the application of an improved terrain-following vertical coordinates on GRAPES model

*chao li[1]

1. NWPC.CMA

Errors caused by topographic feathers of the coordinate planes can be reduced with the Smoothed-level terrain-following coordinate(T-F coordinate for short). On higher layors,coordinate planes of T-F coordinate based on trigonometric function of cos (COS coordinate for short)are horizontal with almost none errors. However,on the lower layers,thickness between planes is too small to keep the model stability.At the same time,it will bring larger calculating errors which result in bad performance of the model.Considering all above,an improved COS coordinate is designed to average the thickness of COS coordinate planes.
Ideal and real case tests are conducted with the GRAPES_Meso model using the improved COS coordinate.The results of the tests indicate that:compared with the COS coordinate, the improved COS coordinate ,on one hand ,keep the planes horizontal on the higher layers ,on the other hand, lead the distribute of the coordinate planes more uniformity , which greatly reduced the errors on the lower layers;The coordinate can reproduce in general the mountain induced gravity waves in comparison to the analytic solution. However, the shapes,vertical structures and intensity of the waves are better simulated by the improved COS coordinate, in the lower levels where the COS coordinate didn’ t behave so better. In the one-month real case tests, the improved COS coordinate gives the better results in terms of smaller forecast bias and root mean square error, and higher anomaly correlation coefficients than the COS coordinate. In conclusion, the improved COS coordinate solves the calculation problems of the COS coordinate ,and improves the prediction ability.

Keywords: GRAPES Model, Terrain-following coordinate, Dynamic Core, Numerical Modelling

©2019. Japan Geoscience Union. All Right Reserved.

Development of a parallel spherical harmonic transform library: design and performance

*Fuyuki SAITO[1]

1. Japan Agency for Marine-Earth Science and Technology

The spherical harmonic transform (SHT) is a typical method to describe the dynamical core in climate models (e.g. MIROC). SHT is a combination of two transformation: a Fourier transformation in longitude and an associate Legendre transformation in latitude. Therefore, a simple way to introduce SHT in parallel computing is to apply domain decomposition in latitudes only, involving a relocation in latitudes before/after the Legendre transformation. However, the number of maximum processors is limited by the size of latitude dimension, which is an obstacle to more efficient computing. Recently the `physics' routines in a climate model have become more and more complex and expensive, thus the heavy computation significantly suffers from the limitation. A new (yet-another) library, Flageolet, has been developed to help parallel processing of SHT in particular for climate models like MIROC, to support more flexible domain decomposition, following the approach adopted in several 3D FFT libraries and also some climate models. As a continuation of last-year's presentation, which reports the design and performance of FFT part, those of SHT part as well as transposition part between FFT and ALT are reported in this study for various sizes of domain around T213 etc, examined on the Earth simulator.

Keywords: spherical harmonic transform

©2019. Japan Geoscience Union. All Right Reserved.

Global data assimilation of multi-species satellite measurements for atmospheric chemistry analysis

*Takashi Sekiya[1], Kazuyuki Miyazaki[2,1], Koji Ogochi[1], Kengo Sudo[3,1], Masayuki Takigawa[1]

1. Japan Agency for Marine-Earth Science and Technology, 2. Jet Propulsion Laboratory/California Institute for Technology, 3. Graduate School of Environmental Studies, Nagoya University

Information on tropospheric ozone and its precursors are important for human health, ecosystem, and climate studies. The combined use of satellite measurements of ozone and its precursors has great potential to provide comprehensive information on the tropospheric chemistry system on various spatial scales. In this study, we present the results of global data assimilation of multi-species measurements (O_3, NO_2, CO, HNO_3, and SO_2) from multi-satellite sensors (OMI, GOME-2, SCIAMACHY, MOPITT, TES, and MLS) using the ensemble Kalman filter approach (Miyazaki et al., 2015). We demonstrated that increasing horizontal resolution from 2.8 to 0.56 degree is necessary for capturing high concentrations of NO_2 in the megacities, whereas 1.1-degree resolution is more suitable for optimizing tropospheric chemistry system on regional and global scales considering the current computational resources (computational cost was larger by a factor of 10 at 0.56-dgree resolution than at 1.1-degree resolution). Using the data assimilation system at 1.1-degree resolution, we constructed an updated version of tropospheric chemistry reanalysis (TCR-2; Miyazaki et al., in prep.) data for 2005—2017, which provide valuable information on decadal changes in air pollutant concentrations and emissions. The estimated NO_x emissions were strongly increased from 2005 to 2011 (+37%/decade) and decreased from 2011 to 2017 (-37%/decade) in China, while the emissions exhibited decreasing trends in Europe (-11%/decade) and the United States (-27%/decade) and an increasing trend in India (+23%/decade) during 2005—2017. A post peta-scale supercomputer such as post-K computer will facilitate the data assimilation calculation to produce tropospheric chemistry reanalysis data at 0.56-degree resolution for air pollutions on a megacity scale globally in a consistent way, which will benefit future study of atmospheric environment on various spatial scales.

Keywords: Data assimilation, Atmospheric chemistry, Atmospheric environment

©2019. Japan Geoscience Union. All Right Reserved.

The sensitivity to WRF shortwave radiation parameterizations in prediction of global horizontal irradiance for investigating interactions of atmosphere with croplands

*Ankur Srivastava[1], Sarita Kumari[1], Rajkumar Dhakar[2]

1. Indian Institute of Technology Delhi, 2. Indian Agriculture Research Institute

The present study intends to evaluate the Advanced Research Weather Research Forecating (ARW) model performance in representing the observed global horizontal irradiance (GHI) measurements while using different shortwave radiation (SWR) parameterization schemes. Two cases are considered, first case is ‘clear sky condition’ which includes model simulation of a clear/ cloudless day and second case is ‘all sky condition’ which includes model simulations of a cloudy and a rainy day. The above two cases are formulated on the basis that amount of incoming SWR will be different in each case owing to the differences in atmospheric conditions.
For the mentioned instances dates of 23rd February, 9th January and 12th March of 2016, which are clear, cloudy and rainy days respectively, are chosen for WRF model simulation. The shortwave radiation schemes that were evaluated are: Dudhia, Community Atmosphere Model (CAM), the updated Rapid Radiative Transfer Model (RRTMG), the updated Goddard and the
Goddard Fluid Dynamics Laboratory (GFDL) schemes. The model generated predictions are verified against the GHI measurements at weather station of Indian Agriculture Research Institute (IARI), New Delhi.
All schemes perform better under ‘clear sky condition’ i.e. for clear/cloudless day. For both the cases Dudhia scheme performs best with Mean Bias (MB) of 62.84 Wm^{-2} for clear day, 86.44 Wm^{-2} for cloudy day and 89.44 Wm^{-2} for rainy day. All-inclusive, the model derived predictions are over estimated in all the schemes.

Keywords: global horizontal irradiance , parameterization, shortwave radiation

©2019. Japan Geoscience Union. All Right Reserved.

The development of an atmospheric aerosol/chemistry–climate model, BCC_AGCM_CUACE2.0, and simulated effective radiative forcing of nitrate aerosols

*QI AN[1,2,4], Hua Zhang[2], Zhili Wang[2], Yi Liu[1,4], Bing Xie[3], Qianxia Liu[3], Zaizhi Wang[3], Sunling Gong[2]

1. LAGEO, IAP, CAS, 2. LaSW, CAMS, 3. NCC,CMA, 4. UCAS

As important components of total anthropogenic aerosols, nitrate aerosols have large impacts on aerosol radiative forcing and climate at regional and seasonal scales, but few current climate models coupled nitrate chemical modules online. This study developed a next-generation atmospheric aerosol/chemistry–climate model, the BCC_AGCM_CUACE2.0. Then, the performance of the model for nitrate was evaluated, and the direct radiative forcing (DRF) and effective radiative forcing (ERF) due to nitrate were simulated for the present day (2010), near future (2030) and middle future (2050) under the Representative Concentration Pathway (RCP) 4.5, 6.0, and 8.5 scenarios relative to the pre-industrial era (1850). The model reproduced the distributions and seasonal changes in nitrate loading well and simulated surface concentrations matched observations in Europe and North America. Current global mean annual loading of nitrates was predicted to increase by 1.12 mg m^{-2} relative to 1850, with the largest increases occurring in East Asia (3.89 mg m^{-2}), Europe (3.6 mg m^{-2}), and South Asia (1.86 mg m^{-2}). The current global mean annual ERF of nitrates was −0.21 W m^{-2} relative to 1850. Due to global reductions in pollutant emissions, the nitrate ERF values were predicted to decrease to −0.17 and −0.20 W m^{-2} in 2030, −0.07 and −0.18 W m^{-2} in 2050 for RCP4.5 and 6.0 relative to 1850, respectively. Under RCP8.5, nitrate ERF values were −0.24 and −0.19 W m^{-2} in 2030 and 2050, respectively. Although global mean nitrate values showed a declining trend, future nitrate loading remained high in East Asia and South Asia.

Keywords: Effective radiative forcing, Nitrate

©2019. Japan Geoscience Union. All Right Reserved.

Impacts of different types and intensities of El Niño events on winter aerosols over China

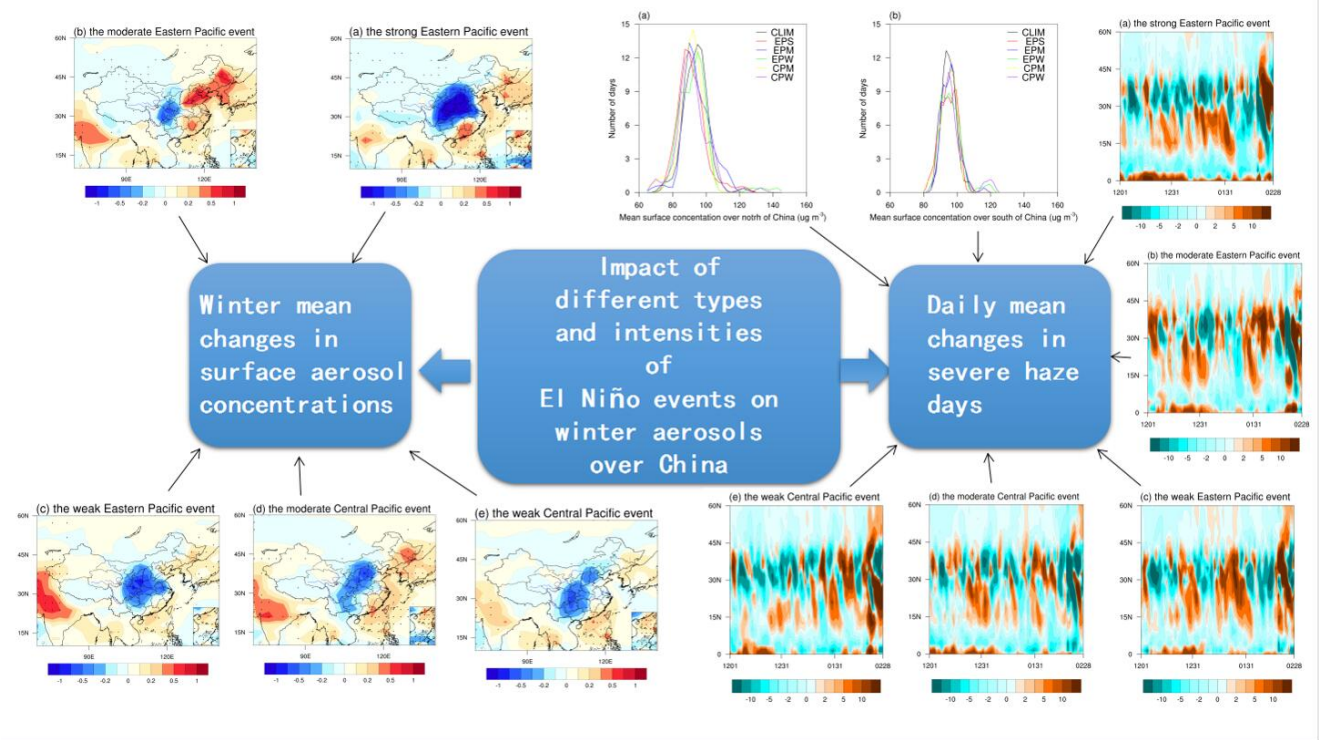
*Xiaochao Yu[1,2], Zhili Wang[2,1], Hua Zhang[2], Shuyun Zhao[3]

1. Collaborative Innovation Center on Forecast and Evaluation of Meteorological Disasters, Nanjing University of Information Science and Technology, Nanjing, 210044, China, 2. State Key Laboratory of Severe Weather and Key Laboratory of Atmospheric Chemistry of CMA, Chinese Academy of Meteorological Sciences, Beijing, 100081, China., 3. National Climate Center, China Meteorological Administration, Beijing, 100081, China

El Niño is a strong signal of interannual climate variability. The occurrence of an El Niño event may have an important impact on atmospheric pollutant concentrations in China through changes to the regional climate. This study quantitatively examines the differences among the effects of different types and intensities of El Niño events on winter mean aerosol concentration and severe haze days in China. It is found that Central Pacific (CP) El Niño events lead to larger increases in the aerosol burden over southern China relative to the same intensity of Eastern Pacific (EP) events. For El Niño events of the same type but with different intensities, moderate events induce large increases in surface aerosol concentrations over the entire eastern China, while strong and weak events lead to obvious decreases in the surface aerosol concentration over northern China. These differences are mainly attributed to changes in atmospheric circulation, with the resulting changes in aerosol mass transport occurring in response to the different types of El Niño event. Except for moderate CP events, all kinds of El Niño events lead to an increase in severe haze days in winter over northern China. Strong and weak EP El Niño events and weak CP El Niño events lead to an increase in severe haze days in winter over southern China. A change in the south-north transport of aerosols caused by El Niño events also play a dominate role in changing the occurrence of winter haze days in China.

Keywords: Eastern Pacific El Niño, Central Pacific El Niño, aerosol concentration, severe haze day

©2019. Japan Geoscience Union. All Right Reserved.



©2019. Japan Geoscience Union. All Right Reserved.

High Cloud Annual Variation and Its Responses to Global Warming in the NICAM AMIP Experiment

*Ying-Wen Chen[1], Masaki Satoh[1,2], Chihiro Kodama[2], Akira Noda[2], Yohei Yamada[2]

1. Atmospheric and Ocean Research Institute, The University of Tokyo , 2. Japan Agency for Marine-Earth Science and Technology

Uncertainties in climate sensitivity mainly come from the ambiguities in simulations of both high- and low-level clouds. The previous studies using NICAM’s short time simulation showed that the both the altitudes and amount of high clouds increase under the global warming condition, while other climate models show high cloud amount contrarily decreases.
Due to the progress in computer performance, long term climate simulation with $x < 20$ km becomes available. A pair of 25-year climate simulation (present and warming climate) with 14-km horizontal resolution (NICAM AMIP-like simulation, Kodama et al. 2015) has been performed by K computer. In this study, we analyze how the annual variation in high clouds is presented in the NICAM AMIP-like simulation. Satellite and in-situ data are used to investigate whether NICAM captures the observed responses of high clouds to the mean sea surface temperature (SST). Regressions between the high cloud amount variation and the SST variation is different with altitudes; positive regressions appear at altitudes above 100 hPa while negative regressions are found in altitudes below 100 hPa. The results are consistent with previous study based on observations (Zelinka and Hartmann 2011). Further analysis showed that the spatial pattern of high clouds is mainly associated with the El Nino response; as SST warmer, the high clouds shift in the eastern Pacific with higher. The increase of high clouds is associated with the increase of ice water content of cloud ice and snow. We argue that the response of high clouds to global warming is also explained by the change in the spatial distribution of the high clouds.

Keywords: Global Warming, Cloud-Resolving Model

©2019. Japan Geoscience Union. All Right Reserved.

Improvements in Simulating the Relationship between ENSO and East Asian Summer Rainfall in the CMIP5 Models

*Yuanhai FU[1], Riyu Lu[1]

1. IAP, CAS

There is a significant relationship between the preceding winter El Niño–Southern Oscillation (ENSO) and the subsequent East Asian summer rainfall (EASR), and this relationship is helpful for seasonal forecasting in East Asia. This study investigated the relationship between the preceding winter ENSO and EASR in the Coupled Model Intercomparison Project Phase 5 (CMIP5) models and compared the results with those from the CMIP3 models. In general, the CMIP5 models capture the ENSO–EASR relationship more realistically than the CMIP3 models. For instance, approximately two-thirds of the CMIP5 models capture the ENSO–EASR relationship, while less than one-third of the CMIP3 models capture the relationship. Further investigation suggests that the improvement could be attributed to simulating the physical processes of ENSO's impact on the EASR more realistically in the CMIP5 models, particularly the effect of ENSO on tropical Indian Ocean SST and the effect of Indian Ocean SST anomalies on the atmospheric convection over the Philippine Sea. However, there is large diversity in the ENSO–EASR relationship in the CMIP5 models, and most of the models underestimate the relationship. This underestimation comes from the underestimation of the physical processes, particularly from the underestimated impact of the atmospheric convection over the Philippine Sea on the EASR. The CMIP5 models that capture the ENSO–EASR relationship well/bad also show high/low skill in representing the physical processes.

Keywords: East Asian summer rainfall, ENSO, CMIP5 model

©2019. Japan Geoscience Union. All Right Reserved.

[E] Poster | A (Atmospheric and Hydrospheric Sciences)：A-OS Ocean Sciences & Ocean Environment

Wed. May 29, 2019 10:45 AM - 12:15 PM JST | Wed. May 29, 2019 1:45 AM - 3:15 AM UTC | Poster Hall International Exhibition Hall8, Makuhari Messe_4

[A-OS08] ECS-Kuroshio and Ryukyu Current System -Observation, modeling and theory-

convener:Hirohiko Nakamura(Kagoshima University, Faculy of Fisheries), Xiao-Hua Zhu(Second Institute of Oceanography)

The East China Sea (ECS) is separated from the North Pacific basin by the Ryukyu Islands. On each side of the Ryukyu Islands, there lies two western boundary currents -the Kuroshio on the northwest and the Ryukyu Current on the southeast. These two currents play an important role in the global substance cycle and have a remarkable impact on the climate and adjacent marginal seas. Our knowledge of the Kuroshio and the Ryukyu Current's dynamics, variability, and impact has advanced significantly over the last decade, because of recent international collaborative field programs, improvement in satellite measurements, and advancement in high-resolution numerical models. This session seeks contributions from ECS-Kuroshio and Ryukyu Current studies and will cover a wide range of topics of observation, modeling and theory. The dynamics of the Kuroshio and the Ryukyu Current's variability at all spatio-temporal scales, the influence of the Kuroshio on typhoons and climate, the interactions among the Kuroshio, Ryukyu Current and eddies, internal waves including near-internal waves and their interactions with background currents, and the water mass exchanges through the gaps between the Ryukyu Islands are welcome to be discussed in this session.

[AOS08-P01] Impact of the mesosacle eddies on the western boundary current over the entire western North Pacific

*Kako Shinichiro[1], Hirohiko Nakamura[2] (1.Graduate School of Science and Engineering, Kagoshima University, 2.Faculty of Fisheries, Kagoshima University)

[AOS08-P02] Glider observations of interleaving layers in the Kuroshio

*Sen Jan[1], Shih-Hong Wang[1], Kai-Chieh Yang[1], Yiing Jang Yang[1], Ming-Huei Chang[1] (1.Institute of Oceanography, National Taiwan Univ.)

[AOS08-P03] Bottom Pressure in the East China Sea -Observation and modeling

*Hua Zheng[1], Xiao-Hua Zhu[1], Hirohiko Nakamura[2], Jae-Hun Park[3], Chanhyung Jeon[4], Ruixiang Zhao[1], Ayako Nishina[2], Chuanzheng Zhang[1], Hanna Na[5], Ze-Nan Zhu[1], Hong Sik Min[6] (1.Second Institute of Oceanography, Ministry of Natural Resources, China, 2.Faculty of Fisheries, Kagoshima University, Kagoshima, Japan, 3.Department of Ocean Sciences, Inha University, Incheon, South Kore, 4.Department of Marine Science and Biological Engineering, Inha University, Incheon, Korea, 5.School of Earth and Environmental Sciences, Seoul National University, Seoul, Korea, 6.Ocean Circulation and Climate Research Center, Korea Institute of Ocean Science and Technology, Busan, Korea)

[AOS08-P04] A numerical study on the dynamics of seasonal velocity variation in the East China Sea

*ZHENLONG ZHANG[1], Nakamura Hirohiko[1], Xiao-Hua Zhu[2] (1.Kagoshima University, 2.Ministry of Natural Resources, CHINA.)

[AOS08-P05] Temporal and spatial velocity variations over the Kuroshio Extension, Kuroshio and Ryukyu Current System in 1982-2014

*YUXIANG QIAO[1], Hirohiko Nakamura[2], AYAKO NISHINA[2] (1.Kagoshima University, Graduate School of Fisheries, 2.Kagoshima University, Faculty of Fishries)

[AOS08-P06] Characteristics of water in the southern Okinawa Trough.

*Ayako Nishina[1], Hirohiko Nakamura[1], Jae-Hun Park[2], Xiao-Hua Zhu[3], Hong Sik Min[4], Hanna Na[5] (1.Kagoshima University, 2.Inha University, 3.Second Institute of Oceanography, 4.Korea Institute of Ocean Science and Technology, 5.Seoul National University)

Impact of the mesosacle eddies on the western boundary current over the entire western North Pacific

*Kako Shinichiro[1], Hirohiko Nakamura[2]

1. Graduate School of Science and Engineering, Kagoshima University, 2. Faculty of Fisheries, Kagoshima University

Although many previous studies have suggested that the mesoscale eddies affect the variations of the Kuroshio and Ryukyu current systems, the generated regions and paths to the western boundary have not been well explained yet. We constructed a mesosacle eddy tracking dataset using FORA-WNP30 in conjunction with Okubo-Weiss parameters to investigate the effects of eddies on the western boundary current over the entire North Pacific. We observed that cyclonic eddies with relatively long durations (>120 days) were mainly generated around the southern Kuroshio Extension region, while anti-cyclonic eddies were generated around the subtropical counter current. In addition, we found that the cyclonic eddies propagate westward along the Kuroshio region and reach the western boundary, while the anti-cyclonic eddies propagate westward from their regions of origin and thereafter reach the Kuroshio recirculation region and Ryukyu current. The comparison of the Ryukyu-current at a depth of 600 m and the number of times the meso-scale eddies passed over the Ryukyu current demonstrated that the weakening (strengthening) of the northward current in the northern part of the Ryukyu region was consistent with the number of times the cyclonic (anti-cyclonic) eddies passed over the northern part of the Ryukyu current.

Keywords: mesoscale eddy, Kuroshio, Ryukyu current

©2019. Japan Geoscience Union. All Right Reserved.

Glider observations of interleaving layers in the Kuroshio

*Sen Jan[1], Shih-Hong Wang[1], Kai-Chieh Yang[1], Yiing Jang Yang[1], Ming-Huei Chang[1]

1. Institute of Oceanography, National Taiwan Univ.

Interleaving layers (or thermohaline intrusions) were sometimes observed by repeated ship-based hydrographic surveys with coarse spacing between adjacent stations in the Kuroshio off Taiwan, but have never been examined in a dynamic context. A Seaglider was navigated along a triangle track east of Taiwan to complete two repeated high-resolution hydrographic observations from December 2016 to March 2017. Prominent interleaving layers were observed between dissimilar intermediate water masses across the Kuroshio. During the observations, a diple eddy pair and a relatively large anticyclonic eddy impinged on the offshore flank of the Kuroshio, respectively, which brought certain impacts on the formation and growth of the interleaving. Aside from the complicated physical processes in the upper 200 m, salinity profiles indicate that interleaving layers appeared within 500 and 800 m with vertical and horizontal length scales of O(50 m) and O(10-100 km), respectively. The time scale for the interleaving layers should be much less than 30 days, inferred from the discrepancy in the interleaving features between the two surveys. The instability analysis together with values of the Turner angle calculated from the hydrographic data suggests that the double-diffusive instability is the primary driving mechanism for the observed interleaving layers.

Keywords: Kuroshio, Interleaving, Double-diffusive instability, Glider observation

©2019. Japan Geoscience Union. All Right Reserved.

Bottom Pressure in the East China Sea -Observation and modeling

*Hua Zheng[1], Xiao-Hua Zhu[1], Hirohiko Nakamura[2], Jae-Hun Park[3], Chanhyung Jeon[4], Ruixiang Zhao[1], Ayako Nishina[2], Chuanzheng Zhang[1], Hanna Na[5], Ze-Nan Zhu[1], Hong Sik Min[6]

1. Second Institute of Oceanography, Ministry of Natural Resources, China, 2. Faculty of Fisheries, Kagoshima University, Kagoshima, Japan, 3. Department of Ocean Sciences, Inha University, Incheon, South Kore, 4. Department of Marine Science and Biological Engineering, Inha University, Incheon, Korea, 5. School of Earth and Environmental Sciences, Seoul National University, Seoul, Korea, 6. Ocean Circulation and Climate Research Center, Korea Institute of Ocean Science and Technology, Busan, Korea

A two-year ocean bottom pressure record acquired between June 2015 and June 2017 observed by two pressure-recording inverted echo sounders (PIESs) and five current and pressure-recording inverted echo sounders (CPIESs) deployed along a section southwest of the Kerama Gap showed a significant 21-day variability. This 21-day bottom pressure variability (P_{bot21}) was particularly strong from July 2016 to January 2017, and it showed a squared coherence of 0.72 with wind stress curl around the Yangtze estuary in the East China Sea (ECS) during this period with a nearly 3-day time lag. A barotropic ocean model demonstrated the generation, spread, and dissipation of P_{bot21}. The modeling results showed that the P_{bot21} was driven by wind stress curl on the continental shelf of the ECS, where depths are shallower than 100 m, and spread southeastward to the Ryukyu Island Chain (RIC). The P_{bot21} was generated and remained on the shallow continental shelf, and only little power spread toward the RIC; thus, whether the signal could be observed by the mooring array was related to where it was generated. Significant P_{bot21} was generated southeast of the Yangtze estuary and measured by the mooring array from July 2016 to January 2017. However, P_{bot21} generated northeast of the Yangtze estuary, far from the mooring section, from January 2016 to April 2016 was exhausted before reaching the mooring array due to the long distance. It is suggested that the spatial pattern of 21-day wind stress curl over the ECS strongly influences P_{bot21} near the RIC.

©2019. Japan Geoscience Union. All Right Reserved.

A numerical study on the dynamics of seasonal velocity variation in the East China Sea

*ZHENLONG ZHANG[1], Nakamura Hirohiko[1], Xiao-Hua Zhu[2]

1. Kagoshima University, 2. Ministry of Natural Resources, CHINA.

In our previous study, we investigated the seasonal velocity variations at different depths over the entire Kuroshio path. It showed that the upper layer (< ~500 m depth) velocity variation over the entire Kuroshio path has a coherent seasonal feature, which reaches a maximum in July and a minimum in autumn or winter, over most of the regions along the Kuroshio path. However, the lower layer velocity (> ~500 m depth, in the continental slope area from the east of Luzon Island to the east of the Ryukyu Island chain) shows a reversed seasonal variation with a maximum in winter. Several numerical experiments were carried out to clarify the essential mechanisms. Although it was shown that the local wind stress upon the current region is a key factor for the seasonal velocity variation in the upper layer, the detailed driving mechanism has been still unknown. Thus, we perform further numerical experiments to clarify the concreate mechanism in this study. Using a rectilinear regional model with idealized continental slope, we have successfully reproduced the seasonal velocity variation of the jet (the Kuroshio) by the seasonal wind stress variation over the jet. It turns out that the velocity of the jet increases (decreases) when the wind stress is directed to downstream (upstream) direction of the jet. We will report the concrete process underlying acceleration and deceleration processes of the upper layer velocity related to the local wind stress.

Keywords: Kuroshio, Seasonal variation

©2019. Japan Geoscience Union. All Right Reserved.

Temporal and spatial velocity variations over the Kuroshio Extension, Kuroshio and Ryukyu Current System in 1982-2014

*YUXIANG QIAO[1], Hirohiko Nakamura[2], AYAKO NISHINA[2]

1. Kagoshima University, Graduate School of Fisheries, 2. Kagoshima University, Faculty of Fishries

Four dimensional variational Ocean ReAnalysis for the Western North Pacific (FORA-WNP30) from 1982 to 2014 is used to investigate temporal and spatial velocity variations over the regions consisting of Kuroshio Extension (KE), Kuroshio and Ryukyu Current System (RCS). In order to identify such temporal and spatial features, we made Hovmöller diagrams at several depths, which display temporal variations of along-stream velocity along the current path from Luzon Island to KE region. In this study, we particularly examine long-term (> 1 year) variations for their regional characteristics (Luzon Island to KE region) and their vertical features (sea surface to 1000 m depth). The results revealed that 1) the KE is dominated by decadal signals while the upstream regions include clearer interannual signals in addition to decadal ones, 2) decadal variations in the KE tends to be almost out of phase to those variations in the upstream regions from Luzon Island to Izu-Ridge, and 3) the velocity variations at the sea surface tend to be similar to those variations at 1000 m depth.

Keywords: Kuroshio, Ryukyu Current, Kuroshio Extension, Velocity, Long-term variations

©2019. Japan Geoscience Union. All Right Reserved.

Characteristics of water in the southern Okinawa Trough.

*Ayako Nishina[1], Hirohiko Nakamura[1], Jae-Hun Park[2], Xiao-Hua Zhu[3], Hong Sik Min[4], Hanna Na[5]

1. Kagoshima University, 2. Inha University, 3. Second Institute of Oceanography, 4. Korea Institute of Ocean Science and Technology, 5. Seoul National University

The Okinawa Trough is a basin within the East China Sea, where maximum depth reaches 2300 m. There are two characteristic water masses in the Okinawa Trough. One is the high salinity water in the sub-surface layer shallower than 300 m and the other is the low salinity water in the intermediate layer from 400 m to 700 m. According to the previous studies, the former water is occupied by the South China Sea Tropical Water (SCSTW) and the Kuroshio Tropical Water (KTW), and the latter is dominated by modified water masses of the North Pacific Intermediate Water (NPIW) and the South China Sea Intermediate Water (SCSIW). However, in the previous studies, the southern part of the Okinawa Trough remains to be observed, and it should be confirmed whether the previous results can apply to the southern part.
In this study, water mass properties in the southern part of the Okinawa Trough are investigated in detail. We mainly used CTD data from T/V Kagoshima-maru cruises in Junes from 2013 to 2018. The high salinity waters in the sub-surface layer were classified into three groups: SCSTW, KTW and the tropical waters in the east of Ryukyu Islands chain. The low salinity water in the intermediate layer had a complicated distribution in which the low salinity water from the east of Taiwan and that from the Kerama Gap.

Keywords: Okinawa Trough, water mass

©2019. Japan Geoscience Union. All Right Reserved.

[E] Poster | A (Atmospheric and Hydrospheric Sciences)：A-OS Ocean Sciences & Ocean Environment

Wed. May 29, 2019 5:15 PM - 6:30 PM JST | Wed. May 29, 2019 8:15 AM - 9:30 AM UTC | Poster Hall International Exhibition Hall8, Makuhari Messe_11

[A-OS08] ECS-Kuroshio and Ryukyu Current System -Observation, modeling and theory-

convener:Hirohiko Nakamura(Kagoshima University, Faculy of Fisheries), Xiao-Hua Zhu(Second Institute of Oceanography)

The East China Sea (ECS) is separated from the North Pacific basin by the Ryukyu Islands. On each side of the Ryukyu Islands, there lies two western boundary currents -the Kuroshio on the northwest and the Ryukyu Current on the southeast. These two currents play an important role in the global substance cycle and have a remarkable impact on the climate and adjacent marginal seas. Our knowledge of the Kuroshio and the Ryukyu Current's dynamics, variability, and impact has advanced significantly over the last decade, because of recent international collaborative field programs, improvement in satellite measurements, and advancement in high-resolution numerical models. This session seeks contributions from ECS-Kuroshio and Ryukyu Current studies and will cover a wide range of topics of observation, modeling and theory. The dynamics of the Kuroshio and the Ryukyu Current's variability at all spatio-temporal scales, the influence of the Kuroshio on typhoons and climate, the interactions among the Kuroshio, Ryukyu Current and eddies, internal waves including near-internal waves and their interactions with background currents, and the water mass exchanges through the gaps between the Ryukyu Islands are welcome to be discussed in this session.

[AOS08-P01] Impact of the mesosacle eddies on the western boundary current over the entire western North Pacific

*Kako Shinichiro[1], Hirohiko Nakamura[2] (1.Graduate School of Science and Engineering, Kagoshima University, 2.Faculty of Fisheries, Kagoshima University)

[AOS08-P02] Glider observations of interleaving layers in the Kuroshio

*Sen Jan[1], Shih-Hong Wang[1], Kai-Chieh Yang[1], Yiing Jang Yang[1], Ming-Huei Chang[1] (1.Institute of Oceanography, National Taiwan Univ.)

[AOS08-P03] Bottom Pressure in the East China Sea -Observation and modeling

*Hua Zheng[1], Xiao-Hua Zhu[1], Hirohiko Nakamura[2], Jae-Hun Park[3], Chanhyung Jeon[4], Ruixiang Zhao[1], Ayako Nishina[2], Chuanzheng Zhang[1], Hanna Na[5], Ze-Nan Zhu[1], Hong Sik Min[6] (1.Second Institute of Oceanography, Ministry of Natural Resources, China, 2.Faculty of Fisheries, Kagoshima University, Kagoshima, Japan, 3.Department of Ocean Sciences, Inha University, Incheon, South Kore, 4.Department of Marine Science and Biological Engineering, Inha University, Incheon, Korea, 5.School of Earth and Environmental Sciences, Seoul National University, Seoul, Korea, 6.Ocean Circulation and Climate Research Center, Korea Institute of Ocean Science and Technology, Busan, Korea)

[AOS08-P04] A numerical study on the dynamics of seasonal velocity variation in the East China Sea

*ZHENLONG ZHANG[1], Nakamura Hirohiko[1], Xiao-Hua Zhu[2] (1.Kagoshima University, 2.Ministry of Natural Resources, CHINA.)

[AOS08-P05] Temporal and spatial velocity variations over the Kuroshio Extension, Kuroshio and Ryukyu Current System in 1982-2014

*YUXIANG QIAO[1], Hirohiko Nakamura[2], AYAKO NISHINA[2] (1.Kagoshima University, Graduate School of Fisheries, 2.Kagoshima University, Faculty of Fishries)

[AOS08-P06] Characteristics of water in the southern Okinawa Trough.

*Ayako Nishina[1], Hirohiko Nakamura[1], Jae-Hun Park[2], Xiao-Hua Zhu[3], Hong Sik Min[4], Hanna Na[5] (1.Kagoshima University, 2.Inha University, 3.Second Institute of Oceanography, 4.Korea Institute of Ocean Science and Technology, 5.Seoul National University)

Impact of the mesosacle eddies on the western boundary current over the entire western North Pacific

*Kako Shinichiro[1], Hirohiko Nakamura[2]

1. Graduate School of Science and Engineering, Kagoshima University, 2. Faculty of Fisheries, Kagoshima University

Although many previous studies have suggested that the mesoscale eddies affect the variations of the Kuroshio and Ryukyu current systems, the generated regions and paths to the western boundary have not been well explained yet. We constructed a mesosacle eddy tracking dataset using FORA-WNP30 in conjunction with Okubo-Weiss parameters to investigate the effects of eddies on the western boundary current over the entire North Pacific. We observed that cyclonic eddies with relatively long durations (>120 days) were mainly generated around the southern Kuroshio Extension region, while anti-cyclonic eddies were generated around the subtropical counter current. In addition, we found that the cyclonic eddies propagate westward along the Kuroshio region and reach the western boundary, while the anti-cyclonic eddies propagate westward from their regions of origin and thereafter reach the Kuroshio recirculation region and Ryukyu current. The comparison of the Ryukyu-current at a depth of 600 m and the number of times the meso-scale eddies passed over the Ryukyu current demonstrated that the weakening (strengthening) of the northward current in the northern part of the Ryukyu region was consistent with the number of times the cyclonic (anti-cyclonic) eddies passed over the northern part of the Ryukyu current.

Keywords: mesoscale eddy, Kuroshio, Ryukyu current

©2019. Japan Geoscience Union. All Right Reserved.

Glider observations of interleaving layers in the Kuroshio

*Sen Jan[1], Shih-Hong Wang[1], Kai-Chieh Yang[1], Yiing Jang Yang[1], Ming-Huei Chang[1]

1. Institute of Oceanography, National Taiwan Univ.

Interleaving layers (or thermohaline intrusions) were sometimes observed by repeated ship-based hydrographic surveys with coarse spacing between adjacent stations in the Kuroshio off Taiwan, but have never been examined in a dynamic context. A Seaglider was navigated along a triangle track east of Taiwan to complete two repeated high-resolution hydrographic observations from December 2016 to March 2017. Prominent interleaving layers were observed between dissimilar intermediate water masses across the Kuroshio. During the observations, a diple eddy pair and a relatively large anticyclonic eddy impinged on the offshore flank of the Kuroshio, respectively, which brought certain impacts on the formation and growth of the interleaving. Aside from the complicated physical processes in the upper 200 m, salinity profiles indicate that interleaving layers appeared within 500 and 800 m with vertical and horizontal length scales of O(50 m) and O(10-100 km), respectively. The time scale for the interleaving layers should be much less than 30 days, inferred from the discrepancy in the interleaving features between the two surveys. The instability analysis together with values of the Turner angle calculated from the hydrographic data suggests that the double-diffusive instability is the primary driving mechanism for the observed interleaving layers.

Keywords: Kuroshio, Interleaving, Double-diffusive instability, Glider observation

©2019. Japan Geoscience Union. All Right Reserved.

Bottom Pressure in the East China Sea -Observation and modeling

*Hua Zheng[1], Xiao-Hua Zhu[1], Hirohiko Nakamura[2], Jae-Hun Park[3], Chanhyung Jeon[4], Ruixiang Zhao[1], Ayako Nishina[2], Chuanzheng Zhang[1], Hanna Na[5], Ze-Nan Zhu[1], Hong Sik Min[6]

1. Second Institute of Oceanography, Ministry of Natural Resources, China, 2. Faculty of Fisheries, Kagoshima University, Kagoshima, Japan, 3. Department of Ocean Sciences, Inha University, Incheon, South Kore, 4. Department of Marine Science and Biological Engineering, Inha University, Incheon, Korea, 5. School of Earth and Environmental Sciences, Seoul National University, Seoul, Korea, 6. Ocean Circulation and Climate Research Center, Korea Institute of Ocean Science and Technology, Busan, Korea

A two-year ocean bottom pressure record acquired between June 2015 and June 2017 observed by two pressure-recording inverted echo sounders (PIESs) and five current and pressure-recording inverted echo sounders (CPIESs) deployed along a section southwest of the Kerama Gap showed a significant 21-day variability. This 21-day bottom pressure variability (P_{bot21}) was particularly strong from July 2016 to January 2017, and it showed a squared coherence of 0.72 with wind stress curl around the Yangtze estuary in the East China Sea (ECS) during this period with a nearly 3-day time lag. A barotropic ocean model demonstrated the generation, spread, and dissipation of P_{bot21}. The modeling results showed that the P_{bot21} was driven by wind stress curl on the continental shelf of the ECS, where depths are shallower than 100 m, and spread southeastward to the Ryukyu Island Chain (RIC). The P_{bot21} was generated and remained on the shallow continental shelf, and only little power spread toward the RIC; thus, whether the signal could be observed by the mooring array was related to where it was generated. Significant P_{bot21} was generated southeast of the Yangtze estuary and measured by the mooring array from July 2016 to January 2017. However, P_{bot21} generated northeast of the Yangtze estuary, far from the mooring section, from January 2016 to April 2016 was exhausted before reaching the mooring array due to the long distance. It is suggested that the spatial pattern of 21-day wind stress curl over the ECS strongly influences P_{bot21} near the RIC.

©2019. Japan Geoscience Union. All Right Reserved.

A numerical study on the dynamics of seasonal velocity variation in the East China Sea

*ZHENLONG ZHANG[1], Nakamura Hirohiko[1], Xiao-Hua Zhu[2]

1. Kagoshima University, 2. Ministry of Natural Resources, CHINA.

In our previous study, we investigated the seasonal velocity variations at different depths over the entire Kuroshio path. It showed that the upper layer (< ~500 m depth) velocity variation over the entire Kuroshio path has a coherent seasonal feature, which reaches a maximum in July and a minimum in autumn or winter, over most of the regions along the Kuroshio path. However, the lower layer velocity (> ~500 m depth, in the continental slope area from the east of Luzon Island to the east of the Ryukyu Island chain) shows a reversed seasonal variation with a maximum in winter. Several numerical experiments were carried out to clarify the essential mechanisms. Although it was shown that the local wind stress upon the current region is a key factor for the seasonal velocity variation in the upper layer, the detailed driving mechanism has been still unknown. Thus, we perform further numerical experiments to clarify the concreate mechanism in this study. Using a rectilinear regional model with idealized continental slope, we have successfully reproduced the seasonal velocity variation of the jet (the Kuroshio) by the seasonal wind stress variation over the jet. It turns out that the velocity of the jet increases (decreases) when the wind stress is directed to downstream (upstream) direction of the jet. We will report the concrete process underlying acceleration and deceleration processes of the upper layer velocity related to the local wind stress.

Keywords: Kuroshio, Seasonal variation

©2019. Japan Geoscience Union. All Right Reserved.

Temporal and spatial velocity variations over the Kuroshio Extension, Kuroshio and Ryukyu Current System in 1982-2014

*YUXIANG QIAO[1], Hirohiko Nakamura[2], AYAKO NISHINA[2]

1. Kagoshima University, Graduate School of Fisheries, 2. Kagoshima University, Faculty of Fishries

Four dimensional variational Ocean ReAnalysis for the Western North Pacific (FORA-WNP30) from 1982 to 2014 is used to investigate temporal and spatial velocity variations over the regions consisting of Kuroshio Extension (KE), Kuroshio and Ryukyu Current System (RCS). In order to identify such temporal and spatial features, we made Hovmöller diagrams at several depths, which display temporal variations of along-stream velocity along the current path from Luzon Island to KE region. In this study, we particularly examine long-term (> 1 year) variations for their regional characteristics (Luzon Island to KE region) and their vertical features (sea surface to 1000 m depth). The results revealed that 1) the KE is dominated by decadal signals while the upstream regions include clearer interannual signals in addition to decadal ones, 2) decadal variations in the KE tends to be almost out of phase to those variations in the upstream regions from Luzon Island to Izu-Ridge, and 3) the velocity variations at the sea surface tend to be similar to those variations at 1000 m depth.

Keywords: Kuroshio, Ryukyu Current, Kuroshio Extension, Velocity, Long-term variations

©2019. Japan Geoscience Union. All Right Reserved.

Characteristics of water in the southern Okinawa Trough.

*Ayako Nishina[1], Hirohiko Nakamura[1], Jae-Hun Park[2], Xiao-Hua Zhu[3], Hong Sik Min[4], Hanna Na[5]

1. Kagoshima University, 2. Inha University, 3. Second Institute of Oceanography, 4. Korea Institute of Ocean Science and Technology, 5. Seoul National University

The Okinawa Trough is a basin within the East China Sea, where maximum depth reaches 2300 m. There are two characteristic water masses in the Okinawa Trough. One is the high salinity water in the sub-surface layer shallower than 300 m and the other is the low salinity water in the intermediate layer from 400 m to 700 m. According to the previous studies, the former water is occupied by the South China Sea Tropical Water (SCSTW) and the Kuroshio Tropical Water (KTW), and the latter is dominated by modified water masses of the North Pacific Intermediate Water (NPIW) and the South China Sea Intermediate Water (SCSIW). However, in the previous studies, the southern part of the Okinawa Trough remains to be observed, and it should be confirmed whether the previous results can apply to the southern part.
In this study, water mass properties in the southern part of the Okinawa Trough are investigated in detail. We mainly used CTD data from T/V Kagoshima-maru cruises in Junes from 2013 to 2018. The high salinity waters in the sub-surface layer were classified into three groups: SCSTW, KTW and the tropical waters in the east of Ryukyu Islands chain. The low salinity water in the intermediate layer had a complicated distribution in which the low salinity water from the east of Taiwan and that from the Kerama Gap.

Keywords: Okinawa Trough, water mass

©2019. Japan Geoscience Union. All Right Reserved.

[E] Poster | A (Atmospheric and Hydrospheric Sciences)：A-OS Ocean Sciences & Ocean Environment

Wed. May 29, 2019 3:30 PM - 5:00 PM JST | Wed. May 29, 2019 6:30 AM - 8:00 AM UTC | Poster Hall International Exhibition Hall8, Makuhari Messe_7

[A-OS11] Continental-Oceanic Mutual Interaction: Planetary scale Material Circulation

convener:Yosuke Alexandre Yamashiki(Earth & Planetary Water Resources Assessment Laboratory Graduate School of Advanced Integrated Studies in Human Survivability Kyoto University), Yukio Masumoto(Graduate School of Science, The University of Tokyo), Swadhin Behera(Climate Variation Predictability and Applicability Research Group, Application Laboratory, JAMSTEC, 3173-25 Showa-machi, Yokohama 236-0001), Takanori Sasaki(Department of Astronomy, Kyoto University)

The main purpose of this session is to promote discussion on mutual interaction between Continental zone and Oceanic zone. The global-scale material circulation induced by River runoff through oceanic general circulation as major topic on Continental-Oceanic Interaction, where the ENSO / IOD influence into continental climate as major topics on Oceanic-Continental Interaction. Numerical simulation and field observation of radionuclide transport from continental zone into ocean and its potential impact is also important topics of this session. The session also extend discussion on planetary hydrology and oceanography focusing on subsurface ocean in Jupiter's moon & Ancient Martian Oceanography & Hydrology by possible application of terrestrial GCM into Ancient Mars.

[AOS11-P01] Remote Sensing of Chlorophyll-a and Submerged Aquatic Vegetation for a Freshwater Lake in Japan

*Shweta Yadav[1], Yamashiki Yosuke[1], Junichi Susaki[1], Kanako Ishikawa[2] (1.Kyoto University, 2.Lake Biwa Environmental Research Institute)

[AOS11-P02] Hydrological and Debris-flow simulation of Martian Surface in Hesperian & early Amazonian epoch

*Hiroaki Sato[2], Yosuke Alexandre Yamashiki[1], Ryusuke Kuroki[1], Hideaki Miyamoto[3], Ryodo Hemmi[3] (1.Earth & Planetary Water Resources Assessment Laboratory Graduate School of Advanced Integrated Studies in Human Survivability Kyoto University, 2.Faculty of Engineering, Kyoto University, 3.Graduate School of Engineering, The University of Tokyo)

[AOS11-P03] Global Lakes & reservoirs Repository and their application for terrestrial surface environment

*Yosuke Alexandre Yamashiki[1], Ryusuke Kuroki[1], Botong Gao[1], Hina Bando[2], Fuka Takagi[3], Shweta Yadav[4] (1.Earth & Planetary Water Resources Assessment Laboratory Graduate School of Advanced Integrated Studies in Human Survivability Kyoto University, 2.Faculty of Science, Kyoto University, 3.Faculty of Agriculture, Kyoto University, 4.Educational Unit for Studies on Connectivity of Hills, Humans and Ocean, Kyoto University)

[AOS11-P04] Numerical simulation of Tidal Heating using SPH and its application to inner sea formation

*keiya murashima[1], Yosuke Alexandre Yamashiki[1], Natsuki Hosono[2] (1.Kyoto University, 2.Japan Agency for Marine-Earth Science and Technology)

Remote Sensing of Chlorophyll-a and Submerged Aquatic Vegetation for a Freshwater Lake in Japan

*Shweta Yadav[1], Yamashiki Yosuke[1], Junichi Susaki[1], Kanako Ishikawa[2]

1. Kyoto University, 2. Lake Biwa Environmental Research Institute

Freshwater lakes, particularly shallow lakes often exhibit alternative vegetative states, a clear-water state dominated by submerged aquatic vegetation (SAV) and a turbid-water state dominated by phytoplankton. Phytoplankton and SAV constitute the base of the aquatic food web and are the primary driver of the biogeochemical process in both the freshwater and coastal water bodies. The abundance of phytoplankton biomass can potentially indicate the degree of eutrophication in a specific waterbody. On the other hand, the massive overgrowth of invasive SAV species can also pose a serious threat to the aquatic ecosystem. Conventional methods (eg. Site-specific Boat survey) used to monitor the large water bodies are often time-consuming and expensive. In this study, we used a remote sensing based approach to monitor SAV and phytoplankton of the Lake. A multi-spectral satellite image (Landsat-8 Operational Land Imager) was used to assess the phytoplankton concentration and SAV biomass. A spectral decomposing algorithm was used to estimate and quantify both phytoplankton and SAV. Based on the peak growth period of SAV in the lake, the estimations were limited to a certain period of the year (i.e. mainly August and September). The image was used to classify and map the SAV coverage area using the spectral mixture analysis. The SAV biomass estimation model was used to determine the biomass of the SAV classified pixels in the lake. The satellite-derived phytoplankton and SAV were validated using the in-situ measured data of the lake. The result indicates the time and location-specific variation in the dominance of the phytoplankton and SAV.

Keywords: Phytoplankton, Submerged Aquatic Vegetation, Remote Sensing, Lake Water Quality

©2019. Japan Geoscience Union. All Right Reserved.

Hydrological and Debris-flow simulation of Martian Surface in Hesperian & early Amazonian epoch

*Hiroaki Sato[2], Yosuke Alexandre Yamashiki[1], Ryusuke Kuroki[1], Hideaki Miyamoto[3], Ryodo Hemmi[3]

1. Earth & Planetary Water Resources Assessment Laboratory Graduate School of Advanced Integrated Studies in Human Survivability Kyoto University, 2. Faculty of Engineering, Kyoto University, 3. Graduate School of Engineering, The University of Tokyo

It is considered that the Mars in Noachian ecoch to early Amazonian was much warmer temperature than current condition, with atmosphere and ocean supported by its magnetic activity. Several valley which seems to be developed by ancient hydrological processes are obsered in Martian surface, is being considered to be built long time before. Some fluvial fun was formed during the following Hesperian to early Amazonian epoch, which is considered as much cooler and drier than Noachian epoch. In this study, we applied Hydro-debris 2D model into Martian surface in Hesperian epoch in order to try develping surface vallay formation throughout hydrological processes.

Sediment transport and associated small-scale debris-flow occurrence may be the key for valley formation, where might be the micro-habitable zone in ancient period. At the same time it is still uncertain how much precipitation and erosion should have been required to formulate such topography. Following the last year’ s calculation we attempted to compare several cases of debris flow experiments by changing hypothetical precipitation rate and erosive coefficients in the initially distributed regolith.

Keywords: Hesperian Epoch, Debris flow

©2019. Japan Geoscience Union. All Right Reserved.

Global Lakes & reservoirs Repository and their application for terrestrial surface environment

*Yosuke Alexandre Yamashiki[1], Ryusuke Kuroki[1], Botong Gao[1], Hina Bando[2], Fuka Takagi[3], Shweta Yadav[4]

1. Earth & Planetary Water Resources Assessment Laboratory Graduate School of Advanced Integrated Studies in Human Survivability Kyoto University, 2. Faculty of Science, Kyoto University, 3. Faculty of Agriculture, Kyoto University, 4. Educational Unit for Studies on Connectivity of Hills, Humans and Ocean, Kyoto University

Global Lakes & Reservoirs Repository (GLR) has been developed in order to list global scale freshwater storage focusing on Lakes & Reservoirs. In this presentation we'll introduce their application, combining this with the ecological model for lakes & reservoirs for their surface environmental assessment under different climatic conditions. A two-layer aquatic ecological model (consisted with three types of phytoplanktons & zooplankton) is linked for a number of global lakes for the evaluation of future trends of aquatic ecosystems, mainly focusing on phytoplankton growth. The application of the database, by coupling it with satellite remote sensing for monitoring aquatic environment, together with the three-dimensional lake & reservoir aquatic environment model, are also introduced in the database.

Keywords: GLR, Remote sensing of aquatic environment

©2019. Japan Geoscience Union. All Right Reserved.

Numerical simulation of Tidal Heating using SPH and its application to inner sea formation

*keiya murashima[1], Yosuke Alexandre Yamashiki[1], Natsuki Hosono[2]

1. Kyoto University, 2. Japan Agency for Marine-Earth Science and Technology

There are some traces of liquid in icy moons, such as a plume of vapor of Europa acquired by Hubble Space Telescope and tiger stripes of Enceladus observed by Cassini. Since liquid water is essential for the origin of life, it can be important to understand the development of inner sea and also the temperature distribution inside of such icy moons.

It is considered that the tidal heating caused by tidal acceleration melts the inner icy layer which results in the presence of liquid water beneath its surface. Thus, we aim at simulating the tidal heating of an icy moon by 3-dimensional numerical fluid calculation in Smoothed Particle Hydrodynamics (SPH) method. As the tidal heating model, we apply the viscosity model which was used for numerical calculation of tidal stripping.

It is confirmed that this viscosity model lead to qualitatively correct result about tidal disruption, but the possibility of its application to tidal heating is not validiated. Therefore, as a first step, we tried to compare the result of this simulation with the result which is estimated theoretically. We made a rotation of a differentiated Titan-sized tidally locked object around a Saturn-mass material point with the radius of orbit being 1.1 times larger than its Roche limit. We also considered how to applicate this simulation to the calculation of actual icy moons. We will report the progress.

Keywords: icy moon, tidal heating

©2019. Japan Geoscience Union. All Right Reserved.

[E] Poster | A (Atmospheric and Hydrospheric Sciences)：A-OS Ocean Sciences & Ocean Environment

Wed. May 29, 2019 5:15 PM - 6:30 PM JST | Wed. May 29, 2019 8:15 AM - 9:30 AM UTC | Poster Hall International Exhibition Hall8, Makuhari Messe_12

[A-OS11] Continental-Oceanic Mutual Interaction: Planetary scale Material Circulation

convener:Yosuke Alexandre Yamashiki(Earth & Planetary Water Resources Assessment Laboratory Graduate School of Advanced Integrated Studies in Human Survivability Kyoto University), Yukio Masumoto(Graduate School of Science, The University of Tokyo), Swadhin Behera(Climate Variation Predictability and Applicability Research Group, Application Laboratory, JAMSTEC, 3173-25 Showa-machi, Yokohama 236-0001), Takanori Sasaki(Department of Astronomy, Kyoto University)

The main purpose of this session is to promote discussion on mutual interaction between Continental zone and Oceanic zone. The global-scale material circulation induced by River runoff through oceanic general circulation as major topic on Continental-Oceanic Interaction, where the ENSO / IOD influence into continental climate as major topics on Oceanic-Continental Interaction. Numerical simulation and field observation of radionuclide transport from continental zone into ocean and its potential impact is also important topics of this session. The session also extend discussion on planetary hydrology and oceanography focusing on subsurface ocean in Jupiter's moon & Ancient Martian Oceanography & Hydrology by possible application of terrestrial GCM into Ancient Mars.

[AOS11-P01] Remote Sensing of Chlorophyll-a and Submerged Aquatic Vegetation for a Freshwater Lake in Japan

*Shweta Yadav[1], Yamashiki Yosuke[1], Junichi Susaki[1], Kanako Ishikawa[2] (1.Kyoto University, 2.Lake Biwa Environmental Research Institute)

[AOS11-P02] Hydrological and Debris-flow simulation of Martian Surface in Hesperian & early Amazonian epoch

*Hiroaki Sato[2], Yosuke Alexandre Yamashiki[1], Ryusuke Kuroki[1], Hideaki Miyamoto[3], Ryodo Hemmi[3] (1.Earth & Planetary Water Resources Assessment Laboratory Graduate School of Advanced Integrated Studies in Human Survivability Kyoto University, 2.Faculty of Engineering, Kyoto University, 3.Graduate School of Engineering, The University of Tokyo)

[AOS11-P03] Global Lakes & reservoirs Repository and their application for terrestrial surface environment

*Yosuke Alexandre Yamashiki[1], Ryusuke Kuroki[1], Botong Gao[1], Hina Bando[2], Fuka Takagi[3], Shweta Yadav[4] (1.Earth & Planetary Water Resources Assessment Laboratory Graduate School of Advanced Integrated Studies in Human Survivability Kyoto University, 2.Faculty of Science, Kyoto University, 3.Faculty of Agriculture, Kyoto University, 4.Educational Unit for Studies on Connectivity of Hills, Humans and Ocean, Kyoto University)

[AOS11-P04] Numerical simulation of Tidal Heating using SPH and its application to inner sea formation

*keiya murashima[1], Yosuke Alexandre Yamashiki[1], Natsuki Hosono[2] (1.Kyoto University, 2.Japan Agency for Marine-Earth Science and Technology)

Remote Sensing of Chlorophyll-a and Submerged Aquatic Vegetation for a Freshwater Lake in Japan

*Shweta Yadav[1], Yamashiki Yosuke[1], Junichi Susaki[1], Kanako Ishikawa[2]

1. Kyoto University, 2. Lake Biwa Environmental Research Institute

Freshwater lakes, particularly shallow lakes often exhibit alternative vegetative states, a clear-water state dominated by submerged aquatic vegetation (SAV) and a turbid-water state dominated by phytoplankton. Phytoplankton and SAV constitute the base of the aquatic food web and are the primary driver of the biogeochemical process in both the freshwater and coastal water bodies. The abundance of phytoplankton biomass can potentially indicate the degree of eutrophication in a specific waterbody. On the other hand, the massive overgrowth of invasive SAV species can also pose a serious threat to the aquatic ecosystem. Conventional methods (eg. Site-specific Boat survey) used to monitor the large water bodies are often time-consuming and expensive. In this study, we used a remote sensing based approach to monitor SAV and phytoplankton of the Lake. A multi-spectral satellite image (Landsat-8 Operational Land Imager) was used to assess the phytoplankton concentration and SAV biomass. A spectral decomposing algorithm was used to estimate and quantify both phytoplankton and SAV. Based on the peak growth period of SAV in the lake, the estimations were limited to a certain period of the year (i.e. mainly August and September). The image was used to classify and map the SAV coverage area using the spectral mixture analysis. The SAV biomass estimation model was used to determine the biomass of the SAV classified pixels in the lake. The satellite-derived phytoplankton and SAV were validated using the in-situ measured data of the lake. The result indicates the time and location-specific variation in the dominance of the phytoplankton and SAV.

Keywords: Phytoplankton, Submerged Aquatic Vegetation, Remote Sensing, Lake Water Quality

©2019. Japan Geoscience Union. All Right Reserved.

Hydrological and Debris-flow simulation of Martian Surface in Hesperian & early Amazonian epoch

*Hiroaki Sato[2], Yosuke Alexandre Yamashiki[1], Ryusuke Kuroki[1], Hideaki Miyamoto[3], Ryodo Hemmi[3]

1. Earth & Planetary Water Resources Assessment Laboratory Graduate School of Advanced Integrated Studies in Human Survivability Kyoto University, 2. Faculty of Engineering, Kyoto University, 3. Graduate School of Engineering, The University of Tokyo

It is considered that the Mars in Noachian ecoch to early Amazonian was much warmer temperature than current condition, with atmosphere and ocean supported by its magnetic activity. Several valley which seems to be developed by ancient hydrological processes are obsered in Martian surface, is being considered to be built long time before. Some fluvial fun was formed during the following Hesperian to early Amazonian epoch, which is considered as much cooler and drier than Noachian epoch. In this study, we applied Hydro-debris 2D model into Martian surface in Hesperian epoch in order to try develping surface vallay formation throughout hydrological processes.

Sediment transport and associated small-scale debris-flow occurrence may be the key for valley formation, where might be the micro-habitable zone in ancient period. At the same time it is still uncertain how much precipitation and erosion should have been required to formulate such topography. Following the last year’ s calculation we attempted to compare several cases of debris flow experiments by changing hypothetical precipitation rate and erosive coefficients in the initially distributed regolith.

Keywords: Hesperian Epoch, Debris flow

©2019. Japan Geoscience Union. All Right Reserved.

Global Lakes & reservoirs Repository and their application for terrestrial surface environment

*Yosuke Alexandre Yamashiki[1], Ryusuke Kuroki[1], Botong Gao[1], Hina Bando[2], Fuka Takagi[3], Shweta Yadav[4]

1. Earth & Planetary Water Resources Assessment Laboratory Graduate School of Advanced Integrated Studies in Human Survivability Kyoto University, 2. Faculty of Science, Kyoto University, 3. Faculty of Agriculture, Kyoto University, 4. Educational Unit for Studies on Connectivity of Hills, Humans and Ocean, Kyoto University

Global Lakes & Reservoirs Repository (GLR) has been developed in order to list global scale freshwater storage focusing on Lakes & Reservoirs. In this presentation we'll introduce their application, combining this with the ecological model for lakes & reservoirs for their surface environmental assessment under different climatic conditions. A two-layer aquatic ecological model (consisted with three types of phytoplanktons & zooplankton) is linked for a number of global lakes for the evaluation of future trends of aquatic ecosystems, mainly focusing on phytoplankton growth. The application of the database, by coupling it with satellite remote sensing for monitoring aquatic environment, together with the three-dimensional lake & reservoir aquatic environment model, are also introduced in the database.

Keywords: GLR, Remote sensing of aquatic environment

©2019. Japan Geoscience Union. All Right Reserved.

Numerical simulation of Tidal Heating using SPH and its application to inner sea formation

*keiya murashima[1], Yosuke Alexandre Yamashiki[1], Natsuki Hosono[2]

1. Kyoto University, 2. Japan Agency for Marine-Earth Science and Technology

There are some traces of liquid in icy moons, such as a plume of vapor of Europa acquired by Hubble Space Telescope and tiger stripes of Enceladus observed by Cassini. Since liquid water is essential for the origin of life, it can be important to understand the development of inner sea and also the temperature distribution inside of such icy moons.

It is considered that the tidal heating caused by tidal acceleration melts the inner icy layer which results in the presence of liquid water beneath its surface. Thus, we aim at simulating the tidal heating of an icy moon by 3-dimensional numerical fluid calculation in Smoothed Particle Hydrodynamics (SPH) method. As the tidal heating model, we apply the viscosity model which was used for numerical calculation of tidal stripping.

It is confirmed that this viscosity model lead to qualitatively correct result about tidal disruption, but the possibility of its application to tidal heating is not validiated. Therefore, as a first step, we tried to compare the result of this simulation with the result which is estimated theoretically. We made a rotation of a differentiated Titan-sized tidally locked object around a Saturn-mass material point with the radius of orbit being 1.1 times larger than its Roche limit. We also considered how to applicate this simulation to the calculation of actual icy moons. We will report the progress.

Keywords: icy moon, tidal heating

©2019. Japan Geoscience Union. All Right Reserved.

[E] Poster | A (Atmospheric and Hydrospheric Sciences)：A-HW Hydrology & Water Environment

Wed. May 29, 2019 3:30 PM - 5:00 PM JST | Wed. May 29, 2019 6:30 AM - 8:00 AM UTC | Poster Hall International Exhibition Hall8, Makuhari Messe_8

[A-HW23] Hydrology & Water Environment

convener:Isao Machida(Geological Survey of Japan), Dai Yamazaki(Institute of Industrial Sciences, The University of Tokyo), Takeshi Hayashi(Faculty of Education and Human Studies, Akita University), Keisuke Fukushi(Institute of Nature & Environmental Technology, Kanazawa University)

We focus on various issues of water cycle and environment and aim to answer questions of hydrological and earth system sciences including 1) surface, subsurface and evapotranspiration processes of water cycle; 2) natural and anthropogenic hydrothermal systems, 3) environments issues and studies on a watershed or global scale, 4) water-related issues with ecological, environmental, and geochemical aspects, and 5) other issues in hydrological sciences. This session welcomes presentations regarding various kinds of approaches and techniques such as field survey, remote sensing, isotope tracers, numerical simulation, and theoretical analysis.

[AHW23-P01] A multiobjective risk management model for real-time reservoir flood control operation

*Juan Chen[1,2], Ping-An Zhong[2], XinYu Wan[2], Yu Zhang[2] (1.College of Earth Sciences and Engineering, Hohai University, 2.College of Hydrology and Water Resources, Hohai University)

[AHW23-P02] Assessment of the Flow Regime of Roanoke River due to Climatic and Anthropogenic Activities

*Rahul Kumar Singh[1], Dr. Manoj Kumar Jain[1] (1.Indian Institute of Technology, Roorkee, India)

[AHW23-P03] Predictive Analysis of Climate, Water, Health and the Environment Nexus

*Abhishek [1], Deepika [2] (1.Technical University Dresden, GERMANY, 2.BPS Government Medical College for Women, Sonepat, INDIA)

[AHW23-P05] Severe droughts provide huge fuel for widespread wildfires in California in USA

*Linghua Qiu[1], Ji Chen[1], Haiyun Shi[2], Liqun Sun[3], Jun Niu[4] (1.the University of Hong Kong, 2.Southern University of Science and Technology, 3.Shenzhen Institutes of Advanced Technology, Chinese Academy of Sciences, 4.China Agricultural University)

[AHW23-P06] A comprehensive evaluation of MODIS-based water use efficiency with global eddy covariance flux data and a process model

*Shanshan YANG[1,2], Jiahua ZHANG[1], Sha ZHANG[1,2], Jingwen WANG[1,2], Yun BAI[1,2], Fengmei YAO[2], Huadong GUO[1] (1.Institute of Remote Sensing and Digital Earth, Chinese Academy of Sciences, 2.University of Chinese Academy of Sciences, Beijing, China)

[AHW23-P07] Impact of variability and anisotropy in the correlation decay distance for precipitation spatial interpolation in China

*yingxian zhang[1] (1.National Climate Center, China Meteorological Administration)

[AHW23-P08] New Record-Breaking Frequency of Annual Maximum Daily Precipitation of 58 stations in the whole Japan, an increasing of extreme values.

*Chhay Ngorn SEANG[1], Tomohito YAMADA[1] (1.Hokkaido University)

[AHW23-P09] Quantifying stemflow to better express its ecohydrological significance

*Shin'ichi Iida[1], Darryl E. Carlye-Moses[2], Sonja Germer[3], Pilar Llorens[4], Beate Michalzik[5], Kazuki Nanko[1], Alexander Tischer[5], Delphis F. Levia[6] (1.Department of Disaster Prevention, Meteorology and Hydrology, Forestry and Forest Products Research Institute, 2.Department of Geography and Environmental Studies, Thompson Rivers University, Kamloops, British Columbia, Canada, 3.Department of Bioengineering,

Leibniz Institute for Agricultural Engineering and Bioeconomy, Potsdam, Germany, 4.Institute of Environmental Assessment and Water Research (IDAEA-CSIC), Barcelona, Spain, 5.Soil Science, Institute of Geography, Friedrich Schiller University Jena, Jena, Germany, 6.Department of Geography and Department of Plant and Soil Sciences, University of Delaware, Newark, DE, USA)

[AHW23-P10] **Hydraulic analysis of overland flow caused by temporally varying rainfall**

*PING-CHENG HSIEH[1], Ming-Chang Wu[1] (1.National Chung Hsing University)

[AHW23-P11] A comparative Study on Water Environment of Isolated Islands - Focusing on Islands in Nagasaki Prefecture - (3)

*Go Yamaki[1], Koji Kodera[2], Kazuki Asami[1], Yoshihiro IGARI[1], Masaki Horiuchi[1] (1.Grad. Student, Hosei Univ., 2.Dep. of Geography, Hosei Univ.)

[AHW23-P12] **Water environment around Kusatsu-Shirane volcano and consideration of the effect of eruption in January 2018**

*Igari Yoshihiro[1], Koji Kodera[2], Kazuki Asami[1] (1.Grad.Student,Hosei Univ., 2.Dep.of Geography Hosei Univ.)

[AHW23-P13] Re-consideration of discharge rate of spring water in Lake Ezu, Kumamoto

*Kimpei Ichiyanagi[1], Kiyoshi Ide[1], Jun Shimada[1], Tsutomu Ichikawa[2] (1.Kumamoto University, 2.Tokai University)

[AHW23-P14] **Evaluating the efficacy of hydrologically and hydrodynamically driven methods of e-flow assessment for Upper Godavari River Basin, India**

*GAURAV KALIDAS PAKHALE[1], Jyoti Punjahari Nale[2], Ashvin Kumar Gosain[3], Rakesh Khosa[3] (1.PhD Research Scholar, Civil Engineering Department, Indian Institute of Technology, Delhi, 2.Project Advisor, IEWP, GIZ India, New Delhi, India, 3.Professor, Civil Engineering Department, Indian Institute of Technology, Delhi)

[AHW23-P15] Presence of pharmaceutical compounds in freshwater lakes and their impact on phytoplankton

*Nandakumar Kanavillil[1], Cassandra Fligg[1], Sreekumari Kurissery[1] (1.Lakehead University, Canada)

[AHW23-P16] **Novel approximate solutions for solute transport due to injections: considering the scale-dependent dispersion and non-integer flow dimension**

*Ye-Chen Lin[1], Hund-Der Yeh[1] (1.National Chiao Tung Univ.)

[AHW23-P17] Experimemtal study on the residual saturation of Porous Media using Pore Doublets Micromodel

*Chun-Wei Peng[1] (1.Taiwan National Chiao Tung University)

[AHW23-P18] Assessment of Synergy between Biomedical Waste and Shallow Groundwater Pollution

*Deepika [1], Abhishek [2] (1.BPS Government Medical College for Women, Sonepat, INDIA, 2.Technical University Dresden, GERMANY)

[AHW23-P19] Erosion and transport processes of earth surface materials in a reservoir-catchment system inferred from atmospheric radionuclides ^{7}Be and ^{210}Pb

*Mikiya Tsuruoka[1], Shinya Ochiai[2], Atsushi Matsuki[2], Seiya Nagao[2] (1.Graduate School of Natural Science and Technology, Kanazawa University, 2.Institute of Nature and Environmental Technology, Kanazawa University)

[AHW23-P20] Fluctuation of groundwater level in a sloping unconfined aquifer due to time varying recharge

*Ming-Chang Wu[1], Ping-Cheng Hsieh[1] (1.National Chung Hsing University)

[AHW23-P21] **Effect of cutoff wall on recharge water storage volume**

*Pei-hsun Tsai[1], Jung-hsing Tai[1] (1.Chaoyang University of Technology)

[AHW23-P22] **Studying Operation Parameters on Flat-Plate Membrane Bioreactor for Sewage Treatment**

*Jen Hung Chiu[1], Wen Chin Chen[1] (1.Studying Operation Parameters on Flat-Plate Membrane Bioreactor for Sewage Treatment)

[AHW23-P23] **Mine-water quality at a tertiary coalfield in India: Characterisation and treatment using novel polyvinyl alcohol (PVA) gel bioreactor**

*Aparna Dutta[1], Sudipta Sarkar[1] (1.Indian Institute of Technology Roorkee)

A multiobjective risk management model for real-time reservoir flood control operation

*Juan Chen[1,2], Ping-An Zhong[2], XinYu Wan[2], Yu Zhang[2]

1. College of Earth Sciences and Engineering, Hohai University, 2. College of Hydrology and Water Resources, Hohai University

Many uncertainties exit in the real-time reservoir flood control operation and bring risks to flood control decisions. A multiobjective optimization model is developed for the real-time risk management for the flood control operation of a reservoir system considering multiple uncertainties such as inflow forecast errors and outflow errors. The two competing objectives considered are: (1) minimizing the risk of reservoir upstream flooding and (2) minimizing the risk of downstream flooding. The optimization model seeks to find the operation schedules that satisfy the flood control objectives and simultaneously minimize the overall risks. The decision variables are the hourly reservoir releases. The formulated multiobjective optimization problem is nonlinear and non-convex, and is solved with an improved Non-dominated Sorting Genetic Algorithm-II (INSGA-II). We use a filtering algorithm to select representative non-dominated solutions from the Pareto front generated by INSGA-II to assist in real-time decision making. The proposed risk management model is applied to the Foziling reservoir in Huaihe river basin of China. The results show that the proposed method can provide a practical way to optimize the real-time flood control operation for risk management of a reservoir.

Keywords: Flood, Reservoir, Flood control operation, Risk assessment, Multiobjective optimization

©2019. Japan Geoscience Union. All Right Reserved.

Assessment of the Flow Regime of Roanoke River due to Climatic and Anthropogenic Activities

*Rahul Kumar Singh[1], Dr. Manoj Kumar Jain[1]

1. Indian Institute of Technology, Roorkee, India

The natural flow regime of many rivers around the world has been significantly altered due to climatic and anthropogenic modifications such as the construction of dams and reservoirs. The natural flow regime plays an important role in the development of the riverine ecosystem. Therefore, quantification of the extent of the alterations in the natural flow regime would be helpful in the river’ s ecological assessment. The Roanoke River in southeastern United States had one of the biggest and least disturbed forest ecosystems but due to climatic changes and anthropogenic actions such as construction of dam, artificial regulations of the natural flow regime, the overall riverine ecosystem has severely impacted. In this study, SWAT (Soil Water Assessment Tool) has been used to reconstruct the long-term unaltered streamflow for a hypothetical no-dam scenario condition, in order to assess the impact of climate change as well as due to construction of the John H Kerr reservoir on Roanoke River streamflow from 1956-2012. In order to simulate the unaltered streamflow series post construction of John H Kerr reservoir, 32 years (1916-1948) of observed gauge inflow prior to anthropogenic disturbance (due to construction of John H Kerr Reservoir) was used for calibration and validation of the parameters of the SWAT model. Historical land use and land cover backcasting data for the year 1938 has been used in the hydrological model to simulate the flow regime prior to construction of the dam and it was kept same during the whole simulation period. The SWAT model simulated observed gauge data with Nash-Sutcliffe efficiency coefficient (NSE) = 0.70, Percent bias (PBIAS) = 0.00 and the determination coefficient (R^2) = 0.73 during the calibration period (1916 - 1936), and performed equally better during the validation period (1937-1948) with NSE = 0.72, PBIAS = 0.00 and R^2 = 0.74. The indicators of hydrologic alteration (IHA) methodology has been used to assess the natural flow regime (no dam or reservoir moderated flow regime) characteristics under a simulated no-reservoir scenario (scenario1) and compare with the IHA results obtained based on the gauged streamflow downstream of the dam (scenario2). Hence, in case of scenario 1, the post-impact period has been taken as the simulated flow series using SWAT model from 1956-2012 and in case of scenario 2 the post-impact period has been taken as the gauged observed streamflow from 1956-2012 at Roanoke Rapids gauging station downstream of the reservoir. The pre-impact period for both the scenario was kept the same i.e. from 1912 to 1949. The results reveal that in case of the IHA assessment based on scenario 1, significant alterations have been observed in 5 out of 32 indicators compared to 13 out 32 indicators in case of scenario 2. The overall hydrologic alteration in case of scenario 1 was 45.65% and it was 55.17% in the case of scenario 2. The alteration during the scenario 1 could be attributed to the overall natural climatic variability. The results also indicate that flow variability in terms of high and low flows were better in scenario 1 compared to scenario 2 where the high flows were completely absorbed including the low pulse count and duration due to regulation in the flow. However, the reservoir operations enhanced the monthly flows including the multiday minima low flows. Thus, the present method can be treated as an easy-to-implement comprehensive approach for designing natural flow regimes to mimic the pre-impact flow condition in order to restore the ecosystem of modified rivers due to anthropogenic interventions.

Keywords: SWAT, IHA, Streamflow, Hydrologic Alteration, Ecosystem

©2019. Japan Geoscience Union. All Right Reserved.

Predictive Analysis of Climate, Water, Health and the Environment Nexus

*Abhishek -[1], Deepika -[2]

1. Technical University Dresden, GERMANY, 2. BPS Government Medical College for Women, Sonepat, INDIA

Amid the major demographic transition of developing world from a rural, agrarian society to an urban, industrial one, there is a need for predictive analytics of impact of the major biotic and abiotic stressors on the environmental constituents. The current study emphasizes the connections between climate, water, environment, and health and their interdependency followed by an impact assessment focusing on an urban environment. A data-driven hybrid framework for water resources assessment and management based on machine learning techniques was developed, calibrated and validated with the ground data for the sub-region scale of North-East Indian regime (mean spatial coordinates: 28° 38' 41.2800" N and 77° 13' 0.1956" E). The remote sensing data for land cover and land change were coupled with the climate model simulations to formulate the health risk assessment framework. The large ensemble of downscaled scenario based outputs including the effects of anthropogenic factors was used to drive the hybrid model framework.

Multi-dimensional Random Walk Metropolis (RWM) algorithms used to optimize the sample observations converged with an RMSE error of 0.18 with a range of 0.006. Pearson Product Moment Correlation coefficient range of all the ensemble members was 0.886-0.904. The prediction accuracy construed from 95 % model uncertainty bounds was 89-91 % for the constituent parameters. The sensitivity analysis revealed that the climate is the key parameter and is the most sensitive for all other linkage units followed by water availability and health factors. Comparative analysis of the simulated- and experimental results enforced comprehensive clarification of the assumptions made therein. By real-time monitoring and forecasting the vital impacts, this research will serve and benefit local policymakers and in the decision-making process, particularly regarding water resources vulnerability and future availability with significant economic consequences. The upscaling of the model form sub-regional to regional scale is well underway.

Keywords: Climate Change, Urbanization, RWM algorithm, Ensemble model

©2019. Japan Geoscience Union. All Right Reserved.

Severe droughts provide huge fuel for widespread wildfires in California in USA

*Linghua Qiu[1], Ji Chen[1], Haiyun Shi[2], Liqun Sun[3], Jun Niu[4]

1. the University of Hong Kong, 2. Southern University of Science and Technology, 3. Shenzhen Institutes of Advanced Technology, Chinese Academy of Sciences, 4. China Agricultural University

The frequently occurred large wildfires in California caught the public’ s attention in recent years and the ability to identify and prevent such disasters is pressing. The study built the rational relationship between soil moisture and vegetation based on remote sensing, hydrology and wildfire data during 2001-2017 in California. The purpose is to estimate the effects of droughts on wildfires and to detect the valid fuel for wildfires. The study results reported that severe droughts could cause huge fuel for wildfires and made them even much more widespread and longer sustained. The consequences could provide significant information for identification and prevention of future wildfires in California and even other regions in the world.

Keywords: Fuel, Wildfires, Droughts, Soil moisture, Vegetation

©2019. Japan Geoscience Union. All Right Reserved.

A comprehensive evaluation of MODIS-based water use efficiency with global eddy covariance flux data and a process model

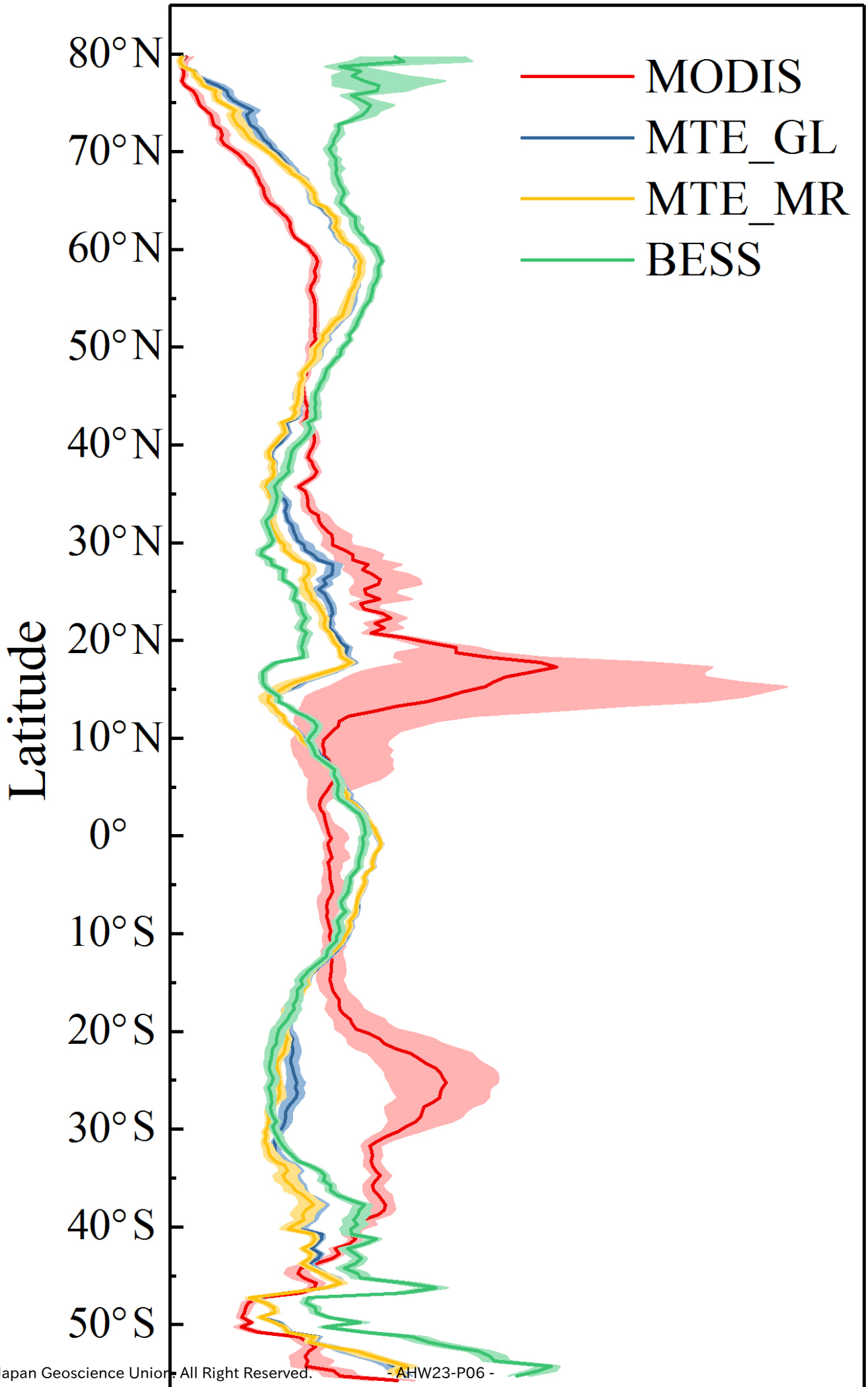
*Shanshan YANG[1,2], Jiahua ZHANG[1], Sha ZHANG[1,2], Jingwen WANG[1,2], Yun BAI[1,2], Fengmei YAO[2], Huadong GUO[1]

1. Institute of Remote Sensing and Digital Earth, Chinese Academy of Sciences, 2. University of Chinese Academy of Sciences, Beijing, China

Ecosystem water use efficiency (WUE), defined as the ratio of gross primary productivity (GPP) to evapotranspiration (ET), is an important indicator to investigate the interaction between the terrestrial carbon and water cycles. The spatiotemporal patterns of WUE inferred from MODIS GPP and ET products and its responses to environmental factors have been analyzed, however, the accuracy of MODIS-derived WUE (MODIS WUE) has not been well evaluated. In this study, we evaluated monthly and annual MODIS WUE using global covariance flux data (FLUXNET2015 dataset) during 2000-2014, and conducted global intercomparisons (2001-2011) among annual WUE from MODIS, gridded FLUXNET (MTE) and a process model (BESS). Site scale (53 sites) evaluation results revealed that MODIS gave reliable estimates for GPP and ET, however, the performances of MODIS WUE was poor for monthly WUE (R2=0.14) and even worse for annual WUE (R2=0.08). MODIS WUE was generally underestimated with a bias of -0.21 gC kg-1 H2O (-8.43%) and RMSE of 1.20 gC kg-1 H2O for monthly WUE, and a bias of -0.28 gC kg-1 H2O (-11.31%) and RMSE of 0.98 gC kg-1 H2O for annual WUE. Among all land cover types, MODIS WUE performed relatively better in savannas and woody savannas for monthly WUE and grasslands for annual WUE, but significantly overestimated WUE in open shrublands. Likewise, MODIS WUE was obviously overestimated in hot and cold semiarid and arid climate zones. The global intercomparison results demonstrated that the spatial pattern of MODIS WUE was broadly similar to that of MTE and BESS WUE, except for the tropical and subtropical arid and semiarid areas. In these regions MODIS WUE showed extremely high values with large uncertainty and different linear trends compared with MTE and BESS WUE. These disagreements were mainly caused by the discrepancies in MODIS ET. Therefore, the uncertainty of MODIS WUE in the tropical arid and semiarid areas should be taken with caution when using MODIS WUE to investigate and interpret how WUE varies spatially and its responses to climate change. Furthermore, the accuracy of MODIS GPP and ET datasets should be paid extra attention since the quality of both GPP and ET would directly affect the WUE accuracy.

Keywords: Water use efficiency (WUE), Evaluation, Intercomparison, MODIS, FLUXNET, BESS

©2019. Japan Geoscience Union. All Right Reserved.



©2019. Japan Geoscience Union. All Right Reserved.

©2019. Japan Geoscience Union. All Right Reserved.

Impact of variability and anisotropy in the correlation decay distance for precipitation spatial interpolation in China

*yingxian zhang[1]

1. National Climate Center, China Meteorological Administration

The correlation decay distance (CDD) plays a key role in the angular-distance weighting (ADW) interpolation technique, being used as the searching radius to select correlated neighbors and to calculate the relative weights. The CDD of daily precipitation in China varies spatially and seasonally, and it presents anisotropic behavior, as a result of topography and the predominant atmospheric circulation. In general, CDD is largest in winter and smallest in summer, except for limited regions such as the Tibetan plateau. From a cross validation analysis, it is found that taking account of spatial and seasonal variations in CDD generally improves the ADW interpolation. Utilization of anisotropic CDDs increases the interpolation skill scores in regions with a dense monitoring network, significant elevation variation (southwestern China) or strongly anisotropic CDDs (Tibetan plateau).

Keywords: daily precipitation, correlation decay distance, ADW interpolation

©2019. Japan Geoscience Union. All Right Reserved.

New Record-Breaking Frequency of Annual Maximum Daily Precipitation of 58 stations in the whole Japan, an increasing of extreme values.

*Chhay Ngorn SEANG[1], Tomohito YAMADA[1]

1. Hokkaido University

The changes in daily temperature extremes in global scale have affected the weather and climate extreme events when there is an increase of greenhouse gas GHG compare to the industrialization in the 19th century (IPCC, 2014). Yamada et al. (2014) illustrate that the water vapor and convective instability follow the Clausius-Clapeyron-like rate of change with 99th percentile hourly precipitation intensity. Lehmann, J. et al. (2015), on another hand, studied globally the characteristic of precipitation change anomaly using a relation of the Clausius-Clapeyron model. By the way, the climate change tends to include another factor, which is more statistical base. The theory of record values in independent and identically distributed (i.i.d) random variable is studied more extensively and is more applicable with an assumption of stationary climate. The Clausius-Clapeyron equation is then also applicable base on the thermodynamic term which illustrates the relation of the temperature, vapor pressure and precipitation formation characteristic which also mentioned in the above previous studies. At the first stage, 58 stations of AMeDAS data with 117-years period across Japan are used for this analysis. The result shows that mean long-term precipitation of these 58 stations is higher than the mean value from theory i.i.d random variable of stationary climate. From this result, it can be implied that the change of precipitation in Japan is influenced by the drift term either of climate change or the heat island. In this case, the Clausius-Clapeyron equation is applied to identify the temperature term of change. This study tries to formulate a theory which more statistical base of climate drifts, non-stationary and non-identically to extreme events in accordance with time series. Clausius-Clapeyron Model and the Linear Drift Model is considered to form an empirical stochastically based on climate trend.

Keywords: Clausius-Clapeyron, New record Breaking, i.i.d

©2019. Japan Geoscience Union. All Right Reserved.

Quantifying stemflow to better express its ecohydrological significance

*Shin'ichi Iida[1], Darryl E. Carlye-Moses[2], Sonja Germer[3], Pilar Llorens[4], Beate Michalzik[5], Kazuki Nanko[1], Alexander Tischer[5], Delphis F. Levia[6]

1. Department of Disaster Prevention, Meteorology and Hydrology, Forestry and Forest Products Research Institute, 2. Department of Geography and Environmental Studies, Thompson Rivers University, Kamloops, British Columbia, Canada, 3. Department of Bioengineering, Leibniz Institute for Agricultural Engineering and Bioeconomy, Potsdam, Germany, 4. Institute of Environmental Assessment and Water Research (IDAEA-CSIC), Barcelona, Spain, 5. Soil Science, Institute of Geography, Friedrich Schiller University Jena, Jena, Germany, 6. Department of Geography and Department of Plant and Soil Sciences, University of Delaware, Newark, DE, USA

Stemflow is the flow of rainwater over the exterior of a tree stem to its base. Due to water balance calculations to obtain interception loss of forest stands, and the sometimes low percentage of stemflow as a function of rainfall, some literature ignores the ecohydrological significance of stemflow. However, stemflow is much more concentrated than throughfall per unit area. In recognition of the extreme amounts of water input to the small area around tree trunks, we advocate for two metrics to better express stemflow in relation to its ecohydrological importance: namely, the stand-scale funneling ratio and the stand-scale infiltration funneling ratio. We calculated these metrics based on measurements carried out in a tropical dry deciduous forest and a subpolar juvenile coniferous stand, and found that these are significantly larger than throughfall on both sites. The data cited from recent papers (n=34) showed that very small stand-scale amount of stemflow (approximately 0.5% on average) were necessary to make the stand-scale funneling ratio to be equal or more than unity. Moreover, the infiltration area of stemflow is generally < 0.2 m^2 due to the high infiltration capacity of top soil of forests, generally resulting in the stand-scale infiltration funneling ratio substantially greater than unity. Thus, stemflow is more effective for soil water recharge than throughfall. We recommend use of these metrics to better express ecohydrological importance of stemflow.

This presentation is based on the published paper as follows:
Carlye-Moses, D.E., Iida, S., Germer, S., Llorens, P., Michalzik, B., Nanko, K., Tischer, A., Levia, D.F. (2018): Expressing stemflow commensurate with its ecohydrological importance. Advances in Water Resources, 121, 472-479. Free open access article to: https://doi.org/10.1016/j.advwatres.2018.08.015

Keywords: Stemflow, Funneling ratio, Forest hydrology

©2019. Japan Geoscience Union. All Right Reserved.

Hydraulic analysis of overland flow caused by temporally varying rainfall

*PING-CHENG HSIEH[1], Ming-Chang Wu[1]

1. National Chung Hsing University

With the development of human civilization and population migration, we use many different types of pervious or impervious materials to cover the original surface. As a result, the surface friction and water permeability are reduced, resulting in increased flow velocity and runoff, and thus increasing the frequency and scale of flood occurrence. Therefore, predicting changes in overland flow caused by rainfall has become an important issue.

This study intends to simulate the overland flow under different rainfall patterns by the theory of diffusion wave model. The diffusion wave equation was used as the governing equation, and an analytical solution of the water depth by the generalized integral transformation method was presented. Since the values of the parameters used in previous research for diffusion wave models vary in an extensive range. In this study, the parameters were adjusted for each location to ensure the rationality of the simulation results according to the law of mass conservation.
The results show that for the non-uniform rainfall, the peak water depth and peak flow due to the post-peak rainfall are the largest, followed by the third quarter peak rainfall; whereas the average flow velocity of the mid-peak rainfall is the largest, followed by the third quarter peak rainfall. The peak water depth, peak flow rate and average flow rate due to the double peak rainfall are the smallest among the six rainfall patterns in this study.

Keywords: overland flow, nonuniform rainfall, diffusion wave

©2019. Japan Geoscience Union. All Right Reserved.

A comparative Study on Water Environment of Isolated Islands - Focusing on Islands in Nagasaki Prefecture - (3)

*Go Yamaki[1], Koji Kodera[2], Kazuki Asami[1], Yoshihiro IGARI[1], Masaki Horiuchi[1]

1. Grad. Student, Hosei Univ., 2. Dep. of Geography, Hosei Univ.

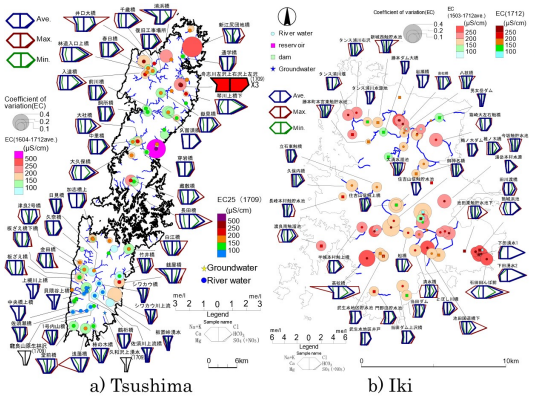
1. Introduction Research on islands in Nagasaki prefecture has hardly been investigated and research has been promoted since 2014 from Goto Island Islands, Tsushima, Iki, Hirado. For this time, we will clarify the water environment in each area from the relationship with land use and climate, and make it a foothold to clarify the material cycle of each island.

2. Target area Iki is rugged with a maximum altitude of 213 m, and there are numerous reservoirs in various parts of the island. In Tsushima, the altitude of the entire island is relatively high, and the mountains occupy about 89%. The Goto Islands Island consists of about 140 large and small islands, with large geological differences on each island. The Hirado Islands have many mountains while the fields are also relatively large. The population penetration rate of wastewater treatment in both areas is as low as 20-40%.

3. Research method Field survey was conducted 2 to 4 times a year from 2014 after organizing and examining existing research. On the site, water temperature, temperature, electric conductivity (EC), pH and RpH, COD were measured, and water was taken to measure the total organic carbon and the main dissolved components.

4. Results and discussion In Iki, the influence of agriculture appears in EC and TOC, but it is interesting that there is almost no effect of nitric acid. On the other hand, although many nitric acid was detected in the Goto Islands, it is thought that factors are due to paddy fields in Iki and upland fields in Goto Islands. Tsushima showed relatively low concentrations of EC and dissolved components, and seasonal changes also appeared. In Hirado Island, especially in the southern part, the geological influence is large in many places, the impact of sea salt is strong in Ikitsuki island and Azuchi Oshima. EC tends to rise in rainwater from October to March, pH tends to decrease. From the above, it is considered that the difference in the quality of the islands is greatly influenced by the difference of geology, topography and agricultural form.

Keywords: Iki island, Tsushima islands, Goto islands, Hirado islands, Water environment



a) Tsushima b) Iki c) Hirado

Fig.1 Water quality

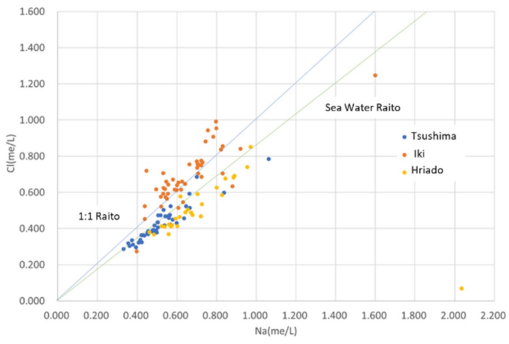


Fig.2 Na / Cl ratio

©2019. Japan Geoscience Union. All Right Reserved.

Water environment around Kusatsu-Shirane volcano and consideration of the effect of eruption in January 2018

*Igari Yoshihiro[1], Koji Kodera[2], Kazuki Asami[1]

1. Grad.Student,Hosei Univ., 2. Dep.of Geography Hosei Univ.

1. Introduction

The eruption (steam explosion) occurred in Mt.Motoshirane (One of Kusatsu-Shirane Volcano) on January 23, 2018. In this area, water quality survey of water environment began in May 2017 before the eruption. In addition to examining the influence on the water quality before and after the eruption, we studied the elution component of volcanic ash and the influence on the water environment. We also attempted to consider water quality forming factors in river water around Kusatsu-Shirane volcano.

2. Research method

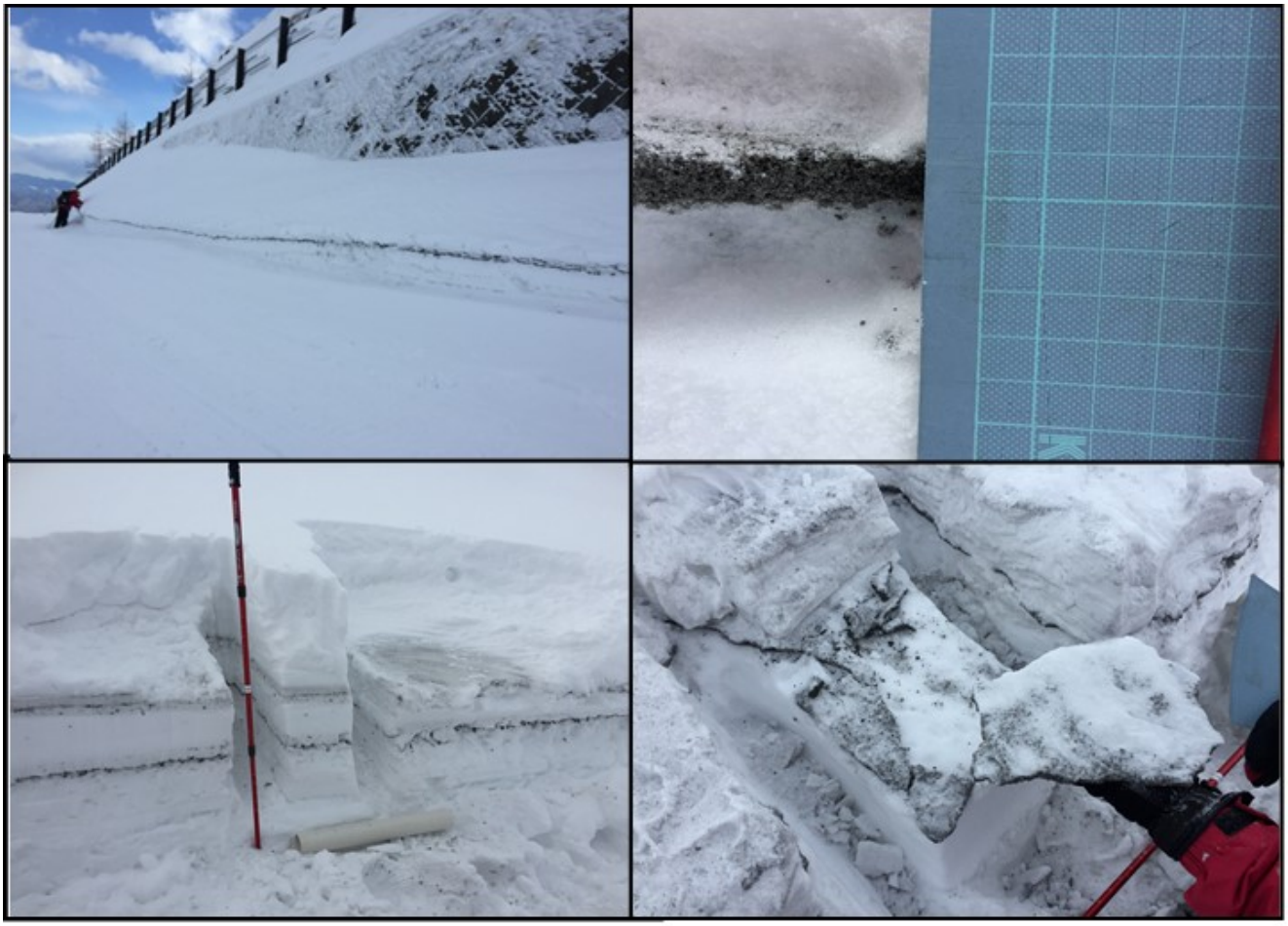
We conducted about 21 field surveys from May 2017 to March 2019. The survey site is about 45 sites, centering on rivers flowing in the east and south of the mountain. Temperature, water temperature, pH, RpH, EC, and flow rate were measured locally, and the sampled sample was analyzed for the main dissolved components. In February 2018, we investigated the deposition situation and ash fall volume of volcanic ash and conducted sampling, and carried out dissolution experiment. In addition to rivers, field surveys and sampling of lakes and precipitation, snow cover, hot spring water were conducted.

3. Results and discussion

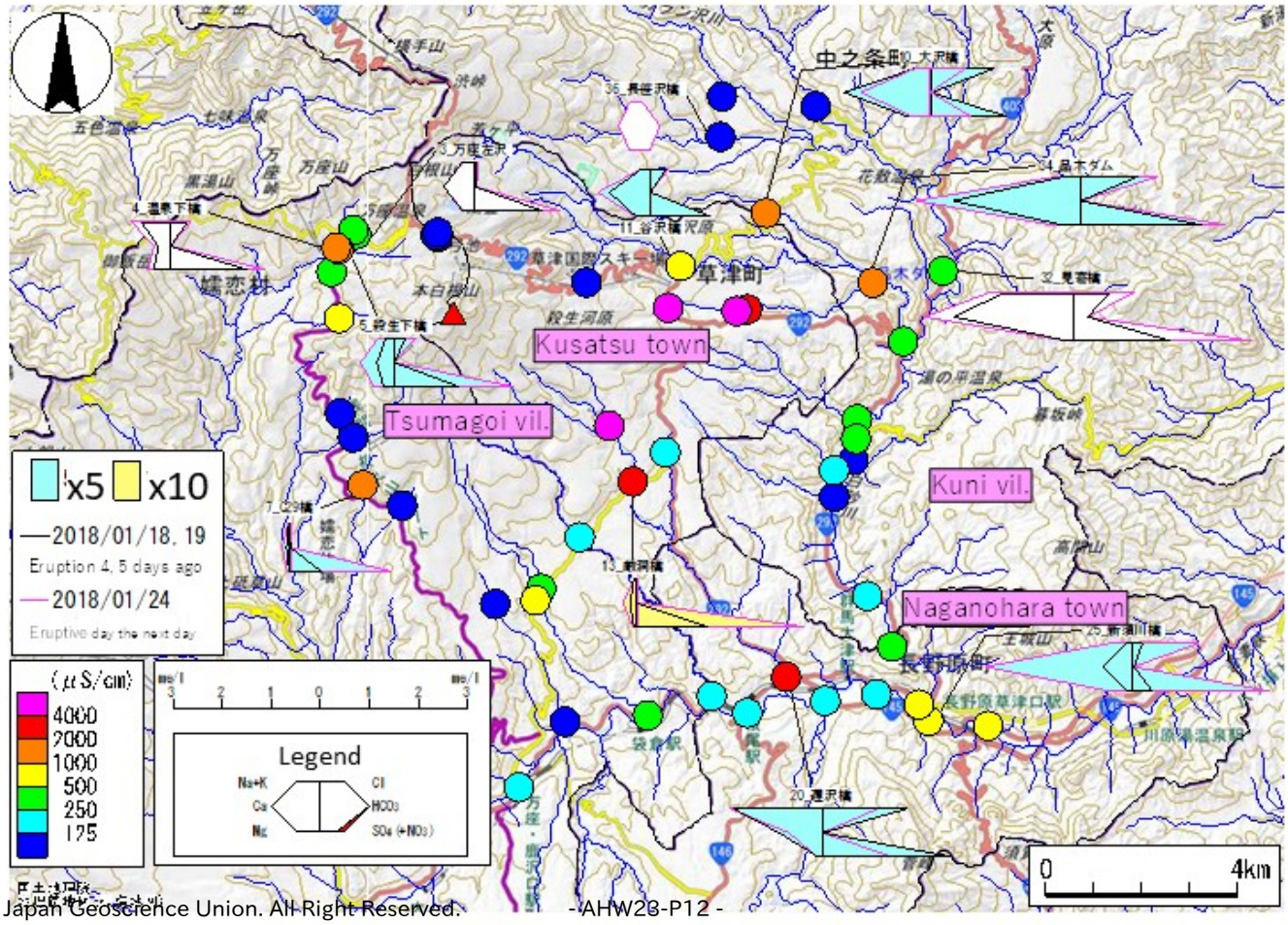
In Shirasuna River flowing to the east side of the mountain, groundwater and river water influenced by hot spring drainage and volcanic activity flow in from the tributary. There are points where the EC value fluctuates greatly, and it is influenced by the discharge and conduction of the dam which stores the neutralizing water of acidic rivers. In the Gando Swamp where the site of sulfur mine is located in the upstream part, the water quality is around pH:2.0, EC:6000 μS/cm. It is conceivable that the deposited volcanic ash affects the quality of the surrounding river due to snow melting water and precipitation.

Keywords: Mt.Kusatsu-Shirane, Volcano, Water environment, Eruption, Hot spring

©2019. Japan Geoscience Union. All Right Reserved.



Picture.1 Ash fall in the east foot of Kusatsu-Shirane volcano (February 6, 2018)



©2019. Japan Geoscience Union. All Right Reserved.

©2019. Japan Geoscience Union. All Right Reserved.

Re-consideration of discharge rate of spring water in Lake Ezu, Kumamoto

*Kimpei Ichiyanagi[1], Kiyoshi Ide[1], Jun Shimada[1], Tsutomu Ichikawa[2]

1. Kumamoto University, 2. Tokai University

In Kumamoto area, 100% of tap water is sourced from abundant groundwater. Recently, there is a great fear of groundwater level decreasing. To estimate discharge rete of spring water in Lake Ezu, the flow rate at 13 sites has been observed every month since December 1991. In previous studies, the total discharge rate of spring water was calculated by flow rates only at the most downstream, the most upper-stream, and incoming streams. In this study, total discharge rate from December 1991 to December 2014 was re-considered as a sum of three zones, that is upper-stream area, Kami-Ezu Lake, and Shimo-Ezu lake. When the discharge rate in each zone became negative, the case 1 where calculation was carried out with minus and the case 2 where it assumed to 0m^3/day were compared. As a result, total discharge rate gradually declined from about 450,000m^3/day in 1992 to about 360,000m^3/day (case 1) and to about 410,000m^3/day (case 2) in 2005. In July 2006, total discharge rate rapidly increased with heavy rainfall. After that, it had fluctuated about 400,000 to 500,000m^3/day in both cases. The discharge rate of Shimo-Ezu Lake sometimes became negative after 2003, and that averaged after July 2006 in case 2 was about 90,000m^3/day more than the case 1. As a result of comparing seasonal variability of discharge rate, monthly mean values of total and Shimo-Ezu Lake are low in April-May and high in October-November. However, monthly mean values of upper-stream area and Kami-Ezu Lake show no significant seasonal fluctuation. Monthly mean values of Shimo-Ezu Lake in August averaged after 2006 was about -14,000m^3/day in case 1 and about 32,000 m^3/day in case 2. Since negative value is not suitable to represent seasonal fluctuation, case 2 is proper to represent the discharge rate of spring water.

Keywords: spring water, Lake Ezu, long-term trend, seasonal variability

©2019. Japan Geoscience Union. All Right Reserved.

Evaluating the efficacy of hydrologically and hydrodynamically driven methods of e-flow assessment for Upper Godavari River Basin, India

*GAURAV KALIDAS PAKHALE[1], Jyoti Punjahari Nale[2], Ashvin Kumar Gosain[3], Rakesh Khosa[3]

1. PhD Research Scholar, Civil Engineering Department, Indian Institute of Technology, Delhi, 2. Project Advisor, IEWP, GIZ India, New Delhi, India, 3. Professor, Civil Engineering Department, Indian Institute of Technology, Delhi

In Peninsular India, pronounced seasonality in the precipitation and tropical semi-arid climate have compelled the tremendous development in the water resources sector. The major proportion of this fertile plateau falls in the rainshadow region of Western Ghats and is rightfully supported through enormous irrigation schemes which include the operation of several large reservoirs. These developments have resulted in alteration of various components of a natural hydrological regime like low as well as high flows. Environmental flows (e-flows), though acknowledged widely for their benefits, have not been attempted vigorously for peninsular river basins due to the prioritised issues related to water scarcity and disputes over water sharing. Also, many of these river streams have historically been known as non-perennial, thus further weakening the case of e-flows. Effectively, many recent e-flow assessments, have been observed to be elementary, quick and based on methods that are less intensive in terms of data and time requirements. In this view, the present study attempts to verify the efficiency of various hydrology and hydrodynamics-based e-flow assessment methods in one of such river basins, Upper Godavari River Basin. For this, hydrological observations of 16 sites with long term record availability (20 years or more) have been used and latest cross section data for these sites have been used for hydrodynamic computations.

Hydrological indices based on concepts like Percentage of Flow (POF) and Range of Variability Approach (RVA) have been estimated using a natural flow regime obtained from SWAT rainfall-runoff modelling. POF approaches like Tennant Method, Tessman Method, Variable Monthly Flow Methods are analysed while RVA approach has been analysed using Indicators of Hydrological Alteration (IHA) platform. These indices have been analysed for their feasibility and acceptability under the natural flow regime to understand the efficacy of these indices in providing optimum e-flow suggestions. Present observed flow regime has been juxtaposed with these indices to assess the present flow health in their comparison.

Hydrodynamic computations have been performed in HEC-RAS using 1-dimensional steady state conditions. Flow discharge versus flow depth, wetted perimeter, etc. relationships obtained for these study sites have been utilised to understand the critical flow levels which ensure the maximum bed inundations preferable for ecological sustainability. Wetted perimeter method of e-flow assessment has been evaluated for its suitability to provide the optimum e-flow suggestions. It has been found that hydrology based simple and quick methods of e-flow assessment fail the basic criteria of feasibility even under natural flow regime while hydrodynamic approach gives site-specific solutions which may not be relatable in longitudinal e-flow implementation.

Keywords: environmental flows, Range of Variability Approach, Wetted perimeter method

©2019. Japan Geoscience Union. All Right Reserved.

Presence of pharmaceutical compounds in freshwater lakes and their impact on phytoplankton

*Nandakumar Kanavillil[1], Cassandra Fligg[1], Sreekumari Kurissery[1]

1. Lakehead University, Canada

Historically, microalgae have been used as bio-indicators of aquatic health and this can be seen in several studies across the world. Often, at the bottom of the food chain microalgae constitute the primary producer of energy of many freshwater ecosystems. Diatoms, a group of microalgae, have been shown to exhibit extreme sensitivity to varying environmental parameters thereby making themselves an excellent candidate for studying the impacts of pollutants such as Pharmaceuticals and Personal Care Products (PPCPs). The contamination by PPCPs is common in our inland water bodies with a potential to get into our drinking water supply. This study explores the presence of PPCPs (Ibuprofen, 17-β Estradiol, and Triclosan) in the nearshore waters of Lake Simcoe, Ontario, Canada and their impacts on microalgal community. The study involved assessment of several environmental and algal parameters in the surrounding freshwater systems of three Waste Water Treatment Plants (WWTPs) that discharge their effluents *via* a creek/water channel to Lake Simcoe. Water samples were also drawn from a control location located away from the WWTPs. The results indicated that 1) PPCPs contamination is prevalent in the water outside of WWTPs (as far as the point of confluence with Lake Simcoe), and 2) The algal parameters varied according to the presence of PPCPs in the surface waters. Thus the study supported the growing concern of pharmaceutical contamination in the freshwater systems and its impacts on primary producers.

Keywords: Water quality, Bioindicators, Freshwater lakes, Pharmaceuticals, Phytoplankton

©2019. Japan Geoscience Union. All Right Reserved.

Novel approximate solutions for solute transport due to injections: considering the scale-dependent dispersion and non-integer flow dimension

*Ye-Chen Lin[1], Hund-Der Yeh[1]

1. National Chiao Tung Univ.

Prior research indicated that the flow dimension in a fractured medium may be of non-integer. In this article, we aim at developing a mathematical model for solute transport problems due to continuous or pulse injection in a non-integer dimensional flow field. The model allows the flow dimension ranging from linear flow to spherical flow. Our model also considers the effect of scale-dependent dispersion. The approximate solutions of the model are derived by applying the arrival times of mean and variance and validated through the comparison with finite-difference solutions of the present model. The results show that the approximate solutions give reasonable predictions when the value of dispersion or flow dimension is not large.

Keywords: solute transport, non-integer flow dimension, approximate solution, scale-dependent dispersion

©2019. Japan Geoscience Union. All Right Reserved.

Experimemtal study on the residual saturation of Porous Media using Pore Doublets Micromodel

*Chun-Wei Peng[1]

1. Taiwan National Chiao Tung University

In this study, we use a micromodel of PDM with different channel diameter ratios to study the fluid entrapment and mobilization. This study focuses on the evolution of the trapping and the amount of residuals saturation in the porous media. We observed the movement of wetting and non-wet liquids during the imbibition and drainage processes.We found that, with the low injection flow rates, the residual amount was strongly related to the contact angle; with the high injection flow rates, viscous force was dominated the trapping process. The results also showed that the liquids were trapped in the small tube for low injection rate, and in the large tube for the high injection rate. Our findings can help to control the residual saturation during water-flooding oil recovery, groundwater remediation, and the storage of carbon dioxide in deep subsurface.

©2019. Japan Geoscience Union. All Right Reserved.

Assessment of Synergy between Biomedical Waste and Shallow Groundwater Pollution

*Deepika -[1], Abhishek -[2]

1. BPS Government Medical College for Women, Sonepat, INDIA, 2. Technical University Dresden, GERMANY

Rapid urbanization and increasing population growth rate followed by the high rates of resource consumption patterns and increased waste generation have had an unintended negative impact on the prevailing environment. In a developing country like India where 50.34 % groundwater resources are not suitable for drinking as per WHO standards (United Nations, 2016), scrutinizing the open dumping of pathogenic biomedical waste becomes of paramount importance. Poor waste management practices pose a huge risk to the health of the public, patients, professionals and contribute to environmental degradation (land, air, and water pollution) if dumped untreated on the open ground. To assess this nexus, a prevalence study of the patients affected with waterborne diseases was conducted in a total of 35 hospitals comprising of government-, government-aided- and private hospitals of Ambala city. With a pronounced steppe climate, Ambala is located in North-Eastern (mean spatial coordinates: 30˚ 22' 41.4480" N and 76˚ 46' 36.1020" E) edge of Haryana, India. The city is drained by non-perennial streams and therefore the inhabitants depend solely on shallow groundwater resources for meeting their domestic water demand.

Data about the sources, quantity produced, treatment facilities, and awareness of biomedical waste, collected by questionnaire method based survey revealed that the mean waste generation was 8.08 kg/day with SD 5.371 kg/day. The biomedical waste consisted of approximately 1.2 % of the total municipal waste generated by the city and the patients affected with waterborne diseases were about 36 % of the total patients recorded. A latin hypercube Pareto distribution coupled with AMALGAM algorithm was employed for the initial sampling states of the proposals from the observed data (no. of patients). Thereafter, posterior estimates were generated using the Markov Chain Monte Carlo (MCMC) methods which showed a close fit with the observed and simulated data with RMSE 0.158. Furthermore, regression analysis with R^2=0.868 construed strong positive linear correlation between two variables viz. the number of patients and biomedical waste generated (and dumped). Recommendations are made for prioritizing the waste segregation and employing the indispensable management processes including waste treatment to avoid the further deterioration of the drinking water quality. The hospital authorities are advised to conduct the periodic seminars for enhancing awareness among the workforce from present 93.3 % to a maximum possible level.

Keywords: Groundwater, Biomedical waste, MCMC methods, Environmental awareness

©2019. Japan Geoscience Union. All Right Reserved.

Erosion and transport processes of earth surface materials in a reservoir-catchment system inferred from atmospheric radionuclides ^{7}Be and ^{210}Pb

*Mikiya Tsuruoka[1], Shinya Ochiai[2], Atsushi Matsuki[2], Seiya Nagao[2]

1. Graduate School of Natural Science and Technology, Kanazawa University, 2. Institute of Nature and Environmental Technology, Kanazawa University

Erosion and transport processes of earth surface materials are related to landform development in river catchment area and material discharge from the land area to the ocean. It is necessary to understand erosion and transport processes of earth surface materials to achieve proper management and prediction of river watershed and coastal area. However, since discharge behavior of earth surface materials in a large-scale river system is complicated by various processes, it is difficult to trace individual processes. On the other hand, earth surface materials eroded from catchment is transported and accumulated in reservoir. Therefore, discharge behavior of earth surface materials from catchment can be observed by monitoring of reservoir sediment. In this study, erosion and transport processes of earth surface materials in catchment were investigated based on atmospheric deposition flux to the catchment and sedimentation flux in the reservoir of ^{7}Be (half-life: 53 days) and ^{210}Pb (half-life: 22.3 years). From July 2016, rain water sample was collected every month with a collecting pan installed on the roof of Noto Atmospheric Observatory in Suzu City. ^{7}Be and ^{210}Pb in rain water were collected on ion exchange resins and measured with a Ge semiconductor detector to obtain atmospheric deposition fluxes. Sediment samples were collected with two sediment traps installed on the bottom of the reservoir (Shin-ike Reservoir) near the Noto Atmospheric Observatory at the same interval with rain sampling. Another trap was also set up in the middle layer (1.5 m above the bottom) since May 2018. Sediment samples were freeze-dried and measured with a Ge semiconductor detector to obtain sedimentation fluxes of ^{7}Be and ^{210}Pb. The atmospheric deposition fluxes of ^{7}Be and ^{210}Pb ranged 1.06-30.7 and 0.334-7.68 Bq/m^{2}/day, respectively. It shows clear seasonal fluctuation with high deposition in winter. The sedimentation fluxes of ^{7}Be in the bottom and middle layers were same level with the deposition flux. This result indicates that the contribution of ^{7}Be from the catchment is small. On the other hand, the sedimentation flux of ^{210}Pb in the middle layer was about 1.7-7.3 times higher than the atmospheric deposition flux of ^{210}Pb. This result suggests that sedimentation flux of ^{210}Pb in the middle layer reflects the contribution of ^{210}Pb from the catchment. The sedimentation flux of ^{210}Pb in the bottom layer was much higher than the atmospheric deposition flux, implying that sedimentation flux in the bottom was largely affected by resuspension in addition to the contribution of ^{210}Pb from the catchment. Residence time of these radionuclides in the reservoir-catchment system was estimated from the ^{7}Be/^{210}Pb$_{ex}$ ratios of rain water and sediment samples. The average residence times of the bottom layer samples and middle layer sample were estimated at 278 days and 141 days, respectively. This difference in the residence time may result from resuspension effect in the reservoir bottom.

Keywords: sediment, reservoir-catchment system, Be-7, Pb-210

©2019. Japan Geoscience Union. All Right Reserved.

Fluctuation of groundwater level in a sloping unconfined aquifer due to time varying recharge

*Ming-Chang Wu[1], Ping-Cheng Hsieh[1]

1. National Chung Hsing University

When a water-permeable slope is recharged by rainfall, the variation of the groundwater level is usually observed by setting up observation wells. However, the point observations are not sufficient to represent the vast domain of an aquifer and are constrained by the high cost of instrumentation and excavated wells. Therefore, the development of mathematical models for groundwater simulations can help us to understand the change of groundwater level more easily.
This study considers the variation of the groundwater level in a sloping aquifer with an impervious bottom. We divided the aquifer into two areas with and without rainfall recharge, and then use the nonlinear Boussinesq equation with a source term derived from the law of mass conservation. Analytical solutions to the nonlinear equation was acquired by the perturbation method for a finite region and a semi-infinite domain. After the transformation of variables, the general integral transformation method was used. The groundwater level varying with time under different factors (such as the dip angle of impervious bed, hydraulic conductivity, storage coefficient and different recharge rates) was discussed.
The present results were compared with the observed data from an observation well, and the difference in between was discussed. It is expected that the research results can better understand the physical mechanism of groundwater level change, and help to manage the groundwater.

Keywords: nonlinear Boussinesq equation, perturbation method, general integral transform method (GITM)

©2019. Japan Geoscience Union. All Right Reserved.

Effect of cutoff wall on recharge water storage volume

*Pei-hsun Tsai[1], Jung-hsing Tai[1]

1. Chaoyang University of Technology

Artificial groundwater recharge is used to increase groundwater in areas with water scarcity. Understanding the hydromechanical features of aquifers during groundwater withdrawal and recharge is necessary for managing groundwater resources effectively. In practice, an artificial pool can be used to collect surface runoff so that it infiltrates the aquifer and recharges groundwater. A cutoff wall can be constructed to seal recharge water and prevent it from flowing from the recharge area. Additional studies are required to understand the effect of the various parameters of cutoff walls on groundwater recharge. This study used the finite difference software FLAC 8.0 to examine the influence of the location and size of gaps of a cutoff wall on recharge water storage volume. Each aquifer was in an unsaturated state before groundwater recharging; therefore, groundwater recharge analyses were simulated by the two-phase flow in unsaturated porous media. The results revealed that when the groundwater layer was sand and the cutoff wall was not extended into the fully impermeable layer, the recharge water completely flowed from the gap between the bottom of the cutoff wall and the fully impermeable layer after stopping groundwater recharge. The recharge water volume related to the size of the gap at the bottom of the cutoff wall. When the cutoff wall was not extended into the groundwater layer, the cutoff wall did not intercept water. The gap at the top of the cutoff wall retained more recharge water compared with the gap at the bottom of the cutoff wall.

Keywords: Groundwater recharge, Cutoff wall, Water storage volume

©2019. Japan Geoscience Union. All Right Reserved.

Studying Operation Parameters on Flat-Plate Membrane Bioreactor for Sewage Treatment

*Jen Hung Chiu[1], Wen Chin Chen[1]

1. Studying Operation Parameters on Flat-Plate Membrane Bioreactor for Sewage Treatment

The flat-plate membrane bioreactor is applied to the domestic sewage treatment, which has a high quality of effluent than the traditional activated sludge process, and decreasing the susceptible of hair entanglement with the hollow fiber membrane. It has become a priority for recent sewage treatment applications.

A flat-plate membrane bioreactor pilot plant with a reaction volume of 4 m^3 was installed in the existing sewage treatment plant. In this research, the parallel treatment of the same influent water quality and hydraulic retention time was carried out to compare the treatment efficiency between the MBR and traditional activated sludge process, and the operational effects of the membrane flux were discussed.

With one year of long-term research, the average removal efficiencies of MBR process, regardless of the COD, SS and E.coli were over 99%, wchih was better than the activated sludge process only 90~95%. Meanwhile, the optimal operation mode of the MBR was obtained in the study. The aeration flow rate in the system was adjusted to 10~13 NL/min per film, the effluent flux was controlled under 50% of the maximum recommended flux of membrane with 9-minute operation and 1 minute stop in a cycle, there is no significant change in operating flux and pressure. These operational mode of MBR can extend the life time of membrane and effectively improve the application of flat-plate MBR to domestic sewage treatment.It is suggested that, in view of water treatment and resource sustainability, the flat plate MBR technology is feasible, and can serve as a green guide to the sewage treatment.

Keywords: Membrane Bioreactor, Flat-Plate Membrane, Sewage

©2019. Japan Geoscience Union. All Right Reserved.

Mine-water quality at a tertiary coalfield in India: Characterisation and treatment using novel polyvinyl alcohol (PVA) gel bioreactor

*Aparna Dutta[1], Sudipta Sarkar[1]

1. Indian Institute of Technology Roorkee

Nearly 78 percent of the total measured (proved) tertiary coal reserves of India is concentrated in the north-eastern state of Assam. The Tertiary coal of North–Eastern Coalfields (NEC) has been found to contain as high as 8% sulphur with varying percentage of pyrite, sulfate, organic and free sulphur. The pyrites are often associated with toxic heavy metals. Acid mine drainage (AMD) is generated when mining activities expose the pyrite and sulfides to atmospheric oxygen, moisture and micro-organisms that catalyse the oxidation process to release large amounts of sulfate into the mine water along with protons and dissolved metals. Microbial dissimilatory sulfate reduction (DSR) in the presence of a suitable organic carbon source can be engineered to treat such water. This study is significant because this region is rich in biodiversity and such mining impacted water may have adverse ecological impact, if discharged without appropriate treatment.The objective of the work is to characterise water samples collected from two open cast mines of Makum coalfield under NEC and evaluate the performance of a novel polyvinyl alcohol (PVA) gel packed bed bioreactor to treat the same. Sample collection, storage and physico-chemical analysis are carried out as per Standard methods of American Public Health Association. The biological treatment process is studied in a cylindrical continuous flow lab scale bioreactor under relevant acidic pH at different feed chemical oxygen demand (COD) to sulfate ratio and hydraulic retention time (HRT). Sludge from a lab scale anaerobic bioreactor treating very high sulfate industrial water is used as inoculum. The sulfate reducing microorganisms are enriched within the bioreactor in fed-batch mode using modified Postgate’ s medium for one month.Oxidation Reduction Potential (ORP), pH, sulfate removal, total inorganic carbon (TIC) and alkalinity produced are measured at the bioreactor outlet to evaluate the process performance. The mine water samples exhibit low pH, high sulfate, conductivity, dissolved solids, hardness, iron and manganese, which indicates the occurrence of AMD. The treatment process reduces the sulfate concentration and increases pH of the treated water. The use of highly porous PVA gel beads as packing material in the bioreactor treating sulfate rich acidic water imparts resilience to operational variation. The study evaluates the novel application of PVA gel beads to bioreactor for treating acidic mine waters from an ecologically important region. The research finding provides an understanding of the process for application to other biological AMD treatment configurations.

Keywords: acid mine drainage (AMD), polyvinyl alcohol (PVA), sulfate, sulfate reducing microorganism (SRM), dissimilatory sulfate reduction(DSR), pyrite

©2019. Japan Geoscience Union. All Right Reserved.

[E] Poster | A (Atmospheric and Hydrospheric Sciences)：A-HW Hydrology & Water Environment

Wed. May 29, 2019 5:15 PM - 6:30 PM JST | Wed. May 29, 2019 8:15 AM - 9:30 AM UTC | Poster Hall International Exhibition Hall8, Makuhari Messe_14

[A-HW23] Hydrology & Water Environment

convener:Isao Machida(Geological Survey of Japan), Dai Yamazaki(Institute of Industrial Sciences, The University of Tokyo), Takeshi Hayashi(Faculty of Education and Human Studies, Akita University), Keisuke Fukushi(Institute of Nature & Environmental Technology, Kanazawa University)

We focus on various issues of water cycle and environment and aim to answer questions of hydrological and earth system sciences including 1) surface, subsurface and evapotranspiration processes of water cycle; 2) natural and anthropogenic hydrothermal systems, 3) environments issues and studies on a watershed or global scale, 4) water-related issues with ecological, environmental, and geochemical aspects, and 5) other issues in hydrological sciences. This session welcomes presentations regarding various kinds of approaches and techniques such as field survey, remote sensing, isotope tracers, numerical simulation, and theoretical analysis.

[AHW23-P01] A multiobjective risk management model for real-time reservoir flood control operation

*Juan Chen[1,2], Ping-An Zhong[2], XinYu Wan[2], Yu Zhang[2] (1.College of Earth Sciences and Engineering, Hohai University, 2.College of Hydrology and Water Resources, Hohai University)

[AHW23-P02] Assessment of the Flow Regime of Roanoke River due to Climatic and Anthropogenic Activities

*Rahul Kumar Singh[1], Dr. Manoj Kumar Jain[1] (1.Indian Institute of Technology, Roorkee, India)

[AHW23-P03] Predictive Analysis of Climate, Water, Health and the Environment Nexus

*Abhishek [1], Deepika [2] (1.Technical University Dresden, GERMANY, 2.BPS Government Medical College for Women, Sonepat, INDIA)

[AHW23-P05] Severe droughts provide huge fuel for widespread wildfires in California in USA

*Linghua Qiu[1], Ji Chen[1], Haiyun Shi[2], Liqun Sun[3], Jun Niu[4] (1.the University of Hong Kong, 2.Southern University of Science and Technology, 3.Shenzhen Institutes of Advanced Technology, Chinese Academy of Sciences, 4.China Agricultural University)

[AHW23-P06] A comprehensive evaluation of MODIS-based water use efficiency with global eddy covariance flux data and a process model

*Shanshan YANG[1,2], Jiahua ZHANG[1], Sha ZHANG[1,2], Jingwen WANG[1,2], Yun BAI[1,2], Fengmei YAO[2], Huadong GUO[1] (1.Institute of Remote Sensing and Digital Earth, Chinese Academy of Sciences, 2.University of Chinese Academy of Sciences, Beijing, China)

[AHW23-P07] Impact of variability and anisotropy in the correlation decay distance for precipitation spatial interpolation in China

*yingxian zhang[1] (1.National Climate Center, China Meteorological Administration)

[AHW23-P08] New Record-Breaking Frequency of Annual Maximum Daily Precipitation of 58 stations in the whole Japan, an increasing of extreme values.

*Chhay Ngorn SEANG[1], Tomohito YAMADA[1] (1.Hokkaido University)

[AHW23-P09] Quantifying stemflow to better express its ecohydrological significance

*Shin'ichi Iida[1], Darryl E. Carlye-Moses[2], Sonja Germer[3], Pilar Llorens[4], Beate Michalzik[5], Kazuki Nanko[1], Alexander Tischer[5], Delphis F. Levia[6] (1.Department of Disaster Prevention, Meteorology and Hydrology, Forestry and Forest Products Research Institute, 2.Department of Geography and Environmental Studies, Thompson Rivers University, Kamloops, British Columbia, Canada, 3.Department of Bioengineering,

Leibniz Institute for Agricultural Engineering and Bioeconomy, Potsdam, Germany, 4.Institute of Environmental Assessment and Water Research (IDAEA-CSIC), Barcelona, Spain, 5.Soil Science, Institute of Geography, Friedrich Schiller University Jena, Jena, Germany, 6.Department of Geography and Department of Plant and Soil Sciences, University of Delaware, Newark, DE, USA)

[AHW23-P10] **Hydraulic analysis of overland flow caused by temporally varying rainfall**

*PING-CHENG HSIEH[1], Ming-Chang Wu[1] (1.National Chung Hsing University)

[AHW23-P11] A comparative Study on Water Environment of Isolated Islands - Focusing on Islands in Nagasaki Prefecture - (3)

*Go Yamaki[1], Koji Kodera[2], Kazuki Asami[1], Yoshihiro IGARI[1], Masaki Horiuchi[1] (1.Grad. Student, Hosei Univ., 2.Dep. of Geography, Hosei Univ.)

[AHW23-P12] **Water environment around Kusatsu-Shirane volcano and consideration of the effect of eruption in January 2018**

*Igari Yoshihiro[1], Koji Kodera[2], Kazuki Asami[1] (1.Grad.Student,Hosei Univ., 2.Dep.of Geography Hosei Univ.)

[AHW23-P13] Re-consideration of discharge rate of spring water in Lake Ezu, Kumamoto

*Kimpei Ichiyanagi[1], Kiyoshi Ide[1], Jun Shimada[1], Tsutomu Ichikawa[2] (1.Kumamoto University, 2.Tokai University)

[AHW23-P14] **Evaluating the efficacy of hydrologically and hydrodynamically driven methods of e-flow assessment for Upper Godavari River Basin, India**

*GAURAV KALIDAS PAKHALE[1], Jyoti Punjahari Nale[2], Ashvin Kumar Gosain[3], Rakesh Khosa[3] (1.PhD Research Scholar, Civil Engineering Department, Indian Institute of Technology, Delhi, 2.Project Advisor, IEWP, GIZ India, New Delhi, India, 3.Professor, Civil Engineering Department, Indian Institute of Technology, Delhi)

[AHW23-P15] Presence of pharmaceutical compounds in freshwater lakes and their impact on phytoplankton

*Nandakumar Kanavillil[1], Cassandra Fligg[1], Sreekumari Kurissery[1] (1.Lakehead University, Canada)

[AHW23-P16] **Novel approximate solutions for solute transport due to injections: considering the scale-dependent dispersion and non-integer flow dimension**

*Ye-Chen Lin[1], Hund-Der Yeh[1] (1.National Chiao Tung Univ.)

[AHW23-P17] Experimemtal study on the residual saturation of Porous Media using Pore Doublets Micromodel

*Chun-Wei Peng[1] (1.Taiwan National Chiao Tung University)

[AHW23-P18] Assessment of Synergy between Biomedical Waste and Shallow Groundwater Pollution

*Deepika [1], Abhishek [2] (1.BPS Government Medical College for Women, Sonepat, INDIA, 2.Technical University Dresden, GERMANY)

[AHW23-P19] Erosion and transport processes of earth surface materials in a reservoir-catchment system inferred from atmospheric radionuclides ^{7}Be and ^{210}Pb

*Mikiya Tsuruoka[1], Shinya Ochiai[2], Atsushi Matsuki[2], Seiya Nagao[2] (1.Graduate School of Natural Science and Technology, Kanazawa University, 2.Institute of Nature and Environmental Technology, Kanazawa University)

[AHW23-P20] Fluctuation of groundwater level in a sloping unconfined aquifer due to time varying recharge

*Ming-Chang Wu[1], Ping-Cheng Hsieh[1] (1.National Chung Hsing University)

[AHW23-P21] **Effect of cutoff wall on recharge water storage volume**

*Pei-hsun Tsai[1], Jung-hsing Tai[1] (1.Chaoyang University of Technology)

[AHW23-P22] **Studying Operation Parameters on Flat-Plate Membrane Bioreactor for Sewage Treatment**

*Jen Hung Chiu[1], Wen Chin Chen[1] (1.Studying Operation Parameters on Flat-Plate Membrane Bioreactor for Sewage Treatment)

[AHW23-P23] **Mine-water quality at a tertiary coalfield in India: Characterisation and treatment using novel polyvinyl alcohol (PVA) gel bioreactor**

*Aparna Dutta[1], Sudipta Sarkar[1] (1.Indian Institute of Technology Roorkee)

A multiobjective risk management model for real-time reservoir flood control operation

*Juan Chen[1,2], Ping-An Zhong[2], XinYu Wan[2], Yu Zhang[2]

1. College of Earth Sciences and Engineering, Hohai University, 2. College of Hydrology and Water Resources, Hohai University

Many uncertainties exit in the real-time reservoir flood control operation and bring risks to flood control decisions. A multiobjective optimization model is developed for the real-time risk management for the flood control operation of a reservoir system considering multiple uncertainties such as inflow forecast errors and outflow errors. The two competing objectives considered are: (1) minimizing the risk of reservoir upstream flooding and (2) minimizing the risk of downstream flooding. The optimization model seeks to find the operation schedules that satisfy the flood control objectives and simultaneously minimize the overall risks. The decision variables are the hourly reservoir releases. The formulated multiobjective optimization problem is nonlinear and non-convex, and is solved with an improved Non-dominated Sorting Genetic Algorithm-II (INSGA-II). We use a filtering algorithm to select representative non-dominated solutions from the Pareto front generated by INSGA-II to assist in real-time decision making. The proposed risk management model is applied to the Foziling reservoir in Huaihe river basin of China. The results show that the proposed method can provide a practical way to optimize the real-time flood control operation for risk management of a reservoir.

Keywords: Flood, Reservoir, Flood control operation, Risk assessment, Multiobjective optimization

©2019. Japan Geoscience Union. All Right Reserved.

Assessment of the Flow Regime of Roanoke River due to Climatic and Anthropogenic Activities

*Rahul Kumar Singh[1], Dr. Manoj Kumar Jain[1]

1. Indian Institute of Technology, Roorkee, India

The natural flow regime of many rivers around the world has been significantly altered due to climatic and anthropogenic modifications such as the construction of dams and reservoirs. The natural flow regime plays an important role in the development of the riverine ecosystem. Therefore, quantification of the extent of the alterations in the natural flow regime would be helpful in the river’ s ecological assessment. The Roanoke River in southeastern United States had one of the biggest and least disturbed forest ecosystems but due to climatic changes and anthropogenic actions such as construction of dam, artificial regulations of the natural flow regime, the overall riverine ecosystem has severely impacted. In this study, SWAT (Soil Water Assessment Tool) has been used to reconstruct the long-term unaltered streamflow for a hypothetical no-dam scenario condition, in order to assess the impact of climate change as well as due to construction of the John H Kerr reservoir on Roanoke River streamflow from 1956-2012. In order to simulate the unaltered streamflow series post construction of John H Kerr reservoir, 32 years (1916-1948) of observed gauge inflow prior to anthropogenic disturbance (due to construction of John H Kerr Reservoir) was used for calibration and validation of the parameters of the SWAT model. Historical land use and land cover backcasting data for the year 1938 has been used in the hydrological model to simulate the flow regime prior to construction of the dam and it was kept same during the whole simulation period. The SWAT model simulated observed gauge data with Nash-Sutcliffe efficiency coefficient (NSE) = 0.70, Percent bias (PBIAS) = 0.00 and the determination coefficient (R^2) = 0.73 during the calibration period (1916 - 1936), and performed equally better during the validation period (1937-1948) with NSE = 0.72, PBIAS = 0.00 and R^2 = 0.74. The indicators of hydrologic alteration (IHA) methodology has been used to assess the natural flow regime (no dam or reservoir moderated flow regime) characteristics under a simulated no-reservoir scenario (scenario1) and compare with the IHA results obtained based on the gauged streamflow downstream of the dam (scenario2). Hence, in case of scenario 1, the post-impact period has been taken as the simulated flow series using SWAT model from 1956-2012 and in case of scenario 2 the post-impact period has been taken as the gauged observed streamflow from 1956-2012 at Roanoke Rapids gauging station downstream of the reservoir. The pre-impact period for both the scenario was kept the same i.e. from 1912 to 1949. The results reveal that in case of the IHA assessment based on scenario 1, significant alterations have been observed in 5 out of 32 indicators compared to 13 out 32 indicators in case of scenario 2. The overall hydrologic alteration in case of scenario 1 was 45.65% and it was 55.17% in the case of scenario 2. The alteration during the scenario 1 could be attributed to the overall natural climatic variability. The results also indicate that flow variability in terms of high and low flows were better in scenario 1 compared to scenario 2 where the high flows were completely absorbed including the low pulse count and duration due to regulation in the flow. However, the reservoir operations enhanced the monthly flows including the multiday minima low flows. Thus, the present method can be treated as an easy-to-implement comprehensive approach for designing natural flow regimes to mimic the pre-impact flow condition in order to restore the ecosystem of modified rivers due to anthropogenic interventions.

Keywords: SWAT, IHA, Streamflow, Hydrologic Alteration, Ecosystem

©2019. Japan Geoscience Union. All Right Reserved.

Predictive Analysis of Climate, Water, Health and the Environment Nexus

*Abhishek -[1], Deepika -[2]

1. Technical University Dresden, GERMANY, 2. BPS Government Medical College for Women, Sonepat, INDIA

Amid the major demographic transition of developing world from a rural, agrarian society to an urban, industrial one, there is a need for predictive analytics of impact of the major biotic and abiotic stressors on the environmental constituents. The current study emphasizes the connections between climate, water, environment, and health and their interdependency followed by an impact assessment focusing on an urban environment. A data-driven hybrid framework for water resources assessment and management based on machine learning techniques was developed, calibrated and validated with the ground data for the sub-region scale of North-East Indian regime (mean spatial coordinates: 28° 38' 41.2800" N and 77° 13' 0.1956" E). The remote sensing data for land cover and land change were coupled with the climate model simulations to formulate the health risk assessment framework. The large ensemble of downscaled scenario based outputs including the effects of anthropogenic factors was used to drive the hybrid model framework.

Multi-dimensional Random Walk Metropolis (RWM) algorithms used to optimize the sample observations converged with an RMSE error of 0.18 with a range of 0.006. Pearson Product Moment Correlation coefficient range of all the ensemble members was 0.886-0.904. The prediction accuracy construed from 95 % model uncertainty bounds was 89-91 % for the constituent parameters. The sensitivity analysis revealed that the climate is the key parameter and is the most sensitive for all other linkage units followed by water availability and health factors. Comparative analysis of the simulated- and experimental results enforced comprehensive clarification of the assumptions made therein. By real-time monitoring and forecasting the vital impacts, this research will serve and benefit local policymakers and in the decision-making process, particularly regarding water resources vulnerability and future availability with significant economic consequences. The upscaling of the model form sub-regional to regional scale is well underway.

Keywords: Climate Change, Urbanization, RWM algorithm, Ensemble model

©2019. Japan Geoscience Union. All Right Reserved.

Severe droughts provide huge fuel for widespread wildfires in California in USA

*Linghua Qiu[1], Ji Chen[1], Haiyun Shi[2], Liqun Sun[3], Jun Niu[4]

1. the University of Hong Kong, 2. Southern University of Science and Technology, 3. Shenzhen Institutes of Advanced Technology, Chinese Academy of Sciences, 4. China Agricultural University

The frequently occurred large wildfires in California caught the public’ s attention in recent years and the ability to identify and prevent such disasters is pressing. The study built the rational relationship between soil moisture and vegetation based on remote sensing, hydrology and wildfire data during 2001-2017 in California. The purpose is to estimate the effects of droughts on wildfires and to detect the valid fuel for wildfires. The study results reported that severe droughts could cause huge fuel for wildfires and made them even much more widespread and longer sustained. The consequences could provide significant information for identification and prevention of future wildfires in California and even other regions in the world.

Keywords: Fuel, Wildfires, Droughts, Soil moisture, Vegetation

©2019. Japan Geoscience Union. All Right Reserved.

A comprehensive evaluation of MODIS-based water use efficiency with global eddy covariance flux data and a process model

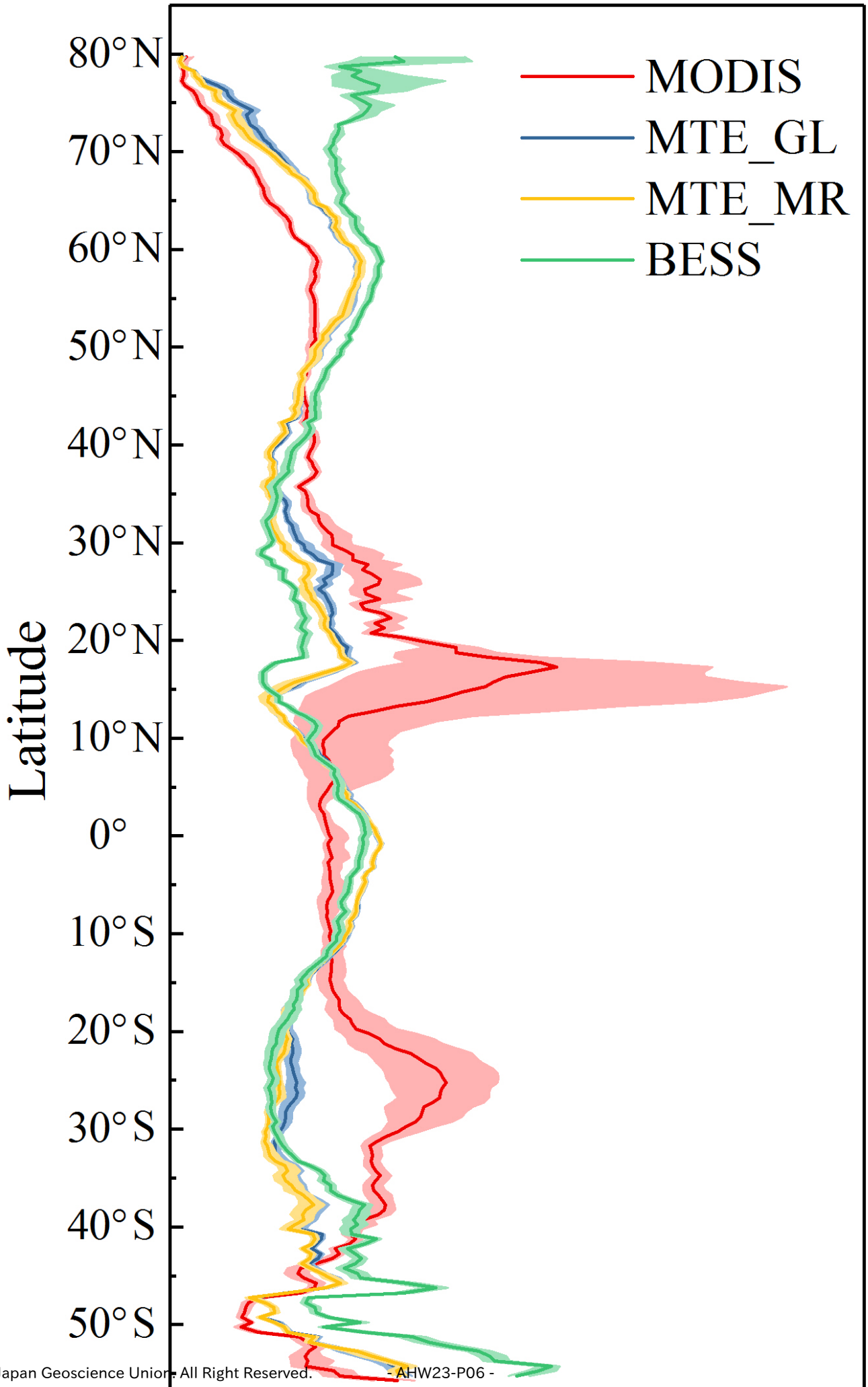
*Shanshan YANG[1,2], Jiahua ZHANG[1], Sha ZHANG[1,2], Jingwen WANG[1,2], Yun BAI[1,2], Fengmei YAO[2], Huadong GUO[1]

1. Institute of Remote Sensing and Digital Earth, Chinese Academy of Sciences, 2. University of Chinese Academy of Sciences, Beijing, China

Ecosystem water use efficiency (WUE), defined as the ratio of gross primary productivity (GPP) to evapotranspiration (ET), is an important indicator to investigate the interaction between the terrestrial carbon and water cycles. The spatiotemporal patterns of WUE inferred from MODIS GPP and ET products and its responses to environmental factors have been analyzed, however, the accuracy of MODIS-derived WUE (MODIS WUE) has not been well evaluated. In this study, we evaluated monthly and annual MODIS WUE using global covariance flux data (FLUXNET2015 dataset) during 2000-2014, and conducted global intercomparisons (2001-2011) among annual WUE from MODIS, gridded FLUXNET (MTE) and a process model (BESS). Site scale (53 sites) evaluation results revealed that MODIS gave reliable estimates for GPP and ET, however, the performances of MODIS WUE was poor for monthly WUE (R2=0.14) and even worse for annual WUE (R2=0.08). MODIS WUE was generally underestimated with a bias of -0.21 gC kg-1 H2O (-8.43%) and RMSE of 1.20 gC kg-1 H2O for monthly WUE, and a bias of -0.28 gC kg-1 H2O (-11.31%) and RMSE of 0.98 gC kg-1 H2O for annual WUE. Among all land cover types, MODIS WUE performed relatively better in savannas and woody savannas for monthly WUE and grasslands for annual WUE, but significantly overestimated WUE in open shrublands. Likewise, MODIS WUE was obviously overestimated in hot and cold semiarid and arid climate zones. The global intercomparison results demonstrated that the spatial pattern of MODIS WUE was broadly similar to that of MTE and BESS WUE, except for the tropical and subtropical arid and semiarid areas. In these regions MODIS WUE showed extremely high values with large uncertainty and different linear trends compared with MTE and BESS WUE. These disagreements were mainly caused by the discrepancies in MODIS ET. Therefore, the uncertainty of MODIS WUE in the tropical arid and semiarid areas should be taken with caution when using MODIS WUE to investigate and interpret how WUE varies spatially and its responses to climate change. Furthermore, the accuracy of MODIS GPP and ET datasets should be paid extra attention since the quality of both GPP and ET would directly affect the WUE accuracy.

Keywords: Water use efficiency (WUE), Evaluation, Intercomparison, MODIS, FLUXNET, BESS

©2019. Japan Geoscience Union. All Right Reserved.



©2019. Japan Geoscience Union. All Right Reserved.

©2019. Japan Geoscience Union. All Right Reserved.

Impact of variability and anisotropy in the correlation decay distance for precipitation spatial interpolation in China

*yingxian zhang[1]

1. National Climate Center, China Meteorological Administration

The correlation decay distance (CDD) plays a key role in the angular-distance weighting (ADW) interpolation technique, being used as the searching radius to select correlated neighbors and to calculate the relative weights. The CDD of daily precipitation in China varies spatially and seasonally, and it presents anisotropic behavior, as a result of topography and the predominant atmospheric circulation. In general, CDD is largest in winter and smallest in summer, except for limited regions such as the Tibetan plateau. From a cross validation analysis, it is found that taking account of spatial and seasonal variations in CDD generally improves the ADW interpolation. Utilization of anisotropic CDDs increases the interpolation skill scores in regions with a dense monitoring network, significant elevation variation (southwestern China) or strongly anisotropic CDDs (Tibetan plateau).

Keywords: daily precipitation, correlation decay distance, ADW interpolation

©2019. Japan Geoscience Union. All Right Reserved.

New Record-Breaking Frequency of Annual Maximum Daily Precipitation of 58 stations in the whole Japan, an increasing of extreme values.

*Chhay Ngorn SEANG[1], Tomohito YAMADA[1]

1. Hokkaido University

The changes in daily temperature extremes in global scale have affected the weather and climate extreme events when there is an increase of greenhouse gas GHG compare to the industrialization in the 19th century (IPCC, 2014). Yamada et al. (2014) illustrate that the water vapor and convective instability follow the Clausius-Clapeyron-like rate of change with 99th percentile hourly precipitation intensity. Lehmann, J. et al. (2015), on another hand, studied globally the characteristic of precipitation change anomaly using a relation of the Clausius-Clapeyron model. By the way, the climate change tends to include another factor, which is more statistical base. The theory of record values in independent and identically distributed (i.i.d) random variable is studied more extensively and is more applicable with an assumption of stationary climate. The Clausius-Clapeyron equation is then also applicable base on the thermodynamic term which illustrates the relation of the temperature, vapor pressure and precipitation formation characteristic which also mentioned in the above previous studies. At the first stage, 58 stations of AMeDAS data with 117-years period across Japan are used for this analysis. The result shows that mean long-term precipitation of these 58 stations is higher than the mean value from theory i.i.d random variable of stationary climate. From this result, it can be implied that the change of precipitation in Japan is influenced by the drift term either of climate change or the heat island. In this case, the Clausius-Clapeyron equation is applied to identify the temperature term of change. This study tries to formulate a theory which more statistical base of climate drifts, non-stationary and non-identically to extreme events in accordance with time series. Clausius-Clapeyron Model and the Linear Drift Model is considered to form an empirical stochastically based on climate trend.

Keywords: Clausius-Clapeyron, New record Breaking, i.i.d

©2019. Japan Geoscience Union. All Right Reserved.

Quantifying stemflow to better express its ecohydrological significance

*Shin'ichi Iida[1], Darryl E. Carlye-Moses[2], Sonja Germer[3], Pilar Llorens[4], Beate Michalzik[5], Kazuki Nanko[1], Alexander Tischer[5], Delphis F. Levia[6]

1. Department of Disaster Prevention, Meteorology and Hydrology, Forestry and Forest Products Research Institute, 2. Department of Geography and Environmental Studies, Thompson Rivers University, Kamloops, British Columbia, Canada, 3. Department of Bioengineering, Leibniz Institute for Agricultural Engineering and Bioeconomy, Potsdam, Germany, 4. Institute of Environmental Assessment and Water Research (IDAEA-CSIC), Barcelona, Spain, 5. Soil Science, Institute of Geography, Friedrich Schiller University Jena, Jena, Germany, 6. Department of Geography and Department of Plant and Soil Sciences, University of Delaware, Newark, DE, USA

Stemflow is the flow of rainwater over the exterior of a tree stem to its base. Due to water balance calculations to obtain interception loss of forest stands, and the sometimes low percentage of stemflow as a function of rainfall, some literature ignores the ecohydrological significance of stemflow. However, stemflow is much more concentrated than throughfall per unit area. In recognition of the extreme amounts of water input to the small area around tree trunks, we advocate for two metrics to better express stemflow in relation to its ecohydrological importance: namely, the stand-scale funneling ratio and the stand-scale infiltration funneling ratio. We calculated these metrics based on measurements carried out in a tropical dry deciduous forest and a subpolar juvenile coniferous stand, and found that these are significantly larger than throughfall on both sites. The data cited from recent papers (n=34) showed that very small stand-scale amount of stemflow (approximately 0.5% on average) were necessary to make the stand-scale funneling ratio to be equal or more than unity. Moreover, the infiltration area of stemflow is generally < 0.2 m^2 due to the high infiltration capacity of top soil of forests, generally resulting in the stand-scale infiltration funneling ratio substantially greater than unity. Thus, stemflow is more effective for soil water recharge than throughfall. We recommend use of these metrics to better express ecohydrological importance of stemflow.

This presentation is based on the published paper as follows:
Carlye-Moses, D.E., Iida, S., Germer, S., Llorens, P., Michalzik, B., Nanko, K., Tischer, A., Levia, D.F. (2018): Expressing stemflow commensurate with its ecohydrological importance. Advances in Water Resources, 121, 472-479. Free open access article to: https://doi.org/10.1016/j.advwatres.2018.08.015

Keywords: Stemflow, Funneling ratio, Forest hydrology

©2019. Japan Geoscience Union. All Right Reserved.

Hydraulic analysis of overland flow caused by temporally varying rainfall

*PING-CHENG HSIEH[1], Ming-Chang Wu[1]

1. National Chung Hsing University

With the development of human civilization and population migration, we use many different types of pervious or impervious materials to cover the original surface. As a result, the surface friction and water permeability are reduced, resulting in increased flow velocity and runoff, and thus increasing the frequency and scale of flood occurrence. Therefore, predicting changes in overland flow caused by rainfall has become an important issue.

This study intends to simulate the overland flow under different rainfall patterns by the theory of diffusion wave model. The diffusion wave equation was used as the governing equation, and an analytical solution of the water depth by the generalized integral transformation method was presented. Since the values of the parameters used in previous research for diffusion wave models vary in an extensive range. In this study, the parameters were adjusted for each location to ensure the rationality of the simulation results according to the law of mass conservation.
The results show that for the non-uniform rainfall, the peak water depth and peak flow due to the post-peak rainfall are the largest, followed by the third quarter peak rainfall; whereas the average flow velocity of the mid-peak rainfall is the largest, followed by the third quarter peak rainfall. The peak water depth, peak flow rate and average flow rate due to the double peak rainfall are the smallest among the six rainfall patterns in this study.

Keywords: overland flow, nonuniform rainfall, diffusion wave

©2019. Japan Geoscience Union. All Right Reserved.

A comparative Study on Water Environment of Isolated Islands - Focusing on Islands in Nagasaki Prefecture - (3)

*Go Yamaki[1], Koji Kodera[2], Kazuki Asami[1], Yoshihiro IGARI[1], Masaki Horiuchi[1]

1. Grad. Student, Hosei Univ., 2. Dep. of Geography, Hosei Univ.

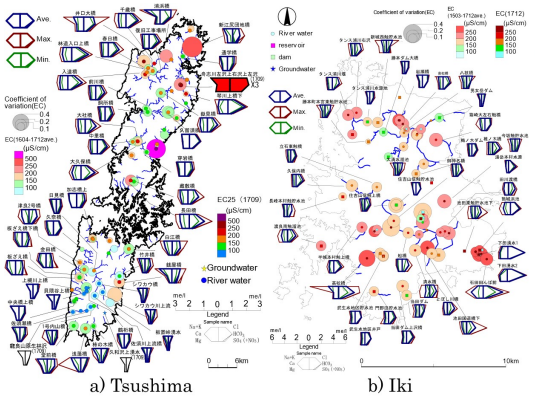
1. Introduction Research on islands in Nagasaki prefecture has hardly been investigated and research has been promoted since 2014 from Goto Island Islands, Tsushima, Iki, Hirado. For this time, we will clarify the water environment in each area from the relationship with land use and climate, and make it a foothold to clarify the material cycle of each island.

2. Target area Iki is rugged with a maximum altitude of 213 m, and there are numerous reservoirs in various parts of the island. In Tsushima, the altitude of the entire island is relatively high, and the mountains occupy about 89%. The Goto Islands Island consists of about 140 large and small islands, with large geological differences on each island. The Hirado Islands have many mountains while the fields are also relatively large. The population penetration rate of wastewater treatment in both areas is as low as 20-40%.

3. Research method Field survey was conducted 2 to 4 times a year from 2014 after organizing and examining existing research. On the site, water temperature, temperature, electric conductivity (EC), pH and RpH, COD were measured, and water was taken to measure the total organic carbon and the main dissolved components.

4. Results and discussion In Iki, the influence of agriculture appears in EC and TOC, but it is interesting that there is almost no effect of nitric acid. On the other hand, although many nitric acid was detected in the Goto Islands, it is thought that factors are due to paddy fields in Iki and upland fields in Goto Islands. Tsushima showed relatively low concentrations of EC and dissolved components, and seasonal changes also appeared. In Hirado Island, especially in the southern part, the geological influence is large in many places, the impact of sea salt is strong in Ikitsuki island and Azuchi Oshima. EC tends to rise in rainwater from October to March, pH tends to decrease. From the above, it is considered that the difference in the quality of the islands is greatly influenced by the difference of geology, topography and agricultural form.

Keywords: Iki island, Tsushima islands, Goto islands, Hirado islands, Water environment



a) Tsushima b) Iki c) Hirado

Fig.1 Water quality

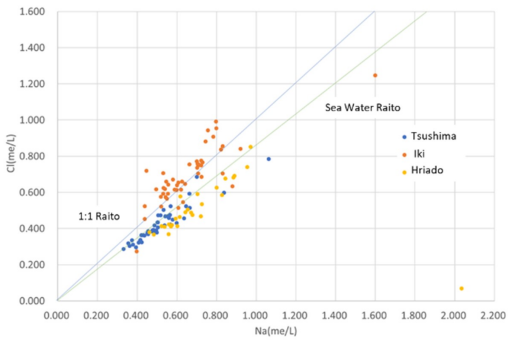


Fig.2 Na / Cl ratio

©2019. Japan Geoscience Union. All Right Reserved.

Water environment around Kusatsu-Shirane volcano and consideration of the effect of eruption in January 2018

*Igari Yoshihiro[1], Koji Kodera[2], Kazuki Asami[1]

1. Grad.Student,Hosei Univ., 2. Dep.of Geography Hosei Univ.

1. Introduction

The eruption (steam explosion) occurred in Mt.Motoshirane (One of Kusatsu-Shirane Volcano) on January 23, 2018. In this area, water quality survey of water environment began in May 2017 before the eruption. In addition to examining the influence on the water quality before and after the eruption, we studied the elution component of volcanic ash and the influence on the water environment. We also attempted to consider water quality forming factors in river water around Kusatsu-Shirane volcano.

2. Research method

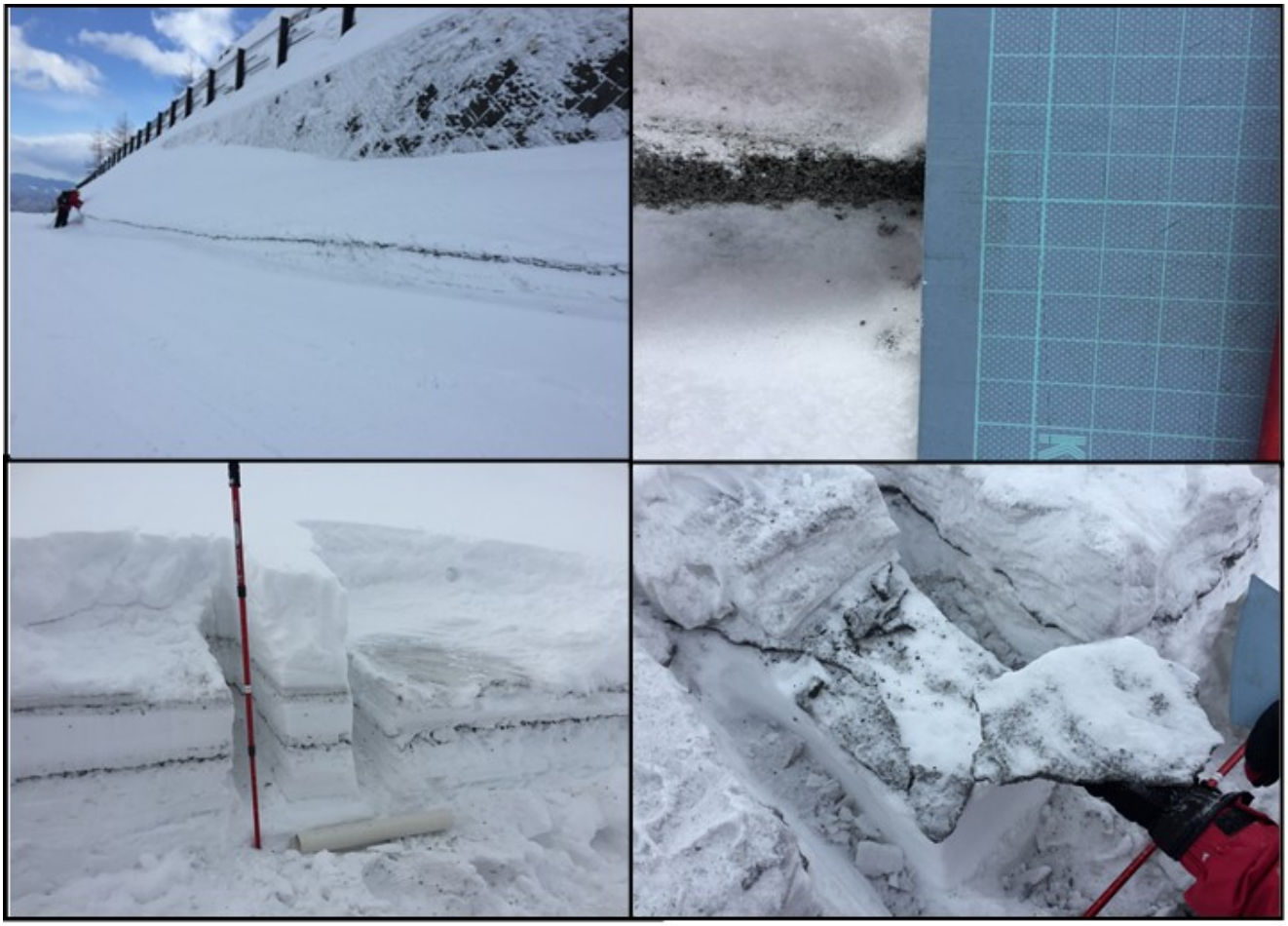
We conducted about 21 field surveys from May 2017 to March 2019. The survey site is about 45 sites, centering on rivers flowing in the east and south of the mountain. Temperature, water temperature, pH, RpH, EC, and flow rate were measured locally, and the sampled sample was analyzed for the main dissolved components. In February 2018, we investigated the deposition situation and ash fall volume of volcanic ash and conducted sampling, and carried out dissolution experiment. In addition to rivers, field surveys and sampling of lakes and precipitation, snow cover, hot spring water were conducted.

3. Results and discussion

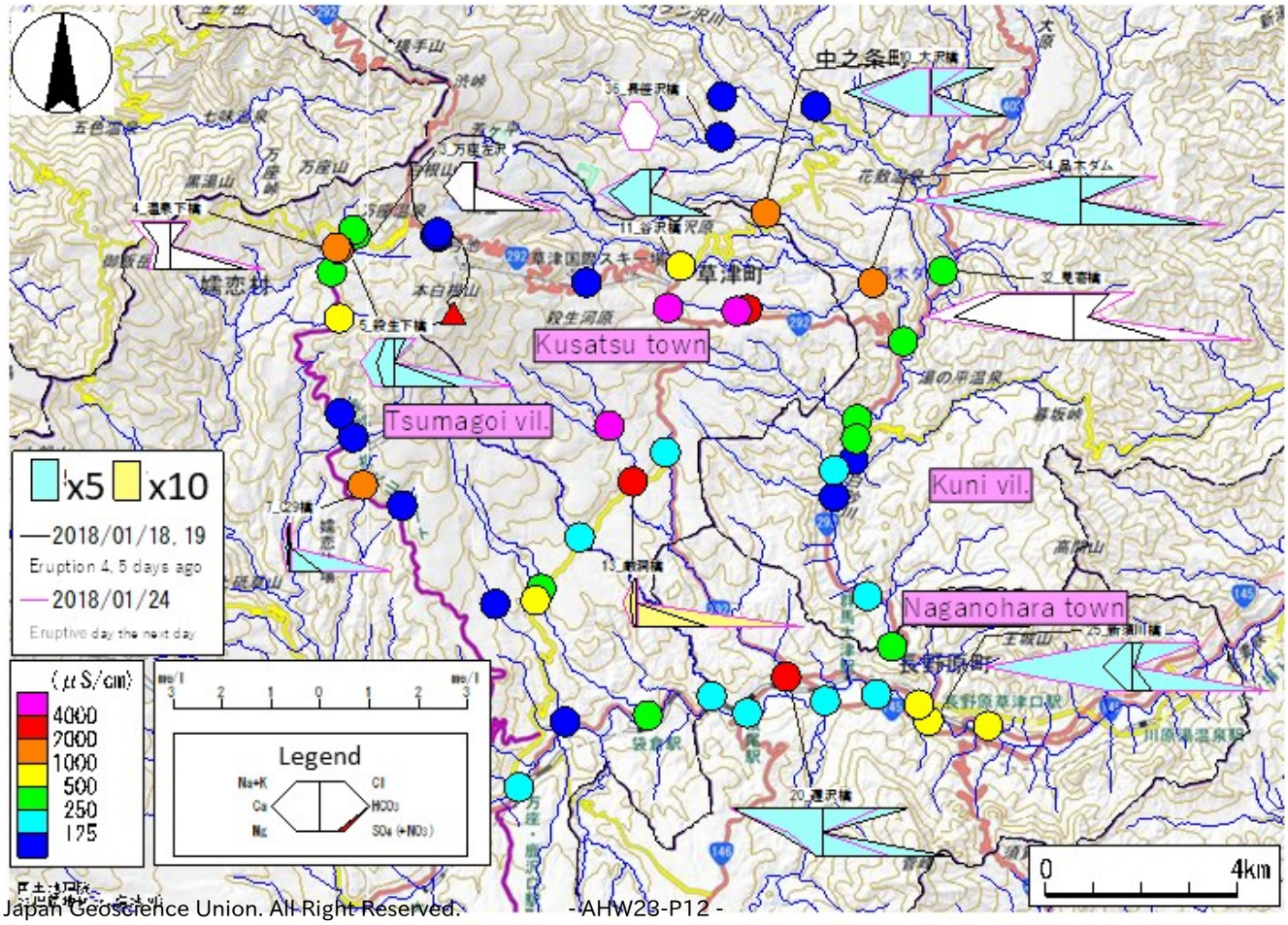
In Shirasuna River flowing to the east side of the mountain, groundwater and river water influenced by hot spring drainage and volcanic activity flow in from the tributary. There are points where the EC value fluctuates greatly, and it is influenced by the discharge and conduction of the dam which stores the neutralizing water of acidic rivers. In the Gando Swamp where the site of sulfur mine is located in the upstream part, the water quality is around pH:2.0, EC:6000 μS/cm. It is conceivable that the deposited volcanic ash affects the quality of the surrounding river due to snow melting water and precipitation.

Keywords: Mt.Kusatsu-Shirane, Volcano, Water environment, Eruption, Hot spring

©2019. Japan Geoscience Union. All Right Reserved.



Picture.1 Ash fall in the east foot of Kusatsu-Shirane volcano (February 6, 2018)



©2019. Japan Geoscience Union. All Right Reserved.

©2019. Japan Geoscience Union. All Right Reserved.

Re-consideration of discharge rate of spring water in Lake Ezu, Kumamoto

*Kimpei Ichiyanagi[1], Kiyoshi Ide[1], Jun Shimada[1], Tsutomu Ichikawa[2]

1. Kumamoto University, 2. Tokai University

In Kumamoto area, 100% of tap water is sourced from abundant groundwater. Recently, there is a great fear of groundwater level decreasing. To estimate discharge rete of spring water in Lake Ezu, the flow rate at 13 sites has been observed every month since December 1991. In previous studies, the total discharge rate of spring water was calculated by flow rates only at the most downstream, the most upper-stream, and incoming streams. In this study, total discharge rate from December 1991 to December 2014 was re-considered as a sum of three zones, that is upper-stream area, Kami-Ezu Lake, and Shimo-Ezu lake. When the discharge rate in each zone became negative, the case 1 where calculation was carried out with minus and the case 2 where it assumed to 0m^3/day were compared. As a result, total discharge rate gradually declined from about 450,000m^3/day in 1992 to about 360,000m^3/day (case 1) and to about 410,000m^3/day (case 2) in 2005. In July 2006, total discharge rate rapidly increased with heavy rainfall. After that, it had fluctuated about 400,000 to 500,000m^3/day in both cases. The discharge rate of Shimo-Ezu Lake sometimes became negative after 2003, and that averaged after July 2006 in case 2 was about 90,000m^3/day more than the case 1. As a result of comparing seasonal variability of discharge rate, monthly mean values of total and Shimo-Ezu Lake are low in April-May and high in October-November. However, monthly mean values of upper-stream area and Kami-Ezu Lake show no significant seasonal fluctuation. Monthly mean values of Shimo-Ezu Lake in August averaged after 2006 was about -14,000m^3/day in case 1 and about 32,000 m^3/day in case 2. Since negative value is not suitable to represent seasonal fluctuation, case 2 is proper to represent the discharge rate of spring water.

Keywords: spring water, Lake Ezu, long-term trend, seasonal variability

©2019. Japan Geoscience Union. All Right Reserved.

Evaluating the efficacy of hydrologically and hydrodynamically driven methods of e-flow assessment for Upper Godavari River Basin, India

*GAURAV KALIDAS PAKHALE[1], Jyoti Punjahari Nale[2], Ashvin Kumar Gosain[3], Rakesh Khosa[3]

1. PhD Research Scholar, Civil Engineering Department, Indian Institute of Technology, Delhi, 2. Project Advisor, IEWP, GIZ India, New Delhi, India, 3. Professor, Civil Engineering Department, Indian Institute of Technology, Delhi

In Peninsular India, pronounced seasonality in the precipitation and tropical semi-arid climate have compelled the tremendous development in the water resources sector. The major proportion of this fertile plateau falls in the rainshadow region of Western Ghats and is rightfully supported through enormous irrigation schemes which include the operation of several large reservoirs. These developments have resulted in alteration of various components of a natural hydrological regime like low as well as high flows. Environmental flows (e-flows), though acknowledged widely for their benefits, have not been attempted vigorously for peninsular river basins due to the prioritised issues related to water scarcity and disputes over water sharing. Also, many of these river streams have historically been known as non-perennial, thus further weakening the case of e-flows. Effectively, many recent e-flow assessments, have been observed to be elementary, quick and based on methods that are less intensive in terms of data and time requirements. In this view, the present study attempts to verify the efficiency of various hydrology and hydrodynamics-based e-flow assessment methods in one of such river basins, Upper Godavari River Basin. For this, hydrological observations of 16 sites with long term record availability (20 years or more) have been used and latest cross section data for these sites have been used for hydrodynamic computations.

Hydrological indices based on concepts like Percentage of Flow (POF) and Range of Variability Approach (RVA) have been estimated using a natural flow regime obtained from SWAT rainfall-runoff modelling. POF approaches like Tennant Method, Tessman Method, Variable Monthly Flow Methods are analysed while RVA approach has been analysed using Indicators of Hydrological Alteration (IHA) platform. These indices have been analysed for their feasibility and acceptability under the natural flow regime to understand the efficacy of these indices in providing optimum e-flow suggestions. Present observed flow regime has been juxtaposed with these indices to assess the present flow health in their comparison.

Hydrodynamic computations have been performed in HEC-RAS using 1-dimensional steady state conditions. Flow discharge versus flow depth, wetted perimeter, etc. relationships obtained for these study sites have been utilised to understand the critical flow levels which ensure the maximum bed inundations preferable for ecological sustainability. Wetted perimeter method of e-flow assessment has been evaluated for its suitability to provide the optimum e-flow suggestions. It has been found that hydrology based simple and quick methods of e-flow assessment fail the basic criteria of feasibility even under natural flow regime while hydrodynamic approach gives site-specific solutions which may not be relatable in longitudinal e-flow implementation.

Keywords: environmental flows, Range of Variability Approach, Wetted perimeter method

©2019. Japan Geoscience Union. All Right Reserved.

Presence of pharmaceutical compounds in freshwater lakes and their impact on phytoplankton

*Nandakumar Kanavillil[1], Cassandra Fligg[1], Sreekumari Kurissery[1]

1. Lakehead University, Canada

Historically, microalgae have been used as bio-indicators of aquatic health and this can be seen in several studies across the world. Often, at the bottom of the food chain microalgae constitute the primary producer of energy of many freshwater ecosystems. Diatoms, a group of microalgae, have been shown to exhibit extreme sensitivity to varying environmental parameters thereby making themselves an excellent candidate for studying the impacts of pollutants such as Pharmaceuticals and Personal Care Products (PPCPs). The contamination by PPCPs is common in our inland water bodies with a potential to get into our drinking water supply. This study explores the presence of PPCPs (Ibuprofen, 17-β Estradiol, and Triclosan) in the nearshore waters of Lake Simcoe, Ontario, Canada and their impacts on microalgal community. The study involved assessment of several environmental and algal parameters in the surrounding freshwater systems of three Waste Water Treatment Plants (WWTPs) that discharge their effluents *via* a creek/water channel to Lake Simcoe. Water samples were also drawn from a control location located away from the WWTPs. The results indicated that 1) PPCPs contamination is prevalent in the water outside of WWTPs (as far as the point of confluence with Lake Simcoe), and 2) The algal parameters varied according to the presence of PPCPs in the surface waters. Thus the study supported the growing concern of pharmaceutical contamination in the freshwater systems and its impacts on primary producers.

Keywords: Water quality, Bioindicators, Freshwater lakes, Pharmaceuticals, Phytoplankton

©2019. Japan Geoscience Union. All Right Reserved.

Novel approximate solutions for solute transport due to injections: considering the scale-dependent dispersion and non-integer flow dimension

*Ye-Chen Lin[1], Hund-Der Yeh[1]

1. National Chiao Tung Univ.

Prior research indicated that the flow dimension in a fractured medium may be of non-integer. In this article, we aim at developing a mathematical model for solute transport problems due to continuous or pulse injection in a non-integer dimensional flow field. The model allows the flow dimension ranging from linear flow to spherical flow. Our model also considers the effect of scale-dependent dispersion. The approximate solutions of the model are derived by applying the arrival times of mean and variance and validated through the comparison with finite-difference solutions of the present model. The results show that the approximate solutions give reasonable predictions when the value of dispersion or flow dimension is not large.

Keywords: solute transport, non-integer flow dimension, approximate solution, scale-dependent dispersion

©2019. Japan Geoscience Union. All Right Reserved.

Experimemtal study on the residual saturation of Porous Media using Pore Doublets Micromodel

*Chun-Wei Peng[1]

1. Taiwan National Chiao Tung University

In this study, we use a micromodel of PDM with different channel diameter ratios to study the fluid entrapment and mobilization. This study focuses on the evolution of the trapping and the amount of residuals saturation in the porous media. We observed the movement of wetting and non-wet liquids during the imbibition and drainage processes.We found that, with the low injection flow rates, the residual amount was strongly related to the contact angle; with the high injection flow rates, viscous force was dominated the trapping process. The results also showed that the liquids were trapped in the small tube for low injection rate, and in the large tube for the high injection rate. Our findings can help to control the residual saturation during water-flooding oil recovery, groundwater remediation, and the storage of carbon dioxide in deep subsurface.

©2019. Japan Geoscience Union. All Right Reserved.

Assessment of Synergy between Biomedical Waste and Shallow Groundwater Pollution

*Deepika -[1], Abhishek -[2]

1. BPS Government Medical College for Women, Sonepat, INDIA, 2. Technical University Dresden, GERMANY

Rapid urbanization and increasing population growth rate followed by the high rates of resource consumption patterns and increased waste generation have had an unintended negative impact on the prevailing environment. In a developing country like India where 50.34 % groundwater resources are not suitable for drinking as per WHO standards (United Nations, 2016), scrutinizing the open dumping of pathogenic biomedical waste becomes of paramount importance. Poor waste management practices pose a huge risk to the health of the public, patients, professionals and contribute to environmental degradation (land, air, and water pollution) if dumped untreated on the open ground. To assess this nexus, a prevalence study of the patients affected with waterborne diseases was conducted in a total of 35 hospitals comprising of government-, government-aided- and private hospitals of Ambala city. With a pronounced steppe climate, Ambala is located in North-Eastern (mean spatial coordinates: 30˚ 22' 41.4480" N and 76˚ 46' 36.1020" E) edge of Haryana, India. The city is drained by non-perennial streams and therefore the inhabitants depend solely on shallow groundwater resources for meeting their domestic water demand.

Data about the sources, quantity produced, treatment facilities, and awareness of biomedical waste, collected by questionnaire method based survey revealed that the mean waste generation was 8.08 kg/day with SD 5.371 kg/day. The biomedical waste consisted of approximately 1.2 % of the total municipal waste generated by the city and the patients affected with waterborne diseases were about 36 % of the total patients recorded. A latin hypercube Pareto distribution coupled with AMALGAM algorithm was employed for the initial sampling states of the proposals from the observed data (no. of patients). Thereafter, posterior estimates were generated using the Markov Chain Monte Carlo (MCMC) methods which showed a close fit with the observed and simulated data with RMSE 0.158. Furthermore, regression analysis with R^2=0.868 construed strong positive linear correlation between two variables viz. the number of patients and biomedical waste generated (and dumped). Recommendations are made for prioritizing the waste segregation and employing the indispensable management processes including waste treatment to avoid the further deterioration of the drinking water quality. The hospital authorities are advised to conduct the periodic seminars for enhancing awareness among the workforce from present 93.3 % to a maximum possible level.

Keywords: Groundwater, Biomedical waste, MCMC methods, Environmental awareness

©2019. Japan Geoscience Union. All Right Reserved.

Erosion and transport processes of earth surface materials in a reservoir-catchment system inferred from atmospheric radionuclides ^{7}Be and ^{210}Pb

*Mikiya Tsuruoka[1], Shinya Ochiai[2], Atsushi Matsuki[2], Seiya Nagao[2]

1. Graduate School of Natural Science and Technology, Kanazawa University, 2. Institute of Nature and Environmental Technology, Kanazawa University

Erosion and transport processes of earth surface materials are related to landform development in river catchment area and material discharge from the land area to the ocean. It is necessary to understand erosion and transport processes of earth surface materials to achieve proper management and prediction of river watershed and coastal area. However, since discharge behavior of earth surface materials in a large-scale river system is complicated by various processes, it is difficult to trace individual processes. On the other hand, earth surface materials eroded from catchment is transported and accumulated in reservoir. Therefore, discharge behavior of earth surface materials from catchment can be observed by monitoring of reservoir sediment. In this study, erosion and transport processes of earth surface materials in catchment were investigated based on atmospheric deposition flux to the catchment and sedimentation flux in the reservoir of ^{7}Be (half-life: 53 days) and ^{210}Pb (half-life: 22.3 years). From July 2016, rain water sample was collected every month with a collecting pan installed on the roof of Noto Atmospheric Observatory in Suzu City. ^{7}Be and ^{210}Pb in rain water were collected on ion exchange resins and measured with a Ge semiconductor detector to obtain atmospheric deposition fluxes. Sediment samples were collected with two sediment traps installed on the bottom of the reservoir (Shin-ike Reservoir) near the Noto Atmospheric Observatory at the same interval with rain sampling. Another trap was also set up in the middle layer (1.5 m above the bottom) since May 2018. Sediment samples were freeze-dried and measured with a Ge semiconductor detector to obtain sedimentation fluxes of ^{7}Be and ^{210}Pb. The atmospheric deposition fluxes of ^{7}Be and ^{210}Pb ranged 1.06-30.7 and 0.334-7.68 Bq/m^{2}/day, respectively. It shows clear seasonal fluctuation with high deposition in winter. The sedimentation fluxes of ^{7}Be in the bottom and middle layers were same level with the deposition flux. This result indicates that the contribution of ^{7}Be from the catchment is small. On the other hand, the sedimentation flux of ^{210}Pb in the middle layer was about 1.7-7.3 times higher than the atmospheric deposition flux of ^{210}Pb. This result suggests that sedimentation flux of ^{210}Pb in the middle layer reflects the contribution of ^{210}Pb from the catchment. The sedimentation flux of ^{210}Pb in the bottom layer was much higher than the atmospheric deposition flux, implying that sedimentation flux in the bottom was largely affected by resuspension in addition to the contribution of ^{210}Pb from the catchment. Residence time of these radionuclides in the reservoir-catchment system was estimated from the ^{7}Be/^{210}Pb$_{ex}$ ratios of rain water and sediment samples. The average residence times of the bottom layer samples and middle layer sample were estimated at 278 days and 141 days, respectively. This difference in the residence time may result from resuspension effect in the reservoir bottom.

Keywords: sediment, reservoir-catchment system, Be-7, Pb-210

©2019. Japan Geoscience Union. All Right Reserved.

Fluctuation of groundwater level in a sloping unconfined aquifer due to time varying recharge

*Ming-Chang Wu[1], Ping-Cheng Hsieh[1]

1. National Chung Hsing University

When a water-permeable slope is recharged by rainfall, the variation of the groundwater level is usually observed by setting up observation wells. However, the point observations are not sufficient to represent the vast domain of an aquifer and are constrained by the high cost of instrumentation and excavated wells. Therefore, the development of mathematical models for groundwater simulations can help us to understand the change of groundwater level more easily.
This study considers the variation of the groundwater level in a sloping aquifer with an impervious bottom. We divided the aquifer into two areas with and without rainfall recharge, and then use the nonlinear Boussinesq equation with a source term derived from the law of mass conservation. Analytical solutions to the nonlinear equation was acquired by the perturbation method for a finite region and a semi-infinite domain. After the transformation of variables, the general integral transformation method was used. The groundwater level varying with time under different factors (such as the dip angle of impervious bed, hydraulic conductivity, storage coefficient and different recharge rates) was discussed.
The present results were compared with the observed data from an observation well, and the difference in between was discussed. It is expected that the research results can better understand the physical mechanism of groundwater level change, and help to manage the groundwater.

Keywords: nonlinear Boussinesq equation, perturbation method, general integral transform method (GITM)

©2019. Japan Geoscience Union. All Right Reserved.

Effect of cutoff wall on recharge water storage volume

*Pei-hsun Tsai[1], Jung-hsing Tai[1]

1. Chaoyang University of Technology

Artificial groundwater recharge is used to increase groundwater in areas with water scarcity. Understanding the hydromechanical features of aquifers during groundwater withdrawal and recharge is necessary for managing groundwater resources effectively. In practice, an artificial pool can be used to collect surface runoff so that it infiltrates the aquifer and recharges groundwater. A cutoff wall can be constructed to seal recharge water and prevent it from flowing from the recharge area. Additional studies are required to understand the effect of the various parameters of cutoff walls on groundwater recharge. This study used the finite difference software FLAC 8.0 to examine the influence of the location and size of gaps of a cutoff wall on recharge water storage volume. Each aquifer was in an unsaturated state before groundwater recharging; therefore, groundwater recharge analyses were simulated by the two-phase flow in unsaturated porous media. The results revealed that when the groundwater layer was sand and the cutoff wall was not extended into the fully impermeable layer, the recharge water completely flowed from the gap between the bottom of the cutoff wall and the fully impermeable layer after stopping groundwater recharge. The recharge water volume related to the size of the gap at the bottom of the cutoff wall. When the cutoff wall was not extended into the groundwater layer, the cutoff wall did not intercept water. The gap at the top of the cutoff wall retained more recharge water compared with the gap at the bottom of the cutoff wall.

Keywords: Groundwater recharge, Cutoff wall, Water storage volume

©2019. Japan Geoscience Union. All Right Reserved.

Studying Operation Parameters on Flat-Plate Membrane Bioreactor for Sewage Treatment

*Jen Hung Chiu[1], Wen Chin Chen[1]

1. Studying Operation Parameters on Flat-Plate Membrane Bioreactor for Sewage Treatment

The flat-plate membrane bioreactor is applied to the domestic sewage treatment, which has a high quality of effluent than the traditional activated sludge process, and decreasing the susceptible of hair entanglement with the hollow fiber membrane. It has become a priority for recent sewage treatment applications.

A flat-plate membrane bioreactor pilot plant with a reaction volume of 4 m^3 was installed in the existing sewage treatment plant. In this research, the parallel treatment of the same influent water quality and hydraulic retention time was carried out to compare the treatment efficiency between the MBR and traditional activated sludge process, and the operational effects of the membrane flux were discussed.

With one year of long-term research, the average removal efficiencies of MBR process, regardless of the COD, SS and E.coli were over 99%, wchih was better than the activated sludge process only 90~95%. Meanwhile, the optimal operation mode of the MBR was obtained in the study. The aeration flow rate in the system was adjusted to 10~13 NL/min per film, the effluent flux was controlled under 50% of the maximum recommended flux of membrane with 9-minute operation and 1 minute stop in a cycle, there is no significant change in operating flux and pressure. These operational mode of MBR can extend the life time of membrane and effectively improve the application of flat-plate MBR to domestic sewage treatment.It is suggested that, in view of water treatment and resource sustainability, the flat plate MBR technology is feasible, and can serve as a green guide to the sewage treatment.

Keywords: Membrane Bioreactor, Flat-Plate Membrane, Sewage

©2019. Japan Geoscience Union. All Right Reserved.

Mine-water quality at a tertiary coalfield in India: Characterisation and treatment using novel polyvinyl alcohol (PVA) gel bioreactor

*Aparna Dutta[1], Sudipta Sarkar[1]

1. Indian Institute of Technology Roorkee

Nearly 78 percent of the total measured (proved) tertiary coal reserves of India is concentrated in the north-eastern state of Assam. The Tertiary coal of North–Eastern Coalfields (NEC) has been found to contain as high as 8% sulphur with varying percentage of pyrite, sulfate, organic and free sulphur. The pyrites are often associated with toxic heavy metals. Acid mine drainage (AMD) is generated when mining activities expose the pyrite and sulfides to atmospheric oxygen, moisture and micro-organisms that catalyse the oxidation process to release large amounts of sulfate into the mine water along with protons and dissolved metals. Microbial dissimilatory sulfate reduction (DSR) in the presence of a suitable organic carbon source can be engineered to treat such water. This study is significant because this region is rich in biodiversity and such mining impacted water may have adverse ecological impact, if discharged without appropriate treatment.The objective of the work is to characterise water samples collected from two open cast mines of Makum coalfield under NEC and evaluate the performance of a novel polyvinyl alcohol (PVA) gel packed bed bioreactor to treat the same. Sample collection, storage and physico-chemical analysis are carried out as per Standard methods of American Public Health Association. The biological treatment process is studied in a cylindrical continuous flow lab scale bioreactor under relevant acidic pH at different feed chemical oxygen demand (COD) to sulfate ratio and hydraulic retention time (HRT). Sludge from a lab scale anaerobic bioreactor treating very high sulfate industrial water is used as inoculum. The sulfate reducing microorganisms are enriched within the bioreactor in fed-batch mode using modified Postgate’ s medium for one month.Oxidation Reduction Potential (ORP), pH, sulfate removal, total inorganic carbon (TIC) and alkalinity produced are measured at the bioreactor outlet to evaluate the process performance. The mine water samples exhibit low pH, high sulfate, conductivity, dissolved solids, hardness, iron and manganese, which indicates the occurrence of AMD. The treatment process reduces the sulfate concentration and increases pH of the treated water. The use of highly porous PVA gel beads as packing material in the bioreactor treating sulfate rich acidic water imparts resilience to operational variation. The study evaluates the novel application of PVA gel beads to bioreactor for treating acidic mine waters from an ecologically important region. The research finding provides an understanding of the process for application to other biological AMD treatment configurations.

Keywords: acid mine drainage (AMD), polyvinyl alcohol (PVA), sulfate, sulfate reducing microorganism (SRM), dissimilatory sulfate reduction(DSR), pyrite

©2019. Japan Geoscience Union. All Right Reserved.

[E] Poster | A (Atmospheric and Hydrospheric Sciences)：A-CG Complex & General

Wed. May 29, 2019 10:45 AM - 12:15 PM JST | Wed. May 29, 2019 1:45 AM - 3:15 AM UTC | Poster Hall International Exhibition Hall8, Makuhari Messe_6

[A-CG35] Projection and detection of global environmental change

convener:Michio Kawamiya(Japan Agency for Marine-Earth Science and Technology), Hiroaki Tatebe(Japan Agency for Marine-Earth Science and Technology), Kaoru Tachiiri(Japan Agency for Marine-Earth Science and Technology)

Anthropogenic forcings on global environment are expected to cause intensification of extreme events, sea level rise, ocean acidification and deoxygenation, as well as large-scale ecosystem changes. The CMIP6 experimental protocol has been established based on which modeling groups across the world are starting to provide environmental projection data toward 6th IPCC assessment report due in 2021. Various new types of studies, such as event attribution and coupling of socio-economic processes and Earth system dynamics, are also emerging in the field of global change projection. In addition, observational studies are becoming increasingly more important for grasping changes in the global environment and evaluating model projections. Interactions and collaborations beyond boundaries of conventional scientific disciplines are desired for dealing with the issue of global changes. This session thus aims to deepen our understanding on global change, from both disciplinary and interdisciplinary viewpoints. This session is co-organized by AIMES - Future Earth project "Analysis, Integration and Modelling of the Earth System" (https://aimesproject.org/).

[ACG35-P01] World Regionalization of Climate Change (1961–2010)

*Shao Sun[1,2], Peijun Shi[2,3,4], Daoyi Gong[2], Tao Zhou[2] (1.National Climate Center, China Meteorological Administration, Beijing 100081, China, 2.State Key Laboratory of Earth Surface Processes and Resource Ecology, Beijing Normal University, Beijing 100875, China, 3.Key Laboratory of Environmental Change and Natural Disaster of Ministry of Education, Beijing Normal University, Beijing 100875, China, 4.Academy of Disaster Reduction and Emergency Management, Ministry of Civil Affairs & Ministry of Education, Beijing 100875, China)

[ACG35-P02] Quantifying and identifying future climate signal, noise, and internal variability at finer temporal scales

*Jongho Kim[1], Manh Van Doi[1] (1.University of Ulsan)

[ACG35-P03] Basic evaluation of MIROC6 and current status of CMIP6 experiments

*Hiroaki Tatebe[1] (1.Japan Agency for Marine-Earth Science and Technology)

[ACG35-P04] Synchronized increase of extreme cold and warm events in China during the recent global warming slowdown

*Xiubao Sun[1,3], Chunzai Wang[1], Guoyu Ren[2,3], Panfeng Zhang[2] (1.State Key Laboratory of Tropical Oceanography (LTO), South China Sea Institute of Oceanology(SCSIO), Chinese Academy of Sciences (CAS), 2.Department of Atmospheric Science, School of Environmental Studies, China University of Geosciences (CUG), 3.Laboratory for Climate Studies, National Climate Center (NCC), China Meteorological Administration (CMA))

[ACG35-P05] Quantification of thermodynamical and dynamical contributions to the anthropogenic influences on tropical cyclone rainfall extremes

*Cheng-Ta Chen[1], Shih-How Lo[1], Chung-Chieh Wang[1], Kazuhisa Tsuboki[2] (1.Department of Earth Sciences, National Taiwan Normal University, 2.Hydrospheric-Atmospheric Research Center, Nagoya University)

[ACG35-P06] Temporal Evolution of the Long-Term Distributional Biases of Climate Models as a Parameter for the Regional Evaluation of the Simulation of Climate Change

*Martin Gomez-Garcia[1], Akiko Matsumura[1], Shiro Hishinuma[1], Daikichi Ogawada[1] (1.Nippon Koei Co. Ltd., Reasearch and Development Center)

[ACG35-P07] A global simulation of bioenergy crop yield

*Zhipin Ai[1], Naota Hanasaki[1] (1.National Institute for Environmental Studies)

[ACG35-P08] Integrated Research Program for Advancing Climate Models - Theme B: national research program in Japan on earth system modeling

*Michio Kawamiya[1], Tomohiro Hajima[1], Kaoru Tachiiri[1], Jun'ichi Tsutsui[2], Tokuta Yokohata[3], Takashi Arakawa[4], Takahiro Inoue[4] (1.Japan Agency for Marine-Earth Science and Technology, 2.Central Research Institute of Electric Power Industry, 3.National Institute for Environmental Studies, 4.Research Organization for Information Science and Technology)

[ACG35-P09] Towards probabilistic climate projections based on the CMIP6 multi-model ensemble

*Junichi Tsutsui[1] (1.Central Research Institute of Electric Power Industry)

[ACG35-P10] Effect on the earth system of realizing 1.5 degree climate target by overshooting after reaching 2 degree level

*Kaoru Tachiiri[1], Herran Diego Silva[2], Xuanming Su[1], Michio Kawamiya[1] (1.Japan Agency for Marine-Earth Science and Technology, 2.Institute for Global Environmental Strategies)

[ACG35-P11] **Historical regional and sectoral contributions to climate change**

*Xuanming Su[1], Kaoru Tachiiri[1], Katsumasa TANAKA[2], Michio Watanabe[1] (1.Japan Agency for Marine-Earth Science and Technology, 2.National Institute for Environmental Studies)

[ACG35-P12] **Future projection of global climate, water, food, bio-energy, and land investigated with MIROC-INTEG: a global bio-geophysical land surface model with human components**

*Tokuta Yokohata[1], Yusuke Satoh[1], Tsuguki Kinoshita[2], Gen Sakurai[3], Yadu Pokhrel[4], Akihiko Ito[1], Etsushi Kato[5], Masashi Okada[1], Naota Hanasaki[1], Tomoko Nitta[6], Seita Emori[1] (1.National Institute for Environmental Studies, 2.Ibaraki University, 3.National Agriculture and Food Research Organization, 4.Michigan State University, 5.The Institute of Applied Energy, 6.University of Tokyo)

[ACG35-P13] **Downscaling a global agricultural land use model to country level for national SSP analysis**

*Wenchao Wu[1], Tomoko Hasegawa[1], Kiyoshi Takahashi[1], Shinichiro Fujimori[2] (1.National Institute for Environmental Studies, 2.Kyoto Univ.)

[ACG35-P14] Extreme Events and Emergent Trends in Marine Ecosystem Stressors under a historical/RCP8.5 Climate Change Pathway

*Keith Bradley Rodgers[1,2], Sarah Schlunegger[3], Richard Slater[3], Burke Hales[4], Axel Timmermann[1,2] (1.IBS Center for Climate Physics, Busan, South Korea, 2.Pusan National University, Busan, South Korea, 3.AOS Program, Princeton University, Princeton NJ, USA, 4.College of Ocean and Atmospheric Sciences, Oregon State Universitym, Corvallis, OR, USA)

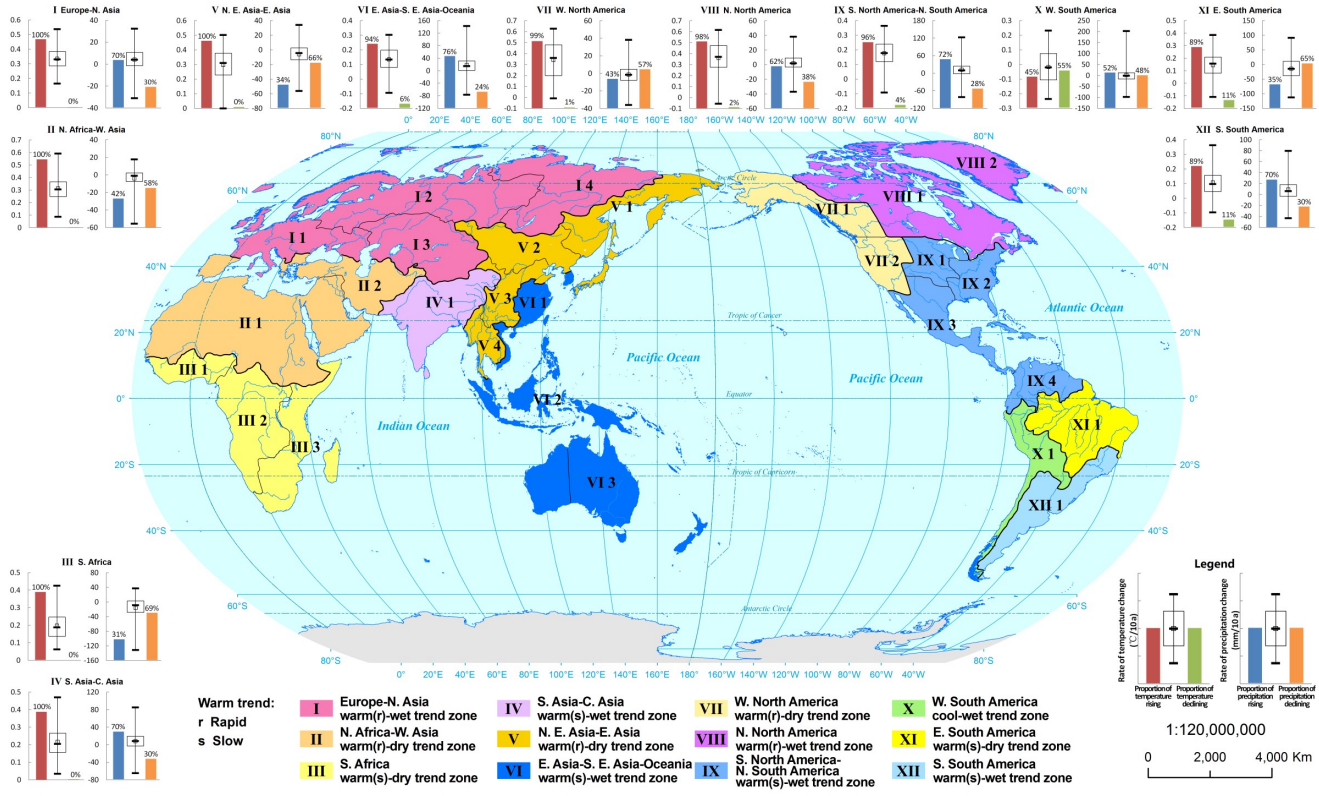
World Regionalization of Climate Change (1961–2010)

*Shao Sun[1,2], Peijun Shi[2,3,4], Daoyi Gong[2], Tao Zhou[2]

1. National Climate Center, China Meteorological Administration, Beijing 100081, China, 2. State Key Laboratory of Earth Surface Processes and Resource Ecology, Beijing Normal University, Beijing 100875, China, 3. Key Laboratory of Environmental Change and Natural Disaster of Ministry of Education, Beijing Normal University, Beijing 100875, China, 4. Academy of Disaster Reduction and Emergency Management, Ministry of Civil Affairs & Ministry of Education, Beijing 100875, China

Existing climate regionalization aims to characterize the regional differences in climate based on years of the mean values of climate indices. However, with the accelerating climate change nowadays, existing climate regionalization cannot represent the regional difference of climate change, nor can it reflect the extreme weather and climate disasters and environmental risks incurred from climate changes. This paper utilizes the tendency value and fluctuation value of temperature and precipitation from 1961 to 2010 to identify the climate change quantitatively, and completes world regionalization of climate change (1961–2010) with administrative subdivisions of countries as the basic unit in combination with world's terrain feature. Level-I regionalization divides world's climate change (1961–2010) into twelve tendency zones based on the tendency of temperature and precipitation; level-II regionalization refers to twenty-eight fluctuation regions based on level-I regionalization according to the fluctuation of temperature and precipitation. Climate change regionalization provides a basis for countries and regions in the world to develop plans for adapting to climate change, especially for managing extreme weather and climate disasters and environmental risks.

Keywords: Climate change, Regionalization, Tendency, Fluctuation, World



©2019. Japan Geoscience Union. All Right Reserved.

Quantifying and identifying future climate signal, noise, and internal variability at finer temporal scales

*Jongho Kim[1], Manh Van Doi[1]

1. University of Ulsan

Quantifying and identifying climate internal variability (CIV) plays an important role in climate change studies because of its irreducible and unpredictable characteristics. A large number of studies have addressed such an issue; however, the issue was only resolved at coarser resolution on the first order moments of few climate variables. Our recent study has estimated CIV of climate variables for a “current” period at finer spatial and temporal scales; however, whether CIV will change or remain constant in the future under the impact of representative concentration pathways (RCP45 and RCP85) is still questionable. To investigate how CIV will change in the future in both spatial pattern and magnitude, CIV is assessed over 30-year periods in both current and future periods with two scenarios in Korea by analyzing an ensemble of 100 simulations generated by an hourly weather generator. In this study, signal to noise ratio (SNR) used to evaluate the model performance will be applied to simulating ensemble for different periods. CIV is then estimated by two methods: “detrended” and “differenced”; SNR is estimated by “analysis of variance” and “trend analysis” methods. Both SNR and CIV are evaluated with four proposed matrices signifying rainfall volume, extremes and occurrence of rainfall. To consider the change of CIV in the future periods, t-test (test for mean difference) and f-test (test for variance difference) are applied to the ensemble of CIV. In this study, analyzing SNR’s values shows that the four proposed matrices are controlled by non-linear stochastic process and the change tend to increase in the future with increase of CO2 concentration. CIV is proved to change in the future periods under impact of CO2 scenarios. Spatial distribution of CIV’s change over future periods of which locations provides the important and useful information for decision making of water resources planning and proposing mitigation measures of disaster protection.

Acknowledgment:

This research was supported by the Water Management Research Program funded by Ministry of Environment of Korean government (127554), and by the Basic Science Research Program of the National Research Foundation of Korea funded by the Ministry of Education (2016R1D1A1B03931886).

Keywords: climate internal variability, signal to noise ratio, t-test, f-test

©2019. Japan Geoscience Union. All Right Reserved.

Basic evaluation of MIROC6 and current status of CMIP6 experiments

*Hiroaki Tatebe[1]

1. Japan Agency for Marine-Earth Science and Technology

The sixth version of the Model for Interdisciplinary Research on Climate (MIROC), called MIROC6, was cooperatively developed by a Japanese climate modeling community. Overall reproducibility of mean climate and internal climate variability in MIROC6 is better than that in the previous version (MIROC5). The tropical climate systems (e.g., summertime precipitation in the western Pacific and the eastward propagating Madden-Julian Oscillation) and the mid-latitude atmospheric circulations (e.g., the westerlies, the polar night jet, and troposphere-stratosphere interactions) are significantly improved in MIROC6. These improvements can be attributed to the newly implemented parameterization for shallow convective processes and to the directly resolved stratosphere. In the present study, simulated mean climate, internal climate variability in MIROC6 are evaluated and briefly summarized in comparison with MIROC5 and observations. Using MIROC6, designated simulations tackling a wide range of climate science issues, as well as seasonal-to-decadal climate predictions and future climate projections, are currently ongoing with an aim towards contributing to the sixth phase of the Coupled Model Intercomparison Project (CMIP6). Preliminary results of historical climate simulations from the middle of the 19th century, climate projections from the present to the end of the 21th century based on future scenarios of the Shared Socio-economic Pathways, and initialized climate predictions on seasonal-to-decadal timescales will be given in this talk.

Keywords: Climate model, CMIP6, climate projections/predictions

©2019. Japan Geoscience Union. All Right Reserved.

Synchronized increase of extreme cold and warm events in China during the recent global warming slowdown

*Xiubao Sun[1,3], Chunzai Wang[1], Guoyu Ren[2,3], Panfeng Zhang[2]

1. State Key Laboratory of Tropical Oceanography (LTO), South China Sea Institute of Oceanology(SCSIO), Chinese Academy of Sciences (CAS), 2. Department of Atmospheric Science, School of Environmental Studies, China University of Geosciences (CUG), 3. Laboratory for Climate Studies, National Climate Center (NCC), China Meteorological Administration (CMA)

From the end of 1990s to the middle of 2010s, global mean temperature experienced a process of warming slowdown. However, global warm extremes did not show the slowdown phenomenon during the recent global warming slowdown. Based on the observation data of 2362 land surface stations in China, we analyzed the cold and warm extremes changes over mainland China between global warming period (1961-1999) and warming slowdown period (2000-2014). Results indicate that the warming trend in the cold season (MAM and DJF) is significantly higher than that in the warm season (JJA and SON) in the period of global warming (1961-1999), while the warming trend in the warm season is significantly higher than that in the cold season in the period of global warming slowdown. That is, the trend of warm season and the cool season in China have reversed. At the same time, we also found that the synchronous increase occurrence of extreme warm events in summer (JJA) and extreme cold events in winter (DJF) leads to the seasonal trend reverse phenomenon, but there are differences in the spatial variation characteristics between cold and warm extremes. The increase of warm extremes in summer is mainly due to the strong increase of warm events in south China, while the increase of cold events in winter is due to the increase of cold events over China. Further, we also found that the variability of extreme temperature has increased more significantly in the warming slowdown period than that in global warming period. East Asian winter monsoon and summer monsoon both show enhanced characteristics during the global warming slowdown period, which indicates that the increase of sea-land temperature difference in summer and winter results in the synchronous increase of extreme cold and warm events by increasing the climate variability in China.

Keywords: Global warming, Global warming slowdown, Extreme warm events, Extreme cold events, Land-sea temperature difference

©2019. Japan Geoscience Union. All Right Reserved.

Quantification of thermodynamical and dynamical contributions to the anthropogenic influences on tropical cyclone rainfall extremes

*Cheng-Ta Chen[1], Shih-How Lo[1], Chung-Chieh Wang[1], Kazuhisa Tsuboki[2]

1. Department of Earth Sciences, National Taiwan Normal University, 2. Hydrospheric-Atmospheric Research Center, Nagoya University

The rainfall extremes and strong winds associated with tropical cyclones lead to significant damages and lost to where they make landfalling. Upward trend in term of financial lost was indicated for the past few decades from the report of major reinsurance firms. Whether the past anthropogenic warming played a significant role in such extreme event and their changes remained very controversial. On one hand, people argue it’s nearly impossible to attribute an individual extreme event to global warming. On the other hand, the increase of heavy rainfall is consistent with the expected effects of climate change on tropical cyclone. To diagnose possible anthropogenic contributions to the odds of heavy rainfall associated with tropical cyclone, we adapt an existing event attribution framework of modeling a ‘world that was’ and comparing it to a modeled ‘world that might have been’ for that same time but for the absence of historical anthropogenic drivers of climate. One limitation for applying such approach to high-impact weather system is that it will require models capable of capturing the essential processes lead to the studied extremes. Using a cloud system resolving model that can properly simulate the complicated interactions between tropical cyclone, large-scale background, topography, we first perform the ensemble ‘world that was’ simulations forced by the high resolution ECMWF YOTC analysis. We then re-simulate with the adjusted ‘world that might have been conditions’ by removing the regional atmospheric and oceanic forcing due to human influences estimated from the CMIP5 model ensemble mean conditions between all forcing and natural forcing only historical runs. Thus our findings are highly conditional on the driving analysis and adjustments therein, but the setup allows us to elucidate possible contribution of anthropogenic forcing to changes in the likelihood of heavy rainfall associated tropical cyclone. With only less than half of degree anthropogenic warming over the study area, we found that this forcing very likely (9 out of 10 cases) increase the risk of heavy rainfall event (grid rainfall greater than 33 mm per hour) by at least 16%. The role of dynamical processes that leads to precipitation extreme increases beyond the moisture content increase will be further analyzed and discussed.

Keywords: Tropical Cyclone, Extreme rainfall, extreme event attribution

©2019. Japan Geoscience Union. All Right Reserved.

Temporal Evolution of the Long-Term Distributional Biases of Climate Models as a Parameter for the Regional Evaluation of the Simulation of Climate Change

*Martin Gomez-Garcia[1], Akiko Matsumura[1], Shiro Hishinuma[1], Daikichi Ogawada[1]

1. Nippon Koei Co. Ltd., Reasearch and Development Center

Owing to the climate variability of the General Circulation Models (GCM), the discrepancy between their outputs and observational datasets at scales that range from hours to years is practically random. Thus, the associated errors need to be evaluated in terms of the long-term (multidecadal) distributional properties of the atmospheric variables. A recently developed bias-correction method corrects the systematic errors (i.e., biases) in the climate mean state and in three distributional measures of the daily and the interannual variability (namely the frequency of extremes, the skewness, and the scale of the variable at each timescale). The adjustment of these biases is done in such a way that the corrections at one timescale do not affect the probability distribution at another. Therefore, this bias-correction method is able to preserve the GCM-simulated climate trends and extensively reproduce the long-term frequency of the observed extreme weather (e.g. 98th percentile of wet days, maximum seasonal mean of surface temperature).

Generally, the bias-correction of GCMs faces the challenge of including the simulated changes of climate, which supposes alterations in not only the mean but also other aspects like the skewness and the frequency of extremes. The abovementioned bias-correction method includes the effect of the simulated climate change in the correction of the distributional biases. However, considering the coarse resolution of the GCMs and the imperfections in the parameterizations of the subgrid physical processes, the fundamental assumption that the distributional biases are predictable (i.e., stationary) is made.

In this study, we explored the possibility of evaluating the sensibility with which GCMs simulate the response of the earth-system components to external forcing (i.e., climate change) by comparing the temporal evolution of the distributional biases at different timescales over specific regions. For the short period in which the observed data was available, our results revealed that many CMIP5 GCMs are indeed able to simulate with a quasi-stationary bias the changes caused by climate change. Moreover, being able to identify the regions in which certain models do not show the errors with a systematic behavior in either the climate mean state, the daily variability or the interannual variability can be useful for the further development of climate models. We expect that with the data of the GCM outputs of the future phases of the CMIP project, the period in which the observed and the modeled data coincide becomes longer and, thus, our conclusions can be supported by more robust evidence.

Keywords: Bias correction of GCMs at different timescales, Climate trends and climate variability, Evaluation of the ability of GCMs to simulate climate change

©2019. Japan Geoscience Union. All Right Reserved.

A global simulation of bioenergy crop yield

*Zhipin Ai[1], Naota Hanasaki[1]

1. National Institute for Environmental Studies

Large-scale development of bioenergy is considered as an effective pathway to achieve the 2 degrees target of the Paris Agreement. To avoid the competition with food crops, so-called the second-generation bioenergy crops such as miscanthus and switchgrass are regarded as potential dedicated biomass crop. However, the models to estimate the yield of miscanthus and switchgrass at a global scale which enable analyzing the effects of irrigation water application are seldom seen as of today. Here, we firstly updated the crop module in the global hydrological model H08 for miscanthus and switchgrass. Then, we conducted a global simulation and validation of the yield for miscanthus and switchgrass at 0.5 degree. The results indicated that the updated H08 have a good ability in simulating the yield of perennial bioenergy crops, which provides a good foundation for further integrated assessment of the impacts of bioenergy crop production on water sector.

Acknowledgement: This research was supported by the Environment Research and Technology Development Fund (S-14-5) of the Environmental Restoration and Conservation Agency.

Keywords: Bioenergy, Crop yield, H08

©2019. Japan Geoscience Union. All Right Reserved.

Integrated Research Program for Advancing Climate Models - Theme B: national research program in Japan on earth system modeling

*Michio Kawamiya[1], Tomohiro Hajima[1], Kaoru Tachiiri[1], Jun'ichi Tsutsui[2], Tokuta Yokohata[3], Takashi Arakawa[4], Takahiro Inoue[4]

1. Japan Agency for Marine-Earth Science and Technology, 2. Central Research Institute of Electric Power Industry, 3. National Institute for Environmental Studies, 4. Research Organization for Information Science and Technology

The Integrated Research Program for Advancing Climate Models, or TOUGOU (abbreviation taken from its Japanese name), is a national project for projection of global change. Its aim to provide information for adaptation and mitigation, based on scientific evaluation of changes including those in extreme events and carbon cycle. The project was launched in April, 2017. While the entire program deals with a wide range of physical aspects and consequent impacts of climate change, Theme B (TOUGOU-B) focuses on the development of a state-of-the-art Earth system model (ESM) incorporating biogeochemical processes, such as sophisticated carbon and nitrogen cycles, as well as its application to exploring future socio-economic pathways of climate change mitigation. MIROC-ESM, an ESM developed under TOUGOU-B (and the previous SOUSEI-B) has been significantly improved since the 5th phase of coupled model intercomparison project (CMIP5), and has started to be run for CMIP6. During the three years since TOUGOU was launched, results have been obtained that may contribute to 6th Assessment Report (AR6) of Intergovernmental Panel on Climate Change (IPCC) including those on impacts of pyrogenic iron on oceanic ecosystem, assessment of the outcome of labor productivity change due to warming, and effects of high dust amount on surface temperature during the Last Glacial Maximum. Besides, efforts to secure ways to disseminate projection data are ongoing under TOUGOU-B. Specifically, collaboration has been established between climate modeling community in Japan and Data Integration and Analysis System (DIAS), a national IT project for environmental data, have been continuing, in order for Japan to participate in Earth System Grid Federation (ESGF). ESGF is an international cooperative activity to construct a data distributing system for climate related data such as CMIP6 outputs. Some of the details of these results will be explained in the presentation.

Keywords: IPCC, Earth system model , carbon cycle, socio-economic scenario, CMIP6, climate mitigation

©2019. Japan Geoscience Union. All Right Reserved.

Towards probabilistic climate projections based on the CMIP6 multi-model ensemble

*Junichi Tsutsui[1]

1. Central Research Institute of Electric Power Industry

Research on climate change mitigation uses a climate model emulator that represents the average and range over a specific multi-model ensemble of complex climate simulations. The Coupled Model Intercomparison Project (CMIP) has provided such multi-model ensembles, and its latest Phase 6 (CMIP6) results are being revealed. As a first step to applying the CMIP6 results to probabilistic climate projections, we focus on the distribution of key parameters representing atmospheric CO_2-induced forcing and transient temperature responses.

In this study, we develop a procedure to determine the forcing-response parameters of a complex climate model. We simultaneously fit a curve built on an impulse response function to the global mean time series of the model's surface temperature anomaly and top-of-atmosphere energy imbalance from two basic CO_2 -forced experiments, i.e., an abrupt quadrupling and a 1%-per-year increase in atmospheric CO_2 concentration. This scheme serves as an improved alternative to the widely-used regression method of Gregory et al. (2004). Furthermore, it makes a complete set of parameters to emulate the target model from which equilibrium climate sensitivity (ECS) and transient climate response (TCR) are derived. The properties of a multi-model ensemble are quantified through a statistical approach including a principal component analysis for the parameters.

The two CO_2-forced experiments are included in the set of common experiments which is designed to maintain continuity across different CMIP phases. Here, we compare the parameters of individual CMIP6 models with those of the previous-phase CMIP5 models. The parameters of the CMIP5 ensemble have several features. The ratio of TCR to ECS is distributed in the range of approximately 0.5 to 0.7, and for models with large ECS, the ratio tends to decrease. The scaling parameter for the effective radiative forcing of CO_2 varies from model to model and tends to be less than a reference value used in a conventional formula of CO_2 radiative forcing. Although the number of CMIP6 models is currently limited, their parameters show similar distributions within the CMIP5 ranges.

Keywords: climate sensitivity, effective radiative forcing, impulse response model, climate model emulator, ensemble climate experiment

©2019. Japan Geoscience Union. All Right Reserved.

Effect on the earth system of realizing 1.5 degree climate target by overshooting after reaching 2 degree level

*Kaoru Tachiiri[1], Herran Diego Silva[2], Xuanming Su[1], Michio Kawamiya[1]

1. Japan Agency for Marine-Earth Science and Technology, 2. Institute for Global Environmental Strategies

By using an Earth system model (ESM) with emissions and land use scenarios consistent with socio-economic projections from an integrated assessment model, the effect of overshooting to 1.5 degree target (in Celsius from pre-industrial periods) after reaching 2 degree level is investigated in selected indicators of the global environment. Unlike the internationally coordinated model intercomparison project, the scenario is developed for a specific climatic model. The ESM output results in delayed achievements for both of 1.5 and 2 degree targets in terms of global surface mean air temperature, but achieved before or around 2100 as expected when we use global mean surface temperature (for which sea surface temperature and surface air temperature are used for ocean and land, respectively) masked with observation areas. In the overshooting scenario more heat is absorbed by the ocean compared to a case without overshooting, but still we found significant difference between the two scenarios in Arctic sea ice, while in both scenarios corals seem difficult to survive the 21st century (when no thermal adaptation is assumed) . The difference in steric sea level rise between the scenarios is only below 2 cm in 2100. In addition, vegetation productivity in broad regions shows slight (~5%) increase. Emission pathways in the scenarios rely on a large amount of carbon sequestration. In the 2 degree scenario CO2 emissions in 2100 are slightly below zero, while for 1.5 degree scenario they are below -20 GtCO2.. When the Earth system has high climate sensitivity and TCRE, to reach the 1.5 degree target we need to take an overshooting temperature pathway, but in case the overshooting is large, difference in some indicators between 1.5 degree and 2 degree scenarios can be non-significant, which is an important indication in implementing adaptive mitigation in the coming decades.

Keywords: Earth system model, integrated assessment model, 1.5 degree target, 2 degree target, stabilization, overshooting

©2019. Japan Geoscience Union. All Right Reserved.

Historical regional and sectoral contributions to climate change

*Xuanming Su[1], Kaoru Tachiiri[1], Katsumasa TANAKA[2], Michio Watanabe[1]

1. Japan Agency for Marine-Earth Science and Technology, 2. National Institute for Environmental Studies

Regional or sectoral contributions to climate change are important in the formulation of climate change policy. After the industrial revolution, developed countries emit CO_2 and non-CO_2 greenhouse gases (GHGs), and the historical emissions are large; while developing countries contribute relative fewer emissions in historical period but increase significantly in recent years or visible future. To assess the contributions to climate change, using cumulative emissions is a general and direct method. However, such method may ignore the lifetime of GHGs since part of the GHGs sink into the biosphere, ocean, soil or diminish during biogeochemical cycles. In this study, we evaluate the historical regional and sectoral contributions to climate change by using an improved version of Simple Climate Model for OPTimization (SCM4OPT) with a normalized marginal method. Based on the results, we analyze ten major GHG emitting countries and 12 sectors.

First, current emissions with relative long lifetime like CO_2 and N_2O, from developing countries increase significantly, like China, India, Mexico and Brazil, however, their contributions to climate change are still relatively smaller, compared with the developed countries such as USA, Japan, Germany, Canada and UK, of which countries the cumulative emissions are in relatively larger scale and current emissions are already under controlled. We can conclude here that the GHGs with relatively long lifetime need to be controlled stringently to reduce the long-term effects on climate change. For CH_4, which has a relatively shorter lifetime, the contributions to climate change are closely related to emissions within recent decades. These imply that reductions on short lifetime emissions can make immediate alleviation regarding climate change.

Second, energy sector contributes most of the CO_2 emissions, and therefore contribute almost half to the climate change among all the sectors. However, for CH_4 and N_2O, agriculture sector contributes most of the emissions and therefore their contributions to climate change are remarkable. Reduction policiesneed to targetthesesectors. In addition, CO_2 from land transportation and CH_4 from waste treatment increase rapidly in recent years, attention also needs to be paid to these sectors for making climate change policies.

Keywords: region emissions, sector emissions, climate change contribution, simple climate model

©2019. Japan Geoscience Union. All Right Reserved.

Future projection of global climate, water, food, bio-energy, and land investigated with MIROC-INTEG: a global bio-geophysical land surface model with human components

*Tokuta Yokohata[1], Yusuke Satoh[1], Tsuguki Kinoshita[2], Gen Sakurai[3], Yadu Pokhrel[4], Akihiko Ito[1], Etsushi Kato[5], Masashi Okada[1], Naota Hanasaki[1], Tomoko Nitta[6], Seita Emori[1]

1. National Institute for Environmental Studies, 2. Ibaraki University, 3. National Agriculture and Food Research Organization, 4. Michigan State University, 5. The Institute of Applied Energy, 6. University of Tokyo

Future climate changes possibly affect water resources, food production, energy supply, and ecosystem services. It is critical to better understand the interactions between the changes in these complicated factors. While earth system models and integrated assessment models are applicable to explore this topic, parts of their natural and/or human processes tend to be simplified depending on their scope. As such, it still remains a challenge to realistically model the human-natural interface. In this context, the MIROC integrated terrestrial model (MIROC-INTEG) was developed. One of the features of MIROC-INTEG is that the natural ecosystem and human activity models are coupled to a global land surface model MATSIRO (Nitta et al. 2014, Journal of Climate), which is a component of a state-of-the-art global climate model, MIROC (Watanabe et al. 2010, Journal of Climate). As a natural ecosystem model, we use a global vegetation model, VISIT (Ito and Inatomi 2012, Biogeosciences). As human activity models, we use a global land-surface model with anthropogenic water regulation modules, HiGW-MAT (Pokhrel et al, 2012, Journal of Hydrometeorology), and a global crop model, PRYSBI2 (Sakurai et al, 2014, Scientific Reports). In HiGW-MAT, models of human water regulations such as water withdrawal from river, dam operation, and irrigation (Hanasaki et al. 2008, Hydrol. Earth Syst. Sci.) are incorporated to the above-mentioned global land surface model, MATSIRO. In PRYSBI2, the growth and yield of four crops (wheat, maize, soybean, rice) are calculated. In addition to these models, a global land use model (Terrestrial Land-use Model, TeLMO) is newly developed in the present study. TeLMO calculate the grid ratio of cropland (food and bio-energy crops), pasture, forest (managed and un-managed), as well as their transition. Output variables of each sub-model are passed to other sub-models during the time integration.
We will present an analysis of historical and future simulations with a focus on the interactions between water, food, energy, and land. In the historical simulations, we validated the model output such as irrigated water, crop yield, ecosystem productions, and cropland area by comparing to the observed or reanalysis data. In the future simulations, we investigated the role of uncertainties in climate (Representative Concentration Pathways) and socio-economic (Shared Socio-economic Pathways) scenarios. We also investigate the role of uncertainties in model parameters, and found that an uncertainty in the fertilization effect of crop growth model PRYSBI2 strongly affect uncertainty in future projection of crop yield and land use change in TeLMO. We found that future changes in precipitation and/or temperature possibly cause decrease in soil moisture, leading to decreases in crop yield (especially in high emission scenario such as RCP8.5). Decrease in crop yield bring about increase in crop land area, which also causes the increase in irrigation demands. Interaction between water, crop yield, and land use, as well as possible impacts on ecosystem service will be discussed in the presentation.

Keywords: Global Climate Model, Earth System Model, Human activity

©2019. Japan Geoscience Union. All Right Reserved.

Downscaling a global agricultural land use model to country level for national SSP analysis

*Wenchao Wu[1], Tomoko Hasegawa[1], Kiyoshi Takahashi[1], Shinichiro Fujimori[2]

1. National Institute for Environmental Studies, 2. Kyoto Univ.

The Shared Socioeconomic Pathways (SSPs) has been part of latest scenario framework developed by the climate change research society in the recent decade, serving the integrated analysis of future climate impacts, vulnerabilities, adaptation, and mitigation, in which the agriculture, food system and land use are important components. Multiple integrated assessment models (IAMs) have been used for the quantitative projections of future agriculture, food system and land use in the global scale. However, the tool and application of IAMs to the quantification of SSPs on regional or national level is limited. Meanwhile, there are growing needs for the quantification of SSPs on regional or national level for a more detailed understanding of agriculture, food, and land use, and their interactions with other nexus, such as energy, water, and biodiversity. One obstacle for such application is the coarse spatial resolution of global IAMs for land use module. This study aims to apply the Asian-Pacific Integrated Model/Platform for Land-Use and Environmental Model (AIM/PLUM) for the quantification of agriculture, food system, and land use in Japan under its national-specific SSPs narratives. To achieve this, a regional land use model, AIM/PLUM-Japan, was developed, by improving the spatial resolution to 0.05˚ (targeting 1km) from global model of 0.5˚. We combined the statistical production area data and spatial land use data to produce a refined base crop map. Agricultural land use could be downscaled to 0.05˚ resolution and gridded agricultural land use information could be generated using this model. Aside from providing quantitative land use information for Japan’ s SSPs, this study also contributes to the IAMs and SSPs societies by testing the applicability and feasibility of global IAMs, especially land use models, to the regional or national extension. For example, regional (national) SSPs quantifications for other regions could be easily implemented by a similar paradigm using AIM/PLUM.

Keywords: downscaling, land use, national SSP

©2019. Japan Geoscience Union. All Right Reserved.

Extreme Events and Emergent Trends in Marine Ecosystem Stressors under a historical/RCP8.5 Climate Change Pathway

*Keith Bradley Rodgers[1,2], Sarah Schlunegger[3], Richard Slater[3], Burke Hales[4], Axel Timmermann[1,2]

1. IBS Center for Climate Physics, Busan, South Korea, 2. Pusan National University, Busan, South Korea, 3. AOS Program, Princeton University, Princeton NJ, USA, 4. College of Ocean and Atmospheric Sciences, Oregon State Universitym, Corvallis, OR, USA

It is important to identify the degree to which climate change will impact ocean ecosystems over the 21st century. Over the last decade there has been increasing application of Earth System Models (ESMs) to project changes in ecosystem stressors (acidification, warming, and de-oxygenation) with a focus on surface and/or thermocline-integrated conditions. Recent efforts have made combined use of CMIP5 models, large ensemble simulations, and/or scenario sensitivity experiments to estimate uncertainties in future projections. Nevertheless very little to date has been done to evaluate how the frequency of extreme events with ecosystem stressors will respond to future climate perturbations. Here we consider for an ensemble suite of simulations with GFDL's ESM2M changes in the frequency of marine ecosystem extreme events over the 21stcentury. We focus on the contrast between the behavior at the ocean's surface vs. base of the ocean's euphotic zone, as these are both important horizons for ocean ecosystems, and on the contrast between the Time of Emergence of decadal trends vs. frequency changes of extreme events, as these are both important ecological timescales. Particular attention is devoted to acidification at the base of the euphotic zone, as this pertains to the life cycle of pteropods. Preliminary results indicate that in addition to the subpolar Northern Oceans and the Southern Ocean, the Large Marine Ecosystems (LME) regions of the eastern Pacific become increasingly exposed to corrosive waters over the 21stcentury.

Keywords: Climate Change, Ecosystem Stressors, Extreme Events, Large Ensemble

©2019. Japan Geoscience Union. All Right Reserved.

[E] Poster | A (Atmospheric and Hydrospheric Sciences)：A-CG Complex & General

Wed. May 29, 2019 5:15 PM - 6:30 PM JST | Wed. May 29, 2019 8:15 AM - 9:30 AM UTC | Poster Hall International Exhibition Hall8, Makuhari Messe_16

[A-CG35] Projection and detection of global environmental change

convener:Michio Kawamiya(Japan Agency for Marine-Earth Science and Technology), Hiroaki Tatebe(Japan Agency for Marine-Earth Science and Technology), Kaoru Tachiiri(Japan Agency for Marine-Earth Science and Technology)

Anthropogenic forcings on global environment are expected to cause intensification of extreme events, sea level rise, ocean acidification and deoxygenation, as well as large-scale ecosystem changes. The CMIP6 experimental protocol has been established based on which modeling groups across the world are starting to provide environmental projection data toward 6th IPCC assessment report due in 2021. Various new types of studies, such as event attribution and coupling of socio-economic processes and Earth system dynamics, are also emerging in the field of global change projection. In addition, observational studies are becoming increasingly more important for grasping changes in the global environment and evaluating model projections. Interactions and collaborations beyond boundaries of conventional scientific disciplines are desired for dealing with the issue of global changes. This session thus aims to deepen our understanding on global change, from both disciplinary and interdisciplinary viewpoints. This session is co-organized by AIMES - Future Earth project "Analysis, Integration and Modelling of the Earth System" (https://aimesproject.org/).

[ACG35-P01] World Regionalization of Climate Change (1961–2010)

*Shao Sun[1,2], Peijun Shi[2,3,4], Daoyi Gong[2], Tao Zhou[2] (1.National Climate Center, China Meteorological Administration, Beijing 100081, China, 2.State Key Laboratory of Earth Surface Processes and Resource Ecology, Beijing Normal University, Beijing 100875, China, 3.Key Laboratory of Environmental Change and Natural Disaster of Ministry of Education, Beijing Normal University, Beijing 100875, China, 4.Academy of Disaster Reduction and Emergency Management, Ministry of Civil Affairs & Ministry of Education, Beijing 100875, China)

[ACG35-P02] Quantifying and identifying future climate signal, noise, and internal variability at finer temporal scales

*Jongho Kim[1], Manh Van Doi[1] (1.University of Ulsan)

[ACG35-P03] Basic evaluation of MIROC6 and current status of CMIP6 experiments

*Hiroaki Tatebe[1] (1.Japan Agency for Marine-Earth Science and Technology)

[ACG35-P04] Synchronized increase of extreme cold and warm events in China during the recent global warming slowdown

*Xiubao Sun[1,3], Chunzai Wang[1], Guoyu Ren[2,3], Panfeng Zhang[2] (1.State Key Laboratory of Tropical Oceanography (LTO), South China Sea Institute of Oceanology(SCSIO), Chinese Academy of Sciences (CAS), 2.Department of Atmospheric Science, School of Environmental Studies, China University of Geosciences (CUG), 3.Laboratory for Climate Studies, National Climate Center (NCC), China Meteorological Administration (CMA))

[ACG35-P05] Quantification of thermodynamical and dynamical contributions to the anthropogenic influences on tropical cyclone rainfall extremes

*Cheng-Ta Chen[1], Shih-How Lo[1], Chung-Chieh Wang[1], Kazuhisa Tsuboki[2] (1.Department of Earth Sciences, National Taiwan Normal University, 2.Hydrospheric-Atmospheric Research Center, Nagoya University)

[ACG35-P06] Temporal Evolution of the Long-Term Distributional Biases of Climate Models as a Parameter for the Regional Evaluation of the Simulation of Climate Change

*Martin Gomez-Garcia[1], Akiko Matsumura[1], Shiro Hishinuma[1], Daikichi Ogawada[1] (1.Nippon Koei Co. Ltd., Reasearch and Development Center)

[ACG35-P07] A global simulation of bioenergy crop yield

*Zhipin Ai[1], Naota Hanasaki[1] (1.National Institute for Environmental Studies)

[ACG35-P08] Integrated Research Program for Advancing Climate Models - Theme B: national research program in Japan on earth system modeling

*Michio Kawamiya[1], Tomohiro Hajima[1], Kaoru Tachiiri[1], Jun'ichi Tsutsui[2], Tokuta Yokohata[3], Takashi Arakawa[4], Takahiro Inoue[4] (1.Japan Agency for Marine-Earth Science and Technology, 2.Central Research Institute of Electric Power Industry, 3.National Institute for Environmental Studies, 4.Research Organization for Information Science and Technology)

[ACG35-P09] Towards probabilistic climate projections based on the CMIP6 multi-model ensemble

*Junichi Tsutsui[1] (1.Central Research Institute of Electric Power Industry)

[ACG35-P10] Effect on the earth system of realizing 1.5 degree climate target by overshooting after reaching 2 degree level

*Kaoru Tachiiri[1], Herran Diego Silva[2], Xuanming Su[1], Michio Kawamiya[1] (1.Japan Agency for Marine-Earth Science and Technology, 2.Institute for Global Environmental Strategies)

[ACG35-P11] **Historical regional and sectoral contributions to climate change**

*Xuanming Su[1], Kaoru Tachiiri[1], Katsumasa TANAKA[2], Michio Watanabe[1] (1.Japan Agency for Marine-Earth Science and Technology, 2.National Institute for Environmental Studies)

[ACG35-P12] **Future projection of global climate, water, food, bio-energy, and land investigated with MIROC-INTEG: a global bio-geophysical land surface model with human components**

*Tokuta Yokohata[1], Yusuke Satoh[1], Tsuguki Kinoshita[2], Gen Sakurai[3], Yadu Pokhrel[4], Akihiko Ito[1], Etsushi Kato[5], Masashi Okada[1], Naota Hanasaki[1], Tomoko Nitta[6], Seita Emori[1] (1.National Institute for Environmental Studies, 2.Ibaraki University, 3.National Agriculture and Food Research Organization, 4.Michigan State University, 5.The Institute of Applied Energy, 6.University of Tokyo)

[ACG35-P13] **Downscaling a global agricultural land use model to country level for national SSP analysis**

*Wenchao Wu[1], Tomoko Hasegawa[1], Kiyoshi Takahashi[1], Shinichiro Fujimori[2] (1.National Institute for Environmental Studies, 2.Kyoto Univ.)

[ACG35-P14] Extreme Events and Emergent Trends in Marine Ecosystem Stressors under a historical/RCP8.5 Climate Change Pathway

*Keith Bradley Rodgers[1,2], Sarah Schlunegger[3], Richard Slater[3], Burke Hales[4], Axel Timmermann[1,2] (1.IBS Center for Climate Physics, Busan, South Korea, 2.Pusan National University, Busan, South Korea, 3.AOS Program, Princeton University, Princeton NJ, USA, 4.College of Ocean and Atmospheric Sciences, Oregon State Universitym, Corvallis, OR, USA)

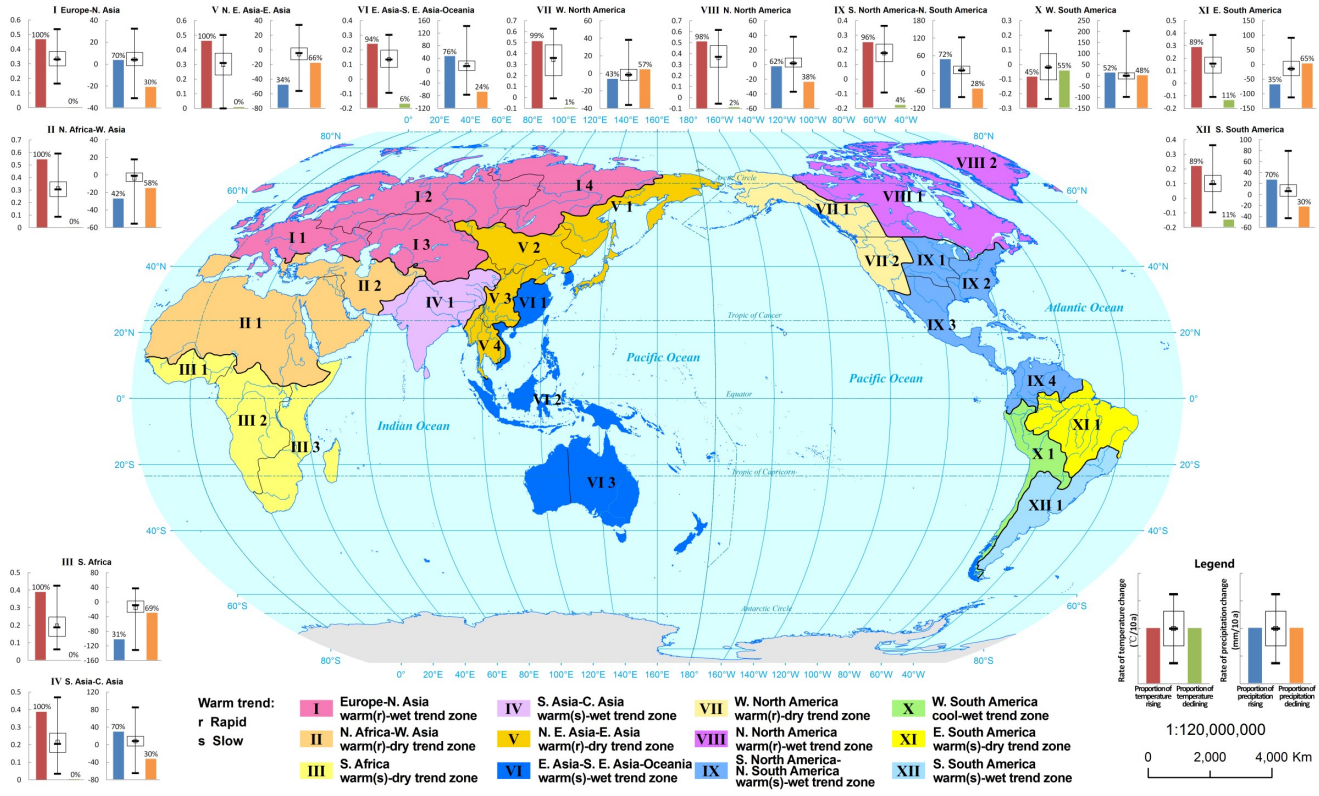
World Regionalization of Climate Change (1961–2010)

*Shao Sun[1,2], Peijun Shi[2,3,4], Daoyi Gong[2], Tao Zhou[2]

1. National Climate Center, China Meteorological Administration, Beijing 100081, China, 2. State Key Laboratory of Earth Surface Processes and Resource Ecology, Beijing Normal University, Beijing 100875, China, 3. Key Laboratory of Environmental Change and Natural Disaster of Ministry of Education, Beijing Normal University, Beijing 100875, China, 4. Academy of Disaster Reduction and Emergency Management, Ministry of Civil Affairs & Ministry of Education, Beijing 100875, China

Existing climate regionalization aims to characterize the regional differences in climate based on years of the mean values of climate indices. However, with the accelerating climate change nowadays, existing climate regionalization cannot represent the regional difference of climate change, nor can it reflect the extreme weather and climate disasters and environmental risks incurred from climate changes. This paper utilizes the tendency value and fluctuation value of temperature and precipitation from 1961 to 2010 to identify the climate change quantitatively, and completes world regionalization of climate change (1961–2010) with administrative subdivisions of countries as the basic unit in combination with world's terrain feature. Level-I regionalization divides world's climate change (1961–2010) into twelve tendency zones based on the tendency of temperature and precipitation; level-II regionalization refers to twenty-eight fluctuation regions based on level-I regionalization according to the fluctuation of temperature and precipitation. Climate change regionalization provides a basis for countries and regions in the world to develop plans for adapting to climate change, especially for managing extreme weather and climate disasters and environmental risks.

Keywords: Climate change, Regionalization, Tendency, Fluctuation, World



©2019. Japan Geoscience Union. All Right Reserved.

Quantifying and identifying future climate signal, noise, and internal variability at finer temporal scales

*Jongho Kim[1], Manh Van Doi[1]

1. University of Ulsan

Quantifying and identifying climate internal variability (CIV) plays an important role in climate change studies because of its irreducible and unpredictable characteristics. A large number of studies have addressed such an issue; however, the issue was only resolved at coarser resolution on the first order moments of few climate variables. Our recent study has estimated CIV of climate variables for a “current” period at finer spatial and temporal scales; however, whether CIV will change or remain constant in the future under the impact of representative concentration pathways (RCP45 and RCP85) is still questionable. To investigate how CIV will change in the future in both spatial pattern and magnitude, CIV is assessed over 30-year periods in both current and future periods with two scenarios in Korea by analyzing an ensemble of 100 simulations generated by an hourly weather generator. In this study, signal to noise ratio (SNR) used to evaluate the model performance will be applied to simulating ensemble for different periods. CIV is then estimated by two methods: “detrended” and “differenced”; SNR is estimated by “analysis of variance” and “trend analysis” methods. Both SNR and CIV are evaluated with four proposed matrices signifying rainfall volume, extremes and occurrence of rainfall. To consider the change of CIV in the future periods, t-test (test for mean difference) and f-test (test for variance difference) are applied to the ensemble of CIV. In this study, analyzing SNR’s values shows that the four proposed matrices are controlled by non-linear stochastic process and the change tend to increase in the future with increase of CO2 concentration. CIV is proved to change in the future periods under impact of CO2 scenarios. Spatial distribution of CIV’s change over future periods of which locations provides the important and useful information for decision making of water resources planning and proposing mitigation measures of disaster protection.

Acknowledgment:

This research was supported by the Water Management Research Program funded by Ministry of Environment of Korean government (127554), and by the Basic Science Research Program of the National Research Foundation of Korea funded by the Ministry of Education (2016R1D1A1B03931886).

Keywords: climate internal variability, signal to noise ratio, t-test, f-test

©2019. Japan Geoscience Union. All Right Reserved.

Basic evaluation of MIROC6 and current status of CMIP6 experiments

*Hiroaki Tatebe[1]

1. Japan Agency for Marine-Earth Science and Technology

The sixth version of the Model for Interdisciplinary Research on Climate (MIROC), called MIROC6, was cooperatively developed by a Japanese climate modeling community. Overall reproducibility of mean climate and internal climate variability in MIROC6 is better than that in the previous version (MIROC5). The tropical climate systems (e.g., summertime precipitation in the western Pacific and the eastward propagating Madden-Julian Oscillation) and the mid-latitude atmospheric circulations (e.g., the westerlies, the polar night jet, and troposphere-stratosphere interactions) are significantly improved in MIROC6. These improvements can be attributed to the newly implemented parameterization for shallow convective processes and to the directly resolved stratosphere. In the present study, simulated mean climate, internal climate variability in MIROC6 are evaluated and briefly summarized in comparison with MIROC5 and observations. Using MIROC6, designated simulations tackling a wide range of climate science issues, as well as seasonal-to-decadal climate predictions and future climate projections, are currently ongoing with an aim towards contributing to the sixth phase of the Coupled Model Intercomparison Project (CMIP6). Preliminary results of historical climate simulations from the middle of the 19th century, climate projections from the present to the end of the 21th century based on future scenarios of the Shared Socio-economic Pathways, and initialized climate predictions on seasonal-to-decadal timescales will be given in this talk.

Keywords: Climate model, CMIP6, climate projections/predictions

©2019. Japan Geoscience Union. All Right Reserved.

Synchronized increase of extreme cold and warm events in China during the recent global warming slowdown

*Xiubao Sun[1,3], Chunzai Wang[1], Guoyu Ren[2,3], Panfeng Zhang[2]

1. State Key Laboratory of Tropical Oceanography (LTO), South China Sea Institute of Oceanology(SCSIO), Chinese Academy of Sciences (CAS), 2. Department of Atmospheric Science, School of Environmental Studies, China University of Geosciences (CUG), 3. Laboratory for Climate Studies, National Climate Center (NCC), China Meteorological Administration (CMA)

From the end of 1990s to the middle of 2010s, global mean temperature experienced a process of warming slowdown. However, global warm extremes did not show the slowdown phenomenon during the recent global warming slowdown. Based on the observation data of 2362 land surface stations in China, we analyzed the cold and warm extremes changes over mainland China between global warming period (1961-1999) and warming slowdown period (2000-2014). Results indicate that the warming trend in the cold season (MAM and DJF) is significantly higher than that in the warm season (JJA and SON) in the period of global warming (1961-1999), while the warming trend in the warm season is significantly higher than that in the cold season in the period of global warming slowdown. That is, the trend of warm season and the cool season in China have reversed. At the same time, we also found that the synchronous increase occurrence of extreme warm events in summer (JJA) and extreme cold events in winter (DJF) leads to the seasonal trend reverse phenomenon, but there are differences in the spatial variation characteristics between cold and warm extremes. The increase of warm extremes in summer is mainly due to the strong increase of warm events in south China, while the increase of cold events in winter is due to the increase of cold events over China. Further, we also found that the variability of extreme temperature has increased more significantly in the warming slowdown period than that in global warming period. East Asian winter monsoon and summer monsoon both show enhanced characteristics during the global warming slowdown period, which indicates that the increase of sea-land temperature difference in summer and winter results in the synchronous increase of extreme cold and warm events by increasing the climate variability in China.

Keywords: Global warming, Global warming slowdown, Extreme warm events, Extreme cold events, Land-sea temperature difference

©2019. Japan Geoscience Union. All Right Reserved.

Quantification of thermodynamical and dynamical contributions to the anthropogenic influences on tropical cyclone rainfall extremes

*Cheng-Ta Chen[1], Shih-How Lo[1], Chung-Chieh Wang[1], Kazuhisa Tsuboki[2]

1. Department of Earth Sciences, National Taiwan Normal University, 2. Hydrospheric-Atmospheric Research Center, Nagoya University

The rainfall extremes and strong winds associated with tropical cyclones lead to significant damages and lost to where they make landfalling. Upward trend in term of financial lost was indicated for the past few decades from the report of major reinsurance firms. Whether the past anthropogenic warming played a significant role in such extreme event and their changes remained very controversial. On one hand, people argue it’s nearly impossible to attribute an individual extreme event to global warming. On the other hand, the increase of heavy rainfall is consistent with the expected effects of climate change on tropical cyclone. To diagnose possible anthropogenic contributions to the odds of heavy rainfall associated with tropical cyclone, we adapt an existing event attribution framework of modeling a ‘world that was’ and comparing it to a modeled ‘world that might have been’ for that same time but for the absence of historical anthropogenic drivers of climate. One limitation for applying such approach to high-impact weather system is that it will require models capable of capturing the essential processes lead to the studied extremes. Using a cloud system resolving model that can properly simulate the complicated interactions between tropical cyclone, large-scale background, topography, we first perform the ensemble ‘world that was’ simulations forced by the high resolution ECMWF YOTC analysis. We then re-simulate with the adjusted ‘world that might have been conditions’ by removing the regional atmospheric and oceanic forcing due to human influences estimated from the CMIP5 model ensemble mean conditions between all forcing and natural forcing only historical runs. Thus our findings are highly conditional on the driving analysis and adjustments therein, but the setup allows us to elucidate possible contribution of anthropogenic forcing to changes in the likelihood of heavy rainfall associated tropical cyclone. With only less than half of degree anthropogenic warming over the study area, we found that this forcing very likely (9 out of 10 cases) increase the risk of heavy rainfall event (grid rainfall greater than 33 mm per hour) by at least 16%. The role of dynamical processes that leads to precipitation extreme increases beyond the moisture content increase will be further analyzed and discussed.

Keywords: Tropical Cyclone, Extreme rainfall, extreme event attribution

©2019. Japan Geoscience Union. All Right Reserved.

Temporal Evolution of the Long-Term Distributional Biases of Climate Models as a Parameter for the Regional Evaluation of the Simulation of Climate Change

*Martin Gomez-Garcia[1], Akiko Matsumura[1], Shiro Hishinuma[1], Daikichi Ogawada[1]

1. Nippon Koei Co. Ltd., Reasearch and Development Center

Owing to the climate variability of the General Circulation Models (GCM), the discrepancy between their outputs and observational datasets at scales that range from hours to years is practically random. Thus, the associated errors need to be evaluated in terms of the long-term (multidecadal) distributional properties of the atmospheric variables. A recently developed bias-correction method corrects the systematic errors (i.e., biases) in the climate mean state and in three distributional measures of the daily and the interannual variability (namely the frequency of extremes, the skewness, and the scale of the variable at each timescale). The adjustment of these biases is done in such a way that the corrections at one timescale do not affect the probability distribution at another. Therefore, this bias-correction method is able to preserve the GCM-simulated climate trends and extensively reproduce the long-term frequency of the observed extreme weather (e.g. 98th percentile of wet days, maximum seasonal mean of surface temperature).

Generally, the bias-correction of GCMs faces the challenge of including the simulated changes of climate, which supposes alterations in not only the mean but also other aspects like the skewness and the frequency of extremes. The abovementioned bias-correction method includes the effect of the simulated climate change in the correction of the distributional biases. However, considering the coarse resolution of the GCMs and the imperfections in the parameterizations of the subgrid physical processes, the fundamental assumption that the distributional biases are predictable (i.e., stationary) is made.

In this study, we explored the possibility of evaluating the sensibility with which GCMs simulate the response of the earth-system components to external forcing (i.e., climate change) by comparing the temporal evolution of the distributional biases at different timescales over specific regions. For the short period in which the observed data was available, our results revealed that many CMIP5 GCMs are indeed able to simulate with a quasi-stationary bias the changes caused by climate change. Moreover, being able to identify the regions in which certain models do not show the errors with a systematic behavior in either the climate mean state, the daily variability or the interannual variability can be useful for the further development of climate models. We expect that with the data of the GCM outputs of the future phases of the CMIP project, the period in which the observed and the modeled data coincide becomes longer and, thus, our conclusions can be supported by more robust evidence.

Keywords: Bias correction of GCMs at different timescales, Climate trends and climate variability, Evaluation of the ability of GCMs to simulate climate change

©2019. Japan Geoscience Union. All Right Reserved.

A global simulation of bioenergy crop yield

*Zhipin Ai[1], Naota Hanasaki[1]

1. National Institute for Environmental Studies

Large-scale development of bioenergy is considered as an effective pathway to achieve the 2 degrees target of the Paris Agreement. To avoid the competition with food crops, so-called the second-generation bioenergy crops such as miscanthus and switchgrass are regarded as potential dedicated biomass crop. However, the models to estimate the yield of miscanthus and switchgrass at a global scale which enable analyzing the effects of irrigation water application are seldom seen as of today. Here, we firstly updated the crop module in the global hydrological model H08 for miscanthus and switchgrass. Then, we conducted a global simulation and validation of the yield for miscanthus and switchgrass at 0.5 degree. The results indicated that the updated H08 have a good ability in simulating the yield of perennial bioenergy crops, which provides a good foundation for further integrated assessment of the impacts of bioenergy crop production on water sector.

Acknowledgement: This research was supported by the Environment Research and Technology Development Fund (S-14-5) of the Environmental Restoration and Conservation Agency.

Keywords: Bioenergy, Crop yield, H08

©2019. Japan Geoscience Union. All Right Reserved.

Integrated Research Program for Advancing Climate Models - Theme B: national research program in Japan on earth system modeling

*Michio Kawamiya[1], Tomohiro Hajima[1], Kaoru Tachiiri[1], Jun'ichi Tsutsui[2], Tokuta Yokohata[3], Takashi Arakawa[4], Takahiro Inoue[4]

1. Japan Agency for Marine-Earth Science and Technology, 2. Central Research Institute of Electric Power Industry, 3. National Institute for Environmental Studies, 4. Research Organization for Information Science and Technology

The Integrated Research Program for Advancing Climate Models, or TOUGOU (abbreviation taken from its Japanese name), is a national project for projection of global change. Its aim to provide information for adaptation and mitigation, based on scientific evaluation of changes including those in extreme events and carbon cycle. The project was launched in April, 2017. While the entire program deals with a wide range of physical aspects and consequent impacts of climate change, Theme B (TOUGOU-B) focuses on the development of a state-of-the-art Earth system model (ESM) incorporating biogeochemical processes, such as sophisticated carbon and nitrogen cycles, as well as its application to exploring future socio-economic pathways of climate change mitigation. MIROC-ESM, an ESM developed under TOUGOU-B (and the previous SOUSEI-B) has been significantly improved since the 5th phase of coupled model intercomparison project (CMIP5), and has started to be run for CMIP6. During the three years since TOUGOU was launched, results have been obtained that may contribute to 6th Assessment Report (AR6) of Intergovernmental Panel on Climate Change (IPCC) including those on impacts of pyrogenic iron on oceanic ecosystem, assessment of the outcome of labor productivity change due to warming, and effects of high dust amount on surface temperature during the Last Glacial Maximum. Besides, efforts to secure ways to disseminate projection data are ongoing under TOUGOU-B. Specifically, collaboration has been established between climate modeling community in Japan and Data Integration and Analysis System (DIAS), a national IT project for environmental data, have been continuing, in order for Japan to participate in Earth System Grid Federation (ESGF). ESGF is an international cooperative activity to construct a data distributing system for climate related data such as CMIP6 outputs. Some of the details of these results will be explained in the presentation.

Keywords: IPCC, Earth system model , carbon cycle, socio-economic scenario, CMIP6, climate mitigation

©2019. Japan Geoscience Union. All Right Reserved.

Towards probabilistic climate projections based on the CMIP6 multi-model ensemble

*Junichi Tsutsui[1]

1. Central Research Institute of Electric Power Industry

Research on climate change mitigation uses a climate model emulator that represents the average and range over a specific multi-model ensemble of complex climate simulations. The Coupled Model Intercomparison Project (CMIP) has provided such multi-model ensembles, and its latest Phase 6 (CMIP6) results are being revealed. As a first step to applying the CMIP6 results to probabilistic climate projections, we focus on the distribution of key parameters representing atmospheric CO_2-induced forcing and transient temperature responses.

In this study, we develop a procedure to determine the forcing-response parameters of a complex climate model. We simultaneously fit a curve built on an impulse response function to the global mean time series of the model's surface temperature anomaly and top-of-atmosphere energy imbalance from two basic CO_2 -forced experiments, i.e., an abrupt quadrupling and a 1%-per-year increase in atmospheric CO_2 concentration. This scheme serves as an improved alternative to the widely-used regression method of Gregory et al. (2004). Furthermore, it makes a complete set of parameters to emulate the target model from which equilibrium climate sensitivity (ECS) and transient climate response (TCR) are derived. The properties of a multi-model ensemble are quantified through a statistical approach including a principal component analysis for the parameters.

The two CO_2-forced experiments are included in the set of common experiments which is designed to maintain continuity across different CMIP phases. Here, we compare the parameters of individual CMIP6 models with those of the previous-phase CMIP5 models. The parameters of the CMIP5 ensemble have several features. The ratio of TCR to ECS is distributed in the range of approximately 0.5 to 0.7, and for models with large ECS, the ratio tends to decrease. The scaling parameter for the effective radiative forcing of CO_2 varies from model to model and tends to be less than a reference value used in a conventional formula of CO_2 radiative forcing. Although the number of CMIP6 models is currently limited, their parameters show similar distributions within the CMIP5 ranges.

Keywords: climate sensitivity, effective radiative forcing, impulse response model, climate model emulator, ensemble climate experiment

©2019. Japan Geoscience Union. All Right Reserved.

Effect on the earth system of realizing 1.5 degree climate target by overshooting after reaching 2 degree level

*Kaoru Tachiiri[1], Herran Diego Silva[2], Xuanming Su[1], Michio Kawamiya[1]

1. Japan Agency for Marine-Earth Science and Technology, 2. Institute for Global Environmental Strategies

By using an Earth system model (ESM) with emissions and land use scenarios consistent with socio-economic projections from an integrated assessment model, the effect of overshooting to 1.5 degree target (in Celsius from pre-industrial periods) after reaching 2 degree level is investigated in selected indicators of the global environment. Unlike the internationally coordinated model intercomparison project, the scenario is developed for a specific climatic model. The ESM output results in delayed achievements for both of 1.5 and 2 degree targets in terms of global surface mean air temperature, but achieved before or around 2100 as expected when we use global mean surface temperature (for which sea surface temperature and surface air temperature are used for ocean and land, respectively) masked with observation areas. In the overshooting scenario more heat is absorbed by the ocean compared to a case without overshooting, but still we found significant difference between the two scenarios in Arctic sea ice, while in both scenarios corals seem difficult to survive the 21st century (when no thermal adaptation is assumed) . The difference in steric sea level rise between the scenarios is only below 2 cm in 2100. In addition, vegetation productivity in broad regions shows slight (~5%) increase. Emission pathways in the scenarios rely on a large amount of carbon sequestration. In the 2 degree scenario CO2 emissions in 2100 are slightly below zero, while for 1.5 degree scenario they are below -20 GtCO2.. When the Earth system has high climate sensitivity and TCRE, to reach the 1.5 degree target we need to take an overshooting temperature pathway, but in case the overshooting is large, difference in some indicators between 1.5 degree and 2 degree scenarios can be non-significant, which is an important indication in implementing adaptive mitigation in the coming decades.

Keywords: Earth system model, integrated assessment model, 1.5 degree target, 2 degree target, stabilization, overshooting

©2019. Japan Geoscience Union. All Right Reserved.

Historical regional and sectoral contributions to climate change

*Xuanming Su[1], Kaoru Tachiiri[1], Katsumasa TANAKA[2], Michio Watanabe[1]

1. Japan Agency for Marine-Earth Science and Technology, 2. National Institute for Environmental Studies

Regional or sectoral contributions to climate change are important in the formulation of climate change policy. After the industrial revolution, developed countries emit CO_2 and non-CO_2 greenhouse gases (GHGs), and the historical emissions are large; while developing countries contribute relative fewer emissions in historical period but increase significantly in recent years or visible future. To assess the contributions to climate change, using cumulative emissions is a general and direct method. However, such method may ignore the lifetime of GHGs since part of the GHGs sink into the biosphere, ocean, soil or diminish during biogeochemical cycles. In this study, we evaluate the historical regional and sectoral contributions to climate change by using an improved version of Simple Climate Model for OPTimization (SCM4OPT) with a normalized marginal method. Based on the results, we analyze ten major GHG emitting countries and 12 sectors.

First, current emissions with relative long lifetime like CO_2 and N_2O, from developing countries increase significantly, like China, India, Mexico and Brazil, however, their contributions to climate change are still relatively smaller, compared with the developed countries such as USA, Japan, Germany, Canada and UK, of which countries the cumulative emissions are in relatively larger scale and current emissions are already under controlled. We can conclude here that the GHGs with relatively long lifetime need to be controlled stringently to reduce the long-term effects on climate change. For CH_4, which has a relatively shorter lifetime, the contributions to climate change are closely related to emissions within recent decades. These imply that reductions on short lifetime emissions can make immediate alleviation regarding climate change.

Second, energy sector contributes most of the CO_2 emissions, and therefore contribute almost half to the climate change among all the sectors. However, for CH_4 and N_2O, agriculture sector contributes most of the emissions and therefore their contributions to climate change are remarkable. Reduction policiesneed to targetthesesectors. In addition, CO_2 from land transportation and CH_4 from waste treatment increase rapidly in recent years, attention also needs to be paid to these sectors for making climate change policies.

Keywords: region emissions, sector emissions, climate change contribution, simple climate model

©2019. Japan Geoscience Union. All Right Reserved.

Future projection of global climate, water, food, bio-energy, and land investigated with MIROC-INTEG: a global bio-geophysical land surface model with human components

*Tokuta Yokohata[1], Yusuke Satoh[1], Tsuguki Kinoshita[2], Gen Sakurai[3], Yadu Pokhrel[4], Akihiko Ito[1], Etsushi Kato[5], Masashi Okada[1], Naota Hanasaki[1], Tomoko Nitta[6], Seita Emori[1]

1. National Institute for Environmental Studies, 2. Ibaraki University, 3. National Agriculture and Food Research Organization, 4. Michigan State University, 5. The Institute of Applied Energy, 6. University of Tokyo

Future climate changes possibly affect water resources, food production, energy supply, and ecosystem services. It is critical to better understand the interactions between the changes in these complicated factors. While earth system models and integrated assessment models are applicable to explore this topic, parts of their natural and/or human processes tend to be simplified depending on their scope. As such, it still remains a challenge to realistically model the human-natural interface. In this context, the MIROC integrated terrestrial model (MIROC-INTEG) was developed. One of the features of MIROC-INTEG is that the natural ecosystem and human activity models are coupled to a global land surface model MATSIRO (Nitta et al. 2014, Journal of Climate), which is a component of a state-of-the-art global climate model, MIROC (Watanabe et al. 2010, Journal of Climate). As a natural ecosystem model, we use a global vegetation model, VISIT (Ito and Inatomi 2012, Biogeosciences). As human activity models, we use a global land-surface model with anthropogenic water regulation modules, HiGW-MAT (Pokhrel et al, 2012, Journal of Hydrometeorology), and a global crop model, PRYSBI2 (Sakurai et al, 2014, Scientific Reports). In HiGW-MAT, models of human water regulations such as water withdrawal from river, dam operation, and irrigation (Hanasaki et al. 2008, Hydrol. Earth Syst. Sci.) are incorporated to the above-mentioned global land surface model, MATSIRO. In PRYSBI2, the growth and yield of four crops (wheat, maize, soybean, rice) are calculated. In addition to these models, a global land use model (Terrestrial Land-use Model, TeLMO) is newly developed in the present study. TeLMO calculate the grid ratio of cropland (food and bio-energy crops), pasture, forest (managed and un-managed), as well as their transition. Output variables of each sub-model are passed to other sub-models during the time integration.
We will present an analysis of historical and future simulations with a focus on the interactions between water, food, energy, and land. In the historical simulations, we validated the model output such as irrigated water, crop yield, ecosystem productions, and cropland area by comparing to the observed or reanalysis data. In the future simulations, we investigated the role of uncertainties in climate (Representative Concentration Pathways) and socio-economic (Shared Socio-economic Pathways) scenarios. We also investigate the role of uncertainties in model parameters, and found that an uncertainty in the fertilization effect of crop growth model PRYSBI2 strongly affect uncertainty in future projection of crop yield and land use change in TeLMO. We found that future changes in precipitation and/or temperature possibly cause decrease in soil moisture, leading to decreases in crop yield (especially in high emission scenario such as RCP8.5). Decrease in crop yield bring about increase in crop land area, which also causes the increase in irrigation demands. Interaction between water, crop yield, and land use, as well as possible impacts on ecosystem service will be discussed in the presentation.

Keywords: Global Climate Model, Earth System Model, Human activity

©2019. Japan Geoscience Union. All Right Reserved.

Downscaling a global agricultural land use model to country level for national SSP analysis

*Wenchao Wu[1], Tomoko Hasegawa[1], Kiyoshi Takahashi[1], Shinichiro Fujimori[2]

1. National Institute for Environmental Studies, 2. Kyoto Univ.

The Shared Socioeconomic Pathways (SSPs) has been part of latest scenario framework developed by the climate change research society in the recent decade, serving the integrated analysis of future climate impacts, vulnerabilities, adaptation, and mitigation, in which the agriculture, food system and land use are important components. Multiple integrated assessment models (IAMs) have been used for the quantitative projections of future agriculture, food system and land use in the global scale. However, the tool and application of IAMs to the quantification of SSPs on regional or national level is limited. Meanwhile, there are growing needs for the quantification of SSPs on regional or national level for a more detailed understanding of agriculture, food, and land use, and their interactions with other nexus, such as energy, water, and biodiversity. One obstacle for such application is the coarse spatial resolution of global IAMs for land use module. This study aims to apply the Asian-Pacific Integrated Model/Platform for Land-Use and Environmental Model (AIM/PLUM) for the quantification of agriculture, food system, and land use in Japan under its national-specific SSPs narratives. To achieve this, a regional land use model, AIM/PLUM-Japan, was developed, by improving the spatial resolution to 0.05˚ (targeting 1km) from global model of 0.5˚. We combined the statistical production area data and spatial land use data to produce a refined base crop map. Agricultural land use could be downscaled to 0.05˚ resolution and gridded agricultural land use information could be generated using this model. Aside from providing quantitative land use information for Japan’ s SSPs, this study also contributes to the IAMs and SSPs societies by testing the applicability and feasibility of global IAMs, especially land use models, to the regional or national extension. For example, regional (national) SSPs quantifications for other regions could be easily implemented by a similar paradigm using AIM/PLUM.

Keywords: downscaling, land use, national SSP

©2019. Japan Geoscience Union. All Right Reserved.

Extreme Events and Emergent Trends in Marine Ecosystem Stressors under a historical/RCP8.5 Climate Change Pathway

*Keith Bradley Rodgers[1,2], Sarah Schlunegger[3], Richard Slater[3], Burke Hales[4], Axel Timmermann[1,2]

1. IBS Center for Climate Physics, Busan, South Korea, 2. Pusan National University, Busan, South Korea, 3. AOS Program, Princeton University, Princeton NJ, USA, 4. College of Ocean and Atmospheric Sciences, Oregon State Universitym, Corvallis, OR, USA

It is important to identify the degree to which climate change will impact ocean ecosystems over the 21st century. Over the last decade there has been increasing application of Earth System Models (ESMs) to project changes in ecosystem stressors (acidification, warming, and de-oxygenation) with a focus on surface and/or thermocline-integrated conditions. Recent efforts have made combined use of CMIP5 models, large ensemble simulations, and/or scenario sensitivity experiments to estimate uncertainties in future projections. Nevertheless very little to date has been done to evaluate how the frequency of extreme events with ecosystem stressors will respond to future climate perturbations. Here we consider for an ensemble suite of simulations with GFDL's ESM2M changes in the frequency of marine ecosystem extreme events over the 21stcentury. We focus on the contrast between the behavior at the ocean's surface vs. base of the ocean's euphotic zone, as these are both important horizons for ocean ecosystems, and on the contrast between the Time of Emergence of decadal trends vs. frequency changes of extreme events, as these are both important ecological timescales. Particular attention is devoted to acidification at the base of the euphotic zone, as this pertains to the life cycle of pteropods. Preliminary results indicate that in addition to the subpolar Northern Oceans and the Southern Ocean, the Large Marine Ecosystems (LME) regions of the eastern Pacific become increasingly exposed to corrosive waters over the 21stcentury.

Keywords: Climate Change, Ecosystem Stressors, Extreme Events, Large Ensemble

©2019. Japan Geoscience Union. All Right Reserved.

[E] Poster | H (Human Geosciences)：H-GM Geomorphology

Wed. May 29, 2019 3:30 PM - 5:00 PM JST | Wed. May 29, 2019 6:30 AM - 8:00 AM UTC | Poster Hall International Exhibition Hall8, Makuhari Messe_11

[H-GM03] Geomorphology

convener:Tsuyoshi Hattanji(Faculty of Life and Environmental Sciences, University of Tsukuba), Masayuki Seto(Fukushima Future Center for Regional Revitalization, Fukushima University)

The main subject of this session is interdisciplinary discussion on the whole range of themes relating to geomorphology, especially geomorphic processes, landform development and its relation to environmental changes, geomorphological hazards and their mitigation, relationships among geomorphic processes, other natural phenomena and human activities, and various techniques of geomorphological measurements and landform classification. All presentations and discussion of this session are made in English.

[HGM03-P01] Honeycomb Weathering (Tafoni) of Sandstone and Environmental Factors in Yonaguni Island, Okinawa Prefecture, Japan

*Takayuki Ogata[1] (1.Disaster Prevention Research Center for Island Regions, University of the Ryukyus)

[HGM03-P02] Colluvial deposits in first-order streams and channel head migration by shallow landslides: Case study in granitic basins, Asaminami, Hiroshima, Japan

*Tsuyoshi Hattanji[1], Ryuya Kodama[2], Takahisa Furuichi[3], Shoji Doshida[4], Yasushi Tanaka[5] (1.Faculty of Life and Environmental Sciences, University of Tsukuba, 2.former College of Geoscience, University of Tsukuba, 3.Hokkaido University, 4.National Research Institute of Fire and Disaster, 5.Komazawa University)

[HGM03-P03] Rock restrictions on topographical features of rivers: model experiment

*Yuta Takase[1], Noritaka Endo[1] (1.Kanazawa University)

[HGM03-P04] Stream power incision model and the stage of topographic equilibrium, using physical experiments

*Imamura Akihiro[1], Noritaka Endo[1] (1.Kanazawa University)

[HGM03-P05] Downstream variation in gravel size of the Tenjin River system

*Kazuaki Hori[1], Kazuya Yonehara[1] (1.Department of Geography, Graduate School of Environmental Studies, Nagoya University)

[HGM03-P06] Talus slope development in the time of deglaciation: a case study of the Rev Valley, SW Spitsbergen

*Krzysztof Senderak[1], Marta Kondracka[1], Bogdan Gądek[1] (1.Faculty of Earth Sciences, University of Silesia)

[HGM03-P07] Distribution of Large Benthic Foraminifers in one of Majuro's Conservation Areas – Drenmeo Island

*Benedict Yamamura[1], Kazuhiko Fujita[2], Melba White[3], Kyotak Ishiguro[3], Hironobu Kan[1] (1.Kyushu University, Integrated Sciences for Global Society - Research Center for Coastal Seafloor , 2.Department of Physics and Earth Sciences, University of the Ryukyus, 3.Marshall Islands Marine Resources Authority)

[HGM03-P08] Luminescence chronology of fluvial and marine records from subsurface sediment cores: An insight into the geomorphic evolution of Kaveri delta, India

*kartika goswami[1], Anbarasu Kumaresan[2], Sivakumar Krishnan[2], Senthil K. Sadasivam[2], Manoj Kumar Jaiswal[1] (1.Department of Earth Sciences, Indian Institute of Science Education and Reserach Kolkata, 2.National College Tiruchirappalli, India)

Honeycomb Weathering (Tafoni) of Sandstone and Environmental Factors in Yonaguni Island, Okinawa Prefecture, Japan

*Takayuki Ogata[1]

1. Disaster Prevention Research Center for Island Regions, University of the Ryukyus

Sandstone surfaces of Yonaguni Island (westernmost of the Ryukyu Arc) often show a honeycomb structure (tafoni) derived from physical disintegration in relation to salt weathering. Miocene sandstone (Yaeyama Group) is extensively exposed on the island surface, and forms sea cliffs along rocky coasts. The honeycomb structure is especially observed along the coasts where wave splashes produce wetting and drying processes assisted by strong wind and active evaporation. The geometry and density of tafoni seem to be controlled by vertical height from the sea level and horizontal distance of the coast line. Field observations at the rocky coasts of Yonaguni Island suggest that larger holes are developed along the north-faced coasts than the south-faced coasts, which depends mainly on the northeastern monsoon during the winter period.

Keywords: weathering, sandstone, rocky coast, tafoni, monsoon, Yaeyama group

©2019. Japan Geoscience Union. All Right Reserved.

Colluvial deposits in first-order streams and channel head migration by shallow landslides: Case study in granitic basins, Asaminami, Hiroshima, Japan

*Tsuyoshi Hattanji[1], Ryuya Kodama[2], Takahisa Furuichi[3], Shoji Doshida[4], Yasushi Tanaka[5]

1. Faculty of Life and Environmental Sciences, University of Tsukuba, 2. former College of Geoscience, University of Tsukuba, 3. Hokkaido University, 4. National Research Institute of Fire and Disaster, 5. Komazawa University

Relationship between dates of colluvial deposits and channel-head migration was examined in granitic mountains where a debris-flow disaster occurred in 2014. Topographic analysis using 1-m grid DEMs before and after the disaster indicates that post-event channel heads were located upslope from pre-event channel heads due to landslide or erosion by debris flow. Post-event channel heads with shallow landslides had strong inverse correlations between local slope and drainage area. Charcoal samples were collected in colluvial deposits of two post-event channel heads (A and B) where the channel heads migrated more than 50 m upslope with shallow landslides. The radiocarbon dates of the samples were 1162–1194 y BP for channel head A and 786 y BP for channel head B. Another sample was collected in colluvial deposits of a post-event channel head (C) with shallow landslide but no migration. The radiocarbon date of the sample at the channel head C was 670 y BP. These radiocarbon data explain contrasting intervals of landslide events in hollows. The channel head A with older radiocarbon dates has the longer interval of landslide events and therefore the valley head has been buried in longer distance (more than 50 m) along the channel since the last landslide event to 2014.

Keywords: High-resolution DEM, Micro-topography, Radiocarbon dating, Valley head

©2019. Japan Geoscience Union. All Right Reserved.

Rock restrictions on topographical features of rivers: model experiment

*Yuta Takase[1], Noritaka Endo[1]

1. Kanazawa University

Landforms of mountainous areas is developed by both downcutting and lateral erosion of rivers. For example, ingrown meanders develop when the lateral erosion is predominant, while entrenched meanders form when the downcutting is dominant. It is a generally accepted understanding that the relative superiority or inferiority between the downcutting and lateral erosion is determined by the uplift rate of the land, rock strength difference, riverbed gradient, deflection of flow in a channel, but the systematic discussion remains insufficient. In this study, we conducted flume experiments to investigate the relationship between bedrock strength and sinuosity, and the relationship between time series pattern of uplift and meandering development. We prepared a single channel that cut a uniform substrate in a two-dimensional flume. The substrates were made of the mixture of fine sand and clay, and we examined two types of substrate, hard and soft ones, which can be formed by changing the ratio of sand and clay (the mixure including more clay is harder). Uplift of the experimental land was realized by lowering a weir set at the downstream end of the channel, i.e. the base-level lowering.

Knickpoints were observed more frequently in the case of hard substrate, which is consistent with previous study (Grimaud, 2016). Sinuosity of the channel tended to be higher for the hard substrate than the soft substrate, which is seemingly opposite the conventional understanding, but can be attributed to sustainability of the channel shape due to erosion resistance of the hard substrate. In all the experiments, the sinuosity tended to be higher after the uplift ceased rather than during the period of uplift.

Keywords: labo, sinuosity, bedrock strength, knickpoint, uplift

©2019. Japan Geoscience Union. All Right Reserved.

Stream power incision model and the stage of topographic equilibrium, using physical experiments

*Imamura Akihiro[1], Noritaka Endo[1]

1. Kanazawa University

Bedrock rivers develop their landforms very slowly, compared with alluvial river, thus bedrock rivers and their surrounding topographies are expected to record long-term environmental changes such as tectonics and climate. The stream power incision model (SPIM) is an empirical model that expresses the erosion rate due to rivers by the product of two power functions of the contributing area and river bed slope. Using this equation with an uplift term, the differential equation of the temporal change in the altitude of riverbed is constituted. When applying the model to a natural drainage basin, the equilibrium state between erosion and uplift is often assumed, partially because the uplift rate is usually unknown. Under the assumption of equilibrium state, SPIM is reduced to the relationship in which the riverbed slope is a power function of the contributing area, known as Flint’s law, which is the basis of “slope-area analysis” to determine the concavity (equivalent to the ratio of two power exponents in SPIM). Usually the two power exponents in SPIM are presumed to be constant if lithology, climate, and other factors are the same. This postulation, however, is difficult to verify for natural landforms, because of heterogeneity of various kind of property within a single drainage basin and difficulty in evaluation of the incision rate.

This study investigates the relation between the incision rate and topographic properties in river basins, through the observation of small-sized physical experiments under well-controlled conditions. A flume used was 90×180 cm, and the substrate to be dissected composed of the uniform mixture of sand and clay was installed. Rainfall was simulated by supplying mist from 10 nozzles. Uplift was realized by lowering a weir that was installed at the downstream end of the flume and determined the base level. The landform was measured by photogrammetry using several hundred photos taken during intermission from rainfall for photographing.

We compared the results of (1) this and (2) the previous studies (Imamura and Endo, 2018) realizing different kinds of uplift: (1) sudden base level lowering from a stable state of basin, to observe the response processes of the landforms until the basin became stable again (about 5 hours); (2) Sudden change in the uplift rate, to observe the change from a stable state under constant uplift of 4.5 mm/h to a new stable state under faster uplift rate of 6.0 mm/h (about 6 hours).

The results of Experiment (1) showed that the incision rate decreased with time (presumably asymptotic to zero), while Experiment (2) always displayed a certain finite value of the incision rate. The power exponents in SPIM, m (for the contributing area) and n (for the slope) did not seem to be constant in both experiments. The ratio m/n also changed, but seemed to converge to a certain value in each experiment.

We evaluated the correlation of the incision rate with the fitted function for each measurement time. In Experiment (1), although the denudation rate decreased with time, the first half of the run time showed good correlations but the latter half showed the worse. By contrast, Experiment (2) exhibited increasing correlations in the latter half of the run. These results suggests that SPIM holds for dynamic equilibrium (tectonic steady state (Montgomery, 2001)) or the early stage of static quasi-equilibrium (erosional stead state (Montgomery, 2001)), but fails for mature or later stages in which a landform proceeds to a

©2019. Japan Geoscience Union. All Right Reserved.

peneplane.

Imamura and Endo, 2018. Incision rate, riverbed slope and contributing area of an experimental drainage basin. JPGU 2018 Abstract.

Montgomery, 2001, Slope distributions, threshold hillslopes, and steady-state topography. American Journal of Science, 301, 432–454.

Keywords: stream power model, laboratory experiment, bedrock river

©2019. Japan Geoscience Union. All Right Reserved.

Downstream variation in gravel size of the Tenjin River system

*Kazuaki Hori[1], Kazuya Yonehara[1]

1. Department of Geography, Graduate School of Environmental Studies, Nagoya University

Many researchers have studied downstream variation in river-bed material size and its controlling factors, because they are important to understand the evolution of fluvial landforms and drainage basin. Many of these studies have focused only on rivers flowing through mountains or alluvial plains. Thus, it is desirable to examine a much broader range, i.e. from head to mouth of a river. We investigated the downstream variation of gravel size and channel gradient in the Tenjin River system (Tenjin, Ogamo, and Mitoku rivers) located in the central part of Tottori prefecture, Japan. The Tenjin River is approximately 34 km in length and major tributaries, the Ogamo and Mitoku rivers, join the Tenjin River at approximately 7 km and 12 km upstream from the mouth, respectively. Mean gravel size tends to decrease toward the downstream between 5 and 23 km upstream from the Tenjin River mouth where exposed gravel bars are easily found. Channel gradient is usually less than 0.03 and its variation is relatively small in this range. On the other hand, exposed gravel bars are uncommon between 23 and 34 km upstream from the mouth. The channel gradient become larger (> 0.06) and shows large variation. Large boulders (> 500 mm) are distributed in the channel. The number of boulders, especially > 1000 mm, seems to be inversely proportional to the distance from the valley wall. Buffers along the rivers regulate the supply of boulders from the valley wall in the upper reaches and reduce the connectivity of sediment supply from the tributaries in the middle and lower reaches. Barriers typified by weirs reduce the connectivity in the longitudinal direction throughout the basin.

Keywords: sediment connectivity, grain size, channel gradient

©2019. Japan Geoscience Union. All Right Reserved.

Talus slope development in the time of deglaciation: a case study of the Rev Valley, SW Spitsbergen

*Krzysztof Senderak[1], Marta Kondracka[1], Bogdan Gądek[1]

1. Faculty of Earth Sciences, University of Silesia

Every high-mountain area is characterized by the occurrence of talus slopes. A process of development this kind of forms depends on among other things climatic conditions. Currently in Spitsbergen, we observe the deglaciation process caused climate changes. This causes that the evolution’ s tempo of all environments linked with glaciers is very high. It also concerns the talus slopes, which, in the last time, are more often used as key element to paleo-environmental reconstructions for last thousands. In this paper, we present the geophysical surveys of talus slopes conducted in the Rev Valley (SW Spitsbergen). The valley was shaped by glacier, which left behind among other things glacial lake and buried glacial ice in mixed slope-moraine material. Nowadays, the talus slopes in this valley develop under the typical conditions of periglacial environment. In the studies of 15 talus slopes we used the ground-penetrating radar (GPR) and electrical resistivity tomography method (ERT). The studies allowed to recognize the internal structure of talus slopes and to determine a character of their elements, such as thickness of slopes, permafrost table and a depth of active layer, present of buried glacial ice, sediementological structures caused by various deposition of material on the slope surface, and finally a shape of bedrock. A comparison obtained results indicates on relevant regularity in the development of internal structure of talus slopes. These are for example visible differences in the terms of present of permafrost, which is located from a depth 2-3 m in the oldest slopes to a depth 4-5 m in the youngest. On the other hands, the studies discovers the deviations from the typical evolution models. The buried glacial ice has not been survived in a younger forms, whereas it is present in these older slopes. Based on the results we created the proposition of model of talus slope evolution developing in a periglacial period. In this time the development of slopes characterize a very high variability, not much lower than in previous paraglacial period. This work was financed from the funds of the National Science Centre in Poland received by Krzysztof Senderak in the Preludium 12 project: Determination of the evolution of slopes of southern Spitsbergen on the background of climate changes (2016/23/N/ST10/00162).

Keywords: talus slope evolution, permafrost, deglaciation, electrical resistivity tomography (ERT), ground-penetrating radar (GPR)

©2019. Japan Geoscience Union. All Right Reserved.

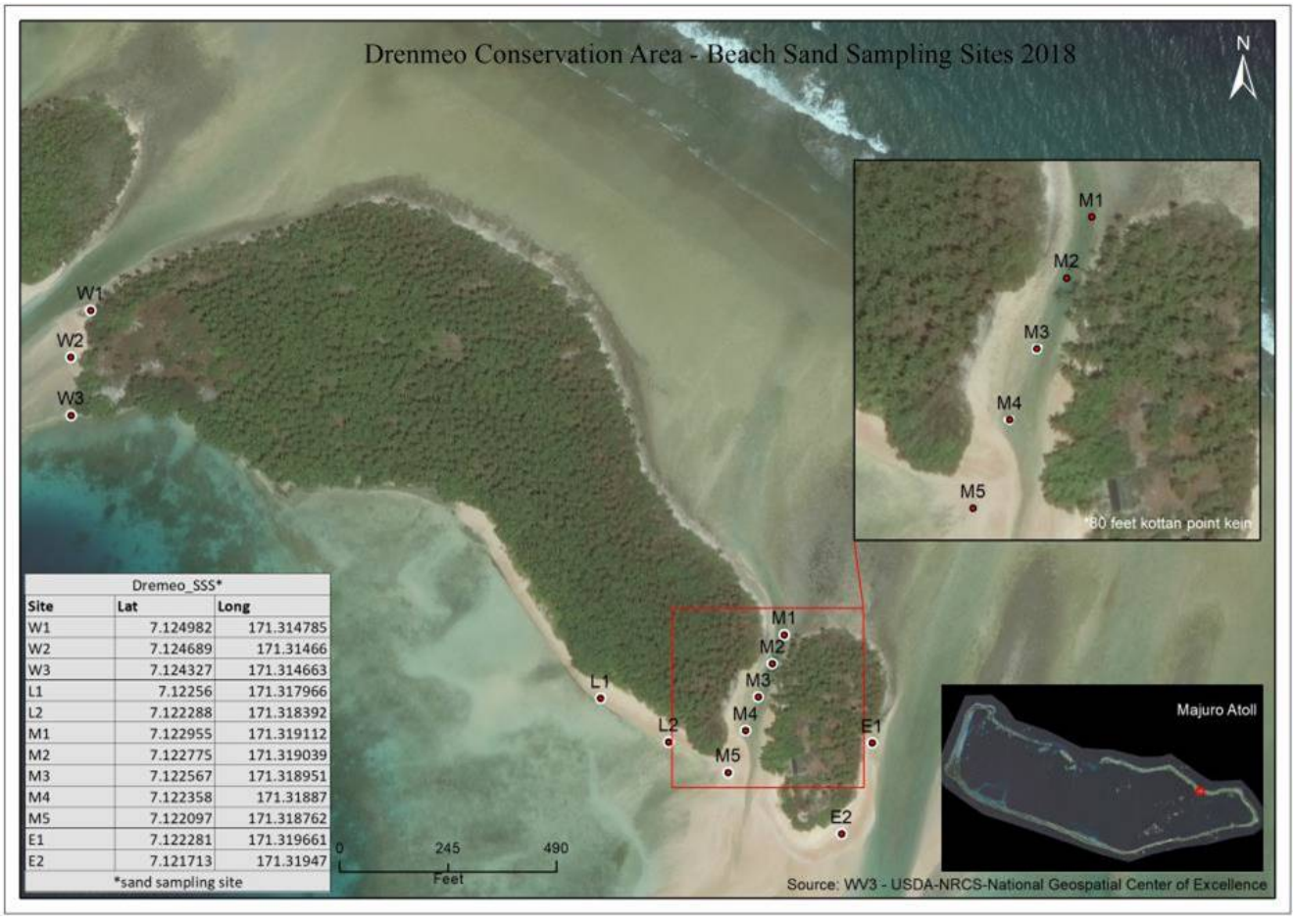
Distribution of Large Benthic Foraminifers in one of Majuro's Conservation Areas –Drenmeo Island

*Benedict Yamamura[1], Kazuhiko Fujita[2], Melba White[3], Kyotak Ishiguro[3], Hironobu Kan[1]

1. Kyushu University, Integrated Sciences for Global Society - Research Center for Coastal Seafloor , 2. Department of Physics and Earth Sciences, University of the Ryukyus, 3. Marshall Islands Marine Resources Authority

Climate change is having a huge impact on the island formation. In this study, we examined the composition and distribution of large benthic foraminifers (LBF) from 12 chosen sample sites (see map) within and outside of Drenmeo islet, one of the designated conservation areas in Majuro atoll. Samples were collected from the area to further investigate the sand built-up between the conservation area and the adjacent islet. The preliminary findings showed that the area is predominantly composed of two island-building LBF, namely *Calcarina sp.* and *Amphistegina sp.* The final results from this study will help stakeholders to amend the management plan to include the adjacent islet under the current management plan.

Keywords: Drenmeo island, conservation area, large benthic foraminifers, management plan



©2019. Japan Geoscience Union. All Right Reserved.

Luminescence chronology of fluvial and marine records from subsurface sediment cores: An insight into the geomorphic evolution of Kaveri delta, India

*kartika goswami[1], Anbarasu Kumaresan[2], Sivakumar Krishnan[2], Senthil K. Sadasivam[2], Manoj Kumar Jaiswal[1]

1. Department of Earth Sciences, Indian Institute of Science Education and Reserach Kolkata, 2. National College Tiruchirappalli, India

Long-term evolution of river deltas is a result of forcings (tectonics, climate, sea level, avulsion, compaction etc). We present the results of luminescence dating of sediments from four sediment cores (VKI, TNR, SY and KKI) of 25 m depth each, retrieved from the Kaveri delta in south India. The coring sites are ~2.5 km, ~11 km, ~17 km and ~20 km away from the present coastline respectively. The cores were analysed for OSL dating, 14C dating, lithology and microfossils and represent various stages of fluvial and marine activity in the region over the last ~150 ka. The chronology of the core closet to the coast (VKI) reflects eight major phases of increased sea level during the late quaternary period (142-140 ka, 104-100 ka, ~121 ka, 87-81 ka, 60-57 ka, 9-6 ka, ~5 ka and ~3 ka) partly coinciding with the global climate cycles MIS 6, MIS 5, MIS 3, MIS 1 respectively. During ~121 ka and 9-6 ka, marine transgression reached the core location to leave marine signatures in the forms of foraminifera. VKI core replicates the quaternary sea level curve, showing strong control of the sea in coastal deposition.

The oldest age of VKI is ~140 ka. The three cores situated further inland give oldest/bottom most ages of~120 ka. This indicates the coastal land has uplifted in the recent years with deeper sediments being encountered at relative shallower depth. The uplift is expected to occur around post 50 ka, creating a basin fill situation for riverine sediments to accumulate and restricting the delta to prograde. This is observed from the sedimentation pattern and robust chronology of the other three inland cores. Analysis of DEM also supported the occurrence of uplift. Thus, the present work examines the geomorphic evolution of Kaveri delta, an archive of fluvial, shoreline and tectonic activities.

Keywords: OSL Dating, Kaveri Delta , GIS, Foraminifera

©2019. Japan Geoscience Union. All Right Reserved.

[E] Poster | H (Human Geosciences)：H-GM Geomorphology

Wed. May 29, 2019 5:15 PM - 6:30 PM JST | Wed. May 29, 2019 8:15 AM - 9:30 AM UTC | Poster Hall International Exhibition Hall8, Makuhari Messe_18

[H-GM03] Geomorphology

convener:Tsuyoshi Hattanji(Faculty of Life and Environmental Sciences, University of Tsukuba), Masayuki Seto(Fukushima Future Center for Regional Revitalization, Fukushima University)

The main subject of this session is interdisciplinary discussion on the whole range of themes relating to geomorphology, especially geomorphic processes, landform development and its relation to environmental changes, geomorphological hazards and their mitigation, relationships among geomorphic processes, other natural phenomena and human activities, and various techniques of geomorphological measurements and landform classification. All presentations and discussion of this session are made in English.

[HGM03-P01] Honeycomb Weathering (Tafoni) of Sandstone and Environmental Factors in Yonaguni Island, Okinawa Prefecture, Japan

*Takayuki Ogata[1] (1.Disaster Prevention Research Center for Island Regions, University of the Ryukyus)

[HGM03-P02] Colluvial deposits in first-order streams and channel head migration by shallow landslides: Case study in granitic basins, Asaminami, Hiroshima, Japan

*Tsuyoshi Hattanji[1], Ryuya Kodama[2], Takahisa Furuichi[3], Shoji Doshida[4], Yasushi Tanaka[5] (1.Faculty of Life and Environmental Sciences, University of Tsukuba, 2.former College of Geoscience, University of Tsukuba, 3.Hokkaido University, 4.National Research Institute of Fire and Disaster, 5.Komazawa University)

[HGM03-P03] Rock restrictions on topographical features of rivers: model experiment

*Yuta Takase[1], Noritaka Endo[1] (1.Kanazawa University)

[HGM03-P04] Stream power incision model and the stage of topographic equilibrium, using physical experiments

*Imamura Akihiro[1], Noritaka Endo[1] (1.Kanazawa University)

[HGM03-P05] Downstream variation in gravel size of the Tenjin River system

*Kazuaki Hori[1], Kazuya Yonehara[1] (1.Department of Geography, Graduate School of Environmental Studies, Nagoya University)

[HGM03-P06] Talus slope development in the time of deglaciation: a case study of the Rev Valley, SW Spitsbergen

*Krzysztof Senderak[1], Marta Kondracka[1], Bogdan Gądek[1] (1.Faculty of Earth Sciences, University of Silesia)

[HGM03-P07] Distribution of Large Benthic Foraminifers in one of Majuro's Conservation Areas – Drenmeo Island

*Benedict Yamamura[1], Kazuhiko Fujita[2], Melba White[3], Kyotak Ishiguro[3], Hironobu Kan[1] (1.Kyushu University, Integrated Sciences for Global Society - Research Center for Coastal Seafloor , 2.Department of Physics and Earth Sciences, University of the Ryukyus, 3.Marshall Islands Marine Resources Authority)

[HGM03-P08] Luminescence chronology of fluvial and marine records from subsurface sediment cores: An insight into the geomorphic evolution of Kaveri delta, India

*kartika goswami[1], Anbarasu Kumaresan[2], Sivakumar Krishnan[2], Senthil K. Sadasivam[2], Manoj Kumar Jaiswal[1] (1.Department of Earth Sciences, Indian Institute of Science Education and Reserach Kolkata, 2.National College Tiruchirappalli, India)

Honeycomb Weathering (Tafoni) of Sandstone and Environmental Factors in Yonaguni Island, Okinawa Prefecture, Japan

*Takayuki Ogata[1]

1. Disaster Prevention Research Center for Island Regions, University of the Ryukyus

Sandstone surfaces of Yonaguni Island (westernmost of the Ryukyu Arc) often show a honeycomb structure (tafoni) derived from physical disintegration in relation to salt weathering. Miocene sandstone (Yaeyama Group) is extensively exposed on the island surface, and forms sea cliffs along rocky coasts. The honeycomb structure is especially observed along the coasts where wave splashes produce wetting and drying processes assisted by strong wind and active evaporation. The geometry and density of tafoni seem to be controlled by vertical height from the sea level and horizontal distance of the coast line. Field observations at the rocky coasts of Yonaguni Island suggest that larger holes are developed along the north-faced coasts than the south-faced coasts, which depends mainly on the northeastern monsoon during the winter period.

Keywords: weathering, sandstone, rocky coast, tafoni, monsoon, Yaeyama group

©2019. Japan Geoscience Union. All Right Reserved.

Colluvial deposits in first-order streams and channel head migration by shallow landslides: Case study in granitic basins, Asaminami, Hiroshima, Japan

*Tsuyoshi Hattanji[1], Ryuya Kodama[2], Takahisa Furuichi[3], Shoji Doshida[4], Yasushi Tanaka[5]

1. Faculty of Life and Environmental Sciences, University of Tsukuba, 2. former College of Geoscience, University of Tsukuba, 3. Hokkaido University, 4. National Research Institute of Fire and Disaster, 5. Komazawa University

Relationship between dates of colluvial deposits and channel-head migration was examined in granitic mountains where a debris-flow disaster occurred in 2014. Topographic analysis using 1-m grid DEMs before and after the disaster indicates that post-event channel heads were located upslope from pre-event channel heads due to landslide or erosion by debris flow. Post-event channel heads with shallow landslides had strong inverse correlations between local slope and drainage area. Charcoal samples were collected in colluvial deposits of two post-event channel heads (A and B) where the channel heads migrated more than 50 m upslope with shallow landslides. The radiocarbon dates of the samples were 1162–1194 y BP for channel head A and 786 y BP for channel head B. Another sample was collected in colluvial deposits of a post-event channel head (C) with shallow landslide but no migration. The radiocarbon date of the sample at the channel head C was 670 y BP. These radiocarbon data explain contrasting intervals of landslide events in hollows. The channel head A with older radiocarbon dates has the longer interval of landslide events and therefore the valley head has been buried in longer distance (more than 50 m) along the channel since the last landslide event to 2014.

Keywords: High-resolution DEM, Micro-topography, Radiocarbon dating, Valley head

©2019. Japan Geoscience Union. All Right Reserved.

Rock restrictions on topographical features of rivers: model experiment

*Yuta Takase[1], Noritaka Endo[1]

1. Kanazawa University

Landforms of mountainous areas is developed by both downcutting and lateral erosion of rivers. For example, ingrown meanders develop when the lateral erosion is predominant, while entrenched meanders form when the downcutting is dominant. It is a generally accepted understanding that the relative superiority or inferiority between the downcutting and lateral erosion is determined by the uplift rate of the land, rock strength difference, riverbed gradient, deflection of flow in a channel, but the systematic discussion remains insufficient. In this study, we conducted flume experiments to investigate the relationship between bedrock strength and sinuosity, and the relationship between time series pattern of uplift and meandering development. We prepared a single channel that cut a uniform substrate in a two-dimensional flume. The substrates were made of the mixture of fine sand and clay, and we examined two types of substrate, hard and soft ones, which can be formed by changing the ratio of sand and clay (the mixure including more clay is harder). Uplift of the experimental land was realized by lowering a weir set at the downstream end of the channel, i.e. the base-level lowering.

Knickpoints were observed more frequently in the case of hard substrate, which is consistent with previous study (Grimaud, 2016). Sinuosity of the channel tended to be higher for the hard substrate than the soft substrate, which is seemingly opposite the conventional understanding, but can be attributed to sustainability of the channel shape due to erosion resistance of the hard substrate. In all the experiments, the sinuosity tended to be higher after the uplift ceased rather than during the period of uplift.

Keywords: labo, sinuosity, bedrock strength, knickpoint, uplift

©2019. Japan Geoscience Union. All Right Reserved.

Stream power incision model and the stage of topographic equilibrium, using physical experiments

*Imamura Akihiro[1], Noritaka Endo[1]

1. Kanazawa University

Bedrock rivers develop their landforms very slowly, compared with alluvial river, thus bedrock rivers and their surrounding topographies are expected to record long-term environmental changes such as tectonics and climate. The stream power incision model (SPIM) is an empirical model that expresses the erosion rate due to rivers by the product of two power functions of the contributing area and river bed slope. Using this equation with an uplift term, the differential equation of the temporal change in the altitude of riverbed is constituted. When applying the model to a natural drainage basin, the equilibrium state between erosion and uplift is often assumed, partially because the uplift rate is usually unknown. Under the assumption of equilibrium state, SPIM is reduced to the relationship in which the riverbed slope is a power function of the contributing area, known as Flint’s law, which is the basis of “slope-area analysis” to determine the concavity (equivalent to the ratio of two power exponents in SPIM). Usually the two power exponents in SPIM are presumed to be constant if lithology, climate, and other factors are the same. This postulation, however, is difficult to verify for natural landforms, because of heterogeneity of various kind of property within a single drainage basin and difficulty in evaluation of the incision rate.

This study investigates the relation between the incision rate and topographic properties in river basins, through the observation of small-sized physical experiments under well-controlled conditions. A flume used was 90×180 cm, and the substrate to be dissected composed of the uniform mixture of sand and clay was installed. Rainfall was simulated by supplying mist from 10 nozzles. Uplift was realized by lowering a weir that was installed at the downstream end of the flume and determined the base level. The landform was measured by photogrammetry using several hundred photos taken during intermission from rainfall for photographing.

We compared the results of (1) this and (2) the previous studies (Imamura and Endo, 2018) realizing different kinds of uplift: (1) sudden base level lowering from a stable state of basin, to observe the response processes of the landforms until the basin became stable again (about 5 hours); (2) Sudden change in the uplift rate, to observe the change from a stable state under constant uplift of 4.5 mm/h to a new stable state under faster uplift rate of 6.0 mm/h (about 6 hours).

The results of Experiment (1) showed that the incision rate decreased with time (presumably asymptotic to zero), while Experiment (2) always displayed a certain finite value of the incision rate. The power exponents in SPIM, m (for the contributing area) and n (for the slope) did not seem to be constant in both experiments. The ratio m/n also changed, but seemed to converge to a certain value in each experiment.

We evaluated the correlation of the incision rate with the fitted function for each measurement time. In Experiment (1), although the denudation rate decreased with time, the first half of the run time showed good correlations but the latter half showed the worse. By contrast, Experiment (2) exhibited increasing correlations in the latter half of the run. These results suggests that SPIM holds for dynamic equilibrium (tectonic steady state (Montgomery, 2001)) or the early stage of static quasi-equilibrium (erosional stead state (Montgomery, 2001)), but fails for mature or later stages in which a landform proceeds to a

©2019. Japan Geoscience Union. All Right Reserved.

peneplane.

Imamura and Endo, 2018. Incision rate, riverbed slope and contributing area of an experimental drainage basin. JPGU 2018 Abstract.

Montgomery, 2001, Slope distributions, threshold hillslopes, and steady-state topography. American Journal of Science, 301, 432–454.

Keywords: stream power model, laboratory experiment, bedrock river

©2019. Japan Geoscience Union. All Right Reserved.

Downstream variation in gravel size of the Tenjin River system

*Kazuaki Hori[1], Kazuya Yonehara[1]

1. Department of Geography, Graduate School of Environmental Studies, Nagoya University

Many researchers have studied downstream variation in river-bed material size and its controlling factors, because they are important to understand the evolution of fluvial landforms and drainage basin. Many of these studies have focused only on rivers flowing through mountains or alluvial plains. Thus, it is desirable to examine a much broader range, i.e. from head to mouth of a river. We investigated the downstream variation of gravel size and channel gradient in the Tenjin River system (Tenjin, Ogamo, and Mitoku rivers) located in the central part of Tottori prefecture, Japan. The Tenjin River is approximately 34 km in length and major tributaries, the Ogamo and Mitoku rivers, join the Tenjin River at approximately 7 km and 12 km upstream from the mouth, respectively. Mean gravel size tends to decrease toward the downstream between 5 and 23 km upstream from the Tenjin River mouth where exposed gravel bars are easily found. Channel gradient is usually less than 0.03 and its variation is relatively small in this range. On the other hand, exposed gravel bars are uncommon between 23 and 34 km upstream from the mouth. The channel gradient become larger (> 0.06) and shows large variation. Large boulders (> 500 mm) are distributed in the channel. The number of boulders, especially > 1000 mm, seems to be inversely proportional to the distance from the valley wall. Buffers along the rivers regulate the supply of boulders from the valley wall in the upper reaches and reduce the connectivity of sediment supply from the tributaries in the middle and lower reaches. Barriers typified by weirs reduce the connectivity in the longitudinal direction throughout the basin.

Keywords: sediment connectivity, grain size, channel gradient

©2019. Japan Geoscience Union. All Right Reserved.

Talus slope development in the time of deglaciation: a case study of the Rev Valley, SW Spitsbergen

*Krzysztof Senderak[1], Marta Kondracka[1], Bogdan Gądek[1]

1. Faculty of Earth Sciences, University of Silesia

Every high-mountain area is characterized by the occurrence of talus slopes. A process of development this kind of forms depends on among other things climatic conditions. Currently in Spitsbergen, we observe the deglaciation process caused climate changes. This causes that the evolution’ s tempo of all environments linked with glaciers is very high. It also concerns the talus slopes, which, in the last time, are more often used as key element to paleo-environmental reconstructions for last thousands. In this paper, we present the geophysical surveys of talus slopes conducted in the Rev Valley (SW Spitsbergen). The valley was shaped by glacier, which left behind among other things glacial lake and buried glacial ice in mixed slope-moraine material. Nowadays, the talus slopes in this valley develop under the typical conditions of periglacial environment. In the studies of 15 talus slopes we used the ground-penetrating radar (GPR) and electrical resistivity tomography method (ERT). The studies allowed to recognize the internal structure of talus slopes and to determine a character of their elements, such as thickness of slopes, permafrost table and a depth of active layer, present of buried glacial ice, sediementological structures caused by various deposition of material on the slope surface, and finally a shape of bedrock. A comparison obtained results indicates on relevant regularity in the development of internal structure of talus slopes. These are for example visible differences in the terms of present of permafrost, which is located from a depth 2-3 m in the oldest slopes to a depth 4-5 m in the youngest. On the other hands, the studies discovers the deviations from the typical evolution models. The buried glacial ice has not been survived in a younger forms, whereas it is present in these older slopes. Based on the results we created the proposition of model of talus slope evolution developing in a periglacial period. In this time the development of slopes characterize a very high variability, not much lower than in previous paraglacial period. This work was financed from the funds of the National Science Centre in Poland received by Krzysztof Senderak in the Preludium 12 project: Determination of the evolution of slopes of southern Spitsbergen on the background of climate changes (2016/23/N/ST10/00162).

Keywords: talus slope evolution, permafrost, deglaciation, electrical resistivity tomography (ERT), ground-penetrating radar (GPR)

©2019. Japan Geoscience Union. All Right Reserved.

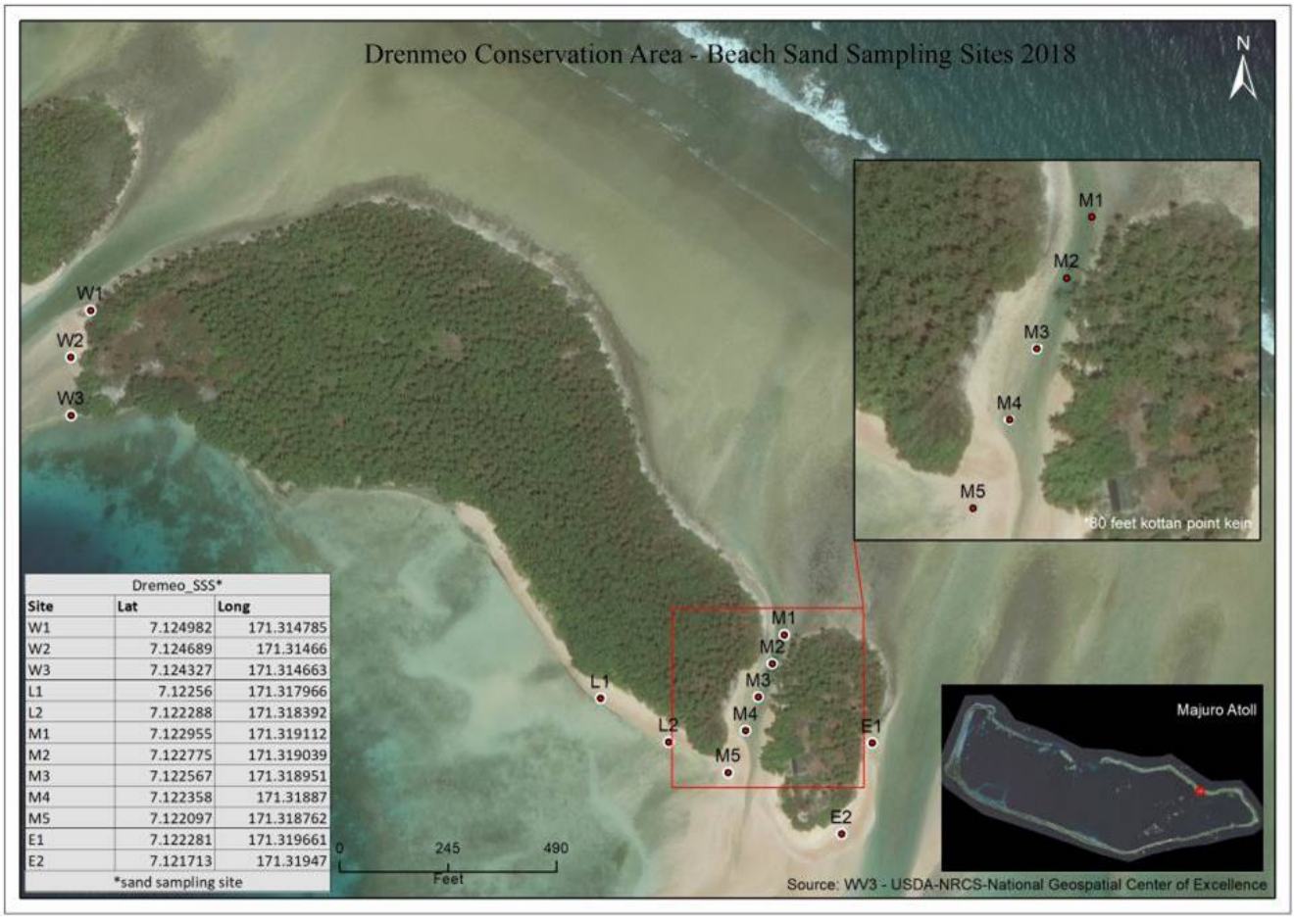
Distribution of Large Benthic Foraminifers in one of Majuro's Conservation Areas –Drenmeo Island

*Benedict Yamamura[1], Kazuhiko Fujita[2], Melba White[3], Kyotak Ishiguro[3], Hironobu Kan[1]

1. Kyushu University, Integrated Sciences for Global Society - Research Center for Coastal Seafloor , 2. Department of Physics and Earth Sciences, University of the Ryukyus, 3. Marshall Islands Marine Resources Authority

Climate change is having a huge impact on the island formation. In this study, we examined the composition and distribution of large benthic foraminifers (LBF) from 12 chosen sample sites (see map) within and outside of Drenmeo islet, one of the designated conservation areas in Majuro atoll. Samples were collected from the area to further investigate the sand built-up between the conservation area and the adjacent islet. The preliminary findings showed that the area is predominantly composed of two island-building LBF, namely *Calcarina sp.* and *Amphistegina sp.* The final results from this study will help stakeholders to amend the management plan to include the adjacent islet under the current management plan.

Keywords: Drenmeo island, conservation area, large benthic foraminifers, management plan



©2019. Japan Geoscience Union. All Right Reserved.

Luminescence chronology of fluvial and marine records from subsurface sediment cores: An insight into the geomorphic evolution of Kaveri delta, India

*kartika goswami[1], Anbarasu Kumaresan[2], Sivakumar Krishnan[2], Senthil K. Sadasivam[2], Manoj Kumar Jaiswal[1]

1. Department of Earth Sciences, Indian Institute of Science Education and Reserach Kolkata, 2. National College Tiruchirappalli, India

Long-term evolution of river deltas is a result of forcings (tectonics, climate, sea level, avulsion, compaction etc). We present the results of luminescence dating of sediments from four sediment cores (VKI, TNR, SY and KKI) of 25 m depth each, retrieved from the Kaveri delta in south India. The coring sites are ~2.5 km, ~11 km, ~17 km and ~20 km away from the present coastline respectively. The cores were analysed for OSL dating, 14C dating, lithology and microfossils and represent various stages of fluvial and marine activity in the region over the last ~150 ka. The chronology of the core closet to the coast (VKI) reflects eight major phases of increased sea level during the late quaternary period (142-140 ka, 104-100 ka, ~121 ka, 87-81 ka, 60-57 ka, 9-6 ka, ~5 ka and ~3 ka) partly coinciding with the global climate cycles MIS 6, MIS 5, MIS 3, MIS 1 respectively. During ~121 ka and 9-6 ka, marine transgression reached the core location to leave marine signatures in the forms of foraminifera. VKI core replicates the quaternary sea level curve, showing strong control of the sea in coastal deposition.

The oldest age of VKI is ~140 ka. The three cores situated further inland give oldest/bottom most ages of~120 ka. This indicates the coastal land has uplifted in the recent years with deeper sediments being encountered at relative shallower depth. The uplift is expected to occur around post 50 ka, creating a basin fill situation for riverine sediments to accumulate and restricting the delta to prograde. This is observed from the sedimentation pattern and robust chronology of the other three inland cores. Analysis of DEM also supported the occurrence of uplift. Thus, the present work examines the geomorphic evolution of Kaveri delta, an archive of fluvial, shoreline and tectonic activities.

Keywords: OSL Dating, Kaveri Delta , GIS, Foraminifera

©2019. Japan Geoscience Union. All Right Reserved.

[E] Poster | H (Human Geosciences)：H-DS Disaster geosciences

Wed. May 29, 2019 10:45 AM - 12:15 PM JST | Wed. May 29, 2019 1:45 AM - 3:15 AM UTC | Poster Hall International Exhibition Hall8, Makuhari Messe_7

[H-DS10] Natural hazards impacts on human society, economics and technological systems

convener:ELENA PETROVA(Lomonosov Moscow State University, Faculty of Geography), Hajime Matsushima(Research Faculty of Agriculture, Hokkaido University)

The last decade set a record for the number and scale of natural disasters and demonstrates high vulnerability of human society and technosphere to their impacts. The most serious consequences have the so-called natural-technological disasters in which natural hazards trigger accidents at technology and infrastructure such as nuclear power and chemical plants, oil refineries and pipelines, power supply systems, buildings, and roads. A distinctive feature of natural-technological events, such as of the 2011 Tohoku earthquake, is their multi-hazard and synergistic nature, which creates cascading impacts, resulting in simultaneous occurrences of myriad catastrophes. The main goal of this multidisciplinary session is to summarize case studies of relationships between natural hazards and technological disasters, their social and economic consequences; and to encourage a discussion about tools and methods to prevent disasters and to minimize their consequences, disaster reconstruction, and tourism for reconstruction, Eco-DRR, and green infrastructure.

[HDS10-P01] The 2018 Activity of Kamchatka Volcanoes and Danger to Aviation

*Olga Girina[1], Dmitry Melnikov[1], Alexander Manevich[1], Anton Nuzhdaev[1], Elena Petrova[2] (1.Institute of Volcanology and Seismology, Far East Division, Russian Academy of Sciences, 2.M.V. Lomonosov Moscow State University)

[HDS10-P02] Planning Methodology on the Effective Use of Green Infrastructure for Disaster Risk Reduction

★Invited Papers

*Keita Aragane[1], Satoshi Funakubo[1] (1.National Institute for Land Infrastructure Management)

[HDS10-P03] EMERGENCY CALL PATTERN IN PETROZAVODSK

*Boris Zalmanovich Belashev[1], Natalia Vladimirovna Krutskikh[1], Anna Aleksandrovna Gerasimova[1] (1.Karelian research center of Russian academy of science)

[HDS10-P04] IDENTIFYING “REGIMES” IN THE TIME SEQUENCES OF PROCESSES

*Boris Zalmanovich Belashev[1] (1.Karelian research center of Russian academy of science)

[HDS10-P05] Investigation of status and demand on public service of earthquake disaster mitigation in China

*Lina Dong[1], Weiping Lian[1], Weitao Chen[1] (1.Development Research Center, China Earthquake Administration)

[HDS10-P06] Analysis of Eco-DRR and Ecological Services using InVEST at the Disaster Areas of Kumamoto Earthquake

*Minghui Tang[1], Naoko Fujita[1] (1.Kyushu University)

[HDS10-P07] Transformation as praxis: Exploring socially just and transdisciplinary pathways to sustainability in marginal environments (TAPESTRY)

*Nobuhito Ohte[1], Lyla Mehta[2], Synne Movik[3], Devanathan Parthasarathy[4] (1.Department of Social Informatics, Graduate School of Informatics, Kyoto University, 2.Institute of Development Studies at the University of Sussex, 3.Department of Urban and Regional Planning, Norwegian University of Life Sciences, 4.Department of Humanities and Social Sciences, Indian Institute of Technology)

[HDS10-P08] Study for the Establishment of the Design for Disaster prevention through the survey of Recognition of tsunami disaster prevention from the viewpoint of green infrastructure in the coastal area of Kyushu-Pacific region.

*Shanshan Xu[1], Naoko Fujita[1], Minghui Tang[1] (1.Kyushu University)

[HDS10-P09] Design for Green Infrastructure: Analysis of Landscape change in the Kumamoto earthquake area

★Invited Papers

*Naoko Fujita[1] (1.Kyushu University)

The 2018 Activity of Kamchatka Volcanoes and Danger to Aviation

*Olga Girina[1], Dmitry Melnikov[1], Alexander Manevich[1], Anton Nuzhdaev[1], Elena Petrova[2]

1. Institute of Volcanology and Seismology, Far East Division, Russian Academy of Sciences, 2. M.V. Lomonosov Moscow State University

Strong explosive eruptions of volcanoes are the most dangerous for aircraft because they can produce in a few hours or days to the atmosphere and the stratosphere till several cubic kilometers of volcanic ash and aerosols. Ash plumes and the clouds, depending on the power of the eruption, the strength and wind speed, can travel thousands of kilometers from the volcano for several days, remaining hazardous to aircraft, as the melting temperature of small particles of ash below the operating temperature of jet engines.

There are 30 active volcanoes in the Kamchatka, and several of them are continuously active. Scientists of KVERT monitor Kamchatkan volcanoes since 1993. In 2018, three of these volcanoes (Sheveluch, Klyuchevskoy, Karymsky) had strong and moderate explosive eruptions.
The eruptive activity of Sheveluch volcano began since 1980 (growth of the lava dome) and is continuing at present. In 2018, strong explosions sent ash up to 10-11 km a.s.l. on 09 January, 26 and 30 December; and up to 6-7 km a.s.l. –on 09 November, and 12, 14, 26-27 and 29 December; ash plumes extended more 2000 km to the different directions of the volcano. Satellite data by KVERT showed a thermal anomaly over the volcano all year. Activity of the volcano was dangerous to international and local aviation.

The moderate explosive events (ash up to 5-6 km a.s.l.) of Klyuchevskoy volcano were observing from 01 till 18 January, on 08 May, and 06 and 15 June. Strong explosions sent ash up to 10.5 km a.s.l. on 14 May. Ash plumes extended more 350 km to the eastern and south-western directions from the volcano. Satellite data by KVERT showed a thermal anomaly over the volcano all year. Activity of the volcano was dangerous to international and local aviation.

The thermal anomaly over Karymsky volcano was recorded on satellite images from time to time, most brightly it manifested in January, May, June-August, September and December. According to visual and satellite data, at this time explosions rose ash up to 6.5 km a.s.l., ash plumes drifted for about 860 km to the different directions from the volcano. The most intense eruptive activity of the volcano was observed on 10, 14-20 and 26-31 July, besides, isolated strong explosive events were observed on 07 and 25 August, on 10-11, 22-23 and 30 September, and 01 December. The size of the ash clouds varied from 5-6 to 240 km. Activity of the volcano was dangerous to local aviation.
This work was supported by the Russian Science Foundation, project No. 16-17-00042.

Keywords: volcano, eruption, Kamchatka, danger to Aviation

©2019. Japan Geoscience Union. All Right Reserved.

Planning Methodology on the Effective Use of Green Infrastructure for Disaster Risk Reduction

*Keita Aragane[1], Satoshi Funakubo[1]

1. National Institute for Land Infrastructure Management

Green Infrastructure (GI) is a concept based on infrastructure development and land utilization that take advantage of natural environments' various functions for creating sustainable and attractive national land or regions. In Japan, since 2015, the concept of GI has been include in National Spatial Strategy, National Land Use Plan, and Priority Plan for Infrastructure Development, etc. Also, lessons learned from the Great East Japan Earthquake raised awareness of the need for more-comprehensive disaster risk reduction strategies in preparing for disasters that surpass worst-case scenarios. Additionally, there is concern over anticipated the Nankai Trough Earthquakes that might cause greater damage in near future, and increasingly frequent urban flooding owing to climate change. Thus, initiative for disaster risks reduction by utilizing GI's multiple functions in addition to approaches focusing on artificial infrastructure has become increasingly important.

This study aims to discuss planning methodology regarding the effective use of GI for disaster risk reduction in urban area by examining the “Green Master Plan (GMP)” through 72 case studies. In Japan, 680 municipal governments have developed GMPs as their basic policy for green space planning, management, and greening. These municipal governments in Japan are recommended to emphasize the viewpoint of disaster risk reduction in their GMPs, and to implement disaster risk reduction systematically through effective use of green spaces such as parks, roadside trees, waterways, private domestic gardens, agricultural land, and woodlands. Result from the case studies revealed that almost all GMPs designated green spaces such as parks as evacuation sites for mega-earthquakes or large-scale fires. Several GMPs were also found to present countermeasures that make effective use of GI for tsunami-related disasters and urban flooding.

Through these findings and through discussions with scholars at a workshop, we published “Technical Note on Green Infrastructure Planning for Urban Resilience” in June 2018. In this technical note, we explain six key points for developing GMPs that enhance the role of GI in disaster risk reduction: (1) combining various measures for disaster risk reduction by utilizing GI from a comprehensive perspective, (2) examining the role and combination of GI and other artificial infrastructure in urban disaster risk reduction, (3) building cooperative relationships with various stakeholders and citizens, (4) taking advantage of multiple functions of GI not only during disasters but also in normal times, (5) establishing a mechanism for maintaining and using GI from a long-term perspective, and (6) considering regional conditions and social situations.

Keywords: Green Infrastructure, Dsaster Risk Reduction, Green Master Plan

©2019. Japan Geoscience Union. All Right Reserved.

EMERGENCY CALL PATTERN IN PETROZAVODSK

*Boris Zalmanovich Belashev[1], Natalia Vladimirovna Krutskikh[1], Anna Aleksandrovna Gerasimova[1]

1. Karelian research center of Russian academy of science

The aim of the study is to analyze the emergency call distribution for Petrozavodsk, Russia, to obtain quantitative disease estimates and to assess the effect of environmental factors on them.

The study was based on medical statistical data and geophysical and geochemical monitoring. Environmental factors, such as magnetic storms and air and urban soil pollution, were assessed. The impersonified catalogue of emergency calls of Petrozavodsk Ambulance from 2015.1.1 to 2017.12.19, database of geomagnetic field variations at Petrozavodsk Geophysical Observatory, data on Kp index monitoring at the Laboratory of Tesis X-ray Astronomy at Lebedev Physical Institute, and the results of geochemical soil sampling in Petrozavodsk were used. Emergency call and geomagnetic activity distributions were constructed and processed in MATLAB computer mathematics system and Qgis software package. Analytical results were demonstrated on cardiovascular diseases.

The number of emergency call for patients with cardiac diseases in 2015-2017 is at about the same level. Seasonal factors affect the time distribution trends of calls for patients with essential hypertension, stenocardia and ischemic cardiac disease and do not affect the distribution trends of myocardial infarction and cerebral crisis. Time distribution spectra display a 25.6 day cycle similar to a geomagnetic activity period, two- and one-week cycles and cycles with periods of about 6, 4 and 3 days. Emergency calls for patients with myocardial infarction reflect the gender and age of the patients. The number of calls on weekends is typically low. On week-days, the number of calls at rush hours is maximum. The number of calls on days close to magnetic storms is not necessarily great. An elevated number of calls on these days for patients with stenocardia and myocardial infarction is observed.

The spatial distribution of the number of emergency calls were obtained using the Ambulance Geoinformation System. The system constructs the spatial distributions of the number of emergency team calls with known diagnoses for the streets and blocks of the city and is used to compare call frequency with district factors. With its help the link of distribution of quantity of calls of ambulance with diagnoses of cardiovascular diseases, bronchial asthma, vegeto-vascular dystonia, new growths, other diseases on districts of the city with the soils contamination indicated by the environmental hazard index –a total of the weighted average concentration values of As, Pb, Zn, Cd, Co, Cu, V, W is studied. No significant correlations between these values have been revealed.

3, 6-daily cycles in the analyzed ranges can be connected to thyroid gland hormone activity and a 4-day cycle to glucocorticoid hormone activity. Circadian rhythms are either thought to be general or to be due to the unwillingness of people to be sent to hospital or call for a doctor on weekends. In case of myocardial infarction, when help is needed urgently, the latter factor does not work, and a one-week cycle in the spectrum, showing the time dependence of the number of calls, is displayed.

This fact and the weekend effect can be understood, based on the properties of hydrocortisone. Stress from production activity stimulates the supply of the hormone into the blood, which rushes to the heart and muscles. When the heart fails to cope with the rush of blood, a cardiac disease becomes more acute.

©2019. Japan Geoscience Union. All Right Reserved.

As the hydrocortisone level in the blood on weekends and holidays declines, the number of emergency calls for patients with cardiovascular diseases decreases.

Peaks in the daily emergency call dynamics distribution on week-days are interpreted to be due to air pollution with car gases at rush hours (9-10 a.m., 1-2 and 6-7 p.m.) and an approximately one-hour delay caused by progress in disease and the need to apply for a doctor.
The emergency call distributions analyzed are highly informative, showing the complete dynamic disease pattern of the urban population.

Keywords: diseases, emergency call, patient, diagnose, magnetic storms, contamination

©2019. Japan Geoscience Union. All Right Reserved.

IDENTIFYING “REGIMES” IN THE TIME SEQUENCES OF PROCESSES

*Boris Zalmanovich Belashev[1]

1. Karelian research center of Russian academy of science

A process is represented as a sequence of “regimes” when describing climatic variations and complex systems, detecting the malfunctioning of instruments and illegal interference in computer and hardware networks. For natural, technological and social processes such representation is comfortable to detect precursors of disastrous events.
The shifts of “regimes” in the sequences are commonly detected by checking statistical hypotheses by Student’s test and tests of non-parametric statistics when comparing the characteristics of the sequence at one or another site. Algorithms often use a priori information, work in unstable fashion over short intervals and at sequences boundaries, find it hard to recognize the shifts and trends of “regimes”.
Widespread R-algorithm [1] analyze data consecutively in a sliding window, operate with a small number of parameters and filter off “red” noise. The boundary regimes it detect may reflect distortions characteristic of the beginning and end of measurements.
The goal of the present study is to develop B-algorithm which automatically recognizes stable “regimes” in time data sequences.
The main stages of the algorithm are clusterization, comparison and optimization. Clusterization preliminary divides a normalized time sequence into “regimes”. While comparing the characteristics of the “regimes”, the division obtained is re-estimated. The final model of division is formed during optimization, which minimizes the variance of deviations from the trends of the “regimes” by varying the internal boundaries of the sites.
The algorithm, developed as a software in the MATLAB computer mathematics system, fulfils procedures automatically, decreases the amount of a priori data, increases operation speed and brings solutions closer to optima.
The operation of B- and R-algorithms is exemplified by the PDO (Pacific Decade Oscillation) sequence of mean January temperatures [2].
In both algorithms the number of “regimes” and their approximate positions coincide. The delay of part of R-“regimes” emphasize the sensitivity of B-algorithm to new “regimes”. Discrepancies are connected with the last “regime” identified by R- and B-algorithms on 2 and 15 members of sequence, respectively.
B- algorithm can operate with constant, linear and complex trends.
B- and R-algorithms, applied to the time sequences of river runoff, solar and seismic activity and the sequences of the annual rings of trees, have provided new information on the stages of processes.
The simplified schematic “regime” representation of a process reveals trends commonly obscured by the abundance of details. B- algorithm identifies stable “regimes” and recognizes the shifts and trends of “regimes”. The use of MATLAB functions increases the potential of the algorithm, admits the fulfilment of procedures by various methods, brings solutions closer to optimum solutions and ensures high operation speed. The ability of the algorithm to automatically process data makes it suitable for working with extensive data in various earth sciences.
References:
1.Rodionov, S. (2006) Use of prewhitening in climate region shift detection. Geophysical Research Letters 33, L12707.
2.Pacific Decadal Oscillation Index Data.
https://www.rdocumentation.org/packages/rpdo/versions/0.2.5.

©2019. Japan Geoscience Union. All Right Reserved.

Keywords: time sequence, shift regime, algorithm, clusterization, comparision, optimization

©2019. Japan Geoscience Union. All Right Reserved.

Investigation of status and demand on public service of earthquake disaster mitigation in China

*Lina Dong[1], Weiping Lian[1], Weitao Chen[1]

1. Development Research Center, China Earthquake Administration

In order to make a comprehensive and systematic evaluation of the status and demands of public service of earthquake disaster mitigation, we launched an investigation with National Bureau of Statistics on the current situation of public service of earthquake disaster mitigation and the demands for it in 2018. The investigation was conducted in 31 provinces of China mainland using the Computer Assisted Telephone Interview(CATI) method and received 20078 valid samples in total.

The results indicate that 52.2% of the population have received the scientific knowledge education for earthquake disaster mitigation in Different levels. It shows that the public still possesses a high expectation of earthquake prediction and farmers have a low level of scientific knowledge of earthquake disaster mitigation. And TV, network, and the new media app such as wechat and weibo become the most important information channels for the public to obtain the earthquake related information. Furthermore, the degree of satisfaction evaluation of public service of earthquake disaster mitigation is marked on 81.22 points (the full mark is 100 points). And the most expectative services for the public are reconstruction, earthquake warning, and house earthquake resilience test. The results of the investigation have provided a scientific evidence for the government to provide better services of earthquake disaster mitigation and to make scientific knowledge popularization in a more scientific way.

Keywords: scientific knowledge popularization of earthquake disaster mitigation, public service, satisfaction evaluation

©2019. Japan Geoscience Union. All Right Reserved.

Analysis of Eco-DRR and Ecological Services using InVEST at the Disaster Areas of Kumamoto Earthquake

*Minghui Tang[1], Naoko Fujita[1]

1. Kyushu University

When compared with other countries in a global point of view, Japan is a country with high number of natural calamities, significant causalities, economic loss and damages by earthquakes, typhoons, and eruption. The damage is especially big when a hazard comes right after another one.

Complex disaster refers to the occurrence of multiple disasters instead of one. Such as, in 2016, Kumamoto prefecture was hit by earthquakes with magnitude as large as 7 and within another 2 months, by heavy rain and the damage was tremendous.

There is a huge number of researches on the eco-application of proceeding in various countries and it is vitally important to verify their validity. Here, InVEST refers to the ArcGIS tool for the integrated review for ecological services and its compensation.

This research focuses on the analysis of the changes of the land cover as reflected in satellite pictures of the whole Kumamoto prefecture taken after the complex disaster, the earthquake in April 2016 and heavy rain in June 2016. Also, it’ s a review on the ecological services with the use of InVEST. A special focus is paid on the review of the soil retention and the quality changes of the eco-habitant as reflection of the disaster damage reduction measures.

In addition, there is an analysis on the change of land coverage on area-unit level with Mashiki-machi, the epicenter, as the target. Furthermore, projection was plotted for the ecological services implemented as the reconstruction plan.

Keywords: Kumamoto Earthquake, Eco-DRR, Ecological services, Complex Disasters, local governments/local communities, InVEST

©2019. Japan Geoscience Union. All Right Reserved.

Transformation as praxis: Exploring socially just and transdisciplinary pathways to sustainability in marginal environments (TAPESTRY)

*Nobuhito Ohte[1], Lyla Mehta[2], Synne Movik[3], Devanathan Parthasarathy[4]

1. Department of Social Informatics, Graduate School of Informatics, Kyoto University, 2. Institute of Development Studies at the University of Sussex, 3. Department of Urban and Regional Planning, Norwegian University of Life Sciences, 4. Department of Humanities and Social Sciences, Indian Institute of Technology

Climate change related uncertainties are the main threats to the sustainability of societies and their environments. To tackle these challenges, systemic transformations are required. Our project focuses on three cases of transformation in marginal environments in India and Bangladesh, and is concerned with: How transformation happens through bottom up processes in these sites; and how they can be scaled up and facilitate wider societal changes. Both require transdisciplinary co-production and the praxis of transformation which presupposes change in social arrangements and reconstruction by individuals. Our project addresses issues concerning governance, wellbeing, identity and quality of life in relation to transformations to sustainability in a lower middle income country (India) and a least developed country (Bangladesh). Our results should help inform processes that ultimately improve the quality of life in marginal environments, and build action and capacity among all partners.

Keywords: Transformation, Sustainability, Marginal environment, Transdisciplinary study, India, Bangladesh

©2019. Japan Geoscience Union. All Right Reserved.

Study for the Establishment of the Design for Disaster prevention through the survey of Recognition of tsunami disaster prevention from the viewpoint of green infrastructure in the coastal area of Kyushu-Pacific region.

*Shanshan Xu[1], Naoko Fujita[1], Minghui Tang[1]

1. Kyushu University

Considering the possibility of Nankai Trough large-scale earthquake predicted to occur in the nearest future, the issue of the tsunami in the coastal area of Kyushu-Pacific region is becoming extremely important. Efforts to utilize the various functions of the ecosystem internationally for the society creation are expanding in recent years, and even in the situation of toughening of the land in Japan, the initiative to incorporate Green Infrastructure (GI) which utilizes the disaster prevention and reduction functions of the natural ecosystem are being observed. Also, during the process of self-help/mutual assistance action and disaster reconstruction at the time of disaster, attention is paid as regional ties are affected, which are being considered as Social capital (SC).

The purpose of this study is to clarify the actual situation of tsunami disaster prevention of Nankai Trough earthquake based on the viewpoint of GI. We conducted a questionnaire survey on tsunami disaster prevention and GI at local governments and local communities. After analyzing the questionnaire, we analyzed the needs of the self-governing president's disaster prevention measures, the problems of the area, and the deviation of the improved situation of municipalities' disaster prevention measures. A correlation analysis was conducted to grasp the relationship between the consciousness concerning GI utilization, the strength of regional linkage SC and the recognition of evacuation.

1. Misalignment between demand and maintenance situation desired by the region

Policy regarding the issue of disaster helpers was extracted as a gap between needs and maintenance situation. Regarding the needs of the soft pattern in disaster prevention, a lot of measures were taken by disaster support supporters, however as it comes from the municipality questionnaire results, the measures related to the introduction of the barrier-free system and evacuation action supporters were introduced only partially. Further improvement is necessary for welfare evacuation sites, measures against supporters requiring evacuation actions, barrier-free formation.

2. SC regarded from the viewpoint of the relationship between intentions to utilize GI and recognition on disaster.

©2019. Japan Geoscience Union. All Right Reserved.

Especially, the correlation coefficient was 0.701 between No.7 and No.6. This shows that those who responded that disaster can happen among residents can respond that regional ties are stronger. For items with a high correlation coefficient between No.3 and No.8, the correlation became 0.437. This means the respondents who answered that evacuation is possible for all area inhabitants including elderly people in case of disaster (flooding, earthquakes, and tsunami) are able to use local well water and spring water in the event of a disaster.

Between No.2 and No.4, the correlation coefficient became 3.380. This is because those who respond that they think they can fully utilize the resources of the area (resources such as firewood, foods that can be harvested in mountains) even in the event of disasters will escape by utilizing the nearby natural landforms such as plateaus and mountains for tsunami evacuation. Between No.2 and No.8, the correlation coefficient became 0.351. This is because it shows those who responded that they thought that they could escape by utilizing nearby plateau and mountains such as mountains during the tsunami evacuation, even if disasters (flood, earthquake, tsunami) occurred, everyone including the elderly in the area evacuated. Between No.2 and No.6, the correlation coefficient became 0.343. This indicates that those who responded that they believe that they can escape by utilizing nearby plateaus and mountains when evacuating the tsunami think that the connection of the community people is strong. Between No.3 and No.6, the correlation coefficient became 0.287. This indicates that those who responded as they thought they could use local well water and spring water at the time of a disaster replied that they think that the regional connection is stronger.

Based on the above, we clarified the SC from the viewpoint of the gap between the request and the maintenance situation the region desires and the relationship between the intention to utilize GI and the perception of disaster. The fact that utilization of natural resources such as well water and spring water and understanding that natural topography can be utilized for evacuation leads to a positive feeling making people believe it is possible for everyone to evacuate even if the tsunami comes, can be suggested from this study.

Keywords: the Design for Disaster prevention, tsunami disaster, green infrastructure, the coastal area of Kyushu-Pacific region, Nankai Trough large-scale earthquake

©2019. Japan Geoscience Union. All Right Reserved.

Design for Green Infrastructure: Analysis of Landscape change in the Kumamoto earthquake area

*Naoko Fujita[1]

1. Kyushu University

The concept of “Green Infrastructure” and “Eco-DRR” is developed in Europe and North America lately, and it started to spread around in Japan after the Tohoku earthquake and tsunami in 2011. Landscape ecology is parallel with this conceptually, as well as in terms of spatial scale. Its successful focused researches and social implementation are becoming pervasive.

The new concept is to solve various problems by local resources and pearls of wisdom, it connects local communities to the world while it’s mainly led by front liners and researchers in engineering and ecological fields that little attention is paid to the aspects of arts and designs. It’s still not well-penetrated despite the validity and functions of the concept are well verified. Thus, it’s vitally important to work on the insufficient.

The purpose of this research is to analyze the reconstruction plan prepared by the affected municipalities of the Kumamoto earthquake and compare the landscape change read from the plan and the actual landscape change actually occurred and make clear how the cities and nature have changed during the reconstruction process.

In this research, we firstly gathered and analyzed the earthquake reconstruction plans created by each local government for all 45 municipalities in Kumamoto prefecture. In this analysis, while studying each municipal original plan, we primarily focused on the background, features, and landscape references of the plan formulation. During this analysis, we grasped the relations between the reconstruction plan and the landscape change, and also clarified what exactly each local government emphasizes independently. As the next step, basing on the field survey, we analyzed the actual state of the landscape changes described in the plan. As a method, we took the photographs at places where the plans adopted by each municipality in Kumamoto prefecture were scheduled or executed, and after recording the current situation and the surrounding landscape, we made a comparison with the photographs taken at the same place in the past. By doing this, we revealed what kind of changes have occurred between the past and the present due to the disaster, and how they affected the surrounding landscape.

Among the 45 municipalities in downtown Kumamoto Prefecture, we found that earthquake reconstruction plan was formulated in 16 municipalities, and 5 municipalities planned to formulate. There were references that "consideration of the landscape when promoting housing improvement and infrastructure development" and "to consider the landscape from the tourism viewpoint". Also, there were plans to utilize the process of reconstruction itself as a resource for tourist attraction. Furthermore, as a result of analyzing the individual plans described in the reconstruction plan, the reference to landscape,

©2019. Japan Geoscience Union. All Right Reserved.

reference to the prediction of landscape change, reference to landscape protection exists in all 16 cities, towns, and villages. Totally 117 relevant plans have been found. Although many of them were intended to cope with the damage at the time of the disaster, there were several plans originally adopted by the local governments to make necessary improvements of the problems they had from the past by conducting disaster recovery.

The field survey was conducted for 16 municipalities in total in Kumamoto Prefecture. One year has passed since the earthquake disaster, and recovery works progressed in a wide range in Kumamoto Prefecture. In the recovery sites in various places, a secondary change of the landscape, which caused the recovery activity aimed at improving the convenience of life and safety, has already been taking place. Moreover, recovery works progressed also in Kumamoto castle which is also cultural asset and tourist attraction, as well as the station and the government office which are the center of town. As a result, we could confirm the change of landscape.

In this research, through the analysis of the reconstruction plan created by the municipalities affected by the Kumamoto earthquake and the field survey, from the viewpoint of Green Infrastructure, we could make clear the process of the landscape change occurred during the process of recovery/reconstruction of the living base, the tourist resources, the natural environment in the affected areas and its influence respectively. Although few local governments have formulated landscape-friendly reconstruction plans, to gain medium- and long-term benefits, we should make landscape-friendly reconstructions from the original planning stage. This is because it is the factor determining the richness of living base, tourism resources, and natural environment.

Keywords: Green Infrastructure, the Kumamoto earthquake , Design

©2019. Japan Geoscience Union. All Right Reserved.

[E] Poster | H (Human Geosciences)：H-DS Disaster geosciences

Wed. May 29, 2019 5:15 PM - 6:30 PM JST | Wed. May 29, 2019 8:15 AM - 9:30 AM UTC | Poster Hall International Exhibition Hall8, Makuhari Messe_21

[H-DS10] Natural hazards impacts on human society, economics and technological systems

convener:ELENA PETROVA(Lomonosov Moscow State University, Faculty of Geography), Hajime Matsushima(Research Faculty of Agriculture, Hokkaido University)

The last decade set a record for the number and scale of natural disasters and demonstrates high vulnerability of human society and technosphere to their impacts. The most serious consequences have the so-called natural-technological disasters in which natural hazards trigger accidents at technology and infrastructure such as nuclear power and chemical plants, oil refineries and pipelines, power supply systems, buildings, and roads. A distinctive feature of natural-technological events, such as of the 2011 Tohoku earthquake, is their multi-hazard and synergistic nature, which creates cascading impacts, resulting in simultaneous occurrences of myriad catastrophes. The main goal of this multidisciplinary session is to summarize case studies of relationships between natural hazards and technological disasters, their social and economic consequences; and to encourage a discussion about tools and methods to prevent disasters and to minimize their consequences, disaster reconstruction, and tourism for reconstruction, Eco-DRR, and green infrastructure.

[HDS10-P01] The 2018 Activity of Kamchatka Volcanoes and Danger to Aviation

*Olga Girina[1], Dmitry Melnikov[1], Alexander Manevich[1], Anton Nuzhdaev[1], Elena Petrova[2] (1.Institute of Volcanology and Seismology, Far East Division, Russian Academy of Sciences, 2.M.V. Lomonosov Moscow State University)

[HDS10-P02] Planning Methodology on the Effective Use of Green Infrastructure for Disaster Risk Reduction

★Invited Papers

*Keita Aragane[1], Satoshi Funakubo[1] (1.National Institute for Land Infrastructure Management)

[HDS10-P03] EMERGENCY CALL PATTERN IN PETROZAVODSK

*Boris Zalmanovich Belashev[1], Natalia Vladimirovna Krutskikh[1], Anna Aleksandrovna Gerasimova[1] (1.Karelian research center of Russian academy of science)

[HDS10-P04] IDENTIFYING “REGIMES” IN THE TIME SEQUENCES OF PROCESSES

*Boris Zalmanovich Belashev[1] (1.Karelian research center of Russian academy of science)

[HDS10-P05] Investigation of status and demand on public service of earthquake disaster mitigation in China

*Lina Dong[1], Weiping Lian[1], Weitao Chen[1] (1.Development Research Center, China Earthquake Administration)

[HDS10-P06] Analysis of Eco-DRR and Ecological Services using InVEST at the Disaster Areas of Kumamoto Earthquake

*Minghui Tang[1], Naoko Fujita[1] (1.Kyushu University)

[HDS10-P07] Transformation as praxis: Exploring socially just and transdisciplinary pathways to sustainability in marginal environments (TAPESTRY)

*Nobuhito Ohte[1], Lyla Mehta[2], Synne Movik[3], Devanathan Parthasarathy[4] (1.Department of Social Informatics, Graduate School of Informatics, Kyoto University, 2.Institute of Development Studies at the University of Sussex, 3.Department of Urban and Regional Planning, Norwegian University of Life Sciences, 4.Department of Humanities and Social Sciences, Indian Institute of Technology)

[HDS10-P08] Study for the Establishment of the Design for Disaster prevention through the survey of Recognition of tsunami disaster prevention from the viewpoint of green infrastructure in the coastal area of Kyushu-Pacific region.

*Shanshan Xu[1], Naoko Fujita[1], Minghui Tang[1] (1.Kyushu University)

[HDS10-P09] Design for Green Infrastructure: Analysis of Landscape change in the Kumamoto earthquake area

★Invited Papers

*Naoko Fujita[1] (1.Kyushu University)

The 2018 Activity of Kamchatka Volcanoes and Danger to Aviation

*Olga Girina[1], Dmitry Melnikov[1], Alexander Manevich[1], Anton Nuzhdaev[1], Elena Petrova[2]

1. Institute of Volcanology and Seismology, Far East Division, Russian Academy of Sciences, 2. M.V. Lomonosov Moscow State University

Strong explosive eruptions of volcanoes are the most dangerous for aircraft because they can produce in a few hours or days to the atmosphere and the stratosphere till several cubic kilometers of volcanic ash and aerosols. Ash plumes and the clouds, depending on the power of the eruption, the strength and wind speed, can travel thousands of kilometers from the volcano for several days, remaining hazardous to aircraft, as the melting temperature of small particles of ash below the operating temperature of jet engines.

There are 30 active volcanoes in the Kamchatka, and several of them are continuously active. Scientists of KVERT monitor Kamchatkan volcanoes since 1993. In 2018, three of these volcanoes (Sheveluch, Klyuchevskoy, Karymsky) had strong and moderate explosive eruptions.
The eruptive activity of Sheveluch volcano began since 1980 (growth of the lava dome) and is continuing at present. In 2018, strong explosions sent ash up to 10-11 km a.s.l. on 09 January, 26 and 30 December; and up to 6-7 km a.s.l. –on 09 November, and 12, 14, 26-27 and 29 December; ash plumes extended more 2000 km to the different directions of the volcano. Satellite data by KVERT showed a thermal anomaly over the volcano all year. Activity of the volcano was dangerous to international and local aviation.

The moderate explosive events (ash up to 5-6 km a.s.l.) of Klyuchevskoy volcano were observing from 01 till 18 January, on 08 May, and 06 and 15 June. Strong explosions sent ash up to 10.5 km a.s.l. on 14 May. Ash plumes extended more 350 km to the eastern and south-western directions from the volcano. Satellite data by KVERT showed a thermal anomaly over the volcano all year. Activity of the volcano was dangerous to international and local aviation.

The thermal anomaly over Karymsky volcano was recorded on satellite images from time to time, most brightly it manifested in January, May, June-August, September and December. According to visual and satellite data, at this time explosions rose ash up to 6.5 km a.s.l., ash plumes drifted for about 860 km to the different directions from the volcano. The most intense eruptive activity of the volcano was observed on 10, 14-20 and 26-31 July, besides, isolated strong explosive events were observed on 07 and 25 August, on 10-11, 22-23 and 30 September, and 01 December. The size of the ash clouds varied from 5-6 to 240 km. Activity of the volcano was dangerous to local aviation.
This work was supported by the Russian Science Foundation, project No. 16-17-00042.

Keywords: volcano, eruption, Kamchatka, danger to Aviation

©2019. Japan Geoscience Union. All Right Reserved.

Planning Methodology on the Effective Use of Green Infrastructure for Disaster Risk Reduction

*Keita Aragane[1], Satoshi Funakubo[1]

1. National Institute for Land Infrastructure Management

Green Infrastructure (GI) is a concept based on infrastructure development and land utilization that take advantage of natural environments' various functions for creating sustainable and attractive national land or regions. In Japan, since 2015, the concept of GI has been include in National Spatial Strategy, National Land Use Plan, and Priority Plan for Infrastructure Development, etc. Also, lessons learned from the Great East Japan Earthquake raised awareness of the need for more-comprehensive disaster risk reduction strategies in preparing for disasters that surpass worst-case scenarios. Additionally, there is concern over anticipated the Nankai Trough Earthquakes that might cause greater damage in near future, and increasingly frequent urban flooding owing to climate change. Thus, initiative for disaster risks reduction by utilizing GI's multiple functions in addition to approaches focusing on artificial infrastructure has become increasingly important.

This study aims to discuss planning methodology regarding the effective use of GI for disaster risk reduction in urban area by examining the “Green Master Plan (GMP)” through 72 case studies. In Japan, 680 municipal governments have developed GMPs as their basic policy for green space planning, management, and greening. These municipal governments in Japan are recommended to emphasize the viewpoint of disaster risk reduction in their GMPs, and to implement disaster risk reduction systematically through effective use of green spaces such as parks, roadside trees, waterways, private domestic gardens, agricultural land, and woodlands. Result from the case studies revealed that almost all GMPs designated green spaces such as parks as evacuation sites for mega-earthquakes or large-scale fires. Several GMPs were also found to present countermeasures that make effective use of GI for tsunami-related disasters and urban flooding.

Through these findings and through discussions with scholars at a workshop, we published “Technical Note on Green Infrastructure Planning for Urban Resilience” in June 2018. In this technical note, we explain six key points for developing GMPs that enhance the role of GI in disaster risk reduction: (1) combining various measures for disaster risk reduction by utilizing GI from a comprehensive perspective, (2) examining the role and combination of GI and other artificial infrastructure in urban disaster risk reduction, (3) building cooperative relationships with various stakeholders and citizens, (4) taking advantage of multiple functions of GI not only during disasters but also in normal times, (5) establishing a mechanism for maintaining and using GI from a long-term perspective, and (6) considering regional conditions and social situations.

Keywords: Green Infrastructure, Dsaster Risk Reduction, Green Master Plan

©2019. Japan Geoscience Union. All Right Reserved.

EMERGENCY CALL PATTERN IN PETROZAVODSK

*Boris Zalmanovich Belashev[1], Natalia Vladimirovna Krutskikh[1], Anna Aleksandrovna Gerasimova[1]

1. Karelian research center of Russian academy of science

The aim of the study is to analyze the emergency call distribution for Petrozavodsk, Russia, to obtain quantitative disease estimates and to assess the effect of environmental factors on them.

The study was based on medical statistical data and geophysical and geochemical monitoring. Environmental factors, such as magnetic storms and air and urban soil pollution, were assessed. The impersonified catalogue of emergency calls of Petrozavodsk Ambulance from 2015.1.1 to 2017.12.19, database of geomagnetic field variations at Petrozavodsk Geophysical Observatory, data on Kp index monitoring at the Laboratory of Tesis X-ray Astronomy at Lebedev Physical Institute, and the results of geochemical soil sampling in Petrozavodsk were used. Emergency call and geomagnetic activity distributions were constructed and processed in MATLAB computer mathematics system and Qgis software package. Analytical results were demonstrated on cardiovascular diseases.

The number of emergency call for patients with cardiac diseases in 2015-2017 is at about the same level. Seasonal factors affect the time distribution trends of calls for patients with essential hypertension, stenocardia and ischemic cardiac disease and do not affect the distribution trends of myocardial infarction and cerebral crisis. Time distribution spectra display a 25.6 day cycle similar to a geomagnetic activity period, two- and one-week cycles and cycles with periods of about 6, 4 and 3 days. Emergency calls for patients with myocardial infarction reflect the gender and age of the patients. The number of calls on weekends is typically low. On week-days, the number of calls at rush hours is maximum. The number of calls on days close to magnetic storms is not necessarily great. An elevated number of calls on these days for patients with stenocardia and myocardial infarction is observed.

The spatial distribution of the number of emergency calls were obtained using the Ambulance Geoinformation System. The system constructs the spatial distributions of the number of emergency team calls with known diagnoses for the streets and blocks of the city and is used to compare call frequency with district factors. With its help the link of distribution of quantity of calls of ambulance with diagnoses of cardiovascular diseases, bronchial asthma, vegeto-vascular dystonia, new growths, other diseases on districts of the city with the soils contamination indicated by the environmental hazard index –a total of the weighted average concentration values of As, Pb, Zn, Cd, Co, Cu, V, W is studied. No significant correlations between these values have been revealed.

3, 6-daily cycles in the analyzed ranges can be connected to thyroid gland hormone activity and a 4-day cycle to glucocorticoid hormone activity. Circadian rhythms are either thought to be general or to be due to the unwillingness of people to be sent to hospital or call for a doctor on weekends. In case of myocardial infarction, when help is needed urgently, the latter factor does not work, and a one-week cycle in the spectrum, showing the time dependence of the number of calls, is displayed.

This fact and the weekend effect can be understood, based on the properties of hydrocortisone. Stress from production activity stimulates the supply of the hormone into the blood, which rushes to the heart and muscles. When the heart fails to cope with the rush of blood, a cardiac disease becomes more acute.

©2019. Japan Geoscience Union. All Right Reserved.

As the hydrocortisone level in the blood on weekends and holidays declines, the number of emergency calls for patients with cardiovascular diseases decreases.

Peaks in the daily emergency call dynamics distribution on week-days are interpreted to be due to air pollution with car gases at rush hours (9-10 a.m., 1-2 and 6-7 p.m.) and an approximately one-hour delay caused by progress in disease and the need to apply for a doctor.
The emergency call distributions analyzed are highly informative, showing the complete dynamic disease pattern of the urban population.

Keywords: diseases, emergency call, patient, diagnose, magnetic storms, contamination

©2019. Japan Geoscience Union. All Right Reserved.

IDENTIFYING “REGIMES” IN THE TIME SEQUENCES OF PROCESSES

*Boris Zalmanovich Belashev[1]

1. Karelian research center of Russian academy of science

A process is represented as a sequence of “regimes” when describing climatic variations and complex systems, detecting the malfunctioning of instruments and illegal interference in computer and hardware networks. For natural, technological and social processes such representation is comfortable to detect precursors of disastrous events.
The shifts of “regimes” in the sequences are commonly detected by checking statistical hypotheses by Student’s test and tests of non-parametric statistics when comparing the characteristics of the sequence at one or another site. Algorithms often use a priori information, work in unstable fashion over short intervals and at sequences boundaries, find it hard to recognize the shifts and trends of “regimes”.
Widespread R-algorithm [1] analyze data consecutively in a sliding window, operate with a small number of parameters and filter off “red” noise. The boundary regimes it detect may reflect distortions characteristic of the beginning and end of measurements.
The goal of the present study is to develop B-algorithm which automatically recognizes stable “regimes” in time data sequences.
The main stages of the algorithm are clusterization, comparison and optimization. Clusterization preliminary divides a normalized time sequence into “regimes”. While comparing the characteristics of the “regimes”, the division obtained is re-estimated. The final model of division is formed during optimization, which minimizes the variance of deviations from the trends of the “regimes” by varying the internal boundaries of the sites.
The algorithm, developed as a software in the MATLAB computer mathematics system, fulfils procedures automatically, decreases the amount of a priori data, increases operation speed and brings solutions closer to optima.
The operation of B- and R-algorithms is exemplified by the PDO (Pacific Decade Oscillation) sequence of mean January temperatures [2].
In both algorithms the number of “regimes” and their approximate positions coincide. The delay of part of R-“regimes” emphasize the sensitivity of B-algorithm to new “regimes”. Discrepancies are connected with the last “regime” identified by R- and B-algorithms on 2 and 15 members of sequence, respectively.
B- algorithm can operate with constant, linear and complex trends.
B- and R-algorithms, applied to the time sequences of river runoff, solar and seismic activity and the sequences of the annual rings of trees, have provided new information on the stages of processes.
The simplified schematic “regime” representation of a process reveals trends commonly obscured by the abundance of details. B- algorithm identifies stable “regimes” and recognizes the shifts and trends of “regimes”. The use of MATLAB functions increases the potential of the algorithm, admits the fulfilment of procedures by various methods, brings solutions closer to optimum solutions and ensures high operation speed. The ability of the algorithm to automatically process data makes it suitable for working with extensive data in various earth sciences.
References:
1.Rodionov, S. (2006) Use of prewhitening in climate region shift detection. Geophysical Research Letters 33, L12707.
2.Pacific Decadal Oscillation Index Data.
https://www.rdocumentation.org/packages/rpdo/versions/0.2.5.

©2019. Japan Geoscience Union. All Right Reserved.

Keywords: time sequence, shift regime, algorithm, clusterization, comparision, optimization

©2019. Japan Geoscience Union. All Right Reserved.

Investigation of status and demand on public service of earthquake disaster mitigation in China

*Lina Dong[1], Weiping Lian[1], Weitao Chen[1]

1. Development Research Center, China Earthquake Administration

In order to make a comprehensive and systematic evaluation of the status and demands of public service of earthquake disaster mitigation, we launched an investigation with National Bureau of Statistics on the current situation of public service of earthquake disaster mitigation and the demands for it in 2018. The investigation was conducted in 31 provinces of China mainland using the Computer Assisted Telephone Interview(CATI) method and received 20078 valid samples in total.

The results indicate that 52.2% of the population have received the scientific knowledge education for earthquake disaster mitigation in Different levels. It shows that the public still possesses a high expectation of earthquake prediction and farmers have a low level of scientific knowledge of earthquake disaster mitigation. And TV, network, and the new media app such as wechat and weibo become the most important information channels for the public to obtain the earthquake related information. Furthermore, the degree of satisfaction evaluation of public service of earthquake disaster mitigation is marked on 81.22 points (the full mark is 100 points). And the most expectative services for the public are reconstruction, earthquake warning, and house earthquake resilience test. The results of the investigation have provided a scientific evidence for the government to provide better services of earthquake disaster mitigation and to make scientific knowledge popularization in a more scientific way.

Keywords: scientific knowledge popularization of earthquake disaster mitigation, public service, satisfaction evaluation

©2019. Japan Geoscience Union. All Right Reserved.

Analysis of Eco-DRR and Ecological Services using InVEST at the Disaster Areas of Kumamoto Earthquake

*Minghui Tang[1], Naoko Fujita[1]

1. Kyushu University

When compared with other countries in a global point of view, Japan is a country with high number of natural calamities, significant causalities, economic loss and damages by earthquakes, typhoons, and eruption. The damage is especially big when a hazard comes right after another one.

Complex disaster refers to the occurrence of multiple disasters instead of one. Such as, in 2016, Kumamoto prefecture was hit by earthquakes with magnitude as large as 7 and within another 2 months, by heavy rain and the damage was tremendous.

There is a huge number of researches on the eco-application of proceeding in various countries and it is vitally important to verify their validity. Here, InVEST refers to the ArcGIS tool for the integrated review for ecological services and its compensation.

This research focuses on the analysis of the changes of the land cover as reflected in satellite pictures of the whole Kumamoto prefecture taken after the complex disaster, the earthquake in April 2016 and heavy rain in June 2016. Also, it’ s a review on the ecological services with the use of InVEST. A special focus is paid on the review of the soil retention and the quality changes of the eco-habitant as reflection of the disaster damage reduction measures.

In addition, there is an analysis on the change of land coverage on area-unit level with Mashiki-machi, the epicenter, as the target. Furthermore, projection was plotted for the ecological services implemented as the reconstruction plan.

Keywords: Kumamoto Earthquake, Eco-DRR, Ecological services, Complex Disasters, local governments/local communities, InVEST

©2019. Japan Geoscience Union. All Right Reserved.

Transformation as praxis: Exploring socially just and transdisciplinary pathways to sustainability in marginal environments (TAPESTRY)

*Nobuhito Ohte[1], Lyla Mehta[2], Synne Movik[3], Devanathan Parthasarathy[4]

1. Department of Social Informatics, Graduate School of Informatics, Kyoto University, 2. Institute of Development Studies at the University of Sussex, 3. Department of Urban and Regional Planning, Norwegian University of Life Sciences, 4. Department of Humanities and Social Sciences, Indian Institute of Technology

Climate change related uncertainties are the main threats to the sustainability of societies and their environments. To tackle these challenges, systemic transformations are required. Our project focuses on three cases of transformation in marginal environments in India and Bangladesh, and is concerned with: How transformation happens through bottom up processes in these sites; and how they can be scaled up and facilitate wider societal changes. Both require transdisciplinary co-production and the praxis of transformation which presupposes change in social arrangements and reconstruction by individuals. Our project addresses issues concerning governance, wellbeing, identity and quality of life in relation to transformations to sustainability in a lower middle income country (India) and a least developed country (Bangladesh). Our results should help inform processes that ultimately improve the quality of life in marginal environments, and build action and capacity among all partners.

Keywords: Transformation, Sustainability, Marginal environment, Transdisciplinary study, India, Bangladesh

©2019. Japan Geoscience Union. All Right Reserved.

Study for the Establishment of the Design for Disaster prevention through the survey of Recognition of tsunami disaster prevention from the viewpoint of green infrastructure in the coastal area of Kyushu-Pacific region.

*Shanshan Xu[1], Naoko Fujita[1], Minghui Tang[1]

1. Kyushu University

Considering the possibility of Nankai Trough large-scale earthquake predicted to occur in the nearest future, the issue of the tsunami in the coastal area of Kyushu-Pacific region is becoming extremely important. Efforts to utilize the various functions of the ecosystem internationally for the society creation are expanding in recent years, and even in the situation of toughening of the land in Japan, the initiative to incorporate Green Infrastructure (GI) which utilizes the disaster prevention and reduction functions of the natural ecosystem are being observed. Also, during the process of self-help/mutual assistance action and disaster reconstruction at the time of disaster, attention is paid as regional ties are affected, which are being considered as Social capital (SC).

The purpose of this study is to clarify the actual situation of tsunami disaster prevention of Nankai Trough earthquake based on the viewpoint of GI. We conducted a questionnaire survey on tsunami disaster prevention and GI at local governments and local communities. After analyzing the questionnaire, we analyzed the needs of the self-governing president's disaster prevention measures, the problems of the area, and the deviation of the improved situation of municipalities' disaster prevention measures. A correlation analysis was conducted to grasp the relationship between the consciousness concerning GI utilization, the strength of regional linkage SC and the recognition of evacuation.

1. Misalignment between demand and maintenance situation desired by the region

Policy regarding the issue of disaster helpers was extracted as a gap between needs and maintenance situation. Regarding the needs of the soft pattern in disaster prevention, a lot of measures were taken by disaster support supporters, however as it comes from the municipality questionnaire results, the measures related to the introduction of the barrier-free system and evacuation action supporters were introduced only partially. Further improvement is necessary for welfare evacuation sites, measures against supporters requiring evacuation actions, barrier-free formation.

2. SC regarded from the viewpoint of the relationship between intentions to utilize GI and recognition on disaster.

©2019. Japan Geoscience Union. All Right Reserved.

Especially, the correlation coefficient was 0.701 between No.7 and No.6. This shows that those who responded that disaster can happen among residents can respond that regional ties are stronger. For items with a high correlation coefficient between No.3 and No.8, the correlation became 0.437. This means the respondents who answered that evacuation is possible for all area inhabitants including elderly people in case of disaster (flooding, earthquakes, and tsunami) are able to use local well water and spring water in the event of a disaster.

Between No.2 and No.4, the correlation coefficient became 3.380. This is because those who respond that they think they can fully utilize the resources of the area (resources such as firewood, foods that can be harvested in mountains) even in the event of disasters will escape by utilizing the nearby natural landforms such as plateaus and mountains for tsunami evacuation. Between No.2 and No.8, the correlation coefficient became 0.351. This is because it shows those who responded that they thought that they could escape by utilizing nearby plateau and mountains such as mountains during the tsunami evacuation, even if disasters (flood, earthquake, tsunami) occurred, everyone including the elderly in the area evacuated. Between No.2 and No.6, the correlation coefficient became 0.343. This indicates that those who responded that they believe that they can escape by utilizing nearby plateaus and mountains when evacuating the tsunami think that the connection of the community people is strong. Between No.3 and No.6, the correlation coefficient became 0.287. This indicates that those who responded as they thought they could use local well water and spring water at the time of a disaster replied that they think that the regional connection is stronger.

Based on the above, we clarified the SC from the viewpoint of the gap between the request and the maintenance situation the region desires and the relationship between the intention to utilize GI and the perception of disaster. The fact that utilization of natural resources such as well water and spring water and understanding that natural topography can be utilized for evacuation leads to a positive feeling making people believe it is possible for everyone to evacuate even if the tsunami comes, can be suggested from this study.

Keywords: the Design for Disaster prevention, tsunami disaster, green infrastructure, the coastal area of Kyushu-Pacific region, Nankai Trough large-scale earthquake

©2019. Japan Geoscience Union. All Right Reserved.

Design for Green Infrastructure: Analysis of Landscape change in the Kumamoto earthquake area

*Naoko Fujita[1]

1. Kyushu University

The concept of “Green Infrastructure” and “Eco-DRR” is developed in Europe and North America lately, and it started to spread around in Japan after the Tohoku earthquake and tsunami in 2011. Landscape ecology is parallel with this conceptually, as well as in terms of spatial scale. Its successful focused researches and social implementation are becoming pervasive.

The new concept is to solve various problems by local resources and pearls of wisdom, it connects local communities to the world while it’s mainly led by front liners and researchers in engineering and ecological fields that little attention is paid to the aspects of arts and designs. It’s still not well-penetrated despite the validity and functions of the concept are well verified. Thus, it’s vitally important to work on the insufficient.

The purpose of this research is to analyze the reconstruction plan prepared by the affected municipalities of the Kumamoto earthquake and compare the landscape change read from the plan and the actual landscape change actually occurred and make clear how the cities and nature have changed during the reconstruction process.

In this research, we firstly gathered and analyzed the earthquake reconstruction plans created by each local government for all 45 municipalities in Kumamoto prefecture. In this analysis, while studying each municipal original plan, we primarily focused on the background, features, and landscape references of the plan formulation. During this analysis, we grasped the relations between the reconstruction plan and the landscape change, and also clarified what exactly each local government emphasizes independently. As the next step, basing on the field survey, we analyzed the actual state of the landscape changes described in the plan. As a method, we took the photographs at places where the plans adopted by each municipality in Kumamoto prefecture were scheduled or executed, and after recording the current situation and the surrounding landscape, we made a comparison with the photographs taken at the same place in the past. By doing this, we revealed what kind of changes have occurred between the past and the present due to the disaster, and how they affected the surrounding landscape.

Among the 45 municipalities in downtown Kumamoto Prefecture, we found that earthquake reconstruction plan was formulated in 16 municipalities, and 5 municipalities planned to formulate. There were references that "consideration of the landscape when promoting housing improvement and infrastructure development" and "to consider the landscape from the tourism viewpoint". Also, there were plans to utilize the process of reconstruction itself as a resource for tourist attraction. Furthermore, as a result of analyzing the individual plans described in the reconstruction plan, the reference to landscape,

©2019. Japan Geoscience Union. All Right Reserved.

reference to the prediction of landscape change, reference to landscape protection exists in all 16 cities, towns, and villages. Totally 117 relevant plans have been found. Although many of them were intended to cope with the damage at the time of the disaster, there were several plans originally adopted by the local governments to make necessary improvements of the problems they had from the past by conducting disaster recovery.

The field survey was conducted for 16 municipalities in total in Kumamoto Prefecture. One year has passed since the earthquake disaster, and recovery works progressed in a wide range in Kumamoto Prefecture. In the recovery sites in various places, a secondary change of the landscape, which caused the recovery activity aimed at improving the convenience of life and safety, has already been taking place. Moreover, recovery works progressed also in Kumamoto castle which is also cultural asset and tourist attraction, as well as the station and the government office which are the center of town. As a result, we could confirm the change of landscape.

In this research, through the analysis of the reconstruction plan created by the municipalities affected by the Kumamoto earthquake and the field survey, from the viewpoint of Green Infrastructure, we could make clear the process of the landscape change occurred during the process of recovery/reconstruction of the living base, the tourist resources, the natural environment in the affected areas and its influence respectively. Although few local governments have formulated landscape-friendly reconstruction plans, to gain medium- and long-term benefits, we should make landscape-friendly reconstructions from the original planning stage. This is because it is the factor determining the richness of living base, tourism resources, and natural environment.

Keywords: Green Infrastructure, the Kumamoto earthquake , Design

©2019. Japan Geoscience Union. All Right Reserved.

[E] Poster | H (Human Geosciences)：H-TT Technology & Techniques

Wed. May 29, 2019 1:45 PM - 3:15 PM JST | Wed. May 29, 2019 4:45 AM - 6:15 AM UTC | Poster Hall International Exhibition Hall8, Makuhari Messe_2

[H-TT21] Non-destructive techniques applied to stone cultural heritage

convener:Chiaki T. Oguchi(Institute for Environmental Science and Technology, Graduate School of Science and Engineering, Saitama University), Celine Elise Thomachot-Schneider(Groupe d'etude des environnements naturels, anthropiques et archeologiques - Universite de Reims-Champagne-Ardenne (France)), Wonsuh Song(Waseda University), Miguel Gomez-Heras(Universidad Autonoma de Madrid)

Non-destructive and non-invasive techniques applying to cultural heritage made of stones, soils and earthen materials have been significantly developed over past years, and thus, the interest in such techniques has greatly increased. Here, we focus the session on new devices, new protocols and new data treatments that allow better understanding of weathering mechanisms, decay states and response to treatments.
A few topics would be listed as follows: 1) The development of new techniques and devices in cultural heritage and new protocols using non-destructive techniques; 2) The application of these techniques and protocols on indoor and outdoor case studies and laboratory studies; 3) The assessment of weathering mechanisms, weathering kinetics, decay state, and response to treatments; and 4) The modeling and simulation of decay processes.

[HTT21-P01] Comparison and Analysis of GNSS-RTK Combined with 3D LiDAR Technology on Monument Maintenance Project

*Lih-Shinn Hwang[1], Chien-Hua Chiu[1], Chien-Wen Wang[1], Hsiao-Hung Chen[1] (1.National Defense Univ.)

[HTT21-P02] Non-destructive field measurement for investigation of deteriorated parts of an artificial cave

Kaisei Sakane[1], *Chiaki T. Oguchi[1], Yasuhiko TAMURA[2] (1.Institute for Environmental Science and Technology, Graduate School of Science and Engineering, Saitama University, 2.The Exective Committee for the Preservation of Taya Cavern)

[HTT21-P03] Ultra-portable thermal cameras for moisture detection

*Miguel Gomez-Heras[1], Laura Lopez-Gonzalez[2], Maria Teresa Gil-Muñoz[3] (1.Universidad Autonoma de Madrid, 2.Artfabrik, 3.Universidad Complutense de Madrid)

[HTT21-P04] A laboratory experiment on stone decay by combination of salt and ice crystallization

*Masato Sato[1], Tsuyoshi Hattanji[2] (1.Graduate School of Life and environmental Sciences, 2.Faculty of Life and EnvironmentalSciences, University of Tsukuba)

[HTT21-P05] Study of the micro-climatic monitoring on the Saint-Remi Basilica (Rheims, France)

*Emilie Huby[1], Celine Elise Thomachot-Schneider[1], Patricia Vazquez[1], Gilles Fronteau[1] (1.Universite de Reims-Champagne-Ardenne)

Comparison and Analysis of GNSS-RTK Combined with 3D LiDAR Technology on Monument Maintenance Project

*Lih-Shinn Hwang[1], Chien-Hua Chiu[1], Chien-Wen Wang[1], Hsiao-Hung Chen[1]

1. National Defense Univ.

The Precision is the first face problem in the restoration and preservation of Monument Maintenance Project. It may be that the initial coordinates of the position cannot be effectively determined by each object of historical antiquities or buildings, which seriously affects the proportional position when the combination is later reconstructed; or because the relative relationship with the natural environment is neglected, the restoration project is time consuming and even there may be errors that cannot be recovered.
Therefore, external reference control points play an important role in the 3D laser scanning operation of historical antiquities or buildings. Especially for long-term monitoring, it almost determines the accuracy of the following article scanning.
However, due to the unexpected situation on the spot, there are often control points lost, and there is a need for a rebuild-point project, which affects the 3D scanning operation of the later cultural relics. Rebuild-point project requires not only consistent precision, but also convenience and speed. This team takes the ancient house of Li-Tengfang, a national monument, as an example. When this term is studying on the restoration and preservation of Monument Maintenance Project, it is, and proposes newly method of rebuild-point project by comparison. A new method based on the viewpoint of engineering measurement is proposed to improve the lack of traditional operations.
The experimental results show that the GNSS-RTK rapidly-precise-positioning technology can replace the traditional static-measurement to practice rebuild-point project, and the 3D LiDAR ground control measurement which accuracy is enough can also be used as a reference for the other control points. Under the premise of high efficiency and constant accuracy, our team not only successfully introduced the concept of engineering measurement into the restoration and preservation of Monument Maintenance Project, but also completed the all 3D laser scanning operation on Li-Tengfang ancient house. All research processes can be provided to relevant units for reference.

Keywords: Monument Maintenance Project, Rebuild-point project, GNSS-RTK rapidly-precise-positioning positioning, 3D LiDAR Ground control measurement

©2019. Japan Geoscience Union. All Right Reserved.

Non-destructive field measurement for investigation of deteriorated parts of an artificial cave

Kaisei Sakane[1], *Chiaki T. Oguchi[1], Yasuhiko TAMURA[2]

1. Institute for Environmental Science and Technology, Graduate School of Science and Engineering, Saitama University, 2. The Exective Committee for the Preservation of Taya Cavern

Non-destructive measurements are useful methods for evaluating weathering degree without any damage on geoarchaeological sites. The present study aims to extract the deteriorated parts by using Silver Schmidt hammer and ultrasonic measurement on the Taya cave in Yokohama city. It is a manmade cave excavated from Kamakura to late Edo periods. Many sculptures and reliefs were carved on the surface of the cave wall made of soft rock. The cave has a complex three-layer structure with a total length of 570 m. Firstly, distribution maps showing cracks and exfoliation parts were created. Then, the points showing low rebound values and slow ultrasonic rates were plotted on the same map. After these on-site measurements, many dangerous parts were turned out within the worship route.

Keywords: Taya Cave, Silver Schmidt Test, Ultrasonic Rate

©2019. Japan Geoscience Union. All Right Reserved.

Ultra-portable thermal cameras for moisture detection

*Miguel Gomez-Heras[1], Laura Lopez-Gonzalez[2], Maria Teresa Gil-Muñoz[3]

1. Universidad Autonoma de Madrid, 2. Artfabrik, 3. Universidad Complutense de Madrid

Thermal imaging technology has grown and costs have decreased exponentially from 1987, when the first portable commercially available radiometric system appeared. Several firms produce nowadays ultra-portable thermal cameras that can be fitted in smartphones and tablets, giving resolutions of thermal images up to 320x240 p at a low cost. This facilitates the use of this tool for practitioners as a part of assessment of the state of conservation of heritage buildings and control and monitoring of conservation measurements. Moisture detection is a particular case in which thermal imaging is useful. This communication presents a case study of ultra-portable thermal camera usage for moisture detection and monitoring in two north-facing chapels in the ambulatory of the 14th to 16th Century Cathedral of Palencia (Spain). [Supported by Top Heritage (P2018/NMT-4372) programe from the Regional Government of Madrid (Spain)]

Keywords: Infrared Termography, Non-Destructive Testing, Moisture

©2019. Japan Geoscience Union. All Right Reserved.

A laboratory experiment on stone decay by combination of salt and ice crystallization

*Masato Sato[1], Tsuyoshi Hattanji[2]

1. Graduate School of Life and environmental Sciences, 2. Faculty of Life and EnvironmentalSciences, University of Tsukuba

A laboratory weathering experiment simulating combination of salt and ice crystallization was carried out using four types of rocks (porous tuff, dense tuff, dense sandstone, and porous andesite) with three types of salts (sodium chloride, sodium sulfate, or magnesium sulfate). The rock specimens were subjected to freeze-thaw cycles in a climatic cabinet where air temperature ranged from -30℃ to 10℃ within 24 hours. Prior to the freeze-thaw experiment, the specimens were immersed in saturated salt solutions at 10˚C or distilled water for 72 hours, and covered with foil for preventing the specimens from drying.
The specimens immersed in saturated salt solutions showed greater weight losses, reductions in Equotip rebound value and longitudinal wave velocity and surface expansion than those immersed in distilled water. Saturated solution of magnesium sulfate induced the greatest damage on rock specimens, although magnesium sulfate has been regarded as an inactive salt in the previous freeze-thaw experiments in which rock specimen were partly immersed in salt solution with dilute or mild concentration. Sodium sulfate induced rock damages comparable with sodium chloride. Sodium and magnesium sulfate crystallized from saturated solution and induced rock expansion prior to freezing. These salt crystals may fill micro-pores in rock and facilitates rock expansion and breakdown due to freezing.

Keywords: alt weathering, frost weathering, freeze-thaw, surface hardness, longitudinal wave velocity, surface expansion

©2019. Japan Geoscience Union. All Right Reserved.

Study of the micro-climatic monitoring on the Saint-Remi Basilica (Rheims, France)

*Emilie Huby[1], Celine Elise Thomachot-Schneider[1], Patricia Vazquez[1], Gilles Fronteau[1]

1. Universite de Reims-Champagne-Ardenne

Historical buildings are subjected to weathering through different factors such as temperature and humidity variations, that have a direct influence on different weathering processes. Insolation produces thermal expansion differences within the stone creating stresses at grain boundaries that can lead to disaggregation. If water is involved, a low temperature can cause the freezing of water inducing ice expansion and cryosuction. These repetitive stresses can damage the stone through fatigue failure. The measurement of environmental parameters on site is essential in order to study the weathering of the stone in its particular environment and anticipate risk areas.
To identify the micro-climatic conditions on a monument, an in situ monitoring was achieved on the Saint-Remi Basilica of Rheims, listed as a UNESCO World Heritage site. A sensor network was set up on the two towers of the monument in December 2017: fourteen temperature-humidity i-Buttons facing different directions, at different heights and recording with a time step of 1 hour, or a time step of 2 minutes for short measurement campaigns.
The data obtained by the sensor network highlighted the microclimates on the building. The height of the measured points had no significant impact on the results, whereas the orientation of the façade had an influence on the surface temperature. This was directly related to the longer solar exposure of the stone throughout the day and allowed to identify micro-climates. The façades exposed to the sun (South, East in the morning, West in the afternoon) present higher temperatures and lower relative humidity compared to the shadowed areas (North, East in the afternoon, West in the morning, other shadowed zones). The relative humidity measured was linked to the temperature: a temperature increase induces a humidity decrease. A mean difference of temperature between South and North of 2,7˚C with a maximum of 18˚C and a mean difference of relative humidity of 4,3% with a maximum of 48% were observed.
Climatic cycles on different time ranges were identified: an annual cycle alternating between winter and summer, a daily cycle due to sun exposure and short cycles identified during short term monitoring. These short abrupt variations of temperature (1-2˚C) on façades lasted between 5 and 40 minutes and were due to cloud cover and/or wind-speed. Four typical days inducing strains were identified: sunny days with a temperature increase superior to 10˚C, rainy days inducing wet/dry cycles, frost days presenting frost/thaw cycles and stormy days where a sudden rain on heated stones caused abrupt temperature and humidity variations. A year can thus be fragmented in those 4 categorized days. This repartition of typical days over a year depended on the micro-climatic variations previously identified: the shadowed zones experienced less sunny days and more rainy days.
This study of climatic monitoring will help anticipate the stone weathering on the Saint-Remi Basilica. The monitoring will continue for the next two years in order to obtain reproducible data and will be coupled with an infrared thermography monitoring. The strains corresponding to the four identified types of day are reproduced through accelerated ageing experiments using the parameters recorded on site. From the repartition of these typical days in one year, this will allow to estimate the behavior of a stone during a year on a sun-exposed façade and on a shadowed zone of the Basilica. The final goal is to be able to anticipate the stone weathering on the monument and identify risk areas.

Keywords: weathering processes, micro-climate, Saint-Remi Basilica, in situ monitoring

©2019. Japan Geoscience Union. All Right Reserved.

©2019. Japan Geoscience Union. All Right Reserved.

[E] Poster | H (Human Geosciences)：H-TT Technology & Techniques

Wed. May 29, 2019 5:15 PM - 6:30 PM JST | Wed. May 29, 2019 8:15 AM - 9:30 AM UTC | Poster Hall International Exhibition Hall8, Makuhari Messe_23

[H-TT21] Non-destructive techniques applied to stone cultural heritage

convener:Chiaki T. Oguchi(Institute for Environmental Science and Technology, Graduate School of Science and Engineering, Saitama University), Celine Elise Thomachot-Schneider(Groupe d'etude des environnements naturels, anthropiques et archeologiques - Universite de Reims-Champagne-Ardenne (France)), Wonsuh Song(Waseda University), Miguel Gomez-Heras(Universidad Autonoma de Madrid)

Non-destructive and non-invasive techniques applying to cultural heritage made of stones, soils and earthen materials have been significantly developed over past years, and thus, the interest in such techniques has greatly increased. Here, we focus the session on new devices, new protocols and new data treatments that allow better understanding of weathering mechanisms, decay states and response to treatments.
A few topics would be listed as follows: 1) The development of new techniques and devices in cultural heritage and new protocols using non-destructive techniques; 2) The application of these techniques and protocols on indoor and outdoor case studies and laboratory studies; 3) The assessment of weathering mechanisms, weathering kinetics, decay state, and response to treatments; and 4) The modeling and simulation of decay processes.

[HTT21-P01] Comparison and Analysis of GNSS-RTK Combined with 3D LiDAR Technology on Monument Maintenance Project

*Lih-Shinn Hwang[1], Chien-Hua Chiu[1], Chien-Wen Wang[1], Hsiao-Hung Chen[1] (1.National Defense Univ.)

[HTT21-P02] Non-destructive field measurement for investigation of deteriorated parts of an artificial cave

Kaisei Sakane[1], *Chiaki T. Oguchi[1], Yasuhiko TAMURA[2] (1.Institute for Environmental Science and Technology, Graduate School of Science and Engineering, Saitama University, 2.The Exective Committee for the Preservation of Taya Cavern)

[HTT21-P03] Ultra-portable thermal cameras for moisture detection

*Miguel Gomez-Heras[1], Laura Lopez-Gonzalez[2], Maria Teresa Gil-Muñoz[3] (1.Universidad Autonoma de Madrid, 2.Artfabrik, 3.Universidad Complutense de Madrid)

[HTT21-P04] A laboratory experiment on stone decay by combination of salt and ice crystallization

*Masato Sato[1], Tsuyoshi Hattanji[2] (1.Graduate School of Life and environmental Sciences, 2.Faculty of Life and EnvironmentalSciences, University of Tsukuba)

[HTT21-P05] Study of the micro-climatic monitoring on the Saint-Remi Basilica (Rheims, France)

*Emilie Huby[1], Celine Elise Thomachot-Schneider[1], Patricia Vazquez[1], Gilles Fronteau[1] (1.Universite de Reims-Champagne-Ardenne)

Comparison and Analysis of GNSS-RTK Combined with 3D LiDAR Technology on Monument Maintenance Project

*Lih-Shinn Hwang[1], Chien-Hua Chiu[1], Chien-Wen Wang[1], Hsiao-Hung Chen[1]

1. National Defense Univ.

The Precision is the first face problem in the restoration and preservation of Monument Maintenance Project. It may be that the initial coordinates of the position cannot be effectively determined by each object of historical antiquities or buildings, which seriously affects the proportional position when the combination is later reconstructed; or because the relative relationship with the natural environment is neglected, the restoration project is time consuming and even there may be errors that cannot be recovered.
Therefore, external reference control points play an important role in the 3D laser scanning operation of historical antiquities or buildings. Especially for long-term monitoring, it almost determines the accuracy of the following article scanning.
However, due to the unexpected situation on the spot, there are often control points lost, and there is a need for a rebuild-point project, which affects the 3D scanning operation of the later cultural relics. Rebuild-point project requires not only consistent precision, but also convenience and speed. This team takes the ancient house of Li-Tengfang, a national monument, as an example. When this term is studying on the restoration and preservation of Monument Maintenance Project, it is, and proposes newly method of rebuild-point project by comparison. A new method based on the viewpoint of engineering measurement is proposed to improve the lack of traditional operations.
The experimental results show that the GNSS-RTK rapidly-precise-positioning technology can replace the traditional static-measurement to practice rebuild-point project, and the 3D LiDAR ground control measurement which accuracy is enough can also be used as a reference for the other control points. Under the premise of high efficiency and constant accuracy, our team not only successfully introduced the concept of engineering measurement into the restoration and preservation of Monument Maintenance Project, but also completed the all 3D laser scanning operation on Li-Tengfang ancient house. All research processes can be provided to relevant units for reference.

Keywords: Monument Maintenance Project, Rebuild-point project, GNSS-RTK rapidly-precise-positioning positioning, 3D LiDAR Ground control measurement

©2019. Japan Geoscience Union. All Right Reserved.

Non-destructive field measurement for investigation of deteriorated parts of an artificial cave

Kaisei Sakane[1], *Chiaki T. Oguchi[1], Yasuhiko TAMURA[2]

1. Institute for Environmental Science and Technology, Graduate School of Science and Engineering, Saitama University, 2. The Exective Committee for the Preservation of Taya Cavern

Non-destructive measurements are useful methods for evaluating weathering degree without any damage on geoarchaeological sites. The present study aims to extract the deteriorated parts by using Silver Schmidt hammer and ultrasonic measurement on the Taya cave in Yokohama city. It is a manmade cave excavated from Kamakura to late Edo periods. Many sculptures and reliefs were carved on the surface of the cave wall made of soft rock. The cave has a complex three-layer structure with a total length of 570 m. Firstly, distribution maps showing cracks and exfoliation parts were created. Then, the points showing low rebound values and slow ultrasonic rates were plotted on the same map. After these on-site measurements, many dangerous parts were turned out within the worship route.

Keywords: Taya Cave, Silver Schmidt Test, Ultrasonic Rate

©2019. Japan Geoscience Union. All Right Reserved.

Ultra-portable thermal cameras for moisture detection

*Miguel Gomez-Heras[1], Laura Lopez-Gonzalez[2], Maria Teresa Gil-Muñoz[3]

1. Universidad Autonoma de Madrid, 2. Artfabrik, 3. Universidad Complutense de Madrid

Thermal imaging technology has grown and costs have decreased exponentially from 1987, when the first portable commercially available radiometric system appeared. Several firms produce nowadays ultra-portable thermal cameras that can be fitted in smartphones and tablets, giving resolutions of thermal images up to 320x240 p at a low cost. This facilitates the use of this tool for practitioners as a part of assessment of the state of conservation of heritage buildings and control and monitoring of conservation measurements. Moisture detection is a particular case in which thermal imaging is useful. This communication presents a case study of ultra-portable thermal camera usage for moisture detection and monitoring in two north-facing chapels in the ambulatory of the 14th to 16th Century Cathedral of Palencia (Spain). [Supported by Top Heritage (P2018/NMT-4372) programe from the Regional Government of Madrid (Spain)]

Keywords: Infrared Termography, Non-Destructive Testing, Moisture

©2019. Japan Geoscience Union. All Right Reserved.

A laboratory experiment on stone decay by combination of salt and ice crystallization

*Masato Sato[1], Tsuyoshi Hattanji[2]

1. Graduate School of Life and environmental Sciences, 2. Faculty of Life and EnvironmentalSciences, University of Tsukuba

A laboratory weathering experiment simulating combination of salt and ice crystallization was carried out using four types of rocks (porous tuff, dense tuff, dense sandstone, and porous andesite) with three types of salts (sodium chloride, sodium sulfate, or magnesium sulfate). The rock specimens were subjected to freeze-thaw cycles in a climatic cabinet where air temperature ranged from -30℃ to 10℃ within 24 hours. Prior to the freeze-thaw experiment, the specimens were immersed in saturated salt solutions at 10˚C or distilled water for 72 hours, and covered with foil for preventing the specimens from drying.
The specimens immersed in saturated salt solutions showed greater weight losses, reductions in Equotip rebound value and longitudinal wave velocity and surface expansion than those immersed in distilled water. Saturated solution of magnesium sulfate induced the greatest damage on rock specimens, although magnesium sulfate has been regarded as an inactive salt in the previous freeze-thaw experiments in which rock specimen were partly immersed in salt solution with dilute or mild concentration. Sodium sulfate induced rock damages comparable with sodium chloride. Sodium and magnesium sulfate crystallized from saturated solution and induced rock expansion prior to freezing. These salt crystals may fill micro-pores in rock and facilitates rock expansion and breakdown due to freezing.

Keywords: alt weathering, frost weathering, freeze-thaw, surface hardness, longitudinal wave velocity, surface expansion

©2019. Japan Geoscience Union. All Right Reserved.

Study of the micro-climatic monitoring on the Saint-Remi Basilica (Rheims, France)

*Emilie Huby[1], Celine Elise Thomachot-Schneider[1], Patricia Vazquez[1], Gilles Fronteau[1]

1. Universite de Reims-Champagne-Ardenne

Historical buildings are subjected to weathering through different factors such as temperature and humidity variations, that have a direct influence on different weathering processes. Insolation produces thermal expansion differences within the stone creating stresses at grain boundaries that can lead to disaggregation. If water is involved, a low temperature can cause the freezing of water inducing ice expansion and cryosuction. These repetitive stresses can damage the stone through fatigue failure. The measurement of environmental parameters on site is essential in order to study the weathering of the stone in its particular environment and anticipate risk areas.
To identify the micro-climatic conditions on a monument, an in situ monitoring was achieved on the Saint-Remi Basilica of Rheims, listed as a UNESCO World Heritage site. A sensor network was set up on the two towers of the monument in December 2017: fourteen temperature-humidity i-Buttons facing different directions, at different heights and recording with a time step of 1 hour, or a time step of 2 minutes for short measurement campaigns.
The data obtained by the sensor network highlighted the microclimates on the building. The height of the measured points had no significant impact on the results, whereas the orientation of the façade had an influence on the surface temperature. This was directly related to the longer solar exposure of the stone throughout the day and allowed to identify micro-climates. The façades exposed to the sun (South, East in the morning, West in the afternoon) present higher temperatures and lower relative humidity compared to the shadowed areas (North, East in the afternoon, West in the morning, other shadowed zones). The relative humidity measured was linked to the temperature: a temperature increase induces a humidity decrease. A mean difference of temperature between South and North of 2,7˚C with a maximum of 18˚C and a mean difference of relative humidity of 4,3% with a maximum of 48% were observed.
Climatic cycles on different time ranges were identified: an annual cycle alternating between winter and summer, a daily cycle due to sun exposure and short cycles identified during short term monitoring. These short abrupt variations of temperature (1-2˚C) on façades lasted between 5 and 40 minutes and were due to cloud cover and/or wind-speed. Four typical days inducing strains were identified: sunny days with a temperature increase superior to 10˚C, rainy days inducing wet/dry cycles, frost days presenting frost/thaw cycles and stormy days where a sudden rain on heated stones caused abrupt temperature and humidity variations. A year can thus be fragmented in those 4 categorized days. This repartition of typical days over a year depended on the micro-climatic variations previously identified: the shadowed zones experienced less sunny days and more rainy days.
This study of climatic monitoring will help anticipate the stone weathering on the Saint-Remi Basilica. The monitoring will continue for the next two years in order to obtain reproducible data and will be coupled with an infrared thermography monitoring. The strains corresponding to the four identified types of day are reproduced through accelerated ageing experiments using the parameters recorded on site. From the repartition of these typical days in one year, this will allow to estimate the behavior of a stone during a year on a sun-exposed façade and on a shadowed zone of the Basilica. The final goal is to be able to anticipate the stone weathering on the monument and identify risk areas.

Keywords: weathering processes, micro-climate, Saint-Remi Basilica, in situ monitoring

©2019. Japan Geoscience Union. All Right Reserved.

©2019. Japan Geoscience Union. All Right Reserved.

[E] Poster | H (Human Geosciences)：H-CG Complex & General

Wed. May 29, 2019 3:30 PM - 5:00 PM JST | Wed. May 29, 2019 6:30 AM - 8:00 AM UTC | Poster Hall International Exhibition Hall8, Makuhari Messe_15

[H-CG25] International Comparison of Landscape Appreciation

convener:Anastasia Petrova(Institute of Oriental Studies of the Russian Academy of Sciences), yoji aoki(Open University of Japan)

Evaluation of landscape has been developed in a variety of fields, such as geography, landscape architecture, nature protection, and some others. Landscape appreciation is a complex and sophisticated psychological phenomenon. There is no consensus among researchers on what the phenomenon of "landscape" truly is, how people physiologically and mentally experience it, which human attributes affect the perception of it, and why it is apprehended the way it is. The concept of landscape appreciation has yet to be clearly defined and there is a lack of agreement on evaluation methods, the factors that determine landscape preferences, the steps in appreciation, and so forth. This session aims to discuss the research findings of landscape evaluation in various fields, including geography, geomorphology, landscape planning, architecture, engineering, social sciences, environmental psychology, meteorology, phenology, and so on.

[HCG25-P01] The Globally Important Agricultural Heritage of Aso from the perspective of landscape and its supporting systems

*REIKO MACHIDA[1] (1.TOKYO UNIVERSITY OF AGRICULTURE)

[HCG25-P02] Hazardous natural phenomena and weather conditions appreciation in Russian landscape painting

*ELENA PETROVA[1] (1.Lomonosov Moscow State University, Faculty of Geography)

[HCG25-P03] Trends of evaluation items to landscape appreciation until 2017 in the English journals

*yoji aoki[1], keisuke mukagai[2], Anastasia Petrova[3] (1.Open University of Japan, 2.Nagano University, 3.Institute of Oriental Studies, Russian Academy of Sciences)

The Globally Important Agricultural Heritage of Aso from the perspective of landscape and its supporting systems

*REIKO MACHIDA[1]

1. TOKYO UNIVERSITY OF AGRICULTURE

Globally Important Agricultural Heritage Systems (GIAHS) is a partnership initiative of the Food and Agriculture Organization of the United Nations which began in 2002 with the aim to identify, support and safeguard remarkable land use systems and landscapes that are rich in globally significant biological diversity evolving from the co-adaptation of a community with its environment and its needs and aspirations for sustainable development. There are 19 countries and 45 areas around the world, and among them 9 areas in Japan that are listed as GIAHS at present.The Aso area located in Northern Kyusyu features the world's largest caldera, which is 25 km wide from north to south and 18 km from east to west and grassland landscapes. The vast grasslands of the Aso area have been managed throughout history by local agricultural activities such as controlled burning, mowing and pasturage since the Heian period. The historical land use in Aso has been a balanced combination of rice fields at the caldera floor, forestry and fungiculture at the foot of the caldera, and grazing pasture at the top of caldera, which is carried out in harmony with the environment. The management of the Aso grasslands for sustainable agriculture have been recognized and certified as Globally Important Agricultural Heritage Systems (GIAHS) in 2013.In terms of landscape, the values of Aso as Globally Important Agricultural Heritage System are the dynamic grassland landscapes of the large caldera, the historical paddies and rice terraces, which vary in size from small to large as a result of the local human activities. There are beautiful rural landscapes on various scales.However, the productivity oriented rural development and the division of land has been having a negative impact on the landscape value of the GIAHS. There are cases of rice paddies and buildings that contribute to the landscape value being lost. From such cases, it is evident that the landscape structures that should be protected since they are GIHS are not recognized widely enough.This study investigated the landscape value and landscape structure as GIAHS and its value supports landscape policy. As a result, it became clear that the landscape structure of Minamiaso village consist of the traditional combination of grasslands and paddy fields retains significant wildlife habitat and picturesque agricultural landscapes. It has become clear that development activities do not influence to landscape in large-scale, however development activities as land readjustment project influenced to landscape in small and medium-scale. "Landscape planning" "Landscape agricultural development plan" can support the landscape structure in small and medium -scale. It is important to plan the land use for the landscape value of GIAHS.

Keywords: Globally Important Agricultural Heritage Systems (GIAHS), Landscape, Landscape Planning

©2019. Japan Geoscience Union. All Right Reserved.

Hazardous natural phenomena and weather conditions appreciation in Russian landscape painting

*ELENA PETROVA[1]

1. Lomonosov Moscow State University, Faculty of Geography

The fixation of various natural phenomena by landscape artists of different historical periods in different regions and countries has not only purely aesthetic interest, but also particular interest to science. During the period of Romanticism that has spread in the European and Russian art in the 19th century, Russian art turned to real living nature. Landscapes of the native country began to play a dominant role in the formation of landscape image. Romanticism aroused interest not only in the picturesque and exotic landscapes, but also in the majestic forces of nature. Volcanic eruptions, earthquakes, storms, thunderstorms, floods, and other natural hazards were new motifs for artists of that time. Romantic artists were inclined to exaggerate the power and destructive forces of natural phenomena they portrayed, elevating any event of this kind to the rank of a natural disaster. Often, they portrayed the rather ordinary storm, thunderstorm, flood as a universal natural catastrophe, comparable, perhaps, only to the biblical flood. What to say about really extraordinary events. Most vividly, the theme of the turbulent, dramatic landscape was developed in the works by Aivazovsky who quite realistically showed the sea element in various stages of its manifestation - from complete calm to the strongest storm. Being in Italy, Russian artists could not disregard such an extraordinary event as the violent eruption of the volcano Vesuvius, which occurred in 1822; many have captured it in their landscape images.

Thanks to the rapid development of scientific knowledge and discoveries in the field of geosciences, including meteorology, artists were encouraged to observe various atmospheric phenomena and weather conditions. Gradually, the sky ceased to be depicted simply as a smooth blue background, as was customary in the tradition of classicism; carefully traced clouds of various types, shapes and shades began to appear in pictures. In addition, various evaporations, fogs, haze, etc. became objects of the landscape image. Romantic artists were little interested in depicting winter and snow, despite the fact that the cold season with a steady snow cover continues in Russia for almost half a year from November to early April. The painting “Russian Winter” (1827) by Nikifore Krylov became perhaps the first winter landscape image in Russian painting. Krylov depicted a somewhat naive, but quite real, winter landscape on the bank of the Tosna River in the vicinity of St. Petersburg, which he painted from life. He was able to reliably convey the atmosphere of the Russian winter: a valley covered with snow, a frozen river, a dark strip of forest in the distance and the peasants with their daily affairs on the road down to the river in the foreground. The first bright and joyful snow-covered landscape image was created, apparently, by Alexey Savrasov in his famous painting “The Rooks Have Come Back” (1871). The spring snow melting and sparkling in the sun became later the favorite motif of the Russian painting. Comparative analysis of landscape pictures can be an important tool, in addition to scientific methods, in studying the nature and dynamics of various hazardous natural processes and phenomena, including hydrological and meteorological ones in conditions of changing climate.

Keywords: hazardous natural phenomena , weather conditions , landscape painting, landscape images

©2019. Japan Geoscience Union. All Right Reserved.

Trends of evaluation items to landscape appreciation until 2017 in the English journals

*yoji aoki[1], keisuke mukagai[2], Anastasia Petrova[3]

1. Open University of Japan, 2. Nagano University, 3. Institute of Oriental Studies, Russian Academy of Sciences

Introduction
We have considered trends of landscape appreciation since JpGU2013-2018. According to the definition of landscape phenomena proposed by Prof. O. Shinohara (Fig. 1), we reported the trends of studies in each part of the phenomena.

Aoki, Y. (1999) described the first landscape evaluation using psychometrical methods to be pioneered by Peterson, G.L. (1967). Before this development, they tried to find the landscape appreciation using various descriptors. They were mostly belonging to the literature or the paintings. As for the literature, the first description of mountain was found in Francesco Petrarca in 1336 of France (Kondo, T. 2002). But his description has no reliable evidence to ensure the landscape. In the field of art, Albrecht Altdorfer drew the first natural landscape in the beginning of 15th century of Germany (Cavaliere, B. 1989). But we could not measure the physical data from his picture. The literature and the art found the beauty of natural landscape by these examples. They recorded the aesthetic beauty in landscape (Thiel, P. 1968).

Jay Appleton (1980) explained the scientific reason of the landscape phenomena with physical data, e.g. geomorphysical data and meteorological data. He explained the landscape phenomena of two pictures, Constable's Weymouth Bay and Constable's sunset study of Hampstead Heath. His approach must be the scientific based explanation to find psychological phenomena of landscape using the geology and meteorology. But the psychological phenomena could deviate by the person observed and the results must be happened statistically. So the process of the landscape phenomena should be explained by stochastic process of psychology. Then scientists developed psychological approach to it.

Here, we summarize the appreciation item (the third component of the landscape phenomena).

1. The developments to establish the psychological scale of appraisal

In the trial of psychometrical method, Ekman & Kuennapas (1962) tested the difference of Nominal scale and Interval scale, and the development of SD method promoted to use many adjectives in the visual complexities (Berlyne & Peckham 1966). Hart & Graham (1967) considered “How to rate & rank landscape”.

In the development of the psychological scale, Heise (1969) tested the scale -3 to 3, and Zube, Anderson & Pitt (1973) used the numerical scale 3 to 14.

2. The psychological evaluation item of preference

Kaplan, Kaplan, & Wendt (1972) proposed to use preference for the landscape appreciation. Compared to the results obtained by SD method, “preference” is easy to understand among different cultural back ground and was popularized in many countries.

©2019. Japan Geoscience Union. All Right Reserved.

3. The developments and the use of SD method

As for the SD method proposed by Osgood & Suci (1955), it employed many pairs of adjectives to evaluate landscape and provided detailed impressions of landscape. The largest number of 240 adjectives was tested by Craik (1975). The results were too complicated and scientists would like to summarize the results. SBE (Terry & Boster 1976), AVQ (Arriaza etc. 2004) and others were statistical aggregation examples of this trial and the example of meaningful aggregation was “Coherence, Complexity, Legibility and Mystery” proposed by Kaplan (1987). These indicators were tested with the relation to the preference and other appreciations by many scientists (Stamps III 2004, and so on.).

4. Method of monetary term evaluation

Monetary term is another evaluation of landscapes and sometimes used in the physical planning (Fukahori & Kubota 2003).

5. Items based on the human behavior of landscape evaluation

The origin of the landscape appreciation was explained from the animal behavior of predation (Appleton 1975). This theory had discussed for a long time. And this behavior might propose a base appreciation of landscape (Aoki & Kitamura 2001). Consideration on the human activities, the reason of visit (Andereck et al. 1989) and the visitability (Abdulkarim & Nasar 2014) were examined and the photographing (Oku & Fukamachi 2006, Sugimoto 2013) were reported.

6. Other appraisals

There are many appreciation descriptors and even now the scientists are finding new descriptors (Collier & Scott 2008). Until now, we could find examples of this trial in absorption (Berlyne 1958), quietness (Womble & Studebaker 1981), beauty (Hull IV, Buhyoff & Daniel 1984), size (Coeterier 1994), fear and stress (Nasar & Jones 1997), positive and negative (Ryan 1998), aggression and violence (Kuo 2001), satisfaction (Kaplan & Austin 2004), overcrowding (Manning & Freimund 2004), openness (Dramstad et al. 2006), ugly (Ruell, Halleux & Teller 2013), and other descriptions.

Keywords: landscape appreciation, appreciation items, until 2017

©2019. Japan Geoscience Union. All Right Reserved.

Table Historical review of landscape appreciation items

Interesting subject	Name of authors	Year
Development of the SD method	Osgood, C.E. and Suci, G.J.	1955
absorption	Berlyne, D.E.,	1958
descriptive appreciation as aesthetic beauty	Thiel, P.,	1961
difference of Nominal scale and Interval scale	Ekman, G. and Kuennapas, T.	1962
SD method	Wright, B. and Rainwater, L.	1962
description	Halprin, L.,	1965
absorption	Berlyne, D.E. and Peckham, S.	1966
description	Noe, S. and Abernathy, B.L.	1966
landscape type	Hart W. J. and William W. Graham,	1967
absorption	Wohlwill, J.F.	1968
numerical scale from -3 to +3	Heise, D.R.,	1969
aesthetic and emotional	Shafer, E.L. and Mietz, J.	1969
objectivity	Craik, K.H.	1972
preference	Kaplan, S., Kaplan, R. and Wendt, J.S.	1972
scaling	Acking, C.A and Sorte, G.J.	1973
numerical scale from 3 to 14	Zube, E.H., Anderson, T. and Pitt, D.	1973
prospect-refuge theory	Appleton, J.	1975
SD method with 240 pairs of adjectives	Craik, K.H.	1975
SBE method; normalization of the results	Daniel, T.C. and Boster, R.S.	1976
monetary	McConnell, K.E.,	1977
SD method	Pedersen, D.M.	1978
SD method	Shuttleworth, S.	1980
preference	Nasar, J.L.,	1981
meaning	Russell, J.A. and Ward, L.M.	1981
quiet	Womble, P. and Studebaker, S.	1981
quiet	Hammitt, W.E.,	1982
preference	Mudrak, L.Y.,	1983
preference	Nasar, J.L.,	1983
SD method	Ruiz, J.P. and Gonzalez-Bernaldez, F.	1983
scenic beauty	Hull IV, R.B., Buhyoff, G.J. and Daniel, T.C.	1984
needs and fears	Talbot, J.F. and Kaplan, R.	1984
preference	Herzog, T.R.	1985
SD method	Abello, R.P., Bernaldez, F.G. and Galiano, E.F.	1986
preference	Talbot, J.F. and Kaplan, R.	1986
survey paper: Coherence, Complexity, Legibility, Mystery	Kaplan, S.	1987
SD method	Kobayashi, M., Higashiyama, J. and Kawasaki, K.	1987
preference	Talbot, J.F., Bardwell, L.V. and Kaplan, R.	1987
monetary	Anderson, L.M. and Cordell, H.K.	1988
preference	Herzog, T. and Smith, G.A.	1988
motivation to visit	Andereck, K. et al.	1989
evaluation by monetary term	Daniel, T.C., et al.	1989
SD method	Kaplan, R., Kaplan, S. and Brown, T.	1989
SD method	Ruiz, M. and Ruiz, J.P.	1989
preference	Gimblett, H.R.	1990
monetary	Green, C.H., et al.	1990
motivation to visit	Uysal, M., McDonald, C.D. and Reid, L.J.	1990
quiet	Ulrich, R.S. et al.	1991
preference	Chokor, B.A	1992
preference	Herzog, T.	1992
refuge provides shelter	Hudson, B.J.	1992
effect to land price	Orland, B., Vinning, J. and Ebreo, A.	1992
familiarity	Purcell, A.T.	1992
description: literature works	Ikeda, T. and Konno, A.	1993
size of space	Coeterier, J.F.,	1994
identity	Hull IV, R.B., Lam, M. and Vigo, G.	1994
preference	Stamps III, A.E.	1994
preference	Strumse, E.	1994
preference	Sullivan III, W.C.,	1994
prospect-refuge theory reviewed	Appleton, J.,	1995
motivation to visit	Cha, S., McCleary, K.W. and Uysal, M.	1995
preference	Mealey, L.	1995
preference on tree form	Sommer, R. and Summit, J.	1995
preference	Herzog, T.R. and Gale, T.A.	1996
scenic preference in Finland	Karjalainen, E.	1996
scaling	Tahvanainen, L., Tyrvainen, L. and Nousiainen, I.	1996
Notation for a Participatory Envirotecture	Thiel, P.,	1996
fear and stress	Nasar, J.L. and Jones, K.M.	1997
landscape preferences of USA, Ireland, Senegal	Newell, P.B.	1997
quiet	Caffyn, A. and Prosser, B.	1998
preference	Herzog, T.R.,	1998
consistency of evaluation by rank order and graphical scale	Karjalainen, E. and Komulainen, M.	1998
preference	Kuo, F.E., Bacaicoa, M. and Sullivan, W.C.	1998
preference and naturalness using Scrub-forest, wide-close view, nature-altered	Purcell, A.T. and Lamb, R.J.	1998
positive and negative scenery of river frontland	Ryan, R.L.	1998
monetary	Tyrvainen, L. and Vaananen, H.	1998
preference	Brown, T.J., Kaplan R. and Quaderer, G.	1999
tranquility and preference	Herzog, T.R. and Barnes, G.J.	1999
preference	Summit, J. and Sommer, R.	1999
landscape preference in Australia	Herzog, T.R. et al	2000
landscape preference in Israel	Misgav, A.	2000
Phylogenic and Ontogenic evolution of landscape appreciation	Aoki, Y. and Kitamura, S.	2001
correlation between preference and likeliness	Hagerhall, C.M.	2001
motivation of ecological behavior	Hartig, T.	2001
aggression and violence	Kuo, F.E.,	2001
preference and danger	Herzog, T.R. and Kutzli, G.E.	2002
landscape preference in Norway	Kaltenborn, B.P. and Bjerke, T.	2002
positive and negative scenery of rural living	Ryan, R.L.,	2002
comparison of VOC and SBE	Franco, D. et al.	2003
cost and amenity level of road scenery	Fukahori, K. and Kubota, Y.	2003
preference	Herzog, T.R. and Leverich, O.L.	2003
AVQ index for visual quality	Arriaza, M. et al.	2004
preference	Herzog, T.R. and Kropscott, L.S.	2004
satisfaction of nature	Kaplan, R. and Austin, M.E.	2004
over crowding by photo montage method	Manning, R.E. and Freimund, W.A	2004
SBE difference 1976-1996	Palmer, J.F.	2004
preference did not correlate to mystery, complexity, legibility, coherence	Stamps, III, A.E.	2004
preference and danger by visibility	Herzog, T.R., & Kirk, K.M.	2005
preference by pair comparison	Rodiek, S.D. and Fried, J.T.	2005
proper openness, student and locals	Dramstad, W.E., et al.	2006
essential features for scenic beauty	Ergin, A., Williams, A.T. and Micallef, A.	2006
landscape preferred in Turkey	Kaplan, A., Taskin, T. and Onenc, A.,	2006
photographing by activity	Oku, H., & Fukamachi, K.	2006
disturbance, naturalness, visual scale, place identity in the photographs	Tveit, M., Ode, A. and Fry, G.	2006
mystery did not affect preference	Herzog, T.R. and Bryce, A.G.,	2007
words interested in the interview	Collier, M.J. and Scott, M.J.	2008
preference of transportation system; vegetation, distance, side fascia affected	Bernasconi, C. et al.	2009
beautiful high mountain, Sherpa appreciate flora, ugly garbage site no vegetation at Everest	Beza, B.B.	2010
species-rich of middle ground affect like of alpine landscape	Lindemann-Matthies, P. et al.	2010
naturalness, unity affect preference of Spruce forest landscape in Turkey	Eroglu, E. and Acar, C.	2011
surprise and Mystery affect preference, Turkey find Mystery at curved street	Nasar, J.L. and Cubukcu, E.	2011
ugly impression of brown fields and montage support improvement in Belgium	Ruelle, C., Halleux, J.-M. & Teller, J.	2013
Visitability	Abdulkarim, D. and Nasar, J. L.	2014
oppressiveness	Asgarzadeh, M. et al.	2014
threat	Chiang, Y-C., Nasal, J. and Ko, C-C.	2014
variance affected by evaluation value	Kalivoda, O. et al.	2014
forest and park affected stress relief	Tyrvainen, L., Ojala, A., Korpela, K. Lanki, T., Tsunetsugu, Y., Kagawa, T.	2014
proper understorey affect preference	van der Wal, R., Miller, D., Irvine, J., Fiorini, S., Amar, A., Yearley, S. Gill, R. & Dandy, N.	2014
openness	Weitkamp, G., Lammeren, R. and Bregt, A.	2014
risk of bushfire	Gill, N. et al.	2015
water use affect landscaping preference	Hayden, L., et al	2015
panorama tree cover density affect to preference	Jiang, B., et al.	2015
green roof affect restorativeness	Lee, K.E., Williams,K.J.H., Sargent, L.D., Williams, N.S.G., Johnson, K.A	2015
aesthetic, morphological condition and ecological integrity	McCormick, A, Fisher, K. and Brierley, G.	2015
water, reed, litter, dead wood affected preference	Eder, R., & Arnberger, A.	2016
tree coverage affect stress recovery	Jiang, B., Li, D., Larsen, L. & Sullivan, W.C.	2016
visual realism and sound affect preference	Lindquist, M., Lange, E. & Kang J.	2016
change of motivation	Shalev, I.	2016
cultural values in visual object	Sowinska-Swierkosz, B.N., Chmielewski, T.J.	2016
visual green reduces noise annoyance	Van Renterghem, T. & Botteldooren, D.	2016
public litter and fishing litter affect preference	Wyles, K.J., Pahl, S. Thomas, K. & Thompson, R.	2016
disorder affect fear of crime	Biasi, Alaina De	2017
nature contact reduce depression, anxiety, stress in outside experience	Brooks, A.M. et al.	2017
biodiversity affected preference	Cracknell, D. et. al.	2017
dead wood affected preference	Gundersen, V., Stange, E.E., Kaltenborn, B.P. Vistad	2017
EAB infestation affect crime, theft, breaking entering, property crime	Kondo, M.C., Han, S., Donovan, G.H., MacDonald, J.M.	2017
preference increase 4bit designed complexinformation entropy values	Kuper, R.	2017
wind generator affect to EEG (electroencephalographic)	Murcia, G. et al.	2017
natural scenery affect change of heart rate by CT scan	Zijlstra, E. et. Al.	2017
attributes affected to landscape aesthetic value of CVM	Dupras, J. et al.	2018
point elements affect preference	Haefner, K. et al.	2018
dense vegetation preferred in city	Harris, V. et al.	2018
motivation of park visit	Hecke, Linde, et al.	2018
firing affect emotional wellbeing	Knez, I. et al.	2018
mature oak with anemone preferred	Nielsen, A.B., Gundersen, V.S. & Jensen, F.S.	2018
traditional landscape preferred by residents in central Alps	Pecher, C., et al.	2018
photo points located by GIS	Sugimoto, K.	2018
setting and arrangement affect restrativeness	Tabrizian, P., et al.	2018
forest preference of 4 seasons	Bravo-Vargas, V. et al.	2019

behavioral consideration
developments in scaling
monetary approaches
use of preference
developments in SD method
other appreciation

©2019. Japan Geoscience Union. All Right Reserved.

[E] Poster | H (Human Geosciences)：H-CG Complex & General

Wed. May 29, 2019 5:15 PM - 6:30 PM JST | Wed. May 29, 2019 8:15 AM - 9:30 AM UTC | Poster Hall International Exhibition Hall8, Makuhari Messe_24

[H-CG25] International Comparison of Landscape Appreciation

convener:Anastasia Petrova(Institute of Oriental Studies of the Russian Academy of Sciences), yoji aoki(Open University of Japan)

Evaluation of landscape has been developed in a variety of fields, such as geography, landscape architecture, nature protection, and some others. Landscape appreciation is a complex and sophisticated psychological phenomenon. There is no consensus among researchers on what the phenomenon of "landscape" truly is, how people physiologically and mentally experience it, which human attributes affect the perception of it, and why it is apprehended the way it is. The concept of landscape appreciation has yet to be clearly defined and there is a lack of agreement on evaluation methods, the factors that determine landscape preferences, the steps in appreciation, and so forth. This session aims to discuss the research findings of landscape evaluation in various fields, including geography, geomorphology, landscape planning, architecture, engineering, social sciences, environmental psychology, meteorology, phenology, and so on.

[HCG25-P01] The Globally Important Agricultural Heritage of Aso from the perspective of landscape and its supporting systems

*REIKO MACHIDA[1] (1.TOKYO UNIVERSITY OF AGRICULTURE)

[HCG25-P02] Hazardous natural phenomena and weather conditions appreciation in Russian landscape painting

*ELENA PETROVA[1] (1.Lomonosov Moscow State University, Faculty of Geography)

[HCG25-P03] Trends of evaluation items to landscape appreciation until 2017 in the English journals

*yoji aoki[1], keisuke mukagai[2], Anastasia Petrova[3] (1.Open University of Japan, 2.Nagano University, 3.Institute of Oriental Studies, Russian Academy of Sciences)

The Globally Important Agricultural Heritage of Aso from the perspective of landscape and its supporting systems

*REIKO MACHIDA[1]

1. TOKYO UNIVERSITY OF AGRICULTURE

Globally Important Agricultural Heritage Systems (GIAHS) is a partnership initiative of the Food and Agriculture Organization of the United Nations which began in 2002 with the aim to identify, support and safeguard remarkable land use systems and landscapes that are rich in globally significant biological diversity evolving from the co-adaptation of a community with its environment and its needs and aspirations for sustainable development. There are 19 countries and 45 areas around the world, and among them 9 areas in Japan that are listed as GIAHS at present.The Aso area located in Northern Kyusyu features the world's largest caldera, which is 25 km wide from north to south and 18 km from east to west and grassland landscapes. The vast grasslands of the Aso area have been managed throughout history by local agricultural activities such as controlled burning, mowing and pasturage since the Heian period. The historical land use in Aso has been a balanced combination of rice fields at the caldera floor, forestry and fungiculture at the foot of the caldera, and grazing pasture at the top of caldera, which is carried out in harmony with the environment. The management of the Aso grasslands for sustainable agriculture have been recognized and certified as Globally Important Agricultural Heritage Systems (GIAHS) in 2013.In terms of landscape, the values of Aso as Globally Important Agricultural Heritage System are the dynamic grassland landscapes of the large caldera, the historical paddies and rice terraces, which vary in size from small to large as a result of the local human activities. There are beautiful rural landscapes on various scales.However, the productivity oriented rural development and the division of land has been having a negative impact on the landscape value of the GIAHS. There are cases of rice paddies and buildings that contribute to the landscape value being lost. From such cases, it is evident that the landscape structures that should be protected since they are GIHS are not recognized widely enough.This study investigated the landscape value and landscape structure as GIAHS and its value supports landscape policy. As a result, it became clear that the landscape structure of Minamiaso village consist of the traditional combination of grasslands and paddy fields retains significant wildlife habitat and picturesque agricultural landscapes. It has become clear that development activities do not influence to landscape in large-scale, however development activities as land readjustment project influenced to landscape in small and medium-scale. "Landscape planning" "Landscape agricultural development plan" can support the landscape structure in small and medium -scale. It is important to plan the land use for the landscape value of GIAHS.

Keywords: Globally Important Agricultural Heritage Systems (GIAHS), Landscape, Landscape Planning

©2019. Japan Geoscience Union. All Right Reserved.

Hazardous natural phenomena and weather conditions appreciation in Russian landscape painting

*ELENA PETROVA[1]

1. Lomonosov Moscow State University, Faculty of Geography

The fixation of various natural phenomena by landscape artists of different historical periods in different regions and countries has not only purely aesthetic interest, but also particular interest to science. During the period of Romanticism that has spread in the European and Russian art in the 19th century, Russian art turned to real living nature. Landscapes of the native country began to play a dominant role in the formation of landscape image. Romanticism aroused interest not only in the picturesque and exotic landscapes, but also in the majestic forces of nature. Volcanic eruptions, earthquakes, storms, thunderstorms, floods, and other natural hazards were new motifs for artists of that time. Romantic artists were inclined to exaggerate the power and destructive forces of natural phenomena they portrayed, elevating any event of this kind to the rank of a natural disaster. Often, they portrayed the rather ordinary storm, thunderstorm, flood as a universal natural catastrophe, comparable, perhaps, only to the biblical flood. What to say about really extraordinary events. Most vividly, the theme of the turbulent, dramatic landscape was developed in the works by Aivazovsky who quite realistically showed the sea element in various stages of its manifestation - from complete calm to the strongest storm. Being in Italy, Russian artists could not disregard such an extraordinary event as the violent eruption of the volcano Vesuvius, which occurred in 1822; many have captured it in their landscape images.

Thanks to the rapid development of scientific knowledge and discoveries in the field of geosciences, including meteorology, artists were encouraged to observe various atmospheric phenomena and weather conditions. Gradually, the sky ceased to be depicted simply as a smooth blue background, as was customary in the tradition of classicism; carefully traced clouds of various types, shapes and shades began to appear in pictures. In addition, various evaporations, fogs, haze, etc. became objects of the landscape image. Romantic artists were little interested in depicting winter and snow, despite the fact that the cold season with a steady snow cover continues in Russia for almost half a year from November to early April. The painting “Russian Winter” (1827) by Nikifore Krylov became perhaps the first winter landscape image in Russian painting. Krylov depicted a somewhat naive, but quite real, winter landscape on the bank of the Tosna River in the vicinity of St. Petersburg, which he painted from life. He was able to reliably convey the atmosphere of the Russian winter: a valley covered with snow, a frozen river, a dark strip of forest in the distance and the peasants with their daily affairs on the road down to the river in the foreground. The first bright and joyful snow-covered landscape image was created, apparently, by Alexey Savrasov in his famous painting “The Rooks Have Come Back” (1871). The spring snow melting and sparkling in the sun became later the favorite motif of the Russian painting. Comparative analysis of landscape pictures can be an important tool, in addition to scientific methods, in studying the nature and dynamics of various hazardous natural processes and phenomena, including hydrological and meteorological ones in conditions of changing climate.

Keywords: hazardous natural phenomena , weather conditions , landscape painting, landscape images

©2019. Japan Geoscience Union. All Right Reserved.

Trends of evaluation items to landscape appreciation until 2017 in the English journals

*yoji aoki[1], keisuke mukagai[2], Anastasia Petrova[3]

1. Open University of Japan, 2. Nagano University, 3. Institute of Oriental Studies, Russian Academy of Sciences

Introduction
We have considered trends of landscape appreciation since JpGU2013-2018. According to the definition of landscape phenomena proposed by Prof. O. Shinohara (Fig. 1), we reported the trends of studies in each part of the phenomena.

Aoki, Y. (1999) described the first landscape evaluation using psychometrical methods to be pioneered by Peterson, G.L. (1967). Before this development, they tried to find the landscape appreciation using various descriptors. They were mostly belonging to the literature or the paintings. As for the literature, the first description of mountain was found in Francesco Petrarca in 1336 of France (Kondo, T. 2002). But his description has no reliable evidence to ensure the landscape. In the field of art, Albrecht Altdorfer drew the first natural landscape in the beginning of 15th century of Germany (Cavaliere, B. 1989). But we could not measure the physical data from his picture. The literature and the art found the beauty of natural landscape by these examples. They recorded the aesthetic beauty in landscape (Thiel, P. 1968).

Jay Appleton (1980) explained the scientific reason of the landscape phenomena with physical data, e.g. geomorphysical data and meteorological data. He explained the landscape phenomena of two pictures, Constable's Weymouth Bay and Constable's sunset study of Hampstead Heath. His approach must be the scientific based explanation to find psychological phenomena of landscape using the geology and meteorology. But the psychological phenomena could deviate by the person observed and the results must be happened statistically. So the process of the landscape phenomena should be explained by stochastic process of psychology. Then scientists developed psychological approach to it.

Here, we summarize the appreciation item (the third component of the landscape phenomena).

1. The developments to establish the psychological scale of appraisal

In the trial of psychometrical method, Ekman & Kuennapas (1962) tested the difference of Nominal scale and Interval scale, and the development of SD method promoted to use many adjectives in the visual complexities (Berlyne & Peckham 1966). Hart & Graham (1967) considered “How to rate & rank landscape”.

In the development of the psychological scale, Heise (1969) tested the scale -3 to 3, and Zube, Anderson & Pitt (1973) used the numerical scale 3 to 14.

2. The psychological evaluation item of preference

Kaplan, Kaplan, & Wendt (1972) proposed to use preference for the landscape appreciation. Compared to the results obtained by SD method, “preference” is easy to understand among different cultural back ground and was popularized in many countries.

©2019. Japan Geoscience Union. All Right Reserved.

3. The developments and the use of SD method

As for the SD method proposed by Osgood & Suci (1955), it employed many pairs of adjectives to evaluate landscape and provided detailed impressions of landscape. The largest number of 240 adjectives was tested by Craik (1975). The results were too complicated and scientists would like to summarize the results. SBE (Terry & Boster 1976), AVQ (Arriaza etc. 2004) and others were statistical aggregation examples of this trial and the example of meaningful aggregation was “Coherence, Complexity, Legibility and Mystery” proposed by Kaplan (1987). These indicators were tested with the relation to the preference and other appreciations by many scientists (Stamps III 2004, and so on.).

4. Method of monetary term evaluation

Monetary term is another evaluation of landscapes and sometimes used in the physical planning (Fukahori & Kubota 2003).

5. Items based on the human behavior of landscape evaluation

The origin of the landscape appreciation was explained from the animal behavior of predation (Appleton 1975). This theory had discussed for a long time. And this behavior might propose a base appreciation of landscape (Aoki & Kitamura 2001). Consideration on the human activities, the reason of visit (Andereck et al. 1989) and the visitability (Abdulkarim & Nasar 2014) were examined and the photographing (Oku & Fukamachi 2006, Sugimoto 2013) were reported.

6. Other appraisals

There are many appreciation descriptors and even now the scientists are finding new descriptors (Collier & Scott 2008). Until now, we could find examples of this trial in absorption (Berlyne 1958), quietness (Womble & Studebaker 1981), beauty (Hull IV, Buhyoff & Daniel 1984), size (Coeterier 1994), fear and stress (Nasar & Jones 1997), positive and negative (Ryan 1998), aggression and violence (Kuo 2001), satisfaction (Kaplan & Austin 2004), overcrowding (Manning & Freimund 2004), openness (Dramstad et al. 2006), ugly (Ruell, Halleux & Teller 2013), and other descriptions.

Keywords: landscape appreciation, appreciation items, until 2017

©2019. Japan Geoscience Union. All Right Reserved.

Table Historical review of landscape appreciation items

Interesting subject	Name of authors	Year
Development of the SD method	Osgood, C.E. and Suci, G.J.	1955
absorption	Berlyne, D.E.,	1958
descriptive appreciation as aesthetic beauty	Thiel, P.,	1961
difference of Nominal scale and Interval scale	Ekman, G. and Kuennapas, T.	1962
SD method	Wright, B. and Rainwater, L.	1962
description	Halprin, L.,	1965
absorption	Berlyne, D.E. and Peckham, S.	1966
description	Noe, S. and Abernathy, B.L.	1966
landscape type	Hart W. J. and William W. Graham,	1967
absorption	Wohlwill, J.F.	1968
numerical scale from -3 to +3	Heise, D.R.,	1969
aesthetic and emotional	Shafer, E.L. and Mietz, J.	1969
objectivity	Craik, K.H.	1972
preference	Kaplan, S., Kaplan, R. and Wendt, J.S.	1972
scaling	Acking, C.A and Sorte, G.J.	1973
numerical scale from 3 to 14	Zube, E.H., Anderson, T. and Pitt, D.	1973
prospect-refuge theory	Appleton, J.	1975
SD method with 240 pairs of adjectives	Craik, K.H.	1975
SBE method; normalization of the results	Daniel, T.C. and Boster, R.S.	1976
monetary	McConnell, K.E.,	1977
SD method	Pedersen, D.M.	1978
SD method	Shuttleworth, S.	1980
preference	Nasar, J.L.,	1981
meaning	Russell, J.A. and Ward, L.M.	1981
quiet	Womble, P. and Studebaker, S.	1981
quiet	Hammitt, W.E.,	1982
preference	Mudrak, L.Y.,	1983
preference	Nasar, J.L.,	1983
SD method	Ruiz, J.P. and Gonzalez-Bernaldez, F.	1983
scenic beauty	Hull IV, R.B., Buhyoff, G.J. and Daniel, T.C.	1984
needs and fears	Talbot, J.F. and Kaplan, R.	1984
preference	Herzog, T.R.	1985
SD method	Abello, R.P., Bernaldez, F.G. and Galiano, E.F.	1986
preference	Talbot, J.F. and Kaplan, R.	1986
survey paper: Coherence, Complexity, Legibility, Mystery	Kaplan, S.	1987
SD method	Kobayashi, M., Higashiyama, J. and Kawasaki, K.	1987
preference	Talbot, J.F., Bardwell, L.V. and Kaplan, R.	1987
monetary	Anderson, L.M. and Cordell, H.K.	1988
preference	Herzog, T. and Smith, G.A.	1988
motivation to visit	Andereck, K. et al.	1989
evaluation by monetary term	Daniel, T.C., et al.	1989
SD method	Kaplan, R., Kaplan, S. and Brown, T.	1989
SD method	Ruiz, M. and Ruiz, J.P.	1989
preference	Gimblett, H.R.	1990
monetary	Green, C.H., et al.	1990
motivation to visit	Uysal, M., McDonald, C.D. and Reid, L.J.	1990
quiet	Ulrich, R.S. et al.	1991
preference	Chokor, B.A	1992
preference	Herzog, T.	1992
refuge provides shelter	Hudson, B.J.	1992
effect to land price	Orland, B., Vinning, J. and Ebreo, A.	1992
familiarity	Purcell, A.T.	1992
description: literature works	Ikeda, T. and Konno, A.	1993
size of space	Coeterier, J.F.,	1994
identity	Hull IV, R.B., Lam, M. and Vigo, G.	1994
preference	Stamps III, A.E.	1994
preference	Strumse, E.	1994
preference	Sullivan III, W.C.,	1994
prospect-refuge theory reviewed	Appleton, J.,	1995
motivation to visit	Cha, S., McCleary, K.W. and Uysal, M.	1995
preference	Mealey, L.	1995
preference on tree form	Sommer, R. and Summit, J.	1995
preference	Herzog, T.R. and Gale, T.A.	1996
scenic preference in Finland	Karjalainen, E.	1996
scaling	Tahvanainen, L., Tyrvainen, L. and Nousiainen, I.	1996
Notation for a Participatory Envirotecture	Thiel, P.,	1996
fear and stress	Nasar, J.L. and Jones, K.M.	1997
landscape preferences of USA, Ireland, Senegal	Newell, P.B.	1997
quiet	Caffyn, A. and Prosser, B.	1998
preference	Herzog, T.R.,	1998
consistency of evaluation by rank order and graphical scale	Karjalainen, E. and Komulainen, M.	1998
preference	Kuo, F.E., Bacaicoa, M. and Sullivan, W.C.	1998
preference and naturalness using Scrub-forest, wide-close view, nature-altered	Purcell, A.T. and Lamb, R.J.	1998
positive and negative scenery of river frontland	Ryan, R.L.	1998
monetary	Tyrvainen, L. and Vaananen, H.	1998
preference	Brown, T.J., Kaplan R. and Quaderer, G.	1999
tranquility and preference	Herzog, T.R. and Barnes, G.J.	1999
preference	Summit, J. and Sommer, R.	1999
landscape preference in Australia	Herzog, T.R. et al	2000
landscape preference in Israel	Misgav, A.	2000
Phylogenic and Ontogenic evolution of landscape appreciation	Aoki, Y. and Kitamura, S.	2001
correlation between preference and likeliness	Hagerhall, C.M.	2001
motivation of ecological behavior	Hartig, T.	2001
aggression and violence	Kuo, F.E.,	2001
preference and danger	Herzog, T.R. and Kutzli, G.E.	2002
landscape preference in Norway	Kaltenborn, B.P. and Bjerke, T.	2002
positive and negative scenery of rural living	Ryan, R.L.,	2002
comparison of VOC and SBE	Franco, D. et al.	2003
cost and amenity level of road scenery	Fukahori, K. and Kubota, Y.	2003
preference	Herzog, T.R. and Leverich, O.L.	2003
AVQ index for visual quality	Arriaza, M. et al.	2004
preference	Herzog, T.R. and Kropscott, L.S.	2004
satisfaction of nature	Kaplan, R. and Austin, M.E.	2004
over crowding by photo montage method	Manning, R.E. and Freimund, W.A	2004
SBE difference 1976-1996	Palmer, J.F.	2004
preference did not correlate to mystery, complexity, legibility, coherence	Stamps, III, A.E.	2004
preference and danger by visibility	Herzog, T.R., & Kirk, K.M.	2005
preference by pair comparison	Rodiek, S.D. and Fried, J.T.	2005
proper openness, student and locals	Dramstad, W.E., et al.	2006
essential features for scenic beauty	Ergin, A., Williams, A.T. and Micallef, A.	2006
landscape preferred in Turkey	Kaplan, A., Taskin, T. and Onenc, A.,	2006
photographing by activity	Oku, H., & Fukamachi, K.	2006
disturbance, naturalness, visual scale, place identity in the photographs	Tveit, M., Ode, A. and Fry, G.	2006
mystery did not affect preference	Herzog, T.R. and Bryce, A.G.,	2007
words interested in the interview	Collier, M.J. and Scott, M.J.	2008
preference of transportation system; vegetation, distance, side fascia affected	Bernasconi, C. et al.	2009
beautiful high mountain, Sherpa appreciate flora, ugly garbage site no vegetation at Everest	Beza, B.B.	2010
species-rich of middle ground affect like of alpine landscape	Lindemann-Matthies, P. et al.	2010
naturalness, unity affect preference of Spruce forest landscape in Turkey	Eroglu, E. and Acar, C.	2011
surprise and Mystery affect preference, Turkey find Mystery at curved street	Nasar, J.L. and Cubukcu, E.	2011
ugly impression of brown fields and montage support improvement in Belgium	Ruelle, C., Halleux, J.-M. & Teller, J.	2013
Visitability	Abdulkarim, D. and Nasar, J. L.	2014
oppressiveness	Asgarzadeh, M. et al.	2014
threat	Chiang, Y-C., Nasal, J. and Ko, C-C.	2014
variance affected by evaluation value	Kalivoda, O. et al.	2014
forest and park affected stress relief	Tyrvainen, L., Ojala, A., Korpela, K. Lanki, T., Tsunetsugu, Y., Kagawa, T.	2014
proper understorey affect preference	van der Wal, R., Miller, D., Irvine, J., Fiorini, S., Amar, A., Yearley, S. Gill, R. & Dandy, N.	2014
openness	Weitkamp, G., Lammeren, R. and Bregt, A.	2014
risk of bushfire	Gill, N. et al.	2015
water use affect landscaping preference	Hayden, L., et al	2015
panorama tree cover density affect to preference	Jiang, B., et al.	2015
green roof affect restorativeness	Lee, K.E., Williams,K.J.H., Sargent, L.D., Williams, N.S.G., Johnson, K.A	2015
aesthetic, morphological condition and ecological integrity	McCormick, A, Fisher, K. and Brierley, G.	2015
water, reed, litter, dead wood affected preference	Eder, R., & Arnberger, A.	2016
tree coverage affect stress recovery	Jiang, B., Li, D., Larsen, L. & Sullivan, W.C.	2016
visual realism and sound affect preference	Lindquist, M., Lange, E. & Kang J.	2016
change of motivation	Shalev, I.	2016
cultural values in visual object	Sowinska-Swierkosz, B.N., Chmielewski, T.J.	2016
visual green reduces noise annoyance	Van Renterghem, T. & Botteldooren, D.	2016
public litter and fishing litter affect preference	Wyles, K.J., Pahl, S. Thomas, K. & Thompson, R.	2016
disorder affect fear of crime	Biasi, Alaina De	2017
nature contact reduce depression, anxiety, stress in outside experience	Brooks, A.M. et al.	2017
biodiversity affected preference	Cracknell, D. et. al.	2017
dead wood affected preference	Gundersen, V., Stange, E.E., Kaltenborn, B.P. Vistad	2017
EAB infestation affect crime, theft, breaking entering, property crime	Kondo, M.C., Han, S., Donovan, G.H., MacDonald, J.M.	2017
preference increase 4bit designed complexinformation entropy values	Kuper, R.	2017
wind generator affect to EEG (electroencephalographic)	Murcia, G. et al.	2017
natural scenery affect change of heart rate by CT scan	Zijlstra, E. et. Al.	2017
attributes affected to landscape aesthetic value of CVM	Dupras, J. et al.	2018
point elements affect preference	Haefner, K. et al.	2018
dense vegetation preferred in city	Harris, V. et al.	2018
motivation of park visit	Hecke, Linde, et al.	2018
firing affect emotional wellbeing	Knez, I. et al.	2018
mature oak with anemone preferred	Nielsen, A.B., Gundersen, V.S. & Jensen, F.S.	2018
traditional landscape preferred by residents in central Alps	Pecher, C., et al.	2018
photo points located by GIS	Sugimoto, K.	2018
setting and arrangement affect restrativeness	Tabrizian, P., et al.	2018
forest preference of 4 seasons	Bravo-Vargas, V. et al.	2019

behavioral consideration
developments in scaling
monetary approaches
use of preference
developments in SD method
other appreciation

©2019. Japan Geoscience Union. All Right Reserved.

[E] Poster | S (Solid Earth Sciences)：S-IT Science of the Earth's Interior & Techtonophysics

Wed. May 29, 2019 10:45 AM - 12:15 PM JST | Wed. May 29, 2019 1:45 AM - 3:15 AM UTC | Poster Hall International Exhibition Hall8, Makuhari Messe_8

[S-IT26] New perspectives on the geodynamics of East Asia

convener:Timothy B Byrne(University of Connecticut), Asuka Yamaguchi(Atomosphere and Ocean Research Institute, The University of Tokyo), Jonny Wu(University of Houston), Kyoko Okino(Atmosphere and Ocean Research Institute, The University of Tokyo)

The Pacific, Indo-Australia and Eurasian plates converge around the Philippine Sea plates in south and East Asia, resulting in one of the most tectonically active regions on earth. The area is also geologically and tectonically complex with numerous active tectonic environments, ranging from subduction to collision, and a long history of plate boundary interactions. The last decade has yielded a wide range of new observations, including detailed geologic data and high resolution crustal to mantle imaging. Here we seek oral and poster presentations that bear on the geologic history and geophysical character of modern and ancient plates in East Asia and their interactions since the Mesozoic. We also invite geodynamic models that integrate these diverse datasets into a more holistic view of this dynamic environment.

[SIT26-P01] Geochemical characteristics of effusive rocks (greenstones) in the Hidaka Belt, Hokkaido, Japan

*Toru Yamasaki[1], Futoshi Nanayama[1] (1.Geol. Survey of Japan (AIST))

[SIT26-P02] Large gas reservoir in continental back-arc basin, revealed by automatic seismic velocity analysis in the Okinawa Trough

*Kota Mukumoto[1], Takeshi Tsuji[1], Andri Hendriyana[1] (1.Kyushu University)

[SIT26-P03] Characterize coseismic deformation of Mw 7.5 Palu earthquake in a triple junction in Sulawesi, Indonesia

*MIN-CHIEN TSAI[1], Ying-Hui Yang[2], Chun-Ying Chiu[3], Jyr-Ching Hu[3] (1.Seismological center, Central Weather Bureau, Taipei, Taiwan, R.O.C., 2.School of Civil Engineering and Architecture, Southwest Petroleum University, Chengdu, China, 3.Department of Geosciences, National Taiwan University, Taipei, Taiwan, R.O.C.)

Geochemical characteristics of effusive rocks (greenstones) in the Hidaka Belt, Hokkaido, Japan

*Toru Yamasaki[1], Futoshi Nanayama[1]

1. Geol. Survey of Japan (AIST)

Igneous rocks in a subduction complex typically occur as greenstones, and petrological and geochemical investigations of such greenstones can provide important insights into the oceanic magmatism, origin of the accretionary complex, and growth of the continental margin. The Hidaka Belt in Central Hokkaido, Japan consists of an early Paleogene subduction complex, referred to as the Hidaka Supergroup (HSG), dominated by clastic rocks. Locally, the terrigenous sediments of the HSG were intruded by the contemporary, normal-type mid-ocean ridge basalts (“*in situ*N-MORBs”) that were formed at an oceanic ridge near the Eurasian continent (Miyashita and Katsushima, 1986: GSJ). The southern area of the HSG has been referred to as the Nakanogawa Group (NKG), which gradually leads to the high-temperature Hidaka metamorphic belt (HMB) in the western part. The lower sequence of the HMB consists mainly of high-grade metabasites, which are assumed to be equivalent to the N-MORBs in the HSG, based on their geochemical features. Recently, Yamasaki and Nanayama (2018a: Lithos) reported about the unique Daimaruyama greenstones from the NKG, formed by an immature intra-oceanic arc-type volcanism. In addition, highly-alkaline basalts, presumably formed at the seamount, exist as exotic blocks in the NKG and are named as Tachiiwa blocks (Owada et al., 1992: JMPEG). In fact, the N-MORBs in the HSG and the Tachiiwa alkaline rocks are characterized by the whole-rock major and minor element geochemistry, but the trace element geochemistry, including the rare earth elements (REEs), has not been reported yet for these rocks. Therefore, we collected 18 samples of greenstones from the entire Hidaka Belt and examined their whole-rock major and trace element geochemistry.

Including those in our previous reports (Yamasaki and Nanayama, 2018a, b: JpGU Abs.), there are three distinct types of greenstones in the Hidaka Belt. The first type are the MORB-type greenstones which show relatively flat chondrite-normalized (CN) REE patterns and N-MORB-normalized (NMN) multi-element patterns with Ti/V = 26–53 and Zr/Nb = 21–117. Although Miyashita and Kiminami (1999: MemGSJ) showed the flat NMN minor element (Nb, P, Zr, Ti, and Y) patterns of basalts from the northern HSG, trace element patterns of the MORB-type rocks in this study show rather light REE (LREE)-rich NMN multi-element patterns. The second type are the ocean island basalt (OIB)-type greenstones. The NMN multi-element and CN REE patterns for this type of greenstones show a gentle slope up to the left, with Ti/V>62 and Zr/Nb<15. The third type are the Daimaruyama greenstones. This type of greenstones show similar NMN multi-element patterns and CN REE patterns to those in the OIB-type, but with a clear relative depletion of Nb, Ta, and Ti. In addition, their Ti-V relations are similar to those in the MORB-type greenstones.

MORB-type greenstones are distributed from the northernmost part of the HSG to the southern Rakko River area in the NKG. OIB-type greenstones occur in the Tachiiwa block and the Rakko River area. Daimaruyama greenstones occur only in the Daimaruyama megablock in the NKG. Since the Tachiiwa and Daimaruyama blocks are presumably derived from the neighboring Tokoro Belt, the absence of the OIB-type and Daimaruyama greenstones in the northern HSG implies a difference in provenance between the HSG and NKG. The MORB-type greenstones do not show the typical N-MORB-type (LREE-depleted) trace element patterns, whereas the metabasite in the HMB shows the typical N-MORB-type geochemical features. In addition, the distribution of the MORB-type greenstones is separated from the metabasites of

©2019. Japan Geoscience Union. All Right Reserved.

the HMB in the southern Hidaka Belt. These lines of evidence suggest that the protolith of the HMB is not an equivalent of the “*in-situ*MORB” in the HSG, and is probably an accreted fragment of the older oceanic plate.

Keywords: Hidaka Belt, greenstones, trace elements

©2019. Japan Geoscience Union. All Right Reserved.

Large gas reservoir in continental back-arc basin, revealed by automatic seismic velocity analysis in the Okinawa Trough

*Kota Mukumoto[1], Takeshi Tsuji[1], Andri Hendriyana[1]

1. Kyushu University

P-wave velocity acquired from seismic reflection data allows us to quantify submarine geological structures. In the Iheya North Knoll of the Okinawa Trough, intense hydrothermal activity occurs due to continental rifting. The hydrothermal system in the Iheya North Knoll has been explored by geophysical surveys, geochemical measurements and drilling campaign. Based on these surveys, gas reservoir could be considered to exist around the Iheya North Knoll. However, gas reservoir around the Iheya North Knoll has not been identified in previous studies. Here we show P-wave velocity structure derived from automatic velocity analysis of multi-channel seismic reflection data. P-wave velocity is sensitive to free gas in sediments. Therefore, P-wave velocity is key information to quantify gas distribution in sediments. Automatic velocity analysis estimated P-wave velocity structure with remarkable high spatial and temporal resolution. The P-wave velocity structure revealed gas reservoirs around the Iheya North Knoll. Although many gas components can be generated by magmatic activity, hydrothermal alteration of organic-rich sediments and biogenic processes, CH_4 and CO_2 could be major gas components which is derived by hydrothermal system in marine sediment. Therefore, main gas components could be CH_4 or CO_2. The strong amplitude reflector above the gas reservoir could be the interface between CH_4 hydrate and gas, because the depth of strong amplitude reflector is well consistent with pressure-temperature conditions of the phase transition. If the main gas component is CH_4, the gas reservoir could be important as resource. Whereas, if the gas reservoir includes CO_2, the gas distribution could be important to consider carbon flux between earth and ocean. Furthermore, widely distributed gas reservoir may influence on the chemical components of hydrothermal fluids in the Iheya North Knoll.

Keywords: Seismic reflection data, Okinawa Trough, Gas reservoir

©2019. Japan Geoscience Union. All Right Reserved.

Characterize coseismic deformation of Mw 7.5 Palu earthquake in a triple junction in Sulawesi, Indonesia

*MIN-CHIEN TSAI[1], Ying-Hui Yang[2], Chun-Ying Chiu[3], Jyr-Ching Hu[3]

1. Seismological center, Central Weather Bureau, Taipei, Taiwan, R.O.C., 2. School of Civil Engineering and Architecture, Southwest Petroleum University, Chengdu, China, 3. Department of Geosciences, National Taiwan University, Taipei, Taiwan, R.O.C.

We first use SAR satellite data to map the coseismic deformation for the 2018 Mw=7.5 strike-slip earthquake of 28 September 2018 in Palu, Sulawesi, Indonesia. The seismogenic fault is a left-lateral a strike-slip event along the Palu-Koro fault at shallow depth that occurred within the interior of the Molucca Sea microplate, which is part of the Sunda plate. We use D-InSAR technique with ALOS-2 descending orbit radar images to characterize coseismic and deformation pattern induced by Palu earthquake.We also plan to use with sub-pixel correlation form Sentinel-2 and Planet imagery to map the surface rupture area and the coseismic offsets in order to provide the near-field deformation data located in decorrelation zone from the D-InSAR result. Thus we can inverse the distribution of slip on the fault patches. In addition, we also calculate the Coulomb stress transfer for assessing the stress increasing and shadow on the major fault systems, such as the active Poso Fault Zone and Mamuju –Lariang Active Fault Zone. In particular, we will assess the seismic potential by Coulomb stress transfer in Minahasa Active Subduction Zone together with two events with Mw 7.9 and Mw 7.0 happened on 1996/01/01 and 1996/07/22. We try to assess the seismogenic potential in terms of interseismic slip rate, slip rate deficit and coupling ratio for the Palu-Koro fault system in a triple junction of the Sulawesi island.

Keywords: InSAR , pixel offset , Palu earthquake, Triple junction

©2019. Japan Geoscience Union. All Right Reserved.

[E] Poster | S (Solid Earth Sciences)：S-IT Science of the Earth's Interior & Techtonophysics

Wed. May 29, 2019 5:15 PM - 6:30 PM JST | Wed. May 29, 2019 8:15 AM - 9:30 AM UTC | Poster Hall International Exhibition Hall8, Makuhari Messe_28

[S-IT26] New perspectives on the geodynamics of East Asia

convener:Timothy B Byrne(University of Connecticut), Asuka Yamaguchi(Atomosphere and Ocean Research Institute, The University of Tokyo), Jonny Wu(University of Houston), Kyoko Okino(Atmosphere and Ocean Research Institute, The University of Tokyo)

The Pacific, Indo-Australia and Eurasian plates converge around the Philippine Sea plates in south and East Asia, resulting in one of the most tectonically active regions on earth. The area is also geologically and tectonically complex with numerous active tectonic environments, ranging from subduction to collision, and a long history of plate boundary interactions. The last decade has yielded a wide range of new observations, including detailed geologic data and high resolution crustal to mantle imaging. Here we seek oral and poster presentations that bear on the geologic history and geophysical character of modern and ancient plates in East Asia and their interactions since the Mesozoic. We also invite geodynamic models that integrate these diverse datasets into a more holistic view of this dynamic environment.

[SIT26-P01] Geochemical characteristics of effusive rocks (greenstones) in the Hidaka Belt, Hokkaido, Japan

*Toru Yamasaki[1], Futoshi Nanayama[1] (1.Geol. Survey of Japan (AIST))

[SIT26-P02] Large gas reservoir in continental back-arc basin, revealed by automatic seismic velocity analysis in the Okinawa Trough

*Kota Mukumoto[1], Takeshi Tsuji[1], Andri Hendriyana[1] (1.Kyushu University)

[SIT26-P03] Characterize coseismic deformation of Mw 7.5 Palu earthquake in a triple junction in Sulawesi, Indonesia

*MIN-CHIEN TSAI[1], Ying-Hui Yang[2], Chun-Ying Chiu[3], Jyr-Ching Hu[3] (1.Seismological center, Central Weather Bureau, Taipei, Taiwan, R.O.C., 2.School of Civil Engineering and Architecture, Southwest Petroleum University, Chengdu, China, 3.Department of Geosciences, National Taiwan University, Taipei, Taiwan, R.O.C.)

Geochemical characteristics of effusive rocks (greenstones) in the Hidaka Belt, Hokkaido, Japan

*Toru Yamasaki[1], Futoshi Nanayama[1]

1. Geol. Survey of Japan (AIST)

Igneous rocks in a subduction complex typically occur as greenstones, and petrological and geochemical investigations of such greenstones can provide important insights into the oceanic magmatism, origin of the accretionary complex, and growth of the continental margin. The Hidaka Belt in Central Hokkaido, Japan consists of an early Paleogene subduction complex, referred to as the Hidaka Supergroup (HSG), dominated by clastic rocks. Locally, the terrigenous sediments of the HSG were intruded by the contemporary, normal-type mid-ocean ridge basalts (“*in situ*N-MORBs”) that were formed at an oceanic ridge near the Eurasian continent (Miyashita and Katsushima, 1986: GSJ). The southern area of the HSG has been referred to as the Nakanogawa Group (NKG), which gradually leads to the high-temperature Hidaka metamorphic belt (HMB) in the western part. The lower sequence of the HMB consists mainly of high-grade metabasites, which are assumed to be equivalent to the N-MORBs in the HSG, based on their geochemical features. Recently, Yamasaki and Nanayama (2018a: Lithos) reported about the unique Daimaruyama greenstones from the NKG, formed by an immature intra-oceanic arc-type volcanism. In addition, highly-alkaline basalts, presumably formed at the seamount, exist as exotic blocks in the NKG and are named as Tachiiwa blocks (Owada et al., 1992: JMPEG). In fact, the N-MORBs in the HSG and the Tachiiwa alkaline rocks are characterized by the whole-rock major and minor element geochemistry, but the trace element geochemistry, including the rare earth elements (REEs), has not been reported yet for these rocks. Therefore, we collected 18 samples of greenstones from the entire Hidaka Belt and examined their whole-rock major and trace element geochemistry.

Including those in our previous reports (Yamasaki and Nanayama, 2018a, b: JpGU Abs.), there are three distinct types of greenstones in the Hidaka Belt. The first type are the MORB-type greenstones which show relatively flat chondrite-normalized (CN) REE patterns and N-MORB-normalized (NMN) multi-element patterns with Ti/V = 26–53 and Zr/Nb = 21–117. Although Miyashita and Kiminami (1999: MemGSJ) showed the flat NMN minor element (Nb, P, Zr, Ti, and Y) patterns of basalts from the northern HSG, trace element patterns of the MORB-type rocks in this study show rather light REE (LREE)-rich NMN multi-element patterns. The second type are the ocean island basalt (OIB)-type greenstones. The NMN multi-element and CN REE patterns for this type of greenstones show a gentle slope up to the left, with Ti/V>62 and Zr/Nb<15. The third type are the Daimaruyama greenstones. This type of greenstones show similar NMN multi-element patterns and CN REE patterns to those in the OIB-type, but with a clear relative depletion of Nb, Ta, and Ti. In addition, their Ti-V relations are similar to those in the MORB-type greenstones.

MORB-type greenstones are distributed from the northernmost part of the HSG to the southern Rakko River area in the NKG. OIB-type greenstones occur in the Tachiiwa block and the Rakko River area. Daimaruyama greenstones occur only in the Daimaruyama megablock in the NKG. Since the Tachiiwa and Daimaruyama blocks are presumably derived from the neighboring Tokoro Belt, the absence of the OIB-type and Daimaruyama greenstones in the northern HSG implies a difference in provenance between the HSG and NKG. The MORB-type greenstones do not show the typical N-MORB-type (LREE-depleted) trace element patterns, whereas the metabasite in the HMB shows the typical N-MORB-type geochemical features. In addition, the distribution of the MORB-type greenstones is separated from the metabasites of

©2019. Japan Geoscience Union. All Right Reserved.

the HMB in the southern Hidaka Belt. These lines of evidence suggest that the protolith of the HMB is not an equivalent of the “*in-situ*MORB” in the HSG, and is probably an accreted fragment of the older oceanic plate.

Keywords: Hidaka Belt, greenstones, trace elements

©2019. Japan Geoscience Union. All Right Reserved.

Large gas reservoir in continental back-arc basin, revealed by automatic seismic velocity analysis in the Okinawa Trough

*Kota Mukumoto[1], Takeshi Tsuji[1], Andri Hendriyana[1]

1. Kyushu University

P-wave velocity acquired from seismic reflection data allows us to quantify submarine geological structures. In the Iheya North Knoll of the Okinawa Trough, intense hydrothermal activity occurs due to continental rifting. The hydrothermal system in the Iheya North Knoll has been explored by geophysical surveys, geochemical measurements and drilling campaign. Based on these surveys, gas reservoir could be considered to exist around the Iheya North Knoll. However, gas reservoir around the Iheya North Knoll has not been identified in previous studies. Here we show P-wave velocity structure derived from automatic velocity analysis of multi-channel seismic reflection data. P-wave velocity is sensitive to free gas in sediments. Therefore, P-wave velocity is key information to quantify gas distribution in sediments. Automatic velocity analysis estimated P-wave velocity structure with remarkable high spatial and temporal resolution. The P-wave velocity structure revealed gas reservoirs around the Iheya North Knoll. Although many gas components can be generated by magmatic activity, hydrothermal alteration of organic-rich sediments and biogenic processes, CH_4 and CO_2 could be major gas components which is derived by hydrothermal system in marine sediment. Therefore, main gas components could be CH_4 or CO_2. The strong amplitude reflector above the gas reservoir could be the interface between CH_4 hydrate and gas, because the depth of strong amplitude reflector is well consistent with pressure-temperature conditions of the phase transition. If the main gas component is CH_4, the gas reservoir could be important as resource. Whereas, if the gas reservoir includes CO_2, the gas distribution could be important to consider carbon flux between earth and ocean. Furthermore, widely distributed gas reservoir may influence on the chemical components of hydrothermal fluids in the Iheya North Knoll.

Keywords: Seismic reflection data, Okinawa Trough, Gas reservoir

©2019. Japan Geoscience Union. All Right Reserved.

Characterize coseismic deformation of Mw 7.5 Palu earthquake in a triple junction in Sulawesi, Indonesia

*MIN-CHIEN TSAI[1], Ying-Hui Yang[2], Chun-Ying Chiu[3], Jyr-Ching Hu[3]

1. Seismological center, Central Weather Bureau, Taipei, Taiwan, R.O.C., 2. School of Civil Engineering and Architecture, Southwest Petroleum University, Chengdu, China, 3. Department of Geosciences, National Taiwan University, Taipei, Taiwan, R.O.C.

We first use SAR satellite data to map the coseismic deformation for the 2018 Mw=7.5 strike-slip earthquake of 28 September 2018 in Palu, Sulawesi, Indonesia. The seismogenic fault is a left-lateral a strike-slip event along the Palu-Koro fault at shallow depth that occurred within the interior of the Molucca Sea microplate, which is part of the Sunda plate. We use D-InSAR technique with ALOS-2 descending orbit radar images to characterize coseismic and deformation pattern induced by Palu earthquake.We also plan to use with sub-pixel correlation form Sentinel-2 and Planet imagery to map the surface rupture area and the coseismic offsets in order to provide the near-field deformation data located in decorrelation zone from the D-InSAR result. Thus we can inverse the distribution of slip on the fault patches. In addition, we also calculate the Coulomb stress transfer for assessing the stress increasing and shadow on the major fault systems, such as the active Poso Fault Zone and Mamuju –Lariang Active Fault Zone. In particular, we will assess the seismic potential by Coulomb stress transfer in Minahasa Active Subduction Zone together with two events with Mw 7.9 and Mw 7.0 happened on 1996/01/01 and 1996/07/22. We try to assess the seismogenic potential in terms of interseismic slip rate, slip rate deficit and coupling ratio for the Palu-Koro fault system in a triple junction of the Sulawesi island.

Keywords: InSAR , pixel offset , Palu earthquake, Triple junction

©2019. Japan Geoscience Union. All Right Reserved.

[E] Poster | S (Solid Earth Sciences)：S-GC Geochemistry

Wed. May 29, 2019 10:45 AM - 12:15 PM JST | Wed. May 29, 2019 1:45 AM - 3:15 AM UTC | Poster Hall International Exhibition Hall8, Makuhari Messe_9

[S-GC40] Volatile Cycles in the Deep Earth - from Subduction Zone to Hot Spot

convener:Hirochika Sumino(Department of Basic Science, Graduate School of Arts and Sciences, The University of Tokyo), Takeshi Hanyu(Japan Agency for Marine-Earth Science and Technology, Department of Solid Earth Geochemistry), Yuji Sano(Division of Ocean and Earth Systems, Atmosphere and Ocean Research Institute, University of Tokyo), Gray E Bebout(Lehigh University)

Volatiles play an important role in the geodynamics and chemical differentiation in the mantle and crust by drastically changing mineral stability and rheological behavior. Fractionation-processes such as partial melting, hydration, and dehydration are all controlled by volatiles in the rocks. A significant portion of the volatiles in the Earth has been thought to be present in the atmosphere and oceans as a consequence of extensive degassing during accretion and subsequent mantle degassing. On the other hand, it has been recently recognized that substantial amounts of volatiles are recycled back into the mantle at subduction zones, where intensive devolatilization of descended materials during arc magma generation was once thought to act as an effective "subduction barrier". However, fundamental questions still remain, such as: how are volatiles species distributed throughout the early and present Earth? What are the mechanisms for, and rate at which, volatiles are fluxed between the atmosphere, crust, and mantle? And what role have volatiles played in driving the evolution of the Earth? The possible role of the core in storing primordial volatiles is also poorly constrained. We therefore welcome contributions from experimental, observational, and modeling studies that help shed light on the deep cycles of volatiles, such as hydrogen, carbon, nitrogen, noble gases, halogens and sulfur. We particularly encourage studies linking the behavior of multiple volatile elements and their isotopic compositions. Studies investigating the linkage between volatile and solid geochemical tracers, the phase equilibria of volatile-bearing mantle assemblages, and the effect of volatiles on the physical properties of the mantle are also welcome.

[SGC40-P01] Continental growth models demystified

*Jun Korenaga[1] (1.Department of Geology and Geophysics, Yale University)

[SGC40-P02] Mass-independent sulfur isotope signature from the 2.7 Ga Belingwe komatiite: Recycling of crustal material in Archean

*Yusuke Kubota[1], Yuichiro Ueno[1,2,3], Kenji Shimizu[3], Fumihiro Matsuura[2], Akira Ishikawa[1,3] (1.Department of Earth and Planetary Sciences, Tokyo Institute of Technology, 2.Earth-Life Science Institute, Tokyo Institute of Technology, 3.Japan Agency for Marine-Earth Science and Technology (JAMSTEC))

[SGC40-P03] Determination of halogens in some standard materials using the neutron irradiation noble gas mass spectrometric technique

*Hirochika Sumino[1], Masahiro Kobayashi[2], Takehiko Saito[3], Keisuke Nagao[3] (1.Department of Basic Science, Graduate School of Arts and Sciences, The University of Tokyo, 2.Tokyo Metropolitan Industrial Technology Research Institute, 3.Geochemical Research Center, Graduate School of Science, University of Tokyo)

[SGC40-P04] FTIR spectroscopy and noble gas mass spectrometry for a single olivine grain

*Sota Niki[1], Hirochika Sumino[2], Masahiro Kobayashi[3], Hiroyuki Kagi[1], Takafumi Hirata[1], Chris J. Ballentine[4] (1.Geochemical Research Center, Grad. School of Science, Univ. of Tokyo, 2.Dept. of Basic Science, Grad. School of Arts and Sciences, Univ. of Tokyo, 3.Tokyo Metropolitan Industrial Technology Research Institute, 4.Dept. of Earth Sciences, Univ. of Oxford)

[SGC40-P05] New halogen incorporation mechanism in serpentine group minerals: Crystal chemical consideration

*Masami Kanzaki[1] (1.Institute for Planetary Matereials, Okayama University)

[SGC40-P06] Mineralogical and geochemical characteristics of cuttings from Taketomi hot spring

*Noriyuki Shingaki[1], Tomohiro Toki[1], Syogo Oshima[2], Masaaki chinen[3], Arito Sakaguchi[4], Naoto Takahata[5], Yuji Sano[5], Shirai Kotaro[5], Kentaro Tanaka[5] (1.University of the Ryukyus , 2.West Japan Engineering Consultants, Inc., 3.MicroRange, 4.Faculty of Science, Yamaguchi University, 5.Atmosphere and Ocean Research Institute, The University of Tokyo)

[SGC40-P07] Variation of helium isotope compositions at Lake Mashu

*Takanori Kagoshima[1], Yuji Sano[1], Atsushi Tanaka[2] (1.Atmosphere and Ocean Research Institute, University of Tokyo, 2.National Institute for Environmental Studies)

[SGC40-P08] Helium isotopes in Tachibana Bay and Shimabara Bay, Nagasaki

*Ma. Teresa Escobar[1], Yama Tomonaga[2], Hajime Obata[1], Shigenobu Takeda[3], Naoto Takahata[1], Yuji Sano[1] (1.Atmosphere and Ocean Research Institute, University of Tokyo, Kashiwanoha, Kashiwa, Chiba, Japan, 2.Eawag,, Swiss Federal Institute of Aquatic Science and Technology, Department of Water Resources and Drinking Water, Überlandstrasse 133 CH-8600 ,Dübendorf, Switzerland, 3.Graduate School of Fisheries and Environmental Sciences, Nagasaki University, Nagasaki, Japan)

Continental growth models demystified

*Jun Korenaga[1]

1. Department of Geology and Geophysics, Yale University

So far proposed models of continental growth exhibit bewildering diversity, but this diversity is rather superficial. By understanding how different growth models are built and what they are meant to constrain, we can gain deeper insight into the evolution of continental crust as well as the dynamics of the early Earth. There are three kinds of growth models: crust-based, mantle-based, and others. Crust-based models provide only the lower bound on net crustal growth, and mantle-based models aim at constraining net crustal growth itself. Other models are also about net crustal growth, but they are subject to greater uncertainty. In the presence of crustal recycling, crust-based models are expected to be different from mantle-based models, and more important, the difference between these two kinds of models provides important constraints on the operation of plate tectonics in the early Earth. Some popular misconceptions in the recent literature are also discussed.

Keywords: Continental crust, Plate tectonics, Chemical differentiation

©2019. Japan Geoscience Union. All Right Reserved.

Mass-independent sulfur isotope signature from the 2.7 Ga Belingwe komatiite: Recycling of crustal material in Archean

*Yusuke Kubota[1], Yuichiro Ueno[1,2,3], Kenji Shimizu[3], Fumihiro Matsuura[2], Akira Ishikawa[1,3]

1. Department of Earth and Planetary Sciences, Tokyo Institute of Technology, 2. Earth-Life Science Institute, Tokyo Institute of Technology, 3. Japan Agency for Marine-Earth Science and Technology (JAMSTEC)

Recycling of the Earth's crustal material has long been discussed mainly through the radiogenic isotopes of modern Ocean Island Basalts (OIB). Recent finding of Sulfur Mass Independent Fractionation (S-MIF) from HIMU and EM I basalts supports recycling of crustal material in mantle (Cabral et al., 2013; Delavault et al., 2016). Since photochemical reactions under reducing Archean atmosphere are thought to be a plausible process of large S-MIF generation (Farquhar et al., 2001; Farquhar and Wings, 2003), these discoveries demonstrated that the S-MIF is a useful signature for tracing Archean crustal material. However, it has been difficult to estimate when the subduction started in the history of the Earth. Here, we report multiple sulfur isotope analysis of the 2.7 Ga Belingwe komatiites and related rocks, which has potential to elucidate earlier subduction or recycling of crustal material before 2.7 Ga. The Belingwe komatiite are one of the best-preserved Archean komatiites in the world. The results show clear S-MIF signature in several komatiites and basalts. Sulfide minerals in the S-MIF bearing samples occur as pyrrhotite and chalcopyrite scattered within groundmass around the quenched olivine and pyroxene crystals, indicating that the sulfides crystalized at the time of eruption. The original nature of the sulfide is also supported by the correlation between sulfur contents and magnesium number. Based on Nd, Sr, and Pb isotope composition measured in the previous study (Shimizu et al., 2005), the S-MIF bearing komatiites and basalts are likely to be derived from depleted mantle source, whereas more enriched samples do not show S-MIF. Therefore, the S-MIF component is not likely derived from assimilated crust at the time of the komatiite volcanism, but originally incorporated in the depleted source mantle. Consequently, our results suggest that subduction of S-MIF bearing surface material into the mantle had been operated at least prior to 2.7 Ga.

Keywords: Sulfur mass independent fractionation, Mantle geochemistry, Komatiite, Archean

©2019. Japan Geoscience Union. All Right Reserved.

Determination of halogens in some standard materials using the neutron irradiation noble gas mass spectrometric technique

*Hirochika Sumino[1], Masahiro Kobayashi[2], Takehiko Saito[3], Keisuke Nagao[3]

1. Department of Basic Science, Graduate School of Arts and Sciences, The University of Tokyo, 2. Tokyo Metropolitan Industrial Technology Research Institute, 3. Geochemical Research Center, Graduate School of Science, University of Tokyo

Halogens are among the most powerful tracers of volatile cycling in subduction zones, because of (i) the large contrast in concentrations between the surface and interior of the Earth [1], (ii) their high affinities to gas- and fluid-phases relative to mineral [2], (iii) distinct elemental and/or isotopic compositions in each reservoir in the Earth [3-7]. However, few analytical techniques can determine trace amounts of halogens, particularly bromine and iodine in mantle-derived samples. Consequently, there have been relatively few previous studies of halogens in mantle-derived samples.

The neutron irradiation noble gas mass spectrometric technique (NI-NGMS) is capable of measuring very low concentrations of halogens (<1 ppb) in very small samples (<1 mg). The NI-NGMS is an extension of the Ar-Ar and I-Xe dating methods [8-10]. Halogens (chlorine, bromine, and iodine) and other elements (potassium, calcium, barium, and uranium) are converted to corresponding isotopes of argon, krypton, and xenon by neutron irradiation in a nuclear reactor. The noble gas isotopes in neutron-irradiated samples are analyzed by noble gas mass spectrometry. Irradiation conditions such as neutron fluence are monitored using standard materials of the Ar-Ar and I-Xe dating methods. Relatively high cross-sections of halogens for neutron capture and high sensitivity of noble gas mass spectrometry enable determination of trace amounts of halogens using NI-NGMS.

We report new halogen concentrations determined for scapolite standards and geological reference materials distributed by Geological Survey of Japan and US Geological Survey using NI-NGMS. Consistent results with those regarded as reference values were obtained from scapolite standards, which indicate that the scapolite standards are reliable in halogen analysis. On the other hand, the halogen concentrations obtained from geological reference materials are systematically lower than the reference values for samples with low concentrations of halogens. The higher concentrations reported for the geological reference materials probably result from contamination on the sample surface during preparation of these reference materials. We also propose a fluorine determination method using NI-NGMS based on neon systematics, although reliable determination of fluorine has been thought to be impossible.

[1] Pyle & Mather, *Chem. Geol.* 2009. [2] Bureau *et al.*, *GCA* 2016. [3] Sumino *et al.*, *EPSL* 2010. [4] Chavrit *et al.*, *GCA* 2016. [5] Kobayashi *et al.*, *EPSL* 2017. [6] Kendrick *et al.*, *Nature Geosci.* 2017. [7] Kobayashi *et al.*, *G-cubed* 2019. [8] Turner, *JGR* 1965. [9] Kendrick, *Chem. Geol.* 2012. [10] Ruzié-Hamilton *et al.*, *Chem. Geol.* 2016.

Keywords: Halogen, Noble gas, Nuetron irradiation, Noble gas mass spectrometry

©2019. Japan Geoscience Union. All Right Reserved.

FTIR spectroscopy and noble gas mass spectrometry for a single olivine grain

*Sota Niki[1], Hirochika Sumino[2], Masahiro Kobayashi[3], Hiroyuki Kagi[1], Takafumi Hirata[1], Chris J. Ballentine[4]

1. Geochemical Research Center, Grad. School of Science, Univ. of Tokyo, 2. Dept. of Basic Science, Grad. School of Arts and Sciences, Univ. of Tokyo, 3. Tokyo Metropolitan Industrial Technology Research Institute, 4. Dept. of Earth Sciences, Univ. of Oxford

Volatiles have been degassed from the mantle and recycled back into the mantle at subduction zones. Water is the main component of volatiles and plays a key role in dynamics of the subduction zones because even a small water content in rocks has an influence on the physical and chemical properties of the rocks (e.g. friction coefficient, melting point, etc.) which are closely related to phenomena studied in earth sciences including volcanic or seismic activities. It is still unclear to what extent of water have been subducted into the mantle and released to the Earth’ s surface. To elucidate the volatile recycling, noble gases are powerful tracers because they have unique compositions in geochemical reservoirs. Previous researches have mainly reported results of bulk analysis of mantle peridotites. On the contrary, in this study, FTIR measurements and noble gas analysis of a single olivine grain were conducted to determine the noble gas concentrations in fluid inclusions.

The olivine samples used for this study were separated from mantle xenoliths collected from an intraplate setting (Hualalai in Hawaii) and two subduction zones (the Avacha volcano in the Kamchatka arc and the Pinatubo volcano in the Luzon arc). The Hualalai olivine was expected to show mantle-derived noble gas compositions (Kobayashi et al., G-cubed 2019) and was used for checking the accuracy of noble gas analysis. The Avacha and Pinatubo olivines contained H_2O-rich fluid inclusions and the noble gas concentrations in the inclusions had been estimated from salinities, and halogen and noble gas compositions (Kobayashi et al., EPSL 2017). The Avacha and Pinatubo olivines were used to confirm the accuracy of the analytical method used in this study for determining the noble gas concentrations in the inclusions.

FTIR measurements were conducted to determine the H_2O concentration in the Avacha and Pinatubo olivines. The mantle xenoliths were crushed into 0.5 to 2 mm and olivine grains were separated. The olivine grains were embedded in resin (Ortho Bright) and polished to a thickness of several hundred micrometers. The weight of samples was 0.7 to 16 mg. The H_2O concentration was calculated from the absorbance at 3404 cm^{-1}. After the FTIR measurements, resin was removed from each grain by heating at 50ºC and dissolving in acetone.

Noble gas analysis was conducted using multicollector noble gas mass spectrometers (Helix SFT and Argus, Thermo Fisher Scientific). After the sample loading into a laser heating cell, the cell was baked out with pumping to desorb atmospheric noble gases to achieve low blank levels required for single-grain analysis. Consequently, noble gases were extracted by laser heating (Fusion Diode Stepped Heating System, Teledyne CETAC) at about 1000 ºC for 5 minutes. The gases released from samples were purified by removing active gases using a getter, and then, absorbed on two cryo-traps (one was for helium and neon and the other was for argon, krypton, and xenon). Each noble gas was desorbed from the trap at a certain temperature and introduced into the mass spectrometers. Helium was measured with Helix SFT and other noble gases were measured with Argus. The abundances and isotopic ratios of noble gases in a

©2019. Japan Geoscience Union. All Right Reserved.

single olivine grain were obtained. The accuracy of the isotopic ratios was checked by the Hualalai samples.

The noble gas concentrations in the inclusions obtained will be compared with the previous bulk analysis to discuss the accuracy of the method in this study. This method of determining the noble gas concentrations in fluid inclusions from single-grain analysis has a potential to clarify the heterogeneity of the mantle volatiles in terms of a single-grain mineral and the flux quantification during the volatile recycling.

Keywords: noble gas, FTIR spectroscopy, mantle

©2019. Japan Geoscience Union. All Right Reserved.

New halogen incorporation mechanism in serpentine group minerals: Crystal chemical consideration

*Masami Kanzaki[1]

1. Institute for Planetary Matereials, Okayama University

Introduction: Recent geochemical studies revealed that serpentinites contain a significant amount of halogens. However, how halogen ions are incorporated into serpentinites is not well understood. Commonly assumed mechanism is "OH^- substitution" in serpentine group minerals (chrysotile, lizardite and antigorite). Although this mechanism will be fine for F, but may not be adequate for larger halogens (Cl, Br, I). Here, I propose new halogen incorporation mechanism in lizardite and antigorite from crystal chemical point of view.

Calculation methods: In order to assess present new incorporation model, first-principles calculation was conducted. Quantum-Espresso package was used to optimize the halogen incooporated model structures. In the present study, lizardite and antigorite (*m*=17 polysome) are considered. For our proposed mechanism, charge balance should be observed; so $Mg^{2+} = X^- + Al^{3+}$ substitution (X^- = halogen) is assumed to introduce halogen to a vacant site. For lizardite, enthalpy difference between two models (OH^- substitution and our model) was calculated for following equation: $Mg_2AlSi_2O_8XH_2 + H_2O = Mg_2AlSi_2O_9XH_4$. Former corresponds to the OH substituted model (with Al introduced), and latter corresponds to our new model. Although this comparison is crude (as free H_2O is included in the equation), it could provide systematic trend with kinds of halogen atoms. Since antigorite has a very large unit cell and many vacant sites, only $Mg^{2+} = Cl^- + Al^{3+}$ substitute in five vacant sites are considered so far.

Results and Discussion: From close inspection of crystal structures of lizardite and antigorite, vacant sites ideal for halogens are identified. The vacant sites are surrounded by four protons (of OH^-) forming elongated tetrahedon (i.e., XH_4^{3+}) if halogen is located. Such vacant sites provide local structure similar to halogen ions in aqueous solution.

In order to further assess present incorporation mechanism, first-principles calculations of lizardite and antigorite containing halogens in those sites were conducted. The structural optimizations confirmed that halogens could be well accommodated into the tetrahedral vacant sites in lizardite. The calculated enthalpy difference between OH substitution and present models in lizardite revealed that larger halogens prefer our model over the OH substitution model. There is sinlge vacant site in lizardite, but antigorite (*m* =17) has 17 crystallographically different vacant sites. Most sites have local structures more or less similar to that of lizardite (locating in 6-membered SiO_4 ring). But there is another kind of vacant site which is locating in 8-membered SiO_4 ring. This local structure is surrounded by six protons, but it can be regareded as two tetrahedral proton sites with edge sharing. Substitution of Cl^- to this site (one of tetrahedral sites) showed lower enthalpy compared to those of other lizardite-like sites, and can accept more larger ions. Therefore, Cl^- (and other larger halogens) will prefet this site in antigorite (*m*=17). Not all antogorite polysomes have this site.

Present study suggests that our new proposed incorporation mechanism is promising, and it should be further studied experimentally. Present new incorporation mechanism would be important to understand elemental partition behavior of halogens in subduction zones.

Keywords: halogen site, serpentine, crystal chemistry, incorporation mechanism, elemental partition

©2019. Japan Geoscience Union. All Right Reserved.

Mineralogical and geochemical characteristics of cuttings from Taketomi hot spring

*Noriyuki Shingaki[1], Tomohiro Toki[1], Syogo Oshima[2], Masaaki chinen[3], Arito Sakaguchi[4], Naoto Takahata[5], Yuji Sano[5], Shirai Kotaro[5], Kentaro Tanaka[5]

1. University of the Ryukyus , 2. West Japan Engineering Consultants, Inc., 3. MicroRange, 4. Faculty of Science, Yamaguchi University, 5. Atmosphere and Ocean Research Institute, The University of Tokyo

It is important to grasp carbon cycle on the earth’ s surface for thinking about global environmental change. A hot spring with a maximum temperature of 64℃ is venting with gas containing 70% of methane from several spots on the seafloor at depth of 22 m at 1 km northeast off Taketomi Island. Based on methane and helium isotope ratios in the venting gas, the influence of magmatic gas has been pointed out. In spite of Taketomi Island located on the trench side from island arc, magmatic gas is venting. It suggests the forearc where magma cannot generate, might form new supply path of carbon from the Earth’ s interior. The mass balance from new supply path of carbon may change estimation of carbon cycle on earth’ s surface. Therefore, the purpose of this study is to elucidate venting mechanism and quantitative grasp of magmatic gas from forearc, and the history of hot spring activities will be investigated to predict future activities.

In 2017, the hot spring was drilled up to depth of 940 m in Taketomi Island. The cuttings with muddy water were sampled every 10 m. The thin sections were prepared from cuttings to be observed using polarization microscope, and the chemical compositions of grains were analyzed by SEM-EDX. The ground samples were analyzed for mineral and chemical compositions by XRD and EDX. The clay minerals gathered by levitation were measured for half-value width of illite using XRD. He and CO_2 contained in samples that were crashed in vacuum were measured for isotope ratios by mass spectrometer. Calcite and dolomite collected from the cuttings were measured for the carbon and oxygen isotope ratios by mass spectrometer. The vitrinite in the cuttings was separated by a heavy liquid, and the reflectance was measured by a reflecting microscope.

In the microscopy, the stratum was roughly divided two formations; cryptocrystalline quartz layer and sand stone layer. Carbonaceous materials were observed in most of the stratum. Dolomite was limitedly observed in the vicinity of 800 m. In the XRD analysis, Quartz was detected at all depth. Calcite was detected at shallower depth than 30 m, and dolomite was detected only around 800 m. As a result of the EDX analysis, silicon was the most dominant in all layers, and especially, it was contained around 0-100 m, 300 m and around 900 m over 80%. There was a layer that contained much calcium. Around 0-30 m, 400-500 m and around 800 m, calcite was contained 15 % or more. The half-value width of illite was large, 0.8 $\Delta^\circ 2\theta$, in only 10 m surface, and as low as 0.2 to 0.4 $\Delta^\circ 2\theta$ below 50 m. Vitrinite reflectance was around 5% in the whole layer, close to measurement limit. The helium content was 10^{-14}-10^{-11} mol per 1g of cuttings, and tended to increase with increasing depth. The highest content was detected at 800 m depth. The helium isotope ratio($^3He/^4He$)have value of 0.4-3.6 times that of atmosphere, and tended to increase with increasing depth. Particularly, it was higher at 100 m, 300-400 m and 700-800 m. The CO_2 content per gram of cuttings, was in the range of 10^{-8}-10^{-6} mol in most layers, but it showed

©2019. Japan Geoscience Union. All Right Reserved.

higher values at 400 m and 800 m depth. the water tended to decrease with increasing depth, and showed especially high values at 400 m and 900 m. The carbon isotope ratio ($\delta^{13}C$) of calcite was -4.7‰ VPDB, and the oxygen isotope ratio ($\delta^{18}O$) is -16.3‰VPDB. The $\delta^{13}C$ value of dolomite was -1‰VPDB, and the $\delta^{18}O$ value was -10.9‰VPDB. The $\delta^{13}C$ value of CO_2 from cuttings at 800 m was -7.3‰VPDB, which contained sufficiently amount of carbon to measure carbon isotope ratio.

Keywords: Taketomi Island, Hot spring, cuttings, vitrinite reflectance, carbon cycle, helium isotope

©2019. Japan Geoscience Union. All Right Reserved.

Variation of helium isotope compositions at Lake Mashu

*Takanori Kagoshima[1], Yuji Sano[1], Atsushi Tanaka[2]

1. Atmosphere and Ocean Research Institute, University of Tokyo, 2. National Institute for Environmental Studies

Helium-3 is one of the most sensitive geochemical tracers which reflects addition of mantle components to gas and fluids in volcanic hydrothermal systems, and $^{3}He/^{4}He$ ratios may be useful to assess temporal change of hydrothermal activity at volcanic lakes. Lake Mashu is a caldera lake which formed around 7000 years ago in Hokkaido. Igarashi et al. (1992) measured He and Ne isotopes in water of Lake Mashu, and concluded that the depth profile of isotopic compositions reflect injection of mantle-derived He due to hot spring activity at the lake bottom. After that, there is no subsequent study reporting He isotope data. The lack of observational data may be due to difficulty of water sampling at caldera lakes. Igarashi et al. (1992) collected water samples into copper tubes. However, this method requires heavy and large sampling tools, and people who can transfer water and seal the tubes properly. In May and September 2017, we investigated Lake Mashu in order to check volcanic activity and practical sampling methods for caldera lakes. We collected water using a Niskin bottle at several depths (surface to 210 m) around the deepest point (211 m). Collected water was immediately transferred into lead-glass containers with vacuum valves at both ends. In Atmosphere and Ocean Research Institute, dissolved gases were extracted by the head space method, and introduced into a purification vacuum line. In the line, He and Ne were purified for isotope analyses. $^{3}He/^{4}He$ and $^{4}He/^{20}Ne$ ratios were measured using Helix-SFT and QMS, respectively. The highest $^{3}He/^{4}He$ ratios were observed at 205-210 m depth, indicating that injection of fluids with the high $^{3}He/^{4}He$ ratio at the bottom. The linear correlation between $^{4}He/^{20}Ne$ and $^{3}He/^{20}Ne$ ratios in water samples indicated mixing of two components: injected fluids and the atmosphere. The estimated $^{3}He/^{4}He$ ratio of the fluid end member was indistinguishable from the value reported by Igarashi et al. (1992), implying a possibility that there was no significant change in volcanic activity at Lake Mashu in the past 30 years.

Keywords: Helium isotope, Volcanic lake, Lake Mashu

©2019. Japan Geoscience Union. All Right Reserved.

Helium isotopes in Tachibana Bay and Shimabara Bay, Nagasaki

*Ma. Teresa Escobar[1], Yama Tomonaga[2], Hajime Obata[1], Shigenobu Takeda[3], Naoto Takahata[1], Yuji Sano[1]

1. Atmosphere and Ocean Research Institute, University of Tokyo, Kashiwanoha, Kashiwa, Chiba, Japan, 2. Eawag,, Swiss Federal Institute of Aquatic Science and Technology, Department of Water Resources and Drinking Water, Ü berlandstrasse 133 CH-8600 ,Dübendorf, Switzerland, 3. Graduate School of Fisheries and Environmental Sciences, Nagasaki University, Nagasaki, Japan

Noble gases are powerful tracers to study physical transport processes in aquatic system. Moreover, helium isotopes have been shown to be very useful to infer the origin of fluids. Shimabara Peninsula is located on western side of the Beppu-Shimabara graben in Kyushu, SW Japan. In the region, there are some hot springs and groundwaters which indicate magmatic helium with high 3He/4He ratio. Although some researchers report helium isotopic ratio on land, there is no data in the sea.

The surrounding bays around Shimabara Peninsula in Nagasaki were recently studied for the existence of hydrothermal springs and vents. Physico-chemical properties characteristic of hydrothermal activity were detected on the seafloor. For this study, we use helium isotopes to detect the occurrence of hydrothermal springs on the seafloor in both Tachibana Bay and Shimabara Bay. Samples were collected using a CTD-CMS system and analyzed using a Noble Gas Mass Spectrometer. Our data supplements the discovery of hydrothermal venting along known faults on the seafloor. We present the results of noble gas measurements conducted on water samples and discuss the relationship between our observations and the tectonic setup of the surrounding region.

Keywords: Helium Isotopes, Hydrothermal vents, Tachibana Bay

©2019. Japan Geoscience Union. All Right Reserved.

[E] Poster | S (Solid Earth Sciences)：S-GC Geochemistry

Wed. May 29, 2019 5:15 PM - 6:30 PM JST | Wed. May 29, 2019 8:15 AM - 9:30 AM UTC | Poster Hall International Exhibition Hall8, Makuhari Messe_31

[S-GC40] Volatile Cycles in the Deep Earth - from Subduction Zone to Hot Spot

convener:Hirochika Sumino(Department of Basic Science, Graduate School of Arts and Sciences, The University of Tokyo), Takeshi Hanyu(Japan Agency for Marine-Earth Science and Technology, Department of Solid Earth Geochemistry), Yuji Sano(Division of Ocean and Earth Systems, Atmosphere and Ocean Research Institute, University of Tokyo), Gray E Bebout(Lehigh University)

Volatiles play an important role in the geodynamics and chemical differentiation in the mantle and crust by drastically changing mineral stability and rheological behavior. Fractionation-processes such as partial melting, hydration, and dehydration are all controlled by volatiles in the rocks. A significant portion of the volatiles in the Earth has been thought to be present in the atmosphere and oceans as a consequence of extensive degassing during accretion and subsequent mantle degassing. On the other hand, it has been recently recognized that substantial amounts of volatiles are recycled back into the mantle at subduction zones, where intensive devolatilization of descended materials during arc magma generation was once thought to act as an effective "subduction barrier". However, fundamental questions still remain, such as: how are volatiles species distributed throughout the early and present Earth? What are the mechanisms for, and rate at which, volatiles are fluxed between the atmosphere, crust, and mantle? And what role have volatiles played in driving the evolution of the Earth? The possible role of the core in storing primordial volatiles is also poorly constrained. We therefore welcome contributions from experimental, observational, and modeling studies that help shed light on the deep cycles of volatiles, such as hydrogen, carbon, nitrogen, noble gases, halogens and sulfur. We particularly encourage studies linking the behavior of multiple volatile elements and their isotopic compositions. Studies investigating the linkage between volatile and solid geochemical tracers, the phase equilibria of volatile-bearing mantle assemblages, and the effect of volatiles on the physical properties of the mantle are also welcome.

[SGC40-P01] Continental growth models demystified

*Jun Korenaga[1] (1.Department of Geology and Geophysics, Yale University)

[SGC40-P02] Mass-independent sulfur isotope signature from the 2.7 Ga Belingwe komatiite: Recycling of crustal material in Archean

*Yusuke Kubota[1], Yuichiro Ueno[1,2,3], Kenji Shimizu[3], Fumihiro Matsuura[2], Akira Ishikawa[1,3] (1.Department of Earth and Planetary Sciences, Tokyo Institute of Technology, 2.Earth-Life Science Institute, Tokyo Institute of Technology, 3.Japan Agency for Marine-Earth Science and Technology (JAMSTEC))

[SGC40-P03] Determination of halogens in some standard materials using the neutron irradiation noble gas mass spectrometric technique

*Hirochika Sumino[1], Masahiro Kobayashi[2], Takehiko Saito[3], Keisuke Nagao[3] (1.Department of Basic Science, Graduate School of Arts and Sciences, The University of Tokyo, 2.Tokyo Metropolitan Industrial Technology Research Institute, 3.Geochemical Research Center, Graduate School of Science, University of Tokyo)

[SGC40-P04] FTIR spectroscopy and noble gas mass spectrometry for a single olivine grain

*Sota Niki[1], Hirochika Sumino[2], Masahiro Kobayashi[3], Hiroyuki Kagi[1], Takafumi Hirata[1], Chris J. Ballentine[4] (1.Geochemical Research Center, Grad. School of Science, Univ. of Tokyo, 2.Dept. of Basic Science, Grad. School of Arts and Sciences, Univ. of Tokyo, 3.Tokyo Metropolitan Industrial Technology Research Institute, 4.Dept. of Earth Sciences, Univ. of Oxford)

[SGC40-P05] New halogen incorporation mechanism in serpentine group minerals: Crystal chemical consideration

*Masami Kanzaki[1] (1.Institute for Planetary Matereials, Okayama University)

[SGC40-P06] Mineralogical and geochemical characteristics of cuttings from Taketomi hot spring

*Noriyuki Shingaki[1], Tomohiro Toki[1], Syogo Oshima[2], Masaaki chinen[3], Arito Sakaguchi[4], Naoto Takahata[5], Yuji Sano[5], Shirai Kotaro[5], Kentaro Tanaka[5] (1.University of the Ryukyus , 2.West Japan Engineering Consultants, Inc., 3.MicroRange, 4.Faculty of Science, Yamaguchi University, 5.Atmosphere and Ocean Research Institute, The University of Tokyo)

[SGC40-P07] Variation of helium isotope compositions at Lake Mashu

*Takanori Kagoshima[1], Yuji Sano[1], Atsushi Tanaka[2] (1.Atmosphere and Ocean Research Institute, University of Tokyo, 2.National Institute for Environmental Studies)

[SGC40-P08] Helium isotopes in Tachibana Bay and Shimabara Bay, Nagasaki

*Ma. Teresa Escobar[1], Yama Tomonaga[2], Hajime Obata[1], Shigenobu Takeda[3], Naoto Takahata[1], Yuji Sano[1] (1.Atmosphere and Ocean Research Institute, University of Tokyo, Kashiwanoha, Kashiwa, Chiba, Japan, 2.Eawag,, Swiss Federal Institute of Aquatic Science and Technology, Department of Water Resources and Drinking Water, Überlandstrasse 133 CH-8600 ,Dübendorf, Switzerland, 3.Graduate School of Fisheries and Environmental Sciences, Nagasaki University, Nagasaki, Japan)

Continental growth models demystified

*Jun Korenaga[1]

1. Department of Geology and Geophysics, Yale University

So far proposed models of continental growth exhibit bewildering diversity, but this diversity is rather superficial. By understanding how different growth models are built and what they are meant to constrain, we can gain deeper insight into the evolution of continental crust as well as the dynamics of the early Earth. There are three kinds of growth models: crust-based, mantle-based, and others. Crust-based models provide only the lower bound on net crustal growth, and mantle-based models aim at constraining net crustal growth itself. Other models are also about net crustal growth, but they are subject to greater uncertainty. In the presence of crustal recycling, crust-based models are expected to be different from mantle-based models, and more important, the difference between these two kinds of models provides important constraints on the operation of plate tectonics in the early Earth. Some popular misconceptions in the recent literature are also discussed.

Keywords: Continental crust, Plate tectonics, Chemical differentiation

©2019. Japan Geoscience Union. All Right Reserved.

Mass-independent sulfur isotope signature from the 2.7 Ga Belingwe komatiite: Recycling of crustal material in Archean

*Yusuke Kubota[1], Yuichiro Ueno[1,2,3], Kenji Shimizu[3], Fumihiro Matsuura[2], Akira Ishikawa[1,3]

1. Department of Earth and Planetary Sciences, Tokyo Institute of Technology, 2. Earth-Life Science Institute, Tokyo Institute of Technology, 3. Japan Agency for Marine-Earth Science and Technology (JAMSTEC)

Recycling of the Earth's crustal material has long been discussed mainly through the radiogenic isotopes of modern Ocean Island Basalts (OIB). Recent finding of Sulfur Mass Independent Fractionation (S-MIF) from HIMU and EM I basalts supports recycling of crustal material in mantle (Cabral et al., 2013; Delavault et al., 2016). Since photochemical reactions under reducing Archean atmosphere are thought to be a plausible process of large S-MIF generation (Farquhar et al., 2001; Farquhar and Wings, 2003), these discoveries demonstrated that the S-MIF is a useful signature for tracing Archean crustal material. However, it has been difficult to estimate when the subduction started in the history of the Earth. Here, we report multiple sulfur isotope analysis of the 2.7 Ga Belingwe komatiites and related rocks, which has potential to elucidate earlier subduction or recycling of crustal material before 2.7 Ga. The Belingwe komatiite are one of the best-preserved Archean komatiites in the world. The results show clear S-MIF signature in several komatiites and basalts. Sulfide minerals in the S-MIF bearing samples occur as pyrrhotite and chalcopyrite scattered within groundmass around the quenched olivine and pyroxene crystals, indicating that the sulfides crystalized at the time of eruption. The original nature of the sulfide is also supported by the correlation between sulfur contents and magnesium number. Based on Nd, Sr, and Pb isotope composition measured in the previous study (Shimizu et al., 2005), the S-MIF bearing komatiites and basalts are likely to be derived from depleted mantle source, whereas more enriched samples do not show S-MIF. Therefore, the S-MIF component is not likely derived from assimilated crust at the time of the komatiite volcanism, but originally incorporated in the depleted source mantle. Consequently, our results suggest that subduction of S-MIF bearing surface material into the mantle had been operated at least prior to 2.7 Ga.

Keywords: Sulfur mass independent fractionation, Mantle geochemistry, Komatiite, Archean

©2019. Japan Geoscience Union. All Right Reserved.

Determination of halogens in some standard materials using the neutron irradiation noble gas mass spectrometric technique

*Hirochika Sumino[1], Masahiro Kobayashi[2], Takehiko Saito[3], Keisuke Nagao[3]

1. Department of Basic Science, Graduate School of Arts and Sciences, The University of Tokyo, 2. Tokyo Metropolitan Industrial Technology Research Institute, 3. Geochemical Research Center, Graduate School of Science, University of Tokyo

Halogens are among the most powerful tracers of volatile cycling in subduction zones, because of (i) the large contrast in concentrations between the surface and interior of the Earth [1], (ii) their high affinities to gas- and fluid-phases relative to mineral [2], (iii) distinct elemental and/or isotopic compositions in each reservoir in the Earth [3-7]. However, few analytical techniques can determine trace amounts of halogens, particularly bromine and iodine in mantle-derived samples. Consequently, there have been relatively few previous studies of halogens in mantle-derived samples.

The neutron irradiation noble gas mass spectrometric technique (NI-NGMS) is capable of measuring very low concentrations of halogens (<1 ppb) in very small samples (<1 mg). The NI-NGMS is an extension of the Ar-Ar and I-Xe dating methods [8-10]. Halogens (chlorine, bromine, and iodine) and other elements (potassium, calcium, barium, and uranium) are converted to corresponding isotopes of argon, krypton, and xenon by neutron irradiation in a nuclear reactor. The noble gas isotopes in neutron-irradiated samples are analyzed by noble gas mass spectrometry. Irradiation conditions such as neutron fluence are monitored using standard materials of the Ar-Ar and I-Xe dating methods. Relatively high cross-sections of halogens for neutron capture and high sensitivity of noble gas mass spectrometry enable determination of trace amounts of halogens using NI-NGMS.

We report new halogen concentrations determined for scapolite standards and geological reference materials distributed by Geological Survey of Japan and US Geological Survey using NI-NGMS. Consistent results with those regarded as reference values were obtained from scapolite standards, which indicate that the scapolite standards are reliable in halogen analysis. On the other hand, the halogen concentrations obtained from geological reference materials are systematically lower than the reference values for samples with low concentrations of halogens. The higher concentrations reported for the geological reference materials probably result from contamination on the sample surface during preparation of these reference materials. We also propose a fluorine determination method using NI-NGMS based on neon systematics, although reliable determination of fluorine has been thought to be impossible.

[1] Pyle & Mather, *Chem. Geol.* 2009. [2] Bureau *et al.*, *GCA* 2016. [3] Sumino *et al.*, *EPSL* 2010. [4] Chavrit *et al.*, *GCA* 2016. [5] Kobayashi *et al.*, *EPSL* 2017. [6] Kendrick *et al.*, *Nature Geosci.* 2017. [7] Kobayashi *et al.*, *G-cubed* 2019. [8] Turner, *JGR* 1965. [9] Kendrick, *Chem. Geol.* 2012. [10] Ruzié-Hamilton *et al.*, *Chem. Geol.* 2016.

Keywords: Halogen, Noble gas, Nuetron irradiation, Noble gas mass spectrometry

©2019. Japan Geoscience Union. All Right Reserved.

FTIR spectroscopy and noble gas mass spectrometry for a single olivine grain

*Sota Niki[1], Hirochika Sumino[2], Masahiro Kobayashi[3], Hiroyuki Kagi[1], Takafumi Hirata[1], Chris J. Ballentine[4]

1. Geochemical Research Center, Grad. School of Science, Univ. of Tokyo, 2. Dept. of Basic Science, Grad. School of Arts and Sciences, Univ. of Tokyo, 3. Tokyo Metropolitan Industrial Technology Research Institute, 4. Dept. of Earth Sciences, Univ. of Oxford

Volatiles have been degassed from the mantle and recycled back into the mantle at subduction zones. Water is the main component of volatiles and plays a key role in dynamics of the subduction zones because even a small water content in rocks has an influence on the physical and chemical properties of the rocks (e.g. friction coefficient, melting point, etc.) which are closely related to phenomena studied in earth sciences including volcanic or seismic activities. It is still unclear to what extent of water have been subducted into the mantle and released to the Earth’ s surface. To elucidate the volatile recycling, noble gases are powerful tracers because they have unique compositions in geochemical reservoirs. Previous researches have mainly reported results of bulk analysis of mantle peridotites. On the contrary, in this study, FTIR measurements and noble gas analysis of a single olivine grain were conducted to determine the noble gas concentrations in fluid inclusions.

The olivine samples used for this study were separated from mantle xenoliths collected from an intraplate setting (Hualalai in Hawaii) and two subduction zones (the Avacha volcano in the Kamchatka arc and the Pinatubo volcano in the Luzon arc). The Hualalai olivine was expected to show mantle-derived noble gas compositions (Kobayashi et al., G-cubed 2019) and was used for checking the accuracy of noble gas analysis. The Avacha and Pinatubo olivines contained H_2O-rich fluid inclusions and the noble gas concentrations in the inclusions had been estimated from salinities, and halogen and noble gas compositions (Kobayashi et al., EPSL 2017). The Avacha and Pinatubo olivines were used to confirm the accuracy of the analytical method used in this study for determining the noble gas concentrations in the inclusions.

FTIR measurements were conducted to determine the H_2O concentration in the Avacha and Pinatubo olivines. The mantle xenoliths were crushed into 0.5 to 2 mm and olivine grains were separated. The olivine grains were embedded in resin (Ortho Bright) and polished to a thickness of several hundred micrometers. The weight of samples was 0.7 to 16 mg. The H_2O concentration was calculated from the absorbance at 3404 cm^{-1}. After the FTIR measurements, resin was removed from each grain by heating at 50ºC and dissolving in acetone.

Noble gas analysis was conducted using multicollector noble gas mass spectrometers (Helix SFT and Argus, Thermo Fisher Scientific). After the sample loading into a laser heating cell, the cell was baked out with pumping to desorb atmospheric noble gases to achieve low blank levels required for single-grain analysis. Consequently, noble gases were extracted by laser heating (Fusion Diode Stepped Heating System, Teledyne CETAC) at about 1000 ºC for 5 minutes. The gases released from samples were purified by removing active gases using a getter, and then, absorbed on two cryo-traps (one was for helium and neon and the other was for argon, krypton, and xenon). Each noble gas was desorbed from the trap at a certain temperature and introduced into the mass spectrometers. Helium was measured with Helix SFT and other noble gases were measured with Argus. The abundances and isotopic ratios of noble gases in a

©2019. Japan Geoscience Union. All Right Reserved.

single olivine grain were obtained. The accuracy of the isotopic ratios was checked by the Hualalai samples.

The noble gas concentrations in the inclusions obtained will be compared with the previous bulk analysis to discuss the accuracy of the method in this study. This method of determining the noble gas concentrations in fluid inclusions from single-grain analysis has a potential to clarify the heterogeneity of the mantle volatiles in terms of a single-grain mineral and the flux quantification during the volatile recycling.

Keywords: noble gas, FTIR spectroscopy, mantle

©2019. Japan Geoscience Union. All Right Reserved.

New halogen incorporation mechanism in serpentine group minerals: Crystal chemical consideration

*Masami Kanzaki[1]

1. Institute for Planetary Matereials, Okayama University

Introduction: Recent geochemical studies revealed that serpentinites contain a significant amount of halogens. However, how halogen ions are incorporated into serpentinites is not well understood. Commonly assumed mechanism is "OH^- substitution" in serpentine group minerals (chrysotile, lizardite and antigorite). Although this mechanism will be fine for F, but may not be adequate for larger halogens (Cl, Br, I). Here, I propose new halogen incorporation mechanism in lizardite and antigorite from crystal chemical point of view.

Calculation methods: In order to assess present new incorporation model, first-principles calculation was conducted. Quantum-Espresso package was used to optimize the halogen incooporated model structures. In the present study, lizardite and antigorite (*m*=17 polysome) are considered. For our proposed mechanism, charge balance should be observed; so $Mg^{2+} = X^- + Al^{3+}$ substitution (X^- = halogen) is assumed to introduce halogen to a vacant site. For lizardite, enthalpy difference between two models (OH^- substitution and our model) was calculated for following equation: $Mg_2AlSi_2O_8XH_2 + H_2O = Mg_2AlSi_2O_9XH_4$. Former corresponds to the OH substituted model (with Al introduced), and latter corresponds to our new model. Although this comparison is crude (as free H_2O is included in the equation), it could provide systematic trend with kinds of halogen atoms. Since antigorite has a very large unit cell and many vacant sites, only $Mg^{2+} = Cl^- + Al^{3+}$ substitute in five vacant sites are considered so far.

Results and Discussion: From close inspection of crystal structures of lizardite and antigorite, vacant sites ideal for halogens are identified. The vacant sites are surrounded by four protons (of OH^-) forming elongated tetrahedon (i.e., XH_4^{3+}) if halogen is located. Such vacant sites provide local structure similar to halogen ions in aqueous solution.

In order to further assess present incorporation mechanism, first-principles calculations of lizardite and antigorite containing halogens in those sites were conducted. The structural optimizations confirmed that halogens could be well accommodated into the tetrahedral vacant sites in lizardite. The calculated enthalpy difference between OH substitution and present models in lizardite revealed that larger halogens prefer our model over the OH substitution model. There is sinlge vacant site in lizardite, but antigorite (*m* =17) has 17 crystallographically different vacant sites. Most sites have local structures more or less similar to that of lizardite (locating in 6-membered SiO_4 ring). But there is another kind of vacant site which is locating in 8-membered SiO_4 ring. This local structure is surrounded by six protons, but it can be regareded as two tetrahedral proton sites with edge sharing. Substitution of Cl^- to this site (one of tetrahedral sites) showed lower enthalpy compared to those of other lizardite-like sites, and can accept more larger ions. Therefore, Cl^- (and other larger halogens) will prefet this site in antigorite (*m*=17). Not all antogorite polysomes have this site.

Present study suggests that our new proposed incorporation mechanism is promising, and it should be further studied experimentally. Present new incorporation mechanism would be important to understand elemental partition behavior of halogens in subduction zones.

Keywords: halogen site, serpentine, crystal chemistry, incorporation mechanism, elemental partition

©2019. Japan Geoscience Union. All Right Reserved.

Mineralogical and geochemical characteristics of cuttings from Taketomi hot spring

*Noriyuki Shingaki[1], Tomohiro Toki[1], Syogo Oshima[2], Masaaki chinen[3], Arito Sakaguchi[4], Naoto Takahata[5], Yuji Sano[5], Shirai Kotaro[5], Kentaro Tanaka[5]

1. University of the Ryukyus , 2. West Japan Engineering Consultants, Inc., 3. MicroRange, 4. Faculty of Science, Yamaguchi University, 5. Atmosphere and Ocean Research Institute, The University of Tokyo

It is important to grasp carbon cycle on the earth’ s surface for thinking about global environmental change. A hot spring with a maximum temperature of 64℃ is venting with gas containing 70% of methane from several spots on the seafloor at depth of 22 m at 1 km northeast off Taketomi Island. Based on methane and helium isotope ratios in the venting gas, the influence of magmatic gas has been pointed out. In spite of Taketomi Island located on the trench side from island arc, magmatic gas is venting. It suggests the forearc where magma cannot generate, might form new supply path of carbon from the Earth’ s interior. The mass balance from new supply path of carbon may change estimation of carbon cycle on earth’ s surface. Therefore, the purpose of this study is to elucidate venting mechanism and quantitative grasp of magmatic gas from forearc, and the history of hot spring activities will be investigated to predict future activities.

In 2017, the hot spring was drilled up to depth of 940 m in Taketomi Island. The cuttings with muddy water were sampled every 10 m. The thin sections were prepared from cuttings to be observed using polarization microscope, and the chemical compositions of grains were analyzed by SEM-EDX. The ground samples were analyzed for mineral and chemical compositions by XRD and EDX. The clay minerals gathered by levitation were measured for half-value width of illite using XRD. He and CO_2 contained in samples that were crashed in vacuum were measured for isotope ratios by mass spectrometer. Calcite and dolomite collected from the cuttings were measured for the carbon and oxygen isotope ratios by mass spectrometer. The vitrinite in the cuttings was separated by a heavy liquid, and the reflectance was measured by a reflecting microscope.

In the microscopy, the stratum was roughly divided two formations; cryptocrystalline quartz layer and sand stone layer. Carbonaceous materials were observed in most of the stratum. Dolomite was limitedly observed in the vicinity of 800 m. In the XRD analysis, Quartz was detected at all depth. Calcite was detected at shallower depth than 30 m, and dolomite was detected only around 800 m. As a result of the EDX analysis, silicon was the most dominant in all layers, and especially, it was contained around 0-100 m, 300 m and around 900 m over 80%. There was a layer that contained much calcium. Around 0-30 m, 400-500 m and around 800 m, calcite was contained 15 % or more. The half-value width of illite was large, 0.8 $\Delta^\circ 2\theta$, in only 10 m surface, and as low as 0.2 to 0.4 $\Delta^\circ 2\theta$ below 50 m. Vitrinite reflectance was around 5% in the whole layer, close to measurement limit. The helium content was 10^{-14}-10^{-11} mol per 1g of cuttings, and tended to increase with increasing depth. The highest content was detected at 800 m depth. The helium isotope ratio($^3He/^4He$)have value of 0.4-3.6 times that of atmosphere, and tended to increase with increasing depth. Particularly, it was higher at 100 m, 300-400 m and 700-800 m. The CO_2 content per gram of cuttings, was in the range of 10^{-8}-10^{-6} mol in most layers, but it showed

©2019. Japan Geoscience Union. All Right Reserved.

higher values at 400 m and 800 m depth. the water tended to decrease with increasing depth, and showed especially high values at 400 m and 900 m. The carbon isotope ratio ($\delta^{13}C$) of calcite was -4.7‰ VPDB, and the oxygen isotope ratio ($\delta^{18}O$) is -16.3‰VPDB. The $\delta^{13}C$ value of dolomite was -1‰VPDB, and the $\delta^{18}O$ value was -10.9‰VPDB. The $\delta^{13}C$ value of CO_2 from cuttings at 800 m was -7.3‰VPDB, which contained sufficiently amount of carbon to measure carbon isotope ratio.

Keywords: Taketomi Island, Hot spring, cuttings, vitrinite reflectance, carbon cycle, helium isotope

©2019. Japan Geoscience Union. All Right Reserved.

Variation of helium isotope compositions at Lake Mashu

*Takanori Kagoshima[1], Yuji Sano[1], Atsushi Tanaka[2]

1. Atmosphere and Ocean Research Institute, University of Tokyo, 2. National Institute for Environmental Studies

Helium-3 is one of the most sensitive geochemical tracers which reflects addition of mantle components to gas and fluids in volcanic hydrothermal systems, and $^{3}He/^{4}He$ ratios may be useful to assess temporal change of hydrothermal activity at volcanic lakes. Lake Mashu is a caldera lake which formed around 7000 years ago in Hokkaido. Igarashi et al. (1992) measured He and Ne isotopes in water of Lake Mashu, and concluded that the depth profile of isotopic compositions reflect injection of mantle-derived He due to hot spring activity at the lake bottom. After that, there is no subsequent study reporting He isotope data. The lack of observational data may be due to difficulty of water sampling at caldera lakes. Igarashi et al. (1992) collected water samples into copper tubes. However, this method requires heavy and large sampling tools, and people who can transfer water and seal the tubes properly. In May and September 2017, we investigated Lake Mashu in order to check volcanic activity and practical sampling methods for caldera lakes. We collected water using a Niskin bottle at several depths (surface to 210 m) around the deepest point (211 m). Collected water was immediately transferred into lead-glass containers with vacuum valves at both ends. In Atmosphere and Ocean Research Institute, dissolved gases were extracted by the head space method, and introduced into a purification vacuum line. In the line, He and Ne were purified for isotope analyses. $^{3}He/^{4}He$ and $^{4}He/^{20}Ne$ ratios were measured using Helix-SFT and QMS, respectively. The highest $^{3}He/^{4}He$ ratios were observed at 205-210 m depth, indicating that injection of fluids with the high $^{3}He/^{4}He$ ratio at the bottom. The linear correlation between $^{4}He/^{20}Ne$ and $^{3}He/^{20}Ne$ ratios in water samples indicated mixing of two components: injected fluids and the atmosphere. The estimated $^{3}He/^{4}He$ ratio of the fluid end member was indistinguishable from the value reported by Igarashi et al. (1992), implying a possibility that there was no significant change in volcanic activity at Lake Mashu in the past 30 years.

Keywords: Helium isotope, Volcanic lake, Lake Mashu

©2019. Japan Geoscience Union. All Right Reserved.

Helium isotopes in Tachibana Bay and Shimabara Bay, Nagasaki

*Ma. Teresa Escobar[1], Yama Tomonaga[2], Hajime Obata[1], Shigenobu Takeda[3], Naoto Takahata[1], Yuji Sano[1]

1. Atmosphere and Ocean Research Institute, University of Tokyo, Kashiwanoha, Kashiwa, Chiba, Japan, 2. Eawag,, Swiss Federal Institute of Aquatic Science and Technology, Department of Water Resources and Drinking Water, Ü berlandstrasse 133 CH-8600 ,Dübendorf, Switzerland, 3. Graduate School of Fisheries and Environmental Sciences, Nagasaki University, Nagasaki, Japan

Noble gases are powerful tracers to study physical transport processes in aquatic system. Moreover, helium isotopes have been shown to be very useful to infer the origin of fluids. Shimabara Peninsula is located on western side of the Beppu-Shimabara graben in Kyushu, SW Japan. In the region, there are some hot springs and groundwaters which indicate magmatic helium with high 3He/4He ratio. Although some researchers report helium isotopic ratio on land, there is no data in the sea.

The surrounding bays around Shimabara Peninsula in Nagasaki were recently studied for the existence of hydrothermal springs and vents. Physico-chemical properties characteristic of hydrothermal activity were detected on the seafloor. For this study, we use helium isotopes to detect the occurrence of hydrothermal springs on the seafloor in both Tachibana Bay and Shimabara Bay. Samples were collected using a CTD-CMS system and analyzed using a Noble Gas Mass Spectrometer. Our data supplements the discovery of hydrothermal venting along known faults on the seafloor. We present the results of noble gas measurements conducted on water samples and discuss the relationship between our observations and the tectonic setup of the surrounding region.

Keywords: Helium Isotopes, Hydrothermal vents, Tachibana Bay

©2019. Japan Geoscience Union. All Right Reserved.

[E] Poster | S (Solid Earth Sciences)：S-CG Complex & General

Wed. May 29, 2019 10:45 AM - 12:15 PM JST | Wed. May 29, 2019 1:45 AM - 3:15 AM UTC | Poster Hall International Exhibition Hall8, Makuhari Messe_10

[S-CG48] Science of slow earthquakes: Toward unified understandings of whole earthquake process

convener:Satoshi Ide(Department of Earth an Planetary Science, University of Tokyo), Hitoshi Hirose(Research Center for Urban Safety and Security, Kobe University), Kohtaro Ujiie(Graduate School of Life and Environmental Sciences, University of Tsukuba), Takahiro Hatano(Earthquake Research Institute, University of Tokyo)

Accumulating observational studies on various types of slow deformation events, such as tectonic tremors, very low frequency events, and slow slip events, portrays some universal characteristics in generally complex behavior, including interaction among events and influence by various outer loadings. Some of these phenomena seem to have causal relation with the occurrence of very large earthquakes. A unified understanding of these slow and fast earthquake processes requires an approach integrating geophysics, seismology, geodesy, geology, and non-equilibrium statistical physics. We welcome presentations based on, but not limited to, geophysical observation, data analysis, analytical theory, numerical simulation, field study, and laboratory experiments.

[SCG48-P01] Off the Kii Peninsula Shallow Low Frequency Earthquake in 2004 revealed by Ocean Bottom Seismometer

*Koji Tamaribuchi[1], Akio Kobayashi[1], Takahito Nishimiya[1], Satoshi Annoura[2] (1.Meteorological Research Institute, 2.Japan Meteorological Agency)

[SCG48-P02] The development of pressure vessel on gouges for rock deformation at seismic rates under water-saturated conditions

*Wei-Ting Lin[1], Li-Wei Kuo[1], Wen-Jie Wu[1], Jia-Jyun Dong[1], Yi-Hung Huang[2] (1.National Central University, 2.MATSUKI HYDRAULIC INDUSTRIAL CO. LTD)

[SCG48-P03] Spatial variations of shallow very low-frequency earthquake activity along the Nankai Trough based on CMT inversion using the 3D heterogeneous model

*Shunsuke Takemura[1], Takanori Matsuzawa[1], Akemi Noda[1], Takashi Tonegawa[2], Youichi Asano[1], Takeshi Kimura[1], Katsuhiko Shiomi[1] (1.National Research Institute for Earth Science and Disaster Resilience, 2.Japan Agency for Marine-Earth Science and Technology)

[SCG48-P04] Evaluation of Magnitude and Characteristics of Seismicity of Low Frequency Earthquakes in Parkfield

*Miki Aso[1,3], Naofumi Aso[2], Satoshi Ide[1] (1.Department of Earth and Planetary Science, The University of Tokyo, 2.Tokyo Institute of Technology, School of Science, 3.OYO RMS Corporation)

[SCG48-P05] Tectonic tremor catalog in the Tohoku-Hokkaido-Oki region using S-net

*Satoshi Ide[1], Tomoaki Nishikawa[2], Takanori Matsuzawa[3], Kazuaki Ohta[2], Naoki Uchida[4], Takuya NISHIMURA[2] (1.Department of Earth an Planetary Science, University of Tokyo, 2.Disaster Prevention Research Institute, Kyoto University, 3.National Research Institute for Earth Science and Disaster Resilience, 4.Graduate School of Science and International Research Institute of Disaster Science, Tohoku University)

[SCG48-P06] Spontaneous Slow Slip and Runaway Slip in Laboratory

*Miki Takahashi[1] (1.Institute of Earthquake and Volcano Geology, Geological Survey of Japan, AIST)

[SCG48-P07] Hydration and amorphization of quartz rocks during high-velocity frictional sliding: An examination of fault gouge from friction experiments of synthetic quartz

*Yuko Onoe[1], Hirotaka Iida[2], Akito Tsutsumi[1], Aki Takigawa[1] (1.Graduate School of Science, Kyoto University, 2.Geothermal Engineering Co., Ltd.)

[SCG48-P08] Constraining S Wave Velocity of the Source Region of Shallow Very Low-Frequency Earthquakes

*Takeshi Akuhara[1], Takashi Tonegawa[2] (1.Earthquake Research Institute, The University of Tokyo, 2.Research and Development center for Earthquake and Tsunami, Japan Agency for Marine-Earth Science and Technology)

[SCG48-P09] **Quantitative relationship between aseismic slip propagation speed and frictional properties**

*Keisuke Ariyoshi[1], Jean-Paul Ampuero[2,3], Roland Burgmann[4], Toru Matsuzawa[5], Akira Hasegawa[5], Ryota Hino[5], Takane Hori[1] (1.Japan Agency for Marine-Earth Science and Technology, 2.Université Côte d'Azur, 3.California Institute of Technology, 4.University of California, Berkeley, 5.Graduate School of Science, Tohoku University)

[SCG48-P10] Comprehensive detection of very low frequency earthquakes off the Pacific coasts of Hokkaido and Tohoku, northeastern Japan

*Satoru Baba[1], Akiko Takeo[1], Kazushige Obara[1], Takanori Matsuzawa[2], Takuto Maeda[3] (1.Earthquake Research Institute, University of Tokyo, 2.National Research Institute for Earth Science and Disaster Resilience, 3.Graduate School of Science and Technology, Hirosaki University)

[SCG48-P11] **Spatio-temporal evolution of long- and short-term slow slip events in the Tokai region, central Japan estimated from a very dense GNSS network, during 1997-2017**

*Hiromu Sakaue[1], Takuya NISHIMURA[2], Jun'ichi Fukuda[3], Teruyuki Kato[4] (1.Graduate School of Science, Kyoto University, 2.Disaster Prevention Research Institute Kyoto University, 3.Earthquake Research Institute,The University of Tokyo, 4.Hot Springs Research Institute of Kanagawa Prefecture)

[SCG48-P12] Broadband excitation of acoustic emission in granular stick-slip : experiments and spectral analyses

*Hidekazu Fukumizu[1], Ikuro Sumita[2] (1.Earth and Environmental Science Course, Division of Natural System, Graduate school of Natural Science and Technology, Kanazawa University, 2.School of Geosciences and Civil Engineering, Kanazawa University)

[SCG48-P13] Episodic tremor and slip silently invades strongly locked megathrust in the Nankai Trough

*Masayuki Kano[1], Aitaro Kato[2], Kazushige Obara[2] (1.Graduate school of science, Tohoku University, 2.Earthquake Research Institute, The University of Tokyo)

[SCG48-P14] Spatial distribution of the electrical resistivity beneath western part of Shikoku Island where long-term SSE events have repeatedly occurred

*Makoto Uyeshima[1], Maki Hata[1], Hiroshi Ichihara[2], Ryokei Yoshimura[3], Koki Aizawa[4] (1.Earthquake Research Institute, The University of Tokyo, 2.Graduate School of Environmental Studies, Nagoya University, 3.Disaster Prevention Research Institute, Kyoto University, 4.Institute of Seismology and Volcanology, Faculty of Sciences, Kyushu University)

[SCG48-P15] Variations of scaling relationships for shallow tremor observed along the Nankai trough

*Masaru Nakano[1], Suguru Yabe[1] (1.Japan Agency for Marine-Earth Science and Technology)

[SCG48-P16] Low-frequency earthquakes triggered by teleseismic surface waves by Ryukyu subduction zone.

Ayumi Kinjo[1], *Mamoru Nakamura[1] (1.Faculty of Science, University of the Ryukyus)

[SCG48-P17] Detection of small surface displacement accompanying deep low-frequency tremor in Shikoku region, southwest Japan

*Yutaro Okada[1], Takao Tabei[2] (1.Faculty of Science, Kochi University, 2.Faculty of Science and Technology, Kochi University)

[SCG48-P18] Long-term temporal change in crustal resistivity beneath western Shikoku

*Futoshi Yamashita[1], Yoshimori Honkura[1] (1.National Research Institute for Earth Science and Disaster Resilience)

[SCG48-P19] Slow decay of postseismic deformation compared with aftershocks following the 2011 Tohoku-oki Earthquake

*Yuta Mitsui[1], Shunsuke Morikami[2] (1.Department of Geosciences, Shizuoka University, 2.Formerly at Graduate School of Science and Technology, Shizuoka University)

[SCG48-P20] Serpentinite dehydration in subduction shear zones formed at source depths of slow earthquakes

*Yasushi Mori[1], Miki Shigeno[1], Kohtaro Ujiie[2], Kazuya Noro[2], Tadao Nishiyama[3] (1.Kitakyushu Museum of Natural History and Human History, 2.University of Tsukuba, 3.Kumamoto University)

[SCG48-P21] Earthquake swarms following very low-frequency earthquakes in the central Ryukyu Trench

*Mamoru Nakamura[1] (1.Faculty of Science, University of the Ryukyus)

[SCG48-P22] Seismic imaging in the central Nankai trough, off Shionomisaki to Kii channel

*Yasuyuki Nakamura[1], Shuichi Kodaira[1], Tetsuo No[1], Yuka Kaiho[1], Gou Fujie[1], Seiichi Miura[1], Kazuya Shiraishi[1] (1.Japan Agency for Marine Earth Science and Technology)

[SCG48-P23] Attempt to Detect Intra-plate SSEs Based on F3 Solution of GEONET

*Yusaku Tanaka[1] (1.Earthquake Research Institute)

[SCG48-P24] A new hydrothermal, low to high speed rotary-shearing apparatus: Reproduction of slow/megathrust earthquakes in laboratory

*Takehiro Hirose[1], Wataru Tanikawa[1], Yohei Hamada[1], Keishi Okazaki[1] (1.Kochi Institute for Core Sample Research, Japan Agency for Marine-Earth Science and Technology)

[SCG48-P25] Very low-frequency earthquakes in western Shikoku remotely triggered by the 2016 Mw5.9 off-Kii Peninsula earthquake

*Masatoshi Miyazawa[1] (1.Disaster Prevention Research Institute, Kyoto University)

[SCG48-P26] **Underground structure around source region of slow earthquakes in western Shikoku obtained by receiver function analysis**

Akira Hikita[1], Aitaro Kato[1], *Kazushige Obara[1], Akiko Takeo[1], Takeshi Akuhara[1] (1.Earthquake Research Institute, The University of Tokyo)

[SCG48-P27] Hypocenter determination of deep low frequency tremors beneath the Kii Peninsula by backprojection of seismic array data

*Kodai Sagae[1], Hisashi Nakahara[1], Takeshi Nishimura[1], Kazutoshi Imanishi[2] (1.Graduate School of Science,Tohoku University, 2.National Institute of Advanced Industrial Science and Technology (AIST))

[SCG48-P28] Triggered tremors and stress perturbations due to surface waves

*Ryohei Ikeda[1], Naoki Suda[1] (1.Hiroshima University)

[SCG48-P29] Numerical modeling of long- and shallow slow slip events including shallow region in Hyuganada and western Nankai, Japan

*Takanori Matsuzawa[1], Bunichiro Shibazaki[2] (1.National Research Institute for Earth Science and Disaster Resilience, 2.Building Research Institute)

[SCG48-P30] Further evidence for the influence of a subducting-ridge on the spatial strain accumulation and release pattern in the shallow eastern Nankai Trough, based on VLFE distribution

*Akiko Toh[1], Chen Wan-Jou [2], Doug Dreger[3], Wu-Cheng Chi[2], Satoshi Ide[1] (1.University of Tokyo, 2.Institute of Earth Sciences, Academia Sinica, 3.UC Berkeley)

[SCG48-P31] Evidence for semi-brittle flow in mantle-wedge serpentinites under high pore fluid pressure and their implications for deep low frequency earthquakes

Kengo Kataoka[1], Yurina Nagata[1], *Ken-ichi Hirauchi[1], Ryosuke Oyanagi[2], Atsushi Okamoto[3], Katsuyoshi Michibayashi[4] (1.Department of Geosciences, Faculty of Science, Shizuoka University, 2.Japan Agency for Marine-Earth Science and Technology, 3.Graduate School of Environmental studies, Tohoku University, 4.Department of Earth and Planetary Sciences, Nagoya University)

[SCG48-P32] Spatial distribution of slow slip events off the Boso peninsula from 1996 to 2018 under sparsity constraints

*Ryoko Nakata[1], Hideitsu Hino[2], Tatsu Kuwatani[3,4], Takahiro Akiyama[5], Shoichi Yoshioka[6], Masato Okada[7], Takane Hori[1] (1.Japan Agency for Marine-Earth Science and Technology, 2.The Institute of Statistical Mathematics, 3.Department of Solid Earth Geochemistry, Japan Agency for Marine-Earth Science and Technology, 4.PRESTO, Japan Science and Technology Agency, 5.Graduate School of Science, Kobe University, 6.Research Center for Urban Safety and Security, Kobe University, 7.Graduate School of Frontier Sciences, The University of Tokyo)

[SCG48-P33] Marine electromagnetic observations around a slow earthquake region in the western Nankai trough

*Hiroshi Ichihara[1], Tada-nori Goto[2], Tetsuo Matsuno[3], Noriko Tada[4], Shinya Sato[2] (1.Earthquake and Volcano Research Center, Nagoya University, 2.Graduate School of Engineering, Kyoto University, 3.Ocean Bottom Exploration Center, Kobe University, 4.JAMSTEC)

[SCG48-P34] Dynamics of precipitating injection fronts inside of structured medium

*Yutaka Sumino[1], Shunsuke Tanaka[1], Miyuki Kunihiro[1] (1.Tokyo University of Science)

[SCG48-P35] Permeability changes of simulated low permeable fault rocks induced by intermediate velocity friction test

*Wataru Tanikawa[1] (1.Japan Agency for Marine-Earth Science and Technology, Kochi Instutute for Core Sample Research)

[SCG48-P36] Modified relation between the coupling and tremor rates around the Shikoku region

*Tadafumi Ochi[1] (1.Institute of Earthquake and Volcano Geology, Geological Survey of Japan, The National Institute of Advanced Industrial Science and Technology)

[SCG48-P37] Spatiotemporal distribution of regular and very low-frequency earthquakes in the northern part of the Ryukyu subduction zone

*Youichi Asano[1], Kazuhiko Goto[2], Hiroshi Yakiwara[3], Shuichiro Hirano[3] (1.National Research Institute for Earth Science and Disaster Resilience, 2.Association for the development of earthquake prediction,

3.Nansei-toko Observatory for Earthquakes and Volcanoes, Kagoshima University)

[SCG48-P38] Possible tectonic tremor activities near the VLFE epicenters in the Sanriku-Oki region in 2011

*Hidenobu Takahashi[1], Ryota Hino[1], Yusaku Ohta[1], Naoki Uchida[1], Syuichi Suzuki[1], Masanao Shinohara[2], Takanori Matsuzawa[3] (1.Graduate school of Science Tohoku University , 2.Earthquake Research Institute, University of Tokyo, 3.National Research Institute for Earth Science and Disaster Resilience)

[SCG48-P39] Heterogeneous structure around a region of slow earthquake activity off Ibaraki prefecture along the Japan Trench

*Kimihiro Mochizuki[1], Tomoaki Yamada[1], Masanao Shinohara[1], Ryota Hino[2], Ryosuke Azuma[2], Yoshihiro Ito[3], Yoshio Murai[4], Kenji Uehira[5], Toshinori Sato[6] (1.ERI, Univ. of Tokyo, 2.Graduate School of Science, Tohoku Univ., 3.DPRI, Kyoto Univ., 4.Faculty of Science, Hokkaido Univ., 5.NIED, 6.Graduate School of Science, Chiba Univ.)

[SCG48-P40] Shallow low-frequency tremor triggered by nearby moderate earthquakes off Sanriku

*Sachiko Tanaka[1], Takanori Matsuzawa[1], Youichi Asano[1] (1.National Research Institute for Earth Science and Disaster Resilience)

[SCG48-P41] Slow slip events in the Bungo Channel over 15 years as inferred from GNSS data (1996-2011)

Takatoshi Yokoi[1], *SHINICHI MIYAZAKI[1], Hiromu Sakaue[1], Jun'ichi Fukuda[2] (1.Graduate School of Science, Kyoto University, 2.Earthquake Research Institute, The University of Tokyo)

[SCG48-P42] Investigations of sensor orientation and a possibility of detecting crustal deformation based on accelerometer records of S-net

*Ryota Takagi[1], Naoki Uchida[1], Takashi NAKAYAMA[1], Ryosuke Azuma[1], Akira Ishigami[1], Tomomi Okada[1], Yusaku Ohta[1], Ryota Hino[1] (1.Research Center for Prediction of Earthquakes and Volcanic Eruptions, Graduate School of Science, Tohoku University)

[SCG48-P43] Spatiotemporal variation of released seismic energy from shallow low-frequency tremor in Hyuga-nada, revealed by ocean bottom seismological observation

*Yusuke Yamashita[1], Saki Watanabe[2], Tomoaki Yamada[3], Masanao Shinohara[3], Takeshi Matsushima[2] (1.Disaster Prevention Research Institute, Kyoto University, 2.Institute of Seismology and Volcanology, Kyushu University, 3.Earthquake Research Institute, The University of Tokyo)

[SCG48-P44] Unified description of fast and slow earthquakes using velocity strengthening patches

*So Ozawa[1], Takahiro Hatano[1] (1.Earthquake Research Institute, the University of Tokyo)

[SCG48-P45] The b-value of the earthquake swarm activities accompanied by the Boso slow slip events

*Yuki Noda[1], Hitoshi Hirose[2,1] (1.Department of Planetology, Faculty of Science, Kobe University , 2.Research Center for Urban Safety and Security, Kobe University)

[SCG48-P46] **Three-dimensional thermal modeling associated with subduction of the Philippine Sea plate at the Ryukyu Trench, and its relation to the occurrence of interplate seismic events**

*Nobuaki Suenaga[1], Shoichi Yoshioka[2,1], Yinfeng Ji[3] (1.Graduate School of Science, Kobe University, Japan, 2.Research Center for Urban Safety and Security, Kobe University, Japan, 3.Chinese Academy of Science, Beijin, China)

Off the Kii Peninsula Shallow Low Frequency Earthquake in 2004 revealed by Ocean Bottom Seismometer

*Koji Tamaribuchi[1], Akio Kobayashi[1], Takahito Nishimiya[1], Satoshi Annoura[2]

1. Meteorological Research Institute, 2. Japan Meteorological Agency

The 2004 off the Kii Peninsula earthquakes (Mj7.1, 7.4) occurred near the Nankai trough axis, southeast off the Kii Peninsula, Japan, on September 5, 2004. After the earthquakes, the Meteorological Research Institute conducted OBS observation to examine the aftershock distribution accurately. Although the analysis was limited to hypocenter relocation of "ordinary aftershocks", no analysis was done for slow events. In this study, it is shown that many low-frequency earthquakes (LFEs) occurred in "ordinary aftershocks" from the detailed inspection of our observation. During the observation period, the frequency of LFE gradually decreased. Since P- and S-arrival times are unclear, it is difficult to determine the distribution of the hypocenter accurately. However, by using the Amplitude Source Location (ASL; Battaglia and Aki, 2003), the LFEs are located between a splay fault and trench axis. The 2004 OBS stations are located east of the DONET, and many LFEs are detected in the 2004 OBS network. In addition, there are many very-low-frequency events (VLFEs) in the F-net waveforms with very-low-frequency band-pass filter (0.02 - 0.05 Hz) during the observation period. We found that the identified LFEs were associated with VLFEs since their amplitudes seemed to be correlated. This means that the LFEs and VLFEs show the same phenomenon. Our observations might contribute to reveal the relationship between ordinary aftershocks, slow-events, and megathrust events such as Nankai trough earthquake.

Keywords: LFE, OBS, 2004 off the Kii Peninsula earthquakes

©2019. Japan Geoscience Union. All Right Reserved.

The development of pressure vessel on gouges for rock deformation at seismic rates under water-saturated conditions

*Wei-Ting Lin[1], Li-Wei Kuo[1], Wen-Jie Wu[1], Jia-Jyun Dong[1], Yi-Hung Huang[2]

1. National Central University, 2. MATSUKI HYDRAULIC INDUSTRIAL CO. LTD

To understand earthquake mechanism and fault behavior during earthquake ruptures, experimentalists commonly conduct rock deformation tests with rotary shear apparatus (e.g., low-to high-velocity rock friction experiment, LHVR) which allow deformed at seismic rates. In general, the materials utilized for rotary shear apparatus are both cohesive rocks (e.g., gabbro and carbonate) and incohesive rocks (natural fault gouges and synthetic rock powders), while the latter are deformed at seismic rates and, commonly at low normal stresses (0.5 to 2 MPa confining with a plastic Teflon ring). However, using Teflon rings has issues of gouge extrusion and chemical contamination, in particular, at high normal stresses (>3MPa) and water-saturated condition, and the obtained mechanical data and associated experimental products seem to be questionable. Here we develop a metal pressure vessel for LHVR to deform gouges at seismic rates and, importantly, expand the normal stress capability (up to 15 MPa) and under water-saturated condition. Our results show the resistance from the pressure vessel itself (metal-to-metal contact) is extremely low (friction coefficient ≈0.02), and the result of kaolinite is similar to the previously published data. In particular, both gouge-extrusion and water-leaking was not observed deformed at a normal stress of 15 MPa and equivalent velocity 1 m/s. The designed pressure vessel could fill the gap of experimental conditions among the current used pressure vessels and complete the understanding of fault ruptures.

Keywords: pressure vessel, water-saturated condition, fault gouge, rotary shear experiment

©2019. Japan Geoscience Union. All Right Reserved.

Spatial variations of shallow very low-frequency earthquake activity along the Nankai Trough based on CMT inversion using the 3D heterogeneous model

*Shunsuke Takemura[1], Takanori Matsuzawa[1], Akemi Noda[1], Takashi Tonegawa[2], Youichi Asano[1], Takeshi Kimura[1], Katsuhiko Shiomi[1]

1. National Research Institute for Earth Science and Disaster Resilience, 2. Japan Agency for Marine-Earth Science and Technology

To reveal structural properties around the Philippine Sea plate boundary, we investigated spatial variation of shallow very low-frequency earthquake (SVLFE) activity along the Nankai Trough. By using F-net velocity seismograms for periods of 20-50s, we conducted centroid moment tensor (CMT) inversion of SVLFEs detected by array analysis of Asano et al. (2008 EPS). Our CMT method is basically same as in Takemura et al. (2018 GRL). Source grids were assumed on the boundary of the Philippine Sea plate at horizontal intervals of 0.1°. Green's functions from source grids to F-net stations were evaluated by finite-difference method simulations of seismic wave propagation within the 3D heterogeneous structure model of Takemura et al. (2019 PAGEOPH).

We applied our CMT method to SVLFEs occurred from June 2003 to May 2018. Almost of CMT solutions are low-angle thrust faulting mechanism occurred around the accretionary prism toe. We evaluated spatial variations of SVLFE activity along the Nankai trough by calculating cumulative moment at each source grid. The areas with large cumulative moments appeared near the trench axis of off the Cape Muroto, the Kii Channel and the southeastern Kii Peninsula. We found spatial correlations between cumulative moment, slip-deficit rate (Noda et al. 2018 JGR) and *S*-wave velocities (Tonegawa et al. 2017 Nature Comm.) around the Philippine Sea plate boundary. Such spatial correlations suggest that SVLFEs are effectively activated by mechanically weakening due to pore fluid at surrounding area of strongly locked zone of the Philippine Sea plate.

Acknowledgement
NIED F-net broadband velocity seismograms were used. The catalogs of slow earthquakes were downloaded from the website of slow earthquake database (Kano et al., 2018 SRL). Finite-different method simulations were conducted on the Earth Simulator at the JAMSTEC.

Keywords: Nankai Trough, Shallow very low-frequency earthquake, CMT inversion, Pore fluid pressure, Slip deficit rate

©2019. Japan Geoscience Union. All Right Reserved.

Evaluation of Magnitude and Characteristics of Seismicity of Low Frequency Earthquakes in Parkfield

*Miki Aso[1,3], Naofumi Aso[2], Satoshi Ide[1]

1. Department of Earth and Planetary Science, The University of Tokyo, 2. Tokyo Institute of Technology, School of Science, 3. OYO RMS Corporation

Over a million tectonic low frequency earthquakes (LFEs) have been found in Parkfield along the San Andreas Fault, as 88 families by Shelly and Hardebeck [2010]. Thanks to enormous event detection, interesting characteristics focusing on their event amplitudes have been reported such as the spatial variation along the fault, the exponential frequency distribution for each family, and the relationship with recurrence time [Shelly and Hardebeck, 2010; Shelly, 2010]. However, the relative size of families has not been quantified accurately, because we have to consider various factors such as radiation pattern depending on focal mechanisms, attenuation during wave propagation, and site amplification effects. For quantitative comparison of scale among differently located events, here we estimate the absolute magnitude of each event considered those effects.

We estimate the seismic moment Mo [Nm] and moment magnitude Mw of all LFE events in the catalog of Shelly [2017]. We first stack seismograms of over one million events in the catalog to improve the signal-to-noise (S/N) ratio. Then, we evaluate the absolute amplitude of the original seismograms using the stacked waveforms. Specifically, we evaluate seismic moment Mo by assuming focal mechanisms of each family, attenuation quality factor, site effect estimated by Aso et al. [2019, submitted to JpGU meeting, “Variations of Focal Mechanisms of Low Frequency Earthquake in Parkfield”], and the source time function estimated by Thomas et al. [2016]. Note that we consider the frequency-limited seismic moment Mo, though it is not exactly the same as the original definition of seismic moment measured at a lower frequency than the minimum frequency contained in one phenomenon.

As previously reported by reported by Shelly and Hardebeck [2010], LFEs in the southern part has larger magnitude. We also find that shallower events are smaller than deeper events.

Similarly, most of the frequency distribution for each family shows an exponential distribution which is also reported for LFEs in Cascadia [Sweet et al., 2014] and New Zealand [Chamberlain et al., 2014].

By comparing size and recurrence interval, the events during LFE burst (seconds interval) tend to be larger than the first event of burst, which occurs after hours-to-days quiescence. A similar tendency is found in tremor burst occurring with a longer time scale (~1-week-long) than that of LFEs (~1-minute-long) [Yabe and Ide, 2014]. These might suggest some temporal change in fault rheology and/or some characteristic spatiotemporal behavior such as Brownian slow earthquake processes [Ide, 2008].

Keywords: San Andreas Fault, Parkfield, seismicity, waveform stacking, low frequency earthquake, amplitude evaluation

©2019. Japan Geoscience Union. All Right Reserved.

Tectonic tremor catalog in the Tohoku-Hokkaido-Oki region using S-net

*Satoshi Ide[1], Tomoaki Nishikawa[2], Takanori Matsuzawa[3], Kazuaki Ohta[2], Naoki Uchida[4], Takuya NISHIMURA[2]

1. Department of Earth an Planetary Science, University of Tokyo, 2. Disaster Prevention Research Institute, Kyoto University, 3. National Research Institute for Earth Science and Disaster Resilience, 4. Graduate School of Science and International Research Institute of Disaster Science, Tohoku University

Recently, various slow earthquakes have discovered in the subduction zone off Tohoku and Hokkaido regions along the Japan Trench. In this presentation, we report the detection of tectonic tremors using the Seafloor Observation Network for Earthquakes and Tsunamis along the Japan Trench (S-net), operated by The National Research Institute for Earth Science and Disaster Resilience (NIED).

We used continuous seismograms from August 2016 to August 2018 recorded by short-period sensors at 150 S-net stations. The original data were converted to envelope waveforms and analyzed using the envelope correlation method coded by Ide (2010), for each 300 s time windows with 150 s overlap. Since the results included many ordinary earthquakes with short durations, we regarded the events with durations longer than 20 s as tremors. This number is twice longer than that used for deep tremors in western Japan, reflecting the long-lasting waves in ocean bottom observation.

We found that the detection completeness is not high due to the high seismic activity in the Japan Trench, especially after the occurrence of large earthquakes, with numerous aftershocks falsely detected. We therefore divided the study area into 18 overlapping sub-regions that cover the locations of tremor activity to solve this problem. We detected tremors in each sub-region and merged the results into one catalogue by removing one of any two events within 10 s and 1 degree of each other, depending on their root-mean-square errors. Some tremor-like signals were found near the triple junction off the Boso Peninsula at approximately 34.8˚N. However, visual inspection revealed these events to be ordinary earthquakes, which we excluded from our tremor catalogue. The resultant tremor catalogue will be available in Slow Earthquake Database (Kano et al., 2018).

Keywords: tectonic tremor, slow earthquake, ocean bottom seismometer, S-net, Japan trench

©2019. Japan Geoscience Union. All Right Reserved.

Spontaneous Slow Slip and Runaway Slip in Laboratory

*Miki Takahashi[1]

1. Institute of Earthquake and Volcano Geology, Geological Survey of Japan, AIST

Earthquake nucleation and propagation involves the acceleration of slip on a fault from a background, quasi-static, low-velocity state towards meter-per-second values. From shear experiments using brine-saturated simulated gouge composed of 80:20 wt.% mixtures of halite and muscovite (following e.g. Niemeijer & Spiers, 2007, JGR), Takahashi et al., [2017, G-cubed] recently reported a switch in the dominant deformation process, from distributed viscous flow (pressure solution creep) to localized brittle deformation, at a critical velocity V_c (~20 μm/sec). The direct effect which is normally observed upon perturbations in sliding rate disappears for $V > V_c$, suggesting that runaway fault-slip may be achieved when the sliding velocity exceeds V_c.
At relatively low shear stress, flow mechanisms, such as pressure solution creep and dislocation creep, will be fast enough to effectively suppress slip acceleration. However, with increasing the shear stress, there may be a velocity range in which flow mechanisms still works but not as effective. Hypothesizing that, under constant shear stress boundary conditions, this may lead to spontaneous acceleration followed by deceleration, analogous to a slow slip event. Moreover, imposing the constant shear stress with equal or larger value of the maximum strength of the simulated gouge, I also hypothesize that slip acceleration may proceed as $V > V_c$, inducing a dynamic weakening.
To address these hypotheses, I conducted torque-controlled rotary shear experiments, using brine-saturated, 80:20 wt % mixtures of halite (grain size < 75 μm) and muscovite (grain size < 33 μm) powders. Approximately 1.65 g of the gouge mixture was sandwiched between two teethed steel piston rings, forming an initially 1 mm thick layer. The piston rings had an inner diameter of 38 mm, and an outer diameter of 50 mm. I used a high-velocity rotary shear apparatus designed by T. Shimamoto [e.g., Togo and Shimamoto, 2012], and now installed at the Geological Survey of Japan (GSJ). The apparatus was modified to enable torque control with an accuracy of ±0.002 in the friction coefficient (μ), at a normal stress of 5 MPa. Rotation displacement is measured using a potentiometer installed close to the piston ring at the rotating side.
A preliminary result shows the velocity evolution after stepwise changes in the shear stress. At low shear stresses, corresponding to the pressure solution creep-controlled regime, transient increasing velocity towards a steady-state values suggests stable sliding. At $\mu \approx 0.6$, the simulated gouge shows spontaneous acceleration to $V \approx 1$ μm/sec, followed by deceleration. Lastly, under a constant shear stress condition equivalent to $\mu = 0.67$, spontaneous slip acceleration occurred followed by dynamic weakening at $V \approx V_c = 20$ μm/sec. More experiments and microstructural observations will help to elucidate the relationship between the critical velocity and the switch among dominant deformation mechanisms.

Keywords: shear stress control test, spontaneous acceleration/deceleration, dynamic weakening

©2019. Japan Geoscience Union. All Right Reserved.

Hydration and amorphization of quartz rocks during high-velocity frictional sliding: An examination of fault gouge from friction experiments of synthetic quartz

*Yuko Onoe[1], Hirotaka Iida[2], Akito Tsutsumi[1], Aki Takigawa[1]

1. Graduate School of Science, Kyoto University, 2. Geothermal Engineering Co., Ltd.

Various types of rocks and fault gouges display weakening of frictional strength at high-velocities, and in many cases, it is caused by high-temperature faulting processes such as frictional melting and thermal decomposition of fault materials. On the other hand, siliceous rocks display weakening of frictional strength at relatively slow slip velocity of ~1 mm/s. This weakening is a specific phenomenon because frictional heat is not sufficient to induce the high-temperature transformation reactions in this slip velocity range [Di Toro et al., 2004]. Goldsby and Tullis [2002] proposed gel lubrication model to explain the weakening of siliceous rocks; in which model frictional weakening likely results from production and shearing of hydrated amorphous silica layer along a fault in quartz rocks. But the relationship between the frictional weakening and hydration and amorphization of fault gouge is not clear yet.

This study aims to elucidate the mechanism of the frictional weakening observed for siliceous rocks. We conducted a series of friction experiments on synthetic quartz samples using a rotary-shear, intermediate-to high-velocity friction testing machine. Experiments were carried out under a constant normal stress condition of 1.5 MPa and at slip velocities of 5 μm/s, 10 μm/s, 105 μm/s, 1 mm/s, 10 mm/s and 105 mm/s. In this study effect of drying the sample on the frictional behavior were examined by introducing dry air to the chamber of the sample. After the friction tests, the gouge material on the slip surfaces were collected and analyzed by FTIR.

The frictional behavior of the synthetic quartz differs between room humidity and dry conditions; velocity weakening was observed for both conditions, however, velocity weakening starts at lower slip velocities for the dry experiments. Under DRY conditions, the frictional weakening occurs at slip velocity around 10 μm/s. From the results of the FTIR analysis, hydration of the gouge is confirmed for all the samples tested in this study. The FTIR result also indicates that the faster the slip velocity, the more the crystal structure of the gouge is destructed.
It is showed that under both DRY and Room Humidity conditions, at least the gouge generated on the friction surface of the sample which showed slip weakening is hydrated, consistent with the weakening model of Goldsby and Tullis [2002].

©2019. Japan Geoscience Union. All Right Reserved.

Constraining S Wave Velocity of the Source Region of Shallow Very Low-Frequency Earthquakes

*Takeshi Akuhara[1], Takashi Tonegawa[2]

1. Earthquake Research Institute, The University of Tokyo, 2. Research and Development center for Earthquake and Tsunami, Japan Agency for Marine-Earth Science and Technology

Shallow very low-frequency earthquakes (VLFEs), which are believed to occur in the vicinity of megathrusts, have been often associated with elevated pore fluid pressure. Lines of evidence for this idea include a small amount of stress drop, high tidal sensitivity, and reduced P wave velocity inferred from active source seismic surveys. Revealing the physical properties of the source region of shallow VLFEs will lead to a better understanding of their generation mechanisms. However, the challenge lies in the difficulty of acquiring S wave velocity in fine resolution.

Recent achievements by the authors may help overcome this issue. Akuhara et al. (2019) developed a robust technique to estimate Green's functions of receiver side structures from offshore seismograms, which are typically ill-conditioned due to water reverberations. Tonegawa et al. (2017) inverted Rayleigh wave admittance (i.e., a ratio of ground displacement to hydraulic pressure) for shallow S wave velocity structures beneath DONET seafloor observatories at the Nankai Trough subduction zone. Their velocity models show low-velocity zones that characterize the source regions of shallow VLFEs. However, a smoothing constraint imposed on the models renders their interpretation somewhat difficult.

This study presents preliminary results from transdimensional inversion of receiver-side Green's function estimated by the method of Akuhara et al. (2019), where we adopt a prior constraint by the velocity models of Tonegawa et al. (2017). Complementary to the Rayleigh admittance, the Green's function approach is sensitive to velocity contrasts and thus will offer an improved resolution.

Keywords: shallow very low frequency earthquake, seismic velocity structure, ocean bottom seismometer, bayesian analysis

©2019. Japan Geoscience Union. All Right Reserved.

Quantitative relationship between aseismic slip propagation speed and frictional properties

*Keisuke Ariyoshi[1], Jean-Paul Ampuero[2,3], Roland Burgmann[4], Toru Matsuzawa[5], Akira Hasegawa[5], Ryota Hino[5], Takane Hori[1]

1. Japan Agency for Marine-Earth Science and Technology, 2. Université Côte d'Azur, 3. California Institute of Technology, 4. University of California, Berkeley, 5. Graduate School of Science, Tohoku University

Recent observations show evidence of propagation of postseismic slip, whose propagation speed may contain information about the mechanical properties of faults. Here, we develop a new analytical relationship between the propagation speed of aseismic slip transients and fault frictional properties, modeled by a rate- and state-dependent friction law. The relationship explains the propagation speed of afterslip in 3-D numerical simulations to first order. Based on this relationship, we identify systematic dependencies of afterslip propagation speed on effective normal stress σ and frictional properties (the coefficients a and a-b which quantify the instantaneous and the steady-state velocity-dependence of friction, respectively, and the characteristic slip distance d_c of fault state evolution). Lower values of the parameter $A=a\sigma$ cause faster propagation in areas where the passage of the postseismic slip front induces large shear stress changes $\Delta\tau$ compared to A, which are typically located near the mainshock rupture. In areas where $\Delta\tau/A$ is small, typically more distant from the mainshock, afterslip propagation speed is more sensitive to (a-b) σ. The propagation speed is proportional to initial slip velocity and inversely proportional to d_c. The relationship developed here should be useful to constrain the frictional properties of faults based on observed propagation speeds, independently of rock laboratory experiments, which can then be used in predictive numerical simulations of aseismic slip phenomena.

Keywords: rate- and state-dependent friction, effective normal stress, stress perturbation

©2019. Japan Geoscience Union. All Right Reserved.

Comprehensive detection of very low frequency earthquakes off the Pacific coasts of Hokkaido and Tohoku, northeastern Japan

*Satoru Baba[1], Akiko Takeo[1], Kazushige Obara[1], Takanori Matsuzawa[2], Takuto Maeda[3]

1. Earthquake Research Institute, University of Tokyo, 2. National Research Institute for Earth Science and Disaster Resilience, 3. Graduate School of Science and Technology, Hirosaki University

Very low frequency earthquakes (VLFEs), classified as one type of slow earthquakes, occur near seismogenic zones. VLFEs off the Pacific coasts of Hokkaido and Tohoku in northeastern Japan occur around subducting plate interfaces near trenches. Asano et al. (2008) found VLFEs in the off-Tokachi region, the southern part of the Pacific coast of Hokkaido along the Kuril Trench, by array signal processing using high-sensitivity accelerometers of Hi-net operated by National Research Institute for Earth Science and Disaster Resilience (NIED). In recent years, VLFEs off the Pacific coast of Tohoku were found by visually checking broadband seismograms of F-net operated by NIED and other events were detected by the matched-filter technique using waveforms of detected events as templates (Matsuzawa et al., 2015). However, the number of detected VLFEs may have been limited because of the small number of the VLFE templates in previous studies. Baba et al. (2018, SSJ) set four virtual epicenters off the Pacific coasts of Hokkaido and Tohoku and detected VLFEs by the matched-filter technique using numerically simulated waveforms as templates. We extended virtual epicentral gridsto make more comprehensive detection of VLFEs.

We used continuous seismograms of F-net seismometers from January 2003 to July 2018 after applying a band-pass filter of 0.02–0.05 Hz. We set 123 virtual epicentral grids off the Pacific coasts of Hokkaido and Tohoku, and computed the synthetic waveform from the source at each virtual epicenter by the finite difference method with a three-dimensional velocity structure model, namely, Japan Integrated Velocity Structure Model (Koketsu et al., 2012). The fault mechanisms were assumed to be consistent with the geometry of the plate boundary and a plate motion model, NUVEL-1A. We then calculated station- and component-averaged cross-correlation coefficients (averaged CC) between synthetic waveforms and the data of F-net seismograms every 1 s, and selected the events which have averaged CC above nine times of the median absolute deviation of the distribution. This method is, however, sensitive to regular earthquakes and teleseismic events as well. We then excluded the signal of regular earthquakes by discarding events with the amplitudes of more than 160 nm/s at 1-2 Hz in vertical components at the nearest stations. Moreover, to remove teleseismic events, we used the USGS earthquake catalog and discarded events with high amplitudes and low averaged cross-correlation coefficients.

VLFE activities in the off-Tokachi and off-Aomori regions show synchronized episodic bursts in the interval of several months. VLFEs in the off-Tokachi region was rapidly increased by the afterslip of the 2003 Tokachi-Oki earthquake. Those in the off-Iwate and off-Ibaraki regions, located out of the coseismic slip area of the 2011 off the Pacific coast of Tohoku Earthquake (hereinafter, the Tohoku earthquake), were also rapidly increased by the afterslip of the Tohoku earthquake. VLFE activity in the off-Miyagi region is characterized by episodic bursts in the interval of several months to one year before the Tohoku earthquake, but it became low since then. VLFE activity in the off-Fukushima region show dramatic increase after an Mw 6.9 earthquake at off-Fukushima on July 19, 2008. In the off-Miyagi and off-Fukushima regions, located within or at the edge of the coseismic slip area of the Tohoku earthquake, VLFE activity has been low since the Tohoku earthquake probably because the earthquake released the

©2019. Japan Geoscience Union. All Right Reserved.

stress almost completely. These results suggest that VLFEs are sensitive to the stress perturbation and can be a slip meter that reflect spatiotemporal change of the interplate slip, as has been indicated by previous studies. Consequently, one possible cause of these episodic VLFE bursts in the off-Tokachi, off-Aomori and off-Miyagi regions may be the intermittent release of small portion of stress accumulated by interplate locking between plates in the interval of several months to one year. The interval of episodic bursts is shorter than a periodicity of slow slips ranging from 1 to 6 years off the Pacific coasts of Tohoku indicated by Uchida et al. (2016).

©2019. Japan Geoscience Union. All Right Reserved.

Spatio-temporal evolution of long- and short-term slow slip events in the Tokai region, central Japan estimated from a very dense GNSS network, during 1997-2017

*Hiromu Sakaue[1], Takuya NISHIMURA[2], Jun'ichi Fukuda[3], Teruyuki Kato[4]

1. Graduate School of Science, Kyoto University, 2. Disaster Prevention Research Institute Kyoto University, 3. Earthquake Research Institute,The University of Tokyo, 4. Hot Springs Research Institute of Kanagawa Prefecture

The long-term slow slip events (SSEs) have been reported on the subducting Philippine Sea Plate in the Tokai region, central Japan during 2001-2005 and 2013-2016. Many short-term slow slip events have been also observed there since 1996. We analyzed GNSS data from 1997 to 2017 to estimate spatiotemporal distribution of interplate slip associated with these SSEs in this study. The GIPSY-OASIS II software (version 6.1) was used to estimate daily coordinates of GNSS stations operated by GSI and JUNCO (the Japanese University Consortium for GPS Research). It is well known that GNSS time series have many systematic signals and noises that do not result from SSEs. They include, for example, seasonal variations, co- and post-seismic deformation of the 2004 southeast off Kii Peninsula earthquakes (M_w 7.3/7.4), the 2008 Ibaraki-ken-oki earthquake (M_w6.9), the 2008 Fukushima-ken-oki earthquake (M_w7.0) and the 2011 Tohoku-oki earthquake (M_w9.0), and crustal deformation of volcanic activity on the northern Izu Islands in 2000. After removing them, we applied a modified Network Inversion Filter (NIF) [Fukuda et al., 2008] to estimate daily slip and slip rate on the subduction plate interface.
Our results suggest that not only long-term SSEs (M_w~7.1 and M_w~6.7) in 2000-2005 and 2013-2016, but also short-term SSEs (M_w<6.1). The maximum estimated daily slip rates for short-term SSEs are an order of magnitude larger than those of the long-term SSE, and peak slip for short-term SSEs migrates along strike with LFTs synchronously. It suggests that LFTs are loaded directly by SSEs, and that slip rate regulates LFT genesis. We will present the change of back slip rate between inter short-term SSEs and characteristics of short-term SSEs (e.g. slip rates and recurrence interval) depending on the occurrence of long-term SSE.

Keywords: slow slip event, Tokai region, GNSS

©2019. Japan Geoscience Union. All Right Reserved.

Broadband excitation of acoustic emission in granular stick-slip : experiments and spectral analyses

*Hidekazu Fukumizu[1], Ikuro Sumita[2]

1. Earth and Environmental Science Course, Division of Natural System, Graduate school of Natural Science and Technology, Kanazawa University, 2. School of Geosciences and Civil Engineering, Kanazawa University

Slow slip and tremor are observed to occur simultaneously (e.g., Rogers and Dragert, Science, 2003). Such observation can be modelled using granular stick-slip experiments which show that the timing of the slips and acoustic emission (AE) are well correlated (e.g., Johnson et al., GRL, 2013, Jiang et al. GRL, 2017). AE waveforms are complex (e.g., Michlmayr & Or, Gran. Matt., 2014), and we do not fully understand the details of the temporal change of AE during the slip. Here we report the results of granular stick-slip experiments which focus on how their spectra depend on the shear rate, particle size and container size.

We shear glass beads contained in a stainless steel beaker using a rotating viscometer to which a vane spindle is attached (Higashi and Sumita, JGR, 2009), and measure the shear stress and AE at 200kHz. We use broadband accelerometers and microphones to measure AE. Four accelerometers are attached at the outer rim of the beaker, and each are separated by an angle of 90 degrees.

We integrate the acceleration to obtain AE velocity –time series data and analyze their characteristics in broad band. We find that although AE has a broad spectrum, the spectra show that there are two characteristic frequency (f) components ; a high-f (of the order of 100 Hz) and a low-f (of the order of 10Hz) components. The velocity waveforms recorded at antipodal positions, show that the high-f components are in phase, whereas the low-f components are of the opposite phase. This indicates that the mechanism which excite these components differ : the high-f component may correspond to AE excited by particle rearrangement, whereas the low-f component may correspond to the translational motion of the container. Indeed we find that the frequency of the low-f component depends on the container size.

We also conducted experiments using a rheometer in a parallel-plate setup and confirmed that these two different components exist. When the particle size becomes larger, the amplitude of the shear stress and the AE velocity increases. Furthermore we find that the mean frequency of the normalized power spectra rose to a higher frequency, thus correlating with the stress increase.

Our experiments indicate that AE is excited in broadband, and that their frequency components can be used to infer the interparticle stress. Such excitation appear to be analogous to tremors and very low frequency earthquakes that are also excited simultaneously.

Keywords: granular matter, stick-slip, acoustic emission, earthquake, tremor

©2019. Japan Geoscience Union. All Right Reserved.

Episodic tremor and slip silently invades strongly locked megathrust in the Nankai Trough

*Masayuki Kano[1], Aitaro Kato[2], Kazushige Obara[2]

1. Graduate school of science, Tohoku University, 2. Earthquake Research Institute, The University of Tokyo

Recent seismic and geodetic observations in subduction zones have revealed that slow earthquakes have preceded some large earthquakes (e.g., Kato et al., 2012; Mavrommatis et al., 2014; Ruiz et al., 2014). Characterization of slow earthquakes and their relation to large earthquakes provides important clues to constrain a wide spectrum of slip rates on tectonic faults. In this study, we report new evidence of a slow slip transient at the downdip edge of the strongly locked seismogenic zone in the western Nankai Trough in southwest Japan based on GNSS time series. This slow slip transient was remotely excited during an episodic tremor and slip at the downdip extension of the locked zone. Through this remote triggering, the frequent occurrence of the deep episodic tremor and slip invades the strongly locked megathrust zone and may intermittently increase the probability of large earthquakes in the Nankai Trough.

Acknowledgments

We used GNSS data provided by the Geospatial Information Authority of Japan. This study was supported by the JSPS KAKENHI Grant Number JP15K17743 in Grant-in-Aid for Young Scientists (B), JP18K03796 in Grant-in-Aid for Scientific Research (C), JP16H06473 and JP16H06474 in Scientific Research on Innovative Areas “Science of Slow Earthquakes.”

Keywords: Slow slip events, Slow earthquakes, Western Shikoku, GNSS

©2019. Japan Geoscience Union. All Right Reserved.

Spatial distribution of the electrical resistivity beneath western part of Shikoku Island where long-term SSE events have repeatedly occurred

*Makoto Uyeshima[1], Maki Hata[1], Hiroshi Ichihara[2], Ryokei Yoshimura[3], Koki Aizawa[4]

1. Earthquake Research Institute, The University of Tokyo, 2. Graduate School of Environmental Studies, Nagoya University, 3. Disaster Prevention Research Institute, Kyoto University, 4. Institute of Seismology and Volcanology, Faculty of Sciences, Kyushu University

In the Bungo channel area at the western margin of the Nankai megathrust rupture zones, the long-term slow slip events (SSE) repeatedly occurred about every 6 or 7 years. Since the last large-scale SSE event occurred in 2010, we will have a next large event soon. In order to obtain the electrical resistivity structure in the vicinity of the SSE area and examine its temporal change, we have started the Network-MT survey in the western part of the Shikoku Island facing the Bungo channel since April, 2016. Just before beginning of the observation, a tiny-scale SSE event occurred in the Bungo-channel (Ozawa, 2017, Hirose et al., 2018). We selected 17 areas in the western part of the Shikoku Island and installed 3 or 4 electrodes in the respective areas. The electrical potential differences with typical electrode spacing of several km are measured by using metallic telephone line network. We also measure the geomagnetic field at two stations in the target region. With the aid of the BIRRP code (Chave and Thomson, 2004), we could estimate the frequency-domain Network-MT response functions of good quality between the voltage difference and the magnetic field. The Network-MT response functions were directly inverted to estimate the 3-D resistivity structure in this area with the aid of the DASOCC Network-MT 3-D inversion code (Siripunvaraporn, Uyeshima & Egbert, 2004).

Conductive portions are commonly detected in the mid-crust of the target region. Their roots are just on the upper surface of the subducting Philippine Sea slab. This may suggest dehydration there. Among the spatial distribution of resistivity, that of seismic P-wave attenuation (Kita and Matsubara, 2016), and that of SSE slips (e.g. Ozawa et al., 2013, Yoshioka et al., 2015, Hirose et al., 2018), some mutually related features are detected. Low Qp (high attenuation) areas tend to correspond to highly conductive areas. The low Qp and highly conductive area are detected just above the subducting slab and outside of the SSE area. Inside the SSE area, while Qp takes generally high values, a patchy conductive area is detected in overall resistive background structure.

This study is supported by JSPS KAKENHI Grand Number JP16H06475 in Scientific Research on Innovative Areas "Science of Slow Earthquakes". It is also partly supported by the Ministry of Education, Culture, Sports, Science and Technology (MEXT) of Japan, under its Earthquake and Volcano Hazards Observation and Research Program. We acknowledge staffs of the Nippon Telegraph and Telephone WEST Corporation for their cordial support in the survey. We also thank H. Abe, A. Takeuchi and Y. Suwa for their help in preparing and installing instruments.

Keywords: slow slip event beneath the Bungo Channel, 3-D resistivity structure, Network-MT observation

©2019. Japan Geoscience Union. All Right Reserved.

Variations of scaling relationships for shallow tremor observed along the Nankai trough

*Masaru Nakano[1], Suguru Yabe[1]

1. Japan Agency for Marine-Earth Science and Technology

Scaling relationships of seismic phenomena is one of keys to understand the source processes. Size distributions of slow earthquakes as low-frequency earthquakes (LFEs), non-volcanic tremor (NVT), very-low-frequency earthquakes (VLFE), and slow-slip events (SSEs) have been studied in many locations. Some studies showed that the size distribution follow an exponential law (e.g. Watanabe et al., 2007; Hiramatsu et al., 2008; Chestler and Creager, 2017), while others showed that power law distributions better explain the observations (e.g. Kao et al., 2010; Bostock et al., 2015; Nakamura and Sunagawa, 2015).

Most of previous studies are for slow earthquakes that occur in regions deeper than the source region of megathrust earthquakes, and only a limited number of studies have been carried out for shallow slow earthquakes beneath accretionary prism as observed along the Nankai trough. Although observed characteristics of shallow and deep ones are very similar, physical conditions as temperature and pressure much differs in these region.

In our previous studies (Nakano et al., 2018SSJ, AGU), we obtained the result that shallow tremor follows a power law distribution with b values of about 1. In this study, we further analyzed tremor activities beneath the Muroto fore-arc basin. using data from DONET2. We estimated the seismic energy of tremor signals using the same method as our previous studies, during intensive activities starting in September 2015, April 2016, February 2017, and February 2018. The source region of each activity is different from each other, spanning between off Shiono-Misaki and off Cape Muroto.

The size distribution of each activity mostly follow power-law distributions, but the b value varies from 0.7 and 1.7. We note that the activity in 2016 is also well fitted by an exponential law, probably due to narrow range of observed event size distribution. Similar result has been obtained in the 2018 activity in Kumano. The size distribution deviate from a power law for largest events as observed in Kumano activities. This deviation at larger events would be due to limited system size, expected from the theoretical stochastic model of tremor by Ide and Yabe (2018). The upper limit of event size, and accordingly the system size, varies from activity to activity.

We also investigated the relation between the seismic energy and duration of tremor events. The relation also follows a power law, with slopes of 2.0 to 2.6 in Kumano, and 1.5 to 3.3 in Muroto. These values are again consistent with the expectation value of 2 from the model of Ide and Yabe (2018).

These investigations represent that the scaling relationships of shallow tremor are mostly consistent with the 2D PCA model by Ide and Yabe (2018). Further studies would be necessary to reproduce the observed variations of the scaling parameters.

Acknowledgments: We used DONET data and JMA and USGS earthquake catalogs in the analysis. This research was supported by JSPS KAKENHI Grant Number 16H06477 in Scientific Research on Innovative Areas “Science of Slow Earthquakes”

Keywords: DONET, Nankai trough, earthquake size distributions

©2019. Japan Geoscience Union. All Right Reserved.

Low-frequency earthquakes triggered by teleseismic surface waves by Ryukyu subduction zone.

Ayumi Kinjo[1], *Mamoru Nakamura[1]

1. Faculty of Science, University of the Ryukyus

We investigated low-frequency earthquakes (LFEs) in the Ryukyu Trench region that were triggered by surface waves from teleseismic earthquakes. Although these LFEs in the southwestern Ryukyu arc have previously been explored by Chao et al. (2016), their hypocenter distribution is not known in detail.

We selected 50 earthquakes from January 2004 to December 2016, which had magnitudes greater than 7.5 and epicentral distances between 9–150˚. We used the waveforms of 6 broadband seismometers in the Ryukyu arc from F-net (NIED) to analyze the surface waves. We also used the waveforms of 20 short-period seismometers in the Ryukyu arc from the Japan Meteorological Agency to detect trace LFEs in Ryukyu Island and determine their hypocenters.

The LFEs in the Yaeyama and Okinawa regions were observed. In the former region, during the passage of the surface waves, spindle-shaped LFE waveforms were first observed at Hateruma (south of Yaeyama Islands), and later at other stations in the Yaeyama region. Similarly, for the latter region, during the passage of the surface waves, spindle-shaped LFE waveforms were first observed at ZMM or Tamagusuku (south of Okinawa Island), and later at other stations in the Okinawa region. These observations suggest that the sources of the triggered LFEs were near or south of Hateruma and Tamagusuku.

We subsequently determined the hypocenters of the triggered LFEs. We computed the LFE travel-time difference between two stations using cross-correlations of the waveforms (Obara, 2002). The travel-time difference of waveforms of the LFEs corresponded to travel-time difference of the S-phase because S-waves were dominant in the LFEs, and P-waves were weak. The hypocenters were determined using the grid search method (Chao et al., 2013). In the Yaeyama region, the LFE hypocenters were mainly distributed near Hateruma Island. In the Okinawa region, they were distributed south of Okinawa Island. These positions are similar to the positions of the LFE hypocenters that accompany very low frequency earthquakes (LFE-VLFEs). This suggests that faulting in a cluster of LFE-VLFEs would be active with dynamic stress change.

In the Okinawa and Yaeyama regions, LFEs are triggered when the peak ground velocity of the surface wave is greater than 0.1 cm/s. This threshold value is similar to that for LFEs in Taiwan (Chao et al., 2013), suggesting that the weak friction coefficient at the plate interface of the Ryukyu Trench is similar to that in Taiwan.

Keywords: low frequency earthquake, surface wave, Ryukyu Trench

©2019. Japan Geoscience Union. All Right Reserved.

Detection of small surface displacement accompanying deep low-frequency tremor in Shikoku region, southwest Japan

*Yutaro Okada[1], Takao Tabei[2]

1. Faculty of Science, Kochi University, 2. Faculty of Science and Technology, Kochi University

In many subduction zones in the world, several types of slow earthquakes occur with different depths on the plate interface and some of them are accompanied by surface displacement. In this study, we focus on small surface displacements coincident with non-volcanic deep low-frequency tremor in Shikoku region in the Nankai subduction zone, southwest Japan.

We use daily coordinates time series from 107 GEONET stations located in Shikoku and tremor catalog compiled by NIED (Maeda and Obara, 2009; Obara et al., 2010) in the period from Jan. 1 2004 to Dec. 31 2008. Since GNSS coordinates changes due to the Bungo Channel long-term slow slip events are well reproduced by S-shaped logistic function, we use the same function to extract small displacement coincident with tremor activity. At first, we convert horizonal components into N50˚W direction after removing annual and semiannual variations and common-mode errors. Next, we fit the logistic function to a data segment with variable time window of 5, 7, and 9 days and estimate an amplitude of the function. The fitting is checked by a correlation coefficient between the observation and calculation. We apply this fitting for entire data period at all stations sliding data segment. Finally, we extract displacement when the amplitude of the fitted logistic function exceeds a certain criterion (1.8 mm in this study) and the correlation coefficient is large enough. If the extracted displacement is coincident with tremor activity within 30 m from the GNSS station, we adopt it as the tremor-related displacement. As a result, 225 events are adopted.

Spatial pattern of the tremor-related displacement seems to be related with the location and mechanism of the tremor event though closer inspection is needed. However, we extract much more small displacements by fitting a logistic function, of which the source is unknown. The logistic function is effective to reproduce transient displacement of the surface but we need to reconsider noise reduction of GNSS time series, time constant of logistic function, time window of the fitting, and so on.

Keywords: GNSS, southwest Japan, Deep low frequency tremor

©2019. Japan Geoscience Union. All Right Reserved.

Long-term temporal change in crustal resistivity beneath western Shikoku

*Futoshi Yamashita[1], Yoshimori Honkura[1]

1. National Research Institute for Earth Science and Disaster Resilience

In southwest Japan, various slow earthquakes such as deep low-frequency tremor and short/long-term slow slip events occur at the subducting plate interface (e.g. Obara and Kato, 2016, Scinence). In western Shikoku, Magneto-telluric (MT) survey was carried out along the dip direction of subducting Philippine Sea plate. The survey revealed an existence of low-resistivity structure in the lower crust in this region (Yamashita and Obara, 2009, AGU). In order to investigate a relationship between this characteristic structure and the activity of slow earthquakes, NIED has been carrying out continuous MT observations in western Shikoku since 2008. Here we show the observational records over 10 years and then discuss a relationship between observed temporal change in crustal resistivity and activity of the long-term slow slip event (L-SSE). Two observational sites KBN and IKT are available as of 2019. Qualities of data recorded at these sites are relatively fine. However, in order to improve the quality for discussing subtle change in MT parameters, we apply a data processing method same as Honkura *et al.* (2013, Nature comm.); we use only data whose coherency between electric and magnetic field is higher than a threshold. The lowest frequency of processed data is 0.00028 Hz. The processed MT parameters, apparent resistivity and phase, do not show any long-term temporal changes at KBN site even after temporal stops of observation over some months. On the other hand, apparent resistivity at IKT site, which is around 10 km southwest away from KBN site, shows temporal reduction at a frequency lower than 0.0022 Hz between 2010 and the middle of 2012. It is known that L-SSE occurred beneath the Bungo Channel in 2010 (e.g. Yoshioka *et al.*, 2015, GJI), which could induce resistivity change in the lower crust and then it might be detected by our MT observation.

Keywords: Crustal resistivity, Long-term slow slip event, Magneto-telluric method

©2019. Japan Geoscience Union. All Right Reserved.

Slow decay of postseismic deformation compared with aftershocks following the 2011 Tohoku-oki Earthquake

*Yuta Mitsui[1], Shunsuke Morikami[2]

1. Department of Geosciences, Shizuoka University, 2. Formerly at Graduate School of Science and Technology, Shizuoka University

In the literature, decays of postseismic deformation rates of large earthquakes were almost comparable to aftershock decays for subduction earthquakes (e.g. Hsu et al. (2006), Lange et al. (2014)). They are characterized by the modified Omori law with p~1, which means "afterslip-triggerred aftershocks". In this study, we focus on the 2011 Tohoku-oki megathrust earthquake using GNSS and seismicity data. On the basis of high-rate analysis of RINEX data and the F3 solution provided by the Geographical Survey Institute (GSI), we clarify the characteristics of postseismic deformation and aftershocks up to five orders of magnitude of time scale. We find that the p value for the postseismic deformation (p_m) is ~0.7, by contrast, that for the aftershocks (p_n) is ~1. Because a rate-and-state-friction model (Helmstetter and Shaw (2009)) predicted $p_m>=p_n$, another or an additional physical mechanism is necessary to explain the data of $p_m<p_n$. One important mechanism is viscoelastic relaxation of asthenosphere, thus we try fitting the postseismic deformation data by combination of afterslip and viscoelastic relaxation (a model of Suito (2017)). The fitting is not poor but fails to reproduce the Omori-like decay. More complex combination models may improve the fitting, but would not make simple Omori-like power-law decays. We need more sophisticated physical model to represent the decay characteristics of postseismic deformation.

Keywords: aftershocks, postseismic deformation, afterslip, viscoelastic relaxation, the 2011 Tohoku Earthquake

©2019. Japan Geoscience Union. All Right Reserved.

Serpentinite dehydration in subduction shear zones formed at source depths of slow earthquakes

*Yasushi Mori[1], Miki Shigeno[1], Kohtaro Ujiie[2], Kazuya Noro[2], Tadao Nishiyama[3]

1. Kitakyushu Museum of Natural History and Human History, 2. University of Tsukuba, 3. Kumamoto University

Long-term slow slip events (L-SSEs) and episodic tremor and slip (ETS) occur along the subduction plate boundary at depths of 30–45 km (Obara, 2002; Shelly et al., 2006). These deep slow earthquakes are probably induced by high pore-fluid pressure. Based on geological study, we propose that the high pore-fluid pressure can be produced by metasomatic dehydration of serpentinite in subduction shear zones at source depths of deep slow earthquakes.

The Nishisonogi metamorphic rocks in Kyushu, Japan, are part of a Late Cretaceous subduction complex metamorphosed at $P \approx 1$ GPa and $T \approx 470$ ˚C. The P-T conditions are close to those of source depths of deep slow earthquakes. Serpentinite mélanges intercalated with the metamorphic rocks contain blocks of metabasite, metapelite and albitite. The mélange matrix consists of chlorite-actinolite schist (CAS), talc schist and schistose serpentinite. Intense shear deformation is concentrated in the CAS, and the serpentinite mélanges have the characteristics of anastomosing shear zones.

Bulk chemical composition of the rocks suggests that the CAS is the metasomatized mixture of serpentinite and metabasite. In addition, chemical mass balance indicates considerable dehydration during the CAS formation, along with a slight increase of solid volume. These findings suggest that the CAS formation involves the build-up of pore-fluid pressure. The high pore-fluid pressure results in the concentration of shear deformation into the weakened CAS.

Dehydration of serpentinite probably plays a key role in deep slow earthquakes (Poulet et al., 2014; Okazaki and Katayama, 2015). Thermal dehydration of serpentinite occurs at ~600 ˚C along the subduction plate boundary (Auzende et al., 2006), which is much higher temperature than that of source depths of deep slow earthquakes. In contrast, metasomatic dehydration of serpentinite described here could occur at source depths of deep slow earthquakes.

Auzende, A-L., et al., 2006, EJM, 18, 21–33. Obara, K., 2002, Science, 296, 1679–1681. Okazaki, K., Katayama, I, 2015, GRL, 42, 1099–1104. Poulet, T., et al., 2014, JGR, 119, 4606–4625. Shelly, D.R., et al., 2006, Nature, 442, 188–191.

Keywords: serpentinite mélange, shear zone, dehydration, pore fluid pressure, Nishisonogi metamorphic rocks, deep slow earthquakes

©2019. Japan Geoscience Union. All Right Reserved.

Earthquake swarms following very low-frequency earthquakes in the central Ryukyu Trench

*Mamoru Nakamura[1]

1. Faculty of Science, University of the Ryukyus

Earthquake swarms occur frequently from Amami Island to Okinawa Island, near the axis of the central Ryukyu Trench. These earthquake swarms recur every few years and typically followed swarms of very-low frequency earthquakes (VLFE) that occur in a similar area. I have investigated the relationship between the VLFEs and the subsequent earthquake swarms in the central Ryukyu Trench, using the earthquake catalog provided by the Japan Meteorological Agency (JMA). For the VLFEs, I used the catalog by Nakamura and Sunagawa (2015) and the extended catalog to December 2018.

Results show that the VLFE swarms occurred approximately one month before the subsequent earthquake swarms began near the trench axis in this region. Previous noteworthy earthquake swarms occurred on August 2005 (with a maximum magnitude of 4.7), April 2009 (with a maximum magnitude of 5.1), May 2016 (with a maximum magnitude of 5.6), and September 2018 (with a maximum magnitude of 6.2).

Prior to the earthquake swarm that occurred in August 2005, a VLFE swarm started near Okinawa Island three months before and its activity moved intermittently from Okinawa Island to Amami Island. In the case of the earthquake swarm that occurred in April 2009, a VLFE swarm started near Amami Island and the subsequent swarm occurred two weeks after the start of the VLFE swarm. The location of the VLFE swarm moved intermittently closer to Okinawa Island. In the case of the earthquake swarm that occurred on May 2016, the VLFE swarm started near Amami Island and its active cluster moved intermittently towards Okinawa Island. The subsequent earthquake swarm started near the trench axis, approximately twenty days after the occurrence of the VLFE swarm. In the case of the earthquake swarm that occurred in September 2018, the VLFE swarm started near Okinoerabu Island (the midpoint between Amami Island and Okinawa Island) and the activity moved intermittently to Okinawa Island. The earthquake swarm occurred approximately twenty-five days after the start of the VLFE swarm. The location of the cluster of the 2018 earthquake swarm was slightly landward from the trench axis.

The faulting associated with these earthquake swarms was of normal type, corresponding to intra-slab earthquakes in the subducting Philippine Sea plate. I calculated the Coulomb Failure Stress (delta-CFS) assuming that a small slow slip event (SSE) occurred on the plate interface. Our results show that the positive delta-CFS that accelerated the normal faulting could not have occurred in the subducted slab near the trench axis until the slip of the SSE had reached close to the trench axis. This suggests that the SSE propagated from Amami Island to Okinawa Island accompanying the activation of the VLFE swarm, the slip of the SSE then propagated close to the trench axis, and the normal-faulting earthquake swarm in the slab was induced by the positive delta-CFS caused by the SSE.

Keywords: Very low frequency earthquake, Ryukyu Trench, Earthquake swarm

©2019. Japan Geoscience Union. All Right Reserved.

Seismic imaging in the central Nankai trough, off Shionomisaki to Kii channel

*Yasuyuki Nakamura[1], Shuichi Kodaira[1], Tetsuo No[1], Yuka Kaiho[1], Gou Fujie[1], Seiichi Miura[1], Kazuya Shiraishi[1]

1. Japan Agency for Marine Earth Science and Technology

Shallow very low frequency events (sVLFE) have been reported in the Nankai Trough subduction zone recently. In the central part of the Nankai trough, sVLFE were observed off Kii channel and Shinomisaki, but not reported in the area between them, off western Kii peninsula. We conducted a seismic survey with R/V *Kaimei* in November and December 2018 in Nankai subduction zone off Kii channel to Shonomisaki to investigate the structural features and its possible relationship to the sVLFE. R/V *Kaimei* fired 10600 inch^3 air gun array at every 50 m and a streamer cable (4.3 km at shortest, 5.7 km at longest) recorded the seismic signals. We acquired 23 seismic profiles with the length of ~ 75 km in dip direction at 4 km line separation and four profiles of ~ 90 km in strike direction at the shallowest part of the subduction zone. In addition, seven dip profiles with the length of 35 km were acquired off Kii channel to cover the lowermost part of the landward slope densely. The streamer cable was towed at a depth of 25 m to relatively enhance the lower frequency signals for better imaging of the deeper structure. Preliminary processed seismic profiles exhibited the structural variation in the survey area. Deformation of the hanging wall sediments and decollement were well imaged especially ~ 20 –30 km from the trough axis. Top of subducting Philippine Sea plate can be observed through ~ 40 –50 km from the trough axis in some of the obtained profiles. A pair of apparently low angle deep strong reflections were imaged at ~ 7 –8 s two-way time around 40 - 50 km from the trough axis off the western Kii peninsula, which was located slightly east and landward of the area with sVLFE. The shallowest part of the subduction zone in the area where the recent sVLFE activity was not reported, a slope basin with younger sediments deposited over the body of the accretionary prism is imaged, and the deformation was not observed in the slope basin. This suggests the thrust faults within the accretionary prism have not been active recently in this area. We will further process acquired data to obtain clearer seismic images and discuss the structural features and its connection to the observed seismological events in the Nankai Trough.

Keywords: Nankai Trough, seismic imaging

©2019. Japan Geoscience Union. All Right Reserved.

Attempt to Detect Intra-plate SSEs Based on F3 Solution of GEONET

*Yusaku Tanaka[1]

1. Earthquake Research Institute

Slow earthquakes have been detected all over the world and providing new insights into earthquakes. However, most of slow slip events (SSEs) were detected only on plate boundaries and intra-plate SSE was detected only once in Hokkaido. Thus, I attempt to detect intra-plate SSEs all over Japan using F3 solution of GEONET by GSI. I analyze the F3 data with six steps, i.e., (1) removing outliers by setting a term of mean + two times standard deviation for 1/4+1/4 year before-and-after each datum except for the datum itself and considering it is an outlier when it is out of the term, (2) removing disconnections estimated from the offsets and linear trends of 60+60 days before-and-after each datum with the least square method, (3) searching statistically significant temporal changes of the trends by using AIC, (4) cheking visually the time series in which the temporal changes are detected, (5) estimating the displacements from the trend chagnes, and (6) verifying the deformations by numerical calculation by setting rectangular faults.

As of 18th Feb 2019, my study has proceeded to the step (4). In the JpGU meeting, I will report the results of this analysis.

Keywords: crustal deformation, slow slip event, geonet

©2019. Japan Geoscience Union. All Right Reserved.

A new hydrothermal, low to high speed rotary-shearing apparatus: Reproduction of slow/megathrust earthquakes in laboratory

*Takehiro Hirose[1], Wataru Tanikawa[1], Yohei Hamada[1], Keishi Okazaki[1]

1. Kochi Institute for Core Sample Research, Japan Agency for Marine-Earth Science and Technology

Earthquakes involve a wide range of slip rates, from slow/aseismic to fast/seismic slip along faults. Thus, frictional properties of faults over wide slip rates (nm/s to m/s), in particular under hydrothermal conditions similar to those expected in seismogenic zones are essential for a unified understanding of all earthquake events. A new hydrothermal, low to high speed rotary-shearing apparatus has been installed at Kochi/JAMSTEC, in order to study the fault constitutive properties at slow to fast slip rates and the physicochemical mechanisms underlying mechanical responses. The apparatus is currently capable of applying slip rates from 100 nm/s to 2 m/s, normal stress up to 55 MPa, fluid pressure up to 120 MPa and temperature up to 450oC with infinite displacement. We have been improving the apparatus to work as we intended. In pilot tests, we used metamorphic rocks (pelitic and green schists) as starting materials that are potentially distributed at and below seismogenic zones along hot and young subduction zones. We will present our preliminary results with the basic design of the apparatus.

Keywords: friction, hydrothermal, slow to fast slip

©2019. Japan Geoscience Union. All Right Reserved.

Very low-frequency earthquakes in western Shikoku remotely triggered by the 2016 Mw5.9 off-Kii Peninsula earthquake

*Masatoshi Miyazawa[1]

1. Disaster Prevention Research Institute, Kyoto University

Slow tectonic events are known to be sensitive to external stress perturbations due to passing seismic waves and earth tides. High-amplitude surface waves from large earthquakes have transiently triggered low-frequency earthquakes (LFEs) and slow slip events (SSEs) in subduction zones. However, dynamic triggering of very low-frequency (VLF) earthquakes during the arrival of seismic waves from a large, distant earthquake has not been observed. Because both the VLF earthquake and the surface wave have similar characteristic periods, remote triggering is not easily detected by using existing methods. We developed a particle filter/smoother for time series analysis combined with Markov chain Monte-Carlo methods, to detect seismic signals and estimate the maximum likelihood source parameters of VLF events that might have been remotely triggered. We apply this method to seismic data from the Mw5.9 earthquake, which occurred on 1 April 2016 (UTC), off Kii Peninsula. We found that six VLF events with magnitudes about 4, likely occurred in the seismogenic regions of ambient LFEs, and were likely triggered by the arrivals of high-amplitude surface waves. The triggering stress changes are from 0.4 to 1.5 kPa, which are similar to the values for LFEs triggering reported previously. Since there were no triggered LFEs in western Shikoku following the 2016 earthquake, these VLF earthquakes are more sensitive to stress changes caused by surface waves from large earthquakes.

Keywords: Very low-frequency earthquake, Remote triggering

©2019. Japan Geoscience Union. All Right Reserved.

Underground structure around source region of slow earthquakes in western Shikoku obtained by receiver function analysis

Akira Hikita[1], Aitaro Kato[1], *Kazushige Obara[1], Akiko Takeo[1], Takeshi Akuhara[1]

1. Earthquake Research Institute, The University of Tokyo

Various types of slow earthquakes have been observed at subduction zones surrounding the Pacific Ocean. It has been suggested that elevated pore fluid pressure plays an essential role in the generation of slow earthquakes because low velocity or high Vp/Vs zones have been also reported along the plate boundaries where they occur. In Tokai region of the Nankai subduction zone, Kato et al. (2010) revealed that long-term slow slip event (SSE) occurs at the boundary between the continental lower crust and the subducting Philippine Sea plate and episodic tremor and slip (ETS) occurs between the mantle wedge and the subducting plate. Kato et al (2010) also revealed that oceanic crust indicates higher Vp/Vs in the long-term SSE region than in the ETS region. In contrast, Toya et al. (2017) reported that the oceanic crust indicates higher Vp/Vs in the ETS region than in the long-term SSE region in western Shikoku of the same subduction zone. In this study, we revealed configurations of continental Moho discontinuity and subducting oceanic crust and investigated relationship between slow earthquakes and the surrounding seismic velocity structure by receiver function analysis using a dense seismic array in western Shikoku.

As a result, continuous continental Moho and oceanic crust are clearly imaged along both north-south and east-west oriented seismic lines. The plate boundary in the south part, where the distinct continental Moho is not imaged, has steeper slope than the north part along the north-south line. ETS occurs between the mantle wedge and the subducting plate, and long-term SSE occurs along a contact between the continental crust and the oceanic crust.
We show that the oceanic crust indicates much higher Vp/Vs than the hanging wall by using also the reverberation phases. This high Vp/Vs means the elevated fluid pore pressure within oceanic crust due to dehydration. Vp/Vs in the oceanic crust is higher in the deep part of the long-term SSE region than in the ETS region like as the case of Tokai. It is assumed that fluid would accumulate within the oceanic crust owing to low permeability of the continental crust in the long-term SSE region. In contrast, serpentinization of the mantle wedge just above the ETS region could reduce fluid pressure in the oceanic crust. Furthermore, Vp/Vs in the oceanic crust becomes lower in the deeper part beyond the ETS depths, suggesting that eclogization is completed at the depths.

Keywords: Receiver function, episodic tremor and slip, long-term slow slip event, low seismic velocity layer

©2019. Japan Geoscience Union. All Right Reserved.

Hypocenter determination of deep low frequency tremors beneath the Kii Peninsula by backprojection of seismic array data

*Kodai Sagae[1], Hisashi Nakahara[1], Takeshi Nishimura[1], Kazutoshi Imanishi[2]

1. Graduate School of Science,Tohoku University, 2. National Institute of Advanced Industrial Science and Technology (AIST)

A seismic array analysis enables us to detect weak signals if they are coherent. In Cascadia, a high accuracy hypocenter determination of tremors has been carried out by using dense seismic arrays (e.g.,Ghosh et al.,2012). In Southwest Japan, previous studies (e.g.,Ueno et al.,2010) applied the **MU**ltiple **SI**gnal **C**lassification (MUSIC) method (Schmidt,1986) to data of surface seismic arrays at Western Shikoku and carried out the hypocenter determination. However, a quantitative threshold for event detection was not considered. Sagae et al.,(2018 SSJ) introduced an event detection threshold based on the coherence of waveforms among stations, and improved tremor detection by using a surface seismic array installed by AIST at the Kii Peninsula. We applied the MUSIC method to this data in times when tremor events were detected and estimated slownesses and arrival azimuths of tremor signals. Their temporal variations suggested tremor migration. However, we did not carry out hypocenter determination. In this study, we determine hypocenters of tremors by backprojection using the estimated slownesses and arrival azimuths.
The surface seismic array installed by AIST at the Kii Peninsula was composed of 39 three component velocity sensors with a natural frequency of 2.0 Hz and a sampling frequency of 200 Hz. This array had an aperture of about 1.5 km and the sensors were arranged in a cross shape with interval spacings of 50~100 m. We analyze data for 1 year (between July 7,2013 and July 7,2014), because the number of sensors is stable in this period.
We focus on a frequency of 3Hz, which is within the tremor's dominant frequency band of 2-10 Hz. Data processing is described as follows. (1) We calculate averaged coherence of waveforms for all station's pairs. (2) We detect tremor events by setting a detection threshold based on the averaged coherence. (3) We estimate slownesses and arrival azimuths by applying the MUSIC method to the data when tremors are detected. (4) We project them back to the plate boundary (Hirose et al.,2008) and determine source locations by using S wave velocity model JMA2001 (Ueno et al.,2002).
We detected 5 periods of high tremor activities during the 1 year period. We compared the hypocenter distributions determined by our method and those of AIST tremor catalogue which were determined from an envelope cross correlation method. Temporal variation of tremors in this study were almost consistent with the AIST catalogue. We were also able to detect about 2.5 times as many events as the AIST catalogue. It is easier to identify temporal variation of tremors in more detail because our study improved temporal resolution up to 10 sec.
We projected temporal variations of tremor distributions into along-strike and along-dip directions. The results show tremors tend to migrate along the strike in time scales of several days with migration velocities of 6.0~9.3 km/day. Along-dip migrations of tremors with a short timescale of several hours are also detected. When we focused on the initial part of tremor activities, tremors tend to start in deeper parts and gradually migrate to shallow parts. These migration velocities were estimated to be about 1.0 km/hr (24 km/day) in the up-dip direction.
In this study, we were able to improve tremor detection by setting the event detection threshold based on the coherence of seismograms for stations pairs in a surface seismic array. Thanks to this, we were able to locate 2.5 times more tremors than the conventional method. We made it easier to keep track of tremor migrations by improving the temporal resolution of hypocenter determination to 10 sec.
We used the plate boundary model (Hirose et al.,2008). We downloaded the AIST catalogue from Slow

©2019. Japan Geoscience Union. All Right Reserved.

Earthquake Database (Kano et al.,2018).

Keywords: Deep low frequency tremor, Seismic array analysis, Backprojection, MUSIC method, Kii Peninsula, Hypocenter determination

©2019. Japan Geoscience Union. All Right Reserved.

Triggered tremors and stress perturbations due to surface waves

*Ryohei Ikeda[1], Naoki Suda[1]

1. Hiroshima University

Surface waves radiated from distant large earthquakes sometimes trigger a series of deep non-volcanic tremors with intervals of 20-30 seconds, which are the same as dominant periods of surface waves [e.g. Miyazawa & Brodsky 2008]. Understanding the triggering mechanism is important because it provides us clues to the slip process occurring along the transition zone of subducting plate interface. Dynamic stress perturbations due to surface waves that triggered tremors were estimated on the order of 1 to 10 kPa [e.g. Chao & Obara 2016]. To study the relationship between triggered tremors and stress perturbations due to surface waves, we computed theoretical dynamic stresses due to surface waves from large earthquakes by using observed and theoretical surface waves.

We focused on the triggered tremors in the western Shikoku region of the Nankai subduction zone. Most of them occurred in two clusters where tectonic tremors actively occur. We computed theoretical dynamic stress perturbations due to surface waves from 106 earthquakes between 2004 and 2016 with moment magnitudes of 7.0 or grater. The receiver points at which the stress components were computed are at the plate boundary below the N.TSAF and N.KWBH stations, which are the nearest stations of the triggered tremors in F-net and Hi-net, respectively. PREM [Dziewonski & Anderson 1981] and Global CMT catalog [Dziewonski et al. 1981; Ekstrom et al. 2012] were used for the Earth model and the seismic sources for computing theoretical surface waves. Source time functions were approximated with triangular functions whose half durations are equal to the centroid time lags.

The stress change at the plate boundary by the surface wave was estimated based on the method of Spudich et al. (1995). This method consists of two stages: (1) Estimate the stress at the surface from the observed ground velocity and (2) Estimate the stress at the plate boundary from the stress at the surface estimated in (1). In these estimations, we used theoretical proportional relations between the ground velocity and the surface stress and those between the surface and the deep stresses in the frequency domain, which were obtained from the theoretical surface waves. We used the N.TSAF and N.KWBH records as the observed ground velocity. The records from the latter were corrected using the method of Maeda et al. (2011).

The stress components in the source coordinates were transformed to the stress normal to the plate interface and the stress along the possible slip direction of tremor source. The normal and slip directions were obtained from the model plate interface [Baba et al. 2002; Nakajima & Hasegawa 2007; Hirose et al. 2008] and plate convergence vectors [Miyazaki & Heki 2001]. We computed waveforms of the Coulomb failure function (ΔCFF) using a frictional coefficient of 0.2 at periods between 20 and 50 seconds.

©2019. Japan Geoscience Union. All Right Reserved.

Results from the N.TSAF records show that the maximum ΔCFF for the events that triggered tremors are greater than 0.5 kPa. The magnitudes of triggering earthquakes are greater than 7.5. ΔCFFs were generally overestimated when we used the corrected N.KWBH records because the correction did not well work, in particular, for the earthquakes with magnitudes less than 7.5. The important point is that not all of the events that provided the stress perturbations greater than 0.5 kPa triggered tremors. This shows that the stress perturbation due to surface waves cannot be the unique triggering condition: other conditions, for example, stress perturbations due to possible background slow slip events and/or high pore fluid pressure are required.

©2019. Japan Geoscience Union. All Right Reserved.

Numerical modeling of long- and shallow slow slip events including shallow region in Hyuganada and western Nankai, Japan

*Takanori Matsuzawa[1], Bunichiro Shibazaki[2]

1. National Research Institute for Earth Science and Disaster Resilience, 2. Building Research Institute

Recent studies reported deep long-term slow slip events (SSEs) in the Hyuganada and western Nankai region (e.g., Kobayashi, 2014; Takagi et al., 2016; Ozawa. 2017). Shallow SSEs are also recently reported with low-frequency tremor and very low-frequency earthquakes (e.g., Araki et al., 2017; Nakano et al., 2018). In our previous study, we have numerically reproduced recurring deep long- and short-term SSEs in the Shikoku region (Matsuzawa et al., 2013), considering the actual distribution of slow earthquakes and configuration of the subducting Philippine Sea plate. We aim to reproduce deep long- and short-term SSEs and shallow SSEs in a single numerical model applying a similar approach in Matsuzawa et al. (2013).

We adopt a rate- and state-dependent friction law (RS-law) with cutoff velocities. We assume that (a-b) value in the RS-law is negative within the deep short-term SSE region, and positive outside that region. The deep short-term SSE region is modeled based on the actual distribution of deep low frequency tremor. Deep long-term SSE region is assumed based on the geodetic observation (Hirose et al., 2011). To focus on the Hyuganada and western Nankai region, we assume stable sliding region with positive (a-b) in the south of the Kyushu-Palau ridge. We also assume low cutoff velocity at the depth shallower than 9 km to reproduce shallow SSEs. Low effective normal stress is assumed at the depth of SSEs. Temporal evolution of slip velocity is numerically simulated, introducing elastic response and realistic configuration of the plate interface.

In terms of deep long-term SSEs in Hyuganada, a simple extension of the long-term SSE region in the Bungo Channel cannot reproduce the segments of observed SSEs. Narrowed long-term SSE region in the dip direction between Bungo and southern Hyuganada can reproduce three observed segments of SSEs, i.e., Bungo, northern Hyuganada, and southern Hyuganada. In addition, recurring shallow SSEs along trench in Hyuganada and off Ashizuri are reproduced in our result. Megathrust earthquakes are divided into two regions; off Shikoku and Hyuganada in our result. The segments of these large earthquakes may be attributed to the long-term SSE region in the Bungo Channel. Our model comprehensively reproduces various SSEs and megathrust earthquakes, including newly found long-term SSEs.

Keywords: Slow Earthquake, Slow Slip Event, Hyuganada

©2019. Japan Geoscience Union. All Right Reserved.

Further evidence for the influence of a subducting-ridge on the spatial strain accumulation and release pattern in the shallow eastern Nankai Trough, based on VLFE distribution

*Akiko Toh[1], Chen Wan-Jou [2], Doug Dreger[3], Wu-Cheng Chi[2], Satoshi Ide[1]

1. University of Tokyo, 2. Institute of Earth Sciences, Academia Sinica, 3. UC Berkeley

We investigated the distribution and focal mechanisms of very low frequency earthquakes (VLFEs) located in the shallow part of the eastern Nankai trough. While they are mainly explained as low angle thrust faulting along the plate boundary (Sugioka et al., 2012; Nakano et al, 2016), along the strike variation in their distribution has also been observed, likely caused by a subducting-ridge (Toh et al., 2018). Such variations could be closely related to the strain release pattern, or the tsunamigenic potential, of this region, thus warrant a further comprehensive study.

We used 3 component records of broadband ocean bottom seismometers equipped in Dense Oceanfloor Network system for Earthquakes and Tsunamis 1 (DONET1). Records of VLFE activities that occurred immediately beneath the network in 2015, 2016 and 2017 for 1-2 weeks each year, are used. Through visual inspections, we detected 335 VLFEs whose signals are observed at least 6 stations on vertical component filtered between 16-32s.

Instead of estimating the source parameters for one after another for all the events, we searched for densely located event groups inferred by similarities of the maximum amplitude variations measured per event, and, so far, worked only on the grouped events. The purpose of this event selection process is to get an overview of the distribution using the simple quantity (i.e. max. amplitude variation) that can be evaluated for every VLFE, and to avoid a bias that may be caused by eliminating events that are merely difficult to process (i.e. do not fit synthetic waveforms) mostly due to complicated long source time functions that characterize VLFEs. The grouping is conducted by a hieratical density-based clustering method HDBSCAN (Campello et al., 2003), and 197 events were grouped into 26 groups that consists of 2 to 35 events.

We determined the centroid origin time, location and 5-component of moment tensor of VLFEs that maximize the normalized variance reduction (VR) between the observed and synthetic velocity waveforms. The waveforms are bandpass filtered either between 16-32s or 20-50s, depending on signal duration and S/N per event. The time and location are grid-searched at intervals of 0.01 degree in horizontal, 1 km in depth between 5 and 10km bsl., and 1 s in time. At each grid, the moment tensor is estimated using the code TDMT_INV (Dreger, 2003) that conducts full-waveform linearized inversion in time domain. Green’s functions are calculated using the code by Herrmann (2013) based on wavenumber integration. We used a 1D structural model based on a 2D model obtained by an active source survey (Nakanishi et al., 2008). Although the 1D structure is assumed, the large variations in station elevation (1.9-4.3 km bsl) are considered in Green’s function calculations.

We obtained 50 events with good VR (>65%). Among the 26 groups, 6 groups ended up with no events of high VR, mostly due to being located outside of the network. Almost all the VLFEs are reasonably explained by low angle thrust faulting. From the obtained distribution, the strong influence of the subduction-ridge located on the northwestern side of DONET1 is inferred. On the southwestern side

©2019. Japan Geoscience Union. All Right Reserved.

where there is no ridge-subduction, VLFEs are distributed beneath outer-ridge toward the trench axis. The estimated depths for the ones located beneath the outer-ridge are deep (7–10km with median at 8km), which are consistent with the depth of the plate boundary of this area. In contrast, on the northeastern side, VLFEs are mostly distributed landward of outer-ridge and their estimated depth are shallow (5–8km with the median at 7km) as previously suggested (To et al., 2015). The shallow depths can be explained by the uplifted plate boundary in this area due to the subducting-ridge. Furthermore, they are located to landward of the peak of the subducting-ridge, which can be reasonably explained by the change in shear stresses and pore pressures caused by the subducting-ridge.

Keywords: Nankai trough, Very low frequency earthquake (VLFE), Accretionary prism, HDBSCAN, Broadband ocean bottom seismometer

©2019. Japan Geoscience Union. All Right Reserved.

Evidence for semi-brittle flow in mantle-wedge serpentinites under high pore fluid pressure and their implications for deep low frequency earthquakes

Kengo Kataoka[1], Yurina Nagata[1], *Ken-ichi Hirauchi[1], Ryosuke Oyanagi[2], Atsushi Okamoto[3], Katsuyoshi Michibayashi[4]

1. Department of Geosciences, Faculty of Science, Shizuoka University, 2. Japan Agency for Marine-Earth Science and Technology, 3. Graduate School of Environmental studies, Tohoku University, 4. Department of Earth and Planetary Sciences, Nagoya University

In southwest Japan, deep low frequency earthquakes occur at the base of the shallow serpentinized mantle wedge. In order to understand deformation styles of the mantle wedge serpentinite, we conducted structural and petrological analysis of a paleo-mantle wedge body that has experienced serpentinization at pressure–temperature conditions corresponding to source areas of low-frequency earthquakes, in the Sanbagawa belt, central Shikoku. The serpentinite body has a block-in-matrix structure that result from pervasive fragmentation. At outcrop and thin section scales, the distribution of blocks follows a power law distribution with exponent $2.32 < D < 2.37$ (2-D). The block has experienced complete serpentinization, characterized by randomly-oriented antigorite aggregates. The matrix also consists of antigorite, which was formed due to dissolution–precipitation process of the block in the presence of H_2O. Antigorite aggregates in the matrix along localized shear planes is characterized by a strong crystallographic preferred orientation with a dominant [010](001) slip system, suggesting dislocation glide on (001) planes. We suggest that deep slow earthquakes occur by semi-plastic deformation of the serpentinized mantle wedge, under low effective normal stresses.

Keywords: slow earthquakes, low frequency earthquake, mantle wedge, serpentinite

©2019. Japan Geoscience Union. All Right Reserved.

Spatial distribution of slow slip events off the Boso peninsula from 1996 to 2018 under sparsity constraints

*Ryoko Nakata[1], Hideitsu Hino[2], Tatsu Kuwatani[3,4], Takahiro Akiyama[5], Shoichi Yoshioka[6], Masato Okada[7], Takane Hori[1]

1. Japan Agency for Marine-Earth Science and Technology, 2. The Institute of Statistical Mathematics, 3. Department of Solid Earth Geochemistry, Japan Agency for Marine-Earth Science and Technology, 4. PRESTO, Japan Science and Technology Agency, 5. Graduate School of Science, Kobe University, 6. Research Center for Urban Safety and Security, Kobe University, 7. Graduate School of Frontier Sciences, The University of Tokyo

We estimated spatial distribution of the six slow slip events (SSEs) off the Boso peninsula, central Japan, from 1996 to 2018. We have applied an inversion method called fused regularization, a type of sparsity constraint, suitable for detecting discontinuous changes in the model parameters, for evaluation function [Nakata et al., 2017]. In this study, to shorten calculation time, we used a type of approximation method by Obuchi and Kabashima [2016] to search hyperparameters, not LOO-CV (leave-one-out cross validation).

From our tentative results, the maximum slips for the 2002, 2011 and 2018 SSEs were large, and the 1996, 2007 and 2013 SSEs were small. The slip distributions of the 2011 and 2018 SSEs seem to be distributed southward than 2002. It is confirmed by numerical experiments that the difference in slip distribution is not due to GNSS station distribution.

Furthermore, we are conducting numerical simulation of earthquake generation cycles, which modelling SSEs off the Boso peninsula and M~8 earthquakes along the Sagami Trough. We will discuss slip distributions of SSEs and locked area during an interseismic period.

©2019. Japan Geoscience Union. All Right Reserved.

Marine electromagnetic observations around a slow earthquake region in the western Nankai trough

*Hiroshi Ichihara[1], Tada-nori Goto[2], Tetsuo Matsuno[3], Noriko Tada[4], Shinya Sato[2]

1. Earthquake and Volcano Research Center, Nagoya University, 2. Graduate School of Engineering, Kyoto University, 3. Ocean Bottom Exploration Center, Kobe University, 4. JAMSTEC

Slow earthquakes have been believed to relate to fraction of pore fluid around plate boundary. Thus, imaging of electrical resistivity (conductivity) distribution is essential to understand slow earthquakes. However, many of SSE areas are distributed beneath the ocean, we need marine electromagnetic (EM) observations. In this presentation, we report preliminary results of marine EM observations in the western part of Nankai Trough (off Miyazaki prefecture and off western Kochi prefecture, Japan) where SSEs, VLF events and regular earthquakes (e.g. 1968 off-Hyuga earthquake, M7.5) are known. We deployed eight ocean bottom electro-magnetometers (OBEMs) and recovered seven of them between 2017 and 2018. In addition to EM fields, two OBEMs measure absolute pressure to detect short period crustal deformations caused by SSE. We estimated high quality magnetotelluric responses based on Chave and Thomson (2004). However, the responses show strong three-dimensionality of resistivity distribution and strong coast effect (e.g. Key and Constable, 2011). They indicate that we need to apply three-dimensional imaging techniques for seafloor magnetotelluric data.

Keywords: Slow earthquake, magnetotelluric, OBEM, Nankai trough, off Miyazaki

©2019. Japan Geoscience Union. All Right Reserved.

Dynamics of precipitating injection fronts inside of structured medium

*Yutaka Sumino[1], Shunsuke Tanaka[1], Miyuki Kunihiro[1]

1. Tokyo University of Science

Recent study on a slow earthquake elucidates that the migration of water within a mantle wedge may play relevant roles[1]. The flow inside of confined geometry, such as within a soil, is often described by the Darcy’s law, where flow velocity is described by the gradient of fluid pressure. Interestingly, however, the water within a mantle wedge contains large amount of solid contents, and hence, a precipitation can be formed within the water[2]. For this reason, the dynamics of fluid flow under the effect of precipitation reaction should be explored.

Based on the above motivation, we explored the 2-dimensional confined chemical garden[3] as an analogue experiment for the fluid flow within a mantle wedge[4]. The system consists of two fluids with a quasi-two dimensional thin cell, so called a Hele-Shaw cell. The cell was filled with a fluid, and the other fluid is injected from the center of the cell. The flow in a Hele-Shaw cell can be described by the Darcy’s law. Furthermore, the mixing of these fluids leads to the precipitation. Thus, the flow observed in 2-dimensional confined chemical garden system is analogous to the one of water in a mantle wedge with precipitation formation.

Our previous study[4] showed that a filamentous pattern appears when the injection speed is high enough, whereas the symmetrical circular front was formed for lower injection speed. This results indicates that the propagation radius of injection front can be drastically different depending on the injection speed. In addition, the number of moving filaments saturate whose value is proportional to the injection speed. Such tendency can be understood with our boundary model adopting the effect Laplace pressure and the conservation of precipitation at the boundary. The model further predicts existence of optimal curvature for the moving front with which the required pressure for the motion is minimum. The curvature, and the speed of the optimal boundary motion is independent of the injection speed. These experimental and theoretical study thus worked well in the 2-dimensional Hele-Shaw cell. However, actual condition in a mantle wedge should have quenched structure, which is absent in a Hele-Shaw cell.

In order to fill the gap between actual condition in a mantle wedge and our analogue experiments, we modified our Hele-Shaw cell to have periodic pillar structure. As a control parameter, we changed the pillar to pillar distance, w, as shown in attached figure. The filament pattern showed meandering motion without pillar structures ($w = \infty$). We found that the filament pattern showed straight motion especially when w agreed with the typical filament width. Our modified mathematical model adopting nonlinear response of permeability with precipitation density numerically reproduced such experimental results. This results indicates that the propagation distance of injected fluid can be modified by the locally quenched disorder within a mantle wedge.

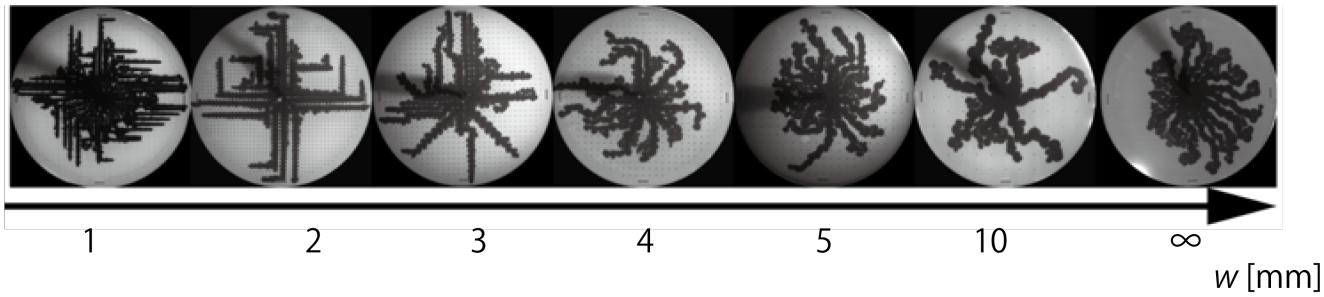
In this paper, we show detailed setup for experiments, as well as mathematical model.

[1] A. Tanaka et al. Earth, Planets and Space 70, 25 (2018).
[2] K. Ujiie, et al., *Geophys. Res. Lett.* **45**, 5371–5379 (2018).

©2019. Japan Geoscience Union. All Right Reserved.

[3] F. Haudin et al., *Proc. Natl. Acad. Sci. U.S.A.* **111**, 17363–17367 (2014).
[4] S. Wagatsuma, et, al., *Phys. Rev. E* **95**,052220 (2017).

Keywords: injection, fluid, precipitation



©2019. Japan Geoscience Union. All Right Reserved.

Permeability changes of simulated low permeable fault rocks induced by intermediate velocity friction test

*Wataru Tanikawa[1]

1. Japan Agency for Marine-Earth Science and Technology, Kochi Instutute for Core Sample Research

Earthquake events often associate with fluctuations of flow rate, pore pressure and pore fluid chemistry at a subsurface of earthquake rupture zones. The co-seismic hydrological changes are explained by changes in fluid permeability of fault zones during earthquakes, and the permeability change plays an important role for dynamic fault processes as well. Therefore, we newly designed a system to estimate water permeability changes during and after low to high velocity shear deformation using a rotary shear apparatus and simulated fault rocks.

A pair of hollow cylindrical samples made by low permeable Belfast dolerite and Aji granite were used as test specimens. To calculate permeability, a radial flow from the inner wall to the outer wall of the specimen was induced by applying a differential pore pressure (0.01 to 0.2 MPa) between inner and outer walls. We performed friction tests at normal stress of 2 MPa, rotation speed from 0.0003 to 0.6 m/s, and slip displacement of 1 m.

The results showed that permeability increased during sliding at every slip velocity condition, and higher velocity friction caused more abrupt increase in permeability. After the end of sliding, permeability gradually decreased with time and then became nearly constant value. Reduction rate of permeability 5 min after slip increased with slip rate. Fiction coefficient was decreased with sliding velocity. Frictional heating is a key to explain slip velocity dependence of permeability (flow rate). Temperature rise caused by frictional heating will reduce fluid viscosity, therefore, apparent permeability reduction after sliding can be explained by an increase in fluid viscosity by cooling. Pore pressure build-up by frictional heating can increase aperture, therefore, this process can explain permeability enhancement during sliding and velocity dependences on permeability increase and friction coefficient.

Keywords: permeability, friction coefficient, frictional heating

©2019. Japan Geoscience Union. All Right Reserved.

Modified relation between the coupling and tremor rates around the Shikoku region

*Tadafumi Ochi[1]

1. Institute of Earthquake and Volcano Geology, Geological Survey of Japan, The National Institute of Advanced Industrial Science and Technology

In Ochi and Takeda (2018, EPS), I examined the relation between the interplate coupling velocity and the number of deep low-frequency tremors in the same place around the Shikoku region, southwest Japan. I found that there were some spot-like points where the coupling and the tremor count were well correlated, and that the regression line required the coupling rate to be the plate convergence rate in this region under conditions of zero tremor count rate. One of the problems to be resolved is the interpretation of the first matter 'spot-like points' mentioned above. According to the pairs of time series of the coupling rate and tremor count rate, some pairs show a time delay, and the others show a small fluctuation in the tremor count rate that seems to be independent of the coupling rate. It is interesting that whether the an ill-correlation just comes from an oversimple model of the linear regression I used in the previous study, or really reflects some physical background. In order to answer this question, I construct the model which allows the fluctuation in the tremor count rate that is independent from the coupling rate and observe the fitness of the model. At this time, some trial models that allow the shorter period fluctuation in the tremor count rate than in the coupling rate and temporal change in the period achieve clear correlations. In the presentation, I will show the results of the various trials.

Keywords: Interplate coupling, Low-frequency tremor

©2019. Japan Geoscience Union. All Right Reserved.

Spatiotemporal distribution of regular and very low-frequency earthquakes in the northern part of the Ryukyu subduction zone

*Youichi Asano[1], Kazuhiko Goto[2], Hiroshi Yakiwara[3], Shuichiro Hirano[3]

1. National Research Institute for Earth Science and Disaster Resilience, 2. Association for the development of earthquake prediction, 3. Nansei-toko Observatory for Earthquakes and Volcanoes, Kagoshima University

We have investigated detailed spatiotemporal distribution of regular and very low-frequency (VLF) earthquakes including an Mw 6.3 interplate event near Tanegashima along the Ryukyu trench on Jun. 08, 2019. This earthquake was followed four Mw4-5 class regular and many VLF earthquakes by the end of Jan., 2019. At first we estimated centroid moment tensors of these regular and several VLF earthquakes, respectively, from broadband seismograms recorded at the NIED F-net and temporally observation stations. In the next step, the known VLF earthquakes were selected to be template events for searching unknown VLF earthquakes from continuous seismograms. If there are several candidates of VLF earth quake, we select the most coherent event with a maximum cross-correlation coefficient averaged over all stations in every 180 seconds. Finally we estimated locations of the selected events from phase shift of the wavelets between the template and these selected events. Obtained result shows that activity of VLF earthquakes after the Mw 6.3 earthquake was started in the adjacent area east of this Mw 6.3 earthquake; however, the following Mw4-5 regular earthquakes occurred south of this area in the period of Jan. 25-30, 2019. In this period, the front of the VLF activity migrated toward east from these Mw4-5 events. Such a spatiotemporal distribution of regular and VLF earthquakes suggests that the after slip of the Mw 6.3 and/or an SSE caused these regular and VLF earthquakes.

Acknowledgment

This study is partly supported by JSPS KAKENHI Grant Number JP16H06473.

Keywords: very low-frequency earthquake, Ryukyu subduction zone

©2019. Japan Geoscience Union. All Right Reserved.

Possible tectonic tremor activities near the VLFE epicenters in the Sanriku-Oki region in 2011

*Hidenobu Takahashi[1], Ryota Hino[1], Yusaku Ohta[1], Naoki Uchida[1], Syuichi Suzuki[1], Masanao Shinohara[2], Takanori Matsuzawa[3]

1. Graduate school of Science Tohoku University , 2. Earthquake Research Institute, University of Tokyo, 3. National Research Institute for Earth Science and Disaster Resilience

Recently various kind of slow earthquakes have been discovered along the Japan Trench subduction zone. Prior to the occurrence of the 2011 Tohoku-oki earthquake, occurrence of slow slip events associated with migration of small earthquake epicenters and tectonic tremors was reported near the hypocenter of the Tohoku-Oki earthquake (e.g. Kato et al., 2012; Ito et al., 2015; Katakami et al., 2018). As a different type of a slow-earthquake family, Very Low Frequency Earthquakes (VLFEs) have been detected in more broad areas (Matsuzawa et al., 2015). Takahashi et al. (in prep.) detected the seismic signals from the VLFEs by short-period ocean bottom seismograms (OBS) deployed in the vicinity of the VLFE epicenters in the Sanriku-Oki region, just after the Tohoku-Oki earthquake. They further identified a number of VLFE-like events, not recognized by the onshore data. Here, we report on possible tectonic tremor activities in the same area based on the OBS data after the 2011 Tohoku-oki earthquake.
We detected four sequences of continuous rises of amplitudes on the OBS records. Each of the sequence has a duration of ~ half a day. The sequences were composed of numerous wave trains with good correlations in their growths and decays in observed amplitudes among the stations, but no distinct P- or S-wave onsets were identified for individual wave trains. Interestingly, the spatial variation of the wave trains amplitudes is similar to those of the previously identified VLFEs. These observations suggest that the sequences were composed of small seismic events closely located each other and to the known VLFEs. It is also notable that some of the VLFE-like events discovered by the OBS data were contained in the sequences. We regard the discovered sequence as a kind of tectonic tremor activity and will inspect their characteristics, such as frequency content and its variability, to clarify their nature and discuss their relevance to slow slip events along the shallow subduction interface, which might promote the activities.

Keywords: tectonic tremor, Sanriku−oki

©2019. Japan Geoscience Union. All Right Reserved.

Heterogeneous structure around a region of slow earthquake activity off Ibaraki prefecture along the Japan Trench

*Kimihiro Mochizuki[1], Tomoaki Yamada[1], Masanao Shinohara[1], Ryota Hino[2], Ryosuke Azuma[2], Yoshihiro Ito[3], Yoshio Murai[4], Kenji Uehira[5], Toshinori Sato[6]

1. ERI, Univ. of Tokyo, 2. Graduate School of Science, Tohoku Univ., 3. DPRI, Kyoto Univ., 4. Faculty of Science, Hokkaido Univ., 5. NIED, 6. Graduate School of Science, Chiba Univ.

Large earthquakes of magnitude (M) ~7 have repeatedly occurred in the Ibaraki-oki region, about 100 km offshore of the Ibaraki prefecture along the Japan Trench, at a constant interval of ~20 years. Mochizuki et al. (2008) conducted a marine seismic survey and revealed that there exists a subducted seamount in the region. They also conducted an offshore seismic observation using ocean bottom seismometers (OBSs) to show that the seismicity in the region can be seen off of the subducted seamount, but not along the plate interface over it. They found that the location of the subducted seamount did not agree with the focal region of the repeating M7 earthquakes. From these results, they argued that the plate interface over the subducted seamount does not constitute an asperity of the repeating M7 earthquakes. Wang and Bilek (2011) introduced an idea that the seamount subduction causes formation of a fracture network within the overriding plate, and such a fracture network would prevent accumulation of large strain energy along the plate interface over the subducted seamount to generate large earthquakes. In addition to the repeating M7 earthquakes, recent studies (e.g. Matsuzawa et al., 2015; Nishikawa and Ide, 2018) have reported activity of slow earthquakes in the region. Relationship between activity of various types of earthquakes and structural features around the plate interface is one of the key topics to better understand controlling factors over earthquake types to be generated.

Recent studies in the Hikurangi subduction margin off the North Island of New Zealand show spatial relationship between variety of fault slips and topographic features of the plate interface. Wallace et al. (2016) successfully observed a large slow slip event just beneath an offshore array of ocean bottom pressure gauges, and precisely determined its slip distribution. They revealed that its slip propagation appeared to have circumvented subducted seamounts that have been imaged by magnetic anomalies as well as seismic reflection sections. Todd et al. (2018), for the first time, detected offshore tremor activity in the Hikurangi margin. The activity appears to have started just after the cessation of the slow slip, and its spatial distribution is only limited within regions of subducted seamounts. These results show that distributions of slow slip and tremor activity do not appear coincident, and thus the physical properties of the plate interface may be different. Further seismic surveys are supposed to provide vital information on structural variations that control physical characteristics of the plate interface.

In February, 2011, we acquired wide-angle reflection and refraction seismic data using 21 OBSs along a 150 km transect in the Ibaraki-oki region during the KH11-2 R/V Hakuho-maru cruise. We also included data from an OBS array that had already been deployed for a long-term seismic observation above the subduction front of the subducted seamount. Thus, we could construct a dense OBS profile above the subducted seamount with a receiver interval of ~3 km to achieve a high spatial resolution, whereas the largest interval is 10 km near both ends of the profile. First arrivals from the airgun sources can be traced up to ~95 km on most of the OBSs. The OBS record sections show significant heterogeneity that may include very rough structural features of the subducting oceanic crust along strike. Such heterogeneity may control seismic activity in the region.

©2019. Japan Geoscience Union. All Right Reserved.

Keywords: Ibaraki-oki, Active source seismic survey, Heterogeneous structure

©2019. Japan Geoscience Union. All Right Reserved.

Shallow low-frequency tremor triggered by nearby moderate earthquakes off Sanriku

*Sachiko Tanaka[1], Takanori Matsuzawa[1], Youichi Asano[1]

1. National Research Institute for Earth Science and Disaster Resilience

In the region off Sanriku, we have observed shallow low-frequency tremor, which occurs between the 12 km and 20 km depth contours of the plate interface, applying an envelope correlation method (Obara, 2002) to the records from the Seafloor observation network for earthquakes and tsunamis along the Japan Trench (S-net) (Tanaka et al., 2018). Several episodes of tremor, each of which lasted for half a day to six days, were detected in 2017, with intervals of one to three months. In the present study, we found tremor triggered by nearby moderate earthquakes. On July 24, 2017, an Mw 5.6 earthquake, showing reverse faulting consistent with the slip on the plate interface, occurred at the downdip end of the tremor zone off Sanriku, which was the largest event within 100 km of that tremor zone in the year. Immediately after the Mw 5.6 earthquake, coherent tremor signals were identified at surrounding stations. These signals continued for 20 hours, and the locations of their sources spanned 40 km along strike and 50 km along dip. Similar triggered tremor was observed following an Mw 5.1 earthquake on July 22, two days before the Mw 5.6 earthquake. This tremor activity was smaller and shorter than that triggered by the Mw 5.6 earthquake; tremor was localized to an area of 20 km by 15 km, and lasted for twelve hours. After a quiescence of nearly one day, the Mw 5.6 earthquake occurred at an adjacent area and triggered tremor was detected again. Triggering of tremor by moderate interplate earthquakes in or very close to the tremor zone we observed may imply small-scale (~ a few kilometers) heterogeneities in frictional properties on the plate interface in the area.

Keywords: shallow low-frequency tremor, triggered tremor, Japan Trench

©2019. Japan Geoscience Union. All Right Reserved.

Slow slip events in the Bungo Channel over 15 years as inferred from GNSS data (1996-2011)

Takatoshi Yokoi[1], *SHINICHI MIYAZAKI[1], Hiromu Sakaue[1], Jun'ichi Fukuda[2]

1. Graduate School of Science, Kyoto University, 2. Earthquake Research Institute, The University of Tokyo

We estimated space-time evolution of inter-plate slip and slip velocity associated with slow slip events (SSE) in the Bungo Channel over 15 years between January 1, 1996 and February 28, 2011, from GNSS data.

We use GNSS time series at 80 stations around the Bungo Channel out of GEONET stations. Time series were obtained with GIPSY-OASIS II software by Nishimura (personal communication). We removed data during SSE and estimated secular velocities, annual and semi-annual seasonal variations, and offsets associated with earthquakes, SSEs and instrumental events. Then we remove contributions of those components from time series with SSE to prepare time series for the inversion. We constructed plate interface based on iso-depth data by Baba et al. (2002) and Hirose et al. (2008), and setup the model region that is 200km long east to west and 280km long north to south. The model region was subdivided into 719 small triangular patches. We employed the inversion method based on the Monte Carlo Mixture Kalman Filter (Fukuda et al. 2008) and estimated slip and slip velocities on the fault continuously over 15 years.

First, Long-term slow slip events (L-SSE hereafter) that lasted for several months were inferred in 1997, 2003 and 2010 as obtained by, such as, Ozawa et al. (2012, 2017) and Yoshioka et al. (2015). In addition to basic characteristics described in these previous studies, short-term slow slip events (S-SSE hereafter) were inferred just before or just after the main slip event. This result suggests that stress perturbations by SSEs trigger other SSEs. Therefore the inferred cumulative moment in this study was smaller than previous studies because we successfully excluded contributions from S-SSEs. Second, S-SSEs have repeatedly occurred with the interval of about three or four months over 15 years. Those S-SSE were located at depths of about 30-40km and associated with low frequency tremors.

In this presentation, we focus space-time evolutions of L-SSE in 2010 and S-SSE in 2005.

Keywords: Slow slip in the Bungo Channel, crustal deformation, Monte Carlo Mixture Kalman Filter

©2019. Japan Geoscience Union. All Right Reserved.

Investigations of sensor orientation and a possibility of detecting crustal deformation based on accelerometer records of S-net

*Ryota Takagi[1], Naoki Uchida[1], Takashi NAKAYAMA[1], Ryosuke Azuma[1], Akira Ishigami[1], Tomomi Okada[1], Yusaku Ohta[1], Ryota Hino[1]

1. Research Center for Prediction of Earthquakes and Volcanic Eruptions, Graduate School of Science, Tohoku University

Seafloor Observation Network for Earthquakes and Tsunamis along the Japan Trench (S-net) of National Research Institute for Earth Science and Disaster Resilience (NIED) will greatly improve our knowledge of subsurface structure beneath offshore region along Japan trench and understanding of regular and slow earthquakes on the subducting plate boundary. We estimated the orientations of S-net sensors that are fundamental information for further data analysis and investigated the possibility of detecting crustal deformation based on accelerometer records.

We determined three parameters of sensor orientations: tilt angle of the long axis of a cable, rotation angle around the long axis, azimuth of the long axis. We estimated the tilt and rotation angles by assuming the DC components of accelerometers record the gravitational acceleration. The tilt and rotation angles slightly vary within the range of 0.01-0.1 degree during the period from 2016 to 2018 except for coseismic steps of rotation angles larger than 1 degree due to the M6.4 off Sanriku earthquake (August 20, 2016) and M7.4 off Fukushima earthquake (November 20, 2016). The long-axis azimuths are estimated by particle motions of long-period Rayleigh waves. We used the accelerometer records in 30-100 s of 7-14 teleseismic earthquakes with Mw 7.0-8.2. The azimuths are constrained in the range of 5-10 degrees. After correcting waveforms based on the estimated sensor orientation, we found coherent waveforms within the whole S-net stations and separation of Rayleigh and Love waves in radial and transverse components.

The capability of the DC components of accelerometers implies a possibility to detect crustal deformation from accelerometer records. We made time series of tilt and rotation angle with the sampling rate of one hour. During the period without offsets partly due to earthquakes, the root-mean-square (RMS) amplitudes of tilt and rotation angles are about 2 micro radians at most stations. The buried stations shallower than 1500 m show smaller variations and RMS amplitudes are about 0.2 micro radians. Some buried stations show tidal response with amplitude of about 1 micro radians. Since the maximum tilt change of land stations by a slow slip event (SSE) near the Boso Peninsula is about 1 micro radians, it might be possible to detect crustal deformation due to similar SSEs based on the accelerometer records.

Acknowledgement: We used continuous records of S-net managed by NIED. We thank NIED for providing the data.

Keywords: S-net, Sensor orientation, Crustal deformation, Slow slip, Tilt observation

©2019. Japan Geoscience Union. All Right Reserved.

Spatiotemporal variation of released seismic energy from shallow low-frequency tremor in Hyuga-nada, revealed by ocean bottom seismological observation

*Yusuke Yamashita[1], Saki Watanabe[2], Tomoaki Yamada[3], Masanao Shinohara[3], Takeshi Matsushima[2]

1. Disaster Prevention Research Institute, Kyoto University, 2. Institute of Seismology and Volcanology, Kyushu University, 3. Earthquake Research Institute, The University of Tokyo

In this study, we estimate the released seismic energy by shallow low-frequency tremors (shallow tremors) and clarify spatiotemporal variation of shallow tremor activity in Hyuga-nada, east off Kyushu. We used the data obtained from the temporal ocean bottom seismological observation for 3 months in 2013 [Yamashita *et al*., 2015] and long-term ocean bottom seismological observation from 2014 to 2017. The source location and released seismic energy of each shallow tremor was simultaneously estimated by Hybrid Envelope Cross-correlation Method [Maeda and Obara, 2009]. Observation data were obtained by the long-term continuous ocean bottom seismic observation in Hyuga-nada from 2013 to 2017. Site amplification factors were estimated by the coda normalization method [e.g., Sato and Fehler, 1998].

Spatial distribution of released seismic energy rate (energy rate) shows a heterogeneity although the average value of that is generally 10^4 J/s. The regions where the energy rate is relatively small are roughly coincident with the subducting or passed areas of the Kyushu-Palau Ridge. This result suggests that the structure and/or shape of the subducting plate such as seamounts or ridges may have an effect on the frictional property of the shallow plate interface. The 2013 activity was similar characteristics of shallow tremor location in space and time as the previous study, including two migrations episode. In addition, the characteristics of the released seismic energy were revealed as follows: (1) the energy rate was large at the both initiation point and the front of the migration, (2) the total released energy amount of the first migration was larger than that of the second migration, (3) both migrations were stopped at the region of small amount of released energy. Migration episode occurred while the 2015 activity and similar characteristics were documented.

Migration speed of shallow tremor is a few times faster, and energy rate of that is one or two orders of magnitude greater than the deep tremor. Applying the model of Ando *et al*. [2010, 2012] and Yabe and Ide [2014] to the result in this study, the average fault strength of shallow tremor is stronger than that of deep tremor, which leads up to a faster fault slip both brittle and ductile area. As a result, migration speed may become to be faster than deep tremor.

Acknowledgements: This study is supported by the research project for compound disaster mitigation on the great earthquakes and tsunami around the Nankai trough region, the MEXT of Japan, and JSPS KAKENHI Grant Number JP16H06471, JP16H06472. We thank Dr. Takuto Maeda for valuable discussions and comments. The observation data in 2013 obtained by T/S Nagasaki-maru. We used the JMA unified earthquake catalog and the seismic data obtained by Kagoshima University.

Keywords: Shallow low frequency tremor, Shallow slow earthquake, Ocean bottom seismological observation

©2019. Japan Geoscience Union. All Right Reserved.

©2019. Japan Geoscience Union. All Right Reserved.

Unified description of fast and slow earthquakes using velocity strengthening patches

*So Ozawa[1], Takahiro Hatano[1]

1. Earthquake Research Institute, the University of Tokyo

In a prevalent view, seismicity in subduction zones is governed by the distribution of the frictional properties of the plate interface. Regions with velocity-weakening (VW) friction generate earthquakes, whereas velocity-strengthening (VS) regions creep aseismically. Although most models consider isolated VW regions (patches) from the idea of asperities (e.g. Dublanchet et al., 2013), isolated VS patches also would exist given the frictional properties on faults are inferred to be complex and hierarchical. Therefore, the role of VS patches is to be studied.

Here we perform 3-D numerical simulation of the seismic cycle of faults governed by the rate and state friction law with the aging law. We distribute randomly circular VS patches on a VW background. We mainly focus on the effect of the ratio of VS and VW areas.

In our preliminary simulation, we identified two important effects. First, the VS patches act as the “stability barriers” during dynamic rupture propagation, which makes the rupture process more complicated than a single propagating crack. Rupture decelerates by encountering a stability barrier, followed by reacceleration due to overcoming the barrier. Such a process gives rise to multiple rupture fronts in the slipping area.

Second, dynamic rupture is inhibited by increasing the number of VS patches, and the fault slips aseismically with strong fluctuation in slip velocity. This is because there are no enough VW regions to accelerate the slip to dynamic rupture. Although a similar mechanism for slow earthquakes is proposed by Skarbek et al. (2012) and Yabe & Ide (2017), our 3-D modeling enables detailed studies on the spatiotemporal evolution of slip. In the presentation, we further discuss our results in the context of the dynamic scaling of rupture growth and the phenomenological law of slow earthquakes.

Keywords: Slow earthquake, Rate and state friction

©2019. Japan Geoscience Union. All Right Reserved.

The b-value of the earthquake swarm activities accompanied by the Boso slow slip events

*Yuki Noda[1], Hitoshi Hirose[2,1]

1. Department of Planetology, Faculty of Science, Kobe University , 2. Research Center for Urban Safety and Security, Kobe University

Slow slip events (SSEs) which are accompanying earthquake swarms repeatedly occur at intervals of about 2 to 7 years off Boso Peninsula (e.g., Sagiya, 2004; Hirose et al., 2012, 2014; Fukuda, 2018). These SSEs and swarms are thought to occur on the upper boundary of the subducting Philippine Sea plate.

As a statistical property of earthquakes, Gutenberg-Righter’ s law is well-known, that is, the relationship between the magnitude and the logarithm of occurrence frequency of earthquakes is expressed well with a straight line a-bM (Gutenberg and Richter, 1944). Although the b-value (slope of the line) often takes values around 1, there are many reports about the temporal changes of the b-value. For example, a decade-scale b-value decrease prior to the 2011 Tohoku Earthquake is reported (Nanjo et al., 2012). Although the relationship between the temporal change of b-value and aseismic slip is suggested, but the lack of near field geodetic observations prevents the direct evidence for the relationship. Here we examine the b-value of the earthquake swarms accompanied by the Boso SSEs, of which the aseismic slip is revealed by geodetic observations.

In this study, we estimate the b-value of the earthquake swarms in 2002, 2007, 2011 and 2014. We use the JMA unified earthquake catalog. As a preliminary analysis, we investigated the earthquakes with focal depths of 5 km to 40 km occurring at 35.05˚ to 35.56˚N in latitude and 140.15˚ to 140.73˚E in longitude. Eventually, “event period” estimated in the previous studies of the crustal deformation by geodetic observation does not necessarily agree with the period of the swarms occurring at the same time. Therefore, in this research, “event period” was redefined from seismic activity and used. In other words, we extracted swarms including a SSE period from crustal deformation studies and the time when the seismicity rate (the number of earthquakes per unit time) is significantly higher than the other time is defined as “event period”. In addition, the period other than the event period is defined as “inter-swarm period”.

We find that the b-values in the event periods tend to be lower than that during inter-swarm period. In more detail, different trends that seem to correspond to the difference in slip zone and location of earthquake activity of each SSE (Hirose et al. 2014) are seen in the b-values for the event periods. A seismic activity near the southern coast of the Boso Peninsula was hardly observed in the 2007 event period, whereas an active seismic activity was seen there in the 2011 event period. In order to clarify the dependence of the b-value on the difference in the location of the earthquakes, we divided the survey area into two areas, that is, the northern area (area A) and the southern area (area B). The seismic activity is observed in all event periods in the area A, whereas an active seismic activity is observed only in the event periods of 2002 and 2011 in the area B. Then a b- value is estimated in each period in the same way. As a result, for the earthquakes occurred in the northern region (area A), there is a tendency that the b-value in each of the event periods is lower by about 0.2-0.4 than that during inter-swarm. On the other hand, such a tendency is not observed in the southern area (area B). Such differences in the northern and southern regions may suggest that the effects of stress changes caused by SSEs vary from region to region.

©2019. Japan Geoscience Union. All Right Reserved.

Keywords: Gutenberg-Richter's law

©2019. Japan Geoscience Union. All Right Reserved.

Three-dimensional thermal modeling associated with subduction of the Philippine Sea plate at the Ryukyu Trench, and its relation to the occurrence of interplate seismic events

*Nobuaki Suenaga[1], Shoichi Yoshioka[2,1], Yinfeng Ji[3]

1. Graduate School of Science, Kobe University, Japan, 2. Research Center for Urban Safety and Security, Kobe University, Japan, 3. Chinese Academy of Science, Beijin, China

Interplate seismic events such as short-term slow slip evens (S-SSEs) (Nakamura, 2017), low-frequency earthquakes (LFEs) (Ando et al., 2012), and shallow very low-frequency earthquakes (VLFEs) (Nakamura et al., 2015) have been identified at the Ryukyu Trench, southwestern Japan. As the specific characteristics of these distributions, depths where S-SSEs and LFEs occur at the plate interface beneath the Okinawa island, whose depth is ranging from 15 km to 25 km, is about 10-20 km shallower than that beneath the Yaeyama islands, whose depth is ranging from 35 km to 50 km.

In this study, we constructed three-dimensional parallelepiped thermal convection model associated with subduction of the Philippine Sea (PHS) plate beneath the Amurian (AM) plate at the Ryukyu subduction zone. We considered subduction history of the PHS plate in the model region, referring to the plate rotation model (Mathews et al., 2016). We performed the numerical simulation as the time-dependent problem in the last 15 Myr to elucidate relationships among calculated thermal structures, dehydrations from the subducting plate, and the interplate seismic events. We used observed heat flow data to constrain thermal structures.

As a result at 0 Ma, we found that interplate temperature where S-SSEs and LFEs occur beneath the Yaeyama islands is lower than that beneath the Okinawa island when compared with the same depth along the direction of the trench axis. This is mainly because the convergence rate (PHS-AM) becomes gradually fast toward the southwest. Therefore, interplate temperatures where S-SSEs and LFEs occur were estimated ranging from 500℃ to 700℃ both beneath the Okinawa island and the Yaeyama islands.

We also calculated water content distribution within the PHS plate, using the calculated thermal structures and the phase diagram of MORB in an oceanic crust (Omori et al., 2008) and ultramafic rock in a slab mantle (Hacker et al., 2003). As for dehydration of MORB, we found that epidote eclogite transforms into amphibole eclogite in the neighboring area where S-SSEs and LFEs occur beneath the Okinawa island, and amphibole eclogite transforms into eclogite beneath the Yaeyama islands. The former and the latter dehydrate a total amount of 1.4 wt% and 0.7 wt% associated with their phase transformations, respectively.

Keywords: three dimensional thermal modeling

©2019. Japan Geoscience Union. All Right Reserved.

[E] Poster | S (Solid Earth Sciences)：S-CG Complex & General

Wed. May 29, 2019 5:15 PM - 6:30 PM JST | Wed. May 29, 2019 8:15 AM - 9:30 AM UTC | Poster Hall International Exhibition Hall8, Makuhari Messe_33

[S-CG48] Science of slow earthquakes: Toward unified understandings of whole earthquake process

convener:Satoshi Ide(Department of Earth an Planetary Science, University of Tokyo), Hitoshi Hirose(Research Center for Urban Safety and Security, Kobe University), Kohtaro Ujiie(Graduate School of Life and Environmental Sciences, University of Tsukuba), Takahiro Hatano(Earthquake Research Institute, University of Tokyo)

Accumulating observational studies on various types of slow deformation events, such as tectonic tremors, very low frequency events, and slow slip events, portrays some universal characteristics in generally complex behavior, including interaction among events and influence by various outer loadings. Some of these phenomena seem to have causal relation with the occurrence of very large earthquakes. A unified understanding of these slow and fast earthquake processes requires an approach integrating geophysics, seismology, geodesy, geology, and non-equilibrium statistical physics. We welcome presentations based on, but not limited to, geophysical observation, data analysis, analytical theory, numerical simulation, field study, and laboratory experiments.

[SCG48-P01] Off the Kii Peninsula Shallow Low Frequency Earthquake in 2004 revealed by Ocean Bottom Seismometer

*Koji Tamaribuchi[1], Akio Kobayashi[1], Takahito Nishimiya[1], Satoshi Annoura[2] (1.Meteorological Research Institute, 2.Japan Meteorological Agency)

[SCG48-P02] The development of pressure vessel on gouges for rock deformation at seismic rates under water-saturated conditions

*Wei-Ting Lin[1], Li-Wei Kuo[1], Wen-Jie Wu[1], Jia-Jyun Dong[1], Yi-Hung Huang[2] (1.National Central University, 2.MATSUKI HYDRAULIC INDUSTRIAL CO. LTD)

[SCG48-P03] Spatial variations of shallow very low-frequency earthquake activity along the Nankai Trough based on CMT inversion using the 3D heterogeneous model

*Shunsuke Takemura[1], Takanori Matsuzawa[1], Akemi Noda[1], Takashi Tonegawa[2], Youichi Asano[1], Takeshi Kimura[1], Katsuhiko Shiomi[1] (1.National Research Institute for Earth Science and Disaster Resilience, 2.Japan Agency for Marine-Earth Science and Technology)

[SCG48-P04] Evaluation of Magnitude and Characteristics of Seismicity of Low Frequency Earthquakes in Parkfield

*Miki Aso[1,3], Naofumi Aso[2], Satoshi Ide[1] (1.Department of Earth and Planetary Science, The University of Tokyo, 2.Tokyo Institute of Technology, School of Science, 3.OYO RMS Corporation)

[SCG48-P05] Tectonic tremor catalog in the Tohoku-Hokkaido-Oki region using S-net

*Satoshi Ide[1], Tomoaki Nishikawa[2], Takanori Matsuzawa[3], Kazuaki Ohta[2], Naoki Uchida[4], Takuya NISHIMURA[2] (1.Department of Earth an Planetary Science, University of Tokyo, 2.Disaster Prevention Research Institute, Kyoto University, 3.National Research Institute for Earth Science and Disaster Resilience, 4.Graduate School of Science and International Research Institute of Disaster Science, Tohoku University)

[SCG48-P06] Spontaneous Slow Slip and Runaway Slip in Laboratory

*Miki Takahashi[1] (1.Institute of Earthquake and Volcano Geology, Geological Survey of Japan, AIST)

[SCG48-P07] Hydration and amorphization of quartz rocks during high-velocity frictional sliding: An examination of fault gouge from friction experiments of synthetic quartz

*Yuko Onoe[1], Hirotaka Iida[2], Akito Tsutsumi[1], Aki Takigawa[1] (1.Graduate School of Science, Kyoto University, 2.Geothermal Engineering Co., Ltd.)

[SCG48-P08] Constraining S Wave Velocity of the Source Region of Shallow Very Low-Frequency Earthquakes

*Takeshi Akuhara[1], Takashi Tonegawa[2] (1.Earthquake Research Institute, The University of Tokyo, 2.Research and Development center for Earthquake and Tsunami, Japan Agency for Marine-Earth Science and Technology)

[SCG48-P09] **Quantitative relationship between aseismic slip propagation speed and frictional properties**

*Keisuke Ariyoshi[1], Jean-Paul Ampuero[2,3], Roland Burgmann[4], Toru Matsuzawa[5], Akira Hasegawa[5], Ryota Hino[5], Takane Hori[1] (1.Japan Agency for Marine-Earth Science and Technology, 2.Université Côte d'Azur, 3.California Institute of Technology, 4.University of California, Berkeley, 5.Graduate School of Science, Tohoku University)

[SCG48-P10] Comprehensive detection of very low frequency earthquakes off the Pacific coasts of Hokkaido and Tohoku, northeastern Japan

*Satoru Baba[1], Akiko Takeo[1], Kazushige Obara[1], Takanori Matsuzawa[2], Takuto Maeda[3] (1.Earthquake Research Institute, University of Tokyo, 2.National Research Institute for Earth Science and Disaster Resilience, 3.Graduate School of Science and Technology, Hirosaki University)

[SCG48-P11] **Spatio-temporal evolution of long- and short-term slow slip events in the Tokai region, central Japan estimated from a very dense GNSS network, during 1997-2017**

*Hiromu Sakaue[1], Takuya NISHIMURA[2], Jun'ichi Fukuda[3], Teruyuki Kato[4] (1.Graduate School of Science, Kyoto University, 2.Disaster Prevention Research Institute Kyoto University, 3.Earthquake Research Institute,The University of Tokyo, 4.Hot Springs Research Institute of Kanagawa Prefecture)

[SCG48-P12] Broadband excitation of acoustic emission in granular stick-slip : experiments and spectral analyses

*Hidekazu Fukumizu[1], Ikuro Sumita[2] (1.Earth and Environmental Science Course, Division of Natural System, Graduate school of Natural Science and Technology, Kanazawa University, 2.School of Geosciences and Civil Engineering, Kanazawa University)

[SCG48-P13] Episodic tremor and slip silently invades strongly locked megathrust in the Nankai Trough

*Masayuki Kano[1], Aitaro Kato[2], Kazushige Obara[2] (1.Graduate school of science, Tohoku University, 2.Earthquake Research Institute, The University of Tokyo)

[SCG48-P14] Spatial distribution of the electrical resistivity beneath western part of Shikoku Island where long-term SSE events have repeatedly occurred

*Makoto Uyeshima[1], Maki Hata[1], Hiroshi Ichihara[2], Ryokei Yoshimura[3], Koki Aizawa[4] (1.Earthquake Research Institute, The University of Tokyo, 2.Graduate School of Environmental Studies, Nagoya University, 3.Disaster Prevention Research Institute, Kyoto University, 4.Institute of Seismology and Volcanology, Faculty of Sciences, Kyushu University)

[SCG48-P15] Variations of scaling relationships for shallow tremor observed along the Nankai trough

*Masaru Nakano[1], Suguru Yabe[1] (1.Japan Agency for Marine-Earth Science and Technology)

[SCG48-P16] Low-frequency earthquakes triggered by teleseismic surface waves by Ryukyu subduction zone.

Ayumi Kinjo[1], *Mamoru Nakamura[1] (1.Faculty of Science, University of the Ryukyus)

[SCG48-P17] Detection of small surface displacement accompanying deep low-frequency tremor in Shikoku region, southwest Japan

*Yutaro Okada[1], Takao Tabei[2] (1.Faculty of Science, Kochi University, 2.Faculty of Science and Technology, Kochi University)

[SCG48-P18] Long-term temporal change in crustal resistivity beneath western Shikoku

*Futoshi Yamashita[1], Yoshimori Honkura[1] (1.National Research Institute for Earth Science and Disaster Resilience)

[SCG48-P19] Slow decay of postseismic deformation compared with aftershocks following the 2011 Tohoku-oki Earthquake

*Yuta Mitsui[1], Shunsuke Morikami[2] (1.Department of Geosciences, Shizuoka University, 2.Formerly at Graduate School of Science and Technology, Shizuoka University)

[SCG48-P20] Serpentinite dehydration in subduction shear zones formed at source depths of slow earthquakes

*Yasushi Mori[1], Miki Shigeno[1], Kohtaro Ujiie[2], Kazuya Noro[2], Tadao Nishiyama[3] (1.Kitakyushu Museum of Natural History and Human History, 2.University of Tsukuba, 3.Kumamoto University)

[SCG48-P21] Earthquake swarms following very low-frequency earthquakes in the central Ryukyu Trench

*Mamoru Nakamura[1] (1.Faculty of Science, University of the Ryukyus)

[SCG48-P22] Seismic imaging in the central Nankai trough, off Shionomisaki to Kii channel

*Yasuyuki Nakamura[1], Shuichi Kodaira[1], Tetsuo No[1], Yuka Kaiho[1], Gou Fujie[1], Seiichi Miura[1], Kazuya Shiraishi[1] (1.Japan Agency for Marine Earth Science and Technology)

[SCG48-P23] Attempt to Detect Intra-plate SSEs Based on F3 Solution of GEONET

*Yusaku Tanaka[1] (1.Earthquake Research Institute)

[SCG48-P24] A new hydrothermal, low to high speed rotary-shearing apparatus: Reproduction of slow/megathrust earthquakes in laboratory

*Takehiro Hirose[1], Wataru Tanikawa[1], Yohei Hamada[1], Keishi Okazaki[1] (1.Kochi Institute for Core Sample Research, Japan Agency for Marine-Earth Science and Technology)

[SCG48-P25] Very low-frequency earthquakes in western Shikoku remotely triggered by the 2016 Mw5.9 off-Kii Peninsula earthquake

*Masatoshi Miyazawa[1] (1.Disaster Prevention Research Institute, Kyoto University)

[SCG48-P26] **Underground structure around source region of slow earthquakes in western Shikoku obtained by receiver function analysis**

Akira Hikita[1], Aitaro Kato[1], *Kazushige Obara[1], Akiko Takeo[1], Takeshi Akuhara[1] (1.Earthquake Research Institute, The University of Tokyo)

[SCG48-P27] Hypocenter determination of deep low frequency tremors beneath the Kii Peninsula by backprojection of seismic array data

*Kodai Sagae[1], Hisashi Nakahara[1], Takeshi Nishimura[1], Kazutoshi Imanishi[2] (1.Graduate School of Science,Tohoku University, 2.National Institute of Advanced Industrial Science and Technology (AIST))

[SCG48-P28] Triggered tremors and stress perturbations due to surface waves

*Ryohei Ikeda[1], Naoki Suda[1] (1.Hiroshima University)

[SCG48-P29] Numerical modeling of long- and shallow slow slip events including shallow region in Hyuganada and western Nankai, Japan

*Takanori Matsuzawa[1], Bunichiro Shibazaki[2] (1.National Research Institute for Earth Science and Disaster Resilience, 2.Building Research Institute)

[SCG48-P30] Further evidence for the influence of a subducting-ridge on the spatial strain accumulation and release pattern in the shallow eastern Nankai Trough, based on VLFE distribution

*Akiko Toh[1], Chen Wan-Jou [2], Doug Dreger[3], Wu-Cheng Chi[2], Satoshi Ide[1] (1.University of Tokyo, 2.Institute of Earth Sciences, Academia Sinica, 3.UC Berkeley)

[SCG48-P31] Evidence for semi-brittle flow in mantle-wedge serpentinites under high pore fluid pressure and their implications for deep low frequency earthquakes

Kengo Kataoka[1], Yurina Nagata[1], *Ken-ichi Hirauchi[1], Ryosuke Oyanagi[2], Atsushi Okamoto[3], Katsuyoshi Michibayashi[4] (1.Department of Geosciences, Faculty of Science, Shizuoka University, 2.Japan Agency for Marine-Earth Science and Technology, 3.Graduate School of Environmental studies, Tohoku University, 4.Department of Earth and Planetary Sciences, Nagoya University)

[SCG48-P32] Spatial distribution of slow slip events off the Boso peninsula from 1996 to 2018 under sparsity constraints

*Ryoko Nakata[1], Hideitsu Hino[2], Tatsu Kuwatani[3,4], Takahiro Akiyama[5], Shoichi Yoshioka[6], Masato Okada[7], Takane Hori[1] (1.Japan Agency for Marine-Earth Science and Technology, 2.The Institute of Statistical Mathematics, 3.Department of Solid Earth Geochemistry, Japan Agency for Marine-Earth Science and Technology, 4.PRESTO, Japan Science and Technology Agency, 5.Graduate School of Science, Kobe University, 6.Research Center for Urban Safety and Security, Kobe University, 7.Graduate School of Frontier Sciences, The University of Tokyo)

[SCG48-P33] Marine electromagnetic observations around a slow earthquake region in the western Nankai trough

*Hiroshi Ichihara[1], Tada-nori Goto[2], Tetsuo Matsuno[3], Noriko Tada[4], Shinya Sato[2] (1.Earthquake and Volcano Research Center, Nagoya University, 2.Graduate School of Engineering, Kyoto University, 3.Ocean Bottom Exploration Center, Kobe University, 4.JAMSTEC)

[SCG48-P34] Dynamics of precipitating injection fronts inside of structured medium

*Yutaka Sumino[1], Shunsuke Tanaka[1], Miyuki Kunihiro[1] (1.Tokyo University of Science)

[SCG48-P35] Permeability changes of simulated low permeable fault rocks induced by intermediate velocity friction test

*Wataru Tanikawa[1] (1.Japan Agency for Marine-Earth Science and Technology, Kochi Instutute for Core Sample Research)

[SCG48-P36] Modified relation between the coupling and tremor rates around the Shikoku region

*Tadafumi Ochi[1] (1.Institute of Earthquake and Volcano Geology, Geological Survey of Japan, The National Institute of Advanced Industrial Science and Technology)

[SCG48-P37] Spatiotemporal distribution of regular and very low-frequency earthquakes in the northern part of the Ryukyu subduction zone

*Youichi Asano[1], Kazuhiko Goto[2], Hiroshi Yakiwara[3], Shuichiro Hirano[3] (1.National Research Institute for Earth Science and Disaster Resilience, 2.Association for the development of earthquake prediction,

3.Nansei-toko Observatory for Earthquakes and Volcanoes, Kagoshima University)

[SCG48-P38] Possible tectonic tremor activities near the VLFE epicenters in the Sanriku-Oki region in 2011

*Hidenobu Takahashi[1], Ryota Hino[1], Yusaku Ohta[1], Naoki Uchida[1], Syuichi Suzuki[1], Masanao Shinohara[2], Takanori Matsuzawa[3] (1.Graduate school of Science Tohoku University , 2.Earthquake Research Institute, University of Tokyo, 3.National Research Institute for Earth Science and Disaster Resilience)

[SCG48-P39] Heterogeneous structure around a region of slow earthquake activity off Ibaraki prefecture along the Japan Trench

*Kimihiro Mochizuki[1], Tomoaki Yamada[1], Masanao Shinohara[1], Ryota Hino[2], Ryosuke Azuma[2], Yoshihiro Ito[3], Yoshio Murai[4], Kenji Uehira[5], Toshinori Sato[6] (1.ERI, Univ. of Tokyo, 2.Graduate School of Science, Tohoku Univ., 3.DPRI, Kyoto Univ., 4.Faculty of Science, Hokkaido Univ., 5.NIED, 6.Graduate School of Science, Chiba Univ.)

[SCG48-P40] Shallow low-frequency tremor triggered by nearby moderate earthquakes off Sanriku

*Sachiko Tanaka[1], Takanori Matsuzawa[1], Youichi Asano[1] (1.National Research Institute for Earth Science and Disaster Resilience)

[SCG48-P41] Slow slip events in the Bungo Channel over 15 years as inferred from GNSS data (1996-2011)

Takatoshi Yokoi[1], *SHINICHI MIYAZAKI[1], Hiromu Sakaue[1], Jun'ichi Fukuda[2] (1.Graduate School of Science, Kyoto University, 2.Earthquake Research Institute, The University of Tokyo)

[SCG48-P42] Investigations of sensor orientation and a possibility of detecting crustal deformation based on accelerometer records of S-net

*Ryota Takagi[1], Naoki Uchida[1], Takashi NAKAYAMA[1], Ryosuke Azuma[1], Akira Ishigami[1], Tomomi Okada[1], Yusaku Ohta[1], Ryota Hino[1] (1.Research Center for Prediction of Earthquakes and Volcanic Eruptions, Graduate School of Science, Tohoku University)

[SCG48-P43] Spatiotemporal variation of released seismic energy from shallow low-frequency tremor in Hyuga-nada, revealed by ocean bottom seismological observation

*Yusuke Yamashita[1], Saki Watanabe[2], Tomoaki Yamada[3], Masanao Shinohara[3], Takeshi Matsushima[2] (1.Disaster Prevention Research Institute, Kyoto University, 2.Institute of Seismology and Volcanology, Kyushu University, 3.Earthquake Research Institute, The University of Tokyo)

[SCG48-P44] Unified description of fast and slow earthquakes using velocity strengthening patches

*So Ozawa[1], Takahiro Hatano[1] (1.Earthquake Research Institute, the University of Tokyo)

[SCG48-P45] The b-value of the earthquake swarm activities accompanied by the Boso slow slip events

*Yuki Noda[1], Hitoshi Hirose[2,1] (1.Department of Planetology, Faculty of Science, Kobe University , 2.Research Center for Urban Safety and Security, Kobe University)

[SCG48-P46] **Three-dimensional thermal modeling associated with subduction of the Philippine Sea plate at the Ryukyu Trench, and its relation to the occurrence of interplate seismic events**

*Nobuaki Suenaga[1], Shoichi Yoshioka[2,1], Yinfeng Ji[3] (1.Graduate School of Science, Kobe University, Japan, 2.Research Center for Urban Safety and Security, Kobe University, Japan, 3.Chinese Academy of Science, Beijin, China)

Off the Kii Peninsula Shallow Low Frequency Earthquake in 2004 revealed by Ocean Bottom Seismometer

*Koji Tamaribuchi[1], Akio Kobayashi[1], Takahito Nishimiya[1], Satoshi Annoura[2]

1. Meteorological Research Institute, 2. Japan Meteorological Agency

The 2004 off the Kii Peninsula earthquakes (Mj7.1, 7.4) occurred near the Nankai trough axis, southeast off the Kii Peninsula, Japan, on September 5, 2004. After the earthquakes, the Meteorological Research Institute conducted OBS observation to examine the aftershock distribution accurately. Although the analysis was limited to hypocenter relocation of "ordinary aftershocks", no analysis was done for slow events. In this study, it is shown that many low-frequency earthquakes (LFEs) occurred in "ordinary aftershocks" from the detailed inspection of our observation. During the observation period, the frequency of LFE gradually decreased. Since P- and S-arrival times are unclear, it is difficult to determine the distribution of the hypocenter accurately. However, by using the Amplitude Source Location (ASL; Battaglia and Aki, 2003), the LFEs are located between a splay fault and trench axis. The 2004 OBS stations are located east of the DONET, and many LFEs are detected in the 2004 OBS network. In addition, there are many very-low-frequency events (VLFEs) in the F-net waveforms with very-low-frequency band-pass filter (0.02 - 0.05 Hz) during the observation period. We found that the identified LFEs were associated with VLFEs since their amplitudes seemed to be correlated. This means that the LFEs and VLFEs show the same phenomenon. Our observations might contribute to reveal the relationship between ordinary aftershocks, slow-events, and megathrust events such as Nankai trough earthquake.

Keywords: LFE, OBS, 2004 off the Kii Peninsula earthquakes

©2019. Japan Geoscience Union. All Right Reserved.

The development of pressure vessel on gouges for rock deformation at seismic rates under water-saturated conditions

*Wei-Ting Lin[1], Li-Wei Kuo[1], Wen-Jie Wu[1], Jia-Jyun Dong[1], Yi-Hung Huang[2]

1. National Central University, 2. MATSUKI HYDRAULIC INDUSTRIAL CO. LTD

To understand earthquake mechanism and fault behavior during earthquake ruptures, experimentalists commonly conduct rock deformation tests with rotary shear apparatus (e.g., low-to high-velocity rock friction experiment, LHVR) which allow deformed at seismic rates. In general, the materials utilized for rotary shear apparatus are both cohesive rocks (e.g., gabbro and carbonate) and incohesive rocks (natural fault gouges and synthetic rock powders), while the latter are deformed at seismic rates and, commonly at low normal stresses (0.5 to 2 MPa confining with a plastic Teflon ring). However, using Teflon rings has issues of gouge extrusion and chemical contamination, in particular, at high normal stresses (>3MPa) and water-saturated condition, and the obtained mechanical data and associated experimental products seem to be questionable. Here we develop a metal pressure vessel for LHVR to deform gouges at seismic rates and, importantly, expand the normal stress capability (up to 15 MPa) and under water-saturated condition. Our results show the resistance from the pressure vessel itself (metal-to-metal contact) is extremely low (friction coefficient ≈0.02), and the result of kaolinite is similar to the previously published data. In particular, both gouge-extrusion and water-leaking was not observed deformed at a normal stress of 15 MPa and equivalent velocity 1 m/s. The designed pressure vessel could fill the gap of experimental conditions among the current used pressure vessels and complete the understanding of fault ruptures.

Keywords: pressure vessel, water-saturated condition, fault gouge, rotary shear experiment

©2019. Japan Geoscience Union. All Right Reserved.

Spatial variations of shallow very low-frequency earthquake activity along the Nankai Trough based on CMT inversion using the 3D heterogeneous model

*Shunsuke Takemura[1], Takanori Matsuzawa[1], Akemi Noda[1], Takashi Tonegawa[2], Youichi Asano[1], Takeshi Kimura[1], Katsuhiko Shiomi[1]

1. National Research Institute for Earth Science and Disaster Resilience, 2. Japan Agency for Marine-Earth Science and Technology

To reveal structural properties around the Philippine Sea plate boundary, we investigated spatial variation of shallow very low-frequency earthquake (SVLFE) activity along the Nankai Trough. By using F-net velocity seismograms for periods of 20-50s, we conducted centroid moment tensor (CMT) inversion of SVLFEs detected by array analysis of Asano et al. (2008 EPS). Our CMT method is basically same as in Takemura et al. (2018 GRL). Source grids were assumed on the boundary of the Philippine Sea plate at horizontal intervals of 0.1°. Green's functions from source grids to F-net stations were evaluated by finite-difference method simulations of seismic wave propagation within the 3D heterogeneous structure model of Takemura et al. (2019 PAGEOPH).

We applied our CMT method to SVLFEs occurred from June 2003 to May 2018. Almost of CMT solutions are low-angle thrust faulting mechanism occurred around the accretionary prism toe. We evaluated spatial variations of SVLFE activity along the Nankai trough by calculating cumulative moment at each source grid. The areas with large cumulative moments appeared near the trench axis of off the Cape Muroto, the Kii Channel and the southeastern Kii Peninsula. We found spatial correlations between cumulative moment, slip-deficit rate (Noda et al. 2018 JGR) and *S*-wave velocities (Tonegawa et al. 2017 Nature Comm.) around the Philippine Sea plate boundary. Such spatial correlations suggest that SVLFEs are effectively activated by mechanically weakening due to pore fluid at surrounding area of strongly locked zone of the Philippine Sea plate.

Acknowledgement
NIED F-net broadband velocity seismograms were used. The catalogs of slow earthquakes were downloaded from the website of slow earthquake database (Kano et al., 2018 SRL). Finite-different method simulations were conducted on the Earth Simulator at the JAMSTEC.

Keywords: Nankai Trough, Shallow very low-frequency earthquake, CMT inversion, Pore fluid pressure, Slip deficit rate

©2019. Japan Geoscience Union. All Right Reserved.

Evaluation of Magnitude and Characteristics of Seismicity of Low Frequency Earthquakes in Parkfield

*Miki Aso[1,3], Naofumi Aso[2], Satoshi Ide[1]

1. Department of Earth and Planetary Science, The University of Tokyo, 2. Tokyo Institute of Technology, School of Science, 3. OYO RMS Corporation

Over a million tectonic low frequency earthquakes (LFEs) have been found in Parkfield along the San Andreas Fault, as 88 families by Shelly and Hardebeck [2010]. Thanks to enormous event detection, interesting characteristics focusing on their event amplitudes have been reported such as the spatial variation along the fault, the exponential frequency distribution for each family, and the relationship with recurrence time [Shelly and Hardebeck, 2010; Shelly, 2010]. However, the relative size of families has not been quantified accurately, because we have to consider various factors such as radiation pattern depending on focal mechanisms, attenuation during wave propagation, and site amplification effects. For quantitative comparison of scale among differently located events, here we estimate the absolute magnitude of each event considered those effects.

We estimate the seismic moment Mo [Nm] and moment magnitude Mw of all LFE events in the catalog of Shelly [2017]. We first stack seismograms of over one million events in the catalog to improve the signal-to-noise (S/N) ratio. Then, we evaluate the absolute amplitude of the original seismograms using the stacked waveforms. Specifically, we evaluate seismic moment Mo by assuming focal mechanisms of each family, attenuation quality factor, site effect estimated by Aso et al. [2019, submitted to JpGU meeting, “Variations of Focal Mechanisms of Low Frequency Earthquake in Parkfield”], and the source time function estimated by Thomas et al. [2016]. Note that we consider the frequency-limited seismic moment Mo, though it is not exactly the same as the original definition of seismic moment measured at a lower frequency than the minimum frequency contained in one phenomenon.

As previously reported by reported by Shelly and Hardebeck [2010], LFEs in the southern part has larger magnitude. We also find that shallower events are smaller than deeper events.

Similarly, most of the frequency distribution for each family shows an exponential distribution which is also reported for LFEs in Cascadia [Sweet et al., 2014] and New Zealand [Chamberlain et al., 2014].

By comparing size and recurrence interval, the events during LFE burst (seconds interval) tend to be larger than the first event of burst, which occurs after hours-to-days quiescence. A similar tendency is found in tremor burst occurring with a longer time scale (~1-week-long) than that of LFEs (~1-minute-long) [Yabe and Ide, 2014]. These might suggest some temporal change in fault rheology and/or some characteristic spatiotemporal behavior such as Brownian slow earthquake processes [Ide, 2008].

Keywords: San Andreas Fault, Parkfield, seismicity, waveform stacking, low frequency earthquake, amplitude evaluation

©2019. Japan Geoscience Union. All Right Reserved.

Tectonic tremor catalog in the Tohoku-Hokkaido-Oki region using S-net

*Satoshi Ide[1], Tomoaki Nishikawa[2], Takanori Matsuzawa[3], Kazuaki Ohta[2], Naoki Uchida[4], Takuya NISHIMURA[2]

1. Department of Earth an Planetary Science, University of Tokyo, 2. Disaster Prevention Research Institute, Kyoto University, 3. National Research Institute for Earth Science and Disaster Resilience, 4. Graduate School of Science and International Research Institute of Disaster Science, Tohoku University

Recently, various slow earthquakes have discovered in the subduction zone off Tohoku and Hokkaido regions along the Japan Trench. In this presentation, we report the detection of tectonic tremors using the Seafloor Observation Network for Earthquakes and Tsunamis along the Japan Trench (S-net), operated by The National Research Institute for Earth Science and Disaster Resilience (NIED).

We used continuous seismograms from August 2016 to August 2018 recorded by short-period sensors at 150 S-net stations. The original data were converted to envelope waveforms and analyzed using the envelope correlation method coded by Ide (2010), for each 300 s time windows with 150 s overlap. Since the results included many ordinary earthquakes with short durations, we regarded the events with durations longer than 20 s as tremors. This number is twice longer than that used for deep tremors in western Japan, reflecting the long-lasting waves in ocean bottom observation.

We found that the detection completeness is not high due to the high seismic activity in the Japan Trench, especially after the occurrence of large earthquakes, with numerous aftershocks falsely detected. We therefore divided the study area into 18 overlapping sub-regions that cover the locations of tremor activity to solve this problem. We detected tremors in each sub-region and merged the results into one catalogue by removing one of any two events within 10 s and 1 degree of each other, depending on their root-mean-square errors. Some tremor-like signals were found near the triple junction off the Boso Peninsula at approximately 34.8˚N. However, visual inspection revealed these events to be ordinary earthquakes, which we excluded from our tremor catalogue. The resultant tremor catalogue will be available in Slow Earthquake Database (Kano et al., 2018).

Keywords: tectonic tremor, slow earthquake, ocean bottom seismometer, S-net, Japan trench

©2019. Japan Geoscience Union. All Right Reserved.

Spontaneous Slow Slip and Runaway Slip in Laboratory

*Miki Takahashi[1]

1. Institute of Earthquake and Volcano Geology, Geological Survey of Japan, AIST

Earthquake nucleation and propagation involves the acceleration of slip on a fault from a background, quasi-static, low-velocity state towards meter-per-second values. From shear experiments using brine-saturated simulated gouge composed of 80:20 wt.% mixtures of halite and muscovite (following e.g. Niemeijer & Spiers, 2007, JGR), Takahashi et al., [2017, G-cubed] recently reported a switch in the dominant deformation process, from distributed viscous flow (pressure solution creep) to localized brittle deformation, at a critical velocity V_c (~20 μm/sec). The direct effect which is normally observed upon perturbations in sliding rate disappears for $V > V_c$, suggesting that runaway fault-slip may be achieved when the sliding velocity exceeds V_c.
At relatively low shear stress, flow mechanisms, such as pressure solution creep and dislocation creep, will be fast enough to effectively suppress slip acceleration. However, with increasing the shear stress, there may be a velocity range in which flow mechanisms still works but not as effective. Hypothesizing that, under constant shear stress boundary conditions, this may lead to spontaneous acceleration followed by deceleration, analogous to a slow slip event. Moreover, imposing the constant shear stress with equal or larger value of the maximum strength of the simulated gouge, I also hypothesize that slip acceleration may proceed as $V > V_c$, inducing a dynamic weakening.
To address these hypotheses, I conducted torque-controlled rotary shear experiments, using brine-saturated, 80:20 wt % mixtures of halite (grain size < 75 μm) and muscovite (grain size < 33 μm) powders. Approximately 1.65 g of the gouge mixture was sandwiched between two teethed steel piston rings, forming an initially 1 mm thick layer. The piston rings had an inner diameter of 38 mm, and an outer diameter of 50 mm. I used a high-velocity rotary shear apparatus designed by T. Shimamoto [e.g., Togo and Shimamoto, 2012], and now installed at the Geological Survey of Japan (GSJ). The apparatus was modified to enable torque control with an accuracy of ±0.002 in the friction coefficient (μ), at a normal stress of 5 MPa. Rotation displacement is measured using a potentiometer installed close to the piston ring at the rotating side.
A preliminary result shows the velocity evolution after stepwise changes in the shear stress. At low shear stresses, corresponding to the pressure solution creep-controlled regime, transient increasing velocity towards a steady-state values suggests stable sliding. At $\mu \approx 0.6$, the simulated gouge shows spontaneous acceleration to $V \approx 1$ μm/sec, followed by deceleration. Lastly, under a constant shear stress condition equivalent to $\mu = 0.67$, spontaneous slip acceleration occurred followed by dynamic weakening at $V \approx V_c = 20$ μm/sec. More experiments and microstructural observations will help to elucidate the relationship between the critical velocity and the switch among dominant deformation mechanisms.

Keywords: shear stress control test, spontaneous acceleration/deceleration, dynamic weakening

©2019. Japan Geoscience Union. All Right Reserved.

Hydration and amorphization of quartz rocks during high-velocity frictional sliding: An examination of fault gouge from friction experiments of synthetic quartz

*Yuko Onoe[1], Hirotaka Iida[2], Akito Tsutsumi[1], Aki Takigawa[1]

1. Graduate School of Science, Kyoto University, 2. Geothermal Engineering Co., Ltd.

Various types of rocks and fault gouges display weakening of frictional strength at high-velocities, and in many cases, it is caused by high-temperature faulting processes such as frictional melting and thermal decomposition of fault materials. On the other hand, siliceous rocks display weakening of frictional strength at relatively slow slip velocity of ~1 mm/s. This weakening is a specific phenomenon because frictional heat is not sufficient to induce the high-temperature transformation reactions in this slip velocity range [Di Toro et al., 2004]. Goldsby and Tullis [2002] proposed gel lubrication model to explain the weakening of siliceous rocks; in which model frictional weakening likely results from production and shearing of hydrated amorphous silica layer along a fault in quartz rocks. But the relationship between the frictional weakening and hydration and amorphization of fault gouge is not clear yet.

This study aims to elucidate the mechanism of the frictional weakening observed for siliceous rocks. We conducted a series of friction experiments on synthetic quartz samples using a rotary-shear, intermediate-to high-velocity friction testing machine. Experiments were carried out under a constant normal stress condition of 1.5 MPa and at slip velocities of 5 μm/s, 10 μm/s, 105 μm/s, 1 mm/s, 10 mm/s and 105 mm/s. In this study effect of drying the sample on the frictional behavior were examined by introducing dry air to the chamber of the sample. After the friction tests, the gouge material on the slip surfaces were collected and analyzed by FTIR.

The frictional behavior of the synthetic quartz differs between room humidity and dry conditions; velocity weakening was observed for both conditions, however, velocity weakening starts at lower slip velocities for the dry experiments. Under DRY conditions, the frictional weakening occurs at slip velocity around 10 μm/s. From the results of the FTIR analysis, hydration of the gouge is confirmed for all the samples tested in this study. The FTIR result also indicates that the faster the slip velocity, the more the crystal structure of the gouge is destructed.
It is showed that under both DRY and Room Humidity conditions, at least the gouge generated on the friction surface of the sample which showed slip weakening is hydrated, consistent with the weakening model of Goldsby and Tullis [2002].

©2019. Japan Geoscience Union. All Right Reserved.

Constraining S Wave Velocity of the Source Region of Shallow Very Low-Frequency Earthquakes

*Takeshi Akuhara[1], Takashi Tonegawa[2]

1. Earthquake Research Institute, The University of Tokyo, 2. Research and Development center for Earthquake and Tsunami, Japan Agency for Marine-Earth Science and Technology

Shallow very low-frequency earthquakes (VLFEs), which are believed to occur in the vicinity of megathrusts, have been often associated with elevated pore fluid pressure. Lines of evidence for this idea include a small amount of stress drop, high tidal sensitivity, and reduced P wave velocity inferred from active source seismic surveys. Revealing the physical properties of the source region of shallow VLFEs will lead to a better understanding of their generation mechanisms. However, the challenge lies in the difficulty of acquiring S wave velocity in fine resolution.

Recent achievements by the authors may help overcome this issue. Akuhara et al. (2019) developed a robust technique to estimate Green's functions of receiver side structures from offshore seismograms, which are typically ill-conditioned due to water reverberations. Tonegawa et al. (2017) inverted Rayleigh wave admittance (i.e., a ratio of ground displacement to hydraulic pressure) for shallow S wave velocity structures beneath DONET seafloor observatories at the Nankai Trough subduction zone. Their velocity models show low-velocity zones that characterize the source regions of shallow VLFEs. However, a smoothing constraint imposed on the models renders their interpretation somewhat difficult.

This study presents preliminary results from transdimensional inversion of receiver-side Green's function estimated by the method of Akuhara et al. (2019), where we adopt a prior constraint by the velocity models of Tonegawa et al. (2017). Complementary to the Rayleigh admittance, the Green's function approach is sensitive to velocity contrasts and thus will offer an improved resolution.

Keywords: shallow very low frequency earthquake, seismic velocity structure, ocean bottom seismometer, bayesian analysis

©2019. Japan Geoscience Union. All Right Reserved.

Quantitative relationship between aseismic slip propagation speed and frictional properties

*Keisuke Ariyoshi[1], Jean-Paul Ampuero[2,3], Roland Burgmann[4], Toru Matsuzawa[5], Akira Hasegawa[5], Ryota Hino[5], Takane Hori[1]

1. Japan Agency for Marine-Earth Science and Technology, 2. Université Côte d'Azur, 3. California Institute of Technology, 4. University of California, Berkeley, 5. Graduate School of Science, Tohoku University

Recent observations show evidence of propagation of postseismic slip, whose propagation speed may contain information about the mechanical properties of faults. Here, we develop a new analytical relationship between the propagation speed of aseismic slip transients and fault frictional properties, modeled by a rate- and state-dependent friction law. The relationship explains the propagation speed of afterslip in 3-D numerical simulations to first order. Based on this relationship, we identify systematic dependencies of afterslip propagation speed on effective normal stress σ and frictional properties (the coefficients a and a-b which quantify the instantaneous and the steady-state velocity-dependence of friction, respectively, and the characteristic slip distance d_c of fault state evolution). Lower values of the parameter $A=a\sigma$ cause faster propagation in areas where the passage of the postseismic slip front induces large shear stress changes $\Delta\tau$ compared to A, which are typically located near the mainshock rupture. In areas where $\Delta\tau/A$ is small, typically more distant from the mainshock, afterslip propagation speed is more sensitive to (a-b) σ. The propagation speed is proportional to initial slip velocity and inversely proportional to d_c. The relationship developed here should be useful to constrain the frictional properties of faults based on observed propagation speeds, independently of rock laboratory experiments, which can then be used in predictive numerical simulations of aseismic slip phenomena.

Keywords: rate- and state-dependent friction, effective normal stress, stress perturbation

©2019. Japan Geoscience Union. All Right Reserved.

Comprehensive detection of very low frequency earthquakes off the Pacific coasts of Hokkaido and Tohoku, northeastern Japan

*Satoru Baba[1], Akiko Takeo[1], Kazushige Obara[1], Takanori Matsuzawa[2], Takuto Maeda[3]

1. Earthquake Research Institute, University of Tokyo, 2. National Research Institute for Earth Science and Disaster Resilience, 3. Graduate School of Science and Technology, Hirosaki University

Very low frequency earthquakes (VLFEs), classified as one type of slow earthquakes, occur near seismogenic zones. VLFEs off the Pacific coasts of Hokkaido and Tohoku in northeastern Japan occur around subducting plate interfaces near trenches. Asano et al. (2008) found VLFEs in the off-Tokachi region, the southern part of the Pacific coast of Hokkaido along the Kuril Trench, by array signal processing using high-sensitivity accelerometers of Hi-net operated by National Research Institute for Earth Science and Disaster Resilience (NIED). In recent years, VLFEs off the Pacific coast of Tohoku were found by visually checking broadband seismograms of F-net operated by NIED and other events were detected by the matched-filter technique using waveforms of detected events as templates (Matsuzawa et al., 2015). However, the number of detected VLFEs may have been limited because of the small number of the VLFE templates in previous studies. Baba et al. (2018, SSJ) set four virtual epicenters off the Pacific coasts of Hokkaido and Tohoku and detected VLFEs by the matched-filter technique using numerically simulated waveforms as templates. We extended virtual epicentral gridsto make more comprehensive detection of VLFEs.

We used continuous seismograms of F-net seismometers from January 2003 to July 2018 after applying a band-pass filter of 0.02–0.05 Hz. We set 123 virtual epicentral grids off the Pacific coasts of Hokkaido and Tohoku, and computed the synthetic waveform from the source at each virtual epicenter by the finite difference method with a three-dimensional velocity structure model, namely, Japan Integrated Velocity Structure Model (Koketsu et al., 2012). The fault mechanisms were assumed to be consistent with the geometry of the plate boundary and a plate motion model, NUVEL-1A. We then calculated station- and component-averaged cross-correlation coefficients (averaged CC) between synthetic waveforms and the data of F-net seismograms every 1 s, and selected the events which have averaged CC above nine times of the median absolute deviation of the distribution. This method is, however, sensitive to regular earthquakes and teleseismic events as well. We then excluded the signal of regular earthquakes by discarding events with the amplitudes of more than 160 nm/s at 1-2 Hz in vertical components at the nearest stations. Moreover, to remove teleseismic events, we used the USGS earthquake catalog and discarded events with high amplitudes and low averaged cross-correlation coefficients.

VLFE activities in the off-Tokachi and off-Aomori regions show synchronized episodic bursts in the interval of several months. VLFEs in the off-Tokachi region was rapidly increased by the afterslip of the 2003 Tokachi-Oki earthquake. Those in the off-Iwate and off-Ibaraki regions, located out of the coseismic slip area of the 2011 off the Pacific coast of Tohoku Earthquake (hereinafter, the Tohoku earthquake), were also rapidly increased by the afterslip of the Tohoku earthquake. VLFE activity in the off-Miyagi region is characterized by episodic bursts in the interval of several months to one year before the Tohoku earthquake, but it became low since then. VLFE activity in the off-Fukushima region show dramatic increase after an Mw 6.9 earthquake at off-Fukushima on July 19, 2008. In the off-Miyagi and off-Fukushima regions, located within or at the edge of the coseismic slip area of the Tohoku earthquake, VLFE activity has been low since the Tohoku earthquake probably because the earthquake released the

©2019. Japan Geoscience Union. All Right Reserved.

stress almost completely. These results suggest that VLFEs are sensitive to the stress perturbation and can be a slip meter that reflect spatiotemporal change of the interplate slip, as has been indicated by previous studies. Consequently, one possible cause of these episodic VLFE bursts in the off-Tokachi, off-Aomori and off-Miyagi regions may be the intermittent release of small portion of stress accumulated by interplate locking between plates in the interval of several months to one year. The interval of episodic bursts is shorter than a periodicity of slow slips ranging from 1 to 6 years off the Pacific coasts of Tohoku indicated by Uchida et al. (2016).

©2019. Japan Geoscience Union. All Right Reserved.

Spatio-temporal evolution of long- and short-term slow slip events in the Tokai region, central Japan estimated from a very dense GNSS network, during 1997-2017

*Hiromu Sakaue[1], Takuya NISHIMURA[2], Jun'ichi Fukuda[3], Teruyuki Kato[4]

1. Graduate School of Science, Kyoto University, 2. Disaster Prevention Research Institute Kyoto University, 3. Earthquake Research Institute,The University of Tokyo, 4. Hot Springs Research Institute of Kanagawa Prefecture

The long-term slow slip events (SSEs) have been reported on the subducting Philippine Sea Plate in the Tokai region, central Japan during 2001-2005 and 2013-2016. Many short-term slow slip events have been also observed there since 1996. We analyzed GNSS data from 1997 to 2017 to estimate spatiotemporal distribution of interplate slip associated with these SSEs in this study. The GIPSY-OASIS II software (version 6.1) was used to estimate daily coordinates of GNSS stations operated by GSI and JUNCO (the Japanese University Consortium for GPS Research). It is well known that GNSS time series have many systematic signals and noises that do not result from SSEs. They include, for example, seasonal variations, co- and post-seismic deformation of the 2004 southeast off Kii Peninsula earthquakes (M_w 7.3/7.4), the 2008 Ibaraki-ken-oki earthquake (M_w6.9), the 2008 Fukushima-ken-oki earthquake (M_w7.0) and the 2011 Tohoku-oki earthquake (M_w9.0), and crustal deformation of volcanic activity on the northern Izu Islands in 2000. After removing them, we applied a modified Network Inversion Filter (NIF) [Fukuda et al., 2008] to estimate daily slip and slip rate on the subduction plate interface.
Our results suggest that not only long-term SSEs (M_w~7.1 and M_w~6.7) in 2000-2005 and 2013-2016, but also short-term SSEs (M_w<6.1). The maximum estimated daily slip rates for short-term SSEs are an order of magnitude larger than those of the long-term SSE, and peak slip for short-term SSEs migrates along strike with LFTs synchronously. It suggests that LFTs are loaded directly by SSEs, and that slip rate regulates LFT genesis. We will present the change of back slip rate between inter short-term SSEs and characteristics of short-term SSEs (e.g. slip rates and recurrence interval) depending on the occurrence of long-term SSE.

Keywords: slow slip event, Tokai region, GNSS

©2019. Japan Geoscience Union. All Right Reserved.

Broadband excitation of acoustic emission in granular stick-slip : experiments and spectral analyses

*Hidekazu Fukumizu[1], Ikuro Sumita[2]

1. Earth and Environmental Science Course, Division of Natural System, Graduate school of Natural Science and Technology, Kanazawa University, 2. School of Geosciences and Civil Engineering, Kanazawa University

Slow slip and tremor are observed to occur simultaneously (e.g., Rogers and Dragert, Science, 2003). Such observation can be modelled using granular stick-slip experiments which show that the timing of the slips and acoustic emission (AE) are well correlated (e.g., Johnson et al., GRL, 2013, Jiang et al. GRL, 2017). AE waveforms are complex (e.g., Michlmayr & Or, Gran. Matt., 2014), and we do not fully understand the details of the temporal change of AE during the slip. Here we report the results of granular stick-slip experiments which focus on how their spectra depend on the shear rate, particle size and container size.

We shear glass beads contained in a stainless steel beaker using a rotating viscometer to which a vane spindle is attached (Higashi and Sumita, JGR, 2009), and measure the shear stress and AE at 200kHz. We use broadband accelerometers and microphones to measure AE. Four accelerometers are attached at the outer rim of the beaker, and each are separated by an angle of 90 degrees.

We integrate the acceleration to obtain AE velocity –time series data and analyze their characteristics in broad band. We find that although AE has a broad spectrum, the spectra show that there are two characteristic frequency (f) components ; a high-f (of the order of 100 Hz) and a low-f (of the order of 10Hz) components. The velocity waveforms recorded at antipodal positions, show that the high-f components are in phase, whereas the low-f components are of the opposite phase. This indicates that the mechanism which excite these components differ : the high-f component may correspond to AE excited by particle rearrangement, whereas the low-f component may correspond to the translational motion of the container. Indeed we find that the frequency of the low-f component depends on the container size.

We also conducted experiments using a rheometer in a parallel-plate setup and confirmed that these two different components exist. When the particle size becomes larger, the amplitude of the shear stress and the AE velocity increases. Furthermore we find that the mean frequency of the normalized power spectra rose to a higher frequency, thus correlating with the stress increase.

Our experiments indicate that AE is excited in broadband, and that their frequency components can be used to infer the interparticle stress. Such excitation appear to be analogous to tremors and very low frequency earthquakes that are also excited simultaneously.

Keywords: granular matter, stick-slip, acoustic emission, earthquake, tremor

©2019. Japan Geoscience Union. All Right Reserved.

Episodic tremor and slip silently invades strongly locked megathrust in the Nankai Trough

*Masayuki Kano[1], Aitaro Kato[2], Kazushige Obara[2]

1. Graduate school of science, Tohoku University, 2. Earthquake Research Institute, The University of Tokyo

Recent seismic and geodetic observations in subduction zones have revealed that slow earthquakes have preceded some large earthquakes (e.g., Kato et al., 2012; Mavrommatis et al., 2014; Ruiz et al., 2014). Characterization of slow earthquakes and their relation to large earthquakes provides important clues to constrain a wide spectrum of slip rates on tectonic faults. In this study, we report new evidence of a slow slip transient at the downdip edge of the strongly locked seismogenic zone in the western Nankai Trough in southwest Japan based on GNSS time series. This slow slip transient was remotely excited during an episodic tremor and slip at the downdip extension of the locked zone. Through this remote triggering, the frequent occurrence of the deep episodic tremor and slip invades the strongly locked megathrust zone and may intermittently increase the probability of large earthquakes in the Nankai Trough.

Acknowledgments

We used GNSS data provided by the Geospatial Information Authority of Japan. This study was supported by the JSPS KAKENHI Grant Number JP15K17743 in Grant-in-Aid for Young Scientists (B), JP18K03796 in Grant-in-Aid for Scientific Research (C), JP16H06473 and JP16H06474 in Scientific Research on Innovative Areas “Science of Slow Earthquakes.”

Keywords: Slow slip events, Slow earthquakes, Western Shikoku, GNSS

©2019. Japan Geoscience Union. All Right Reserved.

Spatial distribution of the electrical resistivity beneath western part of Shikoku Island where long-term SSE events have repeatedly occurred

*Makoto Uyeshima[1], Maki Hata[1], Hiroshi Ichihara[2], Ryokei Yoshimura[3], Koki Aizawa[4]

1. Earthquake Research Institute, The University of Tokyo, 2. Graduate School of Environmental Studies, Nagoya University, 3. Disaster Prevention Research Institute, Kyoto University, 4. Institute of Seismology and Volcanology, Faculty of Sciences, Kyushu University

In the Bungo channel area at the western margin of the Nankai megathrust rupture zones, the long-term slow slip events (SSE) repeatedly occurred about every 6 or 7 years. Since the last large-scale SSE event occurred in 2010, we will have a next large event soon. In order to obtain the electrical resistivity structure in the vicinity of the SSE area and examine its temporal change, we have started the Network-MT survey in the western part of the Shikoku Island facing the Bungo channel since April, 2016. Just before beginning of the observation, a tiny-scale SSE event occurred in the Bungo-channel (Ozawa, 2017, Hirose et al., 2018). We selected 17 areas in the western part of the Shikoku Island and installed 3 or 4 electrodes in the respective areas. The electrical potential differences with typical electrode spacing of several km are measured by using metallic telephone line network. We also measure the geomagnetic field at two stations in the target region. With the aid of the BIRRP code (Chave and Thomson, 2004), we could estimate the frequency-domain Network-MT response functions of good quality between the voltage difference and the magnetic field. The Network-MT response functions were directly inverted to estimate the 3-D resistivity structure in this area with the aid of the DASOCC Network-MT 3-D inversion code (Siripunvaraporn, Uyeshima & Egbert, 2004).

Conductive portions are commonly detected in the mid-crust of the target region. Their roots are just on the upper surface of the subducting Philippine Sea slab. This may suggest dehydration there. Among the spatial distribution of resistivity, that of seismic P-wave attenuation (Kita and Matsubara, 2016), and that of SSE slips (e.g. Ozawa et al., 2013, Yoshioka et al., 2015, Hirose et al., 2018), some mutually related features are detected. Low Qp (high attenuation) areas tend to correspond to highly conductive areas. The low Qp and highly conductive area are detected just above the subducting slab and outside of the SSE area. Inside the SSE area, while Qp takes generally high values, a patchy conductive area is detected in overall resistive background structure.

This study is supported by JSPS KAKENHI Grand Number JP16H06475 in Scientific Research on Innovative Areas "Science of Slow Earthquakes". It is also partly supported by the Ministry of Education, Culture, Sports, Science and Technology (MEXT) of Japan, under its Earthquake and Volcano Hazards Observation and Research Program. We acknowledge staffs of the Nippon Telegraph and Telephone WEST Corporation for their cordial support in the survey. We also thank H. Abe, A. Takeuchi and Y. Suwa for their help in preparing and installing instruments.

Keywords: slow slip event beneath the Bungo Channel, 3-D resistivity structure, Network-MT observation

©2019. Japan Geoscience Union. All Right Reserved.

Variations of scaling relationships for shallow tremor observed along the Nankai trough

*Masaru Nakano[1], Suguru Yabe[1]

1. Japan Agency for Marine-Earth Science and Technology

Scaling relationships of seismic phenomena is one of keys to understand the source processes. Size distributions of slow earthquakes as low-frequency earthquakes (LFEs), non-volcanic tremor (NVT), very-low-frequency earthquakes (VLFE), and slow-slip events (SSEs) have been studied in many locations. Some studies showed that the size distribution follow an exponential law (e.g. Watanabe et al., 2007; Hiramatsu et al., 2008; Chestler and Creager, 2017), while others showed that power law distributions better explain the observations (e.g. Kao et al., 2010; Bostock et al., 2015; Nakamura and Sunagawa, 2015).

Most of previous studies are for slow earthquakes that occur in regions deeper than the source region of megathrust earthquakes, and only a limited number of studies have been carried out for shallow slow earthquakes beneath accretionary prism as observed along the Nankai trough. Although observed characteristics of shallow and deep ones are very similar, physical conditions as temperature and pressure much differs in these region.

In our previous studies (Nakano et al., 2018SSJ, AGU), we obtained the result that shallow tremor follows a power law distribution with b values of about 1. In this study, we further analyzed tremor activities beneath the Muroto fore-arc basin. using data from DONET2. We estimated the seismic energy of tremor signals using the same method as our previous studies, during intensive activities starting in September 2015, April 2016, February 2017, and February 2018. The source region of each activity is different from each other, spanning between off Shiono-Misaki and off Cape Muroto.

The size distribution of each activity mostly follow power-law distributions, but the b value varies from 0.7 and 1.7. We note that the activity in 2016 is also well fitted by an exponential law, probably due to narrow range of observed event size distribution. Similar result has been obtained in the 2018 activity in Kumano. The size distribution deviate from a power law for largest events as observed in Kumano activities. This deviation at larger events would be due to limited system size, expected from the theoretical stochastic model of tremor by Ide and Yabe (2018). The upper limit of event size, and accordingly the system size, varies from activity to activity.

We also investigated the relation between the seismic energy and duration of tremor events. The relation also follows a power law, with slopes of 2.0 to 2.6 in Kumano, and 1.5 to 3.3 in Muroto. These values are again consistent with the expectation value of 2 from the model of Ide and Yabe (2018).

These investigations represent that the scaling relationships of shallow tremor are mostly consistent with the 2D PCA model by Ide and Yabe (2018). Further studies would be necessary to reproduce the observed variations of the scaling parameters.

Acknowledgments: We used DONET data and JMA and USGS earthquake catalogs in the analysis. This research was supported by JSPS KAKENHI Grant Number 16H06477 in Scientific Research on Innovative Areas “Science of Slow Earthquakes”

Keywords: DONET, Nankai trough, earthquake size distributions

©2019. Japan Geoscience Union. All Right Reserved.

Low-frequency earthquakes triggered by teleseismic surface waves by Ryukyu subduction zone.

Ayumi Kinjo[1], *Mamoru Nakamura[1]

1. Faculty of Science, University of the Ryukyus

We investigated low-frequency earthquakes (LFEs) in the Ryukyu Trench region that were triggered by surface waves from teleseismic earthquakes. Although these LFEs in the southwestern Ryukyu arc have previously been explored by Chao et al. (2016), their hypocenter distribution is not known in detail.

We selected 50 earthquakes from January 2004 to December 2016, which had magnitudes greater than 7.5 and epicentral distances between 9–150˚. We used the waveforms of 6 broadband seismometers in the Ryukyu arc from F-net (NIED) to analyze the surface waves. We also used the waveforms of 20 short-period seismometers in the Ryukyu arc from the Japan Meteorological Agency to detect trace LFEs in Ryukyu Island and determine their hypocenters.

The LFEs in the Yaeyama and Okinawa regions were observed. In the former region, during the passage of the surface waves, spindle-shaped LFE waveforms were first observed at Hateruma (south of Yaeyama Islands), and later at other stations in the Yaeyama region. Similarly, for the latter region, during the passage of the surface waves, spindle-shaped LFE waveforms were first observed at ZMM or Tamagusuku (south of Okinawa Island), and later at other stations in the Okinawa region. These observations suggest that the sources of the triggered LFEs were near or south of Hateruma and Tamagusuku.

We subsequently determined the hypocenters of the triggered LFEs. We computed the LFE travel-time difference between two stations using cross-correlations of the waveforms (Obara, 2002). The travel-time difference of waveforms of the LFEs corresponded to travel-time difference of the S-phase because S-waves were dominant in the LFEs, and P-waves were weak. The hypocenters were determined using the grid search method (Chao et al., 2013). In the Yaeyama region, the LFE hypocenters were mainly distributed near Hateruma Island. In the Okinawa region, they were distributed south of Okinawa Island. These positions are similar to the positions of the LFE hypocenters that accompany very low frequency earthquakes (LFE-VLFEs). This suggests that faulting in a cluster of LFE-VLFEs would be active with dynamic stress change.

In the Okinawa and Yaeyama regions, LFEs are triggered when the peak ground velocity of the surface wave is greater than 0.1 cm/s. This threshold value is similar to that for LFEs in Taiwan (Chao et al., 2013), suggesting that the weak friction coefficient at the plate interface of the Ryukyu Trench is similar to that in Taiwan.

Keywords: low frequency earthquake, surface wave, Ryukyu Trench

©2019. Japan Geoscience Union. All Right Reserved.

Detection of small surface displacement accompanying deep low-frequency tremor in Shikoku region, southwest Japan

*Yutaro Okada[1], Takao Tabei[2]

1. Faculty of Science, Kochi University, 2. Faculty of Science and Technology, Kochi University

In many subduction zones in the world, several types of slow earthquakes occur with different depths on the plate interface and some of them are accompanied by surface displacement. In this study, we focus on small surface displacements coincident with non-volcanic deep low-frequency tremor in Shikoku region in the Nankai subduction zone, southwest Japan.

We use daily coordinates time series from 107 GEONET stations located in Shikoku and tremor catalog compiled by NIED (Maeda and Obara, 2009; Obara et al., 2010) in the period from Jan. 1 2004 to Dec. 31 2008. Since GNSS coordinates changes due to the Bungo Channel long-term slow slip events are well reproduced by S-shaped logistic function, we use the same function to extract small displacement coincident with tremor activity. At first, we convert horizonal components into N50˚W direction after removing annual and semiannual variations and common-mode errors. Next, we fit the logistic function to a data segment with variable time window of 5, 7, and 9 days and estimate an amplitude of the function. The fitting is checked by a correlation coefficient between the observation and calculation. We apply this fitting for entire data period at all stations sliding data segment. Finally, we extract displacement when the amplitude of the fitted logistic function exceeds a certain criterion (1.8 mm in this study) and the correlation coefficient is large enough. If the extracted displacement is coincident with tremor activity within 30 m from the GNSS station, we adopt it as the tremor-related displacement. As a result, 225 events are adopted.

Spatial pattern of the tremor-related displacement seems to be related with the location and mechanism of the tremor event though closer inspection is needed. However, we extract much more small displacements by fitting a logistic function, of which the source is unknown. The logistic function is effective to reproduce transient displacement of the surface but we need to reconsider noise reduction of GNSS time series, time constant of logistic function, time window of the fitting, and so on.

Keywords: GNSS, southwest Japan, Deep low frequency tremor

©2019. Japan Geoscience Union. All Right Reserved.

Long-term temporal change in crustal resistivity beneath western Shikoku

*Futoshi Yamashita[1], Yoshimori Honkura[1]

1. National Research Institute for Earth Science and Disaster Resilience

In southwest Japan, various slow earthquakes such as deep low-frequency tremor and short/long-term slow slip events occur at the subducting plate interface (e.g. Obara and Kato, 2016, Scinence). In western Shikoku, Magneto-telluric (MT) survey was carried out along the dip direction of subducting Philippine Sea plate. The survey revealed an existence of low-resistivity structure in the lower crust in this region (Yamashita and Obara, 2009, AGU). In order to investigate a relationship between this characteristic structure and the activity of slow earthquakes, NIED has been carrying out continuous MT observations in western Shikoku since 2008. Here we show the observational records over 10 years and then discuss a relationship between observed temporal change in crustal resistivity and activity of the long-term slow slip event (L-SSE). Two observational sites KBN and IKT are available as of 2019. Qualities of data recorded at these sites are relatively fine. However, in order to improve the quality for discussing subtle change in MT parameters, we apply a data processing method same as Honkura *et al.* (2013, Nature comm.); we use only data whose coherency between electric and magnetic field is higher than a threshold. The lowest frequency of processed data is 0.00028 Hz. The processed MT parameters, apparent resistivity and phase, do not show any long-term temporal changes at KBN site even after temporal stops of observation over some months. On the other hand, apparent resistivity at IKT site, which is around 10 km southwest away from KBN site, shows temporal reduction at a frequency lower than 0.0022 Hz between 2010 and the middle of 2012. It is known that L-SSE occurred beneath the Bungo Channel in 2010 (e.g. Yoshioka *et al.*, 2015, GJI), which could induce resistivity change in the lower crust and then it might be detected by our MT observation.

Keywords: Crustal resistivity, Long-term slow slip event, Magneto-telluric method

©2019. Japan Geoscience Union. All Right Reserved.

Slow decay of postseismic deformation compared with aftershocks following the 2011 Tohoku-oki Earthquake

*Yuta Mitsui[1], Shunsuke Morikami[2]

1. Department of Geosciences, Shizuoka University, 2. Formerly at Graduate School of Science and Technology, Shizuoka University

In the literature, decays of postseismic deformation rates of large earthquakes were almost comparable to aftershock decays for subduction earthquakes (e.g. Hsu et al. (2006), Lange et al. (2014)). They are characterized by the modified Omori law with p~1, which means "afterslip-triggerred aftershocks". In this study, we focus on the 2011 Tohoku-oki megathrust earthquake using GNSS and seismicity data. On the basis of high-rate analysis of RINEX data and the F3 solution provided by the Geographical Survey Institute (GSI), we clarify the characteristics of postseismic deformation and aftershocks up to five orders of magnitude of time scale. We find that the p value for the postseismic deformation (p_m) is ~0.7, by contrast, that for the aftershocks (p_n) is ~1. Because a rate-and-state-friction model (Helmstetter and Shaw (2009)) predicted $p_m>=p_n$, another or an additional physical mechanism is necessary to explain the data of $p_m<p_n$. One important mechanism is viscoelastic relaxation of asthenosphere, thus we try fitting the postseismic deformation data by combination of afterslip and viscoelastic relaxation (a model of Suito (2017)). The fitting is not poor but fails to reproduce the Omori-like decay. More complex combination models may improve the fitting, but would not make simple Omori-like power-law decays. We need more sophisticated physical model to represent the decay characteristics of postseismic deformation.

Keywords: aftershocks, postseismic deformation, afterslip, viscoelastic relaxation, the 2011 Tohoku Earthquake

©2019. Japan Geoscience Union. All Right Reserved.

Serpentinite dehydration in subduction shear zones formed at source depths of slow earthquakes

*Yasushi Mori[1], Miki Shigeno[1], Kohtaro Ujiie[2], Kazuya Noro[2], Tadao Nishiyama[3]

1. Kitakyushu Museum of Natural History and Human History, 2. University of Tsukuba, 3. Kumamoto University

Long-term slow slip events (L-SSEs) and episodic tremor and slip (ETS) occur along the subduction plate boundary at depths of 30–45 km (Obara, 2002; Shelly et al., 2006). These deep slow earthquakes are probably induced by high pore-fluid pressure. Based on geological study, we propose that the high pore-fluid pressure can be produced by metasomatic dehydration of serpentinite in subduction shear zones at source depths of deep slow earthquakes.

The Nishisonogi metamorphic rocks in Kyushu, Japan, are part of a Late Cretaceous subduction complex metamorphosed at $P \approx 1$ GPa and $T \approx 470$ ˚C. The P-T conditions are close to those of source depths of deep slow earthquakes. Serpentinite mélanges intercalated with the metamorphic rocks contain blocks of metabasite, metapelite and albitite. The mélange matrix consists of chlorite-actinolite schist (CAS), talc schist and schistose serpentinite. Intense shear deformation is concentrated in the CAS, and the serpentinite mélanges have the characteristics of anastomosing shear zones.

Bulk chemical composition of the rocks suggests that the CAS is the metasomatized mixture of serpentinite and metabasite. In addition, chemical mass balance indicates considerable dehydration during the CAS formation, along with a slight increase of solid volume. These findings suggest that the CAS formation involves the build-up of pore-fluid pressure. The high pore-fluid pressure results in the concentration of shear deformation into the weakened CAS.

Dehydration of serpentinite probably plays a key role in deep slow earthquakes (Poulet et al., 2014; Okazaki and Katayama, 2015). Thermal dehydration of serpentinite occurs at ~600 ˚C along the subduction plate boundary (Auzende et al., 2006), which is much higher temperature than that of source depths of deep slow earthquakes. In contrast, metasomatic dehydration of serpentinite described here could occur at source depths of deep slow earthquakes.

Auzende, A-L., et al., 2006, EJM, 18, 21–33. Obara, K., 2002, Science, 296, 1679–1681. Okazaki, K., Katayama, I, 2015, GRL, 42, 1099–1104. Poulet, T., et al., 2014, JGR, 119, 4606–4625. Shelly, D.R., et al., 2006, Nature, 442, 188–191.

Keywords: serpentinite mélange, shear zone, dehydration, pore fluid pressure, Nishisonogi metamorphic rocks, deep slow earthquakes

©2019. Japan Geoscience Union. All Right Reserved.

Earthquake swarms following very low-frequency earthquakes in the central Ryukyu Trench

*Mamoru Nakamura[1]

1. Faculty of Science, University of the Ryukyus

Earthquake swarms occur frequently from Amami Island to Okinawa Island, near the axis of the central Ryukyu Trench. These earthquake swarms recur every few years and typically followed swarms of very-low frequency earthquakes (VLFE) that occur in a similar area. I have investigated the relationship between the VLFEs and the subsequent earthquake swarms in the central Ryukyu Trench, using the earthquake catalog provided by the Japan Meteorological Agency (JMA). For the VLFEs, I used the catalog by Nakamura and Sunagawa (2015) and the extended catalog to December 2018.

Results show that the VLFE swarms occurred approximately one month before the subsequent earthquake swarms began near the trench axis in this region. Previous noteworthy earthquake swarms occurred on August 2005 (with a maximum magnitude of 4.7), April 2009 (with a maximum magnitude of 5.1), May 2016 (with a maximum magnitude of 5.6), and September 2018 (with a maximum magnitude of 6.2).

Prior to the earthquake swarm that occurred in August 2005, a VLFE swarm started near Okinawa Island three months before and its activity moved intermittently from Okinawa Island to Amami Island. In the case of the earthquake swarm that occurred in April 2009, a VLFE swarm started near Amami Island and the subsequent swarm occurred two weeks after the start of the VLFE swarm. The location of the VLFE swarm moved intermittently closer to Okinawa Island. In the case of the earthquake swarm that occurred on May 2016, the VLFE swarm started near Amami Island and its active cluster moved intermittently towards Okinawa Island. The subsequent earthquake swarm started near the trench axis, approximately twenty days after the occurrence of the VLFE swarm. In the case of the earthquake swarm that occurred in September 2018, the VLFE swarm started near Okinoerabu Island (the midpoint between Amami Island and Okinawa Island) and the activity moved intermittently to Okinawa Island. The earthquake swarm occurred approximately twenty-five days after the start of the VLFE swarm. The location of the cluster of the 2018 earthquake swarm was slightly landward from the trench axis.

The faulting associated with these earthquake swarms was of normal type, corresponding to intra-slab earthquakes in the subducting Philippine Sea plate. I calculated the Coulomb Failure Stress (delta-CFS) assuming that a small slow slip event (SSE) occurred on the plate interface. Our results show that the positive delta-CFS that accelerated the normal faulting could not have occurred in the subducted slab near the trench axis until the slip of the SSE had reached close to the trench axis. This suggests that the SSE propagated from Amami Island to Okinawa Island accompanying the activation of the VLFE swarm, the slip of the SSE then propagated close to the trench axis, and the normal-faulting earthquake swarm in the slab was induced by the positive delta-CFS caused by the SSE.

Keywords: Very low frequency earthquake, Ryukyu Trench, Earthquake swarm

©2019. Japan Geoscience Union. All Right Reserved.

Seismic imaging in the central Nankai trough, off Shionomisaki to Kii channel

*Yasuyuki Nakamura[1], Shuichi Kodaira[1], Tetsuo No[1], Yuka Kaiho[1], Gou Fujie[1], Seiichi Miura[1], Kazuya Shiraishi[1]

1. Japan Agency for Marine Earth Science and Technology

Shallow very low frequency events (sVLFE) have been reported in the Nankai Trough subduction zone recently. In the central part of the Nankai trough, sVLFE were observed off Kii channel and Shinomisaki, but not reported in the area between them, off western Kii peninsula. We conducted a seismic survey with R/V *Kaimei* in November and December 2018 in Nankai subduction zone off Kii channel to Shonomisaki to investigate the structural features and its possible relationship to the sVLFE. R/V *Kaimei* fired 10600 inch^3 air gun array at every 50 m and a streamer cable (4.3 km at shortest, 5.7 km at longest) recorded the seismic signals. We acquired 23 seismic profiles with the length of ~ 75 km in dip direction at 4 km line separation and four profiles of ~ 90 km in strike direction at the shallowest part of the subduction zone. In addition, seven dip profiles with the length of 35 km were acquired off Kii channel to cover the lowermost part of the landward slope densely. The streamer cable was towed at a depth of 25 m to relatively enhance the lower frequency signals for better imaging of the deeper structure. Preliminary processed seismic profiles exhibited the structural variation in the survey area. Deformation of the hanging wall sediments and decollement were well imaged especially ~ 20 –30 km from the trough axis. Top of subducting Philippine Sea plate can be observed through ~ 40 –50 km from the trough axis in some of the obtained profiles. A pair of apparently low angle deep strong reflections were imaged at ~ 7 –8 s two-way time around 40 - 50 km from the trough axis off the western Kii peninsula, which was located slightly east and landward of the area with sVLFE. The shallowest part of the subduction zone in the area where the recent sVLFE activity was not reported, a slope basin with younger sediments deposited over the body of the accretionary prism is imaged, and the deformation was not observed in the slope basin. This suggests the thrust faults within the accretionary prism have not been active recently in this area. We will further process acquired data to obtain clearer seismic images and discuss the structural features and its connection to the observed seismological events in the Nankai Trough.

Keywords: Nankai Trough, seismic imaging

©2019. Japan Geoscience Union. All Right Reserved.

Attempt to Detect Intra-plate SSEs Based on F3 Solution of GEONET

*Yusaku Tanaka[1]

1. Earthquake Research Institute

Slow earthquakes have been detected all over the world and providing new insights into earthquakes. However, most of slow slip events (SSEs) were detected only on plate boundaries and intra-plate SSE was detected only once in Hokkaido. Thus, I attempt to detect intra-plate SSEs all over Japan using F3 solution of GEONET by GSI. I analyze the F3 data with six steps, i.e., (1) removing outliers by setting a term of mean + two times standard deviation for 1/4+1/4 year before-and-after each datum except for the datum itself and considering it is an outlier when it is out of the term, (2) removing disconnections estimated from the offsets and linear trends of 60+60 days before-and-after each datum with the least square method, (3) searching statistically significant temporal changes of the trends by using AIC, (4) cheking visually the time series in which the temporal changes are detected, (5) estimating the displacements from the trend chagnes, and (6) verifying the deformations by numerical calculation by setting rectangular faults.

As of 18th Feb 2019, my study has proceeded to the step (4). In the JpGU meeting, I will report the results of this analysis.

Keywords: crustal deformation, slow slip event, geonet

©2019. Japan Geoscience Union. All Right Reserved.

A new hydrothermal, low to high speed rotary-shearing apparatus: Reproduction of slow/megathrust earthquakes in laboratory

*Takehiro Hirose[1], Wataru Tanikawa[1], Yohei Hamada[1], Keishi Okazaki[1]

1. Kochi Institute for Core Sample Research, Japan Agency for Marine-Earth Science and Technology

Earthquakes involve a wide range of slip rates, from slow/aseismic to fast/seismic slip along faults. Thus, frictional properties of faults over wide slip rates (nm/s to m/s), in particular under hydrothermal conditions similar to those expected in seismogenic zones are essential for a unified understanding of all earthquake events. A new hydrothermal, low to high speed rotary-shearing apparatus has been installed at Kochi/JAMSTEC, in order to study the fault constitutive properties at slow to fast slip rates and the physicochemical mechanisms underlying mechanical responses. The apparatus is currently capable of applying slip rates from 100 nm/s to 2 m/s, normal stress up to 55 MPa, fluid pressure up to 120 MPa and temperature up to 450oC with infinite displacement. We have been improving the apparatus to work as we intended. In pilot tests, we used metamorphic rocks (pelitic and green schists) as starting materials that are potentially distributed at and below seismogenic zones along hot and young subduction zones. We will present our preliminary results with the basic design of the apparatus.

Keywords: friction, hydrothermal, slow to fast slip

©2019. Japan Geoscience Union. All Right Reserved.

Very low-frequency earthquakes in western Shikoku remotely triggered by the 2016 Mw5.9 off-Kii Peninsula earthquake

*Masatoshi Miyazawa[1]

1. Disaster Prevention Research Institute, Kyoto University

Slow tectonic events are known to be sensitive to external stress perturbations due to passing seismic waves and earth tides. High-amplitude surface waves from large earthquakes have transiently triggered low-frequency earthquakes (LFEs) and slow slip events (SSEs) in subduction zones. However, dynamic triggering of very low-frequency (VLF) earthquakes during the arrival of seismic waves from a large, distant earthquake has not been observed. Because both the VLF earthquake and the surface wave have similar characteristic periods, remote triggering is not easily detected by using existing methods. We developed a particle filter/smoother for time series analysis combined with Markov chain Monte-Carlo methods, to detect seismic signals and estimate the maximum likelihood source parameters of VLF events that might have been remotely triggered. We apply this method to seismic data from the Mw5.9 earthquake, which occurred on 1 April 2016 (UTC), off Kii Peninsula. We found that six VLF events with magnitudes about 4, likely occurred in the seismogenic regions of ambient LFEs, and were likely triggered by the arrivals of high-amplitude surface waves. The triggering stress changes are from 0.4 to 1.5 kPa, which are similar to the values for LFEs triggering reported previously. Since there were no triggered LFEs in western Shikoku following the 2016 earthquake, these VLF earthquakes are more sensitive to stress changes caused by surface waves from large earthquakes.

Keywords: Very low-frequency earthquake, Remote triggering

©2019. Japan Geoscience Union. All Right Reserved.

Underground structure around source region of slow earthquakes in western Shikoku obtained by receiver function analysis

Akira Hikita[1], Aitaro Kato[1], *Kazushige Obara[1], Akiko Takeo[1], Takeshi Akuhara[1]

1. Earthquake Research Institute, The University of Tokyo

Various types of slow earthquakes have been observed at subduction zones surrounding the Pacific Ocean. It has been suggested that elevated pore fluid pressure plays an essential role in the generation of slow earthquakes because low velocity or high Vp/Vs zones have been also reported along the plate boundaries where they occur. In Tokai region of the Nankai subduction zone, Kato et al. (2010) revealed that long-term slow slip event (SSE) occurs at the boundary between the continental lower crust and the subducting Philippine Sea plate and episodic tremor and slip (ETS) occurs between the mantle wedge and the subducting plate. Kato et al (2010) also revealed that oceanic crust indicates higher Vp/Vs in the long-term SSE region than in the ETS region. In contrast, Toya et al. (2017) reported that the oceanic crust indicates higher Vp/Vs in the ETS region than in the long-term SSE region in western Shikoku of the same subduction zone. In this study, we revealed configurations of continental Moho discontinuity and subducting oceanic crust and investigated relationship between slow earthquakes and the surrounding seismic velocity structure by receiver function analysis using a dense seismic array in western Shikoku.

As a result, continuous continental Moho and oceanic crust are clearly imaged along both north-south and east-west oriented seismic lines. The plate boundary in the south part, where the distinct continental Moho is not imaged, has steeper slope than the north part along the north-south line. ETS occurs between the mantle wedge and the subducting plate, and long-term SSE occurs along a contact between the continental crust and the oceanic crust.
We show that the oceanic crust indicates much higher Vp/Vs than the hanging wall by using also the reverberation phases. This high Vp/Vs means the elevated fluid pore pressure within oceanic crust due to dehydration. Vp/Vs in the oceanic crust is higher in the deep part of the long-term SSE region than in the ETS region like as the case of Tokai. It is assumed that fluid would accumulate within the oceanic crust owing to low permeability of the continental crust in the long-term SSE region. In contrast, serpentinization of the mantle wedge just above the ETS region could reduce fluid pressure in the oceanic crust. Furthermore, Vp/Vs in the oceanic crust becomes lower in the deeper part beyond the ETS depths, suggesting that eclogization is completed at the depths.

Keywords: Receiver function, episodic tremor and slip, long-term slow slip event, low seismic velocity layer

©2019. Japan Geoscience Union. All Right Reserved.

Hypocenter determination of deep low frequency tremors beneath the Kii Peninsula by backprojection of seismic array data

*Kodai Sagae[1], Hisashi Nakahara[1], Takeshi Nishimura[1], Kazutoshi Imanishi[2]

1. Graduate School of Science,Tohoku University, 2. National Institute of Advanced Industrial Science and Technology (AIST)

A seismic array analysis enables us to detect weak signals if they are coherent. In Cascadia, a high accuracy hypocenter determination of tremors has been carried out by using dense seismic arrays (e.g.,Ghosh et al.,2012). In Southwest Japan, previous studies (e.g.,Ueno et al.,2010) applied the **MU**ltiple **SI**gnal **C**lassification (MUSIC) method (Schmidt,1986) to data of surface seismic arrays at Western Shikoku and carried out the hypocenter determination. However, a quantitative threshold for event detection was not considered. Sagae et al.,(2018 SSJ) introduced an event detection threshold based on the coherence of waveforms among stations, and improved tremor detection by using a surface seismic array installed by AIST at the Kii Peninsula. We applied the MUSIC method to this data in times when tremor events were detected and estimated slownesses and arrival azimuths of tremor signals. Their temporal variations suggested tremor migration. However, we did not carry out hypocenter determination. In this study, we determine hypocenters of tremors by backprojection using the estimated slownesses and arrival azimuths.
The surface seismic array installed by AIST at the Kii Peninsula was composed of 39 three component velocity sensors with a natural frequency of 2.0 Hz and a sampling frequency of 200 Hz. This array had an aperture of about 1.5 km and the sensors were arranged in a cross shape with interval spacings of 50~100 m. We analyze data for 1 year (between July 7,2013 and July 7,2014), because the number of sensors is stable in this period.
We focus on a frequency of 3Hz, which is within the tremor's dominant frequency band of 2-10 Hz. Data processing is described as follows. (1) We calculate averaged coherence of waveforms for all station's pairs. (2) We detect tremor events by setting a detection threshold based on the averaged coherence. (3) We estimate slownesses and arrival azimuths by applying the MUSIC method to the data when tremors are detected. (4) We project them back to the plate boundary (Hirose et al.,2008) and determine source locations by using S wave velocity model JMA2001 (Ueno et al.,2002).
We detected 5 periods of high tremor activities during the 1 year period. We compared the hypocenter distributions determined by our method and those of AIST tremor catalogue which were determined from an envelope cross correlation method. Temporal variation of tremors in this study were almost consistent with the AIST catalogue. We were also able to detect about 2.5 times as many events as the AIST catalogue. It is easier to identify temporal variation of tremors in more detail because our study improved temporal resolution up to 10 sec.
We projected temporal variations of tremor distributions into along-strike and along-dip directions. The results show tremors tend to migrate along the strike in time scales of several days with migration velocities of 6.0~9.3 km/day. Along-dip migrations of tremors with a short timescale of several hours are also detected. When we focused on the initial part of tremor activities, tremors tend to start in deeper parts and gradually migrate to shallow parts. These migration velocities were estimated to be about 1.0 km/hr (24 km/day) in the up-dip direction.
In this study, we were able to improve tremor detection by setting the event detection threshold based on the coherence of seismograms for stations pairs in a surface seismic array. Thanks to this, we were able to locate 2.5 times more tremors than the conventional method. We made it easier to keep track of tremor migrations by improving the temporal resolution of hypocenter determination to 10 sec.
We used the plate boundary model (Hirose et al.,2008). We downloaded the AIST catalogue from Slow

©2019. Japan Geoscience Union. All Right Reserved.

Earthquake Database (Kano et al.,2018).

Keywords: Deep low frequency tremor, Seismic array analysis, Backprojection, MUSIC method, Kii Peninsula, Hypocenter determination

©2019. Japan Geoscience Union. All Right Reserved.

Triggered tremors and stress perturbations due to surface waves

*Ryohei Ikeda[1], Naoki Suda[1]

1. Hiroshima University

Surface waves radiated from distant large earthquakes sometimes trigger a series of deep non-volcanic tremors with intervals of 20-30 seconds, which are the same as dominant periods of surface waves [e.g. Miyazawa & Brodsky 2008]. Understanding the triggering mechanism is important because it provides us clues to the slip process occurring along the transition zone of subducting plate interface. Dynamic stress perturbations due to surface waves that triggered tremors were estimated on the order of 1 to 10 kPa [e.g. Chao & Obara 2016]. To study the relationship between triggered tremors and stress perturbations due to surface waves, we computed theoretical dynamic stresses due to surface waves from large earthquakes by using observed and theoretical surface waves.

We focused on the triggered tremors in the western Shikoku region of the Nankai subduction zone. Most of them occurred in two clusters where tectonic tremors actively occur. We computed theoretical dynamic stress perturbations due to surface waves from 106 earthquakes between 2004 and 2016 with moment magnitudes of 7.0 or grater. The receiver points at which the stress components were computed are at the plate boundary below the N.TSAF and N.KWBH stations, which are the nearest stations of the triggered tremors in F-net and Hi-net, respectively. PREM [Dziewonski & Anderson 1981] and Global CMT catalog [Dziewonski et al. 1981; Ekstrom et al. 2012] were used for the Earth model and the seismic sources for computing theoretical surface waves. Source time functions were approximated with triangular functions whose half durations are equal to the centroid time lags.

The stress change at the plate boundary by the surface wave was estimated based on the method of Spudich et al. (1995). This method consists of two stages: (1) Estimate the stress at the surface from the observed ground velocity and (2) Estimate the stress at the plate boundary from the stress at the surface estimated in (1). In these estimations, we used theoretical proportional relations between the ground velocity and the surface stress and those between the surface and the deep stresses in the frequency domain, which were obtained from the theoretical surface waves. We used the N.TSAF and N.KWBH records as the observed ground velocity. The records from the latter were corrected using the method of Maeda et al. (2011).

The stress components in the source coordinates were transformed to the stress normal to the plate interface and the stress along the possible slip direction of tremor source. The normal and slip directions were obtained from the model plate interface [Baba et al. 2002; Nakajima & Hasegawa 2007; Hirose et al. 2008] and plate convergence vectors [Miyazaki & Heki 2001]. We computed waveforms of the Coulomb failure function (ΔCFF) using a frictional coefficient of 0.2 at periods between 20 and 50 seconds.

©2019. Japan Geoscience Union. All Right Reserved.

Results from the N.TSAF records show that the maximum ΔCFF for the events that triggered tremors are greater than 0.5 kPa. The magnitudes of triggering earthquakes are greater than 7.5. ΔCFFs were generally overestimated when we used the corrected N.KWBH records because the correction did not well work, in particular, for the earthquakes with magnitudes less than 7.5. The important point is that not all of the events that provided the stress perturbations greater than 0.5 kPa triggered tremors. This shows that the stress perturbation due to surface waves cannot be the unique triggering condition: other conditions, for example, stress perturbations due to possible background slow slip events and/or high pore fluid pressure are required.

©2019. Japan Geoscience Union. All Right Reserved.

Numerical modeling of long- and shallow slow slip events including shallow region in Hyuganada and western Nankai, Japan

*Takanori Matsuzawa[1], Bunichiro Shibazaki[2]

1. National Research Institute for Earth Science and Disaster Resilience, 2. Building Research Institute

Recent studies reported deep long-term slow slip events (SSEs) in the Hyuganada and western Nankai region (e.g., Kobayashi, 2014; Takagi et al., 2016; Ozawa. 2017). Shallow SSEs are also recently reported with low-frequency tremor and very low-frequency earthquakes (e.g., Araki et al., 2017; Nakano et al., 2018). In our previous study, we have numerically reproduced recurring deep long- and short-term SSEs in the Shikoku region (Matsuzawa et al., 2013), considering the actual distribution of slow earthquakes and configuration of the subducting Philippine Sea plate. We aim to reproduce deep long- and short-term SSEs and shallow SSEs in a single numerical model applying a similar approach in Matsuzawa et al. (2013).

We adopt a rate- and state-dependent friction law (RS-law) with cutoff velocities. We assume that (a-b) value in the RS-law is negative within the deep short-term SSE region, and positive outside that region. The deep short-term SSE region is modeled based on the actual distribution of deep low frequency tremor. Deep long-term SSE region is assumed based on the geodetic observation (Hirose et al., 2011). To focus on the Hyuganada and western Nankai region, we assume stable sliding region with positive (a-b) in the south of the Kyushu-Palau ridge. We also assume low cutoff velocity at the depth shallower than 9 km to reproduce shallow SSEs. Low effective normal stress is assumed at the depth of SSEs. Temporal evolution of slip velocity is numerically simulated, introducing elastic response and realistic configuration of the plate interface.

In terms of deep long-term SSEs in Hyuganada, a simple extension of the long-term SSE region in the Bungo Channel cannot reproduce the segments of observed SSEs. Narrowed long-term SSE region in the dip direction between Bungo and southern Hyuganada can reproduce three observed segments of SSEs, i.e., Bungo, northern Hyuganada, and southern Hyuganada. In addition, recurring shallow SSEs along trench in Hyuganada and off Ashizuri are reproduced in our result. Megathrust earthquakes are divided into two regions; off Shikoku and Hyuganada in our result. The segments of these large earthquakes may be attributed to the long-term SSE region in the Bungo Channel. Our model comprehensively reproduces various SSEs and megathrust earthquakes, including newly found long-term SSEs.

Keywords: Slow Earthquake, Slow Slip Event, Hyuganada

©2019. Japan Geoscience Union. All Right Reserved.

Further evidence for the influence of a subducting-ridge on the spatial strain accumulation and release pattern in the shallow eastern Nankai Trough, based on VLFE distribution

*Akiko Toh[1], Chen Wan-Jou [2], Doug Dreger[3], Wu-Cheng Chi[2], Satoshi Ide[1]

1. University of Tokyo, 2. Institute of Earth Sciences, Academia Sinica, 3. UC Berkeley

We investigated the distribution and focal mechanisms of very low frequency earthquakes (VLFEs) located in the shallow part of the eastern Nankai trough. While they are mainly explained as low angle thrust faulting along the plate boundary (Sugioka et al., 2012; Nakano et al, 2016), along the strike variation in their distribution has also been observed, likely caused by a subducting-ridge (Toh et al., 2018). Such variations could be closely related to the strain release pattern, or the tsunamigenic potential, of this region, thus warrant a further comprehensive study.

We used 3 component records of broadband ocean bottom seismometers equipped in Dense Oceanfloor Network system for Earthquakes and Tsunamis 1 (DONET1). Records of VLFE activities that occurred immediately beneath the network in 2015, 2016 and 2017 for 1-2 weeks each year, are used. Through visual inspections, we detected 335 VLFEs whose signals are observed at least 6 stations on vertical component filtered between 16-32s.

Instead of estimating the source parameters for one after another for all the events, we searched for densely located event groups inferred by similarities of the maximum amplitude variations measured per event, and, so far, worked only on the grouped events. The purpose of this event selection process is to get an overview of the distribution using the simple quantity (i.e. max. amplitude variation) that can be evaluated for every VLFE, and to avoid a bias that may be caused by eliminating events that are merely difficult to process (i.e. do not fit synthetic waveforms) mostly due to complicated long source time functions that characterize VLFEs. The grouping is conducted by a hieratical density-based clustering method HDBSCAN (Campello et al., 2003), and 197 events were grouped into 26 groups that consists of 2 to 35 events.

We determined the centroid origin time, location and 5-component of moment tensor of VLFEs that maximize the normalized variance reduction (VR) between the observed and synthetic velocity waveforms. The waveforms are bandpass filtered either between 16-32s or 20-50s, depending on signal duration and S/N per event. The time and location are grid-searched at intervals of 0.01 degree in horizontal, 1 km in depth between 5 and 10km bsl., and 1 s in time. At each grid, the moment tensor is estimated using the code TDMT_INV (Dreger, 2003) that conducts full-waveform linearized inversion in time domain. Green’s functions are calculated using the code by Herrmann (2013) based on wavenumber integration. We used a 1D structural model based on a 2D model obtained by an active source survey (Nakanishi et al., 2008). Although the 1D structure is assumed, the large variations in station elevation (1.9-4.3 km bsl) are considered in Green’s function calculations.

We obtained 50 events with good VR (>65%). Among the 26 groups, 6 groups ended up with no events of high VR, mostly due to being located outside of the network. Almost all the VLFEs are reasonably explained by low angle thrust faulting. From the obtained distribution, the strong influence of the subduction-ridge located on the northwestern side of DONET1 is inferred. On the southwestern side

©2019. Japan Geoscience Union. All Right Reserved.

where there is no ridge-subduction, VLFEs are distributed beneath outer-ridge toward the trench axis. The estimated depths for the ones located beneath the outer-ridge are deep (7–10km with median at 8km), which are consistent with the depth of the plate boundary of this area. In contrast, on the northeastern side, VLFEs are mostly distributed landward of outer-ridge and their estimated depth are shallow (5–8km with the median at 7km) as previously suggested (To et al., 2015). The shallow depths can be explained by the uplifted plate boundary in this area due to the subducting-ridge. Furthermore, they are located to landward of the peak of the subducting-ridge, which can be reasonably explained by the change in shear stresses and pore pressures caused by the subducting-ridge.

Keywords: Nankai trough, Very low frequency earthquake (VLFE), Accretionary prism, HDBSCAN, Broadband ocean bottom seismometer

©2019. Japan Geoscience Union. All Right Reserved.

Evidence for semi-brittle flow in mantle-wedge serpentinites under high pore fluid pressure and their implications for deep low frequency earthquakes

Kengo Kataoka[1], Yurina Nagata[1], *Ken-ichi Hirauchi[1], Ryosuke Oyanagi[2], Atsushi Okamoto[3], Katsuyoshi Michibayashi[4]

1. Department of Geosciences, Faculty of Science, Shizuoka University, 2. Japan Agency for Marine-Earth Science and Technology, 3. Graduate School of Environmental studies, Tohoku University, 4. Department of Earth and Planetary Sciences, Nagoya University

In southwest Japan, deep low frequency earthquakes occur at the base of the shallow serpentinized mantle wedge. In order to understand deformation styles of the mantle wedge serpentinite, we conducted structural and petrological analysis of a paleo-mantle wedge body that has experienced serpentinization at pressure–temperature conditions corresponding to source areas of low-frequency earthquakes, in the Sanbagawa belt, central Shikoku. The serpentinite body has a block-in-matrix structure that result from pervasive fragmentation. At outcrop and thin section scales, the distribution of blocks follows a power law distribution with exponent $2.32 < D < 2.37$ (2-D). The block has experienced complete serpentinization, characterized by randomly-oriented antigorite aggregates. The matrix also consists of antigorite, which was formed due to dissolution–precipitation process of the block in the presence of H_2O. Antigorite aggregates in the matrix along localized shear planes is characterized by a strong crystallographic preferred orientation with a dominant [010](001) slip system, suggesting dislocation glide on (001) planes. We suggest that deep slow earthquakes occur by semi-plastic deformation of the serpentinized mantle wedge, under low effective normal stresses.

Keywords: slow earthquakes, low frequency earthquake, mantle wedge, serpentinite

©2019. Japan Geoscience Union. All Right Reserved.

Spatial distribution of slow slip events off the Boso peninsula from 1996 to 2018 under sparsity constraints

*Ryoko Nakata[1], Hideitsu Hino[2], Tatsu Kuwatani[3,4], Takahiro Akiyama[5], Shoichi Yoshioka[6], Masato Okada[7], Takane Hori[1]

1. Japan Agency for Marine-Earth Science and Technology, 2. The Institute of Statistical Mathematics, 3. Department of Solid Earth Geochemistry, Japan Agency for Marine-Earth Science and Technology, 4. PRESTO, Japan Science and Technology Agency, 5. Graduate School of Science, Kobe University, 6. Research Center for Urban Safety and Security, Kobe University, 7. Graduate School of Frontier Sciences, The University of Tokyo

We estimated spatial distribution of the six slow slip events (SSEs) off the Boso peninsula, central Japan, from 1996 to 2018. We have applied an inversion method called fused regularization, a type of sparsity constraint, suitable for detecting discontinuous changes in the model parameters, for evaluation function [Nakata et al., 2017]. In this study, to shorten calculation time, we used a type of approximation method by Obuchi and Kabashima [2016] to search hyperparameters, not LOO-CV (leave-one-out cross validation).

From our tentative results, the maximum slips for the 2002, 2011 and 2018 SSEs were large, and the 1996, 2007 and 2013 SSEs were small. The slip distributions of the 2011 and 2018 SSEs seem to be distributed southward than 2002. It is confirmed by numerical experiments that the difference in slip distribution is not due to GNSS station distribution.

Furthermore, we are conducting numerical simulation of earthquake generation cycles, which modelling SSEs off the Boso peninsula and M~8 earthquakes along the Sagami Trough. We will discuss slip distributions of SSEs and locked area during an interseismic period.

©2019. Japan Geoscience Union. All Right Reserved.

Marine electromagnetic observations around a slow earthquake region in the western Nankai trough

*Hiroshi Ichihara[1], Tada-nori Goto[2], Tetsuo Matsuno[3], Noriko Tada[4], Shinya Sato[2]

1. Earthquake and Volcano Research Center, Nagoya University, 2. Graduate School of Engineering, Kyoto University, 3. Ocean Bottom Exploration Center, Kobe University, 4. JAMSTEC

Slow earthquakes have been believed to relate to fraction of pore fluid around plate boundary. Thus, imaging of electrical resistivity (conductivity) distribution is essential to understand slow earthquakes. However, many of SSE areas are distributed beneath the ocean, we need marine electromagnetic (EM) observations. In this presentation, we report preliminary results of marine EM observations in the western part of Nankai Trough (off Miyazaki prefecture and off western Kochi prefecture, Japan) where SSEs, VLF events and regular earthquakes (e.g. 1968 off-Hyuga earthquake, M7.5) are known. We deployed eight ocean bottom electro-magnetometers (OBEMs) and recovered seven of them between 2017 and 2018. In addition to EM fields, two OBEMs measure absolute pressure to detect short period crustal deformations caused by SSE. We estimated high quality magnetotelluric responses based on Chave and Thomson (2004). However, the responses show strong three-dimensionality of resistivity distribution and strong coast effect (e.g. Key and Constable, 2011). They indicate that we need to apply three-dimensional imaging techniques for seafloor magnetotelluric data.

Keywords: Slow earthquake, magnetotelluric, OBEM, Nankai trough, off Miyazaki

©2019. Japan Geoscience Union. All Right Reserved.

Dynamics of precipitating injection fronts inside of structured medium

*Yutaka Sumino[1], Shunsuke Tanaka[1], Miyuki Kunihiro[1]

1. Tokyo University of Science

Recent study on a slow earthquake elucidates that the migration of water within a mantle wedge may play relevant roles[1]. The flow inside of confined geometry, such as within a soil, is often described by the Darcy’s law, where flow velocity is described by the gradient of fluid pressure. Interestingly, however, the water within a mantle wedge contains large amount of solid contents, and hence, a precipitation can be formed within the water[2]. For this reason, the dynamics of fluid flow under the effect of precipitation reaction should be explored.

Based on the above motivation, we explored the 2-dimensional confined chemical garden[3] as an analogue experiment for the fluid flow within a mantle wedge[4]. The system consists of two fluids with a quasi-two dimensional thin cell, so called a Hele-Shaw cell. The cell was filled with a fluid, and the other fluid is injected from the center of the cell. The flow in a Hele-Shaw cell can be described by the Darcy’s law. Furthermore, the mixing of these fluids leads to the precipitation. Thus, the flow observed in 2-dimensional confined chemical garden system is analogous to the one of water in a mantle wedge with precipitation formation.

Our previous study[4] showed that a filamentous pattern appears when the injection speed is high enough, whereas the symmetrical circular front was formed for lower injection speed. This results indicates that the propagation radius of injection front can be drastically different depending on the injection speed. In addition, the number of moving filaments saturate whose value is proportional to the injection speed. Such tendency can be understood with our boundary model adopting the effect Laplace pressure and the conservation of precipitation at the boundary. The model further predicts existence of optimal curvature for the moving front with which the required pressure for the motion is minimum. The curvature, and the speed of the optimal boundary motion is independent of the injection speed. These experimental and theoretical study thus worked well in the 2-dimensional Hele-Shaw cell. However, actual condition in a mantle wedge should have quenched structure, which is absent in a Hele-Shaw cell.

In order to fill the gap between actual condition in a mantle wedge and our analogue experiments, we modified our Hele-Shaw cell to have periodic pillar structure. As a control parameter, we changed the pillar to pillar distance, w, as shown in attached figure. The filament pattern showed meandering motion without pillar structures ($w = \infty$). We found that the filament pattern showed straight motion especially when w agreed with the typical filament width. Our modified mathematical model adopting nonlinear response of permeability with precipitation density numerically reproduced such experimental results. This results indicates that the propagation distance of injected fluid can be modified by the locally quenched disorder within a mantle wedge.

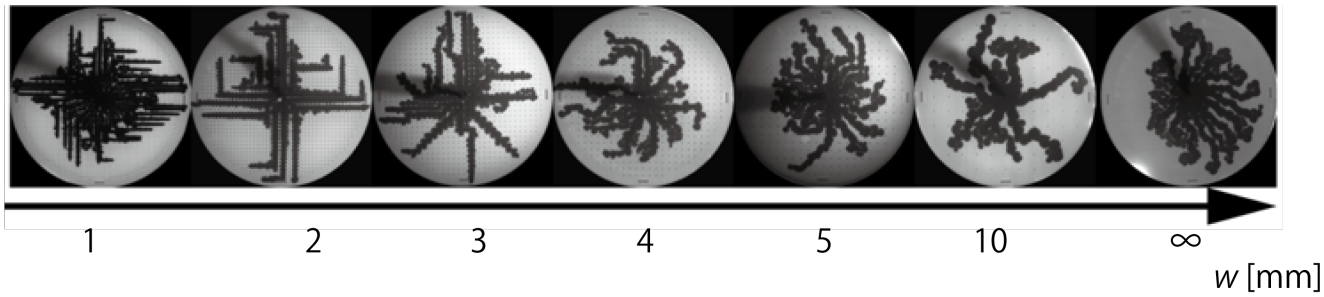
In this paper, we show detailed setup for experiments, as well as mathematical model.

[1] A. Tanaka et al. Earth, Planets and Space 70, 25 (2018).
[2] K. Ujiie, et al., *Geophys. Res. Lett.* **45**, 5371–5379 (2018).

©2019. Japan Geoscience Union. All Right Reserved.

[3] F. Haudin et al., *Proc. Natl. Acad. Sci. U.S.A.* **111**, 17363–17367 (2014).
[4] S. Wagatsuma, et, al., *Phys. Rev. E* **95**,052220 (2017).

Keywords: injection, fluid, precipitation



©2019. Japan Geoscience Union. All Right Reserved.

Permeability changes of simulated low permeable fault rocks induced by intermediate velocity friction test

*Wataru Tanikawa[1]

1. Japan Agency for Marine-Earth Science and Technology, Kochi Instutute for Core Sample Research

Earthquake events often associate with fluctuations of flow rate, pore pressure and pore fluid chemistry at a subsurface of earthquake rupture zones. The co-seismic hydrological changes are explained by changes in fluid permeability of fault zones during earthquakes, and the permeability change plays an important role for dynamic fault processes as well. Therefore, we newly designed a system to estimate water permeability changes during and after low to high velocity shear deformation using a rotary shear apparatus and simulated fault rocks.

A pair of hollow cylindrical samples made by low permeable Belfast dolerite and Aji granite were used as test specimens. To calculate permeability, a radial flow from the inner wall to the outer wall of the specimen was induced by applying a differential pore pressure (0.01 to 0.2 MPa) between inner and outer walls. We performed friction tests at normal stress of 2 MPa, rotation speed from 0.0003 to 0.6 m/s, and slip displacement of 1 m.

The results showed that permeability increased during sliding at every slip velocity condition, and higher velocity friction caused more abrupt increase in permeability. After the end of sliding, permeability gradually decreased with time and then became nearly constant value. Reduction rate of permeability 5 min after slip increased with slip rate. Fiction coefficient was decreased with sliding velocity. Frictional heating is a key to explain slip velocity dependence of permeability (flow rate). Temperature rise caused by frictional heating will reduce fluid viscosity, therefore, apparent permeability reduction after sliding can be explained by an increase in fluid viscosity by cooling. Pore pressure build-up by frictional heating can increase aperture, therefore, this process can explain permeability enhancement during sliding and velocity dependences on permeability increase and friction coefficient.

Keywords: permeability, friction coefficient, frictional heating

©2019. Japan Geoscience Union. All Right Reserved.

Modified relation between the coupling and tremor rates around the Shikoku region

*Tadafumi Ochi[1]

1. Institute of Earthquake and Volcano Geology, Geological Survey of Japan, The National Institute of Advanced Industrial Science and Technology

In Ochi and Takeda (2018, EPS), I examined the relation between the interplate coupling velocity and the number of deep low-frequency tremors in the same place around the Shikoku region, southwest Japan. I found that there were some spot-like points where the coupling and the tremor count were well correlated, and that the regression line required the coupling rate to be the plate convergence rate in this region under conditions of zero tremor count rate. One of the problems to be resolved is the interpretation of the first matter 'spot-like points' mentioned above. According to the pairs of time series of the coupling rate and tremor count rate, some pairs show a time delay, and the others show a small fluctuation in the tremor count rate that seems to be independent of the coupling rate. It is interesting that whether the an ill-correlation just comes from an oversimple model of the linear regression I used in the previous study, or really reflects some physical background. In order to answer this question, I construct the model which allows the fluctuation in the tremor count rate that is independent from the coupling rate and observe the fitness of the model. At this time, some trial models that allow the shorter period fluctuation in the tremor count rate than in the coupling rate and temporal change in the period achieve clear correlations. In the presentation, I will show the results of the various trials.

Keywords: Interplate coupling, Low-frequency tremor

©2019. Japan Geoscience Union. All Right Reserved.

Spatiotemporal distribution of regular and very low-frequency earthquakes in the northern part of the Ryukyu subduction zone

*Youichi Asano[1], Kazuhiko Goto[2], Hiroshi Yakiwara[3], Shuichiro Hirano[3]

1. National Research Institute for Earth Science and Disaster Resilience, 2. Association for the development of earthquake prediction, 3. Nansei-toko Observatory for Earthquakes and Volcanoes, Kagoshima University

We have investigated detailed spatiotemporal distribution of regular and very low-frequency (VLF) earthquakes including an Mw 6.3 interplate event near Tanegashima along the Ryukyu trench on Jun. 08, 2019. This earthquake was followed four Mw4-5 class regular and many VLF earthquakes by the end of Jan., 2019. At first we estimated centroid moment tensors of these regular and several VLF earthquakes, respectively, from broadband seismograms recorded at the NIED F-net and temporally observation stations. In the next step, the known VLF earthquakes were selected to be template events for searching unknown VLF earthquakes from continuous seismograms. If there are several candidates of VLF earth quake, we select the most coherent event with a maximum cross-correlation coefficient averaged over all stations in every 180 seconds. Finally we estimated locations of the selected events from phase shift of the wavelets between the template and these selected events. Obtained result shows that activity of VLF earthquakes after the Mw 6.3 earthquake was started in the adjacent area east of this Mw 6.3 earthquake; however, the following Mw4-5 regular earthquakes occurred south of this area in the period of Jan. 25-30, 2019. In this period, the front of the VLF activity migrated toward east from these Mw4-5 events. Such a spatiotemporal distribution of regular and VLF earthquakes suggests that the after slip of the Mw 6.3 and/or an SSE caused these regular and VLF earthquakes.

Acknowledgment

This study is partly supported by JSPS KAKENHI Grant Number JP16H06473.

Keywords: very low-frequency earthquake, Ryukyu subduction zone

©2019. Japan Geoscience Union. All Right Reserved.

Possible tectonic tremor activities near the VLFE epicenters in the Sanriku-Oki region in 2011

*Hidenobu Takahashi[1], Ryota Hino[1], Yusaku Ohta[1], Naoki Uchida[1], Syuichi Suzuki[1], Masanao Shinohara[2], Takanori Matsuzawa[3]

1. Graduate school of Science Tohoku University , 2. Earthquake Research Institute, University of Tokyo, 3. National Research Institute for Earth Science and Disaster Resilience

Recently various kind of slow earthquakes have been discovered along the Japan Trench subduction zone. Prior to the occurrence of the 2011 Tohoku-oki earthquake, occurrence of slow slip events associated with migration of small earthquake epicenters and tectonic tremors was reported near the hypocenter of the Tohoku-Oki earthquake (e.g. Kato et al., 2012; Ito et al., 2015; Katakami et al., 2018). As a different type of a slow-earthquake family, Very Low Frequency Earthquakes (VLFEs) have been detected in more broad areas (Matsuzawa et al., 2015). Takahashi et al. (in prep.) detected the seismic signals from the VLFEs by short-period ocean bottom seismograms (OBS) deployed in the vicinity of the VLFE epicenters in the Sanriku-Oki region, just after the Tohoku-Oki earthquake. They further identified a number of VLFE-like events, not recognized by the onshore data. Here, we report on possible tectonic tremor activities in the same area based on the OBS data after the 2011 Tohoku-oki earthquake.
We detected four sequences of continuous rises of amplitudes on the OBS records. Each of the sequence has a duration of ~ half a day. The sequences were composed of numerous wave trains with good correlations in their growths and decays in observed amplitudes among the stations, but no distinct P- or S-wave onsets were identified for individual wave trains. Interestingly, the spatial variation of the wave trains amplitudes is similar to those of the previously identified VLFEs. These observations suggest that the sequences were composed of small seismic events closely located each other and to the known VLFEs. It is also notable that some of the VLFE-like events discovered by the OBS data were contained in the sequences. We regard the discovered sequence as a kind of tectonic tremor activity and will inspect their characteristics, such as frequency content and its variability, to clarify their nature and discuss their relevance to slow slip events along the shallow subduction interface, which might promote the activities.

Keywords: tectonic tremor, Sanriku−oki

©2019. Japan Geoscience Union. All Right Reserved.

Heterogeneous structure around a region of slow earthquake activity off Ibaraki prefecture along the Japan Trench

*Kimihiro Mochizuki[1], Tomoaki Yamada[1], Masanao Shinohara[1], Ryota Hino[2], Ryosuke Azuma[2], Yoshihiro Ito[3], Yoshio Murai[4], Kenji Uehira[5], Toshinori Sato[6]

1. ERI, Univ. of Tokyo, 2. Graduate School of Science, Tohoku Univ., 3. DPRI, Kyoto Univ., 4. Faculty of Science, Hokkaido Univ., 5. NIED, 6. Graduate School of Science, Chiba Univ.

Large earthquakes of magnitude (M) ~7 have repeatedly occurred in the Ibaraki-oki region, about 100 km offshore of the Ibaraki prefecture along the Japan Trench, at a constant interval of ~20 years. Mochizuki et al. (2008) conducted a marine seismic survey and revealed that there exists a subducted seamount in the region. They also conducted an offshore seismic observation using ocean bottom seismometers (OBSs) to show that the seismicity in the region can be seen off of the subducted seamount, but not along the plate interface over it. They found that the location of the subducted seamount did not agree with the focal region of the repeating M7 earthquakes. From these results, they argued that the plate interface over the subducted seamount does not constitute an asperity of the repeating M7 earthquakes. Wang and Bilek (2011) introduced an idea that the seamount subduction causes formation of a fracture network within the overriding plate, and such a fracture network would prevent accumulation of large strain energy along the plate interface over the subducted seamount to generate large earthquakes. In addition to the repeating M7 earthquakes, recent studies (e.g. Matsuzawa et al., 2015; Nishikawa and Ide, 2018) have reported activity of slow earthquakes in the region. Relationship between activity of various types of earthquakes and structural features around the plate interface is one of the key topics to better understand controlling factors over earthquake types to be generated.

Recent studies in the Hikurangi subduction margin off the North Island of New Zealand show spatial relationship between variety of fault slips and topographic features of the plate interface. Wallace et al. (2016) successfully observed a large slow slip event just beneath an offshore array of ocean bottom pressure gauges, and precisely determined its slip distribution. They revealed that its slip propagation appeared to have circumvented subducted seamounts that have been imaged by magnetic anomalies as well as seismic reflection sections. Todd et al. (2018), for the first time, detected offshore tremor activity in the Hikurangi margin. The activity appears to have started just after the cessation of the slow slip, and its spatial distribution is only limited within regions of subducted seamounts. These results show that distributions of slow slip and tremor activity do not appear coincident, and thus the physical properties of the plate interface may be different. Further seismic surveys are supposed to provide vital information on structural variations that control physical characteristics of the plate interface.

In February, 2011, we acquired wide-angle reflection and refraction seismic data using 21 OBSs along a 150 km transect in the Ibaraki-oki region during the KH11-2 R/V Hakuho-maru cruise. We also included data from an OBS array that had already been deployed for a long-term seismic observation above the subduction front of the subducted seamount. Thus, we could construct a dense OBS profile above the subducted seamount with a receiver interval of ~3 km to achieve a high spatial resolution, whereas the largest interval is 10 km near both ends of the profile. First arrivals from the airgun sources can be traced up to ~95 km on most of the OBSs. The OBS record sections show significant heterogeneity that may include very rough structural features of the subducting oceanic crust along strike. Such heterogeneity may control seismic activity in the region.

©2019. Japan Geoscience Union. All Right Reserved.

Keywords: Ibaraki-oki, Active source seismic survey, Heterogeneous structure

©2019. Japan Geoscience Union. All Right Reserved.

Shallow low-frequency tremor triggered by nearby moderate earthquakes off Sanriku

*Sachiko Tanaka[1], Takanori Matsuzawa[1], Youichi Asano[1]

1. National Research Institute for Earth Science and Disaster Resilience

In the region off Sanriku, we have observed shallow low-frequency tremor, which occurs between the 12 km and 20 km depth contours of the plate interface, applying an envelope correlation method (Obara, 2002) to the records from the Seafloor observation network for earthquakes and tsunamis along the Japan Trench (S-net) (Tanaka et al., 2018). Several episodes of tremor, each of which lasted for half a day to six days, were detected in 2017, with intervals of one to three months. In the present study, we found tremor triggered by nearby moderate earthquakes. On July 24, 2017, an Mw 5.6 earthquake, showing reverse faulting consistent with the slip on the plate interface, occurred at the downdip end of the tremor zone off Sanriku, which was the largest event within 100 km of that tremor zone in the year. Immediately after the Mw 5.6 earthquake, coherent tremor signals were identified at surrounding stations. These signals continued for 20 hours, and the locations of their sources spanned 40 km along strike and 50 km along dip. Similar triggered tremor was observed following an Mw 5.1 earthquake on July 22, two days before the Mw 5.6 earthquake. This tremor activity was smaller and shorter than that triggered by the Mw 5.6 earthquake; tremor was localized to an area of 20 km by 15 km, and lasted for twelve hours. After a quiescence of nearly one day, the Mw 5.6 earthquake occurred at an adjacent area and triggered tremor was detected again. Triggering of tremor by moderate interplate earthquakes in or very close to the tremor zone we observed may imply small-scale (~ a few kilometers) heterogeneities in frictional properties on the plate interface in the area.

Keywords: shallow low-frequency tremor, triggered tremor, Japan Trench

©2019. Japan Geoscience Union. All Right Reserved.

Slow slip events in the Bungo Channel over 15 years as inferred from GNSS data (1996-2011)

Takatoshi Yokoi[1], *SHINICHI MIYAZAKI[1], Hiromu Sakaue[1], Jun'ichi Fukuda[2]

1. Graduate School of Science, Kyoto University, 2. Earthquake Research Institute, The University of Tokyo

We estimated space-time evolution of inter-plate slip and slip velocity associated with slow slip events (SSE) in the Bungo Channel over 15 years between January 1, 1996 and February 28, 2011, from GNSS data.

We use GNSS time series at 80 stations around the Bungo Channel out of GEONET stations. Time series were obtained with GIPSY-OASIS II software by Nishimura (personal communication). We removed data during SSE and estimated secular velocities, annual and semi-annual seasonal variations, and offsets associated with earthquakes, SSEs and instrumental events. Then we remove contributions of those components from time series with SSE to prepare time series for the inversion. We constructed plate interface based on iso-depth data by Baba et al. (2002) and Hirose et al. (2008), and setup the model region that is 200km long east to west and 280km long north to south. The model region was subdivided into 719 small triangular patches. We employed the inversion method based on the Monte Carlo Mixture Kalman Filter (Fukuda et al. 2008) and estimated slip and slip velocities on the fault continuously over 15 years.

First, Long-term slow slip events (L-SSE hereafter) that lasted for several months were inferred in 1997, 2003 and 2010 as obtained by, such as, Ozawa et al. (2012, 2017) and Yoshioka et al. (2015). In addition to basic characteristics described in these previous studies, short-term slow slip events (S-SSE hereafter) were inferred just before or just after the main slip event. This result suggests that stress perturbations by SSEs trigger other SSEs. Therefore the inferred cumulative moment in this study was smaller than previous studies because we successfully excluded contributions from S-SSEs. Second, S-SSEs have repeatedly occurred with the interval of about three or four months over 15 years. Those S-SSE were located at depths of about 30-40km and associated with low frequency tremors.

In this presentation, we focus space-time evolutions of L-SSE in 2010 and S-SSE in 2005.

Keywords: Slow slip in the Bungo Channel, crustal deformation, Monte Carlo Mixture Kalman Filter

©2019. Japan Geoscience Union. All Right Reserved.

Investigations of sensor orientation and a possibility of detecting crustal deformation based on accelerometer records of S-net

*Ryota Takagi[1], Naoki Uchida[1], Takashi NAKAYAMA[1], Ryosuke Azuma[1], Akira Ishigami[1], Tomomi Okada[1], Yusaku Ohta[1], Ryota Hino[1]

1. Research Center for Prediction of Earthquakes and Volcanic Eruptions, Graduate School of Science, Tohoku University

Seafloor Observation Network for Earthquakes and Tsunamis along the Japan Trench (S-net) of National Research Institute for Earth Science and Disaster Resilience (NIED) will greatly improve our knowledge of subsurface structure beneath offshore region along Japan trench and understanding of regular and slow earthquakes on the subducting plate boundary. We estimated the orientations of S-net sensors that are fundamental information for further data analysis and investigated the possibility of detecting crustal deformation based on accelerometer records.

We determined three parameters of sensor orientations: tilt angle of the long axis of a cable, rotation angle around the long axis, azimuth of the long axis. We estimated the tilt and rotation angles by assuming the DC components of accelerometers record the gravitational acceleration. The tilt and rotation angles slightly vary within the range of 0.01-0.1 degree during the period from 2016 to 2018 except for coseismic steps of rotation angles larger than 1 degree due to the M6.4 off Sanriku earthquake (August 20, 2016) and M7.4 off Fukushima earthquake (November 20, 2016). The long-axis azimuths are estimated by particle motions of long-period Rayleigh waves. We used the accelerometer records in 30-100 s of 7-14 teleseismic earthquakes with Mw 7.0-8.2. The azimuths are constrained in the range of 5-10 degrees. After correcting waveforms based on the estimated sensor orientation, we found coherent waveforms within the whole S-net stations and separation of Rayleigh and Love waves in radial and transverse components.

The capability of the DC components of accelerometers implies a possibility to detect crustal deformation from accelerometer records. We made time series of tilt and rotation angle with the sampling rate of one hour. During the period without offsets partly due to earthquakes, the root-mean-square (RMS) amplitudes of tilt and rotation angles are about 2 micro radians at most stations. The buried stations shallower than 1500 m show smaller variations and RMS amplitudes are about 0.2 micro radians. Some buried stations show tidal response with amplitude of about 1 micro radians. Since the maximum tilt change of land stations by a slow slip event (SSE) near the Boso Peninsula is about 1 micro radians, it might be possible to detect crustal deformation due to similar SSEs based on the accelerometer records.

Acknowledgement: We used continuous records of S-net managed by NIED. We thank NIED for providing the data.

Keywords: S-net, Sensor orientation, Crustal deformation, Slow slip, Tilt observation

©2019. Japan Geoscience Union. All Right Reserved.

Spatiotemporal variation of released seismic energy from shallow low-frequency tremor in Hyuga-nada, revealed by ocean bottom seismological observation

*Yusuke Yamashita[1], Saki Watanabe[2], Tomoaki Yamada[3], Masanao Shinohara[3], Takeshi Matsushima[2]

1. Disaster Prevention Research Institute, Kyoto University, 2. Institute of Seismology and Volcanology, Kyushu University, 3. Earthquake Research Institute, The University of Tokyo

In this study, we estimate the released seismic energy by shallow low-frequency tremors (shallow tremors) and clarify spatiotemporal variation of shallow tremor activity in Hyuga-nada, east off Kyushu. We used the data obtained from the temporal ocean bottom seismological observation for 3 months in 2013 [Yamashita *et al*., 2015] and long-term ocean bottom seismological observation from 2014 to 2017. The source location and released seismic energy of each shallow tremor was simultaneously estimated by Hybrid Envelope Cross-correlation Method [Maeda and Obara, 2009]. Observation data were obtained by the long-term continuous ocean bottom seismic observation in Hyuga-nada from 2013 to 2017. Site amplification factors were estimated by the coda normalization method [e.g., Sato and Fehler, 1998].

Spatial distribution of released seismic energy rate (energy rate) shows a heterogeneity although the average value of that is generally 10^4 J/s. The regions where the energy rate is relatively small are roughly coincident with the subducting or passed areas of the Kyushu-Palau Ridge. This result suggests that the structure and/or shape of the subducting plate such as seamounts or ridges may have an effect on the frictional property of the shallow plate interface. The 2013 activity was similar characteristics of shallow tremor location in space and time as the previous study, including two migrations episode. In addition, the characteristics of the released seismic energy were revealed as follows: (1) the energy rate was large at the both initiation point and the front of the migration, (2) the total released energy amount of the first migration was larger than that of the second migration, (3) both migrations were stopped at the region of small amount of released energy. Migration episode occurred while the 2015 activity and similar characteristics were documented.

Migration speed of shallow tremor is a few times faster, and energy rate of that is one or two orders of magnitude greater than the deep tremor. Applying the model of Ando *et al*. [2010, 2012] and Yabe and Ide [2014] to the result in this study, the average fault strength of shallow tremor is stronger than that of deep tremor, which leads up to a faster fault slip both brittle and ductile area. As a result, migration speed may become to be faster than deep tremor.

Acknowledgements: This study is supported by the research project for compound disaster mitigation on the great earthquakes and tsunami around the Nankai trough region, the MEXT of Japan, and JSPS KAKENHI Grant Number JP16H06471, JP16H06472. We thank Dr. Takuto Maeda for valuable discussions and comments. The observation data in 2013 obtained by T/S Nagasaki-maru. We used the JMA unified earthquake catalog and the seismic data obtained by Kagoshima University.

Keywords: Shallow low frequency tremor, Shallow slow earthquake, Ocean bottom seismological observation

©2019. Japan Geoscience Union. All Right Reserved.

©2019. Japan Geoscience Union. All Right Reserved.

Unified description of fast and slow earthquakes using velocity strengthening patches

*So Ozawa[1], Takahiro Hatano[1]

1. Earthquake Research Institute, the University of Tokyo

In a prevalent view, seismicity in subduction zones is governed by the distribution of the frictional properties of the plate interface. Regions with velocity-weakening (VW) friction generate earthquakes, whereas velocity-strengthening (VS) regions creep aseismically. Although most models consider isolated VW regions (patches) from the idea of asperities (e.g. Dublanchet et al., 2013), isolated VS patches also would exist given the frictional properties on faults are inferred to be complex and hierarchical. Therefore, the role of VS patches is to be studied.

Here we perform 3-D numerical simulation of the seismic cycle of faults governed by the rate and state friction law with the aging law. We distribute randomly circular VS patches on a VW background. We mainly focus on the effect of the ratio of VS and VW areas.

In our preliminary simulation, we identified two important effects. First, the VS patches act as the “stability barriers” during dynamic rupture propagation, which makes the rupture process more complicated than a single propagating crack. Rupture decelerates by encountering a stability barrier, followed by reacceleration due to overcoming the barrier. Such a process gives rise to multiple rupture fronts in the slipping area.

Second, dynamic rupture is inhibited by increasing the number of VS patches, and the fault slips aseismically with strong fluctuation in slip velocity. This is because there are no enough VW regions to accelerate the slip to dynamic rupture. Although a similar mechanism for slow earthquakes is proposed by Skarbek et al. (2012) and Yabe & Ide (2017), our 3-D modeling enables detailed studies on the spatiotemporal evolution of slip. In the presentation, we further discuss our results in the context of the dynamic scaling of rupture growth and the phenomenological law of slow earthquakes.

Keywords: Slow earthquake, Rate and state friction

©2019. Japan Geoscience Union. All Right Reserved.

The b-value of the earthquake swarm activities accompanied by the Boso slow slip events

*Yuki Noda[1], Hitoshi Hirose[2,1]

1. Department of Planetology, Faculty of Science, Kobe University , 2. Research Center for Urban Safety and Security, Kobe University

Slow slip events (SSEs) which are accompanying earthquake swarms repeatedly occur at intervals of about 2 to 7 years off Boso Peninsula (e.g., Sagiya, 2004; Hirose et al., 2012, 2014; Fukuda, 2018). These SSEs and swarms are thought to occur on the upper boundary of the subducting Philippine Sea plate.

As a statistical property of earthquakes, Gutenberg-Righter’ s law is well-known, that is, the relationship between the magnitude and the logarithm of occurrence frequency of earthquakes is expressed well with a straight line a-bM (Gutenberg and Richter, 1944). Although the b-value (slope of the line) often takes values around 1, there are many reports about the temporal changes of the b-value. For example, a decade-scale b-value decrease prior to the 2011 Tohoku Earthquake is reported (Nanjo et al., 2012). Although the relationship between the temporal change of b-value and aseismic slip is suggested, but the lack of near field geodetic observations prevents the direct evidence for the relationship. Here we examine the b-value of the earthquake swarms accompanied by the Boso SSEs, of which the aseismic slip is revealed by geodetic observations.

In this study, we estimate the b-value of the earthquake swarms in 2002, 2007, 2011 and 2014. We use the JMA unified earthquake catalog. As a preliminary analysis, we investigated the earthquakes with focal depths of 5 km to 40 km occurring at 35.05˚ to 35.56˚N in latitude and 140.15˚ to 140.73˚E in longitude. Eventually, “event period” estimated in the previous studies of the crustal deformation by geodetic observation does not necessarily agree with the period of the swarms occurring at the same time. Therefore, in this research, “event period” was redefined from seismic activity and used. In other words, we extracted swarms including a SSE period from crustal deformation studies and the time when the seismicity rate (the number of earthquakes per unit time) is significantly higher than the other time is defined as “event period”. In addition, the period other than the event period is defined as “inter-swarm period”.

We find that the b-values in the event periods tend to be lower than that during inter-swarm period. In more detail, different trends that seem to correspond to the difference in slip zone and location of earthquake activity of each SSE (Hirose et al. 2014) are seen in the b-values for the event periods. A seismic activity near the southern coast of the Boso Peninsula was hardly observed in the 2007 event period, whereas an active seismic activity was seen there in the 2011 event period. In order to clarify the dependence of the b-value on the difference in the location of the earthquakes, we divided the survey area into two areas, that is, the northern area (area A) and the southern area (area B). The seismic activity is observed in all event periods in the area A, whereas an active seismic activity is observed only in the event periods of 2002 and 2011 in the area B. Then a b- value is estimated in each period in the same way. As a result, for the earthquakes occurred in the northern region (area A), there is a tendency that the b-value in each of the event periods is lower by about 0.2-0.4 than that during inter-swarm. On the other hand, such a tendency is not observed in the southern area (area B). Such differences in the northern and southern regions may suggest that the effects of stress changes caused by SSEs vary from region to region.

©2019. Japan Geoscience Union. All Right Reserved.

Keywords: Gutenberg-Richter's law

©2019. Japan Geoscience Union. All Right Reserved.

Three-dimensional thermal modeling associated with subduction of the Philippine Sea plate at the Ryukyu Trench, and its relation to the occurrence of interplate seismic events

*Nobuaki Suenaga[1], Shoichi Yoshioka[2,1], Yinfeng Ji[3]

1. Graduate School of Science, Kobe University, Japan, 2. Research Center for Urban Safety and Security, Kobe University, Japan, 3. Chinese Academy of Science, Beijin, China

Interplate seismic events such as short-term slow slip evens (S-SSEs) (Nakamura, 2017), low-frequency earthquakes (LFEs) (Ando et al., 2012), and shallow very low-frequency earthquakes (VLFEs) (Nakamura et al., 2015) have been identified at the Ryukyu Trench, southwestern Japan. As the specific characteristics of these distributions, depths where S-SSEs and LFEs occur at the plate interface beneath the Okinawa island, whose depth is ranging from 15 km to 25 km, is about 10-20 km shallower than that beneath the Yaeyama islands, whose depth is ranging from 35 km to 50 km.

In this study, we constructed three-dimensional parallelepiped thermal convection model associated with subduction of the Philippine Sea (PHS) plate beneath the Amurian (AM) plate at the Ryukyu subduction zone. We considered subduction history of the PHS plate in the model region, referring to the plate rotation model (Mathews et al., 2016). We performed the numerical simulation as the time-dependent problem in the last 15 Myr to elucidate relationships among calculated thermal structures, dehydrations from the subducting plate, and the interplate seismic events. We used observed heat flow data to constrain thermal structures.

As a result at 0 Ma, we found that interplate temperature where S-SSEs and LFEs occur beneath the Yaeyama islands is lower than that beneath the Okinawa island when compared with the same depth along the direction of the trench axis. This is mainly because the convergence rate (PHS-AM) becomes gradually fast toward the southwest. Therefore, interplate temperatures where S-SSEs and LFEs occur were estimated ranging from 500℃ to 700℃ both beneath the Okinawa island and the Yaeyama islands.

We also calculated water content distribution within the PHS plate, using the calculated thermal structures and the phase diagram of MORB in an oceanic crust (Omori et al., 2008) and ultramafic rock in a slab mantle (Hacker et al., 2003). As for dehydration of MORB, we found that epidote eclogite transforms into amphibole eclogite in the neighboring area where S-SSEs and LFEs occur beneath the Okinawa island, and amphibole eclogite transforms into eclogite beneath the Yaeyama islands. The former and the latter dehydrate a total amount of 1.4 wt% and 0.7 wt% associated with their phase transformations, respectively.

Keywords: three dimensional thermal modeling

©2019. Japan Geoscience Union. All Right Reserved.

[E] Poster | M (Multidisciplinary and Interdisciplinary)：M-GI General Geosciences, Information Geosciences & Simulations

Wed. May 29, 2019 10:45 AM - 12:15 PM JST | Wed. May 29, 2019 1:45 AM - 3:15 AM UTC | Poster Hall International Exhibition Hall8, Makuhari Messe_11

[M-GI30] Data assimilation: A fundamental approach in geosciences

convener:Shin ya Nakano(The Institute of Statistical Mathematics), Yosuke Fujii(Meteorological Research Institute, Japan Meteorological Agency), SHINICHI MIYAZAKI(Graduate School of Science, Kyoto University), Takemasa Miyoshi(RIKEN)

Data assimilation is an inversion approach to estimate the evolution of a system by utilizing a constraint given by a dynamical simulation model. Data assimilation is now widely used not only in meteorology and oceanography but also other fields of geosciences such as hydrology, solid earth science, and space science. This session aims at providing an opportunity for discussion on data assimilation studies among researchers of various field of geosciences. We encourage contributions addressing novel methods and theoretical developments of data assimilation. Contributions dealing with useful applications of data assimilation are also welcome.

[MGI30-P01] Superposition of atmospheric states using information redundancy for Numerical Weather Prediction

*Toshiyuki Ishibashi[1] (1.Meteorological Research Institute/Japan Meteorological Agency)

[MGI30-P02] Numerical Weather Prediction Experiments using a Coupled Atmosphere-Ocean Data Assimilation System in JMA/MRI (3)

*Toshiyuki Ishibashi[1], Takeshi Iriguchi[1], Yosuke Fujii[1], Tamaki Yasuda[1], Yuhei Takaya[1], Naoki Saito[1], Toshikazu Onogi[1] (1.Meteorological Research Institute/Japan Meteorological Agency)

[MGI30-P03] Accurate estimation of posterior error covariance in a 4D-Var inverse analysis

*Yosuke Niwa[1,2], Yosuke Fujii[2,3] (1.National Institute for Environmental Studies, 2.Meteorological Research Institute, Japan Meteorological Agency, 3.The Institute of Statistical Mathematics)

[MGI30-P04] Assimilation CO_2 concentration data in the Kanto region using AIST-MM model and for the estimation of CO_2 emissions

*Yutaka Arai[1], Ryoichi Imasu[1], Hiroaki Kondo[2], Yosuke Niwa[3] (1.Atmosphere and Ocean Research Institute, The University of Tokyo, 2.National Institute of Advanced Industrial Science and Technology, 3.National Institute for Environmental Studies, Independent Administrative Institutions)

[MGI30-P05] Application of data assimilation method on parameter estimation of flow and nutrient behavior in watershed model

*Yosuke Horie[1] (1.Nippon Koei Co., Ltd.)

[MGI30-P06] Bayesian inference of grain growth prediction via multi-phase-field models

*Shin-ichi Ito[1], Hiromichi Nagao[1], Takashi Kurokawa[1], Tadashi Kasuya[1], Junya Inoue[1] (1.The University of Tokyo)

[MGI30-P07] GNSS data assimilation for the Bungo channel Long-term SSEs using Ensemble Kalman Filter (EnKF)

*Megumi Fujita[1], Takuya NISHIMURA[2], Kazuro Hirahara[3], SHINICHI MIYAZAKI[1] (1.Graduate School of Science , Kyoto University, 2.Disaster Prevention Research Institute, Kyoto University, 3.Institute of Education, Research and Regional Cooperation for crisis Management Shikoku, Kagawa University)

[MGI30-P08] A data assimilation library with Python for parallel computing

*Shin ya Nakano[1], Yuya Ariyoshi[2], Tomoyuki Higuchi[1] (1.The Institute of Statistical Mathematics, 2.Faculty of Engineering, Nippon Bunri University)

Superposition of atmospheric states using information redundancy for Numerical Weather Prediction

*Toshiyuki Ishibashi[1]

1. Meteorological Research Institute/Japan Meteorological Agency

Atmospheric state analysis is a difficult scientific problem due to our limited ability in computation and observation, and analysed atmospheric states are fluctuating around the true state. The purpose of this paper is to analyse atmospheric state as a superposition of possible atmospheric states using information redundancy, and evaluate its accuracy in the context of numerical weather prediction (NWP). This atmospheric state analysis approach has two novel aspects. First, it uses only real atmospheric information, and no-artificial perturbations unlike existing ensemble based methods. Second, it does not require specific error structures of our knowledge of the atmosphere. We performed this method on a global numerical weather prediction system of Japan Meteorological Agency. The experimental results show the method can clearly reduce forecast root means square errors about 3-5% in average within 2 day forecast compared to existing methods (CNTL). Furthermore, forecast RMSEs of ensemble means of ensemble forecasts using only a few members generated by this method are significantly smaller than CNTL from the forecast initial time.

©2019. Japan Geoscience Union. All Right Reserved.

Numerical Weather Prediction Experiments using a Coupled Atmosphere-Ocean Data Assimilation System in JMA/MRI (3)

*Toshiyuki Ishibashi[1], Takeshi Iriguchi[1], Yosuke Fujii[1], Tamaki Yasuda[1], Yuhei Takaya[1], Naoki Saito[1], Toshikazu Onogi[1]

1. Meteorological Research Institute/Japan Meteorological Agency

An atmosphere-ocean coupled data assimilation system (CDAS) has been developed at the JMA/MRI to investigate feasibility of a CDAS as a future DAS for seamless numerical prediction including both numerical weather prediction (NWP) and numerical seasonal climate prediction (NCP), and for reanalysis of the atmosphere-ocean. Our CDAS (**MRI-CDA1**) has two features. 1) It composed of the JMA operational systems, the global atmospheric DAS (MRI-NAPEX) based on 4D-Var, the global ocean DAS (MOVE-G2) based on 3D-Var, and the atmosphere- ocean coupled global forecast model (CGCM: JMA/MRI-CGCM2). 2) Coupling strategy is “weak coupling” with two different data assimilation window lengths for the atmosphere and ocean. Here, “weak coupling” denotes the approximation that ignores correlations of atmosphere and ocean background forecast errors. Following the previous reports in JpGU2018 and JpGU-AGU joint meeting 2017 (Ishibashi et al. 2018; 2017), we will report basic property of MRI-CDA1 in NWP.

©2019. Japan Geoscience Union. All Right Reserved.

Accurate estimation of posterior error covariance in a 4D-Var inverse analysis

*Yosuke Niwa[1,2], Yosuke Fujii[2,3]

1. National Institute for Environmental Studies, 2. Meteorological Research Institute, Japan Meteorological Agency, 3. The Institute of Statistical Mathematics

The four-dimensional variational method (4D-Var) is one prominent data assimilation/inversion method. However, it is a non-trivial task for a conventional 4D-Var to estimate a posterior error variance-covariance matrix. This study developed a method to estimate a posterior error variance-covariance matrix especially focusing on its off-diagonal elements, i.e., covariance. Off-diagonal elements are usually difficult to be estimated but provide error correlations that are beneficial for interpreting optimized parameter variations. The method was developed within a 4D-Var framework using a quasi-Newton method with the Broyden–Fletcher–Goldfarb–Shanno (BFGS) formula. This study newly introduces numerical techniques that ensure conjugacy among the set of increment vector pairs in the BFGS formula. Through application to an inverse problem of atmospheric CO_2, the developed method was evaluated with three diagnostic measures and compared against existing methods. The evaluation revealed that the developed method could provide accurate estimates of the posterior variance-covariance matrix, in terms not only of the diagonal but also of the off-diagonal elements. Although far more expensive than optimal state estimation, the computational efficiency was found reasonable for practical use, especially in conjunction with an ensemble approach.

Keywords: inversion, data assimilation, posterior error covariance

©2019. Japan Geoscience Union. All Right Reserved.

Assimilation CO_2 concentration data in the Kanto region using AIST-MM model and for the estimation of CO_2 emissions

*Yutaka Arai[1], Ryoichi Imasu[1], Hiroaki Kondo[2], Yosuke Niwa[3]

1. Atmosphere and Ocean Research Institute, The University of Tokyo, 2. National Institute of Advanced Industrial Science and Technology, 3. National Institute for Environmental Studies, Independent Administrative Institutions

Atmospheric carbon dioxide (CO_2) known as greenhouse gas is the most important gas for global warming. For the reason, there have been many researches about CO_2 such as model calculations, satellite observations and direct observations recently. As computer spec get higher, the CO_2 model has been more improved and 3D distributions of CO_2 has been calculated in more detail. In Japan, the satellite observation has been high resolution by satellite, Greenhouse Observing SATellite-2 (GOSAT-2). But in urban area, CO_2 distributions are complicated because of complexed CO_2 emission source and sink around the area. Especially, in the Kanto district mega city, Tokyo is located, CO_2 emissions from power plants and human activities are very huge. Furthermore, around the city there are forests and mountains which strongly affect to CO_2 concentrations in the atmosphere through their respiration and photosynthesis. In case to calculate such the district with high spatial resolutions, the models are required to be able to represent the temporal and spatial variations of the respiration and photosynthesis of the plants precisely. It has been also pointed out that representativeness of the vertical transport of CO_2 in the models is a key subject. About satellite observations, it is not always possible to observe CO2 distributions because of to be influenced by the weather and the frequencies of them are limited, and what ca be observed are not 3 dimensional but 2 dimensional namely vertical column densities of CO_2. On the other hand, the accuracy of the in-situ observations, is best, but there are very limited observation points. These are obstacles to grasping the detailed behavior of CO_2 concentration.

In this study, a regional transport model, AIST-MM has been used to investigate the behavior of CO_2 concentrations in Kanto district (Kondo et al., 2001). Firstly, AIST-MM computes CO_2 concentrations in the outer area (630 km×550 km), and then calculates CO_2 concentrations in the inner area (216 km×216 km) using the results from the former.
Firstly, the model was improved to be able to calculate the CO_2 seasonal variations through a year in order to estimate CO_2 emission source which contained large error. It was found that AIST-MM had uncertainty in the part of plant activities especially respiration in summer. As the calculation of plant respiration strongly depends on the temperature, when the temperature becomes high, the respiration of plants unrealistically increases. So the plant respiration parameter was tuned.
In order to compensate for the CO_2 influx from outside of the calculation region, the result of a global model, NICAM-TM (GL5) were used as the boundary conditions when calculating outer region. This modification led to improve the calculation of the vertical transport.
Furthermore, constant sea surface temperature was replaced with the satellite observation data derived from AVHRR-AMSR. In order to improve the simulating performance, we adjusted many detailed emission information by distinguishing between holidays and weekdays.
Secondly, Local Ensemble Transform Kalman Filter (LETKF) which is one of data assimilation methods is adapted to the adjusted AIST-MM and try to calculate CO_2 concentrations using in-situ observations, satellite observations, and ground remote sensing observations. In the near future, the CO_2 emissions will be estimated using Kalman smoother method.

©2019. Japan Geoscience Union. All Right Reserved.

Keywords: regional CO2 transport model, plant respiration, data assimilation, Local Ensemble Transform Kalman Filter, Kanto region

©2019. Japan Geoscience Union. All Right Reserved.

Application of data assimilation method on parameter estimation of flow and nutrient behavior in watershed model

*Yosuke Horie[1]

1. Nippon Koei Co., Ltd.

In schemes for nutrient reduction from watershed such as Japanese total volume control framework on nutrient or master plan for sewerage system propagation, hydrologic and nutrient behavior in watershed is critical to make an effective plan to fulfill environmental standard of water body. However, there are many uncertainties in constructing a watershed model as follows. First, observation frequency of concentration of water quality, which is a target of such scheme on nutrient reduction, is not enough because they can be obtained in public water quality observation system only about once a month. Second, pollutant load unit, which is used for quantifying pollutant load from watershed, can be fluctuated from place to place. Third, there are many parameters of watershed models which should be calibrated. To resolve these problems, this study applied EnKF, one of data assimilation method, to SWAT (Soil and Water Assessment Tools) model, which can simulate hydrologic and nutrient cycle in watershed, and conducted parameter estimation to achieve more robust result from watershed model under the uncertainties above.

Keywords: Data assimilation, watershed model, water quality simulation, SWAT

©2019. Japan Geoscience Union. All Right Reserved.

Bayesian inference of grain growth prediction via multi-phase-field models

*Shin-ichi Ito[1], Hiromichi Nagao[1], Takashi Kurokawa[1], Tadashi Kasuya[1], Junya Inoue[1]

1. The University of Tokyo

We propose a Bayesian inference methodology to evaluate unobservable parameters involved in multi-phase-field models with the aim of accurately predicting the observed grain growth, such as in metals and rocks. This approach integrates models and a set of observational image data of grain structures. Since the set of image data is not a time series, directly applying conventional inference techniques that require time series as the input data is difficult. The key idea in our methodology to overcome this difficulty is to construct a time series with an appropriate statistic that characterizes static image data of grain structures. Our methodology implements the empirical Bayes method. It can estimate not only a probability density function of the parameters but also an initial phase-field, which is generally unobservable in real experiments. After validating the proposed method through numerical tests using synthetic data, we apply it to real experimental images of grain structures in a steel alloy. The proposed method properly estimates unobservable parameters together with their uncertainties, and successfully selects the initial phase-field that best explains the experimental data from among candidate initial phase-fields.

Keywords: Grain growth, Bayesian inference, Data assimilation, Phase-field model

©2019. Japan Geoscience Union. All Right Reserved.

GNSS data assimilation for the Bungo channel Long-term SSEs using Ensemble Kalman Filter (EnKF)

*Megumi Fujita[1], Takuya NISHIMURA[2], Kazuro Hirahara[3], SHINICHI MIYAZAKI[1]

1. Graduate School of Science , Kyoto University, 2. Disaster Prevention Research Institute, Kyoto University, 3. Institute of Education, Research and Regional Cooperation for crisis Management Shikoku, Kagawa University

Long-term Slow Slip Events (L-SSEs) in the Bungo channel, southwest Japan occur in the down-dip side of the seismogenic zones on the megathrust plate interface. Although L-SSEs release accumulated strain in the L-SSE zones, they can increase strain in the up-dip seismogenic locked zones. Therefore, better understanding of the temporal evolution of L-SSEs is very important for earthquake hazard assessment. Hirahara, and Nishikiori (JpGU, 2018) developed a method for estimating slip evolution and frictional properties on L-SSE area in the Bungo channel, by applying a data assimilation method EnKF (Ensemble Kalman Filter), which has been developed in meteorology and oceanology, to the synthetic GNSS data. Although they used the surface velocity data as GNSS data, the actual data which we can observe at GNSS station is the surface displacement data, not surface velocity data. In order to apply EnKF to the actual GNSS observational data, we conducted two numerical experiments, as follows.

i)We used the surface velocity data converted from the synthetic surface displacement data as observational data.

ii) We used the surface displacement data, not the surface velocity data as observational data.

We used the same model settings in above two numerical experiments as Hirahara and Nishikiori (2018) did. Firstly, we set a plane fault in homogeneous isotropic elastic body, whose angle of dip is 15 degrees. The frictional force on the plane fault follows a Rate and State Friction (RSF) law with an aging law [Dieterich,1979; Ruina,1983]. We set a velocity weakening (A-B<0) circular patch, whose radius R is 35 km, in the velocity strengthen (A-B>0) fault plane. We reproduced the observed L-SSEs in the Bungo Channel, using the frictional parameters in such a way that R is smaller than the critical nucleation size R_c [Rubin and Ampuero (2005), Chen and Lapusta (2009)]. Secondly, we considered the effect the seismogenic locked zones in the up-dip side of the L-SSEs zone. We set a locked zone at the up-dip of the L-SSE fault, whose back-slip rate is 6.0 cm/yr.

As the common analysis settings, we selected several pairs of frictional parameters in a wide range of parameter space which reproduce L-SSEs for the initial ensemble members of frictional parameters. We made the daily synthetic GNSS surface displacement data for 93 GEONET stations around the Bungo channel by calculating the surface displacements using true synthetic frictional parameters and adding random Gaussian noise. We set the assimilation interval to 10 days.

In experiment i), we calculated 31 day moving averages of the synthetic GNSS displacement data, and we obtained the surface velocities at GNSS stations from the derivatives of a 150-day cubic spline function fitting the moving averaged surface displacements. Then we applied EnKF to the obtained surface velocities and we successfully estimated slip evolution and frictional parameters. This result suggests this method for converting the surface displacement data into the surface velocity data at GNSS stations might be applicable.

©2019. Japan Geoscience Union. All Right Reserved.

In experiment ii), we applied EnKF to the synthetic GNSS displacement data directly. When we conducted experiment ii), we changed some analysis settings for stabilizing the assimilation. Firstly, when the slip velocity at the center of fault plane is low, we added larger random noise to the innovations artificially. Secondly, when the slip velocity at the center of fault plane is high, we reduced the assimilation interval to 1 day and introduced additive inflation to prevent the prediction errors from being too small. As a result, we also successfully estimated slip evolution and frictional parameters using the surface displacements, although the experiment sometime fails depending on the start timing of the analysis. Therefore, this method has not been fully stabilized yet, and we need to improve it for robust estimation.

Finally, we applied EnKF to the real GNSS data before the 2011 Tohoku-oki earthquake in the same settings as experiment i) and ii) respectively. We corrected offsets of major earthquakes and antenna changes in the GNSS data. However, both experiments stopped during the assimilation due to negative slip velocities. It manifests an importance of correction of GNSS data including removing annual and semiannual components for a stable assimilation of real GNSS data. Furthermore, we need to consider the realistic model settings including the geometry of the subducting Philippine Sea plate interface and distribution of both L-SSE and locked zones.

Acknowledgement: We used GNSS of GEONET provided by the Geospatial Information Authority of Japan (GSI).

Keywords: GNSS, Ensemble Kalman Filter (EnKF), Long-term SSEs, the Bungo channel

©2019. Japan Geoscience Union. All Right Reserved.

A data assimilation library with Python for parallel computing

*Shin ya Nakano[1], Yuya Ariyoshi[2], Tomoyuki Higuchi[1]

1. The Institute of Statistical Mathematics, 2. Faculty of Engineering, Nippon Bunri University

Parallel computing is essential to reduce the computational time in the ensemble-based data assimilation. However, it requires skills in parallel programming. It is sometimes a hard task to attain high computational efficiency with ensemble-based data assimilation. In particular, the particle filter (PF) algorithm, which is applicable to nonlinear and/or non-Gaussian problems, contains a procedure difficult to parallelize.
It is thus challenging to achieve high computational efficiency with the PF even for experienced users.

We have developed a Python library named P-cubed (Python Parallelized Particle Filter Library), that enables us to use parallel-ready PF algorithms with high parallel efficiency. Now we are also planning to attach a module of other data assimilation algorithms such as the ensemble Kalman filter to this library. In this presentation, we introduce the parallelized PF algorithms which are already available in P-cubed and explain the design and characteristics of the library. Future prospects of this library will also be discussed.

Keywords: data assimilation, particle filter, parallel computing, Python

©2019. Japan Geoscience Union. All Right Reserved.

[E] Poster | M (Multidisciplinary and Interdisciplinary)：M-GI General Geosciences, Information Geosciences & Simulations

Wed. May 29, 2019 5:15 PM - 6:30 PM JST | Wed. May 29, 2019 8:15 AM - 9:30 AM UTC | Poster Hall International Exhibition Hall8, Makuhari Messe_37

[M-GI30] Data assimilation: A fundamental approach in geosciences

convener:Shin ya Nakano(The Institute of Statistical Mathematics), Yosuke Fujii(Meteorological Research Institute, Japan Meteorological Agency), SHINICHI MIYAZAKI(Graduate School of Science, Kyoto University), Takemasa Miyoshi(RIKEN)

Data assimilation is an inversion approach to estimate the evolution of a system by utilizing a constraint given by a dynamical simulation model. Data assimilation is now widely used not only in meteorology and oceanography but also other fields of geosciences such as hydrology, solid earth science, and space science. This session aims at providing an opportunity for discussion on data assimilation studies among researchers of various field of geosciences. We encourage contributions addressing novel methods and theoretical developments of data assimilation. Contributions dealing with useful applications of data assimilation are also welcome.

[MGI30-P01] Superposition of atmospheric states using information redundancy for Numerical Weather Prediction

*Toshiyuki Ishibashi[1] (1.Meteorological Research Institute/Japan Meteorological Agency)

[MGI30-P02] Numerical Weather Prediction Experiments using a Coupled Atmosphere-Ocean Data Assimilation System in JMA/MRI (3)

*Toshiyuki Ishibashi[1], Takeshi Iriguchi[1], Yosuke Fujii[1], Tamaki Yasuda[1], Yuhei Takaya[1], Naoki Saito[1], Toshikazu Onogi[1] (1.Meteorological Research Institute/Japan Meteorological Agency)

[MGI30-P03] Accurate estimation of posterior error covariance in a 4D-Var inverse analysis

*Yosuke Niwa[1,2], Yosuke Fujii[2,3] (1.National Institute for Environmental Studies, 2.Meteorological Research Institute, Japan Meteorological Agency, 3.The Institute of Statistical Mathematics)

[MGI30-P04] Assimilation CO_2 concentration data in the Kanto region using AIST-MM model and for the estimation of CO_2 emissions

*Yutaka Arai[1], Ryoichi Imasu[1], Hiroaki Kondo[2], Yosuke Niwa[3] (1.Atmosphere and Ocean Research Institute, The University of Tokyo, 2.National Institute of Advanced Industrial Science and Technology, 3.National Institute for Environmental Studies, Independent Administrative Institutions)

[MGI30-P05] Application of data assimilation method on parameter estimation of flow and nutrient behavior in watershed model

*Yosuke Horie[1] (1.Nippon Koei Co., Ltd.)

[MGI30-P06] Bayesian inference of grain growth prediction via multi-phase-field models

*Shin-ichi Ito[1], Hiromichi Nagao[1], Takashi Kurokawa[1], Tadashi Kasuya[1], Junya Inoue[1] (1.The University of Tokyo)

[MGI30-P07] GNSS data assimilation for the Bungo channel Long-term SSEs using Ensemble Kalman Filter (EnKF)

*Megumi Fujita[1], Takuya NISHIMURA[2], Kazuro Hirahara[3], SHINICHI MIYAZAKI[1] (1.Graduate School of Science , Kyoto University, 2.Disaster Prevention Research Institute, Kyoto University, 3.Institute of Education, Research and Regional Cooperation for crisis Management Shikoku, Kagawa University)

[MGI30-P08] A data assimilation library with Python for parallel computing

*Shin ya Nakano[1], Yuya Ariyoshi[2], Tomoyuki Higuchi[1] (1.The Institute of Statistical Mathematics, 2.Faculty of Engineering, Nippon Bunri University)

Superposition of atmospheric states using information redundancy for Numerical Weather Prediction

*Toshiyuki Ishibashi[1]

1. Meteorological Research Institute/Japan Meteorological Agency

Atmospheric state analysis is a difficult scientific problem due to our limited ability in computation and observation, and analysed atmospheric states are fluctuating around the true state. The purpose of this paper is to analyse atmospheric state as a superposition of possible atmospheric states using information redundancy, and evaluate its accuracy in the context of numerical weather prediction (NWP). This atmospheric state analysis approach has two novel aspects. First, it uses only real atmospheric information, and no-artificial perturbations unlike existing ensemble based methods. Second, it does not require specific error structures of our knowledge of the atmosphere. We performed this method on a global numerical weather prediction system of Japan Meteorological Agency. The experimental results show the method can clearly reduce forecast root means square errors about 3-5% in average within 2 day forecast compared to existing methods (CNTL). Furthermore, forecast RMSEs of ensemble means of ensemble forecasts using only a few members generated by this method are significantly smaller than CNTL from the forecast initial time.

©2019. Japan Geoscience Union. All Right Reserved.

Numerical Weather Prediction Experiments using a Coupled Atmosphere-Ocean Data Assimilation System in JMA/MRI (3)

*Toshiyuki Ishibashi[1], Takeshi Iriguchi[1], Yosuke Fujii[1], Tamaki Yasuda[1], Yuhei Takaya[1], Naoki Saito[1], Toshikazu Onogi[1]

1. Meteorological Research Institute/Japan Meteorological Agency

An atmosphere-ocean coupled data assimilation system (CDAS) has been developed at the JMA/MRI to investigate feasibility of a CDAS as a future DAS for seamless numerical prediction including both numerical weather prediction (NWP) and numerical seasonal climate prediction (NCP), and for reanalysis of the atmosphere-ocean. Our CDAS (**MRI-CDA1**) has two features. 1) It composed of the JMA operational systems, the global atmospheric DAS (MRI-NAPEX) based on 4D-Var, the global ocean DAS (MOVE-G2) based on 3D-Var, and the atmosphere- ocean coupled global forecast model (CGCM: JMA/MRI-CGCM2). 2) Coupling strategy is “weak coupling” with two different data assimilation window lengths for the atmosphere and ocean. Here, “weak coupling” denotes the approximation that ignores correlations of atmosphere and ocean background forecast errors. Following the previous reports in JpGU2018 and JpGU-AGU joint meeting 2017 (Ishibashi et al. 2018; 2017), we will report basic property of MRI-CDA1 in NWP.

©2019. Japan Geoscience Union. All Right Reserved.

Accurate estimation of posterior error covariance in a 4D-Var inverse analysis

*Yosuke Niwa[1,2], Yosuke Fujii[2,3]

1. National Institute for Environmental Studies, 2. Meteorological Research Institute, Japan Meteorological Agency, 3. The Institute of Statistical Mathematics

The four-dimensional variational method (4D-Var) is one prominent data assimilation/inversion method. However, it is a non-trivial task for a conventional 4D-Var to estimate a posterior error variance-covariance matrix. This study developed a method to estimate a posterior error variance-covariance matrix especially focusing on its off-diagonal elements, i.e., covariance. Off-diagonal elements are usually difficult to be estimated but provide error correlations that are beneficial for interpreting optimized parameter variations. The method was developed within a 4D-Var framework using a quasi-Newton method with the Broyden–Fletcher–Goldfarb–Shanno (BFGS) formula. This study newly introduces numerical techniques that ensure conjugacy among the set of increment vector pairs in the BFGS formula. Through application to an inverse problem of atmospheric CO_2, the developed method was evaluated with three diagnostic measures and compared against existing methods. The evaluation revealed that the developed method could provide accurate estimates of the posterior variance-covariance matrix, in terms not only of the diagonal but also of the off-diagonal elements. Although far more expensive than optimal state estimation, the computational efficiency was found reasonable for practical use, especially in conjunction with an ensemble approach.

Keywords: inversion, data assimilation, posterior error covariance

©2019. Japan Geoscience Union. All Right Reserved.

Assimilation CO_2 concentration data in the Kanto region using AIST-MM model and for the estimation of CO_2 emissions

*Yutaka Arai[1], Ryoichi Imasu[1], Hiroaki Kondo[2], Yosuke Niwa[3]

1. Atmosphere and Ocean Research Institute, The University of Tokyo, 2. National Institute of Advanced Industrial Science and Technology, 3. National Institute for Environmental Studies, Independent Administrative Institutions

Atmospheric carbon dioxide (CO_2) known as greenhouse gas is the most important gas for global warming. For the reason, there have been many researches about CO_2 such as model calculations, satellite observations and direct observations recently. As computer spec get higher, the CO_2 model has been more improved and 3D distributions of CO_2 has been calculated in more detail. In Japan, the satellite observation has been high resolution by satellite, Greenhouse Observing SATellite-2 (GOSAT-2). But in urban area, CO_2 distributions are complicated because of complexed CO_2 emission source and sink around the area. Especially, in the Kanto district mega city, Tokyo is located, CO_2 emissions from power plants and human activities are very huge. Furthermore, around the city there are forests and mountains which strongly affect to CO_2 concentrations in the atmosphere through their respiration and photosynthesis. In case to calculate such the district with high spatial resolutions, the models are required to be able to represent the temporal and spatial variations of the respiration and photosynthesis of the plants precisely. It has been also pointed out that representativeness of the vertical transport of CO_2 in the models is a key subject. About satellite observations, it is not always possible to observe CO2 distributions because of to be influenced by the weather and the frequencies of them are limited, and what ca be observed are not 3 dimensional but 2 dimensional namely vertical column densities of CO_2. On the other hand, the accuracy of the in-situ observations, is best, but there are very limited observation points. These are obstacles to grasping the detailed behavior of CO_2 concentration.

In this study, a regional transport model, AIST-MM has been used to investigate the behavior of CO_2 concentrations in Kanto district (Kondo et al., 2001). Firstly, AIST-MM computes CO_2 concentrations in the outer area (630 km×550 km), and then calculates CO_2 concentrations in the inner area (216 km×216 km) using the results from the former.
Firstly, the model was improved to be able to calculate the CO_2 seasonal variations through a year in order to estimate CO_2 emission source which contained large error. It was found that AIST-MM had uncertainty in the part of plant activities especially respiration in summer. As the calculation of plant respiration strongly depends on the temperature, when the temperature becomes high, the respiration of plants unrealistically increases. So the plant respiration parameter was tuned.
In order to compensate for the CO_2 influx from outside of the calculation region, the result of a global model, NICAM-TM (GL5) were used as the boundary conditions when calculating outer region. This modification led to improve the calculation of the vertical transport.
Furthermore, constant sea surface temperature was replaced with the satellite observation data derived from AVHRR-AMSR. In order to improve the simulating performance, we adjusted many detailed emission information by distinguishing between holidays and weekdays.
Secondly, Local Ensemble Transform Kalman Filter (LETKF) which is one of data assimilation methods is adapted to the adjusted AIST-MM and try to calculate CO_2 concentrations using in-situ observations, satellite observations, and ground remote sensing observations. In the near future, the CO_2 emissions will be estimated using Kalman smoother method.

©2019. Japan Geoscience Union. All Right Reserved.

Keywords: regional CO2 transport model, plant respiration, data assimilation, Local Ensemble Transform Kalman Filter, Kanto region

©2019. Japan Geoscience Union. All Right Reserved.

Application of data assimilation method on parameter estimation of flow and nutrient behavior in watershed model

*Yosuke Horie[1]

1. Nippon Koei Co., Ltd.

In schemes for nutrient reduction from watershed such as Japanese total volume control framework on nutrient or master plan for sewerage system propagation, hydrologic and nutrient behavior in watershed is critical to make an effective plan to fulfill environmental standard of water body. However, there are many uncertainties in constructing a watershed model as follows. First, observation frequency of concentration of water quality, which is a target of such scheme on nutrient reduction, is not enough because they can be obtained in public water quality observation system only about once a month. Second, pollutant load unit, which is used for quantifying pollutant load from watershed, can be fluctuated from place to place. Third, there are many parameters of watershed models which should be calibrated. To resolve these problems, this study applied EnKF, one of data assimilation method, to SWAT (Soil and Water Assessment Tools) model, which can simulate hydrologic and nutrient cycle in watershed, and conducted parameter estimation to achieve more robust result from watershed model under the uncertainties above.

Keywords: Data assimilation, watershed model, water quality simulation, SWAT

©2019. Japan Geoscience Union. All Right Reserved.

Bayesian inference of grain growth prediction via multi-phase-field models

*Shin-ichi Ito[1], Hiromichi Nagao[1], Takashi Kurokawa[1], Tadashi Kasuya[1], Junya Inoue[1]

1. The University of Tokyo

We propose a Bayesian inference methodology to evaluate unobservable parameters involved in multi-phase-field models with the aim of accurately predicting the observed grain growth, such as in metals and rocks. This approach integrates models and a set of observational image data of grain structures. Since the set of image data is not a time series, directly applying conventional inference techniques that require time series as the input data is difficult. The key idea in our methodology to overcome this difficulty is to construct a time series with an appropriate statistic that characterizes static image data of grain structures. Our methodology implements the empirical Bayes method. It can estimate not only a probability density function of the parameters but also an initial phase-field, which is generally unobservable in real experiments. After validating the proposed method through numerical tests using synthetic data, we apply it to real experimental images of grain structures in a steel alloy. The proposed method properly estimates unobservable parameters together with their uncertainties, and successfully selects the initial phase-field that best explains the experimental data from among candidate initial phase-fields.

Keywords: Grain growth, Bayesian inference, Data assimilation, Phase-field model

©2019. Japan Geoscience Union. All Right Reserved.

GNSS data assimilation for the Bungo channel Long-term SSEs using Ensemble Kalman Filter (EnKF)

*Megumi Fujita[1], Takuya NISHIMURA[2], Kazuro Hirahara[3], SHINICHI MIYAZAKI[1]

1. Graduate School of Science , Kyoto University, 2. Disaster Prevention Research Institute, Kyoto University, 3. Institute of Education, Research and Regional Cooperation for crisis Management Shikoku, Kagawa University

Long-term Slow Slip Events (L-SSEs) in the Bungo channel, southwest Japan occur in the down-dip side of the seismogenic zones on the megathrust plate interface. Although L-SSEs release accumulated strain in the L-SSE zones, they can increase strain in the up-dip seismogenic locked zones. Therefore, better understanding of the temporal evolution of L-SSEs is very important for earthquake hazard assessment. Hirahara, and Nishikiori (JpGU, 2018) developed a method for estimating slip evolution and frictional properties on L-SSE area in the Bungo channel, by applying a data assimilation method EnKF (Ensemble Kalman Filter), which has been developed in meteorology and oceanology, to the synthetic GNSS data. Although they used the surface velocity data as GNSS data, the actual data which we can observe at GNSS station is the surface displacement data, not surface velocity data. In order to apply EnKF to the actual GNSS observational data, we conducted two numerical experiments, as follows.

i)We used the surface velocity data converted from the synthetic surface displacement data as observational data.

ii) We used the surface displacement data, not the surface velocity data as observational data.

We used the same model settings in above two numerical experiments as Hirahara and Nishikiori (2018) did. Firstly, we set a plane fault in homogeneous isotropic elastic body, whose angle of dip is 15 degrees. The frictional force on the plane fault follows a Rate and State Friction (RSF) law with an aging law [Dieterich,1979; Ruina,1983]. We set a velocity weakening (A-B<0) circular patch, whose radius R is 35 km, in the velocity strengthen (A-B>0) fault plane. We reproduced the observed L-SSEs in the Bungo Channel, using the frictional parameters in such a way that R is smaller than the critical nucleation size R_c [Rubin and Ampuero (2005), Chen and Lapusta (2009)]. Secondly, we considered the effect the seismogenic locked zones in the up-dip side of the L-SSEs zone. We set a locked zone at the up-dip of the L-SSE fault, whose back-slip rate is 6.0 cm/yr.

As the common analysis settings, we selected several pairs of frictional parameters in a wide range of parameter space which reproduce L-SSEs for the initial ensemble members of frictional parameters. We made the daily synthetic GNSS surface displacement data for 93 GEONET stations around the Bungo channel by calculating the surface displacements using true synthetic frictional parameters and adding random Gaussian noise. We set the assimilation interval to 10 days.

In experiment i), we calculated 31 day moving averages of the synthetic GNSS displacement data, and we obtained the surface velocities at GNSS stations from the derivatives of a 150-day cubic spline function fitting the moving averaged surface displacements. Then we applied EnKF to the obtained surface velocities and we successfully estimated slip evolution and frictional parameters. This result suggests this method for converting the surface displacement data into the surface velocity data at GNSS stations might be applicable.

©2019. Japan Geoscience Union. All Right Reserved.

In experiment ii), we applied EnKF to the synthetic GNSS displacement data directly. When we conducted experiment ii), we changed some analysis settings for stabilizing the assimilation. Firstly, when the slip velocity at the center of fault plane is low, we added larger random noise to the innovations artificially. Secondly, when the slip velocity at the center of fault plane is high, we reduced the assimilation interval to 1 day and introduced additive inflation to prevent the prediction errors from being too small. As a result, we also successfully estimated slip evolution and frictional parameters using the surface displacements, although the experiment sometime fails depending on the start timing of the analysis. Therefore, this method has not been fully stabilized yet, and we need to improve it for robust estimation.

Finally, we applied EnKF to the real GNSS data before the 2011 Tohoku-oki earthquake in the same settings as experiment i) and ii) respectively. We corrected offsets of major earthquakes and antenna changes in the GNSS data. However, both experiments stopped during the assimilation due to negative slip velocities. It manifests an importance of correction of GNSS data including removing annual and semiannual components for a stable assimilation of real GNSS data. Furthermore, we need to consider the realistic model settings including the geometry of the subducting Philippine Sea plate interface and distribution of both L-SSE and locked zones.

Acknowledgement: We used GNSS of GEONET provided by the Geospatial Information Authority of Japan (GSI).

Keywords: GNSS, Ensemble Kalman Filter (EnKF), Long-term SSEs, the Bungo channel

©2019. Japan Geoscience Union. All Right Reserved.

A data assimilation library with Python for parallel computing

*Shin ya Nakano[1], Yuya Ariyoshi[2], Tomoyuki Higuchi[1]

1. The Institute of Statistical Mathematics, 2. Faculty of Engineering, Nippon Bunri University

Parallel computing is essential to reduce the computational time in the ensemble-based data assimilation. However, it requires skills in parallel programming. It is sometimes a hard task to attain high computational efficiency with ensemble-based data assimilation. In particular, the particle filter (PF) algorithm, which is applicable to nonlinear and/or non-Gaussian problems, contains a procedure difficult to parallelize.
It is thus challenging to achieve high computational efficiency with the PF even for experienced users.

We have developed a Python library named P-cubed (Python Parallelized Particle Filter Library), that enables us to use parallel-ready PF algorithms with high parallel efficiency. Now we are also planning to attach a module of other data assimilation algorithms such as the ensemble Kalman filter to this library. In this presentation, we introduce the parallelized PF algorithms which are already available in P-cubed and explain the design and characteristics of the library. Future prospects of this library will also be discussed.

Keywords: data assimilation, particle filter, parallel computing, Python

©2019. Japan Geoscience Union. All Right Reserved.

[E] Poster | M (Multidisciplinary and Interdisciplinary)：M-TT Technology & Techniques

Wed. May 29, 2019 1:45 PM - 3:15 PM JST | Wed. May 29, 2019 4:45 AM - 6:15 AM UTC | Poster Hall International Exhibition Hall8, Makuhari Messe_6

[M-TT45] Cryoseismology - a new proxy for detecting surface environmental variations of the Earth -

convener:Genti Toyokuni(Research Center for Prediction of Earthquakes and Volcanic Eruptions, Graduate School of Science, Tohoku University), Masaki Kanao(National Institute of Polar Research), Seiji Tsuboi(JAMSTEC, Center for Earth Information Science and Technology)

Several kinds of environmental signals associated with ocean - cryosphere - solid earth systems have recently been detected in bi-polar regions. Ice-related seismic motions for small magnitude events are generally named ice-quakes (ice-shocks) and can be generated by glacially related dynamics. Such kinds of cryoseismic sources are classified into the movements of ice sheets, sea-ice, oceanic tide-cracks, icebergs and the calving fronts of ice caps. Cryoseismic waves are likely to be influenced by variations in environmental conditions, and the continuous study of their time-space variability provides indirect evidence of climate change. As glacial earthquakes are the most prominent phenomena found recently in polar regions, in particular on the Greenland in this 21st century, the new innovative studies from seismology are expected by long-term monitoring under extreme conditions in the Earth's environment.

Taking these issues into account, the conveners are willing to invite many contributions to a special session on "Cryoseismology", which will cover the recent achievements on glacial related seismic events and associated phenomenon observed in polar regions. It is particularly encouraged to have contributions based on seismic signals involving the dynamics of ice sheets, sea-ice, and icebergs and glaciers. Although the glacial earthquakes are the most prominent evidence found recently in polar regions, all related topics involving polar seismology are welcome, such as studies of crust and mantle structure in the area, comparison of tectonic and glacier-related seismicity, recent triggered earthquakes and active volcanoes, glacial isostatic adjustment (GIA), harmonic tremor associated with cryoseismic events, etc. This session has been held every year since 2015, and was held as Union Session last year.

[MTT45-P01] Application of neural network and theoretical seismograms as training data to locate ice quakes

*Seiji Tsuboi[1], DAISUKE SUGIYAMA[1] (1.JAMSTEC, Center for Earth Information Science and Technology)

[MTT45-P02] **P-wave tomography beneath Greenland**

*Takaya Matsuno[1], Genti Toyokuni[1], Dapeng Zhao[1] (1.Research Center for Prediction of Earthquakes and Volcanic Eruptions, Graduate School of Science, Tohoku University)

[MTT45-P03] **Seismic observations in Greenland by a joint USA and Japanese GLISN team (2011–2018)**

*Genti Toyokuni[1], Masaki Kanao[2], Seiji Tsuboi[3], Yoko Tono[4] (1.RCPEVE, Tohoku Univ., 2.NIPR, 3.JAMSTEC, 4.ERI, Univ. Tokyo)

Application of neural network and theoretical seismograms as training data to locate ice quakes

*Seiji Tsuboi[1], DAISUKE SUGIYAMA[1]

1. JAMSTEC, Center for Earth Information Science and Technology

We have applied numerically computed theoretical seismograms and deep machine learning to locate earthquakes. We calculate theoretical seismograms for realistic three-dimensional Earth model and use these seismograms to create seismic wave propagation images at the surface of the Earth. Then we use these images as training dataset of convolutional neural network. We build neural networks for determination of hypocentral parameters, such as epicenter, depth, origin time and magnitude, and applied these networks to actual seismograms to examine if this procedure works to locate earthquake and determine magnitude. Although the number of earthquakes is small and the regional extent is quite limited, the results demonstrate that it is feasible to locate earthquakes by using this approach. Advantages of using this approach to locate earthquakes and determine magnitude are; accuracy of hypocenter parameters can be increased by accumulating theoretical seismograms for various earthquake location and size as learning dataset of deep machine learning; three dimensional Earth structure can be included without additional computational cost to locate earthquakes. Here we will discuss a possibility of applying this methodology to locate ice quakes, which happen in and near the ice sheet.

Keywords: icequakes, hypocenter determination, synthetic seismograms

©2019. Japan Geoscience Union. All Right Reserved.

P-wave tomography beneath Greenland

*Takaya Matsuno[1], Genti Toyokuni[1], Dapeng Zhao[1]

1. Research Center for Prediction of Earthquakes and Volcanic Eruptions, Graduate School of Science, Tohoku University

The Greenland landmass has a long and complex tectonic history (~4 billion years). However, most of the continent is covered by the extensive inland ice cap, so it was hard to access its geology and the underlying tectonics. The Greenland Ice Sheet Monitoring Network (GLISN) is an international project by 11 countries to establish a seismic network in and around Greenland (Toyokuni et al., 2014). The project was initiated in 2009, and now it provides broadband, continuous, and real-time seismic data recorded at 33 stations. In this study we aim to investigate the 3-D upper mantle structure beneath Greenland by using the GLISN data.

We inverted a number of P-wave arrival-time data of both local and teleseismic events, observed at 30 GLISN stations, to estimate a 3-D P-wave velocity (Vp) model beneath Greenland and surrounding regions. All of the GLISN arrival-time data are downloaded from the Bulletins of the International Seismological Centre. We used the seismic tomography method by Zhao et al. (2012).

In the polar region, if grid nodes are arranged on the basis of equatorial coordinates, distance between two adjacent nodes in the same latitude decreases as it gets closer to the pole. To overcome this problem, we converted our study region from the equatorial coordinates to the ecliptic coordinates. This scheme enables us to solve tomographic equations in quasi-Cartesian coordinates (e.g., Kobayashi & Zhao, 2004; Gupta et al., 2009; Takenaka et al., 2017). We set up a 3-D grid with a horizontal grid interval of 2° and a vertical grid interval of 15–30 km (at depths of 5–700 km).

The results of this study are summarized as follows.
(1) There is a prominent low-Vp anomaly beneath Iceland (depth < 500 km), which is related to the current Iceland plume.
(2) In the shallow mantle (40-250 km depths) beneath central and offshore eastern Greenland, Vp is relatively lower than those in the other inland areas of Greenland in the depth range, which may reflect the ancient motion path of the Iceland plume. This feature coincides with known basalt areas at central western and eastern coasts of Greenland.

References:
Kobayashi, R. & D. Zhao (2004) PEPI, 141, 167–181.
Gupta, S., D. Zhao & S. Rai (2009) Gondwana Res, 16, 109–118.
Takenaka, H. et al. (2017) EPS, 69, 67.
Toyokuni, G. et al. (2014) Antarctic Record, 58, 1–18.
Zhao, D. et al. (2012) GJI, 190, 816–828.

Keywords: Seismic tomography, Greenland, Iceland plume, GLISN project

©2019. Japan Geoscience Union. All Right Reserved.

Seismic observations in Greenland by a joint USA and Japanese GLISN team (2011–2018)

*Genti Toyokuni[1], Masaki Kanao[2], Seiji Tsuboi[3], Yoko Tono[4]

1. RCPEVE, Tohoku Univ., 2. NIPR, 3. JAMSTEC, 4. ERI, Univ. Tokyo

The Greenland Ice Sheet (GrIS) is a huge storehouse of water on Earth, and has the potential to raise the global sea level by approximately 7 m if completely melted. Although researchers have been mainly studying the GrIS surface snowmelt as a response to climate warming, recent progress in ice-core drilling, remote sensing, and theoretical analyses has turned a spotlight on its basal conditions. However, the traditional observation techniques, such as ice-core drilling and ice-penetrating radar, provide only discontinuous information in both time and space.

Seismic observation is now drawing widespread attention as an alternative method for monitoring the GrIS. The Greenland Ice Sheet Monitoring Network (GLISN), an international project between 11 countries that began in 2009, now provides broadband, continuous, and real-time seismic data from 33 stations in and around Greenland. Japan is a partner country from when the GLISN project was launched, and has been sending an expedition team every year since 2011. In 2011, a joint USA and Japanese GLISN team installed the dual seismic–GPS station ICESG-GLS2 in the middle of the GrIS. During 2012–2018, we conducted maintenance of three stations on the GrIS (station codes: ICESG-GLS2, DY2G-GLS1, and NEEM-GLS3), and three stations on bedrock in coastal areas (NUUK, DBG, and SOEG). We had succeeded in real-time transmission of broad-band and continuous seismic waveform data from the three ice stations. It was the first time in the world that the seismic data with such a high sampling rate are transferred from the ice sheet. The data is now open to public and available from the IRIS Data Management Center (http://www.iris.edu/ds/nodes/dmc/). This presentation will summarize our field activities for 2011–2018, and introduce the future field plans.

Acknowledgments: The Japanese GLISN team has been supported by research grants from JSPS (24403006).

Keywords: GLISN project, Seismic observation, Greenland Ice Sheet

©2019. Japan Geoscience Union. All Right Reserved.

[E] Poster | M (Multidisciplinary and Interdisciplinary)：M-TT Technology & Techniques

Wed. May 29, 2019 5:15 PM - 6:30 PM JST | Wed. May 29, 2019 8:15 AM - 9:30 AM UTC | Poster Hall International Exhibition Hall8, Makuhari Messe_40

[M-TT45] Cryoseismology - a new proxy for detecting surface environmental variations of the Earth -

convener:Genti Toyokuni(Research Center for Prediction of Earthquakes and Volcanic Eruptions, Graduate School of Science, Tohoku University), Masaki Kanao(National Institute of Polar Research), Seiji Tsuboi(JAMSTEC, Center for Earth Information Science and Technology)

Several kinds of environmental signals associated with ocean - cryosphere - solid earth systems have recently been detected in bi-polar regions. Ice-related seismic motions for small magnitude events are generally named ice-quakes (ice-shocks) and can be generated by glacially related dynamics. Such kinds of cryoseismic sources are classified into the movements of ice sheets, sea-ice, oceanic tide-cracks, icebergs and the calving fronts of ice caps. Cryoseismic waves are likely to be influenced by variations in environmental conditions, and the continuous study of their time-space variability provides indirect evidence of climate change. As glacial earthquakes are the most prominent phenomena found recently in polar regions, in particular on the Greenland in this 21st century, the new innovative studies from seismology are expected by long-term monitoring under extreme conditions in the Earth's environment.

Taking these issues into account, the conveners are willing to invite many contributions to a special session on "Cryoseismology", which will cover the recent achievements on glacial related seismic events and associated phenomenon observed in polar regions. It is particularly encouraged to have contributions based on seismic signals involving the dynamics of ice sheets, sea-ice, and icebergs and glaciers. Although the glacial earthquakes are the most prominent evidence found recently in polar regions, all related topics involving polar seismology are welcome, such as studies of crust and mantle structure in the area, comparison of tectonic and glacier-related seismicity, recent triggered earthquakes and active volcanoes, glacial isostatic adjustment (GIA), harmonic tremor associated with cryoseismic events, etc. This session has been held every year since 2015, and was held as Union Session last year.

[MTT45-P01] Application of neural network and theoretical seismograms as training data to locate ice quakes

*Seiji Tsuboi[1], DAISUKE SUGIYAMA[1] (1.JAMSTEC, Center for Earth Information Science and Technology)

[MTT45-P02] **P-wave tomography beneath Greenland**

*Takaya Matsuno[1], Genti Toyokuni[1], Dapeng Zhao[1] (1.Research Center for Prediction of Earthquakes and Volcanic Eruptions, Graduate School of Science, Tohoku University)

[MTT45-P03] **Seismic observations in Greenland by a joint USA and Japanese GLISN team (2011–2018)**

*Genti Toyokuni[1], Masaki Kanao[2], Seiji Tsuboi[3], Yoko Tono[4] (1.RCPEVE, Tohoku Univ., 2.NIPR, 3.JAMSTEC, 4.ERI, Univ. Tokyo)

Application of neural network and theoretical seismograms as training data to locate ice quakes

*Seiji Tsuboi[1], DAISUKE SUGIYAMA[1]

1. JAMSTEC, Center for Earth Information Science and Technology

We have applied numerically computed theoretical seismograms and deep machine learning to locate earthquakes. We calculate theoretical seismograms for realistic three-dimensional Earth model and use these seismograms to create seismic wave propagation images at the surface of the Earth. Then we use these images as training dataset of convolutional neural network. We build neural networks for determination of hypocentral parameters, such as epicenter, depth, origin time and magnitude, and applied these networks to actual seismograms to examine if this procedure works to locate earthquake and determine magnitude. Although the number of earthquakes is small and the regional extent is quite limited, the results demonstrate that it is feasible to locate earthquakes by using this approach. Advantages of using this approach to locate earthquakes and determine magnitude are; accuracy of hypocenter parameters can be increased by accumulating theoretical seismograms for various earthquake location and size as learning dataset of deep machine learning; three dimensional Earth structure can be included without additional computational cost to locate earthquakes. Here we will discuss a possibility of applying this methodology to locate ice quakes, which happen in and near the ice sheet.

Keywords: icequakes, hypocenter determination, synthetic seismograms

©2019. Japan Geoscience Union. All Right Reserved.

P-wave tomography beneath Greenland

*Takaya Matsuno[1], Genti Toyokuni[1], Dapeng Zhao[1]

1. Research Center for Prediction of Earthquakes and Volcanic Eruptions, Graduate School of Science, Tohoku University

The Greenland landmass has a long and complex tectonic history (~4 billion years). However, most of the continent is covered by the extensive inland ice cap, so it was hard to access its geology and the underlying tectonics. The Greenland Ice Sheet Monitoring Network (GLISN) is an international project by 11 countries to establish a seismic network in and around Greenland (Toyokuni et al., 2014). The project was initiated in 2009, and now it provides broadband, continuous, and real-time seismic data recorded at 33 stations. In this study we aim to investigate the 3-D upper mantle structure beneath Greenland by using the GLISN data.

We inverted a number of P-wave arrival-time data of both local and teleseismic events, observed at 30 GLISN stations, to estimate a 3-D P-wave velocity (Vp) model beneath Greenland and surrounding regions. All of the GLISN arrival-time data are downloaded from the Bulletins of the International Seismological Centre. We used the seismic tomography method by Zhao et al. (2012).

In the polar region, if grid nodes are arranged on the basis of equatorial coordinates, distance between two adjacent nodes in the same latitude decreases as it gets closer to the pole. To overcome this problem, we converted our study region from the equatorial coordinates to the ecliptic coordinates. This scheme enables us to solve tomographic equations in quasi-Cartesian coordinates (e.g., Kobayashi & Zhao, 2004; Gupta et al., 2009; Takenaka et al., 2017). We set up a 3-D grid with a horizontal grid interval of 2° and a vertical grid interval of 15–30 km (at depths of 5–700 km).

The results of this study are summarized as follows.
(1) There is a prominent low-Vp anomaly beneath Iceland (depth < 500 km), which is related to the current Iceland plume.
(2) In the shallow mantle (40-250 km depths) beneath central and offshore eastern Greenland, Vp is relatively lower than those in the other inland areas of Greenland in the depth range, which may reflect the ancient motion path of the Iceland plume. This feature coincides with known basalt areas at central western and eastern coasts of Greenland.

References:
Kobayashi, R. & D. Zhao (2004) PEPI, 141, 167–181.
Gupta, S., D. Zhao & S. Rai (2009) Gondwana Res, 16, 109–118.
Takenaka, H. et al. (2017) EPS, 69, 67.
Toyokuni, G. et al. (2014) Antarctic Record, 58, 1–18.
Zhao, D. et al. (2012) GJI, 190, 816–828.

Keywords: Seismic tomography, Greenland, Iceland plume, GLISN project

©2019. Japan Geoscience Union. All Right Reserved.

Seismic observations in Greenland by a joint USA and Japanese GLISN team (2011–2018)

*Genti Toyokuni[1], Masaki Kanao[2], Seiji Tsuboi[3], Yoko Tono[4]

1. RCPEVE, Tohoku Univ., 2. NIPR, 3. JAMSTEC, 4. ERI, Univ. Tokyo

The Greenland Ice Sheet (GrIS) is a huge storehouse of water on Earth, and has the potential to raise the global sea level by approximately 7 m if completely melted. Although researchers have been mainly studying the GrIS surface snowmelt as a response to climate warming, recent progress in ice-core drilling, remote sensing, and theoretical analyses has turned a spotlight on its basal conditions. However, the traditional observation techniques, such as ice-core drilling and ice-penetrating radar, provide only discontinuous information in both time and space.

Seismic observation is now drawing widespread attention as an alternative method for monitoring the GrIS. The Greenland Ice Sheet Monitoring Network (GLISN), an international project between 11 countries that began in 2009, now provides broadband, continuous, and real-time seismic data from 33 stations in and around Greenland. Japan is a partner country from when the GLISN project was launched, and has been sending an expedition team every year since 2011. In 2011, a joint USA and Japanese GLISN team installed the dual seismic–GPS station ICESG-GLS2 in the middle of the GrIS. During 2012–2018, we conducted maintenance of three stations on the GrIS (station codes: ICESG-GLS2, DY2G-GLS1, and NEEM-GLS3), and three stations on bedrock in coastal areas (NUUK, DBG, and SOEG). We had succeeded in real-time transmission of broad-band and continuous seismic waveform data from the three ice stations. It was the first time in the world that the seismic data with such a high sampling rate are transferred from the ice sheet. The data is now open to public and available from the IRIS Data Management Center (http://www.iris.edu/ds/nodes/dmc/). This presentation will summarize our field activities for 2011–2018, and introduce the future field plans.

Acknowledgments: The Japanese GLISN team has been supported by research grants from JSPS (24403006).

Keywords: GLISN project, Seismic observation, Greenland Ice Sheet

©2019. Japan Geoscience Union. All Right Reserved.

[E] Poster | P (Space and Planetary Sciences)：P-EM Solar-Terrestrial Sciences, Space Electromagnetism & Space Environment

Thu. May 30, 2019 3:30 PM - 5:00 PM JST | Thu. May 30, 2019 6:30 AM - 8:00 AM UTC | Poster Hall International Exhibition Hall8, Makuhari Messe_2

[P-EM15] Study of coupling processes in solar-terrestrial system

convener:Mamoru Yamamoto(Research Institute for Sustainable Humanosphere, Kyoto University), Yasunobu Ogawa(National Institute of Polar Research), Satonori Nozawa(Institute for Space-Earth Environment Research), Akimasa Yoshikawa(Department of Earth and Planetary Sciences, Kyushu University)

The Earth accepts vast input of energy and material from the Sun. The Earth's environment is maintained by the balance between their inputs and outputs. It is therefore important to study energy and mass transport on the Earth. This is an international session that discusses studies of the coupling processes in the Sun-Earth system based on the project "Study of coupling processes in solar-terrestrial system" that was approved by the Master Plan 2011/2014/2017 of Science Council of Japan. We continue proposing the project to the Master Plan 2020. The facilities and networks included are Equatorial MU Radar (EMU) in Indonesia to study the whole equatorial atmosphere, the EISCAT_3D radar system in northern Scandinavia to study detailed structures and elementary processes of the magnetosphere-ionosphere coupling in the polar region, and global networks of various ground-based instruments and observation data. We will show the current status of the project and discuss sciences by soliciting variety papers. This session is open to the world, and we strongly encourage submission of papers related to other facilities and projects, i.e., atmospheric or incoherent scatter radars, observation networks, satellites, and simulation or theoretical studies, etc.

[PEM15-P01] Study on adaptive clutter rejection system using external receiving antennas for the MU radar

*Hiroyuki Hashiguchi[1], Issei Terada[1], Mamoru Yamamoto[1] (1.Research Institute for Sustainable Humanosphere, Kyoto University)

[PEM15-P02] Detached cusp aurora for southward IMF

*Kohei Takasu[1], Satoshi Taguchi[1], Keisuke Hosokawa[2] (1.Department of Geophysics, Graduate School of Science, Kyoto University, 2.Department of Communication Engineering and Informatics, University of Electro-Communications)

[PEM15-P03] Motion of the inverted-V structure during an isolated substorm

*Morio Tanaka[1], Satoshi Taguchi[1], Kohei Takasu[1], Tomokazu Oigawa[1], Keisuke Hosokawa[2] (1.Department of Geophysics, Graduate school of science, Kyoto University, 2.Department of Communication Engineering and Informatics, University of Electro-Communications)

[PEM15-P04] Observation and modeling of Na layer response to energetic particle precipitation

*Takuo T. Tsuda[1], Kyogo Takizawa[1], Ryo Tozu[1], Takuya Kawahara[2], Yoshimasa Tanaka[3], Mitsumu K. Ejiri[3], Takanori Nishiyama[3], Takuji Nakamura[3] (1.The University of Electro-Communications, 2.Shinshu University, 3.National Institute of Polar Research)

[PEM15-P05] Lidar data analysis of the sodium atoms in the thermosphere observed at Tromsoe, Norway

*Takuya Kawahara[1], Satonori Nozawa[2], Norihito Saito[3], Takuo T. Tsuda[4], Toru Takahashi[5], Testuya Kawabata[2], Miki Nishimura[1], Yoshitaka Kobayashi[1] (1.Faculty of Engineering, Shinshu University, 2.ISEE, Nagoya University, 3.RIKEN, Center for Advanced Photonics, 4.The University of Electro-Communications, 5.National Institute of Polar Research)

[PEM15-P06] Spatial-temporal distribution of anomalous enhancement of ambipolar diffusion coefficient observed by meteor radars installed in the polar region

*Toru Takahashi[1], Masaki Tsutsumi[1,2], Yasunobu Ogawa[1,2,3], Satonori Nozawa[3], Chris Hall[4], Hiroshi Miyaoka[1,2] (1.National Institute of Polar Research, 2.SOKENDAI, 3.Institute for Space-Earth Environmental Research, 4.TGO, The Arctic University of Norway)

[PEM15-P07] Progress of ICSWSE and MAGDAS project in recent years

*Shuji Abe[1], Akimasa Yoshikawa[2,1], Teiji Uozumi[1], Akiko Fujimoto[3] (1.International Center for Space Weather Science and Education, Japan, 2.Department of Earth and Planetary Sciences, Kyushu University, 3.Kyushu Institute of Technology)

[PEM15-P08] Status of GNU Radio Beacon Receiver 2 (GRBR2) development

*Mamoru Yamamoto[1], Mayumi Matsunaga[2], Roland Tsunoda[3] (1.Research Institute for Sustainable Humanosphere, Kyoto University, 2.Tokyo University of Technology, 3.SRI International)

[PEM15-P09] Statistical comparison between plasma bubble day-to-day variability and neutral atmosphere by using GPS scintillation and GAIA model

*Mamoru Yamamoto[1], Keigo Kono[1] (1.Research Institute for Sustainable Humanosphere, Kyoto University)

[PEM15-P10] Redevelopment of the MU radar transceiver-module control system

*Mamoru Yamamoto[1], Koki Kurokawa[1], Hiroyuki Hashiguchi[1] (1.Research Institute for Sustainable Humanosphere, Kyoto University)

Study on adaptive clutter rejection system using external receiving antennas for the MU radar

*Hiroyuki Hashiguchi[1], Issei Terada[1], Mamoru Yamamoto[1]

1. Research Institute for Sustainable Humanosphere, Kyoto University

Strong clutter echoes from a hard target such as a mountain or building sometimes cause problems of observations with atmospheric radars. In order to reject or suppress ground clutter echoes, it is effective to use NC-DCMP (Norm Constrained- Directionally Constrained Minimum Power) method, which makes null toward the direction of the clutter, if we can receive signals independently from plural antennas [Nishimura et al., JTech., 2012]. It has been demonstrated that the NC-DCMP method is effective to real observation data with the MU (Middle and Upper atmosphere) radar [Hashiguchi et al., Radio Sci., 2018]. Although NC-DCMP method suppresses clutter echoes with almost maintaining the shape of main lobe to add pseudo-noise compared with the conventional DCMP method, the signal-to-noise ratio (S/N) of atmospheric echoes is somewhat degraded. We studied the clutter suppression method with little S/N degradation by using external antennas.

Four turnstile antennas are installed in the MU radar site. The signal from the antenna is sent to the MU radar observation room through the coaxial cable after amplified by the LNA with the limiter and BPF. It is further amplified by the LNA in the observation room, and then down-converted to intermediate frequency (5 MHz) signal to input to the multi-channel receiving system of the MU radar.

We compared the NC-DCMP method using the each received data of 25 channels, which is a conventional clutter suppression method, and the NC-DCMP method using the simple combination of 25 channels and 4 channels of external antennas. In the former case, the S/N of the atmospheric echoes is somewhat degraded, but in the latter case the main lobe shape is guaranteed by 25 channel simple synthesis, so the S/N degradation is not observed. In the latter case, the clutter suppression is sometimes insufficient. This cause is considered to be that the current positions of external antennas are biased to the north side. Antenna positions should be optimized in the future.

We can apply the achievement of this study to the Equatorial MU radar (EMU), which is proposed to be constructed at West Sumatera, Indonesia. The EMU system is the similar as the MU radar, but its antenna consists of 1045 Yagi antennas with 55 groups and it has 64 receiver channels.

Keywords: Atmospheric radar, Clutter rejection, NC-DCMP method, MU radar

©2019. Japan Geoscience Union. All Right Reserved.

Detached cusp aurora for southward IMF

*Kohei Takasu[1], Satoshi Taguchi[1], Keisuke Hosokawa[2]

1. Department of Geophysics, Graduate School of Science, Kyoto University, 2. Department of Communication Engineering and Informatics, University of Electro-Communications

A poleward-moving aurora is a typical phenomenon in the dayside cusp of the high-latitude ionosphere. This aurora usually originates near the equatorward boundary of the cusp, and diminishes near the poleward boundary of the persistent cusp auroral emissions. In this study we have examined faint poleward-moving auroras that are detached from the persistent cusp emissions by analyzing 630-nm aurora image data from an all-sky imager at Longyearbyen, Svalbard, and precipitating electron data from DMSP spacecraft. These auroras occur for southward IMF, and are located at latitudes higher than 80 MLAT. The intensities are very weak (less than 1 kilo Rayleigh). The result of the analysis shows that the speed of the auroral motion is 1 to 2 km/s, which is faster than typical convection speed in the dayside polar cap. We show the similarities and differences between the faint aurora and the typical poleward moving cusp aurora, and discuss how soft electron precipitation occurs in the region that is well separated from the cusp.

Keywords: Aurora, cusp, plasma convection, IMF

©2019. Japan Geoscience Union. All Right Reserved.

Motion of the inverted-V structure during an isolated substorm

*Morio Tanaka[1], Satoshi Taguchi[1], Kohei Takasu[1], Tomokazu Oigawa[1], Keisuke Hosokawa[2]

1. Department of Geophysics, Graduate school of science, Kyoto University, 2. Department of Communication Engineering and Informatics, University of Electro-Communications

The inverted-V is an energetic electron precipitation event, which can be seen as a V-shape structure in electron flux spectrograms, and causes intense auroral arcs. Previous studies have suggested that the inverted-V structure can move fast poleward or equatorward. However, we still do not understand what drives its motion. In this study we have investigated the detailed characteristics of an inverted-V structure moving poleward, which occurred during an isolated substorm, using simultaneous observations of auroras, precipitating electrons, and field-aligned currents. We analyzed aurora data (630-nm and 557.7-nm) from an all-sky imager at Longyearbyen, Svalbard, and precipitating electrons and magnetic field data from the DMSP spacecraft (F16, F17, F18, F19). One of the interesting characteristics of the poleward-moving inverted-V is the appearance of a downward field-aligned current equatorward of and adjacent to the inverted-V. We discuss how the region of the downward field-aligned current evolves in association with the motion and growth/decay of the inverted V structure, and possibility of a role of the downward field-aligned current for the latitudinal motion of the inverted V.

Keywords: Field-aligned current, aurora, inverted-V, isolated substorm

©2019. Japan Geoscience Union. All Right Reserved.

Observation and modeling of Na layer response to energetic particle precipitation

*Takuo T. Tsuda[1], Kyogo Takizawa[1], Ryo Tozu[1], Takuya Kawahara[2], Yoshimasa Tanaka[3], Mitsumu K. Ejiri[3], Takanori Nishiyama[3], Takuji Nakamura[3]

1. The University of Electro-Communications, 2. Shinshu University, 3. National Institute of Polar Research

Metallic layers, such as Na, Fe, Mg, K, and Ca layers, exist in the mesosphere and lower thermosphere (MLT). The height range of the MLT region corresponds to the ionospheric *D* and *E* regions, and in the polar region energetic particles precipitating from the magnetosphere can often penetrate into the *E* region and even into the *D* region. Therefore, the influence of energetic particles on the metallic layers is of interest regarding changes in atmospheric composition accompanied by auroral activity or geomagnetic activity.

In this study, we have performed a statistical investigation on relationship between Na density and cosmic noise absorption (CNA), which were obtained from 2000 to 2002 at Syowa Station, Antarctic (69.0ºS, 39.6ºE). From the investigation, we found the Na density decrease in accordance with the CNA increase, i.e., increase in the energetic particle precipitation. In the presentation, we will show these observational results, and discuss causality about the observed relationship based on numerical caculations using our Na chemistry model.

Keywords: Na layer, Energetic particle precipitation, Syowa Station, Na chemistry model

©2019. Japan Geoscience Union. All Right Reserved.

Lidar data analysis of the sodium atoms in the thermosphere observed at Tromsoe, Norway

*Takuya Kawahara[1], Satonori Nozawa[2], Norihito Saito[3], Takuo T. Tsuda[4], Toru Takahashi[5], Testuya Kawabata[2], Miki Nishimura[1], Yoshitaka Kobayashi[1]

1. Faculty of Engineering, Shinshu University, 2. ISEE, Nagoya University, 3. RIKEN, Center for Advanced Photonics, 4. The University of Electro-Communications, 5. National Institute of Polar Research

Distribution of low-density Na atoms in the thermosphere is interesting because of the capability of measuring neutral temperature and wind into the lower thermosphere up to 140 km. The thermospheric Na atoms significantly made the altitude range of Na lidar measurements expanded from the 80–105 km to 80–140 km, covering almost the entire E region (Liu et al., GRL, 2016).

The measurements of wind and temperature by a Na lidar in the northern mesosphere (80-105 km) at Tromsoe, Norway (69.6˚N, 19.2˚E) have been carried out in Polar winter season since 2010. However, thermospheric Na has not been seen in our data so far. This is because the automatic analysis program calculates the background signal level using the 140-150 km signals which possibly include a small amount of thermospheric Na signal. Deriving thermospheric Na is done by lowering the background signal level to emphasize thermospheric Na signals. The data at the new moon are selected which have a low background signal. Also, we calculated signal intensity from the Na atoms in the thermosphere based on our lidar parameters such as laser power, a telescope aperture area etc. by using the lidar equation. The results are summarized as follows. (1) Assuming that the Na density is 10 /cm^3, the signal from the Na atoms between 120 and 140 km is expected 300-400 photons, (2) The background signal observed is about 4,400 counts which means the noise level is about 220. So the signal intensity from the Na is nearly comparable to the noise level. (3) Thermospheric Na was not clearly seen in the re-calculated data. However, it depends on the smoothing technique to the original lidar data.

In this talk, we show the results derived by varying the binning time and discuss it.

Keywords: Na lidar, thermosphere, Tromsoe

©2019. Japan Geoscience Union. All Right Reserved.

Spatial-temporal distribution of anomalous enhancement of ambipolar diffusion coefficient observed by meteor radars installed in the polar region

*Toru Takahashi[1], Masaki Tsutsumi[1,2], Yasunobu Ogawa[1,2,3], Satonori Nozawa[3], Chris Hall[4], Hiroshi Miyaoka[1,2]

1. National Institute of Polar Research, 2. SOKENDAI, 3. Institute for Space-Earth Environmental Research, 4. TGO, The Arctic University of Norway

The meteor radar detected echoes of meteor tails as a tracer of neutral wind from 75 to 100 km altitudes (Hall et al., 2005). In addition, by using a decay time of the echo power, the meteor radar also estimated the ambipolar diffusion coefficient, which depends on the ion and electron temperature. The ambipolar diffusion coefficient was utilized to estimate the neutral temperature because the ion and electron temperature are generally in the thermal equilibrium with the neutral temperature. Recently, an anomalous enhancement of the ambipolar diffusion coefficient which could not be explained by the neutral temperature enhancement (hereafter called the anomalous enhancement) was observed by the meteor radar installed at Tromsoe, Norway (69.6 deg. N, 19.2 deg. E)
A previous study compared the anomalous enhancement with the ion velocity and the ion and electron temperature observed by EISCAT radar (Tsutsumi et al. 2017, Proceedings of the 30th Atmospheric Science Symposium, 2017). They reported that the anomalous enhancement tended to appear with the enhancement of ion velocity and electron temperature and frequently appeared at 16 UT. Furthermore, the anomalous enhancement was not seen during an event of the high energy particle precipitation on November 17, 2012 although one case study. Thus, the anomalous enhancement seems to be generated by the intense electric field and the high energy particle precipitation is not always necessary for its generation. As mentioned above, the previous study revealed a fundamental characteristics of the anomalous enhancement, however the generation mechanisms of the anomalous enhancement is still unclear. To clarify this, the comparison the spatial distribution of the anomalous enhancement with the convective electric field are needed. However, to date the latitudinal and local time occurrence of the anomalous enhancement was not revealed in the polar region.
Three meteor radars have been installed at Tromsoe, Bear island (74.5 deg. N, 19.0 deg. E), and Longyearbyen (78.2 deg. N, 16.2 deg. E). These meteor radars almost align on the same longitude line and can provide the spatial distribution of the anomalous enhancement. All meteor radars are a commercially produced VHF system (ENDR8-20) manufactured by ATRAD Pty Ltd. The antennas were produced by the Arctic University of Norway (Nozawa et al., 2012, JGR; Hall et al., 2002, GRL, Hall et al., 2006, JASTP). In this study, the spatial distribution and the occurrence rate of the anomalous enhancement was derived by these meteor radars.
Peaks of occurrence rate was seen at 20-22, 19-21, 16-19 MLT (~UT+3) at Tromsoe, Bear island, and Longyearbyen latitudes, respectively. This indicates that the anomalous enhancement appeared sequentially from high to low latitudes. In the morning sector, the peak of occurrence rate was only seen at 2-6 MLT above Bear island. In the case of high geomagnetic activity (Kp>3), the evening peaks of the occurrence rate shifted to an earlier time. On the other hand, clear peaks of the occurrence rate in the morning sector appeared at 3-5, 4-8, 7-10 MLT, respectively. Furthermore, the anomalous enhancement appeared with high possibility of 90% around 100 km south of Tromsoe. These characteristics which are seen during the time interval of high geomagnetic activity showed good agreement with the geomagnetic activity dependences of convective electric field.

©2019. Japan Geoscience Union. All Right Reserved.

We found another interesting characteristic in the geomagnetic dependence of the occurrence of the anomalous enhancement. The peak of occurrence rate in the evening sector was larger than it observed in the morning sector. This is considered to be related that auroral arcs appearing with intense electric field mainly observed in the evening sector. Thus, the generation of anomalous enhancement seems to relate both the convective electric field and the appearance of auroral arcs.
In this presentation, we will show the spatial distribution, MLT and geomagnetic activity dependence of the anomalous enhancement. We will also intend to present the comparison it with the electric filed observed by EISCAT and EISCAT Svalbard radars

Keywords: meteor radar, Tromsø, EISCAT radar

©2019. Japan Geoscience Union. All Right Reserved.

Progress of ICSWSE and MAGDAS project in recent years

*Shuji Abe[1], Akimasa Yoshikawa[2,1], Teiji Uozumi[1], Akiko Fujimoto[3]

1. International Center for Space Weather Science and Education, Japan, 2. Department of Earth and Planetary Sciences, Kyushu University, 3. Kyushu Institute of Technology

International Center for Space Weather Science and Education (ICSWSE), Kyushu University is the research institute for conducting research and education in space weather. Our magnetometer array named as "MAGDAS/CPMN (MAGnetic Data Acquisition System/Circum-pan Pacific Magnetometer Network)" (Principal Investigator: Dr. A. Yoshikawa) has over seventy fluxgate magnetometers, one induction magnetometer, and four FM-CW (Frequency Modulated Continuous Wave) radars around the world. One of our recent research topics is Equatorial Electrojet (EEJ). We calculate EE-index (Uozumi et al, 2008; Fujimoto et al., 2016) for space weather nowcast/forecast using realtime magnetometer data along the magnetic equator, and update it at each hour on the website (http://data.icswse.kyushu-u.ac.jp/eeindex/). To accelerate the understanding of EEJ structure, we constructed dense magnetometer array near magnetic equator at Peru and Malaysia in recent year. In addition, we finished to install new FM-CW radar at Sicaya, Peru. The instrument works well current now. We are providing our observational information and data including old project via our website (http://data.icswse.kyushu-u.ac.jp/). We also provide them via IUGONET (Inter-university Upper Atmosphere Observation NETwork) Type-A (http://search.iugonet.org/) which is one-stop web service system for researchers to search data, get the information of data, and plot data, and SPEDAS (Space Physics Environment Data Analysis System)/UDAS (iUgonet Data Analysis System). We will provide them via SuperMAG (http://supermag.jhuapl.edu/) in the near future. For accelerating the usage of MAGDAS and its science, we held a tutorial session in International Conference on Space Weather and Satellite Application 2018 at Malaysia, for handling MAGDAS and other data related our research field by using IUGONET system. We believe researchers use MAGDAS data on proper rule and develop their science. We will introduce other research activities in ICSWSE and MAGDAS project, for example, plasma bubble, geomagnetically induced current, and so on.

©2019. Japan Geoscience Union. All Right Reserved.

Status of GNU Radio Beacon Receiver 2 (GRBR2) development

*Mamoru Yamamoto[1], Mayumi Matsunaga[2], Roland Tsunoda[3]

1. Research Institute for Sustainable Humanosphere, Kyoto University, 2. Tokyo University of Technology, 3. SRI International

GNU Radio Beacon Receiver (GRBR) is the very successful digital receiver developed for dual-band (150/400MHz) beacon experiment. We were successfully conducted observations of total-electron content (TEC) of the ionosphere over Japan and in southeast Asia. However, many beacon satellites is now aging, and its number is decreasing. We now have a project to start new satellite-ground beacon experiment with new satellite constellations. One of them is TBEx (Tandem Beacon Explorer), a project by SRI International, to fly a constellation of two 3U cubesats with triband beacon transmitters. Another one is a project of FORMOSAT-7/COSMIC-2 by Taiwan/USA. Well-known mission of COSMIC-2 is GNSS occultation experiment, but the satellites carry triband beacon transmitters. All of these satellites will be placed into low-inclination orbits by the same launch vehicle in 2018, which will give us great opportunities to enhance studies of the low-latitude ionosphere. We develop a new digital receiver, GRBR2, for these new satellite beacon. GRBR2 is a four channel receiver at 150/400/965/1067MHz beacon signals from two satellite constellations. Now The reveiver system was finally fixed. Problem of the project of delay of the satellite launch. But it is now on schedule for launch by 2019 summer. We start deploying GRBR2 in southeast Asian countries. In this presentaiton, we will report GRBR2 system and its performance including results from test experiment in the field.

Keywords: Satellite beacon experiment, Digital receiver development, Total electron content

©2019. Japan Geoscience Union. All Right Reserved.

Statistical comparison between plasma bubble day-to-day variability and neutral atmosphere by using GPS scintillation and GAIA model

*Mamoru Yamamoto[1], Keigo Kono[1]

1. Research Institute for Sustainable Humanosphere, Kyoto University

Equational plasma bubble is one of the most intense irregularities in the ionosphere. The occurrence of the plasma bubble is considered related to weak changes of the underlying atmosphere which is called large-scale wavelike structure (LSWS). The LSWS is expected formed by penetration of the atmospheric wave into the ionosphere. But its real effect is not yet known in detail. The purpose of this research is to investigate the correlation between the neutral atmosphere and day-to-day variability of equatorial plasma bubbles mainly in the Southeast Asia region. We based on the study by Yamamoto et al (2018) that showed relationship between 40-km height temperature variation and S4 index over Kototabang, Indonesia. In this study we tried to extend the observation region and also tried to elucidate atmospheric waves that are related to the plasma bubble. For indicating activity of the plasma bubble, we used S4 index of GPS scintillation measured by ISEE, Nagoya Univ. at Kototabang, Indonesia. Atmospheric data were taken from GAIA database prepared by NICT. We analyzed data from 2003, 2004, 2012, and 2013 where the solar activity was high. Overall correlation between S4 index and the atmospheric temperature showed similar feature throughout these years. However, even when we tried to extract atmospheric wave components from the GAIA data, the correlation between the wave parameter to S4 index did not show large change. This means that the elucidation of the atmospheric wave component was not very successful so far. Further analyses are required.

Reference
Yamamoto, M., Y. Otsuka, H. Jin, Y. Miyoshi (2018) Relationship between day-to-day variability of equatorial plasma bubble activity from GPS scintillation and atmospheric properties from GAIA assimilation, Progress in Earth and Planetary Science, Vol. 5, page 26, doi: 10.1186/s40645-018-0184-7.

©2019. Japan Geoscience Union. All Right Reserved.

Redevelopment of the MU radar transceiver-module control system

*Mamoru Yamamoto[1], Koki Kurokawa[1], Hiroyuki Hashiguchi[1]

1. Research Institute for Sustainable Humanosphere, Kyoto University

The MU radar was installed in Shigaraki, Japan in 1984 as the world first atmospheric radar with active phased-array antenna system. The MU radar consists of 475 Yagi antennas in the circular field of about 100m diameter. By the electronic phase shift of each Yagi, the antenna beam is steered to one of pre-selected 2048 directions in the transmitting pulse-to-pulse basis. Success of the MU radar in the atmospheric/ionospheric research is well known, and its active phased-array configuration was followed by many other radar systems. The phase control of the MU radar is realized by the control of its transceiver-module (TR-module) that are equipped with each Yagi antenna. They are gathered into 25 groups of each 19 modules. One CPU (microcomputer board) is used for control of one group of modules. A weak point of the MU radar exists in this point because we are using the original 8085 CPU board that is connected to the host computer by 1200-baud (!) serial line. This control is very slow, and we could not meet demands for rapid change of observation parameters for long time. This time we tried to re-develop the new TR-module controller by using recent CPU board and electronic devices. In the presentation, we show hardware/software of the newly developed prototype of the MU radar TR-module controller.

Keywords: MU radar, control system, redevelopment

©2019. Japan Geoscience Union. All Right Reserved.

[E] Poster | P (Space and Planetary Sciences)：P-EM Solar-Terrestrial Sciences, Space Electromagnetism & Space Environment

Thu. May 30, 2019 5:15 PM - 6:30 PM JST | Thu. May 30, 2019 8:15 AM - 9:30 AM UTC | Poster Hall International Exhibition Hall8, Makuhari Messe_2

[P-EM15] Study of coupling processes in solar-terrestrial system

convener:Mamoru Yamamoto(Research Institute for Sustainable Humanosphere, Kyoto University), Yasunobu Ogawa(National Institute of Polar Research), Satonori Nozawa(Institute for Space-Earth Environment Research), Akimasa Yoshikawa(Department of Earth and Planetary Sciences, Kyushu University)

The Earth accepts vast input of energy and material from the Sun. The Earth's environment is maintained by the balance between their inputs and outputs. It is therefore important to study energy and mass transport on the Earth. This is an international session that discusses studies of the coupling processes in the Sun-Earth system based on the project "Study of coupling processes in solar-terrestrial system" that was approved by the Master Plan 2011/2014/2017 of Science Council of Japan. We continue proposing the project to the Master Plan 2020. The facilities and networks included are Equatorial MU Radar (EMU) in Indonesia to study the whole equatorial atmosphere, the EISCAT_3D radar system in northern Scandinavia to study detailed structures and elementary processes of the magnetosphere-ionosphere coupling in the polar region, and global networks of various ground-based instruments and observation data. We will show the current status of the project and discuss sciences by soliciting variety papers. This session is open to the world, and we strongly encourage submission of papers related to other facilities and projects, i.e., atmospheric or incoherent scatter radars, observation networks, satellites, and simulation or theoretical studies, etc.

[PEM15-P01] Study on adaptive clutter rejection system using external receiving antennas for the MU radar

*Hiroyuki Hashiguchi[1], Issei Terada[1], Mamoru Yamamoto[1] (1.Research Institute for Sustainable Humanosphere, Kyoto University)

[PEM15-P02] Detached cusp aurora for southward IMF

*Kohei Takasu[1], Satoshi Taguchi[1], Keisuke Hosokawa[2] (1.Department of Geophysics, Graduate School of Science, Kyoto University, 2.Department of Communication Engineering and Informatics, University of Electro-Communications)

[PEM15-P03] Motion of the inverted-V structure during an isolated substorm

*Morio Tanaka[1], Satoshi Taguchi[1], Kohei Takasu[1], Tomokazu Oigawa[1], Keisuke Hosokawa[2] (1.Department of Geophysics, Graduate school of science, Kyoto University, 2.Department of Communication Engineering and Informatics, University of Electro-Communications)

[PEM15-P04] Observation and modeling of Na layer response to energetic particle precipitation

*Takuo T. Tsuda[1], Kyogo Takizawa[1], Ryo Tozu[1], Takuya Kawahara[2], Yoshimasa Tanaka[3], Mitsumu K. Ejiri[3], Takanori Nishiyama[3], Takuji Nakamura[3] (1.The University of Electro-Communications, 2.Shinshu University, 3.National Institute of Polar Research)

[PEM15-P05] Lidar data analysis of the sodium atoms in the thermosphere observed at Tromsoe, Norway

*Takuya Kawahara[1], Satonori Nozawa[2], Norihito Saito[3], Takuo T. Tsuda[4], Toru Takahashi[5], Testuya Kawabata[2], Miki Nishimura[1], Yoshitaka Kobayashi[1] (1.Faculty of Engineering, Shinshu University, 2.ISEE, Nagoya University, 3.RIKEN, Center for Advanced Photonics, 4.The University of Electro-Communications, 5.National Institute of Polar Research)

[PEM15-P06] Spatial-temporal distribution of anomalous enhancement of ambipolar diffusion coefficient observed by meteor radars installed in the polar region

*Toru Takahashi[1], Masaki Tsutsumi[1,2], Yasunobu Ogawa[1,2,3], Satonori Nozawa[3], Chris Hall[4], Hiroshi Miyaoka[1,2] (1.National Institute of Polar Research, 2.SOKENDAI, 3.Institute for Space-Earth Environmental Research, 4.TGO, The Arctic University of Norway)

[PEM15-P07] Progress of ICSWSE and MAGDAS project in recent years

*Shuji Abe[1], Akimasa Yoshikawa[2,1], Teiji Uozumi[1], Akiko Fujimoto[3] (1.International Center for Space Weather Science and Education, Japan, 2.Department of Earth and Planetary Sciences, Kyushu University, 3.Kyushu Institute of Technology)

[PEM15-P08] Status of GNU Radio Beacon Receiver 2 (GRBR2) development

*Mamoru Yamamoto[1], Mayumi Matsunaga[2], Roland Tsunoda[3] (1.Research Institute for Sustainable Humanosphere, Kyoto University, 2.Tokyo University of Technology, 3.SRI International)

[PEM15-P09] Statistical comparison between plasma bubble day-to-day variability and neutral atmosphere by using GPS scintillation and GAIA model

*Mamoru Yamamoto[1], Keigo Kono[1] (1.Research Institute for Sustainable Humanosphere, Kyoto University)

[PEM15-P10] Redevelopment of the MU radar transceiver-module control system

*Mamoru Yamamoto[1], Koki Kurokawa[1], Hiroyuki Hashiguchi[1] (1.Research Institute for Sustainable Humanosphere, Kyoto University)

Study on adaptive clutter rejection system using external receiving antennas for the MU radar

*Hiroyuki Hashiguchi[1], Issei Terada[1], Mamoru Yamamoto[1]

1. Research Institute for Sustainable Humanosphere, Kyoto University

Strong clutter echoes from a hard target such as a mountain or building sometimes cause problems of observations with atmospheric radars. In order to reject or suppress ground clutter echoes, it is effective to use NC-DCMP (Norm Constrained- Directionally Constrained Minimum Power) method, which makes null toward the direction of the clutter, if we can receive signals independently from plural antennas [Nishimura et al., JTech., 2012]. It has been demonstrated that the NC-DCMP method is effective to real observation data with the MU (Middle and Upper atmosphere) radar [Hashiguchi et al., Radio Sci., 2018]. Although NC-DCMP method suppresses clutter echoes with almost maintaining the shape of main lobe to add pseudo-noise compared with the conventional DCMP method, the signal-to-noise ratio (S/N) of atmospheric echoes is somewhat degraded. We studied the clutter suppression method with little S/N degradation by using external antennas.

Four turnstile antennas are installed in the MU radar site. The signal from the antenna is sent to the MU radar observation room through the coaxial cable after amplified by the LNA with the limiter and BPF. It is further amplified by the LNA in the observation room, and then down-converted to intermediate frequency (5 MHz) signal to input to the multi-channel receiving system of the MU radar.

We compared the NC-DCMP method using the each received data of 25 channels, which is a conventional clutter suppression method, and the NC-DCMP method using the simple combination of 25 channels and 4 channels of external antennas. In the former case, the S/N of the atmospheric echoes is somewhat degraded, but in the latter case the main lobe shape is guaranteed by 25 channel simple synthesis, so the S/N degradation is not observed. In the latter case, the clutter suppression is sometimes insufficient. This cause is considered to be that the current positions of external antennas are biased to the north side. Antenna positions should be optimized in the future.

We can apply the achievement of this study to the Equatorial MU radar (EMU), which is proposed to be constructed at West Sumatera, Indonesia. The EMU system is the similar as the MU radar, but its antenna consists of 1045 Yagi antennas with 55 groups and it has 64 receiver channels.

Keywords: Atmospheric radar, Clutter rejection, NC-DCMP method, MU radar

©2019. Japan Geoscience Union. All Right Reserved.

Detached cusp aurora for southward IMF

*Kohei Takasu[1], Satoshi Taguchi[1], Keisuke Hosokawa[2]

1. Department of Geophysics, Graduate School of Science, Kyoto University, 2. Department of Communication Engineering and Informatics, University of Electro-Communications

A poleward-moving aurora is a typical phenomenon in the dayside cusp of the high-latitude ionosphere. This aurora usually originates near the equatorward boundary of the cusp, and diminishes near the poleward boundary of the persistent cusp auroral emissions. In this study we have examined faint poleward-moving auroras that are detached from the persistent cusp emissions by analyzing 630-nm aurora image data from an all-sky imager at Longyearbyen, Svalbard, and precipitating electron data from DMSP spacecraft. These auroras occur for southward IMF, and are located at latitudes higher than 80 MLAT. The intensities are very weak (less than 1 kilo Rayleigh). The result of the analysis shows that the speed of the auroral motion is 1 to 2 km/s, which is faster than typical convection speed in the dayside polar cap. We show the similarities and differences between the faint aurora and the typical poleward moving cusp aurora, and discuss how soft electron precipitation occurs in the region that is well separated from the cusp.

Keywords: Aurora, cusp, plasma convection, IMF

©2019. Japan Geoscience Union. All Right Reserved.

Motion of the inverted-V structure during an isolated substorm

*Morio Tanaka[1], Satoshi Taguchi[1], Kohei Takasu[1], Tomokazu Oigawa[1], Keisuke Hosokawa[2]

1. Department of Geophysics, Graduate school of science, Kyoto University, 2. Department of Communication Engineering and Informatics, University of Electro-Communications

The inverted-V is an energetic electron precipitation event, which can be seen as a V-shape structure in electron flux spectrograms, and causes intense auroral arcs. Previous studies have suggested that the inverted-V structure can move fast poleward or equatorward. However, we still do not understand what drives its motion. In this study we have investigated the detailed characteristics of an inverted-V structure moving poleward, which occurred during an isolated substorm, using simultaneous observations of auroras, precipitating electrons, and field-aligned currents. We analyzed aurora data (630-nm and 557.7-nm) from an all-sky imager at Longyearbyen, Svalbard, and precipitating electrons and magnetic field data from the DMSP spacecraft (F16, F17, F18, F19). One of the interesting characteristics of the poleward-moving inverted-V is the appearance of a downward field-aligned current equatorward of and adjacent to the inverted-V. We discuss how the region of the downward field-aligned current evolves in association with the motion and growth/decay of the inverted V structure, and possibility of a role of the downward field-aligned current for the latitudinal motion of the inverted V.

Keywords: Field-aligned current, aurora, inverted-V, isolated substorm

©2019. Japan Geoscience Union. All Right Reserved.

Observation and modeling of Na layer response to energetic particle precipitation

*Takuo T. Tsuda[1], Kyogo Takizawa[1], Ryo Tozu[1], Takuya Kawahara[2], Yoshimasa Tanaka[3], Mitsumu K. Ejiri[3], Takanori Nishiyama[3], Takuji Nakamura[3]

1. The University of Electro-Communications, 2. Shinshu University, 3. National Institute of Polar Research

Metallic layers, such as Na, Fe, Mg, K, and Ca layers, exist in the mesosphere and lower thermosphere (MLT). The height range of the MLT region corresponds to the ionospheric *D* and *E* regions, and in the polar region energetic particles precipitating from the magnetosphere can often penetrate into the *E* region and even into the *D* region. Therefore, the influence of energetic particles on the metallic layers is of interest regarding changes in atmospheric composition accompanied by auroral activity or geomagnetic activity.

In this study, we have performed a statistical investigation on relationship between Na density and cosmic noise absorption (CNA), which were obtained from 2000 to 2002 at Syowa Station, Antarctic (69.0ºS, 39.6ºE). From the investigation, we found the Na density decrease in accordance with the CNA increase, i.e., increase in the energetic particle precipitation. In the presentation, we will show these observational results, and discuss causality about the observed relationship based on numerical caculations using our Na chemistry model.

Keywords: Na layer, Energetic particle precipitation, Syowa Station, Na chemistry model

©2019. Japan Geoscience Union. All Right Reserved.

Lidar data analysis of the sodium atoms in the thermosphere observed at Tromsoe, Norway

*Takuya Kawahara[1], Satonori Nozawa[2], Norihito Saito[3], Takuo T. Tsuda[4], Toru Takahashi[5], Testuya Kawabata[2], Miki Nishimura[1], Yoshitaka Kobayashi[1]

1. Faculty of Engineering, Shinshu University, 2. ISEE, Nagoya University, 3. RIKEN, Center for Advanced Photonics, 4. The University of Electro-Communications, 5. National Institute of Polar Research

Distribution of low-density Na atoms in the thermosphere is interesting because of the capability of measuring neutral temperature and wind into the lower thermosphere up to 140 km. The thermospheric Na atoms significantly made the altitude range of Na lidar measurements expanded from the 80–105 km to 80–140 km, covering almost the entire E region (Liu et al., GRL, 2016).

The measurements of wind and temperature by a Na lidar in the northern mesosphere (80-105 km) at Tromsoe, Norway (69.6˚N, 19.2˚E) have been carried out in Polar winter season since 2010. However, thermospheric Na has not been seen in our data so far. This is because the automatic analysis program calculates the background signal level using the 140-150 km signals which possibly include a small amount of thermospheric Na signal. Deriving thermospheric Na is done by lowering the background signal level to emphasize thermospheric Na signals. The data at the new moon are selected which have a low background signal. Also, we calculated signal intensity from the Na atoms in the thermosphere based on our lidar parameters such as laser power, a telescope aperture area etc. by using the lidar equation. The results are summarized as follows. (1) Assuming that the Na density is 10 /cm^3, the signal from the Na atoms between 120 and 140 km is expected 300-400 photons, (2) The background signal observed is about 4,400 counts which means the noise level is about 220. So the signal intensity from the Na is nearly comparable to the noise level. (3) Thermospheric Na was not clearly seen in the re-calculated data. However, it depends on the smoothing technique to the original lidar data.

In this talk, we show the results derived by varying the binning time and discuss it.

Keywords: Na lidar, thermosphere, Tromsoe

©2019. Japan Geoscience Union. All Right Reserved.

Spatial-temporal distribution of anomalous enhancement of ambipolar diffusion coefficient observed by meteor radars installed in the polar region

*Toru Takahashi[1], Masaki Tsutsumi[1,2], Yasunobu Ogawa[1,2,3], Satonori Nozawa[3], Chris Hall[4], Hiroshi Miyaoka[1,2]

1. National Institute of Polar Research, 2. SOKENDAI, 3. Institute for Space-Earth Environmental Research, 4. TGO, The Arctic University of Norway

The meteor radar detected echoes of meteor tails as a tracer of neutral wind from 75 to 100 km altitudes (Hall et al., 2005). In addition, by using a decay time of the echo power, the meteor radar also estimated the ambipolar diffusion coefficient, which depends on the ion and electron temperature. The ambipolar diffusion coefficient was utilized to estimate the neutral temperature because the ion and electron temperature are generally in the thermal equilibrium with the neutral temperature. Recently, an anomalous enhancement of the ambipolar diffusion coefficient which could not be explained by the neutral temperature enhancement (hereafter called the anomalous enhancement) was observed by the meteor radar installed at Tromsoe, Norway (69.6 deg. N, 19.2 deg. E)
A previous study compared the anomalous enhancement with the ion velocity and the ion and electron temperature observed by EISCAT radar (Tsutsumi et al. 2017, Proceedings of the 30th Atmospheric Science Symposium, 2017). They reported that the anomalous enhancement tended to appear with the enhancement of ion velocity and electron temperature and frequently appeared at 16 UT. Furthermore, the anomalous enhancement was not seen during an event of the high energy particle precipitation on November 17, 2012 although one case study. Thus, the anomalous enhancement seems to be generated by the intense electric field and the high energy particle precipitation is not always necessary for its generation. As mentioned above, the previous study revealed a fundamental characteristics of the anomalous enhancement, however the generation mechanisms of the anomalous enhancement is still unclear. To clarify this, the comparison the spatial distribution of the anomalous enhancement with the convective electric field are needed. However, to date the latitudinal and local time occurrence of the anomalous enhancement was not revealed in the polar region.
Three meteor radars have been installed at Tromsoe, Bear island (74.5 deg. N, 19.0 deg. E), and Longyearbyen (78.2 deg. N, 16.2 deg. E). These meteor radars almost align on the same longitude line and can provide the spatial distribution of the anomalous enhancement. All meteor radars are a commercially produced VHF system (ENDR8-20) manufactured by ATRAD Pty Ltd. The antennas were produced by the Arctic University of Norway (Nozawa et al., 2012, JGR; Hall et al., 2002, GRL, Hall et al., 2006, JASTP). In this study, the spatial distribution and the occurrence rate of the anomalous enhancement was derived by these meteor radars.
Peaks of occurrence rate was seen at 20-22, 19-21, 16-19 MLT (~UT+3) at Tromsoe, Bear island, and Longyearbyen latitudes, respectively. This indicates that the anomalous enhancement appeared sequentially from high to low latitudes. In the morning sector, the peak of occurrence rate was only seen at 2-6 MLT above Bear island. In the case of high geomagnetic activity (Kp>3), the evening peaks of the occurrence rate shifted to an earlier time. On the other hand, clear peaks of the occurrence rate in the morning sector appeared at 3-5, 4-8, 7-10 MLT, respectively. Furthermore, the anomalous enhancement appeared with high possibility of 90% around 100 km south of Tromsoe. These characteristics which are seen during the time interval of high geomagnetic activity showed good agreement with the geomagnetic activity dependences of convective electric field.

©2019. Japan Geoscience Union. All Right Reserved.

We found another interesting characteristic in the geomagnetic dependence of the occurrence of the anomalous enhancement. The peak of occurrence rate in the evening sector was larger than it observed in the morning sector. This is considered to be related that auroral arcs appearing with intense electric field mainly observed in the evening sector. Thus, the generation of anomalous enhancement seems to relate both the convective electric field and the appearance of auroral arcs.
In this presentation, we will show the spatial distribution, MLT and geomagnetic activity dependence of the anomalous enhancement. We will also intend to present the comparison it with the electric filed observed by EISCAT and EISCAT Svalbard radars

Keywords: meteor radar, Tromsø, EISCAT radar

©2019. Japan Geoscience Union. All Right Reserved.

Progress of ICSWSE and MAGDAS project in recent years

*Shuji Abe[1], Akimasa Yoshikawa[2,1], Teiji Uozumi[1], Akiko Fujimoto[3]

1. International Center for Space Weather Science and Education, Japan, 2. Department of Earth and Planetary Sciences, Kyushu University, 3. Kyushu Institute of Technology

International Center for Space Weather Science and Education (ICSWSE), Kyushu University is the research institute for conducting research and education in space weather. Our magnetometer array named as "MAGDAS/CPMN (MAGnetic Data Acquisition System/Circum-pan Pacific Magnetometer Network)" (Principal Investigator: Dr. A. Yoshikawa) has over seventy fluxgate magnetometers, one induction magnetometer, and four FM-CW (Frequency Modulated Continuous Wave) radars around the world. One of our recent research topics is Equatorial Electrojet (EEJ). We calculate EE-index (Uozumi et al, 2008; Fujimoto et al., 2016) for space weather nowcast/forecast using realtime magnetometer data along the magnetic equator, and update it at each hour on the website (http://data.icswse.kyushu-u.ac.jp/eeindex/). To accelerate the understanding of EEJ structure, we constructed dense magnetometer array near magnetic equator at Peru and Malaysia in recent year. In addition, we finished to install new FM-CW radar at Sicaya, Peru. The instrument works well current now. We are providing our observational information and data including old project via our website (http://data.icswse.kyushu-u.ac.jp/). We also provide them via IUGONET (Inter-university Upper Atmosphere Observation NETwork) Type-A (http://search.iugonet.org/) which is one-stop web service system for researchers to search data, get the information of data, and plot data, and SPEDAS (Space Physics Environment Data Analysis System)/UDAS (iUgonet Data Analysis System). We will provide them via SuperMAG (http://supermag.jhuapl.edu/) in the near future. For accelerating the usage of MAGDAS and its science, we held a tutorial session in International Conference on Space Weather and Satellite Application 2018 at Malaysia, for handling MAGDAS and other data related our research field by using IUGONET system. We believe researchers use MAGDAS data on proper rule and develop their science. We will introduce other research activities in ICSWSE and MAGDAS project, for example, plasma bubble, geomagnetically induced current, and so on.

©2019. Japan Geoscience Union. All Right Reserved.

Status of GNU Radio Beacon Receiver 2 (GRBR2) development

*Mamoru Yamamoto[1], Mayumi Matsunaga[2], Roland Tsunoda[3]

1. Research Institute for Sustainable Humanosphere, Kyoto University, 2. Tokyo University of Technology, 3. SRI International

GNU Radio Beacon Receiver (GRBR) is the very successful digital receiver developed for dual-band (150/400MHz) beacon experiment. We were successfully conducted observations of total-electron content (TEC) of the ionosphere over Japan and in southeast Asia. However, many beacon satellites is now aging, and its number is decreasing. We now have a project to start new satellite-ground beacon experiment with new satellite constellations. One of them is TBEx (Tandem Beacon Explorer), a project by SRI International, to fly a constellation of two 3U cubesats with triband beacon transmitters. Another one is a project of FORMOSAT-7/COSMIC-2 by Taiwan/USA. Well-known mission of COSMIC-2 is GNSS occultation experiment, but the satellites carry triband beacon transmitters. All of these satellites will be placed into low-inclination orbits by the same launch vehicle in 2018, which will give us great opportunities to enhance studies of the low-latitude ionosphere. We develop a new digital receiver, GRBR2, for these new satellite beacon. GRBR2 is a four channel receiver at 150/400/965/1067MHz beacon signals from two satellite constellations. Now The reveiver system was finally fixed. Problem of the project of delay of the satellite launch. But it is now on schedule for launch by 2019 summer. We start deploying GRBR2 in southeast Asian countries. In this presentaiton, we will report GRBR2 system and its performance including results from test experiment in the field.

Keywords: Satellite beacon experiment, Digital receiver development, Total electron content

©2019. Japan Geoscience Union. All Right Reserved.

Statistical comparison between plasma bubble day-to-day variability and neutral atmosphere by using GPS scintillation and GAIA model

*Mamoru Yamamoto[1], Keigo Kono[1]

1. Research Institute for Sustainable Humanosphere, Kyoto University

Equational plasma bubble is one of the most intense irregularities in the ionosphere. The occurrence of the plasma bubble is considered related to weak changes of the underlying atmosphere which is called large-scale wavelike structure (LSWS). The LSWS is expected formed by penetration of the atmospheric wave into the ionosphere. But its real effect is not yet known in detail. The purpose of this research is to investigate the correlation between the neutral atmosphere and day-to-day variability of equatorial plasma bubbles mainly in the Southeast Asia region. We based on the study by Yamamoto et al (2018) that showed relationship between 40-km height temperature variation and S4 index over Kototabang, Indonesia. In this study we tried to extend the observation region and also tried to elucidate atmospheric waves that are related to the plasma bubble. For indicating activity of the plasma bubble, we used S4 index of GPS scintillation measured by ISEE, Nagoya Univ. at Kototabang, Indonesia. Atmospheric data were taken from GAIA database prepared by NICT. We analyzed data from 2003, 2004, 2012, and 2013 where the solar activity was high. Overall correlation between S4 index and the atmospheric temperature showed similar feature throughout these years. However, even when we tried to extract atmospheric wave components from the GAIA data, the correlation between the wave parameter to S4 index did not show large change. This means that the elucidation of the atmospheric wave component was not very successful so far. Further analyses are required.

Reference
Yamamoto, M., Y. Otsuka, H. Jin, Y. Miyoshi (2018) Relationship between day-to-day variability of equatorial plasma bubble activity from GPS scintillation and atmospheric properties from GAIA assimilation, Progress in Earth and Planetary Science, Vol. 5, page 26, doi: 10.1186/s40645-018-0184-7.

©2019. Japan Geoscience Union. All Right Reserved.

Redevelopment of the MU radar transceiver-module control system

*Mamoru Yamamoto[1], Koki Kurokawa[1], Hiroyuki Hashiguchi[1]

1. Research Institute for Sustainable Humanosphere, Kyoto University

The MU radar was installed in Shigaraki, Japan in 1984 as the world first atmospheric radar with active phased-array antenna system. The MU radar consists of 475 Yagi antennas in the circular field of about 100m diameter. By the electronic phase shift of each Yagi, the antenna beam is steered to one of pre-selected 2048 directions in the transmitting pulse-to-pulse basis. Success of the MU radar in the atmospheric/ionospheric research is well known, and its active phased-array configuration was followed by many other radar systems. The phase control of the MU radar is realized by the control of its transceiver-module (TR-module) that are equipped with each Yagi antenna. They are gathered into 25 groups of each 19 modules. One CPU (microcomputer board) is used for control of one group of modules. A weak point of the MU radar exists in this point because we are using the original 8085 CPU board that is connected to the host computer by 1200-baud (!) serial line. This control is very slow, and we could not meet demands for rapid change of observation parameters for long time. This time we tried to re-develop the new TR-module controller by using recent CPU board and electronic devices. In the presentation, we show hardware/software of the newly developed prototype of the MU radar TR-module controller.

Keywords: MU radar, control system, redevelopment

©2019. Japan Geoscience Union. All Right Reserved.

[E] Poster | A (Atmospheric and Hydrospheric Sciences)：A-AS Atmospheric Sciences, Meteorology & Atmospheric Environment

Thu. May 30, 2019 1:45 PM - 3:15 PM JST | Thu. May 30, 2019 4:45 AM - 6:15 AM UTC | Poster Hall International Exhibition Hall8, Makuhari Messe_1

[A-AS02] Advances in Tropical Cyclone Research: Past, Present, and Future

convener:Sachie Kanada(Nagoya University), Akiyoshi Wada(Department of Typhoon and Severe Weather Research, Meteorological Research Institute), Kosuke Ito(University of the Ryukyus), Yoshiaki Miyamoto(Faculty of Environment and Information Studies, Keio University)

Tropical cyclones (TC) sometimes cause destructive disasters in many countries by torrential rainfall, strong wind, storm surge, and high surf. In 2008, the western Japan suffered a record-breaking heavy rainfall related to Typhoon Prapirooon (2018) in July. Furthermore, two Category 4 typhoons, typhoons Jebi (2018) and Trami (2018), made landfalls on the western Japan in September and caused devastating disasters over the Japanese Islands. In the Northern Atlantic, Hurricane Florence caused catastrophic damage in the eastern side of U.S. Recent studies reported a northward shift of the location where a TC achieved the peak intensity and also reported increases in the frequency of rapidly intensifying storms. Thus, understanding the TC processes related to translation, intensity change and precipitation in the changing climate, and to provide more accurate forecasts and long-term projections are essential for the earth and planetary science.
Advances in innovative observations such as meteorological aircraft, weather satellite, supercomputer systems such as the Earth Simulator and K-computer, and introduction of new methods such as the deep-learning, have led to novel development of numerical weather forecasting and understanding of the phenomena related to TCs in the past, present and future climates. In this session, we welcome papers on various aspects of TC studies. We hope that the session will provide a new direction for future TC researches.

[AAS02-P01] Numerical study on lightning frequency in a tropical cyclone

*Yousuke Sato[1,3], Yoshiaki Miyamoto[2,3], Tomita Hirofumi[3] (1.Department of Applied Energy, Nagoya University, 2.Faculty of Environment and Information Studies, Keio University, 3.RIKEN Center for Computational Science)

[AAS02-P02] **Sensitivity of Numerical Simulation of Typhoon Nepartak (2016) to Cloud Condensation Nuclei Concentration**

*Yu-De Wu[1], Jian-Liang Wang[1] (1.Dept. of Environmental Informational and Engineering, Chung Cheng Institute of Technology, National Defense University, Taiwan)

[AAS02-P03] Moisture Budget Analysis for Hurricane Precipitation on Texas

*Satoshi Iizuka[1], Naoki Sakai[1] (1.National Research Institute for Earth Science and Disaster Resilience)

[AAS02-P04] Remote response of a developing tropical cyclone over the western North Pacific to large-scale vapor transport from the Kuroshio in boreal fall

*Keita Fujiwara[1], Ryuichi Kawamura[2], Tetsuya Kawano[2] (1.Graduate School of Science, Kyushu University, 2.Faculty of Science, Kyushu University)

[AAS02-P05] Asymmetrically Intensifying Processes of a Category 4 Super Typhoon Lan (2017) during High Vertical Wind Shear

*Sachie Kanada[1], Akiyoshi Wada[2], Kazuhisa Tsuboki[1] (1.Nagoya University, 2.Meteorological Research Institute)

[AAS02-P06] Roles of preexisting oceanic condition and ocean coupling processes in the intensity prediction during the mature phase of Typhoon Trami (2018)

*Akiyoshi Wada[1] (1.Typhoon Research Department Meteorological Research Institute)

[AAS02-P07] Development and assessment of the probabilistic storm surge forecast system in Taiwan: Case Study of Typhoon Maria in 2018

*Chun-Wei Lin[1], Tso-Ren Wu[1], Yu-Lin Tsai[1], Shu-Chun Chuang[1], Chi-Hao Chu[2], Chuen-Teyr Terng[2] (1.Graduate Institute of Hydrological and Oceanic Sciences, National Central University, Chungli, Taiwan, 2.Marine Meteorology Center, Central Weather Bureau, Taipei, Taiwan)

[AAS02-P08] Basic Data Construction for a Typhoon Disaster Prevention Model : Analysis and Changes by El Nino and La Nina year

*HANA NA[1], Woo-Sik Jung[1] (1.Department of Atmospheric Environment Information Engineering, Atmospheric Environment Information Research Center, Inje University, Gimhae 50834, Korea)

[AAS02-P09] Basic Data Construction for a Typhoon Disaster Prevention Model : Analysis According to the Typhoon Path Type

*HANA NA[1], Woo-Sik JUNG[1] (1.Department of Atmospheric Environment Information Engineering, Atmospheric Environment Information Research Center, Inje University, Gimhae 50834, Korea)

[AAS02-P10] Basic Data Construction for a Typhoon Disaster Prevention Model : Monthly Characteristics of Typhoon Rusa, Maemi, Kompasu, and Bolaven

*HANA NA[1], Woo-Sik Jung[1] (1.Department of Atmospheric Environment Information Engineering, Atmospheric Environment Information Research Center, Inje University, Gimhae 50834, Korea)

[AAS02-P11] The mechanism of typhoon generated in the earth that rotates in the space where the solar wind blows

*Shinji Karasawa[1] (1.Miyagi National College of Technology Professor emeritus)

Numerical study on lightning frequency in a tropical cyclone

*Yousuke Sato[1,3], Yoshiaki Miyamoto[2,3], Tomita Hirofumi[3]

1. Department of Applied Energy, Nagoya University, 2. Faculty of Environment and Information Studies, Keio University, 3. RIKEN Center for Computational Science

This study investigates frequency of lightning in each stage of lifecycle of tropical cyclone (TC) using the next generation weather and climate library called Scalable Computing for Advanced Library and Environment (SCALE; Sato et al. 2015, Nishizawa et al. 2015). Lightning component was developed and implemented into SCALE in this study. An idealized experiment based on an experimental setup of Miyamoto and Takemi (2013) was conducted by SCALE coupled with lightning component. The results of the simulation indicate that the lightning frequency is maximum before rapid intensification (RI) of TC, which supports the report of Price et al. (2009) derived from satellite observation. The frequency of lightning decreases after RI and it keeps small until the TC reaches steady state. Our analyses elucidate that the dependency of the lightning frequency upon the developing stage of TC is originated from the type of convection dominating at each growth stage. Before the RI, the convection generated by consuming convective available potential energy (CAPE) transport hydrometeors upward, and the charge split and the lightning frequently occur. During the steady state, the hydrometeors are mainly transported by the fast rotating flow in the simulated TC, which resulted in the weak charge split and small frequency of lightning.

Keywords: Tropical cyclone, Lightning

©2019. Japan Geoscience Union. All Right Reserved.

Sensitivity of Numerical Simulation of Typhoon Nepartak (2016) to Cloud Condensation Nuclei Concentration

*Yu-De Wu[1], Jian-Liang Wang[1]

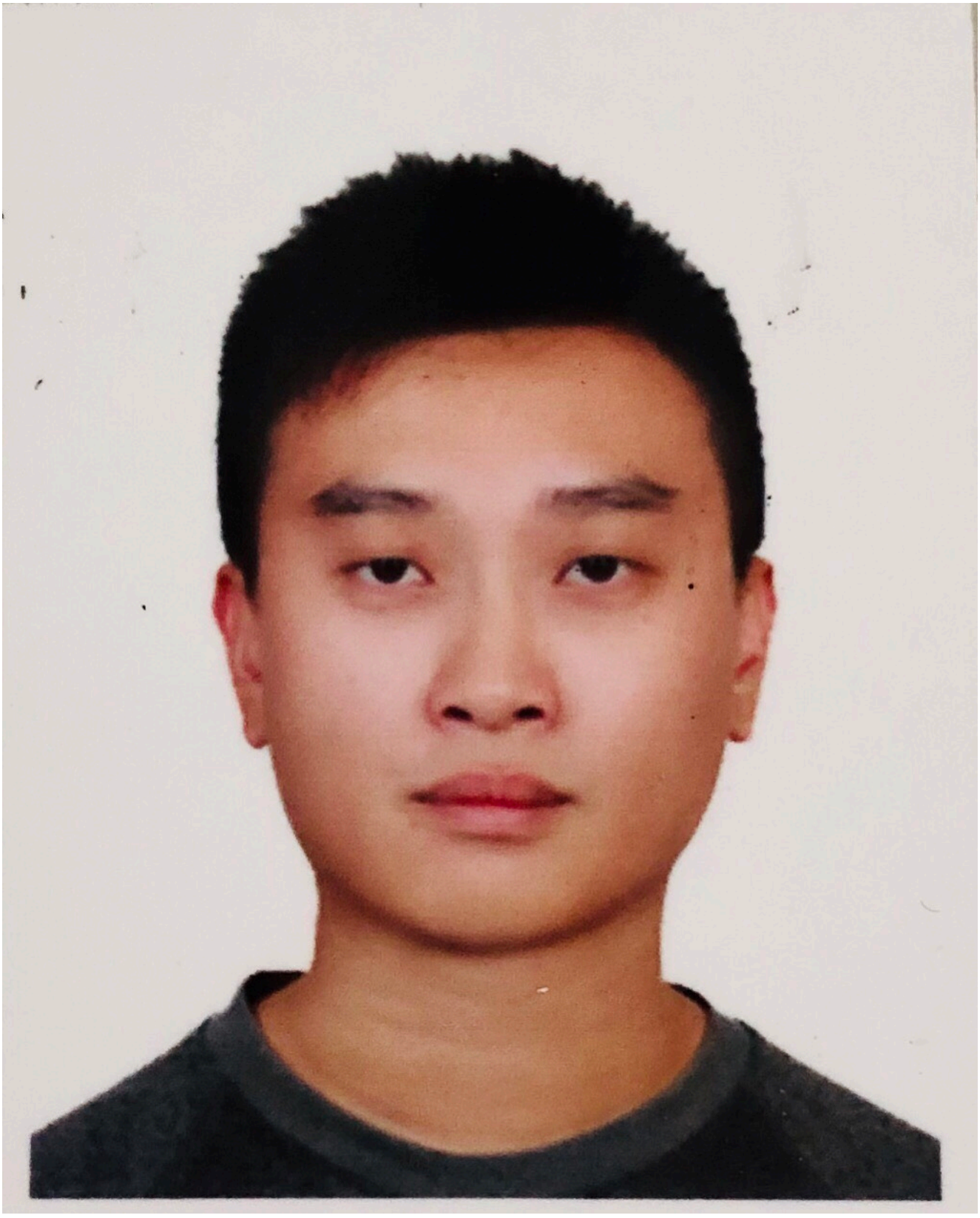
1. Dept. of Environmental Informational and Engineering, Chung Cheng Institute of Technology, National Defense University, Taiwan

The study is carried out using the WRF model and the Cloud Condensation Nuclei, CCN, in the WDM6 microphysics scheme has been modified to test its impacts on typhoon simulations. The simulated track, intensity, and rainfall distribution of Typhoon Nepartak (2016) over Pacific Ocean are compared among numerical experiments of different initial concentration of CCN (wdm6_ctr, wdm6_10, and wdm6_50, where wdm6_10 and wdm6_50 represent that CCN are respectively 10 and 50 times of the value used in wdm6_ctr).

The simulated tracks in three runs are similar, but the intensity and the maximum dBz increase both in wdm6_10 and wdm6_50, but it takes more time for wdm6_50 to intensify. The comparison of mixing ratios of five water species shows that the cloud droplets mixing ratios increase as CCN is increased. The mixing ratios of rain, cloud ice, snow and graupel are enhanced more rapidly in wdm6_10 compared with wdm6_50. The same situation happens in the divergence field and upward motions. It is suggested that the increase of CCN will result in stronger typhoon, but the intensification will be slowed down with too much CCN.

Keywords: Cloud Condensation Nuclei, Typhoon Nepartak, Microphysics Scheme

©2019. Japan Geoscience Union. All Right Reserved.



©2019. Japan Geoscience Union. All Right Reserved.

Moisture Budget Analysis for Hurricane Precipitation on Texas

*Satoshi Iizuka[1], Naoki Sakai[1]

1. National Research Institute for Earth Science and Disaster Resilience

In August 2017, Hurricane Harvey brought the unprecedented amount of rainfall and catastrophic flooding on the Houston metropolitan area, as it stagnated near the coast of Texas for several days after its decline to a tropical storm intensity. The present study compares the moisture budget for rainfall associated with Harvey with those of past hurricanes making landfall on Texas. It seems that the high pressure over the west coast region of the US, along with the meandering of the subtropical jet starting from the periphery of Hawaii and toward the south in Texas, stagnated Hurricane Harvey around the coast of Texas for several days. The meandering of the subtropical jet toward the south in Texas also caused the largest convergence of moisture advected from the Gulf of Mexico efficiently over Texas, although the accompanied high pressure was not extraordinary event. Therefore, it is suggested that surrounding meteorological conditions can greatly affect rainfall related to tropical cyclones.

Keywords: Hurricane Harvey, Precipitation, Moisture Budget

©2019. Japan Geoscience Union. All Right Reserved.

Remote response of a developing tropical cyclone over the western North Pacific to large-scale vapor transport from the Kuroshio in boreal fall

*Keita Fujiwara[1], Ryuichi Kawamura[2], Tetsuya Kawano[2]

1. Graduate School of Science, Kyushu University, 2. Faculty of Science, Kyushu University

A remote linkage between the development of tropical cyclone (TC) over the western North Pacific and moisture transport from the Kuroshio Current due to environmental flow toward TC was examined by using regional cloud resolving model and Lagrangian diagnostics. In this study, we specially highlighted a prototypical TC (Typhoon Chaba 2010), which developed and migrated northward over the Philippines Sea in boreal fall, and conducted sensitivity experiments that modified surface turbulent latent heat flux (LHF) over the Kuroshio. The large-scale environment was characterized by a combination of two synoptic systems, eastward-migrating anticyclone from the Asian continent and TC approaching Japan, bringing low-level northeasterly flows over the Kuroshio through an enhanced meridional pressure gradient in that region. Trajectory analyses suggested that air parcels along the northeasterlies modified by receiving abundant water vapor from the underlying Kuroshio may contribute to latent heating within Chaba’s inner core region as a remote effect, leading to TC development.

When LHF was removed or reduced over the Kuroshio under the dominance of the northwesterly flow, TC intensity attenuated during its developing stage even though TC was fairly far away from the Kuroshio. Since no or little modification of dry air parcels occurred in the atmospheric boundary layer over the Kuroshio, contribution of those parcels to latent heat release around Chaba’s eyewall become small. Furthermore, dry air penetration into TC’s inner core region may act as an inhibitor of convection within that region, resulting in deceleration of the TC development. These findings were consistent with another TC (Typhoon Toakge 2004) with a similar synoptic environment, increasing reliability of remote impact of moisture import from the Kuroshio on TC development.

Keywords: tropical cyclone, moisture transport, Kuroshio Current

©2019. Japan Geoscience Union. All Right Reserved.

Asymmetrically Intensifying Processes of a Category 4 Super Typhoon Lan (2017) during High Vertical Wind Shear

*Sachie Kanada[1], Akiyoshi Wada[2], Kazuhisa Tsuboki[1]

1. Nagoya University, 2. Meteorological Research Institute

On 21 October 2017, Typhoon Lan developed to a Category 4 super typhoon with the minimum central pressure (MCP) of 915 hPa at 25.6 degrees north latitude and maintained the peak intensity until the storm arrived at 29.9˚N under a strong environmental vertical wind shear (VWS) of 14 m s^{-1}. To understand the intensification processes of an intense typhoon with such high VWS, numerical simulations on Typhoon Lan were conducted using a high-resolution three-dimensional atmosphere regional model, the Cloud Resolving Storm Simulator (CReSS; Tsuboki and Sakakibara, 2002). Two sensitivity experiments, 1dO and FO, were conducted with different SST representations. In the 1dO experiment, a simple thermal diffusion model was used to express temperature changes due to ocean vertical mixing. The FO experiment with a time-fixed SST did not consider the evolution of SST. Both experiments used the same initial and boundary conditions and model specifications for the atmosphere, started at 0000 UTC 18 October 2017, and had an integration time of 5 days. The computational domain was 2˚N–37.8˚N and 115˚E–145˚E. The number of horizontal grids in the computational domain was 752×896 with the horizontal grid size of 0.04 longitude by 0.04 latitude.

The typhoon simulated in the 1dO experiment successfully achieved the MCP of 910 hPa at 29.5˚N, exhibiting strong asymmetric precipitation pattern as observed by the satellites. The intensification processes were accompanied by rapid developments of the strong winds and warm core in the low-levels. The strong northeast VWS forced to tilt the storm axis to downshear side (northeast) and, in the downshear quadrants, tall, intense and upstanding eyewall updrafts (CBs) formed from the low-level convergence of the storm travelling northeastward with a relatively fast translation speed of 10 m s^{-1}. Meanwhile, dry subsidence from the upper-levels intensified the low-level warm core in the upshear side of the eye. Despite the inner-core convection and precipitation exhibited strong asymmetric structures, the axisymmetricity of the storm circulation was maintained in the mid-to-low levels and abundant water vapor enclosed in the eye allowed to develop CBs around the radius of the maximum wind speeds. Although the FO storm overestimated the MCP of 879hPa, the similar asymmetric patterns in precipitation and convection were also found in the FO storm. The results indicated that the storm structures of typhoon Lan would be less sensitive to the SST-cooling effect.

Keywords: Typhoon, numerical model

©2019. Japan Geoscience Union. All Right Reserved.

Roles of preexisting oceanic condition and ocean coupling processes in the intensity prediction during the mature phase of Typhoon Trami (2018)

*Akiyoshi Wada[1]

1. Typhoon Research Department Meteorological Research Institute

Typhoon Trami (2018) is one of the typhoons that made landfall in Japan. According to the Regional Specialized Meteorological Center (RSMC) Tokyo best track analysis, the central pressure reached 915 hPa at 18 UTC on 24 September around 20˚N and then rapidly increased by 950 hPa in 18 hours. After the rapid increases in the central pressure, intensity forecasts announced further intensification to 935 hPa, but the typhoon could not intensify again. In order to clarify the impact of the cold eddies over the ocean on this forecast error, we conducted numerical simulations with different oceanic initial conditions (daily data from 19 to 25 September were used so that the number of ensemble members is seven) using a 2 km-mesh nonhydrostatic atmosphere model coupled with ocean surface wave and multilayer ocean models with the Japan Meteorological Agency (JMA) global objective analysis with horizontal resolution of 20 km and the JMA North Pacific Ocean analysis with horizontal resolution of 0.5˚. In addition, a sensitivity numerical experiment was conducted with the oceanic initial condition on 23 September merged with an artificial cold vortex centered at 21˚N, 129˚E of which both a mixed layer and thermocline was 50 m shallower than the control experiment. Moreover, a simulation with a 2 km-mesh nonhydrostatic atmosphere model was performed with the oceanic initial condition on 23 September. The initial time and integration period are 00 UTC on 23 September and 180 hours with the time interval of 3 seconds.

The results of simulated tracks were reasonable compared with the RSMC best track analysis, while the rapid decrease in the central pressure could not be simulated due to a large difference in central pressure at the initial time so that the simulated minimum central pressure was higher than the best track central pressure. From the analysis with the ratio of a difference to the standard deviation obtained from the ensemble experiments, the impact of different oceanic initial conditions on central pressure was different from that on the maximum wind speed particularly from 25 to 27 September when the typhoon passed near the cold eddy. The impact of ocean coupling on simulated central pressure and maximum wind speed was considerably greater than that of the artificial cold eddy and that of different oceanic initial conditions. The impact of the artificial cold eddy was a few times greater than that of different oceanic initial conditions around 26 September. The result indicates that more detailed observation and more accurate analysis regarding the cold eddy over the ocean will contribute to the improvement of typhoon intensity predictions.

Keywords: tropical cyclone, atmosphere-wave-ocean coupled model, intensity forecast, preexisting cold eddy

©2019. Japan Geoscience Union. All Right Reserved.

Development and assessment of the probabilistic storm surge forecast system in Taiwan: Case Study of Typhoon Maria in 2018

*Chun-Wei Lin[1], Tso-Ren Wu[1], Yu-Lin Tsai[1], Shu-Chun Chuang[1], Chi-Hao Chu[2], Chuen-Teyr Terng[2]

1. Graduate Institute of Hydrological and Oceanic Sciences, National Central University, Chungli, Taiwan, 2. Marine Meteorology Center, Central Weather Bureau, Taipei, Taiwan

From the forecast and the analyzed typhoon tracks in Taiwan, it is found that if the forecast track errors are greater than 100 km, roughly a quarter of the length of Taiwan, significant variability of storm surge elevation can be seen.
In order to consider the uncertainty of the atmospheric forecast, this study aims to develop the probabilistic storm surge forecast system. The coastal storm surge model applied in this study is COMCOT-SS (COrnell Multi-Grid COupled Tsunami Model –Storm Surge), which is the kernel of the operating deterministic storm surge forecast system in CWB, Taiwan. It solves nonlinear shallow water equations in the nested-grid scheme. Two ensemble methods are adopted in this study, one is Deterministic Track Error Distribution Method, D-TED Method. The other one is the Ensemble Track Analysis Method, ETA Method. D-TED Method is generated from the deterministic forecast, while the ETA Method obtains typhoon tracks and parameters from the CWB WEPS (CWB WRF Ensemble Prediction System).
From the case study of typhoon Maria in 2018, it shows that as the typhoon approaching Taiwan, the coverage of the tracks from ETA Method would be more convergence comparing to the tracks from D-TED Method, and it provides a more concentrated surge elevation distribution.

Keywords: storm surge, ensemble forecast, COMCOT-SS

©2019. Japan Geoscience Union. All Right Reserved.

Basic Data Construction for a Typhoon Disaster Prevention Model : Analysis and Changes by El Nino and La Nina year

*HANA NA[1], Woo-Sik Jung[1]

1. Department of Atmospheric Environment Information Engineering, Atmospheric Environment Information Research Center, Inje University, Gimhae 50834, Korea

Among the typhoons that affected the Korean Peninsula for approximately 110 years from 1904, when weather observation began until 2018, all of the top five typhoons in terms of the maximum wind speed and property damage record occurred after 2000. This implies that the intensity of typhoons is becoming stronger and the damage is more severe compared to the past. Moreover, typhoons are significantly affected by the sea temperature. The El Nino and La Nina phenomena, in which significant changes in the sea temperature occur, may significantly affect the occurrence and intensity of typhoons affecting the Korean Peninsula. Therefore, this study aims to analyze changes by year, and the years of El Nino and La Nina occurrences by estimating the maximum wind speed that can be generated during typhoon period based on the typhoons that affected the Korean Peninsula. This study was conducted for the period between 2002 and 2015. As a result of analyzing the maximum wind speed of the typhoons that affected the Korean Peninsula by year, high 3-second gusts tended to occur in the Gyeongsang-do area including the southeast coast of the Korean Peninsula from 2002 to 2006. Subsequently, the strong wind area of the 3-second gusts expanded, and high 3-second gusts occurred in the Seoul metropolitan area. Moreover, as a result of investigating the 3-second gust characteristics for the years of El Nino and La Nina occurrences, a higher maximum wind speed was observed from the typhoons that affected the Korean Peninsula in the years of El Nino occurrence.

This research was supported by Basic Science Research Program through the National Research Foundation of Korea(NRF) funded by the Ministry of Education(2017R1D1A3B03036152)

Keywords: Typhoon Disaster Prevention Model, 3-Second gust, El Nino, La Nina

©2019. Japan Geoscience Union. All Right Reserved.

Basic Data Construction for a Typhoon Disaster Prevention Model : Analysis and Changes by El Nino and La Nina year

Hana Na, Woo-Sik Jung

Among the typhoons that affected the Korean Peninsula for approximately 110 years from 1904, when weather observation began until 2018, all of the top five typhoons in terms of the maximum wind speed and property damage record occurred after 2000. This implies that the intensity of typhoons is becoming stronger and the damage is more severe compared to the past. Moreover, typhoons are significantly affected by the sea temperature. The El Nino and La Nina phenomena, in which significant changes in the sea temperature occur, may significantly affect the occurrence and intensity of typhoons affecting the Korean Peninsula. Therefore, this study aims to analyze changes by year, and the years of El Nino and La Nina occurrences by estimating the maximum wind speed that can be generated during typhoon period based on the typhoons that affected the Korean Peninsula. This study was conducted for the period between 2002 and 2015. As a result of analyzing the maximum wind speed of the typhoons that affected the Korean Peninsula by year, high 3-second gusts tended to occur in the Gyeongsang-do area including the southeast coast of the Korean Peninsula from 2002 to 2006. Subsequently, the strong wind area of the 3-second gusts expanded, and high 3-second gusts occurred in the Seoul metropolitan area. Moreover, as a result of investigating the 3-second gust characteristics for the years of El Nino and La Nina occurrences, a higher maximum wind speed was observed from the typhoons that affected the Korean Peninsula in the years of El Nino occurrence.

This research was supported by Basic Science Research Program through the National Research Foundation of Korea(NRF) funded by the Ministry of Education(2017R1D1A3B03036152)

Key words : Typhoon Disaster Prevention Model, WRF, 3-Second gust, El Nino, La Nina

©2019. Japan Geoscience Union. All Right Reserved.

Basic Data Construction for a Typhoon Disaster Prevention Model : Analysis According to the Typhoon Path Type

*HANA NA[1], Woo-Sik JUNG[1]

1. Department of Atmospheric Environment Information Engineering, Atmospheric Environment Information Research Center, Inje University, Gimhae 50834, Korea

In this study, a typhoon disaster prevention model was used to estimate the maximum wind speed during typhoon period by path type from all typhoons that affected the Korean Peninsula from 2002 to 2015. For the typhoon information and upper wind information used as input data, the results of the WRF numerical model, which utilized the Best Track data of the RSMC Tokyo Typhoon Center and the RDAPS data of the Korea Meteorological Administration, were applied. From analyzing the path type impact frequency using all typhoons that affected the Korean Peninsula during the study period (2002–2015), Type 7 that affected the Korean Peninsula through Japan was the most frequent, followed by Type 2 that directly landed on the Korean Peninsula through the southern coast. From analyzing the monthly path types of the typhoons that affected the Korean Peninsula, Type 2 that affected the Korean Peninsula by landing on the southern coast and Type 7 that affected the Korean Peninsula through Japan were the most frequent for the recently increasing September typhoons. The analysis of the maximum wind speed of the 3-second gust that may occur during typhoon period by path type revealed that Type 2 that affected the Korean Peninsula by landing on the southern coast exhibited the highest 3-second gust. As a result of examining the distribution of Type 2, high 3-second gusts occurred throughout the Korean Peninsula, including the southeast coast. As for the path of Type 2 that directly affected the Korean Peninsula by landing on the southern coast, the occurrence frequency was the second highest during the entire study period and the value of the 3-second gust, which was the maximum wind speed that may occur during typhoon period, was the highest.

This research was supported by Basic Science Research Program through the National Research Foundation of Korea(NRF) funded by the Ministry of Education(2017R1D1A3B03036152)

Keywords: Typhoon Path, 3-Second gust, Typhoon Disaster Prevention Model

©2019. Japan Geoscience Union. All Right Reserved.

Basic Data Construction for a Typhoon Disaster Prevention Model : Analysis According to the Typhoon Path Type

Hana Na, Woo-Sik Jung

In this study, a typhoon disaster prevention model was used to estimate the maximum wind speed during typhoon period by path type from all typhoons that affected the Korean Peninsula from 2002 to 2015. For the typhoon information and upper wind information used as input data, the results of the WRF numerical model, which utilized the Best Track data of the RSMC Tokyo Typhoon Center and the RDAPS data of the Korea Meteorological Administration, were applied. From analyzing the path type impact frequency using all typhoons that affected the Korean Peninsula during the study period (2002–2015), Type 7 that affected the Korean Peninsula through Japan was the most frequent, followed by Type 2 that directly landed on the Korean Peninsula through the southern coast. From analyzing the monthly path types of the typhoons that affected the Korean Peninsula, Type 2 that affected the Korean Peninsula by landing on the southern coast and Type 7 that affected the Korean Peninsula through Japan were the most frequent for the recently increasing September typhoons. The analysis of the maximum wind speed of the 3-second gust that may occur during typhoon period by path type revealed that Type 2 that affected the Korean Peninsula by landing on the southern coast exhibited the highest 3-second gust. As a result of examining the distribution of Type 2, high 3-second gusts occurred throughout the Korean Peninsula, including the southeast coast. As for the path of Type 2 that directly affected the Korean Peninsula by landing on the southern coast, the occurrence frequency was the second highest during the entire study period and the value of the 3-second gust, which was the maximum wind speed that may occur during typhoon period, was the highest.

This research was supported by Basic Science Research Program through the National Research Foundation of Korea(NRF) funded by the Ministry of Education(2017R1D1A3B03036152)

Keywords : Typhoon Disaster Prevention Model, WRF, Typhoon Track, 3-Second gust

©2019. Japan Geoscience Union. All Right Reserved.

Basic Data Construction for a Typhoon Disaster Prevention Model : Monthly Characteristics of Typhoon Rusa, Maemi, Kompasu, and Bolaven

*HANA NA[1], Woo-Sik Jung[1]

1. Department of Atmospheric Environment Information Engineering, Atmospheric Environment Information Research Center, Inje University, Gimhae 50834, Korea

According to a typhoon report that summarized the typhoons that had affected the Korean Peninsula for approximately 100 years since the start of weather observation in the Korean Peninsula, the number of typhoons that affected the Korean Peninsula was the highest in August, followed by July, and September. A study that analyzed the period between 1953 and 2003 revealed that the number of typhoons that affected the Korean Peninsula was 62 in August, 49 in July, and 45 in September. As shown, previous studies that analyzed the typhoons that affected the Korean Peninsula by month were primarily focused on the impact frequency. This study aims to estimate the monthly impact frequency of the typhoons that affected the Korean Peninsula as well as the maximum wind speed that accompanied the typhoons. It also aims to construct the basic data of a typhoon disaster prevention model by estimating the maximum wind speed during typhoon period using Typhoon Rusa that resulted in the highest property damage, Typhoon Maemi that recorded the maximum wind speed, Typhoon Kompasu that significantly affected the Seoul metropolitan area, and Typhoon Bolaven that recently recorded severe damages. A typhoon disaster prevention model was used to estimate the maximum wind speed of the 3-second gust that may occur, and the 700 hPa wind speed estimated through WRF(Weather Research and Forecasting) numerical simulation was used as input data.

Unlike the target period reported in the white paper on typhoons (1904–2010), this study analyzed the monthly impact frequency of the typhoons that affected the Korean Peninsula from 2002 and 2015. The result indicated that the impact frequency was the highest in August, followed by July and September. This result was the same as that of the typhoon report. An analysis by year revealed that typhoon period increased in September. The 3-second gust was found to be the highest in September, followed by August and July. When this result was analyzed in relation to the recently increasing autumn typhoons (September and October), the 3-second gust result was the highest in September, indicating disaster prevention must be emphasized. By additionally analyzing the maximum wind speed distributions of Typhoon Rusa, Maemi, Kompasu, and Bolaven, the area with the maximum wind speed varied depending on the typhoon path, and the 3-second gust was higher than 44 m/s based on the typhoon intensity classification and accounted for approximately10%.

This research was supported by Basic Science Research Program through the National Research Foundation of Korea(NRF) funded by the Ministry of Education(2017R1D1A3B03036152)

Keywords: Typhoon Disaster Prevention Model, WRF, 3-Second gust

©2019. Japan Geoscience Union. All Right Reserved.

Basic Data Construction for a Typhoon Disaster Prevention Model : Monthly Characteristics of Typhoon Rusa, Maemi, Kompasu, and Bolaven

Hana Na, Woo-Sik Jung

According to a typhoon report that summarized the typhoons that had affected the Korean Peninsula for approximately 100 years since the start of weather observation in the Korean Peninsula, the number of typhoons that affected the Korean Peninsula was the highest in August, followed by July, and September. A study that analyzed the period between 1953 and 2003 revealed that the number of typhoons that affected the Korean Peninsula was 62 in August, 49 in July, and 45 in September. As shown, previous studies that analyzed the typhoons that affected the Korean Peninsula by month were primarily focused on the impact frequency. This study aims to estimate the monthly impact frequency of the typhoons that affected the Korean Peninsula as well as the maximum wind speed that accompanied the typhoons. It also aims to construct the basic data of a typhoon disaster prevention model by estimating the maximum wind speed during typhoon period using Typhoon Rusa that resulted in the highest property damage, Typhoon Maemi that recorded the maximum wind speed, Typhoon Kompasu that significantly affected the Seoul metropolitan area, and Typhoon Bolaven that recently recorded severe damages. A typhoon disaster prevention model was used to estimate the maximum wind speed of the 3-second gust that may occur, and the 700 hPa wind speed estimated through WRF(Weather Research and Forecasting) numerical simulation was used as input data.

Unlike the target period reported in the white paper on typhoons (1904–2010), this study analyzed the monthly impact frequency of the typhoons that affected the Korean Peninsula from 2002 and 2015. The result indicated that the impact frequency was the highest in August, followed by July and September. This result was the same as that of the typhoon report. An analysis by year revealed that typhoon period increased in September. The 3-second gust was found to be the highest in September, followed by August and July. When this result was analyzed in relation to the recently increasing autumn typhoons (September and October), the 3-second gust result was the highest in September, indicating disaster prevention must be emphasized. By additionally analyzing the maximum wind speed distributions of Typhoon Rusa, Maemi, Kompasu, and Bolaven, the area with the maximum wind speed varied depending on the typhoon path, and the 3-second gust was higher than 44 m/s based on the typhoon intensity classification and accounted for approximately10%.

This research was supported by Basic Science Research Program through the National Research Foundation of Korea(NRF) funded by the Ministry of Education(2017R1D1A3B03036152)

Keywords : Typhoon Disaster Prevention Model, WRF, 3-Second gust, RUSA, MAEMI, KOMPASU, BOLAVEN

©2019. Japan Geoscience Union. All Right Reserved.

The mechanism of typhoon generated in the earth that rotates in the space where the solar wind blows

*Shinji Karasawa[1]

1. Miyagi National College of Technology Professor emeritus

The atmosphere in the upper tropical cyclone (TC) rotates the clock-wise direction by the trade winds and westerlies. The rotation speed near the center increases, because the angular momentum of the atmospheric molecule is transported. The eye of the typhoon is appeared at the place where the centrifugal force of the rotation on the flow exceeds compared with the difference of the pressure. The atmosphere including the vapor of water in the cumulonimbus are mixed with the cold air flow swirling in the clockwise direction at the eye of typhoon, where the water vapors become to the rain, and the cumulonimbus rotates in anticlockwise direction.
The solar wind includes rotational momentum and the rotational momentum of the solar wind generates the trade winds. On the other hand, the westerlies are caused by the solar wind that rotates the tail of Earth's magnetosphere on the opposite side of the Sun in anticlockwise rotation, and it gives the driving force of the westerlies. Ref. S. Karasawa.
https://www.youtube.com/watch?v=bzCup63G8z8&feature=youtu.be

Keywords: tropical cyclone, westerlies, trade winds, solar wind, Earth’ s rotation, Sun’ s rotation

©2019. Japan Geoscience Union. All Right Reserved.

[E] Poster | A (Atmospheric and Hydrospheric Sciences)：A-AS Atmospheric Sciences, Meteorology & Atmospheric Environment

Thu. May 30, 2019 5:15 PM - 6:30 PM JST | Thu. May 30, 2019 8:15 AM - 9:30 AM UTC | Poster Hall International Exhibition Hall8, Makuhari Messe_5

[A-AS02] Advances in Tropical Cyclone Research: Past, Present, and Future

convener:Sachie Kanada(Nagoya University), Akiyoshi Wada(Department of Typhoon and Severe Weather Research, Meteorological Research Institute), Kosuke Ito(University of the Ryukyus), Yoshiaki Miyamoto(Faculty of Environment and Information Studies, Keio University)

Tropical cyclones (TC) sometimes cause destructive disasters in many countries by torrential rainfall, strong wind, storm surge, and high surf. In 2008, the western Japan suffered a record-breaking heavy rainfall related to Typhoon Prapirooon (2018) in July. Furthermore, two Category 4 typhoons, typhoons Jebi (2018) and Trami (2018), made landfalls on the western Japan in September and caused devastating disasters over the Japanese Islands. In the Northern Atlantic, Hurricane Florence caused catastrophic damage in the eastern side of U.S. Recent studies reported a northward shift of the location where a TC achieved the peak intensity and also reported increases in the frequency of rapidly intensifying storms. Thus, understanding the TC processes related to translation, intensity change and precipitation in the changing climate, and to provide more accurate forecasts and long-term projections are essential for the earth and planetary science.
Advances in innovative observations such as meteorological aircraft, weather satellite, supercomputer systems such as the Earth Simulator and K-computer, and introduction of new methods such as the deep-learning, have led to novel development of numerical weather forecasting and understanding of the phenomena related to TCs in the past, present and future climates. In this session, we welcome papers on various aspects of TC studies. We hope that the session will provide a new direction for future TC researches.

[AAS02-P01] Numerical study on lightning frequency in a tropical cyclone

*Yousuke Sato[1,3], Yoshiaki Miyamoto[2,3], Tomita Hirofumi[3] (1.Department of Applied Energy, Nagoya University, 2.Faculty of Environment and Information Studies, Keio University, 3.RIKEN Center for Computational Science)

[AAS02-P02] **Sensitivity of Numerical Simulation of Typhoon Nepartak (2016) to Cloud Condensation Nuclei Concentration**

*Yu-De Wu[1], Jian-Liang Wang[1] (1.Dept. of Environmental Informational and Engineering, Chung Cheng Institute of Technology, National Defense University, Taiwan)

[AAS02-P03] Moisture Budget Analysis for Hurricane Precipitation on Texas

*Satoshi Iizuka[1], Naoki Sakai[1] (1.National Research Institute for Earth Science and Disaster Resilience)

[AAS02-P04] Remote response of a developing tropical cyclone over the western North Pacific to large-scale vapor transport from the Kuroshio in boreal fall

*Keita Fujiwara[1], Ryuichi Kawamura[2], Tetsuya Kawano[2] (1.Graduate School of Science, Kyushu University, 2.Faculty of Science, Kyushu University)

[AAS02-P05] Asymmetrically Intensifying Processes of a Category 4 Super Typhoon Lan (2017) during High Vertical Wind Shear

*Sachie Kanada[1], Akiyoshi Wada[2], Kazuhisa Tsuboki[1] (1.Nagoya University, 2.Meteorological Research Institute)

[AAS02-P06] Roles of preexisting oceanic condition and ocean coupling processes in the intensity prediction during the mature phase of Typhoon Trami (2018)

*Akiyoshi Wada[1] (1.Typhoon Research Department Meteorological Research Institute)

[AAS02-P07] Development and assessment of the probabilistic storm surge forecast system in Taiwan: Case Study of Typhoon Maria in 2018

*Chun-Wei Lin[1], Tso-Ren Wu[1], Yu-Lin Tsai[1], Shu-Chun Chuang[1], Chi-Hao Chu[2], Chuen-Teyr Terng[2] (1.Graduate Institute of Hydrological and Oceanic Sciences, National Central University, Chungli, Taiwan, 2.Marine Meteorology Center, Central Weather Bureau, Taipei, Taiwan)

[AAS02-P08] Basic Data Construction for a Typhoon Disaster Prevention Model : Analysis and Changes by El Nino and La Nina year

*HANA NA[1], Woo-Sik Jung[1] (1.Department of Atmospheric Environment Information Engineering, Atmospheric Environment Information Research Center, Inje University, Gimhae 50834, Korea)

[AAS02-P09] Basic Data Construction for a Typhoon Disaster Prevention Model : Analysis According to the Typhoon Path Type

*HANA NA[1], Woo-Sik JUNG[1] (1.Department of Atmospheric Environment Information Engineering, Atmospheric Environment Information Research Center, Inje University, Gimhae 50834, Korea)

[AAS02-P10] Basic Data Construction for a Typhoon Disaster Prevention Model : Monthly Characteristics of Typhoon Rusa, Maemi, Kompasu, and Bolaven

*HANA NA[1], Woo-Sik Jung[1] (1.Department of Atmospheric Environment Information Engineering, Atmospheric Environment Information Research Center, Inje University, Gimhae 50834, Korea)

[AAS02-P11] The mechanism of typhoon generated in the earth that rotates in the space where the solar wind blows

*Shinji Karasawa[1] (1.Miyagi National College of Technology Professor emeritus)

Numerical study on lightning frequency in a tropical cyclone

*Yousuke Sato[1,3], Yoshiaki Miyamoto[2,3], Tomita Hirofumi[3]

1. Department of Applied Energy, Nagoya University, 2. Faculty of Environment and Information Studies, Keio University, 3. RIKEN Center for Computational Science

This study investigates frequency of lightning in each stage of lifecycle of tropical cyclone (TC) using the next generation weather and climate library called Scalable Computing for Advanced Library and Environment (SCALE; Sato et al. 2015, Nishizawa et al. 2015). Lightning component was developed and implemented into SCALE in this study. An idealized experiment based on an experimental setup of Miyamoto and Takemi (2013) was conducted by SCALE coupled with lightning component. The results of the simulation indicate that the lightning frequency is maximum before rapid intensification (RI) of TC, which supports the report of Price et al. (2009) derived from satellite observation. The frequency of lightning decreases after RI and it keeps small until the TC reaches steady state. Our analyses elucidate that the dependency of the lightning frequency upon the developing stage of TC is originated from the type of convection dominating at each growth stage. Before the RI, the convection generated by consuming convective available potential energy (CAPE) transport hydrometeors upward, and the charge split and the lightning frequently occur. During the steady state, the hydrometeors are mainly transported by the fast rotating flow in the simulated TC, which resulted in the weak charge split and small frequency of lightning.

Keywords: Tropical cyclone, Lightning

©2019. Japan Geoscience Union. All Right Reserved.

Sensitivity of Numerical Simulation of Typhoon Nepartak (2016) to Cloud Condensation Nuclei Concentration

*Yu-De Wu[1], Jian-Liang Wang[1]

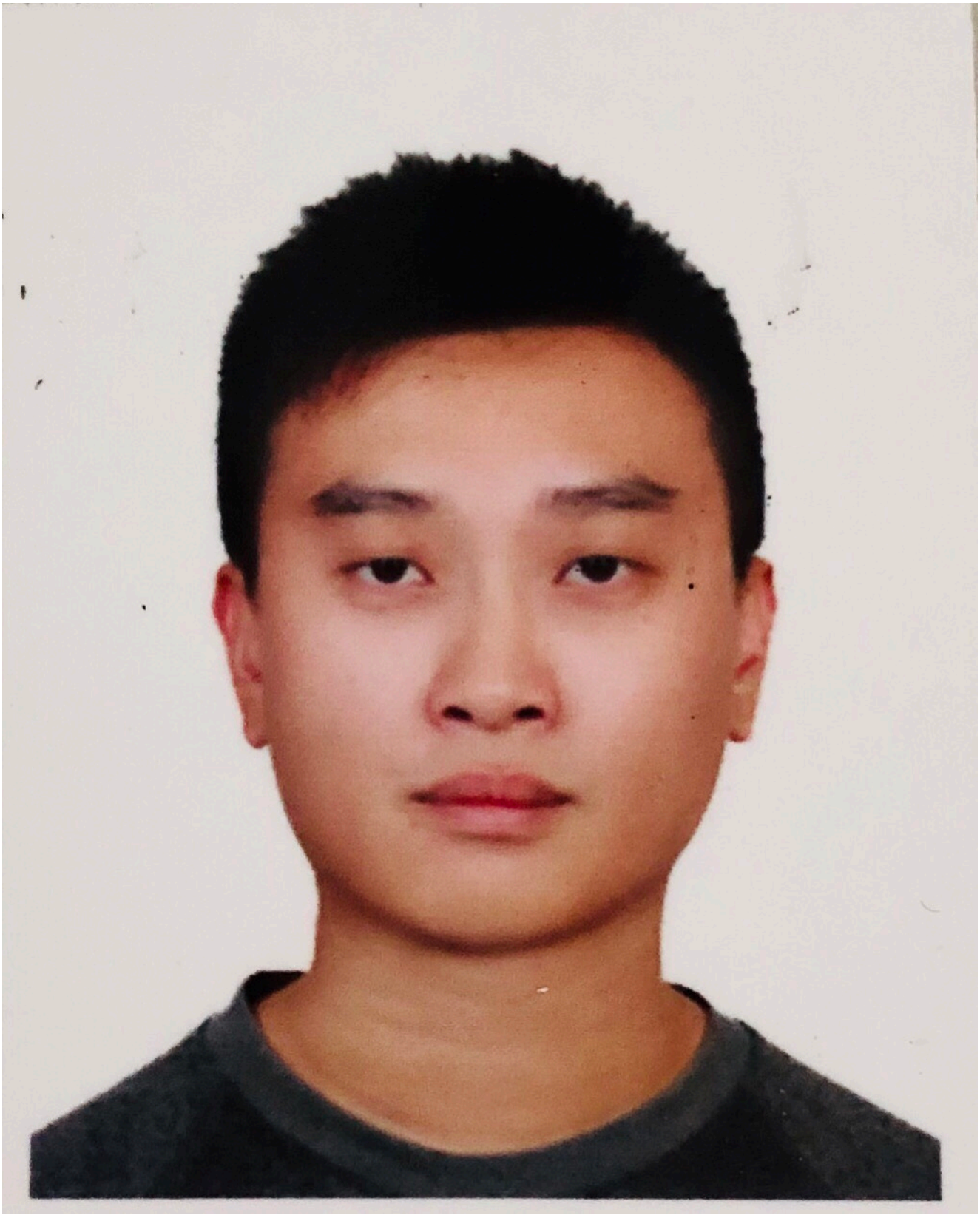
1. Dept. of Environmental Informational and Engineering, Chung Cheng Institute of Technology, National Defense University, Taiwan

The study is carried out using the WRF model and the Cloud Condensation Nuclei, CCN, in the WDM6 microphysics scheme has been modified to test its impacts on typhoon simulations. The simulated track, intensity, and rainfall distribution of Typhoon Nepartak (2016) over Pacific Ocean are compared among numerical experiments of different initial concentration of CCN (wdm6_ctr, wdm6_10, and wdm6_50, where wdm6_10 and wdm6_50 represent that CCN are respectively 10 and 50 times of the value used in wdm6_ctr).

The simulated tracks in three runs are similar, but the intensity and the maximum dBz increase both in wdm6_10 and wdm6_50, but it takes more time for wdm6_50 to intensify. The comparison of mixing ratios of five water species shows that the cloud droplets mixing ratios increase as CCN is increased. The mixing ratios of rain, cloud ice, snow and graupel are enhanced more rapidly in wdm6_10 compared with wdm6_50. The same situation happens in the divergence field and upward motions. It is suggested that the increase of CCN will result in stronger typhoon, but the intensification will be slowed down with too much CCN.

Keywords: Cloud Condensation Nuclei, Typhoon Nepartak, Microphysics Scheme

©2019. Japan Geoscience Union. All Right Reserved.



©2019. Japan Geoscience Union. All Right Reserved.

Moisture Budget Analysis for Hurricane Precipitation on Texas

*Satoshi Iizuka[1], Naoki Sakai[1]

1. National Research Institute for Earth Science and Disaster Resilience

In August 2017, Hurricane Harvey brought the unprecedented amount of rainfall and catastrophic flooding on the Houston metropolitan area, as it stagnated near the coast of Texas for several days after its decline to a tropical storm intensity. The present study compares the moisture budget for rainfall associated with Harvey with those of past hurricanes making landfall on Texas. It seems that the high pressure over the west coast region of the US, along with the meandering of the subtropical jet starting from the periphery of Hawaii and toward the south in Texas, stagnated Hurricane Harvey around the coast of Texas for several days. The meandering of the subtropical jet toward the south in Texas also caused the largest convergence of moisture advected from the Gulf of Mexico efficiently over Texas, although the accompanied high pressure was not extraordinary event. Therefore, it is suggested that surrounding meteorological conditions can greatly affect rainfall related to tropical cyclones.

Keywords: Hurricane Harvey, Precipitation, Moisture Budget

©2019. Japan Geoscience Union. All Right Reserved.

Remote response of a developing tropical cyclone over the western North Pacific to large-scale vapor transport from the Kuroshio in boreal fall

*Keita Fujiwara[1], Ryuichi Kawamura[2], Tetsuya Kawano[2]

1. Graduate School of Science, Kyushu University, 2. Faculty of Science, Kyushu University

A remote linkage between the development of tropical cyclone (TC) over the western North Pacific and moisture transport from the Kuroshio Current due to environmental flow toward TC was examined by using regional cloud resolving model and Lagrangian diagnostics. In this study, we specially highlighted a prototypical TC (Typhoon Chaba 2010), which developed and migrated northward over the Philippines Sea in boreal fall, and conducted sensitivity experiments that modified surface turbulent latent heat flux (LHF) over the Kuroshio. The large-scale environment was characterized by a combination of two synoptic systems, eastward-migrating anticyclone from the Asian continent and TC approaching Japan, bringing low-level northeasterly flows over the Kuroshio through an enhanced meridional pressure gradient in that region. Trajectory analyses suggested that air parcels along the northeasterlies modified by receiving abundant water vapor from the underlying Kuroshio may contribute to latent heating within Chaba’s inner core region as a remote effect, leading to TC development.

When LHF was removed or reduced over the Kuroshio under the dominance of the northwesterly flow, TC intensity attenuated during its developing stage even though TC was fairly far away from the Kuroshio. Since no or little modification of dry air parcels occurred in the atmospheric boundary layer over the Kuroshio, contribution of those parcels to latent heat release around Chaba’s eyewall become small. Furthermore, dry air penetration into TC’s inner core region may act as an inhibitor of convection within that region, resulting in deceleration of the TC development. These findings were consistent with another TC (Typhoon Toakge 2004) with a similar synoptic environment, increasing reliability of remote impact of moisture import from the Kuroshio on TC development.

Keywords: tropical cyclone, moisture transport, Kuroshio Current

©2019. Japan Geoscience Union. All Right Reserved.

Asymmetrically Intensifying Processes of a Category 4 Super Typhoon Lan (2017) during High Vertical Wind Shear

*Sachie Kanada[1], Akiyoshi Wada[2], Kazuhisa Tsuboki[1]

1. Nagoya University, 2. Meteorological Research Institute

On 21 October 2017, Typhoon Lan developed to a Category 4 super typhoon with the minimum central pressure (MCP) of 915 hPa at 25.6 degrees north latitude and maintained the peak intensity until the storm arrived at 29.9˚N under a strong environmental vertical wind shear (VWS) of 14 m s^{-1}. To understand the intensification processes of an intense typhoon with such high VWS, numerical simulations on Typhoon Lan were conducted using a high-resolution three-dimensional atmosphere regional model, the Cloud Resolving Storm Simulator (CReSS; Tsuboki and Sakakibara, 2002). Two sensitivity experiments, 1dO and FO, were conducted with different SST representations. In the 1dO experiment, a simple thermal diffusion model was used to express temperature changes due to ocean vertical mixing. The FO experiment with a time-fixed SST did not consider the evolution of SST. Both experiments used the same initial and boundary conditions and model specifications for the atmosphere, started at 0000 UTC 18 October 2017, and had an integration time of 5 days. The computational domain was 2˚N–37.8˚N and 115˚E–145˚E. The number of horizontal grids in the computational domain was 752×896 with the horizontal grid size of 0.04 longitude by 0.04 latitude.

The typhoon simulated in the 1dO experiment successfully achieved the MCP of 910 hPa at 29.5˚N, exhibiting strong asymmetric precipitation pattern as observed by the satellites. The intensification processes were accompanied by rapid developments of the strong winds and warm core in the low-levels. The strong northeast VWS forced to tilt the storm axis to downshear side (northeast) and, in the downshear quadrants, tall, intense and upstanding eyewall updrafts (CBs) formed from the low-level convergence of the storm travelling northeastward with a relatively fast translation speed of 10 m s^{-1}. Meanwhile, dry subsidence from the upper-levels intensified the low-level warm core in the upshear side of the eye. Despite the inner-core convection and precipitation exhibited strong asymmetric structures, the axisymmetricity of the storm circulation was maintained in the mid-to-low levels and abundant water vapor enclosed in the eye allowed to develop CBs around the radius of the maximum wind speeds. Although the FO storm overestimated the MCP of 879hPa, the similar asymmetric patterns in precipitation and convection were also found in the FO storm. The results indicated that the storm structures of typhoon Lan would be less sensitive to the SST-cooling effect.

Keywords: Typhoon, numerical model

©2019. Japan Geoscience Union. All Right Reserved.

Roles of preexisting oceanic condition and ocean coupling processes in the intensity prediction during the mature phase of Typhoon Trami (2018)

*Akiyoshi Wada[1]

1. Typhoon Research Department Meteorological Research Institute

Typhoon Trami (2018) is one of the typhoons that made landfall in Japan. According to the Regional Specialized Meteorological Center (RSMC) Tokyo best track analysis, the central pressure reached 915 hPa at 18 UTC on 24 September around 20˚N and then rapidly increased by 950 hPa in 18 hours. After the rapid increases in the central pressure, intensity forecasts announced further intensification to 935 hPa, but the typhoon could not intensify again. In order to clarify the impact of the cold eddies over the ocean on this forecast error, we conducted numerical simulations with different oceanic initial conditions (daily data from 19 to 25 September were used so that the number of ensemble members is seven) using a 2 km-mesh nonhydrostatic atmosphere model coupled with ocean surface wave and multilayer ocean models with the Japan Meteorological Agency (JMA) global objective analysis with horizontal resolution of 20 km and the JMA North Pacific Ocean analysis with horizontal resolution of 0.5˚. In addition, a sensitivity numerical experiment was conducted with the oceanic initial condition on 23 September merged with an artificial cold vortex centered at 21˚N, 129˚E of which both a mixed layer and thermocline was 50 m shallower than the control experiment. Moreover, a simulation with a 2 km-mesh nonhydrostatic atmosphere model was performed with the oceanic initial condition on 23 September. The initial time and integration period are 00 UTC on 23 September and 180 hours with the time interval of 3 seconds.

The results of simulated tracks were reasonable compared with the RSMC best track analysis, while the rapid decrease in the central pressure could not be simulated due to a large difference in central pressure at the initial time so that the simulated minimum central pressure was higher than the best track central pressure. From the analysis with the ratio of a difference to the standard deviation obtained from the ensemble experiments, the impact of different oceanic initial conditions on central pressure was different from that on the maximum wind speed particularly from 25 to 27 September when the typhoon passed near the cold eddy. The impact of ocean coupling on simulated central pressure and maximum wind speed was considerably greater than that of the artificial cold eddy and that of different oceanic initial conditions. The impact of the artificial cold eddy was a few times greater than that of different oceanic initial conditions around 26 September. The result indicates that more detailed observation and more accurate analysis regarding the cold eddy over the ocean will contribute to the improvement of typhoon intensity predictions.

Keywords: tropical cyclone, atmosphere-wave-ocean coupled model, intensity forecast, preexisting cold eddy

©2019. Japan Geoscience Union. All Right Reserved.

Development and assessment of the probabilistic storm surge forecast system in Taiwan: Case Study of Typhoon Maria in 2018

*Chun-Wei Lin[1], Tso-Ren Wu[1], Yu-Lin Tsai[1], Shu-Chun Chuang[1], Chi-Hao Chu[2], Chuen-Teyr Terng[2]

1. Graduate Institute of Hydrological and Oceanic Sciences, National Central University, Chungli, Taiwan, 2. Marine Meteorology Center, Central Weather Bureau, Taipei, Taiwan

From the forecast and the analyzed typhoon tracks in Taiwan, it is found that if the forecast track errors are greater than 100 km, roughly a quarter of the length of Taiwan, significant variability of storm surge elevation can be seen.
In order to consider the uncertainty of the atmospheric forecast, this study aims to develop the probabilistic storm surge forecast system. The coastal storm surge model applied in this study is COMCOT-SS (COrnell Multi-Grid COupled Tsunami Model –Storm Surge), which is the kernel of the operating deterministic storm surge forecast system in CWB, Taiwan. It solves nonlinear shallow water equations in the nested-grid scheme. Two ensemble methods are adopted in this study, one is Deterministic Track Error Distribution Method, D-TED Method. The other one is the Ensemble Track Analysis Method, ETA Method. D-TED Method is generated from the deterministic forecast, while the ETA Method obtains typhoon tracks and parameters from the CWB WEPS (CWB WRF Ensemble Prediction System).
From the case study of typhoon Maria in 2018, it shows that as the typhoon approaching Taiwan, the coverage of the tracks from ETA Method would be more convergence comparing to the tracks from D-TED Method, and it provides a more concentrated surge elevation distribution.

Keywords: storm surge, ensemble forecast, COMCOT-SS

©2019. Japan Geoscience Union. All Right Reserved.

Basic Data Construction for a Typhoon Disaster Prevention Model : Analysis and Changes by El Nino and La Nina year

*HANA NA[1], Woo-Sik Jung[1]

1. Department of Atmospheric Environment Information Engineering, Atmospheric Environment Information Research Center, Inje University, Gimhae 50834, Korea

Among the typhoons that affected the Korean Peninsula for approximately 110 years from 1904, when weather observation began until 2018, all of the top five typhoons in terms of the maximum wind speed and property damage record occurred after 2000. This implies that the intensity of typhoons is becoming stronger and the damage is more severe compared to the past. Moreover, typhoons are significantly affected by the sea temperature. The El Nino and La Nina phenomena, in which significant changes in the sea temperature occur, may significantly affect the occurrence and intensity of typhoons affecting the Korean Peninsula. Therefore, this study aims to analyze changes by year, and the years of El Nino and La Nina occurrences by estimating the maximum wind speed that can be generated during typhoon period based on the typhoons that affected the Korean Peninsula. This study was conducted for the period between 2002 and 2015. As a result of analyzing the maximum wind speed of the typhoons that affected the Korean Peninsula by year, high 3-second gusts tended to occur in the Gyeongsang-do area including the southeast coast of the Korean Peninsula from 2002 to 2006. Subsequently, the strong wind area of the 3-second gusts expanded, and high 3-second gusts occurred in the Seoul metropolitan area. Moreover, as a result of investigating the 3-second gust characteristics for the years of El Nino and La Nina occurrences, a higher maximum wind speed was observed from the typhoons that affected the Korean Peninsula in the years of El Nino occurrence.

This research was supported by Basic Science Research Program through the National Research Foundation of Korea(NRF) funded by the Ministry of Education(2017R1D1A3B03036152)

Keywords: Typhoon Disaster Prevention Model, 3-Second gust, El Nino, La Nina

©2019. Japan Geoscience Union. All Right Reserved.

Basic Data Construction for a Typhoon Disaster Prevention Model : Analysis and Changes by El Nino and La Nina year

Hana Na, Woo-Sik Jung

Among the typhoons that affected the Korean Peninsula for approximately 110 years from 1904, when weather observation began until 2018, all of the top five typhoons in terms of the maximum wind speed and property damage record occurred after 2000. This implies that the intensity of typhoons is becoming stronger and the damage is more severe compared to the past. Moreover, typhoons are significantly affected by the sea temperature. The El Nino and La Nina phenomena, in which significant changes in the sea temperature occur, may significantly affect the occurrence and intensity of typhoons affecting the Korean Peninsula. Therefore, this study aims to analyze changes by year, and the years of El Nino and La Nina occurrences by estimating the maximum wind speed that can be generated during typhoon period based on the typhoons that affected the Korean Peninsula. This study was conducted for the period between 2002 and 2015. As a result of analyzing the maximum wind speed of the typhoons that affected the Korean Peninsula by year, high 3-second gusts tended to occur in the Gyeongsang-do area including the southeast coast of the Korean Peninsula from 2002 to 2006. Subsequently, the strong wind area of the 3-second gusts expanded, and high 3-second gusts occurred in the Seoul metropolitan area. Moreover, as a result of investigating the 3-second gust characteristics for the years of El Nino and La Nina occurrences, a higher maximum wind speed was observed from the typhoons that affected the Korean Peninsula in the years of El Nino occurrence.

This research was supported by Basic Science Research Program through the National Research Foundation of Korea(NRF) funded by the Ministry of Education(2017R1D1A3B03036152)

Key words : Typhoon Disaster Prevention Model, WRF, 3-Second gust, El Nino, La Nina

©2019. Japan Geoscience Union. All Right Reserved.

Basic Data Construction for a Typhoon Disaster Prevention Model : Analysis According to the Typhoon Path Type

*HANA NA[1], Woo-Sik JUNG[1]

1. Department of Atmospheric Environment Information Engineering, Atmospheric Environment Information Research Center, Inje University, Gimhae 50834, Korea

In this study, a typhoon disaster prevention model was used to estimate the maximum wind speed during typhoon period by path type from all typhoons that affected the Korean Peninsula from 2002 to 2015. For the typhoon information and upper wind information used as input data, the results of the WRF numerical model, which utilized the Best Track data of the RSMC Tokyo Typhoon Center and the RDAPS data of the Korea Meteorological Administration, were applied. From analyzing the path type impact frequency using all typhoons that affected the Korean Peninsula during the study period (2002–2015), Type 7 that affected the Korean Peninsula through Japan was the most frequent, followed by Type 2 that directly landed on the Korean Peninsula through the southern coast. From analyzing the monthly path types of the typhoons that affected the Korean Peninsula, Type 2 that affected the Korean Peninsula by landing on the southern coast and Type 7 that affected the Korean Peninsula through Japan were the most frequent for the recently increasing September typhoons. The analysis of the maximum wind speed of the 3-second gust that may occur during typhoon period by path type revealed that Type 2 that affected the Korean Peninsula by landing on the southern coast exhibited the highest 3-second gust. As a result of examining the distribution of Type 2, high 3-second gusts occurred throughout the Korean Peninsula, including the southeast coast. As for the path of Type 2 that directly affected the Korean Peninsula by landing on the southern coast, the occurrence frequency was the second highest during the entire study period and the value of the 3-second gust, which was the maximum wind speed that may occur during typhoon period, was the highest.

This research was supported by Basic Science Research Program through the National Research Foundation of Korea(NRF) funded by the Ministry of Education(2017R1D1A3B03036152)

Keywords: Typhoon Path, 3-Second gust, Typhoon Disaster Prevention Model

©2019. Japan Geoscience Union. All Right Reserved.

Basic Data Construction for a Typhoon Disaster Prevention Model : Analysis According to the Typhoon Path Type

Hana Na, Woo-Sik Jung

In this study, a typhoon disaster prevention model was used to estimate the maximum wind speed during typhoon period by path type from all typhoons that affected the Korean Peninsula from 2002 to 2015. For the typhoon information and upper wind information used as input data, the results of the WRF numerical model, which utilized the Best Track data of the RSMC Tokyo Typhoon Center and the RDAPS data of the Korea Meteorological Administration, were applied. From analyzing the path type impact frequency using all typhoons that affected the Korean Peninsula during the study period (2002–2015), Type 7 that affected the Korean Peninsula through Japan was the most frequent, followed by Type 2 that directly landed on the Korean Peninsula through the southern coast. From analyzing the monthly path types of the typhoons that affected the Korean Peninsula, Type 2 that affected the Korean Peninsula by landing on the southern coast and Type 7 that affected the Korean Peninsula through Japan were the most frequent for the recently increasing September typhoons. The analysis of the maximum wind speed of the 3-second gust that may occur during typhoon period by path type revealed that Type 2 that affected the Korean Peninsula by landing on the southern coast exhibited the highest 3-second gust. As a result of examining the distribution of Type 2, high 3-second gusts occurred throughout the Korean Peninsula, including the southeast coast. As for the path of Type 2 that directly affected the Korean Peninsula by landing on the southern coast, the occurrence frequency was the second highest during the entire study period and the value of the 3-second gust, which was the maximum wind speed that may occur during typhoon period, was the highest.

This research was supported by Basic Science Research Program through the National Research Foundation of Korea(NRF) funded by the Ministry of Education(2017R1D1A3B03036152)

Keywords : Typhoon Disaster Prevention Model, WRF, Typhoon Track, 3-Second gust

©2019. Japan Geoscience Union. All Right Reserved.

Basic Data Construction for a Typhoon Disaster Prevention Model : Monthly Characteristics of Typhoon Rusa, Maemi, Kompasu, and Bolaven

*HANA NA[1], Woo-Sik Jung[1]

1. Department of Atmospheric Environment Information Engineering, Atmospheric Environment Information Research Center, Inje University, Gimhae 50834, Korea

According to a typhoon report that summarized the typhoons that had affected the Korean Peninsula for approximately 100 years since the start of weather observation in the Korean Peninsula, the number of typhoons that affected the Korean Peninsula was the highest in August, followed by July, and September. A study that analyzed the period between 1953 and 2003 revealed that the number of typhoons that affected the Korean Peninsula was 62 in August, 49 in July, and 45 in September. As shown, previous studies that analyzed the typhoons that affected the Korean Peninsula by month were primarily focused on the impact frequency. This study aims to estimate the monthly impact frequency of the typhoons that affected the Korean Peninsula as well as the maximum wind speed that accompanied the typhoons. It also aims to construct the basic data of a typhoon disaster prevention model by estimating the maximum wind speed during typhoon period using Typhoon Rusa that resulted in the highest property damage, Typhoon Maemi that recorded the maximum wind speed, Typhoon Kompasu that significantly affected the Seoul metropolitan area, and Typhoon Bolaven that recently recorded severe damages. A typhoon disaster prevention model was used to estimate the maximum wind speed of the 3-second gust that may occur, and the 700 hPa wind speed estimated through WRF(Weather Research and Forecasting) numerical simulation was used as input data.

Unlike the target period reported in the white paper on typhoons (1904–2010), this study analyzed the monthly impact frequency of the typhoons that affected the Korean Peninsula from 2002 and 2015. The result indicated that the impact frequency was the highest in August, followed by July and September. This result was the same as that of the typhoon report. An analysis by year revealed that typhoon period increased in September. The 3-second gust was found to be the highest in September, followed by August and July. When this result was analyzed in relation to the recently increasing autumn typhoons (September and October), the 3-second gust result was the highest in September, indicating disaster prevention must be emphasized. By additionally analyzing the maximum wind speed distributions of Typhoon Rusa, Maemi, Kompasu, and Bolaven, the area with the maximum wind speed varied depending on the typhoon path, and the 3-second gust was higher than 44 m/s based on the typhoon intensity classification and accounted for approximately10%.

This research was supported by Basic Science Research Program through the National Research Foundation of Korea(NRF) funded by the Ministry of Education(2017R1D1A3B03036152)

Keywords: Typhoon Disaster Prevention Model, WRF, 3-Second gust

©2019. Japan Geoscience Union. All Right Reserved.

Basic Data Construction for a Typhoon Disaster Prevention Model : Monthly Characteristics of Typhoon Rusa, Maemi, Kompasu, and Bolaven

Hana Na, Woo-Sik Jung

According to a typhoon report that summarized the typhoons that had affected the Korean Peninsula for approximately 100 years since the start of weather observation in the Korean Peninsula, the number of typhoons that affected the Korean Peninsula was the highest in August, followed by July, and September. A study that analyzed the period between 1953 and 2003 revealed that the number of typhoons that affected the Korean Peninsula was 62 in August, 49 in July, and 45 in September. As shown, previous studies that analyzed the typhoons that affected the Korean Peninsula by month were primarily focused on the impact frequency. This study aims to estimate the monthly impact frequency of the typhoons that affected the Korean Peninsula as well as the maximum wind speed that accompanied the typhoons. It also aims to construct the basic data of a typhoon disaster prevention model by estimating the maximum wind speed during typhoon period using Typhoon Rusa that resulted in the highest property damage, Typhoon Maemi that recorded the maximum wind speed, Typhoon Kompasu that significantly affected the Seoul metropolitan area, and Typhoon Bolaven that recently recorded severe damages. A typhoon disaster prevention model was used to estimate the maximum wind speed of the 3-second gust that may occur, and the 700 hPa wind speed estimated through WRF(Weather Research and Forecasting) numerical simulation was used as input data.

Unlike the target period reported in the white paper on typhoons (1904–2010), this study analyzed the monthly impact frequency of the typhoons that affected the Korean Peninsula from 2002 and 2015. The result indicated that the impact frequency was the highest in August, followed by July and September. This result was the same as that of the typhoon report. An analysis by year revealed that typhoon period increased in September. The 3-second gust was found to be the highest in September, followed by August and July. When this result was analyzed in relation to the recently increasing autumn typhoons (September and October), the 3-second gust result was the highest in September, indicating disaster prevention must be emphasized. By additionally analyzing the maximum wind speed distributions of Typhoon Rusa, Maemi, Kompasu, and Bolaven, the area with the maximum wind speed varied depending on the typhoon path, and the 3-second gust was higher than 44 m/s based on the typhoon intensity classification and accounted for approximately10%.

This research was supported by Basic Science Research Program through the National Research Foundation of Korea(NRF) funded by the Ministry of Education(2017R1D1A3B03036152)

Keywords : Typhoon Disaster Prevention Model, WRF, 3-Second gust, RUSA, MAEMI, KOMPASU, BOLAVEN

©2019. Japan Geoscience Union. All Right Reserved.

The mechanism of typhoon generated in the earth that rotates in the space where the solar wind blows

*Shinji Karasawa[1]

1. Miyagi National College of Technology Professor emeritus

The atmosphere in the upper tropical cyclone (TC) rotates the clock-wise direction by the trade winds and westerlies. The rotation speed near the center increases, because the angular momentum of the atmospheric molecule is transported. The eye of the typhoon is appeared at the place where the centrifugal force of the rotation on the flow exceeds compared with the difference of the pressure. The atmosphere including the vapor of water in the cumulonimbus are mixed with the cold air flow swirling in the clockwise direction at the eye of typhoon, where the water vapors become to the rain, and the cumulonimbus rotates in anticlockwise direction.
The solar wind includes rotational momentum and the rotational momentum of the solar wind generates the trade winds. On the other hand, the westerlies are caused by the solar wind that rotates the tail of Earth's magnetosphere on the opposite side of the Sun in anticlockwise rotation, and it gives the driving force of the westerlies. Ref. S. Karasawa.
https://www.youtube.com/watch?v=bzCup63G8z8&feature=youtu.be

Keywords: tropical cyclone, westerlies, trade winds, solar wind, Earth’ s rotation, Sun’ s rotation

©2019. Japan Geoscience Union. All Right Reserved.

[E] Poster | A (Atmospheric and Hydrospheric Sciences)：A-OS Ocean Sciences & Ocean Environment

Thu. May 30, 2019 10:45 AM - 12:15 PM JST | Thu. May 30, 2019 1:45 AM - 3:15 AM UTC | Poster Hall International Exhibition Hall8, Makuhari Messe_2

[A-OS07] Climate variability and predictability on subseasonal to decadal timescales

convener:Takashi Mochizuki(Japan Agency for Marine-Earth Science and Technology), V Ramaswamy(NOAA GFDL), Doug Smith(Met Office), Yushi Morioka(Japan Agency for Marine-Earth Science and Technology)

Climate variability poses growing threats to human lives and socio-economic activities through changes in frequency and intensity of abnormal weather such as cold/heat waves and floods/droughts. This involves several climate phenomena with a wide range of timescales from subseasonal to decadal variations (e.g. MJO, IOD, ENSO, PDV, AMV). Many efforts have been made for understanding and predicting climate variations on each timescale, but there remain large uncertainties in simulation and prediction of subseasonal to decadal climate variations. This highlights lack of understanding of weather and climate interaction across different spatial and temporal timescales (e.g. tropical cyclones and ENSO) as well as multiple physical processes underlying climate variations (e.g. troposphere-stratosphere coupling, air-sea-ice interaction). This session aims to share current knowledge of subseasonal to decadal climate variability and predictability in order to identify the unresolved issues for better understanding and accurate prediction. This session invites all the abstracts related to the observational, theoretical, process-level and modelling research on subseasonal to decadal climate variability and predictability.

[AOS07-P01] Changes in North American and European Heatwave Characteristics

*Szandra A. Peter[1], Ben Kirtman[1] (1.Rosenstiel School of Marine and Atmospheric Science)

[AOS07-P02] **The effects of the "New Climate" Warming on Western Mediterranean: Situation of the Recent Extreme Events**

*Mohammed-Said KARROUK[1] (1.Hassan II University of Casablanca)

[AOS07-P03] **Month-to-month Difference of the Western Pacific Subtropical High Simulated by CMIP5 Models**

*Xiao Dong[1], Renping Lin[1] (1.Institute of Atmospheric Physics)

[AOS07-P04] Potential regulation on the climatic effect of Tibetan Plateau heating by tropical air–sea coupling

*Ziqian Wang[1], Anmin Duan[2], Song Yang[1] (1.School of Atmospheric Sciences, Sun Yat-sen University, 2.Institute of Atmospheric Physics, Chinese Academy of Sciences)

[AOS07-P05] Intraseasonal variation of the South Asian high and its role in connecting the Indian and East Asian summer monsoons

*Wei Wei[1] (1.Sun Yat-sen University)

[AOS07-P06] Mean Surface Air Temperatures in Japan - Regional Classification and Interranual Variability

*Pascal Oettli[1], Masami Nonaka[1], Swadhin Behera[1] (1.Japan Agency for Marine-Earth Science and Technology)

[AOS07-P07] Inter-Annual Variability of the Indonesian Rainfall and Air-Sea Interaction over the Indian-Pacific Ocean Associated with Regime Shift

*Murni Ngestu Nurutami[1], Tadahiro Hayasaka[1] (1.Center for Atmospheric and Oceanic Studies, Graduate School of Science, Tohoku University)

[AOS07-P08] Exploring synoptic-scale drivers of interannual rainfall variability over Africa

*Piotr Wolski[1], Chris Jack[1], Waarith Abrahams[1], Stefaan Conradie[1] (1.University of Cape Town)

[AOS07-P09] **Effect of El Niño on the response ratio of Hadley circulation to different SST meridional structures**

*Juan Feng[1] (1.Beijing Normal University)

[AOS07-P10] **Novel data-driven approach for ENSO prediction**

*Dmitri Kondrashov[1], Evgeniy Loskutov[2], Andrei Gavrilov[2], Dmitry Mukhin[2], Alexander Feigin[2] (1.University of California, Los Angeles, United States, 2.Institute of Applied Physics of the Russian Academy of Sciences, Nizhny Novgorod, Russian Federation)

[AOS07-P11] Experimental seasonal climate prediction using CFES: Comparison with the SINTEX-F systems

*Nobumasa Komori[1], Bunmei Taguchi[2], Akira Kuwano-Yoshida[3,1], Takeshi Doi[1], Masami Nonaka[1] (1.Japan Agency for Marine-Earth Science and Technology, 2.Research Center for Advanced Science and Technology, The University of Tokyo, 3.Disaster Prevention Research Institute, Kyoto University)

[AOS07-P12] Exploring the SST error growth during ENSO developing phase by using BCC_CSM1.1(m)

*Ben Tian[1], Hongli Ren[1] (1.National Climate Center, China Meteorological Administration)

[AOS07-P13] Role of sea-ice initialization in climate predictability over the Weddell Sea

*Yushi Morioka[1], Takeshi Doi[1], Doroteaciro Iovino[2], Simona Masina[2], Swadhin Behera[1] (1.Japan Agency for Marine-Earth Science and Technology (JAMSTEC), 2.Centro Euro-Mediterraneo sui Cambiamenti Climatici (CMCC))

[AOS07-P14] Observed and hindcasted subdecadal variability of the tropical Pacific climate

*Takashi Mochizuki[1], Masahiro Watanabe[2] (1.Japan Agency for Marine-Earth Science and Technology, 2.Atmosphere-Ocean Research Institute, The University of Tokyo)

Changes in North American and European Heatwave Characteristics

*Szandra A. Peter[1], Ben Kirtman[1]

1. Rosenstiel School of Marine and Atmospheric Science

Heat waves are a serious threat to ecosystems, society and the economies of the world. By calculating specific threshold values from daily maximum 2 m temperatures of the NCEP/NCAR reanalysis data (Kalnay et al. 1996), the frequency of heat waves during summer months (JJA) in Europe and the US is determined for the period of 1982 to 2017. The differences between the first and the second half of the 36-year period are discussed, and the results are compared to the North American Multi-Model Ensemble (NMME) forecast with specific focus on recent heat waves in the Pacific Northwest of North America and Central Europe. The connection between heat waves and known climate variability (i.e., the NAO, PNA) is analyzed. We strive to assess the importance of natural variability, such as the NAO, in the frequency of heat waves by comparing the first and last half of the studied 36-year period. We also examine how well the NMME retrospective and real-time forecasts capture heat waves (and cold spells), and the sources of predictability (i.e., sea surface temperature anomalies, land surface conditions), and how the predictability connects to the various modes of climate variability.

©2019. Japan Geoscience Union. All Right Reserved.

The effects of the "New Climate" Warming on Western Mediterranean: Situation of the Recent Extreme Events

*Mohammed-Said KARROUK[1]

1. Hassan II University of Casablanca

Since the nineties of the last century, climatological research following a great scientific advance in the field of prediction, not the variability and evolution of the different climatic parameters was beginning to be clearer!

But today, since the beginning of 2005, certainly due to oceanic thermal cumulations, and the shift of climatic zones towards poles in selective forms (more intense on the oceans present on the continents); Climatic events do not evolve according to the usual and expected rhythms: atmospheric circulation, precipitation, temperatures, seasonal phenomena, etc. These conditions are a spatiotemporal evolution and distribution, which characterize the new "global climate", by the new atmospheric regime imposing the Meridian Atmospheric Circulation (MAC), alternating the conditions of Freshness (humidity) and Heat (drought) along the year.

In this new situation, Western Mediterranean, located in the climate transition zone, is fully affected by the "New Climate". Usually, the atmospheric response to major climatic events (ENSO) in this region such as "El Niño" was characterized by the establishment of the NAO positive index, stability and drought, due to dominance Zonal Atmospheric Circulation in winter. On the other hand, in the "La Niña" episode, the negative index of the NAO and the predominant Meridian Atmospheric Circulation and precipitation became abundant.

Since the beginning of this century, qualified meteorological events of "exceptional !" causing floods have continued to occur in Western Mediterranean, with increasing recurrence, prompting us to wonder about the "new" mode of hydro-thermal function of the climate system that induces torrential rains, as well as its effect on environments and societies.

Thanks to spatial observation and monitoring of meteorological conditions over the last 15 years, these types of alternating Heat / Cold conditions have become predictable, enabling decision-makers today to prepare adequately for the management of related risks to the "New Climate" warmed.

Keywords: "New Climate" Warmed, New Atmospheric Circulation, Meridian Atmospheric Circulation (MAC) , Western Mediterranean, Heat / Cold, Drought / Flood

©2019. Japan Geoscience Union. All Right Reserved.

Month-to-month Difference of the Western Pacific Subtropical High Simulated by CMIP5 Models

*Xiao Dong[1], Renping Lin[1]

1. Institute of Atmospheric Physics

The western Pacific subtropical high (WPSH) is an important circulation system of the East Asian summer monsoon (EASM). Most previous studies have focused on the variability of summer mean WPSH. Note that the WPSH also experiences subseasonal variation from early to late summer. In this study we examined the month-to-month shift of the WPSH in boreal summer, that is, from June to July and from July to August, simulated by CMIP5 Atmospheric General Circulation Models (AGCMs) and coupled models. Results show that climatologically AGCMs can reproduce the northward shift of the WPSH better than eastward retreat from July to August. Compared with AGCMs, coupled models can improve the month-to-month shift simulation to some extent, indicating that the air-sea coupling processes are also important in subseasonal timescale.

Keywords: western Pacific subtropical high, CMIP5 simulation, month to month variation

©2019. Japan Geoscience Union. All Right Reserved.

Potential regulation on the climatic effect of Tibetan Plateau heating by tropical air–sea coupling

*Ziqian Wang[1], Anmin Duan[2], Song Yang[1]

1. School of Atmospheric Sciences, Sun Yat-sen University, 2. Institute of Atmospheric Physics, Chinese Academy of Sciences

Based on the conventional weather research and forecasting (WRF) model and the air–sea coupled mode WRF-OMLM, we investigate the potential regulation on the climatic effect of Tibetan Plateau (TP) heating by the air–sea coupling over the tropical Indian Ocean and western Pacific. Results indicate that the TP heating significantly enhances the southwesterly monsoon circulation over the northern Indian Ocean and the South Asia subcontinent. The intensified southwesterly wind cools the sea surface mainly through the wind-evaporation-SST (sea surface temperature) feedback. Cold SST anomaly then weakens monsoon convective activity, especially that over the Bay of Bengal, and less water vapor is thus transported into the TP along its southern slope from the tropical oceans. As a result, summer precipitation decreases over the TP, which further weakens the TP local heat source. Finally, the changed TP heating continues to influence the summer monsoon precipitation and atmospheric circulation. To a certain extent, the air–sea coupling over the adjacent oceans may weaken the effect of TP heating on the mean climate in summer. It is also implied that considerations of air–sea interaction are necessary in future simulation studies of the TP heating effect.

Keywords: Air–sea coupling, Tibetan Plateau, Thermal forcing, Regional model

©2019. Japan Geoscience Union. All Right Reserved.

Intraseasonal variation of the South Asian high and its role in connecting the Indian and East Asian summer monsoons

*Wei Wei[1]

1. Sun Yat-sen University

The South Asian high (SAH) is the most intense and persistent upper-level circulation system in the Asian monsoon region during boreal summer. It plays a crucial role in the onset and variation of the Asian summer monsoon. Ample evidence shows that the monsoon onset and activities are closely related to the intraseasonal oscillation (ISO). Previous studies have found that the ISO in the East Asian summer monsoon (EASM) is impacted by the northward or northwestward propagation of the ISO in the South China Sea and the western North Pacific, and the northeastward propagation of the ISO in the tropical Indian Ocean. However, seldom research mentioned the effect of the ISO in the SAH. Our previous studies have shown that the SAH plays an important role in connecting the Indian summer monsoon (ISM) and the EASM on the interannual time scale. However, the effect of the SAH on the connection of the ISM and the EASM on the intraseasonal time scale is still not clear. Actually, the ISO in the SAH is significant in its zonal variation. In this study, we firstly figured out the intraseasonal variation feature of the SAH. And then, we explored the upper-level signal which will lead to the onset, advance and retreat of the EASM. Considering significant ISO in the ISM, we investigated the ISO feature in the ISM and its effect on the ISO in the SAH. Finally, we addressed a new physical process that the ISO in the ISM will impact the ISO in the SAH, and further influence the advance and retreat of the EASM on the intraseasonal time scale. We try to learn about the intraseasonal variation of the EASM in a new view, and propose a new way to improve the short-term climate prediction and the extended-range weather forecast.

©2019. Japan Geoscience Union. All Right Reserved.

Mean Surface Air Temperatures in Japan - Regional Classification and Interranual Variability

*Pascal Oettli[1], Masami Nonaka[1], Swadhin Behera[1]

1. Japan Agency for Marine-Earth Science and Technology

Back to the year 1886, several divisions of the climate of Japan into homogeneous climatic regions have been proposed, following different approaches of the question. This includes the Köppen climate classification (Fukui in 1933; Sekiguchi in 1949), the new Thornthwaite climate classification (Isozaki in 1933; Fukui in 1957) or the similarities of weather conditions. The latter is performed either throughout the year (Nakagawa in 1899; Sekiguchi in 1959; Yoshino in 1980) or during specific seasons (Iwakiri in 1967; Murata and Yoshino in 1988), sometimes with the help of statistical techniques, such as principal component analysis and the cluster analysis (Mikami in 1975; Koizumi and Kato in 2012.)

Using a type of artificial neural network called Self-Organizing Map, or SOM, we propose another division of the climate of Japan, solely based on the mean areal surface air temperature anomalies. SOM has been successfully employed in climate studies for more than a decade and has showed its ability to extract simple features from high-dimensional data. Here, SOM is applied to group 762 AMeDAS stations, taken throughout Japan for the last 30 years, into homogeneous clusters (=regions). Clustering is performed seasonally, with a focus on boreal winter (December to February) and boreal summer (June to August). As a result, eight regions are defined and associated time series of temperature anomalies (=indices) are computed.

Subsequently, possible source(s) of the interannual variability of mean surface air temperature anomalies are explored, for a better understanding of the regional differences. For this, correlation coefficients between indices previously defined and different climatic variable anomaly fields (sea-surface temperatures, outgoing longwave radiation, geopotential height...) are calculated. Hopefully, this work would also lead to a better seasonal forecast, taking into account the specificity of each region in regard to their link to the large-scale variability.

Keywords: Japan, Air temperature, Classification, Interannual variability

©2019. Japan Geoscience Union. All Right Reserved.

Inter-Annual Variability of the Indonesian Rainfall and Air-Sea Interaction over the Indian-Pacific Ocean Associated with Regime Shift

*Murni Ngestu Nurutami[1], Tadahiro Hayasaka[1]

1. Center for Atmospheric and Oceanic Studies, Graduate School of Science, Tohoku University

The inter-annual and inter-decadal variability of the Indonesian rainfall are investigated in association with the interannual climate modes over Indian-Pacific Oceans and the inter-decadal modulation on inter-annual climate variability impact. Rainfall data of the Climate Research Unit (CRU) from 1901 to 2016 and the Global Precipitation Climatology Project (GPCP) from 1979 to 2016 for June –November (JJASON) are used. The empirical orthogonal function (EOF) is used to identify the dominant spatial and temporal variability patterns of rainfall and the standard and partial correlation techniques are used to compare and to quantify the linear relationship between two or more time-series datasets. Based on the first principle component (PC1) of both CRU and GPCP data, the results show that canonical El Niño Southern-Oscillation (canonical ENSO), ENSO Modoki, and Indian Ocean Dipole (IOD) are the major climate modes influencing the inter-annual variability of the Indonesian rainfall, and the Inter-decadal Pacific Oscillation (IPO) is the major decadal phenomenon which affects the decadal variability of Indonesian rainfall. All of the inter-annual climate modes and IPO have negative correlation with the Indonesian rainfall, but the spatial distributions of Indonesian rainfall change associated with each phenomenon are different. During 1970 to 2016, three phases of IPO have been identified which are strongly related to Indonesian rainfall with the correlation coefficient of -0.75. The three phases are a negative phase in 1970-1978, a positive phase in 1979-1997, and another negative phase in 1998-2015. Mostly, these climate modes occur simultaneously, and the impacts of them on rainfall are combined. The driest condition of rainfall occurs when El Niño coincides with positive IOD during positive IPO, and the wettest condition occurs when La Niña –La Niña Modoki coincides with negative IOD during negative IPO over the whole region of Indonesia. The IPO plays a role in modulating the impact of these inter-annual climate modes on their frequencies and magnitudes to Indonesian rainfall from 1970s until present. The responses of the Indonesian rainfall to each inter-annual climate mode modulated by IPO are different as based on their time series correlation coefficient. The negative correlation between canonical ENSO and Indonesian rainfall weakens during negative IPO from early 2000s and intensifies during positive IPO. On the other hand, the negative correlation between ENSO Modoki and Indonesian rainfall and between IOD and Indonesian rainfall increases during negative phase of IPO from late 1990s, and the negative correlation between ENSO Modoki and Indonesian rainfall weakens during positive IPO. Recently, the frequency of ENSO Modoki and IOD and their impacts on Indonesian rainfall increase.

Keywords: Indonesian rainfall variability, El Niño Southern-Oscillation (ENSO), ENSO Modoki, Interannual Variability, Decadal Variability, Interdecadal Pacific Oscillation

©2019. Japan Geoscience Union. All Right Reserved.

Exploring synoptic-scale drivers of interannual rainfall variability over Africa

*Piotr Wolski[1], Chris Jack[1], Waarith Abrahams[1], Stefaan Conradie[1]

1. University of Cape Town

Variability in local climate is a result of an interplay of multi-scale drivers –processes and feedbacks - intertwined within dependency or conditioning chain across spatial scales: from global to synoptic to meso- to local. Resolving these drivers and dependencies can be framed through the following questions: where does a deterministic signal at a particular time scale arise, how does it propagate through space and scales, and how can we maximize our ability to capture it? Here, we report on an exploratory study focusing on the synoptic-scale forcing underlying rainfall variability at the interannual time scale over Africa. In that, we systematically map, over the continent, variables and spatial scales which provide the strongest explanatory power of interannual rainfall variability. In addition, we constrast the explanatory power of mean state of synoptic fields with that of their variance, and of frequency of individual (daily) states. The analyses utilize multiple regression and CCA performed on mean de-orthogonalized fields of q,t,u,v,z at various pressure levels, with daily states of synoptic variables classified using self-organizing maps (SOM). The results are interpreted from the process perspective in terms of their agreement with the current understanding of the role of process chains affecting rainfall over various regions of the contient, and in terms of their implications to statistical downscaling of climate projections and seasonal forecasts.

Keywords: rainfall variability, statistical climatology, Africa, self organizing maps

©2019. Japan Geoscience Union. All Right Reserved.

Effect of El Niño on the response ratio of Hadley circulation to different SST meridional structures

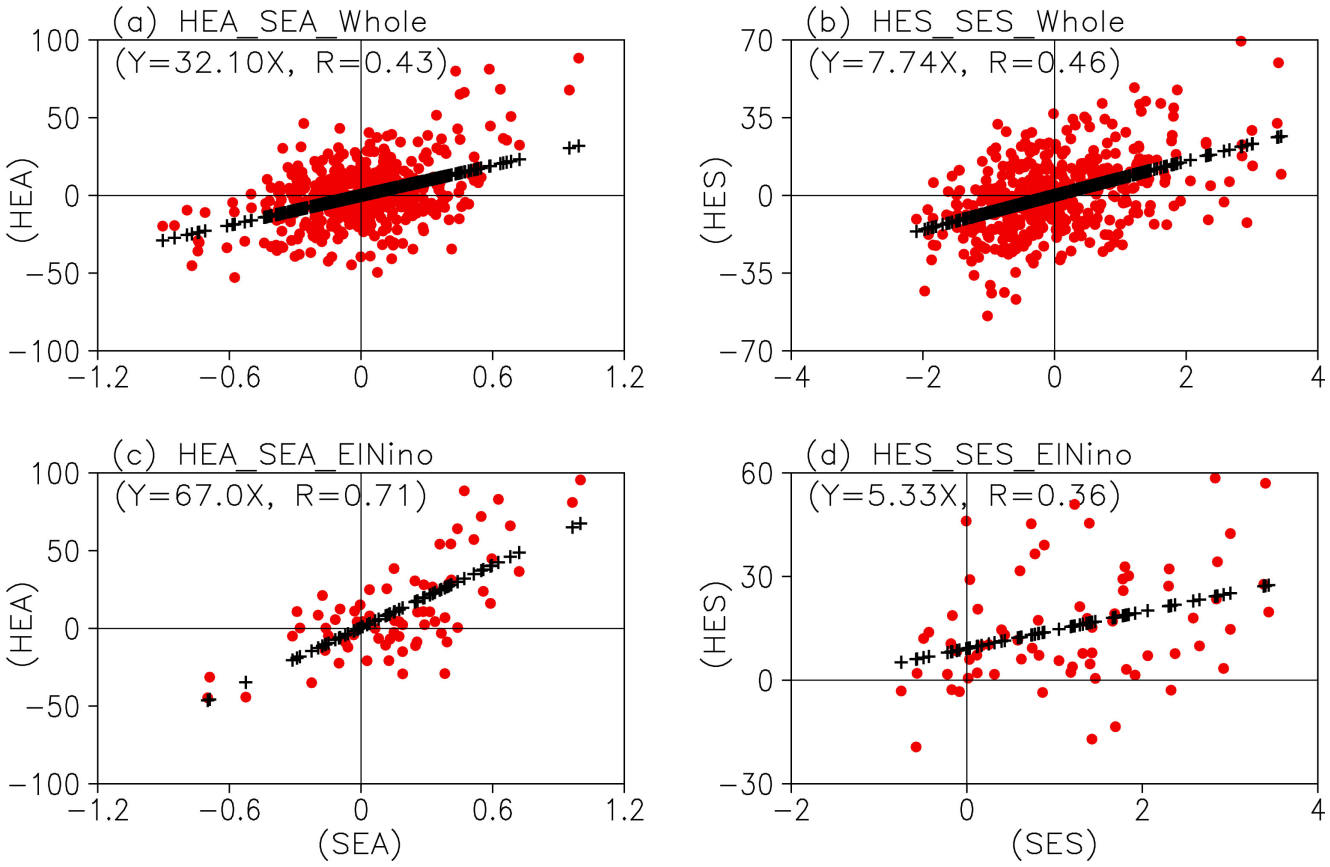
*Juan Feng[1]

1. Beijing Normal University

The role of El Niño in influencing the response ratio of the Hadley circulation (HC) to different tropical sea surface temperature (SST) meridional structures is investigated over the period 1979–2016. The explained variance of the equatorially asymmetric principal mode of HC variability is enhanced during El Niño events that are characterized by equatorially symmetric El Niño SST anomalies. The reason for the enhanced explained variance is examined. It is shown that the response ratio of the HC to different SST meridional structures is greatly enhanced in El Niño events; this is because the SST over the Indo-Pacific warm pool (IPWP) shows inhomogeneous warming in El Niño events, with greater values in the southern IPWP. The asymmetric warming over the IPWP is opposite to the climatological meridional structure of the SST over the IPWP, which intensifies the equatorially symmetric variation of SST, and contributes to the enhanced response ratio of the HC to SST. This point is further verified by the suppression of this enhanced response ratio in El Niño events of the HC to SST when the effects of SST over the IPWP are removed, implying the different warming amplitude within the IPWP during the El Niño events contributes to the enhanced response ratio. The response in La Niña events is also explored, indicating a difference between El Niño and La Niña events. These results may help explain the corresponding variations of the HC during the El Niño events, and highlight the different influences of the El Niño and La Niña events on the response of the HC to SST.

Keywords: Hadley circulation, sea surface temperature, Indo-Pacific warm pool, El Niño

©2019. Japan Geoscience Union. All Right Reserved.



©2019. Japan Geoscience Union. All Right Reserved.

Novel data-driven approach for ENSO prediction

*Dmitri Kondrashov[1], Evgeniy Loskutov[2], Andrei Gavrilov[2], Dmitry Mukhin[2], Alexander Feigin[2]

1. University of California, Los Angeles, United States, 2. Institute of Applied Physics of the Russian Academy of Sciences, Nizhny Novgorod, Russian Federation

We have developed novel data-driven technique for ENSO prediction that combines two existing approaches: linear dynamical mode (LDM) decomposition of spatially distributed data, and multilevel empirical model reduction (EMR) stochastic modeling approach. The nonlinear EMR model that utilizes dynamical variables obtained by empirical orthogonal function (EOF) decomposition of tropical Pacific SST’ s (Kondrashov et al. 2005), had already achieved a very competitive skill in International Research Institute for Climate and Society (IRI) ENSO real-time multi-model plume (Barnston et al. 2012). On the other hand, Gavrilov et al. (2018) have shown that LDM decomposition provides better modes for ENSO forecast than EOFs.

In the presented results we have used LDM modes as dynamical variables at the main level of multilevel linear EMR model. The model was trained on monthly 1960 -- 2014 sea surface temperatures (30S to 30N, 2x2 deg). The results of comparing skill of the retrospective predictions of the SST-based ENSO indices obtained by EMR model with LDM and EOF modes, will be discussed.

1. Kondrashov, D., Kravtsov, S., Robertson, A. W., & Ghil, M. (2005). A Hierarchy of Data-Based ENSO Models. Journal of Climate, 18(21), 4425–4444. doi:10.1175/JCLI3567.1

2. Gavrilov, A., Seleznev, A., Mukhin, D., Loskutov, E., Feigin, A., & Kurths, J. (2018). Linear dynamical modes as new variables for data-driven ENSO forecast. Climate Dynamics, 1–18. http://doi.org/10.1007/s00382-018-4255-7.

3. Barnston, A. G., M. K. Tippett, M. L. Heureux, S. Li, and D. G. DeWitt, 2012: Skill of real-time seasonal ENSO model predictions during 2002–2011 —is our capability improving? *Bulletin of the American Meteorological Society*, **93 (5)**, 631–651, doi:10.1175/BAMS-D-11-00111.1.

Keywords: ENSO, stochastic modeling, prediction

©2019. Japan Geoscience Union. All Right Reserved.

Experimental seasonal climate prediction using CFES: Comparison with the SINTEX-F systems

*Nobumasa Komori[1], Bunmei Taguchi[2], Akira Kuwano-Yoshida[3,1], Takeshi Doi[1], Masami Nonaka[1]

1. Japan Agency for Marine-Earth Science and Technology, 2. Research Center for Advanced Science and Technology, The University of Tokyo, 3. Disaster Prevention Research Institute, Kyoto University

An experimental seasonal climate prediction system has been developed based on the Coupled atmosphere-ocean general circulation model for the Earth Simulator (CFES). Following the well-established systems based on the SINTEX-F model, initial conditions for seasonal climate prediction are constructed by strongly nudging sea surface temperature (SST) to observed one.

At this stage, 12-member ensemble 6-month predictions from the 1st day of March, June, September, and December have been conducted from 1983 through 2018, after 32-years of coupled spin-up integration with SST-nudging to the observed climatology. The experimental system exhibits skill in predicting variability of seasonal-mean 2-m air temperature over the tropical Pacific, and contributes to the improvement of multi-model ensemble prediction with the SINTEX-F systems.

Keywords: experimental seasonal climate prediction, global coupled atmosphere-ocean GCM, atmosphere-ocean interaction, multi-model ensemble

©2019. Japan Geoscience Union. All Right Reserved.

Exploring the SST error growth during ENSO developing phase by using BCC_CSM1.1(m)

*Ben Tian[1], Hongli Ren[1]

1. National Climate Center, China Meteorological Administration

Here we assess the ENSO prediction errors as a function of lead time using the seasonal hindcast of the Beijing Climate Center System Model, BCC_CSM1.1(m). The ensemble mean forecasts seems to be more challenging during the developing years of ENSO, compared with those made towards the decay phase. The composites of SST prediction errors are significantly negative and cover a large area in central-eastern tropical Pacific, thus limiting the model in forecasting the onset and intensity of El Niño. The large-scale errors, at their early stage, are generated gradually by negative anomalies in the subsurface temperature of the central-western equatorial Pacific, a process similar to El Niño decay and then transition to La Nina growth phase. Our results support others' work of "sensitive areas" for ENSO predictions, and emphasize the essential accuracy of initial fields and their early evolution, providing information for further improving the forecasting skill of ENSO.

Keywords: El Nino prediction, error evolution, sea surface temperature

©2019. Japan Geoscience Union. All Right Reserved.

Role of sea-ice initialization in climate predictability over the Weddell Sea

*Yushi Morioka[1], Takeshi Doi[1], Doroteaciro Iovino[2], Simona Masina[2], Swadhin Behera[1]

1. Japan Agency for Marine-Earth Science and Technology (JAMSTEC), 2. Centro Euro-Mediterraneo sui Cambiamenti Climatici (CMCC)

Potential impact of sea-ice initialization on the interannual climate predictability over the Weddell Sea is investigated using a coupled general circulation model. Climate variability in the Weddell Sea is generally believed to have association with remote forcing such as El Niño-Southern Oscillation and the Southern Annual Mode. However, sea-ice variability in the Weddell Sea has been recently suggested to play additional roles in modulating local atmospheric variability through changes in surface air temperature and near-surface baroclinicity. When both the model’s sea-surface temperature (SST) and sea-ice concentration (SIC) are initialized with observations using nudging schemes, reforecast experiments from September 1st show improvements in predicting the observed SIC anomalies in the Weddell Sea up to four months ahead, compared to the other experiments with only SST initialization. During austral spring (Oct-Dec) of lower-than-normal sea-ice years in the Weddell Sea, reforecast experiments with the SST and SIC initializations reasonably predict high surface air temperature anomalies in the Weddell Sea and high sea-level pressure anomalies over the Atlantic sector of the Southern Ocean. These results suggest that accurate initialization of sea-ice conditions during austral winter is necessary for skillful prediction of climate variability over the Weddell Sea during austral spring.

Keywords: Air-sea-ice interaction, Climate predictability, Weddell Sea

©2019. Japan Geoscience Union. All Right Reserved.

Observed and hindcasted subdecadal variability of the tropical Pacific climate

*Takashi Mochizuki[1], Masahiro Watanabe[2]

1. Japan Agency for Marine-Earth Science and Technology, 2. Atmosphere-Ocean Research Institute, The University of Tokyo

The tropical Pacific is highly responsible for controlling the tendencies of global climate. Here, we have found a subdecadal (i.e., 3-year-running means) variation that has been distinctively observed in the 2000s over the tropical Pacific. The warm water that originated from the positive ocean-heat-content (OHC) anomaly over the western Pacific in 2000 slowly extended eastward and stayed at the central equatorial Pacific between 2002-2005, rather than reaching the eastern edge. At the same time, an accompanying anti-cyclonic surface wind anomaly was observed in the off-equatorial North Pacific. This dynamical response of the upper ocean may have contributed to the subsequent warming in the western Pacific. In the preceding decades, in contrast, the observed OHC has usually represented a periodic fluctuation in the tropical Pacific, characterized by anomalous heat input/output in the meridional direction and slow eastward adjustment in the equatorial ocean thermocline. This subdecadal variation in the 2000s is quite distinct from our decadal hindcasts with initialization in Coupled Model Intercomparison Project Phase 5. The model predominantly simulates periodic-type fluctuations in any decade, and the resultant low predictability of the subdecadal variation in the 2000s can work to modulate the predictive skills at a lead time of several years.

Keywords: subdecadal variability, climate prediction, predictability, tropical Pacific

©2019. Japan Geoscience Union. All Right Reserved.

[E] Poster | A (Atmospheric and Hydrospheric Sciences)：A-OS Ocean Sciences & Ocean Environment

Thu. May 30, 2019 5:15 PM - 6:30 PM JST | Thu. May 30, 2019 8:15 AM - 9:30 AM UTC | Poster Hall International Exhibition Hall8, Makuhari Messe_7

[A-OS07] Climate variability and predictability on subseasonal to decadal timescales

convener:Takashi Mochizuki(Japan Agency for Marine-Earth Science and Technology), V Ramaswamy(NOAA GFDL), Doug Smith(Met Office), Yushi Morioka(Japan Agency for Marine-Earth Science and Technology)

Climate variability poses growing threats to human lives and socio-economic activities through changes in frequency and intensity of abnormal weather such as cold/heat waves and floods/droughts. This involves several climate phenomena with a wide range of timescales from subseasonal to decadal variations (e.g. MJO, IOD, ENSO, PDV, AMV). Many efforts have been made for understanding and predicting climate variations on each timescale, but there remain large uncertainties in simulation and prediction of subseasonal to decadal climate variations. This highlights lack of understanding of weather and climate interaction across different spatial and temporal timescales (e.g. tropical cyclones and ENSO) as well as multiple physical processes underlying climate variations (e.g. troposphere-stratosphere coupling, air-sea-ice interaction). This session aims to share current knowledge of subseasonal to decadal climate variability and predictability in order to identify the unresolved issues for better understanding and accurate prediction. This session invites all the abstracts related to the observational, theoretical, process-level and modelling research on subseasonal to decadal climate variability and predictability.

[AOS07-P01] Changes in North American and European Heatwave Characteristics

*Szandra A. Peter[1], Ben Kirtman[1] (1.Rosenstiel School of Marine and Atmospheric Science)

[AOS07-P02] **The effects of the "New Climate" Warming on Western Mediterranean: Situation of the Recent Extreme Events**

*Mohammed-Said KARROUK[1] (1.Hassan II University of Casablanca)

[AOS07-P03] **Month-to-month Difference of the Western Pacific Subtropical High Simulated by CMIP5 Models**

*Xiao Dong[1], Renping Lin[1] (1.Institute of Atmospheric Physics)

[AOS07-P04] Potential regulation on the climatic effect of Tibetan Plateau heating by tropical air–sea coupling

*Ziqian Wang[1], Anmin Duan[2], Song Yang[1] (1.School of Atmospheric Sciences, Sun Yat-sen University, 2.Institute of Atmospheric Physics, Chinese Academy of Sciences)

[AOS07-P05] Intraseasonal variation of the South Asian high and its role in connecting the Indian and East Asian summer monsoons

*Wei Wei[1] (1.Sun Yat-sen University)

[AOS07-P06] Mean Surface Air Temperatures in Japan - Regional Classification and Interranual Variability

*Pascal Oettli[1], Masami Nonaka[1], Swadhin Behera[1] (1.Japan Agency for Marine-Earth Science and Technology)

[AOS07-P07] Inter-Annual Variability of the Indonesian Rainfall and Air-Sea Interaction over the Indian-Pacific Ocean Associated with Regime Shift

*Murni Ngestu Nurutami[1], Tadahiro Hayasaka[1] (1.Center for Atmospheric and Oceanic Studies, Graduate School of Science, Tohoku University)

[AOS07-P08] Exploring synoptic-scale drivers of interannual rainfall variability over Africa

*Piotr Wolski[1], Chris Jack[1], Waarith Abrahams[1], Stefaan Conradie[1] (1.University of Cape Town)

[AOS07-P09] **Effect of El Niño on the response ratio of Hadley circulation to different SST meridional structures**

*Juan Feng[1] (1.Beijing Normal University)

[AOS07-P10] **Novel data-driven approach for ENSO prediction**

*Dmitri Kondrashov[1], Evgeniy Loskutov[2], Andrei Gavrilov[2], Dmitry Mukhin[2], Alexander Feigin[2] (1.University of California, Los Angeles, United States, 2.Institute of Applied Physics of the Russian Academy of Sciences, Nizhny Novgorod, Russian Federation)

[AOS07-P11] Experimental seasonal climate prediction using CFES: Comparison with the SINTEX-F systems

*Nobumasa Komori[1], Bunmei Taguchi[2], Akira Kuwano-Yoshida[3,1], Takeshi Doi[1], Masami Nonaka[1] (1.Japan Agency for Marine-Earth Science and Technology, 2.Research Center for Advanced Science and Technology, The University of Tokyo, 3.Disaster Prevention Research Institute, Kyoto University)

[AOS07-P12] Exploring the SST error growth during ENSO developing phase by using BCC_CSM1.1(m)

*Ben Tian[1], Hongli Ren[1] (1.National Climate Center, China Meteorological Administration)

[AOS07-P13] Role of sea-ice initialization in climate predictability over the Weddell Sea

*Yushi Morioka[1], Takeshi Doi[1], Doroteaciro Iovino[2], Simona Masina[2], Swadhin Behera[1] (1.Japan Agency for Marine-Earth Science and Technology (JAMSTEC), 2.Centro Euro-Mediterraneo sui Cambiamenti Climatici (CMCC))

[AOS07-P14] Observed and hindcasted subdecadal variability of the tropical Pacific climate

*Takashi Mochizuki[1], Masahiro Watanabe[2] (1.Japan Agency for Marine-Earth Science and Technology, 2.Atmosphere-Ocean Research Institute, The University of Tokyo)

Changes in North American and European Heatwave Characteristics

*Szandra A. Peter[1], Ben Kirtman[1]

1. Rosenstiel School of Marine and Atmospheric Science

Heat waves are a serious threat to ecosystems, society and the economies of the world. By calculating specific threshold values from daily maximum 2 m temperatures of the NCEP/NCAR reanalysis data (Kalnay et al. 1996), the frequency of heat waves during summer months (JJA) in Europe and the US is determined for the period of 1982 to 2017. The differences between the first and the second half of the 36-year period are discussed, and the results are compared to the North American Multi-Model Ensemble (NMME) forecast with specific focus on recent heat waves in the Pacific Northwest of North America and Central Europe. The connection between heat waves and known climate variability (i.e., the NAO, PNA) is analyzed. We strive to assess the importance of natural variability, such as the NAO, in the frequency of heat waves by comparing the first and last half of the studied 36-year period. We also examine how well the NMME retrospective and real-time forecasts capture heat waves (and cold spells), and the sources of predictability (i.e., sea surface temperature anomalies, land surface conditions), and how the predictability connects to the various modes of climate variability.

©2019. Japan Geoscience Union. All Right Reserved.

The effects of the "New Climate" Warming on Western Mediterranean: Situation of the Recent Extreme Events

*Mohammed-Said KARROUK[1]

1. Hassan II University of Casablanca

Since the nineties of the last century, climatological research following a great scientific advance in the field of prediction, not the variability and evolution of the different climatic parameters was beginning to be clearer!

But today, since the beginning of 2005, certainly due to oceanic thermal cumulations, and the shift of climatic zones towards poles in selective forms (more intense on the oceans present on the continents); Climatic events do not evolve according to the usual and expected rhythms: atmospheric circulation, precipitation, temperatures, seasonal phenomena, etc. These conditions are a spatiotemporal evolution and distribution, which characterize the new "global climate", by the new atmospheric regime imposing the Meridian Atmospheric Circulation (MAC), alternating the conditions of Freshness (humidity) and Heat (drought) along the year.

In this new situation, Western Mediterranean, located in the climate transition zone, is fully affected by the "New Climate". Usually, the atmospheric response to major climatic events (ENSO) in this region such as "El Niño" was characterized by the establishment of the NAO positive index, stability and drought, due to dominance Zonal Atmospheric Circulation in winter. On the other hand, in the "La Niña" episode, the negative index of the NAO and the predominant Meridian Atmospheric Circulation and precipitation became abundant.

Since the beginning of this century, qualified meteorological events of "exceptional !" causing floods have continued to occur in Western Mediterranean, with increasing recurrence, prompting us to wonder about the "new" mode of hydro-thermal function of the climate system that induces torrential rains, as well as its effect on environments and societies.

Thanks to spatial observation and monitoring of meteorological conditions over the last 15 years, these types of alternating Heat / Cold conditions have become predictable, enabling decision-makers today to prepare adequately for the management of related risks to the "New Climate" warmed.

Keywords: "New Climate" Warmed, New Atmospheric Circulation, Meridian Atmospheric Circulation (MAC) , Western Mediterranean, Heat / Cold, Drought / Flood

©2019. Japan Geoscience Union. All Right Reserved.

Month-to-month Difference of the Western Pacific Subtropical High Simulated by CMIP5 Models

*Xiao Dong[1], Renping Lin[1]

1. Institute of Atmospheric Physics

The western Pacific subtropical high (WPSH) is an important circulation system of the East Asian summer monsoon (EASM). Most previous studies have focused on the variability of summer mean WPSH. Note that the WPSH also experiences subseasonal variation from early to late summer. In this study we examined the month-to-month shift of the WPSH in boreal summer, that is, from June to July and from July to August, simulated by CMIP5 Atmospheric General Circulation Models (AGCMs) and coupled models. Results show that climatologically AGCMs can reproduce the northward shift of the WPSH better than eastward retreat from July to August. Compared with AGCMs, coupled models can improve the month-to-month shift simulation to some extent, indicating that the air-sea coupling processes are also important in subseasonal timescale.

Keywords: western Pacific subtropical high, CMIP5 simulation, month to month variation

©2019. Japan Geoscience Union. All Right Reserved.

Potential regulation on the climatic effect of Tibetan Plateau heating by tropical air–sea coupling

*Ziqian Wang[1], Anmin Duan[2], Song Yang[1]

1. School of Atmospheric Sciences, Sun Yat-sen University, 2. Institute of Atmospheric Physics, Chinese Academy of Sciences

Based on the conventional weather research and forecasting (WRF) model and the air–sea coupled mode WRF-OMLM, we investigate the potential regulation on the climatic effect of Tibetan Plateau (TP) heating by the air–sea coupling over the tropical Indian Ocean and western Pacific. Results indicate that the TP heating significantly enhances the southwesterly monsoon circulation over the northern Indian Ocean and the South Asia subcontinent. The intensified southwesterly wind cools the sea surface mainly through the wind-evaporation-SST (sea surface temperature) feedback. Cold SST anomaly then weakens monsoon convective activity, especially that over the Bay of Bengal, and less water vapor is thus transported into the TP along its southern slope from the tropical oceans. As a result, summer precipitation decreases over the TP, which further weakens the TP local heat source. Finally, the changed TP heating continues to influence the summer monsoon precipitation and atmospheric circulation. To a certain extent, the air–sea coupling over the adjacent oceans may weaken the effect of TP heating on the mean climate in summer. It is also implied that considerations of air–sea interaction are necessary in future simulation studies of the TP heating effect.

Keywords: Air–sea coupling, Tibetan Plateau, Thermal forcing, Regional model

©2019. Japan Geoscience Union. All Right Reserved.

Intraseasonal variation of the South Asian high and its role in connecting the Indian and East Asian summer monsoons

*Wei Wei[1]

1. Sun Yat-sen University

The South Asian high (SAH) is the most intense and persistent upper-level circulation system in the Asian monsoon region during boreal summer. It plays a crucial role in the onset and variation of the Asian summer monsoon. Ample evidence shows that the monsoon onset and activities are closely related to the intraseasonal oscillation (ISO). Previous studies have found that the ISO in the East Asian summer monsoon (EASM) is impacted by the northward or northwestward propagation of the ISO in the South China Sea and the western North Pacific, and the northeastward propagation of the ISO in the tropical Indian Ocean. However, seldom research mentioned the effect of the ISO in the SAH. Our previous studies have shown that the SAH plays an important role in connecting the Indian summer monsoon (ISM) and the EASM on the interannual time scale. However, the effect of the SAH on the connection of the ISM and the EASM on the intraseasonal time scale is still not clear. Actually, the ISO in the SAH is significant in its zonal variation. In this study, we firstly figured out the intraseasonal variation feature of the SAH. And then, we explored the upper-level signal which will lead to the onset, advance and retreat of the EASM. Considering significant ISO in the ISM, we investigated the ISO feature in the ISM and its effect on the ISO in the SAH. Finally, we addressed a new physical process that the ISO in the ISM will impact the ISO in the SAH, and further influence the advance and retreat of the EASM on the intraseasonal time scale. We try to learn about the intraseasonal variation of the EASM in a new view, and propose a new way to improve the short-term climate prediction and the extended-range weather forecast.

©2019. Japan Geoscience Union. All Right Reserved.

Mean Surface Air Temperatures in Japan - Regional Classification and Interranual Variability

*Pascal Oettli[1], Masami Nonaka[1], Swadhin Behera[1]

1. Japan Agency for Marine-Earth Science and Technology

Back to the year 1886, several divisions of the climate of Japan into homogeneous climatic regions have been proposed, following different approaches of the question. This includes the Köppen climate classification (Fukui in 1933; Sekiguchi in 1949), the new Thornthwaite climate classification (Isozaki in 1933; Fukui in 1957) or the similarities of weather conditions. The latter is performed either throughout the year (Nakagawa in 1899; Sekiguchi in 1959; Yoshino in 1980) or during specific seasons (Iwakiri in 1967; Murata and Yoshino in 1988), sometimes with the help of statistical techniques, such as principal component analysis and the cluster analysis (Mikami in 1975; Koizumi and Kato in 2012.)

Using a type of artificial neural network called Self-Organizing Map, or SOM, we propose another division of the climate of Japan, solely based on the mean areal surface air temperature anomalies. SOM has been successfully employed in climate studies for more than a decade and has showed its ability to extract simple features from high-dimensional data. Here, SOM is applied to group 762 AMeDAS stations, taken throughout Japan for the last 30 years, into homogeneous clusters (=regions). Clustering is performed seasonally, with a focus on boreal winter (December to February) and boreal summer (June to August). As a result, eight regions are defined and associated time series of temperature anomalies (=indices) are computed.

Subsequently, possible source(s) of the interannual variability of mean surface air temperature anomalies are explored, for a better understanding of the regional differences. For this, correlation coefficients between indices previously defined and different climatic variable anomaly fields (sea-surface temperatures, outgoing longwave radiation, geopotential height...) are calculated. Hopefully, this work would also lead to a better seasonal forecast, taking into account the specificity of each region in regard to their link to the large-scale variability.

Keywords: Japan, Air temperature, Classification, Interannual variability

©2019. Japan Geoscience Union. All Right Reserved.

Inter-Annual Variability of the Indonesian Rainfall and Air-Sea Interaction over the Indian-Pacific Ocean Associated with Regime Shift

*Murni Ngestu Nurutami[1], Tadahiro Hayasaka[1]

1. Center for Atmospheric and Oceanic Studies, Graduate School of Science, Tohoku University

The inter-annual and inter-decadal variability of the Indonesian rainfall are investigated in association with the interannual climate modes over Indian-Pacific Oceans and the inter-decadal modulation on inter-annual climate variability impact. Rainfall data of the Climate Research Unit (CRU) from 1901 to 2016 and the Global Precipitation Climatology Project (GPCP) from 1979 to 2016 for June –November (JJASON) are used. The empirical orthogonal function (EOF) is used to identify the dominant spatial and temporal variability patterns of rainfall and the standard and partial correlation techniques are used to compare and to quantify the linear relationship between two or more time-series datasets. Based on the first principle component (PC1) of both CRU and GPCP data, the results show that canonical El Niño Southern-Oscillation (canonical ENSO), ENSO Modoki, and Indian Ocean Dipole (IOD) are the major climate modes influencing the inter-annual variability of the Indonesian rainfall, and the Inter-decadal Pacific Oscillation (IPO) is the major decadal phenomenon which affects the decadal variability of Indonesian rainfall. All of the inter-annual climate modes and IPO have negative correlation with the Indonesian rainfall, but the spatial distributions of Indonesian rainfall change associated with each phenomenon are different. During 1970 to 2016, three phases of IPO have been identified which are strongly related to Indonesian rainfall with the correlation coefficient of -0.75. The three phases are a negative phase in 1970-1978, a positive phase in 1979-1997, and another negative phase in 1998-2015. Mostly, these climate modes occur simultaneously, and the impacts of them on rainfall are combined. The driest condition of rainfall occurs when El Niño coincides with positive IOD during positive IPO, and the wettest condition occurs when La Niña –La Niña Modoki coincides with negative IOD during negative IPO over the whole region of Indonesia. The IPO plays a role in modulating the impact of these inter-annual climate modes on their frequencies and magnitudes to Indonesian rainfall from 1970s until present. The responses of the Indonesian rainfall to each inter-annual climate mode modulated by IPO are different as based on their time series correlation coefficient. The negative correlation between canonical ENSO and Indonesian rainfall weakens during negative IPO from early 2000s and intensifies during positive IPO. On the other hand, the negative correlation between ENSO Modoki and Indonesian rainfall and between IOD and Indonesian rainfall increases during negative phase of IPO from late 1990s, and the negative correlation between ENSO Modoki and Indonesian rainfall weakens during positive IPO. Recently, the frequency of ENSO Modoki and IOD and their impacts on Indonesian rainfall increase.

Keywords: Indonesian rainfall variability, El Niño Southern-Oscillation (ENSO), ENSO Modoki, Interannual Variability, Decadal Variability, Interdecadal Pacific Oscillation

©2019. Japan Geoscience Union. All Right Reserved.

Exploring synoptic-scale drivers of interannual rainfall variability over Africa

*Piotr Wolski[1], Chris Jack[1], Waarith Abrahams[1], Stefaan Conradie[1]

1. University of Cape Town

Variability in local climate is a result of an interplay of multi-scale drivers –processes and feedbacks - intertwined within dependency or conditioning chain across spatial scales: from global to synoptic to meso- to local. Resolving these drivers and dependencies can be framed through the following questions: where does a deterministic signal at a particular time scale arise, how does it propagate through space and scales, and how can we maximize our ability to capture it? Here, we report on an exploratory study focusing on the synoptic-scale forcing underlying rainfall variability at the interannual time scale over Africa. In that, we systematically map, over the continent, variables and spatial scales which provide the strongest explanatory power of interannual rainfall variability. In addition, we constrast the explanatory power of mean state of synoptic fields with that of their variance, and of frequency of individual (daily) states. The analyses utilize multiple regression and CCA performed on mean de-orthogonalized fields of q,t,u,v,z at various pressure levels, with daily states of synoptic variables classified using self-organizing maps (SOM). The results are interpreted from the process perspective in terms of their agreement with the current understanding of the role of process chains affecting rainfall over various regions of the contient, and in terms of their implications to statistical downscaling of climate projections and seasonal forecasts.

Keywords: rainfall variability, statistical climatology, Africa, self organizing maps

©2019. Japan Geoscience Union. All Right Reserved.

Effect of El Niño on the response ratio of Hadley circulation to different SST meridional structures

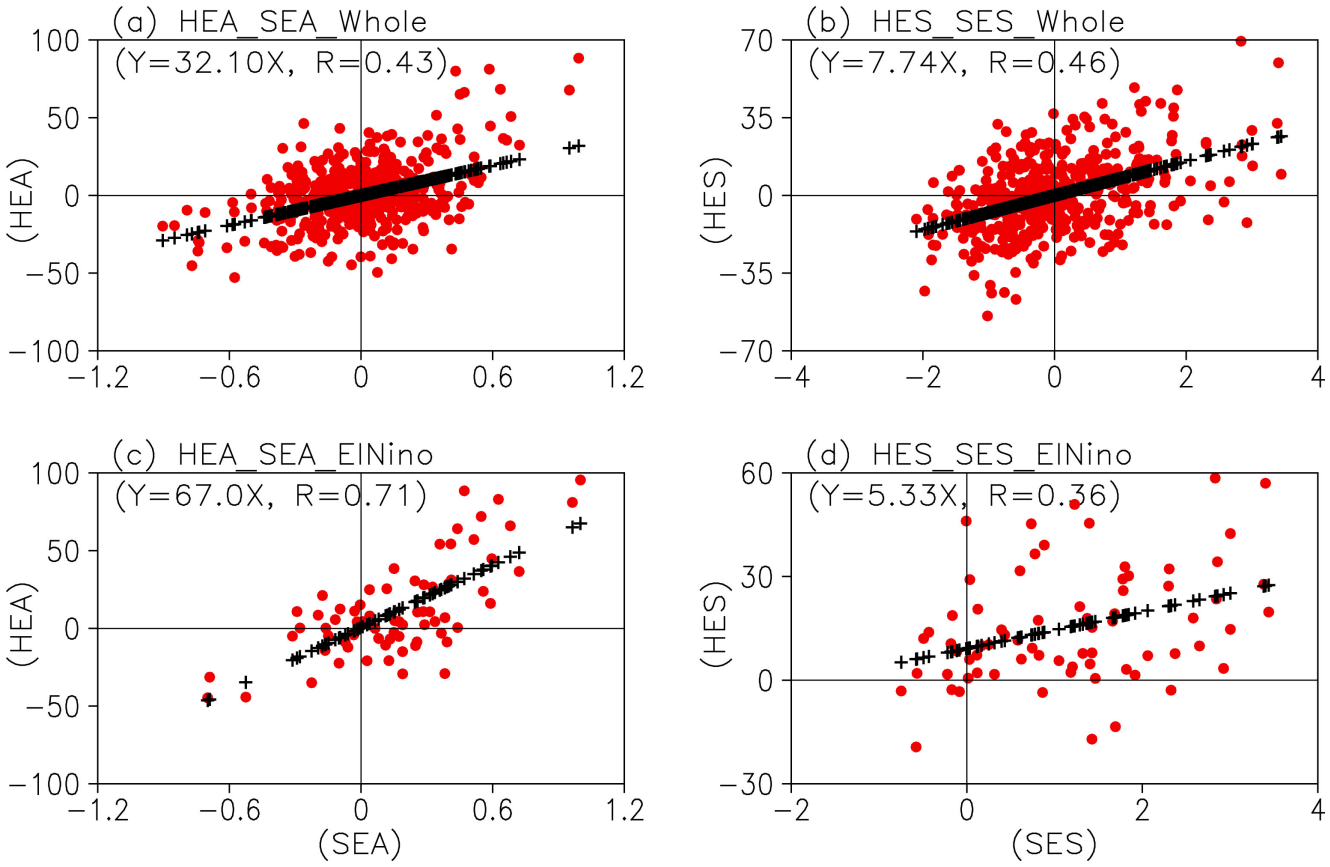
*Juan Feng[1]

1. Beijing Normal University

The role of El Niño in influencing the response ratio of the Hadley circulation (HC) to different tropical sea surface temperature (SST) meridional structures is investigated over the period 1979–2016. The explained variance of the equatorially asymmetric principal mode of HC variability is enhanced during El Niño events that are characterized by equatorially symmetric El Niño SST anomalies. The reason for the enhanced explained variance is examined. It is shown that the response ratio of the HC to different SST meridional structures is greatly enhanced in El Niño events; this is because the SST over the Indo-Pacific warm pool (IPWP) shows inhomogeneous warming in El Niño events, with greater values in the southern IPWP. The asymmetric warming over the IPWP is opposite to the climatological meridional structure of the SST over the IPWP, which intensifies the equatorially symmetric variation of SST, and contributes to the enhanced response ratio of the HC to SST. This point is further verified by the suppression of this enhanced response ratio in El Niño events of the HC to SST when the effects of SST over the IPWP are removed, implying the different warming amplitude within the IPWP during the El Niño events contributes to the enhanced response ratio. The response in La Niña events is also explored, indicating a difference between El Niño and La Niña events. These results may help explain the corresponding variations of the HC during the El Niño events, and highlight the different influences of the El Niño and La Niña events on the response of the HC to SST.

Keywords: Hadley circulation, sea surface temperature, Indo-Pacific warm pool, El Niño

©2019. Japan Geoscience Union. All Right Reserved.



©2019. Japan Geoscience Union. All Right Reserved.

Novel data-driven approach for ENSO prediction

*Dmitri Kondrashov[1], Evgeniy Loskutov[2], Andrei Gavrilov[2], Dmitry Mukhin[2], Alexander Feigin[2]

1. University of California, Los Angeles, United States, 2. Institute of Applied Physics of the Russian Academy of Sciences, Nizhny Novgorod, Russian Federation

We have developed novel data-driven technique for ENSO prediction that combines two existing approaches: linear dynamical mode (LDM) decomposition of spatially distributed data, and multilevel empirical model reduction (EMR) stochastic modeling approach. The nonlinear EMR model that utilizes dynamical variables obtained by empirical orthogonal function (EOF) decomposition of tropical Pacific SST’ s (Kondrashov et al. 2005), had already achieved a very competitive skill in International Research Institute for Climate and Society (IRI) ENSO real-time multi-model plume (Barnston et al. 2012). On the other hand, Gavrilov et al. (2018) have shown that LDM decomposition provides better modes for ENSO forecast than EOFs.

In the presented results we have used LDM modes as dynamical variables at the main level of multilevel linear EMR model. The model was trained on monthly 1960 -- 2014 sea surface temperatures (30S to 30N, 2x2 deg). The results of comparing skill of the retrospective predictions of the SST-based ENSO indices obtained by EMR model with LDM and EOF modes, will be discussed.

1. Kondrashov, D., Kravtsov, S., Robertson, A. W., & Ghil, M. (2005). A Hierarchy of Data-Based ENSO Models. Journal of Climate, 18(21), 4425–4444. doi:10.1175/JCLI3567.1

2. Gavrilov, A., Seleznev, A., Mukhin, D., Loskutov, E., Feigin, A., & Kurths, J. (2018). Linear dynamical modes as new variables for data-driven ENSO forecast. Climate Dynamics, 1–18. http://doi.org/10.1007/s00382-018-4255-7.

3. Barnston, A. G., M. K. Tippett, M. L. Heureux, S. Li, and D. G. DeWitt, 2012: Skill of real-time seasonal ENSO model predictions during 2002–2011 —is our capability improving? *Bulletin of the American Meteorological Society*, **93 (5)**, 631–651, doi:10.1175/BAMS-D-11-00111.1.

Keywords: ENSO, stochastic modeling, prediction

©2019. Japan Geoscience Union. All Right Reserved.

Experimental seasonal climate prediction using CFES: Comparison with the SINTEX-F systems

*Nobumasa Komori[1], Bunmei Taguchi[2], Akira Kuwano-Yoshida[3,1], Takeshi Doi[1], Masami Nonaka[1]

1. Japan Agency for Marine-Earth Science and Technology, 2. Research Center for Advanced Science and Technology, The University of Tokyo, 3. Disaster Prevention Research Institute, Kyoto University

An experimental seasonal climate prediction system has been developed based on the Coupled atmosphere-ocean general circulation model for the Earth Simulator (CFES). Following the well-established systems based on the SINTEX-F model, initial conditions for seasonal climate prediction are constructed by strongly nudging sea surface temperature (SST) to observed one.

At this stage, 12-member ensemble 6-month predictions from the 1st day of March, June, September, and December have been conducted from 1983 through 2018, after 32-years of coupled spin-up integration with SST-nudging to the observed climatology. The experimental system exhibits skill in predicting variability of seasonal-mean 2-m air temperature over the tropical Pacific, and contributes to the improvement of multi-model ensemble prediction with the SINTEX-F systems.

Keywords: experimental seasonal climate prediction, global coupled atmosphere-ocean GCM, atmosphere-ocean interaction, multi-model ensemble

©2019. Japan Geoscience Union. All Right Reserved.

Exploring the SST error growth during ENSO developing phase by using BCC_CSM1.1(m)

*Ben Tian[1], Hongli Ren[1]

1. National Climate Center, China Meteorological Administration

Here we assess the ENSO prediction errors as a function of lead time using the seasonal hindcast of the Beijing Climate Center System Model, BCC_CSM1.1(m). The ensemble mean forecasts seems to be more challenging during the developing years of ENSO, compared with those made towards the decay phase. The composites of SST prediction errors are significantly negative and cover a large area in central-eastern tropical Pacific, thus limiting the model in forecasting the onset and intensity of El Niño. The large-scale errors, at their early stage, are generated gradually by negative anomalies in the subsurface temperature of the central-western equatorial Pacific, a process similar to El Niño decay and then transition to La Nina growth phase. Our results support others' work of "sensitive areas" for ENSO predictions, and emphasize the essential accuracy of initial fields and their early evolution, providing information for further improving the forecasting skill of ENSO.

Keywords: El Nino prediction, error evolution, sea surface temperature

©2019. Japan Geoscience Union. All Right Reserved.

Role of sea-ice initialization in climate predictability over the Weddell Sea

*Yushi Morioka[1], Takeshi Doi[1], Doroteaciro Iovino[2], Simona Masina[2], Swadhin Behera[1]

1. Japan Agency for Marine-Earth Science and Technology (JAMSTEC), 2. Centro Euro-Mediterraneo sui Cambiamenti Climatici (CMCC)

Potential impact of sea-ice initialization on the interannual climate predictability over the Weddell Sea is investigated using a coupled general circulation model. Climate variability in the Weddell Sea is generally believed to have association with remote forcing such as El Niño-Southern Oscillation and the Southern Annual Mode. However, sea-ice variability in the Weddell Sea has been recently suggested to play additional roles in modulating local atmospheric variability through changes in surface air temperature and near-surface baroclinicity. When both the model’s sea-surface temperature (SST) and sea-ice concentration (SIC) are initialized with observations using nudging schemes, reforecast experiments from September 1st show improvements in predicting the observed SIC anomalies in the Weddell Sea up to four months ahead, compared to the other experiments with only SST initialization. During austral spring (Oct-Dec) of lower-than-normal sea-ice years in the Weddell Sea, reforecast experiments with the SST and SIC initializations reasonably predict high surface air temperature anomalies in the Weddell Sea and high sea-level pressure anomalies over the Atlantic sector of the Southern Ocean. These results suggest that accurate initialization of sea-ice conditions during austral winter is necessary for skillful prediction of climate variability over the Weddell Sea during austral spring.

Keywords: Air-sea-ice interaction, Climate predictability, Weddell Sea

©2019. Japan Geoscience Union. All Right Reserved.

Observed and hindcasted subdecadal variability of the tropical Pacific climate

*Takashi Mochizuki[1], Masahiro Watanabe[2]

1. Japan Agency for Marine-Earth Science and Technology, 2. Atmosphere-Ocean Research Institute, The University of Tokyo

The tropical Pacific is highly responsible for controlling the tendencies of global climate. Here, we have found a subdecadal (i.e., 3-year-running means) variation that has been distinctively observed in the 2000s over the tropical Pacific. The warm water that originated from the positive ocean-heat-content (OHC) anomaly over the western Pacific in 2000 slowly extended eastward and stayed at the central equatorial Pacific between 2002-2005, rather than reaching the eastern edge. At the same time, an accompanying anti-cyclonic surface wind anomaly was observed in the off-equatorial North Pacific. This dynamical response of the upper ocean may have contributed to the subsequent warming in the western Pacific. In the preceding decades, in contrast, the observed OHC has usually represented a periodic fluctuation in the tropical Pacific, characterized by anomalous heat input/output in the meridional direction and slow eastward adjustment in the equatorial ocean thermocline. This subdecadal variation in the 2000s is quite distinct from our decadal hindcasts with initialization in Coupled Model Intercomparison Project Phase 5. The model predominantly simulates periodic-type fluctuations in any decade, and the resultant low predictability of the subdecadal variation in the 2000s can work to modulate the predictive skills at a lead time of several years.

Keywords: subdecadal variability, climate prediction, predictability, tropical Pacific

©2019. Japan Geoscience Union. All Right Reserved.

[E] Poster | A (Atmospheric and Hydrospheric Sciences)：A-OS Ocean Sciences & Ocean Environment

Thu. May 30, 2019 3:30 PM - 5:00 PM JST | Thu. May 30, 2019 6:30 AM - 8:00 AM UTC | Poster Hall International Exhibition Hall8, Makuhari Messe_4

[A-OS10] Atlantic climate variability, and its global impacts and predictability

convener:Ingo Richter(JAMSTEC Japan Agency for Marine-Earth Science and Technology), Hiroki Tokinaga(Research Institute for Applied Mechanics, Kyushu University), Noel S Keenlyside(Geophysical Institute Bergen), Carlos R Mechoso(University of California Los Angeles)

The Atlantic Ocean is subject to pronounced climate variations that occur on a wide range of time scales, including interannual variability in the equatorial and subtropical regions, and Atlantic multi-decadal variability (AMV), which has been linked with the Atlantic meridional overturning circulation (AMOC). These are connected to other climate variations across the globe. The AMV, e.g., has long been known to have global impacts, such as changes in the Indian, Asian and South American summer monsoons, and changes in the Pacific associated with the "global hiatus". Interannual variability in the equatorial and subtropical Atlantic has also been shown to influence global climate, including over Asia, while the freshening of the North Atlantic by melting of the Greenland ice cap is expected to influence all ocean basins via atmospheric bridges. Likewise, misrepresentation of the Atlantic can have global ramifications in climate models. Misrepresentation of the AMOC, e.g., has been associated with model biases in the entire Northern Hemisphere.

This session seeks observational, modeling, and theoretical studies on the mechanisms that determine the Atlantic mean climate and variability, as well as the predictability and global impacts of such variability. We also seek studies that evaluate climate model performance in the region. Topics include atmosphere-ocean-cloud interactions in the tropical Atlantic and their remote impacts; relationships between tropical and mid/high latitude variability; air-sea interaction along the Gulf Stream and its influence on cyclones and storm track evolution; variability in the Benguela upwelling region; influence of Agulhas leakage on the South Atlantic; coupled climate models biases in the region and their impacts; AMOC and long-term climate change.

[AOS10-P01] The strengthening of Amazonian precipitation during the wet season driven by tropical sea surface temperature forcing

*Xinyue Wang[1], Xichen Li[1], Jiang Zhu[1], Clemente A S Tanajura[2] (1.Institute of Atmospheric Physics, Chinese Academy of Sciences, 2.Institute of Physics, Federal University of Bahia, Salvador, Brazil)

[AOS10-P02] Linear inverse modeling of the tropical Atlantic

*Ingo Richter[1], Ping Chang[2] (1.JAMSTEC Japan Agency for Marine-Earth Science and Technology, 2.Texas A&M University)

[AOS10-P03] Relationships Among Inter-model Spread and Biases in Tropical Atlantic Sea Surface Temperatures

Elsa - Mohino Harris[1], *Belen Rodriguez-Fonseca[1,2], Teresa - Losada[1], Irene - Polo[1], Roberto - Mechoso[3] (1.Department of Physics of the Earth and Astrophysics, Universidad Complutense de Madrid, 28040, Madrid, Spain. , 2.Institute of Geosciences IGEO,UCM-CSIC, 28040, Madrid, Spain., 3.Department of Atmospheric and Oceanic Sciences, UCLA, Los Angeles, USA)

[AOS10-P04] Revisiting the CMIP5 Thermocline in the Equatorial Pacific and Atlantic Oceans

Antonio - Castaño[1,2], Elsa - Mohino[1], *Belen Rodriguez-Fonseca[1,2], Teresa - Losada[1] (1.Department of Physics of the Earth and Astrophysics, Universidad Complutense de Madrid, 28040, Madrid, Spain., 2.Institute of Geosciences, IGEO, UCM-CSIC 28040, Madrid, Spain.)

[AOS10-P05] Lagged Effects of North Atlantic SST Anomalies on Weather in Remote Areas

*Natalia Gnatiuk[1], Timo Vihma[2], Leonid Bobylev[1] (1.Nansen International Environmental and Remote Sensing Centre, 2.Finnish Meteorological Institute)

[AOS10-P06] SST anomalies in the northern tropical Atlantic as a negative feedback to ENSO development

*Ingo Richter[1], Hiroki Tokinaga[2], Yu Kosaka[3], Takeshi Doi[1] (1.JAMSTEC Japan Agency for Marine-Earth Science and Technology, 2.Kyoto University, 3.University of Tokyo)

The strengthening of Amazonian precipitation during the wet season driven by tropical sea surface temperature forcing

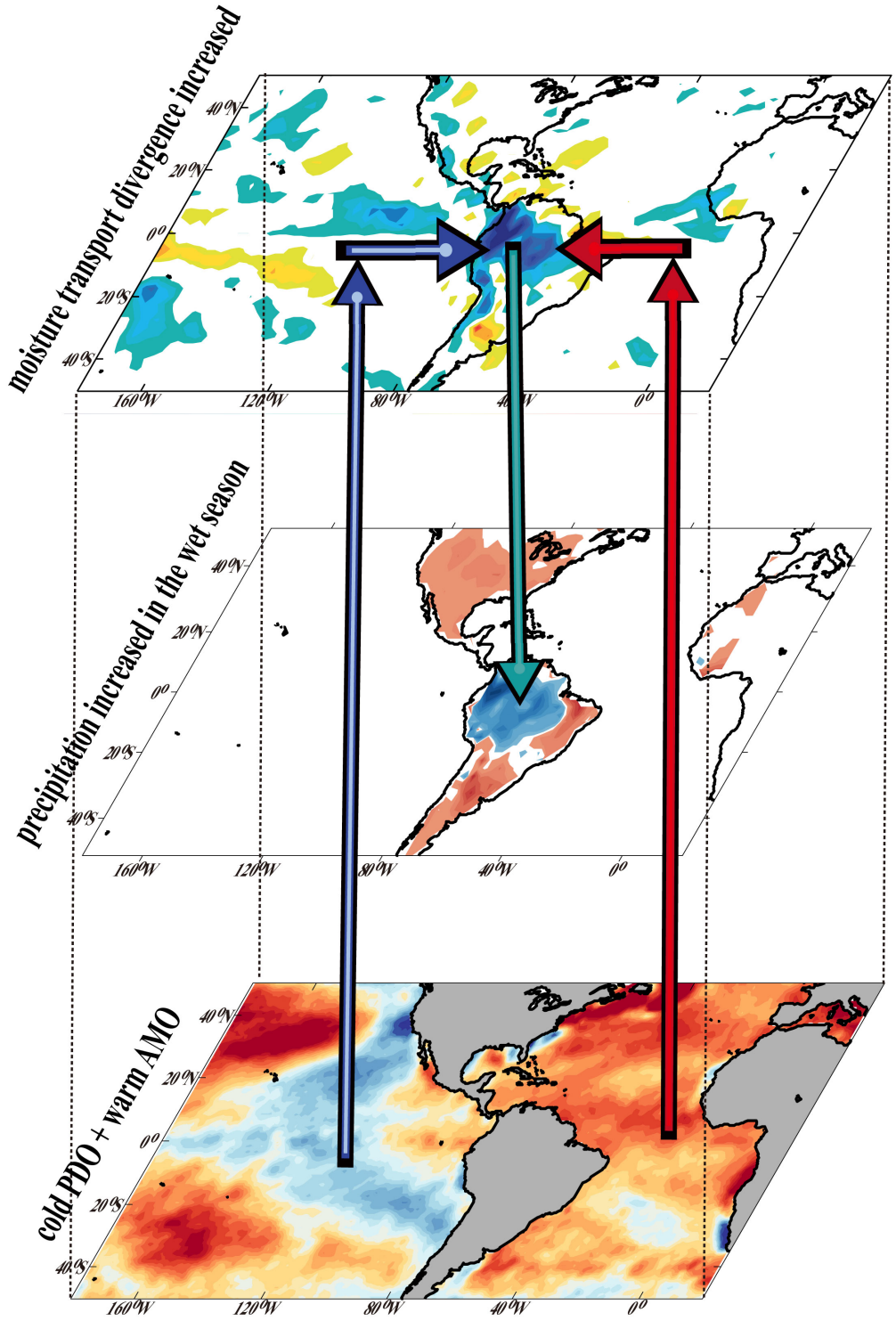
*Xinyue Wang[1], Xichen Li[1], Jiang Zhu[1], Clemente A S Tanajura[2]

1. Institute of Atmospheric Physics, Chinese Academy of Sciences, 2. Institute of Physics, Federal University of Bahia, Salvador, Brazil

Amazonian rainfall plays a critical role in the global climate system and the hydrological cycle. It is thus important to quantify changes in the Amazonian rainfall and clarify its mechanism. Previous studies indicate that the interannual variability of Amazonian precipitation could be largely attributed to variabilities in the South American monsoon system and the El Niño Southern Oscillation. However, the trend of the wet season tropical Amazonian precipitation during recent decades is not very well investigated. In this study, by combining both satellite and in situ observations, it is revealed that tropical Amazonian precipitation has significantly increased by~180 to 600 mm (in different datasets) in the wet season during the satellite era from 1979 to 2015. We then use a state-of-the-art atmospheric model to simulate the impact of the tropical sea surface temperatures (SSTs) on the precipitation changes. Results show that the multidecadal warming of the tropical Atlantic has contributed more than half of this precipitation change over the past three decades, while the east Pacific cooling plays a secondary role. We finally combine the simulation results and the reanalysis data to investigate the mechanisms of this process, i.e. the SST variability dramatically increases the convergence of the moisture transport over the Amazon region. The precipitation changes over the Amazon region largely impact on the local hydrological cycle and the ecosystem, and have important impacts on the global climate system by mediating the teleconnection between the Pacific and the Atlantic oceans. Our results show that the long-term change in the wet season Amazonian precipitation is important and deserves further investigation and discussion.

Keywords: convective precipitation, Amazon, tropical Atlantic, moisture convergence

©2019. Japan Geoscience Union. All Right Reserved.



©2019. Japan Geoscience Union. All Right Reserved.

Linear inverse modeling of the tropical Atlantic

*Ingo Richter[1], Ping Chang[2]

1. JAMSTEC Japan Agency for Marine-Earth Science and Technology, 2. Texas A&M University

The tropical Atlantic features variability at interannual and decadal time scales that is known to have a strong influence on the surrounding continents and possibly other ocean basins. Current prediction systems, however, struggle to skillfully predict sea-surface temperature (SST), let alone its impact on rainfall over the adjacent continents. It is often assumed that this poor prediction skill is due to the severe SST biases and misrepresented variability patterns that most models feature in the region but this has recently been called into question.

In the present study, we construct a simple statistical model of the tropical Atlantic to 1) investigate the influence of model biases on prediction skill, and 2) establish a benchmark to evaluate dynamical model against. Using 35 fully coupled ocean-atmosphere GCMs from the pre-industrial control experiment (piControl) of the Coupled Model Intercomparison Project Phase 5 (CMIP5) we construct a linear inverse model (LIM) for each GCM based on tropical SSTs only. The LIM thus constructed is then used to predict SSTs for the period 2000-2017 from the NCEP/NCAR reanalysis. These predictions are compared to those from a LIM constructed using the NCEP/NCAR reference for the period 1948-1999 as training data. Since each of the model LIMs is constructed from more or less unrealistic variability patterns one would expect to see a clear impact on prediction skill.

The results, however, indicate that prediction skill in the tropical Atlantic is relatively insensitive to the tropical variability patterns of each model. Only some cases see a marked deterioration of prediction skill relative to the reference model. The LIM performs well in the subtropical north and south Atlantic. In the equatorial Atlantic, on the other hand, skill is rather poor at 3 months lead time, though clearly above persistence. Our analysis suggests that in many CMIP5 models misrepresentation of variability should not be a major stumbling block toward skillful prediction. This indicates that the current lack of prediction skill in the region is due to other factors, such as model initialization or inherent predictability limits due to noise.
Comparing several dynamical hindcast experiments with the LIM constructed from observations, we find that the LIM generally has superior prediction skill over most parts of the tropical Atlantic.

Keywords: linear inverse modeling, tropical Atlantic, seasonal prediction

©2019. Japan Geoscience Union. All Right Reserved.

Relationships Among Inter-model Spread and Biases in Tropical Atlantic Sea Surface Temperatures

Elsa - Mohino Harris[1], *Belen Rodriguez-Fonseca[1,2], Teresa - Losada[1], Irene - Polo[1], Roberto - Mechoso[3]

1. Department of Physics of the Earth and Astrophysics, Universidad Complutense de Madrid, 28040, Madrid, Spain. , 2. Institute of Geosciences IGEO,UCM-CSIC, 28040, Madrid, Spain., 3. Department of Atmospheric and Oceanic Sciences, UCLA, Los Angeles, USA

State-of-the-art general circulation models show important systematic errors in their simulation of sea surface temperatures (SST), especially in the Tropical Atlantic. In this work the spread in the simulation of climatological SST in the Tropical Atlantic by 24 CMIP5 models is examined, and its relationship with the mean systematic biases in the region is explored. The modes of inter-model variability are estimated by applying Principal Component (PC) analysis to the SSTs in the region 70ºW-20ºE, 20ºS-20ºN. The inter-model variability is approximately explained by the first three modes. The first mode is related to warmer SSTs in the basin, shows worldwide connections with same-signed loads over most of the tropics and is connected with lower low cloud cover over the eastern parts of the subtropical oceans. The second mode is restricted to the Atlantic, where it shows negative and positive loads to the north and south of the equator, respectively, and is connected to a too weak Atlantic Meridional Overturning Circulation (AMOC). The third mode is related to the double Intertropical Convergence Zone bias in the Pacific and to an interhemispheric asymmetry in the net radiation at the top of the atmosphere. According to the results, the most important of these contributors for SST biases spread in the Tropical Atlantic is the second mode, with models having stronger biases simulating weaker AMOCs.

Keywords: GCM bias, CMIP5, tropical Atlantic, intermodel spread

©2019. Japan Geoscience Union. All Right Reserved.

Revisiting the CMIP5 Thermocline in the Equatorial Pacific and Atlantic Oceans

Antonio - Castaño[1,2], Elsa - Mohino[1], *Belen Rodriguez-Fonseca[1,2], Teresa - Losada[1]

1. Department of Physics of the Earth and Astrophysics, Universidad Complutense de Madrid, 28040, Madrid, Spain., 2. Institute of Geosciences, IGEO, UCM-CSIC 28040, Madrid, Spain.

The thermocline is defined as the ocean layer for which the vertical thermal gradient is maximum. In the equatorial ocean, observations led to the use of the 20˚C isotherm depth (z20) as an estimate of the thermocline. This work compares z20 against the physical thermocline in the Equatorial Atlantic and Pacific Oceans, using SODA reanalysis and CMIP5 Pre-Industrial Control simulations. Our results show that in models z20 is systematically deeper and flatter than the thermocline and does not respond correctly to surface wind stress variations. It is also shown that the annual cycle of z20 is much weaker than that of the physical thermocline. This happens in both equatorial basins and indicates that z20 does not react to the same mechanisms as the thermocline. Possible consequences in the assessment of air-sea coupling in current GCMs and bias reduction strategies are also suggested, as well as possible effects in the representation of upwelling systems in the tropical region.

Keywords: CMIP5, defining thermocline, tropical atlantic, air-sea interactions

©2019. Japan Geoscience Union. All Right Reserved.

Lagged Effects of North Atlantic SST Anomalies on Weather in Remote Areas

*Natalia Gnatiuk[1], Timo Vihma[2], Leonid Bobylev[1]

1. Nansen International Environmental and Remote Sensing Centre, 2. Finnish Meteorological Institute

Polar climate has experienced dramatic changes during observed global warming. These changes in turn have, as hypothesised, strong influences on the mid-latitude weather. Many proposed linkages focus on the effects of changes in sea ice, sea surface temperature or terrestrial snow pack on the air temperature in selected mid-latitude areas. Our hypothesis is that from the point of view of the atmosphere, it does not matter whether the thermal forcing from the surface originates from sea ice melt, terrestrial snow melt, or changes in SST. Most important is to quantify how the atmosphere responds to anomalies in surface temperature, and how the local/regional responses may affect weather patterns in remote areas. By analysing these responses systematically in global scale, we can identify the regions and seasons where/when the response is strongest. Comparing these regions/seasons to observed changes in sea ice, terrestrial snow, and open ocean SST, we will obtain information on the relative importance of forcing from these three factors. For this purpose, we studied the relationships between anomalies in the surface temperature (Ts) in the Northern Hemisphere (on grid 1.5°-1.5°) and 2-m air temperature (T2m) in selected 13 study regions in Europe, Greenland, and parts of Asia and North Africa for the period 1979-2018 based on the ERA-Interim reanalysis. Applying also detrended data, we eliminated spurious correlations resulting from similar trends in the two variables.

We detected significant correlations between the surface temperature over the Labrador Sea, Canadian archipelago and North Atlantic and 2-m air temperature in different study regions for inter-seasonal spring - summer (MAM-JJA) and autumn - winter (SON-DJF) relationships. Among the strongest correlations between the spring Ts and summer T2m were the positive correlations found between Ts in the North Atlantic and T2m in Scandinavia, Ts in the Labrador Sea and T2m in Northeast Europe, and Ts in Norther Sahara and T2m in Urals. As well, among the strongest correlations between the autumn Ts and winter T2m were the positive correlations found between Ts in the North Atlantic and the Labrador Sea and T2m in Scandinavia and Northwest Africa; and the negative correlations found between Ts in the Labrador Sea and the North Atlantic and T2m in Scandinavia, Northeast Europe, Urals, Black Sea region and Northcentral Asia.

In order to identify thermal forcing factors and to assess their relative importance, we analysed the multiyear averages and anomalies of sea-ice concentration, snow cover and surface heat fluxes. According to the results, in all identified cases, changes in SST mostly were an influencing factor.

Another big challenge was to understand the physical mechanisms responsible for the obtained statistical results. For this purpose, we analysed surface pressure, geopotential heights, wind components, air-mass trajectories, incoming solar radiation, cloud cover, and total precipitation for sub-sets of 10 coldest and 10 warmest seasons in the period 1979-2018. There is a detectable effect on anomalies in the atmospheric pressure field and wind components in these regions.

The research is granted by the “ERA.Net RUS Plus” Initiative, ID 166 and national RFBR project No. 18-55-76004; and partly by RSF grant №. 17-17-01151.

©2019. Japan Geoscience Union. All Right Reserved.

Keywords: Sea surface temperature anomalies, Teleconnections, Mid-latitude weather, North Atlantic

©2019. Japan Geoscience Union. All Right Reserved.

SST anomalies in the northern tropical Atlantic as a negative feedback to ENSO development

*Ingo Richter[1], Hiroki Tokinaga[2], Yu Kosaka[3], Takeshi Doi[1]

1. JAMSTEC Japan Agency for Marine-Earth Science and Technology, 2. Kyoto University, 3. University of Tokyo

It has been known for some time that SST anomalies in the equatorial Pacific induce same-signed anomalies in the northern tropical Atlantic (NTA) through changes in the Atlantic trade winds. More recently, it has been suggested that the NTA, in turn, can influence the equatorial Pacific through changes in the surface zonal winds over the western part of the basin. The sign of these wind anomalies, however, would act to force equatorial Pacific SST anomalies that are opposite to those in the NTA. The present study takes a closer look at this apparent conundrum by conducting GCM experiments with prescribed SSTs for the period 1982-2014. In the control experiment, observed SSTs are prescribed globally, while in two sensitivity experiments SST anomalies are removed from either the tropical Atlantic or the tropical Pacific. For the control experiment, analysis suggests that NTA warming is accompanied by SST warming and westerly wind anomalies in the equatorial Pacific. When tropical Pacific SST anomalies are removed, on the other hand, NTA warming coincides with easterly anomalies. Moreover, when SST anomalies are removed from the tropical Atlantic, wind variability over the western equatorial Pacific is enhanced. These results suggest that SST anomalies in the NTA, which are strongly influenced by the tropical Pacific, act as a negative feedback to ENSO development. This interbasin link may be further complicated by other influences on the NTA, such as local air-sea coupling and the North Atlantic Oscillation.

Keywords: tropical Atlantic, ENSO, teleconnections

©2019. Japan Geoscience Union. All Right Reserved.

[E] Poster | A (Atmospheric and Hydrospheric Sciences)：A-OS Ocean Sciences & Ocean Environment

Thu. May 30, 2019 5:15 PM - 6:30 PM JST | Thu. May 30, 2019 8:15 AM - 9:30 AM UTC | Poster Hall International Exhibition Hall8, Makuhari Messe_8

[A-OS10] Atlantic climate variability, and its global impacts and predictability

convener:Ingo Richter(JAMSTEC Japan Agency for Marine-Earth Science and Technology), Hiroki Tokinaga(Research Institute for Applied Mechanics, Kyushu University), Noel S Keenlyside(Geophysical Institute Bergen), Carlos R Mechoso(University of California Los Angeles)

The Atlantic Ocean is subject to pronounced climate variations that occur on a wide range of time scales, including interannual variability in the equatorial and subtropical regions, and Atlantic multi-decadal variability (AMV), which has been linked with the Atlantic meridional overturning circulation (AMOC). These are connected to other climate variations across the globe. The AMV, e.g., has long been known to have global impacts, such as changes in the Indian, Asian and South American summer monsoons, and changes in the Pacific associated with the "global hiatus". Interannual variability in the equatorial and subtropical Atlantic has also been shown to influence global climate, including over Asia, while the freshening of the North Atlantic by melting of the Greenland ice cap is expected to influence all ocean basins via atmospheric bridges. Likewise, misrepresentation of the Atlantic can have global ramifications in climate models. Misrepresentation of the AMOC, e.g., has been associated with model biases in the entire Northern Hemisphere.

This session seeks observational, modeling, and theoretical studies on the mechanisms that determine the Atlantic mean climate and variability, as well as the predictability and global impacts of such variability. We also seek studies that evaluate climate model performance in the region. Topics include atmosphere-ocean-cloud interactions in the tropical Atlantic and their remote impacts; relationships between tropical and mid/high latitude variability; air-sea interaction along the Gulf Stream and its influence on cyclones and storm track evolution; variability in the Benguela upwelling region; influence of Agulhas leakage on the South Atlantic; coupled climate models biases in the region and their impacts; AMOC and long-term climate change.

[AOS10-P01] The strengthening of Amazonian precipitation during the wet season driven by tropical sea surface temperature forcing

*Xinyue Wang[1], Xichen Li[1], Jiang Zhu[1], Clemente A S Tanajura[2] (1.Institute of Atmospheric Physics, Chinese Academy of Sciences, 2.Institute of Physics, Federal University of Bahia, Salvador, Brazil)

[AOS10-P02] **Linear inverse modeling of the tropical Atlantic**

*Ingo Richter[1], Ping Chang[2] (1.JAMSTEC Japan Agency for Marine-Earth Science and Technology, 2.Texas A&M University)

[AOS10-P03] Relationships Among Inter-model Spread and Biases in Tropical Atlantic Sea Surface Temperatures

Elsa - Mohino Harris[1], *Belen Rodriguez-Fonseca[1,2], Teresa - Losada[1], Irene - Polo[1], Roberto - Mechoso[3] (1.Department of Physics of the Earth and Astrophysics, Universidad Complutense de Madrid, 28040, Madrid, Spain. , 2.Institute of Geosciences IGEO,UCM-CSIC, 28040, Madrid, Spain., 3.Department of Atmospheric and Oceanic Sciences, UCLA, Los Angeles, USA)

[AOS10-P04] **Revisiting the CMIP5 Thermocline in the Equatorial Pacific and Atlantic Oceans**

Antonio - Castaño[1,2], Elsa - Mohino[1], *Belen Rodriguez-Fonseca[1,2], Teresa - Losada[1] (1.Department of Physics of the Earth and Astrophysics, Universidad Complutense de Madrid, 28040, Madrid, Spain., 2.Institute of Geosciences, IGEO, UCM-CSIC 28040, Madrid, Spain.)

[AOS10-P05] Lagged Effects of North Atlantic SST Anomalies on Weather in Remote Areas

*Natalia Gnatiuk[1], Timo Vihma[2], Leonid Bobylev[1] (1.Nansen International Environmental and Remote Sensing Centre, 2.Finnish Meteorological Institute)

[AOS10-P06] SST anomalies in the northern tropical Atlantic as a negative feedback to ENSO development

*Ingo Richter[1], Hiroki Tokinaga[2], Yu Kosaka[3], Takeshi Doi[1] (1.JAMSTEC Japan Agency for Marine-Earth Science and Technology, 2.Kyoto University, 3.University of Tokyo)

The strengthening of Amazonian precipitation during the wet season driven by tropical sea surface temperature forcing

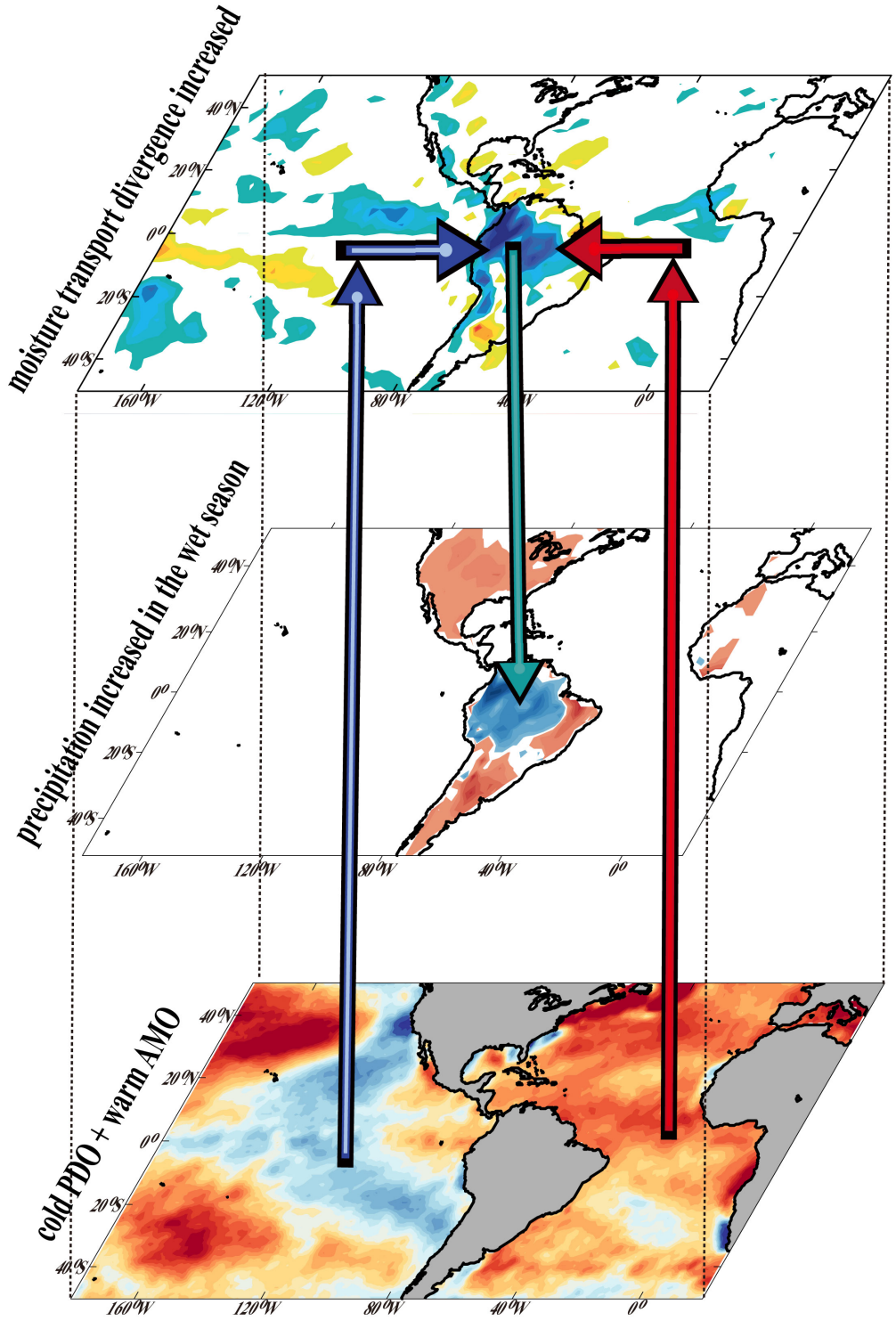
*Xinyue Wang[1], Xichen Li[1], Jiang Zhu[1], Clemente A S Tanajura[2]

1. Institute of Atmospheric Physics, Chinese Academy of Sciences, 2. Institute of Physics, Federal University of Bahia, Salvador, Brazil

Amazonian rainfall plays a critical role in the global climate system and the hydrological cycle. It is thus important to quantify changes in the Amazonian rainfall and clarify its mechanism. Previous studies indicate that the interannual variability of Amazonian precipitation could be largely attributed to variabilities in the South American monsoon system and the El Niño Southern Oscillation. However, the trend of the wet season tropical Amazonian precipitation during recent decades is not very well investigated. In this study, by combining both satellite and in situ observations, it is revealed that tropical Amazonian precipitation has significantly increased by~180 to 600 mm (in different datasets) in the wet season during the satellite era from 1979 to 2015. We then use a state-of-the-art atmospheric model to simulate the impact of the tropical sea surface temperatures (SSTs) on the precipitation changes. Results show that the multidecadal warming of the tropical Atlantic has contributed more than half of this precipitation change over the past three decades, while the east Pacific cooling plays a secondary role. We finally combine the simulation results and the reanalysis data to investigate the mechanisms of this process, i.e. the SST variability dramatically increases the convergence of the moisture transport over the Amazon region. The precipitation changes over the Amazon region largely impact on the local hydrological cycle and the ecosystem, and have important impacts on the global climate system by mediating the teleconnection between the Pacific and the Atlantic oceans. Our results show that the long-term change in the wet season Amazonian precipitation is important and deserves further investigation and discussion.

Keywords: convective precipitation, Amazon, tropical Atlantic, moisture convergence

©2019. Japan Geoscience Union. All Right Reserved.



©2019. Japan Geoscience Union. All Right Reserved.

Linear inverse modeling of the tropical Atlantic

*Ingo Richter[1], Ping Chang[2]

1. JAMSTEC Japan Agency for Marine-Earth Science and Technology, 2. Texas A&M University

The tropical Atlantic features variability at interannual and decadal time scales that is known to have a strong influence on the surrounding continents and possibly other ocean basins. Current prediction systems, however, struggle to skillfully predict sea-surface temperature (SST), let alone its impact on rainfall over the adjacent continents. It is often assumed that this poor prediction skill is due to the severe SST biases and misrepresented variability patterns that most models feature in the region but this has recently been called into question.

In the present study, we construct a simple statistical model of the tropical Atlantic to 1) investigate the influence of model biases on prediction skill, and 2) establish a benchmark to evaluate dynamical model against. Using 35 fully coupled ocean-atmosphere GCMs from the pre-industrial control experiment (piControl) of the Coupled Model Intercomparison Project Phase 5 (CMIP5) we construct a linear inverse model (LIM) for each GCM based on tropical SSTs only. The LIM thus constructed is then used to predict SSTs for the period 2000-2017 from the NCEP/NCAR reanalysis. These predictions are compared to those from a LIM constructed using the NCEP/NCAR reference for the period 1948-1999 as training data. Since each of the model LIMs is constructed from more or less unrealistic variability patterns one would expect to see a clear impact on prediction skill.

The results, however, indicate that prediction skill in the tropical Atlantic is relatively insensitive to the tropical variability patterns of each model. Only some cases see a marked deterioration of prediction skill relative to the reference model. The LIM performs well in the subtropical north and south Atlantic. In the equatorial Atlantic, on the other hand, skill is rather poor at 3 months lead time, though clearly above persistence. Our analysis suggests that in many CMIP5 models misrepresentation of variability should not be a major stumbling block toward skillful prediction. This indicates that the current lack of prediction skill in the region is due to other factors, such as model initialization or inherent predictability limits due to noise.
Comparing several dynamical hindcast experiments with the LIM constructed from observations, we find that the LIM generally has superior prediction skill over most parts of the tropical Atlantic.

Keywords: linear inverse modeling, tropical Atlantic, seasonal prediction

©2019. Japan Geoscience Union. All Right Reserved.

Relationships Among Inter-model Spread and Biases in Tropical Atlantic Sea Surface Temperatures

Elsa - Mohino Harris[1], *Belen Rodriguez-Fonseca[1,2], Teresa - Losada[1], Irene - Polo[1], Roberto - Mechoso[3]

1. Department of Physics of the Earth and Astrophysics, Universidad Complutense de Madrid, 28040, Madrid, Spain. , 2. Institute of Geosciences IGEO,UCM-CSIC, 28040, Madrid, Spain., 3. Department of Atmospheric and Oceanic Sciences, UCLA, Los Angeles, USA

State-of-the-art general circulation models show important systematic errors in their simulation of sea surface temperatures (SST), especially in the Tropical Atlantic. In this work the spread in the simulation of climatological SST in the Tropical Atlantic by 24 CMIP5 models is examined, and its relationship with the mean systematic biases in the region is explored. The modes of inter-model variability are estimated by applying Principal Component (PC) analysis to the SSTs in the region 70ºW-20ºE, 20ºS-20ºN. The inter-model variability is approximately explained by the first three modes. The first mode is related to warmer SSTs in the basin, shows worldwide connections with same-signed loads over most of the tropics and is connected with lower low cloud cover over the eastern parts of the subtropical oceans. The second mode is restricted to the Atlantic, where it shows negative and positive loads to the north and south of the equator, respectively, and is connected to a too weak Atlantic Meridional Overturning Circulation (AMOC). The third mode is related to the double Intertropical Convergence Zone bias in the Pacific and to an interhemispheric asymmetry in the net radiation at the top of the atmosphere. According to the results, the most important of these contributors for SST biases spread in the Tropical Atlantic is the second mode, with models having stronger biases simulating weaker AMOCs.

Keywords: GCM bias, CMIP5, tropical Atlantic, intermodel spread

©2019. Japan Geoscience Union. All Right Reserved.

Revisiting the CMIP5 Thermocline in the Equatorial Pacific and Atlantic Oceans

Antonio - Castaño[1,2], Elsa - Mohino[1], *Belen Rodriguez-Fonseca[1,2], Teresa - Losada[1]

1. Department of Physics of the Earth and Astrophysics, Universidad Complutense de Madrid, 28040, Madrid, Spain., 2. Institute of Geosciences, IGEO, UCM-CSIC 28040, Madrid, Spain.

The thermocline is defined as the ocean layer for which the vertical thermal gradient is maximum. In the equatorial ocean, observations led to the use of the 20˚C isotherm depth (z20) as an estimate of the thermocline. This work compares z20 against the physical thermocline in the Equatorial Atlantic and Pacific Oceans, using SODA reanalysis and CMIP5 Pre-Industrial Control simulations. Our results show that in models z20 is systematically deeper and flatter than the thermocline and does not respond correctly to surface wind stress variations. It is also shown that the annual cycle of z20 is much weaker than that of the physical thermocline. This happens in both equatorial basins and indicates that z20 does not react to the same mechanisms as the thermocline. Possible consequences in the assessment of air-sea coupling in current GCMs and bias reduction strategies are also suggested, as well as possible effects in the representation of upwelling systems in the tropical region.

Keywords: CMIP5, defining thermocline, tropical atlantic, air-sea interactions

©2019. Japan Geoscience Union. All Right Reserved.

Lagged Effects of North Atlantic SST Anomalies on Weather in Remote Areas

*Natalia Gnatiuk[1], Timo Vihma[2], Leonid Bobylev[1]

1. Nansen International Environmental and Remote Sensing Centre, 2. Finnish Meteorological Institute

Polar climate has experienced dramatic changes during observed global warming. These changes in turn have, as hypothesised, strong influences on the mid-latitude weather. Many proposed linkages focus on the effects of changes in sea ice, sea surface temperature or terrestrial snow pack on the air temperature in selected mid-latitude areas. Our hypothesis is that from the point of view of the atmosphere, it does not matter whether the thermal forcing from the surface originates from sea ice melt, terrestrial snow melt, or changes in SST. Most important is to quantify how the atmosphere responds to anomalies in surface temperature, and how the local/regional responses may affect weather patterns in remote areas. By analysing these responses systematically in global scale, we can identify the regions and seasons where/when the response is strongest. Comparing these regions/seasons to observed changes in sea ice, terrestrial snow, and open ocean SST, we will obtain information on the relative importance of forcing from these three factors. For this purpose, we studied the relationships between anomalies in the surface temperature (Ts) in the Northern Hemisphere (on grid 1.5°-1.5°) and 2-m air temperature (T2m) in selected 13 study regions in Europe, Greenland, and parts of Asia and North Africa for the period 1979-2018 based on the ERA-Interim reanalysis. Applying also detrended data, we eliminated spurious correlations resulting from similar trends in the two variables.

We detected significant correlations between the surface temperature over the Labrador Sea, Canadian archipelago and North Atlantic and 2-m air temperature in different study regions for inter-seasonal spring - summer (MAM-JJA) and autumn - winter (SON-DJF) relationships. Among the strongest correlations between the spring Ts and summer T2m were the positive correlations found between Ts in the North Atlantic and T2m in Scandinavia, Ts in the Labrador Sea and T2m in Northeast Europe, and Ts in Norther Sahara and T2m in Urals. As well, among the strongest correlations between the autumn Ts and winter T2m were the positive correlations found between Ts in the North Atlantic and the Labrador Sea and T2m in Scandinavia and Northwest Africa; and the negative correlations found between Ts in the Labrador Sea and the North Atlantic and T2m in Scandinavia, Northeast Europe, Urals, Black Sea region and Northcentral Asia.

In order to identify thermal forcing factors and to assess their relative importance, we analysed the multiyear averages and anomalies of sea-ice concentration, snow cover and surface heat fluxes. According to the results, in all identified cases, changes in SST mostly were an influencing factor.

Another big challenge was to understand the physical mechanisms responsible for the obtained statistical results. For this purpose, we analysed surface pressure, geopotential heights, wind components, air-mass trajectories, incoming solar radiation, cloud cover, and total precipitation for sub-sets of 10 coldest and 10 warmest seasons in the period 1979-2018. There is a detectable effect on anomalies in the atmospheric pressure field and wind components in these regions.

The research is granted by the “ERA.Net RUS Plus” Initiative, ID 166 and national RFBR project No. 18-55-76004; and partly by RSF grant №. 17-17-01151.

©2019. Japan Geoscience Union. All Right Reserved.

Keywords: Sea surface temperature anomalies, Teleconnections, Mid-latitude weather, North Atlantic

©2019. Japan Geoscience Union. All Right Reserved.

SST anomalies in the northern tropical Atlantic as a negative feedback to ENSO development

*Ingo Richter[1], Hiroki Tokinaga[2], Yu Kosaka[3], Takeshi Doi[1]

1. JAMSTEC Japan Agency for Marine-Earth Science and Technology, 2. Kyoto University, 3. University of Tokyo

It has been known for some time that SST anomalies in the equatorial Pacific induce same-signed anomalies in the northern tropical Atlantic (NTA) through changes in the Atlantic trade winds. More recently, it has been suggested that the NTA, in turn, can influence the equatorial Pacific through changes in the surface zonal winds over the western part of the basin. The sign of these wind anomalies, however, would act to force equatorial Pacific SST anomalies that are opposite to those in the NTA. The present study takes a closer look at this apparent conundrum by conducting GCM experiments with prescribed SSTs for the period 1982-2014. In the control experiment, observed SSTs are prescribed globally, while in two sensitivity experiments SST anomalies are removed from either the tropical Atlantic or the tropical Pacific. For the control experiment, analysis suggests that NTA warming is accompanied by SST warming and westerly wind anomalies in the equatorial Pacific. When tropical Pacific SST anomalies are removed, on the other hand, NTA warming coincides with easterly anomalies. Moreover, when SST anomalies are removed from the tropical Atlantic, wind variability over the western equatorial Pacific is enhanced. These results suggest that SST anomalies in the NTA, which are strongly influenced by the tropical Pacific, act as a negative feedback to ENSO development. This interbasin link may be further complicated by other influences on the NTA, such as local air-sea coupling and the North Atlantic Oscillation.

Keywords: tropical Atlantic, ENSO, teleconnections

©2019. Japan Geoscience Union. All Right Reserved.

[E] Poster | A (Atmospheric and Hydrospheric Sciences)：A-HW Hydrology & Water Environment

Thu. May 30, 2019 3:30 PM - 5:00 PM JST | Thu. May 30, 2019 6:30 AM - 8:00 AM UTC | Poster Hall International Exhibition Hall8, Makuhari Messe_5

[A-HW22] Materials transport and nutrient cycles in watersheds; from headwaters to coastal seas

convener:Masahiro Kobayashi(Forestry and Forest Products Research Institute), Seiko Yoshikawa(Institute for Agro-environmental Sciences, National Agriculture and Food Research Organization), Jun Yasumoto(University of the Ryukyus, Faculty of Agriculuture), Adina Paytan(University of California Santa Cruz)

This session aims to synthetize watershed sciences in order to understand dynamical processes of materials transport and nutrient cycles in watersheds from headwaters to coastal seas. The session will be integrating a variety of research disciplines including limnology, ground water hydrology, coastal oceanography, meteorology, pedology, sedimentology, forestry, agriculture, fishery, ecology, social science and more. This session calls for ideas on new methods for the watershed sciences, such as tracer and molecular technique, hydrological modeling, paleontological approaches, laboratory and field experiments, social-scientific evaluation of ecosystem services and social-ecological systems, and so on, in order to elucidate physical, chemical and biological mechanisms for shedding light on natural phenomena and their changes over time in complex and dynamic watershed systems under human and climate impacts. Through this session, we would like to facilitate interdisciplinary collaboration among participants to create new knowledge on watershed sciences.

[AHW22-P01] Phosphate Enrichment Hampers Development of Juvenile Acropora digitifera Coral by Inhibiting Skeleton Formation

Mariko Iijima[1], *Yasumoto Ko[1], Jun Yasumoto[2], Mina Hirose[3], Mitsuru Jimbo[1], Shugo Watabe[1] (1.Kitasato University School of Marine Biosciences, 2.Faculty of Agriculture, University of the Ryukyus, 3.Tropical Technology Plus)

[AHW22-P02] Modeling chlorophyll-a concentration using remote sensing in shallow water systems: Comparison of sensors

*Assefa M Melesse[1], Tara Blakey[1], Mohammad Haji Gholizadeh[1], Mohd Manzar Abbas[1] (1.Florida International University)

[AHW22-P03] Dynamics in groundwater flow system with seasonal water table variation in a coastal and island

*Yusuke Tomozawa[1], Shin-ichi Onodera[1], Mitsuyo Saito[2] (1.Graduate School of Integrated Arts and Sciences Hiroshima University, 2.Graduate School of Environmental and Life Science, Okayama University)

[AHW22-P04] The Tracing of Groundwater Contamination Sources in Indonesian Coastal Alluvial Groundwater using $\delta^{34}S$ and $\delta^{15}N$ Isotopes

*Anna Fadliah Rusydi[1,4], Mitsuyo Saito[2], Seiichiro Ioka[3], Shin-ichi Onodera[1] (1.Graduate School of Integrated Arts and Sciences, Hiroshima University, Japan, 2.Graduate School of Environmental and Life Sciences, Okayama University, Japan, 3.Research Institute for Sustainable Energy, Hirosaki University, Japan, 4.Research Center for Geotechnology, Indonesian Institute of Sciences, Indonesia)

[AHW22-P05] Spatio-temporal dynamics of orthophosphate with implications for limitation of phytoplankton growth in north basin of Lake Biwa, Japan

*Xin Liu[1], Rong Yi[1], Masahiro Maruo[1], Syuhei Ban[1] (1.The University of Shiga Prefecture)

[AHW22-P06] Microbial phase analysis in aquifer of Ryukyu Limestone Zone using next generation sequencer

*Umi Murao[1], Jun Yasumoto[1], Yasumoto Ko[3], Mina Hirose[2], Nanami Mizusawa[3], Ryo Iguchi[4], Bam H.N. Razafindrabe[5], Syugo Watabe[3] (1.University of the Ryukyus, Faculty of Agriculuture Department of Regional Agricultural Engineering, 2.Tropical Tecnology Plus, 3.Kitasato University School of Marine Biosciences, 4.National Institute of Advanced Industrial Science and Technology, 5.University of the Ryukyus, Faculty of Agriculuture Department of Subtropical Agro-Environmental Sciences)

[AHW22-P07] Evaluation for temporal variation in groundwater inflow to the lagoons connected to Lake Biwa by radon (^{222}Rn) tracer analysis

*Mitsuyo Saito[1], Shin-ichi Onodera[2], Yusuke Tomozawa[2], Kunyang Wang[2], Syuhei Ban[3], Noboru Okuda[4] (1.Graduate School of Environmental and Life Science, Okayama University, 2.Graduate School of Integrated Arts and Sciences, Hiroshima University, 3.School of Environmental Sciences, The University of Shiga Prefecture, 4.Research Institute for Humanity and Nature)

[AHW22-P08] Br/Cl ratio characteristics of groundwater in coastal areas in Indonesia

*Seiichiro Ioka[1], Shin-ichi Onodera[2], Mitsuyo Saito[3], Anna Fadliah Rusydi[2,4] (1.Institute of Regional Innovation, Hirosaki University, Japan, 2.Graduate School of Integrated Arts and Sciences, Hiroshima University, Japan, 3.Graduate School of Environmental and Life Sciences, Okayama University, Japan, 4.Research Center for Geotechnology, Indonesian Institute of Sciences, Indonesia)

[AHW22-P09] Estimation of groundwater recharge and phosphorus transport under different precipitation conditions in a suburban catchment, using SWAT model

*Kunyang Wang[1,2], Shin-ichi Onodera[1], Mitsuyo Saito[3], Noboru Okuda[4], Takuya Okubo[5] (1.Graduate School of Integrated Arts and Science, Hiroshima University, 2.Capital Normal University, 3.Okayama University, 4.Research Institute for Humanity and Nature, 5.University of the Shiga Prefecture)

[AHW22-P10] Losses of phosphorus with soil erosion and nitrate with groundwater recharge in an agricultural catchment, subtropical small island

*Shin-ichi Onodera[1], Mitsuyo Saito[2], Yang Cao[1], Anna Fadliah Rusydi[1], Hide Omae[3], Yoshiko Iizumi[4], Yusuke Tomozawa[1] (1.Graduate School of Integrated and Arts Sciences, Hiroshima University, 2.Graduate School of Environmental and Life Science, Okayama University, 3.JIRCAS TARF, 4.JIRCAS HQ)

[AHW22-P11] Phosphate solubilizing bacteria as an indicator of sediment phosphorus in freshwater lakes

*Sreekumari Kurissery[1], Katelynn Crawford[1], Nandakumar Kanavillil[1] (1.Lakehead University, Canada)

[AHW22-P12] A Study on the dynamics of various phosphate forms in soil and groundwater in Ryukyu limestone regions

*Masashi Nozaki[1], Jun Yasumoto[2], Yasumoto Ko[3], Hirose Mina[4], Iijima Mariko[3], Ryuichi Shinjo[5], Bam H.N. Razafindrabe[6] (1.University of The Ryukyus, Graduate School of Agriculture,, 2.University of the Ryukyus, Faculty of Agriculture, Department of Regional Agricultural Engineering, 3.Kitasato University School of Marine Biosciences, 4.Tropical Technology Plus, 5.Department of Physics and Earth Sciences, University of the Ryukyus, 6.University of the Ryukyus, Faculty of Agriculture, Department of Subtropical Agro-Environmental Sciences)

[AHW22-P13] Impacts of highly concentrated turbid water on the groundwater in the Tedori River alluvial fan, Japan

*Yoichi Fujihara[1], Shunsuke Chono[1], Keiji Takase[1], Eiji Ichion[1] (1.Department of Environmental Science, Ishikawa Prefectural University)

[AHW22-P14] Altitude effect of water stable isotopic ratio of ravine water and its contribution to groundwater in alluvial plains - Comparison in east and west side catchments of Lake Biwa –

*Yusuke Tomozawa[1], Kunyang Wang[1], Mitsuyo Saito[2], Syuhei Ban[3], Noboru Okuda[4], Shin-ichi Onodera[1] (1.Graduate School of Integrated Arts and Sciences Hiroshima University, 2.Graduate School of

Environmental and Life Science, Okayama University, 3.School of Environmental Science, The University of Shiga Prefecture, 4.Research Institute for Humanity and Nature)

[AHW22-P15] Calculation of TN and TP concentration coefficients of river water for each land use by a simple watershed model.

*Seiko Yoshikawa[1], Donglai Ma[1,4], Tadamasa Saito[1,5], Kenji Matsumori[2], Yuko Itoh[3], Masahiro Kobayashi[3] (1.Institute for Agro-environmental Sciences, National Agriculture and Food Research Organization, 2.Western Region Agricultural Research Center, National Agriculture and Food Research Organization, 3.Forestry and Forest Products Research Institute, 4.Graduate school,Tsukuba University, 5.Faculty of Agriculture, Ibaraki University)

[AHW22-P16] **Possibility of nutrients transportation from littoral slope for enhancement of phytoplankton growth in north basin of Lake Biwa**

*Syuhei Ban[1], Rong YI[1], Xin Liu[1], Masahiro Maruo[1], Miki Sudo[1], Naoshige Goto[1], Jun Murase[2] (1.The University of Shiga Prefecture, 2.Nagoya University)

[AHW22-P17] SWAT model analysis for confirming the effects of crop growth on the suspended sediment concentration from a settling basin catchment on Ishigaki island

*Yang Cao[1], Shin-ichi Onodera[1], Mitsuyo Saito[2], Hide Omae[3], Yoshiko Iizumi[3] (1.Graduate School of Integrate Arts and Sciences, Hiroshima University, 2.Graduate School of Environmental and life Science, Okayama University, 3.Tropical Agriculture Research Front (TARF), Japan International Research Center for Agricultural Sciences (JIRCAS))

[AHW22-P18] Estimating the runoff of water, sediment, and nutrient using SWAT model in Kikuchi-river watershed, Kumamoto, and the influence of the forest

*Soichiro Fujii[1], Masahiko Kanamori[1], Yuko Nagano[1], Maki Kinoshita[2], Yuta Shimizu[3], Shin-ichi Onodera[4] (1.Japan Forest Technology Association, 2.PASCO Corporation, 3.Western Region Agricultural Research Center, National Agriculture and Food Research Organization, 4.Graduate School of Integrated and Arts Sciences, Hiroshima University)

[AHW22-P19] Atmospheric depositions on forest ecosystems in areas along the Sea of Japan

*Yuko Itoh[1], Keiji Takase[2], Yoichi Fujihara[2], Toru Okamoto[1] (1.Forestry and Forest Products Research Institute, Japan, 2.Ishikawa Prefectural University)

[AHW22-P20] Continuous and simultaneous flux measurement of N_2O and CO_2 from agricultural soil using a portable multi-turn time-of-flight mass spectrometer

*Noriko Nakayama[1], Yusuke Iwai[1], Yo Toma[2], Hiroshi Furutani[1], Ryusuke Hatano[3], Michisato Toyoda[1] (1.Osaka University, 2.Ehime University, 3.Hokkaido University)

[AHW22-P21] Effects of introduction of cyclic irrigation system on mass balances of SS and T-P in Lake Inbanuma, Chiba, Japan

*Tomijiro Kubota[1] (1.National Agriculture and Food Research Organization, Institute for Rural Engineering)

Phosphate Enrichment Hampers Development of Juvenile Acropora digitifera Coral by Inhibiting Skeleton Formation

Mariko Iijima[1], *Yasumoto Ko[1], Jun Yasumoto[2], Mina Hirose[3], Mitsuru Jimbo[1], Shugo Watabe[1]

1. Kitasato University School of Marine Biosciences, 2. Faculty of Agriculture, University of the Ryukyus, 3. Tropical Technology Plus

Coral reef degradation resulting from various types of local stress on corals such as excessive nutrient enrichment in and gravel inflow into coastal waters is of an increasing global concern. Because tropical and subtropical seawaters are generally poor in nutrients and thus oligotrophic, these stresses are thought to result in the decline of environments favorable to coral growth. Inorganic phosphates have been especially considered to possibly inhibit the formation of coral skeleton. Despite many studies available on the effects of nutrients on corals, a clear consensus for how nutrients exert deteriorative effects on the corals has not been established satisfactorily. Recently, we found that biogenic polyamines react with carbon dioxide (CO_2) and accelerate an aragonite formation of calcium carbonate ($CaCO_3$) in seawater. In this study, we examined the effects of phosphates and nitrates on *in vitro* aragonite formation of $CaCO_3$ by using biogenic polyamines and *in vivo* aragonite formation of juvenile coral *Acropora digitifera* skeletons, showing that phosphates clearly inhibited both *in vitro* and *in vivo* $CaCO_3$ formations at similar concentrations. In contrast, nitrates inhibited neither *in vitro* aragonite formation of $CaCO_3$ nor *in vivo* aragonite formation of juvenile coral skeletons. These findings indicate that phosphates have a detrimental effect on bioinorganic coral calcification. Furthermore, the findings that phosphate enrichment inhibits coral skeleton formation led us to conclude that enriched phosphate is adsorbed on juvenile coral skeleton surface and inhibits inorganically normal development of juvenile coral skeleton.

Keywords: phosphate, calcification

©2019. Japan Geoscience Union. All Right Reserved.

Modeling chlorophyll-a concentration using remote sensing in shallow water systems: Comparison of sensors

*Assefa M Melesse[1], Tara Blakey[1], Mohammad Haji Gholizadeh[1], Mohd Manzar Abbas[1]

1. Florida International University

The level of productivity in the upland and coastal water bodies is highly linked to land processes (land use, water management, water and nutrient fluxes). Understanding the linkage between these processes and the level of algal blooms in the water bodies is crucial for improving water quality. A comparative study was conducted using remote sensing data from three different sensors (SeaWIFS, MoDIS and Landsat) to evaluate the capability of reflectance data from these sensors for estimation of chl-a concentrations in three water bodies in the USA (Lake Okeechobee, Florida Bay and Chesapeake Bay). Observed chl-a data were gathered and compared with simulation results. The analysis found that all of the sensors have performed well in deeper water bodies than in shallow sections due to the bottom reflectance from non-algal blooms. For shallow water bodies, selection of the proper bands and band combinations, identification of the non-algal bloom reflectance and the corresponding algorithms can improve the simulation. Seasonality as well as spatial variability (using cross-sections) were evaluated and the results showed that chl-a values were highly variable for the selected summer months. Indicative of the effect of land surface fluxes of nutrients, chl-a values were higher closer to coastal areas in the Florida bay and Chesapeake Bay. The chl-a in the freshwater lake of Okeechobee was simulated using Landsat 8 data and the results found were very good. Comparison of the SeaWIFS and MoDIS chl-a value to that of the measured concentrations in the deeper section of Florida Bay and Chesapeake Bay, respectively showed very good agreement.

Keywords: Chl-a, SeaWIFS, Water qulity modeling, South Florida, Remote sensing

©2019. Japan Geoscience Union. All Right Reserved.

Dynamics in groundwater flow system with seasonal water table variation in a coastal and island

*Yusuke Tomozawa[1], Shin-ichi Onodera[1], Mitsuyo Saito[2]

1. Graduate School of Integrated Arts and Sciences Hiroshima University, 2. Graduate School of Environmental and Life Science, Okayama University

In islands, freshwater water resources are valuable as living and agricultural use, and dug wells water and reservoirs had been utilized for more than 100 years. In order to use such water resources sustainably, it is important to evaluate groundwater flow as well as water budget.

In this research, we examined to confirm the seasonal variation in water stable isotopic ratios in observation boreholes at the coastal lowland in Ikuchi Island Hiroshima prefecture. Moreover, considering that the target area is coastal, Cl^- concentration was analyzed to evaluate the influence of salt fresh water boundary.

The experimental site is located on Ikuchi Island in Hiroshima prefecture. The highest altitude is 456 m. The basement rock is mainly composed of granite. Annual average precipitation is 1058.8 mm. Observation boreholes are located at the coastal lowland in the southeastern part of the island. The upper site (Site U) with the altitude of 5.1 m asl has 3 boreholes with the depths of 2 m, 15 m, 30 m, the lower site (Site D) with 2.5 m asl has 8 with the depth of 1 m, 2 m, 3 m, 10 m, 15 m, 20 m, 30 m, 40 m, respectively. The water sampling was carried out from monthly to half year interval since 2015. Every samples were analyzed for water isotopic ratios by PICARO and anion component by ion chromatography. Especially samples in January in 2019 were analyzed for CFCs and SF6.

Based on the previous study (Saito and Onodera, 2007), the distinct altitude effect of isotopic ratio in precipitation has been confirmed. Due to spatial and temporal variations in isotopic ratios, recharge process to groundwater was suggested as follows, 1) recharge on site to shallow groundwater (2-3m deep) at D ($\delta^{18}O$: -7.8 to - 7.4 ‰), 2) river water contribution to the shallow groundwater (2-15m) at U ($\delta^{18}O$: - 8.3 to - 7.5 ‰), 3) recharge in the mountain slope with the altitude of about 360 m to deep groundwater (30m) at U ($\delta^{18}O$: - 8.4 to - 8.1 ‰), 4) recharge at 400 m on near the mountain top to deep groundwater (10-30 m) at D($\delta^{18}O$: - 8.7 to - 8.4 ‰), 5) recharge of precipitation with lower isotope than in present to deeper groundwater (40 m) at D ($\delta^{18}O$: -8.9 to - 8.8 ‰)

The deepest groundwater (40m) at D had lower isotopic ratios with higher Cl^- concentration (250 to 584 mg / L) during a lower water table in the winter. This indicated the seawater –fresh water boundary rose with water table according to Gyben-Hrzberg concept. These phenomena also suggest to cause the rise of deeper and older groundwater flow line. Consequently, we suggest the lower isotopic ratio in deeper groundwater indicates the immobile water which were recharged in the glacial period. Based on other tracers (CFC, SF 6), we will discuss more.

Keywords: stable isotope, groundwater, coastal

©2019. Japan Geoscience Union. All Right Reserved.

The Tracing of Groundwater Contamination Sources in Indonesian Coastal Alluvial Groundwater using $\delta^{34}S$ and $\delta^{15}N$ Isotopes

*Anna Fadliah Rusydi[1,4], Mitsuyo Saito[2], Seiichiro Ioka[3], Shin-ichi Onodera[1]

1. Graduate School of Integrated Arts and Sciences, Hiroshima University, Japan, 2. Graduate School of Environmental and Life Sciences, Okayama University, Japan, 3. Research Institute for Sustainable Energy, Hirosaki University, Japan, 4. Research Center for Geotechnology, Indonesian Institute of Sciences, Indonesia

The coastal area is one of the Indonesian Government priorities as an archipelago country. The groundwater in the area is one of the most reliable clean water resources, therefore it is crucial to understanding the vulnerability of this resource. Our research area was located at Indramayu, a developing rural coastal area in Indonesia, where, the environment was relatively pristine. This research aimed was to identify the effect of natural condition and human activity to groundwater quality by using stable isotope $\delta^{34}S$ and $\delta^{15}N$.

Totally, there were 20 samples taken from groundwater (18) and river (2). The nitrate and sulfate were detected in a total of 5 and 19 samples, respectively. The isotopes composition for isotope nitrate were -11.2 ‰–+22.22‰ for $\delta^{15}N\text{-}NO_3$ and -3.4 ‰–+17.1‰ for $\delta^{18}O\text{-}NO_3$. Moreover, the values of $\delta^{34}S\text{-}SO_4$ and $\delta^{18}O\text{- }SO_4$ were varied from -4.2 ‰–+28.4‰ and +7.3 ‰–+18.8 ‰, respectively. The isotopic signatures of nitrate suggested that the used of inorganic fertilizer and animal manure give the impact to both groundwater and river. Similarly, the isotopic signatures of sulfur were showing that those detected sulfate in the groundwater were mostly coming from fertilizer. Moreover, the soil was mineralized by organic sulfate as well. At one point, located in the fishery area, the groundwater was indicated the seawater contamination. It was shown by the heavy composition of sulfur isotope (28.4‰ for $\delta^{34}S$ and 18.8‰ for $\delta^{18}O$). Lastly, our results showed those combined isotopes of $\delta^{34}S$ and $\delta^{15}N$ along with land-use evaluation could explain the possible sources of groundwater in coastal area at very early urbanization stage.

Keywords: Sulfur Isotope, Nitrate Isotope, Coastal Groundwater, Indramayu

©2019. Japan Geoscience Union. All Right Reserved.

Spatio-temporal dynamics of orthophosphate with implications for limitation of phytoplankton growth in north basin of Lake Biwa, Japan

*Xin Liu[1], Rong Yi[1], Masahiro Maruo[1], Syuhei Ban[1]

1. The University of Shiga Prefecture

Orthophosphate (PO_4-P) is the main chemical form of phosphorus (P) for phytoplankton growth, often considered as a limiting nutrient for primary production in freshwater ecosystems. However, few information on accurate measurements for PO_4-P concentrations in epilimnion of meso- and oligotrophic lakes due to lower than the detection limit (60 nM) of soluble reactive P using traditional spectrophotometrical method. In the present study, we measured PO_4-P concentrations using ion chromatography with a detection limit of 5 nM, and determined truly vertical distribution of PO_4-P throughout the year with other abiotic and biotic environmental factors in north basin of Lake Biwa, to accurately understand biogeochemical processes of P in this mesotrophic lake.

Field investigations were conducted monthly from April to December 2018 at station K4 (35º19'9.6"N, 136º11'2.7"E; 50 m deep). Phosphate enrichment experiments were also made at each sampling occasion to clarify P limitation for phytoplankton growth. Lake water including phytoplankton assemblage collected from epilimnion (0–20 m) was enriched with 1 μM of PO_4-P (+P) and incubated together with untreated one (control) for 2 days under ambient light and temperature conditions. To evaluate the effect of potentially nutrient-rich bottom water, the filtered bottom water was mixed with untreated epilimnion water including phytoplankton at 1:1 (+B) was incubated at the same conditions as the +P treatment. Phytoplankton growth rate (g) was calculated with equation of $g=\ln(C_t/C_0)/2$, where C_0 and C_t are chlorophyll *a* (chl. *a*) concentrations at start and end of the experiment, respectively.

Water temperature increased in the epilimnion from May, and strict thermocline was developed from June to September. Chl. *a* concentrations increased from June to July in 10–20 m, and from October to November in 0–20 m. PO_4-P concentrations were always low, <20 nM, in the epilimnion from April to June. The concentrations below 30 m increased up to 140 nM in May, but decreased after that until July. In August and September, the concentrations increased up to 30–40 nM even in the epilimnion probably due to disturbance by typhoon. The concentrations below 30 m increased with depth, and the highest values were frequently observed near the bottom, up to 220 nM. On average throughout the water column, PO_4-P concentrations were 24–48 nM from April to June, then slightly increased up to 73 nM until September, being constant, 50–63 nM until December.

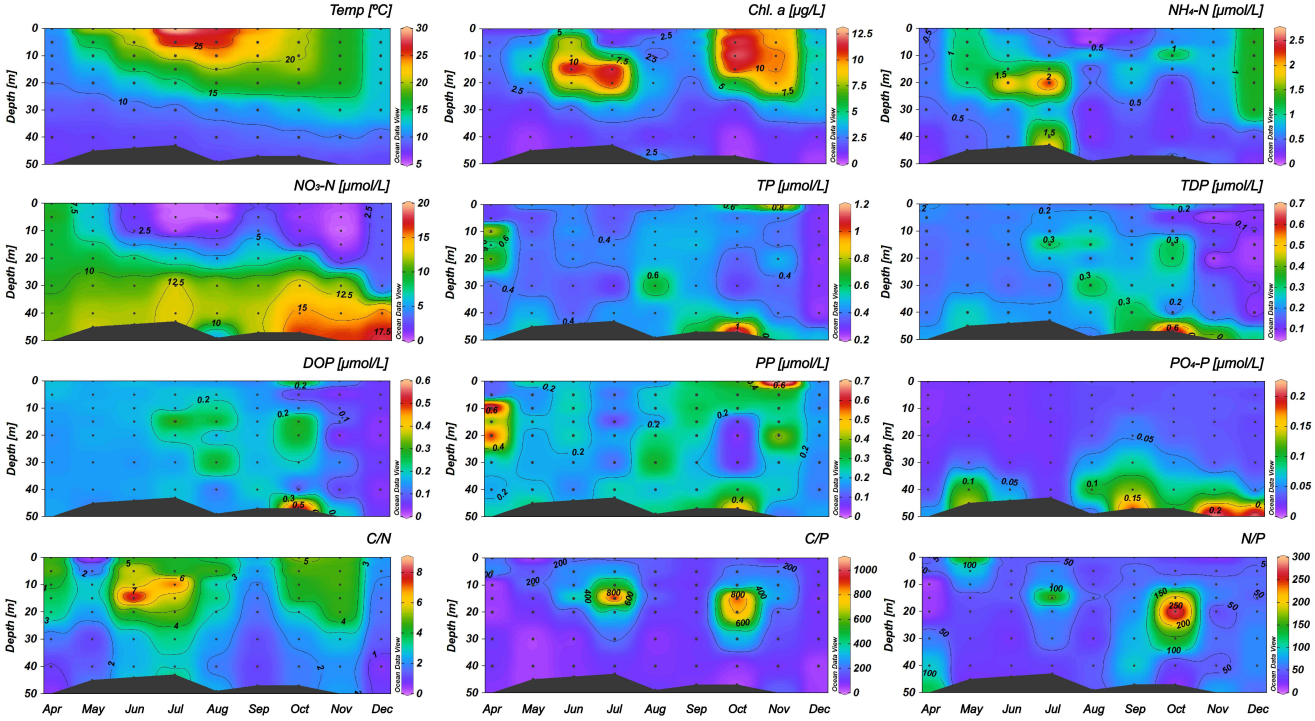
Total P, total dissolved P, dissolved organic P and particulate P exhibited similar spatio-temporal distributions, but different pattern from those of PO_4-P. NH_4-N increased in 10–20 m from May to July, whereas the NO_3-N increased in the hypolimnion as season progressed. Sestonic C:N:P ratios suggested a terrible P deficiency in July and October when phytoplankton biomass increased.

Phosphate enrichment experiments showed that phytoplankton in the epilimnion was mostly limited with P for its growth. Phytoplankton g in control varied −0.05-0.08 d^{-1}, being always lower than those in +P (−0.04-0.44 d^{-1}) and/or +B (−0.04-0.49 d^{-1}) treatments except for November and December. In November, no growth was found even in +P treatment. This might be caused by nitrogen limitation because of <6 μM of NO_3-N in the epilimnion. The g of control was similar as that of +P and +B (ca. 0.1 d^{-1}) in December, indicating that P deficiency for phytoplankton growth was relaxed until December by vertical convection.

©2019. Japan Geoscience Union. All Right Reserved.

We firstly determined completely vertical distributions of PO_4-P in north basin of Lake Biwa from spring to winter, and detected 20–40 nM of PO_4-P in the epilimnion. Phosphate enrichment experiments showed that 20 nM of PO_4-P might be critical concentration for phytoplankton growth in the lake. No phytoplankton growth even in +P treatment in November implied that nitrogen limitation for phytoplankton growth will be possible in Autumn. Further study for clarify this will be needed.

Keywords: Orthophosphate dynamics, Phosphorus limitation, Phytoplankton growth rate, Ion chromatography, Biogeochemical processes, Freshwater ecosystem



©2019. Japan Geoscience Union. All Right Reserved.

Microbial phase analysis in aquifer of Ryukyu Limestone Zone using next generation sequencer

*Umi Murao[1], Jun Yasumoto[1], Yasumoto Ko[3], Mina Hirose[2], Nanami Mizusawa[3], Ryo Iguchi[4], Bam H.N. Razafindrabe[5], Syugo Watabe[3]

1. University of the Ryukyus, Faculty of Agriculuture Department of Regional Agricultural Engineering, 2. Tropical Tecnology Plus, 3. Kitasato University School of Marine Biosciences, 4. National Institute of Advanced Industrial Science and Technology, 5. University of the Ryukyus, Faculty of Agriculuture Department of Subtropical Agro-Environmental Sciences

Clean water and sanitation (Sustainable development Goals (6)) is one of the world's important issues. People use groundwater in many areas as a water source, but various cases of contamination by agricultural activities and substances derived from human and animal excrements have been reported.

On the other hand, genetic analysis techniques using molecular biological methods have been applied to the analysis of microbial phase in the water environment.

In recent years, the method using the latest analysis equipment of next generation Sequencer is established, mainly for microorganisms. In addition, new monitoring indices such as environmental DNA have been developed. It is thought that the microbial phase in groundwater varies depending on the influence of various environmental factors and human activity, but the actual condition is not clear.

The next generation Sequencer is a very powerful tool used to grasp the microbial phase in groundwater. It is thought that the microbial phase can be an important indicator in water resource management of basins in the future.

The purpose of this study is to investigate the microbial species and their coexistence in groundwater in the Ryukyu Limestone area using the next generation sequencer.

Keywords: groundwater, microbial community analysis, genetic analysis

©2019. Japan Geoscience Union. All Right Reserved.

Evaluation for temporal variation in groundwater inflow to the lagoons connected to Lake Biwa by radon (^{222}Rn) tracer analysis

*Mitsuyo Saito[1], Shin-ichi Onodera[2], Yusuke Tomozawa[2], Kunyang Wang[2], Syuhei Ban[3], Noboru Okuda[4]

1. Graduate School of Environmental and Life Science, Okayama University, 2. Graduate School of Integrated Arts and Sciences, Hiroshima University, 3. School of Environmental Sciences, The University of Shiga Prefecture, 4. Research Institute for Humanity and Nature

Primary production in freshwater lakes and reservoirs are usually controlled by phosphorus (P). Lacustrine groundwater discharge (LGD), direct discharge of subsurface water to lake, is regarded as a potential nutrient paths, including phosphorus from a catchment to lake water environment. There are more than 20 lagoons around Lake Biwa which were originally a part of the lake. These lagoons are regarded to have important functions as settling ponds of inflowing loads from the catchments to Lake Biwa, refuges for shallow water ecosystems and so on. Because these lagoons are connected to Lake Biwa, evaluation of nutrient budget is important for the nutrient cycle in the lake. Some researchers have pointed out the presence of LGD in littoral area of Lake Biwa. However, it has not been evaluated for the lagoons around the lake. In the present research, we aimed to evaluate the temporal variation in groundwater inflow to a lagoon connected to Lake Biwa by radon (^{222}Rn) tracer analysis.

The field campaigns were conducted in December 2017, August and October 2018 for the lagoons (Noda-Numa and Hasu-Ike) located on northeastern shore of Lake Biwa. The volume of inflow and outflow, water temperature, electric conductivity, chlorophyll-a and radon (^{222}Rn) concentration were measured in the lagoon. ^{222}Rn is a radioactive element of uranium (^{238}U) series with 3.8 day of half-life. ^{222}Rn is a useful tracer of groundwater discharge because it generally enriched in groundwater than surface water. To examine the temporal variation in groundwater inflow, the time-series ^{222}Rn concentration in water was obtained. Water samples were collected at the inlet, outlet and near the center of the lagoons and natural springs and groundwater wells around the lagoons. Water and ^{222}Rn balance suggest that groundwater inflow is larger in Noda-Numa than Hasu-Ike. The catchment topography may influence on this difference. ^{222}Rn balance-based residence time of lagoon water was estimated 10-20 days in Noda-Numa, and 4-5 days in Hasu-Ike, were similar with that based on water balance. These results suggest the groundwater inflow is a potential phosphorus path to Noda-Numa.

Keywords: Groundwater inflow, Connected lagoons, Lake Biwa, Radon (222Rn)

©2019. Japan Geoscience Union. All Right Reserved.

Br/Cl ratio characteristics of groundwater in coastal areas in Indonesia

*Seiichiro Ioka[1], Shin-ichi Onodera[2], Mitsuyo Saito[3], Anna Fadliah Rusydi[2,4]

1. Institute of Regional Innovation, Hirosaki University, Japan, 2. Graduate School of Integrated Arts and Sciences, Hiroshima University, Japan, 3. Graduate School of Environmental and Life Sciences, Okayama University, Japan, 4. Research Center for Geotechnology, Indonesian Institute of Sciences, Indonesia

The urban development in Indonesia’ s coastal areas has led to an increase of groundwater demand, which then has resulted in groundwater salinization. In this study, we analyze bromide and Br/Cl ratio characteristics, as index of groundwater salinization, in three cities of Indonesian coastal areas, namely: Indramayu, Mataram, and Semarang. Each research site is at different stage of urbanization. Indramayu is in very early stage of urbanization, followed by Mataram as a developing tourism area, and the last one Semarang as a heavy urbanization city. The results show that concentrations of bromide in groundwater are ranged from 0.05 to 38 mg/L in Indramayu, 0.01 to 0.8 mg/L in Mataram, and 0.02 to 8.0 mg/L in Semarang. Furthermore, the occurrence of Br is described in terms of the Br/Cl weight ratio, which allows for small changes in bromide concentrations to be assessed in terms of salinity. Median values of Br/Cl weight ratio in the groundwater of Indramayu, Mataram, and Semarang were approximately 0.0035, 0.0027, and 0.0025, respectively, while the ratio in seawater is generally around 0.0035. The relationship between Br/Cl weight ratio and chloride concentration indicate the groundwater in Indramayu is undergoing salinization due to seawater intrusion compared to the other two areas, meanwhile the groundwater in Semarang is experiencing chloride contamination due to anthropogenic activities based on the study by Andreasen and Fleck (1997).

Keywords: Indonesia, groundwater, Br/Cl ratio, coastal area

©2019. Japan Geoscience Union. All Right Reserved.

Estimation of groundwater recharge and phosphorus transport under different precipitation conditions in a suburban catchment, using SWAT model

*Kunyang Wang[1,2], Shin-ichi Onodera[1], Mitsuyo Saito[3], Noboru Okuda[4], Takuya Okubo[5]

1. Graduate School of Integrated Arts and Science, Hiroshima University, 2. Capital Normal University, 3. Okayama University, 4. Research Institute for Humanity and Nature, 5. University of the Shiga Prefecture

The quantification of the groundwater recharge and phosphorus transport in water is one of the most important indicators of the water cycle in lakes because these processes are related to the transport of large nutrient loads. The Yasu River is one of the important water sources of the Biwa Lake. In this paper, Geographic Information System technology is used to analyze and predict the land use change in the Yasu River Basin. The water balance was simulated using the Soil and Water Assessment Tool. Simulations of different years in different precipitation seasons were carried out. The correlation coefficient and the Nash Sutcliffe coefficient are higher than the reference values. The sensitivity analysis of the parameters reveals the different degrees of sensitivity of the parameters in different water seasons, CN2 always has a high sensitivity during all kinds of water season. The total groundwater recharge and discharge are 180 million m^3 and 179 million m^3 in the normal precipitation season, respectively. The trends differ in the dry and wet seasons. In the dry season of 2007, the groundwater recharge was below 140 million m^3, while it exceeded 240 million m^3 in the rainy season in 2003. In addition, the process of phosphorus loss in the basin and release into Lake Biwa are explained from the perspective of space and time. This is closely related to the spatial distribution of the main channel and the time distribution of precipitation. The total amount of nonpoint source pollution of phosphorus in three years is equivalent to 4.08 kg/ha of paddy fields in the watershed. The spatial distribution of phosphorus loss is related to the stream flow, it is mainly concentrated in the area with paddy fields and urban. The time distribution is related to the distribution of the precipitation. With increasing precipitation, the nonpoint source pollution of phosphorus slightly increases. This is due to the driving effect of precipitation on the phosphorus transfer and erosion of soil.

Keywords: Phosphorus transport, Groundwater recharge, Different precipitation conditions, SWAT model

©2019. Japan Geoscience Union. All Right Reserved.

Losses of phosphorus with soil erosion and nitrate with groundwater recharge in an agricultural catchment, subtropical small island

*Shin-ichi Onodera[1], Mitsuyo Saito[2], Yang Cao[1], Anna Fadliah Rusydi[1], Hide Omae[3], Yoshiko Iizumi[4], Yusuke Tomozawa[1]

1. Graduate School of Integrated and Arts Sciences, Hiroshima University, 2. Graduate School of Environmental and Life Science, Okayama University, 3. JIRCAS TARF, 4. JIRCAS HQ

In tropical and subtropical region, the rainfall intensity is strong and soil erosion in an agricultural land is one of big environmental issues. Especially, the impact of large sediment discharge on the coral reef is serious around small islands, such as Okinawa and Philippines. In case of Okinawa Prefecture, to reduce the sediment discharge and conserve corals, many sediment trap ponds are constructed in a downstream area of agricultural lands. However, sediment deposition rate, variation of trap effect, and component of sediment in a pond have not been confirmed.

To estimate of erosion rate and deposition process of a small pond in an agricultural catchment of a subtropical small island, we examine to observe the sediment deposition in a small pond and monitor water level and chlorophyll a in a pond and runoff and turbidity of an inflow stream in a small catchment with the area of 300m2 in Ishigaki Island, Okinawa Prefecture, Subtropical region. Our monitoring was started from February 2017 after removing all sediment in a pond in January, and up to April 2018. Observation of sediment deposition was conducted with collecting the samples at 5 sites in June 2017 and January 2018. Inflow and outflow water samples were collected every one month.
The sediment deposition was extremely large from January to May 2017, the average erosion rate in all catchment area was estimated to be 6mm. On the other hand, the sediment deposition was nothing from June 2017 to January 2018. Based on the monitoring of stream runoff and turbidity, one big storm event in April with strong intensity mainly contributes to sediment discharge and overflow of the pond occurred. On the other hand, the later period had also big events. This difference is suggested to be the difference of land cover by crops and availability of sediment trap in this pond. In addition, the sediment component mainly was composed of surface soft layer, subsurface sandy layer, and bottom gravel layer. The average thickness was 2cm in surface layer, 100cm in mid sandy layer, and 10cm in gravel layer, respectively. Especially, the surface soft layer had high nutrient content. The dissolved nutrient of inflow stream water and pond water were high concentration. But the 10% of nutrient in the inflow decreased in pond. This means the plankton was produced, using this nutrient and that was deposited later. The soft layer is suggested to be effect of organic fertilizer, it is expected to apply to agricultural lands.

Keywords: Phosphorus, groundwater, nitrate

©2019. Japan Geoscience Union. All Right Reserved.

Phosphate solubilizing bacteria as an indicator of sediment phosphorus in freshwater lakes

*Sreekumari Kurissery[1], Katelynn Crawford[1], Nandakumar Kanavillil[1]

1. Lakehead University, Canada

It has been well documented that phosphorus pollution is one of the most significant factors impeding the overall health of freshwater lakes. Various measures are being taken to reduce phosphorus input into the lakes by anthropogenic activities and thus to maintain a healthy ecosystem. However, it is well known that bioavailable phosphorus tends to bind with substances such as ferric iron and calcium present in the water, become insoluble, and settles into the sediments. The presentstudy has been carried out to understand the relationship between the sediment phosphorus concentration and density of phosphate solubilizing bacteria (PSB) in two lakes in Ontario, Canada, namely, Lake Simcoe and Sparrow Lake. In September 2017, 20cm sediment cores were collected from the nearshore sites of these two lakes to determine the presence of PSB in relation to the sediment phosphorus concentration. PSB could potentially release phosphorus back into the water column through a process called internal phosphorus loading from the inorganic phosphates in the sediment when the right conditions are present. PSB were isolated from the sediment cores at 5 cm intervals by plating on to Pikovskaya’ s agar. Five grams of sediment was used to analyze total reactive phosphorus in the sediment. In Lake Simcoe, PSB ranged from $3x10^1$ to $1.1x10^1$ cfu/g, and the amount of total reactive phosphorus ranged from 0.19 to 0.46 mg/g. In Sparrow Lake, PSB ranged from $4x10^0$ to $3x10^1$ cfu/g and the amount of total reactive phosphorus ranged from 0.21 to 0.39 mg/g. A linear regression was completed to determine the relationship between total reactive phosphorus and PSB for each core. The results showed a negative relationship between these two tested parameters (Lake Simcoe: r^2=0.23, $y = -35.34x + 30.811$ p=0.5206, and Sparrow Lake: r^2 =0.87, $y = -155.9x + 62.322$, p=0.067). While PSB density decreased with core depth, the concentration of reactive phosphorus increased. This indicates that the density of PSB in lake sediment may indicate the concentration of total reactive phosphorus and thus the internal phosphorus loading. More study is recommended to confirm the results.

Keywords: Phosphate Solubilizing Bacteria, Freshwater Lakes , Sediment Phosphorus , Canada

©2019. Japan Geoscience Union. All Right Reserved.

A Study on the dynamics of various phosphate forms in soil and groundwater in Ryukyu limestone regions

*Masashi Nozaki[1], Jun Yasumoto[2], Yasumoto Ko[3], Hirose Mina[4], Iijima Mariko[3], Ryuichi Shinjo[5], Bam H.N. Razafindrabe[6]

1. University of The Ryukyus, Graduate School of Agriculture,, 2. University of the Ryukyus, Faculty of Agriculture, Department of Regional Agricultural Engineering, 3. Kitasato University School of Marine Biosciences, 4. Tropical Technology Plus, 5. Department of Physics and Earth Sciences, University of the Ryukyus, 6. University of the Ryukyus, Faculty of Agriculture, Department of Subtropical Agro-Environmental Sciences

Phosphorus in water environment exists in various forms and size, such as dissolved, particulate, organic and inorganic forms. However, there are many unclear points in Phosphorus in groundwater. In this study, we tried to understand the dynamics of various phosphate forms in soil and groundwater in Ryukyu limestone regions by combining Inductively Coupled Plasma Atomic Emission Spectrometry (ICP-AES) and ^{31}P Nuclear Magnetic Resonance (^{31}P-NMR), in addition to Colorimetric (molybdenum blue method). From August 2017 to August 2018, we took groundwater samples in southern part of Okinawa, Japan, with Ryukyu limestone distribution on a monthly basis. We measured pH, electronic conductivity (EC), Oxidation-Reduction Potential (ORP), dissolved oxygen (DO) and alkalinity (HCO_3^-) on site, and analyzed major dissolved ion (Cl^-, HCO_3^-, NO_2^-, NO_3^-, SO_4^{2-}, Na^+, K^+, Mg^{2+}, Ca^{2+}), suspended solid (SS) and phosphorus concentration. Phosphorus concentration analyzed 3 different method to molybdenum blue method (Col-P), ICP-AES (ICP-P) and Total P (T-P). Phosphate form analysis used ^{31}P-NMR.
We compared Col-P and ICP-P in order to understand dissolved phosphorus spatial distribution. The results show that ICP-P is 1.06~49.24 times larger than Col-P. It is inferred that ICP-P is also measuring fine particulate phosphorus and organic phosphorus. As a result, several forms of phosphate without orthophosphate were found in groundwater. Particulate phosphorus was determined by subtracting ICP-P from T-P. A positive correlation (r= 0.78) was found between P-P and SS. According to these results, it is thought that PP adsorbs various forms of phosphate including orthophosphate. We analyzed the correlation between dissolved phosphorus (Col-P, ICP-P) and all measured value in order to understand the characteristics of seasonal variation to dissolved phosphorus. There was a negative correlation between Col-P to water temperature. When focusing on seasonal variation of Col-P, we found that Col-P concentration decreases when water temperature increases. Moreover, Col-P concentration increases as water temperature increases. Through the analysis of various forms of phosphate in soil and SS by using ^{31}P-NMR, along with orthophosphate, pyrophosphate, pyrophosphate ester, orthophosphate monoester were also detected. It is thus suggested that the phosphate of polymeric or organic forms other than orthophosphate are from plant origin, as a result of microbial activities and microorganism decomposition.

Keywords: Phosphorus, 31P-NMR, Groundwater

©2019. Japan Geoscience Union. All Right Reserved.

Impacts of highly concentrated turbid water on the groundwater in the Tedori River alluvial fan, Japan

*Yoichi Fujihara[1], Shunsuke Chono[1], Keiji Takase[1], Eiji Ichion[1]

1. Department of Environmental Science, Ishikawa Prefectural University

The Tedori River alluvial fan in the Ishikawa prefecture is a representative alluvial fan in the Hokuriku region in Japan. The river water is taken by a headworks located at the top of the alluvial fan and is used for irrigation in paddy fields with a total area of about 7,500 ha. Seepages from the riverbed and percolations from the paddy area are the main sources of groundwater in the Tedori River alluvial fan. In 2015, large-scale landslides in the upper reaches of the Tedori River caused a long period of high turbidity in the river. Highly concentrated turbid water with an average concentration of 585 mg/L (a maximum of 4,012 mg/L) has been discharged continuously into the river since May, 2015. This turbidity has caused concerns about the recharge functions of groundwater in the alluvial fan.

In this study, the measurements of paddy percolations and riverbed seepages, before and after the occurrence of high turbidity, were used to examine the influence of these phenomena on groundwater recharge functions in the alluvial fan. We measured water requirement rates in the paddy area in the Tedori River alluvial fan. The measurements were conducted before and after the midsummer-drainage period at >100 paddy fields. We also measured the river discharges in the cross-sections of the river throughout the alluvial fan. The number of cross-sections was 16 and we estimated the riverbed seepages by calculating the discharge differences between the cross-sections.

The results revealed that the amount of paddy percolation decreased significantly due to the turbidity of the river water. The average percolation in the paddy area was found to be 12.4 mm/day in 2014 and 7.9 mm/day in 2016 before the midsummer-drainage period. Moreover, the average percolation in the paddy was found to be 19.6 mm/day in 2014 and 13.7 mm/day in 2016 after the midsummer-drainage period. The volume of the riverbed seepage was observed to have reduced and the seepage section were also observed to have shortened. The observed seepages from the river bed were 4.72 m3/s in 2009 and 3.33 m3/s in 2016 for the irrigation period, whereas for the non-irrigation period, these values were 5.92 m3/s in 2009 and 1.25 m3/s in 2016. Furthermore, the seepage section was found to shorten from 14.2 km to 8.0 km, due to the high turbidity of the water.

Finally, we estimated the amount of groundwater recharge based on these measurements, which revealed that the groundwater recharge from paddy percolation decreased by 270 mm/year (36%), and the recharge from riverbed decreased by 591 mm/year (61%). The total groundwater recharge decreased by 861 mm/year (36%), a value that corresponded to the groundwater level measurements. From these results, we can conclude that the effects of highly concentrated turbid water on the groundwater are quite serious in the Tedori River alluvial fan.

Keywords: groundwater, paddy percolation, riverbed seepage

©2019. Japan Geoscience Union. All Right Reserved.

Altitude effect of water stable isotopic ratio of ravine water and its contribution to groundwater in alluvial plains - Comparison in east and west side catchments of Lake Biwa –

*Yusuke Tomozawa[1], Kunyang Wang[1], Mitsuyo Saito[2], Syuhei Ban[3], Noboru Okuda[4], Shin-ichi Onodera[1]

1. Graduate School of Integrated Arts and Sciences Hiroshima University, 2. Graduate School of Environmental and Life Science, Okayama University, 3. School of Environmental Science, The University of Shiga Prefecture, 4. Research Institute for Humanity and Nature

The stable isotope ratio of hydrogen and oxygen in water is one of useful tracers for hydrological cycle and processes in the catchment scale as well as global. The typical characteristics are spatial or geographical distribution trend such as “altitude effect” or “inland effect”, which are lower in the higher altitude or more inland. Based on these trend, the groundwater recharge area had been estimated. However, the merger of these effects and additional effect such as the seasonal variation of isotopic ratio in precipitation or vapor causes various trend.
In this study, we examined to confirm the altitude effect of water stable isotope ratio and estimate recharge altitude to groundwater in alluvial plains, with comparing in the east and west side catchments of Lake Biwa .
Sampling of spring water in the Serikawa upstream area on the east side of Lake Biwa was conducted in July 2017, December 2017, August 2018. Sampling of ravine water in the Adogawa / Ukawa upstream area on the west side of Lake Biwa was conducted in August 2018. Water samples of spring in the head water and groundwater in the alluvial plain were collected at 11 and 2 sites in the east and at 13 and 2 in the west with measuring EC, pH and DO, respectively. The water stable isotopic ratios were analyzed by PICARO.
Stable isotopic ratios in groundwater were lower than surface water in both east and west. Altitude effects of spring water in the head water were recognizable. This means the surface water in the alluvial plain was mainly contributed from Lake Biwa, whereas groundwater was from the head water. The altitude effect of oxygen stable isotopic ratio was 0.15 - 0.13 ‰/ 100 m on the east side and 0.15 ‰/ 100 m on the west side (only in the upper stream of the Ado River). In addition, the d value of isotopic ratio in the precipitation was 23‰ in the upper Adokawa in August 2018, 18 ‰in Ugawa, and 20 ‰in Serikawa.
We also estimated groundwater recharge elevation and water contribution rate in the upstream region based on these.

Keywords: stable isotope, altitude effect, groundwater recharge

©2019. Japan Geoscience Union. All Right Reserved.

Calculation of TN and TP concentration coefficients of river water for each land use by a simple watershed model.

*Seiko Yoshikawa[1], Donglai Ma[1,4], Tadamasa Saito[1,5], Kenji Matsumori[2], Yuko Itoh[3], Masahiro Kobayashi[3]

1. Institute for Agro-environmental Sciences, National Agriculture and Food Research Organization, 2. Western Region Agricultural Research Center, National Agriculture and Food Research Organization, 3. Forestry and Forest Products Research Institute, 4. Graduate school,Tsukuba University, 5. Faculty of Agriculture, Ibaraki University

Water quality deterioration of rivers caused by leakage of fertilizer components such as nitrogen and phosphorus from paddy and upland fields is a environmental problem. Also, runoff of fertilizer components are expected to increase with the accelerated water and sediment runoff by intensification and localization of rainfall caused by climate change. Although it is difficult to predict the place and extent of heavy-rainfall-related disasters, we firstly grasp the average concentrations of nitrogen and phosphorus and predict increase and decrease in those concentrations when the way of rain changes. Nitrogen and phosphorus runoff is depend on land use and land cover, conservative measures, topography, climate condition mainly rainfall etc.. Among them, the land use and land cover is expected to be a main factor in normal climate conditions. In order to contribute to the prediction of heavy-rain related disasters in the future, coefficients that indicate the total nitrogen (TN) and total phosphorus (TP) load intensity to rivers of each land use for the river watersheds across the country are calculated using a simple watershed land use model. Watersheds whose lower ends are observation points of water quality, and whose land use ratios were determined by GIS technique using published database of DEM (GSI, 10B) and LULC mesh data (JAXA , ALOS AVNIR-2). The TN and TP concentration coefficients of paddy, upland, forest, and urban were calculated by applying the below multiple regression equation using the land use ratios and published TN and TP data(Ministry of Environment).

$c = a_1 x_1 + a_2 x_2 + a_3 x_3 + a_4 x_4$

C: TN or TP concentration (mg L^{-1}) a_i : TN or TP concentration coefficient for land use *I,* x_i : ratio of land use *I,* Land use: 1;paddy, 2;upland fields, 3;forest, 4;urban

TN concentration coefficient across Japan is 1.67 (from lower limit 95% value 1.34 to upper limit 95% value 2.01), 4.08 (from 3.64 to 4.51), 0.76 (from 0.67 to 0.90), 3.57 (from 3.38 to 3.76) for paddy fields, upland fields, forests and urban areas respectively (n=3256). The TP concentration coefficient is 0.146 (lower limit 95% value 0.119 to upper limit 95% value 0.172), 0.172 (0.138 to 0.206), 0.044 (0.033 to 0.055), 0.267 (0.253 to 0.282) for paddy fields, upland fields, forests and urban areas respectively (n=3256,). Prefectural TN and TP concentration coefficients for paddy and upland fields related only loosely to prefectural surplus N and surplus P. On the other hand, prefectural TN and TP concentration coefficients for forests and urban related to prefectural population densities by logarithmic functions with determination coefficients R^2 from 0.45 to 0.48.

Keywords: watershed land-use model, TN, TP, concentration coefficient

©2019. Japan Geoscience Union. All Right Reserved.

Possibility of nutrients transportation from littoral slope for enhancement of phytoplankton growth in north basin of Lake Biwa

*Syuhei Ban[1], Rong YI[1], Xin Liu[1], Masahiro Maruo[1], Miki Sudo[1], Naoshige Goto[1], Jun Murase[2]

1. The University of Shiga Prefecture, 2. Nagoya University

Nutrient loading from non-point source in a lake ecosystem has not been well recognized yet. In Lake Biwa, total phosphorus (TP) does not decline to the level before eutrophication period, 1960s to 1970s, despite of decreasing the loading from point sources surrounding the lake after that. One of the reasons for no well lowering TP in the lake is attributed to agricultural runoff, in which suspended materials including phosphorus would be deposited to the littoral bottom. In our previous study, subsurface maximum of ammonium as a proxy of dissolved materials from anaerobic interstitial waters in the littoral bottom sediments was found along a transect from littoral to pelagic regions, implying horizontal transportation of nutrients from littoral sediments. There were no such evidences of soluble reactive phosphorus (SRP) yet due to always below the detection limit in the pelagic waters. Recently, we developed modified protocol using an ion chromatography for measuring orthophosphate concentration at nano-molar levels. In this presentation, we' d like to provide several evidences for horizontal transportation of dissolved nutrients including orthophosphate along a transect from littoral to pelagic sites in north basin of Lake Biwa.

Total of the 6 times transect surveys for determining vertical profiles of nutrients, methane and herbicides were made in 2010-2011. Additional two transect surveys for determining those of nutrients including orthophosphate were made in 16 May and 25 July of 2018. During the 2010-2011 campaigns, *in situ* phytoplankton primary production was measured during the stagnation period using light intensity and chlorophyll *a*concentration monitored by sensors attached to a mooring buoy situated at an offshore station in north basin of Lake Biwa and an equation of photosynthesis - light intensity (P-I) curve.

In 2010-2011 campaigns, we detected sub-surface maximum layer, 20-30 m, of ammonium and methane as a proxy of dissolved materials transported from interstitial water in the sediment of littoral slope. Herbicides, which were used in rice paddy during the rice planting and proxy of materials transported from terrestrial environments surrounding the lake, were also detected in 20-30 m even at the offshore regions in the lake. Primary production monitoring suggested that phytoplankton production depended on some environmental variables other than solar irradiance, e.g. nutrients, until summer months. These results suggested that nutrients for enhancing algal growth might be horizontally transported from sediment in the littoral slope, and that the source of the nutrients might be provided from the drainage of rice paddy.

In 2018 campaigns, sub-surface maximum of ammonium was clearly found along a transect from littoral to pelagic sites in both May and July, but no such sub-surface maximum of orthophosphate was found. Several reasons for failure to find sub-surface maximum of orthophosphate might be proposed. Phosphate would be used by both phytoplankton and bacteria, while ammonium would be used by phytoplankton alone in the euphotic layer. In phosphate limited environment, such as pelagic areas in north basin of Lake Biwa, sub-surface maximum could not be easily detected due to rapid absorption by both phytoplankton and bacteria. Or, a transportation of nutrients from the littoral sloop would sporadically occur, and then we simply missed to detect it. This is on-going research project, and then further studies will be conducted to clarify this issue.

©2019. Japan Geoscience Union. All Right Reserved.

Keywords: Horizontal nutrient transportation, non-point source loading, agricultural runoff, Lake Biwa

©2019. Japan Geoscience Union. All Right Reserved.

SWAT model analysis for confirming the effects of crop growth on the suspended sediment concentration from a settling basin catchment on Ishigaki island

*Yang Cao[1], Shin-ichi Onodera[1], Mitsuyo Saito[2], Hide Omae[3], Yoshiko Iizumi[3]

1. Graduate School of Integrate Arts and Sciences, Hiroshima University, 2. Graduate School of Environmental and life Science, Okayama University, 3. Tropical Agriculture Research Front (TARF), Japan International Research Center for Agricultural Sciences (JIRCAS)

Crop growth has a significant effect on soil erosion in small watersheds. Exploring the characteristics and occurrences of soil erosion in small watersheds assists in our understanding of the water and material cycles in agricultural areas. The small catchment on the tropical island of Ishigaki, Japan, was chosen as the research area. The effects of sugarcane growth at different stages on the suspended sediment concentration in the basin from January 2017 to July 2018 were analyzed based on the Soil and Water Assessment Tool (SWAT) model. This study will explore the possible driving factors of these phenomena. The results show that the suspended sediment concentration in the basin reached its highest value on a rainy day near the sugarcane planting period because of the soil relaxation caused by tillage and cultivation. At the end of the sugarcane growth period, the sediment concentration was not at a high level when the rainfall reached 150 mm, because of the effective protection of the soil by sugarcane. The simulated sediment concentration of precipitation per mm showed that the simulated sediment concentration was at its highest during the crop planting period, followed by the period of bare land, and at the lowest during the crop growth period.

Keywords: SWAT model, Small catchment, Sugarcane, Sediment, Ishigaki

©2019. Japan Geoscience Union. All Right Reserved.

Estimating the runoff of water, sediment, and nutrient using SWAT model in Kikuchi-river watershed, Kumamoto, and the influence of the forest

*Soichiro Fujii[1], Masahiko Kanamori[1], Yuko Nagano[1], Maki Kinoshita[2], Yuta Shimizu[3], Shin-ichi Onodera[4]

1. Japan Forest Technology Association, 2. PASCO Corporation, 3. Western Region Agricultural Research Center, National Agriculture and Food Research Organization, 4. Graduate School of Integrated and Arts Sciences, Hiroshima University

Recently, enclosed sea area such as Ariake-sea have severe nutrient enrichment problem and is decreasing the produce of fishery industry. Such enclosed sea area is commonly affected by river water quality discharged from the land area. Therefore, estimating the load of sediment and nutrient from its land area is important. However, most of researches estimating discharge from land area is conducted by simple method using primary load factor. These method only can provide the estimates in annual scale regardless of the land use. On the other hand, the positive effect of forest to water quality in the river, so-called green dam, is paid attention recently, and supposed to play important roll on improvement to sea environment. However, the effect of forest to water quality is not explained enough, and few research has conducted in watershed scale. In this study, we aim to simulate water, sediment, and nutrient runoff in order to provide more detail information about discharge from land area, and to estimate the influence of the forest to water quality. We use Soil and Water Assessment Tool (SWAT) and chose Kikuchi-river as a model watershed, which has the third largest watershed area among the rivers drain into Ariake-sea.

We set Komoda observatory as the most downstream point of Kikuchi-river and the model watershed is the upstream side from there. More than half of this watershed is covered by forest. We collected land use data, soil data, climate data and 30m mesh digital elevation model (DEM) data of this watershed in order to establish the model. In order to calibrate and validate the model performance, observed data of daily stream flow from 2008 to 2016, and sampling data of sediment and nutrient were collected. Moreover, we measured the amount of sediment, phosphorus and nitrogen during flood situation in 2016 and 2017. The parameters in the model were modified according to the result of calibration, and the performance of the model was evaluated from three indices such as Nash-Sutcliffe index.

The model performance was evaluated as more than satisfactory for all materials: water, sediment, phosphorus and nitrogen. Therefore, this model can simulate daily runoff from 2008 to 2017. The runoff rate of sediment and most of nutrient from forest was less than 30% of the annual average in whole watershed, although water discharge was the same level to the rate of forest area, which indicates the function of forest to provide low concentrate water of sediment and nutrient to the river. In conclusion, modelling the runoff from land area using SWAT model has potential to provide detail information about land area discharge and estimate the influence of forest to river water quality.

Keywords: SWAT model, Runoff estimation

©2019. Japan Geoscience Union. All Right Reserved.

Atmospheric depositions on forest ecosystems in areas along the Sea of Japan

*Yuko Itoh[1], Keiji Takase[2], Yoichi Fujihara[2], Toru Okamoto[1]

1. Forestry and Forest Products Research Institute, Japan, 2. Ishikawa Prefectural University

In recent years, concerns about the effects of excess-nitrogen usage by human activities on terrestrial environment, including forest ecosystems, have been increasing at a global scale. The phenomenon of high-nitrate efflux from several forest watersheds has already been reported in the surroundings of metropolitan areas in Japan. Furthermore, concerns regarding the effects of transboundary air pollution on areas along the Sea of Japan with expanding economic activities have been increasing in Asian countries. However, on-site monitoring throughout the year is difficult in most of these areas because of heavy snow, especially in the mountainous area. Therefore, the behaviors of elements within forest ecosystems throughout a year have primarily not yet been elucidated in this district. This study was conducted to determine the influxes and effluxes of elements in this heavy snowy region and to understand the contribution of transboundary air pollution to the quantity of atmospheric deposition. We also carried out rainfall and stream water investigations from the headwater area to the lower stream area in the Tedori River Basin and an inland mountainous area to understand the geographical distribution of the actual conditions of elements' influxes and effluxes in this region. We started monitoring the major and minor elements in a small forested watershed in the middle part of the Tedori River Basin, Ishikawa prefecture, Japan, in 2013. In this study site, we observed a large amount of precipitation throughout the year. Regarding the annual snowfall amount, there were extensive variations among the years. Seasonal fluctuations were observed in the influx of atmospheric deposition; in particular, the distribution of most of the elements increased during winter. The annual deposition average of inorganic nitrogen (NH_4-N + NO_3-N) in this site was 15.8 kg ha^{-1}. The contribution of winter season deposition to the annual inputs was high. The influx of nitrogen by bulk precipitation during winter season was 2.3 times that of summer, and that of sulfur sulfate was 3.7 times. The nitrogen influx quantity was similar to or more than that reported in nitrogen-saturated forested areas of the Kanto district. Therefore, similar to that in the Kanto district, higher nitrogen deposition loads from the atmosphere could also be influenced on the effect of nitrogen dynamics and the increase in nitrogen efflux at these forest watersheds. However, the efflux concentrations of most of the dissolved elements in stream water did not show clear seasonal fluctuations. Stream water nitrate concentration was stable and low. In addition to the seasonal fluctuation of nitrogen and sulfur, the ratios among some trace elements, which are anthropogenic substances (Pb, V, As, etc.), and sea salts and yellow sand could be useful indicators to elucidate the contribution of transboundary air pollution to these regions. We compared the element inputs associated with precipitation during the non-snowy season (July–November) at six locations in the Tedori River Basin and one location in the inland area. The inorganic nitrogen and sulfuric acid sulfur influxes were the largest at the middle reaches of the Tedori River Basin. The inflow amount of inorganic nitrogen and sulfuric acid sulfur at two points in the mountainous area was approximately half or less than that at the middle region and was approximately the same as the inflow amount at the inland mountainous area. Furthermore, we investigated stream water, spring water, and ground water samples from the headwater area to the lower stream area in the Tedori River Basin. The nitrate concentrations in all the samples ranged from 0.00 to 2.93 mgL^{-1} (median value: 0.69 mgL^{-1}). In contrast, the nitrate concentrations of stream water in the Tsukuba experimental forest watershed, which has been reported as a nitrogen-saturated forested area of the Kanto district, were much higher (average value: 7.56 mgL^{-1}) than those in the Tedori River Basin. Compared with the influx, the efflux concentrations of nitrate in the water

©2019. Japan Geoscience Union. All Right Reserved.

samples were generally very low around this basin. Therefore, higher nitrogen depositions have not yet distinctly influenced the nitrate concentrations of stream water in this area. To elucidate the influence of transboundary air pollutant influx on the entire Tedori River Basin, it is necessary to evaluate the inflow amount during the snowy season in the mountainous area. Therefore, it is important to establish a method that can be used to observe the influx and efflux of elements throughout the year even in mountainous areas with heavy snow.

©2019. Japan Geoscience Union. All Right Reserved.

Continuous and simultaneous flux measurement of N_2O and CO_2 from agricultural soil using a portable multi-turn time-of-flight mass spectrometer

*Noriko Nakayama[1], Yusuke Iwai[1], Yo Toma[2], Hiroshi Furutani[1], Ryusuke Hatano[3], Michisato Toyoda[1]

1. Osaka University, 2. Ehime University, 3. Hokkaido University

Agricultural soil is one of the important sources/sinks of greenhouse gases such as N_2O, CO_2, and CH_4. The formation and consumption of such greenhouse gases in agricultural soils are dependent on not only the chemical and biological properties of the soil, but also their variations. Hence continuous monitoring of such greenhouse gases as tracer gases are quite useful to track chemical and biological processes and variations of soil properties.

In this paper, we describe a new field-deployable gas flux measurement system for the continuous monitoring of multiple agricultural soil gases (N_2O, CO_2, and CH_4) using a high resolution multi-turn time-of-flight mass spectrometer (MULTUM) combined with an automated flux chamber system. The new system measured the soil gases every 2.5 min with the precisions of ~6% for N_2O, CH_4, and 2% or better for CO_2 and O_2 at atmospheric concentrations with one relative standard deviation (RSD) for n = 10.

To demonstrate the utility of the continuous multi-gas flux measurement system, we conducted a field study at the Ehime University farm (Ehime, Japan) from September 3rd to 8th, 2018. In the field study, an automated flux chamber was placed in the agricultural field and the soil gas concentrations in the chamber were continuously monitored by the MULTUM system. Soil temperature/moisture sensor were also monitored at the depth of 7.5 cm underground in addition to a weather information (wind speed, precipitation, solar radiation). The continuous measurement had been continued with operators almost unattended except for a daily system check.

For one flux measurement (20 min), eight gas samples were taken every 2.5 min with the flux chamber closed. Gas flux of N_2O and CO_2 had been carried out by applying linear regression to the eight gas measurements. We found that a significant correlation of N_2O flux with soil electrical conductivity and water content, although no significant correlation of CO_2 flux to soil electrical conductivity was observed. Significant and rapid decreases in N_2O and CO_2 flux during rainfall events were also observed. Our preliminary result shows that high time-resolution flux data obtained by MULTUM system is quite useful for tracking the variation in soil properties and biological processes and their activity in soil environment.

Keywords: on-site mass spectorometry, MULTUM, soil-to-atmospher gas flux

©2019. Japan Geoscience Union. All Right Reserved.

Effects of introduction of cyclic irrigation system on mass balances of SS and T-P in Lake Inbanuma, Chiba, Japan

*Tomijiro Kubota[1]

1. National Agriculture and Food Research Organization, Institute for Rural Engineering

Introduction

The introduction of cyclic irrigation has been advanced since 2010 in the Lake Inbanuma as part of the update project of the irrigation facilities. In the present study, mass balances of SS and T-P were examined before and after the introduction of the cyclic irrigation.

Materials and methods

The irrigation block where the cyclic irrigation began in 2015 was selected as the investigation site, and the investigation was executed to the irrigation period in 2014 and 2015. The hydrological and water quality investigation was executed at ① division works of irrigation canal and ② drainage pumping station. Water samples were taken at the two points and the TOC, SS, TN, NO3-N, NO2-N, NH4-N, TP, and PO4-P were analyzed in the regular investigation executed about once a month. Besides regular investigation, water samples were taken once a day (8:00AM or noon) by the automatic water sampler and SS and T-P were analysed. The turbidity and water level were measured every ten minutes by using data loggers at same sites. The turbidity data were converted into the concentration of SS and TP by using the regression curve. The quantity of water intaken from the lake and drainage to the lake were obtained from the records of the facility manager.

Result and discussion

The inflow and outflow loads and the balance were calculated before and after the introduction of the cyclic irrigation. In 2014, before the start of cyclic irrigation, both the outflow loads of SS and T-P were small to compare with those inflow loads. The amount of accumulation of SS and T-P were about 1.3t and 2kg respectively when having no rainfall in the irrigation block. On the other hand, the outflow of SS and T-P were about 3.5t/day and 20kg/day respectively in rainy days. If 2015 year is compared to 2014, it had increased in T-P though the load of irrigation water each day at no rainfall periods and it had not been change in SS though an accurate comparison is difficult according to the missing value. However, after the cyclic irrigation had been started, the amount of the outflow loads had decreased greatly like 35% in SS and 38% in T-P. The balance of the outflow loads during the irrigation periods of 2014 were -470kg/day in SS, which meant the purification type, while +2.6kg/day in T-P. as a result, it was found that the introduction of cyclic irrigation system had worked for water purification in SS and T-P effectively.

Keywords: cyclic irrigation system, water pollution, suspended solid, total phosphorus

©2019. Japan Geoscience Union. All Right Reserved.

[E] Poster | A (Atmospheric and Hydrospheric Sciences)：A-HW Hydrology & Water Environment

Thu. May 30, 2019 5:15 PM - 6:30 PM JST | Thu. May 30, 2019 8:15 AM - 9:30 AM UTC | Poster Hall International Exhibition Hall8, Makuhari Messe_9

[A-HW22] Materials transport and nutrient cycles in watersheds; from headwaters to coastal seas

convener:Masahiro Kobayashi(Forestry and Forest Products Research Institute), Seiko Yoshikawa(Institute for Agro-environmental Sciences, National Agriculture and Food Research Organization), Jun Yasumoto(University of the Ryukyus, Faculty of Agriculuture), Adina Paytan(University of California Santa Cruz)

This session aims to synthetize watershed sciences in order to understand dynamical processes of materials transport and nutrient cycles in watersheds from headwaters to coastal seas. The session will be integrating a variety of research disciplines including limnology, ground water hydrology, coastal oceanography, meteorology, pedology, sedimentology, forestry, agriculture, fishery, ecology, social science and more. This session calls for ideas on new methods for the watershed sciences, such as tracer and molecular technique, hydrological modeling, paleontological approaches, laboratory and field experiments, social-scientific evaluation of ecosystem services and social-ecological systems, and so on, in order to elucidate physical, chemical and biological mechanisms for shedding light on natural phenomena and their changes over time in complex and dynamic watershed systems under human and climate impacts. Through this session, we would like to facilitate interdisciplinary collaboration among participants to create new knowledge on watershed sciences.

[AHW22-P01] Phosphate Enrichment Hampers Development of Juvenile Acropora digitifera Coral by Inhibiting Skeleton Formation

Mariko Iijima[1], *Yasumoto Ko[1], Jun Yasumoto[2], Mina Hirose[3], Mitsuru Jimbo[1], Shugo Watabe[1] (1.Kitasato University School of Marine Biosciences, 2.Faculty of Agriculture, University of the Ryukyus, 3.Tropical Technology Plus)

[AHW22-P02] Modeling chlorophyll-a concentration using remote sensing in shallow water systems: Comparison of sensors

*Assefa M Melesse[1], Tara Blakey[1], Mohammad Haji Gholizadeh[1], Mohd Manzar Abbas[1] (1.Florida International University)

[AHW22-P03] Dynamics in groundwater flow system with seasonal water table variation in a coastal and island

*Yusuke Tomozawa[1], Shin-ichi Onodera[1], Mitsuyo Saito[2] (1.Graduate School of Integrated Arts and Sciences Hiroshima University, 2.Graduate School of Environmental and Life Science, Okayama University)

[AHW22-P04] The Tracing of Groundwater Contamination Sources in Indonesian Coastal Alluvial Groundwater using $\delta^{34}S$ and $\delta^{15}N$ Isotopes

*Anna Fadliah Rusydi[1,4], Mitsuyo Saito[2], Seiichiro Ioka[3], Shin-ichi Onodera[1] (1.Graduate School of Integrated Arts and Sciences, Hiroshima University, Japan, 2.Graduate School of Environmental and Life Sciences, Okayama University, Japan, 3.Research Institute for Sustainable Energy, Hirosaki University, Japan, 4.Research Center for Geotechnology, Indonesian Institute of Sciences, Indonesia)

[AHW22-P05] Spatio-temporal dynamics of orthophosphate with implications for limitation of phytoplankton growth in north basin of Lake Biwa, Japan

*Xin Liu[1], Rong Yi[1], Masahiro Maruo[1], Syuhei Ban[1] (1.The University of Shiga Prefecture)

[AHW22-P06] Microbial phase analysis in aquifer of Ryukyu Limestone Zone using next generation sequencer

*Umi Murao[1], Jun Yasumoto[1], Yasumoto Ko[3], Mina Hirose[2], Nanami Mizusawa[3], Ryo Iguchi[4], Bam H.N. Razafindrabe[5], Syugo Watabe[3] (1.University of the Ryukyus, Faculty of Agriculuture Department of Regional Agricultural Engineering, 2.Tropical Tecnology Plus, 3.Kitasato University School of Marine Biosciences, 4.National Institute of Advanced Industrial Science and Technology, 5.University of the Ryukyus, Faculty of Agriculuture Department of Subtropical Agro-Environmental Sciences)

[AHW22-P07] Evaluation for temporal variation in groundwater inflow to the lagoons connected to Lake Biwa by radon (^{222}Rn) tracer analysis

*Mitsuyo Saito[1], Shin-ichi Onodera[2], Yusuke Tomozawa[2], Kunyang Wang[2], Syuhei Ban[3], Noboru Okuda[4] (1.Graduate School of Environmental and Life Science, Okayama University, 2.Graduate School of Integrated Arts and Sciences, Hiroshima University, 3.School of Environmental Sciences, The University of Shiga Prefecture, 4.Research Institute for Humanity and Nature)

[AHW22-P08] Br/Cl ratio characteristics of groundwater in coastal areas in Indonesia

*Seiichiro Ioka[1], Shin-ichi Onodera[2], Mitsuyo Saito[3], Anna Fadliah Rusydi[2,4] (1.Institute of Regional Innovation, Hirosaki University, Japan, 2.Graduate School of Integrated Arts and Sciences, Hiroshima University, Japan, 3.Graduate School of Environmental and Life Sciences, Okayama University, Japan, 4.Research Center for Geotechnology, Indonesian Institute of Sciences, Indonesia)

[AHW22-P09] Estimation of groundwater recharge and phosphorus transport under different precipitation conditions in a suburban catchment, using SWAT model

*Kunyang Wang[1,2], Shin-ichi Onodera[1], Mitsuyo Saito[3], Noboru Okuda[4], Takuya Okubo[5] (1.Graduate School of Integrated Arts and Science, Hiroshima University, 2.Capital Normal University, 3.Okayama University, 4.Research Institute for Humanity and Nature, 5.University of the Shiga Prefecture)

[AHW22-P10] Losses of phosphorus with soil erosion and nitrate with groundwater recharge in an agricultural catchment, subtropical small island

*Shin-ichi Onodera[1], Mitsuyo Saito[2], Yang Cao[1], Anna Fadliah Rusydi[1], Hide Omae[3], Yoshiko Iizumi[4], Yusuke Tomozawa[1] (1.Graduate School of Integrated and Arts Sciences, Hiroshima University, 2.Graduate School of Environmental and Life Science, Okayama University, 3.JIRCAS TARF, 4.JIRCAS HQ)

[AHW22-P11] Phosphate solubilizing bacteria as an indicator of sediment phosphorus in freshwater lakes

*Sreekumari Kurissery[1], Katelynn Crawford[1], Nandakumar Kanavillil[1] (1.Lakehead University, Canada)

[AHW22-P12] A Study on the dynamics of various phosphate forms in soil and groundwater in Ryukyu limestone regions

*Masashi Nozaki[1], Jun Yasumoto[2], Yasumoto Ko[3], Hirose Mina[4], Iijima Mariko[3], Ryuichi Shinjo[5], Bam H.N. Razafindrabe[6] (1.University of The Ryukyus, Graduate School of Agriculture,, 2.University of the Ryukyus, Faculty of Agriculture, Department of Regional Agricultural Engineering, 3.Kitasato University School of Marine Biosciences, 4.Tropical Technology Plus, 5.Department of Physics and Earth Sciences, University of the Ryukyus, 6.University of the Ryukyus, Faculty of Agriculture, Department of Subtropical Agro-Environmental Sciences)

[AHW22-P13] Impacts of highly concentrated turbid water on the groundwater in the Tedori River alluvial fan, Japan

*Yoichi Fujihara[1], Shunsuke Chono[1], Keiji Takase[1], Eiji Ichion[1] (1.Department of Environmental Science, Ishikawa Prefectural University)

[AHW22-P14] Altitude effect of water stable isotopic ratio of ravine water and its contribution to groundwater in alluvial plains - Comparison in east and west side catchments of Lake Biwa –

*Yusuke Tomozawa[1], Kunyang Wang[1], Mitsuyo Saito[2], Syuhei Ban[3], Noboru Okuda[4], Shin-ichi Onodera[1] (1.Graduate School of Integrated Arts and Sciences Hiroshima University, 2.Graduate School of

Environmental and Life Science, Okayama University, 3.School of Environmental Science, The University of Shiga Prefecture, 4.Research Institute for Humanity and Nature)

[AHW22-P15] Calculation of TN and TP concentration coefficients of river water for each land use by a simple watershed model.

*Seiko Yoshikawa[1], Donglai Ma[1,4], Tadamasa Saito[1,5], Kenji Matsumori[2], Yuko Itoh[3], Masahiro Kobayashi[3] (1.Institute for Agro-environmental Sciences, National Agriculture and Food Research Organization, 2.Western Region Agricultural Research Center, National Agriculture and Food Research Organization, 3.Forestry and Forest Products Research Institute, 4.Graduate school,Tsukuba University, 5.Faculty of Agriculture, Ibaraki University)

[AHW22-P16] **Possibility of nutrients transportation from littoral slope for enhancement of phytoplankton growth in north basin of Lake Biwa**

*Syuhei Ban[1], Rong YI[1], Xin Liu[1], Masahiro Maruo[1], Miki Sudo[1], Naoshige Goto[1], Jun Murase[2] (1.The University of Shiga Prefecture, 2.Nagoya University)

[AHW22-P17] SWAT model analysis for confirming the effects of crop growth on the suspended sediment concentration from a settling basin catchment on Ishigaki island

*Yang Cao[1], Shin-ichi Onodera[1], Mitsuyo Saito[2], Hide Omae[3], Yoshiko Iizumi[3] (1.Graduate School of Integrate Arts and Sciences, Hiroshima University, 2.Graduate School of Environmental and life Science, Okayama University, 3.Tropical Agriculture Research Front (TARF), Japan International Research Center for Agricultural Sciences (JIRCAS))

[AHW22-P18] Estimating the runoff of water, sediment, and nutrient using SWAT model in Kikuchi-river watershed, Kumamoto, and the influence of the forest

*Soichiro Fujii[1], Masahiko Kanamori[1], Yuko Nagano[1], Maki Kinoshita[2], Yuta Shimizu[3], Shin-ichi Onodera[4] (1.Japan Forest Technology Association, 2.PASCO Corporation, 3.Western Region Agricultural Research Center, National Agriculture and Food Research Organization, 4.Graduate School of Integrated and Arts Sciences, Hiroshima University)

[AHW22-P19] Atmospheric depositions on forest ecosystems in areas along the Sea of Japan

*Yuko Itoh[1], Keiji Takase[2], Yoichi Fujihara[2], Toru Okamoto[1] (1.Forestry and Forest Products Research Institute, Japan, 2.Ishikawa Prefectural University)

[AHW22-P20] Continuous and simultaneous flux measurement of N_2O and CO_2 from agricultural soil using a portable multi-turn time-of-flight mass spectrometer

*Noriko Nakayama[1], Yusuke Iwai[1], Yo Toma[2], Hiroshi Furutani[1], Ryusuke Hatano[3], Michisato Toyoda[1] (1.Osaka University, 2.Ehime University, 3.Hokkaido University)

[AHW22-P21] Effects of introduction of cyclic irrigation system on mass balances of SS and T-P in Lake Inbanuma, Chiba, Japan

*Tomijiro Kubota[1] (1.National Agriculture and Food Research Organization, Institute for Rural Engineering)

Phosphate Enrichment Hampers Development of Juvenile Acropora digitifera Coral by Inhibiting Skeleton Formation

Mariko Iijima[1], *Yasumoto Ko[1], Jun Yasumoto[2], Mina Hirose[3], Mitsuru Jimbo[1], Shugo Watabe[1]

1. Kitasato University School of Marine Biosciences, 2. Faculty of Agriculture, University of the Ryukyus, 3. Tropical Technology Plus

Coral reef degradation resulting from various types of local stress on corals such as excessive nutrient enrichment in and gravel inflow into coastal waters is of an increasing global concern. Because tropical and subtropical seawaters are generally poor in nutrients and thus oligotrophic, these stresses are thought to result in the decline of environments favorable to coral growth. Inorganic phosphates have been especially considered to possibly inhibit the formation of coral skeleton. Despite many studies available on the effects of nutrients on corals, a clear consensus for how nutrients exert deteriorative effects on the corals has not been established satisfactorily. Recently, we found that biogenic polyamines react with carbon dioxide (CO_2) and accelerate an aragonite formation of calcium carbonate ($CaCO_3$) in seawater. In this study, we examined the effects of phosphates and nitrates on *in vitro* aragonite formation of $CaCO_3$ by using biogenic polyamines and *in vivo* aragonite formation of juvenile coral *Acropora digitifera* skeletons, showing that phosphates clearly inhibited both *in vitro* and *in vivo* $CaCO_3$ formations at similar concentrations. In contrast, nitrates inhibited neither *in vitro* aragonite formation of $CaCO_3$ nor *in vivo* aragonite formation of juvenile coral skeletons. These findings indicate that phosphates have a detrimental effect on bioinorganic coral calcification. Furthermore, the findings that phosphate enrichment inhibits coral skeleton formation led us to conclude that enriched phosphate is adsorbed on juvenile coral skeleton surface and inhibits inorganically normal development of juvenile coral skeleton.

Keywords: phosphate, calcification

©2019. Japan Geoscience Union. All Right Reserved.

Modeling chlorophyll-a concentration using remote sensing in shallow water systems: Comparison of sensors

*Assefa M Melesse[1], Tara Blakey[1], Mohammad Haji Gholizadeh[1], Mohd Manzar Abbas[1]

1. Florida International University

The level of productivity in the upland and coastal water bodies is highly linked to land processes (land use, water management, water and nutrient fluxes). Understanding the linkage between these processes and the level of algal blooms in the water bodies is crucial for improving water quality. A comparative study was conducted using remote sensing data from three different sensors (SeaWIFS, MoDIS and Landsat) to evaluate the capability of reflectance data from these sensors for estimation of chl-a concentrations in three water bodies in the USA (Lake Okeechobee, Florida Bay and Chesapeake Bay). Observed chl-a data were gathered and compared with simulation results. The analysis found that all of the sensors have performed well in deeper water bodies than in shallow sections due to the bottom reflectance from non-algal blooms. For shallow water bodies, selection of the proper bands and band combinations, identification of the non-algal bloom reflectance and the corresponding algorithms can improve the simulation. Seasonality as well as spatial variability (using cross-sections) were evaluated and the results showed that chl-a values were highly variable for the selected summer months. Indicative of the effect of land surface fluxes of nutrients, chl-a values were higher closer to coastal areas in the Florida bay and Chesapeake Bay. The chl-a in the freshwater lake of Okeechobee was simulated using Landsat 8 data and the results found were very good. Comparison of the SeaWIFS and MoDIS chl-a value to that of the measured concentrations in the deeper section of Florida Bay and Chesapeake Bay, respectively showed very good agreement.

Keywords: Chl-a, SeaWIFS, Water qulity modeling, South Florida, Remote sensing

©2019. Japan Geoscience Union. All Right Reserved.

Dynamics in groundwater flow system with seasonal water table variation in a coastal and island

*Yusuke Tomozawa[1], Shin-ichi Onodera[1], Mitsuyo Saito[2]

1. Graduate School of Integrated Arts and Sciences Hiroshima University, 2. Graduate School of Environmental and Life Science, Okayama University

In islands, freshwater water resources are valuable as living and agricultural use, and dug wells water and reservoirs had been utilized for more than 100 years. In order to use such water resources sustainably, it is important to evaluate groundwater flow as well as water budget.

In this research, we examined to confirm the seasonal variation in water stable isotopic ratios in observation boreholes at the coastal lowland in Ikuchi Island Hiroshima prefecture. Moreover, considering that the target area is coastal, Cl^- concentration was analyzed to evaluate the influence of salt fresh water boundary.

The experimental site is located on Ikuchi Island in Hiroshima prefecture. The highest altitude is 456 m. The basement rock is mainly composed of granite. Annual average precipitation is 1058.8 mm. Observation boreholes are located at the coastal lowland in the southeastern part of the island. The upper site (Site U) with the altitude of 5.1 m asl has 3 boreholes with the depths of 2 m, 15 m, 30 m, the lower site (Site D) with 2.5 m asl has 8 with the depth of 1 m, 2 m, 3 m, 10 m, 15 m, 20 m, 30 m, 40 m, respectively. The water sampling was carried out from monthly to half year interval since 2015. Every samples were analyzed for water isotopic ratios by PICARO and anion component by ion chromatography. Especially samples in January in 2019 were analyzed for CFCs and SF6.

Based on the previous study (Saito and Onodera, 2007), the distinct altitude effect of isotopic ratio in precipitation has been confirmed. Due to spatial and temporal variations in isotopic ratios, recharge process to groundwater was suggested as follows, 1) recharge on site to shallow groundwater (2-3m deep) at D ($\delta^{18}O$: -7.8 to - 7.4 ‰), 2) river water contribution to the shallow groundwater (2-15m) at U ($\delta^{18}O$: - 8.3 to - 7.5 ‰), 3) recharge in the mountain slope with the altitude of about 360 m to deep groundwater (30m) at U ($\delta^{18}O$: - 8.4 to - 8.1 ‰), 4) recharge at 400 m on near the mountain top to deep groundwater (10-30 m) at D($\delta^{18}O$: - 8.7 to - 8.4 ‰), 5) recharge of precipitation with lower isotope than in present to deeper groundwater (40 m) at D ($\delta^{18}O$: -8.9 to - 8.8 ‰)

The deepest groundwater (40m) at D had lower isotopic ratios with higher Cl^- concentration (250 to 584 mg / L) during a lower water table in the winter. This indicated the seawater –fresh water boundary rose with water table according to Gyben-Hrzberg concept. These phenomena also suggest to cause the rise of deeper and older groundwater flow line. Consequently, we suggest the lower isotopic ratio in deeper groundwater indicates the immobile water which were recharged in the glacial period. Based on other tracers (CFC, SF 6), we will discuss more.

Keywords: stable isotope, groundwater, coastal

©2019. Japan Geoscience Union. All Right Reserved.

The Tracing of Groundwater Contamination Sources in Indonesian Coastal Alluvial Groundwater using $\delta^{34}S$ and $\delta^{15}N$ Isotopes

*Anna Fadliah Rusydi[1,4], Mitsuyo Saito[2], Seiichiro Ioka[3], Shin-ichi Onodera[1]

1. Graduate School of Integrated Arts and Sciences, Hiroshima University, Japan, 2. Graduate School of Environmental and Life Sciences, Okayama University, Japan, 3. Research Institute for Sustainable Energy, Hirosaki University, Japan, 4. Research Center for Geotechnology, Indonesian Institute of Sciences, Indonesia

The coastal area is one of the Indonesian Government priorities as an archipelago country. The groundwater in the area is one of the most reliable clean water resources, therefore it is crucial to understanding the vulnerability of this resource. Our research area was located at Indramayu, a developing rural coastal area in Indonesia, where, the environment was relatively pristine. This research aimed was to identify the effect of natural condition and human activity to groundwater quality by using stable isotope $\delta^{34}S$ and $\delta^{15}N$.

Totally, there were 20 samples taken from groundwater (18) and river (2). The nitrate and sulfate were detected in a total of 5 and 19 samples, respectively. The isotopes composition for isotope nitrate were -11.2 ‰–+22.22‰ for $\delta^{15}N\text{-}NO_3$ and -3.4 ‰–+17.1‰ for $\delta^{18}O\text{-}NO_3$. Moreover, the values of $\delta^{34}S\text{-}SO_4$ and $\delta^{18}O\text{- }SO_4$ were varied from -4.2 ‰–+28.4‰ and +7.3 ‰–+18.8 ‰, respectively. The isotopic signatures of nitrate suggested that the used of inorganic fertilizer and animal manure give the impact to both groundwater and river. Similarly, the isotopic signatures of sulfur were showing that those detected sulfate in the groundwater were mostly coming from fertilizer. Moreover, the soil was mineralized by organic sulfate as well. At one point, located in the fishery area, the groundwater was indicated the seawater contamination. It was shown by the heavy composition of sulfur isotope (28.4‰ for $\delta^{34}S$ and 18.8‰ for $\delta^{18}O$). Lastly, our results showed those combined isotopes of $\delta^{34}S$ and $\delta^{15}N$ along with land-use evaluation could explain the possible sources of groundwater in coastal area at very early urbanization stage.

Keywords: Sulfur Isotope, Nitrate Isotope, Coastal Groundwater, Indramayu

©2019. Japan Geoscience Union. All Right Reserved.

Spatio-temporal dynamics of orthophosphate with implications for limitation of phytoplankton growth in north basin of Lake Biwa, Japan

*Xin Liu[1], Rong Yi[1], Masahiro Maruo[1], Syuhei Ban[1]

1. The University of Shiga Prefecture

Orthophosphate (PO_4-P) is the main chemical form of phosphorus (P) for phytoplankton growth, often considered as a limiting nutrient for primary production in freshwater ecosystems. However, few information on accurate measurements for PO_4-P concentrations in epilimnion of meso- and oligotrophic lakes due to lower than the detection limit (60 nM) of soluble reactive P using traditional spectrophotometrical method. In the present study, we measured PO_4-P concentrations using ion chromatography with a detection limit of 5 nM, and determined truly vertical distribution of PO_4-P throughout the year with other abiotic and biotic environmental factors in north basin of Lake Biwa, to accurately understand biogeochemical processes of P in this mesotrophic lake.

Field investigations were conducted monthly from April to December 2018 at station K4 (35º19'9.6"N, 136º11'2.7"E; 50 m deep). Phosphate enrichment experiments were also made at each sampling occasion to clarify P limitation for phytoplankton growth. Lake water including phytoplankton assemblage collected from epilimnion (0–20 m) was enriched with 1 μM of PO_4-P (+P) and incubated together with untreated one (control) for 2 days under ambient light and temperature conditions. To evaluate the effect of potentially nutrient-rich bottom water, the filtered bottom water was mixed with untreated epilimnion water including phytoplankton at 1:1 (+B) was incubated at the same conditions as the +P treatment. Phytoplankton growth rate (g) was calculated with equation of $g=\ln(C_t/C_0)/2$, where C_0 and C_t are chlorophyll *a* (chl. *a*) concentrations at start and end of the experiment, respectively.

Water temperature increased in the epilimnion from May, and strict thermocline was developed from June to September. Chl. *a* concentrations increased from June to July in 10–20 m, and from October to November in 0–20 m. PO_4-P concentrations were always low, <20 nM, in the epilimnion from April to June. The concentrations below 30 m increased up to 140 nM in May, but decreased after that until July. In August and September, the concentrations increased up to 30–40 nM even in the epilimnion probably due to disturbance by typhoon. The concentrations below 30 m increased with depth, and the highest values were frequently observed near the bottom, up to 220 nM. On average throughout the water column, PO_4-P concentrations were 24–48 nM from April to June, then slightly increased up to 73 nM until September, being constant, 50–63 nM until December.

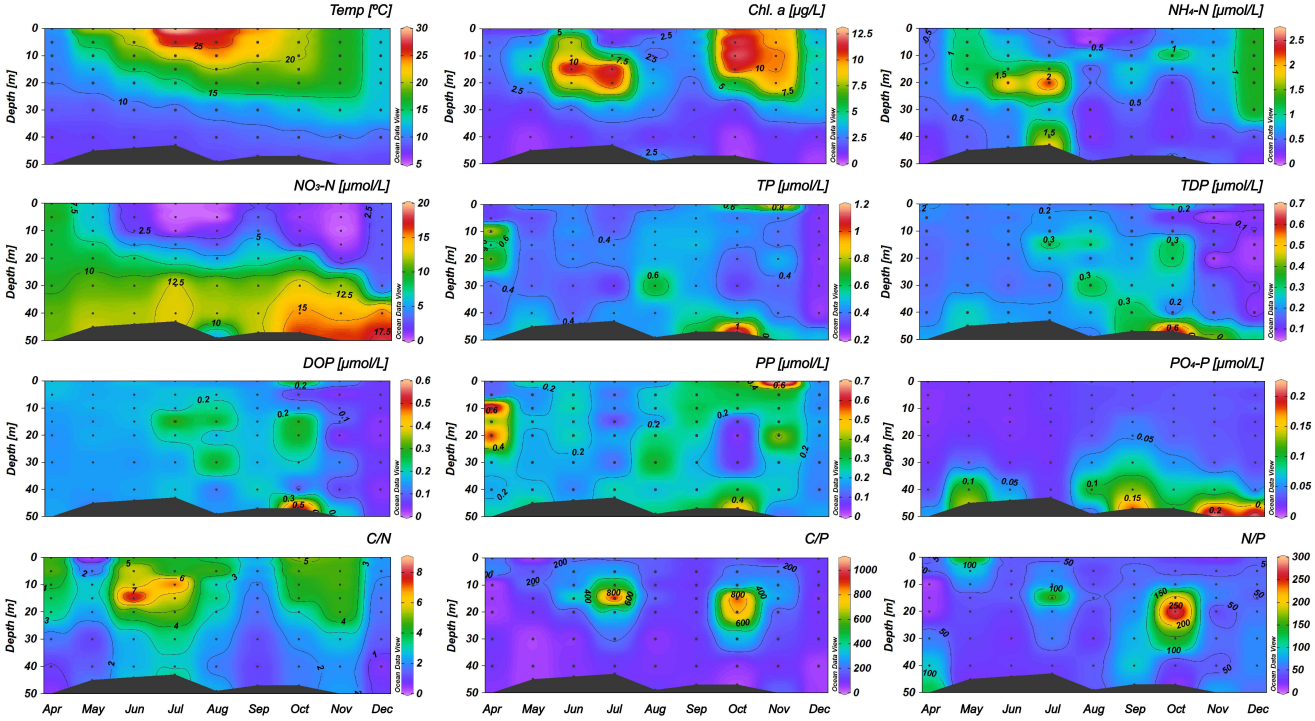
Total P, total dissolved P, dissolved organic P and particulate P exhibited similar spatio-temporal distributions, but different pattern from those of PO_4-P. NH_4-N increased in 10–20 m from May to July, whereas the NO_3-N increased in the hypolimnion as season progressed. Sestonic C:N:P ratios suggested a terrible P deficiency in July and October when phytoplankton biomass increased.

Phosphate enrichment experiments showed that phytoplankton in the epilimnion was mostly limited with P for its growth. Phytoplankton g in control varied −0.05-0.08 d^{-1}, being always lower than those in +P (−0.04-0.44 d^{-1}) and/or +B (−0.04-0.49 d^{-1}) treatments except for November and December. In November, no growth was found even in +P treatment. This might be caused by nitrogen limitation because of <6 μM of NO_3-N in the epilimnion. The g of control was similar as that of +P and +B (ca. 0.1 d^{-1}) in December, indicating that P deficiency for phytoplankton growth was relaxed until December by vertical convection.

©2019. Japan Geoscience Union. All Right Reserved.

We firstly determined completely vertical distributions of PO_4-P in north basin of Lake Biwa from spring to winter, and detected 20–40 nM of PO_4-P in the epilimnion. Phosphate enrichment experiments showed that 20 nM of PO_4-P might be critical concentration for phytoplankton growth in the lake. No phytoplankton growth even in +P treatment in November implied that nitrogen limitation for phytoplankton growth will be possible in Autumn. Further study for clarify this will be needed.

Keywords: Orthophosphate dynamics, Phosphorus limitation, Phytoplankton growth rate, Ion chromatography, Biogeochemical processes, Freshwater ecosystem



©2019. Japan Geoscience Union. All Right Reserved.

Microbial phase analysis in aquifer of Ryukyu Limestone Zone using next generation sequencer

*Umi Murao[1], Jun Yasumoto[1], Yasumoto Ko[3], Mina Hirose[2], Nanami Mizusawa[3], Ryo Iguchi[4], Bam H.N. Razafindrabe[5], Syugo Watabe[3]

1. University of the Ryukyus, Faculty of Agriculuture Department of Regional Agricultural Engineering, 2. Tropical Tecnology Plus, 3. Kitasato University School of Marine Biosciences, 4. National Institute of Advanced Industrial Science and Technology, 5. University of the Ryukyus, Faculty of Agriculuture Department of Subtropical Agro-Environmental Sciences

Clean water and sanitation (Sustainable development Goals (6)) is one of the world's important issues. People use groundwater in many areas as a water source, but various cases of contamination by agricultural activities and substances derived from human and animal excrements have been reported.

On the other hand, genetic analysis techniques using molecular biological methods have been applied to the analysis of microbial phase in the water environment.

In recent years, the method using the latest analysis equipment of next generation Sequencer is established, mainly for microorganisms. In addition, new monitoring indices such as environmental DNA have been developed. It is thought that the microbial phase in groundwater varies depending on the influence of various environmental factors and human activity, but the actual condition is not clear.

The next generation Sequencer is a very powerful tool used to grasp the microbial phase in groundwater. It is thought that the microbial phase can be an important indicator in water resource management of basins in the future.

The purpose of this study is to investigate the microbial species and their coexistence in groundwater in the Ryukyu Limestone area using the next generation sequencer.

Keywords: groundwater, microbial community analysis, genetic analysis

©2019. Japan Geoscience Union. All Right Reserved.

Evaluation for temporal variation in groundwater inflow to the lagoons connected to Lake Biwa by radon (^{222}Rn) tracer analysis

*Mitsuyo Saito[1], Shin-ichi Onodera[2], Yusuke Tomozawa[2], Kunyang Wang[2], Syuhei Ban[3], Noboru Okuda[4]

1. Graduate School of Environmental and Life Science, Okayama University, 2. Graduate School of Integrated Arts and Sciences, Hiroshima University, 3. School of Environmental Sciences, The University of Shiga Prefecture, 4. Research Institute for Humanity and Nature

Primary production in freshwater lakes and reservoirs are usually controlled by phosphorus (P). Lacustrine groundwater discharge (LGD), direct discharge of subsurface water to lake, is regarded as a potential nutrient paths, including phosphorus from a catchment to lake water environment. There are more than 20 lagoons around Lake Biwa which were originally a part of the lake. These lagoons are regarded to have important functions as settling ponds of inflowing loads from the catchments to Lake Biwa, refuges for shallow water ecosystems and so on. Because these lagoons are connected to Lake Biwa, evaluation of nutrient budget is important for the nutrient cycle in the lake. Some researchers have pointed out the presence of LGD in littoral area of Lake Biwa. However, it has not been evaluated for the lagoons around the lake. In the present research, we aimed to evaluate the temporal variation in groundwater inflow to a lagoon connected to Lake Biwa by radon (^{222}Rn) tracer analysis.

The field campaigns were conducted in December 2017, August and October 2018 for the lagoons (Noda-Numa and Hasu-Ike) located on northeastern shore of Lake Biwa. The volume of inflow and outflow, water temperature, electric conductivity, chlorophyll-a and radon (^{222}Rn) concentration were measured in the lagoon. ^{222}Rn is a radioactive element of uranium (^{238}U) series with 3.8 day of half-life. ^{222}Rn is a useful tracer of groundwater discharge because it generally enriched in groundwater than surface water. To examine the temporal variation in groundwater inflow, the time-series ^{222}Rn concentration in water was obtained. Water samples were collected at the inlet, outlet and near the center of the lagoons and natural springs and groundwater wells around the lagoons. Water and ^{222}Rn balance suggest that groundwater inflow is larger in Noda-Numa than Hasu-Ike. The catchment topography may influence on this difference. ^{222}Rn balance-based residence time of lagoon water was estimated 10-20 days in Noda-Numa, and 4-5 days in Hasu-Ike, were similar with that based on water balance. These results suggest the groundwater inflow is a potential phosphorus path to Noda-Numa.

Keywords: Groundwater inflow, Connected lagoons, Lake Biwa, Radon (222Rn)

©2019. Japan Geoscience Union. All Right Reserved.

Br/Cl ratio characteristics of groundwater in coastal areas in Indonesia

*Seiichiro Ioka[1], Shin-ichi Onodera[2], Mitsuyo Saito[3], Anna Fadliah Rusydi[2,4]

1. Institute of Regional Innovation, Hirosaki University, Japan, 2. Graduate School of Integrated Arts and Sciences, Hiroshima University, Japan, 3. Graduate School of Environmental and Life Sciences, Okayama University, Japan, 4. Research Center for Geotechnology, Indonesian Institute of Sciences, Indonesia

The urban development in Indonesia’ s coastal areas has led to an increase of groundwater demand, which then has resulted in groundwater salinization. In this study, we analyze bromide and Br/Cl ratio characteristics, as index of groundwater salinization, in three cities of Indonesian coastal areas, namely: Indramayu, Mataram, and Semarang. Each research site is at different stage of urbanization. Indramayu is in very early stage of urbanization, followed by Mataram as a developing tourism area, and the last one Semarang as a heavy urbanization city. The results show that concentrations of bromide in groundwater are ranged from 0.05 to 38 mg/L in Indramayu, 0.01 to 0.8 mg/L in Mataram, and 0.02 to 8.0 mg/L in Semarang. Furthermore, the occurrence of Br is described in terms of the Br/Cl weight ratio, which allows for small changes in bromide concentrations to be assessed in terms of salinity. Median values of Br/Cl weight ratio in the groundwater of Indramayu, Mataram, and Semarang were approximately 0.0035, 0.0027, and 0.0025, respectively, while the ratio in seawater is generally around 0.0035. The relationship between Br/Cl weight ratio and chloride concentration indicate the groundwater in Indramayu is undergoing salinization due to seawater intrusion compared to the other two areas, meanwhile the groundwater in Semarang is experiencing chloride contamination due to anthropogenic activities based on the study by Andreasen and Fleck (1997).

Keywords: Indonesia, groundwater, Br/Cl ratio, coastal area

©2019. Japan Geoscience Union. All Right Reserved.

Estimation of groundwater recharge and phosphorus transport under different precipitation conditions in a suburban catchment, using SWAT model

*Kunyang Wang[1,2], Shin-ichi Onodera[1], Mitsuyo Saito[3], Noboru Okuda[4], Takuya Okubo[5]

1. Graduate School of Integrated Arts and Science, Hiroshima University, 2. Capital Normal University, 3. Okayama University, 4. Research Institute for Humanity and Nature, 5. University of the Shiga Prefecture

The quantification of the groundwater recharge and phosphorus transport in water is one of the most important indicators of the water cycle in lakes because these processes are related to the transport of large nutrient loads. The Yasu River is one of the important water sources of the Biwa Lake. In this paper, Geographic Information System technology is used to analyze and predict the land use change in the Yasu River Basin. The water balance was simulated using the Soil and Water Assessment Tool. Simulations of different years in different precipitation seasons were carried out. The correlation coefficient and the Nash Sutcliffe coefficient are higher than the reference values. The sensitivity analysis of the parameters reveals the different degrees of sensitivity of the parameters in different water seasons, CN2 always has a high sensitivity during all kinds of water season. The total groundwater recharge and discharge are 180 million m^3 and 179 million m^3 in the normal precipitation season, respectively. The trends differ in the dry and wet seasons. In the dry season of 2007, the groundwater recharge was below 140 million m^3, while it exceeded 240 million m^3 in the rainy season in 2003. In addition, the process of phosphorus loss in the basin and release into Lake Biwa are explained from the perspective of space and time. This is closely related to the spatial distribution of the main channel and the time distribution of precipitation. The total amount of nonpoint source pollution of phosphorus in three years is equivalent to 4.08 kg/ha of paddy fields in the watershed. The spatial distribution of phosphorus loss is related to the stream flow, it is mainly concentrated in the area with paddy fields and urban. The time distribution is related to the distribution of the precipitation. With increasing precipitation, the nonpoint source pollution of phosphorus slightly increases. This is due to the driving effect of precipitation on the phosphorus transfer and erosion of soil.

Keywords: Phosphorus transport, Groundwater recharge, Different precipitation conditions, SWAT model

©2019. Japan Geoscience Union. All Right Reserved.

Losses of phosphorus with soil erosion and nitrate with groundwater recharge in an agricultural catchment, subtropical small island

*Shin-ichi Onodera[1], Mitsuyo Saito[2], Yang Cao[1], Anna Fadliah Rusydi[1], Hide Omae[3], Yoshiko Iizumi[4], Yusuke Tomozawa[1]

1. Graduate School of Integrated and Arts Sciences, Hiroshima University, 2. Graduate School of Environmental and Life Science, Okayama University, 3. JIRCAS TARF, 4. JIRCAS HQ

In tropical and subtropical region, the rainfall intensity is strong and soil erosion in an agricultural land is one of big environmental issues. Especially, the impact of large sediment discharge on the coral reef is serious around small islands, such as Okinawa and Philippines. In case of Okinawa Prefecture, to reduce the sediment discharge and conserve corals, many sediment trap ponds are constructed in a downstream area of agricultural lands. However, sediment deposition rate, variation of trap effect, and component of sediment in a pond have not been confirmed.

To estimate of erosion rate and deposition process of a small pond in an agricultural catchment of a subtropical small island, we examine to observe the sediment deposition in a small pond and monitor water level and chlorophyll a in a pond and runoff and turbidity of an inflow stream in a small catchment with the area of 300m2 in Ishigaki Island, Okinawa Prefecture, Subtropical region. Our monitoring was started from February 2017 after removing all sediment in a pond in January, and up to April 2018. Observation of sediment deposition was conducted with collecting the samples at 5 sites in June 2017 and January 2018. Inflow and outflow water samples were collected every one month.
The sediment deposition was extremely large from January to May 2017, the average erosion rate in all catchment area was estimated to be 6mm. On the other hand, the sediment deposition was nothing from June 2017 to January 2018. Based on the monitoring of stream runoff and turbidity, one big storm event in April with strong intensity mainly contributes to sediment discharge and overflow of the pond occurred. On the other hand, the later period had also big events. This difference is suggested to be the difference of land cover by crops and availability of sediment trap in this pond. In addition, the sediment component mainly was composed of surface soft layer, subsurface sandy layer, and bottom gravel layer. The average thickness was 2cm in surface layer, 100cm in mid sandy layer, and 10cm in gravel layer, respectively. Especially, the surface soft layer had high nutrient content. The dissolved nutrient of inflow stream water and pond water were high concentration. But the 10% of nutrient in the inflow decreased in pond. This means the plankton was produced, using this nutrient and that was deposited later. The soft layer is suggested to be effect of organic fertilizer, it is expected to apply to agricultural lands.

Keywords: Phosphorus, groundwater, nitrate

©2019. Japan Geoscience Union. All Right Reserved.

Phosphate solubilizing bacteria as an indicator of sediment phosphorus in freshwater lakes

*Sreekumari Kurissery[1], Katelynn Crawford[1], Nandakumar Kanavillil[1]

1. Lakehead University, Canada

It has been well documented that phosphorus pollution is one of the most significant factors impeding the overall health of freshwater lakes. Various measures are being taken to reduce phosphorus input into the lakes by anthropogenic activities and thus to maintain a healthy ecosystem. However, it is well known that bioavailable phosphorus tends to bind with substances such as ferric iron and calcium present in the water, become insoluble, and settles into the sediments. The presentstudy has been carried out to understand the relationship between the sediment phosphorus concentration and density of phosphate solubilizing bacteria (PSB) in two lakes in Ontario, Canada, namely, Lake Simcoe and Sparrow Lake. In September 2017, 20cm sediment cores were collected from the nearshore sites of these two lakes to determine the presence of PSB in relation to the sediment phosphorus concentration. PSB could potentially release phosphorus back into the water column through a process called internal phosphorus loading from the inorganic phosphates in the sediment when the right conditions are present. PSB were isolated from the sediment cores at 5 cm intervals by plating on to Pikovskaya’ s agar. Five grams of sediment was used to analyze total reactive phosphorus in the sediment. In Lake Simcoe, PSB ranged from $3x10^1$ to $1.1x10^1$ cfu/g, and the amount of total reactive phosphorus ranged from 0.19 to 0.46 mg/g. In Sparrow Lake, PSB ranged from $4x10^0$ to $3x10^1$ cfu/g and the amount of total reactive phosphorus ranged from 0.21 to 0.39 mg/g. A linear regression was completed to determine the relationship between total reactive phosphorus and PSB for each core. The results showed a negative relationship between these two tested parameters (Lake Simcoe: r^2=0.23, $y = -35.34x + 30.811$ p=0.5206, and Sparrow Lake: r^2 =0.87, $y = -155.9x + 62.322$, p=0.067). While PSB density decreased with core depth, the concentration of reactive phosphorus increased. This indicates that the density of PSB in lake sediment may indicate the concentration of total reactive phosphorus and thus the internal phosphorus loading. More study is recommended to confirm the results.

Keywords: Phosphate Solubilizing Bacteria, Freshwater Lakes , Sediment Phosphorus , Canada

©2019. Japan Geoscience Union. All Right Reserved.

A Study on the dynamics of various phosphate forms in soil and groundwater in Ryukyu limestone regions

*Masashi Nozaki[1], Jun Yasumoto[2], Yasumoto Ko[3], Hirose Mina[4], Iijima Mariko[3], Ryuichi Shinjo[5], Bam H.N. Razafindrabe[6]

1. University of The Ryukyus, Graduate School of Agriculture,, 2. University of the Ryukyus, Faculty of Agriculture, Department of Regional Agricultural Engineering, 3. Kitasato University School of Marine Biosciences, 4. Tropical Technology Plus, 5. Department of Physics and Earth Sciences, University of the Ryukyus, 6. University of the Ryukyus, Faculty of Agriculture, Department of Subtropical Agro-Environmental Sciences

Phosphorus in water environment exists in various forms and size, such as dissolved, particulate, organic and inorganic forms. However, there are many unclear points in Phosphorus in groundwater. In this study, we tried to understand the dynamics of various phosphate forms in soil and groundwater in Ryukyu limestone regions by combining Inductively Coupled Plasma Atomic Emission Spectrometry (ICP-AES) and ^{31}P Nuclear Magnetic Resonance (^{31}P-NMR), in addition to Colorimetric (molybdenum blue method). From August 2017 to August 2018, we took groundwater samples in southern part of Okinawa, Japan, with Ryukyu limestone distribution on a monthly basis. We measured pH, electronic conductivity (EC), Oxidation-Reduction Potential (ORP), dissolved oxygen (DO) and alkalinity (HCO_3^-) on site, and analyzed major dissolved ion (Cl^-, HCO_3^-, NO_2^-, NO_3^-, SO_4^{2-}, Na^+, K^+, Mg^{2+}, Ca^{2+}), suspended solid (SS) and phosphorus concentration. Phosphorus concentration analyzed 3 different method to molybdenum blue method (Col-P), ICP-AES (ICP-P) and Total P (T-P). Phosphate form analysis used ^{31}P-NMR.
We compared Col-P and ICP-P in order to understand dissolved phosphorus spatial distribution. The results show that ICP-P is 1.06~49.24 times larger than Col-P. It is inferred that ICP-P is also measuring fine particulate phosphorus and organic phosphorus. As a result, several forms of phosphate without orthophosphate were found in groundwater. Particulate phosphorus was determined by subtracting ICP-P from T-P. A positive correlation (r= 0.78) was found between P-P and SS. According to these results, it is thought that PP adsorbs various forms of phosphate including orthophosphate. We analyzed the correlation between dissolved phosphorus (Col-P, ICP-P) and all measured value in order to understand the characteristics of seasonal variation to dissolved phosphorus. There was a negative correlation between Col-P to water temperature. When focusing on seasonal variation of Col-P, we found that Col-P concentration decreases when water temperature increases. Moreover, Col-P concentration increases as water temperature increases. Through the analysis of various forms of phosphate in soil and SS by using ^{31}P-NMR, along with orthophosphate, pyrophosphate, pyrophosphate ester, orthophosphate monoester were also detected. It is thus suggested that the phosphate of polymeric or organic forms other than orthophosphate are from plant origin, as a result of microbial activities and microorganism decomposition.

Keywords: Phosphorus, 31P-NMR, Groundwater

©2019. Japan Geoscience Union. All Right Reserved.

Impacts of highly concentrated turbid water on the groundwater in the Tedori River alluvial fan, Japan

*Yoichi Fujihara[1], Shunsuke Chono[1], Keiji Takase[1], Eiji Ichion[1]

1. Department of Environmental Science, Ishikawa Prefectural University

The Tedori River alluvial fan in the Ishikawa prefecture is a representative alluvial fan in the Hokuriku region in Japan. The river water is taken by a headworks located at the top of the alluvial fan and is used for irrigation in paddy fields with a total area of about 7,500 ha. Seepages from the riverbed and percolations from the paddy area are the main sources of groundwater in the Tedori River alluvial fan. In 2015, large-scale landslides in the upper reaches of the Tedori River caused a long period of high turbidity in the river. Highly concentrated turbid water with an average concentration of 585 mg/L (a maximum of 4,012 mg/L) has been discharged continuously into the river since May, 2015. This turbidity has caused concerns about the recharge functions of groundwater in the alluvial fan.

In this study, the measurements of paddy percolations and riverbed seepages, before and after the occurrence of high turbidity, were used to examine the influence of these phenomena on groundwater recharge functions in the alluvial fan. We measured water requirement rates in the paddy area in the Tedori River alluvial fan. The measurements were conducted before and after the midsummer-drainage period at >100 paddy fields. We also measured the river discharges in the cross-sections of the river throughout the alluvial fan. The number of cross-sections was 16 and we estimated the riverbed seepages by calculating the discharge differences between the cross-sections.

The results revealed that the amount of paddy percolation decreased significantly due to the turbidity of the river water. The average percolation in the paddy area was found to be 12.4 mm/day in 2014 and 7.9 mm/day in 2016 before the midsummer-drainage period. Moreover, the average percolation in the paddy was found to be 19.6 mm/day in 2014 and 13.7 mm/day in 2016 after the midsummer-drainage period. The volume of the riverbed seepage was observed to have reduced and the seepage section were also observed to have shortened. The observed seepages from the river bed were 4.72 m3/s in 2009 and 3.33 m3/s in 2016 for the irrigation period, whereas for the non-irrigation period, these values were 5.92 m3/s in 2009 and 1.25 m3/s in 2016. Furthermore, the seepage section was found to shorten from 14.2 km to 8.0 km, due to the high turbidity of the water.

Finally, we estimated the amount of groundwater recharge based on these measurements, which revealed that the groundwater recharge from paddy percolation decreased by 270 mm/year (36%), and the recharge from riverbed decreased by 591 mm/year (61%). The total groundwater recharge decreased by 861 mm/year (36%), a value that corresponded to the groundwater level measurements. From these results, we can conclude that the effects of highly concentrated turbid water on the groundwater are quite serious in the Tedori River alluvial fan.

Keywords: groundwater, paddy percolation, riverbed seepage

©2019. Japan Geoscience Union. All Right Reserved.

Altitude effect of water stable isotopic ratio of ravine water and its contribution to groundwater in alluvial plains - Comparison in east and west side catchments of Lake Biwa –

*Yusuke Tomozawa[1], Kunyang Wang[1], Mitsuyo Saito[2], Syuhei Ban[3], Noboru Okuda[4], Shin-ichi Onodera[1]

1. Graduate School of Integrated Arts and Sciences Hiroshima University, 2. Graduate School of Environmental and Life Science, Okayama University, 3. School of Environmental Science, The University of Shiga Prefecture, 4. Research Institute for Humanity and Nature

The stable isotope ratio of hydrogen and oxygen in water is one of useful tracers for hydrological cycle and processes in the catchment scale as well as global. The typical characteristics are spatial or geographical distribution trend such as “altitude effect” or “inland effect”, which are lower in the higher altitude or more inland. Based on these trend, the groundwater recharge area had been estimated. However, the merger of these effects and additional effect such as the seasonal variation of isotopic ratio in precipitation or vapor causes various trend.
In this study, we examined to confirm the altitude effect of water stable isotope ratio and estimate recharge altitude to groundwater in alluvial plains, with comparing in the east and west side catchments of Lake Biwa .
Sampling of spring water in the Serikawa upstream area on the east side of Lake Biwa was conducted in July 2017, December 2017, August 2018. Sampling of ravine water in the Adogawa / Ukawa upstream area on the west side of Lake Biwa was conducted in August 2018. Water samples of spring in the head water and groundwater in the alluvial plain were collected at 11 and 2 sites in the east and at 13 and 2 in the west with measuring EC, pH and DO, respectively. The water stable isotopic ratios were analyzed by PICARO.
Stable isotopic ratios in groundwater were lower than surface water in both east and west. Altitude effects of spring water in the head water were recognizable. This means the surface water in the alluvial plain was mainly contributed from Lake Biwa, whereas groundwater was from the head water. The altitude effect of oxygen stable isotopic ratio was 0.15 - 0.13 ‰/ 100 m on the east side and 0.15 ‰/ 100 m on the west side (only in the upper stream of the Ado River). In addition, the d value of isotopic ratio in the precipitation was 23‰ in the upper Adokawa in August 2018, 18 ‰in Ugawa, and 20 ‰in Serikawa.
We also estimated groundwater recharge elevation and water contribution rate in the upstream region based on these.

Keywords: stable isotope, altitude effect, groundwater recharge

©2019. Japan Geoscience Union. All Right Reserved.

Calculation of TN and TP concentration coefficients of river water for each land use by a simple watershed model.

*Seiko Yoshikawa[1], Donglai Ma[1,4], Tadamasa Saito[1,5], Kenji Matsumori[2], Yuko Itoh[3], Masahiro Kobayashi[3]

1. Institute for Agro-environmental Sciences, National Agriculture and Food Research Organization, 2. Western Region Agricultural Research Center, National Agriculture and Food Research Organization, 3. Forestry and Forest Products Research Institute, 4. Graduate school,Tsukuba University, 5. Faculty of Agriculture, Ibaraki University

Water quality deterioration of rivers caused by leakage of fertilizer components such as nitrogen and phosphorus from paddy and upland fields is a environmental problem. Also, runoff of fertilizer components are expected to increase with the accelerated water and sediment runoff by intensification and localization of rainfall caused by climate change. Although it is difficult to predict the place and extent of heavy-rainfall-related disasters, we firstly grasp the average concentrations of nitrogen and phosphorus and predict increase and decrease in those concentrations when the way of rain changes. Nitrogen and phosphorus runoff is depend on land use and land cover, conservative measures, topography, climate condition mainly rainfall etc.. Among them, the land use and land cover is expected to be a main factor in normal climate conditions. In order to contribute to the prediction of heavy-rain related disasters in the future, coefficients that indicate the total nitrogen (TN) and total phosphorus (TP) load intensity to rivers of each land use for the river watersheds across the country are calculated using a simple watershed land use model. Watersheds whose lower ends are observation points of water quality, and whose land use ratios were determined by GIS technique using published database of DEM (GSI, 10B) and LULC mesh data (JAXA , ALOS AVNIR-2). The TN and TP concentration coefficients of paddy, upland, forest, and urban were calculated by applying the below multiple regression equation using the land use ratios and published TN and TP data(Ministry of Environment).

$c = a_1 x_1 + a_2 x_2 + a_3 x_3 + a_4 x_4$

C: TN or TP concentration (mg L^{-1}) a_i : TN or TP concentration coefficient for land use *I,* x_i : ratio of land use *I,* Land use: 1;paddy, 2;upland fields, 3;forest, 4;urban

TN concentration coefficient across Japan is 1.67 (from lower limit 95% value 1.34 to upper limit 95% value 2.01), 4.08 (from 3.64 to 4.51), 0.76 (from 0.67 to 0.90), 3.57 (from 3.38 to 3.76) for paddy fields, upland fields, forests and urban areas respectively (n=3256). The TP concentration coefficient is 0.146 (lower limit 95% value 0.119 to upper limit 95% value 0.172), 0.172 (0.138 to 0.206), 0.044 (0.033 to 0.055), 0.267 (0.253 to 0.282) for paddy fields, upland fields, forests and urban areas respectively (n=3256,). Prefectural TN and TP concentration coefficients for paddy and upland fields related only loosely to prefectural surplus N and surplus P. On the other hand, prefectural TN and TP concentration coefficients for forests and urban related to prefectural population densities by logarithmic functions with determination coefficients R^2 from 0.45 to 0.48.

Keywords: watershed land-use model, TN, TP, concentration coefficient

©2019. Japan Geoscience Union. All Right Reserved.

Possibility of nutrients transportation from littoral slope for enhancement of phytoplankton growth in north basin of Lake Biwa

*Syuhei Ban[1], Rong YI[1], Xin Liu[1], Masahiro Maruo[1], Miki Sudo[1], Naoshige Goto[1], Jun Murase[2]

1. The University of Shiga Prefecture, 2. Nagoya University

Nutrient loading from non-point source in a lake ecosystem has not been well recognized yet. In Lake Biwa, total phosphorus (TP) does not decline to the level before eutrophication period, 1960s to 1970s, despite of decreasing the loading from point sources surrounding the lake after that. One of the reasons for no well lowering TP in the lake is attributed to agricultural runoff, in which suspended materials including phosphorus would be deposited to the littoral bottom. In our previous study, subsurface maximum of ammonium as a proxy of dissolved materials from anaerobic interstitial waters in the littoral bottom sediments was found along a transect from littoral to pelagic regions, implying horizontal transportation of nutrients from littoral sediments. There were no such evidences of soluble reactive phosphorus (SRP) yet due to always below the detection limit in the pelagic waters. Recently, we developed modified protocol using an ion chromatography for measuring orthophosphate concentration at nano-molar levels. In this presentation, we' d like to provide several evidences for horizontal transportation of dissolved nutrients including orthophosphate along a transect from littoral to pelagic sites in north basin of Lake Biwa.

Total of the 6 times transect surveys for determining vertical profiles of nutrients, methane and herbicides were made in 2010-2011. Additional two transect surveys for determining those of nutrients including orthophosphate were made in 16 May and 25 July of 2018. During the 2010-2011 campaigns, *in situ* phytoplankton primary production was measured during the stagnation period using light intensity and chlorophyll *a*concentration monitored by sensors attached to a mooring buoy situated at an offshore station in north basin of Lake Biwa and an equation of photosynthesis - light intensity (P-I) curve.

In 2010-2011 campaigns, we detected sub-surface maximum layer, 20-30 m, of ammonium and methane as a proxy of dissolved materials transported from interstitial water in the sediment of littoral slope. Herbicides, which were used in rice paddy during the rice planting and proxy of materials transported from terrestrial environments surrounding the lake, were also detected in 20-30 m even at the offshore regions in the lake. Primary production monitoring suggested that phytoplankton production depended on some environmental variables other than solar irradiance, e.g. nutrients, until summer months. These results suggested that nutrients for enhancing algal growth might be horizontally transported from sediment in the littoral slope, and that the source of the nutrients might be provided from the drainage of rice paddy.

In 2018 campaigns, sub-surface maximum of ammonium was clearly found along a transect from littoral to pelagic sites in both May and July, but no such sub-surface maximum of orthophosphate was found. Several reasons for failure to find sub-surface maximum of orthophosphate might be proposed. Phosphate would be used by both phytoplankton and bacteria, while ammonium would be used by phytoplankton alone in the euphotic layer. In phosphate limited environment, such as pelagic areas in north basin of Lake Biwa, sub-surface maximum could not be easily detected due to rapid absorption by both phytoplankton and bacteria. Or, a transportation of nutrients from the littoral sloop would sporadically occur, and then we simply missed to detect it. This is on-going research project, and then further studies will be conducted to clarify this issue.

©2019. Japan Geoscience Union. All Right Reserved.

Keywords: Horizontal nutrient transportation, non-point source loading, agricultural runoff, Lake Biwa

©2019. Japan Geoscience Union. All Right Reserved.

SWAT model analysis for confirming the effects of crop growth on the suspended sediment concentration from a settling basin catchment on Ishigaki island

*Yang Cao[1], Shin-ichi Onodera[1], Mitsuyo Saito[2], Hide Omae[3], Yoshiko Iizumi[3]

1. Graduate School of Integrate Arts and Sciences, Hiroshima University, 2. Graduate School of Environmental and life Science, Okayama University, 3. Tropical Agriculture Research Front (TARF), Japan International Research Center for Agricultural Sciences (JIRCAS)

Crop growth has a significant effect on soil erosion in small watersheds. Exploring the characteristics and occurrences of soil erosion in small watersheds assists in our understanding of the water and material cycles in agricultural areas. The small catchment on the tropical island of Ishigaki, Japan, was chosen as the research area. The effects of sugarcane growth at different stages on the suspended sediment concentration in the basin from January 2017 to July 2018 were analyzed based on the Soil and Water Assessment Tool (SWAT) model. This study will explore the possible driving factors of these phenomena. The results show that the suspended sediment concentration in the basin reached its highest value on a rainy day near the sugarcane planting period because of the soil relaxation caused by tillage and cultivation. At the end of the sugarcane growth period, the sediment concentration was not at a high level when the rainfall reached 150 mm, because of the effective protection of the soil by sugarcane. The simulated sediment concentration of precipitation per mm showed that the simulated sediment concentration was at its highest during the crop planting period, followed by the period of bare land, and at the lowest during the crop growth period.

Keywords: SWAT model, Small catchment, Sugarcane, Sediment, Ishigaki

©2019. Japan Geoscience Union. All Right Reserved.

Estimating the runoff of water, sediment, and nutrient using SWAT model in Kikuchi-river watershed, Kumamoto, and the influence of the forest

*Soichiro Fujii[1], Masahiko Kanamori[1], Yuko Nagano[1], Maki Kinoshita[2], Yuta Shimizu[3], Shin-ichi Onodera[4]

1. Japan Forest Technology Association, 2. PASCO Corporation, 3. Western Region Agricultural Research Center, National Agriculture and Food Research Organization, 4. Graduate School of Integrated and Arts Sciences, Hiroshima University

Recently, enclosed sea area such as Ariake-sea have severe nutrient enrichment problem and is decreasing the produce of fishery industry. Such enclosed sea area is commonly affected by river water quality discharged from the land area. Therefore, estimating the load of sediment and nutrient from its land area is important. However, most of researches estimating discharge from land area is conducted by simple method using primary load factor. These method only can provide the estimates in annual scale regardless of the land use. On the other hand, the positive effect of forest to water quality in the river, so-called green dam, is paid attention recently, and supposed to play important roll on improvement to sea environment. However, the effect of forest to water quality is not explained enough, and few research has conducted in watershed scale. In this study, we aim to simulate water, sediment, and nutrient runoff in order to provide more detail information about discharge from land area, and to estimate the influence of the forest to water quality. We use Soil and Water Assessment Tool (SWAT) and chose Kikuchi-river as a model watershed, which has the third largest watershed area among the rivers drain into Ariake-sea.

We set Komoda observatory as the most downstream point of Kikuchi-river and the model watershed is the upstream side from there. More than half of this watershed is covered by forest. We collected land use data, soil data, climate data and 30m mesh digital elevation model (DEM) data of this watershed in order to establish the model. In order to calibrate and validate the model performance, observed data of daily stream flow from 2008 to 2016, and sampling data of sediment and nutrient were collected. Moreover, we measured the amount of sediment, phosphorus and nitrogen during flood situation in 2016 and 2017. The parameters in the model were modified according to the result of calibration, and the performance of the model was evaluated from three indices such as Nash-Sutcliffe index.

The model performance was evaluated as more than satisfactory for all materials: water, sediment, phosphorus and nitrogen. Therefore, this model can simulate daily runoff from 2008 to 2017. The runoff rate of sediment and most of nutrient from forest was less than 30% of the annual average in whole watershed, although water discharge was the same level to the rate of forest area, which indicates the function of forest to provide low concentrate water of sediment and nutrient to the river. In conclusion, modelling the runoff from land area using SWAT model has potential to provide detail information about land area discharge and estimate the influence of forest to river water quality.

Keywords: SWAT model, Runoff estimation

©2019. Japan Geoscience Union. All Right Reserved.

Atmospheric depositions on forest ecosystems in areas along the Sea of Japan

*Yuko Itoh[1], Keiji Takase[2], Yoichi Fujihara[2], Toru Okamoto[1]

1. Forestry and Forest Products Research Institute, Japan, 2. Ishikawa Prefectural University

In recent years, concerns about the effects of excess-nitrogen usage by human activities on terrestrial environment, including forest ecosystems, have been increasing at a global scale. The phenomenon of high-nitrate efflux from several forest watersheds has already been reported in the surroundings of metropolitan areas in Japan. Furthermore, concerns regarding the effects of transboundary air pollution on areas along the Sea of Japan with expanding economic activities have been increasing in Asian countries. However, on-site monitoring throughout the year is difficult in most of these areas because of heavy snow, especially in the mountainous area. Therefore, the behaviors of elements within forest ecosystems throughout a year have primarily not yet been elucidated in this district. This study was conducted to determine the influxes and effluxes of elements in this heavy snowy region and to understand the contribution of transboundary air pollution to the quantity of atmospheric deposition. We also carried out rainfall and stream water investigations from the headwater area to the lower stream area in the Tedori River Basin and an inland mountainous area to understand the geographical distribution of the actual conditions of elements' influxes and effluxes in this region. We started monitoring the major and minor elements in a small forested watershed in the middle part of the Tedori River Basin, Ishikawa prefecture, Japan, in 2013. In this study site, we observed a large amount of precipitation throughout the year. Regarding the annual snowfall amount, there were extensive variations among the years. Seasonal fluctuations were observed in the influx of atmospheric deposition; in particular, the distribution of most of the elements increased during winter. The annual deposition average of inorganic nitrogen (NH_4-N + NO_3-N) in this site was 15.8 kg ha^{-1}. The contribution of winter season deposition to the annual inputs was high. The influx of nitrogen by bulk precipitation during winter season was 2.3 times that of summer, and that of sulfur sulfate was 3.7 times. The nitrogen influx quantity was similar to or more than that reported in nitrogen-saturated forested areas of the Kanto district. Therefore, similar to that in the Kanto district, higher nitrogen deposition loads from the atmosphere could also be influenced on the effect of nitrogen dynamics and the increase in nitrogen efflux at these forest watersheds. However, the efflux concentrations of most of the dissolved elements in stream water did not show clear seasonal fluctuations. Stream water nitrate concentration was stable and low. In addition to the seasonal fluctuation of nitrogen and sulfur, the ratios among some trace elements, which are anthropogenic substances (Pb, V, As, etc.), and sea salts and yellow sand could be useful indicators to elucidate the contribution of transboundary air pollution to these regions. We compared the element inputs associated with precipitation during the non-snowy season (July–November) at six locations in the Tedori River Basin and one location in the inland area. The inorganic nitrogen and sulfuric acid sulfur influxes were the largest at the middle reaches of the Tedori River Basin. The inflow amount of inorganic nitrogen and sulfuric acid sulfur at two points in the mountainous area was approximately half or less than that at the middle region and was approximately the same as the inflow amount at the inland mountainous area. Furthermore, we investigated stream water, spring water, and ground water samples from the headwater area to the lower stream area in the Tedori River Basin. The nitrate concentrations in all the samples ranged from 0.00 to 2.93 mgL^{-1} (median value: 0.69 mgL^{-1}). In contrast, the nitrate concentrations of stream water in the Tsukuba experimental forest watershed, which has been reported as a nitrogen-saturated forested area of the Kanto district, were much higher (average value: 7.56 mgL^{-1}) than those in the Tedori River Basin. Compared with the influx, the efflux concentrations of nitrate in the water

©2019. Japan Geoscience Union. All Right Reserved.

samples were generally very low around this basin. Therefore, higher nitrogen depositions have not yet distinctly influenced the nitrate concentrations of stream water in this area. To elucidate the influence of transboundary air pollutant influx on the entire Tedori River Basin, it is necessary to evaluate the inflow amount during the snowy season in the mountainous area. Therefore, it is important to establish a method that can be used to observe the influx and efflux of elements throughout the year even in mountainous areas with heavy snow.

©2019. Japan Geoscience Union. All Right Reserved.

Continuous and simultaneous flux measurement of N_2O and CO_2 from agricultural soil using a portable multi-turn time-of-flight mass spectrometer

*Noriko Nakayama[1], Yusuke Iwai[1], Yo Toma[2], Hiroshi Furutani[1], Ryusuke Hatano[3], Michisato Toyoda[1]

1. Osaka University, 2. Ehime University, 3. Hokkaido University

Agricultural soil is one of the important sources/sinks of greenhouse gases such as N_2O, CO_2, and CH_4. The formation and consumption of such greenhouse gases in agricultural soils are dependent on not only the chemical and biological properties of the soil, but also their variations. Hence continuous monitoring of such greenhouse gases as tracer gases are quite useful to track chemical and biological processes and variations of soil properties.

In this paper, we describe a new field-deployable gas flux measurement system for the continuous monitoring of multiple agricultural soil gases (N_2O, CO_2, and CH_4) using a high resolution multi-turn time-of-flight mass spectrometer (MULTUM) combined with an automated flux chamber system. The new system measured the soil gases every 2.5 min with the precisions of ~6% for N_2O, CH_4, and 2% or better for CO_2 and O_2 at atmospheric concentrations with one relative standard deviation (RSD) for n = 10.

To demonstrate the utility of the continuous multi-gas flux measurement system, we conducted a field study at the Ehime University farm (Ehime, Japan) from September 3rd to 8th, 2018. In the field study, an automated flux chamber was placed in the agricultural field and the soil gas concentrations in the chamber were continuously monitored by the MULTUM system. Soil temperature/moisture sensor were also monitored at the depth of 7.5 cm underground in addition to a weather information (wind speed, precipitation, solar radiation). The continuous measurement had been continued with operators almost unattended except for a daily system check.

For one flux measurement (20 min), eight gas samples were taken every 2.5 min with the flux chamber closed. Gas flux of N_2O and CO_2 had been carried out by applying linear regression to the eight gas measurements. We found that a significant correlation of N_2O flux with soil electrical conductivity and water content, although no significant correlation of CO_2 flux to soil electrical conductivity was observed. Significant and rapid decreases in N_2O and CO_2 flux during rainfall events were also observed. Our preliminary result shows that high time-resolution flux data obtained by MULTUM system is quite useful for tracking the variation in soil properties and biological processes and their activity in soil environment.

Keywords: on-site mass spectorometry, MULTUM, soil-to-atmospher gas flux

©2019. Japan Geoscience Union. All Right Reserved.

Effects of introduction of cyclic irrigation system on mass balances of SS and T-P in Lake Inbanuma, Chiba, Japan

*Tomijiro Kubota[1]

1. National Agriculture and Food Research Organization, Institute for Rural Engineering

Introduction

The introduction of cyclic irrigation has been advanced since 2010 in the Lake Inbanuma as part of the update project of the irrigation facilities. In the present study, mass balances of SS and T-P were examined before and after the introduction of the cyclic irrigation.

Materials and methods

The irrigation block where the cyclic irrigation began in 2015 was selected as the investigation site, and the investigation was executed to the irrigation period in 2014 and 2015. The hydrological and water quality investigation was executed at ① division works of irrigation canal and ② drainage pumping station. Water samples were taken at the two points and the TOC, SS, TN, NO3-N, NO2-N, NH4-N, TP, and PO4-P were analyzed in the regular investigation executed about once a month. Besides regular investigation, water samples were taken once a day (8:00AM or noon) by the automatic water sampler and SS and T-P were analysed. The turbidity and water level were measured every ten minutes by using data loggers at same sites. The turbidity data were converted into the concentration of SS and TP by using the regression curve. The quantity of water intaken from the lake and drainage to the lake were obtained from the records of the facility manager.

Result and discussion

The inflow and outflow loads and the balance were calculated before and after the introduction of the cyclic irrigation. In 2014, before the start of cyclic irrigation, both the outflow loads of SS and T-P were small to compare with those inflow loads. The amount of accumulation of SS and T-P were about 1.3t and 2kg respectively when having no rainfall in the irrigation block. On the other hand, the outflow of SS and T-P were about 3.5t/day and 20kg/day respectively in rainy days. If 2015 year is compared to 2014, it had increased in T-P though the load of irrigation water each day at no rainfall periods and it had not been change in SS though an accurate comparison is difficult according to the missing value. However, after the cyclic irrigation had been started, the amount of the outflow loads had decreased greatly like 35% in SS and 38% in T-P. The balance of the outflow loads during the irrigation periods of 2014 were -470kg/day in SS, which meant the purification type, while +2.6kg/day in T-P. as a result, it was found that the introduction of cyclic irrigation system had worked for water purification in SS and T-P effectively.

Keywords: cyclic irrigation system, water pollution, suspended solid, total phosphorus

©2019. Japan Geoscience Union. All Right Reserved.

[E] Poster | A (Atmospheric and Hydrospheric Sciences)：A-CG Complex & General

Thu. May 30, 2019 1:45 PM - 3:15 PM JST | Thu. May 30, 2019 4:45 AM - 6:15 AM UTC | Poster Hall International Exhibition Hall8, Makuhari Messe_3

[A-CG34] Satellite Earth Environment Observation

convener:Riko Oki(Japan Aerospace Exploration Agency), Yoshiaki HONDA(Center for Environmental Remote Sensing, Chiba University), Yukari Takayabu(Atmosphere and Ocean Research Institute, the University of Tokyo), Tsuneo Matsunaga(Center for Global Environmental Research and Satellite Observation Center, National Institute for Environmental Studies)

In recent years, we cannot avoid facing issues on global environmental changes that occur in various spatiotemporal scales. The earth environmental observation data by satellites became the necessary basic data to tackle and solve those issues. Due to the recent advancement in the observation sensor technique and the data processing technique, the satellite observation has been showing rapid progress, and the time is changing from examining the accuracy of the observation sensor data to the advancement of the data application, leading to broaden potential users. In these days application became synergetic, so we comprehensively pick
up this topic in the Atmospheric and Hydrospheric Sciences Session of this Union Meeting that enables to comprise the atmospheric, oceanic and land sciences; by combining the intelligence and the knowledge of the party, we propose a session that aims to prompt further studies towards the issues on earth environmental change, the advancement in the data application and future plans of Earth Observation missions.

[ACG34-P01] Impact of usage of multiple-satellite sensors on accuracy of daily-mean sea surface wind data

*Ayumi Koizumi[1], Masahisa Kubota[2], Kunio Kutsuwada[3], Hiroyuki Tomita[4], Tsutomu Hihara[5] (1.Tokai University, 2.Tokai University, Institute of Ocean Research and Development, 3.School of Marine Science and Technology, Tokai University, 4.Institute for Space-Earth Environmental, Nagoya University, 5.Japan Agency for Marine-Erth Science and Technology)

[ACG34-P02] Temperature and Size Variability of Warm Pools in the Global Oceans

*ChunYi Lin[1] (1.National Museum of Marine Science & Technology)

[ACG34-P03] Sea surface temperature from SGLI aboard the GCOM-C satellite of JAXA

*Yukio Kurihara[1], Kazunori Ogata[2], Hiroshi Murakami[2], Misako Kachi[2] (1.Tripli-I Co., Ltd., 2.JAXA EORC)

[ACG34-P04] Concept of small satellite UV/visible imaging spectrometer optimized for tropospheric NO_2 measurements in air quality monitoring

*Tamaki Fujinawa[1,5], Katsuyuki Noguchi[2], Akihiko Kuze[3], Andreas Richter[4], John P. Burrows[4], Andreas C. Meier[4], Tomohiro Sato[1], Takeshi Kuroda[1], Naohiro Yoshida[5], YASUKO KASAI[1,5] (1.National Institute of Information and Communications Technology, 2.Nara Women's University, 3.Japan Aerospace Exploration Agency, 4.University of Bremen, 5.Tokyo Institute of Technology)

[ACG34-P05] EarthCARE L2 algorithms for cloud and precipitation

*Kaori Sato[1], Hajime Okamoto[1], Hiroshi Ishimoto[2] (1.Research Institute for Applied Mechanics, Kyushu University, 2.Meteorological Research Institute)

[ACG34-P06] Analysis of the Surface Echo Characteristics Derived from GPM/DPR Wide Swath Observation Experiment

*Kosuke Yamamoto[1], Kinji Furukawa[1], Nobuhiro Takahashi[2], Takuji Kubota[1] (1.Japan Aerospace Exploration Agency, 2.Nagoya University)

[ACG34-P07] The Recent Results from the Global Precipitation Measurement (GPM) mission in Japan

*Riko Oki[1], Takuji Kubota[1], Kinji Furukawa[1], Yuki Kaneko[1], Moeka Yamaji[1], Kosuke Yamamoto[1], Toshio Iguchi[2], Yukari Takayabu[3] (1.Japan Aerospace Exploration Agency, 2.NICT, 3.the University of Tokyo)

[ACG34-P08] **Verification of Global Satellite Mapping of precipitation (GSMaP) for providing its error information**

*Moeka Yamaji[1], Takuji Kubota[1] (1.Earth Observation Research Center, Japan Aerospace Exploration Agency)

[ACG34-P09] Detection of the mixed phase top using the measured dual-frequency ratio of reflectivity with GPM/DPR

*Yuki Kaneko[1], Toshio Iguchi[2] (1.Japan Aerospace Exploration Agency, 2.National Institute of Information and Communications Technology)

[ACG34-P10] **Comparison between high frequency satellite rainfall estimation and APHRODITE-2 ground rain gauge observation**

*Hitoshi Hirose[1], Koichi Toyoshima[1], Atsushi Higuchi[1], Akiyo Yatagai[2], Natsuko Yasutomi[3] (1.Center for Environmental Remote Sensing, Chiba University, 2.Hirosaki University, 3.Disaster Prevention Research Institute, Kyoto University)

[ACG34-P11] Development of the high resolution GSMaP by the Himawari-8

*Tomoaki Mega[1], Tomoo Ushio[1] (1.Tokyo Metropolitan University)

[ACG34-P12] Preliminary results of on-orbit estimation for polarization sensitivity of GCOM-C/SGLI

*Risa Miyazaki[1], Hiroshi Murakami[1], Masahiro Hori[1] (1.Japan Aerospace Exploration Agency)

[ACG34-P13] Analysis of SGLI validation datas based on the effects of the growth and ground types for the AGB development

*Ryota Ishibashi[1], Koji KAJIWARA[1], Yoshiaki HONDA[1] (1.Center for environmental remote sensing, Chiba University)

[ACG34-P14] Remote sensing of aerosol optical properties and water-leaving radiance based on the optimal estimation approach

*Chong Shi[1], Teruyuki Nakajima[1], Makiko Hashimoto[1], Hideaki Takenaka[1] (1.Japan Aerospace Exploration Agency)

[ACG34-P15] Aerosol retrieval and PM2.5 from space using GOSAT/TANSO-CAI

*Makiko Hashimoto[1], Hideaki Takenaka[1], Teruyuki Nakajima[1], Akiko Higurashi[2] (1.Japan Aerospace Explortion Agency, 2.NIES)

[ACG34-P16] **Establishing a high resolution road fugitive dust emission inventory in Kaifeng City, China**

*Yiming Xu[1], Shili Liu[1], Xinyue Cao[1], Xianbao Shen[1], Zhiliang Yao[1] (1.Department of Environmental Science and Engineering, Beijing Technology and Business University)

[ACG34-P17] A Relationship between Diurnal Change Patterns of Land Surface Temperature and Spatial Configuration of the Osaka Metropolitan Area Captured by Himawari-8

*Yuhei Yamamoto[1], Hirohiko Ishikawa[1] (1.Disaster Prevention Research Institute, Kyoto University)

Impact of usage of multiple-satellite sensors on accuracy of daily-mean sea surface wind data

*Ayumi Koizumi[1], Masahisa Kubota[2], Kunio Kutsuwada[3], Hiroyuki Tomita[4], Tsutomu Hihara[5]

1. Tokai University, 2. Tokai University, Institute of Ocean Research and Development, 3. School of Marine Science and Technology, Tokai University, 4. Institute for Space-Earth Environmental, Nagoya University, 5. Japan Agency for Marine-Erth Science and Technology

Most satellites observing sea surface winds have sun-synchronous orbits and provide observation data at the same place two times per a day. We can expect that daily-mean values estimated from these data have some errors when diurnal changes in wind field cannot be neglected. For this problem, use of multiple satellites is helpful. Since the number of sensors used to construct daily-mean data is different among the years, it is expected that the accuracy of a daily-mean value changes from year to year.

The purpose of this study is to describe time variation of accuracy in daily-mean wind data in the Japanese Ocean Flux Data Sets with Use of Remote Sensing Observation (J-OFURO)-3 and to investigate its causes by comparing with in-situ measurement data by moored buoys and calculating three statistical values.

Results reveal that the statistical values are improved with year. To examine the relationship between the yearly statistics and the yearly number of satellite sensors, we plotted a scatter diagram between the number of satellites and three statistical values in each year. We found that the correlations between them are very high. We also focused on a time interval of the satellite wind observation, namely maximum missing time within a day. The result showed that the correlation between three statistical values and maximum missing time intervals is high. Since the relation between these two factors is not independent, we analyzed by considering both factors together. First, we chose five buoys with various standard deviations for a daily-mean value. Next, we picked up data from buoy's hourly data using random numbers, and calculated the daily mean value using the random data, and then determined the number of observations and the maximum missing time interval each day. Assuming the daily mean value calculated from 24 hourly data as a true value, the RMSE between this true value and the daily mean created from random data was calculated. From the result of this analysis, it was found that the value of Root Mean Square Error(RMSE) depends on the maximum missing time interval rather than the number of observations. Furthermore, when RMSE was normalized by standard deviation, the same figures were obtained for all buoys. This result implies that the RMSE of the daily mean value of the buoy station can be estimated if the magnitude of diurnal variation is known by giving the number of satellites used for observation and the maximum missing time interval, Moreover, by applying this result, we think that it is possible to show the optimal number of sensors and observation time for target accuracy. This result gives very breakthrough information to the design of the satellite observation system for sea surface wind.

Keywords: Multiple-satellite sensors, Sea surface wind

©2019. Japan Geoscience Union. All Right Reserved.

Temperature and Size Variability of Warm Pools in the Global Oceans

*ChunYi Lin[1]

1. National Museum of Marine Science & Technology

Using advance satellite-derived Sea surface height anomaly, sea surface temperature (SST) data, and heat flux data, we investigate the thermal variability, temperature and size variability of warm pools in the global oceans, the Pacific, the Atlantic, and the Indian Ocean, respectively. Because of the high density and specific heat of seawater, water can store and transport large amounts of heat. High SST has particular influence on global climate system. Furthermore previous studies focused on the global warming or area warming, in this investigation we present results of warm pool SST binned into 1 ˚C interval. Detecting temperature and size variability of warm pools in the global oceans, it suggests that the high SST area (SST ≧ 28˚C) has faster increasing rate than surrounding area (SST 20˚C - 27˚C) in the global oceans, the Pacific, the Atlantic, and the Indian Ocean, respectively. To understand the role of surface heat flux in the tropical SST fluctuation, we analyze the mixed layer heat balance equation. Upper ocean heat budget between the heat advection and heat diffusion term are compared and heat diffusion processes may be a mechanism for transporting excessive amount of heat that the warm pool through enhancing the SST gradient around the edge of the warm pool. In order to find out dominant period components and the relationship of energy-frequency distribution without influenced induced by nonlinear and nonstationary signals, the Hilbert-Huang Transform applied by ensemble empirical mode decomposition is employed. The ensemble empirical mode decomposition analysis indicates that the interannual component has strong influence on the variability of the warm core pool in the Pacific, presumably because of the presence of El Niño phenomenon, while the annual cycle dominates the variability in the Indian and the Atlantic Ocean.

Keywords: warm pool, SST, heat flux

©2019. Japan Geoscience Union. All Right Reserved.

Sea surface temperature from SGLI aboard the GCOM-C satellite of JAXA

*Yukio Kurihara[1], Kazunori Ogata[2], Hiroshi Murakami[2], Misako Kachi[2]

1. Tripli-I Co., Ltd., 2. JAXA EORC

The Global Change Observation Mission-Climate (GCOM-C) satellite, which is one of two satellites for the GCOM mission of the Japan Aerospace and Exploration Agency (JAXA), was launched on 23 December 2017. The Second Generation Global Imager (SGLI) is the optical sensor aboard GCOM-C which consists of two components: the Visible and Near-infrared Radiometer (VNR) and the Infrared Scanner (IRS). SGLI has switchable spatial resolution from 250 m x 250 m to 1 km x 1 km. The resolution of 250 m x 250 m is expected to reveal complicated structure of geophysical parameters. Sea surface temperature (SST), which is one of the important parameters in the geophysical field, is also determinable by using split window data of SGLI. SGLI SST is retrieved by utilization of newly developed cloud masking method and a modified SST method originally developed for Himawari-8. Considering combined utilization of satellite SSTs, the methods developed for SGLI SST will be applied back to Himawari-8 data as well as the data from the Visible Infrared Imaging Radiometer Suite (VIIRS) aboard the Suomi National Polar-orbiting Partnership (Suomi NPP) satellite. SGLI SST is validated by comparison with buoy data. The comparison result shows RMSD of ~0.4 K, good agreement between SGLI SSTs and buoy data. Triple comparison with Himawari-8 and VIIRS SSTs is being started. Operational retrieval of SGLI SST started at the end of 2018. The products are available at the G-Portal site of JAXA and the JAXA Satellite Monitoring and Environmental Studies (JASMES) site of the Earth Observation Center (EORC) of JAXA.

©2019. Japan Geoscience Union. All Right Reserved.

Concept of small satellite UV/visible imaging spectrometer optimized for tropospheric NO_2 measurements in air quality monitoring

*Tamaki Fujinawa[1,5], Katsuyuki Noguchi[2], Akihiko Kuze[3], Andreas Richter[4], John P. Burrows[4], Andreas C. Meier[4], Tomohiro Sato[1], Takeshi Kuroda[1], Naohiro Yoshida[5], YASUKO KASAI[1,5]

1. National Institute of Information and Communications Technology, 2. Nara Women's University, 3. Japan Aerospace Exploration Agency, 4. University of Bremen, 5. Tokyo Institute of Technology

Satellite observations at nadir can potentially facilitate a better understanding of the emissions and distribution of tropospheric nitrogen dioxide, NO_2. The identification of emissions requires adequate spatiotemporal resolution measurements of the total column amounts of NO_2. The spatial resolution of previous and current observations is insufficient for the identification of NO_2 hot-spots. Switching to a spatial resolution of ~1 km x ~1 km can improve the identification of local sources of NO_2 and their emissions. To investigate the feasibility of observations with such a high spatial resolution, we simulated radiance spectra for different cases under varying parameters, such as area, season, satellite altitude, and surface reflectance by using the radiative transfer model SCIATRAN. We subsequently retrieved NO_2 slant column densities (SCDs) using the differential optical absorption spectroscopy (DOAS) technique with several fit windows. For test cases associated with polluted conditions, we found that the conceptual nadir-observing instrument on a satellite at an altitude of ~300 km involved the lowest retrieval errors for signal-to-noise ratios of around 1000 with accuracy better than the required 5% for tropospheric NO_2 SCD and that the fit window of 425--497 nm met the scientific requirements for both surface reflectance cases.

Keywords: Nitrogen dioxide, Earth observation, Radiative transfer model, Remote sensing

©2019. Japan Geoscience Union. All Right Reserved.

EarthCARE L2 algorithms for cloud and precipitation

*Kaori Sato[1], Hajime Okamoto[1], Hiroshi Ishimoto[2]

1. Research Institute for Applied Mechanics, Kyushu University, 2. Meteorological Research Institute

The EarthCARE (Earth Clouds, Aerosols and Radiation Explorer, JAXA-ESA) mission will carry the first 94GHz Doppler Cloud Profiling Radar (CPR) with a high spectral resolution atmospheric lidar (ATLID) at 355nm. Recent progresses in EarthCARE L2 cloud/precipitation algorithms for the treatment of multiple scattering and cloud particle nonsphericity are presented.

Keywords: spaceborne active sensor, cloud

©2019. Japan Geoscience Union. All Right Reserved.

Analysis of the Surface Echo Characteristics Derived from GPM/DPR Wide Swath Observation Experiment

*Kosuke Yamamoto[1], Kinji Furukawa[1], Nobuhiro Takahashi[2], Takuji Kubota[1]

1. Japan Aerospace Exploration Agency, 2. Nagoya University

The observation from spaceborne precipitation radar has been contributed to better understanding of earth climate system. Global Precipitation Measurement (GPM) core satellite Dual-frequency Precipitation Radar (DPR) provides us 3-dimentional information of precipitation by the scan width of about 250 km, but there have been arguments that to bring systematic impact on the weather monitoring through global rainfall map such as GSMaP, wider swath observation by precipitation radar is necessary.

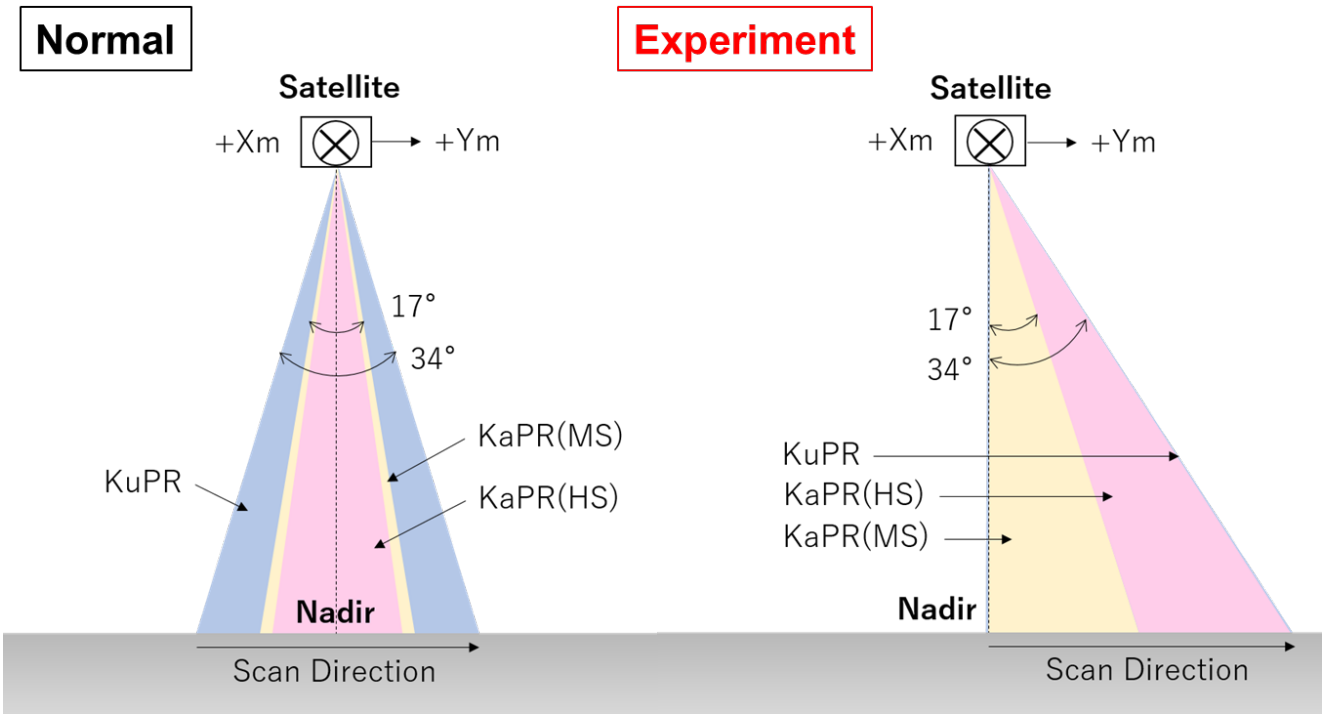
Based on those requirements, the scan pattern of GPM/DPR was experimentally changed for 1 day from 13UTC on September 26th. In this experiment, the scan angle was changed to observe from nadir to about +34˚ assuming future spaceborne precipitation radar with wider swath width, while in the normal observation DPR scans ±17˚. The height and strength of the mainlobe clutter with larger incident angle were assessed statistically to examine the possibility of the rainfall retrieval with wide swath observation by DPR.

In order to examine mainlobe clutter height, it is inevitable to reduce sidelobe and grating lobe effect. In this study, clutter-free observation data is extracted based on following procedures; 1) extract bins above mainlobe clutter; 2) extract bins under non-precipitation condition from 1); 3) extract bins that satisfy |received power −averaged noise power| < 2 sigma of the noise power from 2). Note that this procedure was applied only for KuPR observation since sidelobe and grating lobe clutter is not prominent in KaPR.

The result for KuPR observation shows that the mainlobe clutter top height at the larger incident angle over ocean is somehow suppressed at around 4 km while over land it increases almost linearly up to around 5 km due to the strong surface scattering. The same tendency is found on the KaPR observation, but it has lower clutter top height of around 2.5 km and 3.5 km, over ocean and land respectively. Suppression is clearer over ocean thanks to the specular reflection. The results also indicate that relatively intense rainfall can be retrieved while shallow rainfall with weak echo power may not be acceptable for retrieval because it should be masked by the surface clutter.

Keywords: precipitation radar, radar clutter, GPM core satellite

©2019. Japan Geoscience Union. All Right Reserved.



©2019. Japan Geoscience Union. All Right Reserved.

The Recent Results from the Global Precipitation Measurement (GPM) mission in Japan

*Riko Oki[1], Takuji Kubota[1], Kinji Furukawa[1], Yuki Kaneko[1], Moeka Yamaji[1], Kosuke Yamamoto[1], Toshio Iguchi[2], Yukari Takayabu[3]

1. Japan Aerospace Exploration Agency, 2. NICT, 3. the University of Tokyo

The Global Precipitation Measurement (GPM) mission is an international cooperate satellite project to achieve highly accurate and highly frequent global precipitation observations. The GPM mission consists of the GPM Core satellite jointly developed by the U.S. and Japan and Constellation Satellites that carry microwave radiometers and provided by the GPM partner agencies. The GPM Core satellite carries the Dual-frequency Precipitation Radar (DPR) by the Japan Aerospace Exploration Agency (JAXA) and the National Institute of Information and Communications Technology (NICT) and the GPM Microwave Imager (GMI) provided by National Aeronautics and Space Administration (NASA). The GPM Core satellite was launched in February 2014 and achieved its prime mission period planned for 3 years in 2017.

It has been continuing its observation as the extended mission phase after that.

JAXA develops the DPR Level 1 algorithm and the NASA-JAXA Joint Algorithm Team develops the DPR Level 2 and DPR-GMI combined Level 2 algorithms. The DPR, the DPR-GMI combined algorithms and the latent heating algorithm were updated, and those products were released in October 2018 as Version 0.6. Using dual frequency information of DPR, the latest Level 2 products include information such as precipitation phase at surface, heavy ice precipitation and so on. Also, the calibration factors of TRMM/PR were re-examined to have consistency between DPR/Ku. The same GPM Ku-band radar L2 algorithm now applies to the TRMM/PR, so that the long radar precipitation data exceeding more than 20 years are now available. From May 2018 in the extended mission period, the scan pattern of the Ka-band radar has been changed to realize matched beam observation in full swath. The new algorithm applying to the changed scan pattern is now under development.

JAXA also develops the Global Satellite Mapping of Precipitation (GSMaP), that is hourly and 0.1-degree horizontal resolution global rainfall map. It is available through the “JAXA Global Rainfall Watch” website (https://sharaku.eorc.jaxa.jp/GSMaP/index.htm). GSMaP product family includes different data latency products and rain gauge calibrated products and so on. The GSMaP near-real-time version (GSMaP_NRT) product provides global rainfall map in 4-hour after observation, and an improved version of GSMaP near-real-time gauge-adjusted (GSMaP_Gauge_NRT) product has been released since Dec. 2018.

The GSMaP real-time product called GSMaP_NOW now product is providing data at the earliest timing. It has been realized using the geostationary satellite Himawari-8 operated by the Japan Meteorological Agency (JMA) since November 2015. Since Nov. 2018 the domain of GSMaP_NOW has been extended to the region of the geostationary satellite Meteosat operated by the European Organization for the Exploitation of Meteorological Satellites (EUMETSAT) in November 2018. JAXA is further developing the GSMaP_NOW to provide global real-time rainfall product.

Keywords: GPM, Satellite Remote Sensing, Precipitation

©2019. Japan Geoscience Union. All Right Reserved.

©2019. Japan Geoscience Union. All Right Reserved.

Verification of Global Satellite Mapping of precipitation (GSMaP) for providing its error information

*Moeka Yamaji[1], Takuji Kubota[1]

1. Earth Observation Research Center, Japan Aerospace Exploration Agency

Precipitation is one of the most essential parameters in the Earth system. Due to address water issues like water shortage or floods, JAXA has developed and provided Global Satellite Mapping of Precipitation (GSMaP), which is hourly global precipitation dataset. It is under the Global Precipitation Measurement (GPM) mission and contributes.
GSMaP allows us to capture the hourly horizontal distribution of precipitation with good latency after observation. The spatial resolution is 0.1 x 0.1 degrees latitude/longitude. It has been used for various kinds of utilization purposes.
In terms of accuracy, GSMaP algorithms were updated in several times, and GSMaP has been getting more accurate day by day, however, it is known that the inhomogeneous of accuracy is existed depending on algorithm characteristics. It has been needed to provide information about the uncertainty and accuracy of GSMaP by users.
In this study, verification result of GSMaP near-realtime product version 6 (GSMaP_NRT) is reported. The radar/raingauge analysed precipitation data by Japan Meteorological Agency, which is an hourly rainfall analysis generated from ground-based precipitation radars corrected by automated rain gauges, are used as the reference data. Since the purpose of this study is for providing generalized error information, root mean square errors (RMSE) is statistically calculated for each precipitation level and each reliability flag during May-June-July-August-September-October in 2015-2018. Some initial results showed that the RMSE qualitatively represented the error for each precipitation level and reliability flag. The RMSE ratio to the average precipitation rate got larger as the precipitation rate became smaller while it became stable around 60 –80 % when precipitation rate was more than 10 mm/h. We report the validation results in detail, such as land/ocean difference or sampling dependence, and focus on the effectiveness of it.

Keywords: precipitation, GPM, GSMaP, validation

©2019. Japan Geoscience Union. All Right Reserved.

Detection of the mixed phase top using the measured dual-frequency ratio of reflectivity with GPM/DPR

*Yuki Kaneko[1], Toshio Iguchi[2]

1. Japan Aerospace Exploration Agency, 2. National Institute of Information and Communications Technology

The core observatory of the Global Precipitation Measurement (GPM) mission was launched in 2014 and has been observing rain and snow between 65˚S and 65˚N by the Dual Frequency Precipitation Radar (DPR) and the GPM Microwave Imager (GMI). The DPR provides three-dimensional structure of storms derived from reflected energy from precipitation particles. Precipitation echoes at the two frequencies of the DPR, Ka-band (25GHz) and Ku-band (14GHz), make it possible to infer the mean size and physical property of precipitation particles. The swath width of Ka-band scanning was 125 kilometers centered at nadir and was nested within the Ku-band’ s wider scan width of 254 kilometers. On May 21 2018, the Ka-band scan pattern was changed to match with the Ku-band’ s. Dual frequency radar reflectivity factors are available for full swath of 254 kilometers now.

The classification (CSF) module in the standard DPR level2 algorithm detects a bright band (BB) and classifies precipitation into three types, stratiform, convective, and other. Rain types affect the retrievals of rain amount and latent heating in the DPR algorithm. Accurate classification is also important in the Global Satellite Mapping of Precipitation (GSMaP) algorithm because it affects the rain profile database used in the rain retrieval with microwave radiometers. The BB detectability by the standard CSF algorithm is lower at and near the swath edges than near nadir because only Ku-band data was available in the outer swath before and because slant incidence of radar beams smears the vertical profiles.

As the Ka-band scan pattern has changed to cover the full swath, we can apply a dual-frequency method to detect a BB now. We have developed a method that uses the dual frequency ratio (DFR) to detect the mixed phase top. It looks at the slope of DFR as a function of range to identify the transition height from ice to water. DFR itself is estimated from measured DFR (DFRm) with attenuation correction. Preliminary experiments show that the developed method can detect the BB in stratiform rain over the swath almost uniformly. This method also has a potential to identify the transition height even in some convective cases. In this research we evaluate the performance of the algorithm by comparing the altitude of BB and the transition height with those estimated by using X-band multi-parameter radar (XRAIN) data.

Keywords: GPM, Melting Layer, Precipitation Radar

©2019. Japan Geoscience Union. All Right Reserved.

Comparison between high frequency satellite rainfall estimation and APHRODITE-2 ground rain gauge observation

*Hitoshi Hirose[1], Koichi Toyoshima[1], Atsushi Higuchi[1], Akiyo Yatagai[2], Natsuko Yasutomi[3]

1. Center for Environmental Remote Sensing, Chiba University, 2. Hirosaki University, 3. Disaster Prevention Research Institute, Kyoto University

APHRODITE project collects daily precipitation observation data from ground rain gauges in each country, and then performs appropriate quality control and converts it into gridded data. APHRODITE holds long-term data from the 1960s to the present and focuses on analyzes such as changes in characteristics of extreme rainfall due to long-term climate change. However, ground-based daily rain observations has a problem which end of the day (EOD) in each country is different from each other. To estimate the EOD in each country, we developed a Rain Potential Map (RPM) which is a product that can estimate global rain probability using geostationary meteorological satellites (GEO) (Hirose et al., 2016, JMSJ). In this study, we used the RPM, GSMaP and CMORPH which are global satellite rain estimation data based on microwave satellite and GEO observations.

Since the above satellite rainfall observation data can estimate global precipitation every hour, it is possible to create daily average data in which the average section is shifted by one hour. By correlating the satellite daily precipitation observation time series with the APHRODITE daily precipitation observation time series, the EOD value in each country was estimated from the time when the correlation coefficient is largest. We confirmed that the reliability of this method is high by a verification analysis in the field where true value of EOD is already known. Moreover, we made pseudo hourly rain time series of APHRODITE by inserting APHDOITE daily rain time series to satellite hourly rain time series. By this method, we will try to make a new APHRODITE data that is corrected for the EOD difference between each country.

Keywords: Precipitaition, Satellite, APHRODITE

©2019. Japan Geoscience Union. All Right Reserved.

Development of the high resolution GSMaP by the Himawari-8

*Tomoaki Mega[1], Tomoo Ushio[1]

1. Tokyo Metropolitan University

There is a new generation infrared (IR) imager on new-generation gestationary weather-satellite such as the Himawari-8 and the Geostationary Operational Environmental Satellite-R series. The imagers observe multi-channel passive imaging radiometer. The imagers observe wave a full disk with several km in about ten minutes. In Near-future, the IR imager observation should cover the globe.

Global precipitation information is an important tool for water management or earth science. Spaceborne sensors is one of the most convenient tools of global observation. The sensors cover global and provide uniform quality data. Precipitation estimation use microwave radiometer in low earth orbit (LOE). A microwave radiometer has high spatial resolution. However, one drawback of the microwave radiometer in LOE is narrow observation area. Whole earth observation by a microwave radiometer on a LOE satellite need some days. Therefore, global precipitation map is made from combined satellite data. However, combined data of microwave radiometer on LOE don’ t cover global in one hour. One of the global precipitation map is the Global satellite mapping of Precipitation (GSMaP). Precipitation estimation of the GSMaP made from microwave radiometer data. The GSMaP Moving Vector with Kalmanfilter (MVK) and Near real time compensate precipitation of no observation area by IR information. Spatial and temporal resolution of the GSMaP MVK achives 0.1 degree and one hour. This study shows downscale technique for GSMaP precipitation map by High-spatial and temporal resolution IR data of the Himawari-8. IR datasets of Himawari-8 are available every 2.5 minutes in the Japan region. In the presentation, we will also show validation the high resolution GSMaP and ground-radar network in Japan.

Keywords: Precipitation, GSMaP, Microwave Radiometer, Infrared Radiometer, Algorithm

©2019. Japan Geoscience Union. All Right Reserved.

Preliminary results of on-orbit estimation for polarization sensitivity of GCOM-C/SGLI

*Risa Miyazaki[1], Hiroshi Murakami[1], Masahiro Hori[1]

1. Japan Aerospace Exploration Agency

The GCOM-C has been launched successfully on 23th Dec. 2017 from the Tanegashima Space Center by H-IIA vehicle No.37. After the initial calibration/validation phase of one year after launch, all SGLI standard products have been released from JAXA’s data providing service (G-Portal) from Dec. 20, 2018.

In generally, the radiance reflected by the sea surface and the atmosphere is strongly polarized. When observing a large polarized light, the output radiance vary from the actual radiance because of the polarization sensitivity characteristic of the optical sensor. Especially for ocean color products, it is important to evaluate the effect of polarization sensitivity because it is necessary to extract the weak water-leaving reflectance (<10% of the whole) by the accurate atmospheric correction.
The polarization sensitivity of GCOM-C/SGLI of each NP (Non-Polarization) band has been measured in the pre-launch ground test. The ground test results of polarization sensitivity were shown to be <3.5% on average in the pixel direction in all bands. In this study, we evaluate whether the polarization sensitivity estimated from on-orbit observation data is consistent with the pre-launch test results. In this work, we report on the RED bands (VN07, VN08) and the NIR bands (VN10, VN11) of SGLI.
Polarization sensitivity on-orbit was evaluated based on Gordon and Zhang (1997) and Meister et al. (2005). We use the observation data by SGLI/PL (Polarization) band to estimate the real stokes vector components at the top of atmosphere (TOA). In order to obtain the polarization sensitivity with respect to directly observed radiance at TOA, L1B before inter-pixel sensitivity correction and before inter-telescope sensitivity correction was self-made from L1A data.
We analyzed the observation data of 12 path that PL band is observed nadir direction. The characteristics of the instrument for polarization sensitivity (polarization factor) were estimated by the least squares method. On the east side of the observation image, the error is large because of Sun-Glint. Although the variation in the pixel direction was still large, the estimated polarization factors (3 to 5 %) were consisted with the prelaunch ground test (~ 3.5%). However, sensitivity patterns in the pixel direction could not be identified, so we will continue to improve the evaluation in the future.

Keywords: GCOM-C, SGLI, Polarization sensitivity

©2019. Japan Geoscience Union. All Right Reserved.

Analysis of SGLI validation datas based on the effects of the growth and ground types for the AGB development

*Ryota Ishibashi[1], Koji KAJIWARA[1], Yoshiaki HONDA[1]

1. Center for environmental remote sensing, Chiba University

The effects of the earth of the time variant system should be difficult to detect the influence of the growth types and also the effects of the growth field’s variations. The research may occur the SGLI’s RSRF datas of the calculated AGB data accuracy analysis that observed between every kinds of the growth and also the ground types. The significance area of the SGLI observed, each of detected datas accuracy have to be considered. We show observation ways for the ground truth of the reflectance, LAI and fAPAR. The first case we use is a case of vegetation at the grassland. And then, based of reflectance values, we compare the other type as the Mixed coniferous forest example. The influence of an effect of the type of growth may occur the reflectance of the distributed area. We will detect these effects of the growth type. The influence at the observed area be necessarily to be verified.

The research topic includes the ground truth observation for the accuracy verification of a SGLI data obtained. For development of ground truth, the way to obtain datas were important. This paper explains how to examine growth (such as a second growth forest and other) and the slope factor of the second growth forest area and also the reflectance of each forest types. Then, this paper make ground truth observation scheme for the high accuracy AGB referenced data development at ground cover area. We explain the method of examine the error detection way including observation devices and also the problem of the research topic to be examined. Results may occur an example case of such kinds of the sloped forest and the kinds of the plane. The results shows a typical difference between the sloped and the plane, and then the results may occur the possibility that comparison of standard deviation may be an effective way to detect the volume of the forest type between every ground truth.

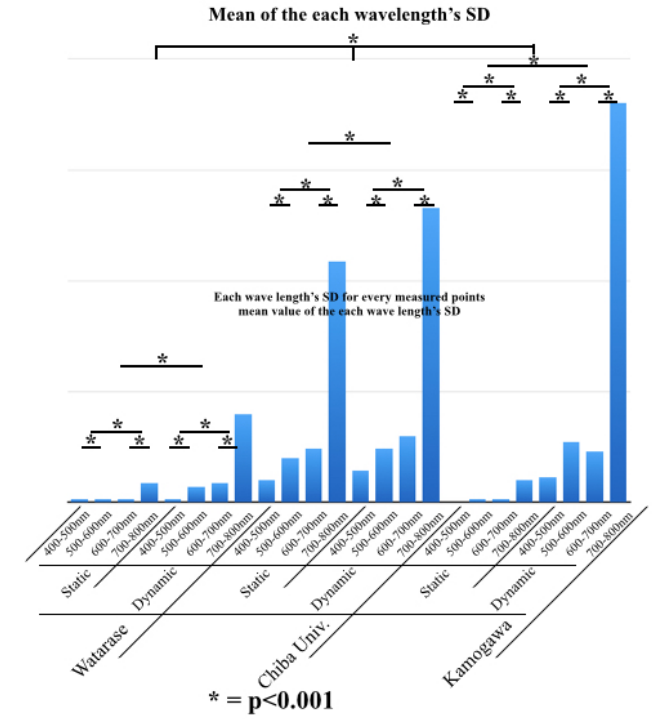
The case of we use as the sloped fields, reflectance of each wavelength were low and then the near 400 to 700 nm area will be higher than other wavelength (ANOVA values of results: $p < 0.001$). And then, we can see the effects of slope should be detected at total values of the reflectance. The reflectance of a wavelength were obtained that aimed to detect the verification of the slope and the growth type’s reflectance. When the mixed coniferous forest, static observation develop same reflectance values but the effect of the sloped factor occur the high value of the standard deviations. Then, our method applied to the method of the SGLI’s data calculation scheme, and then the growth factor of the area be affects the influence of the from 400 to 700 nm wavelength and also the factor of slope region be affects the wavelength of reflectance. SGLI data analysis, the factor of these parameters were used to remake the size of RSRF data from 250 m to 1000 m resolution. The future, we investigate more and then, the mask area of high value difference around the nearest 16 pixels be considered. Datas were significant at some pixels, such as a steep sloped, growth types, or error detected area. Data development of RSRF, the reflectance of each cells are detected as the values of the every ground types by the standard deviation.

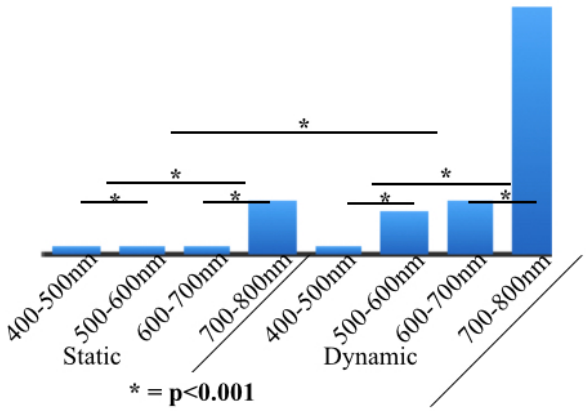
Keywords: SGLI's data verifications, Reflectance maps, Statistical ANOVA analysis

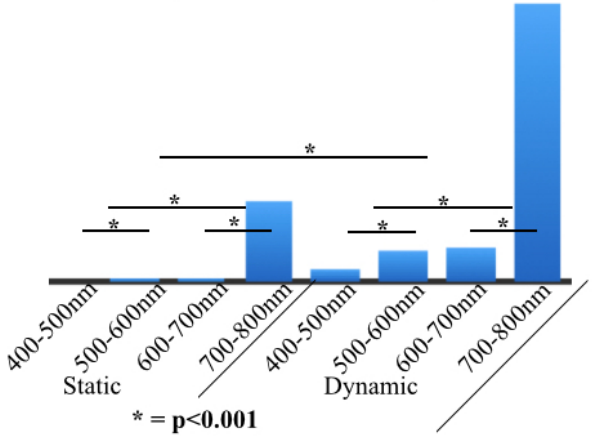
©2019. Japan Geoscience Union. All Right Reserved.

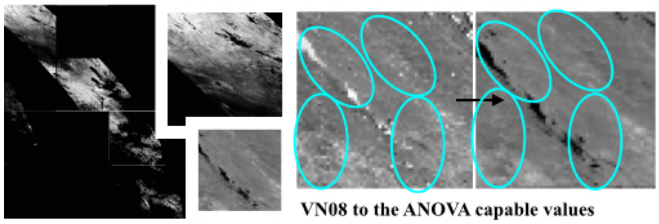
Factor analysis of variable results (Three-way ANOVA)

Sloped factors: Mean values of the SD of each (dynamic/semi-static)
Canopy factors: Difference of each SD of the every SD
Growth typed factors: Difference of each Mean and SD








VN08 to the ANOVA capable values

©2019. Japan Geoscience Union. All Right Reserved.

Remote sensing of aerosol optical properties and water-leaving radiance based on the optimal estimation approach

*Chong Shi[1], Teruyuki Nakajima[1], Makiko Hashimoto[1], Hideaki Takenaka[1]

1. Japan Aerospace Exploration Agency

A flexible inversion algorithm is proposed for jointly retrieving aerosol optical properties and water-leaving radiance from multispectral instrument over the ocean. A combined multi-wavelength and multi-pixel constraint approach is used to estimate aerosol and hydrosol over clear and turbid waters, based on the forward simulation from a coupled atmospher-ocean radiative transfer model. This sort of simultaneous inversion helps to correct the biases induced by the neglect of water-leaving radiance in the traditional aerosol retrieval algorithms, in addition, it can provide more aerosol information than the standard ocean color approach. To investigate the availability of current scheme, we conduct the retrieval in the process of MODIS, GOSAT/CAI and GCOM-C/SGLI instruments.

©2019. Japan Geoscience Union. All Right Reserved.

Aerosol retrieval and PM2.5 from space using GOSAT/TANSO-CAI

*Makiko Hashimoto[1], Hideaki Takenaka[1], Teruyuki Nakajima[1], Akiko Higurashi[2]

1. Japan Aerospace Explortion Agency, 2. NIES

Aerosol in the atmosphere has a great impact not only for the Earth’ s radiation budget and changing the Earth’ s climate, but also on human health. Especially, the fine particle, which is often called PM2.5, has drawn attention as a cause of health damage.

The urban area is a source of anthropogenic aerosol, which is mostly composed of small particles, and the particles are transported to other regions. Satellite remote sensing provides effective means to monitor the atmospheric aerosols in wide area including urban areas.

Accurate retrieval of fine mode aerosol optical thickness (AOT) is necessary to calculate an equivalent value of PM2.5 from space. Therefore, an aerosol retrieval algorithm for satellite remote sensing of urban areas to improve the retrieval accuracy of aerosol properties, which is called MWPM (Multiple wavelengths and pixels method) (Hashimoto and Nakajima, 2017), was developed. The method simultaneously retrieves fine and coarse mode AOT and single scattering albedo by using several wavelengths and spatial difference of surface reflectance. The method is useful for aerosol retrieval over spatially inhomogeneous surface like an urban area.

The algorithm was applied to GOSAT (Greenhouse Gases Observing Satellite) / TANSO-CAI (Cloud and Aerosol Imager, CAI) data. The GOSAT launched ten years ago (on January 23th, 2009) is a satellite to monitor greenhouse gases (GHG) such as carbon dioxide and methane with TANSO-FTS (Fourier Transform Spectrometer, FTS). The CAI is a supplementarysensor of the FTS, detecting cloud and deriving aerosol optical properties.

PM2.5 using retrieved fine mode AOT by MWPM in East Asian region from 2009 was calculated. The poster presents a retrieval result of PM2.5 over the East Asian region from space in several years and discusses the seasonal and annual variations.
Monitoring of aerosol properties such as AOT, PM2.5 and soot mixing ratio over land is added to the mission of GOSAT-2 that was launched on Otober 29th 2018. As a near-future plan, the algorithm will be applied to GOSAT-2/TANSO-CAI-2 data to generate standard PM2.5 data products.

Keywords: Remote sensing , Aerosol

©2019. Japan Geoscience Union. All Right Reserved.

Establishing a high resolution road fugitive dust emission inventory in Kaifeng City, China

*Yiming Xu[1], Shili Liu[1], Xinyue Cao[1], Xianbao Shen[1], Zhiliang Yao[1]

1. Department of Environmental Science and Engineering, Beijing Technology and Business University

Due to the rapid urbanization and industrialization in many Chinese cities, ambient particulate matter pollution such as road fugitive dust pollution becomes a serious environmental problem. However, the emission of road fugitive dust is relatively difficult to quantify as it is of high uncertainty and spatial heterogeneity. The research aims to build a high resolution road fugitive dust emission inventory which is transferrable and applicable to other cities in China. High spatial resolution images were utilized to digitalize whole road network of Kaifeng City, Henan Province, China. Vehicle flows of the whole road network were estimated by incorporating the whole road network, field measured data and GPS data on an hourly, daily, weekly, monthly and yearly basis at city level. By fusing the road network information, vehicle flow, road dust load, average vehicle weight, a high resolution road fugitive dust emission inventory was established. The results showed that the total emissions of PM_{10}, $PM_{2.5}$ and Total Suspended Particulate from road fugitive dust at commuter time and downtown were much higher compared with other time and location in Kaifeng City. The framework of this road fugitive dust emission inventory can be applied to other cities, and it can provide data support and guide fugitive dust management in China.

Keywords: Road Fugitive Dust, High Resolution Remote Sensing, Satellite Data, Air Pollutant Emission Inventory

©2019. Japan Geoscience Union. All Right Reserved.

A Relationship between Diurnal Change Patterns of Land Surface Temperature and Spatial Configuration of the Osaka Metropolitan Area Captured by Himawari-8

*Yuhei Yamamoto[1], Hirohiko Ishikawa[1]

1. Disaster Prevention Research Institute, Kyoto University

Land surface temperature (LST) is a physical quantity that greatly contributes to the formation of an urban thermal environment. Therefore, understanding the spatiotemporal characteristics of LST is necessary for constructing a sustainable urban environment. The spatial distribution relationship between the instantaneous LST and urban land use has been investigated using polar-orbiting satellite/airborne sensors. This study explored how the urban spatial configuration and meteorological field affect the temporal changes of LST by using Japanese geostationary satellite (Himawari-8) sensor.
The study area is the Osaka metropolitan area in Japan and target days are three days that were clear-sky throughout the day in summer (August 12, 2016, July 19, 2018, and August 4, 2018). We used 100 m-mesh urban land use data and ground-based meteorological observation data to examine the urban spatial configuration and meteorological fields, respectively. The temporal changes of LST are the amplitude and phase mainly forming the diurnal change of LST. These two temporal changes were extracted by applying principal component analysis to the diurnal changes of LST represented by the 10-minute LST dataset retrieved from Himawari-8 data.
Our results showed that the spatial variations in the amplitude and phase corresponded to the penetration time and duration of the sea breeze and the thermal inertia of surface materials. Besides, it was found that the LST change during daytime was larger in the high-density low-building areas than in the low-density low-building areas. This result suggests that the increase in building density increases the LST change during the daytime. These findings lead to a deeper understanding of an urban hot environment and are helpful for urban planning to mitigate the deterioration of a hot environment.

Keywords: Land Surface Temperature, Himawari-8, Urban Heat Island

©2019. Japan Geoscience Union. All Right Reserved.

[E] Poster | A (Atmospheric and Hydrospheric Sciences)：A-CG Complex & General

Thu. May 30, 2019 5:15 PM - 6:30 PM JST | Thu. May 30, 2019 8:15 AM - 9:30 AM UTC | Poster Hall International Exhibition Hall8, Makuhari Messe_12

[A-CG34] Satellite Earth Environment Observation

convener:Riko Oki(Japan Aerospace Exploration Agency), Yoshiaki HONDA(Center for Environmental Remote Sensing, Chiba University), Yukari Takayabu(Atmosphere and Ocean Research Institute, the University of Tokyo), Tsuneo Matsunaga(Center for Global Environmental Research and Satellite Observation Center, National Institute for Environmental Studies)

In recent years, we cannot avoid facing issues on global environmental changes that occur in various spatiotemporal scales. The earth environmental observation data by satellites became the necessary basic data to tackle and solve those issues. Due to the recent advancement in the observation sensor technique and the data processing technique, the satellite observation has been showing rapid progress, and the time is changing from examining the accuracy of the observation sensor data to the advancement of the data application, leading to broaden potential users. In these days application became synergetic, so we comprehensively pick
up this topic in the Atmospheric and Hydrospheric Sciences Session of this Union Meeting that enables to comprise the atmospheric, oceanic and land sciences; by combining the intelligence and the knowledge of the party, we propose a session that aims to prompt further studies towards the issues on earth environmental change, the advancement in the data application and future plans of Earth Observation missions.

[ACG34-P01] Impact of usage of multiple-satellite sensors on accuracy of daily-mean sea surface wind data

*Ayumi Koizumi[1], Masahisa Kubota[2], Kunio Kutsuwada[3], Hiroyuki Tomita[4], Tsutomu Hihara[5] (1.Tokai University, 2.Tokai University, Institute of Ocean Research and Development, 3.School of Marine Science and Technology, Tokai University, 4.Institute for Space-Earth Environmental, Nagoya University, 5.Japan Agency for Marine-Erth Science and Technology)

[ACG34-P02] Temperature and Size Variability of Warm Pools in the Global Oceans

*ChunYi Lin[1] (1.National Museum of Marine Science & Technology)

[ACG34-P03] Sea surface temperature from SGLI aboard the GCOM-C satellite of JAXA

*Yukio Kurihara[1], Kazunori Ogata[2], Hiroshi Murakami[2], Misako Kachi[2] (1.Tripli-I Co., Ltd., 2.JAXA EORC)

[ACG34-P04] Concept of small satellite UV/visible imaging spectrometer optimized for tropospheric NO_2 measurements in air quality monitoring

*Tamaki Fujinawa[1,5], Katsuyuki Noguchi[2], Akihiko Kuze[3], Andreas Richter[4], John P. Burrows[4], Andreas C. Meier[4], Tomohiro Sato[1], Takeshi Kuroda[1], Naohiro Yoshida[5], YASUKO KASAI[1,5] (1.National Institute of Information and Communications Technology, 2.Nara Women's University, 3.Japan Aerospace Exploration Agency, 4.University of Bremen, 5.Tokyo Institute of Technology)

[ACG34-P05] EarthCARE L2 algorithms for cloud and precipitation

*Kaori Sato[1], Hajime Okamoto[1], Hiroshi Ishimoto[2] (1.Research Institute for Applied Mechanics, Kyushu University, 2.Meteorological Research Institute)

[ACG34-P06] Analysis of the Surface Echo Characteristics Derived from GPM/DPR Wide Swath Observation Experiment

*Kosuke Yamamoto[1], Kinji Furukawa[1], Nobuhiro Takahashi[2], Takuji Kubota[1] (1.Japan Aerospace Exploration Agency, 2.Nagoya University)

[ACG34-P07] The Recent Results from the Global Precipitation Measurement (GPM) mission in Japan

*Riko Oki[1], Takuji Kubota[1], Kinji Furukawa[1], Yuki Kaneko[1], Moeka Yamaji[1], Kosuke Yamamoto[1], Toshio Iguchi[2], Yukari Takayabu[3] (1.Japan Aerospace Exploration Agency, 2.NICT, 3.the University of Tokyo)

[ACG34-P08] **Verification of Global Satellite Mapping of precipitation (GSMaP) for providing its error information**

*Moeka Yamaji[1], Takuji Kubota[1] (1.Earth Observation Research Center, Japan Aerospace Exploration Agency)

[ACG34-P09] Detection of the mixed phase top using the measured dual-frequency ratio of reflectivity with GPM/DPR

*Yuki Kaneko[1], Toshio Iguchi[2] (1.Japan Aerospace Exploration Agency, 2.National Institute of Information and Communications Technology)

[ACG34-P10] **Comparison between high frequency satellite rainfall estimation and APHRODITE-2 ground rain gauge observation**

*Hitoshi Hirose[1], Koichi Toyoshima[1], Atsushi Higuchi[1], Akiyo Yatagai[2], Natsuko Yasutomi[3] (1.Center for Environmental Remote Sensing, Chiba University, 2.Hirosaki University, 3.Disaster Prevention Research Institute, Kyoto University)

[ACG34-P11] Development of the high resolution GSMaP by the Himawari-8

*Tomoaki Mega[1], Tomoo Ushio[1] (1.Tokyo Metropolitan University)

[ACG34-P12] Preliminary results of on-orbit estimation for polarization sensitivity of GCOM-C/SGLI

*Risa Miyazaki[1], Hiroshi Murakami[1], Masahiro Hori[1] (1.Japan Aerospace Exploration Agency)

[ACG34-P13] Analysis of SGLI validation datas based on the effects of the growth and ground types for the AGB development

*Ryota Ishibashi[1], Koji KAJIWARA[1], Yoshiaki HONDA[1] (1.Center for environmental remote sensing, Chiba University)

[ACG34-P14] Remote sensing of aerosol optical properties and water-leaving radiance based on the optimal estimation approach

*Chong Shi[1], Teruyuki Nakajima[1], Makiko Hashimoto[1], Hideaki Takenaka[1] (1.Japan Aerospace Exploration Agency)

[ACG34-P15] Aerosol retrieval and PM2.5 from space using GOSAT/TANSO-CAI

*Makiko Hashimoto[1], Hideaki Takenaka[1], Teruyuki Nakajima[1], Akiko Higurashi[2] (1.Japan Aerospace Explortion Agency, 2.NIES)

[ACG34-P16] **Establishing a high resolution road fugitive dust emission inventory in Kaifeng City, China**

*Yiming Xu[1], Shili Liu[1], Xinyue Cao[1], Xianbao Shen[1], Zhiliang Yao[1] (1.Department of Environmental Science and Engineering, Beijing Technology and Business University)

[ACG34-P17] A Relationship between Diurnal Change Patterns of Land Surface Temperature and Spatial Configuration of the Osaka Metropolitan Area Captured by Himawari-8

*Yuhei Yamamoto[1], Hirohiko Ishikawa[1] (1.Disaster Prevention Research Institute, Kyoto University)

Impact of usage of multiple-satellite sensors on accuracy of daily-mean sea surface wind data

*Ayumi Koizumi[1], Masahisa Kubota[2], Kunio Kutsuwada[3], Hiroyuki Tomita[4], Tsutomu Hihara[5]

1. Tokai University, 2. Tokai University, Institute of Ocean Research and Development, 3. School of Marine Science and Technology, Tokai University, 4. Institute for Space-Earth Environmental, Nagoya University, 5. Japan Agency for Marine-Erth Science and Technology

Most satellites observing sea surface winds have sun-synchronous orbits and provide observation data at the same place two times per a day. We can expect that daily-mean values estimated from these data have some errors when diurnal changes in wind field cannot be neglected. For this problem, use of multiple satellites is helpful. Since the number of sensors used to construct daily-mean data is different among the years, it is expected that the accuracy of a daily-mean value changes from year to year.

The purpose of this study is to describe time variation of accuracy in daily-mean wind data in the Japanese Ocean Flux Data Sets with Use of Remote Sensing Observation (J-OFURO)-3 and to investigate its causes by comparing with in-situ measurement data by moored buoys and calculating three statistical values.

Results reveal that the statistical values are improved with year. To examine the relationship between the yearly statistics and the yearly number of satellite sensors, we plotted a scatter diagram between the number of satellites and three statistical values in each year. We found that the correlations between them are very high. We also focused on a time interval of the satellite wind observation, namely maximum missing time within a day. The result showed that the correlation between three statistical values and maximum missing time intervals is high. Since the relation between these two factors is not independent, we analyzed by considering both factors together. First, we chose five buoys with various standard deviations for a daily-mean value. Next, we picked up data from buoy's hourly data using random numbers, and calculated the daily mean value using the random data, and then determined the number of observations and the maximum missing time interval each day. Assuming the daily mean value calculated from 24 hourly data as a true value, the RMSE between this true value and the daily mean created from random data was calculated. From the result of this analysis, it was found that the value of Root Mean Square Error(RMSE) depends on the maximum missing time interval rather than the number of observations. Furthermore, when RMSE was normalized by standard deviation, the same figures were obtained for all buoys. This result implies that the RMSE of the daily mean value of the buoy station can be estimated if the magnitude of diurnal variation is known by giving the number of satellites used for observation and the maximum missing time interval, Moreover, by applying this result, we think that it is possible to show the optimal number of sensors and observation time for target accuracy. This result gives very breakthrough information to the design of the satellite observation system for sea surface wind.

Keywords: Multiple-satellite sensors, Sea surface wind

©2019. Japan Geoscience Union. All Right Reserved.

Temperature and Size Variability of Warm Pools in the Global Oceans

*ChunYi Lin[1]

1. National Museum of Marine Science & Technology

Using advance satellite-derived Sea surface height anomaly, sea surface temperature (SST) data, and heat flux data, we investigate the thermal variability, temperature and size variability of warm pools in the global oceans, the Pacific, the Atlantic, and the Indian Ocean, respectively. Because of the high density and specific heat of seawater, water can store and transport large amounts of heat. High SST has particular influence on global climate system. Furthermore previous studies focused on the global warming or area warming, in this investigation we present results of warm pool SST binned into 1 ˚C interval. Detecting temperature and size variability of warm pools in the global oceans, it suggests that the high SST area (SST ≧ 28˚C) has faster increasing rate than surrounding area (SST 20˚C - 27˚C) in the global oceans, the Pacific, the Atlantic, and the Indian Ocean, respectively. To understand the role of surface heat flux in the tropical SST fluctuation, we analyze the mixed layer heat balance equation. Upper ocean heat budget between the heat advection and heat diffusion term are compared and heat diffusion processes may be a mechanism for transporting excessive amount of heat that the warm pool through enhancing the SST gradient around the edge of the warm pool. In order to find out dominant period components and the relationship of energy-frequency distribution without influenced induced by nonlinear and nonstationary signals, the Hilbert-Huang Transform applied by ensemble empirical mode decomposition is employed. The ensemble empirical mode decomposition analysis indicates that the interannual component has strong influence on the variability of the warm core pool in the Pacific, presumably because of the presence of El Niño phenomenon, while the annual cycle dominates the variability in the Indian and the Atlantic Ocean.

Keywords: warm pool, SST, heat flux

©2019. Japan Geoscience Union. All Right Reserved.

Sea surface temperature from SGLI aboard the GCOM-C satellite of JAXA

*Yukio Kurihara[1], Kazunori Ogata[2], Hiroshi Murakami[2], Misako Kachi[2]

1. Tripli-I Co., Ltd., 2. JAXA EORC

The Global Change Observation Mission-Climate (GCOM-C) satellite, which is one of two satellites for the GCOM mission of the Japan Aerospace and Exploration Agency (JAXA), was launched on 23 December 2017. The Second Generation Global Imager (SGLI) is the optical sensor aboard GCOM-C which consists of two components: the Visible and Near-infrared Radiometer (VNR) and the Infrared Scanner (IRS). SGLI has switchable spatial resolution from 250 m x 250 m to 1 km x 1 km. The resolution of 250 m x 250 m is expected to reveal complicated structure of geophysical parameters. Sea surface temperature (SST), which is one of the important parameters in the geophysical field, is also determinable by using split window data of SGLI. SGLI SST is retrieved by utilization of newly developed cloud masking method and a modified SST method originally developed for Himawari-8. Considering combined utilization of satellite SSTs, the methods developed for SGLI SST will be applied back to Himawari-8 data as well as the data from the Visible Infrared Imaging Radiometer Suite (VIIRS) aboard the Suomi National Polar-orbiting Partnership (Suomi NPP) satellite. SGLI SST is validated by comparison with buoy data. The comparison result shows RMSD of ~0.4 K, good agreement between SGLI SSTs and buoy data. Triple comparison with Himawari-8 and VIIRS SSTs is being started. Operational retrieval of SGLI SST started at the end of 2018. The products are available at the G-Portal site of JAXA and the JAXA Satellite Monitoring and Environmental Studies (JASMES) site of the Earth Observation Center (EORC) of JAXA.

©2019. Japan Geoscience Union. All Right Reserved.

Concept of small satellite UV/visible imaging spectrometer optimized for tropospheric NO_2 measurements in air quality monitoring

*Tamaki Fujinawa[1,5], Katsuyuki Noguchi[2], Akihiko Kuze[3], Andreas Richter[4], John P. Burrows[4], Andreas C. Meier[4], Tomohiro Sato[1], Takeshi Kuroda[1], Naohiro Yoshida[5], YASUKO KASAI[1,5]

1. National Institute of Information and Communications Technology, 2. Nara Women's University, 3. Japan Aerospace Exploration Agency, 4. University of Bremen, 5. Tokyo Institute of Technology

Satellite observations at nadir can potentially facilitate a better understanding of the emissions and distribution of tropospheric nitrogen dioxide, NO_2. The identification of emissions requires adequate spatiotemporal resolution measurements of the total column amounts of NO_2. The spatial resolution of previous and current observations is insufficient for the identification of NO_2 hot-spots. Switching to a spatial resolution of ~1 km x ~1 km can improve the identification of local sources of NO_2 and their emissions. To investigate the feasibility of observations with such a high spatial resolution, we simulated radiance spectra for different cases under varying parameters, such as area, season, satellite altitude, and surface reflectance by using the radiative transfer model SCIATRAN. We subsequently retrieved NO_2 slant column densities (SCDs) using the differential optical absorption spectroscopy (DOAS) technique with several fit windows. For test cases associated with polluted conditions, we found that the conceptual nadir-observing instrument on a satellite at an altitude of ~300 km involved the lowest retrieval errors for signal-to-noise ratios of around 1000 with accuracy better than the required 5% for tropospheric NO_2 SCD and that the fit window of 425--497 nm met the scientific requirements for both surface reflectance cases.

Keywords: Nitrogen dioxide, Earth observation, Radiative transfer model, Remote sensing

©2019. Japan Geoscience Union. All Right Reserved.

EarthCARE L2 algorithms for cloud and precipitation

*Kaori Sato[1], Hajime Okamoto[1], Hiroshi Ishimoto[2]

1. Research Institute for Applied Mechanics, Kyushu University, 2. Meteorological Research Institute

The EarthCARE (Earth Clouds, Aerosols and Radiation Explorer, JAXA-ESA) mission will carry the first 94GHz Doppler Cloud Profiling Radar (CPR) with a high spectral resolution atmospheric lidar (ATLID) at 355nm. Recent progresses in EarthCARE L2 cloud/precipitation algorithms for the treatment of multiple scattering and cloud particle nonsphericity are presented.

Keywords: spaceborne active sensor, cloud

©2019. Japan Geoscience Union. All Right Reserved.

Analysis of the Surface Echo Characteristics Derived from GPM/DPR Wide Swath Observation Experiment

*Kosuke Yamamoto[1], Kinji Furukawa[1], Nobuhiro Takahashi[2], Takuji Kubota[1]

1. Japan Aerospace Exploration Agency, 2. Nagoya University

The observation from spaceborne precipitation radar has been contributed to better understanding of earth climate system. Global Precipitation Measurement (GPM) core satellite Dual-frequency Precipitation Radar (DPR) provides us 3-dimentional information of precipitation by the scan width of about 250 km, but there have been arguments that to bring systematic impact on the weather monitoring through global rainfall map such as GSMaP, wider swath observation by precipitation radar is necessary.

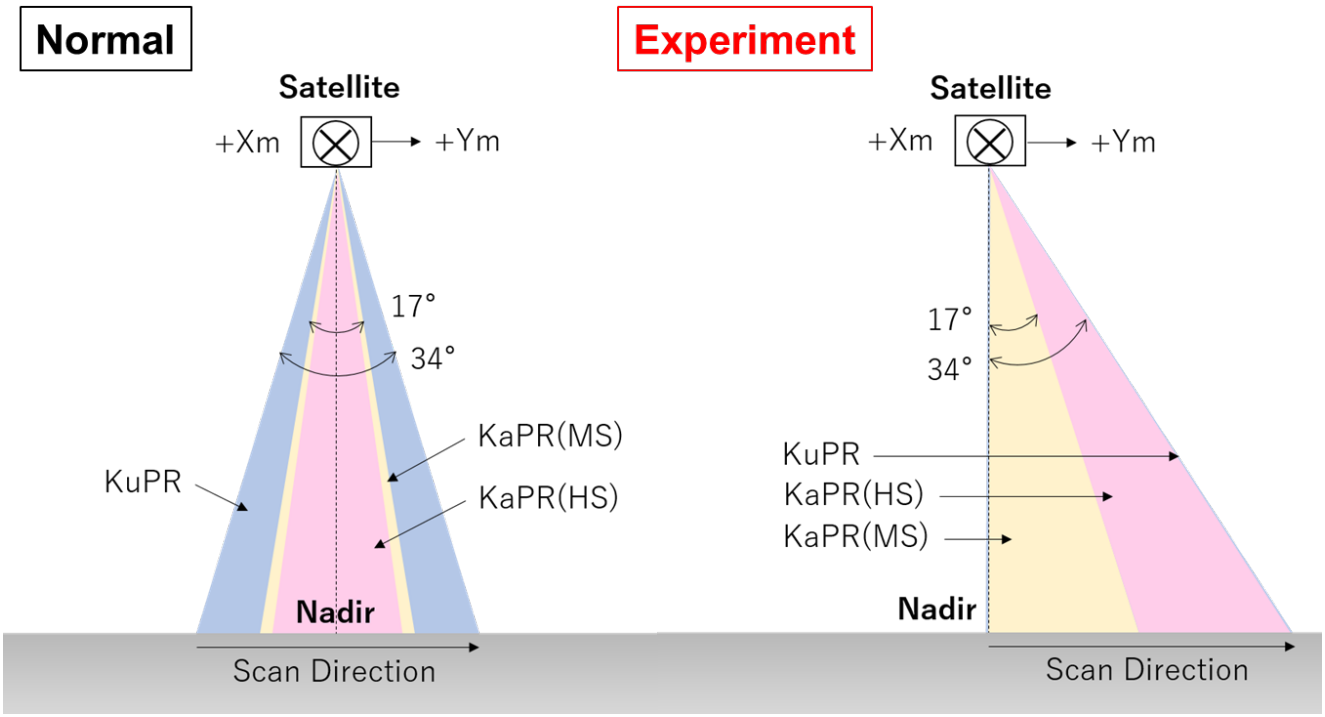
Based on those requirements, the scan pattern of GPM/DPR was experimentally changed for 1 day from 13UTC on September 26th. In this experiment, the scan angle was changed to observe from nadir to about +34˚ assuming future spaceborne precipitation radar with wider swath width, while in the normal observation DPR scans ±17˚. The height and strength of the mainlobe clutter with larger incident angle were assessed statistically to examine the possibility of the rainfall retrieval with wide swath observation by DPR.

In order to examine mainlobe clutter height, it is inevitable to reduce sidelobe and grating lobe effect. In this study, clutter-free observation data is extracted based on following procedures; 1) extract bins above mainlobe clutter; 2) extract bins under non-precipitation condition from 1); 3) extract bins that satisfy |received power −averaged noise power| < 2 sigma of the noise power from 2). Note that this procedure was applied only for KuPR observation since sidelobe and grating lobe clutter is not prominent in KaPR.

The result for KuPR observation shows that the mainlobe clutter top height at the larger incident angle over ocean is somehow suppressed at around 4 km while over land it increases almost linearly up to around 5 km due to the strong surface scattering. The same tendency is found on the KaPR observation, but it has lower clutter top height of around 2.5 km and 3.5 km, over ocean and land respectively. Suppression is clearer over ocean thanks to the specular reflection. The results also indicate that relatively intense rainfall can be retrieved while shallow rainfall with weak echo power may not be acceptable for retrieval because it should be masked by the surface clutter.

Keywords: precipitation radar, radar clutter, GPM core satellite

©2019. Japan Geoscience Union. All Right Reserved.



©2019. Japan Geoscience Union. All Right Reserved.

The Recent Results from the Global Precipitation Measurement (GPM) mission in Japan

*Riko Oki[1], Takuji Kubota[1], Kinji Furukawa[1], Yuki Kaneko[1], Moeka Yamaji[1], Kosuke Yamamoto[1], Toshio Iguchi[2], Yukari Takayabu[3]

1. Japan Aerospace Exploration Agency, 2. NICT, 3. the University of Tokyo

The Global Precipitation Measurement (GPM) mission is an international cooperate satellite project to achieve highly accurate and highly frequent global precipitation observations. The GPM mission consists of the GPM Core satellite jointly developed by the U.S. and Japan and Constellation Satellites that carry microwave radiometers and provided by the GPM partner agencies. The GPM Core satellite carries the Dual-frequency Precipitation Radar (DPR) by the Japan Aerospace Exploration Agency (JAXA) and the National Institute of Information and Communications Technology (NICT) and the GPM Microwave Imager (GMI) provided by National Aeronautics and Space Administration (NASA). The GPM Core satellite was launched in February 2014 and achieved its prime mission period planned for 3 years in 2017.

It has been continuing its observation as the extended mission phase after that.

JAXA develops the DPR Level 1 algorithm and the NASA-JAXA Joint Algorithm Team develops the DPR Level 2 and DPR-GMI combined Level 2 algorithms. The DPR, the DPR-GMI combined algorithms and the latent heating algorithm were updated, and those products were released in October 2018 as Version 0.6. Using dual frequency information of DPR, the latest Level 2 products include information such as precipitation phase at surface, heavy ice precipitation and so on. Also, the calibration factors of TRMM/PR were re-examined to have consistency between DPR/Ku. The same GPM Ku-band radar L2 algorithm now applies to the TRMM/PR, so that the long radar precipitation data exceeding more than 20 years are now available. From May 2018 in the extended mission period, the scan pattern of the Ka-band radar has been changed to realize matched beam observation in full swath. The new algorithm applying to the changed scan pattern is now under development.

JAXA also develops the Global Satellite Mapping of Precipitation (GSMaP), that is hourly and 0.1-degree horizontal resolution global rainfall map. It is available through the “JAXA Global Rainfall Watch” website (https://sharaku.eorc.jaxa.jp/GSMaP/index.htm). GSMaP product family includes different data latency products and rain gauge calibrated products and so on. The GSMaP near-real-time version (GSMaP_NRT) product provides global rainfall map in 4-hour after observation, and an improved version of GSMaP near-real-time gauge-adjusted (GSMaP_Gauge_NRT) product has been released since Dec. 2018.

The GSMaP real-time product called GSMaP_NOW now product is providing data at the earliest timing. It has been realized using the geostationary satellite Himawari-8 operated by the Japan Meteorological Agency (JMA) since November 2015. Since Nov. 2018 the domain of GSMaP_NOW has been extended to the region of the geostationary satellite Meteosat operated by the European Organization for the Exploitation of Meteorological Satellites (EUMETSAT) in November 2018. JAXA is further developing the GSMaP_NOW to provide global real-time rainfall product.

Keywords: GPM, Satellite Remote Sensing, Precipitation

©2019. Japan Geoscience Union. All Right Reserved.

©2019. Japan Geoscience Union. All Right Reserved.

Verification of Global Satellite Mapping of precipitation (GSMaP) for providing its error information

*Moeka Yamaji[1], Takuji Kubota[1]

1. Earth Observation Research Center, Japan Aerospace Exploration Agency

Precipitation is one of the most essential parameters in the Earth system. Due to address water issues like water shortage or floods, JAXA has developed and provided Global Satellite Mapping of Precipitation (GSMaP), which is hourly global precipitation dataset. It is under the Global Precipitation Measurement (GPM) mission and contributes.
GSMaP allows us to capture the hourly horizontal distribution of precipitation with good latency after observation. The spatial resolution is 0.1 x 0.1 degrees latitude/longitude. It has been used for various kinds of utilization purposes.
In terms of accuracy, GSMaP algorithms were updated in several times, and GSMaP has been getting more accurate day by day, however, it is known that the inhomogeneous of accuracy is existed depending on algorithm characteristics. It has been needed to provide information about the uncertainty and accuracy of GSMaP by users.
In this study, verification result of GSMaP near-realtime product version 6 (GSMaP_NRT) is reported. The radar/raingauge analysed precipitation data by Japan Meteorological Agency, which is an hourly rainfall analysis generated from ground-based precipitation radars corrected by automated rain gauges, are used as the reference data. Since the purpose of this study is for providing generalized error information, root mean square errors (RMSE) is statistically calculated for each precipitation level and each reliability flag during May-June-July-August-September-October in 2015-2018. Some initial results showed that the RMSE qualitatively represented the error for each precipitation level and reliability flag. The RMSE ratio to the average precipitation rate got larger as the precipitation rate became smaller while it became stable around 60 –80 % when precipitation rate was more than 10 mm/h. We report the validation results in detail, such as land/ocean difference or sampling dependence, and focus on the effectiveness of it.

Keywords: precipitation, GPM, GSMaP, validation

©2019. Japan Geoscience Union. All Right Reserved.

Detection of the mixed phase top using the measured dual-frequency ratio of reflectivity with GPM/DPR

*Yuki Kaneko[1], Toshio Iguchi[2]

1. Japan Aerospace Exploration Agency, 2. National Institute of Information and Communications Technology

The core observatory of the Global Precipitation Measurement (GPM) mission was launched in 2014 and has been observing rain and snow between 65˚S and 65˚N by the Dual Frequency Precipitation Radar (DPR) and the GPM Microwave Imager (GMI). The DPR provides three-dimensional structure of storms derived from reflected energy from precipitation particles. Precipitation echoes at the two frequencies of the DPR, Ka-band (25GHz) and Ku-band (14GHz), make it possible to infer the mean size and physical property of precipitation particles. The swath width of Ka-band scanning was 125 kilometers centered at nadir and was nested within the Ku-band’ s wider scan width of 254 kilometers. On May 21 2018, the Ka-band scan pattern was changed to match with the Ku-band’ s. Dual frequency radar reflectivity factors are available for full swath of 254 kilometers now.

The classification (CSF) module in the standard DPR level2 algorithm detects a bright band (BB) and classifies precipitation into three types, stratiform, convective, and other. Rain types affect the retrievals of rain amount and latent heating in the DPR algorithm. Accurate classification is also important in the Global Satellite Mapping of Precipitation (GSMaP) algorithm because it affects the rain profile database used in the rain retrieval with microwave radiometers. The BB detectability by the standard CSF algorithm is lower at and near the swath edges than near nadir because only Ku-band data was available in the outer swath before and because slant incidence of radar beams smears the vertical profiles.

As the Ka-band scan pattern has changed to cover the full swath, we can apply a dual-frequency method to detect a BB now. We have developed a method that uses the dual frequency ratio (DFR) to detect the mixed phase top. It looks at the slope of DFR as a function of range to identify the transition height from ice to water. DFR itself is estimated from measured DFR (DFRm) with attenuation correction. Preliminary experiments show that the developed method can detect the BB in stratiform rain over the swath almost uniformly. This method also has a potential to identify the transition height even in some convective cases. In this research we evaluate the performance of the algorithm by comparing the altitude of BB and the transition height with those estimated by using X-band multi-parameter radar (XRAIN) data.

Keywords: GPM, Melting Layer, Precipitation Radar

©2019. Japan Geoscience Union. All Right Reserved.

Comparison between high frequency satellite rainfall estimation and APHRODITE-2 ground rain gauge observation

*Hitoshi Hirose[1], Koichi Toyoshima[1], Atsushi Higuchi[1], Akiyo Yatagai[2], Natsuko Yasutomi[3]

1. Center for Environmental Remote Sensing, Chiba University, 2. Hirosaki University, 3. Disaster Prevention Research Institute, Kyoto University

APHRODITE project collects daily precipitation observation data from ground rain gauges in each country, and then performs appropriate quality control and converts it into gridded data. APHRODITE holds long-term data from the 1960s to the present and focuses on analyzes such as changes in characteristics of extreme rainfall due to long-term climate change. However, ground-based daily rain observations has a problem which end of the day (EOD) in each country is different from each other. To estimate the EOD in each country, we developed a Rain Potential Map (RPM) which is a product that can estimate global rain probability using geostationary meteorological satellites (GEO) (Hirose et al., 2016, JMSJ). In this study, we used the RPM, GSMaP and CMORPH which are global satellite rain estimation data based on microwave satellite and GEO observations.

Since the above satellite rainfall observation data can estimate global precipitation every hour, it is possible to create daily average data in which the average section is shifted by one hour. By correlating the satellite daily precipitation observation time series with the APHRODITE daily precipitation observation time series, the EOD value in each country was estimated from the time when the correlation coefficient is largest. We confirmed that the reliability of this method is high by a verification analysis in the field where true value of EOD is already known. Moreover, we made pseudo hourly rain time series of APHRODITE by inserting APHDOITE daily rain time series to satellite hourly rain time series. By this method, we will try to make a new APHRODITE data that is corrected for the EOD difference between each country.

Keywords: Precipitaition, Satellite, APHRODITE

©2019. Japan Geoscience Union. All Right Reserved.

Development of the high resolution GSMaP by the Himawari-8

*Tomoaki Mega[1], Tomoo Ushio[1]

1. Tokyo Metropolitan University

There is a new generation infrared (IR) imager on new-generation gestationary weather-satellite such as the Himawari-8 and the Geostationary Operational Environmental Satellite-R series. The imagers observe multi-channel passive imaging radiometer. The imagers observe wave a full disk with several km in about ten minutes. In Near-future, the IR imager observation should cover the globe.

Global precipitation information is an important tool for water management or earth science. Spaceborne sensors is one of the most convenient tools of global observation. The sensors cover global and provide uniform quality data. Precipitation estimation use microwave radiometer in low earth orbit (LOE). A microwave radiometer has high spatial resolution. However, one drawback of the microwave radiometer in LOE is narrow observation area. Whole earth observation by a microwave radiometer on a LOE satellite need some days. Therefore, global precipitation map is made from combined satellite data. However, combined data of microwave radiometer on LOE don’ t cover global in one hour. One of the global precipitation map is the Global satellite mapping of Precipitation (GSMaP). Precipitation estimation of the GSMaP made from microwave radiometer data. The GSMaP Moving Vector with Kalmanfilter (MVK) and Near real time compensate precipitation of no observation area by IR information. Spatial and temporal resolution of the GSMaP MVK achives 0.1 degree and one hour. This study shows downscale technique for GSMaP precipitation map by High-spatial and temporal resolution IR data of the Himawari-8. IR datasets of Himawari-8 are available every 2.5 minutes in the Japan region. In the presentation, we will also show validation the high resolution GSMaP and ground-radar network in Japan.

Keywords: Precipitation, GSMaP, Microwave Radiometer, Infrared Radiometer, Algorithm

©2019. Japan Geoscience Union. All Right Reserved.

Preliminary results of on-orbit estimation for polarization sensitivity of GCOM-C/SGLI

*Risa Miyazaki[1], Hiroshi Murakami[1], Masahiro Hori[1]

1. Japan Aerospace Exploration Agency

The GCOM-C has been launched successfully on 23th Dec. 2017 from the Tanegashima Space Center by H-IIA vehicle No.37. After the initial calibration/validation phase of one year after launch, all SGLI standard products have been released from JAXA’s data providing service (G-Portal) from Dec. 20, 2018.

In generally, the radiance reflected by the sea surface and the atmosphere is strongly polarized. When observing a large polarized light, the output radiance vary from the actual radiance because of the polarization sensitivity characteristic of the optical sensor. Especially for ocean color products, it is important to evaluate the effect of polarization sensitivity because it is necessary to extract the weak water-leaving reflectance (<10% of the whole) by the accurate atmospheric correction.
The polarization sensitivity of GCOM-C/SGLI of each NP (Non-Polarization) band has been measured in the pre-launch ground test. The ground test results of polarization sensitivity were shown to be <3.5% on average in the pixel direction in all bands. In this study, we evaluate whether the polarization sensitivity estimated from on-orbit observation data is consistent with the pre-launch test results. In this work, we report on the RED bands (VN07, VN08) and the NIR bands (VN10, VN11) of SGLI.
Polarization sensitivity on-orbit was evaluated based on Gordon and Zhang (1997) and Meister et al. (2005). We use the observation data by SGLI/PL (Polarization) band to estimate the real stokes vector components at the top of atmosphere (TOA). In order to obtain the polarization sensitivity with respect to directly observed radiance at TOA, L1B before inter-pixel sensitivity correction and before inter-telescope sensitivity correction was self-made from L1A data.
We analyzed the observation data of 12 path that PL band is observed nadir direction. The characteristics of the instrument for polarization sensitivity (polarization factor) were estimated by the least squares method. On the east side of the observation image, the error is large because of Sun-Glint. Although the variation in the pixel direction was still large, the estimated polarization factors (3 to 5 %) were consisted with the prelaunch ground test (~ 3.5%). However, sensitivity patterns in the pixel direction could not be identified, so we will continue to improve the evaluation in the future.

Keywords: GCOM-C, SGLI, Polarization sensitivity

©2019. Japan Geoscience Union. All Right Reserved.

Analysis of SGLI validation datas based on the effects of the growth and ground types for the AGB development

*Ryota Ishibashi[1], Koji KAJIWARA[1], Yoshiaki HONDA[1]

1. Center for environmental remote sensing, Chiba University

The effects of the earth of the time variant system should be difficult to detect the influence of the growth types and also the effects of the growth field’s variations. The research may occur the SGLI’s RSRF datas of the calculated AGB data accuracy analysis that observed between every kinds of the growth and also the ground types. The significance area of the SGLI observed, each of detected datas accuracy have to be considered. We show observation ways for the ground truth of the reflectance, LAI and fAPAR. The first case we use is a case of vegetation at the grassland. And then, based of reflectance values, we compare the other type as the Mixed coniferous forest example. The influence of an effect of the type of growth may occur the reflectance of the distributed area. We will detect these effects of the growth type. The influence at the observed area be necessarily to be verified.

The research topic includes the ground truth observation for the accuracy verification of a SGLI data obtained. For development of ground truth, the way to obtain datas were important. This paper explains how to examine growth (such as a second growth forest and other) and the slope factor of the second growth forest area and also the reflectance of each forest types. Then, this paper make ground truth observation scheme for the high accuracy AGB referenced data development at ground cover area. We explain the method of examine the error detection way including observation devices and also the problem of the research topic to be examined. Results may occur an example case of such kinds of the sloped forest and the kinds of the plane. The results shows a typical difference between the sloped and the plane, and then the results may occur the possibility that comparison of standard deviation may be an effective way to detect the volume of the forest type between every ground truth.

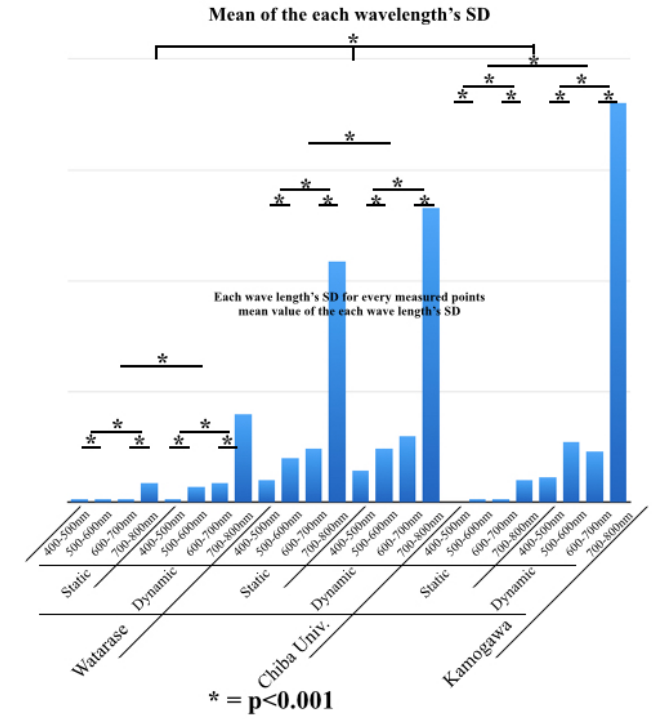
The case of we use as the sloped fields, reflectance of each wavelength were low and then the near 400 to 700 nm area will be higher than other wavelength (ANOVA values of results: $p < 0.001$). And then, we can see the effects of slope should be detected at total values of the reflectance. The reflectance of a wavelength were obtained that aimed to detect the verification of the slope and the growth type’s reflectance. When the mixed coniferous forest, static observation develop same reflectance values but the effect of the sloped factor occur the high value of the standard deviations. Then, our method applied to the method of the SGLI’s data calculation scheme, and then the growth factor of the area be affects the influence of the from 400 to 700 nm wavelength and also the factor of slope region be affects the wavelength of reflectance. SGLI data analysis, the factor of these parameters were used to remake the size of RSRF data from 250 m to 1000 m resolution. The future, we investigate more and then, the mask area of high value difference around the nearest 16 pixels be considered. Datas were significant at some pixels, such as a steep sloped, growth types, or error detected area. Data development of RSRF, the reflectance of each cells are detected as the values of the every ground types by the standard deviation.

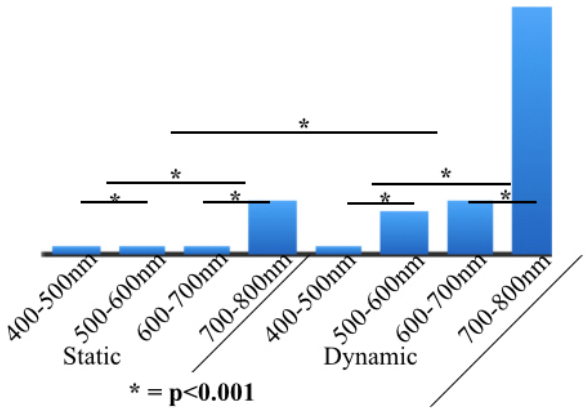
Keywords: SGLI's data verifications, Reflectance maps, Statistical ANOVA analysis

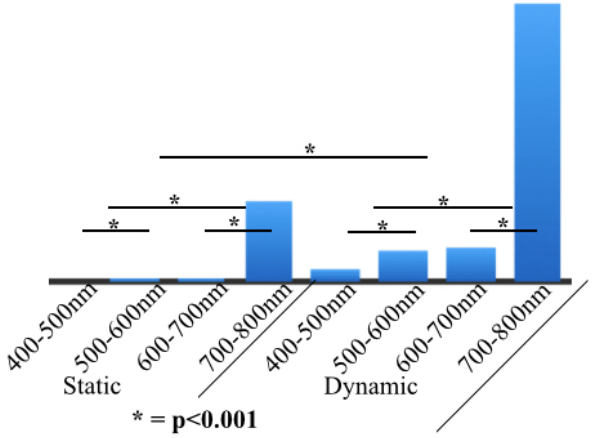
©2019. Japan Geoscience Union. All Right Reserved.

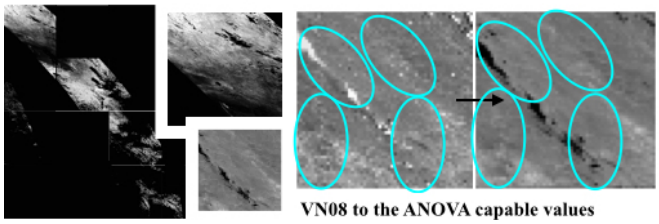
Factor analysis of variable results (Three-way ANOVA)

Sloped factors: Mean values of the SD of each (dynamic/semi-static)
Canopy factors: Difference of each SD of the every SD
Growth typed factors: Difference of each Mean and SD








VN08 to the ANOVA capable values

©2019. Japan Geoscience Union. All Right Reserved.

Remote sensing of aerosol optical properties and water-leaving radiance based on the optimal estimation approach

*Chong Shi[1], Teruyuki Nakajima[1], Makiko Hashimoto[1], Hideaki Takenaka[1]

1. Japan Aerospace Exploration Agency

A flexible inversion algorithm is proposed for jointly retrieving aerosol optical properties and water-leaving radiance from multispectral instrument over the ocean. A combined multi-wavelength and multi-pixel constraint approach is used to estimate aerosol and hydrosol over clear and turbid waters, based on the forward simulation from a coupled atmospher-ocean radiative transfer model. This sort of simultaneous inversion helps to correct the biases induced by the neglect of water-leaving radiance in the traditional aerosol retrieval algorithms, in addition, it can provide more aerosol information than the standard ocean color approach. To investigate the availability of current scheme, we conduct the retrieval in the process of MODIS, GOSAT/CAI and GCOM-C/SGLI instruments.

©2019. Japan Geoscience Union. All Right Reserved.

Aerosol retrieval and PM2.5 from space using GOSAT/TANSO-CAI

*Makiko Hashimoto[1], Hideaki Takenaka[1], Teruyuki Nakajima[1], Akiko Higurashi[2]

1. Japan Aerospace Explortion Agency, 2. NIES

Aerosol in the atmosphere has a great impact not only for the Earth’ s radiation budget and changing the Earth’ s climate, but also on human health. Especially, the fine particle, which is often called PM2.5, has drawn attention as a cause of health damage.

The urban area is a source of anthropogenic aerosol, which is mostly composed of small particles, and the particles are transported to other regions. Satellite remote sensing provides effective means to monitor the atmospheric aerosols in wide area including urban areas.

Accurate retrieval of fine mode aerosol optical thickness (AOT) is necessary to calculate an equivalent value of PM2.5 from space. Therefore, an aerosol retrieval algorithm for satellite remote sensing of urban areas to improve the retrieval accuracy of aerosol properties, which is called MWPM (Multiple wavelengths and pixels method) (Hashimoto and Nakajima, 2017), was developed. The method simultaneously retrieves fine and coarse mode AOT and single scattering albedo by using several wavelengths and spatial difference of surface reflectance. The method is useful for aerosol retrieval over spatially inhomogeneous surface like an urban area.

The algorithm was applied to GOSAT (Greenhouse Gases Observing Satellite) / TANSO-CAI (Cloud and Aerosol Imager, CAI) data. The GOSAT launched ten years ago (on January 23th, 2009) is a satellite to monitor greenhouse gases (GHG) such as carbon dioxide and methane with TANSO-FTS (Fourier Transform Spectrometer, FTS). The CAI is a supplementarysensor of the FTS, detecting cloud and deriving aerosol optical properties.

PM2.5 using retrieved fine mode AOT by MWPM in East Asian region from 2009 was calculated. The poster presents a retrieval result of PM2.5 over the East Asian region from space in several years and discusses the seasonal and annual variations.
Monitoring of aerosol properties such as AOT, PM2.5 and soot mixing ratio over land is added to the mission of GOSAT-2 that was launched on Otober 29th 2018. As a near-future plan, the algorithm will be applied to GOSAT-2/TANSO-CAI-2 data to generate standard PM2.5 data products.

Keywords: Remote sensing , Aerosol

©2019. Japan Geoscience Union. All Right Reserved.

Establishing a high resolution road fugitive dust emission inventory in Kaifeng City, China

*Yiming Xu[1], Shili Liu[1], Xinyue Cao[1], Xianbao Shen[1], Zhiliang Yao[1]

1. Department of Environmental Science and Engineering, Beijing Technology and Business University

Due to the rapid urbanization and industrialization in many Chinese cities, ambient particulate matter pollution such as road fugitive dust pollution becomes a serious environmental problem. However, the emission of road fugitive dust is relatively difficult to quantify as it is of high uncertainty and spatial heterogeneity. The research aims to build a high resolution road fugitive dust emission inventory which is transferrable and applicable to other cities in China. High spatial resolution images were utilized to digitalize whole road network of Kaifeng City, Henan Province, China. Vehicle flows of the whole road network were estimated by incorporating the whole road network, field measured data and GPS data on an hourly, daily, weekly, monthly and yearly basis at city level. By fusing the road network information, vehicle flow, road dust load, average vehicle weight, a high resolution road fugitive dust emission inventory was established. The results showed that the total emissions of PM_{10}, $PM_{2.5}$ and Total Suspended Particulate from road fugitive dust at commuter time and downtown were much higher compared with other time and location in Kaifeng City. The framework of this road fugitive dust emission inventory can be applied to other cities, and it can provide data support and guide fugitive dust management in China.

Keywords: Road Fugitive Dust, High Resolution Remote Sensing, Satellite Data, Air Pollutant Emission Inventory

©2019. Japan Geoscience Union. All Right Reserved.

A Relationship between Diurnal Change Patterns of Land Surface Temperature and Spatial Configuration of the Osaka Metropolitan Area Captured by Himawari-8

*Yuhei Yamamoto[1], Hirohiko Ishikawa[1]

1. Disaster Prevention Research Institute, Kyoto University

Land surface temperature (LST) is a physical quantity that greatly contributes to the formation of an urban thermal environment. Therefore, understanding the spatiotemporal characteristics of LST is necessary for constructing a sustainable urban environment. The spatial distribution relationship between the instantaneous LST and urban land use has been investigated using polar-orbiting satellite/airborne sensors. This study explored how the urban spatial configuration and meteorological field affect the temporal changes of LST by using Japanese geostationary satellite (Himawari-8) sensor.
The study area is the Osaka metropolitan area in Japan and target days are three days that were clear-sky throughout the day in summer (August 12, 2016, July 19, 2018, and August 4, 2018). We used 100 m-mesh urban land use data and ground-based meteorological observation data to examine the urban spatial configuration and meteorological fields, respectively. The temporal changes of LST are the amplitude and phase mainly forming the diurnal change of LST. These two temporal changes were extracted by applying principal component analysis to the diurnal changes of LST represented by the 10-minute LST dataset retrieved from Himawari-8 data.
Our results showed that the spatial variations in the amplitude and phase corresponded to the penetration time and duration of the sea breeze and the thermal inertia of surface materials. Besides, it was found that the LST change during daytime was larger in the high-density low-building areas than in the low-density low-building areas. This result suggests that the increase in building density increases the LST change during the daytime. These findings lead to a deeper understanding of an urban hot environment and are helpful for urban planning to mitigate the deterioration of a hot environment.

Keywords: Land Surface Temperature, Himawari-8, Urban Heat Island

©2019. Japan Geoscience Union. All Right Reserved.

[E] Poster | H (Human Geosciences)：H-TT Technology & Techniques

Thu. May 30, 2019 10:45 AM - 12:15 PM JST | Thu. May 30, 2019 1:45 AM - 3:15 AM UTC | Poster Hall International Exhibition Hall8, Makuhari Messe_3

[H-TT19] Geographic Information Systems and Cartography

convener:Takashi Oguchi(Center for Spatial Information Science, The University of Tokyo), Yuji Murayama(Graduate School of Life and Environmental Sciences), Yoshiki Wakabayashi(Graduate School of Urban Environmental Sciences, Tokyo Metropolitan University)

This session discusses various methods which acquire, store, analyze and visualize geospatial data, and presents the outcomes of empirical studies using GIS or mapping methods. The session also deals with applications of digital data, and GIS, and mapping to various fields of earth and planetary science and human society. All presentations and discussion of this session are made in English.

[HTT19-P01] Monitoring and Simulating Land Use/Cover Changes and its Impact on Land Surface Temperature in Sapporo City, Japan

*RUCI WANG[1], YUJI MURAYAMA[1] (1.University of Tsukuba)

[HTT19-P02] Spatiotemporal Variations of Land Cover/Use and Sustainable Urban Heat Island (UHI) Mitigation Strategies: A Case Study of Chinese Bay Megacities

★Invited Papers

*Fei LIU[1], Yuji MURAYAMA[1] (1. University of Tsukuba)

[HTT19-P03] A LST Study of the Seoul Metropolitan City, South Korea, Based on Landsat Data (1996 – 2017)

*Prabath Priyankara[1,3], Manjula Ranagalage[1,4], DMSLB Dissanayake[1,4], Takehiro Morimoto[1,2], Yuji Murayama[1,2] (1.Graduate School of Life and Environmental Sciences, University of Tsukuba, Japan, 2.Faculty of Life and Environmental Sciences, University of Tsukuba, Japan, 3.Faculty of Agriculture, University of Ruhuna, Sri Lanka, 4.Faculty of Social Sciences and Humanities, Rajarata University of Sri Lanka, Sri Lanka)

[HTT19-P04] Improvement of GIS exercise classes using the GIS open educational resources based on questionnaire surveys

★Invited Papers

*Hiroyuki Yamauchi[1], Takashi Oguchi[1], Yuichi S. Hayakawa[2,1], Kotaro Iizuka[1] (1.Center for Spatial Information Science, The University of Tokyo, 2.Environmental Geography, Faculty of Environmental Earth Science, Hokkaido University)

[HTT19-P05] The Development of COP for Tzu Chi Disaster Prevention System by Using QGIS-Taking 2018 Hualien Earthquake as an Example

*kuan-wen tseng[1], Ming-Ta Tsai[1], Yun-Ching Wang[1], Ming-Chih Wang[1], Chien-Hsien Liu[1] (1.03-3809093)

[HTT19-P06] Comparative study on shape and distribution of landslides caused by the 2012 Northern Kyushu heavy rainfall and the 2016 Kumamoto earthquake in the Aso region, Kumamoto, Japan

*Yasutaka Haneda[1], Takashi Oguchi[2], Kotaro Iizuka[2], Hitoshi SAITO[3,2], Yuichi S. Hayakawa[4,2], Shoichiro Uchiyama[5] (1.Graduate School of Frontier Science, The University of Tokyo, 2.Center for Spatial Information Science, The University of Tokyo, 3.College of Economics, Kanto Gakuin University, 4.Faculty of Environmental Earth Science, Hokkaido University, 5.National Research Institute for Earth Science and Disaster Resilience)

[HTT19-P07] Using GIS and remote sensing to assess relationships between landslides and land cover changes in the Sanbagawa and Mikabu Belts, Shikoku, Japan

*Roxanne Lai[1], Takashi Oguchi[1] (1.University of Tokyo)

[HTT19-P08] **Analysis of Morphometric Parameters for Mountains Ranges and Landslides due to the July 2018 Heavy Rain in Western Japan Using GIS Data**

*Toshikazu Fukuba[1], Takashi Oguchi[2] (1.Department of Earth and Planetary Environmental Science, The University of Tokyo, 2.Center for Spatial Information Science, The University of Tokyo)

[HTT19-P09] Analyzing short-term topographic change in coastal sand dunes using UAS-SfM photogrammetry: A case study in Northern Kujukuri, Japan

*Seulgi Lee[1], Yasutaka Nakata[2], Kotaro Iizuka[3], Takashi Oguchi[3] (1.Graduate School of Frontier Sciences, The University of Tokyo, 2.Forest Research Department, Forestry Research Institute, Hokkaido Research Organization, 3.Center for Spatial Information Science, The University of Tokyo)

[HTT19-P10] **Responses of suspended sediment yield to precipitation, topography and dam control in the Yellow River Basin, China**

*Ruiqi Zhang[1], Takashi Oguchi[2] (1. Department of Natural Environmental Studies, Graduate School of Frontier Sciences, The University of Tokyo, 2.Center for Spatial Information Science, The University of Tokyo)

Monitoring and Simulating Land Use/Cover Changes and its Impact on Land Surface Temperature in Sapporo City, Japan

*RUCI WANG[1], YUJI MURAYAMA[1]

1. University of Tsukuba

In recent years, urban heat island phenomenon (UHI) which prevails in many cities worldwide has caused broad public concern. UHI phenomenon impairs healthy urban development and causes excessive energy consumption, climatic and environmental deterioration. Land use/cover changes are one of the most crucial variables influencing on UHI. Therefore, monitoring and simulating land use/cover changes and analyzing its effects on LST are essential for healthy urban development. This study aims to capture the impact of land use/cover on LST and simulate the LST under various land use/cover scenarios in Sapporo city, Japan. At first, we monitored the land use/cover changes from 1985 to 2015 and detect the change of LST concerning land use/cover distribution. Then, we predicted the future conditions of LST based on various land use/cover scenarios. The results show that the LST differs according to land use/cover types, and the proportion of land use/cover types is the most significant factor affecting LST. The findings also indicate that the built-up area and paddy field have the highest average LST, while the green space and water area help cool the city. In the future, the green area such as urban green parks and grassland should be planned in the city to mitigate the UHI phenomenon. It reveals the spatial characterization of LST which provides significant insights for government and city planners.

Keywords: Geographical information science, Urban heat island, Land surface temperature, Land use/cover change, Sapporo city

©2019. Japan Geoscience Union. All Right Reserved.

Spatiotemporal Variations of Land Cover/Use and Sustainable Urban Heat Island (UHI) Mitigation Strategies: A Case Study of Chinese Bay Megacities

*Fei LIU[1], Yuji MURAYAMA[1]

1. University of Tsukuba

Rapid urbanization significantly affects the urban thermal environment in the context of global climate change. The assessment of surface urban heat island (SUHI) and development of mitigation strategies in megacities have become frontier issues on human health and urban sustainability. In this study, taking of the three Chinese bay megacities, we attempt to 1) disclose the relationship between land surface temperature (LST) and land cover using remote sensing quantified analysis, 2) to clarify the mechanism and characteristics of SUHI formation based on bi-temporal patterns and variations of land cover, and 3) to sustainably regulate and optimize the urban environment and further create urban planning and policies for relieving urban thermal effect. The study target is Guangzhou metropolitan area (GMA), Hangzhou metropolitan area (HMA) and Shanghai Metropolitan area (SMA) in China. The result of this study indicated remarkably different characteristics, arrangement, and variations among different bay thermal environments. Overall, spatial layouts and changes in the thermal environment of these three megacities were substantially identical with their land cover pattern and tendency. Although land covers significantly influenced the LST as a whole, the different areas had different magnitudes of SUHI coming from different land cover compositions and differentials. The results would provide a valuable reference to disentangle spatiotemporal variation of the bay urban thermal environments, and the urbanization-induced land covers temperature dynamics. This study would contribute to the development of future SUHI mitigation solutions.

Keywords: Land Cover/Use , Urban Heat Island (UHI), Mitigation Strategies

©2019. Japan Geoscience Union. All Right Reserved.

A LST Study of the Seoul Metropolitan City, South Korea, Based on Landsat Data (1996 –2017)

*Prabath Priyankara[1,3], Manjula Ranagalage[1,4], DMSLB Dissanayake[1,4], Takehiro Morimoto[1,2], Yuji Murayama[1,2]

1. Graduate School of Life and Environmental Sciences, University of Tsukuba, Japan, 2. Faculty of Life and Environmental Sciences, University of Tsukuba, Japan, 3. Faculty of Agriculture, University of Ruhuna, Sri Lanka, 4. Faculty of Social Sciences and Humanities, Rajarata University of Sri Lanka, Sri Lanka

Rapid urban growth often replaced urban vegetation with impervious surfaces which leads to increase land surface temperature (LST) periodically and tends to form urban heat islands (UHI). This is a serious issue of urbanized cities and the increase of LST badly affects the well-being of the life and environments of the cities. The Seoul Metropolitan City (SMC), South Korea, is one of the developed and rapidly urbanizing metropolitan city in Asia. The aim of this study was to examine the spatiotemporal variations of LST in the SMC and surroundings in the context of the UHI using Landsat data. The study examined the relationship of LST with the normalized difference vegetation index (NDVI) and the normalized difference built-up index (NDBI) at three time periods 1996, 2006, and 2017. Also, the study was investigated the environmentally critical areas based on LST and NDVI by modeling environmental criticality index (ECI). According to the results of the study, there is a negative correlation between LST with NDVI and positive correlation of LST with NDBI across all three time periods. In SMC, most of the environmentally critical areas are located in the central business district (CBD), near the harbor, and along the main transportation network. According to the results of the study, it is recommended that the identified environmentally critical areas to be considered in the urban planning of the city. Green spaces of the city will help to improve the life and environmental well-being of the SMC.

Keywords: Urban Heat Island, Land Surface Temperature, NDVI, NDBI, Environmental Criticality Index, Seoul Metropolitan City

©2019. Japan Geoscience Union. All Right Reserved.

Improvement of GIS exercise classes using the GIS open educational resources based on questionnaire surveys

*Hiroyuki Yamauchi[1], Takashi Oguchi[1], Yuichi S. Hayakawa[2,1], Kotaro Iizuka[1]

1. Center for Spatial Information Science, The University of Tokyo, 2. Environmental Geography, Faculty of Environmental Earth Science, Hokkaido University

Free and open source GIS software has been utilized for GIS education all over the world. However, as far as we recognize, GIS education in many Japanese universities underutilize such software packages. Therefore, we developed GIS exercise materials explaining spatial data analyses using free and open-source GIS. We have been providing these materials for higher education and designated them as the GIS Open Educational Resources. We used the materials in a university exercise class, which was held as an intensive course for three days at The University of Tokyo. During the exercise, we have conducted questionnaire surveys to clarify the three criteria: difficulty, understanding and satisfactory levels of the students. The results showed that the students felt difficulty in some situations such as the utilization of GIS for the first time and complex operations using different types of data. The contents of the exercise syllabus and materials were improved based on the feedback. We conducted another GIS exercise class at the university to verify the utility of improvements. In this presentation, we show the improvements in the exercise syllabus and the comparison of educational effects on students before and after the improvements.

Keywords: GIS education, exercise, Open Educational Resources, Free and open-source GIS

©2019. Japan Geoscience Union. All Right Reserved.

The Development of COP for Tzu Chi Disaster Prevention System by Using QGIS-Taking 2018 Hualien Earthquake as an Example

*kuan-wen tseng[1], Ming-Ta Tsai[1], Yun-Ching Wang[1], Ming-Chih Wang[1], Chien-Hsien Liu[1]

1. 03-3809093

The Hualien earthquake occurred at 23:50 and 41.6 seconds on February 6, 2018. The epicenter was located in the coastal area of Hualien County. The earthquake scale was 6.2 and the Seismic source depth was 6.3 kilometers. The earthquake disaster along the Milun fault was mainly concentrated in Hualien City, and collapsed the first and second floors of the “Tongshuai” building. The “Yunmen Cuidi” Building showed a 45-degree tilt. The lower floors of the residential community building "Baijin Shuangxing" and “Wuzhu Wusu” at Guosheng Sixth Street were destroyed. This study mainly uses the powerful geospatial analysis capabilities of Geographic Information System (GIS) to provide Tzu Chi's plans for disaster mitigation. The projects include: (1) humanitarian cares; (2) visiting and reporting of damage situations around main disaster areas and (3) “Reassuring Homes Visits” in order to provide assistance to Tzu Chi people for operations of disaster mitigation.

Keywords: Millun fault, geographic information system, spatial analysis, Tzu Chi Foundation

©2019. Japan Geoscience Union. All Right Reserved.

Comparative study on shape and distribution of landslides caused by the 2012 Northern Kyushu heavy rainfall and the 2016 Kumamoto earthquake in the Aso region, Kumamoto, Japan

*Yasutaka Haneda[1], Takashi Oguchi[2], Kotaro Iizuka[2], Hitoshi SAITO[3,2], Yuichi S. Hayakawa[4,2], Shoichiro Uchiyama[5]

1. Graduate School of Frontier Science, The University of Tokyo, 2. Center for Spatial Information Science, The University of Tokyo, 3. College of Economics, Kanto Gakuin University, 4. Faculty of Environmental Earth Science, Hokkaido University, 5. National Research Institute for Earth Science and Disaster Resilience

The 2016 Kumamoto earthquake triggered many landslides in the Aso region, southwestern Japan. Previous studies have revealed the processes of some large representative landslides in the western Aso region, but they have not comprehensively dealt with lots of small landslides. Other studies have discussed landslide distribution and relationships with that of the heavy rainfall events in July 2012 in the northern part of the Central Cones of the Aso volcano. However, they have not been investigated the western part of the Aso region which has various topographical and geological characteristics. Therefore, this study compares the formation and distribution of landslides caused by the heavy rainfall and earthquake events in both the central and western part of the Aso region.

The study areas are the western part of the Aso region and the Sensuikyo region at the northern part of the Central Cones (Fig. 1). The western part was divided into three sites: site P (caldera walls and the outer rim), Q (western part of Central Cones), and R (river terrace and talus) based on geomorphological and geological characteristics. The Sensuikyo region is referred to as site S. This study utilized multi-temporal datasets derived from airborne lidar and photogrammetry using UAV photographs: (i) before the heavy rainfall, (ii) between the heavy rainfall and the earthquake, and (iii) after the earthquake. By using digital elevation data and a sediment transportation map, elevation lowering spots caused by the landslides were identified. Then terrain information and the indexes of shape and spatial distribution were analyzed at the elevation lowering spots.

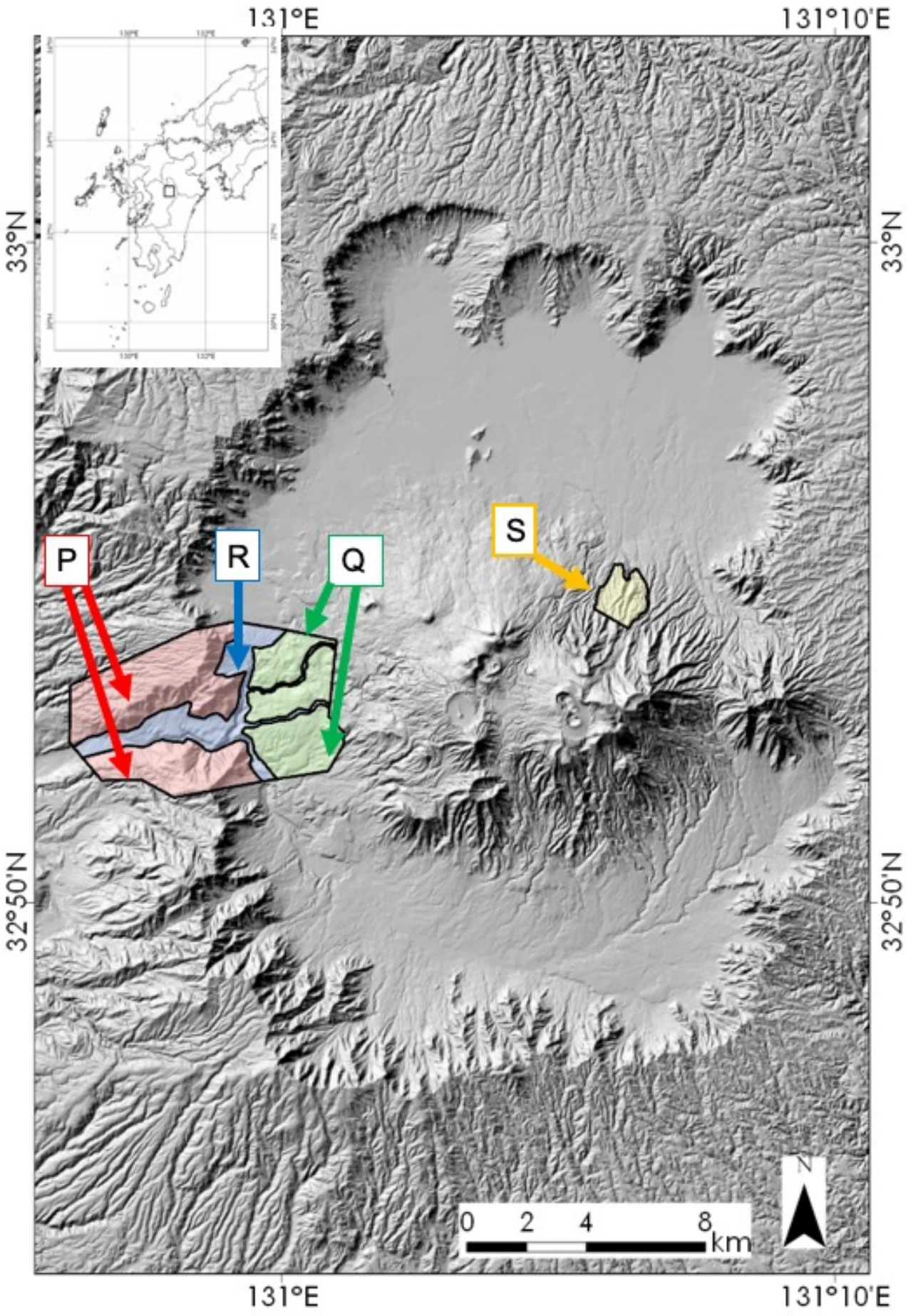
From the analysis, it was found that the heavy rainfall induced 374 landslides and the earthquake triggered 440 landslides. Landslides affected by the two different events were recognized in sites P and S. In site S, the indexes of spatial distribution showed that the earthquake caused the displacement of regolith remained on the upper convex part of the slope. In site P, the shape indexes indicated that the former event led to removal of topsoil, whereas the latter event induced the failure of lava and pyroclastic rocks. In site Q, failed slopes are not as steep as locations where landslides occurred due to past heavy rainfall events, and remained thick unconsolidated topsoil is composed of volcanic ash. It slipped deeply in 2016 due to strong seismic shaking strengthened by topographic site effects on the convex part of the slope. In site R, landslide shapes and comparison with those in site P suggest that collapsed soil directly fell into rivers without erosion of topsoil.

This study has revealed that the distribution of landslides due to the earthquake is related to that by the heavy rainfall in the Sensuikyo region. On the other hand, in the western part of the Aso region, differences in shape and distribution are found between landslides caused by the two events. Moreover, there are differences in the formation of earthquake-induced landslides among the different study sites.

©2019. Japan Geoscience Union. All Right Reserved.

Keywords: The 2016 Kumamoto Earthquake, July 2012 Northern Kyushu Heavy rainfall, landslides

©2019. Japan Geoscience Union. All Right Reserved.



©2019. Japan Geoscience Union. All Right Reserved.

Using GIS and remote sensing to assess relationships between landslides and land cover changes in the Sanbagawa and Mikabu Belts, Shikoku, Japan

*Roxanne Lai[1], Takashi Oguchi[1]

1. University of Tokyo

The Sanbagawa and Mikabu Belts are metamorphic belts that run across Southwest Japan, and are home to numerous large crystalline schist landslides, including the widely-studied slow but continuously moving Zentoku landslide. Villages and communities have been built on these landslide areas due to historical and cultural factors, as well as the fertility of the soil. With changing human needs and social trends, however, changing land uses is becoming an increasingly important issue. In Japan, movement of the population from rural to urban areas have resulted in much land and agricultural land abandonment. As vegetation cover changes after land abandonment, this temporal and spatial effect may have important effects on geomorphic processes such as landslide susceptibility and landslide kinematics.

Here we track long-term land cover changes over vegetated landslide areas of the Sanbagawa and Mikabu Belts of Shikoku Island, Japan, and conduct spatio-temporal analyses to assess relationships between landslides and land cover changes. Given changing land uses, including land abandonment in these landslide areas over time, we use long-term high-resolution land cover vegetation datasets to examine first the long-term land use changes, and then use statistical methods to explore their relationships with landslide susceptibility and kinematics. Mapping of spatial data and their analysis using GIS constitute a core part of the research. The results suggest interconnections between land use changes and land movement.

Keywords: Landslides, Shikoku, GIS , Remote Sensing

©2019. Japan Geoscience Union. All Right Reserved.

Analysis of Morphometric Parameters for Mountains Ranges and Landslides due to the July 2018 Heavy Rain in Western Japan Using GIS Data

*Toshikazu Fukuba[1], Takashi Oguchi[2]

1. Department of Earth and Planetary Environmental Science, The University of Tokyo, 2. Center for Spatial Information Science, The University of Tokyo

Morphometric parameters for mountains ranges have been analyzed in many studies. These studies in recent years used Digital Elevation Models (DEMs) to calculate values of morphometric parameters within mountains and provided consideration on landform evolution. In addition, morphometric parameters calculated by DEMs have been used for producing landslide hazard maps. This study investigates geomorphometric parameters within the Chugoku and Shikoku Mountains, Japan, and the relationships among the parameters. In addition, landslides caused by the July 2018 heavy rain in western Japan is also investigated and the relationships between the landforms of the mountains and the landslides are discussed. Altitude, slope angle, slope aspect and slope curvature are chosen for morphometric parameters to be investigated.

Morphometric parameters for the Chugoku and in Shikoku Mountains computed using DEMs and GIS have some characteristics common to the Japanese Alps. For example, for wide altitudinal zones, slope angle tends to be constant around 30 to 40 degrees even if altitude changes. However, the values of the constant slope angle are not the same, which may be due to geological differences or the difference in the formation age of mountains. Although the frequency distribution of slope aspect is similar to the Chugoku and Shikoku Mountains, anisotropy of slope aspect is different between the two mountains. This may be caused by differences in the formation age, formation mechanism, or geology of the mountains.

Analysis of landslides caused by the July 2018 heavy rain in Hiroshima using landslide data and DEMs revealed that landslides mostly occurred around 300 m in altitude, at 15 to 30 degrees in slope angle, and on concave slopes. Although the characteristics slope angles higher than 30 degrees point to frequent slope failures at high and steep mountain slopes in the Chugoku and Shikoku Mountains, landslides corresponding to one rainfall event do not necessarily follow this, because they depend on the distribution of rainfall during the event. Therefore, possibility of landslides in low and gentle mountains close to populated areas needs to be considered seriously for mitigating landslide disasters.

Keywords: GIS, Mountain landform, Landslide, Morphometric parameters

©2019. Japan Geoscience Union. All Right Reserved.

Analyzing short-term topographic change in coastal sand dunes using UAS-SfM photogrammetry: A case study in Northern Kujukuri, Japan

*Seulgi Lee[1], Yasutaka Nakata[2], Kotaro Iizuka[3], Takashi Oguchi[3]

1. Graduate School of Frontier Sciences, The University of Tokyo, 2. Forest Research Department, Forestry Research Institute, Hokkaido Research Organization, 3. Center for Spatial Information Science, The University of Tokyo

Collection of spatial data is critical for the identification of coastlines and coastal zones and related studies in coastal geomorphology. It is particularly important to obtain high-resolution elevation data in order to observe topographical changes of coastal sand dunes with frequent dynamic movements during a short period of time. Unmanned Aerial System (UAS) photogrammetry combined with Structure from Motion (SfM) offers an effective solution to the acquisition of such data. Kujukuri, facing the Pacific Ocean in Chiba Prefecture, Japan, is a region with a long coastal zone of about 60 km. Although the development of this area since the 1960s has destroyed many natural landscapes, they are relatively preserved in Northern Kujukuri. This study focuses on short-term topographic changes in coastal sand dunes there and discusses the effects of vegetation and wind.
UAV-SfM surveys were conducted seven times from September 2016 to December 2018, and the obtained topographic data were analyzed using GIS software (ArcGIS Pro) to evaluate changes in terrain conditions by season and year. We also analyzed the wind direction data provided by the Japan Meteorological Agency. Vegetation data were obtained from the field surveys and the green-red vegetation index extracted from the UAS images. The following three characteristics were identified: 1) Short-term topographic changes tend to be influenced by specific events such as storm events, and therefore terrain conditions in the same season may be different from year to year. 2) General wind conditions represented by the meteorological data corresponding to the overall change of sand dune topography, especially at seasonal or longer scales. 3) Formation of small sand dunes is affected by vegetation distribution. This study has suggested factors affecting short-term topographic changes of coastal sand dunes based on frequent data acquisition in the field and geospatial technologies.

Keywords: GIS, Coastal sand dunes, UAV, SfM

©2019. Japan Geoscience Union. All Right Reserved.

Responses of suspended sediment yield to precipitation, topography and dam control in the Yellow River Basin, China

*Ruiqi Zhang[1], Takashi Oguchi[2]

1. Department of Natural Environmental Studies, Graduate School of Frontier Sciences, The University of Tokyo, 2. Center for Spatial Information Science, The University of Tokyo

Soil erosion has long been a serious problem in the Yellow River Basin in China. The high sediment load carried by the Yellow River results in deposition along its path, raising the riverbed and increasing the flood risk in the lower reaches. To mitigate this situation, large-scale soil conservation measures have been put into practice such as the construction of dams to effectively trap fluvial sediments. Previous studies on this topic focused on the interannual fluctuation of sediment yield caused by dams and reservoirs. However, few studies focused on their effects on the seasonal variation of sediment yield. In 2002, the Yellow River Conservancy Committee began to implement the water-sediment regulation (WSR) scheme to regulate the river water, which further strengthen the impact of dam control on the seasonality of sediment yield. Therefore, this research aims to integrate natural contributing factors such as topography and precipitation with the WSR-based dam control to analyze the seasonal and spatial variations of sediment yield in the Yellow River, for the years 2008 to 2012. Data of daily suspended sediment concentration, water discharge, and precipitation were downloaded from the Chinese Data Sharing Infrastructure of Earth System Science, and the ASTER GLOBAL DEMs with a resolution of 1 arc-second were downloaded from the U.S. Geological Survey web site. ArcGIS and R software packages are used to analyze the obtained data. Inspection of data quality revealed that consecutive sediment yield and precipitation data for 97 watersheds are usable.

Data analysis indicated the following four basic hydrological characteristics of the watersheds. 1) Water discharge within each watershed is not stable both interannually and seasonally, because it has been affected by the implementation of dam regulation as well as low discharge conditions mostly in spring and winter especially in some small watersheds. 2) The variation of sediment yield in some natural watersheds reflects change in precipitation, leading to sediment yield peaks in summer. 3) In other watersheds, the variation of sediment yield tends to be independent of precipitation. Instead, some artificial conservation measures such as dam control effectively intercept sediments from the upstream area. 4) The correlation between suspended sediment yield and water discharge varies among watersheds, and the correlation coefficient can be used as a parameter representing hydrological characteristics. The DEMs have been also analyzed to relate hydrology and climate with geomorphology. The obtained results may help the policy makers better understand the erosion situations in the Yellow River Basin and regulate the soil conservation measures.

Keywords: Suspended sediment yield, the Yellow River basin, seasonality, precipitation, topography, dam control

©2019. Japan Geoscience Union. All Right Reserved.

[E] Poster | H (Human Geosciences)：H-TT Technology & Techniques

Thu. May 30, 2019 5:15 PM - 6:30 PM JST | Thu. May 30, 2019 8:15 AM - 9:30 AM UTC | Poster Hall International Exhibition Hall8, Makuhari Messe_16

[H-TT19] Geographic Information Systems and Cartography

convener:Takashi Oguchi(Center for Spatial Information Science, The University of Tokyo), Yuji Murayama(Graduate School of Life and Environmental Sciences), Yoshiki Wakabayashi(Graduate School of Urban Environmental Sciences, Tokyo Metropolitan University)

This session discusses various methods which acquire, store, analyze and visualize geospatial data, and presents the outcomes of empirical studies using GIS or mapping methods. The session also deals with applications of digital data, and GIS, and mapping to various fields of earth and planetary science and human society. All presentations and discussion of this session are made in English.

[HTT19-P01] Monitoring and Simulating Land Use/Cover Changes and its Impact on Land Surface Temperature in Sapporo City, Japan

*RUCI WANG[1], YUJI MURAYAMA[1] (1.University of Tsukuba)

[HTT19-P02] Spatiotemporal Variations of Land Cover/Use and Sustainable Urban Heat Island (UHI) Mitigation Strategies: A Case Study of Chinese Bay Megacities

★Invited Papers

*Fei LIU[1], Yuji MURAYAMA[1] (1. University of Tsukuba)

[HTT19-P03] A LST Study of the Seoul Metropolitan City, South Korea, Based on Landsat Data (1996 – 2017)

*Prabath Priyankara[1,3], Manjula Ranagalage[1,4], DMSLB Dissanayake[1,4], Takehiro Morimoto[1,2], Yuji Murayama[1,2] (1.Graduate School of Life and Environmental Sciences, University of Tsukuba, Japan, 2.Faculty of Life and Environmental Sciences, University of Tsukuba, Japan, 3.Faculty of Agriculture, University of Ruhuna, Sri Lanka, 4.Faculty of Social Sciences and Humanities, Rajarata University of Sri Lanka, Sri Lanka)

[HTT19-P04] Improvement of GIS exercise classes using the GIS open educational resources based on questionnaire surveys

★Invited Papers

*Hiroyuki Yamauchi[1], Takashi Oguchi[1], Yuichi S. Hayakawa[2,1], Kotaro Iizuka[1] (1.Center for Spatial Information Science, The University of Tokyo, 2.Environmental Geography, Faculty of Environmental Earth Science, Hokkaido University)

[HTT19-P05] The Development of COP for Tzu Chi Disaster Prevention System by Using QGIS-Taking 2018 Hualien Earthquake as an Example

*kuan-wen tseng[1], Ming-Ta Tsai[1], Yun-Ching Wang[1], Ming-Chih Wang[1], Chien-Hsien Liu[1] (1.03-3809093)

[HTT19-P06] Comparative study on shape and distribution of landslides caused by the 2012 Northern Kyushu heavy rainfall and the 2016 Kumamoto earthquake in the Aso region, Kumamoto, Japan

*Yasutaka Haneda[1], Takashi Oguchi[2], Kotaro Iizuka[2], Hitoshi SAITO[3,2], Yuichi S. Hayakawa[4,2], Shoichiro Uchiyama[5] (1.Graduate School of Frontier Science, The University of Tokyo, 2.Center for Spatial Information Science, The University of Tokyo, 3.College of Economics, Kanto Gakuin University, 4.Faculty of Environmental Earth Science, Hokkaido University, 5.National Research Institute for Earth Science and Disaster Resilience)

[HTT19-P07] Using GIS and remote sensing to assess relationships between landslides and land cover changes in the Sanbagawa and Mikabu Belts, Shikoku, Japan

*Roxanne Lai[1], Takashi Oguchi[1] (1.University of Tokyo)

[HTT19-P08] **Analysis of Morphometric Parameters for Mountains Ranges and Landslides due to the July 2018 Heavy Rain in Western Japan Using GIS Data**

*Toshikazu Fukuba[1], Takashi Oguchi[2] (1.Department of Earth and Planetary Environmental Science, The University of Tokyo, 2.Center for Spatial Information Science, The University of Tokyo)

[HTT19-P09] Analyzing short-term topographic change in coastal sand dunes using UAS-SfM photogrammetry: A case study in Northern Kujukuri, Japan

*Seulgi Lee[1], Yasutaka Nakata[2], Kotaro Iizuka[3], Takashi Oguchi[3] (1.Graduate School of Frontier Sciences, The University of Tokyo, 2.Forest Research Department, Forestry Research Institute, Hokkaido Research Organization, 3.Center for Spatial Information Science, The University of Tokyo)

[HTT19-P10] **Responses of suspended sediment yield to precipitation, topography and dam control in the Yellow River Basin, China**

*Ruiqi Zhang[1], Takashi Oguchi[2] (1. Department of Natural Environmental Studies, Graduate School of Frontier Sciences, The University of Tokyo, 2.Center for Spatial Information Science, The University of Tokyo)

Monitoring and Simulating Land Use/Cover Changes and its Impact on Land Surface Temperature in Sapporo City, Japan

*RUCI WANG[1], YUJI MURAYAMA[1]

1. University of Tsukuba

In recent years, urban heat island phenomenon (UHI) which prevails in many cities worldwide has caused broad public concern. UHI phenomenon impairs healthy urban development and causes excessive energy consumption, climatic and environmental deterioration. Land use/cover changes are one of the most crucial variables influencing on UHI. Therefore, monitoring and simulating land use/cover changes and analyzing its effects on LST are essential for healthy urban development. This study aims to capture the impact of land use/cover on LST and simulate the LST under various land use/cover scenarios in Sapporo city, Japan. At first, we monitored the land use/cover changes from 1985 to 2015 and detect the change of LST concerning land use/cover distribution. Then, we predicted the future conditions of LST based on various land use/cover scenarios. The results show that the LST differs according to land use/cover types, and the proportion of land use/cover types is the most significant factor affecting LST. The findings also indicate that the built-up area and paddy field have the highest average LST, while the green space and water area help cool the city. In the future, the green area such as urban green parks and grassland should be planned in the city to mitigate the UHI phenomenon. It reveals the spatial characterization of LST which provides significant insights for government and city planners.

Keywords: Geographical information science, Urban heat island, Land surface temperature, Land use/cover change, Sapporo city

©2019. Japan Geoscience Union. All Right Reserved.

Spatiotemporal Variations of Land Cover/Use and Sustainable Urban Heat Island (UHI) Mitigation Strategies: A Case Study of Chinese Bay Megacities

*Fei LIU[1], Yuji MURAYAMA[1]

1. University of Tsukuba

Rapid urbanization significantly affects the urban thermal environment in the context of global climate change. The assessment of surface urban heat island (SUHI) and development of mitigation strategies in megacities have become frontier issues on human health and urban sustainability. In this study, taking of the three Chinese bay megacities, we attempt to 1) disclose the relationship between land surface temperature (LST) and land cover using remote sensing quantified analysis, 2) to clarify the mechanism and characteristics of SUHI formation based on bi-temporal patterns and variations of land cover, and 3) to sustainably regulate and optimize the urban environment and further create urban planning and policies for relieving urban thermal effect. The study target is Guangzhou metropolitan area (GMA), Hangzhou metropolitan area (HMA) and Shanghai Metropolitan area (SMA) in China. The result of this study indicated remarkably different characteristics, arrangement, and variations among different bay thermal environments. Overall, spatial layouts and changes in the thermal environment of these three megacities were substantially identical with their land cover pattern and tendency. Although land covers significantly influenced the LST as a whole, the different areas had different magnitudes of SUHI coming from different land cover compositions and differentials. The results would provide a valuable reference to disentangle spatiotemporal variation of the bay urban thermal environments, and the urbanization-induced land covers temperature dynamics. This study would contribute to the development of future SUHI mitigation solutions.

Keywords: Land Cover/Use , Urban Heat Island (UHI), Mitigation Strategies

©2019. Japan Geoscience Union. All Right Reserved.

A LST Study of the Seoul Metropolitan City, South Korea, Based on Landsat Data (1996 –2017)

*Prabath Priyankara[1,3], Manjula Ranagalage[1,4], DMSLB Dissanayake[1,4], Takehiro Morimoto[1,2], Yuji Murayama[1,2]

1. Graduate School of Life and Environmental Sciences, University of Tsukuba, Japan, 2. Faculty of Life and Environmental Sciences, University of Tsukuba, Japan, 3. Faculty of Agriculture, University of Ruhuna, Sri Lanka, 4. Faculty of Social Sciences and Humanities, Rajarata University of Sri Lanka, Sri Lanka

Rapid urban growth often replaced urban vegetation with impervious surfaces which leads to increase land surface temperature (LST) periodically and tends to form urban heat islands (UHI). This is a serious issue of urbanized cities and the increase of LST badly affects the well-being of the life and environments of the cities. The Seoul Metropolitan City (SMC), South Korea, is one of the developed and rapidly urbanizing metropolitan city in Asia. The aim of this study was to examine the spatiotemporal variations of LST in the SMC and surroundings in the context of the UHI using Landsat data. The study examined the relationship of LST with the normalized difference vegetation index (NDVI) and the normalized difference built-up index (NDBI) at three time periods 1996, 2006, and 2017. Also, the study was investigated the environmentally critical areas based on LST and NDVI by modeling environmental criticality index (ECI). According to the results of the study, there is a negative correlation between LST with NDVI and positive correlation of LST with NDBI across all three time periods. In SMC, most of the environmentally critical areas are located in the central business district (CBD), near the harbor, and along the main transportation network. According to the results of the study, it is recommended that the identified environmentally critical areas to be considered in the urban planning of the city. Green spaces of the city will help to improve the life and environmental well-being of the SMC.

Keywords: Urban Heat Island, Land Surface Temperature, NDVI, NDBI, Environmental Criticality Index, Seoul Metropolitan City

©2019. Japan Geoscience Union. All Right Reserved.

Improvement of GIS exercise classes using the GIS open educational resources based on questionnaire surveys

*Hiroyuki Yamauchi[1], Takashi Oguchi[1], Yuichi S. Hayakawa[2,1], Kotaro Iizuka[1]

1. Center for Spatial Information Science, The University of Tokyo, 2. Environmental Geography, Faculty of Environmental Earth Science, Hokkaido University

Free and open source GIS software has been utilized for GIS education all over the world. However, as far as we recognize, GIS education in many Japanese universities underutilize such software packages. Therefore, we developed GIS exercise materials explaining spatial data analyses using free and open-source GIS. We have been providing these materials for higher education and designated them as the GIS Open Educational Resources. We used the materials in a university exercise class, which was held as an intensive course for three days at The University of Tokyo. During the exercise, we have conducted questionnaire surveys to clarify the three criteria: difficulty, understanding and satisfactory levels of the students. The results showed that the students felt difficulty in some situations such as the utilization of GIS for the first time and complex operations using different types of data. The contents of the exercise syllabus and materials were improved based on the feedback. We conducted another GIS exercise class at the university to verify the utility of improvements. In this presentation, we show the improvements in the exercise syllabus and the comparison of educational effects on students before and after the improvements.

Keywords: GIS education, exercise, Open Educational Resources, Free and open-source GIS

©2019. Japan Geoscience Union. All Right Reserved.

The Development of COP for Tzu Chi Disaster Prevention System by Using QGIS-Taking 2018 Hualien Earthquake as an Example

*kuan-wen tseng[1], Ming-Ta Tsai[1], Yun-Ching Wang[1], Ming-Chih Wang[1], Chien-Hsien Liu[1]

1. 03-3809093

The Hualien earthquake occurred at 23:50 and 41.6 seconds on February 6, 2018. The epicenter was located in the coastal area of Hualien County. The earthquake scale was 6.2 and the Seismic source depth was 6.3 kilometers. The earthquake disaster along the Milun fault was mainly concentrated in Hualien City, and collapsed the first and second floors of the “Tongshuai” building. The “Yunmen Cuidi” Building showed a 45-degree tilt. The lower floors of the residential community building "Baijin Shuangxing" and “Wuzhu Wusu” at Guosheng Sixth Street were destroyed. This study mainly uses the powerful geospatial analysis capabilities of Geographic Information System (GIS) to provide Tzu Chi's plans for disaster mitigation. The projects include: (1) humanitarian cares; (2) visiting and reporting of damage situations around main disaster areas and (3) “Reassuring Homes Visits” in order to provide assistance to Tzu Chi people for operations of disaster mitigation.

Keywords: Millun fault, geographic information system, spatial analysis, Tzu Chi Foundation

©2019. Japan Geoscience Union. All Right Reserved.

Comparative study on shape and distribution of landslides caused by the 2012 Northern Kyushu heavy rainfall and the 2016 Kumamoto earthquake in the Aso region, Kumamoto, Japan

*Yasutaka Haneda[1], Takashi Oguchi[2], Kotaro Iizuka[2], Hitoshi SAITO[3,2], Yuichi S. Hayakawa[4,2], Shoichiro Uchiyama[5]

1. Graduate School of Frontier Science, The University of Tokyo, 2. Center for Spatial Information Science, The University of Tokyo, 3. College of Economics, Kanto Gakuin University, 4. Faculty of Environmental Earth Science, Hokkaido University, 5. National Research Institute for Earth Science and Disaster Resilience

The 2016 Kumamoto earthquake triggered many landslides in the Aso region, southwestern Japan. Previous studies have revealed the processes of some large representative landslides in the western Aso region, but they have not comprehensively dealt with lots of small landslides. Other studies have discussed landslide distribution and relationships with that of the heavy rainfall events in July 2012 in the northern part of the Central Cones of the Aso volcano. However, they have not been investigated the western part of the Aso region which has various topographical and geological characteristics. Therefore, this study compares the formation and distribution of landslides caused by the heavy rainfall and earthquake events in both the central and western part of the Aso region.

The study areas are the western part of the Aso region and the Sensuikyo region at the northern part of the Central Cones (Fig. 1). The western part was divided into three sites: site P (caldera walls and the outer rim), Q (western part of Central Cones), and R (river terrace and talus) based on geomorphological and geological characteristics. The Sensuikyo region is referred to as site S. This study utilized multi-temporal datasets derived from airborne lidar and photogrammetry using UAV photographs: (i) before the heavy rainfall, (ii) between the heavy rainfall and the earthquake, and (iii) after the earthquake. By using digital elevation data and a sediment transportation map, elevation lowering spots caused by the landslides were identified. Then terrain information and the indexes of shape and spatial distribution were analyzed at the elevation lowering spots.

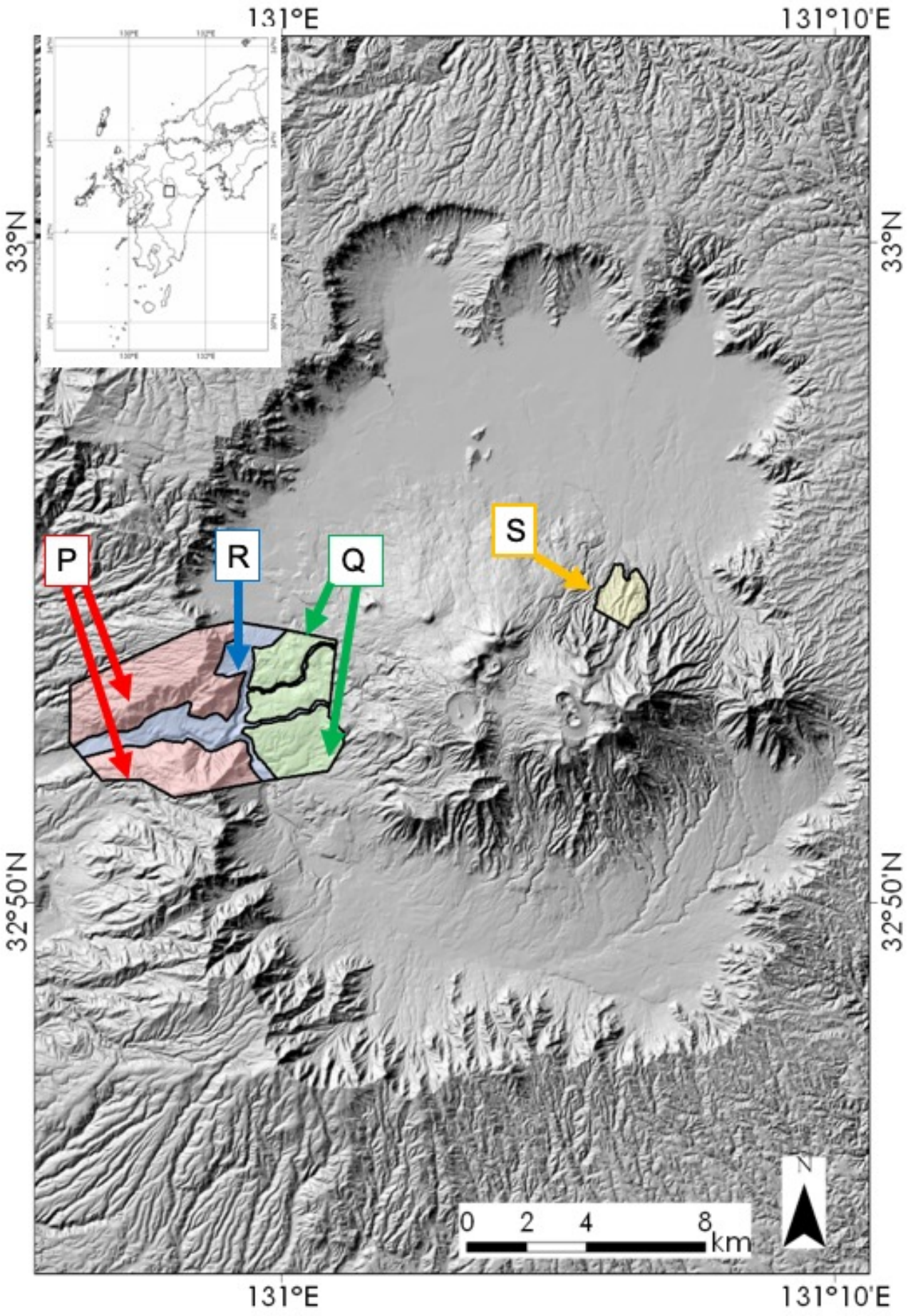
From the analysis, it was found that the heavy rainfall induced 374 landslides and the earthquake triggered 440 landslides. Landslides affected by the two different events were recognized in sites P and S. In site S, the indexes of spatial distribution showed that the earthquake caused the displacement of regolith remained on the upper convex part of the slope. In site P, the shape indexes indicated that the former event led to removal of topsoil, whereas the latter event induced the failure of lava and pyroclastic rocks. In site Q, failed slopes are not as steep as locations where landslides occurred due to past heavy rainfall events, and remained thick unconsolidated topsoil is composed of volcanic ash. It slipped deeply in 2016 due to strong seismic shaking strengthened by topographic site effects on the convex part of the slope. In site R, landslide shapes and comparison with those in site P suggest that collapsed soil directly fell into rivers without erosion of topsoil.

This study has revealed that the distribution of landslides due to the earthquake is related to that by the heavy rainfall in the Sensuikyo region. On the other hand, in the western part of the Aso region, differences in shape and distribution are found between landslides caused by the two events. Moreover, there are differences in the formation of earthquake-induced landslides among the different study sites.

©2019. Japan Geoscience Union. All Right Reserved.

Keywords: The 2016 Kumamoto Earthquake, July 2012 Northern Kyushu Heavy rainfall, landslides

©2019. Japan Geoscience Union. All Right Reserved.



©2019. Japan Geoscience Union. All Right Reserved.

Using GIS and remote sensing to assess relationships between landslides and land cover changes in the Sanbagawa and Mikabu Belts, Shikoku, Japan

*Roxanne Lai[1], Takashi Oguchi[1]

1. University of Tokyo

The Sanbagawa and Mikabu Belts are metamorphic belts that run across Southwest Japan, and are home to numerous large crystalline schist landslides, including the widely-studied slow but continuously moving Zentoku landslide. Villages and communities have been built on these landslide areas due to historical and cultural factors, as well as the fertility of the soil. With changing human needs and social trends, however, changing land uses is becoming an increasingly important issue. In Japan, movement of the population from rural to urban areas have resulted in much land and agricultural land abandonment. As vegetation cover changes after land abandonment, this temporal and spatial effect may have important effects on geomorphic processes such as landslide susceptibility and landslide kinematics.

Here we track long-term land cover changes over vegetated landslide areas of the Sanbagawa and Mikabu Belts of Shikoku Island, Japan, and conduct spatio-temporal analyses to assess relationships between landslides and land cover changes. Given changing land uses, including land abandonment in these landslide areas over time, we use long-term high-resolution land cover vegetation datasets to examine first the long-term land use changes, and then use statistical methods to explore their relationships with landslide susceptibility and kinematics. Mapping of spatial data and their analysis using GIS constitute a core part of the research. The results suggest interconnections between land use changes and land movement.

Keywords: Landslides, Shikoku, GIS , Remote Sensing

©2019. Japan Geoscience Union. All Right Reserved.

Analysis of Morphometric Parameters for Mountains Ranges and Landslides due to the July 2018 Heavy Rain in Western Japan Using GIS Data

*Toshikazu Fukuba[1], Takashi Oguchi[2]

1. Department of Earth and Planetary Environmental Science, The University of Tokyo, 2. Center for Spatial Information Science, The University of Tokyo

Morphometric parameters for mountains ranges have been analyzed in many studies. These studies in recent years used Digital Elevation Models (DEMs) to calculate values of morphometric parameters within mountains and provided consideration on landform evolution. In addition, morphometric parameters calculated by DEMs have been used for producing landslide hazard maps. This study investigates geomorphometric parameters within the Chugoku and Shikoku Mountains, Japan, and the relationships among the parameters. In addition, landslides caused by the July 2018 heavy rain in western Japan is also investigated and the relationships between the landforms of the mountains and the landslides are discussed. Altitude, slope angle, slope aspect and slope curvature are chosen for morphometric parameters to be investigated.

Morphometric parameters for the Chugoku and in Shikoku Mountains computed using DEMs and GIS have some characteristics common to the Japanese Alps. For example, for wide altitudinal zones, slope angle tends to be constant around 30 to 40 degrees even if altitude changes. However, the values of the constant slope angle are not the same, which may be due to geological differences or the difference in the formation age of mountains. Although the frequency distribution of slope aspect is similar to the Chugoku and Shikoku Mountains, anisotropy of slope aspect is different between the two mountains. This may be caused by differences in the formation age, formation mechanism, or geology of the mountains.

Analysis of landslides caused by the July 2018 heavy rain in Hiroshima using landslide data and DEMs revealed that landslides mostly occurred around 300 m in altitude, at 15 to 30 degrees in slope angle, and on concave slopes. Although the characteristics slope angles higher than 30 degrees point to frequent slope failures at high and steep mountain slopes in the Chugoku and Shikoku Mountains, landslides corresponding to one rainfall event do not necessarily follow this, because they depend on the distribution of rainfall during the event. Therefore, possibility of landslides in low and gentle mountains close to populated areas needs to be considered seriously for mitigating landslide disasters.

Keywords: GIS, Mountain landform, Landslide, Morphometric parameters

©2019. Japan Geoscience Union. All Right Reserved.

Analyzing short-term topographic change in coastal sand dunes using UAS-SfM photogrammetry: A case study in Northern Kujukuri, Japan

*Seulgi Lee[1], Yasutaka Nakata[2], Kotaro Iizuka[3], Takashi Oguchi[3]

1. Graduate School of Frontier Sciences, The University of Tokyo, 2. Forest Research Department, Forestry Research Institute, Hokkaido Research Organization, 3. Center for Spatial Information Science, The University of Tokyo

Collection of spatial data is critical for the identification of coastlines and coastal zones and related studies in coastal geomorphology. It is particularly important to obtain high-resolution elevation data in order to observe topographical changes of coastal sand dunes with frequent dynamic movements during a short period of time. Unmanned Aerial System (UAS) photogrammetry combined with Structure from Motion (SfM) offers an effective solution to the acquisition of such data. Kujukuri, facing the Pacific Ocean in Chiba Prefecture, Japan, is a region with a long coastal zone of about 60 km. Although the development of this area since the 1960s has destroyed many natural landscapes, they are relatively preserved in Northern Kujukuri. This study focuses on short-term topographic changes in coastal sand dunes there and discusses the effects of vegetation and wind.
UAV-SfM surveys were conducted seven times from September 2016 to December 2018, and the obtained topographic data were analyzed using GIS software (ArcGIS Pro) to evaluate changes in terrain conditions by season and year. We also analyzed the wind direction data provided by the Japan Meteorological Agency. Vegetation data were obtained from the field surveys and the green-red vegetation index extracted from the UAS images. The following three characteristics were identified: 1) Short-term topographic changes tend to be influenced by specific events such as storm events, and therefore terrain conditions in the same season may be different from year to year. 2) General wind conditions represented by the meteorological data corresponding to the overall change of sand dune topography, especially at seasonal or longer scales. 3) Formation of small sand dunes is affected by vegetation distribution. This study has suggested factors affecting short-term topographic changes of coastal sand dunes based on frequent data acquisition in the field and geospatial technologies.

Keywords: GIS, Coastal sand dunes, UAV, SfM

©2019. Japan Geoscience Union. All Right Reserved.

Responses of suspended sediment yield to precipitation, topography and dam control in the Yellow River Basin, China

*Ruiqi Zhang[1], Takashi Oguchi[2]

1. Department of Natural Environmental Studies, Graduate School of Frontier Sciences, The University of Tokyo, 2. Center for Spatial Information Science, The University of Tokyo

Soil erosion has long been a serious problem in the Yellow River Basin in China. The high sediment load carried by the Yellow River results in deposition along its path, raising the riverbed and increasing the flood risk in the lower reaches. To mitigate this situation, large-scale soil conservation measures have been put into practice such as the construction of dams to effectively trap fluvial sediments. Previous studies on this topic focused on the interannual fluctuation of sediment yield caused by dams and reservoirs. However, few studies focused on their effects on the seasonal variation of sediment yield. In 2002, the Yellow River Conservancy Committee began to implement the water-sediment regulation (WSR) scheme to regulate the river water, which further strengthen the impact of dam control on the seasonality of sediment yield. Therefore, this research aims to integrate natural contributing factors such as topography and precipitation with the WSR-based dam control to analyze the seasonal and spatial variations of sediment yield in the Yellow River, for the years 2008 to 2012. Data of daily suspended sediment concentration, water discharge, and precipitation were downloaded from the Chinese Data Sharing Infrastructure of Earth System Science, and the ASTER GLOBAL DEMs with a resolution of 1 arc-second were downloaded from the U.S. Geological Survey web site. ArcGIS and R software packages are used to analyze the obtained data. Inspection of data quality revealed that consecutive sediment yield and precipitation data for 97 watersheds are usable.

Data analysis indicated the following four basic hydrological characteristics of the watersheds. 1) Water discharge within each watershed is not stable both interannually and seasonally, because it has been affected by the implementation of dam regulation as well as low discharge conditions mostly in spring and winter especially in some small watersheds. 2) The variation of sediment yield in some natural watersheds reflects change in precipitation, leading to sediment yield peaks in summer. 3) In other watersheds, the variation of sediment yield tends to be independent of precipitation. Instead, some artificial conservation measures such as dam control effectively intercept sediments from the upstream area. 4) The correlation between suspended sediment yield and water discharge varies among watersheds, and the correlation coefficient can be used as a parameter representing hydrological characteristics. The DEMs have been also analyzed to relate hydrology and climate with geomorphology. The obtained results may help the policy makers better understand the erosion situations in the Yellow River Basin and regulate the soil conservation measures.

Keywords: Suspended sediment yield, the Yellow River basin, seasonality, precipitation, topography, dam control

©2019. Japan Geoscience Union. All Right Reserved.

[E] Poster | S (Solid Earth Sciences)：S-IT Science of the Earth's Interior & Techtonophysics

Thu. May 30, 2019 3:30 PM - 5:00 PM JST | Thu. May 30, 2019 6:30 AM - 8:00 AM UTC | Poster Hall International Exhibition Hall8, Makuhari Messe_10

[S-IT25] Planetary cores: Structure, formation, and evolution

convener:Hidenori Terasaki(Graduate School of Science, Osaka University), Eiji Ohtani(Department of Earth and Planetary Materials Science, Graduate School of Science, Tohoku University), William F McDonough(University of Maryland College Park), George Helffrich(Earth-Life Science Institute, Tokyo Institute of Technology)

There are fundamental links between the formation and evolution of planets and their satellites to that of their cores. Defining the physical and chemical properties of the cores of these terrestrial bodies are fundamental for understanding their internal structures and thermal profile. Recent advances in experimental and theoretical studies provide new insights and applications to the Earth's cores and other terrestrial bodies. Near-future exploration missions will obtain data on the internal structure of terrestrial planets (e.g., Mars and Mercury) and planet-satellite systems. We anticipate presentations on recent advances on the physical and chemical properties of cores and discussions regarding the latest views of their formation and evolution. We welcome contributions from mineral/rock physics, geophysics, geochemistry, geodynamics, and planetary science.

[SIT25-P01] Stratification of the Earth’s core by SiO_2 crystallisation

*George Helffrich[1], Satoshi Kaneshima[2], Kei Hirose[1,3] (1.Earth-Life Science Institute, Tokyo Institute of Technology, 2.Earth and Planetary Sciences, Kyushu University, 3.Earth and Planetary Sciences Department, University of Tokyo)

[SIT25-P02] Relation between sound velocity and density for liquid iron alloys under Earth’s core pressures by laser-shock compression

*Tatsuhiro Sakaiya[1], Tadashi Kondo[1], Hidenori Terasaki[1], Keisuke Shigemori[2], Yoichiro Hironaka[2] (1.Graduate School of Science, Osaka University, 2.Institute of Laser Engineering, Osaka University)

[SIT25-P03] Geochemical estimates of Earth's core heat content at the end of accretion

*Vincent Clesi[1], Renaud Deguen[1] (1.Laboratoire de Geologie de Lyon - Terre, Planètes, Environnement, Université Claude Bernard Lyon 1, CNRS, ENS-Lyon, 69622 Villeurbanne, France.)

[SIT25-P04] The effect of temperature on density of solid metals

*Asaka Kamiya[1], Hidenori Terasaki[1], Tadashi Kondo[1] (1.Osaka University)

[SIT25-P05] Phase relations in the Fe-Ni-Si system at high pressures and high temperatures

*Daijo Ikuta[1], Eiji Ohtani[1], Saori Kawaguchi[2], Naohisa Hirao[2], Yasuo Ohishi[2] (1.Department of Earth Science, Tohoku University, 2.JASRI)

Stratification of the Earth's core by SiO_2 crystallisation

*George Helffrich[1], Satoshi Kaneshima[2], Kei Hirose[1,3]

1. Earth-Life Science Institute, Tokyo Institute of Technology, 2. Earth and Planetary Sciences, Kyushu University, 3. Earth and Planetary Sciences Department, University of Tokyo

Based on various studies reporting seismic wavespeed deviations from PREM in the outermost outer core, the core appears to be stratified. Compositional layering, where liquids of different densities overlie one another is one stratification possibility. This mechanism, however, inhibits vertical flows in the liquid near the surface of the core implied by models of secular variation of the Earth's magnetic field. To avoid this limitation, we propose a mechanism by which the layering arises in an analogous way to atmospheric cloud formation. If liquid metal containing dissolved Si+O reaches a saturation level in the outermost outer core, SiO_2 will crystallize and rise to the core-mantle boundary (CMB), causing density changes in the liquid by release of latent heat and changing composition. We present an physical model for this process and show that it explains the observed outer core wavespeed variations better than previous parameterizations. For a CMB temperature of 3800 K and a core light element content of 5 wt% Si+O, SiO_2 begins crystallizing 260 km below the CMB through an interval about 160 km thick, yet core liquid can flow freely through the crystallization interval, facilitating magnetic field changes on decadal to century time scales.

©2019. Japan Geoscience Union. All Right Reserved.

Relation between sound velocity and density for liquid iron alloys under Earth's core pressures by laser-shock compression

*Tatsuhiro Sakaiya[1], Tadashi Kondo[1], Hidenori Terasaki[1], Keisuke Shigemori[2], Yoichiro Hironaka[2]

1. Graduate School of Science, Osaka University, 2. Institute of Laser Engineering, Osaka University

Sound velocity at Earth's core conditions are one of the most important physical properties in Earth science because it can be directly compared with the seismological Earth model (PREM: Preliminary Reference Earth Model) [1]. The composition of solid inner core is estimated from the comparison of the model [1] and the extrapolation of sound velocities as a function of density of iron and iron alloys obtained by the static compression experiment [2, 3]. Birch's law, a linear sound velocity–density relation [4], is used to extrapolate sound velocities to densities in the core condition. On the other hand, the composition of liquid outer core is estimated from the partitioning and solubility data in the inner core boundary condition for the composition of solid core. There has been some works for the sound velocity of iron and iron alloys on the Earth's core condition by dynamic techniques using explosive [5], gas gun [5-11], and laser [12-14]. In this study, we measure the sound velocity and density of liquid iron alloys by shock-compression method using high-power laser.
We conducted shock-compression experiments using a High Intensity Plasma Experimental Research (HIPER) system at the GEKKO-XII laser irradiation facility [15] at the Institute of Laser Engineering, Osaka University. The samples were Fe-Ni alloys, pure nickel, Fe-Si alloys, pure silicon, and pyrrhotite. The sound velocities and densities of shock-compressed iron alloys using the high-power laser were measured by x-ray radiography [12-14] at pressures up to 1000 GPa.
Part of this work was performed under the joint research project of the Institute of Laser Engineering, Osaka University and supported by JSPS KAKENHI Grant Number JP16K05541.

References
[1] A. M. Dziewonski and D. L. Anderson, Phys. Earth Planet. Inter. 25, 297-356 (1981).
[2] J. Badro et al., Earth Planet. Sci. Lett. 254, 233-238 (2007).
[3] G. Fiquet et al., Phys. Earth Planet. Inter. 172, 125-129 (2009).
[4] F. Birch, Geophys. J. R. Astron. Soc. 4, 295-311 (1961).
[5] J. M. Brown and R. G. McQueen, J. Geophys. Res. 91, 7485-7494 (1986).
[6] J. H. Nguyen and N. C. Holmes, Nature 427, 339-342 (2004).
[7] J. W. Shaner et al., Shock Waves in Condensed Matter, 135-138 (1988).
[8] H. Huang et al., J. Geophys. Res. 116, B04201 (2010).
[9] H. Huang et al., Nature 479, 513-516 (2011).
[10] Y. Zhang et al., Sci. Rep. 6, 22473 (2016).
[11] H. Huang et al., J. Geophys. Res. 123, 4730 (2018).
[12] K. Shigemori et al., Eur. Phys. J. D 44, 301-305 (2007).
[13] K. Shigemori et al., Rev. Sci. Instrum. 83, 10E529 (2012).
[14] T. Sakaiya et al., Earth Planet. Sci. Lett. 392, 80-85 (2014).
[15] C. Yamanaka et al., Nucl. Fusion 27, 19-30 (1987).

Keywords: sound velocity, shock compression, iron alloy, Earth's core, Birch's law

©2019. Japan Geoscience Union. All Right Reserved.

Geochemical estimates of Earth's core heat content at the end of accretion

*Vincent Clesi[1], Renaud Deguen[1]

1. Laboratoire de Geologie de Lyon - Terre, Planètes, Environnement, Université Claude Bernard Lyon 1, CNRS, ENS-Lyon, 69622 Villeurbanne, France.

The composition of Earth's mantle, when compared to experimentally determined partitioning coefficients, can be used to constrain the conditions of equilibration - pressure *P*, temperature *T*, and oxygen fugacity fO_2 - of the metal and silicates during core-mantle differentiation.
This places constraints on the thermal state of the planet during its accretion, and it is tempting to try to use these data to estimate the heat content of the core at the end of accretion.
To do so, we develop an analytical model of the thermal evolution of the metal phase during its descent through the solid mantle toward the growing core, taking into account compression heating, viscous dissipation heating, and heat exchange with the surrounding silicates. For each impact, the model takes as initial condition the pressure and temperature at the base of the magma ocean, and gives the temperature of the metal when it reaches the core. The growth of the planet results in additional pressure increase and compression heating of the core.
The thermal model is coupled to a Monte-Carlo inversion of the metal/silicates equilibration conditions (*P*, *T*, fO_2) in the course of accretion from the abundance of Ni, Co, V and Cr in the mantle, and provides an estimate of the core heat content at the end of accretion for each geochemically successful accretion.
The core heat content depends on the mean degree of metal-silicates equilibration, on the mode of metal/silicates separation in the mantle (diapirism, percolation, or dyking), but also very significantly on the shape of the equilibration conditions curve (equilibration *P* and *T* vs. fraction of Earth accreted).
We find that many accretion histories which are successful in reproducing the mantle composition yield a core that is colder than its current state.
Imposing that the temperature of the core at the end of accretion is higher than its current values therefore provides strong constraints on the accretion history.
In particular, we find that the core heat content depends significantly on the last stages of accretion

Keywords: Core formation, Model

©2019. Japan Geoscience Union. All Right Reserved.

The effect of temperature on density of solid metals

*Asaka Kamiya[1], Hidenori Terasaki[1], Tadashi Kondo[1]

1. Osaka University

It is reported that sound velocities of several solid metals show drastic non-linear reduction at near the melting temperature. This is called premelting effect. Nadal and Le Poac (2013) reported that the sound velocity (P-wave and S-wave velocities) of solid tin (Sn) decreased drastically just before melting (T/T_m ~0.99) at ambient pressure. They suggested that this decrease is due to reduction of elastic moduli (bulk and shear moduli). To understand the premelting effect more accurately, density data of tin near the melting temperature is also required in addition to sound velocity data. However, the precise density behavior of tin around the melting temperature is still missing. In this study, we measured the density of solid metals (tin and nickel) at ambient pressure and studied the effect of temperature on the density near melting temperature. The densities of solid metals were measured from optical image of the sample in the high-temperature furnace up to 673 K for Sn and 1873 K for fcc-Ni. The densities in this study were measured with error of 0.07 % for Sn and 0.4 % for Ni. Density of Sn decreases linearly with increasing temperature up to 490 K and reduced drastically above 490 K (at T/T_m~0.97). This drastic decrease in density of Sn is likely to relate to the premelting effect suggested from sound velocity measurement. In contrast, density of Ni decreases almost linearly with increasing temperature up to melting point and no drastic density change was observed in solid state.

Keywords: premelting effect, Tin, Ni, density, high temperature, electric furnace

©2019. Japan Geoscience Union. All Right Reserved.

Phase relations in the Fe-Ni-Si system at high pressures and high temperatures

*Daijo Ikuta[1], Eiji Ohtani[1], Saori Kawaguchi[2], Naohisa Hirao[2], Yasuo Ohishi[2]

1. Department of Earth Science, Tohoku University, 2. JASRI

The Earth's core has supposed to be constituted by iron-nickel alloys with some light elements. Silicon is one of the most convincing candidates among the light elements. Therefore, the study of high pressure and high temperature properties and behaviors for the Fi-Ni-Si system is important in understanding and constraining to the properties of the Earth's core. In this study, high pressure and high temperature properties for three different contents of Fe-Ni-Si alloys were investigated by using laser heated diamond anvil cells and in situ X-ray diffraction with synchrotron radiation. We determined the phase relations of $Fe_{(0.94-x)}Ni_{0.06}Si_x$ (x = 0.10, 0.17, 0.26) up to 166 GPa and 2800 K, respectively. According to previous Fe-Si system studies, $Fe_{0.83}Si_{0.17}$ alloys transform from hcp to hcp+B2 and fcc+hcp+B2 phases with increasing temperature in isobaric conditions. We observed the change in temperature increase and positive slope of these boundaries due to the nickel containing effect and the difference in silicon content. We report the details of phase relations in the Fe-Ni-Si system and discuss with the differences from the Fe-Si system.

Keywords: Fe-Ni-Si system, phase relation, high pressure

©2019. Japan Geoscience Union. All Right Reserved.

[E] Poster | S (Solid Earth Sciences)：S-IT Science of the Earth's Interior & Techtonophysics

Thu. May 30, 2019 5:15 PM - 6:30 PM JST | Thu. May 30, 2019 8:15 AM - 9:30 AM UTC | Poster Hall International Exhibition Hall8, Makuhari Messe_21

[S-IT25] Planetary cores: Structure, formation, and evolution

convener:Hidenori Terasaki(Graduate School of Science, Osaka University), Eiji Ohtani(Department of Earth and Planetary Materials Science, Graduate School of Science, Tohoku University), William F McDonough(University of Maryland College Park), George Helffrich(Earth-Life Science Institute, Tokyo Institute of Technology)

There are fundamental links between the formation and evolution of planets and their satellites to that of their cores. Defining the physical and chemical properties of the cores of these terrestrial bodies are fundamental for understanding their internal structures and thermal profile. Recent advances in experimental and theoretical studies provide new insights and applications to the Earth's cores and other terrestrial bodies. Near-future exploration missions will obtain data on the internal structure of terrestrial planets (e.g., Mars and Mercury) and planet-satellite systems. We anticipate presentations on recent advances on the physical and chemical properties of cores and discussions regarding the latest views of their formation and evolution. We welcome contributions from mineral/rock physics, geophysics, geochemistry, geodynamics, and planetary science.

[SIT25-P01] Stratification of the Earth’s core by SiO_2 crystallisation

*George Helffrich[1], Satoshi Kaneshima[2], Kei Hirose[1,3] (1.Earth-Life Science Institute, Tokyo Institute of Technology, 2.Earth and Planetary Sciences, Kyushu University, 3.Earth and Planetary Sciences Department, University of Tokyo)

[SIT25-P02] Relation between sound velocity and density for liquid iron alloys under Earth’s core pressures by laser-shock compression

*Tatsuhiro Sakaiya[1], Tadashi Kondo[1], Hidenori Terasaki[1], Keisuke Shigemori[2], Yoichiro Hironaka[2] (1.Graduate School of Science, Osaka University, 2.Institute of Laser Engineering, Osaka University)

[SIT25-P03] Geochemical estimates of Earth's core heat content at the end of accretion

*Vincent Clesi[1], Renaud Deguen[1] (1.Laboratoire de Geologie de Lyon - Terre, Planètes, Environnement, Université Claude Bernard Lyon 1, CNRS, ENS-Lyon, 69622 Villeurbanne, France.)

[SIT25-P04] The effect of temperature on density of solid metals

*Asaka Kamiya[1], Hidenori Terasaki[1], Tadashi Kondo[1] (1.Osaka University)

[SIT25-P05] Phase relations in the Fe-Ni-Si system at high pressures and high temperatures

*Daijo Ikuta[1], Eiji Ohtani[1], Saori Kawaguchi[2], Naohisa Hirao[2], Yasuo Ohishi[2] (1.Department of Earth Science, Tohoku University, 2.JASRI)

Stratification of the Earth's core by SiO_2 crystallisation

*George Helffrich[1], Satoshi Kaneshima[2], Kei Hirose[1,3]

1. Earth-Life Science Institute, Tokyo Institute of Technology, 2. Earth and Planetary Sciences, Kyushu University, 3. Earth and Planetary Sciences Department, University of Tokyo

Based on various studies reporting seismic wavespeed deviations from PREM in the outermost outer core, the core appears to be stratified. Compositional layering, where liquids of different densities overlie one another is one stratification possibility. This mechanism, however, inhibits vertical flows in the liquid near the surface of the core implied by models of secular variation of the Earth's magnetic field. To avoid this limitation, we propose a mechanism by which the layering arises in an analogous way to atmospheric cloud formation. If liquid metal containing dissolved Si+O reaches a saturation level in the outermost outer core, SiO_2 will crystallize and rise to the core-mantle boundary (CMB), causing density changes in the liquid by release of latent heat and changing composition. We present an physical model for this process and show that it explains the observed outer core wavespeed variations better than previous parameterizations. For a CMB temperature of 3800 K and a core light element content of 5 wt% Si+O, SiO_2 begins crystallizing 260 km below the CMB through an interval about 160 km thick, yet core liquid can flow freely through the crystallization interval, facilitating magnetic field changes on decadal to century time scales.

©2019. Japan Geoscience Union. All Right Reserved.

Relation between sound velocity and density for liquid iron alloys under Earth's core pressures by laser-shock compression

*Tatsuhiro Sakaiya[1], Tadashi Kondo[1], Hidenori Terasaki[1], Keisuke Shigemori[2], Yoichiro Hironaka[2]

1. Graduate School of Science, Osaka University, 2. Institute of Laser Engineering, Osaka University

Sound velocity at Earth's core conditions are one of the most important physical properties in Earth science because it can be directly compared with the seismological Earth model (PREM: Preliminary Reference Earth Model) [1]. The composition of solid inner core is estimated from the comparison of the model [1] and the extrapolation of sound velocities as a function of density of iron and iron alloys obtained by the static compression experiment [2, 3]. Birch's law, a linear sound velocity–density relation [4], is used to extrapolate sound velocities to densities in the core condition. On the other hand, the composition of liquid outer core is estimated from the partitioning and solubility data in the inner core boundary condition for the composition of solid core. There has been some works for the sound velocity of iron and iron alloys on the Earth's core condition by dynamic techniques using explosive [5], gas gun [5-11], and laser [12-14]. In this study, we measure the sound velocity and density of liquid iron alloys by shock-compression method using high-power laser.
We conducted shock-compression experiments using a High Intensity Plasma Experimental Research (HIPER) system at the GEKKO-XII laser irradiation facility [15] at the Institute of Laser Engineering, Osaka University. The samples were Fe-Ni alloys, pure nickel, Fe-Si alloys, pure silicon, and pyrrhotite. The sound velocities and densities of shock-compressed iron alloys using the high-power laser were measured by x-ray radiography [12-14] at pressures up to 1000 GPa.
Part of this work was performed under the joint research project of the Institute of Laser Engineering, Osaka University and supported by JSPS KAKENHI Grant Number JP16K05541.

References
[1] A. M. Dziewonski and D. L. Anderson, Phys. Earth Planet. Inter. 25, 297-356 (1981).
[2] J. Badro et al., Earth Planet. Sci. Lett. 254, 233-238 (2007).
[3] G. Fiquet et al., Phys. Earth Planet. Inter. 172, 125-129 (2009).
[4] F. Birch, Geophys. J. R. Astron. Soc. 4, 295-311 (1961).
[5] J. M. Brown and R. G. McQueen, J. Geophys. Res. 91, 7485-7494 (1986).
[6] J. H. Nguyen and N. C. Holmes, Nature 427, 339-342 (2004).
[7] J. W. Shaner et al., Shock Waves in Condensed Matter, 135-138 (1988).
[8] H. Huang et al., J. Geophys. Res. 116, B04201 (2010).
[9] H. Huang et al., Nature 479, 513-516 (2011).
[10] Y. Zhang et al., Sci. Rep. 6, 22473 (2016).
[11] H. Huang et al., J. Geophys. Res. 123, 4730 (2018).
[12] K. Shigemori et al., Eur. Phys. J. D 44, 301-305 (2007).
[13] K. Shigemori et al., Rev. Sci. Instrum. 83, 10E529 (2012).
[14] T. Sakaiya et al., Earth Planet. Sci. Lett. 392, 80-85 (2014).
[15] C. Yamanaka et al., Nucl. Fusion 27, 19-30 (1987).

Keywords: sound velocity, shock compression, iron alloy, Earth's core, Birch's law

©2019. Japan Geoscience Union. All Right Reserved.

Geochemical estimates of Earth's core heat content at the end of accretion

*Vincent Clesi[1], Renaud Deguen[1]

1. Laboratoire de Geologie de Lyon - Terre, Planètes, Environnement, Université Claude Bernard Lyon 1, CNRS, ENS-Lyon, 69622 Villeurbanne, France.

The composition of Earth's mantle, when compared to experimentally determined partitioning coefficients, can be used to constrain the conditions of equilibration - pressure *P*, temperature *T*, and oxygen fugacity fO_2 - of the metal and silicates during core-mantle differentiation.
This places constraints on the thermal state of the planet during its accretion, and it is tempting to try to use these data to estimate the heat content of the core at the end of accretion.
To do so, we develop an analytical model of the thermal evolution of the metal phase during its descent through the solid mantle toward the growing core, taking into account compression heating, viscous dissipation heating, and heat exchange with the surrounding silicates. For each impact, the model takes as initial condition the pressure and temperature at the base of the magma ocean, and gives the temperature of the metal when it reaches the core. The growth of the planet results in additional pressure increase and compression heating of the core.
The thermal model is coupled to a Monte-Carlo inversion of the metal/silicates equilibration conditions (*P*, *T*, fO_2) in the course of accretion from the abundance of Ni, Co, V and Cr in the mantle, and provides an estimate of the core heat content at the end of accretion for each geochemically successful accretion.
The core heat content depends on the mean degree of metal-silicates equilibration, on the mode of metal/silicates separation in the mantle (diapirism, percolation, or dyking), but also very significantly on the shape of the equilibration conditions curve (equilibration *P* and *T* vs. fraction of Earth accreted).
We find that many accretion histories which are successful in reproducing the mantle composition yield a core that is colder than its current state.
Imposing that the temperature of the core at the end of accretion is higher than its current values therefore provides strong constraints on the accretion history.
In particular, we find that the core heat content depends significantly on the last stages of accretion

Keywords: Core formation, Model

©2019. Japan Geoscience Union. All Right Reserved.

The effect of temperature on density of solid metals

*Asaka Kamiya[1], Hidenori Terasaki[1], Tadashi Kondo[1]

1. Osaka University

It is reported that sound velocities of several solid metals show drastic non-linear reduction at near the melting temperature. This is called premelting effect. Nadal and Le Poac (2013) reported that the sound velocity (P-wave and S-wave velocities) of solid tin (Sn) decreased drastically just before melting (T/T_m ~0.99) at ambient pressure. They suggested that this decrease is due to reduction of elastic moduli (bulk and shear moduli). To understand the premelting effect more accurately, density data of tin near the melting temperature is also required in addition to sound velocity data. However, the precise density behavior of tin around the melting temperature is still missing. In this study, we measured the density of solid metals (tin and nickel) at ambient pressure and studied the effect of temperature on the density near melting temperature. The densities of solid metals were measured from optical image of the sample in the high-temperature furnace up to 673 K for Sn and 1873 K for fcc-Ni. The densities in this study were measured with error of 0.07 % for Sn and 0.4 % for Ni. Density of Sn decreases linearly with increasing temperature up to 490 K and reduced drastically above 490 K (at T/T_m~0.97). This drastic decrease in density of Sn is likely to relate to the premelting effect suggested from sound velocity measurement. In contrast, density of Ni decreases almost linearly with increasing temperature up to melting point and no drastic density change was observed in solid state.

Keywords: premelting effect, Tin, Ni, density, high temperature, electric furnace

©2019. Japan Geoscience Union. All Right Reserved.

Phase relations in the Fe-Ni-Si system at high pressures and high temperatures

*Daijo Ikuta[1], Eiji Ohtani[1], Saori Kawaguchi[2], Naohisa Hirao[2], Yasuo Ohishi[2]

1. Department of Earth Science, Tohoku University, 2. JASRI

The Earth's core has supposed to be constituted by iron-nickel alloys with some light elements. Silicon is one of the most convincing candidates among the light elements. Therefore, the study of high pressure and high temperature properties and behaviors for the Fi-Ni-Si system is important in understanding and constraining to the properties of the Earth's core. In this study, high pressure and high temperature properties for three different contents of Fe-Ni-Si alloys were investigated by using laser heated diamond anvil cells and in situ X-ray diffraction with synchrotron radiation. We determined the phase relations of $Fe_{(0.94-x)}Ni_{0.06}Si_x$ (x = 0.10, 0.17, 0.26) up to 166 GPa and 2800 K, respectively. According to previous Fe-Si system studies, $Fe_{0.83}Si_{0.17}$ alloys transform from hcp to hcp+B2 and fcc+hcp+B2 phases with increasing temperature in isobaric conditions. We observed the change in temperature increase and positive slope of these boundaries due to the nickel containing effect and the difference in silicon content. We report the details of phase relations in the Fe-Ni-Si system and discuss with the differences from the Fe-Si system.

Keywords: Fe-Ni-Si system, phase relation, high pressure

©2019. Japan Geoscience Union. All Right Reserved.

[E] Poster | S (Solid Earth Sciences)：S-VC Volcanology

Thu. May 30, 2019 3:30 PM - 5:00 PM JST | Thu. May 30, 2019 6:30 AM - 8:00 AM UTC | Poster Hall International Exhibition Hall8, Makuhari Messe_12

[S-VC34] Connecting magma dynamics in vent-conduit system with surface expression of volcanic eruption

convener:Takahiro Miwa(National research institute for earth science and disaster prevention), Nobuo Geshi(Geological Survey of Japan, The National Institute of Advanced Industrial Science and Technology)

Magma dynamics within a shallow conduit system control the diversity of behavior of volcanic eruptions. Recent advancements in geophysical, airborne and ground-based observation techniques provide quantitative data about the dynamic behavior of volcanic eruptions. New analytical methods of the macro and microtextures of eruptive products also open new insights on detailed dynamics of magmas within conduit. The aim of this session is the integration of these new techniques to approach the dynamics of magma ascending from a shallow part of conduit to vent. This session seeks submissions that explore magma dynamics controlling the behaviors of volcanic eruption by integrated investigation of 1) degassing, outgassing, crystallization, and fragmentation of ascending magma, 2) emission and recycling of eruptive product, and 3) morphological characterization of the vent-conduit system. We encourage contributions based on textural-petrological analyses of eruptive product, experimental study reproducing magma in the conduit, geophysical observation on surface expression of volcanic eruption, and related numerical modeling.

[SVC34-P01] A new formulation of viscosity-included bubble nucleation rate in ascending magmas and re-estimation of bubble number density (2)

*Mizuki Nishiwaki[1], Atsushi Toramaru[2] (1.Department of Earth and Planetary Sciences, Graduate School of Sciences, Kyushu University, 2.Department of Earth and Planetary Sciences, Faculty of Sciences, Kyushu University)

[SVC34-P02] Kinetic delay of crystal growth controls plagioclase-basaltic melt apparent disequilibrium

*Ryoya Oida[1], Hidemi Ishibashi[1], ATSUSHI YASUDA[2], Natsumi Hokanishi[2] (1.Faculty of Science, Shizuoka University, 2.Earthquake Research Institute, University of Tokyo)

[SVC34-P03] Eruptive trends and dynamics of remote volcanoes detected form space-based thermal data and SO_2 emissions: a comparative analysis of Stromboli, Batu Tara and Tinakula volcanoes

*Corrado CIGOLINI[1], Marco Laiolo[1], Francesco Massimetti[1,2], Maurizio Ripepe[2], Diego Coppola[1] (1.Department of Earth Sciences, University of Torino, Italy, 2.Department of Earth Sciences, University of Firenze, Italy)

[SVC34-P04] The source depth of Strombolian explosions: a multiparametric approach and comparison

*Jacopo Taddeucci[1], Miguel Angel Alatorre-Ibarguengoitia[2], Valeria Cigala[3], Elisabetta Del Bello[1], Damien Gaudin[4], Ulrich Kueppers[4], Tullio Ricci[1], Valentino Salvatore[5], Piergiorgio Scarlato[1] (1.Istituto Nazionale di Geofisica e Vulcanologia, Rome, Italy, 2.Centro de Investigación en Gestión de Riesgo y Cambio Climático, Universidad de Ciencias y Artes de Chiapas, Tuxtla Gutiérrez, Mexico, 3.Department of Geosciences, Università degli Studi di Padova, Padua, Italy, 4.Department of Earth and Environmental Sciences. Ludwig-Maximilians-Universität (LMU). Munich, Germany, 5.Dipartimento di Scienze della Terra, Sapienza Università di Roma, Rome, Italy)

[SVC34-P05] Magmatic aggregate of basaltic ash particles

*Takahiro Miwa[1], Nobuo Geshi[2] (1.National research institute for earth science and disaster prevention, 2.National Institute of Advanced Industrial Science and Technology)

[SVC34-P06] Melt inclusion study on the eruption process of Izu-Omuroyama monogenetic volcano, Japan

Risako Hatada[1], *Hidemi Ishibashi[1], Yusuke Suzuki[2], ATSUSHI YASUDA[3], Natsumi Hokanishi[3] (1.Faculty of Science, Shizuoka University, 2.Izu Peninsula Geopark, 3.Earthquake Research Institute, University of Tokyo)

[SVC34-P07] Time-series variation in the textures of ejecta of the An'ei eruption, Izu-Oshima

*Yuya Ikenaga[1], Fukashi Maeno[1], ATSUSHI YASUDA[1] (1.Earthquake Research Institute, The University of Tokyo)

[SVC34-P08] The textural analysis of pumice from the Plinian eruption of Taupo volcano: implications for tube pumice

*Masatoshi Ohashi[1], Mie Ichihara[2], Fukashi Maeno[2], Ben Kennedy[3], Darren Gravley[3] (1.Department of Earth and Planetary Science, Graduate School of Science, The University of Tokyo, 2.Earthquake Research Institute, The University of Tokyo, 3.Department of Geological Sciences, The University of Canterbury)

A new formulation of viscosity-included bubble nucleation rate in ascending magmas and re-estimation of bubble number density (2)

*Mizuki Nishiwaki[1], Atsushi Toramaru[2]

1. Department of Earth and Planetary Sciences, Graduate School of Sciences, Kyushu University, 2. Department of Earth and Planetary Sciences, Faculty of Sciences, Kyushu University

To evaluate the effect of melt viscosity on bubble nucleation, we newly formulate homogeneous nucleation rate of water bubbles to explicitly include melt viscosity. The viscosity appears in the pre-exponential factor of the nucleation rate in terms of the Péclet number: the ratio of bubble growth timescale by molecular diffusion and viscous relaxation timescale. The pre-exponential factor linearly decreases with increasing viscosity (or decreasing Péclet number) under a given supersaturation. We numerically solve the evolution of bubble nucleation and growth processes in ascending magmas by using the new formula of nucleation rate and a precise approximation of moment equations of bubble size distribution function. In high viscosity or high decompression rate region, the effect of melt viscosity reduces bubble number density by several orders of magnitude compared with the previous study. Because of the lack of experimental data in this high-viscous regime, the reality of this regime will be verified by future experiments.

Keywords: bubble nucleation, bubble growth, BND (Bubble Number Density), BSD (Bubble Size Distribution), Péclet number

©2019. Japan Geoscience Union. All Right Reserved.

Kinetic delay of crystal growth controls plagioclase-basaltic melt apparent disequilibrium

*Ryoya Oida[1], Hidemi Ishibashi[1], ATSUSHI YASUDA[2], Natsumi Hokanishi[2]

1. Faculty of Science, Shizuoka University, 2. Earthquake Research Institute, University of Tokyo

Plagioclase-melt compositional relations sensitively depend on temperature, T, and water content, X_W, of melt. Therefore, the relations are formulated as functions of T and X_W and used as geothermohygrometer (e.g., Putirka, 2008). Plagioclase-melt equilibrium is postulated for applying the thermohygrometer models. However, validity of the assumption is unobvious for microlite crystallization driven by degassing and/or cooling during eruption. Can we apply the thermohygrometers to the plagioclase-melt pairs formed by dynamic crystallization? To examine the issue, the cooling crystallization experiments of the high-Al basaltic melt were carried out and textural and chemical analyses were performed the run samples.

We used the high-Al basalt lava from Waianae, Hawaii Oahu as the starting material for the cooling crystallization experiments. This experiment was conducted using the 1atm fO_2-controlled furnace at University of Hawaii at Manoa. After 3 hours pre-heating at 1180℃, ~30K higher than the liquidus, the samples were cooled at cooling rates, R_c, of 0.1, 0.3, 1, 3, and 10K/min, and then quenched in water at four target temperatures, T_q, of 1150, 1120, 1090, and 1060℃. We used FE-EPMA (JEOL-JXA-8530FPlus) and EPMA (JEOL8800R) at Earthquake Research Institute, University of Tokyo, for textural and chemical analyses of the run samples.

As R_c and/or T_q increase, the abundance and size of plagioclase crystals decrease. As R_c increases, the shape of plagioclase changes from euhedral to dendritic. The R_c-dependent shape change is more obvious at lower T_q. Pyroxene crystallization was suppressed in the run samples coolied at higher R_c. In addition, melt boundary layers are observed around pyroxene in the samples cooled at 0.3-1K/min, quenched at 1090℃ and cooled at 0.3-3K/min, quenched at 1060℃, and around plagioclase in the samples cooled at >3K/min, quenched at <1120℃. Lower diffusivity of Al_2O_3 compared to those of FeO and MgO is responsible for lower threshold cooling rate of melt boundary layer formation around pyroxene.

The maximum An# [=100Ca/(Ca + Na)] of plagioclase was almost the same among all run samples. We applied both plagioclase liquidus and plagioclase-melt An-partitioning thermometers of Putirka (2008) to the pairs of plagioclase rim-boundary layer melt (BLM) and plagioclase rim-far field melt (FFM) to estimate temperatures recorded in their phase compositions. At T_q=1150℃, the estimated temperatures well represent T_q for both BLM and FFM. However, at lower T_q, both of the thermometers estimate temperatures higher than T_q; difference between estimated temperature and T_q, ΔT, increases as decreasing T_q. The two thermometers estimate similar temperatures for each sample, and the differences between the two estimated temperatures do not depend on R_c. These results suggest that the plagioclase-melt partition coefficient of An component does not depend on the R_c. Therefore, the increase of ΔT at lower T_q is not due to the R_c-dependence of the partition coefficient. It is attributed to the kinetic delay of the crystal growth at lower temperature. On the other hand, the coincidence between calculated temperatures and T_q at 1150℃ suggests that kinetic delay of plagioclase crystal growth is small at near liquidus temperature.

©2019. Japan Geoscience Union. All Right Reserved.

Present results show that plagioclase-melt thermometers can be applied regardless of the R_c at higher temperatures, while magmatic temperature tends to be overestimated due to kinetic delay of crystal growth at lower temperature.

Keywords: plagioclase, crystallization, kinetics, basalt, geothermometry

©2019. Japan Geoscience Union. All Right Reserved.

Eruptive trends and dynamics of remote volcanoes detected form space-based thermal data and SO_2 emissions: a comparative analysis of Stromboli, Batu Tara and Tinakula volcanoes

*Corrado CIGOLINI[1], Marco Laiolo[1], Francesco Massimetti[1,2], Maurizio Ripepe[2], Diego Coppola[1]

1. Department of Earth Sciences, University of Torino, Italy, 2. Department of Earth Sciences, University of Firenze, Italy

South-Eastern Pacific has a large number of unmonitored volcanoes that may potentially produce large-scale eruptive events capable to affect highly-populated areas. Therefore, forecasting changes in volcanic activity in the light of historical time-series is a rather intriguing challenge for the space-based earth observations.
Batu Tara (Indonesia) and Tinakula (Solomon Island) are two poorly known volcanic islands with morphologies and reported short-term activities rather similar to the ones observed at Stromboli volcano (Italy). However, thanks to over a decade-long satellite data we are able to effectively compare the activity occurring at Stromboli (a unique natural laboratory and “open-vent” system) with those taking place at the above volcanoes.
We process and analyse the radiant flux (thermal activity) coupled with SO_2 emissions (degassing activity) at these three volcanoes for over a decade. The combined analysis of Volcanic Radiant Power (from MODIS data) and SO_2 burden (from OMI data) reveals different long-term eruptive trends, and contrasting ratio of gas vs. thermal emissions. In fact, the persistent open-vent explosive activity of Stromboli volcano is interrupted by flank effusions that periodically drain the degassed magma stored at shallow levels. On the other hand, the long-lasting exponential decay of both thermal and gas emissions observed at Batu Tara is consistent with the eruption of an “undegassed magma” from a deep, and likely a “closed” magma chamber. Finally, Tinakula volcano exhibits multiple year-long eruptive phases, characterised by evolving gas vs. thermal ratio correlated with an increasing eruptive intensity: thus suggesting the involvement of a volatile-zoned magma chamber with periodic phases of gas/magma accumulations.
Our results suggest that the combined analysis of satellite thermal/gas data is a useful tool for better understanding long-term volcanic dynamics and interpreting volcanic processes occurring at a shorter time-scale. We also stress that large satellite datasets on active volcanoes, available from different platforms, greatly enhance the opportunity to efficiently monitor remote volcanic targets in the attempt to mitigate volcanic risk.

Keywords: Remote volcanoes, satellite datasets, Volcanic Radiative Power, SO2 emissions, volcanic risk

©2019. Japan Geoscience Union. All Right Reserved.

The source depth of Strombolian explosions: a multiparametric approach and comparison

*Jacopo Taddeucci[1], Miguel Angel Alatorre-Ibarguengoitia[2], Valeria Cigala[3], Elisabetta Del Bello[1], Damien Gaudin[4], Ulrich Kueppers[4], Tullio Ricci[1], Valentino Salvatore[5], Piergiorgio Scarlato[1]

1. Istituto Nazionale di Geofisica e Vulcanologia, Rome, Italy, 2. Centro de Investigación en Gestión de Riesgo y Cambio Climático, Universidad de Ciencias y Artes de Chiapas, Tuxtla Gutiérrez, Mexico, 3. Department of Geosciences, Università degli Studi di Padova, Padua, Italy, 4. Department of Earth and Environmental Sciences. Ludwig-Maximilians-Universität (LMU). Munich, Germany, 5. Dipartimento di Scienze della Terra, Sapienza Università di Roma, Rome, Italy

The source depth of an individual explosion during Strombolian-style explosive volcanic activity can be defined as the depth of the region within the volcanic conduit where magma fragmentation occurs and the acceleration of pyroclasts by the expanding gas continuum begins. Source depth is thought to exert a first-order control on the final ejection dynamics of the pyroclasts and the ensuing eruptive styles and hazards. As such, different methods to estimate source depth have been developed in the past.

Here, we used three independent methods to estimate the source depth of some Strombolian explosions from Stromboli and Etna volcanoes (Italy). The first method uses the back-tracking of the trajectories of pyroclasts leaving the vent to infer their minimum release depth. It is a purely geometric method relying on the assumption that pyroclasts follow linear trajectories after fragmentation. The second method uses the time delay between the appearance of pyroclasts at the vent and the arrival of acoustic waves at a recording station at a known distance from the vent. This method relies on several assumptions, including (i) the sound velocity inside the conduit, (ii) the co-location of source depth of pyroclasts and acoustic waves, and (iii) a constant velocity of pyroclasts in the conduit, following the initial acceleration. The third method uses the velocity of pyroclasts progressively exiting the vent. This velocity decays following a non-linear trend which is function of the source depth, as illustrated by previous experimental and theoretical studies. As for the second method, also this last one assumes a constant velocity of pyroclasts rising in the conduit.

For the Etna case, the three methods provide consistent results and a shallow (<20 m) source depth of the explosions. For the Stromboli case, the first and third methods provide shallow (around 6 and 15 m, respectively) source depths while the second method provides depths of around 60 m. The incompatibility of such large depths with the first two methods, and given the relative assumptions, we believe that in the Stromboli case the co-location of the particles and acoustic source is probably the least strong assumption. These results suggest that caution should be used in assessing source depth from a single methodology, and that more investigations are required on the source of acoustic signals from the explosions and on the motion (specifically the acceleration and deceleration) of pyroclasts ascending along the conduit.

Keywords: strombolian, explosion, depth

©2019. Japan Geoscience Union. All Right Reserved.

Magmatic aggregate of basaltic ash particles

*Takahiro Miwa[1], Nobuo Geshi[2]

1. National research institute for earth science and disaster prevention, 2. National Institute of Advanced Industrial Science and Technology

Dynamics of volcanic cloud and jet at the vent is largely controled by a grain size of pyroclast. The grain size is considered to be determined by primary fragmentation of magma, and subsequent breakup of pyroclasts due to therir collsions in upper conduit (Dufek et al. 2012). However, whether the breakup occurs or not depend on viscoelastic responce of magma (Dingwell and Webb, 1989).
In this study, we report aggregate of ash particles which is formed in magmatic temperature. We observed basaltic ash samples from Stromboli volcano, Italy, and Aso volcano, Japan. The “magmatic aggretate” shows texture that numerous small guest particles (< 200 μm) adhere or stick on a host particle (> 1 mm). All the host particles are catergorized to sideromelane having fluidal morphology. The guest particles are on fluidal surface of the host particle, and show fluidal and dense morphology. These characteristics found in the magmatic aggregate can be explaned by collision and aggretation of ash particles in high temperature condition. Here we model formation of the magmatic aggregates as passing of two frying particles bearing viscoelastic nature, by using viscosity of magma estimated (10^4-10^5 Pa s). When the relative velocity of the two particles falls the critical value, the two particles behave as viscous material, coalsece each other, and then form the magmatic aggregate. The result of calculation demonstrates that the critical relative velocity is approximately 10^{-2} m/s, and implies the magmatic aggregation is difficult to occur for silisic magma with highly viscosity. Thus we conclude that the collision can increase average grain size of pyroclast in basaltic system.

Keywords: Eruptive dynamics, Interaction of ash particles, Viscoelastic response of magma

©2019. Japan Geoscience Union. All Right Reserved.

Melt inclusion study on the eruption process of Izu-Omuroyama monogenetic volcano, Japan

Risako Hatada[1], *Hidemi Ishibashi[1], Yusuke Suzuki[2], ATSUSHI YASUDA[3], Natsumi Hokanishi[3]

1. Faculty of Science, Shizuoka University, 2. Izu Peninsula Geopark, 3. Earthquake Research Institute, University of Tokyo

Izu-Omuroyama is one of monogenetic volcanoes in Izu-Tobu volcanic field, which is the largest pyroclastic cone formed by ~4ka eruption with ~450 million tons of tephra and lava (Koyano et al., 1996). Because a monogenetic volcano such as Omuroyama is built by the first eruption of a newly-formed magma plumbing system, phenocrysts and melt inclusions (MIs) in its volcanic products may record information about the initial process of formation of the magma plumbing system. In this study, textural and chemical analyses were performed for phenocrysts and MIs in Strombolian scoria of the Omuroyama eruption to clarify the eruption process of the monogenetic volcano.

According to Koyano et al. (1996), Omuroyama eruption started from sub-plinian phase (stage-A), followed by weak ash-eruption phase (stage-B), and then shifted to the main phase of Strombolian eruption (stage-C). Omuroyama pyroclastic cone was built during the stage-C. In this study, we performed textural and chemical analyses for phenocrysts and MIs in the fall scoria erupted during the stage-C, by using FE-EPMA and EPMA at ERI, Univ. Tokyo, Japan.

The scoria contain ~3.3 vol.% of olivine and ~5.4 vol.% of plagioclase as phenocrysts, and their groundmass include olivine and plagioclase microphenocsyts (MPs) of several tens-100 microns sizes embedded in almost glassy or microlite-rich matrix. Olivine phenocrysts are homogeneous (Fo~74-83 with concentration at 83-84) in each grain except for normal zoned rim. Olivine MPs has compositions similar to Fo-poor phenocrysts. Most of plagioclase phenocrysts show reverse zoning with cores of An~30-60 and rims of An~84 and dusty zones are often found. Plagioclase MPs have compositions identical to those of phenocryst rims. Olivine- and plagioclase-hosted MIs have SiO_2 contents of ~52-60 wt.% and 57-78 wt.%, respectively. Compositions of both olivine- and plagioclase-hosted MIs with SiO_2~57-60 wt.% are identical with glass in microlite-poor groundmass, indicating that the melt was saturated with olivine and plagioclase. Based on the olivine-plagioclase-melt compositional relation, temperature and H_2O content conditions of the melt is estimated to be ~1080ºC and ~2 wt.% (H2O-saturated depth of ~2km), respectively. Majority of MIs in plagioclase phenocrysts are rhyolitic with SiO2~70-74wt.%. FeO content of host plagioclase crystals are consistent with those in equilibrium with the MIs. H_2O contents of the MIs are estimated by melt-plagioclase hygrometer to be ~6.2-9.2 wt.% (H_2O-saturated depth of ~8-14km), under assumption of temperature of 800-850 ºC. In addition, olivine-hosted MIs with $SiO_2 < 57$ wt.% are enriched in SO_3 (~0.3-0.5 wt.%), indicating their origin deeper than those of more evolved MIs ($SO_3 < 0.1$ wt.%).

Present results suggest that (1) deep-derived, olivine-bearing mafc melt ascent, captured plagioclase phenocrysts and rhyolitic melt and mixed with them at 11km depth, and crystallized MPs at 2km depth before the eruption, and (2) rhyolitic melt existed at ~11km depth beneath the volcanic field at ca. 800 years before the first eruption of rhyolitic magma at Kawagodaira volcano.

Keywords: melt inclusion, monogenetic volcano, rhyolite, Izu-Omuroyama, plagioclase

©2019. Japan Geoscience Union. All Right Reserved.

©2019. Japan Geoscience Union. All Right Reserved.

Time-series variation in the textures of ejecta of the An'ei eruption, Izu-Oshima

*Yuya Ikenaga[1], Fukashi Maeno[1], ATSUSHI YASUDA[1]

1. Earthquake Research Institute, The University of Tokyo

In Izu-Oshima, a large-scale eruption called the An’ ei eruption began in 1777. This eruption lasted for 15 years, and scoria and lava flows were strongly ejected before ash eruption period (Nakamura, 1964; Isshiki, 1984; Koyama and Hayakawa, 1996, Tsukui et al, 2009). As for scoria eruption, the transition of the intensity of eruption was unveiled (Ikenaga et al., 2018). Scoria eruption in the initial stage (Unit A) was somewhat weak and scoria is poor in plagioclase phenocrysts (Pl). After the small-scale scoria eruption (Unit B, rich in Pl), the climax stage (Unit C) occurred. Scoria in Unit C is richest in Pl and eruption column height of this unit is inferred to be approximately 10km. The change in the textures of scoriae among these 3 units, however, has not been investigated yet. It becomes clear in this study that there are differences in the textures of scoriae.

The scoria of Unit A (A-scoria) is rich in microlites and the groundmass glass has low transparency. The surface of bubbles is rough and many bubbles are connected each other. On the other hand, the scoria of Unit C (C-scoria) has almost no microlites and the glass is transparent. The shape of bubbles is spherical or ellipsoid, and the surface of bubbles is smooth. The connectivity of bubbles is low. The characteristics of the scoria of Unit B (B-scoria) are intermediate between those of A- and C-scoria. Considering the transition in the intensity of eruption, magma ascent rate of Unit A is expected to have been low than that of Unit C, and the crystallization of microlites and connection of bubbles in Unit A were probably caused because of low decompression rate.

The compositions of Pl, groundmass glass and melt inclusions in Pl of scoriae were measured using EPMA, and there are no difference in these compositions among 3 units. It is inferred from this result that the change in the intensity of 3 units was not caused by injection of undifferentiated magma into magma chamber, but caused by other processes, such as decompression of magma chamber after the eruption of Unit A. It is a future issue to reveal the cause of the change in intensity.

Keywords: Izu-Oshima, Transition in texture, Composition of eruption products

©2019. Japan Geoscience Union. All Right Reserved.

The textural analysis of pumice from the Plinian eruption of Taupo volcano: implications for tube pumice

*Masatoshi Ohashi[1], Mie Ichihara[2], Fukashi Maeno[2], Ben Kennedy[3], Darren Gravley[3]

1. Department of Earth and Planetary Science, Graduate School of Science, The University of Tokyo, 2. Earthquake Research Institute, The University of Tokyo, 3. Department of Geological Sciences, The University of Canterbury

Tube pumice is characterized by aligned highly elongated bubbles and is a common product of explosive silicic eruptions. This bubble texture is thought to reflect shear deformations during flow in a conduit (Marti et al., 1999). Therefore, quantitative measurements of tube pumice texture can inform conduit flow models. Recent development in X-ray tomography allows us to measure bubble shapes in 3D pumice accurately (e.g., Dingwell et al., 2016). In addition to the microscopic structures of individual pumices, the abundance of tube and non-tube pumices in the stratigraphy is important in inferring temporal and spatial variations in a conduit flow. This study aims at quantifying micro-structural and stratigraphic features of pumice from the 1.8 ka eruption of Taupo volcano, New Zealand.

The 1.8 ka eruption is the most recent large eruptive event from Taupo volcano. It is characterized by various eruptive styles, including three phreatomagmatic fall deposits (units 1, 3, 4), Hatepe plinian fall deposit (unit 2), Taupo plinian fall deposit (unit 5), and Taupo ignimbrite (unit 6) (Houghton et al., 2010). Since those deposits show chemically uniform pumices and melt inclusions, the great diversity of bubble textures in pumices may reflect purely physical processes in the eruption. We collected samples from the units of the two plinian eruptions (units 2 and 5) and the ignimbrite (unit 6), and measured bubble textures and vesicularities. Among those units, we focused on unit 5 to investigate the transition from plinian fall to ignimbrite. For this purpose, a detailed sampling of unit 5 was conducted at an outcrop about 25 km away from the vent, where the unit consists of a fine lower part (40 cm) and a coarse upper part (180 cm). We sampled clasts from the bottom to top of the unit 5 layer at 20cm interval. The bubble textures of more than 1000 pumice samples were measured by a digital microscope (VHX-1000, Keyence) with variable illumination function. The illumination was optimized to make good luminance contrast between the flat surface and bubbles for image analysis.

The image analysis shows that bubbles in unit 5 are more elongated than those in unit 2 and less elongated than those in unit 6. The average values of bubble elongation in unit 2 and 6 are proportional to those of vesicularity. In contrast, bubble elongation and vesicularity are uniform within unit 5. The component analysis over unit 5 shows that the weight percentage of lithics is also uniform except in the lowest part. The relatively high lithic content in the lowest part suggests vent widened or shifted location at the beginning of the Taupo plinian event.

Previous studies in other volcanoes suggest that bubbles in the pre-ignimbrite phase become more elongated toward the flow stage (Taddeucci and Wohletz 2001, Polacci et al., 2003). The increased amount of tube pumice is thought to reflect a gradual transition from fallout to ignimbrite, and it was interpreted as a result of increased erosive activity near the conduit wall, or a greater conduit area available for shearing (Polacci et al., 2003). In contrast, no such variation of bubble texture is observed in Taupo plinian event (unit 5), which implies that a steady conduit flow was sustained during the pre-ignimbrite fallout eruption. The ignimbrite (unit 6) might not simply be the result of a collapsing plinian eruption column. It is also possible that the topmost part of unit 5 had been eroded by and/or mixed with the pyroclastic flow that deposited the subsequent ignimbrite (unit 6).

©2019. Japan Geoscience Union. All Right Reserved.

Keywords: bubble texture, tube pumice, Taupo

©2019. Japan Geoscience Union. All Right Reserved.

[E] Poster | S (Solid Earth Sciences)：S-VC Volcanology

Thu. May 30, 2019 5:15 PM - 6:30 PM JST | Thu. May 30, 2019 8:15 AM - 9:30 AM UTC | Poster Hall International Exhibition Hall8, Makuhari Messe_23

[S-VC34] Connecting magma dynamics in vent-conduit system with surface expression of volcanic eruption

convener:Takahiro Miwa(National research institute for earth science and disaster prevention), Nobuo Geshi(Geological Survey of Japan, The National Institute of Advanced Industrial Science and Technology)

Magma dynamics within a shallow conduit system control the diversity of behavior of volcanic eruptions. Recent advancements in geophysical, airborne and ground-based observation techniques provide quantitative data about the dynamic behavior of volcanic eruptions. New analytical methods of the macro and microtextures of eruptive products also open new insights on detailed dynamics of magmas within conduit. The aim of this session is the integration of these new techniques to approach the dynamics of magma ascending from a shallow part of conduit to vent. This session seeks submissions that explore magma dynamics controlling the behaviors of volcanic eruption by integrated investigation of 1) degassing, outgassing, crystallization, and fragmentation of ascending magma, 2) emission and recycling of eruptive product, and 3) morphological characterization of the vent-conduit system. We encourage contributions based on textural-petrological analyses of eruptive product, experimental study reproducing magma in the conduit, geophysical observation on surface expression of volcanic eruption, and related numerical modeling.

[SVC34-P01] A new formulation of viscosity-included bubble nucleation rate in ascending magmas and re-estimation of bubble number density (2)

*Mizuki Nishiwaki[1], Atsushi Toramaru[2] (1.Department of Earth and Planetary Sciences, Graduate School of Sciences, Kyushu University, 2.Department of Earth and Planetary Sciences, Faculty of Sciences, Kyushu University)

[SVC34-P02] Kinetic delay of crystal growth controls plagioclase-basaltic melt apparent disequilibrium

*Ryoya Oida[1], Hidemi Ishibashi[1], ATSUSHI YASUDA[2], Natsumi Hokanishi[2] (1.Faculty of Science, Shizuoka University, 2.Earthquake Research Institute, University of Tokyo)

[SVC34-P03] **Eruptive trends and dynamics of remote volcanoes detected form space-based thermal data and SO_2 emissions: a comparative analysis of Stromboli, Batu Tara and Tinakula volcanoes**

*Corrado CIGOLINI[1], Marco Laiolo[1], Francesco Massimetti[1,2], Maurizio Ripepe[2], Diego Coppola[1] (1.Department of Earth Sciences, University of Torino, Italy, 2.Department of Earth Sciences, University of Firenze, Italy)

[SVC34-P04] The source depth of Strombolian explosions: a multiparametric approach and comparison

*Jacopo Taddeucci[1], Miguel Angel Alatorre-Ibarguengoitia[2], Valeria Cigala[3], Elisabetta Del Bello[1], Damien Gaudin[4], Ulrich Kueppers[4], Tullio Ricci[1], Valentino Salvatore[5], Piergiorgio Scarlato[1] (1.Istituto Nazionale di Geofisica e Vulcanologia, Rome, Italy, 2.Centro de Investigación en Gestión de Riesgo y Cambio Climático, Universidad de Ciencias y Artes de Chiapas, Tuxtla Gutiérrez, Mexico, 3.Department of Geosciences, Università degli Studi di Padova, Padua, Italy, 4.Department of Earth and Environmental Sciences. Ludwig-Maximilians-Universität (LMU). Munich, Germany, 5.Dipartimento di Scienze della Terra, Sapienza Università di Roma, Rome, Italy)

[SVC34-P05] Magmatic aggregate of basaltic ash particles

*Takahiro Miwa[1], Nobuo Geshi[2] (1.National research institute for earth science and disaster prevention, 2.National Institute of Advanced Industrial Science and Technology)

[SVC34-P06] Melt inclusion study on the eruption process of Izu-Omuroyama monogenetic volcano, Japan

Risako Hatada[1], *Hidemi Ishibashi[1], Yusuke Suzuki[2], ATSUSHI YASUDA[3], Natsumi Hokanishi[3] (1.Faculty of Science, Shizuoka University, 2.Izu Peninsula Geopark, 3.Earthquake Research Institute, University of Tokyo)

[SVC34-P07] Time-series variation in the textures of ejecta of the An'ei eruption, Izu-Oshima

*Yuya Ikenaga[1], Fukashi Maeno[1], ATSUSHI YASUDA[1] (1.Earthquake Research Institute, The University of Tokyo)

[SVC34-P08] The textural analysis of pumice from the Plinian eruption of Taupo volcano: implications for tube pumice

*Masatoshi Ohashi[1], Mie Ichihara[2], Fukashi Maeno[2], Ben Kennedy[3], Darren Gravley[3] (1.Department of Earth and Planetary Science, Graduate School of Science, The University of Tokyo, 2.Earthquake Research Institute, The University of Tokyo, 3.Department of Geological Sciences, The University of Canterbury)

A new formulation of viscosity-included bubble nucleation rate in ascending magmas and re-estimation of bubble number density (2)

*Mizuki Nishiwaki[1], Atsushi Toramaru[2]

1. Department of Earth and Planetary Sciences, Graduate School of Sciences, Kyushu University, 2. Department of Earth and Planetary Sciences, Faculty of Sciences, Kyushu University

To evaluate the effect of melt viscosity on bubble nucleation, we newly formulate homogeneous nucleation rate of water bubbles to explicitly include melt viscosity. The viscosity appears in the pre-exponential factor of the nucleation rate in terms of the Péclet number: the ratio of bubble growth timescale by molecular diffusion and viscous relaxation timescale. The pre-exponential factor linearly decreases with increasing viscosity (or decreasing Péclet number) under a given supersaturation. We numerically solve the evolution of bubble nucleation and growth processes in ascending magmas by using the new formula of nucleation rate and a precise approximation of moment equations of bubble size distribution function. In high viscosity or high decompression rate region, the effect of melt viscosity reduces bubble number density by several orders of magnitude compared with the previous study. Because of the lack of experimental data in this high-viscous regime, the reality of this regime will be verified by future experiments.

Keywords: bubble nucleation, bubble growth, BND (Bubble Number Density), BSD (Bubble Size Distribution), Péclet number

©2019. Japan Geoscience Union. All Right Reserved.

Kinetic delay of crystal growth controls plagioclase-basaltic melt apparent disequilibrium

*Ryoya Oida[1], Hidemi Ishibashi[1], ATSUSHI YASUDA[2], Natsumi Hokanishi[2]

1. Faculty of Science, Shizuoka University, 2. Earthquake Research Institute, University of Tokyo

Plagioclase-melt compositional relations sensitively depend on temperature, T, and water content, X_W, of melt. Therefore, the relations are formulated as functions of T and X_W and used as geothermohygrometer (e.g., Putirka, 2008). Plagioclase-melt equilibrium is postulated for applying the thermohygrometer models. However, validity of the assumption is unobvious for microlite crystallization driven by degassing and/or cooling during eruption. Can we apply the thermohygrometers to the plagioclase-melt pairs formed by dynamic crystallization? To examine the issue, the cooling crystallization experiments of the high-Al basaltic melt were carried out and textural and chemical analyses were performed the run samples.

We used the high-Al basalt lava from Waianae, Hawaii Oahu as the starting material for the cooling crystallization experiments. This experiment was conducted using the 1atm fO_2-controlled furnace at University of Hawaii at Manoa. After 3 hours pre-heating at 1180℃, ~30K higher than the liquidus, the samples were cooled at cooling rates, R_c, of 0.1, 0.3, 1, 3, and 10K/min, and then quenched in water at four target temperatures, T_q, of 1150, 1120, 1090, and 1060℃. We used FE-EPMA (JEOL-JXA-8530FPlus) and EPMA (JEOL8800R) at Earthquake Research Institute, University of Tokyo, for textural and chemical analyses of the run samples.

As R_c and/or T_q increase, the abundance and size of plagioclase crystals decrease. As R_c increases, the shape of plagioclase changes from euhedral to dendritic. The R_c-dependent shape change is more obvious at lower T_q. Pyroxene crystallization was suppressed in the run samples coolied at higher R_c. In addition, melt boundary layers are observed around pyroxene in the samples cooled at 0.3-1K/min, quenched at 1090℃ and cooled at 0.3-3K/min, quenched at 1060℃, and around plagioclase in the samples cooled at >3K/min, quenched at <1120℃. Lower diffusivity of Al_2O_3 compared to those of FeO and MgO is responsible for lower threshold cooling rate of melt boundary layer formation around pyroxene.

The maximum An# [=100Ca/(Ca + Na)] of plagioclase was almost the same among all run samples. We applied both plagioclase liquidus and plagioclase-melt An-partitioning thermometers of Putirka (2008) to the pairs of plagioclase rim-boundary layer melt (BLM) and plagioclase rim-far field melt (FFM) to estimate temperatures recorded in their phase compositions. At T_q=1150℃, the estimated temperatures well represent T_q for both BLM and FFM. However, at lower T_q, both of the thermometers estimate temperatures higher than T_q; difference between estimated temperature and T_q, ΔT, increases as decreasing T_q. The two thermometers estimate similar temperatures for each sample, and the differences between the two estimated temperatures do not depend on R_c. These results suggest that the plagioclase-melt partition coefficient of An component does not depend on the R_c. Therefore, the increase of ΔT at lower T_q is not due to the R_c-dependence of the partition coefficient. It is attributed to the kinetic delay of the crystal growth at lower temperature. On the other hand, the coincidence between calculated temperatures and T_q at 1150℃ suggests that kinetic delay of plagioclase crystal growth is small at near liquidus temperature.

©2019. Japan Geoscience Union. All Right Reserved.

Present results show that plagioclase-melt thermometers can be applied regardless of the R_c at higher temperatures, while magmatic temperature tends to be overestimated due to kinetic delay of crystal growth at lower temperature.

Keywords: plagioclase, crystallization, kinetics, basalt, geothermometry

©2019. Japan Geoscience Union. All Right Reserved.

Eruptive trends and dynamics of remote volcanoes detected form space-based thermal data and SO_2 emissions: a comparative analysis of Stromboli, Batu Tara and Tinakula volcanoes

*Corrado CIGOLINI[1], Marco Laiolo[1], Francesco Massimetti[1,2], Maurizio Ripepe[2], Diego Coppola[1]

1. Department of Earth Sciences, University of Torino, Italy, 2. Department of Earth Sciences, University of Firenze, Italy

South-Eastern Pacific has a large number of unmonitored volcanoes that may potentially produce large-scale eruptive events capable to affect highly-populated areas. Therefore, forecasting changes in volcanic activity in the light of historical time-series is a rather intriguing challenge for the space-based earth observations.
Batu Tara (Indonesia) and Tinakula (Solomon Island) are two poorly known volcanic islands with morphologies and reported short-term activities rather similar to the ones observed at Stromboli volcano (Italy). However, thanks to over a decade-long satellite data we are able to effectively compare the activity occurring at Stromboli (a unique natural laboratory and “open-vent” system) with those taking place at the above volcanoes.
We process and analyse the radiant flux (thermal activity) coupled with SO_2 emissions (degassing activity) at these three volcanoes for over a decade. The combined analysis of Volcanic Radiant Power (from MODIS data) and SO_2 burden (from OMI data) reveals different long-term eruptive trends, and contrasting ratio of gas vs. thermal emissions. In fact, the persistent open-vent explosive activity of Stromboli volcano is interrupted by flank effusions that periodically drain the degassed magma stored at shallow levels. On the other hand, the long-lasting exponential decay of both thermal and gas emissions observed at Batu Tara is consistent with the eruption of an “undegassed magma” from a deep, and likely a “closed” magma chamber. Finally, Tinakula volcano exhibits multiple year-long eruptive phases, characterised by evolving gas vs. thermal ratio correlated with an increasing eruptive intensity: thus suggesting the involvement of a volatile-zoned magma chamber with periodic phases of gas/magma accumulations.
Our results suggest that the combined analysis of satellite thermal/gas data is a useful tool for better understanding long-term volcanic dynamics and interpreting volcanic processes occurring at a shorter time-scale. We also stress that large satellite datasets on active volcanoes, available from different platforms, greatly enhance the opportunity to efficiently monitor remote volcanic targets in the attempt to mitigate volcanic risk.

Keywords: Remote volcanoes, satellite datasets, Volcanic Radiative Power, SO2 emissions, volcanic risk

©2019. Japan Geoscience Union. All Right Reserved.

The source depth of Strombolian explosions: a multiparametric approach and comparison

*Jacopo Taddeucci[1], Miguel Angel Alatorre-Ibarguengoitia[2], Valeria Cigala[3], Elisabetta Del Bello[1], Damien Gaudin[4], Ulrich Kueppers[4], Tullio Ricci[1], Valentino Salvatore[5], Piergiorgio Scarlato[1]

1. Istituto Nazionale di Geofisica e Vulcanologia, Rome, Italy, 2. Centro de Investigación en Gestión de Riesgo y Cambio Climático, Universidad de Ciencias y Artes de Chiapas, Tuxtla Gutiérrez, Mexico, 3. Department of Geosciences, Università degli Studi di Padova, Padua, Italy, 4. Department of Earth and Environmental Sciences. Ludwig-Maximilians-Universität (LMU). Munich, Germany, 5. Dipartimento di Scienze della Terra, Sapienza Università di Roma, Rome, Italy

The source depth of an individual explosion during Strombolian-style explosive volcanic activity can be defined as the depth of the region within the volcanic conduit where magma fragmentation occurs and the acceleration of pyroclasts by the expanding gas continuum begins. Source depth is thought to exert a first-order control on the final ejection dynamics of the pyroclasts and the ensuing eruptive styles and hazards. As such, different methods to estimate source depth have been developed in the past.

Here, we used three independent methods to estimate the source depth of some Strombolian explosions from Stromboli and Etna volcanoes (Italy). The first method uses the back-tracking of the trajectories of pyroclasts leaving the vent to infer their minimum release depth. It is a purely geometric method relying on the assumption that pyroclasts follow linear trajectories after fragmentation. The second method uses the time delay between the appearance of pyroclasts at the vent and the arrival of acoustic waves at a recording station at a known distance from the vent. This method relies on several assumptions, including (i) the sound velocity inside the conduit, (ii) the co-location of source depth of pyroclasts and acoustic waves, and (iii) a constant velocity of pyroclasts in the conduit, following the initial acceleration. The third method uses the velocity of pyroclasts progressively exiting the vent. This velocity decays following a non-linear trend which is function of the source depth, as illustrated by previous experimental and theoretical studies. As for the second method, also this last one assumes a constant velocity of pyroclasts rising in the conduit.

For the Etna case, the three methods provide consistent results and a shallow (<20 m) source depth of the explosions. For the Stromboli case, the first and third methods provide shallow (around 6 and 15 m, respectively) source depths while the second method provides depths of around 60 m. The incompatibility of such large depths with the first two methods, and given the relative assumptions, we believe that in the Stromboli case the co-location of the particles and acoustic source is probably the least strong assumption. These results suggest that caution should be used in assessing source depth from a single methodology, and that more investigations are required on the source of acoustic signals from the explosions and on the motion (specifically the acceleration and deceleration) of pyroclasts ascending along the conduit.

Keywords: strombolian, explosion, depth

©2019. Japan Geoscience Union. All Right Reserved.

Magmatic aggregate of basaltic ash particles

*Takahiro Miwa[1], Nobuo Geshi[2]

1. National research institute for earth science and disaster prevention, 2. National Institute of Advanced Industrial Science and Technology

Dynamics of volcanic cloud and jet at the vent is largely controled by a grain size of pyroclast. The grain size is considered to be determined by primary fragmentation of magma, and subsequent breakup of pyroclasts due to therir collsions in upper conduit (Dufek et al. 2012). However, whether the breakup occurs or not depend on viscoelastic responce of magma (Dingwell and Webb, 1989).
In this study, we report aggregate of ash particles which is formed in magmatic temperature. We observed basaltic ash samples from Stromboli volcano, Italy, and Aso volcano, Japan. The “magmatic aggretate” shows texture that numerous small guest particles (< 200 μm) adhere or stick on a host particle (> 1 mm). All the host particles are catergorized to sideromelane having fluidal morphology. The guest particles are on fluidal surface of the host particle, and show fluidal and dense morphology. These characteristics found in the magmatic aggregate can be explaned by collision and aggretation of ash particles in high temperature condition. Here we model formation of the magmatic aggregates as passing of two frying particles bearing viscoelastic nature, by using viscosity of magma estimated (10^4-10^5 Pa s). When the relative velocity of the two particles falls the critical value, the two particles behave as viscous material, coalsece each other, and then form the magmatic aggregate. The result of calculation demonstrates that the critical relative velocity is approximately 10^{-2} m/s, and implies the magmatic aggregation is difficult to occur for silisic magma with highly viscosity. Thus we conclude that the collision can increase average grain size of pyroclast in basaltic system.

Keywords: Eruptive dynamics, Interaction of ash particles, Viscoelastic response of magma

©2019. Japan Geoscience Union. All Right Reserved.

Melt inclusion study on the eruption process of Izu-Omuroyama monogenetic volcano, Japan

Risako Hatada[1], *Hidemi Ishibashi[1], Yusuke Suzuki[2], ATSUSHI YASUDA[3], Natsumi Hokanishi[3]

1. Faculty of Science, Shizuoka University, 2. Izu Peninsula Geopark, 3. Earthquake Research Institute, University of Tokyo

Izu-Omuroyama is one of monogenetic volcanoes in Izu-Tobu volcanic field, which is the largest pyroclastic cone formed by ~4ka eruption with ~450 million tons of tephra and lava (Koyano et al., 1996). Because a monogenetic volcano such as Omuroyama is built by the first eruption of a newly-formed magma plumbing system, phenocrysts and melt inclusions (MIs) in its volcanic products may record information about the initial process of formation of the magma plumbing system. In this study, textural and chemical analyses were performed for phenocrysts and MIs in Strombolian scoria of the Omuroyama eruption to clarify the eruption process of the monogenetic volcano.

According to Koyano et al. (1996), Omuroyama eruption started from sub-plinian phase (stage-A), followed by weak ash-eruption phase (stage-B), and then shifted to the main phase of Strombolian eruption (stage-C). Omuroyama pyroclastic cone was built during the stage-C. In this study, we performed textural and chemical analyses for phenocrysts and MIs in the fall scoria erupted during the stage-C, by using FE-EPMA and EPMA at ERI, Univ. Tokyo, Japan.

The scoria contain ~3.3 vol.% of olivine and ~5.4 vol.% of plagioclase as phenocrysts, and their groundmass include olivine and plagioclase microphenocsyts (MPs) of several tens-100 microns sizes embedded in almost glassy or microlite-rich matrix. Olivine phenocrysts are homogeneous (Fo~74-83 with concentration at 83-84) in each grain except for normal zoned rim. Olivine MPs has compositions similar to Fo-poor phenocrysts. Most of plagioclase phenocrysts show reverse zoning with cores of An~30-60 and rims of An~84 and dusty zones are often found. Plagioclase MPs have compositions identical to those of phenocryst rims. Olivine- and plagioclase-hosted MIs have SiO_2 contents of ~52-60 wt.% and 57-78 wt.%, respectively. Compositions of both olivine- and plagioclase-hosted MIs with SiO_2~57-60 wt.% are identical with glass in microlite-poor groundmass, indicating that the melt was saturated with olivine and plagioclase. Based on the olivine-plagioclase-melt compositional relation, temperature and H_2O content conditions of the melt is estimated to be ~1080ºC and ~2 wt.% (H2O-saturated depth of ~2km), respectively. Majority of MIs in plagioclase phenocrysts are rhyolitic with SiO2~70-74wt.%. FeO content of host plagioclase crystals are consistent with those in equilibrium with the MIs. H_2O contents of the MIs are estimated by melt-plagioclase hygrometer to be ~6.2-9.2 wt.% (H_2O-saturated depth of ~8-14km), under assumption of temperature of 800-850 ºC. In addition, olivine-hosted MIs with $SiO_2 < 57$ wt.% are enriched in SO_3 (~0.3-0.5 wt.%), indicating their origin deeper than those of more evolved MIs ($SO_3 < 0.1$ wt.%).

Present results suggest that (1) deep-derived, olivine-bearing mafc melt ascent, captured plagioclase phenocrysts and rhyolitic melt and mixed with them at 11km depth, and crystallized MPs at 2km depth before the eruption, and (2) rhyolitic melt existed at ~11km depth beneath the volcanic field at ca. 800 years before the first eruption of rhyolitic magma at Kawagodaira volcano.

Keywords: melt inclusion, monogenetic volcano, rhyolite, Izu-Omuroyama, plagioclase

©2019. Japan Geoscience Union. All Right Reserved.

©2019. Japan Geoscience Union. All Right Reserved.

Time-series variation in the textures of ejecta of the An'ei eruption, Izu-Oshima

*Yuya Ikenaga[1], Fukashi Maeno[1], ATSUSHI YASUDA[1]

1. Earthquake Research Institute, The University of Tokyo

In Izu-Oshima, a large-scale eruption called the An’ ei eruption began in 1777. This eruption lasted for 15 years, and scoria and lava flows were strongly ejected before ash eruption period (Nakamura, 1964; Isshiki, 1984; Koyama and Hayakawa, 1996, Tsukui et al, 2009). As for scoria eruption, the transition of the intensity of eruption was unveiled (Ikenaga et al., 2018). Scoria eruption in the initial stage (Unit A) was somewhat weak and scoria is poor in plagioclase phenocrysts (Pl). After the small-scale scoria eruption (Unit B, rich in Pl), the climax stage (Unit C) occurred. Scoria in Unit C is richest in Pl and eruption column height of this unit is inferred to be approximately 10km. The change in the textures of scoriae among these 3 units, however, has not been investigated yet. It becomes clear in this study that there are differences in the textures of scoriae.

The scoria of Unit A (A-scoria) is rich in microlites and the groundmass glass has low transparency. The surface of bubbles is rough and many bubbles are connected each other. On the other hand, the scoria of Unit C (C-scoria) has almost no microlites and the glass is transparent. The shape of bubbles is spherical or ellipsoid, and the surface of bubbles is smooth. The connectivity of bubbles is low. The characteristics of the scoria of Unit B (B-scoria) are intermediate between those of A- and C-scoria. Considering the transition in the intensity of eruption, magma ascent rate of Unit A is expected to have been low than that of Unit C, and the crystallization of microlites and connection of bubbles in Unit A were probably caused because of low decompression rate.

The compositions of Pl, groundmass glass and melt inclusions in Pl of scoriae were measured using EPMA, and there are no difference in these compositions among 3 units. It is inferred from this result that the change in the intensity of 3 units was not caused by injection of undifferentiated magma into magma chamber, but caused by other processes, such as decompression of magma chamber after the eruption of Unit A. It is a future issue to reveal the cause of the change in intensity.

Keywords: Izu-Oshima, Transition in texture, Composition of eruption products

©2019. Japan Geoscience Union. All Right Reserved.

The textural analysis of pumice from the Plinian eruption of Taupo volcano: implications for tube pumice

*Masatoshi Ohashi[1], Mie Ichihara[2], Fukashi Maeno[2], Ben Kennedy[3], Darren Gravley[3]

1. Department of Earth and Planetary Science, Graduate School of Science, The University of Tokyo, 2. Earthquake Research Institute, The University of Tokyo, 3. Department of Geological Sciences, The University of Canterbury

Tube pumice is characterized by aligned highly elongated bubbles and is a common product of explosive silicic eruptions. This bubble texture is thought to reflect shear deformations during flow in a conduit (Marti et al., 1999). Therefore, quantitative measurements of tube pumice texture can inform conduit flow models. Recent development in X-ray tomography allows us to measure bubble shapes in 3D pumice accurately (e.g., Dingwell et al., 2016). In addition to the microscopic structures of individual pumices, the abundance of tube and non-tube pumices in the stratigraphy is important in inferring temporal and spatial variations in a conduit flow. This study aims at quantifying micro-structural and stratigraphic features of pumice from the 1.8 ka eruption of Taupo volcano, New Zealand.

The 1.8 ka eruption is the most recent large eruptive event from Taupo volcano. It is characterized by various eruptive styles, including three phreatomagmatic fall deposits (units 1, 3, 4), Hatepe plinian fall deposit (unit 2), Taupo plinian fall deposit (unit 5), and Taupo ignimbrite (unit 6) (Houghton et al., 2010). Since those deposits show chemically uniform pumices and melt inclusions, the great diversity of bubble textures in pumices may reflect purely physical processes in the eruption. We collected samples from the units of the two plinian eruptions (units 2 and 5) and the ignimbrite (unit 6), and measured bubble textures and vesicularities. Among those units, we focused on unit 5 to investigate the transition from plinian fall to ignimbrite. For this purpose, a detailed sampling of unit 5 was conducted at an outcrop about 25 km away from the vent, where the unit consists of a fine lower part (40 cm) and a coarse upper part (180 cm). We sampled clasts from the bottom to top of the unit 5 layer at 20cm interval. The bubble textures of more than 1000 pumice samples were measured by a digital microscope (VHX-1000, Keyence) with variable illumination function. The illumination was optimized to make good luminance contrast between the flat surface and bubbles for image analysis.

The image analysis shows that bubbles in unit 5 are more elongated than those in unit 2 and less elongated than those in unit 6. The average values of bubble elongation in unit 2 and 6 are proportional to those of vesicularity. In contrast, bubble elongation and vesicularity are uniform within unit 5. The component analysis over unit 5 shows that the weight percentage of lithics is also uniform except in the lowest part. The relatively high lithic content in the lowest part suggests vent widened or shifted location at the beginning of the Taupo plinian event.

Previous studies in other volcanoes suggest that bubbles in the pre-ignimbrite phase become more elongated toward the flow stage (Taddeucci and Wohletz 2001, Polacci et al., 2003). The increased amount of tube pumice is thought to reflect a gradual transition from fallout to ignimbrite, and it was interpreted as a result of increased erosive activity near the conduit wall, or a greater conduit area available for shearing (Polacci et al., 2003). In contrast, no such variation of bubble texture is observed in Taupo plinian event (unit 5), which implies that a steady conduit flow was sustained during the pre-ignimbrite fallout eruption. The ignimbrite (unit 6) might not simply be the result of a collapsing plinian eruption column. It is also possible that the topmost part of unit 5 had been eroded by and/or mixed with the pyroclastic flow that deposited the subsequent ignimbrite (unit 6).

©2019. Japan Geoscience Union. All Right Reserved.

Keywords: bubble texture, tube pumice, Taupo

©2019. Japan Geoscience Union. All Right Reserved.

[E] Poster | S (Solid Earth Sciences)：S-CG Complex & General

Thu. May 30, 2019 3:30 PM - 5:00 PM JST | Thu. May 30, 2019 6:30 AM - 8:00 AM UTC | Poster Hall International Exhibition Hall8, Makuhari Messe_14

[S-CG50] Intraslab and intraplate earthquakes

convener:Saeko Kita(International Institute of Seismology and Earthquake Engineering, BRI), Tomohiro Ohuchi(Geodynamics Research Center, Ehime University), Marcel Thielmann(Bavarian Geoinstitute, University of Bayreuth), Ryo Okuwaki(Research Institute of Earthquake and Volcano Geology, Geological Survey of Japan, National Institute of Advanced Industrial Science and Technology)

The purpose of this session is to share recent advances of geo-scientifical studies for intraslab and shallow-depth intraplate earthquakes. We seek to formulate future directions of the interdisciplinary study of the occurrence of intermediate-depth and deep earthquakes from the viewpoint of seismology, geodynamics and mineral physics. We welcome presentations from a wide variety of scientific disciplines, including seismology, seismotectonics, geodynamics, mineral and rock physics, other geophysics, geology, and numerical modeling.

[SCG50-P01] Changes in seismicity rate, stress orientations, and b-values before and after ETS events in the Philippine sea plate under Kii Peninsula

*Saeko Kita[1], Heidi Houston[2], Sachiko Tanaka[3], Youichi Asano[3], Takuo Shibutani[4], Naoki Suda[5] (1.Building Research Institute, 2.USC, 3.NIED, 4.DPRI, Kyoto University, 5.Hiroshima University)

[SCG50-P02] **Inhomogeneous conduit across slab controlled by intraslab stress heterogeneity in the Nankai subduction zone**

*Makoto Otsubo[1], Ayumu Miyakawa[2], Ikuo Katayama[3], Keishi Okazaki[4] (1.Geological Survey of Japan, Research Institute of Earthquake and Volcano Geology, 2.Geological Survey of Japan, Research Institute of Geology and Geoinformation, 3.Hiroshima University, 4.JAMSTEC)

[SCG50-P03] New insights into the mechanism of deep-focus earthquakes

*Ayako Tsuchiyama[1], Junichi Nakajima[1] (1.Tokyo Institute of Technology)

[SCG50-P04] Faulting in deforming harzburgite under wet conditions

*Tomohiro Ohuchi[1], Xinglin Lei[2], Yuji Higo[3], Yoshinori Tange[3], Takeshi Sakai[1] (1.Geodynamics Research Center, Ehime University, 2.National Institute of Advanced Industrial Science and Technology, 3.Japan Synchrotron Radiation Research Institute)

[SCG50-P05] Semi-brittle behavior of olivine single crystals under the conditions of Earth's mantle transition zone

Yoshihisa Naruse[1], *Tomohiro Ohuchi[1] (1.Geodynamics Research Center, Ehime University)

[SCG50-P06] High-pressure deformation experiments on peridotite gouges under hydrothermal conditions, using a deformation-DIA apparatus

*Maki Semba[1], Ken-ichi Hirauchi[1], Tomohiro Ohuchi[2], Katsuyoshi Michibayashi[3] (1.Department of Geosciences, Faculty of Science, Shizuoka University, 2.Geodynamics Research Center, Ehime University, 3.Department of Earth and Planetary Sciences, Nagoya university)

[SCG50-P07] Stable fault slip in antigorite-olivine aggregates at high pressures

Mai Ikehara[1], *Tomoaki Kubo[1], Takuya Iwasato[2], Yuji Higo[3], Masahiro Imamura[1], Yoshinori Tange[3] (1.Kyushu University, 2.Shin-Nippon Nondestructive Inspection Co., Ltd., 3.JASRI)

[SCG50-P08] Rheology and frictional instability of lawsonite in high pressure deformation experiments

*Rei Shiraishi[1], Jun Muto[1], Akihiro Tsunoda[2], Sando Sawa[1], Akio Suzuki[1] (1.Department of Earth Science, Graduate School of Science, Tohoku University, 2.Earthquake Research Institute, University of Tokyo)

[SCG50-P09] Grain Size Dependency of Olivine-Spinel Phase Transformational Mechanism Responsible for Deep-focus Earthquakes

*Sando Sawa[1], Jun Muto[1], Nobuyoshi Miyajima[2], Hiroyuki Nagahama[1] (1.Department of Earth Science, Tohoku University, 2.Bayerisches Geoinstitut, University of Bayreuth)

[SCG50-P10] **Seismicity and mineral destabilizations in the subducting mantle up to 6 GPa, 200 km depth**

*Thomas P. Ferrand[1] (1.Earthquake Research Institute)

[SCG50-P11] Receiver function imaging of subducting Pacific plate and mantle wedge under Japanese islands using denser network of stations

*HyeJeong Kim[1], Hitoshi Kawakatsu[1], Takeshi Akuhara[1], Masanao Shinohara[1] (1.Earthquake Research Institute, The University of Tokyo)

[SCG50-P12] Strong S-wave attenuation in the mantle wedge beneath the NE Japan and interpretations of high-frequency wave propagation path of intraslab earthquakes

*Takahiro Shiina[1,2], Kei Katsumata[2], Kiyoshi Yomogida[3], Aitaro Kato[1] (1.Earthquake Research Institute, The University of Tokyo, 2.Institute of Seismology and Volcanology, Graduate School of Science, Hokkaido University, 3.Graduate School of Science, Hokkaido University)

Changes in seismicity rate, stress orientations, and b-values before and after ETS events in the Philippine sea plate under Kii Peninsula

*Saeko Kita[1], Heidi Houston[2], Sachiko Tanaka[3], Youichi Asano[3], Takuo Shibutani[4], Naoki Suda[5]

1. Building Research Institute, 2. USC, 3. NIED, 4. DPRI, Kyoto University, 5. Hiroshima University

The slip on the plate interface has the potential to affect the stress field and seismicity within the subducting slab. Several studies have examined the interaction of slow slip phenomena with intraslab earthquakes [Nankai and Tokai regions, Han et al. 2014; Mexico, Radiguet et al. 2018, 2018 JpGU meeting; New Zealand, 2018, Warren-Smith, 2018 AGU meeting]. Kita et al. [2018, SSJ meeting] reported the stress change in the whole slab associated with ETS times based on stress tensor inversion results. However, we find a clear double seismic zone under Kii Peninsula, as also noted in a previous study [e.g. Miyoshi and Ishibashi, 2004]. Therefore, we here examine seismicity rate variations, stress changes, and b-value variations of seismicity separately for the upper plane events and oceanic mantle ones relative to ETS timings beneath the Kii Peninsula. We use the JMA earthquake catalog, the NIED tremor catalog, the upper surface of the Philippine sea plate estimated by Shibutani and Hirahara [2016], P-wave polarity data by NIED, and a stress tensor inversion code [Vavrycuk, 2014].

We determined the timings of ~30 large ETS beneath the Kii Peninsula from 2001 to 2017, and categorized slab seismicity relative to the occurrence times of nearby the ETS (i.e., 60 days before or after). We then combined or stacked the slab seismicity based on these relative occurrence times. The rate of seismicity both in the upper plane events and in the oceanic mantle ones after the ETS timings clearly decreased, compared to the rate before the ETS timings. The peaks of b-values of seismicity both in the upper plane events and oceanic mantle ones were found to occur 1.5 months before ETS. A change in stress orientations before and after the ETS was seen in the oceanic mantle, and a relatively small change was seen for the upper plane events. The stress change in the upper plane events appears to be larger in the region updip of the ETS zone. The results of our study suggest that the aseismic slip on the plate boundary may affect the stress field and the occurrence of seismicity within the subducting slab beneath the Kii Peninsula. Fluid migration from the oceanic slab into the ETS zone on the plate boundary could be related to the interaction of slow slip phenomena with intraslab earthquakes.

Keywords: Intraslab earthquake, ETS, stress change, b-value, time change, Kii peninsula

©2019. Japan Geoscience Union. All Right Reserved.

Inhomogeneous conduit across slab controlled by intraslab stress heterogeneity in the Nankai subduction zone

*Makoto Otsubo[1], Ayumu Miyakawa[2], Ikuo Katayama[3], Keishi Okazaki[4]

1. Geological Survey of Japan, Research Institute of Earthquake and Volcano Geology, 2. Geological Survey of Japan, Research Institute of Geology and Geoinformation, 3. Hiroshima University, 4. JAMSTEC

Non volcanic deep low-frequency tremors and slow slip events occur simultaneously in the transition zone from locked to continuously creeping fault at the down dip portion of the Nankai Trough subduction zone, southwestern Japan. The occurrence of these slow earthquakes is attributed to the effect of high pore pressures on the plate boundaries. The Nankai Trough subduction zone has a discontinuous band of occurrence of these slow earthquakes along the trench. Here we show that spatial variation of intraslab stress can control fluid migration through the subducted Philippine Sea slab to the plate boundary. The tri-axial normal faulting stress detected by the stress tensor inversion by using focal mechanisms in the slab controls anisotropies of permeability trending NNW–SSE sub-horizontal orientation from the subducted Philippine Sea slab to the plate boundary. The inhomogeneous condition controlled by the spatial stress heterogeneities in the subducted Philippine Sea slab represents the intraslab fluid pathway. The hypothesis is consistent with spatial heterogeneity of slow earthquake activities and $^{3}He/^{4}He$ ratio distributions.

Keywords: Fluid, Nankai Trough, Slab, Slow earthquake, Stress

©2019. Japan Geoscience Union. All Right Reserved.

New insights into the mechanism of deep-focus earthquakes

*Ayako Tsuchiyama[1], Junichi Nakajima[1]

1. Tokyo Institute of Technology

Generally, deep-focus earthquakes were generated in subducting slabs and occurred along some specific regions such as Izu-Bonin zone and Tonga-Fiji zone. We have not identified their occurrence mechanisms, even though some plausible hypotheses, dehydration embrittlement, thermal and shear plastic instability, and transformational faulting, were proposed. In this study, we try to obtain new constraints that deepen the understanding of deep-focus earthquakes through waveform analysis of earthquakes in the Izu-Bonin subduction zone.

First, we picked up 460 quakes at a depth range of 300-400 km in 2003-2015 beneath Tokai area from the catalog data provided by Japan Meteorological Agency, and relocated them with double-difference earthquake relocation algorithm (hypoDD; Waldhauser and Ellsworth, 2000). Second, we computed their coherence values between all available pairs of earthquakes with cross-spectrum analysis. Then, we were successful to identify a few earthquake clusters that had a very high coherence value over 0.9 in a long time window of 40 s including P and S waves. Moreover, we relocated these earthquakes with hypoDD again by using precisely-determined differential travel-time data derived from waveform data. As a result, we could find that earthquakes in each cluster occurred on single fault plane with complementary rapture areas.

Additionally, we implemented moment tensor inversion (Gephart and Forsyth, 1984) and estimated the stress field around the region where we discovered a few clusters showing waveform similarities. Moreover, we computed the amount of stress drop of the similar earthquakes with spectrum analysis of seismic wave. Through these waveform analyses, we interpreted that the mechanism of these similar deep-focus earthquakes could be explained by combining two possible mechanisms; dehydration embrittlement that regulates the rupture initiation and thermal and shear plastic instability that controls the rupture propagation along a pre-existing fault.

Keywords: deep-focus earthquakes, intraslab earthquakes

©2019. Japan Geoscience Union. All Right Reserved.

Faulting in deforming harzburgite under wet conditions

*Tomohiro Ohuchi[1], Xinglin Lei[2], Yuji Higo[3], Yoshinori Tange[3], Takeshi Sakai[1]

1. Geodynamics Research Center, Ehime University, 2. National Institute of Advanced Industrial Science and Technology, 3. Japan Synchrotron Radiation Research Institute

The subduction zone produces a major fraction of the Earth's seismic activity. The mechanisms of intermediate-depth (> 40 km depth) and deep-focus (> 300 km) earthquakes are fundamentally different from those of shallow (< 40 km) earthquakes. This is because the frictional strength of silicate rocks exceeds the upper limit of the stress level in the upper mantle (< 300 MPa: Obata and Karato, 1995) at pressures higher than 1 GPa (~30 km depth). Therefore, the cause of intraslab seismicity at intermediate depths has been attributed to dehydration of serpentinite (e.g., Peakock, 2001) because the water released during dehydration reaction of serpentinite reduces the effective confining pressure. The dehydration embrittlement model is now widely accepted, because the location of the double seismic zone in the subducting Pacific slab corresponds to the main dehydration field in the pressure-temperature diagram of the hydrous peridotite (Omori et al., 2002).

To evaluate the effect of water on semi-brittle behavior of harzburgite, we conducted in-situ uniaxial deformation experiments on as-is/water-saturated harzburgite at pressures 1.2-3.0 GPa and temperatures 770-1250 K with a constant displacement rate using a deformation-DIA apparatus. Pressure, stress, and strain were measured in situ by using x-ray diffraction patterns and radiographs. Acoustic emissions (AEs) were also recorded continuously on six sensors, and three-dimensional AE source location were determined.

Formation of throughgoing faults was observed even when differential stress is much lower than the confining pressure (i.e., > 0.3 times of confining pressure) in water-saturated harzburgite. This is contrast to the case of water-saturated dunite (Ohuchi et al., 2018), in which fracture strength exceeds the confining pressure (i.e., Goetze's criterion). Creep strength of water-saturated harzburgite was lower than that of as-is harzburgite (~0.5-1 GPa at each temperature). Weakening of the harzburgite by the aqueous fluid resulted in the reduction in the number of AE events and decrease in fault slip rate (< 3.6E-4 s^{-1} at a stress of < 1.05 GPa). Stress/pressure drop around the timing of a faulting was limited at strains of 1E-4 s^{-1}. The aseismic faulting observed in the water-saturated harzburgite implies that silent slip events around the subduction interface is due to semi-brittle flow of water-saturated harzburgite (i.e., a dehydration product of antigorite).

Keywords: harzburgite, water, semi-brittle flow

©2019. Japan Geoscience Union. All Right Reserved.

Semi-brittle behavior of olivine single crystals under the conditions of Earth’s mantle transition zone

Yoshihisa Naruse[1], *Tomohiro Ohuchi[1]

1. Geodynamics Research Center, Ehime University

The origin of deep-focus earthquakes, which occur at depths of 300-700km in the subducting slabs, fundamentally differs from that of other earthquakes and has been attributed to the pressure-induced phase transition in olivine. Previous studies on Mg_2GeO_4 olivine have shown that grain size reduction induced by the phase transition in olivine causes shear localization (e.g., Burnley et al., 1991; Schubnel et al., 2013). Schubnel et al. (2013) reported intense acoustic emissions around the timing of a faulting which would be induced by shear localization in polycrystalline Mg_2GeO_4 olivine. In order to understand the relationship between fracturing and the phase transition in olivine, we conducted deformation experiments on single crystals of San Carlos olivine (Fo_{91}) at pressure of 10-15 GPa and temperatures of 1000-1100 degC using a deformation-DIA apparatus. Single crystal of olivine was chosen to exclude the effect of grain boundaries on nucleation of high-pressure phases of olivine (i.e., wadsleyite and ringwoodite).

Array of microcrack parallel to either (100), (010) or (110) plane was developed at an ~50 degree to the direction of uniaxial compression. Rotation of olivine axes associating the formation of subgrain boundaries was observed around the microcrack arrays, showing that plastic deformation of the olivine single crystal inevitably associated formation of the microcracks. In most samples, microcracks coalesced and then a few throughgoing fractures were developed. Particles of wadsleyite /ringwoodite having a diameter of a few micrometer or less were preferentially nucleated on the microcrack surfaces. Ultrafine-grained domains, which consist of the wadsleyite /ringwoodite particles, were formed along the throughgoing fractures. Development of a banded ultrafine-grained domain was also observed along a throughgoing fracture, implying that shear localization could occur as a result of semi-brittle flow of olivine and a transition from dislocation creep to grain-size-sensitive creep in subducting slabs at depths > 410 km.

Keywords: olivine, phase transition, semi-brittle flow, microcrack, deep-focus earthquake

©2019. Japan Geoscience Union. All Right Reserved.

High-pressure deformation experiments on peridotite gouges under hydrothermal conditions, using a deformation-DIA apparatus

*Maki Semba[1], Ken-ichi Hirauchi[1], Tomohiro Ohuchi[2], Katsuyoshi Michibayashi[3]

1. Department of Geosciences, Faculty of Science, Shizuoka University, 2. Geodynamics Research Center, Ehime University, 3. Department of Earth and Planetary Sciences, Nagoya university

In subducting oceanic plates, the focal depth of intraslab earthquakes is deeper (>40 km) than that of interplate earthquakes. Since the normal stress on faults (e.g., outer-rise faults) hosting the intraslab earthquakes is too high to generate brittle shear failure, there may be some mechanisms to weaken effective fault strength. In addition, the hypocenter distribution of intraslab earthquakes forms double-planed structure of the deep seismic zone, and the location of the lower plane is in accord with the stability limit of serpentine (antigorite), suggesting shear deformation of antigorite-bearing peridotite gouges in the presence of hydrothermal water. Here, in order to understand the influence of hydrous minerals on the fault strength, we performed deformation experiments on simulated peridotite gouges with compositions of dunite (100% olivine) and harzburgite (70% olivine/30% orthopyroxene) under hydrothermal conditions, using a deformation-DIA apparatus. The experiments were conducted at a temperature of 580˚C, a confining pressure of 2.5 GPa, and shear strain rates of 2.70 $\times 10^{-5}$ to 1.03 $\times 10^{-4}$ s^{-1}. In the deformed peridotite gouges, localized shear zones such as R_1 and B shears were observed, and these shears were accompanied with newly formed hydrous phases (serpentine or talc). Olivine grains have a crystal preferred orientation characterized by a slip system of [001] (010). These results indicate that semi-brittle flow is a major deformation mechanism of the peridotite gouges. Considering low coefficients of friction of serpentine and talc, we can suggest that the infiltration of seawater along outer-rise fault planes and subsequent hydrothermal alteration result in effective shear strengths low enough to produce intraslab earthquakes.

Keywords: deformation-DIA apparatus, peridotite, serpentinization, frictional strength

©2019. Japan Geoscience Union. All Right Reserved.

Stable fault slip in antigorite-olivine aggregates at high pressures

Mai Ikehara[1], *Tomoaki Kubo[1], Takuya Iwasato[2], Yuji Higo[3], Masahiro Imamura[1], Yoshinori Tange[3]

1. Kyushu University, 2. Shin-Nippon Nondestructive Inspection Co., Ltd., 3. JASRI

Intermediate-depth earthquakes are observed to occur within subducting oceanic plates at depths of about 60-300 km where most materials exhibit plastic deformation rather than brittle failure, owing to high pressures and temperatures. Dehydration embrittlement of hydrous minerals, particularly antigorite serpentine, is one of the most popular hypotheses for explaining shear instability under such conditions (e.g., Raleigh and Paterson, 1965). Recent high-pressure deformation experiments, monitoring Acoustic Emission (AE) activities upon syndeformational antigorite dehydration, showed that dehydration embrittlement was not observed on single-phase antigorite (Gasc et al., 2017), whereas dehydration related faulting was formed on antigorite-olivine aggregates with strong AEs (Ferrand et al., 2017). However, most of the previous high-pressure studies have been conducted in axial compression at relatively low pressures (< 3.5 GPa), insufficient to consider intermediate-depth earthquakes. Therefore, in this study, we conducted high-pressure shear deformation experiments on two-phase aggregates of antigorite and olivine, considering partially serpentinized peridotites, in order to investigate possible shear localization and shear instability up to 7 GPa.

Deformation experiments were conducted at 5-7 GPa, 350-700 ℃ using Deformation-DIA apparatuses at SPring-8 (BL04B1). Monochromatic X-rays (50-60 keV) were used to measure dehydration kinetics, shear strain and stress with recording AEs. We used three kinds of starting materials; natural cored antigorite from Kawarakoba in Nagasaki prefecture, forsterite polycrystal, and two-phase sintered mixtures of antigorite and San Carlos olivine (antigorite 10, 30, 50 vol %). The samples were cut into disks having thickness of 300 μm and used for a shear deformation study by being assembled between two 45˚-cut alumina pistons. In shear deformation experiments, the starting disk was compressed to 5 or 7 GPa at room temperature, annealed at 350 or 400 ℃ for 1 h, and then deformed with an anvil displacement rate of 200 μm/h. In some experiments, we increased temperature during shear deformation with a ramping rate of 0.1 ℃/sec to induce dehydration reaction. Microstructures of the recovered samples were examined by an optical microscope and a scanning electron microscope (SEM).

From X-ray radiography images, we observed shear localization in all two-phase samples deformed within the antigorite stability field at 5 GPa. The locallization occurred when homogeneous shear strain γ reached 0.4-0.9 (strain rate 1.3-2.2 $\times 10^{-4}$/s), and then most strains were partitioned to the fault zone with the slip velocity of 4.6-9.1 $\times 10^{-2}$ μm/s. Because no AEs were detected from the sample region, the localized deformation is thought to occur by stable sliding. SEM observations revealed that a thin shear deformation zone was formed along the fault, where the plastic deformation of both antigorite and olivine was significant. Striation and nanograins were observed on the fault plane, suggesting the formation of nanogouge. In contrast, homogeneous deformation was developed during antigorite dehydration with temperature ramping, even in the sample showing shear localization in the antigorite stability field. Under higher pressure condition 7 GPa, shear localization did not occur in all samples regardless of temperature. These results suggest that, although AE activities were detected with the dehydration in the antigorite-olivine aggregates up to 3.5 GPa in the previous study, further increase of pressure inhibits shear instability and shear localization. Thus, other dehydration reactions and/or instability mechanisms are required to explain intermediate-depth earthquakes deeper than ~100 km.

©2019. Japan Geoscience Union. All Right Reserved.

©2019. Japan Geoscience Union. All Right Reserved.

Rheology and frictional instability of lawsonite in high pressure deformation experiments

*Rei Shiraishi[1], Jun Muto[1], Akihiro Tsunoda[2], Sando Sawa[1], Akio Suzuki[1]

1. Department of Earth Science, Graduate School of Science, Tohoku University, 2. Earthquake Research Institute, University of Tokyo

The cause of intermediate-depth earthquakes (50-300 km) in subducting slabs have been proposed to be the dehydration embrittlement (e.g., Raleigh and Paterson, 1965), because there are many kinds of hydrous minerals in a subducting slab and hypocenter distribution coincides with the dehydration boundary determined by high pressure experiments (e.g., Hacker et al., 2003). Many experimental studies on antigorite have been conducted, but a few previous works about dehydration embrittlement of lawsonite-bearing rocks experimentally. Lawsonite, $CaAl_2Si_2O_7(OH)_2H_2O$, is a hydrous mineral which contains 11 wt% water in its structure as both water molecules and a hydroxy group (Cmodi and Zanazzi, 1996). Lawsonite is one of the candidate for dehydration embrittlement in cold subducting slabs, however previous works have apparently contradictory results. Okazaki and Hirth (2016) showed that lawsonite dehydration induced unstable fault slip based on deformation experiments of pure lawsonite using Griggs-type deformation apparatus at 1 GPa. On the other hand, Incel et al. (2017) also investigated deformation properties of lawsonite and glaucophane mixture at 1.5 to 3.0 GPa using deformation-DIA apparatus. They insisted that there is no evidence for a straightforward relation to the dehydration of lawsonite and the brittle failure of samples. So, we have conducted the deformation experiments of lawsonite under the cold slab conditions in order to clarify the deformation property of lawsonite and understand the relationship between dehydration and brittle failure.

Experiments were carried out using Deformation-Cubic Anvil Press (D-CAP) installed at KEK PF AR-NE7A beamline. Pure lawsonite powder (98%) was used as starting materials. Deformation experiments were carried out at a pressure of 6 GPa and temperatures of 300 - 800 ˚C. The temperature was increased at the same time as deformation started. The temperature ramping rate over the strain rate was set the ranges for the real subducting slab, which ranges from 10^2 to 10^4 ˚C (Chernak and Hirth, 2011; Okazaki and Hirth, 2016). During deformation stages, strain, stress and transformation rate were measured for in-situ using a monochromatic X-ray beam with an energy of 60 keV.

Four experiments showed rapid stress drop during temperature ramping before lawsonite dehydration starts. We observed microstructure of recovered samples, there are many through going faults and microcracks but no dehydration products. Our results indicate that brittle process and frictional sliding occur without dehydration of lawsonite. This suggests that the intermediate-depth earthquakes can be caused by the deformation itself of lawsonite without the dehydration of lawsonite.

Keywords: intermediate-depth earthquakes, dehydration embrittlement, Lawsonite

©2019. Japan Geoscience Union. All Right Reserved.

Grain Size Dependency of Olivine-Spinel Phase Transformational Mechanism Responsible for Deep-focus Earthquakes

*Sando Sawa[1], Jun Muto[1], Nobuyoshi Miyajima[2], Hiroyuki Nagahama[1]

1. Department of Earth Science, Tohoku University, 2. Bayerisches Geoinstitut, University of Bayreuth

Deep-focus earthquakes occur at the depth from 440 km to 660 km in the subducting slab. The mechanism responsible for the earthquakes is thought to be different from that of shallow earthquakes, so that previous studies have reported the various mechanisms. By the geophysical observations and deformation experiments, the phase transformational faulting mechanism is presumed as the precursor of deep-focus earthquakes (e.g., Zhan et al., 2014). The phase transformational faulting mechanism is that metastable olivine in the slab undergoes the phase transformation to fine-grained spinel and faulting occurs with strain localization into the fine-grained spinel. This shear instability depends on grain size. Furthermore, the grain size may restrict the pressure- and temperature-conditions where the shear instability occurs, that is, the region of slab where deep-focus earthquakes occur. However, previous studies have conducted deformation experiments with finer grain size than expected in the slab (e.g., Burnley et al., 1991). Hence, the results from the laboratory experiments cannot directly apply to the geophysical observation. In this study, to reveal the grain size dependency on the phase transformational faulting, we conducted the deformation experiments of germanate olivine (about 3 μm), which is an analogue material of silicate olivine, finer-grained than that in previous studies (30 μm). We used a Griggs-type solid-confining media deformation apparatus. The confining pressure, temperature and strain rate are 1.2 GPa, 400~900 ℃ and 2.0×10^{-4} s^{-1}, respectively. Even though deformation experiments were conducted under wider temperature conditions than previous studies, we did not observe any shear instability event with apparent stress drops. Also, Raman spectroscopy clarified that the germanate olivine underwent the transformation to spinel at temperatures higher than 500 ℃. Shear instability does not occur because the difference in grain sizes between olivine and nucleated spinel in this study was smaller than those in previous studies. Also, the transformation temperature in this study was much lower than those in previous study (T > 1000 ℃ in Burnley et al., 1991). Considering the rate equation of the transformation (Chan, 1956), small grain size promotes the transformation, but these fast rates of the transformation cannot be explained only by the effect of the grain size. Therefore, the presence of water such as absorbed water in a starting material can also contribute to promote the transformation. Hence, both small initial grain size and a little amount of water promote the transformation even at lower temperature. These results indicate that the phase transformational faulting mechanism has strong grain size dependency. In summary, the pressure- and temperature-conditions where the faulting occurs depends on the grain size of olivine and amount of water. Because the grain size in the slab is larger than that in the experiments, by extrapolating from these results, we may restrict the region of slab where deep-focus earthquakes occur.

This work was supported by the JSPS Japanese-German Graduate Externship.

[Reference]
Burnley et al. (1991), JGR, vol 96, 425-443.
Chan (1956), Acta Metallurgica, vol 4, 449-459.
Zhan et al. (2014), EPSL, vol 385, 89-96.

©2019. Japan Geoscience Union. All Right Reserved.

Keywords: Deep-focus earthquakes, Griggs type piston-cylinder apparatus, phase transformation

©2019. Japan Geoscience Union. All Right Reserved.

Seismicity and mineral destabilizations in the subducting mantle up to 6 GPa, 200 km depth

*Thomas P. Ferrand[1]

1. Earthquake Research Institute

In the subducting oceanic lithosphere, a significant part of the seismicity is triggered in the mantle, especially along the upper and lower Wadati-Benioff planes. Several studies have investigated the potential involvement of dehydration reactions in the triggering mechanism of mantle earthquakes. Recent experimental results reveal that, under subduction conditions, mechanical instabilities nucleate in strong stable mineral aggregates during the destabilization of minor amounts of antigorite, i.e. the high-temperature serpentine, through a stress transfer, without any fluid overpressure. Here I confront these laboratory results to seismological observations. On one hand, most of the natural hydrous magnesium silicates seem to be known, with experimentally-deduced stability limits up to 7 GPa, at least, available as relatively accurate estimates. On the other hand, recent achievements in thermal structure of subduction zones combined with precise hypocentre relocation give access to pressure and temperature conditions at earthquakes hypocentres. A series of P-T diagrams summarizes the stability limit of minerals that may be part of natural peridotite with variable compositions at pressures from 0.5 to 6 GPa and temperatures from 200 to 950˚C, and compares it with seismicity. Both hydrous and anhydrous phases are considered. A myriad of minor metamorphic reactions could participate in a transformation-driven stress transfer, even if the stability limits of serpentine minerals seem to correlate with most of the observed seismicity.

Keywords: earthquakes, intraslab, DDST, dehydration, transformation, subduction

©2019. Japan Geoscience Union. All Right Reserved.

Receiver function imaging of subducting Pacific plate and mantle wedge under Japanese islands using denser network of stations

*HyeJeong Kim[1], Hitoshi Kawakatsu[1], Takeshi Akuhara[1], Masanao Shinohara[1]

1. Earthquake Research Institute, The University of Tokyo

Receiver function imaging has been frequently used by different groups focusing on different depths of the Japanese subduction zone. The overlying crust (Shiomi and Park, 2008, Bianchi et al, 2015), the Pacific plate before (Kawakatsu et al., 2009) and after subduction (Kawakatsu and Watada, 2007; Wirth and Long, 2012), and the mantle transition zones (Kawakatsu and Yoshioka, 2011; Tauzin et al., 2018) were discussed using the NIED array stations (Hi-net and F-net). Recently, deployment of ocean bottom seismometers (OBSs) enabled studies of subduction zones closer to the trench (e.g., Akuhara and Mochizuki, 2015). Kawakatsu and Kim (2018, SSJ) have obtained a new version of receiver function imaging using 14-year long of Hi-net data. However, there are other land stations (e.g., J-array) that can improve the station coverage. Here, we collect data from available on-land stations deployed in north-eastern Japan to obtain a denser 2-D array of stations. Additionally, data from temporary OBS stations (Shinohara et al. 2012) are gathered to image the subducted Pacific plate in shallower depths than previously available. Continuous imaging from ocean to land will help to constrain transition of the hydrated oceanic crust along subduction that is expressed as a low velocity layer for better understanding of the hydration/dehydration processes during subduction, which might be related to the occurrence of subduction zone earthquakes.

Keywords: subduction zone, receiver function, ccp stacking

©2019. Japan Geoscience Union. All Right Reserved.

Strong S-wave attenuation in the mantle wedge beneath the NE Japan and interpretations of high-frequency wave propagation path of intraslab earthquakes

*Takahiro Shiina[1,2], Kei Katsumata[2], Kiyoshi Yomogida[3], Aitaro Kato[1]

1. Earthquake Research Institute, The University of Tokyo, 2. Institute of Seismology and Volcanology, Graduate School of Science, Hokkaido University, 3. Graduate School of Science, Hokkaido University

For intraslab earthquakes at intermediate-depths in NE Japan, especially at greater than about 100-km depths, it has been often recorded that high-frequency waveform higher than 8 Hz show a remarkable delay of arrival compared with S wave which predominates in a low-frequency band. The magnitude of the delay is little in the forearc region, whereas it increases up to about 40 s in the backarc region. In this study, we investigate the details in the propagation processes of the high-frequency later phase observed for the intraslab earthquakes at the intermediate-depths. To constrain the source location of the high-frequency later phase, we employ the source-scanning algorithm (SSA) [Kao and Shan, 2004] with realistic velocity and attenuation structures, assuming that the high-frequency later phase is generated by the single scattering process. Namely, we estimate a scattering point by using mean-square amplitudes which is synthesized from two horizontal components of the observed waveforms.
Results in frequency bands of 4-32 Hz show that scattering points are distributed beneath the forearc region. The scattering points can reproduce the observed delays of amplitude amplifications associating with the high-frequency later phases. Moreover, similar locations of the scattering points are imaged along the forearc region in the entire NE Japan. These results indicate that high-frequency later phase is a wave scattered at the forearc region and that short wave-length heterogeneity generally developed in the forearc region of NE Japan.
This interpretation well matches implications from previous studies [e.g., Yomogida et al., 2004; Hasemi and Horiuchi, 2010]. Additionally, the obtained distributions of scattering points which appear to surround the highly attenuating mantle wedge suggest that attenuation structure strongly controls propagation paths of seismic wave, in particular, a high-frequency wave. In other words, the identifications of high-frequency later phase may become easy because the amplitude of direct wave crossing the high-attenuation zone decreases. To confirm this consideration, we estimate *Qs* along the direct wave by using the coda-normalization method [e.g., Aki, 1980]. This estimation provides 2-3 times smaller path-averaged *Qs* in seismic records of which rays lay on the backarc and the volcanic front than that of which rays lay on the forearc region. These results support that spatial variation in *QS* produces heterogenous propagations of seismic waves emitted from intraslab earthquakes. It is thus required to take scattering and attenuation structures simultaneously into account to understand complex behaviors of high-frequency waves in a future study.

Keywords: S-wave attenuation, Intraslab earthquakes, High-frequency later phase, Scattered wave

©2019. Japan Geoscience Union. All Right Reserved.

[E] Poster | S (Solid Earth Sciences)：S-CG Complex & General

Thu. May 30, 2019 5:15 PM - 6:30 PM JST | Thu. May 30, 2019 8:15 AM - 9:30 AM UTC | Poster Hall International Exhibition Hall8, Makuhari Messe_26

[S-CG50] Intraslab and intraplate earthquakes

convener:Saeko Kita(International Institute of Seismology and Earthquake Engineering, BRI), Tomohiro Ohuchi(Geodynamics Research Center, Ehime University), Marcel Thielmann(Bavarian Geoinstitute, University of Bayreuth), Ryo Okuwaki(Research Institute of Earthquake and Volcano Geology, Geological Survey of Japan, National Institute of Advanced Industrial Science and Technology)

The purpose of this session is to share recent advances of geo-scientifical studies for intraslab and shallow-depth intraplate earthquakes. We seek to formulate future directions of the interdisciplinary study of the occurrence of intermediate-depth and deep earthquakes from the viewpoint of seismology, geodynamics and mineral physics. We welcome presentations from a wide variety of scientific disciplines, including seismology, seismotectonics, geodynamics, mineral and rock physics, other geophysics, geology, and numerical modeling.

[SCG50-P01] Changes in seismicity rate, stress orientations, and b-values before and after ETS events in the Philippine sea plate under Kii Peninsula

*Saeko Kita[1], Heidi Houston[2], Sachiko Tanaka[3], Youichi Asano[3], Takuo Shibutani[4], Naoki Suda[5] (1.Building Research Institute, 2.USC, 3.NIED, 4.DPRI, Kyoto University, 5.Hiroshima University)

[SCG50-P02] **Inhomogeneous conduit across slab controlled by intraslab stress heterogeneity in the Nankai subduction zone**

*Makoto Otsubo[1], Ayumu Miyakawa[2], Ikuo Katayama[3], Keishi Okazaki[4] (1.Geological Survey of Japan, Research Institute of Earthquake and Volcano Geology, 2.Geological Survey of Japan, Research Institute of Geology and Geoinformation, 3.Hiroshima University, 4.JAMSTEC)

[SCG50-P03] New insights into the mechanism of deep-focus earthquakes

*Ayako Tsuchiyama[1], Junichi Nakajima[1] (1.Tokyo Institute of Technology)

[SCG50-P04] Faulting in deforming harzburgite under wet conditions

*Tomohiro Ohuchi[1], Xinglin Lei[2], Yuji Higo[3], Yoshinori Tange[3], Takeshi Sakai[1] (1.Geodynamics Research Center, Ehime University, 2.National Institute of Advanced Industrial Science and Technology, 3.Japan Synchrotron Radiation Research Institute)

[SCG50-P05] Semi-brittle behavior of olivine single crystals under the conditions of Earth's mantle transition zone

Yoshihisa Naruse[1], *Tomohiro Ohuchi[1] (1.Geodynamics Research Center, Ehime University)

[SCG50-P06] High-pressure deformation experiments on peridotite gouges under hydrothermal conditions, using a deformation-DIA apparatus

*Maki Semba[1], Ken-ichi Hirauchi[1], Tomohiro Ohuchi[2], Katsuyoshi Michibayashi[3] (1.Department of Geosciences, Faculty of Science, Shizuoka University, 2.Geodynamics Research Center, Ehime University, 3.Department of Earth and Planetary Sciences, Nagoya university)

[SCG50-P07] Stable fault slip in antigorite-olivine aggregates at high pressures

Mai Ikehara[1], *Tomoaki Kubo[1], Takuya Iwasato[2], Yuji Higo[3], Masahiro Imamura[1], Yoshinori Tange[3] (1.Kyushu University, 2.Shin-Nippon Nondestructive Inspection Co., Ltd., 3.JASRI)

[SCG50-P08] Rheology and frictional instability of lawsonite in high pressure deformation experiments

*Rei Shiraishi[1], Jun Muto[1], Akihiro Tsunoda[2], Sando Sawa[1], Akio Suzuki[1] (1.Department of Earth Science, Graduate School of Science, Tohoku University, 2.Earthquake Research Institute, University of Tokyo)

[SCG50-P09] Grain Size Dependency of Olivine-Spinel Phase Transformational Mechanism Responsible for Deep-focus Earthquakes

*Sando Sawa[1], Jun Muto[1], Nobuyoshi Miyajima[2], Hiroyuki Nagahama[1] (1.Department of Earth Science, Tohoku University, 2.Bayerisches Geoinstitut, University of Bayreuth)

[SCG50-P10] **Seismicity and mineral destabilizations in the subducting mantle up to 6 GPa, 200 km depth**

*Thomas P. Ferrand[1] (1.Earthquake Research Institute)

[SCG50-P11] Receiver function imaging of subducting Pacific plate and mantle wedge under Japanese islands using denser network of stations

*HyeJeong Kim[1], Hitoshi Kawakatsu[1], Takeshi Akuhara[1], Masanao Shinohara[1] (1.Earthquake Research Institute, The University of Tokyo)

[SCG50-P12] Strong S-wave attenuation in the mantle wedge beneath the NE Japan and interpretations of high-frequency wave propagation path of intraslab earthquakes

*Takahiro Shiina[1,2], Kei Katsumata[2], Kiyoshi Yomogida[3], Aitaro Kato[1] (1.Earthquake Research Institute, The University of Tokyo, 2.Institute of Seismology and Volcanology, Graduate School of Science, Hokkaido University, 3.Graduate School of Science, Hokkaido University)

Changes in seismicity rate, stress orientations, and b-values before and after ETS events in the Philippine sea plate under Kii Peninsula

*Saeko Kita[1], Heidi Houston[2], Sachiko Tanaka[3], Youichi Asano[3], Takuo Shibutani[4], Naoki Suda[5]

1. Building Research Institute, 2. USC, 3. NIED, 4. DPRI, Kyoto University, 5. Hiroshima University

The slip on the plate interface has the potential to affect the stress field and seismicity within the subducting slab. Several studies have examined the interaction of slow slip phenomena with intraslab earthquakes [Nankai and Tokai regions, Han et al. 2014; Mexico, Radiguet et al. 2018, 2018 JpGU meeting; New Zealand, 2018, Warren-Smith, 2018 AGU meeting]. Kita et al. [2018, SSJ meeting] reported the stress change in the whole slab associated with ETS times based on stress tensor inversion results. However, we find a clear double seismic zone under Kii Peninsula, as also noted in a previous study [e.g. Miyoshi and Ishibashi, 2004]. Therefore, we here examine seismicity rate variations, stress changes, and b-value variations of seismicity separately for the upper plane events and oceanic mantle ones relative to ETS timings beneath the Kii Peninsula. We use the JMA earthquake catalog, the NIED tremor catalog, the upper surface of the Philippine sea plate estimated by Shibutani and Hirahara [2016], P-wave polarity data by NIED, and a stress tensor inversion code [Vavrycuk, 2014].

We determined the timings of ~30 large ETS beneath the Kii Peninsula from 2001 to 2017, and categorized slab seismicity relative to the occurrence times of nearby the ETS (i.e., 60 days before or after). We then combined or stacked the slab seismicity based on these relative occurrence times. The rate of seismicity both in the upper plane events and in the oceanic mantle ones after the ETS timings clearly decreased, compared to the rate before the ETS timings. The peaks of b-values of seismicity both in the upper plane events and oceanic mantle ones were found to occur 1.5 months before ETS. A change in stress orientations before and after the ETS was seen in the oceanic mantle, and a relatively small change was seen for the upper plane events. The stress change in the upper plane events appears to be larger in the region updip of the ETS zone. The results of our study suggest that the aseismic slip on the plate boundary may affect the stress field and the occurrence of seismicity within the subducting slab beneath the Kii Peninsula. Fluid migration from the oceanic slab into the ETS zone on the plate boundary could be related to the interaction of slow slip phenomena with intraslab earthquakes.

Keywords: Intraslab earthquake, ETS, stress change, b-value, time change, Kii peninsula

©2019. Japan Geoscience Union. All Right Reserved.

Inhomogeneous conduit across slab controlled by intraslab stress heterogeneity in the Nankai subduction zone

*Makoto Otsubo[1], Ayumu Miyakawa[2], Ikuo Katayama[3], Keishi Okazaki[4]

1. Geological Survey of Japan, Research Institute of Earthquake and Volcano Geology, 2. Geological Survey of Japan, Research Institute of Geology and Geoinformation, 3. Hiroshima University, 4. JAMSTEC

Non volcanic deep low-frequency tremors and slow slip events occur simultaneously in the transition zone from locked to continuously creeping fault at the down dip portion of the Nankai Trough subduction zone, southwestern Japan. The occurrence of these slow earthquakes is attributed to the effect of high pore pressures on the plate boundaries. The Nankai Trough subduction zone has a discontinuous band of occurrence of these slow earthquakes along the trench. Here we show that spatial variation of intraslab stress can control fluid migration through the subducted Philippine Sea slab to the plate boundary. The tri-axial normal faulting stress detected by the stress tensor inversion by using focal mechanisms in the slab controls anisotropies of permeability trending NNW–SSE sub-horizontal orientation from the subducted Philippine Sea slab to the plate boundary. The inhomogeneous condition controlled by the spatial stress heterogeneities in the subducted Philippine Sea slab represents the intraslab fluid pathway. The hypothesis is consistent with spatial heterogeneity of slow earthquake activities and $^{3}He/^{4}He$ ratio distributions.

Keywords: Fluid, Nankai Trough, Slab, Slow earthquake, Stress

©2019. Japan Geoscience Union. All Right Reserved.

New insights into the mechanism of deep-focus earthquakes

*Ayako Tsuchiyama[1], Junichi Nakajima[1]

1. Tokyo Institute of Technology

Generally, deep-focus earthquakes were generated in subducting slabs and occurred along some specific regions such as Izu-Bonin zone and Tonga-Fiji zone. We have not identified their occurrence mechanisms, even though some plausible hypotheses, dehydration embrittlement, thermal and shear plastic instability, and transformational faulting, were proposed. In this study, we try to obtain new constraints that deepen the understanding of deep-focus earthquakes through waveform analysis of earthquakes in the Izu-Bonin subduction zone.

First, we picked up 460 quakes at a depth range of 300-400 km in 2003-2015 beneath Tokai area from the catalog data provided by Japan Meteorological Agency, and relocated them with double-difference earthquake relocation algorithm (hypoDD; Waldhauser and Ellsworth, 2000). Second, we computed their coherence values between all available pairs of earthquakes with cross-spectrum analysis. Then, we were successful to identify a few earthquake clusters that had a very high coherence value over 0.9 in a long time window of 40 s including P and S waves. Moreover, we relocated these earthquakes with hypoDD again by using precisely-determined differential travel-time data derived from waveform data. As a result, we could find that earthquakes in each cluster occurred on single fault plane with complementary rapture areas.

Additionally, we implemented moment tensor inversion (Gephart and Forsyth, 1984) and estimated the stress field around the region where we discovered a few clusters showing waveform similarities. Moreover, we computed the amount of stress drop of the similar earthquakes with spectrum analysis of seismic wave. Through these waveform analyses, we interpreted that the mechanism of these similar deep-focus earthquakes could be explained by combining two possible mechanisms; dehydration embrittlement that regulates the rupture initiation and thermal and shear plastic instability that controls the rupture propagation along a pre-existing fault.

Keywords: deep-focus earthquakes, intraslab earthquakes

©2019. Japan Geoscience Union. All Right Reserved.

Faulting in deforming harzburgite under wet conditions

*Tomohiro Ohuchi[1], Xinglin Lei[2], Yuji Higo[3], Yoshinori Tange[3], Takeshi Sakai[1]

1. Geodynamics Research Center, Ehime University, 2. National Institute of Advanced Industrial Science and Technology, 3. Japan Synchrotron Radiation Research Institute

The subduction zone produces a major fraction of the Earth's seismic activity. The mechanisms of intermediate-depth (> 40 km depth) and deep-focus (> 300 km) earthquakes are fundamentally different from those of shallow (< 40 km) earthquakes. This is because the frictional strength of silicate rocks exceeds the upper limit of the stress level in the upper mantle (< 300 MPa: Obata and Karato, 1995) at pressures higher than 1 GPa (~30 km depth). Therefore, the cause of intraslab seismicity at intermediate depths has been attributed to dehydration of serpentinite (e.g., Peakock, 2001) because the water released during dehydration reaction of serpentinite reduces the effective confining pressure. The dehydration embrittlement model is now widely accepted, because the location of the double seismic zone in the subducting Pacific slab corresponds to the main dehydration field in the pressure-temperature diagram of the hydrous peridotite (Omori et al., 2002).

To evaluate the effect of water on semi-brittle behavior of harzburgite, we conducted in-situ uniaxial deformation experiments on as-is/water-saturated harzburgite at pressures 1.2-3.0 GPa and temperatures 770-1250 K with a constant displacement rate using a deformation-DIA apparatus. Pressure, stress, and strain were measured in situ by using x-ray diffraction patterns and radiographs. Acoustic emissions (AEs) were also recorded continuously on six sensors, and three-dimensional AE source location were determined.

Formation of throughgoing faults was observed even when differential stress is much lower than the confining pressure (i.e., > 0.3 times of confining pressure) in water-saturated harzburgite. This is contrast to the case of water-saturated dunite (Ohuchi et al., 2018), in which fracture strength exceeds the confining pressure (i.e., Goetze's criterion). Creep strength of water-saturated harzburgite was lower than that of as-is harzburgite (~0.5-1 GPa at each temperature). Weakening of the harzburgite by the aqueous fluid resulted in the reduction in the number of AE events and decrease in fault slip rate (< 3.6E-4 s^{-1} at a stress of < 1.05 GPa). Stress/pressure drop around the timing of a faulting was limited at strains of 1E-4 s^{-1}. The aseismic faulting observed in the water-saturated harzburgite implies that silent slip events around the subduction interface is due to semi-brittle flow of water-saturated harzburgite (i.e., a dehydration product of antigorite).

Keywords: harzburgite, water, semi-brittle flow

©2019. Japan Geoscience Union. All Right Reserved.

Semi-brittle behavior of olivine single crystals under the conditions of Earth’s mantle transition zone

Yoshihisa Naruse[1], *Tomohiro Ohuchi[1]

1. Geodynamics Research Center, Ehime University

The origin of deep-focus earthquakes, which occur at depths of 300-700km in the subducting slabs, fundamentally differs from that of other earthquakes and has been attributed to the pressure-induced phase transition in olivine. Previous studies on Mg_2GeO_4 olivine have shown that grain size reduction induced by the phase transition in olivine causes shear localization (e.g., Burnley et al., 1991; Schubnel et al., 2013). Schubnel et al. (2013) reported intense acoustic emissions around the timing of a faulting which would be induced by shear localization in polycrystalline Mg_2GeO_4 olivine. In order to understand the relationship between fracturing and the phase transition in olivine, we conducted deformation experiments on single crystals of San Carlos olivine (Fo_{91}) at pressure of 10-15 GPa and temperatures of 1000-1100 degC using a deformation-DIA apparatus. Single crystal of olivine was chosen to exclude the effect of grain boundaries on nucleation of high-pressure phases of olivine (i.e., wadsleyite and ringwoodite).

Array of microcrack parallel to either (100), (010) or (110) plane was developed at an ~50 degree to the direction of uniaxial compression. Rotation of olivine axes associating the formation of subgrain boundaries was observed around the microcrack arrays, showing that plastic deformation of the olivine single crystal inevitably associated formation of the microcracks. In most samples, microcracks coalesced and then a few throughgoing fractures were developed. Particles of wadsleyite /ringwoodite having a diameter of a few micrometer or less were preferentially nucleated on the microcrack surfaces. Ultrafine-grained domains, which consist of the wadsleyite /ringwoodite particles, were formed along the throughgoing fractures. Development of a banded ultrafine-grained domain was also observed along a throughgoing fracture, implying that shear localization could occur as a result of semi-brittle flow of olivine and a transition from dislocation creep to grain-size-sensitive creep in subducting slabs at depths > 410 km.

Keywords: olivine, phase transition, semi-brittle flow, microcrack, deep-focus earthquake

©2019. Japan Geoscience Union. All Right Reserved.

High-pressure deformation experiments on peridotite gouges under hydrothermal conditions, using a deformation-DIA apparatus

*Maki Semba[1], Ken-ichi Hirauchi[1], Tomohiro Ohuchi[2], Katsuyoshi Michibayashi[3]

1. Department of Geosciences, Faculty of Science, Shizuoka University, 2. Geodynamics Research Center, Ehime University, 3. Department of Earth and Planetary Sciences, Nagoya university

In subducting oceanic plates, the focal depth of intraslab earthquakes is deeper (>40 km) than that of interplate earthquakes. Since the normal stress on faults (e.g., outer-rise faults) hosting the intraslab earthquakes is too high to generate brittle shear failure, there may be some mechanisms to weaken effective fault strength. In addition, the hypocenter distribution of intraslab earthquakes forms double-planed structure of the deep seismic zone, and the location of the lower plane is in accord with the stability limit of serpentine (antigorite), suggesting shear deformation of antigorite-bearing peridotite gouges in the presence of hydrothermal water. Here, in order to understand the influence of hydrous minerals on the fault strength, we performed deformation experiments on simulated peridotite gouges with compositions of dunite (100% olivine) and harzburgite (70% olivine/30% orthopyroxene) under hydrothermal conditions, using a deformation-DIA apparatus. The experiments were conducted at a temperature of 580˚C, a confining pressure of 2.5 GPa, and shear strain rates of 2.70 $\times 10^{-5}$ to 1.03 $\times 10^{-4}$ s^{-1}. In the deformed peridotite gouges, localized shear zones such as R_1 and B shears were observed, and these shears were accompanied with newly formed hydrous phases (serpentine or talc). Olivine grains have a crystal preferred orientation characterized by a slip system of [001] (010). These results indicate that semi-brittle flow is a major deformation mechanism of the peridotite gouges. Considering low coefficients of friction of serpentine and talc, we can suggest that the infiltration of seawater along outer-rise fault planes and subsequent hydrothermal alteration result in effective shear strengths low enough to produce intraslab earthquakes.

Keywords: deformation-DIA apparatus, peridotite, serpentinization, frictional strength

©2019. Japan Geoscience Union. All Right Reserved.

Stable fault slip in antigorite-olivine aggregates at high pressures

Mai Ikehara[1], *Tomoaki Kubo[1], Takuya Iwasato[2], Yuji Higo[3], Masahiro Imamura[1], Yoshinori Tange[3]

1. Kyushu University, 2. Shin-Nippon Nondestructive Inspection Co., Ltd., 3. JASRI

Intermediate-depth earthquakes are observed to occur within subducting oceanic plates at depths of about 60-300 km where most materials exhibit plastic deformation rather than brittle failure, owing to high pressures and temperatures. Dehydration embrittlement of hydrous minerals, particularly antigorite serpentine, is one of the most popular hypotheses for explaining shear instability under such conditions (e.g., Raleigh and Paterson, 1965). Recent high-pressure deformation experiments, monitoring Acoustic Emission (AE) activities upon syndeformational antigorite dehydration, showed that dehydration embrittlement was not observed on single-phase antigorite (Gasc et al., 2017), whereas dehydration related faulting was formed on antigorite-olivine aggregates with strong AEs (Ferrand et al., 2017). However, most of the previous high-pressure studies have been conducted in axial compression at relatively low pressures (< 3.5 GPa), insufficient to consider intermediate-depth earthquakes. Therefore, in this study, we conducted high-pressure shear deformation experiments on two-phase aggregates of antigorite and olivine, considering partially serpentinized peridotites, in order to investigate possible shear localization and shear instability up to 7 GPa.

Deformation experiments were conducted at 5-7 GPa, 350-700 ℃ using Deformation-DIA apparatuses at SPring-8 (BL04B1). Monochromatic X-rays (50-60 keV) were used to measure dehydration kinetics, shear strain and stress with recording AEs. We used three kinds of starting materials; natural cored antigorite from Kawarakoba in Nagasaki prefecture, forsterite polycrystal, and two-phase sintered mixtures of antigorite and San Carlos olivine (antigorite 10, 30, 50 vol %). The samples were cut into disks having thickness of 300 μm and used for a shear deformation study by being assembled between two 45˚-cut alumina pistons. In shear deformation experiments, the starting disk was compressed to 5 or 7 GPa at room temperature, annealed at 350 or 400 ℃ for 1 h, and then deformed with an anvil displacement rate of 200 μm/h. In some experiments, we increased temperature during shear deformation with a ramping rate of 0.1 ℃/sec to induce dehydration reaction. Microstructures of the recovered samples were examined by an optical microscope and a scanning electron microscope (SEM).

From X-ray radiography images, we observed shear localization in all two-phase samples deformed within the antigorite stability field at 5 GPa. The locallization occurred when homogeneous shear strain γ reached 0.4-0.9 (strain rate 1.3-2.2 $\times 10^{-4}$/s), and then most strains were partitioned to the fault zone with the slip velocity of 4.6-9.1 $\times 10^{-2}$ μm/s. Because no AEs were detected from the sample region, the localized deformation is thought to occur by stable sliding. SEM observations revealed that a thin shear deformation zone was formed along the fault, where the plastic deformation of both antigorite and olivine was significant. Striation and nanograins were observed on the fault plane, suggesting the formation of nanogouge. In contrast, homogeneous deformation was developed during antigorite dehydration with temperature ramping, even in the sample showing shear localization in the antigorite stability field. Under higher pressure condition 7 GPa, shear localization did not occur in all samples regardless of temperature. These results suggest that, although AE activities were detected with the dehydration in the antigorite-olivine aggregates up to 3.5 GPa in the previous study, further increase of pressure inhibits shear instability and shear localization. Thus, other dehydration reactions and/or instability mechanisms are required to explain intermediate-depth earthquakes deeper than ~100 km.

©2019. Japan Geoscience Union. All Right Reserved.

©2019. Japan Geoscience Union. All Right Reserved.

Rheology and frictional instability of lawsonite in high pressure deformation experiments

*Rei Shiraishi[1], Jun Muto[1], Akihiro Tsunoda[2], Sando Sawa[1], Akio Suzuki[1]

1. Department of Earth Science, Graduate School of Science, Tohoku University, 2. Earthquake Research Institute, University of Tokyo

The cause of intermediate-depth earthquakes (50-300 km) in subducting slabs have been proposed to be the dehydration embrittlement (e.g., Raleigh and Paterson, 1965), because there are many kinds of hydrous minerals in a subducting slab and hypocenter distribution coincides with the dehydration boundary determined by high pressure experiments (e.g., Hacker et al., 2003). Many experimental studies on antigorite have been conducted, but a few previous works about dehydration embrittlement of lawsonite-bearing rocks experimentally. Lawsonite, $CaAl_2Si_2O_7(OH)_2H_2O$, is a hydrous mineral which contains 11 wt% water in its structure as both water molecules and a hydroxy group (Cmodi and Zanazzi, 1996). Lawsonite is one of the candidate for dehydration embrittlement in cold subducting slabs, however previous works have apparently contradictory results. Okazaki and Hirth (2016) showed that lawsonite dehydration induced unstable fault slip based on deformation experiments of pure lawsonite using Griggs-type deformation apparatus at 1 GPa. On the other hand, Incel et al. (2017) also investigated deformation properties of lawsonite and glaucophane mixture at 1.5 to 3.0 GPa using deformation-DIA apparatus. They insisted that there is no evidence for a straightforward relation to the dehydration of lawsonite and the brittle failure of samples. So, we have conducted the deformation experiments of lawsonite under the cold slab conditions in order to clarify the deformation property of lawsonite and understand the relationship between dehydration and brittle failure.

Experiments were carried out using Deformation-Cubic Anvil Press (D-CAP) installed at KEK PF AR-NE7A beamline. Pure lawsonite powder (98%) was used as starting materials. Deformation experiments were carried out at a pressure of 6 GPa and temperatures of 300 - 800 ˚C. The temperature was increased at the same time as deformation started. The temperature ramping rate over the strain rate was set the ranges for the real subducting slab, which ranges from 10^2 to 10^4 ˚C (Chernak and Hirth, 2011; Okazaki and Hirth, 2016). During deformation stages, strain, stress and transformation rate were measured for in-situ using a monochromatic X-ray beam with an energy of 60 keV.

Four experiments showed rapid stress drop during temperature ramping before lawsonite dehydration starts. We observed microstructure of recovered samples, there are many through going faults and microcracks but no dehydration products. Our results indicate that brittle process and frictional sliding occur without dehydration of lawsonite. This suggests that the intermediate-depth earthquakes can be caused by the deformation itself of lawsonite without the dehydration of lawsonite.

Keywords: intermediate-depth earthquakes, dehydration embrittlement, Lawsonite

©2019. Japan Geoscience Union. All Right Reserved.

Grain Size Dependency of Olivine-Spinel Phase Transformational Mechanism Responsible for Deep-focus Earthquakes

*Sando Sawa[1], Jun Muto[1], Nobuyoshi Miyajima[2], Hiroyuki Nagahama[1]

1. Department of Earth Science, Tohoku University, 2. Bayerisches Geoinstitut, University of Bayreuth

Deep-focus earthquakes occur at the depth from 440 km to 660 km in the subducting slab. The mechanism responsible for the earthquakes is thought to be different from that of shallow earthquakes, so that previous studies have reported the various mechanisms. By the geophysical observations and deformation experiments, the phase transformational faulting mechanism is presumed as the precursor of deep-focus earthquakes (e.g., Zhan et al., 2014). The phase transformational faulting mechanism is that metastable olivine in the slab undergoes the phase transformation to fine-grained spinel and faulting occurs with strain localization into the fine-grained spinel. This shear instability depends on grain size. Furthermore, the grain size may restrict the pressure- and temperature-conditions where the shear instability occurs, that is, the region of slab where deep-focus earthquakes occur. However, previous studies have conducted deformation experiments with finer grain size than expected in the slab (e.g., Burnley et al., 1991). Hence, the results from the laboratory experiments cannot directly apply to the geophysical observation. In this study, to reveal the grain size dependency on the phase transformational faulting, we conducted the deformation experiments of germanate olivine (about 3 μm), which is an analogue material of silicate olivine, finer-grained than that in previous studies (30 μm). We used a Griggs-type solid-confining media deformation apparatus. The confining pressure, temperature and strain rate are 1.2 GPa, 400~900 ℃ and 2.0×10^{-4} s^{-1}, respectively. Even though deformation experiments were conducted under wider temperature conditions than previous studies, we did not observe any shear instability event with apparent stress drops. Also, Raman spectroscopy clarified that the germanate olivine underwent the transformation to spinel at temperatures higher than 500 ℃. Shear instability does not occur because the difference in grain sizes between olivine and nucleated spinel in this study was smaller than those in previous studies. Also, the transformation temperature in this study was much lower than those in previous study (T > 1000 ℃ in Burnley et al., 1991). Considering the rate equation of the transformation (Chan, 1956), small grain size promotes the transformation, but these fast rates of the transformation cannot be explained only by the effect of the grain size. Therefore, the presence of water such as absorbed water in a starting material can also contribute to promote the transformation. Hence, both small initial grain size and a little amount of water promote the transformation even at lower temperature. These results indicate that the phase transformational faulting mechanism has strong grain size dependency. In summary, the pressure- and temperature-conditions where the faulting occurs depends on the grain size of olivine and amount of water. Because the grain size in the slab is larger than that in the experiments, by extrapolating from these results, we may restrict the region of slab where deep-focus earthquakes occur.

This work was supported by the JSPS Japanese-German Graduate Externship.

[Reference]
Burnley et al. (1991), JGR, vol 96, 425-443.
Chan (1956), Acta Metallurgica, vol 4, 449-459.
Zhan et al. (2014), EPSL, vol 385, 89-96.

©2019. Japan Geoscience Union. All Right Reserved.

Keywords: Deep-focus earthquakes, Griggs type piston-cylinder apparatus, phase transformation

©2019. Japan Geoscience Union. All Right Reserved.

Seismicity and mineral destabilizations in the subducting mantle up to 6 GPa, 200 km depth

*Thomas P. Ferrand[1]

1. Earthquake Research Institute

In the subducting oceanic lithosphere, a significant part of the seismicity is triggered in the mantle, especially along the upper and lower Wadati-Benioff planes. Several studies have investigated the potential involvement of dehydration reactions in the triggering mechanism of mantle earthquakes. Recent experimental results reveal that, under subduction conditions, mechanical instabilities nucleate in strong stable mineral aggregates during the destabilization of minor amounts of antigorite, i.e. the high-temperature serpentine, through a stress transfer, without any fluid overpressure. Here I confront these laboratory results to seismological observations. On one hand, most of the natural hydrous magnesium silicates seem to be known, with experimentally-deduced stability limits up to 7 GPa, at least, available as relatively accurate estimates. On the other hand, recent achievements in thermal structure of subduction zones combined with precise hypocentre relocation give access to pressure and temperature conditions at earthquakes hypocentres. A series of P-T diagrams summarizes the stability limit of minerals that may be part of natural peridotite with variable compositions at pressures from 0.5 to 6 GPa and temperatures from 200 to 950˚C, and compares it with seismicity. Both hydrous and anhydrous phases are considered. A myriad of minor metamorphic reactions could participate in a transformation-driven stress transfer, even if the stability limits of serpentine minerals seem to correlate with most of the observed seismicity.

Keywords: earthquakes, intraslab, DDST, dehydration, transformation, subduction

©2019. Japan Geoscience Union. All Right Reserved.

Receiver function imaging of subducting Pacific plate and mantle wedge under Japanese islands using denser network of stations

*HyeJeong Kim[1], Hitoshi Kawakatsu[1], Takeshi Akuhara[1], Masanao Shinohara[1]

1. Earthquake Research Institute, The University of Tokyo

Receiver function imaging has been frequently used by different groups focusing on different depths of the Japanese subduction zone. The overlying crust (Shiomi and Park, 2008, Bianchi et al, 2015), the Pacific plate before (Kawakatsu et al., 2009) and after subduction (Kawakatsu and Watada, 2007; Wirth and Long, 2012), and the mantle transition zones (Kawakatsu and Yoshioka, 2011; Tauzin et al., 2018) were discussed using the NIED array stations (Hi-net and F-net). Recently, deployment of ocean bottom seismometers (OBSs) enabled studies of subduction zones closer to the trench (e.g., Akuhara and Mochizuki, 2015). Kawakatsu and Kim (2018, SSJ) have obtained a new version of receiver function imaging using 14-year long of Hi-net data. However, there are other land stations (e.g., J-array) that can improve the station coverage. Here, we collect data from available on-land stations deployed in north-eastern Japan to obtain a denser 2-D array of stations. Additionally, data from temporary OBS stations (Shinohara et al. 2012) are gathered to image the subducted Pacific plate in shallower depths than previously available. Continuous imaging from ocean to land will help to constrain transition of the hydrated oceanic crust along subduction that is expressed as a low velocity layer for better understanding of the hydration/dehydration processes during subduction, which might be related to the occurrence of subduction zone earthquakes.

Keywords: subduction zone, receiver function, ccp stacking

©2019. Japan Geoscience Union. All Right Reserved.

Strong S-wave attenuation in the mantle wedge beneath the NE Japan and interpretations of high-frequency wave propagation path of intraslab earthquakes

*Takahiro Shiina[1,2], Kei Katsumata[2], Kiyoshi Yomogida[3], Aitaro Kato[1]

1. Earthquake Research Institute, The University of Tokyo, 2. Institute of Seismology and Volcanology, Graduate School of Science, Hokkaido University, 3. Graduate School of Science, Hokkaido University

For intraslab earthquakes at intermediate-depths in NE Japan, especially at greater than about 100-km depths, it has been often recorded that high-frequency waveform higher than 8 Hz show a remarkable delay of arrival compared with S wave which predominates in a low-frequency band. The magnitude of the delay is little in the forearc region, whereas it increases up to about 40 s in the backarc region. In this study, we investigate the details in the propagation processes of the high-frequency later phase observed for the intraslab earthquakes at the intermediate-depths. To constrain the source location of the high-frequency later phase, we employ the source-scanning algorithm (SSA) [Kao and Shan, 2004] with realistic velocity and attenuation structures, assuming that the high-frequency later phase is generated by the single scattering process. Namely, we estimate a scattering point by using mean-square amplitudes which is synthesized from two horizontal components of the observed waveforms.
Results in frequency bands of 4-32 Hz show that scattering points are distributed beneath the forearc region. The scattering points can reproduce the observed delays of amplitude amplifications associating with the high-frequency later phases. Moreover, similar locations of the scattering points are imaged along the forearc region in the entire NE Japan. These results indicate that high-frequency later phase is a wave scattered at the forearc region and that short wave-length heterogeneity generally developed in the forearc region of NE Japan.
This interpretation well matches implications from previous studies [e.g., Yomogida et al., 2004; Hasemi and Horiuchi, 2010]. Additionally, the obtained distributions of scattering points which appear to surround the highly attenuating mantle wedge suggest that attenuation structure strongly controls propagation paths of seismic wave, in particular, a high-frequency wave. In other words, the identifications of high-frequency later phase may become easy because the amplitude of direct wave crossing the high-attenuation zone decreases. To confirm this consideration, we estimate *Qs* along the direct wave by using the coda-normalization method [e.g., Aki, 1980]. This estimation provides 2-3 times smaller path-averaged *Qs* in seismic records of which rays lay on the backarc and the volcanic front than that of which rays lay on the forearc region. These results support that spatial variation in *QS* produces heterogenous propagations of seismic waves emitted from intraslab earthquakes. It is thus required to take scattering and attenuation structures simultaneously into account to understand complex behaviors of high-frequency waves in a future study.

Keywords: S-wave attenuation, Intraslab earthquakes, High-frequency later phase, Scattered wave

©2019. Japan Geoscience Union. All Right Reserved.

[E] Poster | S (Solid Earth Sciences)：S-CG Complex & General

Thu. May 30, 2019 10:45 AM - 12:15 PM JST | Thu. May 30, 2019 1:45 AM - 3:15 AM UTC | Poster Hall International Exhibition Hall8, Makuhari Messe_6

[S-CG51] Role of volatiles on Earth and planetary dynamics

convener:Takayuki Ishii(Bavarian Research Institute, University of Bayreuth), Eiji Ohtani(Department of Earth and Planetary Materials Science, Graduate School of Science, Tohoku University), Michihiko Nakamura(Division of Earth and Planetary Materials Science, Department of Earth Science, Graduate School of Science, Tohoku University), Bjorn Mysen(Geophysical Laboratory, Carnegie Inst. Washington)

This session addresses how volatile species affect dynamics of the
Earth and planets from natural observations, laboratory experiments, and
numerical modeling in the temperature, pressure, and oxygen activity
range from the early stage of the planet formation to the present. The
volatiles can be critical in zones of magma storage and ascent, mantle
upwelling and melting in the fluid-enriched subduction zones, in the
mantle transition zone, in the lower mantle, in the core-mantle boundary,
and in Earth and planetary cores. However, volatiles affect properties
and processes differently depending on their pressure, temperature, and
redox conditions, which vary in time and space.
 This session aims to address how volatiles control the dynamic
processes of the Earth and planets, governed by their geophysical and
geochemical properties. We welcome papers dealing with geological and
laboratory observations coupled with numerical modeling on the role of
volatiles. The topics include (1) Stability relations, chemical and
physical properties of crystalline, molten and fluid phases,
partitioning of volatiles among these phases, (2) Rheological and other
physical properties of minerals, and the effects of intergranular fluid
on the properties, (3) Volatiles and dehydration induced seismicity and
volcanism in various tectonic regions including subduction zones, and (4)
Effects of volatiles in numerical simulation of geo-tectonics, and (5)
Magma outgassing and its control of volcanic eruption dynamics.

[SCG51-P01] Permeability prediction of porous media with the finite difference Stokes solver LaMEM

*Philipp Eichheimer[1], Wakana Fujita[2], Marcel Thielmann[1], Anton Popov[3], Gregor Golabek[1], Boris Kaus[3], Maximilian Kottwitz[3] (1.Bayerisches Geoinstitut, University of Bayreuth, 2.Department of Earth Science, Tohoku University, Sendai, 3.Institute of Geosciences, Johannes Gutenberg University Mainz)

[SCG51-P02] Grain growth-induced fluid localization and permeability reduction

*Wakana Fujita[1], Michihiko Nakamura[1], Kentaro Uesugi[2] (1.Graduate School of Science, Tohoku University, 2.JASRI/SPring-8)

[SCG51-P03] Pargasite stability in the upper mantle at H_2O-undersaturated conditions

*Marija Putak Juricek[1], Hans Keppler[1] (1.BGI)

[SCG51-P04] **Constraining the water content at the top of the mantle transition zone with the elasticity of wadsleyite and olivine**

*Zhongqing Wu[1] (1.University of Science and Technology of China)

[SCG51-P05] ***Single crystal elasticity of Fe-bearing phase E by Brillouin spectroscopy***

*Niccolo Satta[1], Hauke Marquardt [2], Alexander Kurnosov[1], Tiziana Boffa Ballaran [1], Johannes Buchen[3], Catherine McCammon[1], Takaaki Kawazoe[4] (1.Bayerisches Geoinstitut, University of Bayreuth, 95440 Bayreuth, Germany, 2.Department of Earth Sciences, University of Oxford, South Parks Road, Oxford, UK., 3.Seismological Laboratory, California Institute of Technology, Pasadena, CA 91125, USA., 4.Department of Earth and Planetary Systems Science, Hiroshima University, Hiroshima 739-8526, Japan.)

[SCG51-P06] Discovery of two hexagonal phases in (Fe,Al)OOH under the P-T conditions of the deep lower mantle

*Lu Liu[1,2], Li Zhang[1], Hongsheng Yuan[1] (1.Center for High Pressure Science and Technology Advanced Research, 2.University of Science and Technology of China)

[SCG51-P07] **Effect of grid resolution on tectonic regimes in global-scale convection models**

*Enrico Marzotto[1], Marcel Thielmann[1], Gregor Golabek[1] (1.Bayerisches Geoinstitut)

[SCG51-P08] A 3-D crust and uppermost mantle electrical conductivity model of subduction zone beneath NE Japan

*Masahiro Ichiki[1,2], Toshiki Kaida[1], Yasuo Ogawa[3] (1.Graduate School of Science, Tohoku University, 2.International Research Institute of Disaster Science, 3.School of Science, Tokyo Institute of Technology)

[SCG51-P09] *The conditions of sublithospheric diamond formation constrained from ferric iron-rich exsolution from ferropericlase inclusions.*

*Caterina Melai[1], Daniel Frost[1], Tiziana Boffa Ballaran[1], Catherine McCammon[1] (1.Bayerisches Geoinstitute)

[SCG51-P10] **Probing the variation of the oxygen fugacity in diamond anvil cells using the Fe-Ir alloy as redox sensor**

*Serena Dominijanni[1], Catherine McCammon[1], Leonid Dubrovinsky[1], Dan Frost[1], Nobuyoshi Miyajima[1] (1.Bayerisches Geoinstitut)

[SCG51-P11] Goethite behavior at Earth's lower mantle conditions

*Egor Gennadievich Koemets[1], Maxim Bykov[1], George Aprilis[2], Timofey Fedotenko[2], Stella Chariton[1], Saiana Khandarkhaeva[1], Iuliia Koemets[1], Marcel Thielmann[1], Natalia Dubrovinsaia[2], Leonid Dubrovinsky[1] (1.BGI (Bayerisches Geoinstitut), Universität Bayreuth, Germany, 2.Material Physics and Technology at Extreme Conditions, Laboratory of Crystallography, Universität Bayreuth, Germany)

[SCG51-P12] The oxygen content of sulphides in the mantle and a geothermometer for diamond formation

*Sumith Abeykoon[1], Dan Frost[1], Vera Laurenz[1] (1.Bayerisches Geoinstitut, University of Bayreuth)

Permeability prediction of porous media with the finite difference Stokes solver LaMEM

*Philipp Eichheimer[1], Wakana Fujita[2], Marcel Thielmann[1], Anton Popov[3], Gregor Golabek[1], Boris Kaus[3], Maximilian Kottwitz[3]

1. Bayerisches Geoinstitut, University of Bayreuth, 2. Department of Earth Science, Tohoku University, Sendai, 3. Institute of Geosciences, Johannes Gutenberg University Mainz

The flow of fluids through porous media such as groundwater flow or magma migration is one of the most important processes in geological sciences. The property controlling the efficiency of the flow is the permeability of the rock, thus an accurate determination and prediction of its value is of crucial importance. For this reason, permeability of rocks has been measured across different scales. As laboratory measurements exhibit a range of limitations, the numerical prediction of permeability at conditions where laboratory experiments struggle has become an important method to complement laboratory approaches. At high resolutions, this prediction becomes computationally very expensive, which makes it crucial to develop methods that maximize accuracy. In this work we introduce the open-source finite difference solver LaMEM that can be used to numerically predict the permeability of porous media under laminar conditions. We employ a stencil rescaling method to increase accuracy due to a better description of the solid-fluid interface, thus reducing the computational cost. To validate the method, we perform a series of tests employing both analytical solutions for simplified geometries as well as results from other numerical approaches for more complicated geometries. Furthermore we compare our numerical results to laboratory measurements on glass bead samples with porosities ranging from 20% to 2.5%, showing good agreement.

Keywords: Permeability, Numerical modelling, Digital Rock Physics

©2019. Japan Geoscience Union. All Right Reserved.

Grain growth-induced fluid localization and permeability reduction

*Wakana Fujita[1], Michihiko Nakamura[1], Kentaro Uesugi[2]

1. Graduate School of Science, Tohoku University, 2. JASRI/SPring-8

Efficiency of segregation of geological fluids such as aqueous fluids and melts is an essential elementary process for volatile cycles in subduction zones. Permeability is an intrinsic rock property that controls flow rate of fluid. Various permeability models have been presented by numerical models of textually equilibrated rocks (e.g. 1, 2), laboratory measurements on synthetic rocks (e.g. 3) and estimation from cross-sectional area of synthetic rocks (4). However, there exist discrepancies among those models. Because permeability is very sensitive to microscopic geometry of pore fluid, those disagreements may arise from lack of understanding toward three-dimensional (3D) microstructure of fluid network.

Dihedral angle has been considered to be a critical parameter that controls fluid geometry and thus permeability. Beside, some previous studies shed light on the effect of grain growth on fluid distribution because it could induce pore fluid distortion and coalescence (5, 6). These studies suggest that in the actual systems where the microstructure of rocks evolve in dynamic processes, grain growth would be important along with the dihedral angle.

To investigate the effect of grain growth on the fluid distribution and permeability, we present 3D images of quartz–CHO fluid aggregates, containing nominal fluid fractions between 0.03 and 0.10. Samples were synthesized from a powdered mixture of Arkansus quartz and amorphous silica prepared by sol-gel method and hot-pressed in a piston–cylinder apparatus at 900˚C and 1.0 GPa for 192h. The fluid fractions and the dihedral angles were controlled using brucite added in the capsule bottom and oxalic acid dihydrate mixed with SiO_2 powder. 3D images were obtained using synchrotron X-ray microtomography at BL20XU experimental hutch2 of SPring-8. Regardless of dihedral angles (CO_2 content in fluids), both cross-sectional area and 3D images of samples showed grain-scale fluid localization which would be formed by pore fluid coalescence induced by grain growth. Computed permeabilities using numerical model, LaMEM (7) were almost consistent with laboratory measurements by (3) but more than one order of magnitude lower than a numerical model by (2). This would indicate that localized fluids extensively reduce permeability by reducing the diameter of fluid tubes along grain edges, which would suggest transport of water into Earth’ s deep interior by the subducting slab.

Reference:
1. von Bargen and Waff. 1986, J. Geophys. Res. 91, 9261–9276.
2. Rudge, J.F. 2018, Proc. R. Soc. Lond. A 474, 20170639.
3. Wark and Watson. 1998, Earth Planet. Sci. Lett. 164, 591–605.
4. Faul, U.H. 1997, J. Geophys. Res. 102, 10299–10311.
5. Walte et al. 2003, Geology 2003 31, 1009-1012.
6. Yoshino and Watson. 2005, Earth Planet. Sci. Lett. 235, 453–468.
7. Kaus et al. 2016, NIC Symposium 2016

Keywords: Permeability, Quartz, Grain growth, Dihedral angle, Fluid segregation

©2019. Japan Geoscience Union. All Right Reserved.

Pargasite stability in the upper mantle at H_2O-undersaturated conditions

*Marija Putak Juricek[1], Hans Keppler[1]

1. BGI

Amphibole is the most commonly occurring hydrous mineral in mantle xenoliths and the majority of upper mantle amphiboles have compositions close to pargasite end member. Previous experimental work has demonstrated that pargasite stability is sensitive to variations in bulk alkali and water content of the starting material. While it has been successfully shown that addition of more alkali leads to stabilization of pargasite to higher P and T, the effect of water on amphibole stability is not so straightforward.

At H_2O-saturated conditions, alkali elements partition strongly into aqueous fluid and become less available for crystallization of amphibole. As a result, amphibole seemingly becomes stable at higher P and T when less H_2O is added to the starting material. This observation led to the hypothesis that pargasite may be a ubiquitous phase in the upper mantle, which is believed to contain only several hundred ppm of H_2O. However, most of the previous studies determined pargasite stability at H_2 O-saturated conditions where solid phases coexist with an aqueous fluid during experiments. Since such environments are not representative of the nearly dry upper mantle, the purpose of this study is to investigate pargasite stability at H_2O-undersaturated conditions.

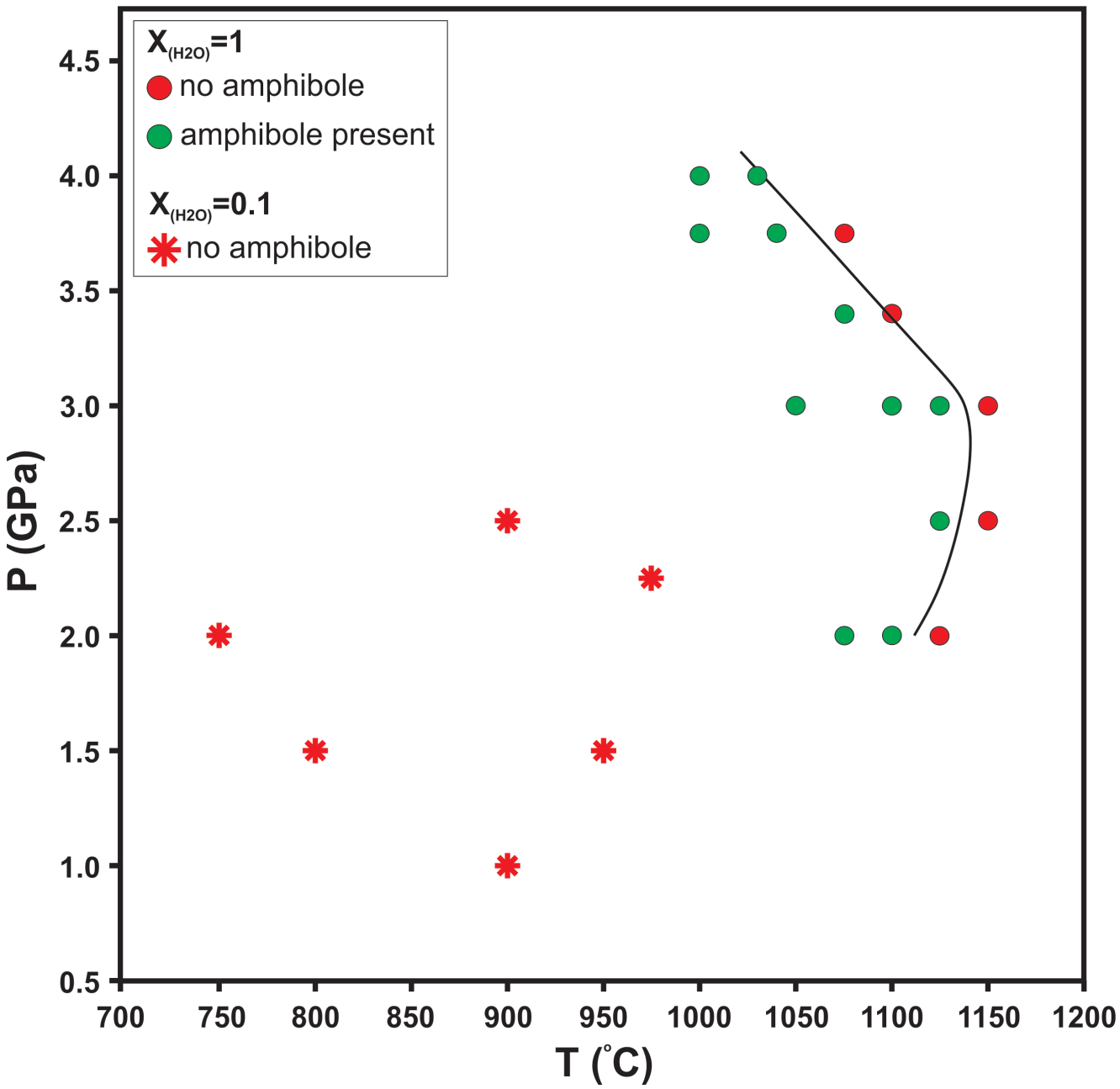
Because of the high specific surface area of powders, adsorption of atmospheric H_2O on fine grained starting materials prevents attaining H_2O-undersaturation by adding small amounts of water to the sample. Instead, H_2O-undersaturated conditions may be precisely controlled by diluting the water in the sample with another component. Under such conditions, solid phases are expected to coexist with a low water activity fluid throughout the experiment. As molecular nitrogen is mostly insoluble in upper mantle minerals, it can be used to adjust the water activity of the fluid to a desired low value.

All experiments were performed in a piston cylinder apparatus. The samples for H_2O-undersaturated experiments were prepared by adding silver azide (AgN_3) and brucite to a synthetic peridotite mixture. In several experiments water was added directly as $H_2O_{(l)}$. The amount of water was kept constant in all experiments (1 wt. percent) and the molar fraction of water in the N_2-H_2O fluid was adjusted to the desired value by weighing an appropriate amount of AgN_3, which decomposed to metallic silver and molecular nitrogen during heating. In H_2O-saturated experiments, no silver azide was added to the peridotite mixture. Experimental products were analyzed using JEOL JXA-8200 electron microprobe.

Preliminary results show that pargasite is not stable in equilibrium with fluids diluted to X_{H2O}=0.1 at pressures above 1 GPa. At H_2O-saturated conditions pargasite stability field can extend to pressures of 4 GPa and above 1100 ℃, depending on bulk alkali and water contents. Results from experiments at X_{H2O} =0.1 and X_{H2O}=1 suggest that pargasite can exist only in regions of the upper mantle which have been affected by high water activity fluids, such as areas in the vicinity of subduction zones. The ambient nominally anhydrous upper mantle, better represented by experiments at H_2O-undersaturated conditions, is not expected to contain pargasite.

Keywords: pargasite, stability, upper, mantle

©2019. Japan Geoscience Union. All Right Reserved.



©2019. Japan Geoscience Union. All Right Reserved.

Constraining the water content at the top of the mantle transition zone with the elasticity of wadsleyite and olivine

*Zhongqing Wu[1]

1. University of Science and Technology of China

Zhongqing Wu[a,b,*], Wenzhong Wang[a,b], Michael J. Walter[c] ,Ye Peng[a,b], Simon Redfern[d],

[a] Laboratory of Seismology and Physics of Earth’ s Interior, School of Earth and Space Sciences, University of Science and Technology of China, Hefei, Anhui 230026, China

[b] Mengcheng National Geophysical Observatory, Anhui, China

[c]School of Earth Sciences, University of Bristol, Bristol BS8 1RJ, UK

[d]Department of Earth Science, University of Cambridge, Cambridge CB2 3EQ, UK

The water content in the mantle transition zone (MTZ) exerts a controlling influence on the dynamical and chemical evolution of Earth, but is poorly known. In principle the water content at the top of the transition zone can be inferred by comparing the velocity and density contrasts across the 410-km seismic discontinuity with predictions based on the phase transition of olivine to wadsleyite. The high-quality elastic data of at pressure and temperature (PT) conditions of the transition zone are crucial but are very challenge for experiments to obtain. Calculating these elastic data at high PT conditions in conventional method are also very expensive. Instead, these elastic data were calculated using the method of Wu and Wentzcovitch (2011), which reduces the computational workload to tenth of the conventional method. All calculations for two phases were conducted using the same computational details as far as possible, which guarantees that the velocity and density differences between two phases have very high precise. All these calculated elastic data agree well with the available experimental data. The iron and water effect on the elasticity are also well described.

With these high-quality elastic data covered the PT condition of the transition zone, we analyze the water and wadsleyite content at the top of the transition zone. We found that the water content of wadsleyite at the top of the transition zone can be well constrained when density and velocities jumps are considered together. For a pyrolitic mantle composition with ~60% olivine, our best fit is ~ 0.5 wt% water at the top of the transition zone. If the transition zone is dry, as suggested by some electrical conductivity models, the upper mantle may only contain ~ 50% olivine.

Wu, Z., Wentzcovitch, R.M., 2011. Quasiharmonic thermal elasticity of crystals: An analytical approach. Phys. Rev. B - Condens. Matter Mater. Phys. 83, 1–8. doi:10.1103/PhysRevB.83.184115

©2019. Japan Geoscience Union. All Right Reserved.

Single crystal elasticity of Fe-bearing phase E by Brillouin spectroscopy

*Niccolo Satta[1], Hauke Marquardt [2], Alexander Kurnosov[1], Tiziana Boffa Ballaran [1], Johannes Buchen[3], Catherine McCammon[1], Takaaki Kawazoe[4]

1. Bayerisches Geoinstitut, University of Bayreuth, 95440 Bayreuth, Germany, 2. Department of Earth Sciences, University of Oxford, South Parks Road, Oxford, UK., 3. Seismological Laboratory, California Institute of Technology, Pasadena, CA 91125, USA., 4. Department of Earth and Planetary Systems Science, Hiroshima University, Hiroshima 739-8526, Japan.

Earth’s deep water cycle plays a key role for the dynamic evolution of our planet and the development of habitable conditions. Surface water can be transported to Earth’s mantle by subduction of oceanic lithosphere. Experimental investigations have shown that water can be efficiently stored in Dense Hydrous Magnesium Silicates (DHMS) in cold subducting slabs. However, quantification of the incoming water budget based on the interpretation of seismological observations is hampered by a lack of elasticity measurements of DHMSs. Here, we report single-crystal elasticity measurements of Fe-bearing phase E, a DHMS that is stable at pressures and temperature of Earth’s mantle transition zone. A very low bulk modulus has been reported for phase E, suggesting that it might produce seismic velocity heterogeneities detectable by seismological investigations. However, the shear modulus of phase E has not been quantified.

We synthesized Fe-bearing phase E single crystals in a multi-anvil apparatus. Chemical composition as well as crystal structure have been determined using electron microprobe analysis, Mössbauer spectroscopy, and single-crystal X-ray diffraction. We derived the full elastic stiffness tensor by Brillouin spectroscopy on two single crystals of selected orientations. We found phase E to have both the lowest bulk modulus and shear modulus among the DHMSs at ambient conditions. Phase E shows very low compressional and shear velocities especially when compared to the other principal minerals likely present in subducting slabs after serpentine breakdown. Modelling of seismic velocities in dry and hydrated upper mantle and transition zone rocks suggests that the presence of even small amounts of phase E can appreciably lower seismic wave velocities. Phase E could be used as seismological indicator for water stored at depth in subducting scenarios. The elasticity of phase E under mantle conditions will be explored in future research.

Keywords: Brillouin scattering, Phase E, Seismic wave velocities

©2019. Japan Geoscience Union. All Right Reserved.

Discovery of two hexagonal phases in (Fe,Al)OOH under the P-T conditions of the deep lower mantle

*Lu Liu[1,2], Li Zhang[1], Hongsheng Yuan[1]

1. Center for High Pressure Science and Technology Advanced Research, 2. University of Science and Technology of China

Deep water can cause a series of complex seismological phenomena by changing the density and thermal stability of lower mantle components. δ-H solid solution phase (AlOOH-$MgSiO_2(OH)$) is stable at lower mantle conditions[1],because the crystallographic frameworks of the phase H is similar to that of the δ-AlOOH phase, with very strong hydrogen bonds[2,3]. δ-AlOOH and ε-FeOOH can also form solid solution[4] (δ - ε solution). It is reasonable to infer that δ - ε solid solution may have similar thermal stability as that of H-δ solution, considering their similar crystal structure[5]. In our experiments, we synthesized the δ - ε solution at 79GPa and 1600K in a laser-heated diamond anvil cell. As the temperature increases to 2100k, the orthorhombic δ - ε solution transformed into a hexagonal-structured phase. By combining powder X-ray diffraction techniques with multigrain indexation[6], we determined its hexagonal lattice with a=b=10.019Å and c=2.614Å. At 79GPa and 2400K, the hexagonal phase transforms into another hexagonal phase, with the lattice parameters of a=b=2.733Å and c=9.343Å. The discovery of these two new phases may provide new insights into the deep-water storage.

References

1.Ohira I, Ohtani E, Sakai T, et al. Stability of a hydrous δ-phase, AlOOH-$MgSiO_2(OH)_2$, and a mechanism for water transport into the base of lower mantle[J].Earth and Planetary Science Letters, 2014, 401: 12-17.
2.Ohtani, E., Amaike, Y., Kamada, S., Sakamaki, T. and Hirao, N. Stability of hydrous phase H $MgSiO_4H_2$ under lower mantle conditions. Geophys. Res. Lett. 41, -8287 (2014).
3.Nishi M,Kuwayama Y,Tsuchiya J,et al.The pyrite-type high-pressure form of FeOOH[J]. Nature,2017,54(7662):205-208.
4.T Kawazoe,I Ohira,T Ishii et al. Single crystal synthesis of δ-(Al,Fe)OOH American Mineralogist. Volume 102, pages 1953–1956, (2017)
5.Gleason A E,Quiroga C E,Suzuki A,et al.Symmetrization driven spin transition in ε-FeOOH at high pressure[J]. Earth and Planetary Science Letters, 2013, 379: 49-55.
6.Zhang L,Yuan H,Meng Y,et al.Discovery of a hexagonal ultradense hydrous phase in (Fe, Al) OOH[J]. Proceedings of the National Academy of Sciences,2018,115(12):2908-2911.

Keywords: High temperature and high pressure experiment, hydrous phase, diamond anvil cell

©2019. Japan Geoscience Union. All Right Reserved.

Effect of grid resolution on tectonic regimes in global-scale convection models

*Enrico Marzotto[1], Marcel Thielmann[1], Gregor Golabek[1]

1. Bayerisches Geoinstitut

Global-scale convection models using a visco-plastic rheology coupled with a temperature-dependent viscosity usually show different tectonic regimes: mobile, episodic or stagnant lid.

In the mobilelidregime, the lid is continuously subducting into the mantle (plate-like behavior). The episodic lid regime is characterized by the stability of the lid until sufficiently large lithospheric stresses break it, causing rapid resurfacing. Finally the stagnant lid regime is defined by an undeformable lid that does not participate in convection

In numerical simulations these three types of regimes can be obtained by varying some target parameters such as: temperature-dependency of viscosity and yield stress.

The yield stress in particular is a key parameter because it sets the stress necessary to cause plastic yielding, hence, in a visco-plastic rheology, the stress necessary to break the cold surface regions. A high yield stress will result in a stagnant lid. On the other hand, a low yield stress causes a weak lid that is constantly broken and sinks into the mantle.Despite the key importance of physical parameters, also numerical parameters have an effect on the tectonic regime, determining different outcomes justby changing the grid resolution.

Here we use the code StagYY (*Tackley, 2008*) in a 2D spherical annulus geometry (*Hernlund & Tackley, 2008*) to determine the resolution-dependent tectonic regime for different yield stresses in global-scale convection models. To assess the effect of grid resolution on lid behavior we use 16 different resolutions keeping all physical parameters unchanged. To make sure that steady state has been reached each simulation is run for 15 Gyrs. Tested resolutions vary from 128x32 to 1024x256 grid points. To understand this influence on the tectonic regime we study the resolution within the lid requiring an appropriate lid definition, based on the thermal and velocity field. Our results show that there is a correspondence between low radial resolution and mobile lid regime and that low aspect ratio cells (azimuthal to radial grid spacing) favor a plate-like behavior of the lid, while for large aspect ratios the mobile lid regime is persistent.

This work is the first part of a larger project, aiming to studyslab stagnation and hydration of the mantle transition zone (MTZ) using self-consistent global-scale mantle convection models, where subducting slabs carry water from the surface into the Earth’ s interior and potentially hydrate the MTZ. We expect that our previous work packages will help us to obtain realistic slab ponding in the MTZ, so we can study the hydration state of this region over time.

References:

Tackley, P. J. (2008). Modelling compressible mantle convection with large viscosity contrasts in a

©2019. Japan Geoscience Union. All Right Reserved.

three-dimensional spherical shell using the yin-yang grid. *Phys. Earth Planet. Int.* 171, 7-18.

Hernlund, J. W. and P. J. Tackley (2008). Modeling mantle convection in the spherical annulus. *Phys. Earth Planet. Int.* 171, 48-54

Keywords: Geodynamical Modelling, StagYY, Grid Resolution

©2019. Japan Geoscience Union. All Right Reserved.

A 3-D crust and uppermost mantle electrical conductivity model of subduction zone beneath NE Japan

*Masahiro Ichiki[1,2], Toshiki Kaida[1], Yasuo Ogawa[3]

1. Graduate School of Science, Tohoku University, 2. International Research Institute of Disaster Science, 3. School of Science, Tokyo Institute of Technology

The crustal fluids beneath NE Japan is originated from dehydration of subducting Pacific slab or from convection in the backarc mantle, as is shown by seismic tomography [e.g. Zhao, 2017]. We investigated the fluid transportation paths from upper mantle to crust of subduction zone using electrical conductivity exploration.

We expanded electromagnetic field observation sites (96 sites) to northern part of NE Japan and obtained magnetotelluric responses and geomagnetic transfer functions in the period range of 20 –30720 seconds (22 periods) by BIRRP code [Chave and Thomson, 2004]. We used WSINV3D [Siripunvaraporn and Egbert, 2009] to invert those responses into three dimensional electrical resistivity model.

The preliminary model gives normalized root mean square misfit 5.87. A prominent conductor appears in the crust to uppermost mantle and the conductor spreads towards backarc direction. In our previous model [Ichiki et al., 2015], we found the overturned shape conductor towards backarc direction in the mantle wedge beneath central part of NE Japan. This study has found it beneath northern part NE Japan as well.

Those imply the crustal fluid and/or melt is transported along the pathway that is the plate boundary beneath the volcanic front to the backarc crust. The fluid transportation can explain the presence of enigmatic backarc volcano in the NE Japan. In this presenation, we speculate and discuss evolution of this pathway in geological time on the basis of the chlonological data of igneous rocks [Yoshida et al., 2013].

Acknouwledgement: This study is financially supported by KAKEN-HI No.26109006.

Keywords: electrical conductivity, resistivity, magnetotelluric, subduction zone

©2019. Japan Geoscience Union. All Right Reserved.

The conditions of sublithospheric diamond formation constrained from ferric iron-rich exsolution from ferropericlase inclusions.

*Caterina Melai[1], Daniel Frost[1], Tiziana Boffa Ballaran[1], Catherine McCammon[1]

1. Bayerisches Geoinstitute

Ferropericlase is apparently one of the more common inclusions to be found in sub-lithospheric diamonds, which are considered to form in the convecting mantle. Although relatively rare, these inclusions have been examined in a number of studies in the hope of providing information on the formation conditions of such deep diamonds, which could potentially be in the transition zone or lower mantle. The wide range of oxide Fe/(Fe+Mg) ratios found has raised the idea that they may form through the oxidation of iron metal. During TEM investigations, however, evidence for the exsolution of Fe_2O_3-rich phases such as magnesioferrite have been found, which implies that a more complex scenario may be involved. Ferropericlase-magnesiowüstite diamond inclusions are most likely some of the deepest available samples from the mantle and they potentially provide the most direct evidence for deep mantle carbon transport processes. The ferric iron contents of such inclusions alone may not provide a direct estimate for the oxygen fugacity at which the inclusions were trapped, particularly if pressure has a strong effect on the fo_2 - Fe^{3+}/Fe_{tot} relationship. However, using experimental data it is possible to determine the oxygen fugacity at which the exsolution observed in the diamond inclusions occurred and coupled with the oxide Fe^{3+}/Fe_{tot} ratio this could be used to estimate the pressure of formation.

The ferropericlase- magnesioferrite system has been investigated by several studies at room pressure but the stability field of the two components has been shown to become more complicated at high pressure due to the formation of mixed valence oxides. We have combined experimental measurements with thermodynamic modelling in order to address two main questions: at which P, T, fO_2 conditions do Fe_2O_3 -rich phases exsolve from ferropericlase? And what is the maximum Fe^{3+}/Fe_{tot} ratio of ferropericlase. To answer these questions, multianvil experiments have been performed between 6 –25 GPa and 1200-1800˚C using a starting composition of $(Mg_{86}Fe_{14})O$ plus 20 % Fe_2O_3. Pt powder was added to the experiments to act as a redox sensor and minor amounts of Ni, Cr, Mn and Na were also added. Samples were then analyzed with the scanning electron microscope, electron microprobe, Mössbauer spectroscopy and X-ray diffraction. In the recovered experiments ferropericlase coexists with magnetite-magnesioferrite solid solution up to 10 GPa and $Mg_2Fe_2O_5$-Fe_4O_5 solid solution at higher pressures. In the calculation of the oxygen fugacity a ferropericlase model in the FeO-$Fe_{2/3}$O-MgO system was employed and exchange of Mg and Fe^{2+} in magnetite was accounted for. Oxygen fugacities at which the phases coexist can be calculated in the magnetite-magnesioferrite field using three different equilibria and a quite simple ferropericlase mixing model results in calculated oxygen fugacities that are within 0.1 log units of each other for all three equilibria. The results show that magnetite-magnesioferrite solid solution should not be in equilibrium with ferropericlase in the diamond stability field. Our results imply that the exsolution of Fe^{3+} rich phases observed in natural samples likely occurred at pressures corresponding to the transition zone or deeper.

©2019. Japan Geoscience Union. All Right Reserved.

Probing the variation of the oxygen fugacity in diamond anvil cells using the Fe-Ir alloy as redox sensor

*Serena Dominijanni[1], Catherine McCammon[1], Leonid Dubrovinsky[1], Dan Frost[1], Nobuyoshi Miyajima[1]

1. Bayerisches Geoinstitut

Understanding the oxygen fugacity (fO_2) in diamond anvil cells (DACs) is an important issue for many reasons, among them reconciling contradictory results that have been obtained for carbonate studies (Cerantola et al., 2017; Dorfman et al., 2018) that might be due to different redox conditions during the experiments. We therefore investigated the fO_2 conditions during DAC experiments using powder X-ray diffraction (beamlines ID15b and ID27) and energy-domain Synchrotron Mössbauer Source (SMS) spectroscopy (beamline ID18) at the European Synchrotron Radiation Facility (Grenoble, France). Double sided laser heating experiments (Aprilis et al., 2017) were carried out at high pressure and temperature using a mixture of synthetic ferropericlase ($Mg_{0.75}Fe_{0.25}$)O and pure iridium powder as a sliding redox sensor (Borisov and Palme, 2000; Swartzendruber, 1984; Taylor et al., 1992). The Fe content in the Fe-Ir alloy, together with the amount of FeO in ferropericlase, allows a calculation of fO_2 during the experiments (Stagno et al., 2011; Woodland and O'Neill, 1997). Preliminary results from powder X-ray diffraction data show that, after heating, an Fe-Ir metal alloy that can be indexed in the Fm-3m space group is formed by the reaction of pure Ir and Fe from ferropericlase according to the reaction:

(Mg,Fe)O + Ir --> (Mg,Fe)O + (Fe,Ir)

The compressibility of the Fe-Ir alloy and ferropericlase was measured up to ~ 60 GPa and SMS data were collected before and after heating. X-ray diffraction results coupled with energy-dispersive X-ray spectroscopy (EDS) measurements and a simple thermodynamic model indicate that the redox conditions during the DAC experiments were close to the iron-wüstite (IW) buffer, although some inhomogeneity was observed. Further chemical analyses and additional experiments are ongoing to understand the variation of oxygen fugacity in a DAC during laser heating.

Keywords: oxygen fugacity , redox sensor, diamond anvil cell

©2019. Japan Geoscience Union. All Right Reserved.

Goethite behavior at Earth's lower mantle conditions

*Egor Gennadievich Koemets[1], Maxim Bykov[1], George Aprilis[2], Timofey Fedotenko[2], Stella Chariton[1], Saiana Khandarkhaeva[1], Iuliia Koemets[1], Marcel Thielmann[1], Natalia Dubrovinsaia[2], Leonid Dubrovinsky[1]

1. BGI (Bayerisches Geoinstitut), Universität Bayreuth, Germany, 2. Material Physics and Technology at Extreme Conditions, Laboratory of Crystallography, Universität Bayreuth, Germany

Water and water-bearing species have a strong impact on numerous processes in Earth’ s interiors. Presence of water affects chemical and physical properties of mantle minerals, changes melting temperatures, sound velocities and viscosity of materials, and causing different global phenomena such as, for example, arc volcanism and plate tectonics. Thereby, the deep Earth’ s regions enriched with water are crucial for understanding our planet’ s geodynamics and geochemistry. Still, mechanisms of water circulation between geospheres remain poorly understood. Recent studies suggest that goethite present in Banded Iron Formations (BIFs) may transfer some quantities of water to the deep Earth interiors with subducting slabs. It was reported that goethite remains stable in the sinking slab until it reaches the base of a lower mantle. By the meaning of in situ powder XRD it was revealed that at pressures corresponding to the depths ~1500-1800 km and moderately high temperatures goethite undergoes a phase transition to form a novel stable pyrite-type phase FeO_2H_x with $0 \leqq x \leqq 1$ (named as Py-phase). Thus, goethite and its HP pyrite-type form became a candidate for water and/or hydrogen transfer and storage to the lower mantle and the core-mantle boundary. Using laser-heating in diamond anvil cells we performed a series of experiments on an investigation of goethite (as a starting material) stability at P-T conditions covering possible range in subducting slabs. By the meaning of sensitive in situ single-crystal XRD in DACs we registered decomposition of goethite and formation of known (such as ι-Fe_2O_3, η-Fe_2O_3, a high-pressure orthorhombic form of Fe_3O_4, Fe_5O_7) and novel iron-oxygen compounds. Results of structure solution and refinement established these compounds to be orthorhombic Fe_7O_{10} and hexagonal non-stoichiometric phase $Fe_{6.31}O_9$. Our results suggest that FeOOH cannot transport water into the deep of Earth’ s mantle.

Keywords: Goethite, Diamond anvil cell, High Pressure, Single-crystal XRD, Subducting slabs

©2019. Japan Geoscience Union. All Right Reserved.

The oxygen content of sulphides in the mantle and a geothermometer for diamond formation

*Sumith Abeykoon[1], Dan Frost[1], Vera Laurenz[1]

1. Bayerisches Geoinstitut, University of Bayreuth

Sulphides are ubiquitous accessory minerals in mantle rocks and form the most prevalent type of inclusion in diamonds. Diamond sulphide inclusions are trapped as sulphide melts that crystallise on cooling to form Fe-Ni monosulphide solid solution (MSS) and ultimately recrystallizes to assemblages containing pyrrhotite, $Fe_{(1-x)}S$ (x = 0 to 0.2), pentlandite, $(Fe,Ni)_9S_8$, and sometimes pyrite (FeS_2). Sulphide inclusions are also found in many xenoliths but those which are hosted by diamonds provide potentially the most pristine samples from the lithospheric mantle and deeper. Previous experiments indicate that oxygen partitions into sulphide melts and although sparse, some measurements of natural sulphide inclusions from mantle xenoliths indeed show measurable and in some cases relatively high oxygen concentrations. If the parameters that control sulphide oxygen concentration can be determined then they could be potentially used to understand conditions in the mantle and in particular in sublithospheric diamonds. The oxygen content of sulphides separating to the core during core formation could have also influenced the oxygen fugacity of the early mantle.
We have measured the oxygen contents of sulphide melts within experimentally produced mantle assemblages at high pressures and temperatures. A series of multi-anvil experiments were conducted to equilibrate a peridotite assemblage with molten sulphide (FeS) at pressures between 3 –11 GPa and temperatures of 1300 ˚C –1700 ˚C. The effects of pressure, temperature, oxygen fugacity and composition have been investigated. Oxygen fugacity was determined in some experiments by saturating the sulphide in Ir to produce a separate Ir-Fe metal alloy, for which the Fe content is a function of oxygen fugacity. The results show that sulphide melt oxygen contents can range up to 16 weight % FeO, at mantle conditions. Moreover, the content of oxygen in the sulphide is found to be not controlled by fO_2 or fS_2, which is in disagreement with previous experimental studies conducted at ambient pressure conditions. The experiments indicate that the oxygen concentration is mainly controlled by the FeO activity in coexisting silicates phases and the temperature, although further work is still required to calibrate effects of Ni and Cu. In order to fit the data and to account for the FeO dependence, we developed a thermodynamic model using an end-member equilibrium between olivine, pyroxene and FeO in the sulphide melt. The resulting relationship can be used as a geothermometer based on sulphide inclusion oxygen contents and could be particularly useful for determining diamond formation temperatures for sub lithospheric diamonds.

Keywords: Sulfide, Oxygen, Geothermometer

©2019. Japan Geoscience Union. All Right Reserved.

[E] Poster | S (Solid Earth Sciences)：S-CG Complex & General

Thu. May 30, 2019 5:15 PM - 6:30 PM JST | Thu. May 30, 2019 8:15 AM - 9:30 AM UTC | Poster Hall International Exhibition Hall8, Makuhari Messe_27

[S-CG51] Role of volatiles on Earth and planetary dynamics

convener:Takayuki Ishii(Bavarian Research Institute, University of Bayreuth), Eiji Ohtani(Department of Earth and Planetary Materials Science, Graduate School of Science, Tohoku University), Michihiko Nakamura(Division of Earth and Planetary Materials Science, Department of Earth Science, Graduate School of Science, Tohoku University), Bjorn Mysen(Geophysical Laboratory, Carnegie Inst. Washington)

This session addresses how volatile species affect dynamics of the
Earth and planets from natural observations, laboratory experiments, and
numerical modeling in the temperature, pressure, and oxygen activity
range from the early stage of the planet formation to the present. The
volatiles can be critical in zones of magma storage and ascent, mantle
upwelling and melting in the fluid-enriched subduction zones, in the
mantle transition zone, in the lower mantle, in the core-mantle boundary,
and in Earth and planetary cores. However, volatiles affect properties
and processes differently depending on their pressure, temperature, and
redox conditions, which vary in time and space.
 This session aims to address how volatiles control the dynamic
processes of the Earth and planets, governed by their geophysical and
geochemical properties. We welcome papers dealing with geological and
laboratory observations coupled with numerical modeling on the role of
volatiles. The topics include (1) Stability relations, chemical and
physical properties of crystalline, molten and fluid phases,
partitioning of volatiles among these phases, (2) Rheological and other
physical properties of minerals, and the effects of intergranular fluid
on the properties, (3) Volatiles and dehydration induced seismicity and
volcanism in various tectonic regions including subduction zones, and (4)
Effects of volatiles in numerical simulation of geo-tectonics, and (5)
Magma outgassing and its control of volcanic eruption dynamics.

[SCG51-P01] Permeability prediction of porous media with the finite difference Stokes solver LaMEM

*Philipp Eichheimer[1], Wakana Fujita[2], Marcel Thielmann[1], Anton Popov[3], Gregor Golabek[1], Boris Kaus[3], Maximilian Kottwitz[3] (1.Bayerisches Geoinstitut, University of Bayreuth, 2.Department of Earth Science, Tohoku University, Sendai, 3.Institute of Geosciences, Johannes Gutenberg University Mainz)

[SCG51-P02] Grain growth-induced fluid localization and permeability reduction

*Wakana Fujita[1], Michihiko Nakamura[1], Kentaro Uesugi[2] (1.Graduate School of Science, Tohoku University, 2.JASRI/SPring-8)

[SCG51-P03] Pargasite stability in the upper mantle at H_2O-undersaturated conditions

*Marija Putak Juricek[1], Hans Keppler[1] (1.BGI)

[SCG51-P04] **Constraining the water content at the top of the mantle transition zone with the elasticity of wadsleyite and olivine**

*Zhongqing Wu[1] (1.University of Science and Technology of China)

[SCG51-P05] ***Single crystal elasticity of Fe-bearing phase E by Brillouin spectroscopy***

*Niccolo Satta[1], Hauke Marquardt [2], Alexander Kurnosov[1], Tiziana Boffa Ballaran [1], Johannes Buchen[3], Catherine McCammon[1], Takaaki Kawazoe[4] (1.Bayerisches Geoinstitut, University of Bayreuth, 95440 Bayreuth, Germany, 2.Department of Earth Sciences, University of Oxford, South Parks Road, Oxford, UK., 3.Seismological Laboratory, California Institute of Technology, Pasadena, CA 91125, USA., 4.Department of Earth and Planetary Systems Science, Hiroshima University, Hiroshima 739-8526, Japan.)

[SCG51-P06] Discovery of two hexagonal phases in (Fe,Al)OOH under the P-T conditions of the deep lower mantle

*Lu Liu[1,2], Li Zhang[1], Hongsheng Yuan[1] (1.Center for High Pressure Science and Technology Advanced Research, 2.University of Science and Technology of China)

[SCG51-P07] **Effect of grid resolution on tectonic regimes in global-scale convection models**

*Enrico Marzotto[1], Marcel Thielmann[1], Gregor Golabek[1] (1.Bayerisches Geoinstitut)

[SCG51-P08] A 3-D crust and uppermost mantle electrical conductivity model of subduction zone beneath NE Japan

*Masahiro Ichiki[1,2], Toshiki Kaida[1], Yasuo Ogawa[3] (1.Graduate School of Science, Tohoku University, 2.International Research Institute of Disaster Science, 3.School of Science, Tokyo Institute of Technology)

[SCG51-P09] *The conditions of sublithospheric diamond formation constrained from ferric iron-rich exsolution from ferropericlase inclusions.*

*Caterina Melai[1], Daniel Frost[1], Tiziana Boffa Ballaran[1], Catherine McCammon[1] (1.Bayerisches Geoinstitute)

[SCG51-P10] **Probing the variation of the oxygen fugacity in diamond anvil cells using the Fe-Ir alloy as redox sensor**

*Serena Dominijanni[1], Catherine McCammon[1], Leonid Dubrovinsky[1], Dan Frost[1], Nobuyoshi Miyajima[1] (1.Bayerisches Geoinstitut)

[SCG51-P11] Goethite behavior at Earth's lower mantle conditions

*Egor Gennadievich Koemets[1], Maxim Bykov[1], George Aprilis[2], Timofey Fedotenko[2], Stella Chariton[1], Saiana Khandarkhaeva[1], Iuliia Koemets[1], Marcel Thielmann[1], Natalia Dubrovinsaia[2], Leonid Dubrovinsky[1] (1.BGI (Bayerisches Geoinstitut), Universität Bayreuth, Germany, 2.Material Physics and Technology at Extreme Conditions, Laboratory of Crystallography, Universität Bayreuth, Germany)

[SCG51-P12] The oxygen content of sulphides in the mantle and a geothermometer for diamond formation

*Sumith Abeykoon[1], Dan Frost[1], Vera Laurenz[1] (1.Bayerisches Geoinstitut, University of Bayreuth)

Permeability prediction of porous media with the finite difference Stokes solver LaMEM

*Philipp Eichheimer[1], Wakana Fujita[2], Marcel Thielmann[1], Anton Popov[3], Gregor Golabek[1], Boris Kaus[3], Maximilian Kottwitz[3]

1. Bayerisches Geoinstitut, University of Bayreuth, 2. Department of Earth Science, Tohoku University, Sendai, 3. Institute of Geosciences, Johannes Gutenberg University Mainz

The flow of fluids through porous media such as groundwater flow or magma migration is one of the most important processes in geological sciences. The property controlling the efficiency of the flow is the permeability of the rock, thus an accurate determination and prediction of its value is of crucial importance. For this reason, permeability of rocks has been measured across different scales. As laboratory measurements exhibit a range of limitations, the numerical prediction of permeability at conditions where laboratory experiments struggle has become an important method to complement laboratory approaches. At high resolutions, this prediction becomes computationally very expensive, which makes it crucial to develop methods that maximize accuracy. In this work we introduce the open-source finite difference solver LaMEM that can be used to numerically predict the permeability of porous media under laminar conditions. We employ a stencil rescaling method to increase accuracy due to a better description of the solid-fluid interface, thus reducing the computational cost. To validate the method, we perform a series of tests employing both analytical solutions for simplified geometries as well as results from other numerical approaches for more complicated geometries. Furthermore we compare our numerical results to laboratory measurements on glass bead samples with porosities ranging from 20% to 2.5%, showing good agreement.

Keywords: Permeability, Numerical modelling, Digital Rock Physics

©2019. Japan Geoscience Union. All Right Reserved.

Grain growth-induced fluid localization and permeability reduction

*Wakana Fujita[1], Michihiko Nakamura[1], Kentaro Uesugi[2]

1. Graduate School of Science, Tohoku University, 2. JASRI/SPring-8

Efficiency of segregation of geological fluids such as aqueous fluids and melts is an essential elementary process for volatile cycles in subduction zones. Permeability is an intrinsic rock property that controls flow rate of fluid. Various permeability models have been presented by numerical models of textually equilibrated rocks (e.g. 1, 2), laboratory measurements on synthetic rocks (e.g. 3) and estimation from cross-sectional area of synthetic rocks (4). However, there exist discrepancies among those models. Because permeability is very sensitive to microscopic geometry of pore fluid, those disagreements may arise from lack of understanding toward three-dimensional (3D) microstructure of fluid network.

Dihedral angle has been considered to be a critical parameter that controls fluid geometry and thus permeability. Beside, some previous studies shed light on the effect of grain growth on fluid distribution because it could induce pore fluid distortion and coalescence (5, 6). These studies suggest that in the actual systems where the microstructure of rocks evolve in dynamic processes, grain growth would be important along with the dihedral angle.

To investigate the effect of grain growth on the fluid distribution and permeability, we present 3D images of quartz–CHO fluid aggregates, containing nominal fluid fractions between 0.03 and 0.10. Samples were synthesized from a powdered mixture of Arkansus quartz and amorphous silica prepared by sol-gel method and hot-pressed in a piston–cylinder apparatus at 900˚C and 1.0 GPa for 192h. The fluid fractions and the dihedral angles were controlled using brucite added in the capsule bottom and oxalic acid dihydrate mixed with SiO_2 powder. 3D images were obtained using synchrotron X-ray microtomography at BL20XU experimental hutch2 of SPring-8. Regardless of dihedral angles (CO_2 content in fluids), both cross-sectional area and 3D images of samples showed grain-scale fluid localization which would be formed by pore fluid coalescence induced by grain growth. Computed permeabilities using numerical model, LaMEM (7) were almost consistent with laboratory measurements by (3) but more than one order of magnitude lower than a numerical model by (2). This would indicate that localized fluids extensively reduce permeability by reducing the diameter of fluid tubes along grain edges, which would suggest transport of water into Earth’ s deep interior by the subducting slab.

Reference:
1. von Bargen and Waff. 1986, J. Geophys. Res. 91, 9261–9276.
2. Rudge, J.F. 2018, Proc. R. Soc. Lond. A 474, 20170639.
3. Wark and Watson. 1998, Earth Planet. Sci. Lett. 164, 591–605.
4. Faul, U.H. 1997, J. Geophys. Res. 102, 10299–10311.
5. Walte et al. 2003, Geology 2003 31, 1009-1012.
6. Yoshino and Watson. 2005, Earth Planet. Sci. Lett. 235, 453–468.
7. Kaus et al. 2016, NIC Symposium 2016

Keywords: Permeability, Quartz, Grain growth, Dihedral angle, Fluid segregation

©2019. Japan Geoscience Union. All Right Reserved.

Pargasite stability in the upper mantle at H_2O-undersaturated conditions

*Marija Putak Juricek[1], Hans Keppler[1]

1. BGI

Amphibole is the most commonly occurring hydrous mineral in mantle xenoliths and the majority of upper mantle amphiboles have compositions close to pargasite end member. Previous experimental work has demonstrated that pargasite stability is sensitive to variations in bulk alkali and water content of the starting material. While it has been successfully shown that addition of more alkali leads to stabilization of pargasite to higher P and T, the effect of water on amphibole stability is not so straightforward.

At H_2O-saturated conditions, alkali elements partition strongly into aqueous fluid and become less available for crystallization of amphibole. As a result, amphibole seemingly becomes stable at higher P and T when less H_2O is added to the starting material. This observation led to the hypothesis that pargasite may be a ubiquitous phase in the upper mantle, which is believed to contain only several hundred ppm of H_2O. However, most of the previous studies determined pargasite stability at H_2 O-saturated conditions where solid phases coexist with an aqueous fluid during experiments. Since such environments are not representative of the nearly dry upper mantle, the purpose of this study is to investigate pargasite stability at H_2O-undersaturated conditions.

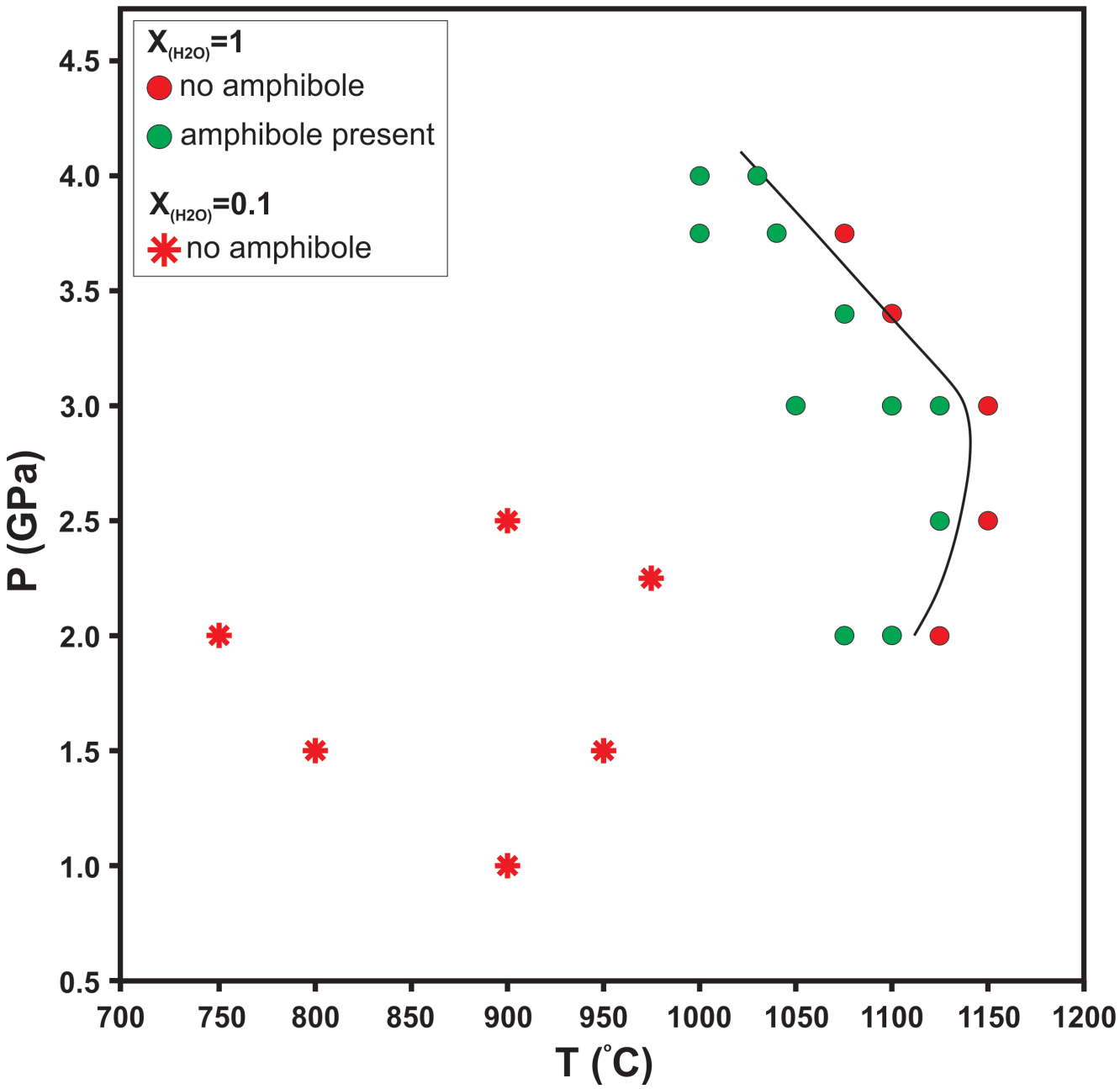
Because of the high specific surface area of powders, adsorption of atmospheric H_2O on fine grained starting materials prevents attaining H_2O-undersaturation by adding small amounts of water to the sample. Instead, H_2O-undersaturated conditions may be precisely controlled by diluting the water in the sample with another component. Under such conditions, solid phases are expected to coexist with a low water activity fluid throughout the experiment. As molecular nitrogen is mostly insoluble in upper mantle minerals, it can be used to adjust the water activity of the fluid to a desired low value.

All experiments were performed in a piston cylinder apparatus. The samples for H_2O-undersaturated experiments were prepared by adding silver azide (AgN_3) and brucite to a synthetic peridotite mixture. In several experiments water was added directly as $H_2O_{(l)}$. The amount of water was kept constant in all experiments (1 wt. percent) and the molar fraction of water in the N_2-H_2O fluid was adjusted to the desired value by weighing an appropriate amount of AgN_3, which decomposed to metallic silver and molecular nitrogen during heating. In H_2O-saturated experiments, no silver azide was added to the peridotite mixture. Experimental products were analyzed using JEOL JXA-8200 electron microprobe.

Preliminary results show that pargasite is not stable in equilibrium with fluids diluted to X_{H2O}=0.1 at pressures above 1 GPa. At H_2O-saturated conditions pargasite stability field can extend to pressures of 4 GPa and above 1100 ℃, depending on bulk alkali and water contents. Results from experiments at X_{H2O} =0.1 and X_{H2O}=1 suggest that pargasite can exist only in regions of the upper mantle which have been affected by high water activity fluids, such as areas in the vicinity of subduction zones. The ambient nominally anhydrous upper mantle, better represented by experiments at H_2O-undersaturated conditions, is not expected to contain pargasite.

Keywords: pargasite, stability, upper, mantle

©2019. Japan Geoscience Union. All Right Reserved.



©2019. Japan Geoscience Union. All Right Reserved.

Constraining the water content at the top of the mantle transition zone with the elasticity of wadsleyite and olivine

*Zhongqing Wu[1]

1. University of Science and Technology of China

Zhongqing Wu[a,b,*], Wenzhong Wang[a,b], Michael J. Walter[c] ,Ye Peng[a,b], Simon Redfern[d],

[a] Laboratory of Seismology and Physics of Earth’ s Interior, School of Earth and Space Sciences, University of Science and Technology of China, Hefei, Anhui 230026, China

[b] Mengcheng National Geophysical Observatory, Anhui, China

[c]School of Earth Sciences, University of Bristol, Bristol BS8 1RJ, UK

[d]Department of Earth Science, University of Cambridge, Cambridge CB2 3EQ, UK

The water content in the mantle transition zone (MTZ) exerts a controlling influence on the dynamical and chemical evolution of Earth, but is poorly known. In principle the water content at the top of the transition zone can be inferred by comparing the velocity and density contrasts across the 410-km seismic discontinuity with predictions based on the phase transition of olivine to wadsleyite. The high-quality elastic data of at pressure and temperature (PT) conditions of the transition zone are crucial but are very challenge for experiments to obtain. Calculating these elastic data at high PT conditions in conventional method are also very expensive. Instead, these elastic data were calculated using the method of Wu and Wentzcovitch (2011), which reduces the computational workload to tenth of the conventional method. All calculations for two phases were conducted using the same computational details as far as possible, which guarantees that the velocity and density differences between two phases have very high precise. All these calculated elastic data agree well with the available experimental data. The iron and water effect on the elasticity are also well described.

With these high-quality elastic data covered the PT condition of the transition zone, we analyze the water and wadsleyite content at the top of the transition zone. We found that the water content of wadsleyite at the top of the transition zone can be well constrained when density and velocities jumps are considered together. For a pyrolitic mantle composition with ~60% olivine, our best fit is ~ 0.5 wt% water at the top of the transition zone. If the transition zone is dry, as suggested by some electrical conductivity models, the upper mantle may only contain ~ 50% olivine.

Wu, Z., Wentzcovitch, R.M., 2011. Quasiharmonic thermal elasticity of crystals: An analytical approach. Phys. Rev. B - Condens. Matter Mater. Phys. 83, 1–8. doi:10.1103/PhysRevB.83.184115

©2019. Japan Geoscience Union. All Right Reserved.

Single crystal elasticity of Fe-bearing phase E by Brillouin spectroscopy

*Niccolo Satta[1], Hauke Marquardt [2], Alexander Kurnosov[1], Tiziana Boffa Ballaran [1], Johannes Buchen[3], Catherine McCammon[1], Takaaki Kawazoe[4]

1. Bayerisches Geoinstitut, University of Bayreuth, 95440 Bayreuth, Germany, 2. Department of Earth Sciences, University of Oxford, South Parks Road, Oxford, UK., 3. Seismological Laboratory, California Institute of Technology, Pasadena, CA 91125, USA., 4. Department of Earth and Planetary Systems Science, Hiroshima University, Hiroshima 739-8526, Japan.

Earth’s deep water cycle plays a key role for the dynamic evolution of our planet and the development of habitable conditions. Surface water can be transported to Earth’s mantle by subduction of oceanic lithosphere. Experimental investigations have shown that water can be efficiently stored in Dense Hydrous Magnesium Silicates (DHMS) in cold subducting slabs. However, quantification of the incoming water budget based on the interpretation of seismological observations is hampered by a lack of elasticity measurements of DHMSs. Here, we report single-crystal elasticity measurements of Fe-bearing phase E, a DHMS that is stable at pressures and temperature of Earth’s mantle transition zone. A very low bulk modulus has been reported for phase E, suggesting that it might produce seismic velocity heterogeneities detectable by seismological investigations. However, the shear modulus of phase E has not been quantified.

We synthesized Fe-bearing phase E single crystals in a multi-anvil apparatus. Chemical composition as well as crystal structure have been determined using electron microprobe analysis, Mössbauer spectroscopy, and single-crystal X-ray diffraction. We derived the full elastic stiffness tensor by Brillouin spectroscopy on two single crystals of selected orientations. We found phase E to have both the lowest bulk modulus and shear modulus among the DHMSs at ambient conditions. Phase E shows very low compressional and shear velocities especially when compared to the other principal minerals likely present in subducting slabs after serpentine breakdown. Modelling of seismic velocities in dry and hydrated upper mantle and transition zone rocks suggests that the presence of even small amounts of phase E can appreciably lower seismic wave velocities. Phase E could be used as seismological indicator for water stored at depth in subducting scenarios. The elasticity of phase E under mantle conditions will be explored in future research.

Keywords: Brillouin scattering, Phase E, Seismic wave velocities

©2019. Japan Geoscience Union. All Right Reserved.

Discovery of two hexagonal phases in (Fe,Al)OOH under the P-T conditions of the deep lower mantle

*Lu Liu[1,2], Li Zhang[1], Hongsheng Yuan[1]

1. Center for High Pressure Science and Technology Advanced Research, 2. University of Science and Technology of China

Deep water can cause a series of complex seismological phenomena by changing the density and thermal stability of lower mantle components. δ-H solid solution phase (AlOOH-$MgSiO_2(OH)$) is stable at lower mantle conditions[1],because the crystallographic frameworks of the phase H is similar to that of the δ-AlOOH phase, with very strong hydrogen bonds[2,3]. δ-AlOOH and ε-FeOOH can also form solid solution[4] (δ - ε solution). It is reasonable to infer that δ - ε solid solution may have similar thermal stability as that of H-δ solution, considering their similar crystal structure[5]. In our experiments, we synthesized the δ - ε solution at 79GPa and 1600K in a laser-heated diamond anvil cell. As the temperature increases to 2100k, the orthorhombic δ - ε solution transformed into a hexagonal-structured phase. By combining powder X-ray diffraction techniques with multigrain indexation[6], we determined its hexagonal lattice with a=b=10.019Å and c=2.614Å. At 79GPa and 2400K, the hexagonal phase transforms into another hexagonal phase, with the lattice parameters of a=b=2.733Å and c=9.343Å. The discovery of these two new phases may provide new insights into the deep-water storage.

References

1.Ohira I, Ohtani E, Sakai T, et al. Stability of a hydrous δ-phase, AlOOH-$MgSiO_2(OH)_2$, and a mechanism for water transport into the base of lower mantle[J].Earth and Planetary Science Letters, 2014, 401: 12-17.
2.Ohtani, E., Amaike, Y., Kamada, S., Sakamaki, T. and Hirao, N. Stability of hydrous phase H $MgSiO_4H_2$ under lower mantle conditions. Geophys. Res. Lett. 41, -8287 (2014).
3.Nishi M,Kuwayama Y,Tsuchiya J,et al.The pyrite-type high-pressure form of FeOOH[J]. Nature,2017,54(7662):205-208.
4.T Kawazoe,I Ohira,T Ishii et al. Single crystal synthesis of δ-(Al,Fe)OOH American Mineralogist. Volume 102, pages 1953–1956, (2017)
5.Gleason A E,Quiroga C E,Suzuki A,et al.Symmetrization driven spin transition in ε-FeOOH at high pressure[J]. Earth and Planetary Science Letters, 2013, 379: 49-55.
6.Zhang L,Yuan H,Meng Y,et al.Discovery of a hexagonal ultradense hydrous phase in (Fe, Al) OOH[J]. Proceedings of the National Academy of Sciences,2018,115(12):2908-2911.

Keywords: High temperature and high pressure experiment, hydrous phase, diamond anvil cell

©2019. Japan Geoscience Union. All Right Reserved.

Effect of grid resolution on tectonic regimes in global-scale convection models

*Enrico Marzotto[1], Marcel Thielmann[1], Gregor Golabek[1]

1. Bayerisches Geoinstitut

Global-scale convection models using a visco-plastic rheology coupled with a temperature-dependent viscosity usually show different tectonic regimes: mobile, episodic or stagnant lid.

In the mobilelidregime, the lid is continuously subducting into the mantle (plate-like behavior). The episodic lid regime is characterized by the stability of the lid until sufficiently large lithospheric stresses break it, causing rapid resurfacing. Finally the stagnant lid regime is defined by an undeformable lid that does not participate in convection

In numerical simulations these three types of regimes can be obtained by varying some target parameters such as: temperature-dependency of viscosity and yield stress.

The yield stress in particular is a key parameter because it sets the stress necessary to cause plastic yielding, hence, in a visco-plastic rheology, the stress necessary to break the cold surface regions. A high yield stress will result in a stagnant lid. On the other hand, a low yield stress causes a weak lid that is constantly broken and sinks into the mantle.Despite the key importance of physical parameters, also numerical parameters have an effect on the tectonic regime, determining different outcomes justby changing the grid resolution.

Here we use the code StagYY (*Tackley, 2008*) in a 2D spherical annulus geometry (*Hernlund & Tackley, 2008*) to determine the resolution-dependent tectonic regime for different yield stresses in global-scale convection models. To assess the effect of grid resolution on lid behavior we use 16 different resolutions keeping all physical parameters unchanged. To make sure that steady state has been reached each simulation is run for 15 Gyrs. Tested resolutions vary from 128x32 to 1024x256 grid points. To understand this influence on the tectonic regime we study the resolution within the lid requiring an appropriate lid definition, based on the thermal and velocity field. Our results show that there is a correspondence between low radial resolution and mobile lid regime and that low aspect ratio cells (azimuthal to radial grid spacing) favor a plate-like behavior of the lid, while for large aspect ratios the mobile lid regime is persistent.

This work is the first part of a larger project, aiming to studyslab stagnation and hydration of the mantle transition zone (MTZ) using self-consistent global-scale mantle convection models, where subducting slabs carry water from the surface into the Earth’ s interior and potentially hydrate the MTZ. We expect that our previous work packages will help us to obtain realistic slab ponding in the MTZ, so we can study the hydration state of this region over time.

References:

Tackley, P. J. (2008). Modelling compressible mantle convection with large viscosity contrasts in a

©2019. Japan Geoscience Union. All Right Reserved.

three-dimensional spherical shell using the yin-yang grid. *Phys. Earth Planet. Int.* 171, 7-18.

Hernlund, J. W. and P. J. Tackley (2008). Modeling mantle convection in the spherical annulus. *Phys. Earth Planet. Int.* 171, 48-54

Keywords: Geodynamical Modelling, StagYY, Grid Resolution

©2019. Japan Geoscience Union. All Right Reserved.

A 3-D crust and uppermost mantle electrical conductivity model of subduction zone beneath NE Japan

*Masahiro Ichiki[1,2], Toshiki Kaida[1], Yasuo Ogawa[3]

1. Graduate School of Science, Tohoku University, 2. International Research Institute of Disaster Science, 3. School of Science, Tokyo Institute of Technology

The crustal fluids beneath NE Japan is originated from dehydration of subducting Pacific slab or from convection in the backarc mantle, as is shown by seismic tomography [e.g. Zhao, 2017]. We investigated the fluid transportation paths from upper mantle to crust of subduction zone using electrical conductivity exploration.

We expanded electromagnetic field observation sites (96 sites) to northern part of NE Japan and obtained magnetotelluric responses and geomagnetic transfer functions in the period range of 20 –30720 seconds (22 periods) by BIRRP code [Chave and Thomson, 2004]. We used WSINV3D [Siripunvaraporn and Egbert, 2009] to invert those responses into three dimensional electrical resistivity model.

The preliminary model gives normalized root mean square misfit 5.87. A prominent conductor appears in the crust to uppermost mantle and the conductor spreads towards backarc direction. In our previous model [Ichiki et al., 2015], we found the overturned shape conductor towards backarc direction in the mantle wedge beneath central part of NE Japan. This study has found it beneath northern part NE Japan as well.

Those imply the crustal fluid and/or melt is transported along the pathway that is the plate boundary beneath the volcanic front to the backarc crust. The fluid transportation can explain the presence of enigmatic backarc volcano in the NE Japan. In this presenation, we speculate and discuss evolution of this pathway in geological time on the basis of the chlonological data of igneous rocks [Yoshida et al., 2013].

Acknouwledgement: This study is financially supported by KAKEN-HI No.26109006.

Keywords: electrical conductivity, resistivity, magnetotelluric, subduction zone

©2019. Japan Geoscience Union. All Right Reserved.

The conditions of sublithospheric diamond formation constrained from ferric iron-rich exsolution from ferropericlase inclusions.

*Caterina Melai[1], Daniel Frost[1], Tiziana Boffa Ballaran[1], Catherine McCammon[1]

1. Bayerisches Geoinstitute

Ferropericlase is apparently one of the more common inclusions to be found in sub-lithospheric diamonds, which are considered to form in the convecting mantle. Although relatively rare, these inclusions have been examined in a number of studies in the hope of providing information on the formation conditions of such deep diamonds, which could potentially be in the transition zone or lower mantle. The wide range of oxide Fe/(Fe+Mg) ratios found has raised the idea that they may form through the oxidation of iron metal. During TEM investigations, however, evidence for the exsolution of Fe_2O_3-rich phases such as magnesioferrite have been found, which implies that a more complex scenario may be involved. Ferropericlase-magnesiowüstite diamond inclusions are most likely some of the deepest available samples from the mantle and they potentially provide the most direct evidence for deep mantle carbon transport processes. The ferric iron contents of such inclusions alone may not provide a direct estimate for the oxygen fugacity at which the inclusions were trapped, particularly if pressure has a strong effect on the fo_2 - Fe^{3+}/Fe_{tot} relationship. However, using experimental data it is possible to determine the oxygen fugacity at which the exsolution observed in the diamond inclusions occurred and coupled with the oxide Fe^{3+}/Fe_{tot} ratio this could be used to estimate the pressure of formation.

The ferropericlase- magnesioferrite system has been investigated by several studies at room pressure but the stability field of the two components has been shown to become more complicated at high pressure due to the formation of mixed valence oxides. We have combined experimental measurements with thermodynamic modelling in order to address two main questions: at which P, T, fO_2 conditions do Fe_2O_3 -rich phases exsolve from ferropericlase? And what is the maximum Fe^{3+}/Fe_{tot} ratio of ferropericlase. To answer these questions, multianvil experiments have been performed between 6 –25 GPa and 1200-1800˚C using a starting composition of $(Mg_{86}Fe_{14})O$ plus 20 % Fe_2O_3. Pt powder was added to the experiments to act as a redox sensor and minor amounts of Ni, Cr, Mn and Na were also added. Samples were then analyzed with the scanning electron microscope, electron microprobe, Mössbauer spectroscopy and X-ray diffraction. In the recovered experiments ferropericlase coexists with magnetite-magnesioferrite solid solution up to 10 GPa and $Mg_2Fe_2O_5$-Fe_4O_5 solid solution at higher pressures. In the calculation of the oxygen fugacity a ferropericlase model in the FeO-$Fe_{2/3}$O-MgO system was employed and exchange of Mg and Fe^{2+} in magnetite was accounted for. Oxygen fugacities at which the phases coexist can be calculated in the magnetite-magnesioferrite field using three different equilibria and a quite simple ferropericlase mixing model results in calculated oxygen fugacities that are within 0.1 log units of each other for all three equilibria. The results show that magnetite-magnesioferrite solid solution should not be in equilibrium with ferropericlase in the diamond stability field. Our results imply that the exsolution of Fe^{3+} rich phases observed in natural samples likely occurred at pressures corresponding to the transition zone or deeper.

©2019. Japan Geoscience Union. All Right Reserved.

Probing the variation of the oxygen fugacity in diamond anvil cells using the Fe-Ir alloy as redox sensor

*Serena Dominijanni[1], Catherine McCammon[1], Leonid Dubrovinsky[1], Dan Frost[1], Nobuyoshi Miyajima[1]

1. Bayerisches Geoinstitut

Understanding the oxygen fugacity (fO_2) in diamond anvil cells (DACs) is an important issue for many reasons, among them reconciling contradictory results that have been obtained for carbonate studies (Cerantola et al., 2017; Dorfman et al., 2018) that might be due to different redox conditions during the experiments. We therefore investigated the fO_2 conditions during DAC experiments using powder X-ray diffraction (beamlines ID15b and ID27) and energy-domain Synchrotron Mössbauer Source (SMS) spectroscopy (beamline ID18) at the European Synchrotron Radiation Facility (Grenoble, France). Double sided laser heating experiments (Aprilis et al., 2017) were carried out at high pressure and temperature using a mixture of synthetic ferropericlase ($Mg_{0.75}Fe_{0.25}$)O and pure iridium powder as a sliding redox sensor (Borisov and Palme, 2000; Swartzendruber, 1984; Taylor et al., 1992). The Fe content in the Fe-Ir alloy, together with the amount of FeO in ferropericlase, allows a calculation of fO_2 during the experiments (Stagno et al., 2011; Woodland and O'Neill, 1997). Preliminary results from powder X-ray diffraction data show that, after heating, an Fe-Ir metal alloy that can be indexed in the Fm-3m space group is formed by the reaction of pure Ir and Fe from ferropericlase according to the reaction:

(Mg,Fe)O + Ir --> (Mg,Fe)O + (Fe,Ir)

The compressibility of the Fe-Ir alloy and ferropericlase was measured up to ~ 60 GPa and SMS data were collected before and after heating. X-ray diffraction results coupled with energy-dispersive X-ray spectroscopy (EDS) measurements and a simple thermodynamic model indicate that the redox conditions during the DAC experiments were close to the iron-wüstite (IW) buffer, although some inhomogeneity was observed. Further chemical analyses and additional experiments are ongoing to understand the variation of oxygen fugacity in a DAC during laser heating.

Keywords: oxygen fugacity , redox sensor, diamond anvil cell

©2019. Japan Geoscience Union. All Right Reserved.

Goethite behavior at Earth's lower mantle conditions

*Egor Gennadievich Koemets[1], Maxim Bykov[1], George Aprilis[2], Timofey Fedotenko[2], Stella Chariton[1], Saiana Khandarkhaeva[1], Iuliia Koemets[1], Marcel Thielmann[1], Natalia Dubrovinsaia[2], Leonid Dubrovinsky[1]

1. BGI (Bayerisches Geoinstitut), Universität Bayreuth, Germany, 2. Material Physics and Technology at Extreme Conditions, Laboratory of Crystallography, Universität Bayreuth, Germany

Water and water-bearing species have a strong impact on numerous processes in Earth’ s interiors. Presence of water affects chemical and physical properties of mantle minerals, changes melting temperatures, sound velocities and viscosity of materials, and causing different global phenomena such as, for example, arc volcanism and plate tectonics. Thereby, the deep Earth’ s regions enriched with water are crucial for understanding our planet’ s geodynamics and geochemistry. Still, mechanisms of water circulation between geospheres remain poorly understood. Recent studies suggest that goethite present in Banded Iron Formations (BIFs) may transfer some quantities of water to the deep Earth interiors with subducting slabs. It was reported that goethite remains stable in the sinking slab until it reaches the base of a lower mantle. By the meaning of in situ powder XRD it was revealed that at pressures corresponding to the depths ~1500-1800 km and moderately high temperatures goethite undergoes a phase transition to form a novel stable pyrite-type phase FeO_2H_x with $0 \leqq x \leqq 1$ (named as Py-phase). Thus, goethite and its HP pyrite-type form became a candidate for water and/or hydrogen transfer and storage to the lower mantle and the core-mantle boundary. Using laser-heating in diamond anvil cells we performed a series of experiments on an investigation of goethite (as a starting material) stability at P-T conditions covering possible range in subducting slabs. By the meaning of sensitive in situ single-crystal XRD in DACs we registered decomposition of goethite and formation of known (such as ι-Fe_2O_3, η-Fe_2O_3, a high-pressure orthorhombic form of Fe_3O_4, Fe_5O_7) and novel iron-oxygen compounds. Results of structure solution and refinement established these compounds to be orthorhombic Fe_7O_{10} and hexagonal non-stoichiometric phase $Fe_{6.31}O_9$. Our results suggest that FeOOH cannot transport water into the deep of Earth’ s mantle.

Keywords: Goethite, Diamond anvil cell, High Pressure, Single-crystal XRD, Subducting slabs

©2019. Japan Geoscience Union. All Right Reserved.

The oxygen content of sulphides in the mantle and a geothermometer for diamond formation

*Sumith Abeykoon[1], Dan Frost[1], Vera Laurenz[1]

1. Bayerisches Geoinstitut, University of Bayreuth

Sulphides are ubiquitous accessory minerals in mantle rocks and form the most prevalent type of inclusion in diamonds. Diamond sulphide inclusions are trapped as sulphide melts that crystallise on cooling to form Fe-Ni monosulphide solid solution (MSS) and ultimately recrystallizes to assemblages containing pyrrhotite, $Fe_{(1-x)}S$ (x = 0 to 0.2), pentlandite, $(Fe,Ni)_9S_8$, and sometimes pyrite (FeS_2). Sulphide inclusions are also found in many xenoliths but those which are hosted by diamonds provide potentially the most pristine samples from the lithospheric mantle and deeper. Previous experiments indicate that oxygen partitions into sulphide melts and although sparse, some measurements of natural sulphide inclusions from mantle xenoliths indeed show measurable and in some cases relatively high oxygen concentrations. If the parameters that control sulphide oxygen concentration can be determined then they could be potentially used to understand conditions in the mantle and in particular in sublithospheric diamonds. The oxygen content of sulphides separating to the core during core formation could have also influenced the oxygen fugacity of the early mantle.
We have measured the oxygen contents of sulphide melts within experimentally produced mantle assemblages at high pressures and temperatures. A series of multi-anvil experiments were conducted to equilibrate a peridotite assemblage with molten sulphide (FeS) at pressures between 3 –11 GPa and temperatures of 1300 ˚C –1700 ˚C. The effects of pressure, temperature, oxygen fugacity and composition have been investigated. Oxygen fugacity was determined in some experiments by saturating the sulphide in Ir to produce a separate Ir-Fe metal alloy, for which the Fe content is a function of oxygen fugacity. The results show that sulphide melt oxygen contents can range up to 16 weight % FeO, at mantle conditions. Moreover, the content of oxygen in the sulphide is found to be not controlled by fO_2 or fS_2, which is in disagreement with previous experimental studies conducted at ambient pressure conditions. The experiments indicate that the oxygen concentration is mainly controlled by the FeO activity in coexisting silicates phases and the temperature, although further work is still required to calibrate effects of Ni and Cu. In order to fit the data and to account for the FeO dependence, we developed a thermodynamic model using an end-member equilibrium between olivine, pyroxene and FeO in the sulphide melt. The resulting relationship can be used as a geothermometer based on sulphide inclusion oxygen contents and could be particularly useful for determining diamond formation temperatures for sub lithospheric diamonds.

Keywords: Sulfide, Oxygen, Geothermometer

©2019. Japan Geoscience Union. All Right Reserved.

[E] Poster | M (Multidisciplinary and Interdisciplinary)：M-IS Intersection

Thu. May 30, 2019 10:45 AM - 12:15 PM JST | Thu. May 30, 2019 1:45 AM - 3:15 AM UTC | Poster Hall International Exhibition Hall8, Makuhari Messe_9

[M-IS03] Evolution and variability of the Asian monsoon in Cenozoic global climate changes

convener:Masanobu Yamamoto(Faculty of Environmental Earth Science, Hokkaido University), Ryuji Tada(Department of Earth and Planetary Science, Graduate School of Science, The Univeristy of Tokyo)

The Asian Monsoon (AM) is a part of interhemispheric atmospheric phenomena that is driven by the thermal gradient between ocean and land. Contrasts of insolation, heat content and latent heat transfer between ocean and land may have affected the behavior of the AM in the past, but the proxy records are occasionally controversial and do not show a clear picture of the AM variability. Recent proxy and modeling studies suggest that glacial pCO2 cycles could be related to the position of southern westerlies, which is sensitive to interhemispheric heat imbalance. Because monsoon is driven by the heat imbalance, knowledge on the variability of the AM is important to understand the behavior of the global climate system. In this session, presentations on the reconstruction of long-term AM variability from various archives such as IODP expedition cores, discussion on its forcing, and the roles of the AM in global climate changes are welcome.

[MIS03-P01] Asian dust source variability since 10 Ma based on grain size specific mineral composition at IODP Site U1425 in the Japan Sea

*Mui Fa Alison Lee[1], Tomohisa Irino[1] (1.Faculty of Environmental Earth Science, Hokkaido University)

[MIS03-P02] Sources and formation environment of biomass burning products in Pliocene and Pleistocene marine sediments in the Japan Sea

*Song Lu[1], Youhei Yamashita[2], Tomohisa Irino[2] (1.Graduate School of Environmental Science, Hokkaido University , 2.Faculty of Environmental Earth Science, Hokkaido University)

[MIS03-P03] Variation of mineral dust flux in peat at a high moor on the Mt. Daisetsu during Holocene

*Tomohisa Irino[1], Keisuke Hirai[1], Osamu Seki[1], James Hooper[2], Samuel Marx[2] (1.Hokkaido University, 2.University of Wollongong)

[MIS03-P04] Variations in sea surface environments recorded by algal biomarkers in the Japan Sea off the western coast of Hokkaido (IODP Site U1422) over the last 250 ka

*Asako Suzuki[1], Ken Sawada[2], Satoshi Furota[3], Yaeko Igarashi[4], Tomohisa Irino[5] (1.Graduate School of Science, Hokkaido University, 2.Department of Earth and Planetary Sciences, Faculty of Science, Hokkaido University, 3.Japan Agency for Marine-Earth Science and Technology, 4.Institute for Paleoenvironment of Northern Regions, 5.Faculty of Environmental Earth Science, Hokkaido University)

[MIS03-P05] **Decadal oscillation in hydrogen stable isotope ratio of long chain fatty acids in Lake Suigetsu sediment core**

*Masaya Inagaki[1], Masanobu Yamamoto[1,2], Takeshi Nakagawa[3] (1.Graduate School of Environmental Science, Hokkaido University, 2.Faculty of Environmental Earth Science, Hokkaido University, 3.Research Center for Palaeoclimatology, Ritsumeikan University)

[MIS03-P06] **Amplitude modulation of sea surface temperature variability in the Bay of Bengal by 400-kyr eccentricity cycle**

*Masanobu Yamamoto[1], Yuko Tsuchiya[1], Steven Clemens[2] (1.Faculty of Environmental Earth Science, Hokkaido University, 2.Department of Earth, Planetary and Environmental Sciences, Brown University)

Asian dust source variability since 10 Ma based on grain size specific mineral composition at IODP Site U1425 in the Japan Sea

*Mui Fa Alison Lee[1], Tomohisa Irino[1]

1. Faculty of Environmental Earth Science, Hokkaido University

Sediments at Integrated Ocean Drilling Program (IODP) Site U1425 in the Japan Sea is under the strong influence of westerly jet stream and winter monsoon wind which transporting a significant amount of aeolian dust from both Taklamakan deserts and Gobi deserts. Aeolian dust from Taklamakan showed very high content of quartz (60-90%) and less plagioclase (5-40%) than from NE Chinese deserts and Loess (Gobi). The lower value of half height width (FWHM) of illite peak in X-ray diffraction (XRD) profile can be used as an indicator higher illite crystallinity. A decreasing trend of illite FWHM (increasing trend of the crystalinity) towards the core of the fold and thrust anticline has been recognized (Robinson et al. 1990; Orozco et al. 1998). Illite is also predominant component of the Chinese loess, and its highly crystallized nature has been interpreted to indicate that the illite was not formed at surface temperature and may have originated from a low temperature metamorphic environment.

In order to reconstruct a long-term changes in dust sources and transport pathways of Asian dust utilizing knowledges above, we examined mineral composition of IODP Site U1425 located at the central Japan Sea. The sediment samples were separated into >4 μm (silt) and <4 μm (clay) fractions by repeated pipette method. Both fractions were used for powder XRD analysis and peak heights of diagnostic peaks of major minerals were regarded as relative abundance of the minerals. FWHM and chemical index of illite were also examined.

In general, a very high quartz content found at Site U1425 may indicate sediments are aeolian source from Taklamakan deserts and higher plagioclase (albite) may infer dust source from Gobi deserts. Intervals around 9.5 Ma, 8.3 Ma, 7.9 Ma and 4.5 Ma showed very high quartz content and less albite at Site U1425, which indicate increases in dust supplied from Taklamakan than Gobi deserts due to stronger westerly wind. During Pliocene to early Pleistocene (4.2-2Ma), Taklamakan dust is still dominant, however the increasing influence of Gobi dust is recognized at 4.1 and 3.4Ma. On the other hand, an abrupt increase of the ratio of albite to quartz from 0.2 at 4.5 Ma to 0.8 at 4.1 Ma is found, which also shows another maximum at 0.6 Ma. In general, increase of albite abundance in sediments at Site U1425 during Pleistocene indicates the increasing dust supplied from NE China and Gobi deserts and the strengthened winter monsoon.

FWHM (crystallinity) of illite in silt fraction at Site U1425 showed low values (high crystallinity) with narrow range around 0.2°2θ during Pleistocene. The illite chemistry index showed values below 0.4 and genrerally around 0.3 during Pleistocene, which represents (Fe, Mg)-rich illites (biotite) characterized for physically eroded or unweathered rocks. The highly crystallized and Fe–Mg rich illites in the silt fraction at Site U1425 in the Japan Sea suggests their aeolian origin which may be derived from pre-existing sediments which eroded from low-grade metamorphic rocks in the northern regions of the Tibetan Plateau. In a longer time-scale, higher crystallinity and lower chemistry index of illite in silt fractions occurred in similar timing at 9.3 Ma and 6.6-2.7 Ma which could be correlated with the active regional uplift and tectonic activities of the northeastern margin of the Tibetan Plateau. Possible changes in source of illite indicates frequent plate tectonic activities near the Taklamakan deserts of North Tibet plateau especially from 6.6-2.7Ma.

©2019. Japan Geoscience Union. All Right Reserved.

Keywords: Aeolian dust, Taklamakan deserts, Quartz, Feldspar , Illite, Gobi deserts

©2019. Japan Geoscience Union. All Right Reserved.

Sources and formation environment of biomass burning products in Pliocene and Pleistocene marine sediments in the Japan Sea

*Song Lu[1], Youhei Yamashita[2], Tomohisa Irino[2]

1. Graduate School of Environmental Science, Hokkaido University , 2. Faculty of Environmental Earth Science, Hokkaido University

Behavior of black carbon (BC) is crucial for the earth surface environment because it could cause global warming by absorbing sunlight in the atmosphere. BC is originated from incomplete combustion of biomass or fossil fuels. Combustion in natural processes is incomplete due to local limitation of oxygen during the fire, which leads to the formation of organic fire residues. Robustness of BC to degradation in the natural environment enables us to use BC as a proxy to study the driving force of frequency and burning temperatures of past wildfire events. But the previous fire researches (paleoclimate rather than modern ecology) did not discuss the control factors for burning temperature or try to rebuild the fire temperature. Objective of this study is to understand factors controlling the thermal/optical/chemical characters of BC with burning temperature, provenance and aging in relation to the variabilities of vegetation in the hinterland. For these purposes, BC was quantified as elemental carbon (EC) in coarse (>2 μm) and fine (<2 μm) fractions of sediment samples using a thermal optical transmittance (TOT) method, and their burning temperatures were estimated for bulk samples through measurement of composition of benzene polycarboxylic acids (BPCAs), molecular markers of fire residues, determined with High Performance Liquid Chromatography (HPLC). In order to examine the relationship between burning temperature and BPCA composition, selected plants were experimentally charred to obtain standard charcoal samples. We also applied TOT and BPCA methods to marine sediments such as the surface sediments collected during KR15-10 cruise off the Wakasa Bay and 63 samples between 0 and 203 m CCSF-D were selected from IODP Site U1423 in the northeastern Japan Sea which covered the last 4.3 Myr. Size dependencies of EC contents and thermal properties will be compared with the contents and composition of BPCAs to examine the influence of sources, transport pathways, and burning temperatures of BCs contained in marine sediments.

Keywords: biomass burning, elemental carbon, benzene polycarboxylic acid

©2019. Japan Geoscience Union. All Right Reserved.

Variation of mineral dust flux in peat at a high moor on the Mt. Daisetsu during Holocene

*Tomohisa Irino[1], Keisuke Hirai[1], Osamu Seki[1], James Hooper[2], Samuel Marx[2]

1. Hokkaido University, 2. University of Wollongong

Mt. Daisetsu, Hokkaido, Japan is located just below the northern route of Asian dust transport and receives a significant amount of dust which dies snow surface brown in spring time every year. This area is also characterized by well-developed high moors on the mountains covering the last 4000 - 7500 yrs, which would continuously record the history of climate change during the middle to late Holocene. Peat collected from these high moor could be also a suitable material for a precise age determination using the radio carbon, and its inorganic fraction might consist of aeolian dust of continental origin and volcanic materials of the local origin which could be easily distinguished from each other.

Asian dust transported to the northern Japan may have a different source from those transported to the southwestern Japan. In spite of this, many of previous dust studies for Asian dust deposition in Japan have been conducted for the paleo-archives collected from the southern area. Therefore, it is necessary to reconstruct the composition and flux of Asian dust transported to the northern Japan in order to understand the spatio-temporal variability of westerly that could have significant influence on the climate in east Asia.

We collected peat cores from the high moor in Mt. Daisetsuzan area, and measured the mineral composition contained in peat. After heat treatment of peat samples, we conducted X-ray diffraction (XRD) analysis on the ash fraction and semi-quantified the minerals. Quartz, illite, and chlorite showed positive correlation among others, while various feldspars showed another positive correlation among others independent from quartz. Amorphous materials exhibited a variability different from quartz or feldspars. High ash content was associated with high feldspars or amorphous. Comparing these mineral compositions with those of aeolian dust deposited in this area and the local riverbed materials, we judged that the inorganic fraction could be explained by mixtures of aeolian dust and two kinds (crystalline and amorphous) of local volcanic materials.

We applied statistical unmixing of these mineral assemblage using PARAFAC algorithm on XRD profiles. Quantification of subcomponents such as Asian dust and local volcanic materials enabled us to estimate the variation of dust flux to this northern region for the last 5000 years. Comparison of our results with previous works for dust depositional history in southwestern region around Japan shows an antiphase variation of dust fluxes between north and south, which suggests the change in meandering pattern or pathway of westerly jet trasporting Asian dust.

Keywords: Asian dust, peat, Mt. Daisetsu, Holocene

©2019. Japan Geoscience Union. All Right Reserved.

Variations in sea surface environments recorded by algal biomarkers in the Japan Sea off the western coast of Hokkaido (IODP Site U1422) over the last 250 ka

*Asako Suzuki[1], Ken Sawada[2], Satoshi Furota[3], Yaeko Igarashi[4], Tomohisa Irino[5]

1. Graduate School of Science, Hokkaido University, 2. Department of Earth and Planetary Sciences, Faculty of Science, Hokkaido University, 3. Japan Agency for Marine-Earth Science and Technology, 4. Institute for Paleoenvironment of Northern Regions, 5. Faculty of Environmental Earth Science, Hokkaido University

The Japan Sea is a marginal sea that is closed by four straits, and the surface and deep waters are characterized by the Tsushima Warm Current (TWC), and Japan Sea Proper Water, respectively. In glacial-interglacial cycle, the sea surface environment in the Japan Sea has repeatedly changed by sea level fluctuation. It is reported that intense cooling of surface waters in the northern Japan Sea occurred caused by intensification of the East Asian Winter Monsoon (EAWM), but there have been few researches in this area. Thus, we analyzed algal biomarkers of a sediment core from the site U1422 (northern Japan Sea) of IODP Exp. 346 for the last 250ka. In particular, we apply the paleothermometer using long-chain alkyl diols, which are thought to be produced by diatoms and eustigmatophyte algae in addition to a proxy for sea surface temperature (SST based on alkenones, which are produced by haptophyte algae. The long-chain alkyl diols were also used as the proxies for upwelling intensity and inflow of fresh water, and thus, can provide multiple information for reconstruction of marine paleoenvironment.

The sediment cores studied were recovered at Site U1422 in the northern part of the Japan Basin (the Japan Sea off the western coast of Hokkaido) at 43°45.99’ N, 138°49.99’ E by Integrated Ocean Drilling Program (IODP) Expedition 346. We focus the duration from the MIS 8 to the present (-ca. 250ka). Lipids were extracted with dichloromethane/methanol, and separated to aliphatic, aromatic and polar fractions. Lipids were identified and quantified by GC-MS and GC-FID.

The SSTs based on alkenones and alkyl diols basically fluctuated along the glacial-interglacial cycles. The alkenone-based SSTs were found to be much higher than the diol-based SSTs during the MIS 2-3. The reasons of the differences are likely to be high contribution of distinctive alkenone producer during these stages. In our study, we calculated not only $U^{K'}_{37}$ but also the index containing tetra-unsaturated alkenone (U^{K}_{37}) in the SST estimate, because the tetra-unsaturated alkenone is abundantly detected in several samples. The U^{K}_{37}-based SSTs generally tend to be lower than those estimated by $U^{K'}_{37}$.

Diol Indices 1 and 2, which are proxies of upwelling intensity, are overall low levels. These results indicate that consistent upwelling system is hardly developed in the northern Japan Sea. However, the indices increase in the MIS 2, implying that vertical mixing was promoted as a result of the surface cooling in this stage. Moreover, the C_{32} 1, 15-diol ratio, which is considered as an indicator of fresh water input into marine environment, tended to increase at the transition periods, such as the glacial to interglacial periods. These results suggest that fresh water arisen by melting of snows and ices accumulated on lands was flowing into the Japan Sea through the rivers during these transitions. The increasing spikes of the diol-based fresh water index are also observed during the glacial periods. This can be attributed to the fresh waters arisen by sea ice melting that came from the northward and/or affected by the inflow of TWC as a result of sea-level falling.

©2019. Japan Geoscience Union. All Right Reserved.

Keywords: Northern Japan Sea, Algal biomarker, Alkenone, Diol, East Asian Monsoon, Quaternary

©2019. Japan Geoscience Union. All Right Reserved.

Decadal oscillation in hydrogen stable isotope ratio of long chain fatty acids in Lake Suigetsu sediment core

*Masaya Inagaki[1], Masanobu Yamamoto[1,2], Takeshi Nakagawa[3]

1. Graduate School of Environmental Science, Hokkaido University, 2. Faculty of Environmental Earth Science, Hokkaido University, 3. Research Center for Palaeoclimatology, Ritsumeikan University

Japanese weathers are affected by the Pacific Decadal Oscillation (PDO), monsoon, and El Niño Southern Oscillation. In this study, we analyzed the hydrogen isotopes of long chain n-fatty acids in sediment cores from Lake Suigetsu in Fukui Prefecture, and reconstructed variability in the isotopic ratio of precipitation from 1362 to 1662 CE and from1852 to 2017 CE. Hydrogen isotopic composition (δ D) showed decadal oscillation ranging from ~-170‰ to ~-120‰. Between 1362 and 1662 CE, this oscillation corresponded to the decadal oscillation seen in the UK37’ -based sea surface temperature (SST) in Beppu Bay. Higher SST corresponded to higher δ D. Because the SST in Beppu Bay corresponds to the PDO, we suppose that variability in the δ D of long chain n-fatty acids in Lake Suigetsu reflected the isotopic ratio of precipitation that responded to the PDO. In Nagoya, the isotope ratio of precipitation is governed by the position of Baiu front. When Baiu front is developed north of Nagoya, the isotope ratio is high. When Baiu front is south of Nagoya, isotope ratio is low (Kurita et al., 2015 Climate of the Past). This suggest that the position of the Baiu front was linked to the PDO from 1362 to 1662 CE. In the conditions of the negative PDO (high SST in Beppu Bay), the Baiu front was tended to be located north of Lake Suigetsu.

Keywords: PDO, isotopic ratio of precipitation, climate change

©2019. Japan Geoscience Union. All Right Reserved.

Amplitude modulation of sea surface temperature variability in the Bay of Bengal by 400-kyr eccentricity cycle

*Masanobu Yamamoto[1], Yuko Tsuchiya[1], Steven Clemens[2]

1. Faculty of Environmental Earth Science, Hokkaido University, 2. Department of Earth, Planetary and Environmental Sciences, Brown University

We generated a 1.7 kyr-resolution TEX_{86}-based sea surface temperature (SST) record from the International Ocean Discovery Program Site U1446 in the Bay of Bengal during the last 1.46 Myr. The SST varied synchronously with LR04 benthic foraminifera $\delta^{18}O$ and deep water $\delta^{13}C$. The cyclicity changed from 41-kyr to 100-kyr around 900 ka. The amplitude of SST variation responded to the 400-kyr cycles of eccentricity. Higher amplitude corresponded to low eccentricity. This suggests that eccentricity forced climate variability independently of the shift of cyclicity of glacial cycles across the Mid-Pleistocene Transition.

Keywords: Bay of Bengal, Sea surface temperature, Mid-Pleistocene Transition

©2019. Japan Geoscience Union. All Right Reserved.

[E] Poster | M (Multidisciplinary and Interdisciplinary)：M-IS Intersection

Thu. May 30, 2019 5:15 PM - 6:30 PM JST | Thu. May 30, 2019 8:15 AM - 9:30 AM UTC | Poster Hall International Exhibition Hall8, Makuhari Messe_34

[M-IS03] Evolution and variability of the Asian monsoon in Cenozoic global climate changes

convener:Masanobu Yamamoto(Faculty of Environmental Earth Science, Hokkaido University), Ryuji Tada(Department of Earth and Planetary Science, Graduate School of Science, The Univeristy of Tokyo)

The Asian Monsoon (AM) is a part of interhemispheric atmospheric phenomena that is driven by the thermal gradient between ocean and land. Contrasts of insolation, heat content and latent heat transfer between ocean and land may have affected the behavior of the AM in the past, but the proxy records are occasionally controversial and do not show a clear picture of the AM variability. Recent proxy and modeling studies suggest that glacial pCO2 cycles could be related to the position of southern westerlies, which is sensitive to interhemispheric heat imbalance. Because monsoon is driven by the heat imbalance, knowledge on the variability of the AM is important to understand the behavior of the global climate system. In this session, presentations on the reconstruction of long-term AM variability from various archives such as IODP expedition cores, discussion on its forcing, and the roles of the AM in global climate changes are welcome.

[MIS03-P01] Asian dust source variability since 10 Ma based on grain size specific mineral composition at IODP Site U1425 in the Japan Sea

*Mui Fa Alison Lee[1], Tomohisa Irino[1] (1.Faculty of Environmental Earth Science, Hokkaido University)

[MIS03-P02] Sources and formation environment of biomass burning products in Pliocene and Pleistocene marine sediments in the Japan Sea

*Song Lu[1], Youhei Yamashita[2], Tomohisa Irino[2] (1.Graduate School of Environmental Science, Hokkaido University , 2.Faculty of Environmental Earth Science, Hokkaido University)

[MIS03-P03] Variation of mineral dust flux in peat at a high moor on the Mt. Daisetsu during Holocene

*Tomohisa Irino[1], Keisuke Hirai[1], Osamu Seki[1], James Hooper[2], Samuel Marx[2] (1.Hokkaido University, 2.University of Wollongong)

[MIS03-P04] Variations in sea surface environments recorded by algal biomarkers in the Japan Sea off the western coast of Hokkaido (IODP Site U1422) over the last 250 ka

*Asako Suzuki[1], Ken Sawada[2], Satoshi Furota[3], Yaeko Igarashi[4], Tomohisa Irino[5] (1.Graduate School of Science, Hokkaido University, 2.Department of Earth and Planetary Sciences, Faculty of Science, Hokkaido University, 3.Japan Agency for Marine-Earth Science and Technology, 4.Institute for Paleoenvironment of Northern Regions, 5.Faculty of Environmental Earth Science, Hokkaido University)

[MIS03-P05] **Decadal oscillation in hydrogen stable isotope ratio of long chain fatty acids in Lake Suigetsu sediment core**

*Masaya Inagaki[1], Masanobu Yamamoto[1,2], Takeshi Nakagawa[3] (1.Graduate School of Environmental Science, Hokkaido University, 2.Faculty of Environmental Earth Science, Hokkaido University, 3.Research Center for Palaeoclimatology, Ritsumeikan University)

[MIS03-P06] **Amplitude modulation of sea surface temperature variability in the Bay of Bengal by 400-kyr eccentricity cycle**

*Masanobu Yamamoto[1], Yuko Tsuchiya[1], Steven Clemens[2] (1.Faculty of Environmental Earth Science, Hokkaido University, 2.Department of Earth, Planetary and Environmental Sciences, Brown University)

Asian dust source variability since 10 Ma based on grain size specific mineral composition at IODP Site U1425 in the Japan Sea

*Mui Fa Alison Lee[1], Tomohisa Irino[1]

1. Faculty of Environmental Earth Science, Hokkaido University

Sediments at Integrated Ocean Drilling Program (IODP) Site U1425 in the Japan Sea is under the strong influence of westerly jet stream and winter monsoon wind which transporting a significant amount of aeolian dust from both Taklamakan deserts and Gobi deserts. Aeolian dust from Taklamakan showed very high content of quartz (60-90%) and less plagioclase (5-40%) than from NE Chinese deserts and Loess (Gobi). The lower value of half height width (FWHM) of illite peak in X-ray diffraction (XRD) profile can be used as an indicator higher illite crystallinity. A decreasing trend of illite FWHM (increasing trend of the crystalinity) towards the core of the fold and thrust anticline has been recognized (Robinson et al. 1990; Orozco et al. 1998). Illite is also predominant component of the Chinese loess, and its highly crystallized nature has been interpreted to indicate that the illite was not formed at surface temperature and may have originated from a low temperature metamorphic environment.

In order to reconstruct a long-term changes in dust sources and transport pathways of Asian dust utilizing knowledges above, we examined mineral composition of IODP Site U1425 located at the central Japan Sea. The sediment samples were separated into >4 μm (silt) and <4 μm (clay) fractions by repeated pipette method. Both fractions were used for powder XRD analysis and peak heights of diagnostic peaks of major minerals were regarded as relative abundance of the minerals. FWHM and chemical index of illite were also examined.

In general, a very high quartz content found at Site U1425 may indicate sediments are aeolian source from Taklamakan deserts and higher plagioclase (albite) may infer dust source from Gobi deserts. Intervals around 9.5 Ma, 8.3 Ma, 7.9 Ma and 4.5 Ma showed very high quartz content and less albite at Site U1425, which indicate increases in dust supplied from Taklamakan than Gobi deserts due to stronger westerly wind. During Pliocene to early Pleistocene (4.2-2Ma), Taklamakan dust is still dominant, however the increasing influence of Gobi dust is recognized at 4.1 and 3.4Ma. On the other hand, an abrupt increase of the ratio of albite to quartz from 0.2 at 4.5 Ma to 0.8 at 4.1 Ma is found, which also shows another maximum at 0.6 Ma. In general, increase of albite abundance in sediments at Site U1425 during Pleistocene indicates the increasing dust supplied from NE China and Gobi deserts and the strengthened winter monsoon.

FWHM (crystallinity) of illite in silt fraction at Site U1425 showed low values (high crystallinity) with narrow range around 0.2°2θ during Pleistocene. The illite chemistry index showed values below 0.4 and genrerally around 0.3 during Pleistocene, which represents (Fe, Mg)-rich illites (biotite) characterized for physically eroded or unweathered rocks. The highly crystallized and Fe–Mg rich illites in the silt fraction at Site U1425 in the Japan Sea suggests their aeolian origin which may be derived from pre-existing sediments which eroded from low-grade metamorphic rocks in the northern regions of the Tibetan Plateau. In a longer time-scale, higher crystallinity and lower chemistry index of illite in silt fractions occurred in similar timing at 9.3 Ma and 6.6-2.7 Ma which could be correlated with the active regional uplift and tectonic activities of the northeastern margin of the Tibetan Plateau. Possible changes in source of illite indicates frequent plate tectonic activities near the Taklamakan deserts of North Tibet plateau especially from 6.6-2.7Ma.

©2019. Japan Geoscience Union. All Right Reserved.

Keywords: Aeolian dust, Taklamakan deserts, Quartz, Feldspar , Illite, Gobi deserts

©2019. Japan Geoscience Union. All Right Reserved.

Sources and formation environment of biomass burning products in Pliocene and Pleistocene marine sediments in the Japan Sea

*Song Lu[1], Youhei Yamashita[2], Tomohisa Irino[2]

1. Graduate School of Environmental Science, Hokkaido University , 2. Faculty of Environmental Earth Science, Hokkaido University

Behavior of black carbon (BC) is crucial for the earth surface environment because it could cause global warming by absorbing sunlight in the atmosphere. BC is originated from incomplete combustion of biomass or fossil fuels. Combustion in natural processes is incomplete due to local limitation of oxygen during the fire, which leads to the formation of organic fire residues. Robustness of BC to degradation in the natural environment enables us to use BC as a proxy to study the driving force of frequency and burning temperatures of past wildfire events. But the previous fire researches (paleoclimate rather than modern ecology) did not discuss the control factors for burning temperature or try to rebuild the fire temperature. Objective of this study is to understand factors controlling the thermal/optical/chemical characters of BC with burning temperature, provenance and aging in relation to the variabilities of vegetation in the hinterland. For these purposes, BC was quantified as elemental carbon (EC) in coarse (>2 μm) and fine (<2 μm) fractions of sediment samples using a thermal optical transmittance (TOT) method, and their burning temperatures were estimated for bulk samples through measurement of composition of benzene polycarboxylic acids (BPCAs), molecular markers of fire residues, determined with High Performance Liquid Chromatography (HPLC). In order to examine the relationship between burning temperature and BPCA composition, selected plants were experimentally charred to obtain standard charcoal samples. We also applied TOT and BPCA methods to marine sediments such as the surface sediments collected during KR15-10 cruise off the Wakasa Bay and 63 samples between 0 and 203 m CCSF-D were selected from IODP Site U1423 in the northeastern Japan Sea which covered the last 4.3 Myr. Size dependencies of EC contents and thermal properties will be compared with the contents and composition of BPCAs to examine the influence of sources, transport pathways, and burning temperatures of BCs contained in marine sediments.

Keywords: biomass burning, elemental carbon, benzene polycarboxylic acid

©2019. Japan Geoscience Union. All Right Reserved.

Variation of mineral dust flux in peat at a high moor on the Mt. Daisetsu during Holocene

*Tomohisa Irino[1], Keisuke Hirai[1], Osamu Seki[1], James Hooper[2], Samuel Marx[2]

1. Hokkaido University, 2. University of Wollongong

Mt. Daisetsu, Hokkaido, Japan is located just below the northern route of Asian dust transport and receives a significant amount of dust which dies snow surface brown in spring time every year. This area is also characterized by well-developed high moors on the mountains covering the last 4000 - 7500 yrs, which would continuously record the history of climate change during the middle to late Holocene. Peat collected from these high moor could be also a suitable material for a precise age determination using the radio carbon, and its inorganic fraction might consist of aeolian dust of continental origin and volcanic materials of the local origin which could be easily distinguished from each other.

Asian dust transported to the northern Japan may have a different source from those transported to the southwestern Japan. In spite of this, many of previous dust studies for Asian dust deposition in Japan have been conducted for the paleo-archives collected from the southern area. Therefore, it is necessary to reconstruct the composition and flux of Asian dust transported to the northern Japan in order to understand the spatio-temporal variability of westerly that could have significant influence on the climate in east Asia.

We collected peat cores from the high moor in Mt. Daisetsuzan area, and measured the mineral composition contained in peat. After heat treatment of peat samples, we conducted X-ray diffraction (XRD) analysis on the ash fraction and semi-quantified the minerals. Quartz, illite, and chlorite showed positive correlation among others, while various feldspars showed another positive correlation among others independent from quartz. Amorphous materials exhibited a variability different from quartz or feldspars. High ash content was associated with high feldspars or amorphous. Comparing these mineral compositions with those of aeolian dust deposited in this area and the local riverbed materials, we judged that the inorganic fraction could be explained by mixtures of aeolian dust and two kinds (crystalline and amorphous) of local volcanic materials.

We applied statistical unmixing of these mineral assemblage using PARAFAC algorithm on XRD profiles. Quantification of subcomponents such as Asian dust and local volcanic materials enabled us to estimate the variation of dust flux to this northern region for the last 5000 years. Comparison of our results with previous works for dust depositional history in southwestern region around Japan shows an antiphase variation of dust fluxes between north and south, which suggests the change in meandering pattern or pathway of westerly jet trasporting Asian dust.

Keywords: Asian dust, peat, Mt. Daisetsu, Holocene

©2019. Japan Geoscience Union. All Right Reserved.

Variations in sea surface environments recorded by algal biomarkers in the Japan Sea off the western coast of Hokkaido (IODP Site U1422) over the last 250 ka

*Asako Suzuki[1], Ken Sawada[2], Satoshi Furota[3], Yaeko Igarashi[4], Tomohisa Irino[5]

1. Graduate School of Science, Hokkaido University, 2. Department of Earth and Planetary Sciences, Faculty of Science, Hokkaido University, 3. Japan Agency for Marine-Earth Science and Technology, 4. Institute for Paleoenvironment of Northern Regions, 5. Faculty of Environmental Earth Science, Hokkaido University

The Japan Sea is a marginal sea that is closed by four straits, and the surface and deep waters are characterized by the Tsushima Warm Current (TWC), and Japan Sea Proper Water, respectively. In glacial-interglacial cycle, the sea surface environment in the Japan Sea has repeatedly changed by sea level fluctuation. It is reported that intense cooling of surface waters in the northern Japan Sea occurred caused by intensification of the East Asian Winter Monsoon (EAWM), but there have been few researches in this area. Thus, we analyzed algal biomarkers of a sediment core from the site U1422 (northern Japan Sea) of IODP Exp. 346 for the last 250ka. In particular, we apply the paleothermometer using long-chain alkyl diols, which are thought to be produced by diatoms and eustigmatophyte algae in addition to a proxy for sea surface temperature (SST based on alkenones, which are produced by haptophyte algae. The long-chain alkyl diols were also used as the proxies for upwelling intensity and inflow of fresh water, and thus, can provide multiple information for reconstruction of marine paleoenvironment.

The sediment cores studied were recovered at Site U1422 in the northern part of the Japan Basin (the Japan Sea off the western coast of Hokkaido) at 43°45.99’ N, 138°49.99’ E by Integrated Ocean Drilling Program (IODP) Expedition 346. We focus the duration from the MIS 8 to the present (-ca. 250ka). Lipids were extracted with dichloromethane/methanol, and separated to aliphatic, aromatic and polar fractions. Lipids were identified and quantified by GC-MS and GC-FID.

The SSTs based on alkenones and alkyl diols basically fluctuated along the glacial-interglacial cycles. The alkenone-based SSTs were found to be much higher than the diol-based SSTs during the MIS 2-3. The reasons of the differences are likely to be high contribution of distinctive alkenone producer during these stages. In our study, we calculated not only $U^{K'}_{37}$ but also the index containing tetra-unsaturated alkenone (U^{K}_{37}) in the SST estimate, because the tetra-unsaturated alkenone is abundantly detected in several samples. The U^{K}_{37}-based SSTs generally tend to be lower than those estimated by $U^{K'}_{37}$.

Diol Indices 1 and 2, which are proxies of upwelling intensity, are overall low levels. These results indicate that consistent upwelling system is hardly developed in the northern Japan Sea. However, the indices increase in the MIS 2, implying that vertical mixing was promoted as a result of the surface cooling in this stage. Moreover, the C_{32} 1, 15-diol ratio, which is considered as an indicator of fresh water input into marine environment, tended to increase at the transition periods, such as the glacial to interglacial periods. These results suggest that fresh water arisen by melting of snows and ices accumulated on lands was flowing into the Japan Sea through the rivers during these transitions. The increasing spikes of the diol-based fresh water index are also observed during the glacial periods. This can be attributed to the fresh waters arisen by sea ice melting that came from the northward and/or affected by the inflow of TWC as a result of sea-level falling.

©2019. Japan Geoscience Union. All Right Reserved.

Keywords: Northern Japan Sea, Algal biomarker, Alkenone, Diol, East Asian Monsoon, Quaternary

©2019. Japan Geoscience Union. All Right Reserved.

Decadal oscillation in hydrogen stable isotope ratio of long chain fatty acids in Lake Suigetsu sediment core

*Masaya Inagaki[1], Masanobu Yamamoto[1,2], Takeshi Nakagawa[3]

1. Graduate School of Environmental Science, Hokkaido University, 2. Faculty of Environmental Earth Science, Hokkaido University, 3. Research Center for Palaeoclimatology, Ritsumeikan University

Japanese weathers are affected by the Pacific Decadal Oscillation (PDO), monsoon, and El Niño Southern Oscillation. In this study, we analyzed the hydrogen isotopes of long chain n-fatty acids in sediment cores from Lake Suigetsu in Fukui Prefecture, and reconstructed variability in the isotopic ratio of precipitation from 1362 to 1662 CE and from1852 to 2017 CE. Hydrogen isotopic composition (δ D) showed decadal oscillation ranging from ~-170‰ to ~-120‰. Between 1362 and 1662 CE, this oscillation corresponded to the decadal oscillation seen in the UK37’ -based sea surface temperature (SST) in Beppu Bay. Higher SST corresponded to higher δ D. Because the SST in Beppu Bay corresponds to the PDO, we suppose that variability in the δ D of long chain n-fatty acids in Lake Suigetsu reflected the isotopic ratio of precipitation that responded to the PDO. In Nagoya, the isotope ratio of precipitation is governed by the position of Baiu front. When Baiu front is developed north of Nagoya, the isotope ratio is high. When Baiu front is south of Nagoya, isotope ratio is low (Kurita et al., 2015 Climate of the Past). This suggest that the position of the Baiu front was linked to the PDO from 1362 to 1662 CE. In the conditions of the negative PDO (high SST in Beppu Bay), the Baiu front was tended to be located north of Lake Suigetsu.

Keywords: PDO, isotopic ratio of precipitation, climate change

©2019. Japan Geoscience Union. All Right Reserved.

Amplitude modulation of sea surface temperature variability in the Bay of Bengal by 400-kyr eccentricity cycle

*Masanobu Yamamoto[1], Yuko Tsuchiya[1], Steven Clemens[2]

1. Faculty of Environmental Earth Science, Hokkaido University, 2. Department of Earth, Planetary and Environmental Sciences, Brown University

We generated a 1.7 kyr-resolution TEX_{86}-based sea surface temperature (SST) record from the International Ocean Discovery Program Site U1446 in the Bay of Bengal during the last 1.46 Myr. The SST varied synchronously with LR04 benthic foraminifera $\delta^{18}O$ and deep water $\delta^{13}C$. The cyclicity changed from 41-kyr to 100-kyr around 900 ka. The amplitude of SST variation responded to the 400-kyr cycles of eccentricity. Higher amplitude corresponded to low eccentricity. This suggests that eccentricity forced climate variability independently of the shift of cyclicity of glacial cycles across the Mid-Pleistocene Transition.

Keywords: Bay of Bengal, Sea surface temperature, Mid-Pleistocene Transition

©2019. Japan Geoscience Union. All Right Reserved.

[E] Poster | M (Multidisciplinary and Interdisciplinary)：M-IS Intersection

Thu. May 30, 2019 10:45 AM - 12:15 PM JST | Thu. May 30, 2019 1:45 AM - 3:15 AM UTC | Poster Hall International Exhibition Hall8, Makuhari Messe_10

[M-IS04] Interdisciplinary studies on pre-earthquake processes

convener:Katsumi Hattori(Department of Earth Sciences, Graduate School of Science, Chiba University), JANN-YENQ Liu(Institute of Space Science, National Central University, Taiwan), Dimitar Ouzounov(Center of Excellence in Earth Systems Modeling & Observations (CEESMO) , Schmid College of Science & Technology Chapman University, Orange, California, USA), Qinghua Huang(Peking University)

This session expands the interdisciplinary discussions on preparation process of earthquake and earthquake predictability by presenting the latest progress in studying the physically based pre-earthquake phenomena. New observations from space and ground have provided
evidences, which may enhance better understanding of tectonic activity. The session anticipates talks that include but not limited to observations and analyses of seismic, electrical, electromagnetic, electro-chemical and thermodynamic processes related to stress changes in the lithosphere along with their statistical and physical validation. Presentations on the latest observational results associated with major earthquakes obtained by different methodologies are welcomed. The topics of the session are as follows but not limited.

-General discussion on earthquake preparation process and the physics of pre-earthquake signals

- Theory, modeling, laboratory experiments, computational simulation for generation and propagation of pre-earthquake signals and their connection with seismic cycle

 - Multi-parameter observations, detection, and validation of pre-earthquake signals

 - Cross-disciplinary studies, practical and technical approaches for better understanding of earthquake preparation processes and their connection with seismicity

[MIS04-P01] Statistical analysis and Evaluation of ULF seismo-magnetic phenomena at Kakioka, Japan, during 1983-2017

*Kei Takahashi[1], Katsumi Hattori[2], Peng Han[3] (1.Faculty of Science, Chiba University, 2.Graduate School of Science, Chiba University, 3.Southern University of Science and Technology, China)

[MIS04-P02] Pre-seismic anomalies on Earth’s magnetic field and ionosphere electron density using Swarm data

*Amune Yamazaki[1], Katsumi Hattori[1], Rui Song[1] (1.Chiba University)

[MIS04-P03] Measurement of radon density in the atmosphere at Okayama, Kochi, Choshi and Kiyosumi, II

*Tohru Okabayashi[1], Kiyotaka Ninagawa[2], Isao Yamamoto[3], Katsumi Hattori[4], Chie Yoshino[4], Haruna Kojima[4], Nobuhiro Maeda (1.Department of Merical Risk and Crisis Management, Faculty of Risk and Crisis Management, Chiba Institute of Science, 2.Faculty of Science, Okayama University of Science, 3.Falcuty of Engineering, Okayama University of Science, 4.Graduate school of Science, Chiba University)

[MIS04-P04] Possible anomalous changes in solar quiet-daily geomagnetic variation *Sq* related to the 2011 off the Pacific coast of Tohoku earthquake (Mw 9.0)

*Xiaocan Liu[1], Katsumi Hattori[2,3], Peng Han[4], Huaran Chen[1] (1.Institute of geophysics China Earthquake Administrition, 2.Graduate School of Science, Chiba University, Chiba, Japan, 3. Center for Environmental Remote Sensing, Chiba University, Chiba, Japan, 4.Department of Earth and Space Sciences, Southern University of Science and Technology, ShenZhen, China)

[MIS04-P05] Co-seismic geomagnetic fluctuations and atmospheric disturbances during the 2018 M6.2 Hualien Earthquake

*Chun-Rong Chen[1], JANN-YENQ Liu[1] (1.Graduate Institute of Space Science, National Central University)

[MIS04-P06] Multi-sensor monitoring network for earthquake precursor study near subduction zone at Boso, Japan

*Katsumi Hattori[1], Chie Yoshino[1], WEIYUN XIE[2], Sanaka Saito[2], Haruna Kojima[2], Rui Song[2], Peng Han[3], Toru Mogi[4], Tada-nori Goto[5], Ichi Takumi[6], Hiroshi Yasukawa[7], Motoaki Mouri[8], Jun Izutsu[9], Tadashi Takano[10], Chihiro Yamanaka[11], Masashi Kamogawa[12], Yoshiaki Ando[13], JANN-YENQ Liu[14], Dimitar Ouzounov[15], Valery Tramutoli[16] (1.Department of Earth Sciences, Graduate School of Science, Chiba University, 2.Graduate School of Science and Engineering, Chiba University, 3.Southern University of Science and Technology, China, 4.Hokkaido University, 5.Kyoto University, 6.Nagoya Institute of Technology, 7.Aichi Prefectural University, 8.Aichi University, 9.Chubu University, 10.Nihon University, 11.Osaka University, 12.Tokyo Gakugei University, 13.The University of Electro-Communications, 14.National Central University, Taiwan, 15.Chapman University, US, 16.University of Basilicagta, Italy)

[MIS04-P07] Transient Effects in Atmosphere and Ionosphere Associated with 2018 Mw 7.5 Sulawesi Indonesia Earthquake and Triggered Tsunami and Volcano Activities

★Invited Papers

*Dimitar Ouzounov[1], Sergey Pulinets[2], Dmitry Davidenko[2], Alexander Rozhnoi[3], Maria Solovieva[3], Tiger Liu[4] (1.Center of Excellence in Earth Systems Modeling & Observations (CEESMO) , Schmid College of Science & Technology Chapman University, Orange, California, USA, 2.Space Research Institute, RAS, Moscow, Russia, 3.The Schmidt Institute of Physics of the Earth, RAS, Moscow, Russia, 4.Center for Astronautical Physics and Engineering, National Central University, Taoyuan City, Taiwan)

[MIS04-P08] Seismicity change and b value variation prior to the Wenchuan earthquake (*Ms 8.0*)

*Peng Han[1], Rui Wang[1], Ying Chang[1], Miao Miao[1], Haixia Shi[2], Lingyuan Meng[2], Xuemei Zhang[2], Weiyun Xie[3], Katsumi Hattori[3] (1.Southern University of Science and Technology, Shenzhen, China, 2.China Earthquake Networks Center, Beijing 100045, China, 3.Chiba University, Chiba, Japan)

Statistical analysis and Evaluation of ULF seismo-magnetic phenomena at Kakioka, Japan, during 1983-2017

*Kei Takahashi[1], Katsumi Hattori[2], Peng Han[3]

1. Faculty of Science, Chiba University, 2. Graduate School of Science, Chiba University, 3. Southern University of Science and Technology, China

To clarify and verify the ultralow frequency (ULF) seismo-magnetic phenomena, we have performed statistical studies on the geomagnetic data observed at the Kakioka (KAK) station, Japan, during 1983-2017. We investigated the energy of ULF geomagnetic signals of the frequency around 0.01 Hz using wavelet transform analysis. To minimize the influences of artificial noises and global magnetic perturbations, we used only the geomagnetic data observed at midnight time (LT 2:30 A.M. to 4:00 A.M.).We define the geomagnetic anomalies when the Z components of geomagnetic data exceeds median + 1.5 IQR, where IQR is the interquartile range. Considering that ionospheric disturbances may also lead to enhancements in the Z component, we exclude the anomaly when the energy of H component exceeds median + 3.0 IQR. Statistical analysis of superposed epoch analysis have indicated that ULF magnetic anomalies are more likely to appear before sizable isolated earthquake events (Es parameter which is higher than 8th power of 10 and no earthquake events during ±45 days) rather than after them, especially 6-10 days before the events. Finally, we have evaluated the precursory information of ULF geomagnetic signals for local sizable earthquakes using Molchan’ s error diagram. The above results have indicated that the ULF seismo-magnetic phenomena at Kakioka clearly contain precursory information and have a possibility of improving forecasting of large earthquakes.

©2019. Japan Geoscience Union. All Right Reserved.

Pre-seismic anomalies on Earth’s magnetic field and ionosphere electron density using Swarm data

*Amune Yamazaki[1], Katsumi Hattori[1], Rui Song[1]

1. Chiba University

An earthquake is a rapid release of stress in the lithosphere and often leads to serious damages on human lives and society. Even though the short-time forecast of earthquake is important, it is not achieved yet. However, many electromagnetic phenomena that may be related to seismic activity have been reported recently. The satellite, one of the useful tools to observe these phenomena, can cover the global areas and can collect a large amount of data related to earthquakes which have large magnitude worldwide in short time. The Swarm satellites mission started to operate on November 22, 2013 by European Space Agency, with the constellation of three satellites (A, B, C) The anomalies preceded to the Ecuador earthquake in 2016 have been reported using the Swarm data. In this paper, in order to validate these results using the magnetic vector Y data by VFM and electron density data by Langmuir probe, we have analyzed the Swarm data related the M6.3~6.9 earthquakes occurred at Lombok Island, Indonesia, in July 28, August 5, and 19, 2018. The study area is a 1000 km square from the epicenter of 20180805 earthquake and the analyzed period is from May 28 to September 27, 2018. In this paper we report night-time orbit data at 18:00-6:00 LT.

As results, we found the following tendencies; (1) positive anomalies on magnetic Y vector about 1-2 weeks before the earthquakes and (2) negative anomalies on electron density from 1 week to 1 month before the earthquakes. We performed the same analysis to the data on the same period in 2016 and 2017 for reference when there were no M6+ earthquakes. We found that the number of anomaly track is only abruptly increased in the short period from the end of June to July in 2018, and that the trend is not able to be found in 2016 and 2017. From this unique trend in 2018, it is suggestive of the existence of the relation between the local seismic activity and in-situ satellite anomalies in the magnetic field and electron density in Lombok area.

©2019. Japan Geoscience Union. All Right Reserved.

Measurement of radon density in the atmosphere at Okayama, Kochi, Choshi and Kiyosumi, II

*Tohru Okabayashi[1], Kiyotaka Ninagawa[2], Isao Yamamoto[3], Katsumi Hattori[4], Chie Yoshino[4], Haruna Kojima[4], Nobuhiro Maeda

1. Department of Merical Risk and Crisis Management, Faculty of Risk and Crisis Management, Chiba Institute of Science, 2. Faculty of Science, Okayama University of Science, 3. Falcuty of Engineering, Okayama University of Science, 4. Graduate school of Science, Chiba University

We report continuous measurement of radon density in atmosphere at Okayama for three years, Kochi, Choshi and Kiyosumi for two years. An increase of radon density in groundwater at Nishinomiya city [1] and in atmosphere [2] at the southern part of Hyogo Prefecture Earthquake in 1995 were reported, respectively. In the case of Tohoku Region Pacific Coast Earthquake, the data obtained the exhaust air monitor that peak duration was long and the peak decreased rapidly before earthquake has been reported at the radiation facility of Fukushima Medical College in Fukushima [3]. On the other hand, a PIN photodiode have been developed and used as a high sensitive alpha ray detector in Super Kamiokande [4]. Since 2016, we also made an experimental setup using PIN photodiode, and measured the radon density in atmosphere. Using a Si PIN photodiode (S3204-09, unsealed, Hamamatsu Photodiode K.K.) as an alpha ray detector, we constructed radon detection setup combined with aluminum pot as an air accumulator, H4083 (Hamamatsu) as a charge amplifier, C4900-01 (Hamamatsu) as a high voltage power supply module, a pulse shaped amplifier with time constant of 10 msec, a multi channel analyzer (MCA-LiteN), and a PC as a data analysis. Obtained alpha spectra of atmosphere showed 4 peaks originated from ^{218}Po, ^{214}Po and ^{210}Po of U series, and ^{212}Po of Th series. Since 2017, we newly started to measure at Kochi, Choshi and Kiyosumi using our apparatus. Details of observed data are discussed in addition the data at Okayama since 2016.

[1] Igarashi G., Saeki S., Takahata N., Sumikawa K., Tasaka S., Sasaki Y., Takahashi M. and Sano Y. : Ground-water radon anomaly before the Kobe earthquake in Japan, Science, 269, 60-61, 1995.
[2] Yasuoka, Y. and Shinogi, M.: Anomaly in atmospheric radon concentration: a possible precursor of the 1995 Kobe, Japan, earthquake. Health Physics, 72, 759-761, 1997.
[3] Nagahama H., Yasuoka Y., Suzuki T., and Homma Y.: Radon Variation in the Air Before the 2011 Tohoku Earthquake (Mw =9.0), Programme and Abstracts, A32-09, The Seismological Society of Japan. 2011, Fall Meeting.
[4] Nemoto, M., Tasaka S., Hori H., Okumura K., Kajita T., and Takeuchi Y. : Development of High Sensitive Radon Detector with Electrostatic Collection. Radioisotopes, 46, 710-719, 1997 (Japanese).

Keywords: radon, atmosphere, earthquake prediction

©2019. Japan Geoscience Union. All Right Reserved.

Possible anomalous changes in solar quiet-daily geomagnetic variation *Sq* related to the 2011 off the Pacific coast of Tohoku earthquake (Mw 9.0)

*Xiaocan Liu[1], Katsumi Hattori[2,3], Peng Han[4], Huaran Chen[1]

1. Institute of geophysics China Earthquake Administrition, 2. Graduate School of Science, Chiba University, Chiba, Japan, 3. Center for Environmental Remote Sensing, Chiba University, Chiba, Japan, 4. Department of Earth and Space Sciences, Southern University of Science and Technology, ShenZhen, China

Seismo-electromagnetic researches have been studied for decades (e.g. Hayakawa and Fujinawa, 1994; Hayakawa and Molchanov, 2002, 2008,2013; Hattori, 2004, Hattori, et al., 2004a, 2004b; Hayakawa et al., 2007;, Hattori et al., 2013; Han et al., 2011, 2014, 2015, 2016, 2017; Huang QH et al., 2011, 2015; Du A, Huang Q et al., 2002, Rong YM et al., 2012, Yuan G.P., Zhang X.M. et al. 2015), and the geomagnetic diurnal variation (GDV) is a stable variation of the geomagnetic field that can be used to detect possible anomalous changes associated with large earthquakes.

We investigated data observed at 20 geomagnetic observatories at longitudes of 130˚E to 150˚E between 2009 and 2012 to detect possible anomalous changes in the geomagnetic solar quiet daily variation (Sq) related to the 2011 off the Pacific coast of Tohoku earthquake (Mw 9.0) occurred on March 11, 2011 in Japan. We selected the 5 quiet days every month and analyzed three component magnetic data with 1 min resolution using the natural orthogonal component (NOC) method to identify Sq variations from observations, and performed the spherical harmonic analysis (SHA) to separate the internal and the external equivalent Sq current systems of Je and Ji. We obtained that, Je and Ji are distorted near the epicenter area on two geomagnetic quiet days of January 23 and 27, 2011. They are about two months before the earthquake. Then, we made backward computation on the external and internal parts of the SHA model geomagnetic fields, Be and Bi, to determine the possible anomalous magnetic field variations at each station. Results show significant differences in daily variation for all components on January 23 and 27, 2011. The other days, we could not recognize any apparent anomalous behaviors, except known secular, seasonal, and solar activity dependences. A possible connection between this anomaly and the very strong Tohoku earthquake, which followed only one and half month after the geomagnetic anomaly is of highest interest for the research on earthquake precursors.

Keywords: geomagnetic solar quiet daily variation (Sq), natural orthogonal component (NOC) method, spherical harmonic analysis (SHA), the 2011 off the Pacific coast of Tohoku earthquak

©2019. Japan Geoscience Union. All Right Reserved.

Co-seismic geomagnetic fluctuations and atmospheric disturbances during the 2018 M6.2 Hualien Earthquake

*Chun-Rong Chen[1], JANN-YENQ Liu[1]

1. Graduate Institute of Space Science, National Central University

The strong ground motion of 6 February 2018 M6.2 Hualien Earthquake triggered a series of co-seismic geomagnetic fluctuations and seismo-traveling atmospheric disturbances (STADs) signatures in infrasonic waves and micro-pressures upon the seismic wave arrival. Networks of 9 QuakeFinder systems, 3 infrasound systems, 2 tiltmeters, 2 micro-barometers, and 11 co-located seismometers are used in this study. Each QuakeFinder system consists of a 3-axes induction magnetometer, an air conductivity sensor, a geophone, and temperature/relative humidity sensors. Co-seismic signatures clearly appear in the induction magnetometers, infrasound systems, and micro-barometers data. The magnetometers register both high- and low-frequency pulsations. Geomagnetic fluctuations occur upon the seismic wave arrival but last a longer duration, while the STADs lag their co-located seismic waves by about 15-45 seconds. The long-lasting fluctuations recorded by both induction and fluxgate magnetometers suggest that the ground/underground water motion play an important role, which is further conformed by low-frequency fluctuations in the tiltmeter data. In general, the amplitude of geomagnetic fluctuations decays as away from the epicenter. However, unusual large co-seismic geomagnetic fluctuations are detected over areas of the abnormal seismic intensity level and/or the magnetic underground structure with anomalously high susceptibilities.

Keywords: Geomagnetic, QuakeFinder, Infrasound, micro-Barometer, Tiltmeter

©2019. Japan Geoscience Union. All Right Reserved.

Multi-sensor monitoring network for earthquake precursor study near subduction zone at Boso, Japan

*Katsumi Hattori[1], Chie Yoshino[1], WEIYUN XIE[2], Sanaka Saito[2], Haruna Kojima[2], Rui Song[2], Peng Han[3], Toru Mogi[4], Tada-nori Goto[5], Ichi Takumi[6], Hiroshi Yasukawa[7], Motoaki Mouri[8], Jun Izutsu[9], Tadashi Takano[10], Chihiro Yamanaka[11], Masashi Kamogawa[12], Yoshiaki Ando[13], JANN-YENQ Liu[14], Dimitar Ouzounov[15], Valery Tramutoli[16]

1. Department of Earth Sciences, Graduate School of Science, Chiba University, 2. Graduate School of Science and Engineering, Chiba University, 3. Southern University of Science and Technology, China, 4. Hokkaido University, 5. Kyoto University, 6. Nagoya Institute of Technology, 7. Aichi Prefectural University, 8. Aichi University, 9. Chubu University, 10. Nihon University, 11. Osaka University, 12. Tokyo Gakugei University, 13. The University of Electro-Communications, 14. National Central University, Taiwan, 15. Chapman University, US, 16. University of Basilicagta, Italy

New observations from ground and space have provided multiple evidences of pre-earthquake signals and the latest studies show their statistical significance, repeatability, and universality. In this project, to understand the preparation process of large earthquakes and slow-slip events in subduction zone, especially to clarify the nucleation stage of the earthquake cycle, we plan to establish a dense observation network in Boso, Japan, where large subduction earthquakes are expected soon. Since the subsurface fluid flow may play an important role in the preparation process of subduction activities, we intend to employ electromagnetic approaches including oceanic and continental MT survey to monitor the underground resistivity structure which is sensitive to the dynamics of fluid. Other geophysical monitoring such as ULF geomagnetic and geoelectrical observations, radon measurements, and inland GPS movements, TIR, and OLR will be incorporated to help to understand the preparation process and evaluate the applicability of various pre-earthquake signals towards short term earthquake forecasting. We call this idea “sensor WEB”. We will show the state of the art and some results in our presentation.
This study is supported by Grand-in-Aids for Scientific Research of Japan Society for Promotion of Science (26249060).

©2019. Japan Geoscience Union. All Right Reserved.

Transient Effects in Atmosphere and Ionosphere Associated with 2018 Mw 7.5 Sulawesi Indonesia Earthquake and Triggered Tsunami and Volcano Activities

*Dimitar Ouzounov[1], Sergey Pulinets[2], Dmitry Davidenko[2], Alexander Rozhnoi[3], Maria Solovieva[3], Tiger Liu[4]

1. Center of Excellence in Earth Systems Modeling & Observations (CEESMO) , Schmid College of Science & Technology Chapman University, Orange, California, USA, 2. Space Research Institute, RAS, Moscow, Russia, 3. The Schmidt Institute of Physics of the Earth, RAS, Moscow, Russia, 4. Center for Astronautical Physics and Engineering, National Central University, Taoyuan City, Taiwan

We analyze retrospectively the transient variations of four different physical parameters of atmosphere/ionosphere during the time of M7.5 od Sept 28, 2018 in Indonesia namely: (i) thermodynamic proprieties in the lower atmosphere, (ii) outgoing earth radiation (OLR) at the TOA, (ii) GPS/TEC and (iv) the very-low-frequency (VLF/LF) signals at the receiving station in Petropavlovsk-Kamchatski (RTK, Russia). We found that in the second part of September 2018 a rapid augment of satellite observed earth radiation in the atmosphere and the anomaly located in close vicinity to the future M7.5 epicenter reached the maximum on Sept 21-22. The GPS/TEC data analysis indicates an augment and variation in electron density reaching a maximum value during the Sept 26-27 periods. Two VLF/LF crossing wave paths - NWC-RTK and JJY-RTK, have shown abnormal behavior of signals during on days Sept 26-28 two days before the earthquake. Our results show coherence between the appearance of pre-earthquake transient’ s effects in atmosphere and ionosphere (with a short time-lag, from hours up to a few days) and the occurrence of 2018 M7.5 in Indonesia. Traveling ionospheric tsunami disturbances (TITDs) in the total electron content (TEC) induced by tsunami waves of the 28 September 2018 Mw 7.5 Sulawesi Indonesia earthquake are detected by of seven ground-based receivers of the global positioning system (GPS) in South Asia, Oceanic, Pacific areas. It is found that the origin is about 100 km North of the epicenter and the horizontal speed is of about 187 m/s.

The pre-earthquake nature of the signals in atmosphere and ionosphere were revealed by simultaneous analysis of satellite, GPS/TEC and VLF/LF observations and suggest that they follow a general temporal-spatial evolution pattern, which has been seen in other large earthquakes worldwide.

Keywords: earthquake, tsunami, volcano, precursor, GPS/TEC, thermal anomaly

©2019. Japan Geoscience Union. All Right Reserved.

Seismicity change and b value variation prior to the Wenchuan earthquake (*Ms 8.0*)

*Peng Han[1], Rui Wang[1], Ying Chang[1], Miao Miao[1], Haixia Shi[2], Lingyuan Meng[2], Xuemei Zhang[2], Weiyun Xie[3], Katsumi Hattori[3]

1. Southern University of Science and Technology, Shenzhen, China, 2. China Earthquake Networks Center, Beijing 100045, China, 3. Chiba University, Chiba, Japan

The Gutenberg-Richter Law describes frequency-magnitude distribution of earthquakes. A number of studies have shown that the slope (b value) of the relationship between frequency and magnitude decreased before large earthquakes. Based on the analysis of the earthquake catalog from January, 2000 to April, 2008, we have investigated seismicity change and b value variation prior to the *Ms* 8.0 Wenchuan earthquake. The results show clear drops of both monthly and quarterly frequency of earthquakes during 2005-2006. The b value exhibits a long-term decrease trend since 2002, and reaches to the minimum just before the onset of the main shock. The temporal variation of b value is quite similar to that prior to the *Mw* 9.0 Tohoku earthquake in Japan, which may reflect the stress evolution during the preparation process of large earthquakes. These results indicate that the b value is an important indicator of an impending great earthquake, and has high potential in terms of predicting a future large quake.

Keywords: Wenchuan earthquake, b value, seismicity

©2019. Japan Geoscience Union. All Right Reserved.

[E] Poster | M (Multidisciplinary and Interdisciplinary)：M-IS Intersection

Thu. May 30, 2019 5:15 PM - 6:30 PM JST | Thu. May 30, 2019 8:15 AM - 9:30 AM UTC | Poster Hall International Exhibition Hall8, Makuhari Messe_35

[M-IS04] Interdisciplinary studies on pre-earthquake processes

convener:Katsumi Hattori(Department of Earth Sciences, Graduate School of Science, Chiba University), JANN-YENQ Liu(Institute of Space Science, National Central University, Taiwan), Dimitar Ouzounov(Center of Excellence in Earth Systems Modeling & Observations (CEESMO) , Schmid College of Science & Technology Chapman University, Orange, California, USA), Qinghua Huang(Peking University)

This session expands the interdisciplinary discussions on preparation process of earthquake and earthquake predictability by presenting the latest progress in studying the physically based pre-earthquake phenomena. New observations from space and ground have provided
evidences, which may enhance better understanding of tectonic activity. The session anticipates talks that include but not limited to observations and analyses of seismic, electrical, electromagnetic, electro-chemical and thermodynamic processes related to stress changes in the lithosphere along with their statistical and physical validation. Presentations on the latest observational results associated with major earthquakes obtained by different methodologies are welcomed. The topics of the session are as follows but not limited.

-General discussion on earthquake preparation process and the physics of pre-earthquake signals

- Theory, modeling, laboratory experiments, computational simulation for generation and propagation of pre-earthquake signals and their connection with seismic cycle

 - Multi-parameter observations, detection, and validation of pre-earthquake signals

 - Cross-disciplinary studies, practical and technical approaches for better understanding of earthquake preparation processes and their connection with seismicity

[MIS04-P01] Statistical analysis and Evaluation of ULF seismo-magnetic phenomena at Kakioka, Japan, during 1983-2017

*Kei Takahashi[1], Katsumi Hattori[2], Peng Han[3] (1.Faculty of Science, Chiba University, 2.Graduate School of Science, Chiba University, 3.Southern University of Science and Technology, China)

[MIS04-P02] Pre-seismic anomalies on Earth’s magnetic field and ionosphere electron density using Swarm data

*Amune Yamazaki[1], Katsumi Hattori[1], Rui Song[1] (1.Chiba University)

[MIS04-P03] Measurement of radon density in the atmosphere at Okayama, Kochi, Choshi and Kiyosumi, II

*Tohru Okabayashi[1], Kiyotaka Ninagawa[2], Isao Yamamoto[3], Katsumi Hattori[4], Chie Yoshino[4], Haruna Kojima[4], Nobuhiro Maeda (1.Department of Merical Risk and Crisis Management, Faculty of Risk and Crisis Management, Chiba Institute of Science, 2.Faculty of Science, Okayama University of Science, 3.Falcuty of Engineering, Okayama University of Science, 4.Graduate school of Science, Chiba University)

[MIS04-P04] Possible anomalous changes in solar quiet-daily geomagnetic variation *Sq* related to the 2011 off the Pacific coast of Tohoku earthquake (Mw 9.0)

*Xiaocan Liu[1], Katsumi Hattori[2,3], Peng Han[4], Huaran Chen[1] (1.Institute of geophysics China Earthquake Administrition, 2.Graduate School of Science, Chiba University, Chiba, Japan, 3. Center for Environmental Remote Sensing, Chiba University, Chiba, Japan, 4.Department of Earth and Space Sciences, Southern University of Science and Technology, ShenZhen, China)

[MIS04-P05] Co-seismic geomagnetic fluctuations and atmospheric disturbances during the 2018 M6.2 Hualien Earthquake

*Chun-Rong Chen[1], JANN-YENQ Liu[1] (1.Graduate Institute of Space Science, National Central University)

[MIS04-P06] Multi-sensor monitoring network for earthquake precursor study near subduction zone at Boso, Japan

*Katsumi Hattori[1], Chie Yoshino[1], WEIYUN XIE[2], Sanaka Saito[2], Haruna Kojima[2], Rui Song[2], Peng Han[3], Toru Mogi[4], Tada-nori Goto[5], Ichi Takumi[6], Hiroshi Yasukawa[7], Motoaki Mouri[8], Jun Izutsu[9], Tadashi Takano[10], Chihiro Yamanaka[11], Masashi Kamogawa[12], Yoshiaki Ando[13], JANN-YENQ Liu[14], Dimitar Ouzounov[15], Valery Tramutoli[16] (1.Department of Earth Sciences, Graduate School of Science, Chiba University, 2.Graduate School of Science and Engineering, Chiba University, 3.Southern University of Science and Technology, China, 4.Hokkaido University, 5.Kyoto University, 6.Nagoya Institute of Technology, 7.Aichi Prefectural University, 8.Aichi University, 9.Chubu University, 10.Nihon University, 11.Osaka University, 12.Tokyo Gakugei University, 13.The University of Electro-Communications, 14.National Central University, Taiwan, 15.Chapman University, US, 16.University of Basilicagta, Italy)

[MIS04-P07] Transient Effects in Atmosphere and Ionosphere Associated with 2018 Mw 7.5 Sulawesi Indonesia Earthquake and Triggered Tsunami and Volcano Activities

★Invited Papers

*Dimitar Ouzounov[1], Sergey Pulinets[2], Dmitry Davidenko[2], Alexander Rozhnoi[3], Maria Solovieva[3], Tiger Liu[4] (1.Center of Excellence in Earth Systems Modeling & Observations (CEESMO) , Schmid College of Science & Technology Chapman University, Orange, California, USA, 2.Space Research Institute, RAS, Moscow, Russia, 3.The Schmidt Institute of Physics of the Earth, RAS, Moscow, Russia, 4.Center for Astronautical Physics and Engineering, National Central University, Taoyuan City, Taiwan)

[MIS04-P08] Seismicity change and b value variation prior to the Wenchuan earthquake (*Ms 8.0*)

*Peng Han[1], Rui Wang[1], Ying Chang[1], Miao Miao[1], Haixia Shi[2], Lingyuan Meng[2], Xuemei Zhang[2], Weiyun Xie[3], Katsumi Hattori[3] (1.Southern University of Science and Technology, Shenzhen, China, 2.China Earthquake Networks Center, Beijing 100045, China, 3.Chiba University, Chiba, Japan)

Statistical analysis and Evaluation of ULF seismo-magnetic phenomena at Kakioka, Japan, during 1983-2017

*Kei Takahashi[1], Katsumi Hattori[2], Peng Han[3]

1. Faculty of Science, Chiba University, 2. Graduate School of Science, Chiba University, 3. Southern University of Science and Technology, China

To clarify and verify the ultralow frequency (ULF) seismo-magnetic phenomena, we have performed statistical studies on the geomagnetic data observed at the Kakioka (KAK) station, Japan, during 1983-2017. We investigated the energy of ULF geomagnetic signals of the frequency around 0.01 Hz using wavelet transform analysis. To minimize the influences of artificial noises and global magnetic perturbations, we used only the geomagnetic data observed at midnight time (LT 2:30 A.M. to 4:00 A.M.).We define the geomagnetic anomalies when the Z components of geomagnetic data exceeds median + 1.5 IQR, where IQR is the interquartile range. Considering that ionospheric disturbances may also lead to enhancements in the Z component, we exclude the anomaly when the energy of H component exceeds median + 3.0 IQR. Statistical analysis of superposed epoch analysis have indicated that ULF magnetic anomalies are more likely to appear before sizable isolated earthquake events (Es parameter which is higher than 8th power of 10 and no earthquake events during ±45 days) rather than after them, especially 6-10 days before the events. Finally, we have evaluated the precursory information of ULF geomagnetic signals for local sizable earthquakes using Molchan’ s error diagram. The above results have indicated that the ULF seismo-magnetic phenomena at Kakioka clearly contain precursory information and have a possibility of improving forecasting of large earthquakes.

©2019. Japan Geoscience Union. All Right Reserved.

Pre-seismic anomalies on Earth’s magnetic field and ionosphere electron density using Swarm data

*Amune Yamazaki[1], Katsumi Hattori[1], Rui Song[1]

1. Chiba University

An earthquake is a rapid release of stress in the lithosphere and often leads to serious damages on human lives and society. Even though the short-time forecast of earthquake is important, it is not achieved yet. However, many electromagnetic phenomena that may be related to seismic activity have been reported recently. The satellite, one of the useful tools to observe these phenomena, can cover the global areas and can collect a large amount of data related to earthquakes which have large magnitude worldwide in short time. The Swarm satellites mission started to operate on November 22, 2013 by European Space Agency, with the constellation of three satellites (A, B, C) The anomalies preceded to the Ecuador earthquake in 2016 have been reported using the Swarm data. In this paper, in order to validate these results using the magnetic vector Y data by VFM and electron density data by Langmuir probe, we have analyzed the Swarm data related the M6.3~6.9 earthquakes occurred at Lombok Island, Indonesia, in July 28, August 5, and 19, 2018. The study area is a 1000 km square from the epicenter of 20180805 earthquake and the analyzed period is from May 28 to September 27, 2018. In this paper we report night-time orbit data at 18:00-6:00 LT.

As results, we found the following tendencies; (1) positive anomalies on magnetic Y vector about 1-2 weeks before the earthquakes and (2) negative anomalies on electron density from 1 week to 1 month before the earthquakes. We performed the same analysis to the data on the same period in 2016 and 2017 for reference when there were no M6+ earthquakes. We found that the number of anomaly track is only abruptly increased in the short period from the end of June to July in 2018, and that the trend is not able to be found in 2016 and 2017. From this unique trend in 2018, it is suggestive of the existence of the relation between the local seismic activity and in-situ satellite anomalies in the magnetic field and electron density in Lombok area.

©2019. Japan Geoscience Union. All Right Reserved.

Measurement of radon density in the atmosphere at Okayama, Kochi, Choshi and Kiyosumi, II

*Tohru Okabayashi[1], Kiyotaka Ninagawa[2], Isao Yamamoto[3], Katsumi Hattori[4], Chie Yoshino[4], Haruna Kojima[4], Nobuhiro Maeda

1. Department of Merical Risk and Crisis Management, Faculty of Risk and Crisis Management, Chiba Institute of Science, 2. Faculty of Science, Okayama University of Science, 3. Falcuty of Engineering, Okayama University of Science, 4. Graduate school of Science, Chiba University

We report continuous measurement of radon density in atmosphere at Okayama for three years, Kochi, Choshi and Kiyosumi for two years. An increase of radon density in groundwater at Nishinomiya city [1] and in atmosphere [2] at the southern part of Hyogo Prefecture Earthquake in 1995 were reported, respectively. In the case of Tohoku Region Pacific Coast Earthquake, the data obtained the exhaust air monitor that peak duration was long and the peak decreased rapidly before earthquake has been reported at the radiation facility of Fukushima Medical College in Fukushima [3]. On the other hand, a PIN photodiode have been developed and used as a high sensitive alpha ray detector in Super Kamiokande [4]. Since 2016, we also made an experimental setup using PIN photodiode, and measured the radon density in atmosphere. Using a Si PIN photodiode (S3204-09, unsealed, Hamamatsu Photodiode K.K.) as an alpha ray detector, we constructed radon detection setup combined with aluminum pot as an air accumulator, H4083 (Hamamatsu) as a charge amplifier, C4900-01 (Hamamatsu) as a high voltage power supply module, a pulse shaped amplifier with time constant of 10 msec, a multi channel analyzer (MCA-LiteN), and a PC as a data analysis. Obtained alpha spectra of atmosphere showed 4 peaks originated from ^{218}Po, ^{214}Po and ^{210}Po of U series, and ^{212}Po of Th series. Since 2017, we newly started to measure at Kochi, Choshi and Kiyosumi using our apparatus. Details of observed data are discussed in addition the data at Okayama since 2016.

[1] Igarashi G., Saeki S., Takahata N., Sumikawa K., Tasaka S., Sasaki Y., Takahashi M. and Sano Y. : Ground-water radon anomaly before the Kobe earthquake in Japan, Science, 269, 60-61, 1995.
[2] Yasuoka, Y. and Shinogi, M.: Anomaly in atmospheric radon concentration: a possible precursor of the 1995 Kobe, Japan, earthquake. Health Physics, 72, 759-761, 1997.
[3] Nagahama H., Yasuoka Y., Suzuki T., and Homma Y.: Radon Variation in the Air Before the 2011 Tohoku Earthquake (Mw =9.0), Programme and Abstracts, A32-09, The Seismological Society of Japan. 2011, Fall Meeting.
[4] Nemoto, M., Tasaka S., Hori H., Okumura K., Kajita T., and Takeuchi Y. : Development of High Sensitive Radon Detector with Electrostatic Collection. Radioisotopes, 46, 710-719, 1997 (Japanese).

Keywords: radon, atmosphere, earthquake prediction

©2019. Japan Geoscience Union. All Right Reserved.

Possible anomalous changes in solar quiet-daily geomagnetic variation *Sq* related to the 2011 off the Pacific coast of Tohoku earthquake (Mw 9.0)

*Xiaocan Liu[1], Katsumi Hattori[2,3], Peng Han[4], Huaran Chen[1]

1. Institute of geophysics China Earthquake Administrition, 2. Graduate School of Science, Chiba University, Chiba, Japan, 3. Center for Environmental Remote Sensing, Chiba University, Chiba, Japan, 4. Department of Earth and Space Sciences, Southern University of Science and Technology, ShenZhen, China

Seismo-electromagnetic researches have been studied for decades (e.g. Hayakawa and Fujinawa, 1994; Hayakawa and Molchanov, 2002, 2008,2013; Hattori, 2004, Hattori, et al., 2004a, 2004b; Hayakawa et al., 2007;, Hattori et al., 2013; Han et al., 2011, 2014, 2015, 2016, 2017; Huang QH et al., 2011, 2015; Du A, Huang Q et al., 2002, Rong YM et al., 2012, Yuan G.P., Zhang X.M. et al. 2015), and the geomagnetic diurnal variation (GDV) is a stable variation of the geomagnetic field that can be used to detect possible anomalous changes associated with large earthquakes.

We investigated data observed at 20 geomagnetic observatories at longitudes of 130˚E to 150˚E between 2009 and 2012 to detect possible anomalous changes in the geomagnetic solar quiet daily variation (Sq) related to the 2011 off the Pacific coast of Tohoku earthquake (Mw 9.0) occurred on March 11, 2011 in Japan. We selected the 5 quiet days every month and analyzed three component magnetic data with 1 min resolution using the natural orthogonal component (NOC) method to identify Sq variations from observations, and performed the spherical harmonic analysis (SHA) to separate the internal and the external equivalent Sq current systems of Je and Ji. We obtained that, Je and Ji are distorted near the epicenter area on two geomagnetic quiet days of January 23 and 27, 2011. They are about two months before the earthquake. Then, we made backward computation on the external and internal parts of the SHA model geomagnetic fields, Be and Bi, to determine the possible anomalous magnetic field variations at each station. Results show significant differences in daily variation for all components on January 23 and 27, 2011. The other days, we could not recognize any apparent anomalous behaviors, except known secular, seasonal, and solar activity dependences. A possible connection between this anomaly and the very strong Tohoku earthquake, which followed only one and half month after the geomagnetic anomaly is of highest interest for the research on earthquake precursors.

Keywords: geomagnetic solar quiet daily variation (Sq), natural orthogonal component (NOC) method, spherical harmonic analysis (SHA), the 2011 off the Pacific coast of Tohoku earthquak

©2019. Japan Geoscience Union. All Right Reserved.

Co-seismic geomagnetic fluctuations and atmospheric disturbances during the 2018 M6.2 Hualien Earthquake

*Chun-Rong Chen[1], JANN-YENQ Liu[1]

1. Graduate Institute of Space Science, National Central University

The strong ground motion of 6 February 2018 M6.2 Hualien Earthquake triggered a series of co-seismic geomagnetic fluctuations and seismo-traveling atmospheric disturbances (STADs) signatures in infrasonic waves and micro-pressures upon the seismic wave arrival. Networks of 9 QuakeFinder systems, 3 infrasound systems, 2 tiltmeters, 2 micro-barometers, and 11 co-located seismometers are used in this study. Each QuakeFinder system consists of a 3-axes induction magnetometer, an air conductivity sensor, a geophone, and temperature/relative humidity sensors. Co-seismic signatures clearly appear in the induction magnetometers, infrasound systems, and micro-barometers data. The magnetometers register both high- and low-frequency pulsations. Geomagnetic fluctuations occur upon the seismic wave arrival but last a longer duration, while the STADs lag their co-located seismic waves by about 15-45 seconds. The long-lasting fluctuations recorded by both induction and fluxgate magnetometers suggest that the ground/underground water motion play an important role, which is further conformed by low-frequency fluctuations in the tiltmeter data. In general, the amplitude of geomagnetic fluctuations decays as away from the epicenter. However, unusual large co-seismic geomagnetic fluctuations are detected over areas of the abnormal seismic intensity level and/or the magnetic underground structure with anomalously high susceptibilities.

Keywords: Geomagnetic, QuakeFinder, Infrasound, micro-Barometer, Tiltmeter

©2019. Japan Geoscience Union. All Right Reserved.

Multi-sensor monitoring network for earthquake precursor study near subduction zone at Boso, Japan

*Katsumi Hattori[1], Chie Yoshino[1], WEIYUN XIE[2], Sanaka Saito[2], Haruna Kojima[2], Rui Song[2], Peng Han[3], Toru Mogi[4], Tada-nori Goto[5], Ichi Takumi[6], Hiroshi Yasukawa[7], Motoaki Mouri[8], Jun Izutsu[9], Tadashi Takano[10], Chihiro Yamanaka[11], Masashi Kamogawa[12], Yoshiaki Ando[13], JANN-YENQ Liu[14], Dimitar Ouzounov[15], Valery Tramutoli[16]

1. Department of Earth Sciences, Graduate School of Science, Chiba University, 2. Graduate School of Science and Engineering, Chiba University, 3. Southern University of Science and Technology, China, 4. Hokkaido University, 5. Kyoto University, 6. Nagoya Institute of Technology, 7. Aichi Prefectural University, 8. Aichi University, 9. Chubu University, 10. Nihon University, 11. Osaka University, 12. Tokyo Gakugei University, 13. The University of Electro-Communications, 14. National Central University, Taiwan, 15. Chapman University, US, 16. University of Basilicagta, Italy

New observations from ground and space have provided multiple evidences of pre-earthquake signals and the latest studies show their statistical significance, repeatability, and universality. In this project, to understand the preparation process of large earthquakes and slow-slip events in subduction zone, especially to clarify the nucleation stage of the earthquake cycle, we plan to establish a dense observation network in Boso, Japan, where large subduction earthquakes are expected soon. Since the subsurface fluid flow may play an important role in the preparation process of subduction activities, we intend to employ electromagnetic approaches including oceanic and continental MT survey to monitor the underground resistivity structure which is sensitive to the dynamics of fluid. Other geophysical monitoring such as ULF geomagnetic and geoelectrical observations, radon measurements, and inland GPS movements, TIR, and OLR will be incorporated to help to understand the preparation process and evaluate the applicability of various pre-earthquake signals towards short term earthquake forecasting. We call this idea “sensor WEB”. We will show the state of the art and some results in our presentation.
This study is supported by Grand-in-Aids for Scientific Research of Japan Society for Promotion of Science (26249060).

©2019. Japan Geoscience Union. All Right Reserved.

Transient Effects in Atmosphere and Ionosphere Associated with 2018 Mw 7.5 Sulawesi Indonesia Earthquake and Triggered Tsunami and Volcano Activities

*Dimitar Ouzounov[1], Sergey Pulinets[2], Dmitry Davidenko[2], Alexander Rozhnoi[3], Maria Solovieva[3], Tiger Liu[4]

1. Center of Excellence in Earth Systems Modeling & Observations (CEESMO) , Schmid College of Science & Technology Chapman University, Orange, California, USA, 2. Space Research Institute, RAS, Moscow, Russia, 3. The Schmidt Institute of Physics of the Earth, RAS, Moscow, Russia, 4. Center for Astronautical Physics and Engineering, National Central University, Taoyuan City, Taiwan

We analyze retrospectively the transient variations of four different physical parameters of atmosphere/ionosphere during the time of M7.5 od Sept 28, 2018 in Indonesia namely: (i) thermodynamic proprieties in the lower atmosphere, (ii) outgoing earth radiation (OLR) at the TOA, (ii) GPS/TEC and (iv) the very-low-frequency (VLF/LF) signals at the receiving station in Petropavlovsk-Kamchatski (RTK, Russia). We found that in the second part of September 2018 a rapid augment of satellite observed earth radiation in the atmosphere and the anomaly located in close vicinity to the future M7.5 epicenter reached the maximum on Sept 21-22. The GPS/TEC data analysis indicates an augment and variation in electron density reaching a maximum value during the Sept 26-27 periods. Two VLF/LF crossing wave paths - NWC-RTK and JJY-RTK, have shown abnormal behavior of signals during on days Sept 26-28 two days before the earthquake. Our results show coherence between the appearance of pre-earthquake transient’ s effects in atmosphere and ionosphere (with a short time-lag, from hours up to a few days) and the occurrence of 2018 M7.5 in Indonesia. Traveling ionospheric tsunami disturbances (TITDs) in the total electron content (TEC) induced by tsunami waves of the 28 September 2018 Mw 7.5 Sulawesi Indonesia earthquake are detected by of seven ground-based receivers of the global positioning system (GPS) in South Asia, Oceanic, Pacific areas. It is found that the origin is about 100 km North of the epicenter and the horizontal speed is of about 187 m/s.

The pre-earthquake nature of the signals in atmosphere and ionosphere were revealed by simultaneous analysis of satellite, GPS/TEC and VLF/LF observations and suggest that they follow a general temporal-spatial evolution pattern, which has been seen in other large earthquakes worldwide.

Keywords: earthquake, tsunami, volcano, precursor, GPS/TEC, thermal anomaly

©2019. Japan Geoscience Union. All Right Reserved.

Seismicity change and b value variation prior to the Wenchuan earthquake (*Ms 8.0*)

*Peng Han[1], Rui Wang[1], Ying Chang[1], Miao Miao[1], Haixia Shi[2], Lingyuan Meng[2], Xuemei Zhang[2], Weiyun Xie[3], Katsumi Hattori[3]

1. Southern University of Science and Technology, Shenzhen, China, 2. China Earthquake Networks Center, Beijing 100045, China, 3. Chiba University, Chiba, Japan

The Gutenberg-Richter Law describes frequency-magnitude distribution of earthquakes. A number of studies have shown that the slope (b value) of the relationship between frequency and magnitude decreased before large earthquakes. Based on the analysis of the earthquake catalog from January, 2000 to April, 2008, we have investigated seismicity change and b value variation prior to the *Ms* 8.0 Wenchuan earthquake. The results show clear drops of both monthly and quarterly frequency of earthquakes during 2005-2006. The b value exhibits a long-term decrease trend since 2002, and reaches to the minimum just before the onset of the main shock. The temporal variation of b value is quite similar to that prior to the *Mw* 9.0 Tohoku earthquake in Japan, which may reflect the stress evolution during the preparation process of large earthquakes. These results indicate that the b value is an important indicator of an impending great earthquake, and has high potential in terms of predicting a future large quake.

Keywords: Wenchuan earthquake, b value, seismicity

©2019. Japan Geoscience Union. All Right Reserved.

[E] Poster | M (Multidisciplinary and Interdisciplinary)：M-IS Intersection

Thu. May 30, 2019 3:30 PM - 5:00 PM JST | Thu. May 30, 2019 6:30 AM - 8:00 AM UTC | Poster Hall International Exhibition Hall8, Makuhari Messe_19

[M-IS06] Conservation of geoparks, natural geosites and cultural heritage: weathering process and damage assessment

convener:Chiaki T. Oguchi(Institute for Environmental Science and Technology, Graduate School of Science and Engineering, Saitama University), Tetsuya Waragai(Graduate School of Science and Engineering, Nihon University), Kuniyasu Mokudai(Tohoku Gakuin University), Magdalini Theodoridou(School of Engineering, Cardiff University)

Geoparks, world heritage sites, natural geosites and cultural heritage structures are considered important natural and/or cultural heritage properties. They have been exposed to weathering not only in geologic time frame but also in human time scale, thus rocks and geological materials are often facing deterioration. In order to preserve these sites conservation measures should be considered. Several studies have taken place on this topic involving a wide range of research fields, such as geomorphology, engineering geology, geoarchaeology, conservation science, geoconservation, materials science, petrophysics, geochemistry, geotechnical engineering etc. However, our knowledge on many aspects is still limited. The session welcomes contributions, presenting original research, discussions as well as case studies on documentation, measurement and monitoring techniques, experimental procedures, predictive models, damage assessment, etc. Papers from all research fields are invited dealing with the broad topic of geosites and cultural heritage.

[MIS06-P01] The artistic qualities of religion reliefs in Taya-cave.Japan

*OGATA KEISUKE[1] (1.TSURUMI UNIVERSITY)

[MIS06-P02] Effect of stress concentration on the Weathering Mechanism of Sandstone Pillars of Angkor Wat, Cambodia by means of numerical simulation

*Takato Takemura[1], Tetsuya Waragai[2] (1.Nihon Univ., 2.Nihon University)

[MIS06-P03] Meaning to preserve evidence of large scale landslide

*Kuniyasu Mokudai[1], Hidekazu Sato[2] (1.Japan Geoservice Incorporated, 2.Mt. Kurikoma Area Geopark)

The artistic qualities of religion reliefs in Taya-cave.Japan

*OGATA KEISUKE[1]

1. TSURUMI UNIVERSITY

The Yaya-csve is located within the Jōsenji-Temle in Taya Town,Sakae ward,Yokohama-shi,Kanagawa Prefecture.The cave is called “Yuga-dou”,which is thought to be the present form in the Edo period, when the Kamakura period entered monks drills as a training ground. As for the religious relief carved in the cave, it is presumed from the record of “Koukoku-chishi” that it was produced for about 20years from 1842 to1862. In addition, “Sekiguchi diary” contains articles on visiting caves in 1859.

Subjects of reliefs are divided into the following areas in order of the route, and about 300 are engraved over 250 meters in total length.

First area:A and Un lions, Up and Doun dragon, Gold wing bird. Ceiling family crest.

Second area:Zodiac image. Ceiling three bats.

Third area:Chichibu 33 Kannon sacred place. Karyou-binga.

Fourth area:Asahina-benzaiten.

Fifth area:Saigoku 33 Kannon sacred place.

Sixth area:Sone Tenman-gū shrine and Takasago pine.

Seventh area:Yakuyoke Kobō-daishi master.

Eighth area:Taizōkai-shugi-mandala. Ceiling crane hemp leaf pattern.

Ninth area:Ichigan Kobō-daishi master. Shikoku 88 sacred place.

Tenth area:Shikoku 88 sacred place. 49in-shugi-mandala. Four Gorin tower.

Eleventh area:Godai-myouou.

Twelfth area:Water Kobō-daishi master. Sadasan one Turtle. Kouya-san Ishidoumaru. Unchū-kuyou bodhisattva.

Thirteenth area:18Rakan.

Fourteenth area:Iwaya-Fudou.

Fifteenth area:Bandou 33 Kannon sacred place.

Regrading the style, religious subjecks such as the Saigoku, bandou, Chichibu 33 Kannon sacred place,

©2019. Japan Geoscience Union. All Right Reserved.

Shikoku 88 sacred place and shugi-mandala are also perfunctory aspects, but “Sone Tenman-gū shrine and Takasago pine” and “Sadasan one Turtle” and 18-Rakan etc are the sculptures with high artistic and strong paintertly elements.

The faith in the 18th century was diverse, especially the common people went around the whole countey sacred place. Also for each of those who can not visit the sacred place a mini sacred place of each sacred place was established in various places. The Taya-cave near the Tokaido must also have collected the faith of the common people as a mini sacred place.

Taya-cave is currently designated as a registered cultural property of Yokohama City as a historic site in 1990. However, due to years of deterioration, it is becoming difficult to preserve and maintain the current situation. Therefore, in 2017 the Taya-cave preservation execution committee was established, we aim to conduct a basic survey in each department of cultural property, engineering and environmental studies, revalidate its value, preserve it as VR digital data in the future, to make it public and utilize.
In 2018, under the auspices of the Japan Society for the Promotion of Science(JSPS), collaborative research with the Italian ISSM/CNR Laboratory began, and in 2019 the research was continued with the subsidy of the Asahi Shimbun Cultural Foundation.

Keywords: History of Jōsenji-Temle and Taya-cave., On the time of religion haut-reliefs prodactionin in Taya-cave., Types and artistic religious reliefs in Taya-cave., From of common people’s belief in Japan in the 18th century., Preservation of Taya-cave and its future use.

©2019. Japan Geoscience Union. All Right Reserved.

Effect of stress concentration on the Weathering Mechanism of Sandstone Pillars of Angkor Wat, Cambodia by means of numerical simulation

*Takato Takemura[1], Tetsuya Waragai[2]

1. Nihon Univ., 2. Nihon University

Since Angkor Wat is located in a tropical monsoon climate, the sandstone building materials are strongly affected by weathering related to high temperatures, heavy rainfall and intense solar radiation. Weathering damage can be observed on a number of pillars, however, the outer pillars exhibit little weathering damage compared to the inner pillars, even though the outer pillars are more exposed to the rain and sunlight than the inner pillars. To understand the effect of stress concentration on the weathering sandstone pillars, we carried out the measurement of the degree of weathering damage of pillars, in-situ measurement of humidity and temperature change near the pillar and the numerical simulation for structural analysis.As a result, the weathering damage is not necessarily only due to the wetting-drying cycle. Since relatively large compressive stress is applied to the base of the inner pillar where the weathering damage is large, therefore, the weathering rate could be accelerated by the compressive stress concentration.

Keywords: Angkor Wat, Stress concentration

©2019. Japan Geoscience Union. All Right Reserved.

Meaning to preserve evidence of large scale landslide

*Kuniyasu Mokudai[1], Hidekazu Sato[2]

1. Japan Geoservice Incorporated, 2. Mt. Kurikoma Area Geopark

There are many mountainous area in Japanese islands. In mountainous area, many natural hazards occured. Visualization of landslide is necessary in order to understand the slope process in the mountains to non-experts. At Mt. Kurikoma Mountain area Geopark, we have been engaged in conservation of large-scale landslide landform, education and information dissemination activities. In order to preserve the landslide phenomenon which is the cause of the slope disaster, a scientific understanding of the landform is necessary. Furthermore, it is necessary to restructure the view of nature of the concerned parties.

Keywords: large scale landslide, geopark, geoconservation

©2019. Japan Geoscience Union. All Right Reserved.

[E] Poster | M (Multidisciplinary and Interdisciplinary)：M-IS Intersection

Thu. May 30, 2019 5:15 PM - 6:30 PM JST | Thu. May 30, 2019 8:15 AM - 9:30 AM UTC | Poster Hall International Exhibition Hall8, Makuhari Messe_36

[M-IS06] Conservation of geoparks, natural geosites and cultural heritage: weathering process and damage assessment

convener:Chiaki T. Oguchi(Institute for Environmental Science and Technology, Graduate School of Science and Engineering, Saitama University), Tetsuya Waragai(Graduate School of Science and Engineering, Nihon University), Kuniyasu Mokudai(Tohoku Gakuin University), Magdalini Theodoridou(School of Engineering, Cardiff University)

Geoparks, world heritage sites, natural geosites and cultural heritage structures are considered important natural and/or cultural heritage properties. They have been exposed to weathering not only in geologic time frame but also in human time scale, thus rocks and geological materials are often facing deterioration. In order to preserve these sites conservation measures should be considered. Several studies have taken place on this topic involving a wide range of research fields, such as geomorphology, engineering geology, geoarchaeology, conservation science, geoconservation, materials science, petrophysics, geochemistry, geotechnical engineering etc. However, our knowledge on many aspects is still limited. The session welcomes contributions, presenting original research, discussions as well as case studies on documentation, measurement and monitoring techniques, experimental procedures, predictive models, damage assessment, etc. Papers from all research fields are invited dealing with the broad topic of geosites and cultural heritage.

[MIS06-P01] The artistic qualities of religion reliefs in Taya-cave.Japan

*OGATA KEISUKE[1] (1.TSURUMI UNIVERSITY)

[MIS06-P02] Effect of stress concentration on the Weathering Mechanism of Sandstone Pillars of Angkor Wat, Cambodia by means of numerical simulation

*Takato Takemura[1], Tetsuya Waragai[2] (1.Nihon Univ., 2.Nihon University)

[MIS06-P03] Meaning to preserve evidence of large scale landslide

*Kuniyasu Mokudai[1], Hidekazu Sato[2] (1.Japan Geoservice Incorporated, 2.Mt. Kurikoma Area Geopark)

The artistic qualities of religion reliefs in Taya-cave.Japan

*OGATA KEISUKE[1]

1. TSURUMI UNIVERSITY

The Yaya-csve is located within the Jōsenji-Temle in Taya Town,Sakae ward,Yokohama-shi,Kanagawa Prefecture.The cave is called “Yuga-dou”,which is thought to be the present form in the Edo period, when the Kamakura period entered monks drills as a training ground. As for the religious relief carved in the cave, it is presumed from the record of “Koukoku-chishi” that it was produced for about 20years from 1842 to1862. In addition, “Sekiguchi diary” contains articles on visiting caves in 1859.

Subjects of reliefs are divided into the following areas in order of the route, and about 300 are engraved over 250 meters in total length.

First area:A and Un lions, Up and Doun dragon, Gold wing bird. Ceiling family crest.

Second area:Zodiac image. Ceiling three bats.

Third area:Chichibu 33 Kannon sacred place. Karyou-binga.

Fourth area:Asahina-benzaiten.

Fifth area:Saigoku 33 Kannon sacred place.

Sixth area:Sone Tenman-gū shrine and Takasago pine.

Seventh area:Yakuyoke Kobō-daishi master.

Eighth area:Taizōkai-shugi-mandala. Ceiling crane hemp leaf pattern.

Ninth area:Ichigan Kobō-daishi master. Shikoku 88 sacred place.

Tenth area:Shikoku 88 sacred place. 49in-shugi-mandala. Four Gorin tower.

Eleventh area:Godai-myouou.

Twelfth area:Water Kobō-daishi master. Sadasan one Turtle. Kouya-san Ishidoumaru. Unchū-kuyou bodhisattva.

Thirteenth area:18Rakan.

Fourteenth area:Iwaya-Fudou.

Fifteenth area:Bandou 33 Kannon sacred place.

Regrading the style, religious subjecks such as the Saigoku, bandou, Chichibu 33 Kannon sacred place,

©2019. Japan Geoscience Union. All Right Reserved.

Shikoku 88 sacred place and shugi-mandala are also perfunctory aspects, but “Sone Tenman-gū shrine and Takasago pine” and “Sadasan one Turtle” and 18-Rakan etc are the sculptures with high artistic and strong paintertly elements.

The faith in the 18th century was diverse, especially the common people went around the whole countey sacred place. Also for each of those who can not visit the sacred place a mini sacred place of each sacred place was established in various places. The Taya-cave near the Tokaido must also have collected the faith of the common people as a mini sacred place.

Taya-cave is currently designated as a registered cultural property of Yokohama City as a historic site in 1990. However, due to years of deterioration, it is becoming difficult to preserve and maintain the current situation. Therefore, in 2017 the Taya-cave preservation execution committee was established, we aim to conduct a basic survey in each department of cultural property, engineering and environmental studies, revalidate its value, preserve it as VR digital data in the future, to make it public and utilize.
In 2018, under the auspices of the Japan Society for the Promotion of Science(JSPS), collaborative research with the Italian ISSM/CNR Laboratory began, and in 2019 the research was continued with the subsidy of the Asahi Shimbun Cultural Foundation.

Keywords: History of Jōsenji-Temle and Taya-cave., On the time of religion haut-reliefs prodactionin in Taya-cave., Types and artistic religious reliefs in Taya-cave., From of common people’s belief in Japan in the 18th century., Preservation of Taya-cave and its future use.

©2019. Japan Geoscience Union. All Right Reserved.

Effect of stress concentration on the Weathering Mechanism of Sandstone Pillars of Angkor Wat, Cambodia by means of numerical simulation

*Takato Takemura[1], Tetsuya Waragai[2]

1. Nihon Univ., 2. Nihon University

Since Angkor Wat is located in a tropical monsoon climate, the sandstone building materials are strongly affected by weathering related to high temperatures, heavy rainfall and intense solar radiation. Weathering damage can be observed on a number of pillars, however, the outer pillars exhibit little weathering damage compared to the inner pillars, even though the outer pillars are more exposed to the rain and sunlight than the inner pillars. To understand the effect of stress concentration on the weathering sandstone pillars, we carried out the measurement of the degree of weathering damage of pillars, in-situ measurement of humidity and temperature change near the pillar and the numerical simulation for structural analysis.As a result, the weathering damage is not necessarily only due to the wetting-drying cycle. Since relatively large compressive stress is applied to the base of the inner pillar where the weathering damage is large, therefore, the weathering rate could be accelerated by the compressive stress concentration.

Keywords: Angkor Wat, Stress concentration

©2019. Japan Geoscience Union. All Right Reserved.

Meaning to preserve evidence of large scale landslide

*Kuniyasu Mokudai[1], Hidekazu Sato[2]

1. Japan Geoservice Incorporated, 2. Mt. Kurikoma Area Geopark

There are many mountainous area in Japanese islands. In mountainous area, many natural hazards occured. Visualization of landslide is necessary in order to understand the slope process in the mountains to non-experts. At Mt. Kurikoma Mountain area Geopark, we have been engaged in conservation of large-scale landslide landform, education and information dissemination activities. In order to preserve the landslide phenomenon which is the cause of the slope disaster, a scientific understanding of the landform is necessary. Furthermore, it is necessary to restructure the view of nature of the concerned parties.

Keywords: large scale landslide, geopark, geoconservation

©2019. Japan Geoscience Union. All Right Reserved.

[E] Poster | M (Multidisciplinary and Interdisciplinary) : M-IS Intersection

Thu. May 30, 2019 3:30 PM - 5:00 PM JST | Thu. May 30, 2019 6:30 AM - 8:00 AM UTC | Poster Hall International Exhibition Hall8, Makuhari Messe_20

[M-IS07] Astrobiology

convener:Hikaru Yabuta(Hiroshima University, Department of Earth and Planetary Systems Science), Seiji Sugita(Department of Earth and Planetary Science, Graduate School of Science Sciece, The University of Tokyo), Misato Fukagawa(National Astronomical Observatory of Japan), Fujishima Kosuke(Tokyo Institute of Technology, Earth-Life Science Institute)

Twenty years have passed since when the field of Astrobiology, which aims to unveil the origins, evolution, and habitability of life by integrating multidisciplinary fields, was established. Individual themes related to Astrobiology, such as chemical evolution in the early Solar System, formation of planetary system, prebiotic chemistry in the early Earth, evolution of life in the Earth's history, extremophile, and habitable planetary environments, has been studied by the knowledge and methods from the multiple fields, which has enabled us to explain "Where we came from" in some ways. However, despite an overwhelming number of investigations and discussions through gathering of the scientists from different fields, there has remained the long-standing unsolved question: How did abiotic materials gain biological function in the Earth and elsewhere in universe? There is still a large gap between prebiotic organic chemistry and biochemistry toward Origins of Life and planetary habitability. Therefore, the JpGU Astrobiology session focuses on pathfinding of "integration of astronomy, geoscience, and biochemistry", which will face an increasing need for the future Astrobiology. In order to enhance our understanding of "What is life", we propose to discuss the biochemical events linked with planetary systems, which is beyond the knowledge in a test tube, by an integration of exoplanets and molecular biology, etc. Through this approach, we will lead the discussions and developments of life-detection strategies for the future exploration of life in universe.

[MIS07-P01] Exoplanets Revealed by High-Precision Infrared Doppler Technique Using IRD: Large Exploration for Planets around Cool M-type Stars Begins

*Masayuki Kuzuhara[1,3], Bunei Sato[4], Motohide Tamura[2,1,3], Takayuki Kotani[1,3,5], Nagayoshi Ohashi[3,6], Masashi Omiya[1,3], Teruyuki Hirano[4], Hiroki Harakawa[6,3,1], Wako Aoki[3,5], Norio Narita[2,1], Yasunori Hori[1,3], Akitoshi Ueda[3,5], Akihiko Fukui[2], Hiroyuki Tako Ishikawa[5,3], Ishizuka Masato[2], Takashi Kurokawa[1,7], Nobuhiko Kusakabe[1,3], Tomoyuki Kudo[6,3,1], Eiichiro Kokubo[3], Mihoko Konishi[1,3], Tadashi Nakajima[1,3,5], Jun Nishikawa[3,5,1], Masahiro Ogihara[3], Takuma Serizawa[7] (1.Astrobiology Center of NINS, 2.The University of Tokyo, Graduate School of Science, 3.National Astronomical Observatory of Japan, 4.Tokyo Institute of Technology, 5.SOKENDAI, 6.Subaru Telescope, 7.Tokyo University of Agriculture and Technology)

[MIS07-P02] Discrimination of organic compounds and mineral particles by fluorescent microscopy for the detection of Martian life.

*Tomoka Okada[1], Yoshitaka Yoshimura[2], Atsuo Miyakawa[3], Yuka Murano[3], Shin-ichi Yokobori[3], Akihiko Yamagishi[3], Kensei Kobayashi[1], Yoko Kebukawa[1] (1.YOKOHAMA National university, 2.Tamagawa University, 3.Tokyo University of Pharmacy and Life Sciences)

[MIS07-P03] Morphological and spectroscopic characteristics of organic matter in Banded Iron Formation, Barberton Greenstone Belt, South Africa

*Hiroki Amemiya[1], Ryo Nakajima[1], Yoko Ohtomo[1], Tsubasa Otake[1], Tsutomu Sato[1] (1.Division of sustainable Resources Engineering, Faculty of Engineering, Hokkaido University)

[MIS07-P04] Understanding peptide sequence selectivity on iron sulfide (FeS) nanoparticle surfaces

*Fujishima Kosuke[1], Norio Kitadai[1], Kenji Kasama[1] (1.Earth-Life Science Institute, Tokyo Institute of Technology)

[MIS07-P05] A process model of L-homochiral peptides formation initiated with L-alanine

*Toratane Munegumi[1], Taisuke Yamaga[1] (1.Department of Science Education, Naruto University of Education)

[MIS07-P06] Possible Formation of Amino Acids and Carboxylic Acids in Slightly-Reducing Primitive Earth Atmospheres

*Miei Kinoshita[1], Shintaro Ikeda[1], Kimitaka Kawamura[2], Bhagawati Kunwar[2], Hitoshi Fukuda[3], Yoshiyuki Oguri[3], Hiromi Shibata[4], Junichi Takahashi[1], Vladimir Airapetian[5], Yoko Kebukawa[1], Kensei Kobayashi[1] (1.Yokohama National University, 2.Chubu University, 3.Tokyo Institute of Technology, 4.Osaka University, 5.NASA Goddard SFC)

[MIS07-P07] Application of Machine learning and software development for initial analysis in the TANPOPO mission

*Kyoko Okudaira[1], Yuto Toda[1], Takashi Sonoke[1], Yuichi Yaguchi[1], Masashi Yoshida[1], Junya Imani[2], Satoshi Sasaki[3], Hajime Yano[4], Hirohide Demura[1], Makoto Tabata[5], Akihiko Yamagishi[6] (1.The University of Aizu, 2.YUKI Precision, 3.Tokyo University of Technology, 4.JAXA, 5.Chiba University, 6.Tokyo University of Pharmacy and Life Science)

[MIS07-P08] Structure analysis of the hyper velocity impact tracks of the particles captured by silica aerogel on the International Space Station

*Mizuho Nishi[1], Akira Tsuchiyama[1], Hajime Yano[2], Hikaru Yabuta[3], Kyoko Okudaira[4], Junya Matsuno[1], Masayuki Uesugi[5], Uesugi Kentaro[5], Nakano Tukasa[6], Takaaki Noguchi[7], MITA Hajime[8], Akihiko Yamagishi[9] (1.Kyoto University, 2.Institute of Space and Astronautical Science, Japan Aerospace Exploration Agency, 3.Hiroshima University, 4.The University of Aizu, 5.JASRI/SPring-8, 6.National Institute of Advanced Industrial Science and Technology, 7.Kyusyu University, 8.Fukuoka Institute of Technology, 9.Tokyo University of Pharmacy and Life Science)

[MIS07-P09] High-Angular-Resolution Observations of Protoplanetary Disks

*Misato Fukagawa[1] (1.National Astronomical Observatory of Japan)

[MIS07-P10] Characterization of high molecular weight amino acid precursors formed in interstellar ice analog

*Soushi Kuramoto[1], Tomohito Sato[1], Hitoshi Fukuda[2], Yoshiyuki Oguri[2], Kotaro Kondo[2], Hiromi Shibata[3], Yoko Kebukawa[1], Kensei Kobayashi[1], Satoshi Yoshida[4] (1.Yokohama National University, 2.Tokyo Institute of Technology, 3.University of Osaka, 4.National Institutes for Quantum Radiological Science and Technology)

[MIS07-P11] Theoretical elucidation of prebiotic formation processes into nucleobases

*Yu Komatsu[1,2], Taiki Suzuki[1,2] (1.Astrobiology Center, 2.National Astronomical Observatory of Japan)

[MIS07-P12] Formation Process of A Glycine's Precursor Candidate, CH3NH2

*Taiki Suzuki[1,2], Liton Majumdar[3], Masatoshi Ohishi[2] (1.National Institutes of Natural Sciences Astrobiology Center, 2.National Astronomical Observatory of Japan, 3.NASA Jet Propulsion Laboratory (JPL))

[MIS07-P13] Numerical study on the stellar atmosphere & wind of Cool Stars

*Takahito Sakaue[1], Kazunari Shibata[1] (1.Kyoto University)

[MIS07-P14] Design of space exposure experiments of organic matter in Tanpopo 2

*Takuya Yokoo[1], tomohito sato[1], Itsuki Sakon[2], Kazumichi Nakagawa[3], Hajime Yano[4], Miki Nakayama[5], Hajime Mita[5], Yoko Kebukawa[1], Kensei Kobayashi[1] (1.Yokohama National University, 2.University of Tokyo, 3.Kobe University, 4.JAXA, 5.Fukuoka Institute of Technology)

Exoplanets Revealed by High-Precision Infrared Doppler Technique Using IRD: Large Exploration for Planets around Cool M-type Stars Begins

*Masayuki Kuzuhara[1,3], Bunei Sato[4], Motohide Tamura[2,1,3], Takayuki Kotani[1,3,5], Nagayoshi Ohashi[3,6], Masashi Omiya[1,3], Teruyuki Hirano[4], Hiroki Harakawa[6,3,1], Wako Aoki[3,5], Norio Narita[2,1], Yasunori Hori[1,3], Akitoshi Ueda[3,5], Akihiko Fukui[2], Hiroyuki Tako Ishikawa[5,3], Ishizuka Masato[2], Takashi Kurokawa[1,7], Nobuhiko Kusakabe[1,3], Tomoyuki Kudo[6,3,1], Eiichiro Kokubo[3], Mihoko Konishi[1,3], Tadashi Nakajima[1,3,5], Jun Nishikawa[3,5,1], Masahiro Ogihara[3], Takuma Serizawa[7]

1. Astrobiology Center of NINS, 2. The University of Tokyo, Graduate School of Science, 3. National Astronomical Observatory of Japan, 4. Tokyo Institute of Technology, 5. SOKENDAI, 6. Subaru Telescope, 7. Tokyo University of Agriculture and Technology

Planets outside the Solar system, so-called exoplanets, are promising as a new window for astrobiology. Among those, planets orbiting cool M-type stars (main-sequence stars with effective temperatures less than about 3000 K) have the great potential to push forward astrobiological studies on exoplanets. The habitable zone (HZ) is the zone where liquid water is sustainable on the surfaces of planets. It is expected that the HZs around cooler stars come closer to the parent stars (Kopparapu et al. 2013, ApJ 765, 131). In addition, the recent exoplanet observations performed by the *Kepler* space telescope have revealed that the occurrence rate of small exoplanets similar to Earth increases as the effective temperatures of stars decrease (e.g., Mulders et al. 2015, ApJ 798, 112). Furthermore, the Doppler technique, one of primary methods for exoplanet observations, can more easily find a planet with the orbit closer to its parent star. Accordingly, targeting cool M-type stars provides a significant advantage in the observations of rocky planets in HZs based on the Doppler technique. Also, the snow line around a cool M-type star is close to the star; this is intriguing in terms of the planet formation process.
Nevertheless, the exoplanet observations for cool M-type stars have not been advanced compared with those for hotter stars, due to their faintness. In particular, the low brightness of a cool M-type star at optical wavelengths makes it problematic to observe its planet based on visible light, which has been mostly used in exoplanet observations. We have therefore developed the InfraRed Doppler (IRD) instrument, which is a high-dispersion spectrograph to enable the exoplanet observations using the high-precision Doppler technique at near-infrared (Kotani et al. 2018, Proc. of the SPIE 10702, 1070211). Near-infrared light is suited for observing cool M-type stars, since their peak flux is located in a near-infrared region. One of bottlenecks to achieve high-precision measurements using the near-infrared Doppler technique is the lack of a reference source that enables us to correctly calibrate a measurement fluctuation caused by the instability of an observation instrument. We use a laser frequency comb (LFC) generated by the system that has been newly developed for IRD as a reference source to calibrate IRD measurements. An LFC spectrum has a number of emission lines with fine sampling intervals and is observed simultaneously with a stellar spectrum, so it works as a correct wavelength calibrator for the stellar spectrum. After our laboratory performance verifications of IRD with its LFC system (Kuzuhara et al. 2018, Proc. of the SPIE 10702, 1070260), the IRD operation started on the Subaru Telescope, whose large primary mirror enables high-sensitivity observations even for cool M-type stars. The use of IRD with the Subaru Telescope significantly helps the discoveries and characterizations of exoplanets around cool M-type stars.
We have planned a large survey for planets around cool M-type stars with IRD on the Subaru Telescope, which actually begins on February, 2019. In this survey, we monitor 60 M-type stars over 175 nights

©2019. Japan Geoscience Union. All Right Reserved.

allocated for 5 years. Our pre-survey simulation prospects more than 60 planet detections; those discoveries include a few dozen Earth-like planets, among which some are expected to locate within HZs. Thus, the IRD survey provides important contributions on improving our current understanding of planet formation models for low-mass stars like cool M-type stars, as well as the provisions of samples for exoplanet characterizations using the future large telescopes such as TMT. Here, we report the result of our ongoing on-sky tests to evaluate the IRD performances such as its measurement precision and stability. Furthermore, we explain the above large program in detail: our science goals, and the target selection and observation strategy for the goals are provided.

Keywords: Exoplanet, Doppler technique, Habitable Zone, IRD, planet formation, M-type star

©2019. Japan Geoscience Union. All Right Reserved.

Discrimination of organic compounds and mineral particles by fluorescent microscopy for the detection of Martian life.

*Tomoka Okada[1], Yoshitaka Yoshimura[2], Atsuo Miyakawa[3], Yuka Murano[3], Shin-ichi Yokobori[3], Akihiko Yamagishi[3], Kensei Kobayashi[1], Yoko Kebukawa[1]

1. YOKOHAMA National university, 2. Tamagawa University, 3. Tokyo University of Pharmacy and Life Sciences

The Viking mission searched life on Mars in 1976, but did not find apparent biological activities[1)]. However, the detection sensitivity of the Viking instrument (GC-MS) has been found to be low, suggesting that organic compounds could exist on Martian surface. Recently the MSL Curiosity by NASA detected organic compounds[2)]. The Phoenix mission discovered H_2O ice[3)] and possible liquid water flows were found at RSL (Recurring Slope Lineae) by MRO (Mars Reconnaissance Orbiter)[4)]. These findings suggested that life might exist on Martian surface.

We have proposed a life search program on the surface of Mars with a fluorescence microscope[5)]. This microscope is called Life detection Microscope (LDM) which detects microorganisms in more than 100 times higher sensitivity than the Viking GC-MS. In this program, we plan to use two fluorescent dyes SYTO 24 and propidium iodide (PI) in LDM. SYTO24 permeates cell membrane and stains organic compounds. PI also stains organic compounds such as nucleic acids, but it doesn’t permeate cell membrane. Therefore, the combination of these two dyes makes it possible to differentiate the organic compounds surrounded by membranes (living cells) and dead cells.

However, there are some mineral particles have autofluorescence, possibly detected as false positives. In this research, in order to discriminate organic compounds from mineral particles, the autofluorescence of minerals were measured under various conditions.

Various kind of mineral specimens were finely ground with a glass pen washed with ethanol. Fluorescent images were obtained with a fluorescence microscope and a digital camera and their fluorescent intensities were measured by image analysis. We also examined fluorescent spectra of mineral particles using a diffraction grating. The results showed the fluorescent intensities and spectra of mineral particles were clearly different from the stained organic compounds. These methods would be useful to detect organic compounds among mineral particles.

1) Navarro-Gonzalez, R., *et al.,* 2006, *PNAS*, 103: 16089-16094. 2) Freissient, C., *et al*., 2015, *J. Geophys. Res. Planets,* 120: 495-514. 3) Feldman, W. C., *et al.,* 2002. *Science*, 297, 75-78. 4) McEwen A. S, *et al.,* 2011, *Science,* 333: 740-743. 5) Yamagishi, A., *et al*., 2010, *Bio. Sci. Space,* 24: 67-82.

Keywords: Mars, Fluorescent microscope, Life Detection

©2019. Japan Geoscience Union. All Right Reserved.

Morphological and spectroscopic characteristics of organic matter in Banded Iron Formation, Barberton Greenstone Belt, South Africa

*Hiroki Amemiya[1], Ryo Nakajima[1], Yoko Ohtomo[1], Tsubasa Otake[1], Tsutomu Sato[1]

1. Division of sustainable Resources Engineering, Faculty of Engineering, Hokkaido University

The emergence of cyanobacteria has been postulated to cause an increase in Earth’ s atmospheric oxygen concentration ~2.45 Ga and oxidation of ferrous iron in a seawater, facilitating the formation of Banded Iron Formations (BIFs) in the Proterozoic era. On the other hand, iron precipitation process in the Archean is still controversial. Previous studies suggest that anoxygenic iron-oxidizing bacteria and/or free oxygen produced by cyanobacteria, was responsible for iron oxidation before ~2.45 Ga. Organic matter preserved in BIFs may provide insights into the iron oxidation process and biological evolution in Archean. However, authenticity of Archaean organic matter has to be first clarified for further investigations due to possible later contamination. Here, we investigated morphological and spectroscopic characteristics of organic matter in ~3.2 Ga BIFs in Sheba mine, Moodies Group, Barberton Green stone Belt, South Africa to estimate the chemical structure combined with a contamination check using Raman spectroscopy.

Organic matter was collected by two different methods: extraction by acid treatment of powder samples and pick up with a micro-manipulator from thin sections. When Raman spectra were obtained using 532 nm wavelength laser, acid-treated organic matter showed two peaks ~1350 and ~1580 cm^{-1} corresponding to disordered and ordered carbon structures, whereas micro-sampled organic matter shows no detectable peak with a high background. Because yellow-green fluorescence was observed in micro-sampled organic matter using a Fluorescence microscope, the fluorescence likely causes a high background in the Raman spectra. Therefore, 785 nm wavelength laser was applied for micro-sampled organic matter. Calculated metamorphic temperature from the Raman spectra obtained by acid-treated and micro-sampled organic matter was from 400 to 540˚C, which is consist with greenschist facies of the Barberton Greenstone Belt. This indicates that the organic matter is not a later contamination. Chemical mapping with an Electron Probe Micro Analyzer shows that micro-sampled organic matter is predominately comprised of carbon with slight contribution of nitrogen (< 0.1wt%). Infrared spectra of the organic matter show absorption peaks corresponding to N-O, C-O, and C=O bonds, suggesting that organic matter remains their functional groups in the structure. Based on the morphology and microstructure observed by Field Emission- Scanning Electron Microscope, the organic matter may have been derived from biofilm because of similarity in the morphology as well as the large size (20 –50 μm). Furthermore, the micro-sampled organic matter has a rough surface while the acid-treated organic matter has a smooth one, which may be due to damages by acid-treatment. Our results suggest that micro-sampling is suitable to observe the detailed morphological and structural features of organic matter preserved in Archean sedimentary rocks.

Keywords: Archean, Microfossils, Barberton Greenstone Belt, Raman spectroscopy, Infrared spectroscopy

©2019. Japan Geoscience Union. All Right Reserved.

Understanding peptide sequence selectivity on iron sulfide (FeS) nanoparticle surfaces

*Fujishima Kosuke[1], Norio Kitadai[1], Kenji Kasama[1]

1. Earth-Life Science Institute, Tokyo Institute of Technology

The emergence and evolution of functional biopolymers on Earth is one of the unsolved key questions regarding the origin of life. Amongst various building blocks of polymers, amino acids are prebiotically abundant and different plausible paths toward forming polypeptides have been previously shown in the context of early Earth environment. However, relationship between a specific geochemical environment and the types of biopolymers that could retain or to propergate in that condition is not yet fully systematically explored. Hence, we have prepared random octapeptide library with a combination of limited set of amino acids (Gly, Ile, His, Asp, Cys, Arg) as a probe to explore the sequence selectivity of iron sulfide (FeS) nanoparticles as a simulant of the geochemical settings that once existed at the deep-sea floor or the surface of early Earth. Experiment was carried out by mixing the FeS nanoparticles and random peptides in pure H_2O solution inside the anoxic chamber to allow adsorption under moderate temperature/pH condition. After extensive rinsing step, peptides that remain bound to the FeS nanoparticles were analyzed directly by MALDI-MS/MS to retrieve sequence information. We will discuss the latest sequence results obtained from screening and discuss sequence selective feature of FeS and its relevance to the iron-sulfur cluster known as a fundamental cofactor in biology.

Keywords: Iron sulfide, peptide adsorption, MALDI-MS/MS, iron-sulfur cluster

©2019. Japan Geoscience Union. All Right Reserved.

A process model of L-homochiral peptides formation initiated with L-alanine

*Toratane Munegumi[1], Taisuke Yamaga[1]

1. Department of Science Education, Naruto University of Education

Hydrogen abstraction from L-alanine by hydroxy radical facilitates alkylation on β-carbon of alanine as well as retention of L-chirality. The reaction rate constant of hydrogen abstraction ($k=6.21\times10^{7}\ M^{-1}s^{-1}$) on β-carbon was about 3.7 times faster than that ($k=1.7\times10^{7}\ M^{-1}s^{-1}$) on α-carbon. The fact supports that alkylation proceeds faster than racemization, and the chirality of product amino acids will be hold. Similar alkylation of oligopeptides will also proceed with a lower level epimerization than alkylation. This research discusses how the lower reaction rate of epimerization than alkylation lead homochiral peptides.

Keywords: L-alanine, peptides, homochirality

©2019. Japan Geoscience Union. All Right Reserved.

Possible Formation of Amino Acids and Carboxylic Acids in Slightly-Reducing Primitive Earth Atmospheres

*Miei Kinoshita[1], Shintaro Ikeda[1], Kimitaka Kawamura[2], Bhagawati Kunwar[2], Hitoshi Fukuda[3], Yoshiyuki Oguri[3], Hiromi Shibata[4], Junichi Takahashi[1], Vladimir Airapetian[5], Yoko Kebukawa[1], Kensei Kobayashi[1]

1. Yokohama National University, 2. Chubu University, 3. Tokyo Institute of Technology, 4. Osaka University, 5. NASA Goddard SFC

Since 1950s, a large number of laboratory experiments have been performed to examine possible formation of bioorganic compounds such as amino acids in primitive Earth atmosphere. Earlier experiments with strongly reducing gas mixtures containing large molar ratio of methane and ammonia, and it was reported that efficient production of amino acids and other important organics were formed in it by spark discharges and other energy sources. It is now estimated, however, that the early Earth atmosphere was only slightly reducing [1]: N_2 and CO_2were the major atmospheric constituents, together with some small amount of reducing carbon species like CH_4 and/or CO. Simulation experiments suggested, however, that amino acid formation was restricted under these conditions [2]. We reported that cosmic rays could facilitate chemical reactions with less reducing model of primitive atmosphere such as a mixture of CO_2, CO, $N_2$and H_2O [3]. However these energy sources have been ignored in experiments with initiation of prebiotic chemistry [4]. Here, we examine possible formation of amino acids from slightly reducing gas mixtures by applying high-energy protons to simulate the action of cosmic rays.

We conducted three sets of laboratory experiments using energetic particles, spark discharge and UV light as dominant energy sources. In these sets of experiments we used 400 mL of gas mixture of N_2, $CO_2$and CH_4introduced to a Pyrex tube together with 5 mL of pure water under 350 Torr of N2 and 350 Torr of mixtures with varied mixing ratios of $CH_4$and CO_2. In order to simulate possible roles of cosmic rays, the gas mixture was irradiated with 2.5 MeV proton beam produced in the Tandem accelerator at Tokyo Tech, Japan. We also exposed the same composition of gas mixtures to spark discharges by using a Tesla coil to simulate lightning. The gas mixtures were also irradiated with UV light (l> 190 nm) from a xenon lamp. Each product was acid-hydrolyzed and was subjected to amino acid analysis by HPLC and GC/MS, both after derivatization. Carboxylic acids were determined by GC/MS after derivatization. Starting and resulting gas mixtures were analyzed with a quadrupole mass spectrometer.

Amino acids were detected in the hydrolyzed products when gas mixtures of N_2, CO_2, $CH_4$and H_2O were irradiated with 2.5 MeV protons at the initial the molar ratio of methane (r_{CH4}) in the starting gas mixture as low as 0.5 %. On the other hand, amino acids were detected only when $r_{CH4}$was greater than 15 % in the case of spark discharges. The experiments with UV irradiation source did not yield amino acids or their precursors even when $r_{CH4}$was 50 %. Very little amino acids were detected in all the products before hydrolysis. It was shown that not free amino acids but amino acid precursors were formed in selected experiments.

Carboxylic acids including formic acid, oxalic acid and glyoxylic acid were detected from unhydrolized products derived from N_2-CO_2gas mixtures exposed to spark discharges and proton irradiation. We show that some free carboxylic acids could be formed in non-reducing atmospheres as well as slightly reducing atmospheres either by proton irradiation or by spark discharges. It was suggested that the mechanism of formation of amino acid precursors from N_2-CO_2-CH_4-H_2O mixtures was quite different from that of

©2019. Japan Geoscience Union. All Right Reserved.

carboxylic acids.

Lightning and solar UV have been considered important energy sources for prebiotic synthesis in primitive Earth atmosphere. We here showed that lightning and solar UV could not singularly synthesize important N-containing organics such as amino acids from slightly reducing primitive Earth atmosphere. On the other hand, cosmic ray could have been an important energy source to synthesize amino acid precursors even if primitive Earth atmosphere was only slightly reducing. It would be of interest to examine whether there are synergetic effects among cosmic rays, UV and thundering.

References:

[1] H. Kuwahara and S. Sugita, *Icarus,* **257**,290-301 (2015).

[2] H. Kuwahara *et al.,Orig. Life Evol. Biosph.,* **42**,533-541(2012).

[3] K. Kobayashi *et al.*, *Orig. Life Evol. Biosph.* **28**, 155-165 (1998).

[4] S. L. Miller and H. C. Urey, *Science,* **130**,245-251 (1957).

Keywords: Primitive Earth Atmospheres, Amino Acids, Solar Energetic Particles

©2019. Japan Geoscience Union. All Right Reserved.

Application of Machine learning and software development for initial analysis in the TANPOPO mission

*Kyoko Okudaira[1], Yuto Toda[1], Takashi Sonoke[1], Yuichi Yaguchi[1], Masashi Yoshida[1], Junya Imani[2], Satoshi Sasaki[3], Hajime Yano[4], Hirohide Demura[1], Makoto Tabata[5], Akihiko Yamagishi[6]

1. The University of Aizu, 2. YUKI Precision, 3. Tokyo University of Technology, 4. JAXA, 5. Chiba University, 6. Tokyo University of Pharmacy and Life Science

One of the goals of the TANPOPO mission is collecting cosmic dust and space debris on the International Space Station [1]. Ultra-low density material “silica aerogel” panels are used as capture media [2]. These panels retrieved from the space are sent to the laboratory and initial analysis has been conducted by a system called “CLOXS”.

CLOXS efficiently covers the processes (1) Automatic imaging the entire panel, 2) Search for penetration track candidates, 3) Mapping of track candidates, 4) Shape data acquisition of tracks, and 5) Automatic sample cutting) up to sample allocation to researchers. However, to reduce researchers’ time and effort, improvement of the software and automation of some processes are required.

In this study, application of machine learning in discrimination of objects in aerogel images taken by CLOXS is mainly reported. The research goal is to classify objects in the images into tracks and dirt using machine learning.

There are morphological varieties in the objects. As for both tracks and dirt, they are classified into 4 types respectively in this study.

Since the contrast of the images are low, the first step of our approach is preprocessing of the images. We compared the results of *Contrast Stretching* and *CLAHE* (Contrast Limited Adaptive Histogram Equalization).

Learning data and test data are prepared respectively, to compare the case that the images are categorized into 4 types and the case that the images of all types are dealt altogether.

Convolutional Neural Network (CNN) is used as a method of machine learning. *Python* is used as programing Language.

In conclusion, as for image processing, *CLAHE* showed higher accuracy when tracks were judged to be tracks, and *Contrast Stretching* was found to yield a better result for dirt. It is probably because, in *Contrast Stretching*, *CNN* was not sufficiently highlighted to capture features, and *CLAHE* was able to improve the contrast sufficiently.

Regarding separating the types of tracks and dirt, the accuracy rate was higher when tracks were categorized into different types and learned.

Although further evaluation and improvements might be needed, our accuracy rates meet the mission requirements, that is, the percentage of identifying track as track should be more than 95 %, while the percentage of identifying dirt as dirt should be more than 70 % (that of NOT identifying true track as dirt

©2019. Japan Geoscience Union. All Right Reserved.

should be less than 30 %).

[1] A. Yamagishi et al., “Tanpopo: Astrobiology exposure and micrometeoroid capture experiments - proposed experiments at the exposure facility of ISS-JEM”, *Trans. JSASS. Aerospace Tech. Jpn.* vol. 12, No. ists29, p. Tk_49-Tk_55, 2014.

[2] M. Tabata, et al. “Ultralow-density double-layer silica aerogel fabrication for the intact capture of cosmic dust in low-Earth orbits” *J. Sol-Gel Sci. Technol.* 77(2), 325-334, 2016.

Keywords: TANPOPO mission, Astrobiology, Initial analysis, Machine learning, Software development

©2019. Japan Geoscience Union. All Right Reserved.

Structure analysis of the hyper velocity impact tracks of the particles captured by silica aerogel on the International Space Station

*Mizuho Nishi[1], Akira Tsuchiyama[1], Hajime Yano[2], Hikaru Yabuta[3], Kyoko Okudaira[4], Junya Matsuno[1], Masayuki Uesugi[5], Uesugi Kentaro[5], Nakano Tukasa[6], Takaaki Noguchi[7], MITA Hajime[8], Akihiko Yamagishi[9]

1. Kyoto University, 2. Institute of Space and Astronautical Science, Japan Aerospace Exploration Agency, 3. Hiroshima University, 4. The University of Aizu, 5. JASRI/SPring-8, 6. National Institute of Advanced Industrial Science and Technology, 7. Kyusyu University, 8. Fukuoka Institute of Technology, 9. Tokyo University of Pharmacy and Life Science

In Japan's first astrobiology experiment “Tanpopo”, attempts have been made to capture cosmic dust by installing ultra-low-density silica aerogel at the Japanese Experiment Module “Kibo” of the International Space Station (ISS) [1]. This mission was conducted with the aim of verifying the hypothesis that the origin of life was supplied from outside the earth [2]. Silica aerogel had been used in NASA’s cometary dust sample return mission “Stardust” [3]. Impact tracks formed by collision of cometary dust against aerogel were classified into 3 types, A, B and C, based on their shapes [4]. The track shapes have useful information for estimating the size and density of dust particles [5]. The purposes of this research are (1) to find impact tracks formed by cosmic dust in Tanpopo aerogel and (2) to describe the three-dimensional shapes of impact tracks with different origins (cosmic dust and space debris) and finally to clarify the relation between the track shape and the origin.

At SPring-8 BL47XU, three-dimensional shapes were obtained with imaging absorption tomography for 8 impact tracks (D1-231, D1-298, D1-362, E1-200, E1-304, F1-328, F1-389, F1-623), which were found in Tanpopo aerogel faced to the space direction. The imaging experiments were made at 7, 8, 9 keV with the voxel size of 0.24 or 0.465 μm. CT images at 8 keV were used to extract track shapes. Track length (L_t), maximum track diameter (D_m), aspect ratio, and other shape properties were obtained. These values were compared with Stardust tracks. Dual-energy tomography (DET) [6] was applied to estimate the materials of particles captured in the tracks. Another track (E2-000) was observed only with an optical microscope. For D1-231, D1-298, D1-362 and E2-000, the aerogel was compressed and real solid particles in the tracks were searched with an optical microscope.

The 9 tracks in total were classified into 5 types based on their shapes. Type 1 (E2-000) is a track formed by cosmic dust, where two pyroxene particles were identified at the tip of the track [7]. The track shape resembles Stardust type B track, but its entrance widely spreads. Type 2 (D1-231) is somewhat similar to Stardust type A track. Type 3 (E1-200 and E1-304) is a track having abundant cracks developed on the wall with a narrow entrance. Type 4 (F1-328 and F1-389) is extremely asymmetrical in its shape and has cracks similar to Type 3. Type 5 (D1-362 and F1-623) is a bowl-shaped track with a large entrance. The relationship between L_t and D_m of these tracks was almost the same as that of Stardust tracks except for Type 5. However, their specific shapes of Types 2, 3 and 4 are significantly different from Stardust tracks. The cracks of these tracks are similar to those seen at the end of Stardust type A and B tracks, indicating that they were formed by a relatively low-speed impact. Similar tracks to Type 5 were reported in the aerogel in the exposure experiment on the Mir Station. They may be due to high-speed collision of weakly-adhered aggregates [8]. From the quantitative analysis of such impact tracks, there is a possibility of obtaining knowledge about new parameter areas which could not be obtained by conventional research. DET results showed that most of fine particles in the tracks do not contain Fe and Ni. Low values of their

©2019. Japan Geoscience Union. All Right Reserved.

linear absorption coefficients are smaller than that of cosmic dust. They should be formed by impact of weekly-adhered aggregates that were broken into very small pieces by the impact and mixed with condensed aerogel. Two particles with relatively high linear absorption coefficient were confirmed in D1-231 and D1-362. They were confirmed by and optical microscope after compressing.

[1] Yamagishi A. et al. 2012. Space Utiliz Res, 28, 220. [2] Chyba C. & Sagan C. 1992. Nature, 355, 125. [3] Brownlee D. et al. 2006. Science, 314, 1711. [4] Hörz et al. 2006. Science, 314, 1716. [5] Tsuchiyama A. et al. 2009. Meteoritics & Planetary Science, 44, 1203. [6] Tsuchiyama A. 2013. Geochimica et Cosmochimica Acta 116, 5. [7] Noguchi T., 2018, Private message. [8] Hörz and Zolensky, 2000, Icarus 147, 559.

Keywords: Tanpopo mission, Cosmic dust

©2019. Japan Geoscience Union. All Right Reserved.

High-Angular-Resolution Observations of Protoplanetary Disks

*Misato Fukagawa[1]

1. National Astronomical Observatory of Japan

The recent progress in understanding of planet-formation process will be reviewed based on the results obtained at high angular resolution with astronomical facilities such as the Atacama Large Millimeter/submillimeter Array (ALMA). Circumstellar disk structures around young stars are birthplaces of planets. The physical and chemical condition in such protoplanetary disks can be linked to some extent to the planetary environment (e.g., atmospheric composition) where further chemical reactions might lead to formation of building blocks of life. This presentation includes the topics on detailed disk density structures at ~5-au or better resolution, gas detections in the later stages of disks where the collisional events in the planetary systems may happen, detections of organic molecules, and the prospects on disk observations in future.

Keywords: Exoplanets, Astronomy

©2019. Japan Geoscience Union. All Right Reserved.

Characterization of high molecular weight amino acid precursors formed in interstellar ice analog

*Soushi Kuramoto[1], Tomohito Sato[1], Hitoshi Fukuda[2], Yoshiyuki Oguri[2], Kotaro Kondo[2], Hiromi Shibata[3], Yoko Kebukawa[1], Kensei Kobayashi[1], Satoshi Yoshida[4]

1. Yokohama National University, 2. Tokyo Institute of Technology, 3. University of Osaka, 4. National Institutes for Quantum Radiological Science and Technology

It is suggested that extraterrestrial organic compounds are important for chemical evolution toward the generation of the first life on the Earth. Bioorganic compounds such as amino acids were found in hydrolyzed extracts of meteorite [1]. The products before hydrolysis referred to as “amino acid precursors” were, however, little known. It has been sometimes claimed that a-amino acids found in meteorites were formed by the Strecker synthesis. If so, aminonitriles and amino acid amides are the precursors, but they have not identified as major precursors yet. Extraterrestrial amino acid precursors were probably synthesized in molecular cloud environments or small celestial bodies. We irradiated possible interstellar media, such as mixture of carbon monoxide, ammonia and water to simulate possible reactions among interstellar media in dense clouds. The irradiation products were analyzed by HPLC and mass spectrometry.

A gaseous mixture (CO and NH_3) was sealed in a Pyrex glass tube with liquid water. The gaseous mixture was irradiated with 2.5 MeV protons from a Tandem accelerator at Tokyo Institute of Technology. Total quantity of electricity was 2 mC. The name of the irradiation products is hereafter called CAW. CAW was fractionated by cation exchange HPLC into several fractions to discriminate the fractions with glycine amide or aminoacetonitrile (the Strecker-type precursors) and those without them. Each fraction was hydrolyzed with 6M HCl at 110 ˚C for 24h and was subjected to amino acid analysis. Molecular weights of CAW were estimated by ultrafiltration (molecular weight cut off: 3000), gel filtration (column: Shodex OHpak SB-802.5 HQ) and mass spectrometry by ESI-TOF-MS.

It was shown that glycine was rarely detected in the fractions with the Strecker-type simple amino acid precursors (aminoacetonitrile, glycine amide). It was suggested that the CAW (an interstellar organics analogue) contained complex amino acid precursors with molecular weights of some thousands. Compared with molecular weights standards (authentic proteins), molecular weights of CAW were estimated 6000 or more by gel filtration chromatography. Peaks of m/z = 1000 or over were detected by mass spectrometry. These results strongly suggested that complex amino acid precursors with large molecular weights could be directly generated from small molecules such as CO in interstellar environments. We are now trying to characterize amino acid precursors formed in interstellar ice analogue (frozen mixture of CH3OH, NH3 and H2O [2]) by heavy ions irradiation.

[1] K. A. Kvenvolden *et al.*, *Nature* 228, 923 (1970).

[2] K. Kobayashi *et al.*, *Electr. Commun.* Jpn. 91, 293 (2008).

Keywords: Chemical evolution, interstellar ice, the Strecker synthesis, amino acid precursor

©2019. Japan Geoscience Union. All Right Reserved.

Theoretical elucidation of prebiotic formation processes into nucleobases

*Yu Komatsu[1,2], Taiki Suzuki[1,2]

1. Astrobiology Center, 2. National Astronomical Observatory of Japan

As argued [1], the comets and meteorites may have provided a large amount of prebiotic molecules to the Early Earth. However, where and how such organic molecules were built is still controversial.

Recently, volatile glycine (NH2CH2COOH) has been detected in the coma of comet 67P/Churyumov-Gerasimenko by the ROSINA mass spectrometer [2], with giving us clues to glycine's interstellar origin. Moreover, in addition to various amino acids, nucleobases, such as purine, uracil, guanine, and xanthine have been identified in the meteorite (e.g., [3]). These studies suggest the formation of prebiotic molecules in the extreme condition prior to the early Earth chemistry.

If prebiotic molecules are built from small atoms or radicals in the cold ISM, the prebiotic molecules must have almost barrier-less formation paths. On the other hand, the bombardment of comets and/or asteroids would have provided very high temperature condition for chemical reactions, which may have led to the decomposition and formation of further complex prebiotic molecules. To understand the formation processes, the quantum chemical calculation is a powerful tool. The previous quantum chemical calculation has already reported the promising chemical paths to amino acids and nucleobases (e.g., [4]).

Here we investigated the possible pathway of pyrimidine, purine, uracil and thymine by the automated exploration of chemical reaction pathways. We have already discovered key dissociations for each molecule. For example, uracil and thymine, the pyrimidine type of nucleobase, have lower barriers to dissociate into an isocyanic acid, which corresponds to the previous laboratory experience, and the rest molecule. Pyrimidine and purine, which are skeleton structures of nucleobases and do not poses any oxygen atoms, have high barriers, implying to require high temperature environment like the bombardment, even though we did not exclude all possibilities of radical reactions. Detailed discussions will be provided on our poster.

References

[1] Ehrenfreund (2002), Rep. Prog. Phys. 65 1427

[2] Altwegg et al. (2016), Sci, 2, e1600285

[3] Simomiya et al. (1990), Geo, 24,343

[4] Ferus et al. (2015), PNAS, 112, 7109

Keywords: Prebiotic Chemistry, Quantum Chemistry, DNA /RNA, Interstellar Chemistry

©2019. Japan Geoscience Union. All Right Reserved.

©2019. Japan Geoscience Union. All Right Reserved.

Formation Process of A Glycine's Precursor Candidate, CH3NH2

*Taiki Suzuki[1,2], Liton Majumdar[3], Masatoshi Ohishi[2]

1. National Institutes of Natural Sciences Astrobiology Center, 2. National Astronomical Observatory of Japan, 3. NASA Jet Propulsion Laboratory (JPL)

As [1] argued, the comets and meteorites may have provided a large amount of prebiotic molecules to the early Earth. An attempt to understand the origins of life must necessarily begin with detailed studies of the formation and evolution of complex organic molecules (COMs), products of complex chemistry that most likely starts in molecular clouds and continues within the protoplanetary disk.
Since the amino acids are the essential building blocks of life, the search for amino acids and their complex organic precursors at different stages of star and planet formation is one of the exciting topics in modern astronomy. Recently, volatile glycine (NH_2CH_2COOH) was detected in the coma of comet 67P/Churyumov-Gerasimenko by the ROSINA mass spectrometer [2], also giving clues about glycine's interstellar origin. However, the survey observations of glycine toward ISM have been not successful. Therefore, revealing the formation pathways to glycine is important for astrochemistry and astrobiology not only to know the promising glycine-rich sources for future surveys but also to understand the general chemical evolution of N-bearing molecules in the ISM.
In this context, we performed the chemical modeling study for the high-mass star, with the possible formation processes of glycine with theoretically and/or experimentally suggested formation paths [3]. We suggested that glycine was efficiently formed through the following reactions: First, the hydrogenation process to HCN leads to the formation of CH_2NH and CH_3NH_2 on interstellar grain surface (HCN + 2H => CH_2NH, and then CH_2NH + 2H => CH_3NH_2). Then, the destruction of CH_3NH_2 by radicals will form CH_2NH_2. Finally, CH_2NH_2 and COOH radical react to form glycine. For this test, a key molecule would be CH_3OH, whose formation process is well known. Both experiments and theoretical works suggested that CH_3OH is built via grain surface hydrogenation processes to CO (CO + 2H => H_2CO, and then H_2CO + 2H => CH_3OH). If CH_3NH_2 is also produced through hydrogenation process, “CH_3NH_2/CH_3OH” ratio should be well reproduced by the modeling. However, it was difficult to test this formation process due to the very limited number of previous CH3NH2 observations.
With this motivation, we performed the observation of CH_3NH_2 and CH_3OH with ALMA toward high mass star-forming regions, G10.47+0.03, NGC6334I, W51 e1/e2, and G31.41+0.3. As a result, both of CH_3OH and CH_3NH_2 were detected toward all sources. The molecular abundances were derived with rotation diagram method. The high excitation temperatures of 100 and 200 K and compact distributions suggest that CH_3NH_2 emissions originate from the hot and dense regions. The observed molecular abundance ratio, “CH_3NH_2/CH_3OH” ranges from 0.2 to 2.1. The low “CH_3NH_2/CH_3OH” ratio of 0.2 is close to our modeling, supporting that CH_3NH_2 is the product of the hydrogenation process in those sources. However, the higher “CH_3NH_2/CH_3OH” ratio of nearly two, observed toward NGC6334I MM1, could not be reproduced with our modeling under the possible parameter range. Thus, our chemical modeling would not correctly reproduce the physics or chemistry of such CH_3NH_2-rich sources. Further studies of such sources will enable us to promote our knowledge of glycine chemistry and provide us with promising sources for future glycine surveys.

Citations:
[1] Ehrenfreund (2002), Rep. Prog. Phys. 65 1427

©2019. Japan Geoscience Union. All Right Reserved.

[2] Altwegg et al. (2016), Sci, 2, e1600285
[3] Suzuki et al, (2018), ApJ, 825, 51

Keywords: radio astronomy, chemical modeling, prebiotic molecules

©2019. Japan Geoscience Union. All Right Reserved.

Numerical study on the stellar atmosphere & wind of Cool Stars

*Takahito Sakaue[1], Kazunari Shibata[1]

1. Kyoto University

Cool stars offer the good opportunities to investigate what environments the Earth-like exoplanets are in, and how they are affected by the host star. TRAPPIST-1 is an ultracool dwarf; the spectral type is M8V (T_{eff} =2559K) with the lower mass of 0.08M_{sun} (radius = 0.11R_{sun}). The star is confirmed to have seven planets (Gillon et al. 2017) and thus greatly interested in not only by stellar astrophysics but also by astrobiology. Here, we report the results of one-dimensional magnetohydrodynamic (MHD) simulation of the stellar wind from TRAPPIST-1. Several solar wind theories, which have been examined observationally, are applied to the case of TRAPPIST-1. Among them, it is the plausible idea that the dissipation of the incompressible MHD wave leads to the heating and driving the stellar wind. For instance, Garraffo et al. 2017 succeeded in the three-dimensional MHD simulation of the stellar wind from TRAPPIST-1, by extending their solar wind model in which the incompressible MHD wave is exhausted by the turbulent dissipation. The incompressible MHD wave, on the other hand, is also affected not only by the turbulent dissipation but also by the nonlinear mode coupling, which leads to the formation of the shock wave and consequently contribute to heating the wind. This nonlinear process has been well investigated to account for the dynamics of the lower solar atmosphere (Kudoh & Shibata 1999) and driving the solar wind (Suzuki & Inutsuka 2005), but not discussed for the stellar wind from TRAPPIST-1. In this study, therefore, we performed the one-dimensional MHD simulation to consider the nonlinear process of the incompressible MHD wave leading to the shock formation, and succeeded in reproducing the stellar wind from TRAPPIST-1.

Keywords: stellar wind, cool stars, TRAPPIST-1

©2019. Japan Geoscience Union. All Right Reserved.

Design of space exposure experiments of organic matter in Tanpopo 2

*Takuya Yokoo[1], tomohito sato[1], Itsuki Sakon[2], Kazumichi Nakagawa[3], Hajime Yano[4], Miki Nakayama[5], Hajime Mita[5], Yoko Kebukawa[1], Kensei Kobayashi[1]

1. Yokohama National University, 2. University of Tokyo, 3. Kobe University, 4. JAXA, 5. Fukuoka Institute of Technology

1. Introduction

Large number of organic compounds have been discovered in molecular clouds and in meteorites. Some of organic compounds required for emergence of life are thought to be synthesized in space. Then, meteorites and interplanetary dust particles could deliver them to the Earth. The first Japanese astrobiology space experiment called “Tanpopo” was conducted to study this hypothesis[1].
The objective of the Tanpopo Mission is to understand bi-directional propagation of microorganisms and organic matter between the Earth and space. In other words, in the Tanpopo Mission, we examine whether life exists only on the earth by evaluating whether microorganisms can escape into space and whether organic matter can reach to the Earth from outer space.
As one of subthemes in this project, amino acids and their precursor compounds including complex interstellar organic matter analog were directly exposed to outer space by utilizing the International Space Station (ISS), and recoveries of these organics were measured to understand degradation of organic compounds under the environment of the outer space. In the Tanpopo experiment, hexatriacontane (HTC) was used to prevent the sample from sublimation during exposure to space at the ISS. However, HTC absorbs ultraviolet light with a wavelength of 160 nm or less. To understand the effects of shorter wavelength UV, the next space experiment "Tanpopo 2" applies a new design for direct exposure of organic compounds without HTC and optical windows. In addition to the aluminum plate same as the one used in Tanpopo, the silicon substrates are also used for exposure the sample to space, in the organic matter exposure experiment of “Tanpopo 2 “. In the Tanpopo Mission, glycine, hydantoin, isovaline, ethylmethylhydantoin, CAW (complex organic matter produced from proton beam irradiation to CO, NH_3, H_2O mixture) were used, and glycine and CAW showed relatively high recoveries [2]. In "Tanpopo 2", glycine and CA (proton beam irradiation product to CO, NH_3 mixture) on the silicon substrates will be directly exposed to space in addition to the same compounds on the same aluminum plate used in the Tanpopo. The recovered samples will be analyzed by FT-IR, XANES, and SEM, in addition to amino acid analysis.
Here we report the design of the space experiment such as preparation method of the space experiment sample.

2. Experimental

(1) A gas mixture of CO (350 Torr) and NH_3 (350 Torr) and a silicon plate (10 mmϕ) were placed in a glass container, and the gas mixture was irradiated with 2.5 MeV proton beam from a tandem accelerator to deposit organic matter on the plate.
(2) The thickness of the organic matter (CA) film on the silicon plate was measured using a three-dimensional microscope.
(3) Structural analysis of organic matter (CA) on the silicon plate was also carried out using FT-IR.
(4) Amino acid analysis was carried out by cation exchange HPLC after hydrolyzing silicon plate with CA with 6 M hydrochloric acid at 110 ˚C for 24 hours.

©2019. Japan Geoscience Union. All Right Reserved.

(5) Glycine is planned to be deposited on a silicon substrate by a vacuum vapor deposition equipment (Fukuoka Institute of Technology).

3. Results and Discussion

The CA deposition thickness was approximately 8 μm, but more sample thickness would be required due to potential loss of the organic materials by atomic oxygen present in low Earth orbit during exposure. Thus, we decided to use non-polished Si substrates instead of polished Si substrate. Because the sample can be kept in the bottom of indentations on the rough surface of non-polished substrate, even if a part of sample surface is lost.
Amino acid analyses of CA by cation exchanged HPLC showed, various amino acids including aspartic acid, threonine, glycine, alanine, -aminoisobutyric acid and serine were detected after acid hydrolysis. Glycine was particularly abundant, whose yield was 827 ±7 nmol from a single CA deposited Si substrate.

4. Conclusions

We will conduct the durability test of our samples on the silicon substrate including the vibration test, cooling test, heating test before launch in 2019 with the space X company to the ISS. We are planning to conduct various analyses from recovered samples. The recovery and degradation of these samples will make a further leap forward our understanding of the possible delivery of organic matter from interplanetary dust particles to the early Earth.

5. References

[1] A. Yamagishi, H. Yano, K. Okudaira, K. Kobayashi, S. Yokobori, M. Tabata, H. Kawai, *Biol. Sci. Space*, **21** : 67-75 (2007).
[2] K. Kobayashi *et al.*, 2018 JpGU meeting, Chiba (2018).

©2019. Japan Geoscience Union. All Right Reserved.

[E] Poster | M (Multidisciplinary and Interdisciplinary)：M-IS Intersection

Thu. May 30, 2019 5:15 PM - 6:30 PM JST | Thu. May 30, 2019 8:15 AM - 9:30 AM UTC | Poster Hall International Exhibition Hall8, Makuhari Messe_37

[M-IS07] Astrobiology

convener:Hikaru Yabuta(Hiroshima University, Department of Earth and Planetary Systems Science), Seiji Sugita(Department of Earth and Planetary Science, Graduate School of Science Sciece, The University of Tokyo), Misato Fukagawa(National Astronomical Observatory of Japan), Fujishima Kosuke(Tokyo Institute of Technology, Earth-Life Science Institute)

Twenty years have passed since when the field of Astrobiology, which aims to unveil the origins, evolution, and habitability of life by integrating multidisciplinary fields, was established. Individual themes related to Astrobiology, such as chemical evolution in the early Solar System, formation of planetary system, prebiotic chemistry in the early Earth, evolution of life in the Earth's history, extremophile, and habitable planetary environments, has been studied by the knowledge and methods from the multiple fields, which has enabled us to explain "Where we came from" in some ways. However, despite an overwhelming number of investigations and discussions through gathering of the scientists from different fields, there has remained the long-standing unsolved question: How did abiotic materials gain biological function in the Earth and elsewhere in universe? There is still a large gap between prebiotic organic chemistry and biochemistry toward Origins of Life and planetary habitability. Therefore, the JpGU Astrobiology session focuses on pathfinding of "integration of astronomy, geoscience, and biochemistry", which will face an increasing need for the future Astrobiology. In order to enhance our understanding of "What is life", we propose to discuss the biochemical events linked with planetary systems, which is beyond the knowledge in a test tube, by an integration of exoplanets and molecular biology, etc. Through this approach, we will lead the discussions and developments of life-detection strategies for the future exploration of life in universe.

[MIS07-P01] Exoplanets Revealed by High-Precision Infrared Doppler Technique Using IRD: Large Exploration for Planets around Cool M-type Stars Begins

*Masayuki Kuzuhara[1,3], Bunei Sato[4], Motohide Tamura[2,1,3], Takayuki Kotani[1,3,5], Nagayoshi Ohashi[3,6], Masashi Omiya[1,3], Teruyuki Hirano[4], Hiroki Harakawa[6,3,1], Wako Aoki[3,5], Norio Narita[2,1], Yasunori Hori[1,3], Akitoshi Ueda[3,5], Akihiko Fukui[2], Hiroyuki Tako Ishikawa[5,3], Ishizuka Masato[2], Takashi Kurokawa[1,7], Nobuhiko Kusakabe[1,3], Tomoyuki Kudo[6,3,1], Eiichiro Kokubo[3], Mihoko Konishi[1,3], Tadashi Nakajima[1,3,5], Jun Nishikawa[3,5,1], Masahiro Ogihara[3], Takuma Serizawa[7] (1.Astrobiology Center of NINS, 2.The University of Tokyo, Graduate School of Science, 3.National Astronomical Observatory of Japan, 4.Tokyo Institute of Technology, 5.SOKENDAI, 6.Subaru Telescope, 7.Tokyo University of Agriculture and Technology)

[MIS07-P02] Discrimination of organic compounds and mineral particles by fluorescent microscopy for the detection of Martian life.

*Tomoka Okada[1], Yoshitaka Yoshimura[2], Atsuo Miyakawa[3], Yuka Murano[3], Shin-ichi Yokobori[3], Akihiko Yamagishi[3], Kensei Kobayashi[1], Yoko Kebukawa[1] (1.YOKOHAMA National university, 2.Tamagawa University, 3.Tokyo University of Pharmacy and Life Sciences)

[MIS07-P03] Morphological and spectroscopic characteristics of organic matter in Banded Iron Formation, Barberton Greenstone Belt, South Africa

*Hiroki Amemiya[1], Ryo Nakajima[1], Yoko Ohtomo[1], Tsubasa Otake[1], Tsutomu Sato[1] (1.Division of sustainable Resources Engineering, Faculty of Engineering, Hokkaido University)

[MIS07-P04] Understanding peptide sequence selectivity on iron sulfide (FeS) nanoparticle surfaces

*Fujishima Kosuke[1], Norio Kitadai[1], Kenji Kasama[1] (1.Earth-Life Science Institute, Tokyo Institute of Technology)

[MIS07-P05] A process model of L-homochiral peptides formation initiated with L-alanine

*Toratane Munegumi[1], Taisuke Yamaga[1] (1.Department of Science Education, Naruto University of Education)

[MIS07-P06] Possible Formation of Amino Acids and Carboxylic Acids in Slightly-Reducing Primitive Earth Atmospheres

*Miei Kinoshita[1], Shintaro Ikeda[1], Kimitaka Kawamura[2], Bhagawati Kunwar[2], Hitoshi Fukuda[3], Yoshiyuki Oguri[3], Hiromi Shibata[4], Junichi Takahashi[1], Vladimir Airapetian[5], Yoko Kebukawa[1], Kensei Kobayashi[1] (1.Yokohama National University, 2.Chubu University, 3.Tokyo Institute of Technology, 4.Osaka University, 5.NASA Goddard SFC)

[MIS07-P07] Application of Machine learning and software development for initial analysis in the TANPOPO mission

*Kyoko Okudaira[1], Yuto Toda[1], Takashi Sonoke[1], Yuichi Yaguchi[1], Masashi Yoshida[1], Junya Imani[2], Satoshi Sasaki[3], Hajime Yano[4], Hirohide Demura[1], Makoto Tabata[5], Akihiko Yamagishi[6] (1.The University of Aizu, 2.YUKI Precision, 3.Tokyo University of Technology, 4.JAXA, 5.Chiba University, 6.Tokyo University of Pharmacy and Life Science)

[MIS07-P08] Structure analysis of the hyper velocity impact tracks of the particles captured by silica aerogel on the International Space Station

*Mizuho Nishi[1], Akira Tsuchiyama[1], Hajime Yano[2], Hikaru Yabuta[3], Kyoko Okudaira[4], Junya Matsuno[1], Masayuki Uesugi[5], Uesugi Kentaro[5], Nakano Tukasa[6], Takaaki Noguchi[7], MITA Hajime[8], Akihiko Yamagishi[9] (1.Kyoto University, 2.Institute of Space and Astronautical Science, Japan Aerospace Exploration Agency, 3.Hiroshima University, 4.The University of Aizu, 5.JASRI/SPring-8, 6.National Institute of Advanced Industrial Science and Technology, 7.Kyusyu University, 8.Fukuoka Institute of Technology, 9.Tokyo University of Pharmacy and Life Science)

[MIS07-P09] High-Angular-Resolution Observations of Protoplanetary Disks

*Misato Fukagawa[1] (1.National Astronomical Observatory of Japan)

[MIS07-P10] Characterization of high molecular weight amino acid precursors formed in interstellar ice analog

*Soushi Kuramoto[1], Tomohito Sato[1], Hitoshi Fukuda[2], Yoshiyuki Oguri[2], Kotaro Kondo[2], Hiromi Shibata[3], Yoko Kebukawa[1], Kensei Kobayashi[1], Satoshi Yoshida[4] (1.Yokohama National University, 2.Tokyo Institute of Technology, 3.University of Osaka, 4.National Institutes for Quantum Radiological Science and Technology)

[MIS07-P11] Theoretical elucidation of prebiotic formation processes into nucleobases

*Yu Komatsu[1,2], Taiki Suzuki[1,2] (1.Astrobiology Center, 2.National Astronomical Observatory of Japan)

[MIS07-P12] Formation Process of A Glycine's Precursor Candidate, CH3NH2

*Taiki Suzuki[1,2], Liton Majumdar[3], Masatoshi Ohishi[2] (1.National Institutes of Natural Sciences Astrobiology Center, 2.National Astronomical Observatory of Japan, 3.NASA Jet Propulsion Laboratory (JPL))

[MIS07-P13] Numerical study on the stellar atmosphere & wind of Cool Stars

*Takahito Sakaue[1], Kazunari Shibata[1] (1.Kyoto University)

[MIS07-P14] Design of space exposure experiments of organic matter in Tanpopo 2

*Takuya Yokoo[1], tomohito sato[1], Itsuki Sakon[2], Kazumichi Nakagawa[3], Hajime Yano[4], Miki Nakayama[5], Hajime Mita[5], Yoko Kebukawa[1], Kensei Kobayashi[1] (1.Yokohama National University, 2.University of Tokyo, 3.Kobe University, 4.JAXA, 5.Fukuoka Institute of Technology)

Exoplanets Revealed by High-Precision Infrared Doppler Technique Using IRD: Large Exploration for Planets around Cool M-type Stars Begins

*Masayuki Kuzuhara[1,3], Bunei Sato[4], Motohide Tamura[2,1,3], Takayuki Kotani[1,3,5], Nagayoshi Ohashi[3,6], Masashi Omiya[1,3], Teruyuki Hirano[4], Hiroki Harakawa[6,3,1], Wako Aoki[3,5], Norio Narita[2,1], Yasunori Hori[1,3], Akitoshi Ueda[3,5], Akihiko Fukui[2], Hiroyuki Tako Ishikawa[5,3], Ishizuka Masato[2], Takashi Kurokawa[1,7], Nobuhiko Kusakabe[1,3], Tomoyuki Kudo[6,3,1], Eiichiro Kokubo[3], Mihoko Konishi[1,3], Tadashi Nakajima[1,3,5], Jun Nishikawa[3,5,1], Masahiro Ogihara[3], Takuma Serizawa[7]

1. Astrobiology Center of NINS, 2. The University of Tokyo, Graduate School of Science, 3. National Astronomical Observatory of Japan, 4. Tokyo Institute of Technology, 5. SOKENDAI, 6. Subaru Telescope, 7. Tokyo University of Agriculture and Technology

Planets outside the Solar system, so-called exoplanets, are promising as a new window for astrobiology. Among those, planets orbiting cool M-type stars (main-sequence stars with effective temperatures less than about 3000 K) have the great potential to push forward astrobiological studies on exoplanets. The habitable zone (HZ) is the zone where liquid water is sustainable on the surfaces of planets. It is expected that the HZs around cooler stars come closer to the parent stars (Kopparapu et al. 2013, ApJ 765, 131). In addition, the recent exoplanet observations performed by the *Kepler* space telescope have revealed that the occurrence rate of small exoplanets similar to Earth increases as the effective temperatures of stars decrease (e.g., Mulders et al. 2015, ApJ 798, 112). Furthermore, the Doppler technique, one of primary methods for exoplanet observations, can more easily find a planet with the orbit closer to its parent star. Accordingly, targeting cool M-type stars provides a significant advantage in the observations of rocky planets in HZs based on the Doppler technique. Also, the snow line around a cool M-type star is close to the star; this is intriguing in terms of the planet formation process.
Nevertheless, the exoplanet observations for cool M-type stars have not been advanced compared with those for hotter stars, due to their faintness. In particular, the low brightness of a cool M-type star at optical wavelengths makes it problematic to observe its planet based on visible light, which has been mostly used in exoplanet observations. We have therefore developed the InfraRed Doppler (IRD) instrument, which is a high-dispersion spectrograph to enable the exoplanet observations using the high-precision Doppler technique at near-infrared (Kotani et al. 2018, Proc. of the SPIE 10702, 1070211). Near-infrared light is suited for observing cool M-type stars, since their peak flux is located in a near-infrared region. One of bottlenecks to achieve high-precision measurements using the near-infrared Doppler technique is the lack of a reference source that enables us to correctly calibrate a measurement fluctuation caused by the instability of an observation instrument. We use a laser frequency comb (LFC) generated by the system that has been newly developed for IRD as a reference source to calibrate IRD measurements. An LFC spectrum has a number of emission lines with fine sampling intervals and is observed simultaneously with a stellar spectrum, so it works as a correct wavelength calibrator for the stellar spectrum. After our laboratory performance verifications of IRD with its LFC system (Kuzuhara et al. 2018, Proc. of the SPIE 10702, 1070260), the IRD operation started on the Subaru Telescope, whose large primary mirror enables high-sensitivity observations even for cool M-type stars. The use of IRD with the Subaru Telescope significantly helps the discoveries and characterizations of exoplanets around cool M-type stars.
We have planned a large survey for planets around cool M-type stars with IRD on the Subaru Telescope, which actually begins on February, 2019. In this survey, we monitor 60 M-type stars over 175 nights

©2019. Japan Geoscience Union. All Right Reserved.

allocated for 5 years. Our pre-survey simulation prospects more than 60 planet detections; those discoveries include a few dozen Earth-like planets, among which some are expected to locate within HZs. Thus, the IRD survey provides important contributions on improving our current understanding of planet formation models for low-mass stars like cool M-type stars, as well as the provisions of samples for exoplanet characterizations using the future large telescopes such as TMT. Here, we report the result of our ongoing on-sky tests to evaluate the IRD performances such as its measurement precision and stability. Furthermore, we explain the above large program in detail: our science goals, and the target selection and observation strategy for the goals are provided.

Keywords: Exoplanet, Doppler technique, Habitable Zone, IRD, planet formation, M-type star

©2019. Japan Geoscience Union. All Right Reserved.

Discrimination of organic compounds and mineral particles by fluorescent microscopy for the detection of Martian life.

*Tomoka Okada[1], Yoshitaka Yoshimura[2], Atsuo Miyakawa[3], Yuka Murano[3], Shin-ichi Yokobori[3], Akihiko Yamagishi[3], Kensei Kobayashi[1], Yoko Kebukawa[1]

1. YOKOHAMA National university, 2. Tamagawa University, 3. Tokyo University of Pharmacy and Life Sciences

The Viking mission searched life on Mars in 1976, but did not find apparent biological activities[1)]. However, the detection sensitivity of the Viking instrument (GC-MS) has been found to be low, suggesting that organic compounds could exist on Martian surface. Recently the MSL Curiosity by NASA detected organic compounds[2)]. The Phoenix mission discovered H_2O ice[3)] and possible liquid water flows were found at RSL (Recurring Slope Lineae) by MRO (Mars Reconnaissance Orbiter)[4)]. These findings suggested that life might exist on Martian surface.

We have proposed a life search program on the surface of Mars with a fluorescence microscope[5)]. This microscope is called Life detection Microscope (LDM) which detects microorganisms in more than 100 times higher sensitivity than the Viking GC-MS. In this program, we plan to use two fluorescent dyes SYTO 24 and propidium iodide (PI) in LDM. SYTO24 permeates cell membrane and stains organic compounds. PI also stains organic compounds such as nucleic acids, but it doesn’t permeate cell membrane. Therefore, the combination of these two dyes makes it possible to differentiate the organic compounds surrounded by membranes (living cells) and dead cells.

However, there are some mineral particles have autofluorescence, possibly detected as false positives. In this research, in order to discriminate organic compounds from mineral particles, the autofluorescence of minerals were measured under various conditions.

Various kind of mineral specimens were finely ground with a glass pen washed with ethanol. Fluorescent images were obtained with a fluorescence microscope and a digital camera and their fluorescent intensities were measured by image analysis. We also examined fluorescent spectra of mineral particles using a diffraction grating. The results showed the fluorescent intensities and spectra of mineral particles were clearly different from the stained organic compounds. These methods would be useful to detect organic compounds among mineral particles.

1) Navarro-Gonzalez, R., *et al.,* 2006, *PNAS*, 103: 16089-16094. 2) Freissient, C., *et al*., 2015, *J. Geophys. Res. Planets,* 120: 495-514. 3) Feldman, W. C., *et al.,* 2002. *Science*, 297, 75-78. 4) McEwen A. S, *et al.,* 2011, *Science,* 333: 740-743. 5) Yamagishi, A., *et al*., 2010, *Bio. Sci. Space,* 24: 67-82.

Keywords: Mars, Fluorescent microscope, Life Detection

©2019. Japan Geoscience Union. All Right Reserved.

Morphological and spectroscopic characteristics of organic matter in Banded Iron Formation, Barberton Greenstone Belt, South Africa

*Hiroki Amemiya[1], Ryo Nakajima[1], Yoko Ohtomo[1], Tsubasa Otake[1], Tsutomu Sato[1]

1. Division of sustainable Resources Engineering, Faculty of Engineering, Hokkaido University

The emergence of cyanobacteria has been postulated to cause an increase in Earth’ s atmospheric oxygen concentration ~2.45 Ga and oxidation of ferrous iron in a seawater, facilitating the formation of Banded Iron Formations (BIFs) in the Proterozoic era. On the other hand, iron precipitation process in the Archean is still controversial. Previous studies suggest that anoxygenic iron-oxidizing bacteria and/or free oxygen produced by cyanobacteria, was responsible for iron oxidation before ~2.45 Ga. Organic matter preserved in BIFs may provide insights into the iron oxidation process and biological evolution in Archean. However, authenticity of Archaean organic matter has to be first clarified for further investigations due to possible later contamination. Here, we investigated morphological and spectroscopic characteristics of organic matter in ~3.2 Ga BIFs in Sheba mine, Moodies Group, Barberton Green stone Belt, South Africa to estimate the chemical structure combined with a contamination check using Raman spectroscopy.

Organic matter was collected by two different methods: extraction by acid treatment of powder samples and pick up with a micro-manipulator from thin sections. When Raman spectra were obtained using 532 nm wavelength laser, acid-treated organic matter showed two peaks ~1350 and ~1580 cm^{-1} corresponding to disordered and ordered carbon structures, whereas micro-sampled organic matter shows no detectable peak with a high background. Because yellow-green fluorescence was observed in micro-sampled organic matter using a Fluorescence microscope, the fluorescence likely causes a high background in the Raman spectra. Therefore, 785 nm wavelength laser was applied for micro-sampled organic matter. Calculated metamorphic temperature from the Raman spectra obtained by acid-treated and micro-sampled organic matter was from 400 to 540˚C, which is consist with greenschist facies of the Barberton Greenstone Belt. This indicates that the organic matter is not a later contamination. Chemical mapping with an Electron Probe Micro Analyzer shows that micro-sampled organic matter is predominately comprised of carbon with slight contribution of nitrogen (< 0.1wt%). Infrared spectra of the organic matter show absorption peaks corresponding to N-O, C-O, and C=O bonds, suggesting that organic matter remains their functional groups in the structure. Based on the morphology and microstructure observed by Field Emission- Scanning Electron Microscope, the organic matter may have been derived from biofilm because of similarity in the morphology as well as the large size (20 –50 μm). Furthermore, the micro-sampled organic matter has a rough surface while the acid-treated organic matter has a smooth one, which may be due to damages by acid-treatment. Our results suggest that micro-sampling is suitable to observe the detailed morphological and structural features of organic matter preserved in Archean sedimentary rocks.

Keywords: Archean, Microfossils, Barberton Greenstone Belt, Raman spectroscopy, Infrared spectroscopy

©2019. Japan Geoscience Union. All Right Reserved.

Understanding peptide sequence selectivity on iron sulfide (FeS) nanoparticle surfaces

*Fujishima Kosuke[1], Norio Kitadai[1], Kenji Kasama[1]

1. Earth-Life Science Institute, Tokyo Institute of Technology

The emergence and evolution of functional biopolymers on Earth is one of the unsolved key questions regarding the origin of life. Amongst various building blocks of polymers, amino acids are prebiotically abundant and different plausible paths toward forming polypeptides have been previously shown in the context of early Earth environment. However, relationship between a specific geochemical environment and the types of biopolymers that could retain or to propergate in that condition is not yet fully systematically explored. Hence, we have prepared random octapeptide library with a combination of limited set of amino acids (Gly, Ile, His, Asp, Cys, Arg) as a probe to explore the sequence selectivity of iron sulfide (FeS) nanoparticles as a simulant of the geochemical settings that once existed at the deep-sea floor or the surface of early Earth. Experiment was carried out by mixing the FeS nanoparticles and random peptides in pure H_2O solution inside the anoxic chamber to allow adsorption under moderate temperature/pH condition. After extensive rinsing step, peptides that remain bound to the FeS nanoparticles were analyzed directly by MALDI-MS/MS to retrieve sequence information. We will discuss the latest sequence results obtained from screening and discuss sequence selective feature of FeS and its relevance to the iron-sulfur cluster known as a fundamental cofactor in biology.

Keywords: Iron sulfide, peptide adsorption, MALDI-MS/MS, iron-sulfur cluster

©2019. Japan Geoscience Union. All Right Reserved.

A process model of L-homochiral peptides formation initiated with L-alanine

*Toratane Munegumi[1], Taisuke Yamaga[1]

1. Department of Science Education, Naruto University of Education

Hydrogen abstraction from L-alanine by hydroxy radical facilitates alkylation on β-carbon of alanine as well as retention of L-chirality. The reaction rate constant of hydrogen abstraction ($k=6.21\times10^{7}\ M^{-1}s^{-1}$) on β-carbon was about 3.7 times faster than that ($k=1.7\times10^{7}\ M^{-1}s^{-1}$) on α-carbon. The fact supports that alkylation proceeds faster than racemization, and the chirality of product amino acids will be hold. Similar alkylation of oligopeptides will also proceed with a lower level epimerization than alkylation. This research discusses how the lower reaction rate of epimerization than alkylation lead homochiral peptides.

Keywords: L-alanine, peptides, homochirality

©2019. Japan Geoscience Union. All Right Reserved.

Possible Formation of Amino Acids and Carboxylic Acids in Slightly-Reducing Primitive Earth Atmospheres

*Miei Kinoshita[1], Shintaro Ikeda[1], Kimitaka Kawamura[2], Bhagawati Kunwar[2], Hitoshi Fukuda[3], Yoshiyuki Oguri[3], Hiromi Shibata[4], Junichi Takahashi[1], Vladimir Airapetian[5], Yoko Kebukawa[1], Kensei Kobayashi[1]

1. Yokohama National University, 2. Chubu University, 3. Tokyo Institute of Technology, 4. Osaka University, 5. NASA Goddard SFC

Since 1950s, a large number of laboratory experiments have been performed to examine possible formation of bioorganic compounds such as amino acids in primitive Earth atmosphere. Earlier experiments with strongly reducing gas mixtures containing large molar ratio of methane and ammonia, and it was reported that efficient production of amino acids and other important organics were formed in it by spark discharges and other energy sources. It is now estimated, however, that the early Earth atmosphere was only slightly reducing [1]: N_2 and CO_2were the major atmospheric constituents, together with some small amount of reducing carbon species like CH_4 and/or CO. Simulation experiments suggested, however, that amino acid formation was restricted under these conditions [2]. We reported that cosmic rays could facilitate chemical reactions with less reducing model of primitive atmosphere such as a mixture of CO_2, CO, $N_2$and H_2O [3]. However these energy sources have been ignored in experiments with initiation of prebiotic chemistry [4]. Here, we examine possible formation of amino acids from slightly reducing gas mixtures by applying high-energy protons to simulate the action of cosmic rays.

We conducted three sets of laboratory experiments using energetic particles, spark discharge and UV light as dominant energy sources. In these sets of experiments we used 400 mL of gas mixture of N_2, $CO_2$and CH_4introduced to a Pyrex tube together with 5 mL of pure water under 350 Torr of N2 and 350 Torr of mixtures with varied mixing ratios of $CH_4$and CO_2. In order to simulate possible roles of cosmic rays, the gas mixture was irradiated with 2.5 MeV proton beam produced in the Tandem accelerator at Tokyo Tech, Japan. We also exposed the same composition of gas mixtures to spark discharges by using a Tesla coil to simulate lightning. The gas mixtures were also irradiated with UV light (l> 190 nm) from a xenon lamp. Each product was acid-hydrolyzed and was subjected to amino acid analysis by HPLC and GC/MS, both after derivatization. Carboxylic acids were determined by GC/MS after derivatization. Starting and resulting gas mixtures were analyzed with a quadrupole mass spectrometer.

Amino acids were detected in the hydrolyzed products when gas mixtures of N_2, CO_2, $CH_4$and H_2O were irradiated with 2.5 MeV protons at the initial the molar ratio of methane (r_{CH4}) in the starting gas mixture as low as 0.5 %. On the other hand, amino acids were detected only when $r_{CH4}$was greater than 15 % in the case of spark discharges. The experiments with UV irradiation source did not yield amino acids or their precursors even when $r_{CH4}$was 50 %. Very little amino acids were detected in all the products before hydrolysis. It was shown that not free amino acids but amino acid precursors were formed in selected experiments.

Carboxylic acids including formic acid, oxalic acid and glyoxylic acid were detected from unhydrolized products derived from N_2-CO_2gas mixtures exposed to spark discharges and proton irradiation. We show that some free carboxylic acids could be formed in non-reducing atmospheres as well as slightly reducing atmospheres either by proton irradiation or by spark discharges. It was suggested that the mechanism of formation of amino acid precursors from N_2-CO_2-CH_4-H_2O mixtures was quite different from that of

©2019. Japan Geoscience Union. All Right Reserved.

carboxylic acids.

Lightning and solar UV have been considered important energy sources for prebiotic synthesis in primitive Earth atmosphere. We here showed that lightning and solar UV could not singularly synthesize important N-containing organics such as amino acids from slightly reducing primitive Earth atmosphere. On the other hand, cosmic ray could have been an important energy source to synthesize amino acid precursors even if primitive Earth atmosphere was only slightly reducing. It would be of interest to examine whether there are synergetic effects among cosmic rays, UV and thundering.

References:

[1] H. Kuwahara and S. Sugita, *Icarus,* **257**,290-301 (2015).

[2] H. Kuwahara *et al.,Orig. Life Evol. Biosph.,* **42**,533-541(2012).

[3] K. Kobayashi *et al.*, *Orig. Life Evol. Biosph.* **28**, 155-165 (1998).

[4] S. L. Miller and H. C. Urey, *Science,* **130**,245-251 (1957).

Keywords: Primitive Earth Atmospheres, Amino Acids, Solar Energetic Particles

©2019. Japan Geoscience Union. All Right Reserved.

Application of Machine learning and software development for initial analysis in the TANPOPO mission

*Kyoko Okudaira[1], Yuto Toda[1], Takashi Sonoke[1], Yuichi Yaguchi[1], Masashi Yoshida[1], Junya Imani[2], Satoshi Sasaki[3], Hajime Yano[4], Hirohide Demura[1], Makoto Tabata[5], Akihiko Yamagishi[6]

1. The University of Aizu, 2. YUKI Precision, 3. Tokyo University of Technology, 4. JAXA, 5. Chiba University, 6. Tokyo University of Pharmacy and Life Science

One of the goals of the TANPOPO mission is collecting cosmic dust and space debris on the International Space Station [1]. Ultra-low density material “silica aerogel” panels are used as capture media [2]. These panels retrieved from the space are sent to the laboratory and initial analysis has been conducted by a system called “CLOXS”.

CLOXS efficiently covers the processes (1) Automatic imaging the entire panel, 2) Search for penetration track candidates, 3) Mapping of track candidates, 4) Shape data acquisition of tracks, and 5) Automatic sample cutting) up to sample allocation to researchers. However, to reduce researchers’ time and effort, improvement of the software and automation of some processes are required.

In this study, application of machine learning in discrimination of objects in aerogel images taken by CLOXS is mainly reported. The research goal is to classify objects in the images into tracks and dirt using machine learning.

There are morphological varieties in the objects. As for both tracks and dirt, they are classified into 4 types respectively in this study.

Since the contrast of the images are low, the first step of our approach is preprocessing of the images. We compared the results of *Contrast Stretching* and *CLAHE* (Contrast Limited Adaptive Histogram Equalization).

Learning data and test data are prepared respectively, to compare the case that the images are categorized into 4 types and the case that the images of all types are dealt altogether.

Convolutional Neural Network (CNN) is used as a method of machine learning. *Python* is used as programing Language.

In conclusion, as for image processing, *CLAHE* showed higher accuracy when tracks were judged to be tracks, and *Contrast Stretching* was found to yield a better result for dirt. It is probably because, in *Contrast Stretching*, *CNN* was not sufficiently highlighted to capture features, and *CLAHE* was able to improve the contrast sufficiently.

Regarding separating the types of tracks and dirt, the accuracy rate was higher when tracks were categorized into different types and learned.

Although further evaluation and improvements might be needed, our accuracy rates meet the mission requirements, that is, the percentage of identifying track as track should be more than 95 %, while the percentage of identifying dirt as dirt should be more than 70 % (that of NOT identifying true track as dirt

©2019. Japan Geoscience Union. All Right Reserved.

should be less than 30 %).

[1] A. Yamagishi et al., “Tanpopo: Astrobiology exposure and micrometeoroid capture experiments - proposed experiments at the exposure facility of ISS-JEM”, *Trans. JSASS. Aerospace Tech. Jpn.* vol. 12, No. ists29, p. Tk_49-Tk_55, 2014.

[2] M. Tabata, et al. “Ultralow-density double-layer silica aerogel fabrication for the intact capture of cosmic dust in low-Earth orbits” *J. Sol-Gel Sci. Technol.* 77(2), 325-334, 2016.

Keywords: TANPOPO mission, Astrobiology, Initial analysis, Machine learning, Software development

©2019. Japan Geoscience Union. All Right Reserved.

Structure analysis of the hyper velocity impact tracks of the particles captured by silica aerogel on the International Space Station

*Mizuho Nishi[1], Akira Tsuchiyama[1], Hajime Yano[2], Hikaru Yabuta[3], Kyoko Okudaira[4], Junya Matsuno[1], Masayuki Uesugi[5], Uesugi Kentaro[5], Nakano Tukasa[6], Takaaki Noguchi[7], MITA Hajime[8], Akihiko Yamagishi[9]

1. Kyoto University, 2. Institute of Space and Astronautical Science, Japan Aerospace Exploration Agency, 3. Hiroshima University, 4. The University of Aizu, 5. JASRI/SPring-8, 6. National Institute of Advanced Industrial Science and Technology, 7. Kyusyu University, 8. Fukuoka Institute of Technology, 9. Tokyo University of Pharmacy and Life Science

In Japan's first astrobiology experiment “Tanpopo”, attempts have been made to capture cosmic dust by installing ultra-low-density silica aerogel at the Japanese Experiment Module “Kibo” of the International Space Station (ISS) [1]. This mission was conducted with the aim of verifying the hypothesis that the origin of life was supplied from outside the earth [2]. Silica aerogel had been used in NASA’s cometary dust sample return mission “Stardust” [3]. Impact tracks formed by collision of cometary dust against aerogel were classified into 3 types, A, B and C, based on their shapes [4]. The track shapes have useful information for estimating the size and density of dust particles [5]. The purposes of this research are (1) to find impact tracks formed by cosmic dust in Tanpopo aerogel and (2) to describe the three-dimensional shapes of impact tracks with different origins (cosmic dust and space debris) and finally to clarify the relation between the track shape and the origin.

At SPring-8 BL47XU, three-dimensional shapes were obtained with imaging absorption tomography for 8 impact tracks (D1-231, D1-298, D1-362, E1-200, E1-304, F1-328, F1-389, F1-623), which were found in Tanpopo aerogel faced to the space direction. The imaging experiments were made at 7, 8, 9 keV with the voxel size of 0.24 or 0.465 μm. CT images at 8 keV were used to extract track shapes. Track length (L_t), maximum track diameter (D_m), aspect ratio, and other shape properties were obtained. These values were compared with Stardust tracks. Dual-energy tomography (DET) [6] was applied to estimate the materials of particles captured in the tracks. Another track (E2-000) was observed only with an optical microscope. For D1-231, D1-298, D1-362 and E2-000, the aerogel was compressed and real solid particles in the tracks were searched with an optical microscope.

The 9 tracks in total were classified into 5 types based on their shapes. Type 1 (E2-000) is a track formed by cosmic dust, where two pyroxene particles were identified at the tip of the track [7]. The track shape resembles Stardust type B track, but its entrance widely spreads. Type 2 (D1-231) is somewhat similar to Stardust type A track. Type 3 (E1-200 and E1-304) is a track having abundant cracks developed on the wall with a narrow entrance. Type 4 (F1-328 and F1-389) is extremely asymmetrical in its shape and has cracks similar to Type 3. Type 5 (D1-362 and F1-623) is a bowl-shaped track with a large entrance. The relationship between L_t and D_m of these tracks was almost the same as that of Stardust tracks except for Type 5. However, their specific shapes of Types 2, 3 and 4 are significantly different from Stardust tracks. The cracks of these tracks are similar to those seen at the end of Stardust type A and B tracks, indicating that they were formed by a relatively low-speed impact. Similar tracks to Type 5 were reported in the aerogel in the exposure experiment on the Mir Station. They may be due to high-speed collision of weakly-adhered aggregates [8]. From the quantitative analysis of such impact tracks, there is a possibility of obtaining knowledge about new parameter areas which could not be obtained by conventional research. DET results showed that most of fine particles in the tracks do not contain Fe and Ni. Low values of their

©2019. Japan Geoscience Union. All Right Reserved.

linear absorption coefficients are smaller than that of cosmic dust. They should be formed by impact of weekly-adhered aggregates that were broken into very small pieces by the impact and mixed with condensed aerogel. Two particles with relatively high linear absorption coefficient were confirmed in D1-231 and D1-362. They were confirmed by and optical microscope after compressing.

[1] Yamagishi A. et al. 2012. Space Utiliz Res, 28, 220. [2] Chyba C. & Sagan C. 1992. Nature, 355, 125. [3] Brownlee D. et al. 2006. Science, 314, 1711. [4] Hörz et al. 2006. Science, 314, 1716. [5] Tsuchiyama A. et al. 2009. Meteoritics & Planetary Science, 44, 1203. [6] Tsuchiyama A. 2013. Geochimica et Cosmochimica Acta 116, 5. [7] Noguchi T., 2018, Private message. [8] Hörz and Zolensky, 2000, Icarus 147, 559.

Keywords: Tanpopo mission, Cosmic dust

©2019. Japan Geoscience Union. All Right Reserved.

High-Angular-Resolution Observations of Protoplanetary Disks

*Misato Fukagawa[1]

1. National Astronomical Observatory of Japan

The recent progress in understanding of planet-formation process will be reviewed based on the results obtained at high angular resolution with astronomical facilities such as the Atacama Large Millimeter/submillimeter Array (ALMA). Circumstellar disk structures around young stars are birthplaces of planets. The physical and chemical condition in such protoplanetary disks can be linked to some extent to the planetary environment (e.g., atmospheric composition) where further chemical reactions might lead to formation of building blocks of life. This presentation includes the topics on detailed disk density structures at ~5-au or better resolution, gas detections in the later stages of disks where the collisional events in the planetary systems may happen, detections of organic molecules, and the prospects on disk observations in future.

Keywords: Exoplanets, Astronomy

©2019. Japan Geoscience Union. All Right Reserved.

Characterization of high molecular weight amino acid precursors formed in interstellar ice analog

*Soushi Kuramoto[1], Tomohito Sato[1], Hitoshi Fukuda[2], Yoshiyuki Oguri[2], Kotaro Kondo[2], Hiromi Shibata[3], Yoko Kebukawa[1], Kensei Kobayashi[1], Satoshi Yoshida[4]

1. Yokohama National University, 2. Tokyo Institute of Technology, 3. University of Osaka, 4. National Institutes for Quantum Radiological Science and Technology

It is suggested that extraterrestrial organic compounds are important for chemical evolution toward the generation of the first life on the Earth. Bioorganic compounds such as amino acids were found in hydrolyzed extracts of meteorite [1]. The products before hydrolysis referred to as “amino acid precursors” were, however, little known. It has been sometimes claimed that a-amino acids found in meteorites were formed by the Strecker synthesis. If so, aminonitriles and amino acid amides are the precursors, but they have not identified as major precursors yet. Extraterrestrial amino acid precursors were probably synthesized in molecular cloud environments or small celestial bodies. We irradiated possible interstellar media, such as mixture of carbon monoxide, ammonia and water to simulate possible reactions among interstellar media in dense clouds. The irradiation products were analyzed by HPLC and mass spectrometry.

A gaseous mixture (CO and NH_3) was sealed in a Pyrex glass tube with liquid water. The gaseous mixture was irradiated with 2.5 MeV protons from a Tandem accelerator at Tokyo Institute of Technology. Total quantity of electricity was 2 mC. The name of the irradiation products is hereafter called CAW. CAW was fractionated by cation exchange HPLC into several fractions to discriminate the fractions with glycine amide or aminoacetonitrile (the Strecker-type precursors) and those without them. Each fraction was hydrolyzed with 6M HCl at 110 ˚C for 24h and was subjected to amino acid analysis. Molecular weights of CAW were estimated by ultrafiltration (molecular weight cut off: 3000), gel filtration (column: Shodex OHpak SB-802.5 HQ) and mass spectrometry by ESI-TOF-MS.

It was shown that glycine was rarely detected in the fractions with the Strecker-type simple amino acid precursors (aminoacetonitrile, glycine amide). It was suggested that the CAW (an interstellar organics analogue) contained complex amino acid precursors with molecular weights of some thousands. Compared with molecular weights standards (authentic proteins), molecular weights of CAW were estimated 6000 or more by gel filtration chromatography. Peaks of m/z = 1000 or over were detected by mass spectrometry. These results strongly suggested that complex amino acid precursors with large molecular weights could be directly generated from small molecules such as CO in interstellar environments. We are now trying to characterize amino acid precursors formed in interstellar ice analogue (frozen mixture of CH3OH, NH3 and H2O [2]) by heavy ions irradiation.

[1] K. A. Kvenvolden *et al.*, *Nature* 228, 923 (1970).

[2] K. Kobayashi *et al.*, *Electr. Commun.* Jpn. 91, 293 (2008).

Keywords: Chemical evolution, interstellar ice, the Strecker synthesis, amino acid precursor

©2019. Japan Geoscience Union. All Right Reserved.

Theoretical elucidation of prebiotic formation processes into nucleobases

*Yu Komatsu[1,2], Taiki Suzuki[1,2]

1. Astrobiology Center, 2. National Astronomical Observatory of Japan

As argued [1], the comets and meteorites may have provided a large amount of prebiotic molecules to the Early Earth. However, where and how such organic molecules were built is still controversial.

Recently, volatile glycine (NH2CH2COOH) has been detected in the coma of comet 67P/Churyumov-Gerasimenko by the ROSINA mass spectrometer [2], with giving us clues to glycine's interstellar origin. Moreover, in addition to various amino acids, nucleobases, such as purine, uracil, guanine, and xanthine have been identified in the meteorite (e.g., [3]). These studies suggest the formation of prebiotic molecules in the extreme condition prior to the early Earth chemistry.

If prebiotic molecules are built from small atoms or radicals in the cold ISM, the prebiotic molecules must have almost barrier-less formation paths. On the other hand, the bombardment of comets and/or asteroids would have provided very high temperature condition for chemical reactions, which may have led to the decomposition and formation of further complex prebiotic molecules. To understand the formation processes, the quantum chemical calculation is a powerful tool. The previous quantum chemical calculation has already reported the promising chemical paths to amino acids and nucleobases (e.g., [4]).

Here we investigated the possible pathway of pyrimidine, purine, uracil and thymine by the automated exploration of chemical reaction pathways. We have already discovered key dissociations for each molecule. For example, uracil and thymine, the pyrimidine type of nucleobase, have lower barriers to dissociate into an isocyanic acid, which corresponds to the previous laboratory experience, and the rest molecule. Pyrimidine and purine, which are skeleton structures of nucleobases and do not poses any oxygen atoms, have high barriers, implying to require high temperature environment like the bombardment, even though we did not exclude all possibilities of radical reactions. Detailed discussions will be provided on our poster.

References

[1] Ehrenfreund (2002), Rep. Prog. Phys. 65 1427

[2] Altwegg et al. (2016), Sci, 2, e1600285

[3] Simomiya et al. (1990), Geo, 24,343

[4] Ferus et al. (2015), PNAS, 112, 7109

Keywords: Prebiotic Chemistry, Quantum Chemistry, DNA /RNA, Interstellar Chemistry

©2019. Japan Geoscience Union. All Right Reserved.

©2019. Japan Geoscience Union. All Right Reserved.

Formation Process of A Glycine's Precursor Candidate, CH3NH2

*Taiki Suzuki[1,2], Liton Majumdar[3], Masatoshi Ohishi[2]

1. National Institutes of Natural Sciences Astrobiology Center, 2. National Astronomical Observatory of Japan, 3. NASA Jet Propulsion Laboratory (JPL)

As [1] argued, the comets and meteorites may have provided a large amount of prebiotic molecules to the early Earth. An attempt to understand the origins of life must necessarily begin with detailed studies of the formation and evolution of complex organic molecules (COMs), products of complex chemistry that most likely starts in molecular clouds and continues within the protoplanetary disk.
Since the amino acids are the essential building blocks of life, the search for amino acids and their complex organic precursors at different stages of star and planet formation is one of the exciting topics in modern astronomy. Recently, volatile glycine (NH_2CH_2COOH) was detected in the coma of comet 67P/Churyumov-Gerasimenko by the ROSINA mass spectrometer [2], also giving clues about glycine's interstellar origin. However, the survey observations of glycine toward ISM have been not successful. Therefore, revealing the formation pathways to glycine is important for astrochemistry and astrobiology not only to know the promising glycine-rich sources for future surveys but also to understand the general chemical evolution of N-bearing molecules in the ISM.
In this context, we performed the chemical modeling study for the high-mass star, with the possible formation processes of glycine with theoretically and/or experimentally suggested formation paths [3]. We suggested that glycine was efficiently formed through the following reactions: First, the hydrogenation process to HCN leads to the formation of CH_2NH and CH_3NH_2 on interstellar grain surface (HCN + 2H => CH_2NH, and then CH_2NH + 2H => CH_3NH_2). Then, the destruction of CH_3NH_2 by radicals will form CH_2NH_2. Finally, CH_2NH_2 and COOH radical react to form glycine. For this test, a key molecule would be CH_3OH, whose formation process is well known. Both experiments and theoretical works suggested that CH_3OH is built via grain surface hydrogenation processes to CO (CO + 2H => H_2CO, and then H_2CO + 2H => CH_3OH). If CH_3NH_2 is also produced through hydrogenation process, “CH_3NH_2/CH_3OH” ratio should be well reproduced by the modeling. However, it was difficult to test this formation process due to the very limited number of previous CH3NH2 observations.
With this motivation, we performed the observation of CH_3NH_2 and CH_3OH with ALMA toward high mass star-forming regions, G10.47+0.03, NGC6334I, W51 e1/e2, and G31.41+0.3. As a result, both of CH_3OH and CH_3NH_2 were detected toward all sources. The molecular abundances were derived with rotation diagram method. The high excitation temperatures of 100 and 200 K and compact distributions suggest that CH_3NH_2 emissions originate from the hot and dense regions. The observed molecular abundance ratio, “CH_3NH_2/CH_3OH” ranges from 0.2 to 2.1. The low “CH_3NH_2/CH_3OH” ratio of 0.2 is close to our modeling, supporting that CH_3NH_2 is the product of the hydrogenation process in those sources. However, the higher “CH_3NH_2/CH_3OH” ratio of nearly two, observed toward NGC6334I MM1, could not be reproduced with our modeling under the possible parameter range. Thus, our chemical modeling would not correctly reproduce the physics or chemistry of such CH_3NH_2-rich sources. Further studies of such sources will enable us to promote our knowledge of glycine chemistry and provide us with promising sources for future glycine surveys.

Citations:
[1] Ehrenfreund (2002), Rep. Prog. Phys. 65 1427

©2019. Japan Geoscience Union. All Right Reserved.

[2] Altwegg et al. (2016), Sci, 2, e1600285
[3] Suzuki et al, (2018), ApJ, 825, 51

Keywords: radio astronomy, chemical modeling, prebiotic molecules

©2019. Japan Geoscience Union. All Right Reserved.

Numerical study on the stellar atmosphere & wind of Cool Stars

*Takahito Sakaue[1], Kazunari Shibata[1]

1. Kyoto University

Cool stars offer the good opportunities to investigate what environments the Earth-like exoplanets are in, and how they are affected by the host star. TRAPPIST-1 is an ultracool dwarf; the spectral type is M8V (T_{eff} =2559K) with the lower mass of 0.08M_{sun} (radius = 0.11R_{sun}). The star is confirmed to have seven planets (Gillon et al. 2017) and thus greatly interested in not only by stellar astrophysics but also by astrobiology. Here, we report the results of one-dimensional magnetohydrodynamic (MHD) simulation of the stellar wind from TRAPPIST-1. Several solar wind theories, which have been examined observationally, are applied to the case of TRAPPIST-1. Among them, it is the plausible idea that the dissipation of the incompressible MHD wave leads to the heating and driving the stellar wind. For instance, Garraffo et al. 2017 succeeded in the three-dimensional MHD simulation of the stellar wind from TRAPPIST-1, by extending their solar wind model in which the incompressible MHD wave is exhausted by the turbulent dissipation. The incompressible MHD wave, on the other hand, is also affected not only by the turbulent dissipation but also by the nonlinear mode coupling, which leads to the formation of the shock wave and consequently contribute to heating the wind. This nonlinear process has been well investigated to account for the dynamics of the lower solar atmosphere (Kudoh & Shibata 1999) and driving the solar wind (Suzuki & Inutsuka 2005), but not discussed for the stellar wind from TRAPPIST-1. In this study, therefore, we performed the one-dimensional MHD simulation to consider the nonlinear process of the incompressible MHD wave leading to the shock formation, and succeeded in reproducing the stellar wind from TRAPPIST-1.

Keywords: stellar wind, cool stars, TRAPPIST-1

©2019. Japan Geoscience Union. All Right Reserved.

Design of space exposure experiments of organic matter in Tanpopo 2

*Takuya Yokoo[1], tomohito sato[1], Itsuki Sakon[2], Kazumichi Nakagawa[3], Hajime Yano[4], Miki Nakayama[5], Hajime Mita[5], Yoko Kebukawa[1], Kensei Kobayashi[1]

1. Yokohama National University, 2. University of Tokyo, 3. Kobe University, 4. JAXA, 5. Fukuoka Institute of Technology

1. Introduction

Large number of organic compounds have been discovered in molecular clouds and in meteorites. Some of organic compounds required for emergence of life are thought to be synthesized in space. Then, meteorites and interplanetary dust particles could deliver them to the Earth. The first Japanese astrobiology space experiment called “Tanpopo” was conducted to study this hypothesis[1].
The objective of the Tanpopo Mission is to understand bi-directional propagation of microorganisms and organic matter between the Earth and space. In other words, in the Tanpopo Mission, we examine whether life exists only on the earth by evaluating whether microorganisms can escape into space and whether organic matter can reach to the Earth from outer space.
As one of subthemes in this project, amino acids and their precursor compounds including complex interstellar organic matter analog were directly exposed to outer space by utilizing the International Space Station (ISS), and recoveries of these organics were measured to understand degradation of organic compounds under the environment of the outer space. In the Tanpopo experiment, hexatriacontane (HTC) was used to prevent the sample from sublimation during exposure to space at the ISS. However, HTC absorbs ultraviolet light with a wavelength of 160 nm or less. To understand the effects of shorter wavelength UV, the next space experiment "Tanpopo 2" applies a new design for direct exposure of organic compounds without HTC and optical windows. In addition to the aluminum plate same as the one used in Tanpopo, the silicon substrates are also used for exposure the sample to space, in the organic matter exposure experiment of “Tanpopo 2 “. In the Tanpopo Mission, glycine, hydantoin, isovaline, ethylmethylhydantoin, CAW (complex organic matter produced from proton beam irradiation to CO, NH_3, H_2O mixture) were used, and glycine and CAW showed relatively high recoveries [2]. In "Tanpopo 2", glycine and CA (proton beam irradiation product to CO, NH_3 mixture) on the silicon substrates will be directly exposed to space in addition to the same compounds on the same aluminum plate used in the Tanpopo. The recovered samples will be analyzed by FT-IR, XANES, and SEM, in addition to amino acid analysis.
Here we report the design of the space experiment such as preparation method of the space experiment sample.

2. Experimental

(1) A gas mixture of CO (350 Torr) and NH_3 (350 Torr) and a silicon plate (10 mmϕ) were placed in a glass container, and the gas mixture was irradiated with 2.5 MeV proton beam from a tandem accelerator to deposit organic matter on the plate.
(2) The thickness of the organic matter (CA) film on the silicon plate was measured using a three-dimensional microscope.
(3) Structural analysis of organic matter (CA) on the silicon plate was also carried out using FT-IR.
(4) Amino acid analysis was carried out by cation exchange HPLC after hydrolyzing silicon plate with CA with 6 M hydrochloric acid at 110 ˚C for 24 hours.

©2019. Japan Geoscience Union. All Right Reserved.

(5) Glycine is planned to be deposited on a silicon substrate by a vacuum vapor deposition equipment (Fukuoka Institute of Technology).

3. Results and Discussion

The CA deposition thickness was approximately 8 μm, but more sample thickness would be required due to potential loss of the organic materials by atomic oxygen present in low Earth orbit during exposure. Thus, we decided to use non-polished Si substrates instead of polished Si substrate. Because the sample can be kept in the bottom of indentations on the rough surface of non-polished substrate, even if a part of sample surface is lost.
Amino acid analyses of CA by cation exchanged HPLC showed, various amino acids including aspartic acid, threonine, glycine, alanine, -aminoisobutyric acid and serine were detected after acid hydrolysis. Glycine was particularly abundant, whose yield was 827 ±7 nmol from a single CA deposited Si substrate.

4. Conclusions

We will conduct the durability test of our samples on the silicon substrate including the vibration test, cooling test, heating test before launch in 2019 with the space X company to the ISS. We are planning to conduct various analyses from recovered samples. The recovery and degradation of these samples will make a further leap forward our understanding of the possible delivery of organic matter from interplanetary dust particles to the early Earth.

5. References

[1] A. Yamagishi, H. Yano, K. Okudaira, K. Kobayashi, S. Yokobori, M. Tabata, H. Kawai, *Biol. Sci. Space*, **21** : 67-75 (2007).
[2] K. Kobayashi *et al.*, 2018 JpGU meeting, Chiba (2018).

©2019. Japan Geoscience Union. All Right Reserved.

[E] Poster | M (Multidisciplinary and Interdisciplinary)：M-AG Applied Geosciences

Thu. May 30, 2019 10:45 AM - 12:15 PM JST | Thu. May 30, 2019 1:45 AM - 3:15 AM UTC | Poster Hall International Exhibition Hall8, Makuhari Messe_11

[M-AG38] Satellite Land Physical Processes Monitoring at Medium/High/Very High Resolution

convener:Jean-Claude Roger(University of Maryland College Park), Shinichi Sobue(Japan Aerospace Exploration Agency), Eric Vermote(NASA Goddard Space Flight Center)

We solicit papers on the land physical processes monitoring. In particular, it will include the inversion and use of land products from medium, high, and very high spatial resolution. For the last years, medium, high, and very high resolutions became a useful and a powerful toll for Earth studies. Topics of interest mainly include (not limited to):
- New developments for data processing, including atmospheric correction and cloud screening;
- Analysis and correction of directional effects in land surface reflectances;
- Use of time series of surface reflectances for land monitoring, including land cover classification and crop yield prediction (including data integration and data harmonization);
- Development and use of new vegetation indices (i.e. red edge) and other products for agriculture applications;
- Theoretical studies for sensors capabilities enhancements to future sensors at high/medium resolutions;
- Use of products in agricultural monitoring applications (such as crop area, crop type, crop growing, yield estimation and prediction, damage assessment);
- Agriculture monitoring algorithm description;
- Evaluation or validation of potential products with ground measurements, official statistics;
- International initiative to enhance Earth-Observing-based agricultural information.

Depending on outcome, we think about a special issue.

[MAG38-P01] Improving the AVHRR LTDR BRDF correction

*Jose Luis Villaescusa[1,2], Belen Franch[1,2], Jean-Claude Roger[1,2], Eric Vermote[2] (1.University of Maryland College Park, 2.NASA Goddard Space Flight Center)

[MAG38-P02] Winter wheat yield model based on remote sensing data

*Belen Franch[1,2], Eric Vermote[2,1], Sergii Skakun[1,2], Jean-Claude Roger[1,2], Inbal Becker-Reshef[1], Chris Justice[1] (1.Department of Geographical Sciences, University of Maryland, 2.NASA Goddard Space Flight Center)

[MAG38-P03] Agricultural monitoring from Optical and SAR data

*Andrés Eduardo Santamaría-Artigas[1,2], Sergii Skakun[1,2], Belen Franch[1,2], Jean-Claude Roger[1,2], Eric Vermote[2] (1.University of Maryland College Park, 2.NASA Goddard Space Flight Center)

[MAG38-P04] Eco-hydrological modeling using field-based and Earth Observations to assess water use efficiency and support agricultural water resources management

pierre Guillevic[2,1], *Jean-Claude Roger[1,2] (1.University of Maryland, College Park, USA, 2.NASA Goddard Space flight Center, Greenbelt, USA)

[MAG38-P05] Detecting and quantifying forest dynamics using SAR time-series data in Indonesia

*Pedro Rodriguez-Veiga[1,2,3], Narumasa Tsutsumida[3] (1.Centre for Landscape and Climate Research, University of Leicester, Leicester, UK, 2.NERC National Centre for Earth Observation (NCEO), Leicester, UK, 3.Graduate School of Global Environmental Studies, Kyoto University, Japan)

Improving the AVHRR LTDR BRDF correction

*Jose Luis Villaescusa[1,2], Belen Franch[1,2], Jean-Claude Roger[1,2], Eric Vermote[2]

1. University of Maryland College Park, 2. NASA Goddard Space Flight Center

The Advanced Very High Resolution Radiometer (AVHRR) sensors aboard the different NOAA satellites provide a unique global remote sensing dataset that ranges from the 1980s to the present. Using these data, the NASA funded Long Term Data Record (LTDR) project aims to develop a quality and consistent Climate Data Record (CDR) of AVHRR data with the use of the Moderate Resolution Imaging Spectrometer (MODIS) instrument as a reference. This product retrieves the BRDF corrected land surface reflectance using the VJB method (Vermote et al., 2009), which corrects the anisotropic effects by obtaining Volumetric (V) and Geometrical (R) parameters, defined in the Roujean model (Roujean et al., 1992), as a function of the Normalized Difference Vegetation Index (NDVI). Inaccuracies regarding the AVHRR atmospheric correction and calibration in the red band for the pre-MODIS era (1982-2000), propagate towards the surface reflectance’ s BRDF correction. However, with the use of the less noisy Near-Infrared (NIR) band we can reduce said errors by finding an empirical relationship between the red-NIR V and R parameters. This study aims to find said relationship using the MODIS sensor, which is an already established and accurate product (Justice et al., 2002; Liang et al., 2002), to then apply it to the noisy AVHRR data and reduce the BRDF errors in the red band.

Keywords: AVHRR, VJB, MODIS, BRDF, LTDR

©2019. Japan Geoscience Union. All Right Reserved.

Winter wheat yield model based on remote sensing data

*Belen Franch[1,2], Eric Vermote[2,1], Sergii Skakun[1,2], Jean-Claude Roger[1,2], Inbal Becker-Reshef[1], Chris Justice[1]

1. Department of Geographical Sciences, University of Maryland, 2. NASA Goddard Space Flight Center

Accurate and timely crop yield forecasts are critical for making informed agricultural policies and investments, as well as increasing market efficiency and stability. Earth observation data from space can contribute to agricultural monitoring, including crop yield assessment and forecasting. This work presents a new EO-based empirical winter wheat yield model. It is based on the un-mixing of the wheat signal from a coarse resolution EO data at 1 km by using yearly crop type masks to a pure wheat signal (100% of wheat within the pixel). *This wheat signal is used to calibrate the model using as inputs the seasonal amplitude and length of the Difference Vegetation Index (DVI) peak extracted from Moderate Resolution Imaging Spectroradiometer (MODIS) data and the average of the evaporative fraction (EF) 30 days after the peak. The three regressors proposed are focused on the reproduction stage of the wheat (DVI amplitude and length) and the grain filling process (EF 30-days average). The model is calibrated at subnational level using historical statistics from 2001 to 2016. In each administrative unit, a different calibration coefficient (based on all possible combination of the three regressors in a linear model) is selected depending on the statistical significance of each variable. The model was applied to estimate the national and subnational winter wheat yield in the United States, Ukraine, Russia and France from 2001 to 2017. At the subnational level the model shows very good performance with a coefficient of determination higher than 0.7 and Root Mean Square Error (RMSE) lower than 15%. At the national level the model provides a strong coefficient of determination higher than 0.8 and a RMSE lower than 8%, which demonstrates good performance of the models at this scale. Additionally, it was also able to capture low winter wheat yields during years with extreme weather events, for example 2002 in US and 2003 in Ukraine.*

Keywords: Yield model, MODIS , agriculture

©2019. Japan Geoscience Union. All Right Reserved.

Agricultural monitoring from Optical and SAR data

*Andrés Eduardo Santamaría-Artigas[1,2], Sergii Skakun[1,2], Belen Franch[1,2], Jean-Claude Roger[1,2], Eric Vermote[2]

1. University of Maryland College Park, 2. NASA Goddard Space Flight Center

Vegetation indices derived from optical remote sensing data are a valuable source of information for agricultural monitoring. However, cloud cover over some areas reduces the number of valid observations, which can difficult the detection of changes in crop condition. In this context, synthetic aperture radar (SAR) systems are an interesting alternative due to their low sensitivity to clouds. In this work, we analyze the relationship between SAR backscatter from Sentinel-1 and vegetation indices derived from the Harmonized Landsat-8 Sentinel-2 (HLS) product with data from the year 2017 over 6 land cover classes in Ukraine: Winter crops, summer crops, bare land, grasslands, forest, and water. Results show that SAR data from Sentinel-1 could be used to complement optical indices for certain land covers. In the case of winter crops (rapeseed and wheat), the ratio between Sigma-0 VV and VH polarization showed the highest relationship with the Normalized Difference Vegetation Index (NDVI) while for summer crops (maize, sugar beet, sunflower, and soybean) the highest relationship was shown by the Sigma-0 VH polarization and NDVI. Further work is being developed to exploit more complex SAR models which account for other variables that affect the backscatter signal such as soil moisture.

Keywords: agricultural monitoring, crop condition, synthetic aperture radar, HLS, normalized difference vegetation index

©2019. Japan Geoscience Union. All Right Reserved.

Eco-hydrological modeling using field-based and Earth Observations to assess water use efficiency and support agricultural water resources management

pierre Guillevic[2,1], *Jean-Claude Roger[1,2]

1. University of Maryland, College Park, USA, 2. NASA Goddard Space flight Center, Greenbelt, USA

The objective of this NASA project is to develop an integrated modeling platform using Earth Observations to simulate large-scale hydrological processes and food production in support of water use decision and agricultural policy. The decision tool will provide timely and relevant assessments of crop growth, agricultural water use and available water supply from local to regional scales, with the capability to predict the impact of different climate and water resources management scenarios on food production. The approach is based on the use of field and Earth observations to calibrate an eco-hydrological model, and climate simulations to forecast crop condition and yield through the crop season. The expected primary outcomes and results for stakeholders is potential best water management practices to improve water use efficiency and prevent excessive losses of water and nitrogen to the environment. These will be provided to in-country end-users within various relevant Ministries and Departments, in order to inform regional and national decisions. Changing precipitation patterns, droughts of increasing duration and severity and growing demand for food have significant implications on water management practices, spurring an increased need for irrigation in a sustainable manner and better monitoring of water resources for the agricultural sector in general. Understanding the context and water resource constraints that stakeholders and smallholder farmers face in climate sensitive regions is critical to target and understand the potential impact of water use management. We focus on a diverse set of regional pilot cases in Argentina, South Africa, Tanzania and the United States that are representative of a range of agricultural systems, water issues and climate impacts. The application is integrated in the GEOGLAM project, an existing widely-used web-based platform which will aid synthesizing the project outcomes and expert domain knowledge to provide timely and actionable water resources and crop condition information to assist local, regional and national water management decisions. At the end, the application will be interactive and will offer the end-user organizations the possibility to submit new water resource management scenarios online for impact evaluation.

Earth Observations are critical to characterize and monitor the different components of agricultural ecosystems and change (forests, croplands and marginal lands availability, for example) across temporal and spatial scales. Satellite data in the shortwave, thermal infrared and microwave spectral domains from US (MODIS, VIIRS, Landsat, SMAP) and European (Sentinel 1 and 2) sensors will be used to characterize changes in land surfaces and water use from 2000 to the present in support of agricultural planning decisions. In a research context, the potential of new satellite missions (i.e., ECOSTRESS, SWOT and SAOACOM) to derive surface hydrology information will be evaluated. The Agricultural Policy/Environmental eXtender (APEX) watershed model is proposed as the modeling tool to understand the biophysical and human-decision processes associated with the food-energy-water nexus. Model simulations will use climate data from the NASA Goddard Earth Observing System Model (GEOS-5) Atmosphere-Ocean General Circulation Model: MERRA-2 for simulation of past conditions and seasonal (6-month) forecasts for projections in the future. The study focus on large, key agricultural regions where agricultural ecosystems are vulnerable to demographic expansion and/or climate variability and change including drought and flood events.

©2019. Japan Geoscience Union. All Right Reserved.

Keywords: water resources, hydrologycal modelling , remote sensing

©2019. Japan Geoscience Union. All Right Reserved.

Detecting and quantifying forest dynamics using SAR time-series data in Indonesia

*Pedro Rodriguez-Veiga[1,2,3], Narumasa Tsutsumida[3]

1. Centre for Landscape and Climate Research, University of Leicester, Leicester, UK, 2. NERC National Centre for Earth Observation (NCEO), Leicester, UK, 3. Graduate School of Global Environmental Studies, Kyoto University, Japan

Satellite Earth Observation (EO) data allows the generation of forest disturbance maps that can improve greenhouse gas (GHG) monitoring at local and national scales, and provide information that can be used for land use planning and management. Mapping forest biomass stocks, deforestation, forest degradation and enhancement is crucial in order to determine the loss of carbon stocks due to disturbances (e.g. deforestation, fires) or the gain due to new forest or growth. Time-series observations identify decreasing or increasing trends of aboveground biomass carbon, and separate anthropogenic related changes from seasonal changes of vegetation. This is important for understanding the terrestrial carbon cycle and for supporting better forest management and policies. This study uses time-series data from L-band Synthetic Aperture Radar (SAR) JAXA’s ALOS PALSAR and ALOS-2 PALSAR-2 to quantify carbon loss and gain trajectories (emission / sequestration) of existing forests in West Java (Indonesia).

Keywords: deforestation, SAR, time-series, forest dynamics

©2019. Japan Geoscience Union. All Right Reserved.

[E] Poster | M (Multidisciplinary and Interdisciplinary)：M-AG Applied Geosciences

Thu. May 30, 2019 5:15 PM - 6:30 PM JST | Thu. May 30, 2019 8:15 AM - 9:30 AM UTC | Poster Hall International Exhibition Hall8, Makuhari Messe_43

[M-AG38] Satellite Land Physical Processes Monitoring at Medium/High/Very High Resolution

convener:Jean-Claude Roger(University of Maryland College Park), Shinichi Sobue(Japan Aerospace Exploration Agency), Eric Vermote(NASA Goddard Space Flight Center)

We solicit papers on the land physical processes monitoring. In particular, it will include the inversion and use of land products from medium, high, and very high spatial resolution. For the last years, medium, high, and very high resolutions became a useful and a powerful toll for Earth studies. Topics of interest mainly include (not limited to):
- New developments for data processing, including atmospheric correction and cloud screening;
- Analysis and correction of directional effects in land surface reflectances;
- Use of time series of surface reflectances for land monitoring, including land cover classification and crop yield prediction (including data integration and data harmonization);
- Development and use of new vegetation indices (i.e. red edge) and other products for agriculture applications;
- Theoretical studies for sensors capabilities enhancements to future sensors at high/medium resolutions;
- Use of products in agricultural monitoring applications (such as crop area, crop type, crop growing, yield estimation and prediction, damage assessment);
- Agriculture monitoring algorithm description;
- Evaluation or validation of potential products with ground measurements, official statistics;
- International initiative to enhance Earth-Observing-based agricultural information.

Depending on outcome, we think about a special issue.

[MAG38-P01] Improving the AVHRR LTDR BRDF correction

*Jose Luis Villaescusa[1,2], Belen Franch[1,2], Jean-Claude Roger[1,2], Eric Vermote[2] (1.University of Maryland College Park, 2.NASA Goddard Space Flight Center)

[MAG38-P02] Winter wheat yield model based on remote sensing data

*Belen Franch[1,2], Eric Vermote[2,1], Sergii Skakun[1,2], Jean-Claude Roger[1,2], Inbal Becker-Reshef[1], Chris Justice[1] (1.Department of Geographical Sciences, University of Maryland, 2.NASA Goddard Space Flight Center)

[MAG38-P03] Agricultural monitoring from Optical and SAR data

*Andrés Eduardo Santamaría-Artigas[1,2], Sergii Skakun[1,2], Belen Franch[1,2], Jean-Claude Roger[1,2], Eric Vermote[2] (1.University of Maryland College Park, 2.NASA Goddard Space Flight Center)

[MAG38-P04] Eco-hydrological modeling using field-based and Earth Observations to assess water use efficiency and support agricultural water resources management

pierre Guillevic[2,1], *Jean-Claude Roger[1,2] (1.University of Maryland, College Park, USA, 2.NASA Goddard Space flight Center, Greenbelt, USA)

[MAG38-P05] Detecting and quantifying forest dynamics using SAR time-series data in Indonesia

*Pedro Rodriguez-Veiga[1,2,3], Narumasa Tsutsumida[3] (1.Centre for Landscape and Climate Research, University of Leicester, Leicester, UK, 2.NERC National Centre for Earth Observation (NCEO), Leicester, UK, 3.Graduate School of Global Environmental Studies, Kyoto University, Japan)

Improving the AVHRR LTDR BRDF correction

*Jose Luis Villaescusa[1,2], Belen Franch[1,2], Jean-Claude Roger[1,2], Eric Vermote[2]

1. University of Maryland College Park, 2. NASA Goddard Space Flight Center

The Advanced Very High Resolution Radiometer (AVHRR) sensors aboard the different NOAA satellites provide a unique global remote sensing dataset that ranges from the 1980s to the present. Using these data, the NASA funded Long Term Data Record (LTDR) project aims to develop a quality and consistent Climate Data Record (CDR) of AVHRR data with the use of the Moderate Resolution Imaging Spectrometer (MODIS) instrument as a reference. This product retrieves the BRDF corrected land surface reflectance using the VJB method (Vermote et al., 2009), which corrects the anisotropic effects by obtaining Volumetric (V) and Geometrical (R) parameters, defined in the Roujean model (Roujean et al., 1992), as a function of the Normalized Difference Vegetation Index (NDVI). Inaccuracies regarding the AVHRR atmospheric correction and calibration in the red band for the pre-MODIS era (1982-2000), propagate towards the surface reflectance’ s BRDF correction. However, with the use of the less noisy Near-Infrared (NIR) band we can reduce said errors by finding an empirical relationship between the red-NIR V and R parameters. This study aims to find said relationship using the MODIS sensor, which is an already established and accurate product (Justice et al., 2002; Liang et al., 2002), to then apply it to the noisy AVHRR data and reduce the BRDF errors in the red band.

Keywords: AVHRR, VJB, MODIS, BRDF, LTDR

©2019. Japan Geoscience Union. All Right Reserved.

Winter wheat yield model based on remote sensing data

*Belen Franch[1,2], Eric Vermote[2,1], Sergii Skakun[1,2], Jean-Claude Roger[1,2], Inbal Becker-Reshef[1], Chris Justice[1]

1. Department of Geographical Sciences, University of Maryland, 2. NASA Goddard Space Flight Center

Accurate and timely crop yield forecasts are critical for making informed agricultural policies and investments, as well as increasing market efficiency and stability. Earth observation data from space can contribute to agricultural monitoring, including crop yield assessment and forecasting. This work presents a new EO-based empirical winter wheat yield model. It is based on the un-mixing of the wheat signal from a coarse resolution EO data at 1 km by using yearly crop type masks to a pure wheat signal (100% of wheat within the pixel). *This wheat signal is used to calibrate the model using as inputs the seasonal amplitude and length of the Difference Vegetation Index (DVI) peak extracted from Moderate Resolution Imaging Spectroradiometer (MODIS) data and the average of the evaporative fraction (EF) 30 days after the peak. The three regressors proposed are focused on the reproduction stage of the wheat (DVI amplitude and length) and the grain filling process (EF 30-days average). The model is calibrated at subnational level using historical statistics from 2001 to 2016. In each administrative unit, a different calibration coefficient (based on all possible combination of the three regressors in a linear model) is selected depending on the statistical significance of each variable. The model was applied to estimate the national and subnational winter wheat yield in the United States, Ukraine, Russia and France from 2001 to 2017. At the subnational level the model shows very good performance with a coefficient of determination higher than 0.7 and Root Mean Square Error (RMSE) lower than 15%. At the national level the model provides a strong coefficient of determination higher than 0.8 and a RMSE lower than 8%, which demonstrates good performance of the models at this scale. Additionally, it was also able to capture low winter wheat yields during years with extreme weather events, for example 2002 in US and 2003 in Ukraine.*

Keywords: Yield model, MODIS , agriculture

©2019. Japan Geoscience Union. All Right Reserved.

Agricultural monitoring from Optical and SAR data

*Andrés Eduardo Santamaría-Artigas[1,2], Sergii Skakun[1,2], Belen Franch[1,2], Jean-Claude Roger[1,2], Eric Vermote[2]

1. University of Maryland College Park, 2. NASA Goddard Space Flight Center

Vegetation indices derived from optical remote sensing data are a valuable source of information for agricultural monitoring. However, cloud cover over some areas reduces the number of valid observations, which can difficult the detection of changes in crop condition. In this context, synthetic aperture radar (SAR) systems are an interesting alternative due to their low sensitivity to clouds. In this work, we analyze the relationship between SAR backscatter from Sentinel-1 and vegetation indices derived from the Harmonized Landsat-8 Sentinel-2 (HLS) product with data from the year 2017 over 6 land cover classes in Ukraine: Winter crops, summer crops, bare land, grasslands, forest, and water. Results show that SAR data from Sentinel-1 could be used to complement optical indices for certain land covers. In the case of winter crops (rapeseed and wheat), the ratio between Sigma-0 VV and VH polarization showed the highest relationship with the Normalized Difference Vegetation Index (NDVI) while for summer crops (maize, sugar beet, sunflower, and soybean) the highest relationship was shown by the Sigma-0 VH polarization and NDVI. Further work is being developed to exploit more complex SAR models which account for other variables that affect the backscatter signal such as soil moisture.

Keywords: agricultural monitoring, crop condition, synthetic aperture radar, HLS, normalized difference vegetation index

©2019. Japan Geoscience Union. All Right Reserved.

Eco-hydrological modeling using field-based and Earth Observations to assess water use efficiency and support agricultural water resources management

pierre Guillevic[2,1], *Jean-Claude Roger[1,2]

1. University of Maryland, College Park, USA, 2. NASA Goddard Space flight Center, Greenbelt, USA

The objective of this NASA project is to develop an integrated modeling platform using Earth Observations to simulate large-scale hydrological processes and food production in support of water use decision and agricultural policy. The decision tool will provide timely and relevant assessments of crop growth, agricultural water use and available water supply from local to regional scales, with the capability to predict the impact of different climate and water resources management scenarios on food production. The approach is based on the use of field and Earth observations to calibrate an eco-hydrological model, and climate simulations to forecast crop condition and yield through the crop season. The expected primary outcomes and results for stakeholders is potential best water management practices to improve water use efficiency and prevent excessive losses of water and nitrogen to the environment. These will be provided to in-country end-users within various relevant Ministries and Departments, in order to inform regional and national decisions. Changing precipitation patterns, droughts of increasing duration and severity and growing demand for food have significant implications on water management practices, spurring an increased need for irrigation in a sustainable manner and better monitoring of water resources for the agricultural sector in general. Understanding the context and water resource constraints that stakeholders and smallholder farmers face in climate sensitive regions is critical to target and understand the potential impact of water use management. We focus on a diverse set of regional pilot cases in Argentina, South Africa, Tanzania and the United States that are representative of a range of agricultural systems, water issues and climate impacts. The application is integrated in the GEOGLAM project, an existing widely-used web-based platform which will aid synthesizing the project outcomes and expert domain knowledge to provide timely and actionable water resources and crop condition information to assist local, regional and national water management decisions. At the end, the application will be interactive and will offer the end-user organizations the possibility to submit new water resource management scenarios online for impact evaluation.

Earth Observations are critical to characterize and monitor the different components of agricultural ecosystems and change (forests, croplands and marginal lands availability, for example) across temporal and spatial scales. Satellite data in the shortwave, thermal infrared and microwave spectral domains from US (MODIS, VIIRS, Landsat, SMAP) and European (Sentinel 1 and 2) sensors will be used to characterize changes in land surfaces and water use from 2000 to the present in support of agricultural planning decisions. In a research context, the potential of new satellite missions (i.e., ECOSTRESS, SWOT and SAOACOM) to derive surface hydrology information will be evaluated. The Agricultural Policy/Environmental eXtender (APEX) watershed model is proposed as the modeling tool to understand the biophysical and human-decision processes associated with the food-energy-water nexus. Model simulations will use climate data from the NASA Goddard Earth Observing System Model (GEOS-5) Atmosphere-Ocean General Circulation Model: MERRA-2 for simulation of past conditions and seasonal (6-month) forecasts for projections in the future. The study focus on large, key agricultural regions where agricultural ecosystems are vulnerable to demographic expansion and/or climate variability and change including drought and flood events.

©2019. Japan Geoscience Union. All Right Reserved.

Keywords: water resources, hydrologycal modelling , remote sensing

©2019. Japan Geoscience Union. All Right Reserved.

Detecting and quantifying forest dynamics using SAR time-series data in Indonesia

*Pedro Rodriguez-Veiga[1,2,3], Narumasa Tsutsumida[3]

1. Centre for Landscape and Climate Research, University of Leicester, Leicester, UK, 2. NERC National Centre for Earth Observation (NCEO), Leicester, UK, 3. Graduate School of Global Environmental Studies, Kyoto University, Japan

Satellite Earth Observation (EO) data allows the generation of forest disturbance maps that can improve greenhouse gas (GHG) monitoring at local and national scales, and provide information that can be used for land use planning and management. Mapping forest biomass stocks, deforestation, forest degradation and enhancement is crucial in order to determine the loss of carbon stocks due to disturbances (e.g. deforestation, fires) or the gain due to new forest or growth. Time-series observations identify decreasing or increasing trends of aboveground biomass carbon, and separate anthropogenic related changes from seasonal changes of vegetation. This is important for understanding the terrestrial carbon cycle and for supporting better forest management and policies. This study uses time-series data from L-band Synthetic Aperture Radar (SAR) JAXA’s ALOS PALSAR and ALOS-2 PALSAR-2 to quantify carbon loss and gain trajectories (emission / sequestration) of existing forests in West Java (Indonesia).

Keywords: deforestation, SAR, time-series, forest dynamics

©2019. Japan Geoscience Union. All Right Reserved.

[E] Poster | M (Multidisciplinary and Interdisciplinary)：M-AG Applied Geosciences

Thu. May 30, 2019 3:30 PM - 5:00 PM JST | Thu. May 30, 2019 6:30 AM - 8:00 AM UTC | Poster Hall International Exhibition Hall8, Makuhari Messe_25

[M-AG40] CTBT IMS Technologies for Detecting Nuclear Explosion and Their Applications to Earth Science

convener:Nurcan Meral Ozel(Comprehensive Nuclear-Test-Ban Treaty Organization), Hiroyuki Matsumoto(Japan Agency for Marine-Earth Science and Technology), Yosuke Naoi(Japan Atomic Energy Agency)

The Comprehensive Nuclear-Test-Ban Treaty Organization (CTBTO) was founded in 1996 in response to the adaption of the Treaty in 1996 by the United Nations General Assembly, which bans nuclear explosions on the Earth's surface, in the atmosphere, underwater and underground. The Treaty has a unique and comprehensive verification regime to make sure that no nuclear explosion goes undetected. The regime is supported by International Monitoring Systems (IMS) composed of the four state-of-art technologies; 1) Seismic, 2) Hydroacoustic, 3) Infrasound, and 4) Radionuclide, by the International Data Centre (IDC), and by the On-Site Inspections (OSI).
IMS will, when complete, consists of 337 facilities worldwide to monitor the planet for signs of nuclear explosion. Around 90 % of the facilities are in operation and sending the data to the IDC in Vienna, Austria.
The huge amount of data collected by the stations can be used for other purposes such as civil and scientific applications in addition to detecting nuclear explosions. They can provide Tsunami Warning centres with near real-time information about an underwater earthquake. During the Fukushima Daiichi Power Plant accident, in March 2011, the IMS network's radionuclide stations tracked the dispersion of radioactivity on a global scale. The data could also help better understand the oceans, volcanos, climate change, the movement of marine mammals, and many other issues.
This session will provide the overview of CTBTO and its IMS, the scientific discussion on each technology, and its outcomes. The session welcomes young scientists and engineers who are interested in four IMS technologies.

[MAG40-P01] Overview of the Japanese National Data Centre-1 (NDC-1)

*RYOHEI EMURA[1], Takayuki Otsu[1], Toyomi Sakamoto[1], Soshi Iwata[1], Takanari Fujii[1], Mami Nogami[1], Makiko Iwakuni[1], Masashi Motohashi[1] (1.Japan Weather Association)

[MAG40-P02] Challenging to utilize the infrasound technologies for civil and science application

*Masashi Motohashi[1], Nobuo Arai[2], Takayuki Otsu[1], Mami Nogami[1], Makiko Iwakuni[1], Ryohei Emura[1] (1.Japan Weather Association, 2.Disaster Mitigation Research Center, Nagoya Unicersity)

[MAG40-P03] CTBT IMS hydroacoustic signal detections from the Ioto volcanic island in the northwest Pacific Ocean

*Hiroyuki Matsumoto[1,2], Mario Zampolli[1], Georgios Haralabus[1], Jerry Stanley[1], James Mattila[1], Nurcan Meral Ozel[1] (1.Comprehensive Nuclear-Test-Ban Treaty Organization (CTBTO), 2.Japan Agency for Marine-Earth Science and Technology (JAMSTEC))

[MAG40-P04] Installation of a floating hydrophone system within the SOFAR channel

*Hiroko Sugioka[1], Masayuki Obayashi[2] (1.Kobe University, 2.JAMSTEC)

[MAG40-P05] Fin whale signals observed at S-net seismic stations

*Takeshi Nakamura[1], Ryoichi Iwase[2] (1.National Research Institute for Earth Science and Disaster Resilience, 2.Japan Agency for Marine-Earth Science and Technology)

[MAG40-P06] Implementation of integrated observation from seafloor through atmosphere – past, current, and future plans

*Keisuke Ariyoshi[1], Akira Nagano[1], Hiroyuki Matsumoto[1], Nurcan Meral Ozel[2] (1.Japan Agency for Marine-Earth Science and Technology, 2.Comprehensive Nuclear-Test-Ban Treaty Organization)

Overview of the Japanese National Data Centre-1 (NDC-1)

*RYOHEI EMURA[1], Takayuki Otsu[1], Toyomi Sakamoto[1], Soshi Iwata[1], Takanari Fujii[1], Mami Nogami[1], Makiko Iwakuni[1], Masashi Motohashi[1]

1. Japan Weather Association

Japan Weather Association (JWA) is working as the Comprehensive Nuclear-Test-Ban Treaty (CTBT) National Data Centre-1 (NDC-1) of Japan which is in charge of analysis on waveform data, operation and maintenance of seismic and infrasound stations in Japan. There are two main roles of NDC-1: 1: technical adviser to the national authority (MOFA) from the view point of seismic and infrasound analysis, and 2: station operator of IMS stations (PS22, AS51-AS55 and IS30). And there are three main activities of NDC-1 as technical adviser: 1: if the suspicious event would occur, we would try to clarify its characteristics and report its results to the MOFA via the secretariat, 2: we sometimes do 1-week integrated operational exercise hosted by the secretariat on the assumption that the situation would be, and 3: we are paying efforts to improve our analytical capability of SHI data and explanation capability by using the national exercises.

This poster introduces the integrated operational exercise and the event discrimination analysis results of the 6th DPRK nuclear test as of the real analysis results in particular.

The integrated operational exercise is conducted by NDCs, integrating the data and analysis addressed by NDCs, and reporting to the CTBT National Operating System of Japan. These exercises have been implemented 27 times since 2009 and 30areas were selected for regions and countries. And our event discrimination analysis takes mainly three methods: 1: regional P/S ratio, 2: P/S spectral ratio and 3: mb: Ms.

Keywords: CTBT, National Data Centre, seismic, infrasound, waveform analysis, event discrimination analysis

©2019. Japan Geoscience Union. All Right Reserved.

Challenging to utilize the infrasound technologies for civil and science application

*Masashi Motohashi[1], Nobuo Arai[2], Takayuki Otsu[1], Mami Nogami[1], Makiko Iwakuni[1], Ryohei Emura[1]

1. Japan Weather Association, 2. Disaster Mitigation Research Center, Nagoya Unicersity

Japan Weather Association (JWA) is working as the Comprehensive Nuclear-Test-Ban Treaty (CTBT) National Data Centre-1 (NDC-1) of Japan which is in charge of analysis on waveform data, operation and maintenance of infrasound and seismic stations in Japan.

We observed infrasonic signals two times from underground nuclear test in DPRK. From the perspective of nuclear test monitoring, it is important to analyze and study the infrasonic signals from a variety of natural phenomena to discriminate the signal from explosion. On the other hand, that kind of studies are also important for civil and science application of infrasound technologies. We also observed infrasound from large tsunami at the time of 2011 off the Pacific coast of Tohoku Earthquake. If the signals from such hazardous phenomena can be detected immediately, it will be very helpful to alert the occurrence of disaster or approach of hazardous phenomena.

This triggered us to build our own observation network in Japan. We are challenging to utilize the infrasound technologies for civil and science application as well as nuclear test monitoring.

Keywords: Barometer, Infrasound, CTBT

©2019. Japan Geoscience Union. All Right Reserved.

CTBT IMS hydroacoustic signal detections from the Ioto volcanic island in the northwest Pacific Ocean

*Hiroyuki Matsumoto[1,2], Mario Zampolli[1], Georgios Haralabus[1], Jerry Stanley[1], James Mattila[1], Nurcan Meral Ozel[1]

1. Comprehensive Nuclear-Test-Ban Treaty Organization (CTBTO), 2. Japan Agency for Marine-Earth Science and Technology (JAMSTEC)

In-situ observation in terms of seismicity suggested that the volcanic activity of Ioto (formerly Iwojima), a volcanic island offshore Japan in the northwest Pacific Ocean increased in early September in 2018. Discolored waters and a splash were confirmed in the nearshore by a local flyover observation. Although these visual signs evidenced a connection between undersea eruptions and recorded seismic activity, there still remained uncertainty as to what portion of the *in-situ* recorded seismic activity was associated with volcanic tremors vs. undersea eruptive events.
During the same period, a large number of underwater acoustic (hydroacoustic) signals were recorded by the Comprehensive Nuclear-Test-Ban Treaty’s (CTBT) International Monitoring System (IMS) hydroacoustic (HA) station HA11 Wake Island. A set of three hydrophone sensors forming a triplet makes it possible to compute the back-azimuth uniquely for wave packets with a good signal-to-noise ratio. We analyzed the data of the IMS hydrophone triplets during the month of September 2018 and compared them with *in-situ* seismic observations in Ioto for the same period.
The IMS hydrophone triplet data made it possible to discriminate the hydroacoustic signals associated with the Ioto volcanic activity. The direction-of-arrival (DOA) was estimated during the entire period of relatively high volcanic activity using cross-correlation analysis. The arrivals from Ioto at the IMS HA station and the *in-situ* observations showed good correlation. The present study suggests that two-thirds of the arrivals of hydroacoustec signals were associated with volcanic tremors and one-third with the undersea eruptions.

Keywords: Internataional Monitoring System (IMS), Hydrophone triplet, Ioto

©2019. Japan Geoscience Union. All Right Reserved.

Installation of a floating hydrophone system within the SOFAR channel

*Hiroko Sugioka[1], Masayuki Obayashi[2]

1. Kobe University, 2. JAMSTEC

Unequal geographical data coverage continues to fundamentally limit the quality of tomographic reconstructions of seismic wave speeds in the interior of the Earth. Only at great cost can geophysicists overcome the difficulties of placing seismographs on the two thirds of the Earth’ s surface that is covered by oceans. The lack of spatial data coverage strongly hampers the determination of the structure of the Earth in the uncovered regions. Therefore, three-dimensional Earth models are marked by blank spots in areas where little or no information can be obtained. Improving this problem requires the observation of seismic waves in the oceans. Ocean bottom seismometers are capable of addressing the coverage gap, but they are expensive to manufacture and deploy using vessels.

Oceanographers had designed robotic floating instruments, floats that spend their lives at depth but surface periodically, using a pump and bladder, to make temperature and salinity profile measurements (the large-scale international Argo project). Such low-cost Sounding Oceanographic Lagrangian Observers (SOLO) (Davis et al., 2001) could be equipped with a hydrophone to record water pressure variations induced by compressional waves. Such a floating seismometer would surface upon detection of a useful seismic event, determine a GPS location, and transmit the waveforms to a satellite, which is nicknamed MERMAID for ‘mobile earthquake recorder in marine areas by independent divers’. The great promise of this technology has been demonstrated since the first voyage in 2003, clearly illustrates its contributions to global seismology.

We installed five MERMAID floats in the South Pacific Ocean in late December of 2018 to early January of 2019 during the MR18-06 Leg 1 cruise from Japan to Chile using the R/V Mirai of JAMSTEC under an international project of SPPIM (South Pacific Plume Imaging with MERMAIDs). The launching locations for MERMAIDs are (01-42.256N,146-12.472W), (03-19.696S, 139-31.973W), (15-55.626S, 120-07.688W), (18-31.285S, 114-57.378W) and (20-59.832S, 109-59.513W), respectively. All floats have been drifting to almost west since the deployment as recording to transfer the land at sea surface every 10 days. So far, MERMAID detected several seismic events, for example, the Mw 6.8 Brazil deep focus earthquake at depth of 575 km on January 5. MERMAID recorded a clear incoming P-wave whose precise arrival time can be determined to within a fraction of a second. In addition to recording teleseismic P-waves, they would pick up hydroacoustic phases (T-waves) trapped waves propagating in the SOFAR (Sound Fixing and Ranging) channel. They might be complementary to the global seismic network including CTBTO stations to recognize unknown enigmatic events.

Keywords: SOFAR channel, Hydroacoustic waves

©2019. Japan Geoscience Union. All Right Reserved.

Fin whale signals observed at S-net seismic stations

*Takeshi Nakamura[1], Ryoichi Iwase[2]

1. National Research Institute for Earth Science and Disaster Resilience, 2. Japan Agency for Marine-Earth Science and Technology

Real-time earthquake and tsunami seafloor station network called “S-net” (Seafloor observation network for earthquakes and tsunamis along the Japan Trench) was developed by National Research Institute for Earth Science and Disaster Resilience (NIED) in water depths of 100-7,830 m in northeastern Japan. The network consists of 150 observation stations off Boso to Kushiro and Aomori areas (Kanazawa et al., 2016; Uehira et al. 2016; Mochizuki et al., 2016). Each station has seismic sensors and pressure gauges to observe broadband signals from seismic event and tsunami. In this study, we show fin whale signals detected from the S-net data and present the seasonal variation of the signals and the migratory behavior of the whales.

We analyzed seismic station data of S-net from 2016 to 2018. We found characteristic signals with the spectral peak in the frequency bands of 15-25 Hz. One of remarkable features in the signals is that the band width that can be identified as signal is limited in a very narrow range; the signal level is very low or below the noise level in the frequency bands of less than 10 Hz that are typical bands in seismic waves and T-phases. Another feature is that the signals have a short duration of about 1 second and are repeatedly found at regular intervals of several tens of seconds. These are consistent with the features of acoustic signals from fin whales as found in observation data at IMS hydroacoustic stations (e.g., Lawrence, 2004) and also as shown in previous studies such as Iwase (2014) and Sugioka et al. (2015) that analyzed seafloor station data off the Kushiro-Tokachi cable sensor system. We thus assume that the characteristic signals observed at S-net stations are ones associated with fin whale activities. Most of the signals were detected at stations off Kushiro and Aomori areas in cold winter. The signals were also detected at stations deployed in the outer rise area. We suppose that integrated scientific studies across marine biology to geophysics using S-net data could contribute to developing our understandings of various signal sources observed in seafloor areas and of ecological behavior of marine mammals and also to real-time monitoring of their activities and safe navigation of ships by the monitoring.

Keywords: seafloor observation, S-net, fin whale

©2019. Japan Geoscience Union. All Right Reserved.

Implementation of integrated observation from seafloor through atmosphere –past, current, and future plans

*Keisuke Ariyoshi[1], Akira Nagano[1], Hiroyuki Matsumoto[1], Nurcan Meral Ozel[2]

1. Japan Agency for Marine-Earth Science and Technology, 2. Comprehensive Nuclear-Test-Ban Treaty Organization

The authors have challenged to promote our understandings of global dynamics associated with ocean physics particularly by the simultaneous observation through the seafloor to the atmosphere. We have initiated the total station using both D/V ‘Chikyu’ and the seafloor observatory network ‘DONET’ in the Nankai trough. This total station has clarified the Kuroshio current variation in this region by using both the ambient pressure at DONET and the surface current measurement at D/V ‘Chikyu’. This observation performed at the point where D/V ‘Chikyu’ was in operation for a few months, and therefore there still remained some difficulties to extend to areal and long-term observation. Now, we try to extend our proposed total station to the nearshore network from the point of view of not only scientific application but also civil use for natural disaster mitigation such as earthquake, tsunami, and high-tide caused by storm. On the other hand, a global permanent observation network has been developed and operated by the Comprehensive Nuclear-Test-Ban Treaty Organization (CTBTO) since the 2000s as the International Monitoring System (IMS) regime for the real-time monitoring of nuclear explosion’s test in the underground, underwater, and above surface up to the atmosphere. Four technologies with over 330 stations will cover the entire Earth after certification of all of stations. Three categories of geophysical observations of four technologies such as seismic (50 primary and 120 auxiliary stations), infrasound (60 stations), and hydro-acoustic (11 stations) network operated globally may be beneficial and of interest for our proposed integrated observations. In the presentation, we introduce the preliminary results on our integrated observation of total stations and our drawing blue print of future plans.

Keywords: seismic observation, seafloor cabled network, disaster mitigation

©2019. Japan Geoscience Union. All Right Reserved.

[E] Poster | M (Multidisciplinary and Interdisciplinary)：M-AG Applied Geosciences

Thu. May 30, 2019 5:15 PM - 6:30 PM JST | Thu. May 30, 2019 8:15 AM - 9:30 AM UTC | Poster Hall International Exhibition Hall8, Makuhari Messe_45

[M-AG40] CTBT IMS Technologies for Detecting Nuclear Explosion and Their Applications to Earth Science

convener:Nurcan Meral Ozel(Comprehensive Nuclear-Test-Ban Treaty Organization), Hiroyuki Matsumoto(Japan Agency for Marine-Earth Science and Technology), Yosuke Naoi(Japan Atomic Energy Agency)

The Comprehensive Nuclear-Test-Ban Treaty Organization (CTBTO) was founded in 1996 in response to the adaption of the Treaty in 1996 by the United Nations General Assembly, which bans nuclear explosions on the Earth's surface, in the atmosphere, underwater and underground. The Treaty has a unique and comprehensive verification regime to make sure that no nuclear explosion goes undetected. The regime is supported by International Monitoring Systems (IMS) composed of the four state-of-art technologies; 1) Seismic, 2) Hydroacoustic, 3) Infrasound, and 4) Radionuclide, by the International Data Centre (IDC), and by the On-Site Inspections (OSI).
IMS will, when complete, consists of 337 facilities worldwide to monitor the planet for signs of nuclear explosion. Around 90 % of the facilities are in operation and sending the data to the IDC in Vienna, Austria.
The huge amount of data collected by the stations can be used for other purposes such as civil and scientific applications in addition to detecting nuclear explosions. They can provide Tsunami Warning centres with near real-time information about an underwater earthquake. During the Fukushima Daiichi Power Plant accident, in March 2011, the IMS network's radionuclide stations tracked the dispersion of radioactivity on a global scale. The data could also help better understand the oceans, volcanos, climate change, the movement of marine mammals, and many other issues.
This session will provide the overview of CTBTO and its IMS, the scientific discussion on each technology, and its outcomes. The session welcomes young scientists and engineers who are interested in four IMS technologies.

[MAG40-P01] Overview of the Japanese National Data Centre-1 (NDC-1)

*RYOHEI EMURA[1], Takayuki Otsu[1], Toyomi Sakamoto[1], Soshi Iwata[1], Takanari Fujii[1], Mami Nogami[1], Makiko Iwakuni[1], Masashi Motohashi[1] (1.Japan Weather Association)

[MAG40-P02] Challenging to utilize the infrasound technologies for civil and science application

*Masashi Motohashi[1], Nobuo Arai[2], Takayuki Otsu[1], Mami Nogami[1], Makiko Iwakuni[1], Ryohei Emura[1] (1.Japan Weather Association, 2.Disaster Mitigation Research Center, Nagoya Unicersity)

[MAG40-P03] CTBT IMS hydroacoustic signal detections from the Ioto volcanic island in the northwest Pacific Ocean

*Hiroyuki Matsumoto[1,2], Mario Zampolli[1], Georgios Haralabus[1], Jerry Stanley[1], James Mattila[1], Nurcan Meral Ozel[1] (1.Comprehensive Nuclear-Test-Ban Treaty Organization (CTBTO), 2.Japan Agency for Marine-Earth Science and Technology (JAMSTEC))

[MAG40-P04] Installation of a floating hydrophone system within the SOFAR channel

*Hiroko Sugioka[1], Masayuki Obayashi[2] (1.Kobe University, 2.JAMSTEC)

[MAG40-P05] Fin whale signals observed at S-net seismic stations

*Takeshi Nakamura[1], Ryoichi Iwase[2] (1.National Research Institute for Earth Science and Disaster Resilience, 2.Japan Agency for Marine-Earth Science and Technology)

[MAG40-P06] Implementation of integrated observation from seafloor through atmosphere – past, current, and future plans

*Keisuke Ariyoshi[1], Akira Nagano[1], Hiroyuki Matsumoto[1], Nurcan Meral Ozel[2] (1.Japan Agency for Marine-Earth Science and Technology, 2.Comprehensive Nuclear-Test-Ban Treaty Organization)

Overview of the Japanese National Data Centre-1 (NDC-1)

*RYOHEI EMURA[1], Takayuki Otsu[1], Toyomi Sakamoto[1], Soshi Iwata[1], Takanari Fujii[1], Mami Nogami[1], Makiko Iwakuni[1], Masashi Motohashi[1]

1. Japan Weather Association

Japan Weather Association (JWA) is working as the Comprehensive Nuclear-Test-Ban Treaty (CTBT) National Data Centre-1 (NDC-1) of Japan which is in charge of analysis on waveform data, operation and maintenance of seismic and infrasound stations in Japan. There are two main roles of NDC-1: 1: technical adviser to the national authority (MOFA) from the view point of seismic and infrasound analysis, and 2: station operator of IMS stations (PS22, AS51-AS55 and IS30). And there are three main activities of NDC-1 as technical adviser: 1: if the suspicious event would occur, we would try to clarify its characteristics and report its results to the MOFA via the secretariat, 2: we sometimes do 1-week integrated operational exercise hosted by the secretariat on the assumption that the situation would be, and 3: we are paying efforts to improve our analytical capability of SHI data and explanation capability by using the national exercises.

This poster introduces the integrated operational exercise and the event discrimination analysis results of the 6th DPRK nuclear test as of the real analysis results in particular.

The integrated operational exercise is conducted by NDCs, integrating the data and analysis addressed by NDCs, and reporting to the CTBT National Operating System of Japan. These exercises have been implemented 27 times since 2009 and 30areas were selected for regions and countries. And our event discrimination analysis takes mainly three methods: 1: regional P/S ratio, 2: P/S spectral ratio and 3: mb: Ms.

Keywords: CTBT, National Data Centre, seismic, infrasound, waveform analysis, event discrimination analysis

©2019. Japan Geoscience Union. All Right Reserved.

Challenging to utilize the infrasound technologies for civil and science application

*Masashi Motohashi[1], Nobuo Arai[2], Takayuki Otsu[1], Mami Nogami[1], Makiko Iwakuni[1], Ryohei Emura[1]

1. Japan Weather Association, 2. Disaster Mitigation Research Center, Nagoya Unicersity

Japan Weather Association (JWA) is working as the Comprehensive Nuclear-Test-Ban Treaty (CTBT) National Data Centre-1 (NDC-1) of Japan which is in charge of analysis on waveform data, operation and maintenance of infrasound and seismic stations in Japan.

We observed infrasonic signals two times from underground nuclear test in DPRK. From the perspective of nuclear test monitoring, it is important to analyze and study the infrasonic signals from a variety of natural phenomena to discriminate the signal from explosion. On the other hand, that kind of studies are also important for civil and science application of infrasound technologies. We also observed infrasound from large tsunami at the time of 2011 off the Pacific coast of Tohoku Earthquake. If the signals from such hazardous phenomena can be detected immediately, it will be very helpful to alert the occurrence of disaster or approach of hazardous phenomena.

This triggered us to build our own observation network in Japan. We are challenging to utilize the infrasound technologies for civil and science application as well as nuclear test monitoring.

Keywords: Barometer, Infrasound, CTBT

©2019. Japan Geoscience Union. All Right Reserved.

CTBT IMS hydroacoustic signal detections from the Ioto volcanic island in the northwest Pacific Ocean

*Hiroyuki Matsumoto[1,2], Mario Zampolli[1], Georgios Haralabus[1], Jerry Stanley[1], James Mattila[1], Nurcan Meral Ozel[1]

1. Comprehensive Nuclear-Test-Ban Treaty Organization (CTBTO), 2. Japan Agency for Marine-Earth Science and Technology (JAMSTEC)

In-situ observation in terms of seismicity suggested that the volcanic activity of Ioto (formerly Iwojima), a volcanic island offshore Japan in the northwest Pacific Ocean increased in early September in 2018. Discolored waters and a splash were confirmed in the nearshore by a local flyover observation. Although these visual signs evidenced a connection between undersea eruptions and recorded seismic activity, there still remained uncertainty as to what portion of the *in-situ* recorded seismic activity was associated with volcanic tremors vs. undersea eruptive events.
During the same period, a large number of underwater acoustic (hydroacoustic) signals were recorded by the Comprehensive Nuclear-Test-Ban Treaty’s (CTBT) International Monitoring System (IMS) hydroacoustic (HA) station HA11 Wake Island. A set of three hydrophone sensors forming a triplet makes it possible to compute the back-azimuth uniquely for wave packets with a good signal-to-noise ratio. We analyzed the data of the IMS hydrophone triplets during the month of September 2018 and compared them with *in-situ* seismic observations in Ioto for the same period.
The IMS hydrophone triplet data made it possible to discriminate the hydroacoustic signals associated with the Ioto volcanic activity. The direction-of-arrival (DOA) was estimated during the entire period of relatively high volcanic activity using cross-correlation analysis. The arrivals from Ioto at the IMS HA station and the *in-situ* observations showed good correlation. The present study suggests that two-thirds of the arrivals of hydroacoustec signals were associated with volcanic tremors and one-third with the undersea eruptions.

Keywords: Internataional Monitoring System (IMS), Hydrophone triplet, Ioto

©2019. Japan Geoscience Union. All Right Reserved.

Installation of a floating hydrophone system within the SOFAR channel

*Hiroko Sugioka[1], Masayuki Obayashi[2]

1. Kobe University, 2. JAMSTEC

Unequal geographical data coverage continues to fundamentally limit the quality of tomographic reconstructions of seismic wave speeds in the interior of the Earth. Only at great cost can geophysicists overcome the difficulties of placing seismographs on the two thirds of the Earth’ s surface that is covered by oceans. The lack of spatial data coverage strongly hampers the determination of the structure of the Earth in the uncovered regions. Therefore, three-dimensional Earth models are marked by blank spots in areas where little or no information can be obtained. Improving this problem requires the observation of seismic waves in the oceans. Ocean bottom seismometers are capable of addressing the coverage gap, but they are expensive to manufacture and deploy using vessels.

Oceanographers had designed robotic floating instruments, floats that spend their lives at depth but surface periodically, using a pump and bladder, to make temperature and salinity profile measurements (the large-scale international Argo project). Such low-cost Sounding Oceanographic Lagrangian Observers (SOLO) (Davis et al., 2001) could be equipped with a hydrophone to record water pressure variations induced by compressional waves. Such a floating seismometer would surface upon detection of a useful seismic event, determine a GPS location, and transmit the waveforms to a satellite, which is nicknamed MERMAID for ‘mobile earthquake recorder in marine areas by independent divers’. The great promise of this technology has been demonstrated since the first voyage in 2003, clearly illustrates its contributions to global seismology.

We installed five MERMAID floats in the South Pacific Ocean in late December of 2018 to early January of 2019 during the MR18-06 Leg 1 cruise from Japan to Chile using the R/V Mirai of JAMSTEC under an international project of SPPIM (South Pacific Plume Imaging with MERMAIDs). The launching locations for MERMAIDs are (01-42.256N,146-12.472W), (03-19.696S, 139-31.973W), (15-55.626S, 120-07.688W), (18-31.285S, 114-57.378W) and (20-59.832S, 109-59.513W), respectively. All floats have been drifting to almost west since the deployment as recording to transfer the land at sea surface every 10 days. So far, MERMAID detected several seismic events, for example, the Mw 6.8 Brazil deep focus earthquake at depth of 575 km on January 5. MERMAID recorded a clear incoming P-wave whose precise arrival time can be determined to within a fraction of a second. In addition to recording teleseismic P-waves, they would pick up hydroacoustic phases (T-waves) trapped waves propagating in the SOFAR (Sound Fixing and Ranging) channel. They might be complementary to the global seismic network including CTBTO stations to recognize unknown enigmatic events.

Keywords: SOFAR channel, Hydroacoustic waves

©2019. Japan Geoscience Union. All Right Reserved.

Fin whale signals observed at S-net seismic stations

*Takeshi Nakamura[1], Ryoichi Iwase[2]

1. National Research Institute for Earth Science and Disaster Resilience, 2. Japan Agency for Marine-Earth Science and Technology

Real-time earthquake and tsunami seafloor station network called “S-net” (Seafloor observation network for earthquakes and tsunamis along the Japan Trench) was developed by National Research Institute for Earth Science and Disaster Resilience (NIED) in water depths of 100-7,830 m in northeastern Japan. The network consists of 150 observation stations off Boso to Kushiro and Aomori areas (Kanazawa et al., 2016; Uehira et al. 2016; Mochizuki et al., 2016). Each station has seismic sensors and pressure gauges to observe broadband signals from seismic event and tsunami. In this study, we show fin whale signals detected from the S-net data and present the seasonal variation of the signals and the migratory behavior of the whales.

We analyzed seismic station data of S-net from 2016 to 2018. We found characteristic signals with the spectral peak in the frequency bands of 15-25 Hz. One of remarkable features in the signals is that the band width that can be identified as signal is limited in a very narrow range; the signal level is very low or below the noise level in the frequency bands of less than 10 Hz that are typical bands in seismic waves and T-phases. Another feature is that the signals have a short duration of about 1 second and are repeatedly found at regular intervals of several tens of seconds. These are consistent with the features of acoustic signals from fin whales as found in observation data at IMS hydroacoustic stations (e.g., Lawrence, 2004) and also as shown in previous studies such as Iwase (2014) and Sugioka et al. (2015) that analyzed seafloor station data off the Kushiro-Tokachi cable sensor system. We thus assume that the characteristic signals observed at S-net stations are ones associated with fin whale activities. Most of the signals were detected at stations off Kushiro and Aomori areas in cold winter. The signals were also detected at stations deployed in the outer rise area. We suppose that integrated scientific studies across marine biology to geophysics using S-net data could contribute to developing our understandings of various signal sources observed in seafloor areas and of ecological behavior of marine mammals and also to real-time monitoring of their activities and safe navigation of ships by the monitoring.

Keywords: seafloor observation, S-net, fin whale

©2019. Japan Geoscience Union. All Right Reserved.

Implementation of integrated observation from seafloor through atmosphere –past, current, and future plans

*Keisuke Ariyoshi[1], Akira Nagano[1], Hiroyuki Matsumoto[1], Nurcan Meral Ozel[2]

1. Japan Agency for Marine-Earth Science and Technology, 2. Comprehensive Nuclear-Test-Ban Treaty Organization

The authors have challenged to promote our understandings of global dynamics associated with ocean physics particularly by the simultaneous observation through the seafloor to the atmosphere. We have initiated the total station using both D/V ‘Chikyu’ and the seafloor observatory network ‘DONET’ in the Nankai trough. This total station has clarified the Kuroshio current variation in this region by using both the ambient pressure at DONET and the surface current measurement at D/V ‘Chikyu’. This observation performed at the point where D/V ‘Chikyu’ was in operation for a few months, and therefore there still remained some difficulties to extend to areal and long-term observation. Now, we try to extend our proposed total station to the nearshore network from the point of view of not only scientific application but also civil use for natural disaster mitigation such as earthquake, tsunami, and high-tide caused by storm. On the other hand, a global permanent observation network has been developed and operated by the Comprehensive Nuclear-Test-Ban Treaty Organization (CTBTO) since the 2000s as the International Monitoring System (IMS) regime for the real-time monitoring of nuclear explosion’s test in the underground, underwater, and above surface up to the atmosphere. Four technologies with over 330 stations will cover the entire Earth after certification of all of stations. Three categories of geophysical observations of four technologies such as seismic (50 primary and 120 auxiliary stations), infrasound (60 stations), and hydro-acoustic (11 stations) network operated globally may be beneficial and of interest for our proposed integrated observations. In the presentation, we introduce the preliminary results on our integrated observation of total stations and our drawing blue print of future plans.

Keywords: seismic observation, seafloor cabled network, disaster mitigation

©2019. Japan Geoscience Union. All Right Reserved.